Every Decker book is accompanied by a CD-ROM.

BC Decker Inc is committed to providing high-quality electronic publications that complement traditional information and learning methods.

Physiologic Basis of Respiratory Disease is accompanied by a dual-platform CD-ROM, which features the complete text and full-color images. The fully searchable PDF files facilitate the exploration of need-to-know information. The disc is also ideal for printing pertinent information necessary for patient education.

The book and disc are sold only as a package; neither are available independently, and no prices are available for the items individually. We trust you will find the book/CD package invaluable and invite your comments and suggestions.

Access information. Acquire knowledge. Please visit www.bcdecker.com for a complete list of titles in your discipline. Our innovative approach to meeting the informational needs of healthcare professionals ensures that Decker products belong in your library and on your computer.

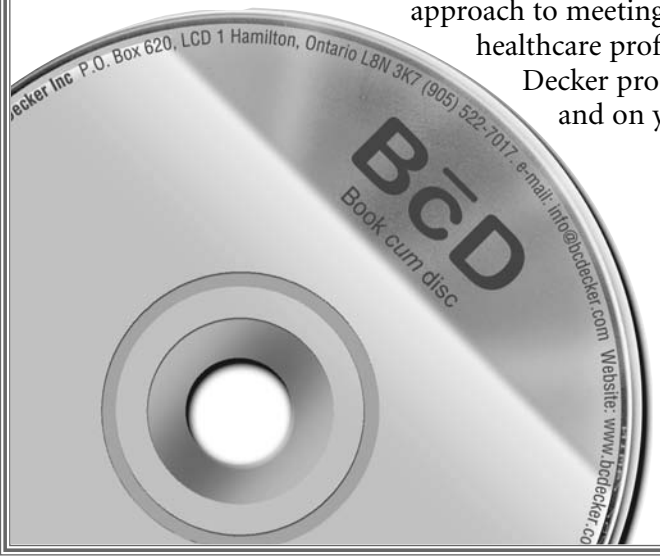

Brian C. Decker
CEO and Publisher

BC Decker

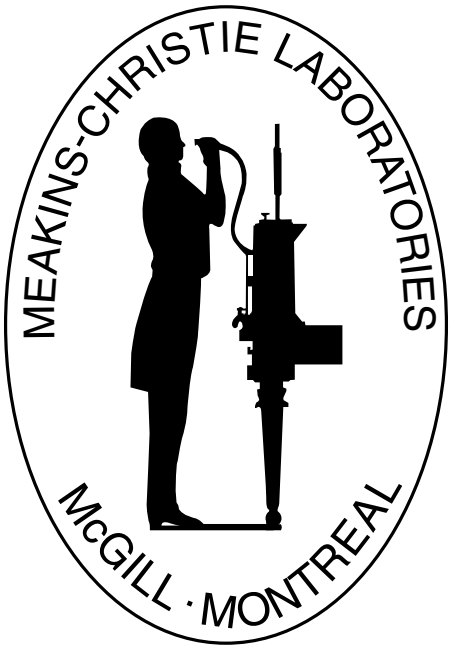
MEAKINS-CHRISTIE LABORATORIES
McGILL · MONTREAL

PHYSIOLOGIC BASIS *of* RESPIRATORY DISEASE

Qutayba Hamid, MD, PhD, MRCP, FRCPath
Professor of Medicine
Department of Medicine
McGill University
Montreal, Quebec

Joanne Shannon, MD
Postdoctoral Fellow
Meakins-Christie Laboratories
McGill University
Montreal, Quebec

James Martin, MD, DSc
Professor of Medicine
Department of Medicine
McGill University
Montreal, Quebec

2005
BC Decker Inc
Hamilton

Exit

BC Decker Inc
P.O. Box 620, L.C.D. 1
Hamilton, Ontario L8N 3K7
Tel: 905-522-7017; 800-568-7281
Fax: 905-522-7839; 888-311-4987
E-mail: info@bcdecker.com
www.bcdecker.com

05 06 07 08/WPC/9 8 7 6 5 4 3 2 1

ISBN 1-55009-236-7
Printed in the United States of America

Sales and Distribution

United States
BC Decker Inc
P.O. Box 785
Lewiston, NY 14092-0785
Tel: 905-522-7017; 800-568-7281
Fax: 905-522-7839; 888-311-4987
E-mail: info@bcdecker.com
www.bcdecker.com

Canada
BC Decker Inc
20 Hughson Street South
P.O. Box 620, LCD 1
Hamilton, Ontario L8N 3K7
Tel: 905-522-7017; 800-568-7281
Fax: 905-522-7839; 888-311-4987
E-mail: info@bcdecker.com
www.bcdecker.com

Foreign Rights
John Scott & Company
International Publishers' Agency
P.O. Box 878
Kimberton, PA 19442
Tel: 610-827-1640
Fax: 610-827-1671
E-mail: jsco@voicenet.com

Japan
Igaku-Shoin Ltd.
Foreign Publications Department
3-24-17 Hongo
Bunkyo-ku, Tokyo, Japan 113-8719
Tel: 3 3817 5680
Fax: 3 3815 6776
E-mail: fd@igaku-shoin.co.jp

UK, *Europe, Scandinavia, Middle East*
Elsevier Science
Customer Service Department
Foots Cray High Street
Sidcup, Kent
DA14 5HP, UK
Tel: 44 (0) 208 308 5760
Fax: 44 (0) 181 308 5702
E-mail: cservice@harcourt.com

Singapore, Malaysia, Thailand, Philippines, Indonesia, Vietnam, Pacific Rim, Korea
Elsevier Science Asia
583 Orchard Road
#09/01, Forum
Singapore 238884
Tel: 65-737-3593
Fax: 65-753-2145

Australia, New Zealand
Elsevier Science Australia
Customer Service Department
STM Division
Locked Bag 16
St. Peters, New South Wales, 2044
Australia
Tel: 61 02 9517-8999
Fax: 61 02 9517-2249
E-mail: stmp@harcourt.com.au
www.harcourt.com.au

Mexico and Central America
ETM SA de CV
Calle de Tula 59
Colonia Condesa
06140 Mexico DF, Mexico
Tel: 52-5-5553-6657
Fax: 52-5-5211-8468
E-mail: editoresdetextosmex@prodigy.net.mx

Brazil
Tecmedd Importadora E Distribuidora De Livros Ltda.
Avenida Maurílio Biagi, 2850
City Ribeirão, Ribeirão Preto – SP – Brasil
CEP: 14021-000
Tel: 0800 992236
Fax: (16) 3993-9000
E-mail: tecmedd@tecmedd.com.br

India, Bangladesh, Pakistan, Sri Lanka
Elsevier Health Sciences Division
Customer Service Department
17A/1, Main Ring Road
Lajpat Nagar IV
New Delhi – 110024, India
Tel: 91 11 2644 7160-64
Fax: 91 11 2644 7156
E-mail: esindia@vsnl.net

CONTENTS

FOREWORD

Physiology has played a crucial role in our understanding of common respiratory diseases, particularly asthma and chronic obstructive pulmonary disease. The Meakins-Christie Laboratories have been at the forefront of this understanding since 1972. This book brings together an extraordinary range of contributions to this field by past and present members of this internationally renowned organization. The historical origins of the Meakins-Christie Laboratories are beautifully described by Peter Macklem, who has done so much to establish a world-class research center. The range of technologies encompassed by the various contributors is quite astounding, indicating how much physiology relates to other scientific approaches to understanding the complexities of lung disease. It is this multidisciplinary approach to lung diseases that has proved to be so successful in elucidating the complex mechanisms involved in many pulmonary diseases and which has been pioneered by the Meakins-Christie Laboratories.

The Meakins-Christie Laboratories have led the way in many areas of research into pulmonary diseases. Linking pathology to function seems so obviously important now. It was pioneered by investigators at Meakins-Christie Laboratories, such as William "Whitey" Thurlbeck, and this tradition has been admirably developed and advanced by Jim Hogg and Manuel Cosio. Respiratory epidemiology, and its strong presence at the Laboratories, can trace its origins to the pioneering work of Margaret Becklake. But it is in "hard" physiology where the Meakins-Christie Laboratories have excelled and led the world. This book brings together the contributions of many of the international leaders in respiratory physiology. Not surprisingly, many of them were trained at the Meakins-Christie Laboratories. As such, this book covers a vast range of aspects of respiratory physiology: mechanics, ventilation, gas exchange, respiratory muscles, control of breathing, sleep-disordered breathing, and exercise physiology, as well as the clinical applications of respiratory physiology. The fact that all of the authors are present or past members of the Meakins-Christie Laboratories gives the book an extraordinary coherence; Qutayba Hamid, Joanne Shannon, and Jim Martin have done a superb job in bringing together all this expertise in such a well-ordered manner.

In recent years there has been less emphasis on physiology, as funding has largely switched to cell and molecular biology, with the result that many physiology departments have downsized or even closed. Cloning of the human genome was rightly hailed as a great step forward in science, but only now is it recognized that identifying genes is only a small step toward understanding complex diseases. Interest is swinging back toward physiology, as the field integrates advances in cell and molecular biology with functional changes in whole organisms. It is recognized that physiology is of vital importance in making sense of all the advances in basic science, and the field is now re-emerging as functional genomics and systems biology. The Meakins-Christie Laboratories have always maintained an interest in cell and molecular biology, which is reflected in many chapters of this book, and this institution has been among the first to integrate this into whole animal physiology and its clinical application. This institution has kept the flag of physiology alive, while many other scientific institutions have sacrificed physiology to follow scientific fashion, now to their great regret!

This book covers the whole range of respiratory physiology, from relevant basic cell physiology to human respiratory physiology, and includes the important applications of physiology in clinical practice. I cannot think of any other institution in the world whose own associates could cover this topic so comprehensively and effectively. This volume will be of enormous value to all academic respiratory physicians as well as those involved in all aspects of research into pulmonary medicine. I have always been impressed on my visits to the Meakins-Christie Laboratories by the active discussion and interaction taking place between the different research groups-a perfect environment for research. The Meakins-Christie Laboratories have trained scientists from all over the world who have themselves become international leaders, and this is well reflected in the authorship of the chapters. Sadly, some of the prominent acolytes, including Ann Woolcock, Ludwig Engel, and David Flenley, are no longer with us, but the spirit of the Meakins-Christie Laboratories is alive and well. The Meakins-Christie Laboratories have played a major international role in pulmonary research under the leadership of Peter Macklem, Joseph Milic-Emili, and now Jim Martin. This book is an excellent summary of all of these achievements and illustrates how the Meakins-Christie Laboratories have maintained their position at the cutting edge of respiratory science.

PETER BARNES
London, UK
March 2005

PREFACE

The research interests of the Meakins-Christie Laboratories have evolved from the excellence in respiratory physiology at McGill University initiated by Dr. Ronald Christie many years ago. Its legacy of excellence has been upheld by physiologists such as David Bates, Margaret Becklake, Peter Macklem, and Joseph Milic-Emili. The research performed in the Meakins-Christie Laboratories has always been motivated by its potential clinical relevance. Attempts to develop tests to identify early peripheral airway disease in smokers and the evaluation of the contribution of the respiratory muscles to ventilatory failure are but two examples of the enthusiasm for patient-related issues.

In recent years remarkable strides have been made in exploring the cellular and molecular physiology of the lungs and the respiratory skeletal muscles, and the mechanisms underlying respiratory disease have been greatly clarified. The elucidation of the pathobiologic basis for disease has not replaced the need to understand "classical respiratory physiology." The respiratory physician still requires a familiarity with the fundamental mechanisms of abnormal gas exchange and altered respiratory system mechanics in common diseases such as asthma, chronic obstructive pulmonary disease (COPD), and pulmonary fibrosis. The cardinal symptoms of these diseases are largely attributable to gas exchange and respiratory system mechanics.

The muscles of the respiratory pump, a term coined by Macklem, Roussos, and coworkers, are affected by altered geometry of the respiratory system such that their pressure-generating capacities are compromised. Whether true muscle fatigue occurs is still uncertain, but it has been a logical approach to provide rehabilitation with a view to improving respiratory muscle function. However, attempts to rehabilitate patients with advanced obstructive lung disease have been confounded by skeletal muscle deconditioning and dysfunction, revealing unsuspected systemic effects of COPD on both respiratory and peripheral skeletal muscle. Understanding skeletal muscle biology has therefore become a necessity for the respiratory physician.

In this book we have attempted to address most of the currently clinically relevant pulmonary physiology and pathophysiology that the respiratory physician should be familiar with. We have not attempted to be encyclopedic in our approach, and one may argue that the book is not even-handed in its treatment of the subject. The book has inevitable biases resulting from the fact that the authors are, for the most part, former fellows of the Meakins-Christie Laboratories or have been closely associated with the Laboratories. We believe that this bias does not detract from the intrinsic clinical pertinence of the contents.

We gratefully acknowledge the generosity of our colleagues for their contributions to this book. We wish also to acknowledge the patience and encouragement provided by the staff of BC Decker Inc. We hope that the reader will enjoy the read as we have enjoyed the process of creating this book the and renewing our association with our fellow Meakins-Christie Laboratories alumni and other colleagues dedicated to respiratory physiology.

Q. HAMID
J. SHANNON
J.G. MARTIN

CONTRIBUTORS

Nicholas R. Anthonisen, MD, PhD, FRCP
Professor Emeritus
Department of Internal Medicine
University of Manitoba
Winnipeg, Manitoba

Walter Araujo Zin, MD, PhD
Professor of Physiology
Carlos Chagas Filho Institute of Biophysics
Federal University of Rio de Janeiro
Rio de Janeiro, Brazil

Michel Aubier, MD
Professor of Pneumology
Department of Pneumology
Faculté Xavier Bichat. Université Paris 7
Paris, France

Simonetta Baraldo, PhD
Postdoctoral Fellow
Cardiothoracic and Vascular Sciences
University of Padua
Padua, Italy

Jason H. T. Bates, PhD, DSc
Professor of Medicine
Vermont Lung Center
University of Vermont
Burlington, Vermont

Margaret Becklake, MB, BCh, MD, FRCP(E)
Professor of Medicine
Departments of Medicine and Epidemiology,
Biostatistics and Occupational Health
McGill University
Montreal, Quebec

François Bellemare, PhD
Research Associate
Department of Pneumology
Sleep Laboratory Hôtel Dieu of CHUM
Montreal, Quebec

Yves Berthiaume, MD
Professeur Titulaire
Département de Médecine
Université de Montreal
Montreal, Quebec

Jorge Boczkowski, MD, PhD
Principal Investigator
U700
INSERM
Paris, France

Gisella Borzone, MD
Associate Professor
Pontificia Universidad Catolica de Chile
Santiago, Chile

Jean Bourbeau, MD
Assistant Professor of Medicine
Department of Medicine
McGill University
Montreal, Quebec

Peter T. P. Bye, MBBS, FRACP, PhD
Clinical Associate Professor
Department of Medicine
University of Sydney
Sydney, New South Wales

Peter M. A. Calverley, MB, ChB, FRCP, FRCP(E)
Professor of Medicine
University of Liverpool
Liverpool, United Kingdom

Paolo Carbonara, MD
Research Fellow
Meakins-Christie Laboratories
McGill University
Montreal, Quebec

Koji Chihara, MD, PhD
Chief of Thoracic Surgery
Shizuoka City Shizuoka Hospital
Shizuoka, Japan

Alain S. Comtois, PhD
Associate Professor
Kinanthropologie
Université du Quebec a Montreal
Montreal, Quebec

Manuel G. Cosio, MD
Professor of Medicine
Respiratory Division
McGill University
Montreal, Quebec

David J. Cotton, MD, FRCP(C)
Professor of Medicine
Department of Internal Medicine
College of Medicine University of Saskatchewan
Saskatoon, Saskatchewan

Steven Robert Couglin, MSc, PhD
Research Fellow
Department of Medicine
University of Liverpool
Liverpool, United Kingdom

Guy Czaika, PhD
University of Montreal
Montreal, Quebec

Edgardo D'Angelo, MD
Professor of Human Physiology
Istituto di Fisiologia Umana I
Univeresità degli Studi di Milano
Milan, Italy

Richard Debigaré, PT, PhD
Assistant Professor
Department of Medicine
Université Laval
Montreal, Quebec

Marc Decramer, MD, PhD
Professor of Medicine
Department of Pneumology
Katholieke Universiteit Leauveu
Leuven, Belgium

Jerome A. Dempsey, PhD
Professor of Medicine
Department of Population Health Sciences
University of Wisconsin-Madison
Madison, Wisconsin

Orlando Díaz, MD
Associate Professor
Pontificia Universidad catolica de Chile
Santiago, Chile

Nicholas C. Duffy, MBChB, MRCP
Lecturer
Department of Medicine
University of Liverpool
Liverpool, United Kingdom

David H. Eidelman
Professor of Medicine
Respiratory Division
McGill University
Montreal, Quebec

Marlowe W. Eldridge, MD
Assistant Professor of Medicine
Population Health Sciences
University of Wisconsin-Madison
Madison, Wisconsin

Mark R. Elkins, MHSci
Honorary Associate
School of Physiotherapy
University of Sydney
Sydney, New South Wales

Antoni Ferrer, MD
Senior Associate Physician
Servei de Pneumologia
Hospital de Sabadell Institut
Institut Universitari Corporació Parc Taulí
Universitat Autònoma de Barcelona
Barcelona, Spain

Pierre-Olivier Fiset
Department of Medicine
McGill University
Montreal, Quebec

Elizabeth D. Fixman, PhD
Assistant Professor
Department of Medicine
McGill University
Montreal, Quebec

Felicity S. Flack, PhD
Division of Clinical Sciences
Telethon Institute for Child Health Research
University of Western Australia
Perth, Western Australia

Richard Fraser, MDCM, FRCP(C)
Professor of Pathology
Department of Pathology
McGill University
Montreal, Quebec

Ghislaine Gayan-Ramirez, PhD
Department of Pneumology
Katholieke Universiteit Leauveu
Leuven, Belgium

R. Heberto Ghezzo, PhD, FRSS
Research Associate
Department of Medicine
McGill University
Montreal, Quebec

Peter Goldberg, MDCM
Associate Professor of Medicine
Respiratory Medicine
McGill University
Montreal, Quebec

Anne Gonzalez, MD
Meakins-Christie Laboratories
McGill University
Montreal, Quebec

Rik Gooselink, PT, PhD
Professor of Medicine
Katholieke Universiteit Leauveu
Leuven, Belgium

Brian L. Graham, PhD
Professor of Medicine
Department of Medicine
College of Medicine University of Saskatchewan
Saskatoon, Saskatchewan

Alejandro Grassino, MD
Professor of Medicine
Department of Medicine
University of Montreal
Montreal, Quebec

David A. Hall, PhD, MD
Respiratory and Clinical Care Fellow
Department of Respirology and Critical Care Medicine
University of Toronto
Toronto, Ontario

Qutayba Hamid, MD, PhD, MRCP, FRCPath
Professor of Medicine
Department of Medicine
McGill University
Montreal, Quebec

John W. Hanrahan, PhD
Professor of Physiology
Department of Physiology
McGill University
Montreal, Quebec

Zoltán Hantos, MSc, PhD, CSc, DSc
Professor of Medicine
Medical Informatics
Albert Szent-Gyorgyi Medical University
Szeged, Hungary

Hans C. Haverkamp, MS
Predoctoral Fellow
Population Health Sciences
University of Wisconsin-Madison
Madison, Wisconsin

Sabah N. A. Hussain, MD, PhD
James McGill Professor
Department of Medicine
McGill University
Montreal, Quebec

Charles G. Irvin, PhD
Professor and Director
Vermont Lung Center
University of Vermont
Burlington, Vermont

Tian-Xi Jiang, MD
Research Associate
Department of Medicine
University of British Columbia
Vancouver, British Columbia

R. John Kimoff, MD, FRCP(C)
Associate Professor
Department of Medicine
McGill University
Montreal, Quebec

Malcolm King, PhD, FCCP
Professor of Medicine
Department of Medicine
University of Alberta
Edmonton, Alberta

Tom Kotsimbos, MD, FRACP
Associate Professor
Department of Medicine
Monash University
Melbourne, Victoria

Nickolaos G. Koulouris, MD, PhD
Associate Professor in Respiratory Medicine
Department of Respiratory Medicine
University of Athens
Athens, Greece

Jennifer S. Landry, MD, FRCP(C)
Assistant Professor
Department of Medicine
McGill University
Montreal, Quebec

Sophie Lanone, PhD
U700
INSERM
Paris, France

Anne-Marie Lauzon, PhD
Assistant Professor
Department of Medicine
McGill University
Montreal, Quebec

Catherine Lemière, MD, MSc
Associate Professor
Department of Medicine
University of Montreal
Montreal, Quebec

Carmen Lisboa, MD
Professor of Medicine
Pontificia Universidad catolica de Chile
Santiago, Chile

Mara S. Ludwig, MD
Professor of Medicine
Meakins-Christie Laboratories
McGill University
Montreal, Quebec

Peter T. Macklem, MD, CM, FRCP(C), FRSC
Professor Emeritus
Department of Medicine
McGill University
Montreal, Quebec

Sheldon Magder, MD, FRCP(C)
Professor of Medicine and Physiology
Department of Medicine and Physiology
McGill University
Montreal, Quebec

François Maltais, MD
Associate Professor of Medicine
Department of Medicine
Université Laval
Montreal, Quebec

Jure Manfreda, MD
Associate Professor
Internal Medicine
University of Manitoba
Winnipeg, Manitoba

James G. Martin, MD, DSc
Professor of Medicine
Department of Medicine
McGill University
Montreal, Quebec

Stefan Matecki, MD, PhD
Fellow
Meakins-Christie Laboratories
McGill University
Montreal, Quebec

Bruce Mazer, MD
Associate Professor of Pediatrics
Department of Pediatrics
McGill University
Montreal, Quebec

Brent E. McParland, MSc, PhD
Postdoctoral Fellow
Department of Medicine
University of British Columbia
Vancouver, British Columbia

René P. Michel, MD, CM, FRCP(C)
Professor of Pathology
Department of Pathology
McGill University
Montreal, Quebec

Marie-Claire Michoud, MSc, PhD
Research Associate
Department of Medicine
McGill University
Montreal, Quebec

Joseph Milic-Emili, CM, MD, FRSC
Professor Emeritus
Department of Physiology
McGill University
Montreal, Quebec

Jordan D. Miller, MS
Predoctoral Fellow
Population Health Sciences
University of Wisconsin-Madison
Madison, Wisconsin

Michiaki Mishima, MD, PhD
Professor and Chairman
Respiratory Medicine
Postgraduate School of Medicine, Kyoto University
Kyoto, Japan

Zöe Müller
Research Assistant
Department of Medicine
McGill University
Montreal, Quebec

Takahide Nagase, MD
Professor of Medicine
Department of Respiratory Medicine
University of Tokyo, The Graduate School of Medicine
Tokyo, Japan

Ronald Olivenstein, MD, FRCP(C)
Assistant Professor of Medicine
Department of Medicine
McGill University
Montreal, Quebec

Manuel Paiva, PhD
Professor of Medicine
Laboratoire de Physique Biomédical
Université Libre de Bruxelles
Brussels, Belgium

Peter Paré, MD, FRCP
Professor of Medicine
Department of Medicine
University of British Columbia
Vancouver, British Columbia

Hélène Perrault, PhD
Professor and Chair
Kinesiology and Physical Education
McGill University
Montreal, Quebec

Basil J. Petrof, MD, FRCP(C)
Associate Professor
Department of Medicine
McGill University
Montreal, Quebec

Claude Poirier, MD, FRCP(C)
Chargé d'enseignement
University of Montreal
Montreal, Quebec

William S. Powell, PhD
Professor of Medicine
Department of Medicine
McGill University
Montreal, Quebec

Immanuela Ravé Moss, MD, PhD, FAAP
Professor of Medicine
Departments of Pediatrics and Physiology
McGill University
Montreal, Quebec

W. Darlene Reid, BMR(PT), PhD
Associate Professor
School of Rehabilitation Sciences
University of British Columbia
Vancouver, British Columbia

Paolo Renzi, MD, FCCP, FRCP(C)
Professor of Research
Department of Medicine
University of Montreal
Montreal, Quebec

Jeremy Road, MD, FRCP(C)
Professor of Medicine
Department of Medicine
University of British Columbia
Vancouver, British Columbia

Robert Rodriguez-Roisin, MD, FRCP(E)
Professor of Medicine
Department of Medicine
Universitat de Barcelona
Barcelona, Spain

Lee M. Romer, PhD
Lecturer
Sport Sciences
Brunel University
Uxbridge, Middlesex

Charis Roussos, MD, PhD
Professor of Intensive Care Medicine
Critical Care and Pulmonary Services
University of Athens Medical School
Athens, Greece

Marina Saetta, MD
Professor of Medicine
Department of Cardiothoracic and Vascular Sciences
University of Padua
Padua, Italy

Andrew Sanford, PhD
Associate Professor of Medicine
Department of Medicine
University of British Columbia
Vancouver, British Columbia

Dean E. Schraufnagel, MD, FCCP
Professor of Medicine
Division of Pulmonary, Critical Care and Sleep Medicine
University of Illinois at Chicago
Chicago, Illinois

Chun Y. Seow, PhD
Associate Professor
Pathology/Laboratory Medicine
University of British Columbia
Vancouver, British Columbia

Joanne Shannon, MD
Postdoctoral Fellow
Meakins-Christie Laboratories
McGill University
Montreal, Quebec

Stephanie A. Shore, PhD
Senior Lecturer in Physiology
Department of Environmental Health
Harvard School of Public Health
Boston, Massachussets

Peter D. Sly, MD, DSc, FRACP
Professor of Medicine
Centre for Child Health Research
University of Western Australia
Perth, Western Australia

Duncan Stewart, MDCM, FRCP, FACC, FAHA
Professor of Medicine
Department of Cardiology
University of Toronto
Toronto, Ontario

Rame Taha, MD
Research Scientist
Department of Anesthesia
University of Montreal
Montreal, Quebec

Camille Taillé
Research Fellow
U700
INSERM
Paris, France

Salem al-Tamemi, MD, FRCP(C)
Clinical and Research Fellow
Department of Clinical Immunology
McGill University
Montreal, Quebec

Claudio Tantucci, MD
Professor of Respiratory Medicine
Scienze Mediche e Chirurgiche
University of Brescia
Brescia, Italy

Scott James Tebbutt, PhD
Clinical Assistant Professor
Department of Medicine
University of British Columbia
Vancouver, British Columbia

Robert S. Tepper, MD, PhD
Professor of Pediatrics
Department of Pediatrics
Indiana University
Indianapolis, Indiana

Barbara Tolloczko, PhD
Research Associate
Department of Medicine
McGill University
Montreal, Quebec

Thierry Troosters, PT, PhD
Professor of Pulmonary Rehabilitation
Department of Rehabilitation Sciences
Katholieke Universiteit Leauveu
Leuven, Belgium

André de Troyer, MD, PhD
Professor of Physiology
Department of Cardiorespiratory Physiology
Brussels School of Medicine
Brussels, Belgium

Meri K. Tulic, PhD
Research Fellow
Meakins-Christie Laboratories
McGill University
Montreal, Quebec

Debra Turner, PhD
Adjunt Senior Lecturer
Telethon Institute for Child Health Research
University of Western Australia
Perth, West Australia

Sylvia Verbanck, PhD
Respiratory Division
Vrye Universiteit Brussel
Brussels, Belgium

Peter D. Wagner, MD
Professor of Medicine and Bioengineering
Division of Physiology
University of California San Diego
La Jolla, California

Xiangyu Wang, MD
Postdoctoral Fellow
School of Rehabilitation Sciences
University of British Columbia
Vancouver, British Columbia

Michael Ward, PhD, MD, FRCP(C)
Associate Professor of Medicine
Department of Medicine
University of Toronto
Toronto, Ontario

Spyros Zakynthinos, MD
Associate Professor of Intensive Care Medicine
Critical Care and Pulmonary Services
University of Athens Medical School
Athens, Greece

HISTORY OF THE MEAKINS-CHRISTIE LABORATORIES

Peter T. Macklem

The first quarter of the twentieth century marks the beginning of the history of the Meakins-Christie Laboratories for Respiratory Research. Shortly before his death in 1919, Sir William Osler, then Regius Professor of Medicine at Oxford University, the world's most renowned physician and McGill University's most distinguished graduate, wrote to the dean of the faculty of medicine recommending that McGill appoint a full-time chairman of the Department of Medicine who would establish research in the hospital as an essential part of academic medical activities. Until that time the teachers at McGill's medical school were all part-time physicians who had private practices outside the teaching hospitals.

It took the dean some time to act on Sir William's recommendation, but in 1924 Dr. Jonathan Meakins arrived from the University of Edinburgh to take up his appointment as physician-in-chief of the Royal Victoria Hospital (RVH) and the first full-time chairman of medicine in Canada. Dr. Meakins more than fulfilled his mandate to establish clinical research at the RVH. He wrested control of clinical laboratory services away from the Department of Pathology, so the clinical biochemistry and hematology laboratories became part of the Department of Medicine and provided the department with an extremely valuable research infrastructure. This extraordinary accomplishment made the RVH almost unique in the world. Traditionally, clinical laboratory services are supplied by clinical pathologists, but at the RVH they are supplied by internists. Although this organizational structure has frustrated hospital administrators, it is directly responsible for the tradition of hospital-based clinical research that has made the RVH such a renowned academic institution. Meakins' efforts to develop research in the RVH did not stop at biochemistry and hematology. In the early 1930s he recruited Ronald Christie for a postdoctoral fellowship at the RVH. Together they published a series of classic papers dealing with the mechanics of breathing in emphysema and mitral stenosis and with blood gas abnormalities in pulmonary edema.[1–3]

Dr. Jonathan Meakins

After 7 years in Montreal, Christie returned to England to take up an academic position at St. Bartholomew's Hospital Medical School, where he rose to the rank of professor and chairman. In the meantime, the Department of Medicine at the RVH had fallen into disarray with the appointment of one individual as physician-in-chief and another as departmental chairman. These two individuals did not see eye-to-eye on any issue, and the department was tainted by acrimony. An interim departmental head was chosen, while a search committee was established by the hospital's board of directors to find a permanent solution. The solution turned out to be Ronald Christie.

Christie had visited McGill at the request of the search committee and had been offered the job. He returned to London confident that the offer would be withdrawn because of the almost impossible conditions he had put on his acceptance, including a whole new wing for the Department of Medicine to match the one recently built for the Department of Surgery. He was therefore surprised to see Mr. David Muir, president of the Bank of Montreal and chairman of the RVH board, waiting outside his office in London one day. All of his conditions had been agreed to, and Christie accepted the job.

Ronald Christie returned to Montreal as physician-in-chief of the RVH and chairman of the McGill Department of Medicine in 1955, when I was a final year medical student. Shortly after he arrived, he gave a professional lecture to the faculty. Not many people can recall the details of a lecture delivered 50 years previously, but I remember Christie's well.

Dr. Ronald Christie

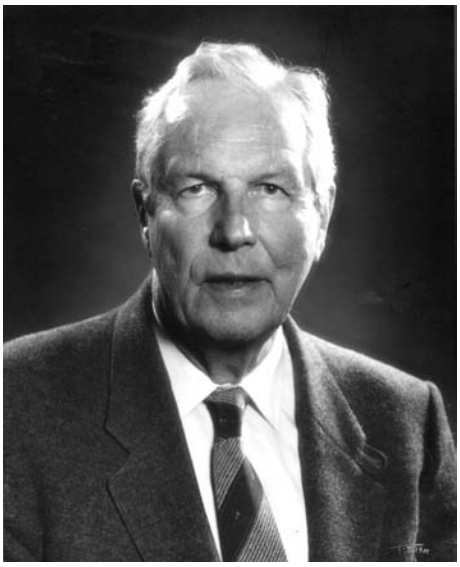

Dr. Peter Paré

He talked about lung compliance and resistance and how the two combined made up the work of ventilating the lung. He showed how these parameters changed systematically with changes in tidal volume and breathing frequency. He showed that in diseases affecting the mechanical properties of the lung, there was a particular tidal volume and frequency for a given minute ventilation that resulted in minimal work, and this was the breathing pattern.

I was entranced. While I understood diseases of other systems, I totally lacked a cohesive framework to understand diseases of the respiratory system. Although I had been taught about complemental air and supplemental air, these terms were never talked about during my clinical years, and classification of lung diseases into obstructive and resistive abnormalities was still in the future. Finally, someone had constructed a framework in which I could begin to understand respiratory function in disease.

In retrospect, this lecture was to have an enormous influence on my future. It took some years before I chose to pursue the challenge of respirology, but there is no doubt that Christie's lecture engendered my interest in this field.

When Christie arrived in 1955, there was already a strong infrastructure in place at the RVH. Peter Paré was a young internist who had specialized in respiratory medicine and who had recently joined the attending staff. Darrell "Dag" Munro was an outstanding thoracic surgeon, and Bob Fraser was a young star of the radiology department.

Christie brought Dr. David Bates with him. In 1956 and he appointed him director of the newly created respiratory division. Bates and Christie went on to do an extraordinary job of recruiting: Maurice McGregor and his wife Margaret Becklake, from South Africa; William "Whitey" Thurlbeck, another South African pathologist, who was on the staff of the Massachusetts General Hospital; and Joseph Milic-Emili, from the Harvard School of Public Health. Nick Anthonisen, who came from the United States for residency training, stayed and joined the faculty. Charlie Bryan came from the RCAF to do his PhD degree under Bates. All of these people were to become world leaders in their respective fields.

Bates and Christie wrote *Respiratory Function in Disease*, which became a medical best seller. The title is a tribute to Meakins and Davies, who wrote a book of the same name in the 1920s, of which I have a copy, a treasured gift from Dr. Christie when the Meakins-Christie Laboratories opened. David Bates and Maurice McGregor formed the joint cardiorespiratory service of the RVH and the Montreal Children's Hospital (MCH). Margaret Becklake established excellence in respiratory epidemiology at McGill, a legacy that persists today and to which she is contributing as much as ever. Milic is world renowned for his contributions to respiratory physiology, particularly for his groundbreaking work on regional lung function using xenon 133 and his studies on the control of breathing. Thurlbeck established McGill as one of the leading centers of respiratory pathology and lung morphometry. Nick Anthonisen, a renowned physician, physiologist, and epidemiologist, went on to become dean of medicine at the University of Manitoba, and Charlie Bryan made many contributions to pediatric respirology, including the introduction of high-frequency oscillatory ventilation for the treatment of acute respiratory distress syndrome of infancy. Those who were already in place also made extraordinary contributions. Bob Fraser became the world's leading pulmonary radiologist. Peter Paré was renowned for his excellence as a clinician and teacher. He has been responsible for inspiring and instilling clinical excellence in a vast number of respirologists in Canada and around the world. Fraser and Pare wrote *Diagnosis of Diseases of the Chest*, the book by which all other clinical texts of respiratory disease were judged. Dag Munro performed the world's second lung transplant. It was a heady time.

David Bates deserves great credit for developing respiratory research at McGill in an inclusive multidisciplinary program including clinical, fundamental, and epidemiologic research in both the Royal Victoria and Montreal Children's Hospitals and spanning the disciplines of respiratory medicine, pathology,

Dr. David Bates

epidemiology, cardiology, and radiology. The joint cardiorespiratory service of the RVH and MCH rapidly became world famous. Respiratory research at McGill rivaled that of similar research centers at Harvard, Johns Hopkins, the State University of New York at Buffalo, the University of California, San Francisco, and elsewhere.

By 1962, following in Meakins' footsteps, Christie had become dean of the McGill Faculty of Medicine. In 1967 he retired. Maurice McGregor replaced him as dean, and David Bates became chairman of the Department of Physiology. I was appointed director of the Respiratory Division at the RVH.

Almost as soon as I was appointed, Peter Paré, my lifelong friend and professional colleague, told me that his brother, Paul Paré, then a vice president of Imperial Tobacco, was going to be made president. He suggested that we approach Paul to support respiratory research at the RVH. Our pitch was that the tobacco industry was causing lung disease and that since it was incapable of undertaking research into the diseases it was causing, it should support the research of scientists who could investigate how smoking led to disease. Paul, a man of great integrity, agreed. This led to negotiations with the Canadian Tobacco Manufacturer's Council, the consortium of Canadian tobacco companies. They agreed to donate $300,000 to McGill to build new laboratories for respiratory research and to provide overhead costs for the first 10 years of operation.

Today, this amount seems minuscule, but we were able to tap into federal resources to match those funds, so we had $600,000 to work with. After much discussion and some initial setbacks, we scaled our plans and settled on a two-storey addition to the Pathological Institute, conveniently located adjacent to Thurlbeck's lung morphometry laboratory. The plans were sent to tender, the contract was awarded, and work began. The egg was fertilized and the Meakins-Christie Laboratories were conceived.

I had a pretty fair idea of how I wanted the laboratories to operate. I had spent an unforgettable year and a half with Jere Mead and Jim Whittenberger at the Harvard School of Public Health and had also spent time in Dick Reilly's department at the Johns Hopkins School of Hygiene working with Don Proctor and Sol Permutt. The attitude in both institutions was identical and wonderful—that work should be fun. In both places much of the day was spent exploring, discussing, and dissecting new ideas. The idea of change and innovation was not only welcomed, it was fostered. Almost daily, furious arguments (but neverquarrels) would break out, out of which spectacularly stupid and, more than occasionally, spectacularly brilliant ideas would emerge. And we had the academic freedom to pursue them. When I was in Boston, Jere Mead and I would drive to and from work every day. We would argue about the hot topic of the time and decide what we were going to play with that day. One such morning we were arguing hotly about the role of airway wall compliance in limiting expiratory flow, when Jere had an idea. He suggested that we push a catheter into the lung, push it right through the parenchyma and the visceral pleura, and then continue pulling it until the other end, which was widened into a bell shape, caught in a small airway. Then we could measure the pressure in small airways and partition the pressure drop and the resistance between central and peripheral airways. Such was the spirit of academic freedom in the laboratories that Jim Whittenberger directed, that we were able to start on this idea within half an hour, and within a week we had most of the methodologic problems solved.

This was science heaven. This was what I wanted for the Meakins-Christie Laboratories.

To achieve this, the laboratories were designed for procedures, not as individual private fiefdoms. There was a laboratory for animal mechanics, another for human mechanics, an exposure chamber, a gas exchange laboratory, and radioactive gas laboratories for both animals and humans. The sharing of laboratories, although it presented problems in scheduling and the setting up of equipment, promoted interactions among scientists with similar interests, which I hoped would stimulate new and exciting ideas. I was convinced that creative people interacting with other creative people with common interests would come up with more original ideas than they would conducting their science in isolation. One big room, the chief technician's domain, had tables and chairs and always fresh coffee. Everyone—technicians, secretaries, research fellows, and research directors—was encouraged to eat lunch in that room. One day, I arrived late; every seat was taken, but a junior research fellow from France immediately stood up and offered me his seat. One of the technicians piped up, "What are you doing that for?!" I was pleased. That was exactly the sort of atmosphere I had hoped to establish.

Large blackboards were put up in every room to encourage expression and discussion. The fellows' offices were adjacent to the research directors' offices. Doors were kept open, appointments unnecessary. Talking is one of the strongest stimuli to innovation. Thus, our weekly research seminar was the highlight of the week's activities. In order to embolden shy research trainees to comment and ask

Dr. Paul Paré

questions, beer was freely available to loosen their tongues. Although probably the research directors drank more than the trainees, this worked. The beer seminars were held in the evening and were open-ended. Many memorable ones went on past midnight. One visiting VIP said, "I'm told that here I won't get past my first slide, so I'm going to start with my second." This was a great compliment.

From the beginning, the laboratories were designed to be interdisciplinary, and physiologists, physicians, epidemiologists, pathologists, radiologists, and biomedical engineers were invited to participate. The laboratories were open in the sense that anyone who wanted to collaborate with one of the scientists working there was welcome to do so.

After a long gestation period, the Meakins-Christie Laboratories for Respiratory Research were born in August 1972. At the opening ceremonies we were tackled by the media about the propriety of accepting tainted tobacco money. When the reporters heard that the money was given carte blanche, with no strings attached, to investigate, among other things, how smoking damaged the lungs, this issue was resolved.

In creating the laboratories, we tried to make the concept that research should be fun, that secrecy was anti-innovative, and that free and open discussion was essential, the core of our philosopy. Judging from the list of distinguished scientists who have contributed to this book, I think we succeeded. I pay homage to some exceptional people with whom I collaborated, who were extraordinarily creative and who even after death command immense influence over their survivors. They stand as proof of the vitality of freedom, openness, and creativity in science. In particular, I am talking about Whitey Thurlbeck, Ann Woolcock, Harold Menkes, Fred Douglas, David Flenley, and Ludwig Engel. These people enriched my life extraordinarily and would have similarly enriched this book if they were still with us. During their time at McGill they promoted the vision of intellectual freedom and openness, so they deserve much credit for not only persistence of this vision in the Meakins-Christie Laboratories but also for promoting it in their own institutions. I cannot finish without pointing out that Jim Higg contributed hugely to the early years of the laboratories. He and Ann Woolcock were among my first research fellows. What a start that was!

I directed the Meakins-Christie Laboratories from 1972 until 1979, when I resigned to take up new challenges. The leadership of the Meakins-Christie Laboratories passed into the capable hands of Joseph Milic-Emili and then Jim Martin. It has continued to grow in size, influence, and contributions to new knowledge. Clearly, it is in wise and capable hands.

REFERENCES

1. Christie RV, Mclntosh CA. The measurement of intrapleural pressure in man and its significance. J Clin Invest 1934;13:279.
2. Christie RV. The elastic properties of the emphysematous lung and their clinical significance. J Clin Invest 1934;13:295.
3. Christie RV, Meakins JC. The intrapleural pressure in congestive heart failure and its clinical significance. J Clin Invest 1934;13:323.

CHAPTER 1

HISTOLOGY AND GROSS ANATOMY OF THE RESPIRATORY TRACT

Richard S. Fraser

The lower respiratory tract extends from the larynx to the most distal portions of the lung parenchyma. Its airways can be considered in two groups: *conducting* and *transitional*.[1,2] The former comprises those whose walls do not contain alveoli and are thick enough to prevent gas diffusing into the adjacent lung parenchyma. They include the trachea, bronchi, and membranous (nonalveolated) bronchioles; the latter are defined structurally by the absence of cartilage in their walls. These airways, along with their accompanying arteries and veins, lymphatic vessels, nerves, interlobular septa, and pleura, constitute the nonparenchymal portion of the lung. As the name suggests, transitional airways have both conductive and respiratory functions. They consist of respiratory bronchioles and alveolar ducts; in addition to conducting gas to and from the most peripheral portion of the lung, each has alveoli on its wall that serve in gas exchange. Alveoli associated with the transitional airways and with the more distal alveolar sacs constitute the lung *parenchyma*. It has been estimated that approximately 87% of the total lung volume is alveolar, 6% of which is composed of tissue, and the remainder of which is gas.[3]

Both the right and the left lung are enveloped by a thin layer of connective tissue (the visceral pleura), which focally extends into the parenchyma, dividing it into several lobes (upper, middle, and lower on the right side and upper and lower on the left). A potential space (the pleural cavity) separates the visceral pleura from the parietal pleura, which lines the chest wall, mediastinum, and diaphragm.

CONDUCTING AIRWAYS

The basic branching pattern of the conducting zone is dichotomous (that is, the parent branch divides into two parts). As a general rule, the angles made by daughter branches with their parent vary with their diameter[1]: when the branches are of equal size, the angles tend to be equal; when the branches are of different size, the smaller branch usually makes a larger angle with the parent. Through common usage, the designation *main bronchi* is applied to the bronchi arising at the bifurcation of the trachea and extending to the origin of the upper lobe bronchus on each side; the terms *upper*, *middle,* and *lower lobe bronchi* are used for the corresponding bronchi supplying individual lobes, and the term *intermediate bronchus* is applied to the airway segment between the right upper lobe bronchus and the origins of the right middle and lower lobe bronchi.

The basic morphology of the conducting airways is similar and consists of a surface epithelium composed largely of ciliated and secretory cells overlying subepithelial tissue that consists predominantly of connective tissues and glands (Figure 1-1). The proportion and type of these elements vary at different levels of the conducting system.

EPITHELIUM

The tracheal and proximal bronchial epithelium are composed predominantly of tall, columnar ciliated and goblet cells, and smaller, somewhat triangular, basal cells (Figure 1-2).[4] *Ciliated cells* are about five times more numerous than goblet cells in the central airways, and the ratio is even greater peripherally.[5] They have thin, tapering bases that are attached firmly to the underlying basal lamina. The cells are also attached to one another at their apical surfaces by tight junctions,[6] forming a barrier physically impermeable to most substances,[7] and laterally to one another and to basal cells by desmosomes. Intercellular spaces containing numerous microvilli are present between the cells, especially at their basal aspects.[8] Emanating from the surface of each ciliated cell are approximately 200 to 250 cilia, as well as numerous shorter microvilli (Figure 1-3), which, in addition to microvilli located in the intercellular space, are important in the transepithelial movement of fluid and electrolytes.[9]

Goblet cells account for about 20 to 30% of cells in the more proximal airways[5] and decrease in number distally, so that only occasional cells are present in normal membranous bronchioles.[10] Ultrastructurally, the apical portion of the cytoplasm is distended by numerous membrane-bound, electron-lucent secretory granules. Histochemical studies

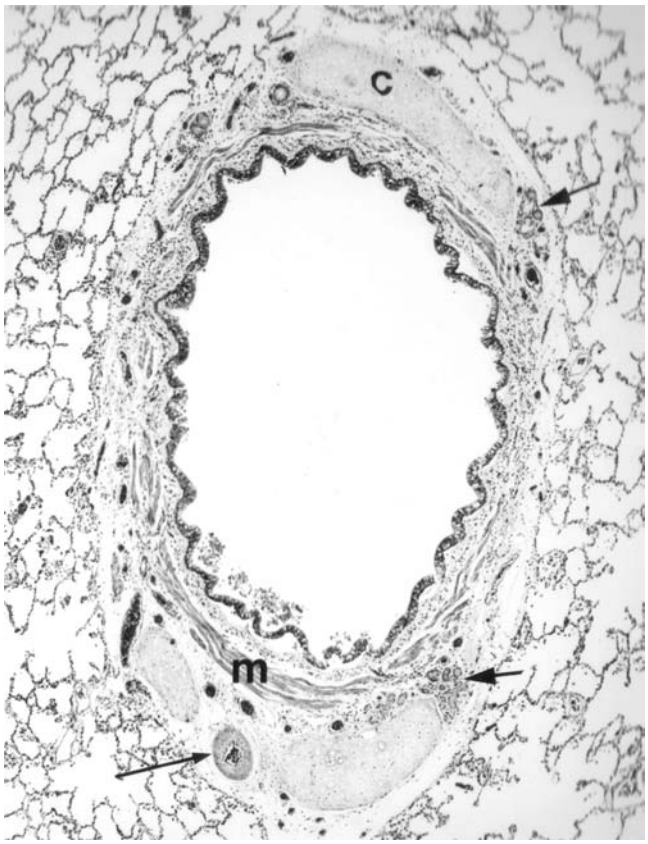

FIGURE 1-1 Conducting airway (hematoxylin-eosin stain). Subsegmental bronchus showing cartilage (c), mucous glands (*short arrows*), bronchial artery (*long arrow*), and muscle (m). Reproduced with permission from Fraser RS, Müller NL, Colman N, Paré PD, Diagnosis of Diseases of the Chest, IV edition. Philadelphia: WB Saunders; 1999.

have shown these to contain predominantly neutral mucin and sulfomucins.[11] However, variation in both ultrastructural and histochemical features has been demonstrated in different airways, and cells with a large proportion of non-sulfated sialomucins have also been identified.[12]

Basal cells are relatively small, somewhat triangular cells whose bases are attached to the basement membrane and whose apices normally do not reach the airway lumen. They are more abundant in the proximal airways, where they form a more or less continuous layer, and gradually diminish in number distally, so that they are difficult to identify in bronchioles.[13,14] They function as a reserve from which the epithelium is repopulated, both normally and after airway injury,[14] and are involved in the attachment of columnar epithelial cells to the basement membrane.[15]

Clara cells (nonciliated bronchiolar secretory cells) are found primarily in membranous bronchioles, in which they constitute the majority of the epithelium along with ciliated cells.[16] They are columnar or (in the more distal airways) cuboidal in shape and bulge somewhat into the airway lumen, slightly projecting above the surrounding ciliated cells. The cytoplasm contains a prominent Golgi apparatus, abundant granular endoplasmic reticulum and mitochondria, and numerous membrane-bound, electron-dense granules. The latter contain a number of lipids and proteins,[17] including a 10 kDa protein known as *Clara cell-specific*

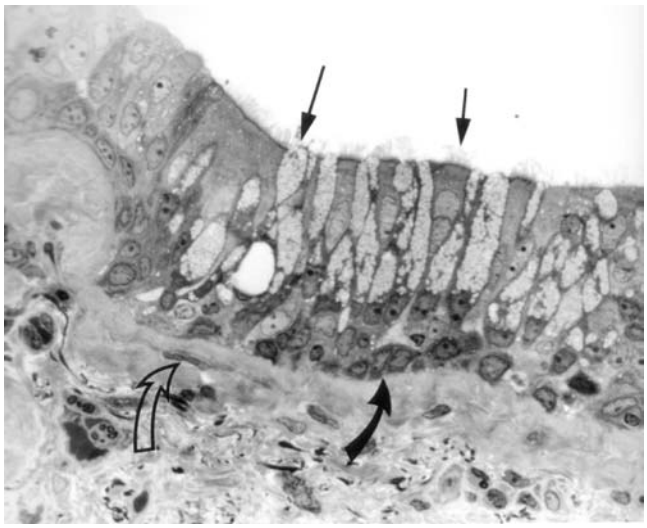

FIGURE 1-2 Conducting airway epithelium and lamina propria (electron micrograph). Ciliated cell (*short straight arrow*), goblet cell (*long straight arrow*), basal cell (*black curved arrow*), and subepithelial fibroblast (*empty curved arrow*).

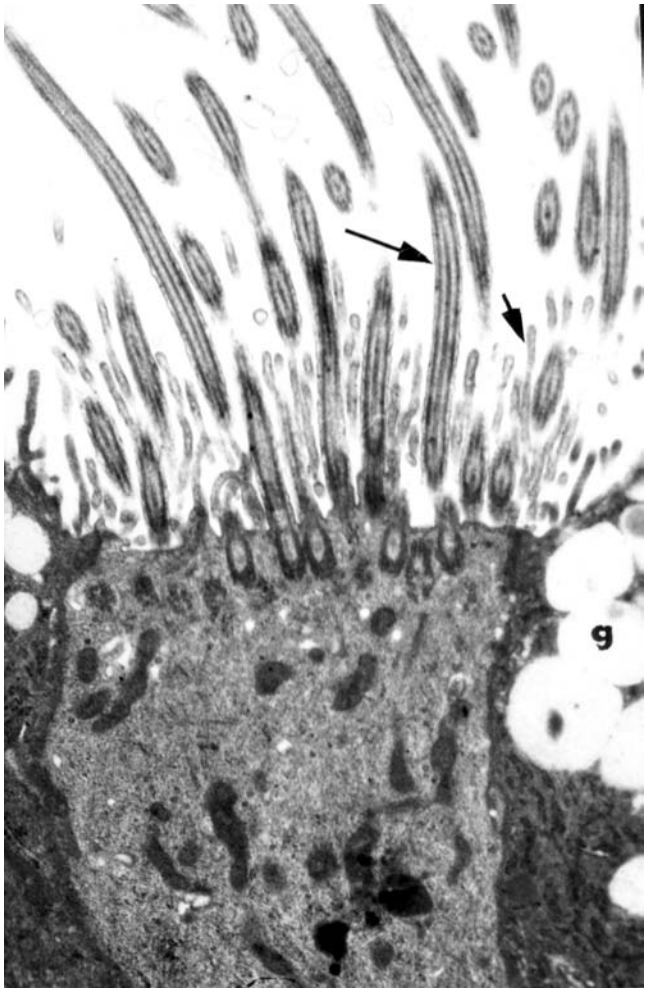

FIGURE 1-3 Ciliated cell (electron micrograph). Apical portion of cell showing cilia (*long arrow*) and microvilli (*short arrow*). Secretory granules (g) of a goblet cell can be seen in the adjacent cell. Reproduced with permission Fraser RS, Müller NL, Colman N, Paré PD, Diagnosis of Diseases of the Chest, IV edition. Philadelphia: WB Saunders; 1999.

protein (CC10, CC16, Protein 1) that may have a role in the regulation of local inflammatory and immune reactions,[18] several surfactant apoproteins,[19] and a leukocyte protease inhibitor.[20] In addition to these secretory functions, there is evidence that Clara cells act as progenitor cells in the regeneration of damaged bronchiolar epithelium.[21]

Neuroendocrine cells constitute about 1 to 2% of bronchial epithelial cells in neonates[22] and 0.5% in adults.[23] They are attached at their bases to the basement membrane and have tapering apices that extend toward and may or may not reach the airway surface. Ultrastructurally, the cytoplasm contains numerous membrane-bound, electron-dense neurosecretory granules (Figure 1-4) that contain a variety of peptides, including gastrin-releasing peptide (bombesin), calcitonin, calcitonin gene–related peptide, somatostatin, substance P, endothelin, and enkephalin.[24] These peptides appear to be secreted mostly at the basal aspect of the cell, although some may also be released via lateral cytoplasmic processes to affect adjacent epithelial cells, or into the airway lumen itself. The principal functions of the cells are believed to be related to the local effects of these secreted peptides. The cells appear as early as 8 weeks in the human fetus and increase in number thereafter,[25] suggesting a role in the control of lung development.

Cells of the immune system are present within the epithelium of all conducting airways. *Dendritic* and *Langerhans' cells* are structurally similar cells that possess elongated cytoplasmic extensions and an organelle-rich cytoplasm; Langerhans' cells have characteristic pentalaminar cytoplasmic structures termed *Birbeck granules*.[26] Dendritic cells are found throughout the lung, including the alveolar septa, peribronchiolar connective tissue, and bronchus-associated lymphoid tissue[26]; Langerhans' cells appear to be present only within airway epithelium. In this location, their number is considerably greater in proximal than in distal branches.[27] Langerhans' cells express cell surface receptors for immunoglobulins,[26] and it is believed that they act as antigen-processing and antigen-presenting cells and as stimulators of T-cell proliferation.[28] *Lymphocytes* (predominantly T cells) are present throughout the conducting airway epithelium, usually singly.[29] Although they are undoubtedly involved in processing and reacting to inhaled antigens, it is also possible that they have a role in modifying airway epithelial cell function. Greater numbers of lymphocytes can be seen as lymphoid aggregates in the lamina propria and submucosa (bronchus-associated lymphoid tissue), usually in the setting of acute or chronic airway injury. *Mast cells* are also found in small numbers within the airway epithelium.[30]

A *basement membrane* underlies the epithelium over its entire basal aspect. Its primary function is to provide an attachment for the epithelium to the underlying connective tissue. On the epithelial side, this attachment is mediated by adhesion molecules and by hemidesmosomal junctions with basal cells[31]; on the opposite side, anchoring fibrils emanate from the basement membrane and intertwine with collagen fibers in the upper lamina propria.

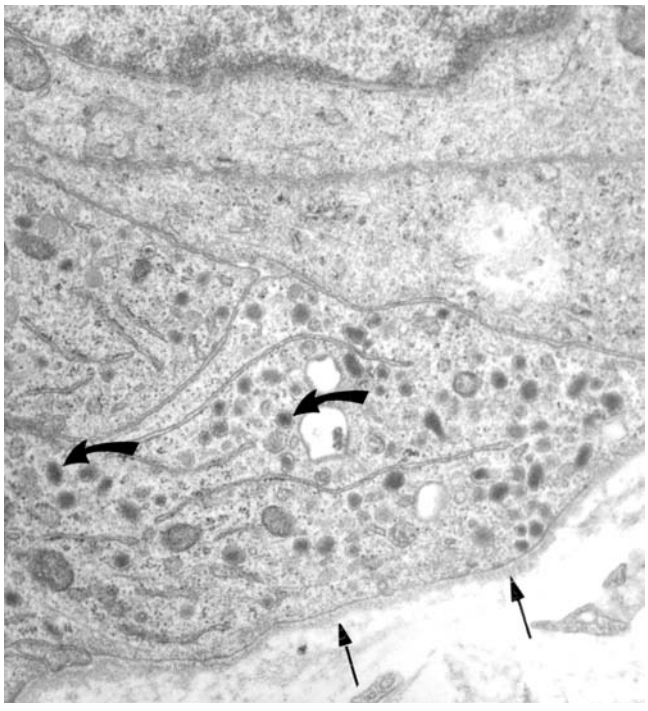

FIGURE 1-4 Neuroendocrine cell (electron micrograph). Basal portion of two cells, one of which is adjacent to the basement membrane (*straight arrows*). The cytoplasm contains numerous electron-dense neurosecretory granules (*curved arrows*). Reproduced with permission from Fraser RS, Müller NL, Colman N, Paré PD, Diagnosis of Diseases of the Chest, IV edition. Philadelphia: WB Saunders; 1999.

Submucosa and Lamina Propria

The subepithelial tissue can be subdivided into a lamina propria, situated between the basement membrane and the muscularis mucosa, and a submucosa, consisting of all the remaining airway tissue. The *lamina propria* consists principally of a network of capillaries, a meshwork of reticulin fibers continuous with the basement membrane, and bundles of elastic and nerve fibers. Ultrastructural examination shows the presence of a population of fibroblasts located immediately beneath the basement membrane (the attenuated fibroblast sheath) that have been speculated to be capable of interaction with adjacent epithelial cells and to be involved with the regulation of local inflammatory and reparative processes.[32] The *submucosa* contains cartilage, muscle, and other supportive connective tissue elements, as well as the major portion of the tracheobronchial glands. The airway wall can also be considered as being composed of inner and outer layers, the former extending from the lumen to the outermost layer of smooth muscle and the latter from the smooth muscle to the airway adventitial–parenchymal boundary.[33]

Tracheal *cartilage* plates consist of about 16 to 20 U-shaped structures oriented in a horizontal plane with their open ends directed posteriorly.[34] The posterior (membranous) portion of the wall is free of cartilage. The spaces between the plates contain smooth muscle, tracheal glands, and collagenous and elastic tissue. The U-shape of the cartilage plates is maintained in the main bronchi; however, they become smaller and irregular in shape in lobar and segmental bronchi and disappear altogether in membranous bronchioles.

Elastic tissue in the lamina propria tends to be clustered in bundles oriented in a longitudinal direction. These bundles are especially well developed in the posterior portion of the trachea and main bronchi, where they form well-defined ridges.[35] Prominent elastic thickening is also present in the lamina propria at bronchial branch points. The cartilage plates are connected by bundles of fibroelastic tissue arranged predominantly in a longitudinal direction. At numerous sites, particularly in smaller airways, elastic fibers emanating from these longitudinally arranged bundles intermingle with the elastic tissue of the lamina propria.[1] These fibers are believed to help transmit to the more rigid and stronger cartilaginous fibrous tissue the tension that arises in the airway epithelium and lung parenchyma during breathing.

Tracheal muscle is found predominantly in the membranous portion, where it is organized in both longitudinal and transverse bundles (Figure 1-5); the latter are attached to the inner perichondrium close to the tip of the cartilaginous rings (the bundles joining each ring posteriorly).[36] Although somewhat less prominent, transverse fibers can also be found between the cartilage rings in the anterior portion. In the bronchi, muscle is organized in bundles close to the epithelium adjacent to the lamina propria. In the larger airways, the orientation is mainly circumferential, as in the trachea. In the more distal branches, the muscle is obliquely oriented and arranged in branching and anastomosing bundles that form irregular spirals in the airway wall. The proportion of muscle relative to airway diameter is greater in smaller airways.[37]

Loose connective tissue consisting of proteoglycans and mature collagen occupies much of the remainder of the submucosa. This tissue is continuous with connective tissue in the adjacent pulmonary arteries as well as that in the perivenous tissue near the hilum and in the interlobular and pleural interstitium. This interdependence of connective tissue is important in maintaining the overall structure of the lung and in providing a scaffold for the more delicate connective tissue of the parenchyma.

Tracheobronchial glands are specialized extensions of the airway surface epithelium into the submucosa. Both the number and size of the glands are greater in the more proximal airways,[38] and they are absent altogether in the smallest bronchi and bronchioles. The secretory portion of the gland is connected to the surface by a duct of variable length whose lining is similar to that of the surface airway epithelium (Figure 1-6). Multiple branched secretory tubules arise from the collecting duct. They are lined proximally by mucus-secreting cells that contain several histochemically different types of mucin and distally by serous cells.[39] The latter have been shown to contain a variety of substances that are potentially important in local airway defense, including lysozyme, lactoferrin, transferrin, and a protease inhibitor. Myoepithelial cells are present between the basement membrane and both types of epithelial cell[40] and are presumably responsible in part for expulsion of glandular secretions.

Many cells concerned with airway defense are found in the airway lamina propria and submucosa. *Lymphocytes* can be identified either singly or in clusters, the latter being variously termed lymphoid nodules, lymphoid aggregates, or bronchus-associated lymphoid tissue (BALT).[41] Lymphoid aggregates are composed of well-defined but unencapsulated

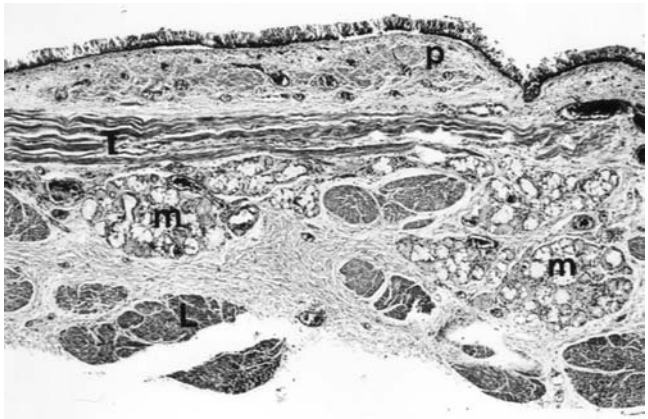

FIGURE 1-5 Posterior tracheal wall (hematoxylin-eosin stain). Lamina propria (p), transverse muscle bundle (T), longitudinal muscle bundle (L), and mucous glands (m).

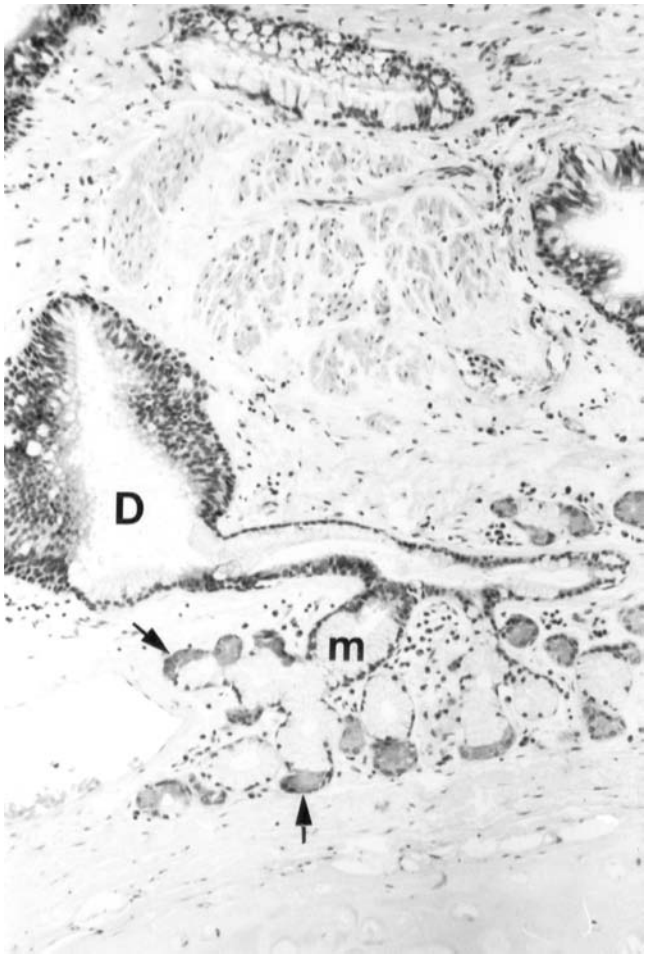

FIGURE 1-6 Bronchial gland (hematoxylin-eosin stain). Collecting duct (D), mucous cells (m), and serous cells (*arrows*).

clusters of mature lymphocytes, with smaller numbers of dendritic cells and lymphoblasts. The cells extend into the overlying epithelium, which is often flattened and lacks mucus or ciliary differentiation. Small, thin-walled blood vessels are present within the aggregates, possibly serving as a site for cell migration to and from the circulation. *Plasma cells*, primarily IgA and IgG in type, are common in the tracheobronchial wall, particularly in proximal bronchi in association with tracheobronchial glands, and in the lamina propria close to the basement membrane.[42] Isolated *macrophages* can be found throughout the lamina propria and submucosa and tend to be more numerous in individuals exposed to noxious materials such as cigarette smoke and inorganic dust. *Mast cells* can be found throughout the lung in airway, alveolar, pleural, and interlobular interstitial tissue, as well as in airway epithelium.[43] Although the cells are structurally similar, there appear to be differences in mediator content between them, suggesting variable functions.[44]

TRANSITIONAL AIRWAYS

The number and length of airways from the terminal membranous bronchiole to the alveolar sac as well as the pattern of their branching are quite variable.[45,46] Some of this irregularity may be related to spatial constraints imposed by pleura, interlobular septa, and larger airways and vessels. On average, however, there are probably about two to three respiratory bronchioles and four to six alveolar ducts between the terminal bronchiole and the alveolar sacs.

The surface of respiratory bronchioles is lined by a low columnar to cuboidal epithelium that gradually decreases in extent as the number of alveoli increases. In first- and second-order bronchioles, it is usually complete on one side, where it overlies a lamina propria and muscle continuous with that of the terminal bronchiole (Figure 1-7). As the number of alveoli increases, the lamina propria diminishes; however, muscle and elastic tissue continue in a spiral fashion surrounding the alveolar mouths.[47] Bronchiolar-type epithelium and lamina propria are absent in alveolar ducts. The contribution of transitional airways to gas exchange is probably substantial; in one investigation, approximately 35% to 40% of all alveoli in three acini were found to be located in these structures.[45]

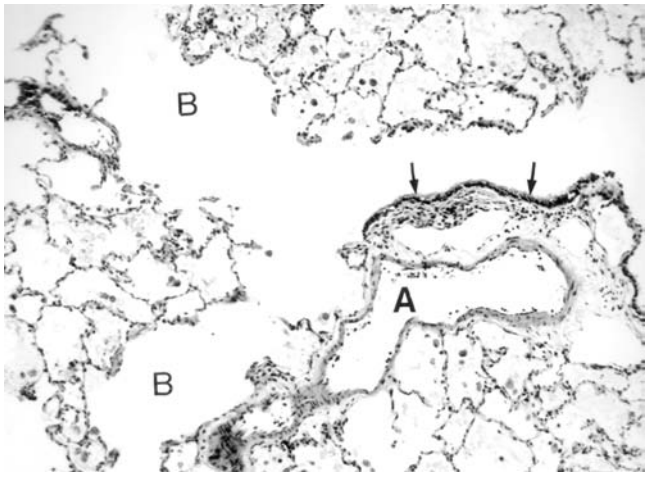

FIGURE 1-7 Respiratory bronchiole (hematoxylin-eosin stain). Epithelium (*arrows*), pulmonary artery (A), and distal branches (B). Reproduced with permission from Fraser RS, Müller NL, Colman N, Paré PD, Diagnosis of Diseases of the Chest, IV edition. Philadelphia: WB Saunders; 1999.

RESPIRATORY TISSUE

Alveoli are demarcated by septa composed of a continuous layer of epithelial cells overlying a thin interstitium (Figure 1-8). The former consists principally of two morphologically distinct cells, type I and type II; alveolar macrophages are also present on the epithelial surface. The interstitium contains capillaries involved in gas exchange, as well as connective tissue and a variety of cells responsible for maintaining alveolar shape and defense.

Type I alveolar cells cover approximately 95% of the alveolar septal surface.[48] The nucleus of this cell type is small and covered by a thin rim of cytoplasm containing few organelles. The rest of the cytoplasm extends as a broad

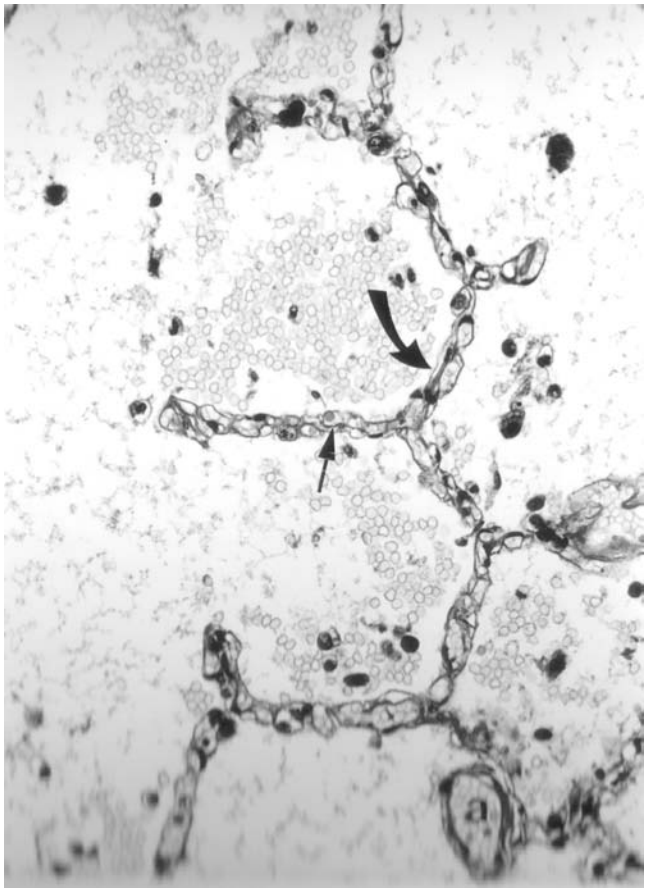

FIGURE 1-8 Alveoli (hematoxylin-eosin stain). Septa are composed of capillaries and a small amount of connective tissue (*short arrow*). In some foci (*curved arrow*), the latter appears to be thicker. Precapillary arteriole (a). (Airspaces contain fluid and red blood cells secondary to left heart failure.) Reproduced with permission from Fraser RS, Müller NL, Colman N, Paré PD, Diagnosis of Diseases of the Chest, IV edition. Philadelphia: WB Saunders; 1999.

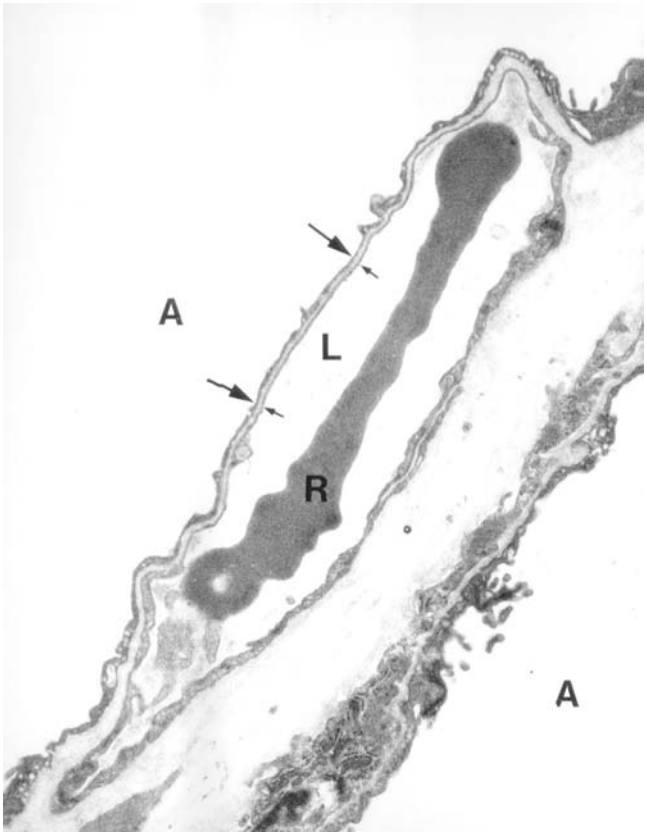

FIGURE 1-9 Air–blood barrier (electron micrograph). Red blood cell (R), capillary lumen (L), and alveolar airspace (A). Type I epithelial cytoplasm (*long arrows*) and endothelial cytoplasm (*short arrows*) are separated by a small amount of fused epithelial–endothelial basement membrane. (The interstitial tissue adjacent to the capillary is abnormally thickened by collagen.)

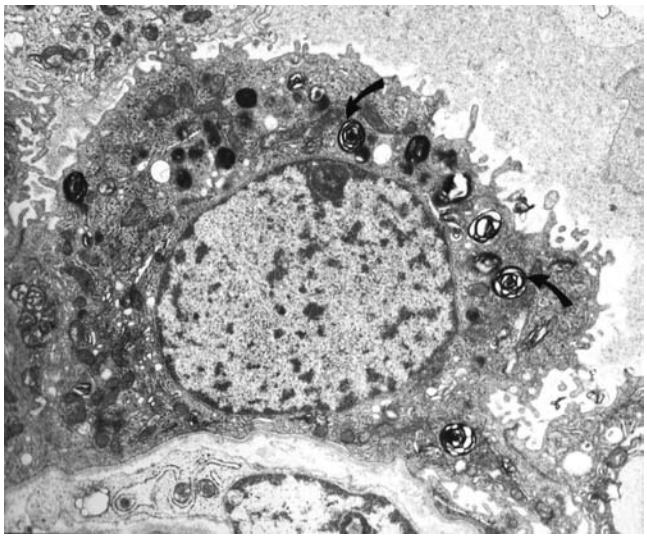

FIGURE 1-10 Type II epithelial cell (electron micrograph). Secretory granules with lamellar inclusions (*arrows*).

sheet 50 μm or more over the alveolar surface and is about 0.3 to 0.4 μm thick (Figure 1-9). Adjacent type I cells are joined to one another by tight junctions that provide a more or less complete barrier to the diffusion of fluid and water-soluble substances into the alveolar airspace.[49] The cell cytoplasm contains pinocytotic vesicles that can theoretically transport material in either direction across the air–blood barrier.

Type II epithelial cells tend to be located near corners where alveoli meet.[50] Their cytoplasm contains a well-developed endoplasmic reticulum, a prominent Golgi complex, and numerous membrane-bound, secretory granules (Figure 1-10). The latter contain characteristic lamellar inclusions that are the source of surfactant, the substance responsible for modifying alveolar surface tension.[51] Type II cells have a number of other important functions. A small number are mitotically active and are able to differentiate into type I cells, repopulating the alveolar surface as the latter die. There is also evidence that type II cells synthesize a variety of substances involved in alveolar structure and defense, including fibronectin and α_1-antitrypsin,[52,53] and are able to suppress lymphocyte proliferation and enhance macrophage function in the alveolar septa.[54]

Surfactant can be identified on transmission electron microscopy as an extremely thin (4 nm) layer of osmiophilic material that covers the alveolar epithelial surface.[55] It appears to consist of two components: (1) a film facing the alveolar airspace, which is composed of densely spaced, highly surface-active phospholipids, and (2) a deep layer containing surface-active phospholipids in a different physicochemical configuration and linked to proteins. Components of the superficial layer are thought to be recruited from the deeper layer (hypophase) during expansion of the lung and may reenter it at low lung volumes. The hypophase contains aggregates of lipid termed *tubular myelin* that have a characteristic fingerprint-like pattern.

A more or less continuous basement membrane is present adjacent to the type I and type II cells. Focally, it is fused with the basement membrane underlying the endothelial cells of the alveolar capillaries. Connective tissue, as well as endothelial and epithelial cell nuclei, tend to be absent from this region of basement membrane fusion. This portion of the septum—consisting of the thin type I cell sheet, the endothelial cell cytoplasm, and the fused basement membranes—is about 0.4 to 0.5 μm thick and is the principal site of gas exchange across the air–blood barrier. Elsewhere, endothelial and epithelial basement membranes are separated by an interstitial space of variable width that contains connective tissue (including elastic and collagen fibers) and a variety of cells.[56] The most prominent of these is the *myofibroblast* (*contractile interstitial cell*), which, as the name suggests, has ultrastructural features suggestive of both fibroblast and muscle differentiation (Figure 1-11).[57] Possible functions of these cells include local regulation of alveolar gas exchange ($\dot{V}/\dot{Q}$) (their contraction resulting in a reduction in capillary bloodflow), regulation of the fluid content of the alveolar interstitium, and production of connective tissue, both in the normal state and in pathologic alveolar fibrosis.[56,57]

Scattered *macrophages* are present in the alveolar interstitium and on its epithelial surface. Ultrastructurally, they have prominent surface microvilli and an abundance of membrane-bound primary and secondary lysosomes.[58]

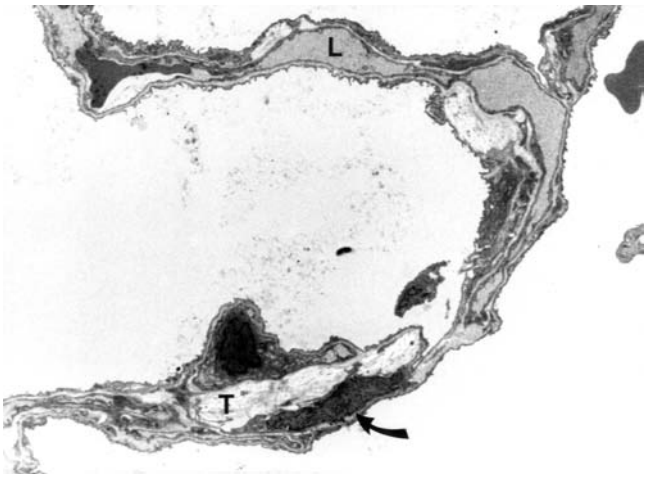

FIGURE 1-11 Alveolus with interstitial cell (electron micrograph). Interstitial cell nucleus (arrow), collagen (T), and capillary lumen (L).

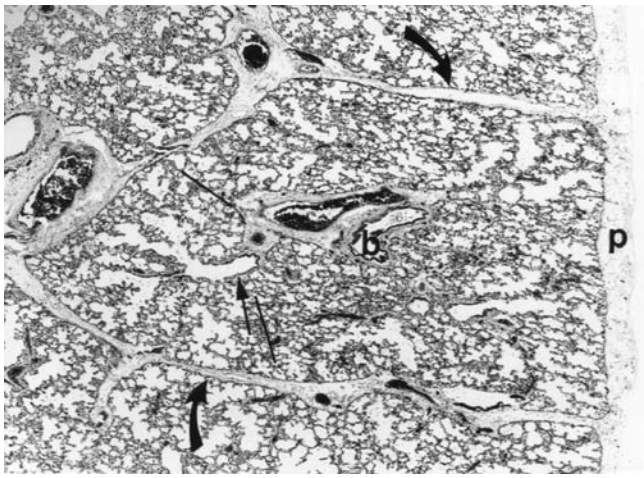

FIGURE 1-12 Secondary lobule and acinus (hematoxylin-eosin stain). Interlobular septa (*curved arrows*), pleura (p), central bronchiole (b), and respiratory bronchiole (*straight arrow*). The tissue between straight lines corresponds approximately to an acinus. Reproduced with permission from Fraser RS, Müller NL, Colman N, Paré PD, Diagnosis of Diseases of the Chest, IV edition. Philadelphia: WB Saunders; 1999.

Although they are morphologically similar, it is possible that these and other pulmonary macrophages have different functional capabilities. In fact, they have been considered to form several groups on the basis of their anatomic location[59]: (1) the *airway* macrophage, situated on or beneath the epithelial lining of conducting airways; (2) the *alveolar interstitial* macrophage; (3) the *alveolar surface* macrophage; (4) the *intravascular* macrophage, located adjacent to the capillary endothelial cell[60]; and (5) the *pleural* macrophage.[61] In addition to macrophages, a variety of other cells involved in parenchymal defense can be found in the alveolar interstitium, including *mast cells*,[62] *lymphocytes*, and *CD4, Ia+ dendritic cells*.[63]

Numerically, the alveolar macrophage is the most important nonepithelial cell in the parenchyma. Bronchoalveolar lavage of normal human airspaces yields a cell population including approximately 95% macrophages; dendritic cells (0.5%), lymphocytes (1 to 2%), monocyte-like cells of uncertain nature (2%), and polymorphonuclear leukocytes (less than 1%) account for the remainder.[63]

The number of alveoli in the adult human lung has been estimated to be about 300×10^6.[64] However, one group documented considerable variation in this figure among different individuals, with computed values ranging from 212×10^6 to 605×10^6.[65] In adults, both maximal diameter and depth of the alveolus (measured from the opening at the alveolar duct or sac to the base) are about 250 to 300 μm.[66]

LUNG UNIT

The most widely accepted subdivisions of lung parenchyma that have been proposed as the fundamental "unit" of lung structure are the secondary lobule and the pulmonary acinus. The former can be defined as the smallest discrete portion of the lung surrounded by connective tissue septa (Figure 1-12). It is somewhat polyhedral in shape, usually measures 1 to 2.5 cm in diameter, and contains a central membranous bronchiole, which gives rise to several respiratory bronchioles. Interlobular septa are best developed in the periphery of the lung, where they are continuous with the pleura (Figure 1-13). They are most numerous in the apical, anterior, and lateral aspects of the upper lobe and in the lateral and anterior regions of the lower lobes. In the central regions of the lung, septa are often difficult to identify or absent altogether. Because of this deficiency, there is an alternative definition of the lobule as consisting of pulmonary parenchyma supplied by a cluster of three to five terminal bronchioles.[67]

The pulmonary acinus comprises all lung tissue distal to the terminal bronchiole and is composed of respiratory bronchioles, alveolar ducts, alveolar sacs, alveoli, and their accompanying vessels and connective tissue (see Figure 1-12).

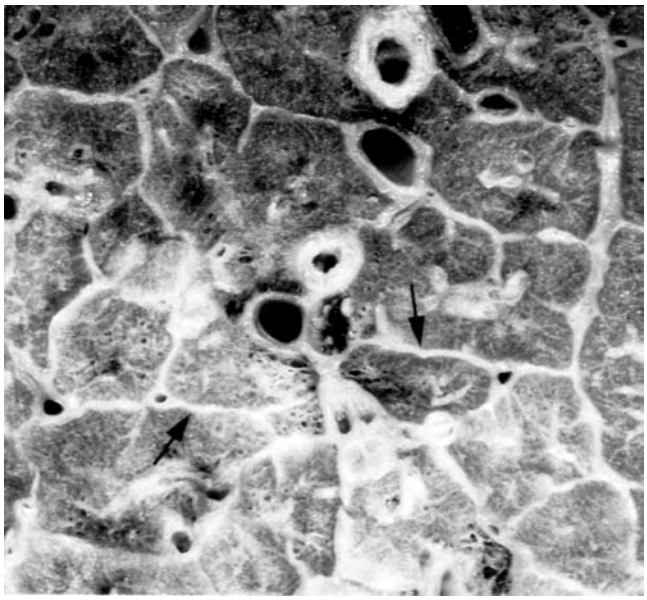

FIGURE 1-13 Interlobular septa (electron micrograph). Septa (*arrows*) are clearly evident as a result of thickening by carcinoma.

Measurements of acinar diameter vary between 6 and 10 mm, depending to some extent on the technique and the pressure at which the lung is inflated.[68]

CHANNELS OF PERIPHERAL AIRWAY AND ACINAR COMMUNICATION

The best understood of these structures are *alveolar pores*, small discontinuities in the alveolar septa also known as *pores of Kohn*. The size of the aperture is usually between 2 and 10 μm, and there are as many as 5 to 20 pores per alveolus.[69,70] They are generally round, and their edges are lined by type I epithelial cells. By transmission electron microscopy, they are usually free of cellular or other material in airway-fixed material; however, in vascular-perfused tissue, they are typically occluded by a thin film of surfactant.[69] Since it is probable that vascular-perfused tissue more closely represents the normal state of the alveolar airspace, the presence of this surfactant casts some doubt on the significance of the pores as a mechanism for collateral ventilation.

Direct communications between alveolar sacs and membranous bronchioles (*canals of Lambert*)[71] consist of epithelial-lined tubular structures that, in lungs fixed in deflation, range in diameter from practically "closed" to 30 μm in diameter. It is not known whether they provide accessory communication solely within acini or whether interacinar connections capable of subserving collateral ventilation occur as well. The results of experimental studies in both animals and humans indicate that particles considerably larger than either alveolar pores or most canals of Lambert are able to pass through collateral channels in lung parenchyma.[72] The precise anatomic correlate of these pathways is unclear.

PULMONARY VASCULATURE

Pulmonary Arteries

Pulmonary arteries are intimately related to the airways and divide with them, a branch accompanying the adjacent airway to the level of the respiratory bronchioles. In addition to these "conventional" vessels, many accessory branches arise at points other than corresponding airway divisions and extend directly into the adjacent lung parenchyma (Figure 1-14). *Elastic arteries* include the main pulmonary artery and its lobar, segmental, and subsegmental branches extending approximately to the junction of bronchi and bronchioles. The elastic laminae are located in the media and are organized in layers, which become less numerous as the vessels decrease in size. At a diameter of about 1,000 to 500 μm, only two layers—internal and external—can be identified, at which point the vessels are considered *muscular arteries*. Beginning at a diameter of about 100 μm, the arteries gradually lose their medial smooth muscle to become *arterioles*, so that, at a diameter of about 70 μm, the vessels are composed solely of a thin intima and a single elastic lamina that is continuous with the external elastic lamina of the parent artery. Arterioles continue to divide within the acinus, some accompanying bronchioles and alveolar ducts to the level of the alveolar sacs and others penetrating the adjacent parenchyma directly.[73] The smaller branches ramify to form the capillary network of the alveoli.

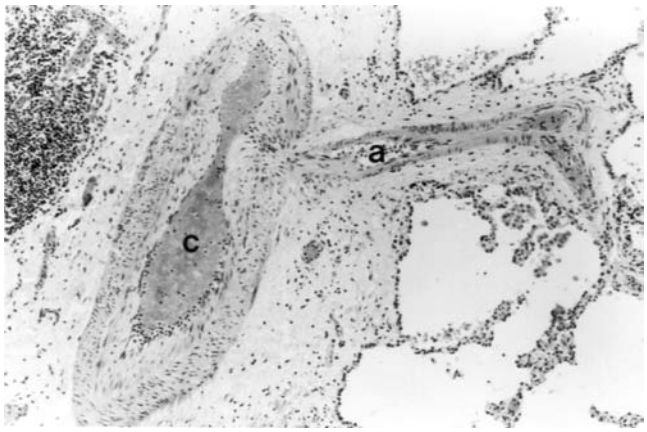

FIGURE 1-14 Pulmonary artery (hematoxylin-eosin stain). Conventional (c) and accessory (a) branches.

The pulmonary capillaries form a dense network of short interconnecting segments (Figure 1-15).[64] Measurements of the external diameter of these segments in fresh lung average about 8.6 μm; assuming the average thickness of the capillary endothelium to be about 0.3 μm, the average internal capillary diameter is thus about 8 μm. However, these values vary substantially with both lung volume and capillary pressure.[74,75] The average axial length of capillary segments is about 10 μm.

At all levels of the arterial tree, the *intima* is very thin, consisting of an endothelial cell layer and its adjacent basement membrane. The endothelial cells tend to be organized in an interlocking mosaic.[76] Like type I epithelial cells, they possess cytoplasm that extends as thin, plate-like processes measuring as little as 0.1 to 0.3 μm in thickness. Short, microvillus-like projections are present on the luminal surface, particularly in arteries.[77] These greatly increase the cell

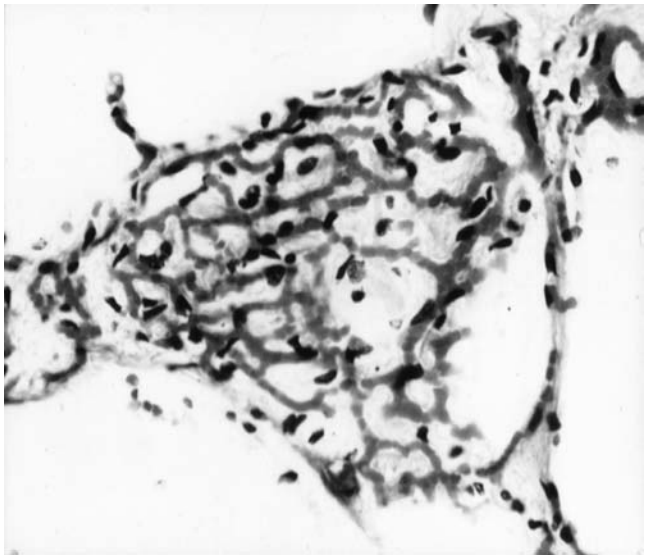

FIGURE 1-15 Pulmonary capillaries (hematoxylin-eosin stain). En face view of an alveolar wall shows numerous interconnecting capillary segments.

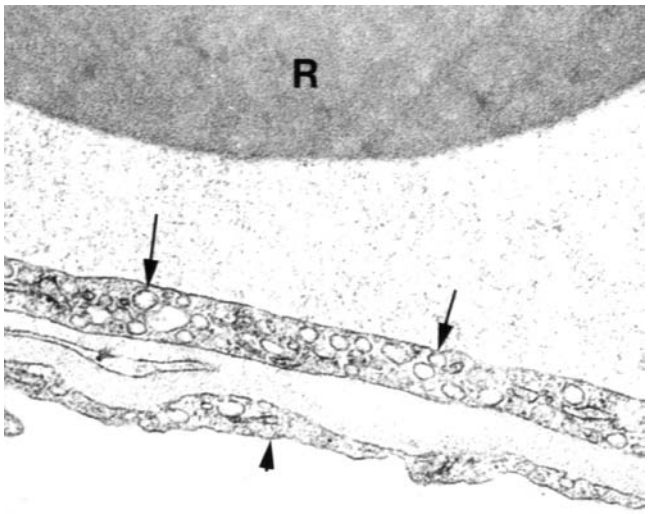

FIGURE 1-16 Pulmonary capillary endothelial cell (electron micrograph). Red blood cell (R), endothelial cell caveolae (*long arrows*), and type I epithelial cell (*short arrow*).

surface area and may play a role in the metabolism of various blood substances as well as facilitating metabolite transfer between the blood and the endothelial cells.

Small vesicles (*caveolae intracellulare*) can also be seen in endothelial cells, particularly those lining alveolar capillaries (Figure 1-16). In the latter, they are most prominent in the relatively thick, non–gas-exchanging part of the cell, at either the luminal or the abluminal surface.[78] Small electron-dense granules, considered to represent enzyme complexes responsible for various metabolic functions, can be seen at the bases of the vesicles. In addition to metabolic activity, the vesicles are believed to function in the transport of fluid and proteins between blood and interstitial tissues and across the air–blood barrier.[79]

Adjacent endothelial cells are joined by tight junctions.[79] For the most part, these are continuous; however, occasional intercellular clefts measuring up to 4 nm in thickness can be observed in alveolar capillaries. As determined by freeze–fracture techniques, these junctions are less complex than those of the alveolar epithelium, suggesting that the main site of solute impermeability in the air–blood barrier is the epithelium. The complexity of the endothelial junctions is variable in different parts of the vasculature, being greater in arterioles than in the more permeable venules, and greater in the base than at the apex of the lung.[80]

Several cell types can be found within the arterial–arteriolar wall in addition to smooth muscle and endothelial cells. *Pericytes* are located between the basement membrane and endothelial cells, predominantly in capillaries but also to some extent in arterioles. They have thin microfilament-containing processes that extend toward and attach to the endothelial cell surface.[81] *Mast cells* are also present in the connective tissue adjacent to pulmonary vessels, where they have been hypothesized to function as mediators of hypoxic vasoconstriction.[82]

Pulmonary Veins

Unlike pulmonary arteries, pulmonary veins and venules are not associated with airways and course instead in the parenchyma or in the connective tissue septa that delimit the secondary lobules. As in the pulmonary arterial system, numerous supernumerary vessels join the veins as they run to the hilum.[83] Histologically, pulmonary venules are indistinguishable from arterioles. Veins have a variable number of elastic laminae, between which are small bundles of smooth muscle cells. No valves are present within venous lumina. However, regularly spaced annular constrictions related to local accumulations of smooth muscle have been identified in the veins of some animals and have been hypothesized to be important in the control of pulmonary bloodflow.[84]

BRONCHIAL VASCULATURE

Most individuals have two to four bronchial arteries, a relatively common pattern being one on the right (originating from the third intercostal artery) and two on the left (arising directly from the aorta).[85] At the hila, the vessels form an intercommunicating circular arc around the main bronchi from which several branches (usually two or three on opposite sides of the airway wall) extend into the peribronchial connective tissue (see Figure 1-1). These branches send smaller twigs into the bronchial wall that ramify to form a vascular plexus in the submucosa. The latter can comprise as much as 10 to 20% of the volume of the normal subepithelial tissue, and it has been hypothesized that significant airway narrowing may occur when these vessels become congested.[86] Most arteries stop at the level of the terminal bronchioles.

The bronchial circulation has a dual venous drainage. One portion, related to the trachea and proximal bronchi, drains into the bronchial veins to the right side of the heart via the azygos and hemiazygos veins. The other, which drains the major portion of the intrapulmonary bronchial flow,[87] originates in anastomoses with small precapillary and postcapillary pulmonary vessels and courses via the pulmonary veins into the left atrium.

LYMPHATIC SYSTEM

Lymph flows along two major pathways in the lung, one located in the peribronchovascular connective tissue and the other in interlobular septal connective tissue (Figure 1-17).[88] Anastomotic channels up to 4 cm long connect the two pathways, particularly in the basal portion of the lower lobes. Lymphatic capillaries originate in the region of the distal respiratory bronchioles.[89] Some lymphatics are located immediately adjacent to alveolar airspaces in the interlobular, peribronchial, and perivascular connective tissue. These channels have been termed *juxtaalveolar* lymphatics because of their close topographic and possible functional relationship with the alveolar airspaces.[90]

Histologically, pulmonary lymphatics can be divided into capillaries and collecting channels, the latter defined by the presence of mural smooth muscle cells or valves. With the use of scanning electron microscopy, three types of vessel have been distinguished[91]: (1) relatively broad, ribbon-like structures that are closely linked to lymphatic capillaries (reservoir lymphatics); (2) tubular structures that may

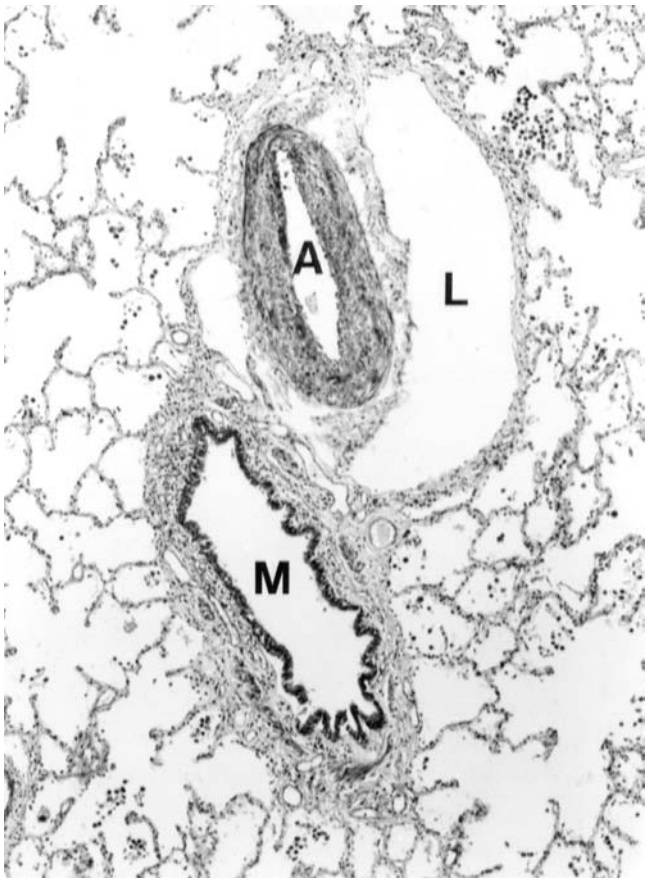

FIGURE 1-17 Perivascular lymphatic (hematoxylin-eosin stain). Membranous bronchiole (M), pulmonary artery (A), and lymphatic distended by fluid (L).

contain valves and extend for long distances without side branches (conduit lymphatics); and (3) complexes of plexiform vessels that surround the arteries, veins, and bronchi (sacculotubular lymphatics).

The basement membrane beneath lymphatic capillary endothelial cells is discontinuous, and intercellular junctions are absent between some endothelial cells. The resulting gaps in the vessel wall provide a relatively easy route for interstitial fluid that has leaked from alveolar septal capillaries to enter the lymphatic capillary lumen. The cytoplasm of the endothelial cells contains numerous microfilaments, which have been hypothesized to constitute an actin-like contractile system that regulates opening or closing of the intercellular gaps.[89]

Numerous valves 1 to 2 mm apart direct lymph flow in both the pleural and intrapulmonary lymphatics. Although they appear to be bicuspid in two-dimensional histologic sections, stereomicroscopic studies have shown most to be monocuspid and shaped like a funnel.[89] They are well adapted to unidirectional flow since they cannot be inverted and are easily occluded by flow in an abnormal direction.

PLEURA

The pleural space is enclosed by the visceral pleura, which covers the lungs, and by the parietal pleura, which lines the chest wall, diaphragm, and mediastinum.[92] The two join at the hila. Extensions of visceral pleura into the underlying lung form fissures (one major and one minor on the right and a single major one on the left) that divide the lung into lobes.

The visceral pleura can be considered to consist of three layers (Figure 1-18): (1) a superficial *endopleura*, composed of a continuous layer of mesothelial cells overlying a thin network of collagen and elastic fibers; (2) an *external elastic lamina*, which consists of a layer of collagen and elastic tissue whose thickness varies,[93] possibly as a result of differences in pleural stress during the respiratory cycle; and (3) a *vascular* (*interstitial*) layer that consists of connective tissue containing lymphatic and blood vessels. The last-named is continuous with the interstitial tissue of the interlobular septa and overlies a thin internal elastic lamina that encases the entire lung parenchyma and separates alveoli from the pleura, interlobular septa, and bronchovascular bundles.

The parietal pleura consists of a layer of connective tissue adjacent to the endothoracic fascia of the chest wall. It is divided into two parts by a layer of fibroblastic tissue, with most of the vessels being located in the part furthest from the pleura.

Mesothelial cells form a continuous layer overlying the entire visceral and parietal pleural surface. Their size and shape vary with transpulmonary pressure, the cells becoming more flattened as the lung expands.[92] Characteristically, the cell surface is covered by numerous long, thin microvilli. Fine strands approximately 150 nm in diameter emanate from the surface glycocalyx and extend between the microvilli; it has been suggested that fluid trapped in compartments formed by these strands and by the microvilli themselves protects the mesothelial cells from the trauma of normal pleural movement.[94]

Mesothelial cells are metabolically active and appear to have several functions. They are likely to be responsible, at least in part, for regulating the composition and amount of pleural fluid, and there is evidence that they have the ability to produce components of the submesothelial connective tissue.[95] Surface-active phospholipids similar to alveolar

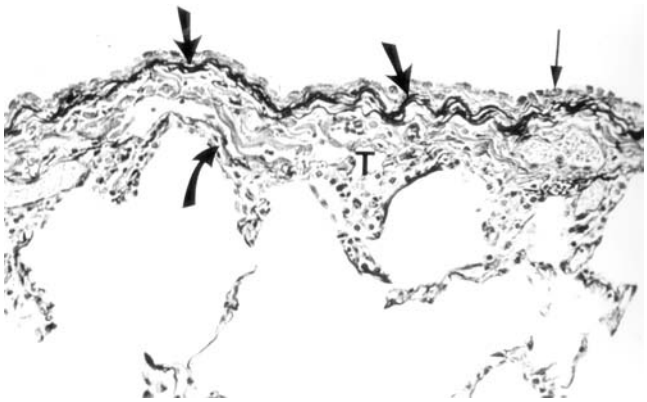

FIGURE 1-18 Visceral pleura (elastic van Giesen stain). Mesothelial cells (*thin arrow*), external elastic lamina (*thick arrows*), internal elastic lamina (*curved arrow*), and interstitial layer (T).

surfactant, most likely produced by mesothelial cells, have been found in the pleural space, where they may act as lubricants to facilitate pleural surface movement.[96]

PULMONARY INNERVATION

The lung is innervated by fibers that travel in the vagus nerve and in nerves derived from the second to fifth thoracic ganglia of the sympathetic trunk.[97] These fibers carry afferents and efferents of the parasympathetic and sympathetic autonomic nervous systems. In addition, there is pharmacologic and physiologic evidence for a nonadrenergic, noncholinergic, neural inhibitory efferent system (*nonadrenergic inhibitory system*), the anatomic pathway of which has not been well defined.[98] Although both excitatory and inhibitory components have been demonstrated in rodents, the human lung does not seem to have an excitatory pathway.

The vagus nerve contains preganglionic, parasympathetic efferent fibers and afferent fibers from various lung receptors. The sympathetic fibers are largely postganglionic efferent in type. Fibers of these two systems enter the hila, join with branches from the cardiac autonomic plexus, and form large posterior and smaller anterior plexuses in the peribronchovascular connective tissue. From these plexuses arise peribronchial and perivascular nerve fibers that extend distally. These connect with ganglia in the airway wall (Figure 1-19), where the vagal preganglionic fibers synapse with postganglionic neurons. At numerous points along their course, the airway nerves send out branches into the submucosa and mucosa that terminate in bronchial muscle, mucous glands, and small blood vessels.

Thicker fibers thought to be largely of an afferent sensory type bypass the ganglia. Some of these originate in receptors within the airway epithelium and lamina propria, tracheobronchial smooth muscle, the perichondrial tissue of large airways, the pulmonary parenchyma, and the pulmonary and bronchial arteries and veins.[99] Afferent receptors themselves have been divided into three groups on the basis of their distribution and physiologic response to various stimuli. The *irritant* or *cough receptors* are located predominantly in the trachea and large bronchi, their number decreasing progressively as the smaller peripheral airways are approached.[100] They are highly arborized myelinated nerve fibers with numerous free nerve endings that terminate in the airway epithelium. Their stimulation results in reflex bronchoconstriction, and their role is probably to inhibit inhalation of toxic material.[101]

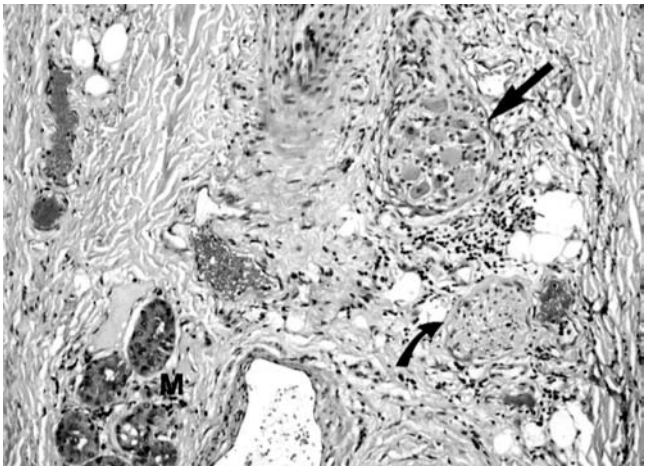

FIGURE 1-19 Bronchial wall innervation (hematoxylin-eosin stain). Connective tissue in the periphery of an airway wall shows a nerve (*curved arrow*) and ganglion (*straight arrow*). M = mucus gland.

The second major group of myelinated afferent nerves originates in *stretch receptors*. The latter are found in airway smooth muscle, where they are organized in tendril-like structures closely applied to the surface of individual muscle cells. They are responsible for sending information regarding lung volume to the respiratory center; integration of their input results in "off-switch" activity in the respiratory center. The third type of lung afferent originates in the *J* (*juxtacapillary*) *receptor*.[102] The nerve endings of these small, nonmyelinated fibers are situated in the lung parenchyma adjacent to alveolar septa and pulmonary capillaries and in the walls of the conducting airways.

Efferent innervation of the lung includes preganglionic fibers from vagal nuclei, which descend in the vagus to synapse with postganglionic neurons in the ganglia around the airways, and postganglionic fibers from the cervical sympathetic ganglia. Postganglionic cholinergic fibers supply the mucous glands of the large airways and the goblet cells, their stimulation causing an increase in secretion in both structures. Vagal efferent fibers also supply airway smooth muscle as well as pulmonary and bronchial vascular smooth muscle; stimulation of these cholinergic fibers causes airway smooth muscle contraction (resulting in airway narrowing) and vascular smooth muscle relaxation (leading to pulmonary and bronchial vascular dilatation).

The nerves to the pulmonary arteries run in the perivascular adventitia as far as parenchymal arterioles and connect extensively with the peribronchial nerves. Two plexuses of cholinergic fibers have been identified in the larger vessels, one located in the outer adventitia, and the other at the adventitia–media junction; in smaller vessels, only a single (inner) plexus is present.[103] Many nerves related to the pulmonary veins extend into the inner media, where they form a complex subendothelial network. The bronchial arteries contain a prominent nerve plexus at the media–adventitia junction, presumably consisting of efferent supply to the smooth muscles of these vessels; this plexus also sends numerous branches to the bronchial mucous glands.

RESPIRATORY MUSCLES

The respiratory muscles can be divided into four groups, each with different functions and mechanisms of action—the upper airway muscles, the diaphragm, the intercostal and accessory inspiratory muscles, and the abdominal muscles. These muscles can be considered to be "primary" (those that routinely contract during tidal breathing in normal individuals) and "accessory" (those that are not normally active during tidal breathing but are recruited when the demand for ventilation increases). The diaphragm is the

principal primary muscle of inspiration[104]; others include the scalene, parasternal, and external intercostal muscles. The accessory inspiratory muscles include the sternocleidomastoid, pectoralis, serratus anterior, trapezius, and latissimus dorsi muscles. The expiratory muscles include the abdominal, internal intercostal, and triangularis sterni muscles. The abdominal muscles include the rectus and transverse abdominis muscles and the external and internal oblique muscles; although these muscles are generally regarded as expiratory in function, they may also play an active role in inspiration.[105]

The diaphragm has a complex three-dimensional structure. Its central portion (the central tendon) consists of a sheet of connective tissue fibers that has a shape similar to that of a broad-bladed boomerang. The costal (chest wall) muscle fibers arise anteriorly from the xyphoid process and around the convexity of the thorax from ribs 7 to 12. Additional crural fibers arise from the lateral margins of the lumbar vertebrae. All these fibers converge toward the central tendon and are inserted into it nearly perpendicular to its margin. The greatest respiratory excursion occurs in the posterolateral portion of the hemidiaphragms, where the muscle fibers are longest.

There is evidence that the diaphragm is, in fact, two distinct muscles that have separate nervous and vascular supplies, as well as functions. The costal portion of the diaphragm is mechanically in series with the intercostal and accessory muscles, and its contraction can result in both descent of the diaphragm and elevation of the rib cage; by contrast, the crural portion is in parallel with the costal portion of the diaphragm, and its contraction results in descent of the diaphragm without elevation of the rib cage.[106]

The diaphragm is composed of three types of muscle fiber that have different histochemical profiles, related to the different myosin heavy-chain isotypes expressed by the cells[107]: (1) slow-twitch oxidative fatigue-resistant units (type 1); (2) fast-twitch oxidative glycolytic fatigue-resistant units (type 2a); and (3) fast-twitch glycolytic fatigable units (type 2b). Type 1 represents approximately 50% of the muscle fibers, type 2a about 20%, and type 2b about 30%. The relative proportions of the different types of motor fibers present in the diaphragm may be important in the pathogenesis of muscle fatigue and ventilatory failure. Histologically, the muscular portion comprises multiple muscle fascicles of variable size containing individual muscle fibers that also have different ultrastructural characteristics.[108]

The diaphragm has an abundant blood supply derived from the phrenic and intercostal arteries and from branches of the internal thoracic (mammary) arteries. Flow can increase to approximately 250 mL/min/100 g of muscle during maximal activation (about half of the maximal blood-flow to the heart).[109] An extensive lymphatic network drains fluid via collecting vessels into mediastinal channels.[108]

REFERENCES

1. Von Hayek H. The human lung. New York: Hafer; 1960.
2. Nagaishi C. Functional anatomy and histology of the lung. Baltimore: University Park Press; 1972.
3. Stone KC, Mercer RR, Freeman BA, et al. Distribution of lung cell numbers and volumes between alveolar and nonalveolar tissue. Am Rev Respir Dis 1992;146:454.
4. Gail DB, Lenfant CJM. State of the art—cells of the lung: biology and clinical implications. Am Rev Respir Dis 1983; 127:366.
5. Rhodin JAG. The ciliated cell: ultrastructure and function of the human tracheal mucosa. Am Rev Respir Dis 1966;93:1.
6. Godfrey RWA, Severs NJ, Jeffrey PK. Freeze–fracture morphology and quantification of human bronchial epithelial tight junctions. Am J Respir Cell Mol Biol 1992;6:453.
7. Herard AL, Zahm JM, Pierrot D, et al. Epithelial barrier integrity during *in vitro* wound repair of the airway epithelium. Am J Respir Cell Mol Biol 1996;15:624.
8. Widdicombe JH, Gashi AA, Basbaum CB, et al. Structural changes associated with fluid absorption by dog tracheal epithelium. Exp Lung Res 1986;10:57.
9. Nathanson I, Nadel JA. Movement of electrolytes and fluid across airways. Lung 1984;162:125.
10. Ebert RV, Terracio MJ. The bronchiolar epithelium in cigarette smokers: observations with the scanning electron microscope. Am Rev Respir Dis 1975;111:4.
11. Marsan C, Cava E, Roujeau J, et al. Cytochemical and histochemical characterization of epithelial mucins in human bronchi. Acta Cytol 1978;22:562.
12. Spicer SS, Schulte BA, Chakrin LW. Ultrastructural and histochemical observations of respiratory epithelium and gland. Exp Lung Res 1983;4:137.
13. Tamai S. Basal cells of the human bronchiole. Acta Pathol Jpn 1983;33:125.
14. Boers JE, Ambergen AW, Thunnissen FBJM. Number and proliferation of basal and parabasal cells in normal human airway epithelium. Am J Respir Crit Care Med 1988;157:2000.
15. Evans MJ, Cox RA, Shami SG, et al. Junctional adhesion mechanisms in airway basal cells. Am J Respir Cell Mol Biol 1990;3:341.
16. Widdicombe JG, Pack RJ. The Clara cell. Eur J Respir Dis 1982;63:202.
17. Massaro GD, Singh G, Mason R, et al. Biology of the Clara cell. Am J Physiol 1994;266:L101.
18. Jorens PG, Sibille Y, Goulding NJ, et al. Potential role of Clara cell protein, an endogenous phospholipase A_2 inhibitor, in acute lung injury. Eur Respir J 1995;8:1647.
19. Phelps DS, Floros J. Localization of pulmonary surfactant proteins using immunohistochemistry and tissue *in situ* hybridization. Exp Lung Res 1991;17:985.
20. DeWater R, Willems LNA, Van Muijen GNP, et al. Ultrastructural localization of bronchial antileukoprotease in central and peripheral human airways by a gold-labeling technique using monoclonal antibodies. Am Rev Respir Dis 1986;133:882.
21. Evans MJ, Cabral-Anderson LJ, Freeman G. Role of the Clara cell in renewal of the bronchiolar epithelium. Lab Invest 1978;38:648.
22. Ito T, Nakatani Y, Nagahara N, et al. Quantitative study of pulmonary endocrine cells in anencephaly. Lung 1987;165:297.
23. Boers JE, den Brok JL, Koudstaal J, et al. Number and proliferation of neuroendocrine cells in normal human airway epithelium. Am J Respir Crit Care Med 1996;154:758.
24. Becker KL. The coming of age of a bronchial epithelial cell. Am Rev Respir Dis 1993;148:1166.
25. Watanabe H. Pathological studies of neuroendocrine cells in human embryonic and fetal lung. Light microscopical, immunohistochemical and electron microscopical approaches. Acta Pathol Jpn 1988;38:59.
26. Hance AJ. Pulmonary immune cells in health and disease. Dendritic cells and Langerhans' cells. Eur Respir J 1993; 6:1213.

27. Schon-Hegrad MA, Oliver J, McMenamin PG, et al. Studies on the density, distribution, and surface phenotype of intraepithelial class II major histocompatibility complex antigen (Ia)-bearing dendritic cells (DC) in the conducting airways. J Exp Med 1991;173:1345.
28. Van Haarst JM, Verhoeven GT, de Wit HJ, et al. CD1a+ and CD1a− accessory cells from human bronchoalveolar lavage differ in allostimulatory potential and cytokine production. Am J Respir Cell Mol Biol 1996;15:752.
29. Erle DJ, Pabst R. Intraepithelial lymphocytes in the lung. A neglected lymphocyte population. Am J Respir Cell Mol Biol 2000;22:398–400.
30. Lamb D, Lumsden A. Intraepithelial mast cells in human airway epithelium: evidence for smoking-induced changes in their frequency. Thorax 1982;37:334.
31. Mette SA, Pilewski J, Buck CA, et al. Distribution of integrin cell adhesion receptors on normal bronchial epithelial cells and lung cancer cells *in vitro* and *in vivo*. Am J Respir Cell Mol Biol 1993;8:562.
32. Evans MJ, Van Winkle LS, Fanucchi MV, Plopper CG. The attenuated fibroblast sheath of the respiratory tract epithelial–mesenchymal trophic unit. Am J Respir Cell Mol Biol 1999;21:655–7.
33. Bai A, Eidelman DH, Hogg JC, et al. Proposed nomenclature for quantifying subdivisions of the bronchial wall. J Appl Physiol 1994;77:1011.
34. Reid L. Visceral cartilage. J Anat 1976;122:349.
35. Monkhouse WS, Whimster WF. An account of the longitudinal mucosal corrugations of the human tracheo-bronchial tree, with observations on those of some animals. J Anat 1986; 122:681.
36. Hakansson CH, Mercke U, Sonesson B, et al. Functional anatomy of the musculature of the trachea. Acta Morphol Neerl Scand 1976;14:291.
37. Matsuba K, Thurlbeck WM. A morphometric study of bronchial and bronchiolar walls in children. Am Rev Respir Dis 1972; 105:908.
38. Whimster WF, Lord P, Biles B. Tracheobronchial gland profiles in four segmental airways. Am Rev Respir Dis 1984;129:985.
39. Lamb D, Reid L. Histochemical types of acidic glycoprotein produced by mucous.
40. Meyrick B, Sturgess JM, Reid L. A reconstruction of the duct system and secretory tubules of the human bronchial submucosal gland. Thorax 1969;24:729.
41. Holt PG. Development of bronchus associated lymphoid tissue (BALT) in human lung disease: a normal host defense mechanism awaiting therapeutic exploitation? Thorax 1993;48:1097.
42. Soutar CA. Distribution of plasma cells and other cells containing immunoglobulin in the respiratory tract of normal man and class of immunoglobulin contained therein. Thorax 1976;31:158.
43. Brinkman GL. The mast cell in normal bronchus and lung. J Ultrastruct Res 1968;23:115.
44. Caughey GH. Serine proteinases of mast cell and leukocyte granules. A league of their own. Am J Respir Crit Care Med 1994;150:S138.
45. Pump KK. Morphology of the acinus of the human lung. Dis Chest 1969;56:126.
46. Parker H, Horsfield K, Cumming G. Morphology of distal airways in the human lung. J Appl Physiol 1971;31:386.
47. Young CD, Moore GW, Hutchins GM. Connective tissue arrangement in respiratory airways. Anat Rec 1980;198: 245.
48. Crapo JD, Barry BE, Gehr P, et al. Cell number and cell characteristics of the normal human lung. Am Rev Respir Dis 1982;125:332.
49. Bartels H. The air–blood barrier in the human lung: a freeze–fracture study. Cell Tissue Res 1979;198:269.
50. Parra SC, Burnette R, Rice HP, et al. Zonal distribution of alveolar macrophages, type II pneumocytes, and alveolar septal connective tissue gaps in adult human lungs. Am Rev Respir Dis 1986;133:908.
51. Bakewell WE, Viviano CJ, Dixon D, et al. Confocal laser scanning immunofluorescence microscopy of lamellar bodies and pulmonary surfactant protein A in isolated alveolar type II cells. Lab Invest 1991;65:87.
52. Crouch EC, Moxley MA, Longmore W. Synthesis of collagenous proteins by pulmonary type II epithelial cells. Am Rev Respir Dis 1987;135:1118.
53. Boutten A, Venembre P, Seta N, et al. Oncostatin M is a potent stimulator of α_1-antitrypsin secretion in lung epithelial cells: modulation by transforming growth factor-β and interferon-γ. Am J Respir Cell Mol Biol 1998; 18:511.
54. Paine R III, Mody CH, Chavis A, et al. Alveolar-epithelial cells block lymphocyte proliferation *in vitro* without inhibiting activation. Am J Respir Cell Mol Biol 1991;5:221.
55. Hawgood S, Shiffer K. Structures and properties of the surfactant-associated proteins. Annu Rev Physiol 1991;53:375.
56. Weibel ER, Bachofen H. Structural design of the alveolar septum and fluid exchange. In: Fishman AP, Renkin EM, editors. Pulmonary edema. Bethesda, MD: American Physiological Society; 1979. p. 1.
57. Kapanci Y, Assimacopoulos A, Irle C, et al. "Contractile interstitial cells" in pulmonary alveolar septa: a possible regulator of ventilation/perfusion ratio? J Cell Biol 1974;60:375.
58. Pratt SA, Smith MH, Ladman AJ, et al. The ultrastructure of alveolar macrophages from human cigarette smokers and nonsmokers. Lab Invest 1971;24:331.
59. Brain JD, Sorokin SP, Godleski JJ. Quantification, origin, and fate of pulmonary macrophages. In: Brain JD, Proctor DF, Reid LM, editors. Respiratory defense mechanisms. New York: Marcel Dekker; 1977. p. 849.
60. Dehring DJ, Wismar BL. Intravascular macrophages in pulmonary capillaries of humans. Am Rev Respir Dis 1989;139: 1027.
61. Frankenberger M, Passlick B, Hofer T, et al. Immunologic characterization of normal human pleural macrophages. Am J Respir Cell Mol Biol 2000;23:419–26.
62. Fox B, Bull TB, Gut A. Mast cells in the human alveolar wall: an electron microscopic study. J Clin Pathol 1981;34: 1333.
63. Van Haarst JMW, Hoogsteden HC, De Wit HJ, et al. Dendritic cells and their precursors isolated from human bronchoalveolar lavage: immunocytologic and functional properties. Am J Respir Cell Mol Biol 1994;11:344.
64. Weibel ER, Gomez DM. Architecture of the human lung. Science 1962;137:577.
65. Angus GE, Thurlbeck WM. Number of alveoli in the human lung. J Appl Physiol 1972;32:483.
66. Weibel ER. Morphometry of the human lung. New York: Academic Press; 1963.
67. Reid L. The secondary lobule in the adult human lung, with special reference to its appearance in bronchograms. Thorax 1968;13:110.
68. Lui YM, Taylor JR, Zylak CJ. Roentgen-anatomical correlation of the individual human pulmonary acinus. Radiology 1973;109:1.
69. Takaro T, Price HP, Parra SC. Ultrastructural studies of apertures in the interalveolar septum of the adult human lung. Am Rev Respir Dis 1979;119:425.
70. Kawakami M, Takizawa T. Distribution of pores within alveoli in the human lung. J Appl Physiol 1987;63:1866.

71. Lambert MW. Accessory bronchiole–alveolar communications. J Pathol Bacteriol 1955;70:311.
72. Martin HB. Respiratory bronchioles as the pathway for collateral ventilation. J Appl Physiol 1966;21:1443.
73. Pump KK. The circulation in the peripheral parts of the human lung. Dis Chest 1966;49:119.
74. Kendall MW, Eissmann E. Scanning electron microscopic examination of human pulmonary capillaries using a latex replication method. Anat Rec 1980;196:275–83.
75. Glazier JB, Hughes JMB, Maloney JE, et al. Measurements of capillary dimensions and blood volume in rapidly frozen lungs. J Appl Physiol 1969;26:65.
76. Heath D, Smith P. The pulmonary endothelial cell. Thorax 1979;34:200.
77. Smith U, Ryan JW, Michie DD, et al. Endothelial projections as revealed by scanning electron microscopy. Science 1971;173:925.
78. Smith U, Ryan JW. Substructural features of pulmonary endothelial caveolae. Tissue Cell 1972;4:49.
79. Schneeberger EE. Structural basis for some permeability properties of the air–blood barrier. Fed Proc 1978;37:2471.
80. Yoneda K. Regional differences in the intercellular junctions of the alveolar-capillary membrane in the human lung. Am Rev Respir Dis 1982;126:893.
81. Meyrick B, Reid L. Ultrastructural findings in lung biopsy material from children with congenital heart defects. Am J Pathol 1980;101:527.
82. Nadziejko CE, Loud AV, Kikkawa Y. Effect of alveolar hypoxia on pulmonary mast cells in vivo. Am Rev Respir Dis 1989;140:743.
83. Hislop A, Reid L. Fetal and childhood development of the intrapulmonary veins in man: branching pattern and structure. Thorax 1973;28:313.
84. Schraufnagel DR, Patel KR. Sphincters in pulmonary veins: an anatomic study in rats. Am Rev Respir Dis 1990;141:721.
85. Cudkowicz L. Bronchial arterial circulation in man: normal anatomy and responses to disease. In: Moser KM, editor. Pulmonary vascular diseases. New York: Marcel Dekker; 1979. p. 111.
86. Mariassy AT, Gazeroglu H, Wanner A. Morphometry of the subepithelial circulation in sheep airways: effect of vascular congestion. Am Rev Respir Dis 1991;143:162.
87. Deffebach ME, Charan NB, Lakshminarayan S, et al. The bronchial circulation—small, but a vital attribute of the lung. Am Rev Respir Dis 1987;135:463.
88. Lauweryns JM. The blood and lymphatic microcirculation of the lung. In: Sommers SC, editor. Pulmonary pathology decennial; 1966–1975. New York: Appleton-Century-Crofts; 1975. p. 1.
89. Lauweryns JM, Baert JH. Alveolar clearance and the role of the pulmonary lymphatics. State of the art. Am Rev Respir Dis 1977;115:625.
90. Lauweryns JM. The juxta-alveolar lymphatics in the human adult lung. Histologic studies in 15 cases of drowning. Am Rev Respir Dis 1970;102:877.
91. Scfraufnagel DE. Forms of lung lymphatics: a scanning electron microscopic study of casts. Anat Rec 1992;233:547.
92. Wang N-S. Anatomy and physiology of the pleural space. Clin Chest Med 1985;6:3.
93. Mariassy AT, Wheeldon EB. The pleura: a combined light microscopic, scanning, and transmission electron microscopic study in the sheep: I. Normal pleura. Exp Lung Res 1983;4:293.
94. Andrews PM, Porter KR. The ultrastructural morphology and possible functional significance of mesothelial microvilli. Anat Rec 1973;177:409.
95. Rennard SI, Jaurand M-C, Bignan J, et al. Role of pleural mesothelial cells in the production of the submesothelial connective tissue matrix of lung. Am Rev Respir Dis 1984;130:267.
96. Hills BA. Graphite-like lubrication of mesothelium by oligolamellar pleural surfactant. J Appl Physiol 1992;73:1034.
97. Spencer H, Leof D. The innervation of the human lung. J Anat 1964;98:599.
98. Richardson JB. Nonadrenergic inhibitory innervation of the lung. Lung 1981;195:315.
99. Sant'Ambrogio G. Nervous receptors of the tracheobronchial tree. Annu Rev Physiol 1987;49:611.
100. Laitinen A. Ultrastructural organization of intraepithelial nerves in the human airway tract. Thorax 1985;40:488.
101. Sant'Ambrogio G. Information arising from the tracheobronchial tree of mammals. Physiol Rev 1982;62:531.
102. Fox B, Bull TB, Guz A. Innervation of alveolar walls in the human lung: an electron microscopic study. J Anat 1980;131:6832.
103. Amenta F, Cavallotti C, Ferrante F, et al. Cholinergic innervation of the human pulmonary circulation. Acta Anat 1983;117:58.
104. De Troyer A, Loring SH. Actions of the respiratory muscles. In: Roussos C, editor. The thorax. In: Lenfant C, editor. Lung biology in health and disease. New York: Marcel Dekker; 1995. p. 535–63.
105. De Troyer A. Mechanical role of the abdominal muscles in relation to posture. Respir Physiol 1998;53:341.
106. Supinski G, DiMarco AF, Hussein F, et al. Analysis of the contraction of series and parallel muscles working against elastic loads. Respir Physiol 1995;87:141.
107. Edwards RHT, Faulkner JA. Structure and function of the respiratory muscles. In: Roussos C, editor. The thorax. In: Lenfant C, editor. Lung biology in health and disease. New York: Marcel Dekker; 1995. p. 185–217.
108. Leak LV. Gross and ultrastructural morphologic features of the diaphragm. Am Rev Respir Dis 1979;119 Suppl:3.
109. Comtois AS, Rochester DF. Respiratory muscle blood flow. In: Roussos C, editor. The thorax. In: Lenfant C, editor. Lung biology in health and disease. New York: Marcel Dekker; 1995. p. 633–61.

CHAPTER 2

STATICS OF THE RESPIRATORY SYSTEM

Edgardo D'Angelo, Joseph Milic-Emili

The static mechanical properties of the respiratory system and its component parts are studied by determining the corresponding volume–pressure (*V–P*) relationships. These relationships are usually represented as single functions, implying that pressures depend on volume alone and that the pressure across any respiratory structure is represented by a single value. Neither of these assumptions is correct since static pressures differ depending on the previous volume and time history of the respiratory system. Thus, the quasistatic *V–P* curves that are obtained as volume is changed in progressive steps from residual volume (RV) to total lung capacity (TLC) and back again are loops. Plastoelastic and, in most instances, viscoelastic properties of the lung and chest wall, as well as differences in the sequence of recruitment and derecruitment of lung units between inflation and deflation, are responsible for the presence of these loops. Moreover, the static pressure across the lung and chest wall varies at different sites because of the effects of gravity and because of the different shapes of these structures.[1] Also, the static pressure across the respiratory system may become nonuniform under conditions involving airway closure. Nevertheless, for the sake of simplicity, the quasistatic *V–P* relationships will be hereafter considered as single functions.

V–P RELATIONSHIPS DURING RELAXATION

Respiratory System

During relaxation of the respiratory muscles, the net pressure developed by the respiratory system (P_{rs}) results from the forces exerted by its elastic elements and equals the difference between alveolar pressure (P_{alv}) with the airway opening closed, or mouth pressure with the glottis open, and body surface pressure (P_{bs}). Conversely, P_{rs} indicates the pressure that the respiratory muscles must exert to maintain that lung volume with open airways. This applies, however, only when the shape of the respiratory system is the same whether the respiratory muscles are active or not. For a given volume, the elastic energy, and hence the elastic pressure, is minimal for the configuration occurring during relaxation and is increased whenever that configuration is changed.

The *V–P* curve of the relaxed respiratory system is shown in Figure 2-1. In the middle volume range, the relationship is almost linear, whereas it curves markedly above 85% and below 15% of vital capacity (VC). The tangent to the *V–P* curve represents the compliance of the respiratory system (C_{rs}). The volume at $P_{alv} = 0$ is the resting volume of the respiratory system: during quiet breathing, it usually corresponds to the lung volume at the end of a spontaneous expiration, which is, by definition, the functional residual capacity (FRC).

Measurements of lung volume and mouth pressure do not normally pose major technical problems. However, voluntary relaxation of the respiratory muscles is difficult to obtain, and there is evidence that tonic respiratory muscle activity is often present in awake subjects.[2] Certainly, the quasistatic *V–P* relationships obtained in the paralyzed subject better reflect the elastic forces that develop in the respiratory system and its component parts. Their comparison with those in the awake subject is, however, problematic (see below).

Lung and Chest Wall

Because the chest wall (w) and lung (L) are placed pneumatically in series, the volume changes of the chest wall (ΔV_w) and the lung (ΔV_L) should be the same (except for shifts of blood) and equal to that of the respiratory system (ΔV_{rs}), whereas, under static, relaxed conditions, $P_{rs} = P_{alv} = P_w + P_L$. It follows that the reciprocal of the compliance of the respiratory system equals the sum of the reciprocals of lung and chest wall compliance. Because P_w indicates the pressure exerted by the relaxed chest wall, it follows that when the respiratory muscles contract at fixed volumes, $P_{alv} = P_w + P_L + P_{mus}$.

The pressure exerted by the lung is the difference between alveolar and pleural surface pressure, $P_L = P_{alv} - P_{pl}$; that exerted by the chest wall is the difference between pleural surface and body surface pressure, $P_w = P_{pl} - P_{bs}$. Thus, during relaxation, $P_w = P_{pl}$, whereas during muscle contraction at constant lung volume, $P_{pl} = P_w + P_{mus}$ and $P_{pl} = P_{alv} - P_L$. In humans, P_{pl} is usually obtained from esophageal pressure measurements; the interpretation of these measures requires, however, some caution.[3,4]

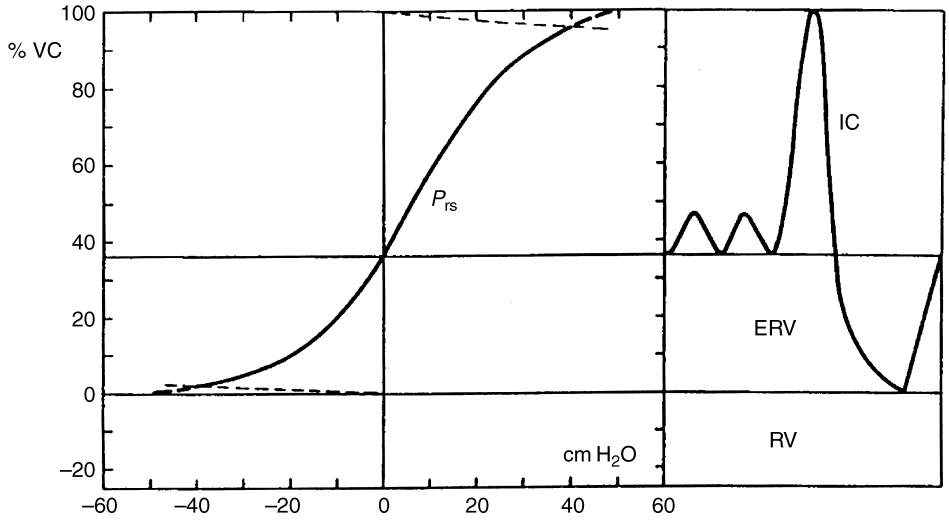

FIGURE 2-1 Quasistatic *V–P* curve of the total respiratory system during relaxation in a sitting posture, with a spirogram showing subdivisions of lung volume. The *broken lines* indicate the volume change due to gas compression at total lung capacity and the expansion at residual volume (RV) during relaxation against an obstruction. ERV = expiratory reserve volume; IC = inspiratory capacity; VC = vital capacity. Adapted from Agostoni E and Hyatt R.[2]

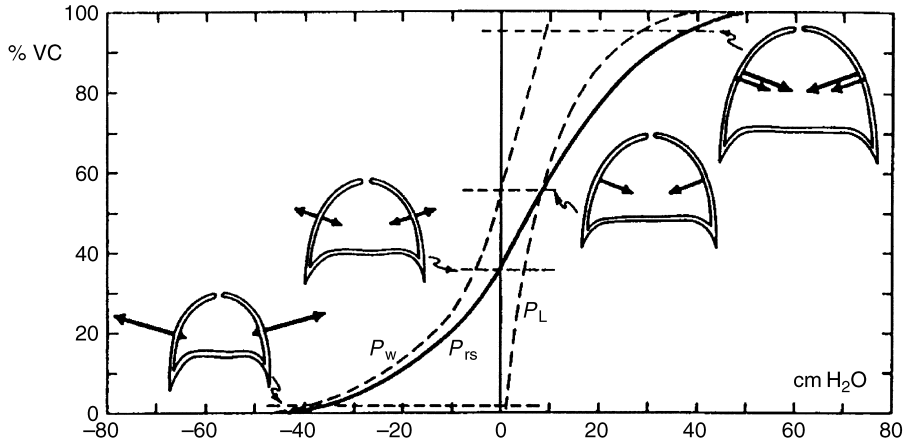

FIGURE 2-2 Quasistatic *V–P* curves of lung (P_L), chest wall (P_w), and total respiratory system (P_{rs}) during relaxation in a sitting posture. The static forces of lung and chest wall are indicated by the *arrows* in the drawings. The dimensions of the arrows are not to scale; the volume corresponding to each drawing is indicated by the horizontal broken lines. VC = vital capacity. Adapted from Agostoni E and Hyatt R.[2]

The *V–P* relationships of the lung and chest wall in the sitting position are shown in Figure 2-2: the former increases its curvature with increasing lung volume, whereas the opposite is true for the latter. The fall in C_{rs} at high lung volumes is therefore mainly due to the decrease in C_L, whereas at low lung volume it reflects the decreased C_w. In the tidal volume range, the *V–P* relationships of both the lung and chest wall are nearly linear, and C_L and C_w are about the same. In the sitting posture, they amount to 4% VC per 1 cm H_2O, or 0.2 L/cm H_2O. In normal young subjects, the resting volume of the lung ($P_L = 0$) is close to RV, and the lung recoils inward over nearly all the VC. Hence, the resting volume of the respiratory system occurs when the inward recoil of the lung is balanced by the outward recoil of the chest wall, that is, $P_w + P_L = 0$. This volume depends on posture (see below). A detailed description of the quasistatic behavior of the lung is given elsewhere in this book (see Chapter 3, "Statics of the Lung").

Rib Cage, Diaphragm, and Abdominal Wall

Lung volume changes occur because of the displacement of the rib cage facing the lung (rc,L) and of the diaphragm–abdomen (di-ab). From this viewpoint, these two structures may be considered to operate in parallel: hence $P_w = P_{rc,L} = P_{di\text{-}ab}$, and $\Delta V_w = \Delta V_{rc,L} + \Delta V_{di\text{-}ab}$. Wade[5] and Agostoni and colleagues[6] computed these volumes by means of geometric approaches, which, however, involve questionable assumptions. The *V–P* curves obtained with these procedures are shown in Figure 2-3. They indicate that (1) the volume contributed by the diaphragm–abdomen displacement is greater than that contributed by the displacement of the pulmonary part of the rib cage; (2) the volume contributed by the pulmonary part of the rib cage at FRC is about the same in the supine and erect postures, changes in FRC with posture being therefore essentially due to displacement of the diaphragm–abdomen; (3) at any given lung volume, the contribution of the pulmonary part of the rib cage is larger in the

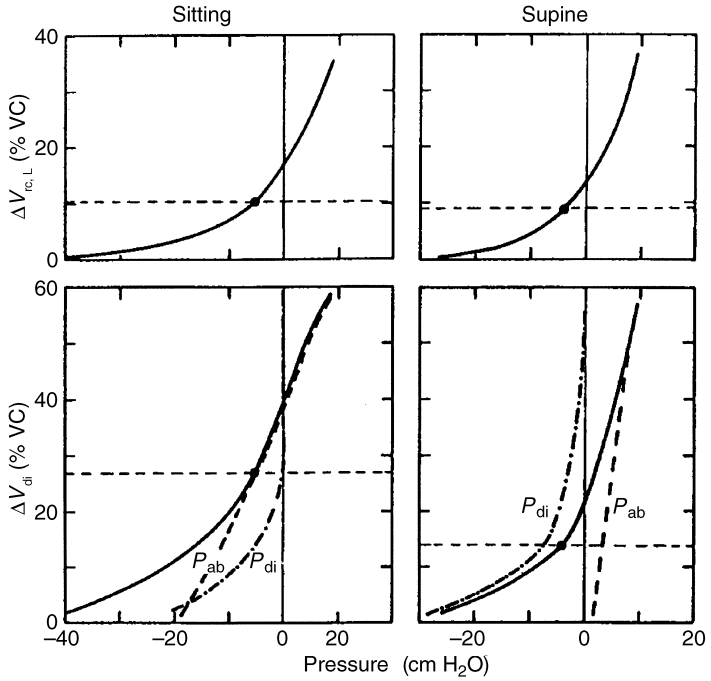

FIGURE 2-3 Quasistatic *V–P* curves of pulmonary rib cage (*upper diagrams*) and abdomen–diaphragm (*lower diagrams*) during relaxation in sitting (*left diagrams*) and supine postures (*right diagrams*). The abdomen–diaphragm is thought to be placed in parallel with the pulmonary rib cage, that is, that facing the lung. Data on the volume contribution of the pulmonary rib cage ($\Delta V_{rc,L}$) and diaphragm (ΔV_{di}) and those on pressures of the chest wall (P_w), diaphragm (P_{di}), and abdomen (P_{ab}) are from Agostoni and Hyatt.[2] The *horizontal broken line* indicates the volume at functional residual capacity.

supine than in the erect posture; (4) the compliance of the pulmonary part of the rib cage ($C_{rc,L}$) and of the diaphragm–abdomen ($C_{di\text{-}ab}$) decreases progressively below FRC, whereas $C_{rc,L}$ increases more than $C_{di\text{-}ab}$ with increasing lung volume above FRC; and (5) the *V–P* curve of the pulmonary part of the rib cage does not change its shape with posture, whereas that of the diaphragm–abdomen becomes markedly more concave in the erect posture, probably because of postural tonus of the abdominal muscles, and greater distortion of the abdominal wall due to the greater top-to-bottom difference in abdominal pressure in the erect than in the supine posture.[7]

Konno and Mead showed that partitioning of chest wall volume could be achieved without any assumptions being made when the two parallel pathways were represented by the rib cage (rc) and the abdominal wall (ab,w): hence $\Delta V_w = \Delta V_{rc} + \Delta V_{ab,w}$, whereas the pressures across the two pathways are P_w and abdominal pressure (P_{ab}), respectively.[8,9] Figure 2-4 shows the *V–P* curves obtained with this approach. They confirm some conclusions reached with the aforementioned approach: (1) the volume of the rib cage or of its pulmonary part at FRC is nearly the same in all postures, despite different lung volumes; and (2) the relationship between the volume contributed by the two parts over the VC shifts rightward when the subject moves from the supine to the erect posture. Because of the lifting and expansion of the rib cage, $\Delta V_{di\text{-}ab}$ (Wade and Agostoni approach) is shared partly by rib cage and partly by abdominal wall displacement (Konno and Mead approach); a comparison between the volume partitioning obtained with the two approaches suggests that the fraction of the volume displaced by the diaphragm not shared by the abdominal wall is roughly 0.5 during a VC maneuver.

Mead redefined the pressure acting on the rib cage, taking into account that (1) this structure is facing both the lungs and the abdominal contents, being affected partly by P_{pl} and partly by P_{ab}, and (2) the diaphragm operates in series with the rib cage, insofar as transdiaphragmatic pressure ($P_{di} = P_w - P_{ab}$) acts to move the ribs out and up.[10] Hence, in Mead's model, the pressure exerted by the passive rib cage should be given by $P_{rc} = (1-f)\ P_w + fP_{ab} - kP_{di}$, where f is the fraction of the internal surface of the rib cage not facing the lung, and k, which includes the pertinent geometric features, is the fraction of transdiaphragmatic pressure acting on the rib cage; setting $K = f + k$, $P_{rc} = (1-K)\ P_w + KP_{ab}$. When $P_{di} = 0$ and, hence, $P_w = P_{ab}$, as in the erect posture at or above FRC, $P_{rc} = P_w$, which was the primitive definition of the pressure developed by the passive rib cage. On the other hand, when $P_{di} \neq 0$, as in the erect posture below FRC, or in the supine posture over most of the VC, P_{rc} should be higher than P_w and closer to P_{ab} the smaller the lung volume since f increases with decreasing lung volume. Indeed, it appears that $P_{rc} = P_{ab}$ when $K = 1$, as should be the case near RV, owing to the cranial position of the diaphragm. Unfortunately, the values of K and their dependence on lung volume are not known with precision, particularly in the supine posture. However, assuming that K changes linearly from 0.9 to 0.2 between RV and TLC, in both the standing and supine postures, it appears that, with decreasing lung volume, no progressive decrease in rib cage compliance occurs in Mead's model, implying that the increasing stiffness of the chest wall observed below FRC is due essentially to the diaphragm, particularly in the supine posture. On the other hand, as in the previous models, there

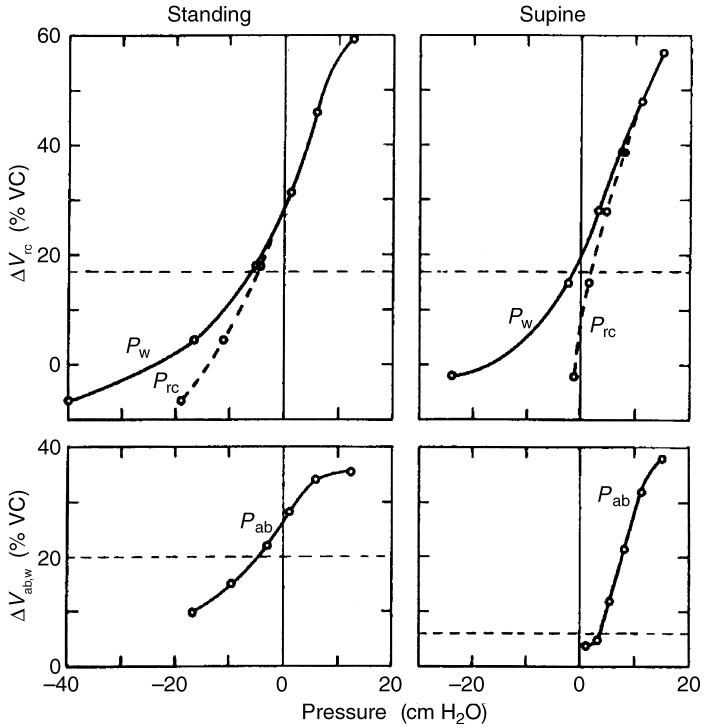

FIGURE 2-4 Quasistatic *V–P* curves of rib cage (*upper diagrams*) and abdominal wall (*lower diagrams*) during relaxation in standing (*left diagrams*) and supine (*right diagrams*) postures, according to Mead's model of the chest wall (see text). Data on the volume contribution of the rib cage (ΔV_{rc}) and abdominal wall ($\Delta V_{ab,w}$) and those on pressures of the chest wall (P_w) and abdomen (P_{ab}) are from Konno and Mead.[9] The effective pressure developed by the passive rib cage (P_{rc}) was computed with use of the equation $P_{rc} = (1 - K)\ P_w + KP_{ab}$, on the assumption that K varied linearly from 0.9 to 0.2 over the vital capacity range in both postures (see text). The *horizontal broken line* indicates the volume at functional residual capacity.

is a rightward displacement of the curve when the subject changes from the erect to the supine posture.

Other models of the chest wall have been proposed in addition to those mentioned above, yet it can be shown that in all of them the same force balance equations apply for the rib cage and the abdominal compartment, respectively.[11–13] Indeed, common to all models are the assumptions that (1) the rib cage and the abdominal wall can move independently, that is, $\Delta V_{ab,w}$ and ΔV_{rc} are unique functions of P_{ab} and ΔP_{rc}, respectively, thus allowing the compliance to be obtained as the ratio between the changes in compartmental volume and pressure, and (2) the relaxed rib cage and abdomen move with one degree of freedom, that is, without significant distortion. Although some results suggest that coupling between the rib cage and the abdominal wall can be ignored, it is questionable whether forces acting on small areas of the rib cage surface, such as diaphragmatic tension, should be considered to affect the rib cage motion in the same manner as those acting on relatively large fractions of the rib cage surface, such as $(1 - f)\ P_w$ or fP_{ab}.[14,15] In fact, distortion of the relaxed rib cage should be expected to take place whenever $P_w \neq P_{ab}$, and hence $P_{di} \neq 0$, as in the supine posture or in the erect posture below FRC. Indeed, rib cage distortion occurs with contraction of the diaphragm in tetraplegic subjects, with electrophrenic stimulation both in animals and humans, and in normal subjects during voluntary and involuntary respiratory acts.[16–21] In the dog, the relationships between indices of pulmonary rib cage motion and P_w, as well as between indices of abdominal wall motion and P_{ab}, obtained during isolated diaphragm contractions, fall close to their respective relaxation lines, thus indicating high rib cage flexibility and, hence, negligible mechanical coupling between pulmonary and abdominal rib cage compartments.[17,22,23] The pattern of motion of the relaxed rib cage during immersion in seated subjects suggests that rib cage flexibility is fairly large also in humans.[14] On the other hand, Ward and colleagues concluded that in human subjects, coupling between the pulmonary and abdominal rib cage should ensure transmission to the pulmonary rib cage of a substantial fraction of the force acting on the abdominal rib cage.[24] These authors, however, pointed out the several theoretical and technical limitations of their approach.

Effects of Posture

As shown in Figure 2-5, the *V–P* curve of the lung does not change appreciably with posture, whereas that of the chest wall does, mainly because of the effect of gravity on the abdomen. Indeed, when the effect of gravity in the erect posture is simulated in the supine subject by applying negative pressure around the lower abdomen, the *V–P* curve of the respiratory system becomes almost equal to that in the sitting posture.[16]

The relaxed abdomen has been likened to a container filled with liquid, in which part of the wall is distensible.[25] The level at which the abdominal pressure is equal to ambient pressure, the "zero level," depends on the equilibrium

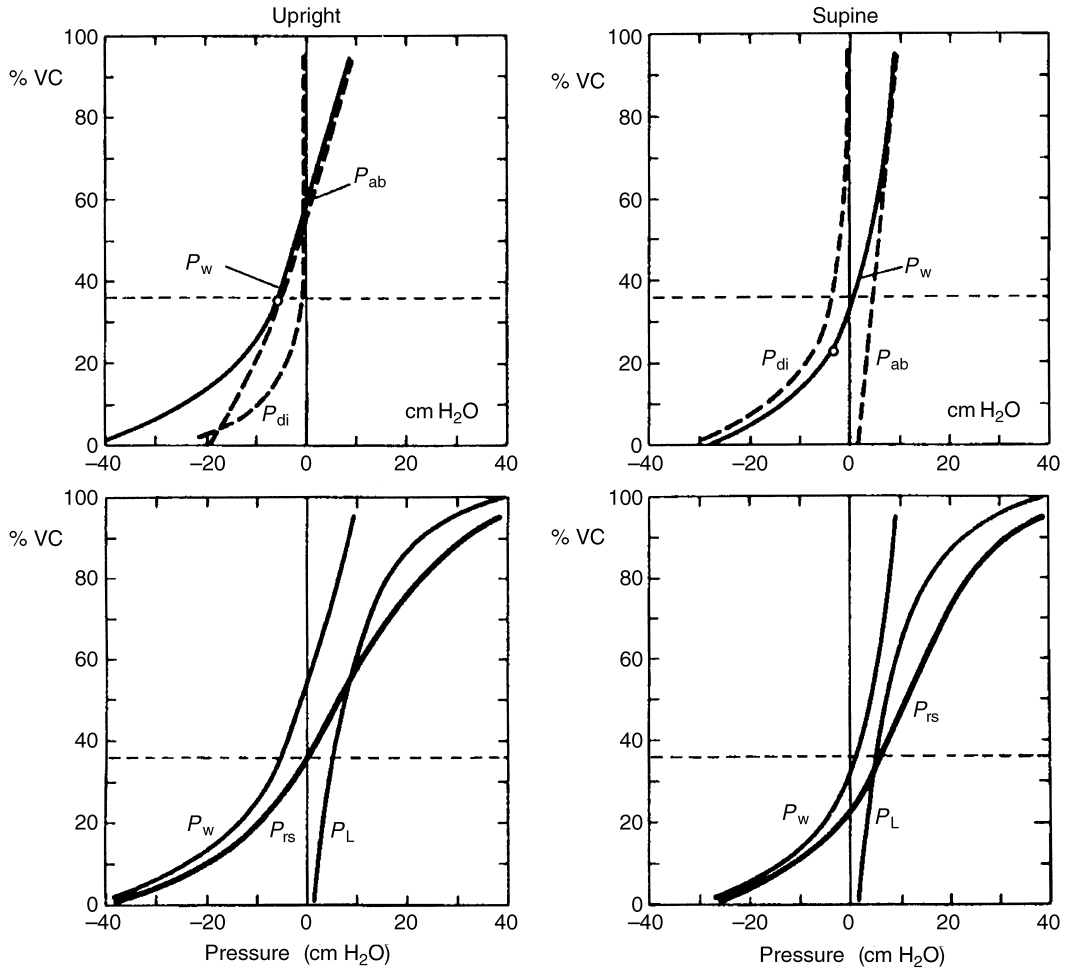

FIGURE 2-5 Pressure contributed by various parts of the respiratory system in the sitting and supine postures. The *upper diagrams* show the *V–P* relationships of the chest wall and the pressures contributed by the diaphragm and abdomen. The *circles* indicate the resting volume of the respiratory system. The *lower diagrams* show the *V–P* relationships of chest wall, lung, and total respiratory system. Adapted from Agostoni E and Hyatt R.[2]

among the elastic forces of the abdominal wall, diaphragm, rib cage, and lung and the gravitational force of the abdominal contents. The position of the zero level with respect to the lung height determines whether gravity exerts inflationary or deflationary effects on the respiratory system. At the end of a normal expiration, that is, at the resting volume of the respiratory system, the zero level of P_{ab} is about 3 to 4 cm vertically beneath the diaphragmatic dome in the erect posture, close to the ventral and dorsal wall of the abdomen in the supine and prone postures, respectively, and midway between the two sides in the lateral decubitus.[25] As a consequence, the resting volumes of both the chest wall and respiratory system decrease from the erect posture, to the lateral, prone, and supine postures.

The zero level of abdominal pressure shifts, however, with lung volume, but by different degrees in the standing and horizontal postures. In erect posture, the hydrostatic pressure applied on the abdominal surface of the diaphragm is about -20 cm H_2O at RV and nil at about 55% VC (the resting volume of the chest wall), whereas at higher volumes it is above atmospheric pressure. In the supine position, as in the other horizontal postures, changes in P_{ab} over the VC are nearly half those occurring in the upright posture, and shift of the zero level with lung volume is accordingly smaller, whereas $\Delta V_{ab,w}$ is larger in the erect posture. The reduced compliance of the abdominal wall in the erect posture should, in turn, be attributed to the larger average hydrostatic pressure applied to the anterior abdominal wall. In the lateral posture, the action of gravity on the abdomen-diaphragm is expiratory in the lower part and inspiratory in the upper part. Because the two lungs have different sizes, the *V–P* relationships should therefore differ somewhat between the right and left lateral decubitus. Indeed, in anesthetized paralyzed subjects, FRC was found to be 0.24 L (2% VC) larger in the right than in the left lateral decubitus.[26]

Effects of Aging

The static behavior of the respiratory system—lungs and chest wall—changes throughout life. From young adulthood on, the VC decreases almost linearly with age, the decrease being due to an increase in the RV, as TLC remains essentially unchanged.[27–29] The recoil of the lung decreases with

age, particularly at high lung volume, whereas its resting volume increases substantially.[28–31] On the other hand, the recoil of the chest wall increases and its resting volume decreases with age: hence, the *V–P* curve of the chest wall becomes less steep, pivoting around a point at about mid–lung volume, where its recoil remains the same.[29] The increase of FRC with age is therefore mainly due to the decrease of lung recoil and is less marked than that of RV. Since in the mid-volume range the compliance of the lung increases whereas that of the chest wall decreases, the compliance of the respiratory system becomes only slightly smaller with age.[29]

Effects of Anesthesia and Paralysis

The most evident effect of general anesthesia in normal supine subjects is the fall in FRC: according to Rehder and Marsh, this is given by $\Delta FRC = 10.2 - 0.23 \times age - 47 \times weight/height$, where ΔFRC is expressed as a percentage of awake FRC and age, weight, and height are given in years, kilograms, and centimeters, respectively.[32] Such a decrease occurs also in the prone posture, but not in the sitting posture, and probably in the lateral decubitus.[26,33]

The tonic activity of both inspiratory rib cage muscles and diaphragm has been suggested to augment the chest wall recoil in awake subjects.[34–36] However, this tone is minimal in the supine position, when ΔFRC is larger, and larger in the erect posture, when ΔFRC is zero, and the presence of diaphragmatic tone is controversial.[35,36] Perhaps tonic activity affects only the shape of the diaphragm, as recent studies have documented changes in the shape of the diaphragm not followed by any evident cephalad displacement with induction of anesthesia and paralysis.[36–38] Expiratory activity that appears in abdominal muscles with anesthesia does not seem to be a major factor in lowering FRC since the latter does not decrease further with muscular paralysis.[39,40] The shape of the chest wall also changes with anesthesia: the anteroposterior diameters of both the rib cage and abdomen decrease, and the transverse diameters increase, but it is unclear whether the volume of the thoracic cavity is effectively reduced because of these dimensional changes.[36,41–43]

Increases in intrathoracic blood volume up to 0.3 L have been reported to occur with anesthesia–paralysis.[36,42] Although this might account for part of the fall in FRC, the lack of an established relationship between the increases in intrathoracic blood volume and the concurrent reductions in FRC precludes any firm conclusion concerning their impact.

Figure 2-6 shows the *V–P* curves of the respiratory system, lung, and chest wall obtained in supine, normal subjects before and after anesthesia and after anesthesia and paralysis. They indicate that the decrease in FRC with anesthesia reflects the increase in the elastic recoil of the respiratory system that takes place at all lung volumes. This increase is independent of the depth of anesthesia, is not affected by muscle paralysis or prevented by large, repeated lung inflations, and does not change with time.[40,44] Similar to the FRC changes, those changes in mechanical properties of the respiratory system also exhibit large intersubject variability, suggesting that the same factors could be responsible for both changes.

The decrease in C_{rs} is mainly due to changes in lung mechanics.[40,45] Several mechanisms can lower C_L, such as increased smooth muscle tone or stimulation of other contractile elements in the airways or lung parenchyma, atelectasis or small airway closure, and changes in surfactant function. It is presently impossible to tell which of these mechanisms is the main cause of the decrease in C_L. Lung *V–P* curves on inflation from FRC are often S-shaped, a fact that could be indicative of alveolar recruitment (see Chapter 3, "Statics of the Lung"). In normal supine anesthetized paralyzed subjects, atelectasis developing at FRC is eliminated with positive end-expiratory pressure.[46] Such alveolar recruitment can quantitatively account for both the increase in C_L and the leftward shift of the static *V–P* curve of the lung observed with positive end-expiratory pressure in some normal supine anesthetized paralyzed subjects.[47] However, similar changes in lung mechanics have been observed also in normal seated subjects after maintained hyperinflation and have been attributed to changes in either pulmonary blood volume or airway muscle tone.[48–50] It is also still unclear whether the decrease in C_L during anesthesia is

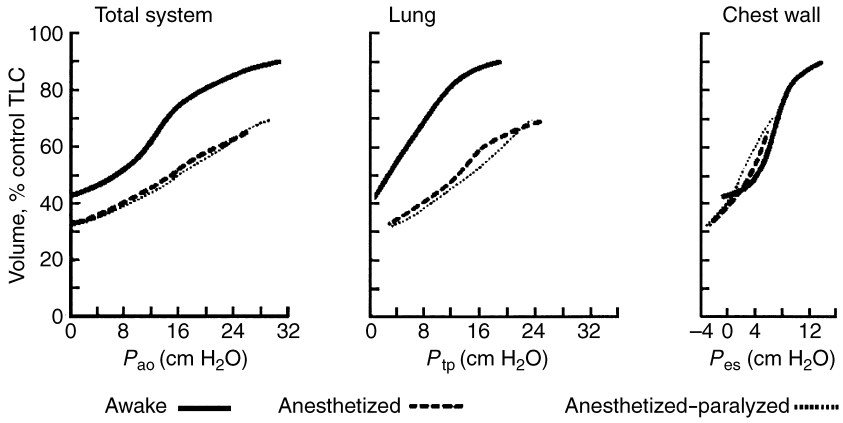

FIGURE 2-6 Mean quasistatic *V–P* curves of the respiratory system, lung, and chest wall from five normal subjects on deflation from airway opening pressure (P_{ao}) of 30 cm H_2O while awake, anesthetized, and anesthetized and paralyzed. P_{es} = esophageal pressure; P_{tp} = transpulmonary pressure; TLC = total lung capacity. Adapted from Westbrook PR et al.[40]

primarily due to any of the mechanisms mentioned above. It has been suggested that changes in C_L are, in fact, secondary to changes in chest wall function leading to volume reduction as conditions where ventilation occurs at low lung volumes are eventually associated with decreases in compliance, probably due to higher surface tension.[40,51] This sequence of events contrasts, however, with the observation that in supine anesthetized paralyzed subjects, C_L, although increased with positive end-expiratory pressure, remains substantially lower than that reported for awake supine subjects at comparable lung volumes.[2,47]

The *V–P* relationship of the chest wall seems to undergo only minor changes with anesthesia and paralysis in the supine posture. Static compliance in the mid-volume range is similar to that reported for awake supine subjects during relaxation, but the static *V–P* curve either shifts to the right or becomes less curved at low lung volumes.[2,40,45,47,52] Indeed, the increase in chest wall compliance with positive end-expiratory pressure in anesthetized paralyzed subjects is only one-fourth of that occurring over the same range of lung volume during relaxation in awake supine subjects.[2,47]

V–P RELATIONSHIPS DURING STATIC MUSCULAR EFFORT

Alveolar Pressure

Figure 2-7 shows the maximum static inspiratory and expiratory pressures exerted for 1 to 2 seconds in the lung at different volumes in the upright posture. The horizontal distance between the outer, solid curves, and the relaxation curve gives the net pressure exerted by the contraction of the respiratory muscles, represented by the broken lines. The expiratory pressures are larger when the chest is inflated, whereas the inspiratory pressures are larger when it is deflated. This behavior depends upon the mechanical advantage and the force–length relationship of the agonist muscles, besides being influenced by the mechanical features of the passive structures involved, by the action of the antagonist muscles, and by possible inhibition of the effort. Indeed, the length of the expiratory muscles increases with lung volume, the opposite being true for the inspiratory muscles.

The maximum inspiratory pressure exerted by children is nearly the same as that of adults at most lung volumes. This has been related to the smaller radius of curvature of the rib cage of the diaphragm and of the abdominal wall in the children.[53,54] At large lung volumes, however, the maximum expiratory pressures exerted by adults are markedly greater than those of children, probably because of greater development of accessory expiratory muscles in adults. Women do not develop as high maximum pressures as men of similar age.[54] Some of this difference seems to be due to the difference in strength of the accessory muscles, but use might be important as respiratory muscle strength can be increased by training.[55,56] The decrease in the maximum respiratory pressures with age, their difference between sexes, and their scattering among subjects parallel those observed for the maximum strength of other groups of muscles in the body.[55]

Pressure swings during respiratory effort are inversely related to the compliance of the fluid that fills the respiratory system. Because of the dependence of gas compliance upon absolute pressure, differences in pressure swings may become very large if the same efforts are made at low ambient pressure. At high altitude, therefore, the *V–P* diagram is very much curtailed, although the actual mechanics of the chest are not changed.[57]

Abdominal and Thoracic Pressures

Whereas transthoracic pressure measurements give the resultant of the actions of all muscles that act simultaneously, a separation of the contributions of inspiratory and expiratory muscles may be done through transdiaphragmatic (P_{di}) and transabdominal (P_{ab}) pressure measurements. The pressures on the thoracic and abdominal sides of the diaphragm at different lung volumes during static inspiratory, expiratory, and expulsive efforts are shown in Figure 2-8. During maximum inspiratory effort, P_{ab} remains roughly as at relaxation in

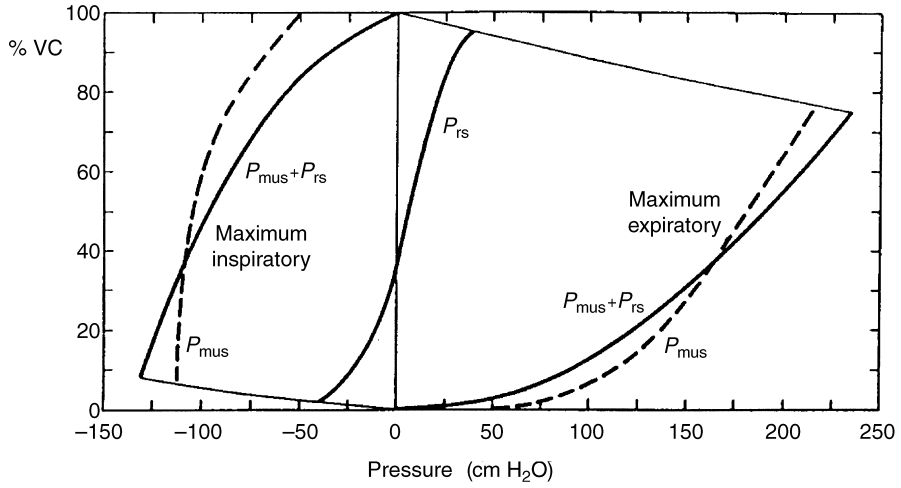

FIGURE 2-7 *V–P* relationships during maximum static inspiratory and expiratory efforts ($P_{mus} + P_{rs}$) and during relaxation (P_{rs}) in the sitting posture. The *broken lines* indicate the net pressure contributed by muscles. Adapted from Agostoni E and Hyatt R.[2]

trained subjects. Up to about 60% VC, P_{di} remains almost constant as the volume increases, and then it decreases progressively. Hence, maximum P_{di} (horizontal distance between solid and broken lines) is similar to maximum transthoracic pressure (horizontal distance between solid line and ordinate at zero pressure). In untrained subjects, however, P_{ab} often increases at high lung volumes because of abdominal muscle contraction, as revealed by electromyography.[58–62] In these subjects, P_{di} is roughly the same at all lung volumes. During a moderate expiratory effort above resting volume, P_{di} is nil as the diaphragm is relaxed. During a maximum effort, there is an abdominal–thoracic pressure difference (see Figure 2-8).[63] Since at these volumes the diaphragm is not passively distended, this pressure is attributable to diaphragmatic contraction. With decreasing lung volumes, the pressure contributed by diaphragm contraction increases progressively.[64]

During expulsive efforts, the muscles of the abdominal wall contract more vigorously than during maximum expiratory efforts, and the diaphragm also increases its activity. P_{ab} reaches its maximum and P_{pl} is smaller than during maximum expiratory efforts, suggesting that, in this instance, the action of the muscles of the abdominal wall on the rib cage is more than balanced by diaphragmatic contraction. The pressure differences between maximum expulsive and expiratory efforts decrease with lung volume, disappearing at RV. At large and mid–lung volumes, the values of P_{di} are generally higher during maximum expulsive than during maximum inspiratory efforts, indicating that the diaphragm yields the largest abdominal–thoracic pressure difference when the lower ribs are pulled down and in by the contraction of the muscles of the abdominal wall.[53] Indeed, the lateral diameter of the rib cage at the xiphoid level, relative to its value at the same lung volume during relaxation, is reduced by the activity of the expiratory muscles and increased by the inspiratory muscles.[65]

Bellemare and Bigland-Ritchie showed, with single-twitch occlusion, that the diaphragm is maximally activated during maximum expulsive efforts at end-expiration.[66] When reporting a similar study, Gandevia and McKenzie concluded that the same applies to the diaphragm during inspiratory efforts at end-expiration.[67] Maximal activation of the diaphragm during maximum expulsive efforts, but not during maximum inspiratory efforts, was also shown by Hershenson and colleagues.[68] Differences in P_{di} between the two maneuvers seem, however, to be caused by the different length and/or shape of the contracted diaphragm, rather than by level of activation. Indeed, from fluoroscopic examination of the diaphragm during maximal diaphragmatic inspiratory efforts with or without superimposed maximum expulsive efforts, Hillman and colleagues concluded that diaphragmatic length is greater during the combined maximum efforts and that the greater length was responsible for the associated larger P_{di}.[69] Moreover, from the records of change in the configuration of the rib cage and abdomen, they inferred that the diaphragm is being stretched for the entire duration (3 to 5 seconds) of the combined maximum efforts and suggested that pleiometric contraction of the diaphragm provides an additional explanation for the larger P_{di} during this maneuver. Similarly, Gandevia and colleagues, using digital sequential radiography, found that the diaphragm length decreased by about 20% during maximal inspiratory efforts but was essentially unchanged during maximal expulsive efforts with the glottis open.[70]

Upper Volume Extreme

A balance between the elastic force, which rises markedly at both volume extremes, and that of the agonist muscles, which decreases at both extremes (see Figure 2-7), seems to set the upper volume limit in those subjects in whom, at the end of maximum inspiration, the abdominal muscles do not contract.[71] In some subjects, however, the abdominal muscles contract at full inspiration, as shown by their marked electrical activity.[59–62] Hence, in these subjects, the limit to the upper volume extreme (TLC) is set also by the contraction of the antagonist muscles. It is difficult to assess whether the decrease in the force of the agonist muscles at high lung volumes depends only on mechanical disadvantage or also on a reflex inhibition of the effort.[72] Marked increases of TLC have been reported to occur during acute asthmatic attacks.[73–76] Most of these results are probably due

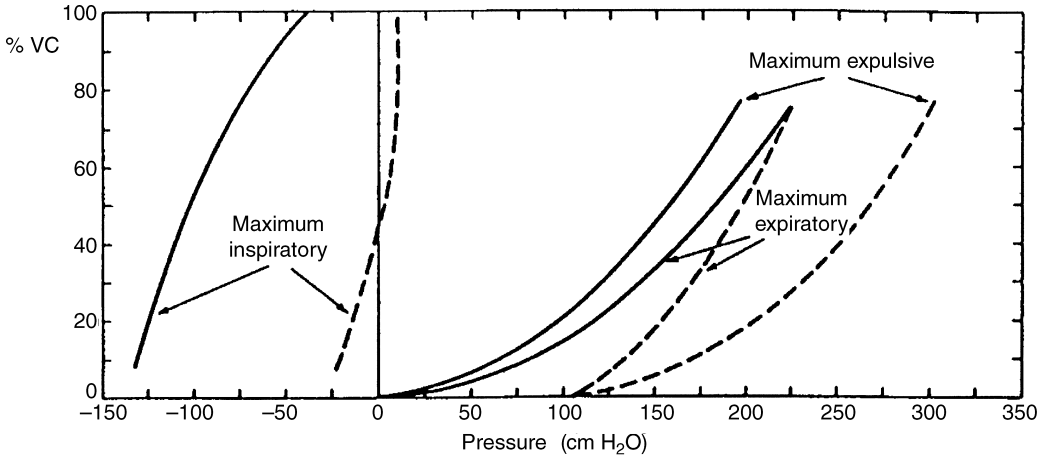

FIGURE 2-8 Lung volume against pressure above (*continuous line*) and below (*broken line*) the diaphragmatic dome during maximum static inspiratory, expiratory, and expulsive efforts. Adapted from Agostoni E and Hyatt R.[2]

to technical artefacts.[77–79] Those increases that do occur are, in general, caused by loss of lung recoil since increased strength of the inspiratory muscles could be demonstrated in only one subject.[79] Finally, small but significant increases in TLC were found in normal subjects breathing 6% carbon dioxide; the mechanism was unclear, but since lung recoil was unaltered, changes in the chest wall were probably responsible.[80]

Lower Volume Extreme

In normal adults, the RV is determined by a static balance between the elastic force exerted by the respiratory system and that of the respiratory muscles. The patency of most airways at RV is shown by the finding that a positive expiratory pressure rapidly applied to the respiratory system at or near RV produces a sudden expiration of a volume of air greater than that which could be squeezed from the intrathoracic airways.[81] The diaphragm is contracted at RV, as shown both by the presence of electrical activity and by a P_{di} that is higher than at relaxation (see Figure 2-8).[64,82] The marked contraction of the diaphragm seems to be related to the simultaneous activation of the abdominal muscles rather than to a reflex because it is negligible when the lung volume is reduced to the same extent by an external force.[83]

In elderly humans, the static balance described above does not occur because expiration at low lung volume proceeds so slowly that it is ended by an abrupt inspiration before the expiratory flow has ceased, and, therefore, no static balance is achieved.[81] In these subjects, however, the main cause of the increased RV is airway closure, which occurs over a much greater portion of the lung than in young subjects.[84] Airway closure also affects the setting of RV indirectly. When airway closure involves a large fraction of the lung, the communicating lung units will have to have a lower volume to the same extent that the closed units have a higher volume. Hence, the open units reach a flow-limiting condition, thus contributing to the flow-time–limited RV of old subjects.[84]

REFERENCES

1. Agostoni E. Mechanics of the pleural space. Physiol Rev 1972;52:57–128.
2. Agostoni E, Hyatt R. Static behavior of the respiratory system. In: Macklem PT, Mead J, editors. Handbook of physiology. The respiratory system, mechanics of breathing. Vol. III. Bethesda, MD: American Physiological Society; 1986. p. 113–30.
3. D'Angelo E. Techniques for studying the mechanics of the pleural space. In: Otis AB, editor. Techniques in life science, part II. Vol. P415. Amsterdam: Elsevier; 1984. p. 1–32.
4. Milic-Emili J. Measurements of pressures in respiratory physiology. In: Otis AB, editor. Techniques in life science, part II. Vol. P412. Amsterdam: Elsevier; 1984. p. 1–22.
5. Wade OL. Movements of the thoracic cage and diaphragm in respiration. J Physiol (Lond) 1954;124:193–212.
6. Agostoni E, Mognoni P, Torri G, et al. Relation between changes of rib cage circumference and lung volume. J Appl Physiol 1965;20:1179–86.
7. Strohl KP, Mead J, Banzett RB, et al. Regional differences in abdominal muscle activity during various maneuvers in humans. J Appl Physiol 1981;51:1471–6.
8. Konno K, Mead J. Measurement of the separate volume changes of rib cage and abdomen during breathing. J Appl Physiol 1967;22:407–22.
9. Konno K, Mead J. Static volume–pressure characteristics of the rib cage and abdomen. J Appl Physiol 1968;24:544–8.
10. Mead J. Mechanics of the chest wall. In: Hutas I, Debreczeni LA, editors. Advances in physiological sciences. Vol. 10. Oxford: Pergamon Press; 1981. p. 3–11.
11. Macklem PT, Macklem DM, De Troyer A. A model of inspiratory muscle mechanics. J Appl Physiol 1983;55:547–57.
12. Hillman DR, Markos J, Finucane K. Effect of abdominal compression on maximum transdiaphragmatic pressure. J Appl Physiol 1990;68:2296–304.
13. Boynton BR, Barnas GM, Dadmun JT, et al. Mechanical coupling of the rib cage, abdomen, and diaphragm through their area of apposition. J Appl Physiol 1991;70: 1235–44.
14. Agostoni E, Gurtner G, Torri C, et al. Respiratory mechanics during submersion and negative-pressure breathing. J Appl Physiol 1966;21:251–8.
15. Deschamps C, Rodarte JR, Wilson TA. Coupling between rib cage and abdominal compartments of the relaxed chest wall. J Appl Physiol 1998;65:2265–9.
16. Zechman FW, Musgrave FS, Mains RC, et al. Respiratory mechanics and pulmonary diffusing capacity with lower body negative pressure. J Appl Physiol 1967;22:247–50.
17. D'Angelo E, Sant'Ambrogio G. Direct action of the contracting diaphragm on the rib cage in rabbits and dogs. J Appl Physiol 1974;36:715–19.
18. Danon J, Druz WS, Goldberg NB, et al. Function of isolated paced diaphragm and cervical accessory muscles in C1 quadriplegics. Am Rev Respir Dis 1979;119:909–19.
19. D'Angelo E. Cranio-caudal rib cage distortion with increasing inspiratory airflow in man. Respir Physiol 1981;44:215–37.
20. Crawford ABH, Dodd D, Engel LA. Change in rib cage shape during quiet breathing, hyperventilation and single inspirations. Respir Physiol 1983;54:197–209.
21. McCool FD, Loring SH, Mead J. Rib cage distortion during voluntary and involuntary breathing acts. J Appl Physiol 1985;58:1703–12.
22. Jiang J, Demedts M, Decramer M. Mechanical coupling of upper and lower canine rib cages and its functional significance. J Appl Physiol 1998;64:620–6.
23. D'Angelo E, Michelini S, Miserocchi G. Local motion of the chest wall during passive and active expansion. Respir Physiol 1973;19:47–59.
24. Ward ME, Ward JW, Macklem PT. Analysis of human chest wall motion using a two-compartment rib cage model. J Appl Physiol 1992;72:1338–47.
25. Duomarco JL, Rimini R. La presion intrabdominal en el hombre. Buenos Aires: El Ateneo; 1947.
26. Hedenstierna C, Bindslev L, Santesson J, et al. Airway closure in each lung of anesthetized human subjects. J Appl Physiol 1981;50:55–64.
27. Needham CB, Rogan MC, McDonald I. Normal standard for lung volumes, intrapulmonary gas mixing and maximum breathing capacity. Thorax 1954;9:313–25.
28. Pierce JA, Ebert RV. The elastic properties of the lungs in the aged. J Lab Clin Med 1958;51:63–71.
29. Turner JM, Mead J, Wohl MB. Elasticity of human lungs in relation to age. J Appl Physiol 1968;25:664–71.
30. Frank NR, Mead J, Ferris BC Jr. The mechanical behaviour of the lungs in healthy elderly persons. J Clin Invest 1957;36:1680–7.
31. Gibson CJ, Pride NB, O'Cain C, et al. Sex and age differences in pulmonary mechanics in normal nonsmoking subjects. J Appl Physiol 1976;41:20–5.

32. Rehder K, Marsh M. Respiratory mechanics during anesthesia and mechanical ventilation. In: Macklem PT, Mead J, editors. Handbook of physiology. The respiratory system, mechanics of breathing. Vol. III. Bethesda, MD: American Physiological Society; 1986. p. 737–52.
33. Rehder K, Sittipong R, Sessler AD. The effects of thiopental–meperidine anesthesia with succinylcholine paralysis on functional residual capacity and dynamic lung compliance in normal sitting man. Anesthesiology 1972;37: 395–8.
34. Muller N, Volgyesi G, Becker L, et al. Diaphragmatic muscle tone. J Appl Physiol 1979;47:279–284.
35. Druz WS, Sharp JT. Activity of respiratory muscles in upright and recumbent humans. J Appl Physiol 1981;51:1552–61.
36. Krayer S, Rehder K, Beck KC, et al. Quantification of thoracic volumes by three-dimensional imaging. J Appl Physiol 1987;62:591–8.
37. Krayer S, Rehder K, Vettermann J, et al. Position and motion of the human diaphragm during anesthesia–paralysis. Anesthesiology 1989;70:891–8.
38. Drummond GB, Allan PL, Logan MR. Changes in diaphragmatic position in association with the induction of anaesthesia. Br J Anaesth 1986;58:1246–51.
39. Freund F, Roos A, Dodd RB. Expiratory activity of the abdominal muscles in man during general anesthesia. J Appl Physiol 1964;19:693–7.
40. Westbrook PR, Stubbs SE, Sessler AD, et al. Effects of anesthesia and muscle paralysis on respiratory mechanics in normal man. J Appl Physiol 1973;34:81–6.
41. Vellody VP, Nassery M, Dius WS, et al. Effects of body position change on thoracoabdominal motion. J Appl Physiol 1978;45:581–9.
42. Hedenstierna G, Löfström B, Lundh R. Thoracic gas volume and chest–abdomen dimensions during anesthesia and muscle paralysis. Anesthesiology 1981;55:499–506.
43. Hedenstierna G, Strandberg A, Brismar B, et al. Functional residual capacity, thoracoabdominal dimensions, and central blood volume during general anesthesia with muscle paralysis and mechanical ventilation. Anesthesiology 1985;62:247–54.
44. Rehder K, Mallow JE, Fibuch EE, et al. Effects of isoflurane anesthesia and muscle paralysis on respiratory mechanics in normal man. Anesthesiology 1974;41:477–85.
45. D'Angelo E, Robatto F, Calderini E, et al. Pulmonary and chest wall mechanics in anesthetized paralyzed humans. J Appl Physiol 1991;70:2602–10.
46. Brismar B, Hedenstierna G, Lundquist H, et al. Pulmonary densities during anesthesia with muscular relaxation—a proposal of atelectasis. Anesthesiology 1985;62:422–8.
47. D'Angelo E, Calderini E, Tavola M, et al. Effect of PEEP on respiratory mechanics in anesthetized paralyzed humans. J Appl Physiol 1992;73:1736–42.
48. Goldberg HS, Mitzner W, Adams K, et al. Effect of intrathoracic pressure on pressure–volume characteristics of the lung in man. J Appl Physiol 1975;38:411–17.
49. Hillman DR, Finucane KE. The effect of hyperinflation on lung elasticity in healthy subjects. Respir Physiol 1983;54: 295–305.
50. Duggan CJ, Castle WD, Berend N. Effects of continuous positive airway pressure breathing on lung volume and distensibility. J Appl Physiol 1990;68:1121–6.
51. Young SL, Tierney DF, Clements JA. Mechanism of compliance change in excised rat lungs at low transpulmonary pressure. J Appl Physiol 1970;29:780–5.
52. Sharp JT, Johnson FN, Goldberg NB, et al. Hysteresis and stress adaptation in the human respiratory system. J Appl Physiol 1967;23:487–97.
53. Agostoni E, Mead J. Statics of the respiratory system. In: Fenn WO, Rahn H, editors. Handbook of physiology. Respiration. Vol. I. Washington, DC: American Physiological Society; 1964. p. 387–409.
54. Cook CD, Mead J, Orzalesi MM. Static volume–pressure characteristics of the respiratory system during maximal efforts. J Appl Physiol 1964;19:1016–22.
55. Ringqvist T. The ventilatory capacity in healthy subjects. An analysis of causal factors with special reference to the respiratory forces. Scand J Clin Lab Invest Suppl 1966; 88:5–179.
56. Leith DB, Bradley M. Ventilatory muscle strength and endurance training. J Appl Physiol 1976;41:508–16.
57. Rahn H, Otis AB, Chadwick LB, et al. The pressure–volume diagram of the thorax and lung. Am J Physiol 1946; 146:161–78.
58. De Troyer A, Estenne M. Limitation of measurements of transdiaphragmatic pressure in detecting diaphragmatic weakness. Thorax 1981;36:169–74.
59. Mills JN. The nature of the limitation of maximal inspiratory and expiratory efforts. J Physiol (Lond) 1950;111:376–81.
60. Campbell EJM. An electromyographic study of the role of the abdominal muscles in breathing. J Physiol (Lond) 1952;117: 222–33.
61. Campbell EJM, Green JH. The variations in intra-abdominal pressure and the activity of the abdominal muscles during breathing; a study in man. J Physiol (Lond) 1953; 122:282–90.
62. Delhez L, Petit JM, Milic-Emili J. Influence des muscles expirateurs dans la limitation de l'inspiration. (Etude electromyographique chez l'homme.) Rev Franc Etud Clin Biol 1959;4:815–18.
63. Agostoni E, Rahn H. Abdominal and thoracic pressures at different lung volumes. J Appl Physiol 1960;15:1087–92.
64. Agostoni E, Torri G. Diaphragm contraction as a limiting factor to maximum expiration. J Appl Physiol 1962;17:427–8.
65. Agostoni E, Mognoni P. Deformation of the chest wall during breathing efforts. J Appl Physiol 1966;21:1827–32.
66. Bellemare F, Bigland-Ritchie B. Assessment of human diaphragm strength and activation using phrenic nerve stimulation. Respir Physiol 1984;58:263–77.
67. Gandevia SC, McKenzie DK. Activation of the human diaphragm during maximal static efforts. J Physiol (Lond) 1985;367:45–56.
68. Hershenson MB, Kikuchi Y, Loring SH. Relative strengths of the chest wall muscles. J Appl Physiol 1988;65:852–62.
69. Hillman DR, Markos J, Finucane KE. Effect of abdominal compression on maximum transdiaphragmatic pressure. J Appl Physiol 1990;68:2296–304.
70. Gandevia SC, Gorman RB, McKenzie DK, et al. Dynamic changes in human diaphragm length: maximal inspiratory and expulsive efforts studied with sequential radiography. J Physiol (Lond) 1992;457:167–76.
71. Mead J, Milic-Emili J, Turner JM. Factors limiting depth of a maximal inspiration in human subjects. J Appl Physiol 1963;18:295–6.
72. Agostoni E. Statics. In: Campbell EJM, Agostoni E, Newson-Davis J, editors. The respiratory muscles. Mechanics and neural control. London: Lloyd-Luke; 1970. p. 48–79.
73. Woolcock AJ, Mead J. Lung volume in exacerbations of asthma. Am J Med 1966;41:259–73.
74. Anderson SD, McBvoy JDS, Bianco S. Changes in lung volumes and airway resistance after exercise in asthmatic subjects. Am Rev Respir Dis 1972;106:30–7.
75. Freedman S, Tattersfield AE, Pride NB. Changes in lung mechanics during asthma induced by exercise. J Appl Physiol 1975;38:974–82.

76. Peress L, Sybrecht C, Macklem PT. The mechanism of increase in total lung capacity during acute asthma. Am J Med 1976;61:165–9.
77. Brown R, Ingram RH Jr, McFadden BR Jr. Problems in the plethysmographic assessment of changes in total lung capacity in asthma. Am Rev Respir Dis 1978;118:685–92.
78. Shore S, Milic-Emili J, Martin C. Reassessment of body plethysmographic technique for the measurement of thoracic gas volume in asthmatics. Am Rev Respir Dis 1982;126:515–20.
79. Stanescu DC, Rodenstein D, Cauberghs M, et al. Failure of body plethysmography in bronchial asthma. J Appl Physiol 1982;52:939–48.
80. Rodarte JR, Hyatt RB. Effect of acute exposure to CO_2 on lung mechanics in normal man. Respir Physiol 1973;17:135–45.
81. Leith DE, Mead J. Mechanisms determining residual volume of the lungs in normal subjects. J Appl Physiol 1967;23:221–7.
82. Delhez L, Troquet J, Damoiseau J, et al. Influence des modalites d'execution des maneuvres d'expiration forcee et hyperpression thoraco-abdominale sur l'activite electrique du diaphragme. Arch Int Physiol Biochem 1964;72:76–94.
83. Agostoni E, Gurtner G, Torri C, Rahn H. Respiratory mechanics during submersion and negative-pressure breathing. J Appl Physiol 1966;21:251–8.
84. Davis C, Campbell EJM, Openshaw P, et al. Importance of airway closure in limiting maximal expiration in normal man. J Appl Physiol 1980;48:695–701.

CHAPTER 3

STATICS OF THE LUNG

Joseph Milic-Emili, Edgardo D'Angelo

Pulmonary mechanics has been reviewed extensively in the literature.[1–3] Since then, however, it has been recognized that gravity plays an important role in determining the behavior of the lungs in the intact thorax. In the present account, we review first the static behavior of isolated lungs and then that of the lungs in the intact thorax. The effect of gravity on respiratory mechanics is also discussed in greater detail elsewhere in the book (see Chapter 2, "Statics of the Respiratory System" and Chapter 14, "Ventilation Distribution"). In this chapter, we focus mainly on the major determinants of the morphology of the lung volume–pressure (*V–P*) relationship, such as the critical closing and opening pressures of the peripheral airways and airspaces, and the concurrent derecruitment and recruitment of lung units during volume cycling. This information is presently of considerable clinical relevance because the current "open-lung strategy," which is designed to keep the airways and alveoli open in mechanically ventilated patients, is based on the analysis of the morphology of the quasistatic *V–P* relationships of the lung, or its surrogate, the respiratory system.

STATIC BEHAVIOR OF THE ISOLATED LUNG

Static *V–P* Curves

Static *V–P* curves of the excised lungs were first obtained in 1849 by Hutchinson, who studied two human lungs immediately postmortem.[4] Since then, many such studies on the lungs of different species have been reported, but adequate data pertaining to normal human lungs are still lacking. Accordingly, the lungs of other mammals will be used for purposes of illustration.

V–P relationships vary somewhat among species and are dependent on experimental parameters such as temperature and prior volume history. When these sources of variability are held constant, however, *V–P* relationships are highly reproducible. Typical quasistatic *V–P* behavior is illustrated in Figure 3-1.

When starting from the completely degassed (atelectatic) state, a high transpulmonary pressure is needed to begin inflation (see Figure 3-1), the critical pressures for opening atelectatic units being in the order of 30 cm H_2O. With repeated cycling between 0 and 30 cm H_2O airway pressure (P_{aw}), the *V–P* loops become consistent, undergoing about a five-fold volume change between minimal (V_0) and maximal (V_{30}) inflation. This volume range is approximately that which a subject would achieve between residual volume (RV) and a maximal inspiratory effort to achieve total lung capacity (TLC). At the high end, the lung stiffens, presumably due to both connective tissue stiffness and increasing surface tension. With inflation to $P_{aw} > 30$ cm H_2O, volume will continue to increase, although at a relatively low rate, until the lung ruptures and leaks develop. An upper P_{aw} limit of less than 25 cm H_2O would significantly underestimate maximum physiologic volume. This would be particularly likely when lungs were being studied after atelectasis because opening of atelectatic alveoli might still be incomplete. Small volume cycles (see Figure 3-1), such as occur during tidal breathing in vivo, require small pressure changes and involve little hysteresis. When the lung is filled with saline (see Figure 3-1), there is much less recoil than with air filling because of the absence of surface forces.

Figure 3-2 shows static *V–P* curves of a freshly excised dog lung with repeated cycling between P_{aw} of -5 and 30 cm H_2O. Inspection of this figure reveals several features that will be described below. In this analysis, the absence of atelectasis is assumed.

Static *V–P* Hysteresis

The *V–P* curve during lung deflation is not the same as during lung inflation, reflecting static hysteresis. This may involve three main mechanisms: plastic behavior of tissue elements and true tissue hysteresis; surface hysteresis; and differences in the sequence of recruitment and derecruitment of lung units between inflation and deflation.[5–7]

Resting Lung Volume

This is the volume at zero P_{aw}, which is commonly referred to as "minimal volume" or "minimal air." These terms are misnomers because if P_{aw} is decreased to below zero, there is a further decrease in lung volume (see Figure 3-2). The term "resting volume of lung" ($V_{r,L}$) seems to be more appropriate. The magnitude of $V_{r,L}$ varies with the animal species. During deflation, in the example in Figure 3-2, $V_{r,L}$ amounts to about 16% of the volume at a transpulmonary pressure of 30 cm H_2O (V_{30}). In exsanguinated dog and cat

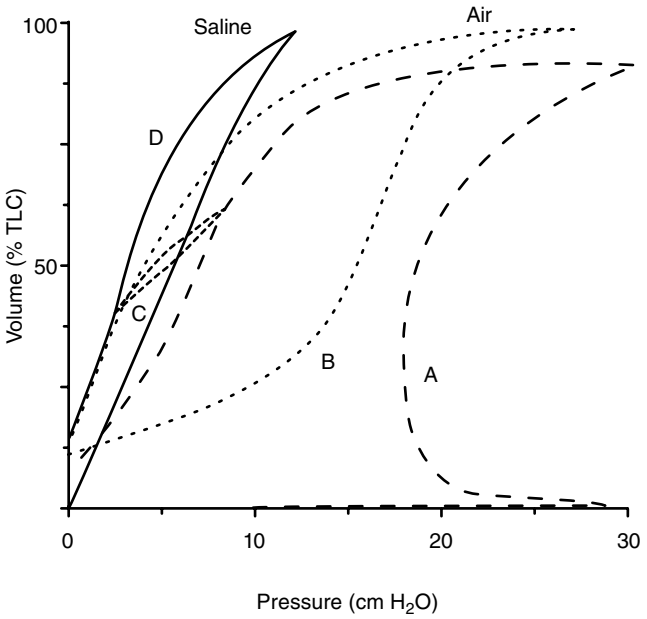

FIGURE 3-1 Four inflation–deflation maneuvers in an excised rabbit lung generating characteristic *V–P* curves. *A*, Inflation from the degassed (atelectatic) state shows that transpulmonary pressures of 30 cm H_2O are required before there is substantial reopening of alveoli. On deflation to 0 cm H_2O, emptying is incomplete. *B*, Repeated cycles between 0 and 30 cm H_2O show stable curves: the lung is now much more easily inflated than in (A) but still becomes relatively stiff near 30 cm H_2O. *C*, Small volume cycles (such as in tidal breaths in vivo) occur between 3 and 8 cm H_2O. *D*, With air replaced by saline, the lung shows much less recoil over the same volume range. Adapted from Hoppin FG et al.[5]

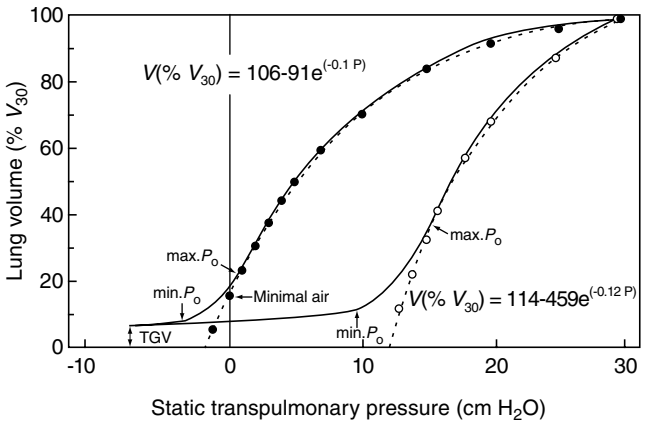

FIGURE 3-2 Quasistatic *V–P* curves obtained with a freshly excised dog lung. Lung gas volume is expressed as a percentage of the volume at a transpulmonary pressure of 30 cm H_2O (% V_{30}). *Filled and open circles:* exponential relationships during lung deflation and inflation, respectively. P_c = maximum airway closing pressure; P_o = maximum airway opening pressure; TGV = trapped gas volume. In excised lung preparations, airway pressure corresponds to transpulmonary pressure. Adapted from Glaister DH et al.[6]

lungs, $V_{r,L}$ amounts to 10 to 20% of V_{30}, but higher values have been reported in humans.[2,6] For example, in the study by Stigol and colleagues, $V_{r,L}$ ranged between 18 and 60% V_{30}, which suggests that these results may not represent normal behavior but have probably been influenced by the presence of stable foam in the airways.[8] The variability of pulmonary blood content may also affect the "minimal volume." In studies on excised cat lungs, Frank, repeating an earlier observation by von Basch, found that, with pulmonary vascular engorgement, $V_{r,L}$ increases by a small amount.[9,10]

$V_{r,L}$ depends, among other factors, on the previous volume history of the lungs. As shown in Figures 3-1 and 3-2, it is lower during inflation than during deflation.

Trapped-gas Volume

In older texts, where the term "minimal air" is used to define the volume of gas in the freely collapsed lung, it is stated that this gas is trapped by closure of noncartilaginous airways, the assumption being that, at zero P_{aw}, the airways leading to all pulmonary alveoli are closed. Kleinman and colleagues were the first to point out that at $V_{r,L}$ some airways must remain patent throughout their length.[11] In fact, when P_{aw} is decreased to below zero, there is a further decrease in lung volume (see Figure 3-2). When a critical P_{aw} of about −3 to −5 cm H_2O is reached, however, expulsion of gas from the lung ceases, suggesting that all pulmonary pathways are now closed.[6] The volume of gas trapped behind the closed airways is generally referred to as *trapped-gas volume* (TGV). Hughes and colleagues demonstrated that it was the terminal bronchioles that closed.[12]

Airway Closing Pressure

The critical transpulmonary pressure (P_L) at which lung emptying ceases has been termed the *minimum airway closing pressure* ($P_{c,min}$). Since some airways begin to close at P_L values higher than $P_{c,min}$, the term *maximum airway closing pressure* ($P_{c,max}$) should refer to the P_L at which airway closure begins during deflation.[6] In excised dog lungs, $P_{c,min}$ is in the order of −2.5 cm H_2O, whereas in excised "normal" human lungs, it is close to zero.[6,8] In open-chest rabbits, cats, and dogs, $P_{c,min}$ ranges between −1 and −2 cm H_2O.[13] Less information is available with regard to $P_{c,max}$. Some inferences can, however, be drawn from the analysis of the shape of the static deflation *V–P* relationships of the lung.

Exponential Character of *V–P* Curves

As shown in Figure 3-2, in the volume range between V_{30} and about 20% V_{30}, the relationship between volume and pressure during deflation can be described with good approximation by the following exponential function:

$$V = V_{max} - b \cdot e^{-KP_L} \qquad (3\text{-}1)$$

where V_{max} is the predicted volume at infinite P_L, P_L is static transpulmonary pressure, K is a constant, and b is the difference between V_{max} and the predicted lung volume at zero P_L.[6] Thus, above 20% of V_{30}, the static deflation *V–P* curve is of exponential character, as defined by Equation 3-1. Such a function has also been shown to fit in vivo *V–P* relationships in humans.[14] The nonlinearity of the *V–P* curves makes it difficult to use accepted terms such as compliance, which presuppose a linear system. Instead, we may use Equation 3-1 to describe a curve above the inflection

point, and, in particular, we may consider the constant K to be an *index* of the compliance of the lung or lobe.

At volumes lower than 20% of V_{30}, the experimental relationship during lung deflation deviates to the left of the exponential function as a result of progressive airway closure, beginning at the point where the experimental curve starts to deviate from the exponential function (inflection point indicated as max P_c on the deflation *V–P* curve in Figure 3-2). Clearly, when the airways leading to parts of the lung close, a greater change in P_L will be required to produce a given volume change, and hence the overall lung compliance will be reduced, resulting in a shift to the left of the *V–P* curve. If this interpretation is correct, the P_L at the inflection point on the deflation curve should represent maximum P_c, and the pressure at which TGV is reached reflects the minimum P_c. In view of the complexities of the multitudinous pathways within the lung, it seems reasonable for there to be a range of P_c values rather than a unique value pertinent to all airways, the difference between maximum and minimum P_c reflecting the range of P_c inhomogeneity within the lung. Similar inhomogeneity is found within single lobes.

The maximum P_c has been found to correspond to the "closing volume" measured with single-breath tests, supporting the notion that it reflects airway closure.[15] The finding of negative $P_{c,min}$ indicates that, at low volumes, at least some of the peripheral airways offer resistance to collapse. A full discussion of the factors stabilizing the peripheral airways can be found elsewhere.[16]

The closing pressures for airways are less negative than those for alveoli. Indeed, in experiments on rabbits, cats, and dogs, Cavagna and colleagues demonstrated that $P_{c,min}$ for the airways amounts to -1 to -2 cm H_2O, whereas that for the alveoli ranges between -3 and -6 cm H_2O.[13] As a result, during lung deflation, TGV is usually reached before onset of atelectasis. This is a useful functional feature because smaller values of P_L are required to reopen closed airways than to reopen closed alveoli (compare curves A and B in Figure 3-1).

Airway Opening Pressure

The P_L necessary to reopen a closed airway would be expected to be greater than that required to close it because surface forces would be different under the two circumstances.[16] Indeed, as shown in the example of Figure 3-2, during lung inflation from TGV there is very little volume change until a critical P_L of about 10 cm H_2O is reached. This pressure probably represents the *minimum* airway opening pressure ($P_{o,min}$). As for closing pressure, different airways also appear to have a range of opening pressures. An estimate of the *maximum* airway opening pressure ($P_{o,max}$) may be possible by analysis of the inflation *V–P* curves of the lung.

In the range between the lung volume corresponding to $P_{o,min}$ (about 10 cm H_2O of P_L) and about 36% of V_{30}, the slope of the inflation curve increases progressively (see Figure 3-2). This phenomenon probably reflects, at least in part, progressive opening of closed airways, that is, progressive recruitment of lung units that were initially at their TGV. At lung volumes higher than about 36% of V_{30}, the relationship between volume and pressure again fits an exponential function of the type described by Equation 3-1. The point where the experimental curve joins the exponential function (inflection point on the inflation curve in Figure 3-2) probably reflects $P_{o,max}$, the latter being about 5 cm H_2O higher than $P_{o,min}$.

Isotropic Behavior of the Lung

Isotropic behavior implies that all parts of the lung fill or empty proportionately.[2] In studies on excised dog lobes, Frank has shown that there is a small difference in the static *V–P* relationships between the upper and lower lobes but not between the right and left upper lobes or the right and left lower lobes.[17] This has also been demonstrated in dogs and rabbits, but not in humans.[18–20] However, some indirect evidence suggests that in humans there may also be differences similar to those observed in dogs and rabbits.[21] Morphometric studies in isolated lungs of various species have shown that the alveoli expand relatively uniformly over most of the *V–P* curve, in the sense that all undergo a proportional increase in size and that this increase is equal in all directions.[22–25] In experiments on excised dog lungs, Hughes and colleagues found that during lung inflation and deflation the percentage changes of bronchial length and diameter for airways of different sizes were approximately the same and that changes in length, and in many cases of diameter, were reasonably well correlated with changes in the cube root of absolute lung volume.[26] All of these findings are consistent with the notion that in the absence of airspace or airway closure, the isolated lungs or lobes expand relatively uniformly. However, studies with radioactive xenon have shown that at times there may be substantial differences in static mechanical behavior between and within lobes of dogs and monkeys.[6,15] This is associated with substantial inhomogeneity in both critical opening and closing pressures.[6,15]

The fact that the bulk elastic properties of whole lobes are exponential when all units are ventilating implies that the individual respiratory units also have exponential properties. In this context, the inhomogeneity of opening and closing pressures is unimportant as the exponential properties are descriptive of the ventilation range beyond that where sequential opening and closing is occurring.

If the units comprising a lobe have different values of K, then the lobe cannot be homogeneous and isotropic. It is not possible, however, to detect any such inhomogeneity within a lobe from its *V–P* curve. Such inhomogeneity may instead be detected by studying the distribution of ventilation and washout characteristics of an inspired bolus of tracer gas.[27]

Previous Volume History

The effect of different inflation volumes (ie, different previous inflation volume history) on the quasistatic *V–P* curves of an isolated dog lung can be seen in Figure 3-3. Similar curves are obtained when studying the individual lobes.[6] Figure 3-3A shows the effect of ventilating the lung between 30 cm H_2O (V_{30}) and successively lower end-deflation pressures from 20 to 2.5 cm H_2O. The traces were obtained as a continuous recording through five cycles. In this pressure range, lungs

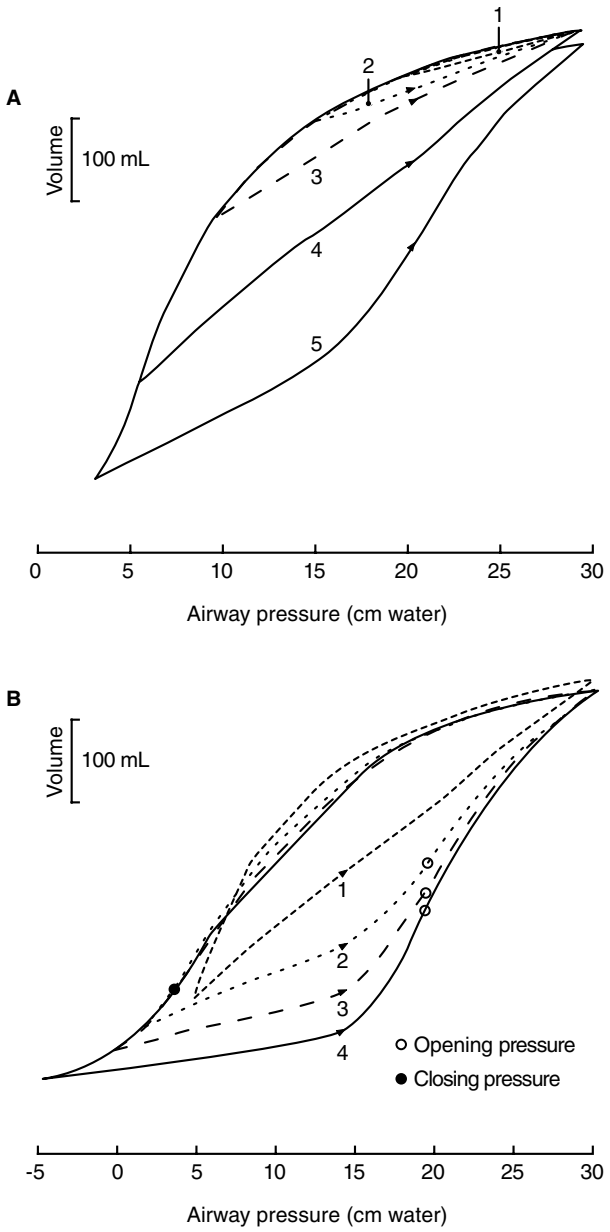

FIGURE 3-3 Quasistatic *V–P* curves obtained by cycling a freshly excised dog lung between a transpulmonary pressure of 30 cm H_2O and successively lower end-deflationary pressures. For clarity, this figure has been divided in two panels, curve 1 of *B* being the same as curve 4 of *A*. The maximal opening and closing pressures are indicated. Note the different scales on the abscissae in *A* and *B*. Adapted from Glaister DH et al.[6]

adapted in a single cycle. Figure 3-3B shows the effect of ventilating the same lung between V_{30} and successively reduced airway pressures from +5 to −5 cm H_2O.

So long as the preparation is cycled between V_{30} and volumes above $P_{c,max}$, the behavior shown in Figure 3-3A (curves 1 to 4) is always observed: all *V–P* curves have a common deflation limb, and the separate inflation limbs are fairly straight. In contrast, as soon as the end-deflationary pressure is allowed to fall below $P_{c,max}$ (curve 5), the *V–P* characteristics are altered. The curve exhibits the classic sigmoid shape, the progressive reduction in compliance reflecting airway closure; that is, the more units are closed, the smaller is the overall volume change for a given pressure change. In this case, the inflation curves exhibit a distinct "knee," which may be explained by reopening of most of the units closed during deflation. The initial inflation phase below the "knee" in the curve should reflect inflation of the units still open at the end of the deflation, coupled possibly with the reopening of a relatively small number of closed units. In the vicinity of the knee, there is rapid reopening of most of the closed units.

During lung deflation, the onset of airway closure ($P_{c,max}$) occurs at the same pressure and volume at all ventilation ranges (see Figure 3-3B). This suggests that the presence or absence of airway closure during ventilation can be closely gauged by relating the end-deflationary pressure to $P_{c,max}$.

The progressive decrease in compliance during the initial part of the inflation curves mimics the increasing degree of closure as the end-deflationary pressure is reduced. Interestingly, the opening pressures of all curves are approximately the same, even though the corresponding lung volumes are highly sensitive to the ventilation range. The increase in volume between inflation curves 1 to 4 in Figure 3-3B probably mainly reflects a progressively greater number of units with open airways as the end-deflationary pressure is increased from $P_{c,min}$ to $P_{c,max}$.

The pattern of opening of units can also be seen in Figure 3-4, which depicts *V–P* loops as the dog lung in Figure 3-3 is cycled between TGV and successively higher end-inflation volumes. Between −5 and +12 cm H_2O, there is virtually no hysteresis and the compliance is constant because virtually all units are closed and we are simply observing the compliance of the airways between the trachea and the site of closure. As the inflation range is increased to +20 cm H_2O, just above the knee on the curve, there is a change in behavior. The first inflation is curve 2a, and deflation is along curve 2. During subsequent inflations, the steady-state curve 2b is attained. The deflation limb of the cycle does not alter during this period. We can attribute this behavior to the changing pattern of opening of units. During the first cycle, all units tend to resist opening until a pressure of about 17 cm H_2O, and then, at the knee of curve 2a, massive opening occurs. During deflation, units initially decrease in volume, with a few closing; massive closure then occurs below the inflection point. During subsequent inflations, there is a much greater distribution of opening pressures, and hence the knee is less sharply defined. Similarly, the first inflation to 25 cm H_2O (curve 3a) exhibits a sharp knee just above the previous highest inflation pressure as units not hitherto opened are opened up, but again, on repeated inflation to the same pressure (curve 3b), these units open more readily, and the sharp knee is smoothed out. A further increase in inflation pressure to 30 cm H_2O (curves 4a and 4b) shows the same features, suggesting that the airways subtending some units were still closed at an inflation pressure of 25 cm H_2O. This, however, may also reflect recruitment of atelectatic alveoli (microatelectasis), which could not be visually detected on the lung surface of the excised lung.

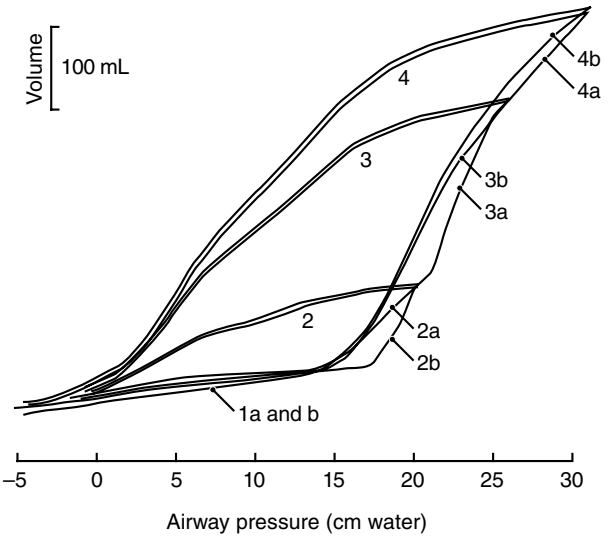

FIGURE 3-4 Quasistatic *V–P* curves obtained by cycling the same excised dog lung as in Figure 3-3 between a transpulmonary pressure of $-5\,cm\,H_2O$ and successively higher end-inflationary pressures. Adapted from Glaister DH et al.[6]

The "knee" on the inflation curve of the lung (see Figures 3-3 and 3-4) has been commonly termed "lower inflection point." This, however, is a misnomer because an inflection point is said to occur where the slope of a curve changes direction (from increasing to decreasing or vice versa). Thus, in reality, the "knee" reflects the point on the inflation *V–P* curve where the rate of change in the slope dV/dP_L is highest, as a result of substantial but not complete airway opening.

In studies on mechanically ventilated patients, it has often been assumed that the "knee" reflects reopening of atelectatic alveoli, whereas in reality it reflects reopening of closed airways. For reopening, atelectatic alveoli transpulmonary pressures of the order of 30 cm H_2O are required (see Figure 3-1, curve A).

Prolonged Volume Cycling

As long as cycling occurs at volumes above $P_{c,max}$, the lung adopts, in a single cycle, a new consistent configuration of the *V–P* curve when the inflation volume is changed (see Figure 3-1, curves A and B). In experiments on open-chest dogs and rabbits, ventilated with physiologic tidal volumes and positive end-expiratory pressure (PEEP) above $P_{c,max}$, it has been shown that such consistency is maintained also during prolonged volume cycling (up to 4 h).[28–30] In fact, under these conditions, there were no changes in lung statics or dynamics.

In contrast, when PEEP was reduced below $P_{c,max}$ there was a significant time-dependent increase in lung elastance, airway resistance, and tissue resistance, which can be attributed to concurrent peripheral airway closure and increase in surface forces.[29,30] After 3 to 4 hours of such low-volume ventilation, both lung elastance and tissue resistance could be returned to the initial control values by administration of three to five full lung inflations followed by mechanical ventilation with PEEP. In contrast, airway resistance remained high, and there was histologic evidence of injury in respiratory and membranous bronchioles, characterized by epithelial necrosis and sloughing.[30] Thus, mechanical ventilation of normal open-chest rabbits at low lung volume (zero end-expiratory pressure), which entails cyclic airway reopening and closure, may result in damage to the noncartilaginous airways and a concurrent increase in airway resistance. Such a phenomenon has been previously shown after low-volume ventilation in both an ex vivo model of lavaged rat lung and in closed-chest rabbits with surfactant-depleted lungs.[31,32] The latter results, which were obtained with abnormal lungs, have been used to explain the *low-volume* injury that may occur in patients with the adult respiratory distress syndrome during mechanical ventilation without PEEP.[33] In this connection, it is tempting to speculate that bronchiolar injury may also occur in other diseases characterized by the presence of peripheral airway closure during tidal breathing, such as chonic obstructive pulmonary disease (COPD) and obesity (see Chapter 58, "Spirometric Predictions of Exercise Limitation in Patients with Chronic Obstructive Pulmonary Disease"). Persistent cyclic bronchiolar reopening and closure may, in fact, eventually lead to destruction of the peripheral airways, manifested by centrilobular emphysema in COPD, and by the unexplained increase of airway resistance reported in some obese subjects.[34]

Low-volume breathing also affects the distribution of ventilation and gas exchange within the lung (see Chapter 2, "Statics of the Respiratory System").

Nature of Lung Hysteresis

In the absence of airway closure (see Figure 3-3A, curves 1 to 4), the hysteresis exhibited by the *V–P* loops reflects surface phenomena, plastic behavior of tissue elements, and true tissue hysteresis.[5–7] In the presence of airway closure, the hysteresis becomes much more pronounced (see Figure 3-3B) and may involve considerable work during lung inflation that is not recovered during lung deflation. On deflation, peripheral airways are c1osed with a liquid plug as a result of the surface tension forces operating on the liquid lining of the bronchioles. These airways will only open again on inflation at a considerably higher transmural pressure than that at which closure occurred. As each unit opens, it inflates rapidly to the volume it would have achieved had it been open from the start; thereafter, it inflates normally. In this way, the shape of the *V–P* curve is determined by the sequence of opening and closing of units superimposed on normal elastic stress–strain relationships.

This model may be modified by the presence of collateral ventilation. Airway closure may occur but be undetected in the *V–P* curve, so long as collateral channels remain open. This is because the distal units would be in indirect communication with central airways and other patent lung units. Thus, closing pressures as estimated may reflect both collateral and primary airway closure. A similar situation will potentially occur on inflation.

In the absence of collateral ventilation, atelectasis could only be obtained in situ by absorption of alveolar gas (after a period of oxygen breathing) into the bloodstream. This is

because, in normal lung, $P_{c,min}$ is lower for the alveoli than for the peripheral airways (see above). Collateral ventilation, however, offers another route for gas to reach the alveoli with closed airways.

STATIC BEHAVIOR OF THE LUNG IN SITU

In the absence of airspace or airway closure, the isolated lungs or lobes expand relatively uniformly[35]; this is not the case when the lungs are inside the thorax.[18,19,25,36] This different behavior can probably be accounted for by the fact that, whereas in excised preparations the pleural surface pressure (P_{pl}) is uniform, this is not the case in the intact thorax. Indeed, it is well recognized that, in situ, the pleural surface pressure is not uniform but that there is a vertical gradient in P_{pl}, with the more negative values at the upper parts. As a result of this gradient, the static transpulmonary pressure (P_L), that is, the difference between the static alveolar pressure (P_{alv}) and P_{pl}, is greater in upper lung zones, and consequently the upper lung units are normally more expanded than those in the lower zones.

The effects of the vertical gradient of P_L on regional ventilation distribution and on regional gas exchange are described elsewhere in the book (see Chapter 14, "Ventilation Distribution"). Here we briefly consider the implications of airway closure on conventional measurements of the static *V–P* properties of the lung in humans.

Figure 3-5 shows the static *V–P* curves of a normal subject measured in situ using the esophageal balloon technique.[35] As in Figure 3-2, the exponential *V–P* relationships during lung deflation and inflation are also found at high lung volumes. However, maximal P_c occurs at a higher volume (~50% TLC) than in the isolated lung (~20% V_{30}) because of the vertical gradient in pleural surface pressure. Furthermore, with an intact thorax, some of the airways remain patent even at full expiration. Thus, in situ, the morphology of the static *V–P* curves of the lung is markedly altered by the pleural pressure gradient.[15,36] It should be noted, however, that in situ artifacts in esophageal pressure measurements probably also affect the measured *V–P* curves of the lung, particularly in the supine position.[15,37]

The effect of the P_{pl} gradient on lung mechanics has also been extensively described by Glaister and colleagues in excised dog and monkey lungs and lobes subjected to an artificial "normal" gradient in pleural surface pressure.[15] This study also showed that, under these conditions, the differences between minimal and maximal values of closing and opening pressures are much greater than in the absence of the gradient.

In conclusion, from the clinical standpoint, peripheral airway closure is one of the most important hallmarks of pulmonary statics. In fact, when the static end-expiratory transpulmonary pressure is lower than $P_{c,max}$, there are the following effects: (1) gas trapping, characterized by a "knee" on the static lung inflation *V–P* curve and an inflection point ($P_{c,max}$) on the deflation curve; (2) increased hysteresis with a concomitant increase in hysteresis-related work (as reflected by increased hysteresis area); (3) time-related changes in respiratory mechanics; (4) cyclic reopening and closure of peripheral airways, with a risk of bronchiolar injury; and (5) maldistribution of ventilation and impaired gas exchange with the lung. Accordingly, assessment of pulmonary statics is important, particularly during mechanical ventilation.

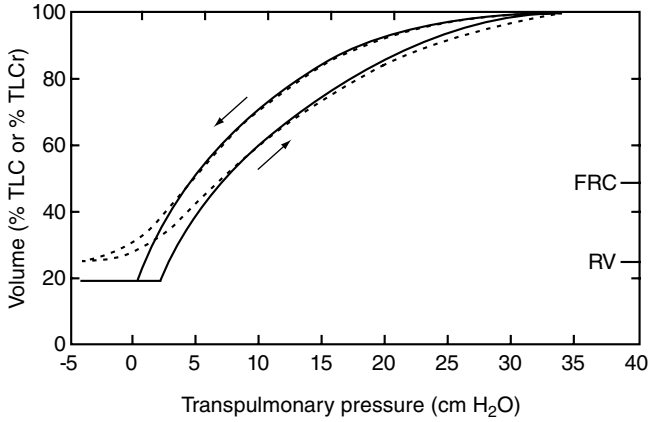

FIGURE 3-5 Quasistatic pulmonary *V–P* curves of a normal, seated subject. Lung gas volume is expressed as a percentage of total lung capacity (%TLC) and regional total lung capacity (%TLCr). *Broken lines* represent experimental relationships derived from measurements of esophageal pressure. *Solid lines* represent relationships that should be obtained in the absence of the vertical gradient in transpulmonary pressure due to gravity. It is assumed that in the absence of such a gradient, small airway closure would not occur even at residual volume (RV). FRC = functional residual capacity. The points at which the experimental relationships during deflation and inflation deviate from the corresponding exponential curves indicate the maximal closing ($P_{c,max}$) and opening ($P_{o,max}$) pressures. Adapted from Sutherland PW et al.[36]

REFERENCES

1. Mead J. Mechanical properties of lungs. Physiol Rev 1961;41:281–330.
2. Radford EP Jr. Static mechanical properties of mammalian lungs. In: Fenn WO, Rahn H, editors. Handbook of physiology. Respiration. Vol. I. Washington, DC: American Physiological Society; 1964. p. 429–49.
3. Clements JA, Tierney DF. Alveolar instability associated with altered surface tension. In: Fenn WO, Rahn H, editors. Handbook of physiology. Respiration. Vol. II. Washington, DC: American Physiological Society; 1964. p. 1565–83.
4. Hutchinson J. Thorax. In: Todd RB, editor. Encyclopaedia of anatomy and physiology 4. London: Longmans; 1849–1852. p. 1059.
5. Hoppin FG Jr, Stothert JC Jr, Greaves IA, et al. Lung recoil: elastic and rheological properties. In: Macklem P, Mead J, editors. Handbook of physiology: the respiratory system. Vol. III, Part I. Bethesda, MD: American Physiological Society; 1986. p. 195–215.
6. Glaister DH, Schroter RC, Sudlow MF, et al. Bulk elastic properties of excised lungs and the effect of transpulmonary pressure gradient. Respir Physiol 1973;17:347–64.
7. Hoppin FG. Sources of lung recoil. In: Milic-Emili J, editor. Respiratory mechanics. Respir Monogr 1999;12:33–53.
8. Stigol LC, Vawter GF, Mead J. Studies on the elastic recoil of the lung in pediatric population. Am Rev Respir Dis 1972;105:552–63.

9. Frank NR. Influence of acute pulmonary congestion on recoiling force of excised cat's lung. J Appl Physiol 1959; 14:905–8.
10. von Basch S. Ueber eine Function des Capillardruckes in den Lungen alveoli. Wien Med Blatter 1887;10:465–7.
11. Kleinman LE, Poulos DA, Siebens AA. Minimal air in dogs. J Appl Physiol 1964;19:204–6.
12. Hughes JMB, Rosenzweig DY, Kivitz PB. Site of airway closure in excised dog lungs: histologic demonstration. J Appl Physiol 1970;29:340–4.
13. Cavagna GA, Stemmler EJ, DuBois AB. Alveolar resistance to atelectasis. J Appl Physiol 1967;22:441–52.
14. Milic-Emili J, Henderson JAM, Dolovich MB, et al. Regional distribution of inspired gas in the lung. J Appl Physiol 1966;21:749–59.
15. Glaister DH, Schroter RC, Sudlow MF, et al. Transpulmonary pressure gradient and ventilation distribution in excised lungs. Respir Physiol 1973;17:365–85.
16. Macklem PT, Proctor DF, Hogg JC. The stability of peripheral airways. Respir Physiol 1969;8:191–203.
17. Frank NR. A comparison of static volume–pressure relations of excised pulmonary lobes of dogs. J Appl Physiol 1963; 18:274–8.
18. Faridy EE, Kidd R, Milic-Emili J. Topographical distribution of inspired gas in excised lobes of dogs. J Appl Physiol 1967; 22:760–6.
19. D'Angelo E. Local alveolar size and transpulmonary pressure *in situ* and in isolated lungs. Respir Physiol 1972;14: 251–66.
20. Berend N, Shoog C, Thrulbeck WM. Exponential analysis of lobar pressure–volume characteristics. Thorax 1981;36:452–5.
21. Bake B, Bjure J, Grimby G, et al. Regional distribution of inspired gas in supine man. Scand J Respir Dis 1967;48: 189–96.
22. Dunnill MS. Effect of lung inflation on alveolar surface area in the dog. Nature 1967;214:1013–4.
23. Forrest JB. The effect of changes in lung volume on the size and shape of alveoli. J Physiol (Lond) 1970;210: 533–47.
24. Kuno K, Staub NC. Acute mechanical effects of lung volume changes on artificial microholes in alveolar walls. J Appl Physiol 1968;24:83–92.
25. D'Angelo E. Stress–strain relationships during uniform and non-uniform expansion of isolated lungs. Respir Physiol 1975;23:87–108.
26. Hughes JMB, Hoppin FG Jr, Mead J. Effect of lung inflation on bronchial length and diameter in excised lungs. J Appl Physiol 1972;32:25–35.
27. Anthonisen NR. Closing volume. In: West JB, editor. Regional differences in the lung. New York: Academic Press; 1977. p. 451–82.
28. Dechman G, Lauzon AM, Bates JHT. Mechanical behaviour of canine respiratory system at very low lung volumes. Respir Physiol 1994;95:119–39.
29. Taskar V, Evander JJ, Wollmer P, et al. Healthy lungs tolerate repetitive collapse and reexpansion. Acta Anaesthesiol Scand 1995;39:370–6.
30. D'Angelo E, Pecchiari M, Baraggia P, et al. Low volume ventilation induces peripheral airway injury and increased airway resistance in normal open-chest rabbits. J Appl Physiol 2002;92:949–56.
31. Muscedere JG, Mullen JBM, Gan K, et al. Tidal ventilation at low airway pressure can augment lung injury. Am J Respir Crit Care Med 1994;149:1327–34.
32. Taskar V, Evander JJ, Robertson B, et al. Surfactant dysfunction makes lungs vulnerable to repetitive collapse and reexpansion. Am J Respir Crit Care Med 1997;155:313–20.
33. Koutsoukou A, Bekos B, Sotiropoulou C, et al. Effects of positive end-expiratory pressure on gas exchange and expiratory flow limitation in adult respiratory distress syndrome. Crit Care Med 2002;30:1941–9.
34. Yap JCH, Watson RA, Gilbey S, Pride NB. Effects of posture on respiratory mechanics in obesity. J Appl Physiol 1995; 79:1199–205.
35. Katsura T, Rosenzwaig R, Sutherland PW, et al. Effect of external support on regional alveolar expansion in excised dog lungs. J Appl Physiol 1970;25:133–7.
36. Sutherland PW, Katsura T, Milic-Emili J. Previous volume history of the lung and regional distribution of gas. J Appl Physiol 1968;25:566–74.
37. Milic-Emili J, Mead J, Turner JM. Topography of esophageal pressure as a function of posture in man. J Appl Physiol 1964;19:212–6.

CHAPTER 4

ACT OF BREATHING: DYNAMICS

Peter T. Macklem

The branch of mechanics that deals with motion, the forces or pressures, that produce it, and the resistances that must be overcome is called dynamics. This chapter deals with the dynamics of the lung during breathing, but it is beyond our scope to consider the dynamics of the chest wall and respiratory muscles. This is addressed in part elsewhere in this book (see Chapter 7, "Act of Breathing: The Ventilatory Pump"). A superb, timeless review of the dynamics of breathing is contained in Mead's *Physiological Review* article.[1]

To analyze breathing dynamics, one needs to know the volume of gas inspired and expired at the mouth, the flow rates, and the pressures required to move the lungs. With this information, one can calculate the resistances to motion of the lungs. In health, under most circumstances, there are three types of resistance: (1) the resistance to the flow of air along the upper airway and the tracheobronchial tree between the mouth and the alveoli, determined by the physical properties of the gas, how fast the gas is flowing, and the geometry of the airways; (2) the elastic resistance of the alveoli, which is determined by the size of the breath, the elastic properties of the alveolar walls, and the surface tension of the alveolar lining liquid; and (3) the resistance due to tissue viscance. The last is also a property of the alveolar walls and results from the fact that the lung exhibits hysteresis, so that the pressures required to inflate the lung are greater than those at the same volume on deflation. When breathing is very rapid, the lung's inertial properties may lead to additional resistance to motion. Inertance depends primarily on the mass of gas in the airways and how quickly the gas is accelerated and decelerated, given by the rate of change of airflow at the mouth. Finally, in certain disease states, the respiratory muscles, which produce the pressures required to inflate the lung, must overcome a "threshold" load that is similar in effect to the inertial loads that skeletal muscles must overcome when lifting an object. These muscles initially contract isometrically and develop a force equal to the weight of the object being lifted before any motion of the object takes place. Similarly, when the respiratory muscles have to overcome a threshold load, they must develop a finite pressure before any inspiratory flow starts.

THEORY

Equation of Motion of the Lung

The pressure difference across the lung between the mouth or airway opening and the pleural space, or transpulmonary pressure (P_L), is the agency that moves the lung:

$$P_L = P_{ao} - P_{pl} \tag{4-1}$$

where P_{pl} is pleural pressure and P_{ao} is the pressure at the airway opening. The alveoli lie between the airway opening and the pleural space, and they have a pressure inside them (P_A) that may be different from either P_{ao} or P_{pl}. Thus:

$$P_L = P_{ao} - P_A + P_A - P_{pl} \tag{4-2}$$

$P_{ao} - P_A$ is the pressure drop across the airways and thus is the pressure producing flow of air in and out of the lung. This is the pressure that overcomes the flow resistance of the upper airway and tracheobronchial tree (P_{fr}):

$$P_{fr}{}^{*} = P_{ao} - P_A \tag{4-3}$$

$P_A - P_{pl}$ is the pressure difference between the alveoli and the pleural space, which contains tissue viscance and the elastic recoil pressure of the lung (P_{el}). Ignoring tissue viscance for the time being:

$$P_{el} = P_A - P_{pl} \tag{4-4}$$

Substituting in Equation 4-2:

$$P_L = P_{fr} + P_{el} \tag{4-5}$$

This is illustrated in Figure 4-1.

P_{fr} is in phase with flow, whereas, when tidal volumes are small and hysteresis can be neglected, P_{el} is in phase with volume. The relationships between flow, volume, P_{fr}, P_{el}, and P_L are shown in Figure 4-2.

If one considers that one complete respiratory cycle constitutes 360° (like a circle), then one observes that flow is one-quarter of a cycle or 90° ahead of volume. Similarly, P_{fr}, which is in phase with flow, is 90° ahead of P_{el}, which is

*During spontaneous inspiration, this pressure is positive and alveolar pressure is negative, whereas during expiration, it is negative and alveolar pressure is positive.

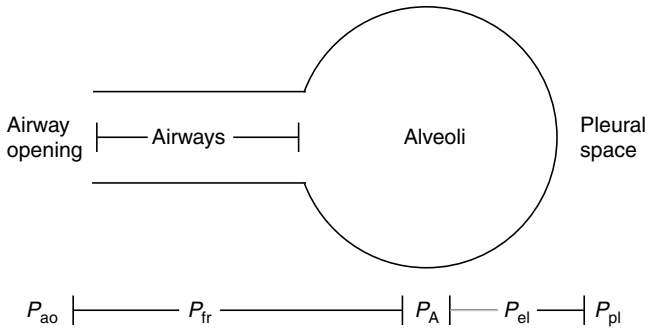

FIGURE 4-1 Simple one-compartment model of the lung in which the upper airway and tracheobronchial tree are represented by a single tube and the parenchyma by a single alveolus. The pressure producing flow (P_{fr}) is the difference between the pressure at the airway opening and the pressure in the alveoli ($P_{ao} - P_A$). The elastic recoil pressure (P_{el}) is the pressure difference between P_A and the pressure in the pleural space ($P_A - P_{pl}$).

in phase with volume. The bottom panel of Figure 4-2 shows how P_L can be calculated as the sum of P_{el} and P_{fr}, where P_{fr} is the hatched area between P_L and P_{el}.

Each of the variables flow (V'), volume (V), P_{fr}, P_{el}, and P_L has both a magnitude (its size) and a phase (when it occurs). It can be seen that the phase of P_L lags behind that of V' and P_{fr} but leads V and P_{el}. I will show that the phase and magnitude of P_L in relation to the other variables depend, upon the lungs' elastic, flow-resistive, and inertial properties, tidal volume (V_T), V', and respiratory rate (f_B). To have the phase and magnitude of a single variable depend on so many other variables may sound complicated. In reality, as will be seen, it is quite straightforward with the use of vector analysis.

By definition, the resistance to flow of air into and out of the lung, airway resistance (R_{aw}), is given by P_{fr}/V' and:

$$P_{fr} = R_{aw}V' \tag{4-6}$$

The elastic properties of the lung are characterized in part by lung compliance (C_L):

$$C_L = V_T/\Delta P_{el}{}^{\dagger} \tag{4-7}$$

and

$$\Delta P_{el} = V_T/C_L$$

Equation 4-5 can be rewritten:

$$\Delta P_L = P_{fr}{}^{\ddagger} + \Delta P_{el} \tag{4-8}$$

Substituting for P_{fr} and ΔP_{el}:

$$\Delta P_L = V_T/C_L + R_{aw}V' \tag{4-9}$$

If breathing is quasisinusoidal, V_T and f_B must obviously determine V'. This is given by the formula $V' = 2\pi f_B \cdot j \cdot V_T$, where $j = \sqrt{-1}$ and is used to indicate V and V' are 90° out of phase. The quantity $2\pi f_B$ is denoted by the Greek letter omega. Thus:

$$\Delta P_L = V_T/C_L + R_{aw} \cdot \omega \cdot j \cdot V_T \tag{4-10}$$

For most purposes, Equations 4-9 and 4-10 can be used as equations of motion of the lung. Equation 4-10 can be used when breathing is nearly sinusoidal, and Equation 4-9 when it is not. However, at $f_B > 1.5$ Hz, the lung's inertial properties come into play. Lung inertance (I_L) depends upon the rate of change of flow or acceleration (V''). Again, if breathing is quasisinusoidal:

$$V'' = j \cdot \omega \cdot V' = j^2 \cdot \omega^2 \cdot V_T = -\omega^2 \cdot V_T$$

because $(\sqrt{-1})^2 = -1$

This is illustrated in Figure 4-3. As V' passes through zero, V'' is maximal; when V' is maximal and for a brief instant it is not changing, V'' is zero. It can be seen that V_L and V'' are 180° out of phase. The inertial pressure (P_{in}) is in phase with

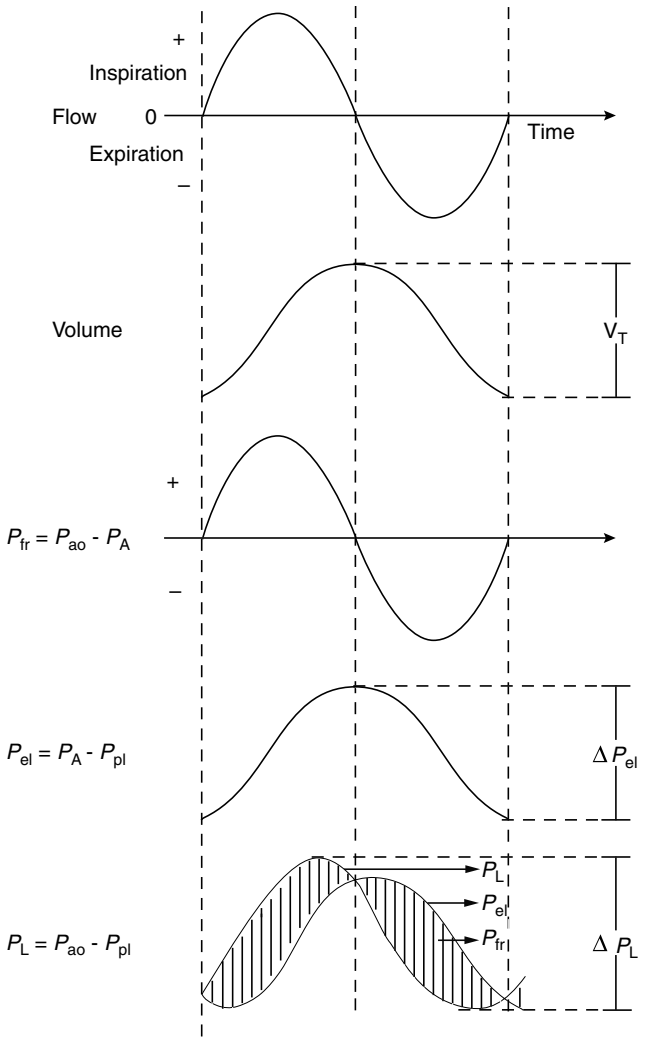

FIGURE 4-2 Relationships between flow, P_{fr}, ΔP_{el}, and the pressure difference across the lung, transpulmonary pressure (P_L). P_{fr} is in phase with flow; ΔP_{el} is in phase with volume; and ΔP_L is the sum of P_{fr} and ΔP_{el}, and its phase is between that of P_{fr} and ΔP_{el}. At zero flow points at the beginning and end of a breath, $P_{fr} = 0$ and $P_{el} = P_L$. V_T = tidal volume; other symbols as in Figure 4-1.

[†] Every lung volume has its particular values of P_{el}, depending on lung volume history (Chapter 3, "Statics of the Lung"). Here I am referring exclusively to the change in P_{el} over the tidal volume range, not absolute P_{el}; hence the use of the delta symbol.

[‡] P_{fr} and V' both cycle in phase around zero, and therefore no delta sign is required.

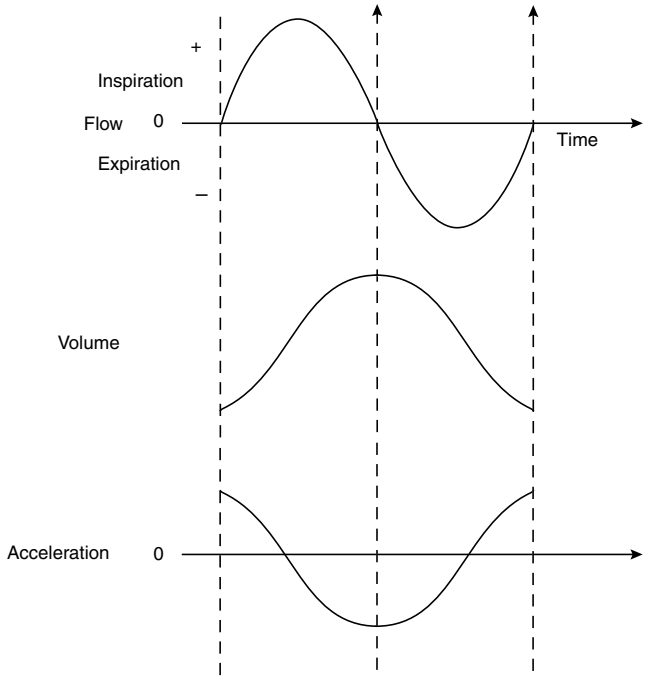

FIGURE 4-3 Phase relationships between flow, volume, and acceleration for a sinusoidal breathing pattern.

V'', and therefore P_{el} and P_{in} are 180° out of phase. Thus, at breathing frequencies >1.5 Hz, P_{in} subtracts from P_{el} in the determination of P_L, and the equation of motion becomes:

$$\Delta P_L = V_T/C_L + \omega \cdot j \cdot R_{aw} \cdot V_T - \omega^2 I_L V_T$$

or

$$\Delta P_L = V_T(1/C_L + \omega \cdot j \cdot R_{aw} - \omega^2 I_L) \qquad (4\text{-}11)$$

Vector Analysis of the Equation of Motion

Circular Motion Imagine a frictionless pendulum with a pen at the bottom producing a tracing of its motion on a strip of paper moving at right angles to the pendular motion. The tracing would be a sine wave. If the paper speed were just right, the amplitude of the pendulum could be precisely equal to the period of one complete cycle, as shown in Figure 4-4A. If the time axis or direction of the paper changed every time the pendulum reached the midpoint of its motion, so that the tracing returned to its point of origin (Figure 4-4B), the pendular motion would be described as a trajectory traveling in a counterclockwise circle. The pendulum's amplitude would be given by the circle's diameter and

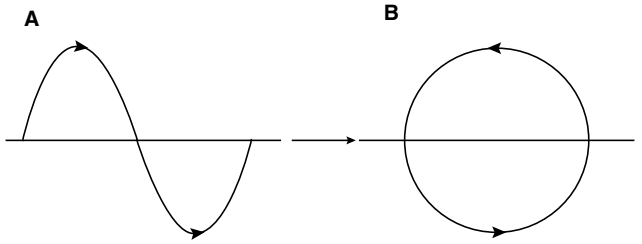

FIGURE 4-4 *A*, Pendular motion represented by a sine wave. *B*, Pendular motion represented by a circle. See text for further explanation.

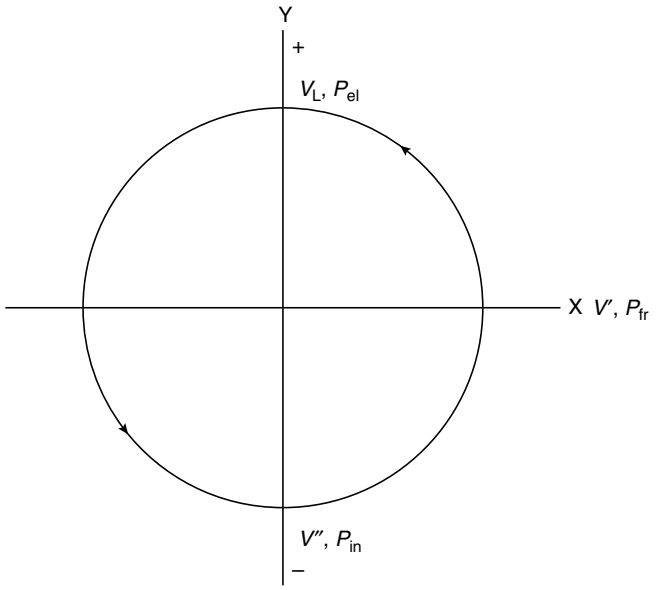

FIGURE 4-5 Determination of the phase relationships between lung volume (V_L), P_{el}, flow (V'), P_{fr}, acceleration (V''), and inertial pressure (P_{in}). See text for further explanation.

its phase at any instant by its position on the 360° of the circle's circumference. It was from this sort of analysis that we concluded that V_T and ΔP_{el} lag V' and P_{fr} by 90° and that ΔP_{el} and P_{in} are 180° out of phase.

The representation of a variable undergoing sinusoidal motion by a circle in which both amplitude and phase of the variable can be determined is called vector analysis. Vectors have both amplitude and phase. If, at any instant in time, V' were to be aligned with the x-axis, then P_{fr}, in phase with it, would also be aligned on the x-axis. Both V_L and P_{el}, which lag V' and P_{fr} by 90°, would be aligned along the y-axis at positive values of y, whereas V'' and P_{in} would also be aligned along the y-axis at negative values of y. This is illustrated in Figure 4-5.

Determination of Phase and Amplitude of Respiratory Variables Knowing V_T, f_B, R_{aw}, C_L, and I_L, how does one measure the phase and amplitude of ΔP_{el}, P_{fr}, and P_{in} by vector analysis?

Assume a V_T of 0.5 L and an f_B of 15/min = 0.25/s, an R_{aw} of 1.5 cm H_2O/L/s, and a C_L of 0.2 L/cm H_2O. Then, $\omega V_T = 0.785$ L/s, $P_{fr} = 1.178$ cm H_2O, and $\Delta P_{el} = 2.5$ cm H_2O. When these values are plotted on the vector graph with V' (closed square) and P_{fr} (open square) on the x-axis and V_T (closed circle) and ΔP_{el} (open circle) on the y-axis, the results shown in Figure 4-6 are obtained. Remember that the amplitude is the diameter of the circle, not the radius. Thus, the V_T intersects the ordinate at a value of 0.25 not 0.5. Study this graph carefully until it is understood. It is the key to all the vector analysis that follows. The vector sum of ΔP_{el} and P_{fr} provides the solution for the phase and magnitude of ΔP_L (outermost circle). ΔP_L is given by the intersection of the horizontal projection of ΔP_{el} with the vertical projection of P_{fr} (point X on the graph). Its length from the origin to point X is half of its amplitude, and its phase is

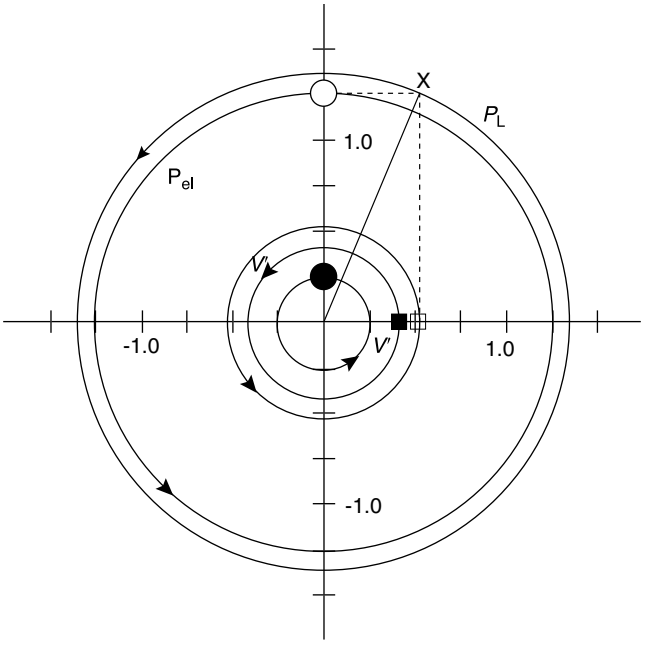

FIGURE 4-6 Vector analysis of the dynamics of breathing. For explanation, see text.

the number of degrees by which it lags V' and P_{fr}. Note that the magnitude of ΔP_L is greater than that of either ΔP_{el} or P_{fr}, and for the values of V_T, f_B, C_L and R_{aw} chosen, the phase of ΔP_L is closer to that of ΔP_{el} than of P_{fr}.

If breathing had been extremely slow, so that $f_B \rightarrow 0$, then ωV_T would also be small, and ΔP_L would be almost in phase with volume and would have a magnitude almost equal to ΔP_{el}, as shown in Figure 4-7A (we do not need the circles any more). On the other hand, if breathing had been very rapid, say 1 Hz, and V_T small, then ΔP_L would be nearly in phase with V' and almost equal in magnitude to P_{fr} (Figure 4-7B). The phase and magnitude of ΔP_L depend importantly on the pattern of breathing.

Because the amplitude of ΔP_{el} is determined in part by C_L (Equation 4-7) and the amplitude of P_{fr} by R_{aw} (Equation 4-6), which are independent of the pattern of breathing, the mechanical properties of the lung are also important determinants of the phase and amplitude of ΔP_L. This is illustrated in Figure 4-8. When the lungs are stiff with pulmonary fibrosis or pulmonary edema, C_L is small and ΔP_{el} is large. The effect on ΔP_L is similar to the effect of a large V_T and small f_B (Figure 4-8A). On the other hand, with airways obstruction, as in asthma or chronic obstructive pulmonary disease (COPD), P_{fr} is large, and the result is similar to a rapid shallow breathing pattern (Figure 4-8B).

If one knows the breathing pattern, lung compliance, and airways resistance, one can calculate the phase and amplitude of transpulmonary pressure, the pressure that is moving the lung, and partition it into its two components, P_{fr} and P_{el}, due to flow resistance and lung elastic recoil, respectively.

Conversely, if one measures V_T, f_B, and P_L (the usual measurements made when assessing lung mechanics), one can calculate C_L and R_{aw} as illustrated in Figure 4-9. The measured variables, V_T and f_B, from which V' is calculated, and the measured values of phase and amplitude of ΔP_L are plotted on the graph, from which P_{el} (open circle) and P_{fr} (closed circle) are obtained by dropping perpendiculars from P_L to the y- and x-axes, respectively. Knowledge of P_{el}, P_{fr}, V_T, and ωV_T then allows calculation of lung compliance and airways resistance.

In practice, this approach has been used infrequently to measure the mechanical properties of lungs, probably

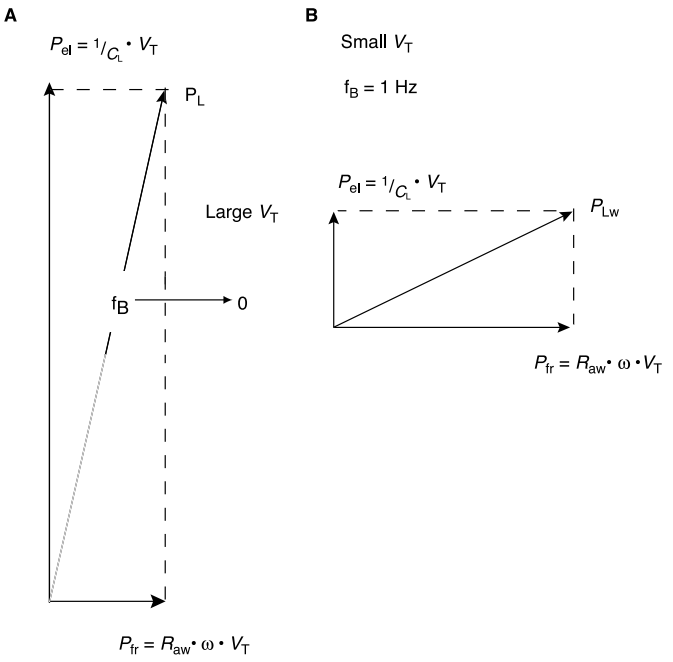

FIGURE 4-7 Influence of (*A*) slow, deep breathing and (*B*) rapid, shallow breathing on the phase and magnitude of P_L.

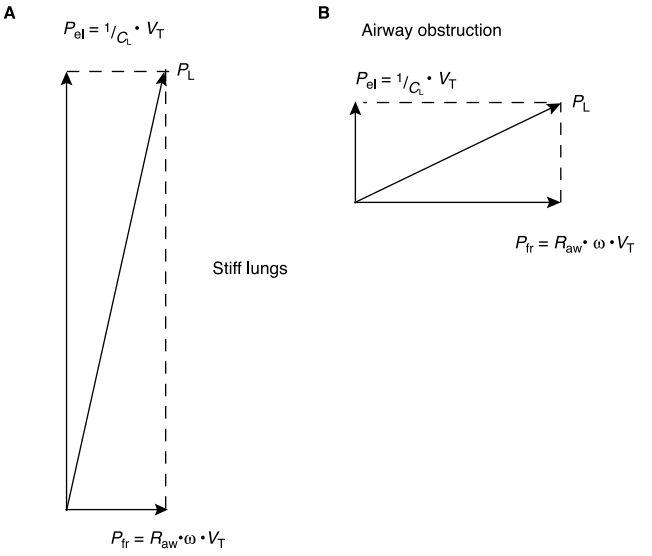

FIGURE 4-8 Vector analysis showing the effect of stiff lungs (*A*) and airways obstruction (*B*) on P_{el}, P_{fr}, and P_L. When the lungs are stiff, C_L is low and P_{el} is large. The effect on P_L is similar to that of slow, deep breathing (see Figure 4-7A). Conversely, when the airways are obstructed, R_{aw} is large and the effect on P_L is similar to that of rapid, shallow breathing (see Figure 4-7B).

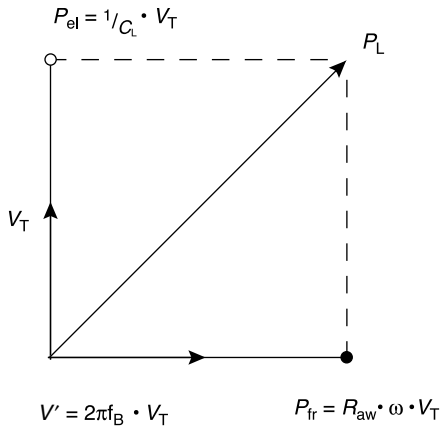

FIGURE 4-9 Vector analysis solving for ΔP_{el} and P_{fr}, knowing V_T, V', and ΔP_L.

because breathing is not really sinusoidal. Determination of how accurately ωV_T predicts measured flow would show how applicable vector analysis might be in the measurement of the dynamics of breathing. Certainly, the assumption that breathing is sinusoidal has been very useful in modeling the mechanics of breathing.

At breathing frequencies >1.5 Hz, inertia cannot be ignored. Consider that P_{in} is given by $\omega^2 I_L V_T$, whereas P_{el} is independent of ω. For a given V_T, P_{in} increases rapidly with breathing frequency, but ΔP_{el} remains constant. Because P_{in} is 180° out of phase with P_{el} and subtracts directly from P_{el}, the vector sum of ΔP_{el} and P_{in} affects the phase and magnitude of ΔP_L. This is illustrated in Figure 4-10A. As P_{in} increases at constant ΔP_{el}, P_L moves closer and closer to the phase of P_{fr}.

It is evident that, at a particular value of ω, ΔP_{el} and P_{in} will be equal and opposite. The resulting vector sum of the two will be zero. Under these circumstances, P_{fr} is the only determinant of ΔP_L, which becomes in phase with and of equal magnitude to P_{fr} (Figure 4-10B), and the equation of motion reduces to $\Delta P_L = R_{aw}\omega V_T = P_{fr}$. When this occurs,

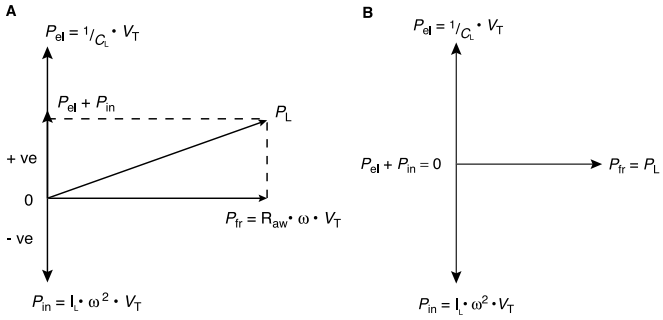

FIGURE 4-10 *A*, Vector diagram illustrating the importance of inertia at high breathing frequencies. When f_B is greater than 90/min, P_{in} cannot be ignored. Because ΔP_{el} and P_{in} are 180° out of phase, P_{in} subtracts from ΔP_{el}, which makes P_{fr} the dominant vector determining the phase and magnitude of P_L. *B*, Vector diagram illustrating resonant frequency when ΔP_{el} and P_{in} are equal and opposite, canceling each other out, and leaving P_{fr} as the only component of ΔP_L.

$V_T/C_L = \omega^2 I_L V_T$ and $f_B = {}^{1}/_{2\pi}\,(C_L \cdot I_L)^{-1/2}$. This is the resonant frequency of the lung, and it is about 6 Hz. This is the frequency at which the impedance to the flow of air is minimal. It is also the frequency at which dogs pant.

HYSTERESIVITY

Until now, I have ignored the problem of the resistance due to tissue viscance or hysteresivity. When P_L is measured, it is not simply $P_{ao} - P_A + P_{el}$. This is because $P_A - P_{pl}$ contains a term not in phase with volume. This is most easily seen when one measures the static pressure–volume curve of the lung. At any lung volume, P_{el} is greater on inflation from residual volume (RV) than it is on deflation from total lung capacity (TLC). Thus, the inflation pressure–volume curve is displaced to the right of the deflation curve. The pressure difference between inflation and deflation leads volume by 90° and is therefore in phase with flow. For this reason, the resulting pressure–volume curve has been thought to result from the viscous resistance of lung tissue. However, it is not flow dependent. The phenomenon is called hysteresis, and it quantifies the difference between the energy that is the product of pressure and volume stored in the lung on inflation and that recovered during deflation. This difference is the area contained between the two pressure–volume curves or, in other words, the energy dissipated in a respiratory cycle. Although the dissipated energy is greatest for vital capacity breaths, it is still finite during quiet breathing. The hysteretic pressure is well described by the expression:

$$P = j\eta V_T/C_L \qquad (4\text{-}12)$$

where j is the mathematical device indicating that P is 90° out of phase with volume and η is hysteresivity defined as the dimensionless ratio of the hysteretic pressure difference at mid–tidal volume to the change in elastic recoil pressure for that particular breath, as shown in Figure 4-11.[2] Equation 4-12 shows that the pressure is dependent on both tidal volume and $1/C_L$ or lung elastance, and thus it specifically couples the energy dissipated by hysteresis to the lung's elastic properties, which reflect the stress-bearing elements. How can this be? Fredberg and Stamenovic give several examples.[2] Attached crossbridges in smooth muscle make the muscle stiffer. However, if the muscle is stretched during inspiration, some crossbridges may break, thereby dissipating stored energy and leading to hysteresis, but with the breakage, the muscle becomes more compliant. When atelectatic alveoli inflate, it takes a substantial pressure to overcome the surface tension and viscosity of the liquid lining the airspaces and allow them to open. When opened, they tend to remain open, so the energy required to open them is dissipated, but once the airspaces are open, the lung becomes more compliant. A third example of dissipative and elastic coupling is via the surface-lining layer of surfactant at the alveolar air–liquid interface. On inflation, the number of surface-active molecules lining the surface film may be inadequate to cover the film over the whole increase in surface area that occurs. As a result, the surface film breaks, and molecules with a higher surface tension form the lining layer until new surface-active molecules are

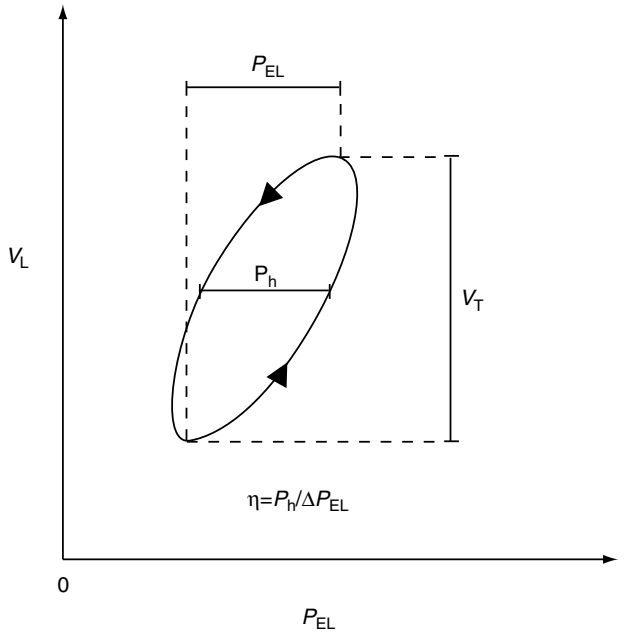

FIGURE 4-11 Static P_{el}–V_L pressure–volume loop illustrating hysteresis. Hysteresivity (η) is the ratio of the difference in P_{el} at mid-V_T (P_h) and the difference in P_{el} at zero flow points: $\eta = P_h/\Delta P_{el}$.

adsorbed onto the surface from the hypophase. Thus, elastic recoil pressures are greater on lung expansion, and it takes greater force to expand the surface. On deflation, there is an excess of surface molecules, so that, as surface area decreases, the surface film may actually resist compression, so that it buckles and the surface-active molecules are forced into the hypophase, from whence they must be subsequently recruited during the following inspiration. In these ways, one obtains insight into how elastic and dissipative properties become linked in the lung.[2]

In order to take hysteresivity into account, the equation of motion of the lung must be modified to:

$$\Delta P_L = V_T/C_L + j\eta V_T/C_L + \omega j R_{aw} V_T - \omega^2 I_L V_T$$

or

$$\Delta P_L = V_T[^1/C_L + j(\eta/C_L + \omega R_{aw}) - \omega^2 I_L] \quad (4\text{-}13)$$

To express Equation 4-12 in terms of absolute P_L, one writes:

$$P_L = P_{Lo} + V_T[1/C_L + j(\eta/C_L + \omega R_{aw}) - \omega^2 I_L] \quad (4\text{-}14)$$

where P_{Lo} is the absolute transpulmonary pressure at end-expiratory volume.

From Equations 4-13 and 4-14, it can be seen that tidal volume, which, along with breathing frequency, determines flow and acceleration, affects every term in the equation of motion except P_{Lo}, which, during quiet breathing, is transpulmonary pressure at functional residual capacity (FRC).

There are two terms in the equation of motion that are 90° out of phase with volume. When one uses the difference between mouth and esophageal pressure to measure transpulmonary pressure, the ratio of pressure in phase with flow and flow is called pulmonary resistance. This includes $\eta V_T/C_L$, which has nothing to do with the resistance to flow along the airways. The error induced in estimating airways resistance from pulmonary resistance can be substantial, particularly if tidal volumes are large and compliance low.[3,4] The error can become very large if one is attempting to measure the resistance of only the peripheral airways because $\eta V_T/C_L$ is large relative to $\omega R_{aw} V_T$.[5] The error can be minimized by using small tidal volumes, which is an attractive feature of the forced oscillation technique, in which the lungs are oscillated by a loudspeaker.[5,6] Furthermore, if one wishes to measure flow-resistive pressure only during inspiration or expiration, then one can avoid pressures due to hysteresis by measuring the difference between the static inflation or deflation pressures and the dynamic pressures at the same volume.[5]

Nevertheless, the dependence of hysteretic pressures on $\eta V_T/C_L$ means that there are substantial errors in the older literature where pulmonary resistance was used to estimate the effects on the airways of interventions such as drugs, changes in lung volume, and disease. The situation becomes further complicated in that η is not assumed to be constant but could vary with tidal volume and elastance, the reciprocal of compliance.[4,7]

Hysteretic and flow-resistive effects have been experimentally separated in tissue strips and by the direct measurement of alveolar pressure with the use of alveolar capsules. These two methods provided results that were in agreement with each other, and the roles of tidal stretching of alveolar walls, lung volume history,[8] elastance,[4] and hysteresivity[3] have been measured. However, care should be taken in comparing the behavior of tissue strips with lung volume changes in the former. The forces required for stretching are determined by the shear modulus, whereas the pressures required for volume change are determined by the bulk modulus. The two moduli are not the same.

The results of pharmacologic experiments proved surprising. Almost every intervention that influenced airway resistance also increased hysteresis.[3,8–12] In some instances, the major effects of the drug appeared to be on the lung parenchyma rather than on the airways, so that interpreting pulmonary resistance in terms of bronchoconstriction can be misleading. In tissue strips, pharmacologic agents induced changes of stiffness and also changed η. However, the relationship between the two was different for different agents.[4] The authors pointed out that their experiments "demonstrated the existence of distinct mechanical states that differed according to the specific agonist by which the tissues were stimulated." In whole lungs, elastance and hysteresis were changed by changing lung volume history and by pharmacologic interventions. These alterations were separated into two distinct components, changes in η and changes in elastance. Again, changes in η and elastance were dissociated. With changes in volume history, elastance changed but η did not, whereas with smooth muscle agonists, both changed.[13] When lungs were saline filled, to eliminate the surface effects, and elastance was altered by changing lung volume, hysteresis was still tightly coupled to elastance, but η remained constant.[11]

These experiments reveal a fundamental property of lung tissue and the parenchymal air–liquid interface, namely the coupling of dissipative properties to the stress-bearing elements of the lung responsible for their elastic properties. They also point out the importance of separating airway from lung tissue properties in disease states and in pharmacologic interventions. Too often, changes in the properties of one could mask or appear to indicate artifactual changes in the other.

Unfortunately, very few attempts have been made to separate airway from parenchymal dissipative properties in living human lungs. The technology exists to do such experiments: whole body plethysmography can be used to measure alveolar pressure and airways resistance, and the difference between alveolar and esophageal pressure can be used to obtain the elastic pressure–volume curve. Thus, it should be possible to investigate the coupling of dissipative and elastic properties of the parenchyma, as well as to separate airway from parenchymal effects. This needs to be done particularly when the actions of pharmacologic agents and disease states on the human lung are being evaluated.

MEASUREMENT OF LUNG MECHANICS

The measurement of the mechanical properties of lungs entails the measurement of flow, volume, and pressure.[14] Flow is measured with a pneumotachygraph, and frequently this is integrated to obtain volume. The measurement of flow is accurate and reasonably straightforward, although care must be taken when gas physical properties, particularly viscosity change, and when very rapid flow transients need to be accurately measured. This usually requires a mouthpiece and noseclip, and thus the measurement of flow poses a problem when a mouthpiece and noseclip are either undesirable or impossible. The same problems apply to the measurement of volume, as discussed below.

Lung Volume Measurements

As mentioned above, lung volume change is frequently measured by integrating a tracing of flow at the mouth. Volumes can also be measured with a spirometer or a bag-in-box system connected to the mouth. None of these is entirely satisfactory. All integrators suffer from integrator drift, so absolute changes in lung volume, such as those that occur with exercise, cannot be measured accurately. Rebreathing from a spirometer requires scrubbing of carbon dioxide and, for a stable tracing, addition of oxygen at exactly the rate at which oxygen is taken up by the pulmonary capillaries. This is not usually possible. A bag-in-box system allows one to breathe in from a bag enclosed in a box with a spirometer attached to it, and then out into the box, because the inspiratory and expiratory lines are separated by valves. This provides a stable tracing without the need to scrub carbon dioxide or add oxygen. However, the time over which volume can be measured is determined by the volume of gas contained within the bag. When this is exhausted, the measurement of volume stops.

Volume displacement or variable-flow whole body plethysmographs provide accurate measurements of changes in body volume that, during normal quiet breathing, closely reflect the volumes of gas breathed in and out of the mouth. However, under circumstances when there are large swings in alveolar pressure, there may be significant compression and decompression of alveolar gas. When this occurs, changes in body volume (measured by plethysmography) are greater than the volumes exchanged at the mouth. This is a very useful feature in the measurement of maximal expiratory flow–volume curves because maximal expiratory flow is determined by absolute lung volume and not merely the volume expired at the mouth.[15] During a forced expiration there is substantial gas compression, so the absolute lung volume is less than the volume of gas expired at the mouth. Thus, whenever the latter is used to measure flow–volume curves, maximal expiratory flow at the measured volume is underestimated. This can lead to substantial errors in the measurement of flow–volume curves if there is marked hyperinflation and the expiratory alveolar pressures are high.[16] This is usually the case in COPD, when the errors can be very large indeed.[16] Although these errors are avoided when volumes are measured by whole body plethysmography, the stability of the tracings is affected by heating and humidification. Furthermore, it is obvious that whole body plethysmography cannot yet be used during exercise or easily during sleep.

Surprisingly in this era of high technology, the requirement for a mouthpiece and noseclip makes it remarkably difficult to measure ventilation in such conditions as sleep, phonation, and infancy and in critically ill patients. The same considerations apply to changes in absolute lung volume during exercise, for example. This problem has resulted in attempts to measure breathing based on body surface measurements. Two of these methods, magnetometry and inductance plethysmography, depend upon the abdomen and the rib cage, each acting as compartments with a single degree of freedom.[17] This is an approximation leading to significant errors (generally ignored in the literature) when breathing exceeds the rather strict limits established by Konno and Mead.[17] Furthermore, calibration changes with posture. This can be dealt with in part by measuring xiphipubic distance. However, the control of posture and respiratory effort necessary for reasonably accurate measurements renders these methods of limited value.

A new technology, optoelectronic plethysmography, involves placing of reflective markers over the surface of the chest wall, tracking each one in three dimensions, and then reconstructing the whole chest wall, and its compartments, to measure volume changes dynamically without mouthpiece and noseclip.[18,19] It has undergone extensive evaluation and appears to be highly accurate.[20] It can be used to measure ventilation in all the problem situations listed above (not yet tried in infants). It requires no assumptions with regard to the number of degrees of freedom of the rib cage and abdomen. Because it measures chest wall volume, in contrast to whole body plethysmography, which measures body volume, it is sensitive not only to gas compression and decompression but also to blood shifts from the trunk to the extremities. This new feature has been used to demonstrate substantial blood shifts during exercise with

expiratory flow–limitation, when expiratory pressures can be markedly positive.[21] Although this technology has great promise, it is expensive and requires advanced electronic computations that need to be made user-friendly before the method will gain widespread use.

Another new noninvasive method, phonospirometry, estimates tracheal flow from tracheal breath sounds, obtained simply with a microphone placed on the neck.[22] It appears to be at least as accurate as magnetometry and inductance plethysmography but less sensitive to chest wall distortions and changes in posture. Considerably more research will be necessary to determine its applicability to clinical situations such as sleep-disordered breathing and investigation of the sudden infant death syndrome.

Pressure Measurements

Esophageal pressure is an accurate measure of pleural pressure (P_{pl}). Esophageal pressure is equal to the pressure outside the esophagus, or P_{pl} if there is no pressure difference across the esophageal wall. This is generally true if the esophagus is not distended by the pressure-measuring probe. For details concerning esophageal pressure measurements, see Baydur and colleagues[23] (see also Chapter 55, "Esophageal Pressure Measurement")

From the measurement of the static pressure–volume curve of the lung, which defines P_{el} as a function of lung volume, and the dynamic pressure–volume curve, which encircles the static curve over the tidal volume range, one can obtain an approximate measure of P_A as the difference between the static and the dynamic pressures at the same lung volume as shown in Figure 4-12.

An accurate measurement of P_A in intact humans requires the use of whole body plethysmography. In excised lungs or open-chested experimental animals, it can be measured directly with capsules glued on the surface of the visceral pleura; the pleura contain holes, so that the capsule connects directly with the subpleural alveoli.

The principle of measuring P_A from whole body plethysmography is most easily understood when one considers what happens when one rebreathes while sitting inside a constant-volume box. Assuming isothermal conditions and negligible humidification of inspired air (conditions that are satisfactorily met during panting), box pressure can only change to the extent that there is compression and expansion of alveolar gas. In a constant-volume plethysmograph, compression of alveolar gas requires expansion of gas within the box and thus a fall in box pressure. In order to find how much expansion is required to explain a given change in box pressure, a calibration procedure is performed in which a known volume of gas is introduced into and removed from the box with a syringe, and the resulting pressure changes are measured. Then box pressure and pressure at the mouth are measured while the subject pants against a closed airway. From Boyle's law, the product of box pressure and box volume change (calculated from the calibration procedure) equals the product of mouth pressure (equal to alveolar pressure because no air is flowing) and lung gas volume. The last is the only unknown. This is the basis of measurement of absolute thoracic gas volume by whole body plethysmography. However, this measurement also serves to calibrate the relationship between box pressure, P_A, and the degree of alveolar gas compression and expansion. Subsequently, the subject rebreathes to and from the box by panting through a pneumotachygraph while box pressure is measured, the magnitude of alveolar gas compression and expansion is calculated, and, because absolute thoracic gas volume is known, P_A is derived. The ratio between P_A and the measured flow then provides R_{aw}.

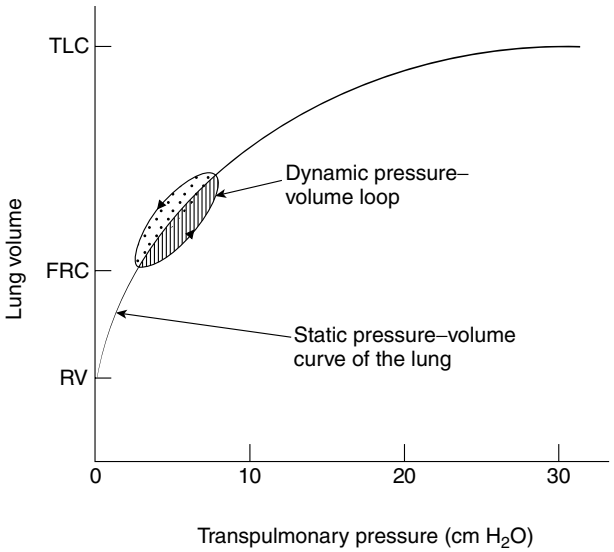

FIGURE 4-12 Static pressure–volume curve of the lung with superimposed dynamic pressure–volume loop. The hatched region represents the flow-resistive and hysteretic pressures during inspiration, and the dotted region represents the same pressures during expiration. The areas of these regions quantify the net work performed on the lung by the respiratory muscles.

RELATIONSHIP BETWEEN LUNG MECHANICS AND VENTILATION DISTRIBUTION

Time Constants

Up to this point, I have considered the lung as a single tube representing the conducting airways and a single alveolus representing the millions of gas-exchanging airspaces making up the lung parenchyma. This model cannot be applied to the distribution of ventilation to multiple airspaces arranged in parallel. Let us pose the question: what determines how fast such a lung will fill when transpulmonary pressure is increased? Imagine a step square wave increase in transpulmonary pressure ΔP_L. Neglecting inertia, at the instant this pressure is applied to the lung, P_{fr} will equal ΔP_L, so that:

$$\Delta P_L = P_{fr} = R_{aw}V'$$

Once the lung has completely filled, flow will cease, P_{fr} will equal zero, and ΔP_L will equal ΔP_{el}, so that:

$$\Delta P_L = \Delta P_{el} = \Delta V/C_L$$

and

$$R_{aw}V' = \Delta V/C_L$$

Cross-multiplying:

$$R_{aw}C_L = \text{time}$$

The product of airway resistance and lung compliance has the units of time, and its value is the lung's time constant. The time constant is the parameter that determines how rapidly a lung will fill when P_L increases.[24] What it states is actually rather obvious. As airway resistance increases and flow decreases at a given P_{fr}, it takes longer and longer to fill the lungs, and as compliance increases at a given flow, it takes longer to inflate the lung because it requires more volume to do so for a given ΔP_{el}. When both increase, the effects are more than additive; they are multiplicative.

However, the lungs have many parallel airspaces, each with its own compliance and flow resistance. Therefore, each parallel airspace, whether or not one is considering a single acinus, lobule, segment, or lobe, has its own time constant. If these are markedly different one from another, as occurs in some diseases, then some units will lag behind their neighbors. The fast units will fill and start to empty before the slow units have finished filling.[24] Thus, part of the latter's inspired volume will be alveolar gas that their neighbors are expiring. Furthermore, because slow units will not have the time to fill completely before they start emptying, their tidal volume will fall, so that the fast units receive a larger fraction of the total tidal volume. This situation becomes progressively worse as breathing frequency increases and the respiratory cycle time progressively decreases relative to the time constants.[24] This would be an unfortunate way to breathe, and it does not normally occur. What, then, is the condition for each of the parallel airspaces to fill and empty in synchrony with all its neighbors?

For this to occur at all breathing frequencies, it is necessary for all the time constants of all similar-sized parallel airspaces, large or small, to be equal.[24] Such a constraint is difficult to achieve. The pathways to perihilar airspaces are much shorter than those to the base of the lung posteriorly. Owing to the gravity-determined gradient in pleural pressure, both the resistance to the flow of air and the compliance of airspaces are less in superior lung regions than in dependent ones. Presumably, the time constants of parallel airspaces are not all equal, and they do not have to be for the airspaces in the lung to fill and empty synchronously at physiologic breathing frequencies. As long as the time constants are short relative to the respiratory cycle time, there can be inequality of time constants.[5]

Direct measurements of intrabronchial pressure have shown that in normal lungs most of the resistance to airflow is in the large central airways, and very little resistance is offered by the peripheral airways.[5,25] The resistance common to parallel airspaces, namely the central airways for airspaces distal to the peripheral airways, plays no role in generating asynchrony among these peripheral units. Thus, the pertinent resistances that make up the time constants are the resistances of the peripheral airways. Because these are small, the time constants are small, on the order of 0.02 to 0.04 seconds. These are about two orders of magnitude less than the respiratory cycle times of 2 to 4 seconds at physiologic breathing frequencies, which normally range from 15/min at rest to 30/min at maximal exercise. This allows for considerable inequality among the time constants of peripheral lung units with very little asynchrony or reduction in tidal volume of the slower units. However, even if time constant inequality were sufficient to lead to asynchrony, there are two powerful influences promoting synchrony in both normal and diseased lungs: interdependence among parallel lung units[26] and collateral ventilation.[27]

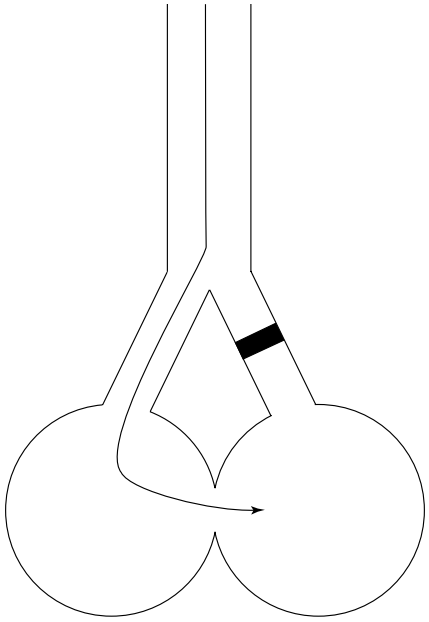

FIGURE 4-13 Two-compartment lung model illustrating collateral ventilation in the presence of complete airway obstruction to one compartment. Inspired air follows the route shown by the arrow and exchanges gas in the unobstructed airspace before entering the collaterally ventilated airspace, which receives alveolar gas. The time required to ventilate the obstructed airspace is determined by the time constant for collateral ventilation, which is the product of the resistance of the channels connecting the two compartments and the effective compliance of the collaterally ventilated space. For further explanation see text.

Collateral Ventilation

When airways become occluded, gas can enter into the subtended airspaces via collateral channels. In excised dog lungs, collateral ventilation is extremely rapid, providing normal tidal volumes to airspaces beyond completely obstructed airways at breathing frequencies as high as 1 Hz.[28] A model of this situation is shown in Figure 4-13. The time taken for gas to flow from unobstructed airspaces into obstructed ones via collateral channels is given by the time constant for collateral ventilation (T_{col}), or the product of the flow resistance of the collateral channels (R_{col}) and the compliance of the collaterally ventilated space (C_{col}). The fact that collateral channels deliver a normal tidal volume to airspaces beyond completely obstructed airspaces at a breathing frequency of 1 Hz indicates that T_{col} in excised dog lungs must be considerably less than 1 second. This has been experimentally verified.[27]

One can measure R_{col} by wedging a catheter in a bronchus, passing air through it at a known constant rate (V'_{col}), and measuring the pressure at the catheter tip.[29] If the flow is suddenly turned off, the pressure decays in a quasiexponential way. In most studies there is no sudden pressure drop, indicating that the resistance between the catheter tip and the alveoli beyond is negligible at the flow rate used. Thus, the pressure producing collateral flow (P_{col}) is given by the pressure difference between the catheter tip and alveolar pressure in the rest of the lung: $R_{col} = P_{col}/V'_{col}$. The quasiexponential fall in pressure at the catheter tip when flow is suddenly switched off allows the measurement of T_{col} as the time needed for the pressure to fall by 63% of its initial value. Dividing T_{col} by R_{col} gives C_{col}. C_{col} measured in this way is considerably less than predicted by the estimated amount of lung tissue beyond the obstructed airways. The explanation for this is given below. For the present, the essential message is that the low value of C_{col} is one of the major reasons why T_{col} is surprisingly short.

The time constant for collateral ventilation depends on a variety of variables, including species, lung volume, the size of the airway obstructed,[27] oxygen and carbon dioxide concentrations in the airways,[30,31] surface forces,[32] and airway smooth muscle tone in the collateral channels.[33]

The lungs of large animals such as horses cattle, and swine are completely lobulated. Because each lobule is completely separated from its neighbors by connective tissue, there is no collateral ventilation between lobules. The lungs of smaller animals such as dogs, cats, and rabbits are nonlobulated and have extensive collateral ventilation. Human lungs lie between these extremes. They are partially lobulated, so that collateral ventilation occurs between lobules but is considerably slower than in nonlobulated lungs.[27] Although, so far as I am aware, no direct comparisons of T_{col} have been made in lungs in living animals and excised lungs, the literature strongly suggests that T_{col} is substantially longer in living lungs in situ than after they are excised. The reasons for this are not known.

T_{col} is highly dependent on lung distending pressure and volume, more so even than airway resistance.[27,34] Furthermore, the greater the volume of lung beyond the obstructed airway, the longer is T_{col}.[29,35] Thus, it takes longer to collaterally ventilate a part of the lung beyond an obstructed large airway than an obstructed small airway. Presumably, this reflects the external surface area/volume ratio of the collaterally ventilated space. The surface area available for collateral ventilation should be a major determinant of R_{col} because it should determine the number of parallel collateral channels entering the obstructed units. As the surface area/volume ratio increases as the volume of the space decreases, it is to be expected that T_{col} will be less with small airway occlusion than with large airway occlusion. However, with increases in lung volume, the surface area/volume ratio decreases. Thus, it seems likely that the caliber of collateral channels increases considerably more than is necessary to offset the decrease in surface area/volume ratio.

The collateral channels are probably not the pores of Kohn[36] but are more likely to be the canals of Lambert and alveolar ducts that extend between lobules and acini. Evidently, they are lined with smooth muscle because R_{col} is sensitive to both smooth muscle agonists and antagonists,[33,34] as well as oxygen and carbon dioxide concentrations.[30,31]

Interdependence

Transpulmonary pressure or the pressure difference between the mouth and pleural space is somehow transmitted to all the airspaces and airways completely surrounded by lung tissue because in healthy lungs all alveoli expand and contract in synchrony with changes in transpulmonary pressure. This pressure is transmitted deep within lung tissue by tension transmitted by stretched alveolar walls to neighboring alveoli. At the pleural surface, the pressure applied to the visceral pleura by the attached alveolar walls is the sum of the forces transmitted by each alveolar wall divided by the surface area of the pleura over which they act, that is, $\Sigma F/A$. The same ratio defines the pressure applied to the external surface of any structure or group of structures completely surrounded by lung tissue.[26] To the extent that the lung is isotropic, this ratio should be the same throughout the lung. The pressure applied at the pleural surface is counterbalanced by P_{pl}, which keeps the lung applied to the chest wall and diaphragm, so that $\Sigma F/A = -P_{pl}$. Thus, if $\Sigma F/A$ equals $-P_{pl}$ and is the same throughout the lung, P_{pl} is applied to the outer surface of all intrapulmonary structures, whether they are blood vessels, airways, acini, or lobules. This appears to be very nearly true.[26]

However, as discussed elsewhere in this book (see Chapter 14, "Ventilation Distribution"), there is a gravity-determined gradient in P_{pl}. Thus, within any given horizontal slice of healthy lung tissue, all airspaces, bronchi, bronchioles, and blood vessels are distended by very nearly the same transpulmonary pressure. Any normal variation in transpulmonary pressure is essentially in the vertical direction from top to bottom.

As the lung expands, both ΣF and A increase. But because P_{pl} becomes more negative, ΣF must increase more than A. Now imagine what happens if one group of airspaces becomes smaller relative to its neighbors. Under these circumstances, its surface area decreases while the alveolar walls attached to its surface are stretched: $\Sigma F/A$ increases owing both to an increase in the numerator and a decrease in the denominator. Conversely, if the airspaces expand relative to their neighbors, ΣF decreases while A increases. The interdependence of lung parenchyma tends to conserve the size of all structures within the parenchyma by increasing or decreasing the local distending pressure to maintain the homogeneity of lung parenchyma.[26,37,38]

Synchrony of Healthy Lungs

In healthy lungs, all alveoli expand and contract in near synchrony at physiologic breathing frequencies. This is known because, as discussed above, dynamic lung compliance is the same as static lung compliance and does not change with breathing frequency,[24] even in the presence of moderate time constant inequalities.

In the presence of more substantial time constant inequalities, the filling and emptying of units with long time

constants will be delayed.[24] However, any delay will make these units smaller than their neighbors on inflation and larger on deflation, immediately bringing into play forces of interdependence. These forces will make the alveolar pressures in the delayed airspaces more negative on inflation and more positive on deflation than in the rest of the lung. This, in turn, will increase the flow through the airways serving the delayed spaces and create a flow across the collateral channels. The collateral flow will be determined by the difference in alveolar pressure between the normal and the delayed airspaces and the resistance to collateral flow.[27,28] The increased negativity of alveolar pressure in the collaterally ventilated space due to interdependence decreases the time needed for collateral ventilation to take place and explains the decrease in measured C_{col}. Interdependence acts to make the compliance of the collaterally ventilated space seem less than it really is. Thus, the low value of C_{col} is really an "effective" compliance resulting from interdependence of lung tissue.[27,37–39] When time constant inequalities are such that delays occur, interdependence and collateral ventilation combine to act in concert to minimize phase lags in an attempt to maintain nearly synchronous filling and emptying of all alveoli.[39]

Effects of Airways Obstruction on Ventilation Distribution

The conservative mechanisms that maintain the normal synchrony fail in disease. If the peripheral airways only comprise 10% of airways resistance or ~0.1 cm H_2O/L/s, compared to central airways with a resistance of ~0.9 cm H_2O/L/s, and half of them become blocked, peripheral airway resistance will double to 0.2 cm H_2O/L/s. The resistance of central airways, where no structural changes have occurred, will remain the same at 0.9 cm H_2O/L/s. Total resistance, which is the sum of the two, will increase from 1.0 to 1.1 cm H_2O/L/s, as illustrated in Figure 4-14. This change is within the error of measurement. The obstruction is therefore difficult to detect by measuring either maximal expiratory flows or airway resistance. Nevertheless, the pathophysiologic process is severe because the airways to half of the gas-exchanging region of the lung are completely blocked. For this reason, the peripheral airways are called the lung's quiet zone[40] because considerable disease may be present within them with only minimal effects on the usual tests of lung function.[41] How can these structural alterations be detected by tests of lung function?

Figure 4-13 illustrates this problem. It can be seen that the airspaces beyond the obstruction can receive gas only from the unobstructed airspace where gas exchange has already occurred. In the case of the excised dog lobes discussed above, the measured pulmonary resistance was only minimally increased as a result of small beads obstructing about half of the peripheral airways. There was no change in vital capacity or the static pressure–volume curves, and dynamic compliance did not change with frequency.[28] Yet all fresh air breathed in had to enter the unobstructed airspaces before traversing the collateral channels and entering into obstructed ones. It is unlikely that the obstructed airspace will receive any fresh gas. It will be ventilated by gas that has already exchanged oxygen and carbon dioxide. The distribution of inspired gas should be markedly abnormal.

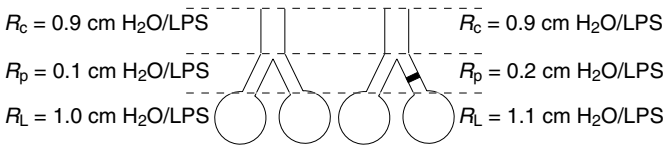

FIGURE 4-14 Two-compartment lung model illustrating the effect of complete occlusion of half of the peripheral airways on airways resistance. *Left panel*: unobstructed peripheral airways. *Right panel*: half of all peripheral airways completely obstructed. Because peripheral airway resistance is only ~10% of total flow resistance, obstructing half the peripheral airways increases total flow resistance by only 10%. LPS = liters per second.

When one considers the possibility that there could be a phase lag between the two airspaces shown in Figure 4-13, it is evident that if T_{col} is finite the obstructed airspace must lag behind the unobstructed one because it takes time for gas to cross the collateral channels and fill the obstructed space. However, if respiratory cycle time is long compared to T_{col}, the phase lag will be small; the obstructed units could have a normal tidal volume, but an alveolar ventilation that approaches zero. The tidal volume, and alveolar ventilation of the unobstructed alveoli will be twice normal, but a volume of gas equal to half the tidal volume will escape across the collateral channels, and the alveoli will not be overdistended. The ventilation/perfusion ratio of the unobstructed units should be abnormally high and the obstructed units abnormally low, resulting in a broad and abnormal distribution of these ratios. Thus, one would predict that airways obstruction in the lung's quiet zone should lead to measurable abnormalities of gas exchange and ventilation distribution.

Finally, if T_{col} is higher than in dogs, as it is in humans, one would predict that the obstructed airspaces would lag behind the unobstructed ones and that the lag would become progressively worse as T_{col} became a progressively greater fraction of respiratory cycle time as breathing frequency increased. Accompanying the phase lag, there would be insufficient time for a normal tidal volume to cross the collateral channels. Whereas the total tidal volume might remain unchanged, the unobstructed units would become progressively overdistended, and the obstructed units progressively underdistended, as breathing frequency increased. An increased tidal volume of some airspaces requires an increased swing in P_{el}. However, the increase in the elastic recoil pressure swings would not be accompanied by an increased total tidal volume, so dynamic compliance would decrease, and this decrease should be progressive with increased breathing frequency.

All of these predictions have been confirmed. Dogs with blocked airways have abnormalities in the distribution of inspired gas[42] and gas exchange.[43,44] Among smokers whose routine lung function tests are normal, a substantial percentage have abnormal gas mixing in the lung,[45] abnormalities of gas exchange,[46] and frequency dependence of compliance.[47] The combination of a normal static

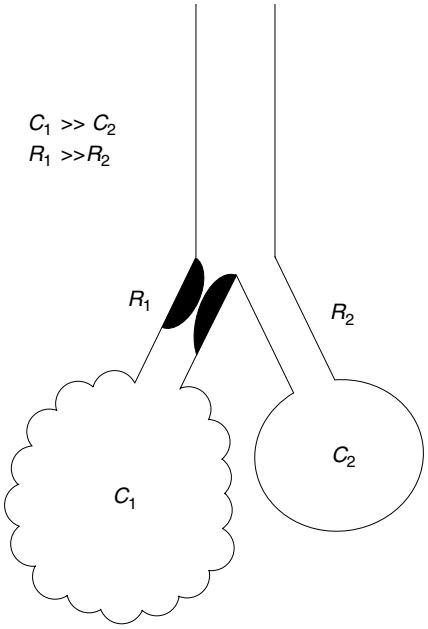

FIGURE 4-15 Two-compartment lung model illustrating mechanical abnormalities in emphysema. The left-hand airspace is a large hypercompliant emphysematous region with an obstruction in the peripheral airways leading to it. The right-hand airspace represents normal unobstructed lung tissue. During slow breathing, the obstruction (R_1) has little effect on the distribution of inspired air. Under these conditions, the relative compliance of the two compartments (C_1 and C_2) determines the distribution of inspired air. Because $C_1 > C_2$, the emphysematous space is better ventilated than the normal airspace. As breathing frequency increases, the distribution of inspired air will become more and more dependent on the time constants (R_1C_1 and R_2C_2) of the two compartments. Because $R_1C_1 > R_2C_2$, the normal lung compartment will become progressively more ventilated as breathing frequency increases. For further discussion see text.

pressure–volume curve and pulmonary resistance with abnormal ventilation distribution, gas exchange and frequency dependence of compliance indicates peripheral airway obstruction. There are claims in the literature that abnormally low maximal expiratory flows at low lung volumes are also diagnostic of small airway obstruction, but there is no evidence that this is so, and there are cogent reasons to believe that changes in the lung's elastic properties could account for this abnormality.

In more advanced disease, when the forced expiratory volume in 1 second (FEV_1) and forced vital capacity (FVC) become abnormal, all these abnormalities become more pronounced. In addition, the alveolar destruction caused by COPD increases lung compliance where alveolar destruction is present, leaving other more normal regions relatively unaffected. During a slow inspiration, inspired gas should be preferentially distributed to the most compliant (ie, the most diseased) regions. However, as illustrated in Figure 4-15, because these regions have a high compliance as well as obstructed small airways serving them, they will be the units with the longest time constants. As a result, at rapid breathing frequencies they will become less well ventilated compared to their less diseased neighbors. This leads to major problems in the interpretation of ventilation and ventilation–perfusion scanning with the use of technetium or other contrast agents. Breathing frequency is rarely controlled in these tests. The situation is further complicated because a significant percentage of smokers have subclinical emphysema that is not suspected during life.

The alveolar destruction of COPD also decreases the resistance to collateral ventilation, so that it can become less than airways resistance.[48,49] In this manner, collateral channels can become major ventilatory pathways in emphysema. This has led to the suggestion that the mechanics of breathing in patients with emphysema might be improved if they breathed through spiracles or tubes entering the lungs directly through the rib cage.[50] Preliminary results in excised human emphysematous lungs removed during transplant surgery show that substantial volumes of trapped gas that cannot be removed through the airways can be removed via spiracles (unpublished data). This increases the vital capacity while decreasing the RV/TLC ratio. In addition, these preliminary studies indicate that the distribution of inspired gas through the spiracles is as good as, and sometimes better than, the distribution through the airways. Cooper has tried this procedure in a few patients with end-stage COPD, although he brilliantly inserted the spiracle by making a hole in an airway wall directly into the lung parenchyma instead of through the rib cage (J. Cooper, personal communication). This converts a major surgical operation into a relatively minor therapeutic bronchoscopic procedure. To date, the results are encouraging, but it must be stressed that this experimental therapy is very much in the earliest stages of development. It will be several years, if ever, before it becomes an established therapy for emphysema.

REFERENCES

1. Mead J. The mechanical properties of lungs. Physiol Rev 1961;41:281–330.
2. Fredberg JJ, Stamenovic D. On the imperfect elasticity of lung tissue. J Appl Physiol 1989;67:2408–19.
3. Ludwig MS, Robatto FM, Simard S, et al. Lung tissue resistance during contractile stimulation: structural damping decomposition. J Appl Physiol 1992;72:1332–7.
4. Fredberg JJ, Bunk D, Ingenito E, Shore SA. Tissue resistance and the contractile state of lung parenchyma. J Appl Physiol 1993;74:1387–97.
5. Macklem PT, Mead J. Resistance of central and peripheral airways measured by a retrograde catheter. J Appl Physiol 1967; 22:395–401.
6. Vincent NJ, Knudson R, Leith DE, et al. Factors influencing pulmonary resistance. J Appl Physiol 1970;29:236–43.
7. Kimmel E, Seri M, Fredberg JJ. Lung tissue resistance and hysteretic moduli of lung parenchyma. J Appl Physiol 1995; 79:461–6.
8. Ludwig MS, Dreshaj I, Solway J, et al. Partitioning of pulmonary resistance during constriction in the dog: effects of volume history. J Appl Physiol 1987;62:807–15.
9. Ludwig MS, McNamara JJ, Castile RG, et al. Lung inflation does not increase maximal expiratory flow during induced obstruction in the dog. J Appl Physiol 1988;65:415–21.
10. Nagase T, Dallaire MJ,Ludwig MS. Airway and tissue behavior during early response in sensitized rats: role of 5-HT and LTD4. J Appl Physiol 1996;80:583–90.

11. Navajas D, Moretto A, Rotger M, et al. Dynamic elastance and tissue resistance of isolated liquid-filled rat lungs. J Appl Physiol 1995;79:1595–600.
12. Nagase T, Martin JG, Ludwig MS. Comparative study of mechanical interdependence: effect of lung volume on Raw during induced constriction. J Appl Physiol 1993;75:2500–5.
13 Robatto FM, Simard S, Orana H, et al. Effect of lung volume on plateau response of airways and tissue to methacholine in dogs. J Appl Physiol 1992;73:1908–13.
14. Mead J, Whittenberger JL. Physical properties of human lungs measured during spontaneous respiration. J Appl Physiol 1953;5:779–96.
15. Mead J, Turner JM, Macklem PT, Little JB. Significance of the relationship between lung recoil and maximum expiratory flow. J Appl Physiol 1967;22:95–108.
16. Ingram RH Jr, Schilder DP. Effect of gas compression on pulmonary pressure, flow, and volume relationship. J Appl Physiol 1966;21:1821–6.
17. Konno K, Mead J. Measurement of the separate volume changes of rib cage and abdomen during breathing. J Appl Physiol 1967;22:407–22.
18. Ferrigno G, Carnevali P, Aliverti A, et al. Three-dimensional optical analysis of chest wall motion. J Appl Physiol 1994;77: 1224–31.
19. Carnevali P, Ferrigno G, Aliverti A, Pedotti A. A new method for 3D optical analysis of chest wall motion. Technol Health Care 1996;4:43–65.
20. Cala SJ, Kenyon CM, Ferrigno G, et al. Chest wall and lung volume estimation by optical reflectance motion analysis. J Appl Physiol 1996;81:2680–9.
21. Iandelli I, Aliverti A, Kayser B, et al. Determinants of exercise performance in normal men with externally imposed expiratory flow limitation. J Appl Physiol 2002;92:1943–52.
22. Que CL, Kolmaga C, Durand LG, et al. Phonospirometry for noninvasive measurement of ventilation: methodology and preliminary results. J Appl Physiol 2002;93:1515–26.
23. Baydur A, Behrakis PK, Zin WA, et al. A simple method for assessing the validity of the esophageal balloon technique. Am Rev Respir Dis 1982;126:788–91.
24. Otis AB, McKerrow CB, Bartlett RA, et al. Mechanical factors in the distribution of ventilation. J Appl Physiol 1956;8: 427–43.
25. Hogg JC, Macklem PT, Thurlbeck WM. Site and nature of airway obstruction in chronic obstructive lung disease. N Engl J Med 1968;278:1355–60.
26. Mead J, Takashima T, Leith D. Stress distribution in the lung: a model of pulmonary elasticity. J Appl Physiol 1970; 596–608.
27. Woolcock AJ, Macklem PT. Mechanical factors influencing collateral ventilation in human, dog, and pig lungs. J Appl Physiol 1971;30:99–115.
28. Brown R, Woolcock AJ, Vincent NJ, Macklem PT. Physiological effects of experimental airway obstruction with beads. J Appl Physiol 1969;27:328–35.
29. Menkes H, Lindsay D, Gamsu G, et al. Measurement of sublobar lung volume and collateral flow resistance in dogs. J Appl Physiol 1973;35:917–21.
30. Traystman RJ, Batra GK, Menkes HA. Local regulation of collateral ventilation by oxygen and carbon dioxide. J Appl Physiol 1976;40:819–23.
31. Traystman RJ, Terry PB, Menkes HA. Carbon dioxide—a major determinant of collateral ventilation. J Appl Physiol 1978; 45:69–74.
32. Menkes H, Gardiner A, Gamsu G, et al. Influence of surface forces on collateral ventilation. J Appl Physiol 1971;31:544–9.
33. Smith LJ, Inners CR, Terry PB, et al. Effects of methacholine and hypocapnia on airways and collateral ventilation in dogs. J Appl Physiol 1979;46:966–72.
34. Kaplan J, Koehler RC, Terry PB, et al. Effect of lung volume on collateral ventilation in the dog. J Appl Physiol 1980;49:9–15.
35. Woolcock AJ, Macklem PT, Hogg JC, et al. The response of central and peripheral airways to vagal stimulation in dogs. Aspen Emphysema Conf 1967;10:275–85.
36. Menkes H, Macklem PT. Collateral flow. In: Macklem PT, Mead J, editors. Handbook of physiology: the respiratory system; mechanics of breathing. Bethesda, MD: American Physiological Society; 1986. p. 337–55.
37. Menkes H, Lindsay D, Wood L, et al. Interdependence of lung units in intact dog lungs. J Appl Physiol 1972;32:681–6.
38. Menkes H, Gamsu G, Schroter R, Macklem PT. Interdependence of lung units in isolated dog lungs. J Appl Physiol 1972; 32:675–80.
39. Macklem PT. Airway obstruction and collateral ventilation. Physiol Rev 1971;51:368–436.
40. Mead J. The lung's "quiet zone." N Engl J Med 1970;282:1318–9.
41. Hogg JC, Williams J, Richardson JB, et al. Age as a factor in the distribution of lower-airway conductance and in the pathologic anatomy of obstructive lung disease. N Engl J Med 1970;282:1283–7.
42. Hogg W, Brunton J, Kryger M, et al. Gas diffusion across collateral channels. J Appl Physiol 1972;33:568–75.
43. Flenley DC, Picken J, Welchel L, et al. Blood gas transfer after small airway obstruction in the dog and minipig. Respir Physiol 1972;15:39–51.
44. Flenley DC, Welchel L, Macklem PT. Factors affecting gas exchange by collateral ventilation in the dog. Respir Physiol 1972;15:52–69.
45. Dosman J, Bode F, Ghezzo RH, et al. The relationship between symptoms and functional abnormalities in clinically healthy cigarette smokers. Am Rev Respir Dis 1976;114: 297–304.
46. Levine G, Housley E, MacLeod P, Macklem PT. Gas exchange abnormalities in mild bronchitis and asymptomatic asthma. N Engl J Med 1970;282:1277–82.
47. Woolcock AJ, Vincent NJ, Macklem PT. Frequency dependence of compliance as a test for obstruction in the small airways. J Clin Invest 1969;48:1097–106.
48. Hogg JC, Macklem PT, Thurlbeck WM. The resistance of collateral channels in excised human lungs. J Clin Invest 1969; 48:421–31.
49. Terry PB, Traystman RJ, Newball HH, et al. Collateral ventilation in man. N Engl J Med 1978;298:10–5.
50. Macklem PT. Collateral ventilation. N Engl J Med 1978; 298:49–50.

CHAPTER 5

RESPIRATORY MECHANICS IN INFANTS AND CHILDREN

Peter D. Sly, Felicity S. Flack, Zoltán Hantos

Pediatricians recognize that children are not miniature adults and that the structural and mechanical proportions of their respiratory apparatus change with growth and development throughout childhood. Children approximately double in body size from birth to 18 months of age, double again by 5 years of age, and double again to achieve their adult size. The shape, size, and composition of the respiratory system also change dramatically throughout childhood, with increases in lung volume paralleling the increases in body size. Alterations in the configuration of the rib cage, maturation and stiffening of the chest wall, development of the skeletal muscles of respiration, and changes in lung structure all occur within the first few years after birth. A human child has approximately 10% of the adult complement of alveoli present at birth. The first 18 postnatal months represent the period of rapid alveolarization, with increases in lung volume after this being accomplished mainly by increases in alveolar size.[1,2]

The changes occurring with growth and development of the respiratory system are accompanied by changes in the mechanical properties of the respiratory system. This chapter reviews recent data on respiratory mechanics in infants and children. For data from classic studies, the reader is referred to the excellent review by Bryan and Wohl in the 1986 edition of the *Handbook of Physiology*.[3]

STATIC PRESSURE–VOLUME CURVES

The classic studies of Agostoni[4] showed that the static pressure–volume (*P–V*) curve of a newborn infant's respiratory system was substantially different from that of an adult. The outward recoil of the infant's chest wall was very small and the inward recoil of the infant's lung slightly lower than that of an adult. This resulted in the static balance of forces, that is, the static equilibrium of the infant's respiratory system, occurring at a much lower proportion of total lung capacity (TLC) (approximately 10%) than in an adult (approximately 40% of TLC). The lack of chest wall stiffness may be necessary to facilitate passage through the birth canal. Clinically, the elastance of the infant's chest wall can be recognized as sternal retraction. This is seen normally during breathing in the early postnatal period and is exaggerated by any lung disease in infants. Although Agostoni[4] did not study premature infants, sternal retraction during tidal respiration is more prominent in these infants, suggesting that their chest wall is even more compliant than that of infants born at term.

Recently, Tepper and colleagues[5] measured quasistatic *P–V* curves from near TLC to the passively determined static equilibrium point of the respiratory system (ie, passive functional residual capacity [FRC]) in 49 healthy infants ranging in age from 1 to 104 weeks. The infants were studied during spontaneous breathing under chloral hydrate sedation. Respiratory muscle relaxation was achieved by inflating the infant's respiratory system several times to an airway pressure of 30 cm H_2O. The volume exhaled from 30 cm H_2O (V_{30}) was calculated from passive deflations. In addition, passive expiration was interrupted at various points during deflation, and quasistatic *P–V* curves were constructed. The quasistatic compliance of the respiratory system (C_{rs}) was calculated by linear regression of the data points between 5 and 15 cm H_2O, the linear part of the *P–V* curve.

Tepper and colleagues[5] reported increases in V_{30} and in C_{rs} with increasing length but a decrease in specific compliance (C_{rs}/V_{30}) with increasing length. They also reported a lower V_{30} in infants born to smoking mothers but no difference in specific compliance between the infants of smoking and nonsmoking mothers. These data highlight the complexity of the changes in the respiratory system occurring in the early postnatal period and show that these changes are not simply due to a change in lung volume during this period.

Lanteri and Sly[6] measured respiratory mechanics in 51 children with healthy lungs during general anesthesia and muscle relaxation. C_{rs} was calculated from quasistatic *P–V* curves constructed with the use of multiple occlusions during relaxed expiration. The authors reported that C_{rs} increased with increasing height, with a linear relationship being seen on a log–log plot (Figure 5-1). These authors also concluded that specific compliance decreased with increasing height, suggesting that the changes occurring in lung structure with growth continue to influence respiratory mechanics until adolescence.[6]

CHEST WALL EFFECTS

The mechanical properties of the chest wall have a major impact on the overall mechanical behavior of the respiratory

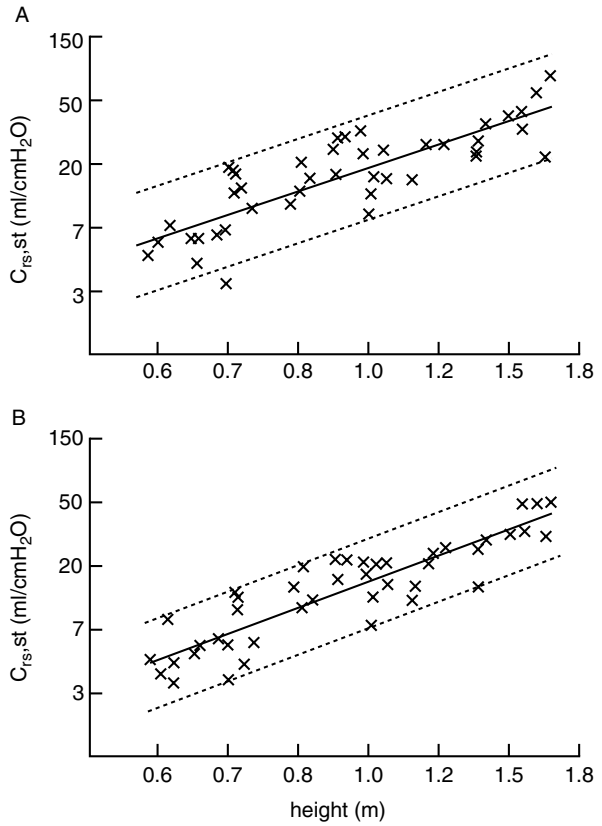

FIGURE 5-1 Natural log of compliance plotted against natural log of height for all subjects. *X*, mean C_{rs} measurement in one child; *solid line*, model best fitting these data; *dotted lines*, 85% confidence intervals of fit. Both axes are plotted with a natural log scale but are labeled with absolute numbers for clarity. *A*, ln $C_{rs,st}$ versus ln height. *B*, ln dynamic C_{rs} ($C_{rs,dyn}$) versus ln height. Reproduced with permission from Lanteri CJ and Sly PD.[6]

system in infants and children and change substantially in early life. Papastamelos and colleagues[7] measured C_{rs}, lung compliance (C_L), and chest wall compliance (C_W) in the tidal volume range, with respiratory muscles relaxed, in 40 sedated infants ranging in age from 2 weeks to 3.5 years. They found that the chest wall, relative to body size, stiffened progressively during early life, with a linear decrease in C_W/kg with increasing age ($r = -0.495$, slope -0.037, $p = .001$). Average C_W was 16.5 ± 7.5 mL/cm H_2O (2.80 mL/cm H_2O/kg) in children <1 year old and 20.1 ± 7.7 mL/cm H_2O (2.04 mL/cm H_2O/kg) for children >1 year old. Furthermore, the chest wall was nearly three times as compliant as the lungs ($C_W/C_L = 2.9 \pm 1.1$) in infants during the first year of life. In the older children studied, the chest wall had stiffened to the point that the compliances of the chest wall and lung were approximately equal. These data are consistent with those reported by Nicolai and colleagues,[8] who found that the chest wall contributed approximately 19% to the overall elastic behavior of the respiratory system in a small group of infants studied under general anesthesia. In premature infants, C_W has been reported to vary from 3 to 10 mL/cm $H_2O^{-1} \cdot kg^{-1}$ and to decrease with increasing gestational age.[9]

Using a modification of the forced oscillation technique (FOT) that includes low frequencies (see next section for details), Hantos and Sly (unpublished data) have examined the contribution of the chest wall to respiratory impedance, measured between 0.5 and 21 Hz. Low-frequency impedance spectra were measured in six infants (aged 6 to 18 months) at a transrespiratory pressure of 20 cm H_2O. The constant-phase model (see next section) was fitted to the impedance spectra to obtain estimates of airway and parenchymal mechanics. Esophageal pressure was measured with a miniature pressure transducer to separate Z_{rsS} into Z_L and Z_W components. At 20 cm H_2O, the lungs contributed the majority of newtonian resistance ($82 \pm 9\%$) and inertance ($68 \pm 24\%$), whereas the contributions of lung and chest wall to the coefficients of tissue damping and tissue elastance were approximately equal (lungs contributing $42 \pm 6\%$ and $50 \pm 6\%$, respectively).

AIRWAY AND PARENCHYMAL MECHANICS

Lanteri and Sly[6] measured respiratory mechanics in 51 children with normal lungs, aged 3 weeks to 15 years, under general anesthesia, using multilinear regression to calculate dynamic respiratory system compliance ($C_{dyn,rs}$) and resistance (R_{rs}), and a midexpiratory airway occlusion to calculate R_{aw} from the postocclusion changes in airway opening pressure. They reported linear decreases in both R_{rs} and R_{aw}, when plotted on a log–log plot, with increasing height. The slopes of the decreases were -1.706 for R_{rs} and -1.285 for R_{aw}[6] (Figure 5-2).

Following midexpiratory airway occlusion, a biphasic change in P_{ao} is seen.[10] Immediately after the occlusion, a rapid increase in P_{ao} is seen, representing the resistive pressure drop across the conducting airways. This is followed by a secondary, slower increase in P_{ao}, attributable to stress recovery in the respiratory tissues (a manifestation of viscoelasticity), together with any gas redistribution due to ventilation inhomogeneity. This secondary change in pressure has been called P_{dif} and is used to reflect viscoelastic properties of the lung tissues and chest wall.[10] In the above study, Lanteri and Sly[6] reported a biphasic change in P_{dif} with age (Figure 5-3). P_{dif} was highest in the youngest children, falling rapidly during the first year of life. The authors attributed this decrease to the rapid increase in the number of alveoli occurring during this period. They also reported that P_{dif} increased after approximately 5 years of age; they speculated that this might be due to increasing influence of the viscoelastic properties of the chest wall.

A major limitation of the interrupter technique is that it requires mechanical ventilation and muscle relaxation to produce reliable data. A variety of FOTs have been used over the years to measure the mechanical properties of the respiratory system under conditions that more closely resemble normal "working" conditions. This methodology is essentially noninvasive as it does not rely on active subject cooperation. Forced oscillation, as used in most human studies, measures input impedance by applying a pressure waveform (forcing function) to the airway opening and measuring the resultant flow produced at the airway opening. The resulting impedance

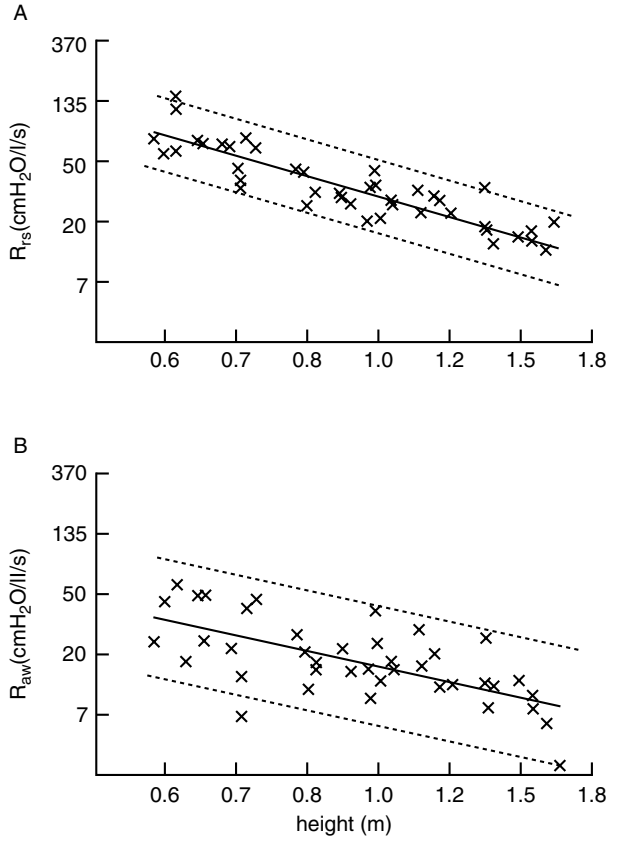

FIGURE 5-2 Natural log of resistance plotted against natural log of height. *x*, mean resistance measurement for one child; *solid line*, model best fitting these data; *dotted lines*, 95% confidence interval of this fit. Both axes are plotted with a natural log scale but are labeled with absolute numbers for clarity. *A*, ln respiratory system resistance (R_{rs}) versus ln height. *B*, ln airway resistance (R_{aw}) measured at 50% of expired volume versus ln height. Reproduced with permission from Lanteri CJ and Sly PD.[6]

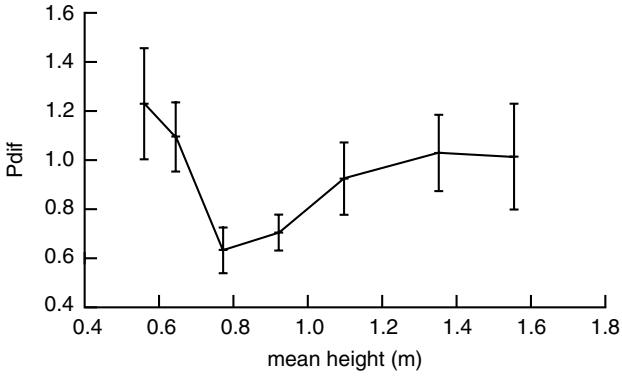

FIGURE 5-3 Group mean values ± standard error of secondary pressure difference (P_{dif}; in cm H_2O) versus height. Reproduced with permission from Lanteri CJ and Sly PD.[6]

reflects the complex viscoelastic resistance of the respiratory system (Z_{rs}). Lung impedance (Z_L) can be estimated by measuring transpulmonary pressure. Recent developments in this field have led to new methods that allow low-frequency forced oscillation to be used to partition Z_L into airway and tissue components. The constant-phase model[11] has provided an adequate description of the lungs in several species. This model consists of an airway component, represented by a frequency-independent airway resistance (R_{aw}) and airway inertance (I_{aw}), and a constant-phase tissue component $[(G - jH)/\omega^{\alpha}$, where G and H are coefficients for tissue damping and elastance, respectively, ω is angular frequency, and α determines the frequency dependence of the real (pressure change in phase with flow) and imaginary (pressure change in phase with volume) parts of the impedance]. Thus:

$$Z_{rs} = R + j\omega I + [(G - jH)/\omega^{\alpha} \qquad (5\text{-}1)$$

In an initial study,[12] we demonstrated that measurements of Z_{rs} could be made in infants between 0.5 and 21 Hz during short pauses in spontaneous breathing achieved by invoking the infant's Hering–Breuer inflation reflex to inhibit respiratory muscle activity temporarily. Infants were studied supine, with the neck supported in the midline in slight extension following an oral dose of chloral hydrate (80 mg/kg). The Hering–Breuer reflex was invoked by inflating the infant's lungs to a transrespiratory pressure of 20 cm H_2O with a pump and closing a valve at the airway opening with the lungs inflated. This produced sufficient suppression of breathing efforts (6 to 10 s) to allow measurement of Z_{rs}. At the end of each measurement, the occlusion valve was opened, allowing passive exhalation, and the infants resumed breathing immediately.

The reproducibility of the measurements within an infant was very good at all frequencies, except those coinciding with the heart rate and its harmonics.[12] The parameter values were reasonably consistent between the infants studied, the group mean values being as follows: $R_{aw} = 10.0 \pm 2.1$ cm H_2O/s/L; $I_{aw} = 61.2 \pm 13.8$ cm H_2O/s^2/L; $G = 28.6 \pm 4.9$ cm H_2O/L; and $H = 141.0 \pm 55.0$ cm H_2O/L.

The normal pattern of growth and development of the respiratory system, in particular the relative growth of airways and lung tissues, was examined in 37 normal infants aged 7 weeks to 2 years, with use of the low-frequency FOT.[13] Normality was defined as no history of asthma or bronchiolitis and fewer than three lower respiratory illnesses. All infants had been free of any respiratory illness for at least 4 weeks at the time of measurement. When plotted as a function of body length, both tissue parameters G and H showed a quasihyperbolic decrease with increasing length. In contrast, R showed a quasilinear decrease with increasing length (Figures 5-4 to 5-6). In addition, these studies have shown that changes in tissue mechanical properties occur at a more rapid rate than airway mechanics in the first 2 years of life and are consistent with the notion that airways and lung parenchyma grow at different rates.

VOLUME DEPENDENCE

Respiratory mechanical properties are known to be volume dependent in experimental animals and in adults. The volume dependence of low-frequency mechanics was studied in 8 infants (aged 7 to 26 months) by making measurements at the volumes achieved with transrespiratory pressures of 0,

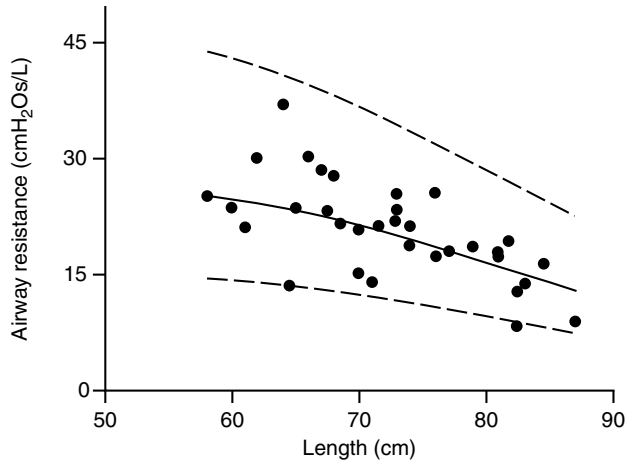

FIGURE 5-4 R_{aw} plotted against body length. The *solid line* represents the fitted regression line; the *long dashed line* represents the 95% confidence interval for the individual data. Mean measurements for each child are also shown. The *solid lines* connecting individual data points represent those infants with repeated measurements showing tracking of airway mechanics. Reproduced with permission from Hall GL et al.[13]

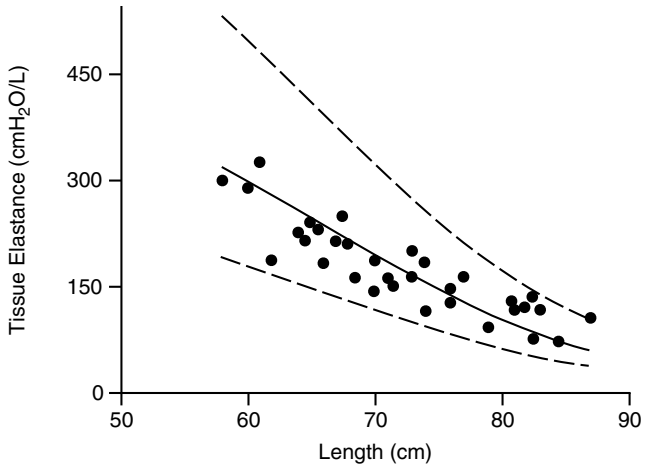

FIGURE 5-6 *H* versus body length. The *solid line* represents the fitted regression line; the *long dashed line* represents the 95% confidence interval for the individual data. Mean measurements for each child are also shown (*closed circles*). Individual data connected by solid lines are included, indicating those infants with repeated measurements showing tracking of tissue elastance. Reproduced with permission from Hall GL et al.[13]

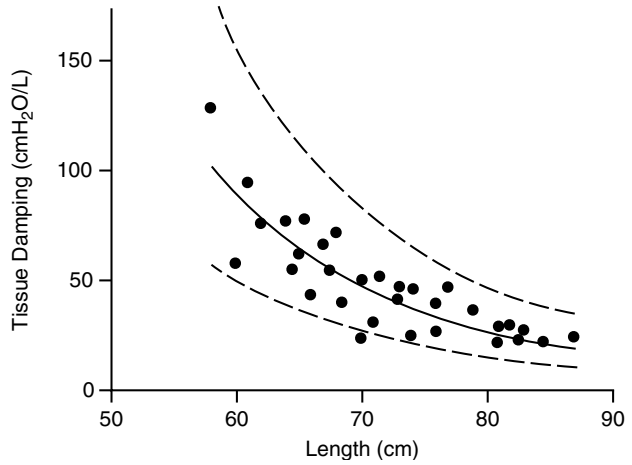

FIGURE 5-5 *G* plotted against body length. The *solid line* represents the fitted regression line; the *long dashed line* represents the 95% confidence interval for the individual data. Mean measurements for each child are also shown (*closed circles*). Individual data connected by solid lines are included, indicating those infants with repeated measurements showing tracking of tissue mechanics. Reproduced with permission from Hall GL et al.[13]

10, and 20 cm H_2O.[14] Volume dependence of Z_{rs} was demonstrated, with a similar pattern being evident in all infants studied. R_{aw} decreased progressively with increasing lung volume, from a group mean of 20.6 ± 4.9 cm H_2O/s/L at FRC (transrespiratory pressure of 0 cm H_2O) to 12.5 ± 2.7 cm H_2O/s/L at 10 cm H_2O and 8.7 ± 2.4 cm H_2O/s/L at 20 cm H_2O, reflecting the increases in airway diameter with lung volume. There were no consistent changes in I_{aw}. The values of *G* and *H* were the smallest at 10 cm H_2O; that is, the minima of tissue resistance and elastance are reached in the tidal volume range. The changes seen in both the airway and tissue parameters are consistent with the results of previous studies, in both animals and humans (usually adults), in which different methodologies have been used. The mechanical parameters estimated from oscillations imposed at FRC or at moderate inflation volumes (eg, that achieved at 10 cm H_2O) are more relevant to the conditions characterizing spontaneous respiration and theoretically are preferable to those obtained at higher volumes (eg, that achieved at 20 cm H_2O). However, from a practical point of view, making measurements of low-frequency mechanics at the volume achieved at a transrespiratory pressure of 20 cm H_2O is advocated as these measurements can be more reliably obtained and are more likely to be obtained in infants with lung disease.

The clinical importance of volume dependence frequently becomes manifest during mechanical ventilation. As demonstrated by Kano and colleagues,[15] the linear portion of the *P–V* curve is relatively small in infants and young children. It is easy to "push" them onto the flattened upper portion of the curve when using clinically necessary ventilator settings. This phenomenon was demonstrated by investigating the influence of nonlinearities on the *P–V* curves obtained during mechanical ventilation on the estimates of respiratory mechanics obtained from multilinear regression analyses. When the children's lungs were overdistended, the fits obtained by multilinear regression were improved significantly by the inclusion of a volume-dependent elastance term in the regression model, that is:

$$P_{ao} = (E_1 + E_2V)V + R_{rs}V' + P_{A,ee} \qquad (5\text{-}2)$$

where P_{ao} is the airway opening pressure, V is the volume excursion during tidal ventilation, $E_1 + E_2V$ represents the total elastance over the tidal volume range, E_1 represents

the volume-independent portion of elastance, E_2V represents the volume-dependent portion of elastance (the change in elastance with increasing volume), and $P_{A,ee}$ is the alveolar pressure at end-expiration. The authors concluded that measuring the volume-dependent behavior of the respiratory system by including a volume-dependent elastance term in the multilinear regression model provided a useful method for estimating respiratory system overdistention during mechanical ventilation.[15]

FREQUENCY DEPENDENCE

Studies in both animals[16] and adult humans[17] in which sinusoidal forcing at different frequencies was employed have demonstrated characteristic changes in the resistive and elastic properties of the respiratory system with frequency. Frequency dependence can also be studied by making measurements at different ventilation frequencies, keeping tidal volume and inspiratory/expiratory ratio constant. Nicolai and colleagues[8] demonstrated frequency dependence of the mechanical properties of the respiratory system, lungs, and chest wall in children aged 2 to 56 months undergoing cardiac surgery. Dynamic elastance (E_{rs}) and resistance (R_{rs}) of the respiratory system and of the lung (E_L and R_L) were calculated with the use of a multilinear regression technique under anesthesia prior to the onset of surgery, and the procedure was repeated with the chest wall opened via a midline sternotomy. Esophageal pressure (P_{es}) was measured with the chest wall intact to allow partitioning of E_{rs} and R_{rs} into components representing the mechanical properties of the lung and chest wall. The total respiratory system and lungs exhibited typical frequency-dependent behavior, with elastance increasing and resistance decreasing with increasing ventilation frequency. The pattern of frequency dependence was essentially the same whether the chest wall was intact or opened, suggesting that this is not solely a property of the chest wall but that the lungs contribute as well.

Kano and colleagues[18] demonstrated that the respiratory mechanics of a group of newborn infants (mean gestational age 37 ± 2.7 weeks) showed the same pattern of frequency dependence as described in the previous paragraph. When ventilation frequency was increased from 30 to 80 breaths per minute, E_{rs} increased by a mean of 8.3% and R_{rs} decreased by a mean of 17.5%. The data presented by Nicolai and colleagues[8] and by Kano and colleagues[18] show the clinical importance of understanding the frequency dependence of respiratory mechanics. Ventilator settings are most commonly changed in response to changes in disease status. These changes in ventilator setting will result in changes in the estimates of respiratory mechanics obtained during ventilations and can complicate the interpretation of changes in lung function.

The frequency dependence of respiratory mechanics can most readily be explored using FOTs. As discussed above, small amplitude oscillations containing multiple frequency components simultaneously applied can be used to measure Z_{rs}. Forced oscillations applied over a wide range of frequencies in infants have revealed that the mechanical behavior of the respiratory system is dominated at lower frequencies (<5 Hz) by the lung tissues and at higher frequencies (>10 Hz) by the airways.[12–14,19]

UPPER AIRWAY/NASAL CONTRIBUTION

Infants are preferential nose-breathers, and the mechanical properties of the nose and upper airway therefore play an important part in determining the mechanical behavior of the respiratory system. Using the FOT described above,[12] Hall and colleagues[19] demonstrated that the nasal pathway contributed approximately half of the airway resistance (mean 44.6% $\pm$ 4.9%) and most of the respiratory system inertance (mean 71.7% $\pm$ 3.5%) in infants aged 8 to 25 months.

When the forced oscillations are applied at the airway opening to measure Z_{rs}, the upper airway can act as a shunt for the oscillatory flow. Attempts have been made to minimize this effect by using a head generator, in which the subject's head and neck are enclosed in a rigid chamber and pressures are varied around the head rather than applied directly to the airway opening.[20] Modifications of this technique have been used to measure Z_{rs} in spontaneously breathing infants[21] and preschool children.[22] These studies were difficult to perform and did not produce reliable data within a frequency range encompassing normal breathing frequency. They did show, however, that the mechanical properties of the upper airway wall do contribute to respiratory system behavior and need to be considered.

SEX DIFFERENCE IN RESPIRATORY MECHANICS

The differences in respiratory mechanics between males and females have been reviewed extensively recently[23] and are discussed further elsewhere in this book (see Chapter 52, "Sex and Gender Differences in Airway Behavior Across the Human Lifespan"). This chapter highlights the gender differences described in respiratory mechanics in infants and young children.

Gender differences in spirometric measurements of lung function are well recognized in children, with gender-specific normative equations being a standard feature of commercially available lung function equipment. Lanteri and Sly[6] published gender-specific equations for dynamic and static measurements of compliance and resistance, measured under general anesthesia in children aged 3 weeks to 15 years (Table 5-1). The differences in the regression of respiratory mechanics and height failed to reach statistical significance, presumably because of the relatively small numbers of boys ($n = 29$) and girls ($n = 22$) studied.

Gender has been shown to be an important determinant of forced expiration in infants, especially when data from large numbers of infants are reported.[24] Gender was an important predictor of the maximal flow at FRC ($V'_{max\,FRC}$), measured from forced expiratory maneuvers performed at the end of a tidal inspiration, with $V'_{max\,FRC}$ being, on average, 20% higher in girls during the first 9 months of life. The authors concluded that "failure to use sex-specific prediction equations for $V'_{max\,FRC}$ may preclude detection of

Table 5-1 Gender-Specific Regression Equations for the Natural Log of Respiratory Mechanics versus the Natural Log of Height

y	*a*	*b*	*R*
Girls			
$C_{rs,st}$, mL/cm H_2O (0.313)	2.858	2.039 (0.225)	0.846
$C_{rs,dyn}$, mL/cm H_2O (0.275)	2.760	2.184 (0.169)	0.903
R_{rs}, cm H_2O/mL/s (0.290)	−3.607	−1.834 (0.178)	0.855
$R_{aw\ 50\%}$, cm H_2O/mL/s (0.431)	−4.243	−1.485 (0.304)	0.646
Boys			
$C_{rs,st}$, mL/cm H_2O (0.437)	2.927	1.592 (0.259)	0.593
$C_{rs,dyn}$, mL/cm H_2O (0.275)	2.703	1.987 (0.227)	0.756
R_{rs}, cm H_2O/mL/s (0.290)	−3.504	−1.560 (0.183)	0.743
$R_{aw\ 50\%}$, cm H_2O/mL/s (0.545)	−4.157	−1.063 (0.350)	0.285

Values in parentheses are standard errors. Equations take the following form: ln $y = a + b$(ln height). $R_{aw\ 50\%}$ represents the airway resistance calculated from an airway interruption occurring during expiration after 50% of the volume has been exhaled. Reproduced with permission from Lanteri CJ and Sly PD.[6]

clinically significant changes in girls and lead to false reports of diminished airway function in boys." Stocks and colleagues[25] demonstrated that these gender differences were also present in infants born prematurely, with $V'_{max\,FRC}$ tending to be higher in girls born prematurely (115 vs 94 mL/s [95% CI − 5–47]) than in boys when studied on discharge from the neonatal unit (mean gestational age 33 weeks; mean age at study 19 days postnatal). Although no systematic study of gender differences in airway differentiation in utero has been reported, these data suggest that these differences in lung function are the result of developmental differences rather than of sex-specific environmental effects.

SUMMARY AND CONCLUSIONS

Just as children are not miniature adults, their lungs are not miniature versions of adult lungs. The lungs undergo enormous growth and development during the first few years of life, and marked changes also occur in the mechanical properties. Specific compliance of the respiratory system falls, and the chest wall stiffens during early life. Low-frequency forced oscillations allow the partitioning of respiratory mechanics into components representing the airways and tissues. The use of these techniques reveals that the changes in the parenchymal mechanical properties occur at a more rapid rate than changes in airway mechanics in the first 2 years of life.

REFERENCES

1. Dunnill MS. Postnatal growth of the lung. Thorax 1962; 17:329–33.
2. Thurlbeck WM. Postnatal human lung growth. Thorax 1982;37: 564–71.
3. Bryan AC, Wohl MEB. Respiratory mechanics in children. In: Fishman AP, editor. Handbook of physiology, Vol. III. Part 1. Bethesda (MD): American Physiological Society; 1986. p. 179–91.
4. Agostoni E. Volume–pressure relationships of the thorax and lung in the newborn. J Appl Physiol 1959;14:909–13.
5. Tepper RS, Williams T, Kisling J, Castile R. Static compliance of the respiratory system in healthy infants. Am J Respir Crit Care Med 2001;163:91–4.
6. Lanteri CJ, Sly PD. Changes in respiratory mechanics with age. J Appl Physiol 1993;74:369–78.
7. Papastamelos C, Panitch HB, England SE, Allen JL. Developmental changes in chest wall compliance in infancy and early childhood. J Appl Physiol 1995;78:179–84.
8. Nicolai T, Lanteri CJ, Sly PD. Frequency dependence of elastance and resistance in ventilated children with and without the chest opened. Eur Respir J 1993;6:1340–6.
9. Allen JL, Sivan S. Measurements of chest wall function. In: Stocks J, Sly PD, Tepper RS, Morgan WJ, editors. Infant respiratory function testing. New York: Wiley-Liss; 1996. p. 329–53.
10. Bates JH, Ludwig MS, Sly PD, et al. Interrupter resistance elucidated by alveolar pressure measurement in open-chest normal dogs. J Appl Physiol 1988;65:408–14.
11. Hantos Z, Daróczy B, Suki B, et al. Input impedance and peripheral inhomogeneity of dog lungs. J Appl Physiol 1992;72:168–78.
12. Sly P, Hayden M, Petak F, Hantos Z. Measurement of low-frequency respiratory impedance in infants. Am J Respir Crit Care Med 1996;154:161–6.
13. Hall GL, Hantos Z, Petak F, et al. Airway and respiratory tissue mechanics in normal infants. Am J Respir Crit Care Med 2000;162:1397–402.
14. Petak F, Hayden MJ, Hantos Z, Sly PD. Volume dependence of respiratory impedance in infants. Am J Respir Crit Care Med 1997;156:1172–7.
15. Kano S, Lanteri CJ, Duncan AW, Sly PD. Influence of nonlinearities on estimates of respiratory mechanics using multilinear regression analysis. J Appl Physiol 1994;77: 1185–97.
16. Bates JHT, Shardonofsky F, Stewart DE. The low-frequency dependence of respiratory system resistance and elastance in normal dogs. Respir Physiol 1989;78:369–82.
17. Barnas GM, Mills PJ, Mackenzie CF, et al. Dependencies of respiratory system resistance and elastance on amplitude and frequency in the normal range of breathing. Am Rev Respir Dis 1991;143:240–4.
18. Kano S, Lanteri CJ, Pemberton PJ, et al. Fast versus slow ventilation for neonates. Am Rev Respir Dis 1993;148:578–84.
19. Hall GL, Hantos Z, Wildhaber JH, Sly PD. Contribution of nasal pathways to low frequency respiratory impedance in infants. Thorax 2002;57:396–9.
20. Peslin R, Duvivier C, Jardin P. Upper airway walls impedance measured with head plethysmograph. J Appl Physiol 1984; 57:596–600.
21. Desager KN, Cauberghs M, Naudts J, van de Woestijne KP. Influence of upper airway shunt on total respiratory impedance in infants. J Appl Physiol 1999;87:902–9.
22. Mazurek H, Willim G, Marchal F, et al. Input respiratory impedance measured by head generator in preschool children. Pediatr Pulmonol 2000;30:47–55.
23. Becklake MR, Kauffmann F. Gender differences in airway behaviour over the human life span [comment]. Thorax 1999;54:1119–38.
24. Hoo AF, Dezateux C, Hanrahan JP, et al. Sex-specific prediction equations for Vmax(FRC) in infancy: a multicenter collaborative study. Am J Respir Crit Care Med 2002;165: 1084–92.
25. Stocks J, Henschen M, Hoo AF, et al. Influence of ethnicity and gender on airway function in preterm infants. Am J Respir Crit Care Med 1997;156:1855–62.

CHAPTER 6

PHYSICS OF EXPIRATORY FLOW LIMITATION

Jason H. T. Bates

Clinical assessment of lung function is most commonly based on a phenomenon known as expiratory flow limitation,[1,2] in which the magnitude of the flow leaving the lungs does not increase indefinitely with the expiratory pressure generated by the respiratory muscles. Rather, flow approaches a maximum value that cannot be exceeded regardless of how much extra effort is exerted. The maximum expiratory flow that can be achieved decreases markedly with lung volume and, in fact, is beyond the reach of the respiratory muscles in a healthy subject near total lung capacity. Over about 80% of the vital capacity range, however, the muscles of a healthy individual can generate sufficient pressure to achieve maximal expiratory flow.[1] This maximal flow is influenced by the elastic recoil pressure of the lung and by airway diameter and is decreased in diseases such as asthma and bronchitis. Consequently, the shape and position of the plot of flow ($\dot{V}$) versus volume (V) during a maximal expiratory effort is diagnostic of lung disease. The most commonly used parameter derived from the phenomenon of flow limitation is the volume of air expired in the first second of a forced expiration following a maximal inspiration, known as FEV_1.

Maximal flow decreases with decreasing airway radius, which explains why individuals with narrowed airways (as in asthma or chronic obstructive pulmonary disease) have a reduced FEV_1 compared with normal individuals. Maximal flow also decreases as the airway wall becomes less stiff. Consequently, maximal flow decreases with decreasing lung volume as a result of the decreased tension in the alveolar walls that tether the pulmonary airways. FEV_1 is thus reduced in subjects with abnormally compliant airways, such as in emphysema.[3]

FEV_1 is a sensitive parameter for the diagnosis of lung disease, but its specificity is limited by the fact that a lower-than-expected value can indicate either that the airways are not as patent as they should be (obstructive pulmonary disease) or that there was a problem in expanding the lungs properly in the preceding maximal inspiration (restrictive pulmonary disease). When FEV_1 is coupled with a measure of the total volume of gas expired during an entire forced expiration, known as forced vital capacity (FVC), one can differentiate between obstructive disease (both FEV_1 and the ratio FEV_1/FVC are lower than normal) and restrictive disease (FVC is lower than normal but FEV_1/FVC is normal).[1,2,4]

The great advantage of the forced expiratory maneuver from a clinical standpoint is that it is completely noninvasive and requires only that the subject be able to inhale maximally and then exhale forceably. It is thus applicable to all patients except young children (typically less than 5 years of age) and patients with certain neuromuscular pathologies. For the same reason, however, forced expiratory maneuvers have limited utility as research tools in laboratory animals.

Linking changes in FEV_1 and FVC to abnormalities in lung structure is also nontrivial, although some computational modeling studies have produced realistic simulations.[5,6] In order to make this link, it is necessary to understand the physics underlying the phenomenon of expiratory flow limitation. Reviewing the basics of this physics is the purpose of the present chapter, and the focus is on deriving the important concepts from first principles. This is particularly needed with regard to wave speed theory as the wave speed formula is widely accepted as being a central determinant of maximal flow and appears in basic physiology texts (eg, Leff and Schumacker[7]), yet the assumptions inherent in its derivation are less well appreciated by the physiology community.

VISCOUS MECHANISMS

At the simplest level, flow limitation can be understood in terms of the viscous effects of gas flowing along a collapsible airway[8] as follows. Suppose that the alveolar regions of the lung behave as a single compartment exiting through a single conduit representing the conducting airways. The expiratory muscles act to force air from this structure by applying a positive pressure (pleural pressure, P_{pl}) to both the alveolar compartment and the outside of the airway (Figure 6-1). The alveolar compartment is compliant, so an increase in P_{pl} causes an increase in alveolar pressure (P_A) relative to the pressure at the airway opening (P_{ao}). The result is a pressure gradient that drives flow out along the airway. If the airway is rigid, the rate at which air flows along the airway ($\dot{V}$) will increase, in principle without limit, as P_A increases. In such a situation, there is no finite maximal flow.

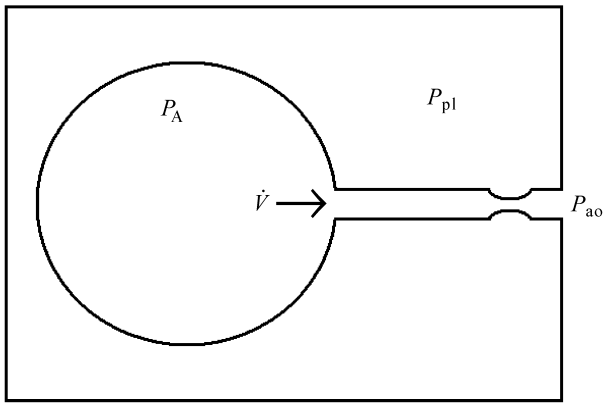

FIGURE 6-1 Stylized model of the respiratory system featuring an elastic alveolar unit, internal pressure P_A, emptying through an airway to an outside pressure of P_{ao}. Both alveolar unit and airways are encased in a chest wall compartment that applies a pressure P_{pl} to both.

The situation is different, however, if the conduit is compliant because now it will tend to narrow in the presence of an inward-acting transmural pressure across its walls. The pressure inside the conduit decreases from P_A at its distal end to P_{ao} at its proximal end because of the viscous pressure drop present in the flowing stream of air. Consequently, the transmural pressure increases from $P_{pl} - P_A$ to $P_{pl} - P_{ao}$ (see Figure 6-1). Increasing P_{pl} has two opposing effects; it increases the upstream driving pressure, which tends to increase $\dot{V}$, and it narrows the conduit, which increases its resistance and decreases flow. If the latter effect ever gets to the point of matching or exceeding the former, $\dot{V}$ will not be able to increase despite increases in P_{pl}. Flow thus becomes limited when any further increases in the driving pressure along the airway are offset by increased luminal narrowing. The precise point along the airway where this limiting process takes place in an actual lung (the so-called choke point) varies with the mechanical properties of the airways and parenchyma and moves from the large extrapulmonary airways at high lung volume to the lung periphery as volume decreases.[9]

BERNOULLI EFFECT

The explanation just given for flow limitation is based on the flow resistance of the airway. This arises purely from the viscosity of air when flow is laminar, although air density makes a contribution when flow becomes turbulent. This is not the only way of getting flow limitation, however. An alternative explanation is based on the Bernoulli effect, which depends only on the density (ρ) of air. If air is flowing at a rate $\dot{V}$ along a conduit of cross-sectional area A, the pressure at any point in the conduit measured perpendicular to the direction of flow (so-called lateral pressure) is less than the pressure driving flow at that point by an amount (P_b) proportional to the axial flow velocity (u):

$$P_b = \frac{\beta\rho u^2}{2} = \frac{\beta\rho\dot{V}^2}{2A^2} \tag{6-1}$$

where β is a constant that depends on the flow velocity profile.[10,11] We will assume from now on that β equals 1.0, which corresponds to uniform flow where velocity is independent of radial position in the conduit. The Bernoulli effect is a manifestation of the conservation of energy; because fluid mass (ie, volume) is conserved, narrowing the conduit for a given $\dot{V}$ will cause the fluid's velocity to increase.[12] This is achieved, however, without any addition of external energy, and so must be offset by a decrease in the potential energy of the fluid, which is reflected in a decrease in its lateral pressure.

As air flows along a compliant airway, the decreased lateral pressure due to the Bernoulli effect results in an increased transmural pressure. This effectively sucks the airway walls inward, which tends to narrow the airway lumen (ie, reduce A in Equation 6-1). For a given $\dot{V}$, this narrowing increases u, which further decreases lateral pressure, which, in turn, further decreases A. By this mechanism, it is possible, depending on the elastic characteristics of the airway wall, to have complete collapse of the airway. As soon as this happens, of course, flow ceases altogether, so the Bernoulli effect disappears and the airway opens up again, only to have the process repeat itself. This may lead to audible airway flutter.

To see how the Bernoulli effect can lead to flow limitation from a mathematical point of view, suppose that in the flexible conduit carrying the flow there is a linear relationship between its transmural pressure (P_{tm}) and A. The slope of the relationship is dP_{tm}/dA, so:

$$P_{tm} = \frac{dP_{tm}}{dA}(A_0 - A) \tag{6-2}$$

where A_0 is the tube area at zero P_{tm}. If we neglect viscous effects (ie, let airway resistance be zero), then P_{tm} is equal simply to P_b, given by Equation 6-1. We can thus write:

$$\frac{\rho\dot{V}^2}{2A^2} = \frac{dP_{tm}}{dA}(A_0 - A) \tag{6-3}$$

or

$$\dot{V} = \sqrt{\frac{2A^2}{\rho}\frac{dP_{tm}}{dA}(A_0 - A)} \tag{6-4}$$

This equation defines the functional relationship between $\dot{V}$ and A. Inspection of Equation 6-4 reveals that $\dot{V}$ equals zero when A is equal to either zero or A_0. Furthermore, when A starts to become smaller than A_0 (ie, when the airway starts to narrow), the above expression becomes different from zero. This means that the magnitude of $\dot{V}$ must reach a maximum for some value of A between A_0 and zero, as is clearly shown in Figure 6-2, which is a plot of $\dot{V}$ versus A defined by Equation 6-4. The slope of this relationship is zero at the maximum, so we can find the exact value of A at which it occurs by differentiating $\dot{V}$ with respect to A and setting the result equal to zero. The derivative is the following rather complicated expression:

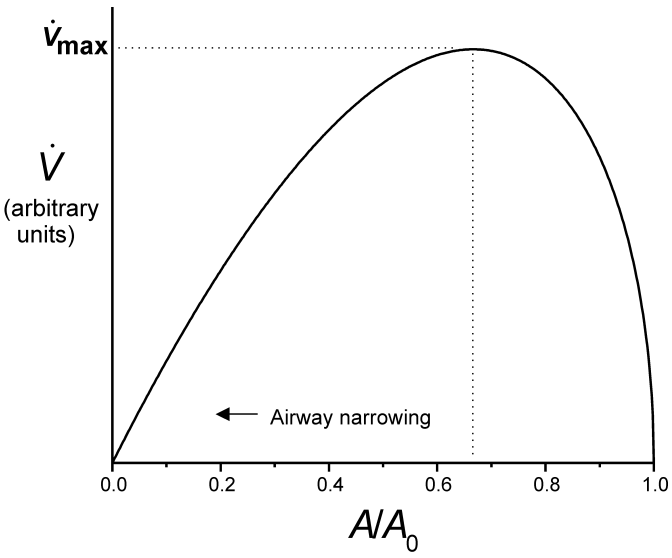

FIGURE 6-2 Plot of Equation 6-4 showing that $\dot{V}$ achieves a maximum at $A/A_0 = 2/3$.

$$\frac{d\dot{V}}{dA} = \frac{\left(2A_0 - 3A\right)\frac{A}{\rho}\frac{dP_{tm}}{dA}}{\sqrt{\frac{2A^2}{\rho}\frac{dP_{tm}}{dA}(A_0 - A)}} = 0 \tag{6-5}$$

Fortunately, making this expression equal zero is simply a matter of choosing a value for A that makes the numerator zero. There are two possible choices; either A is zero, in which case $\dot{V}$ is itself zero, or the bracketed quantity $(2A_0 - 3A)$ is zero, in which case:

$$A = \frac{2}{3}A_0 \tag{6-6}$$

Using this expression to replace A_0 in Equation 6-4 provides the value for the maximal $\dot{V}$ as:

$$\dot{V}_{max} = A\sqrt{\frac{A}{\rho}\frac{dP_{tm}}{dA}} \tag{6-7}$$

This equation, which is derived in a more general setting by Dawson and Elliot,[13] shows how the Bernoulli effect imposes a certain functional dependence of $\dot{V}_{max}$ on airway area, the density of air, and the elastic behavior of the airway wall. It is clear from this equation, for example, that a decrease in airway stiffness (ie, dP_{tm}/dA) will reduce $\dot{V}_{max}$, as in emphysema, whereas an increase in A will increase $\dot{V}_{max}$, as occurs with bronchodilatation. It is also clear from Equation 6-7 that $\dot{V}_{max}$ should be greater when a subject breathes a less dense gas, as is indeed the case with a helium–oxygen mixture in normal lungs.[14]

WAVE SPEED

Another concept that is considered to be central to the determination of maximal expiratory flow is that of wave speed.[15] The theory of wave speed was originally introduced to the respiratory community by Dawson and Elliot,[13] who adapted the concept from previous work on the flow of urine along the urethra. To understand wave speed theory, it is instructive to see how the equations governing wave propagation can be derived from first principles.[16] First, consider the flow of air through a rigid conduit. (Actually, the walls of such a conduit can never be perfectly rigid, but what is important here is that they are rigid compared to the compressibility of the gas inside the conduit.) If an aliquot of air is introduced at one end of the conduit, the pressure at that end increases accordingly, and this sends a pressure pulse to the other end at the speed of sound. This establishes the pressure gradient necessary to drive the aliquot along the conduit. For a structure the size of a human lung, this is effectively instantaneous compared to the time scales of normal respiratory events. Furthermore, there is, in principle, no limit to how big the aliquot of air can be and thus no limit to the flow that is produced.

Now consider a conduit with walls that are compliant compared to the air inside it, so that we may consider the air to be incompressible. When an aliquot of air is introduced into such a conduit, it is initially accommodated by lateral expansion of the conduit's upstream walls. This expansion then propagates toward the other end of the conduit at a rate determined not by the speed of sound but by the much lower speed of movement of the elastic deformation of the wall. To accommodate a steady stream of air in this way, the conduit walls must move in a continuous wave, meaning that each point in the wall must oscillate radially either side of its relaxed position. Because the air is moved along by the wave motion of the conduit walls, the velocity of propagation of the air equals the speed of these elastic waves. The actual flow transmitted is given by the product of this velocity and the amplitude of the oscillations. Obviously, once these oscillations reach an amplitude equal to the conduit radius, the opposing walls will bump into each other at the peak of their inward excursions, thereby limiting the flow that can be carried in this way.

To see how this works mathematically, suppose we have a perfectly cylindrical compliant airway. From the circular symmetry of the situation, we can reduce the problem to a single dimension and consider oscillations in an elastic string representing a thin strip of width α cut axially along the airway (Figure 6-3A). Let the relaxed (equilibrium) position of this string be at a distance r_0 from the center of the airway and the axial distance along the string be x (Figure 6-3B). Suppose, now, that a parcel of air is positioned so as to displace a portion of the string laterally from its equilibrium position, so that radius r becomes a function of x. As the string is actually part of an elastic tube, this generates a tension of magnitude αT in the displaced portion of the string, where T is the tension per unit circumferential distance around the tube wall. We will assume that the tension at each point along the string is proportional to the magnitude of the lateral displacement (ie, $r - r_0$) at that point. That is:

$$\alpha T = \alpha E(r - r_0) \tag{6-8}$$

where E is the specific elastance of the airway wall.

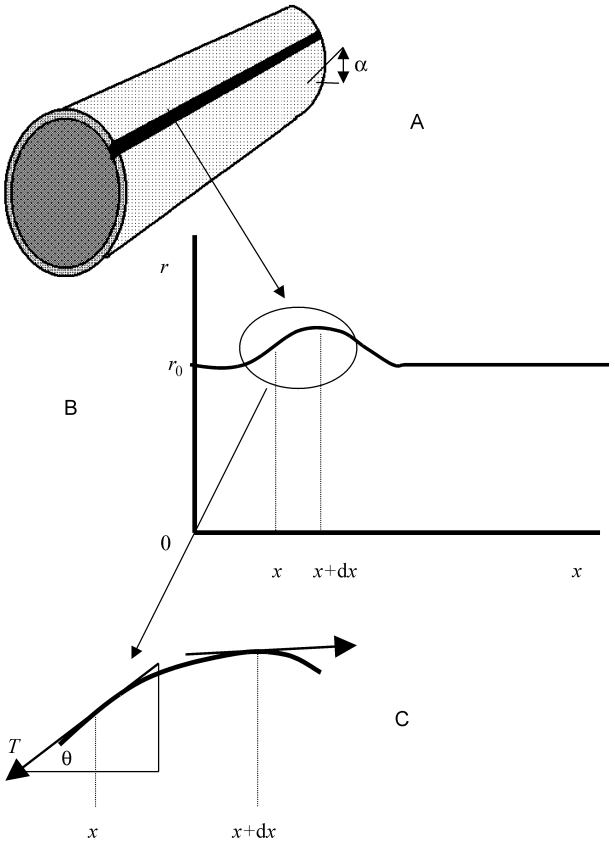

FIGURE 6-3 *A*, A thin string of width α is cut axially from an elastic tube. *B*, The elastic string is displaced radially from its equilibrium position of r_0. *C*, The string has tension at any point proportional to its displacement from r_0 at that point. The tension in the string at positions x and $x + dx$ has vertical components whose difference gives the net force acting on the intervening section (Equation 6-9).

We now focus our attention on the infinitesimal region between axial positions x and $x + dx$ (Figure 6-3C). The tension in the string at position x has a vertical component equal to $\alpha T \sin\theta$ (see Figure 6-3C), which acts to pull down on the segment of string between x and $x + dx$. Similarly, an upward force is applied by the vertical component of tension at position $x + dx$. The net force (F) acting upward between x and $x + dx$ is thus the difference between the vertical components of tension at $x + dx$ and x. If the slope of the string at both positions is small (that is, the height of the parcel of air is small compared to its length), then $\sin\theta$ is approximately equal to the derivative of r with respect to x, so we can write:

$$F = \alpha E(r - r_0)\left[\left(\frac{\partial r}{\partial x}\right)_{x+dx} - \left(\frac{\partial r}{\partial x}\right)_x\right] \tag{6-9}$$

where we have used partial derivatives to denote the slope of the string because the position of each point along the string (ie, the function r) varies with both x and t. Note that the above expression is only an exact equality because dx is infinitesimal. If dx were of finite extent, it would be only approximately true. Note, also, that we are only considering radial displacements of the string. When displacements are large, it is possible to have a point on the string move axially as well, but we will ignore these effects here.

F acts vertically on the mass of the string between x and $x + dx$ and on the small column of air between the string and r_0. We will assume the string mass to be negligible compared with the mass of the air column, which is:

$$M = \alpha(r - r_0)\rho dx \tag{6-10}$$

where ρ is the density of air. The radial acceleration, $\partial^2 r/\partial t^2$, of this mass of air is provided by F according to Newton's law of motion:

$$F = M\frac{\partial^2 r}{\partial t^2} \tag{6-11}$$

Substituting Equations 6-9 and 6-10 into Equation 6-11 and rearranging gives:

$$\frac{\left[\left(\frac{\partial r}{\partial x}\right)_{x+dx} - \left(\frac{\partial r}{\partial x}\right)_x\right]}{dx} = \frac{\partial^2 r}{\partial x^2} = \frac{\rho}{E}\frac{\partial^2 r}{\partial t^2} \tag{6-12}$$

This equation can be expressed as:

$$\frac{\partial^2 r}{\partial t^2} = v^2\frac{\partial^2 r}{\partial x^2} \tag{6-13}$$

where

$$v = \sqrt{\frac{E}{\rho}} \tag{6-14}$$

Equation 6-13 involves derivatives of r with respect to both x and t and is therefore a partial differential equation. In fact, it is the one-dimensional version of a very famous and important partial differential equation—the wave equation—which appears in various guises throughout physics. Fortunately, the wave equation is solvable analytically; that is, its solution can be written as an exact formula. The formula is actually quite simple. It was found by the mathematician d'Alembert[16] over 250 years ago to be:

$$r(x,t) = r(x \pm vt) \tag{6-15}$$

What this means is that r can be any function that is desired, provided that the variables x and t always appear together in the combination $x \pm vt$. For example, r could be a function such as $(x - vt) + 5(x - vt)^2 + \log(x - vt)$ but not a function such as $x + 5vt^2 + \log(x - t)$. To see that this is true, just try substituting these various expressions into Equation 6-13; every time you differentiate $r(x - vt)$ with respect to t you get another factor of $-v$ (because of the chain rule), whereas differentiating with respect to x does not produce a factor of v. Differentiating twice with respect to t gives the factor v^2 that appears in Equation 6-13.

What does the solution given by Equation 6-15 mean? It describes a traveling wave, a function that moves either to the right (if the argument is $x - vt$) or the left (if the

argument is $x + vt$) without changing shape. Furthermore, the speed with which this wave moves is v. To see this, notice simply that if a wave moving to the right starts out at $t = 0$ being described by the function $r(x)$, at a time t seconds later it is described by $r(x - vt)$. This is still the same function r (that is, it has not changed shape), but it has been displaced to the right by the distance vt, so v must be its velocity.

Finally, we want to express v in terms of the variables related to flow through a conduit, namely the cross-sectional area (A) of the conduit and P_{tm}. First, we note that:

$$E = \frac{dT}{dr} \tag{6-16}$$

Since $A = \pi r^2$, we have:

$$dA = 2\pi r dr \tag{6-17}$$

Next, we recall that the pressure in the conduit due to tension in its curved walls is given by the Laplace law[17] as $P_{tm} = 2T/r$. Assuming that the changes in r involved are small, this gives:

$$dP = \frac{2dT}{r} \tag{6-18}$$

Substituting Equations 6-17 and 6-18 into Equation 6-16, and then putting the result into Equation 6-14, gives the wave speed as:

$$\begin{aligned} v &= \sqrt{\frac{\pi r^2}{\rho}\frac{dP}{dA}} \\ &= \sqrt{\frac{A}{\rho}\frac{dP}{dA}} \end{aligned} \tag{6-19}$$

Once the amplitude of elastic waves in the string considered above reaches r_0, the inward movement of opposing walls prevents further excursions. This is equivalent to having the circular cross-section of the tube going to zero at the nadir of each oscillation, corresponding to a wave amplitude for the entire tube of A. This gives a maximal flow of:

$$\dot{V}_{max} = A\sqrt{\frac{A}{\rho}\frac{dP}{dA}} \tag{6-20}$$

Note, however, that such large excursions of the airway wall are at odds with the requirement invoked in the above derivation that changes in r be small, so Equation 6-20 can only be an approximation of what actually happens. In any case, Equation 6-20 is the oft-quoted formula for the $\dot{V}_{max}$ predicted by wave speed theory.[1,8]

The limiting effects of wave speed can also be understood from the perspective of what happens when the downstream pressure in an airway is lowered. In order for the lowering of downstream pressure to have an effect on $\dot{V}$, the mechanical perturbations produced by the lowering of the pressure must be transmitted to the upstream end of the airway. In other words, an increase in $\dot{V}$ can only occur if the delivery of air to the upstream end is increased, and this only takes place if the upstream end knows that pressure has been lowered at the downstream end. However, this transmission of information takes place at wave speed, so if the gas is already flowing downstream at this rate, the perturbations never have a chance to reach the upstream end of the airway.[8] This is reminiscent of water flowing over a waterfall; lowering the downstream level of the waterfall does nothing to change the flow over the waterfall, similar to the way that a Starling resistor works.[18]

An interesting thing about the $\dot{V}_{max}$ specified by Equation 6-20 is that it is exactly the same as the $\dot{V}_{max}$ determined by Equation 6-7, implying that wave speed and the Bernoulli effect are expressions of the same phenomenon. Indeed, both are descriptions of the effects of convective acceleration of gas along the airway based on Newton's law and the conservation of mass and energy.

It is important to note that the above wave speed formula was obtained by making a number of assumptions, including that the amplitude of the elastic wave is small compared to its wavelength, the radial excursions of the airway wall are small, the air in the airway is incompressible and inviscid, and the airway wall is linearly elastic and massless. These assumptions are, of course, not realized in a real lung. Indeed, some may not even be close, such as the small-amplitude requirement. Consequently, the wave speed formula should be viewed more as providing physical insight into the determinants of expiratory flow limitation rather than accurately predicting actual $\dot{V}_{max}$. For example, Equation 6-20 shows that $\dot{V}_{max}$ decreases with reductions in A, as occur in asthma, and with reductions in airway wall stiffness (dP/dA), as occur in emphysema. More accurate predictions of exactly how $\dot{V}_{max}$ depends on these quantities could be achieved by relaxing some or all of the assumptions invoked in deriving the above equations, but the mathematics involved rapidly become rather involved.[19] Also, the airways of the lung are, of course, not a single conduit but rather form a heterogeneous branching tree structure. Nevertheless, the theory outlined above does provide valuable insight into the key physical determinants of maximal expiratory flow and indeed has been applied with some success to anatomically accurate computational models of the airway tree that appear to give reasonable predictions of the phenomenon of flow limitation.[5,6]

SUMMARY AND CONCLUSIONS

We have discussed the physical mechanisms responsible for determining maximal, effort-independent expiratory flow in the lungs, with an emphasis on deriving the fundamental concepts from first principles. There are considered to be two distinct phenomena involved: the mechanism based on gas viscosity that leads to compressive collapse at the choke point and the mechanism based on gas density that involves the Bernoulli effect and wave speed theory. It is thought that the viscous mechanism dominates at low lung volumes and the density-dependent mechanism is more important at high lung volumes.[1] However, it is important to note that these mechanisms are invariably presented in texts and review articles in a highly idealized and simplified fashion (the present chapter included). In reality, these two mechanisms are not independent because viscous dissipation and

convective acceleration occur simultaneously throughout the airway tree, as discussed by Mead.[20] Furthermore, numerous physical realities exist in an actual lung that potentially complicate matters greatly, such as area-dependent airway compliance, complex flow velocity profiles, and excursions of the airway wall that may be large at the flow-limiting site (in contrast to the small-amplitude assumption necessary for the derivation of the wave speed formula). Nevertheless, the idealized theory does serve to delineate those factors (ie, airway caliber, airway wall stiffness, and gas density) that play the major roles in determining maximal expiratory flow and as such are invaluable in providing physical insight into a process whose importance for clinical respiratory medicine cannot be overestimated.

REFERENCES

1. Hyatt R. Forced expiration. In: Macklem P, Mead J, editors. Handbook of physiology. Section 3: The respiratory system. Bethesda, MD: American Physiological Society; 1986. p. 295–314.
2. Fish J. Bronchial challenge testing. In: Middleton E, Reed CE, Ellis EF, et al, editors. Allergy: principles and practice, 4th ed. St Louis, MO: Mosby-Year Book; 1993. p. 613–27.
3. Du Toit JI, Woolcock AJ, Salome CM, et al. Characteristics of bronchial hyperresponsiveness in smokers with chronic air-flow limitation. Am Rev Respir Dis 1986;134:498–501.
4. Cherniak R. Pulmonary function testing. Philadelphia: WB Saunders; 1977.
5. Polak AG, Lutchen KR. Computational model for forced expiration from asymmetric normal lungs. Ann Biomed Eng 2003;31:891–907.
6. Lambert RK. Simulation of the effects of mechanical nonhomogeneities on expiratory flow from human lungs. J Appl Physiol 1990;68:2550–63.
7. Leff A, Schumacker P. Respiratory physiology. Basics and applications. Philadelphia: Saunders; 1993.
8. Wilson T, Rodarte J, Butler J. Wave-speed and viscous flow limitation. In: Macklem P, Mead J, editors. Handbook of physiology. Section 3: The respiratory system. Bethesda, MD: American Physiological Society; 1986. p. 55–61.
9. Macklem PT, Mead J. Factors determining maximum expiratory flow in dogs. J Appl Physiol 1968;25:159–69.
10. Bates JH, Sly PD, Sato J, et al. Correcting for the Bernoulli effect in lateral pressure measurements. Pediatr Pulmonol 1992;12:251–6.
11. Chang H. Flow dynamics in the respiratory tract. In: Chang H, Paiva M, editors. Respiratory physiology—an analytical approach. New York: Dekker; 1989. p. 57–138.
12. Pedley T, Drazen J. Aerodynamic theory. In: Macklem P, Mead J, editors. Handbook of physiology. Section 3: The respiratory system. Bethesda, MD: American Physiological Society; 1986. p. 41–54.
13. Dawson SV, Elliott EA. Wave-speed limitation on expiratory flow—a unifying concept. J Appl Physiol 1977; 43:498–515.
14. Mink S, Ziesmann M, Wood LD. Mechanisms of increased maximum expiratory flow during HeO2 breathing in dogs. J Appl Physiol 1979;47:490–502.
15. Elliott EA, Dawson SV. Test of wave-speed theory of flow limitation in elastic tubes. J Appl Physiol 1977;43:516–22.
16. Weinberger H. A first course in partial differential equations. New York: Wiley; 1965.
17. West J. Respiratory physiology. The essentials. 6th ed. Philadelphia: Lippincott Williams & Wilkins; 1999.
18. Pride NB, Permutt S, Riley RL, Bromberger-Barnea B. Determinants of maximal expiratory flow from the lungs. J Appl Physiol 1967;23:646–62.
19. Zamir M. In: The physics of pulsatile flow. New York: Springer-Verlag; 2000. p. 113–46.
20. Mead J. Expiratory flow limitation: a physiologist's point of view. Fed Proc 1980;39:2771–5.

CHAPTER 7

ACT OF BREATHING: THE VENTILATORY PUMP*

Peter T. Macklem

In order to breathe, we must continuously contract and relax our respiratory muscles about 30,000 times a day, or a billion times for a lifetime of 90 years. Such extreme demands are not made of any other skeletal muscles. The respiratory muscles move the parts of the chest wall that form the boundaries of the thoracic cavity, either enlarging or contracting its volume and thereby ventilating the lungs. This ventilatory pump is obviously essential for life. The main function of the lung is to exchange gas, whereas the main function of the ventilatory pump is to replenish the alveoli with fresh air and to expel alveolar gas from the lung.

VENTILATORY PUMP

The ventilatory pump consists of the following: (1) the respiratory muscles, which expand and contract the thoracic cavity; (2) the compartments of the chest wall that the muscles displace when they contract, namely the rib cage and abdomen; (3) the cortical and brainstem centers that control the respiratory muscles; and (4) the intervening neural connections.

What are the respiratory muscles, and how do they accomplish their task?

Ignoring the upper airway muscles, which contract to maintain airway patency, the main respiratory muscles are as follows: (1) the diaphragm, divided into its costal and crural parts, which have different actions, anatomic origins, and cervical segmental innervations[1,2]; (2) the abdominal muscles, of which the transversus muscle appears to be the most important in breathing[3]; (3) the inspiratory muscles of the rib cage, including the external intercostal muscles, the parasternal muscles, the scalene muscles, and the sternocleidomastoid muscles[4–7]; and (4) the expiratory muscles of the rib cage, including the internal intercostal muscles and the triangularis sterni muscle.[8] A complete description of the respiratory muscles can be found elsewhere in this book (see Chapter 22, "Actions of the Respiratory Muscles").

The compartments displaced by the respiratory muscles are the rib cage and the abdomen.[9] Outward displacements of the abdominal wall and expansion of the rib cage are inspiratory, and vice versa. When these two compartments move in opposite directions, with expansion of one and contraction of the other, there is very little interaction between the two.[9,10] However, what interaction there is cannot be ignored,[11,12] as is discussed below.

A substantial part of the internal surface of the rib cage is directly apposed to the diaphragm.[13] As a result, one can model the rib cage as being composed of two subcompartments, the part that is apposed to the lung, the pulmonary rib cage, and the part apposed to the diaphragm, the abdominal rib cage.[14] The boundary between the two compartments is at the level of the xiphisternum at functional residual capacity (FRC). Ribs 1 to 6 are tightly attached to the sternum and thus form part of the pulmonary rib cage. Ribs 7 to 12 are loosely attached to the sternum through considerably longer costal cartilages. The parts of them below the level of the xiphisternum form part of the abdominal rib cage.

AGENCIES ACTING ON CHEST WALL COMPARTMENTS

The reason why it is useful to describe the rib cage as two compartments is that the forces acting on each are quite different. The pulmonary rib cage is exposed on its inner surface to pleural pressure (P_{pl}) over the surface of the lung. As P_{pl} becomes more negative with inspiration, it acts to contract the pulmonary rib cage. To prevent paradoxical displacements, inspiratory rib cage muscles must be recruited. These act on the pulmonary rib cage, but not on the abdominal rib cage. Of all the inspiratory rib cage muscles, only the external intercostal muscles are attached to both the pulmonary and abdominal rib cage compartments, and the fibers inserting on the ribs in the abdominal compartment only become activated at high levels of exercise.[7] Under most circumstances, they remain electrically silent. All other inspiratory rib cage muscles only insert on the pulmonary rib cage.

* Modified with permission from Macklem PT. The act of breathing. In: Aliverti A, Brusasco V, Macklem PT, Pedotti A, editors. Mechanics of breathing: pathophysiology, diagnosis and treatment. Milan: Springer-Verlag; 2002. p. 3–11.

Probably the most important expiratory rib cage muscle is the triangularis sterni muscle, which originates from the lateral border of the sternum and runs axially and laterally in a cephalad direction to insert into the lower border of the ribs of the pulmonary rib cage.[8]

The abdominal rib cage is exposed on its inner surface to P_{pl} over the surface of the diaphragm. This pressure, in contrast to P_{pl} over the surface of the lung, generally rises during inspiration. This reflects the rise in abdominal pressure (P_{ab}) when the diaphragm contracts and pushes down on the abdominal contents, displacing the abdomen outward. P_{ab} is transmitted through the costal diaphragmatic fibers to the pleural space in the area of apposition and acts to expand the abdominal rib cage.[13] In addition, the costal diaphragmatic fibers originate from ribs 7 to 11 and run axially in the area of apposition to insert on the central tendon. Thus, with diaphragmatic contraction there is a cephalad force acting on the abdominal rib cage in concert with P_{ab} to expand it.[15,16] The abdominal muscles are also attached to the abdominal rib cage, and when they are recruited, they act to contract it.[3]

Apart from a small slip of the costal part of the diaphragm attached to the sternum, the diaphragm has no attachments on the pulmonary rib cage and therefore has no direct action on it. Therefore, to a reasonable approximation, the agencies acting on the pulmonary rib cage in the absence of rib cage distortion are P_{pl} over the surface of the lung and the pressures developed by the rib cage muscles (P_{rcm}). At equilibrium, these agencies must be balanced by the elastic recoil pressure of the pulmonary rib cage ($P_{rc,p}$): $P_{rc,p} = P_{rcm} + P_{pl}$. In contrast, the agencies acting on the abdominal rib cage in the absence of rib cage distortion are P_{ab}, a fraction of transdiaphragmatic pressure ($P_{di} = P_{ab} - P_{pl}$), called the insertional component of P_{di} (xP_{di}, where $1 \geq x \geq 0$),[15–17] and a fraction of the pressure developed by the abdominal muscles (P_{abm}), called the insertional component of P_{abm} (yP_{abm}, where $1 \geq y \geq 0$).[17] At equilibrium, these agencies must be balanced by the elastic recoil of the abdominal rib cage ($P_{rc,a}$): $P_{rc,a} = xP_{di} + P_{ab} - yP_{abm}$ (yP_{abm} is given a negative sign because its action is deflationary, whereas xP_{di} and P_{ab} are inflationary). Although the rib cage can be easily distorted,[18–20] in quiet breathing and exercise this does not occur to any significant extent.[21] Therefore:

$$P_{rc,p} = P_{rc,a} = P_{rcm} + P_{pl} = xP_{di} + P_{ab} - yP_{abm}$$

and by rearranging:

$$P_{rcm} = (x + 1)P_{di} - yP_{abm} \qquad (7\text{-}1)$$

In a similar manner to the rib cage, motion of the abdomen can be described by the motion of two subcompartments: the cephalad portion of the abdomen wall is attached to the costal margin and moves when the costal margin moves[9,12]; the caudal portion of the abdominal wall is not moved by the costal margin. Thus, the cephalad portion is the only part of the abdominal wall that can be pulled outward with an inspiratory action as a result of muscle contraction. But this muscular action is primarily on the rib cage, not the abdomen. No abdominal muscles act to expand the abdominal wall. Thus, the caudal part of the abdominal wall always expands passively, either as a result of an increase in abdominal pressure due to diaphragmatic contraction or because of relaxation of abdominal muscle contraction, when abdominal pressure can actually fall during abdominal expansion.[17]

ACTIONS OF INDIVIDUAL RESPIRATORY MUSCLE GROUPS

Let us consider the actions of the abdominal muscles. Among them, the rectus abdominis muscle does not seem to be important for breathing. The most important is the transversus muscle, and the oblique muscles are probably both postural and respiratory.[3] These muscles form the anterolateral abdominal wall and insert into the costal margin; they can therefore act on the abdominal rib cage.[3,21] When they contract by themselves, they displace the abdominal wall inward, compress the abdominal contents, increase P_{ab}, and passively stretch the relaxed diaphragm.

Their action on the rib cage is considerably more complex. In the upright posture, the abdominal muscles are passively stretched by gravity acting ventrally on the abdominal contents and demonstrate tonic electrical activity.[22,23] Therefore, the abdominal muscles must have a restrictive action on the abdominal rib cage during inspiration.[21] In the supine posture, on the other hand, gravity acts dorsally rather than ventrally, and the abdominal muscles are electrically silent,[22,23] so that they have no action on the abdominal rib cage. This postural change in the forces acting on the rib cage has not been well studied.

When the abdominal muscles contract in isolation, they passively stretch the diaphragm. The passively stretched costal fibers exert an inflationary action on the abdominal rib cage, as does the increase in P_{ab}, which is transmitted through the diaphragm to its inner surface. However, the tension transmitted from the abdominal muscles at the costal margin tends to deflate this part of the rib cage. The increase in P_{ab} is transmitted to the pleural space to increase P_{pl} but is reduced by whatever passive P_{di} is present. The increase in P_{pl} acts to inflate the pulmonary rib cage, while it deflates the lung. To a close approximation, the volume of abdominal contents is constant. The movable surfaces of the abdomen are the ventral and lateral surfaces of the abdominal wall and the diaphragm, which forms the abdomen's cephalad boundary. Thus, the volume displaced by the cephalad displacement of the diaphragm must equal the volume swept by inward displacement of the abdominal wall. This is greater than the increase in chest wall volume due to pulmonary rib cage expansion. Thus, the actions of the abdominal muscles on both the lungs and abdomen are deflationary. They are expiratory muscles.

The forces acting on the pulmonary and abdominal parts of the rib cage during isolated abdominal muscle contraction are likely to be different, producing a distortion of the rib cage away from its relaxation configuration. To the

extent that the rib cage resists bending, there will be an interaction between the two rib cage compartments, tending to minimize distortions.[14] Although, almost certainly, both rib cage compartments expand, the displacements and distortions between the two rib cage compartments have not yet been studied in detail.

Now let us see what happens when the inspiratory muscles of the rib cage contract in isolation. These muscles, of which the most important are the scalene muscles and parasternal muscles,[4,5] also include whatever external intercostal muscles are activated during breathing and the sternocleidomastoid muscles. As pointed out above, these muscles insert almost exclusively into the pulmonary rib cage.

Contracting the inspiratory rib cage muscles therefore has a direct action in expanding the pulmonary rib cage, making P_{pl} more negative, inflating the lung and sucking the diaphragm in a cephalad direction, passively stretching it. Because the diaphragm is relaxed, the negative P_{pl} is transmitted to the abdomen, so that P_{ab} falls as well, but not by as much as P_{pl}, because of the passive P_{di} resulting from the stretching of the diaphragmatic fibers. The fall in P_{ab} acts to displace the abdominal wall and the abdominal rib cage inward, whereas the passively stretched costal diaphragmatic fibers tend to expand the abdominal rib cage. The net effect on the abdomen is expiratory, whereas the net effect on the whole chest wall is inspiratory. Hence, the expiratory displacement of the abdominal wall, which equals the cephalad displacement of the diaphragm, is not as great as the inspiratory displacement of the pulmonary rib cage. Again, the effect on the abdominal rib cage is not straightforward, and the precise displacements and distortions have not yet been accurately measured.

What happens when the diaphragm, often referred to as the most important respiratory muscle, is the only muscle contracting? The diaphragm's connections with the rib cage are all at the costal margin on ribs 7 to 12 in the abdominal rib cage (except for a tiny slip at the bottom of the sternum). Thus, it has only a minimal direct action on the pulmonary rib cage. When it contracts, its fibers exert a force on the central tendon, which is displaced caudally, compressing the abdominal contents, increasing P_{ab}, and displacing the abdominal wall outward.[24] At the same time, the fibers originating from the costal margin exert a cephalad force on the abdominal rib cage through ribs 7 to 12, and this is augmented by the increase in P_{ab} acting in the area of apposition of diaphragm to rib cage.[15,24] The purpose of diaphragmatic contraction is to develop a pressure difference across the muscle, so that as P_{ab} increases, P_{pl} decreases, thereby inflating the lung. Thus, the action of the diaphragm on both the abdomen and the lung is purely inspiratory, but the decrease in P_{pl} has an expiratory effect on the pulmonary rib cage. If the diaphragm contracts against a closed glottis, when, to a close approximation, chest wall and lung volume remain constant, the pulmonary rib cage is displaced inward as the abdomen is displaced outward.[20] Whereas the increase in P_{ab} and the tension developed in the costal fibers act to expand the abdominal rib cage, this is almost exactly counterbalanced by the expiratory displacement of the pulmonary rib cage and the resistance of the rib cage to bending, so that no net movement of the abdominal rib cage occurs, and considerable rib cage distortion takes place.[21]

The motions occurring when the diaphragm is the only muscle contracting and air is free to flow into the lung have not yet been studied with precision, but it is likely that significant rib cage distortions would also take place. The pulmonary rib cage would be caught between the expiratory force of the fall in P_{pl} acting over its whole inner surface and the inspiratory action of the expanding abdominal rib cage taking the pulmonary rib cage along with it. As most of the force developed by the diaphragm on the rib cage would go into distorting it, and only a small fraction into expanding it,[20] this would be an inefficient way to breathe. Rib cage distortions are costly,[20] so a good way to breathe is to avoid them altogether. As discussed above, rib cage distortions are minimal during breathing in normal subjects, even during heavy exercise.

Rib cage distortions have not been studied to any significant extent in disease, but in airways obstruction with hyperinflation, one might expect a decrease in the area of apposition, and with extreme hyperinflation, a change in the direction of force exerted by the diaphragm at the costal margin from axial to radial. If this was the case, the diaphragm would tend to deflate the abdominal rib cage, both because this part of the rib cage would now be exposed to the deflationary action of P_{pl} over the surface of the lung and because of the radial direction of tension in the costal fibers acting at the costal margin.

QUIET BREATHING AT REST

Normally, humans breathe both at rest and during exercise, in such a way that the rib cage does not distort.[21] The undistorted configuration of the pulmonary and abdominal rib cage compartments occurs when the pressure acting on both compartments is the same. This occurs during relaxation with all muscles relaxed and $P_{pl} = P_{ab}$. During quiet breathing at rest, equal pressures acting on both compartments require that the inspiratory rib cage muscles contract to the extent that the net inflationary pressure acting on the pulmonary rib cage is identical to the net inflationary pressure produced by the agencies acting on the abdominal rib cage. This situation is described above by Equation 7-1. The inspiratory rib cage muscles must overcome the deflationary action of the fall in P_{pl} on the pulmonary rib cage and develop an inflationary pressure equal to the combined effects of the direct action of the diaphragm on the abdominal rib cage, given by xP_{di}, and P_{ab} acting at its inner surface, minus the deflationary pressure developed by the passively stretched abdominal muscles. The fact that the measured P_{rcm} is only about half of P_{di} during quiet breathing[12,14] suggests that yP_{abm} is substantial.

BREATHING DURING EXERCISE

A quite different pattern of breathing emerges during exercise. As soon as exercise starts, there is an immediate

recruitment of expiratory muscles, even at zero workload.[12] The abdominal muscles are the main ones recruited; the expiratory rib cage muscles are recruited to a lesser extent. The expiratory muscles are recruited cyclically, starting at the beginning of expiration and increasing the pressure that they develop throughout expiration, which reaches its maximal value at end-expiration. Then they do not relax right away, but slowly throughout inspiration (Figure 7-1). This results in a P_{ab} that is high at the beginning of inspiration but falls progressively throughout inspiration, in striking contrast to breathing at rest, when P_{ab} increases throughout inspiration.[12] The pressures developed by the various respiratory muscle groups during quiet breathing and as a function of exercise workload are shown in Figure 7-2. At rest, only the diaphragm and the inspiratory rib cage muscles are active. At the onset of exercise, even at zero workload, the abdominal and expiratory rib cage muscles are recruited. Surprisingly, P_{di} decreases from quiet breathing to zero workload exercise, and as exercise workload increases, P_{di} only increases modestly. At zero workload and above, P_{abm} and P_{rcm} are considerably greater than P_{di}.

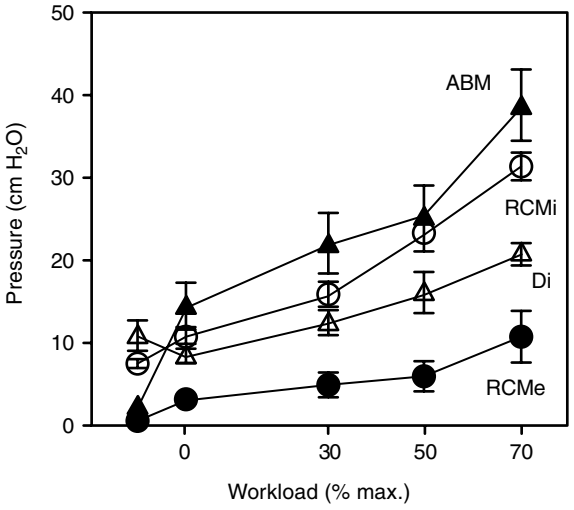

FIGURE 7-2 Pressures developed by the diaphragm (Di; open triangles), the abdominal muscles (ABM: *closed triangles*), and the inspiratory and expiratory rib cage muscles (RCMi: *open circles*; RCMe: *closed circles*, respectively) during quiet breathing (QB) and during exercise at 0, 30, 50, and 70% maximal exercise workload. Reproduced with permission from Aliverti A et al.[17]

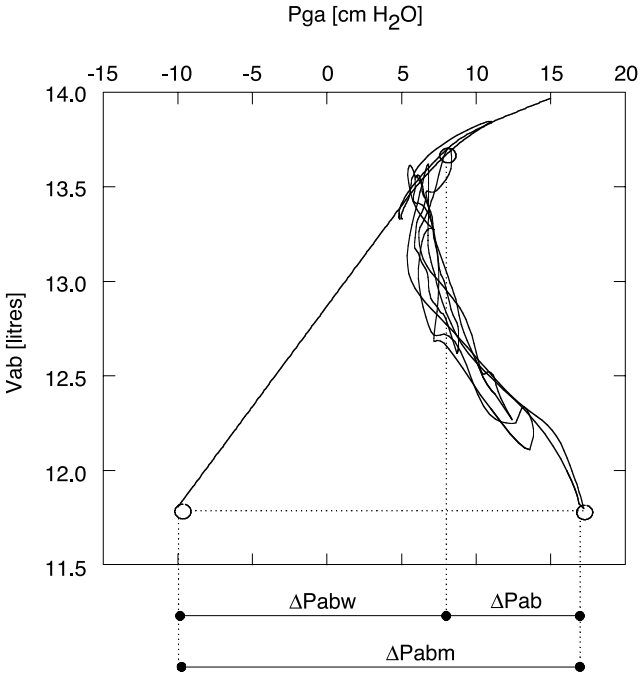

FIGURE 7-1 Pressure volume diagram of the abdomen during relaxation, quiet breathing, and various levels of exercise. V_{ab}, volume displaced by the abdominal wall. P_{ga}, gastric pressure, used as an index of abdominal pressure (P_{ab}). The straight line with a positive slope at lower values of V_{ab} and bending to the right at high V_{ab} is the relaxation pressure-volume curve of the abdomen and P_{abw} is the elastic recoil pressure of the abdomen. The heavy curve along the relaxation line ending in the open circle is the abdominal pressure-volume curve during quiet breathing. The curved lines with negative slopes are dynamic abdominal pressure-volume curves during various levels of exercise. The open circle at the bottom end of the largest of these curves is a zero-flow point at end-expiration. The upper open circle is a zero-flow point at end-inspiration. The pressure generated by the abdominal muscles (P_{abm}) at any V_{ab} is the horizontal distance between the relaxation and dynamic curves at that V_{ab}. Reproduced with permission from Aliverti A et al.[17]

Evidently, as soon as exercise starts, there is an immediate change in the central drive to the respiratory muscles. This drive activates the muscles to produce power, the product of the flow they generate and the pressure they produce. But how this power is partitioned between flow and pressure is not determined by the central drive; it is a unique function of the load that the muscle acts against. During breathing at rest, P_{ab} rises and P_{pl} falls throughout inspiration, progressively increasing the load on the diaphragm, because both pressures act to impede diaphragmatic descent. The increase in P_{ab} and decrease in P_{pl} represent the interaction between the activation of the diaphragm produced by the central drive and the elastic loads of the lung and chest wall that the diaphragm is acting against. For a given degree of activation, as these loads increase during inspiration, more of the central drive to the diaphragm is converted into P_{di} and less is converted into flow.

Quite the opposite situation pertains during exercise. The decrease in P_{ab} during inspiration shown in Figure 7-1 parallels the decrease in P_{pl}. If $\Delta P_{ab} = \Delta P_{pl}$, then the diaphragm would contract quasi-isotonically, and the elastic loads would disappear. Thus, the gradual relaxation of abdominal muscles throughout inspiration unloads the diaphragm so that more of the central drive is converted to flow and less to pressure. This is illustrated in Figure 7-3, which shows that most of the diaphragm's power during exercise is expressed as flow rather than pressure. Indeed, the fold increases in power developed by the inspiratory rib cage muscles, the abdominal muscles, and the diaphragm as a function of exercise workload are all about the same (Figure 7-4). The fact that inspiratory P_{rcm} and P_{abm} exceed P_{di} indicates that the diaphragm's role during exercise is primarily as a flow generator, whereas the

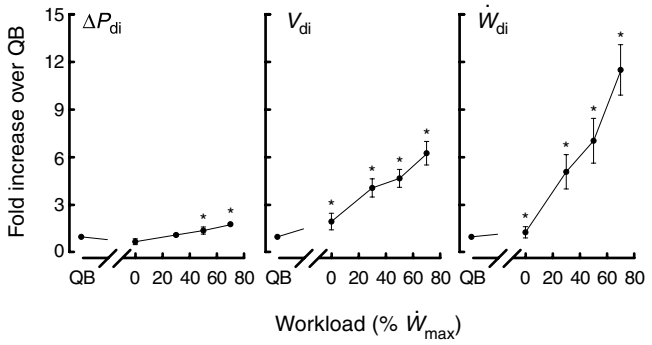

FIGURE 7-3 Fold increases over quiet breathing of transdiaphragmatic pressure (*left panel*), velocity of shortening (*middle panel*), and power (*right panel*) developed by the diaphragm as a function of exercise workload. Reproduced with permission from Aliverti A et al.[17]

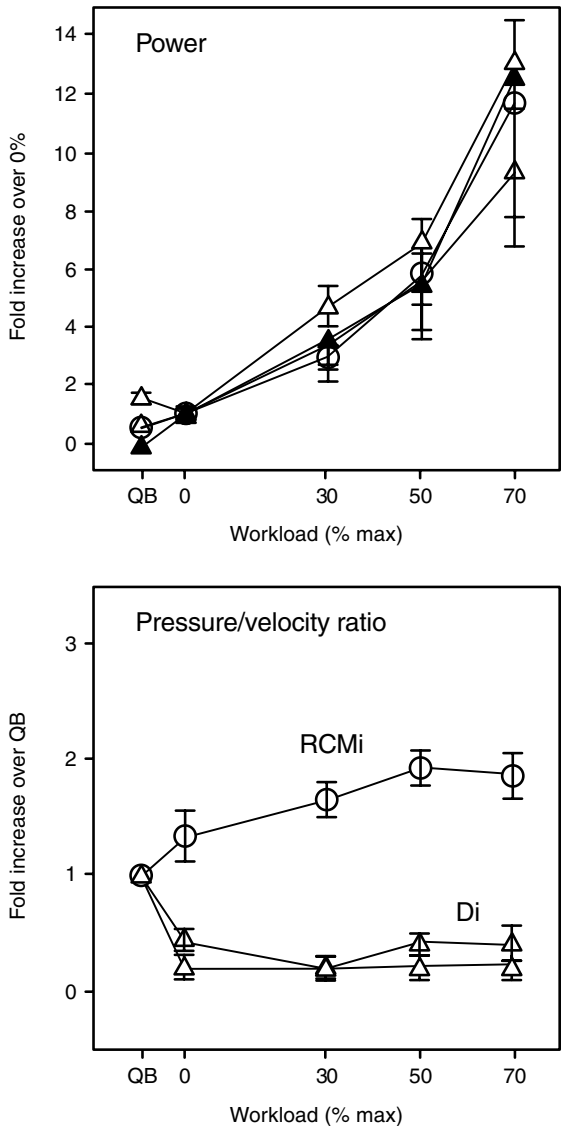

FIGURE 7-4 Power and its partitioning into pressure and flow during quiet breathing (QB) and as a function of exercise workload. *Upper panel:* Power developed by the diaphram (*open triangles*), inspiratory rib cage muscles (*open circles*), and abdominal muscles (*closed triangles*); *lower panel:* partitioning of power of the inspiratory rib cage muscles and the diaphragm. Reproduced with permission from Aliverti A et al.[17]

inspiratory rib cage and abdominal muscles are primarily pressure generators acting to displace the rib cage and abdomen, respectively. This is shown for the diaphragm and inspiratory rib cage muscles in the lower panel of Figure 7-4, in which the power developed by these muscles is partitioned into its pressure and flow components as the ratio between pressure and velocity of shortening.

During exercise, the conditions for no rib cage distortion are the same as in Equation 7-1, except that P_{abm} is both active and passive. Expressing Equation 7-1 in terms of changes gives:

$$\Delta P_{rcm} = (x + 1)\,\Delta P_{di} - y\Delta P_{abm} \qquad (7\text{-}2)$$

P_{rcm} now includes both inspiratory and expiratory rib cage muscles. The condition for *both* lack of rib cage distortion *and* isotonic diaphragm contraction is obtained by setting $\Delta P_{di} = 0$ in Equation 7-2:

$$P_{rcm} = -\,yP_{abm} \qquad (7\text{-}3)$$

Equation 7-3 states that a simple control system by which the central drive to the combined inspiratory and expiratory rib cage muscles is exactly 180° out of phase with the drive to the abdominal muscles, with a constant of proportionality equal to y, accomplishes two remarkable things: it prevents costly rib cage distortions and removes the elastic load from the diaphragm, allowing it to act as a flow generator.[12] The plot of P_{rcm} versus P_{abm} during exercise is shown in Figure 7-5 and confirms that the pressures developed by these two muscle groups are, in fact, nearly 180° out of phase.[12]

In addition to preventing rib cage distortions and allowing the diaphragm to act as a flow generator, the

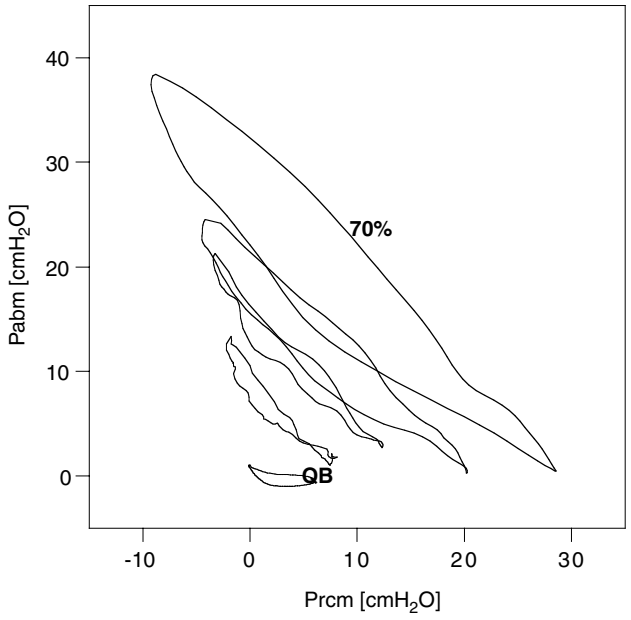

FIGURE 7-5 Relationship between the pressures developed by the abdominal muscles (P_{abm}) and those developed by the rib cage muscles (P_{rcm}) during quiet breathing (QB) and at increasing levels of exercise to a maximum of 70% maximal power output (70%). During all levels of exercise, these pressures are nearly 180° out of phase. Reproduced with permission from Aliverti A et al.[17]

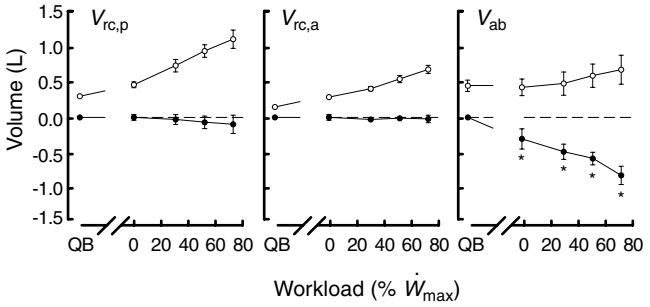

FIGURE 7-6 Volume changes of the lung-apposed rib cage ($V_{rc,p}$), the diaphragm-apposed rib cage ($V_{rc,a}$), and the abdomen (V_{ab}) during quiet breathing and as a function of exercise workload. On the ordinate, the volumes are referenced to functional residual capacity (FRC) during quiet breathing (0.0). *Open circles:* end-inspiratory volume; *closed circles:* end-expiratory volume. Reproduced with permission from Aliverti A et al.[17]

abdominal muscles play another important role: end-expiratory lung volume progressively decreases as exercise workload increases. This allows elastic energy to be stored in the system below FRC that can be released to perform useful external work during inspiration. Furthermore, the reduction in end-expiratory lung volume is entirely accomplished by a reduction in the volume of the abdominal compartment; there is no decrease in the volume of the rib cage at end-expiration, whereas all the increase in lung volume takes place in the rib cage compartment. This is shown in Figure 7-6. As the volume of the abdomen is the main determinant of diaphragmatic fiber length,[25] its inward displacement lengthens the diaphragm fibers, allowing it to generate more power for a given degree of central activation.

SUMMARY AND CONCLUSIONS

There are three sets of respiratory muscles, namely the diaphragm, the abdominal muscles, and the rib cage muscles. Each has a unique action on the three compartments comprising the chest wall, namely the pulmonary or lung-apposed rib cage, the abdominal or diaphragm-apposed rib cage, and the abdomen. Although it is possible to breathe with only one of these three, isolated contraction of each has unwanted effects on at least one of the compartments. To prevent these effects, coordinated recruitment of two or three sets of muscles is required. During breathing at rest, this is accomplished by the coordinated activity of the diaphragm and inspiratory rib cage muscles. Normally, no expiratory muscles are used. During exercise, the abdominal muscles, and to a lesser extent the expiratory rib cage muscles, are immediately recruited. The abdominal muscles, in concert with the rib cage muscles, play a double role of preventing costly rib cage distortions and unloading the diaphragm so that it acts as a flow generator, whereas the rib cage and abdominal muscles take on the task of developing the pressures required to move the rib cage and abdomen, respectively. The abdominal muscles play a third role in decreasing end-expiratory lung volume by decreasing the volume of the abdomen. This stores elastic energy in the respiratory system that can be released during inspiration to perform useful external work. It also lengthens diaphragmatic fibers so that they develop more power for a given level of activation.

REFERENCES

1. De Troyer A, Sampson M, Sigrist S, Macklem PT. The diaphragm: two muscles. Science 1981;213:237–8.
2. De Troyer A, Sampson M, Sigrist S, Macklem PT. Action of costal and crural parts of the diaphragm on the rib cage in dog. J Appl Physiol 1982;53:30–9.
3. De Troyer A, Sampson A, Sigrist S, Kelly S. How the abdominal muscles act on the rib cage. J Appl Physiol 1983;54: 465–9.
4. De Troyer A, Estenne M. Coordination between rib cage muscles and diaphragm during quiet breathing in humans. J Appl Physiol 1984;57:899–906.
5. Legrand A, Schneider E, Gevenois PA, De Troyer A. Respiratory effects of the scalene and sternomastoid muscles in humans. J Appl Physiol 2003;94:1467–72.
6. De Troyer A, Kelly S, Macklem PT, Zin WA. Mechanics of intercostal space and actions of external and internal intercostal muscles. J Clin Invest 1985;75:850.
7. Whitelaw WA, Feroah T. Patterns of intercostal muscle activity in humans. J Appl Physiol 1989;67:2087–94.
8. De Troyer A, Ninane V, Gilmartin JJ, et al. Triangularis sterni muscle use in supine humans. J Appl Physiol 1987;62: 919–25.
9. Konno K, Mead J. Measurement of the separate volume changes of rib cage and abdomen during breathing. J Appl Physiol 1967;22:407–22.
10. Deschamps C, Rodarte JR, Wilson TA. Coupling between rib cage and abdominal compartments of the relaxed chest wall. J Appl Physiol 1988;65:2265–9.
11. Mead J, Loring SH. Analysis of volume displacement and length changes of the diaphragm during breathing. J Appl Physiol 1982;53:750–5.
12. Aliverti A, Iandelli I, Duranti R, et al. Respiratory muscle dynamics and control during exercise with externally imposed expiratory flow limitation. J Appl Physiol 2002;92:1953–63.
13. Mead J. Functional significance of the area of apposition of diaphragm to rib cage. Am Rev Respir Dis 1979;119 (2 Pt 2):31–2.
14. Ward ME, Ward JW, Macklem PT. Analysis of human chest wall motion using a two compartment rib cage model. J Appl Physiol 1992;72:1338–47.
15. Loring SH, Mead J. Action of the diaphragm on the rib cage inferred from a force-balance analysis. J Appl Physiol 1982;53:756–60.
16. Mead J, Loring SH. Analysis of volume displacement and length changes of the diaphragm during breathing. J Appl Physiol 1982;53:750–5.
17. Aliverti A, Cala SJ, Duranti R, et al. Human respiratory muscle actions and control during exercise. J Appl Physiol 1997;83:1256–69.
18. Reid MB, Loring SH, Banzett RB, Mead J. Passive mechanics of upright human chest wall during immersion from hips to neck. J Appl Physiol 1986;60:1561–70.
19. McCool FD, Loring SH, Mead J. Rib cage distortion during voluntary and involuntary breathing acts. J Appl Physiol 1985;58:1703–12.
20. Chihara K, Kenyon CM, Macklem PT. Human rib cage distortability. J Appl Physiol 1996;81:437–47.

21. Kenyon CM, Cala SJ, Yan S, et al. Rib cage mechanics during quiet breathing and exercise in humans. J Appl Physiol 1997;83:1242–55.
22. De Troyer A. Mechanical role of the abdominal muscles in relation to posture. Respir Physiol 1983;53:341–53.
23. Loring SH, Mead J. Abdominal muscle use during quiet breathing and hyperpnea in uninformed subjects. J Appl Physiol 1982;52:700–4.
24. Macklem PT, Macklem DM, De Troyer A. A model of inspiratory muscle mechanics. J Appl Physiol 1983; 55:547–57.
25. Aliverti A, Ghidoli G, Dellaca RL, et al. Chest wall kinematic determinants of diaphragm length by optoelectronic plethysmography and ultrasonography. J Appl Physiol 2003;94:621–30.

CHAPTER 8

PULMONARY STATICS IN DISEASE

Paolo Carbonara, David H. Eidelman

Although once at the cutting edge of clinical pulmonary physiology, the measurement of static pressure–volume (*P–V*) curves of the lung has now fallen somewhat into disfavor. The advent of computed tomography (CT) scanning has led to a decrease in interest in the use of the *P–V* curve as a clinical diagnostic tool or even as an adjunct to research. Nevertheless, the concepts underlying the measurement of static lung mechanics are essential for understanding and interpreting other pulmonary function tests and for clinically important measurements in the intensive care unit. Moreover, there are still niches where the *P–V* curve can make an important contribution to solving diagnostic problems. The *P–V* curve is above all an attempt to evaluate the elasticity of the lung. Although it is possible to consider both the dynamic and static lung elasticity, this chapter focuses on the static *P–V* curve, with the goal of reviewing its clinical applications and how its measurement has contributed to our understanding of disease pathophysiology.

MEASUREMENT OF THE *P–V* CURVE

The overall aim of *P–V* curve measurement is to infer the elastic properties of the lung from changes in transpulmonary pressure (ie, the difference between airway opening pressure and pleural pressure) and changes in lung volume. This requires some means of estimating pleural pressure changes. Although there have been reports of measuring pleural pressure directly,[1] the esophageal balloon technique, which is based on the notion that swings in esophageal pressure reflect those in the pleura, has long been the standard method for constructing *P–V* curves in humans. The details and pitfalls of the esophageal balloon technique are discussed elsewhere in this book (see Chapter 55, "Esophageal Pressure Measurement"). Although it is theoretically possible to measure the full scale of the *P–V* relationship from residual volume (RV) to total lung capacity (TLC) and back to RV, in clinical practice *P–V* curves are usually measured between functional residual capacity (FRC) and TLC. Moreover, there is evidence to suggest that deflation curves are more reproducible than inflation curves,[2] and most publications on clinical applications of *P–V* curves focus on the deflation curve from TLC to FRC. Therefore, in this chapter we largely restrict ourselves to discussions of the deflation *P–V* curve.

P–V CURVE INTERPRETATION

From a clinical standpoint, interpretation of the *P–V* curve requires a systematic analysis of its component parts, pressure and volume. The mechanical relationship between changes in pressure and volume may be plotted in several ways, but, traditionally, volume as a percentage of predicted TLC is plotted on the ordinate and transpulmonary pressure in cm H_2O or kPa on the abscissa (Figure 8-1). Plotting the TLC in terms of its predicted value has the immediate advantage that abnormalities in lung volume can be seen at a glance. Thus, restriction or hyperinflation can be diagnosed directly from the graph as displacements of the curve to lower or higher volumes, respectively. In contrast, there is no need to display the transpulmonary pressure in terms of predicted values as there is little variation in the *range* of pressures among healthy individuals or even across species. For example, the maximal transpulmonary pressure in a mouse is of the same magnitude as in a human,[3] although the scale of the lung volume is clearly much different.

INSPECTION

Much of the diagnostic information in a *P–V* curve can be gleaned from inspection. The TLC and FRC can be determined by looking at the volume range of the curve. Similarly, the position of the curve on the abscissa yields information about overall stiffness. The maximum transpulmonary pressure ($P_{L,max}$) achieved is a measure of the maximal elastic recoil pressure against which lung inflation takes place. As $P_{L,max}$ is increased in cases of parenchymal lung restriction, such, as pulmonary fibrosis, and decreased in emphysema, this index provides some information about overall lung elasticity. It is, however, dependent on muscle

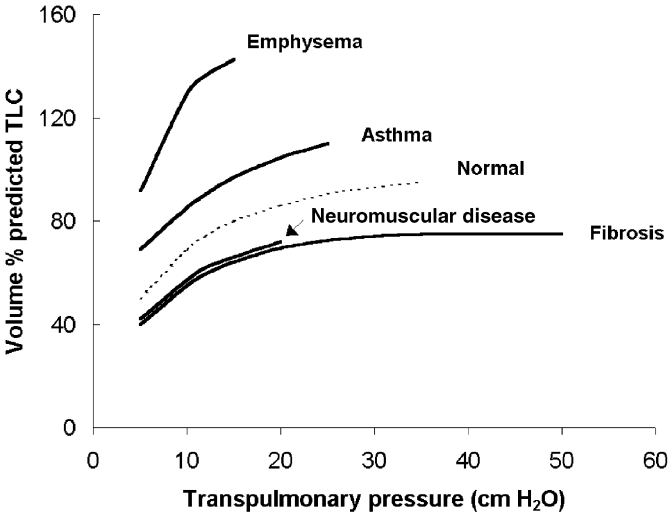

FIGURE 8-1 Examples of prototype *P–V* curves under different clinical conditions. Adapted from Hughes JMB, Pride NB, editors. Lung function tests: physiological principles and clinical applications. 1st ed. Philadelphia: WB Saunders; 1999. p. 49.

activity, and decreases in $P_{L,max}$ can reflect neuromuscular function or effort as well as decreased lung stiffness. The overall position and shape are very helpful diagnostically. Shifts to the left (lower P_L), particularly when accompanied by increased curvature and verticality, are strongly suggestive of emphysema (Figures 8-1 and 8-2A). Conversely, curves with high $P_{L,max}$ that are shifted downward and to the right are diagnostic of restriction due to increased parenchymal stiffness (Figures 8-1 and 8-2B). Normally shaped and positioned curves with decreased $P_{L,max}$ are suggestive of neuromuscular dysfunction.

P–V Indices

Although inspection may be useful for clinical purposes, it does not lend itself to comparisons among individuals, particularly in population studies. Furthermore, in some cases, the appearance of the *P–V* curve is ambiguous, with a shape that does not fully satisfy the criteria for emphysema, for example. To address this problem, a number of indices calculated from the *P–V* curve have been proposed as objective measures of lung elasticity. Each of these measures represents an attempt to deal with the characteristic nonlinearity of the *P–V* curve. Although many indices have been proposed for clinical and research use, this chapter focuses on the three most important: compliance, exponential analysis, and the use of transpulmonary pressures at multiple lung volumes.

Compliance Static compliance (C_{st}) is usually defined as the ratio of the change in volume to the change in pressure over a fixed volume range. Compliance is, in fact, the slope of the *P–V* curve when plotted with volume on the ordinate and transpulmonary pressure on the abscissa. This is referred to as a static compliance because the measurements of pressure and volume are made under conditions of zero flow. Measurements made during active breathing, with non-zero airflow, are referred to as *dynamic*. Dynamic compliance includes energy losses due to the viscoelastic properties of the lung, as well as those related to ventilatory inhomogeneity,[4] and are thus systematically different from static measurements.

Because of the nonlinear relationship between volume and pressure, compliance is not constant at all lung volumes. It is therefore necessary to calculate compliance over a limited portion of the *P–V* curve that is approximately linear. For practical reasons, the region near FRC is conventionally used as it provides a clinically relevant estimate

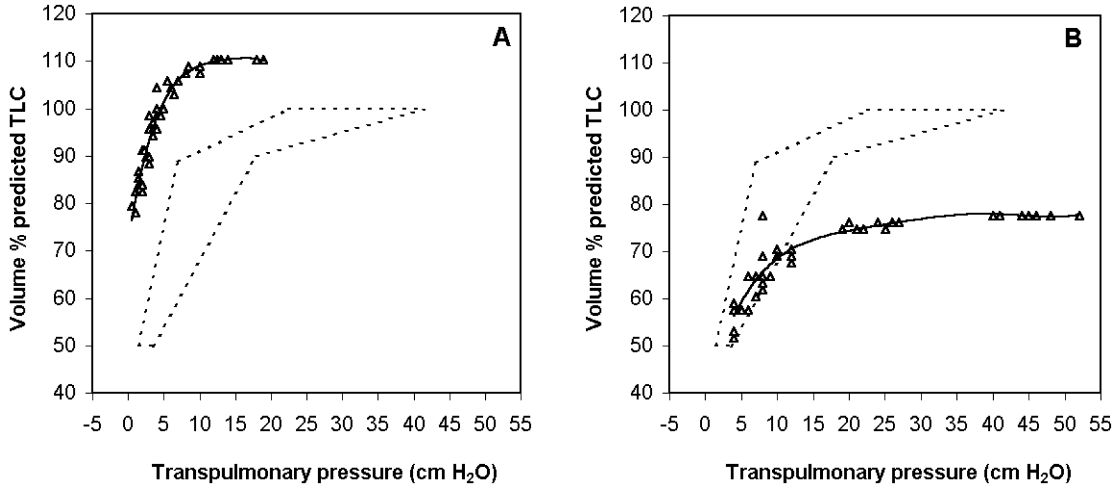

FIGURE 8-2 Examples of *P–V* curves in emphysema *A* and fibrosis *B* plotted as percentage predicted total lung capacity (TLC) versus transpulmonary pressure.[7] Single points represent individual measurements of pressure and volume. *Dashed lines* represent predicted normal range. The *P–V* indices for *A* were as follows: $C_{stat} = 0.973$ L/cm H_2O (247% predicted); $P_{L90} = 8$ cm H_2O (58.9% predicted); $P_{L,max} = 19$ cm H_2O (59.4% predicted); TLC = 7.5 L (110.3% predicted); $k = 0.2859$ (192.9% predicted). The *P–V* indices for *A* were as follows: $C_{stat} = 0.20$ L/cm H_2O (70% predicted); $P_L90 = 7$ cm H_2O (49.3% predicted); $P_{L,max} = 52$ cm H_2O (164.1% predicted); TLC = 5.3 L (76.1% predicted); $k = 0.1491$ (88.2% predicted).

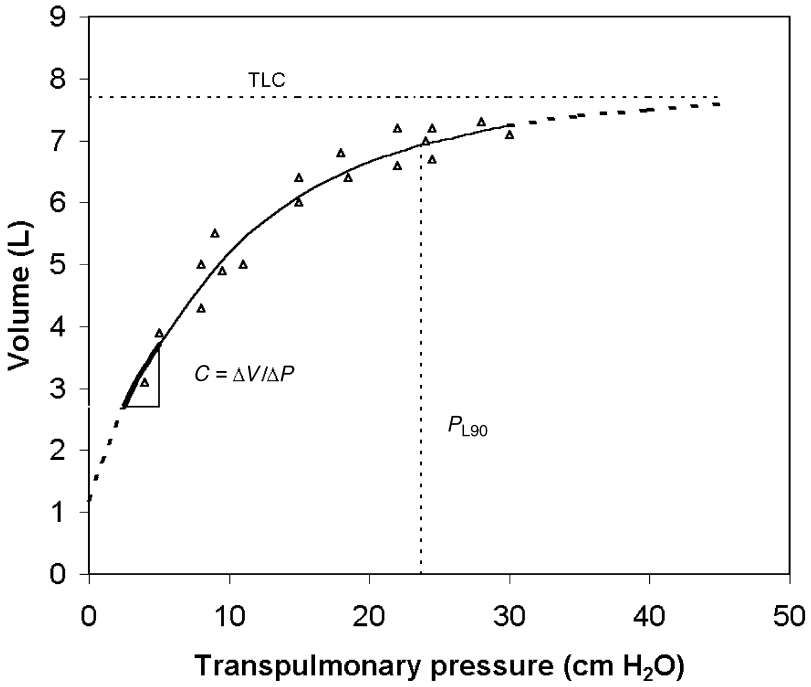

FIGURE 8-3 Demonstration of *P–V* indices. Volume is plotted on the ordinate and pressure on the abscissa. Each point represents one measurement of the *P–V* relationship. The *solid curve* is the result of fitting the equation $V = A - Be^{-kP}$, where V is lung volume and P is transpulmonary pressure. The *thick segment* represents the range over which compliance (C) is calculated as the slope of the *P–V* curve from FRC. The *vertical dashed line* represents the transpulmonary pressure at 90% of TLC (P_{L90}).

of lung stiffness in the tidal volume range (Figure 8-3). Most commonly, the ratio of the change in volume between FRC and FRC + 0.5 L, and the change in transpulmonary pressure over this volume range, is used:

$$C_{st} = \frac{\Delta V}{\Delta P}$$

C_{st} is reasonably useful, but because it scales proportionately to resting lung volume, it is subject to variation if FRC is not held constant. It is also difficult to compare individuals whose FRCs differ greatly. This is particularly important when comparing adults with children or when making comparisons across species. For this reason, it has been proposed to calculate a specific compliance (C_{sp}), in which the lung compliance is "corrected" by dividing by the resting lung volume (FRC).[5] The resulting value is somewhat more robust when comparisons across differently sized individuals are made and has been used to allow comparisons across species.

Exponential Analysis Another approach to dealing with the nonlinearity of the *P–V* curve has been to fit *P–V* data to nonlinear models and then describe the curve based on the parameters of this function. By far the most successful of these approaches is to fit *P–V* curve data to an exponential function, which reliably describes the *P–V* relationship between FRC and TLC, with the asymptote being close to TLC (see Figure 8-3). Since this is a nonlinear relationship, one needs to use either logarithmic transformation or an iterative fitting technique to do the calculations. Although several formulations for the exponential function have been proposed, the most widely used relationship, based on an approach first reported by Salazar and Knowles,[6] is shown here:

$$V = A - Be^{-kP}$$

In this equation, V is the lung volume, P is the transpulmonary pressure, and A describes the asymptote of the exponential which, in principle, should be slightly greater than the achieved TLC. The parameter B is the difference in volume between A and the intercept of the function with the ordinate. The parameter of greatest interest is k. Sometimes termed the shape constant, k is a dimensionless number that provides a measure of the curvilinearity of the curve. The more concave downward the curve, the greater the k value. Thus, in emphysematous patients, k is increased, whereas in fibrotic patients, it is low.

An important characteristic of k is that it is independent of lung volume. In principle, this means that similar values of k may be expected among individuals of differing size, making it an attractive candidate for a volume-independent measure of overall *P–V* curve shape. More importantly, since it describes the shape of the entire *P–V* curve, k is potentially very useful in population studies as an objective and quantitative measurement of the *P–V* relationship.

Multiple Transpulmonary Pressure Measurements Although indices such as C_{st} and k aim to encapsulate the

P–V curve in a single number, another approach to handling the nonlinear *P–V* curve has been to break it down into segments, describing it by a set of transpulmonary pressures at fixed proportions of the TLC. The *P–V* curve is thus described by the transpulmonary pressure at 90% of TLC ($P_{L,90}$), 80% of TLC ($P_{L,80}$), and so on down to $P_{L,40}$. Turner and colleagues[7] used this approach to report predicted values for normal *P–V* curves. Of these, $PL_{,90}$ appears to be the most robust, particularly as a marker of loss of elastic recoil, where it is more reproducible than measurements of $P_{L,max}$.[2]

CLINICAL APPLICATIONS

Emphysema and Chronic Obstructive Lung Disease

Although measurement of the static *P–V* curve has been applied clinically to a variety of lung diseases, the greatest interest has been in obstructive lung disease, particularly in cases of emphysema. It has long been known that emphysematous lungs exhibit diminished elastic recoil and that this decrease in stiffness is of great pathophysiologic importance. Although the advent of spirometry made it simple to detect airflow obstruction, confirmation of the diagnosis of emphysema was exceedingly difficult before CT scanning became available. Although bullae and widespread lung destruction can be detected on plain radiographs of the chest, emphysema has been considered a pathologic diagnosis that is confirmed only at autopsy or after surgery. This led to the hope that investigations of lung elasticity would be a helpful indicator of emphysema.

Before the invention of the esophageal balloon technique, measurement of the transpulmonary pressure was a key obstacle to the investigation of lung elasticity in emphysema. Christie was among the first to address this directly, by taking advantage of the practice of inducing therapeutic pneumothorax as a treatment for tuberculosis. In a classic publication, Christie[1] combined direct measurements of pleural pressure obtained through needles placed in the pleural space with spirometric measurements of lung volume to estimate pulmonary compliance in patients with emphysema. Christie laid the groundwork for future studies by demonstrating the feasibility of studying lung mechanics in vivo. Further advances in this area had to await the end of World War II, when electronic transducers and materials suitable for the construction of esophageal balloon catheter systems became available. By the early 1960s, the notion that emphysematous lung is significantly more compliant than normal lung, with a static *P–V* curve shifted leftward and upward (see Figure 8-2A), was well established in the literature.[8]

Attempts to relate compliance measurements to other features suggestive of emphysema have not been very successful. For example, Yip and colleagues[9] failed to find much evidence of correlation between increases in FRC and compliance in patients with stable chronic obstructive pulmonary disease (COPD). In contrast, the correlation between FRC and $P_{L,max}$ was much more significant, suggesting that data from the entire *P–V* curve are needed to adequately describe the changes in mechanics in emphysema, rather than limiting the measurements to the region near to FRC. This was consistent with a study by Silvers and colleagues,[10] who demonstrated the importance of loss of elastic recoil as a marker of emphysema even in cases of mild or minimal disease. The use of the shape factor *k* as a marker of mild or early emphysema has been evaluated in several studies. The results of studies in patients with emphysema did confirm increases in *k*,[11] but correlations with other markers of emphysema[2,12] or, later, with anatomic evidence of emphysema on CT scans was not as good as expected,[13] particularly in mild cases.

The lack of sensitivity of *P–V* curves in practice has not been completely explained. Several confounding factors certainly contribute. There is a natural loss of elasticity with age, independent of emphysema, so that in older subjects losses of recoil may be out of proportion to the degree of anatomic emphysema actually detected. Another problem relates to the heterogeneous nature of emphysema in most cases. Whereas the *P–V* curve represents the overall elastic behavior of the entire lung, emphysema typically causes regional destruction of the lungs. Measurement of average esophageal pressure changes and total lung volume may not be an effective way to investigate the behavior of the upper lobes that have been damaged by centrilobular emphysema. Under these conditions, the mechanical behavior of the most affected areas, where the ventilation is minimal and which make a negligible contribution to the vital capacity (VC), cannot be detected from the *P–V* curve. As Greaves and Colebatch pointed out,[11] the *P–V* curve and especially the *k* factor are most likely to reflect the less diseased parts of the lung, whereas anatomic measures of emphysema map the most damaged areas. This view is supported by classic physiologic–radiologic correlations carried out by Macklem and colleagues,[14] who used tantalum bronchograms to demonstrate the importance of the preserved areas of emphysematous lungs in determining their mechanical properties. In their studies, it was the nonemphysematous part of the lung that determined the compliance of the lung rather than the bullae. Furthermore, somewhat counterintuitively, the bullae exhibited low compliance, rather than the high compliance usually associated with emphysema.

Chest Wall For many years, it was believed that emphysema could lead, in at least some cases, to a decrease in chest wall compliance that, in some instances, would be sufficient to decrease overall respiratory system compliance. Although this has been found in several studies,[15,16] these investigations suffered from technical problems related to the difficulty in achieving full relaxation of the inspiratory muscles during the maneuver in often intensely dyspneic patients. Nevertheless, any decrease in chest wall compliance would have the dual effect of increasing the work of breathing and acting as a limiting factor in lung hyperinflation. In a careful study, Sharp and colleagues[17] demonstrated that the measured decrease in chest wall compliance in COPD patients is artifactual. They eliminated any inspiratory muscle activity with the use of neuromuscular

blockade, so that the purely passive static behavior of the chest wall could be measured. With fully relaxed musculature, they were able to inflate the lungs to volumes never reached in normal subjects, well above the normal TLC. They concluded that the thoracic wall compliance does not change significantly in emphysematous patients across the entire range of volumes that they explored. Thus, chest wall mechanics do not limit pulmonary hyperinflation in COPD patients.

Imaging The development of modern imaging techniques such as CT has revolutionized the study of emphysema pathophysiology. It has become possible to make anatomic assessments in living subjects and correlate them with measures of lung elasticity and other pulmonary function tests. High-resolution computed tomography (HRCT) can detect emphysema with high sensitivity and lends itself to the development of numerical algorithms for the quantification of disease extent and the relative importance of airway and parenchymal disease. Several approaches to this have been taken, ranging from subjective, visual scores of emphysema extent to objective scores based on the percentage of lung area occupied by pixels with low attenuation values. Indices based on the latter have been shown to be quite reproducible, providing a useful quantitative measure of emphysema. The results of studies in which imaging has been compared with pathologic assessments of emphysema have shown excellent correlations.

A few attempts have been made to relate HRCT evaluation and indices of lung elasticity, but they have yielded discrepant results. The results of some studies have demonstrated a poor correlation between the decrease in lung elastic recoil and emphysema score,[18] whereas those of others have shown a more significant correlation.[19] A major problem in interpreting the results of these studies is the lack of consistency of the indices used for both mechanics and imaging. For example, in some studies, $P_{L,max}$ was compared to a qualitative visual CT score,[18] whereas in others, k,[19] $P_{L,90}$,[19] and the natural logarithm of k have been used.[19] These difficulties have been compounded by variations in the patient populations.[13]

Most recently, Baldi and colleagues[13] carried out a detailed study in which all the main indices of lung mechanics (k factor, ln k, $P_{L,max}$, $P_{L,90}$) were compared to mean CT number and a quantitative CT emphysema score in 24 COPD patients with moderate-to-severe airflow obstruction. Only a weak correlation was found between loss of elastic recoil and the extent of emphysema, failing to reach statistical significance, although when indices of mechanics were plotted against the mean CT number, a measure of average tissue density, a significant correlation was found. These results parallel the studies on anatomic emphysema quantitation cited above, underscoring the inability of the *P–V* curve to reveal the most damaged areas of the lung. Instead, changes in the *P–V* curve seem to reflect what is going on in the relatively preserved, nonemphysematous parenchyma. Taken together, these findings tend to confirm that the *P–V* curve is not a useful measure of extent or severity of disease in emphysema.

Early Disease As the *P–V* curve seems to be highly influenced by those parts of the lung that are not yet greatly affected by anatomic emphysema, it is not unreasonable to hypothesize that measurement of *P–V* curves might be useful in detecting early changes in the lung parenchyma, before well-defined anatomic emphysema is present. Perhaps the real correlation between structure and function will be found at a more subtle level. Indeed, Cosio and colleagues[20] have presented evidence that there are significant microscopic changes in the lung parenchyma of healthy, "pre-emphysematous" smokers, in whom increases in the size of alveolar fenestrae were demonstrated. These lesions corresponded anatomically to the regions where centrilobular emphysematous changes would be typically seen in smokers. Indices of elastic recoil, in particular $P_{L,90,}$ correlated significantly with the mean area of the fenestrae. These findings led to the concept of "ultramicroscopic emphysema," which refers to increased size, irregular shape, and increased numbers of alveolar pores and fenestrae in smokers with negligible or absent gross emphysema. It is of note that these findings have recently been reproduced experimentally in guinea pigs exposed to cigarette smoke,[21] where a correlation was found between the number of pores and static compliance measured between 0 and 15 cm H_2O of transpulmonary pressure, as well as with TLC, FRC, and RV.

Another approach to the detection of early lung destruction in emphysema, again from the Cosio laboratory, was the development of the destructive index (DI), introduced as a light microscopic index of parenchymal damage in smokers.[22] Using point counting, Saetta and colleagues[22] calculated the ratio between the percentage of destroyed space and the total alveolar and ductal space. DI was able to differentiate the lungs of smokers from those of nonsmokers and was more sensitive than a preexisting index, the mean linear intercept (L_m). DI also showed a fair correlation with the functional indices, including the elastic properties. This index was refined further by Eidelman and colleagues,[23] who demonstrated that DI could be separated into two components: DI_b, which measures the breaks in alveolar septa, and DI_e, which measures the true emphysematous spaces. Only DI_b was significantly increased in the lungs of smokers and thus appeared to be a microscopic precursor of the subsequent gross destruction of the proximal portion of the lobulus.[23] This finding again reinforces the importance of heterogeneity of lung destruction in emphysema.

What of the relationship between lung mechanics and destruction? In 1989, Eidelman and colleagues reported a systematic study of heterogeneity of mechanical properties of the lung in smokers and subjects with α_1-antitrypsin deficiency.[24] Although some smokers exhibited the expected decrease in elastic recoil, increased compliance, and changes in shape of the *P–V* curve, as described by Macklem and Becklake[8] and similar to that seen in the α_1-antitrypsin–deficient subjects, others, despite decreased elastic recoil pressure, showed a significantly less accentuated slope of their *P–V* curves. In other words, they exhibited reduced rather than increased compliance. Similarly, the k factor was not increased in these subjects. It is of interest that the

patients whose lungs appeared to be stiffer also showed the most severe airflow limitation. This observation suggested the hypothesis that lung destruction in the smokers may be heterogeneous in a manner corresponding to the anatomic abnormalities present. Those with *P–V* curves resembling that seen in α_1-antitrypsin deficiency might have evidence of panlobular emphysema in their lungs, whereas the others could have a predominantly centrilobular pattern. Kim and colleagues[25] investigated this at a microscopic level, confirming the presence of centrilobular and panlobular patterns. Subsequent studies suggested that those individuals with the unexpected decrease in compliance all had the centrilobular variant.[26,27] These finding are consistent with the notion that distribution, rather than the severity of emphysema, influences the shape of the *P–V* curve.

Asthma

The notion that pulmonary mechanics may be abnormal in asthma is more controversial than it is for emphysema. Asthma is generally considered to be primarily an airway disease in which inflammation leads to increased capacity for airway smooth muscle shortening and intermittent bronchoconstriction. Although there is some evidence that the peribronchial parenchyma is inflamed in asthma,[28,29] asthma remains a disease of the tracheobronchial tree. Nevertheless, there is a long history of reports of abnormal lung mechanics in asthmatic patients. More than 30 years ago, Woolcock and Read[30] reported that VC is reduced in asthma. This change was associated with increased RV, FRC, and TLC, as might also be found in emphysema patients (see Figure 8-1). In our experience, in the present-day world of frequent use of inhaled corticosteroids, increases in TLC are rare among asthmatic patients. Nevertheless, the central issue, from the point of view of pulmonary elastic properties, is whether the increases in lung volume that may occur in uncontrolled asthma merely represent gas trapping behind closed airways or rather reflect loss of elastic recoil as occurs in emphysema.

There have been reports of abnormal *P–V* curves in asthma, both in remission and during acute exacerbations, with the principal finding being loss of elastic recoil. Decreases in recoil have been described as transient, reverting to normal after therapy with corticosteroids.[31] Among reports of lung static mechanical properties in asthma, there is a consensus that the compliance in the tidal volume range is unchanged, with a normal slope at FRC. When alterations are seen, they tend to affect the recoil at higher lung volumes.[31–35] A limitation of many studies of elastic recoil in asthma relates to technical difficulties with plethysmographic measurements of lung volumes in the setting of airflow obstruction. These limitations were not recognized until the 1980s, after many of these studies were completed. Nevertheless, Gelb and colleagues[36] have presented new interesting data in this regard. In a group of patients with moderate-to-severe chronic persistent asthma undergoing optimal treatment, and with no signs of emphysema, there is actually a marked loss of elastic recoil, and this loss of elastic recoil accounted for 34 to 50% of the decrease in maximum expiratory flow at 70 and 80% TLC. Based on these data, the authors have hypothesized that airflow limitation in asthma may result from mechanisms in the far periphery of the lung, involving structural changes in the parenchyma and distal airways, rather than being limited to the more proximal airways. These findings are consistent with observations from the Denver group, who have described inflammatory involvement of the alveolar and distal airways in transbronchial biopsy specimens from asthmatic subjects.[28,29,37] Macrophages, $CD4^+$ lymphocytes and eosinophils were detected, and in some cases[28,29] there was a correlation between alveolar infiltrate and decline in lung function. It is certainly conceivable that inflammation in the lung periphery could ultimately lead to damage or disruption of stromal components of the lung, including elastic fibers, and this would account for the loss of elastic recoil, whereas bronchoconstriction per se has been shown to increase the dynamic elastance without affecting the static *P–V* curve.[38] Changes in lung stiffness have the potential to alter coupling between the lung and the airways, leading to enhanced responsiveness, particularly in the supine position[39] or at night.[40]

Another mechanism of potential relevance occurring in asthma involves the important role of surfactant as a determinant of pulmonary mechanical behavior. Murine data suggest that surfactant may be altered in allergic inflammation,[41] and this suggestion is supported by a modest amount of data from humans.[42] It is known that alveolar surfactant, through the action of its components surfactant protein-B (SP-B) and, to a lesser extent, SP-C, contributes to the mechanical stability of the alveoli and distal airways, thus preventing air trapping through distal airway closure. In heterozygous SP-B–deficient mice, airway closure is enhanced, leading to increased RV, whereas their homozygous counterparts die soon after birth.[43] Moreover, Th2 cytokines prominent in asthma, such as interleukin-4 (IL-4) and IL-5, may alter the function of SP-B[44] and SP-C.[45] Finally, in addition to their implications for lung mechanics, changes in surfactant could have immunomodulatory implications; some components of surfactant bind allergens, so these are not available to bind IgE.

Fibrotic Lung Disease

Although idiopathic pulmonary fibrosis (IPF) is the prototype of these disorders, there are many etiologic categories of fibrosis that share the mechanical consequence of decreased lung volumes (restriction) with increased lung recoil or decreased compliance. IPF is characterized by progressive distortion of the lung architecture, with inflammation and accumulation of fibrotic tissue, eventually leading to the development of what is termed "end-stage lung." In its advanced stages, this type of lung disease is characterized by the so-called "honeycomb" pattern, with diffuse fibrosis, loss of recognizable architectural organization, cystic lesions, and traction bronchiectasis. The functional counterpart of these changes is decreased TLC, usually accompanied by a reduction in RV.[46,47] The mechanical similarities among these diseases lead to similarities in the appearance of the *P–V* curve, which is shifted downward and to the right (see Figure 8-2B).

It is noteworthy that the decrease in the volume of the airspaces is accompanied by an increase in tissue volume, due to collagen deposition, and so the total intrathoracic volume might in some cases be less altered than would be predicted from the gas volume evaluation alone.[4] Although compliance is decreased, the shape of the *P–V* curve is less affected, at least as reflected in the *k* factor calculated from exponential curve fitting.[46]

As with emphysema, the diagnostic utility of measuring the *P–V* curve in parenchymal restrictive disease is less of an issue than in the past. The high-resolution CT scan is now central to the diagnosis of interstitial lung diseases, including IPF. Nevertheless, the *P–V* curve can be a sensitive and effective approach to diagnosis, particularly in difficult cases with multiple disease processes. For example, in a group of patients with progressive systemic sclerosis, none of whom had signs of pulmonary involvement shown by standard radiography or reduction of TLC, the static compliance was reduced in one-third of cases.[48]

Extrapulmonary Diseases

In neuromuscular diseases resulting in weakness of the respiratory muscles, the involvement of inspiratory and expiratory muscles results primarily in changes in lung volumes, typically a decrease in both VC and TLC,[49,50] the severity of which correlates with the degree of muscle impairment. However, reduction in the amplitude of volume excursion is not the only feature of the *P–V* curve in neuromuscular disease. A decrease in the slope of the *P–V* curve can often be observed (see Figure 8-1), suggesting a reduction in lung compliance, the principal determinant of which appears to be the frequent presence of microatelectasis within the parenchyma. A change in the passive properties of the chest wall has also been reported, and in children, in particular, an increase in chest wall compliance has been demonstrated.[51] This change, probably attributable to the higher amount of cartilage in the thoracic cage,[52] can represent a potential determinant of thoracic deformation. In elderly subjects, however, the chest wall is stiffened, possibly through accumulation of fibrotic tissue among the muscle fibers, leading to a reduction in chest wall compliance. The rib cage in quadriplegic patients also appears to be significantly stiffer than in normal subjects.[53] In addition, it has been suggested that patients with chronic neuromuscular disease eventually develop a decrease in chest wall outward elastic recoil (or increase in transthoracic pressure),[54] which can result in a decrease in FRC, often observed in these patients.[49,50] An alternative or complementary explanation of the decrease in FRC is that the measured FRC does not represent the true relaxation volume of the respiratory system in patients with neuromuscular disease but rather a lower volume actively reached by the subjects, so that the subsequent inspiration can benefit from the descent of the diaphragm and the relaxation of the abdominal muscles.[4] Deformities of the thoracic cage, such as severe scoliosis or pleural thickening, can also impair ventilatory function directly by impairing pulmonary inflation, resulting in a restrictive syndrome. It remains unclear, however, whether some of these abnormalities can be attributed to changes in the elastic properties of the lung.[4]

CONCLUSIONS

Although the measurement of *P–V* curves has gone out of fashion, this remains a useful technique for the measurement of the functional state of the lung. Particularly in the context of emphysema research, the *P–V* curve appears to be a relatively simple means of detecting evidence of lung destruction before it is evident on CT scans and of differentiating among patterns of destruction in the lung that may be of pathophysiologic importance. In difficult cases with mixed radiologic patterns of disease, the *P–V* curve may be the only means to determine the physiologic basis of a patient's disordered breathing.

ACKNOWLEDGMENTS

The authors wish to thank Professor Joseph Milic-Emili, Dr Susumu Isogai, and Cliff Pavlovic of the Meakins-Christie Laboratories, McGill University, Montreal, Canada, for their help and advice in the preparation of the chapter and Dr Sabah Hussain, Meakins-Christie Laboratories, director of the Pulmonary Function Laboratory, Royal Victoria Hospital, Montreal, Canada, for providing pulmonary function tests and *P–V* curves from patients.

REFERENCES

1. Christie RV. The elastic properties of the emphysematous lung and their clinical significance. J Clin Invest 1934; 13:245–321.
2. Osborne S, Hogg JC, Wright JL, et al. Exponential analysis of the pressure–volume curve. Correlation with mean linear intercept and emphysema in human lungs. Am Rev Respir Dis 1988;137:1083–8.
3. Tankersley CG, Rabold R, Mitzner W. Differential lung mechanics are genetically determined in inbred murine strains. J Appl Physiol 1999;86:1764–9.
4. Pride NB, Macklem PT. Lung mechanics in disease. In: Macklem PT, Mead J, editors. Handbook of physiology. Section 3: The respiratory system. Vol. III. Mechanics of breathing. Bethesda, MD: American Physiological Society; 1986. p. 659–92.
5. Lyons HA, Chiang ST. Specific compliance of pulmonary compartments. In: Current research in chronic respiratory disease: proceedings of 11th Aspen Emphysema Conference. Arlington, VA: US Health Services and Mental Health Administration. Chronic Respiratory Diseases Control Program; 1968. p. 257–68.
6. Salazar E, Knowles JH. An analysis of pressure–volume curve characteristics in the lung. J Appl Physiol 1964;19:97–104.
7. Turner JM, Mead J, Wohl ME. Elasticity of human lungs in relation to age. J Appl Physiol 1968;25:664–71.
8. Macklem PT, Becklake MR. The relationship between the mechanical and diffusing properties of the lung in health and disease. Am Rev Respir Dis 1963;87:45–55.
9. Yip CK, Epstein H, Goldring RM. Relationship of functional residual capacity to static pulmonary mechanics in chronic obstructive pulmonary disease. Am J Med Sci 1984; 287:3–6.
10. Silvers GW, Petty TL, Stanford RE. Elastic recoil changes in early emphysema. Thorax 1980;35:490–5.
11. Greaves IA, Colebatch HJ. Elastic behavior and structure of normal and emphysematous lungs post mortem. Am Rev Respir Dis 1980;121:127–36.

12. Pare PD, Brooks LA, Bates J, et al. Exponential analysis of the lung pressure–volume curve as a predictor of pulmonary emphysema. Am Rev Respir Dis 1982;126:54–61.
13. Baldi S, Miniati M, Bellina CR, et al. Relationship between extent of pulmonary emphysema by high-resolution computed tomography and lung elastic recoil in patients with chronic obstructive pulmonary disease. Am J Respir Crit Care Med 2001;164:585–9.
14. Macklem PT, Thurlbeck WM, Fraser RG. Chronic obstructive disease of small airways. Ann Intern Med 1971;74: 167–77.
15. Ting EV, Lyons HA. Pressure–volume relations of lung and thoracic cage in pulmonary emphysema. J Appl Physiol 1961;16:517–21.
16. Cherniack RM, Hodson A. Compliance of the chest wall in chronic bronchitis and emphysema. J Appl Physiol 1963;18:707–11.
17. Sharp JT, van Lith P, Nuchprayoon C, et al. The thorax in chronic obstructive lung disease. Am J Med 1968;44:39–46.
18. Morrison NJ, Abboud RT, Ramadan F, et al. Comparison of single breath carbon monoxide diffusing capacity and pressure–volume curves in detecting emphysema. Am Rev Respir Dis 1989;139:1179–87.
19. Gugger M, Gould G, Sudlow MF, et al. Extent of pulmonary emphysema in man and its relation to the loss of elastic recoil. Clin Sci (Lond) 1991;80:353–8.
20. Cosio MG, Shiner RJ, Saetta M, et al. Alveolar fenestrae in smokers. Relationship with light microscopic and functional abnormalities. Am Rev Respir Dis 1986;133:126–31.
21. Wright JL. The importance of ultramicroscopic emphysema in cigarette smoke-induced lung disease. Lung 2001;179:71–81.
22. Saetta M, Shiner RJ, Angus GE, et al. Destructive index: a measurement of lung parenchymal destruction in smokers. Am Rev Respir Dis 1985;131:764–9.
23. Eidelman DH, Ghezzo H, Kim WD, Cosio MG. The destructive index and early lung destruction in smokers. Am Rev Respir Dis 1991;144:156–9.
24. Eidelman DH, Ghezzo H, Kim WD, et al. Pressure–volume curves in smokers. Comparison with alpha-1-antitrypsin deficiency. Am Rev Respir Dis 1989;139:1452–8.
25. Kim WD, Eidelman DH, Izquierdo JL, et al. Centrilobular and panlobular emphysema in smokers. Two distinct morphologic and functional entities. Am Rev Respir Dis 1991;144: 1385–90.
26. Saetta M, Kim WD, Izquierdo JL, et al. Extent of centrilobular and panacinar emphysema in smokers' lungs: pathological and mechanical implications. Eur Respir J 1994;7:664–71.
27. Finkelstein R, Fraser RS, Ghezzo H, Cosio MG. Alveolar inflammation and its relation to emphysema in smokers. Am J Respir Crit Care Med 1995;152:1666–72.
28. Kraft M, Martin RJ, Wilson S, et al. Lymphocyte and eosinophil influx into alveolar tissue in nocturnal asthma. Am J Respir Crit Care Med 1999;159:228–34.
29. Kraft M, Djukanovic R, Wilson S, et al. Alveolar tissue inflammation in asthma. Am J Respir Crit Care Med 1996;154:1505–10.
30. Woolcock AJ, Read J. Lung volumes in exacerbations of asthma. Am J Med 1966;41:259–73.
31. Gold WM, Kaufman HS, Nadel JA. Elastic recoil of the lungs in chronic asthmatic patients before and after therapy. J Appl Physiol 1967;23:433–8.
32. Woolcock AJ, Read J. The static elastic properties of the lungs in asthma. Am Rev Respir Dis 1968;98:788–94.
33. Finucane KE, Colebatch HJ. Elastic behavior of the lung in patients with airway obstruction. J Appl Physiol 1969;26: 330–8.
34. Buist AS, Ghezzo H, Anthonisen NR, et al. Relationship between the single-breath N test and age, sex, and smoking habit in three North American cities. Am Rev Respir Dis 1979;120:305–18.
35. Zapletal A, Desmond KJ, Demizio D, Coates AL. Lung recoil and the determination of airflow limitation in cystic fibrosis and asthma. Pediatr Pulmonol 1993;15:13–18.
36. Gelb AF, Licuanan J, Shinar CM, Zamel N. Unsuspected loss of lung elastic recoil in chronic persistent asthma. Chest 2002;121:715–2.
37. Sutherland ER, Martin RJ. Distal lung inflammation in asthma. Ann Allergy Asthma Immunol 2002;89:119–24.
38. Pellegrino R, Wilson O, Jenouri G, Rodarte JR. Lung mechanics during induced bronchoconstriction. J Appl Physiol 1996;81: 964–75.
39. Irvin CG, Pak J, Martin RJ. Airway–parenchyma uncoupling in nocturnal asthma. Am J Respir Crit Care Med 2000;161:50–6.
40. Shardonofsky FR, Martin JG, Eidelman DH. Effect of body posture on concentration–response curves to inhaled methacholine. Am Rev Respir Dis 1992;145:750–5.
41. Liu M, Wang L, Enhorning G. Surfactant dysfunction develops when the immunized guinea-pig is challenged with ovalbumin aerosol. Clin Exp Allergy 1995;25:1053–60.
42. Hohlfeld JM, Ahlf K, Enhorning G, et al. Dysfunction of pulmonary surfactant in asthmatics after segmental allergen challenge. Am J Respir Crit Care Med 1999;159: 1803–9.
43. Clark JC, Weaver TE, Iwamoto HS, et al. Decreased lung compliance and air trapping in heterozygous SP-B-deficient mice. Am J Respir Cell Mol Biol 1997;16:46–52.
44. Jain-Vora S, Wert SE, Temann UA, et al. Interleukin-4 alters epithelial cell differentiation and surfactant homeostasis in the postnatal mouse lung. Am J Respir Cell Mol Biol 1997; 17:541–51.
45. Mishra A, Weaver TE, Beck DC, Rothenberg ME. Interleukin-5-mediated allergic airway inflammation inhibits the human surfactant protein C promoter in transgenic mice. J Biol Chem 2001;276:8453–9.
46. Gibson GJ, Pride NB, Davis J, Schroter RC. Exponential description of the static pressure–volume curve of normal and diseased lungs. Am Rev Respir Dis 1979;120: 799–811.
47. Gibson GJ, Pride NB. Pulmonary mechanics in fibrosing alveolitis: the effects of lung shrinkage. Am Rev Respir Dis 1977;116:637–47.
48. Gupta D, Aggarwal AN, Sud A, Jindal SK. Static lung mechanics in patients of progressive systemic sclerosis without obvious pulmonary involvement. Indian J Chest Dis Allied Sci 2001;43:97–101.
49. De Troyer A, Borenstein S, Cordier R. Analysis of lung volume restriction in patients with respiratory muscle weakness. Thorax 1980;35:603–10.
50. Gibson GJ, Pride NB, Davis JN, Loh LC. Pulmonary mechanics in patients with respiratory muscle weakness. Am Rev Respir Dis 1977;115:389–95.
51. Papastamelos C, Panitch HB, Allen JL. Chest wall compliance in infants and children with neuromuscular disease. Am J Respir Crit Care Med 1996;154:1045–8.
52. Gozal D. Pulmonary manifestations of neuromuscular disease with special reference to Duchenne muscular dystrophy and spinal muscular atrophy. Pediatr Pulmonol 2000; 29:141–50.
53. Estenne M, De Troyer A. The effects of tetraplegia on chest wall statics. Am Rev Respir Dis 1986;134:121–4.
54. De Troyer A, Estenne M. The respiratory system in neuromuscular disorders. In: Roussos C, editor. The thorax. 2nd ed. New York: Marcel-Dekker; 1995. p. 2177–212.

CHAPTER 9

STRUCTURE–FUNCTION CORRELATIONS IN PULMONARY FIBROSIS

Anne Gonzalez, Mara S. Ludwig

Idiopathic pulmonary fibrosis (IPF), or cryptogenic fibrosing alveolitis, is a specific form of chronic fibrosing interstitial pneumonia of unknown cause limited to the lung and associated with a histologic pattern of usual interstitial pneumonia (UIP).[1,2] True "idiopathic" pulmonary fibrosis must be distinguished from interstitial lung disease associated with an underlying connective tissue disorder, pneumoconiosis, hypersensitivity pneumonitis, or granulomatous involvement of the lung parenchyma. In addition, the "idiopathic interstitial pneumonias" comprise a broad group of conditions with widely varying natural histories and responses to treatment. As knowledge and understanding have evolved, so have the classification schemes. This chapter reviews the current literature on correlations of structure and function in patients with pulmonary fibrosis. Functional parameters include standard pulmonary function tests and measures of gas exchange, as well as more detailed studies of lung tissue mechanics. To put the studies in their "historic" context, we first briefly review histopathologic definitions and their implications. Finally, the contribution of data from animal models to the understanding of structure–function correlations in IPF is examined.

PATHOLOGIC DEFINITIONS AND THEIR IMPLICATIONS

UIP, the histologic pattern central to a diagnosis of IPF, is characterized by spatial heterogeneity, with areas of normal lung tissue alternating with fibrosis in a predominantly subpleural distribution, and temporal heterogeneity, with end-stage fibrosis and honeycombing abutting areas of proliferating fibroblasts ("fibroblastic foci") (Figure 9-1). The histopathologic patterns of desquamative interstitial pneumonia (DIP), respiratory bronchiolitis-associated interstitial lung disease (RB-ILD), nonspecific interstitial pneumonia (NSIP), lymphoid interstitial pneumonia, acute interstitial pneumonia, and idiopathic bronchiolitis obliterans organizing pneumonia represent separate entities, to be distinguished from IPF. This subclassification, based on clinicopathologic criteria, has important prognostic and therapeutic implications. IPF has a worse response to therapy and prognosis.[3] However, the recognition of separate histopathologic subgroups is recent, and our understanding of IPF and idiopathic interstitial pneumonias has changed significantly since the original description of rapidly progressive, diffuse interstitial fibrosis by Hamman and Rich in 1944.[4]

In 1978, Carrington and colleagues[5] histologically classified patients with interstitial pneumonia into "desquamative" and "usual" types and found a dramatically better 5-year survival with DIP (95%) than with UIP (55%). In a retrospective analysis published in 1980, Turner-Warwick and colleagues[6,7] noted that cellularity and less fibrosis on lung biopsy (without criteria of DIP) were associated with longer survival and steroid responsiveness. The hypothesized pathogenesis of IPF at the time was that it began as an alveolitis, with inflammatory cell infiltration, and progressed to fibrosis.[8,9] There was debate as to whether patients with pulmonary fibrosis should be split "artificially" into two morphologic groups, DIP and UIP, or whether one (DIP) represented an earlier stage, with predominant alveolitis, and the other (UIP) a later stage of IPF.[10] More recently, the worse 5-year survival of patients with UIP (20%) compared with other histopathologic subsets, including NSIP (70%) and DIP/RB-ILD (80%), has been clearly demonstrated.[11] The results of a recent study of patients with UIP showed that the extent and severity of cellularity or fibrosis were not predictors of survival.[12]

There has been an evolution in our understanding of the pathogenesis of IPF. Earlier workers hypothesized that the disease progressed linearly from cellular to fibrotic stages, and it was suggested that medical intervention at an earlier stage might halt disease progression. There was a specific clinical rationale for the identification of structure–function correlations in pulmonary fibrosis: physiologic studies that reflected the underlying cellular or fibrotic structure would allow assessment of prognosis and response to treatment.[8] Functional studies that could monitor the fibrotic process over time would obviate the need for repeated lung biopsies. This was the driving force behind many of the studies of

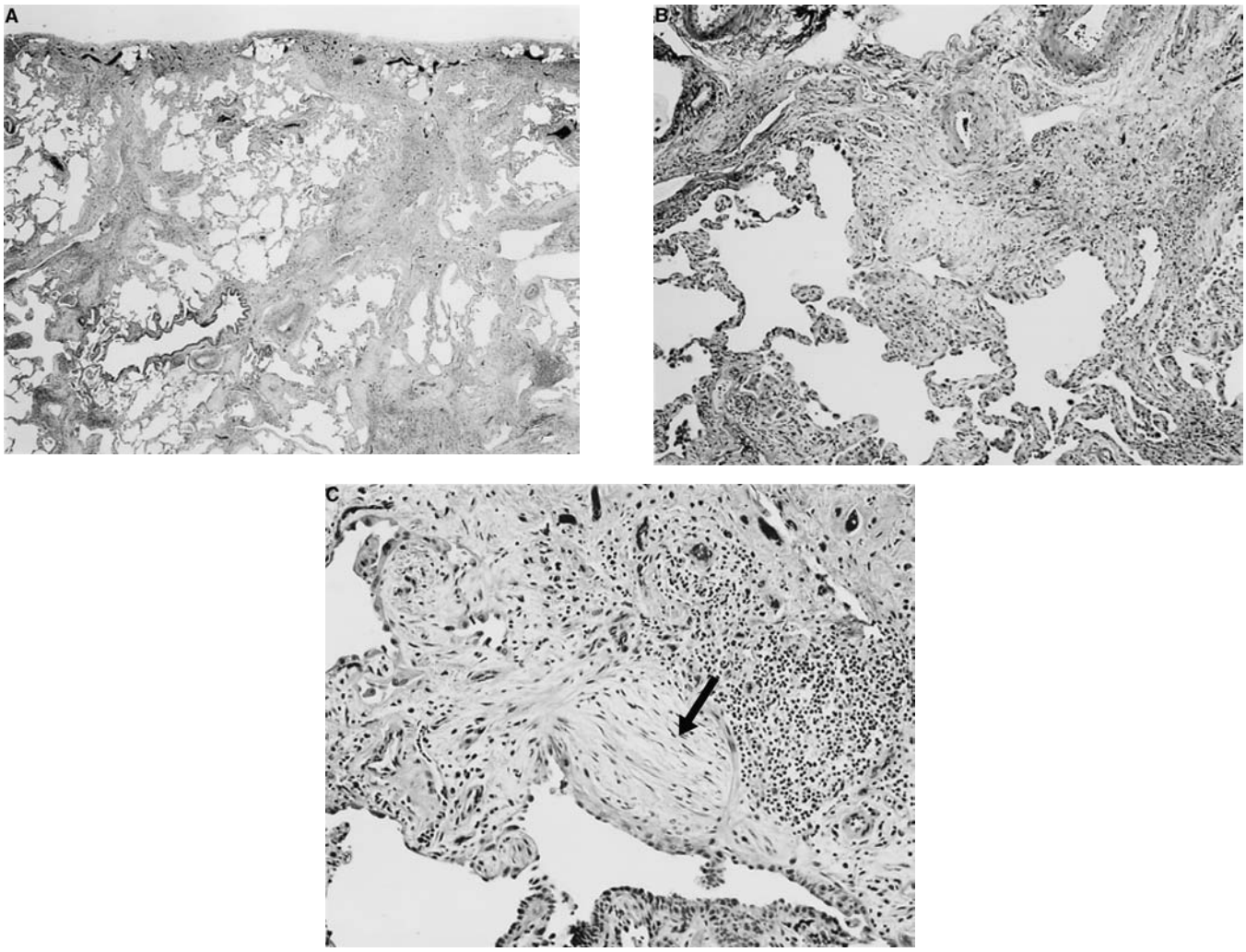

FIGURE 9-1 Photomicrographs from patients with pulmonary fibrosis. *A*, Usual interstitial pneumonia showing patchy fibrosis with a subpleural distribution. *B*, Area of dense collagenous scarring adjacent to cystic changes. *C*, Fibroblastic focus of loose connective tissue (*arrow*). Reproduced with permission from American Thoracic Society / European Respiratory Society.[1]

structure–function correlations in IPF that are reviewed in this chapter. It must be kept in mind that many of the patients considered to have IPF in these studies would probably not meet today's stricter clinicopathologic criteria, and most studies therefore include patients with a variety of subtypes of idiopathic interstitial pneumonia.

STANDARD PULMONARY FUNCTION TESTS

The typical findings of pulmonary function tests in pulmonary fibrosis are well established: restrictive impairment with reduced vital capacity (VC) and total lung capacity (TLC), normal airflow, reduced diffusing capacity for carbon monoxide (DLco), and mild resting hypoxemia that worsens with exertion.[1,10] In a description of the findings in 29 patients with IPF, Crystal and colleagues[8] noted a mean TLC of 62.9% of that predicted and a mean DLco of 46.8% of that predicted. However, two patients had normal lung volumes and one patient a normal DLco, despite morphologic evidence of mild-to-moderate fibrosis. The mean forced expiratory volume in 1 second (FEV_1) was 97.6% of that predicted. The average patient with IPF had resting arterial hypoxemia (arterial partial pressure of oxygen [P_aO_2] = 63.9 mm Hg), although four patients had normal resting P_aO_2.[8] Beyond their contribution to the diagnosis of IPF, how do these findings correlate with the severity of the underlying structural abnormality? Both earlier and later studies have provided disappointing results.

Gaensler and Carrington[13] graded 146 lung biopsies of interstitial pneumonias, of which one-third were pneumoconioses, using an overall histologic index of 0 to 5. They found the correlation of percentage predicted VC with the histologic index to be good in the pneumoconioses and only fair in the UIP cases. Similarly, when they compared UIP and DIP, Carrington and colleagues[5] noted that a moderately good correlation existed between the pathologist's estimate of severity and reduction of lung volume in UIP (forced vital capacity [FVC], $r = -.40$; TLC, $r = -.44$) but not in DIP (FVC, $r = -.07$; TLC, $r = -.16$). Gaensler and Carrington[14] published a larger review of 358 patients who had undergone open lung biopsy for a variety of diffuse infiltrative lung diseases and found a similar correlation of FVC ($r = -.39$) and TLC ($r = -.34$) with estimates of pathologic severity. These represent modest correlations at best.

Beyond a general index of pathologic severity, other investigators sought to identify correlations between the degree of cellularity or fibrosis and functional impairment. In general, the lung volumes were found to bear no relationship to the extent of the alveolitis in IPF. The reduction in lung volumes roughly paralleled the fibrosis of the disease, but the correlations were weak to moderate at best. Green and colleagues[15] noted that the degree of fibrosis appeared to be more closely related to functional changes than either interstitial mononuclear cell infiltration or vessel wall enlargement: the coefficient of correlation (r) of the fibrosis grade with VC was 0.45. Fulmer and colleagues[9] graded the severity of fibrosis and degree of cellularity in lung biopsy specimens of 23 patients with IPF and compared these parameters to a variety of physiologic measures. None of the standard physiologic test results (VC, TLC, functional residual capacity [FRC] or DLco) correlated significantly with either the morphologic assessment of degree of fibrosis or degree of cellularity. VC showed a trend toward correlation with the degree of fibrosis but accounted for only about 17% of total variability ($r = .422$, $r^2 = .168$).

In more recent studies, further attempts have been made to clarify the relationship between pulmonary function tests and degree of cellular infiltration and fibrosis in IPF. Chinet and colleagues[16] studied 21 patients with diffuse lung fibrosis, of whom 2 had connective tissue diseases and 7 had pneumoconioses. The pathologic data were correlated with TLC and FVC in both groups of patients. In the patients with fibrosing alveolitis, TLC was inversely correlated with both fibrosis ($r = -.735$) and cellular infiltration ($r = -.705$), whereas FVC was inversely correlated with fibrosis ($r = -.598$) but not cellular infiltration ($r = -.201$). Interestingly, the findings of cellular infiltration and fibrosis were themselves positively correlated ($r = .573$, $p < .02$). Cherniack and colleagues[17] evaluated 96 patients with biopsy-confirmed IPF and scored lung pathology according to a previously described system[18] based on four factors: fibrosis, cellularity, "desquamation," and granulation/connective tissue. TLC and FVC were found to correlate with the cellularity factor score ($r = -.374$ and $-.477$, respectively). The authors postulated that these correlations could explain the previously reported finding of lower FVCs in patients who responded to corticosteroid therapy than in those who did not.[19]

DLco is another widely used measurement in the evaluation and monitoring of patients with IPF. Reduced DLco has been commonly reported in cases of interstitial lung disease, even when the lung volumes were normal.[19] However, in several studies no correlation has been found between DLco and histopathologic changes.[5,9,13] In their study of histopathologic grading and function, Cherniack and colleagues[17] found a weak correlation of DLco with the "desquamation" factor ($r = -.363$) and total pathology score ($r = -.354$). Chinet and colleagues[16] noted a correlation of DLco with pathologic grade ($r = -.707$) but not with DLco corrected for alveolar volume ($DLco/V_A$).

Thus, despite being commonly used in clinical practice, measurements of lung volumes and DLco show limited and variable correlations with the severity of pulmonary fibrosis. Several factors may explain this finding. In the studies in which pulmonary function tests have been evaluated in IPF, lung biopsy has been used as the "gold standard." However, biopsies are done routinely only once during a patient's clinical course; no correlation of function and structure for an individual patient is done over time.[10] Furthermore, the biopsy findings are assumed to be representative of the disease process throughout the lung, even though IPF, by its nature, is a relatively heterogeneous process, and sampling errors are likely. Nonetheless, this assumption is considered reasonable as long as the surgeon avoids biopsy of the areas with greatest radiographic involvement (and unrecognizable end-stage disease) and favors biopsy of "average lung."[14] Additionally, measurements of lung structure have been largely observational; morphometric techniques, which quantify morphologic changes, have rarely been applied. Finally, the effect of smoking on lung function measurements has not been systematically taken into account in these patients.

In their 1995 study, Cherniack and colleagues[17] considered the influence of smoking on pulmonary function in a group of untreated patients with biopsy-confirmed IPF. TLC and FVC in current smokers were higher than in those who had never smoked, whereas $DLco/V_A$ was lower in current smokers than in those who had never smoked, as was the FEV_1/FVC ratio. The coefficient of elastic retraction (maximal static transpulmonary pressure divided by the TLC) was also lower in current smokers than in those who had never smoked. In an earlier study, Schwartz and colleagues[20] found that smokers with IPF had higher lung volumes (TLC, RV, and FRC) and lower DLco, yet, surprisingly, the FEV_1/FVC ratio was not significantly related to either smoking status or pack-years of cigarette smoking. In another study[21] it was found that smokers with IPF had higher lung volumes, whereas their FEV_1/FVC ratio and specific airway conductance were significantly lower. In smokers with IPF, the coefficient of retraction was significantly lower than in the nonsmokers. In the 1978 study by Carrington and colleagues,[5] 24% of patients with UIP had significant obstructive impairment, defined as $FEV_1/FVC < 70\%$, with 12 of the 13 patients being smokers with chronic bronchitis. These findings explain part of the difficulty of establishing structure–function correlations in patients with IPF and point out the need to consider the effect of smoking when interpreting functional parameters.

The situation is even more complex because smoking cannot entirely explain the airflow obstruction observed in this disease process. Classically, the FEV_1/FVC ratio is described as being normal or increased in patients with IPF.[1,10] The reduced FEV_1/FVC ratio described above in smokers and the finding of gas trapping have been attributed by investigators to the concomitant presence of emphysema and interstitial fibrosis: smoking and IPF appear to have opposite effects on airway function and, by implication, airway structure.[20] But airflow obstruction can occur in IPF in the absence of concurrent smoking-related obstructive airways disease. In fact, although IPF is classically considered to be an alveolar disease, small airway fibrosis was noted in the original description of Hamman and Rich.[4] Ostrow and Cherniack[22] compared the lung elastic recoil and maximal expiratory flow–volume relationships of

11 patients with diffuse interstitial lung disease (of whom 7 were diagnosed as having IPF) and normal control subjects. Total lung volume was reduced and lung elastic recoil was increased in all patients. The relationship between maximal expiratory flow ($\dot{V}_{max}$) and lung elastic recoil, representative of airway resistance upstream from the equal-pressure point,[23] was compared between patients and controls. Despite increased lung elastic recoil, $\dot{V}_{max}$ was not found to be greater than normal, suggesting increased airway resistance in patients with IPF. Fulmer and colleagues[24] attempted to correlate morphologic and physiologic observations of small airways in patients with IPF. All 18 patients had normal airway function according to the results of standard physiologic studies (FEV_1/FVC and airway resistance by plethysmography[25]). On lung biopsy, 17 of 18 patients (94%) had peribronchiolar fibrosis or peribronchiolar inflammation or bronchiolitis; 67% had an overall estimate of small airways diameter as "narrowed," 59% had frequency-dependent dynamic compliance, and 50% had abnormal maximum expiratory flow–volume curves. These authors found a significant correlation between the measurements of dynamic compliance and maximum flow–volume curves with the overall estimate of small airways diameter.

GAS EXCHANGE

Measurements of P_aO_2 and alveolar–arterial differences in oxygen partial pressures [$P_{A-a}O_2$], both resting and with exercise, have been correlated with disease severity in cases of pulmonary fibrosis. The resting P_aO_2 bears a loose relationship to the extent of disease as individuals with early disease tend to have a P_aO_2 close to normal, and with disease progression, there may be resting hypoxemia.[10] Green and colleagues[15] noted that the resting P_aO_2 was the single best predictor of pulmonary pathology, with a correlation coefficient of 0.50 with the fibrosis grade. However, most authors have failed to demonstrate a significant correlation of resting P_aO_2 with morphologic data.[5,9,16,17] In contrast, studies of gas exchange with exercise have provided more sensitive functional tests of the disease process in IPF.

Gaensler and Carrington[13] found a strong correlation between the $P_{A-a}O_2$ measured during exercise and the overall histologic index ($r = .67$). In their study of UIP and DIP, Carrington and colleagues[5] compared measured physiologic deficits with the pathologist's overall estimate of functional impairment. The best correlations were with exercise P_aO_2 ($r = -.59$ for UIP and $r = -.54$ for DIP) and exercise $P_{A-a}O_2$. Whereas these authors favored the measurement of P_aO_2 and $P_{A-a}O_2$ with exercise, Fulmer and colleagues[9] found that adjusting the absolute change in P_aO_2 between rest and maximum exercise for the amount of work accomplished (oxygen consumption [$\dot{V}O_2$] with exercise minus $\dot{V}O_2$ at rest) correlated best with overall disease severity. There was also a strong correlation of disease severity with the change in $P_{A-a}O_2$ per liter of oxygen consumed. Various authors have attempted to dissect out the contribution of alveolitis and fibrosis to the impairment of gas exchange. Chinet and colleagues[16] showed a closer correlation of pathologic changes with exercise P_aO_2 and $P_{A-a}O_2$ than with resting oxygen values, but the fibrosis and cellular infiltration grades were similarly correlated with the gas exchange data. A further issue is the contribution of smoking in these studies. The correlation of fibrosis index with $P_{A-a}O_2$ at maximal exercise becomes significant when smoking history is taken into account[17] (Figure 9-2).

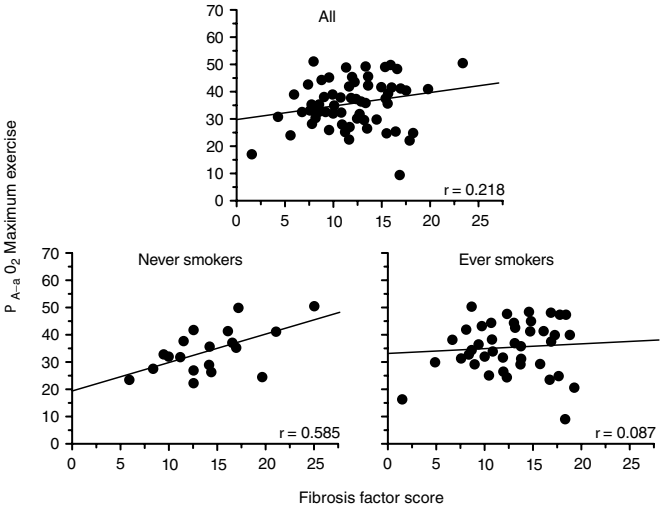

FIGURE 9-2 Contribution of smoking history to the relationship between fibrosis index and $P_{A-a}O_2$ during maximal exercise. Reproduced with permission from Cherniack RM et al.[17]

The hypoxemia of pulmonary fibrosis was initially attributed to the thickened alveolar interstitium forming an anatomic barrier to the diffusion of oxygen—hence the term "alveolar–capillary block."[26] In 1962, Finley and colleagues[27] suggested that the major cause of resting hypoxemia in these patients was not a barrier to the diffusion of oxygen but was, rather, secondary to ventilation–perfusion mismatching. In 1976, Wagner and colleagues,[28] using the technique of multiple inert gas elimination to measure ventilation–perfusion ratio distributions, noted that all of the resting hypoxemia was explained adequately by $V/\dot{Q}$ inequalities. However, with exercise, diffusion limitation contributed to the hypoxemia: they estimated that approximately 20% of the $P_{A-a}O_2$ was due to a diffusion barrier, with $V/\dot{Q}$ inequality remaining the most important factor accounting for the low P_aO_2.

LUNG TISSUE MECHANICS

Standard pulmonary function tests and measures of gas exchange appear to reflect changes in the underlying lung structure in IPF incompletely and inconsistently. Potential limitations of such physiologic testing have already been discussed. An additional problem is that the results of standard pulmonary function tests generally reflect pathology in the entire respiratory system, that is, respiratory muscles, chest wall, airways, and parenchymal tissues. Investigators therefore turned to methods that more directly sampled the mechanical behavior of the lung parenchymal tissues, the major site of disease pathology.

As early as 1956, Marshall and DuBois[29] reported on measurements of viscous resistance of lung tissue in patients with pulmonary disease, using a novel approach[30] in which the

difference between total pulmonary resistance, measured with the esophageal balloon technique, and airway resistance, measured plethysmographically, was calculated. Lung compliance was also measured. The subjects included eight patients with sarcoidosis, six with pneumoconiosis, and five with other types of pulmonary infiltrations, of which three were considered to represent pulmonary fibrosis (not biopsy proven). The authors found a moderate increase in tissue viscous resistance and diminished lung compliance in patients with sarcoidosis and pulmonary fibrosis. Bachofen and Scherrer[31] measured total pulmonary resistance, airway resistance, and lung tissue resistance in 10 patients with diffuse interstitial pulmonary fibrosis. The lung tissue resistance, was found to be an average of four-fold higher in patients with lung fibrosis than in healthy persons of the same age. There was an inverse correlation between VC, or compliance, and the lung tissue resistance in patients with lung fibrosis, suggesting a coupling between the increase in tissue resistance and the decrease of compliance. After comparing tissue resistance relative to VC between patients and controls, the authors concluded that, in patients with lung fibrosis, the increase in lung tissue resistance could not be completely attributed to the loss of normally compliant lung tissue.

Gibson and Pride[32,33] studied the pulmonary mechanics in pulmonary fibrosis, with the aim of distinguishing the effect of lung "shrinkage" from abnormal distensibility of functioning alveoli. Others had noted the downward and rightward shift of the transpulmonary pressure–volume (*P–V*) curve in patients with pulmonary fibrosis, felt to reflect the extent of fibrosis, with stiffening of peripheral lung units.[8–10] By modeling *P–V* and maximal flow–*V* curves, the authors showed that if some lung units were replaced by nondistensible fibrous tissue, then conventional measurements of compliance would be decreased relative to lung volume, and values of transpulmonary pressure at a given percentage of predicted TLC would be higher than normal. Therefore, the measurement of lung compliance could not distinguish between reduction in the number of functioning alveoli (lung "shrinkage") and abnormal distensibility of the alveoli. In most patients, however, static compliance was low even when corrected for the decreased lung volume. In addition, reduced distensibility of functioning alveoli was likely if maximal expiratory flow was excessive in relation to lung volume as a percentage of VC.

In a similar manner, Sansores and colleagues[34] analyzed the relationship between the degree of lung fibrosis and the shape of the *P–V* curve. The *P–V* data above FRC were fitted to the exponential equation $V = A - Be^{-kP}$, where k is an exponential constant that describes the shape of the curve and is related to specific compliance.[35] They studied 33 patients with chronic interstitial lung disease, of whom 19 had pigeon breeder's disease and 14 had IPF (although the morphologic changes described may have represented DIP or NSIP). The degree of pulmonary fibrosis was assessed on lung biopsy using a semiquantitative grading scheme. When k was expressed as a percentage of that predicted for age, there was a modest but statistically significant correlation with the severity of lung fibrosis ($r = -.38$, $p < .05$). Nonuniformity of lung damage and variability in the assessment of pathology and lung function were some of the reasons invoked for this relatively poor correlation.

More recently, Verbeken and colleagues[36] examined, functionally and morphometrically, 13 human lungs with generalized fibrosis at autopsy and compared the data with those from normal lungs. After fixation, the mean internal chord of airspaces (L_{ma}), transection length of alveolar walls (L_{mw}), and internal diameter (d) and density of membranous bronchioles (n/cm^2) were determined. The fibrotic lungs were characterized structurally by an increase in L_{mw} and d. L_{mw} was correlated negatively with TLC and VC and was correlated positively with elastic recoil pressure (P_L), at 80 and 90% of TLC. The fibrotic lungs had a *P–V* curve that was shifted downward and to the right. However, when the volumes were expressed as a percentage of measured TLC, the differences in *P–V* curves between normal and fibrotic lungs disappeared. These data suggest that the shift of the *P–V* curve was the result of replacement of a number of lung units by nondistensible fibrous tissue ("shrinkage"), whereas the remaining units functioned relatively normally.[33]

Finally, Nava and Rubini[37] reported the first systematic measurements of resistance and elastance of the total respiratory system, lung, and chest wall during mechanical ventilation in patients with end-stage pulmonary fibrosis. Respiratory mechanics were monitored, after adequate sedation and paralysis, in seven patients being ventilated for acute respiratory failure. Both static and dynamic elastance of the respiratory system were significantly increased; this was due to abnormal lung elastance. The resistance of the respiratory system was also markedly increased compared with the values reported for normal subjects, with lung resistance accounting for most of the total resistance. All patients had biopsy-proven IPF, but no structural correlations were established. These abnormal mechanical properties were significantly correlated with the degree of hypercapnia.

The correlation of structure with function as assessed by various measurements of lung tissue mechanics, such as tissue resistance or shape of the *P–V* curve, appears to be somewhat better than that with standard pulmonary function tests or measures of gas exchange. One question raised is whether the downward and rightward shift of the *P–V* curve represents increased stiffness of the functioning alveoli or simply a decrease in alveolar volume: this is a somewhat theoretical consideration as both conditions probably contribute. It remains to be demonstrated whether tools that directly sample dynamic tissue mechanical properties, such as measurement of complex impedance,[38,39] would be more useful than standard physiologic testing in the evaluation and monitoring of patients throughout the course of their disease.

ANIMAL STUDIES

There are several advantages to using animal models to evaluate the relationship between structure and function in disease. First, the time of onset and cause of the disease are known, and tissue samples can be easily obtained at any time throughout the course of the illness. Inbred animals comprise a relatively homogeneous group, and control animals are readily available. However, there are many limitations to

this approach, including difficulties in establishing appropriate animal models and in performing adequate pulmonary function testing. Several different animal models have been used in the study of pulmonary fibrosis, including bleomycin-induced lung fibrosis (Figure 9-3) and radiation-induced fibrosis.[40–42] More recently, transgenic models in which various proteins involved in the pathogenesis of pulmonary fibrosis are up- or down-regulated have been used.[43,44] Most of the data in the literature comparing structure and function have been obtained with the bleomycin model of pulmonary fibrosis.

Initial reports describing bleomycin as an agent for the induction of pulmonary fibrosis in hamsters and baboons were published in the late 1970s.[41,42,45,46] Physiologic and morphologic changes were carefully characterized in a series of studies and included many of the same features evident in human IPF. The results of physiologic studies showed restrictive lung disease with reduced lung volumes and diffusing capacity and a rightward shift of the *P–V* curve. The results of morphologic studies showed fibrotic reactions and increases in the levels of specific extracellular matrix proteins, collagen and elastin. However, the authors were unable to document significant correlations between changes in the physiologic parameters and alterations in the levels of specific matrix proteins. They did, however, show significant correlations between various lung volumes and lung compliance and more general indices of lung disease.[41,45] In later studies in rabbits,[47] similar difficulties in demonstrating correlations between structure and function in bleomycin-induced disease were evident. Although changes in lung volume were significantly correlated with indices reflecting alveolar wall thickness and fibrosis neither diffusing capacity corrected for alveolar volume nor the exponent *k* derived from the *P–V* curve correlated with indices of structural changes.

Some of the problems in establishing correlations between structure and function in the bleomycin model may relate to disease heterogeneity. As discussed by Goldstein and colleagues,[45] diseased lung units may contribute minimally to the mechanical behavior of the system as only the more normal lung units participate in the physiologic measurements. Moreover, the cellular and fibrotic response can be very heterogeneously distributed throughout the lung because of the method of intratracheal bleomycin instillation. A further explanation is that mechanisms other than fibrosis per se may contribute to the abnormal physiology. Horiuchi and colleagues[48] have shown that the physical properties of surfactant are abnormal in rats treated with bleomycin, and this contributes to the increased elastic recoil observed in this model.

One potential approach to obviate these problems is to study structure–function correlations in a model system that more directly reflects the specific site of injury of the disease process. We recently published the results of studies in which we used lung parenchymal strips from rats previously given bleomycin.[49,50] Physiologic measurements are made in the organ bath and morphometric quantitation of collagen, elastin, and proteoglycans (PGs) in the parenchymal strips obtained. The contribution of the air–liquid interface to the physiologic measurements is excluded as the preparation is fluid-filled. Furthermore, the anatomic make-up of the tissue in which the physiologic changes are measured can be directly examined. Using this approach, we have shown significant correlations between changes in tissue resistance, elastance, and hysteresivity (an index of mechanical friction in the tissues) and the levels of collagen (Figure 9-4) and the small leucine-rich PG, biglycan. Faffe and colleagues[51] studied a murine model of silicosis, measuring physiologic parameters of parenchymal strips in the organ bath and collagen and elastic fiber content in the same tissues. They also demonstrated significant correlations between mechanical parameters and extracellular matrix molecules.

Difficulties remain, however, with the appropriateness of the animal models employed to date. As mentioned above, there are problems with the bleomycin-induced fibrosis model related to the distribution of agent, as well as the nature of the injury provoked. More recently, transgenic animal models have been introduced, which more closely reproduce the mechanistic insults of IPF. Transforming

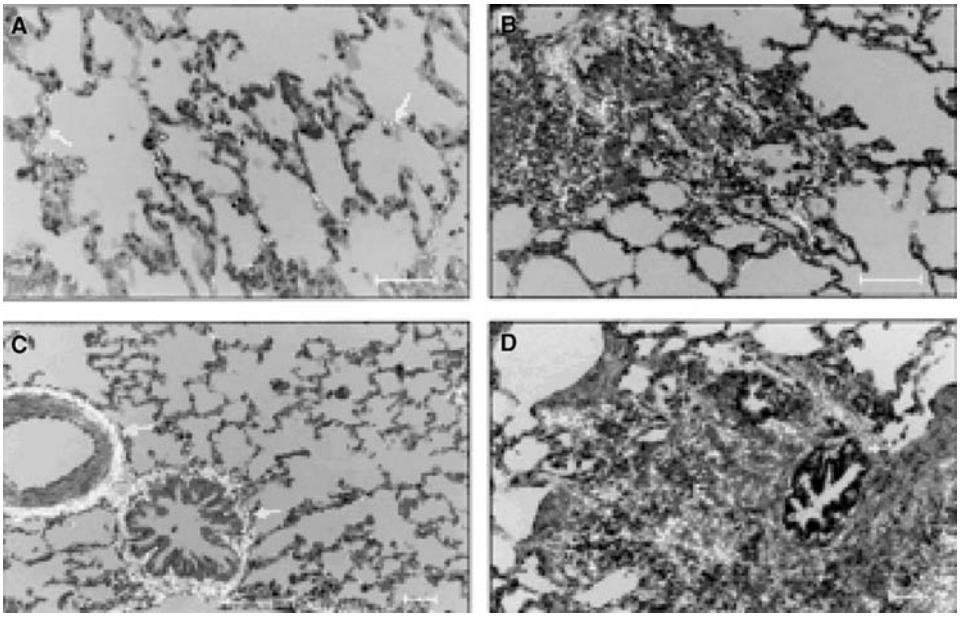

FIGURE 9-3 Photomicrograph of parenchymal strips from saline-exposed (*A*, *C*) and bleomycin-exposed (*B*, *D*) rats stained with Sirius red with polarization for collagen. Note peribronchiolar fibrosis in (*D*). Reproduced with permission from Dolhnikoff M et al.[49]

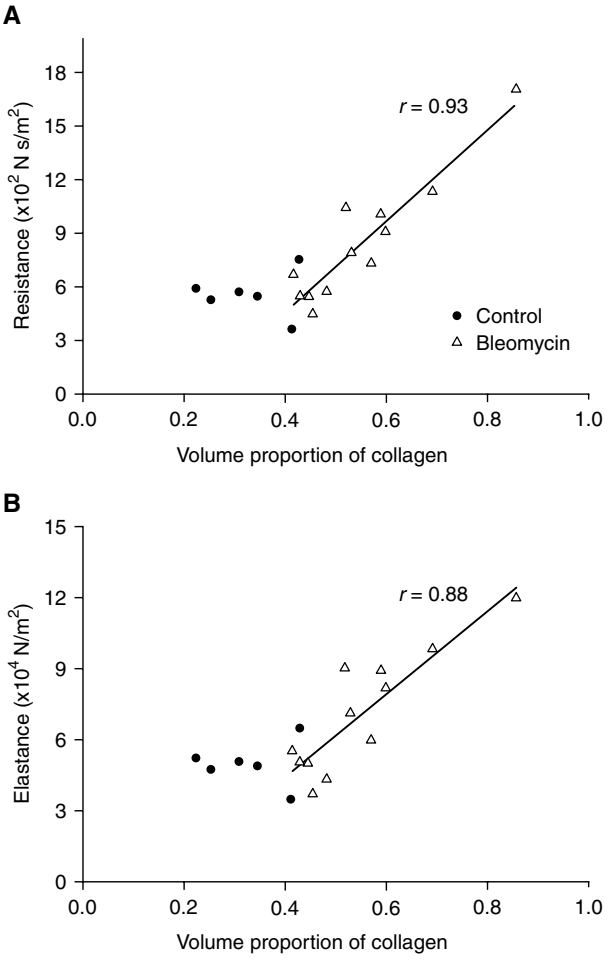

FIGURE 9-4 Correlation between volume proportion of collagen and (A) resistance and (*B*) elastance of isolated parenchymal strips from saline-exposed control and bleomycin-exposed rats. Linear regression for bleomycin data only is shown. Reproduced with permission from Dolhnikoff M et al.[49]

growth factor (TGF)-β is a critical cytokine involved in the pathogenesis of human IPF.[52,53] Animal models in which upregulation of TGF-β, as well as other cytokines, is used to provoke pulmonary fibrosis represent a significant advance in the study of IPF. Physiologic–morphologic studies need to be carried out in these model systems.

CONCLUSIONS

The study of structure–function correlations in IPF is hampered by several factors. First, the recognition of IPF as a specific type of idiopathic interstitial pneumonia with the histologic pattern of usual interstitial pneumonia is recent, and most of the clinical studies performed to date have included patients who do not meet these strict diagnostic criteria. Evolving hypotheses regarding the pathogenesis of IPF are reflected in the many studies in which attempts have been made to establish functional correlates of predominant fibrosis or cellularity in lung biopsy specimens. The lack of a standardized pathologic scoring system severely limits the comparability of the various studies; moreover, morphometric techniques, which are more quantitative, have been rarely applied. The effect of smoking has not been consistently taken into account. Studies in which tissue mechanics have been directly measured have yielded slightly better results. Although animal studies have thus far contributed little to the clarification of structure–function correlations in pulmonary fibrosis, the recent development of transgenic models and refocusing of attention on tissue mechanics offer some potential for advancement in this area.

There is a clear need for further studies of structure and function in pulmonary fibrosis, done in accordance with current histopathologic definitions and using physiologic methods that more specifically sample the site of disease. A method of partitioning airway and tissue mechanics by measuring complex impedance in human subjects has been recently developed and successfully applied in patients with asthma.[38,39] Similar studies in patients with pulmonary fibrosis might be helpful in establishing more accurate correlates of structure and function. Such studies would hopefully lead to the development of improved tools for establishing prognosis and monitoring the course of pathology in patients afflicted with this poorly characterized disease process.

REFERENCES

1. American Thoracic Society/European Respiratory Society. International multidisciplinary consensus classification of idiopathic interstitial pneumonias: general principles and recommendations. Am J Respir Crit Care Med 2002; 165:277–304.
2. King TE Jr, Costabel U, Cordier J-F. Idiopathic pulmonary fibrosis: diagnosis and treatment. Am J Respir Crit Care Med 2000;161:646–64.
3. Collard HR, King TE Jr. Demystifying idiopathic interstitial pneumonia. Arch Intern Med 2003;163:17–29.
4. Hamman L, Rich A. Acute diffuse interstitial fibrosis of the lung. Bull Johns Hopkins Hosp 1944;74:177–212.
5. Carrington CB, Gaensler EA, Coutu RE, et al. Natural history and treated course of usual and desquamative interstitial pneumonia. N Engl J Med 1978;298:801–9.
6. Turner-Warwick M, Burrows B, Johnson A. Cryptogenic fibrosing alveolitis: clinical features and their influence on survival. Thorax 1980;35:171–80.
7. Turner-Warwick M, Burrows B, Johnson A. Cryptogenic fibrosing alveolitis: response to corticosteroid treatment and its effect on survival. Thorax 1980;35:593–9.
8. Crystal RG, Fulmer JD, Roberts WC, et al. Idiopathic pulmonary fibrosis. Clinical, histologic, radiographic, physiologic, scintigraphic, cytologic, and biochemical aspects. Ann Intern Med 1976;85:769–88.
9. Fulmer JD, Roberts WC, von Gal ER, Crystal RG. Morphologic–physiologic correlates of the severity of fibrosis and degree of cellularity in idiopathic pulmonary fibrosis. J Clin Invest 1979;63:665–76.
10. Keogh BA, Crystal RG. Clinical significance of pulmonary function tests. Pulmonary function testing in interstitial pulmonary disease. What does it tell us? Chest 1980;78:856–65.
11. Bjoraker JA, Ryu JH, Edwin MK, et al. Prognostic significance of histopathologic subsets in idiopathic pulmonary fibrosis. Am J Respir Crit Care Med 1998;157:199–203.
12. King TE Jr, Schwarz MI, Colby TV, et al. Idiopathic pulmonary fibrosis: relationship between histopathologic features and mortality. Am J Respir Crit Care Med 2001;164:1025–32.
13. Gaensler EA, Carrington CB. Radiographic–physiologic–pathologic correlations in interstitial pneumonias. Prog Respir Res 1975;8:223–41.

14. Gaensler EA, Carrington CB. Open biopsy for chronic diffuse infiltrative lung disease: clinical, roentgenographic, and physiological correlations in 502 patients. Ann Thorac Surg 1980;30:411–26.
15. Green GM, Graham WG, Hanson JS, et al. Correlated studies of interstitial pulmonary disease. Chest 1976;69:S263.
16. Chinet T, Jaubert F, Dusser D, et al. Effects of inflammation and fibrosis on pulmonary function in diffuse lung fibrosis. Thorax 1990;45:675–8.
17. Cherniack RM, Colby TV, Flint A, et al. Correlation of structure and function in idiopathic pulmonary fibrosis. Am J Respir Crit Care Med 1995;151:1180–8.
18. Cherniack RM, Colby TV, Flint A, et al. Quantitative assessment of lung pathology in idiopathic pulmonary fibrosis. The BAL Cooperative Group Steering Committee. Am Rev Respir Dis 1991;144:892–900.
19. Rudd RM, Haslam PL, Turner-Warwick M. Cryptogenic fibrosing alveolitis. Relationships of pulmonary physiology and bronchoalveolar lavage to response to treatment and prognosis. Am Rev Respir Dis 1981;124:1–8.
20. Schwartz DA, Merchant RK, Helmers RA, et al. The influence of cigarette smoking on lung function in patients with idiopathic pulmonary fibrosis. Am Rev Respir Dis 1991;144: 504–6.
21. Hanley ME, King TE Jr, Schwarz MI, et al. The impact of smoking on mechanical properties of the lungs in idiopathic pulmonary fibrosis and sarcoidosis. Am Rev Respir Dis 1991;144:1102–6.
22. Ostrow D, Cherniack RM. Resistance to airflow in patients with diffuse interstitial lung disease. Am Rev Respir Dis 1973;108:205–10.
23. Mead J, Turner JM, Macklem PT, Little JB. Significance of the relationship between lung recoil and maximum expiratory flow. J Appl Physiol 1967;22:95–108.
24. Fulmer JD, Roberts WC, von Gal ER, Grystal RG. Small airways in idiopathic pulmonary fibrosis. Comparison of morphologic and physiologic observations. J Clin Invest 1977;60: 595–610.
25. DuBois AB, Botelho SY, Comroe JH Jr. A new method for measuring airway resistance in man using a body plethysmograph: values in normal subjects and in patients with respiratory disease. J Clin Invest 1956;35:327–35.
26. Austrain R, McClement JH, Renzetti AD Jr, et al. Clinical and physiologic features of some types of pulmonary diseases with impairment of alveolar–capillary diffusion; the syndrome of "alveolar–capillary block." Am J Med 1951;11: 667–85.
27. Finley TN, Swenson EW, Comroe JH Jr. The cause of arterial hypoxemia at rest in patients with "alveolarcapillary block syndrome." J Clin Invest 1962;41:618–22.
28. Wagner PD, Dantzker DR, Dueck R, et al. Distribution of ventilation–perfusion ratios in patients with interstitial lung disease. Chest 1976;69:256–7.
29. Marshall R, DuBois AB. The measurement of the viscous resistance of the lung tissues in normal man. Clin Sci (Lond) 1956;15:161–70.
30. DuBois AB, Marshall R. The viscous resistance of lung tissue in patients with pulmonary disease. Clin Sci (Lond) 1956; 15:473–83.
31. Bachofen H, Scherrer M. Lung tissue resistance in diffuse interstitial pulmonary fibrosis. J Clin Invest 1967;46:133–40.
32. Gibson GJ, Pride NB. A reappraisal of lung mechanics in fibrosing alveolitis. Chest 1976;69:S256.
33. Gibson GJ, Pride NB. Pulmonary mechanics in fibrosing alveolitis: the effects of lung shrinkage. Am Rev Respir Dis 1977;116:637–47.
34. Sansores RH, Ramirez-Venegas A, Perez-Padilla R, et al. Correlation between pulmonary fibrosis and the lung pressure–volume curve. Lung 1996;174:315–23.
35. Colebatch HJ, Ng CK, Nikov N. Use of an exponential function for elastic recoil. J Appl Physiol 1979;46:387–93.
36. Verbeken EK, Cauberghs M, Lauweryns JM, van de Woestijne KP. Structure and function in fibrosing alveolitis. J Appl Physiol 1994;76:731–42.
37. Nava S, Rubini F. Lung and chest wall mechanics in ventilated patients with end stage idiopathic pulmonary fibrosis. Thorax 1999;54:390–5.
38. Kaczka DW, Ingenito EP, Suki B, Lutchen KR. Partitioning airway and lung tissue resistances in humans: effects of bronchoconstriction. J Appl Physiol 1997;82:1531–41.
39. Kaczka DW, Ingenito EP, Israel E, Lutchen KR. Airway and lung tissue mechanics in asthma. Effects of albuterol. Am J Respir Crit Care Med 1999;159:169–78.
40. Fine A, Goldstein RH. Animal models of pulmonary fibrosis. In: Crystal RG, West JB, Weibel ER, Barnes PJ, editors. The lung. Philadelphia: Scientific Foundations; 1997. p. 2525–35.
41. Snider GL, Celli BR, Goldstein RH, et al. Chronic interstitial pulmonary fibrosis produced in hamsters by endotracheal bleomycin. Lung volumes, volume–pressure relations, carbon monoxide uptake, and arterial blood gas studied. Am Rev Respir Dis 1978;117:289–97.
42. Snider GL, Hayes JA, Korthy AL. Chronic interstitial pulmonary fibrosis produced in hamsters by endotracheal bleomycin: pathology and stereology. Am Rev Respir Dis 1978;117: 1099–108.
43. Lee CG, Homer RJ, Zhu Z, et al. Interleukin-13 induces tissue fibrosis by selectively stimulating and activating transforming growth factor beta(1). J Exp Med 2001;194: 809–21.
44. Kolb M, Margetts PJ, Sime PJ, Gauldie J. Proteoglycans decorin and biglycan differentially modulate TGF-beta-mediated fibrotic responses in the lung. Am J Physiol Lung Cell Mol Physiol 2001;280:L1327–34.
45. Goldstein RH, Lucey EC, Franzblau C, and Snider GL. Failure of mechanical properties to parallel changes in lung connective tissue composition in bleomycin-induced pulmonary fibrosis in hamsters. Am Rev Respir Dis 1979; 120:67–73.
46. McCullough B, Collins JF, Johanson WG Jr, Grover FL. Bleomycin-induced diffuse interstitial pulmonary fibrosis in baboons. J Clin Invest 1978;61:79–88.
47. Berend N, Feldsien D, Cederbaums D, Cherniack RM. Structure–function correlation of early stages of lung injury induced by intratracheal bleomycin in the rabbit. Am Rev Respir Dis 1985;132:582–9.
48. Horiuchi T, Ikegami M, Cherniack RM, Mason RJ. Increased surface tension of the lung and surfactant in bleomycin-induced pulmonary fibrosis in rats. Am J Respir Crit Care Med 1996;154:1002–5.
49. Dolhnikoff M, Mauad T, Ludwig MS. Extracellular matrix and oscillatory mechanics of rat lung parenchyma in bleomycin-induced fibrosis. Am J Respir Crit Care Med 1999;160(Pt 1): 1750–7.
50. Ebihara T, Venkatesan N, Tanaka R, Ludwig MS. Changes in extracellular matrix and tissue viscoelasticity in bleomycin-induced lung fibrosis. Temporal aspects. Am J Respir Crit Care Med 2000;162:1569–76.
51. Faffe DS, Silva GH, Kurtz PM, et al. Lung tissue mechanics and extracellular matrix composition in a murine model of silicosis. J Appl Physiol 2001;90:1400–6.
52. Khalil N, Bereznay O, Sporn M, Greenberg AH. Macrophage production of transforming growth factor beta and fibroblast collagen synthesis in chronic pulmonary inflammation. J Exp Med 1989;170:727–37.
53. Khalil N, O'Connor RN, Unruh HW, et al. Increased production and immunohistochemical localization of transforming growth factor-beta in idiopathic pulmonary fibrosis. Am J Respir Cell Mol Biol 1991;5:155–62.

CHAPTER 10

STRUCTURE–FUNCTION RELATIONSHIPS IN CHRONIC OBSTRUCTIVE PULMONARY DISEASE

Manuel G. Cosio, Marina Saetta, Heberto Ghezzo, Simonetta Baraldo

Since flow is the result of a driving pressure (elastic recoil of the lung parenchyma) and of an opposing resistance that constrains flow (obstruction of the airways), a reduction in flow can be due either to a reduced driving pressure or to an increased resistance. In smokers, when pathologic changes involve the small airways they will contribute to airflow limitation by narrowing and obliterating the lumen and therefore increasing the resistance. Active constriction of the airways further compounds the problem. Conversely, when pathologic changes are localized in the lung parenchyma, they will contribute to airflow limitation by reducing the elastic recoil of the lung through parenchymal destruction, as well as by reducing the elastic load applied to the airways through destruction of alveolar attachments, therefore reducing the airway lumen further. Because small airway abnormalities and emphysema coexist in the lungs of smokers, their complex interaction will govern the pathophysiology of chronic obstructive pulmonary disease (COPD).

The present chapter focuses on the relationship between structural abnormalities in small airways and lung parenchyma and pulmonary function in COPD in an attempt to highlight the possible mechanisms contributing to airflow limitation in this disease. Special attention will be paid to the inflammatory component in the lungs of smokers, possibly the key component in the causation of disease. We will see how studies correlating morphology, including inflammation and function, have gone a long way toward improving our understanding of the possible mechanisms by which cigarette smoking might produce COPD.

EVOLUTION OF THE UNDERSTANDING OF COPD

COPD is a very old disease, perhaps one of the oldest lung diseases ever suffered. In 1972, a mummy of an old woman, who had lived in Alaska 1,600 years ago, was discovered. Her lungs showed abundant anthracotic deposits along with areas of centrilobular emphysema (CLE).[1] This is probably the oldest known case of COPD, most likely produced by biomass (open fires) exposure. COPD secondary to exposure to open wood fires while cooking is still an important cause of COPD in many countries[2] and probably has been a cause of COPD ever since fire was introduced for cooking. Most likely, the Alaskan woman coughed, produced sputum, and was dyspneic during exercise. Probably many women were! Similar findings were reported in Egyptian mummies.[1] However, it took many centuries for physicians to understand COPD, and this introduction explains briefly how concepts evolved.

The word "emphysema" is derived from the Greek "to blow into" and therefore is used to mean "air containing" or "inflated." Although the first mention of emphysema dates back to the early seventeenth century, with Bonet (1617) describing a case with "voluminous lungs," progress in our understanding of lung disease due to chronic airflow obstruction has been sporadic and painfully slow.[3] The first description of enlarged airspaces in emphysema in humans, together with illustrations, was provided by Ruysh in 1721.[4] Watson,[5] in 1764, gave a complete anatomic description of a case of emphysema: "The lungs were enormously distended with air . . . this air was extravasate and had burst through the extremities of the bronchi and vesicular substance . . . In a word, the lung was truly emphysematous. In several parts this had formed large bladders . . . The air getting loose in the substance of the lungs cannot be parted with expiration; it subsequently is retained there and the space it occupies prevents as much of the external air being received into the lungs as its own quantity." Morgagni, in his "De sedibus et causis morborum per anatomen indagatis" (1769), described several cases in which the lungs were

turgid, particularly from air.[6] Baillie in 1799[7] and 1807[8] provided a very clear description of emphysema. In his textbook, he states that emphysematous lungs did not collapse at postmortem and filled the pleural cavities and that the alveoli ("cells") were full of air.

The contribution of Laennec in 1826[9] is a crucial one. He recognized that fixation by inflation was essential for the proper examination of the lungs for the presence of disease. He was the first to distinguish between interstitial emphysema and enlarged air sacs, or "emphysema proper." He appreciated that airspaces enlarge with increasing age, and he distinguished these physiologic changes from emphysema. More importantly, he related the structural abnormalities to the clinical syndrome as he recognized that cough, mucus production, airflow obstruction, and shortness of breath on effort were the clinical correlates, in life, of the finding of emphysema at autopsy. He recognized that air trapping and increased collateral ventilation were features of emphysematous lungs and that the peripheral airways were the primary site of obstruction in emphysema. He also speculated that loss of elastic recoil was a factor in diminished flow from the lungs. Interestingly, he recognized that emphysema was associated with chronic bronchitis, which he considered to be the chief causative factor. The relationship between chronic bronchitis and emphysema was also discussed by Louis in 1838,[10] Hasse in 1846,[11] and Waters[12] in 1862. Within a few years, arguments began as to whether the symptoms were always caused by emphysema or whether disease of the conducting airways without emphysema could also cause this syndrome. This is a question that we are still concerned with.

During those same years, the first microscopic descriptions of emphysema appeared, based on plastic casts or on thick sections, which underlined the changes in collagen and elastic fibers. Microscopic examination of the lungs underscored the presence of three consistent findings in emphysematous lungs: the presence of fenestrae in the alveolar walls, the reduction of the capillary bed, and alterations in pulmonary elastic fibers. According to Laennec's theory, hyperinflation of the alveoli appeared to be the first event, and further discussion centered on the mechanisms by which the destruction of the alveolar walls occurred. The predominant opinion was that chronic or repeated hyperinflation led to enlargement of the preexisting interalveolar pores of Kohn or formation of tears in the alveolar wall. Alternative hypotheses favored the role of structural or functional abnormalities of elastic fibers or of compression of the capillaries with resultant ischemic atrophy of the alveolar walls.

Our present knowledge of the pathologic anatomy of pulmonary emphysema dates almost entirely from the middle of the twentieth century, when Gough and Wentworth[13] introduced the use of whole lung sections fixed in inflation and mounted on paper. With this technique, they found "two fundamentally different" types of emphysema, now usually called centrilobular or centriacinar emphysema (CLE) and panlobular or panacinar (PLE) emphysema. Gough's report was based on a study of 140 emphysematous lungs, of which 75 showed CLE.[14] All lungs with CLE had chronic bronchiolitis, and inflammatory changes extended distally to the level where emphysematous expansion occurred. Narrowing of the bronchioles was present in 60% of lesions, whereas dilated or normal airways led to the emphysematous spaces in the remaining 40%. There was no recognizable respiratory bronchiolitis in generalized emphysema (PLE), a finding in marked contrast to that in CLE.

Strikingly absent in all work published prior to 1952 is any illustration of, or reference to, what now might be interpreted as CLE. In view of the excellence of some of the illustrations and the use of inflated lungs by the earlier workers, it seems valid to wonder whether CLE has rapidly increased in frequency in the twentieth century in the same way that bronchogenic cancer has.

The history of chronic bronchitis is far less known than that of emphysema, probably because the term "bronchitis" was used in many different senses. In 1717, Sydenham gave the first description of what could be regarded as chronic bronchitis.[15] Laennec recognized chronic bronchitis, using the term "chronic mucous catarrh," emphasized hypersecretion, and also observed that it could end fatally ("suffocative catarrh"). The term "chronic bronchitis" was introduced by Stokes,[16] who recognized its association with emphysema and also distinguished between mucoid and mucopurulent sputum. Florey and colleagues in 1932[17] described both the increased size of bronchial mucous glands and goblet cell metaplasia as essential features of chronic bronchitis. Reid in 1954[18] provided a comprehensive description of the morphologic alterations of the lungs and airways of patients with chronic bronchitis, with a particular focus on abnormalities of mucous glands, which for many years have been considered a histologic hallmark for the recognition of bronchitis.

The link between cigarette smoking and lung disease took longer to be recognized. Not until the late 1800s did Mendelssohn[19] report that smoking had a deleterious effect on the respiratory system. These early studies were hampered by the lack of sensitive physiologic tests of lung function and relied heavily on differences between smokers and nonsmokers in the prevalence of respiratory symptoms.

Measurements of lung capacity were available after Hutchinson invented the spirometer in 1846. Hutchinson[20] reported a population study in more than 2,000 people of the different subdivisions of vital capacity. Interestingly, Hutchinson believed at the outset that his technique was useful only for the early diagnosis of pulmonary tuberculosis. This indication was taken seriously in many countries, and by 1930 it was still recommended in many European countries to perform spirometry in schools and military compounds for the early detection of tuberculosis.[1]

Not until the 1920s did clinicians become interested in measurements of the disturbance in function that occurs in disease, and the techniques of physiologic measurement moved from laboratory animals to human subjects. Simple spirometers such as Pescher's bottle were commonly used because of simplicity and low cost. The volume of water displaced from the bottle after a forced expiration was a good indication of the vital capacity. With use of these devices, it was then learned that the mean expiratory

volume was decreased in emphysema, pleurisy, fibrothorax, and tuberculosis.[1]

The classic study by Christie in 1933 showed the relationship between lung volume and pressure in normal subjects and that there was loss of lung elasticity in patients with clinical emphysema, a cause of airflow limitation in COPD, as we now know.[21] Shortly afterwards, Cournand and colleagues advanced the notion that emphysema was obstructive.[22] They noted the expiratory slowing that occurred in their patients, as well as the air trapping that occurred as breathing frequency increased. Measurements of the vital capacity ensued, and after years of testing and discussion, the volume fraction of the vital capacity expired in 1 second (the FEV_1) was established, thus forming the basis for the most important present-day physiologic test in the assessment of airflow obstruction. Dayman's[23] classic analysis of expiration indicated that bronchi, bronchioles, or emphysema could obstruct flow.

As clinical pulmonary physiology assumed greater importance and became the dominant science in pulmonary medicine, the previous knowledge of the simple morphology of emphysema was found inadequate, and the usual pathologic methods of examining the lung were deemed unsatisfactory. A better way to visualize and quantitate the disease was needed in order to keep pace with the advances in the understanding of the physiology of the disease. As mentioned above, Gough and Wentworth[13] provided the needed improvement for the study of the disease by developing a technique by which examination of sections of entire inflated lungs became possible and simple. In doing so, Gough[14] laid the foundation of modern knowledge of the pathologic anatomy of pulmonary emphysema. Study of the correlations between the new knowledge of physiologic derangements and the morphology of the disease could now begin.

MORPHOLOGY–FUNCTION CORRELATIONS IN EMPHYSEMA: THE FIRST ATTEMPTS

In the earlier studies correlating morphology and function (1960 to the 1970s), macroscopic diagnosis was used to determine the extent of emphysema, usually in whole lungs obtained at autopsy. Thurlbeck[24] discussed at length the problems associated with the macroscopic diagnosis of emphysema, a subjective method "which may be affected by the opinions and emotions of the observer" and is not improved by the use of point counting. It should also be noted that the standardization of pulmonary function testing had not been achieved in those years. Lung volumes were measured mainly with gas dilution techniques, which may account for some of the differences found among these early studies. However, much work by many authors correlating the morphology and the associated function in emphysema was published between 1960 and the mid-1970s, establishing an overall association between the extent of disease and different functional parameters. The first reported work used maximum voluntary ventilation, a function of the FEV_1, as the physiologic measurement, and it was significantly correlated with the extent of macroscopic emphysema[25] in 31 patients. Two other series found a close relationship, -0.76[26] and -0.74,[27] between the FEV_1% predicted and extent of emphysema, whereas two authors failed to show any significant difference between flows and extent of emphysema.[28,29] Not surprisingly, the best relationships were shown in series that contained high proportions of patients with little airflow obstruction and a wide spectrum of severity of emphysema in their lungs.[26,27,30,31] Correlation coefficients of greater than -0.7 were found in only 3 of the 11 series reviewed here, so it could be concluded that whereas emphysema has an important relationship with expiratory flow rates, this relationship is not precise enough to indicate the amount of emphysema. Subdivisions of lung volumes were no better at predicting the severity of emphysema,[25,26,28–30,32,33] and only the correlation between residual volume (RV)/total lung capacity (TLC) and emphysema was found to be reasonably good by most, but not all, authors.[26,29,33]

The test that all authors have found to be related to the extent of emphysema is the diffusing capacity for carbon monoxide. In the nine series reviewed, correlation coefficients ranged between -0.60 and -0.88. Thus, diffusion capacity remains the test of pulmonary function most closely related to the extent and severity of emphysema. However, as reviewed above, no one test or combination of tests predicts accurately the amount of emphysema in the lungs of living subjects.[34]

We can suitably end this review of the early attempts at correlating lung disease with function in smokers by citing a revealing passage in Thurlbeck[24] heralding things to come. He comments on the remarkable drop in flows found in some patients with trivial emphysema: "We originally attributed this drop to chronic bronchitis, since it seemed unlikely to us that these amounts of emphysema would lower flow rates to this extent. However, the flow rates of other patients with trivial emphysema who had no bronchitis were just as impaired as were those in the patients in the same group who had bronchitis. It thus seems that mild or moderate emphysema may be associated with marked decrease in flow rates."

Not until a few years later, when the concept of small airways dysfunction was re-introduced (Gough had already described the bronchiolitis that accompanied CLE), did an explanation for Thurlbeck's comments start to become apparent.

STRUCTURE–FUNCTION RELATIONSHIP IN NORMAL AIRWAYS: STATIC MEASUREMENTS FOR A DYNAMIC FUNCTION

The small airways of the lung or membranous bronchioles are key in the pathophysiology of COPD. Total airway resistance represents the contribution of the resistance of the various levels of the airway from the larynx and large cartilaginous airways down to respiratory bronchioles. The site of major airway resistance has been studied in dogs[35] and in human lungs[36] with the use of a retrograde catheter technique to partition the contribution of the large cartilaginous and the small airways less than 2 mm in diameter.

These studies revealed that peripheral airway resistance was only a small proportion of the resistance of the entire tracheobronchial tree. In addition, as lung volume changed, total resistance increased near TLC.[37] The low resistance in the small airways was related to their large overall cross-sectional area in the lung periphery. However, other authors, using different techniques to partition central and peripheral resistance, have questioned the original findings[36] and have shown significantly higher peripheral resistance in normal lungs.[37,38]

According to the Poiseuille equation, airway resistance depends upon the number, length, and cross-sectional area of the conducting airways. The number of airways in the normal lung is determined by the pattern of branching, which is established by the sixteenth week of fetal life. The airway length varies considerably from person to person, depending upon age and body size; airway length also varies within an individual, depending upon the phase of ventilation, increasing during inspiration as lung volume increases and decreasing during expiration. Because resistance to airflow in a given airway changes according to the fourth power of the radius of the airway, the cross-sectional area within the tracheobronchial tree is by far the dominant determinant of airway resistance. The cross-sectional area of any given airway is determined by the balance between two opposing forces: those forces tending to distend the walls and those tending to contract the walls, primarily the tension exerted by airway smooth muscle and elastic elements. Airways change in length and diameter during breathing, and in general both dimensions change in proportion to the lung volume. This outward force is provided from the attached lung parenchyma in the case of terminal bronchioles or from the indirect effects of pleural pressure in the case of intrapulmonary conducting airways. Changes in lung volume above functional residual capacity (FRC) have little effect on airway resistance, but between FRC and RV airway resistance increases rapidly and approaches infinity at RV as airway closure occurs. Although it is useful to relate measurements of airway resistance to those of lung volume, the determinant of the relationship between lung volume and airway resistance is the elastic recoil at the given lung volume.[39]

Changes in the geometry of normal bronchi depend not only on the transmural pressure across their walls but also on the distensibility of the elements composing the walls. These constitutive properties of the airway are reflected in the diameter–pressure relationships of the airways. The results of studies fall into two general categories: one in which most of the changes occur at relatively low distending pressures (6 to 10 cm H_2O)[40] and one in which both length and diameter change continuously over the full range of pressures.[41] These discrepant results can be explained by differences in bronchial smooth muscle tone at the time when the experiments were conducted.[42] When bronchomotor tone is absent, the airways become relatively floppy and distend almost fully at low pressures. In contrast, when tone is present, the airways distend more slowly and continuously during inflation.

Airway caliber and, therefore, resistance is also influenced by complex neurohumoral control. Both intra- and extrathoracic airways respond to changes in lung volumes, as described above, but a portion of the lung volume effect is reflexively mediated and is attenuated by prior administration of atropine.[43] In addition, there are active stimuli for both bronchodilatation and bronchoconstriction. Airway caliber is under reflex control through afferent lung receptors and efferent autonomic cholinergic, adrenergic, and "purinergic" nerves. Local changes in gas tension, either hypoxia[44] or hypercapnia,[45] can narrow airways. The resultant decrease in ventilation to areas of low oxygen partial pressure (PO_2) or carbon dioxide partial pressure (PCO_2) represents a compensatory mechanism that serves to promote a match between ventilation and perfusion; as such, it is analogous to, although less important than, hypoxic vasoconstriction.

It is obvious from the above that, no matter how accurate the morphometry and other experimental pathology methods used, the results obtained by analyzing "static" microscopic sections will provide only part of the picture. However, a good morphometric analysis of the possible abnormalities might help reveal the abnormal dynamic behavior of the airways.

MORPHOLOGY–FUNCTION CORRELATION OF THE SMALL AIRWAYS IN SMOKERS

The so-called "small airways" comprise both the membranous bronchioles (less than 2 mm in diameter) and the respiratory bronchioles. When they involve inflammatory processes, the changes are termed "bronchiolitis" and "respiratory bronchiolitis" respectively. The terms "small airways" and "membranous bronchioles," and "small airway disease" and "bronchiolitis," are used interchangeably in this chapter.

As mentioned above, contrary to previous beliefs, Macklem and Mead,[35] by using the novel technique of the retrograde catheter, demonstrated that airways less than 2 mm in diameter (small airways) contributed no more than one-quarter of the total airway resistance in dog lungs. Hogg and colleagues,[36] applying the same technique to human lungs, found that in excised normal lungs only 25% of the total airways resistance was contributed by airways less than 2 to 3 mm in diameter. However, in smokers with mild emphysema, there was a fourfold increase in peripheral airway resistance, whereas total airway resistance remained largely unchanged. More severe degrees of emphysema resulted in a marked increase in total airway resistance due almost entirely to the increase in the peripheral airway component. This work established the then new, and still prevailing, concept that peripheral airways are the major site of increased resistance and disease in smoke-induced obstructive lung disease and that significant increases in the resistance of these airways can be present without measurable changes in the total airway resistance of the lung—hence the term coined by Mead[46] to describe the small airways, "the silent zone of the lung."

Niewoehner and colleagues[47] were the first to demonstrate that definite pathologic abnormalities could already be present in the peripheral airways of young smokers. Membranous bronchioles had denuded epithelium and

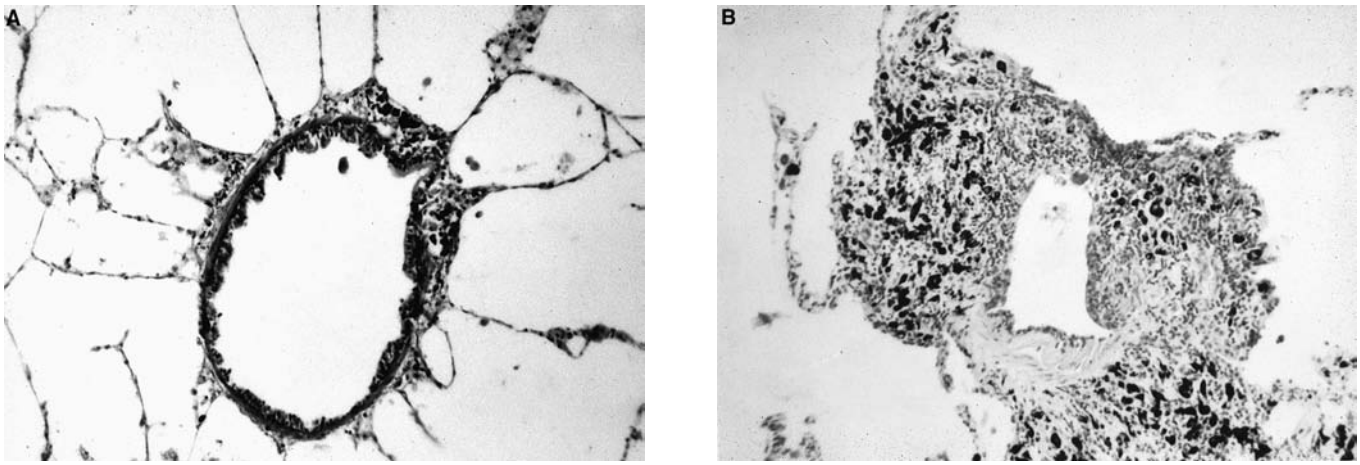

FIGURE 10-1 *A,* Normal small airway. *B*, Abnormal small airway in a smoker (surgical specimen) showing epithelial and wall inflammatory changes. ×100 original magnification.

increased numbers of intramural inflammatory cells. This study demonstrated a definite association between cigarette smoking and pathologic changes in the peripheral airways, and it was hypothesized that these lesions are responsible for the subtle physiologic abnormalities observed in young smokers and may be the precursor of more severe anatomic lesions.

The observations of the early structural changes and site of airflow limitation in smokers in the small airways created enthusiasm for tests of small airway function. The results of such tests, it was hoped, would become abnormal before flow limitation indicated by a decrease in FEV_1 was obvious, and this could identify the smokers most likely to progress to chronic airflow limitation. This was based, in turn, on the hypothesis that structural changes in the small airways preceded the development of COPD. If small airway disease preceded the development of emphysema and COPD, it was not unreasonable to hope that tests of small airway function could be used to identify the susceptible smoker who would develop clinically significant COPD. In order to test this important hypothesis, it was first necessary to demonstrate that the tests of small airway function indeed reflected pathologic abnormalities in the small airways, before performing population studies.

By studying smokers who had tests of pulmonary function, including those sensitive to small airways dysfunction, before undergoing resection for lung tumors, investigators at the Meakins-Christie Laboratories at McGill University[48] developed a pathologic score to describe the microscopic changes in the small airways and to relate them to lung function. Specifically, they scored luminal occlusion, goblet cell metaplasia, squamous cell metaplasia, mucosal ulcers, muscle hypertrophy, inflammatory cell infiltrate, and fibrosis of and pigment deposition in the walls of airways less than 2 mm in diameter. This study showed that these patients had similar but much more extensive abnormalities in the small airways than those described by Niewoehner and colleagues.[47] The abnormalities that could be seen in the older smokers from the McGill study were changes in the epithelium with squamous metaplasia and a chronic inflammatory infiltrate and slight increases in the amount of connective tissue in the walls of the small airways (Figure 10-1). As the pathologic and functional abnormalities progressed, the cellular inflammatory infiltrate changed little, but there was a progressive increase in the amount of connective tissue pigment and muscle in the airway wall. Significant goblet cell metaplasia could be seen in the most severely affected airways (Figure 10-2).

Comparison of the physiologic measurements reflecting small airway abnormalities, such as the nitrogen washout test, volume of isoflow (V_{isoV}) (the volume at which maximum expiratory flows during helium–oxygen breathing and air breathing and ΔV_{max50} become equal), and the results of other function tests, such as the percentage of forced vital capacity in 1 second (FEV_1/FVC), midflow rate, and RV, with the pathologic score showed a progressive deterioration as the score for the morphologic abnormalities increased (Figure 10-3). The striking correlation between the progression of physiologic impairment and the degree of small airway disease suggested that inflammatory changes of the small airways made an important contribution to the functional deterioration seen in COPD, even in the presence

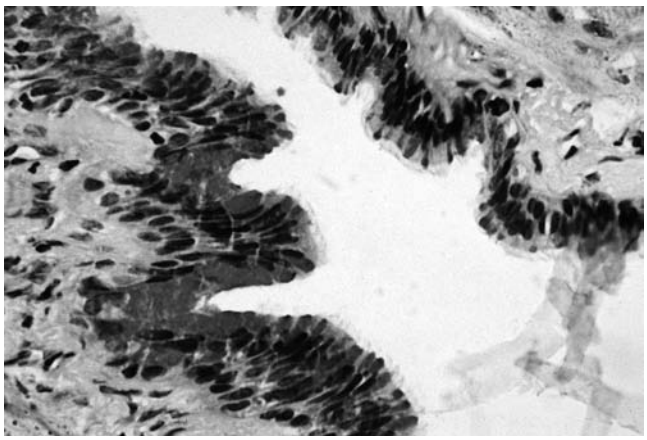

FIGURE 10-2 Goblet cell metaplasia in a small airway of a smoker (surgical specimen). HPS-PAS stain ×250 original magnification.

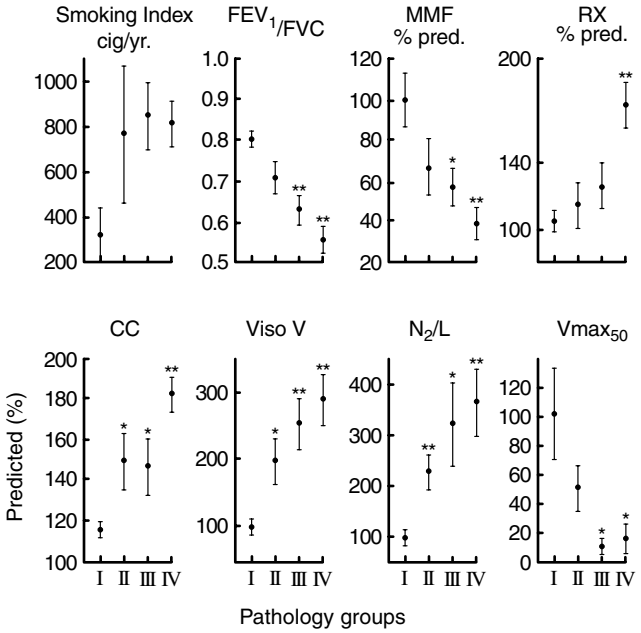

FIGURE 10-3 Correlation of the "small airways" pulmonary functions with the pathologic severity of the small airways (airways score). Cases have been placed into four groups of increasing severity score from I to IV. Reproduced with permission from Hoppin FG et al.[48]

of emphysema. Furthermore, in subjects with normal FEV_1/FVC ratios, two tests of small airway function, the slope of phase III of the nitrogen washout and the volume of isoflow of the air–helium flow–volume curves, were able to detect mild abnormalities of the small airways at a time when the results of other spirometric tests were normal.[48]

Other investigators later confirmed the above findings using lungs obtained either during surgery or at autopsy. Berend and colleagues[49] showed that results of the tests of small airway function correlated best with the total pathologic score of the small airways and, in particular, with the inflammatory score. They also found that the closing volume and the mid–maximum expiratory flow correlated significantly with a measure of airway luminal size.[50] Determining maximal expiratory flow–volume curves in excised human lungs, Berend and colleagues,[51] in another study, showed that flow at the trachea correlated significantly with the total pathologic score of the small airways, as well as with the inflammation, fibrosis, and emphysema scores. Petty and colleagues[52] performed lung function tests on lungs obtained at autopsy and observed that lungs with an abnormal closing capacity had higher total pathologic, inflammation, and fibrosis scores. Wright and colleagues[53] also examined the morphologic basis of small airway obstruction in COPD and attempted to determine the usefulness of tests of lung function in identifying early airway disease. In particular, they divided their group of 96 patients into those with a normal FEV_1 and those with an FEV_1 below 80% predicted. When the FEV_1 was normal, the results of several abnormal tests of small airway function were associated with increasing fibrosis scores in membranous bronchioles and with worsening intraluminal and mural inflammatory scores of respiratory bronchioles (respiratory bronchiolitis).

These studies demonstrated that smokers develop abnormalities of the small airways early in life, that these abnormalities are reflected in vivo by tests sensitive to small airway disease, and that the pathologic abnormalities increase as lung function deteriorates further. The scene was then set to investigate whether abnormalities in the results of tests of small airways early in the lives of smokers could predict those who would eventually develop COPD. Buist and colleagues[54] reported a 9- to 10-year follow-up of two groups of smokers in whom spirometry and the single-breath nitrogen test were used throughout the follow-up period to determine the usefulness of the single-breath nitrogen test in identifying smokers who experienced a rapid decline in FEV_1 and were therefore at risk of developing chronic airflow limitation. Eighty-seven percent of the smokers who developed an abnormal FEV_1 during the follow-up had an abnormal single-breath nitrogen test result and subsequently an increased rate of decline of FEV_1. It was therefore useful in identifying smokers at risk of developing chronic airflow limitation; however, its usefulness was diminished by the high proportion of smokers who had mild functional abnormalities but did not progress to develop chronic airflow limitation.

In summary, cigarette smoke seems to elicit an inflammatory reaction in the membranous and respiratory bronchioles early in life, and this abnormality can be detected by tests of small airway function such as the slope of phase III of the nitrogen washout test. However, the early pathologic and physiologic abnormalities do not progress in all smokers, and physiologic abnormalities in the small airways do not allow us to predict the 15 to 20% of smokers who progress to chronic airflow limitation. Further physiologic deterioration is accompanied by progressive pathologic abnormalities—goblet cell metaplasia, fibrosis, muscle, narrowing of the airways, and emphysema. A complex interaction between airflow limitation and changes in airway structure and in the lung parenchyma, still not well understood today, had emerged.

PROGRESSION OF SMALL AIRWAY ABNORMALITIES IN COPD

The striking correlation between the progression of physiologic impairment and the degree of small airway disease suggests that inflammation of the small airways makes an important contribution to the functional deterioration seen in COPD, even when emphysema is present.

Many studies have since addressed the pathologic changes of the small airways in smokers and their relationship with the flow limitation found in established COPD. Of special interest are studies comparing the airway changes in smokers with various degrees of emphysema and COPD with nonsmokers since they give a perspective not only on the effects of smoking and emphysema but also on the effect of aging on the airways.

In one such study, Cosio and colleagues[55] compared abnormalities in the small airways in smokers and in

nonsmokers who suffered accidental death. Pulmonary function status was not known; however, the degrees of both macroscopic emphysema and microscopic emphysema, assessed with the mean linear intercept, were no different in smokers and nonsmokers, suggesting that, in most cases, the effects of cigarettes were mild. Nonetheless, abnormalities in the membranous and respiratory bronchioles of smokers were quite apparent, with increased numbers of goblet cells and cellular inflammatory infiltrates and muscle and respiratory bronchiolitis, in comparison with nonsmokers. The overall mean diameter of airways less than 2 mm was similar in both groups, but smokers had a significantly greater proportion of bronchioles smaller than 400 μm than nonsmokers, and this proportion was closely related to the total score of airway abnormalities. Several other studies have indicated that there is a better relationship between airflow limitation and the proportion of very narrow airways 0.2 mm and 0.35 mm in diameter.[52,56,57]

Wright and colleagues[58] studied lungs of nonsmokers, smokers, and ex-smokers and reported no significant differences in individual values for total pathologic scores for membranous bronchioles between current and former smokers. Wright and colleagues[59] also found that the wall thicknesses of membranous and respiratory bronchioles for each bronchiolar diameter were increased in almost all size ranges in smokers when compared with lifetime nonsmokers, indicating that smoking is associated with an increase in airway wall thickness independent of airway size and regardless of the presence or absence of emphysema. However, for the same level of function, the degree of airway abnormalities was quite variable, suggesting that other abnormalities, probably elastic recoil losses, influenced the degree of flow limitation.

Hale and colleagues[60] added another group of 18 lungs of patients dying with documented COPD to the population of smokers and nonsmokers in the study of Cosio and colleagues.[55] This study is of interest since it clearly shows the progression of the small airway pathologic changes from nonsmoking older individuals to smokers with mild disease and finally to smokers dying with COPD (Figure 10-4). The cellular inflammatory infiltrate, fibrosis, and muscle in the airway wall increased significantly in a stepwise fashion in the three groups, and, as expected from our initial study, the number of airways less than 400 μm increased accordingly. The mean diameter of the small airways tended to decrease, but the range of diameters was so large that no statistical differences could be found even between patients with the most severe COPD and nonsmokers. A similarly wide range was found for all the airway inflammatory abnormalities measured in the two groups of smokers, indicating that not every smoker reacts in the same way to cigarette smoke and that some smokers are more prone to develop small airway abnormalities than are others.

Not surprisingly, smokers dying of COPD have more emphysema in their lungs than nonsmokers and patients with mild COPD. The degree of emphysema assessed macroscopically correlates with all abnormalities found in the small airways. With this large degree of intercorrelation, it would not be surprising if in severe COPD, the degree of

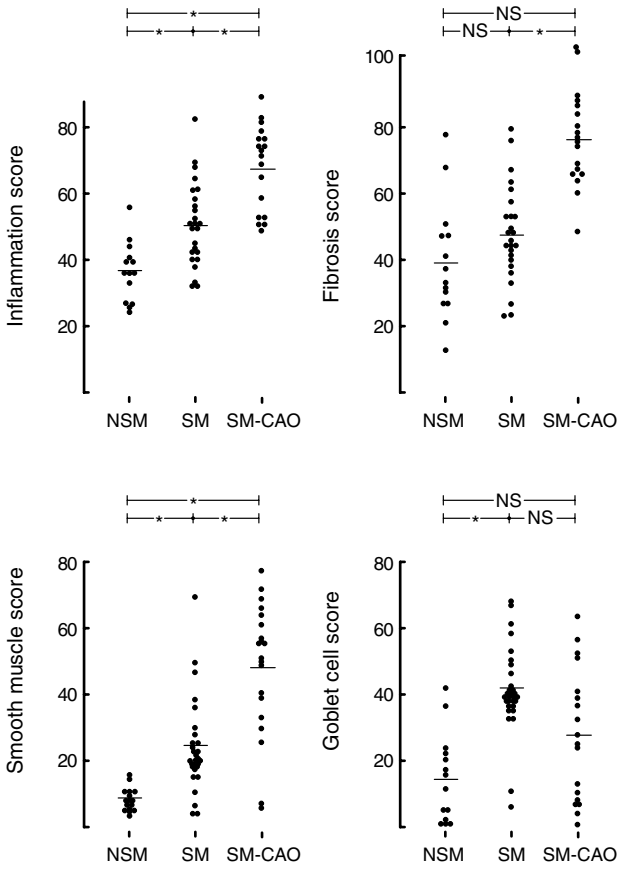

FIGURE 10-4 The progression of the small airway abnormalities in smokers. Groups shown are nonsmokers (NSM), smokers without known chronic obstructive pulmonary disease (COPD) (SM), and smokers with COPD (SM-CAO). All cases are autopsy cases. Reproduced with permission from Cosio MG et al.[55]

emphysema might override correlations between morphology of the small airways and function. Nonetheless, Hale and colleagues[60] found that the degree of airflow limitation correlated not only with emphysema but also with the average airway diameter and the proportion of airways smaller than 400 μm, a function of the total pathologic score of the small airways.

Similar results were obtained by Nagai and colleagues[61] in patients dying with COPD. In their study, flow rates antemortem correlated with the degree of macroscopic emphysema but also with the proportion of airways less than 400 μm in diameter and the degree of deformity of bronchioles. They attributed the decreases in flow to both emphysema causing loss of elastic recoil and airway obstruction caused by an excess number of very small bronchioles and deformity of bronchiolar lumens. It was also clear from this study that, for the same degree of airflow limitation, smokers with lesser degrees of emphysema had more diseased small airways, suggesting that the combined effect of loss of recoil secondary to emphysema and increase in airways resistance secondary to small airway abnormalities produces the airflow limitation in COPD.

The relationship between small airway diameters, a function of the proportion of the very small airways less than 400 μm in diameter in the lung, and lung disease in smokers is of interest. Smokers have a significant excess of

airways less than 400 μm in diameter when compared with nonsmokers, and this proportion correlates with the severity of pathologic abnormalities in these airways, suggesting that the inflammatory reactions in the airways result in an excess of airways less than 400 μm in diameter. However, this explanation may not fully account for the relationship between disease and the caliber of the small airways. The mean bronchiolar diameter and the percentage of airways less than 400 μm in diameter are highly variable even in nonsmokers.[55,62] Small airway caliber may be constitutionally determined or altered because of diseases in childhood, or both, and perhaps persons with smaller airways, because of constitution or childhood illness, are more susceptible to developing disease in these airways when exposed to cigarette smoke or other irritants.

Beyond Morphometry: Mechanisms of Airway Inflammation and Airway Constriction

As discussed above, airway dimensions are smaller in smokers than in nonsmokers. However, these differences seem to be minimal and only evident through calculation of the proportion of airways smaller than 400 μm and, by themselves, may not account for the large increases in airway resistance found in the lungs of smokers. It was explained above how the conducting system of the lung, the airways, does not consist merely of passive tubes, as is assumed for morphometry, but is composed of structures able to change in size during the respiratory cycle and in response to stimuli. It would then seem reasonable to assume that the in vitro measurements of airway diameter might not accurately reflect the airway dimensions in vivo. The main reasons for this discrepancy could be as follows: (1) airway diameters in vitro are measured at TLC, whereas expiratory flows depend on the behavior of the airways during a full lung deflation from TLC to RV, and (2) active constriction of the airways in vivo will not necessarily be evident in fixed human lungs. Hence, the in vitro measurements may not detect these events.

There is ample evidence demonstrating that the airways of smokers react to nonspecific stimuli by constricting, causing an increased resistance and a decreased FEV_1. Many authors[63–69] believe that smokers might have hyperreactive airways and that this hyperreactivity might contribute to the natural history of COPD. Furthermore, the inflammatory abnormalities found in the airways of smokers could contribute to the constriction of normal airway smooth muscle. Hence, regardless of the presence or absence of muscle hyperresponsiveness, muscle constriction in smokers is most likely an important component of airflow limitation in COPD. In support of the role of muscle hyperresponsiveness in the mechanism of COPD are the results of a recent and comprehensive population survey in which smokers showed a relationship between airway responsiveness to methacholine and the rate of decline of lung function[70]; the greater the degree of airway responsiveness at baseline evaluation, the steeper the decline in FEV_1 in response to smoking, a finding consistent with the Dutch hypothesis.

Several pathologic changes could be responsible for active muscle constriction and airway narrowing in COPD. These include (1) airway epithelial damage resulting in increased epithelial permeability and impairment of other epithelial functions, (2) chronic airway inflammation, (3) fibrotic changes in the airway wall, (4) increased amounts of smooth muscle with altered smooth muscle sensitivity and contractility, and (5) loss of alveolar attachments. The role of the epithelium and inflammation may be the key to the pathogenesis of airway narrowing.

Role of the Epithelium in Airway Inflammation and Narrowing

Effects of Altered Permeability The protective barrier formed by the airway epithelium is altered by cigarette smoke. Denuded epithelium, mucosal ulcers, and goblet and squamous cell metaplasia are consistently found in the airways of smokers. Cigarette smoke is cytotoxic to epithelial cells, and the extent of injury is directly related to the concentration of smoke to which the cells are exposed.[71] Numerous studies have shown that cigarette smoke causes airway epithelium to become more permeable to electron-dense tracers, with damage to junctional complexes being demonstrated in smoke-exposed guinea pigs.[72–74] The altered epithelial permeability leaves underlying afferent nerve endings and irritant receptors exposed to bronchoconstrictor and other proinflammatory substances. Thus, the dysfunction of the epithelial cells could contribute to bronchoconstriction and airway inflammation. Finally, altered integrity of the epithelial barrier permits access of plasma exudate to the airway lumen and has mechanical and inflammatory effects on the small airways.

Effects of Luminal Fluid Once across the epithelial barrier, plasma exudate and its associated macromolecules immediately fill the interstices between epithelial projections.[75] Liquid-filled interstices could amplify the degree of luminal compromise in at least two ways. First, the luminal cross-sectional area is reduced as the interstices fill with fluid.[76] Second, plasma proteins may alter the surface tension of the airway lining fluid, and this can further compromise the airway lumen.[77] Macklem and colleagues[78] have reasoned that if the interstices fill with liquid, the surface tension of the airway lining liquid increases, and the radius of curvature of the interfaces joining the tips of epithelial projections increases. At the point where the curvatures of the interfaces joining projections match the curvature of the airway lumen, a point of instability is reached and airways could close. This has been suggested as a physical mechanism that could contribute to airway hyperresponsiveness. Any such effect will be enhanced through impairment of the surface-active properties of surfactant.

Inflammatory Effects of Epithelial Disruption The present evidence suggests that, by sending "danger" signals in response to cigarette smoke, the epithelium is responsible for the initiation and possibly maintenance of the innate inflammatory immune response seen in smokers. Over 2,000 different xenobiotic compounds have been identified

in cigarette smoke, and it has been estimated that there are 10^{14} free radicals in each puff of cigarette smoke,[79] a considerable xenobiotic and oxidant burden on the respiratory epithelium, which is the first line of defense against inhaled substances. Not surprisingly, the defense role comes at a price as cigarette smoke can harm the epithelium and produce apoptosis and necrosis of epithelial cells.[71] There is now ample evidence that, once injured, the epithelium, by increasing permeability and by the production of inflammatory mediators such as interleukin-8 (IL-8), IL-1β, tumor necrosis factor-α (TNF-α), granulocyte–macrophage colony-stimulating factor, and intercellular adhesion molecule-1, could be a potent stimulator of an innate immune reaction.[80,81]

Another consequence of injury to the epithelium caused by cigarette smoke and the resultant increase in epithelial permeability[82,83] is the production and release of tachykinins (substance P and neurokinin-A). These neuropeptides are synthesized by sensory neurons and stored in the terminal parts of the axon collaterals found beneath and within the epithelium, around blood vessels, around submucosal glands, and within the muscle layer of the airways. The release of tachykinins from sensory nerves can be evoked by a variety of stimuli, including cigarette smoke,[84,85] producing bronchoconstriction and modulating a number of important immunologic functions, such as T-cell proliferation,[86] lymphocyte traffic,[87] and production of cytokines, including IL-1, IL-3, IL-6, IL-10, IL-12, and TNF-α.[88,89]

The inflammatory effects of the tachykinins are, in part, controlled by neutral endopeptidase, an enzyme on the surface of the specific cells that are the site of action of tachykinins, and that cleaves and inactivates them. Neutral endopeptidase activity is found specifically in epithelium, glands, nerves, and smooth muscle.[90] The abolition of neutral endopeptidase activity by stripping the epithelium or by inhibition of this enzyme by specific inhibitors is known to increase smooth muscle responses to bronchoconstrictor substances.[91] If airway epithelium is shed or altered, any effects of tachykinins may be more pronounced, not only on airway smooth muscle but also on the inflammatory effects of tachykinins in the mucosa and submucosa.

Endogenous Bronchodilator Effects Respiratory epithelium seems to directly modulate the responsiveness of bronchial smooth muscle by the release of inhibitory factors. In fact, the respiratory epithelium has a high density of β-adrenoreceptors, higher than that in bronchial smooth muscle.[92] The increased smooth muscle relaxation in response to isoproterenol in bronchial rings with intact epithelium compared with preparations denuded of epithelium highlights the importance of the β-adrenoreceptors in the epithelium–smooth muscle interaction.[92,93] Airway mucus, often increased in COPD, may inactivate some epithelium-derived factors.[94]

In summary, the integrity of the epithelial surface seems to be necessary for the normal function and regulation of the airways. Loss of the epithelium and/or possible replacement of normal epithelial ciliated cells by goblet or squamous cells may be one of the initial events in the development of an inflammatory reaction and airway narrowing in smokers. The chronicity of the stimulation could perpetuate the process and enhance the progress of the pathologic changes in smokers.

Airway Wall Contribution to Airway Narrowing

It has been shown that as obstruction worsens, so does the associated degree of airway fibrosis.[48,53,95] This, along with the inflammatory infiltrate, will contribute to the increase in the thickness of the airway wall and the decrease in the thickness of the airway lumen. The amount of muscle in the airway wall is also increased in smokers compared with nonsmokers,[55] and this increase becomes more pronounced as a function of worsening airflow obstruction. It may contribute to airway narrowing through active constriction or through encroachment on the luminal area.

The walls, both internal and external to the smooth muscle layer, are thicker in smokers with airflow limitation than in smokers without airflow limitation, and increasing thickness is associated with smaller airway diameters.[96] Thickening decreases the airway lumen and also has an important effect on the mechanical behavior of the small airways. Moreno and colleagues[97] and Wiggs and colleagues[98] elegantly showed that as the muscle constricts, the thickness of the wall increases, causing the wall to encroach on the lumen in such a way that the thicker the airway wall internal to the muscle, the greater the narrowing resulting from a given degree of smooth muscle shortening. Wiggs and colleagues[98] expanded upon the ideas of Moreno and colleagues and examined the effects of airway wall thickening, loss of elastic recoil, and airway smooth muscle shortening on the increase in airway resistance, using a model of the human tracheobronchial tree. This analysis showed that moderate amounts of airway wall thickening, which has little effect on baseline resistance, can profoundly affect the airway narrowing caused by smooth muscle shortening—especially if the wall thickening is localized to peripheral airways.[96,98]

Fibrosis is not confined to the internal part of the airway but also occurs external to the smooth muscle layer.[97] The mechanical effects of fibrosis and increased airway wall thickness external to airway smooth muscle are different from those of increased thickness of the internal wall. In normal airways, the data of Gunst and colleagues[99] suggest that the lung elastic recoil provides an elastic afterload to peripheral airway smooth muscle and impedes its ability to shorten. This elastic load increases as lung volume increases. According to the interdependence theory, the pressure applied to the outer surface of intrapulmonary airways is equal to the sum of forces applied to the outer surface of the airway by the attached alveolar walls expressed as a fraction of the external surface area of the airway. As the airway wall thickens, the attached alveolar walls become shorter, the forces on the airway wall decrease, the outer airway surface area increases, and hence the pressure applied to the airway decreases.[100] In support of these theories are the findings of Ding and colleagues[101] and Bellofiore and colleagues[102] in elastase-induced emphysema in rats, showing the importance of elastic recoil in smooth muscle shortening in these animals.

Alveolar Attachments

From the previous discussion, it is apparent that loss of the alveolar support around the airways, if it were to occur in smokers, ought to have an important effect on the patency of the small airways and consequently on lung function.

Anderson and Foraker were the first investigators to link pulmonary parenchymal and small airway disease in smokers.[103] They postulated that inflammation of the small airways extends to the parenchyma, leading to weakening of the alveolar walls with destruction. The loss of alveolar attachments to bronchiolar walls will lead to a reduction in the caliber of the airways due to loss of radial traction forces (Figure 10-5). Saetta and colleagues[104] tested this hypothesis and indeed demonstrated a strong association between loss of alveolar attachments and bronchiolar narrowing in the lungs of subjects with mild chronic airflow obstruction. As postulated by Anderson and Foraker,[103] the inflammation of the small airway walls correlated closely with the number of abnormal alveolar attachments.[104] Functionally, the loss of alveolar attachments was found to correlate significantly with loss of elastic recoil, an increase in the closing volume, and a decrease in FEV_1.[104,105] Nagai and colleagues[106] examined lungs obtained at autopsy from patients with moderate-to-severe chronic airflow obstruction and emphysema and found that the loss of normal alveolar attachments was closely related to emphysema. The deformity index, used to describe the irregularity in shape and deformity of peripheral airways, was related to the loss of alveolar attachments and to the decreases in flow in these patients. Thus, it seems apparent that emphysematous changes around the airways will significantly interact with airway patency in the production of airflow limitation.

FIGURE 10-5 Small airway in chronic obstructive pulmonary disease, showing decreased alveolar attachments and narrowed lumen.

STRUCTURE–FUNCTION RELATIONSHIP IN THE LUNG PARENCHYMA

Microscopic Findings in the Lung Parenchyma in COPD: The Doughnut Effect

The traditional method for the study of emphysema has been naked-eye observation (with or without a dissecting microscope or magnifying lenses) of lung slices, either in thin paper-mounted sections or barium-impregnated thick slices floated in water. The focus of these studies has been the identification of holes (or bullae), that is, the terminally destroyed lung in which the type of emphysema producing the hole (CLE versus PLE) is often difficult to identify, especially in severe emphysema cases. There is ample evidence, both functional and microscopic,[107,108] that the so-called normal lung found between the emphysematous holes (the doughnut) is not normal, and microscopic emphysematous lesions have been found. It follows that the "doughnut" will be intimately related to the "hole," that is, the emphysema found under the microscope in the macroscopically apparently normal lung will give rise to the hole as emphysema progresses. Furthermore, in an emphysematous lung, the function will probably be determined in large part by the properties of the apparently normal lung, "the doughnut," found between the holes, something that can be assessed by microscopy. This concept has been elegantly demonstrated by Hogg and colleagues.[109] In excised human lungs with CLE, they measured lung volumes with radiologic methods, in which the emphysematous spaces could be visualized and measured, combined with measurements of pressure, thus obtaining the compliance of the centrilobular emphysematous spaces along with the compliance of the rest of the lung. They found that in the range of RV to TLC, emphysematous spaces changed very little in size with changes in elastic pressure (very low compliance), indicating that there is little if any contribution of these spaces to lung emptying. The mechanical characteristics of the rest of the non–obviously emphysematous lung were much more normal, and the compliance was higher.[109]

It should be evident by now that the pathophysiology of COPD is a complex interplay of pathologic abnormalities in the airways and lung parenchyma. Therefore, in order to understand the deranged function in COPD, we need to study the morphology of the airways and parenchyma and correlate them with the functional abnormalities.

Relationship Between Small Airway Abnormalities and Emphysema in Smokers

Physiologic evidence suggesting that smokers could develop two different types of emphysema was provided by Eidelman and colleagues.[110] They found that smokers with COPD had different patterns of functional abnormalities. Some exhibited pressure–volume curves typical of emphysema, which resembled those seen in α_1-antiprotease deficiency, with high compliance and low elastic recoil pressure at high lung volumes. However, about one-half of their subjects had low or normal compliance and, despite similar elastic recoil, had lower FEV_1 values and pressure–volume curves not typical of emphysema.

Based on these findings, Kim and colleagues[111] reasoned that such dissimilar functional behavior ought to correspond to different parenchymal morphologic abnormalities: PLE for the smokers with mechanical characteristics similar to those seen with α_1-antiprotease deficiency and CLE for the others. They tested this hypothesis in 34 patients undergoing lung resection who had pulmonary function

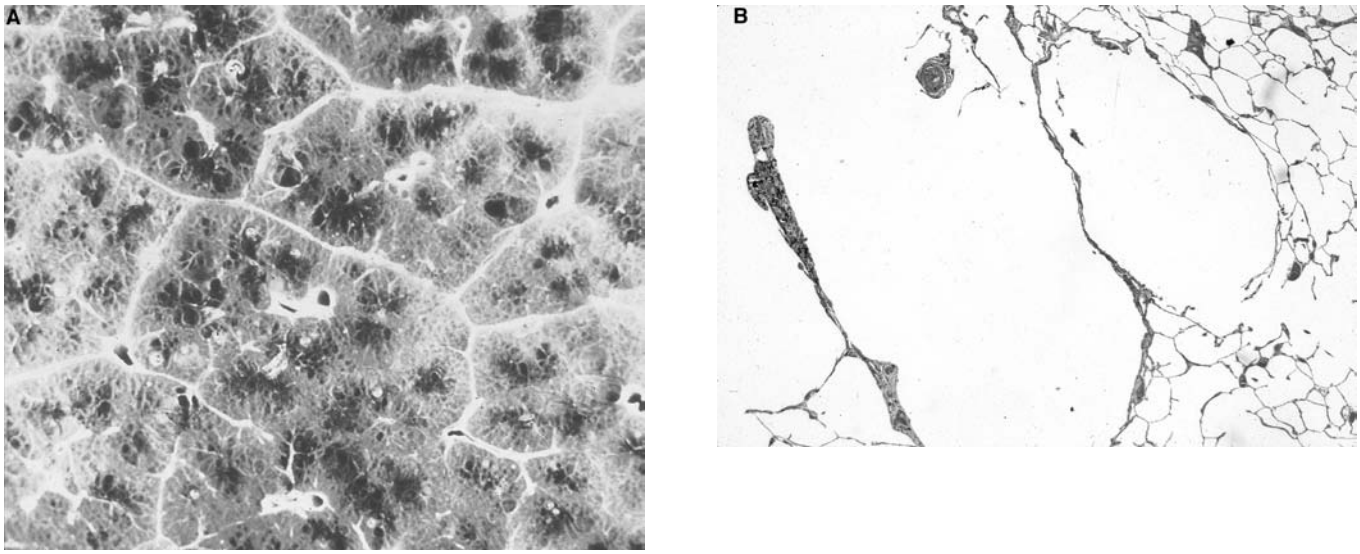

FIGURE 10-6 *A*, Macroscopic view of centrilobular emphysematous areas in the center of the acinus are surrounded by a normal-looking lung. *B*, Micrograph of a lung section showing centrilobular emphysema; similarly, emphysematous destruction is surrounded by normal alveoli.

tests performed before surgery. Emphysema was assessed microscopically and characterized as CLE (Figure 10-6) or PLE (Figure 10-7) with the use of available definitions; it was quantitated by means of the mean linear intercept. Both types of emphysema could be found in this population of smokers; 18 patients had pure or predominant CLE, and 16 had PLE. The mechanical properties were found to be different in both types of emphysema. Patients with PLE had a higher compliance and a higher constant of elasticity (*K*) than patients with CLE. As the emphysema worsened, compliance, *K,* and the elastic recoil at 90% of TLC worsened in PLE but did not change in CLE. Furthermore, losses of elasticity correlated significantly with the extent of emphysema in lungs with PLE but not in those with CLE (Figure 10-8). These findings suggest that mechanical properties are different in the two types of emphysema, and these differences become more marked with the progression of the airspace enlargement, suggesting that the two types of lung destruction are different from the start.

There is further evidence in the literature, beyond the simple microscopic morphology, of the differences between CLE and PLE, and these differences could have important effects on parenchymal function in the two types of emphysema. Substantial evidence exists that elastic fibers undergo proteolytic destruction in the lungs in pulmonary emphysema.[112] Wright[112] compared the three-dimensional architecture of 200 to 300 μm–thick sections of normal and emphysematous lungs and observed that elastic fibers in emphysema were attenuated, separated from each other, and retracted at the unattached ends. Damaged elastic fibers were generally associated with alveolar wall fenestrae, loss of capillaries, and a slight increase in the amount of fibrous tissue. Fukuda and colleagues[113] studied the structure of the elastic network of the lung in CLE and PLE and found important differences between the two emphysema types. In

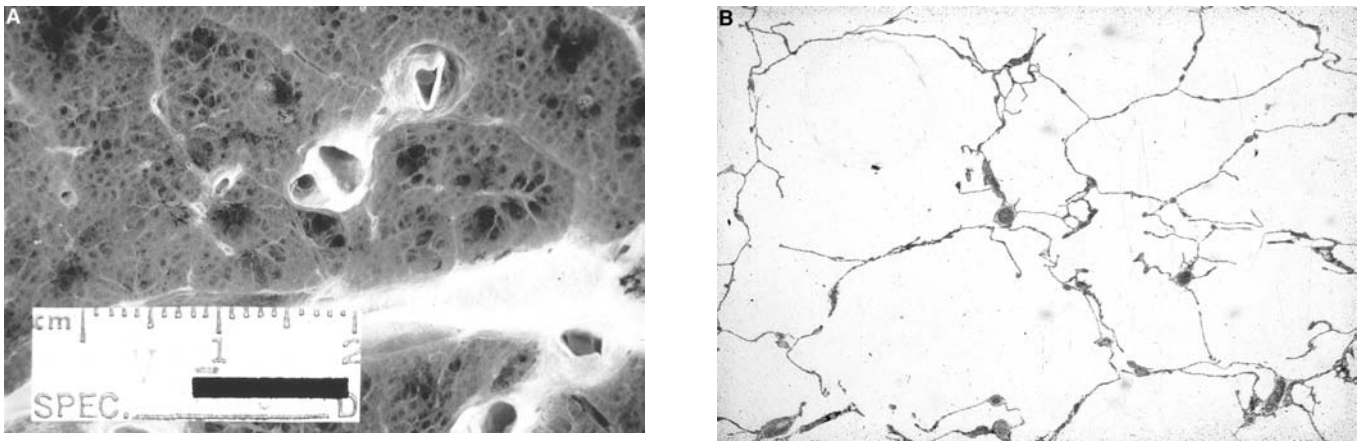

FIGURE 10-7 *A*, Macroscopic view of panlobular emphysema (PLE). The whole acinus is abnormal. *B*, Micrograph of a lung section showing PLE. All airspaces are enlarged, and the size of the alveoli approaches the size of the alveolar ducts.

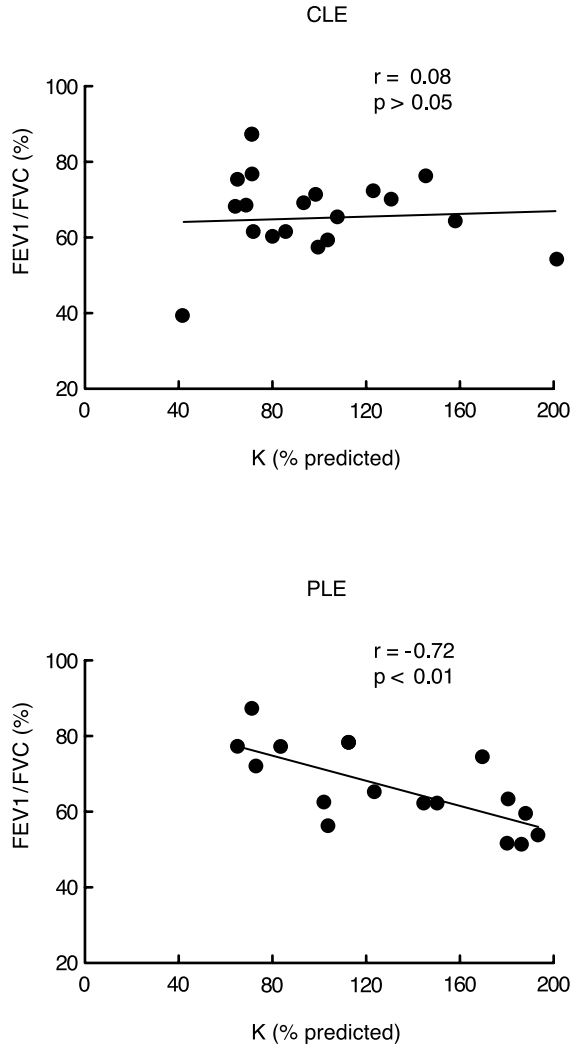

FIGURE 10-8 Correlation between elastic recoil (*K*) and flow (FEV_1/FVC) in smokers with centrilobular emphysema and panlobular emphysema. Pulmonary function was measured prior to surgery in 38 smokers undergoing lung resection for lung nodules. Reproduced with permission from Kim WD et al.[111]

the lungs of patients with PLE, fragmented elastic fibers were observed frequently in alveolar walls and occasionally in bronchioles. At the electron microscopic level, the amorphous component of the elastic fiber appeared to be disrupted, with a fine granularity and a diminished electron density in comparison to normal elastic fibers. In contrast, the lungs of patients with CLE contained few of the disrupted elastic fibers observed in lungs with PLE.

The study of alveolar fenestrae in emphysema also shows how the ultrastructural anatomy of emphysema varies. In our laboratory, we have studied the numbers, size, and distribution of these fenestrae in lungs with CLE and PLE. In CLE, larger fenestrae are found in the center of the acinus, probably destroying respiratory bronchioles and possibly alveolar ducts (Figure 10-9). Fenestrae in the periphery of the acinus are smaller and less numerous. In PLE, however, the fenestrae are smaller than in CLE and distributed equally throughout the acinus.[114,115]

These findings emphasize the distinctiveness of the two types of emphysema that smokers develop. PLE is diffuse,

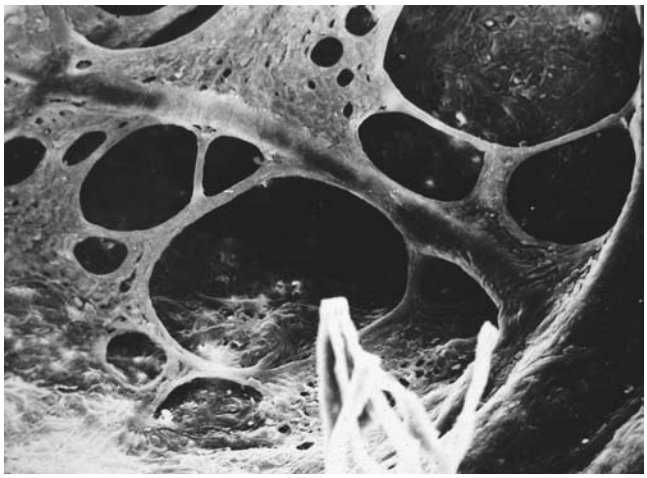

FIGURE 10-9 Scanning electron microscopy of an alveolar wall in a case of centrilobular emphysema, showing prominent fenestrae in the "near" portion of the acinus. Reproduced with permission from Angus GE et al.[114]

affecting all the structures in the acinus evenly and preferentially destroying the elastic network of the lung. In CLE, the destruction is preferentially in the center of the acinus, where inflammatory and mechanical changes (negative pressure generated with lung inflation, more marked in the upper parts of the lung) probably act synergistically to increase the fenestrae size; the fenestrae eventually coalesce, destroying the lung parenchyma. In this type of emphysema, the elastic fibers seem to be less damaged but are rearranged around large emphysematous spaces. Such dissimilar behavior ought to have important functional consequences that are of interest when correlative studies of emphysema and function in smokers are being considered.

Another important difference between the two types of emphysema found by Kim and colleagues[111] was the extent of the small airway abnormalities, later confirmed by Saetta and colleagues[116] and Finkelstein and colleagues.[117] Lungs with CLE had higher total pathologic scores of the small airways than lungs with PLE. The higher scores were mainly ascribable to increased amounts of muscle and fibrosis in the airway wall. Probably as a result of the more severe pathologic involvement, lungs with CLE had more airways smaller than 400 μm in diameter than lungs with PLE (Figure 10-10). Not surprisingly, the pathophysiology of flow limitation in smokers, a function of airway resistance and elastic recoil pressures, differs between the two types of emphysema. Flow decreases as airway abnormalities increase in CLE, but there is no relationship between flow and airway disease in PLE (Figure 10-11). In contrast, flow decreases significantly as elasticity decreases in PLE but not in CLE (Figure 10-12). These findings clarify the pathogenesis of airflow limitation in smokers and indicate that in CLE, loss of flow is primarily a function of airway abnormalities, with elastic recoil loss playing an additive role. By contrast, in patients with PLE, the flow limitation seems to be mainly a function of reduced elastic recoil, and added airway abnormalities could worsen flows even further in these cases.

The studies of Kim and colleagues,[111] Saetta and colleagues,[116] and Finkelstein and colleagues[117] are of interest

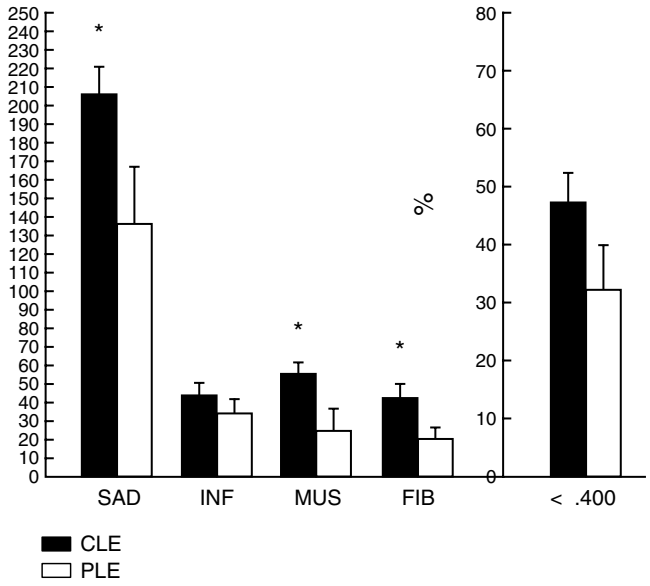

FIGURE 10-10 Pathologic score and proportion of airway diameters smaller than 400 μm in 38 smokers' lungs with either centrilobular emphysema or panlobular emphysema. Reproduced with permission from Kim WD et al.[111]

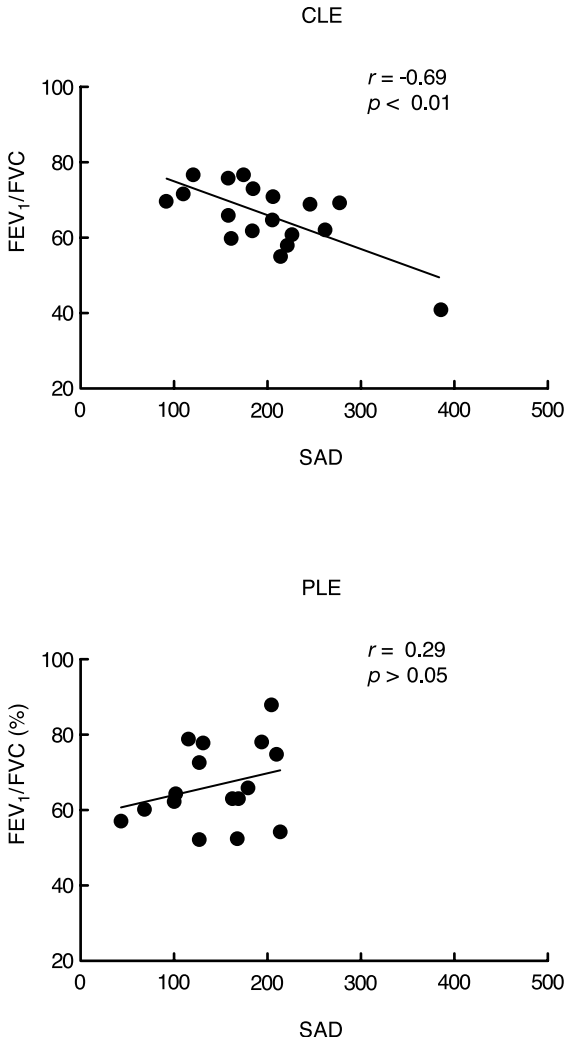

FIGURE 10-11 Correlation between the pathology of the small airways (SAD) and flow (FEV_1/FVC) in smokers with centrilobular emphysema and panlobular emphysema. Reproduced with permission from Kim WD et al.[111]

because they not only clarify the mechanisms of airflow limitation and the role of the bronchioles in COPD but also confirm the possibility of smokers developing two diseases with different pathogenetic mechanisms. The diffuse parenchymal destruction seen in PLE may result from a blood-borne mechanism. On the other hand, the uneven pattern of lung destruction seen in CLE is associated with more severe abnormalities in the small airways, suggesting that centrilobular destruction is related to airborne factors and intimately related to the airway inflammatory process. In support of this hypothesis are the findings of Saetta and colleagues,[116] who found a close correlation between the inflammation of the airways and the parenchymal destruction in lungs with CLE, but not in lungs with PLE. Thus, it is likely that the inflammatory reaction seen in and around small airways and respiratory bronchioles spreads to the parenchyma surrounding these airways and eventually destroys the alveolar walls attached to the airways and the respiratory bronchioles and alveolar ducts. The preservation of alveolar structure and size with concomitant destruction of alveolar ducts and respiratory bronchioles in CLE supports this possibility. Leopold and Gough[118] also showed that the small airways were usually inflamed in lungs with CLE but seldom in patients with predominant PLE. Similar observations were reported by Anderson and Foraker,[119] who felt that CLE and PLE were two different diseases.

These studies provided a new basis for the investigation of lung disease in smokers. If the pathogenetic mechanisms in the two types of emphysema in smokers are different, as the evidence suggests, the study of cigarette-induced lung disease as a single entity will delay even further the understanding of COPD.

Inflammatory Component in COPD: Parenchyma and Airways

The recognition that inflammatory cells play a key role in the pathogenesis of COPD is now so widespread that it has led to the inclusion of the term "abnormal inflammatory response" in the disease definition. In fact, according to the most recent guidelines, COPD is defined as "a disease state characterised by not fully reversible airflow limitation that is usually both progressive and associated with an abnormal inflammatory response of the lungs to noxious particles or gases."[120]

Indeed, the earliest and more constant pathologic abnormality in the airway and parenchyma of smokers is the cellular inflammatory infiltrate. Cellular inflammation, per se, may be responsible for mild airflow limitation,[52,55,94] and it has been suggested that inflammation may lead to functional bronchiolar constriction by releasing bronchoactive mediators.[121] The chronicity of inflammation would, in turn, produce other changes, such as fibrosis of the airway, and could possibly increase the smooth muscle either directly as a result of inflammation or indirectly as a result of chronically increased muscle tone. The stimuli for this abnormality are not precisely known, but it seems that injury to the epithelium, the first structure encountered by cigarette smoke, could promote and perpetuate an inflammatory reaction in the lung.

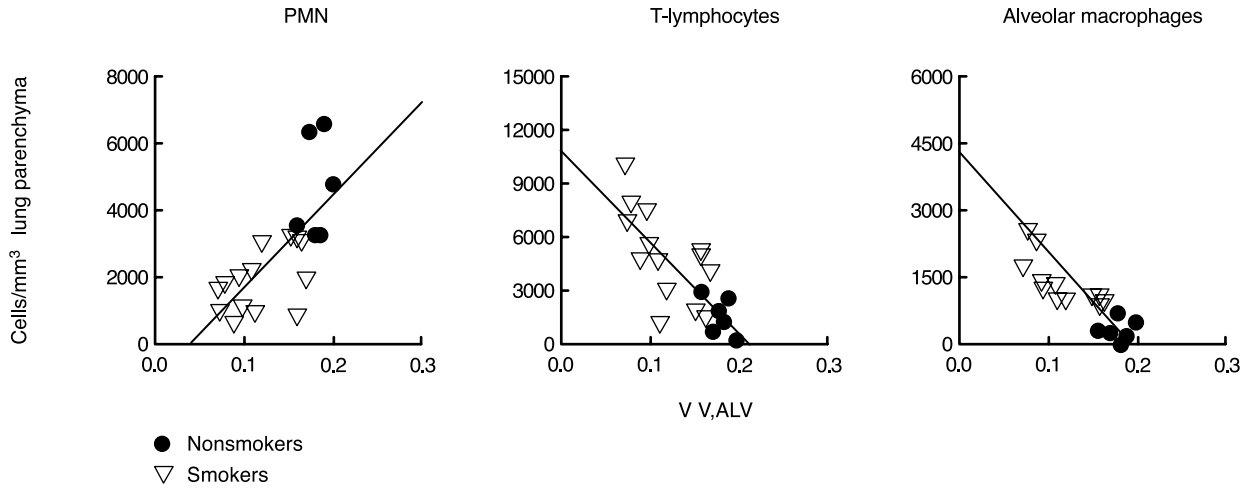

FIGURE 10-12 Correlation of the number of inflammatory cells/mm^3 in the alveolar wall (neutrophils, CD3$^+$ T cells, alveolar macrophages) with the extent of emphysema (V_{VA} = volume of alveolar wall decreases as emphysema increases) in smokers' lungs obtained at surgery. Reproduced with permission from Finkelstein R et al.[117]

In most of the early studies of small airways in smokers, the inflammation of the airways was analyzed in a quantitative fashion. Qualitative morphometric studies of the airways and the lung parenchyma took some time to come, but when they did they changed the way in which we think about the cellular inflammatory mechanism of COPD.

Bosken and colleagues[122] were some of the first investigators to study qualitatively the airway inflammation in smokers with chronic airflow obstruction, and they demonstrated that the number of submucosal neutrophils correlated significantly with the number of cigarettes smoked. They also found that B lymphocytes and CD4$^+$ T cells were most numerous in the adventitia, and there were more CD8$^+$ cells in the epithelium than in the inner wall or the adventitia. B lymphocytes in the entire wall and the adventitia accounted for about 15% of the inflammatory cells and constituted the only cell type that was statistically increased in number in the airways of smokers with obstruction when compared with those without airflow obstruction. Later, Fournier and colleagues[123] and Saetta and colleagues,[124] when studying the large airways of smokers with chronic bronchitis, found increased numbers of CD3$^+$, CD4$^+$, and CD8$^+$ lymphocytes in the bronchial wall. CD8$^+$ lymphocytes predominated over CD4$^+$ lymphocytes, reflecting previously described changes in bronchoalveolar lavage (BAL) fluid and peripheral blood.

Eidelman and colleagues[125] and Saetta and colleagues[126] reasoned that morphometric analysis of the inflammatory cell load in the alveolar wall in smokers would be more informative than BAL fluid. They showed that smokers' lungs had increased cellularity in the alveolar walls, the intensity of which was correlated with the extent of parenchymal destruction. However, the number of neutrophils in the alveolar wall decreased as the alveolar destruction increased, indicating that cells other than the neutrophils were involved in the mechanism of lung destruction. These authors also showed an important correlation between the extent of lung destruction, measured by the destructive index, and losses of lung recoil.

The study that initiated the present interest in the T cell as a possible important cell in the pathogenesis of COPD in general and emphysema in particular was carried out by Finkelstein and colleagues in 1995.[127] Following the findings described above,[125,126] showing a correlation of the number of inflammatory cells, other than neutrophils, with alveolar wall destruction, they investigated which other inflammatory cells could be potentially involved in the production of emphysema. Using immunochemistry, the authors identified the inflammatory cells infiltrating the alveolar wall, and by morphometry they defined the extent of emphysema in smokers and nonsmokers undergoing lung resection. Their findings were surprising at the time as they reported that the most prominent inflammatory cells in the lung parenchyma of smokers were CD3$^+$ T lymphocytes, which increased in number from a mean of 1,546 cells/mm^3 in nonsmokers to 10,000 cells/mm^3 in some smokers. Furthermore, a clear correlation between the number of CD3$^+$ T cells and the extent of emphysema was found, suggesting a role for T lymphocytes in the pathogenesis of emphysema in smokers (see Figure 10-12). Emphysema was also associated with the presence of increased numbers of alveolar macrophages, which significantly correlated with the numbers of T cells, suggesting an interaction between these cells in the inflammatory process leading to emphysema, possibly mediated by a Th1 type of T-cell response (interferon-γ [IFN-γ], TNF-α, and IL-2 cytokine profile). They also confirmed the previous finding that the number of neutrophils in the alveolar wall decreased as the emphysema increased.

Abundant but variable numbers of T cells (CD3$^+$), together with other inflammatory cells, are also found in the small airways of smokers. Finkelstein and colleagues investigated the inflammatory infiltrates in the airways in a series of smokers and nonsmokers in whom airway reactivity had

been measured before lung resection.[117] Smokers were divided according to the type of emphysema in the lung, CLE or PLE. Owing to the large variability in the numbers of inflammatory cells in the airways (from 0 to 500,000/mm^3), no statistical difference was found in the numbers of the different inflammatory cells between the airways of nonsmokers and smokers. However, the degree of airway reactivity correlated with the load of T cells in the airways in smokers with CLE but not in smokers with PLE or nonsmokers. Because similar total numbers of CD3$^+$ T cells were present in the three groups, they suggested that the T cells in CLE were behaving differently, possibly because they were of a different phenotype (Th2 vs Th1). In support of this possibility is the finding that mRNA of the Th2-type cytokines IL-4 and IL-5 (cytokines found in asthma) is abundantly expressed by inflammatory cells in the walls of large airways in smokers with chronic bronchitis and COPD.[128] These cytokines play an important role in the development of asthma, a disease characterized by an increase in airway reactivity; hence, it is possible that clones of T cells in smokers with CLE could express a Th2 cytokine profile that might induce airway reactivity in these cases. Furthermore, IL-4 has been shown to have profibrotic effects by stimulating fibroblasts to proliferate and secrete collagen,[129] and this profibrotic role might be of relevance to the increased remodeling with fibrosis in the small airways and in the increased fibrosis in areas of emphysema found commonly in patients with CLE.[117] Further characterization of the T-cell Th phenotype in the small airways of patients with COPD will be necessary to confirm these possibilities.

Following the report by Finkelstein and colleagues[127] proposing a role for T cells in COPD, Saetta and colleagues identified the CD8$^+$ T cell as the predominant lymphocyte in the small airways[130] of smokers with COPD. This study showed that the only significant difference in the inflammatory cell infiltrate between asymptomatic smokers and smokers with COPD was the increase in CD8$^+$ T cells in patients with COPD. Furthermore, the number of CD8$^+$ T cells was negatively correlated with the degree of airflow obstruction, as measured by the FEV_1, again suggesting a possible role for these cells in the pathogenesis of the disease. This important study introduced the prevailing concept that the development of CD8$^+$ T-cell inflammation in response to smoking is one of the important factors predisposing to the development of COPD. O'Shaughnessy and colleagues found similar T-cell inflammation in the large airways.[131]

Chemokines and T-cell receptors in smokers' lungs have been reported recently by Saetta and colleagues,[132] and their findings indicate that the T cells found in the lungs of patients with COPD are activated, with significant expression of the CXCR3 receptor in the T cells infiltrating the lung, which is not found in nonsmokers. Furthermore, IFN-γ was coexpressed with CXCR3, and the IFN-induced protein-10, a ligand for the CXCR3 receptor, was strongly expressed in the airways and pulmonary arterioles in smokers with COPD but not in other smokers and nonsmoker controls. Importantly, the number of T cells expressing CXCR3, a chemokine receptor restricted to activated T cells and natural killer cells, in the lung[133,134] was correlated inversely with the FEV_1/FVC ratio in smokers, suggesting that as the activated T cells expressing CXCR3 and IFN-γ in the lung increase, there is an increase in lung damage and worsening of the lung function.

The CD4$^+$ T cells are also found, albeit in smaller numbers, in the airways of smokers with COPD, and these cells express activated STAT-4, a transcription factor that is essential for activation and commitment of the Th1 lineage. Not surprisingly, the number of CD4$^+$ T cells expressing activated STAT-4 was associated with the number of cells expressing IFN-γ, and the number of activated STAT-4 lymphocytes correlated with the degree of airflow obstruction.[135] The findings in these two studies strongly support the idea that COPD is mediated by an active Th1 immune reaction in the lung, comprising both CD8$^+$ and CD4$^+$ T cells.

The CD8$^+$ T cells are also the predominant T cells infiltrating the alveolar wall in smokers with COPD, although the numbers of CD4$^+$ T cells are also increased.[136–138] Majo and colleagues,[136] when studying lungs from nonsmokers and smokers obtained at surgery, found that, similar to the airways,[130] the only measurable difference between smokers with and without COPD was a substantial increase in the number of total T cells (CD3$^+$) and CD8$^+$ T cells in the alveolar walls of smokers with COPD (Figure 10-13). Furthermore, the total number of T cells, both CD8$^+$ and CD4$^+$, increased with the number of cigarettes smoked in smokers with COPD but not in healthy smokers, suggesting that the CD4$^+$ T cell is also involved in the inflammatory process in COPD. Majo and colleagues,[136] reasoning that as cytolytic CD8$^+$ T cells were involved, apoptosis should be present, quantitated and found an increased number of apoptotic cells in the lungs of smokers with COPD, which correlated with the numbers of CD8$^+$ cytolytic T cells in the alveolar wall. This and other reports showing an increased number of structural lung cells undergoing apoptosis in emphysematous lungs[139–141] support the idea that CD8$^+$

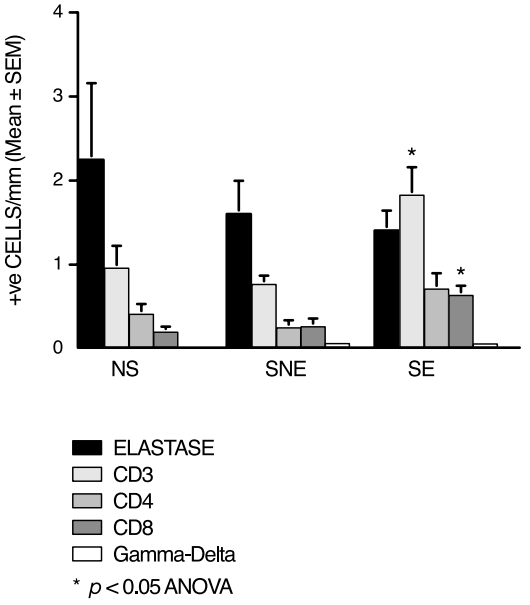

FIGURE 10-13 Cell counts in the alveolar walls of nonsmokers, smokers without emphysema, and smokers with emphysema. All surgical lungs. Reproduced with permission from Majo J et al.[136]

T cells induce apoptosis of endothelial and epithelial cells in emphysema.

Recent studies on smokers with severe COPD demonstrated that the relatively mild infiltration with $CD8^+$ and $CD4^+$ T cells found in patients with mild-to-moderate disease increases markedly in the lungs[138] and airways[142] of severely diseased patients. The numbers of all inflammatory cells, except B lymphocytes, were found to be increased in the lungs of patients with severe emphysema, even though these patients had not smoked more than the control subjects. By far the most numerous cells were $CD4^+$ T cells ($330 \pm 58 \times 10^{12}$) and $CD8^+$ T cells ($250 \pm 51 \times 10^{12}$), but neutrophils, macrophages, and even eosinophils were also increased in number. A relationship between the degree of emphysema and the numbers of each cell type present in the tissue, strongest ($R^2 > 0.8$) for $CD4^+$, $CD8^+$, and alveolar macrophages, was found.[137,138] These studies are of importance because they show that, in COPD, inflammation with an abundance of T lymphocytes and other inflammatory cells continues and even increases late into the disease process.

Recently, we have shown that some mouse strains exposed to cigarette smoke can develop emphysema, and that the severity of emphysema, as assessed by the airspace enlargement and loss of recoil, seems to depend on the ability of the strain to sustain an innate immune response and to mount an adaptive immune response, with $CD4^+$ and $CD8^+$ T cells expressing a Th1 type of cytokine.[143] The finding of animal models that follow the same pattern of disease as humans when exposed to cigarette smoke would be important as it would simplify the investigation of the pathogenic factors in general, and the role of the T cells in particular, in the pathogenesis of COPD in humans.

There is, as we have seen, overwhelming evidence for the presence of T cells in the lungs in COPD and for the activation of these cells. According to the present concepts of T-cell physiology, if the T cells, alone or together with other inflammatory cells, were responsible for the lung injury and progression of COPD, it would be as a response to an antigenic stimulus originating in the lung. Hence, COPD would have to be considered an autoimmune disease triggered by smoking, as previously suggested.[136,144–146]

CONCLUSIONS

Studies correlating the structure of the lung and different measurements of function, from physiologic to cellular and molecular, have been done over the years and are responsible for our present understanding of the pathophysiology of COPD. These studies have revealed that the pathophysiology of COPD is very complex. For the very basic question of how much of the altered function in COPD is due to emphysema, to losses of elastic recoil, and to pathologic and functional abnormalities in the airways, there is not yet a clear answer. However, it is clear that no single one of these abnormalities acts alone and that interactions between the three are responsible.

An important finding is that smokers can develop either CLE or PLE in a pure or clearly predominant form in their lungs in response to cigarette smoking. The different types of emphysema affect the lung parenchyma, the elastic recoil pressure of the lung, and the airways differently. In PLE there are more abnormal and clearly destroyed elastic fibers, more pronounced losses of lung recoil, and less remodeling in the small airways than in CLE. Furthermore, airway reactivity is increased and related to the airway remodeling in CLE but not in PLE. It is our impression that the Dutch hypothesis may well have validity for the patients with COPD who preferentially develop CLE and significant airway remodeling. Thus, COPD should not be considered a homogeneous entity resulting from smoking since CLE and PLE could be fairly different entities, a concept put forward many years ago by Anderson and Foraker.[103] The importance of this paradigm is that if COPD is considered as a single entity, especially from the pathologic point of view, it will take longer to understand the disease. Likewise, studies correlating morphology and function in COPD ought to assess not only the small airways and their abnormalities but also the type and extent of emphysema in order to determine the different contributions of these abnormalities to the pathophysiology of the disease. We believe that such studies would be rewarding.

Looking at the lungs, we have learned to appreciate, quantitate, and identify the cellular inflammatory component in COPD. These studies have broadened the long-standing protease–antiprotease paradigm in the mechanism of emphysema. The discovery of T cells in the lungs of smokers and their correlation with the extent of emphysema and the degree of abnormality in pulmonary function have provided new, more realistic, possibilities for the mechanism of COPD involving an adaptive immune reaction. The consequences of these studies are very important since they are changing the old ideas about the pathogenesis of COPD and are providing avenues for exploration that may explain why only some smokers develop COPD.

We conclude this chapter by inviting readers to consider these last thoughts. If we accept that T cells form part of the inflammatory component of the disease, we have to accept the reason why T cells are in the lung, that is, they are responding to an antigen challenge originating in the lung. If this is the case, we do not think we can escape the conclusion that COPD is a disease produced, at least in part, by antigens (self or modified self) from the lung (autoimmune) secondary to smoking, as we have suggested before.[146] Of course, none of this could be possible without a significant, and persistent, innate immune inflammation, comprising neutrophils and macrophages. Exploring this possibility may lead us to a better understanding and thus to new, and perhaps more effective therapeutic approaches to the disease.

REFERENCES

1. Sauvet J. EPOC un viaje a traves del tiempo. Healthnet SL, editor. Barcelona: Boerhinger Ingehleim; 2000.
2. Pérez-Padilla R, Regalado J, Vedal S. Exposure to biomass smoke and chronic airway disease in Mexican women. A case-control study. Am J Respir Crit Care Med 1996;154:701–6.
3. Bonet T. Sepulchretum sive anatomia practica ex cadaveribus morbo denatis, proponens historias observationes omium

pene humani corporis affectuum, ipsorumoue causas reconditas revelans. Geneva: 1679.
4. Ruysh F. Obervationes anatomica–chirurgicae. In: Tractatio anatomica. Amsterdam: 1721.
5. Watson W. An account on what happened on opening the body of an asthmatic person. Philos Trans R 1764;54:239–45.
6. Morgagni GB. The seats and causes of disease. Investigated by anatomy: in five books, containing a great variety of dissections, with remarks. London: Johnson and Payne; 1769.
7. Baillie M. A series of engravings, accompanied with explanations which are intended to illustrate the morbid anatomy of some of the most important parts of the human body divided into 10 fascicule. London: W. Bulmer; 1799.
8. Baillie M. The morbid anatomy of some of the most important parts of the human body. London: W. Bulmer; 1807.
9. Laennec RTH. A treatise on the diseases of the chest and on mediate ausculation. London: Longmans; 1834.
10. Louis PCA. Researches on emphysema of the lungs. In: Waldie A, editor. Gunglinson's American medical library. Philadelphia: 1838. p. 491–552.
11. Hasse CE. An anatomical description of the diseases of the organs of circulation and respiration. London: Sydenham Society; 1846.
12. Waters ATH. Researches on the nature, pathology and treatment of emphysema of the lungs and its relations with other diseases of the chest. London: Churchill; 1862.
13. Gough J, Wentworth JW. The use of thin sections of entire organs in morbid anatomical studies. J R Microsc Soc 1949; 69:231–5.
14. Gough J. Discussion on the diagnosis of pulmonary emphysema. The pathological diagnosis of emphysema. Proc R Soc Med 1952;45:576–7.
15. Syndenham T. The whole works of that excellent physician, Dr Thomas Syndenham: wherein not only the history and cures of acute diseases are treated of, after a new and accurate method; but also the shortest and safest way of curing most chronic diseases. London: Wellington; 1717.
16. Stokes W. A treatise on the diagnosis and treatment of diseases of the chest—Part 1. The New Sydenham Society; 1882. p. 150–75.
17. Florey HW, Carleton HM, Well OA. Mucus secretion in the trachea. Br J Exp Pathol 1932;13:269–84.
18. Reid L. The pathology of chronic bronchitis. Proc R Soc Med 1954;49:771–3.
19. Mendelssohn A. The effect of smoking on the health. Journal of the Russia National Health Society. Lancet 1887;ii:952–3.
20. Hutchinson J. On the capacity of the lungs and on the respiratory functions, with a view of establishing a precise and easy method of detecting disease by the spirometer. Med Chir Soc Trans 1846;VII:137–45.
21. Christie RV. The elastic properties of the emphysematous lung and their clinical significance. Am Soc Clin Invest 1933; 295–321.
22. Courmand A, Richards DW Jr, Darling RC. Graphic tracings of respiration in studies of pulmonary disease. Annu Rev Tuberc 1939;40:487–516.
23. Dayman H. Mechanics of airflow in health and in emphysema. J Clin Invest 1951;30:1175–90.
24. Thurlbeck WM. Chronic airflow obstruction in lung disease. In: Bennington JL, editor. Major problems in pathology. Vol. 5. Philadelphia: WB Saunders; 1976.
25. Sweet HC, Wyatt JP, Kinsella PW. Correlation of lung macrosections with pulmonary function in emphysema. Am J Med 1960;29:277–81.
26. Watanabe S, Mitchell M, Renzetti AD Jr. Correlation of structure and function in chronic pulmonary disease. Am Rev Respir Dis 1965;92:221–7.
27. Ryder RC, Lyons JP, Campbell H, Gough J. Emphysema in coal workers' pneumoconiosis. BMJ 1970;3:481–7.
28. Burrows B, Fletcher CM, Heard BE, et al. The emphysematous and bronchial types of chronic airways obstruction: a clinicopathological study of patients in London and Chicago. Lancet 1966;830–5.
29. Jenkins DE, Greenberg SD, Boushy SF, et al. Correlation of morphologic emphysema with pulmonary function parameters. Trans Assoc Am Phys 1965;78:218–30.
30. Thurlbeck WM, Henderson JA, Fraser RG, Bates DV. Chronic obstructive lung disease. A comparison between clinical, roentgenologic, functional and morphologic criteria in chronic bronchitis, emphysema, asthma and bronchiectasis. Medicine 1970;49:81–145.
31. McKenzie HI, Glick M, Outbred KG. Chronic bronchitis in coal miners: ante-mortem–post-mortem comparisons. Thorax 1969;24:527–35.
32. Boushy SF, Aboumrad MH, North LB, Helgason AH. Lung recoil pressure, airway resistance and forced flows related to morphologic emphysema. Am Rev Respir Dis 1971;104: 551–61.
33. Park SS, Janis M, Shim CS, Williams MH Jr. Relationship of bronchitis and emphysema to altered pulmonary function. Am Rev Respir Dis 1970;102:927–36.
34. Thurlbeck WM, Fraser RG, Bates DV. The correlation between pulmonary structure and function in chronic bronchitis, emphysema and asthma. Med Thorax 1965;22:295–303.
35. Macklem PT, Mead J. Resistance of central and peripheral airways measured by a retrograde catheter. J Appl Physiol 1967;22:395–401.
36. Hogg JC, Macklem PT, Thurlbeck WM. Site and nature of airway obstruction in chronic obstructive lung disease. N Engl J Med 1968;273:1355–60.
37. Van Brabandt H, Cauberghs M, Verbeken E, et al. Partitioning of pulmonary impedance in excised human and canine lungs. J Appl Physiol 1983;55:1733–42.
38. Hoppin FG Jr, Green M, Morgan MS. Relationship of central and peripheral airway resistance to lung volume in dogs. J Appl Physiol 1978;44:728–37.
39. Stubbs SE, Hyatt RE. Effect of increased lung recoil pressure on maximal expiratory flow in normal subjects. J Appl Physiol 1972;32:325–31.
40. Hyatt RE, Flath RE. Influence of lung parenchyma on pressure–diameter behavior of dog bronchi. J Appl Physiol 1966;21: 1448–52.
41. Hughes JMB, Hoppin FG Jr, Mead J. Effect of lung inflation on bronchial length and diameter in excised lungs. J Appl Physiol 1972;32:25–35.
42. Hahn HL, Graf PD, Nadel JA. Effect of vagal tone on airway diameters and on lung volume in anesthetized dogs. J Appl Physiol 1976;41:581–9.
43. Inners CR, Terry PB, Traystman RJ, Menkes HA. Effects of lung volume on collateral and airways resistance in man. J Appl Physiol 1979;46:67–73.
44. Saunders NA, Betts MF, Pengelly LD, Rebuck AS. Changes in lung mechanics induced by acute isocapnic hypoxia. J Appl Physiol 1977;42:413–9.
45. Widdicombe JH, Gashi AA, Basbaum CB, Nathanson IT. Structural changes associated with fluid absorption by dog tracheal epithelium. Exp Lung Res 1986;10:57–69.
46. Mead J. The lung's "quiet zone." N Engl J Med 1970;282:1318–9.
47. Niewoehner DE, Kleinerman J, Rice DB. Pathologic changes in the peripheral airways of young cigarette smokers. N Engl J Med 1974;291:755–8.
48. Cosio M, Ghezzo H, Hogg JC, et al. The relations between structural changes in small airways and pulmonary function tests. N Engl J Med 1978;298:1277–81.

49. Berend N, Wright JL, Thurlbeck WM, et al. Small airways disease: reproducibility of measurements and correlation with lung function. Chest 1981;79:263–8.
50. Berend N, Woolcock AJ, Marlin GE. Correlation between the function and structure of the lung in smokers. Am Rev Respir Dis 1979;119:695–705.
51. Berend N, Skoog C, Thurlbeck WM. Single-breath nitrogen test in excised human lungs. J Appl Physiol 1981;51: 1568–73.
52. Petty TL, Silvers GW, Stanford RE, et al. Small airway pathology is related to increased closing capacity and abnormal slope of phase III in excised human lungs. Am Rev Respir Dis 1980;121:449–56.
53. Wright JL, Lawson LM, Paré PD, et al. The detection of small airways disease. Am Rev Respir Dis 1984;129:989–94.
54. Buist AS, Vollmer WM, Johnson LR, McCamant LE. Does the single-breath N_2 test identify the smoker who will develop chronic airflow limitation? Am Rev Respir Dis 1988;137: 293–301.
55. Cosio MG, Hale KA, Niewoehner DE. Morphologic and morphometric effects of prolonged cigarette smoking on the small airways. Am Rev Respir Dis 1980;122:265–71.
56. Bignon J, Khoury F, Even P, et al. Morphometric study in chronic obstructive bronchopulmonary disease. Pathologic, clinical, and physiologic correlations. Am Rev Respir Dis 1969;99:669–95.
57. Matsuba K, Thurlbeck WM. The number and dimensions of small airways in emphysematous lungs. Am J Pathol 1972; 67:265–76.
58. Wright JL, Lawson LM, Pare PD, et al. Morphology of peripheral airways in current smokers and ex-smokers. Am Rev Respir Dis 1983;127:474–7.
59. Wright JL, Hobson J, Wiggs BR, et al. Effect of cigarette smoking on structure of the small airways. Lung 1987;165:91–100.
60. Hale KA, Ewing SL, Gosnell BA, Niewoehner DB. Lung disease in long-term cigarette smokers with and without chronic airflow obstruction. Am Rev Respir Dis 1984;130:718–21.
61. Nagai A, West WW, Paul JL, Thurlbeck WM. The National Institutes of Health Intermittent Positive Pressure Breathing trial: pathology studies. I. Interrelationship between morphologic lesions. Am Rev Respir Dis 1985;132:937–45.
62. Niewoehner DE, Knoke JD, Kleinerman J. Peripheral airways as a determinant of ventilatory function in the human lung. J Clin Invest 1977;60:131–51.
63. Ramsdale EH, Morris MM, Roberts RS, Hargreave FE. Bronchial responsiveness to methacholine in chronic bronchitis: relationship to airflow obstruction and cold air responsiveness. Thorax 1984;39:912–8.
64. Yan K, Salome CM, Woolcock AJ. Prevalence and nature of bronchial hyperresponsiveness in subjects with chronic obstructive pulmonary disease. Am Rev Respir Dis 1985; 132:25–9.
65. Arnup ME, Mendella LA, Anthonisen NR. Effects of cold air hyperpnea in patients with chronic obstructive lung disease. Am Rev Respir Dis 1983;128:236–9.
66. Benson MK. Bronchial responsiveness to inhaled histamine and isoprenaline in patients with airway obstruction. Thorax 1978;33:211–3.
67. Woolcock AJ, Peat JK, Salome CM, et al. Prevalence of bronchial hyper-responsiveness and asthma in a rural adult population. Thorax 1987;42:361–8.
68. Welty C, Weiss ST, Tager IB, et al. The relationship of airways responsiveness to cold air, cigarette smoking and atopy to respiratory symptoms and pulmonary function in adults. Am Rev Respir Dis 1984;130:198–203.
69. Sparrow D, O'Connor G, Colton T, et al. The relationship of nonspecific bronchial responsiveness to the occurrence of respiratory symptoms and decreased levels of pulmonary function. The normative aging study. Am Rev Respir Dis 1987;135:1255–60.
70. Tashkin DP, Altose MD, Connett JE, et al. Methacholine reactivity predicts changes in lung function over time in smokers with early chronic obstructive pulmonary disease. The Lung Health Study Research Group. Am J Respir Crit Care Med 1996;153(6 Pt 1):1802–11.
71. Sun W, Wu R, Last JA. Effects of exposure to environmental tobacco smoke on a human tracheobronchial epithelial cell line. Toxicology 1995;100:163–74.
72. Simani IAS, Inove S, Hogg JC. Penetration of the respiratory epithelium of guinea pigs following exposure to cigarette smoke. Lab Invest 1974;31:75–87.
73. Boucher RC, Johnston J, Inove S, et al. The effect of cigarette smoke on the permeability of guinea pig airways. Lab Invest 1980;43:94–100.
74. Walker DC, Mackenzie A, Hulbert WC, Hogg JC. Cigarette smoke exposure and tight junctions of the epithelial cells of guinea pig trachea. Am Rev Respir Dis Suppl 1982;125:264.
75. Yager D, Shore S, Drazen JM. Airway luminal liquid. Sources and role as an amplifier of bronchoconstriction. Am Rev Respir Dis 1991;143:S52–4.
76. Yager D, Butler JP, Bastacky J, et al. Amplification of airway constriction due to liquid-filling of airway interstices. J Appl Physiol 1989;66:2873–84.
77. Phang PT, Keough MW. Inhibition of pulmonary surfactant by plasma from normal adults and from patients having cardiopulmonary bypass. J Thorac Cardiovasc Surg 1986; 91:248–51.
78. Macklem PT, Proctor DF, Hogg JC. The stability of peripheral airways. Respir Physiol 1970;8:191–203.
79. Rahman I, Smith CA, Lawson MF, et al. Induction of gamma-glutamylcysteine synthetase by cigarette smoke is associated with AP-1 in human alveolar epithelial cells. FEBS Lett 1996;396:21–5.
80. Mills PR, Davies RJ, Devalia JL. Airway epithelial cells, cytokines, and pollutants. Am J Respir Crit Care Med 1999;160:S38–43.
81. Mio T, Romberger DJ, Thompson AB, et al. Cigarette smoke induces interleukin-8 release from human bronchial epithelial cells. Am J Respir Crit Care Med 1997;155:1770–6.
82. Rusznak C, Bayram H, Devalia JL, Davies RJ. Impact of the environment on allergic lung diseases. Clin Exp Allergy 1997;27 Suppl 1:26–35.
83. Jones JG, Minty BD, Lawler P, et al. Increased alveolar epithelial permeability in cigarette smokers. Lancet 1980;1:66–8.
84. Joos GF, De Swert KO, Pauwels RA. Airway inflammation and tachykinins: prospects for the development of tachykinin receptor antagonists. Eur J Pharmacol 2001;429:239–50.
85. Maghni K, Taha R, Afif W, et al. Dichotomy between neurokinin receptor actions in modulating allergic airway responses in an animal model of helper T cell type 2 cytokine-associated inflammation. Am J Respir Crit Care Med 2000; 162:1068–74.
86. Payan DG, Brewster DR, Goetzl EJ. Specific stimulation of human T lymphocytes by substance P. J Immunol 1983;131:1613–5.
87. Moore TC, Whitley GA, Lami JL, Said SI. Substance P increases and prolongs increased output of T4 (CD4) lymphocytes from lymph nodes of sheep in vivo: is it a mediator of immunological memory? Immunopharmacology 1990;20: 207–16.
88. Rameshwar P, Ganea D, Gascon P. In vitro stimulatory effect of substance P on hematopoiesis. Blood 1993;81:391–8.
89. Derocq JM, Segui M, Blazy C, et al. Effect of substance P on cytokine production by human astrocytic cells and blood mononuclear cells: characterization of novel tachykinin receptor antagonists. FEBS Lett 1996;399:321–5.

90. Johnson AR, Ashton J, Schultz WW, Erdos EG. Neutral metalloendopeptidases in human lung tissue and cultured cells. Am Rev Respir Dis 1985;132:564–8.
91. Frossard N, Rhoden KJ, Barnes PJ. Influence of epithelium on guinea pig airway responses to tachykinins: role of endopeptidase and cyclooxygenase. J Pharmacol Exp Ther 1989;248:292–8.
92. Xue Q-F, Maurer R, Engel G. Selective distribution of beta- and alpha$_1$-adrenoreceptors in rat lung visualized by autoradiography. Arch Int Pharmacodyn Ther 1983;266:308–14.
93. Holroyde MC. The influence of epithelium on the responsiveness of guinea-pig isolated trachea. Br J Pharmacol 1986;87:501–7.
94. Vanhoutte PM. Airway epithelium and bronchial reactivity. Can J Physiol Pharmacol 1987;65:448–50.
95. Wright JL, Wiggs BJ, Hogg JC. Airway disease in upper and lower lobes in lungs of patients with and without emphysema. Thorax 1984;39:282–5.
96. Bosken CH, Wiggs BR, Paré PD, Hogg JC. Small airway dimensions in smokers with obstruction to airflow. Am Rev Respir Dis 1990;142:563–70.
97. Moreno RH, Hogg JC, Paré PD. Mechanics of airway narrowing. Am Rev Respir Dis 1986;133:1171–80.
98. Wiggs BR, Bosken C, Paré PD, et al. A model of airway narrowing in asthma and in chronic obstructive pulmonary disease. Am Rev Respir Dis 1992;145:1251–8.
99. Gunst SJ, Warner DO, Wilson TA, Hyatt RE. Parenchymal interdependence and airway response to methacholine in excised dog lobes. J Appl Physiol 1988;65:2490–7.
100. Macklem PT. Factors determining bronchial smooth muscle shortening. Am Rev Respir Dis 1991;143:S47–8.
101. Ding DJ, Martin JG, Macklem PT. Effects of lung volume on maximal methacholine-induced bronchial constriction in normal humans. J Appl Physiol 1987;62:1324–30.
102. Bellofiore S, Eidelman DH, Macklem PT, Martin JG. Effects of elastase-induced emphysema on airway response to methacholine in rats. J Appl Physiol 1990;66:606–12.
103. Anderson AE, Foraker AG. Relative dimensions of bronchioles and parenchymal spaces in lungs from normal subjects and emphysematous patients. Am J Med 1962;32:218–26.
104. Saetta M, Ghezzo H, Kim WD, et al. Loss of alveolar attachments in smokers. A morphometric correlate of lung function impairment. Am Rev Respir Dis 1985;132:894–900.
105. Petty TL, Silvers GW, Stanford RE. Radial traction and small airways disease in excised human lungs. Am Rev Respir Dis 1986;133:132–5.
106. Nagai A, Yamawaki I, Takizawa T, Thurlbeck WM. Alveolar attachments in emphysema of human lungs. Am Rev Respir Dis 1991;144:888–91.
107. Berend N, Skoog C, Thurlbeck WM. Exponential analysis of lobar pressure–volume characteristics. Thorax 1981;36:452–5.
108. Berend N, Skoog C, Thurlbeck WM. Lobar pressure–volume characteristics of excised human lungs. Thorax 1981;36:290–5.
109. Hogg JC, Nepszy SJ, Macklem PT, Thurlbeck WM. Elastic properties of the centrilobular emphysematous space. J Clin Invest 1969;48:1306–12.
110. Eidelman DH, Ghezzo H, Kim WD, et al. Pressure–volume curves in smokers. Comparison with alpha-1-antitrypsin deficiency. Am Rev Respir Dis 1989;139:1452–8.
111. Kim WD, Eidelman DH, Izquierdo JL, et al. Centrilobular and panlobular emphysema in smokers. Two distinct morphologic and functional entities. Am Rev Respir Dis 1991;144: 1385–90.
112. Wright RR. Elastic tissue of normal and emphysematous lungs. A tridimensional histologic study. Am J Pathol 1961;39:355–63.
113. Fukuda Y, Masuda Y, Ishizaki M, et al. Morphogenesis of abnormal elastic fibers in lungs of patients with panacinar and centriacinar emphysema. Hum Pathol 1989;20:652–9.
114. Angus GE, Saetta M, Wang N-S, et al. SEM morphometric description of emphysema type. Am Rev Respir Dis 1984;129:A321.
115. Cosio MG, Shiner RJ, Saetta M, et al. Alveolar fenestrae in smokers. Relationship with light microscopic and functional abnormalities. Am Rev Respir Dis 1986;133:126–31.
116. Saetta M, Izquierdo JL, Kim WD, Cosio MG. Centrilobular and panacinar emphysema in smokers. Two different diseases. Am Rev Respir Dis 1990;141:A713.
117. Finkelstein R, Ma HD, Ghezzo H, et al. Morphometry of small airways in smokers and its relationship to emphysema type and hyperresponsiveness. Am J Respir Crit Care Med 1995; 152:267–76.
118. Leopold JC, Gough J. The centrilobular form of hypertrophic emphysema and its relation to chronic bronchitis. Thorax 1957;12:219–25.
119. Anderson AE, Foraker AG. Centrilobular emphysema and panlobular emphysema: two different diseases. Thorax 1973; 27:547–50.
120. Pauwels RA, Buist AS, Ma P, et al. Global strategy for the diagnosis, management, and prevention of chronic obstructive pulmonary disease. National Heart, Lung, and Blood Institute and World Health Organization Global Initiative for Chronic Obstructive Lung Disease (GOLD): Executive Summary. Respir Care 2001;46:798–825.
121. Berend N. Lobar distribution of bronchiolar inflammation in emphysema. Am Rev Respir Dis 1981;124:218–20.
122. Bosken CH, Hards J, Gatter K, Hogg JC. Characterization of the inflammatory reaction in the peripheral airways of cigarette smokers using immunocytochemistry. Am Rev Respir Dis 1992;145:911–7.
123. Fournier M, Lebargy F, Le Roy Ladurie F, et al. Intraepithelial T-lymphocyte subsets in the airways of normal subjects and of patients with chronic bronchitis. Am Rev Respir Dis 1989;140:737–42.
124. Saetta M, Di Stefano A, Maestrelli P, et al. Activated T-lymphocytes and macrophages in bronchial mucosa of subjects with chronic bronchitis. Am Rev Respir Dis 1993; 147:301–6.
125. Eidelman DH, Ghezzo H, Kim WD, Cosio MG. The Destructive Index and early lung destruction in smokers. Am Rev Respir Dis 1991;144:156–9.
126. Saetta M, Shiner RJ, Angus GE, et al. Destructive Index (DI): a measurement of lung parenchymal destruction in smokers. Am Rev Respir Dis 1985;131:764–9.
127. Finkelstein R, Fraser RS, Ghezzo H, Cosio MG. Alveolar inflammation and its relation to emphysema in smokers. Am J Respir Crit Care Med 1995;152:1666–72.
128. Zhu J, Majumdar S, Qiu Y, et al. Interleukin-4 and interleukin-5 gene expression and inflammation in the mucus-secreting glands and subepithelial tissue of smokers with chronic bronchitis. Lack of relationship with CD8(+) cells. Am J Respir Crit Care Med 2001;164:2220–8.
129. Sempowski GD, Beckmann MP, Derdak S, Phipps RP. Subsets of murine lung fibroblasts express membrane-bound and soluble IL-4 receptors. Role of IL-4 in enhancing fibroblast proliferation and collagen synthesis. J Immunol 1994;152: 3606–14.
130. Saetta M, Di Stefano A, Turato G, et al. CD8+ T-lymphocytes in peripheral airways of smokers with chronic obstructive pulmonary disease. Am J Respir Crit Care Med 1998;157: 822–6.
131. O'Shaughnessy TC, Ansari TW, Barnes NC, Jeffery PK. Inflammation in bronchial biopsies of subjects with chronic bronchitis: inverse relationship of CD8+ T lymphocytes with FEV1. Am J Respir Crit Care Med 1997;155:852–7.
132. Saetta M, Mariani M, Panina-Bordignon P, et al. Increased expression of the chemokine receptor CXCR3 and its ligand

CXCL10 in peripheral airways of smokers with chronic obstructive pulmonary disease. Am J Respir Crit Care Med 2002;165:1404–9.
133. Loetscher M, Gerber B, Loetscher P, et al. Chemokine receptor specific for IP10 and mig: structure, function, and expression in activated T-lymphocytes. J Exp Med 1996;184:963–9.
134. Qin S, Rottman JB, Myers P, et al. The chemokine receptors CXCR3 and CCR5 mark subsets of T cells associated with certain inflammatory reactions. J Clin Invest 1998;101: 746–54.
135. Di Stefano A, Caramori G, Capelli A, et al. STAT4 activation in smokers and patients with chronic obstructive pulmonary disease. Eur Respir J 2004;24:78–85.
136. Majo J, Ghezzo H, Cosio MG. Lymphocyte population and apoptosis in the lungs of smokers and their relation to emphysema. Eur Respir J 2001;17:946–53.
137. Saetta M, Baraldo S, Corbino L, et al. CD8+ve cells in the lungs of smokers with chronic obstructive pulmonary disease. Am J Respir Crit Care Med 1999;160:711–7.
138. Retamales I, Elliott WM, Meshi B, et al. Amplification of inflammation in emphysema and its association with latent adenoviral infection. Am J Respir Crit Care Med 2001;164: 469–73.
139. Kasahara Y, Tuder RM, Cool CD, et al. Endothelial cell death and decreased expression of vascular endothelial growth factor and vascular endothelial growth factor receptor 2 in emphysema. Am J Respir Crit Care Med 2001;163: 737–44.
140. D'Armiento J, Franke T, Imai K. Apoptosis in human emphysema lungs. Implication for novel therapeutic strategies. Am J Respir Crit Care Med 2000;161:A812.
141. Yokohori N, Aoshiba K, Yasui S, Nagai A. Epithelial apoptosis in a murine model of elastase-induced pulmonary emphysema. Am J Respir Crit Care Med 2000;161:A817.
142. Turato G, Zuin R, Miniati M, et al. Airway inflammation in severe chronic obstructive pulmonary disease: relationship with lung function and radiologic emphysema. Am J Respir Crit Care Med 2002;166:105–10.
143. Guerrassimov A, Takubo Y, Turcotte A, et al. The development of emphysema in cigarette smoke exposed mice is strain dependent. Am J Respir Crit Care Med 2004;170:1–8.
144. Cosio MG, Majo J, Cosio MG. Inflammation of the airways and lung parenchyma in COPD: role of T cells. Chest 2002; 121:160S–5S.
145. Augusti A, MacNee W, Donaldson K, Cosio M. Hypothesis: does COPD have an autoimmune component? Thorax 2003; 58:832–4.
146. Cosio MG. Autoimmunity, T-cells and STAT-4 in the pathogenesis of chronic obstructive pulmonary disease. Eur Respir J 2004;24:3–5.

CHAPTER 11

STRUCTURE–FUNCTION CORRELATIONS IN ASTHMA

Mara Ludwig

It is axiomatic that changes in lung structure will necessarily lead to changes in lung function. This is generally true in asthma. Changes in the structure of the airway wall have been well documented in asthma.[1,2] From a theoretical standpoint, it is reasonable to predict that such anatomic changes will result in alterations in airflow resistance and, hence, expiratory flow. In addition, a thickened airway wall should affect the consequences of airway smooth muscle shortening and, hence, bronchial hyperresponsiveness. However, the data on structural remodeling of the asthmatic airway and the resultant effects on airway function are somewhat controversial.

The effects of parenchymal changes in asthma are less clear. There is evidence in animal models of alterations in parenchymal structure, but fewer data are available for human disease. Furthermore, the contribution of the lung parenchyma to alterations in lung function in asthma is still being defined. Establishment of the precise link between changes in parenchymal structure and function will require further study.

In this chapter, I examine the changes in lung structure at the level of the conducting airways and more distal lung in asthma, the theory predicting how such changes should affect lung mechanical behavior, and the actual data documenting changes in physiology. Studies in both humans and animals are addressed.

STRUCTURAL CHANGES IN THE AIRWAY

The airway wall consists of several layers, including the epithelial layer, the basement membrane and subepithelium, and the airway smooth muscle layer. In addition, mucous glands and small vessels form part of the structure of the airway wall. Changes in all of these components have been described in asthma.

Damage to the epithelium has been described in both postmortem and endobronchial biopsy specimens from asthmatic central airways[3] (Figure 11-1). Some controversy has arisen as to whether some of these alterations may relate to sampling artifacts as opposed to actual in situ abnormalities. Nonetheless, increased epithelial shedding seems to be a feature of asthmatic airways, especially in more severe disease. The functional alterations arising from these changes are more likely due to alterations in epithelial-derived mediators, for example, nitric oxide,[4] rather than alterations in lung mechanics per se.

Recently, a great deal of attention has been paid to structural alterations in the basement membrane and subepithelial layer in asthma. Some of this attention can be attributed to the fact that, with endoscopic biopsy, this portion of the airway tree can be readily sampled. Roche and colleagues[5] performed some of the initial studies with this approach to examine the epithelial basement membrane and subepithelium in mildly asthmatic subjects. They showed that the reticular basement membrane was primarily affected, the loose network of collagen fibrils having been replaced by a much denser one. Fibronectin, a glycoprotein, was up-regulated, especially in the subepithelial region. This report spurred a number of studies on patients with asthma of varying severity, in which extensive changes in this layer of the airway wall were documented. Further reports have identified increases in specific collagen subtypes[6] and in the glycoprotein tenascin.[7] Mauad and colleagues[8] examined potential changes in the elastic fiber system in the airways of patients dying from fatal asthma. These authors showed elastosis in central airways; elastic fiber content was significantly decreased. We have been interested in potential changes in proteoglycans, a class of extracellular matrix molecules that are involved in the regulation of tissue hydration and turgor and that interact with various cytokines and growth factors, for example, transforming growth factor (TGF)-β, known to be up-regulated in the asthmatic airway wall.[9–11] In a study conducted in mild, atopic asthmatic patients, the amounts of various proteoglycans, including versican, lumican, and biglycan, were increased in the subepithelial layer of the asthmatic airway wall compared with that of control subjects[12] (Figure 11-2). Whereas we did not document changes in the small proteoglycan decorin, a molecule that has been shown to interact directly with TGF-β,[13] Redington and colleagues[14] were able to demonstrate colocalization of TGF-β and decorin in bronchial biopsy specimens from patients with mild asthma. Roberts[15] has

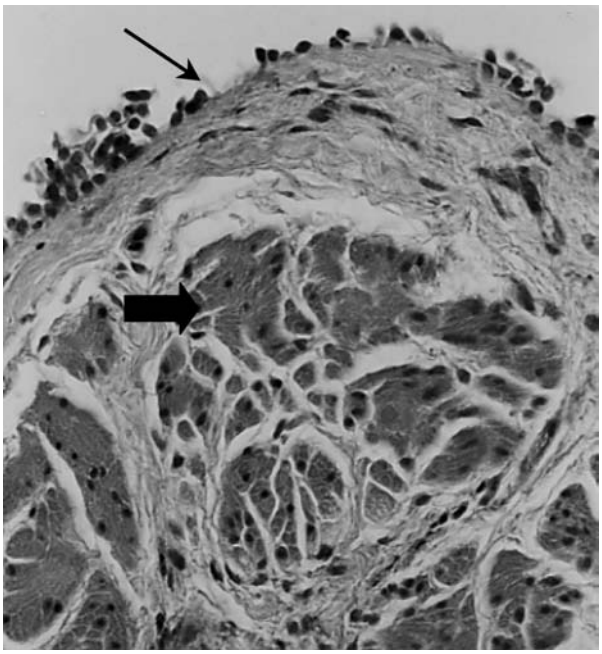

FIGURE 11-1 Epithelial damage (*thin arrow*) and increased airway smooth muscle (*thick arrow*) in an endobronchial biopsy specimen of an asthmatic patient Hematoxylin-eosin stain; ×200 original magnification. Reproduced with permission from Hamid Q. Gross pathology and histopathology in asthma. J Allergy Clin Immunol 2003;111:431–2.

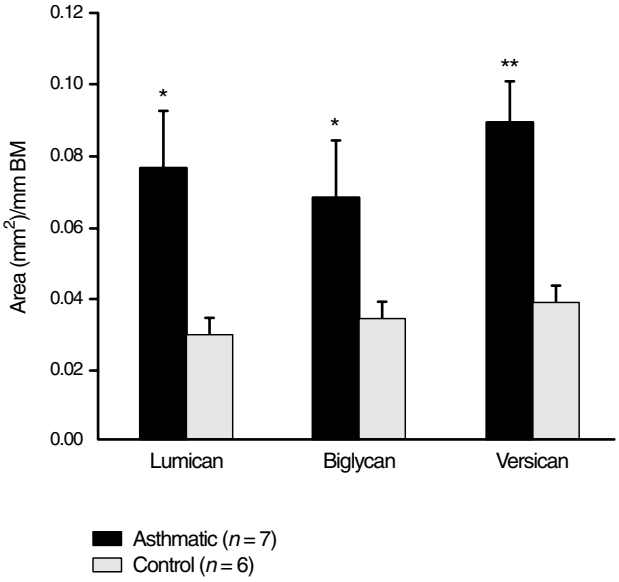

FIGURE 11-2 Increases in immunostaining for lumican, biglycan, and versican in endobronchial biopsy specimens from asthmatic patients versus normal controls. $*p < .05$; $**p < .01$. BM-basement membrane. Reproduced with permission from Huang J et al.[12]

reported an abundance of versican and decorin in postmortem specimens of airways in patients who died of fatal asthma. Insofar as these molecules are known to affect the biomechanical characteristics of the matrix,[9] alterations in their deposition in the asthmatic airway wall may have greater significance than simply their effect on the amount of airway wall thickening, as is discussed below.

The putative cell responsible for these alterations in the extracellular matrix is the myofibroblast. The myofibroblast has both synthetic and contractile phenotypes. The number of myofibroblasts has been shown to be increased in the collagen layer of the asthmatic airway wall.[16] Furthermore, Gizycki and colleagues[17] have shown that, in asthmatic patients, allergen inhalation can result in an influx of myofibroblast-like cells into the airway wall 24 hours postchallenge. The precise nature of the myofibroblast is, however, somewhat controversial. Whether this cell represents a dedifferentiated smooth muscle cell or fibroblast, or a separate cell type entirely, is not clear.

There is abundant evidence in the literature that airway smooth muscle mass is increased in asthma (see Figure 11-1). Data have been gathered from cases of asthma of varying severity, including fatal asthma, and changes have been noted in airways of different dimensions.[18–20] Similar results have been obtained from animal models in which "asthma" has been induced via sensitization.[21] In addition to the potential effect of increased smooth muscle mass on airway constriction, these cells also have synthetic properties and the capacity to affect the extracellular matrix, especially that in the region of the smooth muscle layer.[22] Hence, alterations in airway smooth muscle may also affect airway function via an effect on matrix deposition.

It has been reported that the bronchial vascular area is increased in both fatal and nonfatal asthma.[23] Changes have been described primarily in the submucosal area. Li and colleagues[24,25] found increases in the number and size of bronchial vessels in asthmatic airway walls. However, Carroll and colleagues[26] found no change in the total number of blood vessels or the total area occupied by vessels corrected for square millimeter of submucosa. These authors did show that the area and number of large blood vessels in cartilaginous airways were increased; however, the vasculature in the smaller airways was unchanged. More recently, Tanaka and colleagues[27] have reported on a novel technique, high-magnification bronchovideoscopy, which permits direct visualization of airway vasculature in situ. Using this approach, the authors found increases in subepithelial vascularity in the airway walls of both recently diagnosed and more chronic asthmatics.

Finally, mucous gland hypertrophy is well described in asthma and is thought to be important in the excessive production of mucus encountered in these patients. Carroll and colleagues[18] have shown that the area of mucous glands is increased throughout the airway tree; airways of patients with fatal asthma showed a greater increase in mucous gland area than did airways of patients with nonfatal asthma. Both were increased relative to airways of control subjects. Asthmatic patients who die of their disease often have airways occluded with mucus.

HOW STRUCTURAL CHANGES LEAD TO FUNCTIONAL CHANGES

Theoretical Considerations

Extensive work has been done to model the effects of a thickened airway wall on airway mechanics. Two effects require consideration. One is the effect of a thickened airway

on airway resistance due to a decrease in the lumen of the airway. Under laminar flow conditions, resistance is proportional to the inverse of the radius to the fourth power ($1/r^4$). Therefore, a relatively small decrease in the diameter of the airway lumen will have a large impact on airflow resistance. The second issue relates to the effect of a thickened airway wall on induced airway narrowing. Moreno and colleagues[28,29] generated a model that made possible an examination of the effects of airway wall thickening on both airway resistance and induced airway narrowing. Essentially, this model predicts that, as the airway wall thickens, the amount of luminal narrowing as a consequence of airway smooth muscle shortening will be greatly enhanced. Although the effect on baseline airway resistance may be modest, the effect on the resistance of the constricted airway will be substantial[30] (Figure 11-3). Furthermore, because of the airway wall thickening in asthmatic airways, less airway smooth muscle shortening is required for the airways to occlude.[31] Subsequent analysis by this same group, using this modeling approach and morphometric measurements taken from asthmatic patients, implicated increased smooth muscle mass as a primary determinant of the increased airway resistance in response to constrictor stimuli in asthmatic patients.[32] Hence, remodeling and thickening of the subepithelial and smooth muscle layer, such as has been demonstrated in asthmatic airways, should have important consequences in terms of the physiologic function of the airways.

Other aspects of the changes in the airway wall structure also need to be included in these types of analyses. The folding of the basement membrane that occurs as a consequence of bronchoconstriction requires energy. The basement membrane buckles into folds—the number of folds may affect the bronchial response measured during induced constriction.[33] Therefore, remodeling of the basement membrane has the potential to affect airway responsiveness via effects on mucosal folding. Lambert and colleagues[34] suggested that the increased basement membrane thickness observed in asthma has the potential to function in a protective fashion, by decreasing airway constriction in response to a contractile stimulus via this mechanism. This point raises the issue of whether remodeling in the asthmatic airway wall is necessarily a negative outcome.

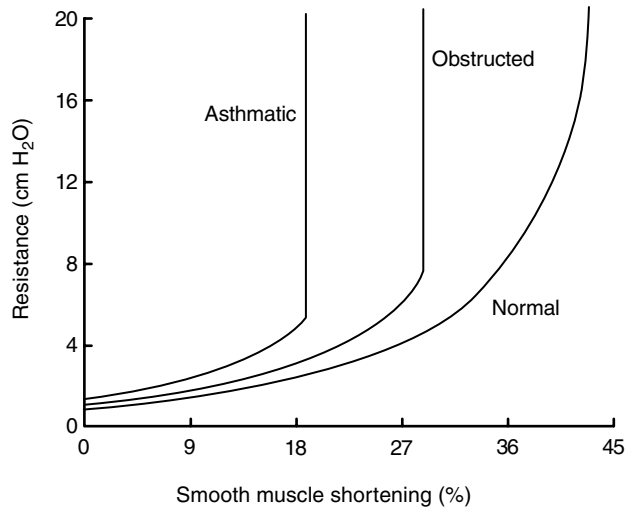

FIGURE 11-3 Pulmonary resistance, calculated with use of the model of Moreno and colleagues, versus airway smooth muscle shortening. Wall thickening, which modestly increases baseline resistance, has profound effects on airway smooth muscle shortening and, hence, airway responsiveness. Reproduced with permission from Paré PD et al.[30]

A further consideration is the potential change in the mechanical characteristics or viscoelastic properties of the airway wall with the airway remodeling observed in asthma. As mentioned above, extensive changes have been described in collagen and proteoglycans in the submucosal layer. These molecules are important in determining the viscoelastic properties of the extracellular matrix and hence may alter the overall mechanical properties of the airway wall. Collagen is well known to contribute to the elastic properties of extracellular matrices. More recently, we published data demonstrating that proteoglycans contribute to the viscoelastic properties of lung tissue.[35] Digestion of glycosaminoglycan side chains of proteoglycan molecules led to alterations of mechanical properties in peripheral lung strips. More recent data from work on decorin-deficient mice—decorin is important in collagen fiber assembly—showed that elastic properties were altered and that airway resistance was decreased in these animals.[36] Hence, alterations in the deposition of these molecules in the airway wall have the potential to affect airway elastance. As airway smooth muscle constricts against the load offered by the airway wall, changes in the mechanical properties of the airway wall will have consequences for airway smooth muscle shortening and airway narrowing. Some data are available on this precise question. Bramley and colleagues[37] used collagenase, a nonspecific proteolytic enzyme that degrades various extracellular matrix components, to alter the viscoelastic properties of human bronchial strips. Shortening in response to electric field stimulation and histamine was markedly enhanced. In a bronchial specimen obtained from an asthmatic patient undergoing lobectomy, the elastance of the airway was less than that of airways obtained from control subjects; active shortening was increased.[38] However, whether asthmatic patients generally have decreased airway elastance is not clear. One might predict that increased collagen and proteoglycan deposition should lead to increased elastance. A recent report by Brackel and colleagues[39] on 10 asthmatic patients supports this notion; airway compliance (the inverse of elastance) measured in vivo with a pressure probe (the Pitot probe) was decreased in the asthmatic patients compared with controls; that is, the airways were indeed stiffer.

Although the precise nature of the change in the vasculature in the airway wall is not entirely clear, vascular engorgement could theoretically cause narrowing of the lumen and airway obstruction. However, investigation of this hypothesis in animals[40] has failed to establish this mechanism. A further consideration is the effect of edema fluid on airway narrowing. Airway interstices could be filled with edema fluid, resulting in a decrease in luminal area; alternatively, the surface properties of the surfactant layer could be

compromised, leading to small airway collapse.[41] Again, studies in animals have not confirmed the importance of this mechanism in enhanced bronchoconstriction.[42] Finally, remodeling of the airways could affect airway narrowing because of the mechanism of airway–parenchymal interdependence. In addition to airway smooth muscle contracting against the load offered by the elastance of the airway, the smooth muscle must shorten against the load offered by the parenchymal attachments tethering the airway wall.[43] Changes in the adventitia, the layer to which the parenchyma is attached, could affect the transmission of load to the airway wall. Alternatively, changes in the viscoelastic properties of the airway wall could affect the mechanical interaction between the alveolar attachments and the airway wall.

Clinical Data

As delineated above, there is compelling evidence that the airway wall is substantially remodeled in asthmatic patients and that, theoretically, such remodeling should result in physiologic changes in airway behavior, in terms of both baseline airway resistance and sensitivity to induced constriction. However, the clinical data that support this association are not conclusive. There are conflicting reports on whether increases in submucosal thickness result in altered airway responsiveness and whether inhaled corticosteroids have a modulating effect on the observed structural changes in the airway wall remodeling, coincident with the documented improvements in physiology. There is some clinical evidence that thickened airways function differently from normal. Minshall and colleagues[11] showed that subepithelial fibrosis was inversely correlated with forced expiratory volume in 1 second (FEV_1) (% predicted) (Figure 11-4). In a

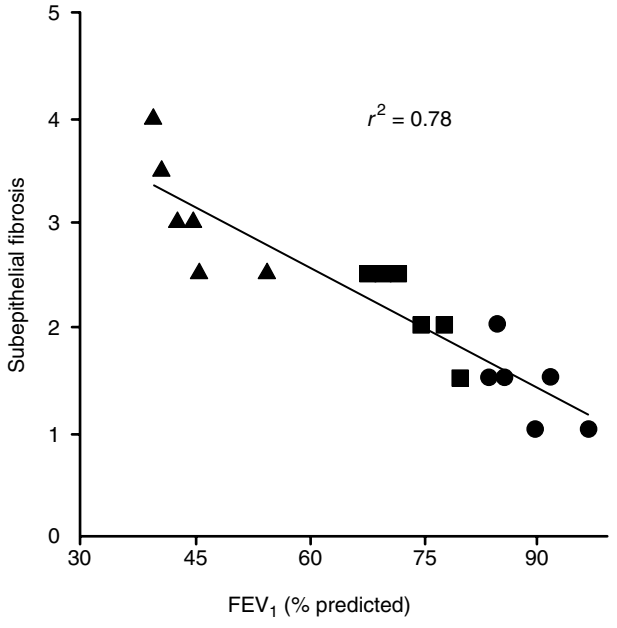

FIGURE 11-4 Correlation between subepithelial fibrosis and FEV_1 (% predicted) in the airway wall of asthmatic subjects. r = regression coefficient. Reproduced with permission from Minshall EM et al.[11]

further study by this group,[44] collagen subtypes were characterized. There was a "dose–response" relationship between severity of asthma, as defined by FEV_1 (% predicted), and the amounts of both collagen I and collagen III in the subepithelium. In the study on proteoglycans in the asthmatic airway wall, there was a significant inverse correlation between the area of positive immunostaining for the proteoglycans lumican and biglycan and the PC_{20} (provocative concentration required to cause a fall in FEV_1 of 20%) to methacholine.[12] Westergren-Thorsson and colleagues[45] examined the production of proteoglycans by fibroblasts isolated from endobronchial biopsy specimens from subjects with mild, atopic asthma. They showed a significant negative correlation between perlecan, versican, biglycan, and small heparan sulfate proteoglycan and PC_{20} to methacholine. These data support the hypothesis that proteoglycans may be responsible for the enhanced airway responsiveness of these mildly asthmatic patients. The mechanism could involve resultant airway wall thickening or proteoglycan effects on mechanical behavior and load of the airway wall. Supporting this hypothesis are the data of Vignola and colleagues,[46] who showed that the matrix metalloproteinase-9 (MMP-9)/tissue inhibitor of metalloproteinase-1 (TIMP-1) ratio was correlated with FEV_1 (% predicted). MMP-9 is a matrix metalloproteinase that has the capacity to degrade extracellular matrix proteins, and TIMP-1 is its inhibitor. The interpretation offered by these authors is that the relative amounts of these two enzymes can impact on airway remodeling and, hence, airway function.

On the other hand, some investigators have been unable to document such a link between structure and function. Chu and colleagues[6] reported on subjects with asthma of varying severity, again differentiated by FEV_1 (% predicted), but also by use of inhaled and/or oral corticosteroids. They found no correlation between collagen deposition and FEV_1 (% predicted) or between collagen deposition and duration of asthma. One might argue that these data are more difficult to interpret because of the potential effects of steroids on airway remodeling, but, as we shall discuss, the effects of steroids on the remodeling process are far from clear. A further study concerning this question is one in which the effects of age and asthma duration on airway structure were examined in airways from patients with fatal asthma.[47] Over time, the airway obstruction of asthma tends to become irreversible.[48] One might predict that the mechanism for this fixed obstruction would be a chronically remodeled airway. The results are somewhat inconclusive. Whereas overall airway narrowing was more severe in older asthmatic patients, subepithelial collagen and connective tissue matrix within the airway smooth muscle layer were similar in both young and old asthmatic patients; there was a trend toward more smooth muscle in the older group. Surprisingly, young asthmatic patients who succumbed to their disease had little change in the dimensions of the airway wall compared with age-matched controls. This suggests that other factors, such as smooth muscle constriction, may contribute to the fatal outcome rather than airway remodeling per se.

Relatively few data are available on the question of changes in airway smooth muscle and severity of asthma.

The lack of data is largely due to a sampling problem, that is, the relative inaccessibility of the smooth muscle layer to biopsy techniques. Recently, Benayoun and colleagues[49] published a study on subjects with asthma of different severity in which the airway smooth muscle was sampled, as were mucous glands, subepithelial basement membrane, fibroblasts, etc. Airways of patients with severe asthma were distinguished by larger numbers of fibroblasts, increased mucous gland size, increased airway smooth muscle area, and increased cell size, compared with those of patients with less severe asthma, controls, and patients with chronic obstructive pulmonary disease. Moreover, airflow obstruction was inversely correlated with fibroblast number and airway smooth muscle cell size. This is the first study linking changes in airway smooth muscle with indices of altered physiology.

Further information can be gleaned from studies on the effects of inhaled steroids on airway remodeling and lung function. If airway remodeling results in altered physiology, then abrogation of airway remodeling by steroid therapy should result in improvements in mechanical behavior. The results are conflicting. First, there are discrepant data concerning whether inhaled corticosteroids cause reversal of remodeling. Jeffrey and colleagues[50] were able to show changes in inflammatory cells in the airway wall of asthmatics treated with inhaled budesonide but no difference in thickening of the reticular basement membrane. Other investigators have shown a steroid effect on remodeling. In various studies,[7,51,52] decreases in tenascin, collagen type III, and basement membrane thickness have been described after steroid treatment durations ranging from 4 weeks to 4 months. Several explanations have been offered for these discrepant findings, including variations in type of inhaled steroid, dosage, and treatment duration. One suggestion that is particularly interesting is that treatment must be provided before remodeling is established. Vanacker and colleagues[53] investigated this hypothesis in an animal model, the Brown Norway rat model of allergen-induced asthma. They showed that inhaled steroids affected subsequent allergen-induced airway remodeling only if steroids were administered concomitantly with the allergic stimulus. Steroids delivered after the fact, that is, after airway remodeling was established, had no impact.

If one accepts the notion that steroids can modulate airway remodeling, then the next question is whether changes in the structure are mirrored by changes in physiologic function. Again, discrepant results are reported in the literature. Whereas Olivieri and colleagues[51] found changes in both basement membrane thickness and bronchial responsiveness (as measured by PC_{20}), Trigg and colleagues[52] found no differences in FEV_1 or PC_{20} despite decreases in their index of remodeling (collagen type III deposition in the lamina reticularis). In a study conducted in the rat model of asthma,[53] differences in both fibronectin deposition and airways responsiveness were found. In none of these studies was an attempt made to directly correlate changes in the two parameters, that is, airway remodeling and function. In one study, an attempt was made to define steroid-induced changes in vascularity.[54] Asthmatic patients receiving beclomethasone were shown to have reduced numbers of vessels in the lamina propria compared with asthmatic patients not receiving inhaled steroids. Furthermore, the authors attempted to correlate numbers of vessels with airway responsiveness and bronchodilator response. They found an inverse relationship between steroids and PD_{20} and a positive relationship between steroids and salbutamol-induced bronchodilatation. These data, although preliminary (r^2 values were of the order of .14 and .24, respectively), are provocative.

Although there is some information available on remodeling of the submucosa and submucosal vessels and changes in function with steroid therapy, little is known about steroid-induced changes in the smooth muscle layer and changes in airway function. This again relates to the tendency to sample only the more superficial layer of the airway wall with endoscopic biopsy.

AIRWAY REMODELING: A POSITIVE OUTCOME?

Finally, the idea that airway remodeling may represent an adaptive or protective response deserves some discussion. As outlined above, alterations in the matrix of the airway wall could impact on constriction-induced airway narrowing in a modulating fashion. Changes in the viscoelastic properties of the airway wall, at the level of the submucosa, the smooth muscle, or the adventitia, could all affect the load against which the airway smooth muscle must shorten. Increased resistance and/or elastance of the tissues would render shortening of the airway smooth muscle more difficult. Changes in the reticular basement membrane could alter the folding tendencies of the bronchial mucosa and hence the decrease in airway lumen with induced constriction. Finally, alterations in the viscoelastic properties of the matrix could impact on the response of the airway smooth muscle to volume perturbations, such as occur with a deep breath. In subjects with mild asthma, a deep breath can modify airway smooth muscle constriction, whereas in those with more severe asthma, a deep breath can have a bronchoconstricting effect.[55] A matrix with different viscoelastic properties could affect the transmission of strain to the smooth muscle cell. Perhaps one of the key differences between people with mild and more severe asthma lies in the ability of the matrix to remodel in the appropriate way. This may also serve to account for many of the discrepant clinical findings documented in this review.

STRUCTURAL CHANGES IN THE DISTAL LUNG OR LUNG PARENCHYMA AND POTENTIAL EFFECTS ON LUNG FUNCTION

The role of the distal lung or lung parenchyma in contributing to asthmatic disease has received renewed attention in recent years. In part, this is because of new techniques for sampling the mechanical behavior of this portion of the lung. The alveolar capsule has permitted measurement of alveolar pressure and, hence, partitioning of lung resistance into airway and tissue components, at least in animal models of asthma.[56,57] Measurement of complex impedence of the lung with the use of multifrequency input signals has

allowed measurement of tissue mechanical properties in patients with asthma.[58] In addition, investigators have begun to sample distal lung tissue with transbronchial biopsy to identify pathologic changes at the alveolar level in asthmatic patients.[59] Two reviews have addressed the issue of the contribution of the distal lung and parenchymal tissues to the asthmatic response.[60,61]

The observation that the mechanical behavior of the lung tissues is altered in asthma was made several years ago by Woolcock and Read,[62] who described decreased lung recoil in asthmatic patients compared with normal subjects. This observation was confirmed by other investigators,[63,64] but a structural explanation for the observed increase in compliance was lacking. Gelb and colleagues[65] followed patients with chronic moderate and severe persistent asthma over several years and demonstrated that the changes in recoil persisted over time. In addition to the documented changes in the elastic properties of the lung, recent studies have defined alterations in the resistive properties of the lung parenchyma. Using complex impedance to measure tissue damping or resistance, Kaczka and colleagues[66] showed that certain subgroups of asthmatic patients had increased tissue resistance, which accounted in part for overall increases in lung resistance. Kaminsky and colleagues[67] used a more indirect approach to sample the resistive behavior of the lung tissues but also showed a change in the tissue resistive properties in asthmatic patients exposed to hyperpnea challenge.

Limited data are available on alterations in the structure of the lungs at the alveolar level. Studies in which transbronchial biopsy has been used to obtain alveolar tissue have focused primarily on inflammation in the alveolar wall.[61,68,69] Studies in patients with nocturnal and severe asthma have shown an influx of eosinophils, lymphocytes, and neutrophils at the alveolar level (Figure 11-5). Perhaps most intriguing was the correlation between the decrement in FEV_1 and number of alveolar inflammatory cells.[61,68] Unfortunately, potential changes in the structural cells or matrix components of the alveolar wall were not addressed by these investigators.

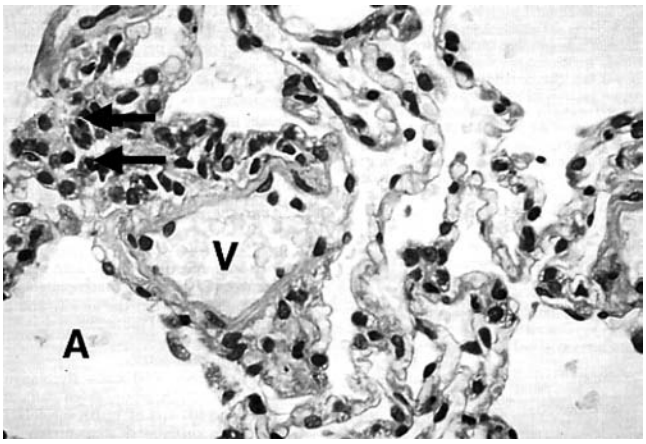

FIGURE 11-5 Photomicrograph of a transbronchial biopsy specimen from a subject with nocturnal asthma, showing eosinophilic infiltration into the alveolar wall (*arrows*). A-alveolar space; V-vessel. Reproduced with permission from Kraft M.[61]

Some information is available from animal models of asthma. Models of allergy that have been used to approach this question include the Brown Norway rat model and the BALB/c mouse.[57,70] In the rat model, measurements of parenchymal mechanics have been made with the alveolar capsule technique and the isolated parenchymal tissue strip.[57,71,72] The latter is a preparation that includes primarily alveolar wall,[73] and it has been extensively used to examine the mechanical and pharmacologic properties of the distal lung.[74,75] Using this model, investigators from our laboratory have shown that a large component of both the early and late asthmatic responses to inhaled ovalbumin in intact sensitized rats is attributable to changes in lung tissue resistance.[57] Further experiments in vitro confirmed that this response was occurring at the parenchymal level and did not simply reflect heterogeneous airway constriction. Addition of ovalbumin to the parenchymal strip in the organ bath elicited significant increases in the resistive and hysteretic behavior of the preparation.[72] Data from the ovalbumin-sensitized BALB/c mouse have confirmed these findings.[70] Tissue resistance was obtained with use of both the alveolar capsule and measurement of complex impedance. In the ovalbumin-sensitized mice, methacholine responsiveness was increased compared with nonsensitized animals; moreover, the bronchoconstrictor response occurred primarily at the level of the lung parenchyma. Another model that has been used is that of hyperpnea-induced bronchoconstriction in the guinea pig.[76,77] Experiments with this model, in which parenchymal mechanics were sampled with the alveolar capsule, again demonstrated that much of the constrictor response was occurring at the parenchymal level.

The anatomic changes occurring at the parenchymal level that give rise to the enhanced bronchoconstrictor response are unclear. Two possible mechanisms have been suggested. The first is contraction of "contractile interstitial cells" or myofibroblasts at the level of the alveolus or alveolar duct.[78,79] Work in our laboratory on parenchymal tissue strips obtained from surgical human specimens has shown that contractile responses to acetylcholine can occur in lung tissue that is essentially devoid of small airways.[79] The second mechanism that has been reported is distortion of the parenchymal tissues and alterations in alveolar geometry with induced constriction[57,80] (Figure 11-6). In the sensitized Brown Norway rat exposed to ovalbumin, the index of lung tissue distortion was significantly correlated ($r^2 = .89$) with the degree of the tissue resistance response. These data confirm a link between changes in structure and function at the parenchymal level. Whether substantial remodeling, such as has been defined in the airway wall, is occurring has not been addressed but certainly warrants investigation.

Finally, alterations in the structure of the parenchyma could have implications for airway function via the mechanism of airway–parenchyma interdependence.[81,82] As mentioned above, airway smooth muscle must contract against the load offered by the parenchymal attachments tethering the airway wall. Ding and colleagues,[82] in studies conducted in normal human volunteers, showed that changing the

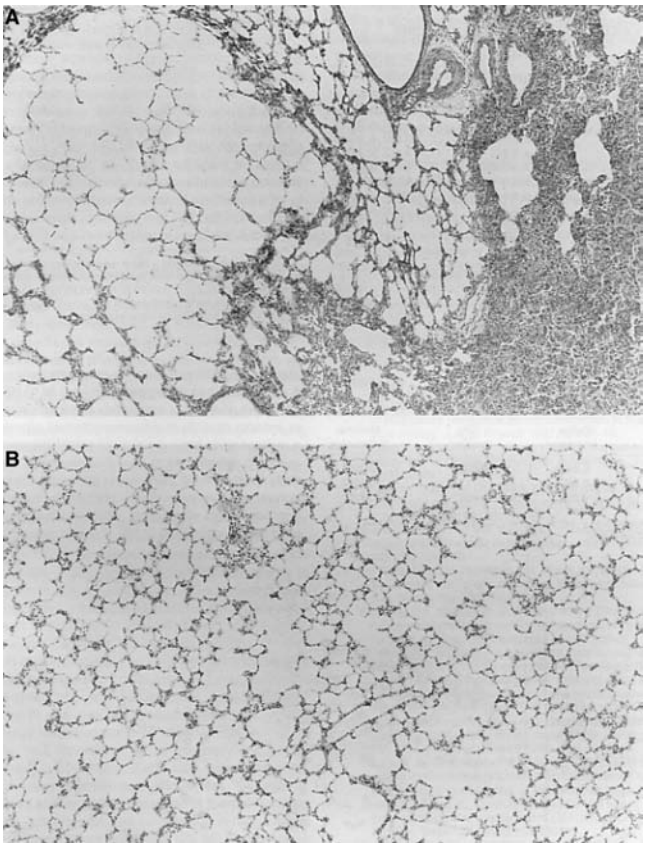

FIGURE 11-6 Photomicrograph of lung tissue from an ovalbumin-challenged sensitized Brown Norway rat (*A*) and a saline-challenged sensitized control (*B*). Note the distortion and atelectasis in the ovalbumin-challenged lung. Hemotoxylin-eosin stain; × 63 original magnification. Reproduced with permission from Nagase T et al.[57]

magnitude of the elastic recoil acting on the airways, by altering lung volume, had substantial effects on induced airway constriction. Alterations in the viscoelastic properties of the parenchymal attachments could impact on airway narrowing via this mechanism. The data showing changes in elastic recoil and tissue resistance in asthmatic patients[62,66] imply a change in the structural composition of the alveolar wall. Inflammation in the alveolar wall in asthmatic patients is now well documented.[61,68] That this inflammatory stimulation results in remodeling of the extracellular matrix such as occurs in the airway wall seems likely.

SUMMARY AND CONCLUSIONS

Remodeling of the airway wall in asthma is a well-established phenomenon. Theoretically, the described changes should result in enhancement of the airway narrowing observed in asthmatic disease, in terms of both baseline airway resistance and the response to induced constriction. However, there are also theoretical arguments to support the notion that remodeling could result in modulation of airway narrowing. The clinical data that support the association between changes in structure and function are somewhat discrepant, perhaps reflecting the fact that the nature of the remodeling that occurs, rather than the amount of remodeling per se, may be the critical determinant of the functional consequences. More detailed descriptions of asthmatic airway remodeling and its functional impact are required. The contribution of the distal lung or lung parenchyma to asthmatic disease is less evident. Well-deserved attention is now being paid to this compartment of the lung and its contribution to asthmatic pathology. Further investigation of the precise structural alterations in the lung parenchyma that take place in asthma, and their effects on both the functional behavior of the parenchyma and airway narrowing, is warranted.

REFERENCES

1. Jeffrey PK. Remodeling in asthma and chronic obstructive lung disease. Am J Respir Crit Care Med 2001;164:S28–38.
2. Bousquet J, Jeffrey PK, Busse WW, et al. From bronchoconstriction to airways inflammation and remodeling. Am J Respir Crit Care Med 2000;161:1720–45.
3. Laitinen LA, Heino M, Laitinen, et al. Damage of the airway epithelium and bronchial reactivity in patients with asthma. Am Rev Respir Dis 1985;131:599–606.
4. Hamid Q, Springall DR, Riveros-Moreno V, et al. Induction of nitric oxide synthase in asthma. Lancet 1993;342:1510–3.
5. Roche WR, Beasley R, Williams JH, Holgate ST. Subepithelial fibrosis in the bronchi of asthmatics. Lancet 1989;1:520–4.
6. Chu HW, Halliday JL, Martin RJ, et al. Collagen deposition in large airways may not differentiate severe asthma from milder forms of the disease. Am J Respir Crit Care Med 1998;158:1936–44.
7. Laitinen A, Altraja A, Kämpe M, et al. Tenascin is increased in airway basement membrane of asthmatics and decreased by an inhaled steroid. Am J Respir Crit Care Med 1997;156:951–8.
8. Mauad T, Xavier ACG, Saldiva PHN, Dolhnikoff M. Elastosis and fragmentation of fibers of the elastic system in fatal asthma. Am J Respir Crit Care Med 1999;160:968–75.
9. Iozzo RV. Matrix proteoglycans: from molecular design to cellular function. Annu Rev Biochem 1998;67:609–52.
10. Vignola AM, Chanez P, Chiappara G, et al. Transforming growth factor-β expression in mucosal biopsies in asthma and chronic bronchitis. Am J Respir Crit Care Med 1997;156:591–9.
11. Minshall EM, Leung DYM, Martin RS, et al. Eosinophil associated TGF-β_1 mRNA expression and airways fibrosis in bronchial asthma. Am J Respir Cell Mol Biol 1997;17:326–33.
12. Huang J, Olivenstein R, Taha R, et al. Enhanced proteoglycan deposition in the airway wall of atopic asthmatics. Am J Respir Crit Care Med 1999;160:725–9.
13. Yamaguchi Y, Mann DM, Ruoslahti E. Negative regulation of transforming growth factor-β by the proteoglycan decorin. Nature 1990;346:281–4.
14. Redington AE, Roche WR, Holgate ST, Howarth PH. Co-localization of immunoreactive transforming growth factor-beta1 and decorin in bronchial biopsies from asthmatic and normal subjects. J Pathol 1998;186:410–5.
15. Roberts CR. Is asthma a fibrotic disease? Chest 1995;107:111S–7S.
16. Brewster CEP, Howarth PH, Djukanovic R, et al. Myofibroblasts and subepithelial fibrosis in bronchial asthma. Am J Respir Cell Mol Biol 1990;3:507–11.
17. Gizycki MJ, Adelroth E, Rogers AV, et al. Myofibroblast involvement in the allergen-induced late response in mild atopic asthma. Am J Respir Cell Mol Biol 1997;16:664–73.
18. Carroll N, Elliot J, Morton A, James A. The structure of large and small airways in nonfatal and fatal asthma. Am Rev Respir Dis 1993;147:405–10.

19. Dunnill MS, Massarella GR, Anderson JA. A comparison of the quantitative anatomy of the bronchi in normal subjects, in status asthmaticus, in chronic bronchitis and in emphysema. Thorax 1969;24:176–9.
20. Saetta M, Di Stefano A, Rosina C, et al. Quantitative structural analysis of peripheral airways and arteries in sudden fatal asthma. Am Rev Respir Dis 1991;143:138–43.
21. Sapienza S, Du T, Eidelman DH, et al. Structural changes in the airways of sensitized Brown Norway rats after antigen challenge. Am Rev Respir Dis 1991;144:423–7.
22. Johnson PRA, Black JL, Carlin S, et al. The production of extracellular matrix proteins by human passively sensitized airway smooth-muscle cells in culture. Am J Respir Crit Care Med 2000;162:2145–51.
23. Kuwano K, Bosken CH, Pare PD, et al. Small airways dimensions in asthma and in chronic obstructive pulmonary disease. Am Rev Respir Dis 1993;148:1220–5.
24. Li X, Wilson JW. Increased vascularity of the bronchial mucosa in mild asthma. Am J Respir Crit Care Med 1997;156:229–33.
25. Orsida BE, Ward C, Li X, et al. Effect of a long acting β_2-agonist over three months on airway wall vascular remodeling in asthma. Am J Respir Crit Care Med 2001;164:117–21.
26. Carroll NG, Cooke C, James AL. Bronchial blood vessel dimensions in asthma. Am J Respir Crit Care Med 1997;155: 689–95.
27. Tanaka H, Yamada G, Saikai T, et al. Increased airway vascularity in newly diagnosed asthma using a high-magnification bronchovideoscope. Am J Respir Crit Care Med 2003;168: 1495–9.
28. Moreno RH, Hogg JC, Paré PD. Mechanics of airway narrowing. Am Rev Respir Dis 1986;133:1171–80.
29. Wiggs BR, Moreno R, Hogg JC, et al. A model of the mechanics of airway narrowing. J Appl Physiol 1990;69:849–60.
30. Paré PD, Wiggs BR, James A, et al. The comparative mechanics and morphology of airways in asthma and in chronic obstructive pulmonary disease. Am Rev Respir Dis 1991; 143:1189–93.
31. James AL, Parć PD, Hogg JC. The mechanics of airway narrowing in asthma. Am Rev Respir Dis 1989;139:242–6.
32. Lambert RK, Wiggs BR, Kuwano K, et al. Functional significance of increased airway smooth muscle in asthma and COPD. J Appl Physiol 1993;74:2771–81.
33. Lambert RK. Role of bronchial basement membrane in airway collapse. J Appl Physiol 1991;71:666–73.
34. Lambert RK, Codd SL, Alley MR, Pack RJ. Physical determinants of bronchial mucosal folding. J Appl Physiol 1994; 77:1206–16.
35. Al Jamal R, Roughley PJ, Ludwig MS. Effect of glycosaminoglycan degradation on lung tissue viscoelasticity. Am J Physiol Lung Cell Mol Physiol 2001;280:L306–15.
36. Fust A, Iozzo R, Ludwig MS. Alterations in lung mechanics in decorin deficient mice. Am J Physiol Lung Cell Mol Physiol 2005 (in press).
37. Bramley AM, Roberts CR, Schellenberg RR. Collagenase increases shortening of human bronchial smooth muscle *in vitro*. Am J Respir Crit Care Med 1995;152:1513–7.
38. Bramley AJ, Thomson RJ, Roberts CR, Schellenberg RR. Hypothesis: excessive bronchoconstriction in asthma is due to decreased airway elastance. Eur Respir J 1994;7: 337–41.
39. Brackel HJL, Pederson OF, Mulder PGH, et al. Central airways behave more stiffly during forced expiration in patients with asthma. Am J Respir Crit Care Med 2000; 162:896–904.
40. Wagner EM, Mitzner W. Effects of bronchial vascular engorgement on airway dimensions. J Appl Physiol 1996;81: 293–301.
41. Yager D, Butler JP, Bastacky J, et al. Amplification of airway constriction due to liquid filling of airway interstices. J Appl Physiol 1989;66:2873–84.
42. Wagner EM. Effects of edema on small airway narrowing. J Appl Physiol 1997;83:784–91.
43. Macklem PT. Mechanical factors of determining maximum bronchoconstriction. Eur Respir J 1989;2(Suppl 6):516s–9s.
44. Minshall E, Chakir J, Laviolette M, et al. IL-11 expression is increased in severe asthma: association with epithelial cells and eosinophils. J Allergy Clin Immunol 2000;105: 232–83.
45. Westergren-Thorsson G, Chakir J, Lafreniere-Allart MJ, et al. Correlation between airways responsiveness and proteoglycan production by bronchial fibroblasts from normal and asthmatic subjects. Int J Biochem Cell Biol 2002;34: 1256–67.
46. Vignola AM, Riccobono L, Mirabella A, et al. Sputum metalloproteinase-9/tissue inhibitor of metalloproteinase-1 ratio correlates with airflow obstruction in asthma and chronic bronchitis. Am J Respir Crit Care Med 1998;158:1945–50.
47. Bai TR, Cooper J, Koelmeyer T, et al. The effect of age and duration of disease on airway structure in fatal asthma. Am J Respir Crit Care Med 2000;162:663–9.
48. Lange P, Parner J, Vestbo P, et al. A 15-year follow-up study of ventilatory function in adults with asthma. N Engl J Med 1998;339:1194–200.
49. Benayoun L, Druilhe A, Dombret MC, et al. Airway structural alterations selectively associated to severe asthma. Am J Respir Crit Care Med 2003; 167:1360–8.
50. Jeffrey PK, Godfrey RW, Ädelroth E, et al. Effects of treatment on airway inflammation and thickening of basement membrane reticular collagen in asthma. A quantitative light and electron microscopic study. Am Rev Respir Dis 1992; 145:890–9.
51. Olivieri D, Chetta A, Del Donno M, et al. Effect of short-term treatment with low-dose inhaled fluticasone propionate on airway inflammation and remodeling in mild asthma: a placebo-controlled study. Am J Respir Crit Care Med 1997;155:1864–71.
52. Trigg CJ, Manolitsas ND, Wang J, et al. Placebo-controlled immunopathologic study of four months of inhaled corticosteroids in asthma. Am J Respir Crit Care Med 1994; 150:17–22.
53. Vanacker NJ, Palmans E, Kips JC, Pauwels RA. Fluticasone inhibits but does not reverse allergen-induced structural airway changes. Am J Respir Crit Care Med 2001;163:674–9.
54. Orsida BE, Li X, Hickey B, et al. Vascularity in asthmatic airways: relation to inhaled steroid dose. Thorax 1999;54: 289–95.
55. Gayrard P, Orehek J, Grimaud C, Charpin J. Bronchoconstrictor effects of a deep inspiration in patients with asthma. Am Rev Respir Dis 1975;111:433–9.
56. Fredberg JJ, Ingram RH, Castile R, et al. Nonhomogeneity of lung response to inhaled histamine assessed with alveolar capsules. J Appl Physiol 1985;58:1914–22.
57. Nagase T, Moretto A, Dallaire MJ, et al. Airway and tissue responses to antigen challenge in sensitized Brown Norway rats. Am J Respir Crit Car Med 1994;150:218–26.
58. Lutchen KR, Sullivan A, Arbogast FT, et al. Use of transfer impedance measurements for clinical assessment of lung mechanics. Am J Respir Crit Care Med 1998;157:435–46.
59. Kraft M, Djukanovic R, Wilson S, et al. Alveolar tissue inflammation in asthma. Am J Respir Crit Care Med 1996;154: 1505–10.
60. Ludwig MS. Role of lung parenchyma. In: Barnes PJ, Grunstein MM, Leff AR, Woolcock AS, editors. Asthma. Philadelphia: Lippincott-Raven; 1997. p. 1319–34.

61. Kraft M. The distal airways: are they important in asthma? Eur Respir J 1999;14:1403–17.
62. Woolcock AJ, Read J. The static elastic properties of the lungs in asthma. Am Rev Respir Dis 1968;98:788–94.
63. Finucane KE, Colebatch HJH. Elastic behavior of the lung in patients with airway obstruction. J Appl Physiol 1969;26: 330–8.
64. Colebatch HJH, Finucane KE, Smith MM. Pulmonary conductance and elastic recoil relationships in asthma and emphysema. J Appl Physiol 1973;34:143–53.
65. Gelb A, Licuanan J, Shinar CM, et al. Unsuspected loss of lung elastic recoil in chronic persistent asthma. Chest 2002;121: 715–21.
66. Kaczka DW, Ingenito EP, Israel E, et al. Airway and lung tissue mechanics in asthma. Effects of albuterol. Am J Respir Crit Care Med 1999;159:169–78.
67. Kaminsky DA, Wenzel S, Carcano C, et al. Hyperpnea-induced changes in parenchymal lung mechanics in normal subjects and in asthmatics. Am J Respir Crit Care Med 1997;155: 1260–6.
68. Kraft M, Martin RJ, Wilson S, et al. Lymphocyte and eosinophil influx into alveolar tissue in noctural asthma. Am J Respir Crit Care Med 1999;159:228–34.
69. Wenzel SE, Szefler SJ, Leung DYM, et al. Bronchoscopic evaluation of severe asthma. Persistent inflammation associated with high dose glucocorticoids. Am J Respir Crit Care Med 1997;156:737–43.
70. Tomioka S, Bates JHT, Irvin C. Airway and tissue mechanics in a murine model of asthma: alveolar capsule vs. forced oscillations. J Appl Physiol 2002;93:263–70.
71. Nagase T, Fukuchi Y, Dallaire J, et al. In vitro airway and tissue response to antigen in sensitized rats. Am J Respir Crit Care Med 1995;152:81–6.
72. Nagase T, Ludwig MS. Antigen-induced responses in lung parenchymal strips during sinusoidal oscillation. Can J Physiol Pharmacol 1998;76:176–81.
73. Salerno FG, Dallaire M, Ludwig MS. Does the anatomic makeup of parenchymal lung strips affect oscillatory mechanics during induced constriction? J Appl Physiol 1995;79:66–72.
74. Lulich KM, Mitchell HW, Sparrow MP. The cat lung strip as an in vitro preparation of peripheral airways: a comparison of β-adrenoceptor agonists, autacoids and anaphylactic challenge on the lung strip and trachea. Br J Pharmacol 1976;58:71–9.
75. Goldie RG, Bertram JF, Papadimitriou JM, Patterson JW. The lung parenchyma strip. TIPS 1984;5:7–9.
76. Nagase T, Dallaire MJ, Ludwig MS. Airway and tissue responses during hyperpnea-induced constriction in guinea pigs. Am J Respir Crit Care Med 1994;149:1342–7.
77. Nagase T, Ohga E, Katayama H, et al. Roles of calcitonin gene-related peptide (CGRP) in hyperpnea-induced constriction in guinea pigs. Am J Respir Crit Care Med 1996;154:1551–6.
78. Kapanci Y, Assimacopoulos A, Irle C, et al. Contractile interstitial cells in pulmonary alveolar septa: a possible regulator of ventilation/perfusion ratio? J Cell Biol 1974;60:375–92.
79. Dolhnikoff M, Morin J, Ludwig MS. Human lung parenchyma responds to contractile stimulation. Am J Respir Crit Care Med 1998;158:1607–12.
80. Nagase T, Lei M, Robatto FM, et al. Tissue viscance during induced constriction in rabbit lungs: morphological–physiological correlations. J Appl Physiol 1992;73:1900–7.
81. Mead J, Takishima T, Leith D. Stress distribution in lungs: a model of pulmonary elasticity. J Appl Physiol 1970;28: 596–608.
82. Ding DJ, Martin JG, Macklem PT. Effects of lung volume on maximal metacholine-induced bronchoconstriction in normal humans. J Appl Physiol 1987;62:1324–30.

CHAPTER 12

STRUCTURE–FUNCTION RELATIONSHIPS IN AIRWAY DISEASE: ANALYSIS BY COMPUTED TOMOGRAPHIC IMAGING

Michiaki Mishima

Asthma and chronic obstructive pulmonary disease (COPD) are the most prevalent lung diseases, and they contribute an enormous burden of morbidity.[1,2] In both diseases, environmental factors such as allergens, viruses, and bacteria, as well as personal, occupational, and atmospheric exposures, appear to cause an exaggerated immune/inflammatory response in genetically susceptible individuals.[3] The inflammatory response leads to a variety of structural changes in the tissues of the airways and the lung parenchyma, such as destruction of alveolar walls resulting in emphysema and airway wall remodeling. The complex changes in the airways, which involve hyperplasia and hypertrophy of a number of tissues, such as epithelium, airway smooth muscle, glands, and blood vessels, result in considerable thickening of these structures.

Lung remodeling in disease has been investigated in experimental animals and in humans through the examination of autopsy tissues, surgically resected lung tissues, and airway mucosal bronchoscopic biopsy specimens. However, modern imaging techniques also permit the examination of remodeling in a noninvasive manner. Much useful information can be derived through the analysis of the distribution of low-attenuation areas (LAAs) in the lung caused by emphysema, and airway remodeling can be examined through the measurement of airway dimensions by using computed tomography (CT) images. In this chapter, we summarize the results of recent work in this area as it pertains to structure–function relationships in patients with COPD and asthma.

DISTRIBUTION OF LAAS: FRACTAL ANALYSIS

COPD

Increases in the LAAs in the lung regions of chest CT images in patients with COPD have been reported to reflect the development of pathologic emphysema.[4–7] Nevertheless, previous methods of analyzing lung CT images are limited to general clinical diagnostic purposes[8] because the size and spatial distribution of LAAs are not taken into account. Uppaluri and colleagues[9] found that a texture analysis could differentiate between normal and emphysematous tissue with 100% accuracy. However, it was not clear whether this method would detect early emphysema. Mishima and colleagues examined the statistical properties of LAA clusters (spatially continuous LAA on CT images) in COPD patients and in normal subjects.[10] A comparison between the original and LAA images in a representative COPD subject is shown in Figures 12-1A and 12-1B. In COPD patients, the percentage of the lung field occupied by LAAs (LAA%) spanned a large range, from 2.6 to 67.6%, whereas LAA% was always $<30\%$ in healthy subjects. The values of LAA% for normal subjects spanned a narrower range: 15.6 ± 8.0. Thus, COPD patients may fall in the normal range or have elevated LAA%. For purposes of comparison, we classified COPD-affected subjects into two groups, those with normal LAA% ($<30\%$), designated COPD 30, and those with elevated LAA% ($>30\%$), termed COPD >30. The LAA images of a normal subject and of a COPD 30 subject with a similar LAA% (7%) are compared in Figures 12-1C and 12-1D. These images show that the COPD patient had fewer but somewhat larger clusters of LAAs than the normal subject. The cumulative distribution of the size of the LAA clusters (the number of the LAA clusters whose size was larger than the threshold size) followed a power law characterized by an exponent D (Figure 12-2). D was shown to be a measure of the complexity of the terminal airspace geometry. The D values correlated with the diffusing capacity of the lung (Figure 12-3).

The COPD patients with normal LAA% had significantly smaller D values than the healthy subjects, suggesting that D might provide an index of early alveolar damage and the accompanying changes in lung architecture. Insights into the

potential mechanisms of the evolution of alveolar damage were obtained with the use of a mechanical model of the lung parenchyma. A large elastic spring network model was used, and with this model it was demonstrated that the neighboring smaller LAA clusters tended to coalesce and form larger clusters as the weak elastic fibers separating them broke under tension (Figure 12-4). This process leaves LAA% unchanged but reduces the number of small clusters. This, in turn, results in a reduction in *D* similar to that observed in patients with early emphysema. These findings suggest that *D* is a sensitive and powerful parameter for the detection of the terminal airspace enlargement that occurs in patients with early emphysema.

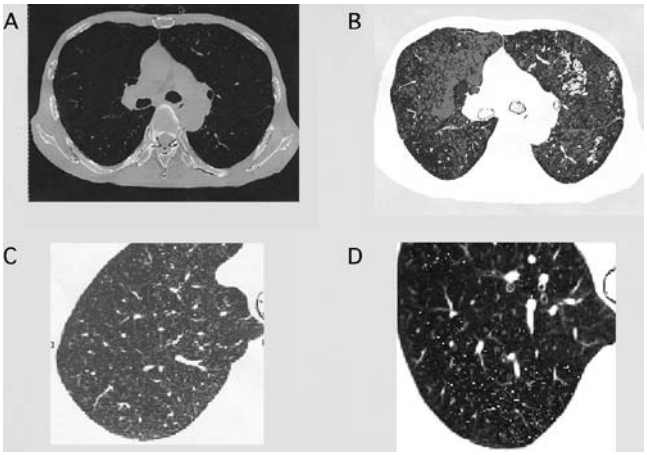

FIGURE 12-1 *A*, Original CT image of the middle lung slice in a representative COPD patient. LAA% is 55.1%. *B*, The same image as in *A*, but the individual clusters comprising contiguous LAA regions are shown in different gray scales. The lung field was identified from the rest of the image, and the lumen of the trachea and large bronchi were excluded. The white regions are smaller airways and vessels. *C*, LAA image of a normal subject. *D*, LAA image of a COPD patient. The LAA% and exponent *D* of the cluster distribution of the two images in *C* and *D* are 7.2% versus 7.1% and 2.97 versus 1.71, respectively.

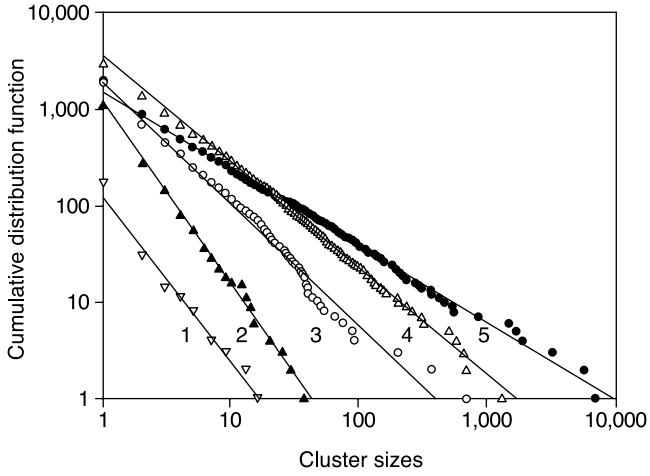

FIGURE 12-2 Log–log plot of representative cumulative frequency distributions of LAA size. The five lung slices analyzed had LAA% values of 5.1% (1), 15.6% (2), 30.9% (3), 42.3% (4), and 60.4% (5). Each data set was fitted to the plots by linear regression. In these five cases, *r* is .991, .997, .987, .998, and .998, respectively. The corresponding *D* values are 1.71, 1.87, 1.26, 1.10, and 0.64, respectively.

Asthma

The nature of asthma as a chronic inflammatory disease of the airways has been well described.[11] Asthma was considered to be an essentially reversible disorder, but chronic inflammation in asthma can also lead to structural alterations.[12] Airway and lung parenchymal changes associated

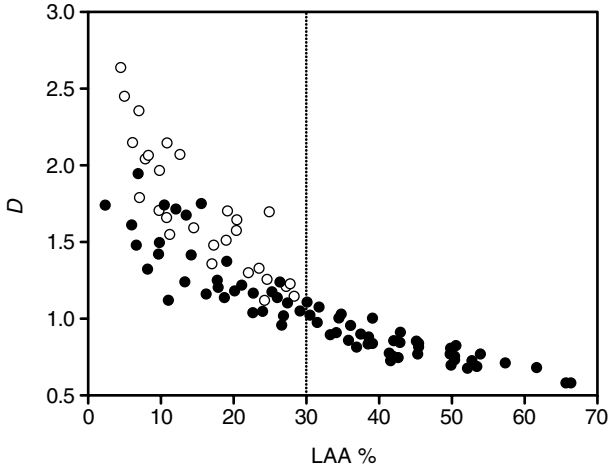

FIGURE 12-3 Relationship between LAA% and *D*. *Open and closed circles* represent normal subjects and COPD patients, respectively. The LAA% in the normal subjects is <30 (*dotted line*).

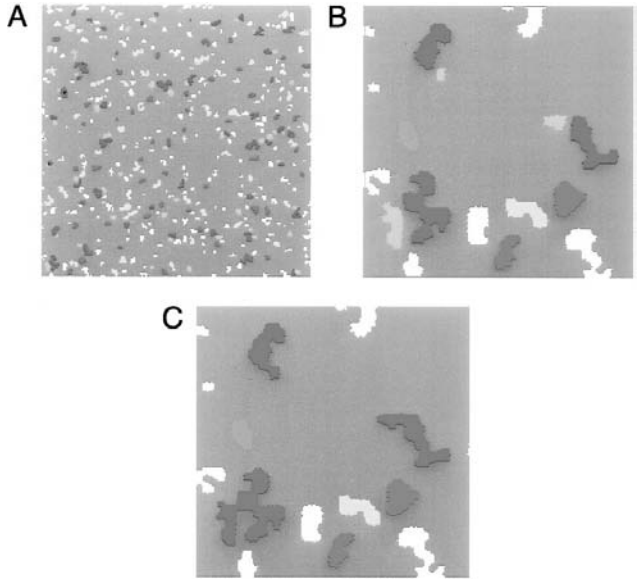

FIGURE 12-4 Images obtained from simulations in which a square lattice (500×500) of nodes connected by springs was used. The lattice constant is 1. The gray areas represent LAA clusters in which several nodes have been removed from the network. *A*, A 250×250 zoom into the lattice. *B*, Zoom into a small area (50×50) of the lattice in *A*. Notice that the three larger gray clusters and the smaller gray clusters are separated by tissue (*gray*). *C*, The same network as in *B* but after 554 additional springs (whose tension was higher than 80% of the maximum tension) have been cut out of the 500×500 network. The tension in the walls separating the larger and smaller gray clusters in *B* was high, and the alveolar walls broke. As a result, the smaller gray clusters now form part of the larger gray clusters.

with asthma are considered to be responsible for irreversible airway obstruction, an outcome that is frequently observed in subjects with severe asthma.[13,14]

Mitsunobu and colleagues found that the relative area of the lung with attenuation values lower than −950 Hounsfield Units (HU) (RA950) correlated with airflow limitation, lung volume, and severity of asthma but not the diffusing capacity in nonsmoking patients with asthma.[15] HU (CT number) is defined as −1,000 for air and 0 for water. Thus, an area with −950 HU is a very-low-density area. The purpose of this study was to investigate whether asthma affected the size distribution of LAA clusters and the development of emphysema.

Mitsunobu and colleagues quantified the size distribution of LAA clusters in nonsmoking subjects with asthma and compared it with those in both nonsmoking healthy subjects and subjects with asthma with a smoking history. In addition, they investigated how asthma severity influenced LAA clusters.[16] The values of LAA% and *D* in subjects with asthma with a smoking history differed significantly from those in nonsmoking subjects with asthma and in control subjects. In nonsmoking subjects with asthma, both parameters differed significantly between those with severe asthma and those with mild or moderate asthma. The LAA% differed significantly between subjects with moderate asthma and those with mild asthma, but *D* did not. For mild and moderate asthma, a highly significant correlation between LAA% and *D* was observed in subjects with a smoking history but not in nonsmoking subjects with asthma (Figures 12-5 to 12-7). The results suggest that the decrease in *D* is mostly related to emphysematous change, and the increase in LAA% results from both hyperinflation and emphysematous change. Thus, measurements of both LAA% and *D* may provide useful information for the characterization of LAAs in subjects with asthma.

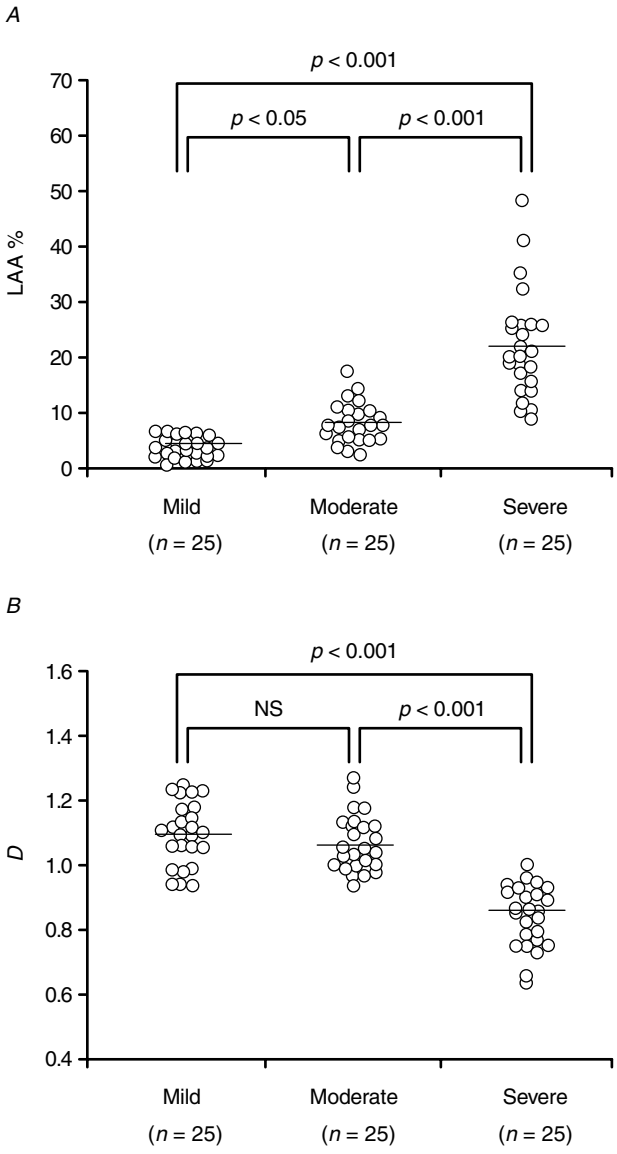

FIGURE 12-5 Relationships between disease severity and LAA% (*A*) or *D* (*B*) in subjects with asthma without a smoking history. LAA% values were significantly higher in severe asthma than in mild ($p < .001$) and moderate ($p < .001$) asthma and in moderate asthma than in mild asthma ($p < .05$). *D* values were significantly lower in severe asthma than in mild ($p < .001$) or moderate ($p < .001$) asthma. However, no significant difference was observed between mild and moderate asthma.

AIRWAY DIMENSIONS

COPD

Recently, CT has been used to measure airway wall dimensions. Patients with asthma have thicker airways on CT scans than healthy controls, and the degree of thickening is related to the severity of disease and airflow obstruction.[17–22] The resolution of the technique is generally limited to the segmental bronchus. Nakano and colleagues developed a semi-automatic digital analysis method for the measurement of airway dimensions. They measured the dimensions of the apical segmental bronchus in 114 smokers (94 COPD patients and 20 asymptomatic control subjects).[23] With the apical bronchus identified by three expert pulmonologists, the following parameters were measured automatically on the computer (Figure 12-8): luminal area (A_i), short radius (SR) and long radius (LR) of the lumen, and airway wall thickness. The following procedures were performed: (1) the lumen of the bronchus was identified with the use of a threshold of −500 HU[24]; the area of the lumen was considered to be A_I; (2) SR and LR were defined as the shortest and longest distances from the centroid point of the lumen to the edge; (3) from the centroid point of the lumen, 128 rays fanning out over 360° were examined, to determine the wall thickness along the rays[25,26]; and (4) those rays that projected onto the adjacent vessel were excluded. Wall thickness was calculated from the nonexcluded rays.

Nakano and colleagues found that A_i was smaller and the airway wall area percentage (percent ratio of wall area to total airway area) was greater in COPD patients than in asymptomatic control subjects (Table 12-1). They tested whether the wall area percentage added value to the prediction of pulmonary function tests beyond a high-resolution computed tomography (HRCT) estimate of the severity of emphysema [(percent LAA / total lung area) × 100 (LAA%)]. Although both wall area percentage and LAA% correlated with measurements of lung function, the combination of wall area percentage and LAA% improved the estimate of

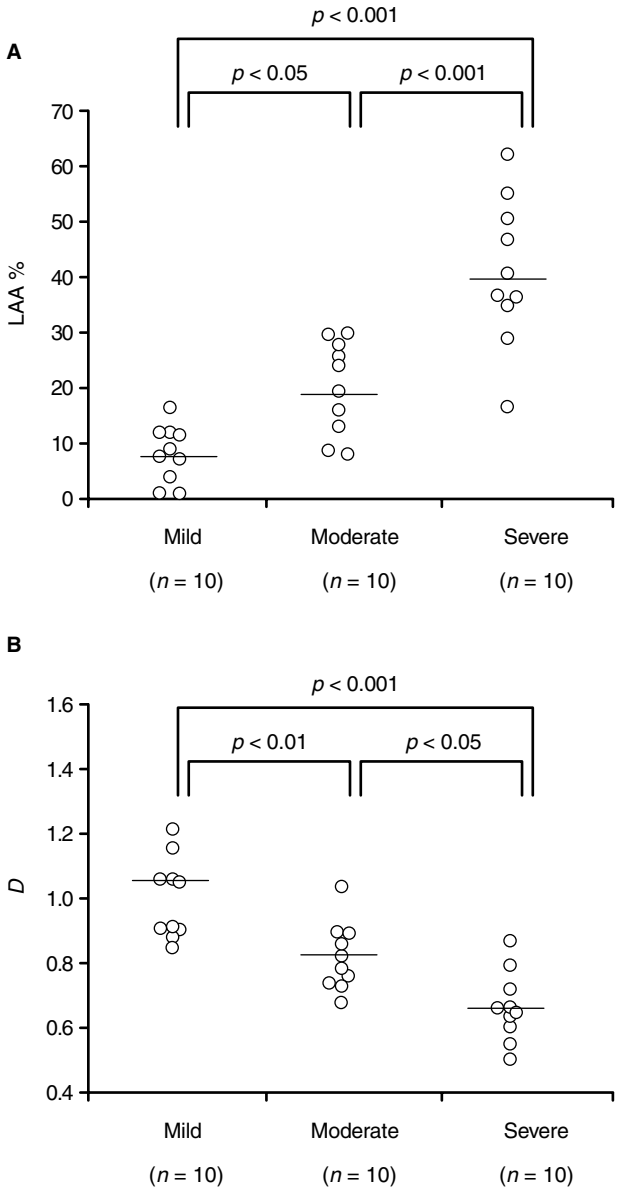

FIGURE 12-6 Relationships between asthma severity and LAA% (*A*) or *D* (*B*) in subjects with asthma with a smoking history. LAA% values were significantly higher in severe asthma than in mild ($p < .001$) or moderate ($p < .001$) asthma and in moderate asthma than in mild asthma ($p < .05$). *D* values were significantly lower in severe asthma than in mild ($p < .001$) or moderate ($p < .05$) asthma, and in moderate asthma than in mild asthma ($p < .01$).

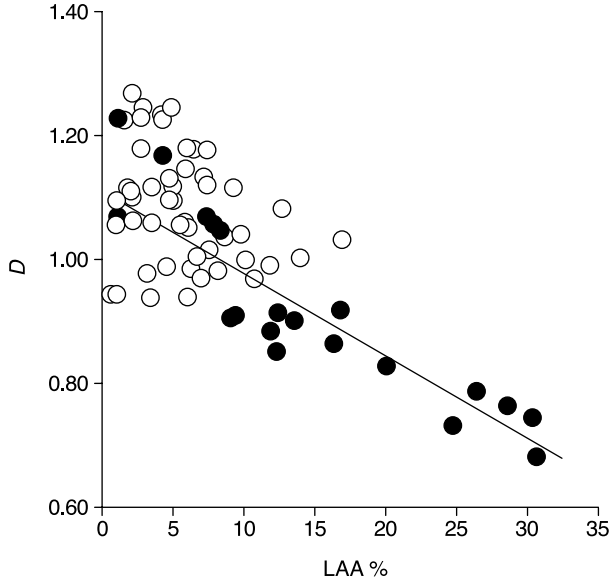

FIGURE 12-7 Relationship between LAA% and *D* in patients with mild and moderate asthma. *Open circles* and *closed circles* represent patients without and with a smoking history, respectively. There was a highly significant correlation between LAA% and *D* ($r = -.907$, $p < .0001$) in patients with a smoking history but not in those without a smoking history.

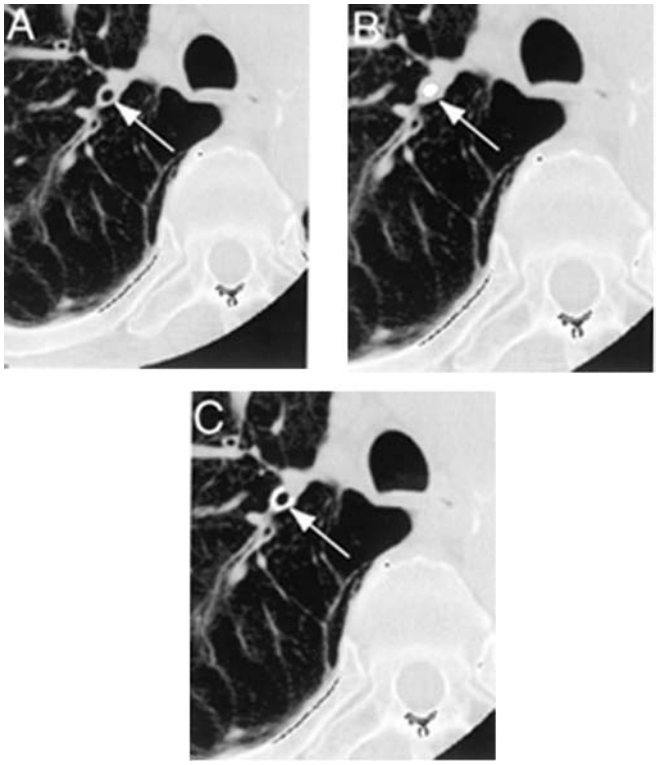

FIGURE 12-8 A representative case showing the process of airway analysis. Using a helical CT image containing the apical bronchus to the upper lobe (*A*), the algorithm defines the luminal area (*B*) and wall thickness (*C*). Note that identification of the airway wall thickness was successful even when the pulmonary blood vessel ran parallel to the bronchus.

pulmonary function abnormalities. In a multivariate model, Nakano and colleagues found that they could more accurately predict forced expiratory volume in 1 second (FEV_1), forced vital capacity (FVC), FEV_1/FVC, and peak expiratory flow, but not diffusing capacity of the lung for carbon monoxide, when both the estimate of airway wall thickening and the extent of LAAs were included in a statistical model (Table 12-2). They also found that they could divide COPD-affected subjects into groups that had a predominant loss of lung attenuation or thickening and narrowing of the apical segmental bronchus using LAA% and wall area percentage (Figure 12-9). Although many subjects had both decreased lung attenuation consistent with emphysema and

Table 12-1 Large Airway Dimensions in Chronic Obstructive Pulmonary Disease (COPD) Measured Using High-Resolution Computed Tomography (HRCT)*

Subject Variables	*Control* (n = 20)	*COPD* (n = 94)
Age (years)	64 ± 17	69 ± 7
Smoking (pack years)	58 ± 45	74 ± 42
FEV_1 (% predicted)	100 ± 13	37 ± 15†
A_i (mm^2)	22 ± 6	16 ± 8†
A_i (%)	59 ± 5	66 ± 8†

*Values given as mean ± SD. Data modified with permission from Nakano et al.[23]
†$p < .01$ compared to asymptomatic smokers.
A_i = luminal area; A_w = wall area; FEV_1 = forced expiratory volume in 1 second.

airway wall thickening, there were individuals with similar degrees of obstruction whose abnormalities appeared to be predominantly the result of airway remodeling and others in whom abnormalities appeared to be predominantly related to the loss of lung parenchyma. Interestingly, Nakano and colleagues also found that A_i was related to FEV_1, whereas Niimi and colleagues failed to find any relationship between A_i and the severity of asthma.[20] The different patterns of remodeling found in these two studies may reflect fundamental differences in the inflammatory processes in asthma and COPD and could influence the reversibility of the narrowing.

Asthma

CT findings, including airway wall thickening, have been evaluated in asthmatic patients.[27] However, most interpretations have been subjective,[27,28] and in only a few studies has CT been used to quantitatively analyze airway wall thickness

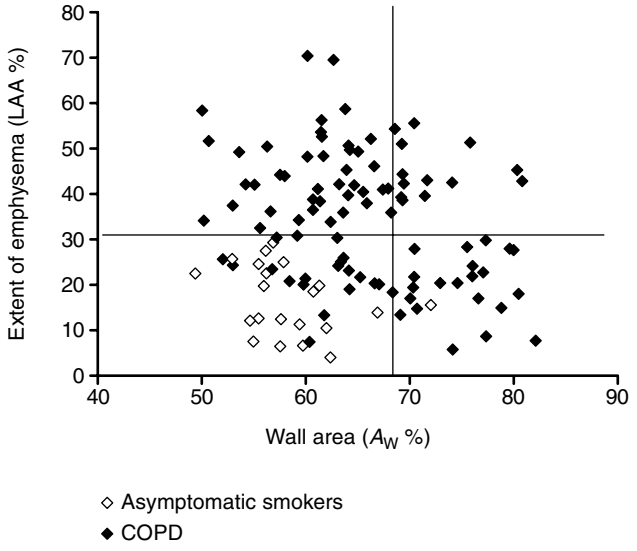

FIGURE 12-9 Relationship between airway wall area percentage and extent of emphysema (LAA%) in 94 COPD patients and 20 asymptomatic smokers. The *horizontal line* shows the mean +2SD of LAA% of the asymptomatic smokers. The *vertical line* shows the mean +2 SD of wall area percentage of the asymptomatic smokers. With use of these cutoff values, COPD patients can be divided into groups: an airway remodeling-dominant group (high wall area percentage and low LAA%), an emphysema-dominant group (low wall area percentage and high LAA%), and a mixed group (high wall area percentage and high LAA%).

Table 12-2 Correlation Coefficients (*r* Values) of Univariate and Stepwise Multiple Regression Analyses for Pulmonary Function Test

	Univariate regression analysis		*Multiple regression analysis*
Variables	*LAA%*	*A_w%*	*LAA% and A_w%*
FVC (% predicted)	−0.159*	−0.437†	0.482†
FEV_1 (% predicted)	−0.529†	−0.338†	0.659†
FEV_1/FVC (%)	−0.650†	−0.192†	0.700†
PEFR (% predicted)	−0.395†	−0.487†	0.660†
RV/TLC (%)	0.378†	0.422†	0.597†
DLco/V_A (mL/min/mm Hg/L)	−0.683†	0.030*	NA

Data reprinted with permission from Nakano et al.[23]
A_w = wall area; DLco/V_A = diffusing capacity of the lung for carbon monoxide/alveolar volume; FEV_1 = forced expiratory volume in 1 second; FVC = forced vital capacity; LAA = low-attenuation area; NA = stepwise multiple regression analysis showed no additional predictive value of including A_w%; PEFR = peak expiratory flow rate; RV/TLC = residual volume/total lung capacity.
*Not significant; *p* values were adjusted for multiple comparisons.
†$p < .001$.

in patients with asthma.[17,18] Okazawa and colleagues[18] and Awadh and colleagues[19] have shown that the airways of asthmatic patients are thicker than those of normal controls, whereas Boulet and colleagues[17] failed to show such a difference. The presence and significance of airway wall thickening as assessed by CT in asthmatic patients thus remain to be clarified.

Niimi and colleagues[20] analyzed 81 asthmatic subjects (13 mild persistent, 39 moderate persistent, 22 severe persistent, and 7 intermittent) and compared them with 28 healthy volunteers. The representative CT images are shown in Figure 12-10. They found that the airway wall area (A_w) was increased in patients with asthma without a decrease in A_i. A_w was correlated positively with the duration and clinical severity of asthma (Figure 12-11), whereas wall area percentage was negatively related to FEV_1 (% predicted), FEV_1/FVC (%) and forced expiratory flow over the middle hall of the vital capacity (% predicted). Matsumoto and colleagues measured serum eosinophil cationic protein (ECP) levels, which reflect ongoing eosinophilic airway inflammation and serve as a marker for asthma activity, in 113 asthmatic patients during exacerbation. ECP levels, however, may not be elevated in some asthmatic patients, even when they are symptomatic. Such patients with low ECP levels were significantly older, had longer disease duration, and had lower serum IgE levels. They had a greater degree of airway wall thickening than those with higher ECP levels. Thus, mechanisms other than eosinophilic inflammation, such as airway remodeling, may be involved in asthma exacerbation in these patients.[29]

The relationship between airway wall thickness and inducible airway narrowing or AHR (airway hyperresponsiveness) has rarely been investigated. Boulet and colleagues[17] and Little and colleagues[30] compared airway wall thickness, as assessed by CT, with AHR in asthmatic patients. AHR was measured as the provocative concentration of methacholine[31] that produced a 20% fall in FEV_1 (PC_{20}-FEV_1). In one study,[17] a positive correlation of AHR with airway wall thickness was found in a subgroup of

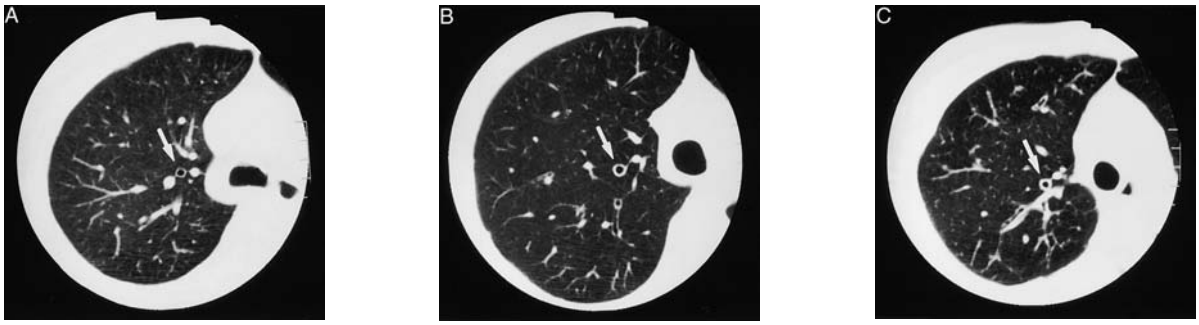

FIGURE 12-10 Representative CT images of (*A*) a control subject, (*B*) a patient with mild persistent asthma, and (*C*) a patient with severe persistent asthma. The views of the apical bronchus of the right upper lobe are indicated by *arrows*.

patients, whereas in the other,[30] no significant relationship was found. Niimi and colleaguess addressed these inconsistent findings by studying the relationship between airway wall thickness, assessed with CT, and AHR, evaluated by inhalation of methacholine,[31] in stable asthmatic subjects with ($n = 23$) and without ($n = 22$) inhaled steroid treatment. As compared with a provocation test with FEV_1 as the sole index of AHR, the latter method enables the separate evaluation of the two distinct and possibly independent components of AHR: airway sensitivity and airway reactivity or exaggerated airway narrowing.[32,33] Airway hypersensitivity is represented by the leftward shift of the methacholine–respiratory resistance dose–response curve. Airway hyperreactivity is represented by the steeper slope of the dose–response curve. In both groups of patients, airway sensitivity was not related to airway reactivity. Airway sensitivity was related to eosinophil count ($r = .57$ in the steroid-positive group and $r = .49$ in the steroid-negative group) but not to airway wall thickness. In contrast, airway reactivity was negatively correlated with airway wall thickness ($r = -.56$ and $r = -.55$) (Figure 12-12) but not with eosinophil count. These results suggest that airway wall thickening may attenuate airway reactivity in asthmatic patients. These findings may have important implications for the pathophysiology and treatment of airway remodeling.

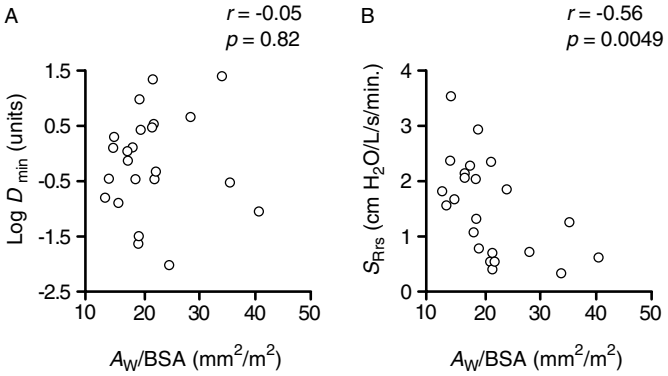

FIGURE 12-12 Relationship between airway sensitivity (*A*), reactivity (*B*), and airway wall thickness in patients treated with inhaled steroid. D_{min} is a marker of airway sensitivity (the cumulative dose of inhaled methacholine at the inflection point at which respiratory resistance begins to increase). Lower D_{min} values indicate higher sensitivity to methacholine. S_{Rrs} is a measure of airway reactivity (the slope of the methacholine–respiratory resistance dose–response curve). Higher S_{Rrs} values indicate higher reactivity to methacholine. Log D_{min} was not significantly related to wall area (A_w)/body surface area (BSA) in either the steroid-positive group or the steroid-negative asthmatic groups. S_{Rrs} was negatively correlated with wall area/BSA. The results were the same in steroid-negative patients.

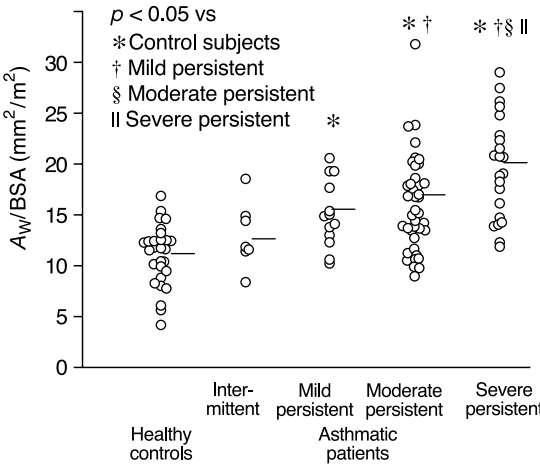

FIGURE 12-11 The distribution of wall area (A_w)/body surface area (BSA) in the control and four asthmatic groups. Bars represent means. The difference among the groups was significant by ANOVA ($p < .001$).

CONCLUSIONS

In patients with COPD, the cumulative size distribution of the LAA clusters followed a power law characterized by an exponent *D*, which was shown to be a measure of the complexity of the terminal airspace geometry. The COPD patients with normal LAA% had significantly lower *D* values than the healthy subjects, and the *D* values did not correlate with the results of pulmonary function tests, except for the diffusing capacity of the lung. These results were examined with the use of a large elastic spring network model, and it was found that the neighboring smaller LAA clusters tend to coalesce and form larger clusters as the weak elastic fibers separating them break under tension. This process leaves LAA% unchanged, whereas it decreases the number of small clusters and increases the number of large clusters, which results in a reduction in *D* similar to that observed in early emphysema patients. These findings suggest that *D* is a sensitive and powerful parameter for the detection of the

terminal airspace enlargement that occurs in early emphysema. This study was limited to centrilobular emphysema. However, Cosio and colleagues suggested that LAAs on CT images could be used as an in vivo indicator of microscopic emphysema or other types of emphysema, such as panlobular emphysema.[34,35] The fractal analysis may also provide further information on these types of emphysema.

In nonsmoking subjects with asthma, both LAA% and *D* differed significantly between severe asthma and mild or moderate asthma. The LAA% differed significantly between moderate and mild asthma, but *D* did not. For mild and moderate asthma, a highly significant correlation between LAA% and *D* was observed in patients with a smoking history but not in nonsmoking subjects with asthma. These results suggest that a decrease in *D* is mostly related to emphysematous change, and measurements of both LAA% and *D* may provide useful information for the characterization of LAAs in patients with asthma.

With regard to the assessment of airway dimensions, in patients with COPD the outcome was as follows: (1) A_w was increased and A_i was decreased; (2) wall area percentage and LAA% (percent ratio of LAA and total lung area; estimator of emphysematous lesion) can together explain the airflow limitation in COPD; and (3) COPD patients can be divided into groups, one with predominant loss of lung attenuation and one with thickening and narrowing of the apical segmental bronchus, with the use of LAA% and wall area percentage; the emphysema-dominant group without airway wall thickening may be good candidates for lung volume reduction surgery or antielastase therapy, whereas the airway-dominant group may be better suited to vigorous therapy with bronchodilators or antiinflammatory agents.

In patients with asthma, the results were as follows: (1) A_w was increased without a decrease in A_I; (2) A_w was correlated positively with the duration and severity of asthma; (3) airway sensitivity was related to sputum eosinophil count but not to airway wall thickness; and (4) airway reactivity was negatively correlated with airway wall thickness but not with eosinophil count.

In conclusion, digital analysis of the CT images obtained in cases of COPD and asthma may contribute much to the management of these diseases. The phenotyping of COPD with the use of LAA and airway dimensions may be a useful method with which to investigate the pathogenesis of COPD and may lead to tailor-made therapy. Analysis of LAAs in patients with asthma will allow emphysema to be distinguished from hyperinflation. The measurement of airway dimensions will have an important role in the strategy of asthma therapy. For example, it may help to solve the question of whether early intervention with inhaled corticosteroids or other medications can prevent airway remodeling.

REFERENCES

1. Pauwels RA, Buist AS, Calverley PM, et al. Global strategy for the diagnosis, management, and prevention of chronic obstructive pulmonary disease: NHLBI/WHO Global Initiative for Chronic Obstructive Pulmonary Disease (GOLD) Workshop summary. Am J Respir Crit Care Med 2001;163:1256–76.
2. American Thoracic Society. Standards for the diagnosis and care of patients with chronic obstructive pulmonary disease (COPD) and asthma. Am Rev Respir Dis 1987;136:225–44.
3. Nakano Y, Müller NL, King GG, et al. Quantitative assessment of airway remodeling using high-resolution CT. Chest 2002;122:271s–5s.
4. Godard PR, Nicholson EM, Laszlo F, et al. Computed tomography in pulmonary emphysema. Clin Radiol 1982;33:379–87.
5. Hayhurst MD, MacNee W, Wellenstein DE. Diagnosis of pulmonary emphysema by computerised tomography. Lancet 1984;2:320–3.
6. Bergin C, Müler NI, Nichols DM, et al. The diagnosis of emphysema. A computed tomographic–pathologic correlation. Am Rev Respir Dis 1986;133:541–6.
7. Gevenois PA, Maertelaer V, Vuyst PA, et al. Comparison of computed density and macroscopic morphometry in pulmonary emphysema. Am J Respir Crit Care Med 1995;152:653–7.
8. Gelb AF, Scein M, Kuei J, et al. Limited contribution of emphysema in advanced chronic obstructive pulmonary disease. Am Rev Respir Dis 1993;147:1157–61.
9. Uppaluri R, Mitsa T, Sonka M, et al. Quantification of pulmonary emphysema from lung computed tomography images. Am J Respir Crit Care Med 1997;156:248–54.
10. Mishima M, Hirai T, Itoh H, et al. Complexity of terminal airspace geometry assessed by lung computed tomography in normal subjects and patients with chronic obstructive pulmonary disease. Proc Natl Acad Sci U S A 1999;396:8829–34.
11. Roche W. Inflammatory and structural changes in the small airways in bronchial asthma. Am J Respir Crit Care Med 1998; 157:191S–4S.
12. Park JW, Hong YK, Kim CW, et al. High-resolution computed tomography in patients with bronchial asthma: correlation with clinical features, pulmonary functions and bronchial hyperresponsiveness. J Investig Allergol Clin Immunol 1997;7:186–92.
13. Paganin F, Seneterre E, Chanez P, et al. Computed tomography of the lungs in asthma: influence of disease severity and etiology. Am J Respir Crit Care Med 1996;153:110–4.
14. Mitsunobu F, Mifune T, Ashida K, et al. Low-attenuation areas of the lungs on high-resolution computed tomography in asthma. J Asthma 2001;38:355–64.
15. Mitsunobu F, Mifune T, Ashida K, et al. The influence of age and disease severity on high resolution CT lung densitometry in asthma. Thorax 2001;56:851–6.
16. Mitsunobu F, Ashida K, Hosaki Y, et al. Complexity of terminal airspace geometry assessed by computed tomography in asthma. Am J Respir Crit Care Med 2003;167:411–7.
17. Boulet L-P, Belanger M, Carrier G. Airway responsiveness and bronchial wall thickness in asthma with or without fixed airflow obstruction. Am J Respir Crit Care Med 1995;152:865–71.
18. Okazawa M, Müller N, McNamara AE, et al. Human airway narrowing measured using high resolution computed tomography. Am J Respir Crit Care Med 1996;154:1557–62.
19. Awadh N, Müller NL, Park CS, et al. Airway wall thickness in patients with near fatal asthma and control groups: assessment with high resolution computed tomographic scanning. Thorax 1998;53:248–53.
20. Niimi A, Matsumoto H, Amitani R, et al. Airway wall thickness in asthma assessed by computed tomography. Relation to clinical indices. Am J Respir Crit Care Med 2000;162:1518–23.
21. Kasahara K, Shiba K, Ozawa T, et al. Correlation between the bronchial subepithelial layer and whole airway wall thickness in patients with asthma. Thorax 2002;57:242–6.
22. Little SA, Sproule MW, Cowan MD, et al. High resolution computed tomographic assessment of airway wall thickness in chronic asthma: reproducibility and relationship with lung function and severity. Thorax 2002;57:247–53.

23. Nakano Y, Muro S, Sakai H, et al. Computed tomographic measurements of airway dimensions and emphysema in smokers: correlation with lung function. Am J Respir Crit Care Med 2000;162:1102–8.
24. McNitt-Gray MF, Goldin JG, Johnson TD, et al. Development and testing of image-processing methods for the quantitative assessment of airway hyperresponsiveness from high-resolution CT images. J Comput Assist Tomogr 1997;21: 939–47.
25. Amirav I, Kramer SS, Grunstein MM, et al. Assessment of methacholine-induced airway constriction by ultrafast high-resolution computed tomography. J Appl Physiol 1997; 75:2239–50.
26. Reinhardt JM, D'Souza ND, Hoffman EA, et al. Accurate measurement of intrathoracic airways. IEEE Trans Med Imaging 1997;16:820–7.
27. Lynch DA, Newell JD, Tschomper BA, et al. Uncomplicated asthma in adults: comparison of CT appearance of the lungs in asthmatic and healthy subjects. Radiology 1993; 188:829–33.
28. Greiner P, Mourey-Gerosa I, Benali K, et al. Abnormalities of the airways and lung parenchyma in asthmatics: CT observations in 50 patients and inter- and intraobserver variability. Eur J Radiol 1996;6:199–206.
29. Matsumoto H, Niimi A, Minakuchi M, et al. Serum eosinophil cationic protein levels measured during exacerbation of asthma: characteristics of patients with low titres. Clin Exp Allergy 2001;31:637–43.
30. Little SA, Sproule MW, Cowan MD, et al. High resolution computed tomographic assessment of airway wall thickness in chronic asthma: reproducibility and relationship with lung function and severity. Thorax 2002;57:247–53.
31. Takishima T, Hida W, Sasaki H, et al. Direct-writing recorder of the dose–response curves of the airway to methacholine. Chest 1981;80:600–6.
32. Sterk PJ, Bel EH. Bronchial hyperresponsiveness: the need for a distinction between hypersensitivity and excessive airway narrowing. Eur Respir J 1989;2:267–74.
33. Lotvall J, Inman M, O'Byrne P. Measurement of airway hyperresponsiveness: new considerations. Thorax 1998;53: 419–24.
34. Gevenous PA, De Vuyst P, Cosio MG, et al. Comparison of computed density and microscopic morphometry in pulmonary emphysema. Am J Respir Crit Care Med 1996; 154:187–92.
35. Kim WD, Eidelman DH, Cosio MG, et al. Centrilobular and panlobular emphysema in smokers. Two distinct morphologic and functional entities. Am Rev Respir Dis 1991;144: 1385–90.

CHAPTER 13

BREATHING STRATEGIES IN ASTHMA AND CHRONIC OBSTRUCTIVE LUNG DISEASE

James G. Martin

Asthma and chronic obstructive lung disease are among the commonest conditions for which patients are referred to the respirologist. Although the gas exchange function of the lungs is paramount in importance to the host, it is often only in the advanced stages of the disease that gas exchange is compromised in a way that has any clinical significance. The symptom of dyspnea, which often drives patients to see a physician, often has little or nothing to do with impairment of gas exchange. Arterial blood gas analysis may show gas exchange to be perfectly adequate at times when dyspnea is considerable. Understanding the cardinal symptom of dyspnea and the functional impairment suffered by patients with chronic obstructive pulmonary disease (COPD) and asthma requires that we understand the mechanics of breathing in these conditions. Much of the breathlessness associated with acute asthmatic attacks, chronic asthma, and COPD is caused by the impact of abnormal respiratory system mechanics on the respiratory muscles, which, in turn, give rise to an exaggerated and uncomfortable sense of the effort needed to breathe. This topic has been recently reviewed by Banzett and colleagues.[1]

Asthma and COPD have certain alterations in the mechanics of breathing in common. One of the important differences is that the changes in respiratory system mechanics in asthma occur acutely, whereas there is a slowly progressive evolution of lung dysfunction in COPD. Slow progress of the disease process allows time for adaptive changes that are no doubt responsible for the fact that symptomatic COPD usually does not come to medical attention until there is much more marked airflow limitation than is usually associated with symptomatic asthma. In other words, for a given degree of airflow limitation, the asthmatic subject is generally more symptomatic than the subject with COPD. Here we review the mechanics of breathing in both diseases under conditions of rest and, to a lesser extent, during exercise, with a view to better understanding the basis for symptoms such as dyspnea in COPD and asthma.

ASTHMA

Bronchoconstriction and Mechanical Impedance to Breathing

In most asthmatic subjects, lung function is normal or close to normal between attacks. During an acute attack of asthma, bronchoconstriction causes a variety of alterations in respiratory system mechanics that lead to an increase in the impedance to breathing.[2] The most important change in lung function that affects the mechanical impedance to breathing and that stresses the capacity of the asthmatic subject to sustain minute ventilation is hyperinflation. The term hyperinflation is often used loosely in reference to changes in lung volume in obstructive lung diseases. Hyperinflation, defined as an increase in the functional residual capacity (FRC), is the most physiologically relevant form of hyperinflation because it is closely linked to the respiratory system impedance encountered during tidal breathing. It needs to be distinguished from the term hyperinflation employed by the radiologist to describe a (frequently) subjective impression of an increase in lung volume on a chest radiograph taken at total lung capacity (TLC). An increase in TLC is caused by loss of lung elastic recoil and is an infrequent finding in asthmatic subjects. However, it has been well documented, not only by body plethysmography, which is sensitive to artifactual increases in estimates of lung volume based on delays in the transmission of alveolar pressure to the mouth when airway resistance is high,[3] but also by the helium dilution technique of measurement of absolute lung volumes,[4] which tends to give underestimates of lung volume. When a persistent increase in the TLC is present in asthma, it is a marker of severity.[5] Hyperinflation should also not be confused with air trapping, which is reflected in an increase in residual volume (RV). Even though an increase in RV, if of sufficient magnitude, would force an increase in FRC, it happens that RV and FRC change in parallel and therefore are independently determined.

Hyperinflation in asthma results from an increase in expiratory airflow resistance, but it is surprisingly complex in its etiology. Both the lung mechanical properties and the pattern of use of the respiratory muscles are important determinants of the degree of hyperinflation.[6] The determinants of FRC are usually cited as the inward elastic recoil of the lung and the opposing outward elastic recoil of the chest wall, whereby FRC is set by the balance of these passive forces. However, this is, strictly speaking, infrequently true. Only in normal subjects breathing quietly at rest does the FRC appear as a first approximation to be determined by the balance of the above-mentioned elastic forces. Under these circumstances, there is a brief end-expiratory pause. However, only if one includes respiratory muscle "tone" as a component of chest wall recoil does the notion of a static balance of elastic forces hold true. When the respiratory muscles are paralyzed in normal subjects, there is a fall in FRC. In respiratory disease, there is a departure from "quiet" breathing that results in the FRC being dynamically determined more often than not.[7]

The deviation of the FRC from the normal value in obstructive lung diseases can be easily understood intuitively. When an inspiration is taken, a return to FRC requires that the expiratory flow and the time required for the complete expiration are adequate. If airway narrowing occurs, then the time constant for emptying of the lungs will increase and the time available for expiration may not be sufficient to allow the subject to return to FRC by the end of expiration. Contrary to common belief among clinicians that expiration is prolonged in obstructive diseases, a notion based on a prolonged audible expiration, the ratio of inspiratory to expiratory duration changes little with airflow obstruction. Adjustments to expiration are therefore not among the strategies used to defend end-expiratory lung volume. We can imagine the process of hyperinflation in the following manner. If an increase in airway resistance is imposed as a step change at the end of inspiration, and if there is no change in breathing pattern or recruitment pattern of the respiratory muscles, the subject will have a discrepancy between the inspired and expired volumes. In other words, the end-expiratory lung volume will rise. The next breath will be taken from a higher lung volume and will be succeeded by an expiration that again may or may not be equal to the inspired volume, depending on the degree of airway narrowing. This process will continue until such time as a new stable end-expiratory volume, FRC, is achieved. This new equilibrium will be reached because an increase in lung volume leads to an increase in the elastic pressures exerted on the airways by the alveolar attachments, relieving airway obstruction as well as assisting expiration through the provision of increased respiratory system recoil. The difference between the usual FRC and the relaxed end-expiratory lung volume (V_r) can be described by the following equation:

$$\text{FRC} - V_r = V_t e^{-T_e/\tau} \qquad (13\text{-}1)$$

where V_t is tidal volume, T_e is the expiratory time, e is the natural logarithm, and τ is the time constant of the respiratory system, given by the product of respiratory system resistance and compliance. The high resistance caused by bronchoconstriction can be offset by an increase in lung stiffness (reduced compliance) caused by hyperinflation. Of course, this equation deals only with the behavior of a passive respiratory system.

The respiratory system does not behave passively during expiration in the setting of increased impedance to breathing. Even when there is expiratory airflow obstruction, the expiratory flow rates can be modulated by respiratory muscle activity, as long as flow limitation is not present during tidal breathing. Persistence of inspiratory muscle activity into expiration, so-called postinspiratory activity of the diaphragm and the inspiratory rib cage muscles, often occurs and serves to slow expiration.[6,8,9] This phenomenon is referred to as expiratory braking. Narrowing of the laryngeal aperture can also retard expiratory airflow but is more important in neonates as a mechanism employed in the defense of FRC.[10]

Despite the complex regulation of expiratory airflow in asthma, there is a correlation between the magnitude of hyperinflation and the degree of airflow obstruction as measured by both pulmonary resistance and, the more usual measure in clinical practice, the forced expiratory volume in 1 second (FEV_1). The relationship is linear and quite tight for pulmonary resistance (Figure 13-1) but shows a more variable relationship with the FEV_1. The relationship of hyperinflation to airflow obstruction is also quite variable from subject to subject, so that certain subjects show a greater predisposition to hyperinflate than others during an asthma attack of equal severity, as measured by resistance or maximum expiratory flow.[11] The explanation for the variability in hyperinflation has not been entirely explored, but it is contributed to by differences in the patterns of respiratory muscle recruitment, as are discussed in detail below.

Respiratory Muscles and Acute Asthma

One might assume that because asthma is a disease that causes expiratory airflow obstruction, recruitment of the expiratory muscles would dominate the alterations in respiratory muscle recruitment. However, this is not the case. In fact, the major change in muscle recruitment involves the inspiratory muscles, in particular the muscles of the rib cage. We can obtain substantial insights into respiratory muscle recruitment by examining pleural pressure changes during breathing. The tidal volume and pleural pressure changes for a subject in whom a very mild degree of bronchoconstriction is induced by an inhalation of an aerosol of histamine are shown in Figure 13-2. The tidal volume changes a little, but there is a more obvious increase in the end-expiratory lung volume as hyperinflation takes place. There is a concurrent increase in the swings in pleural pressure, indicating that there is an increase in respiratory muscle recruitment. Of note is the fact that the swing in the pleural pressure is more prominent in the inspiratory direction and there is a minimal increase in the swing in the expiratory direction.[6] The greater fall in inspiratory pleural pressure is a reflection of the increase in inspiratory impedance to breathing caused by bronchoconstriction. The increased impedance is a function of airway narrowing that

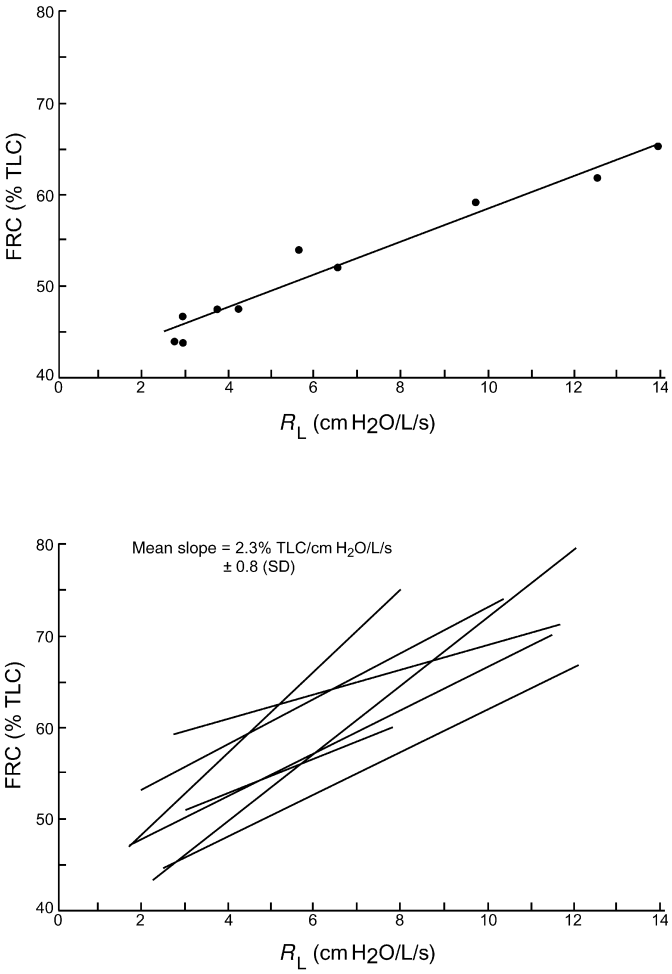

FIGURE 13-1 The relationship between functional residual capacity (FRC), expressed as percentage total lung capacity (% TLC), and the degree of airflow obstruction is shown at different degrees of histamine-induced bronchoconstriction for a single subject (*upper panel*) and for seven different subjects (*lower panel*). Airflow obstruction is quantified as pulmonary resistance (R_L). FRC and R_L are linearly related in each subject, but the slopes of the relationships are variable. Redrawn with permission from Martin et al 1980[6].

causes an increase in resistive impedance, whereas hyperinflation moves the respiratory system to a part of the volume–pressure relationship that is flatter and where the recoil of the system is greater. This latter causes an increase in elastic impedance. Many asthmatic subjects, when asked to rate the difficulty in inspiring and expiring, describe greater difficulty in inspiration.[4,12]

The pleural pressure trace in expiration is noteworthy for the fact that the pressure does not become markedly positive, such as one might expect in the setting of vigorous expiratory muscle recruitment. Pleural pressure decays from its value at end inspiration to a progressively more positive value. However, this value is less than would be expected if the relaxation of the inspiratory muscles were complete and if the elastic recoil of the chest wall were allowed to exert itself. The explanation for this phenomenon is that the inspiratory muscles relax gradually and incompletely during expiration, exerting a braking effect on the expiratory flow. The gradual relaxation of the inspiratory muscles during

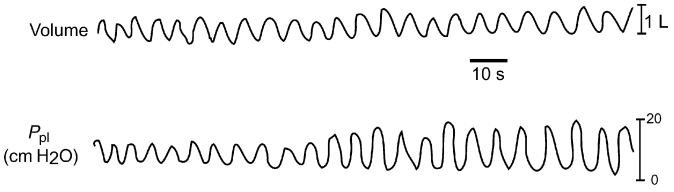

FIGURE 13-2 The tidal volume and pleural pressure changes during the inhalation of histamine by an asthmatic subject are shown. The end-expiratory lung volume, the tidal volume, and the frequency of breathing can all be seen to increase as bronchoconstriction develops. The pleural pressure swings increase in magnitude, predominantly as a result of a progressively more negative pressure during inspiration. The peak pressure during expiration is only slightly more positive than it was during quiet tidal breathing prior to provocation.

expiration makes the transition between inspiratory and expiratory flows a smooth event, but since it is a form of expiratory braking, it will also reduce expiratory flows and may worsen hyperinflation. The teleologic explanation of such a strategy of deployment of the respiratory musculature is not clear, but it will certainly tend to prevent tidal breathing occurring at a lung volume where flow limitation is more likely to occur. Indeed, asthmatic subjects seem to avoid the development of flow limitation during tidal breathing (Figure 13-3),[13] in contrast to many patients with COPD, who are flow-limited at rest (see Chapter 58, "Spirometric Predictions of Exercise Limitation in Patients with Chronic Obstructive Pulmonary Disease").

The rate of expiration can also be regulated by altering the glottic aperture. Narrowing of the glottis slows airflow in expiration and is a mechanism that is not energetically costly for adjusting end-expiratory lung volume. Indeed, asthma provoked by histamine is associated with glottic narrowing.[14]

Work of Breathing in Asthma

Bronchoconstriction causes an increase in resistive impedance to breathing and increases elastic impedance by causing hyperinflation. Inspiratory muscle activity is not confined to inspiration but spills over into the expiratory phase of the breathing cycle, as a persistent postinspiratory braking. In order to quantify the impact of an increase in respiratory impedance on the respiratory muscles, it is necessary to consider the relationship between the pleural pressure and lung volume during breathing. This method of plotting volume–pressure relationships for a graphical analysis of the mechanics of breathing is called the Campbell diagram, after the eminent respirologist, E. J. Moran Campbell. Such a plot is shown for quiet breathing and following an induced asthma attack in Figure 13-4. The small swings in pleural pressure during tidal breathing prior to the induction of bronchospasm are in striking contrast to those during bronchospasm. The work of breathing that is done in inflating the lungs is given by the product of pleural pressure and volume, where pressure refers to the difference between the measured pressure and atmospheric pressure. The product of pressure and volume, where pressure is referred to the chest wall relaxation line, represents the net work of breathing done by the respiratory system. The

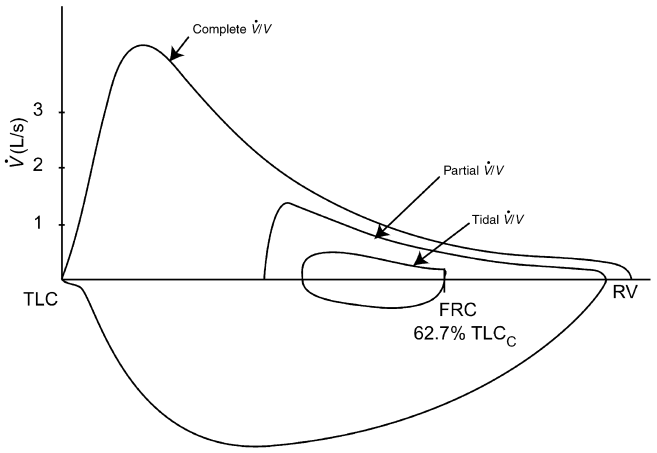

FIGURE 13-3 Maximum expiratory flow–volume curves from total lung capacity (TLC) (complete), partial (end-inspiratory lung volume close to an end-tidal inspiration), and tidal breathing for an asthmatic subject following histamine inhalation. The tidal flows are less than the partial maximal flows, which are, in turn, less than the maximal flows. The subject was hyperinflated, as indicated by the fact that functional residual capacity (FRC) was 62.7% of the control TLC. FRC is usually about 50% of TLC.

latter is more pertinent to the effort needed to breathe because it is the work that needs to be done by the respiratory muscles during breathing. This work comprises the work done to overcome elastic resistance and also flow-resistive resistance in displacing the lungs and the chest wall. The inspiratory work of breathing, calculated for asthmatic subjects during histamine-induced asthma, showed a substantial increase even for a modest degree of bronchoconstriction. However, the work also changes as a function of bronchoconstriction, as measured by the FEV_1, in a very variable manner from person to person (Figure 13-5).[2] The chest wall relaxation line was taken from published data[15] since it is extremely difficult to measure it in untrained subjects.

The elastic work and the resistive work of breathing done per minute were also calculated for the same asthmatic subjects. Work rate was calculated in preference to work per breath because, as ventilation increases with bronchoconstriction, not only does the work of breathing increase per breath, but the breathing frequency usually increases also. For example, in this same study in which the FEV_1 fell by a mean of 51% following histamine administration, minute ventilation increased from 12.1 L/min to 19.7 L/min. Hyperinflation, an increase in physiologic dead space, and an increase in the drive to breathe all contribute to this response, which increases inspiratory muscle work rate more than the work done per breath. The total work rate rose more than 10-fold from 6.7 J/min prior to bronchoconstriction to 71.4 J/min at a level of bronchoconstriction that

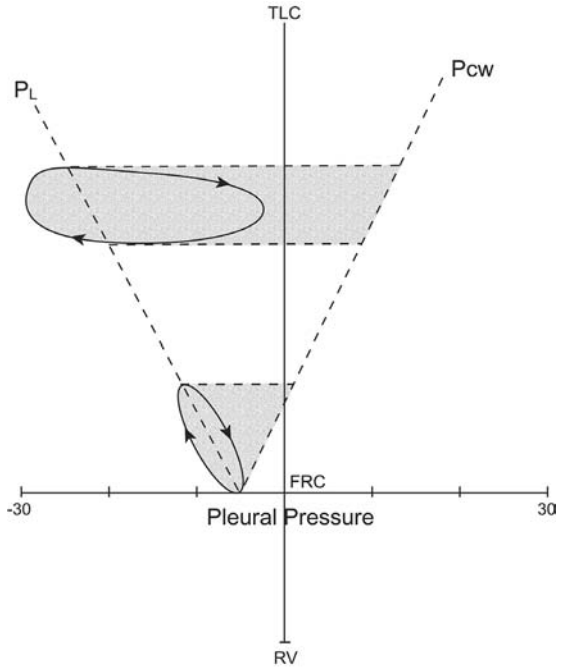

FIGURE 13-4 Campbell diagram showing the changes in pleural pressure (abscissa) during quiet breathing and during bronchoconstriction. The volume (expressed as percentage total lung capacity) is shown on the ordinate. The small tidal breathing loop contrasts with the marked increase in pressure swings during bronchoconstriction. The cross-hatched areas indicate the inspiratory work of breathing. Note that the expiratory pleural pressure does not reach the relaxation pressure of the chest wall, which means that there was a net inspiratory action of the respiratory muscles during expiration. This is expiratory braking, and it contributes to hyperinflation.

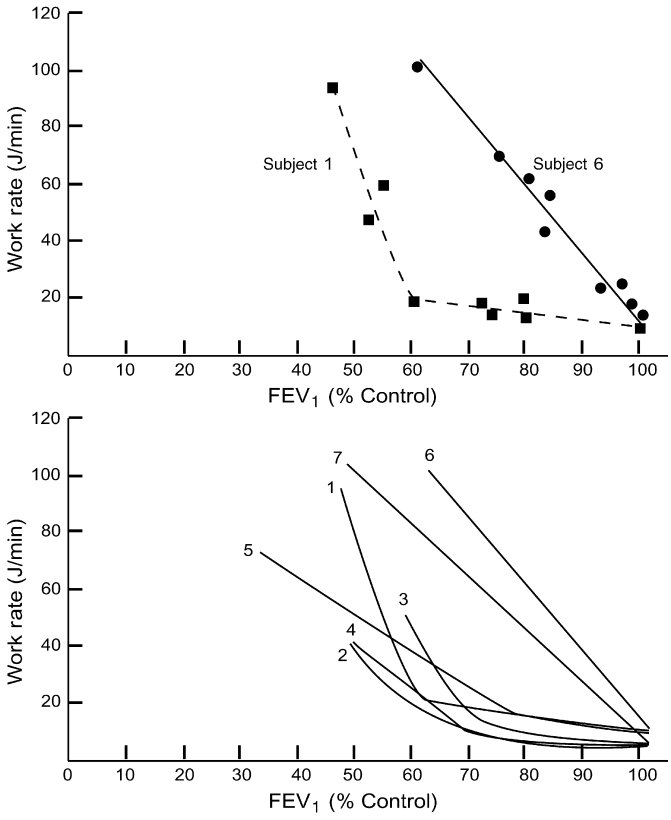

FIGURE 13-5 The work of breathing performed by the inspiratory muscles was calculated from the Campbell diagrams constructed from tidal volume and pleural pressure changes for seven asthmatic subjects at various degrees of bronchoconstriction induced by aerosols of histamine. The chest wall relaxation characteristics necessary for the calculation of work were taken from published data on normal subjects. The *upper panel* shows the relationship between work and FEV_1 for two illustrative subjects. The *lower panel* shows linear regression plots for all seven subjects. Redrawn with permission from Martin et al 1983[2].

resulted in a fall in FEV_1 of 51%. Both the elastic and resistive work increased, but the proportion of the work that was performed in overcoming elastic forces was 69% of the total work during quiet breathing and 57% of the total at maximal bronchoconstriction. The fact that elastic work still represents the major part of the work is explained by the occurrence of hyperinflation. The variable increases in the work of breathing from subject to subject during an asthma attack relate in substantial degree to the variability in the magnitude of hyperinflation in individual subjects. There is an additional component of the elastic work of breathing that is attributable to inhomogeneous ventilation. Unequal expansion of different parts of the lung leads to an increase in elastic impedance since some areas of lung that are well ventilated contribute more to the tidal volume than other, less well-ventilated, areas. It is also the phenomenon that probably accounts for the tearing of the lungs during attacks of asthma that causes pneumomediastinum.

Partitioning the Work of Breathing Between the Diaphragm and the Rib Cage Muscles

During quiet breathing in normal subjects, it is argued that most of the work of breathing is attributable to the diaphragm and that other muscles make a minor contribution to the energetics of breathing. The recruitment of the inspiratory muscles increases when the impedance to breathing increases. There is, in general, a relatively greater recruitment of the inspiratory muscles of the rib cage than the diaphragm as respiratory system impedance increases. External mechanical loads have frequently been used to simulate the loading of disease, and patterns of muscle recruitment have been examined. Both elastic and resistive inspiratory loads cause an increase in inspiratory muscle activity, and a preferential recruitment of the rib cage muscles is observed.[16]

It is difficult to assess quantitatively the contributions of the diaphragm and the rib cage muscles to breathing. However, the patterns of recruitment of the rib cage muscles and the diaphragm can be deduced by examining the displacements of the rib cage and abdominal compartments of the chest wall and related pressures such as the pleural and abdominal pressure changes, as well as the difference between these pressures, the transdiaphragmatic pressure.[17,18] However, a precise quantitative assessment of the contributions to breathing of the rib cage muscles and the diaphragm is difficult because the diaphragm has complex effects on both the rib cage and abdominal compartments of the chest wall. The insertion of the diaphragm onto the lower ribs causes a cephalad force on the rib cage. In addition, the increase in intraabdominal pressure that its contraction causes is transmitted across the zone of apposition of the diaphragm to the lower rib cage. This pressure is also inspiratory in action. Precise displacements of the diaphragm are therefore hard to measure. This topic is discussed elsewhere in this book (see Chapter 7, "Act of Breathing: The Ventilatory Pump") and has been the subject of several publications.[19–22]

In order to assess the relative energy costs of the contractions of the rib cage muscles and the diaphragm in induced asthma, the pressure–time products for all the respiratory muscles and for the diaphragm have been calculated during induced bronchoconstriction of asthmatic subjects. The pressure–time product has been shown to be a better predictor of oxygen consumption by the myocardium than external mechanical work.[23] It is also a useful predictor of the oxygen costs of skeletal respiratory muscular contractions.[24] It is easier to calculate for the respiratory muscles than is the external mechanical work done by these muscles and should also be closely related to oxygen consumption by these muscles. In the asthmatic subjects undergoing histamine provocation, the pressure–time product for the diaphragm measured over 1 minute increased three-fold, whereas the net inspiratory muscle pressure–time product (inclusive of rib cage muscles and diaphragm) increased almost five-fold. This indicates that the diaphragm is protected from the increase in the work of breathing by the transfer of inspiratory work to the rib cage muscles.

Although a consideration of the pleural pressure changes alone does not suggest any activation of the expiratory muscles during induced asthma, a comparison of the changes in intraabdominal pressure (measured by placing a balloon in the stomach) during quiet breathing and during bronchoconstriction, coupled with measurements of the abdominal wall displacements, indicates that the abdominal muscles are recruited[25] and have an important role to play in breathing in asthma. During quiet breathing, the gastric pressure rises during inspiration as the diaphragm contracts, descends, and displaces the abdominal contents downward and outward (Figure 13-6). Subsequently, during expiration, the abdominal wall moves inward as the gastric pressure falls, and the diaphragm returns to its former position. As bronchoconstriction worsens, the abdominal wall excursions diminish and the gastric pressure changes become biphasic, showing an increase in both inspiration and in expiration. The rise in pressure during inspiration reflects diaphragmatic contraction, whereas the rise in expiration reflects abdominal muscle contraction. This pattern of pressure change indicates that the abdominal muscles are active in expiration, but because the contraction of the abdominal muscles is often not sufficient to cause pleural pressure to become more positive than that achieved by passive recoil of the chest wall, it is difficult to conclude that their function is primarily as expiratory muscles. What, then, might their function be? This question is addressed below. It is, of course, also true that the persistence of inspiratory muscle activity in expiration, particularly that of the rib cage muscles, is underestimated from a consideration of pleural pressure–lung volume relationships.

When the abdominal muscles contract during expiration, they displace the abdominal wall inward and force the diaphragm upward into the chest. When the subject is upright, the relaxation of the abdominal muscles at the onset of inspiration lowers intraabdominal pressure and acts as an assist for the diaphragm. This action has been previously noted during exercise and has led to the concept of the abdominal muscles as accessory muscles of inspiration.[25] A similar strategy enables subjects with complete diaphragmatic paralysis to breathe without paradoxical abdominal movements in the upright posture,[26] whereas such a strategy does not work in the recumbent

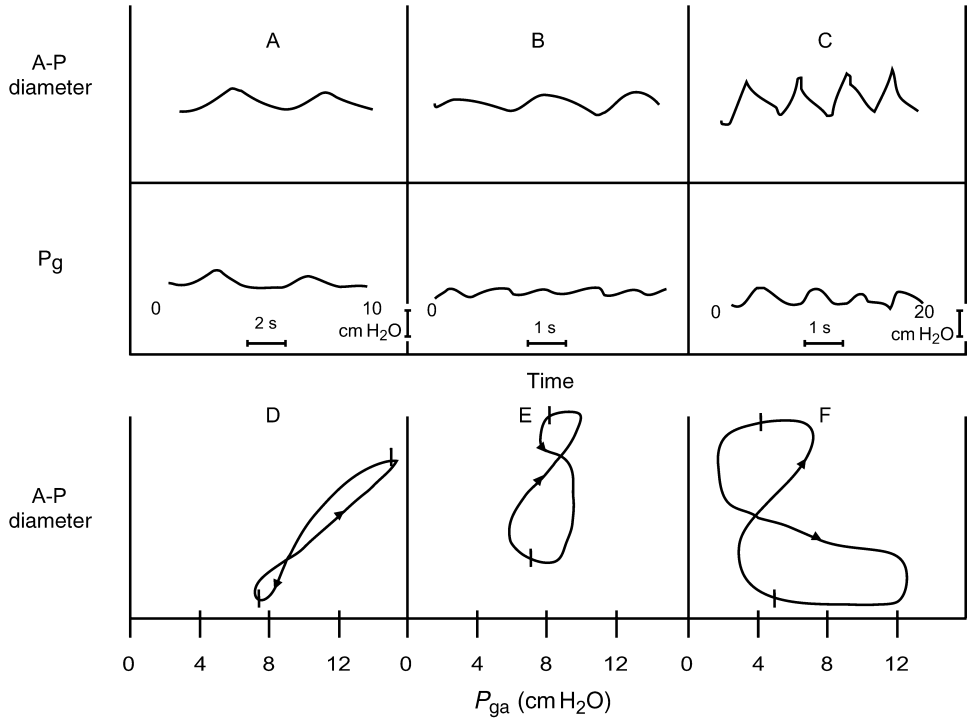

FIGURE 13-6 The changes in the anteroposterior (A-P) diameter of the abdomen were monitored with a pair of magnetometers, and gastric pressure (P_{ga}) was monitored with a balloon catheter in the stomach. Traces of the changes in A-P dimensions and P_{ga} are shown during quiet tidal breathing (*A*) and during two successive levels of bronchoconstriction induced by histamine (*B*, *C*). *x*–*y* plots of the A-P dimension of the abdomen against P_{ga} are shown in (*D*), (*E*), and (*F*). For explanations see text. Redrawn with permission from Martin et al 1980[6].

posture because the action of gravity on the abdominal wall is not in an inspiratory direction in this posture.

Chest Wall Displacements During Breathing with Induced Asthma

The partitioning of the work of breathing between the diaphragm and the rib cage muscles can be appreciated by considering the movements of the chest wall compartments during breathing. Several techniques are available for the measurement of the movements of the rib cage and abdominal compartments. The early investigations were performed using magnetometers, which were electronic devices attached to the anterior and posterior aspects of the rib cage and abdomen that permitted the measurement of the distance between the two probes. From these signals, the movements of the chest wall were followed. In trained subjects, it was possible to show that following a breath to TLC and with relaxed respiratory muscles, the chest wall deflated from TLC to FRC with the relative contributions of the rib cage and abdomen following a reproducible pattern. The relationship between rib cage and abdominal volume during a relaxation maneuver is illustrated in Figure 13-7, and the term frequently used to describe the relationship is the relaxation line. During quiet tidal breathing, the rib cage and abdomen inflate and deflate in such a way as to follow the relaxation line. This is the most economic way to inflate the respiratory system, and any deviation from this configuration leads to an increase in the work of breathing.[25]

There are few measurements of the changes in rib cage and abdominal volume during acute asthma.[27] In one such study, the changes in rib cage and abdominal volumes during histamine-induced asthma were examined.[28] The major portion of the tidal volume is usually attributable to displacement of the rib cage and in the asthmatic subjects prior to bronchoconstriction was approximately 70%. After bronchoconstriction, the rib cage excursion contributed almost 96% of the tidal volume. These measurements are consistent with the conclusions drawn from the analysis of respiratory pressures that the inspiratory muscles acting on the rib cage are preferentially recruited during acute asthma. Hyperinflation in asthma occurs in some subjects predominantly through expansion of the rib cage and in other subjects through outward displacement of the abdomen, reflecting descent of the diaphragm. Subjects who breathe with the rib cage during tidal breathing have an increase in FRC through an inspiratory displacement of the rib cage, whereas those who breathe with a predominant displacement of the abdomen favor an inspiratory displacement of the abdomen. The fact that the distribution of volume change through the rib cage and abdomen corresponds to the distribution of volume change during quiet tidal breathing suggests that the chest wall configuration at FRC may correspond to the relaxation configuration; the rib cage and abdomen follow the relaxation configuration during quiet breathing (see Figure 13-7). The "strategy" of breathing that results in hyperinflation through the abdominal compartment of the chest wall is likely to be a very unfavorable one from the point of view of diaphragmatic function.[29] The costal and crural portions of the diaphragm seem to work as two separate muscles, usually working mechanically in parallel to

generate pressure. A parallel mechanical interaction is well suited to pressure generation. However, hyperinflation appears to uncouple the two parts of the diaphragm, causing them to act mechanically in series.[30] This causes them to be less able to cope with the increased demand for inspiratory pressure generation that is seen in asthma. This situation does seem to evoke a corrective strategy because during bronchoconstricted breathing the chest wall movements are usually almost exclusively through the rib cage, and the abdomen does not expand much beyond its configuration at end-expiration (see Figure 13-7). This pattern of deployment of the inspiratory muscles limits the excursion of the diaphragm, whose mechanical efficiency is impaired by excessive shortening.

It is also remarkable that during exercise or hyperventilation induced by breathing carbon dioxide, the increase in the excursion of the abdominal compartment of the chest wall is usually only in the expiratory direction, whereas the end-inspiratory position of the abdominal wall changes little[25] (see Figure 13-7). This action of the abdominal muscles, by reducing the FRC, allows the outward recoil of the chest wall to increase, reducing the inspiratory work of breathing. It also lengthens the diaphragmatic muscle fibers, placing them on a more favorable portion of their length–tension curve. This results in more force generation for a given neural output to the diaphragm. Finally, the timely relaxation of the abdominal muscles allows the weight of the abdominal contents to provide an inspiratory force. Respiratory muscles other than the diaphragm absorb the increased work of breathing resulting from the deformation of the chest wall. The coordinate action of the rib cage and abdominal muscles defends the diaphragm against fatiguing loads, keeping its configuration and fiber length optimal while at the same time distributing the work of breathing to other respiratory muscles. A similar strategy seems to apply in the use of the respiratory muscles in asthma. Although this pattern of respiratory muscle action may protect the diaphragm from excessive loading, it is possible that it may be associated with a more intense sense of the effort needed to breathe.

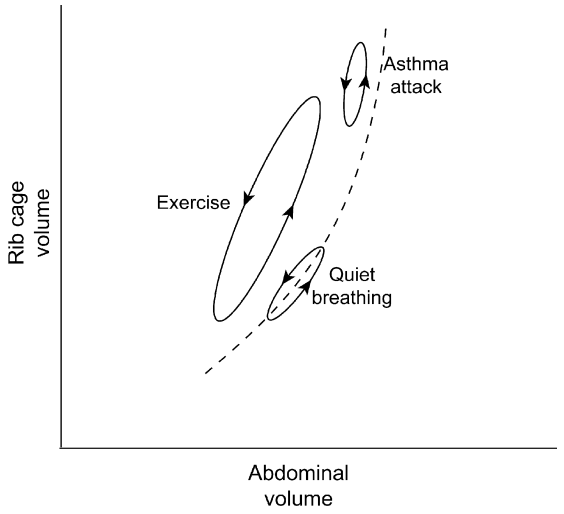

FIGURE 13-7 The changes in rib cage and abdominal dimensions are shown during a passive expiration from total lung capacity (TLC) to functional residual capacity (FRC) and during a passive inspiration from residual volume (RV) to FRC (*dotted line*). The rib cage is more compliant ($\partial V/\partial P$) than the abdomen, so that more of the volume change is accommodated by the excursion of the rib cage. The changes in volume of the rib cage are plotted against the changes in abdominal volume during a maneuver involving an inspiratory rib cage maneuver or abdominal inspiratory maneuver with the glottis closed. The changes in volume are therefore reciprocally related and equal in magnitude. The loops represent the excursions of the rib cage and abdomen during quiet breathing, exercise, and an asthma attack.

COPD

Mechanical Impedances

The strategy of breathing required in COPD bears similarities to that needed in asthma because the abnormal loads faced by the respiratory muscles are similar. Both resistive and elastic impedances are increased in COPD, and the changes in respiratory mechanics are also substantially influenced by hyperinflation. An important difference between the two conditions is that chronic changes in FRC are more frequently present in COPD. However, there are also changes that occur during acute exacerbations of the condition and also during exercise that challenge the respiratory muscles in a manner similar to acute asthma. The increases in FRC in some patients with COPD are very large indeed and sometimes exceed the value of the predicted TLC. Since the chest wall has an outward recoil up to the lung volume corresponding to 60 to 70% of the TLC, any increase in lung and chest wall volume beyond this value requires the activity of the inspiratory muscles. In other words, the FRC cannot be determined by a static balance of forces but must be determined by active and dynamic mechanisms involving the inspiratory muscles. Expiration is not achieved by a passive balance of forces of the elastic recoil of lungs and chest wall because expiration is interrupted by the onset of the activity of the inspiratory muscles. Immediately prior to the cessation of airflow in expiration, alveolar pressure is positive, often substantially so. This pressure is predominantly the result of the recoil of the respiratory system but may be enhanced by expiratory muscle recruitment. The parallel between the positive alveolar pressure toward end-expiration and externally applied positive end-expiratory pressure (PEEP) has led to the term intrinsic PEEP (PEEPi). This positive alveolar pressure needs to be offset by inspiratory muscle activity before expiration can be terminated and inspiration initiated. As such, PEEPi is a threshold load that needs to be overcome before inspiratory muscle action can cause flow of air into the lungs. One of the consequences of the positive alveolar pressure in expiration is pulmonary hypertension that results from the compression of alveolar capillaries and is a feature of both COPD[31] and asthma.[32] The results of recent studies on normal subjects, in which external expiratory loads have been used to mimic flow limitation, have suggested a potential for cardiovascular consequences of exercise-induced hyperinflation and high expiratory pressures.[33]

The increase in FRC in COPD is one of the causes of an increased mechanical load in the act of breathing in this

condition. As in asthma, the inspiratory load in COPD is composed of elastic and resistive components. However, loss of lung elastic recoil is more frequent in COPD than in asthma, so that the elastic load is likely to be somewhat less. The passive chest wall mechanical properties seem to be unaffected in COPD patients, so that breathing at high lung volume will also require muscle force to overcome the elastic recoil of the chest wall. Intrinsic PEEP leads to an additional threshold load that needs to be overcome before inspiration can take place. This is also a feature of asthma, although it has received little attention in this condition. However, it appears to be a contributor to dyspnea in asthma[34] as well as in COPD.[35]

Respiratory Muscle Recruitment

The mechanical impedance in COPD requires that inspiratory muscle recruitment increase so as to maintain minute ventilation. The rib cage muscles are activated in COPD, including the scalene and sternocleidomastoid muscles. The abdominal muscles are also frequently active during the expiratory cycle. The diaphragm is disadvantaged by the hyperinflation of COPD because not only are its muscle fiber lengths reduced, but the flattening that it experiences should result in it being a less effective inspiratory muscle. Indeed, the results of experimental studies suggest that the diaphragm may become expiratory in action at very high lung volumes.[36] However, studies of diaphragmatic function in patients with COPD indicate that the mechanical responses of the diaphragm to phrenic nerve stimulation are quite well preserved. There appear to be adaptive responses such that the diaphragm compensates well for the length changes caused by hyperinflation; all things considered, it is at least as effective, and in some cases more effective, than the diaphragm in a normal subject operating at the same lung volume.[37]

The abdominal muscles are usually not very active during quiet breathing in the supine posture but are active in upright subjects with COPD. In some cases, this activity is associated with a sufficiently positive pleural pressure during expiration to cause flow limitation. Although recruitment of the abdominal muscles may allow the diaphragmatic configuration to be improved and may also cause diaphragm fiber lengthening,[38] the generation of expiratory pressures that exceed those necessary to cause maximal expiratory flows is unhelpful. Indeed, flow limitation is often associated with a greater sense of dyspnea than that experienced when it is absent.[39] It has been postulated that pursed-lip breathing is a strategy designed to relieve discomfort caused by airflow limitation. However, the mechanism of the relief of dyspnea by pursed-lip breathing seems likely to be related to the prolongation of expiration and the decrease in end-expiratory chest wall volume[40] rather than airway mechanics. Attempts to confirm that expiratory muscle recruitment in COPD is associated with more effective generation of pressure by the diaphragm have not been successful. The pressure output of the diaphragm for a given electrical activation, as measured by the electromyogram, was not different among COPD subjects with and without phasic abdominal muscle contraction during tidal breathing.[41]

During exercise, many COPD patients experience an increase in FRC as a result of the effects of an increase in minute ventilation.[38,42] Indeed, without an increase in FRC, those patients who have expiratory flow limitation at rest are unable to increase minute ventilation. An increase in tidal volume and/or breathing frequency (reduction in expiratory time) causes an increase in FRC. This change in FRC is in contrast to the behavior of normal subjects, who usually experience a fall in FRC. It is likely that asthmatic subjects will also, on occasion, have an increase in FRC, depending on the severity of the lung function abnormality. The degree of hyperinflation in exercising subjects with COPD may result in the end-inspiratory lung volume approaching TLC and is often associated with intense dyspnea[43] and a marked degree of activation of the diaphragm.[42] The compromise of respiratory function associated with hyperinflation seems to contribute[44] to the development of hypercapnia during exercise. A measurement of the inspiratory capacity provides a simple and useful way of assessing the degree of hyperinflation that is induced by an exacerbation of obstructive lung disease or in association with dynamic hyperinflation caused by exercise. It is strongly associated with dyspnea but has thus far not been incorporated into clinical practice.

CONCLUSIONS

Asthma and COPD are two common diseases that are associated with abnormalities in respiratory system mechanics involving expiratory airflow limitation during forced expiration and hyperinflation during tidal breathing. Expiratory airflow limitation is often present in COPD during quiet tidal breathing but not in asthma. Hyperinflation is associated with an increased energy cost of breathing and disadvantaged inspiratory muscle function. It is also associated with marked dyspnea as well as occult effects such as pulmonary hypertension. Increases in inspiratory swings in pleural pressure result in such clinical signs as pulsus paradoxus and intercostal indrawing and account for pneumomediastinum, when tearing of the alveoli occurs. Changes in patterns of muscle recruitment occur when subjects are faced with increases in respiratory impedance. These involve an increase in recruitment of rib cage muscles and an increase in the contribution of the displacement of the rib cage to tidal volume. These changes are similar to those observed during exercise in normal subjects. It is perhaps not surprising that the strategy of use and recruitment of the respiratory muscles during asthmatic attacks and in COPD resembles that used to cope with the physiologic stimulus of exercise. The human subject has evolved to cope with the physiologic stress of exercise but not necessarily disease processes.

ACKNOWLEDGMENTS

The author wishes to acknowledge the assistance of Mr Pierre Fiset in the preparation of the figures for this chapter. Many publications that have contributed to our understanding of this topic have not been referenced, but the contributions that they have made are gratefully acknowledged.

REFERENCES

1. Banzett RB, Dempsey JA, O'Donnell DE, Wamboldt MZ. Symptom perception and respiratory sensation in asthma. Am J Respir Crit Care Med 2000;162:1178–82.
2. Martin JG, Shore SA, Engel LA. Mechanical load and inspiratory muscle action during induced asthma. Am Rev Respir Dis 1983;128:455–60.
3. Shore S, Milic-Emili J, Martin JG. Reassessment of body plethysmographic technique for the measurement of thoracic gas volume in asthmatics. Am Rev Respir Dis 1982;126:515–20.
4. Woolcock AJ, Read J. Lung volumes in exacerbation of asthma. Am J Med 1966;41:259–73.
5. Gelb AF, Zamel N, Hogg JC, et al. Pseudophysiologic emphysema resulting from severe small-airways disease. Am J Respir Crit Care Med 1998;158:815–19.
6. Martin JG, Powell E, Shore S, et al. The role of the respiratory muscles in the hyperinflation of bronchial asthma. Am Rev Respir Dis 1980;121:441–7.
7. De Troyer A, Martin JG. Respiratory muscle tone and the control of functional residual capacity. Chest 1983;84:3–4.
8. Martin JG, Habib M, Engel LA. Inspiratory muscle activity during induced hyperinflation. Respir Physiol 1980;39:303–13.
9. Muller N, Bryan AC, Zamel N. Tonic inspiratory muscle-activity as a cause of hyper-inflation in histamine induced asthma. Fed Proc 1980;39:278.
10. Kosch PC, Stark AR. Dynamic maintenance of end-expiratory lung-volume in full-term infants. J Appl Physiol 1984; 57:1126–33.
11. Tantucci C, Ellaffi M, Duguet A, et al. Dynamic hyperinflation and flow limitation during methacholine-induced bronchoconstriction in asthma. Eur Respir J 1999;14:295–301.
12. Lougheed MD, Lam M, Forkert L. Breathlessness during acute bronchoconstriction in asthma. Pathophysiologic mechanisms. Am Rev Respir Dis 1993;148:1452–9.
13. Tantucci C, Ellaffi M, Duguet A, et al. Dynamic hyperinflation and flow limitation during methacholine-induced bronchoconstriction in asthma. Eur Respir J 1999;14:295–301.
14. Collett P, Brancatisano T, Engel LA. Contribution of the larynx to air-flow obstruction in bronchial-asthma. Aust N Z J Med 1982;12:221–2.
15. Johnson L, Mead J. Volume–pressure relationships during pressure breathing and voluntary relaxation. J Appl Physiol 1963;18:505–8.
16. Mengeot PM, Bates JH, Martin JG. Effect of mechanical loading on displacements of chest wall during breathing in humans. J Appl Physiol 1985;58:477–84.
17. Goldman MD, Mead J. Mechanical interaction between diaphragm and rib cage. J Appl Physiol 1973;35:197–204.
18. Konno K, Mead J. Measurement of separate volume changes of rib cage and abdomen during breathing. J Appl Physiol 1967;22:407–22.
19. Macklem PT, Gross D, Grassino A, Roussos C. Partitioning of inspiratory pressure swings between diaphragm and intercostal-accessory muscles. J Appl Physiol 1978;44:200–8.
20. Macklem PT, Roussos C, Derenne JP, Delhez L. Interaction between the diaphragm, intercostal-accessory muscles of inspiration and the rib cage. Respir Physiol 1979;38:141–52.
21. Macklem PT. Mathematical and graphical analysis of inspiratory muscle action. Respir Physiol 1979;38:153–71.
22. Ward ME, Ward JW, Macklem PT. Analysis of human chest-wall motion using a 2-compartment rib cage model. J Appl Physiol 1992;72:1338–47.
23. Sarnoff SJ, Braunwald E, Welch GH, et al. Hemodynamic determinants of oxygen consumption of the heart with special reference to the tension–time index. Am J Physiol 1958;192:148–56.
24. McGregor M, Becklake MR. Relationship of oxygen cost of breathing to respiratory mechanical work and respiratory force. J Clin Invest 1961;40:971–80.
25. Grimby G, Goldman M, Mead J. Respiratory muscle action inferred from rib cage and abdominal V–P partitioning. J Appl Physiol 1976;41:739–51.
26. Chen IY, Armstrong JD. Value of fluoroscopy in patients with suspected bilateral hemidiaphragmatic paralysis. AJR Am J Roentgenol 1993;160:29–31.
27. Marazzini L, Rizzato G. Rib cage and abdomen–diaphragm in bronchial asthma—relative contributions to air displacement. Am Rev Respir Dis 1971;103:285–6.
28. Lennox S, Mengeot PM, Martin JG. The contributions of rib cage and abdominal displacements to the hyperinflation of acute bronchospasm. Am Rev Respir Dis 1985;132:679–84.
29. Chen RC, Kayser B, Yan S, Macklem PT. Twitch transdiaphragmatic pressure depends critically on thoracoabdominal configuration. J Appl Physiol 2000;88:54–60.
30. Macklem PT, Macklem DM, Detroyer A. A model of inspiratory muscle mechanics. J Appl Physiol 1983;55:547–57.
31. Pepe PE, Marini JJ. Occult positive end-expiratory pressure in mechanically ventilated patients with air-flow obstruction—the auto-Peep effect. Am Rev Respir Dis 1982;126:166–70.
32. Permutt S. Relation between pulmonary arterial pressure and pleural pressure during the acute asthmatic attack. Chest 1973;63 Suppl:25S–8S.
33. Iandelli I, Aliverti A, Kayser B, et al. Determinants of exercise performance in normal men with externally imposed expiratory flow limitation. J Appl Physiol 2002;92:1943–52.
34. Lougheed MD, Webb KA, O'Donnell DE. Breathlessness during induced lung hyperinflation in asthma—the role of the inspiratory threshold load. Am J Respir Crit Care Med 1995; 152:911–20.
35. O'Donnell DE, Revill SM, Webb KA. Dynamic hyperinflation and exercise intolerance in chronic obstructive pulmonary disease. Am J Respir Crit Care Med 2001;164:770–7.
36. Sant'Ambrogio G, Saibene F. Contractile properties of diaphragm in some mammals. Respir Physiol 1970;10:349–57.
37. Similowski T, Yan S, Gauthier AP, et al. Contractile properties of the human diaphragm during chronic hyperinflation. N Engl J Med 1991;325:917–23.
38. Dodd DS, Brancatisano T, Engel LA. Chest wall mechanics during exercise in patients with severe chronic air-flow obstruction. Am Rev Respir Dis 1984;129:33–8.
39. Eltayara L, Ghezzo H, Milic-Emili J. Orthopnea and tidal expiratory flow limitation in patients with stable COPD. Chest 2001;119:99–104.
40. Bianchi R, Gigliotti F, Rontagnoli I, et al. Chest wall kinematics and breathlessness during pursed-lip breathing in patients with COPD. Chest 2004;125:459–65.
41. Yan S, Sinderby C, Bielen P, et al. Expiratory muscle pressure and breathing mechanics in chronic obstructive pulmonary disease. Eur Respir J 2000;16:684–90.
42. Sinderby C, Spahija J, Beck J, et al. Diaphragm activation during exercise in chronic obstructive pulmonary disease. Am J Respir Crit Care Med 2001;163:1637–41.
43. O'Donnell DE, Revill SM, Webb KA. Dynamic hyperinflation and exercise intolerance in chronic obstructive pulmonary disease. Am J Respir Crit Care Med 2001;164:770–7.
44. O'Donnell DE, D'Arsigny C, Fitzpatrick M, Webb KA. Exercise hypercapnia in advanced chronic obstructive pulmonary disease. Am J Respir Crit Care Med 2002;166:663–8.

CHAPTER 14

VENTILATION DISTRIBUTION

Joseph Milic-Emili

The first section of this chapter deals with the static regional distribution of gas in the lung. Next, the dynamic distribution is reviewed. Because of space limitations, this account focuses on normal, awake humans. Additional information can be found elsewhere in this book (see Chapter 3, "Statics of the Lung") and in other sources.[1–6]

STATIC DISTRIBUTION OF GAS

In the absence of atelectasis or airway closure, alveolar expansion in isolated lungs or lobes appears to be relatively uniform.[7–10] This is not the case when the lungs are inside the thorax. The first direct demonstration that there is a vertical gradient of alveolar expansion in the intact thorax was provided in 1966 by measuring the regional distribution of gas within the lungs with xenon^{133} and external scintillation counters.[11] The radioactive xenon techniques for measuring regional volumes are based on the gas dilution principle.[12–14] The individual lung fields from which radiation is obtained consist of slices or cylinders of lung tissue whose size depends on the characteristics of the scintillation counters. These fields bear little relationship to anatomic subdivisions of the lung, and hence the term *regional* is used to describe measurements made in such counter fields. The volume of these regions is often expressed as a fraction of the regional volume at total lung capacity (TLC). Because, in normal humans, at TLC the alveoli are nearly equal in size throughout the lungs (that is, the TLC per alveolus [TLC_{alv}] is uniform[11]), expression of regional volumes as a fraction of the volume of each region at TLC (V_r/TLC_r) is a particularly useful baseline for comparison. Indeed, regional differences in V_r/TLC_r reflect differences in size (volume) of the alveoli. Similarly, regional differences in $\Delta V_r/TLC_r$ reflect differences in volume change per alveolus.

REGIONAL SUBDIVISIONS OF LUNG VOLUME

Figure 14-1 shows the distribution of gas at functional residual capacity (FRC) and residual volume (RV) in eight seated, normal adults.[15] Regional volumes are expressed as a percentage of TLC_r (lower abscissa). It is apparent that at both RV and FRC, the apical alveoli are more expanded than those in the basilar zones. Whereas the regional FRC/TLC ratio decreases approximately linearly with distance down the lung, the regional RV/TLC ratio decreases progressively from the top of the lung to roughly the middle of the lung, thereafter being essentially constant at a value of approximately 19% TLC_r. Similar relationships between regional FRC/TLC and vertical lung distance have been found in other studies on seated subjects.[11,16–21] In contrast, the relationship between regional RV/TLC and vertical distance down the lung does not always exhibit the behavior shown in Figure 14-1. Several investigators have shown that, in many subjects, the relationship between regional RV/TLC and vertical height is nearly linear over the entire lung.[11,16,22,23] This discrepant behavior may relate to age differences among subjects, different methods, or different procedures. In erect humans, no significant differences in expansion were found at constant lung height between the left lung and right lung at both RV and FRC.

Kaneko and colleagues[24] found that in horizontal postures there is also a vertical gradient of alveolar expansion at both RV and FRC. In that study, no systematic differences in lung expansion could be detected at constant lung height in any of the positions studied. Subsequent studies have confirmed that in horizontal positions there is a vertical gradient of alveolar expansion at RV and FRC.[20,21,23,25] In most instances, however, there was also a smaller but appreciable apex-to-base difference in regional FRC/TLC, with the apical regions being more expanded.

The existence of a vertical gradient of alveolar expansion was confirmed by freezing whole dogs, thus fixing the lungs in situ, and measuring alveolar sizes with morphometric techniques[9] or by lung density.[26] Glazier and colleagues[9] found a marked vertical gradient of alveolar size in head-up dogs frozen at FRC. No significant difference in size was found when the head-up dogs were frozen with their lungs inflated to a transpulmonary pressure of 30 cm H_2O because at this distending pressure the lungs are on a flat part of their static volume–pressure (V–P) curve, so that the existing regional differences in pleural surface pressure make little difference to alveolar volume. These results agree with those of other animal studies[7,26] and support the notion that, at full inflation, the alveoli are expanded nearly uniformly throughout the lung.

Glazier and colleagues[9] also found that at FRC in the horizontal posture the canine alveoli were more expanded in upper than in dependent lung regions, but no differences in alveolar size were found at a given lung height. These results do not conform with the apex-to-base gradient of regional FRC/TLC found in horizontal humans by some

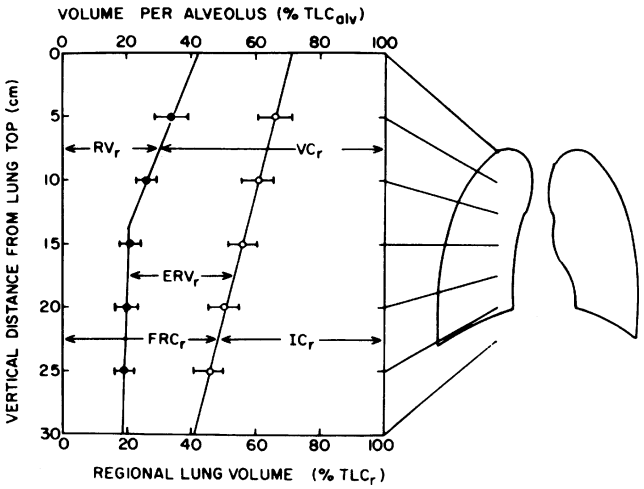

FIGURE 14-1 Average ± SE regional subdivisions of lung volume in eight healthy seated men (aged 31 to 45 years) at residual volume (RV) (*filled circles*) and functional residual capacity (FRC) (*open circles*). Reproduced with permission from Milic-Emili J.[2] ERV_r = regional expiratory reserve volume; FRC_r = regional FRC; IC_r = regional inspiratory capacity; RV_r = regional residual volume; TLC_r = regional total lung capacity; TLC_{alv} = alveolar volume at TLC; VC_r = regional vital capacity.

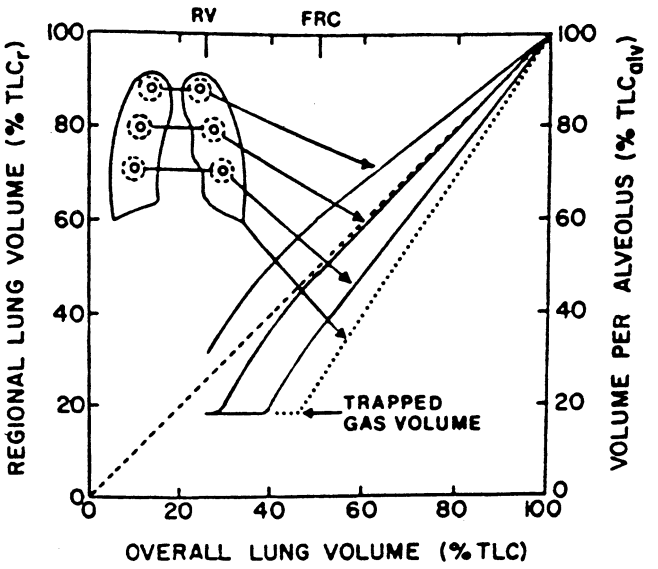

FIGURE 14-2 Average relationships between regional (or alveolar) and overall lung volumes in four seated healthy men aged 33 to 39 years. *Solid lines* indicate the results from three lung regions (4.5, 13.8, and 22.5 cm from the lung top). The *dotted line* indicates the predicted relationship for the lowermost lung zones. The *dashed line* (line of identity) indicates regional (or alveolar) percentile expansion equal to overall lung expansion. Reproduced with permission from Milic-Emili J.[4] FRC = functional residual capacity; RV = residual volume; TLC = total lung capacity; TLC_{alv} = alveolar volume at TLC; TLC_r = regional TLC.

investigators[20,23,25] but are similar to the results of Kaneko and colleagues.[24]

RELATIONSHIP BETWEEN REGIONAL AND OVERALL LUNG EXPANSION

A more complete description of the static distribution of gas within the lungs is obtained by measuring regional volumes at different overall lung volumes, encompassing the entire range of the vital capacity.[15] Such results are shown in Figure 14-2. Regional volumes (V_r) at three different vertical levels of the lung are plotted against the overall lung volume (V). If all lung regions expanded uniformly, the volume of each region (expressed as a percentage of TLC_r) should always equal the overall lung volume (expressed as a percentage of TLC); that is, the data would fall along the identity line (slope = 1). This is not the case: the upper lung units are more expanded than those in the lower zones at all lung volumes, except at full inspiration, and the maximum differences in regional lung expansion occur just below FRC.

In upright humans, the previous volume history of the lung has relatively little effect on the regional static distribution of gas, in the sense that the relationships shown in Figure 14-2 pertain to both inflation from RV and deflation from TLC,[15] provided that there is no prolonged breath-hold at RV.[27] Accordingly, the slopes dV_r/dV of the curves in Figure 14-2 indicate the relative rates of change in volume of the alveoli of various lung regions during static or quasi-static lung inflation and deflation. At lung volumes above FRC, the relationships between regional and overall lung volumes are approximately linear, indicating that, in this range of volumes, the relative rates of filling or emptying of the various lung zones should be essentially fixed (that is, the lungs fill and empty nonsequentially). However, the slopes of the curves are greater in dependent lung zones, indicating that the dependent alveoli undergo greater volume changes. These results suggest that when a normal subject takes a slow breath from FRC, the ventilation per alveolus should be greater in dependent than in upper lung regions, but that the relative distribution of ventilation should be independent of the volume inspired; that is, the difference in ventilation between upper and dependent alveoli should be proportionately the same whether the subject takes a resting tidal breath or a maximal inspiration.

Below FRC, the relationships between regional and overall lung volume are not linear (see Figure 14-2). When the volume of a region reaches a value of approximately 19% TLC_r, it remains constant despite further reduction in overall lung volume. This probably corresponds to the regional trapped-gas volume (ie, the regional volume at which the regional peripheral airways close, trapping gas behind them). When the lung volume is reduced below FRC, airway closure begins in the most dependent parts of the lung (which are exposed to more positive pleural surface pressure) and progresses upward until RV is reached.[28,29] If the airways to part of the lung close, the slope dV_r/dV of the remainder of the lung must increase. At low lung volumes, the slopes of the curves relating regional to overall volume are steeper in the upper than in the dependent zones. Therefore, during slow inspiration from RV, the upper alveoli initially receive relatively greater ventilation; however, the proportion of gas delivered into the upper units

decreases progressively as inspiration proceeds, whereas the opposite is true in the dependent zones. Thus, at low lung volumes, not only is the distribution of inspired gas during slow inspiration reversed, but the various regions fill and empty sequentially.

Static relationships between regional and overall lung volumes for the sitting position have been reported by several investigators.[11,16,21,30] Their results generally agree with those in Figure 14-2, except that the relationships between V_r and V above FRC appear to be less linear in some reports[16,21] than in others. A similar discrepancy between different studies is also found for horizontal postures. According to Kaneko and colleagues,[24] the general pattern in the supine, prone, and lateral decubitus positions is similar to that in Figure 14-2, but other investigators have found that, above FRC, there are appreciable curvilinearities in the V_r versus V relationships, particularly in the lateral decubitus position.[16,21,31] In view of the experimental errors inherent in the radioactive gas techniques, such discrepancies are more apparent than real: because of the complexity of the lung structure and its support, deviations in V_r versus V relationships from linearity may be expected, but the resolution of regional volume measurements based on radioactive gas techniques is inherently inadequate to resolve this problem.

FACTORS GOVERNING THE STATIC DISTRIBUTION OF GAS

Unlike the lungs of many mammals, which may exhibit significant differences in elastic properties between the upper and lower lobes,[7,8] the human lungs appear to have relatively uniform static mechanical properties.[11,15,32] Therefore, it follows that the nonuniform alveolar expansion (see Figures 14-1 and 14-2) must be caused primarily by regional differences in pleural surface pressure (P_{pl}). Indeed, in the absence of regional differences in P_{pl}, the relationships between V_r and V (Figure 14-2) should fall along the line of identity. Thus, the observed differences in alveolar expansion imply that static P_{pl} (and hence transpulmonary pressure, P_L) is not uniform in the intact thorax. The transpulmonary pressure (P_L) is the difference between the pressure at the airway opening (P_{aw}) and P_{pl}.

Quantitatively, the regional differences in alveolar expansion depend on the intrinsic static *V–P* characteristics of the lung and the regional differences in P_L.

Intrinsic Static V–P Relationships

Such relationships may be obtained from measurements on excised lungs[32,33] or can be derived by relating the regional volumes determined with radioactive gases to the corresponding regional transpulmonary pressure.[11,15,24]

Figure 14-3 shows the intrinsic static *V–P* relationship of the lungs obtained with the latter approach by Sutherland and colleagues.[15] The curve pertains to lung deflation from TLC and is the average obtained in the four normal seated adults of Figure 14-2. Since the static mechanical properties appear to be relatively uniform in normal humans, this curve should apply to each individual lung region.[11,15] In the P_L range between 40 and -0.5 cm H_2O, the static *V–P* relationship is closely described by an exponential function[33]:

$$V = V_0 + V_{max}\,(1 - e^{-KP_L}) \qquad (14\text{-}1)$$

where V is volume, V_0 and V_{max} are predicted volumes at zero and infinite static P_L, and K is a constant. If P_L is reduced to below -0.5 cm H_2O, no further change in volume is observed because the peripheral airways (presumably the terminal bronchioles) close, and gas is trapped behind the closed airways.[28,29,33] The P_L at which the peripheral airways close (-0.5 cm H_2O in Figure 14-3) is termed the critical closing pressure. The trapped-gas volume corresponds to approximately 19% of regional TLC (Figures 14-2 and 14-3).

To reopen the closed airways, a critical P_L of about $+2$ cm H_2O is required in normal adults. In elderly subjects (65 to 75 years old), both the critical closing and opening pressures are higher (0 and $+4.5$ cm H_2O, respectively).[29] This suggests that the airways of aged lungs offer less resistance to collapse, but the reasons are not presently known.[34] Predictably, the regional trapped-gas volume also increases with age.[29,34] It should be stressed that once gas is trapped behind closed airways, its volume does not necessarily remain constant but decreases with time. Ruff and colleagues[27] demonstrated that during a breath-hold of approximately 30 seconds at RV (mouth closed), the RV_r/TLC_r ratio in the dependent lung zones decreased significantly compared with results obtained without a breath-hold. This was associated with an increase of RV_r/TLC_r in the upper lung zones. They attributed this phenomenon to the fact that at RV some of the small airways in the dependent lung zones remain patent[22]; this allows gas to escape slowly via collateral ventilation or diffusion from units with closed airways into units with open airways and hence into the upper lung zones. The results of Ruff and colleagues[27] may explain the different regional distributions of gas at RV found by different investigators (see "Regional Subdivisions of Lung Volume"). The data in Figure 14-1 were obtained without a breath-hold at RV, whereas in other studies a variable breath-hold was made. Engel and colleagues[22] have demonstrated that in humans at RV not all the small airways in the dependent lung zones are closed. Because of the complexities of the multitudinous pathways within the lung, there is probably a range of closing pressures for small airways rather than a unique value, as implied by Figure 14-3; the same also applies to the opening pressures for the airways (see Chapter 3, "Statics of the Lung").

Topography of Pleural Surface Pressure

In experimental animals, the topography of pleural surface pressure has been studied extensively with the use of direct measurements.[35,36] These studies have confirmed the presence of a gradient in P_{pl} along the vertical axis of the lung (ie, in the direction of gravity), whereas along the horizontal axis, P_{pl} is, in general, relatively uniform. Direct measurement of P_{pl} is not feasible in humans. However, useful information has been obtained with the indirect method introduced by Milic-Emili and colleagues.[11] This approach is based on the principle that when the regional static distribution of gas

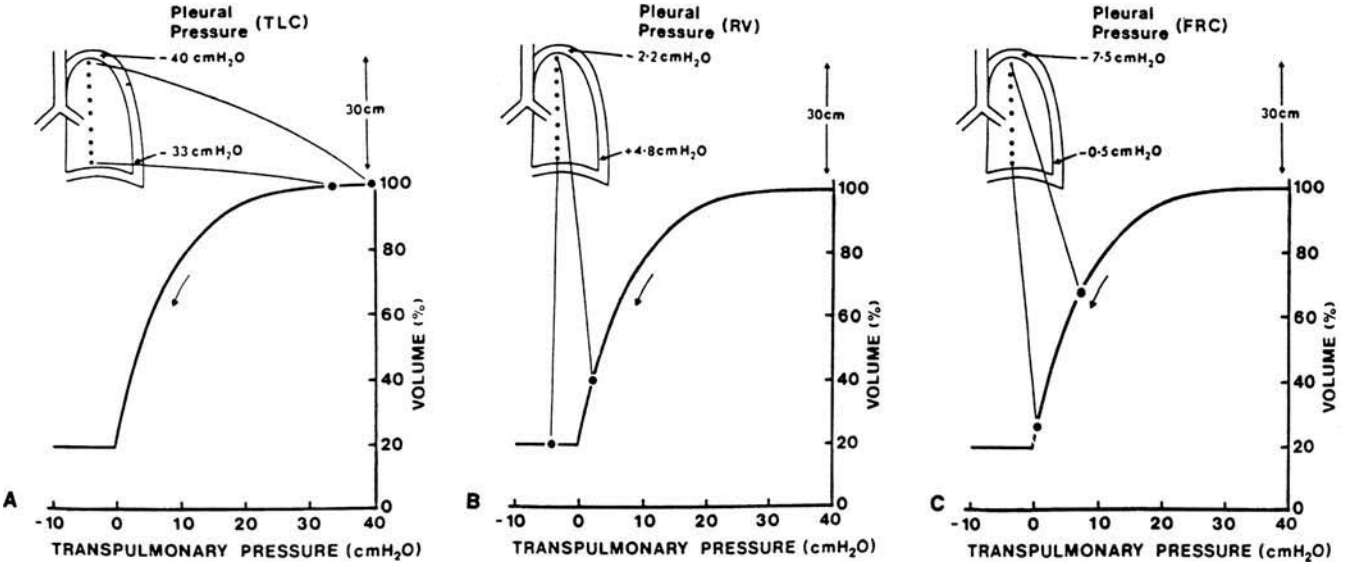

FIGURE 14-3 Effect of a vertical gradient of pleural surface pressure on the static distribution of gas within the lung during deflation. The intrinsic static mechanical properties of the lung (*heavy line*) are assumed to be uniform. At full inspiration (*A*) all regions are expanded virtually uniformly, despite the difference in pleural surface pressure down the lung, but at residual volume (RV) (*B*) and functional residual capacity (FRC) (*C*) the pleural surface pressure gradient causes upper regions to be more expanded than lower zones. These diagrams also show the indirect method for determining regional pleural pressures (see text). Reproduced with permission from Milic-Emili J.[2] TLC = total lung capacity.

and the intrinsic static mechanical properties are known, the regional distribution of P_{pl} can be determined. This method has limitations because any errors in measurement of regional lung volumes or static *V–P* curves will be reflected in the estimates of regional P_{pl}. It should be noted, however, that direct measurement of P_{pl} is technically complex, and its validity is often questionable.

The indirect approach for estimating regional P_{pl} is illustrated in Figure 14-3. The regional volumes at RV and FRC, such as shown in Figure 14-2, are fitted to the static *V–P* curve in Figure 14-3. This allows estimation of local P_L and hence of local P_{pl} (which in this case equals $-P_L$ because the mouth pressure was zero).

When this approach is used, the relationship between lung height and static P_{pl} in seated humans appears to be nearly linear, with a gradient of approximately 0.25 cm H_2O/cm, which seems to be independent of lung volume.[11,15] The latter is important because it indicates that the static changes in P_{pl} with lung volume are relatively uniform. Using the same method, Kaneko and colleagues[24] found a volume-independent vertical gradient of P_{pl} ranging from 0.16 to 0.18 cm H_2O/cm in normal adults in lateral, supine, and prone postures.

The observation that under static conditions the gradient in P_{pl} does not change substantially with lung volume is important. Indeed, the linear relationships between regional and overall lung volume, such as seen in Figure 14-2, at lung volumes higher than FRC (ie, in the range where gas trapping is absent) can only be explained by a combination of a fixed vertical gradient in P_{pl} and uniform static mechanical properties, characterized by an exponential function (Equation 14-1).[11,15] These are stringent requirements. Small departures from perfect exponential behavior, small inhomogeneities in static mechanical properties, and small changes in P_{pl} gradient with lung volume may explain the observation that during quasistatic inflation and deflation, the lungs exhibit some sequential behavior also at lung volumes higher than FRC[31,37–39] rather than the nonsequential pattern implied by Figure 14-2. Such sequential behavior contributes to the slope of phase III during the closing volume tests (see below).

As illustrated in Figure 14-3, the regional differences in alveolar expansion are determined by the interaction of regional differences in P_{pl} with the static mechanical properties of the lung. This model provides a useful basis for explaining the static distribution of gas under a variety of conditions.

In seated humans, Bryan and colleagues[30] found that the vertical gradients of P_{pl} and alveolar size increased proportionally with increased headward acceleration, becoming nil when the data were extrapolated to zero gravity. Clearly, gravity plays an important role in determining the regional differences in P_{pl}. Gravity may act through distortion of lung tissue by its own weight or indirectly via changes in thoracoabdominal configuration. In humans, unlike in animals,[35,36] lung weight appears to play a more important role in determining regional differences in P_{pl} (and hence regional lung expansion) than distortion of the chest wall. This is particularly true in the upright position, in which the regional distribution of gas is not influenced appreciably by a wide range of thoracoabdominal shapes[18] or by the weight of the abdominal contents.[19] Only extreme deformations of the chest wall produced either by externally applied forces or by strong muscle contractions cause appreciable changes in regional gas distribution and, by implication, in P_{pl}.[17] The smaller role of the chest wall in humans than in animals in

determining the regional distribution of gas has been interpreted as being due to the stiffer rib cage, which is more resistant to deformation.[18]

In humans, the most deformable part of the chest wall is its diaphragmatic boundary, and hence a greater potential for distortion exists in horizontal postures because of the abdominal pressure gradient. Indeed, muscle paralysis during anesthesia in lateral decubitus results in significantly greater vertical differences of alveolar expansion than in the awake state.[21] This is thought to be caused by removal of diaphragmatic tone, allowing transmission of abdominal pressure across the paralyzed diaphragm. By contrast, a contracted diaphragm should isolate the lungs from the abdominal contents, thus reducing transmission of abdominal pressure. Indeed, strong selective contraction of the diaphragm in lateral decubitus can virtually abolish the vertical gradient of alveolar size.[31] Thus, in the horizontal positions, factors other than lung weight may play a role in determining the static distribution of gas. In upright humans, however, lung weight appears to be the major determinant.

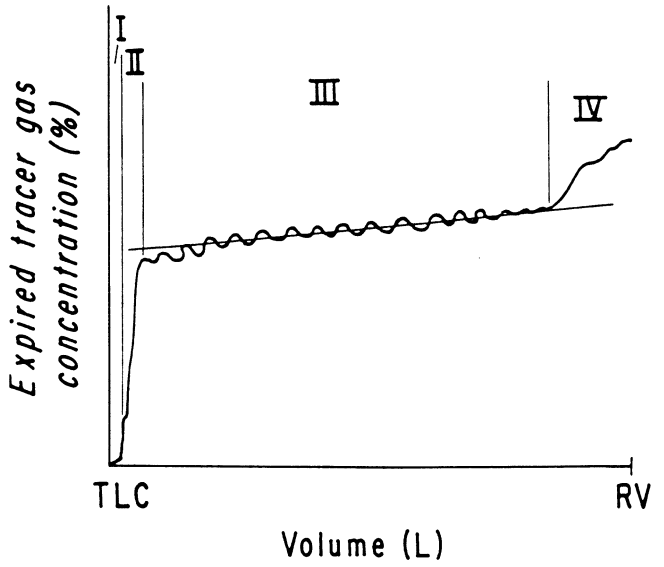

FIGURE 14-4 Idealized representation of closing volume test. Phases I to IV are indicated. The junction between phase III and phase IV reflects the closing volume. The straight line through phase III indicates the slope of phase III. Also seen in this figure are the cardiac oscillations in expired tracer gas. RV = residual volume; TLC = total lung capacity.

Closing Volume

The closing volume measurements, which are described in detail elsewhere,[34] can be obtained with the bolus and resident gas methods. The former consists of administering a bolus of trace gas (eg, argon, SF_6, ^{133}Xe) at RV while air is slowly inhaled to TLC. Since at RV the airways in the dependent lung zones are closed (Figure 14-3A), the tracer gas is delivered preferentially to the upper lung regions. During the subsequent slow expiration from TLC to RV, a critical volume (closing volume) is reached at which the airways in the lower lung regions begin to close; as expiration progresses, closure spreads toward the middle lung zones. As a result, the contribution of the lower zones to the expirate decreases with a progressive increase in the expired tracer concentration, as shown in Figure 14-4. The closing volume corresponds to the junction between phase III and IV.

The resident gas technique is similar, except that in this case a difference in tracer gas concentration (nitrogen) between the upper and lower lung regions is obtained by the inhalation of pure oxygen from RV to TLC. Since RV_r is larger in the upper lung regions (Figure 14-1), the nitrogen (resident gas) concentration at TLC is higher in upper than lower lung zones. As a result, during subsequent slow expiration from TLC to RV, a record similar to that in Figure 14-4 is obtained. Thus, closing volume tracings obtained under normal gravitational conditions can be accounted for by the simple model in Figure 14-3. Such a model also predicts that in the absence of gravity, when topographic gradients in P_{pl} should be absent, airway closure should disappear because RV_r should exceed the regional trapped-gas volume (TGV_r) throughout the lung. A study by Guy and colleagues[40] carried out in conditions of microgravity in Spacelab SLS-1 did not entirely confirm the above prediction. Compared to the standing measurements in normal gravity made pre- and postflight, there was a marked decrease in ventilatory inhomogeneity during microgravity, as evidenced by a significant reduction in cardiogenic oscillations, slope of phase III, and height of phase IV, for both nitrogen and argon. However, in four of the seven subjects studied, there was an apparent closing volume with argon but not nitrogen. The latter finding suggests that in microgravity there are no appreciable regional differences in RV_r, and the former finding is probably due to the fact that the critical closing pressure (P_o) is not discrete, as implied in Figure 14-3. In fact, although direct evidence is lacking, it is likely that in human lungs and lobes there is a range of critical closing (and opening) pressures, as in the excised lungs and lobes of rabbits, cats, dogs, and monkeys (see Chapter 3, "Statics of the Lung"). Thus, to the extent that airway closure may occur at low lung volumes in microgravity, a closing volume should be present. In this connection, it should be noted that in microgravity there is a significant reduction of overall RV relative to normal gravity,[41] which should promote airway closure at low lung volumes. Indeed, if the end-expiratory lung volumes were not limited by the chest wall, the RV should correspond to the TGV. This is the case for excised lung preparations, in which expiration is not limited by the chest wall, and hence the whole lung can be emptied until airway closure is present throughout the lung.[33] In fact, in many excised lobes and lungs of both dogs and monkeys, a distinct closing volume was found with the bolus method in the absence of a vertical gradient in P_{pl}.[42] However, when the same lungs or lobes were subjected to an artificially created vertical gradient in P_{pl}, there was a marked increase in the height of phase IV. These results are analogous to those found under both normal conditions and microgravity.

Under normal conditions, the gravity contribution of sequential regional lung emptying to the nitrogen slope of phase III obtained with the resident gas technique does not

exceed about 20%.[43] In microgravity, such an effect may be even smaller, as reflected by the reduction in the slope of phase III.

DYNAMIC DISTRIBUTION OF GAS

The distribution of gas by convection (bulk flow) is governed by (1) regional compliance (C), resistance (R), and time constant ($\tau = RC$) and (2) regional differences in dynamic changes in P_{pl}. If τ were the same in all regions, and dynamic ΔP_{pl} were in phase and uniform, the dynamic distribution of gas would be the same as the static distribution; that is, it would simply reflect regional differences in compliance. Accordingly, the various lung regions would fill and empty synchronously, the distribution of gas being independent of flow and frequency of breathing.[44] In that case, the static relationships in Figure 14-2 would also exist under dynamic conditions. There is good evidence, however, that τ is not uniform. Furthermore, under some conditions, dynamic ΔP_{pl} appears to vary substantially from one region to another. As a result, the dynamic distribution of gas is complex, and, not surprisingly, conflicting results have been reported by different investigators. This topic has been reviewed in detail elsewhere.[5,6] Only a brief account is provided here.

Otis and colleagues[44] were the first to propose the theory that the time constants of different parallel pathways within the lung determine whether or not the pathways behave synchronously during inflation and deflation. During sinusoidal cycling, a two-compartment lung model with different time constants, representing upper and lower lung regions of normal subjects, predicts very little flow and frequency dependence of tidal volume distribution if the transpulmonary pressure swings are in phase and of equal magnitude.[45] Departure from the sinusoidal waveform also makes little difference.[46] The validity of these predictions is supported by the results of studies in which regional ventilation per unit volume was measured at fixed tidal volume but increased frequency.[47,48]

By contrast, Pedley and colleagues[49] predicted that the distribution of a bolus of ^{133}Xe inhaled at constant flow should be markedly flow dependent. Their analysis, which pertains to erect humans inhaling from FRC, predicts that (1) at the onset of constant-flow inflation ($t = 0$), the apex-to-base ratio of ventilation per alveolus ($\dot{V}_a/\dot{V}_b$) will equal R_b/R_a, and (2) in the interval between $t = 0$ and a critical time (t_{crit}), which depends on the magnitude of the apical and basilar τ, there is a gradual redistribution of flow toward the lung bases, such that for $t > t_{crit}$, $\dot{V}_a/\dot{V}_b$ should approximate C_a/C_b. In short, this analysis shows that during the interval between $t = 0$ and t_{crit}, the distribution of gas changes continuously with time (asynchronous filling), departing from the static distribution, which is governed by C_a/C_b.

Based on anatomic and mechanical considerations, Pedley and colleagues[49] predicted that in erect humans (1) R_a/R_b should equal unity; (2) consistent with the vertical gradient in P_{pl} (Figure 14-3), C_a/C_b should be less than 1; and (3) t_{crit} should amount to about 0.4 seconds. Point (3) allows us to compute the volume of inspired gas that is distributed asynchronously at various rates ($\dot{V}$) of constant-flow inflation. This critical volume is given by $\Delta V_{crit} = t_{crit}\dot{V}$. For $\dot{V} > 0.4$ L/s, ΔV_{crit} amounts to less than 0.16 L. This is less than the combined volume of the anatomic and equipment dead space in most studies in which radioactive gases were inhaled either as boluses or as tidal breaths. It follows that, for $\dot{V} > 0.4$ L/s, asynchronous filling should pertain solely to the dead space air, whereas the gas labeled with ^{133}Xe should be distributed according to regional compliances, closely approximating the static distribution of gas shown in Figure 14-2.[49] In fact, Sutherland and colleagues[15] found that in seated humans the distribution of a 0.7 L breath taken at low flow from FRC is consistent with the static distribution of gas.

The predictions of Pedley and colleagues[49] are also supported by Dollfuss and colleagues.[28] They asked normal erect subjects to perform vital capacity inspirations at constant $\dot{V}$ ranging from 0.5 to 1 L/s. At different preset volumes, they injected a bolus of ^{133}Xe into the inspirate and measured the regional distribution of ventilation per alveolus. This was fully consistent with the static distribution of gas; that is, the boluses were distributed in accordance with the slopes dV_r/dV in Figure 14-2. This is not surprising because in these experiments the ^{133}Xe boluses were administered at times that largely exceeded t_{crit}.[50] By contrast, as shown in Figure 14-5, if a ^{133}Xe bolus is inhaled from FRC, its distribution departs from the static distribution at lower flows than those used by Dollfuss and colleagues because in this case the bolus is delivered into the alveoli within the $t = 0$ to t_{crit} period as soon as $\dot{V}$ exceeds about 0.4 L/s. The results shown in Figure 14-5 are consistent with the predictions of Pedley and colleagues[49]: the $\dot{V}_a/\dot{V}_b$ ratio increases progressively with inspiratory flow (reflecting the fact that the ^{133}Xe bolus is distributed at a time progressively closer to onset of inspiration) and tends to asymptote toward unity (consistent with $R_a = R_b$).

The results of these and other studies[47,48,51–54] support the notion that in upright humans, the uneven regional distribution of ventilation during normal breathing basically results from regional differences in lung mechanics caused by the gravity-dependent gradient in pleural surface pressure, whereas the dynamic changes in P_{pl} are probably relatively uniform. In the horizontal postures, however, unequal driving pressures seem to play an important role in determining the regional distribution of ventilation,[20] as suggested by Sybrecht and colleagues.[23] Using ^{133}Xe boluses inhaled from the same lung volume, they found that the flow dependence of apex-to-base gas distribution was more marked in the supine than in the sitting position. Because, along the craniocaudal axis, regional expansion and hence time constants should be more uniform in the supine than in the sitting posture,[25] the greater flow dependence could only be interpreted in terms of unequal swings in driving pressure.

It should be noted that even small regional differences in the magnitude of ΔP_{pl} may substantially influence the regional ventilation distribution and its flow dependence.[46] In all body postures, nonuniform changes in P_{pl} sufficient to cause substantial changes in the distribution of ventilation

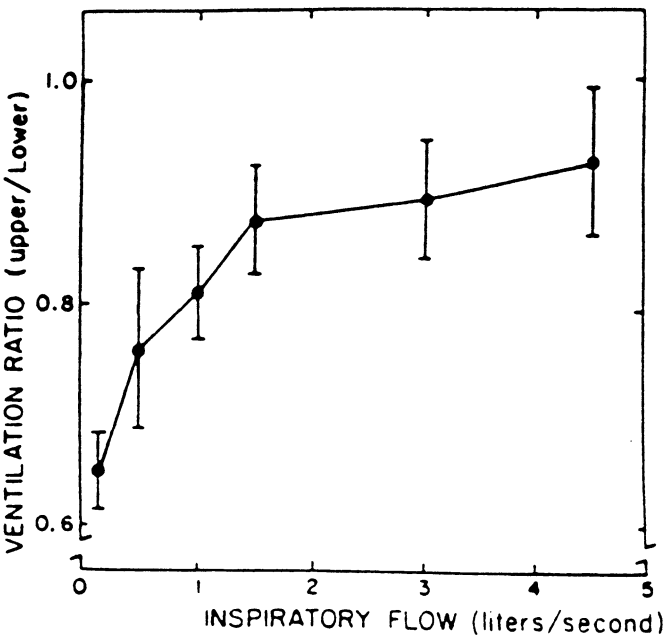

FIGURE 14-5 Apex-to-base ratio of ventilation per alveolus plotted against flow during constant-flow inflation. Mean ± SE for seven normal seated subjects (24 to 36 years old) inhaling ^{133}Xe boluses from functional residual capacity. Reproduced with permission from Bake B et al.[51]

can be achieved by selective voluntary contraction of different respiratory muscles,[38,55–58] by strapping of the lower rib cage,[59] and with high inspiratory resistance.[17] The nature of these changes, which result from lung–chest wall interaction, has been elegantly discussed by Engel.[6] It should be stressed, however, that in the upright position the regional distribution of ventilation during natural breathing movements appears to be governed mainly by regional differences in lung mechanics rather than unequal driving pressures.

Marked flow dependence of the regional distribution of inspired gas is found not only at high but also at low lung volumes. Indeed, boluses of ^{133}Xe inhaled from RV by erect subjects at low flow rates (0.2 to 0.3 L/s) are distributed preferentially to apical lung regions, but faster inspiration produces a more even distribution, the redistribution occurring at flows between 0.3 and 2.5 L/s.[60] Higher flow rates cause little further change in the distribution of the labeled gas. As mentioned earlier, at RV the airways in dependent lung zones are closed, and hence during a low inspiration from RV, the lower units do not receive inspired gas until the transpulmonary pressure reaches the critical value required to reopen the closed airways. During slow inspiration from RV, the lower regions open after the ^{133}Xe bolus has been inhaled, so little or no ^{133}Xe enters the dependent lung zones. Because of the increased transpulmonary pressure associated with increasing $\dot{V}$, the lower airways open earlier during rapid inspiration, and hence the ventilation in dependent lung zones increases. The fact that almost no further change in bolus distribution is evident at $\dot{V} > 2.5$ L/s suggests that "maximum airway opening is obtained at the transpulmonary pressure required to generate this flow rate."[60] This critical P_L has been estimated to be about 7 cm H_2O.[3]

Clearly, further studies are needed before the factors determining the static and dynamic distributions of gas within different regions of the lungs are fully understood. Nevertheless, the present knowledge has been useful in explaining the abnormalities in the regional distribution of ventilation and gas exchange in a variety of pulmonary and cardiac disorders.[3,5,34]

Finally, it should be stressed that in normal subjects during normal tidal breathing in the upright posture, the primary determinants of ventilatory inhomogeneity are not gravitational in origin. Indeed, under these conditions, the overall distribution of ventilation is only slightly less inhomogeneous than in microgravity.[61] By contrast, transition from a standing to a supine position at normal gravity results in markedly increased inhomogeneity of ventilation distribution, particularly in elderly subjects, as peripheral airway closure is present during tidal breathing from the age of about 45 years.[62] Indeed, the increased difference in alveolar and arterial partial oxygen pressures ($P_{A-a}O_2$) seen in normal subjects with advancing age[63] is probably due almost entirely to the presence of peripheral airway closure during tidal breathing. As a result of airway closure, there is a ventilation–perfusion imbalance, the lower parts of the lungs being relatively underventilated and overperfused, with a concurrent increase in $P_{A-a}O_2$. Such a phenomenon is also seen in many diseases characterized by decreased FRC and/or increased closing volume (eg, obesity, heart failure, goiter). However, a full account of the role of regional abnormalities of ventilation distribution in disease is beyond the scope of the present chapter, which is concerned with physiologic aspects. Similarly, the nonregional aspects of ventilation heterogeneity can be found elsewhere.[64]

In conclusion, studies based on radioactive gases have provided considerable insight into the basic mechanisms that govern the regional function of normal lungs. As indicated in this chapter, there are still many aspects that need to be clarified with the use of more precise measurements. Much further work is also needed to describe regional lung function in patients with respiratory disorders.

ACKNOWLEDGMENT

I thank Ms Lisa Shearer for typing the manuscript.

REFERENCES

1. Knipping H, von Bolt H, Venrath H, et al. Eine neue Methode zur Prüfung der Herz- und Lugenfunktion. Dtsch Med Wochenschr 1955;80:1146–7.
2. Milic-Emili J. Pulmonary statics. In: Widdicombe JG, editor. Respiratory physiology I. Vol 2. International Review of Physiology Series. Baltimore: Butterworth; 1974. p. 105–37.
3. Milic-Emili J. Ventilation. In: West JB, editor. Regional differences in lung. New York: Academic Press; 1977. p. 167–99.
4. Milic-Emili J. Static distribution of lung volumes. In: Macklem PT, Mead J, editors. Handbook of physiology; mechanics of breathing. Vol 2. Bethesda, MD: American Physiological Society; 1986. p. 561–74.

5. Hughes JMB, Amis TC. Regional ventilation distribution. In: Engel LA, Paiva M, editors. Gas mixing and distribution in the lung. New York: Marcel Dekker; 1985. p. 177–220.
6. Engel LA. Dynamic distribution of gas flow. In: Macklem PT, Mead J, editors. Handbook of physiology: mechanics of breathing. Vol 2. Bethesda, MD: American Physiological Society; 1986. p. 575–93.
7. D'Angelo E. Local alveolar size and transpulmonary pressure in situ and in isolated lungs. Respir Physiol 1972;14:251–66.
8. Faridy EE, Kidd R, Milic-Emili J. Topographical distribution of inspired gas in excised lobes of dogs. J Appl Physiol 1967;22:760–6.
9. Glazier JB, Hughes JMB, Maloney JE, West JB. Vertical gradient of alveolar size in lungs of dogs frozen intact. J Appl Physiol 1967;23:694–705.
10. Klingele TG, Staub NC. Alveolar shape changes with volume in isolated, air-filled lobe of cat lung. J Appl Physiol 1970; 28:411–4.
11. Milic-Emili J, Henderson JAM, Dolovich MB, et al. Regional distribution of inspired gas in the lung. J Appl Physiol 1966; 21:749–59.
12. Ball CW Jr, Stewart P, Newsham B, Bates DV. Regional pulmonary function studied with xenon-133. J Clin Invest 1962; 41:4519–31.
13. Milic-Emili J. Radioactive xenon in the evaluation of regional lung function. Semin Nucl Med 1971;1:246–62.
14. West JB. Radioactive methods. In: West JB, editor. Regional differences in the lung. New York: Academic Press; 1977. p. 33–84.
15. Sutherland PW, Katsura T, Milic-Emili J. Previous volume history of the lung and regional distribution of gas. J Appl Physiol 1968;25:566–74.
16. Demets M. Regional distributions of lung volumes, ventilation and transpulmonary pressure [PhD thesis]. Leuven: Catholic University of Leuven; 1978.
17. Grassino AE, Anthonisen NR. Chest wall distortion and regional lung volume distribution in erect humans. J Appl Physiol 1975;39:1004–7.
18. Grassino AE, Bake B, Martin RR, Anthonisen NR. Voluntary changes of thoracoabdominal shape and regional lung volumes in humans. J Appl Physiol 1975;39:997–1003.
19. Greene RJ, Hughes JMB, Sudlow MF, Milic-Emili J. Regional lung volumes during water immersion to the xiphoid in seated man. J Appl Physiol 1974;36:734–6.
20. Amis NR, Jones HA, Hughes JMB. Effect of posture on interregional distribution of pulmonary ventilation in man. Respir Physiol 1984;56:145–67.
21. Rehder K, Sessler AD, Rodarte JR. Regional intrapulmonary gas distribution in awake and anesthetized-paralyzed man. J Appl Physiol 1977;42:391–402.
22. Engel LA, Grassino A, Anthonisen NR. Demonstration of airway closure in man. J Appl Physiol 1975;38:1117–25.
23. Sybrecht G, Landau L, Martin R, et al. Influence of posture on flow dependence of distribution of inhaled ^{133}Xe boli. J Appl Physiol 1976;41:489–96.
24. Kaneko K, Milic-Emili J, Dolovich MB, et al. Regional distribution of ventilation and perfusion as a function of body position. J Appl Physiol 1966;21:767–77.
25. Bake B, Bjure J, Grimby G, et al. Regional distribution of inspired gas in supine man. Scand J Respir Dis 1967;48:189–96.
26. Hogg JC, Nepszy S. Regional lung volume and pleural pressure gradient estimated from lung density in dogs. J Appl Physiol 1969;27:198–203.
27. Ruff F, Martin RR, Milic-Emili J. Previous volume history of the lung and regional distribution of residual volume. J Appl Physiol 1981;51:313–20.
28. Dollfuss RE, Milic-Emili J, Bates DV. Regional ventilation of the lung studied with boluses of ^{133}xenon. Respir Physiol 1967;2:234–46.
29. Holland J, Milic-Emili J, Macklem PT, Bates DV. Regional distribution of pulmonary ventilation and perfusion in elderly subjects. J Clin Invest 1968;47:81–92.
30. Bryan AC, Milic-Emili J, Pengelly D. Effect of gravity on the distribution of pulmonary ventilation. J Appl Physiol 1966;21:778–84.
31. Roussos CS, Martin RR, Engel LA. Diaphragmatic contraction and the gradient of alveolar expansion in the lateral posture. J Appl Physiol 1977;43:32–8.
32. Berend N, Skoog C, Thurlbeck WM. Lobar pressure–volume characteristics of excised human lungs. Thorax 1981; 36:290–5.
33. Glaister DH, Schorter RC, Sudlow MF, Milic-Emili J. Bulk elastic properties of excised lungs and the effect of a transpulmonary pressure gradient. Respir Physiol 1973;17:347–64.
34. Anthonisen NR. Closing volume. In: West JB, editor. Regional differences in the lung. New York: Academic Press; 1977. p. 451–82.
35. Agostoni E. Mechanics of the pleural space. Physiol Rev 1972;52:57–128.
36. Agostoni E. Transpulmonary pressure. In: West JB, editor. Regional differences in the lung. New York: Academic Press; 1977. p. 245–80.
37. Anthonisen NR, Robertson PC, Ross WRD. Gravity-dependent sequential emptying of lung regions. J Appl Physiol 1970;28:589–95.
38. Roussos CS, Fixley M, Genest J, et al. Voluntary factors influencing the distribution of inspired gas. Am Rev Respir Dis 1977;116:457–67.
39. Roussos CS, Fukuchi Y, Macklem PT, Engel LA. Influence of diaphragmatic contraction on ventilation distribution in horizontal man. J Appl Physiol 1976;40:417–24.
40. Guy HJB, Prisk GK, Elliott AR, et al. Inhomogeneity of pulmonary ventilation during sustained microgravity as determined by single-breath washouts. J Appl Physiol 1994;76:1719–29.
41. Elliott AR, Prisk GK, Guy HJB, West JB. Lung volumes during sustained microgravity on Spacelab SLS-1. J Appl Physiol 1994;77:2005–14.
42. Gleister DH, Schroter RC, Sudlow MF, Milic-Emili J. Transpulmonary pressure gradient and ventilation distribution in excised lungs. Respir Physiol 1973;17:365–85.
43. Verbanck S, Paiva M. Gas washout and aerosol bolus techniques: non-invasive measures of lung structure and ventilation heterogeneity. In: Aliverti A, Brusasco V, Macklem PT, Pedotti A, editors. Mechanics of breathing. Milan: Springer-Verlag; 2002. p. 129–45.
44. Otis AB, McKerrow CB, Bartlett RA, et al. Mechanical factors in distribution of pulmonary ventilation. J Appl Physiol 1955; 8:427–43.
45. Chang HK, Shykoff BE. A model simulation of ventilation distributions. Bull Eur Physiopathol Respir 1982;18:329–38.
46. Shykoff BC, Van Grondelle A, Chang HK. Effects of unequal pressure swings and different waveforms on distribution of ventilation: a nonlinear model simulation. Respir Physiol 1982;48:157–68.
47. Forkert L, Anthonisen NR, Wood LDH. Frequency dependence of regional lung washout. J Appl Physiol 1978;45:161–70.
48. Jones RL, Overton TR, Sproule BJ. Frequency dependence of ventilation distribution in normal and obstructed lungs. J Appl Physiol 1977;42:548–53.
49. Pedley TJ, Sudlow MF, Milic-Emili J. A nonlinear theory of the distribution of pulmonary ventilation. Respir Physiol 1972;15:1–38.

50. Bates JHT, Rossi A, Milic-Emili J. Analysis of the behavior of the respiratory system with constant inspiratory flow. J Appl Physiol 1985;58:1840–8.
51. Bake B, Wood L, Murphy B, et al. Effect of inspiratory flow rate on regional distribution of inspired gas. J Appl Physiol 1974;37:8–17.
52. Connolly T, Bake B, Wood L, Milic-Emili J. Regional distribution of a ^{133}Xe labeled gas volume inspired at constant flow rates. Scand J Respir Dis 1975;56:150–9.
53. Hughes JMB, Grant BJB, Greene RE, et al. Inspiratory flow rate and ventilation distribution in normal subjects and in patients with simple chronic bronchitis. Clin Sci 1972;43: 583–95.
54. Grant BJB, Jones HA, Hughes JMB. Sequence of regional filling during a tidal breath in man. J Appl Physiol 1974;37:158–65.
55. Fixley MS, Roussos CS, Murphy B, et al. Flow dependence of gas distribution and the pattern of inspiratory muscle contraction. J Appl Physiol 1978;45:733–41.
56. Roussos CS, Siegler DIM, Engel LA. Influence of diaphragmatic contraction and expiratory flow on the pattern of lung emptying. Respir Physiol 1976;27:157–67.
57. Chevrolet JC, Emrich J, Martin RR, Engel LA. Voluntary changes in ventilation distribution in the lateral posture. Respir Physiol 1979;38:313–23.
58. Chevrolet JC, Martin JG, Flood R, et al. Topographical ventilation and perfusion distribution during IPPB in the lateral posture. Am Rev Respir Dis 1978;118:847–54.
59. Forkert L. Effect of regional chest wall restriction on regional lung function. J Appl Physiol 1980;49:655–62.
60. Robertson PC, Anthonisen NR, Ross D. Effect of inspiratory flow rate on regional distribution of inspired gas. J Appl Physiol 1969;26:438–43.
61. Prisk GK, Guy HJB, Elliott AR, et al. Ventilatory inhomogeneity determined from multiple-breath washouts during sustained microgravity on Spacelab SLS-1. J Appl Physiol 1995;78:597–607.
62. Leblanc P, Ruff F, Milic-Emili J. Effect of age and body position on airway closure in man. J Appl Physiol 1970; 28:448–51.
63. Sorbini CA, Grassi V, Solinas E, Muiesan G. Arterial oxygen tension in relation to age in healthy subjects. Respiration 1968;25:3–13.
64. Verbanck S, Paiva M. Gas washout and aerosol bolus techniques: non-invasive measures of lung structure and ventilation heterogeneity. In: Aliverti A, Brusasco V, Macklem PT, Pedotti A, editors. Mechanics of breathing: pathophysiology, diagnosis and treatment. Milan: Springer-Verlag; 2002. p. 129–45.

CHAPTER 15

GAS CONVECTION AND DIFFUSION

Manuel Paiva, Sylvia Verbanck

Convective and diffusive gas transport in the lungs are described here from the perspective of a noninvasive test of ventilation distribution that is able to distinguish between structural changes affecting the proximal and peripheral lung zones. This will lead us to a new interpretation of an old ventilation distribution test, the multiple-breath inert gas washout (MBW). First, we present the basic concepts necessary to the interpretation of the MBW, then we describe this test in detail, and, finally, we show its clinical applications.

BASIC CONCEPTS: CONVECTION AND DIFFUSION

Convective or bulk flow refers to the movement of all gas species at the mean velocity of the airstream and is the principal mechanism of gas transport in the conducting airways during normal tidal breathing. The convective flow of air requires the presence of a pressure gradient. The increase in total cross-sectional area of the conducting airways as a function of distance from the mouth results in a progressive fall of convective velocity, despite the narrowing of individual pathways with axial length. The convective velocity at the end of the alveolar sacs is necessarily zero, as a result of their cul-de-sac structure. For all these reasons, gas transport in the lungs is quite peculiar.

The process of molecular diffusion is the principal mechanism of gas mixing in the lung periphery. In contrast to convective transport, diffusion requires the presence of a concentration gradient. Gaseous diffusion is due to the random motion of individual gas molecules and results in a net transfer of a given gas species from a region of high concentration to one of low concentration. Unlike with convection, there is no net transport of matter. Between the zones dominated by convective and diffusive transport, an intermediate zone must exist where both mechanisms play a role. We will see that this zone corresponds anatomically to the terminal bronchioles and the first generations of the acini and plays a major role in gas transport mechanisms.

In a steady state, the diffusive flow (Φ_{Dif}) of a gas per unit of time across an area S is defined by Fick's (first) law of diffusion:

$$\Phi_{Dif} = -DS(dC/dx) \qquad (15\text{-}1)$$

where C is the concentration of the gas species, x is the one-dimensional spatial coordinate, and D is the diffusion coefficient dependent on the gas species and quantifies the amount of gas diffusing across a unit area in unit of time per unit gradient of concentration (cm^2/s). For a mixture of two gases, diffusion is characterized by a binary diffusion coefficient (D). In the lung, there are usually five gases present (nitrogen, oxygen, carbon dioxide, argon, and water vapor); under experimental conditions, additional gases may be introduced. However, in most physiologic and experimental conditions, the diffusion of any given gas species under study can usually be characterized by an effective binary diffusion coefficient with the remainder of the gas mixture. It can be shown that molecular diffusion in the lung can be realistically described by assuming that radial diffusion in the ducts is instantaneous.[1,2] The axial diffusion in a duct of constant cross-section is then described by the classic diffusion equation:

$$\partial C/\partial t = D(\partial^2 C/\partial x^2) \qquad (15\text{-}2)$$

where t is time and x is the distance to a fixed point in the duct. Equation 15-2 is also called Fick's second law of diffusion, and it is nothing more than the combination of Fick's first law with matter balance (the rate of concentration variation in an arbitrary small element of volume is given by the difference between incoming and outgoing gas per unit of time and unit of volume of the element considered).

The symbol ∂ is traditionally used (instead of d) to indicate the derivative of C with respect to one variable (first derivative with respect to time and second derivative with respect to distance). Because of this, Equation 15-1 is called a partial differential equation and not an ordinary differential equation, as would be the case if C depended on one variable only. The implementation of partial differential equations in the lung structure, with all its complexity, is not straightforward, and this may be why some physiologists have been reluctant to accept models of gas transport in the lung. Furthermore, the model predictions of gas mixing in the peripheral lung can only be tested indirectly by comparing simulated gas concentrations at the model exit with experimental gas concentration curves obtained at a subject's mouth. Neither the most advanced medical imaging techniques nor intrapulmonary probes as yet allow direct measurements of gas concentration in the lung periphery.

To obtain a solution for Equation 15-2, two conditions have to be specified: the initial and the boundary conditions. For example, if we want to describe how oxygen molecules, all located at a given point (chosen as the coordinates of the origin), diffuse in nitrogen molecules, the initial condition is $\delta(x)$, that is, the function that represents all oxygen at the same point at time zero. For an infinite tube, the boundary conditions correspond to zero concentration at the two ends. With $D = 0.22$ cm^2/s, the analytic solution of Equation 15-2 is the well-known gaussian function. Unfortunately, this is not relevant for any realistic simulation in the airways, which are not infinite tubes, and $\delta(x)$ as the initial condition is not pertinent to the inspiration of oxygen.

In 1963, Weibel proposed a model of the lung[3] that paved the way for much more realistic simulations, namely a symmetric bronchial tree of equal pathway lengths, which allows the airways to be lumped together into a trumpet-shaped figure representing the relationship between axial lung length and summed airway cross-sectional area. Two equivalent equations were published in 1972[4,5] to describe gas transport and mixing with the use of this symmetric model. In their simplest form, both equations can be written as:

$$(\partial C/\partial t) = [D(s/S)(\partial^2 C/\partial x^2)] + [(D/S)(ds/dx)(\partial C/\partial x)] - u(\partial C/\partial x) \quad (15\text{-}3)$$

where C, D, t, and x have the same meaning as in Equation 15-2, u is the convective velocity, and s and S are the cross-sectional area of the conducting airways alone and the total cross-sectional area of airways plus alveoli, respectively. Equation 15-3 corresponds to a model with rigid walls. It is as if all the volume changes took place at the origin of the coordinates (end of the alveolar sacs). The use of a model that will expand equally in all directions introduces minor computational changes that do not contribute to the interpretation of MBW.

There are three main differences between Equation 15-3 and Equation 15-2, the latter merely describing diffusive mixing in a cylinder of constant cross-sectional area: (1) D is multiplied by the factor s/S, which is the ratio between the duct cross-sectional area without and with alveoli—it represents the delay in the axial spread of the molecules due to the reflections from the alveolar septa, and is only different from unity in the alveolar zone; (2) the second term of Equation 15-3 reflects the spatial change in airway cross-sectional area along the bronchial tree; and (3) the third term of Equation 15-3 simulates the convective displacement of all molecules with the mean velocity u. If convective and diffusive gas transport in the complex three-dimensional structure of the bronchial tree can be represented using only one spatial coordinate (x), it is because of the assumption of instantaneous radial diffusion and the use of a symmetric model. The trade-off for this simplification is that, as we have only one spatial variable, we cannot distinguish between different pathways, and the model cannot simulate transport in an asymmetric structure.

It is indeed surprising that transport in such a complex structure as the human bronchial tree can be described by such a simple equation. We present here only the solutions of Equation 15-3 corresponding to a 2-second inspiration of oxygen followed by a 2-second expiration with a constant flow of 250 mL/s.[6] The origin of the coordinates (x_0) from which the distance is taken is chosen as the end of the alveolar sacs (twenty-third generation). The entry of the model (x_1) corresponds to the eleventh generation. We assume that the first 10 generations only introduce a delay equal to the ratio between the volume of those generations and the convective flow. For simplicity, the inspired and the residual gas concentrations are assumed to be equal to 1 and 0, respectively. We also neglect gas exchange. Therefore, the initial condition is $C(x, t = 0) = 0$. The boundary conditions during inspiration are $\partial C/\partial x = 0$ at $x = 0$ (reflexive condition at the end of the alveolar sacs) and $C(x_1, t) = 1$ for $t_1 \leq t \leq 2$ seconds, t_1 being the time needed for the inspired gas to cross the first 10 generations. During expiration, the velocity is reversed, and the concentration at the entry of the model is given by the solution of Equation 15-3.

Figure 15-1 shows solutions of Equation 15-3 for the conditions described. Curves 1 to 10 are the solutions $C(x, t)$ for $t = 0.4n$ seconds, $n = 1, 2, \ldots, 10$, that is, every 0.4 seconds. The inspired gas concentration is plotted as a function of the distance to the origin of coordinates (lower abscissa) or the Weibel generation (upper abscissa). Generation 16 corresponds to terminal bronchioles and defines the acinar entry. Curves 1 to 5 correspond to the inspiration and curves 6 to 10 to the expiration, curves 5 and 10 being the end of inspiration and expiration, respectively. Curves 2 to 5 are almost stationary. This striking behavior means that, insofar as this model represents the real system, the gas concentration in the lung does not change during most of the inspiration when the flow is constant. Also, only the last 8 mm of the bronchial tree present a concentration different from the inspired one. The concentration profile represented by curves 2 to 5 is usually called the diffusion front. Instead of showing oxygen, we could have used nitrogen concentration: $1 - C(x, t)$. The diffusion front can then be understood as a balance between nitrogen bulk flow toward the lung periphery and nitrogen diffusive flow in the opposite direction. This elegant concept was described in detail by Engel et al.[7]

The concentration during most of the period of expiration (curves 7 to 10) is constant, and the Bohr dead space (V_D) can be computed from the equation:

$$V_D/V_T = (C_{ET} - C_E)/C_{ET} \quad (15\text{-}4)$$

where V_T is tidal volume and C_E and C_{ET} are mean expired and end-tidal (or alveolar) gas concentration, respectively. Because the expired concentration in Figure 15-1 is almost constant, Bohr dead space is similar to Fowler dead space. In the present simulation, it is equal to 115 mL, including the volume of the trachea. The vertical line in Figure 15-1 is such that the volume proximal to this line corresponds to the computed dead space. For the flow and tidal volume considered, the model indeed behaves as if there were two compartments: one with a volume equal to 115 mL and no mixing at all, and another compartment where the mixing is perfect. This concept is explained in the next section. The concept of diffusion front has found many applications,

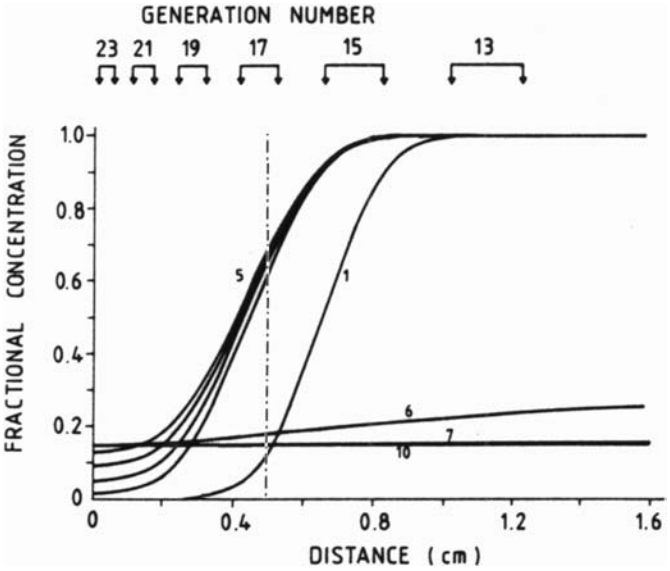

FIGURE 15-1 Solutions of Equation 15-3 for the conditions described. Curves 1 to 10 are the solutions $C(x, t)$ for $t = 0.4n$ seconds, $n = 1, 2, \ldots, 10$, that is, every 0.4 seconds. The concentration is plotted as a function of the distance to the origin of coordinates (*lower abscissa*) or the Weibel generation (*upper abscissa*). The *vertical line* is placed such that the volume proximal to it is the computed dead space.

particularly in the interpretation of tests using inert gases with different diffusion coefficients: simulations with helium and sulfur hexafluoride (SF_6) show a more proximal diffusion front for helium and provide the basis for the interpretation of a larger dead space for sulfur hexafluoride.[1,2] The same concept has been recently extended to the study of nitric oxide (NO) transport in the lung, and it has been shown how compartmental models neglecting NO axial diffusion underestimate NO excretion in the airways.[8]

MBW TEST

Bearing in mind the above concept of the diffusion front during an oxygen inspiration in a nitrogen-filled lung, we now consider what happens during an MBW test, that is, 20 to 25 consecutive oxygen inspirations. Figure 15-2 shows volume and nitrogen concentration tracings, as a function of time, obtained from a typical MBW test in a normal adult.[9] This test requires a regular breathing pattern with a V_T of approximately 1 L, starting from functional residual capacity (FRC) and using pure oxygen for inspiration. The valve switch occurs during an exhalation, and the subject was instructed to watch a screen during each inspiration, inhale to an indicator line, and then exhale freely back to FRC. The first and the twentieth expiration are represented (inset) as a function of expired volume. If, at the end of the test, the inspired gas is switched back to air, a nitrogen washin can be obtained. The information content of nitrogen washins is almost the same, and we consider here only nitrogen washouts. The lung can also first be equilibrated with other mixtures containing gases of different diffusivities such as helium and sulfur hexafluoride, which are then washed out.

In the traditional analysis of MBW, only end-tidal or mean expired nitrogen concentrations are used. When plotted as a function of breath number or lung turnover (TO), they are referred to as the expired nitrogen washout curve. However, various changes in anatomy or lung function can lead to similar alterations of the nitrogen washout curve. In particular, the expired nitrogen washout curves do not provide any information about the magnitude of lung units or mechanisms involved in the ventilation inhomogeneity that develops following the structural alterations caused by disease processes. However, it was suggested[10] that the identification of specific mechanisms could be achieved using the MBW if the slope of phase III or alveolar plateau (dN_2/dV) were also computed for each breath. The feasibility of this technique was first demonstrated for normal subjects with gases of different diffusivities,[11] and the sensitivity of the MBW to different variables was studied: preexpiratory breath-hold time,[12] tidal volume,[13] preinspiratory lung volume,[14] airway closure[15] and gravity.[16] MBW was also performed in normal subjects after intravenous atropine[17] and bronchoprovocation with histamine.[17] Finally, patients with chronic obstructive pulmonary disease (COPD)[18] and asthma[19] were studied before and after administration of salbutamol.[19] The clinical relevance of being able to identify different ventilation distribution mechanisms via the MBW is that these mechanisms are intrinsically linked to different anatomic units in which structural defects can be detected.

Figure 15-3 shows the normalized phase III slopes (slopes divided by the mean expired nitrogen concentrations) from a hyperresponsive subject under control conditions (solid symbols) and following bronchoprovocation (open symbols), as a function of TO, defined as the cumulative expired volume divided by FRC. The normalized slopes obtained after bronchoprovocation are used to define the two indices derived from the MBW that are thought to represent ventilation distribution in conductive (S_{cond}) and acinar (S_{acin}) lung zones: S_{cond} is the normalized slope difference per TO determined by linear regression between TO = 1.5 and TO = 6, and S_{acin} is the normalized slope of the first expiration minus S_{cond} after dividing it by the number of breaths per TO. The rationale for these definitions is explained below.

SIMPLEST MBW MODEL

The simplest model allowing a quantitative description of an MBW is shown in Figure 15-4A. It consists of a perfect mixing compartment and a dead space (no mixing) with volumes equal to V_0 and VD, respectively ($V_0 + VD = FRC$). For simplicity, we assume a nitrogen concentration equal to 80% before the first oxygen inspiration. Figure 15-4B shows the nitrogen concentration at the model entry and lung volume (V_L) as a function of time, for a constant flow of 0.5 L/s and $V_T = 1$ L. During each inspiration, $[N_2] = 0$ and a volume $V_T - V_D$ of oxygen mixes with the nitrogen present in V_0. At the onset of each expiration, a volume V_D of oxygen is first expired, followed by a constant nitrogen concentration. This process leads to an exponential decrease or a linear decrease of the logarithm of the nitrogen concentration

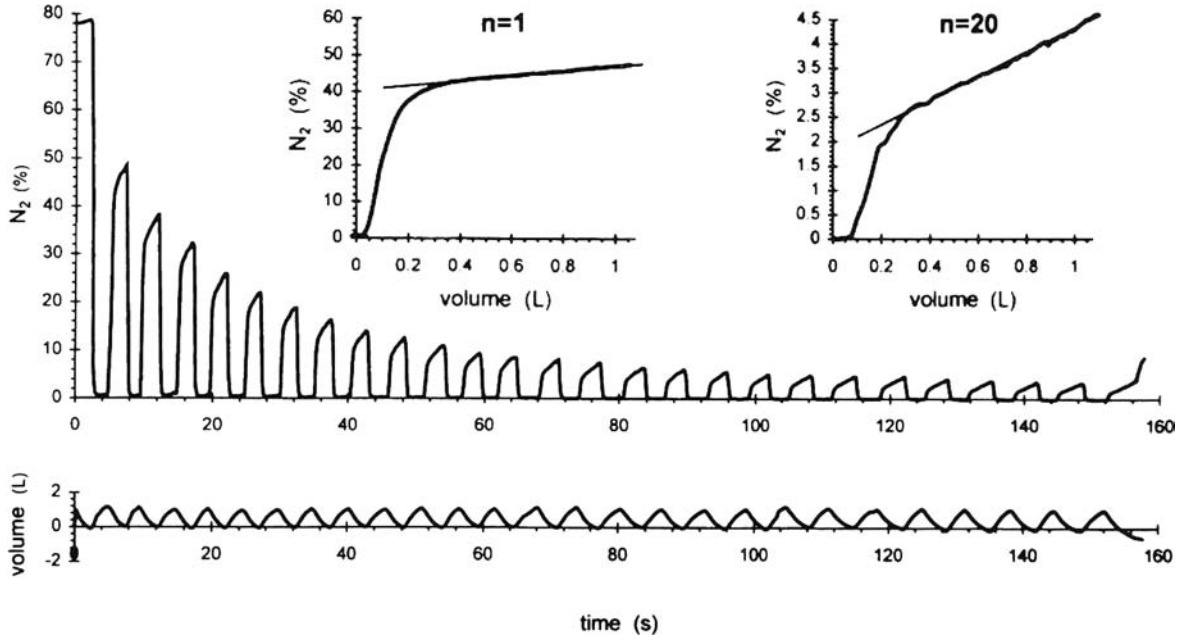

FIGURE 15-2 Nitrogen concentration and volume tracings as a function of time during a multiple-breath washout (MBW) test from a normal subject during a bronchoprovocation test with histamine, which greatly increases the slopes, particularly at the end of the MBW. *Inset*: alveolar slope versus expired volume from breaths 1 and 20 plotted using an equivalent scaling with respect to mean expired nitrogen concentrations of breaths 1 and 20, respectively. Reproduced with permission from Verbanck S et al.[9]

(Figure 15-4C) and zero (normalized) slope of the alveolar plateau (dots in Figure 15-4D). These computations were done with $V_0 = 3$ L, which corresponds to three breaths per TO. The gray line in Figure 15-4D corresponds to the mean values obtained (experimentally) in normal subjects.[1]

An interesting observation from experimental MBW is that mean or end-expired nitrogen concentration can closely approach an exponential, whereas zero normalized slopes are never observed. If the model in Figure 15-4A is used to fit experimental data with known V_T, it is possible to compute FRC and V_D. However, the model values of FRC and V_D may not correspond to the physiologic ones. The fitting procedure incorporates in these two fitted parameters all the other physical processes that take place in the complex structure of the lung.

Even though, for some applications, gas transport in the lung can be approached with a simple model such as that shown in Figure 15-4A, it is known from the work of Milic-Emili and colleagues[20] that the lung is not ventilated homogeneously, the dependent regions (bottom zone in the upright posture) being ventilated more. This is attributed to the action of gravity and led to the concept of so-called topographic ventilation inhomogeneity. In the meantime, experiments performed in microgravity[16] demonstrated that heterogeneous distribution of ventilation also takes place among lung units much smaller than the topographic lung regions. Concentration measurements made by intrapulmonary sampling in open-chest dogs have also shown large ventilation inhomogeneities within small lung regions.[21] These results were interpreted using a model with two parallel units following different pressure–volume curves.[22] The first direct observation of nonuniformity of volume changes within small lung regions came from the work of Olson and Rodarte.[23] These authors implanted parenchymal markers in isolated dog lobes and measured the deformation of tetrahedrons (the volume defined by four noncoplanar markers)

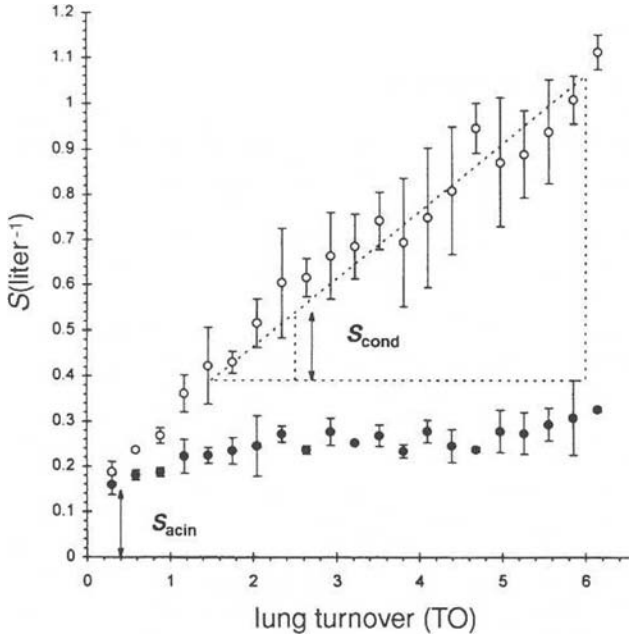

FIGURE 15-3 Normalized slopes (slopes divided by mean expired nitrogen concentrations) as a function of lung turnover (TO) under control conditions (*solid symbols*) and following bronchoprovocation (*open symbols*). Data are means ± SD of the results of three (control) or two (provocation) MBW tests. In the case of the provocation curve, the derivation of S_{acin} and S_{cond} is shown. Details are given in the text. Reproduced with permission from Verbanck S et al.[9]

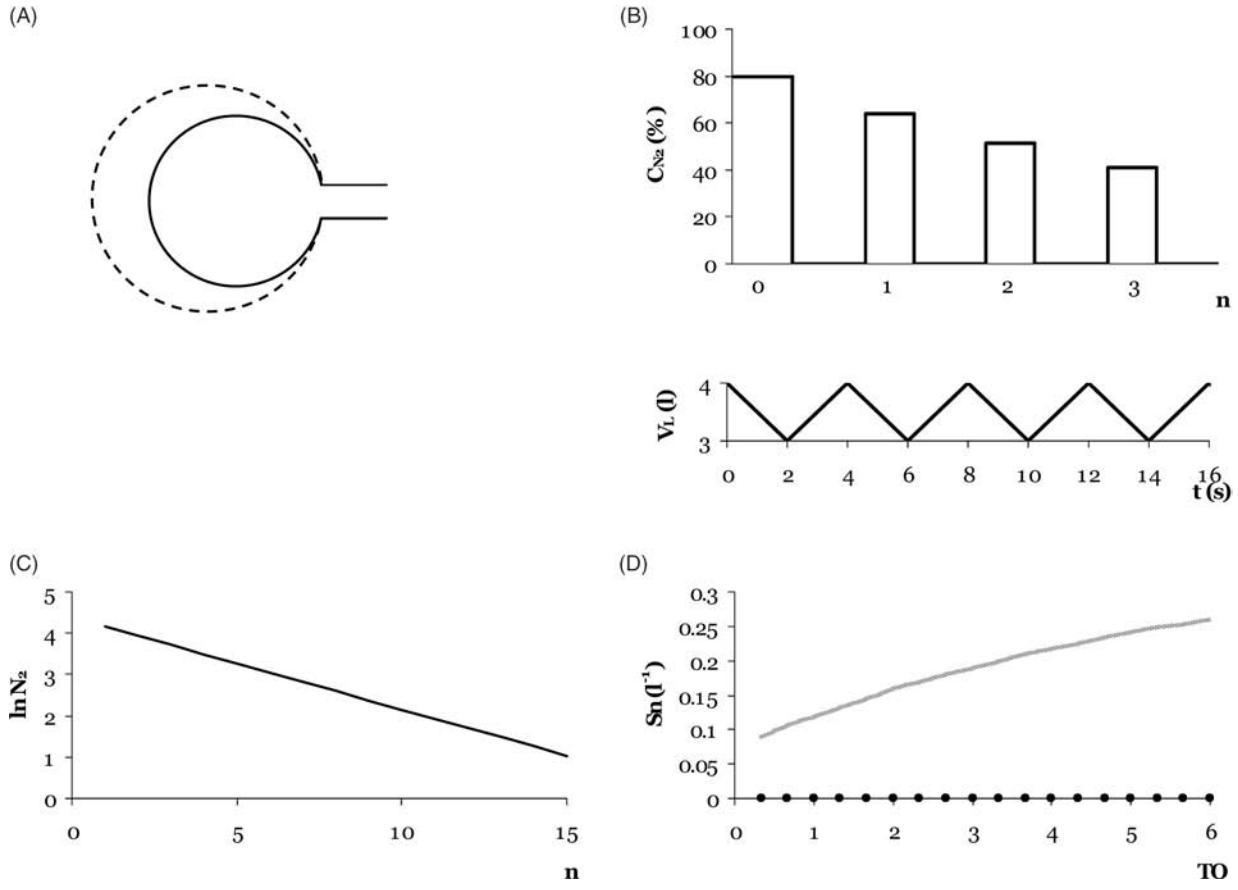

FIGURE 15-4 *A*, One-compartment model of the lung used in MBW simulations with a perfect mixing unit of volume V_0, with a dead space of volume V_D, and for a tidal volume V_T. *B*, Nitrogen concentration and model volume as a function of breath number and time, respectively. *C*, Continuous line drawn over the expired nitrogen concentration as a function of breath number. *D*, Normalized slopes as a function of lung turnover (TO). The *continuous gray line* is the mean experimental value obtained in normal subjects[1] and the *dots* are the model simulations.

with volumes ranging from 0.2 to 25.1 cm^3 at total lung capacity. They demonstrated considerable nonuniformity of volume changes. Furthermore, the variability of volume expansions did not follow any topographic orientation. The same behavior was also present in saline-filled lobes, suggesting that the major determinant of the inhomogeneities is related to the properties of the parenchyma itself and not to the effects of surfactant.

Whatever the exact location and size of these lung units, a more realistic model should take into account some degree of heterogeneity in gas transport between parallel spaces. Each parallel unit again consists of a perfectly mixed compartment and an associated dead space. Since the transport mechanism bringing inspired oxygen to these parallel lung units is convection, any such ventilatory inhomogeneities are called convection-dependent inhomogeneities (CDIs). For this concept to hold true, the units under study should not be too small, as otherwise the concentration would equilibrate between these parallel units by molecular diffusion. In adult humans, and under normal breathing conditions, CDI is thought to occur between lung units at least as big as acini, that is, the set of units subtended by a terminal bronchiole.

CDI MODEL

The simplest model allowing a quantitative description of gas transport in parallel units is shown in Figure 15-5A. We discuss later the physiologic or anatomic meaning of the two units in Figure 15-5A. That part of the lung volume where inspired gases mix perfectly with the resident ones is now divided in two units of volume, each $V_0/2$, and V_T is divided into two different volumes, V_{T1} and V_{T2}, with $V_{T1} < V_{T2}$. V_D is divided into a common dead space (V_{DC}) and two dead spaces leading to the ventilatory units (V_{D1}, V_{D2}). For simplicity, we used the following values in the computations $V_D = 200\ cm^3$ $V_{DC} = 100\ cm^3$, and $V_{D1} = V_{D2} = 50\ cm^3$ (the appropriate values for the different dead spaces depend on the specific anatomic zones that they ventilate). In the example of Figure 15-5A, the upper lung unit is less ventilated than the lower one.

It is simple to compute the nitrogen concentration in each of the two compartments of the model of Figure 15-5A at every subsequent expiration, that is, to determine an expired nitrogen washout curve for each unit. Each one follows an exponential curve as for the one-compartment model (dashed lines), and the expired nitrogen washout

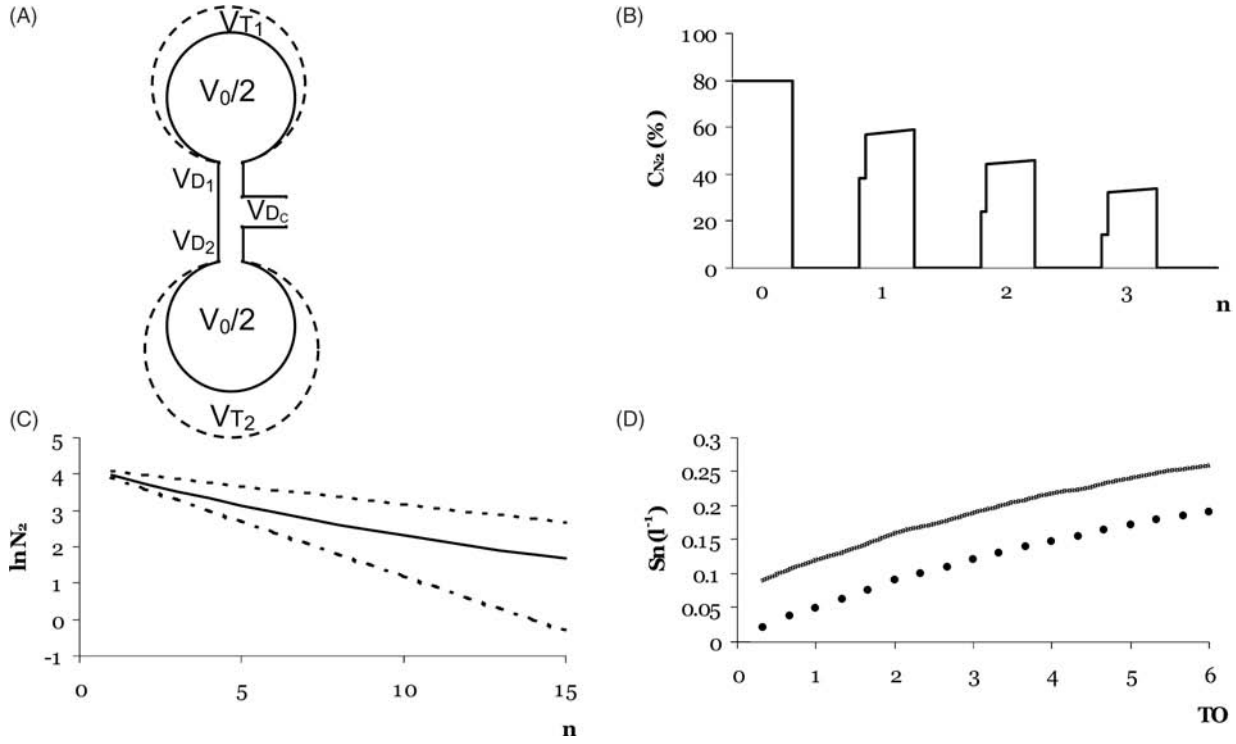

FIGURE 15-5 *A*, Two-compartment model of the lung used in MBW simulations with two perfect mixing units, a common dead space, and two dead spaces leading to each mixing unit. *B*, Nitrogen concentration and model volume as a function of breath number and time respectively. *C*, Continuous line drawn over the expired nitrogen concentration as a function of breath number. *D*, Normalized slopes as a function of lung turnover (TO). The *continuous gray line* is the mean experimental value obtained in normal subjects[1] and the *dots* are the model simulations. In *C*, the nitrogen concentration in each unit is represented by a *dashed line*.

curve resulting from the two units combined (solid line) shows a biexponential nitrogen decay. An interesting aspect of this simple two-compartment model is that the influence of flow sequence on the washout profile of Figure 15-5C (continuous line) is minor. In other words, although the continuous line of Figure 15-5C is no longer a monoexponential curve (not linear on a log scale), its nonlinearity is not a parameter that is sensitive to temporal variations in emptying pattern. Furthermore, different types of inhomogeneity—spatial or temporal—can lead to the same curve, showing its lack of specificity.

In contrast to the expired washout curves, the slope of the nitrogen phase III in each expiration is crucially determined by the expiratory flow profile of each unit upon emptying. In this respect, the nitrogen phase III slope gives information not only on the spatial but also on the temporal ventilation inhomogeneities. If the two units empty synchronously, the slope of the nitrogen alveolar plateau is zero, whatever the concentration difference between them. The fact that nitrogen slopes are always positive during an experimental MBW (Figure 15-2) has a direct implication (in the framework of a CDI model): whatever the anatomic origin of these units, the better-ventilated one (lower unit in Figure 15-5A, where nitrogen concentration is lower) necessarily empties more (with respect to the other unit) at the beginning of the expiration.

An MBW simulated with the two-compartment model, with a (linear) flow sequence between the two units, is shown in Figure 15-5B. The beginning of the expiration does not go directly from zero to the phase III plateau because of the different transit times through dead spaces V_{D1} and V_{D2}, but this is a trivial effect. A large number of (asymmetric) units, as in the real lung, would, in fact, lead to a smooth phase II. This effect was studied in detail by Horsfield and Cumming[24] and is not addressed here. We are interested in the simulations of phase III slopes. Not only are they not zero, but when normalized (divided) by the mean expired nitrogen concentrations of each expiration, they have a characteristic shape shown by the dots of Figure 15-5D: the normalized slopes parallel the experimental curves (continuous gray curve), with the extrapolation to $n = 0$ being equal to zero (the simulations were performed with the specific volume parameters given above for the model in Figure 15-5A and with a flow sequence chosen to parallel the experimental values).

It can be understood intuitively why the normalized slopes increase (ultimately reaching a constant value for large n): normalizing the slopes corresponds to considering the concentration differences with respect to their mean value. Because the overall concentration decreases exponentially, the relative concentration–difference increases progressively. In fact, it is maximal when the best-ventilated unit is completely washed out (nitrogen concentration equal to zero in that unit).

The fact that the extrapolations of phase III slopes to $n = 0$ (or TO = 0) are significantly different from zero is a

feature of the experimental MBW curve (Figure 15-2) that is not, and cannot, be represented by a CDI model (Figure 15-5D). Thus far, the only model that has been able to simulate a non-zero extrapolation to $n = 0$ is one that takes into account convection and diffusion simultaneously. Hence, it is referred to as a model of diffusion–convection-dependent inhomogeneities (DCDIs).

DCDI MODEL

In this section, we describe in more detail what happens in the lung periphery and show why the one-compartment model of Figure 15-4A is not satisfactory, even if the lung is expanding homogeneously. A structural characteristic of the bronchial tree plays a crucial role in the interpretation of the MBW: the asymmetry of the last lung generations is schematically represented in Figure 15-6A (the numbers of branches and generations have been reduced for clarity). The duct m subtends two groups of ducts, one (upper) with 7 ducts and the other (lower) with 14 ducts, in which the concentrations are determined by the number of molecules crossing the sections S_1 and S_2, respectively (for simplicity, duct m is represented as a terminal bronchiole). Hereafter, we define the sets of 7 and 14 ducts as units 1 and 2, respectively. If all ducts have the same volume, the volume ratio of these two units is $V_1/V_2 = 1/2$. Asymmetry has been characterized[25] by $(1 - V_1/V_2)$ in order to have its value increased when the difference between V_1 and V_2 increases (if the subtended volumes are equal, asymmetry is equal to zero).

For simplicity, we consider here only two gases, oxygen and nitrogen, and assume that at the beginning of inspiration there is no oxygen in the lung. Any other constant value can be assumed (such as 15% or 20% for oxygen), and concentrations can be renormalized to obtain the actual values. Because of the two-component mixture used, computations can be done for one gas only, the value for the other gas being the difference from 100%. To describe the amount of oxygen reaching units 1 and 2 after an inspiration of oxygen, we need to consider the two mechanisms of transport: convection and diffusion. We present here a simplified mathematical description of this complex process, but the exact formulation can be found, for example, in Dutrieue and colleagues.[26]

Inspiration

Although the convective transport and diffusive transport of gases operate simultaneously, the mathematical treatment can be done separately because they are caused by two

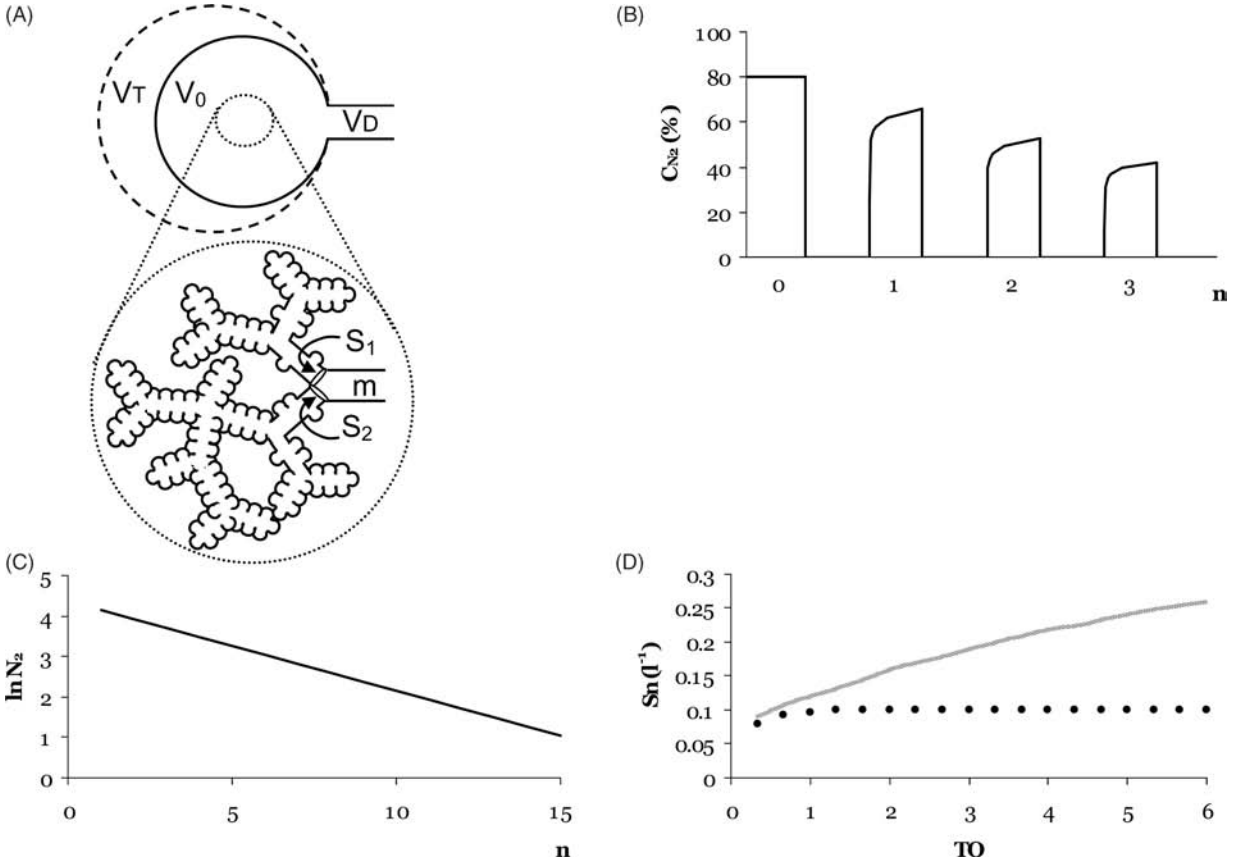

FIGURE 15-6 *A*, Model of the lung periphery used to describe convection–diffusion-dependent inhomogeneities (DCDIs). Duct m subtends two groups of ducts, the molecules reaching each one through cross-sections S_1 and S_2, respectively. *B*, Nitrogen concentration and model volume as a function of breath number and time, respectively. *C*, Continuous line drawn over the expired nitrogen concentration as a function of breath number. *D*, Normalized slopes as a function of lung turnover (TO). The *continuous gray line* is the mean experimental value obtained in normal subjects[1] and the *dots* are the model simulations.

independent physical mechanisms: a pressure gradient for convection and (random) molecular movement for diffusion.

Convective Flow (Φ_{Conv}). During inspiration and for a mass flow in duct m equal to $\dot{V}_m$ and oxygen concentration equal to C_m, the amount of oxygen reaching units 1 and 2 is given by:

$$\Phi_{Conv1} = \dot{V}_1 C_m \tag{15-5}$$

and

$$\Phi_{Conv2} = \dot{V}_2 C_m \tag{15-6}$$

respectively, with:

$$\dot{V}_m = \dot{V}_1 + \dot{V}_2 \tag{15-7}$$

and $\dot{V}_1$ and $\dot{V}_2$ proportional to V_1 and V_2, respectively, (homogeneous expansion), that is:

$$\dot{V}_1 = \dot{V}_m V_1/(V_1 + V_2) \tag{15-8}$$

and

$$\dot{V}_2 = \dot{V}_m V_2/(V_1 + V_2) \tag{15-9}$$

For an inspiration time T_i, the oxygen concentrations in units 1 and 2 (Figure 15-5A) are:

$$\begin{aligned} C_1 &= T_i \dot{V}_1 C_m/(V_1 + T_i \dot{V}_1) \\ &= [T_i C_m/(V_1 + T_i \dot{V}_1)] \\ &\quad \times [\dot{V}_m V_1/(V_1 + V_2)] \end{aligned} \tag{15-10}$$

and

$$\begin{aligned} C_2 &= T_i \dot{V}_2 C_m/(V_2 + T_i \dot{V}_2) \\ &= [T_i C_m/(V_2 + T_i \dot{V}_2)] \\ &\quad \times [\dot{V}_m V_2/(V_1 + V_2)] \end{aligned} \tag{15-11}$$

A simple calculation shows that $C_1 = C_2$.

If only convective gas transport occurs, the same oxygen concentration in both units is anticipated. In other words, convective flow in a homogeneous expansile lung does not create concentration inhomogeneities. We show now that the situation is quite different (and more complex) when diffusion plays a role.

Diffusive Flow (Φ_{Dif}). A very important consequence of Equation 15-1 is that there is diffusive flow only when there is a concentration gradient. During inspiration, the first airway generations are rapidly filled with oxygen. Therefore, oxygen concentration is 100%, and as the derivative of a constant is zero, there is no diffusive flow and this mechanism is not relevant for the branch points of the first airway generations: the corresponding branch points (roughly generations 1 to 14)[25,26] generate CDI only. Alternatively, considering the very last generations (roughly generations 21 to 23), diffusion equilibrates the concentration and the concentration gradient is also zero. Intermediate between the proximal lung, where convection predominates, and the peripheral lung, where diffusion is predominant, roughly between generations 16 and 20, there are concentration gradients. Let us assume that such a concentration gradient exists at the level of the entrance of units 1 and 2 in Figure 15-5A, in which case both convection and diffusion are involved in the transport.

During inspiration:

$$\Phi_{Dif1} = -DS_1 (dC_m/dx_1) \tag{15-12}$$

and

$$\Phi_{Dif2} = -DS_2 (dC_m/dx_2) \tag{15-13}$$

where x_1 and x_2 are distances measured from the entry of ducts of section S_1 and S_2, respectively. The key to understanding this process is that Φ_{Dif1} and Φ_{Dif2} are not in proportion to the volumes of the subtended units 1 and 2, respectively. Although the computation of the exact diffusion flows requires knowledge of the dimensions of each duct (including the cross-sections), the Φ_{Dif1}/Φ_{Dif2} ratio is larger than V_1/V_2. A direct consequence is that oxygen concentration in unit 1 (of volume V_1) is higher than that in unit 2 (of volume V_2). Therefore, the nitrogen concentration is higher in unit 2. This result is counterintuitive as diffusion is always seen as a process equalizing concentrations, a consequence of the probabilistic approach of perfect gas theory or of the second law of thermodynamics.

Finally, we need to add both convection and diffusion flows in each group of units to enable the computation of concentrations:

$$\Phi_{Total} = \Phi_{Conv} + \Phi_{Dif} \tag{15-14}$$

or

$$\Phi_{Total1} = \dot{V}_1 C_m - DS_1 (dC_m/dx_1) \tag{15-15}$$

and

$$\Phi_{Total2} = \dot{V}_2 C_m - DS_2 (dC_m/dx_2) \tag{15-16}$$

Where are these units that have inhomogeneous concentrations, even though their expansion is homogeneous? They are subtended by branch points where diffusion and convective flow are of the same order of magnitude, which in adult lungs correspond to the first acinar generations. Because these units are close to each other, much of the concentration difference generated during inspiration would equilibrate during an end-inspiratory breath-hold. We consider here only the situation where expiration immediately follows the end of inspiration.

Expiration

The same mathematical equations apply for diffusion and convection during expiration, but a qualitative approach is more helpful for understanding the mechanisms leading to the slope of the nitrogen alveolar plateau. We reason in terms of nitrogen concentration (nitrogen concentration is larger in unit 2 at the end of inspiration). On expiration, convection from the larger unit (unit 2) first brings nitrogen-rich gas to the branch point, where it diffuses back (in the opposite direction to the convective flow) into the smaller unit (unit 1). However, oxygen does not diffuse back into the larger unit as effectively, due to the larger convective

flow out of this unit. Because of the back-diffusion of nitrogen into the smaller unit (diffusion flow is always from the larger to the smaller concentration), less nitrogen appears at the mouth at the beginning of expiration. The nitrogen back-diffusion decreases during expiration as the concentration differences between units decrease, with the consequence that more nitrogen molecules are expired, which results in a positive slope of the alveolar plateau. This is shown in the first expiration represented in Figure 15-6B. There is a smooth transition between phase I (zero nitrogen concentration) and phase III (alveolar plateau), due to axial diffusion in the airways.

All previous explanations describe gas transport in the ducts represented in Figure 15-6A. Although not explicitly demonstrated here, it is easy to accept that an MBW leads to a monoexponential nitrogen curve as represented in Figure 15-6C. It can also be shown[11] that the normalized slopes (S_n) of a simulated MBW (Figure 15-6D) are almost independent of the breath number (or TO). The main reason for this very different behavior from the two-compartment model (Figure 15-4A) is that, whereas in the two-compartment model the concentrations decrease exponentially in each compartment (because they are diffusion independent), nitrogen concentrations decrease almost to the same extent in the units of Figure 15-6A.

The almost constant S_n as a function of breath number or TO is a very fortunate result for it allows the separation of the two mechanisms (CDI and DCDI) as described in Figure 15-3. To obtain S_{acin}, one simply subtracts the CDI contribution, taking advantage of the approximately linear portion (dashed line) of S to compute it: for TO = 1.5 and 6, S is equal to 0.39 and 1.04 L^{-1}, respectively. For the MBW in Figure 15-2, 4.5 TO correspond to 15 breaths, which leads to a CDI contribution per breath of $(1.04 - 0.39)/15 = 0.043\ L^{-1}$. This is the value to be subtracted from the phase III slope of the first breath, and gives $S_{acin} = 0.152\ L^{-1}$. S_{cond} is defined as the CDI contribution per TO[9]: $S_{cond} = (1.05 - 0.39)/4.5 = 0.147\ L^{-1}$/TO. Despite the fact that the dimensions of S_{acin} and S_{cond} are the same and expressed in L^{-1}, they cannot be compared directly as S_{cond} is normalized per TO and S_{acin} is a difference of slopes. This precludes a direct comparison between S_{cond} and S_{acin}. In fact, because of the very different mechanisms associated with S_{cond} (CDI) and S_{acin} (DCDI), these indices are intrinsically independent. The advantage of using TO instead of breath number is mainly for MBW comparisons with different lung and/or tidal volumes, which is important, particularly in infants (a more refined definition of TO is the cumulative expired volume, excluding dead space, divided by FRC minus dead space).

The results presented here are a consequence of a theoretical approach, which consisted of applying classic physical laws in a branching structure. The best indication so far that the DCDI mechanism gives a realistic description of what goes on in the lung periphery comes from comparisons between simulations[27] of washouts performed in rat lungs[28] and the corresponding experiments. In these small mammals, gravity should play a negligible role, and the anatomy is known in much greater detail than in humans. When we simply substituted the human lung geometry for the rat lung geometry and used the same diffusion–convection equations, the simulations showed excellent quantitative agreement with experimental data without any parameter of the model being fitted. Furthermore, the model also predicted larger phase III slopes for helium than for sulfur hexafluoride, which had been the most unexpected experimental observation in rat lungs. The larger slope for helium than for sulfur hexafluoride in rats, as opposed to humans, could be entirely accounted for by the differential pattern of branching asymmetry at the level of their respective diffusion fronts.

An important contribution to the understanding of the respective roles of CDIs and DCDIs in humans came from recent MBW experiments performed in space. Contrary to general expectations, MBW-normalized phase III slopes showed small differences from those obtained on the ground, demonstrating a minor effect of gravity. Despite this demonstration of gravity-independent inhomogeneity, it is not yet known where these lung units are located or what mechanisms are involved, although inhomogeneous elastic properties of the lung parenchyma probably play a role. The fact that, on earth, the CDI contribution to the phase III slope in humans is greater than that in other mammals, such as rats[28] and steers,[29] suggests that the particular orientation of the lung with respect to the gravity field may also play a role. It is clearly established that, in both humans and steers, gravity-dependent topographic ventilation inhomogeneities do exist. However, the flow sequence between these units during respiration is probably very small, implying that its CDI contribution to the slope of phase III is negligible.

CLINICAL APPLICATIONS

For many years, model simulations have been focused on vital capacity single-breath washout (SBW) tests, from the perspective of using them as a tool for detection of early lung disease, such as cigarette smoke–induced airway alterations.[30–32] Ventilation distribution tests that reflect heterogeneity of airway change, rather than an overall airway change, could indeed be expected to be more sensitive to lung disease in its initial stages. However, it became apparent that in the case of SBW, the different mechanisms influencing its phase III slope were also critically dependent on lung volume, particularly near residual volume (RV) and total lung capacity (TLC). For instance, airway closure, which is expected to be enhanced in lung disease, not only generates a phase IV but also affects the slope of phase III of an SBW.[33] By the use of a modified SBW test with a 1 L inspiration from FRC, some of these effects can be avoided, and its potential has been recently demonstrated in heart–lung transplant patients, in whom the helium phase III slopes of the modified SBW test became abnormal approximately 1 year before the forced expiratory volume in 1 second (FEV_1) decrease was seen to reflect a rejection episode.[34]

Besides the advantage of reducing the lung volume dependence of ventilation distribution near RV and TLC, the MBW is less affected by gravity than the vital capacity

SBW.[16,35] This makes the MBW test more sensitive to intrinsic structural lung changes. More importantly, however, the possibility of using an MBW to distinguish convection- from diffusion-dependent mechanisms provides a direct link to lung structure in the conductive and acinar lung zones, respectively. In the controversy surrounding the role of the small airways in various lung pathologies, the small airway location in the conductive or acinar lung zone is probably a relevant distinction to make.

Before discussing the results obtained from MBW tests in various clinical settings, we should point out that the MBW phase III slope analysis can be adapted to other mammalian species, to distinguish proximal lung structure, where convection dominates gas transport, from peripheral lung structure, where convection–diffusion interaction occurs. The cutoff between these two entities will be determined by the location of the diffusion front, which can be computed for any given lung geometry, as was done for the rat lung.[27] These simulations facilitate the interpretation of actual correlations between phase III slopes and histomorphometric results obtained in rats with induced emphysema.[36] Experimental studies showing a differential response of proximal and peripheral MBW indices to oleic acid–induced edema in mongrel dogs, where only the peripheral MBW index was affected,[37] lend further support to the potential of the MBW test to distinguish between proximal and peripheral lung structural alterations.

In human subjects, smoking-induced lung disease has been studied by means of SBW[30–32] and MBW[38,39] tests. In most ventilation distribution studies in smokers, use has been made of the vital capacity SBW maneuver, where increased phase III slopes were often unduly referred to as an indication of peripheral alterations only. Reports of the decline in mean expired MBW curves in smokers with relatively normal lung function also revealed impaired ventilation distribution, again without indicating the location of structural alterations. In an MBW study linking peripheral ventilation distribution to peripheral aerosol behavior,[40] 12 smokers with normal lung function were studied and showed significantly greater S_{acin} values than 12 subjects who had never smoked (although S_{cond} showed a tendency to increase, it did not do so significantly). A more extended MBW data set, obtained from 122 smokers pooled per decade of smoking history and compared with 63 histamine provocation test–negative subjects who had never smoked, indicated that from 10 pack-years onward, both S_{acin} and S_{cond} become abnormal, whereas none of the spirometric indices showed any abnormality before 20 pack-years.[41] This concomitant S_{cond} and S_{acin} behavior points to the early involvement of small airways around the acinar entrance. Furthermore, a comparison between the asymptomatic smokers and overt COPD patients showed how S_{acin} and S_{cond} behavior diverged, depending on the presence of emphysematous lesions. The strength of the indices S_{acin} and S_{cond} lies in their ability to noninvasively monitor the smoker's lung, covering the entire spectrum of smoking-induced lung change from its earliest stages to the most advanced disease state.

Patients with overt COPD have generally shown the greatest values of S_{acin} in all adult patient groups studied thus far. This probably stems from the added contribution of parenchymal destruction (emphysema) to a marked change in the asymmetry of the peripheral lung structure, in addition to that produced by small airways inflammation at the level of the acinar entrance. In a group of COPD patients with various degrees of airway obstruction [$FEV_1/FVC = 52 \pm 11$(SD)%] and transfer factor for carbon monoxide (TLco) = 77 ± 25(SD)%, the relationship of S_{cond} and S_{acin} to standard lung function indices was evaluated by means of a principal components factor analysis, which linked correlated indices with independent factors accounting for 81% of the total variance within the COPD group.[18] S_{acin} was linked to the so-called acinar lung zone factor, comprising also diffusing capacity measurements. S_{cond} was linked to the so-called conductive lung zone factor, comprising also specific airway conductance and forced expiratory flows. The fact that S_{cond} and S_{acin} were linked to independent factors is a statistical confirmation of the hypothesis that S_{cond} and S_{acin} do reflect independent lung alterations, corresponding to different functional lung units. FEV_1/FVC was the only variable linked to both the conductive and the acinar lung zone factor, indicating a combined conductive and acinar contribution to airways obstruction in these COPD patients.

In asthma patients, in whom diffusing capacity is usually normal, there is an additional benefit of an index such as S_{acin} to reflect the acinar airspaces, comprising both nonalveolated bronchioles and alveolated ducts. In a study of 20 patients with moderate-to-severe asthma, with an average FEV_1 of 73 ± 14(SD)% predicted,[19] baseline S_{acin} values were found to be abnormal; S_{acin} values were intermediate between those obtained in normal subjects and in COPD patients. Baseline S_{cond} was also abnormal in the asthma patients but similar to that obtained in the COPD patients. After salbutamol inhalations, significant decreases in S_{cond} and S_{acin} were observed in the asthma group but not in the COPD group. These results indicate significant—but partially reversible—acinar airways impairment in asthma patients compared with the more severe baseline acinar airways impairment in COPD patients, none of which was reversible after salbutamol inhalation. In an attempt to maximize S_{cond} and S_{acin} reversibility in asthma patients with a β_2 agonist, a study was undertaken in a group of patients with mild asthma[42] with an average baseline FEV_1 of 92 ± 21(SD)% predicted. This study showed that the mildly asthmatic lung has the ability to reverse relatively mildly elevated baseline S_{acin} values to normal, whereas S_{cond} remained significantly abnormal at all times. These findings point to non–β_2-reversible conductive airways alterations in the early stages of asthma, which could be part of the much discussed airway remodeling in the pathogenesis of asthma. Also, a comparison with the results of the study on patients with moderate-to-severe asthma[19] indicates that, despite similar S_{cond} values across different degrees of asthma severity, S_{acin} abnormality and irreversibility appear to be hallmarks of more severe asthma. Ventilation distribution has also been previously investigated in asthma patients in terms of nitrogen phase III slope of the SBW[43–45] or of MBW expired

concentration washout curves,[46] with a general observation of decreased overall lung ventilation heterogeneity after inhalation of β_2-mimetic drugs. However, those studies did not provide any indication of anatomic location of the implicated lung units.

Even in normal subjects, the site of action of commonly used provoking agents such as histamine and methacholine is still uncertain. An MBW study clearly showed that, even in hyperresponsive but nonasthmatic subjects, only the conducting airways are implicated.[9] For an average FEV_1 decrease of 26% after a 2 mg cumulative dose of histamine, S_{cond} was shown to increase by 390%, whereas there was no significant change in S_{acin}, indicating that during provocation large CDI-type ventilation heterogeneities occur and that the airways affected by the provocation process are situated proximal to the entrance of the acinar lung zone. The inequality in response of parallel airways, superimposed on global airway narrowing, could reflect density differences in muscarinic receptors and/or cholinergic innervation between parallel airways located at a given lung depth in addition to the proximal versus peripheral density differences along the bronchial tree. Since the conducting airways (as reflected in S_{cond}) constitute the main source of ventilation heterogeneity during bronchoprovocation, and because this component is only poorly represented in the SBW phase III slope, this could explain the moderate SBW phase III slope increases observed by others after provocation.[47,48] Although it is intrinsically impossible to determine the contribution from acinar and conductive airspaces by only studying the decline in mean expired concentration in an MBW test, several such reports in the case of bronchoprovocation[49,50] did speculate on an important contribution from convection-dependent ventilation heterogeneity. A comparative study of two nonspecific bronchoprovocation aerosols[51] revealed an apparent paradox of greater ventilation heterogeneity (largest S_{cond} increase) for the bronchoprovoking agent (methacholine) that induced the least deterioration of spirometry, at least in terms of FEV_1. It was suggested that the differential action of histamine and methacholine is confined to the conducting airways, where histamine probably causes the greatest overall airway narrowing and methacholine induces the largest parallel heterogeneity in airway narrowing, probably at the level of the large and small conducting airways, respectively. In any case, the observed ventilation heterogeneities predict a risk for dissociation between ventilation–perfusion mismatch and spirometry, particularly after methacholine challenge, as has been observed experimentally by others.[52]

CONCLUSIONS

Although ventilation distribution tests such as the MBW can obviously not replace tests of standard lung function, they do appear to provide a considerable amount of complementary information. On the one hand, S_{acin} has the potential to detect and isolate airway alterations at the level of acinar airspaces, which is impossible with lung function tests, unless significant parenchymal destruction is involved. This MBW index evolved from the understanding of a mechanism of DCDI at the level of the diffusion front. On the other hand, S_{cond} is particularly prone to heterogeneity of lung filling and emptying, potentially generated by heterogeneity in the progression of structural changes. This MBW index derives from the understanding of CDIs generated proximal to the diffusion front. Finally, the MBW-derived indices, which rely so heavily on asymmetry or heterogeneity of lung structure and its expansion characteristics, are particularly useful for early detection when structural changes are still potentially reversible.

ACKNOWLEDGMENTS

This work was supported by Belgian Program PRODEX.

REFERENCES

1. Paiva M, Engel LA. Gas mixing in the lung periphery. In: Chang HK, Paiva M, editors. Respiratory physiology: an analytical approach. New York: Dekker; 1989. p. 245–76.
2. Paiva M, Engel LA. Theoretical studies of gas mixing and ventilation distribution in the lung. Physiol Rev 1987;67: 750–96.
3. Weibel ER. Morphometry of the human lung. New York: Springer Verlag; 1963.
4. Paiva M. Computation of the boundary conditions for diffusion in the human lung. Comput Biomed Res 1972;5:585–95.
5. Scherer PW, Shendalman LH, Greene NM. Bull Math Biophys 1972;34:393–412.
6. Paiva M. Gas transport in the human lung. J Appl Physiol 1973;35:401–10.
7. Engel LA, Uts G, Wood LDH, Macklem P. Gas mixing during inspiration. J Appl Physiol 1973;35:18–24.
8. Van Muylem A, Noël C, Paiva M. Modeling of impact of gas molecular diffusion on nitric oxide expired profile. J Appl Physiol 2003;94:119–27.
9. Verbanck S, Schuermans D, Van Muylem A, et al. Ventilation distribution during histamine provocation. J Appl Physiol 1997;83:1907–16.
10. Paiva M. Two new pulmonary functional indexes suggested by a simple mathematical model. Respiration 1975;32: 389–403.
11. Crawford ABH, Makowska M, Paiva M, Engel LA. Convection- and diffusion-dependent ventilation maldistribution in normal subjects. J Appl Physiol 1985;59:838–46.
12. Crawford ABH, Makowska M, Kelly S, Engel LA. Effect of breath holding on ventilation maldistribution during tidal breathing in normal subjects. J Appl Physiol 1986;61:2108–15.
13. Crawford ABH, Makowska M, Engel LA. Effect of tidal volume on ventilation maldistribution. Respir Physiol 1986;66:11–25.
14. Crawford ABH, Cotton DS, Paiva M, Engel, LA. Effect of lung volume on ventilation distribution. J Appl Physiol 1989;66:2502–10.
15. Crawford ABH, Cotton DS, Paiva M, Engel LA. Effect of airway closure on ventilation distribution. J Appl Physiol 1989; 66:2511–5.
16. Prisk GK, Elliott AR, Guy HJB, et al. Multiple-breath washin of helium and sulfurhexafluoride in sustained microgravity. J Appl Physiol 1998;84:244–52.
17. Crawford ABH, Makowska M, Engel LA. Effect of bronchomotor tone on static mechanical properties and ventilation distribution. J Appl Physiol 1987;63:2278–85.
18. Verbanck S, Schuermans D, Van Muylem A, et al. Conductive and acinar lung-zone contributions to ventilation inhomogeneity in COPD. Am J Respir Crit Care Med 1998;157:1573–7.

19. Verbanck S, Schuermans D, Noppen M, et al. Evidence of acinar airways involvement in asthma. Am J Respir Crit Care Med 1999;159:1545–50.
20. Milic-Emili J, Henderson JAM, Dolovich MB, et al. Regional distribution of ventilation of inspired gas in the lung. J Appl Physiol 1966;21:749–59.
21. Engel LA, Utz J, Wood LDH, Macklem PT. Ventilation distribution in anatomical lung units. J Appl Physiol 1974;37:194–200.
22. Fukuchi Y, Cosio M, Murphy B, Engel LA. Intraregional basis for sequential filling and emptying of the lung. Respir Physiol 1980;41:253–66.
23. Olson LE, Rodarte JR. Regional differences in expansion in excised dog lung lobes. J Appl Physiol 1984;57:1710–4.
24. Horsfield K, Cumming G. Functional consequences of airway morphology. J Appl Physiol 1968;24:384–90.
25. Paiva M, Engel LA. The anatomical basis for the sloping N_2 plateau. Respir Physiol 1981;44:325–37.
26. Dutrieue B, Vanholsbeeck F, Verbanck S, Paiva M. A human acinar structure for simulation of realistic alveolar plateau slopes. J Appl Physiol 2000;89:1859–67.
27. Verbanck S, Weibel ER, Paiva M. Simulations of washout experiments in postmortem rat lungs. J Appl Physiol 1993;75:441–51.
28. Verbanck S, Gonzalez Mangado N, Peces-Barba Romero G, Paiva M. Multiple-breath washout experiments in rat lungs. An evaluation of intraregional ventilation distribution. J Appl Physiol 1991;71:847–54.
29. Rollin F, Desmecht S, Verbanck S, et al. Multiple-breath washout and washin experiments in steers. J Appl Physiol 1996;81:957–63.
30. Georg J, Lassen NA, Mellemgaard K, Vinther A. Diffusion in the gas phase of the lungs in normal and emphysematous subjects. Clin Sci 1965;29:525–32.
31. Cosio M, Ghezzo H, Hogg JC, et al. The relations between structural changes in small airways and pulmonary-function tests. N Engl J Med 1978;298:1277–81.
32. Dosman JA, Cotton DJ, Graham BL, et al. Sensitivity and specificity of early diagnostic tests of lung function in smokers. Chest 1981;79:6–11.
33. Dutrieue B, Lauzon AM, Verbanck S, et al. Helium and sulfur hexafluoride bolus washin in short-term microgravity. J Appl Physiol 1999;86:1594–602.
34. Estenne M, Van Muylem A, Knoop C, Antoine M. Detection of obliterative bronchiolitis after lung transplantation by indexes of ventilation distribution. Am J Respir Crit Care Med 2000;162:1047–51.
35. Guy HJ, Prisk GK, Elliott AR, et al. Inhomogeneity of pulmonary ventilation during sustained microgravity as determined by single-breath washouts. J Appl Physiol 1994;76:1719–29.
36. Rubio ML, Sanchez-Cifuentes MV, Peces-Barba G, et al. Intrapulmonary gas mixing in panacinar and centri-acinar induced emphysema in rats. Am J Respir Crit Care Med 1998;157:237–45.
37. Tsang JY, Emery MJ, Hlastala MP. Ventilation inhomogeneity in oleic acid-induced pulmonary edema. J Appl Physiol 1997;82:1040–5.
38. Fleming GM, Chester EH, Saniie B, Saidel GM. Ventilation inhomogeneity using multibreath nitrogen washout: comparison of moment ratios and other indexes. Am Rev Respir Dis 1980;121:789–94.
39. Ericsson CH, Svartengren M, Mossberg B, Camner P. Bronchial reactivity, lung function, and serum immunoglobulin E in smoking-discordant monozygotic twins. Am Rev Respir Dis 1993;147:296–300.
40. Verbanck S, Schuermans D, Vincken W, Paiva M. Saline aerosol bolus dispersion. The effect of acinar airway alteration. J Appl Physiol 2001;90:1754–62.
41. Verbanck S, Schuermans D, Meysman M, et al. Early detection of lung damage in smokers: tests of ventilation heterogeneity. Am J Respir Crit Care Med 2003;167:A655.
42. Verbanck S, Schuermans D, Paiva M, Vincken W. Nonreversible conductive airway ventilation heterogeneity in mild asthma. J Appl Physiol 2003;94:1380–6.
43. Fairshter RD, Wilson AF. Relationship between the site of airflow limitation and localization of the bronchodilator response in asthma. Am Rev Respir Dis 1980;122:27–32.
44. Olofsson J, Bake B, Blomqvist N, Skoogh BE. Effect of increasing bronchodilatation on the single breath nitrogen test. Bull Eur Physiopathol Respir 1985;21:31–6.
45. Cooper DM, Mellins RB, Mansell AL. Ventilation distribution and density dependence of expiratory flow in asthmatic children. J Appl Physiol 1983;54:1125–30.
46. Lutchen KR, Habib RH, Dorkin HL, Wall MA. Respiratory impedance and multibreath N_2 washout in healthy, asthmatic, and cystic fibrosis subjects. J Appl Physiol 1990;68:2139–49.
47. Nielsen J, Dahlqvist M, Welinder H, et al. Small airways function in aluminium and stainless steel welders. Int Arch Occup Environ Health 1993;65:101–5.
48. Scano G, Stendardi L, Bracamonte M, et al. Site of action of inhaled histamine in asymptomatic asthmatic patients. Clin Allergy 1982;12:281–8.
49. Harris EA, Buchanan PR, Whitlock RML. Human alveolar gas-mixing efficiency for gases of differing diffusivity in health and airflow limitation. Clin Sci 1987;73:351–9.
50. Langley F, Horsfield K, Burton G, et al. Effect of inhaled methacholine on gas mixing efficiency. Clin Sci 1988;74:187–92.
51. Verbanck S, Schuermans D, Noppen M, et al. Methacholine versus histamine: paradoxical response of spirometry and ventilation distribution. J Appl Physiol 2001;91:2587–94.
52. Rodriguez-Roisin R, Ferrer A, Navajas D, et al. Ventilation–perfusion mismatch after methacholine challenge in patients with mild bronchial asthma. Am Rev Respir Dis 1991;144:88–94.

CHAPTER 16

LUNG VASCULATURE: FUNCTIONAL INFERENCES FROM MICROSTRUCTURE

Dean E. Schraufnagel

The lung is principally a gas exchange organ, so it is not surprising that the lung is well adapted for matching ventilation and perfusion. Gas exchange occurs across an alveolar capillary membrane that may be as thin as 0.5 μm. The lung distributes its deoxygenated blood to capillaries that have well-oxygenated gas on the other side of this membrane, which keeps the air and blood compartments separate. The air compartment remains relatively dry. Excessive fluid is quickly and efficiently removed to preserve the gas exchange area. The lung maintains this arrangement despite constant movement and an airborne assault of particles and gases. To protect the alveolar wall's integrity, the pulmonary vasculature operates at low pressure. It can, however, respond quickly to a diminished bloodflow caused, for example, by thromboembolism. A new blood supply can be rapidly sluiced from the high-pressure bronchial circulation to avert necrosis.

Although many cells, chemicals, and physical principles are required for lungs to work properly, this chapter relates its function to the microstructural design of the basic vascular components, the pulmonary arteries, capillaries, and veins, the bronchial vessels, and the lymphatics. It is based on observations of and inferences drawn from the scanning electron microscopic images of casts of these structures. Most of the work has been done on rats, but humans, mice, sheep, pigs, dogs, and hamsters have also been studied. Usually, there is insufficient information to allow a discussion of differences among species and to know for certain how much of the animal data applies to humans. Interspecies variation is common in vein morphology.[1]

SCANNING MICROSCOPY OF VASCULAR CASTS

Corrosion casting for scanning electron microscopy is usually done with methylmethacrylate resin, which sets quickly after the addition of an accelerator and can withstand the electron beam when it hardens. A corrosive agent, such as aqueous sodium hydroxide, can effectively remove the tissue to prepare the casts for viewing. Although there is slight uniform shrinkage, the casts faithfully replicate structures less than a micrometer in size. Despite its viscosity, methylmethacrylate fills all parts of the pulmonary vascular tree, including the lymphatics, in conditions of pulmonary edema. Its major advantage is that removal of tissue allows an unobstructed view of these structures. Scanning electron microscopy offers higher magnification, sharper images, and three-dimensional exposure. The casts should be studied with light microscopy as the two techniques are complementary.[2]

PULMONARY ARTERIES

Anatomy

The pulmonary arteries travel with the airways and bronchial arteries in the center of the lung lobule and then branch beyond it (Figure 16-1). Consistent with their goal of supplying blood to alveoli, large pulmonary arteries only branch to distribute bloodflow to lung segments and alveoli. Although pulmonary arteries taper in diameter as they follow the airways and divide to match their airway companions, they do not give off capillaries until they branch into short segments just before the alveoli (Figure 16-2). In arteries larger than 1 mm, about 75% of their branches come off one at a time, with their diameters being about 80 to 90% of that of the stem. Arteries between 200 and 300 μm have only about 50% of their branches single, and their average branch-to-stem diameter ratio is about 50%.[3]

Pulmonary Artery Constriction

Pulmonary arteries remain straight and have smooth, luminal surfaces. Oval impressions seen in methylmethacrylate casts are caused by endothelial cell nuclei. The nucleus of an endothelial cell is the least compliant area of the cell, and the pressure used to cast the arteries distends the nonnuclear area slightly more than the area occupied by the cell nuclei, giving a characteristic indentation that extends in the long axis of the vessel. Normally, pulmonary arteries are relaxed. When they constrict, the infolding is broad and

extends over an area that is usually 30 μm or more in length[4] (see Figure 16-1). In hypoxia, pulmonary hypertension, and other conditions, the lumen may narrow extensively and unevenly.[5]

Decreased oxygen level in the airway is a potent stimulus to pulmonary artery constriction. This constriction decreases bloodflow to a lung, lobe, or segment and represents a "coarse gain" mechanism in the control of gas exchange. This is useful for airway occlusion but may act against the host in conditions of global hypoxia, such as seen at high altitude. The mechanism is quite different from the "fine-tuning" mechanism of the pulmonary veins, which may depend on the amount of oxygen in the blood as it exits the capillaries. In comparison to airway oxygen level, decreased blood oxygen level is a weak stimulus for contraction of the pulmonary arteries.

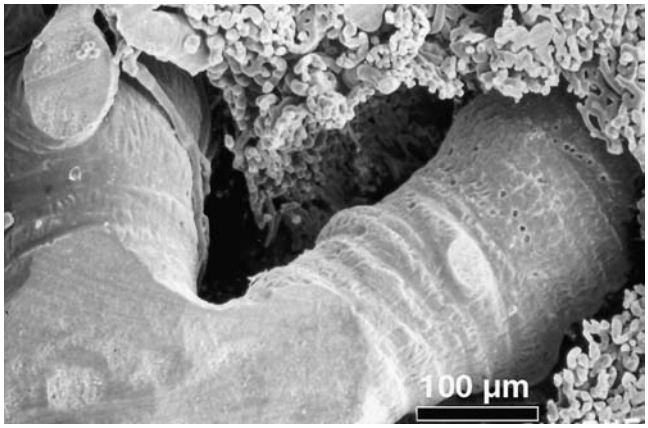

FIGURE 16-1 Scanning electron micrograph showing a cast of a normal rat pulmonary artery contracting. Pulmonary arteries are usually relaxed. When they contract, they do so over a long running length. Reproduced with permission from Schraufnagel DE and Patel KR.[4]

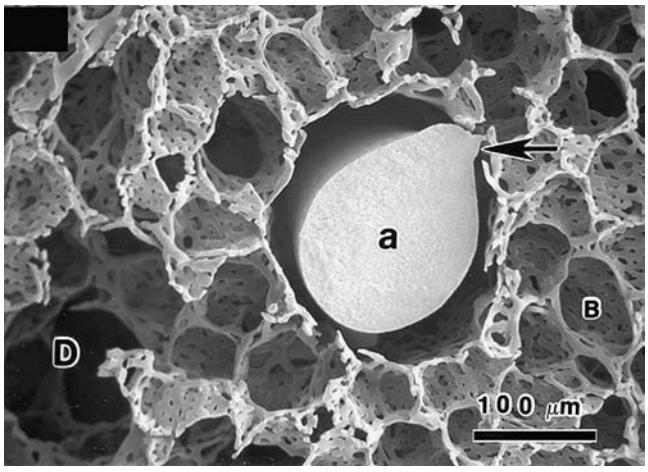

FIGURE 16-2 Scanning electron micrograph showing a cast of a small pulmonary artery (a) surrounded by alveoli. Arteries of this size give off short branches before dividing into capillaries. The alveolar baskets (B) and alveolar ducts (D) are more prominent than normal in this rat, which was given intratracheal elastase to cause emphysema. Reproduced with permission from Schraufnagel DE.[2]

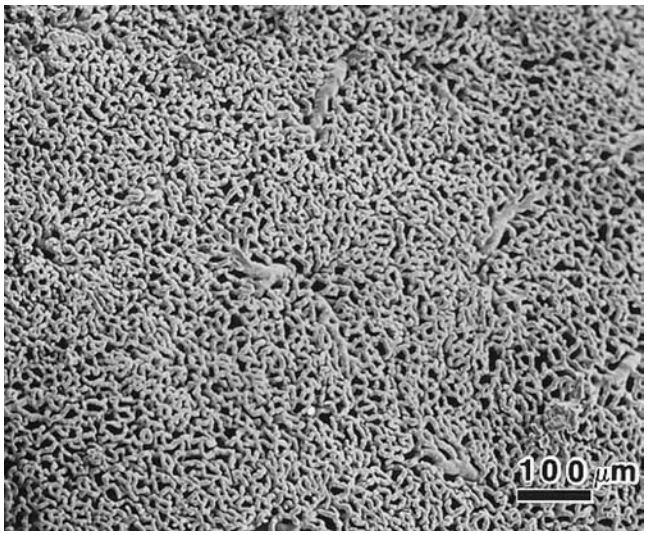

FIGURE 16-3 Scanning electron micrograph showing a cast of capillaries on the pleural surface of a normal rat. The capillaries are less dense than alveolar capillaries. No arteries or veins are seen on the normal pleural surface. Reproduced with permission from Schraufnagel DE.[2]

The caliber and length of the pulmonary arteries both decrease with expiration and increase with inspiration. This causes bloodflow to increase with inspiration and enhances the pulsatility of flow in these vessels.

PULMONARY CAPILLARIES

Anatomy

Capillaries account for most of the vasculature in the lung and have a distinct appearance, regardless of their size. They do not change caliber with distance or branching and have no directionality, although their diameter may vary at bends and other places. They branch sharply, at nearly right angles, which facilitates the slow lateral flow of blood as it exchanges gases and solutes. Right-angle branching conserves pressure in a low-pressure system such as the pulmonary circulation[6] and can cause significant focal variation in hematocrit.

Scanning electron microscopy of pulmonary capillary casts shows that they are arranged in two patterns, alveolar (see Figure 16-2) and pleural (Figure 16-3). Alveolar capillaries form baskets around alveoli[7] and cover about 75% of their surface area[8] (Figure 16-4). Alveolar capillaries come together in pentagonal rings. The center of each ring is about 4 μm in diameter in normal rats at low lung volumes,[9] which is space enough for a single cell. Contractile myofibroblasts in these sites might contract to control alveolar bloodflow.[10] One capillary supplies more than one alveolus,[11] and capillary branching is extensive within an alveolus. In the rat, normal alveolar capillaries have about 16 branches per 100 μm of length.[9] Capillaries may attach directly to large veins but not to arteries.

The capillaries on the pleural surface, around bronchioles, and in the bronchovascular bundle (Figure 16-5) are less dense, making up about 67% of the surface.[8] They are planar and branch less often, having only about 11 branches

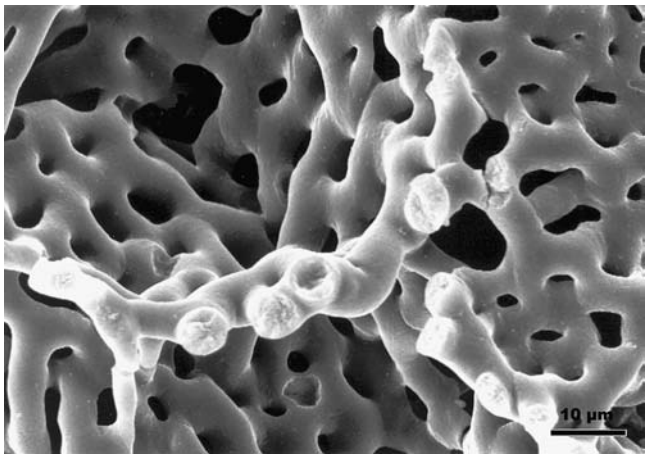

FIGURE 16-4 Scanning electron micrograph showing a cast of alveolar baskets in a rat given elastase to cause emphysema. Reproduced with permission from Schraufnagel DE and Schmid A.[8]

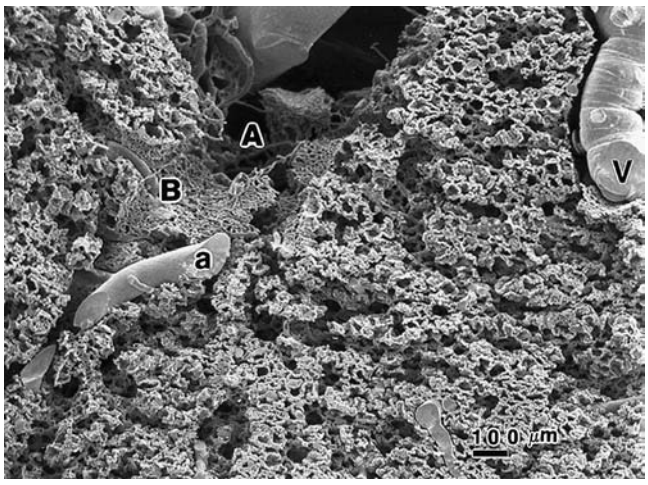

FIGURE 16-5 Scanning electron micrograph showing the relationships between the airway (A), artery (a), and vein (v) in a rat. The capillaries in the bronchovascular bundle have a pattern similar to that of pleural capillaries. Reproduced with permission from Schraufnagel DE.[2]

per 100 µm.[9] Pleural capillaries are less likely than alveolar capillaries to have flattened and widened areas at bends.

Capillary Control of Ventilation–Perfusion Matching

Alveolar capillaries fold and unfold during breathing. The change in resistance to bloodflow may affect perfusion–ventilation matching. At low alveolar volume, especially in an atelectatic state, capillaries are kinked (Figure 16-6). The increased microvascular resistance caused by the bending greatly reduces bloodflow in these capillaries. As inspiration begins from functional residual capacity, the capillaries unfold, enhancing bloodflow.[12] The fall in downstream pressure that results from the increased diameter of the capillaries and veins augments bloodflow. During tidal breathing, the alveoli that expand the most receive the most blood and air. Alveoli that are already expanded at the beginning of

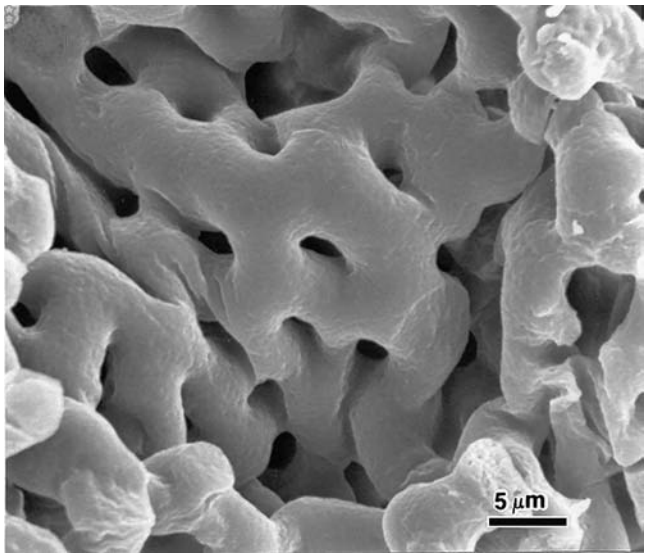

FIGURE 16-6 Scanning electron micrograph showing normal rat alveolar capillaries cast at low lung volume. The bending capillaries increase resistance to bloodflow. Reproduced with permission from Schraufnagel DE et al.[9]

inspiration, such as those at the top of the lung or in emphysema, are stretched and have narrowed capillary lumens (Figure 16-7). Indeed, they may not fill at all.[8] Capillary folding may decrease bloodflow on expiration.

Response to Injury and Angiogenesis

Structurally, pulmonary capillaries have limited responses to injury. They can increase in diameter—but not much without rupturing. They are increased in the adult respiratory distress syndrome,[13] hepatic cirrhosis,[14] and lung fibrosis.[9] The enlarged diameter appears not to increase the overall alveolar–capillary surface area.[9] The density of the lung

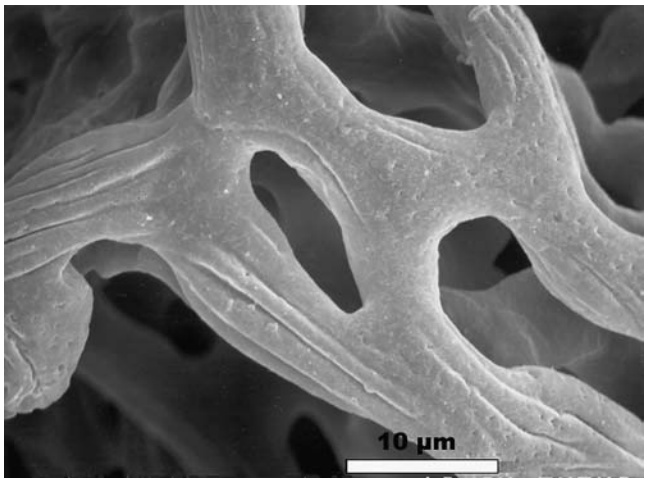

FIGURE 16-7 Scanning electron micrograph showing capillaries at total lung capacity of a rat given elastase. The capillaries were cast at functional residual volume. The lungs were inflated to total lung capacity before the resin set. Narrowed capillaries in fully expanded lungs have increased resistance to bloodflow. Reproduced with permission from Schraufnagel DE and Schmid A.[8]

capillaries may decrease in different disease states.[15] The capillaries of the lungs of rats with elastase-induced emphysema have large alveolar baskets, vessels that end abruptly near areas of destruction,[8] and decreased branching.[9] Light microscopic observations of human lungs provide similar findings. Most lung disease and experimental conditions are heterogeneous, with patchy capillary involvement (Figure 16-8).

Angiogenesis of pulmonary capillaries is less well described than that of bronchial capillaries but occurs in response to capillary endothelial injury caused by mitomycin in humans.[16] As native capillaries are destroyed, new capillaries replace them but in a haphazard manner (Figure 16-9).

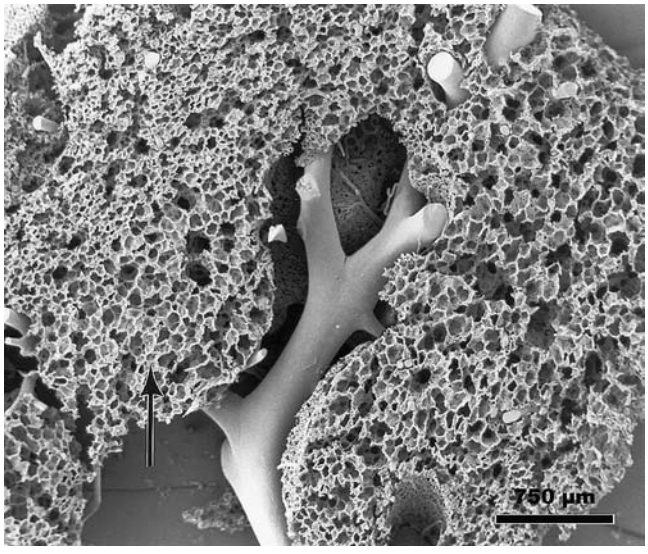

FIGURE 16-8 Scanning electron micrograph of the cast vasculature of a rat given elastase to cause emphysema, showing heterogeneity of the reaction. The capillary baskets in the left upper part of the micrograph are smaller than those closer to the artery and airway, where elastase was insufflated. Reproduced with permission from Schraufnagel DE and Schmid A.[8]

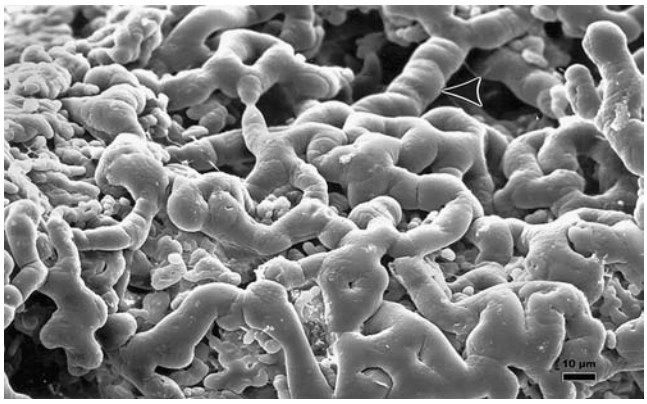

FIGURE 16-9 Scanning electron micrograph of cast pulmonary capillaries, showing the vascular remodeling that had taken place in a woman who was given mitomycin and developed progressive pulmonary hypertension over about a 3-month period. At autopsy, the native capillaries were distorted and shrunken, and new capillaries had grown to replace them. The *arrowhead* shows a capillary segment coming from an adjacent alveolus. Reproduced with permission from Schraufnagel DE et al.[16]

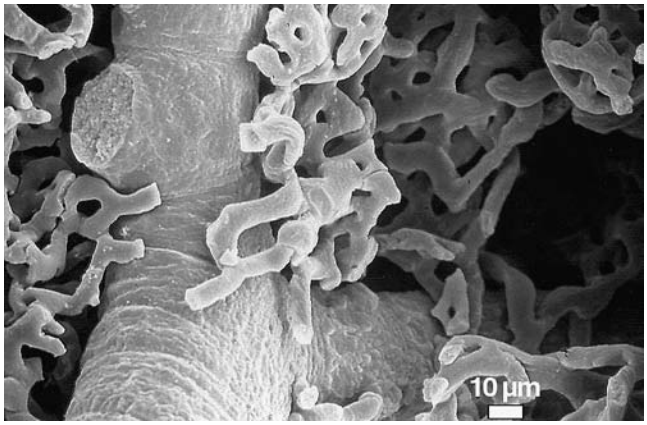

FIGURE 16-10 Scanning electron micrograph showing the cast of a normal rat vein with the characteristic features of round endothelial nuclear impressions and banding. Reproduced with permission from Schraufnagel DE et al.[18]

PULMONARY VEINS

Anatomy

In contrast to light microscopy, scanning electron microscopy of casts can distinguish pulmonary veins from arteries at any size. Cast veins have round endothelial cell nuclear impressions that have no orientation with respect to the long axis of the vessel[17] (Figure 16-10). Cast veins have less space between their surfaces and adjacent capillaries than do arteries because of thinner vessel walls. Within the lung (in humans and rats), they do not travel with the airways.[1] Veins up to at least 100 µm in diameter may receive capillaries.[18] The lumens of pulmonary veins have regular small indentations (rings).[19] These rings are narrow (1 to 3 µm in width), generally circumferential constrictions, occurring about every 20 to 50 µm, just after the site of entry of tributaries. They are caused by smooth muscle bundles[20] and constrict in response to the neural discharge of a head blow[4] (Figure 16-11).

Venous Ventilation–Perfusion Matching

The constrictions of the pulmonary veins may work in concert with capillaries to exert fine control of ventilation and perfusion at the alveolar level. There are extensive interconnections between capillaries and hundreds of potential paths for erythrocytes to take from the beginning of the capillaries to the vein (see Figure 16-2). The small ring constrictions in the vein at the sites of entrance of capillaries can direct bloodflow in this low-resistance system. Resistance is proportional to the length of the tube and the viscosity of the fluid and inversely proportional to the fourth power of the radius. According to this relationship, a small contraction (<3% of the diameter) of the smallest veins could greatly affect capillary bloodflow. These fine quivers can be seen with the use of in vivo microscopy (in dogs).

Veins are downstream from the critical event of oxygenation of erythrocytes. Pulmonary capillary endothelial cells produce nitric oxide,[21] which is differentially absorbed and

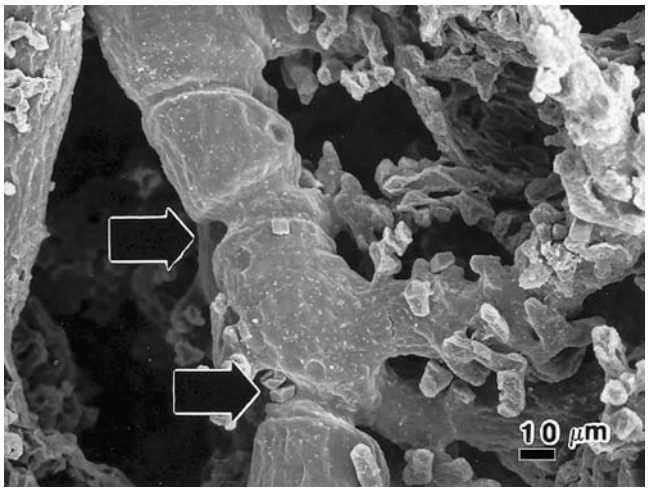

FIGURE 16-11 This cast of a rat vein after a head blow shows deep constrictions (*thick arrows*) regularly and at sites that could control inflow. Reproduced with permission from Schraufnagel DE.[2]

metabolized by hemoglobin and myoglobin.[22,23] Nitric oxide is also absorbed and metabolized differentially by oxygenated hemoglobin, deoxygenated hemoglobin, and carboxyhemoglobin.[24] Deoxygenated hemoglobin and carboxyhemoglobin may scavenge the nitric oxide produced by capillary endothelial cells. If the venous muscle myoglobin does not come into contact with a sufficient amount of nitric oxide, its muscle may retain its resting tone.[25] The resulting slight constriction would slow the return of desaturated blood from that capillary segment. On the other hand, if oxygenated hemoglobin were present at the end pulmonary capillary segment and the nitric oxide had less affinity for it than for the deoxygenated form, then nitric oxide might be available to interact with the venous muscle myoglobin, which would relax the muscle and allow unimpeded bloodflow. Although this is an attractive and straightforward hypothesis, there are several factors that make it more complicated. The affinity of nitric oxide for the heme compounds depends on the local pH,[26] the relative fluxes of other reactive oxygen species,[27] and protein interactions.[28] Carbon monoxide could participate in these reactions[29] and be a potent mediator on its own.

Nitric oxide synthase–knockout mice have more pulmonary hypertension than wild-type mice[30] and more severe pulmonary hypertension when exposed to hypoxia.[31] The venous contraction hypothesis could also partly explain the observation of erythrocytes passing through capillaries at different velocities, although interactions with endothelial surface molecules are also important.

Neurogenic Pulmonary Edema

A corollary of the hypothesis stated above is that exuberant dysfunction of these venous sphincters may cause neurogenic pulmonary edema. Neurogenic pulmonary edema has been recognized to be associated with brain injury since at least the nineteenth century.[32] This form of pulmonary edema can occur in healthy persons after head trauma, hanging, or an epileptic seizure. Its postmortem appearance can be more florid and hemorrhagic than in people suffering from chronic congestive heart failure. Abrupt contraction of venous smooth muscle has been considered to be a logical mechanism for neurogenic pulmonary edema. Pulmonary venous muscle tone is under sympathetic neural control, and sympathetic stimulation increases pulmonary vascular resistance.[33] Venous resistance is increased in neurogenic edema,[34] and α-adrenergic antagonists attenuate the edema.[35]

Injection of methylmethacrylate into the pulmonary vasculature of rats with neurogenic pulmonary edema was found to be not possible, and the cast of the microvasculature could only be studied if a head blow was given immediately after the vasculature was cast. The head blow caused a deepening of the muscular venous sphincters[4] (see Figure 16-11). Treatment of the rats with the α-antagonists prazosin and phentolamine caused a reduction of the constriction.[36] Endothelin-1 may also be involved because it constricts the sphincters[37] and may influence regional perfusion in the lung.[38]

Pulmonary resistance is increased if the vasculature is perfused in the reverse direction,[33] and this resistance is increased by applying sympathetic agents,[33] suggesting a forward-pumping action by the veins. There are species differences in the pumping ability of pulmonary veins,[1] but in all species the pumping action of veins is less than that of arteries, which is consistent with their muscular structures.

Flow in a Low-Pressure System

A low-pressure system must have low resistance. The low resistance of the pulmonary veins results partly from their having no valves. Neurally controlled venous muscle could allow active control of perfusion with lower resistance than a system with valves. The problems with a valveless system include pooling with gravity and reverse flow under conditions of high downstream pressures, such as left heart failure or mitral stenosis (Figure 16-12).

Although pulmonary bloodflow has long been known to be gravity dependent and to increase from apex to base,

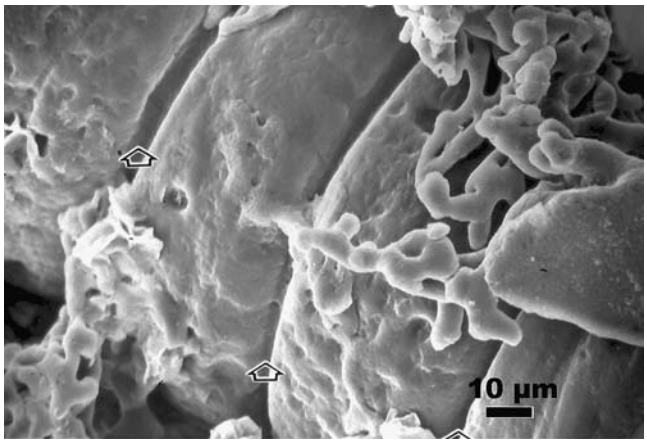

FIGURE 16-12 Scanning electron micrograph of a cast vein of rat given a head blow, showing constrictions. The capillaries that drain into the veins are bulging, suggesting that back-pressure may have distended them. Reproduced with permission from Schraufnagel DE and Patel KR.[4]

Anthonisen and Milic-Emili showed that the flow is actually decreased at the very bottom of the lungs, a phenomenon termed a zone 4 condition.[39] Hakim and colleagues later showed that it was not a vertical flow gradient but a central-to-peripheral gradient. The proximal flow pattern held true for breath-holding human subjects,[40] thereby refuting the argument that distal capillaries have less supporting structure than the central lung and are, therefore, more likely to be pinched off by changes in alveolar architecture with inspiration.

Scanning electron microscopic observations of capillary casts offer a suitable explanation. The extensive branching of the alveolar capillaries presents many short-circuit routes that blood can take in reaching veins. In the low-pressure and low-flow pulmonary capillaries with near right-angle branching, short circuits are favored over the distal routes at rest (see Figures 16-2 and 16-5). With exercise, the increased flow would be expected to extend the perfusion to more peripheral capillaries, thus recruiting distal sites. The muscle tone in small pulmonary veins would aid the recruitment and prevent haphazard or reverse flow.

Reverse Flow

Spontaneously hypertensive rats[41] and certain cattle have well-developed venous musculature and deep venous constrictions in their casts.[1,42] This finding was especially true of the older spontaneously hypertensive rats, which often develop cardiac failure. Venous muscular hypertrophy occurs in human states of high downstream pressure, such as chronic congestive heart failure and mitral stenosis.

The venous constrictions could protect against backflow and be actively controlled by neural, humoral, or cytokine mechanisms. The sphincters could provide a valve function without adding to the impedance of valves. Aharinejad and colleagues found that initial lymphatics were located adjacent to these venous muscle tufts, suggesting that their contraction could also facilitate lymphatic flow.[43]

High downstream pressure may be more likely to be transmitted retrogradely without venous valves. The high pressure in conditions such as mitral stenosis, congenital heart disease, and congestive heart failure and the squeeze provided by the pulmonary arteries no doubt push blood into the lung interstitium and lymphatics, giving the characteristic pathologic picture seen in these conditions. The muscular arteries undergo medial hypertrophy, and the arterioles become muscular. The lungs become heavy with edema and blood. Collagen is laid down in the interstitium and muscular coat of the arteries and veins. These changes are greater in the dependent lungs, but the intimal fibrosis that arteries undergo may occur in the upper parts of the lungs. Pulmonary veins develop a substantial media that separates the intima and adventitia, causing them to look like arteries. Hemosiderin-laden macrophages and iron-encrusted elastic fibers mark the remains of the trapped erythrocytes in these lungs. This hemosiderosis gives the lungs a brown, indurated appearance. Lymphatic hypertrophy and widened interlobular septa are common.

The cardiac muscle present in the pulmonary veins may hypertrophy. Venous cardiac muscle contracts with systole. In humans, this muscle extends only about a few centimeters from the ostium, but in other species it extends well into the lung. These autorhythmic cells may be the source of atrial arrhythmias and must be identified for successful ultrasonic ablation therapy.

BRONCHIAL CIRCULATION

Anatomy

Almost all blood coming through the pulmonary arteries is destined to be oxygenated. To allow this, the bronchial arteries must supply the lung structures not involved with gas exchange, such as the walls of the pulmonary vessels, airways proximal to the terminal bronchioles, and the pleura in many species. In all species, bronchial arteries at their origins are much smaller than pulmonary arteries but taper less and become about the same size at about 100 μm in diameter.[44] Bronchial vessels branch and anastomose as they weave through the bronchovascular bundle (Figure 16-13). Casts of the bronchial arteries have deep longitudinal grooves resulting from contracted smooth muscle. Their thicker walls lead to there being more space between the cast artery and the surrounding capillaries or lymphatics. Bronchial arteries are generally not difficult to distinguish from pulmonary arteries, although the bronchial artery loses many of its distinguishing features as it approaches capillary size (<50 μm).

Bronchial veins collect blood that comes from the large airways and mediastinal tissue. Like other systemic veins, they have leaflet valves to prevent the backflow of blood.

Bronchial Circulation with Pulmonary Artery Occlusion

Many studies have shown that the bronchial arteries fill pulmonary capillaries and veins. The vasa vasorum coming from the bronchial arteries can empty into the pulmonary arteries.[45] In pathologic conditions, such as cirrhosis, the anastomoses of the two circulations become exaggerated and can involve any vascular component.[46] So interconnected are these circulations that bronchial arteries can

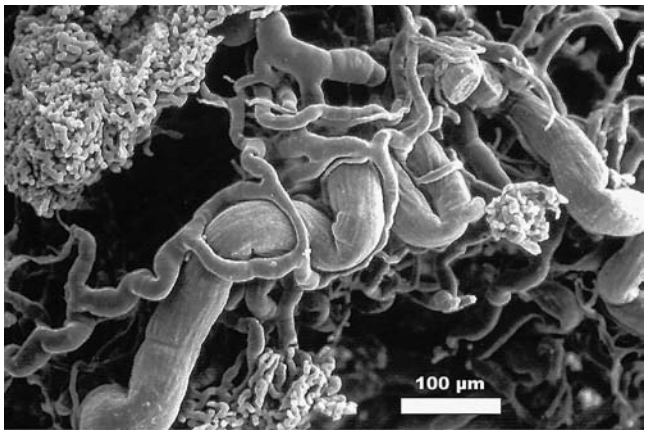

FIGURE 16-13 Scanning electron micrograph of the vasa vasorum of a sheep injected through the bronchial artery. Note that it weaves in the bronchovascular bundle and supplies the larger artery. Reproduced with permission from Schraufnagel DE et al.[44]

rescue the lung from infarction after complete occlusion of the pulmonary artery.[47] The bronchial circulation must immediately expand its flow to do this, and its pressure must be reduced to avoid damage to the alveolar membranes. After ligation of the pulmonary artery, a large pressure drop occurs in the bronchial arteries greater than 350 μm in diameter.[48] Casts of these vessels show that they have deep constrictions and sharp-angled turns that create high resistance[44] (Figure 16-14). It is interesting that bronchial arteries can contract one side preferentially[44] (Figure 16-15).

The most common cause of occlusion of pulmonary arteries is thromboembolism, and pulmonary infarction occurs in only about 31% of pulmonary emboli. It appears that pulmonary infarction may be a failure of the bronchial circulation to supply the lung segment, which no longer receives its pulmonary bloodflow.[49] Pulmonary infarction is correlated with the number of lobes involved, left ventricular failure, and a greater number of small pulmonary arteries being affected by emboli.[49]

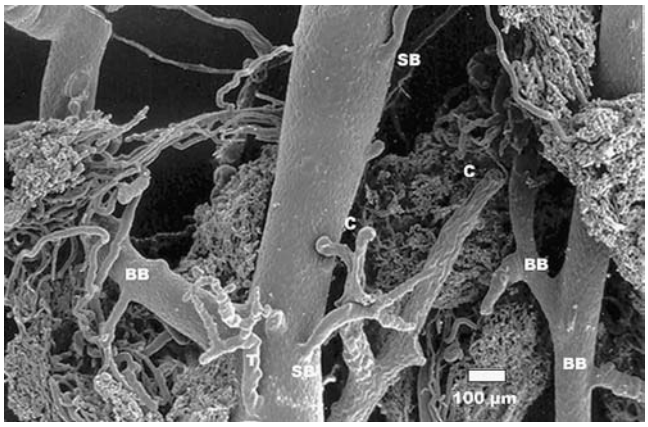

FIGURE 16-14 Scanning electron micrograph showing casts of bronchial arteries of a sheep. Bronchial arteries can brake their high pressures by sharp branches (SB), deep constrictions (C), backward branching (BB), and twisting (T).

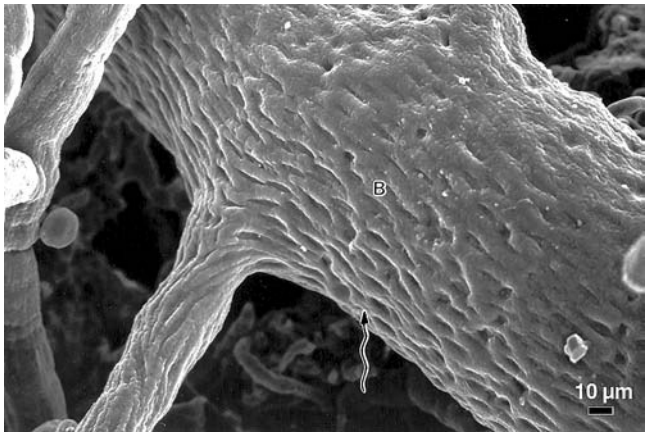

FIGURE 16-15 Bronchial arteries may constrict on one side more than on the other, as shown in this cast of a sheep bronchial artery. Note the deep furrows of the endothelial cell nuclei (*wavy arrow*) on the side giving off the branch. Reproduced with permission from Schraufnagel DE et al.[44]

Angiogenesis and the Bronchial and Pulmonary Circulations

The bronchial circulation has been recognized as the major source of angiogenesis in the lung. It supplies the new blood vessels found in bronchiectasis and airway inflammation, but the pulmonary circulation may also undergo angiogenesis.[16] New vessels develop in response to an angiogenic stimulus; this may be hypoxia, which causes the production of vascular endothelial growth factor,[50] sphingosine 1-phosphate,[51] or other angiogenic factors. In flat capillary beds,[52] such as are found in the embryonic lung, new vessels may develop by intussusception,[53] a mechanism whereby capillary walls pinch down and fuse, producing an intercapillary peg. This creates a capillary division that serves as a point for growth of new vessels. An alternative to intussusceptive growth is growth by sprouting. The tracheobronchial circulation can sprout tiny hair-like capillaries in response to ischemia or other stimuli[9] (Figure 16-16). The capillaries join randomly, establish flow, enlarge, and remodel to form mature vessels (Figure 16-17). The first small capillaries are too small to allow the flow of erythrocytes.

LYMPHATICS

Anatomy

Under conditions of increased permeability, methylmethacrylate resin injected into the vascular system seeps into the lymphatics and casts them. Scanning electron micrographs of these casts show several characteristic structures. The interstitial spaces or tissue planes that receive fluid from capillaries or alveoli and the interstitial space beneath the pleura have been called prelymphatics by von Hayek[54] and others. When preparations are cast, these tissue planes of the lung fill well and have a characteristic appearance. At low magnification, they appear as a film contained by the visceral pleura or within the bronchovascular bundles or interlobular septa. Casts of prelymphatics have connective tissue strands across their surfaces. Although it appears

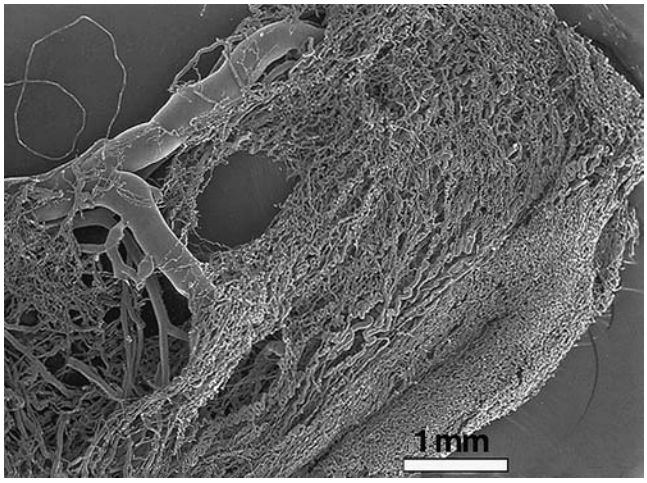

FIGURE 16-16 Scanning electron micrograph showing tracheal revascularization 7 days after a rat had a three-ring segment sectioned, resutured, and covered with transforming growth factor-α. Many hair-like vessels arise and connect.

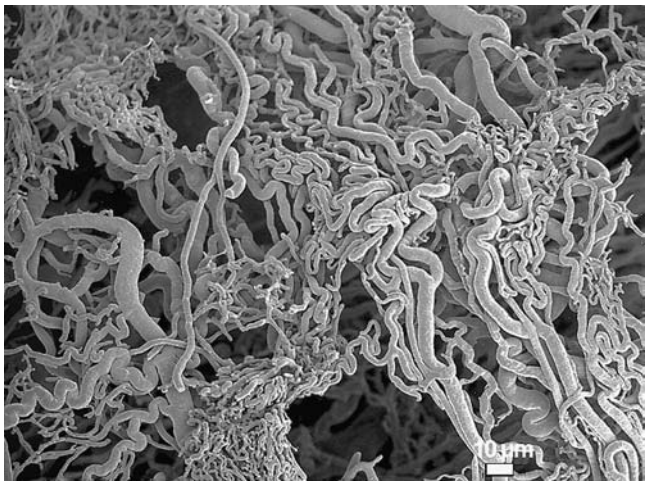

FIGURE 16-17 Scanning electron micrograph showing new vessels along a suture line of a rat on day 6 after it had undergone the procedure described in Figure 16-16. New capillaries grow tortuously. Reproduced with permission from Schraufnagel DE et al.[58]

that prelymphatics occasionally drain directly into conduit lymphatics, they usually connect to other structures, which have been termed reservoir lymphatics.[55] These flat structures are about 15 to 40 µm wide and have small pouches branching laterally from their long axes. Their leaf-like side branches end blindly (Figure 16-18). Although reservoir lymphatics have a linear dimension, it is often difficult to distinguish them from prelymphatics because of the gradual transition from one to the other. The rough surfaces of prelymphatics and reservoir lymphatics distinguish them from blood capillaries. Reservoir lymphatics connect to the conduit lymphatic vessels.[55]

Cast conduit lymphatic vessels are irregularly cylindrical on the pleural surface and are about the same size as the small adjacent blood vessels, but their diameters vary several-fold, from less than 5 µm to more than 35 µm, within a few hundred micrometers (Figure 16-19). The lymphatic walls contain actin and myosin. It is unclear whether focal contraction results in the formation of the pouches proximal to valves. Conduit lymphatics on the pleural surface may wind around companion blood vessels.

Within the lung, especially in the interlobular septae, conduit lymphatics are flat, with less variation in diameter than the pleural vessels. The casts often have longitudinal grooves on their inner sides and joints at the sites of valves (Figure 16-20). Conduit lymphatics that come from large peribronchial (Figure 16-21) or perivascular saccular lymphatics are rounder. Conduit lymphatics rarely accept tributaries or give off branches. Lymphatics are not found around individual alveoli.[55]

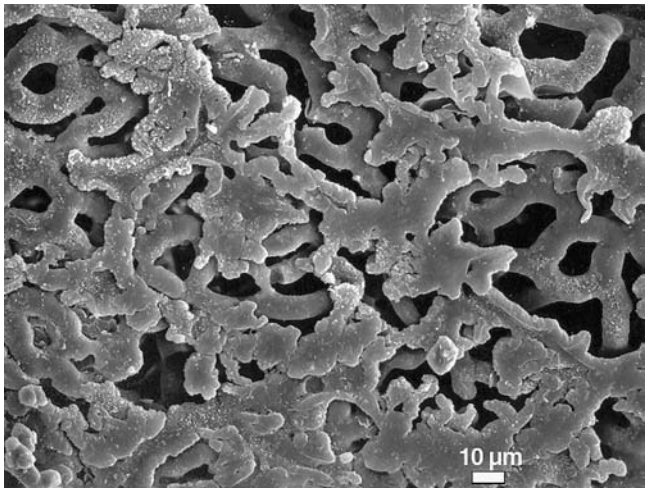

FIGURE 16-18 Scanning electron micrograph of a cast of rat reservoir lymphatics. Reservoir lymphatics are the first lymphatics to have a tubular pattern. They are often mixed with prelymphatics and generally drain into a conduit lymphatic. Pleural blood capillaries with their even round surfaces can be seen underneath the pleural reservoir lymphatics, especially on the right. This rat was exposed to 85% oxygen for 7 days.

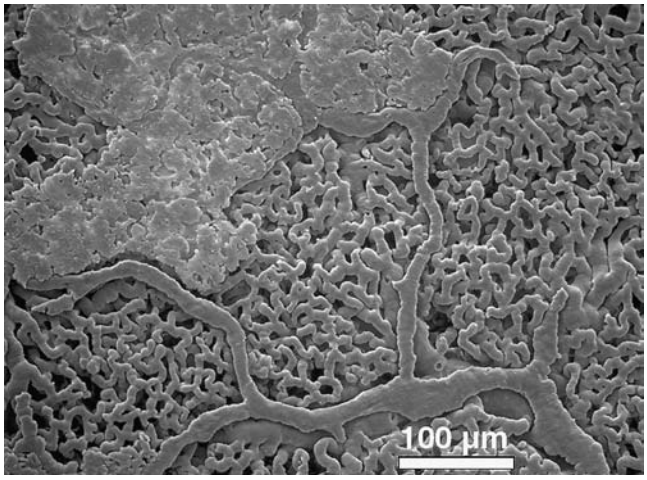

FIGURE 16-19 Scanning electron micrograph showing a cast of a conduit pleural lymphatic draining a prelymphatic area in a rat exposed to 85% oxygen for 7 days. Note the irregularity of the diameter of the lymphatic vessel compared to the blood capillaries below it. Reproduced with permission from Schraufnagel DE et al.[59]

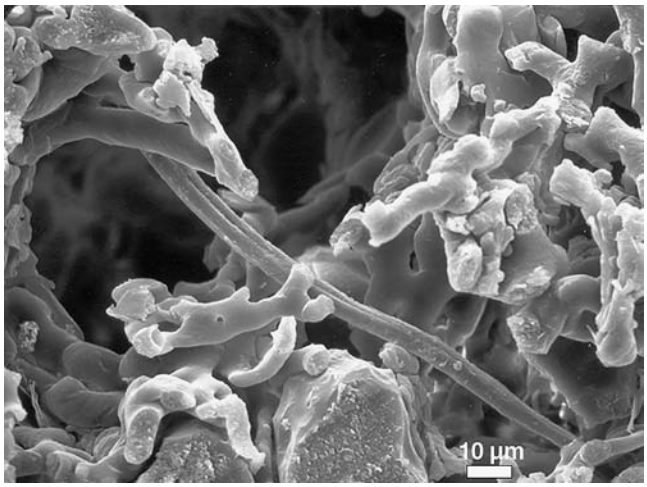

FIGURE 16-20 Scanning electron micrograph showing another intrapulmonary conduit lymphatic. Characteristic of these ribbon-like structures are the central longitudinal grooves. This rat was exposed to 85% oxygen for 7 days.

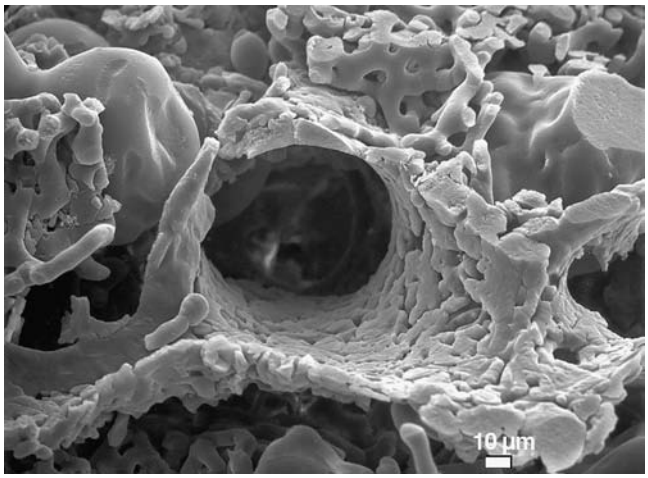

FIGURE 16-21 Scanning electron micrograph showing a cast of the bronchial saccular lymphatics, which have an identical appearance to perivascular saccular lymphatics. This rat was exposed to 85% oxygen for 7 days. Reproduced with permission from Schraufnagel DE et al.[59]

Large blood vessels and airways have broad tubulosaccular lymphatics, which differ from the other forms in being sac-like arrangements that have surrounded a vessel or airway (see Figure 16-21). The saccules can be more than 10 times wider than conduit lymphatics and are more heterogeneous than reservoir lymphatics. The size of the saccular component of these lymphatics ranges widely from 10 µm to more than 100 µm, yet their walls are thin.[55]

Prelymphatics, reservoir lymphatics, and saccular lymphatics are not difficult to distinguish from blood vessels because they lack their strict tubular shape. The irregular surfaces of reservoir lymphatics are caused by projections into the lymphatic vessel lumen. Conduit lymphatics are tubular and may be similar in size to blood vessels, but the variation in their diameter and lack of branches and tributaries set them apart.

Casting Lymphatics

In the normal state, lymphatics are collapsed and difficult to cast, but with brief lung injury the lymphatics rapidly dilate.[56] Prolonged rinsing with hypo-osmotic solution, avoiding fixation before casting, and use of a lower-viscosity resin increase the ability to cast lymphatics.

Function of Reservoir Lymphatics

Reservoir lymphatics could keep alveoli dry by holding fluid until the conduit lymphatic traffic decreases. Their fronds suggest that they may have an absorptive function, and their linearity suggests that they are itineraries for lymph. The storage concept of reservoir and tubulosaccular lymphatics fits the data on lymph accumulation in the lung.[57]

SUMMARY

Study of the lung microvascular structure through scanning electron microscopy of vascular casts shows how its functions could be carried out. The extensive capillary paths and the constrictions on the smallest veins, coupled with a signaling theory for the detection of deoxygenated blood, provide plausible explanations for intricate ventilation–perfusion matching. It is also not difficult to surmise that an exuberance of this process may result in lung damage caused by neurogenic pulmonary edema or congestive heart failure. The shape of individual alveolar capillaries with lung inflation may affect their filling and ventilation–perfusion matching. The enormous number of pathways that blood can take through alveolar capillaries and the resistance, flow, and branching may explain the physiologic puzzle of decreased bloodflow at the lung bases and capillary recruitment with exercise. Study of the lymphatic casts in a variety of conditions shows how they can rescue the lung by rapid expansion to control pulmonary edema. Finally, the bronchial circulation is structured to respond rapidly with a new blood supply to prevent lung necrosis after vascular occlusion.

REFERENCES

1. Kay JM. Pulmonary vasculature and nerves. Comparative morphologic features of the pulmonary vasculature in mammals. Am Rev Respir Dis 1983;128:S53–7.
2. Schraufnagel DE. The lung microstructure. In: Motta PM, Murakami T, Fujita H, editors. Scanning electron microscopy of vascular casts: method and applications. Norwell, MA: Kluwer Academic Publishers; 1992. p. 123–37.
3. Albertine KH, Wiener-Kronish JP, Koike K, Staub N. Quantification of damage by air embolization to lung microvessels in anesthetized sheep. J Appl Physiol 1984;57:1360–8.
4. Schraufnagel DE, Patel KR. Sphincters in pulmonary veins: an anatomic study in rats. Am Rev Respir Dis 1990;141:721–6.
5. Hijiya K, Okada Y. Scanning electron microscope study of the cast of the pulmonary capillary vessels in rats. J Electron Microsc (Tokyo) 1978;27:49–53.
6. Sobin SS, Intaglietta M, Frasher WGJ, Herta M. The geometry of the pulmonary microcirculation. Angiology 1966;17:24–30.
7. Ohtani O. Microvasculature of the rat lung as revealed by scanning electron microscopy of corrosion casts. Scanning Electron Microsc 1980;(Pt 3):349–56.
8. Schraufnagel DE, Schmid A. Capillary structure in elastase-induced emphysema. Am J Pathol 1988;130:126–35.
9. Schraufnagel DE, Mehta D, Harshbarger R, et al. Capillary remodeling in bleomycin-induced pulmonary fibrosis. Am J Pathol 1986;125:97–106.
10. Kapanci Y, Assimacopoulos A, Irle C, et al. "Contractile interstitial cells" in pulmonary alveolar septa: a possible regulator of ventilation–perfusion ratio? Ultrastructural, immunofluorescence, and in vitro studies. J Cell Biol 1974;60:375–92.
11. Ryan SF. The structure of the interalveolar septum of the mammalian lung. Anat Record 1969;165:467–84.
12. Assimacopoulos A, Guggenheim R, Kapanci Y. Changes in alveolar capillary configuration at different levels of lung inflation in the rat. An ultrastructural and morphometric study. Lab Invest 1976;34:10–22.
13. Tomashefski JF Jr, Davies P, Boggis C, et al. The pulmonary vascular lesions of the adult respiratory distress syndrome. Am J Pathol 1983;112:112–26.
14. Schraufnagel DE, Malik R, Goel V, et al. Lung capillary changes in hepatic cirrhosis in the rat. Am J Physiol (Lung Cell Mol Physiol) 1997;272:L139–47.
15. Schraufnagel DE. Corrosion casting of the lung for scanning electron microscopy. In: Schraufnagel DE, editor. Electron

microscopy of the lung. New York: Marcel Dekker; 1990. p. 257–97.
16. Schraufnagel DE, Sekosan M, McGee T, Thakkar MB. Human alveolar capillaries undergo angiogenesis in pulmonary veno-occlusive disease. Eur Respir J 1996;9:346–50.
17. Miodonski A, Hodde KC, Bakker C. Rasterelektronen-mikroskopie. Morphologische Unterschiede zwischen Arterien und Venen. Beitr Elektronenmikroskop Direktabb Oberfl 1976; 9:435–42.
18. Schraufnagel DE. Microvascular casting of the lung: a state-of-the-art review. Scanning Microsc 1987;1:1733–47.
19. Takino M, Miyake S. Über die Besonderheiten der Arteria und Vena pulmonalis bei verschiedenen Tieren, besonders beim Menschen. Acta Scholae Med Univ Imp Kyoto 1936;18:226–45.
20. Aharinejad S, Böck P. Appearance of venous sphincters in the pulmonary microvascular bed of normotensive and spontaneously hypertensive rats. Scanning Microsc 1992;6:865–75.
21. Ignarro LJ, Byrns RE, Buga GM, Wood KS. Endothelium-derived relaxing factor from pulmonary artery and vein possesses pharmacologic and chemical properties identical to those of nitric oxide radical. Circ Res 1987;61:866–79.
22. Doyle MP, Hoekstra JW. Oxidation of nitrogen oxides by bound dioxygen in hemoproteins. J Inorg Biochem 1981;14:351–8.
23. Eich RF, Li T, Lemon DD, et al. Mechanism of NO-induced oxidation of myoglobin and hemoglobin. Biochemistry 1996; 35:6976–83.
24. Spencer NY, Zeng H, Patel RP, Hogg N. Reaction of S-nitrosoglutathione with the heme group of deoxyhemoglobin. J Biol Chem 2000;275:36562–7.
25. Stamler JS, Jia L, Eu JP, et al. Blood flow regulation by S-nitrosohemoglobin in the physiological oxygen gradient. Science 1997;276:2034–7.
26. Herold S, Exner M, Nauser T. Kinetic and mechanistic studies of the NO*-mediated oxidation of oxymyoglobin and oxyhemoglobin. Biochemistry 2001;40:3385–95.
27. Jourd'heuil D, Mills L, Miles AM, Grisham MB. Effect of nitric oxide on hemoprotein-catalyzed oxidative reactions. Nitric Oxide 1998;2:37–44.
28. Kharitonov VG, Sharma VS, Magde D, Koesling D. Kinetics of nitric oxide dissociation from five- and six-coordinate nitrosyl hemes and heme proteins, including soluble guanylate cyclase. Biochemistry 1997;36:6814–8.
29. Sharma VS, Traylor TG, Gardiner R, Mizukami H. Reaction of nitric oxide with heme proteins and model compounds of hemoglobin. Biochemistry 1987;26:3837–43.
30. Steudel W, Ichinose F, Huang PL, et al. Pulmonary vasoconstriction and hypertension in mice with targeted disruption of the endothelial nitric oxide synthase (NOS 3) gene. Circ Res 1997;81:34–41.
31. Steudel W, Scherrer-Crosbie M, Bloch KD, et al. Sustained pulmonary hypertension and right ventricular hypertrophy after chronic hypoxia in mice with congenital deficiency of nitric oxide synthase 3. J Clin Invest 1998;101:2468–77.
32. Carson W. Pulmonary apoplexy. In: Pepper W, editor. System of medicine. Vol 3. Diseases of the respiratory, circulatory and haemopoietic systems. Philadelphia: Lea and Co.; 1885. p. 293–5.
33. Daly ID, Ramsay DJ, Waaler BA. The site of action of nerves in the pulmonary vascular bed in the dog. J Physiol 1970; 209:317–39.
34. Maron MB, Dawson CA. Pulmonary venoconstriction caused by elevated cerebrospinal fluid in the dog. J Appl Physiol Respir Environ Exercise Physiol 1980;49:73–8.
35. Brashear RE, Ross JC. Hemodynamic effects of elevated cerebrospinal fluid pressure: alterations with adrenergic blockade. J Clin Invest 1970;49:1324–33.
36. Schraufnagel DE, Thakkar MB. Pulmonary venous sphincter constriction is attenuated by α-adrenergic antagonism. Am Rev Respir Dis 1993;148:477–82.
37. Aharinejad S, Marks SC Jr, Schraufnagel DE. Endothelin-1 focally constricts pulmonary veins in rats. J Thorac Cardiovasc Surg 1995;110:148–56.
38. Onizuka M, Miyauchi T, Mitsui K, et al. Endothelin-1 mediates regional blood flow during and after pulmonary operations. J Thorac Cardiovasc Surg 1992;104:1696–701.
39. Anthonisen NR, Milic-Emili J. Distribution of pulmonary perfusion in erect man. J Appl Physiol 1966;21:760–6.
40. Hakim TS, Lisbona R, Dean GW. Gravity-independent inequality in pulmonary blood flow in humans. J Appl Physiol 1987;63:1114–21.
41. Aharinejad S, Schraufnagel DE, Böck P, et al. Spontaneously hypertensive rats develop pulmonary hypertension and hypertrophy of pulmonary venous sphincters. Am J Pathol 1996;148:281–90.
42. Aharinejad S, Egerbacher F, Nourani P, et al. Pulmonary venous sphincters in cattle. Anat Rec 1996;246:356–63.
43. Aharinejad S, Böck P, Firbas W, Schraufnagel DE. Pulmonary lymphatics and their spatial relationship to venous sphincters. Anat Rec 1995;242:531–44.
44. Schraufnagel DE, Pearse DB, Mitzner WA, Wagner EM. Three-dimensional structure of the bronchial microcirculation in sheep. Anat Rec 1995;243:357–66.
45. Schraufnagel DE. Microvascular casting of the lung—bronchial versus pulmonary filling. Scanning Microsc 1989;3:575–8.
46. Schraufnagel DE, Kay JM. Structural and pathological changes in the lung vasculature in chronic liver disease. Clin Chest Med 1996;17:1–15.
47. Virchow R. Über die Standpunkte in der Wissenschaftlichen Medizen. Virchows Arch [A] 1847;1:1–19.
48. Kelly SM, Taylor AE, Michel RP. Bronchial collateral vessel micropuncture pressure in postobstructive pulmonary vasculopathy. J Appl Physiol 1992;73:1914–24.
49. Schraufnagel DE, Tsao MS, Yao YT, Wang NS. Factors associated with pulmonary infarction: a discriminant analysis study. Am J Clin Pathol 1985;85:15–18.
50. Neuffeld G, Cohen T, Gengrinovitch S, Poltorak Z. Vascular endothelial growth factor (VEGF) and its receptors. FASEB J 1999;13:9–22.
51. English D, Brindley DN, Spiegel S, Garcia JG. Lipid mediators of angiogenesis and the signalling pathways they initiate. Biochim Biophys Acta 2002;1582:228–39.
52. Patan S, Alvarez MJ, Schittny JC, Burri PH. Intussusceptive microvascular growth: a common alternative to capillary sprouting. Arch Histol Cytol 1992;55:65–75.
53. Caduff JH, Fischer LC, Burri PH. Scanning electron microscope study of the developing microvasculature in the postnatal rat lung. Anat Record 1986;216:154–64.
54. Von Hayek H. The human lung. New York: Hafner; 1960.
55. Schraufnagel DE. Forms of lung lymphatics: a scanning electron microscopic study of casts. Anat Record 1992; 233:547–54.
56. Schraufnagel DE, Agaram NP, Faruqui A, et al. Pulmonary lymphatics and edema accumulation after brief lung injury. Am J Physiol Lung Cell Mol Physiol 2003;284:L891–7.
57. Havill AM, Gee MH. Role of interstitium in clearance of alveolar fluid in normal and injured lungs. J Appl Physiol 1984; 57:1–6.
58. Schraufnagel DE, Arzouman DA, Sekosan M, Ho YK. The effect of transforming growth factor alpha on airway angiogenesis. J Thorac Cardiovasc Surg 1992;104:1582–8.
59. Schraufnagel DE, Llopart Basterra J, Hainis K, Sznajder JI. Lung lymphatics increase after hyperoxic lung injury: an ultrastructural study of casts. Am J Pathol 1994;144:1393–402.

CHAPTER 17

VENTILATION–PERFUSION RELATIONSHIPS

Peter D. Wagner

STRUCTURAL AND FUNCTIONAL BASIS OF VENTILATION, PERFUSION, AND GAS EXCHANGE

The lung exists for gas exchange, that is, the transfer of oxygen from the air to the blood and carbon dioxide from the blood to the air. Its basic structural unit is the alveolus—a roughly polygonal gas-filled tissue "bubble" whose walls are filled with capillaries. The human lung contains some 300 million alveoli, and their diameters average about 300 μm. The strategy of dividing the lung up into a massive number of very small units keeps the total gas volume low enough for the lungs to fit inside the chest while at the same time creating an enormous interfacial surface area for exchange of oxygen and carbon dioxide between gas and blood.

To enable gas exchange, alveoli are supplied with both inspired gas via the airways and venous blood from the right side of the heart. The gas and blood must be kept in very close proximity to one another for gas exchange to occur, but they must still remain physically completely separated. Separation is accomplished via the blood–gas barrier—a thin (about 0.3 μm) layer of cells and supporting matrix. Oxygen and carbon dioxide exchange occurs by diffusion through the blood–gas barrier along partial pressure gradients between alveolar gas and capillary blood.

As a gas exchanger, the lung is the servant of the body tissues. Under steady-state conditions, the lungs absorb from the air exactly that amount of oxygen per minute needed to support tissue metabolism—no more and no less. This is true also for the elimination of carbon dioxide produced by metabolism. The first step in this process is ventilation, a process of sequential inhalation and exhalation of gas. During each inspiration, oxygen is inhaled from the air, at a concentration of about 21% (or partial pressure, PO_2, of about 150 mm Hg). Inhalation is accomplished by the fall in alveolar gas pressure to below atmospheric pressure following contraction of the diaphragm and chest wall muscles, which expand the thoracic cavity, thus reducing intrathoracic pressure. When intrathoracic pressure falls, so too does alveolar pressure. As alveolar pressure falls below atmospheric pressure, air flows from the environment along the airways to reach the alveoli, where it mixes with alveolar gas remaining from prior breaths. Because oxygen molecules move continually across the blood–gas barrier into the pulmonary capillary blood, the alveolar oxygen level from prior breaths is considerably lower than inspired. The freshly inhaled oxygen thus "tops up" the alveolar oxygen store, replacing the molecules that have moved into the blood. This process serves to stabilize the alveolar oxygen concentration over time at about 14%, or about 100 mm Hg.

An analogy would be adding 1 gallon of gasoline every 20 miles to the tank of a car that does 20 miles per gallon: the amount of gasoline in the tank will oscillate around 0.5 gallons about a constant level as long as topping up is continued. Each gallon added is the equivalent of each breath raising alveolar oxygen levels; continued driving depletes the fuel level at a steady rate, much as oxygen molecules constantly move into the blood to supply the cells of the body. If the fuel tank is large relative to the 1-gallon "tidal volume" of gasoline, the fuel level oscillations are relatively small, allowing a simple view of the tank as having an essentially constant amount of gasoline over time.

Since tidal volume is normally only about 500 mL, whereas functional residual capacity (FRC) is some 4,000 mL, the oscillations of oxygen about the mean are indeed very small. Thus, if average alveolar PO_2 is about 100 mm Hg, each inspiration raises this to about 102 mm Hg. During each expiration, it is obvious that no oxygen can move from the air to the alveoli, but oxygen still moves from the alveolar gas into the blood, reducing the alveolar PO_2 to about 98 mm Hg by the end of the exhalation. For most purposes, it is entirely satisfactory to consider the alveolar PO_2 to be constant over time, despite the tidal nature of breathing and the ± 2 mm Hg PO_2 oscillation.[1]

Once oxygen has moved across the blood–gas barrier into the pulmonary capillary blood, a process of passive diffusion,[2] almost all of it ($>98\%$) binds to hemoglobin in the red blood cells. The remainder is physically dissolved in the water of the plasma and red cells. These cells spend only about 0.75 seconds[3] in the pulmonary microcirculation taking on oxygen molecules. This period of time reflects the high rate of bloodflow through the pulmonary vascular bed (about 6 L/min) and the small capillary blood volume at any instant (about 75 mL). The ratio of capillary volume to

bloodflow [75 mL/(6 L/min)] is the average transit time, and this indeed comes to 0.75 seconds. In normal lungs at rest, the time required to fully load oxygen onto hemoglobin is only about 0.25 seconds,[4] and thus there is considerable reserve capacity in the "oxygen-diffusing capacity" of the lung. This is explained by the very large alveolar wall surface area through which the oxygen diffuses, some 80 m^2 in all, and the very short diffusion distance separating alveolar gas from capillary blood, both mentioned above.

The end result is that in normal lungs at rest, the PO_2 in the blood exiting the pulmonary capillary network is virtually equal to that of the alveolar gas (100 mm Hg) and diffusion equilibration is said to be complete. The PO_2 in the blood leaving the lungs is thus also about 100 mm Hg. Because of the shape of the oxygen–hemoglobin dissociation curve, essentially all oxygen-binding sites (98 of every 100) contain oxygen at this pressure of 100 mm Hg. In other words, the oxygen saturation of blood leaving the lungs is 98%.

Whereas the process of ventilation is "tidal," with sequential inspiration and expiration occurring through the same system of airways, bloodflow through the lung vasculature is unidirectional. Thus, the right ventricle pumps partially deoxygenated blood returned from the various body tissues through the pulmonary arterial tree to the capillary bed, where reoxygenation takes place as described. The oxygenated blood then is collected in the pulmonary veins, which forward the blood to the left heart for distribution to the tissues. What enables passive diffusion to accomplish the transfer of oxygen from alveolar gas into the blood is the fact that alveolar PO_2 is much higher (at 100 mm Hg) than the PO_2 of the blood returning from the tissues (normally about 40 mm Hg). The fall in PO_2 from 100 (arterial) to 40 mm Hg (venous) as blood traverses the body reflects the extraction of oxygen by each tissue to support its metabolic needs.

Figure 17-1 depicts the entire process in a homogeneous or "one-compartment" lung. The processes of ventilation, diffusion, and bloodflow are indicated, along with the normal oxygen and carbon dioxide partial pressures in alveolar gas and pulmonary arterial and venous blood.

The gas exchange process is intrinsically inefficient. Thus, exhaled alveolar gas has considerable oxygen in it (14% of expired gas is oxygen, equivalent to 100 mm Hg as mentioned), and inspired air contains 21% oxygen at 150 mm Hg. Thus, only about one-third of the inhaled oxygen is absorbed, and considerable ventilatory effort is therefore wasted (compared with a hypothetically perfectly efficient lung, in which all of the inhaled oxygen would be taken up). Similarly, since blood returning from the tissues still has a PO_2 of 40 mm Hg (which corresponds to an oxygen–hemoglobin saturation of about 75%), only about 25% of the oxygen in each red blood cell is transferred to the tissues to support metabolism. Considerable cardiac contractile effort is therefore wasted as well.

In addition, the process of diffusion appears overendowed, when we consider that the transit time, at 0.75 seconds, is three times as long as required. One could hypothetically survive the removal of two-thirds of the lung tissue and still have sufficient time for diffusion equilibration (at rest).

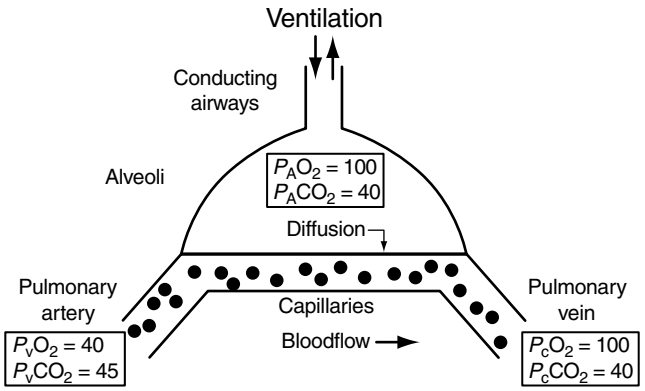

FIGURE 17-1 The principal structures involved in pulmonary gas exchange and their functions. Gas exchange is an integrated process involving ventilation, bloodflow, and diffusion.

There are reasons, however, why the body imposes these "taxes" on itself. First, maintaining alveolar PO_2 at 100 mm Hg is important because when the arterial blood reaches the various tissue beds, the unloading of oxygen is, as in the lung, a process of passive diffusion. This requires a high incoming PO_2 in the arterial blood to provide the diffusion gradient to the tissues. Thus, when arterial PO_2 is reduced, such as at altitude, exercise capacity is also reduced, in large part because of the reduction in the blood–tissue gradient of oxygen driving diffusion. Second, the reserve capacity in capillary transit time seen at rest reflects the need for greatly increased oxygen uptake during exercise. If the lungs were not "overbuilt" for resting conditions, little exercise could be accomplished because during exercise oxygen would not be able to be transferred from alveolar gas to capillary blood sufficiently quickly. Third, the low tissue extraction rate of 25% noted above also reflects the need to be able to extract more oxygen from each red cell during exercise to support much higher metabolic rates.

CHALLENGES TO GAS EXCHANGE CAUSED BY THE STRUCTURE OF THE LUNGS

In the section above, I pointed out intrinsic inefficiencies, seen at rest, based on the need to provide the body with sufficient oxygen when metabolic needs increase. However, the fact that the lung accomplishes gas exchange by a process dependent on ventilation, passive diffusion, and bloodflow has led to pulmonary structural characteristics that have considerable potential to interfere with gas exchange, even in the healthy lung. These potential problems are thus additional to those described above. That such interferences rarely seem to happen in health is remarkable. However, they collectively form the basis of why gas exchange can be so severely compromised in pulmonary disease (see Chapter 18, "Ventilation–Perfusion Distributions in Disease").

The potentially deleterious effects of lung structure on gas exchange include the following.

Lung Collapse: Pneumothorax

Because breathing is a tidal process, a mechanism is required for alternately inflating and deflating the lungs with each

breath. The left and right lungs lie in physically separate parts of the thoracic cavity. The intrapleural space between the surface of the lungs and the inner surface of the chest wall contains only a thin film of liquid. Since the lungs are elastic, they have a natural tendency to collapse away from the chest wall. The lungs are kept inflated and do not collapse, by virtue of the subatmospheric pressure in the intrapleural space. This pressure is below atmospheric because the lungs tend to collapse whereas the chest wall tends to spring out. These opposing tendencies create a stable state of lung inflation with a negative intrapleural pressure. If the integrity of the intrapleural space on either side of the chest is violated (as may happen in chest wall trauma or with spontaneous pneumothorax), the lung on that side will collapse like a punctured balloon. In such a situation, breathing efforts will be ineffectual, and thus the lung will remain unventilated, obviously compromising gas exchange, with potentially fatal consequences. The need for sequential inflation and deflation in a system where gas exchange occurs by diffusion through very thin alveolar–capillary membranes imposes constraints on lung structure that result in a delicate tissue framework susceptible to pneumothorax.

Dead Space

Because gas exchange occurs by passive diffusion, a very large alveolar surface area is needed in order for sufficient oxygen to reach the pulmonary capillaries. Suppose that the lung, with a volume (V) at FRC of 4,000 mL, were a single spherical large alveolus. Since volume is given by the formula $V = (4/3) \times x \times r^3$, the radius, r, would be about 10 cm. Since the surface area (A) of this sphere is given by the formula $A = 4 \times x \times r^2$, total surface area would be about 1,200 cm^2. Given the thickness (about 0.3 μm) of the blood–gas barrier, it was noted above that an area of about 80 m^2 is required to enable the rates of oxygen uptake required for heavy exercise. This is 800,000 cm^2. Thus, a single large alveolus would have more than 600-fold too small a surface area to support gas exchange during exercise.

From the above area and volume formulae, it should be apparent that the surface area/volume ratio of a sphere (A/V) increases as its diameter is reduced. Thus, to achieve a sufficient surface area for gas exchange within a 4 L total volume, the lung must be constructed not as a single sphere but rather as a parallel collection of many smaller "spheres"—the alveoli. It turns out that to have an 80 m^2 surface area with a 4 L total volume, about 300 million spheres of diameter about 300 μm would be needed.

The consequence of this requirement is the herculean task of ventilating each alveolus with relatively equal amounts of air on each breath. Much like a bunch of grapes on a branched stem, the alveoli (grapes) are connected to a branched system of conducting airways (stem). This tree-trunk-like system of airways has to branch some 23 times in order to supply such a large number of alveoli.

The total volume of these conducting airways is considerable, and it should be clear that all inhaled air must negotiate these airways before it reaches the alveoli where gas exchange takes place. Down to about the sixteenth branch point, the airways are constructed robustly only for delivery of air, and no oxygen crosses the thick walls of these first 16 branches to contribute to overall oxygen uptake. The total volume of these 16 generations of airways in the average person is about 150 mL[5] and is called the anatomic dead space.

Of every tidal breath taken, normally about 500 mL, only 350 mL of fresh air will reach the alveoli and take part in oxygen uptake. If there are 15 breaths/min, total ventilation will be 15×500 mL/min, or 7.5 L/min. However, alveolar ventilation (that amount of fresh air reaching the alveoli) is only $15 \times (500 - 150)$ mL/min, or 5.3 L/min. The normal dead space is thus about 30% of the tidal volume, and the ventilation associated with it (2.2 L/min in this example) is termed wasted ventilation.

One must ventilate some 40% more to achieve a given level of oxygen uptake than if there were no conducting airway system. This requirement may be problematic in patients with severe lung disease and is the basis for the use of transtracheal catheter administration of air or oxygen to patients with impaired ventilation. Direct insufflation of air into the trachea functionally eliminates that part of the anatomic dead space above the trachea (the larynx and oropharynx). This reduces the amount of ventilation needed to support a given metabolic rate.

Airway Infection/Inflammation

The progressive branching of the airways imposes not only dead space but also ever-narrowing and increasing numbers of airways with each generation (or branching). In the small bronchioles, because of their enormous number, the total cross-sectional area is so high that the linear velocity of gas becomes very low. This favors the settling out of large, inhaled particles (such as dust particles, bacteria, or viruses), which may adhere to the airway wall and initiate inflammation. Here, as elsewhere in the airways, edema and secretions can develop. In the small airways in particular, the lumen cross-section can then be significantly reduced, impairing distal alveolar ventilation.

Ventilation and Perfusion Inequality Resulting from Multiple Branching

Yet another intrinsic disadvantage of such a progressively branching airway system is that the dimensions of all members of each generation cannot be identical. Since these airways are arranged in parallel with one another, those airways that are for some reason longer and narrower than others will impose higher resistance to airflow, and thus there may be inequality in the distribution of ventilation to distal alveoli. This concept applies equally to the pulmonary vascular tree, which also branches progressively and will give rise to inequality in the distribution of alveolar bloodflow.

Dynamic Compression of the Airways

Yet another consequence of the branching airway system is that smaller peripheral airways (which lack cartilage in their walls), in particular, become susceptible to compression during exhalation. During quiet breathing at rest this does not occur, but during forceful exhalations, such as seen during

exercise, the resulting positive intrapleural pressure can compress these airways, resulting in limitation of airflow. This problem is known as dynamic compression. To the extent that this phenomenon occurs unevenly throughout the lung, as a result of both gravitational and nongravitational influences, it will add to the possibility of inequality of ventilation. In young healthy people, it is not of much concern. It is seen more with advancing age, as the elastic recoil of the lungs diminishes,[6] and is a hallmark of emphysema, where elastic recoil is greatly reduced. Reduced elastic recoil is a factor because dynamic compression is to some extent counteracted by outward radial traction imposed on airways by alveoli connected to them, and the strength of such radial traction depends on elastic recoil.

Alveolar Collapse

The alveolar epithelial surface is wet, as are all body tissues. Yet this surface, on the inside of each alveolus, is in direct contact with air. This creates a (roughly spherical) air–liquid interface, and surface tension must therefore exist. As with soap bubbles, such surface tension acts to reduce the surface area of the interface, so that alveoli are intrinsically prone to collapse. The law of LaPlace shows that the smaller the alveolar radius, the greater will be the tendency for collapse to occur because of this surface tension. Thus, having a great many small "bubbles" rather than fewer large ones may serve gas exchange well but puts the lungs at risk of collapse. Without special molecules that greatly reduce the surface tension of the alveolar lining fluid (surfactant), widespread lung collapse would occur. This is indeed seen clinically in premature infants, whose surfactant system is immature, and in acute lung injury at any age, when the surfactant system malfunctions.

Pulmonary Edema

The balance of hydrostatic and osmotic forces between the blood in the pulmonary capillaries and the fluid in the interstitium around them is such that there is a net force driving fluid out of the capillaries into the interstitium of the blood–gas barrier. Were this fluid to accumulate, the blood–gas barrier would thicken, and this would reduce the rate of diffusive equilibration for oxygen and carbon dioxide between the alveolar gas and capillary blood. It would also make affected alveolar walls stiffer and thus more difficult to inflate during inspiration. That such fluid does not normally accumulate is because of the pulmonary lymphatic system, which collects such fluid and facilitates its transport back into the systemic venous system along a lymph vessel tree that follows the airway branching pattern centrally and ends in the superior vena cava.

Lymphatic obstruction or overwhelming the system with high rates of fluid transudation does, in fact, cause pulmonary edema, and lung function can accordingly be impaired.

Capillary Integrity

Finally, the very delicate nature of the blood–gas barrier (about 0.3 μm thick) makes it vulnerable to disruption when stressed.[7] This can result from high intracapillary blood pressure (as happens frequently in race horses when they are galloping, for example[8]). It could also possibly result from excessive stretch of the alveolar wall (as happens during mechanical ventilation of ill patients when inflation pressures are excessive). Since the blood–gas barrier is predominantly formed of capillary walls (mated to alveolar epithelium), its disruption leads to local inflammation, edema, and, when severe, even frank hemorrhage of blood into the alveoli. Any of these effects may impair gas exchange.

It is remarkable that in the face of all these challenges, gas exchange proceeds as smoothly as it does, even in health. It is testament to the success of evolutionary countermeasures to these problems—phenomena such as making the alveoli support each other mechanically by being physically joined together; reducing surface tension by surfactant production; clearing inhaled particles by means of scavenger cells (macrophages) and the mucociliary airway clearance system; and a pulmonary microvasculature that keeps blood pressures low (when flow is increased) by mechanisms of recruitment and distention of blood vessels.

GRAVITATIONAL DETERMINANTS OF VENTILATION–PERFUSION DISTRIBUTION

As if these challenges were not enough, the presence of gravity imposes systematic gradients in the distribution of ventilation and bloodflow in the lung. These gradients are in the same direction but are unequal in magnitude. Thus, (1) both bloodflow and ventilation are generally higher in dependent than in nondependent regions, and (2) the inequality of bloodflow considerably exceeds that of ventilation. As a result, the ratio of ventilation to bloodflow, a critical determinant of gas exchange, is not uniform. In the upright lung, it is systematically higher at the apex than at the base.[9] The gradient in ventilation can be explained by the weight of the lung itself causing some "sagging" of the lung within the thorax. Thus, the nondependent alveoli will be more expanded than the dependent alveoli, much like a "slinky," or coiled spring, hanging under its own weight: the upper coils are further apart than the lower coils, due to its weight. This uneven expansion is considered in the context of the pressure–volume behavior of the lung. More expanded alveoli, further up the pressure–volume curve, are stiffer than less expanded alveoli. Thus, the larger, nondependent alveoli expand less with each breath and thus receive less ventilation than their dependent neighbors. As a result, the ventilation of alveoli near the bottom of the upright human lung is about twice the ventilation of alveoli near the top.

Gravity also explains the gradient in perfusion, wherein the bloodflow in alveoli at the bottom of the upright human lung is perhaps 10 times higher than at the top of the lung. This is explained in large part by the hydrostatic properties of a column of liquid and Ohm's law. Ohm's law states that flow will vary directly with pressure (assuming constant resistance). Since pulmonary artery pressure falls by 1 cm H_2O with each centimeter increase in height up the lung, because blood has a density of about 1 g/cm, bloodflow will fall with increasing height up the lung. This concept suffices for the general explanation of bloodflow variation with vertical

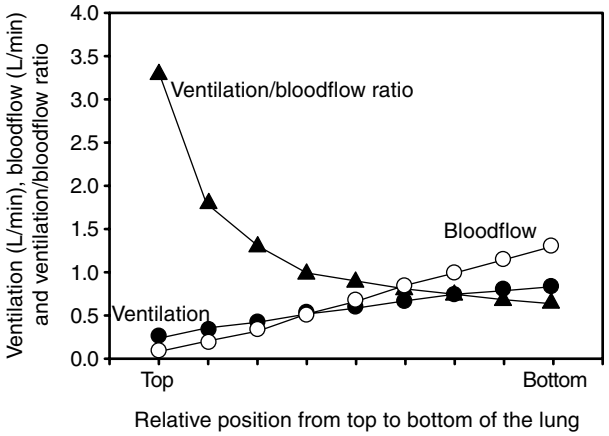

FIGURE 17-2 Data from West[9] showing the systematic changes in ventilation, bloodflow, and their ratio with distance up and down the upright human lung. Whereas ventilation and bloodflow are both lower at the top than the bottom, there is relatively more ventilation than bloodflow at the top and relatively more bloodflow than ventilation at the bottom. As a result, ventilation/perfusion ratios are higher at the top than at the bottom.

position throughout the lung, but the details are more complex because the blood vessels are exposed to alveolar gas pressure. Accordingly, as first described by West and Dollery,[10] lung perfusion is functionally described by relationships among three pressures: pulmonary arterial, pulmonary venous, and alveolar. In this way, three functional "zones" are defined. But from the operational point of view, one sees an essentially linear fall in bloodflow across zones from the bottom to the top of the upright lung.

Figure 17-2 shows this classic variation in ventilation, bloodflow, and the ratio between them with vertical distance, drawn from the data of West.[9] Figure 17-2 reminds us that the systematic variation in ventilation and bloodflow implies obligate variation in the *ratio* of ventilation ($\dot{V}_A$) to bloodflow ($\dot{Q}$) with vertical distance, also shown in Figure 17-2. This critical concept is discussed later.

NONGRAVITATIONAL DETERMINANTS OF $\dot{V}_A/\dot{Q}$ DISTRIBUTION

It has been known for almost 40 years that gravity is not the only factor responsible for uneven distribution of ventilation and bloodflow in the lungs. For example, ventilation and bloodflow fall off serially with distance along the airways, independently of gravity.[11] Variation in ventilation and bloodflow at a given horizontal level also occurs because of intrinsic anatomic variation in airway and vascular geometry, and there may also be random or even systematic differences in airway and vascular smooth muscle responses that further modify distribution. Furthermore, the repeated branching pattern of the airways and blood vessels gives rise to fractal behavior in distribution, such that spatial correlation of both ventilation and bloodflow occurs.[12] That is, there is clustering such that adjacent areas of the lung are generally more similar with regard to both ventilation and bloodflow than are distant areas. The degree of variation in both ventilation and bloodflow has been shown to be substantial, and it has been claimed that, as a result, nongravitational causes of both ventilation and perfusion inequality are more important than those based on gravity. If that were true, it would imply that whereas ventilation and bloodflow were each nonuniform, variations in each must correlate, such that the nonuniformity in their ratio (ventilation/perfusion ratio) is far less. This conclusion is based on the fact that the gravitational gradient in ventilation/perfusion ratios accounts for the majority of the normal alveolar–arterial PO_2 difference,[9] leaving very little that can be due to other, nongravitational causes.

PRINCIPLES OF PULMONARY GAS EXCHANGE

A central theme emerging from the preceding discussion is the importance of the ratio of ventilation to bloodflow (the ventilation/perfusion or $\dot{V}_A/\dot{Q}$ ratio) in determining gas exchange. This section provides the quantitative basis for this claim. It relies on a single, fundamental, yet simple principle: conservation of mass. The most well-known treatises on the subject can be found in the literature of the immediate post–World War II period. This is when Riley and Cournand[13] and Rahn and Fenn[14] separately laid out the principles of gas exchange, converting them into useful relationships that have given us our current understanding of how gas exchange takes place and what factors are involved.

The problem is approached by recognizing that oxygen is taken out of the respired air at a rate exactly equal to the rate of its uptake into the pulmonary capillary blood, so long as the lung exchange process is in a steady state. With this explicit assumption, we can write one equation depicting the removal of oxygen from respired gas and a second depicting its uptake into capillary blood, as follows:

$$\dot{V}O_2 = \dot{V}_I F_I O_2 - \dot{V}_A F_A O_2 \qquad (17\text{-}1)$$

$$\dot{V}O_2 = \dot{Q} C_a O_2 - \dot{Q}\ C_v O_2 \qquad (17\text{-}2)$$

In these two equations, $\dot{V}O_2$ represents the rate of oxygen uptake, which is equal to the body metabolic rate, $\dot{V}_I$ and $\dot{V}_A$ are, respectively, inspired and expired alveolar ventilation, and F_IO_2 and F_AO_2 are, respectively, inspired and expired fractional alveolar oxygen concentrations. Equation 17-1 thus states that the amount of oxygen taken out of respired air per minute is the amount inhaled per minute ($\dot{V}_I F_I O_2$) minus the amount exhaled ($\dot{V}_A F_A O_2$). Equation 17-2 is very similar but refers to the blood. Thus, $\dot{Q}$ is total pulmonary bloodflow (essentially equal to cardiac output), and C_aO_2 and C_vO_2 are, respectively, the oxygen concentrations in arterial and mixed venous blood. Here, oxygen taken into the blood is the difference between the rate at which oxygen leaves the lungs ($\dot{Q}\, C_aO_2$) and the rate at which it enters ($\dot{Q}\, C_vO_2$). Because of the steady-state assumption, the $\dot{V}O_2$ values in the two equations are identical.

Thus, Equations 17-1 and 17-2 can themselves be equated:

$$\dot{V}_I F_I O_2 - \dot{V}_A F_A O_2 = \dot{Q} C_a O_2 - \dot{Q} C_v O_2 \qquad (17\text{-}3)$$

If we assume for simplicity that $\dot{V}_I$ and $\dot{V}_A$ are numerically identical (and they normally differ by no more than 1%), we

can replace $\dot{V}_I$ with $\dot{V}_A$ and simplify Equation 17-3 as follows:

$$\dot{V}_A(F_IO_2 - F_AO_2) = \dot{Q}\ (C_aO_2 - C_vO_2) \qquad (17\text{-}4)$$

This can be rearranged, yielding:

$$\dot{V}_A/\dot{Q} = (C_aO_2 - C_vO_2)/(F_IO_2 - F_AO_2) \qquad (17\text{-}5)$$

It is more usual to convert the fractional concentrations F_IO_2 and F_AO_2 to their corresponding partial pressures P_IO_2 and P_AO_2 (using Dalton's Law of Partial Pressures), which simply involves a proportionality constant that we can call k, such that:

$$\dot{V}_A/\dot{Q} = k(C_aO_2 - C_vO_2)/(P_IO_2 - P_AO_2) \qquad (17\text{-}6)$$

Exactly the same reasoning leads to a similar equation for carbon dioxide:

$$\dot{V}_A/\dot{Q} = k(C_vCO_2 - C_aCO_2)/(P_ACO_2 - P_ICO_2) \qquad (17\text{-}7)$$

Both the numerator and denominator terms are reversed for carbon dioxide, simply reflecting the fact that whereas oxygen moves from air to blood, carbon dioxide moves from blood to air. In addition, P_ICO_2 is so low (air normally contains only 0.03% carbon dioxide) that it can be neglected.

Equations 17-6 and 17-7 describe the necessary quantitative relationships between $\dot{V}_A/\dot{Q}$ ratio and gas concentrations in the alveolar gas and capillary blood. It is critical to understanding these equations to realize that they contain both independent and dependent variables. Most commonly, we use Equation 17-6 to find, for given values of $\dot{V}_A/\dot{Q}$ ratio and of mixed venous and inspired oxygen levels (the independent variables), what the alveolar (and hence end-capillary) oxygen levels (the dependent variables) must be to satisfy the equation. The same applies for P_ACO_2 in Equation 17-7.

The answer is given in Figure 17-3. Here, the numerical solution to Equation 17-6 is presented for all possible values of $\dot{V}_A/\dot{Q}$, using normal values for inspired and mixed venous PO_2. The lowest possible $\dot{V}_A/\dot{Q}$ value is zero, corresponding to a perfused alveolus that has no ventilation (ie, a shunt). Such a unit exchanges no gas, and so the end-capillary blood leaving that unit has a PO_2 equal to that of mixed venous blood (40 Torr in this example). The highest possible $\dot{V}_A/\dot{Q}$ value is infinite, representing a ventilated alveolus without any bloodflow (called alveolar dead space). This unit also exchanges no gas, and thus the alveolar PO_2 equals that of the inspired gas (150 Torr in this case). Between these extremes, there is a smooth relationship where P_AO_2 increases nonlinearly with increasing $\dot{V}_A/\dot{Q}$ ratio as shown.

A major assumption in solving Equation 17-6 is that the alveolar and end-capillary PO_2 values are the same. This implies complete equilibration by diffusion for oxygen across the blood–gas barrier. A justification for this assumption, at least at rest, was provided earlier. Identical assumptions are used for carbon dioxide in solving Equation 17-7.

Figure 17-4 shows the solution to Equation 17-7 for carbon dioxide in a manner similar to Figure 17-3 for oxygen. Again, the extremes of $\dot{V}_A/\dot{Q}$ ratio produce PCO_2 values corresponding to that of mixed venous blood when the $\dot{V}_A/\dot{Q}$ ratio is zero and to that of inspired gas (essentially zero) when the $\dot{V}_A/\dot{Q}$ ratio is infinite, whereas between there is a smooth relationship, with PCO_2 falling as $\dot{V}_A/\dot{Q}$ is increased.

Equations 17-6 and 17-7 are very useful. Under the prevailing major assumptions (steady-state conditions and complete diffusion equilibration), they show that alveolar (and thus end-capillary) PO_2 and PCO_2 values are determined by three interacting factors. These are (1) the $\dot{V}_A/\dot{Q}$ ratio, (2) the so-called "boundary" conditions—mixed venous and inspired oxygen and carbon dioxide levels, and (3) the oxygen–hemoglobin and carbon dioxide dissociation curves because they determine the relationships between oxygen and carbon dioxide concentrations (numerator of Equations 17-6 and 17-7) and partial pressures (denominator of Equations 17-6 and 17-7). Alterations in any one of these three factors thus have the potential to affect alveolar and hence arterial PO_2. Figures 17-3 and 17-4 showed how the first of these three ($\dot{V}_A/\dot{Q}$ ratio) affects PO_2 and PCO_2. Figure 17-5 shows how changes in mixed venous PO_2 and

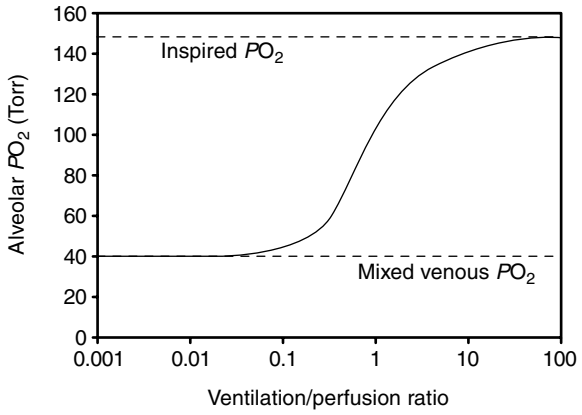

FIGURE 17-3 Dependence of alveolar PO_2 on ventilation/perfusion ($\dot{V}_A/\dot{Q}$) ratio. At low $\dot{V}_A/\dot{Q}$, alveolar PO_2 is close to mixed venous PO_2; at high $\dot{V}_A/\dot{Q}$, it is close to inspired PO_2. Alveolar PO_2 is most sensitive to $\dot{V}_A/\dot{Q}$ in the normal range ($\dot{V}_A/\dot{Q}$ of about 1).

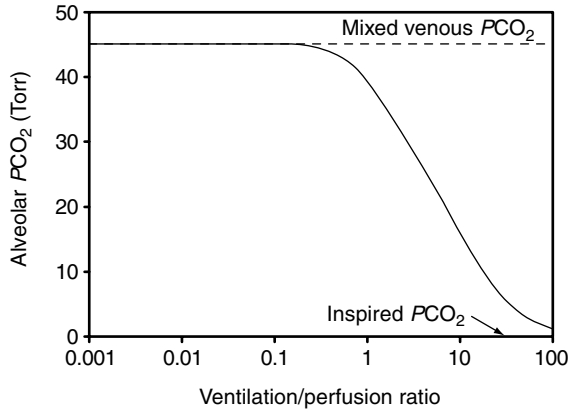

FIGURE 17-4 Dependence of alveolar PCO_2 on ventilation/perfusion ($\dot{V}_A/\dot{Q}$) ratio. At low $\dot{V}_A/\dot{Q}$, alveolar PCO_2 is close to mixed venous PCO_2; at high $\dot{V}_A/\dot{Q}$, it is close to inspired PCO_2. Alveolar PO_2 is most sensitive to $\dot{V}_A/\dot{Q}$ in the above-normal range ($\dot{V}_A/\dot{Q}$ of about 1 to 10).

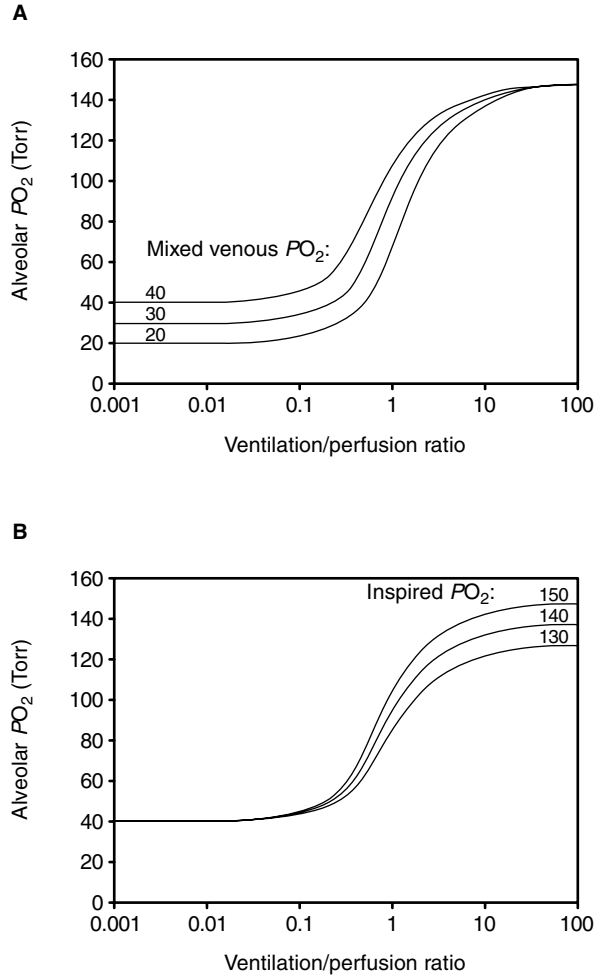

FIGURE 17-5 Relationship of alveolar PO_2 to $\dot{V}_A/\dot{Q}$ depends on both mixed venous PO_2 (*A*) and inspired PO_2 (*B*). In particular, PO_2 in areas of low $\dot{V}_A/\dot{Q}$ reflects mixed venous PO_2, whereas areas of high $\dot{V}_A/\dot{Q}$ reflect inspired PO_2.

inspired PO_2 affect PO_2. A fall in mixed venous PO_2 reduces alveolar PO_2 in all alveoli, but much more so in alveoli whose $\dot{V}_A/\dot{Q}$ ratio is low. Such units have their PO_2 "tied to" that of mixed venous blood, as shown. Correspondingly, a fall in inspired PO_2 also reduces alveolar PO_2, but more so when $\dot{V}_A/\dot{Q}$ ratio is high. The curve for carbon dioxide behaves correspondingly when venous or inspired PCO_2 is changed. Figure 17-6 shows how changes in the PO_2 corresponding to hemoglobin oxygen saturation of 50% (P_{50}) affect alveolar PO_2 when mixed venous and inspired PO_2 are maintained at normal values. Thus, a fall in P_{50} leads to a higher alveolar PO_2 at any $\dot{V}_A/\dot{Q}$ ratio, and vice versa. The effects are clearly greatest in the normal range of $\dot{V}_A/\dot{Q}$ and are negligible when $\dot{V}_A/\dot{Q}$ is either very low or very high.

Solving Equations 17-6 and 17-7 by hand or graphically, as done originally,[14] is very laborious, due mostly to the nonlinear and interdependent nature of the oxygen and carbon dioxide dissociation curves. Today, these equations are easily solved by computer, and the necessary algorithms are well established[15,16] and available.

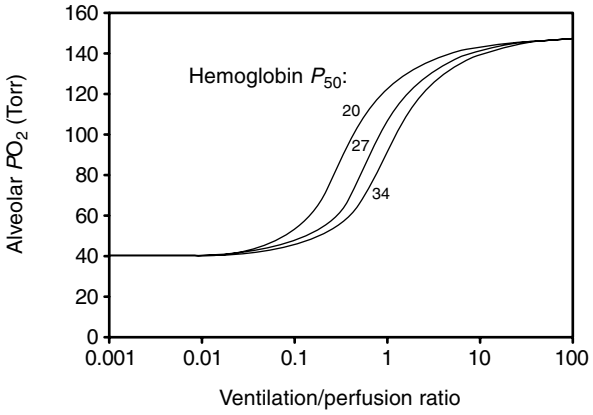

FIGURE 17-6 Dependence of alveolar PO_2 on hemoglobin P_{50}. As P_{50} varies, alveolar PO_2 changes (at given mixed venous and inspired PO_2). Changes in P_{50} affect alveolar PO_2 mostly in the normal range of $\dot{V}_A/\dot{Q}$, around 1.

GAS EXCHANGE IN THE PERFECTLY HOMOGENEOUS LUNG

To apply these concepts to the lungs, it is useful to begin with an ideal lung that is completely homogeneous. Even though the lungs of young healthy subjects contain $\dot{V}_A/\dot{Q}$ inequality from several sources, as discussed above, the degree of inequality normally present has very little detrimental effect on arterial PO_2 and PCO_2. Commonly, arterial PO_2 is only about 5 to 10 Torr below alveolar PO_2; this has negligible effects on arterial oxygen saturation and concentration and no measurable effect on arterial PCO_2. Thus, the normal lung is not far from being homogeneous in terms of overall gas exchange, and the following analysis therefore can be used with little error.

Once again, it is the concept of which variables in the system are independent and which are dependent that should first be considered when applying Equations 17-1 through 17-7. Restating Equations 17-1 and 17-2, we have:

$$\dot{V}O_2 = \dot{V}_I F_I O_2 - \dot{V}_A F_A O_2 = k\dot{V}_A(P_I O_2 - P_A O_2) \quad (17\text{-}8)$$

(remember that taking $\dot{V}_I = \dot{V}_A$ is reasonable; k converts fractional concentration F to partial pressure P) and

$$\dot{V}O_2 = \dot{Q}(C_a O_2 - C_v O_2) \quad (17\text{-}9)$$

When considering Equation 17-8, recall that the lung remains the "servant of the body," such that the body, not the lung, sets $\dot{V}O_2$ as an independent variable in the current context. Likewise, $P_I O_2$ is set by the environmental conditions, and $\dot{V}_A$ is determined by the integrated respiratory control system and mechanical properties of the lungs and chest wall. Thus, the single dependent variable is alveolar PO_2 ($P_A O_2$). What Equation 17-8 tells us is as follows: given the $\dot{V}O_2$, $P_I O_2$, and amount of alveolar ventilation ($\dot{V}_A$), the alveolar PO_2 takes a unique, dependent value that must satisfy Equation 17-8. These are the only determinants of alveolar PO_2 in a homogeneous lung.

Let us now proceed to Equation 17-9. The same value of $\dot{V}O_2$ must exist as for Equation 17-8. Total pulmonary blood-flow will also be determined, like ventilation, by complex

control systems external to the lungs. Given that alveolar and end-capillary (here = arterial) PO_2 are equal in this homogeneous lung, arterial oxygen concentration (C_aO_2) must be that value read off the oxygen–hemoglobin dissociation curve for the value of alveolar PO_2 determined from Equation 17-8. Hence, the remaining unknown, mixed venous oxygen concentration must be that value that satisfies Equation 17-9.

In sum, Equation 17-8 shows that it is only metabolic rate, ventilation, and inspired PO_2 that together influence arterial PO_2 when the lungs are completely homogeneous. Cardiac output does not influence arterial PO_2 under such circumstances but does affect mixed venous PO_2. Again, these conclusions pertain only to steady-state conditions and when there is complete diffusion equilibration across the blood–gas barrier. Although this is strictly true only for a homogeneous lung, these conclusions are also approximately correct for the normal human lung, as discussed above.

When this approach is taken, and as can be inferred from Figures 17-3 and 17-4, we can see that normal arterial PO_2 is about 100 Torr, and arterial PCO_2 is about 40 Torr. This is based on (1) alveolar ventilation at 5 to 6 L/min and cardiac output at 5 to 6 L/min, such that overall $\dot{V}_A/\dot{Q}$ ratio is close to 1, and (2) a metabolic rate resulting in a $\dot{V}O_2$ of 300 mL/min and a $\dot{V}CO_2$ of 240 mL/min.

GAS EXCHANGE IN THE PRESENCE OF $\dot{V}_A/\dot{Q}$ INEQUALITY

$\dot{V}_A/\dot{Q}$ inequality is defined as the state wherein not all alveoli enjoy the same $\dot{V}_A/\dot{Q}$ ratio. However, all of the principles laid out in Equations 17-1 to 17-7 apply when $\dot{V}_A/\dot{Q}$ inequality develops, just as in the homogeneous lung. In the presence of $\dot{V}_A/\dot{Q}$ inequality, these equations can be applied in turn to each different $\dot{V}_A/\dot{Q}$ ratio unit in the lung. The performance of the whole lung is then found simply by summing the contributions from each unit. In reality, there are (as stated earlier) some 300 million alveoli in the lungs. However, due to their small size and anatomic proximity to each other, it is thought that many adjacent alveoli together form a functional unit of gas exchange. Evidence points to the acinus (all alveoli distal to the last terminal bronchiole) as the anatomic basis of a functional unit,[17] and there are about 100,000 such acini in the lung, consistent with about 17 generations[18] of dichotomously branching airways up to the last terminal bronchiole ($2^{17} = 131{,}072$). Although this number is very much lower than 300 million, it is still far too high to deal with experimentally. Since each unit is characterized by two independent variables (ventilation and bloodflow), it would take some 260,000 measurements to fully describe the functional $\dot{V}_A/\dot{Q}$ distribution! We have neither the technology nor the resources to do this, and thankfully it turns out not to be necessary to understand $\dot{V}_A/\dot{Q}$ inequality in the lung. In fact, the simplest model of inequality, the two-compartment model, is quite adequate for illustration of how $\dot{V}_A/\dot{Q}$ inequality affects gas exchange. I show this below.

To work through this more difficult analysis, it is most instructive to use particular examples. It is easiest to start from the homogeneous lung and then use the above equations to determine how a two-compartment model with a defined degree of $\dot{V}_A/\dot{Q}$ mismatch affects gas exchange. What will be found is that $\dot{V}_A/\dot{Q}$ inequality causes hypoxemia, hypercapnia, and reductions in the rates of both oxygen uptake and carbon dioxide elimination. Such a result is not compatible with life in the long term because the lung cannot supply enough oxygen for the metabolic needs of the body or keep up with the associated rate of carbon dioxide elimination. Usually, the body employs one or more compensatory mechanisms (discussed below), which can return $\dot{V}O_2$ and $\dot{V}CO_2$ to levels matching the tissue metabolic rate. However, sometimes this does not happen. And, occasionally, the degree of inequality may be too severe for available compensatory mechanisms to cope with. In either case, death will ensue.

I will begin with a homogeneous lung, using values for the variables that correspond to those of a typical normal resting adult breathing air at sea level. I will stipulate the following independent variables: $F_IO_2 = 0.21$; $F_ICO_2 = 0$; barometric pressure = 760 Torr; $\dot{V}O_2 = 300$ mL/min; $\dot{V}CO_2 = 240$ mL/min; alveolar ventilation = 5.2 L/min; cardiac output = 6.0 L/min. Additional secondary information required includes hemoglobin concentration (taken to be normal, 15 g/dL), hemoglobin P_{50} (normal at 27 Torr), and acid–base status, which will also be taken to be normal. That is, there is no metabolic acidosis or alkalosis.

Applying first Equations 17-1 and 17-2 for oxygen and using the corresponding approach simultaneously for carbon dioxide, we find that, for the given $\dot{V}_A/\dot{Q}$ ratio of 5.2/6.0, or 0.87, $P_AO_2 = 100$ Torr and $P_ACO_2 = 40$ Torr. This is compatible with Figures 17-3 and 17-4. Mixed venous PO_2 is about 40 Torr, and mixed venous PCO_2 is 46 Torr. These unique values (here rounded to the nearest integer) fit the equations and allow for the requisite $\dot{V}O_2$ and $\dot{V}CO_2$ specified above.

Figure 17-7 shows these results in diagrammatic form, where the lung is drawn as two "alveoli" that are equally perfused and equally ventilated. Thus, although two "alveoli" are drawn, they have the same $\dot{V}_A/\dot{Q}$ ratio, and thus the system is really a homogeneous lung. The "trachea" is represented by the single vertical line at the top of the figure. It divides into two "bronchi" that connect the "trachea" to the two circular "alveoli." Beneath each alveolus is its vasculature, drawn as a curved "vessel" on each side that touches its alveolus, forming the "blood–gas barrier" at the points of contact. Blood flows from the outside inwards for each "alveolus," and the two "blood vessels" join at the foot of the figure to form the "left atrial" and hence "systemic arterial" bloodstreams.

Suppose we now suddenly create severe airway obstruction in the "bronchus" of the left-hand "alveolus." This could, in fact, happen, for example, from inhalation of a foreign body into a main bronchus, and is depicted in Figure 17-8. If we analyze the effects of this inequality, assuming first that the mixed venous blood oxygen and carbon dioxide levels remain normal, the results are as shown in Figure 17-8A. The large black dot indicates the obstruction, which has reduced ventilation on the left side from 2.6 to just

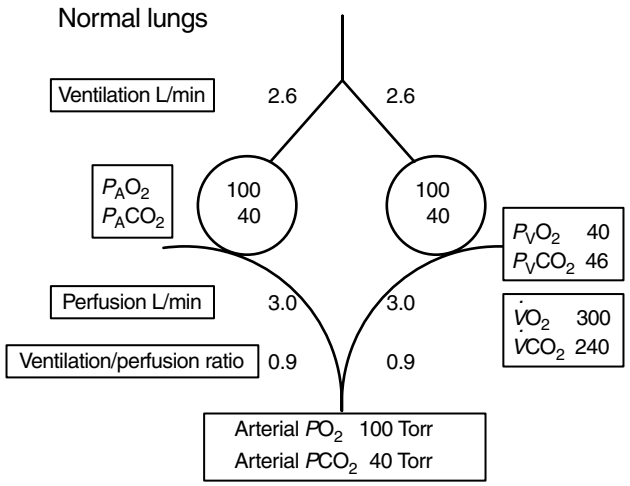

FIGURE 17-7 Gas exchange function in a homogeneous lung that is normally perfused and ventilated. Arterial PO_2 and PCO_2 are 100 and 40 Torr, respectively, and the lung is able to take up the normal amount of oxygen (300 mL/min) and eliminate the normal amount of carbon dioxide (240 mL/min). These results all come from solving the mass conservation equations (Equations 17-1 and 17-2 for oxygen and the corresponding equations for carbon dioxide).

0.3 L/min. As a result, the rest of the ventilation is diverted to the right side, keeping total ventilation constant. In reality, both ventilation and mixed venous gas levels would change, as too may cardiac output, and these changes are discussed below. However, to understand the effects of $\dot{V}_A/\dot{Q}$ inequality on gas exchange, we will first assume no changes in any of these variables.

The redistribution of ventilation gives rise to two different $\dot{V}_A/\dot{Q}$ ratios, as Figure 17-8 shows: 0.1 on the left and 1.6 on the right. Since overall ventilation and bloodflow are unchanged, the overall $\dot{V}_A/\dot{Q}$ ratio remains at 5.2/6.0, or 0.87. Note that the $\dot{V}_A/\dot{Q}$ ratio of the left side is lower, and that of the right side is higher, than this overall value. At first sight, one might think that, for this reason, the two would offset one another, and overall gas exchange would be unaffected. This is not the case, as the following analysis demonstrates.

When Equations 17-1 and 17-2 are applied separately to both "alveoli," the resulting alveolar PO_2 values are, as shown, 47 and 119 Torr (see Figure 17-3). Similar calculations for carbon dioxide reveal that alveolar PCO_2 values are 46 and 35 Torr, respectively (see Figure 17-4). The bloodflow remains equally distributed between the alveoli (3 L/min each), and so the mixed arterial blood is a 50:50 mixture of the bloodstreams from the two alveoli. Because the oxygen dissociation curve is so nonlinear, this mixture does not produce a PO_2 halfway between the two alveolar PO_2 values of 47 and 119 (which would be 83) but gives rise to a much lower PO_2, 58 Torr.

Similar calculations for carbon dioxide give a rather different result: because the carbon dioxide dissociation curve is nearly linear, the PCO_2 of mixed arterial blood is essentially the average of the two alveolar PCO_2 values, at 41 Torr. Although this is a small absolute increase from normal (of only about 1 Torr), even a 1-Torr increase is a significant percentage (about 20%) of the mixed venous–arterial PCO_2 difference, suggesting that carbon dioxide elimination is indeed compromised, even though the change in arterial PCO_2 seems trivial.

Thus, in this particular model, where the primary lesion corresponds to areas of greatly reduced $\dot{V}_A/\dot{Q}$ ratio, the effects on arterial PO_2 are shown to be far greater than those on arterial PCO_2. These results also imply that total oxygen uptake must have been reduced (same mixed venous PO_2 but lower than normal arterial PO_2), and Figure 17-8A indicates this, with $\dot{V}O_2$ falling from its normal value of 300 mL/min (Figure 17-7) to 200 mL/min, a 33% reduction. There is also a reduction in carbon dioxide elimination as implied above, from 240 mL/min in the normal lung to 210 mL/min here, but the interference is less than for oxygen, a reduction of only 13%.

The next step in the analysis is to determine the effect of this hypoxic and (slightly) hypercapnic blood on oxygen transport to (and carbon dioxide transport from) the peripheral tissues. Since tissue metabolic rate continues unchanged, the tissues will attempt to extract sufficient oxygen from the blood for their metabolic needs. Extracting the same amount of oxygen from arterial blood with a lower PO_2 must result in a fall in venous PO_2 draining the tissues. This must cause a fall in mixed venous PO_2 in the pulmonary artery. Returning to Figure 17-5A, it becomes clear that this fall in mixed venous PO_2 must reduce alveolar PO_2, especially in the low-$\dot{V}_A/\dot{Q}$ "alveolus," which will further lower systemic arterial PO_2 as well. However, this strategy does enable restoration of $\dot{V}O_2$ to normal. Figure 17-8B shows the result of this process, and it can be seen that $\dot{V}O_2$ is indeed restored to 300 mL/min, but the penalty is a fall in both mixed venous and arterial PO_2 (to 33 and 48 Torr, respectively). In a similar manner, because arterial PCO_2 was increased by $\dot{V}_A/\dot{Q}$ inequality, adding all the metabolically produced carbon dioxide to tissue blood raises mixed venous PCO_2, which will lead to a further increase in arterial PCO_2. Arterial PCO_2 is now 45 Torr, up from 41 Torr. However, as for oxygen, the lungs are again able to eliminate all of the carbon dioxide produced (240 mL/min). Figure 17-8B shows this as well.

We thus have what at first sight appears to be a paradox: overall lung function (ie, $\dot{V}O_2$ and $\dot{V}CO_2$) has been restored, but the hypoxemia and hypercapnia are both worse than before the changes in venous PO_2 and PCO_2 that allowed $\dot{V}O_2$ and $\dot{V}CO_2$ to be normalized. Actually, this is typical of other functional systems in the body and is not a paradox. For example, in stable chronic renal failure, the total amount of urea excreted in the urine per unit time exactly matches tissue urea production, but this can happen only in the case of a higher than normal blood urea level when some nephrons are diseased and functionally compromised.

To this point, the body tissues have been protected ($\dot{V}O_2$ and $\dot{V}CO_2$ normalized), but hypoxemia and hypercapnia are both significant. The next likely response is therefore an increase in ventilation resulting from chemoreceptor activation in response to the low PO_2 and high PCO_2. Figure 17-8C shows that if the normal (right-hand) alveolus has its ventilation increased by just 0.6 L/min (ie, by just 12%), arterial PCO_2 is returned to the normal value of 40 Torr, even if the

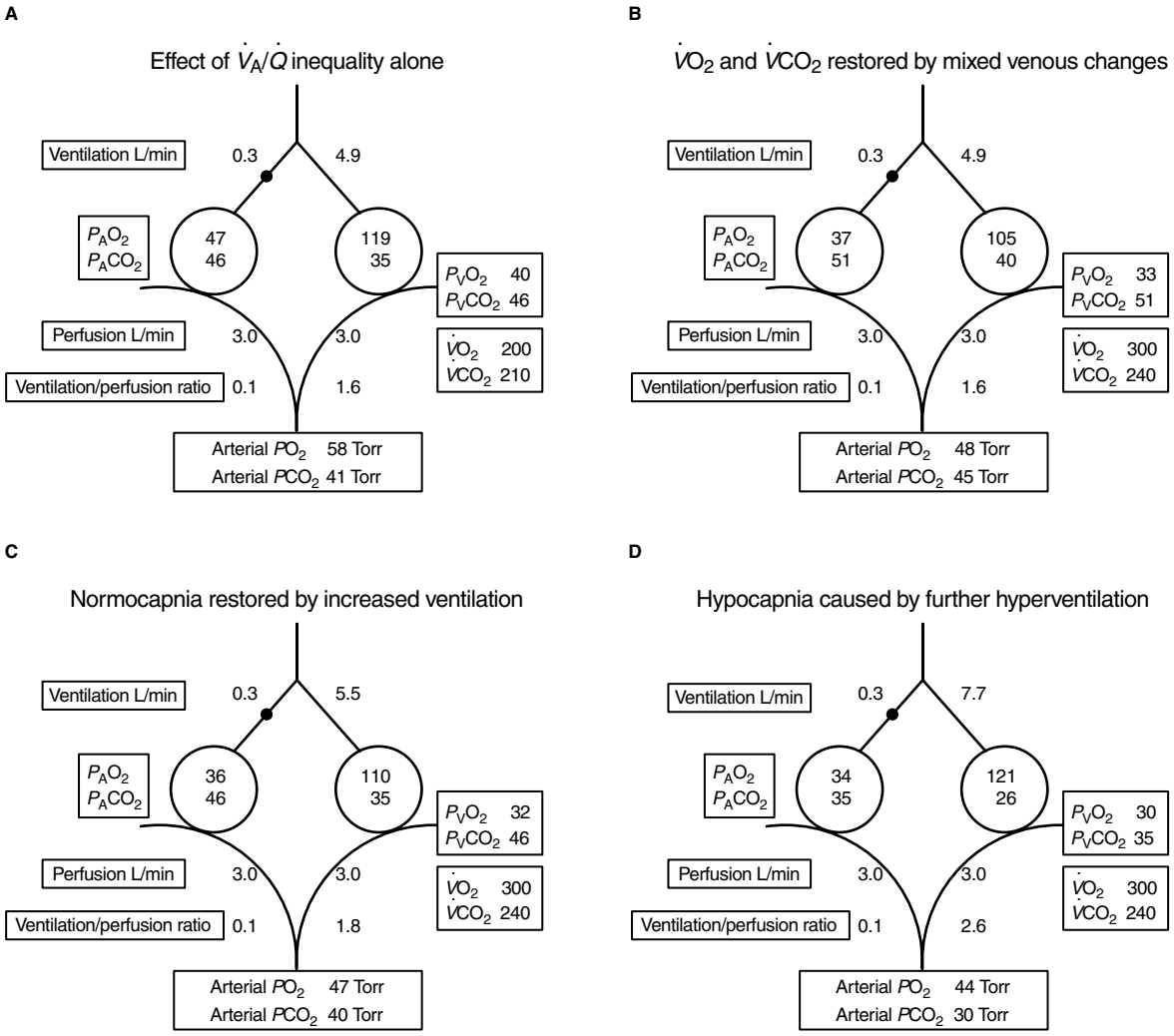

FIGURE 17-8 Effect on gas exchange of severe unilateral airway obstruction causing inequality of ventilation distribution. *A*, Without change in total ventilation, bloodflow, or inspired/mixed venous composition, there is moderate hypoxemia, slight hypercapnia, and diminished oxygen uptake and carbon dioxide elimination. *B*, There will be an immediate fall in mixed venous PO_2 and rise in PCO_2. This allows normalization of $\dot{V}O_2$ and $\dot{V}CO_2$, but at a cost of further hypoxemia and hypercapnia. *C*, Hypercapnia and hypoxemia will stimulate respiration, normalizing arterial PCO_2. Hypoxemia is not corrected, however. *D*, With arterial PO_2 still low after ventilation has increased, there may be a further increase in ventilation, now leading to hypocapnia but still not alleviating hypoxemia.

obstruction on the left side is unaltered. This is a trivial increase in ventilation, and thus in respiratory effort, and normally will take place rapidly. However, note that this increase in ventilation has no significant effect on arterial PO_2, as Figure 17-8 indicates. Improving alveolar PO_2 on the right side increases oxygen concentration in the blood negligibly because the oxygen dissociation curve is flat in this region. PO_2 on the left side is essentially unchanged because there has been no relief of the airway obstruction. Thus, there is little effect on arterial PO_2. In fact, PO_2 in this example has actually fallen (even if by only 1 Torr), despite the increase in ventilation. This is explained by the Bohr effect of carbon dioxide on the oxygen dissociation curve. In this particular model, further increases in ventilation on the right side are futile. Even reducing arterial PCO_2 to 30 Torr by increasing ventilation on the right side to 7.7 L/min (Figure 17-8D) fails to improve arterial PO_2. The patient can survive the obstruction in terms of overall gas exchange and can overcome the initial hypercapnia quite easily. However, hypoxemia remains severe and refractory to increases in ventilation.

It is very instructive to contrast the behavior of this particular model (severe airway obstruction) with its symmetric counterpart of severe vascular obstruction, as might occur as a result of pulmonary thromboembolism. Figure 17-9 shows such a two-compartment model, with the same overall ventilation and cardiac output as in the normal lung. In this case, bloodflow on the left-hand side is impaired, essentially as severely as was ventilation in the prior model of airway obstruction (see Figure 17-8). We can apply exactly the same principles to calculate how oxygen and carbon dioxide exchange will be affected, using the relationships in Figures 17-3 and 17-4 and the particular values for $\dot{V}_A/\dot{Q}$ shown in Figure 17-9A. At this point, the assumption of unchanged mixed venous PO_2 and PCO_2 will again be made, as in Figure 17-8A. Note again that in this example,

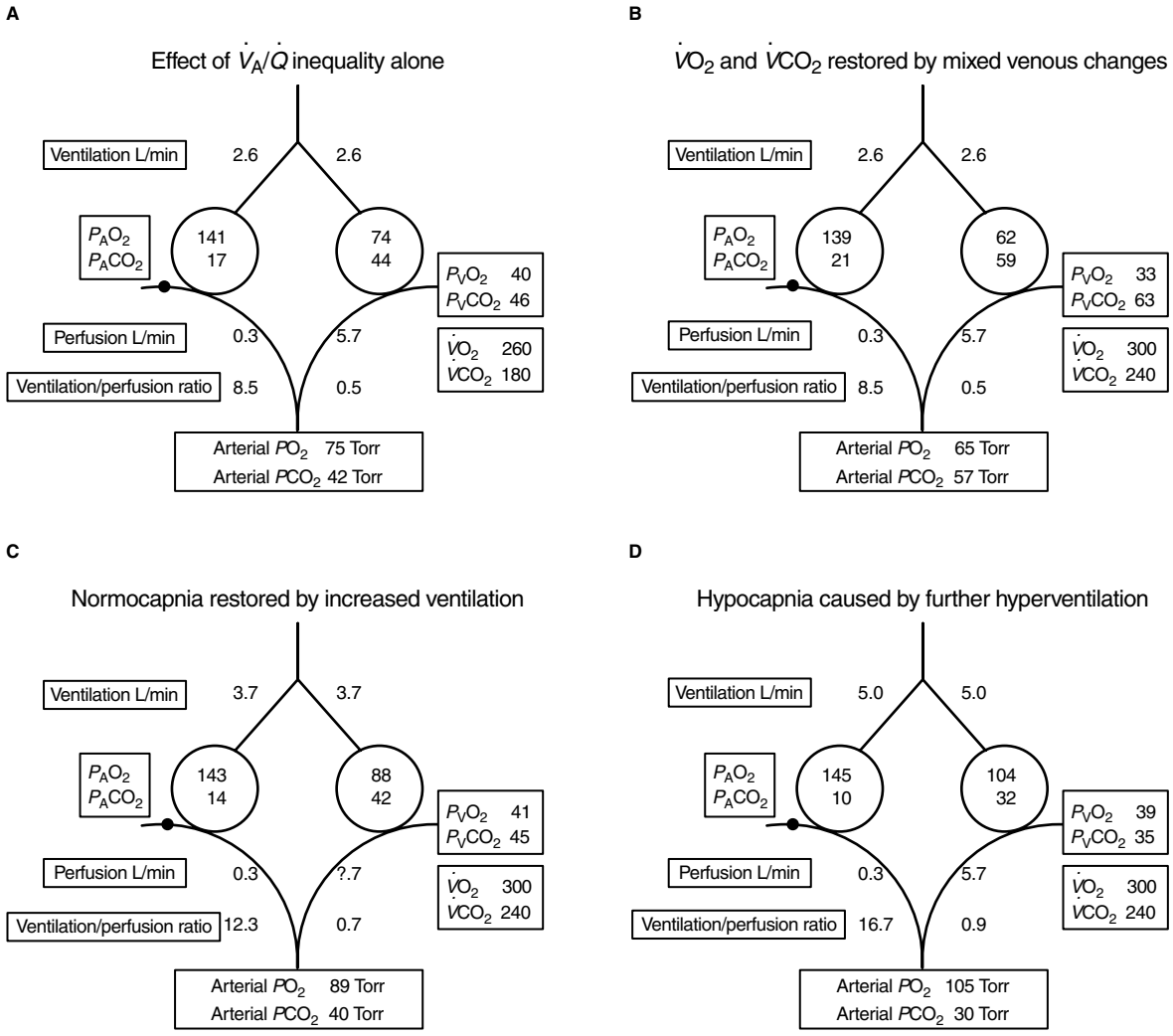

FIGURE 17-9 Effect on gas exchange of severe unilateral vascular obstruction causing inequality of bloodflow distribution. *A*, Without change in total ventilation, bloodflow, or inspired/mixed venous composition, there is mild hypoxemia, slightly more hypercapnia than in the airway obstruction model, and diminished oxygen uptake and carbon dioxide elimination. In this model, the effects on carbon dioxide are more prominent than for airway obstruction. *B*, As in Figure 17-8, there will be an immediate fall in mixed venous PO_2 and a rise in PCO_2. This normalizes $\dot{V}O_2$ and $\dot{V}CO_2$, but at the cost of further hypoxemia and, especially, hypercapnia. *C*, Hypercapnia (in particular) and hypoxemia will stimulate respiration, which normalizes arterial PCO_2. Hypoxemia is essentially corrected. *D*, Any further increase in ventilation, were it to occur, would be able to raise arterial PO_2 above normal.

one side has a $\dot{V}_A/\dot{Q}$ ratio lower than normal, and the other has a $\dot{V}_A/\dot{Q}$ ratio higher than normal—just as for the airway obstruction model. The different values result in different numbers, and in this case, whereas arterial PO_2 has been less affected than in the case of airway obstruction, arterial PCO_2 has increased twice as much as in the prior model—by 2 Torr. $\dot{V}O_2$ has fallen from 300 mL/min to 260 mL/min, a reduction of only 13%, whereas $\dot{V}CO_2$ has fallen from 240 to 180 mL/min, or by 25%. Thus, carbon dioxide has been affected more than oxygen in this analog of pulmonary embolism.

As with the prior model, the tissues will extract the necessary oxygen from the venous blood and add all of the carbon dioxide produced, causing venous PO_2 to fall and PCO_2 to rise. As before, this will cause arterial PO_2 to fall further and PCO_2 to rise further, but this will again allow normalization of $\dot{V}O_2$ and $\dot{V}CO_2$, as shown in Figure 17-9B. Note here that arterial hypercapnia is severe, whereas hypoxemia is relatively mild, consistent with the greater effects of such a $\dot{V}_A/\dot{Q}$ pattern on carbon dioxide than on oxygen.

Stimulation of the chemoreceptors will thus occur and lead to an increase in ventilation. Figure 17-9C shows that a small increase in ventilation of just over 2 L/min (from 5.2 to 7.4 L/min) will suffice to completely normalize arterial PCO_2. In stark contrast to the airway obstruction model, in which half the lung (in terms of bloodflow) could not be ventilated and was very hypoxic, almost all of the lung (again in terms of bloodflow) is well ventilated. Thus, arterial PO_2 is essentially normalized (to 89 Torr) by this modest level of increased ventilation. In fact, a small further increase in ventilation to just 10 L/min would produce an above-normal arterial PO_2 of over 100 Torr (Figure 17-9D), along with an arterial PCO_2 of 30 Torr.

These two models illustrate the spectrum of gas exchange disturbances. They show that, based on straightforward principles of mass balance, it is possible to understand how

$\dot{V}_A/\dot{Q}$ inequality affects the ability of the lungs to exchange the required amounts of oxygen and carbon dioxide and the penalties that must be paid in terms of arterial blood gas aberrations to achieve this. They also illustrate the important concept that the degree to which oxygen and carbon dioxide are differently affected by $\dot{V}_A/\dot{Q}$ inequality depends on the pattern of that inequality.

METHODS FOR QUANTIFYING GAS EXCHANGE ABNORMALITIES

To this point, the focus has been on understanding how gas exchange takes place and how $\dot{V}_A/\dot{Q}$ inequality perturbs gas exchange. This is necessary for learning about the process, but simply understanding the concepts is not sufficient when one wishes to approach altered gas exchange in patients with lung disease. Accordingly, much work over the last half century has dealt with attempts to measure altered gas exchange and abnormal ventilation–perfusion relationships in particular. The most common approaches are now described, in order of increasing complexity.

Arterial PO_2, Arterial PCO_2, and the P_aO_2/F_IO_2 Ratio

The simplest parameters of gas exchange are the arterial PO_2 and PCO_2 themselves. Normal values have been established by sampling arterial blood from large numbers of normal subjects.[19–21] The results are consistent with all of the above theory. Arterial PO_2 is normally greater than 90 Torr (at sea level), and arterial PCO_2 is normally 40 Torr (also at sea level). There is variability in both PO_2 and PCO_2. This is due to both biologic and instrumental variance. A common cause of biologic variance is hyperventilation during the sampling procedure as a result of the anxiety-provoking arterial puncture itself. Reasonable values for total variance with well-functioning blood gas electrodes are about 3 to 5 Torr (1 SD) for PO_2 and 1 to 2 Torr for PCO_2.

Both arterial PO_2 and PCO_2 fall with altitude,[22] due to the reduction in inspired PO_2 and its concomitant effect of increasing ventilation. Thus, the altitude at which blood is sampled is important for interpretation of the data. Another factor is age since PO_2 falls gradually (if slightly) with age. The changes in healthy nonsmokers are small, and octogenarians typically have a PO_2 in the range of 80 to 85 Torr.[19–21] PCO_2, on the other hand, appears to remain constant with age.

Measuring arterial PO_2 and PCO_2 is simple and is very commonly done, but these variables represent the entire integrated result of all gas exchange processes in the lung ($\dot{V}_A/\dot{Q}$ relationships, shunting, diffusion limitation) and the above-mentioned compensatory responses in mixed venous blood, in ventilation, and in cardiac output. Thus, the information obtained, although clinically very useful, is limited in terms of the insights provided into the alterations in physiology.

In situations where inspired oxygen levels may vary, such as in the intensive care unit, an extensively used alternative to the direct use of arterial PO_2 is the ratio of arterial to inspired PO_2 (or arterial PO_2 to F_IO_2). This ratio is intended to allow comparisons of arterial PO_2 even as F_IO_2 is therapeutically altered. It represents an attempt to control for the expected changes in arterial PO_2 when F_IO_2 is changed, so that the lungs can be compared irrespective of F_IO_2. The physiologic basis of this is reasonable under some but not all conditions, as Figure 17-10 shows.

Figure 17-10A shows arterial PO_2 itself as a function of F_IO_2, over the range from air ($F_IO_2 = 0.21$) to pure oxygen ($F_IO_2 = 1.0$) in three theoretical models of the lung. They reflect a normal lung, a lung containing a 20% shunt but no $\dot{V}_A/\dot{Q}$ inequality, and a lung with severe $\dot{V}_A/\dot{Q}$ inequality but no shunt. Arterial PO_2 changes with F_IO_2 substantially in all three examples, but at different rates.

Figure 17-10 shows the same arterial PO_2 values now divided by F_IO_2. The normal lung and the lung with only a shunt show quite different ratios that are roughly constant

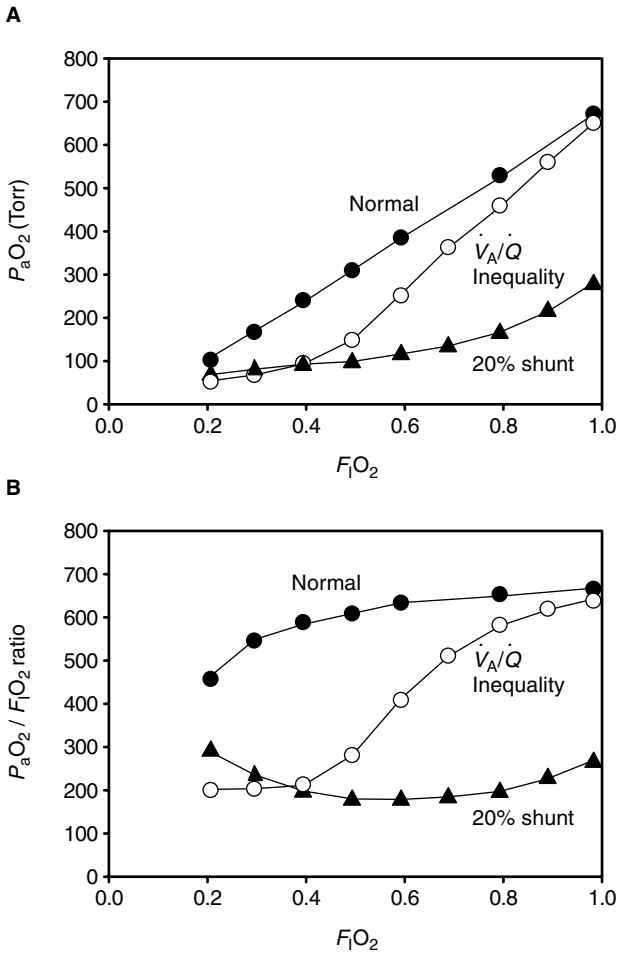

FIGURE 17-10 Response of arterial PO_2 (*A*) and the ratio of arterial PO_2 to F_IO_2 (*B*) to increases in F_IO_2 in three different lungs. *Closed circles* indicate a normal lung, *triangles* indicate a lung with a 20% shunt but no $\dot{V}_A/\dot{Q}$ inequality, and *open circles* indicate a lung with severe $\dot{V}_A/\dot{Q}$ inequality but no shunt.The normal lung and the lung with a pure shunt show essentially constant but very different P_aO_2/F_IO_2 ratios, providing a rationale for the use of this ratio in assessing gas exchange when F_IO_2 is subject to change (as in critically ill patients). However, the response in the third lung, which has $\dot{V}_A/\dot{Q}$ inequality rather than shunt, is very different. This lung looks like the lung with a shunt at lower F_IO_2 but like the normal lung at high F_IO_2. This points out the limitations in the use of this ratio.

over a wide F_IO_2 range. Certainly, the mean values of about 600 (normal) and 200 (20% shunt) are very different, and the variability, especially above an F_IO_2 of 0.3 to 0.4, is modest. The problem with the P_aO_2/F_IO_2 ratio is seen in lungs with $\dot{V}_A/\dot{Q}$ inequality but no shunt, where between room air and 40% inspired oxygen, the P_aO_2/F_IO_2 ratio is about 200, similar to that of the lung with a 20% shunt. However, at high F_IO_2 values, the P_aO_2/F_IO_2 ratio rises rapidly and is not different from normal above about 90% inspired oxygen. Consequently, the P_aO_2/F_IO_2 ratio must be used with care when significant $\dot{V}_A/\dot{Q}$ inequality is present.

Alveolar–Arterial PO_2 Difference

The alveolar–arterial PO_2 difference ($P_{A-a}O_2$) is the calculated difference between the "ideal" (essentially, the mean) alveolar PO_2[13] and the measured arterial PO_2. The $P_{A-a}O_2$ is more informative than just PO_2 and PCO_2 alone for more than one reason. First, it accounts for hyperventilation and hypoventilation because these processes affect both PO_2 and PCO_2 in a well-defined manner, such that $P_{A-a}O_2$ does not change much. In other words, an increase or decrease in ventilation will not per se affect $P_{A-a}O_2$ significantly, even though PO_2 and PCO_2 will each change. Thus, $P_{A-a}O_2$ reflects the integrated effects of ventilation–perfusion inequality, shunting, and diffusion limitation. As a result, it marks the degree of pulmonary dysfunction better than do absolute values of PO_2 and PCO_2. Second, it allows for changes in inspired PO_2 because that variable is explicitly a part of the formula.

$P_{A-a}O_2$ is calculated from a formula derived from Equation 17-8 and the corresponding equation for carbon dioxide. Recall that Equation 17-8 was given as:

$$\dot{V}O_2 = \dot{V}_IF_IO_2 - \dot{V}_AF_AO_2 = k\dot{V}_A(P_IO_2 - P_AO_2)$$

The corresponding equation for carbon dioxide, assuming no significant carbon dioxide in inspired gas, is:

$$\dot{V}CO_2 = \dot{V}_AF_ACO_2 = k\dot{V}_A(P_ACO_2) \qquad (17\text{-}10)$$

If we now simply divide Equation 17-10 by Equation 17-8 and define the ratio of carbon dioxide eliminated ($\dot{V}CO_2$) to oxygen taken up ($\dot{V}O_2$) as the respiratory exchange ratio, R, we have:

$$R = P_ACO_2/(P_IO_2 - P_AO_2) \qquad (17\text{-}11)$$

This is rearranged to define alveolar PO_2:

$$P_AO_2 = P_IO_2 - P_ACO_2/R \qquad (17\text{-}12)$$

$P_{A-a}O_2$ is now just the difference between P_AO_2 from Equation 17-12 and arterial PO_2 (P_aO_2):

$$P_{A-a}O_2 = P_IO_2 - P_ACO_2/R - P_aO_2 \qquad (17\text{-}13)$$

This is called the alveolar gas equation. Because we used the approximation that $\dot{V}_I = \dot{V}_A$ in developing Equation 17-8, Equation 17-13 is also based on that assumption. We can take account of the fact that, in general, $\dot{V}_I$ and $\dot{V}_A$ are slightly different. When this is done, Equation 17-13 becomes:

$$P_{A-a}O_2 = P_IO_2 - P_ACO_2/R - P_aO_2 + P_ACO_2F_IO_2(1 - R)/R \qquad (17\text{-}14)$$

If normal values for all of the variables are inserted into Equation 17-14, we can calculate that the additional term in Equation 17-14 is very small, usually about 2 Torr. For clinical purposes, it can be neglected, and the simpler form, Equation 17-13, is used. For research purposes, however, Equation 17-14 is preferred.

Three important limitations should be kept in mind when using either form of the alveolar gas equation. The first is that the equation applies only when gas exchange is in a steady state. The second is that R needs to be known if $P_{A-a}O_2$ is to be accurate. Measuring R in clinical circumstances is uncommon. It is found by determining $\dot{V}O_2$ and $\dot{V}CO_2$ from analysis of expired gas. Under most circumstances, assuming $R = 0.85$ is reasonable. The third limitation is that alveolar PCO_2 (P_ACO_2 in Equations 17-13 and 17-14) is taken to be the same as arterial PCO_2. This is reasonable under many conditions, especially when areas of low, but not high, $\dot{V}_A/\dot{Q}$ ratio are prominent. However, when high $\dot{V}_A/\dot{Q}$ ratio regions are significant, alveolar PCO_2 can be considerably lower than arterial PCO_2, causing an underestimation of $P_{A-a}O_2$. The two examples discussed above in the two-compartment analysis of $\dot{V}_A/\dot{Q}$ inequality are consistent with this conclusion.

$P_{A-a}O_2$ is thus a compromise parameter, balancing simplicity against both limitations resulting from the required assumptions and the depth of information revealed. Hypoventilation (or hyperventilation) alone will not increase $P_{A-a}O_2$, but whether an abnormal $P_{A-a}O_2$ is caused by $\dot{V}_A/\dot{Q}$ inequality, shunting, or diffusion limitation alone or in combination cannot be determined.

Normally, $P_{A-a}O_2$ is 5 to 10 Torr in young healthy subjects. Because it is the difference between two large numbers (alveolar PO_2, about 100 Torr, and arterial PO_2, about 90 to 95 Torr), the variance in $P_{A-a}O_2$ resulting from measurement errors is quite large. Negative values are not uncommonly found but should not be considered intrinsically problematic because of the large variance.

Two- and Three-Compartment Models of $\dot{V}_A/\dot{Q}$ Inequality

Given the limitations of the $P_{A-a}O_2$, efforts have been made to find more informative ways of quantifying gas exchange. Some 50 years ago, Riley and Cournand[13] devised a three-compartment model that is still clinically useful today, especially in critically ill patients. The lungs are imagined as consisting of just three alveoli. One alveolus is unventilated but is perfused, and thus is a shunt. A second alveolus is ventilated but unperfused and is therefore a dead space. The third, normal, compartment is both ventilated and perfused and is responsible for all of the oxygen uptake and carbon dioxide elimination by the patient. These three alveoli together account for all of the ventilation and all of the bloodflow, and the model is applied by using measured arterial and mixed venous oxygen concentration data to divide the total bloodflow into two fractions—that in the shunt and that in the normal compartment. In a corresponding manner, the arterial and mixed expired PCO_2 values are then used to divide the total ventilation into two fractions—that in the dead space and that in the normal compartment. The

Riley three-compartment model is thus really a pair of two-compartment models in which the normal compartment is shared. The bloodflow fraction in the shunt compartment is called physiologic shunt (or, equivalently, venous admixture), and the ventilation fraction in the dead space is called physiologic dead space (or, equivalently, wasted ventilation).

The calculations of physiologic shunt and dead space are based on mass conservation principles (as was all of the preceding discussion on gas exchange), as follows.

Arterial oxygen concentration, C_aO_2, must be the bloodflow-weighted average of the concentrations of oxygen in the normal (called "ideal," i) alveolus, C_iO_2, and that of mixed venous blood passing through the shunt, C_vO_2, as follows, where S is fractional perfusion in the shunt compartment:

$$C_aO_2 = (1-S)C_iO_2 + SC_vO_2 \qquad (17\text{-}15)$$

If arterial and mixed venous oxygen levels are measured, and C_iO_2 is calculated from the oxygen dissociation curve with knowledge of P_iO_2 (the PO_2 of the normal alveolus calculated using the alveolar gas equation), S can be computed by rearranging Equation 17-15:

$$S = (C_iO_2 - C_aO_2)/(C_iO_2 - C_vO_2) \qquad (17\text{-}16)$$

In normal lungs, S should be very close to zero and not more than 0.01 to 0.02. This is because there are essentially no unventilated alveoli in normal lungs. Thus, any value greater than about 0.02 would be interpreted as abnormal.

There is a very important limitation to the use of Equation 17-16. It explicitly requires knowledge of the mixed venous oxygen concentration. As the preceding discussion of two-compartment models of $\dot{V}_A/\dot{Q}$ inequality has shown, mixed venous PO_2 can vary considerably, so that assuming any particular value may be problematic. Thus, unless C_vO_2 is measured, S may contain substantial errors.

From principles similar to those underlying calculation of physiologic shunt, mixed expired PCO_2 ($P_{exp}CO_2$) must be the weighted average of the PCO_2 in the normal (ideal) alveolus (P_iCO_2) and zero (which is the PCO_2 of the ventilated but unperfused, dead space alveolus; see Figure 17-3). If V_D is the fraction of the total ventilation in the dead-space alveolus, we have:

$$P_{exp}CO_2 = (V_D \times 0) + (1 - V_D)P_iCO_2 \qquad (17\text{-}17)$$

On rearrangement, this becomes:

$$V_D = (P_iCO_2 - P_{exp}CO_2)/P_iCO_2 \qquad (17\text{-}18)$$

As with the alveolar gas equation above, it is common practice to assume that the ideal PCO_2 is equal to the arterial value (P_aCO_2), such that Equation 17-18 now becomes:

$$V_D = (P_aCO_2 - P_{exp}CO_2)/P_aCO_2 \qquad (17\text{-}19)$$

In Equation 17-19, V_D is often called "V_D/V_T" or dead-space/tidal volume ratio. Note that to measure mixed expired PCO_2, we must collect several entire exhalations and measure mean PCO_2 in that mixed, exhaled gas. The conducting airways will clearly contribute to the dilution of carbon dioxide in mixed expired gas because the mixed expirate contains gas that filled the conducting airways at the end of inspiration—that is, inspired gas, normally devoid of carbon dioxide. Thus, the normal value of V_D is about 0.3 because conducting airway volume is about 30% of the total tidal volume under normal conditions. An increase above 0.3 therefore marks abnormal exchange. This warning sign requires further consideration because the normal value of V_D can vary greatly as tidal volume varies. Thus, with a constant conducting airway volume of 150 mL, a fall in tidal volume from 500 to 300 mL/breath would increase V_D from 0.3 to 0.5. Thus, in applying Equation 17-19, it is critical to know actual tidal volume. We can assume that conducting airway volume is about 1 mL per pound of body weight (in a nonobese patient). Once tidal volume is known, the fraction of V_D that should be attributable to conducting airway volume can be easily computed, and what is left is then the measure of the ventilation of unperfused alveoli.

In applying both Equation 17-16 for physiologic shunt and Equation 17-19 for physiologic dead space, the lungs have been modeled by Riley as a three-compartment structure. This is a gross oversimplication in many if not most cases. Of course, if there actually is only a true shunt present (as, for example, in atelectasis, or via a right-to-left intracardiac shunt), the calculated physiologic shunt will be accurate. The same holds true for physiologic dead space—it will be accurate if the actual situation is one of completely unperfused alveoli. However, in most patients, there is a distribution of $\dot{V}_A/\dot{Q}$ ratios present—low but greater than zero and/or high but less than infinite. In such circumstances, S from Equation 17-16 and V_D from Equation 17-19 will systematically underestimate the fractions of bloodflow and ventilation (respectively) associated with these low- and high-$\dot{V}_A/\dot{Q}$ regions. Nevertheless, these are very useful indices of abnormal gas exchange that have withstood the tests of time. They represent the equivalent fractional shunt and dead space necessary to explain arterial and expired gas concentrations and as such are useful measures of the degree of pulmonary abnormality.

Distribution of Ventilation/Perfusion Ratios

Theoretical Basis The limitations of the $P_{A-a}O_2$, the P_aO_2/F_IO_2 ratio, and the Riley three-compartment model discussed above have led workers to search for better methods for assessing gas exchange. Just as Riley and Cournand used measurements of arterial and expired oxygen and carbon dioxide levels to determine parameters of simple three-compartment models of ventilation and bloodflow, it has been shown that measurements of arterial and expired levels of foreign inert gases can also be used to determine parameters of the ventilation/perfusion ratio distribution. The principles of such inert gas methods are identical to those used by Riley and Cournand, but by simultaneously exposing the lungs to a mixture of many inert gases, one can go from simple three-compartment models to a smooth approximation of the entire $\dot{V}_A/\dot{Q}$ distribution.

The difference between Riley's three-compartment model and the $\dot{V}_A/\dot{Q}$ distribution derived from inert gases is essentially only quantitative; the basis is the same. Riley used oxygen to determine the division of bloodflow between two

compartments and carbon dioxide to divide ventilation between two compartments. Using a mixture of several inert gases allows one to divide both ventilation and bloodflow among the entire possible spectrum of $\dot{V}_A/\dot{Q}$ units. The only other differences are that (1) changes in the levels of F_IO_2, total ventilation, and cardiac output affect the parameters obtained in the Riley analysis for the same actual $\dot{V}_A/\dot{Q}$ distribution, and (2) the level of oxygen (and possibly also of carbon dioxide) can affect how ventilation and bloodflow are distributed, thus making the three-compartment model sensitive to values of the variables used to measure it. If inert gases are applied at trace (parts per million) levels, they do not affect the distribution and thus provide a more reliable picture of $\dot{V}_A/\dot{Q}$ relationships.

To understand inert gas methods, one needs to understand the objective of using them: to describe the way in which $\dot{V}_A/\dot{Q}$ ratios are distributed within the lung. The image is one of a lung that consists of a spectrum of gas exchange units, each of which is a homogeneous unit with a particular $\dot{V}_A/\dot{Q}$ ratio. These particular $\dot{V}_A/\dot{Q}$ ratios are selected objectively to adequately represent the whole possible $\dot{V}_A/\dot{Q}$ range (from zero to infinity), just as in a human population survey only a small fraction of the actual population is used to represent the whole population. The question then becomes how bloodflow (and, separately, how ventilation) is distributed among these many $\dot{V}_A/\dot{Q}$ units.

An analogy would be the distribution of weight/height ratios in a group of people. One would take the members of the group and measure their weight and height. One would then aggregate members into small weight/height ranges (such as 30 to 32 kg/m or 32 to 34 kg/m) and plot the number of members in each such range (*y*-axis) against weight/height group ratio midpoint on the *x*-axis. With a large enough number of subjects, one would probably end up with a smooth, bell-shaped curve, with most subjects near the mean and the numbers decreasing on either side with increasing distance from the mean. This kind of plot is called a frequency distribution and is the most succinct and complete description of the population of height/weight ratios.

To apply this to the lung, we need such frequency distributions: one for ventilation and the other for bloodflow. Figure 17-11A illustrates the principle. Two curves are shown for a hypothetical $\dot{V}_A/\dot{Q}$ distribution, one for how ventilation is distributed among units of varying $\dot{V}_A/\dot{Q}$ ratio and the other for bloodflow. The *x*-axis depicts the $\dot{V}_A/\dot{Q}$ ratio, which in this example runs from 0.001 to 1,000. Note that units with $\dot{V}_A/\dot{Q}$ of zero [a shunt: perfused ($\dot{Q} > 0$) but not ventilated ($\dot{V}_A = 0$)] are absent in this case; units with an infinite $\dot{V}_A/\dot{Q}$ ratio [dead space: ventilated ($\dot{V}_A > 0$) but unperfused ($\dot{Q} = 0$)] are also not present. However, both shunt and dead space could be placed on Figure 17-11A, were they present. Figure 17-11A indicates the pattern of ventilation and bloodflow across the range of $\dot{V}_A/\dot{Q}$ ratios, and the key point is that real lungs will have units with any or all $\dot{V}_A/\dot{Q}$ ratios in between the extremes, as shown by the curves. A special feature of the $\dot{V}_A/\dot{Q}$ distribution is that because the $\dot{V}_A/\dot{Q}$ ratio is defined as the ratio of ventilation to bloodflow, any points on the ventilation and bloodflow curves at the same *x*-axis value of $\dot{V}_A/\dot{Q}$ are numerically related:

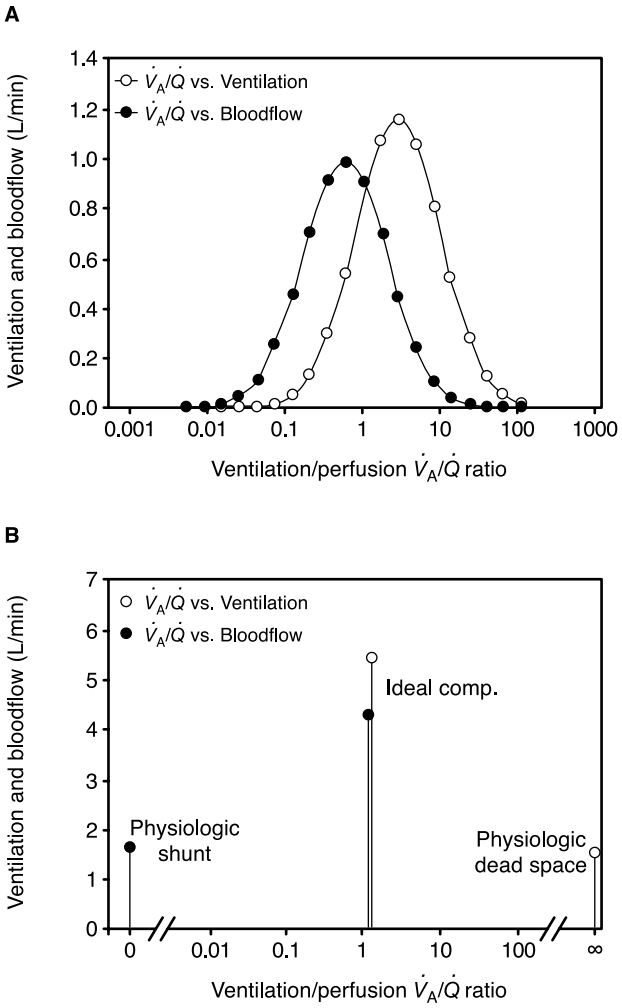

FIGURE 17-11 Concept of the distribution of ventilation/perfusion ratios. *A* shows a continuous distribution of both ventilation and bloodflow. It succinctly describes the relative amounts of ventilation and bloodflow associated with lung regions of different $\dot{V}_A/\dot{Q}$ ratio from 0.001 to 1,000. This is the information necessary to explain how well or poorly the lung exchanges oxygen and carbon dioxide. *B* shows the Riley three-compartment equivalent of this particular distribution and indicates how this model, although clinically useful, greatly oversimplifies the actual situation.

$$\dot{V}_A = Q\dot{V}_A/\dot{Q} \qquad (17\text{-}20)$$

Thus, if we know the bloodflow distribution ($\dot{Q}$ vs. $\dot{V}_A/\dot{Q}$), we also know the ventilation distribution ($\dot{V}_A$ vs. $\dot{V}_A/\dot{Q}$), and vice versa.

In Figure 17-11B, the Riley three-compartment model obtained from the same distribution shown in Figure 17-11A is projected onto this platform. Figure 17-11B shows three virtual compartments with $\dot{V}_A/\dot{Q}$ ratios of 0, the ideal value (about 1.2 in this case), and infinity, with the bloodflow split between the first two and the ventilation split between the latter two. Physiologic shunt and dead space are each a little less than 2 L/min. It is evident how the Riley model, although clinically useful, greatly oversimplifies the actual lungs by representing a broad distribution as a three-compartment equivalent.

Figure 17-11A depicts ventilation and bloodflow, respectively, at a series of 20 equally spaced $\dot{V}_A/\dot{Q}$ ratios (equally spaced on a logarithmic scale, which is more useful than a linear scale for a distribution of ratios). Using a discrete set of $\dot{V}_A/\dot{Q}$ ratios (be it 20 or 50 or some other number) is a very convenient way to describe the distribution and turns out to be both simpler and more flexible than trying to work with a truly continuous mathematical function. What is key is to select the $\dot{V}_A/\dot{Q}$ ratios evenly across the $\dot{V}_A/\dot{Q}$ scale, as has been done in Figure 17-11A.

Based on this concept of the $\dot{V}_A/\dot{Q}$ distribution, we can now proceed to examine the behavior of a single inert gas in any one of the $\dot{V}_A/\dot{Q}$ compartments and then in the distribution as a whole, as in Figure 17-11A. Going back to Equations 17-1 and 17-2, which described mass conservation for the uptake of oxygen by the lungs, we can apply the same principles to an inert gas of solubility λ. Since inert gases obey Henry's law, the concentration in blood (C_{ig}) is directly proportional to partial pressure (P_{ig}):

$$C_{ig} = \lambda P_{ig} \tag{17-21}$$

The constant of proportionality is the solubility, λ, and since inert gases equilibrate very rapidly across the blood–gas barrier, alveolar (P_{Aig}) and end-capillary (P_{cig}) inert gas partial pressures are identical. Equations 17-1 and 17-2 then become:

$$\dot{V}_{ig} = \dot{V}_l P_{lig} - \dot{V}_A P_{Aig} \tag{17-22}$$

and

$$\dot{V}_{ig} = \dot{Q}(C_{cig} - C_{vig}) = Q\lambda(P_{Aig} - P_{vig}) \tag{17-23}$$

The inert gases are presented to the lungs dissolved in saline or dextrose by way of constant intravenous infusion. In this way, they are being eliminated by the lungs, just as for carbon dioxide. P_{lig} is therefore zero by design, simplifying the equations. Equating Equations 17-22 and 17-23 and dropping the subscript "ig" for simplicity, we have:

$$\dot{V}_A P_A = \dot{Q}\lambda(P_v - P_A) \tag{17-24}$$

Isolating P_A and dividing by both $\dot{Q}$ and P_v yields:

$$P_A/P_v = P_c/P_v = \lambda/(\lambda + \dot{V}_A/\dot{Q}) \tag{17-25}$$

The units for λ are such that it becomes what is called the blood/gas partition coefficient of the gas. The partition coefficient is the ratio of the equilibrium concentrations of the inert gas in the blood and gas phases and describes the solubility of the gas in blood. Remember that P_A is alveolar, P_c is end-capillary, and P_v is mixed venous partial pressure of the inert gas.

Equation 17-25 is very useful. The ratio P_c/P_v for a gas being eliminated by the lungs is its fractional retention. Thus, if 100 molecules were infused and 80 were eliminated by ventilation, retention would be 0.2 (or 20%). Equation 17-25 shows that retention is a simple function of only the partition coefficient and the $\dot{V}_A/\dot{Q}$ ratio. Retention falls with increasing $\dot{V}_A/\dot{Q}$ ratio for a given value of λ; it also falls as λ is reduced for a given value of $\dot{V}_A/\dot{Q}$. This equation can be applied to each $\dot{V}_A/\dot{Q}$ ratio unit in the entire $\dot{V}_A/\dot{Q}$ distribution. Suppose that we simultaneously infused six inert gases and wished to use the retention data to construct the $\dot{V}_A/\dot{Q}$ distribution. We could set up a lung having six predetermined (ie, known) $\dot{V}_A/\dot{Q}$ ratios (equally spaced across the $\dot{V}_A/\dot{Q}$ range in Figure 17-11A). The task would be to determine how total pulmonary bloodflow is distributed among the six compartments. We apply the same mass conservation logic as for physiologic shunt (Equation 17-15). That logic means that, for any one inert gas, its retention fraction measured in mixed systemic arterial blood must be a bloodflow-weighted average of the six compartmental retentions. If $R = P_c/P_v$, we can write for any one gas:

$$R_j \text{ (retention in } \dot{V}_A/\dot{Q} \text{ compartment j)} = \lambda/(\lambda + \dot{V}_A/\dot{Q}_j) \tag{17-26}$$

Then, systemic arterial R would be:

$$R = \dot{Q}_1 R_1 + \dot{Q}_2 R_2 + \dot{Q}_3 R_3 + \dot{Q}_4 R_4 + \dot{Q}_5 R_5 + \dot{Q}_6 R_6 \tag{17-27}$$

Here the six values of $\dot{Q}_j$ are fractional bloodflow values that sum to 1.0. It is these values that are unknown and that we need to determine, given the measured value of R and the calculated values of all R_j. If six different gases were simultaneously infused and their systemic arterial retentions (R values on the left side of Equation 17-27) were measured, each of the six gases would generate one equation similar to Equation 17-27. In each of these six equations, we already know λ as the measured partition coefficient and have specified the six values of $\dot{V}_A/\dot{Q}$. Thus, each value of R_j for each gas can be calculated. What we now have is a set of six simultaneous linear equations in six unknowns—the six compartmental bloodflow fractions. Such an equation system is easily and uniquely solved—there is only one set of six values of fractional $\dot{Q}$ that satisfies all six equations. It is no accident that in this example there is the same number of gases as $\dot{V}_A/\dot{Q}$ compartments. That is required for a conventional solution to such a set of equations.

We now can plot the paired values of bloodflow and $\dot{V}_A/\dot{Q}$ ratio compartment by compartment, as in Figure 17-11A, and we have found the distribution of $\dot{V}_A/\dot{Q}$ ratios, at least as a six-compartment model.

This process has been described to give a feel for the basic principles. However, there are three major limitations to the use in practice of such a simple system:

1. In being limited to the same number of $\dot{V}_A/\dot{Q}$ compartments as we have gases, six in this example, we may have a too coarse sampling of the $\dot{V}_A/\dot{Q}$ axis to properly fit the results. Six gases are about all that can be measured simultaneously in a reasonable time frame. Modeling research has shown that the $\dot{V}_A/\dot{Q}$ domain needs to be divided into at least 20 compartments (plus shunt and dead space) to overcome this limitation in practice. It would be infeasible in practice to expose the lungs to 20 different gases to enable a 20-compartment analysis.
2. There is no guarantee that the six compartments will end up having positive values for bloodflow when the equations are solved. However, negative bloodflow has no physiologic meaning, and therefore bloodflow in

every compartment must be constrained to be non-negative (ie, greater than or equal to zero).

3. Such a system, in which the number of compartments and the number of gases are equal, turns out to be quite sensitive to inevitable random experimental errors. Thus, the allocation of bloodflow among the six compartments may jump around between duplicate samples, due to experimental error. It would be desirable to be able to solve the equations in such a way as to return a stable set of compartmental bloodflows from duplicate data sets that differed because of random error only. This would reduce concern that two apparently different results from two data sets reflected a real difference in the lungs and at the same time increase confidence that an observed difference in results was a true biologic change.

Fortunately, mathematical methods exist that can overcome these limitations.[23,24] The present formulation of the multiple inert gas elimination technique (MIGET) uses an infusion of six inert gases whose partition coefficients (λ) span the range from very low (sulfur hexafluoride [SF_6], $\lambda = 0.005$) to very high (acetone, $\lambda = 300$). The four intervening gases are ethane ($\lambda = 0.1$), cyclopropane ($\lambda = 0.5$), enflurane ($\lambda = 2.5$), and ether ($\lambda = 12$). A 50 $\dot{V}_A/\dot{Q}$ compartmental discretization of the $\dot{V}_A/\dot{Q}$ axis is used with this set of six gases. Although the number of compartments (50) exceeds the number of gases (6), by incorporation of a smoothing constraint on the process for solving the equations, the $\dot{V}_A/\dot{Q}$ distribution can be found in a manner that is stable to normal levels of experimental error. It limits the results to smooth frequency distributions, thereby acknowledging that fine resolution in the shape of the $\dot{V}_A/\dot{Q}$ distribution cannot be determined. Given the likelihood that there are some 100,000 individual acini (essentially the unit of gas exchange) in a lung, it is highly unlikely that actual $\dot{V}_A/\dot{Q}$ distributions are ragged or jagged. Imagine the frequency distribution of height in a population of 100,000 people. With this many points, it would be a smooth curve. Thus, limiting the outcome to smooth curves is unlikely to impose a significant constraint.

To understand the concept of smoothing, a good analogy is the task of mapping the location of, say, 50 tennis balls thrown randomly onto a tennis court. It would take precisely 50 independent measurements to locate all 50 balls. However, if the 50 balls were first threaded onto a rope, each ball separated by, say, no more than 12 inches from its neighbor, and the rope of balls was thrown randomly onto the court, the task of mapping the location of all 50 balls would be far easier. Mapping every, say, eighth ball would allow the approximate locations of the remainder to be identified without further measurements. This is because the string of 50 balls would have to form a relatively smooth line because of the short distances between adjacent balls.

The details of the mathematical process (including the non-negativity requirement, which involves a different process from that of smoothing) used for the MIGET can be found in a series of publications[23,24] and are not further presented here. Papers analyzing the limits on the information that the method provides have also been published.[25–27] Many published studies show the findings in a variety of cardiopulmonary diseases and are discussed in Chapter 18, "Ventilation–Perfusion Distributions in Disease."

$\dot{V}_A/\dot{Q}$ Distribution in Health The first question one might have concerning the MIGET is what is found in normal young adult subjects. Figure 17-12 shows the $\dot{V}_A/\dot{Q}$ distribution typically found in such a subject.[28] It is symmetric about its mean $\dot{V}_A/\dot{Q}$ (which is very close to 1.0). It is narrow, with almost all ventilation and bloodflow confined to a single $\dot{V}_A/\dot{Q}$ decade (between about 0.3 and 3.0), as Figure 17-12 shows. Thus, there are no regions of very low or very high $\dot{V}_A/\dot{Q}$ ratio. There is no shunt, and dead space is about 30% (of total ventilation). It is interesting that when this pattern is compared with that reconstructed from topographic measurements made with radioactive tracers (see Figure 17-2), there is little difference. Thus, most of the functional $\dot{V}_A/\dot{Q}$ inequality in the young, normal lung can be explained by gravitational variance in $\dot{V}_A/\dot{Q}$ ratios. Although ventilation and bloodflow are both apparently nonuniform in a given horizontal plane, there must be considerable covariance between them. Otherwise, this nonuniformity would add considerably to the functional $\dot{V}_A/\dot{Q}$ inequality observed with the MIGET.

Whereas the curves shown in Figure 17-12 represent the full picture of how ventilation and bloodflow are distributed functionally, summary parameters of this distribution are frequently used, just as for any group of observations. The first three moments of the distribution are most commonly used for this. The first moment is the mean $\dot{V}_A/\dot{Q}$ ratio; the second moment (about the mean) reflects dispersion. For a perfectly symmetric, logarithmically normal curve similar to that in Figure 17-12, the second moment yields the standard deviation, such that about 68% of the total ventilation and bloodflow falls between the mean -1 SD and the mean $+1$ SD. For nonsymmetric curves, the second moment gives a

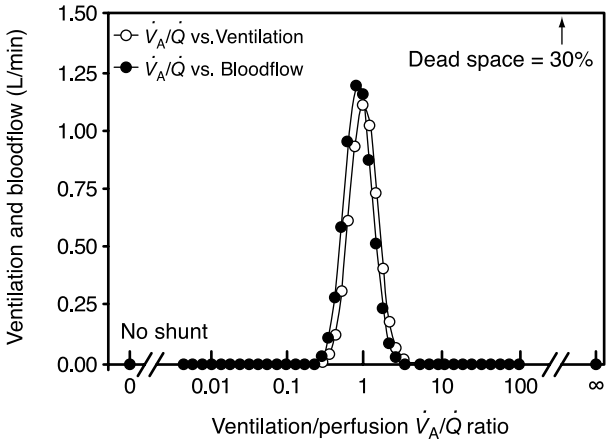

FIGURE 17-12 $\dot{V}_A/\dot{Q}$ distribution typical of a young, normal, upright human subject. The distribution is narrow, symmetric, and confined to the $\dot{V}_A/\dot{Q}$ decade between about 0.3 and 3. There is no shunt or dead space. See text for further analysis.

useful quantitative index of dispersion, but it should not strictly be called the standard deviation. The third moment (about the mean) depicts the curves' symmetry. A third moment equal to zero indicates a symmetric distribution; skewing to the left or right is manifested by a third moment different from zero.

A large body of work over the years has established that the second moment has a normal range that runs from about 0.3 to 0.6 (95% confidence limits).[19,29–31] A completely homogeneous lung (which does not exist) would have a value of zero. A patient with severe lung disease in an intensive care unit on a ventilator might have a second moment of 2 to 2.5. Thus, mildly abnormal values run from 0.6 to about 0.8. Moderately abnormal values run from 0.8 to about 1.2, and severe $\dot{V}_A/\dot{Q}$ inequality produces a second moment above 1.2. The highest values seen are about 2.5.

The distribution shown in Figure 17-11A has a second moment of 1.25, whereas that of the normal subject in Figure 17-12 has a second moment of 0.40.

Note that neither shunt nor dead space, which are explicitly recovered by the MIGET, along with the rest of the distribution, is included in the second moment calculation because the formula requires taking the logarithm of the $\dot{V}_A/\dot{Q}$ ratio of each compartment in the distribution. The logarithms of zero and of infinity are not definable, so shunt and dead space are excluded and reported separately as fractions of total pulmonary bloodflow and ventilation respectively.

Additional Information Available from the MIGET

Determination of the frequency distribution of ventilation and bloodflow with use of the MIGET allows the analysis of gas exchange in considerable detail. The very shape of the distribution can yield mechanistic insights into how gas exchange is regulated and affected as conditions change. Changes in the degree of inequality with interventions are useful in assessing their mechanisms. However, two additional categories of information can be obtained when the method is used: (1) determining the role, if any, of diffusion limitation in oxygen uptake and (2) determining the modifying roles of any "extrapulmonary" influences on gas exchange.[32]

Assessment of Diffusion Limitation of Oxygen Uptake

Diffusion limitation is inferred as follows. All nonreactive inert gases are essentially invulnerable to reduced elimination by limited diffusion across the blood–gas barrier, no matter what conditions prevail.[4] Oxygen, however, can be diffusion limited, especially during exercise and at altitude.[30,33,34] This means that if diffusion limitation for oxygen exists, there will be more severe hypoxemia than expected from the degree of $\dot{V}_A/\dot{Q}$ inequality alone as determined by the MIGET. Comparison of the actual with the expected arterial PO_2 reflects the extent of diffusion limitation for oxygen.

The expected arterial PO_2 is determined with the use of principles already described. First, Equations 17-1 and 17-2 are used to find alveolar PO_2 and the corresponding end-capillary oxygen concentration for each $\dot{V}_A/\dot{Q}$ ratio unit in the $\dot{V}_A/\dot{Q}$ distribution. This computation is performed with the explicit assumption that oxygen exchange across the blood–gas barrier is *not* diffusion limited. Then, mass conservation rules are used to compute the mixed arterial oxygen concentration as a bloodflow-weighted average of oxygen concentrations from all units in the particular $\dot{V}_A/\dot{Q}$ distribution under consideration. Mixed arterial PO_2 is then determined from the arterial oxygen concentration with use of the hemoglobin dissociation curve. If there is no diffusion limitation for oxygen, the arterial PO_2 calculated in this way will agree with the arterial PO_2 that was actually measured. However, if oxygen is, in fact, diffusion limited, the actual arterial PO_2 will be lower than that predicted by the MIGET. The difference between the actual and the predicted arterial PO_2 values then can be used to calculate the oxygen-diffusing capacity of the lungs necessary to explain the difference.[35]

With this approach, diffusion limitation of oxygen uptake is rarely seen, even in lung disease—measured and expected arterial PO_2 values are in agreement. The only condition in which diffusion limitation is seen consistently in lung disease is pulmonary fibrosis during exercise.[36] Diffusion limitation is actually more commonly observed in health, but only during the heaviest of exercise, especially in athletes, where pulmonary capillary red cell transit time is presumed to be reduced to the point of causing diffusion limitation. Exercise at altitude accentuates diffusion limitation for oxygen, so that it is seen in essentially all normal subjects, not just athletes.[30,33] At altitude, it can have an enormous negative impact on arterial oxygenation and thus tissue oxygen availability.[37]

Role of Extrapulmonary Factors in Modulating Arterial PO_2

Returning to the basic principles of pulmonary gas exchange discussed above, it should be clear that, in addition to the intrapulmonary factors ($\dot{V}_A/\dot{Q}$ inequality, shunts, and diffusion limitation), additional factors can influence arterial PO_2. These are the so-called "extrapulmonary" factors. They include the inspired oxygen level, metabolic rate, total ventilation, cardiac output, features of the hemoglobin dissociation curve (total hemoglobin concentration and P_{50}), body temperature, and acid–base state. All of these factors influence local alveolar PO_2 through the way in which they affect the solutions to the basic equations for gas exchange (Equations 17-1 and 17-2).

The MIGET is well suited to elucidating the quantitative roles of such factors, especially when more than one may change at a time in a given patient. Many examples can be imagined. One of the earliest applications was explaining how the bronchodilator isoproterenol affected gas exchange in patients with asthma.[38] It was shown that the drug caused preferential vasodilatation in areas of reduced $\dot{V}_A/\dot{Q}$ ratio (presumably by releasing prior hypoxic vasoconstriction), such that $\dot{V}_A/\dot{Q}$ inequality was actually made acutely worse by the increased bloodflow through these poorly ventilated regions. However, the expected fall in arterial PO_2 was

attenuated by the concomitant increase in cardiac output because of an increase in mixed venous PO_2 (see Figure 17-5A). Another example is reconciling the mild hypoxemia usually seen in asthmatic patients with the much more severe hypoxemia seen in patients with large myocardial infarcts and pulmonary edema resulting from associated heart failure.[39] With use of the MIGET, the actual fractional perfusion of poorly ventilated regions is often greater in asthmatic patients than in patients with heart failure. This apparent paradox is explained by the fact that cardiac output is often above normal in asthmatic patients, whereas it is considerably reduced in patients with heart failure, with consequent effects on mixed venous PO_2. Thus, maintaining a high mixed venous PO_2 is effective in preventing severe hypoxemia in asthma, whereas failure to keep mixed venous PO_2 levels normal leads to substantial hypoxemia even when $\dot{V}_A/\dot{Q}$ inequality is not that severe. Further situations in which extrapulmonary factors may change arterial oxygenation can be imagined. A simple case is when inspired oxygen levels are changed. Arterial PO_2 will change as a result, and the MIGET allows one to answer the question of whether or not the change in PO_2 is as expected for the particular change in F_IO_2. One needs to know the distribution of $\dot{V}_A/\dot{Q}$ ratios for this, because the expected change is very dependent on the underlying pattern of $\dot{V}_A/\dot{Q}$ inequality. One uses the method much as described above in the context of assessing diffusion limitation. If the change in PO_2 is not as expected, the MIGET will identify the reason, be it a change in $\dot{V}_A/\dot{Q}$ relationships or something else.

SUMMARY

This chapter has focused on how ventilation and bloodflow are distributed to the very large number of alveoli in the lung and laid out the structural basis of why these distributions are not uniform, even in health. What is remarkable is that, despite the great potential for severe maldistribution of both ventilation and bloodflow, the overall amount of $\dot{V}_A/\dot{Q}$ inequality is very small and has a negligible impact on gas exchange and arterial PO_2 and PCO_2. The relationship between how much oxygen (and carbon dioxide) is exchanged in a unit of lung and the $\dot{V}_A/\dot{Q}$ ratio of that unit is developed with the use of basic principles of mass conservation. This is then used to explain how nonuniformity in the distribution of either ventilation or bloodflow in disease impairs gas exchange and how the body adjusts to maintain overall oxygen and carbon dioxide transport between the environment and the tissues. These same relationships are then used in reverse as tools to characterize the degree of $\dot{V}_A/\dot{Q}$ inequality on the basis of simple two- and three-compartment models. This is done by taking measurements of oxygen and carbon dioxide exchange and using them to partition bloodflow and ventilation among the compartments. Finally, because of the limitations of these models, the MIGET is presented in some depth. This method is a tool for determining not only the distribution of ventilation/perfusion ratios but also the roles of diffusion limitation of oxygen uptake and of potential extrapulmonary factors that can significantly modulate arterial PO_2 and PCO_2 when $\dot{V}_A/\dot{Q}$ inequality is present.

REFERENCES

1. Dubois AB. Alveolar CO_2 and O_2 during breath holding, expiration, and inspiration. J Appl Physiol 1952;5:1–12.
2. Barcroft JA, Cooke A, Hartridge H, et al. The flow of oxygen through the pulmonary epithelium. J Physiol (Lond) 1920;53:450–72.
3. Roughton FJW, Forster RE. Relative importance of diffusion and chemical reaction rates determining rate of exchange of gases in the human lung with special reference to true diffusing capacity of pulmonary membrane and volume of blood in the lung capillaries. J Appl Physiol 1957;11: 290–302.
4. Wagner PD. Diffusion and chemical reaction in pulmonary gas exchange. Physiol Rev 1977;57:257–312.
5. Fowler WS. Lung function studies. II. The respiratory dead space. Am J Physiol 1948;154:405–16.
6. Johnson BD, Badr MS, Dempsey JA. Impact of the aging pulmonary system on the response to exercise. Clin Chest Med 1994;15:229–46.
7. West JB, Tsukimoto K, Mathieu-Costello O, et al. Stress failure in pulmonary capillaries. J Appl Physiol 1990;70:1731–42.
8. West JB, Mathieu-Costello O, Jones JH, et al. Stress failure of pulmonary capillaries in racehorses with exercise-induced pulmonary hemorrhage. J Appl Physiol 1993;75:1097–109.
9. West JB. Regional differences in gas exchange in the lung of erect man. J Appl Physiol 1962;17:893–8.
10. West JB, Dollery CT. Distribution of blood flow in isolated lung: relation to vascular and alveolar pressures. J Appl Physiol 1964;19:713–24.
11. Wagner PD, McRae J, Read J. Stratified distribution of blood flow in secondary lobule of the rat lung. J Appl Physiol 1967;22:1115–23.
12. Glenny RW, Robertson HT. Fractal modeling of pulmonary blood flow heterogeneity. J Appl Physiol 1991;70:1024–30.
13. Riley RL, Cournand A. "Ideal" alveolar air and the analysis of ventilation/perfusion relationships in the lung. J Appl Physiol 1949;1:825–47.
14. Rahn H, Fenn WO. A graphical analysis of the respiratory gas exchange. Washington, DC: American Physiological Society; 1955.
15. West JB. Ventilation/perfusion inequality and overall gas exchange in computer models of the lung. Respir Physiol 1969;7:88–110.
16. West JB, Wagner PD. Pulmonary gas exchange. In: West JB, editor. Bioengineering aspects of the lung. Vol 3. New York: Marcel Dekker; 1977. p. 361–458.
17. Young IH, Mazzone RW, Wagner PD. Identification of functional lung unit in the dog by graded vascular embolization. J Appl Physiol 1980;49:132–41.
18. Weibel ER. Morphometry of the human lung. New York: Springer-Verlag; 1963.
19. Cardús J, Burgos F, Diaz O, et al. Increase in pulmonary ventilation/perfusion inequality with age in healthy individuals. Am J Respir Crit Care Med 1997;156:648–53.
20. Sorbini CA, Grassi V, Solinas E, et al. Arterial oxygen tension in relation to age in healthy subjects. Respiration 1968; 25:3–10.
21. Raine JM, Bishop JM. A–a difference in O_2 tension and physiological dead space in normal man. J Appl Physiol 1963; 18:284–8.
22. Rahn H, Otis AB. Man's respiratory response during and after acclimatization to high altitude. Am J Physiol 1949;157: 445–62.
23. Evans JW, Wagner PD. Limits on $\dot{V}_A/\dot{Q}$ distributions from analysis of experimental inert gas elimination. J Appl Physiol 1977;42:889–98.

24. Wagner PD. Estimation of distributions of ventilation/perfusion ratios. Ann Biomed Eng 1981;9:543–56.
25. Ratner ER, Wagner PD. Resolution of the multiple inert gas method for estimating $\dot{V}_A/\dot{Q}$ maldistribution. Respir Physiol 1982;49:293–313.
26. Olszowka AJ. Does inert gas exchange data provide enough information to recover $\dot{V}_A/\dot{Q}$ distributions present in the lung? Physiologist 1975;18:339.
27. Olszowka A, Wagner PD. Numerical analysis in gas exchange. In: West JB, editor. Pulmonary gas exchange. New York: Academic Press; 1980. p. 263–306.
28. Wagner PD, Laravuso RB, Uhl RR, et al. Continuous distributions of ventilation–perfusion ratios in normal subjects breathing air and 100% O_2. J Clin Invest 1974; 54:54–68.
29. Gale GE, Torre-Bueno JR, Moon RE, et al. Ventilation/perfusion inequality in normal humans during exercise at sea level and simulated altitude. J Appl Physiol 1985; 58:978–88.
30. Wagner PD, Gale GE, Moon RE, et al. Pulmonary gas exchange in humans exercising at sea level and simulated altitude. J Appl Physiol 1986;61:260–70.
31. Wagner PD, Hedenstierna G, Bylin G. Ventilation–perfusion inequality in chronic asthma. Am Rev Respir Dis 1987; 136:605–12.
32. Wagner PD, West JB. Ventilation–perfusion relationships. In: West JB, editor. Ventilation, blood flow and diffusion. Vol 1. New York: Academic Press; 1980. p. 219–62.
33. Torre-Bueno JR, Wagner PD, Saltzman HA, et al. Diffusion limitation in normal humans during exercise at sea level and simulated altitude. J Appl Physiol 1985;58:989–95.
34. Lilienthal Jr JL, Riley RI, Proemel DD, et al. An experimental analysis in man of the oxygen pressure gradient from alveolar air to arterial blood during rest and exercise at sea level and at altitude. Am J Physiol 1946;147:199–216.
35. Hammond MD, Hempleman SC. Oxygen diffusing capacity estimates derived from measured $\dot{V}_A/\dot{Q}$ distributions in man. Respir Physiol 1987;69:129–47.
36. Agustí AGN, Roca J, Gea J, et al. Mechanisms of gas exchange impairment in idiopathic pulmonary fibrosis. Am Rev Respir Dis 1991;143:219–25.
37. Wagner PD, Sutton JR, Reeves JT, et al. Operation Everest II: pulmonary gas exchange during a simulated ascent of Mt Everest. J Appl Physiol 1987;63:2348–59.
38. Wagner PD, Dantzker DR, Iacovoni VE, et al. Ventilation–perfusion inequality in asymptomatic asthma. Am Rev Respir Dis 1978;118:511–24.
39. Bencowitz HZ, LeWinter MM, Wagner PD. Effect of sodium nitroprusside on ventilation/perfusion mismatching in heart failure. JACC 1984;4:918–22.

CHAPTER 18

VENTILATION–PERFUSION DISTRIBUTIONS IN DISEASE

Antoni Ferrer, Robert Rodriguez-Roisin

The inception of the multiple inert gas elimination technique (MIGET)[1,2] at the University of California in San Diego at the beginning of the 1970s initiated a major breakthrough in respiratory pathophysiology, introducing the current gold standard for the detailed investigation of ventilation–perfusion ($\dot{V}_A/\dot{Q}$) imbalance and its interplay with the extrapulmonary factors (ie, overall ventilation, cardiac output, and oxygen output) governing pulmonary gas exchange. Before the development of the MIGET, the assessment of pulmonary gas exchange was exclusively based on the three-compartment model of the lung described by Riley and Cournand,[3] still broadly used in the clinical arena because of its usefulness and simplicity.

The three-compartment model of the lung allows the calculation of the alveolar–arterial partial pressure oxygen difference ($P_{A-a}O_2$) through measurement of the partial pressures of oxygen (P_aO_2) and carbon dioxide (P_aCO_2) in arterial blood, along with the venous admixture ratio ($\dot{Q}_S/\dot{Q}_T$) and the physiologic dead space ($\dot{V}_D/\dot{V}_T$). However, the $\dot{Q}_S/\dot{Q}_T$ cannot differentiate true intrapulmonary shunt (nonventilated or zero $\dot{V}_A/\dot{Q}$ ratio) from low $\dot{V}_A/\dot{Q}$ units, just as the $\dot{V}_D/\dot{V}_T$ cannot differentiate between high $\dot{V}_A/\dot{Q}$ units and true physiologic dead space (unperfused or infinite $\dot{V}_A/\dot{Q}$ ratio). The MIGET is a multicompartment approach that facilitates the differentiation of all these concepts because it can discriminate 50 compartments with different $\dot{V}_A/\dot{Q}$ ratios ranging from zero (shunt) to infinity (dead space). In addition to the graphical representation of the $\dot{V}_A/\dot{Q}$ distributions, the MIGET provides quantitative information on numerous physiologic descriptors of pulmonary gas exchange. Central to the quantification of $\dot{V}_A/\dot{Q}$ inequality are the log SD Q (log standard deviation or dispersion of pulmonary bloodflow) and log SD V (dispersion of alveolar ventilation), key descriptors of the amounts of low and high $\dot{V}_A/\dot{Q}$ units, respectively. The upper 95% confidence limit in normal subjects at age 20 years for log SD Q is 0.60 and that for log SD V is 0.65. At age 70 years, the corresponding upper limits are 0.70 and 0.75, respectively.[4]

The MIGET also provides information on the role of the diffusion limitation for oxygen in disease states. The computer calculations based on the theoretical mathematical model of the MIGET allow us to determine the predicted (estimated) P_aO_2 that results from the measured $\dot{V}_A/\dot{Q}$ distributions, with the implicit assumption that there is no oxygen diffusion limitation for inert gases. If the measured (actual) P_aO_2 is significantly lower than the predicted P_aO_2, which reflects $\dot{V}_A/\dot{Q}$ imbalance and intrapulmonary shunt alone, it can be inferred that there is coexisting alveolar–capillary diffusion limitation for oxygen.

The work of different groups of investigators using MIGET in several clinical and experimental conditions over the last 30 years has provided a clear view of pulmonary gas exchange in health and disease.[5] This chapter reviews gas exchange abnormalities in the setting of numerous clinical categories of lung diseases based on this experimental approach.

BRONCHIAL ASTHMA

Persistent Asthma (Table 18-1)

The first study[6] of $\dot{V}_A/\dot{Q}$ distributions in asthmatic patients was carried out in a small series of patients with stable, mild-to-moderate asthma. The distributions of $\dot{V}_A/\dot{Q}$ ratios (Figure 18-1) were typically characterized by a bimodal pattern in bloodflow distribution, with a significant proportion of the cardiac output (approximately 25%) perfusing lung units with low $\dot{V}_A/\dot{Q}$ ratios (< 0.1). There was no shunt and there were no areas with high $\dot{V}_A/\dot{Q}$ ratios, and dead space was normal. In this study, the amount of $\dot{V}_A/\dot{Q}$ imbalance was greater than in subsequent publications, despite the similar severity of airways obstruction, probably because of differences in patient selection and/or their medical treatment. The bimodal pattern of bloodflow distribution was attributed to the effectiveness of collateral ventilation, which prevented complete airways occlusion by mucus plugging, edema, and/or bronchoconstriction. This explains the absence of the development of shunt and the failure of the low $\dot{V}_A/\dot{Q}$ units to collapse beyond the occluded airways.[7] Likewise, it is consistent with the hypothesis that the changes involved in abnormalities of pulmonary gas exchange take place peripherally rather than centrally, where collateral ventilation is less likely to play a major

Table 18-1 Gas Exchange Abnormalities in Different Clinical Types of Asthma

Clinical type of asthma	*Reference*	*No. of patients*	*FEV_1 (% predicted)*	*P_aO_2 (mm Hg)*	*Log SD Q*	*Log SD V*
Stable, mild asthma	11	16	92 ± 5	88.1 ± 2.7	0.71 ± 0.09	0.57 ± 0.04
Stable, moderately severe, chronic asthma	9	26	72 ± 5	89.8 ± 2.3	0.74 ± 0.05	0.58 ± 0.03
Stable, severe, chronic asthma	13	11	39 ± 3	77.3 ± 2.4	0.77 ± 0.03	0.72 ± 0.02
Acute severe asthma (in the emergency room)						
Discharged patients	16	9	46.0 ± 5.8	73.1 ± 3.0	0.92 ± 0.11	0.60 ± 0.05
Hospitalized patients	16	9	31.3 ± 3.3	52.5 ± 3.6	1.28 ± 0.11	0.80 ± 0.09
Acute severe asthma (hospitalized)	15	19	41 ± 3	70.7 ± 2.9	1.18 ± 0.08	0.77 ± 0.03
Acute severe asthma (hospitalized)	14	10	33.0 ± 5.4	50.5 ± 2.6	1.41 ± 0.12	0.78 ± 0.04
Acute severe asthma requiring mechanical ventilation	17	8	*	*	1.65 ± 0.28	1.01 ± 0.24

Values are mean ± SEM. *Patients under mechanical ventilation at maintenance F_iO_2.
Upper 95% confidence limits at age 20 years are 0.60 for log SD *Q* and 0.65 for log SD *V*. At age 70 years, the upper limits of reference are 0.70 for log SD *Q* and 0.75 for log SD *V*.[4]

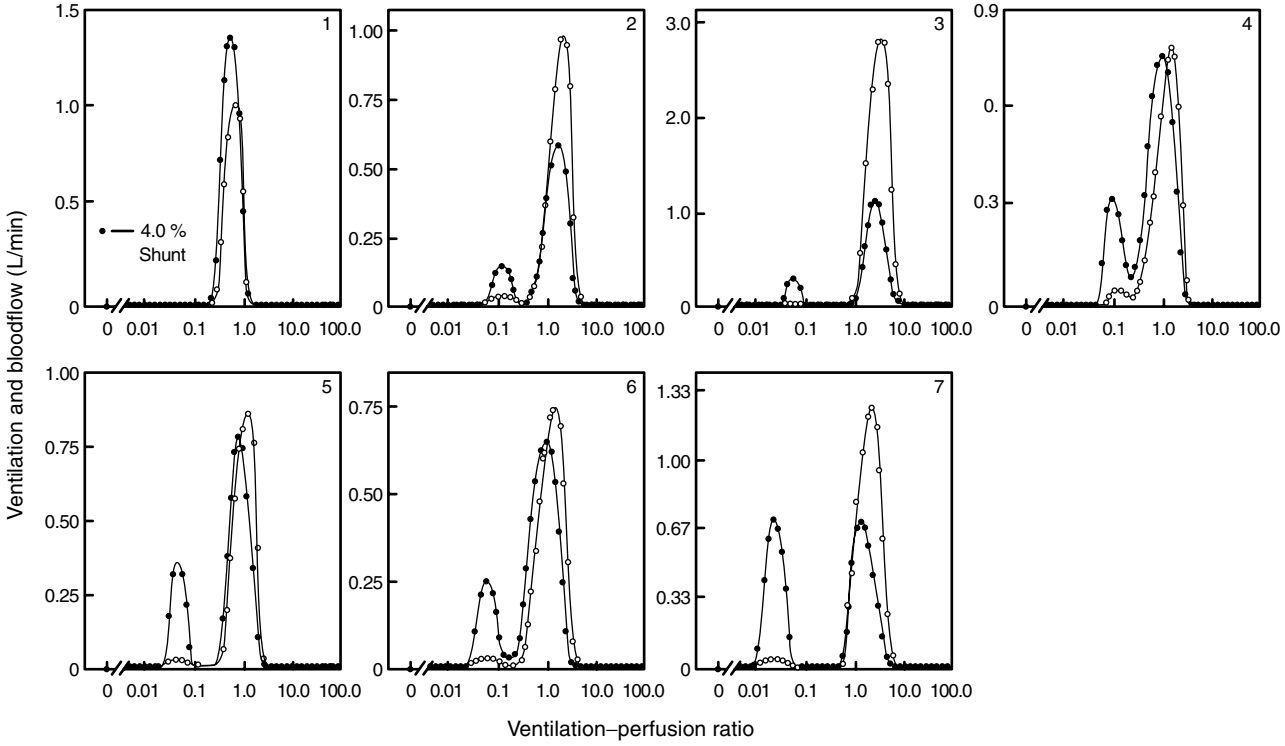

FIGURE 18-1 Representative distributions of ventilation–perfusion ratios of the seven patients with asthma described by Wagner and colleagues.[6] In patients 1 to 6, forced expiratory volume in 1 second (FEV_1) ranged from 60 to 105% predicted, and P_aO_2 was normal or slightly decreased (78 to 109 mm Hg). Patient 7 was experiencing an acute asthmatic episode (FEV_1, 11% predicted; P_aO_2, 52 mm Hg). Open circles = ventilation. Solid circles = bloodflow.

role. Although a bimodal pattern of bloodflow distribution can also be reproduced after methacholine challenge,[8] where central bronchoconstriction is predominant, the presence of this bimodal pattern with modest or no airflow limitation is most consistent with persistent peripheral airways involvement.

Wagner and colleagues[9] also assessed the prevalence and variability of $\dot{V}_A/\dot{Q}$ distributions in a larger sequential study of stable, symptomatic patients with moderately severe asthma followed weekly over a 2-month period. Bimodal distributions were found in only one-third of the measurements, but all but two patients showed bimodality in at least one of the measurements. The principal finding was a widening of bloodflow distribution, although a few patients had normal bloodflow distributions. Unlike the increased log SD *Q*, the log SD *V* was much less abnormal, hence confirming that regions of high $\dot{V}_A/\dot{Q}$ ratio are not a common feature of asthma. Patients in this study were regularly

treated with inhaled glucocorticosteroids, probably resulting in less airways inflammation and in keeping with a low prevalence of bimodal bloodflow distribution. Other studies[7,10,11] involving patients with stable, mild asthma included individuals with intermittent or moderate disease treated with β_2-agonists on demand, with or without inhaled steroids and/or oral theophylline. Although baseline $\dot{V}_A/\dot{Q}$ distributions were mostly unimodal and very narrow, some displayed broader unimodal perfusion and ventilation profiles or just a modest bimodal bloodflow profile. As in previous studies, intrapulmonary shunt was conspicuously absent or negligible, and the areas of high $\dot{V}_A/\dot{Q}$ ratio and dead space were either within normal limits or reduced.

In patients with stable severe asthma,[12,13] the $\dot{V}_A/\dot{Q}$ distributions were broad and unimodal, without shunt or areas with low or high $\dot{V}_A/\dot{Q}$ ratio. The amount of $\dot{V}_A/\dot{Q}$ inequality was modest, and dead space was normal or decreased. Despite the severity of airways obstruction in these patients, they could maintain near-normal P_aO_2, with relatively little $\dot{V}_A/\dot{Q}$ imbalance, presumably because peripheral airways had undergone less inflammatory change, or there was more active hypoxic pulmonary vasoconstriction, or both.

Acute Severe Asthma

Patients with acute severe asthma ("status asthmaticus") have been studied under different clinical circumstances, ranging from their stay at the emergency room to their management in intensive care.[14–17] The $\dot{V}_A/\dot{Q}$ profile was similar to that of those with less severe disease, although with a predominant bimodal bloodflow pattern. A large amount of blood was perfusing areas with low $\dot{V}_A/\dot{Q}$ ratios, but shunt was absent or very modest. The efficacy of the standard treatment facilitated a return to baseline conditions, close to that of healthy individuals (Figure 18-2). All in all, these studies showed a clear dissociation between maximal airflow rates and the amount of $\dot{V}_A/\dot{Q}$ inequality,[14] thereby suggesting that whereas reduced airflow rates predominantly reflect greater airways bronchoconstriction, $\dot{V}_A/\dot{Q}$ mismatch is more related to obstructive changes in peripheral, small airways due to mucus plugging and bronchial wall edema. The patients who were discharged from the emergency room, because of less severe attacks, showed fewer $\dot{V}_A/\dot{Q}$ abnormalities in comparison with those who needed hospitalization, a more intensely affected group.[16] The rate of improvement of expiratory flow rates was, however, similar in discharged and hospitalized patients. Notwithstanding this, whereas the rate of recovery of $\dot{V}_A/\dot{Q}$ imbalance in discharged patients ran in parallel with reduced airflow rates, the pattern in hospitalized patients was substantially delayed in relation to the progressive improvement in airflow rates (Figure 18-3). These findings suggest that the more severe the asthma attack, the more severe the obstructive changes involving peripheral airways for any given degree of diffuse airway narrowing. Patients requiring mechanical ventilation[17] showed the most abnormal gas exchange characteristics of the $\dot{V}_A/\dot{Q}$ spectrum observed in asthma but essentially the same profile as in patients with less severe disease. These patients showed a high level of hypoxic pulmonary vascular response. Interestingly, they

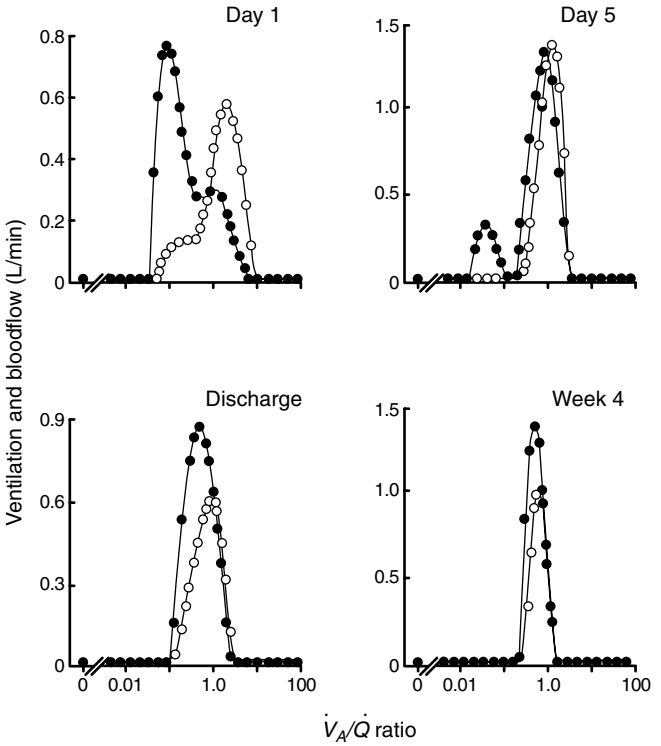

FIGURE 18-2 Evolution of $\dot{V}_A/\dot{Q}$ ratio distributions in a representative patient with acute severe asthma during hospitalization (days 1 and 5), at discharge, and 1 month later. This patient shows a typical bimodal bloodflow distribution at day 1, which still persists, although more discreetly, at day 5, becoming broadly unimodal distribution at discharge. One month later, $\dot{V}_A/\dot{Q}$ distributions are indistinguishable from those of a normal subject. Open circles = ventilation. Solid circles = bloodflow. Reproduced with permission from Roca J et al.[14]

exhibited mild-to-moderate increases in intrapulmonary shunt while breathing 100% oxygen, suggesting the presence of resorption atelectasis.

It has been emphasized that, in addition to the lack of correlation between reduced airflow rates and inert gases, the relationship between arterial blood gases and the indices of $\dot{V}_A/\dot{Q}$ inequality was poor or absent. Although the greater the $\dot{V}_A/\dot{Q}$ mismatch, the lower the P_aO_2, the relatively well-preserved P_aO_2 for the different degrees of $\dot{V}_A/\dot{Q}$ mismatch can be attributed to the high levels of ventilation and cardiac output found in most of the studies, two key extrapulmonary factors governing arterial oxygenation. In all the studies alluded to above, predicted P_aO_2 (according to the MIGET) was always close to measured (actual) P_aO_2, hence excluding oxygen diffusion limitation, even in the most life-threatening forms of asthma.

Bronchial Challenge

Gas exchange has been studied after several types of inhalational challenge.[7,11,18,19] All of the challenges provoked moderate-to-severe bronchoconstriction and a mild-to-moderate fall in P_aO_2, essentially caused by $\dot{V}_A/\dot{Q}$ mismatching. The latter was characterized by mild-to-moderate broad unimodal bloodflow distributions, occasionally bimodal, without associated intrapulmonary shunt.

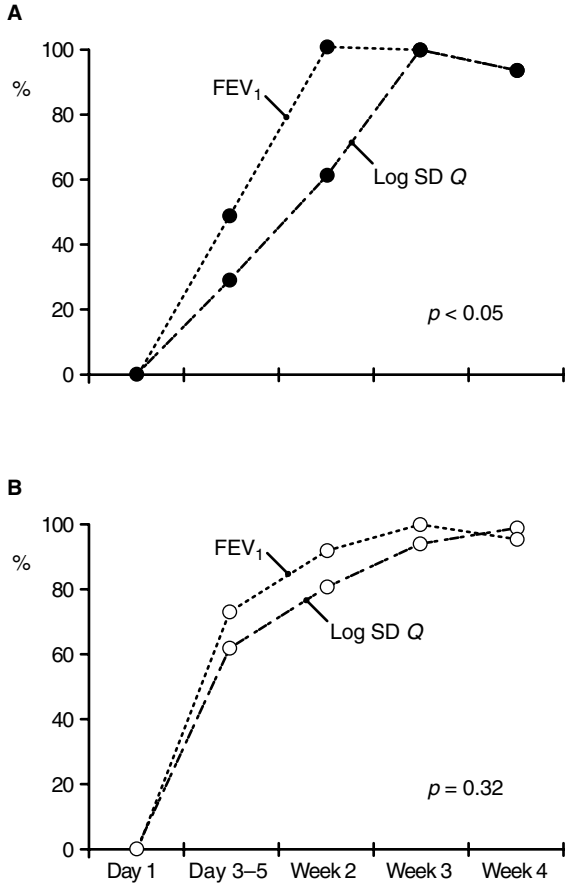

FIGURE 18-3 Time courses of the improvement in forced expiratory volume in 1 second (FEV_1) and $\dot{V}_A/\dot{Q}$ mismatch (measured as the dispersion of bloodflow, log SD Q) in patients with acute severe asthma initially seen in the emergency room. *A*, Patients who required hospitalization. *B*, Patients who could be discharged. Reproduced with permission from Ferrer A et al.[16]

Although all variables had returned to baseline at the completion of the exposure to the provoking agent, the recovery of airflow rates was always more rapid than that of pulmonary gas exchange during methacholine,[11] histamine,[18] and allergen[7] challenges, resembling the recovery from spontaneous acute asthma. Some of the patients developed a late-phase reaction with deterioration of flow rates and $\dot{V}_A/\dot{Q}$ relationships during allergen challenge. It is noteworthy that during a cysteinyl-leukotriene (LTD_4) challenge,[19] there is no dissociation between spirometric and gas exchange disturbances, suggesting that all changes are, rather, related to the intense, widespread bronchoconstriction.

The inhalation of platelet-activating factor (PAF), in patients with mild asthma[20] and in healthy individuals,[21] resulted in moderate-to-severe $\dot{V}_A/\dot{Q}$ disturbances in a pattern similar to that commonly observed in patients with spontaneous moderate-to-severe asthma, probably related to abnormally increased airway permeability. Salbutamol,[22] but not ipratropium bromide,[23] prevented all PAF-induced systemic and pulmonary effects, thereby reinforcing the important role of airway microvascular leakage. However, PAF antagonists have had limited value when added to the standard treatment of acute asthma. Altogether, these findings argue against a potential pathogenic role for PAF as one of the relevant mediators of airway inflammation in bronchial asthma. By contrast, in exercise-induced asthma,[10] $\dot{V}_A/\dot{Q}$ changes returned to baseline values before normalization of airflow rates. This reversed recovery pattern in relation to the other challenges alluded to, or to spontaneous asthma, suggests that in this condition the underlying physiologic mechanisms are different, probably because the sites of the major responses are the large airways, where drying, cooling, and fluid osmotic changes are more pronounced and rapidly reversed.

MIGET studies in asthmatic children have also been performed during exercise[24] and histamine challenge,[25] and both studies showed a different pattern from adults, characterized by the presence of high $\dot{V}_A/\dot{Q}$ areas with a shift of the main bloodflow mode to the left of the $\dot{V}_A/\dot{Q}$ distributions, responsible for the observed hypoxemia. The investigators speculated that chronically narrowed airways capable of producing areas with low $\dot{V}_A/\dot{Q}$ ratio may not be as prevalent in children and that the changes could be due to a valve mechanism causing patchy gas trapping, resulting in hyperinflation and gas trapping, and reduction of bloodflow to these regions.

Oxygen Breathing

Arterial hypoxemia in asthma can be rapidly and efficiently reversed by moderate increases in the fraction of inspired oxygen (F_IO_2) since it is essentially induced by $\dot{V}_A/\dot{Q}$ mismatch. However, although the net balance is an increase in P_aO_2, breathing 100% oxygen causes a deterioration in $\dot{V}_A/\dot{Q}$ mismatch in both chronic[12,13] and acute asthma.[14,15,17] This response is characterized by a widening of the $\dot{V}_A/\dot{Q}$ distributions, more specifically an increased perfusion to low $\dot{V}_A/\dot{Q}$ regions, suggesting release of hypoxic pulmonary vasoconstriction. Only in the most severe patients, namely those who need mechanical ventilation,[17] does collateral ventilation fail to prevent the development of moderate amounts of shunt while a hyperoxic mixture is being breathed (see above).

Response to Bronchodilators

Early studies with conventional arterial blood gases showed that the inhalation of nonselective β-adrenergic agents by patients with chronic airway obstruction often resulted in a transient decrease in P_aO_2 without major changes in P_aCO_2, despite concomitant bronchodilatation.[26,27] Originally, isoproterenol, a relatively short-acting nonselective β-adrenergic agent with both β_1- and β_2-adrenergic properties, was the agent most frequently administered. The comparison of isoproterenol and fenoterol, a more selective but also more potent β_2-agonist, showed that P_aO_2 changes were more marked after isoproterenol, and, although usually small, occasionally the changes were as great as 10 mm Hg. This β-adrenergic–induced transient hypoxemia, so-called "paradoxical hypoxemia," was basically attributed to the potent vasodilator effects of these agents mediated via β_2-receptors releasing hypoxic vasoconstriction and increasing bloodflow to alveoli with altered $\dot{V}_A/\dot{Q}$ areas. The study[6] showed increases in perfusion to areas with low $\dot{V}_A/\dot{Q}$ ratios

and in cardiac output and decreases in P_aO_2, 5 minutes after administration of isoproterenol, suggesting that the release of hypoxic vasoconstriction was the principal mechanism underlying further $\dot{V}_A/\dot{Q}$ worsening. These changes returned to baseline values just 10 minutes after drug administration, whereas expiratory flow rates continued to improve, indicating that the increase in perfusion to relatively underventilated areas was greater than the increase in ventilation to these alveoli. We have shown that, in patients with acute asthma[15] and also in those with stable, severe, persistent asthma,[13] inhaled salbutamol, the cornerstone of selective β_2-agonist treatment, did not alter $\dot{V}_A/\dot{Q}$ imbalance or P_aO_2 15 minutes after the drug was given. The administration of salbutamol by intravenous infusion in patients with acute severe asthma further worsened $\dot{V}_A/\dot{Q}$ relationships without modifying P_aO_2 because the cardiovascular effects of salbutamol, specifically an inordinately increased cardiac output, counterbalanced the deleterious effects of $\dot{V}_A/\dot{Q}$ imbalance on P_aO_2.[15] Although there are no studies on long-acting adrenergic agents with the MIGET, both short-acting and long-acting adrenergic agents may induce small degrees of oxygen desaturation that can be easily offset by conventional oxygen therapy. These mild-to-moderate decreases in P_aO_2 are of the order of 5 mm Hg as a mean in the vast majority of studies, although in a few cases these decrements can be more prominent. It is of note that in a randomized controlled trial, intravenous aminophylline, given within the therapeutic range, in patients with acute asthma, did not cause a deterioration of $\dot{V}_A/\dot{Q}$ mismatching.[28]

CHRONIC OBSTRUCTIVE PULMONARY DISEASE

STABLE CONDITIONS

Wagner and colleagues[29] were also the first to assess $\dot{V}_A/\dot{Q}$ relationships using the MIGET in a subset of 23 patients with stable, severe chronic obstructive pulmonary disease (COPD). They demonstrated an increased dispersion in the distributions of bloodflow and in those of alveolar ventilation and identified three different patterns of $\dot{V}_A/\dot{Q}$ distributions (H, L, and HL). The type H (high) pattern was characterized by the presence of lung units with a high $\dot{V}_A/\dot{Q}$ ratio that produced a bimodal ventilation distribution, containing little bloodflow (almost all of the bloodflow in these patients was in regions with lower $\dot{V}_A/\dot{Q}$ ratios). The type L (low) pattern was characterized by the presence of lung units with very low $\dot{V}_A/\dot{Q}$ ratios that produced a bimodal bloodflow distribution. The type HL (high, low) pattern had the associated features of both. In addition, this study clearly demonstrated that $\dot{V}_A/\dot{Q}$ inequality accounted almost exclusively for all of the observed arterial hypoxemia and that other intrapulmonary mechanisms influencing P_aO_2 (ie, increased intrapulmonary shunt and oxygen diffusion impairment) were negligible. Although the H pattern appeared to be more prevalent in patients with the characteristic emphysematous type of COPD, no other consistent correlations between abnormal $\dot{V}_A/\dot{Q}$ inequalities and clinical characteristics of the patients could be established. Subsequently, other investigators evaluated the $\dot{V}_A/\dot{Q}$ distributions in clinically stable COPD patients, encompassing a wide range of disease severity.[30–44] As shown in Table 18-2, all these studies have consistently documented $\dot{V}_A/\dot{Q}$ disturbances and, despite a wide variation in the degree of airflow obstruction among the different studies, the reported differences in both log SD Q and log SD V were less pronounced than in asthma. Figure 18-4 shows the relationships between forced expiratory volume in 1 second (FEV_1) and log SD Q and log SD V in 89 COPD patients found in different studies by our group.[36,37,41–44] Note that although almost all patients had abnormally high values of log SD Q and log SD V and that the correlations with FEV_1 were significant, the data were widely scattered. Even in patients without airflow obstruction and with normal P_aO_2 but with evidence of

Table 18-2 Ventilation–Perfusion Distributions in Stable Chronic Obstructive Pulmonary Disease

		FEV_1								
Reference	*N*	*L*	*% pred*	*PaO_2 (mm Hg)*	*P_aCO_2 (mm Hg)*	*$P_{A-O}O_2$ (mm Hg)*	*Log SD Q*	*Log SD V*	*Shunt $\%\dot{Q}_T$*	*Dead space $\%\dot{V}_E$*
Wagner et al (1977)[29]	23	NR	40 ± 11	58 ± 9	45 ± 10	NR	1.12 ± 0.30	1.27 ± 0.35	2.1 ± 5.0	36 ± 5
Melot et al (1983)[30]	6	0.80 ± 0.13	NR	52 ± 4	46 ± 3	43 ± 2	0.97 ± 0.07	1.23 ± 0.20	1.7 ± 0.7	47 ± 6
Melot et al (1984)[31]	6	0.89 ± 0.20	NR	52 ± 4	44 ± 3	45 ± 2	0.92 ± 0.06	1.02 ± 0.11	3.5 ± 1.9	55 ± 5
Castaing et al (1985)[32]	14	NR	NR	55 ± 9	51 ± 6	NR	0.78 ± 0.20	1.08 ± 0.41	4.2 ± 4.1	45 ± 11
Dantzker and D'Alonzo (1986)[33]	7	0.56 ± 0.05	NR	76 ± 10	56 ± 6	NR	0.73 ± 0.20	NR	NR	NR
Roca et al (1987)[34]	7	NR	NR	60 ± 3	48 ± 2	NR	0.91 ± 0.06	0.99 ± 0.10	0	46 ± 3
Ringsted et al (1989)[35]	6	0.33 ± 0.14	16 ± 4	50 ± 10	48 ± 7	NR	0.81 ± 0.12	1.43 ± 0.25	3.3 ± 3.0	40 ± 11
Agusti et al (1990)[36]	8	1.15 ± 0.12	36 ± 3	76 ± 2	39 ± 2	28 ± 2	0.90 ± 0.06	1.03 ± 0.11	0.6 ± 0.3	29 ± 3
Barbera et al (1994)[38]	20	2.30 ± 0.51	72 ± 12	77 ± 9	37 ± 3	29 ± 9	0.87 ± 0.24	0.73 ± 0.25	1.0 ± 0.9	32 ± 9
Andrivet et al (1994)[39]	8	0.85 ± 0.11	24 ± 4	70 ± 4	58 ± 5	30 ± 4	0.66 ± 0.18	0.87 ± 0.20	2.6 ± 0.8	56 ± 3
Moinard et al (1994)[40]	14	0.89 ± 0.38	NR	59 ± 10	44 ± 8	NR	1.20 ± 0.30	1.00 ± 0.40	1.7 ± 1.3	52 ± 9
Barbera et al (1996)[41]	13	0.90 ± 0.06	28 ± 2	56 ± 2	46 ± 1	35 ± 3	1.11 ± 0.08	0.96 ± 0.04	2.7 ± 0.9	35 ± 3
Viegas et al (1996)[42]	24	0.93 ± 0.46	30 ± 14	65 ± 8	41 ± 7	37 ± 8	1.11 ± 0.24	0.98 ± 0.25	0.7 ± 1.3	35 ± 11
Barbera et al (1997)[43]	13	0.91 ± 0.19	29 ± 6	60 ± 11	44 ± 6	NR	0.96 ± 0.27	1.08 ± 0.30	1.3 ± 1.7	43 ± 9
Roger et al (1997)[44]	9	1.19 ± 0.07	39 ± 2	72 ± 3	41 ± 1	28 ± 4	0.92 ± 0.09	0.84 ± 0.08	0.5 ± 0.1	37 ± 3

Adapted from Barbera JA.[47] FEV_1 = forced expiratory volume in 1 second; log SD Q = dispersion of bloodflow distribution; log SD V = dispersion of ventilation distribution; N = number of patients in the study; NR = not reported; P_aCO_2 = arterial carbon dioxide tension; P_aO_2 = arterial oxygen tension; $P_{A-a}O_2$ = alveolar–arterial oxygen PO_2 difference; $\dot{Q}_T$ = cardiac output; $\dot{V}_E$ = minute ventilation; Shunt: perfusion to alveolar units with $\dot{V}_A\dot{Q}$ ratios <0.005. Dead space: ventilation to units with $\dot{V}_A\dot{Q}$ ratios >100. Dispersions are either standard deviation or standard error of the mean.

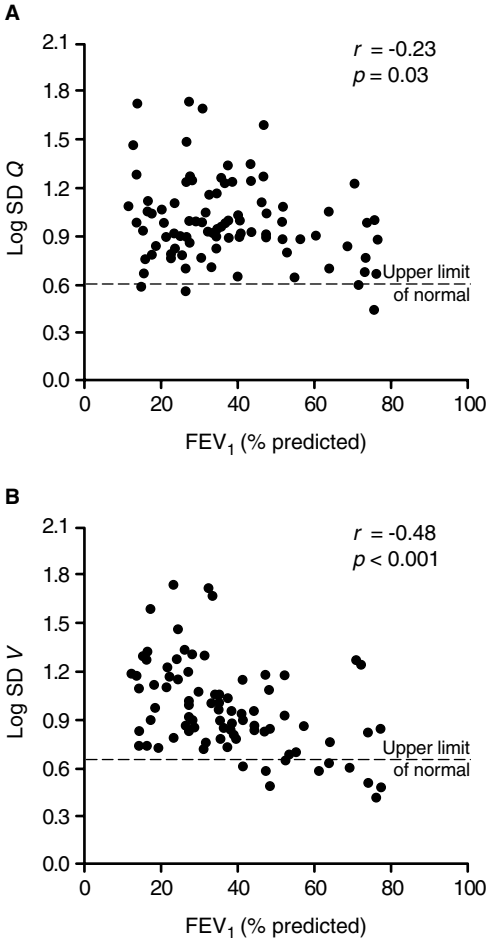

FIGURE 18-4 Relationship between (*A*) dispersion of bloodflow distribution (log SD *Q*) and forced expiratory volume in 1 second (FEV_1, percent predicted) and (*B*) dispersion of ventilation distribution (log SD *V*) and FEV_1 in 89 patients with chronic obstructive pulmonary disease. *Dashed lines* indicate the normal upper 95% confidence limits of log SD *Q* and log SD *V*. Reproduced with permission from Barbera JA.[47]

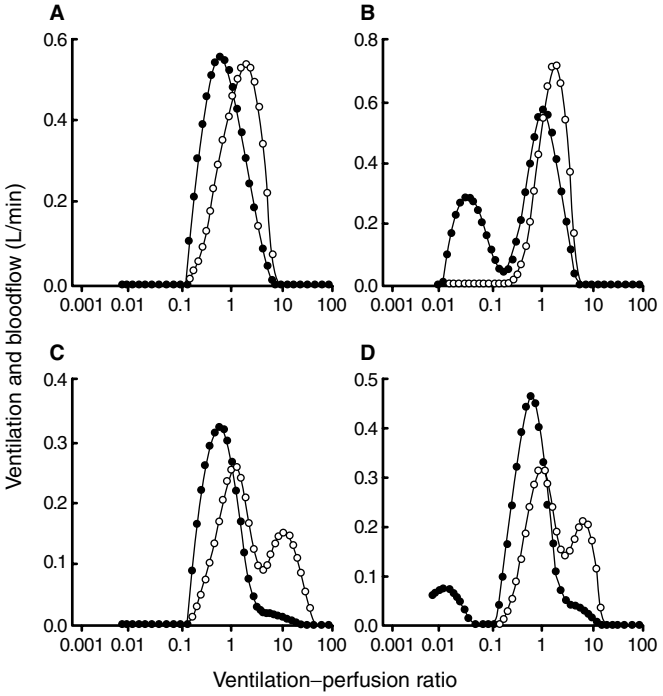

FIGURE 18-5 Patterns of ventilation–perfusion ($\dot{V}_A\dot{Q}$) distribution in patients with chronic obstructive pulmonary disease. *A*, Broad unimodal distributions of both bloodflow and ventilation. *B*, Bimodal distribution of bloodflow with a significant amount of perfusion diverted to areas with low $\dot{V}_A\dot{Q}$ ratios. *C*, Bimodal distribution of ventilation with a significant amount of ventilation diverted to areas with high $\dot{V}_A\dot{Q}$ ratios. *D*, Bimodal distribution of both bloodflow and ventilation. Values of shunt and dead space are not shown. The frequency of presentation of each pattern is discussed in the text. Open circles = ventilation. Solid circles = bloodflow. Reproduced with permission from Barbera JA.[47]

small airways dysfunction,[45] there was a small but significant increase in $P_{A-a}O_2$ with modestly abnormal $\dot{V}_A/\dot{Q}$ relationships, similar to those observed in patients with early COPD and mild airflow obstruction.[37,38] Although the patients with the most severe airflow obstruction tended to show the greatest degrees of $\dot{V}_A/\dot{Q}$ inequality, patients with similar values of FEV_1 could show different degrees of $\dot{V}_A/\dot{Q}$ mismatching. This dissociation between the degree of airflow obstruction and abnormal $\dot{V}_A/\dot{Q}$ indices has also been observed in patients with bronchial asthma,[14] indicating that the structural and functional determinants of airflow rates and gas exchange may be different. As shown in Table 18-2, intrapulmonary shunt is rarely seen in COPD. Thus, its detection should suggest alternative diagnoses (such as atelectasis, pneumonia, pulmonary edema, and/or abnormal pulmonary vascular or cardiac communications).

The "high" and "low" profiles of $\dot{V}_A/\dot{Q}$ distributions originally described[29] can be identified in some patients, but the suggested association between the H pattern and the emphysematous phenotype has never been confirmed subsequently.[46] Moreover, the association between the pattern of $\dot{V}_A/\dot{Q}$ mismatch and the clinical characteristics of COPD has not been addressed in other studies. Cumulative experience with the MIGET indicates that the most frequent pattern of $\dot{V}_A/\dot{Q}$ distributions in COPD was a broadened, unimodal distribution of both bloodflow and ventilation. A retrospective analysis[47] of the patterns of $\dot{V}_A/\dot{Q}$ distribution in 94 patients with stable COPD,[34,36,37,41–44] covering a wide clinical spectrum of COPD, identified four different patterns of $\dot{V}_A/\dot{Q}$ distributions (Figure 18-5). Broad unimodal distributions of bloodflow and ventilation were shown in 45% of the patients; a bimodal distribution of bloodflow, with normal and low $\dot{V}_A/\dot{Q}$ areas, was shown in 23%; a bimodal distribution of ventilation, with normal and high $\dot{V}_A/\dot{Q}$ areas, was shown in 18%; and the remaining 14% showed both bimodal bloodflow and ventilation. This diversity in the pattern of $\dot{V}_A/\dot{Q}$ distributions presumably reflects the heterogeneity of pulmonary pathologic abnormalities and also of the efficiency of compensatory mechanisms (see below).

Exacerbations

Episodes of exacerbation in COPD are characterized by hypoxemia with or without associated hypercapnia. We studied the outcomes resulting from disturbed $\dot{V}_A/\dot{Q}$ relationships during exacerbations that required hospitalization.[43] Both hypoxemia and hypercapnia were related to

further $\dot{V}_A/\dot{Q}$ worsening, characterized by increased perfusion to poorly ventilated areas (low $\dot{V}_A/\dot{Q}$ ratios). Increased intrapulmonary shunt was almost negligible (most commonly <10% of cardiac output), probably because of the absence of complete airways occlusion, the efficiency of collateral ventilation, and/or an active hypoxic vascular response. These results are consistent with widespread airway narrowing provoked by inflammation, bronchospasm, and/or inspissated mucus hypersecretion. Even though hypoxemia was primarily produced by increased $\dot{V}_A/\dot{Q}$ inequality, this effect was amplified by an increase in oxygen consumption, probably attributable to increased work of the respiratory muscles and/or bronchodilator overtreatment resulting in a decreased mixed venous PO_2. The abnormality was, however, counterbalanced, at least in part, by an increased cardiac output; in contrast, minute ventilation was not an influence. An analysis of the factors contributing to the reduction of P_aO_2 during exacerbation[43] indicated that 46% of this reduction can be caused by further $\dot{V}_A/\dot{Q}$ imbalance, 28% by the combined changes of increased oxygen consumption and cardiac output, and the remaining 26% by the amplifying effect on $\dot{V}_A/\dot{Q}$ mismatch that a decreased mixed venous PO_2 had in further decreasing end-capillary PO_2. It is of note that $\dot{V}_A/\dot{Q}$ inequalities during exacerbations are moderate, such that the dispersion of pulmonary bloodflow (log SD Q), one of the best $\dot{V}_A/\dot{Q}$ descriptors, rarely exceeds 1.30,[43,48–51] a threshold of severe $\dot{V}_A/\dot{Q}$ deterioration. By contrast, this $\dot{V}_A/Q$ index is greater in acute severe asthma, with values well above 1.30.[14,17] Even in patients with extremely acute COPD requiring mechanical ventilation,[49–51] the amount of $\dot{V}_A/\dot{Q}$ inequality is less than that found in acute asthma not requiring mechanical support. This implies that acute airway narrowing in asthma attacks is much more pronounced than in COPD exacerbations, leading to the development of a greater proportion of alveolar units with low $\dot{V}_A/\dot{Q}$ ratios. Presumably, acute airway changes are more centrally located in COPD exacerbations than in acute asthma.

Factors Influencing Gas Exchange

Extrapulmonary Factors Patients with COPD may have different values of P_aO_2 for a given degree of $\dot{V}_A/\dot{Q}$ inequality because of the influence of extrapulmonary determinants of gas exchange (overall ventilation, cardiac output, and oxygen consumption). The increase in alveolar ventilation facilitates an increase in the mean $\dot{V}_A/\dot{Q}$ ratio of bloodflow distribution and optimizes P_aO_2, other things being equal. Alveolar units with high $\dot{V}_A/\dot{Q}$ ratios have a greater PO_2 and a lower PCO_2 in the alveoli, such that the increased ventilation to these areas offsets the deleterious influence of areas with low $\dot{V}_A/\dot{Q}$ ratios on P_aO_2. The impact of the breathing pattern on gas exchange is particularly relevant during exacerbations with or without the need for mechanical ventilation (see below). Cardiac output may modify gas exchange, basically through its effect on the oxygen content of mixed venous blood. A decrease in cardiac output will reduce mixed venous PO_2, and a rise in cardiac output will increase it. Accordingly, P_aO_2 will increase or decrease in parallel with the behavior of mixed venous PO_2. This important role of cardiac output in gas exchange has already been alluded to.[43]

Pulmonary Hypoxic Vasoconstriction This phenomenon plays a crucial role in matching alveolar ventilation to pulmonary blood flow in COPD. Its release (inhibition) through the administration of vasodilators,[31,36] 100% oxygen breathing,[38,51] and, occasionally, β_2-adrenergics[35] (see below) will result in decreased pulmonary vascular tone, with increased perfusion to lung units with low $\dot{V}_A/\dot{Q}$ ratios.

Exercise

Arterial PO_2 during exercise may fall, remain unchanged, or even rise, depending on the interactions between the intrapulmonary and extrapulmonary determinants governing gas exchange. In principle, exercise never causes a deterioration in $\dot{V}_A/\dot{Q}$ inequality in COPD: the degree of mismatch present at rest either improves[36,44,52] or remains unaltered,[29,33] depending on the severity of airflow limitation. Arterial PO_2 decreases in severe COPD during exercise, essentially due to the inability of ventilation and cardiac output to increase to meet the expected demands. Whereas healthy subjects show 10-fold increases,[53] patients with severe COPD show only a 2-fold increase in ventilation and cardiac output, essentially because of their ventilatory limitation.[29] Patients with mild COPD are in an intermediate position.[52] There is no oxygen diffusion limitation during exercise.[29,33,44]

Structure–Function Relationships

These have been investigated in patients with mild-to-moderate COPD[37,38,52] who have undergone resectional lung surgery for small nodules. It was shown that the severity of emphysema correlated with P_aO_2, $P_{A-a}O_2$, and bloodflow and ventilation distributions.[37] The correlation between emphysema severity and bloodflow distribution suggests that poorly ventilated alveolar units associated with emphysema may represent one of the structural determinants of hypoxemia in COPD patients. In emphysematous lungs, the reduction of alveolar attachments to membranous bronchioles causes distortion and narrowing of small airways impairing the ventilation in dependent alveolar units and leading to the development of lung units with low $\dot{V}_A/\dot{Q}$ ratios and arterial deoxygenation. As pulmonary emphysema is characterized by destruction of alveolar walls, the enlargement of airspaces and loss of pulmonary capillary network would lead to the development of lung units with greater ventilation than perfusion and intraregional variations in ventilation, that is, areas with high $\dot{V}_A/\dot{Q}$ ratios. The "high pattern," originally described in patients with the clinical characteristics of the emphysematous COPD phenotype,[29] would then be a magnification of this phenomenon. By contrast, small airway abnormalities were only correlated with the dispersion of ventilation,[37] and this has been attributed to heterogeneous distribution of inspired air. However, the absence of correlation between small airway abnormalities with the dispersion of bloodflow and with the percentage of perfusion

to areas with low $\dot{V}_A/\dot{Q}$ ratios cannot be extrapolated to the usual $\dot{V}_A/\dot{Q}$ findings shown in patients with more advanced COPD, particularly during exacerbations.[43,48,50,51] Under these circumstances, a bimodal bloodflow pattern distribution may be more common and can be attributed to the superposition of acute airway changes that are potentially reversible, such as bronchial wall edema and/or mucus plugging, on chronic airways abnormalities. The most characteristic trait of pulmonary vessels was thickening of the intimal layer of pulmonary muscular arteries,[38,54] was related to P_aO_2 values and to the degree of $\dot{V}_A/\dot{Q}$ inequality, and more pronounced in the small arteries that exhibited poor vascular reactivity.[38] The severity of intimal thickening in the pulmonary arteries in COPD patients was linearly correlated with the severity of the inflammatory infiltrate in small airways, suggesting a common inflammatory process affecting both structural abnormalities.[38]

Mechanical Ventilation

The effect of different modes of mechanical ventilation on $\dot{V}_A/\dot{Q}$ distributions in COPD has not been extensively documented. During weaning from mechanical ventilation,[51] the development of a rapid shallow breathing pattern is accompanied by a shift of $\dot{V}_A/\dot{Q}$ distributions toward areas of low $\dot{V}_A/\dot{Q}$ ratios and further $\dot{V}_A/\dot{Q}$ deterioration. As a result, P_aO_2 decreases and P_aCO_2 increases. The beneficial effect of increased cardiac output on P_aO_2 that results from the reduced intrathoracic pressures when patients are disconnected from the ventilator is offset by the detrimental changes in breathing pattern.

We have shown that during weaning from invasive mechanical ventilation,[55] pressure-support ventilation limited $\dot{V}_A/\dot{Q}$ worsening in the transition from positive-pressure ventilation to spontaneous breathing. Hemodynamics, arterial blood gases, and $\dot{V}_A/\dot{Q}$ mismatch were not different between assist-control ventilation and pressure-support ventilation when both modalities provided similar levels of ventilatory assistance. The application of a low level of external positive end-expiratory pressure (PEEP) (equivalent to 50% of intrinsic PEEP) in mechanically ventilated COPD patients[50] shifted $\dot{V}_A/\dot{Q}$ distributions toward areas with high $\dot{V}_A/\dot{Q}$ ratios and improved hypoxemia, but when external PEEP was increased up to the value of intrinsic PEEP, no further improvement in gas exchange was observed. When intrinsic PEEP was reduced by increasing the expiratory time and reducing minute ventilation, a pattern used in controlled mechanical hypoventilation, $\dot{V}_A/\dot{Q}$ distributions shifted toward units with low $\dot{V}_A/\dot{Q}$ ratios, P_aO_2 decreased, and P_aCO_2 increased. However, oxygen delivery to the tissues increased because of the increase in cardiac output induced by the reduction in intrathoracic pressures. In a study with noninvasive ventilation,[48] it was shown that the improvement in hypoxemia and hypercapnia was essentially due to amelioration of alveolar ventilation and not to $\dot{V}_A/\dot{Q}$ amelioration, indicating that an efficient breathing pattern rather than high inspiratory pressures should be the primary goal to improve overall gas exchange during noninvasive ventilation.

Bronchodilators

Both short-acting and long-acting β_2-agonists may induce small decreases in oxygen saturation, which are easily counterbalanced with conventional oxygen therapy. These mild-to-moderate deleterious gas exchange effects, of the order of 5 mm Hg, on average, in most of the studies, are subclinical and well tolerated. In patients with advanced COPD and mild chronic respiratory failure,[35] intravenous terbutaline increased cardiac output, mixed venous PO_2, and oxygen delivery, whereas P_aO_2, systemic blood pressure and pulmonary vascular resistance decreased in the face of an improvement in FEV_1 and minute ventilation. In parallel, there was further $\dot{V}_A/\dot{Q}$ worsening (the perfusion to areas with low $\dot{V}_A/\dot{Q}$ ratios increased) that was not counterbalanced by the simultaneous increase in minute ventilation or an active reduction in pulmonary vascular tone. In the patients with more severe disease, that is, those with more airflow obstruction, hypoxemia, hypercapnia, and also more pronounced pulmonary hypertension, cardiac output increased without pulmonary vascular changes, ventilation increased modestly, and P_aO_2 and the underlying $\dot{V}_A/\dot{Q}$ mismatching remained unaltered. These patients did not alter their basal gas exchange profile after drug administration, conceivably because hypoxic vasoconstriction was weaker or even absent due to more intense chronic alveolar hypoxia and/or to anatomic alterations in the pulmonary vasculature. This would be in keeping with the concept that the progressive increase in pulmonary vascular resistance seen in advanced COPD is due not only to irreversible structural vascular lesions but also to a reversible vascular component.[54] In more severe advanced COPD, the pulmonary vascular tone seems to be more affected, being more rigid and fixed, such that it is less liable to be relaxed (vasodilated) by selective β-agonists. The short-term effect of fenoterol, a selective β_2-agonist, on gas exchange was compared with that of ipratropium bromide in a double-blinded, placebo-controlled study including COPD patients who were mildly to moderately hypoxemic[42]; fenoterol slightly decreased P_aO_2, due to further $\dot{V}_A/\dot{Q}$ worsening. Gas exchange remained stable after ipratropium administration, suggesting that the pulmonary vascular tone was altered after fenoterol administration, resulting in further $\dot{V}_A/\dot{Q}$ inequalities. The effects of intravenous aminophylline on $\dot{V}_A/\dot{Q}$ relationships have also been studied in patients recovering from an exacerbation.[56] Aminophylline improved spirometry but did not affect hypoxemia or the underlying $\dot{V}_A/\dot{Q}$ abnormalities. Although therapeutic doses of aminophylline can increase $\dot{V}_A/\dot{Q}$ inequality in some patients, the overall effect is, in general, modest and of little clinical significance.

Oxygen

As in bronchial asthma, breathing 100% oxygen always causes a deterioration in $\dot{V}_A/\dot{Q}$ relationships subclinically in COPD patients.[29,38,41,51,56,57] Bloodflow is diverted to lung units with lower $\dot{V}_A/\dot{Q}$ ratios, due to the release of hypoxic pulmonary vasoconstriction resulting in increased log SD $\dot{Q}$. By contrast, during hyperoxic breathing, the increase in intrapulmonary shunt due to alveolar collapse resulting

from denitrogenation is almost negligible, rarely exceeding 5% of cardiac output,[29,38,41,51,57] reflecting the fact that most alveolar units have $\dot{V}_A/\dot{Q}$ ratios above their inspired critical value. The effect of oxygen breathing at low concentrations, routinely used in the clinical setting, on $\dot{V}_A/\dot{Q}$ distributions remains undetermined. In one study, the administration of 26% oxygen increased $\dot{V}_A/\dot{Q}$ mismatch,[32] whereas others have failed to demonstrate significant changes in $\dot{V}_A/\dot{Q}$ inequality during breathing of 28% and 40% oxygen.[58]

Vasodilators

Pulmonary hypertension, a cardiovascular complication of COPD that may aggravate its prognosis, can be controlled with long-term oxygen therapy and might be potentially ameliorated by vasodilators. However, systemic vasodilators inhibit hypoxic pulmonary vasoconstriction and have a deleterious impact on $\dot{V}_A/\dot{Q}$ relationships. Nifedipine, a calcium channel blocker, induced a decrease in pulmonary vascular resistance but also a significant fall in P_aO_2, due to increased perfusion of areas with low $\dot{V}_A/\dot{Q}$ ratios, suggesting that the drug releases hypoxic vasoconstriction actively.[31] This detrimental effect of acute administration of systemic vasodilators on $\dot{V}_A/\dot{Q}$ distributions in COPD has been confirmed by others with similar or different vasodilators, such as felodipine,[59] nifedipine,[36] prostaglandin E,[58] and atrial natriuretic factor.[39] In only one study, in which diltiazem was used, was there no deleterious effect on $\dot{V}_A/\dot{Q}$ distributions.[58] The detrimental effect of nifedipine on $\dot{V}_A/\dot{Q}$ mismatch has also been shown during exercise.[36] Inhaled nitric oxide (NO) has a selective vasodilator action on pulmonary circulation. The lack of systemic vasodilatation is due to its inactivation when combined with hemoglobin, for which it has a very high affinity. In a dose–response study of the gas exchange effects of inhaled NO in COPD patients,[60] there was a significant decrease in pulmonary artery pressure at concentrations as low as 5 parts per million (ppm) and, at higher doses, there was a further decrease in pulmonary artery pressure. By contrast, changes in P_aO_2 were modest and shown at concentrations of 40 ppm only. In another study,[40] inhaled NO produced only a moderate decrease in pulmonary artery pressure, whereas P_aO_2 and $\dot{V}_A/\dot{Q}$ distributions remained unchanged. This lack of effect of NO on gas exchange could be explained by the low dose of NO used. We investigated 13 patients with advanced COPD while they were breathing NO (40 ppm) and also 100% oxygen.[41] NO inhalation produced a moderate decrease in pulmonary artery pressure and in P_aO_2 due to further $\dot{V}_A/\dot{Q}$ worsening (ie, increases in log SD $\dot{Q}$ and in the percentage of areas with low $\dot{V}_A/\dot{Q}$ ratios). Oxygen breathing reduced mean pulmonary artery pressure to a lesser extent than NO but caused greater $\dot{V}_A/\dot{Q}$ mismatch. This detrimental effect of inhaled NO on gas exchange in COPD has been confirmed by others[44,61] and attributed to the inhibition of hypoxic vasoconstriction in areas with low $\dot{V}_A/\dot{Q}$ ratios to which the gas has also access, leading to an effect similar to that of systemic vasodilators. NO inhalation decreased pulmonary artery pressure both at rest and during exercise,[44] but the net effect of NO on P_aO_2 was more beneficial during exercise. During exercise, P_aO_2 decreased during breathing of room air, whereas it remained essentially unchanged during NO inhalation. In parallel, $\dot{V}_A/\dot{Q}$ relationships improved during exercise while room air and NO were being breathed, due to reduced ventilation dispersion. The prevention of exercise-induced P_aO_2 fall by NO can be explained by a preferential distribution of NO to well-ventilated alveolar units with faster time constants and more balanced $\dot{V}_A/\dot{Q}$ ratios.

Vasoconstrictors

Pulmonary vasoconstrictors have the theoretical capability to improve $\dot{V}_A/\dot{Q}$ relationships. Of the three studies in COPD patients[30,49,62] on the effect of almitrine, a peripheral chemoreceptor stimulant with pulmonary vasoconstricting effects,[63] two[30,62] showed a beneficial effect on $\dot{V}_A/\dot{Q}$ distributions that was probably related to enhancement of hypoxic pulmonary vasoconstriction, and this was confirmed in dogs[64] and in normal humans.[65] The third study[49] further confirmed these effects in mechanically ventilated COPD patients. This small beneficial effect on gas exchange in patients with COPD comes at the cost of some unwanted effects, such as peripheral neuropathy and body weight loss, which are particularly noticeable during long-term administration of the drug.

INTERSTITIAL LUNG DISEASES

Characteristic of patients with interstitial lung disease (ILD) are dyspnea on exertion, decreased lung volumes, reduced carbon monoxide diffusing capacity (DLco), and mild arterial hypoxemia with hypocapnia at rest that worsens on exercise. The mechanisms of hypoxemia in these disorders have been assessed by means of MIGET in four studies carried out in patients with various ILDs, such as idiopathic pulmonary fibrosis (IPF), asbestosis, and sarcoidosis.[66–68] Altogether, these studies show that $\dot{V}_A/\dot{Q}$ distributions at rest are generally well preserved, narrow, and unimodal and distributed around a $\dot{V}_A/\dot{Q}$ ratio of 1.0, with very modest shunt and bloodflow to units with low $\dot{V}_A/\dot{Q}$ ratios. However, $\dot{V}_A/\dot{Q}$ abnormalities can be mildly increased in more hypoxemic patients. Resting low P_aO_2 was fully explained by $\dot{V}_A/\dot{Q}$ inequality, without evidence of oxygen diffusion limitation; during exercise, part of the increased $P_{A-a}O_2$ (about 20%) was attributed to oxygen diffusion limitation.[66] Our group observed that the pattern of response to exercise can vary with the different categories of ILD.[69] Whereas patients with IPF had a dramatic decrease in P_aO_2 during exercise, patients with asbestosis did not. Therefore, the mechanisms leading to arterial deoxygenation during exercise could also be different. In one of our studies, IPF patients at rest had moderate $\dot{V}_A/\dot{Q}$ imbalance (only 2 to 4% of the cardiac output perfused poorly or unventilated lung units) but also diffusion limitation, both at rest and during exercise. At rest, approximately 20% of arterial hypoxemia was due to diffusion limitation, whereas 80% was induced by $\dot{V}_A/\dot{Q}$ mismatch. During exercise, $\dot{V}_A/\dot{Q}$ mismatch did not worsen, or even improved, but the contribution of the diffusion component to hypoxemia was superior, representing 40% of the $P_{A-a}O_2$, being more intense in the most hypoxemic patients.

There have been similar findings in patients with stage II and III sarcoidosis,[67] where the reported contributions of diffusion limitation to $P_{A-a}O_2$ were 30 and 50%, at rest and during exercise, respectively. The study in IPF patients[68] also showed that the abnormalities of the pulmonary vasculature are key in the modulation of gas exchange, particularly during exercise. Patients with higher pulmonary vascular tone, having greater release of hypoxic vasoconstriction while breathing 100% oxygen, showed less pulmonary hypertension during exercise, less $\dot{V}_A/\dot{Q}$ mismatching at rest and during exercise, and a superior P_aO_2 while exercising. Accordingly, the coexistence of an active pulmonary vascular response to oxygen breathing minimizes gas exchange abnormalities; by contrast, a poor or absent pulmonary vascular tone always coexists with more gas exchange impairment. It is of note that the DLco corrected for alveolar volume (Kco) closely correlated with the magnitude of $\dot{V}_A/\dot{Q}$ disturbances, with the amount of diffusion limitation, and also with the increase in pulmonary vascular resistance elicited by exercise.

PULMONARY VASCULAR DISEASES

In this section we include diseases in which there is a change in pulmonary vascular impedance originating either in the lumen or in the wall of the pulmonary arteries. Here, we focus on the clinical conditions in which vascular obstruction of the pulmonary arterial bed is the main finding, either acutely (pulmonary embolism [PE]) or chronically (chronic thromboembolic pulmonary hypertension [CTPH] and primary pulmonary hypertension [PPH]). The most characteristic disorder associated with a decreased pulmonary vascular tone is the hepatopulmonary syndrome [HPS].

Acute Pulmonary Embolism

Arterial blood gases in PE generally show hypoxemia with increased $P_{A-a}O_2$ and hypocapnia. The mechanisms responsible for these abnormalities have been investigated with the use of the MIGET in several animal models of PE in dogs[70–73] and also in clinical studies.[74–76] These studies have shown that PE can produce different patterns of $\dot{V}_A/\dot{Q}$ inequality, from slightly broadened, unimodal distributions to bimodal distributions of ventilation and/or bloodflow, with different levels of increased dead space and shunt[77,78] (Figure 18-6). These studies have also shown that PE influences most of the intrapulmonary and extrapulmonary factors implicated in pulmonary gas exchange and that the effects of treatment with anticoagulant therapy[76,78] may rapidly reverse the hemodynamic and gas exchange disturbances in these patients.

Ventilation–perfusion inequality is the key mechanism of hypoxemia in PE. The lung units affected by the occlusion

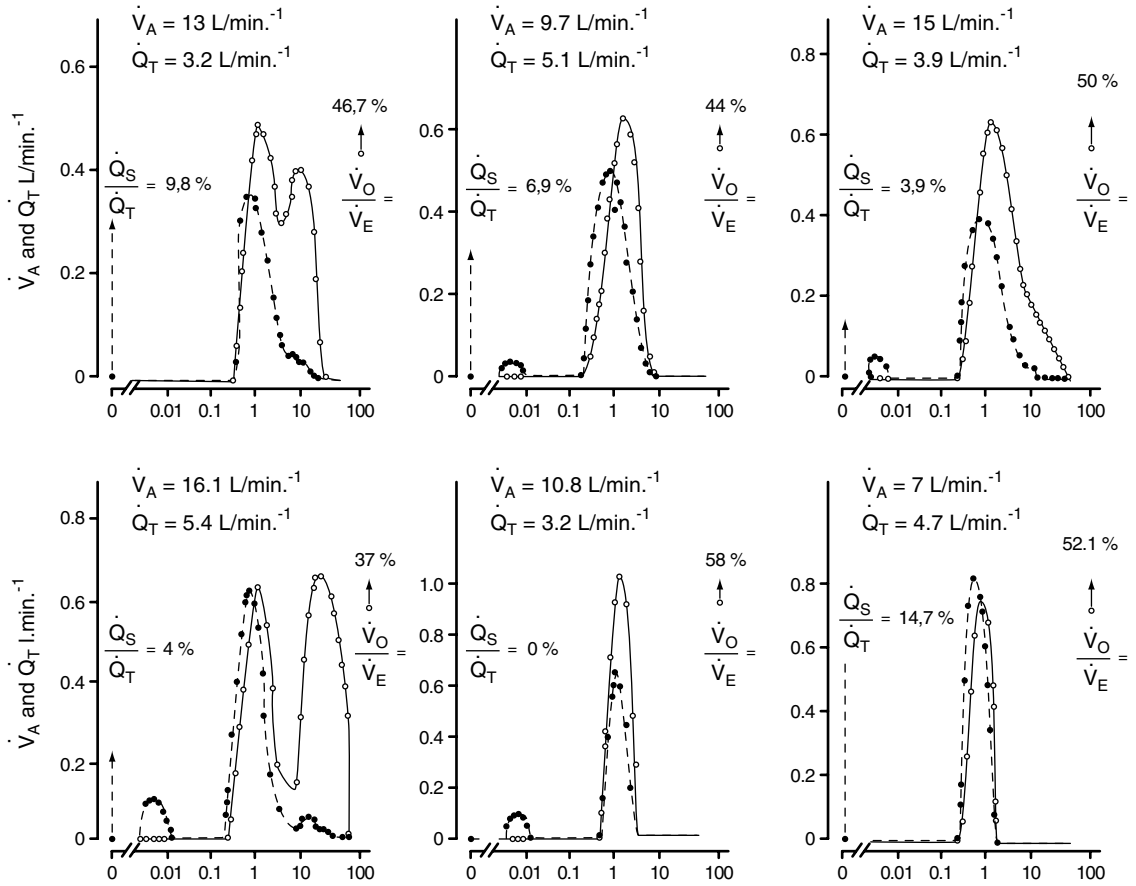

FIGURE 18-6 Different patterns of ventilation–perfusion ($\dot{V}_A\dot{Q}$) distribution in patients with acute pulmonary embolism. The distributions can oscillate from slightly widened unimodal distributions to bimodal distributions of ventilation and/or bloodflow, with different amounts of increased dead space and shunt. Open circles = ventilation. Solid triangles = perfusion. Adapted from Manier G et al.[75]

of their blood vessels by emboli evolve to become areas of net dead space. If vascular occlusion is complete, perfusion is absent and the $\dot{V}_A/\dot{Q}$ ratio equals to infinity or to areas with high $\dot{V}_A/\dot{Q}$ ratios. If vascular occlusion is incomplete, due to small emboli, perfusion is reduced in relation to ventilation, such that the $\dot{V}_A/\dot{Q}$ ratio will increase. However, none of these $\dot{V}_A/\dot{Q}$ changes cause hypoxemia. On the contrary, hypoxemia develops because bloodflow is diverted to the areas with normal $\dot{V}_A/\dot{Q}$ ratios, developing alveolar units in which bloodflow is superior to ventilation, such that their $\dot{V}_A/\dot{Q}$ ratios decrease. The extent of low-$\dot{V}_A/\dot{Q}$ areas depends on the extent of the embolized areas. If these are small, the development of areas with low $\dot{V}_A/\dot{Q}$ ratio will be limited and the degree of hypoxemia modest, whereas if the extent of the embolized regions increases, the areas with low $\dot{V}_A/\dot{Q}$ ratio will expand, resulting in a further decrease in P_aO_2. These $\dot{V}_A/\dot{Q}$ abnormalities may be modulated by other factors, such as the release of hypoxic pulmonary vasoconstriction, which enhances the development of areas with low $\dot{V}_A/\dot{Q}$ ratios,[73] and also by hypocapnic bronchoconstriction, which prevents the development of both areas with high $\dot{V}_A/\dot{Q}$ ratio and increased dead space. There is no evidence of oxygen diffusion limitation.

In acute PE, the presence of increased intrapulmonary shunt appears to be negligible, with values averaging less than 5% of cardiac output.[74–76] However, values up to 39% of cardiac output have also been observed in cases of massive PE.[74] As alluded to, the reduction of bloodflow to regions with occluded pulmonary vessels will redistribute bloodflow to the remaining ones with normal $\dot{V}_A/\dot{Q}$ ratios, hence decreasing the $\dot{V}_A/\dot{Q}$ ratio in nonoccluded areas. Accordingly, the presence of intrapulmonary shunt has to be explained by other causes, such as atelectasis, commonly identified on chest radiographs, or localized pulmonary edema. Atelectasis has been attributed to altered surfactant in embolized areas and to hypocapnic bronchoconstriction in areas with high $\dot{V}_A/\dot{Q}$ ratios. Pulmonary hypertension, and presumably a relative inhibition of hypoxic pulmonary vasoconstriction, can increase the perfusion to atelectatic regions.[73] Increased intrapulmonary shunt may also develop as a result of interstitial or alveolar edema induced by the release of vasoactive mediators from the impacted clots. Large amounts of intrapulmonary shunt have also been observed experimentally in animals after embolization with polystyrene[70] or glass[72] beads, provoked by massive pulmonary edema, a rare finding in human PE. This mechanism seems to be apparently related to the size of the embolus. Embolization with 100 μm glass beads in dogs caused an increased shunt, whereas embolization with 1,000 μm glass beads did not.[71] Thus, fragmentation of emboli into small particles could be the cause of increased shunt in some patients. Severe pulmonary hypertension with right heart failure can open the foramen ovale, resulting in right-to-left intracardiac shunt, which can further decrease P_aO_2.

Dead space is either normal ($< 35\%$ of alveolar ventilation) or moderately elevated.[74–76] The frequent absence of increased dead space after significant embolization suggests that complete occlusion of bloodflow occurs very seldom. There is evidence that the amount of dead space may be related to the size of the emboli. Whereas canine PE with small glass[71] or polystyrene[70] beads and with autologous clots[79] decreases dead space, increases in the size of autologous clots result in increased dead space. These differences can be explained by different mechanisms, such as recruitment of poorly perfused lung units due to pulmonary hypertension, common incomplete vascular obstruction, redistribution of alveolar ventilation from embolized lung regions induced by variably increased bronchial tone, and/or the efficiency of collateral ventilation. Small emboli can generate great differences in the perfusion of neighboring lung units that can be partially ventilated through collateral channels, hence generating areas with high $\dot{V}_A/\dot{Q}$ ratios in the face of normal dead space. Large emboli can also completely interrupt bloodflow to more lung units that cannot be ventilated through collateral ventilation, thus increasing dead space. Regarding ventilation redistribution, regional ventilation and perfusion radioisotopic scans indicate, in patients with PE, reduced ventilation in the embolized lung segments.[76]

Hyperventilation is an important clinical characteristic of PE and causes hypocapnia, a common feature in these patients. Although its precise mechanism has not been completely elucidated, it has been related to stimulation of receptors sensitive to high pulmonary artery pressures. Mixed venous PO_2 is also decreased, essentially due to decreased cardiac output,[76] although increased oxygen consumption may contribute to hypoxemia in some patients. Decreased mixed venous PO_2 is an additional mechanism that can lower P_aO_2, particularly in the presence of both increased intrapulmonary shunt and areas with low $\dot{V}_A/\dot{Q}$ ratio, regions in which end-capillary blood PO_2 approaches mixed venous PO_2 values, thereby more likely contributing to venous admixture. It is important to underline that hyperventilation decreases the hypoxemic effect of a lowered mixed venous PO_2.

Chronic Thromboembolic Pulmonary Hypertension

CTPH is characterized by widespread central obstruction of the pulmonary arteries with organized thrombus and thereby differs substantially from other forms of pulmonary hypertension. Kapitan and colleagues[80] showed that all patients but one were moderately hypoxemic and pulmonary hypertensive, whereas cardiac index and mixed venous PO_2 were reduced. The $\dot{V}_A/\dot{Q}$ distributions were moderately increased, with a broadened unimodal pattern in most patients, whereas the remainder had a broadened central pattern with either a small low or high $\dot{V}_A/\dot{Q}$ mode. Intrapulmonary shunt was not increased, and dead space was slightly above the upper limit of normal. Areas of low or high $\dot{V}_A/\dot{Q}$ ratio and oxygen diffusion limitation were absent. A decreased cardiac output and a low mixed venous PO_2 were responsible for approximately one-third of the increased $P_{A-a}O_2$. Following thromboendarterectomy,[81] $\dot{V}_A/\dot{Q}$ distributions narrowed to near normal, whereas the cardiac index increased.

Primary Pulmonary Hypertension

Dantzker and colleagues[82–84] studied a few patients with chronic obliteration of the pulmonary vascular bed due to idiopathic pulmonary hypertension or to recurrent pulmonary emboli. All the patients had increased $P_{A-a}O_2$ and modest hypoxemia. $\dot{V}_A/\dot{Q}$ relationships were only minimally abnormal; namely, the perfusion to low $\dot{V}_A/\dot{Q}$ units averaged 10%, dead space was normal, and diffusion limitation was absent. Significant hypoxemia occurred only when $\dot{V}_A/\dot{Q}$ inequality was combined with a low mixed venous PO_2. During exercise,[83] there was a significant fall in P_aO_2 and a widened $P_{A-a}O_2$, without an influence on $\dot{V}_A/\dot{Q}$ inequality. Interestingly, P_aO_2 worsening was due to the fall in the mixed venous PO_2 expected during exercise, typically shown in this disease entity. Pulmonary vascular tone contributed to the maintenance of $\dot{V}_A/\dot{Q}$ matching in these patients, as shown by the administration of oxygen, or vasodilators,[84,85] which produced a fall in pulmonary vascular resistance in some patients and an increase in the bloodflow to areas with low $\dot{V}_A/\dot{Q}$ ratios and/or intrapulmonary shunt. However, its detrimental effect on arterial oxygenation was frequently attenuated by increased mixed venous oxygen content due to increased cardiac output.

Portopulmonary hypertension is a pulmonary vascular constrictive/obliterative process that occurs in the context of portal hypertension with or without intrinsic liver disease.[86] No MIGET studies have been done, but respiratory blood gases have been investigated in two studies,[87,88] essentially showing mild-to-moderate hypoxemia. $\dot{V}_A/\dot{Q}$ mismatch was suggested as the most likely mechanism for hypoxemia, although a small effect due to increased intrapulmonary shunt could not be ruled out.

Hepatopulmonary Syndrome

HPS is a well-defined clinical entity[86] characterized by a clinical triad including chronic liver disease, a defect in arterial oxygenation, and intrapulmonary vascular dilatations. The mechanisms of hypoxemia in patients with liver cirrhosis were revisited and clarified with use of the MIGET,[89–93] well before the current consensus definition of HPS.[86] These studies showed increased intrapulmonary shunt, $\dot{V}_A/\dot{Q}$ mismatch, and diffusion disequilibrium for oxygen reflecting a diffusion–perfusion defect; together, these contribute to the different levels of hypoxemia. So far, the only proven effective therapy for HPS is liver transplantation, in that $\dot{V}_A/\dot{Q}$ imbalance is normalized while systemic and pulmonary vascular abnormalities are reversed. Interestingly, DLco after liver transplantation remains unchanged, which is an intriguing finding; the mechanism of this remains undetermined.[86]

ACUTE RESPIRATORY FAILURE

Lung disorders resulting in severe acute respiratory failure in previously healthy subjects may result from primary infectious lung process (severe bacterial pneumonia) or a more widespread, noninfectious process, named either acute lung injury (ALI) or acute respiratory distress syndrome (ARDS). This syndrome is characterized by severe hypoxemia refractory to high concentrations of inspired oxygen.[94]

In ARDS, hypoxemia is basically due to an increased intrapulmonary shunt,[95–97] expressed as an "all or none" phenomenon. Pulmonary bloodflow is distributed predominantly to effective gas-exchanging units or to shunt areas, although some patients may have increased perfusion to lung units with low $\dot{V}_A/\dot{Q}$ ratios. The reported shunt averages about 20 to 30% of cardiac output in most of the studies, although they can reach levels as high as 68%.[95] The mechanisms leading to intrapulmonary shunt include gas absorption caused by complete distal airway occlusion, a reduction in ventilation to units with inspired $\dot{V}_A/\dot{Q}$ ratios below a critical level, absent or deficient surfactant, and lung tissue compression caused by the weight of adjacent lung tissue. These abnormalities can be modulated by changes in F_IO_2, cardiac output, or mixed venous PO_2 and by the effects of vasoactive agents. It is accepted that patients with ALI develop reabsorption atelectasis while breathing 100% oxygen, due to alveolar denitrogenation in units with very low $\dot{V}_A/\dot{Q}$ ratios (so-called "critical $\dot{V}_A/\dot{Q}$ ratio"). This occurs when oxygen uptake by the blood exceeds alveolar ventilation in the absence of the protective action of alveolar nitrogen against collapse. The critical $\dot{V}_A/\dot{Q}$ level below which alveoli are vulnerable to collapse increases with high F_IO_2. Lung units with $\dot{V}_A/\dot{Q}$ ratios less than 0.08 are likely to collapse with 100% oxygen. In ALI, oxygen breathing moderately increases the amount of intrapulmonary shunt (approximately by 35–40%)[57] at a high rate; this then plateaus without modulating the distribution of pulmonary bloodflow. Whereas in patients with ALI, oxygen breathing increases shunt because of the development of reabsorption atelectasis, in patients with COPD, alveolar collapse does not occur because the major mechanism of worsening in gas exchange is further $\dot{V}_A/\dot{Q}$ imbalance due to release of hypoxic vasoconstriction.

The application of PEEP with or without the use of high tidal volumes decreases cardiac output and intrapulmonary shunt without altering the overall pattern of $\dot{V}_A/\dot{Q}$ distributions. This suggests that decreased cardiac output, along with the implementation of several ventilatory strategies, reduces shunt in ARDS. However, in another study, in which cardiac output was maintained by means of a dopamine infusion,[96] the beneficial effects of PEEP on gas exchange were not mitigated. By contrast, there was a redistribution of pulmonary blood toward the main $\dot{V}_A/\dot{Q}$ areas. The application of PEEP increased P_aO_2 and mixed venous PO_2 and efficiently redistributed bloodflow. Thus, shunt decreased substantially (by almost half), whereas the perfusion to units with normal $\dot{V}_A/\dot{Q}$ ratios increased by the same amount. In parallel, dead space increased slightly with PEEP, but no additional high $\dot{V}_A/\dot{Q}$ areas emerged. The application of multiple PEEP trials[97] demonstrated that when P_aO_2 improves, PEEP can induce a reduction in shunt alone, a reduction in low $\dot{V}_A/\dot{Q}$ units alone, or a redistribution in bloodflow from shunt to areas of low or normal $\dot{V}_A/\dot{Q}$ ratios. In these trials, if P_aO_2 remained unchanged, the decrease in bloodflow distribution to shunt

or low $\dot{V}_A/\dot{Q}$ units did not occur. In patients with ARDS, a decrease in mixed venous PO_2 can cause a marked decrease in P_aO_2. Acute respiratory failure–induced pulmonary hypertension can be minimized by vasodilators, but their effects differ with class and route of administration. Intravenous administration of prostanoids, such as prostaglandin E_1 (PGE_1)[98] and prostacyclin (PGI_2),[99,100] calcium antagonists (diltiazem), and ketanserin and sodium nitroprusside,[101] releases hypoxic pulmonary vasoconstriction, increases intrapulmonary shunt, and worsens $\dot{V}_A/\dot{Q}$ mismatch, thereby reducing P_aO_2. However, inhalation of NO[100,102,103] and of aerosolized PGI_2[102] and PGE_1[103] at low concentrations induces pulmonary vasodilatation selectively in ventilated lung regions, hence redistributing bloodflow adequately from nonventilated alveoli (predominantly with increased intrapulmonary shunt) to ventilated lung units and improving $\dot{V}_A/\dot{Q}$ imbalance, with decreased shunt and increased P_aO_2. This happens because these inhaled agents cannot release hypoxic pulmonary vasoconstriction in nonventilated lung units. In a small series of ARDS patients,[104] intravenous infusion of almitrine produced a very rapid increase in P_aO_2, while decreasing the venous admixture ratio. Intrapulmonary shunt fell dramatically in most patients (by 50%), most of the bloodflow being diverted to alveolar units with normal $\dot{V}_A/\dot{Q}$ ratios. The effect was transient, ending as soon as the administration of the drug ceased, and the redistribution of pulmonary bloodflow was associated with a small but significant increase in pulmonary artery pressure. The infusion of almitrine combined with NO inhalation in patients with ARDS had additive effects on the improvement in pulmonary gas exchange, with a mild decrease in pulmonary artery pressure.

In patients with ARDS needing mechanical ventilation and PEEP, a substantial amount of the ventilation takes place in poorly or nonperfused lung zones.[95–97] The increase in dead space and in areas with high $\dot{V}_A/\dot{Q}$ ratios, associated with carbon dioxide retention, can be in part explained by overdistention of well-ventilated alveoli caused by PEEP and/or the application of high tidal volumes. In a canine model of ALI, ventilation with high inflation pressures produced compression of alveolar vessels in nondependent lung units, as evidenced by histologic examination of rapidly frozen lung tissue, which showed that alveolar capillaries were closed in the uppermost, poorly perfused regions, whereas alveolar corner vessels remained open. These changes could explain the increased dead space and the presence of areas of high $\dot{V}_A/\dot{Q}$ ratios. Presumably, the presence of bloodflow in the corner vessels prevents these units being measured as dead space. Alternatively, redistribution of bloodflow caused by reduced cardiac output could be a coexisting mechanism.[95] Large PEEP increments, above 25 cm H_2O or more, do not always elevate dead space or areas with high $\dot{V}_A/\dot{Q}$ ratios.[95] If cardiac output is not reduced, either with appropriate fluid support to maintain adequate cardiac filling[97] or with the use of inotropic drugs,[96] the application of PEEP does not increase the extent of areas of high $\dot{V}_A/\dot{Q}$ ratios, and dead space remains unchanged or only slightly increased.

Ventilatory Strategies

Over the last 10 years, the use of a protective ventilatory strategy (PVS), in which an increase in P_aCO_2 is allowed if necessary (permissive hypercapnia), has been developed so that ventilator-associated lung injury (VALI) can be avoided in the management of patients with ALI/ARDS. The 1998 International Consensus Conference on VALI[105] defined this entity as lung damage with characteristic features of ARDS occurring in patients receiving mechanical ventilation. Preexisting pulmonary disease, such as ARDS per se, appears to constitute a risk factor for VALI. The two most important mechanical causative factors for VALI are (1) the association of alveolar overdistention and high transpulmonary pressure and (2) repeated alveolar collapse and reopening, owing to ventilation at inappropriate tidal ranges of transpulmonary pressure.

The prevention of alveolar overdistention by reducing tidal volume has been investigated using either standardized relatively low levels of PEEP or high levels of PEEP. A MIGET study[106] demonstrated that the induction of permissive hypercapnia, by reducing tidal volume and maintaining constant standard levels of PEEP, increased cardiac output, decreased P_aO_2, increased intrapulmonary shunt, and had no effect on the distribution of bloodflow. In another MIGET study,[107] permissive hypercapnia in patients with ARDS, with or without hyperdynamic sepsis, increased shunt but without concomitant decreases in P_aO_2 because mixed venous PO_2 increased due to increased cardiac output. In septic patients, P_aO_2 remained unchanged, but in nonseptic patients, P_aO_2 increased. In parallel, dead space, the dispersion of bloodflow, and the dispersion of alveolar ventilation remained constant in both subsets of patients. A PVS approach, combining low tidal volume (to avoid alveolar overdistention) and high levels of PEEP (to prevent repeated collapse and reopening of alveolar units throughout the ventilatory cycle), has also been proposed as an alternative mode of ventilation to decrease VALI.[108] We have studied the effects on this PVS strategy,[109] showing that it markedly improved pulmonary gas exchange in early ARDS (Figure 18-7), essentially by recruitment of previously collapsed alveoli and redistribution of pulmonary bloodflow from nonventilated alveoli to areas of normal lung. During PVS, P_aO_2 improved, whereas intrapulmonary shunt decreased. Recruitment of previously collapsed alveolar units was the central factor explaining the reduction in intrapulmonary shunt. The beneficial effects of PVS on pulmonary gas exchange fully overcame the deleterious effect of permissive hypercapnia on arterial oxygenation, namely the decline in alveolar PO_2. Moreover, the increase in cardiac output during PVS, due to systemic vasodilatation, did not result in a proportional increase in intrapulmonary shunt, as one would expect in patients with ARDS,[95] probably because pulmonary bloodflow was appropriately redistributed to normal alveolar units, as a result of concomitant efficient alveolar recruitment. The reduction in the log SD $\mathcal{Q}$ during PVS was probably caused by the fall in overall $\dot{V}_A/\dot{Q}$ ratio resulting from the concomitant effects of both the decrease in alveolar ventilation and the increase in cardiac output provoked by this ventilatory modality.

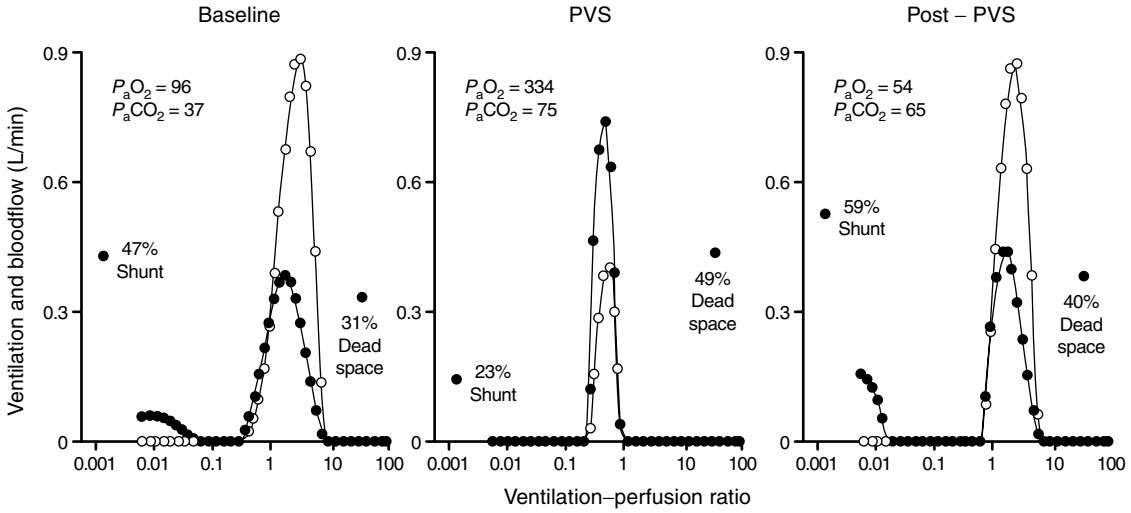

FIGURE 18-7 $V_A\dot{Q}$ distributions in a representative sample of patient with acute respiratory distress syndrome at baseline (P_aO_2 96 mm Hg, P_aCO_2 37 mm Hg), during protective ventilatory strategy (PVS) (P_aO_2 334 mm Hg, P_aCO_2 75 mm Hg), and post-PVS (P_aO_2 54 mm Hg, P_aCO_2 65 mm Hg). The decrease in intrapulmonary shunt during PVS explained the improvement in arterial PO_2. The increase in dead space due to both low tidal volume and high positive end-expiratory pressure values results from the permissive hypercapnia approach used in these patients. Open circles = ventilation. Solid circles = bloodflow. Reproduced with permission from Mancini M et al.[109]

However, a more efficient distribution of pulmonary bloodflow toward areas with normal $\dot{V}_A/\dot{Q}$ ratios could not be ruled out. Likewise, the marked increase in dead space observed during PVS was explained by the combined effect of decreased alveolar ventilation and increased functional residual capacity resulting from high levels of PEEP. This study[109] also showed a strong relationship between improvement in alveolar gas exchange and the amount of PEEP-induced alveolar recruitment, the central role of the decreased intrapulmonary shunt in optimizing arterial oxygenation, and increased systemic oxygen delivery resulting from the rise in cardiac output. All in all, these findings strongly suggest that a PVS with both low tidal volume and high PEEP is the most appropriate therapeutic approach to combine prevention of VALI and enhanced pulmonary and peripheral gas exchange in patients with acute respiratory failure (ARF), at least at an early stage. Before the general consensus on the advantages of PVS with permissive hypercapnia, the inverse inspiratory-to-expiratory ratio (I/E) mechanical ventilation was used as an alternative ventilatory technique in patients with ARDS to improve oxygenation at lower than conventional peak airway pressure. We investigated the effect on gas exchange of inverse I/E ratio ventilation[110] and showed that although short-term pressure-controlled inverse I/E ratio ventilation improves carbon dioxide clearance, the lung becomes less efficient as an oxygen exchanger.

In ARDS patients, alveolar collapse is mainly caused by the pressure of the lung on adjacent dependent areas of lung, such that the periodic change from the supine to the prone position should decompress and reopen these lung units. In a study in which the MIGET was used, patients with ARDS were evaluated before, during, and after 2 hours of pressure-controlled mechanical ventilation with the patient in the prone position.[111] Whereas two-thirds of the patients had an improvement in P_aO_2 of more than 10 mm Hg 30 minutes after adopting the prone position (responders), one-third reacted to positional changes with a deterioration in arterial oxygenation (nonresponders). Whereas the nonresponders did not show altered $\dot{V}_A/\dot{Q}$ distributions during the study, in responders the prone position caused a significant decrease in intrapulmonary shunt, with a concomitant increase in the extent of areas with normal $\dot{V}_A/\dot{Q}$ ratios, without changing the number of areas with low $\dot{V}_A/\dot{Q}$ ratios. Returning the patient to the supine position reversed the improvements in gas exchange. These changes suggest that bloodflow redistribution away from shunt areas is most likely caused by the recruitment of previously atelectatic but nondiseased areas through altered gravitational forces. Continuous axial rotation might be another method for an acute reduction of $\dot{V}_A/\dot{Q}$ mismatch in patients with ALI/ARDS, as demonstrated in another study,[112] where continuous axial rotation on a kinetic treatment table reduced intrapulmonary shunt and log SD $\dot{Q}$, without causing changes in low-$\dot{V}_A/\dot{Q}$ units, while improving arterial oxygenation. This positive response of the continuous rotation was only demonstrated in patients with mild-to-moderate lung injury; in patients presenting with progressive ARDS, the acute positive response was limited.

The different modalities of partial mechanical ventilatory support can be used to wean patients from mechanical ventilation while providing stable ventilatory assistance of a desired degree during acute respiratory failure. Pressure support ventilation (PSV) provides mechanical assistance for each inspiratory effort, supplying a breath-by-breath synchronized insufflation of the lungs until inspiratory gas flow decreases to 25% of the peak flow value. Airway pressure-release ventilation (APRV), which is equivalent to biphasic positive airway pressure, ventilates by periodic switching between two levels of continuous positive airway pressure (CPAP). Spontaneous breathing in any phase of the mechanical ventilator cycle is possible with APRV, which provides a constant degree of ventilatory support

by time-cycled switching between two CPAP levels. When spontaneous breathing is abolished, APRV is not different from conventional pressure-controlled mechanical ventilation. Persisting spontaneous breathing has been considered to improve the distribution of ventilation to dependent lung areas and thereby $\dot{V}_A/\dot{Q}$ matching, presumably through diaphragmatic contraction opposing alveolar compression. A comparison of the effects of APRV and PSV on $\dot{V}_A/\dot{Q}$ ratio distributions in patients with ARDS[113] showed that spontaneous breathing with APRV improved $\dot{V}_A/\dot{Q}$ matching, as evidenced by decreases in intrapulmonary shunt, dead space, log SD Q, and log SD V. The use of PSV did not improve $\dot{V}_A/\dot{Q}$ distributions in comparison to APRV without spontaneous breathing. These findings indicate that uncoupling of spontaneous and mechanical ventilation during APRV improves $\dot{V}_A/\dot{Q}$ matching in ARDS, presumably by recruiting nonventilated lung units. Apparently, mechanical assistance at each inspiration during PSV is not sufficient to counteract the $\dot{V}_A/\dot{Q}$ maldistribution caused by alveolar collapse in patients with ARDS and does not provide any advantage in cardiopulmonary function or gas exchange compared with controlled mechanical ventilation.

SEVERE PNEUMONIA

The most common pattern of $\dot{V}_A/\dot{Q}$ mismatch in patients with bacterial pneumonia requiring mechanical ventilation is a combination of increased intrapulmonary shunt and increased perfusion to low $\dot{V}_A/\dot{Q}$ units.[114] Our group[115] confirmed these results in mechanically ventilated patients and extended them to spontaneously breathing patients with less intense disease. There were no differences between measured P_aO_2 and predicted P_aO_2, ruling out the coexistence of oxygen diffusion limitation. Breathing 100% oxygen did not increase intrapulmonary shunt but worsened bloodflow distribution, suggesting a release of hypoxic pulmonary vasoconstriction. In patients with unilateral lung disease, such as bacterial pneumonia, a lateral position with the good lung dependent ("down") improves P_aO_2. This is induced by improving $\dot{V}_A/\dot{Q}$ imbalance because the perfusion is directed toward the nondependent good lung. Use of the MIGET has confirmed that positional changes cause either a reduction of intrapulmonary shunt, a reduction in the extent of areas with low $\dot{V}_A/\dot{Q}$ ratios, or both.[116]

CONCLUSIONS

In this chapter we have extensively reviewed the pulmonary gas exchange status in the most important chronic airway disorders, while patients are stable and during acute worsening (exacerbations), as well as considered the effects of different key interventions, that is, oxygen breathing or bronchodilator administration, from a comprehensive inert gas perspective (using the MIGET). The MIGET is a tool that has the unique ability not only to reveal the complexity of alveolar ventilation and pulmonary blood distributions but also to unravel the interactive links between the latter variables and ventilation, cardiac output, and oxygen consumption as the principal extrapulmonary determinants of pulmonary gas exchange. The natural histories of other less common conditions, such as diffuse interstitial lung and pulmonary vascular disorders, the majority under stable conditions, are also revisited.

Even though all these chronic "dry" pulmonary disease states share ventilation–perfusion imbalance as the pivotal intrapulmonary determinant of arterial hypoxemia, with or without hypercapnia, extrapulmonary factors interact very influentially with the latter pathophysiologic mechanism, ultimately modulating the levels of arterial and mixed venous blood gases. Likewise, the major acute "wet" respiratory conditions, namely ALI and/or ARDS, are also addressed once more, highlighting the key role of increased intrapulmonary shunt, while giving special attention to the influence of high oxygen concentration and different ventilatory strategies. Like chronic respiratory processes, acute pulmonary disorders also exhibit a dynamic interplay between their key gas exchange intrapulmonary component, that is, increased shunt, and the extrapulmonary ones, among which changes in ventilation and cardiac output predominate.

REFERENCES

1. Wagner PD, Saltzman HA, West JB. Measurement of continuous distributions of ventilation–perfusion ratios: theory. J Appl Physiol 1974;36:588–99.
2. Wagner PD, Naumann PF, Laravuso RB. Simultaneous measurement of eight foreign gases in blood by gas chromatography. J Appl Physiol 1974;36:600–5.
3. Riley RL, Cournand A. "Ideal" alveolar air and the analysis of ventilation–perfusion relationships in the lungs. J Appl Physiol 1949;1:825–47.
4. Cardus J, Burgos F, Diaz O, et al. Increase in pulmonary ventilation–perfusion inequality with age in healthy individuals. Am J Respir Crit Care Med 1997;156:648–53.
5. Roca J, Wagner PD. Contribution of multiple inert gas elimination technique to pulmonary medicine. 1. Principles and information content of the multiple inert gas elimination technique. Thorax 1994;49:815–24.
6. Wagner PD, Dantzker DR, Iacovoni VE, et al. Ventilation–perfusion inequality in asymptomatic asthma. Am Rev Respir Dis 1978;118:511–24.
7. Lagerstrand L, Larsson K, Ihre E, et al. Pulmonary gas exchange response following allergen challenge in patients with allergic asthma. Eur Respir J 1992;5:1176–83.
8. Schmekel B, Hedenstrom H, Kampe M, et al. The bronchial response, but not the pulmonary response to inhaled methacholine is dependent on the aerosol deposition pattern. Chest 1994;106:1781–7.
9. Wagner PD, Hedenstierna G, Bylin G. Ventilation–perfusion inequality in chronic asthma. Am Rev Respir Dis 1987;136:605–12.
10. Young IH, Corte P, Schoeffel RE. Pattern and time course of ventilation–perfusion inequality in exercise-induced asthma. Am Rev Respir Dis 1982;125:304–11.
11. Rodriguez-Roisin R, Ferrer A, Navajas D, et al. Ventilation–-perfusion mismatch after methacholine challenge in patients with mild bronchial asthma. Am Rev Respir Dis 1991;144:88–94.
12. Corte P, Young IH. Ventilation–perfusion relationships in symptomatic asthma. Response to oxygen and clemastine. Chest 1985;88:167–75.

13. Ballester E, Roca J, Ramis L, et al. Pulmonary gas exchange in severe chronic asthma. Response to 100% oxygen and salbutamol. Am Rev Respir Dis 1990;141:558–62.
14. Roca J, Ramis L, Rodriguez-Roisin R, et al. Serial relationships between ventilation–perfusion inequality and spirometry in acute severe asthma requiring hospitalization. Am Rev Respir Dis 1988;137:1055–61.
15. Ballester E, Reyes A, Roca J, et al. Ventilation–perfusion mismatching in acute severe asthma: effects of salbutamol and 100% oxygen. Thorax 1989;44:258–67.
16. Ferrer A, Roca J, Wagner PD, et al. Airway obstruction and ventilation–perfusion relationships in acute severe asthma. Am Rev Respir Dis 1993;147:579–84.
17. Rodriguez-Roisin R, Ballester E, Roca J, et al. Mechanisms of hypoxemia in patients with status asthmaticus requiring mechanical ventilation. Am Rev Respir Dis 1989;139:732–9.
18. Echazarreta AL, Gomez FP, Ribas J, et al. Pulmonary gas exchange responses to histamine and methacholine challenges in mild asthma. Eur Respir J 2001;17:609–14.
19. Echazarreta AL, Dahlen B, Garcia G, et al. Pulmonary gas exchange and sputum cellular responses to inhaled leukotriene D(4) in asthma. Am J Respir Crit Care Med 2001;164:202–6.
20. Felez MA, Roca J, Barbera JA, et al. Inhaled platelet-activating factor worsens gas exchange in mild asthma. Am J Respir Crit Care Med 1994;150:369–73.
21. Rodriguez-Roisin R, Felez MA, Chung KF, et al. Platelet-activating factor causes ventilation–perfusion mismatch in humans. J Clin Invest 1994;93:188–94.
22. Roca J, Felez MA, Chung KF, et al. Salbutamol inhibits pulmonary effects of platelet activating factor in man. Am J Respir Crit Care Med 1995;151:1740–4.
23. Diaz O, Barbera JA, Marrades R, et al. Inhibition of PAF-induced gas exchange defects by beta-adrenergic agonists in mild asthma is not due to bronchodilation. Am J Respir Crit Care Med 1997;156:17–22.
24. Freyschuss U, Hedlin G, Hedenstierna G. Ventilation–-perfusion relationships during exercise-induced asthma in children. Am Rev Respir Dis 1984;130:888–94.
25. Hedlin G, Freyschuss U, Hedenstierna G. Histamine-induced asthma in children: effects on the ventilation–perfusion relationship. Clin Physiol 1985;5:19-34.
26. Knudson RJ, Constantine HP. An effect of isoproterenol on ventilation–perfusion in asthmatic versus normal subjects. J Appl Physiol 1967;22:402–6.
27. Tai E, Read J. Response of blood gas tensions to aminophylline and isoprenaline in patients with asthma. Thorax 1967;22:543–9.
28. Montserrat JM, Barbera JA, Viegas C, et al. Gas exchange response to intravenous aminophylline in patients with a severe exacerbation of asthma. Eur Respir J 1995;8:28–33.
29. Wagner PD, Dantzker DR, Dueck R, et al. Ventilation–perfusion inequality in chronic obstructive pulmonary disease. J Clin Invest 1977;59:203–16.
30. Melot C, Naeije R, Rothschild T, et al. Improvement in ventilation–perfusion matching by almitrine in COPD. Chest 1983; 83:528–33.
31. Melot C, Hallemans R, Naeije R, et al. Deleterious effect of nifedipine on pulmonary gas exchange in chronic obstructive pulmonary disease. Am Rev Respir Dis 1984;130:612–6.
32. Castaing Y, Manier G, Guenard H. Effect of 26% oxygen breathing on ventilation and perfusion distribution in patients with cold. Bull Eur Physiopathol Respir 1985;21:17–23.
33. Dantzker DR, D'Alonzo GE. The effect of exercise on pulmonary gas exchange in patients with severe chronic obstructive pulmonary disease. Am Rev Respir Dis 1986; 134:1135–9.
34. Roca J, Montserrat JM, Rodriguez-Roisin R, et al. Gas exchange response to naloxone in chronic obstructive pulmonary disease with hypercapnic respiratory failure. Bull Eur Physiopathol Respir 1987;23:249–54.
35. Ringsted CV, Eliasen K, Andersen JB, et al. Ventilation–perfusion distributions and central hemodynamics in chronic obstructive pulmonary disease. Effects of terbutaline administration. Chest 1989;96:976–83.
36. Agusti AG, Barbera JA, Roca J, et al. Hypoxic pulmonary vasoconstriction and gas exchange during exercise in chronic obstructive pulmonary disease. Chest 1990;97:268–75.
37. Barbera JA, Ramirez J, Roca J, et al. Lung structure and gas exchange in mild chronic obstructive pulmonary disease. Am Rev Respir Dis 1990;141:895–901.
38. Barbera JA, Riverola A, Roca J, et al. Pulmonary vascular abnormalities and ventilation–perfusion relationships in mild chronic obstructive pulmonary disease. Am J Respir Crit Care Med 1994;149:423–9.
39. Andrivet P, Chabrier PE, Defouilloy C, et al. Intravenously administered atrial natriuretic factor in patients with COPD. Effects on ventilation–perfusion relationships and pulmonary hemodynamics. Chest 1994;106:118–24.
40. Moinard J, Manier G, Pillet O, Castaing Y. Effect of inhaled nitric oxide on hemodynamics and VA/Q inequalities in patients with chronic obstructive pulmonary disease. Am J Respir Crit Care Med 1994;149:1482–7.
41. Barbera JA, Roger N, Roca J, et al. Worsening of pulmonary gas exchange with nitric oxide inhalation in chronic obstructive pulmonary disease. Lancet 1996;347:436–40.
42. Viegas CA, Ferrer A, Montserrat JM, et al. Ventilation–perfusion response after fenoterol in hypoxemic patients with stable COPD. Chest 1996;110:71–7.
43. Barbera JA, Roca J, Ferrer A, et al. Mechanisms of worsening gas exchange during acute exacerbations of chronic obstructive pulmonary disease. Eur Respir J 1997;10:1285–91.
44. Roger N, Barbera JA, Roca J, et al. Nitric oxide inhalation during exercise in chronic obstructive pulmonary disease. Am J Respir Crit Care Med 1997;156:800–6.
45. Barbera JA, Roca J, Rodriguez-Roisin R, et al. Gas exchange in patients with small airways dysfunction. Eur Respir J 1988; 1:27s.
46. Marthan R, Castaing Y, Manier G, Guenard H. Gas exchange alterations in patients with chronic obstructive lung disease. Chest 1985;87:470–5.
47. Barbera JA. Chronic obstructive pulmonary disease. In: Roca J, Rodriguez-Roisin R, Wagner PD, editors. Pulmonary and peripheral gas exchange in health and disease. New York: Marcel Dekker; 2000. p. 229–61.
48. Diaz O, Iglesia R, Ferrer M, et al. Effects of noninvasive ventilation on pulmonary gas exchange and hemodynamics during acute hypercapnic exacerbations of chronic obstructive pulmonary disease. Am J Respir Crit Care Med 1997;156: 1840–5.
49. Castaing Y, Manier G, Guenard H. Improvement in ventilation–perfusion relationships by almitrine in patients with chronic obstructive pulmonary disease during mechanical ventilation. Am Rev Respir Dis 1986;134:910–6.
50. Rossi A, Santos C, Roca J, et al. Effects of PEEP on VA/Q mismatching in ventilated patients with chronic airflow obstruction. Am J Respir Crit Care Med 1994;149:1077–84.
51. Torres A, Reyes A, Roca J, et al. Ventilation–perfusion mismatching in chronic obstructive pulmonary disease during ventilator weaning. Am Rev Respir Dis 1989;140:1246–50.
52. Barbera JA, Roca J, Ramirez J, et al. Gas exchange during exercise in mild chronic obstructive pulmonary disease. Correlation with lung structure. Am Rev Respir Dis 1991; 144:520–5.

53. Wagner PD, Gale GE, Moon RE, et al. Pulmonary gas exchange in humans exercising at sea level and simulated altitude. J Appl Physiol 1986;61:260–70.
54. Peinado VI, Barbera JA, Ramirez J, et al. Endothelial dysfunction in pulmonary arteries of patients with mild COPD. Am J Physiol 1998;274:L908–13.
55. Ferrer M, Iglesia R, Roca J, et al. Pulmonary gas exchange response to weaning with pressure-support ventilation in exacerbated chronic obstructive pulmonary disease patients. Intensive Care Med 2002;28:1595–9.
56. Barbera JA, Reyes A, Roca J, et al. Effect of intravenously administered aminophylline on ventilation/perfusion inequality during recovery from exacerbations of chronic obstructive pulmonary disease. Am Rev Respir Dis 1992; 145:1328–33.
57. Santos C, Ferrer M, Roca J, et al. Pulmonary gas exchange response to oxygen breathing in acute lung injury. Am J Respir Crit Care Med 2000;161:26–31.
58. Guénard H, Castaing Y, Mélot C, Naeije R. Gas exchange during acute respiratory failure in patients with chronic obstructive pulmonary disease. In: Derenne JP, Whitelaw WA, Similowski T, editors. Acute respiratory failure in chronic obstructive pulmonary disease. New York: Marcel Dekker; 1996. p. 227–66.
59. Bratel T, Hedenstierna G, Nyquist O, Ripe E. The use of a vasodilator, felodipine, as an adjuvant to long-term oxygen treatment in COLD patients. Eur Respir J 1990;3:46–54.
60. Adnot S, Kouyoumdjian C, Defouilloy C, et al. Hemodynamic and gas exchange responses to infusion of acetylcholine and inhalation of nitric oxide in patients with chronic obstructive lung disease and pulmonary hypertension. Am Rev Respir Dis 1993;148:310–6.
61. Katayama Y, Higenbottam TW, Diaz de Atauri MJ, et al. Inhaled nitric oxide and arterial oxygen tension in patients with chronic obstructive pulmonary disease and severe pulmonary hypertension. Thorax 1997;52:120–4.
62. Castaing Y, Manier G, Varene N, Guenard H. Effects of oral almitrine on the distribution of VA/Q ratio in chronic obstructive lung diseases. Bull Eur Physiopathol Respir 1981;17:917–32.
63. Naeije R, Melot C, Mols P, et al. Effects of almitrine in decompensated chronic respiratory insufficiency. Bull Eur Physiopathol Respir 1981;17:153–61.
64. Romaldini H, Rodriguez-Roisin R, Wagner PD, West JB. Enhancement of hypoxic pulmonary vasoconstriction by almitrine in the dog. Am Rev Respir Dis 1983;128:288–93.
65. Melot C, Dechamps P, Hallemans R, et al. Enhancement of hypoxic pulmonary vasoconstriction by low dose almitrine bismesylate in normal humans. Am Rev Respir Dis 1989; 139:111–9.
66. Jernudd-Wilhelmsson Y, Hornblad Y, Hedenstierna G. Ventilation–perfusion relationships in interstitial lung disease. Eur J Respir Dis 1986;68:39–49.
67. Eklund A, Broman L, Broman M, Holmgren A. V/Q and alveolar gas exchange in pulmonary sarcoidosis. Eur Respir J 1989;2: 135–44.
68. Agusti AG, Roca J, Gea J, et al. Mechanisms of gas-exchange impairment in idiopathic pulmonary fibrosis. Am Rev Respir Dis 1991;143:219-25.
69. Agusti AG, Roca J, Rodriguez-Roisin R, et al. Different patterns of gas exchange response to exercise in asbestosis and idiopathic pulmonary fibrosis. Eur Respir J 1988;1:510–6.
70. Young I, Mazzone RW, Wagner PD. Identification of functional lung unit in the dog by graded vascular embolization. J Appl Physiol 1980;49:132–41.
71. Delcroix M, Melot C, Vachiery JL, et al. Effects of embolus size on hemodynamics and gas exchange in canine embolic pulmonary hypertension. J Appl Physiol 1990;69: 2254–61.
72. Delcroix M, Melot C, Lejeune P, et al. Effects of vasodilators on gas exchange in acute canine embolic pulmonary hypertension. Anesthesiology 1990;72:77–84.
73. Delcroix M, Melot C, Vermeulen F, Naeije R. Hypoxic pulmonary vasoconstriction and gas exchange in acute canine pulmonary embolism. J Appl Physiol 1996;80: 1240–8.
74. D'Alonzo GE, Bower JS, DeHart P, Dantzker DR. The mechanisms of abnormal gas exchange in acute massive pulmonary embolism. Am Rev Respir Dis 1983;128: 170–2.
75. Manier G, Castaing Y, Guenard H. Determinants of hypoxemia during the acute phase of pulmonary embolism in humans. Am Rev Respir Dis 1985;132:332–8.
76. Santolicandro A, Prediletto R, Fornai E, et al. Mechanisms of hypoxemia and hypocapnia in pulmonary embolism. Am J Respir Crit Care Med 1995;152:336–47.
77. Manier G, Castaing Y. Contribution of multiple inert gas elimination technique to pulmonary medicine—4. Gas exchange abnormalities in pulmonary vascular and cardiac disease. Thorax 1994;49:1169–74.
78. Mélot C, Naeije C. Pulmonary vascular diseases. In: Roca J, Rodriguez-Roisin R, Wagner PD, editors. Pulmonary and peripheral gas exchange in health and disease. New York: Marcel Dekker; 2000. p. 285–302.
79. Delcroix M, Melot C, Vanderhoeft P, Naeije R. Embolus size affects gas exchange in canine autologous blood clot pulmonary embolism. J Appl Physiol 1993;74:1140–8.
80. Kapitan KS, Buchbinder M, Wagner PD, Moser KM. Mechanisms of hypoxemia in chronic thromboembolic pulmonary hypertension. Am Rev Respir Dis 1989;139:1149–54.
81. Kapitan KS, Clausen JL, Moser KM. Gas exchange in chronic thromboembolism after pulmonary thromboendarterectomy. Chest 1990;98:14–9.
82. Dantzker DR, Bower JS. Mechanisms of gas exchange abnormality in patients with chronic obliterative pulmonary vascular disease. J Clin Invest 1979;64:1050–5.
83. Dantzker DR, D'Alonzo GE, Bower JS, et al. Pulmonary gas exchange during exercise in patients with chronic obliterative pulmonary hypertension. Am Rev Respir Dis 1984;130:412–6.
84. Dantzker DR, Bower JS. Pulmonary vascular tone improves VA/Q matching in obliterative pulmonary hypertension. J Appl Physiol 1981;51:607–13.
85. Melot C, Naeije R, Mols P, et al. Effects of nifedipine on ventilation/perfusion matching in primary pulmonary hypertension. Chest 1983;83:203–7.
86. Rodriguez-Roisin R, Krowka MJ, Herve Ph, Fallon MB. Pulmonary–hepatic vascular disorders. Eur Respir J 2004; 29:861–80.
87. Kuo PC, Plotkin JS, Johnson LB, et al. Distinctive clinical features of portopulmonary hypertension. Chest 1997;112: 980–6.
88. Swanson KL, Krowka MJ. Arterial oxygenation associated with portopulmonary hypertension. Chest 2002;121:1869–75.
89. Rodriguez-Roisin R, Roca J, Agusti AG, et al. Gas exchange and pulmonary vascular reactivity in patients with liver cirrhosis. Am Rev Respir Dis 1987;135:1085–92.
90. Melot C, Naeije R, Dechamps P, et al. Pulmonary and extrapulmonary contributors to hypoxemia in liver cirrhosis. Am Rev Respir Dis 1989;139:632–40.
91. Hedenstierna G, Soderman C, Eriksson LS, Wahren J. Ventilation–perfusion inequality in patients with non-alcoholic liver cirrhosis. Eur Respir J 1991;4:711–7.
92. Edell ES, Cortese DA, Krowka MJ, Rehder K. Severe hypoxemia and liver disease. Am Rev Respir Dis 1989;140: 1631–5.

93. Castaing Y, Manier G. Hemodynamic disturbances and VA/Q matching in hypoxemic cirrhotic patients. Chest 1989;96: 1064–9.
94. Bernard GR, Artigas A, Brigham KL, et al. The American–European Consensus Conference on ARDS. Definitions, mechanisms, relevant outcomes, and clinical trial coordination. Am J Respir Crit Care Med 1994;149:818–24.
95. Dantzker DR, Brook CJ, Dehart P, et al. Ventilation–perfusion distributions in the adult respiratory distress syndrome. Am Rev Respir Dis 1979;120:1039–52.
96. Matamis D, Lemaire F, Harf A, et al. Redistribution of pulmonary blood flow induced by positive end-expiratory pressure and dopamine infusion in acute respiratory failure. Am Rev Respir Dis 1984;129:39–44.
97. Ralph DD, Robertson HT, Weaver LJ, et al. Distribution of ventilation and perfusion during positive end-expiratory pressure in the adult respiratory distress syndrome. Am Rev Respir Dis 1985;131:54–60.
98. Melot C, Lejeune P, Leeman M, et al. Prostaglandin E1 in the adult respiratory distress syndrome. Benefit for pulmonary hypertension and cost for pulmonary gas exchange. Am Rev Respir Dis 1989;139:106–10.
99. Radermacher P, Santak B, Wust HJ, et al. Prostacyclin for the treatment of pulmonary hypertension in the adult respiratory distress syndrome: effects on pulmonary capillary pressure and ventilation–perfusion distributions. Anesthesiology 1990;72:238–44.
100. Rossaint R, Falke KJ, Lopez F, et al. Inhaled nitric oxide for the adult respiratory distress syndrome. N Engl J Med 1993; 328:399–405.
101. Radermacher P, Huet Y, Pluskwa F, et al. Comparison of ketanserin and sodium nitroprusside in patients with severe ARDS. Anesthesiology 1988;68:152–7.
102. Walmrath D, Schneider T, Schermuly R, et al. Direct comparison of inhaled nitric oxide and aerosolized prostacyclin in acute respiratory distress syndrome. Am J Respir Crit Care Med 1996;153:991–6.
103. Putensen C, Hormann C, Kleinsasser A, Putensen-Himmer G. Cardiopulmonary effects of aerosolized prostaglandin E1 and nitric oxide inhalation in patients with acute respiratory distress syndrome. Am J Respir Crit Care Med 1998; 157:1743–7.
104. Reyes A, Roca J, Rodriguez-Roisin R, et al. Effect of almitrine on ventilation–perfusion distribution in adult respiratory distress syndrome. Am Rev Respir Dis 1988;137:1062–7.
105. American Thoracic Society. Medical Section of the American Lung Association. International Consensus Conferences in Intensive Care Medicine: Ventilator-associated lung injury in ARDS. Am J Respir Crit Care Med 1999;160:2118–24.
106. Feihl F, Eckert P, Brimioulle S, et al. Permissive hypercapnia impairs pulmonary gas exchange in the acute respiratory distress syndrome. Am J Respir Crit Care Med 2000;162: 209–15.
107. Pfeiffer B, Hachenberg T, Wendt M, Marshall B. Mechanical ventilation with permissive hypercapnia increases intrapulmonary shunt in septic and nonseptic patients with acute respiratory distress syndrome. Crit Care Med 2002; 30:285–9.
108. Amato MB, Barbas CS, Medeiros DM, et al. Effect of a protective-ventilation strategy on mortality in the acute respiratory distress syndrome. N Engl J Med 1998;338: 347–54.
109. Mancini M, Zavala E, Mancebo J, et al. Mechanisms of pulmonary gas exchange improvement during a protective ventilatory strategy in acute respiratory distress syndrome. Am J Respir Crit Care Med 2001;164:1448–53.
110. Zavala E, Ferrer M, Polese G, et al. Effect of inverse I:E ratio ventilation on pulmonary gas exchange in acute respiratory distress syndrome. Anesthesiology 1998;88:35–42.
111. Pappert D, Rossaint R, Slama K, et al. Influence of positioning on ventilation–perfusion relationships in severe adult respiratory distress syndrome. Chest 1994;106:1511–6.
112. Bein T, Reber A, Metz C, et al. Acute effects of continuous rotational therapy on ventilation–perfusion inequality in lung injury. Intensive Care Med 1998;24:132–7.
113. Putensen C, Mutz NJ, Putensen-Himmer G, Zinserling J. Spontaneous breathing during ventilatory support improves ventilation–perfusion distributions in patients with acute respiratory distress syndrome. Am J Respir Crit Care Med 1999;159:1241–8.
114. Lampron N, Lemaire F, Teisseire B, et al. Mechanical ventilation with 100% oxygen does not increase intrapulmonary shunt in patients with severe bacterial pneumonia. Am Rev Respir Dis 1985;131:409–13.
115. Gea J, Roca J, Torres A, et al. Mechanisms of abnormal gas exchange in patients with pneumonia. Anesthesiology 1991;75:782–9.
116. Gillespie DJ, Rehder K. Body position and ventilation–-perfusion relationships in unilateral pulmonary disease. Chest 1987;91:75–9.

CHAPTER 19

PULMONARY EDEMA

René P. Michel, Peter Goldberg

Pulmonary edema is defined as an increase in extravascular lung water, which collects in two principal compartments, the interstitium and the alveoli; when water accumulates in the latter, gas exchange is severely compromised, with life-threatening consequences. Pulmonary edema is generally divided into two main pathogenetic types: (1) hydrostatic (commonly cardiogenic), also termed hemodynamic or high pressure, and (2) permeability edema, also termed "normal pressure" or noncardiogenic, encompassing predominantly acute respiratory distress syndrome (ARDS) and acute lung injury (ALI). Hydrostatic edema results from alterations in the "pressure" parameters in the Starling equation (below), most commonly microvascular pressure. The principal etiologies are shown in Table 19-1. In contrast, permeability edema, characterized by the elevation of microvascular permeability, is currently synonymous with ARDS and ALI. Each, as proposed by the American–European Consensus Conference (AECC), is defined as "a syndrome of inflammation and increasing permeability that is associated with a constellation of clinical, radiographic, and physiologic abnormalities that cannot be explained by, but may coexist with, left atrial or pulmonary capillary hypertension." ALI and ARDS differ only in severity, and their defining criteria are given in Table 19-2[1]; all patients with ARDS have ALI, but not all patients with ALI have ARDS. The classification of ARDS (Table 19-3) separates it into *direct* and *indirect* etiologies. Some investigators have used the terms *pulmonary* and *extrapulmonary*, based on differences in respiratory mechanics and response to positive end-expiratory pressure (PEEP), with predominant consolidation (implying a pneumonic process) in pulmonary ARDS versus prevalent edema and hyaline membranes, that is, diffuse alveolar damage (DAD) (see below), in extrapulmonary ARDS.[2,3] The time frame for the "acute" in ALI/ARDS is "less than 7 days from the onset of the critical illness."[4]

This chapter presents the authors' personal view of pulmonary edema in the adult. We focus on the definitions and classification, the basic pathogenetic mechanisms, including molecular, that result in pulmonary edema, the pathways of fluid movement in the lung, the imaging and pathologic appearances, and the pathophysiologic consequences for lung function and gas exchange. We open small windows on therapeutic vistas and their complications. Animal models are used as appropriate to explain mechanisms.

STARLING EQUATION AND NORMAL FLUID BALANCE

To understand pulmonary edema, it is important to consider the "Starling equation." Although Starling[5] enunciated the concepts of fluid exchange across vascular walls over a century ago, he provided no actual equation in his publication; rather, succeeding authors and investigators designed and refined several variants. One oft-quoted version is $J_v = LS[(P_{mv} - P_{pmv}) - \sigma(\Pi_{mv} - \Pi_{is})]$,[6] in which (with approximately normal values for the lung in parentheses) J_v is net transvascular fluid flow (mL/min); L is specific vascular hydraulic conductance or permeability, dependent on endothelial pore size; S is the vascular surface area of those vessels participating in fluid exchange; LS is K_f or fluid filtration coefficient, a measure of permeability to fluid and vascular surface area (≈0.2 mL/min/100 g/mm Hg); P_{mv} is microvascular (≈capillary) hydrostatic pressure (≈5 to 10 mm Hg); P_{pmv} is perimicrovascular or interstitial hydrostatic pressure (≈ −5 to −7 mm Hg); σ is the osmotic reflection coefficient, determining the relative contribution of the oncotic pressure gradient across the vasculature to the net driving pressure—expressly a measure of the permeability of a specified membrane (eg, endothelial) to a particular solute (eg, albumin), varying between 0 when the membrane is totally permeable, to 1 when it is totally impermeable; in the lung, σ is ≈0.75 to 0.80; Π_{mv} is the oncotic pressure of the blood in the microvasculature of the lung (≈24 mm Hg); and Π_{pmv} is the oncotic pressure in the perimicrovascular interstitium (≈14 mm Hg).

Of the parameters of the Starling equation, P_{mv} and Π_{mv} are those most easily measured or calculated as detailed below: both are measurable in experimental animals but not in humans, except for estimates of Π_{pmv} calculated from the protein level in alveolar fluid from patients with fulminant pulmonary edema.[7] Similarly, J_v, LS, and σ must be determined in animals or calculated from the other parameters (see Granger and colleagues[6] for a comprehensive discussion).

Under normal circumstances, the lung and, in particular, the alveoli are kept optimally hydrated or "dry" and

Table 19-1 Classification of Hydrostatic Edema

Cardiogenic
High cardiac output
Anemia
Shunts (cardiac, pulmonary, peripheral)
Beriberi
Hyperthyroidism
Systolic dysfunction (low cardiac output)
Ischemia
Hypertension
Idiopathic (cardiomyopathy)
Tachycardia-induced
Peripartum
Toxin
Viral
Diastolic dysfunction (normal-to-high cardiac output)
Ischemia
Hypertension
Noncardiogenic
Volume overload, eg, renal failure
Low oncotic pressure, eg, hypalbuminemia, dilutional from crystalloid overinfusion
Pulmonary venous diseases
Pulmonary venoocclusive disease
Mediastinal fibrosis

Inspired in part by Poppas and Rounds.[262]

Table 19-2 Definition of ARDS According to the American–European Consensus Conference, 1994[1]

Acute onset
Hypoxemia (P_aO_2, in mm Hg/$FiO_2 \leq 200$) regardless of PEEP
Bilateral infiltrates on frontal chest radiograph
Pulmonary capillary wedge pressure ≤ 18 mm Hg or no evidence of left atrial hypertension

Acute lung injury differs only in having a $P_aO_2/FiO_2 \leq 300$.

protected against edema by several physiologic safety factors, including the following:

1. Low pulmonary P_{mv} compared to systemic capillaries ($\approx$25 mm Hg).
2. Low P_{pmv} compared to P_{alv} (alveolar pressure $\approx$0 mm Hg), so that filtered fluid preferentially enters the interstitium (negative P_{pmv}) rather than alveoli. As fluid builds up in the interstitium, P_{pmv} rises, acting as negative feedback in the Starling equation.
3. A normally low Π_{pmv}, approximately 50% of Π_{mv}, estimated from protein concentrations in pulmonary edema.[8]
4. The interstitium, able to accommodate a $\approx$50% increase in extravascular lung water, largely proportional to glycosaminoglycans.[9]
5. Lymphatics that drain the interstitial space and whose flow can increase 10 to 15 times acutely or 20 times chronically.
6. As J_v rises, as long as LS and σ are normal, the Π_{pmv}/Π_{mv} ratio drops because the endothelium sieves proteins.
7. An epithelial barrier substantially less permeable than the endothelial barrier because of tighter interepithelial junctions forming a more effective barrier to the passage of solutes and proteins (effective pore radii of 0.5 to 0.9 nm in epithelium vs 6.5 to 7.5 nm in capillary endothelium), affording protection against alveolar flooding.[10]

In general, edema results when the filtered fluid J_v rises beyond the capacity of the lymphatics and other mechanisms to remove it.

Microvascular Pressure

An understanding of the measurement and factors affecting P_{mv} remains critical in the investigation of hydrostatic and

Table 19-3 Classification of Permeability Pulmonary Edema (Acute Respiratory Distress Syndrome and Acute Lung Injury

Direct lung injury
Infections (pneumonia)
Bacterial
Viral (eg, cytomegalovirus, adenovirus, herpes, SARS-associated coronavirus)
Fungal (eg, *Aspergillus*, *Pneumocystis carinii*)
Inhalation
Aspiration of gastric contents
Toxic gases and chemicals (eg, smoke, Cl_2, NH_4, NO_2, O_2, SO_2)
Near-drowning
Injury, traumatic (pulmonary contusion)
Intravascular
Embolism (air, amniotic fluid, fat)
Iatrogenic
Drugs
Anticancer drugs (eg, bleomycin, busulfan, all-*trans* retinoic acid)
Antibiotics
Antiarrhythmics (eg, amiodarone)
Irradiation
Idiopathic
Acute eosinophilic pneumonia
Acute interstitial pneumonia
Immunologic
Acute lupus pneumonitis
Goodpasture's syndrome
Cryptogenic organizing pneumonia/bronchiolitis obliterans organizing pneumonia
Hypersensitivity pneumonitis
Idiopathic pulmonary hemosiderosis
Ischemia–reperfusion-mediated edema (eg, after embolectomy or lung transplantation)
Infiltration by malignancy
Lymphangitic carcinomatosis
Leukemic or lymphomatous infiltration
Indirect lung injury
Sepsis
Multiple fractures, severe trauma with shock
Cardiopulmonary bypass
Major burns
Drug overdose
Acute pancreatitis
Multiple transfusions of blood products
Disseminated intravascular coagulation
High altitude*
Neurogenic*

*With a hydrostatic component. Inspired in part by Lesur and colleagues,[263] Murray and colleagues,[198] Steinberg and Hudson,[82] and Ware and Matthay.[264]

permeability forms of edema. Unlike its counterpart in the systemic circulation, P_{mv} is difficult to measure in the lung; its value depends directly on the distribution of pulmonary vascular resistance (PVR). In experimental animals, P_{mv} has been measured indirectly and, more recently, directly; in the clinical setting, only indirect measurements are possible. In normal lungs, P_{mv} has generally been measured or assumed to be close to the midpoint between pulmonary arterial and venous pressure (or left atrial pressure, P_{la}).[8] Gaar and colleagues[11] determined in isolated perfused canine lobes, using the isogravimetric method, that 56% of total PVR was in arteries and 44% in veins. This led to a widely quoted equation for the calculation of P_{mv}, using the assumption that 40% of resistance was in the veins, such that $P_{mv} = P_w + 0.4(P_{pa} - P_w)$, in which P_{pa} is pulmonary arterial pressure and P_w pulmonary arterial wedge pressure. The principal methods used for the estimation of P_{mv} have included (1) wedge catheters; (2) the isogravimetric method; (3) arterial, venous, or double occlusion; and (4) micropuncture.

Wedge catheters, introduced in 1948 (reviewed by Levy[12]), are employed extensively in clinical practice to measure P_w, an indirect measure of left ventricular end-diastolic pressure, although recently their benefits have been seriously questioned.[13] The principle guiding the measurement of P_w is occlusion of a small-to-medium pulmonary arterial branch, approximately 1.5 to 3.0 mm,[14] by inflation of the catheter's balloon, thereby "wedging" it; as flow distal to the balloon stops, the pressure measured at the tip of the catheter equals the pressure along the vascular tree supplied by that artery until a vein of about the same size is reached, wherein bloodflow resumes. The pressure measured at the tip of the catheter approximates left atrial and ventricular end-diastolic pressures, provided that (1) there is a continuous column of blood into the left atrium and, at end-diastole, into the left ventricle (ie, the lung is in zone 3), and (2) resistance of the large pulmonary veins is low.

In abnormal lungs, particularly in ARDS, with hypoxia or activation of the inflammatory cascade, release of mediators such as histamine, leukotrienes, platelet-activating factor (PAF), and thromboxanes may alter pulmonary arterial and venous resistances, and the relationship between P_{mv} and P_w and reduce the validity of P_w measurements in the estimation of P_{mv}. These considerations impact directly on the management of patients with ARDS, in whom a delicate balance must be maintained between an adequate filling pressure and minimizing pressure-related fluid filtration, and they prompted detailed studies on the distribution of PVR.

In 1979, Hakim and colleagues[15] first used the venous occlusion technique in isolated canine lung lobes to examine the distribution of resistance across the pulmonary vascular bed. The technique, extended to arterial and venous occlusion (AVO) in sequence, generated a simple model in which PVR was partitioned into relatively indistensible arterial and venous segments, each contributing 40% to 45% of the total, separated by a more compliant middle segment contributing 10 to 15%.[16] These segmental resistances and the P_{mv} values dependent on them vary with the physiologic environment, pharmacologic stimuli, and pathologic conditions. For example: (1) the relative proportion of arterial and venous resistance rises with bloodflow and venous pressure; (2) middle segmental resistance increases with airway pressure and hypoxia[17,18]; (3) arterial segmental resistance increases with serotonin level; (4) venous segmental resistance rises with levels of histamine, leukotrienes,[19] PAF,[20] and thromboxane[21]; (4) systemic-to-pulmonary shunts raise mainly the arterial segmental resistance,[22] and fibrosis increases middle segmental resistance.[23]

Nearly simultaneously with the introduction of the occlusion technique, Bhattacharya and Staub[24] measured for the first time pressures by micropuncture in subpleural pulmonary arteries and veins, 10 to 50 μm in diameter, of isolated canine lobes and found that 45% of total resistance was in alveolar wall vessels, with most of the balance of resistance being in small arteries. A dozen years later, similar data were obtained by Negrini and colleagues[25] in intact animals by puncturing the pleura. These and subsequent findings, recently reviewed,[26] reveal that one-third to one-half of the total pressure drop from pulmonary artery to left atrium takes place in alveolar capillaries.

The findings of the micropuncture studies are difficult to reconcile with the occlusion data. Explanations for the discrepancies include (1) technical considerations related to the vascular and alveolar pressures under which micropuncture measurements are made[27] and (2) the notion that subpleural vessels differ morphologically and may not be representative of the entire lung because of their relatively low density and reduced bloodflows.[28,29] In a study in which both techniques were compared,[30] a pressure gradient of only 0.5 mm Hg between 30 and 50 μm arteries and veins, and a large pressure gradient in arteries and veins > 0.9 mm, were found. Nagasaka and colleagues[31,32] reported that, in feline lungs, there was a substantial gradient in arterial and venous vessels and that their relative contributions to the total gradient were flow dependent, consistent with the notion that at low flows, or in vessels with intrinsically lower flow rates, such as in the subpleural region, the contribution of the middle capillary segment to total PVR may be unduly high. One criticism leveled against the occlusion data is the uncertainty concerning the anatomic size limits of each of the segments: Hakim and Kelly[30] addressed this point and concluded that AVO measured pressures in vessels 50 to 900 μm in diameter, probably in the vicinity of 100 μm; a similar size estimate was obtained in a structure–function study of a model of chronic unilateral pulmonary artery ligation.[33] Although the discrepancies between the micropuncture and occlusion data are incompletely resolved, the evidence appears to favor the notion that, for the lung in its entirety, the majority of the resistance lies in the larger arterial and venous vessels, ensuring protection from both arterial overperfusion and elevations in venous pressure. Moreover, a distinct advantage of occlusion is that it offers an experimental model and theoretical framework for the measurement of P_{mv} in patients at the bedside.

Indeed, the AVO techniques have been adapted for use in intact animals and humans, under conditions of pulsatile flow[34–37]: in animals, pressure transients recorded immediately after occlusion has been caused by inflation of the Swan-Ganz catheter's balloon are analyzed to obtain estimates of P_{mv}, yielding values linearly related to those obtained by the isogravimetric method and by double occlusion over a range of pressures. In patients, the methods of analysis and results of the occlusion technique vary with the clinical situation, as discussed elsewhere.[37,38] In one study, Collee and colleagues[39] made 34 estimates of P_{mv} in 15 patients with acute respiratory failure, using arterial occlusion, and found the following: (1) there was elevated total PVR; (2) P_{mv} was significantly higher than P_w; and (3) PVR varied considerably between the arteries and veins (for example, venous resistance ranged between 0.2 and 0.7 of total, a wide scatter from the assumed value of 0.4 in the aforementioned Gaar equation).

To summarize, the clinical measurement of P_{mv} remains difficult, particularly in ARDS, because of (1) regional disparities in severity of disease; (2) difficulties in interpretation of occlusion pressure measurements because of respiratory movements; (3) high levels of PEEP, so that arterial pressure tracings reflect alveolar rather than vascular pressure (ie, zone 1); (4) subjectivity of measurements; and (5) the relatively long time needed for the occlusion to appear on the tracings.[12] In both hydrostatic and permeability edema, the key message is that the fluid filtration pressure P_{mv} is substantially higher than the frequently measured P_w. In particular, the AECC criterion for P_w of 18 mm Hg (see Table 19-2) is relatively high since the corresponding P_{mv} in normal lungs is 23 to 24 mm Hg,[40] above which lung water rises in linear fashion even in normal lungs[41] (see below). Perturbations in the distribution of PVR in ARDS caused by cytokines and mediators, as indicated above, increase the likelihood of an even greater differential between P_{mv} and P_w.[39]

Other Pressures in the Starling Equation

The intravascular oncotic pressure Π_{mv}, counterbalancing P_{mv}, can be measured directly with an osmometer, calculated from equations originally described by Landis and Pappenheimer, with knowledge of the plasma concentrations of albumin and globulins, or read directly from a nomogram.[8] The Π_{mv} is also subject to change, for example, in disease states associated with hypoproteinemia: when the protein concentration falls by about half, patients are at risk of developing pulmonary edema because of the reduced threshold for P_{mv}.[42] In hydrostatic edema, the normal Π_{pmv}/Π_{mv} ratio of about 50% may fall to 30% under conditions of high filtration as long as the sieving properties of the microvascular barrier are maintained.[8]

The P_{pmv} varies with location in the pulmonary parenchyma. Bhattacharya and colleagues[43] found, in normal lungs, that $P_{pmv} \approx -3$ cm H_2O at interalveolar junctions, to which is added the gradient between the perimicrovascular space in the subpleural and parenchymal areas and the hilar interstitial tissues ($\approx$5 cm H_2O), driving fluid toward the hilum. Alterations in P_{pmv} with hydrostatic edema are discussed below.

EDEMA: SOURCES AND PATHWAYS OF LEAKAGE, SEQUENCE AND SITES OF ACCUMULATION, AND CLEARANCE

Sources and Pathways of Fluid Leakage

In the systemic circulation, particularly under conditions of increased permeability, it is accepted that venules are the most leaky vessels.[44] However, in the lung, demonstration of a gradient of vascular permeability between capillaries, small arteries and veins has been difficult, prompting Staub[40] to advocate the term "microvascular" over "capillary" to describe sites of fluid filtration. Morphologic studies with tracers have shown that much of the leakage occurs from capillaries, with lesser amounts from small nonmuscular arteries and veins.[45] Physiologic data show edema leaks from extraalveolar as well as alveolar vessels: alveolar vessels, that is, those subject to alveolar pressure, include the majority of alveolar capillaries but also some small arteries and veins vessels in the extraalveolar compartment, in contrast, are those whose liquid pressure is influenced by pleural pressure and anatomically are composed of most of the arteries and veins and of capillaries at alveolar corners.[8,18] An important variable in the ascertainment of sources and relative amounts of fluid filtered is vascular surface area. As summarized by Staub,[8] morphometric studies of the pulmonary vasculature in humans have shown that 90 to 95% of the vascular surface area is provided by capillaries, with the small balance being provided by arteries and veins. These data suggest that at high alveolar pressure (zone 1 conditions), there should be 10 to 20 times less fluid filtered than under zone 3 conditions; in fact, there is only a twofold difference, reflecting continued filtration in zone 1 by extraalveolar vessels, particularly capillaries in alveolar corners. This reasoning is true if we assume that filtration is directly proportional to surface area, but this has not been demonstrated in pathologic states of permeability edema or even in hydrostatic edema.

Where does the fluid move after its filtration? From capillaries, it enters the thick part of the alveolar–capillary septum[46] and tracks to the "juxtaalveolar region" (junction between alveolar and extraalveolar interstitial spaces), where it enters the initial lymphatics,[47] the movement being driven by passive interstitial hydrostatic pressure gradients facilitated by respiration. As referred to above, the pressure gradient from the alveolar–capillary septum to the interalveolar junctions of -3 cm H_2O[43] is added to a further 1.5 cm H_2O to the initial lymphatics, for a total interstitial pressure gradient from capillaries to lymphatics of 4 to 5 cm H_2O. From there, fluid moves to the hilar interstitial tissues and lymphatics within them.

Sequence and Sites of Edema Fluid Accumulation

When the lymphatics are unable to cope with the demands of filtration, fluid accumulates first in the interstitium around arteries, veins, and airways and in interlobular septa (Figures 19-1 and 19-2), protecting the lung against the final stage, alveolar edema.[48] Studies in which quantitative morphology was used to investigate the distribution of interstitial fluid in hydrostatic and in permeability edema induced

FIGURE 19-1 Part of a frozen canine lung slice after induction of hydrostatic edema: note artery (A) and vein (V) surrounded by fluid cuffs (*arrows*); B = airway.

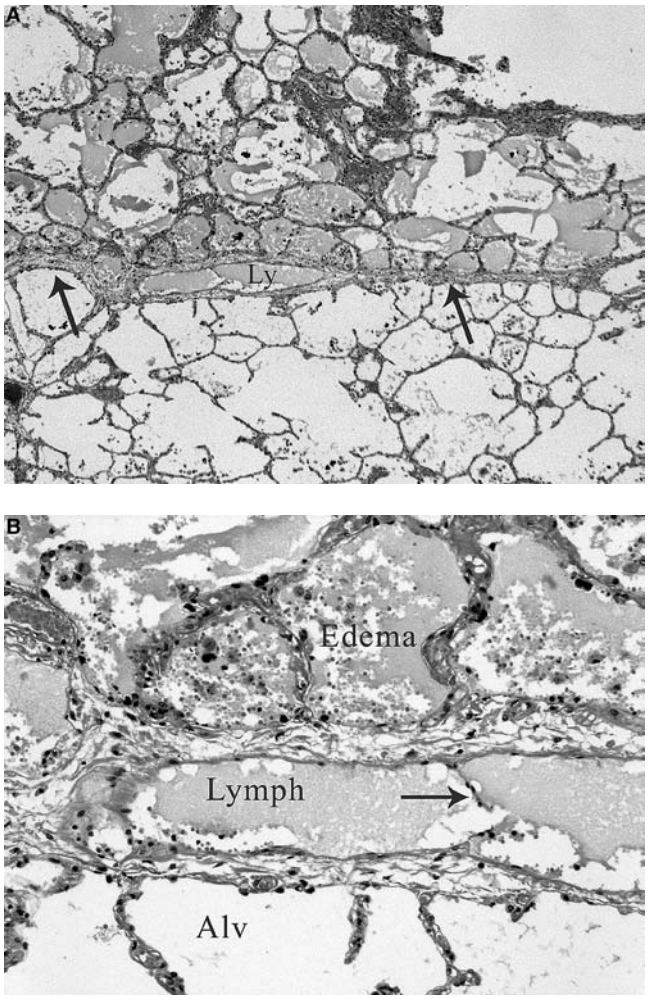

FIGURE 19-2 Light photomicrograph of lung from a patient with cardiogenic pulmonary edema. *A*, Low-power view, showing fluid in the interlobular septum (*arrows*) and adjacent alveoli. Hematoxylin-eosin stain; ×50 original magnification. *B*, Higher-power view, showing dilated lymphatic (Lymph) with its valve (*arrow*) and edema in some alveoli (Alv). Hematoxylin-eosin stain; ×250 original magnification.

by α-naphthylthiourea (ANTU) have shown preferential fluid accumulation around arteries over veins and around larger vessels[49–51]; in bronchovascular bundles, more fluid collects around arteries than around airways (see Figure 19-1), with none around bronchioles. These preferred sites of fluid collection result from differences in compliance of the interstitial spaces and their hydrostatic pressures. Several authors have shown (reviewed by Lai-Fook[52]) that the distribution of edema in the lung depends on gradients of interstitial pressures, resistance and compliance. Peribronchial pressures are less negative than perivascular pressures and rise relative to pleural pressure with inflation because peribronchial pressure follows intrabronchial pressure, which rises with alveolar pressure; in contrast, perivascular pressures are more negative than pleural and peribronchial pressures and reflect the mechanical stress exerted on the vessels by the pulmonary parenchyma. Movement of fluid in the peribronchovascular interstitium also depends on tissue resistance, determined by hyaluronan and the extent of hydration: resistance to fluid flow drops with increasing edema or when hyaluronidase is added.[52]

Interstitial fluid cuffs protect against alveolar flooding by acting as reservoirs. Their volume can rise to 2 to 3 mL/g dry lung weight and in proportion to lung volume.[53,54] Consequently, the lung can augment its wet weight by 50% prior to the onset of alveolar flooding, with the proviso that the alveolar epithelium remains intact. In permeability edema, this reservoir function appears to be much less effective since alveolar flooding may occur early and in some instances bypass altogether the interstitial edema phase.[55]

In interesting morphologic and physiologic studies, primarily in the 1980s, the relationships between the fluid in large peribronchovascular interstitial cuffs and lymphatic drainage were examined; it was found that lymph flow is more closely related to fluid filtration rate from pulmonary microvessels (ie, predominantly to P_{mv}) than to the amount of lung water. It has been demonstrated in morphologic studies that tracers injected intravenously emerge in lymphatic vessels within minutes, whereas their appearance in perivascular interstitial cuffs is delayed in proportion to their distance from the site of filtration.[45,54] In a physiologic model of hydrostatic lung edema, lymph flow was proportional to vascular pressure[56]; when the latter was normalized, lymph flow returned to control values, despite the presence of considerable edema in the lung, consistent with a two-compartment model of the pulmonary interstitium: a perimicrovascular compartment, in direct contact with the filtering vessels, and a second compartment, consisting of "sequestered" spaces around larger bronchovascular bundles and in interlobular septa. This relationship may not hold true in permeability edema, as shown in ANTU-induced edema by Pine and colleagues,[57] who found abundant alveolar edema with little interstitial edema and low lymphatic flow rates.

In hydrostatic edema, the question of precisely how fluid enters alveoli from a filled interstitium remains unanswered. Staub[8] suggested an "overflowing bathtub theory," but the exact site of passage is not clear: morphologic evidence points to the epithelia of alveoli, alveolar ducts, and respiratory

bronchioles as sites of passage,[58] possibly via normally tight interepithelial junctions forced open by the pressure. The terminal respiratory airway epithelium is particularly susceptible to damage,[59] and it is thought that the pores between the interstitium and the alveoli must be fairly large, that is, about 10 to 12 nm, because the protein concentration in alveolar liquid approaches that in the interstitium.

Clearance of Alveolar Edema

The important and clinically relevant topic of the resolution of alveolar edema came to the forefront of research about 20 years ago, when studies provided evidence that alveolar fluid balance in the lung was regulated through active ion transport mechanisms by pulmonary alveolar and distal airway epithelium. The current model for the mechanism of the clearance of water and ions is that active transepithelial transport of salt drives water movement and supplants the passive forces of the Starling equation.[60] Although the alveolar epithelium, with its large surface area (99% of respiratory epithelial area), is the favored site of fluid reabsorption, the precise contribution of each segment of pulmonary epithelium remains undefined. Clara cells and nonciliated cuboidal cells in airways <200 μmin diameter are capable of transporting Na^+ and Cl^- ions and, despite their relatively small numbers, may contribute to alveolar fluid clearance; new evidence suggests that some fluid may be removed by convective surface active forces that propel it into the distal airways, with absorption occurring across respiratory bronchiolar epithelial cells. These cells, along with type II and possibly type I pneumocytes, have their ion transporters distributed asymmetrically on the apical and basal surfaces, enabling unidirectional transport of Na^+ ions. The specific mechanisms involve Na^+ uptake on the alveolar side of epithelial cells via amiloride-sensitive and amiloride-insensitive channels and active pumping from the basolateral surface into the pulmonary interstitium by Na^+/K^+-ATPase.

Supporting the importance of active clearance of alveolar edema are demonstrations that (1) in uninjured lungs, variations in transpulmonary airway pressure resulting from ventilation play a relatively small role in fluid clearance—for example, elimination of ventilation to one lung did not change the rate of fluid clearance in sheep,[61] and similar results in dogs obtained with the use of computed tomography (CT) of frozen lungs and light microscopy showed that ventilation had little effect on the clearance of alveolar edema and acted primarily by aerating alveoli[62]; and (2) clearance is inhibited by hypothermia in several models in different species, including humans.[60]

In contrast, the clearance of alveolar *protein* across the alveolar–epithelial barrier, which is much slower than that of water and solutes, is mediated chiefly by restricted diffusion, with added contributions from endocytosis and transcytosis[63]: in nonanesthetized spontaneously breathing sheep, Matthay and colleagues[60] found that [^{125}I]albumin cleared at a slow constant rate of 1%/h; in contrast, in the first 4 hours, water was removed at 8.3%/h, gradually slowing to 1.4% at 24 hours, due to the increasing osmotic pressure of the residual alveolar protein.

Clearance of fluid differs in hydrostatic and in permeability edema. In clinical studies of hydrostatic edema due to left heart failure, in which the epithelium remains intact, fluid was cleared in most patients within 4 hours of intubation and positive pressure ventilation. In one study, 75% of patients had intact fluid clearance, and the inability to clear fluid in the remaining patients was unrelated to the elevated vascular pressures.[64] In permeability edema, clearance of alveolar fluid is impaired and associated with prolonged respiratory failure and elevated mortality: only those patients who clear fluid quickly have a higher survival rate,[65] consistent with the notion that an intact distal pulmonary epithelium is coupled to a better prognosis in patients with ALI. The subject of the clearance of pulmonary edema is discussed in greater detail elsewhere in this book (see Chapter 38, "Epithelial Function in Lung Injury").

HYDROSTATIC PULMONARY EDEMA

Epidemiology

The epidemiology of hydrostatic pulmonary edema is intimately related to that of congestive heart failure (CHF). The American Heart Association reports about 550,000 new cases each year in the United States, and CHF contributed to approximately 287,200 deaths in 1999.[66] Recent data from the Framingham Heart Study on 3,757 male and 4,472 female subjects free of CHF at baseline, from 1971 to 1996, revealed that, at age 40 years, the lifetime risk for CHF was 21.0% for men and 20.3% for women, remaining at this level with advancing index age because of rapidly increasing CHF incidence rates[67]; the lifetime risk for CHF doubled for subjects with blood pressure $>160/100$ versus $<140/90$ mm Hg, and in those subjects without antecedent myocardial infarction, the lifetime risk for CHF at age 40 years was 11.4% for men and 15.4% for women. Therefore, hypertension and myocardial infarction are the major antecedents of heart failure, including hydrostatic pulmonary edema. In another recent study of 10,311 eligible Framingham Heart Study subjects, Levy and colleagues[66] reported CHF in 1,075 (10.4%) subjects between 1950 and 1999; over those 50 years, the incidence of heart failure declined among women but not among men, and survival after onset of CHF has improved in both sexes. It remains the case that hydrostatic edema as part of CHF is a formidable health problem and that the prognosis after development of CHF is poor, with a median survival of 1.7 years in men and 3.2 years in women.[68]

Pathogenesis

The major causes of hydrostatic pulmonary edema are cardiac, generally left ventricular failure. The customary initiating event is a fall in ventricular ejection fraction, elevating end-diastolic volume and then pressure; this raises P_{la} to maintain output, with passive transmission to the pulmonary venous and microvascular network. According to the Starling equation, this rise in P_{mv} increases J_v directly and vascular surface area S indirectly by recruitment. As first shown in the seminal study of Guyton and Lindsey,[41] raising P_{la} above 24 mm Hg produces a linear rise in lung water as

determined by wet/dry weight ratios; similar findings have been reported in humans.[69] It is noteworthy that in the definition of ARDS (see Table 19-2), the threshold value for P_{mv}, as estimated from P_w, is generally set at a lower level, that is, approximately 18 mm Hg. This relatively high pressure threshold reflects the action of the two principal safety factors: (1) lymph flow (an indirect measure of J_v), which increases to clear fluid in direct proportion to P_{la} and P_{mv}, up to approximately double normal P_{mv}, and (2) an osmotic feedback mechanism, with a proportionate reduction in protein osmotic pressure of the interstitium (Π_{pmv}) and lymph due to sieving of proteins at the endothelial barrier, which, at pressures under ≈40 mm Hg (cf. West and colleagues—later in this chapter), remains intact and reduces fluid filtration by approximately 50%.

Notably, when the right heart also fails, the elevation of systemic venous pressure abrogates part of the safety factor provided by the lymphatics: these enter the neck veins, so that their downstream pressure is increased, reducing their flow rate and accentuating the edema.[40,70] Drake and colleagues[71] found that increases in systemic venous pressure >11 mm Hg produced by heart failure in sheep interfered more with lymph flow from the caudal mediastinal lymph node (which drains predominantly pulmonary lymph) than with lymph flow with zero outflow pressure. Similarly, 20 mm Hg PEEP, which increases central venous pressure, impedes pulmonary lymph flow, and facilitates the formation of hydrostatic pulmonary edema, was reversed by an external thoracic duct fistula, isolating this important source of pulmonary drainage from the elevated venous pressure.[72]

Pathology and Imaging

In the acute stage, the first alteration as P_{mv} rises is pulmonary vascular congestion with distention and recruitment, increasing surface area; as it increases further and the lymphatics are overwhelmed, fluid accumulates, first in the interstitium (interlobular septa and peribronchovascular spaces, and interalveolar septa) and then in alveoli (Figures 19-1 to 19-4). On hematoxylin and eosin (H&E)-stained histologic sections, the interstitial and alveolar spaces are distended by thin eosinophilic fluid (reflecting a lower protein content) that may contain small amounts of blood.

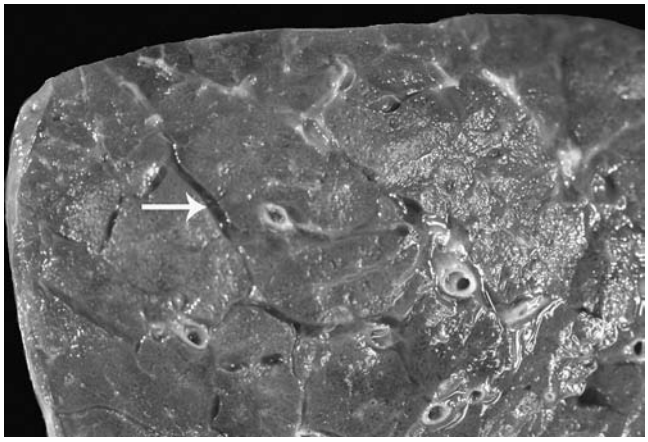

FIGURE 19-3 Part of a lung slice from a patient with hydrostatic edema, showing dilated interlobular septa (one at *arrow*), some extending to pleura (corresponding to Kerley B lines on a chest radiograph).

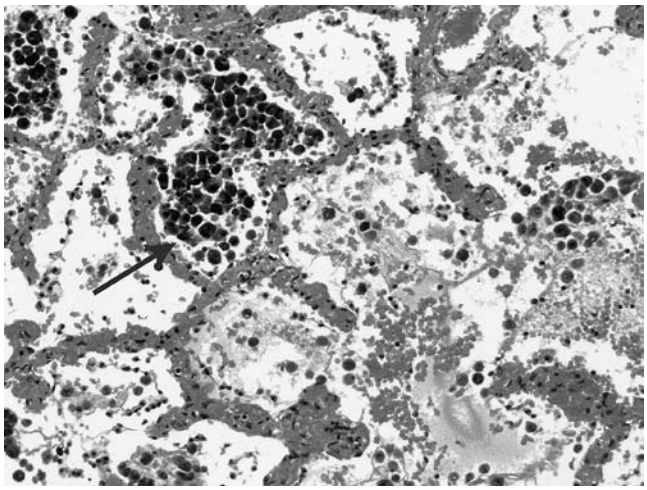

FIGURE 19-4 Medium-power light micrograph of lung from patient with aortic stenosis, long-standing heart failure, and acute on chronic pulmonary edema. Note the markedly congested capillaries in alveolar–capillary septa, alveoli filled with fresh erythrocytes mixed with edema, and aggregates of hemosiderin-laden macrophages (*arrow*), evidence of prior bouts of edema. Hematoxylin-eosin stain; ×250 original magnification.

The findings of imaging studies mirror the pathologic alterations (Figure 19-5). The sequential alterations on chest radiographs are (1) vascular "redistribution" to and distention of upper pulmonary veins; (2) enlargement and loss of definition of hilar structures; (3) septal lines in the lower lung, termed Kerley A and B lines; (4) peribronchial

FIGURE 19-5 Chest radiograph showing hydrostatic edema resulting from heart failure after recent myocardial infarct superimposed on long-standing aortic stenosis in a 74-year-old male. Note distended upper zone vessels, prominent interstitial markings, and fluffy airspace edema in lower lung fields.

and perivascular cuffing with widening and blurring of the margins; and (5) thickening of interlobar fissures with subpleural fluid accumulation.[73,74] Cardiomegaly and pleural effusions are frequent. There are gradients of distribution of edema, both gravity dependent and gravity independent. Several studies have confirmed that, because of the balance of forces favoring fluid filtration, there is more interstitial and alveolar edema in the dependent portions of the lung,[75,76] with variable preferential distribution of fluid in central rather than peripheral zones of the lung (see Figure 19-5), in a so-called "batwing" or "butterfly" pattern.[14]

Chronic or repeated episodes of elevated pulmonary venous pressures may lead to characteristic vascular and parenchymal alterations that include "brown induration of the lung" with abundant hemosiderin-laden alveolar macrophages (see Figure 19-4), mild interstitial and alveolar fibrosis, "arterialization" of veins, and arterial medial thickening, the last of these leading to secondary pulmonary hypertension.[14]

At the ultrastructural level, in isolated perfused canine lobes, descriptive and morphometric studies of acute hydrostatic edema have revealed (1) widening of the air–blood barrier at the thick part of the alveolar–capillary septum, leaving intact its thin part, where endothelial and epithelial basement membranes are fused (and where gas exchange occurs), and (2) increased density of pinocytotic vesicles in capillary endothelium and in alveolar type I pneumocytes and more open interendothelial junctions[77]; in *intact* dogs, however, endothelial vesicular densities are normal, and edema fluid is seen only in the extraalveolar connective tissue spaces,[78] probably as a result of differences in P_{pmv}, Π_{pmv}, or lymph flow rates. More recent studies in excised and perfused rabbit lungs have shown blebs or frank disruptions of epithelium with rare endothelial lesions, distributed in an apical–basal gradient and present in fluid-filled alveoli.[76,79]

In chronic heart failure or mitral stenosis, electron microscopy of lungs from experimental animals or patients shows (1) edema, degeneration, and even reduplication of endothelial cells (ECs); (2) edema of epithelial cells and of the thick part of the alveolar–capillary septum; (3) proliferation of dense connective tissue around capillaries and of type II pneumocytes; and (4) increased numbers of intraalveolar macrophages.[14,80] This remodeling has been associated with an elevation of PVR, a fall in vascular compliance, and, as dictated by the Laplace equation, a reduction in stress on capillaries with an increased threshold for high vascular pressure–induced injury. Mechanisms for the remodeling, reviewed by West and Mathieu-Costello,[81] involve increased expression of genes for extracellular matrix proteins, such as various procollagens and fibronectin, and for growth factors, for example, fibroblast growth factor-2 (FGF-2) and transforming growth factor-β_1 (TGF-β_1).

PERMEABILITY PULMONARY EDEMA

EPIDEMIOLOGY

Although the exact yearly incidence of ALI/ARDS has not been established, estimates in the United States have ranged from highs of 75 in 100,000 to lows of 1.5 to 8.4 in 100,000.[82] More recent data from the ARDS Network study of low-tidal-volume ventilation have suggested rates ranging from 16 to 96 cases of ALI/ARDS per 100,000 population.[83,84] This wide range reflects both the difficulties in conducting such epidemiologic studies and the absence of a specific diagnostic test. The mortality associated with ALI/ARDS, despite over three decades of intensive investigation into causes and treatment, remains disturbingly high, at approximately 50%, and although beneficial effects of low-volume ventilatory management have been reported, numerous pharmacologic agents tested have failed to significantly improve this outcome.

Much of the early literature regarding ALI reported discrepant defining criteria, making comparisons between studies difficult. Although designed to address this lack of uniformity, the AECC criteria for ALI/ARDS (see Table 19-2) were rendered suspect by a recent report of poor interobserver agreement in the radiographic interpretation of ARDS.[85] There are similar concerns about the other criteria for ARDS since hypoxemia and oxygenation are altered by PEEP or alveolar recruitment maneuvers, and measurements of P_w to exclude hydrostatic edema are complicated by concurrent heart failure, application of PEEP, and other variables. Furthermore, the classification of ARDS is hampered by the lack of unique defining criteria: the pathologic characteristics of ARDS are encompassed by DAD as detailed below, but attempts to correlate DAD with the clinical presentation of ARDS have led to frustration. Indeed, in a retrospective study, Patel and colleagues[86] reported that in 57 patients meeting AECC criteria, a specific histologic diagnosis other than DAD was revealed by open-lung biopsy in 60%, underscoring the severe limitations of the AECC definition, and any clinical studies examining pathophysiology and treatment of ALI/ARDS.

Adding to this confusion, data from Gattinoni and colleagues[2] identified two distinct subgroups of ALI: among their 21 patients, 12 were deemed to have suffered a direct pulmonary injury, and in 9 an extrapulmonary cause was thought to be responsible. Although overall respiratory system elastance was similar in both subgroups, differences emerged after its partition into different categories: (1) lung elastance was significantly higher in the pulmonary group, whereas chest wall elastance and abdominal pressure were higher in the extrapulmonary group, and (2) PEEP increased respiratory system elastance in the pulmonary group but failed to recruit any additional lung volume when set to 15 cm H_2O, whereas PEEP decreased elastance in the extrapulmonary group and recruited additional lung volume. The authors explained these results by the consolidation in pulmonary ALI and by the edema and collapse in extrapulmonary ALI.

Given this lack of specificity and of readily available histologic confirmation, plasma markers would be useful to identify the syndrome, similar to troponin in acute coronary syndromes. To date, this search has been unsuccessful. Von Willebrand factor antigen, produced primarily by endothelial cells and, to a lesser extent, by platelets, has been variably identified as a diagnostic and prognostic indicator of

ALI: Ware and colleagues[87] reported that very high levels (>450%) have a greater than 80% positive predictive value for death in ALI, although they stressed that its high plasma-to-pulmonary edema ratio strongly supports the notion that its release reflects a generalized systemic endothelial activation/injury rather than specific lung injury.

More particular to the lung, and perhaps more promising as a diagnostic aid, is the bedside assessment of the activity of pulmonary endothelium-bound angiotensin-converting enzyme (ACE): Orfanos and colleagues[88] found reduced activity of the enzyme early in the course of ALI and an inverse relationship between its activity and the severity of lung injury as characterized by the Murray score. If this assay is to gain clinical credibility, it will have to be assessed both in conditions characterized by systemic endothelial injury, such as sepsis, and in those where lung disease other than ALI plays a prominent role, for example, pneumonia.

To quantify the risk of developing ALI following the onset of specific predisposing conditions, three large prospective studies were conducted, with similar qualifying criteria being used in each, although prior to the AECC definition. Pepe and colleagues[89] followed prospectively 136 patients with sepsis, aspiration of gastric contents, pulmonary contusion, multiple red cell transfusions, multiple major fractures, near-drowning, pancreatitis, and prolonged hypotension: 38% of patients with sepsis and 30% with aspiration developed ALI. Fowler and colleagues[90] similarly followed 993 patients with eight prospectively defined risk factors and identified 68 patients who developed ALI: aspiration carried the greatest risk (36%), and only 4% of the 239 patients with established bacteremia developed ALI. These findings contrast sharply with those of Pepe and colleagues[89]; this could be partly explained, perhaps, by the fact that their definition of sepsis included both infection (but not necessarily bacteremia) and a systemic response to that infection. More recently, Hudson and colleagues[91] prospectively followed patients with eight predefined conditions: ≈41% of patients with sepsis, 36% of patients following multiple blood transfusions, and 22% of patients with pulmonary contusion or gastric aspiration developed ALI. Together, these three studies also revealed that multiple risk factors markedly increase the incidence of ALI, and that ≈85% of patients who develop ALI do so within 72 hours of the onset of the risk factor, with those patients with aspiration tending to do so earlier than those with sepsis or trauma.

The mortality of ARDS in the three aforementioned studies[89,90,91] and a later review[92] ranged from 41 to >60%, and in two of the studies mortality was two- to threefold higher in those patients who developed the syndrome than in those patients at risk who failed to do so.[90,91] Although median survival has been reported to be ≈13 days from onset of ARDS,[90] most studies have shown no relationship between respiratory failure and death. In their retrospective analyses, Montgomery and colleagues[93] reported that only 16% of patients with ALI who died did so because of irreversible respiratory failure; most deaths after 72 hours were due to multiple organ failure and sepsis (interestingly, principally of pulmonary origin). Moreover, even those deaths attributed to respiratory failure had sepsis as a major contributing factor, and cardiac dysfunction, deemed the second leading cause of death, was also complicated by sepsis in 80% of cases. Even the more recent studies have been able to link only a minority of deaths with respiratory failure,[94] a finding with critical implications for any lung-directed pharmacotherapy.

A recent interesting prospective study from Argentina conducted over 15 months identified 235 patients who met AECC criteria for ARDS[95]: sepsis was the main risk factor in 44% (particularly secondary to pneumonia) and aspiration in 10%. Although the arterial partial pressure of oxygen (P_aO_2)/fraction of inspired oxygen (FiO_2) on day 1 did not differentiate survivors from nonsurvivors, by day 2 survivors exhibited significantly improved oxygenation compared to nonsurvivors; additionally, increased mortality was significantly associated with (1) sequential organ failure assessment score at 72 hours; (2) the degree of hypoxemia at 72 hours; and (3) the presence of severe comorbidities. In this study, despite the suggestion from several recent controlled interventional trials of improved survival, a very high mortality rate of 58% was found. It also reinforced the concept that patients with ARDS die *with*, not *from*, the disease, in that only 15% of patients died of refractory hypoxemia, whereas multiple organ dysfunction syndrome (MODS) and sepsis were deemed to be responsible for death in 69% and 66% of patients, respectively.

Other investigators identified additional factors predictive of increased mortality in ALI/ARDS. Monchi and colleagues[96] found in 259 patients that the following factors were associated with an elevated risk of death that overall reached 65%: (1) the SAPS II and McCabe scores; (2) the prior duration of mechanical ventilation and the oxygenation index; (3) the presence of direct (over indirect) lung injury; (4) right ventricular dysfunction; and especially (5) cirrhotic liver disease. Nuckton and colleagues[97] confirmed the importance of the SAPS II score and found that an elevated dead space measured during the first several hours of ARDS was the most sensitive prognostic indicator of death. Two recent preliminary reports have linked an increased hematocrit[98] and numerous red blood cell transfusions[99] to an increased risk of death in patients with ALI, findings all the more intriguing given the recent controversy over transfusion requirements in the critically ill patient.[100]

Pathogenesis

The final common pathway of permeability edema is endothelial and epithelial injury resulting from a variety of insults, causing predominant alveolar flooding that contrasts with the orderly sequence of edema accumulation in hydrostatic edema.[55,101] Filtration occurs independently of P_{mv}, although it is aggravated by its elevation, and the fluid has a high protein concentration, ≈70% of plasma.

Sepsis frequently predisposes to ARDS, and there has been considerable recent interest in a "two-hit hypothesis" for pulmonary (and other organ) injury in sepsis leading to ARDS[102]: the first hit, for example, sepsis, damages the gut–blood barrier; gram-negative bacteria move through the epithelium and enter the bloodstream, and cytokines such

as interleukin (IL)-1, IL-6, and tumor necrosis factor-α (TNF-α) are released, initiating the systemic inflammatory response syndrome (SIRS). This first hit renders the lung susceptible to a second more direct hit (eg, thoracic trauma, ischemia, pulmonary infection, ventilator-induced injury), producing ARDS.

Role of Cells in ARDS

Endothelial Cells ECs have always occupied a central role in the pathogenesis of pulmonary edema, either through their simple function as a barrier in hydrostatic edema or through their injury in ARDS and other forms of permeability edema. ECs can be injured directly and indirectly by endotoxin via polymorphonuclear neutrophils (PMNs), as shown by Meyrick and Brigham[103]: in vivo, a single infusion of *Escherichia coli* endotoxin into sheep causes margination of PMNs and B and T lymphocytes, with pulmonary hypertension at 15 minutes, migration of leukocytes into the interstitium by 30 minutes, and interstitial edema and focal EC damage by 60 minutes. In vitro, endotoxin causes direct dose-dependent damage to bovine pulmonary endothelial monolayers, with retraction, pyknosis, and sloughing, increased prostacyclin production, lactic dehydrogenase release, and heightened permeability to small solutes; electron microscopy shows widened intercellular junctions and cellular contraction at 30 and 60 minutes and cell death beyond 2 hours.[104] More recently, cultured human pulmonary artery ECs were also found to be injured by low concentrations of endotoxin.[105] It is noteworthy that pulmonary ECs from large arteries are more sensitive to endotoxin than are microvascular cells, indicating endothelial phenotypic heterogeneity within the lung.[106] Therefore, endotoxin can injure pulmonary endothelium directly, and this injury is enhanced by complement and granulocyte activation.

Other mediators injurious to ECs and found in increased amounts in bronchoalveolar lavage fluid (BALF) from ARDS patients include TNF-α and angiostatin, a cleavage product of plasminogen,[107] and markers of endothelial dysfunction such as ACE, which decreases in level early in ALI and correlates with the clinical severity of lung injury.[88] Endothelial dysfunction is also manifest in its reduced ability to metabolize the potent vasoconstrictor endothelin-1 (ET-1), contributing to pulmonary hypertension complicating ARDS.[108] In patients with ARDS, the arteriovenous ratio for ET-1 is increased, probably because of a combination of increased secretion and reduced clearance by the lung.[108,109] In an autopsy study of ARDS, tissue immunostaining for ET-1 in vascular ECs, alveolar macrophages, smooth muscle, and airway epithelium was augmented compared with lungs of patients dying without ARDS; immunostaining for both endothelial nitric oxide synthase (NOS) and inducible NOS in the lung was concomitantly reduced.[110]

In addition to their passive role as bystanders or victims, ECs participate actively in the defense against and mediation of lung damage by their activation in response to stimuli such as endotoxin, cytokines, thrombin, and others involved in ARDS.[111] ECs also release and metabolize vasoactive and inflammatory molecules such as serotonin, bradykinin, prostaglandins, ET, NO, and cytokines. Endothelial activation is critical for initiation of the inflammatory response and occurs through the expression of adhesion and signaling molecules and inducible enzymes recognized by different classes of leukocytes, particularly PMNs. For example, when stimulated with lipopolysaccharide (LPS), IL-1, or TNF-α, ECs express E-selectin and IL-8, with adhesion and signaling of PMNs.[112] Other substances expressed by pulmonary ECs in ARDS include epithelial–neutrophil-activating peptide-78 (ENA-78), one of the C-X-C chemokines, the enzyme COX-2, and P-selectin, all implicated in interactions with PMNs.[112] In a recent immunohistochemical study of adhesion molecules in autopsy lungs of patients with ARDS, it was found that intercellular adhesion molecule (ICAM)-1 was up-regulated in all pulmonary vessels (compared with normal subjects), whereas E-selectin and vascular cell adhesion molecule (VCAM) were strongly expressed in larger vessels, with only weak mosaic-like expression in capillary ECs; platelet endothelial adhesion molecule (PECAM/CD31) strongly stained ECs of control and ARDS lungs.[113] It is also of interest that pulmonary microvascular ECs cultured from ARDS patients retain the ability to express increased adhesion molecules such as ICAM-1 and VCAM and secrete more of the cytokines IL-6 and IL-8 compared with cells from control lungs.

In relation to macrophages, as detailed below, macrophage migration inhibitory factor (MIF) is enhanced in ECs in ARDS and causes a modest rise in the expression of aquaporin 1, one of a family of newly discovered water channel proteins, in ECs of lungs from ARDS patients and in cultured ECs, suggesting a role in transcellular fluid movement in this condition.[114]

As detailed below, hyaline membranes and intravascular thrombi are histologic hallmarks of DAD in ARDS, and fibrin is an important component of these, suggesting a dysfunctional coagulation cascade at least locally in the lung: the procoagulant response is increased, related to tissue factor associated with factor VII/VIIa, with concurrent depression of fibrinolytic activity secondary to tissue plasminogen activator and urokinase plasminogen activator (uPA).[115] ECs, as well as epithelial cells and leukocytes, play an important role in these processes: the deposited intra- or extravascular fibrin and its proteolytic fragments and fibrinolytic proteases can independently amplify the inflammatory response, elevate vascular permeability, and activate fibroproliferative processes through complex interactions with cytokines and the kinin and complement systems.[115] Supporting the important role of the coagulation cascade in ARDS, anticoagulant therapy with activated protein C has shown promise in reducing mortality in sepsis.[116] Ware and colleagues[117] very recently reported that in patients with septic and nonseptic ALI/ARDS, levels of protein C in plasma were significantly lower than in normal subjects and similarly critically ill patients with cardiogenic pulmonary edema and that their levels correlated directly with survival and ventilator-free days. The level of protein C was also lower in edema fluid than in simultaneously measured plasma samples, and the lower level was associated with greater respiratory impairment. Moreover, the authors found higher levels of thrombomodulin in the edema fluid of

patients with ALI than in patients with heart failure and consistently higher levels in the edema fluid than in simultaneously measured plasma samples, suggesting local intrapulmonary production; it was demonstrated that alveolar type II cells in vitro, stimulated by various cytokines, released thrombomodulin into the media. Additionally, levels of plasminogen activator inhibitor-1 were found to be higher in plasma and edema fluid from patients with ALI than in patients with heart failure and predicted a poor outcome.[118] These data suggest that in ALI/ARDS the alveolus provides a procoagulant antifibrinolytic environment. The topic of activation of the coagulation system in ALI/ARDS is further covered in recent reviews.[115,116,119]

Clinically and pathogenetically important soluble products of EC activation have been measured in plasma from patients with ARDS: Moss and colleagues[120] found that levels of von Willebrand factor antigen, soluble ICAM-1, and soluble E-selectin were higher in patients at risk for or with ARDS who had sepsis rather than trauma as the predisposing factor, consistent with the notion of differential EC activity. A recent review further details the involvement of ECs in sepsis.[121]

Polymorphonuclear Neutrophils An impressive body of literature generated over the past two decades implicates polymorphonuclear neutrophils (PMNs) as pivotal players in the pathogenesis of ALI. Several groups have documented, by histology, increased accumulation of PMNs within capillaries (rather than venules, as in the systemic vascular bed) and in interstitial and alveolar edema fluid of the injured lung compared with either normal volunteers or patients with respiratory failure not due to ALI[122,123] (Figure 19-6). PMNs dominate other cells in BALF obtained from patients with ARDS.[111] Martin and colleagues[124] reported increased numbers of PMNs in BALF from patients with early ALI (approximately 90% of cells recovered) compared with 3 to 10% in normal subjects, and Fowler and

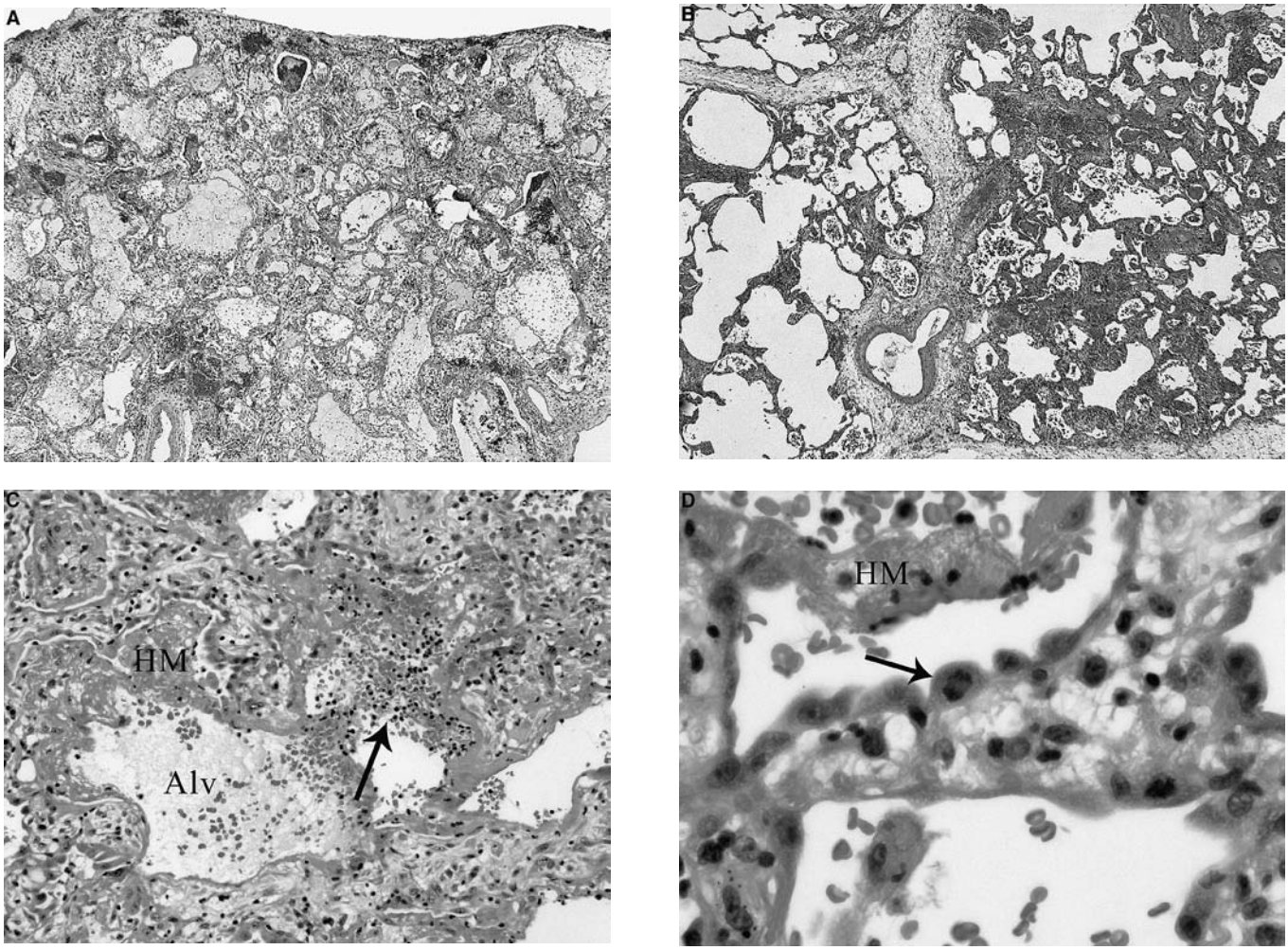

FIGURE 19-6 Light photomicrographs of lung biopsy done 12 days after the onset of respiratory failure resulting from sepsis in a 64-year-old female treated with azathioprine for Crohn's disease. *A*, Low-power view, showing diffuse alveolar damage, with alveoli uniformly filled with exudate, including hyaline membranes. H&E stain; ×50 original magnification. *B*, Low-power view of another area, showing heterogeneous involvement on either side of the interlobular septum. The alveoli on the left are better aerated, contrasting with the poorly aerated airspaces with early fibroproliferation on the right. H&E stain; ×50 original magnification. *C*, Medium-power view, showing alveoli (Alv) filled with proteinaceous exudate, hyaline membranes (HM), hemorrhage, and neutrophils (*arrow*). H&E stain; ×250 original magnification. *D*, High-power view, showing alveoli with hyaline membrane (HM), with erythrocytes, and lined by hyperplastic type II pneumocytes, one with a mitotic figure (*arrow*). H&E stain; ×1,000 original magnification.

colleagues[125] documented increased numbers of PMNs in BALF from patients at risk for development of ARDS compared with normal subjects. Concentrations of PMNs have been correlated with poor prognosis and mortality in sepsis, although not in trauma-related ALI or in ALI due to other causes.[126] Conversely, in survivors, BALF levels of protein and PMNs decrease and levels of macrophages increase with time.[126] It is of interest that moderate-to-severe hypoxemia, an important consequence of ARDS, in and of itself increases degranulation and delays apoptosis of PMNs in human volunteers.[127]

The sequence of events in neutrophil-mediated injury, gleaned from recent reviews,[123,128,129] can be summarized as follows. The first is sequestration of PMNs in pulmonary capillaries, which is necessary but not sufficient to cause lung injury but causes leukopenia, secondary to inhibition of the normal deformation required for passage in pulmonary capillaries, because of altered biomechanical and adhesive properties: inflammatory mediators such as TNF-α, IL-1β, and IL-8 are thought to stiffen PMNs by inducing the assembly of soluble G-actin to F-actin filaments, thereby increasing the formation of cytoskeleton at the cell's periphery. More recent data reveal, however, that pure cytokine-mediated activation generates transient sequestration whose stability depends on PMN–EC interactions, mediated by adhesion molecules such as L-selectin (expressed on PMNs) and CD11/CD18 (β_2 integrin).

The second event is adhesion mediated predominantly through interactions between β_2 integrins on the surfaces of PMNs and ICAM-1 on the surfaces of ECs and by the β_1 integrins, the latter particularly after activation. Adhesion also plays a role in activation and initiates a cascade of events critical in PMN function. Third, PMNs migrate out of the microvessels into the parenchyma, principally via interendothelial junctions on the thick side of the alveolar–capillary barrier. Migration is either mediated by CD11/CD18 (eg, upon endotoxin stimulation) or is independent of it (eg, upon *Streptococcus pneumoniae* or C5a stimulation), being mediated via undiscovered mechanisms.[123]

The fourth event, PMN activation, intimately related to adhesion, is mediated principally by the integrins and results in migration, phagocytosis and the respiratory burst, degranulation, and production of oxidants and cytokines. Activation is associated with increased PMN cross-sectional area regardless of location (circulating, marginated, or adherent).[130] The mechanisms of activation involve bidirectional signals between the surface and the inside of the PMN, from which signal transduction occurs through kinases such as the Src kinases, mitogen-activated protein (MAP) kinases, MEK (MAP/extracellular signal-regulated kinase [ERK] kinase), and phosphoinositide-3-OH kinase (PI 3-K). It is of interest that different stimuli of PMN activation (eg, endotoxin, PAF, and TNF-α) each trigger different kinases, contributing to the heterogeneity of cellular effects. The importance of activation is confirmed by a report that the degree of PMN activation in patients with ALI correlates with the degree of lung injury and levels of TNF-α, IL-6, and IL-8.[131]

Once activated, PMNs injure the lung through diverse mechanisms: (1) generation of reactive oxygen species (hydrogen peroxide, hydroxyl radicals, and superoxide anions), via either NADPH oxidase or, as suggested more recently, the NOS pathway, and (2) secretion of proteolytic enzymes such as PMN elastase, cathepsin G, and the matrix metalloproteinases (MMPs) gelatinase A and B (MMP-2 and -9, respectively). Gelatinase B, released in a latent proform from PMNs, is activated principally by PMN elastase and plays a role in the migration of these cells across the basement membrane by degrading collagen IV.[132] Both gelatinase B and gelatinase A (a product of epithelial, endothelial, and fibroblastic cells) have been found in the epithelial lining fluid of patients with ARDS, correlating with indices of lung injury.[133]

The PMN-mediated damage must be regulated if the resolution of the edema is to proceed. One mechanism is through rapid apoptosis (programmed cell death), mediated by pathways involving PI 3-K and ERK, as well as p38 MAP kinase. PMNs undergoing apoptosis lose surface adhesion molecules and the ability to secrete their granular contents and are promptly ingested by macrophages, minimizing their damaging effects. In patients with ARDS, inhibition of apoptosis of PMNs is mediated by the growth factors granulocyte colony-stimulating factor (G-CSF) and granulocyte–macrophage colony-stimulating factor (GM-CSF) and the mediators endotoxin, IL-2, IL-6, interferon (IFN)-γ, and leukotriene B_4 (LTB_4).[134] Delays in the onset of apoptosis could explain the development or persistence of ARDS: a randomized controlled trial showed that patients with pneumonia receiving G-CSF had higher levels of blood PMNs, faster radiographic improvement, and a lower incidence of ARDS.[135] Recently, Matute-Bello and colleagues[134] found that the antiapoptotic effect of ARDS BALF on normal PMNs was highest in early ARDS and decreased later and that the concentrations of G-CSF and GM-CSF in BALF from patients with ARDS paralleled the antiapoptotic effect of ARDS BALF, supporting the concept that the life span of PMNs in airspaces is modulated during acute inflammation. Also, the presence of GM-CSF in airspaces was associated with improved survival in ARDS, although there was no association between alterations in the antiapoptotic properties of BALF and the clinical outcome of patients with ARDS, suggesting the involvement of more complex processes.[136]

Notwithstanding the aforementioned evidence, the role of PMNs in ALI/ARDS remains somewhat confusing: for example, ARDS occurs in patients with profound neutropenia[137] (Figure 19-7), and some experimental models of ARDS are independent of PMNs.[123] Martin and colleagues[138] demonstrated that injection of LTB_4, a potent PMN chemoattractant, into the lungs of normal volunteers caused significant recruitment of PMNs into the airspaces without increased permeability of the epithelial barrier to protein. Wiener-Kronish and colleagues[139] elegantly demonstrated in sheep that although intravenous *E. coli* endotoxin significantly increased lung vascular permeability, it failed to alter epithelial permeability when administered either intravenously or intraalveolarly, despite a robust neutrophilic

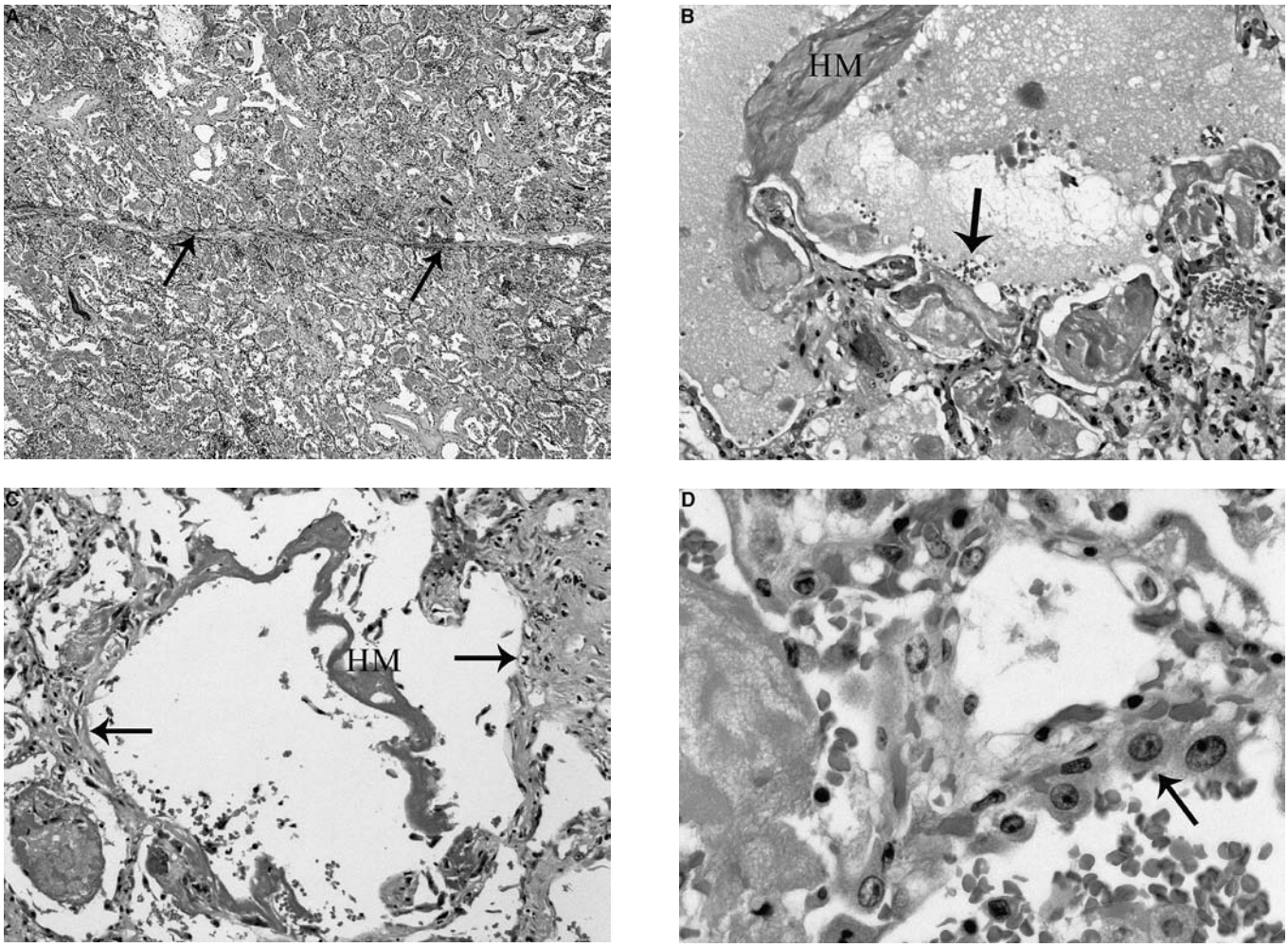

FIGURE 19-7 Light photomicrographs of diffuse alveolar damage in lung from a markedly neutropenic 61-year-old female who died from ARDS following chemotherapy for acute myeloid leukemia. *A*, Low-power view, showing alveoli filled with dense exudate and a thin interlobular septum (*arrows*) without edema. H&E stain; ×50 original magnification. *B*, Medium-power view of alveoli with hyaline membrane (HM), and dense edema fluid admixed with erythrocytes (*arrows*) but entirely devoid of neutrophils. H&E stain; ×250 original magnification. *C*, Medium-power view, showing hyaline membrane (HM) loosely lining an otherwise denuded alveolus (*arrows*), and an absence of neutrophils. H&E stain; ×250 original magnification. *D*, High-power view, showing dense fibrinous edema fluid (*left*) and proliferating type II pneumocytes lining the alveolus (*arrow*). There are no PMNs, only erythrocytes at the bottom. H&E stain; ×1,000 original magnification.

response in airspaces. Therefore, even with an apparently similar initial response to a particular insult, the ultimate development of ALI/ARDS must depend on other, as yet unidentified, factors, and it may be that PMNs are essential but not sufficient for its development. Indeed, PMNs may be beneficial in ARDS, providing an adaptive response in host defense and perhaps explaining the lack of success of a number of antiinflammatory therapeutic strategies.

Macrophages Although numerically less important than PMNs, macrophages, normally found in the interstitium and alveoli and constituting the majority of cells in BALF, have been implicated in ARDS, and indeed may be responsible for the pulmonary damage in ARDS in neutropenic patients. First, alveolar macrophages constitute the earliest line of defense against direct or indirect injury: in response to endotoxin, they rapidly produce TNF-α and IL-1β, mediated by Toll-like receptors, activation of transcription factors such as nuclear factor kappa B (NF-κB), and downstream events; the cytokines then activate other cells, including ECs, that initiate the recruitment of PMNs.[119,140] As the acute phase proceeds, the alveolar mononuclear phagocyte population expands,[126] primarily by recruitment of peripheral blood monocytes into the lung rather than by local proliferation[141]; these recruited cells are recognized by the high-level immunophenotypic expression of CD14, CD11b, and 27E10 (identifying inflammatory acute-phase monocytes) and the low-level expression of CD71, HLA-DR, and 25F9 (a marker of mature tissue macrophages). Rosseau and colleagues[141] followed 49 patients with ARDS by performing sequential BALs, and distinguished two groups, one in which monocyte influx fell and recruited cells matured and a second in which there was sustained monocyte recruitment. The latter phenotype correlated with persistent up-regulation of monocyte chemoattractant protein-1, one of the C-C chemokines responsible for recruitment and subsequent activation of monocytes, and with severity of respiratory failure. Macrophages also appear to be

involved in proximal activation of the numerous cytokines that are produced simultaneously in ARDS and are associated with adverse outcome, such as IL-1β, TNF-α, IL-6, and IL-8[142]: they do this through activation of nuclear transcriptional regulatory proteins, particularly NF-κB, which binds to enhancer/promoter sequences of the proinflammatory cytokines and increases their expression.[143] DNA binding and transactivation by NF-κB are strongly induced by hydrogen peroxide, superoxide, endotoxin, cytokines such as TNF-α and IL-1β, and ischemia–reperfusion injury.[144]

It has been suggested that MIF, a recently rediscovered cytokine expressed by anterior pituitary cells and monocyte–macrophage cells, counterbalances the antiinflammatory properties of glucocorticoids.[145] MIF has attracted attention as a mediator in ARDS, with enhanced expression in alveolar capillary ECs, infiltrating macrophages in lung tissue from ARDS patients and stimulating the release of proinflammatory cytokines such as TNF-α and IL-8; anti-MIF antibody attenuates this response.[146] In addition, MIF induced significant MIF and TNF-α synthesis in cultured ECs, and treatment with anti-MIF or glucocorticoids attenuated pulmonary pathology and the synthesis of MIF or TNF-α in mice with LPS-induced acute lung injury, data all consistent with the notion that MIF induces TNF-α production via an amplifying proinflammatory loop.[114] As intimated above, in addition to proinflammatory effects, macrophages have a potential role in the resolution of ALI: relative and absolute numbers of macrophages in BALF have been correlated with resolution of lung injury and improved survival.[126]

Second, macrophages have an important role in progression from the acute to the fibroproliferative phase of ARDS. They secrete a variety of mediators and growth factors (FGF-2, TGF-β, platelet-derived growth factor, TNF-α, IL-1, IGF-1, and fibronectin) that lead to mesenchymal cell proliferation and migration and to deposition of extracellular matrix, stimulated by cytokines such as GM-CSF, IL-1β, IFN-γ, TNF-α, and TGF-β_1, thereby perpetuating a vicious circle, by paracrine or autocrine action, leading to deposition of connective tissue in several fibrotic lung disorders, including ARDS.[147] In a recent study, it was found that there was increased immunohistochemical staining for insulin-like growth factor-I (IGF-I) and its receptor in alveolar and interstitial macrophages and mesenchymal cells in fibroproliferative ARDS compared with controls that correlated with enhanced immunoreactivity for collagens I and III and proliferating cell nuclear antigen.[148]

Third, in addition to their proinflammatory and profibrotic roles, monocytes and macrophages from patients with SIRS and sepsis can be induced to become tolerant to bacterial endotoxin (LPS), consistent with an immune dysregulation rendering patients with SIRS and MODS more susceptible to infections: this "LPS-tolerant" phenotype is characterized by inhibition of LPS-stimulated TNF production, altered IL-1 and IL-6 release, COX-2 activation, inhibition of MAP kinase activation, and impaired NF-κB translocation.[149] Certain mediators, for example, interleukins-4, -10, -11, and -13, TGF-β, and colony-stimulating factors, profoundly alter monocyte function, including antigen-presenting activity, and inhibit T- and B-lymphocyte activity, resulting in immune suppression manifested clinically as anergy and increased susceptibility to infection. Therefore, as elegantly summarized by Bone,[150] a battle rages between pro- and antiinflammatory mediators: if they achieve a balance to overcome the injurious insult, homeostasis is restored; if not, mediators enter the systemic circulation, producing either the proinflammatory SIRS or a "compensatory anti-inflammatory reaction syndrome" (CARS).

Epithelial Cells Epithelial cells, like ECs, are important targets in ARDS, and damage to them is critical in the development of alveolar edema. Even in early ARDS, type II pneumocytes proliferate; upon resolution, they are removed through extensive apoptosis, as indicated by specific labeling of nuclear DNA fragments.[151] The time frame of the apoptotic response varies with etiology and degree of injury. Apoptosis of type II pneumocytes in DAD is associated with increased expression of p53, WAF1 (p27), and BAX, the latter two induced by p53; the antiapoptotic protein BCL2 is found only in interstitial cells, suggesting that it may play a role in the fibroproliferative stage.[152] Adamson and colleagues[153] found an increased proliferation index in type II pneumocytes and interstitial cells in DAD that correlated with patient survival, with increased expression of c-Myc and cyclin D1, both potentially contributing to dysregulated cellular proliferation and apoptosis in DAD. As summarized above, epithelial cells also play a crucial role in the clearance of pulmonary edema. Further details of the role of epithelial cells in ARDS, including in relation to surfactant and cytokines, are given elsewhere in this book (see Chapter 38, "Epithelial Function in Lung Injury").

Role of Selected Cytokines and Chemokines in ARDS Cytokines are soluble extracellular peptides produced by inflammatory and other cells that act at very low concentrations (10^{-15} M) by binding to surface receptors, in either an autocrine or a paracrine manner. Chemokines, related to cytokines, activate leukocytes and cause them to alter their shape, follow a chemotactic stimulus, and adhere to ECs. The relationship between levels of cytokines in BALF and the pathophysiology and outcome of ALI is complex, being affected by the animal model studied, the techniques used to measure the cytokines, and the specific clinical condition associated with ALI. Although still controversial, the consensus is that the predominant cytokines and chemokines implicated in ALI are IL-1β, IL-8, and TNF-α[154] and that these are produced locally in the lung.[155]

Suter and colleagues[156] studied BALF and plasma levels of cytokines over time in patients with ALI: they found elevated levels of TNF-α in BALF, rising significantly from those at risk, reaching very high levels during early ALI (12 to 36 h after onset), and falling significantly by day 3, whereas plasma levels rose modestly, suggesting intrapulmonary secretion. Surprisingly, they also noted little biologic activity of these levels of TNF-α, which they attributed to high levels of the TNF-α inhibitors, sTNF-RI and -RII, found in the same BALF samples. They also found increased production of IL-1β. BALF levels of IFN-α and elastase, both thought to

be released by PMNs, increased with the severity of the lung injury. It is of interest that none of the plasma levels of these cytokines correlated with disease activity.

Several groups have described a relationship between the levels of pulmonary cytokines and outcome. Meduri and colleagues[157] measured significantly and persistently higher levels of TNF-α, IL-1β, IL-6, and IL-8 in patients with ARDS who did not survive than in those who did. One problem in chronicling the role of various cytokines in ALI/ARDS is the difficulty in differentiating between concentration and biologic activity. To address this, several investigators focused on evaluating the overall inflammatory milieu of the lung in ALI by determining not only the levels of the cytokines but also the levels of their specific and nonspecific antagonists. The latter include α_2-macroglobulin and IL-10, whereas specific antagonists include IL-1 receptor antagonist (IL-1ra), soluble IL-1 receptor II (sIL-1RII), and soluble TNF receptors I and II (sTNF-RI, sTNF-RII). Park and colleagues[158] showed that although the bioactivity of TNF-α and IL-1β was elevated in patients with ARDS compared with normals, the bioactivity of IL-6, an antiinflammatory cytokine, was also increased, so that an overall antiinflammatory milieu predominated in the lungs of these patients. Furthermore, the level of antiinflammatory activity appeared to confer a degree of protection, in that both lung compliance and the degree of injury improved with an increased antiinflammatory environment. Similarly, Donnelly and colleagues[159] found increased concentrations of IL-10 and IL-1ra in the BALF of patients with ARDS and noted an association between low levels of these antiinflammatory cytokines and mortality. Taken together, these data suggest that the injured lung is capable of limiting a potentially overwhelming proinflammatory response and that the net state of inflammation must be considered if we are to understand the complexity of the response.

The role of IL-8 is similarly complicated. Although IL-8 is a known chemoattractant of PMNs to the lung in ALI, data relating to its role as a marker of disease and of its severity are controversial. One group of investigators reported significantly increased BALF levels of IL-8 in patients at risk and progressing to ARDS compared with those patients failing to progress.[160,161] Kurdowska and colleagues[162] were unable to find any such correlation, and although they documented a relationship between IL-8 and the number of PMNs in the BALF of patients beyond day 1 in ALI, IL-8 levels failed to distinguish between survivors and nonsurvivors. However, levels of IL-8 complexed with anti-IL-8, the latter attributed to intrapulmonary production by B cells, were significantly increased in those patients at the onset of ARDS compared with those at risk and were initially higher on day 1 of the established syndrome in survivors than in nonsurvivors, falling significantly in survivors. Subsequently, the same group of investigators reported that in patients at risk, those with lower BALF levels of free IL-8 failed to go on to the full-blown syndrome, whereas of those patients with elevated levels, only those with elevated levels of IL-8–anti-IL-8 complexes in the BALF went on to develop ARDS,[163] supporting the counterintuitive notion that these antibodies, when complexed, enhance disease activity.

Poly (ADP–ribose-1) polymerase (PARP-1), a nuclear DNA-binding enzyme participating in DNA repair, has been implicated in lung injury following the overwhelming oxidative stress that occurs with endotoxin in ARDS. Activation of PARP-1 occurs by breaks in single-stranded DNA, results in depletion of NAD^+ levels, and ultimately leads to cell death. PAPR-1 has also been implicated in the generation of the inflammatory cascade through stimulation of the NFκB pathway. Recently, in a model of LPS-induced lung injury, PMN infiltration, the elaboration of TNF-α, IL-1β, and IL-6 and of the chemokines MIP-1 and MIP-2, the generation of NO, protein leakage, and lipid peroxidation were all significantly diminished by either pharmacologic inhibition of PARP-1 or by its genetic elimination (in PARP-1–deficient mice).[164]

Pathology and Imaging

The pathologic abnormalities of ARDS arise from the damage inflicted on the lungs and the subsequent cascade of pathogenetic events, differing substantially from those observed in hydrostatic edema (Table 19-4). The alterations of ARDS have been summarized in several studies[165–167] and have been divided into those (1) general to ARDS and several forms of permeability edema and (2) reflecting a specific etiology. The general pathologic abnormalities, specifically at the light microscopic level, are encompassed by the term "diffuse alveolar damage" and separated into an acute exudative phase lasting approximately 1 week, a fibroproliferative or organizing phase lasting another 2 weeks, and, beyond 3 to 4 weeks, a fibrotic phase.

In the acute exudative phase, macroscopically the lungs are heavy, at least twice normal and often up to 2,000 g combined weight, dark red and solid, with variably frequent secondary findings such as pneumonia and thromboemboli (Figure 19-8). The cut surface is hemorrhagic and indurated, and close inspection reveals spaces about 1 mm in diameter, corresponding to widened alveolar ducts, surrounded by dense parenchyma.

Light microscopy (see Figures 19-6 and 19-7) initially shows capillary congestion, hemorrhage, and deeply eosinophilic interstitial and alveolar edema, followed by the appearance of characteristic homogeneous, dense, eosinophilic "hyaline membranes" composed of cellular debris, including necrotic epithelial cells (predominantly type I pneumocytes), admixed with fibrin, other plasma proteins, and variable numbers of PMNs. Hyaline membranes typically line alveolar ducts, as well as alveoli and respiratory bronchioles. Interstitial edema is less prominent than in hydrostatic edema (see Figure 19-7A), overshadowed by the alveolar phase secondary to the severe damage to type I pneumocytes, which occupy most of the alveolar surface area.[55]

Several studies, most published between 1965 and 1985, have detailed the ultrastructure of the exudative phase of ARDS.[86,122,168,169] Capillary lumina contain predominantly neutrophils, lower numbers of erythrocytes, and few platelets. The endothelium shows swelling, blebs, widened intercellular junctions with formation of folds or flaps, increased numbers of pinocytotic vesicles, and, rarely,

Table 19-4 Contrasting Features of Hydrostatic Pulmonary Edema and Acute Respiratory Distress Syndrome (ARDS)

Parameter	*Hydrostatic edema*	*Permeability edema (ARDS)*
Etiology and pathogenesis	Elevated P_{mv}, normal endothelium and epithelium	Inflammatory cells and mediators; damage to endothelium and epithelium, elevated permeability
Protein content of edema fluid	Low versus plasma, due to sieving	High with fibrin
Sequence of fluid accumulation	Orderly: congestion, then IS edema, alveolar edema	Prominent early alveolar flooding, less IS edema
Imaging (especially chest radiographs)	Interlobular septal thickening with Kerley A and B lines; edema in perihilar distribution; associated cardiomegaly, vascular redistribution or distention, pleural effusion	Diffuse homogeneous bilateral dense infiltrates; often peripheral
Macroscopy	Spongy lung, frothy fluid on cut surface; wide interlobular septa	Lungs consolidated, hemorrhagic
Light microscopy	More prominent congestion, IS edema, less alveolar edema	Alveolar edema, hyaline membranes, inflammatory cells, ±microemboli
Electron microscopy	Generally normal endothelium and epithelium	Endothelium and epithelium with blebs, damage; inflammatory cells
Chronic effects	"Brown induration," mild fibrosis	May progress to fibroblastic and type II pneumocyte proliferation, severe fibrosis; increased procollagen peptides in edema fluid
Long-term prognosis	Resolution if cause treated	Depends on associated organ failure and extent of lung damage, fibrosis

Modified from Lesur O et al.[263]

disruption and necrosis with exposure of the underlying basal lamina and intravascular fibrin accumulation. Neutrophils, erythrocytes, and platelets frequently emigrate with edema fluid between ECs, widening the interalveolar interstitium, primarily on the thick side of the alveolar–capillary septum, although fibrin deposits may be seen beneath ECs even in the thin part of the septum.[122] The ultrastructural alterations in ECs are subtle compared with those in epithelial cells, which exhibit prominent sloughing of necrotic type I pneumocytes and become admixed with fibrin to form the hyaline membranes. Although type II pneumocytes may also be damaged, they are tougher than type I pneumocytes and indeed replace them in the proliferative phase of ARDS. Ultrastructural morphometric studies have revealed increased interstitial and epithelial cellular volumes, the latter related to transformation of the alveolar lining from type I to type II pneumocytes, and a reduction in capillary volume.[122]

FIGURE 19-8 Lung slice from a patient who died with ARDS 7 days after the onset of respiratory failure. It is solid, with areas of edema and hemorrhage.

In the absence of resolution, a fibroproliferative phase ensues. Macroscopically, the lung becomes firmer and less hemorrhagic, with reorganization of the alveoli into large spaces separated by fibrous tissue (Figure 19-9). In the advanced fibrotic phase, a "honeycomb" pattern may be seen, with reorganized airspaces, 3 to 12 mm in diameter, being visible on chest radiographs and high-resolution CT scans (Figure 19-10), and with a cobblestone pattern on the pleura.

By light microscopy, the fibroproliferative phase is characterized by large numbers of cuboidal type II pneumocytes with abundant cytoplasm, large nuclei with mitoses and prominent nucleoli proliferating along the previously denuded alveolar lining, and replacing lost type I pneumocytes and hyaline membranes (Figure 19-11). If disruption of the lung architecture is significant, distal small airway epithelial cells proliferate and enter adjacent alveoli, and type II pneumocytes may undergo squamous metaplasia.[167] In concert with epithelial regeneration, hyaline membranes organize, with proliferation of granulation tissue composed of myofibroblasts and abundant acid mucopolysaccharides: these may extend into alveoli and form "fibroblastic foci" (also termed Masson bodies) in alveolar ducts to produce so-called alveolar duct fibrosis[165] or less commonly into respiratory bronchioles and bronchioles, to assume the appearance of bronchiolitis obliterans. If repair extends

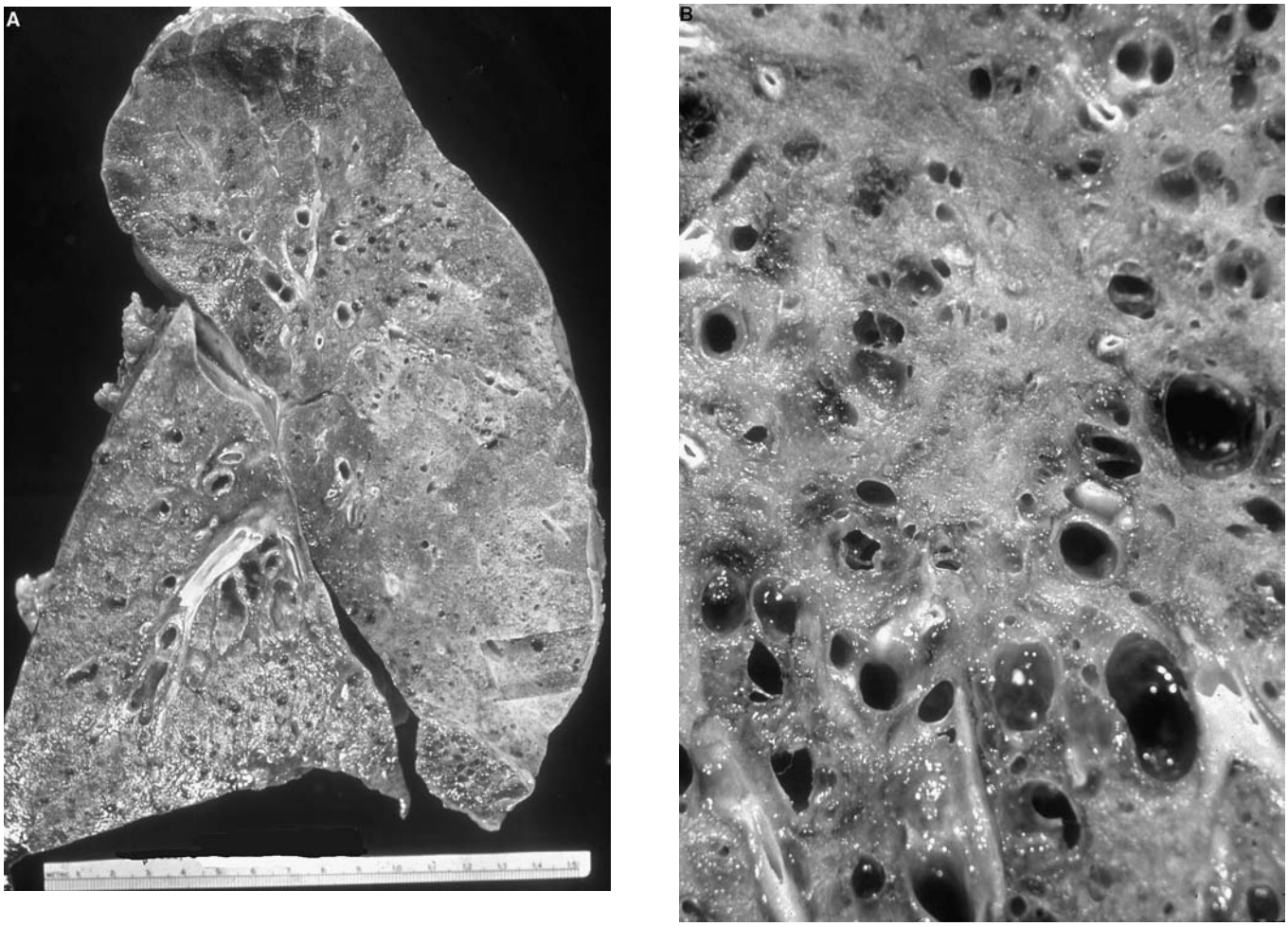

FIGURE 19-9 *A*, Lung slice showing the fibroproliferative stage from a patient who died with ARDS 3 weeks after the onset of respiratory failure. It is dense, with reorganized cystic airspaces, best seen in the lower left and upper right, alternating with solid, more uniform, areas. *B*, Close-up of another slice, showing reorganized honeycomb-like cystic spaces.

beyond ≈3 weeks, fibroblastic foci mature into dense paucicellular fibrous tissue, and destroyed and collapsed alveoli and alveolar ducts are replaced by large simplified spaces lined with hyperplastic type II pneumocytes and separated by thick walls of connective tissue, with collagen, extracellular matrix, and inflammatory cells. In advanced stages, the lung may assume the appearance of usual interstitial pneumonia, with variable parenchymal honeycombing. Immunohistochemical studies[170,171] have revealed albumin, fibrinogen, immunoglobulins, complement and surfactant apoprotein in hyaline membranes in the exudative phase, and fibronectin in the proliferative phases, with type II pneumocytes expressing TNF-α and surfactant apoprotein.

In addition to the relatively nonspecific, albeit characteristic, pathologic alterations of DAD in ARDS, several forms of permeability edema have specific patterns recognizable with the use of light microscopy.[166] Notable in this respect are the infectious etiologies: bacterial pneumonias associated with ARDS are distinguished on light microscopy (in addition to microbiologic findings) by large numbers of PMNs filling alveoli, usually seen in relatively small numbers in ARDS; in *Pneumocystis carinii* pneumonia, in BALF or lung biopsies, there is a distinctive intraalveolar foamy exudate containing the organisms, demonstrated by histochemical silver stain; in viral pneumonias, there are inclusions, for example, of cytomegalovirus, herpesvirus, or adenovirus, visible with H&E or immunohistochemical stains. It is of considerable interest that severe acute respiratory syndrome (SARS) caused by SARS-associated coronavirus produces a histologic picture of DAD in both its acute and proliferative phases; no definite viral inclusions have been seen, but multinucleated cells, of either epithelial or macrophage origin, have been described, although their significance is unclear. This syndrome is reviewed in detail elsewhere.[172] In aspiration pneumonia, aspirated material is frequently identified associated with a foreign body giant cell reaction. With fat embolism, lipid globules obstruct capillaries, giving them an empty appearance, devoid of erythrocytes, and there is an associated variable macrophage-rich inflammatory response. Some drugs may also produce relatively specific reactions, for example, amiodarone, which may cause foamy macrophages to fill alveoli.

When DAD is idiopathic, it is considered to be synonymous with acute interstitial pneumonia (AIP), a rapidly progressive form of pulmonary fibrosis whose histologic

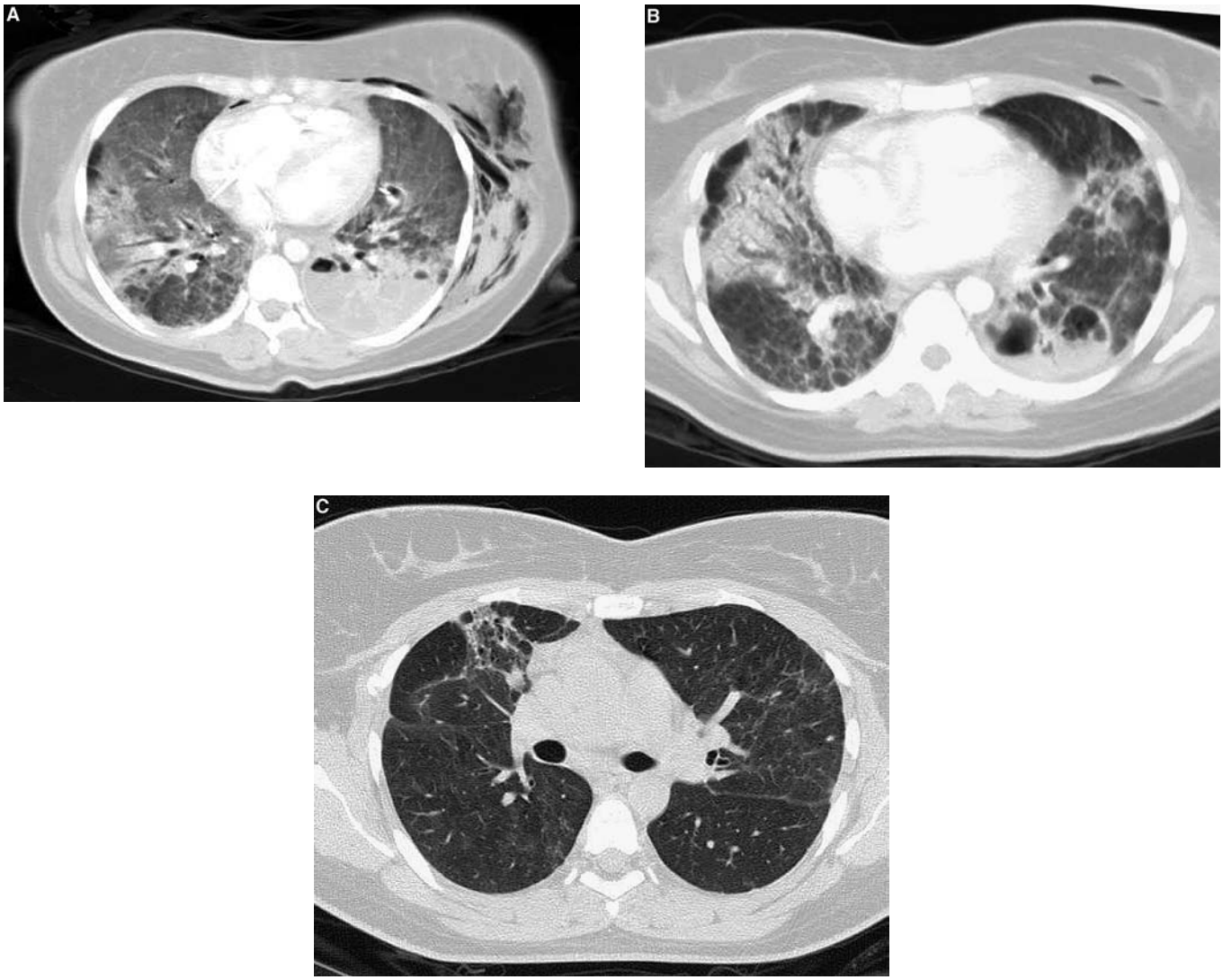

FIGURE 19-10 Sequential chest CT scans of a 39-year-old female with ARDS due to acute pneumococcal pneumonia. *A*, First scan, 6 days after onset. Note the diffuse ground-glass opacification, consolidation with early abscess in the left lower lobe, and subcutaneous emphysema in the left lateral chest soft tissue. *B*, Three weeks after onset: note increased heterogeneity in opacities, abscesses in the left posterior lung and cystic spaces in the right posterior lung. *C*, Scan taken just under 4 months after onset, showing residual irregular fibrosis in the right anterior lung field. The patient was then at home, asymptomatic, and had normal pulmonary function test findings.

features are identical to those of the fibroproliferative phase of DAD and that probably corresponds to the Hamman–Rich syndrome.[166] One noteworthy difference in AIP is that the duration of symptoms prior to the onset of ARDS may be longer than the accepted 7 days; also, the likelihood of progression to end-stage fibrosis is greater and the prognosis is poorer than in other forms of ARDS.

The pulmonary vascular lesions in ARDS, particularly evident on postmortem angiograms and under light microscopy, have been detailed in several elegant studies.[167,173] In the acute phase, thrombi or thromboemboli, generally macrothrombi, are observed in up to 95% of patients. Microthrombi are also frequent, either the hyaline platelet–fibrin type in capillaries and arterioles or the laminated fibrin type in larger arteries. The overall mean external diameter of partially muscular and muscular arteries is reduced in ARDS, with dilatation of intraacinar muscular arteries. In the early proliferative phase of ARDS, fibrocellular intimal proliferation mainly affects small and medium muscular arteries (an obliterative endarteritis) but also veins and lymphatics, with a concentric or eccentric arrangement of fibrin, myointimal cells, hyperplastic endothelial cells, mucopolysaccharides, and collagen, explaining the reduced vascular luminal area and background filling observed on postmortem arteriograms (see Figure 19-11C,D). In the late stages of ARDS, arteriograms show decreased peripheral arterial filling, extension of smooth muscle into normally nonmuscular pulmonary arteries, and medial thickening of preacinar arteries, the last-mentioned becoming tortuous and stretched around dilated airspaces; moreover, the pulmonary capillary bed creates a background ground-glass haze, associated with an increased vascular density that probably mirrors the combined effects of crowded and abnormally dilated and tortuous vessels rather than true pulmonary arterial angiogenesis.

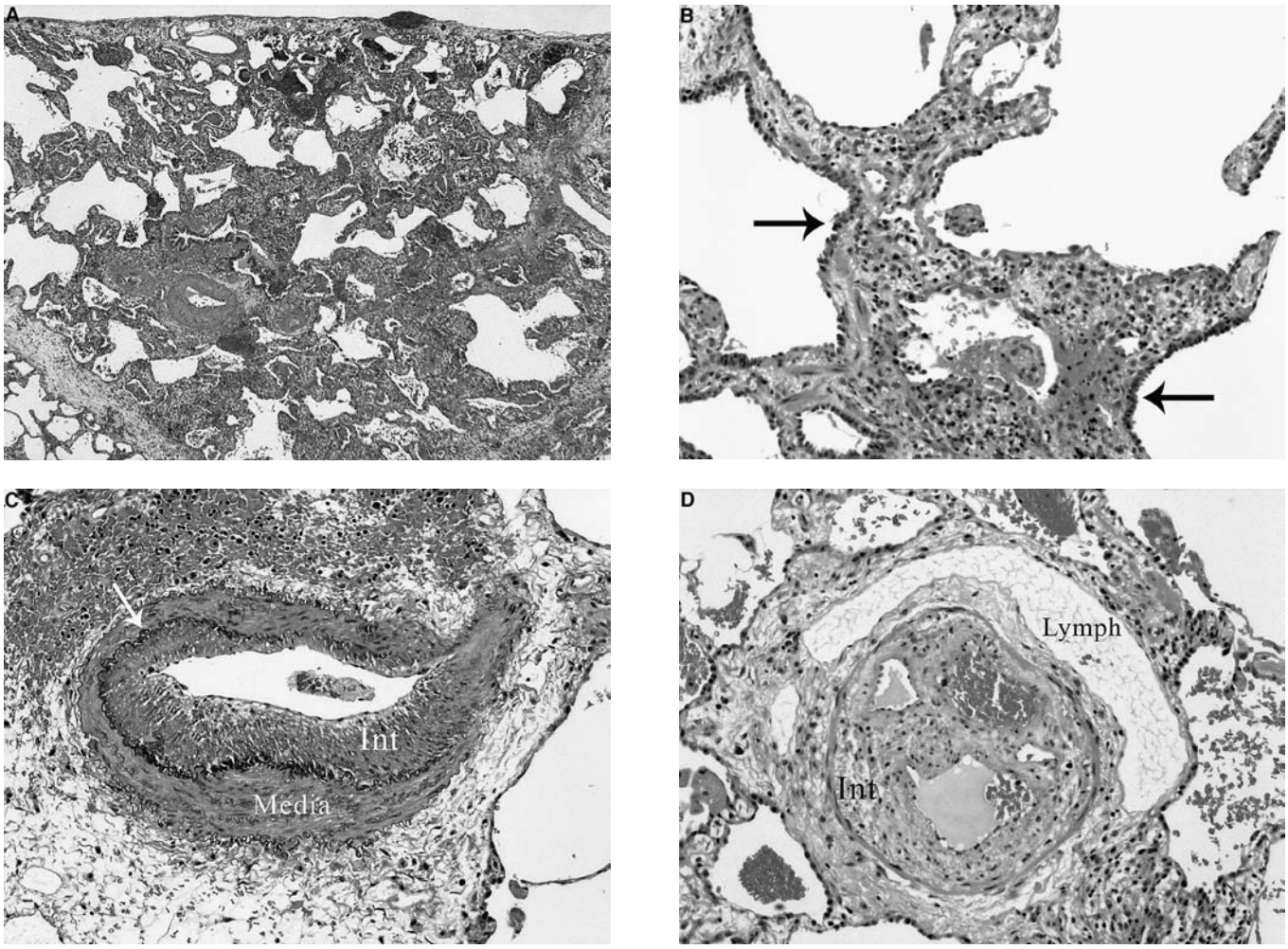

FIGURE 19-11 Photomicrographs of the fibroproliferative phase in the same patient as in Figure 19-6. *A*, Low-power view of septa thickened by fibrous tissue. H&E stain; ×50 original magnification. *B*, Higher-power view, showing interalveolar septa thickened by fibroblasts admixed with inflammatory cells and alveoli lined by regularly aligned type II pneumocytes (*arrows*). H&E stain; ×250 original magnification. *C*, Remodeled medium-sized pulmonary artery with thick media and intima (Int) separated by inner elastic lamina (*arrow*). Verhoeff's elastic stain; ×250 original magnification. *D*, Medium-sized artery showing recanalization after thrombotic or embolic occlusion with proliferating intimal (Int) cells; it is surrounded by a dilated lymphatic vessel. H&E stain; ×250 original magnification.

The pathogenetic mechanisms responsible for the thrombotic vascular lesions include thromboembolism resulting from systemic venous thrombi, in situ thrombosis related to EC injury, and platelet sequestration with localized intrapulmonary or disseminated intravascular coagulation.[167] The chronic vascular remodeling parallels the parenchymal fibrotic process, with similar mechanisms (detailed above), and superimposed hypoxia associated with ARDS and hyperoxia resulting from the therapy. Additionally, the pulmonary hypertension, resulting from vasoconstriction and the aforementioned thrombotic and other vascular lesions, completes the vicious circle of vascular remodeling.

On imaging studies, the evolution of ARDS, detailed elsewhere,[174] has been shown to be more disorderly than that of hydrostatic edema. Although in the early stages the chest radiograph may be normal, it typically progresses rapidly from initial bilateral symmetric hazy opacities, with or without air bronchograms, or occasionally an interstitial pattern as in cardiogenic edema, to dense homogeneous opacities, obscuring pulmonary vessels, cardiac margins, and diaphragm and culminating in the characteristic "white-out" of the lungs (Figure 19-12), with a tendency to peripheral accentuation. Although frequently symmetric, the distribution may be inhomogeneous. In the chronic phase, the chest radiograph shows a more heterogeneous distribution of densities, with linear or reticular patterns (see Figure 19-12). In the latest stage of fibrosis, which develops in 10 to 15% of survivors, radiographs show low lung volumes with irregular round areas of hyperinflation due to reorganized architecture related not only to ARDS but also to complications such as barotrauma, superimposed infections, and vascular events. Complications of therapy as manifested on radiographs are reviewed elsewhere.[174]

The reliability of the chest radiograph in distinguishing hydrostatic from permeability edema with the use of a variety of criteria has been controversial, and although several authors have reported success rates of 70 to 85%, Goodman[174] concludes that the value of the chest radiograph in making this distinction is limited and that clinical

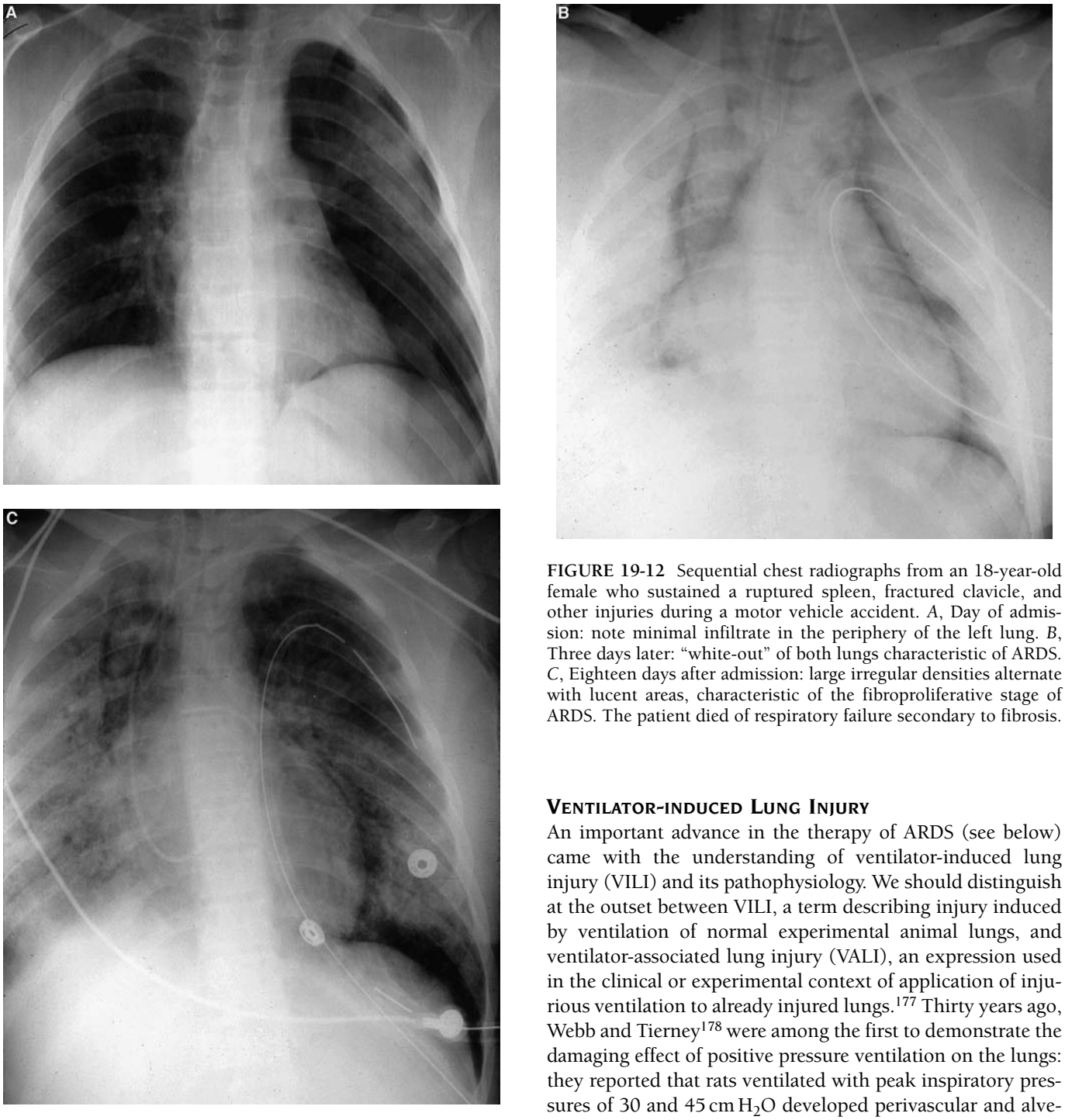

FIGURE 19-12 Sequential chest radiographs from an 18-year-old female who sustained a ruptured spleen, fractured clavicle, and other injuries during a motor vehicle accident. *A*, Day of admission: note minimal infiltrate in the periphery of the left lung. *B*, Three days later: "white-out" of both lungs characteristic of ARDS. *C*, Eighteen days after admission: large irregular densities alternate with lucent areas, characteristic of the fibroproliferative stage of ARDS. The patient died of respiratory failure secondary to fibrosis.

assessment and ancillary diagnostic tests must be taken into account.

CT scans (see Figure 19-10), which are not used routinely, have nevertheless contributed to our understanding of ARDS by (1) emphasizing the heterogeneity of lung involvement; (2) documenting the effects of prone positioning on the distribution of opacification[175]; (3) revealing complications of ARDS, particularly emphysema and abscesses; and (4) enabling follow-up of long-term survivors of ARDS. Desai and colleagues[176] described a coarse reticular pattern of pulmonary fibrosis anteriorly in 23 of 27 patients, perhaps attributable to alveolar overdistention in the acute stages.

Ventilator-Induced Lung Injury

An important advance in the therapy of ARDS (see below) came with the understanding of ventilator-induced lung injury (VILI) and its pathophysiology. We should distinguish at the outset between VILI, a term describing injury induced by ventilation of normal experimental animal lungs, and ventilator-associated lung injury (VALI), an expression used in the clinical or experimental context of application of injurious ventilation to already injured lungs.[177] Thirty years ago, Webb and Tierney[178] were among the first to demonstrate the damaging effect of positive pressure ventilation on the lungs: they reported that rats ventilated with peak inspiratory pressures of 30 and 45 cm H_2O developed perivascular and alveolar edema, respectively, and that the latter suffered from severe hypoxemia and decreased dynamic compliance and died within 1 hour; animals ventilated at 14 cm H_2O had normal lungs. They were also perhaps the first to report the salutary effect of PEEP, in that animals exposed to both 45 cm H_2O of peak pressure and 10 cm H_2O of PEEP failed to develop alveolar edema and hypoxemia.

Subsequently, Kolobow and colleagues[179] mechanically ventilated normal sheep at tidal volumes of 50 to 70 mL/kg and peak inflating pressures of 50 cm H_2O and observed marked lung injury not seen in controls ventilated at volumes of 10 mL/kg and pressures of 15 to 20 cm H_2O; interestingly, the injury was attenuated by ventilation with higher levels of carbon dioxide. Tsuno and colleagues[180]

provocatively suggested that mechanical ventilation rather than the underlying disease process could be primarily responsible for the histopathologic changes deemed to be pathognomonic of ALI. Despite these results, the question of whether the parenchymal damage was due to the applied pressure or to the resulting alveolar stretch remained unanswered. In further studies, it was determined that the injury resulted from lung overdistention[181] and that similar amounts of edema were induced whether lung volume was increased through application of positive or negative pressure.[182] Dreyfuss and Saumon[183] suggested that edema in VILI is more a function of end-inspiratory lung volume than either tidal volume or level of PEEP alone because experimentally it could be induced by combining modest increases in both tidal volume and PEEP that, applied independently, did not produce those increases.

Although an emerging consensus favors alveolar stretch in the pathogenesis of VILI, the mechanisms of injury remain unclear. One theory implicates the increased lung volume and its impact on PVR, whereas the second maintains that injurious forms of mechanical ventilation lead to the elaboration of inflammatory mediators indistinguishable from those found in other models of lung injury, such as LPS-induced ALI.

In support of the first theory, Broccard and colleagues[184] demonstrated in an isolated perfused rabbit lung model that mean airway pressure rather than tidal volume determines lung injury, through an increase in PVR, particularly of the middle segment, known to accompany rises in lung volume above functional residual capacity. The authors underlined the importance of extraalveolar vessels in the pathogenesis of the increased lung water, given that these are subject to greater increases in transmural vascular pressure at high lung volume than are alveolar vessels. Additionally, they demonstrated that, for a given transpulmonary distending pressure, animals with higher pulmonary bloodflow rates suffered more lung injury and that the mitigating effect of PEEP on lung water was due primarily to altered hemodynamics.[185] Another effect of high lung volume and increased PVR is the increased capillary wall strain that causes, as discussed below, capillary stress failure with increased permeability.[186]

Despite these findings, the studies linking PEEP and lung injury are partly contradictory. Notwithstanding the aforementioned observation of worsening pulmonary injury in rats in whom PEEP of 15 cm H_2O was applied to a tidal volume not injurious by itself,[183] Muscedere and colleagues[187] reported that PEEP applied at levels above the inflection point prevented the worsening lung injury seen in those animals exposed to lower levels of PEEP. In this regard, it should be noted that of the initial four studies determining whether or not a protective ventilatory strategy is beneficial,[188–191] the only study giving positive results was one that targeted PEEP therapy to the lower inflection point.[189]

Two additional findings from the study by Muscedere and colleagues[187] merit mention: (1) despite a lack of perfusion in this model, hyaline membranes formed, which is surprising in view of the accepted notion that activation of PMNs with release of proteolytic enzymes and oxygen radicals is necessary for their development, and (2) the location of the injury within the lung depended on the level of PEEP. Indeed, at zero PEEP (ZEEP), most of the injury lay in respiratory and membranous bronchioles, whereas at higher levels of PEEP (although still below the inflection point), the injury was mostly distal in alveolar ducts. This topographic distribution supports the hypothesis that repeated closure and opening of small airways and the failure to maintain the lung open beyond its inflection point are responsible for the lung injury.

With regard to the second theory concerning mechanisms of injury in VILI, several groups have shown a relationship between alveolar stretch and the elaboration of inflammatory cytokines. Tremblay and colleagues,[192,193] in rat lungs ventilated ex vivo with injurious patterns of mechanical ventilation, demonstrated (1) significantly elevated expression of TNF-α and IL-6, originating primarily from the epithelium of airways and alveoli; (2) increased lung lavage levels of protein, inflammatory and antiinflammatory cytokines, and mRNA levels of TNF-α and *c-fos*, the latter being a representative immediate-early response gene with a stretch-responsive promoter; (3) increased release of TNF-α and macrophage inflammatory protein-2, but not of IL-1β, IL-6, interferon-γ, or IL-10, in LPS-sensitized rats; and (4) the greatest injury, produced by a ventilatory strategy combining high transpulmonary distending pressures and ZEEP.

Pursuing these investigations in patients, Zhang and colleagues[194] exposed PMNs of normal volunteers to the supernatant of BALF from patients with ALI after approximately 40 hours of mechanical ventilation with and without a protective ventilatory strategy and found in the latter significant increases in release of elastase, PMN oxidant activity, surface expression of CD18 and CD63, and shed L-selectin.

A recent and intriguing theory is that ventilatory strategies not only induce local pulmonary inflammation but also promote widespread systemic inflammation. Testing this theory in patients with ARDS, Ranieri and colleagues[195] compared two ventilatory strategies. A control group was ventilated to maintain normocapnia with PEEP titrated to achieve a saturation of oxygen (SaO_2) of ≈90% (3 to 15 cm H_2O), and a second group was ventilated with the use of a lung-protective strategy. In the latter group, there were reductions in the levels of PMN, TNF-α, IL-1β, IL-6, and IL-8 in BALF and of the first three mediators in plasma, whereas the levels of these cytokines rose with time in the control group. The authors suggested that, because the majority of ALI patients who die do so secondary to MODS, the systemic inflammatory changes elicited by injurious ventilatory modes may be ultimately responsible for the development of MODS. A further mechanism whereby ventilation could contribute to SIRS is through translocation of bacteria from airspaces to the circulation, as shown experimentally, and analogous to what takes place in the gut.[177]

Hypercapnia, alluded to above, has been advanced as an additional important factor in the attenuation of injurious ventilatory strategies, over and above mechanical

considerations.[179] In rabbit lungs, hypercapnic respiratory acidosis prevented the increased pulmonary microvascular permeability induced by ischemia–reperfusion and oxidant injury, mediated by inhibition of xanthine oxidase activity, whereas buffering of hypercapnic acidosis diminished its protective effects,[196] and hypocapnic respiratory alkalosis potentiated lung injury.[197] The same authors reported that although hypercapnic acidosis was more protective than metabolic acidosis, both inhibited xanthine oxidase to a similar extent, so that as yet unidentified mechanisms probably accounted for their differential effects on lung injury.[196]

Clinical and Therapeutic Issues

ALI and ARDS are characterized by severe hypoxemia, due principally to a large right-to-left shunt, and by stiff, noncompliant lungs, both resulting from alveolar edema. Although the AECC radiographic criteria require only the presence of bilateral pulmonary infiltrates, Murray and colleagues[198] had previously proposed a Lung Injury Score to stratify radiographic findings, in which the disturbance of respiratory mechanics was offered as a reference against which radiographs from various clinical trials of ALI could be compared.

Oxygenation ALI and ARDS are characterized by inhomogeneity of parenchymal involvement, which is well visualized on CT scans (see Figure 19-10), so that only limited portions of the diseased lungs actively participate in ventilation. This concept, in turn, led to (1) the suggestion that a maximum plateau pressure of 35 cm H_2O be applied in the ventilatory management of these patients[199]; (2) the positive trial on low-lung-volume ventilation[83]; and (3) an understanding of the heterogeneous impact of PEEP.[200] CT scans have also lent graphic support to the concept that positioning these patients in the prone position could improve oxygenation.

PEEP Because right-to-left shunt is the fundamental pathophysiologic mechanism that impairs oxygenation,[201] the major therapeutic challenge in this syndrome, the efficacy of high levels of exogenous oxygen, is severely limited, and the attendant toxicity may be considerable. To improve oxygenation, various mechanical ventilatory modes and maneuvers have been attempted. PEEP, by far the most commonly used method to diminish shunt, acts by increasing functional residual capacity through the recruitment of lung units for gas exchange[200] and by decreasing perfusion to unventilated parts of the lung.[201] Despite the consensus that PEEP should be applied to mitigate the effects of high levels of inspired oxygen, there is no agreement on what level of oxygen poses a toxic threat or on the level of PEEP to apply. Traditionally, PEEP has been set at a level yielding acceptable arterial and venous oxygen saturations. Recently, convincing experimental data have emerged, discussed more fully below, suggesting that allowing the lung to repeatedly fall below its lower inflection point is harmful,[187] and in at least one clinical trial in which the amount of PEEP was targeted to just above the lower inflection point, improved survival was observed compared with a conventionally managed ventilator group.[202] Detection of that inflection point, however, is labor intensive, its reproducibility and interobserver variability are controversial, and whether to use the inflation or the deflation portion of the curve is debated.[203]

Furthermore, despite this strong supporting evidence, there are as yet no definitive data on this "open-lung" approach. To date, three trials have addressed this issue: two, one in Canada and the other in France, are ongoing. Although not yet published, the results of the third, with 550 patients in the United States, reviewed recently (R. Brower, personal communication, April 2002), demonstrate that high levels of PEEP are no better than low levels.

It is noteworthy that PEEP may, in fact, increase shunt by the relative overexpansion of previously normal parts of the lung and failure to recruit diseased areas[204]; also, PEEP does not reduce lung water and may even cause it to rise.[205] Despite the apparent beneficial effects of low–lung-volume ventilation,[83] it results in alveolar derecruitment and worsening hypoxemia in many patients, even when PEEP is held near or just above the lower inflection point.[206] To counter this trend and reverse the derecruitment during suctioning, for example, several investigators have proposed various recruitment maneuvers, including sustained inflation at 30 to 45 cm H_2O for 20 seconds and periodic sighs.[207] Regardless of the apparently improved oxygenation achieved by these maneuvers, however, there are as yet no data on their potential for exacerbating lung injury.

Inverse Ratio Ventilation Unfortunately, there are no randomized trials to support the efficacy of this strategy to enhance gas exchange. The only available data come from small studies in which inverse ratio ventilation (IRV) has been compared with conventional ventilation, and the results vary. Huang and colleagues[208] reported that at constant mean airway pressure, both arterial and venous oxygenation deteriorated on IRV, whereas both oxygen delivery and consumption remained unaltered. In contrast, Abraham and Yoshihara[209] reported that in nine patients with ALI before and after the institution of pressure-controlled IRV, oxygenation improved significantly on IRV, whereas peak airway pressure fell, albeit nonsignificantly, and hemodynamic variables remained unchanged.

Liquid Ventilation Liquid ventilation with perfluorocarbon was introduced because of this compound's unique physical properties, which include low surface tension, high solubility of oxygen and carbon dioxide, and the capacity for lung recruitment (liquid PEEP).[210] Although the results of animal studies and uncontrolled studies in humans suggested physiologic and clinical efficacy, a large randomized study in which partial liquid ventilation at two different doses was compared with conventional mechanical ventilation failed to demonstrate any clinical benefit.[210]

High-Frequency Oscillatory Ventilation The application of high-frequency oscillatory ventilation to adult patients with ALI stemmed from its successful use in the neonatal and pediatric populations and from data implicating

mechanical ventilation in aggravating lung injury. As in the early studies with NO, preliminary results demonstrated improvements in oxygenation,[211] but results from the one controlled multicenter trial failed to show benefit in duration of mechanical ventilation or survival.[212]

Prone Position The effect of a change in body position on lung volumes has been appreciated since Moreno and Lyons[213] documented an increased functional residual capacity in the prone compared with the supine position. It took another 25 years for the improvement in oxygenation accompanying these position changes to be widely appreciated, but numerous studies have now documented the efficacy of the prone position in improving gas exchange. Although the literature suggests that 50 to 75% of patients with ALI respond to the change in position, the mechanisms are far from clear.[175,214] In an experimental study, the transition from the supine to the prone position was accompanied by a fall in right-to-left shunt due to increased dorsal regional ventilation rather than to altered bloodflow.[215] A recent review of the topic concluded that the improved oxygenation stems from a more homogeneous distribution of ventilation and perfusion.[175] Despite the high number of responders, however, two randomized controlled trials failed to demonstrate a significant survival benefit.[216,217]

Nitric Oxide NO would seem conceptually to be the perfect treatment for ALI because (1) it is delivered by inhalation, so its vasodilator effects on the pulmonary vasculature should be confined to those alveolar units participating in ventilation, and (2) its half-life is measured in seconds, eliminating any effects on the systemic circulation.[218] Although the number of articles chronicling its benefits on gas exchange has increased greatly since the first report in 1993,[219] four controlled trials failed to demonstrate a significant survival benefit compared with controls, despite an initial transient increase in oxygenation.[220–223] In a post hoc analysis, however, Dellinger and colleagues[221] reported a significant increase in the number of patients alive and off mechanical ventilation by day 28 in the group given 5 ppm NO.

Recently, Gerlach and colleagues[224] confirmed the initial ephemeral improvement in gas exchange but also described a leftward shift in both the oxygenation and pulmonary vascular responses to NO: although all patients had a peak response to 10 ppm initially, the peak response in those receiving continuous treatment with 10 ppm NO fell to 1 ppm by day 4, and gas exchange actually deteriorated in some of these patients; the control group continued to demonstrate a peak response at 10 ppm. The authors suggested that the negative results of randomized trials in which a constant dose of NO was used might have been due, at least in part, to the failure to appreciate this phenomenon.

Surfactant Although surfactant dysfunction is not considered to be the primary abnormality, as in the infant respiratory distress syndrome, it still plays an important role in ARDS.[225] As reviewed by Lewis and Brackenbury,[226] despite several case reports and uncontrolled trials supporting its use, four large randomized controlled trials have yielded variable results. In the first, the synthetic surfactant Exosurf failed to modify ventilator-free days or mortality, but there may have been a design flaw in the study, whereby little surfactant reached distal alveoli. In a smaller trial, a modified natural surfactant, Survanta, was instilled directly into the airways and caused a significant reduction in mortality. Finally, in two larger trials, a recombinant surfactant protein C-based preparation was instilled directly into the airway but failed to change ventilator-free days or mortality, even with significantly improved oxygenation.[225] Post hoc analyses revealed significantly lower mortality rates in those patients with ALI resulting from a direct insult, pneumonia, and aspiration.[226]

Ventilation Given the results of the studies in animals linking large tidal volumes and lung injury, as detailed above, four small clinical studies were undertaken to determine whether a protective ventilatory strategy would yield a measurable clinical benefit in patients with ALI[188–191]: of these, only one demonstrated a mortality benefit.[189] However, in 2000, the Acute Respiratory Distress Syndrome Network (ARDS Net) published its results on the beneficial effects of a protective ventilatory strategy in 800 patients with ALI.[83] This strategy, which consisted of a maximum plateau pressure of 30 cm H_2O and a tidal volume of 6 mL/kg predicted body weight, was compared with a traditional ventilatory strategy of 12 mL/kg predicted body weight and a plateau pressure $<$50 cm H_2O. The trial was terminated prematurely because of efficacy: the authors found that mortality in the protective strategy group fell by approximately 10% (39.8% vs 31%), for a relative decrease of approximately 25%. Furthermore, ventilator-free days at day 28 were significantly greater in the protective strategy group. Although this study has generated much controversy concerning the safety of low–tidal-volume ventilation,[227] it appears that ventilation with large tidal volumes ($>$10 mL/kg) and high plateau pressures ($>$32 cm H_2O) should be avoided and that permissive hypercapnia up to 90 mm Hg, and perhaps higher, is safe.[228]

Fluid and Pulmonary Vascular Pressure Management Although, as detailed above, microvascular pressures (ie, P_{mv}) are thought to remain relatively normal in ALI/ARDS, edema formation is exquisitely sensitive to P_{mv} because of the rise in K_f and fall in σ. Knowing this, several investigators have examined the impact of manipulating P_{mv} and/or Π_{mv} on edema formation in various models of lung injury. Ali and colleagues[229] reported that in dogs with oleic acid–induced edema, furosemide improved oxygenation and intrapulmonary shunt without changing P_w, plasma oncotic pressure or, indeed, the amount of pulmonary edema; they concluded that furosemide acted by dilating the pulmonary vasculature.

A series of clinical studies that followed appeared to support the conclusion that a strategy of "fluid restriction to seek the lowest P_w consistent with adequate cardiac output" is beneficial in patients with ALI.[229] A retrospective analysis of patients with sepsis identified initial protein levels and

their change over time as the most significant predictors of weight gain, prolonged mechanical ventilation, development of ALI, and mortality[230]; Humphrey and colleagues[231] reported a significant survival advantage in those patients with ALI in whom P_w was aggressively lowered by at least 25%.

In a prospective study of patients with ALI, a fluid strategy in which P_w was kept at <18 mm Hg was compared with one aimed at maintaining extravascular lung water (EVLW) at <7 mL/kg[232]: EVLW decreased significantly over time in the EVLW group but not in the P_w group, and by 24 hours and beyond, cumulative fluid balance was significantly lower in the former group; importantly, the study demonstrated that the EVLW group spent significantly fewer days on mechanical ventilation, with a trend toward a lower mortality. Pursuing this line of inquiry, Martin,[233] in a randomized trial of patients with ALI and hypoproteinemia (≤ 5 g/dL), compared one group receiving thrice-daily infusions of 25 g of albumin and continuous infusion of furosemide with a second group treated conventionally: the treatment group experienced increased diuresis and a decrease in weight, accompanied by significantly improved oxygenation within the first 24 hours, with a clear trend toward a reduced need for mechanical ventilation.

Other Therapeutic Strategies With the recognition of the importance of tissue injury and inflammation in ARDS, corticosteroids were studied early on but were found not to be of any benefit in the initial stages.[234] More recently, Meduri and colleagues[235] prospectively examined the effects of methylprednisolone (2 mg/kg starting on day 9 for ≈32 days) on the fibroproliferative stages of ARDS: treated patients had significant improvements in gas exchange, lung injury score, multiple organ dysfunction scores, and rate of successful extubation and significantly decreased rates of intensive care unit and hospital mortality. Although impressive, the results of the study must be tempered by the very small sample size. This therapeutic approach is presently being addressed in a study sponsored by the National Institutes of Health.

The inflammation of ARDS also severely tips the prooxidant–antioxidant balance in favor of the former. Bernard and colleagues[236] reported that plasma and red blood cell levels of the antioxidant glutathione and its precursor cysteine were low in their subjects with ARDS. They compared the effects of therapy with two antioxidants, *N*-acetylcysteine and L-2-oxothiazolidine-4-carboxylate (Procysteine), with those of placebo: although they failed to yield any survival benefit, antioxidants nevertheless appeared to provide clinical benefit by significantly reducing the duration of ALI and, although the effect was not quite significant, by decreasing the number of new organ failures. Considering the relatively small number of patients in this trial and the positive results of a previous study,[237] a larger trial may yield more impressive results.

In conclusion, there has been a striking and frustrating lack of efficacy of these many and varied interventions. Possible reasons for this are the diagnostic imprecision in their definition and the heterogeneous groups of patients serving as subjects. Another possible explanation is the lack of power in many of these trials: in this regard, the ARDS Net trial on low–lung-volume ventilation included over 800 patients.[83] Third, when these trials are being designed, end points must be framed with respect to "best practice": specifically, although overall mortality in ALI still approximates 50% in the uncontrolled setting, it has proven to be considerably less in the context of the randomized trial, in which the control arm is highly structured, raising the question of the impact of highly structured conventional "best practice" therapy alone on mortality. Finally, it must be remembered that, in numerous studies, patients die not *from* ARDS but rather *with* ARDS, so that it may be naive to expect a treatment designed to improve oxygenation to give a major survival advantage to those patients dying from MODS and sepsis.

MIXED AND OTHER FORMS OF PULMONARY EDEMA

Pathogenesis

Although it is convenient to distinguish hydrostatic and permeability edema, in practice they may overlap and interact. Generally, etiologies of edema can be determined, and most forms of permeability edema, at least in the early stages, do not involve substantial elevations in pulmonary vascular pressures. Several issues, however, deserve consideration, as follows.

Some models of lung injury and clinical forms of permeability pulmonary edema are associated with transient or sustained pulmonary hypertension. For example, in sepsis, a major causal association of ARDS, there is formation of microemboli and/or release of mediators that raise pulmonary vascular pressures.

The difficulty of correctly estimating P_{mv} in states of elevated pulmonary vascular permeability is substantial because the distribution of PVR may be altered. As discussed above, mediators and microemboli may preferentially constrict or block arterial, venous, or microvascular segments of the pulmonary circulation, reducing the reliability of measurements of P_w with the Swan-Ganz catheter.

Hydrostatic pressure is at least additive with permeability in producing edema, in both the experimental and the clinical setting. For example, in perfused canine lungs in situ, Huchon and colleagues[75] found that elevation of P_{la} to 18 mm Hg for 1 hour did not significantly raise lung water above the normal 2.4 g/kg, that oleic acid with low P_{la} (0 mm Hg) for 1 hour increased lung water to 6.4 g/kg, and that both oleic acid and high P_{la} elevated lung water to 10.1 g/kg, consistent with a significant synergistic interaction between increased permeability and hydrostatic pressure.

Over the last 10 to 12 years, the distinction between hydrostatic and permeability edema has become further blurred through the elegant studies of West and colleagues, reviewed recently,[81,186] who championed the notion that microvascular pressures over ≈40 mm Hg can raise permeability. The pulmonary blood–gas barrier, composed of endothelial and epithelial cells, basement membrane, and

interstitium, must be both extremely thin (0.2 to 0.3 μm on the thin side of the barrier in humans) for efficient gas exchange and very strong to withstand the enormous stresses in the capillary wall; the latter property has been attributed largely to type IV collagen in the basement membranes. As described by West and colleagues, when the capillary wall stresses and/or intraluminal pressure rise to very high levels, the phenomenon of "stress failure" occurs, characterized by damage demonstrable on ultrastructural examination. Stress failure occurs (1) under physiologic conditions such as strenuous exercise in elite human athletes; (2) in pathologic conditions such as neurogenic pulmonary edema (NPE), high-altitude pulmonary edema (HAPE), severe left heart failure, and mitral stenosis; and (3) in therapeutic maneuvers with overinflation of the lung, for example, in VILI. The stresses to which the capillary (and adjacent epithelium) are subjected may be either circumferential, related to the capillary transmural pressure, or longitudinal, associated with inflation. The characteristic alterations seen in capillary stress failure reported by West and Mathieu-Costello[81] include the following: (1) there are disruptions of ECs, most probably transcellular, some at intercellular junctions, and attachment of platelets to the exposed basement membrane; (2) there are breaks in alveolar type I pneumocytes measuring ≈4 by 1 μm, generally not at intercellular junctions, suggesting that these have considerable mechanical strength; (3) the number of endothelial and epithelial disruptions per millimeter of cell boundary increases with intravascular pressure; (4) the breaks are rapidly reversible, with about 70% of both endothelial and epithelial breaks closing within minutes. Of note, the basement membranes remain generally intact, consistent with their superior strength. In keeping with Laplace's law, stress failure of capillaries occurs at different pressures in different species, for example, 39 mm Hg in the rabbit, 67 mm Hg in the dog, and 96 mm Hg in the horse. The result of capillary stress failure is leakage of proteinaceous fluid and erythrocytes into the interstitium and alveoli, that is, increased permeability edema. It is also of interest that lung inflation lowers the threshold for development of capillary stress failure: for example, in their rabbit model, West and colleagues[81] found that, with a capillary pressure of 20 mm Hg and a transpulmonary pressure of 5 cm H_2O, there were few breaks, but these increased markedly at a transpulmonary pressure of 20 cm H_2O.

High-Altitude Pulmonary Edema

HAPE, also reviewed elsewhere,[238–240] occurs in susceptible persons who ascend to altitudes $>$2,500 m, generally rapidly, although it may occur at lower altitudes.[241] Symptoms characteristically develop 2 to 3 days following ascent, often after strenuous activity or exposure to cold, and include dyspnea, cough, weakness and limitation of physical activity, dizziness, and nausea. There are crackles, tachypnea and tachycardia on physical examination, infiltrates on chest radiographs, generally bilateral, either central or peripheral, and hypoxemia.[238] Recovery typically occurs with descent to sea level, and the rare fatalities are usually related to the unavailability of oxygen or the inability to descend to lower altitudes. In 1991, a consensus committee at the Inter-national Hypoxia Symposium defined HAPE, in the setting of a recent gain in altitude, as the presence of at least two symptoms (dyspnea at rest, cough, weakness, decreased exercise performance, chest tightness or congestion) plus two signs (rales or wheezing, central cyanosis, tachycardia or tachypnea).[242] The same committee proposed a functional grading of disability. The incidence of HAPE is about 5% but varies with altitude, gender, and age (more frequent in males and children); subclinical cases are more frequent.[238] Physiologic parameters show elevated P_{pa} and PVR, normal P_w, reduced cardiac output, mean systemic arterial pressure, and arterial oxygen saturation. Pathologic findings in 26 cases summarized by Hultgren[238] include lung weights ≈2.5 times normal, bloody and foamy edema, macro- or microthrombi, hyaline membranes, and infiltration with PMNs consistent with permeability edema. Although incompletely understood, the putative mechanisms for HAPE involve hypoxic vasoconstriction with high altitude as the initiating stimulus, resulting in inhomogeneous obstruction of the pulmonary vascular bed and perhaps thromboses. With increased activity, cardiac output rises, the unobstructed areas of the pulmonary vasculature are subjected to a high P_{mv}[243], and, via mechanisms proposed by West[186] and enunciated above, permeability edema with high protein content ensues. Additional proposed contributory factors are endothelial dysfunction, a defect in alveolar transepithelial Na^+ transport,[239] increased ET-1 or reduced NO production,[244] and exaggerated sympathetic activation[245] in HAPE-susceptible subjects during acute hypoxia. This susceptibility to HAPE, as recently reported by Droma and colleagues,[246] may be explained by the discovery that two polymorphisms of the endothelial NOS (eNOS) gene were significantly associated with HAPE, underlying impaired synthesis of NO by pulmonary vessels.

Neurogenic Pulmonary Edema

NPE shares some pathogenetic similarities with HAPE but also exhibits differences. Its incidence determined from postmortem studies ranges from 33 to 71%, and it develops in various conditions and injuries of the central nervous system that produce increased intracranial pressure or cerebral ischemia. These lead to a massive sympathetic nervous discharge and catecholamine release,[247] which result in severe systemic vascular vasoconstriction and translocation of blood from the systemic to the pulmonary circulation; this raises P_{pa} and P_w (unlike in HAPE) and produces a variably protein-rich edema.[248] Indeed, the controversy, as in the case of HAPE, has been whether NPE is of the permeability or hydrostatic type: the answer appears to be that when the pressures rise sufficiently, microvascular stress failure and increased permeability follow.[186] Clinical measurements on patients and experimental studies have shown that P_{pa} and P_w can reach 70 to 80 mm Hg and 40 to 70 mm Hg, respectively, consistent with the presence of an important element of cardiac dysfunction being added to the pulmonary hypertension. Further observations

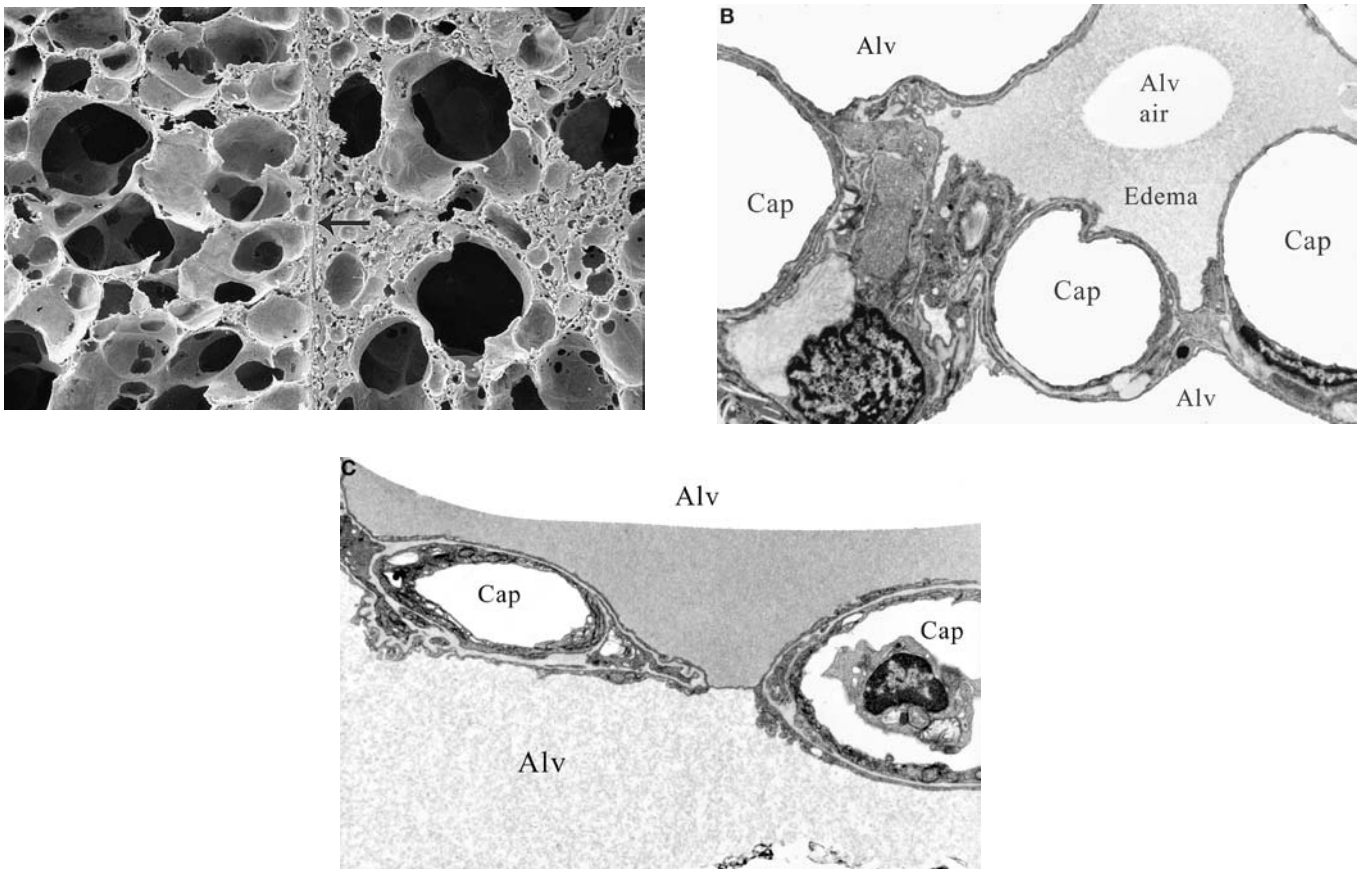

FIGURE 19-13 Ultrastructure of heterogeneity in hydrostatic edema induced in rabbits by fluid infusion (methods detailed elsewhere[76]). *A*, Low-power scanning electron micrograph showing alveoli on the left side of the interlobular septum (*arrow*) with less edema than those on the right, which contain more fluid and are partly collapsed (×150 original magnification). *B*, Medium-power transmission electron micrograph showing one partly flooded alveolus and two empty ones; capillaries (Cap) are empty because of vascular fixation (×9,300 original magnification) *C*, High-power electron micrograph showing alveolar (Alv) edema, with different densities and protein contents on either side of the alveolar–capillary septum (×13,500 original magnification). Cap = capillaries.

favoring a primary hydrostatic mechanism (albeit very severe) include the rapidity of onset and reversibility, the variable protein concentrations in the edema fluid, including some within the range of hydrostatic edema,[249] and the absence of endothelial damage as determined with electron microscopy.[250]

HETEROGENEITY IN PULMONARY EDEMA

Despite a perception of diffuse involvement in pulmonary edema and the aforementioned definition of ARDS and ALI, which includes "diffuse bilateral infiltrates on chest radiographs," there is substantial heterogeneity in pulmonary edema, which remains largely unexplained. The specifics are as follows:

1. As indicated by the AECC in 1994, the definition of ARDS already entails considerable heterogeneity of etiologies, mechanisms, and associations.[1]
2. Despite the sizeable population of patients at risk of developing ALI/ARDS, relatively few do so: as detailed above, Hudson and colleagues[91] reported an overall incidence of 26% of patients admitted to the intensive care unit, suggesting a role for genetic influences, among others, in differences in susceptibility.[251]
3. As is particularly well visualized on CT scans, some lung regions in ARDS have densities of solid tissue because of consolidation, edema, or atelectasis, whereas others retain normal air density and are apparently free of disease[252]; in addition to the systematic dorsal-to-ventral (or other gravity-dependent) gradients explained by hydrostatic forces, there are gravity-independent central-to-peripheral pulmonary heterogeneities whose mechanisms remain incompletely understood.
4. Heterogeneity, both macroscopic and microscopic, is also evident pathologically, in both hydrostatic and permeability edema, since the lung is not affected uniformly by edema; temporal heterogeneity also exists[76,253] (see Figures 19-6C, 19-12B, and 19-13C).
5. Heterogeneities at the cellular level could partly explain those observed on a wider scale. For example, significant regional differences in normal EC ultrastructure exist in the different vascular segments (alveolar and extraalveolar): mean EC thickness is significantly greater in the muscular than in other microvessels, whereas vesicular numerical densities are significantly greater in ECs of capillaries than in those of nonmuscular, partially muscular and muscular vessels, and in venules than arterioles.[254] Endothelial responses to

stimuli such as endotoxin show considerable variation between species, between organs within species, between pulmonary and systemic vessels, and between large and small vascular ECs.[105]

6. The many mediators, cytokines, growth factors, and transcription factors produced by the varieties of cells in the lung are alternative sources of heterogeneity.
7. Important inhomogeneities exist in ventilation/perfusion ratios,[255] probably as a result of heterogeneous pulmonary arterial and venous constriction and airway closure, factors that could alter the distribution of edema.
8. Heterogeneity in lung injury is in part responsible for the amplification of mechanical forces that precipitate VALI: preferential distribution of a positive pressure tidal breath to normally aerated areas renders them vulnerable to overdistention.[177]
9. The reported rates of recovery from ARDS vary considerably, and there is no clear explanation for this.[256]

Therefore, one of the goals of future research, both basic and clinical, as aptly pointed out in a recent publication of the AECC,[257] should be to "progress from clinical syndromes, as presently defined, to more specific entities that are delineated by alterations in specific immunologic or biochemical pathways." To this should be added genetic predispositions and pathologic findings. One immensely successful example of this approach, albeit in a totally different domain, is the latest World Health Organization classification of neoplasms of hematopoietic and lymphoid tissues (leukemias and lymphomas),[258] in which combined clinical, pathologic, immunologic, genetic, and molecular approaches have led to clearly defined entities with specific therapeutic approaches and prognostic implications. This is a challenge of major proportions in ALI/ARDS because obtaining tissue for many of these studies is fraught with difficulty. Nevertheless, the ability to biopsy small samples of tissue and to subject them to increasingly complex analyses, both morphologic and molecular, is rapidly improving and is a definite goal for the future. We have come full circle nearly 30 years after Murray's statement that "lumping these disorders together serves no useful purpose and has the disadvantage of detracting from important and distinctive differences in pathogenesis, therapy and prognosis."[259] Perhaps we could start by splitting off those entities that do not correspond to DAD-associated ARDS.

SUMMARY AND CONCLUSIONS

Although the Starling equation remains a key determinant of our classification and approach to the physiology and management of pulmonary edema, its application and scope have been substantially enlarged and complicated by the acquisition of vast amounts of cellular and molecular biologic data that must be integrated into its basic parameters. The notion that edema can be simply divided into hydrostatic and permeability types has been compromised, for example, by studies showing that markedly elevated hydrostatic pressures induce capillary stress failure and permeability edema. Interactions between the two forms of edema complicate the management of such patients, as does the existence of mixed forms of pulmonary edema. Therefore, a clear understanding of the principles guiding the balance of forces and pressures in the lung circulation, airways, and interstitium is required to integrate the advances made by modern biologic approaches into a coherent whole.

Still, in most instances, major differences remain between hydrostatic and permeability forms of edema. Hydrostatic edema, caused by an elevation of microvascular pressure, mainly in the setting of heart failure, is characterized by a transudate with a low protein concentration relative to plasma, an intact alveolar–capillary septal barrier, and an orderly sequence of fluid accumulation that starts in the interstitium before flooding alveoli and that is readily reversible, provided that the stimulus responsible for the elevation in pressure is treated. Furthermore, even repeated episodes of this form of edema leave the lung with little more than hemosiderin-laden macrophages in the alveoli, mild interstitial fibrosis, and generally mild vascular remodeling.

In contrast, the permeability edema of ALI/ARDS is much more problematic. With its varied etiologies and associations, it is characterized by damage to pulmonary endothelium and epithelium with rapid and predominant alveolar flooding by a protein-rich exudate, causing early compromise of gas exchange. Mechanisms of damage involve activation of a variety of parenchymal and inflammatory cells and production or activation of many cytokines, chemokines and other mediators, growth and transcription factors, receptors, and signal transduction molecules, with multifaceted and complex interactions. Unlike in hydrostatic edema, failure to secure prompt resolution by appropriate therapeutic maneuvers results in activation of a fibroproliferative phase that may terminate in pulmonary fibrosis, with potentially devastating or even fatal consequences.

For these reasons, the major challenges for the future in pulmonary edema lie in the sphere of ALI and ARDS.[260] As mentioned earlier, the definition of ALI/ARDS does not take into account the heterogeneity of disorders and patient populations, so that different diagnostic entities may have to be separated off from the umbrella term, each with specific diagnostic, therapeutic, and prognostic implications. Also, the criteria of the AECC may be difficult to apply consistently. One of the concerns is the lack of a diagnostically accurate biochemical marker and reliable noninvasive measure of alveolar–capillary injury or permeability: specifically, there is a vital need for a marker of lung injury analogous to CPK-MB or troponin in acute myocardial infarction or to serologic tests for the infectious diseases. Furthermore, although considerable progress has been made in our understanding of the mechanisms of injury in ARDS, our knowledge of the interactions and balances between mediators and modulators of inflammation remains incomplete; similarly, the search for reliable markers of severity and mortality has been fraught with obstacles. One area of major progress, as detailed above, is the recognition of VILI and VALI, with the subsequent undertaking of clinical trials demonstrating the value of lung-protective ventilatory strategies in reducing mortality in ALI/ARDS.

Major challenges and directions for future research in ALI are summarized in a recent report from a National Heart, Lung, and Blood Institute Working Group.[261] Some examples of promising avenues for exploration include the following: (1) in epithelial cells, the factors regulating cytokine production in response to injury and mechanisms of protection; (2) in ECs, the molecular mechanisms that regulate responses to injury and interactions with epithelial cells; their diversity also awaits further exploration; (3) mechanisms governing apoptosis and necrosis, responses of fibroblasts and other mesenchymal cells, to shed light on the remodeling of parenchyma and vessels in the fibroproliferative and fibrotic phases of ARDS; (4) in VILI and VALI, the molecular mechanisms of mechanosensing and mechanotransduction during stretching, and how they affect cellular interactions in injured lungs; also the detailed mechanisms whereby injurious ventilatory strategies lead to translocation of mediators, endotoxin and bacteria from the lung to the systemic circulation; and (5) detailed understanding of molecular signaling mechanisms by cells of the immune system and how cells involved in hemostasis and thrombosis are dysregulated in ARDS/ALI; for example, the roles of Toll-like receptors, of NFκB, and of other transcription factors require further scrutiny, as does the role of anticoagulants in the modulation of the injurious effects of ARDS.

With regard to these challenges, a combination of genomic and proteomic approaches and genetic and epidemiologic methods, correlated with traditional physiologic parameters and outcome measures in clinical trials, should substantially advance our knowledge base in this group of complex disorders, supplant the current physiologic and radiographic criteria, and deal with the substantial phenotypic heterogeneity of these disorders.

ACKNOWLEDGMENT

The research done by the authors has been supported in large part by the Canadian Institute of Health Research.

REFERENCES

1. Bernard GR, Artigas A, Brigham KL, et al. The American–European Consensus Conference on ARDS. Definitions, mechanisms, relevant outcomes, and clinical trial coordination. Am J Respir Crit Care Med 1994;149:818–24.
2. Gattinoni L, Pelosi P, Suter PM, et al. Acute respiratory distress syndrome caused by pulmonary and extrapulmonary disease. Different syndromes? Am J Respir Crit Care Med 1998;158:3–11.
3. Pelosi P, Gattinoni L. Acute respiratory distress syndrome of pulmonary and extra-pulmonary origin: fancy or reality? Intensive Care Med 2001;27:457–60.
4. Moss M, Thompson BT. Definitions and clinical risk factors. In: Matthay MA, editor. Acute respiratory distress syndrome. New York: Marcel Dekker; 2003. p. 7–36.
5. Starling EH. On the absorption of fluids from the connective tissue spaces. J Physiol 1896;19:312–26.
6. Granger HJ, Laine GA, Barnes GE, Lewis RE. Dynamics and control of transmicrovascular fluid exchange. In: Staub NC, Taylor AE, editors. Edema. New York: Raven Press; 1984. p. 189–228.
7. Gropper MA, Wiener-Kronish JP, Hashimoto S. Acute cardiogenic pulmonary edema. Clin Chest Med 1994;15:501–15.
8. Staub NC. Pathophysiology of pulmonary edema. In: Staub NC, Taylor AE, editors. Edema. New York: Raven Press; 1984. p. 719–46.
9. Drake RE, Doursout MF. Pulmonary edema and elevated left atrial pressure: four hours and beyond. News Physiol Sci 2002;17:223–6.
10. Inoue S, Michel RP, Hogg JC. Zonulae occludentes in alveolar epithelium and capillary endothelium of dog lung studies with the freeze–fracture technique. J Ultrastruct Res 1976; 56:215–25.
11. Gaar KA, Taylor AE, Owens LJ, Guyton AC. Pulmonary capillary pressure and filtration coefficient in the isolated perfused lung. Am J Physiol 1967;213:910–4.
12. Levy MM. Pulmonary capillary pressure. Clinical implications. Crit Care Clin 1996;12:819–39.
13. Sandham JD, Hull RD, Brant RF, et al. A randomized, controlled trial of the use of pulmonary-artery catheters in high-risk surgical patients. N Engl J Med 2003;348:5–14.
14. Harris P, Heath D. The human pulmonary circulation. 2nd ed. Edinburgh: Churchill Livingstone; 1977.
15. Hakim TS, Dawson CA, Linehan JH. Hemodynamic responses of dog lung lobe to lobar venous occlusion. J Appl Physiol 1979;47:145–52.
16. Hakim TS, Michel RP, Chang HK. Partitioning of pulmonary vascular resistance in dogs by arterial and venous occlusion. J Appl Physiol 1982;52:710–5.
17. Hakim TS, Michel RP, Minami H, Chang HK. Site of pulmonary hypoxic vasoconstriction studied with arterial and venous occlusion. J Appl Physiol 1983;54:1298–302.
18. Hakim TS, Michel RP, Chang HK. Effect of lung inflation on pulmonary vascular resistance by arterial and venous occlusion. J Appl Physiol 1982;53:1110–5.
19. Albert RK, Lamm WJE, Henderson WR, et al. Effect of leukotrienes B4, C4, and D4, on segmental pulmonary vascular pressures. J Appl Physiol 1989;66:458–64.
20. Cheng-Ren C, Voelkel NF, Shih-Wen C. PAF potentiates protamine-induced lung edema: role of pulmonary venoconstriction. J Appl Physiol 1990;68:1059–68.
21. Wakerlin GE, Benson GV, Pearl RG. A thromboxane analog increases pulmonary capillary pressure but not permeability in the perfused rabbit lung. Anesthesiology 1991;75:475–80.
22. Michel RP, Hakim TS, Hanson RE, et al. Distribution of lung vascular resistance after chronic systemic-to-pulmonary shunts. Am J Physiol 1985;249:H1106–13.
23. Michel RP, Hakim TS, Freeman CR. Distribution of pulmonary vascular resistance in experimental fibrosis. J Appl Physiol 1988;65:1180–90.
24. Bhattacharya J, Staub NC. Direct measurement of microvascular pressures in the isolated perfused dog lung. Science 1980;210:327–8.
25. Negrini D, Gonano C, Miserocchi G. Microvascular pressure profile in intact in situ lung. J Appl Physiol 1992;72:332–9.
26. Bhattacharya J. Physiological basis of pulmonary edema. In: Matthay MA, Ingbar DH, editors. Pulmonary edema. New York: Marcel Dekker; 1998. p. 1–36.
27. Miserocchi G, Negrini D, Passi A, De Luca G. Development of lung edema: interstitial fluid dynamics and molecular structure. News Physiol Sci 2001;16:66–71.
28. DeFouw DO, Shumko JZ. Pulmonary microcirculation: differences in endothelia of subpleural and alveolar capillaries. Microvasc Res 1986;32:348–58.
29. Hakim TS. Is flow in subpleural region typical of the rest of the lung? A study using laser-Doppler flowmetry. J Appl Physiol 1992;72:1860–7.
30. Hakim TS, Kelly S. Occlusion pressures vs. micropipette pressures in the pulmonary circulation. J Appl Physiol 1989;67: 1277–85.

31. Nagasaka Y, Ishigaki M, Hazu R, et al. Lung microvascular pressure profile in acute lung injury. Tohoku J Exp Med 1996;179:81–92.
32. Nagasaka Y, Ishigaki M, Okazaki H, et al. Effect of pulmonary blood flow on microvascular pressure profile determined by micropuncture in perfused cat lungs. J Appl Physiol 1994;77:1834–9.
33. Michel RP, Hakim TS. Increased resistance in postobstructive pulmonary vasculopathy: structure–function relationships. J Appl Physiol 1991;71:601–10.
34. Holloway H, Perry M, Downey J, Taylor AE. Estimation of effective pulmonary capillary pressure in intact lungs. J Appl Physiol 1983;54:846–51.
35. Hakim TS, Maarek JM, Chang HK. Estimation of pulmonary capillary pressure in intact dog lungs using the arterial occlusion technique. Am Rev Respir Dis 1989;140:217–24.
36. Maarek JM, Hakim TS, Chang HK. Analysis of pulmonary arterial pressure profile after occlusion of pulsatile blood flow. J Appl Physiol 1990;68:761–9.
37. O'Leary CE, Fiori R, Hakim TS. Perioperative distribution of pulmonary vascular resistance in patients undergoing coronary artery surgery. Anesth Analg 1996;82:958–63.
38. Cope DK, Grimbert F, Downey JM, Taylor AE. Pulmonary capillary pressure: a review. Crit Care Med 1992;20:1043–56.
39. Collee GG, Lynch KE, Hill RD, Zapol WM. Bedside measurement of pulmonary capillary pressure in patients with acute respiratory failure. Anesthesiology 1987;66:614–20.
40. Staub NC. Pulmonary edema. Physiol Rev 1974;54:678–811.
41. Guyton AC, Lindsey AW. Effect of elevated left atrial pressure and decreased plasma protein concentration on the development of pulmonary edema. Circ Res 1959;7: 649–57.
42. Weaver LJ, Carrico CJ. Congestive heart failure and edema. In: Staub NC, Taylor AE, editors. Edema. New York: Raven Press; 1984. p. 543–62.
43. Bhattacharya J, Gropper MA, Staub NC. Interstitial fluid pressure gradient measured by micropuncture in excised dog lung. J Appl Physiol 1984;56:271–7.
44. Majno G, Palade GE, Schoefl GI. Studies on inflammation. II. Site of action of histamine and serotonin on the vascular tree: a topographic study. J Biophys Biochem Cytol 1961;11:607–26.
45. Michel RP. Lung microvascular permeability to dextran in alpha-naphthylthiourea-induced edema. Sites of filtration, patterns of accumulation, and effects of fixation. Am J Pathol 1985;119:474–84.
46. DeFouw DO, Ritter AB, Chinard FP. Alveolar microvessels in isolated perfused dog lungs: structural and functional studies after production of moderate and severe hydrodynamic edema. Exp Lung Res 1985;8:67–79.
47. Weibel ER, Bachofen H. Structural design of the alveolar septum and fluid exchange. In: Fishman AP, Renkin EM, editors. Pulmonary edema. Bethesda (MD): American Physiological Society; 1979. p. 1–20.
48. Staub NC, Nagano H, Pearce ML. Pulmonary edema in dogs, especially the sequence of fluid accumulation in lungs. J Appl Physiol 1967;22:227–40.
49. Michel RP, Smith TT, Poulsen RS. Distribution of fluid in bronchovascular bundles with permeability lung edema induced by alpha-naphthylthiourea in dogs. A morphometric study. Lab Invest 1984;51:97–103.
50. Michel RP, Hakim TS, Smith TT, Poulsen RS. Quantitative morphology of permeability lung edema in dogs induced by alpha-naphthylthiourea. Lab Invest 1983;49:412–19.
51. Michel RP, Meterissian S, Poulsen RS. Morphometry of the distribution of hydrostatic pulmonary oedema in dogs. Br J Exp Pathol 1986;67:865–77.
52. Lai-Fook SJ. Mechanical factors in lung liquid distribution. Annu Rev Physiol 1993;55:155–79.
53. Gee M, Williams DO. Effect of lung inflation on perivascular cuff fluid volume in isolated dog lung lobes. Microvasc Res 1979;17:192–201.
54. Conhaim RL, Lai-Fook SJ, Staub NC. Sequence of perivascular liquid accumulation in liquid-inflated dog lung lobes. J Appl Physiol 1986;60:513–20.
55. Vassilyadi M, Michel RP. Pattern of fluid accumulation in NO2-induced pulmonary edema in dogs. A morphometric study. Am J Pathol 1988;130:10–21.
56. Mitzner W, Sylvester JT. Lymph flow and lung weight in isolated sheep lungs. J Appl Physiol 1986;61:1830–5.
57. Pine M, Beach P, Cottrell T, et al. The relationship between right duct lymph flow and extravascular lung water in dogs given a-naphthylthiourea. J Clin Invest 1976;58:482–92.
58. Conhaim RL. Airway level at which edema liquid enters the air space of isolated dog lungs. J Appl Physiol 1989;67:2234–42.
59. Gordon RE, Case BW, Kleinerman J. Acute NO2 affects penetration and transport of horseradish peroxidase in hamster respiratory epithelium. Am Rev Respir Dis 1983; 128:528–33.
60. Matthay MA, Folkesson HG, Clerici C. Lung epithelial fluid transport and the resolution of pulmonary edema. Physiol Rev 2002;82:569–600.
61. Sakuma T, Pittet JF, Jayr C, Matthay MA. Alveolar liquid and protein clearance in the absence of blood flow or ventilation in sheep. J Appl Physiol 1993;74:176–85.
62. Iancu DM, Zwikler MP, Michel RP. Distribution of alveolar edema in ventilated and unventilated canine lung lobes. Invest Radiol 1996;31:423–32.
63. Folkesson HG, Matthay MA, Westrom BR, et al. Alveolar epithelial clearance of protein. J Appl Physiol 1996;80: 1431–45.
64. Verghese GM, Ware LB, Matthay BA, Matthay MA. Alveolar epithelial fluid transport and the resolution of clinically severe hydrostatic pulmonary edema. J Appl Physiol 1999; 87:1301–12.
65. Ware LB, Matthay MA. Alveolar fluid clearance is impaired in the majority of patients with acute lung injury and the acute respiratory distress syndrome. Am J Respir Crit Care Med 2001;163:1376–83.
66. Levy D, Kenchaiah S, Larson MG, et al. Long-term trends in the incidence of and survival with heart failure. N Engl J Med 2002;347:1397–402.
67. Lloyd-Jones DM, Larson MG, Leip EP, et al. Lifetime risk for developing congestive heart failure: the Framingham Heart Study. Circulation 2002;106:3068–72.
68. Lloyd-Jones DM. The risk of congestive heart failure: sobering lessons from the Framingham Heart Study. Curr Cardiol Rep 2001;3:184–90.
69. Yu PN. Lung water in congestive heart failure. Mod Concepts Cardiovasc Dis 1971;40:27–32.
70. Gabel JC, Drake RE. Increased venous pressure causes increased thoracic duct pressure in awake sheep. J Appl Physiol 1992;73:654–6.
71. Drake RE, Dhother S, Teague RA, Gabel JC. Lymph flow in sheep with rapid cardiac ventricular pacing. Am J Physiol 1997;272:R1595–8.
72. Allen SJ, Drake RE, Laine GA, Gabel JC. Effect of thoracic duct drainage on hydrostatic pulmonary edema and pleural effusion in sheep. J Appl Physiol 1991;71:314–6.
73. Kerley P. Cardiac failure. In: Shank SC, Kerley P, editors. A textbook of x-ray diagnosis. London: Lewis; 1962. p. 97–108.
74. Heitzman ER, Ziter FMJ. Acute interstitial pulmonary edema. AJR Am J Roentgenol 1966;98:291–9.

75. Huchon GJ, Hopewell PC, Murray JF. Interactions between permeability and hydrostatic pressure in perfused dogs' lungs. J Appl Physiol 1981;50:905–11.
76. Bachofen H, Schurch S, Michel RP, Weibel ER. Experimental hydrostatic pulmonary edema in rabbit lungs. Morphology. Am Rev Respir Dis 1993;147:989–96.
77. DeFouw DO. Morphologic study of the alveolar septa in normal and edematous isolated dog lungs fixed by vascular perfusion. Lab Invest 1980;42:413–9.
78. DeFouw DO, Cua WO, Chinard FP. Morphometric and physiological studies of alveolar microvessels in dog lungs in vivo after sustained increases in pulmonary microvascular pressures and after sustained decreases in plasma oncotic pressures. Microvasc Res 1983;25:56–67.
79. Bachofen H, Schurch S, Weibel ER. Experimental hydrostatic pulmonary edema in rabbit lungs. Barrier lesions. Am Rev Respir Dis 1993;147:997–1004.
80. Townsley MI, Fu Z, Mathieu-Costello O, West JB. Pulmonary microvascular permeability. Responses to high vascular pressure after induction of pacing-induced heart failure in dogs. Circ Res 1995;77:317–25.
81. West JB, Mathieu-Costello O. Structure, strength, failure, and remodeling of the pulmonary blood–gas barrier. Annu Rev Physiol 1999;61:543–72.
82. Steinberg KP, Hudson LD. Acute lung injury and acute respiratory distress syndrome. The clinical syndrome. Clin Chest Med 2000;21:401–17.
83. The Acute Respiratory Distress Syndrome Network. Ventilation with lower tidal volumes as compared with traditional tidal volumes for acute lung injury and the acute respiratory distress syndrome. N Engl J Med 2000;342:1301–8.
84. Goss CH, Browser RG, Hudson LD, Rubenfeld GD. Incidence of acute lung injury in the United States. Crit Care Med 2003;31:1607–11.
85. Rubenfeld GD, Caldwell E, Granton J, et al. Interobserver variability in applying a radiographic definition for ARDS. Chest 1999;116:1347–53.
86. Patel SR, Karmpaliotis D, Ayas NT, et al. The role of open lung biopsy in the acute respiratory distress syndrome. Chest 2004;125:197–202.
87. Ware LB, Conner ER, Matthay MA. von Willebrand factor antigen is an independent marker of poor outcome in patients with early acute lung injury. Crit Care Med 2001;29: 2325–31.
88. Orfanos SE, Armaganidis A, Glynos C, et al. Pulmonary capillary endothelium-bound angiotensin-converting enzyme activity in acute lung injury. Circulation 2000;102: 2011–8.
89. Pepe PE, Potkin RT, Holtman D, Carrico CJ. Clinical predictors of the adult respiratory distress syndrome. Am J Surg 1982; 144:124–30.
90. Fowler AA, Hamman RF, Good JT, et al. Adult respiratory distress syndrome: risk with common predispositions. Ann Intern Med 1983;98:593–7.
91. Hudson LD, Milberg JA, Anardi D, Maunder RJ. Clinical risks for development of the acute respiratory distress syndrome. Am J Respir Crit Care Med 1995;151:293–301.
92. Hudson LD, Steinberg KP. Epidemiology of acute lung injury and ARDS. Chest 1999;116(1 Suppl):74S–82S.
93. Montgomery AB, Stager MA, Carrico CJ, Hudson LD. Causes of mortality in patients with the adult respiratory distress syndrome. Am Rev Respir Dis 1985;132:485–9.
94. Anzueto A, Baughman RP, Guntupalli KK, et al. Aerosolized surfactant in adults with sepsis-induced acute respiratory distress syndrome. Exosurf Acute Respiratory Distress Syndrome Sepsis Study Group. N Engl J Med 1996;334: 1417–21.
95. Estenssoro E, Dubin A, Laffaire E, et al. Incidence, clinical course, and outcome in 217 patients with acute respiratory distress syndrome. Crit Care Med 2002;30:2450–6.
96. Monchi M, Bellenfant F, Cariou A, et al. Early predictive factors of survival in the acute respiratory distress syndrome. A multivariate analysis. Am J Respir Crit Care Med 1998;158: 1076–81.
97. Nuckton TJ, Alonso JA, Kallet RH, et al. Pulmonary dead-space fraction as a risk factor for death in the acute respiratory distress syndrome. N Engl J Med 2002;346:1281–6.
98. Atabai K, Ancukiewicz M, Malhotra A, et al. Increasing hematocrit (Hct) levels are associated with increased mortality in patients with acute lung injury (ALI). Am J Respir Crit Care Med 2003;167:A739.
99. Gong MN, Thompson BT, Pothier L, Christiani DC. Mortality in ARDS: potential role of red cell transfusion. Am J Respir Crit Care Med 2003;167:A739.
100. Hebert PC, Wells G, Blajchman MA, et al. A multicenter, randomized, controlled clinical trial of transfusion requirements in critical care. Transfusion Requirements in Critical Care Investigators, Canadian Critical Care Trials Group. N Engl J Med 1999;340:409–17.
101. Montaner JS, Tsang J, Evans KG, et al. Alveolar epithelial damage. A critical difference between high pressure and oleic acid-induced low pressure pulmonary edema. J Clin Invest 1986;77:1786–96.
102. Moore FA, Moore EE, Read RA. Postinjury multiple organ failure: role of extrathoracic injury and sepsis in adult respiratory distress syndrome. New Horiz 1993;1:538–49.
103. Meyrick B, Brigham KL. Acute effects of *Escherichia coli* endotoxin on the pulmonary microcirculation of anesthetized sheep structure:function relationships. Lab Invest 1983;48: 458–70.
104. Meyrick BO, Ryan US, Brigham KL. Direct effects of *E coli* endotoxin on structure and permeability of pulmonary endothelial monolayers and the endothelial layer of intimal explants. Am J Pathol 1986;122:140–51.
105. Meyrick B, Berry LC Jr, Christman BW. Response of cultured human pulmonary artery endothelial cells to endotoxin. Am J Physiol 1995;268:L239–44.
106. Meyrick B, Hoover R, Jones MR, et al. In vitro effects of endotoxin on bovine and sheep lung microvascular and pulmonary artery endothelial cells. J Cell Physiol 1989;138: 165–74.
107. Hamacher J, Lucas R, Lijnen HR, et al. Tumor necrosis factor-alpha and angiostatin are mediators of endothelial cytotoxicity in bronchoalveolar lavages of patients with acute respiratory distress syndrome. Am J Respir Crit Care Med 2002;166:651–6.
108. Langleben D, DeMarchie M, Laporta D, et al. Endothelin-1 in acute lung injury and the adult respiratory distress syndrome. Am Rev Respir Dis 1993;148:1646–50.
109. Fagan KA, McMurtry IF, Rodman DM. Role of endothelin-1 in lung disease. Respir Res 2001;2:90–101.
110. Albertine KH, Wang ZM, Michael JR. Expression of endothelial nitric oxide synthase, inducible nitric oxide synthase, and endothelin-1 in lungs of subjects who died with ARDS. Chest 1999;116(1 Suppl):101S–2S.
111. Pittet JF, Mackersie RC, Martin TR, Matthay MA. Biological markers of acute lung injury: prognostic and pathogenetic significance. Am J Respir Crit Care Med 1997;155: 1187–205.
112. Zimmerman GA, Albertine KH, Carveth HJ, et al. Endothelial activation in ARDS. Chest 1999;116:18S–24S.
113. Muller AM, Cronen C, Muller KM, Kirkpatrick CJ. Heterogeneous expression of cell adhesion molecules by endothelial cells in ARDS. J Pathol 2002;198:270–5.

114. Lai KN, Leung JC, Metz CN, et al. Role for macrophage migration inhibitory factor in acute respiratory distress syndrome. J Pathol 2003;199:496–508.
115. Idell S. Endothelium and disordered fibrin turnover in the injured lung: newly recognized pathways. Crit Care Med 2002;30(5 Suppl):S274–80.
116. Bernard GR, Vincent JL, Laterre PF, et al. Recombinant human protein CWEiSSsg. Efficacy and safety of recombinant human activated protein C for severe sepsis. N Engl J Med 2001;344:699–709.
117. Ware LB, Fang X, Matthay MA. Protein C and thrombomodulin in human acute lung injury. Am J Physiol 2003;285:L514–21.
118. Prabhakaran P, Ware LB, White KE, et al. Elevated levels of plasminogen activator inhibitor-1 in pulmonary edema fluid are associated with mortality in acute lung injury. Am J Physiol 2003;285:L20–8.
119. Manzo ND, Waxman AB. Pathogenesis of acute lung injury. Experimental studies. In: Matthay MA, editor. Acute respiratory distress syndrome. New York: Marcel Dekker; 2003. p. 115–46.
120. Moss M, Gillespie MK, Ackerson L, et al. Endothelial cell activity varies in patients at risk for the adult respiratory distress syndrome. Crit Care Med 1996;24:1782–6.
121. Aird WC. The role of the endothelium in severe sepsis and multiple organ dysfunction syndrome. Blood 2003;101: 3765–77.
122. Bachofen M, Bachofen H, Weibel ER. Lung edema in the adult respiratory distress syndrome. In: Fishman AP, Renkin EM, editors. Pulmonary edema. Bethesda (MD): American Physiological Society; 1979. p. 241–52.
123. Lee WL, Downey GP. Neutrophil activation and acute lung injury. Curr Opin Crit Care 2001;7:1–7.
124. Martin TR, Pistorese BP, Hudson LD, Maunder RJ. The function of lung and blood neutrophils in patients with the adult respiratory distress syndrome. Implications for the pathogenesis of lung infections. Am Rev Respir Dis 1991;144: 254–62.
125. Fowler AA, Hyers TM, Fisher BJ, et al. The adult respiratory distress syndrome. Cell populations and soluble mediators in the air spaces of patients at high risk. Am Rev Respir Dis 1987;136:1225–31.
126. Steinberg KP, Milberg JA, Martin TR, et al. Evolution of bronchoalveolar cell populations in the adult respiratory distress syndrome. Am J Respir Crit Care Med 1994;150: 113–22.
127. Tamura DY, Moore EE, Partrick DA, et al. Acute hypoxemia in humans enhances the neutrophil inflammatory response. Shock 2002;17:269–73.
128. Lee WL, Downey GP. Leukocyte elastase: physiological functions and role in acute lung injury. Am J Respir Crit Care Med 2001;164:896–904.
129. Doerschuk CM. Neutrophil rheology and transit through capillaries and sinusoids. Am J Respir Crit Care Med 1999;159:1693–5.
130. Gee MH, Albertine KH. Neutrophil–endothelial cell interactions in the lung. Annu Rev Physiol 1993;55:227–48.
131. Chollet-Martin S, Jourdain B, Gibert C, et al. Interactions between neutrophils and cytokines in blood and alveolar spaces during ARDS. Am J Respir Crit Care Med 1996;154: 594–601.
132. Delclaux C, Delacourt C, D'Ortho MP, et al. Role of gelatinase B and elastase in human polymorphonuclear neutrophil migration across basement membrane. Am J Respir Cell Mol Biol 1996;14:288–95.
133. Delclaux C, D'Ortho MP, Delacourt C, et al. Gelatinases in epithelial lining fluid of patients with adult respiratory distress syndrome. Am J Physiol 1997;272:L442–51.
134. Matute-Bello G, Liles WC, Radella F, et al. Modulation of neutrophil apoptosis by granulocyte colony-stimulating factor and granulocyte/macrophage colony-stimulating factor during the course of acute respiratory distress syndrome. Crit Care Med 2000;28:1–7.
135. Nelson S, Belknap SM, Carlson RW. A randomized controlled trial of filgrastim as an adjunct to antibiotics for treatment of hospitalized patients with community-acquired pneumonia. J Infect Dis 1998;178:1075–80.
136. Abraham E. What role does neutrophil apoptosis play in acute respiratory distress syndrome? Crit Care Med 2000;28: 253–4.
137. Ognibene FP, Martin SE, Parker MM. Adult respiratory distress syndrome in patients with severe neutropenia. N Engl J Med 1986;315:547–51.
138. Martin TR, Pistorese BP, Chi EY, et al. Effects of leukotriene B4 in the human lung. J Clin Invest 1989;84:1609–19.
139. Wiener-Kronish JP, Albertine KH, Matthay MA. Differential responses of the endothelial and epithelial barriers of the lung in sheep to E*scherichia coli* endotoxin. J Clin Invest 1991;88:864–75.
140. Zimmerman GA, Albertine KH, McIntyre TM. Pathogenesis of sepsis and septic-induced lung injury. In: Matthay MA, editor. Acute respiratory distress syndrome. New York: Marcel Dekker; 2003. p. 245–87.
141. Rosseau S, Hammerl P, Maus U, et al. Phenotypic characterization of alveolar monocyte recruitment in acute respiratory distress syndrome. Am J Physiol 2000;279:L25–35.
142. Meduri GU, Headley S, Tolley E, et al. Plasma and BAL cytokine response to corticosteroid rescue treatment in late ARDS. Chest 1995;108:1315–25.
143. Schwartz MD, Moore EE, Moore FA, et al. Nuclear factor-kappa B is activated in alveolar macrophages from patients with acute respiratory distress syndrome. Crit Care Med 1996;24:1285–92.
144. Baeuerle PA, Henkel T. Function and activation of NF-kappa B in the immune system. Annu Rev Immunol 1994;12: 141–79.
145. Bucala R. MIF rediscovered: cytokine, pituitary hormone, and glucocorticoid-induced regulator of the immune response. FASEB J 1996;10:1607–13.
146. Donnelly SC, Haslett C, Reid PT, et al. Regulatory role for macrophage migration inhibitory factor in acute respiratory distress syndrome. Nat Med 1997;3:320–3.
147. Lasky JA, Brody AR. Interstitial fibrosis and growth factors. Environ Health Perspect 2000;108 Suppl 4:751–62.
148. Krein PM, Sabatini PJ, Tinmouth W, et al. Localization of insulin-like growth factor-I in lung tissues of patients with fibroproliferative acute respiratory distress syndrome. Am J Respir Crit Care Med 2003;167:83–90.
149. West MA, Heagy W. Endotoxin tolerance: a review. Crit Care Med 2002;30:S64–73.
150. Bone RC. Sir Isaac Newton, sepsis, SIRS, and CARS. Crit Care Med 1996;24:1125–8.
151. Bardales RH, Xie SS, Schaefer RF, Hsu SM. Apoptosis is a major pathway responsible for the resolution of type II pneumocytes in acute lung injury. Am J Pathol 1996;149:845–52.
152. Guinee D Jr, Brambilla E, Fleming M, et al. The potential role of BAX and BCL-2 expression in diffuse alveolar damage. Am J Pathol 1997;151:999–1007.
153. Adamson A, Perkins S, Brambilla E, et al. Proliferation, C-myc, and cyclin D1 expression in diffuse alveolar damage: potential roles in pathogenesis and implications for prognosis. Hum Pathol 1999;30:1050–7.
154. Pittet JF, Brenner TJ, Modelska K, Matthay MA. Alveolar liquid clearance is increased by endogenous catecholamines in hemorrhagic shock in rats. J Appl Physiol 1996;81:830–7.

155. Miller EJ, Cohen AB, Matthay MA. Increased interleukin-8 concentrations in the pulmonary edema fluid of patients with acute respiratory distress syndrome from sepsis. Crit Care Med 1996;24:1448–54.
156. Suter PM, Suter S, Girardin E, et al. High bronchoalveolar levels of tumor necrosis factor and its inhibitors, interleukin-1, interferon, and elastase, in patients with adult respiratory distress syndrome after trauma, shock, or sepsis. Am Rev Respir Dis 1992;145:1016–22.
157. Meduri GU, Kohler G, Headley S, et al. Inflammatory cytokines in the BAL of patients with ARDS. Persistent elevation over time predicts poor outcome. Chest 1995;108:1303–14.
158. Park WY, Goodman RB, Steinberg KP, et al. Cytokine balance in the lungs of patients with acute respiratory distress syndrome. Am J Respir Crit Care Med 2001;164:1896–903.
159. Donnelly SC, Strieter RM, Reid PT, et al. The association between mortality rates and decreased concentrations of interleukin-10 and interleukin-1 receptor antagonist in the lung fluids of patients with the adult respiratory distress syndrome. Ann Intern Med 1996;125:191–6.
160. Donnelly SC, Strieter RM, Kunkel SL, et al. Interleukin-8 and development of adult respiratory distress syndrome in at-risk patient groups. Lancet 1993;341:643–7.
161. Hirani N, Antonicelli F, Strieter RM, et al. The regulation of interleukin-8 by hypoxia in human macrophages—a potential role in the pathogenesis of the acute respiratory distress syndrome (ARDS). Mol Med 2001;7:685–97.
162. Kurdowska A, Miller EJ, Noble JM, et al. Anti-IL-8 autoantibodies in alveolar fluid from patients with the adult respiratory distress syndrome. J Immunol 1996;157:2699–706.
163. Kurdowska A, Noble JM, Grant IS, et al. Anti-interleukin-8 autoantibodies in patients at risk for acute respiratory distress syndrome. Crit Care Med 2002;30:2335–7.
164. Liaudet L, Pacher P, Mabley JG, et al. Activation of poly(ADP-ribose) polymerase-1 is a central mechanism of lipopolysaccharide-induced acute lung inflammation. Am J Respir Crit Care Med 2002;165:372–7.
165. Pratt PC, Vollmer RT, Shelburne JD, Crapo JD. Pulmonary morphology in a multihospital collaborative extracorporeal membrane oxygenation project. I. Light microscopy. Am J Pathol 1979;95:191–214.
166. Travis WD, Colby TV, Koss MN, et al. Non-neoplastic disorders of the lower respiratory tract. Washington, DC: American Registry of Pathology and Armed Forces Institute of Pathology; 2002.
167. Tomashefski JF Jr. Pulmonary pathology of acute respiratory distress syndrome. Clin Chest Med 2000;21:435–66.
168. Tomashefski JF Jr, Davies P, Boggis C, et al. The pulmonary vascular lesions of the adult respiratory distress syndrome. Am J Pathol 1983;112:112–26.
169. Albertine KH. Ultrastructural abnormalities in increased-permeability pulmonary edema. Clin Chest Med 1985;6:345–69.
170. Kobashi Y, Manabe T. The fibrosing process in so-called organized diffuse alveolar damage. An immunohistochemical study of the change from hyaline membrane to membranous fibrosis. Virchows Arch A Pathol Anat Histopathol 1993;422:47–52.
171. Fukuda Y, Ishizaki M, Masuda Y, et al. The role of intraalveolar fibrosis in the process of pulmonary structural remodeling in patients with diffuse alveolar damage. Am J Pathol 1987;126:171–82.
172. Ware LB. Severe acute respiratory syndrome. In: Matthay MA, editor. Acute respiratory distress syndrome. New York: Marcel Dekker; 2003. p. 633–44.
173. Snow RL, Davies P, Pontoppidan H, et al. Pulmonary vascular remodeling in adult respiratory distress syndrome. Am Rev Respir Dis 1982;126:887–92.
174. Goodman PC. Radiographic findings in patients with acute respiratory distress syndrome. Clin Chest Med 2000;21:419–33.
175. Pelosi P, Brazzi L, Gattinoni L. Prone position in acute respiratory distress syndrome. Eur Respir J 2002;20:1017–28.
176. Desai SR, Wells AU, Rubens MB, et al. Acute respiratory distress syndrome: CT abnormalities at long-term follow-up. Radiology 1999;210:29–35.
177. Frank JA, Imai Y, Slutsky AS. Pathogenesis of ventilator-induced lung injury. In: Matthay MA, editor. Acute respiratory distress syndrome. New York: Marcel Dekker; 2003. p. 201–44.
178. Webb HH, Tierney DF. Experimental pulmonary edema due to intermittent positive pressure ventilation with high inflation pressures. Protection by positive end-expiratory pressure. Am Rev Respir Dis 1974;110:556–65.
179. Kolobow T, Moretti MP, Fumagalli R, et al. Severe impairment in lung function induced by high peak airway pressure during mechanical ventilation. An experimental study. Am Rev Respir Dis 1987;135:312–5.
180. Tsuno K, Miura K, Takeya M, et al. Histopathologic pulmonary changes from mechanical ventilation at high peak airway pressures. Am Rev Respir Dis 1991;143:1115–20.
181. Hernandez LA, Peevy KJ, Moise AA, Parker JC. Chest wall restriction limits high airway pressure-induced lung injury in young rabbits. J Appl Physiol 1989;66:2364–8.
182. Dreyfuss D, Soler P, Basset G, Saumon G. High inflation pressure pulmonary edema. Respective effects of high airway pressure, high tidal volume, and positive end-expiratory pressure. Am Rev Respir Dis 1988;137:1159–64.
183. Dreyfuss D, Saumon G. Role of tidal volume, FRC, and end-inspiratory volume in the development of pulmonary edema following mechanical ventilation. Am Rev Respir Dis 1993;148:1194–203.
184. Broccard AF, Hotchkiss JR, Suzuki S, et al. Effects of mean airway pressure and tidal excursion on lung injury induced by mechanical ventilation in an isolated perfused rabbit lung model. Crit Care Med 1999;27:1533–41.
185. Broccard AF, Hotchkiss JR, Kuwayama N, et al. Consequences of vascular flow on lung injury induced by mechanical ventilation. Am J Respir Crit Care Med 1998;157:1935–42.
186. West JB. Pulmonary capillary stress failure. J Appl Physiol 2000;89:2483–9.
187. Muscedere JG, Mullen JB, Gan K, Slutsky AS. Tidal ventilation at low airway pressures can augment lung injury. Am J Respir Crit Care Med 1994;149:1327–34.
188. Brochard L, Roudot-Thoraval F, Roupie E, et al. Tidal volume reduction for prevention of ventilator-induced lung injury in acute respiratory distress syndrome. The Multicenter Trial Group on Tidal Volume reduction in ARDS. Am J Respir Crit Care Med 1998;158:1831–8.
189. Amato MB, Barbas CS, Medeiros DM, et al. Effect of a protective-ventilation strategy on mortality in the acute respiratory distress syndrome. N Engl J Med 1998;338:347–54.
190. Brower RG, Shanholtz CB, Fessler HE, et al. Prospective, randomized, controlled clinical trial comparing traditional versus reduced tidal volume ventilation in acute respiratory distress syndrome patients. Crit Care Med 1999;27:1492–8.
191. Stewart TE, Meade MO, Cook DJ, et al. Evaluation of a ventilation strategy to prevent barotrauma in patients at high risk for acute respiratory distress syndrome. N Engl J Med 1998;338:355–61.
192. Tremblay LN, Miatto D, Hamid Q, et al. Injurious ventilation induces widespread pulmonary epithelial expression of tumor necrosis factor-alpha and interleukin-6 messenger RNA. Crit Care Med 2002;30:1693–700.

193. Tremblay L, Valenza F, Ribeiro SP, et al. Injurious ventilatory strategies increase cytokines and *c-fos* m-RNA expression in an isolated rat lung model. J Clin Invest 1997;99:944–52.
194. Zhang H, Downey GP, Suter PM, et al. Conventional mechanical ventilation is associated with bronchoalveolar lavage-induced activation of polymorphonuclear leukocytes: a possible mechanism to explain the systemic consequences of ventilator-induced lung injury in patients with ARDS. Anesthesiology 2002;97:1426–33.
195. Ranieri VM, Suter PM, Tortorella C, et al. Effect of mechanical ventilation on inflammatory mediators in patients with acute respiratory distress syndrome: a randomized controlled trial. JAMA 1999;282:54–61.
196. Laffey JG, Engelberts D, Kavanagh BP. Buffering hypercapnic acidosis worsens acute lung injury. Am J Respir Crit Care Med 2000;161:141–6.
197. Laffey JG, Engelberts D, Kavanagh BP. Injurious effects of hypocapnic alkalosis in the isolated lung. Am J Respir Crit Care Med 2000;162:399–405.
198. Murray JF, Matthay MA, Luce JM, Flick MR. An expanded definition of the adult respiratory distress syndrome. Am Rev Respir Dis 1988;138:720–3.
199. Slutsky AS. Mechanical ventilation. American College of Chest Physicians' Consensus Conference. Chest1993;104:1833–59.
200. Gattinoni L, D'Andrea L, Pelosi P, et al. Regional effects and mechanism of positive end-expiratory pressure in early adult respiratory distress syndrome. JAMA 1993;269: 2122–7.
201. Dantzker DR, Brook CJ, Dehart P, et al. Ventilation–perfusion distributions in the adult respiratory distress syndrome. Am Rev Respir Dis 1979;120:1039–52.
202. Amato MB, Barbas CS, Medeiros DM, et al. Beneficial effects of the "open lung approach" with low distending pressures in acute respiratory distress syndrome. A prospective randomized study on mechanical ventilation. Am J Respir Crit Care Med 1995;152:1835–46.
203. Mehta S, Stewart TE, MacDonald R, et al. Temporal change, reproducibility, and interobserver variability in pressure–volume curves in adults with acute lung injury and acute respiratory distress syndrome. Crit Care Med 2003;31: 2118–25.
204. Ranieri VM, Eissa NT, Corbeil C, et al. Effects of positive end-expiratory pressure on alveolar recruitment and gas exchange in patients with the adult respiratory distress syndrome. Am Rev Respir Dis 1991;144:544–51.
205. Hopewell PC. Failure of positive end-expiratory pressure to decrease lung water content in alloxan-induced pulmonary edema. Am Rev Respir Dis 1979;120:813–9.
206. Richard JC, Maggiore SM, Jonson B, et al. Influence of tidal volume on alveolar recruitment. Respective role of PEEP and a recruitment maneuver. Am J Respir Crit Care Med 2001; 163:1609–13.
207. Moran I, Zavala E, Fernandez R, et al. Recruitment manoeuvres in acute lung injury and acute respiratory distress syndrome. Eur Respir J 2003;42 Suppl:37S–42S.
208. Huang CC, Shih MJ, Tsai YH, et al. Effects of inverse ratio ventilation versus positive end-expiratory pressure on gas exchange and gastric intramucosal PCO(2) and pH under constant mean airway pressure in acute respiratory distress syndrome. Anesthesiology 2001;95:1182–8.
209. Abraham E, Yoshihara G. Cardiorespiratory effects of pressure controlled inverse ratio ventilation in severe respiratory failure. Chest 1989;96:1356–9.
210. Wiedemann HP. Partial liquid ventilation for acute respiratory distress syndrome. Clin Chest Med 2000;21:543–54.
211. Mehta S, Lapinsky SE, Hallett DC, et al. Prospective trial of high-frequency oscillation in adults with acute respiratory distress syndrome. Crit Care Med 2001;29:1360–9.
212. Derdak S, Mehta S, Stewart TE, et al. High-frequency oscillatory ventilation for acute respiratory distress syndrome in adults: a randomized, controlled trial. Am J Respir Crit Care Med 2002;166:801–8.
213. Moreno F, Lyons HA. Effect of body posture on lung volumes. J Appl Physiol 1961;16:27–9.
214. Albert RK. Prone ventilation. Clin Chest Med 2000;21:511–17.
215. Albert RK, Leasa D, Sanderson M, et al. The prone position improves arterial oxygenation and reduces shunt in oleic-acid-induced acute lung injury. Am Rev Respir Dis 1987; 135:628–33.
216. Gattinoni L, Tognoni G, Pesenti A, et al. Effect of prone positioning on the survival of patients with acute respiratory failure. N Engl J Med 2001;345:568–73.
217. Mancebo J, Rialp G, Fernandez R, et al. Prone vs supine position in ARDS patients. Results of a randomized multicenter trial. Am J Respir Crit Care Med 2003;167:A180.
218. Payen DM. Inhaled nitric oxide and acute lung injury. Clin Chest Med 2000;21:519–29.
219. Rossaint R, Falke KJ, Lopez F, et al. Inhaled nitric oxide for the adult respiratory distress syndrome. N Engl J Med 1993; 328:399–405.
220. Troncy E, Collet JP, Shapiro S, et al. Inhaled nitric oxide in acute respiratory distress syndrome: a pilot randomized controlled study. Am J Respir Crit Care Med 1998;157:1486–8.
221. Dellinger RP, Zimmerman JL, Taylor RW, et al. Effects of inhaled nitric oxide in patients with acute respiratory distress syndrome: results of a randomized phase II trial. Inhaled Nitric Oxide in ARDS Study Group. Crit Care Med 1998;26:15–23.
222. Payen D, Vallet B, Geno A. Results of the French prospective multicentric randomized double blind placebo controlled trial on inhaled nitric oxide in ARDS. Clin Chest Med 2000;21:S166.
223. Lundin S, Mang H, Smithies M, et al. Inhalation of nitric oxide in acute lung injury: results of a European multicentre study. The European Study Group of Inhaled Nitric Oxide. Intensive Care Med 1999;25:911–9.
224. Gerlach H, Keh D, Semmerow A, et al. Dose–response characteristics during long-term inhalation of nitric oxide in patients with severe acute respiratory distress syndrome: a prospective, randomized, controlled study. Am J Respir Crit Care Med 2003;167:1008–15.
225. Spragg RG. Acute respiratory distress syndrome. Surfactant replacement therapy. Clin Chest Med 2000;21:531–41.
226. Lewis JF, Brackenbury A. Role of exogenous surfactant in acute lung injury. Crit Care Med 2003;31:S324–8.
227. Eichacker PQ, Gerstenberger EP, Banks SM, et al. Meta-analysis of acute lung injury and acute respiratory distress syndrome trials testing low tidal volumes. Am J Respir Crit Care Med 2002;166:1510–4.
228. Hickling KG, Henderson SJ, Jackson R. Low mortality associated with low volume pressure limited ventilation with permissive hypercapnia in severe adult respiratory distress syndrome. Intensive Care Med 1990;16:372–7.
229. Ali J, Chernicki W, Wood LD. Effect of furosemide in canine low-pressure pulmonary edema. J Clin Invest 1979;64:1494–504.
230. Mangialardi RJ, Martin GS, Bernard GR, et al. Hypoproteinemia predicts acute respiratory distress syndrome development, weight gain, and death in patients with sepsis. Ibuprofen in Sepsis Study Group. Crit Care Med 2000;28: 3137–45.
231. Humphrey H, Hall J, Sznajder I, et al. Improved survival in ARDS patients associated with a reduction in pulmonary capillary wedge pressure. Chest 1990;97:1176–80.
232. Mitchell JP, Schuller D, Calandrino FS, Schuster DP. Improved outcome based on fluid management in critically ill patients requiring pulmonary artery catheterization. Am Rev Respir Dis 1992;145:990–8.

233. Martin GS. Fluid balance and colloid osmotic pressure in acute respiratory failure: emerging clinical evidence. Crit Care 2000;4 Suppl 2:S21–5.
234. Bernard GR, Luce JM, Sprung CL, et al. High-dose corticosteroids in patients with the adult respiratory distress syndrome. N Engl J Med 1987;317:1565–70.
235. Meduri GU, Headley AS, Golden E, et al. Effect of prolonged methylprednisolone therapy in unresolving acute respiratory distress syndrome: a randomized controlled trial. JAMA 1998;280:159–65.
236. Bernard GR, Wheeler AP, Arons MM, et al. A trial of antioxidants N-acetylcysteine and procysteine in ARDS. The Antioxidant in ARDS Study Group. Chest 1997;112:164–72.
237. Suter PM, Domenighetti G, Schaller MD, et al. N-Acetylcysteine enhances recovery from acute lung injury in man. A randomized, double-blind, placebo-controlled clinical study. Chest 1994;105:190–4.
238. Hultgren HN. High-altitude pulmonary edema. In: Matthay MA, Ingbar DH, editors. Pulmonary edema. New York: Marcel Dekker; 1998. p. 355–78.
239. Scherrer U, Sartori C, Lepori M, et al. High-altitude pulmonary edema: from exaggerated pulmonary hypertension to a defect in transepithelial sodium transport. Adv Exp Med Biol 1999;474:93–107.
240. Hackett PH, Roach RC. High-altitude illness. N Engl J Med 2001;345:107–14.
241. Gabry AL, Ledoux X, Mozziconacci M, Martin C. High-altitude pulmonary edema at moderate altitude (<2,400 m; 7,870 feet): a series of 52 patients. Chest 2003;123:49–53.
242. Hackett P, Oelz O. The Lake Louise Consensus of the definition and quantification of altitude sickness. In: Sutton J, Coates G, Houston C, editors. Hypoxia and mountain medicine. Burlington, VT: Queen City Printers; 1992. p. 327–30.
243. Maggiorini M, Melot C, Pierre S, et al. High-altitude pulmonary edema is initially caused by an increase in capillary pressure. Circulation 2001;103:2078–83.
244. Busch T, Bartsch P, Pappert D, et al. Hypoxia decreases exhaled nitric oxide in mountaineers susceptible to high-altitude pulmonary edema. Am J Respir Crit Care Med 2001;163:368–73.
245. Duplain H, Vollenweider L, Delabays A, et al. Augmented sympathetic activation during short-term hypoxia and high-altitude exposure in subjects susceptible to high-altitude pulmonary edema. Circulation 1999;99:1713–8.
246. Droma Y, Hanaoka M, Ota M, et al. Positive association of the endothelial nitric oxide synthase gene polymorphisms with high-altitude pulmonary edema. Circulation 2002;106:826–30.
247. Sarnoff SJ, Sarnoff LC. Neurohemodynamics of pulmonary edema. II. The role of sympathetic pathways in the elevation of pulmonary and systemic vascular pressures following the intracistrenal injection of fibrin. Circulation 1952;6:51–62.
248. Maron MB, Pilati CF. Neurogenic pulmonary edema. In: Matthay MA, Ingbar DH, editors. Pulmonary edema. New York: Marcel Dekker; 1998. p. 319–54.
249. Smith WS, Matthay MA. Evidence for a hydrostatic mechanism in human neurogenic pulmonary edema. Chest 1997;111:1326–33.
250. Weidner WJ, Jones TA, Townsley MI, DeFouw DO. Ultrastructural analysis of sheep lungs after increased intracranial pressure and development of pulmonary edema. Microcirc Endothelium Lymphatics 1986;3:397–410.
251. Marshall RP. Genetic factors in acute lung injury. In: Matthay MA, editor. Acute respiratory distress syndrome. New York: Marcel Dekker; 2003. p. 355–82.
252. Brower RG, Fessler HE. Mechanical ventilation in acute lung injury and acute respiratory distress syndrome. Clin Chest Med 2000;21:491–510.
253. Tomashefski JF Jr. Pulmonary pathology of the acute respiratory distress syndrome. Diffuse alveolar damage. In: Matthay MA, editor. Acute respiratory distress syndrome. New York: Marcel Dekker; 2003. p. 75–114.
254. DeFouw DO. Structural heterogeneity within the pulmonary microcirculation of the normal rat. Anat Rec 1988;221:645–54.
255. Lamm WJ, Graham MM, Albert RK. Mechanism by which the prone position improves oxygenation in acute lung injury. Am J Respir Crit Care Med 1994;150:184–93.
256. Ingbar DH. Mechanisms of repair and remodeling following acute lung injury. Clin Chest Med 2000;21:589–616.
257. Abraham E, Matthay MA, Dinarello CA, et al. Consensus conference definitions for sepsis, septic shock, acute lung injury, and acute respiratory distress syndrome: time for a reevaluation. Crit Care Med 2000;28:232–5.
258. Jaffe ES, Harris NL, Stein H, Vardiman JW. Pathology and genetics of tumours of haematopoietic and lymphoid tissues. Lyon: IARC Press; 2001.
259. Murray JF. The adult respiratory distress syndrome (may it rest in peace). Am Rev Respir Dis 1975;111:716–8.
260. Matthay MA. Acute lung injury. Recent progress and promising directions for future research. In: Matthay MA, editor. Acute respiratory distress syndrome. New York: Marcel Dekker; 2003. p. 645–53.
261. Matthay MA, Zimmerman GA, Esmon C, et al. Future research directions in acute lung injury. Summary of a National Heart, Lung, and Blood Institute Working Group. Am J Respir Crit Care Med 2003;167:1027–35.
262. Poppas A, Rounds S. Congestive heart failure. Am J Respir Crit Care Med 2002;165:4–8.
263. Lesur O, Berthiaume Y, Blaise G, et al. Acute respiratory distress syndrome: 30 years later. Can Respir J 1999;6:71–86.
264. Ware LB, Matthay MA. The acute respiratory distress syndrome. N Engl J Med 2000;342:1334–49.

CHAPTER 20

OXYGEN REGULATION OF VASOMOTOR TONE

David Hall, Duncan Stewart, Michael Ward

Hypoxia occurs commonly in patients with cardiopulmonary diseases, patients who are in shock, and normal individuals during ascent to high altitude. The reduction in oxygen tension experienced by both the pulmonary and systemic circulations under these conditions elicits changes in vascular tone mediated by local and neurohumoral mechanisms that redistribute bloodflow to enhance pulmonary gas exchange and tissue oxygen extraction,[1] respectively. In addition, both endothelial and smooth muscle phenotypes are determined by their ambient oxygen tensions, and the changes in vascular function that result from altered expression of vasoregulatory enzymes during prolonged hypoxia alter the efficacy of these compensatory responses and hence the ability to preserve tissue oxygenation. Moreover, redox status is an important determinant of cell cycle progression, and many vasoregulatory mediators released in response to hypoxia also modulate vascular cell proliferation and differentiation and so influence vascular structure.

The vascular response to hypoxia varies among vascular beds, and both the pulmonary and systemic circulations are affected. The cells of the ductus arteriosus constitute a special case. These specialized cells must respond rapidly to a change from fetal to mature circulation, heralded by an increase in oxygen tension. The response involves an acute change in vascular smooth muscle tone and subsequent structural remodeling. Knowledge regarding the mechanisms by which the ductus arteriosus senses and responds to altered oxygen tension provides important insights that help us understand the nature of these responses in the pulmonary and systemic circulations.

This chapter reviews current knowledge of the molecular bases for these changes, their impact on pulmonary function in disease states, and the role of the direct effects of hypoxia on the vascular tissues in limiting the capacity of systemic circulatory reflexes to preserve the relationship between tissue oxygen delivery and metabolic demand.

PULMONARY CIRCULATION

Acute Hypoxic Pulmonary Vasoconstriction

Von Euler and Liljestrand[2] first made the observation that both hypercapnic and hypoxic inspired gases increase pulmonary artery pressure without increasing left atrial pressure in anesthetized cats.[2] The recognition of the role that this process may play in certain disease states has subsequently led to a large body of research into the cellular mechanisms by which it is mediated. The adaptive role of hypoxic pulmonary vasoconstriction (HPV) is to match pulmonary capillary perfusion to alveolar oxygen tension so as to reduce ventilation–perfusion mismatch and minimize physiologic shunt and dead space volume. The pathophysiologic consequences may result from either an ineffective or an inappropriately exuberant response. Impairment of the HPV response results in worsening hypoxemia. The converse result may have effects that vary from mild elevation of pulmonary vascular resistance (PVR) to severe pulmonary hypertension and right heart failure, depending on the severity of alveolar hypoxia and the amount of the pulmonary vasculature that is affected.

As a physiologic response, HPV serves to decrease perfusion to hypoxic regions of the lungs. Although most obviously of importance in compensating for regional alterations in ventilation, it serves a similar purpose in the setting of global hypoxia since studies of ventilation and perfusion in individuals living at high altitude indicate that perfusion is more homogeneous than in those who live at sea level.[3] This results from increased perfusion of the better-ventilated lung apices in those individuals living at reduced ambient oxygen tension. Even in normal individuals, this mechanism is active in matching ventilation to perfusion on a breath-by-breath basis since vasodilatory drugs that impair HPV (eg, sublingual nitroglycerine[4]) increase the alveolar–arterial oxygen gradient in subjects without pulmonary disease breathing normoxic gas mixtures.[3] Before birth, when oxygen is supplied via the placenta, the same response maintains a high PVR, diverting blood away from the lungs through the ductus arteriosus to the systemic circulation.

The main locus of HPV is the smaller (60 to 700 μm diameter) distal pulmonary arteries,[5,6] although larger conduit pulmonary arteries and even pulmonary veins are known to respond to hypoxia.[7] The response is graded such that smaller arteries are more sensitive and/or demonstrate a greater response than larger vessels.[8] In vivo, hypoxia causes a monophasic rise in PVR that reaches a sustained plateau

within 20 minutes and falls promptly to normal levels on return to normoxic conditions. The magnitude of the response is inversely related to the alveolar partial pressure of oxygen (PO_2) and is magnified by concurrent acidemia.[9] Although studies addressing this issue are limited, available evidence suggests that reductions in systemic oxygen delivery contribute to the response only to the extent that decreases in the oxygen content of venous blood alter the PO_2 in the alveolar space.[10]

The HPV response persists in isolated pulmonary arteries[11] and therefore involves mechanisms that are intrinsic to the pulmonary vasculature and independent of circulating humoral and neuronal inputs. Differences exist, however, between the in vivo and in vitro responses. For example, HPV can be elicited in intact animals when the alveolar PO_2 falls below 50 to 60 mm Hg, whereas in isolated pulmonary artery preparations, more severe reductions in PO_2 (<40 mm Hg) are required.[7] The magnitude of the response is also greater in vivo and in blood-perfused lungs than during saline perfusion, presumably because reactivity is enhanced by neurohumoral factors that affect the basal level of smooth muscle tone. The monophasic change in PVR seen in intact blood-perfused lungs is replaced, in isolated pulmonary arteries, by a biphasic constrictor response with a transient initial phase superimposed on a more slowly developing but sustained constriction, which has been variably reported to depend on the presence of an intact endothelium.[12,13] Caution is therefore needed in extrapolating mechanistic conclusions drawn from the in vitro studies since these responses are clearly subject to modulation by the effects of superimposed physiologic stimuli. From a clinical perspective, the activation of the HPV response at PO_2 values in the 40 to 60 mm Hg range corresponds well with the observed sensitivity to supplemental oxygen of progression of pulmonary hypertension in patients with hypoxemia. Oxygen therapy is currently indicated for persistent arterial PO_2 values below 55 mm Hg since its use above this range has no effect on long-term outcome. This presumably reflects the negligible contribution of reversible vasoconstriction to the pathophysiology of elevated pulmonary vascular resistance at higher oxygen tensions.

To date, no endothelium-derived factor has been found to be indispensable for HPV; however, several lines of evidence suggest that expression of the full response requires endothelial involvement through the production of substances that modulate hypoxia-induced smooth muscle contraction. The role of the endothelium in facilitating the smooth muscle response to hypoxia could reflect either inhibition of the release of a vasodilator substance or stimulation of the release of a vasoconstrictor. The role of changes in pulmonary endothelial nitric oxide release during hypoxia has been investigated in several studies, and data have been presented to support both an increase and a decrease in nitric oxide production.[14,15] Similarly, evidence both for and against involvement of the prostanoid vasodilator prostacyclin in the pulmonary vascular response to hypoxia has been obtained.[16,17] Such variability suggests that altered release of these mediators is not directly responsible for HPV. Studies of vasoconstrictor agents released from pulmonary endothelial cells during hypoxia have been focused on the role of endothelin-1. Hypoxia increases endothelin-1 production by cultured pulmonary artery endothelial cells,[18] and in isolated lungs[19] and in pulmonary vessels in which HPV has been blocked by endothelial denudation, pretreatment with endothelin-1 restores the response to hypoxia.[20] Conflicting conclusions have been drawn, however, from studies in which endothelin receptor antagonists were used to define its physiologic role. Although in porcine and rat pulmonary arteries,[20,21] antagonists active at the endothelin A receptor have been shown to block HPV, they have had no effect in other studies.[22] These findings, and the observation that the time course of the vasoconstrictor response to endothelin-1 is too long to account for rapid breath-to-breath regional adjustments in pulmonary arteriolar tone, have led to the proposal that although endothelin may not be the initiating factor, full expression of HPV requires its basal release. This is consistent with the results of earlier studies, demonstrating synergy between the effects of endothelin and hypoxia on membrane potential,[23] cytoplasmic Ca^{2+} concentration,[23] and Ca^{2+} sensitivity of the smooth muscle cell.[24] It has also been clearly demonstrated that HPV requires the presence of elevated wall tension (tone).[13,25] Since both agonist and mechanically induced preconstriction have similar effects on the hypoxic response, it is more likely that it is not the tone per se that is important but the activation of intracellular signaling pathways, whether by agonists or by mechanical stimulation, that synergize with the mechanisms that are activated in smooth muscle by hypoxia.

Angiotensin-II (ANG-II) has also been implicated as a pulmonary vasoconstrictor. Angiotensin-I is converted to ANG-II by angiotensin-converting enzyme (ACE) in the pulmonary epithelium[26] and hence is well positioned to modulate the reactivity of this circulation. In normal human volunteers and in humans with an activated renin–angiotensin system subjected to acute hypoxia, treatment with an ANG-II blocker resulted in pulmonary vasodilatation and inhibition of the HPV response.[27,28] Marshall and colleagues[29] recently reported a positive correlation between the presence of a specific restriction fragment length polymorphism of the ACE gene associated with elevated ACE levels and the risk of acute respiratory distress syndrome (ARDS). The exact mechanism by which this polymorphism influences the pathogenesis of ARDS is not yet clear; however, dysfunction of the renin–angiotensin system with impairment of HPV may accentuate ventilation–perfusion ($\dot{V}/\dot{Q}$) mismatch and hypoxemia in this disease.

Recently, a novel hypoxia-inducible gene *FIZZ1* (found in inflammatory zone 1) was identified in a mouse chronic hypoxia model of pulmonary hypertension.[30] Produced by bronchial epithelial cells and type II alveolar pneumocytes, this protein stimulates both pulmonary artery smooth muscle cell vasoconstriction and proliferation through mechanisms involving activation of the phosphoinositol-3-kinase/protein kinase B pathway. Effector molecules produced extrinsic to the circulation, in response to activation of oxygen-sensing mechanisms in the lung parenchyma, may therefore also be involved in both the vasoconstrictor and remodeling

Table 20-1 Soluble Mediators Involved in the Acute Pulmonary Vascular Response to Hypoxia

Mediator	*Vasoactive effect*	*Reference*
Nitric oxide	Dilatation	Fagan et al[15]
Prostacyclin	Dilatation	Martin et al[16]
Endothelin-1	Constriction	Liu et al[20]
Angiotensin-II	Constriction	Kiely et al[130]
FIZZ1	Constriction	Teng et al[131]

responses, and this may provide a link, analogous to metabolic feedback mechanisms of vascular control in the systemic circulation, between lung parenchymal oxygenation and regional bloodflow regulation. Studies to explore the pathophysiologic implications and clinical application of this finding are currently under way.

The observations that hypoxia causes pulmonary artery vasoconstriction in pulmonary artery segments denuded of endothelium and isolated from the influence of neurohumoral factors[5] and stimulates contraction[1] and a rise in intracellular Ca^{2+} concentration ($[Ca^{2+}]_i$)[32,33] in myocytes isolated from other cell types strongly implicate the smooth muscle cell as the primary site of initiation of HPV. Smooth muscle cell contraction during hypoxia is triggered by the concurrent activation of multiple pathways. Increased $[Ca^{2+}]_i$ results from Ca^{2+} release from the sarcoplasmic reticulum[34–36] and from influx of extracellular Ca^{2+} due to inhibition of hyperpolarizing (outward) K^+ currents with subsequent activation of L-type Ca^{2+} channels.[37,38] The impact of increased $[Ca^{2+}]_i$ on tone is further enhanced by increased Ca^{2+} sensitivity of the contractile myofilaments.[13,39]

Hypoxia has been found to depolarize pulmonary artery smooth muscle cells by an average of 10 mV.[40] Since the resting membrane potential in these cells is −50 to −60 mV,[41] and since voltage-regulated Ca^{2+} channels have an activation threshold of about −30 mV,[42] this by itself is insufficient to activate contraction. Thus, rather than being the primary stimulus, the depolarizing effect of hypoxia may serve to shift the membrane potential, reducing the ability of the cell to counteract a second activating agency. Nevertheless, it is an important factor in initiation of the response, and the ionic mechanisms that link changes in pulmonary artery smooth muscle membrane potential to fluctuations in ambient oxygen tension have been extensively investigated. Pulmonary arterial smooth muscle cells express a large number of K^+ channel subunits, many of which are voltage gated (K_v channels) and contribute to voltage-regulated transmembrane currents in many species. These channels normally conduct outward (hyperpolarizing) K^+ currents, which serve to maintain the negative resting membrane potential. Their inhibition moves the membrane potential in the positive direction, closer to the activation potential for voltage-gated Ca^{2+} entry. Hypoxia inhibits the conductance of several of these channels when they are expressed in heterologous expression systems.[40–43] Moreover, inhibition of the $K_{v1.5}$[38] and $K_{v2.1}$[36] channels by intracellular administration of specific antibody and by genetic deletion[44] decreases pulmonary artery smooth muscle sensitivity to hypoxia. Such findings strongly support a primary role for these channels as an effector mechanism for hypoxic depolarization in pulmonary vascular smooth muscle.[37,45,46]

Depolarization of the smooth muscle cell membrane may directly activate synthesis of inositol-1,4,5-triphosphate and release of Ca^{2+} from ryanodine-sensitive intracellular stores.[47] In addition, Ca^{2+} entry, triggered by depolarization of the cell membrane, causes secondary Ca^{2+} release from the sarcoplasmic reticulum through the process of Ca^{2+}-induced Ca^{2+} release.[48] The endogenous activator of ryanodine receptors, cADP–ribose, has also been found to be elevated by hypoxia in rat pulmonary arteries[49] and contributes to the rise in $[Ca^{2+}]_i$. The depletion of the sarcoplasmic reticulum Ca^{2+} stores, in turn, activates cation channels that mediate Ca^{2+} influx, in part through pathways that are insensitive to blockers of the L-type channel.[50] A process known as capacitative, store-operated, or store-depletion Ca^{2+} entry creates a positive feedback mechanism to reinforce both depolarization and contraction.

After an initial rise in $[Ca^{2+}]_i$, tension continues to increase during hypoxia in rat pulmonary arteries without corresponding changes in Ca^{2+} concentration, suggesting that hypoxia sensitizes the contractile proteins to Ca^{2+}.[51] This has been attributed, in part, to an effect of hypoxia of the small cytosolic G-protein RhoA. RhoA translocates to the cell membrane, where it activates RhoA-associated kinase, which, in turn, acts to inhibit myosin phosphatase localization to the thick myofilament and so promotes activation of the actin-activated myofibrillar ATPase that drives crossbridge cycling and contraction.[52] Y-27632, a specific inhibitor of Rho-associated kinase, was found to inhibit HPV and to exert a greater effect on the Ca^{2+}-independent second phase of the response[51] than on the initial contraction. In addition, the mitogen-activated protein kinases (MAP kinases), particularly the p38 and ERK1/ERK2 extracellular signal–regulated kinases, regulate vascular smooth muscle, which regulate smooth muscle force, through phosphorylation of the thin filament–associated protein caldesmon[53] and through modulation of phosphorylation of the 20 kDa myosin regulatory light chain.[54] MAPKs have been shown to be activated by hypoxia in rat pulmonary artery rings and to play a role in the development of sustained force during the second phase of the HPV response.[39]

The molecular identity of the pulmonary arterial smooth muscle cell oxygen sensor remains the most controversial aspect of the HPV response. It is not yet even clear whether a single oxygen sensor in the smooth muscle cell is responsible for altering K^+ channel activity, Ca^{2+} release, Ca^{2+} sensitivity, and gene expression or different oxygen sensors mediate specific biochemical effects. Early studies focused on the premise that oxygen, acting as a substrate for biochemical reactions, could impart a rate-limiting effect on mitochondrial electron transport during hypoxia, compromising the energy state of the cell and somehow signaling contraction. Classically, however, mitochondrial respiration has been found to remain unchanged until intracellular PO_2 falls below a critical threshold of 5 mm Hg,[55] and it seems unlikely that myocyte energy supply would become oxygen-limited at oxygen tensions in the range of 40 mm Hg, where HPV is activated. Others have pointed out that the K_m of

mitochondrial cytochrome oxidase is too low to permit detection of hypoxia in the physiologic range[56] through this mechanism. Later studies in isolated lungs and pulmonary arteries[57,58] confirmed that the energy state of the cell does not decrease during hypoxia in either of these systems. Furthermore, general metabolic inhibitors, such as azide, cyanide, and 2-deoxyglucose, and reducing agents do not reproduce the hypoxic effect, and the hypoxic conditions that generate the signal are not sufficiently stressful to induce the expression of "stress genes."[28] The overwhelming accumulated evidence, therefore, is that HPV is not triggered by a decrease in the energy state as a consequence of hypoxia-induced inhibition of mitochondrial electron transport. Accordingly, a dedicated molecular oxygen sensor(s) capable of responding to physiologically relevant levels of hypoxia has been sought.

The involvement of heme proteins capable of reversibly binding oxygen and in so doing undergoing conformational change has received much attention[56] and is supported by the observation that the O_2-like molecules CO and NO, which bind avidly to heme-containing proteins, generate signals that oppose the effects of hypoxia on gene expression in vascular cells.[59] Similarly, transition metals (eg, cobalt and nickel), which can substitute for iron in the heme structure but which cannot bind oxygen, simulate some of the effects of hypoxic exposure.[60] Although several candidate heme proteins have been proposed, none has so far withstood systematic investigation of its potential direct involvement in the acute HPV response. Whether oxygen regulation of membrane potential is due to the oxygen sensitivity of the K^+ channels themselves or is mediated by a separate oxygen sensor also remains controversial. Some K^+ channels are rich in cysteine residues, which provide oxidation targets and thus a mechanism by which the function of the protein may respond to the local redox environment. Based on this observation, Weir and Archer[5] have proposed a mechanism for the regulation of pulmonary arterial smooth muscle membrane potential in which reactive oxygen species (ROS) derived either from the mitochondria during early steps in the electron transport chain or from membrane-associated NADPH oxidase maintain K_v channels in the oxidized open configuration and become inhibited under reducing (hypoxic) conditions. This has been difficult to reconcile, however, with recent observations that the release of ROS from mitochondria is enhanced during hypoxia[61] and plays a critical role in hypoxic induction of specific gene expression.[62] Final conclusions regarding the involvement of ROS in the regulation of pulmonary artery smooth muscle membrane potential and other aspects of smooth muscle cell function, as well as their source during exposure to physiologic levels of hypoxia, must therefore await the results of ongoing investigation.

Pulmonary Vascular Effects of Prolonged Hypoxia

During prolonged alveolar hypoxia, as occurs in many pulmonary diseases, HPV is sustained and accompanied by vascular remodeling. This results in the development of progressive pulmonary hypertension, significantly worsening the prognosis. That tonic smooth muscle contraction continues to contribute to pulmonary hypertension in chronic hypoxia is evidenced by the findings that pulmonary arterial pressure falls acutely in response to inhaled oxygen and vasodilatory agents.[63] Although pulmonary arteries from chronically hypoxic animals demonstrate increased reactivity to agonists,[64] the acute HPV response is impaired after chronic hypoxic exposures.[64–66] This observation is of clinical and physiologic significance because patients with chronic hypoxia not only suffer the deleterious effect of sustained pulmonary hypertension on right ventricular function and the ability to enhance oxygen delivery by increasing cardiac output but also lose the ability to optimize ventilation–perfusion matching in response to superimposed acute changes in alveolar PO_2. The discrepancy between the response to agonists and that to hypoxia has been interpreted as indicative of impairment of the oxygen-sensing mechanism rather than contractile function as the cause of decreased effectiveness of the HPV response.

Endothelin-1 levels are elevated in the pulmonary circulation following prolonged hypoxia, and the increase in basal pulmonary artery tone in chronically hypoxic animals and humans is at least in part due to increased expression of this agonist.[67,68] Even in the absence of external stimuli, however, pulmonary artery smooth muscle cells from chronically hypoxic animals are depolarized relative to cells from normoxic animals. Voltage-gated K^+ currents[69,70] are inhibited in pulmonary artery smooth muscle after chronic hypoxia, and expression of the channels by which they are conducted is down-regulated,[65] which would tend to impair the response to superimposed additional hypoxic insults while raising resting tone. Vasoconstriction in response to 4-aminopyridine, an inhibitor of this channel, is preserved during chronic hypoxia, supporting the suggestion that the loss of hypoxic vasoconstriction is due to decreased function of the oxygen-sensing mechanism that activates these channels rather than to decreased expression of the proteins themselves.[65] $[Ca^{2+}]_i$ is elevated in pulmonary artery smooth muscle cells from chronically hypoxic animals, suggesting that abnormalities of Ca^{2+} handling also contribute to the abnormality; however, antagonists of the voltage-gated (L-type) Ca^{2+} channel were not effective in reducing it,[26] nor were they effective in preventing the development of pulmonary hypertension secondary to chronic hypoxia.[71] These findings suggest that other Ca^{2+} regulatory pathways independent of membrane potential may be affected by chronic hypoxia.

The mechanisms involved in the alterations in pulmonary vascular function during chronic hypoxia may be even more complex than suspected since they may not represent changes in a single cell type. Hypoxia is a stimulus for pulmonary arterial smooth muscle growth, and Frid and colleagues have reported that in cells from bovine pulmonary artery exposed to chronic hypoxia, the proliferative response primarily affects a specific subpopulation of immature smooth muscle cells.[72] These cells were also found to secrete a factor that acted in a paracrine fashion to induce proliferation of neighboring smooth muscle.[73] At least four subtypes of pulmonary artery smooth muscle cell have been

identified,[74] with varying proliferative potential and electrophysiologic properties.[5] The change in smooth muscle cell function may, therefore, reflect the expansion of specific cell types or even the emergence of a totally new phenotype.

Chronic hypoxia, both in disease states and in individuals residing at high altitudes,[75] results in structural changes in the pulmonary vasculature, with the result that the increase in pulmonary vascular resistance becomes fixed and less amenable to reversal by restoration of normoxia or vasodilatory agents. The pathologic hallmark of chronic alveolar hypoxia is the muscularization of the peripheral portions of the pulmonary arterial tree.[75] The development of inner muscular tubes composed of longitudinally oriented smooth muscle is also seen in the intima of small pulmonary arteries and pulmonary arterioles[75] and contributes to the reduction in luminal diameter.[75] Remodeling is not limited to arterioles but also involves the veins and venules,[75] which undergo a similar process of enhanced muscularization that adds to the increase in pulmonary vascular resistance. Van Suylen and colleagues have reported on a strain of mice with an angiotensin-converting enzyme (ACE) allele that renders them partially ACE-deficient (plasma ACE activity 34% of wild-type controls).[76] After 4 weeks of hypoxia ($F_IO_2 = 0.1$), they found a significant difference in the muscularization of small arterioles in the ACE-deficient mice, indicating that ANG-II plays a central role in the remodeling process.

In addition to proliferation, modulation of programmed cell death (apoptosis) is an important site of regulation of pulmonary vascular remodeling in response to chronic hypoxia. Taraseviciene-Stewart and colleagues recently reported on the effect of vascular endothelial growth factor receptor-2 (VEGFR-2) blockade and chronic hypoxia (simulated altitude of 5,000 m) on rat lungs.[77] VEGF is thought to be not only an important endothelial cell growth factor but also important for endothelial cell survival.[78] In rats exposed to hypoxia, in the presence of VEGFR-2 blockade, significant proliferation of pulmonary endothelial cells was observed, leading to precapillary luminal obliteration.[77] In chronically hypoxic rats that were not treated with VEGFR-2 antagonist, only pulmonary artery medial thickening was observed. To reconcile these findings, it was proposed that VEGF receptor blockade leads to endothelial cell apoptosis and that chronic hypoxia selects for apoptosis-resistant cells with a hyperproliferative phenotype.[78] Interestingly, Lee and colleagues[79] reported differences in the phenotype and proliferative responsiveness of pulmonary endothelial cells from patients with primary pulmonary hypertension compared with those with pulmonary hypertension due to cardiac or pulmonary disease, supporting a primary role for the endothelial cell in the development of fixed pulmonary hypertension.

Pulmonary hypertension is a common complication of chronic obstructive pulmonary disease (COPD). The increase in pulmonary artery pressures is often mild to moderate, but some patients may suffer from severe pulmonary hypertension and present with a progressively downhill clinical course because of right-sided heart failure added to ventilatory handicap. The cause of pulmonary hypertension in COPD is generally assumed to be hypoxic pulmonary vasoconstriction leading to permanent medial hypertrophy. However, the results of recent pathologic studies point, rather, to extensive remodeling of the pulmonary arterial walls, with prominent intimal changes. These aspects account for minimal reversibility with supplemental oxygen. There may be a case for pharmacologic treatment of pulmonary hypertension in selected patients with advanced COPD and right-sided heart failure. Candidate drugs include prostacyclin derivatives, endothelin antagonists, and inhaled nitric oxide, all of which have been reported to be of clinical benefit in primary pulmonary hypertension and/or pulmonary hypertension associated with rheumatologic disorders. In randomized controlled trials, however, it has been a challenge to overcome the difficulties of the diagnosis of right ventricular failure and the definition of a relevant primary end point in pulmonary hypertensive COPD patients. Antagonists of the L-type Ca^{2+} channel, which do block hypoxic pulmonary vasoconstriction in normal individuals during ascent to high altitude, have had variable success in COPD patients because of their adverse effects on right ventricular contractility and arterial oxygen saturation resulting from alterations in ventilation–perfusion matching.

DUCTUS ARTERIOSUS

In the fetus, the ductus arteriosus is tonically relaxed by its hypoxic environment, permitting blood to bypass the unventilated lungs. As a result of increasing oxygen tension as respiration begins after parturition, it constricts. Failure of the ductus arteriosus to close (patent ductus arteriosus) occurs in 10% of neonates and may result in significant morbidity. In this setting, vasoconstriction of the ductus arteriosus is caused not by hypoxia but rather increasing oxygen tension.[48] Although modulated by the endothelium, oxygen constriction persists ex vivo after endothelial denudation, indicating that, as in the pulmonary circulation, the response is intrinsic to the smooth muscle.[80] Endothelin-1 has been proposed as an oxygen-regulated modulator of ductus arteriosus closure[81]; however, using genetically modified mice that were $-/-$, $+/-$, or $+/+$ for endothelin A receptor, Coceani and colleagues demonstrated that endothelin contributes to but is not required for closure of the ductus arteriosus after birth.[81] Similarly, Michelakis and colleagues demonstrated that in ductus arteriosus segments in vitro, acute constriction in response to normoxia is unaffected by endothelin A receptor antagonists.[82] Nevertheless, ductus arteriosus cells have been shown to produce endothelin-1 in response to hypoxia, and it is thought that endothelin-1 may play a role in the later stages of remodeling of the ductus arteriosus wall[82] and in maintaining contraction in the closed ductus arteriosus when, in the absence of luminal flow, the smooth muscle cells of the ductus arteriosus experience a hypoxic environment (see below). Vasodilator prostaglandins are widely recognized as being important in preventing ductus arteriosus closure in humans, and indomethacin has therefore been used clinically to accomplish closure of the ductus arteriosus in the neonate.[83]

Based on the observations that inhibition of voltage-gated K^+ channels leads to vasoconstriction of the ductus arteriosus

and that inhibitors of mitochondrial electron transport inhibit both the formation of ROS and oxygen constriction, Michelakis and colleagues[84] offered a mechanistic explanation that parallels the one suggested for the mediation of hypoxic vasoconstriction in the pulmonary circulation. Specifically, they propose that ROS produced in the proximal electron transport chain in response to oxygen serve as mediators that link the mitochondrial oxygen sensor to K^+ conductance and, hence, to membrane potential. This was supported by the results of studies on ductus arteriosus arterial smooth muscle cells,[85] in which administration of catalase (the enzyme that catalyzes the degradation of hydrogen peroxide to oxygen and water) inhibited the increase in ROS, the decrease in K^+ current, and the depolarization of the cell membrane that occur on restoration of normoxia. The effects of hypoxia on K^+ current and membrane potential, furthermore, were mimicked by the administration of exogenous peroxides. The specific channels that mediate depolarization in response to oxygen in ductus arteriosus smooth muscle cells have yet to be identified; however, their regulation by cellular redox status must differ significantly from the regulation of those that effect the HPV response for this mechanism to be shared between tissues demonstrating such diametrically opposed responses to the same stimulus.

In the postnatal period, after the acute closure of the ductus arteriosus has been accomplished, remodeling occurs that ensures that it remains closed. Kajino and colleagues[86] suggested that remodeling of the ductus arteriosus, which involves both proliferation and apoptosis, may be driven by hypoxia of the media. According to their hypothesis, constriction causes loss of luminal perfusion and hence impaired diffusional oxygenation, as well as compression of the vasa vasorum and decreased medial perfusion. This is consistent with the observation that remodeling of the preterm ductus arteriosus does not occur unless the acute vasoconstrictor response results in complete obliteration of the lumen.[86]

SYSTEMIC CIRCULATION

During acute hypoxia, cardiac output increases, ventilation increases, blood catecholamine levels are elevated, and systemic vascular reflexes are activated that redistribute bloodflow toward the heart, respiratory muscles, brain, liver, and adrenal cortex and away from resting skeletal muscles and other metabolically inactive tissues.[87] Concomitantly, microvascular responses are activated that optimize intraparenchymal bloodflow distribution and increase the capacity for tissue oxygen extraction.[88] These responses are well developed in all mammals and are highly conserved across species. The adjustments in vascular tone that are required to redirect flow in this way are mediated by both local and neurohumoral mechanisms. The small preterminal arterioles, which represent the primary site of regulation of transvascular resistance, dilate in response to hypoxia, promoting enhanced perfusion and oxygen transport in areas in which metabolic demand exceeds oxygen delivery. Both the redistribution of bloodflow and the enhancement of oxygen extraction, however, are also dependent on adrenergically mediated responses,[1,87] which reduce bloodflow to areas in which oxygen availability exceeds metabolic need, permitting nutritive perfusion to be optimized.

With prolonged hypoxia, sympathetic tone and circulating catecholamine levels gradually return to normal levels whereas cardiac output remains elevated and the preferential perfusion of vital organs persists.[89,90] This coincides with remodeling of the circulation, characterized by increased capillarity (angiogenesis)[91,92] in metabolically active tissues, which permits the enhanced level of perfusion to these vital areas to be maintained without a sustained increase in sympathetic activity. This is accompanied, however, by alterations in systemic vascular endothelial and smooth muscle function that impair the acute responses and hence limit the capacity to preserve vital organ function in the event of superimposed hemodynamic instability or further acute reductions in oxygen delivery.[93–95]

Direct measurement of the PO_2 of blood within the lumen of arteries, with the use of oxygen–sensitive microelectrodes, has shown that the PO_2 decreases from 70 mm Hg in conduit arteries to 20 mm Hg in terminal arterioles, due to diffusion of oxygen across the arteriolar wall into the surrounding parenchyma.[96] In working cardiac or skeletal muscle, the capillary PO_2 is maintained at 20 mm Hg, whereas the PO_2 within the sarcoplasm of the muscle cell is 2 mm Hg, providing a steep concentration gradient for oxygen supply to these cells.[97] The smooth muscle of the artery wall is separated from the blood by the very thin tunica intima. Since intravascular and extravascular PO_2 are very similar, the smooth muscle PO_2 must be very close to the intravascular value. Consequently, the primary supply of oxygen to arterial smooth muscle in thin-walled arterioles is by diffusion from blood within the lumen. When the arterial smooth muscle layer is thicker than 0.9 to 1 mm, as in larger conduit vessels, diffusion is inadequate for those cells in the outer part of the media, and oxygen supply is supplemented by perfusion of the vascular wall through the vasa vasorum. In the human aorta, for example, vasa vasorum are found in the outer two-thirds of the media.[98]

Acute Hypoxic Vasodilatation

Acute exposure to hypoxia sufficient to lower arterial PO_2 to less than 40 mm Hg elicits the local release of both vasoconstrictor and vasodilator substances from vascular cells, the release of metabolic byproducts from the surrounding parenchyal tissue, and direct effects on the function of systemic vascular smooth muscle. With the notable exception of the internal mammary artery, which constricts under the influence of an endothelium-derived prostanoid,[99] the net effect of these factors in the human systemic circulation is relaxation. The dilatory response demonstrates longitudinal heterogeneity, being inversely related to vessel diameter.[100]

The smooth muscle cells within the vascular media are positioned midway in the diffusion path between the lumen and the surrounding parenchyma, so the PO_2 that these cells experience will be directly influenced by the degree of parenchymal deoxygenation. Since tissue oxygenation is ultimately determined by the relationship between oxygen utilization and delivery, an oxygen-sensing mechanism that

resides within the cells of the parenchyma and regulates perfusion through feedback on the feeding vessels is attractive from a teleologic standpoint. During continuous sympathetic nerve stimulation or catecholamine infusion, bloodflow to skeletal muscle initially falls, due to arteriolar vasoconstriction, but then returns toward control levels, a response termed "sympathetic escape."[101] Superfusion of the muscle with oxygenated buffer, which increases parenchymal PO_2 without significantly altering the PO_2 of the perfusing blood, blocks the vasodilatory response, indicating that sympathetic escape is mediated by a fall in parenchymal cell PO_2.[101] Similarly, hypoxia inhibits agonist- and depolarization-induced coronary artery contraction to a greater degree in the presence of adherent myocardium than when the vessels are dissected free of adherent tissue.[102] Although it is generally accepted that expression of the full integrated response to hypoxia requires the participation of the surrounding parenchyma, the mediator(s) that provides the signal for matching bloodflow to metabolic demand has varied among vascular beds and may depend on the specific parenchymal cell type that is involved. Thus, evidence can be found to support the involvement of K^+ ions, H^+ ions, inorganic phosphates, adenosine metabolites, prostaglandins, and nitric oxide, although none of these play a universal role.[58,102–104]

The P450 hydroxylases comprise a family of enzymes that produce vasoactive products and that require molecular oxygen to catalyze the formation of the vasoconstrictor 20-hydroxyeicosatetranoic acid from arachidonic acid. The 4A isoform of this enzyme is expressed in rat renal and skeletal muscle microvessels and their surrounding parenchymal tissues[105] and is sensitive to oxygen availability over a relatively high range of PO_2 values. Substrate analogs of this reaction, moreover, have been found to attenuate arteriolar constriction in response to increasing PO_2 in rat cremasteric muscle.[105] Further work is therefore needed to evaluate the contribution of this pathway in mediating the hypoxic response of both vascular and parenchymal cells.

In arterioles from some circulations, hypoxic vasodilatation is entirely dependent on the presence of an intact endothelium.[106–108] Based primarily on the results of pharmacologic studies, vasodilatory prostaglandins, nitric oxide, serotonin, ATP, adenosine, and an as yet unidentified endothelium-derived hyperpolarizing factor[106–111] have been advanced as the endothelial mediator of this response. In other arteries, the hypoxic vasorelaxation is not endothelium dependent and is mediated by direct effects on smooth muscle cell membrane potential and Ca^{2+} entry.[112,113] As in the pulmonary circulation, systemic vascular tone is oxygen sensitive over a physiologic range of PO_2 values above those that would be expected to limit energy availability. Measurements carried out in rabbit aorta indicate that at PO_2 values that inhibit contractions in response to potassium chloride and phenylephrine, smooth muscle concentrations of ATP do not fall to levels that would affect the activity rate of either myosin light-chain kinase, which mediates phosphorylation of the regulatory light chain and enables actin–myosin interaction, or the myofibrillar ATPase in the myosin head that provides the energy for crossbridge cycling.[114] Nevertheless, ATP concentrations do approach levels that may limit the inositol phospholipid transduction system,[114] and hypoxic inhibition of norepinephrine-stimulated contraction is associated with a four- to five-fold increase in the phosphatidylinositol 4-phosphate pool in rabbit aorta.[115] This suggests that phosphatidylinositol-4-phosphate kinase may become a rate-limiting step under hypoxic conditions in some vessels.

Systemic Vascular Effects of Prolonged Hypoxia

Prolonged hypoxia causes profound changes in systemic arterial and arteriolar endothelial and smooth muscle function,[93,94] which result in loss of pressure-sensitive "myogenic" arteriolar tone, impaired reactivity to potassium chloride and adrenoceptor agonists in both resistance and conductance vessels,[93–95] and impairment of endothelium-dependent vasorelaxation[116] (Figures 20-1 and 20-2). Arteriolar myogenic reactivity determines the capacity to autoregulate bloodflow and transcapillary fluid flux. Preferential perfusion of vital organs and optimization of oxygen extraction are effected by adrenergic reflexes.[87] Endothelium-dependent flow dilation in conduit and resistance vessels is required to maximize perfusion. Thus, the

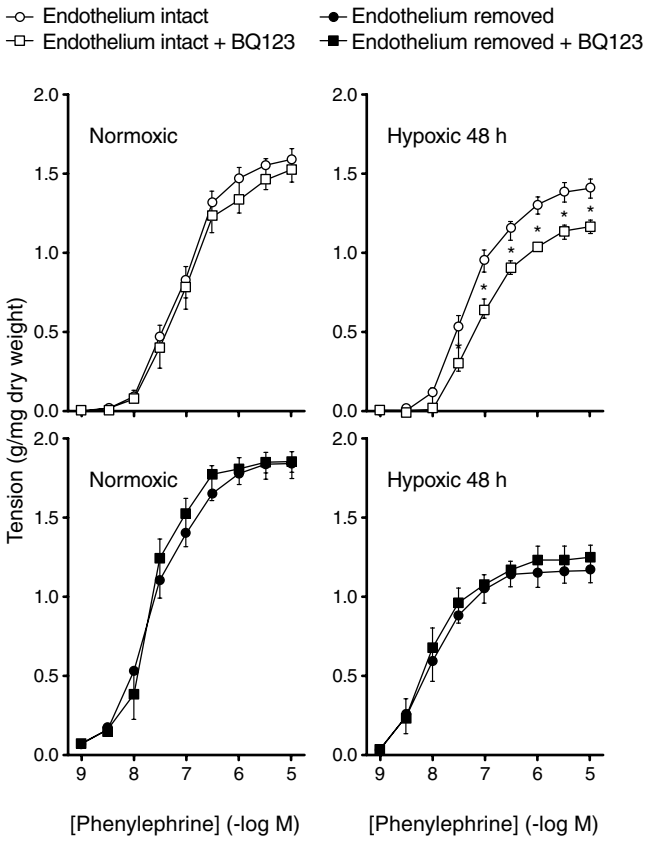

FIGURE 20-1 Phenylephrine concentration–response relationships in aortic rings from normoxic rats and rats exposed to hypoxia for 48 hours. Contraction is impaired after hypoxic exposure. In normoxic animals, contraction is greater after endothelial ablation, indicating that it normally exerts an inhibitory influence. After hypoxia, contraction is greater in the presence of an intact endothelium, indicating that vasoconstrictor release predominates. The constrictor effect of the endothelium is abolished by the endothelin A antagonist BQ123.

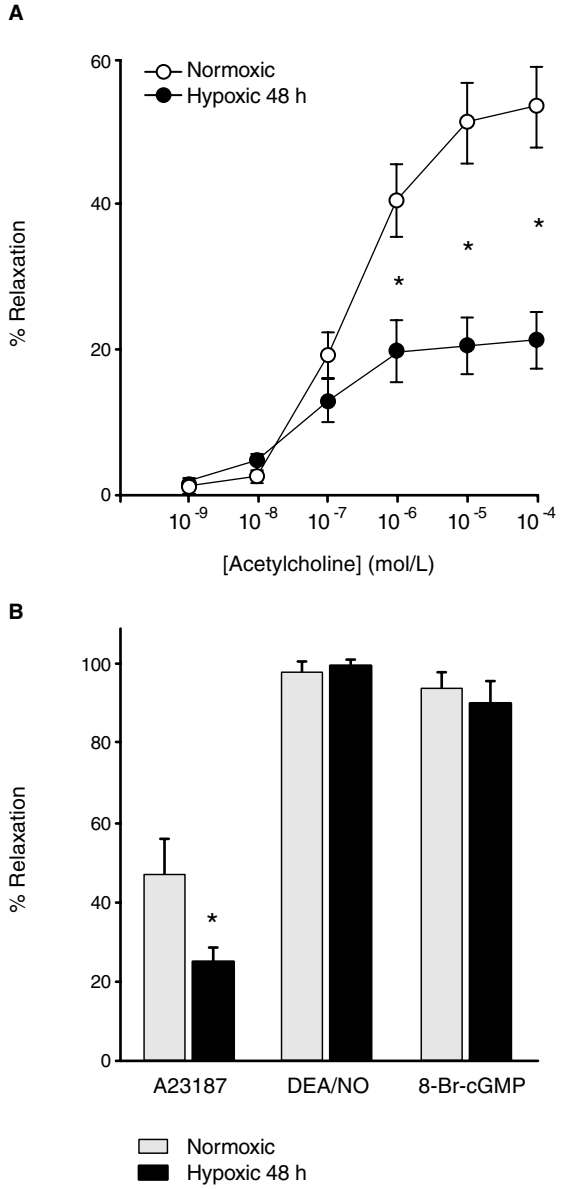

FIGURE 20-2 *A*, Acetylcholine concentration–response relationships in endothelium-intact phenylephrine-precontracted aortic rings from normoxic rats and from rats exposed to hypoxia for 48 hours. Endothelium-dependent acetylcholine-induced relaxation is impaired after hypoxia. *B*, Relaxation of endothelium-intact phenylephrine-precontracted rings from normoxic and hypoxia-exposed rats by acetylcholine, the nitric oxide donor DEA/NO, and cell-permeable 8-bromo-cGMP. Endothelium-dependent (acetylcholine) relaxation is impaired after hypoxia, but endothelium-independent (NO and cGMP) relaxation is not affected.

continued ability to preserve vital organ oxygenation by means of local and sympathetically mediated reflex responses ultimately becomes limited by the effects of hypoxia on the vascular tissues themselves. These effects occur within 12 hours, progress over the ensuing 48 hours, and persist for at least 12 hours after restoration of normoxia.[94,117] Consequently, they are relevant to the pathophysiology of numerous cardiopulmonary diseases (eg, pneumonia, congestive heart failure, COPD exacerbations) that evolve over this time frame.[118]

The molecular mechanisms underlying the hypoxia-induced change in endothelial function have been studied in rat aorta[116] and mesenteric artery.[119,120] In rat aorta, prolonged exposure to hypoxia (12 to 48 hours) results in decreased expression of the endothelial isoform of nitric oxide synthase, impaired smooth muscle formation of cyclic GMP in response to stimulation with acetylcholine, and reduced capacity for endothelium-dependent relaxation of phenylephrine-induced contraction.[116] Aortic endothelial production of endothelin-1 protein is elevated (Figure 20-3), and pharmacologic antagonists of the endothelin A receptor decrease phenylephrine-induced contraction in endothelium-intact aortic rings from hypoxia-exposed but not normoxic rats.[121] These alterations in endothelial protein expression account for the change from a vasodilatory to a vasoconstrictor function. In the rat mesenteric circulation, the endothelium contributes to inhibition of contraction after hypoxia. This is not mediated by changes in nitric oxide bioavailability but by the release of a mediator that acts to hyperpolarize the smooth muscle cell membrane.[120] The effect is sensitive to inhibition by the heme analog tin

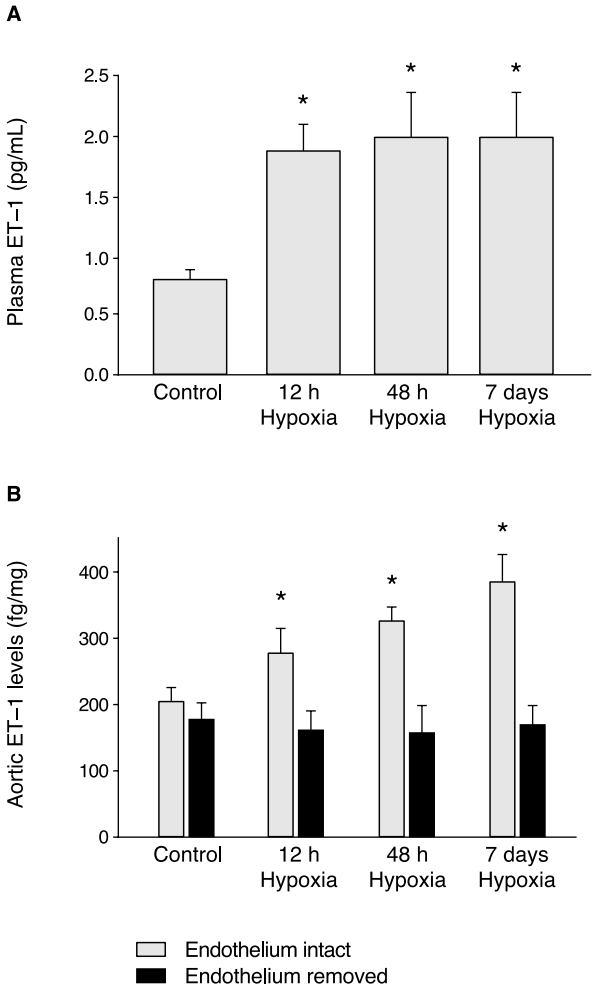

FIGURE 20-3 Plasma (*A*) and aortic (*B*) levels of endothelin-1 (measured by radioimmunoassay) in normoxic rats and rats exposed to hypoxia for 48 hours. Endothelin-1 levels are increased in plasma and in aortic tissue. The increase in aortic endothelin-1 protein levels is localized to the endothelium.

protoporphyrin IX, suggesting the involvement of enzymes involved in heme metabolism. One possible candidate for this role is hemeoxygenase, which catalyzes the release of carbon monoxide during heme degradation.[122] Carbon monoxide shares many of the biochemical properties of nitric oxide,[123] and since hemeoxygenase expression has been shown to be hypoxia inducible in other tissues,[124] it is possible that the hemeoxygenase–carbon monoxide–cGMP pathway becomes an important regulator of mesenteric oxygenation under conditions of reduced systemic oxygen delivery. Figure 20-4 illustrates the effect of hypoxic exposure on aortic endothelial expression of hemeoxygenase isoform 2. The levels of this isoform increase in the aorta after 16 hours of hypoxic exposure and return to control values after 48 hours. It is of interest that this isoform is involved in altered systemic vascular reactivity, even if transiently, because its expression is generally considered to be constitutive.

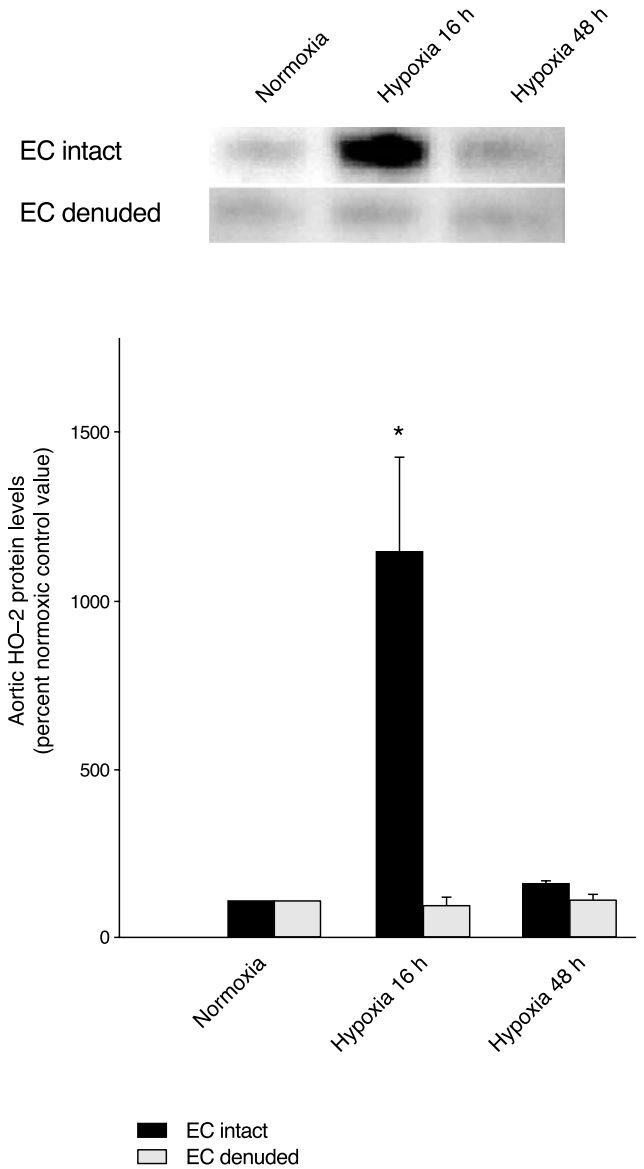

FIGURE 20-4 Effect of hypoxia on aortic expression of hemeoxygenase-2 (HO-2). HO-2 expression is increased at 16 hours but returns to control levels by 48 hours. The signal is abolished after endothelial denudation, indicating that expression is localized to the endothelial cell layer.

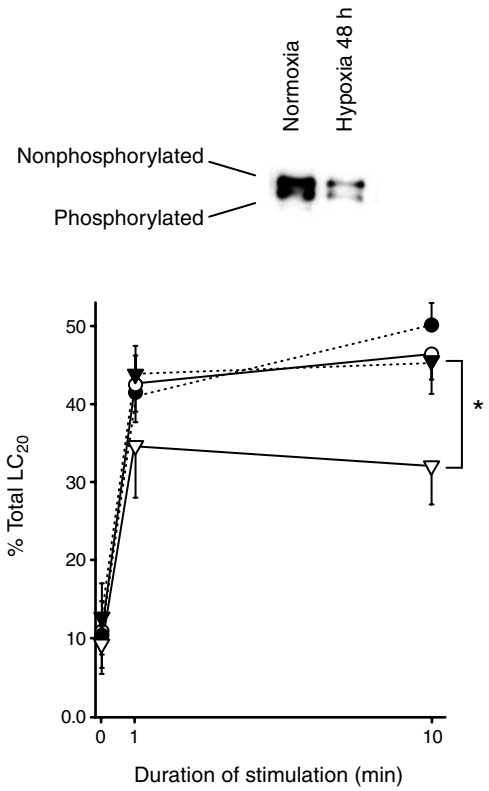

FIGURE 20-5 Phosphorylation of the 20 kDa myosin regulatory light chain (LC_{20}) was measured in aortic strips from normoxic rats (○, ●) and rats exposed to hypoxia for 48 hours (▽, ▼) after 0 min, 1 min, and 10 min stimulation with 10 μmol/L phenylephrine in the presence and absence of DMSO (○, ▽) or the myosin light-chain phosphatase inhibitor Microcystin-LR, 50 nmol/L (●, ▼). *$p < 0.05$ vs corresponding DMSO group. The phosphorylated form of LC_{20} runs faster in a nondenaturating gel because of its charge and conformational change. Phosphorylation is measured as the ratio of nonphosphorylated to total LC_{20}. Hypoxia impairs the capacity to phosphorylate and, therefore, activates myosin through an increase in the activity of myosin light-chain phosphatase.

Prolonged hypoxia affects systemic vascular smooth muscle function at multiple sites.[125] Abnormalities of regulatory light-chain phosphorylation (Figure 20-5), myofibrillar ATPase activity, and myofilament composition have been identified.[125] Phosphorylation of the myosin regulatory light chain is the primary activation step in agonist-induced smooth muscle contraction and is regulated by the relative activities of the Ca^{20}-sensitive myosin light-chain kinase and its opposing myosin light-chain phosphatase. The impairment of aortic smooth muscle activation that occurs after prolonged hypoxic exposure may be attributed to an increase in localization of phosphatase catalytic activity from the cytosol to the thick filament[126] (Figure 20-6). This is mediated by up-regulation of smooth muscle cell expression of a myosin-binding protein (MYPT1) that, by virtue of the presence of specific protein interaction sites, is able to simultaneously bind both the catalytic subunit of protein phosphatase 1 and the myosin heavy chain.[126] The stability of the phosphatase complex is, in turn, regulated by phosphorylation of MYPT1 by rho-associated protein kinase and

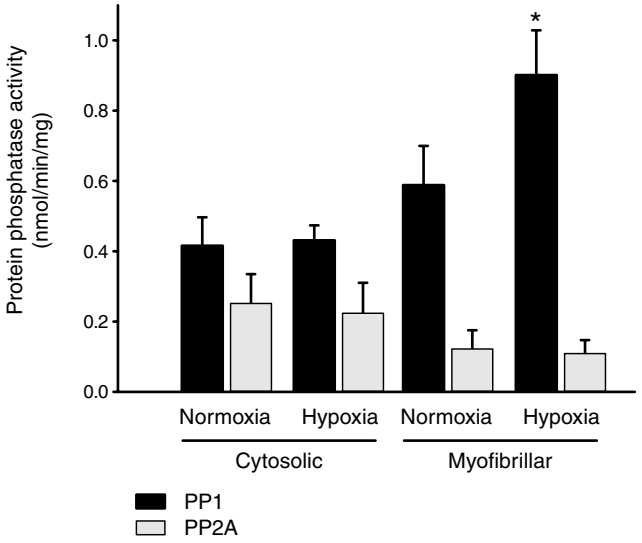

FIGURE 20-6 Protein phosphatase type 1 and type 2A (PP1 and PP2A) activities in aortic cytosolic and myofibrillar fractions from normoxic rats and rats exposed to hypoxia for 48 hours. After hypoxia, increased PP1 activity is localized to the thick myofilament.

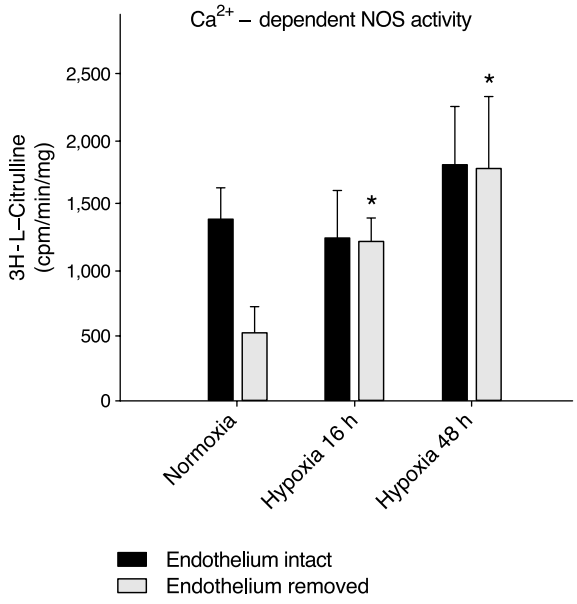

FIGURE 20-7 Ca^{20}-dependent nitric oxide synthase activity in endothelium-intact and -denuded aortic rings from normoxic rats and rats exposed to hypoxia for 48 hours. Endothelial nitric oxide synthase activity declines, whereas the locus of nitric oxide formation shifts to the vascular smooth muscle.

by cGMP-dependent kinase. This brings the activation step under the influence of nitric oxide and carbon monoxide through their effects on the activity of the soluble guanylyl cyclase. Preliminary evidence suggests that the impairment of activation may also reflect an increase in smooth muscle synthesis of these signaling molecules because of hypoxic induction of the expression of their respective synthases (Figures 20-7 and 20-8).[127,128]

Activity of the myofibrillar ATPase located in the head of the myosin heavy chain is regulated not only by light-chain

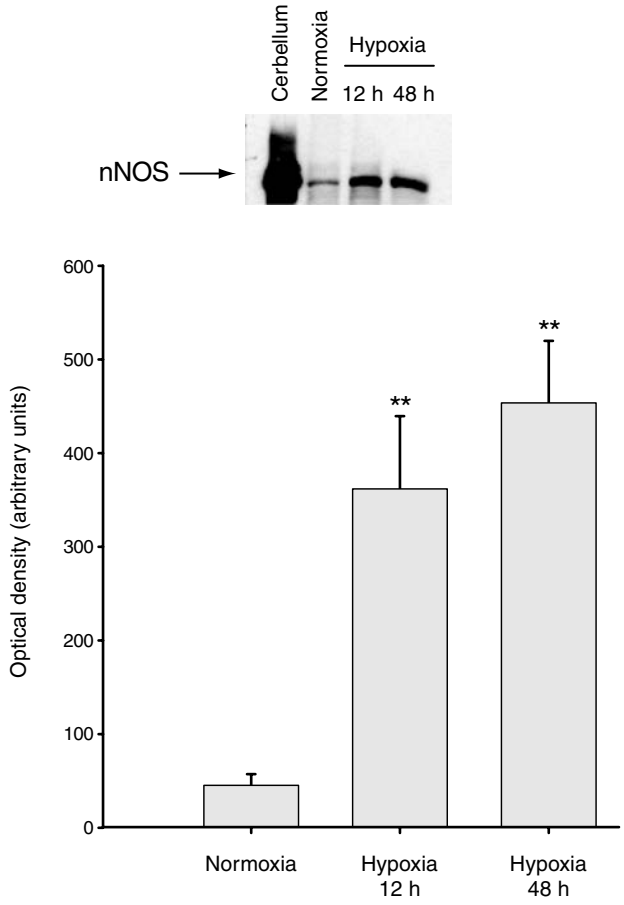

FIGURE 20-8 Western blot showing neuronal nitric oxide synthase (nNOS) protein levels in aortas from normoxic rats and rats exposed to hypoxia for 12 or 48 hours. Aortic nNOS protein expression is increased in hypoxia-exposed rats compared with the normoxic controls.

phosphorylation status but also by the proteins that, along with actin polymer, comprise the thin filament. Caldesmon and calponin both interact with the myosin-binding sites on actin polymer and inhibit actin-activated ATPase activity. Reversal of this inhibitory effect through phosphorylation of these proteins by MAP kinase and by protein kinase C is an important mechanism regulating the Ca^{2+} sensistivity of the contractile myofilaments during agonist-induced contractions. The levels of these proteins are increased in rat aorta, and their phosphorylation levels are decreased,[125,126] providing an explanation for the altered capacity for ATP hydrolysis observed in vascular smooth muscle from rats exposed to hypoxia.[125]

SUMMARY AND CONCLUSIONS

The vasculature is sensitive to changes in blood and tissue PO_2. The importance of identifying the cellular oxygen sensor(s) lies in the fact that the vascular response to oxygen is a vital and highly adaptive physiologic response that matches tissue oxygen delivery to metabolic demand. Inability of the vasculature to respond to elevations in metabolic oxygen demand, for example, during exercise, can lead to tissue ischemia and cell death. Conversely, overperfusion

of a vascular bed leads to vasoconstriction and, over the long term, loss of microvessels (rarefaction) and hypertension.[129] Similarly, hypo- or hyperresponsiveness of the pulmonary vasculature or ductus arteriosus to changes in oxygen tension has major consequences for gas exchange and leads to significant morbidity, as a result of either pulmonary hypertension or worsening hypoxemia. Of particular importance is the recent recognition that the vasculature is among those vital organs whose function is compromised if oxygen deprivation is prolonged and that the oxygen sensitivity of the circulation may be altered by the effects of hypoxia on the vascular tissues themselves. The implications of this are that the adaptive responses of both the pulmonary and systemic circulations are progressively impaired as hypoxia is sustained, with deterioration of pulmonary gas exchange, progressive tissue hypoxia, and hemodynamic instability. The challenge, as the molecular basis of these changes becomes apparent, will be to exploit this understanding to develop novel therapeutic approaches that will reduce organ system dysfunction and the need for the administration of toxic oxygen concentrations in patients with cardiopulmonary disease and refractory hypoxemia.

REFERENCES

1. Cain SM, Chapler CK. O_2 extraction by canine hindlimb during alpha-adrenergic blockade and hypoxic hypoxia. J Appl Physiol 1980;48:630–5.
2. von Euler U, Liljestrand G. Observations on the pulmonary arterial blood pressure in the cat. Acta Physiol Scand 1946;12:301–20.
3. Cutaia M, Rounds S. Hypoxic pulmonary vasoconstriction. Physiologic significance, mechanism, and clinical relevance. Chest 1990;97:706–18.
4. Hales CA, Westphal D. Hypoxemia following the administration of sublingual nitroglycerin. Am J Med 1978;65:911–8.
5. Weir EK, Archer SL. The mechanism of acute hypoxic pulmonary vasoconstriction: the tale of two channels. FASEB J 1995;9:183–9.
6. Fishman AP. Hypoxia on the pulmonary circulation: how and where it acts. Circ Res 1976;38:221–31.
7. Ward JPT, Aaronson PI. Mechanisms of hypoxic pulmonary vasoconstriction: can anyone be right? Respir Physiol 199;115:261–71.
8. Archer SL, Huang JMC, Reeve HL, et al. Differential distribution of electrophysiologically distinct myocytes in conduit and resistance arteries determines their response to nitric oxide and hypoxia. Circ Res 1996;78:431–42.
9. Lejeune P, Brimioulle S, Leeman M, et al. Enhancement of hypoxic pulmonary vasoconstriction by metabolic acidosis in dogs. Anaesthesiology 1990;73:256–64.
10. Pearse RD, Benumof JL, Trousdale FR. PAO_2 and PVO_2 interaction on hypoxic pulmonary vasoconstriction. J Appl Physiol 1982;53:134–9.
11. Madden JA, Dawson CA, Harder DR. Hypoxia-induced activation in small pulmonary arteries from the cat. J Appl Physiol 1985;59:113–8.
12. Leach RM, Hill HM, Snetkov VA, et al. Divergent roles of glycolysis and the mitochondrial electron transport chain in hypoxic pulmonary vasoconstriction of the rat: identity of the hypoxic sensor. J Physiol 2001;536:211–24.
13. Ward JPT, Robertson TP. The role of the endothelium in hypoxic pulmonary vasoconstriction. Exp Physiol 1995;80:793–801.
14. Hampl V, Cornfield DN, Cowan NJ, Archer SL. Hypoxia potentiates nitric oxide synthesis and transiently increases cytosolic calcium levels in pulmonary artery endothelial cells. Eur Respir J 1995;8:515–22.
15. Fagan KA, Tyler RC, Sato K, et al. Relative contributions of endothelial, inducible, and neuronal NOS to tone in the murine pulmonary circulation. Am J Physiol 1999;277: L472–8.
16. Martin LD, Barnes SD, Wetzel RC. Acute hypoxia alters eicosanoid production of perfused pulmonary artery endothelial cells in culture. Prostaglandins 1992;43:371–82.
17. Madden MC, Vender RL, Friedman M. Effect of hypoxia on prostacyclin production in cultured pulmonary artery endothelium. Prostaglandins 1986;31:1049–62.
18. Kourembanas S, Marsden PA, McQuillan LP, Faller DV. Hypoxia induces endothelin gene expression and secretion in cultured human endothelium. J Clin Invest 1991;88:1054–7.
19. Helset E, Kjaeve J, Bjertnaes L, Lundberg JM. Acute alveolar hypoxia increases endothelin-1 release but decreases release of calcitonin gene-related peptide in isolated perfused rat lungs. J Clin Lab Invest 1995;55:369–76.
20. Liu Q, Sham JS, Shimoda LA, Sylvester JT. Hypoxic constriction of porcine distal pulmonary arteries: endothelium and endothelin dependence. Am J Physiol Lung Cell Mol Physiol 2001;280:L856–65.
21. Oparil S, Chen SJ, Meng QC, et al. Endothelin-A receptor antagonist prevents acute hypoxia-induced pulmonary hypertension in the rat. Am J Physiol 1995;268:L95–100.
22. Lazor R, Feihl F, Waeber B, et al. Endothelin-1 does not mediate the endothelium-dependent hypoxic contractions of small pulmonary arterial smooth muscle. Chest 1996;110: 189–97.
23. Kozlowski RZ. Ion channels, oxygen sensation and signal transduction in pulmonary arterial smooth muscle. Cardiovasc Res 1995;30:318–25.
24. Robertson TP, Aaronson PI, Ward JP. Hypoxic vasoconstriction and intracellular Ca^{2+} in pulmonary arteries: evidence for PKC-independent Ca^{2+} sensitization. Am J Physiol 1995; 268:H301–7.
25. Ozaki M, Marshall C, Amaki Y, Marshall BE. Role of wall tension in hypoxic responses of isolated rat pulmonary arteries. Am J Physiol 1998;275:L1069–77.
26. Shimoda LA, Sham JS, Shimoda TH, Sylvester JT. L-type Ca^{2+} channels, resting $[Ca^{2+}]_i$ and ET-1 induced responses in chronically hypoxic pulmonary myocytes. Am J Physiol 2000;279:L884–94.
27. Kiely DG, Cargill RI, Lipworth BJ. Angiotensin II receptor blockade and effects on pulmonary hemodynamics and hypoxic pulmonary vasoconstriction in humans. Chest 1996;110: 698–703.
28. Cargill RI, Lipworth BJ. Lisinopril attenuates acute hypoxic pulmonary vasoconstriction in humans. Chest 1996;109: 424–9.
29. Marshall RP, Webb S, Bellingan GJ, et al. Angiotensin converting enzyme insertion/deletion polymorphism is associated with susceptibility and outcome in acute respiratory distress syndrome. Am J Respir Crit Care Med 2002;166:646–50.
30. Teng X, Li D, Champion HC, Johns RA. FIZZ1/RELMα, a novel hypoxia-induced mitogenic factor in lung with vasoconstrictive and angiogenic properties. Circ Res 2003;92:1065–7.
31. Murray TR, Chen L, Marshall BE, Macarak EJ. Hypoxic contraction of cultured pulmonary vascular smooth muscle cells. Am J Res Cell Mol Biol 1990;3:457–65.
32. Bakhramov A, Evans AM, Kozlowski RZ. Differential effects of hypoxia on the intracellular Ca^{2+} concentration of myocytes isolated from different regions of the rat pulmonary arterial tree. Exp Physiol 1998;83:337–47.

33. Cornfield DN, Stevens T, McMurtry IF, et al. Acute hypoxia causes membrane depolarization and calcium influx in fetal pulmonary artery smooth muscle cells. Am J Physiol 1994;266:L469–75.
34. Gelband CH, Gelband H. Ca^{2+} release from intracellular stores is an essential step in hypoxic pulmonary vasoconstriction of rat pulmonary artery resistance vessels. Circulation 1997;96:3647–54.
35. Jar RI, Toland H, Gelband CH, et al. Prominent role of intracellular Ca^{2+} release in hypoxic vasoconstriction of canine pulmonary artery. Br J Pharmacol 1997;122:21–30.
36. Wilson HL, Dipp M, Thomas JM, et al. ADP–ribosyl cyclase and cyclic ADP–ribose hydrolase act as a redox sensor: a primary role for cADPR in hypoxic pulmonary vasoconstriction. Arch Biochem Biophys 2001;151:180–7.
37. Post JM, Gelband CH, Hume JR. $[Ca^{2+}]_i$ inhibition of K^+ channels in canine pulmonary artery. Novel mechanism for hypoxia-induced membrane depolarisation. Circ Res 1995; 77:131–9.
38. Archer SL, Souil E, Dinh-Xuan AT, et al. Molecular identification of the role of voltage-gated K^+ channels, Kv1.5 and Kv2.1 in hypoxic pulmonary vasoconstriction and control of resting membrane potential in rat pulmonary artery myocytes. J Clin Invest 1998;101:2319–30.
39. Karamsetty MR, Klinger JR, Hill NS. Evidence for the role of p38 MAP kinase in hypoxia-induced pulmonary vasoconstriction. Am J Lung Cell Mol Physiol 2002;283: L859–66.
40. Osipenko ON, Evans AM, Gurney AM. Regulation of the resting potential of rabbit pulmonary artery myocytes by a low threshold, O_2-sensing potassium current. Br J Pharmacol 1997;120:1461–70.
41. McCulloch KM, Osipenko ON, Gurney AM. Oxygen-sensing potassium currents in pulmonary artery. Gen Pharmacol 1999;32:403–11.
42. Clapp LH, Gurney AM. Modulation of calcium movements by nitroprusside in isolated vascular smooth muscle cells. Pflugers Arch 1991;418:462–70.
43. Hulme JT, Coppock EA, Felipe A, et al. Oxygen sensitivity of cloned voltage-gated K^+ channels expressed in the pulmonary vasculature. Circ Res 1999;85:489–97.
44. Archer SL, London B, Hampl V, et al. Impairment of hypoxic pulmonary vasoconstriction in mice lacking the voltage-gated potassium channel Kv1.5. FASEB J 2001;15:1801–3.
45. Yuan XJ. Voltage-gated K^+ currents regulate resting membrane potential and $[Ca^{2+}]_i$ in pulmonary arterial myocytes. Circ Res 1995;77:370–8.
46. Archer SL, Weir EK, Reeve HL, Michelakis E. Molecular identification of O_2 sensors and O_2-sensitive potassium channels in the pulmonary circulation. Adv Exp Med Biol 2000; 475:219–40.
47. Itoh T, Seki N, Suzuki S, et al. Membrane hyperpolarization inhibits agonist-induced synthesis of inositol 1,4,5-triphosphate in rabbit mesenteric artery. J Physiol (Lond) 1992;451:307–28.
48. Weir EK, Reeve HL, Peterson DA, et al. Pulmonary vasoconstriction, oxygen sensing, and the role of ion channels: Thomas A. Neff lecture. Chest 1998;114(1 Suppl):17S–22S.
49. Wilson HL, Dipp M, Thoas JM, et al. ADP–ribosyl cyclase and cyclic ADP–ribose hydrolase act as a redox sensor. A primary role for ADP–ribose in hypoxic pulmonary vasoconstriction. J Biol Chem 2001;276:11180–8.
50. Ng L-C, Gurney AM. Store-operated channels mediate Ca^{2+} influx and contraction in rat pulmonary artery. Circ Res 2001;89:923–9.
51. Robertson TP, Dipp M, Ward JP, et al. Inhibition of sustained hypoxic vasoconstriction by Y-27632 in isolated intrapulmonary arteries and perfused lung of the rat. Br J Pharmacol 2000;131:5–9.
52. Gong MC, Fujihara H, Somlyo AV, Somlyo AP. Translocation of rhoA associated with Ca^{2+} of smooth muscle. J Biol Chem 1997;272:10704–9.
53. Hedges JC, Oxhorn B, Carity M, et al. Phosphorylation of caldesmon by ERK MAP kinases in smooth muscle. Am J Physiol Cell Physiol 2000;278:C718–26.
54. D'Angelo G, Adam LP. Inhibition of ERK attenuates force development by lowering myosin light chain phosphorylation. Am J Physiol Heart Circ Physiol 2002;282:H602–10.
55. Jones DP, Kennedy FG. Intracellular oxygen supply during hypoxia. Am J Physiol 1982;243:C247–53.
56. Bunn HF, Poyton RO. Oxygen sensing and molecular adaptation to hypoxia. Physiol Rev 1996;76:839–85.
57. Buescher PC, Pearse DB, Pillai RP, et al. Energy state and vasomotor tone in hypoxic pig lungs. J Appl Physiol 1991;70:1874–81.
58. Leach RM, Sheehan DW, Chacko VP, Sylvester JT. Energy state, pH, and vasomotor tone during hypoxia in precontracted pulmonary and femoral arteries. Am J Physiol Lung Cell Mol Physiol 2000;278:L294–304.
59. Kourembanos S, McQuillan LP, Leung GK, Faller DV. Nitric oxide regulates the expression of vasoconstrictors and growth factors by vascular endothelium under both normoxia and hypoxia. J Clin Invest 1993;92:99–104.
60. Sandrey J, Bunn HF. In vivo and in vitro regulation of erythropoietin mRNA: measurement by competitive polymerase chain reaction. Blood 1993;81:617–23.
61. Chandel NS, Maltepe E, Goldwasser E, et al. Mitochondrial reactive oxygen species trigger hypoxia-induced transcription. Proc Natl Acad Sci U S A 1998;95:11715–20.
62. Waypa GB, Schumacker PT. O(2) sensing in hypoxic pulmonary vasoconstriction: the mitochondrial door re-opens. Respir Physiol Neurobiol 2002;132:81-91.
63. Shimoda LA, Sham JSK, Sylvester JT. Altered pulmonary vasoreactivity in the chronically hypoxic lung. Physiol Res 2000;49:549–60.
64. McMurtry IF, Petrun MD, Reeves JT. Lungs from chronically hypoxic rats have decreased pressor response to acute hypoxia. Am J Physiol 1978;235:H104–9.
65. Reeve HL, Michelakis E, Nelson DP, et al. Alterations in a redox oxygen sensing mechanism in chronic hypoxia. J Appl Physiol 2001;90:2249–56.
66. McMurtry IF, Morris KG, Petrun MD. Blunted hypoxic vasoconstriction in lungs from short-term high-altitude rats. Am J Physiol 1978;238:H849–57.
67. Chen YF, Oparil S. Endothelial dysfunction in the pulmonary vascular bed. Am J Med Sci 2000;320:223–32.
68. Shimoda LA, Sham JS, Liu Q, Sylvester JT. Acute and chronic hypoxic pulmonary vasoconstriction: a central role for endothelin-1? Respir Physiol Neurobiol 2002;132:93–106.
69. Smirnov SV, Robertson TP, Ward JPT, Aaronson PI. Chronic hypoxia is associated with reduced delayed rectifier K^+ current in rat pulmonary artery muscle cells. Am J Physiol 1994;266:H365–70.
70. Suzuki H, Twarog BM. Membrane properties of smooth muscle cells in pulmonary hypertensive rats. Am J Physiol 1982;242:H907–15.
71. Oka M, Morris KG, McMurtry IF. NIP-121 is more effective than nifedipine in acutely reversing chronic hypoxic pulmonary hypertension. J Appl Physiol 1993;75:1074–80.
72. Frid MG, Aldashev AA, Cabirac GF, et al. Hypoxia stimulates proliferation of a unique cell population isolated from the bovine vascular media. Chest 1998;114(1 Suppl): 28S–9S.
73. Frid MG, Dempsey EC, Durmowicz AG, Stenmark KR. Smooth muscle cell heterogeneity in pulmonary and systemic

vessels. Importance in vascular disease. Arterioscler Thromb Vasc Biol 1997;17:1203–9.
74. Frid MG, Aldashev AA, Dempsey EC, Stenmark KR. Smooth muscle cells isolated from discrete compartments of the mature vascular media exhibit unique phenotypes and distinct growth capabilities. Circ Res 1997;81:940–52.
75. Hasleton PS, Spencer H. Spencer's pathology of the lung. 5th ed. New York: McGraw-Hill, Health Professions Division; 1996.
76. van Suylen RJ, Aartsen WM, Smits JF, Daemen MJ. Dissociation of pulmonary vascular remodeling and right ventricular pressure in tissue angiotensin-converting enzyme-deficient mice under conditions of chronic alveolar hypoxia. Am J Respir Crit Care Med 2001;163:1241–5.
77. Taraseviciene-Stewart L, Kasahara Y, Alger L, et al. Inhibition of the VEGF receptor 2 combined with chronic hypoxia causes cell death-dependent pulmonary endothelial cell proliferation and severe pulmonary hypertension. FASEB J 2001; 15:427–38.
78. Voelkel NF, Cool C, Taraceviene-Stewart L, et al. Janus face of vascular endothelial growth factor: the obligatory survival factor for lung vascular endothelium controls precapillary artery remodeling in severe pulmonary hypertension. Crit Care Med 2002;30(5 Suppl):S251–6.
79. Lee SD, Shroyer KR, Markham NE, et al. Monoclonal endothelial cell proliferation is present in primary but not secondary pulmonary hypertension. J Clin Invest 1998;101:927–34.
80. Tristani-Firouzi M, Reeve HL, Tolarova S, et al. Oxygen-induced constriction of the rabbit ductus arteriosus occurs via inhibition of a 4-aminopyridine-sensitive potassium channel. J Clin Invest 1996;98:1959–65.
81. Coceani F, Liu Y, Seidlitz E, et al. Endothelin A receptor is necessary for O(2) constriction but not closure of ductus arteriosus. Am J Physiol 1999;277(4 Pt 2):H1521–31.
82. Michelakis E, Rebeyka I, Bateson J, et al. Voltage-gated potassium channels in human ductus arteriosus. Lancet 2000; 356:134–7.
83. Seidner SR, Chen YQ, Oprysko PR, et al. Combined prostaglandin and nitric oxide inhibition produces anatomic remodeling and closure of the ductus arteriosus in the premature newborn baboon. Pediatr Res 2001;50: 365–73.
84. Michelakis ED, Rebeyka I, Wu X, et al. O_2 sensing in the human ductus arteriosus: regulation of voltage-gated K^+ channels in smooth muscle cells by a mitochondrial redox sensor. Circ Res 2002;91:478–86.
85. Reeve HL, Tolarova S, Nelson DP, et al. Redox control of oxygen sensing in the rabbit ductus arteriosus. J Physiol 2001;533(Pt 1):253–61.
86. Kajino H, Goldbarg S, Roman C, et al. Vasa vasorum hypoperfusion is responsible for medial hypoxia and anatomic remodeling in the newborn lamb ductus arteriosus. Pediatr Res 2002;51:228–35.
87. Doherty JU, Liang S-S. Arterial hypoxia in awake dogs: role of the sympathetic nervous system in mediating the systemic hemodynamic and regional blood flow responses. J Lab Clin Med 1984;104:665–7.
88. Cain SM. Oxygen delivery and uptake in dogs during anemic and hypoxic hypoxia. J Appl Physiol 1977;74:228–34.
89. Kuwahira I, Gonzalez NC, Heisler N, Piiper J. Changes in regional blood flow distribution and oxygen supply during hypoxia in conscious rats. J Appl Physiol 1993;74: 211–4.
90. Borgia JF, Horvath SM. Effects of acute prolonged hypoxia on cardiovascular dynamics in dogs. J Appl Physiol 1977;43: 784–9.
91. Fisher AJ, Schrader NW, Klitzman B. Effects of chronic hypoxia on capillary flow and hematocrit in rat skeletal muscle. Am J Physiol Heart Circ Physiol 1992;31:H1877–83.
92. Snyder GK, Farelly C, Cuelho JR. Adaptations in skeletal muscle capillarity following changes in oxygen supply and changes in oxygen demands. Eur J Appl Physiol 1992;65: 158–63.
93. Toporsian M, Ward ME. Hyporeactivity of rat diaphragmatic arterioles following exposure to hypoxia in-vivo: role of the endothelium. Am J Respir Crit Care Med 1997;156:1572–8.
94. Auer G, Ward ME. Impaired reactivity of rat aorta to phenylephrine and KCl after prolonged hypoxia: role of the endothelium. J Appl Physiol 1998;85:411–7.
95. Doyle MP, Walker BR. Attenuation of systemic vasoreactivity in chronically hypoxic rats. Am J Physiol Regul Integr Comp Physiol 1991;260:R1114–22.
96. Duling BR, Berne RM. Longitudinal gradients in periarteriolar oxygen tension. Circ Res 1970;27:669–78.
97. Wittenberg BA, Wittenberg JB. Transport of oxygen in muscle. Annu Rev Physiol 1989;51: 857–78.
98. Tsikaras DP, Natsis K, Hytiroglu P, et al. Microanatomy of the vasa vasorum of the human thoracic aorta: a study utilizing a polyester resin casting technique. Morphologie 1997;252: 21–2.
99. Pearson PJ, Lin PJ, Evora PR, Schaff HV. Endothelium-dependent response of human internal mammary artery to hypoxia. Am J Physiol Heart Circ Physiol 1993;264: H376–80.
100. Hutchins PM, Bond RF, Green HD. Participation of oxygen in the local control of skeletal muscle microvasculature. Circ Res 1974;34:85–93.
101. Boeghold MA, Johnson PC. Periarteriolar and tissue PO_2 during sympathetic escape in skeletal muscle. Am J Physiol 1988; 254:H929–36.
102. Kekkhof CJM, van der Linden PJW, Sipkema P. Role of myocardium and endothelium in coronary vascular smooth muscle responses to hypoxia. Am J Physiol Heart Circ Physiol 2002;282:H1296–303.
103. Liao JK, Zulueta JJ, Yu FS, et al. Regulation of bovine endothelial constitutive nitric oxide synthase by oxygen. J Clin Invest 1995;96:2661–6.
104. Liu Q, Flavahan NA. Hypoxic dilatation of porcine small coronary arteries: role of endothelium and KATP channels. Br J Pharmacol 1997;120:728–34.
105. Harder DR, Narayanan J, Birks EK, et al. Identification of a putative microvascular oxygen sensor. Circ Res 1996;79: 54–61.
106. Messina EJ, Sun D, Koller A, et al. Increases in oxygen tension evoke arteriolar constriction by inhibiting endothelial prostaglandin synthesis. Microvasc Res 1994;48: 151–60.
107. Ward ME. Dilation of rat diaphragmatic arterioles by flow and hypoxia: roles of nitric oxide and prostaglandins. J Appl Physiol 1999;86:1644–50.
108. Ward ME, Hussain SNA. Effect of inhibition of nitric oxide release on the diaphragmatic oxygen delivery–consumption relationship. J Crit Care 1994;9:90–9.
109. Burnstock G, Lincoln J, Feher E, et al. Serotonin is localized in endothelial cells of coronary arteries and released during hypoxia: a possible new mechanism for hypoxia-induced vasodilation in rat heart. Experientia 1988;44:705–7.
110. Wei HM, Kang YH, Merrill GF. Canine coronary vasodepressor responses to hypoxia are abolished by 8-phenyltheophylline. Am J Physiol Heart Circ Physiol 1989;257:H1043–8.
111. Tateishi J, Faber JE. ATP-sensitive K^+ channels mediate a_{2D}-adrenergic receptor contraction of arteriolar smooth muscle and reversal of contraction by hypoxia. Circ Res 1994;76:53–63.
112. Grote J, Siegel G, Zimmer K, Adler A. The influence of oxygen tension on membrane potential and tone of canine carotid artery smooth muscle. Am J Physiol 1980;222:481–7.

113. Pearce WJ, Ashwal S, Long DM, Cuevas J. Hypoxia inhibits calcium influx in rabbit basilar and carotid arteries. Am J Physiol Heart Circ Physiol 1992;262:H106–13.
114. Moreland S, Coburn RF, Baron CB, Moreland RS. Mechanical and biochemical events during hypoxia-induced relaxations of rabbit aorta. In: Moreland RS, editor. Regulation of smooth muscle contraction. New York: Plenum Press; 1991. p. 147–57.
115. Coburn RF, Baron C, Papadopoulos MT. Phosphoinositide metabolism and metabolism–contraction coupling in rabbit aorta. Am J Physiol 1998;255:H1476–82.
116. Toporsian M, Govindaraju K, Nagi M, et al. Downregulation of endothelial nitric oxide synthase in rat aorta after prolonged hypoxia in vivo. Circ Res 2000;86:671–5.
117. Heistad DD, Wheeler RC, Aorki VS. Reflex cardiovascular responses after 36 hr of hypoxia. Am J Physiol 1971;220: 1673–6.
118. Heistad DD, Abboud FM, Mark AL, Schmid PG. Impaired reflex vasoconstriction in chronically hypoxemic patients. J Clin Invest 1972;51:331–7.
119. Gonzales RJ, Walker BR. Role of CO in attenuated vasoconstrictor reactivity of mesenteric resistance arteries after chronic hypoxia. Am J Physiol Heart Circ Physiol 2002;282: H30–7.
120. Earley S, Nair JS, Walker BR. 48-h hypoxic exposure results in endothelium-dependent systemic vascular smooth muscle cell hyperpolarization. Am J Physiol Regul Integr Comp Physiol 2002;283:R79–85.
121. Zacour ME, Toporsian M, Auer G, et al. Enhancement of aortic contractility by endothelin following prolonged hypoxia in vivo. Pulmonary Pharmacol Ther 1998;11:197–9.
122. Maines MD. Heme oxygenase: function, regulatory mechanisms, and clinical applications. FASEB J 1988;2:2557–68.
123. Morita T, Perella MA, Lee M-E, Kourembanas S. Smooth muscle cell-derived carbon monoxide is a regulator of vascular cGMP. Proc Natl Acad Sci U S A 1995;92:1475–9.
124. Panchenko MV, Farber HW, Korn JH. Induction of hemeoxygenase-1 by hypoxia and free radicals in human dermal fibroblasts. Am J Physiol 2000;278:C92–101.
125. Zacour ME, Teoh H, Halayko AJ, Ward ME. Mechanisms of aortic smooth muscle hyporeactivity after prolonged hypoxia in rats. J Appl Physiol 2002;92:2625–32.
126. Teoh H, Zacour M, Wener A, et al. Increased myofibrillar protein phosphatase-1 activity impairs rat aortic smooth muscle activation after hypoxia. Am J Physiol (Heart Circ Physiol) 2003;284:H1182–9.
127. Toporsian M, Govindaraju V, Giaid A, Ward ME. Neuronal nitric oxide synthase expression in rat aortic smooth muscle following *in-vivo* hypoxia. Circ Res 1998;98:147–54.
128. Govindaraju V, Ward ME. Endothelial expression of hemeoxygenase-1 in rat aorta following hypoxia. Am J Respir Crit Care Med 1999;159:A347.
129. Lombard JH, Hinojosa-Laborde C, Cowley AW. Hemodynamic and microcirculatory alterations in reduced renal mass hypertension. Hypertension 1989;13:128–38.
130. Kiely DG, Cargill RI, Lipworth BJ. Angiotensin II receptor blockade and effects on pulmonary hemodyamics and hypoxic pulmonary vasoconstriction in humans. Chest 1996;110: 698–703.
131. Teng X, Li D, Champion HC, Johns RA. F1221/RELM alpha, a novel hypoxia-induced mitogenic factor in lung with vasoconstrictive and angiogenic properties. Circ Res 2003; 92:1065–7.

CHAPTER 21

NEURAL CONTROL OF BREATHING

Immanuela Ravé Moss

In this chapter, current concepts concerning the regulation of respiration in the mammal are reviewed, with special emphasis on the human whenever possible. The approach is to take this subject from the fundamental neuronal network currently thought to be the prime generator of central respiratory activity, the putative pacemaker region in the rostral medulla, to respiratory patterns and reflexes in relation to behavioral state in the whole organism. The chapter is organized as follows:

1. The pre-Bötzinger complex—location, structure, function, connectivity, and ontogeny
2. Other respiratory-related brain regions—location, structure, function, connectivity, and ontogeny
3. Respiratory patterns in relation to sleep–wake states throughout ontogeny
4. Respiratory reflexes in relation to sleep–wake states throughout ontogeny

Most of the work that defines the central respiratory network has been performed in fetal or neonatal in vitro preparations. As respiratory patterns and reflexes show changes with maturation, respiratory control is treated as a continuum throughout ontogeny, in which plasticity from fetal life through postnatal development to the mature stage of life is considered. Clinical correlates of pathophysiologic aspects of respiratory control are also presented.

PRE-BÖTZINGER COMPLEX: LOCATION, STRUCTURE, FUNCTION, CONNECTIVITY, AND ONTOGENY

The question of where respiratory rhythm originates has been haunting neurobiologists for many years. Under normal circumstances, this rhythm is robust and regular, and it is modulated by environmental, sleep–wake, emotional, and volitional factors. Over the years, and involving many experimental approaches, several models of central respiratory control have been proposed. The particulars of these models have been largely superseded by the current concepts described in this chapter. Nevertheless, a concept common to these models, which still stands today, is that the efferent central respiratory activity that drives the various respiratory muscles is the summation of a central respiratory drive generated in some respiratory-related brainstem region(s). The fundamental question, however, has been where and precisely how this activity is generated. Does this central activity result from mere oscillatory reciprocal activation–deactivation among various neuronal groups? If this is the case, then how was this activity initiated in the first place? Furthermore, would not such breathing activity, with any mishap, halt at a particular phase in the ongoing breathing cycle, with there being no apparent mechanism for restarting the respiratory oscillation? Because of these and other questions, an alternative hypothesis has been advanced, according to which each breath is generated from a pacemaker. This theory proposes that a neuron or group of pacemaker neurons, endowed with intrinsic membranous ion channel characteristics, depolarize, fire, and repolarize in a rhythmic fashion. This endogenous oscillatory activity can be modulated by afferent inputs, generating an efferent output that is translated into a respiratory drive.

Pacemaker neurons have been well characterized in invertebrates. This is because invertebrates do not have a single central nervous system but instead have several neuronal ganglia, each endowed with a small number of large, distinct, and easily manipulated neurons. Among these are pacemaker neurons controlling motor functions, whose properties have been defined extensively.[1–3] By contrast, the search for a respiratory pacemaker in the multineuronal and highly interconnected mammalian brain has been a very difficult task. Nevertheless, this search has culminated in the seminal study of Smith and colleagues,[4] who identified a group of neurons in the rostral portion of the neonatal rat medulla in vitro that displayed several characteristics required for their definition as pacemakers. To briefly summarize the findings from this and subsequent investigations, these specialized neurons, approximately 600 in number in the adult rat, have been identified in the pre-Bötzinger complex located next to the ambigual nucleus in the rostral ventrolateral medulla. These neurons display bursting activities that are intrinsic and occur in phase with the respiratory cycle, as registered from more peripheral nerves or muscles

(Figure 21-1). A lesion or disruption of synaptic activity within this region can abolish respiratory rhythm. By contrast, the same disruptions occurring caudally to these neurons do not have the same effect.[4–8] This observation demonstrates the importance of this locus for the generation of respiratory drive.

Evidence for the existence and characteristics of the pre-Bötzinger complex neurons has been obtained from a variety of fetal and neonatal in vitro preparations in rodents and from in vivo experiments in anesthetized, decerebrate, and even awake animals of several species.

As elsewhere in the brain, communication between the pre-Bötzinger complex neurons and other regions relies on the presence of excitatory and inhibitory neurotransmitters and neuromodulators. Of great importance in this respect are the G protein–coupled excitatory neurokinin-1 (NK-1) and inhibitory μ-opioid receptor systems. These systems not only have a neuromodulatory role in this pacemaker complex but also seem to define it anatomically in the rat brain. Thus, in addition to displaying intrinsic bursts at respiratory frequency rates, the pre-Bötzinger complex neurons have been shown to express NK-1 receptors that are specific for the excitatory neuropeptide substance P.[9–11] The function of the pacemaker neurons in wild-type versus NK-1-knockout mice was assessed with the use of in vitro preparations and NK-1 antagonists.[12] In conscious rats, the pacemaker regions of the pre-Bötzinger complex were identified by specific chemical lesions that targeted and destroyed the neurons expressing NK-1 receptors, thus producing severe respiratory arrhythmia.[10] The identification of the pacemaker neurons within the pre-Bötzinger complex has been proposed to further require a colocalization of the NK-1 receptors with μ-opioid receptors,[9] the inhibitory endogenous neuropeptides which comprise endomorphin 1 and 2, β-endorphin, and, to some extent, enkephalins. Whereas there are some reports of the presence of several excitatory and inhibitory neurotransmitters in the pre-Bötzinger complex,[13] in other detailed studies it has been found that the only abundant rapidly acting neurochemical in this region is the excitatory neurotransmitter glutamate.[14,15]

The general current theory of the manner in which the pre-Bötzinger pacemaker neurons function is that they are propriomedullary interneurons; that is, they are confined locally and do not by themselves send long axons peripherally. These pacemaker neurons are connected to each other, however, both ipsilaterally and bilaterally. They are also connected to other nearby ventrolateral respiratory column neurons, to cranial motor neurons that supply the respiratory upper airway muscles, and to paraambigual premotor neurons. The latter send efferent axons to spinal motor neurons that, in turn, innervate the major inspiratory and expiratory muscles. Thus, this hybrid pacemaker network provides efferent rhythmic excitation that generates the respiratory oscillation we see as regular breathing.[7,8,14,16]

Very recent findings, however, have cast doubt on this model of the respiratory rhythm generator. As the basic definition of the pre-Bötzinger pacemakers includes their dependence on an intrinsic persistent Na^+ current,[17,18] inhibition of this current would be expected to stop both pacemaker activity and all peripheral respiratory function. However, such experimental inhibition, although arresting the rhythmic bursting activity of the pacemakers, does not perturb hypoglossal respiratory motor activity.[18] This finding suggests that other loci or mechanisms must also participate in the generation of respiratory drive. In this context, it is noteworthy that there is still some controversy as to whether respiratory activity under extreme circumstances, such as gasping during autoresuscitation, involves the pattern generator or another pathway.[8]

Does the pre-Bötzinger complex change during development? This is hard to determine as the in vitro work to define its characteristics has been done in fetal or neonatal rodent preparations, which, by nature, are quite immature, and there have been no attempts in intact animals to define

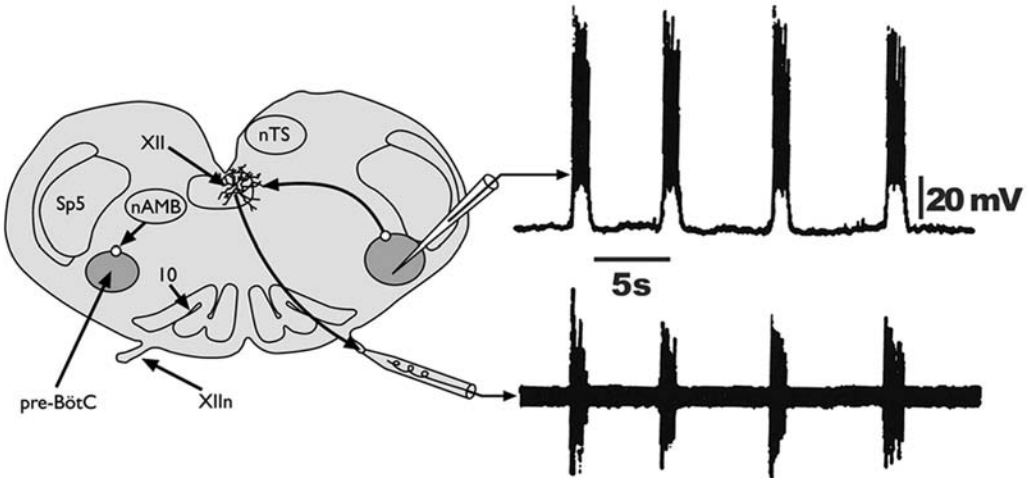

FIGURE 21-1 Schematic representation of the medulla at the level of the pre-Bötzinger complex (pre-BötC) in the in vitro rat preparation. The pre-Bötzinger complex sends signals to the hypoglossal (XII) nucleus, which, in turn, drives the hypoglossal nerve (XII n). Note that the intrinsic oscillatory activity recorded intracellularly from a pre-Bötzinger complex neuron occurs simultaneously with the extracellular inspiratory activity recorded from the hypoglossal nerve. IO = inferior olive; nAMB = ambigual nucleus; nTS = solitary tract nucleus; Sp5 = spinal trigeminal nucleus. Adapted from Smith JC et al[4] and Feldman JL and McCrimmon DR.[81]

its function throughout maturation. Anatomically, however, Ellenberger[19] has found that the neonatal rat has relatively more premotor neurons within the pre-Bötzinger complex than does the adult rat, perhaps indicating continued pacemaker neuronal division in early rodent life. Another clue to possible developmental differences can perhaps be found in the studies of Thoby-Brisson and Ramirez,[17,20] which have revealed two types of pacemaker neuron in neonatal (ie, immature) mouse slice preparation—one group that is cadmium (Cd^{2+}) sensitive and another that is not. The sensitivity to Cd^{2+} presumably indicates the ionic currents operating in these neurons, in which Cd^{2+} sensitivity implies persistent Na^{+} currents and Cd^{2+} insensitivity implies an activation of Ca^{2+} currents. Unlike the Cd^{2+}-insensitive neurons, which respond to anoxia with increased activity, the Cd^{2+}-sensitive neurons respond to anoxia with complete arrest of respiratory activity. Equivalent responses in the intact subject might be, respectively, respiratory stimulation, typical of the mature response to hypoxia, versus apnea, typical of the fetal response to hypoxia. Therefore, one might hypothesize that, with maturation, the pacemaker neuronal activity gradually changes from relying on persistent Na^{+} currents to becoming dependent on Ca^{2+} current activation, thus contributing to the maturation of the respiratory response to hypoxia.

OTHER RESPIRATORY-RELATED BRAIN REGIONS: LOCATION, STRUCTURE, FUNCTION, CONNECTIVITY, AND ONTOGENY

The establishment of the pre-Bötzinger complex as the probable kernel of respiratory drive does not mean that it is the only brain region important for respiratory control. In fact, there are many respiratory-related regions, both in the brainstem and above it, that are of great importance in receiving and integrating afferent input and in mediating or modulating respiratory drive. The most important of these regions are the ventral respiratory group, arranged rostrocaudally in the ventrolateral medulla in association with the ambigual nucleus, and the dorsal respiratory group, located on the dorsal aspect of the medulla and concentrated in the ventrolateral portion of the solitary tract nucleus (Figure 21-2).

The ventral respiratory group, aside from containing the pre-Bötzinger complex, is largely composed of premotor neurons that make connections with the following groups of motor neurons: (1) monosynaptically, with the inspiratory motor neurons in the phrenic nuclei at the C2 to C4 level that supply the diaphragm; (2) monosynaptically, with the inspiratory motor neurons in the cranial nuclei that innervate the respiratory laryngeal, tongue, and pharyngeal upper airway muscles; (3) polysynaptically, with inspiratory motor neurons in the thorax at T1 to T12 that transmit the drive to external intercostal muscles; and (4) polysynaptically, with expiratory motor neurons in the thorax and abdomen that supply expiratory muscles such as the internal intercostal and abdominal muscles (Figure 21-3). Although these premotor neuronal groups have relatively distinct locations along the ambigual/paraambigual nucleus, there is also a great deal of intermingling among them.[19,21,22]

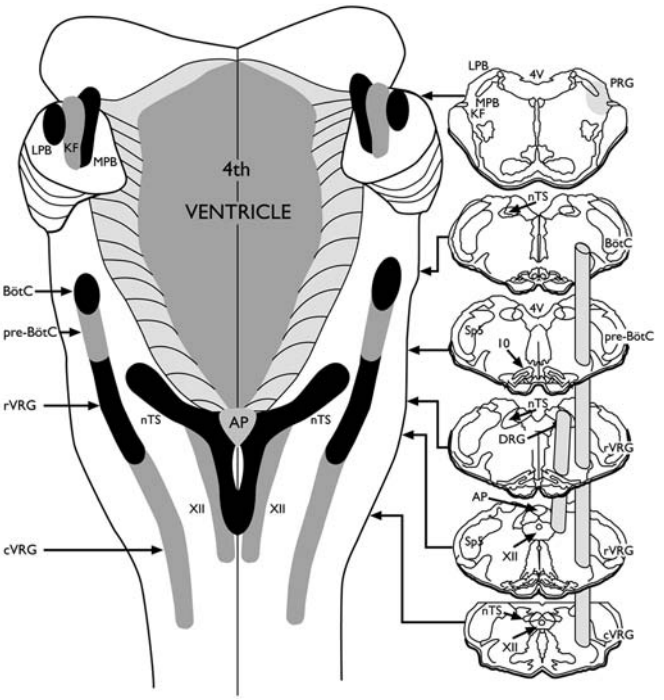

FIGURE 21-2 Schematic representation of a dorsal view of the pons and medulla (cerebellum removed) on the left and of brain sections at several selected levels of the brainstem on the right. The major brainstem respiratory regions, from rostral to caudal, are as follows: (1) in the pons, pontine respiratory group (PRG), including lateral parabrachial nucleus (LPB), medial parabrachial nucleus (MPB), and Kölliker–Fuse nucleus (KF); and (2) in the medulla, paraambigual Bötzinger complex (BötC), pre-Bötzinger complex (pre-BötC), rostral ventral respiratory group (rVRG), caudal ventral respiratory group (cVRG), and solitary tract nucleus–related dorsal respiratory group (DRG). AP = area postrema; IO = inferior olive; nTS = solitary tract nucleus; Sp5 = spinal trigeminal nucleus; 4V = 4th ventricle; XII = hypoglossal nucleus. Adapted from Feldman JL and McCrimmon DR[81] and Feldman JL and Smith JC.[82]

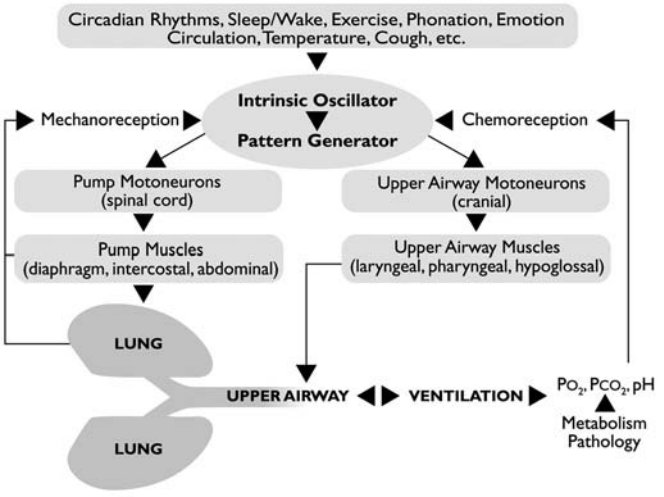

FIGURE 21-3 Schematic representation of the respiratory control system, showing efferent and afferent pathways between the respiratory oscillator (the pre-Bötzinger complex) and the effector organ (the upper airway and the lung), as well as many other influences on breathing behavior. Adapted from Feldman JL and McCrimmon DR.[81]

The dorsal respiratory group in the ventrolateral solitary tract nucleus also contains premotor neurons that supply inspiratory motor neurons (see Figure 21-2). In addition, this region is the recipient of important afferent stimuli, most notably from peripheral and central chemoreceptors and from stretch receptors in the lung (see Figure 21-3). Because there are also many synaptic connections between this region and the ventral respiratory group, the solitary tract nucleus is considered to be a major integrative region for respiratory control. The connectivity between the dorsal and ventral respiratory groups shows species variability; for example, it is less in the rat than in the cat.[22] The importance of this dorsal region to respiratory control, even in the rat, has been recently documented in experiments in which a specific lesion of this region in rats resulted in loss of responsiveness to hypoxemia.[23]

An even more impressive testament to the importance of the dorsal respiratory group in respiratory rhythmogenesis is a report[24] of a 52-year-old woman who was diagnosed with metastatic adenocarcinoma of unknown primary origin. The patient was unexpectedly found dead 10 weeks after the initial diagnosis. A detailed pathologic examination of her brain revealed a previously undetected 2.0×1.3 mm tumor in the right medulla, replacing the solitary tract nucleus at that location (Figure 21-4*A*). The authors suggested that this small tumor, located in a crucial integrative location unilaterally, was sufficient to cause respiratory arrest. The vulnerability of respiratory rhythmogenic mechanisms to central nervous system pathology has been observed frequently and reported extensively.[25]

Aside from the medullary ventral and dorsal respiratory groups, there are other respiratory-related regions in the brainstem that are also important in normal breathing but are only mentioned here. These include the lateral paragigantocellular, the lateral reticular and the cranial trigeminal, facial and hypoglossal nuclei in the medulla, and the parabrachial and Kölliker–Fuse nuclei in the pons (see Figure 21-2). Additional brainstem regions that are pertinent to the relationship between sleep–wake states and respiration include the locus coeruleus in the pons and the reticular raphé nuclei. However, this is not a complete list of respiratory-related brain regions. Suprapontine brain regions, that is, regions above the brainstem, are thought to exert important modulatory influences on the major brainstem regions, especially when there are specific physiologic requirements and/or in stressful situations.[26] Several such diencephalic and midbrain nuclei are activated, for example, by chemical stimuli such as hypoxia and hypercapnia[26–29] or by exercise.[30] The putative respiratory role of these regions was indicated by electrophysiologic activation in rat brain slice neurons in vitro in response to gaseous perturbations in the bathing liquid or by immunostaining for the early gene c-*fos* in response to gaseous exposure or exercise stimuli in intact rats. The regions and nuclei thus identified include the suprapontine lateral and posterior hypothalamus and the periaqueductal gray.

A developmental pattern in some of these responses was also discerned. Caudal hypothalamic neurons of neonatal rats showed lower sensitivity to hypoxia than did those of mature rats, expressed as lower electrical responsiveness in rat brain slices studied in vitro,[27] and lack of c-*fos* activation in brains from rats exposed to hypoxia in vivo.[28]

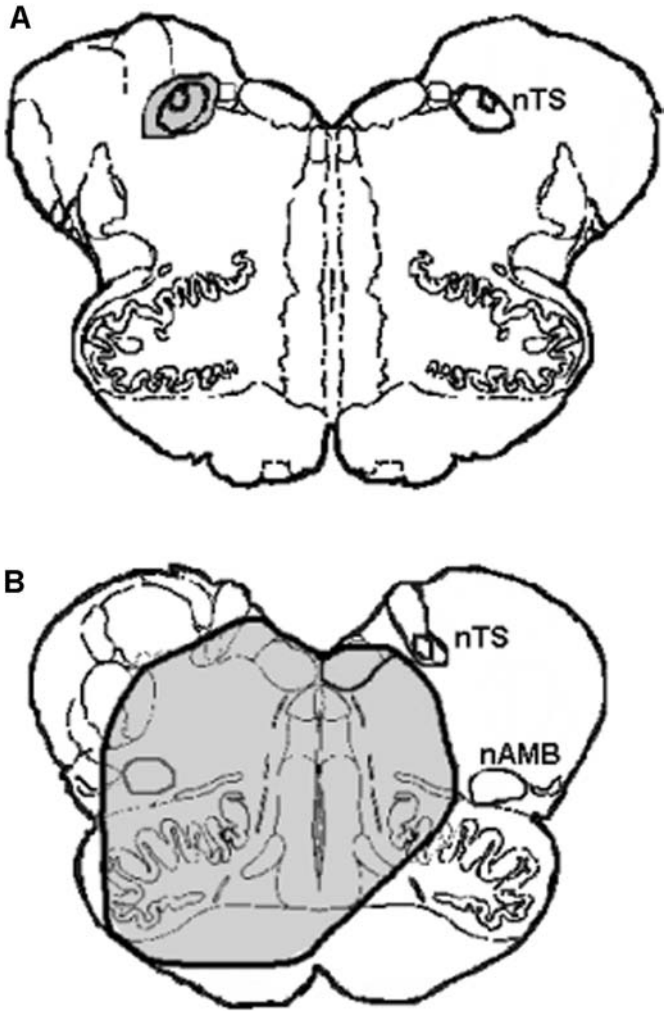

FIGURE 21-4 *A*, Schematic representation of the rostral medulla (dorsal side up), depicting a normal solitary tract nucleus on the right side and a metastatic tumor replacing that nucleus on the left side (*shaded*). In this case, the tumor affected respiratory rhythmicity. Adapted from Rhodes RH and Wightman HR.[24] *B*, Schematic representation of the rostral medulla (dorsal side up) in another patient; the extent of a metastatic tumor is indicated by shading. Despite the location and tumor size, the pathophysiologic effect was on efferent respiratory drive rather than on rhythmogenesis. nAMB = ambigual nucleus; nTS = solitary tract nucleus. Adapted from Corne S et al.[33]

It is important to emphasize that respiration is a behavior and thus is under volitional control. The drive to breathe during speaking, singing, breath-holding, or expulsive maneuvers originates in the cortex (see Figure 21-3).[31] The cortex, too, reacts to hypoxia with c-*fos* activation.[32]

Another illustrative case[33] is that of a 67-year-old man who had a metastasis from a pulmonary adenocarcinoma in his brainstem that was much more extensive than the one described in the previous patient. This tumor (Figure 21-4B) replaced a significant portion of the ambigual and solitary tract nuclei, at least unilaterally, as shown by magnetic reso-

nance imaging (although the precise extent of the tumor was not confirmed pathologically). Despite the extent and crucial location of the tumor, this patient did not display any disturbances in rhythmogenesis. Instead, he developed hypercarbic respiratory failure, during which his respiratory frequency increased appropriately, indicating normal respiratory rhythm, whereas his respiratory effort per breath, expressed as transdiaphragmatic pressure swings, was very much diminished. This reduced respiratory effort remained low even when he volitionally attempted a maximal inspiratory effort. Importantly, the precise location of the pre-Bötzinger complex in humans is not known, and it is presumed that this "kernel" of respiratory rhythm was spared in this case. As such, the findings in this patient may be explained by a disruption in the cortical respiratory motor outflow that normally passes through the autonomic respiratory-related regions on its way to the respiratory muscles. This report is instructive in showing the value of respiratory function studies in the assessment of pathophysiologic processes and in indicating how essential the various respiratory brain nuclei and regions are to the overall sustenance of normal breathing.

Much effort has been exerted by respiratory neurophysiologists in recording and classifying the pattern and timing of the electrophysiologic activities of the respiratory premotor neurons in the major ventral and dorsal respiratory regions and of the neurons in the respiratory modulatory regions. To summarize, these neurons have been found to have ramp-like increasing activities or a rapid rise in activity, followed by a gradual decrease. When their activity has been correlated with peripheral respiratory activities from recordings of phrenic or hypoglossal nerves, the premotor neurons have been found to fire either just before, early on, or during inspiration or expiration. Other neurons have been defined as "phase-spanning," that is, starting to fire during one phase of the respiratory cycle and continuing to fire into the next phase.[8]

There has also been a considerable amount of research aimed at defining the role of neurotransmitter and neuromodulator systems in determining respiratory drive. There is no question that the brain as a whole, including the respiratory-related regions mentioned here, is endowed with a host of such systems (approximately 70 in number), each comprising endogenous ligands and their respective receptors. Therefore, it is not surprising that many agonists or antagonists will often elicit some respiratory-related response when they are injected systemically, microinjected into specific brain loci, or deposited on brain slices.

Caution, however, must be exercised in making the huge jump between such effects and assigning a physiologic role to that transmitter–modulator system in respiratory control. For such a role to be assigned, trials must first be conducted in conscious, intact (including chronically instrumented), and healthy subjects. Second, such trials must be conducted throughout ontogeny as the role of such systems changes with maturation and aging. Third, for each system, reliable assignment as a physiologic player necessitates a variety of experimental approaches carried out throughout ontogeny. These include (1) a significant and dose-dependent response to physiologic concentrations of an agonist—this will establish the presence of the receptor in the region of interest; (2) a significant and dose-dependent response to physiologic concentrations of an antagonist—this will establish that the receptor in that region is normally active and functioning; (3) mapping and quantification of the receptor and ligand in the region of interest; (4) a physiologic respiratory response to a stimulus purported to affect this system and a reversal of the expected physiologic response with an antagonist; and (5) a neuroendocrinologic change in this system in response to the same stimulus that explains the physiologic response.[34] Application of these strict criteria will provide the required assurance that a particular transmitter–modulator system is important in the physiologic control of breathing.

It is widely accepted (although some disputes exist, at least in some situations) that three major rapid neurotransmitters serve as emissaries in sending information to and from the neuronal components of respiratory control: glutamate, as the universal excitatory neurotransmitter, and γ-aminobutyric acid and glycine, as the inhibitory neurotransmitters, each with its respective postsynaptic receptor(s).

More complicated are the functions of the slower-acting neuromodulators. These often coexist with neurotransmitters in the same vesicles and either alter neuronal activity directly or modify the release/activity of the rapid neurotransmitters. Neuromodulators with attributed influences on breathing comprise adenosine, monoamines, including catecholamines and 5-hydroxytryptamine (serotonin), neuropeptides, including opioids, somatostatin, substance P, thyrotropin-releasing hormone, and steroids, including sex hormones. Of these, serotonin, substance P, and opioids have attracted the most interest.

Whereas serotonin and its multiple receptors are widely, albeit heterogeneously, represented in many respiratory regions, respiratory responses to serotonin agonists or antagonists have been variable and inconsistent; in some cases there has been stimulation of respiration and in others respiratory depression.[35] Most recently, interest has focused on the role of this system in producing long-term facilitation in respiration following repeated exposure to hypoxia.[36] In anesthetized, paralyzed, and ventilated adult rats breathing hyperoxic air, interrupted by three 5-minute exposures to hypoxia, the phrenic nerve response 20 to 60 minutes after the hypoxic exposures increases gradually to a level above baseline, and this response has been shown to be serotonin dependent.[37] In awake rats, however, repetitive hypoxia is followed by a very modest increase in ventilation[38,39] and only over a narrow range of hypoxia, above or below which no respiratory facilitation occurs at all.[39] Moreover, repeated hypoxic exposure, similar to that used in the anesthetized rats, does not elicit any posthypoxic respiratory facilitation in healthy adult men, either awake or asleep,[37] nor does repetitive hypoxia elicit any long-term facilitation in healthy awake men or women, either in minute ventilation or in upper airway dilatory genioglossal muscle activity.[40] Only men diagnosed with regular snoring, inspiratory flow limitation, or obstructive sleep apnea have shown facilitation after repeated hypoxia similar to that seen in anesthetized rats.[37] One might conclude that posthypoxic long-term respiratory facilitation is not significant in the overall normal respiratory

response to repeated hypoxia and that this phenomenon, which is influenced by serotonin, may occur only under pathologic conditions of airway obstruction.

With regard to the excitatory neuropeptide substance P, various experimental approaches have convincingly established this neuropeptide system as a true modifier of breathing control throughout ontogeny.[41–43] Research into the physiologic role of the inhibitory opioid systems in respiratory control has established their natural influence during development, according to all the criteria elaborated above. Specifically, the μ-opioid system, in particular, provides attenuation of breathing in the early postnatal period, and this influence diminishes with maturation.[41–43] In contrast, this opioid system has shown little influence on breathing in conscious healthy adult mammalian subjects. This influence appears to resume, however, in adult patients suffering from chronic obstructive lung disease, in whom μ-opioid antagonists stimulate breathing.[44]

RESPIRATORY PATTERNS IN RELATION TO SLEEP–WAKE STATES THROUGHOUT ONTOGENY

The function of ventilation is to maintain homeostasis in H^+ concentration and in partial pressures of carbon dioxide and oxygen. In the mature mammal, the central respiratory neuronal network described in the previous sections, with the help of afferent inputs to be described below, sends efferent outputs to the respiratory muscles, which, in turn, contract and relax rhythmically, thus producing a breathing pattern that maintains such homeostasis. This breathing pattern is modulated by centrally determined factors such as behavioral states and circadian cycles[45,46] (see Figure 21-3). Moreover, both the basic pattern and these modulations vary with development.

Unlike the regular respiratory pattern seen in the healthy adult, breathing during early development is not continuous. In the fetus, weak and irregular breathing movements can already be registered at the end of the first quarter of human gestation. Later in gestation, these breathing movements become gradually stronger and coalesce into periods of breathing activity alternating with periods of apnea, both of which are crucially correlated with particular sleep–wake states. The regulation and expression of these states involve the participation of various brain structures along the neuraxis, such as the brainstem and cortex for rapid eye movement (REM) sleep, or active sleep, and the thalamus, subcortex, and neocortex for non-REM (NREM) sleep, or quiet sleep. Fetal apnea is correlated with NREM sleep, which is characterized by high-voltage, low-frequency electrocortical activity, some nuchal electromyographic activity, and no eye movements. In turn, fetal breathing is correlated primarily with REM sleep and wakefulness. REM sleep is characterized by low-voltage, high-frequency electrocorticographic activity, absent nuchal electromyographic activity, and frequent rapid eye movements. In wakefulness, low-voltage, high-frequency electrocorticographic activity, high nuchal electromyographic activity, and variable eye movements are observed.[42]

Despite the absence in utero of environmental cues such as light or social interactions, the human fetus may already have a functional internal circadian clock at birth that starts to gradually shift the neonatal sleep–wake cycles from an ultradian (less than 24 h) to a circadian (approximately 24 h) rhythm.[47] The postulated functional internal circadian clock at birth is supported by the presence of receptors for the hormone melatonin in the fetal brain. Melatonin is important for setting the circadian rhythm, and it has been shown that maternal melatonin traverses the placenta and is able to interact with these receptors.[48] Indeed, chronically instrumented baboon fetuses, in late gestation, have been found to manifest a 24-hour periodicity in their sleep–wake and breathing behavior, with a preponderance of active sleep and breathing movements at midday (2:00 pm).[49]

At birth, the breathing pattern in the full-term human infant becomes continuous, probably in response to hypercarbic and hypoxic chemosensory stimulation caused by placental separation, and is strengthened by central arousal resulting from multiple environmental stimuli, such as low temperature, light, sound, pressure, or pain. If birth is premature, however, the breathing pattern can be intermediate between fetal and neonatal breathing, that is, a continuous pattern interrupted by periodic breathing. Such periodicity diminishes gradually as the premature infant ages.[42]

Throughout ontogeny, sleep–wake states are known to affect respiratory functions. This is most easily shown in the adult subject, where minute and alveolar ventilation are lower during quiet sleep than in either active sleep or wakefulness, resulting in a slight relative increase in arterial PCO_2 in that state.[50] The finding of relative hypoventilation during quiet sleep is consistent across species, although the specific respiratory function affected may vary among species, for example, respiratory frequency in the adult rat[51] and tidal volume in the adult human.[50] Of interest is the recent finding in unrestrained rats that circadian rhythms, independently of sleep–wake states, also affect respiratory indices and that the influences of the circadian rhythm and sleep–wake states on respiration are additive.[51]

Active (REM) sleep has been of great interest to both sleep and respiratory neurophysiologists. This is because of the peculiar effects of this sleep state on neuronal and respiratory functions, its significant plasticity during ontogeny, and its poorly understood physiologic purpose. As noted above, fetal breathing is largely associated with this sleep state in later gestation. It is possible that the development of this state provides the excitatory stimulus necessary for the emergence of episodic breathing activity in the fetus,[42] as it does in the adult cat.[52] It is interesting that REM sleep is associated with the excitation of many brain loci, including pontogeniculate, hypothalamic, thalamic, and cortical structures, and with decreased neuronal activity on the ventral medullary surface.[53] This paradoxically decreased activity on the medullary surface, which connects with chemoreceptor respiratory input (see below) on the one hand and with efferent neuronal respiratory activity on the other, may partially interrupt the excitation associated with this sleep state, thus producing the well-known atonia in respiratory and postural muscles. Several neurotransmitters, including serotonin, appear to be important in REM sleep activity.[54]

Another important aspect of breathing patterns is the coordination among respiratory muscles. Not only must the major inspiratory or expiratory muscles contract at the same time, regardless of their activity profile, but there must be careful coordination between the upper airway muscles and the major "pump" muscles.[55] The physiologic task of this coordination is to dilate the upper airway in preparation for the oncoming breath during inspiration and to provide adequate braking and maintenance of functional residual capacity during expiration. Accordingly, the timing and pattern of the neuronal activation of the upper airway muscles are of crucial importance to the success of normal breathing. In general, whereas the expiratory upper airway muscles contract at least throughout the expiratory period, the inspiratory upper airway muscles, under normal conditions, start to contract before the major inspiratory pump muscles.[55]

Such coordination normally exists in the mature healthy subject, but what happens in immature subjects? It seems that this coordination also undergoes development, as suggested from the results of experiments in the chronically instrumented, conscious piglet.[56] This animal model is optimal for the assessment of maturational processes because its stage of autonomic brain development at birth is equivalent to that of humans at birth.[57] Electromyographic recordings from such piglets indicate that young age and male gender promote incoordination between the dilatory posterior cricoarytenoid muscle and the diaphragm, in which the former contracts simultaneously with, or even after, the latter.[56] Interestingly, such incoordination is predominant in REM sleep,[56] perhaps explaining why upper airway obstruction is more likely during that sleep–wake state. In adult sleeping rats, REM sleep has been shown to suppress the activity of yet another inspiratory upper airway muscle, the genioglossus, while sparing that of the diaphragm, providing yet another situation that may promote upper airway obstruction even in the healthy adult subject.[58]

Inasmuch as sleep-disordered breathing, including sleep apnea, is the subject of later chapters, it must be noted here that a subset of this affliction occurs due to failure of central respiratory control mechanisms. The case history of the patient presented earlier in this chapter is an extreme example of such failure. During development, apneic episodes due to a temporary cessation of central respiratory drive are much more common, however, and have been termed apnea of prematurity or central infantile apnea.[42] Even more subtle are the findings, again in conscious piglets, of an occasional cessation of electromyographic activity in just one of the recorded respiratory muscles while the other muscle(s) continue(s) to function.[56] These phenomena of immaturity can perhaps be ascribed to incomplete connectivity within the complex central neuronal network for respiratory control.

RESPIRATORY REFLEXES IN RELATION TO SLEEP–WAKE STATES THROUGHOUT ONTOGENY

The most important respiratory reflexes are those emanating from the lung and from chemosensory structures. The reflexes stemming from the lung involve slowly adapting receptors, rapidly adapting receptors and C-fibers and include their afferent pathways, central connections, efferent pathways, and overall reflex actions.

The slowly adapting receptors[59,60] are mechanical receptors associated with the smooth muscle of the tracheobronchial tree that respond to stretch. Under physiologic conditions, such stretch would occur during inspiration, leading to activation of afferent myelinated vagal nerve fibers. This increased activity, when it reached a threshold level, would result in inspiratory activity being switched off at the solitary tract nucleus, leading to the termination of inspiration and the onset of expiration. This reflex is therefore very important in setting respiratory timing. It is easy to imagine that any increase in smooth muscle tone (eg, during bronchoconstriction) or decrease in lung compliance (eg, in restrictive lung disease) would enhance the activation of the slowly adapting receptors and their reflex pathways and, in turn, would increase respiratory frequency.[60] This reflex can be tested by (a) hyperinflating the lung at the height of inspiration, thus producing a prolonged expiratory pause, or (b) inflating the lung during the course of inspiration, thus terminating that breath early. The slow adapting stretch reflex can be elicited more easily during anesthesia or sleep than in wakefulness. In infants, this reflex is exquisitely sensitive as mere airway occlusion at end-inspiration produces prolonged cessation of respiratory activity. A greater inflation volume is required to terminate inspiration in 1-year-old infants than in newborns, indicating postnatal maturation of this reflex.[61] In awake normal adults, this reflex can only be elicited if the subjects are unaware of the stimulus.[62]

In contrast to the slowly adapting receptors, the rapidly adapting receptors arise from unmyelinated filaments located in the epithelium of the tracheobronchial tree. Their activity is carried centrally via thin myelinated vagal fibers that fire irregularly, at various portions of the respiratory cycle, and in response to a great variety of stimuli. These stimuli range from primarily mechanical and irritant in the upper airway to predominantly chemical and irritant in the lower airway. Making central connections in the solitary tract nucleus, the efferent responses range from cough, brief expiration, augmented breaths (sighs), and hyperventilation to laryngeal and bronchial constriction and mucus secretion. In contrast to the reflexes from slowly adapting receptors, which are facilitated by lack of consciousness, those from the rapidly adapting receptors appear to be suppressed during sleep or anesthesia. The rapidly adapting receptors and afferent nerves, as well as their associated reflexes, seem to be scant in early life and to develop with age.[63] Indeed, it is well known that young infants with simple upper respiratory infections do not cough and that cough in a 2-month-old infant spells significant lung pathology.

The last important lung reflexes that need to be mentioned are those from bronchopulmonary C-fibers. These unmyelinated afferent nerve fibers comprise 75% of all lung afferents and innervate the airway mucosa throughout the bronchopulmonary tree. These afferents are primarily sensitive to stimulation by exogenous chemicals (eg, nicotine), endogenous inflammatory mediators (eg, histamine), and

protons/hydroxyl radicals or by increased interstitial fluid volume/pressure due to edema, inflammation, or embolus. The response of the C-fibers to such stimulants is further enhanced by prostanoids and bradykinin. In turn, the C-fibers either produce local axonal effects via neurokinin release or carry the afferent information centrally, predominantly via the vagus nerves, to the solitary tract nucleus and to the rest of the central respiratory network. Centrally mediated responses to C-fiber stimulation include increased breathing frequency, reduced tidal volume, bronchoconstriction, mucus secretion, and, perhaps, a sensation of breathlessness. These responses might be regarded as pulmonary defense mechanisms[64] that appear to be already present in early ontogeny.[65,66] It is important to note that there is some overlap between the C-fibers and the other lung receptors, particularly the rapidly adapting receptors, in both the specific stimuli and responses. Therefore, the total respiratory response via the respiratory pump, upper airway motor neurons, and parasympathetic/sympathetic efferents[67] is considered to be the sum total of all these lung receptor reflexes.

Of the chemosensory reflexes, those that respond to hypoxia include the peripheral chemoreceptors,[68–70] primarily in the carotid body. Adult subjects respond to hypoxia by increasing the afferent activity in the carotid sinus nerve via glossopharyngeal fibers, making connections at the solitary tract nucleus and other respiratory-related regions, resulting in arousal and in a rapid increase in ventilation that is largely sustained throughout the hypoxic exposure. In principle, the same afferent sequence also occurs in the fetus and newborn, except that the activity and sensitivity of the carotid body to hypoxia increase with maturation. The breathing response of the fetus and neonate to acute hypoxia, however, is very different from that in the mature subject in that it is apnea in the first case and initial hyperventilation followed by a decrease in ventilation (the "biphasic response") in the second.[41] Whereas the extent of this late ventilatory decline diminishes with maturation, a slight decline may still be seen in meticulous recordings of respiratory responses to acute continuous hypoxia in adult subjects.[42] This shifting respiratory response to acute hypoxia serves as an example of the plasticity of the respiratory control system during ontogeny and in its response to stressors. Despite these well-established phenomena, several aspects of the response to hypoxia are the subject of much active research and still evoke controversy. These include chemosensory transduction in the carotid body, central hypoxic chemosensitivity, and central hypoxic depression in relation to facilitation in response to episodic hypoxia.

The major carotid body components are the glomus (type I) cells, the afferent nerve fibers, and the sustentacular (type II) cells enveloping them. The predominant view is that the glomus cells, originating in the neural crest, are the receptive organs for oxygen. Chemosensory transduction is thought to be triggered by an inhibition of specific K^+ channels, either by a direct interaction of oxygen with the K^+ channel protein or via a biochemical event associated with a heme protein, thus producing glomus cell depolarization. This depolarization increases intracellular $[Ca^{2+}]$, which, in turn, causes neurotransmitter release and afferent nerve excitation.[69,70] Maturation of this chemosensory function is first and foremost dependent on the sharp, stepwise increase in arterial PO_2 upon fetal exposure to ambient air at birth. Development is accompanied by a postnatal increase in the number of afferent nerve terminals and in a hypoxia-induced increase in K^+ currents, intracellular $[Ca^{2+}]$, catecholamine secretion, and catecholamine receptor genetic expression. Carotid extirpation or denervation in a vulnerable postnatal period produces severe respiratory hypoventilation, apnea, or death in several species, leading to the hypothesis that a pathologic decrease in peripheral chemoreceptor activity could be one of the mechanisms leading to unexpected death in infants.[70]

The declining ventilatory response to acute hypoxia in neonates has been primarily attributed to depression by central mechanisms as the peripheral chemoreceptors, being slowly adapting receptors, continue to excite the chemosensory afferent nerves throughout the hypoxic exposure. Respiratory depression is also seen during repeated hypoxic exposures in neonates, whether the hypoxia is continuous or intermittent.[71,72] Although several mechanisms have been proposed to explain this central depression by hypoxia, one mechanism might involve a hypoxia-induced change in the balance between excitatory and inhibitory neuromodulator influences on respiratory drive, favoring inhibition.[73] Such relative hypoventilation may pose an additional risk for vulnerable infants exposed repeatedly to hypoxia.

As noted previously, there is still some controversy as to whether or not, in adult subjects, recurrent hypoxic exposure produces respiratory facilitation. It appears that such facilitation is found most incontrovertibly in mature animals exposed to recurrent hypoxia under anesthesia or in patients suffering from chronic partial upper airway obstruction or obstructive sleep apnea.[37] Such facilitation would not pose a pathophysiologic risk, however.

The question of central oxygen sensitivity is a subject that will be discussed in conjunction with the physiologic responses to carbon dioxide. The hypercarbic ventilatory reflex is of great relevance to the practice of respiratory medicine in both adults and children as this reflex is blunted especially during sleep in chronic illnesses such as obesity, hypoventilation syndrome,[74] chronic airway obstruction,[75] and central alveolar hypoventilation syndrome (Figure 21-5A, B).[76]

It is well known that only a minor portion of the physiologic response to carbon dioxide is transmitted centrally from peripheral chemoreceptors and that the majority of the reflex emanates from central carbon dioxide detection. The current concept is that this central detection is not restricted to the previously delineated regions on, or just beneath, the surface of the ventral medulla[77] but, rather, that many regions, both at the level of the brainstem and above it, are involved in carbon dioxide chemoreception. Electrophysiologic recordings from in vitro brain slices and other reduced animal preparations, or immunostaining for the expression of early genes in brains of animals that had been exposed to hypercarbia, have been used in studies aimed at demonstrating such widespread chemoreception. Whereas responses to manipulation of carbon dioxide and,

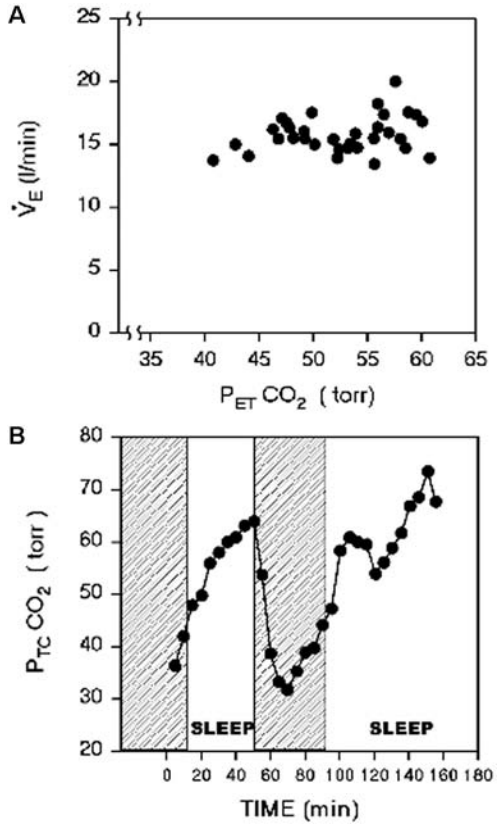

FIGURE 21-5 *A*, Blunted ventilatory responsiveness to hyperoxic carbon dioxide rebreathing in a 25-year-old woman diagnosed with congenital central hypoventilation syndrome at the age of 14 months. *B*, Increased transcutaneous PCO_2 during sleep compared with wakefulness (*shaded*) in a 13-day-old girl who has inherited the congenital central hypoventilation syndrome from her mother, the patient illustrated in Figure 22-5*A*. $P_{ET}CO_2$ = end-tidal partial pressure of carbon dioxide; $P_{TC}CO_2$ = transcutaneous partial pressure of carbon dioxide; *V*dot$_E$ = minute ventilation. Adapted from Sritippayawan S et al.[76]

notably, of oxygen have indeed implied the participation of brain regions other than the "classic" ones, there is still controversy as to whether the activated brain regions signify pure chemosensitivity or auxiliary reactions to the chemical perturbations.[78]

With the use of magnetic resonance imaging[79] and positron emission scanning,[80] healthy human adults have also been shown to exhibit activation of many brain regions in the brainstem, midbrain, hypothalamus, cerebellum, and motor cortex in response to carbon dioxide. Such activation, measured either during steady-state carbon dioxide inhalation or at intervals several minutes after the commencement of the gas exposure, does not, however, necessarily attest to the presence of carbon dioxide chemosensors in all these regions. Rather, it illustrates the behavioral respiratory response to carbon dioxide, which includes chemoreception, integration, arousal, perception, agitation, local changes in cerebral bloodflow, and a combination of autonomic and volitional respiratory responses. This constellation, nonetheless, may be the most important aspect of the responsiveness to carbon dioxide. Indeed, an inability to stage such a complex response is what may doom some patients with an acquired or inherent inability to sense carbon dioxide or a subset of infants who succumb to the sudden infant death syndrome.

Like sensitivity to hypoxia, carbon dioxide responsiveness undergoes significant changes during ontogeny. In the mature ovine fetus, the threshold for this response is high, and the sensitivity is low.[42] During postnatal development, the carbon dioxide threshold decreases and the hypercarbic responsiveness increases, reaching maturation at a stage equivalent to early human childhood.[42]

SUMMARY AND CONCLUSIONS

In the field of the neural control of breathing, great advances have been made in the delineation of participating brain structures and pathways, as well as in the understanding of mechanisms of action. There is also mounting awareness of the plasticity in various respiratory control elements during maturation/senescence and in response to specific situations/stressors. This progress has been made with the use of methodologic approaches ranging from investigations at the cellular and molecular level involving in vitro preparations to studies in animal models, with an increasing emphasis on the use of chronically instrumented and conscious subjects. Whereas genetic "knockouts" have been recently added to the methodologic armamentarium, careful restriction of such genetic manipulations to specific brain regions at selected times in development has the potential to provide a better understanding of the physiology of breathing.

It is important, however, to realize that the greater the amount of knowledge acquired, the larger the need for its confirmation in humans. Detailed pulmonary function testing and innovative imaging techniques will probably enhance the translation of findings from the bench to diagnosis at the bedside.

ACKNOWLEDGMENTS

The writing of this chapter was supported by the Canadian Institutes of Health Research. The author is indebted to Mr. André Laferrière for assistance in literature search, critical review of the manuscript, helpful suggestions, and skillful drawing of some of the figures.

REFERENCES

1. Mendelson M. Oscillator neurons in crustacean ganglia. Science 1971;171:1170–3.
2. Massabuau JC, Meyrand P. Modulation of a neural network by physiological levels of oxygen in lobster stomatogastric ganglion. J Neurosci 1996;16:3950–9.
3. Thoby-Brisson M, Simmers J. Neuromodulatory inputs maintain expression of a lobster motor pattern-generating network in a modulation-dependent state: evidence from long-term decentralization in vitro. J Neurosci 1998;18:2212–25.
4. Smith JC, Ellenberger HH, Ballanyi K, et al. Pre-Bötzinger complex, a brainstem region that may generate respiratory rhythm in mammals. Science 1991;254:726–9.

5. Johnson SM, Koshiya N, Smith JC. Isolation of the kernel for respiratory rhythm generation in a novel preparation: the pre-Bötzinger complex "island." J Neurophysiol 2001;85: 1772–6.
6. Rekling JC, Feldman JL. PreBötzinger complex and pacemaker neurons—hypothesized site and kernel for respiratory rhythm generation. Annu Rev Physiol 1998;60:385–405.
7. Smith JC, Butera RJ Jr, Koshiya N, et al. Respiratory rhythm generation in neonatal and adult mammals, the hybrid pacemaker–network model. Respir Physiol 2000;122:131–47.
8. Ramirez J-M, Zuperku EJ, Alheid GF, et al. Respiratory rhythm generation: converging concepts from in vitro and in vivo models. Respir Physiol Neurobiol 2002;131:43–56.
9. Gray PA, Rekling JC, Bocchiaro CM, Feldman JL. Modulation of respiratory frequency by peptidergic input to rhythmogenic neurons in the preBötzinger complex. Science 1999;286:1566–8.
10. Gray PA, Janczewski WA, Mellen N, et al. Normal breathing requires preBötzinger complex neurokinin-1 receptor-expressing neurons. Nat Neurosci 2001;4:927–30.
11. Guyenet PG, Wang H. Pre-Bötzinger neurons with preinspiratory discharges "in vivo" express NK1 receptors in the rat. J Neurophysiol 2001;86:438–46.
12. Telgkamp P, Cao YQ, Basbaum AI, Ramirez J-M. Long-term deprivation of substance P in PPT-A mutant mice alters the anoxic response of the isolated respiratory network. J Neurophysiol 2002;88:206–13.
13. Liu Y-Y, Ju G, Wong-Riley MTT. Distribution and co-localization of neurotransmitters and receptors in the pre-Bötzinger complex of rats. J Appl Physiol 2001;901:1387–95.
14. Wang H, Stornetta RL, Rosin DL, Guyenet PG. Neurokinin-1 receptor-immunoreactive neurons of the ventral respiratory group in the rat. J Comp Neurol 2001;434:128–46.
15. Guyenet PG, Sevigny CP, Weston MC, Stornetta RL. Neurokinin-1 receptor-expressing cells of the ventral respiratory group are functionally heterogeneous and predominantly glutamatergic. J Neurosci 2002;22:3806–16.
16. Pilowsky PM, Feldman JL. Identifying neurons in the preBötzinger complex that generate respiratory rhythm: visualizing the ghost in the machine. J Comp Neurol 2001;434:125–7.
17. Thoby-Brisson M, Ramirez JM. Identification of two types of inspiratory pacemaker neurons in the isolated respiratory neural network of mice. J Neurophysiol 2001;86:104–12.
18. Del Negro CA, Morgado-Valle C, Feldman JL. Respiratory rhythm: an emergent network property? Neuron 2002; 34:821–30.
19. Ellenberger HH. Nucleus ambiguus and bulbospinal ventral respiratory group neurons in the neonatal rat. Brain Res Bull 1999;50:1–13.
20. Thoby-Brisson M, Ramirez JM. Role of inspiratory pacemaker neurons in mediating the hypoxic response of the respiratory network in vitro. J Neurosci 2000;20:5858–66.
21. Ellenberger HH, Feldman JL. Brainstem connections of the rostral ventral respiratory group of the rat. Brain Res 1990;513:35–42.
22. Ellenberger HH, Feldman JL. Subnuclear organization of the lateral tegmental field of the rat. I: Nucleus ambiguus and ventral respiratory group. J Comp Neurol 1990;294:202–11.
23. Cheng Z, Guo SZ, Lipton AJ, Gozal D. Domoic acid lesions in nucleus of the solitary tract: time-dependent recovery of hypoxic ventilatory response and peripheral afferent axonal plasticity. J Neurosci 2002;22:3215–26.
24. Rhodes RH, Wightman HR. Nucleus of the tractus solitarius metastasis: relationship to respiratory arrest? Can J Neurol Sci 2000;27:328–32.
25. Plum FL, Leigh RJ. Abnormalities of central mechanisms. In: Hornbein TF, editor. Regulation of breathing: lung biology in health and disease series. Vol 17. New York: Marcel Dekker; 1981. p. 989–1067.
26. Horn EM, Waldrop TG. Suprapontine control of respiration. Respir Physiol 1998;114:201–11.
27. Horn EM, Dillon GH, Fan Y-P, Waldrop TG. Developmental aspects and mechanisms of rat caudal hypothalamic neural responses to hypoxia. J Neurophysiol 1999;81:1949–59.
28. Horn EM, Kramer JM, Waldrop TG. Development of hypoxia-induced Fos expression in rat caudal hypothalamic neurons. Neuroscience 2000;99:711–20.
29. Bodineau L, Larnicol N. Brainstem and hypothalamic area activated by tissue hypoxia: fos-like immunoreactivity induced by carbon monoxide inhalation in the rat. Neuroscience 2001;108:643–53.
30. Ichiyama RM, Gilbert AB, Waldrop TG, Iwamoto GA. Changes in exercise activation of diencephalic and brainstem cardiorespiratory areas for training. Brain Res 2002;947:225–33.
31. Demoule A, Verin E, Ross E, et al. Intracortical inhibition and facilitation of the response of the diaphragm to transcranial magnetic stimulation. J Clin Neurophysiol 2003;20:59–64.
32. Sica AL, Greenberg HE, Scharf SM, Ruggiero DA. Immediate-early gene expression in cerebral cortex following exposure to chronic-intermittent hypoxia. Brain Res 2000;870:204–10.
33. Corne S, Webster K, McGinn G, et al. Medullary metastasis causing impairment of respiratory pressure output with intact respiratory rhythm. Am J Respir Crit Care Med 1999;159:315–20.
34. Moss IR, Inman JG. Neurochemicals and respiratory control during development. J Appl Physiol 1989;67:1–13.
35. McCrimmon DR, Mitchell GS, Dekin MS. Glutamate, GABA, and serotonin in ventilatory control. In: Dempsey JA, Pack AI, editors. Regulation of breathing. 2nd ed. New York: Marcel Dekker; 1995. p. 151–218.
36. Mitchell GS, Baker TL, Nanda SA, et al. Intermittent hypoxia and respiratory plasticity. J Appl Physiol 2001;90:2466–75.
37. Behan M, Zabka AG, Mitchell GS. Age and gender effects on serotonin-dependent plasticity in respiratory motor control. Respir Physiol Neurobiol 2002;131:65–77.
38. Olson EB, Bohne CJ, Dwinell MR, et al. Ventilatory long-term facilitation in unanesthetized rats. J Appl Physiol 2001; 91:709–16.
39. McGuire M, Zhang Y, White DP, Ling L. Effect of hypoxic episode number and severity on ventilatory long-term facilitation in awake rats. J Appl Physiol 2002;93:2155–61.
40. Jordan AS, Catcherside PG, O'Donoghue FJ, McEvoy RD. Long-term facilitation of ventilation is not present during wakefulness in healthy men or women. J Appl Physiol 2002; 93:2129–36.
41. Moss IR. Respiratory responses to single and episodic hypoxia during development: mechanisms of adaptation. Respir Physiol 2000;121:185–97.
42. Moss IR. Maturation of respiratory control in the behaving mammal. A Frontiers Review. Respir Physiol Neurobiol 2002;132:131–44.
43. Moss IR, Laferrière A. Central neuropeptide systems and respiratory control during development. Respir Physiol Neurobiol 2002;131:15–27.
44. Dempsey JA, Olson EB Jr, Skatrud JB. Hormones and neurochemicals in the regulation of breathing. In: Handbook of physiology. The respiratory system. Control of breathing. Section 3. Vol II. Bethesda, MD: American Physiological Society; 1986. p. 181–221.
45. Herzog ED, Schwartz WJ. A neural clockwork for encoding circadian time. J Appl Physiol 2002;92:401–8.

46. Dijk D-J, Lockley SW. Integration of human sleep–wake regulation and circadian rhythmicity. J Appl Physiol 2002; 92:852–62.
47. Lohr B, Siegmund R. Ultradian and circadian rhythms of sleep–wake and food-intake behavior during early infancy. Chronobiol Int 1999;16:129–48.
48. Thomas L, Drew JE, Abramovich DR, Williams LM. The role of melatonin in the human fetus. Int J Mol Med 1998;1:539–43.
49. Stark RI, Garland M, Daniel S, Myers MM. Diurnal rhythm of fetal behavioral state. Sleep 1998;21:167–76.
50. Caruana-Montaldo B, Gleeson K, Zwillich CW. The control of breathing in clinical practice. Chest 2000;117:205–25.
51. Stephenson R, Liao KS, Hamrahi H, Horner RL. Circadian rhythms and sleep have additive effects on respiration in the rat. J Physiol 2001;536:225–35.
52. Orem J, Lovering AT, Dunin-Barkowski W, Vidruk EH. Endogenous excitatory drive to the respiratory system in rapid eye movement sleep in cats. J Physiol 2000; 527:365–76.
53. Richard CA, Rector D, Harper RK, Harper RM. Optical imaging of the ventral medullary surface across sleep–wake states. Am J Physiol 1999;277:R1239–45.
54. Horner RL, Sanford LD, Annis D, et al. Serotonin at the laterodorsal tegmental nucleus suppresses rapid-eye-movement sleep in freely behaving rats. J Neurosci 1997;17:7541–52.
55. Kuna S, Remmers JE. Anatomy and physiology of upper airway obstruction. In: Kryger MH, Roth T, Dement WC, editors. Principles and practice of sleep medicine. 3rd ed. Philadelphia, PA: WB Saunders; 2000. p. 840–58.
56. Scott SC, Inman JDG, Moss IR. Ontogeny of sleep and cardiorespiratory behavior in unanesthetized piglets. Respir Physiol 1990;80:83–102.
57. Dobbing J. The later development of the brain and its vulnerability. In: Davis JA, Dobbing J, editors. Scientific foundations of paediatrics. Baltimore: University Park Press; 1982. p. 744–59.
58. Horner RL, Liu X, Gill H, et al. Effects of sleep–wake state on the genioglossus vs. diaphragm muscle responses to CO_2 in rats. J Appl Physiol 2002;92:878–87.
59. Widdicombe J. Airway receptors. Respir Physiol 2001;125:3–15.
60. Schelegle ES, Green JF. An overview of the anatomy and physiology of slowly adapting pulmonary stretch receptors. Respir Physiol 2001;125:17–31.
61. Rabbette PS, Stocks J. Influence of volume dependency and timing of airway occlusions on the Hering–Breuer reflex in infants. J Appl Physiol 1998;85:2033–9.
62. BuSha BF, Judd BG, Manning HL, et al. Identification of respiratory vagal feedback in awake normal subjects using pseudorandom unloading. J Appl Physiol 2001; 90:2330–40.
63. Sant'Ambrogio G, Widdicombe J. Reflexes from airway rapidly adapting receptors. Respir Physiol 2001;125:33–45.
64. Lee L-Y, Pisarri TE. Afferent properties and reflex functions of bronchopulmonary C-fibers. Respir Physiol 2001;125:47–65.
65. Kou YR, Lin YS, Ho C-Y, Lin C-Z. Neonatal capsaicin treatment alters immediate ventilatory responses to inhaled wood smoke in rats. Respir Physiol 1999;116:115–23.
66. Diaz V, Arsenault J, Praud J-P. Consequences of capsaicin treatment on pulmonary vagal reflexes and chemoreceptor activity in lambs. J Appl Physiol 2000;89:1709–18.
67. Jordan D. Central nervous pathways and control of the airways. Respir Physiol 2001;125:67–81.
68. Lahiri S, Acker H. Oxygen sensing in the body. Respir Physiol 1999;115:115–260.
69. Prabhakar NR. Oxygen sensing by the carotid body chemoreceptors. J Appl Physiol 2000;88:2287–95.
70. Donnally DF. Developmental aspects of oxygen sensing by the carotid body. J Appl Physiol 2000;88:2296–301.
71. Waters KA, Beardsmore C, Paquette J, et al. Respiratory responses to rapid-onset, repetitive vs continuous hypoxia in piglets. Respir Physiol 1996;105:135–42.
72. Waters KA, Paquette J, Laferrière A, et al. Curtailed respiration by repeated *vs.* isolated hypoxia in maturing piglets is unrelated to NTS ME or SP levels. J Appl Physiol 1997;83:522-9.
73. Laferrière A, Liu J-K, Moss IR. Neurokinin-1 vs mu-opioid receptor binding in rat nucleus tractus solitarius after single and recurrent intermittent hypoxia. Brain Res Bull 2003;59:307–13.
74. Berger KI, Ayappa I, Chatr-Amontri B, et al. Obesity hypoventilation syndrome as a spectrum of respiratory disturbances during sleep. Chest 2001;120:1231–8.
75. Marcus CL. Sleep-disordered breathing in children. Am J Respir Crit Care Med 2001;164:16–30.
76. Sritippayawan S, Hamutcu R, Kun SS, et al. Mother–daughter transmission of congenital central hypoventilation syndrome. Am J Respir Crit Care Med 2002;166:367–9.
77. Okada Y, Chen Z, Jiang W, et al. Anatomical arrangement of hypercapnia-activated cells in the superficial ventral medulla of rats. J Appl Physiol 2002;93:427–39.
78. Putnam RW, Dean JB, Ballantyne D, editors. Central chemosensitivity. Respir Physiol 2001;129:1–278.
79. Harper RM, Gozal D, Bandler R, et al. Regional brain activation in humans during respiratory and blood pressure challenges. Clin Exp Pharmacol Physiol 1998;25:483–6.
80. Brannan S, Liotti M, Egan G, et al. Neuroimaging of cerebral activations and deactivations associated with hypercapnia and hunger for air. Proc Natl Acad Sci U S A 2000;98:2029–34.
81. Feldman JL, McCrimmon DR. Neural control of breathing. In: Squire LR, Bloom FE, McConnell SK, et al., editors. Fundamental neuroscience. Amsterdam: Academic Press; 2003. p. 967–90.
82. Feldman JL, Smith JC. Neural control of respiratory pattern in mammals: an overview. In: Dempsey JA, Pack AI, editors. Regulation of breathing. Lung biology in health and disease. Vol 79. New York: Marcel Dekker; 1995. p. 39–69.

CHAPTER 22

ACTIONS OF THE RESPIRATORY MUSCLES

André de Troyer

The so-called respiratory muscles are those muscles that provide the motive power for the act of breathing. Thus, although many of these muscles are involved in a variety of activities, such as speech production, cough, vomiting, and trunk motion, their primary task is to displace the chest wall rhythmically to pump gas in and out of the lungs. The present chapter, therefore, starts with a discussion of the basic mechanical structure of the chest wall in humans. Then, the action of each group of muscles is analyzed. For the sake of clarity, the functions of the diaphragm, the intercostal muscles, the muscles of the neck, and the muscles of the abdominal wall are analyzed sequentially. However, since all these muscles normally work together in a coordinated manner, the most critical aspects of their mechanical interactions are also emphasized.

CHEST WALL

The chest wall can be thought of as consisting of two compartments—the rib cage and the abdomen—separated from each other by a thin musculotendinous structure, the diaphragm[1] (Figure 22-1). These two compartments are mechanically arranged in parallel. Expansion of the lungs, therefore, can be accommodated by expansion of either the rib cage or the abdomen or of both compartments simultaneously.

The displacements of the rib cage during breathing are essentially related to the motion of the ribs. Each rib articulates by its head with the bodies of its own vertebra and of the vertebra above and by its tubercle with the transverse process of its own vertebra. The head of the rib is very closely connected to the vertebral bodies by radiate and intraarticular ligaments, such that only slight gliding movements of the articular surfaces on one another can take place. Also, the neck and tubercle of the rib are bound to the transverse process of the vertebra by short ligaments that limit the movements of the costotransverse joint to slight cranial and caudal gliding. As a result, the costovertebral and costotransverse joints together form a hinge, and the respiratory displacements of the rib occur primarily through a rotation around the long axis of its neck, as shown in Figure 22-2A. However, this axis is oriented laterally, dorsally, and caudally. In addition, the ribs are curved and slope caudally and ventrally from their costotransverse articulations, such that their ventral ends and the costal cartilages are more caudal than their dorsal parts (Figure 22-2B, C). When the ribs are displaced in the cranial direction, their ventral ends move laterally and ventrally as well as cranially, the cartilages rotate cranially around the chondrosternal junctions, and the sternum is displaced ventrally. Consequently, there is usually an increase in both the lateral and the dorsoventral diameters of the rib cage (see Figure 22-2B, C). Conversely, a displacement of the ribs in the caudal direction is usually associated with a decrease in rib cage diameters. As a corollary, the muscles that elevate the ribs as their primary action have an inspiratory effect on the rib cage, whereas the muscles that lower the ribs have an expiratory effect on the rib cage.

It is notable, however, that although all the ribs move predominantly by rotation around the long axis of their necks, the costovertebral joints of ribs 7 to 10 have less constraint on their motion than the costovertebral joints of ribs 1 to 6. The long cartilages of ribs 8 to 10 also articulate with one another by small synovial cavities rather than with the sternum. Hence, whereas the upper ribs tend to move as a unit with the sternum, the lower ribs have some freedom to move independently. In both animals and humans, deformations of the rib cage may therefore occur under the influence of muscle contraction or other forces.

The respiratory displacements of the abdominal compartment are more straightforward than those of the rib cage because if one neglects the 100 to 300 mL of abdominal gas, its contents are virtually incompressible. This implies that any local inward displacement of its boundaries results in an equal outward displacement elsewhere. Furthermore, many of these boundaries, such as the spine dorsally, the pelvis caudally, and the iliac crests laterally, are virtually fixed. The parts of the abdominal container that can be displaced are thus largely limited to the ventral abdominal wall and the diaphragm. When the diaphragm contracts during inspiration (see below), its descent usually results in an outward displacement of the ventral abdominal wall; conversely, when the abdominal muscles contract, they cause in general an inward displacement of the belly wall, resulting in a cranial motion of the diaphragm into the thoracic cavity.

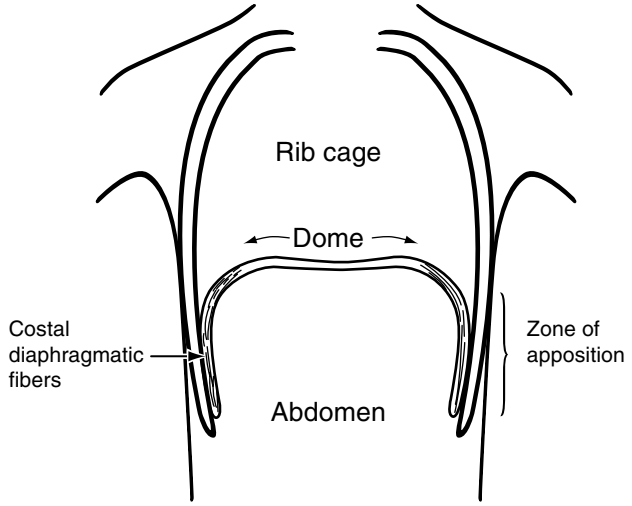

FIGURE 22-1 Frontal section of the chest wall at end-expiration. Note the cranial orientation of the costal diaphragmatic fibers and their apposition to the inner aspect of the lower rib cage (zone of apposition).

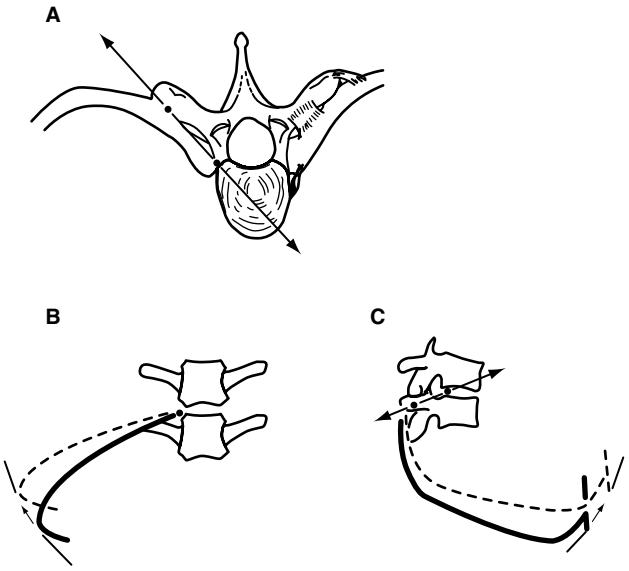

FIGURE 22-2 Respiratory displacements of the rib cage. *A*, Diagram of a typical thoracic vertebra and a pair of ribs (viewed from above). Each rib articulates with both the body and the transverse process of the vertebra (*closed circles*) and is bound to it by strong ligaments (*right*). The motion of the rib, therefore, occurs primarily through a rotation around the axis defined by these articulations (*solid line* and *double arrowhead*). From these articulations, however, the rib slopes caudally and ventrally (*B, C*). As a result, when it becomes more horizontal in inspiration (*dotted line*), it causes an increase in both the transverse (*B*) and the anteroposterior (*C*) diameter of the rib cage (*small arrows*). Reproduced with permission from De Troyer A. Respiratory muscle function. In: Shoemaker WC, Ayres SM, Grenvik A, Holbrook PR, editors. Textbook of critical care. Philadelphia: WB Saunders; 2000. p. 1172–84.

DIAPHRAGM

Functional Anatomy

Anatomically, the diaphragm is unique among skeletal muscles in that its muscle fibers radiate from a central tendon to insert peripherally into skeletal structures. The crural (or vertebral) portion of the diaphragmatic muscle inserts on the ventrolateral aspect of the first three lumbar vertebrae and on the aponeurotic arcuate ligaments, and the costal portion inserts on the xiphoid process of the sternum and the upper margins of the lower six ribs. From their insertions, the costal fibers run cranially, so that they are directly apposed to the inner aspect of the lower rib cage (see Figure 22-1); this is the so-called "zone of apposition" of the diaphragm to the rib cage.[2] Although the older literature suggested the possibility of an intercostal motor innervation of some portions of the diaphragm, it is now clearly established that its only motor supply is through the phrenic nerves, which, in humans, originate in the third, fourth, and fifth cervical segments.

Actions of the Diaphragm

As the muscle fibers of the diaphragm are activated during inspiration, they develop tension and shorten. As a result, the axial length of the apposed diaphragm diminishes and the dome of the diaphragm, which essentially corresponds to the central tendon, descends relative to the costal insertions of the muscle. The dome of the diaphragm remains relatively constant in size and shape during breathing, but its descent has two effects. First, it expands the thoracic cavity along its craniocaudal axis. Hence, pleural pressure falls and, depending on whether the airways are open or closed, lung volume increases or alveolar pressure falls. Second, it produces a caudal displacement of the abdominal viscera and an increase in abdominal pressure, which, in turn, pushes the ventral abdominal wall outward.

In addition, because the muscle fibers of the costal diaphragm insert onto the upper margins of the lower six ribs, they also apply a force on these ribs when they contract, and the cranial orientation of these fibers is such that this force is directed cranially. It therefore has the effect of lifting the ribs and rotating them outward (Figure 22-3). The fall in pleural pressure and the rise in abdominal pressure that result from diaphragmatic contraction, however, act simultaneously on the rib cage, which probably explains why the action of the diaphragm on the rib cage has been controversial for so long.

Action of the Diaphragm on the Rib Cage

When the diaphragm in anesthetized dogs is activated selectively by electrical stimulation of the phrenic nerves, the upper ribs move caudally, and the cross-sectional area of the upper portion of the rib cage decreases.[3] In contrast, the cross-sectional area of the lower portion of the rib cage increases. If a bilateral pneumothorax is subsequently introduced, so that the fall in pleural pressure is eliminated, isolated contraction of the diaphragm causes a greater expansion of the lower rib cage, but the dimensions of the upper rib cage now remain unchanged.[3] Thus, the diaphragm contracting alone in the dog has two opposing effects on the rib cage. On the one hand, it has an expiratory action on the upper rib cage,

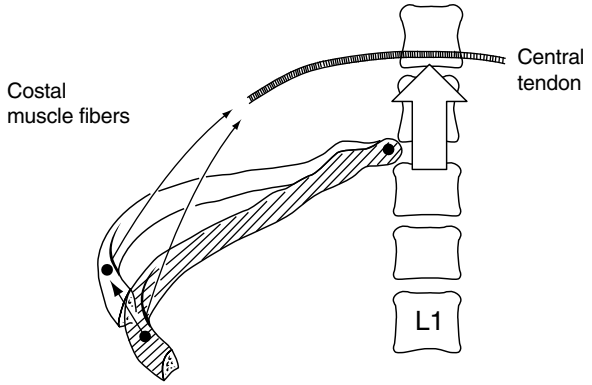

FIGURE 22-3 Insertional component of diaphragmatic action. During inspiration, as the fibers of the costal diaphragm contract, they exert a force on the lower ribs (*arrow*). If the abdominal visceral mass effectively opposes the descent of the diaphragmatic dome (*open arrow*), this force is oriented cranially. Consequently, the lower ribs are lifted and rotate outward. Reproduced with permission from De Troyer A. Mechanics of the chest wall muscles. In: Miller AD, Bishop B, Bianchi AL, editors. Neural control of the respiratory muscles. Boca Raton (FL): CRC Press; 1996. p. 59–73.

and the fact that this action is abolished by a pneumothorax indicates that it is exclusively the result of the fall in pleural pressure. On the other hand, the diaphragm also has an inspiratory action on the lower rib cage. Although the cross-sectional shape of the rib cage in humans differs from that in the dog, measurements of thoracoabdominal motion during phrenic nerve pacing in subjects with transection of the upper cervical cord[4,5] and during spontaneous breathing in subjects with traumatic transection of the lower cervical cord[6,7] have established that the diaphragm contracting alone in humans also has both an expiratory action on the upper rib cage and an inspiratory action on the lower rib cage; this inspiratory action is such that the lower rib cage expands more along its transverse diameter than along its anteroposterior diameter.[7]

Experimental and theoretical studies have confirmed that the inspiratory action of the diaphragm on the lower rib cage results, in part, from the force that the muscle applies on the ribs by way of its insertions; this force is conventionally referred to as the "insertional" force.[8,9] Indeed, the crural portion of the diaphragm has no direct attachments to the ribs, and its selective stimulation in dogs induces a smaller expansion of the lower rib cage than does stimulation of the costal portion.[8] The inspiratory action of the diaphragm on the lower rib cage, however, is also related to the existence of the zone of apposition (see Figure 22-1). This zone makes the lower rib cage, in effect, part of the abdominal container, and measurements in dogs have established that, during breathing, the changes in pressure in the pleural recess between the apposed diaphragm and the rib cage are almost equal to the changes in abdominal pressure.[10] Pressure in this pleural recess rises, rather than falls, during inspiration, thus indicating that the rise in abdominal pressure is truly transmitted through the apposed diaphragm to expand the lower rib cage. The force thus developed by the diaphragm on the lower rib cage through the rise in abdominal pressure has been called the "appositional" force,[8,9] and its magnitude depends, in part, on the size of the zone of apposition. The greater area of apposed diaphragm at the sides of the rib cage compared with the front presumably accounts for the fact that isolated contraction of the diaphragm in humans distorts the lower rib cage to a more elliptical shape.[7]

It should be appreciated, however, that the insertional and appositional forces are largely determined by the resistance provided by the abdominal contents to diaphragmatic descent. If this resistance is high (ie, if abdominal compliance is low), the dome of the diaphragm descends less, the zone of apposition remains significant throughout inspiration, and the rise in abdominal pressure is greater. Therefore, for a given diaphragmatic activation, the appositional force is increased. A dramatic illustration of this phenomenon is provided by quadriplegic subjects given an external abdominal compression; in such subjects, when passive mechanical support to the abdomen is provided by a pneumatic cuff or an elastic binder, the expansion of the lower rib cage during inspiration is accentuated.[4,5] Conversely, if the resistance provided by the abdominal contents is small (ie, if the abdomen is very compliant), the dome of the diaphragm descends more easily, the zone of apposition decreases more, and the rise in abdominal pressure is smaller. Consequently, the inspiratory action of the diaphragm on the rib cage is decreased. Should the resistance provided by the abdominal contents be eliminated, the zone of apposition would disappear in the course of inspiration, but, in addition, the contracting diaphragmatic muscle fibers would become oriented transversely inward at their insertions onto the ribs, such that the insertional force would have an expiratory, rather than an inspiratory, action on the lower rib cage. Indeed, when a dog is eviscerated, the diaphragm causes a decrease, rather than an increase, in lower rib cage dimensions.[3,8]

Influence of Lung Volume

The balance between pleural pressure and the insertional and appositional forces of the diaphragm is markedly affected by changes in lung volume. As lung volume decreases from functional residual capacity (FRC) to residual volume (RV), the zone of apposition increases[9] and the fraction of the rib cage exposed to pleural pressure decreases. As a result, the appositional force increases while the effect of pleural pressure diminishes, and hence the inspiratory action of the diaphragm on the rib cage is enhanced. Conversely, as lung volume increases above FRC, the zone of apposition decreases and a larger fraction of the rib cage becomes exposed to pleural pressure. The inspiratory action of the diaphragm on the rib cage is therefore diminished.[3,8,9] When lung volume approaches total lung capacity (TLC), the zone of apposition all but disappears, and the diaphragmatic muscle fibers become oriented transversely inward as well as cranially. As in the eviscerated animal, the insertional force of the diaphragm is then expiratory, rather than inspiratory, in direction. These two effects of increasing lung volume account for the inspiratory decrease in the transverse diameter of the lower rib cage that is commonly observed in subjects with emphysema and severe hyperinflation (Hoover's sign).

Changes in lung volume affect not only the action of the diaphragm on the rib cage but also its inspiratory effect on the lung. When lung volume in supine dogs, cats, and rabbits is passively increased from FRC to TLC, the fall in pleural pressure induced by selective stimulation of the phrenic nerves decreases gradually and continuously.[11–14] At TLC, in fact, the pressure fall is almost abolished, and when the respiratory system in these animals is inflated to a lung volume greater than ~104% TLC, the pressure fall is even reversed to become a pressure rise.[11,14] Such an expiratory action of the diaphragm on the lung has not been observed in humans, but studies in subjects with transection of the upper cervical cord and phrenic nerve pacing,[4] as well as phrenic nerve stimulation experiments in normal subjects,[15] have shown a similar decline in the lung-inflating action of the human diaphragm with increasing lung volume. As in animals, the diaphragm in humans virtually ceases to generate an inspiratory pressure at TLC.

The adverse effect of hyperinflation on the pressure-generating ability of the diaphragm is primarily related to the decrease in muscle length. Indeed, when lung volume in animals and in humans is increased from RV to TLC, the diaphragmatic muscle fibers shorten by 30 to 40%. In accordance with the length–tension characteristics of the muscle, the force exerted in response to a given stimulation thus decreases markedly. On the other hand, the shape of the diaphragm silhouette hardly changes over the range of a normal vital capacity,[16,17] and as Smith and Bellemare[15] have pointed out, the relationship between lung volume and the pressure across the diaphragm (transdiaphragmatic pressure, P_{di}) obtained during bilateral stimulation of the phrenic nerves in humans is very similar to the length–tension relationship of diaphragmatic muscle fibers in vitro; if an increase in the radius of curvature (flattening of the diaphragm) contributed to the decrease in P_{di} at high lung volumes (Laplace's equation), the decrease in P_{di} should be greater than anticipated on the basis of the decrease in muscle length alone. At very high lung volumes in animals, however, the dome of the diaphragm does become excessively flattened, such that the muscle can no longer expand the abdomen when it contracts. The constriction of the entire rib cage that the contracting diaphragm induces at such lung volumes presumably accounts for the lung-deflating action of the muscle.

Influence of Posture

Because of the effect of gravity on the abdominal contents and abdominal wall, a change from the seated to the supine posture in humans is associated with a marked increase in abdominal compliance.[18] Consequently, the resistance provided by the abdominal contents to diaphragmatic descent is less effective in this posture, and the two forces developed by the diaphragm to expand the lower rib cage are reduced. Thus, whereas the contracting diaphragm in seated quadriplegic subjects causes an increase in the anteroposterior diameter of the lower rib cage, in the supine posture it produces a decrease in this diameter.[4–7] The increase in the transverse diameter of the lower rib cage is also less in this posture.

With a change from the seated to the supine posture, the action of gravity on the abdominal contents also induces a reduction in FRC and a lengthening of the diaphragmatic muscle fibers. Although the concomitant increase in abdominal compliance should cause these fibers to shorten more for a given activation, the force generated by the contracting diaphragm might therefore increase. Studies in patients with transection of the upper cervical cord, in whom bilateral pacing of the phrenic nerves allows the degree of diaphragmatic activation to be maintained constant, have confirmed the influence of posture on the lung-expanding action of the diaphragm.[4,5] When the patients were supine, the unassisted paced diaphragm was able to generate an adequate tidal volume. However, when the patients were gradually tilted head-up, the change in airway pressure and the tidal volume produced by pacing were progressively and markedly reduced.

Interaction between the Left and Right Hemidiaphragms

Both in the dog and in humans, each phrenic nerve supplies its own hemidiaphragm, including all the fibers in the crural segment on its own side of the esophageal hiatus. However, when the left and right phrenic nerves in the dog are stimulated simultaneously at a frequency of 10 Hz, the fall in pleural pressure is 10% greater than the sum of the pressure falls obtained during separate left and right stimulation.[19] The difference between the pressure change produced by the canine left and right hemidiaphragms contracting simultaneously and the sum of the individual pressures, in fact, increases gradually to 40 to 50% as the stimulation frequency increases to 35 to 50 Hz.[14,19] In humans, the change in P_{di} obtained during simultaneous stimulation of the left and right phrenic nerves with single twitches is similarly greater than the sum of the P_{di} values obtained during separate left and right stimulation.[20] Thus, the left and right hemidiaphragms have a synergistic interaction on the lung, and this implies that the pressure loss induced by hemidiaphragmatic paralysis is greater than anticipated on the basis of the pressure generated by one hemidiaphragm alone. The frequency dependence of the synergism further implies that this additional pressure loss should be particularly prominent when an increase in respiratory neural drive is needed, such as during exercise.

This peculiar interaction results, in part, from the fact that the diaphragmatic muscle fibers shorten more during unilateral contraction than during bilateral contraction.[19] Consequently, the force exerted during contraction is smaller in the first instance than in the second. However, the main determinant of this interaction is related to the configuration of the muscle. That is, during unilateral diaphragmatic contraction, the inactive hemidiaphragm is stretched and develops passive tension, which reduces the caudal displacement of the central portion of the dome and impedes the descent of the contracting hemidiaphragm. As a result, the volume displaced (and the pressure generated) by this particular hemidiaphragm is reduced relative to the volume that it displaces when the contralateral hemidiaphragm contracts simultaneously.[19]

INTERCOSTAL MUSCLES

Functional Anatomy

The intercostal muscles are two thin muscle layers occupying each of the intercostal spaces. The external intercostal muscles extend from the tubercles of the ribs dorsally to the costochondral junctions ventrally, with their fibers oriented obliquely caudad and ventrally from the rib above to the rib below. In contrast, the internal intercostal muscles extend from the angles of the ribs dorsally to the sternocostal junctions ventrally, with their fibers running caudad and dorsally from the rib above to the rib below. Thus, although the intercostal spaces contain two layers of intercostal muscle in their lateral portion, they contain a single layer in their ventral and dorsal portions. Ventrally, between the sternum and the chondrocostal junctions, the only fibers are those of the internal intercostal muscles; because of its location and particular function (see below), this portion of the internal intercostal muscles is usually called the "parasternal intercostal muscles." Dorsally, from the angles of the ribs to the vertebrae, the only fibers come from the external intercostal muscles. These latter, however, are duplicated in each interspace by a thin, spindle-shaped muscle that runs from the tip of the transverse process of the vertebra cranially to the angle of the rib caudally; this muscle is the "levator costae." All intercostal muscles are innervated by the intercostal nerves.

Actions of Intercostal Muscles on the Ribs and the Lung

The actions of the intercostal muscles have conventionally been regarded according to the theory proposed by Hamberger,[21] as shown in Figure 22-4. When an intercostal muscle contracts in one interspace, it pulls the upper rib down and the lower rib up. However, as the fibers of the external intercostal muscle slope caudad and ventrally from the rib above to the rib below, their lower insertion is more distant from the center of rotation of the ribs (ie, the costovertebral articulations) than their upper insertion. Consequently, when this muscle contracts, the torque acting on the lower rib is greater than that acting on the upper rib, so its net effect would be to raise the ribs and to inflate the lung. In contrast, as the fibers of the internal intercostal muscle slope caudad and dorsally from the rib above to the rib below, their lower insertion is less distant from the center of rotation of the ribs than the upper one. As a result, when this muscle contracts, the torque acting on the lower rib is smaller than that acting on the upper rib, so its net effect would be to lower the ribs and to deflate the lung. Hamberger further concluded that the action of the parasternal intercostal muscles should be referred to the sternum rather than to the spine; although these muscles form part of the internal intercostal layer, their contraction would therefore raise the ribs and inflate the lung.

In agreement with this theory, selective activation of the canine parasternal intercostal muscles by electrical stimulation elicits a large cranial displacement of the ribs and an increase in lung volume.[22,23] Measurements of the respiratory displacements of the costal cartilages and the sternum

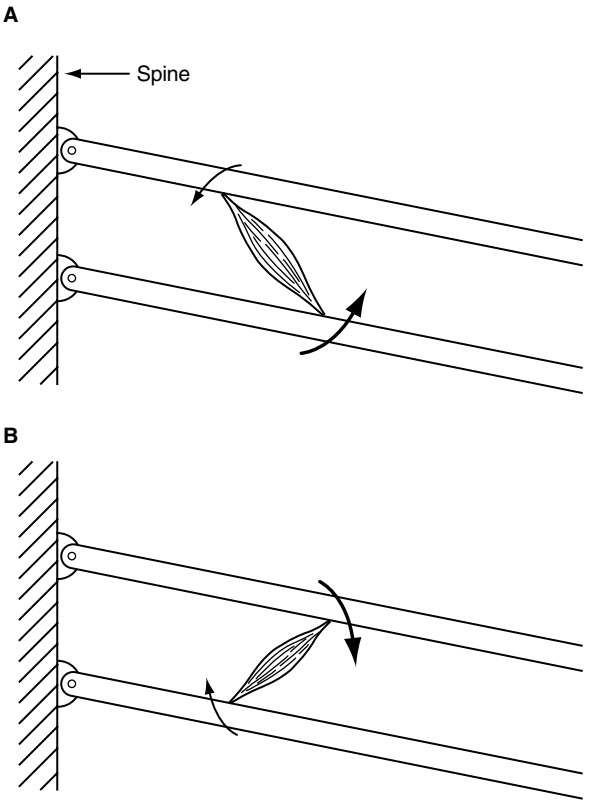

FIGURE 22-4 Diagram illustrating the actions of the intercostal muscles, as proposed by Hamberger.[21] The *hatched area* in each panel represents the spine, and the *two bars* oriented obliquely represent two adjacent ribs; these are linked to each other by the sternum (*right*). The external (*A*) and internal interosseous (*B*) intercostal muscles are depicted as single bundles, and the torques acting on the ribs during contraction of these muscles are represented by *arrows*. See text for further explanation.

in normal subjects have indicated that the human parasternal intercostal muscles, particularly those situated in the second and third interspaces, also have an inspiratory effect on the lung.[24] However, when either the external or the internal interosseous intercostal muscle in a single interspace is selectively stimulated at FRC in the dog, both ribs move closer together, but the cranial displacement of the rib below is always greater than the caudal displacement of the rib above.[25,26] More importantly, both in the dog[27] and in humans,[28] the external and internal interosseous intercostal muscles show marked topographic differences in their actions on the lung. Specifically, in the dog, the external intercostal muscles in the dorsal portion of the upper interspaces have a significant inspiratory effect, but this effect decreases rapidly both toward the costochondral junctions and toward the base of the rib cage (Figure 22-5). As a result, the external intercostal muscles in the ventral portion of the lower interspaces have an expiratory, rather than an inspiratory, effect. The canine internal interosseous intercostal muscles in the dorsal portion of the lower interspaces have a large expiratory effect, but this effect decreases ventrally and cranially, such that, in the ventral half of the first and second interspaces, it is reversed into an inspiratory effect. The respiratory effects of the external and internal

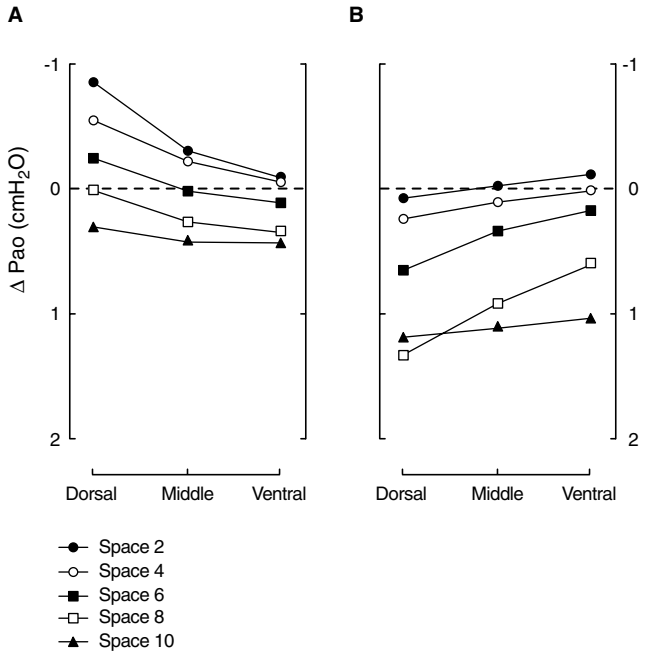

FIGURE 22-5 Actions of the canine external (*A*) and internal interosseous (*B*) intercostal muscles on the lung. These data are the maximal changes in airway pressure (ΔP_{ao}) that the muscles in the dorsal, middle, and ventral portions of the second, fourth, sixth, eighth, and tenth interspaces can generate when contracting against a closed airway. A negative ΔP_{ao} indicates an inspiratory effect, whereas a positive ΔP_{ao} indicates an expiratory effect. Reproduced with permission from De Troyer A et al.[27]

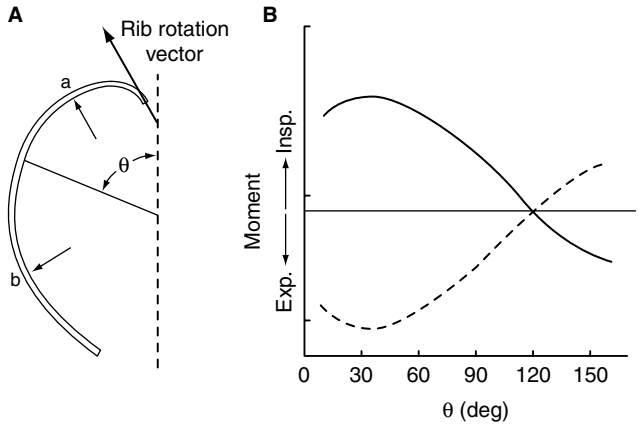

FIGURE 22-6 Effects of rib curvature on the net moment exerted by an intercostal muscle. The plan form of a typical rib in the dog and its axis of rotation (bold vector) are shown in (*A*). At point "a," the distances between the points of attachment of an intercostal muscle on the lower and upper ribs and the axes of rotation of the ribs are different, and the muscle exerts a net moment on the ribs. At point "b," however, the distances between the points of attachment of an intercostal muscle on the lower and upper ribs and the axes of rotation of the ribs are equal, and the muscle exerts no net moment. Thus, the net moment exerted by the muscle depends on the angular position (θ) around the rib, as shown in *B*. The external intercostal muscle (*continuous line*) has the greatest inspiratory moment in the dorsal portion of the rib cage (θ between 15° and 60°); this inspiratory moment then decreases as one moves around the rib cage (θ between 60° and 120°) and is reversed into an expiratory moment in the vicinity of the costochondral junction (θ greater than 120°). The internal intercostal muscle (*dashed line*) shows a similar gradient in expiratory moment.

intercostal muscles in humans show qualitatively similar topographic distributions,[28] although the expiratory effect of the human internal intercostal muscles is greatest in the ventral, rather than the dorsal, portion of the lower interspaces.

The theory of Hamberger cannot explain such dorsoventral and rostrocaudal gradients, and this is because it is based on a two-dimensional model of the rib cage. Indeed, the model is planar, and the ribs are modeled as straight bars rotating around axes that lie perpendicular to the plane of the ribs (see Figure 22-4). Also, the theory of Hamberger contains the implicit assumptions that all the ribs have equal compliances and are equally coupled to the lung.

Real ribs are curved, however, and this curvature has critical effects on the moments exerted by the intercostal muscles,[27,29] as shown in Figure 22-6A. Because the axis of rib rotation is oriented dorsally and laterally, at point "a" on the rib, the tangent plane of the rib cage is perpendicular to the axis of rotation. For the external intercostal muscle, therefore, the distance between the point of attachment of the muscle on the lower rib and the axis of rotation is greater than the distance between the point of attachment of the muscle on the upper rib and the axis of rotation. Consequently, at point "a," the moment exerted by the muscle on the lower rib is greater than the moment exerted on the upper rib, and the net moment is inspiratory. However, at point "b," the tangent plane of the rib cage lies parallel to the axis of rib rotation, so the distances between the points of attachment of the muscle on the two ribs and the axes of rib rotation are equal, and the net moment exerted by the muscle is zero. Thus, the net inspiratory moment of the external intercostal muscle is maximal in the dorsal region of the rib cage, decreases to zero at point "b," and is reversed to an expiratory moment in the ventral region of the rib cage (Figure 22-6B). The net expiratory moment of the internal intercostal muscle is similarly maximal in the dorsal region, decreases in magnitude as one moves away from the spine, and becomes an inspiratory moment in the vicinity of the sternum (Figure 22-6B). Although the difference between the expiratory effect of the internal interosseous intercostal muscles in the dorsal region of the rib cage and the inspiratory effect of the parasternal intercostal muscles was already inferred by Hamberger, it was not appreciated that the differences between the actions of the muscles in the dorsal and ventral regions are the result of gradual transitions, not abrupt changes of mechanism at the costochondral junctions.

In addition, in contrast to the model of Hamberger, the radii of curvature of the ribs increase from the top to the base of the rib cage, the rotational compliances of the different ribs are different,[23,28] and the coupling of the different ribs to the lung varies from the top to the base of the rib cage as well.[30] Specifically, in the dog at FRC, the change in lung volume produced by a given rib displacement increases gradually with increasing rib number in the upper half of the cage, whereas in the lower half of the cage, the change in lung volume produced by a given rib displacement decreases

rapidly with increasing rib number. As a result of these topographic differences in rib compliance and rib–lung coupling, both the external and internal interosseous intercostal muscles in the upper interspaces tend to have an inspiratory effect on the lung. In contrast, in the lower interspaces, both intercostal muscles tend to have an expiratory effect.[30] As shown in Figure 22-5, the location of the muscles along the rostrocaudal axis of the rib cage is the single most important determinant of their respiratory effects, and the orientation of the muscle fibers primarily operates to modulate these effects. That is, for a given muscle mass, the external intercostal muscle in an upper interspace has a larger inspiratory effect on the lung than the internal intercostal muscle, and the external intercostal muscle in a lower interspace has a smaller expiratory effect than the internal intercostal muscle.[30]

Respiratory Function of Intercostal Muscles

These topographic differences in respiratory effects imply that the actions of the muscles on the lung during breathing are largely determined by the topographic distribution of neural drive. Electromyographic studies in dogs,[22] cats,[31,32] baboons,[33] and humans[34–36] have clearly established that the parasternal intercostal muscles invariably contract during the inspiratory phase of the breathing cycle. These muscles, therefore, have a definite inspiratory action on the lung during breathing. Similarly, the external intercostal muscles in animals and in humans are active only during inspiration.[31–34,37,38] However, external intercostal muscle inspiratory activity is found exclusively in the muscle areas with an inspiratory mechanical advantage, and the topographic distribution of this activity is closely matched with the topographic distribution of inspiratory effect.[37–39] Both in the dog and in humans, inspiratory activity in the external intercostal muscles is thus greatest in the dorsal portion of the upper interspaces, that is, in the areas where the muscles have the greatest inspiratory effect. Inspiratory activity then declines gradually in the caudal and the ventral directions, as does the inspiratory effect. The external intercostal muscles with an expiratory effect, that is, in the ventral portion of the lower interspaces, are never active during breathing, including when the demand placed on the respiratory muscle pump is increased by carbon dioxide–enriched gas mixtures or by external mechanical loads.[38] This distribution of neural drive confers to the external intercostal muscles an inspiratory action on the lung during breathing.

On the other hand, the internal interosseous intercostal muscles are active only during expiration, and the topographic distribution of expiratory activity in these muscles mirrors the topographic distribution of expiratory effect. In the dog, internal intercostal muscle expiratory activity is thus greatest in the dorsal portion of the lower interspaces and decreases progressively in the cranial and ventral directions.[38] The areas of internal interosseous intercostal muscle with an inspiratory effect, that is, in the ventral portion of the upper interspaces, are never active during breathing. This distribution of neural drive must confer on the internal interosseous intercostal muscles an expiratory action on the lung during breathing. Thus, the external and internal interosseous intercostal muscles do have opposite actions on the lung during breathing, as conventionally thought, but it must be appreciated that these opposite actions are primarily the result of selective regional activation of the muscles rather than the orientations of the muscle fibers.

Although the external intercostal muscles (including the levator costae) in the upper interspaces and the parasternal intercostal muscles contract together during inspiration, several observations indicate that in anesthetized animals these two muscle groups contribute differently to the cranial displacement of the ribs and the expansion of the lung. First, in anesthetized dogs and cats, the inspiratory cranial displacement of the ribs occurs together with a caudal displacement of the sternum, and this results from the action of the parasternal intercostal muscles.[22,40,41] Indeed, isolated contraction of these muscles causes the sternum to move caudally,[22] whereas isolated contraction of the external intercostal muscles displaces the sternum cranially.[41,42] Second, when the parasternal intercostal muscle in a single interspace is selectively denervated in supine dogs[43] and in upright baboons,[33] the normal inspiratory shortening of the muscle is virtually abolished. Third, when the canine parasternal intercostal muscles in all interspaces are denervated, there is a compensatory increase in external intercostal muscle inspiratory activity, yet the inspiratory cranial displacement of the ribs is markedly reduced.[44] Denervation of the parasternal intercostal muscles in all interspaces in dogs with diaphragmatic paralysis also elicits a large decrease in tidal volume.[41] In contrast, when the canine external intercostal muscles in all interspaces are severed and the parasternal intercostal muscles are left intact, the inspiratory cranial displacement of the ribs and tidal volume show only moderate reductions, although parasternal muscle inspiratory activity remains unchanged.[41,44] In anesthetized animals, therefore, the contribution of the parasternal intercostal muscles to resting breathing is much greater than that of the external intercostal muscles.

However, whereas the parasternal intercostal muscles in the dog are thicker than the external intercostal muscles, in humans the external intercostal muscles are thicker, and the total mass of external intercostal muscle is about six times greater than the parasternal intercostal muscle mass.[28] As a result, the potential inspiratory effect of the external intercostal muscles in humans is about five times greater.[28] In addition, the results of recent electromyographic studies have shown that during resting breathing in normal subjects, the external intercostal muscle in the dorsal portion of the third interspace and the parasternal intercostal muscle in the same interspace start firing simultaneously at the onset of inspiration, but the external intercostal muscle motor units fire with greater discharge rates at the peak of inspiration.[39] This suggests that, in humans, the dorsal areas of the external intercostal muscle receive greater neural drive than the parasternal intercostal muscles and make a greater contribution to lung inflation.

Influence of Lung Volume

In the dog, the length–tension relationship of the parasternal and external intercostal muscles is contracted on its length axis compared with that of the diaphragm.[45]

Therefore, if the parasternal intercostal and external intercostal muscles in the upper interspaces shortened as much as the diaphragm during passive inflation above FRC, their force-generating ability would decrease more. However, whereas the diaphragm shortens by 30 to 40% during inflation from FRC to TLC, the parasternal and upper external intercostal muscles shorten by only ~10%.[23,27] In addition, whereas the resting FRC length of the diaphragm in supine dogs is close to or a little shorter than the muscle optimal length (L_o),[46,47] the canine parasternal intercostal muscles at FRC are 10 to 15% longer than L_o.[45] Consequently, increasing lung volume above FRC causes the diaphragm and the upper external intercostal muscles to move away from L_o but causes the parasternal intercostal muscles to move toward L_o. The net result of these changes is that the force-generating ability of the upper external intercostal muscles should diminish as volume is increased from FRC to TLC; in contrast, the force-generating ability of the canine parasternal intercostal muscles remains unchanged or slightly increases.[48,49]

The fall in pleural pressure produced by the contracting parasternal and external intercostal muscles, however, is determined by the interaction between the force developed by the muscles and the ability of the ribs to move cranially and outward. In the dog, the impedance of the ribs to cranial displacement increases as lung volume is increased above FRC.[25] Moreover, as the ribs become more horizontal with inflation, one would expect that a given cranial rib displacement would lead to a smaller outward displacement. Such alterations in rib displacement should add to the length–tension characteristics of the muscles to reduce the lung-expanding action of the external intercostal muscles at high lung volumes; they might reduce the lung-expanding action of the parasternal intercostal muscles as well, even though the force developed by them might be greater than at FRC. Indeed, DiMarco and colleagues[50] have shown in dogs that the fall in pleural pressure induced by tetanic, simultaneous stimulation of the parasternal and interosseous (external and internal) intercostal muscles in the upper six or seven interspaces decreases gradually as lung volume is increased above FRC. Thus, the change in pressure obtained during stimulation at TLC was ~30% of the change obtained during stimulation at FRC, and similar observations were made during isolated stimulation of the interosseous intercostal muscles.[50] Ninane and Gorini[51] also observed that the fall in pleural pressure produced by selective contraction of the canine parasternal intercostal muscles decreases progressively as lung volume is increased above FRC. The effect of lung volume on the human intercostal muscles, however, is unknown.

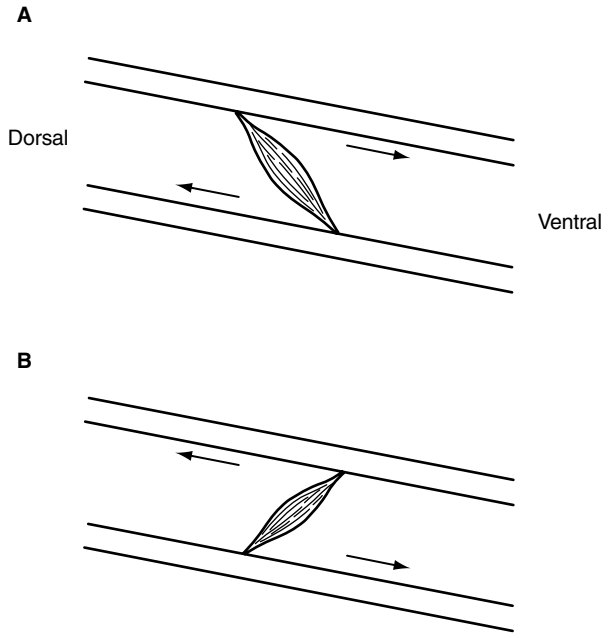

FIGURE 22-7 Diagram of an intercostal space on the right side of the chest (lateral view), illustrating the actions of the external (*A*) and internal interosseous (*B*) intercostal muscles during rotations of the trunk. As in Figure 22-4, the two bars oriented obliquely represent two adjacent ribs, and the muscles are depicted as single bundles. The *arrows* indicate the component of tension vector acting along the ribs. Adapted from De Troyer A. Mechanics of the chest wall muscles. In: Miller AD, Bishop B, Bianchi AL, editors. Neural control of the respiratory muscles. Boca Raton (FL): CRC Press; 1996. p. 59–73.

Nonrespiratory Function of Intercostal Muscles

The insertions and orientations of the external and internal intercostal muscles suggest that these muscles would also be able to twist the rib cage (Figure 22-7). Thus, contraction of the external intercostal muscles on one side of the sternum would rotate the ribs in a transverse plane, so that the upper ribs would move ventrally whereas the lower ribs would move dorsally. In contrast, contraction of the internal intercostal muscles on one side of the sternum would move the upper ribs dorsally and the lower ribs ventrally. In agreement with this idea, Decramer and colleagues[52] have found in anesthetized dogs that the external and internal interosseous intercostal muscles show large, reciprocal changes in length during passive rotations of the thorax. When the animal's trunk was twisted to the left, the external intercostal muscles on the right side and the internal interosseous intercostal muscles on the left side shortened. At the same time, the external intercostal muscles on the left side and the internal intercostal muscles on the right side lengthened. The opposite pattern was seen when the animal's trunk was twisted to the right, with a marked shortening of the right internal and left external intercostal muscles and a lengthening of the left internal muscles and right external muscles. Thus, the length of these muscles changed in the way expected if they were producing the rotations, and indeed, electromyographic studies in normal humans have shown that the external intercostal muscles on the right side of the chest are activated when the trunk is rotated to the left, whereas they remain silent when the trunk is rotated to the right[53]; conversely, the internal intercostal muscles on the right side contracted only when the trunk was rotated to the right.

Triangularis Sterni

The triangularis sterni, also called the transversus thoracis, is not conventionally included among the intercostal muscles. However, this muscle lies deep to the parasternal

intercostal muscles, and its fibers are nearly perpendicular to the latter, running from the dorsal aspect of the caudal half of the sternum to the inner surface of the costal cartilages of the third to seventh ribs. In contrast to the parasternal intercostal muscles, therefore, its selective stimulation in the dog induces a large caudal displacement of the ribs with a small cranial displacement of the sternum and a decrease in lung volume.[54] The triangularis sterni also receives its motor supply from the intercostal nerves.

In quadrupeds, the triangularis sterni invariably contracts during the expiratory phase of the breathing cycle.[54–56] In so doing, it pulls the ribs caudally and deflates the rib cage below its neutral (resting) position.[54] Consequently, when the muscle relaxes at the end of expiration, there is a passive rib cage expansion and an increase in lung volume that precedes the onset of inspiratory muscle contraction. In these animals, the triangularis sterni thus shares the work of breathing with the inspiratory muscles and helps the parasternal and upper external intercostal muscles produce the rhythmic inspiratory expansion of the rib cage.[54] In humans, however, the muscle is thin and usually inactive during resting breathing.[57] Therefore, even though it contracts during expiratory efforts such as coughing, laughing, and speech,[57] its expiratory effect on the lung is small compared with that of the internal intercostal muscles.[24,28]

MUSCLES OF THE NECK

Scalene Muscles

The scalene muscles in humans comprise three muscle heads that run from the transverse processes of the lower five cervical vertebrae to the upper surfaces of the first two ribs. Although they have traditionally been considered to be "accessory" muscles of inspiration, electromyographic studies with concentric needle electrodes have established that, in normal humans, these muscles invariably contract during inspiration, including when the increase in lung volume is very small.[35,36,58,59]

When the scalene muscles are selectively activated by electrical stimulation in the dog, they produce a large cranial displacement of the ribs and sternum, an increase in rib cage anteroposterior diameter, and an increase in lung volume.[60] Since there is no clinical setting that causes paralysis of all the inspiratory muscles without also affecting the scalene muscles, the isolated action of these muscles on the human rib cage cannot be defined precisely. Two observations, however, indicate that contraction of the scalene muscles is an important determinant of the expansion of the upper rib cage during breathing. First, when normal subjects attempt to inspire with the diaphragm alone, there is a marked, selective decrease in scalene muscle activity associated with either less inspiratory increase or a paradoxical decrease in anteroposterior diameter of the upper rib cage.[36] Second, the inspiratory inward displacement of the upper rib cage characteristic of quadriplegia is usually not observed when scalene muscle function is preserved after lower cervical cord transection.[7] As the scalene muscles are innervated from the lower five cervical segments, persistent inspiratory contraction is frequently seen in subjects with a transection at the C7 level or below. In such subjects, the anteroposterior diameter of the upper rib cage tends to remain constant or to increase slightly during inspiration. The fall in pleural pressure produced by a maximal, isolated contraction of these muscles in normal humans would be similar to that caused by the parasternal intercostal muscles in all interspaces.[61]

Sternocleidomastoid Muscles and other Accessory Muscles of Inspiration

Many additional muscles, such as the pectoralis minor, the trapezius, the erector spinae, the serrati, and the sternocleidomastoid muscles, can elevate the ribs when they contract. These muscles, however, run between the shoulder girdle and the rib cage, between the spine and the shoulder girdle, or between the head and the rib cage. Therefore, they have primarily postural functions. In healthy individuals, they contract only during increased inspiratory efforts; in contrast to the scalene muscles, therefore, they are true "accessory" muscles of inspiration.

Of all these muscles, only the sternocleidomastoid muscles, which descend from the mastoid process to the ventral surface of the manubrium sterni and the medial third of the clavicle, have been thoroughly studied. The pressure-generating ability of the sternocleidomastoid muscles in normal humans is about the same as that of the scalene muscles,[61] and their action on the rib cage has been inferred from measurements of chest wall motion in subjects with transection of the upper cervical cord. Indeed, in such subjects, the diaphragm, intercostal muscles, scalene muscles, and abdominal muscles are paralyzed, but the sternocleidomastoid muscles (the motor innervation of which largely depends on the eleventh cranial nerve) are spared and contract forcefully during unassisted inspiration.[4,62] When breathing spontaneously, these subjects show a prominent inspiratory cranial displacement of the sternum and a large inspiratory expansion of the upper rib cage, particularly in its anteroposterior diameter. This prominent cranial displacement of the sternum, however, combined with the fall in intrathoracic pressure, elicits a decrease in the transverse diameter of the lower rib cage[4,62] (Figure 22-8).

ABDOMINAL MUSCLES

Functional Anatomy

The four abdominal muscles with significant respiratory function in humans make up the ventrolateral wall of the abdomen. The rectus abdominis muscle is the most ventral of these muscles. It originates from the ventral aspect of the sternum and the fifth, sixth, and seventh costal cartilages and runs caudally along the whole length of the abdominal wall to insert into the pubis. The muscle is enclosed in a sheath formed by the aponeuroses of the three muscles situated laterally. The most superficial of these is the external oblique muscle, which originates by fleshy digitations from the external surface of the lower eight ribs, well above the costal margin, and directly covers the lower ribs and intercostal muscles. Its fibers radiate caudally to the iliac crest and inguinal ligament and medially to the linea alba. The

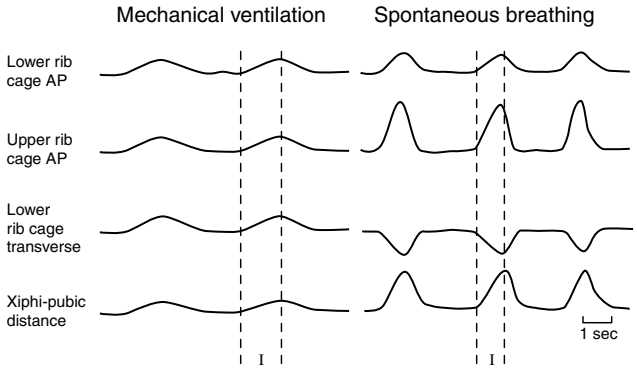

FIGURE 22-8 Pattern of rib cage motion during mechanical ventilation (*left*) and during spontaneous breathing (*right*) in a quadriplegic subject with a traumatic transection of the upper cervical cord (C_1). Each panel shows, from top to bottom, the respiratory changes in anteroposterior (AP) diameter of the lower rib cage, the changes in AP diameter of the upper rib cage, the changes in transverse diameter of the lower rib cage, and the changes in xiphipubic distance. Upward deflections correspond to an increase in diameter or an increase in xiphipubic distance (ie, a cranial displacement of the sternum); I indicates the duration of inspiration. Note that all rib cage diameters and the xiphipubic distance increase in phase during mechanical inflation. During spontaneous inspiration, however, the xiphipubic distance and the upper rib cage AP diameter increase more than the lower rib cage AP diameter, and the lower rib cage transverse diameter decreases.

internal oblique muscle lies deep to the external oblique muscle. Its fibers arise from the iliac crest and inguinal ligament and diverge to insert on the costal margin and an aponeurosis contributing to the rectus sheath down to the pubis. The transversus abdominis muscle is the deepest of the muscles of the lateral abdominal wall. It arises from the inner surface of the lower six ribs, where it interdigitates with the costal insertions of the diaphragm. From this origin, and from the lumbar fascia, the iliac crest, and the inguinal ligament, its fibers run circumferentially around the abdominal visceral mass and terminate ventrally in the rectus sheath.

Actions of the Abdominal Muscles

These four muscles have important functions as flexors (rectus abdominis muscle) and rotators (external oblique and internal oblique muscles) of the trunk, but as respiratory muscles, they have two main actions. First, as they contract, they pull the abdominal wall inward and produce an increase in abdominal pressure. As a result, there is a cranial motion of the diaphragm into the thoracic cavity, leading to an increase in pleural pressure and a decrease in lung volume. Second, these four muscles displace the rib cage through their insertions on the ribs. These insertions would suggest that the action of all abdominal muscles is to pull the ribs caudally and to deflate the rib cage, another expiratory action. Measurements of rib cage motion during electrical stimulation of the individual muscles in dogs have shown, however, that these muscles also have an inspiratory action on the rib cage.[63,64] Indeed, the rise in pleural pressure resulting from the cranial displacement of the diaphragm tends to expand the portion of the rib cage apposed to the lung. Furthermore, by forcing the diaphragm cranially and stretching it, the contracting abdominal muscles induce both an increase in size of the zone of apposition of the diaphragm to the rib cage (see Figure 22-1) and an increase in passive diaphragmatic tension. This passive tension tends to raise the lower ribs and to expand the lower rib cage in the same way as does an active diaphragmatic contraction ("insertional" force).

The action of the abdominal muscles on the rib cage is thus determined by the balance between the insertional, expiratory force of the muscles and the inspiratory force related to the rise in pleural and abdominal pressures. Isolated contraction of the external oblique muscle in humans produces a small caudal displacement of the sternum and a large decrease in the rib cage transverse diameter, but the rectus abdominis muscle, while causing a marked caudal displacement of the sternum and a large decrease in the anteroposterior diameter of the rib cage, also produces a small increase in the rib cage transverse diameter.[65] The isolated actions of the internal oblique and transversus abdominis muscles on the human rib cage are not known. The anatomic arrangement of the transversus abdominis muscle, however, would suggest that, among the abdominal muscles, this muscle has the smallest insertional, expiratory action on the ribs and the greatest effect on abdominal pressure. Isolated contraction of the transversus abdominis muscle should therefore produce little or no expiratory rib cage displacement.

Respiratory Function of the Abdominal Muscles

Irrespective of their actions on the rib cage, the abdominal muscles are primarily expiratory muscles through their action on the diaphragm and the lung, and they play important roles in activities such as coughing and speaking. However, these muscles may also assist inspiration, and the horse breathing at rest provides a dramatic illustration of this inspiratory action.[66] As shown in Figure 22-9, this animal displays a biphasic airflow pattern during both expiration and inspiration. The first part of expiration results from the relaxation of the inspiratory muscles and is, therefore, essentially passive. As expiration proceeds, however, there is strong contraction of the abdominal muscles, which deflates the respiratory system below its relaxation volume and generates a second peak of expiratory airflow. At the onset of the subsequent inspiration, the abdominal muscles relax. In so doing, they promote passive descent of the diaphragm and induce an increase in lung volume as the respiratory system returns toward its relaxation volume; this phenomenon accounts for the first peak of inspiratory airflow. After inspiratory flow diminishes, the inspiratory muscles contract, producing a second peak of inspiratory flow. Although such a flow pattern is rather characteristic of the horse, dogs use a similar strategy of breathing. When anesthetized dogs are placed in the head-up or the prone posture, relaxation of the abdominal muscles at end-expiration accounts for up to 40 to 60% of tidal volume.[67,68]

Healthy humans do not use such a breathing strategy at rest. However, phasic expiratory contraction of the abdominal muscles does occur whenever the demand placed on the

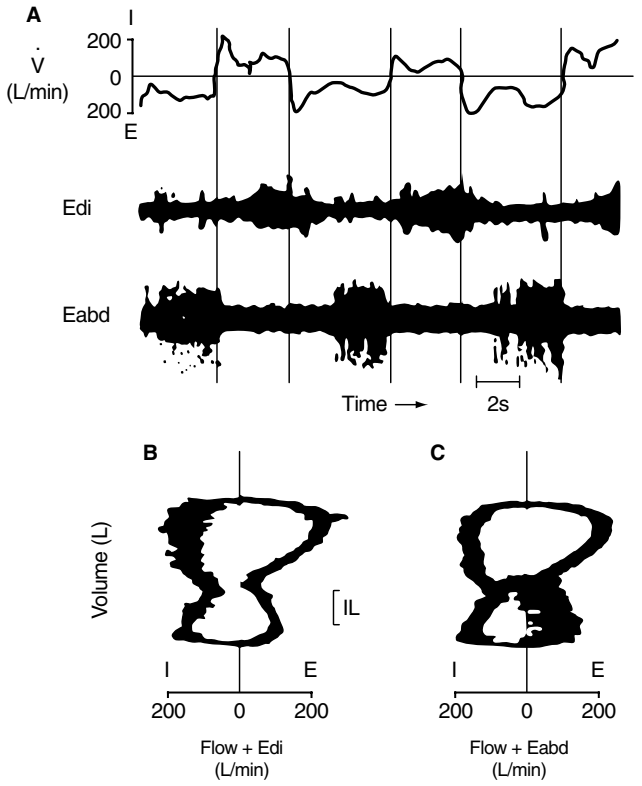

FIGURE 22-9 Strategy of breathing in the horse. *A*, Traces of airflow ($\dot{V}$), electromyogram of the diaphragm (E_{di}), and electromyogram of the abdominal internal oblique muscle (E_{abd}) versus time. Note that the onset of inspiratory flow clearly precedes the onset of E_{di} and that the onset of expiratory flow precedes the onset of E_{abd}. *B*, The corresponding flow–volume loop, in which the raw E_{di} signal has been electrically added to the flow tracing, also shows that most of the E_{di} signal is in the second phase of inspiration. *C*, The flow–volume loop with the raw E_{abd} signal electrically added to the flow tracing further shows that the E_{abd} signal is confined to the second phase of expiration. Reproduced with permission from Koterba AM et al.[66]

inspiratory muscles is increased, such as during exercise or during the breathing of carbon dioxide-enriched gas mixtures. It is noteworthy that, in these conditions, the transversus abdominis muscle is recruited well before activity can be recorded from either the rectus abdominis muscle or the external oblique muscle.[69,70] In view of the actions of these muscles, this preferential recruitment of the transversus abdominis muscle further strengthens the idea that the effect of the abdominal muscles on abdominal pressure is far more important in the act of breathing than is their action on the rib cage.

Influence of Lung Volume

Whereas passive inflation causes shortening of the diaphragm and inspiratory intercostal muscles, it induces lengthening of the abdominal muscles, particularly the transversus abdominis and internal oblique muscle. In supine, anesthetized dogs, these two muscles lengthen by 15 to 25% during inflation from FRC to TLC, whereas the rectus abdominus and external oblique muscles lengthen by only 1 to 3%.[71] With passive inflation, therefore, the force produced by the contracting abdominal muscles increases, and in dogs and rabbits, the rise in abdominal pressure obtained during selective, tetanic stimulation of the muscles at TLC is ~25% greater than the pressure rise obtained for the same stimulation at FRC.[64] A similar observation has been made during magnetic stimulation of the abdominal muscles in normal humans and in quadriplegic subjects.[72] In addition, passive inflation induces a decrease in the passive diaphragmatic tension, particularly when the subjects are in the supine posture. As a result, the rise in abdominal pressure generated by the abdominal muscles is better transmitted to the pleural cavity, which further enhances the lung-deflating action of the muscles.[64]

SUMMARY AND CONCLUSIONS

Although the diaphragm is the main respiratory muscle in humans, movement of the chest wall during breathing is an integrated process that involves many muscles. During spontaneous quiet breathing, the parasternal intercostal muscles, the external intercostal muscles in the dorsal portion of the upper interspaces, and the scalene muscles contract in a coordinated manner during inspiration to lift the ribs and expand the upper half of the rib cage. Relaxation of these muscles at end-inspiration allows the respiratory system to return, through its passive elastic properties, to its neutral (resting) position. During exercise, however, as the production of carbon dioxide by the locomotor muscles is augmented, the regulation of chest wall muscle activation becomes even more complex, involving not only increased activation of the muscles already active during resting breathing but also the recruitment of additional muscles that augment chest wall expansion (the so-called "accessory" muscles). In addition, exercise hyperpnea is associated with phasic expiratory contraction of muscles, such as the transversus abdominis muscle, the triangularis sterni muscle, and the internal interosseous intercostal muscles in the lower interspaces, that deflate the abdomen and the rib cage and increase expiratory airflow, so as to bring rhythmically the respiratory system below its resting volume. Although these muscles have an expiratory action on the lungs, their relaxation at end-expiration causes an increase in lung volume; they therefore reduce the load on the inspiratory muscles and help them meet the increased ventilatory requirements.

Breathing is primarily an automatic process, and the pattern of respiratory muscle activation is to a large extent "hard-wired" to the central respiratory controller. Thus, essentially similar adaptations take place when the work of breathing is increased by disease. When some respiratory muscle groups are weak or paralyzed, the remaining muscles have to overcome the entire resistive and elastic load; the strain imposed on them is consequently greater than normal. Similarly, when airflow resistance is abnormally elevated or when dynamic pulmonary and/or chest wall compliance is abnormally reduced, the inspiratory muscles have to generate a greater reduction in pleural pressure to inflate the lungs. The presence of static or dynamic hyperinflation places an additional load on these muscles by making

them operate at shorter than normal lengths and by reducing their ability to lower pleural pressure. When breathing at rest, patients with severe obstructive or restrictive pulmonary impairment will therefore use their muscles in much the same way as normal subjects do during exercise. In such patients, however, as in patients with respiratory muscle paralysis, some of the contracting muscles may have little or no beneficial effect on the act of breathing.

REFERENCES

1. Konno K, Mead J. Measurement of the separate volume changes of rib cage and abdomen during breathing. J Appl Physiol 1967;22:407–22.
2. Mead J. Functional significance of the area of apposition of diaphragm to rib cage. Am Rev Respir Dis 1979;119:31–2.
3. D'Angelo E, Sant'Ambrogio G. Direct action of contracting diaphragm on the rib cage in rabbits and dogs. J Appl Physiol 1974;36:715–9.
4. Danon J, Druz WS, Goldberg NB, Sharp JT. Function of the isolated paced diaphragm and the cervical accessory muscles in C_1 quadriplegics. Am Rev Respir Dis 1979;119:909–19.
5. Strohl KP, Mead J, Banzett RB, et al. Effect of posture on upper and lower rib cage motion and tidal volume during diaphragm pacing. Am Rev Respir Dis 1984;130:320–1.
6. Mortola JP, Sant'Ambrogio G. Motion of the rib cage and the abdomen in tetraplegic patients. Clin Sci Mol Med 1978;54:25–32.
7. Estenne M, De Troyer A. Relationship between respiratory muscle electromyogram and rib cage motion in tetraplegia. Am Rev Respir Dis 1985;132:53–9.
8. De Troyer A, Sampson M, Sigrist S, Macklem PT. Action of costal and crural parts of the diaphragm on the rib cage in dog. J Appl Physiol 1982;53:30–9.
9. Loring SH, Mead J. Action of the diaphragm on the rib cage inferred from a force–balance analysis. J Appl Physiol 1982;53:756–60.
10. Urmey WF, De Troyer A, Kelly SB, Loring SH. Pleural pressure increases during inspiration in the zone of apposition of diaphragm to rib cage. J Appl Physiol 1988;65:2207–12.
11. Sant'Ambrogio G, Saibene F. Contractile properties of the diaphragm in some mammals. Respir Physiol 1970;10:349–57.
12. Pengelly LD, Alderson AM, Milic-Emili J. Mechanics of the diaphragm. J Appl Physiol 1971;30:797–805.
13. Kim MJ, Druz WS, Danon J, et al. Mechanics of the canine diaphragm. J Appl Physiol 1976;41:369–82.
14. Minh VD, Dolan GF, Konopka RF, Moser KM. Effect of hyperinflation on inspiratory function of the diaphragm. J Appl Physiol 1976;40:67–73.
15. Smith J, Bellemare F. Effect of lung volume on in vivo contraction characteristics of human diaphragm. J Appl Physiol 1987;62:1893–900.
16. Braun NMT, Arora NS, Rochester DF. Force–length relationship of the normal human diaphragm. J Appl Physiol 1982;53:405–12.
17. Gauthier AP, Verbanck S, Estenne M, et al. Three dimensional reconstruction of the in vivo human diaphragm shape at different lung volumes. J Appl Physiol 1994;76:495–506.
18. Estenne M, Yernault JC, De Troyer A. Rib cage and diaphragm–abdomen compliance in humans: effects of age and posture. J Appl Physiol 1985;59:1842–8.
19. De Troyer A, Cappello M, Meurant N, Scillia P. Synergism between the canine left and right hemidiaphragms. J Appl Physiol 2003;94:1757–65.
20. Bellemare F, Bigland-Ritchie B, Woods JJ. Contractile properties of the human diaphragm in vivo. J Appl Physiol 1986; 61:1153–61.
21. Hamberger GE. De Respirationis Mechanismo et usu genuino. Iena; 1749.
22. De Troyer A, Kelly S. Chest wall mechanics in dogs with acute diaphragm paralysis. J Appl Physiol 1982;53:373–9.
23. De Troyer A, Legrand A, Wilson TA. Rostrocaudal gradient of mechanical advantage in the parasternal intercostal muscles of the dog. J Physiol (Lond) 1996;495:239–46.
24. De Troyer A, Legrand A, Gevenois PA, Wilson TA. Mechanical advantage of the human parasternal intercostal and triangularis sterni muscles. J Physiol (Lond) 1998;513:915–25.
25. De Troyer A, Kelly S, Macklem PT, Zin WA. Mechanics of intercostal space and action of external and internal intercostal muscles. J Clin Invest 1985;75:850–7.
26. Ninane V, Gorini M, Estenne M. Action of intercostal muscles on the lung in dogs. J Appl Physiol 1991;70:2388–94.
27. De Troyer A, Legrand A, Wilson TA. Respiratory mechanical advantage of the canine external and internal intercostal muscles. J Physiol (Lond) 1999;518:283–9.
28. Wilson TA, Legrand A, Gevenois PA, De Troyer A. Respiratory effects of the external and internal intercostal muscles in humans. J Physiol (Lond) 2000;530:319–30.
29. Wilson TA, De Troyer A. Respiratory effect of the intercostal muscles in the dog. J Appl Physiol 1993;75:2636–45.
30. De Troyer A, Wilson TA. Coupling between the ribs and the lung in dogs. J Physiol (Lond) 2002;540:231–6.
31. Greer JJ, Martin TP. Distribution of muscle fiber types and EMG activity in cat intercostal muscles. J Appl Physiol 1990; 69:1208–11.
32. Sears TA. Efferent discharges in alpha and fusimotor fibres of intercostal nerves of the cat. J Physiol (Lond) 1964; 174:295–315.
33. De Troyer A, Farkas GA. Contribution of the rib cage inspiratory muscles to breathing in baboons. Respir Physiol 1994;97:135–45.
34. Taylor A. The contribution of the intercostal muscles to the effort of respiration in man. J Physiol (Lond) 1960; 151: 390–402.
35. Delhez L. Contribution électromyographique à l'étude de la mécanique et du contrôle nerveux des mouvements respiratoires de l'homme. Liège: Vaillant-Carmanne; 1974.
36. De Troyer A, Estenne M. Coordination between rib cage muscles and diaphragm during quiet breathing in humans. J Appl Physiol 1984;57:899–906.
37. Bainton CR, Kirkwood PA, Sears TA. On the transmission of the stimulating effects of carbon dioxide to the muscles of respiration. J Physiol (Lond) 1978;280:249–72.
38. Legrand A, De Troyer A. Spatial distribution of external and internal intercostal activity in dogs. J Physiol (Lond) 1999; 518:291–300.
39. De Troyer A, Gorman R, Gandevia SG. Distribution of inspiratory drive to the external intercostal muscles in humans. J Physiol (Lond) 2003;546:943–54.
40. Da Silva KMC, Sayers BMA, Sears TA, Stagg DT. The changes in configuration of the rib cage and abdomen during breathing in the anaesthetized cat. J Physiol (Lond) 1977;266:499–521.
41. De Troyer A, Wilson TA. The canine parasternal and external intercostal muscles drive the ribs differently. J Physiol (Lond) 2000;523:799–806.
42. Loring SH, Woodbridge JA. Intercostal muscle action inferred from finite-element analysis. J Appl Physiol 1991;70:2712–8.
43. De Troyer A, Farkas GA, Ninane V. Mechanics of the parasternal intercostals during occluded breaths in the dog. J Appl Physiol 1988;64:1546–53.

44. De Troyer A. The inspiratory elevation of the ribs in the dog: primary role of the parasternals. J Appl Physiol 1991;70:1447–55.
45. Farkas GA, Decramer M, Rochester DF, De Troyer A. Contractile properties of intercostal muscles and their functional significance. J Appl Physiol 1985;59:528–35.
46. Road J, Newman S, Derenne JP, Grassino A. In vivo length–force relationship of canine diaphragm. J Appl Physiol 1986; 60:63–70.
47. Farkas GA, Rochester DF. Functional characteristics of canine costal and crural diaphragm. J Appl Physiol 1988;65:2253–60.
48. Decramer M, Jiang TX, Demedts M. Effects of acute hyperinflation on chest wall mechanics in dogs. J Appl Physiol 1987;63:1493–8.
49. Jiang TX, Deschepper K, Demedts M, Decramer M. Effects of acute hyperinflation on the mechanical effectiveness of the parasternal intercostals. Am Rev Respir Dis 1989;139:522–8.
50. DiMarco AF, Romaniuk JR, Supinski GS. Mechanical action of the interosseous intercostal muscles as a function of lung volume. Am Rev Respir Dis 1990;142:1041–6.
51. Ninane V, Gorini M. Adverse effect of hyperinflation on parasternal intercostals. J Appl Physiol 1994;77:2201–6.
52. Decramer M, Kelly S, De Troyer A. Respiratory and postural changes in intercostal muscle length in supine dogs. J Appl Physiol 1986;60:1686–91.
53. Whitelaw WA, Ford GT, Rimmer KP, De Troyer A. Intercostal muscles are used during rotation of the thorax in humans. J Appl Physiol 1992;72:1940–4.
54. De Troyer A, Ninane V. Triangularis sterni: a primary muscle of breathing in the dog. J Appl Physiol 1986;60:14–21.
55. Hwang JC, Zhou D, St John WM. Characterization of expiratory intercostal activity to triangularis sterni in cats. J Appl Physiol 1989;67:1518–24.
56. Smith CA, Ainsworth DM, Henderson KS, Dempsey JA. Differential responses of expiratory muscles to chemical stimuli in awake dogs. J Appl Physiol 1989;66:384–91.
57. De Troyer A, Ninane V, Gilmartin JJ, et al. Triangularis sterni muscle use in supine humans. J Appl Physiol 1987;62:919–25.
58. Raper AJ, Thompson WT Jr, Shapiro W, Patterson JL Jr. Scalene and sternomastoid muscle function. J Appl Physiol 1966;21:497–502.
59. Gandevia SC, Leeper JB, McKenzie DK, De Troyer A. Discharge frequencies of parasternal intercostal and scalene motor units during breathing in normal and COPD subjects. Am J Respir Crit Care Med 1996;153:622–8.
60. De Troyer A, Kelly S. Action of neck accessory muscles on rib cage in dogs. J Appl Physiol 1984;56:326–32.
61. Legrand A, Schneider E, Gevenois PA, De Troyer A. Respiratory effects of the scalene and sternomastoid muscles in humans. J Appl Physiol 2003;94:1467–72.
62. De Troyer A, Estenne M, Vincken W. Rib cage motion and muscle use in high tetraplegics. Am Rev Respir Dis 1986;133: 1115–19.
63. De Troyer A, Sampson M, Sigrist S, Kelly S. How the abdominal muscles act on the rib cage. J Appl Physiol 1983;54:465–9.
64. D'Angelo E, Prandi E, Bellemare F. Mechanics of the abdominal muscles in rabbits and dogs. Respir Physiol 1994;97: 275–91.
65. Mier A, Brophy C, Estenne M, et al. Action of abdominal muscles on rib cage in humans. J Appl Physiol 1985;58: 1438–43.
66. Koterba AM, Kosch PC, Beech J, Whitlock T. Breathing strategy of the adult horse (Equus caballus) at rest. J Appl Physiol 1988;64:337–46.
67. Farkas GA, Estenne M, De Troyer A. Expiratory muscle contribution to tidal volume in head-up dogs. J Appl Physiol 1989;67:1438–42.
68. Farkas GA, Schroeder MA. Mechanical role of expiratory muscles during breathing in prone anesthetized dogs. J Appl Physiol 1990;69:2137–42.
69. De Troyer A, Estenne M, Ninane V, et al. Transversus abdominis muscle function in humans. J Appl Physiol 1990;68:1010–16.
70. Abe T, Kusuhara N, Yoshimura N, Easton PA. Differential respiratory activity of four abdominal muscles in humans. J Appl Physiol 1996;80:1379–89.
71. Leevers AM, Road JD. Mechanical response to hyperinflation of the two abdominal muscle layers. J Appl Physiol 1989;66: 2189–95.
72. Estenne M, Pinet C, De Troyer A. Abdominal muscle strength in patients with tetraplegia. Am J Respir Crit Care Med 2000;161:707–12.

CHAPTER 23

BIOLOGY OF THE RESPIRATORY MUSCLES

Ghislaine Gayan-Ramirez, Marc Decramer

The mammalian respiratory pump is a multimuscle system involving the actions of many ventilatory muscles to provide ventilation appropriate to metabolic demands. Respiratory muscles, like other skeletal muscles, are extremely plastic and can adapt their function in response to environmental circumstances or disease by modifying their structure. In this process, the different elements composing the muscles at the molecular level are subjected to changes that, in turn, alter muscle function. The stimulus leading to muscle alterations may be physiologic, pathologic, or traumatic. The changes in muscle cellular structure and function are observed in the contractile properties (muscle mass, dimensions and proportion of muscle fibers, length and number of sarcomeres, myosin heavy-chain isoforms), capillary density, and metabolic content (energy production, mitochondrial amount, content and activity of the oxidative and glycolytic enzymes). These changes are caused by alterations in muscle gene expression (growth factor expression, myogenic regulatory factors, and type Id inhibitor of DNA-binding protein expression).

In this chapter, we review the cellular structure and function of the diaphragm and rib cage muscles under normal conditions and provide an overview of cellular adaptations occurring in these muscles in patients with chronic obstructive pulmonary disease (COPD). Adaptations occurring in response to other pulmonary diseases have been only scantily studied. Efforts have been made to focus on human data, but, where necessary, animal data are also described. In the first part of this chapter, we review the cellular and molecular basis for respiratory muscle adaptations. In the second part, we address the normal respiratory muscle cell biology and adaptations occurring in patients with COPD.

CELLULAR AND MOLECULAR BASIS OF MUSCLE ADAPTATIONS

Changes in gene expression due to environmental circumstances or disease result in alterations in muscle structure and function. As described below, these adaptations may be observed at the level of the contractile apparatus and the metabolism of the muscle.

Contractile Apparatus

The structural elements primarily involved in adaptations of muscle function include sarcomeres, myosin, sarcoplasmic/endoplasmic reticulum Ca^{2+}-ATPase (SERCA) pumps, growth factors, myogenic regulatory factors, and inhibitors of DNA-binding proteins.

Sarcomeres The sarcomere is the functional unit of muscle contraction in skeletal muscle, including respiratory muscles. The sarcomere contains two types of myofilaments: the thick filament (myosin) and the thin filament (actin).[1] According to the sliding filament concept, the force of contraction is developed by the crossbridges where the thick and thin elements overlap. Most properties of muscle are length dependent; maximal force is developed at the optimal length (Figure 23-1). For the diaphragm, the optimal length occurs at a lung volume below functional residual capacity (FRC), whereas for the parasternal intercostal muscles, the optimal length occurs near total lung capacity (TLC).[2] Evidently, when lung volume changes chronically (ie, chronic hyperinflation), some respiratory muscles are placed at a mechanical disadvantage and adapt so as to attempt to restore their optimal length. To this extent, sarcomere adaptation may occur as further described in this chapter.

Myosin The components of myosin have recently received particular attention and are now commonly used to classify muscle fibers. Myosin is composed of two myosin heavy chains (MHCs) and two myosin light chains (MLCs).[3] MHCs and MLCs exist as multiple isoforms (slow and fast), and coexpression of different MHC isoforms within the same muscle fiber is common, even in normal muscle. MHCs determine the intrinsic properties of muscle fibers, and MLCs seem to affect the maximal shortening velocity.[4] The main MHC isoforms are the slow isoform MHC-I and the three fast isoforms MHC-IIa, MHC-IIx, and MHC-IIb. The main MLC isoforms are the slow isoform MLC-1s and the two fast isoforms MLC-1f and MLC-3f.

SERCA Pumps The SERCA pumps belong to the Ca^{2+}-ATPase family and play a key role in the regulation of

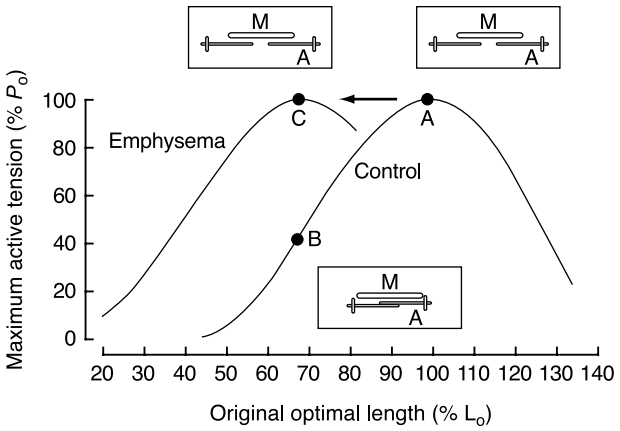

FIGURE 23-1 The effects of acute and chronic diaphragmatic shortening are highlighted in terms of maximal force generation and sarcomere length. Point A represents the original state. Point B represents the acutely shortened muscle, where reduction in the muscle's force-producing capacity is due to reduced sarcomere length. Point C represents chronic diaphragmatic shortening in emphysematous hamsters, where loss in sarcomeres due to chronic shortening occurs, such that the remaining sarcomeres operate at their optimal length. As a result, the length–tension curve of the diaphragm from emphysematous hamsters is displaced to the left of the control curve. A = actin; L_o = optimal length; M = myosin; P_o = maximal tetanic tension. Reproduced with permission from Farkas GA.[2]

skeletal muscle function.[5] Indeed, by pumping Ca^{2+} from the myoplasm into the sarcoplasmic reticulum and thus lowering sarcoplasmic Ca^{2+} concentration, they induce relaxation. Three separate genes (*SERCA1*, *SERCA2*, and *SERCA3*) encode the SERCA family Ca^{2+} pumps.[5,6] The adult form of *SERCA1* (*SERCA1a*) is exclusively expressed in fast-twitch skeletal muscle and is regulated by sarcolipin.[7] Indeed, at low Ca^{2+} concentrations, sarcolipin shifts the K_m for Ca^{2+} of *SERCA1* to higher values and thereby acts as an inhibitor of the pump. But at higher Ca^{2+} concentrations saturating *SERCA1*, sarcolipin behaves as a stimulator of the pump by increasing V_{max}. *SERCA2a* is characteristic of slow-twitch skeletal muscle, cardiac muscle, and smooth muscle and is regulated by phospholamban.[5] When phospholamban is phosphorylated (by cAMP-dependent protein kinase or by Ca^{2+}/calmodulin-dependent protein kinase), the affinity of *SERCA2* for Ca^{2+} is increased. Finally, expression of *SERCA3* is confined to platelets, lymphoid cells, mast cells, and epithelial and endothelial cells of various organs.[8]

Metabolism[9]

The structural characteristics of skeletal muscles are dependent on the proportion and types of the different fibers present in these muscles. Classification systems have designated single fibers as type I, type IIa, type IIb, or type IIx, based on myofibrillar ATPase activity, or as MHC-I, IIa, IIb, or IIx, based on electrophoretic mobility. Each fiber type has its own properties that can be used to assess adaptations of a muscle in a given situation. Thus, the type I fibers are slow-twitch fibers, with a high myoglobin concentration and mitochondrial density and hence high oxidative potential (and consequently low glycolytic potential). These fibers have low myosin ATPase activity and are highly resistant to fatigue. In contrast, the type IIb fibers are fast-twitch fibers with a low myoglobin concentration and mitochondrial density and thus have low oxidative potential but high glycolytic potential and high fatigability. The type IIa fibers are intermediate. To evaluate the oxidative or glycolytic potential of a muscle, mitochondrial content and key enzymes are measured in the muscle: citrate synthase (CS), and 3-hydroxylacyl-A dehydrogenase (HAD) for the oxidative capacity, and lactate dehydrogenase (LDH), phosphofructokinase (PFK) and hexokinase (HK) for the glycolytic capacity. Capillary density is also a parameter often used as maximum bloodflow is high for type I and IIa fibers and low for type IIb fibers.

Muscle Gene Expression

Growth Factors Among the most important growth factors involved in cell growth and regeneration, insulin-like growth factor-I and -II (IGF-I, IGF-II) seem to be the most relevant. Both IGFs can stimulate division and fusion of skeletal muscle satellite cells,[10] and they have been shown to be involved in muscle hypertrophy.[11–13] These growth factors act not only in an endocrine but also in an autocrine/paracrine manner.[11,14] The levels of free IGFs are modulated by the degree of binding to the insulin-like growth factor binding proteins (IGFBPs), so the regulation of the IGFBPs should be taken into account when IGF expression is being examined.

Another growth factor of interest is the growth-related differentiation factor-8 (GDF-8 or myostatin), particularly because this growth factor is exclusively expressed in skeletal muscles.[15] Marked increases in muscle mass and hypertrophy have been reported when the gene encoding for this growth factor is disrupted.[16]

Myogenic Regulatory Factors and Type Id Inhibitors of DNA-Binding Proteins To further unravel the mechanisms of muscle plasticity, the potential role of the myogenic regulatory factors and of the type Id inhibitor of DNA-binding proteins should be investigated as they may modulate the actions of the growth factors. Myogenic factors and the type Id inhibitor of DNA-binding proteins belong to the helix–loop–helix protein family, but whereas myogenic factors contain a basic DNA domain essential for binding to muscle-specific genes to induce transcription, the type Id inhibitor of DNA-binding proteins does not[17] (Figure 23-2). In fact, the type Id inhibitor of DNA-binding proteins inhibits myogenesis directly by forming inactive heterodimers with the E-proteins (ubiquitous basic helix–loop–helix proteins such as E12 and E47) and indirectly by chelating the E-proteins, thereby inhibiting the myogenic-mediated transcription by competitive binding to their dimerization partners (see Figure 23-2). The myogenic regulatory factors (MyoD, myogenin, myf-5, and MRF4) are key regulatory proteins, exclusively expressed in skeletal muscles; their up-regulation is associated with muscle hypertrophy, in contrast to the type Id inhibitor of DNA-binding proteins, whose up-regulation results in muscle atrophy.

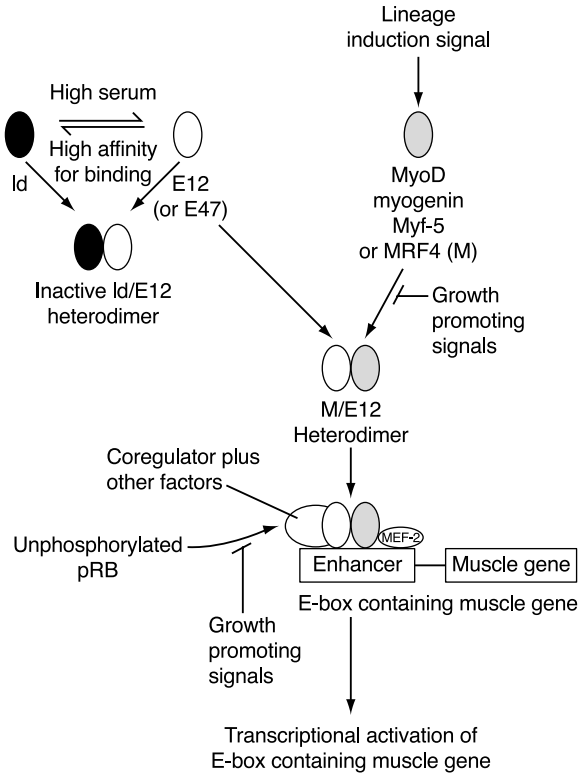

FIGURE 23-2 Proposed interactions of the myogenic regulatory factors with other positive and negative regulatory factors in the transcriptional activation of muscle-specific genes. The members of the basic helix–loop–helix superfamily (MyoD, myogenin, Myf-5, MRF4) can form homodimers or heterodimers by binding with other members of this family, in particular the E-proteins (E12 and E47). This homo- or heterodimer then binds to a conserved DNA sequence (the E-box) found in the regulatory regions of most muscle-specific genes, thereby activating transcription. Proteins that contain the helix–loop–helix domain but lack the basic region, such as the Id-protein, function as negative regulators of E-box–mediated transcription. They also inhibit the myogenic regulatory factor–mediated transcription by competitive binding to their dimerization partners (such as the E-proteins). Adapted from Dias P et al.[17]

MOLECULAR AND CELLULAR BIOLOGY OF THE DIAPHRAGM

The diaphragm is the primary inspiratory muscle, being continuously active throughout life, in contrast to other skeletal muscles, with bursts of high activity during coughing, singing, and exercising. Therefore, diaphragm fibers are resistant to fatigue, their oxidative capacities are elevated, their capillary density is high, and bloodflow to the diaphragm is important because the oxygen requirements of the working diaphragm are met mainly by increasing bloodflow.

The characteristics of the diaphragm under normal conditions are described first, and subsequently we address the adaptations occurring in COPD.

Normal Conditions

Contractile Apparatus

Diaphragm Dimensions Diaphragm muscle mass in normal humans (260 g) represents 95% of the total weight of the diaphragm (280 g). The diaphragm thickness is about 35 mm, whereas the muscle area is 750 cm^2.[18–20] Diaphragm weight has been reported to be higher in males than in females[21] and is correlated positively with body weight.[21,22] Similarly, a linear relationship between body weight and either diaphragm thickness or area has been demonstrated.[23,24] Caution should, however, be exercised when these data are extrapolated to live subjects as they pertain to diaphragm biopsy specimens obtained from cadavers, and several factors, including rigidity, may have influenced the diaphragm dimensions.

Sarcomere Length Diaphragm sarcomere length was reported to be 2.27 ±0.15 μm in subjects with normal spirometry findings[25] (Figure 23-3; Table 23-1). Interestingly, the presence of disrupted sarcomeres (damaged sarcomeres) in the human diaphragm has been shown to be common even in subjects with normal lung function.[26] Whether this is a function of age still remains to be determined.

Myosin and Fiber Types In postmortem studies in which biopsy specimens were obtained from healthy subjects

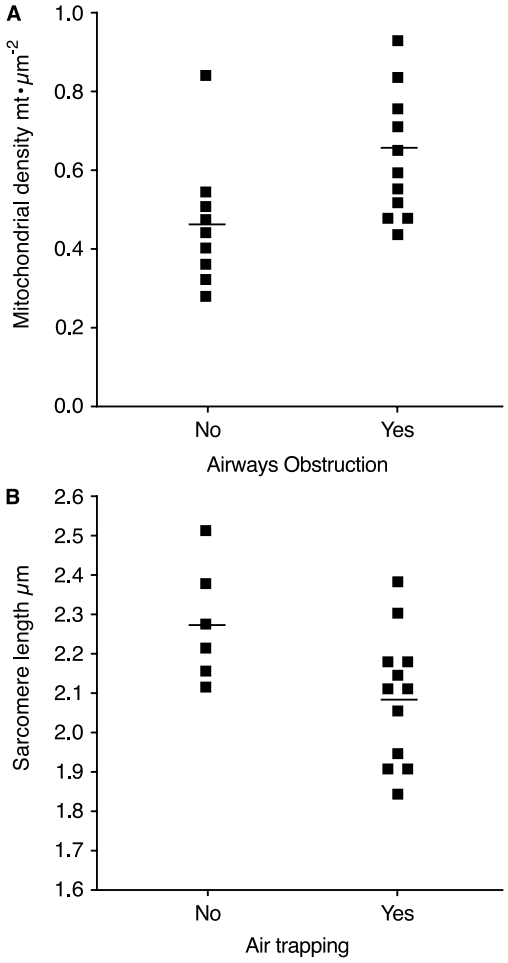

FIGURE 23-3 Mitochondrial density (*A*) and sarcomere length (*B*) in the diaphragm in relation to airways obstruction. No = subjects with normal spirometry; Yes = patients with chronic obstructive pulmonary disease. $p < .05$ for both. Reproduced with permission from Orozco-Levi M et al.[25]

Table 23-1 Diaphragm Contractile Apparatus Characteristics in Controls and Patients with Chronic Obstructive Pulmonary Disease (COPD)

		Control	*COPD*
Diaphragm sarcomere length (μm)		2.27 ± 0.15	2.08 ± 0.16
Diaphragm myosin heavy chain (%)	I	45 ± 2	64 ± 3
	IIa	39 ± 2	29 ± 3
	IIx/b	17 ± 1	8 ± 1
Diaphragm myosin light chain (%)	1sa	3.7 ± 0.5	5.5 ± 0.6
	1sb	14.7 ± 1.6	19.3 ± 1.1
	1f	19.4 ± 1.1	15 ± 0.7
	2s	26.3 ± 2.3	34.2 ± 1.3
	2f	25.4 ± 2.0	19 ± 0.6
	3f	10.2 ± 0.9	7.3 ± 1.8
Diaphragm capillary density (number)	Type I fiber	4–6	Increases proportionally to airway obstruction severity
	Type IIa–IIb fiber	3–5	
Metabolic activity	Oxidative capacity		Citrate synthase activity unchanged
	Glycolytic capacity		Phosphofructokinase activity decreases

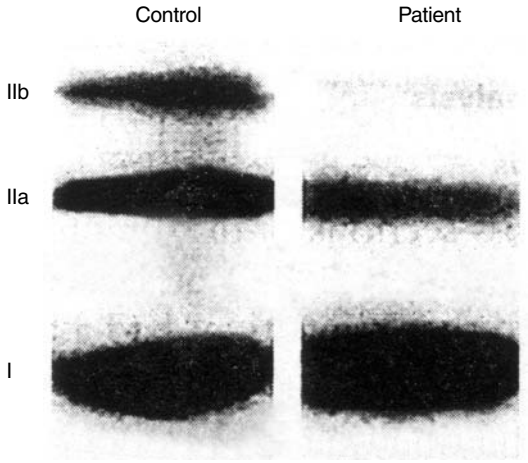

FIGURE 23-4 Western blots of MHC-I, MHC-IIa, and MHC-IIb of the costal part of the diaphragm from a representative control subject and a patient with chronic obstructive pulmonary disease. Adapted from Levine S et al.[35]

who died suddenly, the mean relative proportion of type I fibers was found to be about 50%, the remaining proportion being evenly divided into type IIa and type IIb fibers.[27,28] The average fiber size (cross-sectional area) in the costal diaphragm is 2,200 μm^2 in control subjects,[27,28] type I being slightly larger than both type IIa and type IIb.[29] In patients with normal ventilatory function (FRC, TLC, residual volume [RV], forced expiratory volume in 1 second [FEV_1]) from whom biopsy specimens were taken during thoracotomy, the proportion of type I is about 54%, and those of type IIa and type IIb are each 21%.[30–33] The costal and crural parts of the diaphragm seem to have similar regional distributions of fiber types, although the costal part has a 15% larger fiber diameter than the crural part.[31]

With regard to MHC and MLC presence in the diaphragm, the available information pertains to data obtained in controls such as brain-dead organ donors,[34,35] patients with mild impairment of pulmonary function,[35,36] or patients with cancer.[37] These data reveal that the proportions of diaphragm fibers containing MHC-I and MHC-IIa are similar, whereas the proportion of fibers containing MHC-IIb is low[34,35,37] (Figure 23-4) (see Table 23-1). In fact, it appears that the fibers previously identified as containing MHC-IIb correspond to fibers expressing MHC-IIx.[36,37] Surprisingly, in humans who had suffered sudden accidental death, the proportion of slow-twitch fibers was demonstrated to be almost twice that of either the fast-twitch-a or the fast-twitch-b fibers, the relative proportions of these fast-twitch fibers being similar.[27] Finally, recent data have revealed the presence of developmental MHCs (embryonic and neonatal) in the adult human diaphragm, occurring predominantly in diaphragmatic fibers expressing MHC-IIa[36] (Figure 23-5). The human diaphragm fibers contain six different isoforms of MLC, with the same proportions of MLC-2s and MLC-2f,

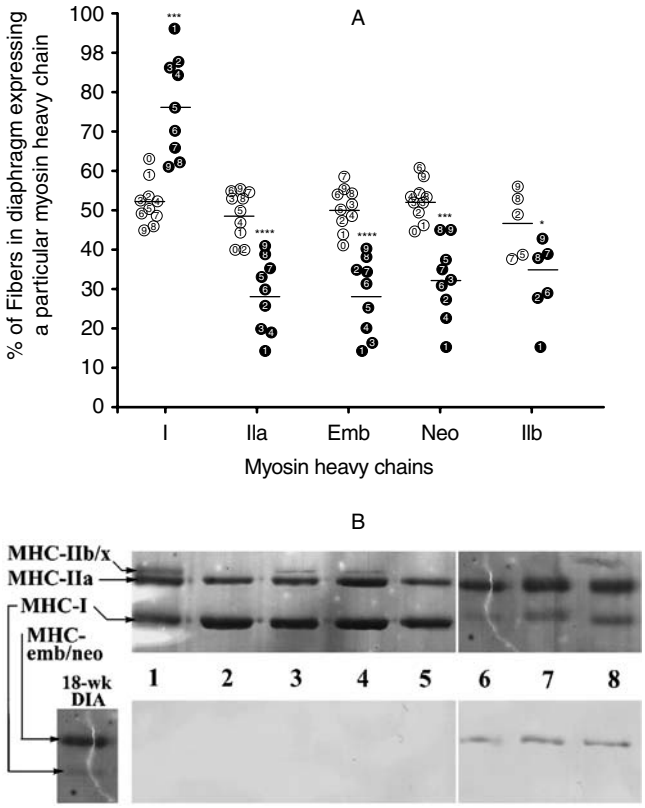

FIGURE 23-5 *A*, Proportions of diaphragm (DIA) fibers in control subjects (*open circles*) and patients with chronic obstructive pulmonary disease (*solid circles*) containing slow (I), type IIa, embryonic (Emb), neonatal (Neo), and type IIb MHCs, as determined by immunocytochemistry. *B*, Representative SDS-PAGE (*top panel*) and immunoblotting against embryonic MHC (*bottom panel*) of diaphragms from control subject (lanes 1, 3, and 4), patient with chronic obstructive pumonary disease (lanes 2 and 5), 18-week-old fetus (lane 6), and 28-week-old fetus (lanes 7 and 8). $*p < .05$, $***p < .001$, and $****p < .0001$. Reproduced with permission from Nguyen T et al.[36]

these proportions being close to that of MLC-1f[34,35,38] (see Table 23-1).

Interestingly, the diaphragm fibers of the rat mainly contain the isoform MHC-IIx and similar proportions of the isoforms MHC-I and MHC-IIa.[39,40] In addition, the rat diaphragm is essentially composed of MLC-1f and MLC-2f.[40] Thus, the fiber composition of the rat diaphragm differs from the fiber composition of the human diaphragm in the sense that the proportion of MHC-I is smaller but the proportion of MHC-IIx is higher. This should be taken into account when extrapolating data from the rat diaphragm to the human diaphragm.

Capillary Density Data from postmortem subjects who were healthy prior to sudden accidental death show that the mean number of capillaries per muscle fiber is about 1.9 ± 0.1 (range 1.5 to 2.4).[27] Type I fibers are surrounded by four to six capillaries and type IIa and type IIb fibers by only three to five capillaries[29] (Figure 23-6) (see Table 23-1). The diffusion distances between capillaries and muscle fibers are less for type I than for type II fibers.[27,29]

SERCA Pumps Because the diaphragm contracts rhythmically during life, the need for the diaphragm to return to a stable resting position at the end of each relaxation is fundamental. Although the clinical implications of impaired diaphragmatic relaxation are obvious, the molecular mechanisms involved has been poorly studied. The expression of SERCA isoforms in the diaphragm has been studied only in animals, including the rat.[41–45] However, discrepancies in the relative levels of the two SERCA isoforms exist between the different studies, probably because of methodologic problems. Thus, *SERCA1* mRNA in the rat diaphragm was reported to represent 90%[41,42] or 75% (N. Viirès, personal communication) of all SERCA mRNA, whereas Sayen and colleagues[43] reported a *SERCA1* fraction of 50%, as we did.[45] We also showed that only the adult form, *SERCA1a*, was expressed in the adult diaphragm.[45] Like us,[45] Wu and colleagues[41,42] demonstrated the presence of *SERCA2a* mRNA in the rat diaphragm. We also noticed the presence of phospholamban mRNA,[45] in contrast to Viirès and colleagues,[46] who could not detect phospholamban with dot blot, a less sensitive technique than the polymerase chain reaction used in our experiment. Interestingly, we demonstrated for the first time the presence of sarcolipin mRNA in the rat diaphragm[45]; until then, sarcolipin had been reported to be expressed mainly in fast-twitch muscles.[47] Thus, like other skeletal muscles, the SERCA pumps of the diaphragm are probably regulated by phospholamban and sarcolipin. Both may play a major role in regulating the kinetics of diaphragm contraction.

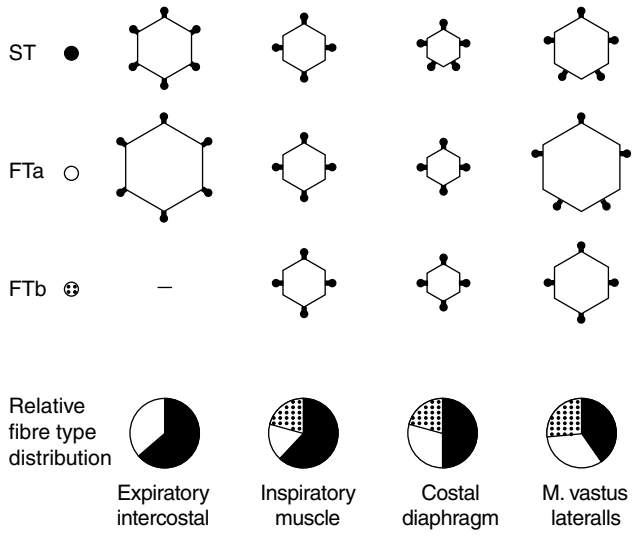

FIGURE 23-6 Schematic illustration of relative cross-sectional areas and proportions of different fibers and number of capillaries in expiratory and inspiratory intercostal muscles, costal diaphragm, and vastus lateralis muscle of normal subjects.[27] ST = slow-twitch fiber; FTa = fast-twitch-a fiber; FTb = fast-twitch-b fiber. Reproduced with permission from Mizuno M.[29]

Metabolism In patients with normal ventilatory function, HAD activity was shown to be slightly higher in the costal part of the diaphragm than in both the external intercostal muscles and the expiratory internal intercostal muscles.[48] CS and glycolytic activities were, however, similar among these muscles.[48,49]

In rats, bioenergetic enzyme activities have been examined in all respiratory muscles.[40] This study showed that the metabolic properties of the costal and crural parts of the diaphragm differ from those of other respiratory muscles, such that they exhibit the highest mitochondrial activities (CS), with the costal part having a 20% higher oxidative capacity than the crural part.[40] Conversely, LDH activity was very low in the diaphragm compared with the other respiratory muscles.[40] As a consequence, the lower LDH/CS ratio in the diaphragm is indicative of high oxidative capacity and relatively low glycolytic capacity. Myofibrillar ATPase activity was significantly lower in the costal and crural parts of the diaphragm than in all other respiratory muscles, but it was related to enzyme activity.[40] Finally, this study revealed that the enzymic activities within the other respiratory muscles were very similar.

Muscle Gene Expression To date, no data on growth factors are available for the human diaphragm. However, in normal rats, IGF-I[50–53] IGF-II[50,51] and myostatin (GDF-8)[54] mRNA are expressed in the diaphragm. In the same species, the presence of the transcription factors and the type Id inhibitor of DNA-binding-proteins[55–58] has also been reported.

The importance of IGF-I in myogenesis and in the maintenance of the growth/integrity of muscle fibers has been underlined in IGF-I-knockout models. Indeed, the body weight of IGF-I-knockout mice was only 60% of that of the wild type, and most of them died at or soon after birth, possibly because of ventilatory failure.[59,60] Recently, Fournier and Lewis showed that the cross-sectional area of all fiber types in the diaphragm of IGF-I–deficient mice was reduced, as were diaphragm thickness, the number of fibers spanning its entire thickness, and the number of capillaries per fiber.[61] It was concluded that muscle hypoplasia reflected the importance of IGF-I for cell proliferation, differentiation,

and apoptosis during development, although the reduced cell size highlights also the importance of IGF-I for the rate and/or maintenance of diaphragm fiber growth in the postnatal state. Succinate dehydrogenase activity was increased in all three types; the enhanced oxidative capacity probably reflects diaphragm compensatory mechanisms in IGF-I-knockout mice.[61] We demonstrated the expression of IGF-I and also IGF-II in the diaphragm in different rat models,[50–53] and preliminary data also confirm the presence of IGF-I mRNA in the human diaphragm (unpublished data).

GDF-8, or myostatin, is an attractive growth factor as it is exclusively expressed in skeletal muscle and seems to be a specific negative genetic regulator of skeletal muscle mass. Indeed, mice with null mutations of the myostatin gene have increased muscle mass,[15] and in HIV-infected men with weight loss, the intramuscular concentrations of myostatin immunoreactive protein are increased compared with healthy men, this concentration being, moreover, inversely correlated with fat-free mass index.[62] Interestingly, we showed that undernutrition was associated with up-regulation of myostatin in the rat diaphragm,[54] suggesting a potential role for myostatin in the diaphragm atrophy observed after undernutrition.

The role in the human diaphragm of the myogenic regulatory factors and the type Id inhibitor of DNA-binding proteins remains to be determined, but our recent data obtained in rats suggest a determinant role for these factors in diaphragm growth regulation.[57,58] Indeed, we recently reported alterations in MyoD and myogenin expression in the diaphragms of mechanically ventilated rats in which diaphragm function was altered and diaphragm fiber dimensions were reduced.[63] In fact, the potential roles of MyoD and myogenin as regulators of fiber phenotype had already been demonstrated, although caution must be exercised in extrapolation because the role of MyoD and myogenin in regulating phenotype expression is model dependent.[64]

COPD

Contractile Apparatus

Diaphragm Dimensions Studies of the human diaphragm dimensions in COPD patients have yielded variable results. Diaphragm mass and thickness have been reported to be greater in COPD patients with normal body weight than in chronically ill underweight patients without COPD.[65,66] By contrast, diaphragm volume and thickness were reduced in underweight patients with chronic bronchitis compared with normal-weight patients without COPD.[67] A reduction in diaphragm weight was observed in patients with emphysema, and, interestingly, this reduction was greater than could be accounted for by the loss of body weight.[21] However, according to Arora and Rochester,[68] the gross dimensions of the diaphragm were similar to those in patients without chronic lung disease, although the possibility that patients with more severe emphysema could have shortened diaphragms was not excluded.

Sarcomere Length Sarcomere length has been reported to be reduced in the diaphragms of COPD patients compared to subjects with normal spirometry[25,69] (see Figure 23-3 and Table 23-1). In addition, the length of the sarcomere was shown to be correlated with the degree of hyperinflation, such that an inverse correlation was found with %TLC and %RV.[69] The greater the lung volume, the shorter the length of the sarcomere.[25] This structural change was associated with the preservation of the capacity to generate force,[25] probably by displacing the diaphragmatic length–tension curve (see Figure 23-1). In fact, Similowski and colleagues had already demonstrated that the diaphragms of COPD patients generated a force similar to or even higher than that generated by the diaphragms of normal subjects at equivalent lung volumes.[70] Finally, although disrupted sarcomeres (damaged sarcomeres) are commonly present in the normal diaphragm, the presence of disruption is more prevalent in the diaphragms of COPD patients, suggesting that contractile molecules are impaired in the diaphragms of COPD patients.[26]

Myosin and Fiber Types From thoracotomy biopsy specimens, it was shown that the proportions of slow-twitch fibers (54%), fast-twitch-a fibers (21%), and fast-twitch-b fibers (21%) in the diaphragms of COPD patients were similar to those in patients with normal ventilatory function.[30–33] This is, however, in contrast to recent data showing that COPD diaphragms had a larger proportion of type I fibers ($71 \pm 5\%$ vs $42 \pm 2\%$), a lower proportion of type IIax fibers ($21 \pm 3\%$ vs $27 \pm 3\%$), and the same proportion of type IIa fibers as controls.[71] No differences in the regional distribution of diaphragm fiber types were found between the costal and crural parts, as in patients with normal lung function, although larger fiber diameters were observed in the costal than in the crural part.[31]

By contrast, recent data obtained from COPD patients showed that the proportion of the diaphragm fibers containing MHC-I increased whereas the proportion of the diaphragm fibers containing the MHC-IIa and MHC-IIb isoforms decreased[35–37,72] (see Figure 23-4 and Table 23-1). This shift toward a fiber type with increased resistance to muscle fatigue is a classic adaptive phenomenon in muscles that face a chronically increased load, as is the case for the diaphragm in COPD patients. In addition, the proportion of the MHC-I isoform in the diaphragms of COPD patients has been shown to be positively correlated with TLC and FRC and negatively correlated with FEV_1.[37] Recently, Nguyen and colleagues demonstrated the presence of developmental MHC isoforms that were not indicative of the presence of new fiber formation in the diaphragms of severe COPD patients.[36] The function of these developmental MHC isoforms remains to be elucidated.

As for the MHCs, the proportion of the slow MLCs increases at the expense of the fast MLCs.[35] Along the same lines, the molar ratio of the slow isoforms MLC-1sa and MLC-2s has been shown to be increased in the diaphragms of COPD patients, whereas that of the fast isoforms MLC-1f and MLC-2f decreased[38] (see Table 23-1). The same holds true for the other contractile proteins, such as troponin and troponin–tropomyosin. Thus, the phenotypic adaptation of

the MLCs follows that of the MHCs, but the functional significance of this adaptation is not yet known for the MLCs. With use of the ATPase technique, fiber diameters appear to be smaller in the diaphragms of COPD patients than in subjects with normal lung function.[30,31] This decreased diameter is, moreover, correlated with vital capacity and FEV_1,[30,31] and this relationship was present in the costal part[30,31] but not in the crural part.[31] Decreases in type I cross-sectional area (−41%) were also recently reported in the diaphragms of COPD patients compared with controls with mild pulmonary impairment.[71]

Capillary Density In COPD patients, the capillary content of the diaphragm increases proportionally with the severity of airway obstruction (see Table 23-1), such that a correlation exists between the number of capillaries and $\%FEV_1$.[72,73] This change probably represents structural remodeling in response to chronically increased muscle load.

SERCA Pumps Unfortunately, no attempts have been made to examine the changes in SERCA pumps in the diaphragms of COPD patients, although this is of conceptual interest. Indeed, fatigue may be present in these patients, in whom the rate of diaphragm relaxation decreases when the diaphragm becomes fatigued.[74,75] Moreover, abnormal Ca^{2+} handling and intracellular Ca^{2+} overload may lead to cell death, and impaired SERCA pump expression has been observed in animal models of hypo- and hyperthyroidism,[43] as well as in cardiomyopathy.[44] In humans, loss of *SERCA1a* Ca^{2+} pump function is one cause of exercise-induced impairment of skeletal muscle relaxation, the major diagnostic feature of Brody's disease.[76] In fact, SERCA pump expression in the diaphragm has been examined only in animal models not closely related to COPD. However, it is worth mentioning that in cardiomyopathic hamsters, *SERCA1* expression was decreased in the diaphragm, whereas *SERCA2* expression remained unchanged.[77] In rats chronically treated with corticosteroids, Aubier and Viirès noticed a nonsignificant increase in *SERCA2* expression and no changes in phospholamban, the regulatory protein of *SERCA2*, in the diaphragm[5] (unpublished data). By contrast, we recently demonstrated that in rats acutely treated with corticosteroids, resulting in selective type II atrophy in the diaphragm, *SERCA1* mRNA but mainly *SERCA2* mRNA were down-regulated.[45] This was associated with down-regulation of phospholamban and up-regulation of sarcolipin.[45] This should be taken into account in COPD patients treated with corticosteroids.

Metabolism In COPD patients, both HK and LDH activities in the costal part of the diaphragm are lower than those in the intercostal muscles, whereas CS and HAD activities are similar.[48] However, the metabolic capacity of the diaphragm is enhanced in COPD patients, in whom the mitochondrial concentration has been shown to be increased (see Figure 23-3), this increase being inversely related to the level of airflow obstruction and positively correlated with the level of hyperinflation.[25] Moreover, preliminary data revealed that the activity of PFK (an enzyme of the glycolytic pathway) was reduced in the diaphragms of severe COPD patients, whereas that of CS (an enzyme of the oxidative pathway) was unchanged[78] (see Table 23-1). The activity of PFK (glycolytic capacity) was inversely correlated with static lung volume (RV/TLC) and the percentage of type II fibers in the diaphragm.[78] Finally, the PFK/CS ratio was inversely correlated with static lung volume and positively correlated with FEV_1.[78] The conclusion from these studies is that oxidative capacity is preserved and glycolytic activity is reduced in the diaphragms of severe COPD patients. Finally, in COPD patients, mitochondrial oxidative capacity relative to ATP demand is increased in each diaphragm fiber type, such that the ratio of succinate dehydrogenase/myofibrillar (m) ATPase increased as a consequence of increased succinate dehydrogenase levels and decreased mATPase.[71] The metabolic adaptations elicited in the diaphragm by severe COPD are similar to those observed during endurance exercise training in limb muscles. This suggests that the increased diaphragm work rate in COPD patients probably results from continuous long-term endurance training due to COPD.

Muscle Gene Expression No data on growth factors, myogenic regulatory factor, and type Id inhibitor of DNA-binding protein expression are available from COPD patients. However, growth hormone has been administered to COPD patients in an attempt to reverse the weight loss present in these patients[79,80] as this hormone is known to induce protein anabolism and muscle growth, either directly or indirectly through IGF-I.[81,82] The results of these studies show an increase in body weight associated with either an increase in maximal inspiratory pressure[79] or no change in peripheral and respiratory muscle strength.[80] The expression of IGF-I in the diaphragm was not examined in any of these studies.

MOLECULAR AND CELLULAR BIOLOGY OF THE RIB CAGE MUSCLES

The diaphragm interacts with other respiratory muscles, such as rib cage muscles. The latter include inspiratory muscles (external intercostal muscles and accessory muscles such as the scalene muscles, the sternocleidomastoid muscles, and the trapezoid muscles) and expiratory muscles (internal intercostal muscles). It is, however, important to mention that the original classification of the external intercostal muscles as inspiratory and the internal intercostal muscles as expiratory may be questioned as it has been shown that the external intercostal muscles may have an expiratory function as well, depending on the interspace they belong to and whether they are laterally or medially located. The same holds true for the internal intercostal muscles, which may also have an inspiratory function (see Chapter 22, "Actions of the Respiratory Muscles"). Therefore, the fiber morphology and capillary supply of the intercostal muscles are linked to functional differences rather than to an anatomic classification as external or internal.

External Intercostal Muscles

These muscles play an important role when respiratory resistance is increased, as in COPD patients, or when ventilatory demands are increased, as during exercise.

In subjects with normal pulmonary function or in apparently healthy subjects who died suddenly, the fiber proportions of the external intercostal muscle were reported to range between 55 and 62% for type I, 17 and 33% for type IIa, and 12 and 22% for type IIb[27,49,83] (see Figure 23-6). These proportions are very similar to those of the internal intercostal muscles.[27,49] The three fiber types are identical in size[49] (see Figure 23-6). The mean cross-sectional area is similar to that of the inspiratory internal intercostal muscles and smaller than that of the expiratory internal intercostal muscles.[29] The number of capillaries per fiber was shown to be 1.6 ± 0.1,[27] lower than in the expiratory internal intercostal muscles (see Figure 23-6) but similar to that in the parasternal muscles (inspiratory internal intercostal muscles).[49] On the other hand, the expiratory external intercostal muscles have the longest diffusion distances of all the respiratory muscles.[27] Oxidative and glycolytic enzyme activities were identical to those of the intercostal muscles,[40,49] whereas HAD activity was lower than that in the diaphragm.[48]

In severe COPD, the proportions of the type II fibers and fast MHCs increase.[83,84] The percentage of type II fibers correlates inversely with the degree of airflow obstruction.[83] It should be mentioned that this adaptation of the external intercostal muscles in COPD patients is totally different to that observed in the diaphragms of these patients. On the other hand, the diameter of the external intercostal fibers is similar in COPD and in normal subjects,[72] and there are no significant differences in fiber size between the dominant and nondominant sides.[85] Type II atrophy has, however, been reported,[32,86] as well as reductions in muscle metabolites,[32] ATP, and phosphocreatine.[86] The reduction in phosphocreatine correlates with the degree of airflow obstruction.[86] Similarly, there is a correlation between maximal inspiratory pressure (P_{Imax}) and the dimensions of the external intercostal muscle.[87] Inverse correlations have also been demonstrated between the minimum diameter of the type I fibers and inspiratory muscle pressure–time index (PTI), as well as between the minimum diameter of type II fibers and strength parameters.[88] The number of capillaries per fiber increases (3.0 ± 0.6 vs 2.3 ± 0.5), and this increase is inversely related to FEV_1.[89] As in the internal intercostal muscles, oxidative enzyme activities and HK activity are increased in the external intercostal muscles of COPD patients.[90] Recent data, however, have shown no changes in the activity of CS (an enzyme of the oxidative pathway), whereas the capacity of the glycolytic pathway increases, as both PFK and LDH activities are enhanced in the external intercostal muscles of COPD patients compared with control subjects.[64] In addition, RV is directly related to glycolytic activity ($r = .716$ with PFK and $r = .697$ with LDH).[64]

Scalene Muscles

In humans, it is well accepted that the scalene muscles are primary inspiratory muscles. In contrast, in the hamster, these muscles function as accessory muscles. The data on muscle fiber composition are poor, and data on muscle cell characteristics are not available, although it has been shown that increased electromyographic activity and motor unit firing frequencies of the scalene muscles occur in COPD patients,[91,92] suggesting adaptation of these muscles at the cellular level.

Autopsy data show that the scalene muscles are composed of 59% type I fibers, 22% type IIa fibers, and 17% type IIb fibers.[28] The fiber cross-sectional area ($1{,}900\ \mu m^2$) is smaller than that reported for the other respiratory muscles, due to the smaller cross-sectional area of the type II fibers.[28]

In control patients (mainly male), the anterior scalene muscle has been shown to have an equal distribution of type I and II fibers, with neither fiber type predominating. Type II fibers are slightly larger than type I fibers.[93] By contrast, others have reported a 70% type I fiber predominance, with a greater size of type I fibers in the anterior scalene muscles of female control patients.[94] Whether these discrepant results are related to gender or to the types of control is difficult to determine. In normal rats, the scalenus medius muscle has the highest LDH activity of all the respiratory muscles.[40] Interestingly, in emphysematous hamsters, inspiratory electromyographic activity is recorded during spontaneous breathing, whereas this muscle is silent in normal hamsters.[95] This is associated with a greater proportion of MHC-IIa at the expense of the MHC-IIx, whose cross-sectional area is also smaller.[95] Thus, with emphysema, the scalene muscles in hamsters not only become primary-like inspiratory muscles but also adapt to enhanced phasic recruitment.

Sternocleidomastoid Muscles

Very few data are available concerning these muscles. Autopsy data show that the sternocleidomastoid muscles have a smaller proportion of type I fibers (35%) compared with other respiratory muscles.[96] However, according to data obtained from a few female control patients, these muscles should be composed of about 50% type I fibers.[93] The sternocleidomastoid muscle fibers have been reported to be smaller in COPD patients than in normal subjects.[97] By contrast, others have shown that the sternocleidomastoid muscles are essentially normal in terms of cross-sectional area in patients with severe COPD compared with control subjects.[98] The reasons for this discrepancy are not known. To the best of our knowledge, there have been no studies in animals in which the sternocleidomastoid muscles have been examined.

Internal Intercostal Muscles

Little information is available concerning the cellular composition of the internal intercostal muscles. It seems that in healthy subjects who have suffered accidental death, these muscles are composed of 64% slow-twitch fibers, 35% fast-twitch-a fibers, and 1% fast-twitch-b fibers (see Figure 23-6), this proportion being similar to that in the external intercostal muscles.[27,49] Interestingly, the inspiratory internal intercostal muscles contain fewer fast-twitch-a fibers (22%) than the expiratory internal intercostal muscles.[27,28] The fast-twitch-a fibers are the largest[49] (see Figure 23-6). The mean cross-sectional area of the expiratory internal

intercostal muscles is larger (4,300 μm^2) than that of the inspiratory internal intercostal muscles and external intercostal muscles (2,900 μm^2),[29] due to the greater areas of both slow-twitch and fast-twitch-a fibers.[27] On the other hand, the glycolytic and oxidative enzyme activities in the internal intercostal muscles are similar to those in the external intercostal muscles,[40,49,90] but HAD activity is lower in the expiratory internal intercostal muscles than in the diaphragm.[48] The number of capillaries per fiber has been reported to be 2.3 ± 0.1 in the expiratory internal intercostal muscles[27] (see Figure 23-6), which is higher than the number in the inspiratory internal and external intercostal muscles.[49]

Interestingly, as for "normal" subjects, the fiber proportions in these muscles in COPD patients have been reported to be similar to those in the external intercostal muscles.[86] In these patients, type II atrophy has been described,[32,86] and this atrophy has been shown to be correlated with all indices of airway obstruction.[32,86] There was, moreover, a depletion of muscle metabolites,[32] as well as ATP and phosphocreatine.[86] Oxidative enzyme activities and HK activity are increased in the internal intercostal muscles of the COPD patients.[90]

SUMMARY AND CONCLUSIONS

Whereas the human diaphragm is composed of about 50% type I fibers, the proportion of these fibers is higher (60%) in the intercostal and scalene muscles, and the proportion has still to be confirmed for the sternocleidomastoid muscles (35% to 50%). Except for the internal intercostal muscles, where type IIb fibers are absent, all the respiratory muscles contain an equal proportion of type II fibers. Capillary supply is highest in the internal intercostal muscles, followed by the diaphragm and the external intercostal muscles, and is not yet determined for the scalene muscles. The diaphragm has the highest oxidative capacity of all the respiratory muscles, whereas glycolytic capacities are similar in all these muscles.

In the diaphragms of COPD patients, the proportion of fibers containing MHC-I increases, whereas the proportion of fibers containing MHC-IIa and MHC-IIb decreases. The same holds true for the MLCs. Moreover, whereas sarcomere length shortens with increasing lung volume, the amount of disrupted sarcomeres is increased in the diaphragms of COPD patients. However, disrupted sarcomeres are also common in control diaphragms. The capillary content of the diaphragm increases in proportion to the severity of airflow obstruction, whereas increased mitochondrial concentration is related to the level of hyperinflation. In contrast to the diaphragm, the proportions of the type II fibers and the fast MHCs in the external intercostal muscles increase in COPD, whereas fiber proportion remains unchanged in the internal intercostal muscles.

The potential role of the growth factors, the myogenic regulatory factors, and the type Id inhibitor of DNA-binding proteins in determining muscle mass and contractile properties remains to be determined in the human diaphragm, but preliminary data from animals are promising.

ACKNOWLEDGMENTS

The studies presented in this chapter were supported by the "Fonds voor Wetenschappelijk Onderzoek-Vlaanderen" grants G.0237.01 and G.0237.03, KULeuven Research Foundation OT 98/44, and Astra-Zeneca Pharmaceuticals.

REFERENCES

1. Schiaffino S, Reggiani C. Molecular diversity of myofibrillar proteins: gene regulation and functional significance. Physiol Rev 1996;76:371–423.
2. Farkas GA. Functional characteristics of the respiratory muscles. Semin Respir Med 1991;12:247–57.
3. Pette D, Staron RS. Cellular and molecular diversities of mammalian skeletal muscle fibers. Rev Physiol Biochem Pharmacol 1990;116:1–76.
4. Sieck GC, Han Y-S, Prakash YS, Jones KA. Cross-bridge cycling kinetics, actomyosin ATPase activity and myosin heavy chain isoforms in skeletal and smooth respiratory muscles. Comp Biochem Physiol 1998;119:435–50.
5. Aubier M, Viires N. Calcium ATPase and respiratory muscle function. Eur Respir J 1998;11:758–66.
6. Wuytack F, Raeymaekers L, Eggermont JA, et al. Isoform diversity and regulation of organellar-type Ca^{2+}-transport ATPases. In: Andersen JP, editor. Advances in molecular and cell biology. Greenwich, CT: JAI Press; 1998. p. 205–48.
7. Odermatt A, Becker S, Khanna VK, et al. Sarcolipin regulates the activity of SERCA1, the fast-twitch skeletal muscle sarcoplasmic reticulum Ca^{2+}-ATPase. J Biol Chem 1998;273:12360–9.
8. Wuytack F, Papp B, Verboomen H, et al. A sarco/endoplasmic reticulum Ca^{2+}-ATPase 3-type Ca^{2+} pump is expressed in platelets, in lymphoid cells, and in mast cells. J Biol Chem 1994;269:1410–6.
9. Edwards RHT, Faulkner JA. Structure and function of the respiratory muscles. In: Roussos C, editor. The thorax. Part B. Applied physiology. New York: Marcel Dekker; 1995. p. 185–217.
10. Dodson MV, Allen RE, Hossner KL. Ovine somatomedin, multiplication-stimulating activity, and insulin promote skeletal muscle satellite cell proliferation in vitro. Endocrinology 1985;117:2357–63.
11. DeVol DL, Rotwein P, Sadow JL, et al. Activation of insulin-like growth factor gene expression during work-induced skeletal muscle growth. Am J Physiol 1990;259:E89–95.
12. Vandenburgh HH, Karlisch P, Shansky J, Feldstein R. Insulin and IGF-I induce pronounced hypertrophy of skeletal myofibers in tissue culture. Am J Physiol 1991;260:C475–84.
13. Adams GR, Haddad F. The relationships among IGF-I, DNA content, and protein accumulation during skeletal muscle hypertrophy. J Appl Physiol 1996;81:2509–16.
14. Turner JD, Rotwein P, Novakofski J, Bechtel PJ. Induction of mRNA for IGF-I and -II during growth hormone-stimulated muscle hypertrophy. Am J Physiol 1988;255:E513–7.
15. McPherron AC, Lawler AM, Lee S-J. Regulation of skeletal muscle mass in mice by a new TGF-beta superfamily member. Nature 1997;387:83–90.
16. Grobet L, Royo Martin LJ, Poncelet D, et al. A deletion in the bovine myostatin gene causes the double-muscled phenotype in cattle. Nat Genet 1997;17:71–4.
17. Dias P, Dilling M, Houghton P. The molecular basis of skeletal muscle differentiation. Semin Diagn Pathol 1994;11:3–14.
18. Orozco-Levi M, Molina LI, Felez M, et al. Ultrasonographic assessment of the human diaphragm contraction. Eur Respir J 1995;8:190s.

19. Hoppeler H. Exercise induced ultrastructural changes in skeletal muscle. Int J Sports Med 1986;7:187–204.
20. Williams RS, Caron MG, Daniel K. Skeletal muscle β-adrenergic receptors: variations due to fiber type and training. Am J Physiol 1984;246:160–7.
21. Thurlbeck WM. Diaphragm and body weight in emphysema. Thorax 1978;33:483–7.
22. Arora NS, Rochester DF. Effect of body weight and muscularity on human diaphragm muscle mass, thickness and area. J Appl Physiol 1982;52:64–70.
23. Rochester DF. Respiratory muscles: structure, size and adaptative capacity. In: Jones NL, Killian KJ, editors. Breathlessness. The Campbell Symposium. Hamilton, ON: Boehringer Ingelheim; 1992. p. 2–12.
24. Caskey CI, Zerhouni EA, Fishman EK, Rahmouni AD. Aging of the diaphragm: a CT study. Radiology 1989;171:385–9.
25. Orozco-Levi M, Gea J, Lloretay JL, et al. Subcellular adaptation of the human diaphragm in chronic obstructive pulmonary disease. Eur Respir J 1999;13:371–8.
26. Orozco-Levi M, Gea J, Aguar C, et al. Sarcomere disruption in the diaphragm of COPD patients; a sign of muscle injury? Am J Respir Crit Care Med 2001;155:A510.
27. Mizuno M, Secher NH. Histochemical characteristics of human expiratory and inspiratory intercostal muscles. J Appl Physiol 1989;67:592–8.
28. McKenzie DK, Gandevia SC, Shorey CD. A histochemical study of human inspiratory muscles. Proc Int Un Physiol 1983;XV:351.
29. Mizuno M. Human respiratory muscles: fibre morphology and capillary supply. Eur Respir J 1991;4:587–601.
30. Sanchez J, Derenne JP, Debesse B, et al. Typology of the respiratory muscles in normal men and in patients with moderate chronic respiratory diseases. Bull Eur Physiopathol Respir 1982;18:901–14.
31. Sanchez J, Medrano G, Debesse B, et al. Muscle fibre types in costal and crural diaphragm in normal men and in patients with moderate chronic respiratory disease. Bull Eur Physiopathol Respir 1985;21:351–6.
32. Hughes RL, Katz H, Sahgal V, et al. Fiber size and energy metabolites in five separate muscles from patients with chronic obstructive lung disease. Respiration 1983;44: 321–8.
33. Lieberman DA, Faulkner JA, Maxwell LC. Performance and histochemical composition of guinea pig and human diaphragm. J Appl Physiol 1973;34:233–7.
34. Tikunov BA, Mancini D, Levine S. Changes in myofibrillar protein composition of human diaphragm elicited by congestive heart failure. J Mol Cell Cardiol 1996;28:2537–41.
35. Levine S, Kaiser L, Leferovich J, Tikunov B. Cellular adaptations in the diaphragm in chronic obstructive pulmonary disease. N Engl J Med 1997;337:1799–806.
36. Nguyen T, Shrager J, Kaiser L, et al. Developmental myosin heavy chains in the adult human diaphragm: coexpression patterns and effect of COPD. J Appl Physiol 2000;88: 1446–56.
37. Mercadier JJ, Schwartz K, Schiaffino S, et al. Myosin heavy chain gene expression changes in the diaphragm of patients with chronic lung hyperinflation. Am J Physiol 1998; 274:L527–34.
38. Tikunov BA, Kaiser L, Nguyen T, Levine S. Myosin light chain and regulatory protein composition of lateral costal diaphragm in normal subjects and in patients with chronic obstructive pulmonary disease. Am J Respir Crit Care Med 1997;155:A510.
39. LaFramboise WA, Watchko JF, Brozanski BS, et al. Myosin heavy chain expression in respiratory muscles of the rat. Am J Respir Cell Mol Biol 1992;6:335–9.
40. Powers SK, Demirel HA, Coombes JS, et al. Myosin phenotype and bioenergetic characteristics of rat respiratory muscles. Med Sci Sports Exerc 1997;12:1573–9.
41. Wu K-D, Lytton J. Molecular cloning and quantification of sarcoplasmic reticulum Ca^{2+}-ATPase isoforms in rat muscles. Am J Physiol 1993;264:C333–41.
42. Wu K-D, Lee W-S, Wey J, et al. Localization and quantification of endoplasmic reticulum Ca^{2+}-ATPase isoform transcripts. Am J Physiol 1995;269:C775–84.
43. Sayen MR, Rohrer DK, Dillmann WH. Thyroid hormone response of slow and fast sarcoplasmic reticulum Ca^{2+} ATPase mRNA in striated muscle. Mol Cell Endocrinol 1992; 87:87–93.
44. Anger M, Lambert F, Chemla D, et al. Sarcoplasmic reticulum Ca^{2+} pumps in heart and diaphragm of cardiomyopathic hamster: effects of perindopril. Am J Physiol 1995;268: H1947–53.
45. Gayan-Ramirez G, Vanzeir L, Wuytack F, Decramer M. Corticosteroids decrease mRNA levels of SERCA pumps, whereas they increase sarcolipin mRNA in the rat diaphragm. J Physiol (Lond) 2000;524:387–97.
46. Viirès N, Govela M, Zedda C, et al. Corticosteroids modify the sarcoplasmic reticulum Ca^{2+}-ATPase (SERCA) expression in the rat diaphragm. Am J Respir Crit Care Med 1997;155:A921.
47. Odermatt A, Taschner PEM, Scherer SW, et al. Characterization of the gene encoding human sarcolipin (SLN), a proteolipid associated with SERCA1: absence of structural mutations in five patients with Brody disease. Genomics 1997;45:541–53.
48. Sanchez J, Bastien C, Medrano G, et al. Metabolic enzymatic activities in the diaphragm of normal men and patients with moderate chronic obstructive pulmonary disease. Bull Eur Physiopathol Respir 1984;20:535–40.
49. Mizuno M, Niels H, Saltin B. Fibre types, capillary supply and enzyme activities in human intercostal muscles. Clin Physiol 1985;5:121–35.
50. Gayan-Ramirez G, Van de Casteele M, Rollier H, et al. Biliary cirrhosis induces type IIx/b atrophy in rat diaphragm and skeletal muscle, and decreases IGF-I mRNA in the liver but not in muscle. J Hepatol 1998;29:241–9.
51. Gayan-Ramirez G, Vanderhoydonc F, Verhoeven G, Decramer M. Acute treatment with corticosteroids decreases IGF-I and IGF-II expression in the rat diaphragm and gastrocnemius. Am J Respir Crit Care Med 1999;159:283–9.
52. Gayan-Ramirez G, Rollier H, Vanderhoydonc F, et al. Nandrolone decanoate does not enhance training effects, but stimulates insulin-like growth factor-I expression in rat diaphragm. J Appl Physiol 2000;88:26–34.
53. Stassijns G, Gayan-Ramirez G, De Leyn P, et al. Systolic ventricular dysfunction causes selective diaphragm atrophy in rats. Am J Respir Crit Care Med 1998;158:1963–7.
54. Gayan-Ramirez G, Vanderhoydonc F, Verhoeven G, Decramer M. Corticosteroid treatment decreases expression of insulin-like growth factors but does not affect growth/differentiation factor-8 in rat diaphragm. Eur Respir J 1998;12:453s.
55. Kraus B, Pette D. Quantification of MyoD, myogenin, MRF4 and Id-1 by reverse-transcriptase polymerase chain reaction in rat muscles. Effects of hypothyroidism and chronic low-frequency stimulation. Eur J Biochem 1997;247:98–106.
56. Weis J. Jun, Fos, MyoD1, and myogenin proteins are increased in skeletal muscle fiber nuclei after denervation. Acta Neuropathol 1994;87:63–70.
57. Gayan-Ramirez G, Decramer M. Regulation of muscle regulatory factor and Id-protein mRNA levels in the rat diaphragm after corticosteroid treatment and undernutrition. Am J Respir Crit Care Med 2001;163:A148.
58. Racz G, Gayan-Ramirez G, de Paepe K, et al. Short-term mechanical ventilation is associated with alterations in

transcription factor and Id-protein mRNA in rat diaphragm. Eur Respir J 2001;68:420s.
59. Liu JP, Baker J, Perkins AS, et al. Mice carrying null mutations of the genes encoding insulin-like growth factor-I and type 1 IGF receptor. Cell 1993;75:59–72.
60. Powell-Braxton L, Hollingshead P, Warburton C, et al. IGF-1 is required for normal embryonic growth in mice. Genes Dev 1993;7:2609–17.
61. Fournier M, Lewis MI. Influences of IGF-I gene disruption on the cellular profile of the diaphragm. Am J Physiol Endocrinol Metab 2000;278:E707–15.
62. Gonzalez-Cadavid NF, Taylor WE, Yarasheski K, et al. Organization of the human myostatin gene and expression in healthy men and HIV-infected men with muscle wasting. Proc Natl Acad Sci U S A 1998;95:14938–43.
63. Racz G, Gayan-Ramirez G, Testelmans D, et al. Early changes in rat diaphragm biology with mechanical ventilation. Am J Respir Crit Care Med 2003;168:297–304.
64. Talmadge RJ. Myosin heavy chain isoform expression following reduced neuromuscular activity: potential regulatory mechanisms. Muscle Nerve 2000;23:661–79.
65. Ishikawa S, Hayes JA. Functional morphometry of the diaphragm in patients with chronic obstructive lung disease. Am Rev Respir Dis 1973;198:135–8.
66. Scott KWM, Hoy J. The cross-sectional area of diaphragmatic muscle fiber in emphysema, measured by an automated image analysis system. J Pathol 1976;120:121–8.
67. Steele RH, Heard BE. Size of the diaphragm in chronic bronchitis. Thorax 1973;28:55–60.
68. Arora NS, Rochester DF. COPD and human diaphragm muscle dimensions. Chest 1987;91:719–24.
69. Orozco-Levi M, Gea J, Aguar C, et al. Ultrastructural changes in the diaphragm of COPD patients: sarcomere adaptability. Am J Respir Crit Care Med 1995;151:A806.
70. Similowski T, Yan S, Gauthier AP, et al. Contractile properties of the human diaphragm during chronic hyperinflation. N Engl J Med 1991;325:917–23.
71. Levine S, Gregory C, Nguyen T, et al. Bioenergetic adaptation of individual human diaphragmatic fibers to severe COPD. J Appl Physiol 2002;92:1205–13.
72. Orozco-Levi M, Gómez DM. Estrutura de los musculos respiratorios en sujetos sanos y sus cambios en pacientes con enfermedad pulmonar obstructiva crónica. Arch Bronchoneumol 2000;36:202–7.
73. Orozco-Levi M, Gea J, Aguar C, et al. Changes in the capillary content in the diaphragm of COPD patients: a sort of muscle remodelling? Am J Respir Crit Care Med 1996;153:A298.
74. Esau SA, Bellemare F, Grassino A, et al. Changes in relaxation rate with diaphragmatic fatigue in humans. J Appl Physiol 1983;54:1353–60.
75. Esau SA, Bye PTP, Pardy RL. Changes in rate of relaxation of sniffs with diaphragmatic fatigue in humans. J Appl Physiol 1983;55:731–75.
76. Odermatt A, Taschner PE, Khanna VK, et al. Mutations in the gene-encoding SERCA1, the fast-twitch skeletal muscle sarcoplasmic reticulum Ca^{2+} ATPase, are associated with Brody disease. Nat Genet 1996;14:191–4.
77. Anger M, Lambert F, Chemla D, et al. Sarcoplasmic reticulum Ca^{2+} pumps in heart and diaphragm of the cardiomyopathic hamster: effects of perindopril. Am J Physiol 1995; 268:H1947–53.
78. Gea J, Felez M, Carmona MA, et al. Oxidative capacity is preserved but glycolytic activity is reduced in the diaphragm of severe COPD. Am J Respir Crit Care Med 1999;159:A579.
79. Pape GS, Friedman M, Underwood LE, Clemmons DR. The effect of growth hormone on weight gain and pulmonary function in patients with chronic obstructive lung disease. Chest 1991;99:1495–500.
80. Burdet L, de Muralt B, Schutz Y, et al. Administration of growth hormone to underweight patients with chronic obstructive pulmonary disease. Am J Respir Crit Care Med 1997;156: 1800–6.
81. Press M. Growth hormone and metabolism. Diabetes Metab Rev 1988;4:391–414.
82. Fryburg DA, Gelfand RA, Barrett EJ. Growth hormone acutely stimulates forearm muscle protein synthesis in normal humans. Am J Physiol 1991;260:E499–504.
83. Gea J, Orozco-Levi M, Aguar C, et al. Adaptive changes concerning the type of fibres and isoforms of myosin in the external intercostal muscle of COPD patients. Eur Respir J 1996;9:160s.
84. Orozco-Levi M, Gea J, Aguar C, et al. Expression of myosin heavy chain isoform in external intercostals of COPD patients. Am J Respir Crit Care Med 1997;155:A510.
85. Jimenez-Fuentes MA, Gea J, Felez M, et al. Morfometría fibrilar del músculo intercostal externo. Comparación entre los lados dominante y no dominante en pacientes con EPOC severa. Arch Bronchoneumol 1998;34:189–93.
86. Campbell JA, Hughes RL, Sahgal V, et al. Alterations in intercostal muscle morphology and biochemistry in patients with obstructive lung disease. Am Rev Respir Dis 1980;122:679–86.
87. Sauleda J, Gea J, Orozco-Levi M, et al. Structure and function relationships of the respiratory muscles. Eur Respir J 1998; 11:906–11.
88. Aguar C, Gea J, Orozco-Levi M, et al. Structural changes and function of intercostal muscles in COPD patients: an outpatient model of biopsy. Am J Respir Crit Care Med 1995; 151:A806.
89. Jimenez-Fuentes MA, Gea J, Aguar C, et al. Densidad capilar y función respiratoria en el músculo intercostal externo. Arch Bronchoneumol 1999;35:471–6.
90. Sanchez J, Brunet A, Medrano G, et al. Metabolic enzymatic activities in the intercostal and serratus muscles and in the latissimus dorsi of middle-aged normal men and patients with moderate obstructive pulmonary disease. Eur Respir J 1988;1:376–83.
91. De Troyer A, Peche R, Yernault JC, Estenne M. Neck muscle activity in patients with severe chronic obstructive pulmonary disease. Am J Respir Crit Care Med 1994;150:41–7.
92. Gandevia SC, Leeper JB, McKenzie DK, De Troyer A. Discharge frequencies of parasternal intercostal and scalene motor units during breathing in normal and COPD subjects. Am J Respir Crit Care Med 1996;153:622–8.
93. Sanders RJ, Ratzin-Jackson CG, Banchero N, Pearce WH. Scalene muscle abnormalities in traumatic thoracic outlet syndrome. Am J Surg 1990;159:231–6.
94. Machleder HI, Moll F, Verity A. The anterior scalene muscle in thoracic outlet compression syndrome. Arch Surg 1986; 121:1141–4.
95. Fournier M, Lewis MI. Functional, cellular, and biochemical adaptations to elastase-induced emphysema in hamster medial scalene. J Appl Physiol 2000;88:1327–37.
96. Johnson MA, Polgar J, Appleton D. Data on the distribution of fibre types in thirty six human muscles. An autopsy study. J Neurol Sci 1973;18:111–29.
97. Arora NS, Rochester DF. Effect of chronic pulmonary disease on sternocleidomastoid muscle. Am Rev Respir Dis 1982; 125:252.
98. Peche R, Estenne M, Genevois PA, et al. Sternomastoid muscle size and strength in patients with severe chronic obstructive pulmonary disease. Am J Respir Crit Care Med 1996;153:422–5.

CHAPTER 24

RESPIRATORY MUSCLE FATIGUE

Spyros Zakynthinos, Charis Roussos

Skeletal muscle fatigue is defined as a loss of the capability of the muscle to generate force and/or the velocity of contraction in response to a load and is accompanied by recovery during rest.[1] Respiratory muscle fatigue may be defined analogously as an inability to continue to generate sufficient pressure to maintain alveolar ventilation in the face of the respiratory loading imposed by lung disease, thus resulting in ventilatory failure. A single measurement of force is necessarily inadequate to detect fatigue, and muscle force-generating or shortening capability must be demonstrated to fall during serial measurements over time. Furthermore, a demonstration that force rises subsequent to rest would be necessary to fully satisfy the definition of fatigue and to exclude the possibility that a given fall in force did not represent muscle injury (the latter does not improve with short periods of rest). Therefore, muscle fatigue can be distinguished from muscle injury (ie, a slowly reversible or irreversible decrement in muscle contractility) and muscle weakness (ie, a reduction in force generation that is fixed and not reversible by rest).

Theoretically, fatigue may occur at any point along the extensive chain of command involved in voluntary muscle contraction, beginning with the brain and ending with the contractile machinery (Figure 24-1). Fatigue is subdivided into two types, representing different biophysical mechanisms of fatigue development and having different physiologic characteristics: failure to generate force because of reduced central motor output (central fatigue) and failure to generate force because of fatigue at the neuromuscular junction or distal to this structure (peripheral or contractile fatigue). Davies and colleagues, the first researchers to study respiratory muscle fatigue, affirmed the existence of both types of fatigue, central and peripheral, when the respiratory system is presented with a fatiguing load.[2] It seems that roughly equal proportions of the force decline during diaphragmatic fatigue can be attributed to reduced central motor drive and peripheral muscle contractile failure.[1,3] Furthermore, this depression of the central motor drive seems to represent a protective adaptation of the central nervous system (CNS) to changes in the contracting muscle, intended to prevent an undue reduction of intrinsic muscle fiber strength.[4]

MUSCLE FUNCTION AND THE PATHOPHYSIOLOGY OF FATIGUE

Force Generation

In the case of voluntary contractions, there is a long chain of command, extending from the motor cortex down to the eventual interaction of actin and myosin within the muscle fiber (see Figure 24-1). These events can be broadly divided into three categories: (1) pathways concerned with delivering sufficient electrical activation of the muscle by the CNS; (2) the metabolic and enzymic processes providing energy to the contractile mechanism; and (3) the excitation–contraction coupling processes that link these two.

Muscle tension can be altered either by varying the firing frequency of each of the active motor units or by varying the number of motor units that are active. At low intensities of muscle contraction, force is developed largely by recruitment of motor units; at moderate and high levels of voluntary contraction, the number of additional motor units recruited during a given increment in force decreases sharply, and force is generated through an increase in the firing frequency of each motor unit.[5]

It is possible experimentally to determine the effectiveness of various firing rates in generating force.[5] As the frequency increases from a single stimulus to a high-frequency train, the muscle responds with a brief twitch (unitary activity), followed by an unfused (oscillatory) contraction, and, finally, when the frequency of stimulation is high enough, by a fused tetanus. Thus, the force–frequency characteristics of a muscle can be conveniently and effectively recorded by programmed electrical stimulation of the nerve in an isolated human nerve–muscle preparation in both limb[6] and respiratory muscles[7] (Figure 24-2). In Figure 24-2, it can be seen in the control (preload) pressure–frequency curve that pressure increases markedly in response to small changes in low-frequency stimulation, whereas pressure is affected very little by large changes in high-frequency stimulation. The importance of this curve is that central factors affecting muscle performance do not influence it. Furthermore, the manner in which it changes shape after loading gives insight into the mechanisms of fatigue. Selective loss of force at high stimulation frequencies (high-frequency fatigue), accompanied by a

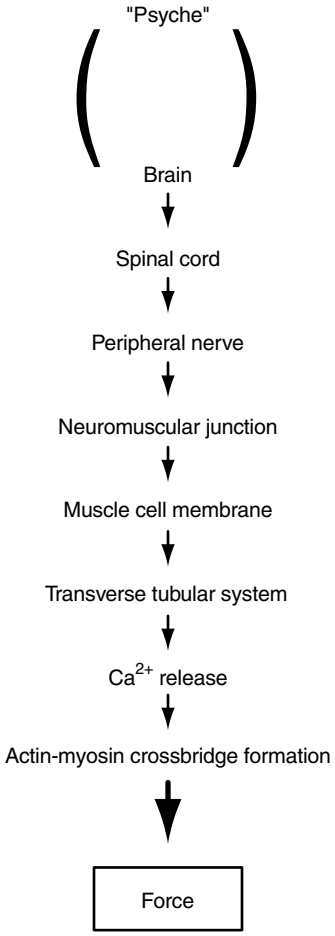

FIGURE 24-1 Command chain for voluntary contraction of skeletal muscle.

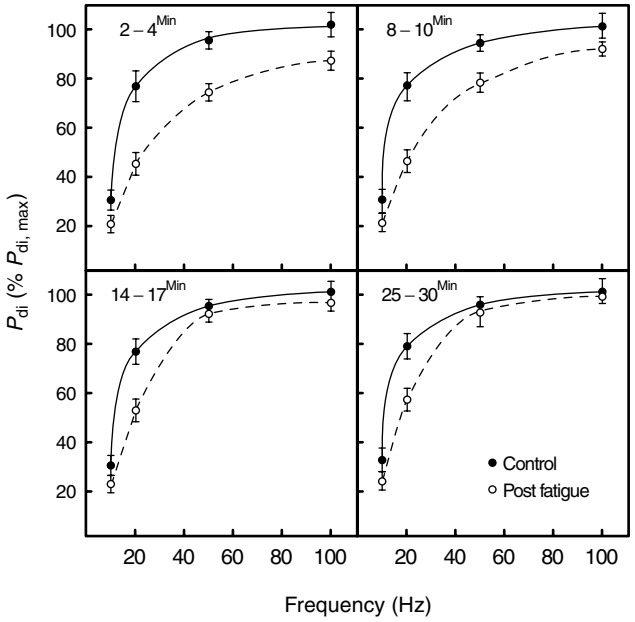

FIGURE 24-2 Pressure–frequency relationships for the human diaphragm at various time points after a loaded breathing trial (ie, a breathing trial in which an external resistive load was applied to increase the work done by the diaphragm and simulate the effects of lung disease). Diaphragm pressure generation was measured through determination of the transdiaphragmatic pressure gradient (P_{di}) generated in response to electrical stimulation of both phrenic nerves; P_{di} (expressed as a percentage of P_{di} generated with supramaximal phrenic nerve stimulation at a frequency of 100 Hz; % $P_{di,max}$) is shown on the ordinate, and phrenic stimulation frequency is shown on the abscissa. The time at which each set of curves was obtained is shown in the upper left-hand corner of each panel. For reference, each panel contains both a postload pressure–frequency curve obtained at the designated time (*dashed line*) and a control preload pressure–frequency curve (*solid line*). At 2 to 4 minutes postloading, there was a large decrement in pressure generation in response to phrenic stimulation at 20 to 100 Hz (*top left panel*), indicating diaphragm fatigue. Over time, the pressures generated in response to high-frequency stimulation increased, so that at 25 to 30 minutes postloading, pressure generation in response to 50 and 100 Hz stimulation had returned to preloading levels (*bottom right panel*). In contrast, however, the response to 20 Hz stimulation remained depressed 25 to 30 minutes postloading. Obviously, both low- and high-frequency peripheral diaphragm fatigue were present 2 to 4 minutes postloading, with rapid resolution of the high-frequency component of fatigue and persistence of the low-frequency component at 25 to 30 minutes. Data from Aubier M et al.[7]

decrease in the amplitude of surface-recorded action potentials of the muscle, indicates fatigue of neuromuscular transmission and/or impaired membrane excitation. Selective loss of force at low stimulation frequencies, not accompanied by a decrease in the amplitude of surface action potentials (low-frequency fatigue), is thought to be due to impairment of excitation–contraction coupling.[6]

Site and Mechanism of Fatigue

Central Fatigue Central fatigue refers to the condition in which muscle force generation during sustained or repetitive contraction decreases owing to reduced central motor output. Central fatigue is judged to be present either when a maximal electrical stimulation is superimposed on a truly maximal voluntary contraction and force generation is still increased or when a certain maximal voluntary effort produces less force than one generated by direct electrical stimulation.[3,8]

The technique of twitch occlusion, originally introduced by Merton in peripheral muscles,[9] was used by Bellemare and Bigland-Ritchie[3,8] in the diaphragm to distinguish central from peripheral fatigue of the respiratory muscles during respiratory loading. They initially observed that it is possible for well-motivated individuals to fully activate the rested diaphragm during voluntary contractions when making a maximal effort (that is, superimposed electrical stimulation of the diaphragm during such maximal maneuvers does not result in an increase in force generation above that achieved voluntarily)[8] (Figure 24-3). As a result, evidence that maximal activation of the diaphragm during a maximal voluntary effort can never be achieved after a period of exercise (that is, the superimposed electrical stimulation can always evoke an increase in force generation) constitutes evidence of central fatigue. Bellemare and Bigland-Ritchie subsequently measured transdiaphragmatic pressure (P_{di}) generation over time before, during, and after inspiratory resistive loading in normal human subjects and employed superimposed electrical phrenic stimulation at

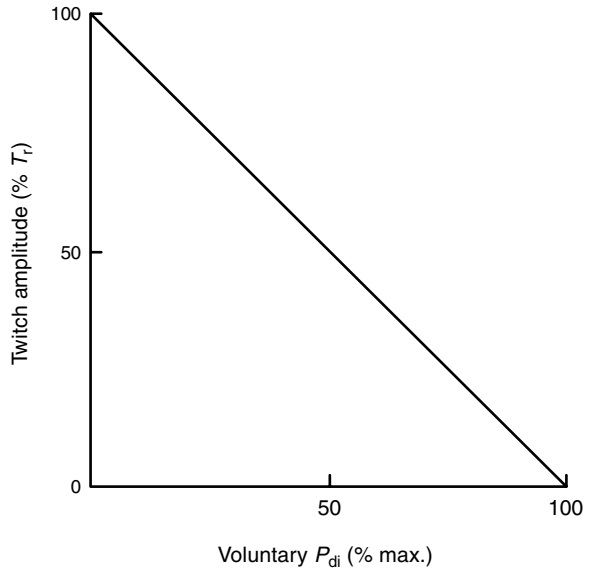

FIGURE 24-3 The relationship between voluntary P_{di} (expressed as a percentage of $P_{di,max}$) and superimposed twitch amplitude (expressed as a percentage of twitch amplitude of the relaxed diaphragm, T_r). As voluntary P_{di} increases, the magnitude of the superimposed twitch increases. Data from Bellemare F and Bigland-Ritchie B.[8]

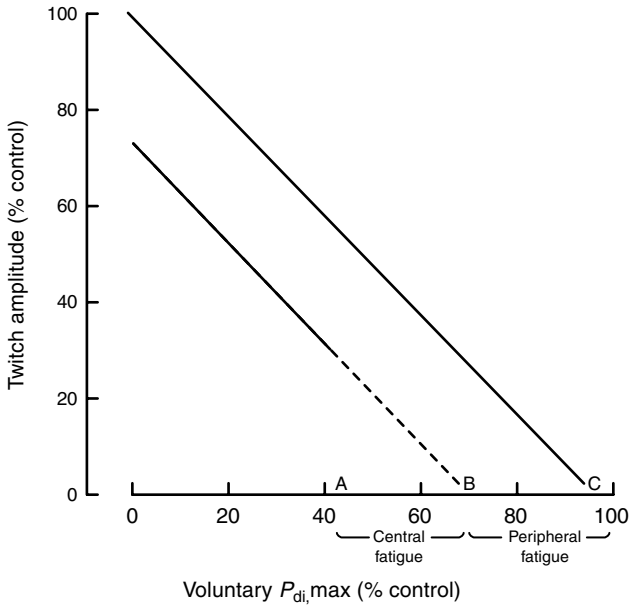

FIGURE 24-4 The relationship between voluntary $P_{di,max}$ and superimposed twitch amplitude (expressed as a percentage of control values, ie, values obtained before inspiratory resistive loading) during control experiments performed prior to loading (*upper line*) and during loading after the limits of endurance had been reached (*lower line*). The difference between the point where the lower line intersects the *x*-axis (predicted voluntary $P_{di,max}$ if the diaphragm was fully activated [point B]) and the actual maximal voluntary P_{di} (point A) represents the contribution of the lack of central drive (central fatigue) to the generation of $P_{di,max}$ (the difference between points A and B). The difference between the point where the upper line interacts the *x*-axis, which is the unfatigued $P_{di,max}$ (point C), and the point where the lower line intersects the *x*-axis (point B) represents the contribution of peripheral muscle fatigue to the generation of $P_{di,max}$ (the difference between points B and C). Data from Bellemare F and Bigland-Ritchie B.[3]

various times during the experiment to determine whether subjects were capable of fully activating the diaphragm.[3] At the start of the study, no superimposed force could be detected during the imposition of electrical stimuli on maximal voluntary efforts, indicating that these subjects were capable of maximally activating the diaphragm before respiratory loading. During the course of loading, however, the extent to which the diaphragm could be activated decreased progressively.[3] At the end of the study, maximal voluntary efforts had decreased by 50%, whereas twitch occlusion restored half of this decrease[3] (Figure 24-4), indicating that even though peripheral fatigue was present, a significant portion of the reduction in force was due to failure of the CNS to activate the diaphragm completely.[3] The results of several later studies have also suggested development of central fatigue during respiratory loading.[10–15]

Central fatigue must not be confused with the progressive decrease in firing rate during maximal contraction, during which superimposed, supramaximal, electrical, tetanic stimulation does not increase muscle force.[16] This decrease in firing frequency is possibly an adaptive, protective mechanism, responding to alteration of muscle contractile characteristics and aimed at preventing muscle exhaustion.[1,16] Such an adaptation would be beneficial as it would avoid the failure of impulse propagation associated with high-frequency fatigue, as well as the complete depletion of vital chemicals within the muscle cell that might occur if high-frequency excitation were maintained. Central fatigue is associated with an even greater decrease in firing rate than can be justified by muscle contractile characteristics. It seems likely that activation of muscle afferents by some fatigue-induced change within the muscle inhibits motor neuron activity and reduces the latter's firing rates.[17] For the diaphragm, it has been shown that afferent information via small (type 3 and type 4) fibers of the phrenic nerve affects the central respiratory controller's discharge in terms of firing rate, firing time, and frequency of breathing.[18,19] These sensory fibers are activated primarily by extracellular metabolic changes, for example, low pH, ischemia, and increased osmolarity, and by some substances (phenyldiguanide, capsaicin). It has been shown that the reduction in central respiratory output during respiratory loading is signaled by small fiber afferents, which are stimulated by lactic acid accumulation and the fall in pH in the respiratory muscles[14] (Figure 24-5).

Central fatigue may be the result of a decrease in central respiratory motor output in response to endogenous opioid (endorphin) elaboration in the CNS, with the endorphin being generated as a consequence of the stress of loaded breathing.[11,13,14] In animals, adequate evidence supports this concept.[11,13,14,20] It was demonstrated that resistive loading resulted in a progressive reduction in tidal volume, which was partially reversed by administration of the opioid antagonist naloxone[11] (Figure 24-6). An increase in β-endorphin in the cisternal cerebrospinal fluid was also detected.[11] In humans, in support of this concept, it was demonstrated

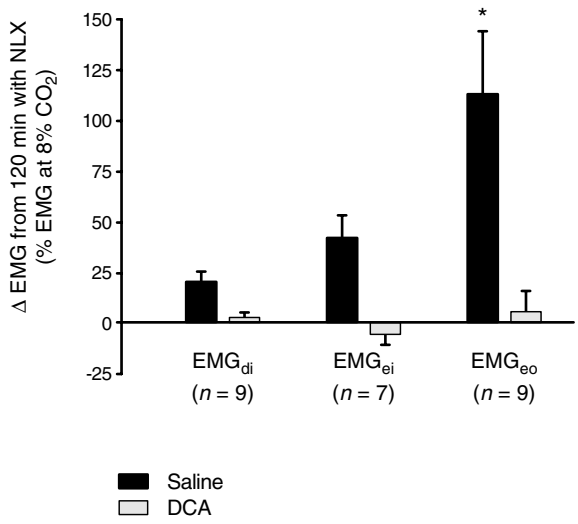

FIGURE 24-5 Respiratory muscle electromyographic responses to naloxone (NLX) after 120 minutes of exposure to saline or dichloroacetate (DCA). $*p < .05$ vs EMG_{di}. During 2 hours of inspiratory flow-resistive loading, goats were exposed to a constant infusion of either saline or DCA, a compound that enhances the activity of pyruvate dehydrogenase and thus lessens the accumulation of lactic acid. NLX was given at the conclusion of the loading period. In the goats given saline, NLX significantly increased the electromyographic activity of the diaphragm (EMG_{di}), external oblique muscles (EMG_{eo}), and external intercostal muscles (EMG_{ei}). DCA infusion completely blocked the NLX effect on respiratory activity. These findings suggest that lactic acid accumulation (and pH fall) in the respiratory muscles is the stimulus signaling activation of the endogenous opioid system, which results in reduction of central respiratory output during inspiratory, flow-resistive loading. Data from Petrozzino JJ et al.[14]

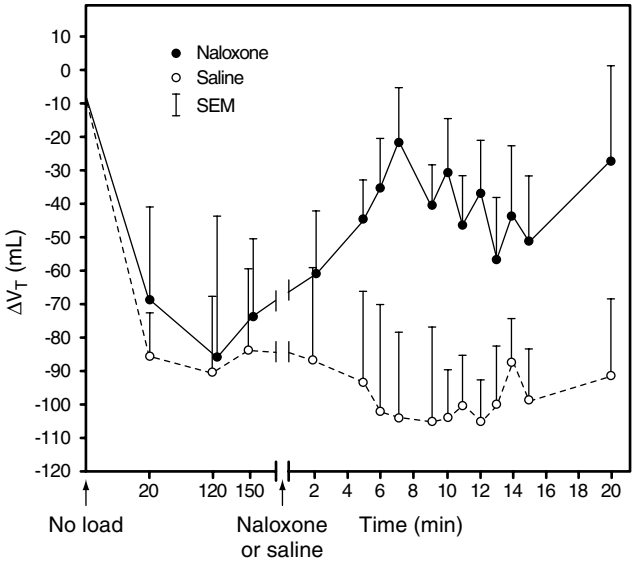

FIGURE 24-6 Tidal volume response of unanesthetized goats to 2.5 hours of high-inspiratory, flow-resistive loading prior to and following administration of naloxone. Tidal volume, which fell considerably during loading, increased significantly but transiently after naloxone administration, whereas saline had no effect. (Note the change in time scale on the *x*-axis.) These data indicate that an increase in airway resistance can activate the endogenous opioid system. Furthermore, the increase in tidal volume immediately following naloxone administration suggests that these potentially fatiguing loads reduce tidal volume prior to the onset of overt muscle fatigue by a mechanism that, in addition to the direct mechanical effect of the load, involves the endogenous opioid system. Data from Scardella A et al.[11]

that naloxone could restore the load compensatory reflex in patients with chronic obstructive pulmonary disease (COPD) in whom it was initially absent.[13] It was postulated that, in such patients, endogenous opioids were elaborated in response to the stress of chronically increased airway resistance, resulting in attenuation of respiratory compensation, perhaps acting as a mechanism to reduce dyspnea.[13] Moreover, in asthmatic subjects after methacholine challenge inducing severe reductions in forced expiratory volume in 1 second (FEV_1), naloxone pretreatment resulted in increased breathing frequency, occlusion pressure, and mean inspiratory flow rate.[15] Endorphin elaboration in the CNS seems to be signaled by small fiber afferents.[14] In addition, it is possible that CNS endorphin production is also stimulated by circulating cytokines, especially interleukin-6 (IL-6), which is produced by the inspiratory muscles when they are working intensely.[20–22]

In summary, during fatiguing loaded breathing, the central discharge firing rate decreases, resulting in force decline (central fatigue) as an adaptation to altered chemistry and/or contractile characteristics of the respiratory muscles, in an effort to prevent their self-destruction through excessive activation. During loaded breathing in various clinical states, this response also includes changes in the timing of breathing (firing time, frequency). These changes of central respiratory controller activity seem to be mediated by afferents (via the small fibers) and blood IL-6, which modulate endogenous opioids. Such a strategy, representing an adaptive response much in the way that opioids are generated in response to chronic pain, certainly minimizes breathlessness and may avoid or delay the onset of respiratory muscle peripheral fatigue, protecting the ventilatory pump from exhaustion. However, it may result in hypoventilation and the development of hypercapnia.

Peripheral Fatigue Peripheral fatigue refers to failure of transmission at the neuromuscular junction or distal to this structure and is judged to be present when muscle force output or velocity falls in response to direct electrical stimulation. This type of fatigue may occur either because of failure of impulse propagation across the neuromuscular junction and/or over the muscle surface membrane (transmission fatigue) or because of failure of the contractile apparatus of muscle fibers (impaired excitation–contraction coupling). The former is also called high-frequency fatigue as fatigue results in depression of force generation in response to high-frequency electrical stimulation (eg, in humans 50 to 100 Hz), and the latter is called low-frequency fatigue since force generation in response to low-frequency stimuli (ie, 1 to 20 Hz) is reduced (see Figure 24-2). Low-frequency fatigue can occur in isolation, but high-frequency fatigue is invariably associated with some alterations in muscle force generation at lower frequencies.

High-frequency fatigue attributed to transmission failure is constantly produced experimentally during artificial stimulation of a motor neuron, when muscle force declines in association with decline in action potential amplitude. From a teleologic point of view, transmission block could be beneficial as failure at the neuromuscular junction or in excitation of the cell membrane may protect the muscle from excessive depletion of its ATP stores, which would lead to damage.[23] High-frequency fatigue has been demonstrated in the diaphragms of normal humans after a trial of high-intensity inspiratory resistive loading; it resolves extremely quickly after cessation of strenuous muscle contractions.[7]

Low-frequency fatigue is attributed to impaired excitation–contraction coupling, a term that includes all processes linking electrical activation of muscle fibers and the various metabolic and enzymic processes providing energy to contractile machinery. Typically, loss of force is not accompanied by a parallel decline in electrical activity[9] and is long-lasting, recovery taking at least 24 hours.[24] It is characterized by selective loss of force at low frequencies of stimulation, despite maintenance of force generated by high frequencies of stimulation, thereby indicating that contractile proteins are capable of generating force provided that sufficient Ca^{2+} is released by the sarcoplasmic reticulum. Therefore, this type of fatigue may result from reduced Ca^{2+} availability due to alterations in sarcoplasmic reticulum function and/or reduced Ca^{2+} sensitivity of myofilaments at submaximal Ca^{2+} concentrations. Both changes have been demonstrated experimentally.[25,26] Reduced myofilament Ca^{2+} sensitivity is caused by increased inorganic phosphate (P_i) concentration and acidosis.[25,27] The reason for reduced Ca^{2+} release by the sarcoplasmic reticulum during contractions is less clear but may be related to declining ATP[25] levels or increased production of oxygen-derived free radicals.[28–30]

Low-frequency fatigue occurs during high-force contractions, and it appears likely that muscle ischemia and reliance on anaerobic metabolism are important factors in its generation. Indeed, low-frequency diaphragmatic fatigue occurs in dogs during cardiogenic or septic shock[31,32]; despite a three-fold increase in integrated electromyographic activity, P_{di} decreased (Figure 24-7). Low-frequency fatigue has been demonstrated in the diaphragm and sternocleidomastoid muscles of normal subjects breathing against high inspiratory resistive loads.[4,33] Low-frequency diaphragmatic fatigue has also been shown to develop in normal subjects asked to sustain maximum voluntary ventilation for 2 minutes.[34]

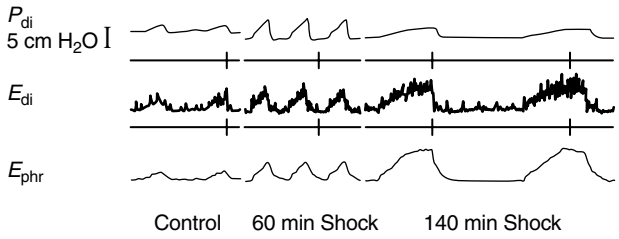

FIGURE 24-7 Tracings from a dog in cardiogenic shock show typical evolution of transdiaphragmatic pressure (P_{di}), integrated electrical activity of the diaphragm (E_{di}), and integrated electrical activity of the phrenic nerve (E_{phr}). The *left panel* represents a control. The *middle panel* shows a reading made 60 minutes after the onset of cardiogenic shock. The *right panel* shows a reading made 140 minutes after the onset of cardiogenic shock and just before death from respiratory arrest. E_{di} and E_{phr} continue to increase, but P_{di} decreases. This finding indicates that the decrease in P_{di} is not due to transmission failure but rather to impaired excitation–contraction coupling (low-frequency fatigue). Data from Aubier M et al.[31]

Metabolic Considerations in Muscle Fatigue

Skeletal muscle is analogous to an engine; it converts chemical energy into heat and work. If the chemical energy available becomes limited or the ability of the muscle to use chemical energy is impaired, the muscle will fail as a force generator.

The authors of most studies have concluded that the major factors underlying fatigue occur within the muscle fibers and mainly result from depletion of muscle energy stores or from pH changes caused by lactate accumulation.[1] Substances directly involved in the transformation of chemical energy into mechanical work in skeletal muscle are ATP, ADP, P_i, hydrogen ions (H^+), magnesium ions (Mg^{2+}), and phosphocreatine (PCr). ATP leaves mitochondria and diffuses into the contractile machinery, where ATPase enzymes hydrolyze one of the pyrophosphate bonds, liberating large quantities of energy in the process:

$$MgATP + H_2O \xrightarrow[ATPases]{} MgADP + P_i + H^+ + Energy$$

In general, metabolic changes can cause fatigue either through a reduction in the amount of high-energy compounds (eg, PCr and ATP) or through accumulation of breakdown products (eg, P_i and H^+). Figure 24-8 shows some important metabolic changes that occur during fatiguing stimulation. Important changes are the breakdown of PCr, with the concomitant formation of P_i, and the formation of lactate, which is usually accompanied by accumulation of H^+ and thus also by reduced intracellular pH.

A great deal of attention has been focused on the role that lactic acid plays in the development of fatigue as a result of the firm correlation that exists between lactic acid accumulation in the muscle and contractile force. It has been shown that respiratory muscles produce great amounts of lactic acid if they are working under fatiguing conditions.[35] However, there is no direct evidence that lactic acid produced by respiratory muscles is the culprit in fatigue.[4] The effects of lactic acid on force generation are believed to be mediated by lowering of the pH. Of all the breakdown products of energy metabolism, H^+ and P_i have the greatest effect on the contractile apparatus.[25,27] An increased P_i concentration and acidosis result in both reduced maximum tension production (ie, tension at saturating Ca^{2+} concentrations) and reduced myofibrillar Ca^{2+} sensitivity[25] (Figure 24-9). Furthermore, H^+ ions exert a direct negative effect on the contractile process itself, which is not related to pH.[25]

In addition to lactic acid accumulation and acidosis of every kind, glycogen depletion,[4] inability to use blood-borne substances,[4] a decrease in the rate of ATP hydrolysis,[36,37] and increased, oxygen-derived free radical production[28–30]

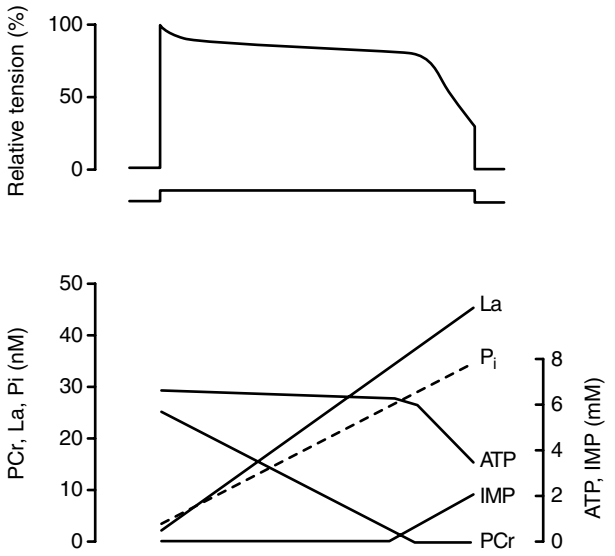

FIGURE 24-8 Characteristic pattern of tension decline (*upper panel*) and metabolic changes (*lower panel*) during fatigue produced by repeated tetanic stimu1ation of *Xenopus* fibers. The tension trace is the envelope of the peak force of a large number of tetanic stimulations. The period of fatiguing stimulation is indicated below the tension record; the duration of this period depends on the fiber's fatigue resistance and pattern of stimu1ation (ie, duration of tetanic stimulation vs rest period between stimulations). The metabolites are lactate (La), inorganic phosphate (P_i), ATP, inosine monophosphate (IMP), and phosphocreatine (PCr). Easily fatigued fibers of *Xenopus* have a very low oxidative capacity, and, during a period of increased energy consumption, they therefore depend on the breakdown of high-energy phosphates (PCr and ATP) and anaerobic glycolysis. The latter process results in accumulation of lactate ions and acidosis. Note that the level of ATP does not start to decline until the store of PCr is almost fully depleted. Note also that the final rapid tension reduction coincides with the reduction in the level of ATP. Data from Nagesser AS et al[36] and Westerblad H and Lannergren J.[37]

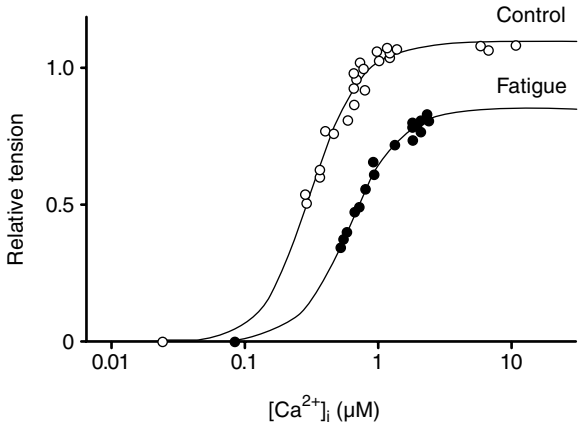

FIGURE 24-9 Relationship between tension expressed as a percentage of maximum and intracellular Ca^{2+} concentration ($[Ca^{2+}]_i$) obtained in controls and during late fatigue in a single mouse muscle fiber. During fatigue, there is both a marked reduction in the stable tension at high $[Ca^{2+}]_i$ (ie, reduced maximum tension) and a marked rightward shift of the data points (ie, reduced Ca^{2+} sensitivity), most likely caused by the combined effect of increased P_i concentration and acidosis. In addition to these two factors, reduced Ca^{2+} release from the sarcoplasmic reticulum may contribute to fatigue. The cause of this factor is less clear, but it may be related to declining ATP levels. Data from Westerblad H and Allen DG.[25]

probably all play a part in causing loss of force during fatigue. However, the exact interplay of all these factors has not yet been identified in either the diaphragm or the other skeletal muscles.[4]

Integrated View of Respiratory Muscle Fatigue

Fatigue is likely to result from a dynamic process in which compensatory mechanisms are overwhelmed in a closed-loop system consisting of central motor drive, peripheral impulse propagation, excitation–contraction coupling, depletion of energy substrates and/or metabolite accumulation, and feedback-modulating reflexes.[1] Although the three types of fatigue, that is, central, peripheral high frequency, and peripheral low frequency, are usually separately considered, it is likely that they do not occur in isolation but coexist when respiratory muscles face an excessive workload, with the relative importance of each depending on duration of respiratory loading and other physiologic variables (eg, arterial pressure and arterial blood gas concentrations). Indeed, for an individual muscle, a close relationship exists between excitation and energy metabolism, representing a protective mechanism, so that when depletion of fuel and/or metabolite accumulation occurs (impaired excitation–contraction coupling or low-frequency peripheral fatigue), the activation system fails; in extreme fatigue, this prevents muscle destruction, which would happen if ATP concentrations fell to zero. A decrease in excitation may result from failure of the neuromuscular junction[7,23] (transmission fatigue or high-frequency peripheral fatigue), reduced rate of firing by the CNS[17] (central fatigue), or both. In the respiratory system, in addition to a reduction in firing frequency, the CNS may respond by altering the timing of breathing (firing time, frequency).[18,19] Such alterations in the responses of the central controllers could be brought about by afferents from fatigued respiratory muscles and the chest wall. In particular, free nerve endings within the muscle might inhibit motor neuron activity in response to muscle stretch and fatigue. Afferent information via small (type 3 and type 4) fibers, stimulated by the heavy work (ergoreceptors, type 3) or by noxious substances such as lactic acid (nociceptors, type 4), reduces central respiratory output by modulating endorphins as an adaptive response to avoid or delay respiratory muscle peripheral fatigue.

ENERGY BALANCE: DETERMINANTS OF A CRITICAL TASK

Muscle fatigue develops when the mean rate of energy demand ($\dot{U}_d$) exceeds the mean rate of energy supply ($\dot{U}_s$), that is, $\dot{U}_d > \dot{U}_s$.[38] Thus, since $E = \dot{W}/\dot{U}_d$ and $\dot{U}_d = \dot{W}/E$, $\dot{W}/E > \dot{U}_s$ or $\dot{W} > \dot{U}_s E$, where $\dot{W}$ is mean muscle power and E is efficiency. Clearly, when $\dot{W} \leq \dot{U}_s E$, the muscle can continue to work indefinitely, but when $\dot{W} > \dot{U}_s E$, there will be a finite endurance time limit. Thus, decreases in either efficiency or energy supplies should encourage fatigue, as

would an increase in muscle power. The threshold of fatigue is the lowest level of exercise and/or mechanical loading that cannot be sustained indefinitely. In other words, the threshold of fatigue corresponds to the lowest $\dot{W}$, where $\dot{W} > \dot{U}_s E$. For a given value of E, $\dot{W}$ and $\dot{U}_s$ at the point where $\dot{W} = \dot{U}_s E$ are named "critical" power ($\dot{W}_{crit}$) and rate of energy supply ($\dot{U}_{s,crit}$), respectively.

For inspiratory muscles during resistive breathing with mouth pressure developed in a square wave manner, $\dot{W}_{crit}$ equals 6 to 8 kg/min.[39] In this situation, $\dot{W} = PV_T f = PV_T(1/T_T)$, where P is mean inspiratory pressure, V_T is tidal volume, f is frequency of breathing, and T_T is total breath time. When numerator and denominator are multiplied by inspiratory time (T_I), the equation becomes $\dot{W} = P(V_T/T_I)(T_I/T_T)$, where V_T/T_I is mean inspiratory flow and T_I/T_T is duty cycle. Duty cycle approximates duration of inspiratory muscle contraction as a proportion of the total duration of the breathing cycle. Therefore, $\dot{W}_{crit} = P(V_T/T_I)(T_I/T_T)$, indicating that the $\dot{W}_{crit}$ of respiratory muscles can be obtained through a variety of combinations of P, V_T/T_I, and T_I/T_T. P can be expressed as a percentage of the maximal pressure. It was found that the critical pressure of all inspiratory muscles is 50 to 70% of the maximal inspiratory pressure ($P_{i,max}$)[39] and that for the diaphragm alone, critical P_{di} is 40% of maximal P_{di} ($P_{di,max}$)[40] for V_T/T_I of 0.6 to 0.9 L/s, and T_I/T_T of 0.3 to 0.4. Furthermore, under conditions of predominant diaphragmatic recruitment, critical P_{di} decreases as T_I/T_T increases at constant V_T/T_I.[41] In other words, when the proportion of the time spent in inspiration increases, the pressure that can be sustained falls. When the product $(P_{di}/P_{di,max})(T_I/T_T)$, called the pressure–time index of the diaphragm (PT_{di}), exceeds the critical value of 0.15 to 0.18, there is a finite endurance time limit that is inversely related to PT_{di}.[41] Below this critical value, breathing can be sustained without evidence of fatigue.[41] A critical value has also been demonstrated for the pressure–time index of inspiratory rib cage muscles other than the diaphragm (PT_{rc}); it amounts to 0.30 when inspiratory intercostal/accessory muscles are predominantly recruited.[42] Finally, in keeping with the above-mentioned determinants of $\dot{W}_{crit}$, it was shown that the critical value of the esophageal pressure–time index (PT_{es}) [used as a measure of global inspiratory muscle pressure output and defined as the product $(P_{es}/P_{es,max})(T_I/T_T)$, where P_{es} is mean esophageal pressure generated per tidal breath, equivalent to P_{tidal}, and $P_{es,max}$ is maximal esophageal pressure, equivalent to $P_{i,max}$] is inversely related to V_T/T_I over a wide range of flows.[43]

One would predict that if $\dot{U}_s E$ is decreased (by decreasing $\dot{U}s$, E, or both), critical values of P or a combination of P, V_T/T_I, and T_I/T_T, composing $\dot{W}$, will decrease (Figure 24-10). For example, decreasing $\dot{U}_s$ by reducing cardiac output in dogs readily results in diaphragmatic fatigue[31] (see Figure 24-7). Similarly, decreasing the bloodflow to the diaphragm in dogs causes fatigue that is reversed by restoring normal perfusion[44] or by hyperperfusion.[45] Furthermore, a decrease in E, as might occur with resistive breathing (as opposed to unobstructed hyperventilation), may substantially alter $\dot{W}_{crit}$. In fact, it was found that $\dot{W}_{crit}$ during hyperventilation[46]

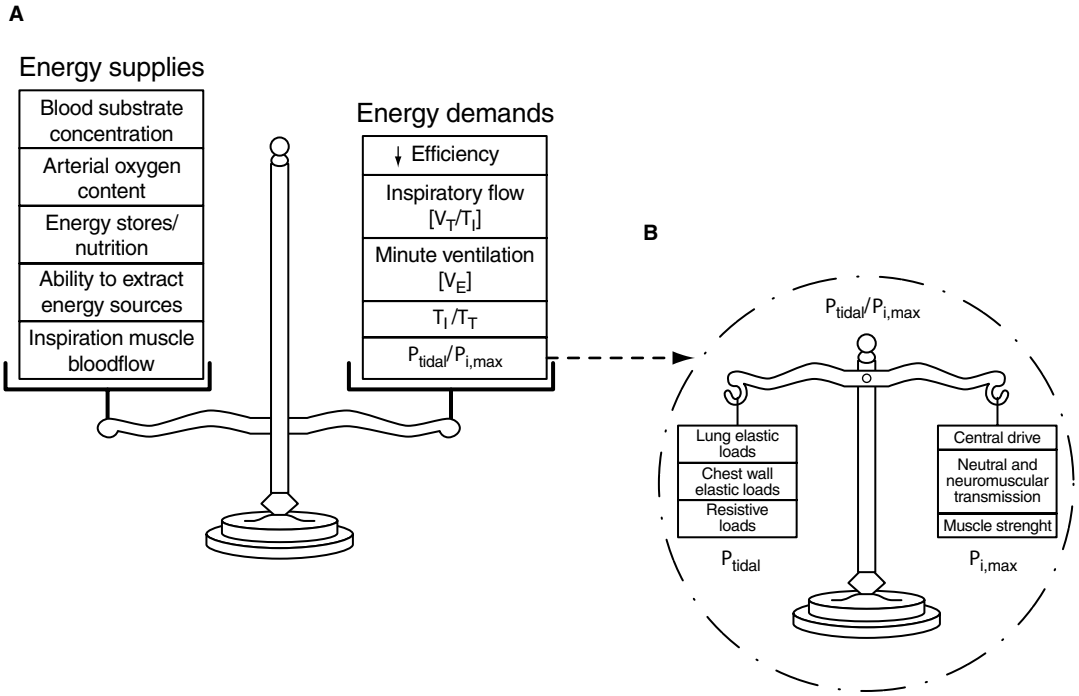

FIGURE 24-10 The various determinants of energy supply, energy demand, and neuromuscular competence are schematically represented. Respiratory muscle endurance is determined by the balance between energy supplies and demands (*A*). Normally, the supplies meet the demands and a large reserve exists. Whenever this balance is in favor of demands, the respiratory muscles ultimately become fatigued. The $P_{tidal}/P_{i,max}$ ratio is one of the determinants of energy demands, which are shown in *B* as a balance between the load per tidal breath (P_{tidal}) and the neuromuscular competence of the ventilatory pump ($P_{i,max}$).

is at least four times greater than the $\dot{W}_{crit}$ of 6 to 8 kg/min during resistive breathing in normal subjects.[39] If the diaphragm operates at shorter lengths during acute hyperinflation, a similar argument may account for a smaller critical P_{di}, when a given force requires much greater excitation.[47] At half inspiratory capacity, E can be reduced by as much as 50%.[47]

In summary, there is clear evidence of the existence of a critical pressure, which, if exceeded, results in fatigue. However, this critical pressure is affected by many factors, including the relative duration of contraction and relaxation per breath (pressure–time index), velocity of contraction, operational length, energy supply, efficiency, and state of muscle training.

DETECTION OF INSPIRATORY MUSCLE FATIGUE

Fatigue is conveniently and conventionally defined in terms of loss of force.[1] However, other changes in physiologic function (eg, electromyographic spectral shift, slowing of muscle relaxation rate) can be useful indicators that the fatigue process is under way.

Because muscle fatigue is a complex phenomenon, a test that is well suited to detect one type of fatigue may be incapable of detecting another.[48] Moreover, the need for serial measurements of an index of muscle force generation over time to detect fatigue is a particular problem in the respiratory system because many variables (ie, lung volume, thoracoabdominal configuration, muscle interaction) can vary over time; all of these factors can influence the relationship between muscle force and pressure generation.[48] For example, consider the utility of measuring $P_{i,max}$ serially to detect respiratory muscle fatigue.[48] This parameter is highly effort dependent, and time-dependent reductions could represent lack of motivation, central fatigue, peripheral high-frequency fatigue, or simply an alteration in lung volume and a resultant mechanical change in the transduction of muscle force into pressure.[48] In addition, failure of $P_{i,max}$ to change does not exclude the development of fatigue because this test would not be suitable for the detection of low-frequency fatigue.[48] As a result, one must keep in mind the potential limitations of a given test for detection of muscle fatigue. Most tests are suitable for detecting the presence of only one component of muscle fatigue, and complete characterization of fatigue requires a complex series of assessments.[48]

Measurement of Force (or Pressure)

Voluntary Maximal Pressures In accordance with the definition of respiratory muscle fatigue, it can potentially be documented by measuring a decrease in voluntary maximal respiratory pressures, with demonstration of recovery with rest. Therefore, to detect inspiratory muscle fatigue, either maximal static inspiratory pressure, maximal transdiaphragmatic pressure, or maximal sniff pressure can be measured (see Chapter 60, "Assessment of Respiratory Muscles").

Maximal static inspiratory pressure ($P_{i,max}$) is measured at the mouth, and its transient fall indicates fatigue of inspiratory muscles as a whole. Such a fall in $P_{i,max}$ has been demonstrated after breathing against external loads,[39] maximal voluntary hyperpnea,[49] marathon running,[50] and labor.[51] The major limitation of $P_{i,max}$ as a test of fatigue is its total dependence on the subject's maximal voluntary effort.[48] Although $P_{i,max}$ is reliable in highly motivated subjects, it cannot be obtained with certainty in patients.[48] Another drawback of $P_{i,max}$ is the potential lack of sensitivity for fatigue detection. Because a maximal static effort is associated with high neuronal firing rate, it reflects mainly high-frequency fatigue and may be a poor indicator of low-frequency fatigue.[48] Therefore, $P_{i,max}$ can be used to detect fatigue in motivated volunteers but has limited utility in patients because of difficulties in ensuring a maximal effort. Twitch interpolation techniques[3,8] provide a potential means of solving this problem.[48]

Maximal transdiaphragmatic pressure ($P_{di,max}$) is measured with balloon-catheter systems, and its transient fall indicates fatigue of the diaphragm. Such a fall in $P_{di,max}$ has been documented after breathing with an emphasis on diaphragmatic recruitment against external loads,[12,40] voluntary hyperpnea,[49] or high-intensity exercise.[52] $P_{di,max}$ has the same types of limitation as $P_{i,max}$ in the detection of fatigue, but, additionally, it is invasive, requiring an even more complex maneuver for reliable measurement than that required to measure $P_{i,max}$. Therefore, $P_{di,max}$ can be used to detect diaphragmatic fatigue in motivated volunteers but cannot be recommended for use in clinical settings.[48]

Maximal sniff P_{di}[53] can be used to assess diaphragmatic strength, whereas global inspiratory muscle strength can be assessed either with maximal sniff esophageal pressure[54] or with maximal sniff nasal inspiratory pressure (SNIP).[55,56] A sniff maneuver is easily performed by almost all subjects and patients, whereas, additionally, the measurement of SNIP is noninvasive, often yielding higher pressures than $P_{i,max}$.[54] However, the usefulness of measuring a transient fall of maximal sniff pressures to detect fatigue in patients remains to be established.[48]

Muscle Response to External Stimulation

Pressure–Frequency Relationship Peripheral fatigue can be most specifically detected by recording the pressure–frequency or force–frequency curve of a muscle in response to electrical motor nerve stimulation. Of the respiratory muscles, the diaphragm[7] (see Figure 24-2) and the sternocleidomastoid muscles[33] are most amenable to this form of testing (see Chapter 60, "Assessment of Respiratory Muscles" and Chapter 67, "Diaphragmatic Responses to Stimulation"). This technique is nonvolitional, thus overcoming the difficulties associated with voluntary efforts. In addition, the response of a particular muscle can be studied in isolation, providing information on the underlying mechanisms of peripheral fatigue (see Figure 24-2). However, this is a difficult test to perform. Tetanic electrical stimulation can also be uncomfortable. To overcome this problem, partial pressure–frequency curves may be constructed with the use of twin pulses and variation of the intervals between the pulses.[57,58] This is better tolerated than tetanic stimulation and can provide comparable information regarding the presence of high- and low-frequency fatigue. Partial pressure–frequency curves may

also be constructed with the use of magnetic stimulation.[59] Therefore, although construction of a pressure–frequency curve provides a means of directly detecting the development of muscle fatigue, the applicability of this approach is limited by patient discomfort associated with high-frequency stimulation, equipment expense and complexity, and the need to carefully control for variation in body position, lung volume, and electrode–nerve interface.[48] Advances in magnetic stimulation techniques may allow a variation of this form of testing to have more widespread clinical use in the future, but this test is currently limited to research applications.[48]

Single-Twitch Stimulation Recording of muscle twitches in response to single nerve shocks can be used to detect the presence of low-frequency fatigue.[57,60] Twitch responses are much easier to obtain but are more variable than tetanic responses and are subject to additional variations caused by twitch potentiation.[24,61] This technique is nonvolitional and produces much less patient discomfort than construction of the force–frequency relationship. However, application of this test in clinical settings is relatively difficult, partly because, in the case of the diaphragm, stimulation of both phrenic nerves is required but also because it is critical for supramaximality to be attained during electrical stimulation for this test to be useful. Magnetic stimulation[62] seems to overcome some of these difficulties, making it a promising technique for obtaining an objective index of the development of muscle fatigue.[24,48,60]

Electromyography

Time Domain Analysis For respiratory muscles, as for any other skeletal muscles, a nearly linear relationship exists between muscle electrical activity and the pressure generated; the slope is related to muscle length. As a result, for a given muscle length, a decrease in the ratio respiratory muscle pressure/integrated electromyographic activity (pressure-to-integrated electromyographic activity ratio) indicates decreased muscle contractility due to the development of fatigue (see Figure 24-7). As the decrease in pressure is not accompanied by decreased integrated electromyographic activity, a decrease in this ratio indicates that neural or neuromuscular transmission factors are not responsible for the decrease in pressure, which is rather due to impaired excitation–contraction coupling.[31]

For this index to be valid, other factors affecting respiratory muscle contractility, such as muscle length, chest wall configuration, or lung volume, should be controlled or kept constant. The applicability of this method to the respiratory system is limited by the difficulty of recording the electromyographic activity of all muscles involved in normal or augmented breathing that contribute to the measured pressure.[48] Moreover, their relative contributions to the generated pressure are known to change during fatigue development.[12,39,63] In practice, the pressure-to-integrated electromyographic activity ratio can be evaluated in the diaphragm, sternocleidomastoid muscles, and abdominal muscles because their electrical activity and force production can be more easily recorded without interference from other muscles. If special precautions are not taken, electromyographic signals (particularly those recorded from the diaphragm with an esophageal electrode) can be subject to artifactual changes caused by variations in lung volume or chest wall configuration.[64] Techniques have been described in recent reports that exclude many of the artifacts associated with esophageal diaphragmatic recording, that is, electrocardiographic, electrode motion, noise, and esophageal peristalsis artifacts.[65–68] Moreover, because multielectrode arrays are used in these techniques, they reliably measure the diaphragm electromyographic amplitude and power spectrum in such a way that these variables are not affected by chest wall configuration and/or diaphragm length.[65] It is obvious that even if electromyographic activity can be accurately recorded, respiratory muscle pressures must also be reliably assessed for the pressure-to-integrated electromyographic activity ratio to be meaningful.[48] Nevertheless, time domain electromyographic assessment in patients enables the detection of fatigue during spontaneous breathing, without the need for special efforts by the patients,[31] and provides a means of determining whether observed reductions in respiratory muscle pressure are due to alterations in action potential transmission or to intrinsic alterations in peripheral muscle function (ie, impaired excitation–contraction coupling or contractile protein myofilament function).[48]

Frequency Domain Analysis Frequency domain analysis of electromyographic signals from the respiratory muscles allows detection of the occurrence of respiratory muscle fatigue because the power spectrum of electromyographic signals typically shifts to lower frequencies during fatiguing contractions.[69] Several indices of the power spectrum have been used for this purpose, including an assessment of the "center" or "centroid" frequency of the power spectrum and a "power ratio" of a high-frequency band over a low-frequency one.[48] Both of these indices decrease with fatigue and increase with recovery. With appropriate instrumentation, these analyses can be done "on-line" in spontaneously breathing subjects or patients. Shifts in the electromyographic power spectrum indicative of diaphragmatic fatigue have been documented during severe whole body exercise,[70] during loaded breathing in normal subjects,[69] in female patients during delivery,[51] and in ventilator-dependent patients during weaning failure.[71] As the electromyographic power spectral shift occurs in the diaphragm before there is failure to develop adequate force, this is a useful objective measure with which to predict the onset of fatigue[1,4] (Figure 24-11). However, the etiology of power spectral shifts with fatigue is still controversial, and the underlying cellular mechanisms remain unknown.[1,4,48] Moreover, power spectral shifts are rapidly reversed on rest or with reduced activity, even though the muscle may remain in a fatigued state. Therefore, this test cannot be taken as a reliable index of the development of muscle fatigue.[48]

Respiratory Muscle Relaxation Rate

On cessation of contraction, skeletal muscles relax at a rate determined by their relative proportions of fast and slow fibers. When muscles fatigue, their relaxation rate declines as a result of slower uptake of Ca^{2+} previously released from

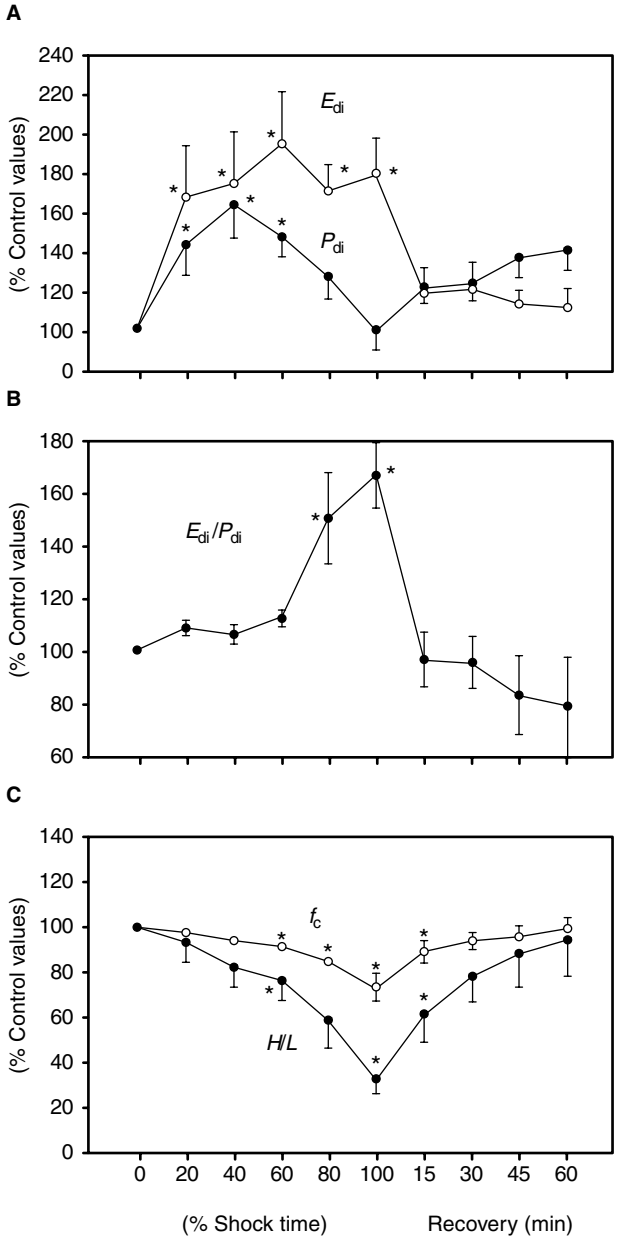

FIGURE 24-11 Changes in the peak values of integrated spontaneous electromyographic activity of the diaphragm (E_{di}) and the corresponding spontaneous transdiaphragmatic pressure (P_{di}) (*A*), ratio of E_{di} to P_{di} (E_{di}/P_{di}) (*B*), and centroid frequency (f_c) and ratio of high and low frequencies of diaphragmatic electromyographic activity (*H/L*) (*C*) during shock induced by balloon inflation in the inferior vena cava in a canine model and recovery. Means ± SE. $p < .05$ compared with control values. Although E_{di}/P_{di} rose at 80 and 100% of shock time only, both f_c and *H/L* declined immediately and progressively after decline in arterial pressure. Data from Hussain S et al.[96]

the sarcoplasmic reticulum. During various types of intermittent contraction, the rates of decay of P_{es} and P_{di} reflect the relaxation rate of the global inspiratory muscles and the diaphragm, respectively. Relaxation rate typically declines before the occurrence of muscle failure, following a time course similar to that of the change in electromyographic power spectrum.[48] On cessation of loading, relaxation rate recovers quickly and reaches baseline values within 5 to 10 minutes.[72,73] The relaxation rate of P_{es} or P_{di} can be measured during intermittent contractions against loads,[72] during sniffs with airway occlusion[73] or without airway occlusion,[74] and during phrenic nerve stimuation.[73] The most useful and simple maneuver is the unoccluded sniff, which is easy to perform for most subjects and provides large and consistent changes in relaxation rate after fatigue.[75] Inspiratory muscle relaxation rate can also be assessed in a less invasive manner by measuring nasopharyngeal or mouth pressure during sniffs with balloons positioned in these locations[74] or entirely noninvasively by using SNIP.[76] However, these less invasive techniques have been validated only in normal subjects; the transmission of brief pressure swings from the alveoli to the upper airways is likely to be dampened in patients with abnormal lung mechanics.[48]

Relaxation rate change is determined from the change in maximal relaxation rate (MRR), which is calculated as the first derivative of pressure with respect to time (dP/dt) over the first half of the relaxation curve. Because MRR increases with the amplitude of pressure swing, it is usual to normalize the MRR and to express it as a percentage of pressure fall in 10 ms.[72,75] The range of normal values for MRR is wide, with overlap between the fresh and fatigued states. Serial measurements are thus required to detect the onset of inspiratory muscle fatigue in an individual.[75]

Measurement of MRR can be used with confidence as an early sign of fatigue in healthy humans subjected to high external inspiratory loads[72–75] or to high-level hyperpnea.[76] MRR can also be used to detect fatiguing contractions during exercise in patients with COPD[77] or during trials of weaning from mechanical ventilation.[78] Because interpretation of changes in MRR is not straightforward, this test can be considered useful only for clinical research.[48]

Pressure–Time Index of Inspiratory Muscles

As previously reported in this section, PT_{es}, PT_{di}, and PT_{rc} (ie, pressure–time index of the global inspiratory muscles, diaphragm, and inspiratory muscles other than the diaphragm, respectively) characterize the operational conditions of the inspiratory muscles with respect to their fatigue threshold. Therefore, these indices may allow assessment of the risk of fatigue before actual task failure occurs.[48] However, as their critical values were established in healthy subjects breathing against external loads, critical thresholds may be different in clinical circumstances, in which a number of pathologic factors (eg, levels of tissue perfusion, presence of hypoxemia) may influence muscle performance.[48] In addition, pressure–time index assessment is dependent on accurate measurement of maximal muscle pressure (eg, $P_{di,max}$ for PT_{di}), which is often difficult in patients. Moreover, the shortening velocity of muscle fibers, that is, inspiratory flow pattern, strongly influences critical values of the pressure–time index.[43] Finally, some clinical conditions (malnutrition, steroid myopathy) change the muscle fiber populations, altering the relationship between muscle strength and fatigability.[48] For example, conditions that result in a shift to a greater concentration of slow fibers in muscle may well result in better tolerance of a given

absolute level of pressure–time index and an increase in critical pressure–time index. Therefore, as fatigue thresholds have been reported only in patients with COPD,[79,80] remaining largely untested in other pathologies, the pressure–time index should be considered a measure of inspiratory load rather than an instrument for the clinical diagnosis of fatigue.

Clinical Detection of Fatigue

Breathing Pattern: Tidal Volume and Breathing Frequency Rapid shallow breathing, characterized by high breathing frequency and low tidal volume, commonly develops in progressive respiratory failure or in unsuccessful attempts to wean patients from mechanical ventilation. These conditions are associated with increased ventilatory load and/or reduced respiratory muscle capacity and therefore potentially may lead to respiratory muscle fatigue (see Figure 24-10). However, the relationship between fatigue and breathing pattern is complex, and rapid, shallow breathing is most likely a reflex response to an increase in respiratory workload and not the consequence of respiratory muscle fatigue per se.[81] Thus, although rapid, shallow breathing may accompany respiratory muscle fatigue,[1] it cannot be considered a specific marker of fatigue.[48]

Thoracoabdominal Motion Analysis of breathing movements gives some insight into the level of recruitment and function of the respiratory muscles (in particular of the diaphragm, rib cage inspiratory muscles, and abdominal muscles).[48] Two unusual patterns of muscle recruitment may be observed in healthy subjects subjected to fatiguing inspiratory loads.[39] The first is increased variability in compartmental contributions to tidal volume, with breaths characterized by clear rib cage predominance alternating with other breaths in which abdominal motion predominates (alternating breathing or respiratory alternans)[39] (Figure 24-12). This pattern reflects alternate predominant recruitment of the inspiratory rib cage (intercostal/accessory) muscles and of the diaphragm. Because fatigue may develop separately in the diaphragm and in the inspiratory rib cage muscles,[41,42] such alternation may represent a way to postpone respiratory muscle failure.[4,39] The second pattern is paradoxical movement of one compartment, generally the abdomen, that is, an inward movement of the abdominal wall during inspiration (abdominal paradox). Abdominal paradox indicates weak, absent, or inefficient contraction of the diaphragm. These two patterns may also be observed in patients breathing against loads that might lead to fatigue,[4] as well as in patients who cannot be weaned from the ventilator[71] (Figure 24-13). However, these abnormal patterns of thoracoabdominal motion are not specific for respiratory muscle fatigue as respiratory alternans and abdominal paradox can appear immediately after institution of loaded breathing due predominantly to increased respiratory load rather than muscle fatigue.[63] Furthermore, these

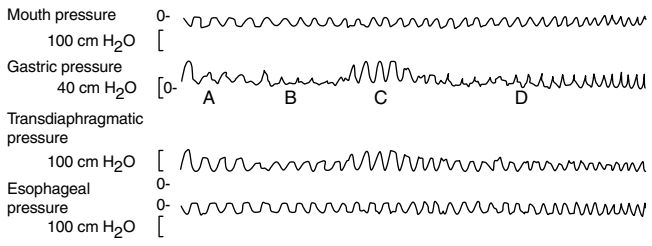

FIGURE 24-12 Tracings of an experimental run in a man breathing against an inspiratory resistive load. With each breath, the subject generated 75% of maximum mouth pressure. All pressures, except for transdiaphragmatic pressure, were measured relative to atmospheric pressure. Only gastric and transdiaphragmatic pressure varied: mouth and esophageal pressures remained constant throughout the run. Gastric pressures increased during periods A and C and declined during periods B and D, indicating alternation of inspiratory muscle recruitment. Data from Roussos C et al.[39]

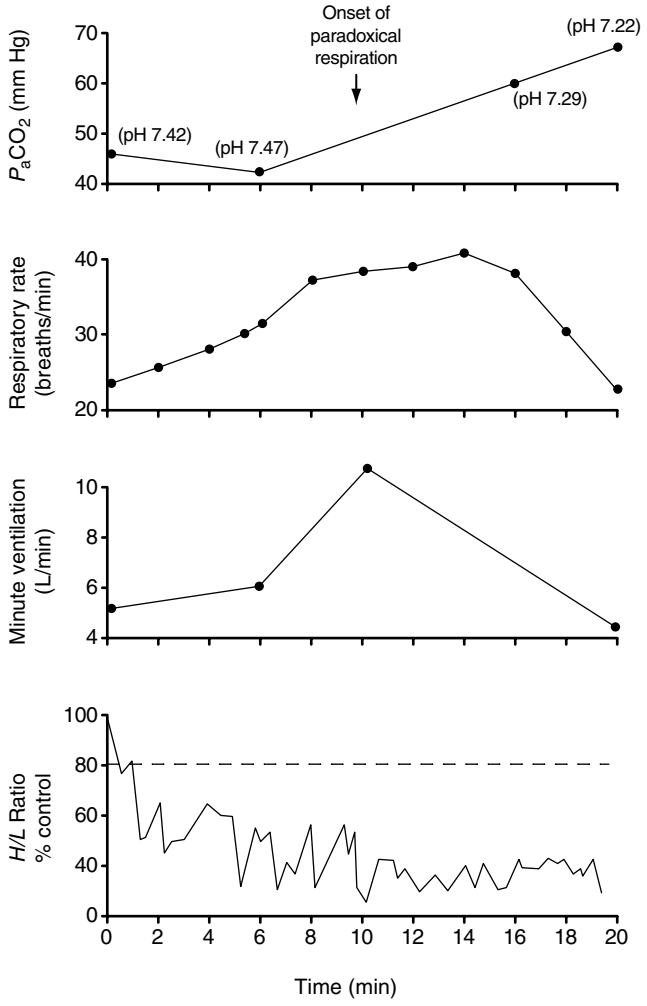

FIGURE 24-13 Sequence of changes in P_aCO_2, respiratory rate, minute ventilation, and high-frequency/low-frequency (*H/L*) ratio of the diaphragm in a patient during a 20-minute attempt at discontinuation of mechanical assistance. The initial change was the fall in *H/L* (indicating fatigue), and this was followed by a progressive increase in respiratory rate. The P_aCO_2 initially fell, and the patient became alkalemic. Paradoxical abdominal displacements were not noted until after there had been substantial increases in respiratory rate and minute ventilation. Hypercapnia and respiratory acidosis did not develop until after abdominal paradox and alternation between rib cage and abdominal breaths were noted. Just before the artificial ventilation was reinstituted, there was a sharp fall in respiratory frequency and in minute ventilation. Data from Cohen C et al.[71]

patterns can also occur, albeit to a lesser degree, during application of low, nonfatiguing respiratory loads.[63] Therefore, abnormal thoracoabdominal motion should be viewed as reflecting specific forms of respiratory muscle dysfunction (eg, diaphragmatic paresis) and/or increased ventilatory load, which in itself may or may not induce respiratory muscle fatigue.[48]

Conclusions

Of the measures and indices described, breathing pattern and thoracoabdominal motion analysis, as well as pressure–time index measurement, are useful but nonspecific tests of fatigue. Serial measurement of maximal voluntary pressures, assessment of maximum relaxation rates, time domain and frequency domain electromyographic analysis, and measurement of respiratory muscle pressures in response to electrical or magnetic nerve stimulation are all techniques that can be used to assess the evolution of respiratory muscle fatigue in the research environment. Of these techniques, serial measurement of respiratory muscle pressures in response to electrical or magnetic nerve stimulation is arguably the best technique with which to directly assess the development of respiratory muscle fatigue at the present time, and it offers the greatest promise for assessment in the clinical setting.[48]

MANAGEMENT OF RESPIRATORY MUSCLE FATIGUE

Experimental muscle fatigue develops when demands on the respiratory pump exceed pump energy supply (see Figure 24-10). However, it is not yet clear whether, in the clinical setting of ventilatory failure, overt peripheral muscle fatigue develops or whether an adaptive feedback reduction of central drive avoids such fatigue, albeit at the cost of hypoventilation.[1,4] The three components of the system (demand, supply, and neuromuscular competence) (see Figure 24-10) are closely linked, and for the patient proceeding to ventilatory failure, a small alteration in one variable may crucially determine outcome. It is rational, therefore, to direct therapeutic efforts at minimizing demand, maximizing neuromuscular competence by improving contractility and optimizing respiratory drive, and increasing energy supply to the respiratory muscles.

Decreasing the Demands on the Respiratory Muscles

If either the work of breathing or the pressure–time index increases to such a point that it exceeds a critical value, energy requirements will increase excessively and fatigue may develop. This explains the inability of normal subjects to maintain high levels of ventilation for long periods[46] or to sustain normal ventilation when the work of breathing is excessive. Therefore, in patients with increased work of breathing, fatigue may be avoided with therapy if it reduces the load on the ventilatory pump to below the fatigue threshold. In the clinical situation, this is most often achieved by treatment directed at reducing airway resistance and increasing lung compliance.

Muscle strength is an important factor influencing muscle energy demands. Therefore, pressure should be normalized by expressing it as a fraction of $P_{i,max}$ at the same fiber length (for example, P_{tidal} should be expressed as a fraction of $P_{i,max}$ measured at functional residual capacity [FRC]). The greater the work required to sustain adequate ventilation, the greater the value of $P_{tidal}/P_{i,max}$ and the greater the energy demand (see Figure 24-10). Thus, at constant pressure, energy demand will increase as $P_{i,max}$ decreases. This is of considerable physiologic significance since $P_{i,max}$ is a function of fiber length; for the respiratory muscles, therefore, it is determined in part by lung volume. Dynamic hyperinflation strongly predisposes respiratory muscles to fatigue, not only by increasing P_{tidal} but also by decreasing $P_{i,max}$.[8,39] Furthermore, if the efficiency of the respiratory muscles decreases, which occurs with an increase in airway resistance,[39,47] the oxygen cost of breathing and energy demands increase for the same muscle power, further predisposing them to fatigue. Airway obstruction frequently leads to dynamic hyperinflation, which further decreases the efficiency of the respiratory muscles by shortening fiber length, by altering the geometry of the diaphragm, and by obliging the muscles to perform an isometric contraction at the beginning of inspiration in order to overcome intrinsic positive end-expiratory pressure ($PEEP_i$).

Improving the Contractility and Endurance of the Respiratory Muscles

Rational therapy for respiratory muscle fatigue includes training, nutritional repletion, rest, and muscle pharmacotherapy. These measures prevent fatigue by improving the contractility and endurance of respiratory muscles and thereby increasing their capacity. Furthermore, as weak muscles are susceptible to fatigue, treatable or avoidable causes of weakness must not be ignored. These include hypercapnia, acidosis, hypocalcemia, hypokalemia, and hypophosphatemia, as well as inflammatory-, thyroid-, alcohol-, steroid-, and drug-induced myopathies.[1]

Pharmacologic Agents Respiratory muscle function can be modulated pharmacologically either by action at the level of excitation–contraction coupling process or by an increase in energy supply to the muscles. Drugs that act at the level of excitation–contraction coupling are xanthines[82,83] and digitalis,[84] and those that increase energy supply are isoproterenol[83] and dopamine.[85] It has been shown in many studies that theophylline at a therapeutic dose enhances respiratory muscle contractility and restores the ability of fatigued muscles to generate force, thus increasing their endurance. The effects of theophylline appear to be greater in the fatigued than in the nonfatigued state and at shorter muscle lengths (eg, during hyperinflation). Theophylline acts by facilitating the influx of Ca^{2+} through slow channels and perhaps activates Ca^{2+}-induced Ca^{2+} release from the sarcoplasmic reticulum.[82]

Training Specific training of the respiratory muscles, like that of other skeletal muscles, can enhance their strength and endurance, the latter being most relevant to patients

with chronic ventilatory loads or weaning difficulties. Respiratory muscle strength has been increased by 55% in subjects performing repeated maximal static inspiratory and expiratory pressure maneuvers.[86] When inspiratory muscle strength is increased, pressure developed per breath expressed as a fraction of the maximum will diminish, thus reducing vulnerability to fatigue.

Inspiratory resistive training in a gradually increasing, conditioning protocol constitutes the most direct approach to improving the strength and endurance of patients with ventilatory failure who are unable to stop using mechanical ventilation in order to facilitate their weaning.[87] Respiratory muscles, like limb muscles, usually respond to high-frequency/low-load contractions with an endurance-conditioning response and to low-frequency/high-load contractions with a strength-conditioning response.[4] Under some circumstances, however, specificity of conditioning is not so precise, and dual-response (ie, endurance and strength) conditioning may occur in response to a single conditioning stimulus.[86] Dual-response conditioning is most likely to occur when muscles are severely deconditioned, as may occur in ventilatory muscles following prolonged periods of mechanical ventilation, total bed rest, undernutrition, debilitating disease, or surgical trauma.[87] Thus, in mechanically ventilated patients with difficulties in weaning, less precise forms of conditioning stimuli, such as low-frequency and low-load activities, may produce improvements in both endurance and strength.[87] Nevertheless, as controlled trials are lacking, administration of training for difficult-to-wean patients is not yet standard practice.

Nutritional Repletion Malnutrition is a very important complicating factor in critically ill patients requiring mechanical ventilation, as well as in patients with a variety of chronic lung diseases. It has been shown to be associated with impaired respiratory muscle structure and function in humans; nutritional repletion can improve the strength and endurance of the ventilatory pump.[1]

Rest A logical approach to the restoration of the contractility and endurance of a fatigued muscle would be to allow the muscle to rest. Available data clearly demonstrate long-term benefit, as evidenced by improvements in the arterial partial pressure of carbon dioxide (P_aCO_2) and maximal respiratory muscle pressures, in patients with either chronic neuromuscular and chest wall disorders or severe stable COPD and carbon dioxide retention ventilated with positive- or negative-pressure noninvasive mechanical ventilation.[88,89] Although such mechanical ventilation rests the respiratory muscles, the mechanism whereby respiratory function, ventilatory failure, and symptoms are improved is not yet clear. The hypothesis that improvement in these patients is a result of respiratory muscle rest reversing muscle fatigue remains speculative.[1] This is because reduction in P_aCO_2 during periods off the ventilator may be due to resetting of the carbon dioxide setpoint, resulting from the forced reduction in P_aCO_2 in the ventilation phase, and improvement in maximal respiratory muscle pressures may be secondary to better P_aCO_2 and P_aO_2 and to a general improvement in well-being attributable to better sleep and/or to resolution of cor pulmonale.[1,4,89]

FATIGUE AS CAUSE OF VENTILATORY FAILURE

Respiratory muscle fatigue is recognized as a cause of ventilatory failure in animal studies of shock, either cardiogenic[31] or septic.[32] However, in clinical conditions with ventilatory failure, clear evidence is lacking, and fatigue remains a very likely cause of hypoventilation. Because hypercapnia occurs either acutely, as in cardiogenic shock with pulmonary edema, or chronically, as in COPD, it follows that if fatigue plays a role in carbon dioxide retention, it may do so either acutely or chronically.

Acute Hypercapnia

Fatigue and, in turn, hypercapnia of acute onset are usually due to a combination of increased mechanical load on the lung, reduced muscle strength, decreased efficiency, and reduced energy supplies to the inspiratory muscles. The mechanisms responsible for carbon dioxide retention are a decrease in minute ventilation (V_E) and an increase in dead space to V_T fraction (V_D/V_T). The sequence of events is as follows. In patients with weak and/or loaded respiratory muscles, V_T is reduced by lowering of the central discharge firing rate and inspiratory time, in order to reduce pressure per breath (P_{tidal}) and energy demand per breath (expressed by the pressure–time index) (central fatigue). In addition, according to this strategy, the respiratory muscles operate at a more optimal length that will not substantially affect their geometry since large tidal breaths force greater shortening of the muscles than small tidal breaths. This reduction in V_T is compensated for, at least in the beginning, by an increase in breathing frequency, such that V_E is maintained or increased. Consequently, since such a pattern of breathing increases V_D/V_T, P_aCO_2 will increase if V_E is preserved or may remain stable if V_E is increased proportionately. Such a frequency of breathing, however, is no longer optimal, and, for the same alveolar ventilation, energy demand will increase. Thus, although nonoptimal frequency seems to be a better option than long T_I, when coupled with the inadequate energy supply, it will finally lead to respiratory muscle peripheral fatigue. Pressure will then decrease and, as a result, V_T and V_E will decrease while V_D/V_T further increases. The reduction in pressure will obviously decrease the pressure–time index and energy demands per breath, but alveolar ventilation will be further reduced and P_aCO_2 will rise. At a later stage (eg, in patients during weaning failure or in animal models with shock), via central mechanisms, T_I increases again and respiratory frequency gradually decreases, resulting in a drop in V_E[31,71] (see Figures 24-7 and 24-13). Finally, in extreme fatigue, the CNS reduces the output signals per breath, further reducing tidal pressure and V_T, and eventually leading to respiratory arrest.

In asthma and exacerbations of COPD, which are common causes of acute hypercapnic respiratory failure, severe airway obstruction results in increased flow resistance and in rapid, shallow breathing. These factors increase the work of breathing and energy demand, leading to breathlessness

and potentially to fatigue. The latter is a very probable hazard as dynamic hyperinflation, which reduces respiratory muscle strength and efficiency, can be severe. At the same time, P_{tidal} increases excessively due to $PEEP_i$ and high resistive and elastic inspiratory loads. Hyperinflation decreases $P_{i,max}$, and, hence, $P_{tidal}/P_{i,max}$ substantially increases, potentially leading to fatigue. The blood supply to the respiratory muscles may eventually be impaired as muscular contractions become very strong, impairing bloodflow. Finally, severe lung disease may lead to hypoxemia and may reduce the amount of energy available, resulting in lactic acid production. Therefore, a constellation of factors decreases $P_{tidal}/P_{i,max}$, leading to dyspnea, fatigue, or both. Such a situation forces alveolar hypoventilation by reducing V_T, either as a way of protecting the muscles or as a consequence of failure (fatigue) of the muscles. It must be noted that, because of hyperinflation, values of $P_{tidal}/P_{i,max}$ lower than those needed at FRC are adequate to cause fatigue of the respiratory muscles.[39]

In cardiogenic shock, there is an increase in energy demand (stiff lungs, hyperventilation) and a decrease in the supply of blood to the respiratory muscles. In such a disease state, the respiratory muscles may fail. The condition has been well described in animal models, with respiratory muscle fatigue leading to severe alveolar hypoventilation, followed by bradypnea and respiratory arrest[31] (see Figure 24-7). In noncardiogenic pulmonary edema, patients need increased pressure and energy to ventilate the lungs. Coexistent severe hypoxemia due to lung damage may reduce the energy supply to the muscles. Furthermore, weakness of the respiratory muscles may be present as a result of malnutrition or sepsis. This imbalance between the capacity of the ventilatory pump and the demands placed on it may again lead to alveolar hypoventilation.

Despite the above-mentioned considerations, data on respiratory muscle function and fatigue in clinical conditions with acute ventilatory failure are sparse. A useful clinical model of acute ventilatory failure is provided by patients who are failing to sustain spontaneous breathing after discontinuation of mechanical ventilation. Recent results indicate that, in at least some patients, high inspiratory load accompanied by hyperinflation or other detrimental factors (eg, high inspiratory flow, hypoperfusion) may lead to inspiratory muscle fatigue[90] (Figure 24-14). Therefore, respiratory muscle fatigue may result in or contribute to severe acute respiratory failure requiring mechanical ventilation.

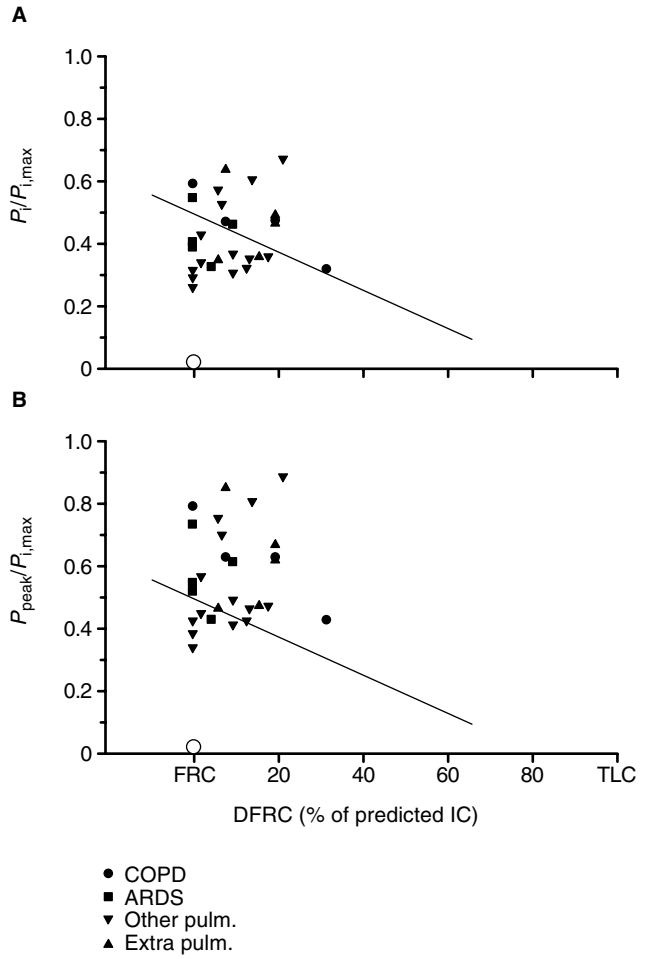

FIGURE 24-14 Pressure–volume diagram similar to that of Roussos and colleagues,[39] in which $P_i/P_{i,max}$ (A) and $P_{peak}/P_{i,max}$ (B) are plotted against dynamic increase in FRC (DFRC), expressed as a percentage of predicted inspiratory capacity (IC), in ventilator-dependent patients. $P_i/P_{i,max}$ and $P_{peak}/P_{i,max}$ are mean and peak inspiratory pressure per breath, respectively, expressed as a fraction of maximum. Each closed symbol refers to a patient. *Open circles* represent the mean values of mean and peak esophageal pressure, respectively, expressed as a fraction of maximum in 10 normal subjects. ARDS = adult respiratory distress syndrome; COPD = exacerbated chronic obstructive pulmonary disease; Extra pulm. = acute respiratory failure of extrapulmonary origin; Other pulm. = other pulmonary diseases. The *solid line* was constructed with the use of data from normal subjects, and represents the critical inspiratory pressures above which fatigue may occur. At normal FRC, the critical inspiratory pressure per breath above which fatigue may occur in normal subjects is about 50% of maximum inspiratory pressure, whereas at FRC+ $^1/_2$ IC, this critical pressure is 25 to 30% of maximum. All patients had excessively high values of both ratios, clustering around the critical line, rather than away from it, as happens in normal subjects. Data from Zakynthinos S et al.[90]

Chronic Hypercapnia

Patients who insidiously retain carbon dioxide invariably need to generate a high inspiratory pressure per breath (P_{tidal}) that is a large fraction of their $P_{i,max}$. The pressure is generated to overcome forces imposed by the chest wall (kyphoscoliosis, thoracoplasty, pleural thickening, severe obesity), by the lung (bronchitis, emphysema, bronchiectasis), or by both (scleroderma, polymyositis). In one category of patients, P_{tidal}, although normal, may be a large fraction of $P_{i,max}$ since the latter is reduced (neuromuscular disorders). It is difficult to determine the mechanism of carbon dioxide retention in such patients. However, reduction of V_T is a frequent feature and therefore may be the common pathway to carbon dioxide retention through an increase in V_D/V_T. The sequence of events is as follows. As disease progresses, P_{tidal}, $P_{tidal}/P_{i,max}$, pressure–time index, or the power required to maintain adequate ventilation increases, and the muscles become more vulnerable to dyspnea and fatigue. In

this process, the CNS may set a lower level of ventilation or may alter the pattern of breathing in order to avoid dyspnea or exhaustion (central fatigue).

When COPD patients who retain carbon dioxide were compared with those who do not, it was found that V_T and T_I were reduced in carbon dioxide retainers, whereas frequency was increased.[91] At equal V_E, V_D/V_T was higher in carbon dioxide retainers, and hence carbon dioxide levels increased. Increased V_D/V_T may be explained as follows. Patients who retain carbon dioxide have lower FEV_1 and $P_{i,max}$ values and higher effective impedance, weight, FRC, and FRC/total lung capacity (TLC) than do nonretainers of carbon dioxide[91,92] (Figure 24-15). At equal driving force ($P_{0.1}$), such a patient is better off terminating T_I early and taking a small V_T, thus avoiding substantial deviations from the optimal length and, perhaps, avoiding the substantial geometric alterations of the diaphragm and intercostal muscles that might occur with a large V_T (long T_I). In the latter case, at the end of inspiration, this type of patient may have to develop pressure approaching or exceeding the critical inspiratory pressure, leading to severe dyspnea or fatigue. In fact, although hypercapnia can be reduced in COPD patients by a voluntary change in the breathing pattern, that is, increasing V_T and decreasing frequency, it has been shown that this type of breathing cannot be tolerated for more than a few minutes before inspiratory muscle fatigue occurs.[79] In this regard, patients with COPD and severe hypercapnia developed a P_{tidal} that was 27% of $P_{i,max}$, whereas P_{tidal} in patients with no carbon dioxide retention was only 10% of $P_{i,max}$.[88] Using the results from normal subjects, in which the critical pressure for the development of fatigue at FRC is about 50% of $P_{i,max}$ and the critical pressure at FRC plus one-half inspiratory capacity is 25 to 30% of $P_{i,max}$,[39] we may place carbon dioxide retainers above or into the critical zone of fatigue, whereas nonretainers remain in the nonfatiguing zone (Figure 24-16). In patients with COPD and P_aCO_2 values of less than 45 mm Hg, this was especially evident.[92] $P_{tidal}/P_{i,max}$ was 10%, and residual volume (RV)/TLC was 50%[92]; that is, patients were certainly below the critical zone for the development of fatigue. In contrast, in patients who retained carbon dioxide, RV/TLC was 67% and $P_{tidal}/P_{i,max}$ was 27%,[92] that is, a value very likely to predispose the muscles to fatigue. Thus, in some patients, the combination of increased work of breathing due to lung disease and/or obesity, decreased mechanical efficiency due to hyperinflation and/or airway resistance, and muscle weakness due to hyperinflation and/or atrophy and undernutrition pushes the respiratory muscle to its limits. In such a predicament, central controllers (through feedback mechanism mediated by endogenous opioids and afferents via small fibers) reduce T_I and V_T, and hence P_{tidal} (central fatigue). Therefore, inspiratory muscle peripheral fatigue is avoided. In this regard, hypercapnic patients weigh their options and choose hypoventilation rather than respiratory muscle peripheral fatigue.[4,48,92]

In many other diseases characterized by chronic hypercapnia (eg, severe obesity and kyphoscoliosis), the mechanism leading to carbon dioxide retention seems to be the same as or similar to that in COPD patients.

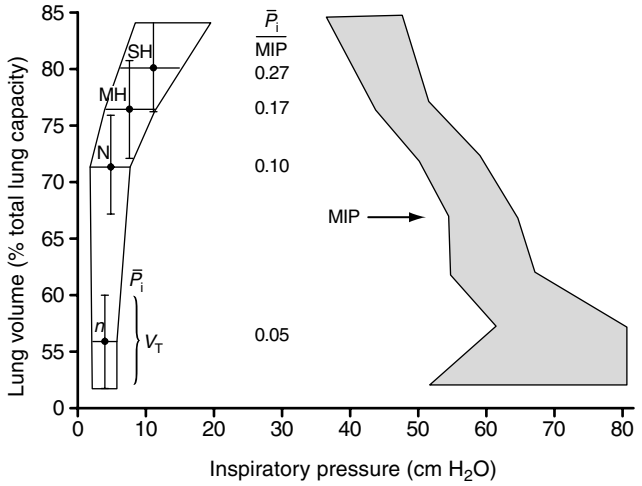

FIGURE 24-15 Relationships among lung volume, tidal pressures, and maximal inspiratory pressures (MIP) in normocapnic and hypercapnic groups of patients with COPD. The *shaded area* on the right was produced from MIP values plus 95% confidence intervals obtained at FRC in all patients and plotted against their FRC/TLC values. On the left, *vertical bars* represent the tidal volume (V_T) excursions and *horizontal bars* represent the mean (± SD) inspiratory transpulmonary pressure swing ($\bar{P}_i$) for the normocapnic (N), moderately hypercapnic (MH), and severely hypercapnic (SH) groups. A subgroup of 15 patients from the normocapnic group with the smallest FRC/TLC, with values near normal, is shown in the left lower corner. The line enclosing the area on the left connects the SD values for each group. The inspiratory muscle load ($\bar{P}_i$/MIP) for each group is given at the level of the midinspiratory volume. Data from Begin P and Grassino A.[92]

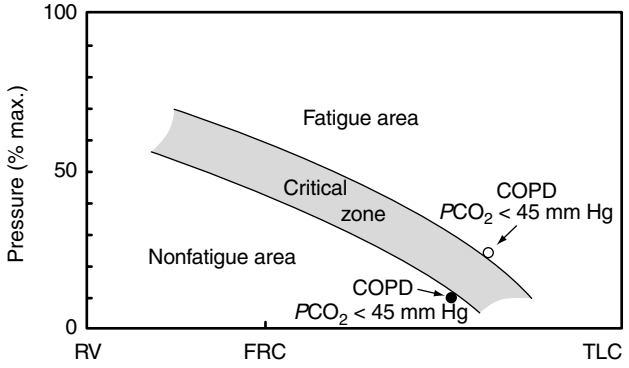

FIGURE 24-16 Effect of lung volume on critical pressure of the respiratory muscles. The diagram was constructed from findings in normal subjects breathing against high inspiratory resistance. Subjects who, at functional residual capacity (FRC) or higher lung volume, generate per-breath pressure (mouth and/or transdiaphragmatic) above the critical zone become fatigued; in contrast, in subjects whose pressure is below the critical zone, fatigue does not occur. Note that patients with chronic obstructive pulmonary disease (COPD) and carbon dioxide retention ($PCO_2 > 45$ mm Hg) are above or barely within the upper limit of the critical zone, whereas patients with no carbon dioxide retention ($PCO_2 < 45$ mm Hg) are below or barely within the lower limit of the critical zone. RV = residual volume; TLC = total lung capacity.

Weaning Failure and Fatigue

The muscles that are used most often, such as the inspiratory muscles (particularly the diaphragm), atrophy the fastest. Artificial ventilation can induce inspiratory muscle atrophy.[93] In addition, many ventilator-supported patients are malnourished, and this will further contribute to atrophy.[94] Thus, patients who are not weaned usually have inspiratory muscle weakness,[60] which leads to shortness of breath and predisposes to fatigue.[71] The question of whether respiratory muscle fatigue occurs in weaning failure patients is of major clinical importance, partly because the development of peripheral fatigue might superimpose structural injury on the already weak respiratory muscles, adversely affecting final weaning outcome.[60] However, the presence of respiratory muscle fatigue during weaning failure remains uncertain, mainly because of technical difficulties, especially in the clinical setting.[48] Indeed, the development of inspiratory muscle fatigue has been shown in several studies[71,78,88,90,95] (Figures 24-13, 24-14, 24-17, and 24-18), but most of the experimental techniques used were nonspecific,[48] raising doubt as to whether fatigue truly occurred. In a recent study, it was shown that weaning failure was not accompanied by low-frequency fatigue of the diaphragm, with the use of the best current technique of serial measurement of P_{di} in response to phrenic nerve stimulation.[60] However, the presence of neither central nor high-frequency fatigue could be excluded in this study.[60] Moreover, during weaning trials in clinical practice, mechanical ventilation is invariably resumed prior to inspiratory muscle exhaustion in patients failing to wean since many symptoms and clinical signs presage the onset of overt fatigue and task failure. Peripheral fatigue could eventually ensue, at least in many patients, in a limited time period had patients with clinical signs of weaning failure been allowed to breathe for longer.

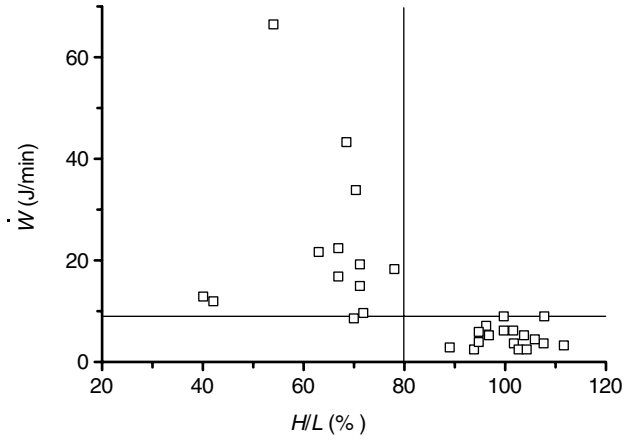

FIGURE 24-17 Plot of individual values of the respiratory muscle power ($\dot{W}$) against the *H/L* ratio of the diaphragm during weaning trials. The *H/L* ratio was expressed as a fraction of its initial value in each period. Two regions can be distinguished: (1) above a certain value of $\dot{W}$ (horizontal line), values of *H/L* were in the zone of fatigue (vertical line), and attempts to wean patients were failing; (2) below this value of $\dot{W}$, no evidence of fatigue occurred, and patients were weaned successfully. Data from Brochard L et al.[95]

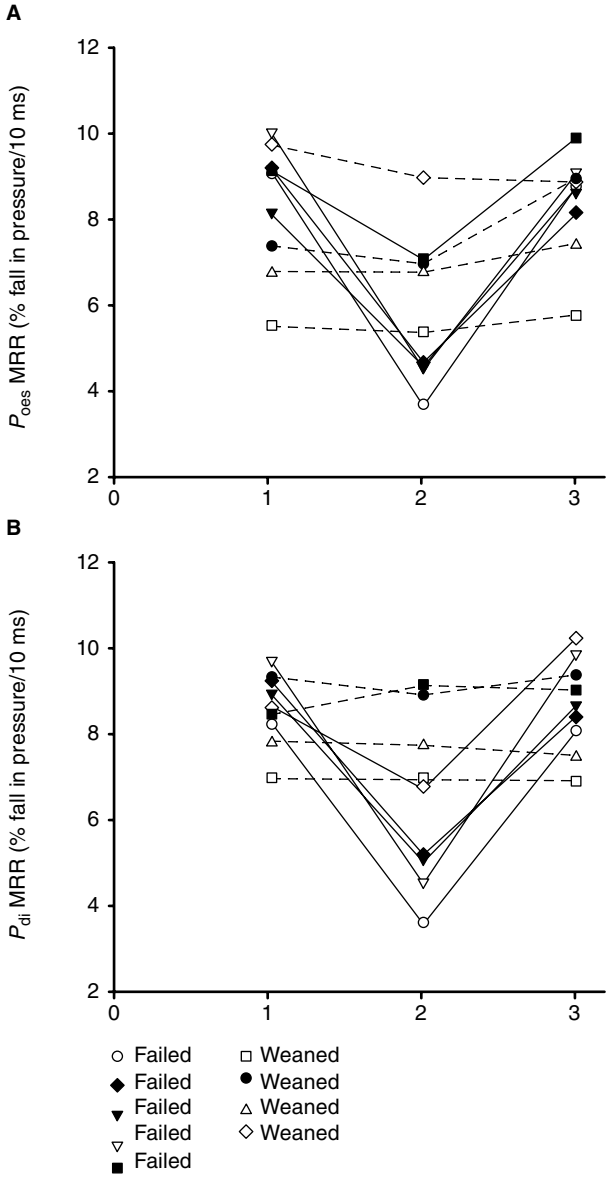

FIGURE 24-18 Sniff esophageal and transdiaphragmatic pressure maximum relaxation rates (MRRs) in nine patients undergoing a weaning tria1. MRR was measured before (1), during (2), and after (3) the weaning tria1. MRR slowed in the five patients who were not weaned, returning to normal when mechanical ventilation was resumed. In the four patients who were weaned successfully, MRR remained unchanged. Data from Goldstone JC et al.[75]

CONCLUSIONS

The inability of respiratory muscles to generate pressure, caused by fatigue and leading to ventilatory failure, is well documented only in shock. For the remaining patients with hypercapnia—acute or chronic—the evidence is not as clear. It seems that, as the work of breathing increases (eg, decreased lung and/or chest wall compliance), $P_{i,max}$ decreases (eg, neuromuscular disease, hyperinflation), or both occur concurrently (eg, acute asthma attack), and then P_{tidal} becomes a large fraction of $P_{i,max}$. The central discharge firing rate and inspiratory time are thereby reduced, and a

decrease in V_T ensues. This strategy possibly involves the small type 3 and type 4 afferents from the muscles and the endogenous opioids (central fatigue), avoids high values of P_{tidal}, and therefore minimizes dyspnea and, ultimately, peripheral fatigue. Peripheral fatigue may occur if this strategy fails.

REFERENCES

1. NHLBI Workshop. Respiratory muscle fatigue: report of the respiratory muscle fatigue workshop group. Am Rev Respir Dis 1990;142:474–80.
2. Davies WH, Haldane JS, Priestly JG. The response to respiratory resistance. J Physiol (Lond) 1919;53:60–9.
3. Bellemare F, Bigland-Ritchie B. Central components of diaphragmatic fatigue assessed by phrenic nerve stimulation. J Appl Physiol 1987;62:1307–16.
4. Roussos C, Zakynthinos S. Fatigue of the respiratory muscles. Intensive Care Med 1996;22:134–55.
5. Milner-Brown HS, Stein RB, Yemm R. The orderly recruitment of human motor units during voluntary isometric contractions. J Physiol (Lond) 1973;230:359–70.
6. Moulds RFW, Young A, Jones DA, Edwards RHT. A study of the contractility, biochemistry and morphology of an isolated preparation of human skeletal muscle. Clin Sci Mol Med 1971;50:291–7.
7. Aubier M, Farkas G, De Troyer A, et al. Detection of diaphragmatic fatigue in man by phrenic stimulation. J Appl Physiol 1981;50:538–44.
8. Bellemare F, Bigland-Ritchie B. Assessment of human diaphragm strength and activation using phrenic nerve stimulation. Respir Physiol 1984;58:263–77.
9. Merton PA. Voluntary strength and fatigue. J Physiol (Lond) 1954;13:553–64.
10. McKenzie DK, Bigland-Ritchie B, Gorman RB, Gandevia SC. Central and peripheral fatigue of human diaphragm and limb muscles assessed by twitch interpolation. J Physiol (Lond) 1992;454:643–56.
11. Scardella A, Santiago T, Edelman N. Naloxone alters the early response to an inspiratory flow-resistive load. J Appl Physiol 1989;67:1747–53.
12. Allen GM, Gandevia SC, McKenzie DK Reliability of measurements of muscle strength and voluntary activation using twitch interpolation. Muscle Nerve 1995;18:593–600.
13. Santiago T, Remolina C, Scoles V, Edelman N. Endorphins and control of breathing; ability of naloxone to restore the impaired flow-resistive load compensation in chronic obstructive pulmonary disease. N Engl J Med 1981;304: 1190–5.
14. Petrozzino JJ, Scardella A, Santiago T, Edelman N. Dichloracetate blocks endogenous opioid effects during inspiratory flow-resistive loading. J Appl Physiol 1992;72: 590–6.
15. Bellofiore S, DiMaria G, Privitera S, et al. Endogenous opioids modulate the increase in ventilatory output and dyspnea during severe acute bronchoconstriction. Am Rev Respir Dis 1990;142:812–6.
16. Bigland-Ritchie B, Johansson R, Lippold OCL, Woods JJ. Contractile speed and EMG changes during fatigue of sustained maximal voluntary contractions. J Neurophysiol 1983;50:313–24.
17. Hannerz J, Grimby L. The afferent influence on the voluntary firing rate of individual motor units in man. Muscle Nerve 1979;2:414–22.
18. Jammes Y, Buchler B, Delpierre S, et al. Phrenic afferents and their role in inspiratory control. J Appl Physiol 1986;60: 854–60.
19. Hussain SN, Magder AC, Roussos C. Chemical activation of thin fiber phrenic afferents: respiratory responses. J Appl Physiol 1990;69:1002–11.
20. Vassilakopoulos T, Zakynthinos S, Roussos C. Strenuous resistive breathing induces proinflammatory cytokines and stimulates the HPA axis in humans. Am J Physiol 1999;277: R1013–9.
21. Vassilakopoulos T, Katsaounou P, Karatza M-H, et al. Strenuous resistive breathing induces plasma cytokines. Role of antioxidants and monocytes. Am J Respir Crit Care Med 2002;166:1572–8.
22. Kosmidou I, Vassilakopoulos T, Xagorari A, et al. Production of interleukin-6 by skeletal myotubes. Role of reactive oxygen species. Am J Respir Cell Moll Biol 2002;26:587–93.
23. Kugelberg E, Lindergren B. Transmission and contraction fatigue of rat motor units in relation to succinate dehydrogenase activity of motor unit fibers. J Physiol (Lond) 1979; 288:285–300.
24. Laghi F, D'Alfonso N, Tobin MJ. Pattern of recovery from diaphragmatic fatigue over 24 hours. J Appl Physiol 1995; 79:539–46.
25. Westerblad H, Allen DG. Changes of myoplasmic calcium concentration during fatigue in single mouse muscle fibers. J Gen Physiol 1991;98:615–35.
26. Westerblad H, Lannergren J, Allen DG. Fatigue of striated muscles: metabolic aspects. In: Roussos C, editor. The thorax. 2nd ed. New York: Marcel Dekker; 1995. p. 219–31.
27. Nosek TM, Leal-Cardoso JH, McLaughlin M, Godt RE. Inhibitory influence of phosphate and arsenate on contraction of skinned skeletal and cardiac muscle. Am J Physiol 1990;259:C933–9.
28. Shindoh C, DiMarco A, Thomas A, et al. Effect of N-acetylcysteine on diaphragm fatigue. J Appl Physiol 1990;68:2107–13.
29. Anzueto A, Andrade PH, Maxwell LC, et al. Resistive breathing activates the glutathione redox cycle and impairs performance of the rat diaphragm. J Appl Physiol 1992;72:529–34.
30. Anzueto A, Supinski GS, Levine SM, Jenkinson SG. Mechanisms of disease: are oxygen-derived free radicals involved in diaphragmatic dysfunction? Am J Crit Care Med 1994;149:1048–52.
31. Aubier M, Trippenbach T, Roussos C. Respiratory muscle fatigue during cardiogenic shock. J Appl Physiol 1981;51:449–508.
32. Hussain S, Simkus G, Roussos C. Respiratory muscle fatigue: a cause of ventilatory failure in septic shock. J Appl Physiol 1985;58:2033–40.
33. Moxham J, Wiles CM, Newman D, Edwards RHT. Sternomastoid muscle function and fatigue in man. Clin Sci Mol Med 1980;59:463–8.
34. Hamnegerd C, Wragg S, Kyroussis D, et al. Diaphragm fatigue following maximal ventilation in man. Eur Respir J 1996; 9:241–7.
35. Jardim J, Farkas G, Prefaut C, et al. The failing inspiratory muscles under normoxic and hypoxic conditions. Am Rev Respir Dis 1981;124:274–9.
36. Nagesser AS, van der Laarse WJ, Elzinga G. Metabolic changes with fatigue in different types of single muscle fibres of *Xenopus laevis*. J Physiol 1992;448:511–23.
37. Westerblad H, Lannergren J. The relation between force and intracellular pH in fatigued, single Xenopus muscle fibres. Acta Physiol Scand 1988;133:83–9.
38. Monod H, Scherrer J. The work capacity of a synergistic muscular group. Ergonomics 1965;8:329–37.
39. Roussos C, Fixley M, Gross D, Macklem PT. Fatigue of inspiratory muscles and their synergic behavior. J Appl Physiol 1979;46:897–904.
40. Roussos C, Macklem PT. Diaphragmatic fatigue in man. J Appl Physiol 1977;43:189–97.

41. Bellemare F, Grassino A. Effect of pressure and timing of contraction on human diaphragm fatigue. J Appl Physiol 1982;53:1190–5.
42. Zocchi L, Fitting JW, Majani U, et al. Effect of pressure and timing of contraction on human rib cage muscle fatigue. Am Rev Respir Dis 1993;147:857–64.
43. McCool FD, Tzelepis GE, Leith DE, Hoppin FC. Oxygen cost of breathing during fatigued inspiratory resistive loads. J Appl Physiol 1989;66:2045–55.
44. Comtois A, Hu F, Grassino A. Restriction of regional blood flow and diaphragm contractibility. J Appl Physiol 1991;70: 2439–47.
45. Supinski G, Dimarco A, Ketai L, et al. Reversibility of diaphragm fatigue by mechanical hyperperfusion. Am Rev Respir Dis 1988;138:604–9.
46. Tenney SM, Reese RE. The ability to sustain great breathing effort. Respir Physiol 1968;5:187–201.
47. Collet PW, Engel LA. Influence of lung volume on oxygen cost of resistive breathing. J Appl Physiol 1986;61:16–24.
48. ATS/ERS. Statement on respiratory muscle testing. Assessment of respiratory muscle fatigue. Am J Respir Crit Care Med 2002;166:571–9.
49. Bai TR, Rabinovitch J, Pardy RL. Near-maximal voluntary hyperpnea and ventilatory muscle function. J Appl Physiol 1984;57:1742–8.
50. Loke J, Mahler DA, Virgulto JA. Respiratory muscle fatigue after marathon running. J Appl Physiol 1982;52:821–4.
51. Nava S, Zanotti E, Ambrosino N, et al. Evidence of acute diaphagmatic fatigue in a "natural" condition: the diaphragm during labor. Am Rev Respir Dis 1992;146:1226–30.
52. Bye PTP, Esau SA, Walley KR, et al. Ventilatory muscles during exercise in air and oxygen in normal men. J Appl Physiol 1984;56:464–71.
53. Miller JM, Moxham J, Green M. The maximal sniff in the assessment of diaphragm function in man. Clin Sci 1985; 69:91–6.
54. Laroche CM, Mier AK, Moxham J, Green M. The value of sniff esophageal pressures in the assessment of global inspiratory muscle strength. Am Rev Respir Dis 1988; 138:598–603.
55. Heritier F, Rahm P, Pasche P, Fitting JW. Sniff nasal inspiratory pressure: a noninvasive assessment of inspiratory muscle strength. Am J Respir Crit Care Med 1994;150:1678–83.
56. Uldry C, Fitting JW. Maximal values of sniff nasal inspiratory pressure in healthy subjects. Thorax 1995;50:371–5.
57. Yan S, Gauthier AP, Similowski T, et al. Force–frequency relationships of in vivo human and in vitro diaphragm using paired stimuli. Eur Respir J 1993;6:211–8.
58. Polkey MI, Kyroussis D, Hamnegard CH, et al. Paired phrenic nerve stimuli for the detection of diaphragm fatigue in humans. Eur Respir J 1997;10:1859–64.
59. Polkey MI, Hamnegard CH, Hughes PD, et al. Influence of acute lung volume change on contractile properties of human diaphragm. J Appl Physiol 1998;85:1322–8.
60. Laghi F, Cattapan SE, Jubran A, et al. Is weaning failure caused by low-frequency fatigue of the diaphragm? Am J Respir Crit Care Med 2003;167:120–7.
61. Wragg S, Hamnegard C, Road J, et al. Potentiation of diaphragmatic twitch after voluntary contraction in normal subjects. Thorax 1994;49:1234–7.
62. Similowski T, Fleury B, Launois S, et al. Cervical magnetic stimulation: a new painless method for bilateral phrenic nerve stimulation in conscious humans. J Appl Physiol 1989;67: 1311–8.
63. Tobin MJ, Perez W, Guenther SM, et al. Does rib cage-abdominal paradox signify respiratory muscle fatigue? J Appl Physiol 1987;63:851–60.
64. Gandevia SC, McKenzie DK. Human diaphragmatic EMG: changes with lung volume and posture during supramaximal phrenic stimulation J Appl Physiol 1986;60:1420–8.
65. Beck J, Sinderby C, Weinberg J, Grassino A. Effects of muscle-to-electrode distance on the human diaphragm electromyogram. J Appl Physiol 1995;79:975–85.
66. Sinderby C, Lindstrom L, Comtois N, Grassino A. Effects of diaphragm shortening on the mean action potential conduction velocity in canines. J Physiol (Lond) 1996;490: 207–14.
67. Sinderby CA, Comtois A, Thomson R, Grassino AE. Influence of the bipolar electrode transfer function on the electromyogram power spectrum. Muscle Nerve 1996;19: 290–301.
68. Sinderby C, Lindstrom L, Grassino AE. Automatic assessment of electromyogram quality. J Appl Physiol 1995;79: 1803–15.
69. Gross D, Grassino A, Ross WRD, Macklem PT. Electromyogram pattern of diaphragmatic fatigue. J Appl Physiol 1979;46:1–7.
70. Pardy RL, Bye PTP. Diaphragmatic fatigue in normoxia and hyperoxia. J Appl Physiol 1985;58:738–42.
71. Cohen C, Zagelbaum G, Gross D, et al. Clinical manifestations of inspiratory muscle fatigue. Am J Med 1982;73: 308–16.
72. Esau SA, Bellemare F, Grassino A, et al. Changes in relaxation rate with diaphragmatic fatigue in humans. J Appl Physiol 1983;54:1353–60.
73. Esau SA, Bye PTP, Pardy RL. Changes in rate of relaxation of sniffs with diaphragmatic fatigue in humans. J Appl Physiol 1983;55:731–5.
74. Koulouris N, Vianna LG, Mulvey DA, et al. Maximal relaxation rates of esophageal, nose, and mouth pressures during a sniff reflect inspiratory muscle fatigue. Am Rev Respir Dis 1989;193:1213–7.
75. Mador MJ, Kufel TJ. Effect of inspiratory muscle fatigue on inspiratory muscle relaxation rates in healthy subjects. Chest 1992;102:1767–73.
76. Kyroussis D, Mills G, Hamnegard CH, et al. Inspiratory muscle relaxation rate assessed from sniff nasal pressure. Thorax 1994;49:1127–33.
77. Kyroussis D, Polkey MI, Keilty SEJ, et al. Exhaustive exercise slows inspiratory muscle relaxation rate in chronic obstructive pulmonary disease. Am J Respir Crit Care Med 1996;153:787–93.
78. Goldstone JC, Green M, Moxham J. Maximum relaxation rate of the diaphragm during weaning from mechanical ventilation. Thorax 1994;49:54–60.
79. Bellemare F, Grassino A. Force reserve of the diaphragm in patients with chronic obstructive pulmonary disease. J Appl Physiol 1983;55:8–15.
80. Vassilakopoulos T, Zakynthinos S, Roussos C. The tension–time index and frequency–tidal volume ratio are the major pathophysiologic determinants of weaning failure and success. Am J Respir Crir Care Med 1988;158:378–85.
81. Tobin MJ, Perez W, Guenther SM, et al. The pattern of breathing during successful and unsuccessful trials of weaning from mechanical ventilation. Am Rev Respir Dis 1986; 134:1111–8.
82. Aubier M, Murciano D, Viires N, et al. Diaphragmatic contractility enhanced by aminophylline: role of extracellular calcium. J Appl Physiol 1983;54:460–4.
83. Howell S, Roussos C. Isoproterenol and aminophylline improve contractility of fatigued canine diaphragm. Am Rev Respir Dis 1984;129:118–24.
84. Aubier M, Viires N, Murciano D, et al. Effects of digoxin on diaphragmatic strength generation. J Appl Physiol 1986; 6:1767–74.

85. Aubier M, Murciano D, Menu Y, et al. Dopamine effects on diaphragmatic strength during acute respiratory failure in chronic obstructive pulmonary disease. Ann Intern Med 1989;110:107–23.
86. Leith DE, Bradley M. Ventilatory muscle strength and endurance training. J Appl Physiol 1976;41:508–16.
87. Aldrich TK, Karpel JP, Uhrlass RM, et al. Weaning from mechanical ventilation: adjunctive use of inspiratory muscle resistive training. Crit Care Med 1989;17:143–7.
88. Goldstein RS, Molotiu N, Skrastins R, et al. Reversal of sleep-induced hypoventilation and chronic respiratory failure by nocturnal negative pressure ventilation in patients with restrictive ventilatory impairment. Am Rev Respir Dis 1987; 135:1049–55.
89. Elliott MW, Mulvey DA, Moxham J, et al. Domiciliary nocturnal nasal intermittent positive pressure ventilation in COPD: mechanisms underlying changes in arterial blood gas tensions. Eur Respir J 1991;4:1049–52.
90. Zakynthinos S, Vassilakopoulos T, Roussos C. The load of inspiratory muscles in patients needing mechanical ventilation. Am J Respir Crit Care Med 1995;152:1248–55.
91. Sorli J, Grassino A, Loragne G, Millic-Emili J. Control of breathing in patients with chronic obstructive lung disease. Clin Sci Mol Med 1978;54:295–304.
92. Begin P, Grassino A. Inspiratory muscle dysfunction and chronic hypercapnia in chronic obstructive pulmonary disease. Am Rev Respir Dis 1991;143:905–12.
93. Sassoon CS, Ciaozzo VJ, Manka A, Sieck GC. Altered diaphragm contractile properties with controlled mechanical ventilation. J Appl Physiol 2002;92:2585–95.
94. Lewis MI, Lorusso TJ, Zhan WZ, Sieck GC. Interactive effects of denervation and malnutrition on diaphragm structure and function. J Appl Physiol 1996;81:2165–72.
95. Brochard L, Harf A, Lorino H, Lemaire F. Inspiratory pressure support prevents diaphragmatic fatigue during weaning from mechanical ventilation. Am Rev Respir Dis 1989;139: 513–21.
96. Hussain S, Marcotte JE, Burnet H, et al. Relationship among EMG and contractile responses of the diaphragm elicited by hypotension. J Appl Physiol 1988;65:649–56.

CHAPTER 25

VENTILATORY MUSCLE INJURY

Xiangyu Wang, Tian-Xi Jiang, W. Darlene Reid, Jeremy Road

Our current understanding of ventilatory muscle injury has largely been derived from morphologic observations. Early attempts at phrenic pacing showed that high-frequency stimulation led to morphologic evidence of myopathy or injury in the diaphragm.[1] However, it was not until Reid and colleagues[2] showed diaphragmatic injury in hamsters with tracheal banding, causing a resistive load to breathing, that it became clear that injury can occur with physiological phrenic motor neuron firing rates. Muscle injury in skeletal muscles has been related to the strength of the contraction, the type of contraction (eccentric more than concentric), and the resting condition of the muscle.[3] The diaphragm has been shown to be activated at high levels during loaded breathing[4,5] and to contract in a nonuniform way in different regions, which could predispose to injury.[6] In addition, a variety of muscle disorders can promote injury in the ventilatory muscles.

Contraction-induced muscle injury has been defined as a structural alteration of the muscle as evidenced by disrupted and degenerating cytoplasm, internal nuclei, broadened interstitium, and increased nuclearity representing inflammatory and/or regenerative cells. Ultrastructurally, sarcolemmal defects, swollen organelles, and disruptions of the sarcomere, including the cytoskeleton, have been shown. In limb muscles, a delayed-onset muscle soreness, reduced force, and increased muscle protein levels in the blood have been demonstrated; however, the time course of each of these events is often not correlated with the degree of muscle injury.

Muscle fatigue is defined by loss of force that recovers with rest. With contraction-induced muscle injury, there is a considerable force loss, and it can persist. Indeed, the main force loss occurs several days after the initial injury, is termed secondary muscle injury, and is associated with muscle inflammation.[7] Force loss at this time is evidenced by reduced responses to both high-frequency and low-frequency stimulation, and therefore low-frequency fatigue and muscle injury are dissimilar. Recovery from injury is slow and is associated with regeneration. In many instances, the regenerated muscle undergoes changes that render it less susceptible to repeated injury.[8]

Fatigue, weakness, and muscle injury can all manifest as reduced force output. Clinically, it is difficult to differentiate among these three causes of reduced diaphragmatic force output, and it is quite possible for these three entities to occur coincidentally in the same patient. Determining the underlying cause of poor ventilatory muscle function is necessary to specifically delineate therapeutic interventions to improve weaning success, to minimize ventilatory failure, and to decrease dyspnea.

Recently, much has been learned about the prevalence of muscle injury in clinical conditions, whether it is exertion overload or muscle disease. Exertion has definitively been shown to induce diaphragm injury in animal models. This association between exertion or overuse and muscle diaphragm injury is more tenuous for human subjects, and other factors, such as medications, aging, and comorbid conditions, may contribute to the ventilatory muscle morphologic abnormalities observed. The development of serum muscle protein assays, such as for troponin and myosin,[9,10] may expand our ability to detect ventilatory muscle injury at the bedside in the future.

The evidence for diaphragm muscle injury in animal models and diaphragm injury in human subjects is discussed in the following sections, followed by a summary of the factors that can contribute to the development of ventilatory muscle injury, the clinical implications of ventilatory muscle injury, and some proposed strategies for intervention.

EVIDENCE OF DIAPHRAGM MUSCLE INJURY IN ANIMAL MODELS

Because of the difficulty in obtaining human diaphragmatic muscle samples, animal models have been used to show ventilatory muscle injury. In addition, other extraneous variables can be more easily controlled in these models than in human studies. Ventilatory muscle injury in animal models using electrical stimulation, resistive loading, experimental

emphysema, corticosteroids, aging, ischemia–reperfusion, sepsis, and diaphragm inactivity are discussed.

Electrical Stimulation

Direct electrical stimulation of the diaphragm or phrenic nerve can produce muscle injury.[11,12] In an in vivo model, stimulating electrodes were apposed directly to the hamster diaphragm. The most remarkable feature of this model was the profound influx of neutrophils observed infiltrating the muscle tissue within 30 minutes and invading individual muscle fibers within a few hours after stimulation.[13] In a rabbit model, 1 and 2 days after phrenic nerve stimulation, inflammation and injury were observed in the diaphragm. In this model, the cellular infiltrate appeared to be primarily mononuclear rather than polymorphonuclear in nature. The amount of injury varied between regions and among animals, with the sternal region being affected to the greatest degree.

The amount of diaphragm injury has been shown to be directly related to the tension–time index (TT_{di}), a parameter that increases as a function of the intensity and duration of contractions; this index is calculated from the mean tension × total stimulation time of the contraction. In an in vitro model, diaphragm strips from Sprague-Dawley rats were set at optimal length for force generation and were stimulated electrically while being superfused with a physiologic solution containing procion orange for the identification of cells whose sarcolemmal membranes were disrupted. Various values of TT_{di} were produced by stimulation with 100 Hz for 3 minutes. A significant positive correlation between TT_{di} and the percentage of fibers with injured sarcolemma was seen. The capacity to recover force was inversely proportional to the number of injured fibers.[14]

Resistive Loading

Injury and force loss have been demonstrated in the rabbit diaphragm after inspiratory resistive loading with a target airway opening pressure of 45 cm H_2O for 1.5 hours. The pressure–time index at this level of load corresponds to ~0.23, which is well above the fatigue threshold of 0.15 reported in the literature.[14] Three days after the bout of resistive loading, muscle biopsy specimens taken from the diaphragm and intercostal muscles demonstrated significant secondary muscle injury in the resistive loading group compared with the controls. The biopsy specimens showed necrotic muscle fibers, inflammatory cells, and widening of the interstitium, which also contained inflammatory cells (Figure 25-1). The cross-sectional areas of the abnormal muscles and connective tissue in the diaphragms of the resistive loading group were higher than those in the controls. The area fractions of abnormal muscle and connective tissue in the resistive loading group averaged 7.3 ± 1.3% and 8.0±0.6%, respectively, compared with control values of 1.1 ± 0.2% and 5.7 ± 0.2%.[15]

In another study[7] in which the rabbits were subjected to the same level of inspiratory resistive loading (IRL), the in vivo diaphragmatic muscle function was measured 3 days after the loading, as reflected by the transdiaphragmatic pressure (P_{di}) swings during bilateral supramaximal stimulation of the phrenic nerves. To minimize the effect of changes in chest wall and diaphragm configuration during phrenic nerve stimulation, the upper part of the abdomen, including the lower part of the rib cage, was bound with an inflated cuff.[7] The P_{di}– frequency values in the IRL group were approximately 30% lower than control values at both high and low frequencies ($p < .01$ at most of the stimulation frequencies). In vitro diaphragm physiologic studies showed similar diaphragmatic force loss (30 to 40%) as found in vivo.[16]

The amount of force loss (30 to 40%) far exceeded the amount of morphologic abnormality (6%). This phenomenon is also seen in limb muscle injury and is not well explained. It is speculated that the disproportionately greater force loss compared with the amount of diaphragm tissue injury seen on histologic examination is probably due to the following reasons. First, light microscopy of muscle sections may not reveal the ultrastructural abnormalities and molecular abnormalities that occurred with injury. Second, muscle injury may occur focally within a myofiber, so that a single tissue cross-section would not show the total proportion of muscle fibers injured at other points along the length of the muscle.[7]

Another model used to induce ventilatory muscle injury is tracheal banding of rodents for several days. After 6 days of tracheal banding of hamsters, hypoxemia and respiratory acidosis were noted.[2] Hematoxylin and eosin (H&E)-stained cross-sections showed a higher area fraction of abnormal muscle in the costal and crural regions of the diaphragm of banded animals. Electron micrographs showed disorganization of the myofibrils, loss of distinct A and I bands, and Z-band streaming. The diaphragm of banded hamsters showed increased rates of degradation of tropomyosin and α-actin.[2] The degree of diaphragm injury and inflammation peaked at 3 days after banding.[17] This temporal pattern coincides with the secondary muscle injury observed in limb muscles.[18]

A study of tracheal banding for 30 days in hamsters also showed deterioration in arterial blood gases and structural abnormalities in the diaphragm. The diaphragm demonstrated evidence of injury and repair, as shown by increased abnormal and inflamed muscle, and a greater variation in fiber size. The diaphragm showed reduced stress in vitro that was attributable to abnormal muscle structure and, to a lesser extent, an increased proportion of type I fibers, a decreased proportion of type 2b fibers, and a tendency for an increase in connective tissue.[19]

Experimental Emphysema

Experimental emphysema induced by a transtracheal injection of elastase in hamsters for 5 weeks[2,20] or 6 months[21–23] has been employed as an animal model to study the effect of pulmonary hyperinflation on diaphragm function and morphology. In a 5-week model, some abnormalities were observed on H&E-stained diaphragm cross-sections from hamsters with experimental emphysema, but stereologic analysis of injury by point counting of H&E-stained cross-sections did not show any significant differences in the area fractions of abnormal and inflamed muscle compared with control values.[2]

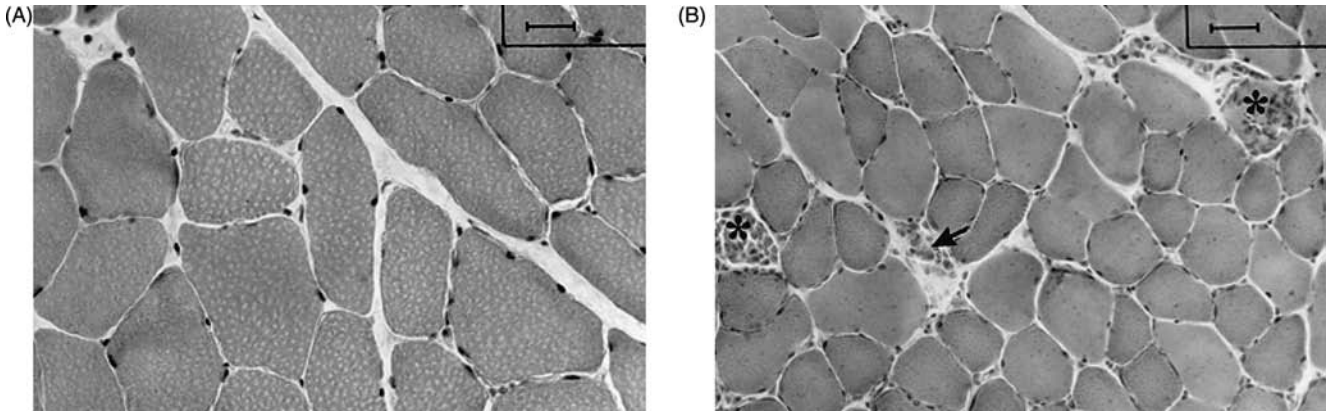

FIGURE 25-1 Light photomicrographs of H&E-stained cross-sections of costal diaphragm from a control rabbit (*A*) and a rabbit subjected to high-intensity inspiratory resistive loading (IRL) (*B*). In *A*, scale bar = 25 μm; in *B*, scale bar = 50 μm. Note necrotic fibers (*), fiber degeneration, and influx of inflammatory cells (*arrows*) in the diaphragm cross-sections (*B*) from the IRL rabbit.

In a 6-month model, optimal diaphragm length for force generation was significantly shorter in the emphysematous hamster than in the control diaphragms. Maximal specific force (ie, force per unit area) was 25% lower in emphysematous hamsters than in control diaphragms. Cross-sectional areas of type II fibers were 30% greater in emphysematous hamsters than in control diaphragms. The number of capillaries surrounding both type I and II fibers increased in the diaphragms of emphysematous hamsters, but in proportion to the hypertrophy of these fibers.[24] In old animals with emphysema, twitch and tetanic forces were reduced by 28% and 14%, respectively, compared with age-matched controls. The diaphragms in emphysematous hamsters showed distinct muscle fiber damage, including Z-line dislocation, disarray of myofibrils, misaligned sarcomeres, focal degeneration, focal necrosis, and segmental necrosis and more signs of suboptimal regeneration (fiber splitting and forking) and abortive regeneration.[25]

Corticosteroids

Depending on the type of steroid, the dose, and the duration of treatment, the corticosteroid-induced defects range from alterations in energy metabolism to muscle weakness with underlying muscle wasting and histologic abnormalities.[26,27] Myonecrosis, vacuolization, excess of internal nuclei, and larger than normal variation of fiber type diameter were observed after administration of cortisone acetate,[28] prednisolone, and triamcinolone.[29] Wilcox and colleagues[30] showed angulated fibers and a more aggregate staining pattern of succinate dehydrogenase but no necrosis after triamcinolone administration. Nava and colleagues[31] observed no necrotic and myogenic changes in the diaphragm after 5 days of prednisolone or triamcinolone administration.

Examination of diaphragm function after the administration of fluorinated and nonfluorinated steroids has provided equivocal results.[29,30,32–38] The reasons for these discrepancies are unclear but may relate to the type, dose, and duration of treatment and the different experimental protocols used to measure diaphragm force.

Aging

Age-related changes in the diaphragm in animal models include atrophy of type IIb fibers, changes in myosin heavy-chain composition,[39] increased fiber grouping suggestive of denervation and innervation,[39,40] increases in both collagen concentration and content of nonreducible collagen cross-linking,[41] and decreased capillary density.[39] Diaphragmatic force-generating capacity has been shown to decrease with age.[41,42] The aged diaphragm becomes more resistant to fatigue in vitro but at the expense of slower contraction.[43] The susceptibility of postnatal day 15 and adult rat diaphragms to acute injury after repetitive activations was examined in vitro. At maximal activation (75 Hz and a lengthening velocity of 1.0 optimal length/s), the maximum force measured during the isometric phase and that measured during the isovelocity lengthening phase were both greater in adult diaphragms than in 15-day-old diaphragms, but both declined to a greater extent in adults with repetitive activation. Ultrastructural analysis showed a greater prevalence of Z-line streaming and sarcomeric disruption in the adult. Diaphragms from older rats were more susceptible to injury than those from young adults.[44]

Although skeletal muscle has the capacity to regenerate itself, this process is not activated by the gradual age-related loss of muscle fibers.[45] The endocrine, autocrine, and paracrine environment in old muscle is less supportive of protein synthesis, re-innervation of muscle fibers, and satellite cell activation, proliferation, and differentiation. There is little information on the effects of aging on the repair and regenerative capacity of the respiratory muscles.

Ischemia–Reperfusion Injury

Tissue damage occurring during revascularization following a prolonged period of critical ischemia is termed reperfusion injury. Nearly all of the ischemia–reperfusion injuries investigated in skeletal muscle studies have been in limb muscle. Does ischemia–reperfusion injury occur in respiratory muscle? It seems unlikely that the blood supply to the diaphragm is ever totally occluded because this muscle is supplied by a number of interconnected arteries.[46] It does

seem, possible, however, that segments of this muscle may be appreciably underperfused during periods of severe systemic hypotension. Another factor that may affect the susceptibility of the diaphragm to partial ischemia is higher levels of xanthine oxidase in the diaphragm than in the heart or limb skeletal muscle.[47] In addition, the ischemic contracting diaphragm produces large quantities of hypoxanthine, the substrate for the reaction catalyzed by xanthine oxidase.[48] As a result, both the substrate and enzyme responsible for generating free radicals during reperfusion may be present in relatively high concentrations in the diaphragm during significant systemic hypotension. Thus, there are reasons to believe that the diaphragm may, in some way, be especially susceptible to ischemia–reperfusion injury, and the mechanisms responsible for ischemia–reperfusion-induced limb muscle injury may also result in ischemia–reperfusion-induced diaphragm injury.

Aubier and colleagues reported that the ventilatory failure in cardiogenic shock was due to an impairment of the contractile process of the respiratory muscle.[49] Supinski and colleagues reported that periods of ischemia, followed by reperfusion, produced a downward shift of the diaphragm force–frequency relationship and also markedly increased diaphragm fatigability.[50] Interestingly, the diaphragm is also susceptible to ischemia–reperfusion injury of distant organs. The lower torso ischemia–reperfusion injury, secondary to temporary aortic cross-clamping in Sprague-Dawley rats, resulted in significant diaphragmatic twitch and tetanic dysfunction.[51]

Thus, diaphragmatic ischemia or mediators released as a result of ischemia elsewhere may impair diaphragm function. To date, however, injury secondary to ischemia–reperfusion has not been demonstrated morphologically in the diaphragm.

Sepsis

It has been well established that sepsis, endotoxemia, and bacteremia are associated with significant diaphragmatic dysfunction and sarcolemmal injury in animal models.[52–55] The proposed mechanisms include failure of neuromuscular transmission, failure of excitation–contraction coupling, the cytotoxic effect of nitric oxide and its metabolites, free radicals, and ubiquitin–proteasome proteolysis.[56–58] Diaphragm sarcolemmal injury has been shown to occur after both acute (4 h) intraarterial endotoxin administration and subacute (24 h) peritonitis induced by cecal ligation and perforation, as indicated by hyperpermeability of myofibers to a low-molecular-weight tracer dye.[52] This finding was consistent with sepsis-induced sarcolemmal damage and consequent impairment of myofiber structural integrity. Sarcolemmal injury was significantly correlated with reductions in the resting membrane potential (E_m) of single diaphragm myofibers. Macrophages were seen in the septic muscles, primarily in perivascular areas but also in the endomysial space.[52] Finally, the early use of mechanical ventilation has been found to decrease the sarcolemmal injury and attenuate the associated diaphragmatic dysfunction.[55] The relationship between the sarcolemmal injury reported in these studies and the muscle injury described previously with associated necrosis is not clear. They may represent a spectrum of pathology, with the early changes reflecting damage to the sarcolemma.

Diaphragmatic Inactivity/Mechanical Ventilation

Several researchers have demonstrated the detrimental effects of controlled mechanical ventilation (CMV) on diaphragm force-generating capacity,[59–62] and in one study[59] these effects were isolated from the confounding factors of anesthesia, neuromuscular junction-blocking agent, and positive end-expiratory pressure.

The diaphragmatic myofibril damage observed after 3 days of CMV was inversely correlated with maximal diaphragmatic force.[63] Down-regulation of the diaphragm insulin-like growth factor-I and MyoD/myogenin messenger ribonucleic acid occurred after 24 hours and diaphragmatic oxidative stress and increased protease activity after 18 hours. In keeping with these findings, diaphragm fiber atrophy was shown after 12 hours of CMV and reduced diaphragm mass after 48 hours.[63] After mechanical ventilation, electron microscopic observations of the diaphragm muscle revealed disrupted myofibrils, increased numbers of lipid vacuoles in the sarcoplasm, and smaller mitochondria with focal membrane disruptions suggestive of early muscle injury. The volumetric and numerical densities of the mitochondria were significantly lower in the CMV group than in the control group. A study of mitochondrial respiration showed minor changes in oxidative phosphorylation coupling in diaphragmatic mitochondria.[64] Nerve conduction and neuromuscular transmission were not affected during 5 days of prolonged mechanical ventilation.[61]

All the studies consistently showed a profound reduction in diaphragm force-generating capacity after CMV. The most recent study showed that 18 hours of mechanical ventilation enhanced diaphragmatic fatigue resistance but impaired diaphragmatic specific tension.[65] In comparison with the control group, diaphragms from CMV-treated animals generated less absolute specific force throughout the fatigue protocol. It is noteworthy that although some alterations in myofibrillar proteins and cellular structure were found, no overt inflammation was reported in these models of reduced diaphragm activity.

DIAPHRAGM INJURY IN HUMAN SUBJECTS

There are many clinical conditions that produce ventilatory muscle weakness, adversely affecting the function of ventilatory muscles and predisposing ventilatory muscles to injury via a variety of mechanisms, such as by increasing the work of breathing. Table 25-1 summarizes the clinical conditions and the potential mechanisms by which they may contribute to ventilatory muscle injury.

More recently, diaphragm injury has been examined in patients with a broad range of airflow limitation. Furthermore, the amount of injury has been quantified at both the light microscopic and ultrastructural levels. In contrast, early studies examining ventilatory muscle injury included small samples[66] or case reports of adults,[67] large samples of infants,[66,68] or observations of the accessory

Table 25-1 Conditions and Mechanisms That May Contribute to Ventilatory Muscle Injury

Clinical disorders	*Examples*	*Possible mechanisms*
Obstructive lung disease	Chronic bronchitis, emphysema, bronchiectasis, cystic fibrosis, asthma, and bronchiolitis	Altered diaphragm geometry, hypoxia, hypercapnia, low pH, and increased work of breathing
Restrictive lung disease	Pulmonary fibrosis, diseases of the pleura or chest wall	Increased work of breathing and hypoxia
Neuromuscular disease	Amyotrophic lateral sclerosis, myasthenia gravis, muscular dystrophies, various myopathies (congenital, metabolic, and inflammatory)	Ventilatory muscle weakness, muscle inflammation, deficiency of dystrophin, decreased compliance, increased work of breathing, hypoxia, hypercapnia, low pH
Sepsis	Bacterial infection/septic shock	Effects of endotoxin and cytokines on muscles
Immobilization	Patients receiving neuromuscular blockade, long-term bed rest, mechanical ventilation	Ventilatory muscle atrophy and weakness; increased degradation
Malnutrition	COPD, starvation	Muscle atrophy and weakness
Aging	Weakened diaphragm in aged patients or animals	Increased susceptibility to muscle injury; inhibition of muscle repair and regeneration capacity
Toxin- and drug-induced myopathies	Use of corticosteroids, alcohol, opiates, lipid-lowering drugs, venom, d-penicillin, and many others	Muscle weakness, myopathies with inflammation, multifocal necrosis, phagocytosis, regeneration

COPD = chronic obstructive pulmonary disease.

muscles of respiration in individuals with relatively mild-to-moderate airflow limitation.[69,70]

Diaphragm injury was found to be related to increasing airflow limitation in a group of patients with a wide range of forced expiratory volume in 1 second values (16 to 122% of predicted).[71] Most of the patients in this cohort had undergone a thoracotomy for lung resection of cancer, and a few had undergone resection of emphysematous regions. The most common abnormality was internally nucleated fibers, and relatively little inflammation was observed. Diaphragm injury was quantified using computer-assisted point counting of H&E-stained cross-sections, and the combined percentage of connective tissue and abnormal muscle was found to be 34% of the cross-sectional area.

Orozco-Levi and colleagues[72] examined sarcomeric disruption in the diaphragms of patients with and without chronic obstructive pulmonary disease (COPD) attending for thoracotomy or abdominal surgery. They found that this type of injury was common, and the range of values was wide 1.3 to 17.3%. The effect of inspiratory loading (an incremental threshold loading test) was examined in a subset of seven COPD and five control patients. The subjects breathed against incremental loads until the maximal pressure was reached. The greatest amount of sarcomeric disruption in the diaphragm was found in COPD patients who had undergone prior inspiratory threshold loading, followed by COPD patients who had not undergone prior inspiratory threshold loading. Hyperinflation was directly correlated with the amount of diaphragm injury. Interestingly, they reported that signs of necrosis, inflammatory cells, or specific fiber type groupings were not observed in the diaphragms of their groups of patients.

Diaphragm injury has also been shown in patients with heart failure compared with control subjects.[73] Common features were tubular aggregates, internal nuclei, abnormal myosin staining, and cores. These abnormalities were more common in the diaphragm than in the other muscles examined, which included the quadriceps femoris, sternothyroid, and pectoralis major muscles. The authors also found that patients with idiopathic dilated cardiomyopathy had the greatest number of abnormalities.

Postmortem examination of the diaphragm has revealed many abnormalities. In a sample of 59 subjects, increased connective tissue and internal nuclei in myofibers were common morphologic abnormalities observed in the diaphragm. Figures 25-2 and 25-3 show the most common abnormalities observed in the human diaphragm. Men with acute respiratory disease had more abnormal diaphragms than men without respiratory disease. Macrophages were the most common leukocyte type observed.[74] In a continuation of this study, a more selective group of patients was examined; midcostal biopsies from six COPD patients and six age- and gender-matched subjects without respiratory disease were obtained.[75] The COPD diaphragms had a greater area fraction of collagen than those without respiratory disease (mean $\pm$ SE: $24.2 \pm 1.0\%$ vs $18.6 \pm 1.1\%$, $p < .001$) and a greater proportion of abnormal muscle fibers ($28.4 \pm 7.2\%$ vs $12.0 \pm 1.3\%$, $p < .05$). The COPD diaphragms displayed features of acute and chronic injury, including necrosis, degenerated cytoplasm, and fibrosis. Further examination of differences between muscles showed that the area fraction of collagen in the crural diaphragm was smaller than in the midcostal diaphragm ($18.0 \pm 0.6\%$ vs $20.9 \pm 0.6\%$, $p < .01$), as was the proportion of abnormal fibers ($11.9 \pm 2.5\%$ vs $14.6 \pm 2.6\%$). The psoas muscle had a lower proportion of abnormal fibers ($8.3 \pm 2.2\%$) and a lower area fraction of collagen ($12.3 \pm 0.5\%$) than the midcostal ($p < .01$) and crural ($p < .001$) diaphragms.

In two large-scale studies, the diaphragms of infants were examined, 125 neonates[66] and 242 infants who had died from sudden infant death syndrome (SIDS).[68] Contraction band necrosis, which is characterized by myofibrillar disorganization with hypercontracted fibers, was the most common finding in the neonates,[66] whereas coagulative necrosis was the most common finding in the SIDS infants.[68] The characteristics of coagulative necrosis have been described as intense eosinophilia, a glassy appearance, and diminished or absent striations affecting parts of the cell. Other abnormal features included inflammatory cells, atrophy, hypertrophied and rounded fibers, and fibrous scarring.[68]

Injury to the accessory muscles of inspiration has been examined by two different groups.[69,70] Both groups examined

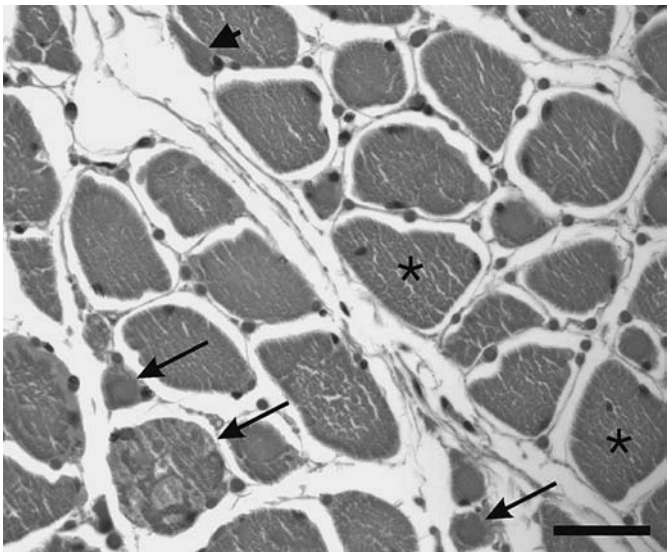

FIGURE 25-2 Light photomicrograph of abnormal morphology in H&E-stained cross-section of human diaphragm. *Arrows* indicate muscle fibers with abnormal cytoplasm; the *arrowhead* indicates an atrophic fiber; *asterisks* indicate centrally nucleated fibers. Scale bar = 50 μm.

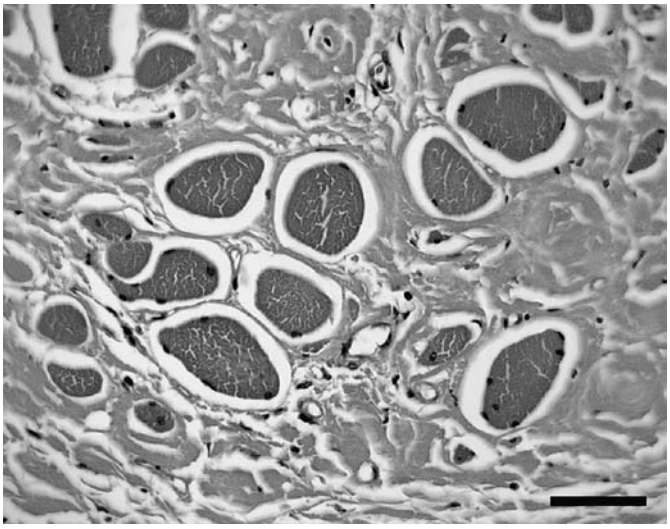

FIGURE 25-3 Light photomicrograph of H&E-stained cross-section of human diaphragm. Note the increased connective tissue surrounding normal-sized and several very atrophic fibers. Scale bar = 50 μm.

the internal and external intercostal muscles and the latissimus dorsi muscle in patients undergoing thoracotomy. The abnormalities observed included variations in fiber size, angular fibers, targeting, inflammatory cells, necrotic fibers, basophilic fibers, fiber splitting, internal nuclei, ragged red fibers, Z-banding streaming, and fiber grouping. Both groups of investigators quantified abnormalities by the presence or absence of the feature rather than the proportion of the cross-sectional area affected. Hards and colleagues[69] found the greatest amount of abnormal features in the external intercostal muscles, whereas Campbell and colleagues[70] found that most abnormalities were in the internal intercostal muscles.

A variety of drugs and toxins can produce muscle injury, and there is no reason to suspect that the ventilatory muscles are not similarly affected. For example, the statins inhibit electron transport by inhibiting hydroxymethylglutaryl coenzyme A reductase and can produce profound rhabdomyolysis.[76] Toxins such as alcohol can produce acute rhabdomyolysis.[77] Systemic diseases can cause myopathy. These diseases can affect the respiratory muscles and include dermatomyositis, polymyositis, and inclusion body myositis.[78–83] Myositis due to graft-versus-host disease can produce diaphragmatic weakness.[84]

In the intensive care unit, the concomitant administration of muscle relaxants and glucocorticoids to mechanically ventilated individuals can cause muscle damage and result in "critical illness myopathy." More than two-thirds of such patients are affected. Initially, after discontinuation of the muscle relaxants, there is a period of denervation and loss of muscle excitation.[85,86] Subsequently, a slowly recovering myopathy occurs. The myopathy shows a selective loss of thick filaments (myosin) and patchy necrosis.[87] To date, there have been no morphologic studies of the diaphragm or other ventilatory muscles in these patients. However, affected patients are known to have significant weakness of the ventilatory muscles that can impede weaning from mechanical ventilation.[86]

The underlying mechanisms contributing to diaphragm injury are probably multifactorial. Overloading of the diaphragm due to increased ventilatory demands, as commonly seen in patients with increased airflow limitation,[71] COPD, and COPD combined with threshold loading,[72] has been related to diaphragm injury in humans. Other factors, such as reduced bloodflow, disuse, aging, and medications, that have myopathic effects may also contribute to disruptions in diaphragm muscle at the light microscopic and ultrastructural levels. It is worth noting that positive adaptations of the inspiratory muscles have been shown in patients with chronic airflow limitation. Levine and colleagues[88] and Mercadier and colleagues[89] found an increase in the slow-twitch characteristics of the diaphragm, which would increase fatigue resistance in COPD patients compared with control individuals. Inspiratory muscle training increased the proportion of type I fibers (by 38%) and the size of type II fibers (by 21%) in the external intercostal muscles of patients with COPD.[90] It would appear that injury and incomplete repair require an exertional overload combined with other compounding factors. Finally, the specific subgroups of patients who are most susceptible to the deleterious effects of overwhelming injury resulting in fibrosis rather than muscle regeneration have yet to be determined.

INTERVENTION STRATEGIES

As described in previous sections, ventilatory muscle injury can be produced under different circumstances, such as following a relatively long period of chronic low-intensity respiratory loading or a short period of acute high-intensity IRL in animal models and was found to be present in patients with respiratory disorders characterized by

Table 25-2 Interventions and Mechanisms That Prevent or Attenuate Muscle/Diaphragm Injury[91–104]

Intervention	*Mechanisms of action*	*Examples*	*References*
Exercise training	Adaptation/conditioning effect, lasting up to 6 months, but overloading can induce muscle injury as well	Bouts of exercise at appropriate intervals	Nosaka et al[91]
Nonsteroidal agents	Antiinflammatory effects	Diclofenac (Voltaren) Indomethacin	O'Grady et al[92] Salminen and Kihlstrom[93]
Anabolic agents	Increases in muscle mass; enhancing muscle cell regeneration	Nandrolone	Verheul et al[94]
Steroids	Antiinflammatory effect and promotes myotube formation in regenerating muscle, but long-term use or high dose can result in muscle injury or myopathy	Prednisone; deflazacort (an oxazoline derivative of prednisolone)	Jacobs et al[95] Anderson et al[96] Anderson and Vargas[97]
β_2-Adrenoceptor agonists	Reduce dystrophic muscle degeneration	Clenbuterol	Zeman et al[98]
Sex hormone	Antioxidant characteristics and increases in membrane stability	Estrogen	Carter et al[99] Bar et al[100]
Free radical scavengers	Scavenge free radicals in the diaphragm	Polyethylene glycol superoxide dismutase, *N*-acetylcysteine, mannitol	Jiang et al[16]
Dietary/nutritional supplements	Increase antioxidant activity in the muscles	Vitamin E, vitamin C	Goldfarb[101]
Ca^{2+} channel blockers	Affect the flux of Ca^{2+} over the sarcoplasmic membrane and protect the muscle from injury	Dantrolene sodium, nifedipine	Amelink et al[102] Duarte et al[103]
Myostatin blockade	Inhibition of the myostatin gene product, to increase muscle mass and strength, and to improve phenotype in myopathies	Intraperitoneal injections of blocking antibodies	Bogdanovich et al[104]

increased work of breathing, such as COPD. Since ventilatory muscle injury has been demonstrated to have negative functional implications in animal models, such as reduced diaphragm force-generating capacity, it is of clinical and therapeutic importance to explore the intervention strategies to prevent the development of respiratory muscle injury or attenuate the respiratory muscle injury.

To this end, some studies have been conducted to explore the intervention strategies that might prevent exertion-induced injury in skeletal muscles. However, all the intervention measures proposed so far are largely experimental in nature and require further investigation. Nevertheless, these proposed measures and potential mechanisms to prevent or attenuate muscle injury in one way or another are summarized in Table 25-2.[91–104]

SUMMARY AND CONCLUSIONS

There is abundant evidence that the ventilatory muscles, particularly the diaphragm, can be damaged during loaded breathing in animal models. Evidence is emerging that this damage also occurs in a variety of clinical situations. Exertion-induced muscle injury may also occur at lower levels of exertion in conditions where the muscle is more susceptible, that is, myopathies and dystrophies, or in the presence of sepsis or after prolonged immobilization by mechanical ventilation. Injury can lead to muscle regeneration, and this regenerated muscle is more resistant to injury during repeated loading. However, muscle regeneration is not guaranteed. The balance between muscle injury and the muscle's ability to regenerate will determine whether the ventilatory muscles can maintain their contractile properties.

REFERENCES

1. Ciesielski TE, Fukuda Y, Glenn WW, et al. Response of the diaphragm muscle to electrical stimulation of the phrenic nerve. A histochemical and ultrastructural study. J Neurosurg 1983;58:92–100.
2. Reid WD, Huang J, Bryson S, et al. Diaphragm injury and myofibrillar structure induced by resistive loading. J Appl Physiol 1994;76:176–84.
3. Faulkner JA, Brooks SV, Opiteck JA. Injury to skeletal muscle fibers during contractions: conditions of occurrence and prevention. Phys Ther 1993;73:911–21.
4. Road JD, Cairns AM. Phrenic motoneuron firing rates before, during, and after prolonged inspiratory resistive loading. J Appl Physiol 1997;83:776–83.
5. Sinderby C, Spahija J, Beck J, et al. Diaphragm activation during exercise in chronic obstructive pulmonary disease. Am J Respir Crit Care Med 2001;163:1637–41.
6. Wakai Y, Leevers AM, Road JD. Regional diaphragm shortening measured by sonomicrometry. J Appl Physiol 1994;77:2791–6.
7. Jiang TX, Reid WD, Road JD. Delayed diaphragm injury and diaphragm force production. Am J Respir Crit Care Med 1998;157(3 Pt 1):736–42.
8. Proske U, Morgan DL. Muscle damage from eccentric exercise: mechanism, mechanical signs, adaptation and clinical applications. J Physiol 2001;537(Pt 2):333–45.
9. Sorichter S, Mair J, Koller A, et al. Skeletal troponin I as a marker of exercise-induced muscle damage. J Appl Physiol 1997;83:1076–82.
10. Simpson JA, Labugger R, Hesketh GG, et al. Differential detection of skeletal troponin I isoforms in serum of a patient with rhabdomyolysis: markers of muscle injury? Clin Chem 2002;48:1112–14.
11. Reid WD, Blogg T, Wiggs BJ, et al. Diaphragmatic plate electrode stimulation of the hamster diaphragm. J Appl Physiol 1989;67:1341–8.

12. Dechman G, Belzberg A, Reid WD. Single-photon emission computed tomography imaging of diaphragm overuse injury in rabbits. Am J Respir Crit Care Med 1998;153: A600.
13. Reid WD, MacGowan NA. Respiratory muscle injury in animal models and humans. Mol Cell Biochem 1998;179:63–80.
14. Zhu E, Comtois AS, Fang L, et al. Influence of tension time on muscle fiber sarcolemmal injury in rat diaphragm. J Appl Physiol 2000;88:135–41.
15. Jiang TX, Reid WD, Belcastro A, et al. Load dependence of secondary diaphragm inflammation and injury after acute inspiratory loading. Am J Respir Crit Care Med 1998; 157:230–6.
16. Jiang TX, Reid WD, Road JD. Free radical scavengers and diaphragm injury following inspiratory resistive loading. Am J Respir Crit Care Med 2001;164:1288–94.
17. Reid WD, Belcastro AN. Time course of diaphragm injury and calpain activity during resistive loading. Am J Respir Crit Care Med 2000;162:1801–6.
18. Friden J, Sjostrom M, Ekblom B. Myofibrillar damage following intense eccentric exercise in man. Int J Sports Med 1983; 4:170–6.
19. Reid WD, Belcastro AN. Chronic resistive loading induces diaphragm injury and ventilatory failure in the hamster. Respir Physiol 1999;118:203–18.
20. Oliven A, Supinski GS, Kelsen SG. Functional adaptation of diaphragm to chronic hyperinflation in emphysematous hamsters. J Appl Physiol 1986;60:225–31.
21. Heunks LM, Bast A, van Herwaarden CL, et al. Effects of emphysema and training on glutathione oxidation in the hamster diaphragm. J Appl Physiol 2000;88:2054–61.
22. van Balkom RH, Dekhuijzen PN, van der Heijden HF, et al. Effects of anabolic steroids on diaphragm impairment induced by methylprednisolone in emphysematous hamsters. Eur Respir J 1999;13:1062–9.
23. Van Der Heijden HF, Dekhuijzen PN, Folgering H, et al. Long-term effects of clenbuterol on diaphragm morphology and contractile properties in emphysematous hamsters. J Appl Physiol 1998;85:215–22.
24. Lewis MI, Zhan WZ, Sieck GC. Adaptations of the diaphragm in emphysema. J Appl Physiol 1992;72:934–43.
25. Machiels HA, Verheul AJ, Croes HJ, et al. Ultrastructural changes in the diaphragm of aged emphysematous hamsters. Basic Appl Myol 2002;12:203–10.
26. LaPier TK. Glucocorticoid-induced muscle atrophy. The role of exercise in treatment and prevention. J Cardiopulm Rehabil 1997;17:76–84.
27. Van Balkom RH, van der Heijden HF, van Herwaarden CL, Dekhuijzen PN. Corticosteroid-induced myopathy of the respiratory muscles. Neth J Med 1994;45:114–22.
28. Ferguson GT, Irvin CG, Cherniack RM. Effect of corticosteroids on respiratory muscle histopathology. Am Rev Respir Dis 1990;142:1047–52.
29. Dekhuijzen PN, Gayan-Ramirez G, de Bock V, et al. Triamcinolone and prednisolone affect contractile properties and histopathology of rat diaphragm differently. J Clin Invest 1993;92:1534–42.
30. Wilcox PG, Hards JM, Bockhold K, et al. Pathologic changes and contractile properties of the diaphragm in corticosteroid myopathy in hamsters: comparison to peripheral muscle. Am J Respir Cell Mol Biol 1989;1:191–9.
31. Nava S, Gayan-Ramirez G, Rollier H, et al. Effects of acute steroid administration on ventilatory and peripheral muscles in rats. Am J Respir Crit Care Med 1996;153(6 Pt 1):1888–96.
32. Moore BJ, Miller MJ, Feldman HA, Reid MB. Diaphragm atrophy and weakness in cortisone-treated rats. J Appl Physiol 1989;67:2420–6.
33. Viires N, Pavlovic D, Pariente R, Aubier M. Effects of steroids on diaphragmatic function in rats. Am Rev Respir Dis 1990;142:34–38.
34. Van Balkom RH, van der Heijden HF, van Moerkerk HT, et al. Effects of different treatment regimens of methylprednisolone on rat diaphragm contractility, immunohistochemistry and biochemistry. Eur Respir J 1996;9:1217–23.
35. Van Balkom RH, Dekhuijzen PN, Folgering HT, et al. Effects of long-term low-dose methylprednisolone on rat diaphragm function and structure. Muscle Nerve 1997;20:983–90.
36. Dekhuijzen PN, Gayan-Ramirez G, Bisschop A, et al. Rat diaphragm contractility and histopathology are affected differently by low dose treatment with methylprednisolone and deflazacort. Eur Respir J 1995;8:824–30.
37. Sasson L, Tarasiuk A, Heimer D, Bark H. Effect of dexamethasone on diaphragmatic and soleus muscle morphology and fatigability. Respir Physiol 1991;85:15–28.
38. Van Balkom RH, Zhan WZ, Prakash YS, et al. Corticosteroid effects on isotonic contractile properties of rat diaphragm muscle. J Appl Physiol 1997;83:1062–7.
39. Tolep K, Kelsen SG. Effect of aging on respiratory skeletal muscles. Clin Chest Med 1993;14:363–78.
40. Bass A, Gutmann E, Hanzlikova V. Biochemical and histochemical changes in energy supply enzyme pattern of muscles of the rat during old age. Gerontologia 1975;21:31–45.
41. Gosselin LE, Johnson BD, Sieck GC. Age-related changes in diaphragm muscle contractile properties and myosin heavy chain isoforms. Am J Respir Crit Care Med 1994;150: 174–8.
42. Criswell D, Powers S, Herb R, et al. Mechanism of specific force deficit in the senescent rat diaphragm. Respir Physiol 1997;107:149–55.
43. Rodrigues CJ, Rodrigues Junior AJ, Bohm GM. Effects of aging on muscle fibers and collagen content of the diaphragm: a comparison with the rectus abdominis muscle. Gerontology 1996;42:218–28.
44. Watchko JF, Johnson BD, Gosselin LE, et al. Age-related differences in diaphragm muscle injury after lengthening activations. J Appl Physiol 1994;77:2125–33.
45. Welle S. Cellular and molecular basis of age-related sarcopenia. Can J Appl Physiol 2002;27:19–41.
46. Comtois A, Gorczyca W, Grassino A. Anatomy of diaphragmatic circulation. J Appl Physiol 1987;62:238–44.
47. Khalidi V, Chaglasssian T. The species distribution of xanthine oxidase. Biochem J 1965;97:318–20.
48. Ketai LH, Grum CM, Supinski GS. Tissue release of adenosine triphosphate degradation products during shock in dogs. Chest 1990;97:220–6.
49. Aubier M, Trippenbach T, Roussos C. Respiratory muscle fatigue during cardiogenic shock. J Appl Physiol 1981;51: 499–508.
50. Supinski G, Stofan D, DiMarco A. Effect of ischemia–reperfusion on diaphragm strength and fatigability. J Appl Physiol 1993;75:2180–7.
51. McLaughlin R, Kelly CJ, Kay E, Bouchier-Hayes D. Diaphragmatic dysfunction secondary to experimental lower torso ischaemia–reperfusion injury is attenuated by thermal preconditioning. Br J Surg 2000;87:201–5.
52. Lin MC, Ebihara S, El Dwairi Q, et al. Diaphragm sarcolemmal injury is induced by sepsis and alleviated by nitric oxide synthase inhibition. Am J Respir Crit Care Med 1998;158(5 Pt 1):1656–63.
53. El-Dwairi Q, Comtois A, Guo Y, et al. Endotoxin-induced skeletal muscle contractile dysfunction: contribution of nitric oxide synthases. Am J Physiol 1998;274(3 Pt 1):C770–9.
54. Comtois AS, Barreiro E, Huang PL, et al. Lipopolysaccharide-induced diaphragmatic contractile dysfunction and

sarcolemmal injury in mice lacking the neuronal nitric oxide synthase. Am J Respir Crit Care Med 2001;163: 977–82.
55. Ebihara S, Hussain SN, Danialou G, et al. Mechanical ventilation protects against diaphragm injury in sepsis: interaction of oxidative and mechanical stresses. Am J Respir Crit Care Med 2002;165:221–8.
56. Hussain SN. Respiratory muscle dysfunction in sepsis. Mol Cell Biochem 1998;179:125–34.
57. Callahan LA, Nethery D, Stofan D, et al. Free radical-induced contractile protein dysfunction in endotoxin-induced sepsis. Am J Respir Cell Mol Biol 2001;24:210–17.
58. Laghi F. Curing the septic diaphragm with the ventilator. Am J Respir Crit Care Med 2002;165:145–6.
59. Sassoon CS, Caiozzo VJ, Manka A, Sieck GC. Altered diaphragm contractile properties with controlled mechanical ventilation. J Appl Physiol 2002;92:2585–95.
60. Anzueto A, Peters JI, Tobin MJ, et al. Effects of prolonged controlled mechanical ventilation on diaphragmatic function in healthy adult baboons. Crit Care Med 1997;25: 1187–90.
61. Radell PJ, Remahl S, Nichols DG, Eriksson LI. Effects of prolonged mechanical ventilation and inactivity on piglet diaphragm function. Intensive Care Med 2002;28: 358–64.
62. Powers SK, Shanely RA, Coombes JS, et al. Mechanical ventilation results in progressive contractile dysfunction in the diaphragm. J Appl Physiol 2002;92:1851–8.
63. Gayan-Ramirez G, Decramer M. Effects of mechanical ventilation on diaphragm function and biology. Eur Respir J 2002; 20:1579–86.
64. Bernard N, Matecki S, Py G, et al. Effects of prolonged mechanical ventilation on respiratory muscle ultrastructure and mitochondrial respiration in rabbits. Intensive Care Med 2003;29:111–8.
65. Shanely RA, Coombes JS, Zergeroglu AM, et al. Short-duration mechanical ventilation enhances diaphragmatic fatigue resistance but impairs force production. Chest 2003;123: 195–201.
66. Silver M, Smith CR. Diaphragmatic contraction band necrosis in a perinatal and infantile autopsy population. Human Pathol 1992;23:817–27.
67. Lloreta J, Orozco M, Gea J, et al. Selective diaphragmatic mitochondrial abnormalities in a patient with marked air flow obstruction. Ultrastruct Pathol 1996;20:67–71.
68. Kariks J. Diaphragmatic muscle fibre necrosis in SIDS. Forensic Sci Int 1989;43:281–91.
69. Hards JM, Reid WD, Pardy RL, et al. Respiratory muscle fiber morphometry: correlation with pulmonary function and nutrition. Chest 1990;97:1037–44.
70. Campbell JA, Hughes RL, Sahgal V, et al. Alterations in intercostal muscle morphology and biochemistry in patients with obstructive lung disease. Am Rev Respir Dis 1980;122: 679–86.
71. Macgowan NA, Evans KG, Road JD, Reid WD. Diaphragm injury in individuals with airflow obstruction. Am J Respir Crit Care Med 2001;163:1654–9.
72. Orozco-Levi M, Lloreta J, Minguiella J, et al. Injury of the human diaphragm associated with exertion and chronic obstructive pulmonary disease. Am J Respir Crit Care Med 2001;164:1734–9.
73. Lindsay DC, Lovegrove CA, Dunn MJ, et al. Histological abnormalities of muscle from limb, thorax and diaphragm in chronic heart failure. Eur Heart J 1996;17:1239–50.
74. Reid WD, Jiang TX, Road J, Elliot WM. Human diaphragm injury, size variation, and inflammation [ID#1255]. In: International Congress of Physiological Sciences; 2001 August; Chirstchurch, New Zealand. Available at: www.iups2001.org.nz (accessed May 01, 2003).
75. Scott A, Road JD, Reid WD. Collagen and injury in the diaphragm of chronic obstructive pulmonary disease patients postmortem. Am J Respir Crit Care Med 2003;167:A413.
76. Pierce LR, Wysowski DK, Gross TP. Myopathy and rhabdomyolysis associated with lovastatin–gemfibrozil combination therapy. JAMA 1990;264:71–5.
77. Pascuzzi RM. Drugs and toxins associated with myopathies. Curr Opin Rheumatol 1998;10:511–20.
78. Lundberg I, Ulfgren AK, Nyberg P, et al. Cytokine production in muscle tissue of patients with idiopathic inflammatory myopathies. Arthritis Rheum 1997;40:865–74.
79. Dalakas MC. Polymyositis, dermatomyositis and inclusion-body myositis. N Engl J Med 1991;325:1487–98.
80. Schiavi EA, Roncoroni AJ, Puy RJ. Isolated bilateral diaphragmatic paresis with interstitial lung disease. An unusual presentation of dermatomyositis. Am Rev Respir Dis 1984;129:337–9.
81. Selva-O'Callaghan A, Sanchez-Sitjes L, Munoz-Gall X, et al. Respiratory failure due to muscle weakness in inflammatory myopathies: maintenance therapy with home mechanical ventilation. Rheumatology (Oxf) 2000;39:914–6.
82. Cohen R, Lipper S, Dantzker DR. Inclusion body myositis as a cause of respiratory failure. Chest 1993;104:975–7.
83. Rubin LA, Urowitz MB. Shrinking lung syndrome in SLE—a clinical pathologic study. J Rheumatol 1983;10:973–6.
84. Stephenson AL, Mackenzie IR, Levy RD, Road J. Myositis associated graft-versus-host-disease presenting as respiratory muscle weakness. Thorax 2001;56:82–4.
85. Rich MM, Teener JW, Raps EC, et al. Muscle is electrically inexcitable in acute quadriplegic myopathy. Neurology 1996;46: 731–6.
86. Road J, Mackie G, Jiang TX, et al. Reversible paralysis with status asthmaticus, steroids, and pancuronium: clinical electrophysiological correlates. Muscle Nerve 1997;20: 1587–90.
87. Lacomis D, Giuliani MJ, Van Cott A, et al. Acute myopathy of intensive care: clinical, electromyographic, and pathological aspects. Ann Neurol 1996;40:645–54.
88. Levine S, Kaiser L, Leferovich J, Tikunov B. Cellular adaptations in the diaphragm in chronic obstructive pulmonary disease. N Engl J Med 1997;337:1799–806.
89. Mercadier JJ, Schwartz K, Schiaffino S, et al. Myosin heavy chain gene expression changes in the diaphragm of patients with chronic lung hyperinflation. Am J Physiol 1998; 274(4 Pt 1):L527–34.
90. Ramirez-Sarmiento A, Orozco-Levi M, Guell R, et al. Inspiratory muscle training in patients with chronic obstructive pulmonary disease: structural adaptation and physiologic outcomes. Am J Respir Crit Care Med 2002; 166:1491–7.
91. Nosaka K, Sakamoto K, Newton M, Sacco P. How long does the protective effect on eccentric exercise-induced muscle damage last? Med Sci Sports Exerc 2001;33:1490–5.
92. O'Grady M, Hackney AC, Schneider K, et al. Diclofenac sodium (Voltaren) reduced exercise-induced injury in human skeletal muscle. Med Sci Sports Exerc 2000;32:1191–6.
93. Salminen A, Kihlstrom M. Protective effect of indomethacin against exercise-induced injuries in mouse skeletal muscle fibers. Int J Sports Med 1987;8:46–9.
94. Verheul AJ, Ennen L, Hafmans T, Dekhuijzen PNR. Effects of anabolic steroids on diaphragm muscle injury in aged emphysematous hamsters. Am J Respir Crit Care Med 2003; 167(7 Suppl):A415.
95. Jacobs SC, Bootsma AL, Willems PW. Prednisone can protect against exercise-induced muscle damage. J Neurol 1996; 243:410–6.

96. Anderson JE, McIntosh LM, Poettcker R. Deflazacort but not prednisone improves both muscle repair and fiber growth in diaphragm and limb muscle in vivo in the mdx dystrophic mouse. Muscle Nerve 1996;19: 1576–85.
97. Anderson JE, Vargas C. Correlated NOS-Imu and myf5 expression by satellite cells in mdx mouse muscle regeneration during NOS manipulation and deflazacort treatment. Neuromusc Disord 2003;13:388–96.
98. Zeman RJ, Peng H, Danon MJ, Etlinger JD. Clenbuterol reduces degeneration of exercised or aged dystrophic (mdx) muscle. Muscle Nerve 2000;23:521–8.
99. Carter A, Dobridge J, Hackney AC. Influence of estrogen on markers of muscle tissue damage following eccentric exercise. Fiziol Cheloveka 2001;27:133–7.
100. Bar PR, Amelink GJ, Oldenburg B, Blankenstein MA. Prevention of exercise-induced muscle membrane damage by oestradiol. Life Sci 1988;42:2677–81.
101. Goldfarb AH. Nutritional antioxidants as therapeutic and preventive modalities in exercise-induced muscle damage. Can J Appl Physiol 1999;24:249–66.
102. Amelink GJ, Van der Kallen CJ, Wokke JH, Bar PR. Dantrolene sodium diminishes exercise-induced muscle damage in the rat. Eur J Pharmacol 1990;179:187–92.
103. Duarte JA, Soares JM, Appell HJ. Nifedipine diminishes exercise-induced muscle damage in mouse. Int J Sports Med 1992;13:274–7.
104. Bogdanovich S, Krag TO, Barton ER, et al. Functional improvement of dystrophic muscle by myostatin blockade. Nature 2002;420:418–21.

CHAPTER 26

RESPIRATORY CONSEQUENCES OF NEUROMUSCULAR DISEASE

Stefan Matecki, Basil J. Petrof

The diaphragm and other respiratory muscles constitute the ventilatory pump upon which the act of breathing depends. In many neuromuscular disorders, muscle weakness involves the respiratory muscles to an equal or even greater extent than other skeletal muscles. The degree of limb muscle weakness cannot be used as a reliable guide to the presence of respiratory muscle impairment since the correlation between the two may be quite poor.[1,2] Respiratory symptoms are often initially minimal because of the inherently large reserve of the respiratory system. Respiratory muscle involvement may also be masked because patients with weak limb muscles spontaneously decrease their overall activity level, thereby reducing the daily physiologic challenge faced by the respiratory system. For all of these reasons, it is not unusual for respiratory muscle weakness to go undetected until overt respiratory failure is precipitated by an acute episode of pulmonary aspiration or infection. Accordingly, the clinician must be vigilant with regard to the possible presence of respiratory muscle weakness in any patient with a known neuromuscular disorder or unexplained exertional dyspnea. Other common symptoms found in patients with neuromuscular disease involving the respiratory muscles include orthopnea, cough during swallowing, weak cough, fatigue, hypersomnolence, morning headaches, insomnia, nightmares, and decreased intellectual performance. Respiratory muscle weakness may be caused by a large and diverse number of diseases affecting the central nervous system, the spinal cord, the nerves, the neuromuscular junction, or the muscle itself. A list of some of the more common or prototypical disorders is shown in Table 26-1, but a comprehensive review of specific disease entities is beyond the scope of this chapter. Instead, our purpose is to discuss general pathophysiologic mechanisms as well as principles of evaluation and treatment that are broadly applicable to most neuromuscular diseases affecting the respiratory system.

OVERVIEW OF PATHOPHYSIOLOGIC MECHANISMS IN CHRONIC VENTILATORY INSUFFICIENCY

Direct Consequences of Respiratory Muscle Weakness

It is not unusual for the pressure produced by the respiratory muscles to be decreased by up to 50% before the appearance of a reduction in vital capacity (VC).[3] Similarly, hypercapnia does not appear in most neuromuscular diseases until the maximum inspiratory pressure (MIP) at the mouth reaches a level below 30% of normal predicted values.[3] These observations underscore the large reserve capacity of the respiratory system, which may, in turn, mask involvement of the respiratory muscles until late in the course of neuromuscular disease.

Respiratory muscle weakness caused by neuromuscular disorders may be associated with increased susceptibility to superimposed respiratory muscle fatigue. The major distinction between simple weakness and fatigue is that the latter is reversible by rest, whereas the former is not. In normal subjects, the diaphragm becomes at risk for the development of fatigue when the pressure–time index (defined as the product of two fractions: inspiratory time/total respiratory cycle time [T_i/T_{tot}] and mean transdiaphragmatic pressure/maximum transdiaphragmatic pressure [P_{di}/P_{dimax}]) exceeds a critical "fatigue threshold" value of 0.15.[4] Based on this calculation, it is apparent that the existence of baseline diaphragmatic weakness (ie, a reduced P_{dimax}) will favor the development of diaphragmatic fatigue. Patients may adopt a breathing pattern that minimizes inspiratory time and transdiaphragmatic pressure (and hence tidal volume) in order to avoid fatigue of the diaphragm, but at the cost of an increase in arterial partial pressure of carbon dioxide (PCO_2).[5,6] In addition, there is evidence that the fatigue threshold value may actually be lower in patients with neuromuscular disorders. Hence, in quadriplegics the fatigue

Table 26-1 Neuromuscular Diseases

Muscular dystrophies
Duchenne muscular dystrophy
Becker muscular dystrophy
Limb-girdle muscular dystrophy
Myotonic dystrophy
Fascioscapulohumeral muscular dystrophy
Congenital muscular dystrophy
Metabolic diseases of muscle
Acid maltase deficiency
Mitochondrial myopathies
Carnitine palmityl transferase deficiency
Other myopathies
Polymyositis or dermatomyositis
Hypothyroidism or hyperthyroidism
Corticosteroid induced
Systemic lupus erythematosus
Diseases of the neuromuscular junction
Myasthenia gravis
Eaton–Lambert syndrome
Botulism
Diseases of peripheral nerve
Charcot–Marie–Tooth disease (also known as hereditary motor and sensory neuropathy)
Friedreich's ataxia
Chronic inflammatory femyelinating polyneuropathy
Guillain–Barré syndrome
Diseases of the motor neuron
Amyotrophic lateral sclerosis
Postpolio syndrome
Infantile progressive spinal muscular atrophy (also known as SMA type 1, Werdnig–Hoffman)
Intermediate spinal muscular atrophy (also known as SMA type 2)
Juvenile spinal muscular atrophy (also known as SMA type 3, Kugelberg–Welander)
Other diseases involving the spinal cord
Traumatic injury
Syringomyelia
Multiple sclerosis

threshold value for the diaphragm is actually reduced (0.10 to 0.12) compared with the value of 0.15 reported for normal individuals.[7] Similarly, a recent study has shown that when the same relative load (expressed as a percentage of maximal strength) is imposed on the respiratory system, the inspiratory muscles of patients with Duchenne dystrophy may be more susceptible to fatigue than those of healthy subjects.[8]

There are few data available concerning the contribution of expiratory muscle weakness to ventilatory failure in neuromuscular disorders. In one study it was found that decreased maximum expiratory pressure (MEP) at the mouth is not an independent predictor of hypercapnia.[9] Nonetheless, in patients with severe expiratory muscle weakness who are unable to generate an effective cough, there is an increased risk of developing atelectasis and pulmonary infection. In patients with neuromuscular disorders, the lowest value of MEP consistent with production of a satisfactory cough is on the order of 50 to 60 cm H_2O.[9,10]

Alterations in Respiratory System Mechanics

The degree of pulmonary restriction found in neuromuscular diseases is frequently greater than would be predicted from the decrement in inspiratory muscle force alone.[11] Increased elastic recoil of both the chest wall and pulmonary parenchyma have been documented.[12] The precise mechanisms underlying these changes are not well understood but are probably multifactorial in nature. For instance, the chronically diminished amplitude of respiratory excursions in patients with neuromuscular weakness may lead to ankylosis of costosternal and costovertebral joints, thereby producing a gradual stiffening of the rib cage. Fibrosis of rib cage muscles (eg, in muscular dystrophy) or connective tissue elements and spinal deformities can also cause a reduction in chest wall compliance.[13] Microatelectasis has been found at autopsy in patients with neuromuscular disorders such as Duchenne dystrophy and spinal muscular atrophy.[14] Once again, it has been hypothesized that this could be related to a lack of spontaneous deep breaths, which normally help re-inflate atelectatic regions of the lung,[15] as well as inefficient cough and clearance of secretions due to expiratory muscle weakness. On the other hand, computed tomography imaging of the lungs failed to confirm the presence of increased atelectasis in a group of patients with Duchenne muscular dystrophy.[16] Impaired activity of surfactant or alterations in the mechanical properties of elastin and collagen fibers within the lungs have also been proposed as possible explanations for reduced lung compliance.[16] Interestingly, in infants and children with neuromuscular disorders, chest wall compliance may actually be increased due to adverse effects on proper development of the chest wall.[17]

Abnormal respiratory mechanics are not limited to the lungs and chest wall but may also involve the upper airway in neuromuscular disorders. In this regard, pharyngeal muscle weakness is observed in neuromuscular disorders such as Duchenne dystrophy,[18] motor neuron disease,[19] and myasthenia gravis.[20] Because weakness of pharyngeal dilator muscles decreases upper airway caliber, there is an increase in upper airway resistance during inspiration. The latter imposes a higher mechanical load on the diaphragm and other inspiratory muscles, thereby increasing the work of breathing.[21] When combined with the decrease in upper airway motor tone normally found during sleep (especially rapid eye-movement [REM] sleep), pharyngeal dilator muscle weakness favors the development of sleep-related hypoventilation and obstructive sleep apnea.

Abnormal Central Control of Breathing

Many neuromuscular disorders that cause respiratory muscle weakness (eg, Duchenne dystrophy, myotonic dystrophy, and Friedrich's ataxia) are also associated with abnormalities of central nervous system function. This raises the question of whether central respiratory control centers within the brain could also be dysfunctional in some of these disorders.[22] Traditional measures of central respiratory drive, such as the ventilatory responses to hypercapnia and hypoxia, or the measurement of inspiratory pressure generated at the mouth 0.1 second after an inspiratory occlusion ($P_{0.1}$),[23] are difficult to interpret in patients with neuromuscular disease. This is because these parameters are affected not only by central ventilatory responsiveness but also by respiratory muscle weakness and abnormal respiratory mechanics. Accordingly, it is often difficult to know what

the "appropriate" values are in such patients, given their other abnormalities of respiratory function.[24] For example, in myotonic dystrophy there is a tendency for carbon dioxide retention that is out of proportion to the degree of respiratory muscle weakness or altered mechanics, suggesting that central respiratory drive is abnormally reduced.[25] In addition, there is a reduction in the ventilatory response to hypercapnia and hypoxia.[26] On the other hand, some studies have reported normal or elevated values of $P_{0.1}$ in these patients,[26–28] suggesting that central drive is not depressed and may even be increased.

There is compelling evidence that sleep-disordered breathing, which is common in patients with neuromuscular disease, can lead to important secondary alterations in central respiratory drive. More specifically, it is postulated that nocturnal hypoventilation and attendant bicarbonate retention lead to a so-called "resetting" of the central carbon dioxide setpoint. Under these conditions, patients with chronic nocturnal hypoventilation develop a reduced central sensitivity to carbon dioxide, which eventually becomes manifest during the daytime. Importantly, it has been demonstrated that such chronic carbon dioxide retention during the daytime can be reversed or ameliorated in many patients by instituting artificial ventilation at night to prevent nocturnal hypoventilation.[29–34] Whether the changes in the carbon dioxide setpoint are due solely to modifications of acid–base status or whether other factors, such as sleep deprivation[35] and hypoxemia, also play a role remains to be determined.

Nonrespiratory Factors Contributing to Chronic Respiratory Impairment

Cardiac involvement occurs in several forms of neuromuscular disease that involve the respiratory system, and is particularly frequent in the muscular dystrophies.[36] In the more advanced stages of Duchenne dystrophy, impaired cardiac function and respiratory insufficiency generally coexist. Left ventricular pump failure with attendant pulmonary venous congestion may cause decreased pulmonary compliance, thereby increasing the work of breathing as well as ventilation–perfusion mismatching and abnormal gas exchange. In addition, there is evidence that respiratory muscle bloodflow is impaired in patients with heart failure, which may further predispose to the development of respiratory muscle dysfunction.[37] As with other conditions characterized by chronic hypoventilation and hypoxemia, pulmonary arterial hypertension and right heart failure may also be present.

Poor nutrition is a common problem among patients with neuromuscular disease.[38,39] Obesity is frequent in patients with neuromuscular disorders because of a variety of factors, including poor dietary habits, sedentary status, and medications (eg, corticosteroids). The presence of obesity places an additional respiratory mechanical burden upon the weakened respiratory muscles and also favors the development of nocturnal hypoventilation and obstructive sleep apnea. Undernutrition may also be a problem, especially late in the disease course, at which time disorders of the alimentary system (impaired swallowing, aspiration, gastroparesis, constipation, etc.) may play an important role. For instance, undernutrition has been reported to occur in approximately half of patients with Duchenne dystrophy.[39] To the extent that undernutrition has also been found to cause atrophy of the diaphragm, particularly within the fast-twitch fiber population,[40] this may also lead to further aggravation of respiratory muscle weakness and dysfunction.

TESTS FOR THE EVALUATION OF RESPIRATORY MUSCLE FUNCTION

Several different tests are currently available to help evaluate the degree of respiratory muscle weakness in patients with neuromuscular disease. Irrespective of the neuromuscular disease in question, the history and physical examination of the patient should serve as the primary guide for determining the nature as well as the frequency of respiratory muscle function testing. A simple measurement of VC with standard spirometry undoubtedly offers the most accessible index of overall ventilatory impairment in neuromuscular disorders, and in many cases it is also the best predictor of survival. Evaluation of respiratory function during sleep (polysomnography) is also important in patients with advanced disease, who are at particular risk for the development of nocturnal hypoventilation and hypoxemia. The more specialized techniques, which specifically measure respiratory muscle function, can be used to confirm a diagnosis of respiratory muscle weakness in uncertain cases. Additional research is needed to determine whether these specialized tests should also be used in following the patient with neuromuscular disease and established respiratory muscle weakness.

Standard or General Tests of Respiratory Function

Spirometry and Lung Volumes As mentioned earlier, spirometry is not a sensitive indicator of respiratory muscle weakness in the early stages of disease, and VC usually remains normal or near-normal until there is a major decline (about 50%) in respiratory muscle strength.[1,3] It should also be noted that in the presence of kyphoscoliosis, it is often preferable to use armspan instead of height to obtain reference values.[41] Despite these limitations, spirometry is the best known predictor of respiratory morbidity and mortality in patients with neuromuscular disease. For example, in Duchenne muscular dystrophy, a VC below 1 L is associated with subsequent mortality,[42] and a VC below 40% of the normal predicted value is significantly correlated with sleep hypoventilation.[43]

Respiratory muscle weakness characteristically induces a restrictive ventilatory defect. The forced expiratory volume in 1 second (FEV_1)/forced vital capacity ratio is generally normal or supranormal, with reductions in total lung capacity and, to a lesser extent, functional residual capacity.[3,14,44] The inspiratory capacity and expiratory reserve volume are typically decreased, reflecting the presence of inspiratory and expiratory muscle weakness, respectively. Significant expiratory muscle weakness, if present, will result in an elevation of residual volume (RV).[3] This may serve as a clue pointing toward a neuromuscular etiology since most other restrictive disorders are associated with reductions in RV.

Another sign of expiratory muscle weakness is when the peak expiratory flow rate, which occurs over the early effort-dependent portion of the forced expiratory curve, is disproportionately reduced in comparison to the FEV_1, VC, and mid-expiratory flows ($MEF_{25–75}$).

Measuring lung volumes with the subject in different body positions is also useful since a large fall in VC upon going from a sitting to a supine posture strongly suggests significant diaphragmatic weakness. In the presence of major diaphragmatic weakness, the weight of the abdominal contents is no longer effectively opposed by the flaccid diaphragm muscle when the patient lies down. Normal subjects demonstrate a mean postural decrease in VC of less than 10% after lying down.[45] In patients with neuromuscular disorders, a postural drop in VC of greater than 25% points to major diaphragmatic weakness with a high degree of sensitivity (79%) and specificity (90%).[46] In addition, it has been reported that the postural fall in VC correlates with respiratory symptoms in amyotrophic lateral sclerosis,[47] as well as the magnitude of oxyhemoglobin desaturation during rapid eye movement (REM) sleep in various neuromuscular disorders.[48]

Flow–Volume Curve Analysis In addition to simple spirometry, a more detailed analysis of the flow–volume curve can provide additional clues to the presence of respiratory muscle weakness. Characteristic features include a delay in reaching peak expiratory flow, truncation of the peak expiratory flow rate, and an abnormally abrupt fall in expiratory flow at the end of expiration (Figure 26-1).[49,50] These changes reflect the fact that the peak expiratory flow rate and flow rates during the final portion of expiration are largely strength dependent. On the other hand, the mid-expiratory flows are less strength dependent and more closely correlated with lung elastic recoil. Accordingly, normal or even supranormal flow rates may be observed in the mid-expiratory portion of the flow–volume curve, consistent with the fact that increased lung recoil contributes to the restrictive ventilatory defect. Inspiratory muscle weakness may be manifested by truncation of the peak inspiratory flow rate.[49] Furthermore, in patients with bulbar or upper airway muscle involvement by neuromuscular diseases (particularly Parkinson's disease), abnormal oscillations of inspiratory and/or expiratory flow may be visible on the flow–volume curve (Figure 26-2).[50] These appear to be the result of dynamic instability of upper airway caliber and in one patient with Parkinson's disease could be largely eliminated by administration of L-dopa.[51]

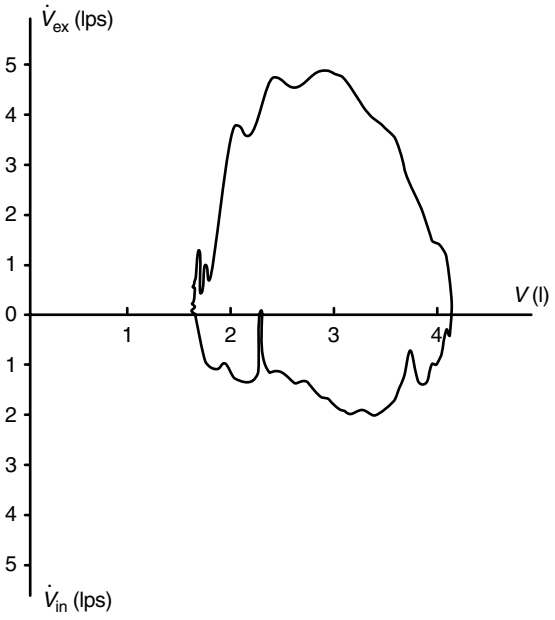

FIGURE 26-1 Flow–volume curve obtained from a patient with neuromuscular disease. Note the abnormal delay in reaching peak expiratory flow as well as the abrupt fall in expiratory flow at end-expiration. Reproduced with permission from Vincken WG et al.[50]

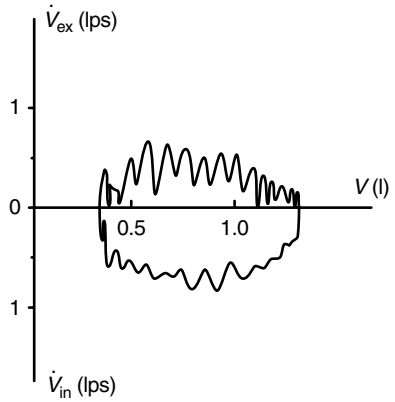

FIGURE 26-2 Flow–volume curve obtained from a patient with an extrapyramidal disorder, demonstrating marked oscillations of both inspiratory and expiratory flow, or so-called "respiratory flutter." Reproduced with permission from Vincken WG et al.[50]

Maximal Inspiratory and Expiratory Mouth Pressures Because of the relative insensitivity of standard spirometry and blood gases to respiratory muscle weakness, it is essential to formally assess respiratory muscle strength in all patients with neuromuscular disorders that potentially affect the respiratory muscles. The simplest direct way of measuring inspiratory muscle strength is to record the pressure generated at the mouth during a maximal inspiratory effort against a closed airway, the MIP.[52,53] Depending upon the neuromuscular disorder in question, the relationship between MIP and outcomes such as nocturnal hypoventilation, mortality, and quality of life is variable. For example, an MIP of approximately 30% predicted has been associated with significantly increased mortality in amyotrophic lateral sclerosis,[54–56] whereas in Duchenne muscular dystrophy a poor correlation was found between MIP values and mortality.[42,43] On the other hand, a significant correlation was reported between reductions in MIP and the fall in VC observed in patients with Duchenne muscular dystrophy.[53] One problem is that, even in normal subjects, there is considerable variability in the MIP measurement.[57] This variability is likely to be even more important in patients with

neuromuscular disease, due to factors such as poor mouth seal caused by facial weakness, or, in some cases, inadequate comprehension of the maneuver because of cognitive impairment associated with the disease.[58] Maximal expiratory mouth pressure measurement against an occluded airway, or MEP, suffers from much the same technical limitations as just described for the MIP. Accordingly, these considerations reinforce the importance of attention to technical details by laboratory personnel, as well as the need for patients to practice the maneuver beforehand, in order to obtain the most reliable results possible.

Arterial Blood Gas Analysis Arterial blood gas analysis is insensitive for either detecting disease or evaluating disease progression in the early to intermediate phases of respiratory muscle weakness. However, blood gas assessment should be performed once the VC has fallen to below 50% of reference values and/or when the MIP is reduced to 30% of normal. It is not unusual to find a mild degree of hyperventilation up until shortly before the development of overt hypercapnic ventilatory insufficiency. Patients may also have normal daytime blood gases despite significant hypoxia and hypercapnia during sleep.

Sleep Study Evaluation (Polysomnography) Sleep-disordered breathing is frequent in patients with neuromuscular disorders.[59] Not only are such patients at increased risk for developing nocturnal hypoventilation with attendant hypoxemia, but there is also an increased prevalence of obstructive sleep apnea. The latter can be related to pharyngeal dilator muscle weakness as well as the presence of significant obesity, which is fairly common given the sedentary status of most neuromuscular patients.[60] Patients with neuromuscular disease are especially prone to develop hypoventilation and oxyhemoglobin desaturation during REM sleep (Figure 26-3).[48] This is because REM sleep is associated with neurally mediated inhibitory mechanisms that greatly reduce the activity level of respiratory muscles other than the diaphragm.[61,62] Accordingly, the impact of REM-associated reductions in intercostal and accessory muscle activation is particularly severe in patients with underlying diaphragmatic weakness since the diaphragm is no longer able to effectively compensate for the loss of the other inspiratory muscles under these conditions. Interestingly, there is evidence that the inhibitory influences of REM sleep on nondiaphragmatic respiratory muscles are blunted in certain patients with diaphragmatic weakness, possibly as a compensatory protective mechanism.[63] In patients with neuromuscular disorders, it can also be difficult to distinguish between hypoventilation and obstructive sleep apnea since the diaphragm and other inspiratory muscles may be too weak to generate the negative suction forces needed to produce the classic signs of obstruction. Under these conditions, direct assessment of respiratory effort during sleep with an esophageal balloon catheter (see below) may be necessary to differentiate between the two entities.[59]

Although attempts have been made in a number of studies to use pulmonary function tests (spirometry, MIP, MEP) and daytime blood gases in order to predict the need for polysomnography in neuromuscular patients, the results have been mixed and seem to vary with the specific disease in question. In Duchenne muscular dystrophy, an FEV_1 $<$40% was found to be a sensitive (91%) but not specific (50%) indicator of sleep hypoventilation, whereas a base excess of $>$4 mmol/L was highly specific (100%) but less sensitive (55%).[43] As a general guideline, one should strongly consider performing a sleep study to rule out significant sleep-disordered breathing when (1) the VC has fallen to below 50% of reference values and/or when the MIP is reduced to 30% of normal; (2) significant abnormalities of daytime blood gases are present; or (3) there are symptoms suggestive of sleep-disordered breathing, such as morning headaches, hypersomnolence, nocturia, insomnia, nightmares, and decreased intellectual performance.

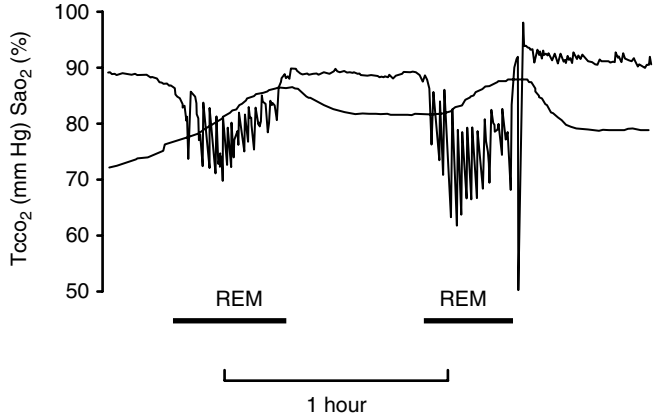

FIGURE 26-3 Polysomnographic tracing showing marked oxyhemoglobin desaturation (SaO_2) along with increases in transcutaneous carbon dioxide ($TcCO_2$) during REM sleep in a patient with neuromuscular weakness. Reproduced with permission from Bye PT et al.[48]

Specialized Tests of Respiratory Muscle Function

Maximal Sniff Nasal Pressure Maximal sniff nasal pressure (sniff P_{imax}) is a relatively new test of inspiratory muscle strength and involves measurement of the pressure generated within an occluded nostril during a maximal sniff maneuver through the contralateral, unoccluded nostril (Figure 26-4).[64] Because the technique does not require a mouthpiece and the sniff is a very familiar maneuver for most individuals, it avoids some of the technical difficulties encountered with the classic MIP measurement. In patients with neuromuscular disorders, it has been reported that sniff P_{imax} values are statistically equivalent to the classic MIP measurement, but with the advantage of being easier to obtain in patients with neuromuscular disorders.[64,65] Furthermore, the correlation between VC and sniff P_{imax} appears to be higher than that between VC and MIP in neuromuscular patients.[65] The technical limitations of sniff P_{imax} include the need for an airtight nasal plug, sufficient pressure generation to cause airflow limitation in the contralateral nostril, and the absence of major nasal congestion.

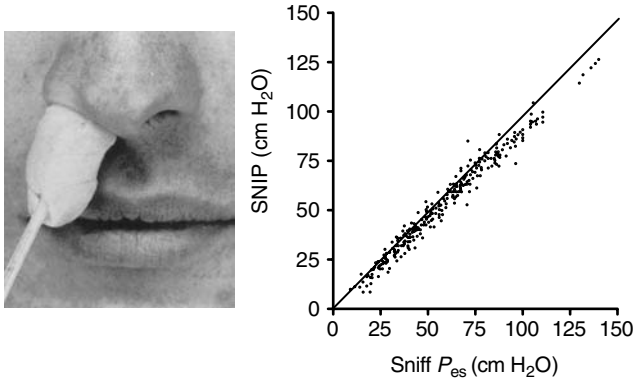

FIGURE 26-4 Measurement of sniff nasal inspiratory pressure (SNIP). *Left*: A nasal plug fitted around the tip of a catheter is inserted into one nostril. *Right*: Relationship between SNIP and sniff esophageal pressure (sniff P_{es}) in normal subjects. Reproduced with permission from Heritier F et al.[64]

Transdiaphragmatic Pressure The ability of the diaphragm to effectively generate negative pressure in the thorax during inspiration can be assessed directly by measuring the pressure difference across the diaphragm, or P_{di}. Pressure changes on either side of the diaphragm in the abdominal (P_{ab}) and pleural (P_{pl}) spaces, respectively, are measured by placing balloon catheters into the stomach and midesophagus. During a maximal inspiratory effort, maximal P_{di} can then be calculated as $P_{dimax} = P_{ab} - P_{pl}$ (Figure 26-5).[66] However, depending upon the particular maneuver employed to generate the maximal inspiratory effort, both the magnitude and the variability of normative values will differ. For example, absolute values obtained during maximal sniff and Müller (through the mouth against a closed glottis) maneuvers are similar (approximately 120 cm H_2O), but the coefficient of variation is substantially lower with a sniff.[67,68] When complete diaphragmatic paralysis is present, the diaphragm is sucked up into the chest during inspiration, so that both P_{ab} and P_{pl} become negative during inspiration and effectively cancel each other out (ie, $P_{di} = 0$). This pattern of pressure generation also gives rise to paradoxical inward motion of the abdominal wall during inspiration, which can be detected clinically when the patient is placed in the supine body position or quantified using respiratory inductance plethysmography and related techniques for measuring thoracoabdominal motion.[69]

Additional information can be gained by combining measurements of P_{di} with phrenic nerve stimulation. Direct electrical stimulation of the phrenic nerves removes the need for patient cooperation in the performance of a maximal inspiratory effort. In addition, the time between imposition of the stimulus and appearance of the compound action potential at the level of the diaphragm (normally about 6 to 10 ms, recorded from surface EMG electrodes placed over the lower rib cage) can be measured, thereby providing an index of phrenic nerve conduction time.[70] In normal subjects, bilateral phrenic nerve twitch (ie, a single impulse) stimulation results in P_{di} values that are approximately 20% of maximal sniff P_{di} values.[67] Similar values are obtained with cervical magnetic stimulation of the phrenic nerve, which is technically easier and also better tolerated by most patients than conventional electrical stimulation[71] since the current intensities required for the latter are often painful.

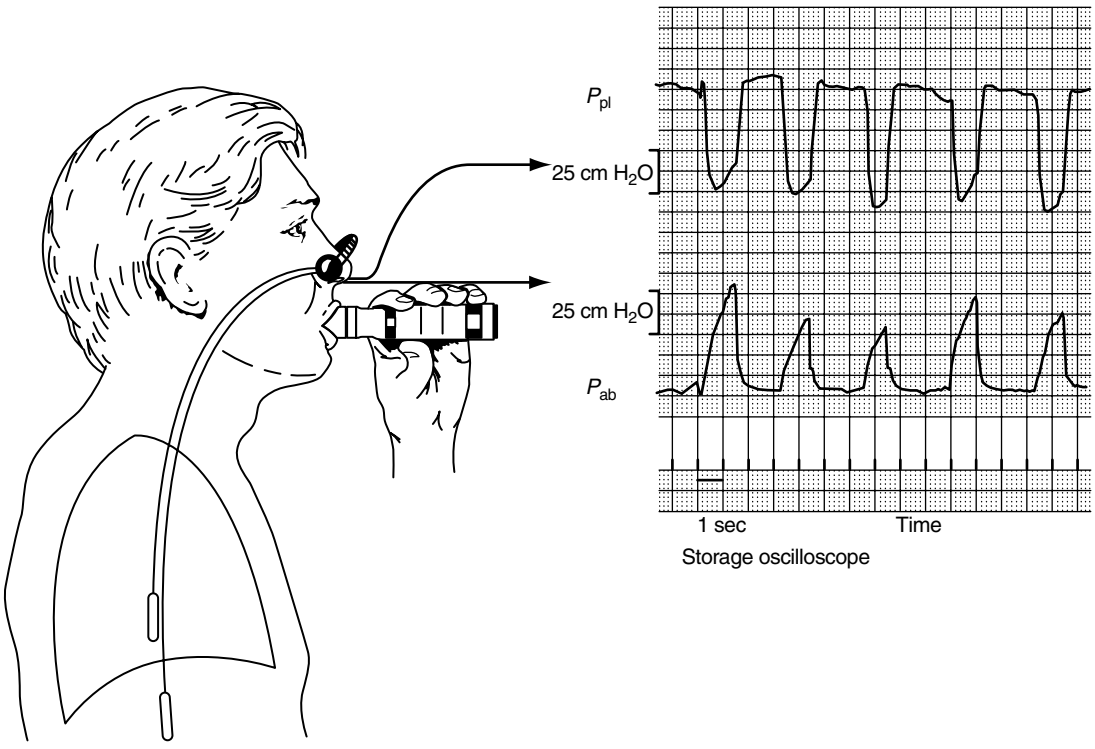

FIGURE 26-5 Method for determining maximal transdiaphragmatic pressure in humans. Balloon catheters placed into the esophagus and stomach are used to measure pleural (P_{pl}) and abdominal (P_{ab}) pressures, respectively. Reproduced with permission from Laporta D and Grassino A.[66]

Tests of Respiratory Muscle Endurance Respiratory muscle endurance has been evaluated by a number of different methods in patients with neuromuscular disorders. Although not a pure test of respiratory muscle endurance alone, the classic maximal voluntary ventilation (MVV) maneuver was found to be reduced in neuromuscular diseases, even when the VC was normal.[24,72,73] Others have measured the maximal sustainable ventilation or pressure produced by the respiratory muscles over various predetermined periods of time[74,75] or the maximal time for which a subject is able to sustain a predetermined percentage of the MVV or P_{dimax}.[76,77] The proper role of respiratory muscle endurance testing for patients with neuromuscular disorders remains to be determined. One potential application is in evaluating the effectiveness of therapeutic interventions. An important technical issue is that, for satisfactory reproducibility of respiratory muscle endurance test results, the subject must learn to adopt a standardized breathing pattern.[78] In addition, there is a theoretical risk of precipitating respiratory muscle fatigue and failure in severely affected patients. Therefore, it is probably only feasible to perform tests of respiratory muscle endurance in a subset of neuromuscular patients who do not suffer from significant cognitive dysfunction or severe respiratory muscle weakness.

RESPIRATORY MANAGEMENT

General Measures

An impaired ability to cough and clear airway secretions places patients with neuromuscular disease at particularly high risk for the development of pulmonary infections. In many cases, there is also an increased propensity to aspirate food or pharyngeal secretions, due to weakness or a lack of coordination of the upper airway muscles. Moreover, it appears that even relatively mild upper respiratory tract infections can lead to major additional reductions in respiratory muscle strength.[79] Therefore, any respiratory tract infection in the patient with severe neuromuscular disease has the potential to trigger an episode of full-blown respiratory failure requiring mechanical ventilatory assistance. For this reason, it is imperative that aggressive measures be taken to both prevent and treat respiratory infections in such patients. This includes the appropriate use of vaccinations against influenza and pneumoccocal pneumonia, aggressive antibiotic treatment of suspected bacterial infections of the respiratory tract, and chest physiotherapy for removal of airway secretions. In addition, either manual or mechanically assisted expulsive maneuvers can be successful in increasing cough efficiency.[80]

Orthotic devices to brace the spine have not been demonstrated to be effective in improving pulmonary function in neuromuscular patients with kyphoscoliosis and may, in fact, worsen pulmonary restriction. Surgical procedures to correct scoliosis are similarly unhelpful in slowing the decline of pulmonary function, at least in patients with Duchenne muscular dystrophy, in whom this issue has been specifically addressed.[81–83] Nonetheless, spinal stabilization may improve comfort and quality of life if instituted early after the loss of ambulation and before the onset of severe scoliosis or contractures. It is important to recognize, however, that surgical stabilization of the spine is associated with a substantial risk of perioperative pulmonary and cardiac complications in such patients and may even be fatal. In one study, approximately half of the patients with a preoperative FVC value of less than 35% suffered from postoperative complications.[83] Therefore, candidates for such surgery should be carefully evaluated in order to exclude those with significant cardiomyopathy, and if undertaken, the intervention should ideally be performed before the VC has fallen to below 50% of its predicted value.[83]

Ventilatory Muscle-directed Measures

Respiratory Muscle Training The rationale for respiratory muscle training is that by increasing strength and endurance, it could help improve exercise tolerance, reduce dyspnea, augment cough efficiency, and increase the ability of the respiratory muscles to tolerate acute increases in respiratory mechanical load associated with pulmonary infections. On the other hand, there is at least a theoretical risk of increasing the rate of disease progression by overtraining, particularly in those disorders (eg, Duchenne dystrophy, postpolio syndrome) in which overuse has been implicated in disease pathogenesis.[84,85] To date, the majority of studies evaluating the effectiveness of respiratory muscle training in neuromuscular disorders have been heavily weighted toward patients with Duchenne muscular dystrophy, although benefits in multiple sclerosis,[86,87] postpolio syndrome,[88] and quadriplegia[89] have also been reported. Most investigations in Duchenne patients,[76,77,90–93] but not all,[74,75] have shown improvements in respiratory muscle strength or endurance after periods of training ranging from approximately 6 weeks to 24 months. Another study also showed a significant reduction in respiratory load perception after training,[94] and it was suggested that this might translate into reduced dyspnea. In general, the reported improvements in respiratory muscle function after training were not associated with changes in VC. In addition, respiratory muscle training appears to offer little or no benefit in Duchenne muscular dystrophy patients with very severe baseline ventilatory impairment (VC $<$ 25% predicted).[76,90] Another potential application of respiratory muscle training, which differs conceptually from those outlined above, is to selectively train nonaffected muscles capable of playing a compensatory role. Hence, in patients who have lost the use of expiratory abdominal and intercostal muscles due to lower cervical spinal cord injury, it is possible to restore a degree of expiratory muscle function by selectively training the clavicular portion of the pectoralis major muscle, which retains innervation under these conditions.[95]

At the present time, there is no clear consensus regarding the role of respiratory muscle training in the management of patients with neuromuscular disorders. Indeed, it should be noted that a similar situation exists even with respect to training of nonrespiratory skeletal muscles in this patient population.[84] Although the overall approach appears promising, questions remain regarding the degree to which the

observed improvements represent true training effects versus learning. Furthermore, it will be important to ascertain whether any improvements in respiratory muscle function induced by training translate into decreased respiratory morbidity or mortality. Finally, given the great heterogeneity of the target diseases in question, future research will need to better identify the most effective training parameters (stimulus intensity, duration, inspiratory versus expiratory, etc.) for specific neuromuscular disorders.

Mechanical Ventilation There is considerable evidence that patients with chronic and progressive ventilatory failure due to neuromuscular diseases benefit from the use of noninvasive ventilatory support, particularly during sleep.[34] Such therapy can consist of either negative pressure (eg, cuirass, body suit or poncho, tank respirator) or positive pressure (eg, via a mask or mouthpiece) delivery methods. Although negative pressure ventilation popularized the use of noninvasive ventilatory support for neuromuscular disease during the poliomyelitis epidemics, this approach has fallen out of favor due to the somewhat cumbersome nature of the devices (ie, difficulty getting into and out of the devices, limited access to the patient during treatment), as well as the increased risk of upper airway obstruction during sleep.[30,96] Positive pressure ventilation is generally delivered via a tight-fitting nasal or full-face (eg, to prevent mouth leak) mask. Potential complications of noninvasive positive pressure ventilation (NIPPV) include facial pressure sores, eye irritation from air leaks, mouth dryness, and gastric distention. As a general rule, the more invasive tracheostomy is reserved for specific circumstances, such as severe bulbar dysfunction, excessive oropharyngeal or pulmonary secretions that require frequent suctioning, or an essentially continuous 24-hour need for ventilatory support.

Several investigations have shown that nocturnal ventilatory support can improve daytime arterial blood gases[29–33] (Figure 26-6), as well as quality of life or survival.[97–99] The use of NIPPV may also decrease pulmonary morbidity and hospitalization rates.[98,100–102] On the other hand, there is no convincing evidence that NIPPV is able to mitigate the progressive loss of respiratory muscle strength or otherwise slow the rate of decline of pulmonary function. In fact, a reduction in respiratory muscle strength was reported after a median period of only 42 hours on NIPPV,[100] suggesting that NIPPV could lead to deconditioning of the respiratory muscles in some patients.[103] Such a concern argues against the use of NIPPV as a prophylactic measure, that is, before the actual onset of alveolar hypoventilation. Indeed, in one study that specifically addressed the issue of prophylactic NIPPV in Duchenne dystrophy, not only was a lack of benefit for this intervention found, but, for unclear reasons, there was actually increased mortality in the group treated with preventive ventilation.[104]

As discussed earlier, hypoventilation often begins during sleep and may manifest itself as insomnia or nightmares as well as more classic symptoms such as fatigue, daytime hypersomnolence, and morning headache. The clearest indication for the institution of NIPPV is when such symptoms are present and associated with documented

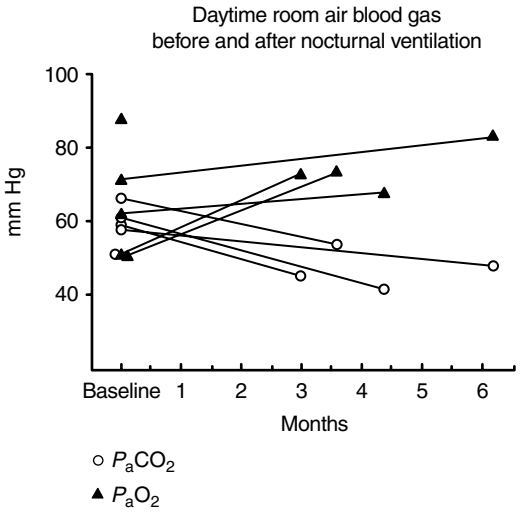

FIGURE 26-6 Daytime arterial blood gas measurements on room air before and after treatment with noninvasive positive pressure ventilation (NIPPV) in a group of patients with neuromuscular disease. Circles = arterial partial pressure of carbon dioxide. Triangles = arterial partial pressure of oxygen. Reproduced with permission from Kerby GR et al.[32]

hypoventilation. A recent consensus conference has suggested that NIPPV be offered in symptomatic patients with at least one of the following: (1) daytime arterial PCO_2 greater than 45 mm Hg; (2) nocturnal level of oxyhemoglobin saturation less than 88% for over five consecutive minutes; or (3) severe underlying pulmonary function abnormalities (MIP < 60 cm H_2O or FVC $< 50\%$ predicted).[34] There is no consensus for specific threshold values of spirometric or blood gas measurements after which NIPPV should be offered in asymptomatic patients, and this will undoubtedly be influenced by the particular disease entity in question and other components of the overall clinical context.

Finally, research suggests that physicians' perceptions of quality of life on NIPPV, and hence their attitudes in offering such therapy to patients, are frequently more negative than reported by patients actually undergoing NIPPV.[105,106] Therefore, an overly negative attitude to ventilatory support on the part of the physician, even in the face of progressive neuromuscular disease, is not appropriate. However, it is imperative that the issue of NIPPV be discussed with patients and their families well before the need for such therapy arises, and these decisions need to be reevaluated on a periodic basis.[107]

ACKNOWLEDGMENTS

This work was supported by the Canadian Institutes of Health Research, Muscular Dystrophy Association, Inc., Association Francaise Contre les Myopathies, and the Fonds de la Recherche en Sante du Quebec.

REFERENCES

1. Black LF, Hyatt RE. Maximal static respiratory pressures in generalized neuromuscular disease. Am Rev Respir Dis 1971;103:641–50.

2. Vincken W, Elleker MG, Cosio MG. Determinants of respiratory muscle weakness in stable chronic neuromuscular disorders. Am J Med 1987;82:53–8.
3. Braun NM, Arora NS, Rochester DF. Respiratory muscle and pulmonary function in polymyositis and other proximal myopathies. Thorax 1983;38:616–23.
4. Bellemare F, Grassino A. Effect of pressure and timing of contraction on human diaphragm fatigue. J Appl Physiol 1982;53:1190–5.
5. Lanini B, Misuri G, Gigliotti F, et al. Perception of dyspnea in patients with neuromuscular disease. Chest 2001;120:402–8.
6. Misuri G, Lanini B, Gigliotti F, et al. Mechanism of CO_2 retention in patients with neuromuscular disease. Chest 2000; 117:447–53.
7. Nava S, Rubini F, Zanotti E, Caldiroli D. The tension–time index of the diaphragm revisited in quadriplegic patients with diaphragm pacing. Am J Respir Crit Care Med 1996; 153:1322–7.
8. Matecki S, Topin N, Hayot M, et al. A standardized method for the evaluation of respiratory muscle endurance in patients with Duchenne muscular dystrophy. Neuromusc Disord 2001;11:171–7.
9. Polkey MI, Lyall RA, Green M, et al. Expiratory muscle function in amyotrophic lateral sclerosis. Am J Respir Crit Care Med 1998;158:734–41.
10. Szeinberg A, Tabachnik E, Rashed N, et al. Cough capacity in patients with muscular dystrophy. Chest 1988;94:1232–5.
11. De Troyer A, Borenstein S, Cordier R. Analysis of lung volume restriction in patients with respiratory muscle weakness. Thorax 1980;35:603–10.
12. De Troyer A, Deisser P. The effects of intermittent positive pressure breathing on patients with respiratory muscle weakness. Am Rev Respir Dis 1981;124:132–7.
13. Estenne M, Heilporn A, Delhez L, et al. Chest wall stiffness in patients with chronic respiratory muscle weakness. Am Rev Respir Dis 1983;128:1002–7.
14. Smith PEM, Calverley PMA, Edwards RHT, et al. Practical problems in the respiratory care of patients with muscular dystrophy. N Engl J Med 1987;316:1197–204.
15. Schmidt-Nowara WW, Altman AR. Atelectasis and neuromuscular respiratory failure. Chest 1984;85:792–5.
16. Estenne M, Gevenois PA, Kinnear W, et al. Lung volume restriction in patients with chronic respiratory muscle weakness: the role of microatelectasis. Thorax 1993;48: 698–701.
17. Papastamelos C, Panitch HB, Allen JL. Chest wall compliance in infants and children with neuromuscular disease. Am J Respir Crit Care Med 1996;154:1045–8.
18. Khan Y, Heckmatt JZ. Obstructive apnoeas in Duchenne muscular dystrophy. Thorax 1994;49:157–61.
19. Garcia-Pachon E, Marti J, Mayos M, et al. Clinical significance of upper airway dysfunction in motor neuron disease. Thorax 1994;49:896–900.
20. Putman MT, Wise RA. Myasthenia gravis and upper airway obstruction. Chest 1996;109:400–4.
21. Vincken W, Guilleminault C, Silvestri L, et al. Inspiratory muscle activity as a trigger causing the airways to open in obstructive sleep apnea. Am Rev Respir Dis 1987;135: 372–7.
22. Veale D, Cooper BG, Gilmartin JJ, et al. Breathing pattern awake and asleep in patients with myotonic dystrophy. Eur Respir J 1995;8:815–8.
23. Whitelaw WA, Derenne JP, Milic-Emili J. Occlusion pressure as a measure of respiratory center output in conscious man. Respir Physiol 1975;23:181–99.
24. Gilmartin JJ, Walls TJ, Stone TN, Gibson GB. Relationship between ventilatory and mouth occlusion pressure responses to carbon dioxide in normal subjects and patients with muscle weakness. Thorax 1980;35:716–21.
25. Begin P, Mathieu J, Almirall J, Grassino A. Relationship between chronic hypercapnia and inspiratory-muscle weakness in myotonic dystrophy. Am J Respir Crit Care Med 1997;156:133–9.
26. Begin R, Bureau MA, Lupien L, Lemieux B. Control and modulation of respiration in Steinert's myotonic dystrophy. Am Rev Respir Dis 1980;121:281–9.
27. Begin R, Bureau MA, Lupien L, et al. Pathogenesis of respiratory insufficiency in myotonic dystrophy: the mechanical factors. Am Rev Respir Dis 1982;125:312–8.
28. Baydur A. Respiratory muscle strength and control of ventilation in patients with neuromuscular disease. Chest 1991;99: 330–8.
29. Mellies U, Ragette R, Schwake C, et al. Sleep-disordered breathing and respiratory failure in acid maltase deficiency. Neurology 2001;57:1290–5.
30. Ellis ER, Bye PT, Bruderer JW, Sullivan CE. Treatment of respiratory failure during sleep in patients with neuromuscular disease. Positive-pressure ventilation through a nose mask. Am Rev Respir Dis 1987;135:148–52.
31. Goldstein RS, Molotiu N, Skrastins R, et al. Reversal of sleep-induced hypoventilation and chronic respiratory failure by nocturnal negative pressure ventilation in patients with restrictive ventilatory impairment. Am Rev Respir Dis 1987; 135:1049–55.
32. Kerby GR, Mayer LS, Pingleton SK. Nocturnal positive pressure ventilation via nasal mask. Am Rev Respir Dis 1987; 135:738–40.
33. Piper AJ, Sullivan CE. Effects of long-term nocturnal nasal ventilation on spontaneous breathing during sleep in neuromuscular and chest wall disorders. Eur Respir J 1996; 9:1515–22.
34. Consensus Conference. Clinical indications for noninvasive positive pressure ventilation in chronic respiratory failure due to restrictive lung disease, COPD, and nocturnal hypoventilation. A Consensus Conference Report. Chest 1999;116:521–34.
35. White DP, Douglas NJ, Pickett CK, et al. Sleep deprivation and the control of ventilation. Am Rev Respir Dis 1983;128: 984–6.
36. Cox GF, Kunkel LM. Dystrophies and heart disease. Curr Opin Cardiol 1997;12:329–43.
37. Mancini DM, Henson D, LaManca J, Levine S. Respiratory muscle function and dyspnea in patients with chronic congestive heart failure. Circulation 1992;86:909–18.
38. Cameron A, Rosenfeld J. Nutritional issues and supplements in amyotrophic lateral sclerosis and other neurodegenerative disorders. Curr Opin Clin Nutr Metab Care 2002;5: 631–43.
39. Willig TN, Carlier L, Legrand M, et al. Nutritional assessment in Duchenne muscular dystrophy. Dev Med Child Neurol 1993;35:1074–82.
40. Prezant DJ, Richner B, Aldrich TK, et al. Effect of long-term undernutrition on male and female rat diaphragm contractility, fatigue, and fiber types. J Appl Physiol 1994;76:1540–7.
41. Hibbert ME, Lanigan A, Raven J, Phelan PD. Relation of armspan to height and the prediction of lung function. Thorax 1988; 43:657–9.
42. Phillips MF, Quinlivan RC, Edwards RH, Calverley PM. Changes in spirometry over time as a prognostic marker in patients with Duchenne muscular dystrophy. Am J Respir Crit Care Med 2001;164:2191–4.
43. Hukins CA, Hillman DR. Daytime predictors of sleep hypoventilation in Duchenne muscular dystrophy. Am J Respir Crit Care Med 2000;161:166–70.

44. Rideau Y, Jankowski LW, Grellet J. Respiratory function in the muscular dystrophies. Muscle Nerve 1981;4:155–64.
45. Allen SM, Hunt B, Green M. Fall in vital capacity with posture. Br J Dis Chest 1985;79:267–71.
46. Fromageot C, Lofaso F, Annane D, et al. Supine fall in lung volumes in the assessment of diaphragmatic weakness in neuromuscular disorders. Arch Phys Med Rehabil 2001;82: 123–8.
47. Varrato J, Siderowf A, Damiano P, et al. Postural change of forced vital capacity predicts some respiratory symptoms in ALS. Neurology 2001;57:357–9.
48. Bye PT, Ellis ER, Issa FG, et al. Respiratory failure and sleep in neuromuscular disease. Thorax 1990;45:241–7.
49. Vincken WG, Elleker MG, Cosio MG. Flow–volume loop changes reflecting respiratory muscle weakness in chronic neuromuscular disorders. Am J Med 1987;83:673–80.
50. Vincken WG, Gauthier SG, Dollfuss RE, et al. Involvement of upper-airway muscles in extrapyramidal disorders. A cause of airflow limitation. N Engl J Med 1984;311:438–42.
51. Vincken WG, Darauay CM, Cosio MG. Reversibility of upper airway obstruction after levodopa therapy in Parkinson's disease. Chest 1989;96:210–2.
52. Griggs RC, Donohoe KM, Utell MJ, et al. Evaluation of pulmonary function in neuromuscular disease. Arch Neurol 1981;38:9–12.
53. Hahn A, Bach JR, Delaubier A, et al. Clinical implications of maximal respiratory pressure determinations for individuals with Duchenne muscular dystrophy. Arch Phys Med Rehabil 1997;78:1–6.
54. Vitacca M, Clini E, Facchetti D, et al. Breathing pattern and respiratory mechanics in patients with amyotrophic lateral sclerosis. Eur Respir J 1997;10:1614–21.
55. Gay PC, Westbrook PR, Daube JR, et al. Effects of alterations in pulmonary function and sleep variables on survival in patients with amyotrophic lateral sclerosis. Mayo Clin Proc 1991;66:686–94.
56. Bourke SC, Shaw PJ, Gibson GJ. Respiratory function vs sleep-disordered breathing as predictors of QOL in ALS. Neurology 2001;57:2040–4.
57. Wilson SH, Cooke NT, Edwards RH, Spiro SG. Predicted normal values for maximal respiratory pressures in Caucasian adults and children. Thorax 1984;39:535–8.
58. Hinton VJ, De Vivo DC, Nereo NE, et al. Poor verbal working memory across intellectual level in boys with Duchenne dystrophy. Neurology 2000;54:2127–32.
59. Labanowski M, Schmidt-Nowara W, Guilleminault C. Sleep and neuromuscular disease: frequency of sleep-disordered breathing in a neuromuscular disease clinic population. Neurology 1996;47:1173–80.
60. Smith PE, Calverley PM, Edwards RH. Hypoxemia during sleep in Duchenne muscular dystrophy. Am Rev Respir Dis 1988; 137:784–5.
61. Stradling JR, Kozar LF, Dark J, et al. Effect of acute diaphragm paralysis on ventilation in awake and sleeping dogs. Am Rev Respir Dis 1987;136:633–7.
62. Tabachnik E, Muller NL, Bryan AC, Levison H. Changes in ventilation and chest wall mechanics during sleep in normal adolescents. J Appl Physiol 1981;51:557–64.
63. Arnulf I, Similowski T, Salachas F, et al. Sleep disorders and diaphragmatic function in patients with amyotrophic lateral sclerosis. Am J Respir Crit Care Med 2000;161:849–56.
64. Heritier F, Rahm F, Pasche P, Fitting JW. Sniff nasal inspiratory pressure. A noninvasive assessment of inspiratory muscle strength. Am J Respir Crit Care Med 1994;150:1678–83.
65. Stefanutti D, Benoist MR, Scheinmann P, et al. Usefulness of sniff nasal pressure in patients with neuromuscular or skeletal disorders. Am J Respir Crit Care Med 2000; 162:1507–11.
66. Laporta D, Grassino A. Assessment of transdiaphragmatic pressure in humans. J Appl Physiol 1985;58:1469–76.
67. Mier A, Brophy C, Moxham J, Green M. Twitch pressures in the assessment of diaphragm weakness. Thorax 1989;44:990–6.
68. Miller JM, Moxham J, Green M. The maximal sniff in the assessment of diaphragm function in man. Clin Sci (Lond) 1985;69:91–6.
69. Perez A, Mulot R, Vardon G, et al. Thoracoabdominal pattern of breathing in neuromuscular disorders. Chest 1996;110: 454–61.
70. Similowski T, Mehiri S, Duguet A, et al. Comparison of magnetic and electrical phrenic nerve stimulation in assessment of phrenic nerve conduction time. J Appl Physiol 1997;82:1190–9.
71. Similowski T, Fleury B, Launois S, et al. Cervical magnetic stimulation: a new painless method for bilateral phrenic nerve stimulation in conscious humans. J Appl Physiol 1989;67: 1311–8.
72. Burke SS, Grove NM, Houser CR, Johnson DM. Respiratory aspects of pseudohypertrophic muscular dystrophy. Am J Dis Child 1971;121:230–4.
73. Fallat RJ, Jewitt B, Bass M, et al. Spirometry in amyotrophic lateral sclerosis. Arch Neurol 1979;36:74–80.
74. Smith PEM, Coakley JH, Edwards RHT. Respiratory muscle training in Duchenne muscular dystrophy. Muscle Nerve 1988;11:784–5.
75. Stern LM, Martin AJ, Jones N, et al. Training inspiratory resistance in Duchenne dystrophy using adapted computer games. Dev Med Child Neurol 1989;31:494–500.
76. Wanke T, Toifl K, Merkle M, et al. Inspiratory muscle training in patients with Duchenne muscular dystrophy. Chest 1994;105:475–82.
77. Vilozni D, Bar-Yishay E, Gur I, et al. Computerized respiratory muscle training in children with Duchenne muscular dystrophy. Neuromusc Disord 1994;4:249–55.
78. Smith K, Cook DJ. Respiratory muscle training in chronic airflow limitation: a meta-analysis. Am Rev Respir Dis 1992; 145:533–9.
79. Poponick JM, Jacobs I, Supinski G, Dimarco AF. Effect of upper respiratory tract infection in patients with neuromuscular disease. Am J Respir Crit Care Med 1997;156:659–64.
80. Bach JR. Mechanical insufflation–exsufflation. Comparison of peak expiratory flows with manually assisted and unassisted coughing techniques. Chest 1993;104:1553–62.
81. Miller F, Moseley CF, Koreska J, Levison H. Pulmonary function and scoliosis in Duchenne dystrophy. J Pediatr Orthop 1988;8:133–7.
82. Kennedy JD, Staples AJ, Brook PD, et al. Effect of spinal surgery on lung function in Duchenne muscular dystrophy. Thorax 1995;50:1173–8.
83. Miller F, Moseley CF, Koreska J. Spinal fusion in Duchenne muscular dystrophy. Dev Med Child Neurol 1992;34:775–86.
84. Petrof BJ. The molecular basis of activity-induced muscle injury in Duchenne muscular dystrophy. Mol Cell Biochem 1998;179:111–23.
85. Pachter BR, Eberstein A. A rat model of the post-polio motor unit. Orthopedics 1991;14:1367–73.
86. Gosselink R, Kovacs L, Kovacs L, et al. Respiratory muscle weakness and respiratory muscle training in severely disabled multiple sclerosis patients. Arch Phys Med Rehabil 2000;81:747–51.
87. Klefbeck B , Hamrah NJ. Effect of inspiratory muscle training in patients with multiple sclerosis. Arch Phys Med Rehabil 2003;84:994–9.

88. Klefbeck B, Lagerstrand L, Mattsson E. Inspiratory muscle training in patients with prior polio who use part-time assisted ventilation. Arch Phys Med Rehabil 2000;81: 1065–71.
89. Rutchik A, Weissman AR, Almenoff PL, et al. Resistive inspiratory muscle training in subjects with chronic cervical spinal cord injury. Arch Phys Med Rehabil 1998;79: 293–7.
90. Dimarco AF, Kelling JS, Dimarco MS, et al. The effects of inspiratory resistive training on respiratory muscle function in patients with muscular dystrophy. Muscle Nerve 1985;8: 284–90.
91. Koessler W, Wanke T, Winkler G, et al. 2 Years' experience with inspiratory muscle training in patients with neuromuscular disorders. Chest 2001;120:765–9.
92. Topin N, Matecki S, Le Bris S, et al. Dose-dependent effect of individualized respiratory muscle training in children with Duchenne muscular dystrophy. Neuromusc Disord 2002;12: 576–83.
93. Martin AJ, Stern L, Yeates J, et al. Respiratory muscle training in Duchenne muscular dystrophy. Dev Med Child Neurol 1986;28:314–8.
94. Gozal D, Thiriet P. Respiratory muscle training in neuromuscular disease: long-term effects on strength and load perception. Med Sci Sports Exerc 1999;31:1522–7.
95. Estenne M, Knoop C, Vanvaerenbergh J, et al. The effect of pectoralis muscle training in tetraplegic subjects. Am Rev Respir Dis 1989;139:1218–22.
96. Levy RD, Bradley TD, Newman SL, et al. Negative pressure ventilation. Effects on ventilation during sleep in normal subjects. Chest 1989;95:95–9.
97. Simonds AK, Muntoni F, Heather S, Fielding S. Impact of nasal ventilation on survival in hypercapnic Duchenne muscular dystrophy. Thorax 1998;53:949–52.
98. Vianello A, Bevilacqua M, Salvador V, et al. Long-term nasal intermittent positive pressure ventilation in advanced Duchenne's muscular dystrophy. Chest 1994;105:445–8.
99. Lyall RA, Donaldson N, Fleming T, et al. A prospective study of quality of life in ALS patients treated with noninvasive ventilation. Neurology 2001;57:153–6.
100. Aboussouan LS, Khan SU, Banerjee M, et al. Objective measures of the efficacy of noninvasive positive-pressure ventilation in amyotrophic lateral sclerosis. Muscle Nerve 2001; 24:403–9.
101. Bach JR. Amyotrophic lateral sclerosis: prolongation of life by noninvasive respiratory AIDS. Chest 2002;122:92–8.
102. Leger P, Bedicam JM, Cornette A, et al. Nasal intermittent positive pressure ventilation. Long-term follow-up in patients with severe chronic respiratory insufficiency. Chest 1994; 105:100–5.
103. Vassilakopoulos T, Petrof BJ. Ventilator-induced diaphragmatic dysfunction. Am J Respir Crit Care Med 2004;169:336–41.
104. Raphael JC, Chevret S, Chastang C, Bouvet F. Randomised trial of preventive nasal ventilation in Duchenne muscular dystrophy. French Multicentre Cooperative Group on Home Mechanical Ventilation Assistance in Duchenne de Boulogne Muscular Dystrophy. Lancet 1994;343:1600–4.
105. Gibson B. Long-term ventilation for patients with Duchenne muscular dystrophy: physicians' beliefs and practices. Chest 2001;119:940–6.
106. Bach JR, Campagnolo DI, Hoeman S. Life satisfaction of individuals with Duchenne muscular dystrophy using long-term mechanical ventilatory support. Am J Phys Med Rehabil 1991;70:129–35.
107. Silverstein MD, Stocking CB, Antel JP, et al. Amyotrophic lateral sclerosis and life-sustaining therapy: patients' desires for information, participation in decision making, and life-sustaining therapy. Mayo Clin Proc 1991;66:906–13.

CHAPTER 27

RESPIRATORY MUSCLES IN SEPSIS

Camille Taillé, Sophie Lanone, Jorge Boczkowski, Michel Aubier

Sepsis is an important medical problem and is an increasingly common cause of morbidity and mortality, particularly in elderly, immunocompromised, and critically ill patients. In fact, severe sepsis is currently the most common cause of death in noncoronary intensive care units in the United States.[1]

From the time when the sepsis phenomenon was first observed, it has been evident that respiratory failure is a major manifestation of this pathologic condition. In fact, 35 years ago, Clowes and colleagues[2] reported that "life-threatening respiratory insufficiency frequently accompanies extensive infections located in other parts of the body." From that moment until now, respiratory failure during sepsis has been traditionally related to secondary lung injury, defined by Petty and Ashbaug[3] in the early 1970s as the adult respiratory distress syndrome (ARDS). Although it is not the sole cause of ARDS, sepsis remains the most common condition precipitating this catastrophic complication, which is associated, in septic patients, with mortality rates as high as 60 to 80%.[4]

Recent experimental data suggest that ARDS is not the only cause of respiratory failure during sepsis. In fact, a large body of experimental evidence has become available in the last 10 to 15 years that failure of the respiratory muscles during sepsis may be an important factor. Since maintenance of ventilation depends on the ability of the respiratory muscles to generate force, dysfunction of these muscles during sepsis can lead to hypoventilation and respiratory failure.

In this chapter, we review the effects of sepsis on respiratory muscle function and the possible mechanisms involved in the genesis of this phenomenon.

PRELIMINARY CONSIDERATIONS

Until quite recently, the term "sepsis" was a source of considerable confusion in animal models and clinical studies because it referred to different conditions in different studies. In order to clarify this situation, a consensus definition of sepsis and its related conditions was proposed recently.[1] From a clinical standpoint, sepsis can be defined as the systemic inflammatory response to infection, manifested by two or more of the following conditions as the result of infection: (1) temperature $>38°C$ or $<36°C$; (2) heart rate >90 beats/min; (3) respiratory rate >20 breaths/min or arterial partial pressure of carbon dioxide (P_aCO_2) <32 mm Hg; and (4) white blood cell count $>12{,}000/mm^3$, $<4{,}000/mm^3$, or $>10\%$ immature forms. Sepsis and its sequelae represent a continuum of clinical and physiopathologic severity. In this context, "septic shock" is defined as sepsis-induced hypotension, persisting despite adequate fluid resuscitation, along with the presence of hypoperfusion abnormalities and organ dysfunction.[1]

These definitions were established for use in clinical practice. In this chapter we focus primarily on animal studies, so we adapt the definitions cited above to the experimental setting. For the purpose of this review, we follow Wichterman and colleagues,[5] for whom "sepsis" refers to an infectious episode wherein an animal is toxic (febrile, weak, anorexic, lethargic, etc.) because of an invasive infection. "Septic shock" refers to the effects of sepsis leading to circulatory collapse. Consequently, we will consider septic shock as a subset of the septic condition, and the term "sepsis" will be used to refer to both situations unless specified otherwise.

EFFECTS OF SEPSIS ON RESPIRATORY MUSCLE FUNCTION

The physiopathology of organ dysfunction during sepsis is a multifactorial process. We have chosen to consider the abnormalities of muscle function in chronologic order because it seems that different physiopathologic aspects of muscle dysfunction predominate at different periods after the beginning of the septic process.

Immediate Effects of Sepsis on Respiratory Muscle Function

Nearly 20 years ago, Hussain and colleagues[6] first demonstrated, in spontaneously breathing dogs, that endotoxic shock resulted in respiratory muscle fatigue, which, in turn,

was the main factor responsible for respiratory failure and death in this experimental model of septic shock. The occurrence of respiratory muscle dysfunction in endotoxic shock was also demonstrated in our laboratory, in mechanically ventilated rats.[7] In this study, we observed a decrease in diaphragmatic strength restricted to the transdiaphragmatic pressure (P_{di}) generated at high frequencies of phrenic nerve stimulation (50 and 100 Hz), whereas twitch and low-frequency P_{di}, as well as muscle relaxation rate, remained unchanged. The endurance capacity of the diaphragm was curtailed in endotoxemic animals. Contractile dysfunction was associated with a decreased diaphragmatic resting membrane potential. This phenomenon, which was found in critically ill patients with various diseases[8] and in septic animal models,[9] could impair action potential generation, resulting in failure of neuromuscular transmission due to postsynaptic membrane depolarization as well as impaired propagation of electrical excitation along diaphragmatic fibers.

A major point in common between the two studies cited above is that blood pressure was significantly reduced in septic animals. It is well known that blood pressure is a major determinant of muscle metabolic substrate delivery and contractile function. In fact, the results of Hussain and colleagues[6] are very similar to those reported by Aubier and colleagues[10] in nonseptic hypotensive spontaneously breathing dogs. The similarity in findings raises the question of the role of hypotension in the physiopathology of the immediate effects of sepsis on respiratory muscle function.

Murphy and colleagues[11] evaluated the role of bacterial products in muscle dysfunction in 4-week-old piglets. These authors investigated, in spontaneously breathing animals, the effects on diaphragmatic strength of a continuous infusion of group B streptococcus at a level that caused a decrease in cardiac output but that avoided hypotension. Diaphragmatic strength was evaluated by measuring P_{di} generated during bilateral phrenic stimulation. The main result of this study was that P_{di} remained unchanged in septic animals over a 4-hour period. However, another study in the same laboratory[11] showed that increasing the dose of streptococcus did not cause significant hypotension but resulted in a transitory but significant decrease in diaphragmatic strength. Hurtado and colleagues[12] investigated the role of hypotension in peripheral muscle dysfunction during sepsis. These authors evaluated the effects of similar levels of septic and nonseptic hypotension on peripheral muscle metabolism and strength generation in rabbits. Blood pressure decreased by approximately 22% of baseline values in both groups of animals. This study showed that by the end of the experiment (180 minutes after the onset of hypotension), hindlimb force was significantly reduced in septic animals for all the frequencies of stimulation. However, a similar reduction was observed in nonseptic animals. Collectively, these studies suggest that both hypotension and bacterial products make individual contributions to the genesis of the immediate deleterious effects of sepsis on respiratory and peripheral muscle function.

Late Effects of Sepsis on Respiratory Muscle Function

Once the first reports on the immediate effects of sepsis on respiratory muscle function were published, investigators focused on the consequences of septic processes lasting several days. Using an in vivo rat model, we evaluated the modifications of diaphragmatic function 3 days after *Streptococcus pneumoniae* injection[13] and 2 days after inoculation of *Escherichia coli* endotoxin.[14] Both inoculations were performed subcutaneously, and both models of sepsis were nonlethal, with no changes in blood pressure, serum electrolytes, or acid–base status. The results of these studies were similar: 2 or 3 days of experimental sepsis in rats impaired diaphragmatic function, without affecting muscle mass and histology. Contractile force in response to phrenic stimulation was reduced without a concomitant decrease in the electrical activity of the muscle. Muscle relaxation rate was prolonged, and the diaphragms of septic animals became fatigued rapidly in response to a stimulation regimen that was without effect on the diaphragms of control animals.

Shindoh and colleagues[15] made similar findings in *E. coli* endotoxin-inoculated hamsters. More recently, Krause and colleagues[16] and Matuszczak and colleagues[17] showed decreased diaphragmatic force in experimental models of pancreatitis, suggesting that patients suffering from such disease could be susceptible to respiratory muscle failure.

The deleterious effects of 2 to 3 days of sepsis on muscular function are not limited to the respiratory muscles. With the use of an in vitro preparation, it was shown in rats that the strength of the soleus and extensor digitorum longus limb muscles was reduced after 3 days of pneumococcal sepsis.[18] In this study, limb muscle mass decreased significantly. When limb muscle tension was corrected for muscle mass, it was still reduced, indicating contractile impairment out of proportion to muscle wasting.

Chronic Effects of Sepsis on Respiratory Muscle Function

Finally, Drew and colleagues[19] examined the effects of a chronic infection lasting for several weeks, visceral leishmaniasis, on the function of the diaphragm and the soleus and plantaris peripheral muscles. Muscular function was assessed in vitro. Infected animals (intracardiac inoculation of *Leishmania donovani* amastigotes) were maintained for 7 to 12 weeks until advanced disease, characterized by anorexia, weight loss, and weakness, was evident. Body weight and the mass of the diaphragm, soleus muscles, and plantaris muscles were reduced in septic animals. Absolute contractile force of the diaphragm and soleus muscles was moderately reduced, only to the extent that muscle mass was decreased. Force normalized to muscle mass or cross-sectional area was not impaired. In contrast, the force of the plantaris muscle, a fast-twitch muscle, was severely reduced even after correction for loss of muscle mass. The effects of leishmaniasis on the diaphragm and soleus muscles were not different from those of semistarvation, with equivalent weight loss, but these models of sepsis produced much greater loss in plantaris muscle force than occurred with semistarvation.

MECHANISMS OF RESPIRATORY MUSCLE DYSFUNCTION DURING SEPSIS

The underlying mechanisms of respiratory muscle dysfunction occurring during the early phase and after several days of sepsis are certainly different. Indeed, energetic impairment appears to be a major pathophysiologic determinant of the dysfunction that develops early. This hypothesis is supported by the fact that early respiratory muscle dysfunction is closely related to the presence of hypotension, which can lead to decreased muscle bloodflow[20] and, thus, a reduction in the delivery of muscle metabolic substrates. In contrast, the late respiratory muscle dysfunction is clearly independent of hypotension. Indeed, muscle metabolic alterations during sepsis are complex and long-lasting, and it is plausible that metabolic alterations could be involved in the genesis of muscular dysfunction, not only in the short term but also in the long term. Indeed, metabolic alterations are triggered by mediators released as a part of the host response to the infectious aggression. We discuss, therefore, the mechanisms involved in respiratory muscle dysfunction during sepsis by considering first the energetic and metabolic aspects and, second, the role of inflammatory mediators (Figure 27-1).

ENERGETICS

From a general point of view, respiratory muscle dysfunction is thought to occur when the blood supply to the muscle is not sufficient to meet the muscle's metabolic needs.[21] The efficiency of uptake of substrates by these muscles mainly depends upon the total bloodflow that reaches them, the conditions of perfusion of the microvascular network, and the ability of muscle cells to use substrates. Sepsis can alter all of these processes.

The septic state is characterized by generalized bloodflow maldistribution among the different organs, including the respiratory muscles. However, this phenomenon is modulated by the degree of contractile activity of the muscle. Indeed, either immediately or late after the beginning of the septic process, if the diaphragm is at rest, its bloodflow decreases,[6] whereas if it contracts, bloodflow increases.[22] The increase in respiratory muscle bloodflow during septic shock can reach high levels, resulting in reduced bloodflow to the brain, the gastrointestinal tract, and other skeletal muscles.[6] It is predictable that, in this state, the function of the vital organs other than the respiratory muscles will be compromised. However, in spite of this finding, the values for diaphragmatic bloodflow observed during septic shock are much lower than the maximum reported in normotensive conditions[6] and are also lower than the maximum theoretical values that this parameter could reach for comparable levels of blood pressure, as estimated by Reid and Johnson's mathematical modeling.[23] Therefore, although diaphragmatic bloodflow is significantly increased during sepsis, a limitation of the maximal bloodflow related to sepsis is operational. This limitation could be situated at the microcirculatory level. Indeed, using an in vivo experimental model in rats, we showed that the number of perfused diaphragmatic capillaries decreased significantly after *E. coli* endotoxin inoculation.[24] This finding did not appear to be attributable to the low arterial pressure observed in this condition since the percentage of nonperfused capillaries did not increase in hypotensive nonseptic control subjects. The impaired capillary perfusion could be due to capillary obstruction by granulocytes[25] and/or to endothelial cell swelling.[25] This finding of a large functional capillary derecruitment may have important functional implications for metabolic substrate exchange and the oxygen extraction capacity of diaphragmatic myofibrils.

In addition to the microcirculatory limitation in the delivery of subtrates to the respiratory muscles, the ability of muscle cells to use subtrates is compromised in sepsis. *E. coli* endotoxin inoculation in rats induces an impairment in diaphragmatic mitochondrial respiration associated with increased production of hydrogen peroxide.[26,27] These alterations are secondary to induction of the inducible isoform of nitric oxide (NO) synthase (NOS-II) in the muscle (see below).

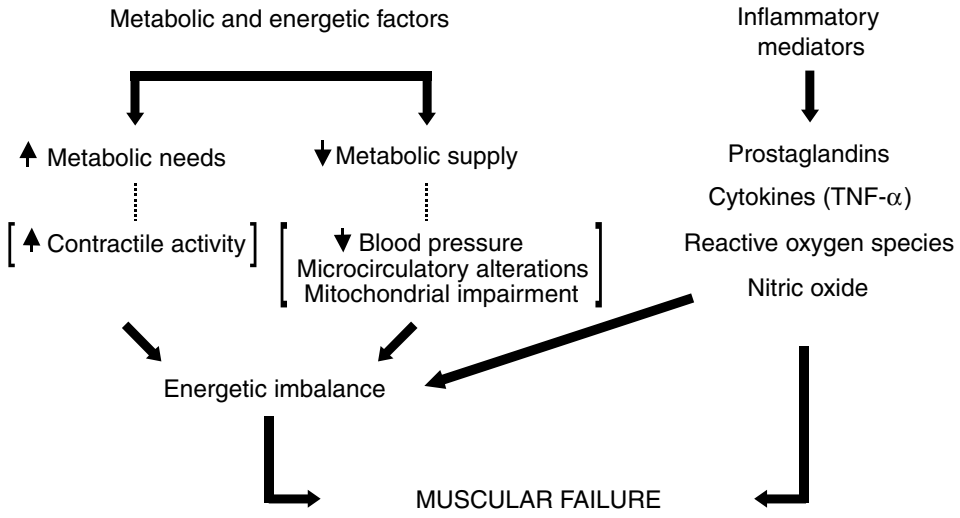

FIGURE 27-1 Mechanisms involved in respiratory muscle dysfunction during sepsis. TNF = tumor necrosis factor.

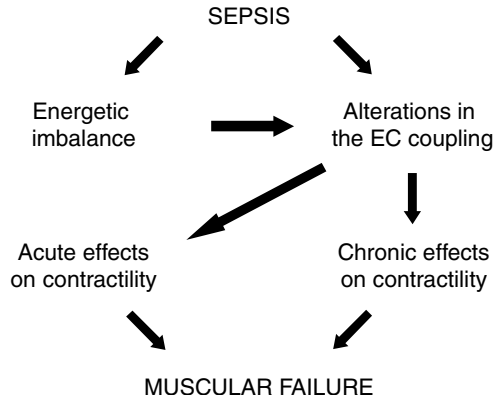

FIGURE 27-2 Respiratory muscle dysfunction during sepsis can be ascribed to the actions of endogenously produced mediators.

MEDIATORS

For many years, it has been recognized that the septic process is the result of extensive triggering of the body's defense mechanisms by the invading microorganisms and their products. These defense mechanisms include the release of cytokines into the circulation, activation of neutrophils and monocytes, and activation of plasma protein cascade systems such as the complement system, the intrinsic (contact system) and extrinsic pathways of coagulation, and the fibrinolytic system. In addition, these inflammatory mediators can act on target cells through locally produced molecules such as prostaglandins or NO. Studies performed in the last 10 years have shown that respiratory muscle dysfunction during sepsis can be ascribed to the actions of endogenously produced mediators, such as prostaglandins, cytokines, reactive oxygen species (ROS), and NO (Figure 27-2). In this section, we review these studies and discuss the mechanism(s) of action of each mediator.

Prostaglandins Several studies have indicated that prostaglandins play a role in the development of peripheral skeletal muscle dysfunction during sepsis.[18] Indeed, elevated prostaglandin E_2 levels have been found in the peripheral muscles of septic animals,[28,29] and pharmacologic inhibition of prostaglandin synthesis has been shown to protect septic animals from peripheral skeletal muscle impairment.[18] Similarly, the cyclooxygenase inhibitor indomethacin prevents the reduction in diaphragmatic strength found in animals with *E. coli* endotoxemia.[14] In addition, this agent prevents peripheral muscle atrophy. Similar results have been reported[30] for septic piglets. In this last study, systemic administration of thromboxane A_2 mimicked the reduction in diaphragmatic strength observed in septic animals.

Cytokines and Other Monocyte Inflammatory Mediators

Several laboratories have evaluated the effects of tumor necrosis factor-α (TNF-α) on respiratory muscle function. In vitro studies showed a dose-dependent decrease in diaphragmatic strength elicited by incubation of muscular fibers with murine or human TNF-α.[31] Incubation of diaphragmatic fibers for 1 hour in endotoxin-stimulated monocyte supernatant medium, which contained 146 ng/mL of TNF-α (a concentration that alone did not impair diaphragmatic contractility) and 30,000 U/mL of interleukin-1β (IL-1β),[32] also decreased diaphragmatic strength. This suggests a synergistic effect between TNF-α and IL-1β on diaphragmatic contractility. Furthermore, in vivo TNF-α induced a significant decrease in diaphragmatic force in dogs, beginning 4 hours after administration.[33] Although in the latter study cardiac output tended to decrease after TNF-α administration, it was maintained within normal values by fluid administration. However, no information on blood pressure was provided. Inoculation of rats with *E. coli* endotoxin induced TNF-α mRNA expression in the diaphragm, along with decreased force.[34] Pretreatment of the animals with an antimurine TNF-α antibody prevented the deterioration in diaphragmatic contractile properties.[34] Collectively, these findings suggest that TNF-α induces a decrease in diaphragmatic force generation. Different mechanisms could explain the effects of TNF-α on diaphragmatic contractility. Wilcox and colleagues[35] showed a role for prostaglandins, and Reid and colleagues[36] demonstrated that TNF-α decreases force by blunting the response of muscle myofilaments to activation by Ca^{2+}. Whether these effects are mediated directly by TNF-α or indirectly by the induction of molecules such as ROS and/or NO (see below) merits further investigation.

Reactive Oxygen Species

Sources of ROS During Sepsis ROS are produced by all aerobic organisms as a consequence of oxygen consumption and cell respiration. They have a role as intracellular mediators at physiologic concentrations. However, under conditions of stress, increasing production of ROS can lead to cellular injury. Under normal conditions, small amounts of ROS are produced in skeletal fibers in response to muscular activity by several cellular sources, such as NAD(P)H-dependent mitochondrial electron transport chains, membrane-bound oxidoreductases, cytosolic xanthine oxidase, arachidonic acid metabolism, and membrane-associated NAD(P)H oxidase.[37] The diaphragmatic muscle contains a large number of mitochondria and thus has a highly oxidative metabolism.[38] During sepsis, the rate of ROS production by respiratory muscles increases, releasing large amounts of superoxide anions, hydroxyl radicals, and hydrogen peroxide.[39] The toxic effects of these ROS on skeletal muscles are indicated by high levels of lipid peroxidation and protein carbonylation.[40] This enhanced ROS production comes from different cellular compartments: part of it depends on mitochondrial respiratory chain impairment following hemodynamic failure,[41] and another part comes from sepsis-activated constitutive skeletal muscle NAD(P)H oxidase.[37] White cells infiltrating skeletal muscle during sepsis contribute to the generation of oxidative stress to a lesser extent.[42]

Effects of ROS on Respiratory Muscle Function The participation of ROS in septic diaphragmatic failure has been clearly demonstrated in experimental models by the protective effect of antioxidant treatments, such as *N*-acetylcysteine,[43] catalase, and superoxide dismutase.[15]

Among the different ROS, superoxide, associated with NO and nitrogen species (see below), and the hydroxyl radical are the two species that play a central role in reducing fiber Ca^{2+} sensitivity and altering contractile protein capacity.[44] ROS reduce skeletal muscle force-generating capacity by inhibiting mitochondrial oxygen consumption.[27] In septic patients, an association between antioxidant depletion, mitochondrial dysfunction and organ failure, and outcome was found,[45] supporting the importance of oxidative stress in generating energetic failure. Oxidants can structurally alter different components of the excitation–contraction coupling system: T-tubules, sarcoplasmic reticulum Ca^{2+} ATPase, and the myosin head (leading to inhibition of actin–myosin binding). Protein oxidation in skeletal muscle occurs early during sepsis and is significantly correlated with the decline in mitochondrial respiration. Moreover, oxidized proteins are more sensitive to degradation. Proteolysis plays a role in the development of muscular weakness observed in sepsis. Finally, myoglobin oxidation decreases the oxygen storage capacity of the muscle.

Antioxidant Defenses Oxidative stress results from an increase in ROS production, as described before, and inadequate antioxidant defenses. Diaphragmatic muscle, because of its high oxidative capacity, also has abundant antioxidant systems. One of the most powerful of them is heme oxygenase (HO), the heme-degrading enzyme. HO produces carbon monoxide, bilirubin, and iron in equimolar concentrations.[46] Two HO isoforms, the inducible HO-1 and the constitutive HO-2, are expressed in skeletal muscles, but HO-1 is expressed in greater amounts in muscles with high oxidative metabolism, such as the diaphragm, soleus muscles, or myocardium.[47] HO-1 is extremely sensitive to a variety of agents that cause oxidative stress and is a powerful protective cellular system in several pathologic conditions, including sepsis. HO-1 is strongly induced in skeletal muscles during endotoxemia.[48] Moreover, pharmacologic activation of the HO pathway during sepsis completely prevents diaphragmatic oxidative stress and contractile failure,[48] whereas inhibition of HO activity enhances diaphragmatic dysfunction and inhibits the functional recovery usually observed 48 hours after endotoxemia. The exact mechanism of the protective effect of HO on muscular function is unknown, but it is possible that the ROS scavenger properties of HO-derived bilirubin and pro-oxidant free heme elimination are responsible for the decrease in oxidative stress. Furthermore, HO can protect against the deleterious effects of nitrogen reactive species by down-regulation of inducible nitric oxide synthase (iNOS) expression through the degradation of heme, an essential cofactor for iNOS protein assembly and activity.[46]

However, despite abundant antioxidants, the antioxidant capacity of the diaphragm is decreased during the first hours of sepsis.[49] This transient deficiency may be due to inactivation of antioxidant enzymes by NO and peroxynitrite, as described for HO-2, the constitutive form of HO.[50] In endotoxin-treated animals, diaphragmatic HO activity decreases during the first 12 hours, with no change in HO isoform expression, suggesting posttranslational modifications. HO activity increases after 24 hours, and this increase directly reflects HO-1 induction (since no change is observed in HO-2 expression).[48]

Despite their abundance, endogenous antioxidant defenses are not sufficient to counteract the high levels of ROS produced during sepsis and to prevent the occurrence of respiratory muscle failure. Interestingly, oxidative damage to diaphragmatic function can be limited by other treatments, such as mechanical ventilation.[51] Recent data have shown that mechanical ventilation can prevent sarcolemmal damage and improve diaphragmatic force, not by decreasing oxidative stress but by abrogating an injurious interaction between oxidative and mechanical stress imposed on the sarcolemma.

Nitric Oxide NO is a secondary messenger molecule that participates in numerous biologic processes, including vasodilatation, neurotransmission, and bronchodilatation. NO is synthesized by a group of enzymes named nitric oxide synthase (NOS), which are responsible for the conversion of L-arginine to L-citrulline and NO in the presence of oxygen. Three NOS isoforms (I to III) have been identified so far, and they all are expressed in respiratory muscles, particularly in the diaphragm.[52–54] NOS-I is mainly expressed in the sarcolemma of type II muscle fibers,[53] whereas NOS-III is localized to the mitochondria of skeletal muscle fibers[55] and the endothelium of diaphragmatic vessels.[53] In animal models of sepsis, it has been extensively demonstrated that NOS-II expression is induced in the diaphragm, at both the mRNA and protein levels, with a resultant increase in NO production.[54,56,57] Interestingly, NOS-II localization varies with the time since lipopolysaccharide (LPS) injection; it is present in the inflammatory cells at 6 and 12 hours after LPS injection, whereas the protein is expressed in skeletal myocytes in a diffuse cytoplasmic pattern from 12 to 24 hours and disappears after 48 hours.

Several lines of evidence suggest that impaired diaphragmatic contractility is a result of NO overproduction during sepsis. Boczkowski and colleagues[52] were the first to propose a link between in vivo induction of diaphragmatic NOS-II and its involvement in the genesis of diaphragmatic contractile dysfunction after *E. coli* endotoxin inoculation in rats. First, this study showed that the time course of NOS-II induction in diaphragmatic myocytes and that of the decrease in diaphragmatic force are similar. Indeed, when NOS-II was expressed in the clusters of inflammatory cells located in diaphragmatic venules and infiltrating the perivascular space of the muscle, no diaphragmatic contractile failure was observed. Altered diaphragmatic force was only seen when NOS-II was expressed in the diaphragmatic myocytes. Second, inhibition of NO synthesis by either NG-monomethyl-L-arginine (L-NMMA), an inhibitor of NOS activity, or dexamethasone, an inhibitor of NOS-II induction, significantly improves the decrease in diaphragmatic force observed in endotoxemic animals. Similar results were obtained by El-Dwairi and colleagues,[58] who used *S*-methylisothiourea as a NOS activity inhibitor. Interestingly, in the former study, the protection was observed for both diaphragmatic peak twitch and maximal

Table 27-1 Summary of the Results Obtained by Comtois and Collaborators[56,60] Showing a More Pronounced Alteration of Diaphragmatic Contractile Function in Response to LPS in NOS I and NOS II Knockout Mice

	NOS protein expression (KO vs WT animals)		*Total NOS activity (KO vs WT animals)*		*Diaphragmatic contractile function (KO vs WT animals)*	
	Basal	*LPS-induced*	*Basal*	*LPS-induced*	*Basal*	*LPS-induced*
NOS-I KO mice	NOS-II: not expressed NOS-III: no difference	NOS-II: less induced NOS-III: no difference	Less	No induction	No difference	More altered
NOS-II KO mice	NOS-I: less NOS-III: not done	NOS-I: more NOS-III: not done	No difference	More	No difference	More altered

KO = knockout; LPS = lipopolysaccharide; NOS = nitric oxide synthase; WT = wild type.

tetanic tension, whereas in the latter, inhibition of muscle NOS activity restored the LPS-induced decline in diaphragmatic force for the low stimulation frequencies (10 and 50 Hz) but not for the maximal frequency used (120 Hz). The discrepancies observed between the results of these different studies could be explained by the lack of exact specificity of the inhibitors used.

In an attempt to define the exact role of the different NOS isoforms in LPS-induced diaphragmatic contractile injury, Comtois and colleagues investigated their role in genetically engineered mice knockouts (KO) for either NOS-II or NOS-I. Table 27-1 summarizes the main results obtained in those two studies.[59,60]

Taken together, those studies tend to suggest that both NOS-I and NOS-II isoforms play protective roles in attenuating LPS-induced reduction in diaphragmatic contractile function, despite leading, respectively, to a decrease and an increase in NO synthesis. Interestingly, another study in NOS-II KO mice[61] showed that LPS injection induced less tyrosine nitration than in wild-type mice, although deficiencies in NOS-I or NOS-III did not affect this protein modification. This highlights the importance of the environment in which NO is synthesized. However, the mechanism(s) by which NO participates in the alteration of diaphragmatic contractile function remains to be determined.

The pharmacologic approach used by several authors has provided insights into the exact role that NO could play in the alteration of respiratory muscle function. Indeed, inhibition of NOS activity by administration of L-NMMA significantly reduced LPS-induced diaphragm sarcolemmal injury and altered resting membrane potential in rats,[57] and administration of another NOS inhibitor, NG-nitroarginine methyl ester (L-NAME), led to protection against the reduction in myofiber Ca^{2+} sensitivity observed in endotoxemic rats.[44] This could have a direct effect on muscular function. Another mediator of interest could be cGMP as it is widely known that NO activates soluble guanylyl cyclase, leading to cGMP synthesis.[62] Kobzik and colleagues[53] demonstrated that agents capable of increasing intracellular cGMP content, such as 8-bromo-cGMP, reverse the protective effect of NOS inhibitors on muscular force. However, in another study,[54] the activation of guanylyl cyclase observed in diaphragmatic muscle after LPS inoculation showed a biphasic time course; early activation appeared to be due to NO synthesized by NOS-II, whereas late activation was independent of NO. Thus, the exact role of cGMP in mediating the effects of NO in sepsis-induced diaphragmatic contractile dysfunction still remains to be elucidated.

NO by itself has a deleterious effect on mitochondrial respiration, with the inhibition of several enzymes, such as aconitase and cytochrome oxidase.[55,63] This effect of NO could contribute to the poor oxygen extraction observed in sepsis and thus participate in causing altered muscular function. Moreover, NO could produce its deleterious effects through its reaction with superoxide anion to form peroxynitrite anion ($ONOO^-$), a very strong oxidizing agent,[64] which targets various molecules such as thiols, lipids, and proteins containing aromatic amino acids and irreversibly inhibits several mitochondrial enzymes such as aconitase, NADH dehydrogenase, succinate dehydrogenase, and superoxide dismutase.[65–67] Several authors have described peroxynitrite formation in the diaphragm of endotoxemic animals,[54,58,61] mainly in the mitochondrial and membrane fractions of LPS-treated rat diaphragms,[61] treatment with L-NMMA leading to diminished nitration of diaphragmatic mitochondrial proteins.[26] Finally, studies aimed at determining the exact role of peroxynitrite in diaphragmatic contractile function showed that in vitro exposure of muscle samples to peroxynitrite itself or peroxynitrite-generating agents led to decreased force generation.[68] It must be pointed out, however, that exogenously generated peroxynitrite, because of its short half-life at physiologic pH,[68] may not react in the same way as endogenously produced peroxynitrite. The exact relationship between peroxynitrite generation and contractile function impairment is not entirely clear, but one explanation could be the oxidating and nitrating properties of peroxynitrite, which can lead to alterations in the proteins involved in the contractile process, such as actin[69] and the sarcoplasmic reticulum Ca^{2+}-ATPase.[70]

Clearly, more detailed evaluation of the role of NO release in modulating respiratory muscle contractile performance during sepsis is still needed.

CONCLUSION AND PERSPECTIVES

Clearly, sepsis impairs the function of respiratory muscles in different animal models. This impairment is observed soon after the onset of the septic process, and it may still be present after several weeks, depending on the duration of the infection. The dysfunction is strongly related to the hypotension that can be present in this condition. In contrast, the later effects (days to weeks) appear to be independent

of hemodynamic alterations and are related to physiopathologic processes that need some time (days to weeks) to develop.

Changes in respiratory energetic metabolism during sepsis may partly explain the observed decline in contractile function of the respiratory muscles. Delayed respiratory muscle dysfunction during sepsis appears to be related to the action of mediators such as prostaglandins, reactive oxygen and nitrogen metabolites, and TNF, acting alone or in concert. This is a new and rapidly growing field of research, and the exact mechanisms by which prostaglandins, oxidative metabolites, and TNF impair muscular function remain to be elucidated, as do the roles of other inflammatory molecules.

It can be postulated that sepsis impairs respiratory muscle function by acting at two levels. The first comprises disturbances at different steps of the chain of muscle energy supply: bloodflow and metabolic substrate extraction and utilization. The second is a direct impairment of the contractile process. These effects of sepsis probably result from the action of septic mediators. The result is a complex series of effects on the respiratory muscles that have potentially profound clinical consequences.

REFERENCES

1. Bone RC, Balk RA, Cerra FB, et al. Definitions for sepsis and organ failure and guidelines for the use of innovative therapies in sepsis. Chest 1992;101:1644–55.
2. Clowes GH Jr, Zuschneid W, Dragacevic S, Turner M. The nonspecific pulmonary inflammatory reactions leading to respiratory failure after shock, gangrene, and sepsis. J Trauma 1968;8:899–914.
3. Petty TL, Ashbaugh DG. The adult respiratory distress syndrome. Clinical features, factors influencing prognosis and principles of management. Chest 1971;60:233–9.
4. Montgomery AB, Stager MA, Carrico, CJ, Hudson LD. Causes of mortality in patients with the adult respiratory distress syndrome. Am Rev Respir Dis 1985;132:485–9.
5. Wichterman KA, Baue AE, Chaudry IH. Sepsis and septic shock—a review of laboratory models and a proposal. J Surg Res 1980;29:189–201.
6. Hussain SNA, Simkus G, Roussos C. Respiratory muscle fatigue: a cause of ventilatory muscle failure in septic shock. J Appl Physiol 1985;58:2033–40.
7. Leon A, et al. Effects of endotoxic shock on diaphragmatic function in mechanically ventilated rats. J Appl Physiol 1992;72:1466–72.
8. Cunningham JN Jr, Carter NW, Rector FC, Seldin D. Resting transmembrane potential difference of skeletal muscle in normal subjects and severely ill patients. J Clin Invest 1971;50:49–59.
9. Illner HP, Shires GT. Membrane defect and energy status of rabbit skeletal muscle cells in sepsis and septic shock. Arch Surg 1981;116:1302–5.
10. Aubier M, Trippenbach T, Roussos C. Respiratory muscle failure during cardiogenic shock. J Appl Physiol 1981;51:499–508.
11. Murphy TD, Mayock DE, Standaert TA, et al. Group B streptococcus has no effect on piglet diaphragmatic force generation. Am Rev Respir Dis 1992;145:471–5.
12. Hurtado FJ, Gutierrez AM, Silva N, et al. Role of tissue hypoxia as the mechanism of lactic acidosis during E. coli endotoxemia. J Appl Physiol 1992;72:1895–901.
13. Boczkowski J, Durevil B, Branger C, et al. Effects of sepsis on diaphragmatic function in rats. Am Rev Respir Dis 1988; 138:260–5.
14. Boczkowski J, Durevil B, Pariente R, Aubier M, et al. Preventive effects of indomethacin on diaphragmatic contractile alterations in endotoxemic rats. Am Rev Respir Dis 1990;142: 193–8.
15. Shindoh C, Dimarco A, Nethery D, Supinski G, et al. Effect of PEG-superoxide dismutase on the diaphragmatic response to endotoxin. Am Rev Respir Dis 1992;145:1350–4.
16. Krause KM, Moody MR, Andrade FH, et al. Peritonitis causes diaphragm weakness in rats. Am J Respir Crit Care Med 1998;157(4 Pt 1):1277–82.
17. Matuszczak Y, Vlires N, Allamedin H, et al. Alteration in diaphragmatic function induced by acute necrotizing pancreatitis in a rodent model. Am J Respir Crit Care Med 1999;160(5 Pt 1):1623–8.
18. Ruff RL, Secrist D. Inhibitors of prostaglandin synthesis or cathepsin B prevent muscle wasting due to sepsis in the rat. J Clin Invest 1984;73:1483–6.
19. Drew JS, Farkas GA, Pearson RD, Rochester DF, et al. Effects of a chronic wasting infection on skeletal muscle size and contractile properties. J Appl Physiol 1988;64:460–5.
20. Hussain SN, Roussos C, Magder S. Autoregulation of diaphragmatic blood flow in dogs. J Appl Physiol 1988;64:329–36.
21. Supinski G. Control of respiratory muscle blood flow. Am Rev Respir Dis 1986;134:1078–9.
22. Ferguson JL, Spitzer JJ, Miller HI. Effects of endotoxin on regional blood flow in the unanesthetized guinea pig. J Surg Res 1978;25:236–43.
23. Reid M, Johnson RL. Efficiency, maximal blood flow and aerobic work capacity of canine diaphragm. J Appl Physiol 1983;54:763–72.
24. Boczkowski J, Vicaut E, Aubier M. In vivo effects of E*scherichia coli* endotoxemia on diaphragmatic microcirculation in rats. J Appl Physiol 1992;72:2219–24.
25. Harlan JM. Leukocyte–endothelial interaction. Blood 1985;65: 513–25.
26. Boczkowski J, Lisdero C, Lanone S, et al. Endogenous peroxynitrite mediates mitochondrial dysfunction in rat diaphragm during endotoxemia. FASEB J 1999;13:1637–46.
27. Callahan L, Stofan D, Sweda L, et al. Free radicals alter maximal diaphragmatic mitochondrial oxygen consumption in endotoxin-induced sepsis. Free Radical Biol Med 2001;30: 129–38.
28. Turinsky J, Loegering DJ. Prostaglandin E2 and muscle protein turnover in P*seudomonas aeruginosa* sepsis. Biochim Biophys Acta 1985;840:137–40.
29. Hasselgren PO, Talamini M, LaFrance R, et al. Effect of indomethacin on proteolysis in septic muscle. Ann Surg 1985;202:557–62.
30. Murphy TD, Gibson RL, Standaert TA, Woodrum DL, et al. Diaphragmatic failure during group B streptococcal sepsis in piglets: the role of thromboxane A2. J Appl Physiol 1995;78:491–8.
31. Hopkins PM. Human recombinant TNF alpha affects rat diaphragm muscle in vitro. Intensive Care Med 1996;22: 359–62.
32. Wilcox PG, Bressler B. Effects of tumor necrosis factor α on in vitro hamster diaphragm contractility. Am Rev Respir Dis 1992;145:A457.
33. Wakai Y, Wilcox P, Cooper J et al. The effect of tumor necrosis factor α (TNF α) on diaphragmatic contractility in anesthetized dogs. Am Rev Respir Dis 1991;143:A560.
34. Shindoh C, Hida W, Ohkawara Y, et al. TNF-alpha mRNA expression in diaphragm muscle after endotoxin administration. Am J Respir Crit Care Med 1995;152(5 Pt 1):1690–6.

35. Wilcox P, Milliken C, Bressler B. High-dose tumor necrosis factor alpha produces an impairment of hamster diaphragm contractility. Attenuation with a prostaglandin inhibitor. Am J Respir Crit Care Med 1996;153:1611–5.
36. Reid MB, Lannergren J, Westerblad H. Respiratory and limb muscle weakness induced by tumor necrosis factor-alpha: involvement of muscle myofilaments. Am J Respir Crit Care Med 2002;166:479–84.
37. Javesghani D, Magder SA, Barreiro E, et al. Molecular characterization of a superoxide-generating NAD(P)H oxidase in the ventilatory muscles. Am J Respir Crit Care Med 2002; 165:412–8.
38. Poole DC, Sexton WL, Farkas GA, et al. Diaphragm structure and function in health and disease. Med Sci Sports Exerc 1997;29:738–54.
39. Nethery D, DiMarco A, Stofan D, Supinski G, et al. Sepsis increases contraction-related generation of reactive oxygen species in the diaphragm. J Appl Physiol 1999;87: 1279–86.
40. Supinski G, Stofan D, Callahan LA, et al. Peroxynitrite induces contractile dysfunction and lipid peroxidation in the diaphragm. J Appl Physiol 1999;87:783–91.
41. Poderoso JJ, Peralta J, Lisdero C, et al. Nitric oxide regulates oxygen uptake and hydrogen peroxide release by the isolated beating rat heart. Am J Physiol 1998;274:C112–9.
42. Supinski G, Stofan D, Nethery D, et al. Apocynin improves diaphragmatic function after endotoxin administration. J Appl Physiol 1999;87:776–82.
43. Callahan L, Nethery D, Stofan D, et al. Free radical-induced contractile protein dysfunction in endotoxin-induced sepsis. Am J Respir Cell Mol Biol 2001;24:210–7.
44. Brealey D, Brand M, Hargreaves I, et al. Association between mitochondrial dysfunction and severity and outcome of septic shock. Lancet 2002;360:219–23.
45. Foresti R, Motterlini R. The heme oxygenase pathway and its interaction with nitric oxide in the control of cellular homeostasis. Free Radic Res 1999;1–17.
46. Taillé C, Lanone S, Aubier M, et al. Stress oxydant et diaphragme: rôle dans la défaillance contractile au cours du sepsis. Rev Mal Respir 2002;19:593–9.
47. Llesuy S, Evelson P, Gonzalez-Flecha B, et al. Oxidative stress in muscle and liver of rats with septic syndrome. Free Radic Biol Med 1994;16:445–51.
48. Ding Y, McCoubrey WK Jr, Maines MD. Interaction of heme oxygenase-2 with nitric oxide donors. Is the oxygenase an intracellular "sink" for NO? Eur J Biochem 1999;264:854–61.
49. Ebihara S, Hussain S, Danialov G, et al. Mechanical ventilation protects against diaphragm injury in sepsis. Interaction of oxidative and mechanical stresses. Am J Respir Crit Care Med 2002;165:221–8.
50. El Dwairi Q, Guo Y, Comtois A, et al. Ontogenesis of nitric oxide synthases in the ventilatory muscles. Am J Respir Cell Mol Biol 1998;18:844–52.
51. Kobzik L, Reid MB, Bredt DS, Stamler JS, et al. Nitric oxide in skeletal muscle. Nature 1994;372:546–8.
52. Boczkowski J, Lanone S, Ungureanu-Longrois D, et al. Induction of diaphragmatic nitric oxide synthase after endotoxin administration in rats. J Clin Invest 1996;98:1550–9.
53. Kobzik L, Stinger B, Balligand JL, et al. Endothelial type nitric oxide synthase in skeletal muscle fibers: mitochondrial relationships. Biochem Biophy Res Commun 1995;211: 375–81.
54. Hussain S, Giaid A, El Dwairi Q, et al. Expression of nitric oxide synthases and GTP cyclohydrolase I in the ventilatory and limb muscles during endotoxemia. Am J Respir Cell Mol Biol 1997;17:173–80.
55. Lin M-C, Ebihara S, El Dwairi Q, et al. Diaphragm sarcolemmal injury is induced by sepsis and alleviated by nitric oxide synthase inhibition. Am J Respir Crit Care Med 1998;158: 1656–63.
56. Comtois A, Barreiro E, Huang P, et al. Lipopolysaccharide-induced diaphragmatic contractile dysfunction and sarcolemmal injury in mice lacking the neuronal nitric oxide synthase. Am J Respir Crit Care Med 2001;163:977–82.
57. Liu S, Lai J, Yang R, Lin-Shiau S. Nitric oxide is not involved in the endotoxemia-induced alterations in Ca^{2+} and ryanodine responses in mouse diaphragms. Naunyn Schmiedebergs Arch Pharmacol 2002;366:327–34.
58. El Dwairi Q, Comtois A, Guo Y, Hussain S. Endotoxin-induced skeletal muscle contractile dysfunction: contribution of nitric oxide synthases. Am J Physiol 1998;274:C770–9.
59. Gath I, Gödtel-Armbrust U, Föstermann U. Expressional down-regulation of neuronal-type NO synthase I in guinea pig skeletal muscle in response to bacterial lipopolysaccharide. FEBS Lett 1997;410:319–23.
60. Comtois A, El Dwairi Q, Laubach V, Hussain S, Lipopolysaccharide-induced diaphragmatic contractile dysfunction in mice lacking the inducible nitric oxide synthase. Am J Respir Crit Care Med 1999;159:1975–80.
61. Moncada S, Higgs A. The L-arginine–nitric oxide pathway. N Engl J Med 1993;329:2002–12.
62. Cleeter MWJ, Copper JM, Darley-Usmar VM, et al. Reversible inhibition of cytochrome c oxidase, the terminal enzyme of the mitochondrial respiratory chain, by nitric oxide. FEBS Lett 1994;345:50–4.
63. Beckman JS, Beckman TW, Chen J, et al. Apparent hydroxyl radical production by peroxynitrite: implications for endothelial injury from nitric oxide and superoxide. Proc Natl Acad Sci U S A 1990;87:1620–4.
64. Radi R, Rodriguez M, Castro L, Telleri R, et al. Inhibition of mitochondrial electron transport by peroxynitrite. Arch Biochem Biophys 1994;308:89–95.
65. Ischiropoulos H, Zhu L, Chen J, et al. Peroxynitrite-mediated tyrosine nitration catalyzed by superoxide dismutase. Arch Biochem Biophys 1992;298:431–7.
66. Poderoso JJ, Carreras MC, Lisden C, et al. Nitric oxide inhibits electron transfer and increases superoxide radical production in rat heart mitochondria and submitochondrial particles. Arch Biochem Biophys 1996;328:85–92.
67. Barreiro E, Comtois A, Gea J, et al. Protein tyrosine nitration in the ventilatory muscles. Role of nitric oxide synthases. Am J Respir Cell Mol Biol 2002;26:438–46.
68. Brunelli L, Crow JP, Beckman JS. The comparative toxicity of nitric oxide and peroxynitrite to *Escherichia coli*. Arch Biochem Biophys 1995;316:327–34.
69. Hantler PD, Gratzer WB. Effects of specific chemical modification of actin. Eur J Biochem 1975;60:67–72.
70. Viner RI, Huhmer AFR, Bigelow DJ, Schoneich C. The oxidative inactivation of sarcoplasmic reticulum Ca^{2+}-ATPase by peroxynitrite. Free Radic Res 1996;24:243–59.

CHAPTER 28

REHABILITATION OF SKELETAL MUSCLES IN CHRONIC OBSTRUCTIVE PULMONARY DISEASE

Thierry Troosters, Rik Gosselink, Marc Decramer

RATIONALE FOR TRAINING THE SKELETAL MUSCLES IN CHRONIC OBSTRUCTIVE PULMONARY DISEASE

Skeletal muscle function is frequently impaired in patients with chronic obstructive pulmonary disease (COPD),[1] even in those persons affected by mild disease.[2] Whether the abnormalities are mainly due to deconditioning are more related to a systemic effect of the disease, or, indeed, result from its treatment with corticosteroids is still a matter for discussion. The main abnormalities that are described are skeletal muscle weakness, atrophy, muscle damage, excessive cell death by apoptosis, and myopathy. This topic is discussed in more detail elsewhere in this book (see Chapter 49, "Peripheral Muscle Dysfunction in Chronic Obstructive Pulmonary Disease").

Muscle weakness is associated with significant disability and can affect the overall prognosis. First, muscle weakness contributes to exercise intolerance in COPD.[3,4] Second, patients with frequent hospital admissions show a greater degree of impairment of muscle strength than do patients who make less use of health care resources.[5] Finally, patients with steroid-induced myopathy have a reduced survival rate.[6] Recently, Marquis and colleagues[7] have shown that reduced muscle bulk, as measured by midthigh cross-sectional area, is an important contributor to survival, even in patients with moderate COPD. These observations suggest that reversing skeletal muscle weakness should be a target of therapy for COPD. In this chapter, the extent to which muscle dysfunction can be improved, and the strategies by which to do so, are discussed.

EFFECT OF EXERCISE TRAINING ON SKELETAL MUSCLES

The effects of exercise training on physiologic outcomes and health-related quality of life in COPD have been well established in randomized controlled studies.[8] Exercise training can be studied at the level of the intact muscle, at the level of the muscle fiber, and at the level of the molecular mechanisms of function of the muscle fiber.

Exercise training (see below) in patients with COPD enhances muscle strength and isolated muscle endurance. In addition to increased strength, increased muscle mass has been reported, especially when resistance training is added to the program. This suggests that hypertrophy can be achieved with exercise training in COPD, especially if these programs include a resistance training component. Whole body endurance, skeletal muscle endurance, and quadriceps fatigability improve considerably after exercise training, even when no specific resistance training is performed.[2,9]

Approaches to Skeletal Muscle Training in COPD

Exercise training is intended to restore skeletal muscle strength, muscle bulk, muscle endurance, muscular efficiency, muscle bioenergetics, and, at the cellular level, the oxidative capacity. In this chapter, the main focus is on the skeletal muscle. The effects of exercise training on other organ systems are not dealt with here, but adaptations of these systems also probably contribute to the effects of exercise training.

Exercise training programs generally consist of endurance training, interval training, and/or resistance training. The evidence suggests that the minimal time needed to achieve the clinically relevant benefits of exercise training in COPD is 8 weeks of three sessions/week. Sufficient stress on the working muscle is a prerequisite in order to achieve exercise training effects. Exercise training should be conducted at high workloads if physiologic benefits are the desired outcome.[10] Owing to ventilatory constraints, it may be difficult to stress the working muscle of COPD patients sufficiently. This led to the early misconception that COPD patients were difficult, if not impossible,

to train.[11] However, about two-thirds of patients referred to pulmonary rehabilitation derive significant physiologic benefits from exercise training.[12] The different exercise training modalities are discussed below.

Resistance Training* This form of exercise training consists of lifting adjusted weights. Generally, training intensity is set at 70% of the weight that a patient can lift once, over the full range of motion. From a review of the literature, McDonagh and Davies[13] concluded that, to improve strength, a load of at least 66% of the maximum weight that can be lifted once (the one repetition maximum; 1RM) was required and had to be lifted at least 10 times. In addition, the higher the workload, the greater the training effect. Empirically, most training programs use 20 to 30 repetitions. Although the training modality was introduced in 1945,[14] there have been few studies in which this intervention has been attempted in COPD patients. The interesting aspect of this form of exercise training is that relatively small muscle groups are put to work. This allows the imposition of relatively high workloads, without exceeding the ventilatory capacity of the patient.[15] The findings of studies on COPD[16–18] and other chronic diseases[19,20] have unanimously confirmed that weight-lifting results in improved muscle strength. There has been only one investigation of the effect of resistance training on muscle cross-sectional area in COPD patients, and the results showed an added effect of resistance training to that of regular endurance training in COPD in improving muscle cross-sectional area.[21] In healthy elderly subjects, specific resistance training is a valuable tool and superior to endurance training for restoring muscle bulk.[22–24] Interestingly, the effects of strength training are not confined to improved muscle strength. In patients with COPD,[16–18] as well as in healthy elderly subjects, beneficial effects of resistance training on whole body endurance[25] and health-related quality of life[17] have been shown. In healthy elderly subjects, resistance training has also been shown to improve muscle oxidative capacity. Furthermore, Jubrias and colleagues showed improved mitochondrial volume density after resistance training and a faster phosphocreatine recovery time as measured with ^{31}P-magnetic resonance spectroscopy,[24] both undisputed markers of improved mitochondrial oxidative capacity. These improvements are generally not seen in younger individuals. In healthy, untrained elderly subjects, oxidative capacity is impaired,[26] and atrophy is present. In animal models of aging, even apoptotic changes are seen.[27] In patients with congestive heart failure (CHF), apoptosis of skeletal myocytes is associated with lower exercise tolerance. Resistance training appears to diminish these derangements, both in healthy subjects and in subjects with chronic disease. In addition, resistance training may have a positive effect on bone mineral density, as has been demonstrated in healthy elderly subjects.[28,29] Since osteoporosis is frequent in COPD, this ancillary effect merits further investigation in COPD.

*Resistance training (or strength training) consists of small muscle group training by lifting weights. This form of training should be distinguished from whole body exercise on ergometers. For this latter form of exercise, we use in this chapter "endurance training" or "interval training."

The effect of resistance training on the adaptations at the level of muscle fibers in patients with COPD has not yet been investigated in any studies. However, since the effects of this modality of training are largely comparable to the effects obtained in healthy elderly subjects and in patients with CHF, one can speculate that the effects at the muscle fiber level are equivalent to those observed in healthy elderly subjects. In elderly subjects, resistance training is associated with a relative increase in the proportion of type I and IIa muscle (oxidative) fibers and a relative decrease in the number of type IIb fibers,[30,31] which is consistent with the improved oxidative capacity.

Resistance training may also impact on markers of systemic inflammation. Recently, it was hypothesized that systemic inflammation and overexpression of tumor necrosis factor-α (TNF-α) may play a role in the onset of muscle weakness.[1] In addition, apoptosis, seen in the quadriceps muscle of low body mass index (BMI) COPD patients, may also be influenced by the presence of TNF-α.[32] It was convincingly shown, in an intriguing study by Greiwe and colleagues,[33] that myocytes of frail elderly subjects produced TNF-α and that resistance training reduced TNF-α expression. Similarly, Conraads and colleagues showed reduced concentrations of circulating TNF-α receptor levels after combined endurance and resistance training in subjects with CHF.[34] What happens to the increased TNF-α expression observed in skeletal muscle from COPD patients[35] after resistance training remains to be studied. Both high- and low-intensity resistance training may have protective effects against oxidative stress.[36] These findings are of the utmost importance to patients with COPD. If resistance training in subjects with COPD could have similar effects, that is, reduction in systemic inflammation and protection against oxidative stress, this therapy would be able to modify the pathogenesis and onset of muscle weakness in COPD, especially in fragile, low-BMI patients.

Recently, the question of whether neuromuscular electrostimulation could be a way to stimulate the skeletal muscle adequately was investigated in two studies.[37,38] Electrical stimulation was delivered with the use of bipolar interferential current or low-frequency current (symmetric biphasic).[38,39] The results of both studies suggest that this form of exercise may be a useful tool for improving muscle strength and endurance capacity.

In summary, resistance training, applied through weight-lifting, is an appealing way to impose a high load on specific muscles without exceeding the ventilatory capacity of patients with COPD. The beneficial effects of resistance training include improved strength and endurance properties of the skeletal muscle. Resistance training is therefore a useful tool in the exercise training programs of patients with COPD.

Whole Body Exercise Training The most common type of clinical exercise training in COPD and other chronic diseases is dynamic exercise training. This form of exercise training is generally performed on cycle ergometers and treadmills. Some investigators have also used free walking as a mode of exercise.[40] In the latter case, the intensity is,

however, poorly controlled. The upper limbs can be trained with the use of specific arm ergometers. As with resistance training, the goal of this form of exercise training is to provide a training stimulus to the working muscle with the added benefit of also generating adaptations of the cardiovascular and respiratory systems. Exercises should be performed for at least 30 minutes, three times per week, if the goal is to improve exercise capacity.[41] In addition, physiologic improvements are only achieved when the training is performed at high intensity.[10,40] Initially, it was believed that the training intensity needed to be above the lactic threshold,[42] but later publications reported clear physiologic training effects, even in the absence of lactic acid production (measured in the blood), provided that a high relative workload ($>$60% of the maximal workload) was imposed.[43,44] It is recommended that training intensity be targeted at 60 to 70% of the peak work rate of the patient. Careful design of the incremental exercise test is, however, critical[45] since the choice of the increments may determine the duration of the exercise test and the achieved peak power. The correct training intensity can be confirmed by using symptom scores (Borg rating) of about 4/10 to 6/10. This level of respiratory sensation is associated with an exercise intensity of about 80% of the peak exercise capacity. It was confirmed in a recent study that dyspnea ratings for a given relative work rate do not change throughout a 6-week training program.[46] Adopting this strategy, we showed statistically and clinically relevant effects of exercise training.[47] There are some important limitations to these tools; for example, patients may experience a "learning curve" in using the Borg scores for symptoms and may quickly become desensitized to dyspnea.[48]

Patients with more severe disease may also have more difficulty in meeting the criterion of 30 minutes of continuous exercise.[49] Training programs can be adjusted without the focus of the high training intensity being lost. Cutting the 30 minutes into shorter intervals of high-intensity exercise has been reported to result in similar training effects to those of endurance training.[50,51] Even periods as short as 30 seconds of high-intensity exercise alternating with rest have been used as a training modality. Use of this modality may indeed result in lower symptom scores during exercise training.[52] Further research, however, needs to be focused on the effects of these programs on the skeletal muscles. Most of the effects described below have been studied with the use of endurance training at high intensity.

The effects of cycle ergometer or whole body exercise training on peripheral muscles have been well studied in COPD patients, and the evidence for its usefulness is strong.[53] The aim of implementing dynamic endurance training is to improve the skeletal muscle endurance capacity. This goal is met through an improvement of the overall oxidative capacity of the skeletal muscle and a reduction in fatigability. No improvements are seen in the oxygen delivery to the working skeletal muscles with exercise,[54] in contrast to what is observed in healthy controls. In a well-designed study by Sala and colleagues[54] (Figure 28-1), the effects of endurance training on skeletal muscle oxidative capacity were clearly shown in healthy subjects and patients with COPD. From the results of this study, it can be concluded that patients with COPD are able to restore the extraction ratio of the lower limbs after exercise training, which is indicative of improved oxidative capacity at submaximal work loads. Peak oxygen consumption (VO_2), however, cannot increase to a large extent as patients with ventilatory constraints may not be able to increase their peak oxygen delivery to the same degree as healthy subjects. The results of Sala and colleagues also confirm that endurance training in patients with COPD improves oxidative capacity. This was demonstrated by the increased intramuscular pH, a better preserved intramuscular phosphocreatine (PCr) pool—indicated by a lower inorganic phosphate concentration ($[P_i]$)/[PCr] ratio—at submaximal work rates after training, and a faster [PCr] recovery time.

The improved oxidative capacity of skeletal muscles after endurance training may be mediated by many factors. Maltais and colleagues showed an increased concentration of citrate synthase and 3-hydroxyacyl-CoA dehydrogenase, two enzymes important in oxidative phosphorylation, reflecting the oxidative capacity of the skeletal muscle.[55] In addition, these investigators showed a specific increase in the cross-sectional area of oxidative muscle fibers type I and IIa.[56] An improved oxidative capacity of the skeletal muscle will lead to less rapid onset of lactate accumulation and will result in a reduction of minute ventilation (and hence dyspnea) for an identical level of oxygen consumption. Lactate production is not a prerequisite for the achievement of training effects. Frequently, patients with severe COPD are

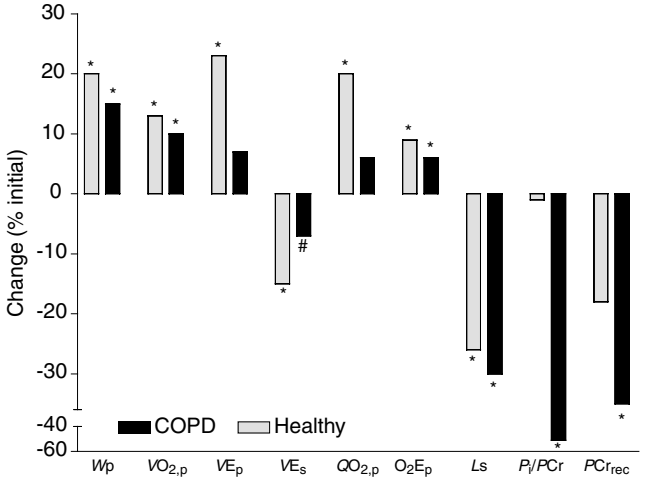

FIGURE 28-1 Overview of training effects. All effects of exercise training are displayed as a percentage of the initial value. Effects are displayed for healthy control subjects and COPD patients (FEV_1 43 ± 9% of predicted). Peak work rate (W_p), peak VO_2 ($VO_{2,p}$), peak ventilation (VE_p), and peak oxygen delivery to the leg ($QO_{2,p}$) are unchanged in COPD after training. Submaximal ventilation (VE_s) tended to decrease. A training effect in terms of oxidative capacity of the muscle is evidenced by increased peak oxygen extraction ratio (O_2E_p), calculated as (arterial oxygen content − femoral venous oxygen content)/arterial oxygen content, reduced lactate level at submaximal isowork (L_s), ratio of inorganic phosphate/phosphocreatine (P_i/PCr), and time to replace half of the available phosphocreatine (PCr_{rec}). *$p < .05$, #$p = .12$, one tail). Adapted from Sala E et al.[54]

limited by ventilatory factors during an incremental exercise test, without demonstrating significant lactate production. These patients may, however, also benefit from dynamic exercise training.[49] The physiologic effect of endurance training in patients not producing lactate can be appreciated from faster oxygen uptake kinetics,[44] and reductions in fatigability of the quadriceps muscle.[9]

It is important to acknowledge that in patients with COPD, as in healthy subjects, training effects are specific. One of the important benefits to patients is the improved mechanical efficiency achieved by practice. Therefore, patients will achieve a higher power output, even without improving peak VO_2. Generally, the effects of exercise training on peak work rate are 20 to 25%, whereas peak VO_2 improves by 10 to 15%. We analyzed data from 22 patient groups from 16 independent studies (total $n = 498$) in which the effect of exercise training in COPD was investigated.[9,18,21,44,47,51,52,54–61] The effects found in each of these studies for $VO_{2,peak}$ and peak work rate are summarized in Figure 28-2. The mean change in peak work rate, weighted for the number of subjects studied, was $20 \pm 41\%$, and the mean change in peak VO_2 was $8 \pm 25\%$. This analysis again shows the improved mechanical efficiency as in all studies the change in peak work rate is larger than the change in peak VO_2.

Although the mean effects of endurance and interval training are undisputed, about one-third of patients may not respond as expected to this intervention[12]; the reasons for this are not yet understood. It is possible that these patients have less muscle weakness before starting the exercise training, are more ventilatory limited, or are less compliant with therapy.[12] These variables, however, allow prediction of

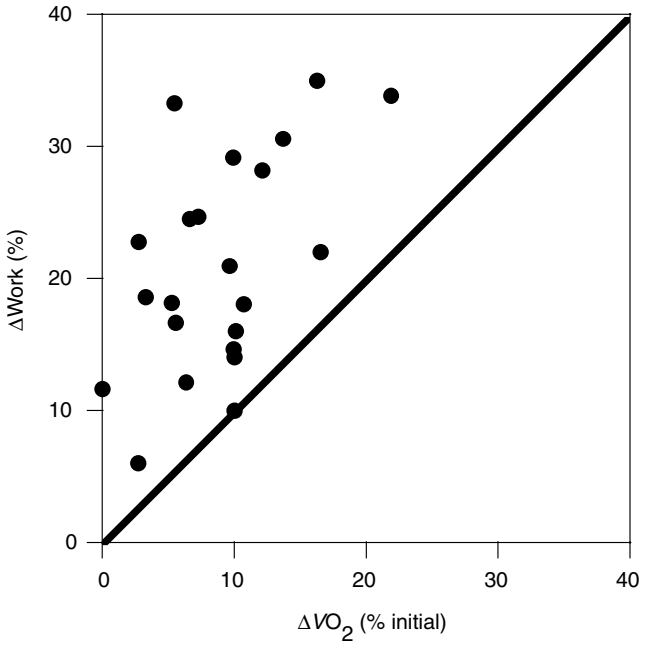

FIGURE 28-2 Results for 22 patient groups from 16 independent studies in which the effects of different training programs in patients with COPD were investigated. The results of every study showed a greater increase in work rate than in peak oxygen uptake.

training response for only about 40%. Other variables may therefore further explain the poor response to exercise training. Rabinovich and colleagues[58] studied the effect of endurance training on skeletal muscle redox capacity and observed that some patients (especially those with a low BMI) have impaired muscle redox capacity after a daily exercise training program. These patients become more susceptible to oxidative stress after exercise training. It remains largely unstudied whether exercise training increases oxidative stress in selected patients. In addition, further studies are required to investigate the role of antioxidants in preventing oxidative stress.

Effect of Combining Resistance and Dynamic Training Modalities Exercise programs that combine resistance and dynamic training modalities may improve muscle strength and general exercise capacity[47,62]; however, the literature in this area is still sparse. The results of two studies, in particular, have confirmed the additive effect of a program combining resistance and endurance training in patients with COPD.[18,21] Consequently, exercise training in patients with COPD should include endurance or interval dynamic exercises and resistance training. A 40-minute program consisting of endurance (20 min) and resistance (20 min) training proved to be superior to 40 minutes of exercise training in each of the modalities separately.[18]

Training the Upper Limbs in Patients with COPD

Although most research has been focused on the effects of lower limb exercise training, it is important to recognize that COPD patients may encounter problems in carrying out the activities of daily living with the upper limbs.[63] Carefully conducted research, however, has revealed that the upper limb muscles (ie, shoulder girdle) may suffer less from the deconditioning generally seen in the lower limb[64] and that the mechanical efficiency of upper limb activities is relatively well preserved compared with the mechanical efficiency observed in healthy subjects.[65] Despite these relatively favorable conditions, COPD patients report excessive symptoms during upper limb activities. The main reason is the coupling of respiration to the muscles involved in upper limb movement. Upper limb exercises do impact on the breathing pattern.[66] This is even more the case during unsupported arm exercises, where relatively more load is shifted toward the diaphragm.[67] Hence, at isoventilation, more dyspnea is reported during upper limb exercises compared with lower limb exercise in COPD patients, especially during unsupported upper limb exercises.[68] Upper limb exercise training programs can be used to reduce dyspnea during upper limb activities.[69] Lower limb exercise training will not improve upper limb performance,[70] so that, if improving upper limb performance is the aim of the training program, specific upper limb exercises should be included. Exercise programs including upper arm exercises reduce the ventilatory requirements for arm elevation.[71,72] Martinez and colleagues suggested that unsupported arm exercises are to be preferred over ergometer training as an exercise modality as they mimic more accurately the activities of daily living.[73]

STRATEGIES FOR "DIFFICULT-TO-TRAIN PATIENTS"

In recent years, efforts have been made to improve the outcome of exercise training in patients who are difficult to train. Generally, the methods used can be placed into two categories: (1) methods that enhance training intensity and (2) methods that stimulate muscle growth. These are summarized in Table 28-1.

Some of these methods are briefly discussed below, but the evidence to support these strategies is limited, and the interventions should be restricted to particular patient subgroups. Proper patient selection seems to be key to the efficient use of resources.

Methods to Enhance Training Intensity

Since there seems to be a dose–response effect of exercise training, enhancing training intensity should result in increased training effects. Owing to the severe mechanical limitations of the ventilatory system, it may be difficult to achieve high workloads in some patients. Indeed, Richardson and colleagues[15] showed, in a small group of very severe COPD patients (forced expiratory volume in 1 second [FEV_1] 0.97 L), that the skeletal muscle had considerable metabolic reserve and that it could cope with higher metabolic loads when the ventilatory limitation was alleviated with the use of 100% oxygen or a helium–oxygen gas mixture (Heliox).

Oxygen acutely improves peak exercise performance in selected COPD patients. It is generally accepted that oxygen supplements reduce ventilatory requirements, both at rest and during exercise. In addition, oxygen supplementation clearly increases oxygen delivery, especially in hypoxemic patients. The consequence of this is that higher work rates can be achieved for the same level of ventilation. Therefore, the use of oxygen breathing may improve training intensity and therefore may impact on the training effect. Although the theoretical concept seems appealing, data are scarce concerning the benefits of oxygen supplementation in exercise training. To the best of our knowledge, three studies have been published so far.[74–76] None has shown beneficial effects of oxygen supplementation. However, the patients studied by Rooyackers and colleagues were only mildly hypoxemic at maximal exercise,[74] and in the study by Garrod and colleagues,[75] only a short-term exercise training program was applied, at very low work rates (unloaded pedaling). Exercise intensity with the use of oxygen supplementation was carefully investigated in a recent double-blind prospective exercise training study; the results confirmed higher training intensities and more pronounced training effects in the group that received oxygen.[77] As a clinical guideline, we suggest that oxygen supplementation be used in those patients in whom the capacity for high-intensity training is clearly increased. Very often, it is claimed that oxygen should be administered to maintain oxygen saturation above an arbitrary certain level (89 to 90%). This concept, however reasonable it may appear, is not evidence based as brief periods of hypoxemia have not been shown to result in adverse effects,[78] and training with hypoxemia may even be beneficial for the muscle if an adequate training stimulus can be provided.

A second way to unload the ventilatory system is through the application of noninvasive mechanical ventilation (NIMV). When properly applied, ventilatory help with techniques such as proportional assist ventilation (PAV) or bilevel positive airway pressure (BiPaP) increases the exercise capacity of COPD patients[79] and may be effective in preventing diaphragmatic fatigue during high-intensity exercise.[80] Indeed, a higher training load can be achieved in patients with severe COPD[81] when PAV is used, resulting in more pronounced training effects. In patients with less severe disease, however, application of NIMV does not result in enhanced training effects.[82] Since the application of NIMV is time-consuming and adjustment of the ventilator settings to the needs of the patient during variable exercise is difficult, this intervention will probably be restricted to highly selected patients.

A last, and potentially appealing, way to reduce the work of breathing, and hence improve ventilatory capacity, is through the breathing of gas mixtures of lower density than air.[83] An often-used mixture is helium 79%/oxygen 21% (Heliox, HeO_2). This combination of gases increases peak exercise performance for whole body exercise,[15] resulting in a possible enhanced training effect. This strategy has been investigated in only one study, and no significant effects were found.[84] In this study, HeO_2 was administered at a maximal flow rate of only 10 L/min, and training was only conducted twice a week for 6 weeks. Despite these limitations, the authors showed a trend for more improvement when HeO_2 was administered during exercise training ($37 \pm 33\%$ in the group breathing room air vs $72 \pm 51\%$ in the group breathing HeO_2, $p = .07$). This study warrants confirmation in a setting where HeO_2 is delivered in an unrestricted manner during high-intensity exercise training three times a week and for a sufficient period of time (>8 weeks).

It should be noted that the above-mentioned strategies are only relevant in selected patients. These options should be considered only after the less invasive and more traditional approaches have been exhausted. In particular, ventilatory capacity in COPD patients may also be improved by optimizing medication (including instructions on how to use inhaler devices correctly and enhancing compliance with medications[85]). Although some drugs have only limited impact on FEV_1, they may substantially reduce dynamic

Table 28-1 Interventions That Can Be Used to Increase Training Intensity or May Stimulate Muscle Growth or Muscle Function

Increasing training intensity	*Stimulating muscle growth or muscle function*
Maximal bronchodilatation	Anabolic steroids
Oxygen	Growth hormone, insulin-like growth factor-I
Helium–oxygen	Nutritional supplements
Noninvasive mechanical ventilation	
Pursed-lips breathing	
Arm bracing	
Reduction in amount of working muscle	

hyperinflation during exercise and hence improve exercise performance.[86] Pursed-lip breathing,[87] and the adoption of a leaning-forward posture with arm bracing, is yet another low-cost intervention that, in selected patients, may improve the ability to cope with high-intensity exercises. It is obvious that these relatively simple and low-cost interventions should be explored first, before more complex, labor-intensive interventions are attempted.

Methods to Stimulate Muscle Growth

Several investigators have tried to restore muscle function by giving nutritional supplements or anabolic stimulants to patients. These strategies should only be used as an adjunct to a pulmonary rehabilitation program in which exercise training is offered. Supplements that have been used in COPD are growth hormone, anabolic steroids, and nutritional supplements (including creatine supplements).

Impressive results have been achieved with the use of anabolic steroids (testosterone,[88] nandrolone decanoate,[89] and oxandrolone[90]) in patients with COPD. Although the focus of studies has been on patients with low BMI, low testosterone levels were not an inclusion criterion. In addition, the studies involved regular exercise training, but no specific strength training was included. Typically, anabolic steroid treatment is used to improve skeletal muscle strength, in combination with strength training.[91] Casaburi and colleagues used testosterone in patients with low baseline testosterone levels.[92] These authors showed a benefit of anabolic steroids in combination with resistance training in improving muscle strength but not exercise performance. Similar observations were made in healthy elderly patients,[93] where testosterone administration in combination with resistance training led to a mean change in muscle cross-sectional area compared with resistance training alone ($4.51 \pm 1.69\,cm^2$ vs $0.61 \pm 1.41\,cm^2$). In this study, testosterone administration and megestrol acetate (an appetite stimulant) ingestion, without resistance training, could not prevent the loss of skeletal muscle cross-sectional area induced by megestrol ($-4.44 \pm 1.66\,cm^2$). Therefore, in selected patients, anabolic steroids or testosterone may be useful agents for the restoration of skeletal muscle strength when resistance training is performed.

Another intervention that can be used together with exercise training is administration of growth hormone. The administration of growth hormone in growth hormone–deficient patients results in enhanced breakdown and oxidative utilization of fat but, more importantly, in muscle hypertrophy through up-regulation of insulin-like growth factor-I (IGF-I).[94] This growth factor induces muscle regeneration through myoblast proliferation.[95–97] In healthy elderly subjects, however, growth hormone does not provide additional beneficial effects over a regular strength training program.[94,98,99] Growth hormone, independently of resistance training, resulted in a greater predominance of muscle (glycolytic) fiber type IIx without altering the functional outcomes (ie, cross-sectional area and muscle strength). In addition, the results of this study showed a large number of side effects. In underweight COPD patients and patients with CHF,[100] this strategy also proved to be largely ineffective in increasing muscle strength or exercise capacity.[101,102] It is of note that in ≈60% of patients suffering from cardiac cachexia, growth hormone resistance has been reported.[103] Hence, administration of growth hormone will lead to less pronounced increases in the levels of autocrine IGF-I and may cause only minimal muscle proliferation. The local application of IGF-I to old muscle effectively counteracts immobilization-induced atrophy.[104] This strategy merits further investigation as it bypasses the possibly blunted IGF-I response to growth hormone supplementation. Other interventions, such as interleukin-15 (IL-15) treatment, are currently under investigation. IL-15 may be a potent promoter of myofibrillar protein accumulation and may be effective in preventing atrophy. In vitro and animal model studies[105,106] are needed to examine the proinflammatory action of IL-15 before experiments in humans can be conducted.

Finally, nutritional supplements such as creatine, or amino acids such as L-carnitine and glutamate, have not been studied extensively in COPD patients. These supplements have been used in healthy subjects, in conjunction with exercise training, with variable success.[107,108] It remains to be determined whether these supplements are useful in COPD patients. There are theoretical backgrounds for supplementation with creatine and protein supplements. COPD patients have low levels of intramuscular substrate[109] and may lack specific amino acids.[110] Although this opens a window of opportunity for the use of nutritional supplements in COPD patients, in combination with exercise training, our preliminary experience with creatine supplements has been rather disappointing.[111]

SUMMARY

Skeletal muscle weakness and reduced oxidative capacity are clear hallmarks of the systemic impact of COPD. Impaired muscle function, unlike airflow limitation, can be partially reversed. This leads to clear improvements in exercise capacity, activities of daily living, and health-related quality of life. Exercise training is a potent therapy for the restoration of muscle function in COPD patients, but programs should be adapted to individual needs. Endurance training, interval training, and resistance training should all be considered when these programs are being developed. In all of these programs, the targeted muscle should be stressed at high intensity. In selected patients, exercise therapy can be supported by oxygen supplementation, NIMV, and/or neuromuscular electrical stimulation. In addition, anabolic stimulants (growth hormone, IGF-I, or anabolic steroids) may be useful in selected patients, but patient subgroups for these therapies need to be better defined.

REFERENCES

1. American Thoracic Society and European Respiratory Society. Skeletal muscle dysfunction in chronic obstructive pulmonary disease. A statement of the American Thoracic Society and European Respiratory Society. Am J Respir Crit Care Med 1999;159:S1–40.

2. Clark CJ, Cochrane L, Mackay E. Low intensity peripheral muscle conditioning improves exercise tolerance and breathlessness in COPD. Eur Respir J 1996;9:2590–6.
3. Gosselink R, Troosters T, Decramer M. Peripheral muscle weakness contributes to exercise limitation in COPD. Am J Respir Crit Care Med 1996;153:976–80.
4. Hamilton AL, Killian KJ, Summers E, Jones NL. Symptom intensity and subjective limitation to exercise in patients with cardiorespiratory disorders. Chest 1996;110:1255–63.
5. Decramer M, Gosselink R, Troosters T, et al. Muscle weakness is related to utilization of health care resources in COPD patients. Eur Respir J 1997;10:417–23.
6. Decramer M, De Bock V, Dom R. Functional and histologic picture of steroid-induced myopathy in chronic obstructive pulmonary disease. Am J Respir Crit Care Med 1996;153: 1958–64.
7. Marquis K, Debigare R, Lacasse Y, et al. Midthigh muscle cross-sectional area is a better predictor of mortality than body mass index in patients with chronic obstructive pulmonary disease. Am J Respir Crit Care Med 2002;166:809–13.
8. Lacasse Y, Brosseau L, Milne S, et al. Pulmonary rehabilitation for chronic obstructive pulmonary disease. Cochrane Database Syst Rev 2002;CD003793.
9. Mador MJ, Kufel TJ, Pineda AL, et al. Effect of pulmonary rehabilitation on quadriceps fatiguability during exercise. Am J Respir Crit Care Med 2001;163:930–5.
10. Casaburi R, Patessio A, Ioli F, . Reductions in exercise lactic acidosis and ventilation as a result of exercise training in patients with obstructive lung disease. Am Rev Respir Dis 1991;143:9–18.
11. Belman MJ, Kendregan BA. Exercise training fails to increase skeletal muscle enzymes in patients with chronic obstructive pulmonary disease. Am Rev Respir Dis 1981;123:256–61.
12. Troosters T, Gosselink R, M. Decramer M. Exercise training in COPD; how to distinguish responders from nonresponders. J Cardiopulm Rehabil 2001;21:10–7.
13. McDonagh MJN, Davies CTM. Adaptive responses of mammalian skeletal muscle to exercise with high loads. Eur J Appl Physiol 1984;52:139–55.
14. DeLorme TL. Restoration of muscle power by heavy resistance exercise. J Bone Joint Surg 1945;27:645–67.
15. Richardson RS, Sheldon J, Poole DC, et al. Evidence of skeletal muscle metabolic reserve during whole body exercise in patients with chronic obstructive pulmonary disease. Am J Respir Crit Care Med 1999;159:881–5.
16. Simpson K, Killian K, McCartney N, et al. Randomised controlled trial of weightlifting exercise in patients with chronic airflow limitation. Thorax 1992;47:70–5.
17. Spruit MA, Gosselink R, Troosters T, et al. Resistance versus endurance training in patients with COPD and skeletal muscle weakness. Eur Respir J 2002;19:1072–8.
18. Ortega F, Toral J, Cejudo P, et al. Comparison of effects of strength and endurance training in patients with chronic obstructive pulmonary disease. Am J Respir Crit Care Med 2002;166:669–74.
19. Headley S, Germain M, Mailloux P, et al. Resistance training improves strength and functional measures in patients with end-stage renal disease. Am J Kidney Dis 2002;40:355–64.
20. Pu CT, Johnson MT, Forman DE, et al. Randomized trial of progressive resistance training to counteract the myopathy of chronic heart failure. J Appl Physiol 2001;90:2341–50.
21. Bernard S, Whittom F, LeBlanc P, et al. Aerobic and strength training in patients with chronic obstructive pulmonary disease. Am J Respir Crit Care Med 1999;159:896–901.
22. Sipila S, Suominen H. Effects of strength and endurance training on thigh and leg muscle mass and composition in elderly women. J Appl Physiol 1995;78:334–40.
23. Tracy BL, Ivey FM, Hurlbut D, et al. Muscle quality. II. Effects of strength training in 65- to 75-yr-old men and women. J Appl Physiol 1999;86:195–201.
24. Jubrias SA, Esselman PC, Price LB, et al. Large energetic adaptations of elderly muscle to resistance and endurance training. J Appl Physiol 2001;90:1663–70.
25. Vincent KR, Braith RW, Feldman RA. Improved cardiorespiratory endurance following 6 months of resistance exercise in elderly men and women. Arch Intern Med 2002;162:673–8.
26. Conley KE, Jubrias SA, Esselman PC. Oxidative capacity and ageing in human muscle. J Physiol 2000;526(Pt 1):203–10.
27. Dirks A, Leeuwenburgh C. Apoptosis in skeletal muscle with aging. Am J Physiol Regul Integr Comp Physiol 2002; 282:R519–27.
28. Yarasheski KE, Campbell JA, Kohrt WM. Effect of resistance exercise and growth hormone on bone density in older men. Clin Endocrinol (Oxf) 1997;47:223–9.
29. Vincent KR, Braith RW. Resistance exercise and bone turnover in elderly men and women. Med Sci Sports Exerc 2002;34:17–23.
30. Hagerman FC, Walsh SJ, Staron RS, et al. Effects of high-intensity resistance training on untrained older men. I. Strength, cardiovascular, and metabolic responses. J Gerontol A Biol Sci Med Sci 2000;55:B336–46.
31. Sharman MJ, Newton RU, Triplett-McBride T, et al. Changes in myosin heavy chain composition with heavy resistance training in 60- to 75-year-old men and women. Eur J Appl Physiol 2001;84:127–32.
32. Agusti AG, Sauleda J, Miralles C, et al. Skeletal muscle apoptosis and weight loss in chronic obstructive pulmonary disease. Am J Respir Crit Care Med 2002;166:485–9.
33. Greiwe JS, Cheng B, Rubin DC, et al. Resistance exercise decreases skeletal muscle tumor necrosis factor alpha in frail elderly humans. FASEB J 2001;15:475–82.
34. Conraads VM, Beckers P, Bosmans J, et al. Combined endurance/resistance training reduces plasma TNF-alpha receptor levels in patients with chronic heart failure and coronary artery disease. Eur Heart J 2002;23:1854–60.
35. Rabinovich RA, Figueras M, Ardite E, et al. Increased TNFalfa plasma levels during moderate intensity exercise in COPD patients. Eur Respir J 2003;21:789–94.
36. Vincent KR, Vincent HK, Braith RW, et al. Resistance exercise training attenuates exercise-induced lipid peroxidation in the elderly. Eur J Appl Physiol 2002;87:416–23.
37. Neder JA, Sword D, Ward SA, et al. Home based neuromuscular electrical stimulation as a new rehabilitative strategy for severely disabled patients with chronic obstructive pulmonary disease (COPD). Thorax 2002;57:333–7.
38. Bourjeily-Habr G, Rochester C, Palermo F, et al. Randomised controlled trial of transcutaneous electrical muscle stimulation of the lower extremities in patients with chronic obstructive pulmonary disease. Thorax 2002;57:1045–9.
39. Bircan C, Senocak O, Peker O, et al. Efficacy of two forms of electrical stimulation in increasing quadriceps strength: a randomized controlled trial. Clin Rehabil 2002;16:194–9.
40. Puente-Maestu L, Sanz ML, Sanz P, et al. Comparison of effects of supervised versus self-monitored training programmes in patients with chronic obstructive pulmonary disease. Eur Respir J 2000;15:517–25.
41. American College of Sports Medicine Position Stand. Exercise and physical activity for older adults. Med Sci Sports Exerc 1998;30:992–1008.
42. Wasserman K, Sue DJ, Casaburi R, Moricca RB. Selection criteria for exercise training in pulmonary rehabilitation. Eur Respir J 1989;7:604s–10s.
43. Punzal PA, Ries AL, Kaplan RW, Prewit LMt. Maximum intensity exercise training in patients with chronic obstructive pulmonary disease. Chest 1991;100:618–23.

44. Casaburi R, Porszasz J, Burns MR, et al. Physiologic benefits of exercise training in rehabilitation of patients with severe chronic obstructive pulmonary disease. Am J Respir Crit Care Med 1997;155:1541–51.
45. Debigare R, Maltais F, Mallet M, et al. Influence of work rate incremental rate on the exercise responses in patients with COPD. Med Sci Sports Exerc 2000;32:1365–8.
46. Mahler DA, Ward J, Mejia-Alfaro R. Stability of dyspnea ratings after exercise training in patients with COPD. Med Sci Sports Exerc 2003;35:1083–7.
47. Troosters T, Gosselink R, Decramer M. Short- and long-term effects of outpatient rehabilitation in patients with chronic obstructive pulmonary disease: a randomized trial. Am J Med 2000;109:207–12.
48. Belman MJ, Brooks LR, Ross DJ, Mohsenifar Z. Variability of breathlessness measurement in patients with chronic obstructive pulmonary disease. Chest 1991;99:566–71.
49. Maltais F, LeBlanc P, Jobin J. Intensity of training and physiological adaptation in patients with chronic obstructive pulmonary disease. Am J Respir Crit Care Med 1997;155: 555–61.
50. Gosselink R, Troosters T, Decramer M. Effects of exercise training in COPD patients; interval versus endurance training. Eur Respir J 1998;12:2S.
51. Coppoolse R, Schols AM, Baarends EM, et al. Interval versus continuous training in patients with severe COPD: a randomized clinical trial. Eur Respir J 1999;14:258–63.
52. Vogiatzis I, Nanas S, Roussos C. Interval training as an alternative modality to continuous exercise in patients with COPD. Eur Respir J 2002;20:12–9.
53. Lacasse Y, Guyatt GH, Goldstein RS. The components of a respiratory rehabilitation program: a systematic overview. Chest 1997;111:1077–88.
54. Sala E, Roca J, Marrades RM, et al. Effects of endurance training on skeletal muscle bioenergetics in chronic obstructive pulmonary disease. Am J Respir Crit Care Med 1999;159: 1726–34.
55. Maltais F, LeBlanc P, Simard C, et al. Skeletal muscle adaptation to endurance training in patients with chronic obstructive pulmonary disease. Am J Respir Crit Care Med 1996; 154:442–7.
56. Whittom F, Jobin J, Simard PM, et al. Histochemical and morphological characteristics of the vastus lateralis muscle in patients with chronic obstructive pulmonary disease. Med Sci Sports Exerc 1998;30:1467–74.
57. O'Donnell DE, McGuire M, Samis L, Webb KA. The impact of exercise reconditioning on breathlessness in severe chronic airflow limitation. Am J Respir Crit Care Med 1995; 152:2005–13.
58. Rabinovich RA, Ardite E, Troosters T, et al. Reduced muscle redox capacity after endurance training in patients with chronic obstructive pulmonary disease. Am J Respir Crit Care Med 2001;164:1114–8.
59. Larson JL, Covey MK, Wirtz SE, et al. Cycle ergometer and inspiratory muscle training in chronic obstructive pulmonary disease. Am J Respir Crit Care Med 1999;160:500–7.
60. Dekhuijzen PN, van Herwaarden CL, Cox NJ, Folgering HT. Exercise training during pulmonary rehabilitation in chronic obstructive pulmonary disease. Lung 168 Suppl: 481–8.
61. Clini E, Foglio K, Bianchi L, et al. In-hospital short-term training program for patients with chronic airway obstruction. Chest 2001;120:1500–5.
62. O'Donnell DE, McGuire M, Samis L, Webb KA. General exercise training improves ventilatory and peripheral muscle strength and endurance in chronic airflow limitation. Am J Respir Crit Care Med 1998;157:1489–97.
63. Tangri S, Woolf CR. The breathing pattern in chronic obstructive lung disease during the performance of some common daily activities. Chest 1973;63:126–7.
64. Gea JG, Pasto M, Carmona MA, et al. Metabolic characteristics of the deltoid muscle in patients with chronic obstructive pulmonary disease. Eur Respir J 2001;17:939–45.
65. Franssen FM, Wouters EF, Baarends EM, et al. Arm mechanical efficiency and arm exercise capacity are relatively preserved in chronic obstructive pulmonary disease. Med Sci Sports Exerc 2002;34:1570–6.
66. Celli BR, Rassulo J, Make BJ. Dysynchronous breathing during arm but not leg exercise in patients with chronic airflow obstruction. N Engl J Med 1986;314:1485–90.
67. Criner GJ, Celli BR. Effect of unsupported arm exercise on ventilatory muscle recruitment in patients with severe chronic airflow obstruction. Am Rev Respir Dis 1988;138: 856–61.
68. McKeough ZJ, Alison JA, Bye PT. Arm exercise capacity and dyspnea ratings in subjects with chronic obstructive pulmonary disease. J Cardiopulm Rehabil 2003;23:218–25.
69. Ries AL, Ellis B, Hawkins RW. Upper extremity exercise training in chronic obstructive pulmonary disease. Chest 1988;93: 688–92.
70. Lake FR, Henderson K, Briffa T, et al. Upper-limb and lower-limb exercise training in patients with chronic airflow obstruction. Chest 1990;97:1077–82.
71. Couser JI Jr, Martinez FJ, Celli BR. Pulmonary rehabilitation that includes arm exercise reduces metabolic and ventilatory requirements for simple arm elevation. Chest 1993;103: 37–41.
72. Epstein SK, Celli BR, Martinez FJ, et al. Arm training reduces the VO2 and VE cost of unsupported arm exercise and elevation in chronic obstructive pulmonary disease. J Cardiopulm Rehabil 1997;17:171–7.
73. Martinez FJ, Vogel PD, Dupont DN, et al. Supported arm exercise vs unsupported arm exercise in the rehabilitation of patients with severe chronic airflow obstruction. Chest 1993;103:1397–402.
74. Rooyackers JM, Dekhuijzen PN, van Herwaarden CL, Folgering HT. Training with supplemental oxygen in patients with COPD and hypoxaemia at peak exercise. Eur Respir J 1997;10:1278–84.
75. Garrod R, Paul EA, Wedzicha JA. Supplemental oxygen during pulmonary rehabilitation in patients with COPD with exercise hypoxaemia. Thorax 2000;55:539–43.
76. Wadell K, Henriksson-Larsen K, Lundgren R. Physical training with and without oxygen in patients with chronic obstructive pulmonary disease and exercise-induced hypoxaemia. J Rehabil Med 2001;33:200–5.
77. Emtner M, Porszasz J, Burns M, et al. Benefits of supplemental oxygen in exercise training in non-hypoxemic chronic obstructive pulmonary disease patients. Am J Respir Crit Care Med 2003;168:1034–42.
78. Smith RP, Johnson MK, Ashley J, et al. Effect of exercise induced hypoxaemia on myocardial repolarisation in severe chronic obstructive pulmonary disease. Thorax 1998;53:572–6.
79. Bianchi L, Foglio K, Pagani M, et al. Effects of proportional assist ventilation on exercise tolerance in COPD patients with chronic hypercapnia. Eur Respir J 1998;11:422–7.
80. Babcock MA, Pegelow DF, Harms CA, Dempsey JA. Effects of respiratory muscle unloading on exercise-induced diaphragm fatigue. J Appl Physiol 2002;93:201–6.
81. Hawkins P, Johnson LC, Nikoletou D, et al. Proportional assist ventilation as an aid to exercise training in severe chronic obstructive pulmonary disease. Thorax 2002; 57:853–9.

82. Bianchi L, Foglio K, Porta R, et al. Lack of additional effect of adjunct of assisted ventilation to pulmonary rehabilitation in mild COPD patients. Respir Med 2002;96:359–67.
83. Oelberg DA, Kacmarek RM, Pappagianopoulos PP, et al. Ventilatory and cardiovascular responses to inspired He-O2 during exercise in chronic obstructive pulmonary disease. Am J Respir Crit Care Med 1998;158:1876–82.
84. Johnson JE, Gavin DJ, Adams-Dramiga S. Effect of training with Heliox and noninvasive positive pressure ventilation on exercise ability in patients with severe COPD. Chest 2002;122:464–72.
85. Berg J, Dunbar-Jacob J, Rohay JM. Compliance with inhaled medications: the relationship between diary and electronic monitor. Ann Behav Med 1998;20:36–8.
86. O'Donnell DE, Lam M, Webb KA. Measurement of symptoms, lung hyperinflation, and endurance during exercise in chronic obstructive pulmonary disease. Am J Respir Crit Care Med 1998;158:1557–65.
87. Casciari RJ, Fairshter RD, Harrison A, et al. Effects of breathing retraining in patients with chronic obstructive pulmonary disease. Chest 1981;79:393–8.
88. Ferreira IM, Verreschi IT, Nery LE, et al. The influence of 6 months of oral anabolic steroids on body mass and respiratory muscles in undernourished COPD patients. Chest 1998;114:19–28.
89. Schols AM, Soeters PB, Mostert R, et al. Physiologic effects of nutritional support and anabolic steroids in patients with chronic obstructive pulmonary disease. A placebo-controlled randomized trial. Am J Respir Crit Care Med 1995;152:1268–74.
90. Yeh SS, DeGuzman B, Kramer T. Reversal of COPD-associated weight loss using the anabolic agent oxandrolone. Chest 2002;122:421–8.
91. Dawson RT. Drugs in sport—the role of the physician. J Endocrinol 2001;170:55–61.
92. Casaburi R, Bhasin S, Cosentino L, et al. Effects of testosterone and resistance training in men with chronic obstructive pulmonary disease. Am J Respir Crit Care Med 2004;170:870–8.
93. Lambert CP, Sullivan DH, Freeling SA, et al. Effects of testosterone replacement and/or resistance exercise on the composition of megestrol acetate stimulated weight gain in elderly men: a randomized controlled trial. J Clin Endocrinol Metab 2002;87:2100–6.
94. Lange KH, Andersen JL, Beyer N, et al. GH administration changes myosin heavy chain isoforms in skeletal muscle but does not augment muscle strength or hypertrophy, either alone or combined with resistance exercise training in healthy elderly men. J Clin Endocrinol Metab 2002;87:513–23.
95. Barton-Davis ER, Shoturma DI, Musaro A, et al. Viral mediated expression of insulin-like growth factor I blocks the aging-related loss of skeletal muscle function. Proc Natl Acad Sci U S A 1998;95:15603–7.
96. Musaro A, McCullagh K, Paul A, et al. Localized Igf-1 transgene expression sustains hypertrophy and regeneration in senescent skeletal muscle. Nat Genet 2001;27:195–200.
97. Zdanowicz MM, Moyse J, Wingertzahn MA, et al. Effect of insulin-like growth factor I in murine muscular dystrophy. Endocrinology 1995;136:4880–6.
98. Yarasheski KE, Zachwieja JJ, Campbell JA, Bier DM. Effect of growth hormone and resistance exercise on muscle growth and strength in older men. Am J Physiol 1995;268: E268–76.
99. Taaffe DR, Jin IH, Vu TH, et al. Lack of effect of recombinant human growth hormone (GH) on muscle morphology and GH-insulin-like growth factor expression in resistance-trained elderly men. J Clin Endocrinol Metab 1996; 81:421–5.
100. Osterziel KJ, Strohm O, Schuler J, et al. Randomised, double-blind, placebo-controlled trial of human recombinant growth hormone in patients with chronic heart failure due to dilated cardiomyopathy. Lancet 1998;351:1233–7.
101. Burdet L, de Muralt B, Schutz Y, et al. Administration of growth hormone to underweight patients with chronic obstructive pulmonary disease. A prospective, randomized, controlled study. Am J Respir Crit Care Med 1997;156:1800–6.
102. Pape GS, Friedman M, Underwood LE, Clemmons DR. The effect of growth hormone on weight gain and pulmonary function in patients with chronic obstructive pulmonary disease. Arch Intern Med 1990;150:1225–39.
103. Anker SD, Volterrani M, Pflaum C, et al. Acquired growth hormone resistance in patients with chronic heart failure: implications for therapy with growth hormone. J Am Coll Cardiol 2001;38:443–52.
104. Chakravarthy MV, Davis BS, Booth FW. IGF-I restores satellite cell proliferative potential in immobilized old skeletal muscle. J Appl Physiol 2000;89:1365–79.
105. Quinn LS, Anderson BG, Drivdahl RH. Overexpression of interleukin-15 induces skeletal muscle hypertrophy in vitro: implications for treatment of muscle wasting disorders. Exp Cell Res 2002;280:55–63.
106. Carbo N, Lopez-Soriano J, Costelli P, et al. Interleukin-15 antagonizes muscle protein waste in tumour-bearing rats. Br J Cancer 2000;83:526–31.
107. Lemon PW. Dietary creatine supplementation and exercise performance: why inconsistent results? Can J Appl Physiol 2002;27:663–81.
108. Brass EP. Supplemental carnitine and exercise. Am J Clin Nutr 2000;72:618S–23S.
109. Jakobsson P, Jorfeldt L, Brundin A. Skeletal muscle metabolites and fibre types in patients with advanced chronic obstructive pulmonary disease (COPD), with and without chronic respiratory failure. Eur Respir J 1990;3:192–6.
110. Engelen MP, Schols AM. Altered amino acid metabolism in chronic obstructive pulmonary disease: new therapeutic perspective? Curr Opin Clin Nutr Metab Care 2002;6: 73–8.
111. Gosselink R, Spruit M, Troosters T, et al. Oral creatine supplementation in COPD exercise training: a randomized double blind placebo controlled trial. Am J Respir Crit Care Med 2003;167:A961.

CHAPTER 29

GENETICS OF RESPIRATORY DISEASE

Scott J. Tebbutt, Andrew J. Sandford, Peter D. Paré

It is beyond the scope of a single book chapter to provide a comprehensive summary of the role that genetics plays in the pathogenesis of pulmonary disease. In this overview, we have limited ourselves to giving a broad synopsis of the various types of genetic disease, ranging from the relatively rare single-gene mendelian disorders (eg, cystic fibrosis [CF] and α_1-antitrypsin deficiency) to the much more common complex diseases that constitute the major burden of pulmonary disease and that have strong environmental influences (eg, chronic obstructive pulmonary disease [COPD] and asthma). We provide a brief explanation of the various methodologies used to find genes, gene polymorphisms, and mutations that contribute to disease. We then concentrate in more detail on specific respiratory disorders for which recent advances in molecular genetics have resulted in significant progress in our understanding of the genetic basis of the disease, specifically, asthma, pulmonary hypertension, COPD, and CF. Finally, with the dawn of the "genomics" era, we briefly describe some of the new "microarray"-based studies of respiratory diseases.

TYPES OF PULMONARY GENETIC DISEASE

Genetic diseases can be divided into two major categories: single-gene mendelian disorders, in which a single mutated gene is both necessary and sufficient to cause disease, and so-called complex genetic diseases, in which the heritable trait is the susceptibility to a disease state given exposure to specific environmental factors. Single-gene disorders are relatively rare since the major detrimental phenotype that they cause imparts a survival disadvantage, and thus evolutionary pressure tends to eliminate the alleles from the population. The classic example of a single-gene mendelian disorder is CF: individuals who have two mutant copies of the *CFTR* gene will inevitably develop disease.[1,2]

Much more common are the complex genetic diseases, in which multiple polymorphic susceptibility genes and environmental exposure are necessary for the disease phenotype to develop. In addition, it is likely that different combinations of polymorphic susceptibility genes increase the risk for the same disease in different families; thus, there is genetic heterogeneity. Although these disorders show familial concordance that cannot wholly be attributed to shared environment, the polygenic nature and the requirement for appropriate environmental exposure cause a pattern of inheritance that does not follow simple mendelian rules, such as dominant, recessive, or sex linked. Complex genetic diseases are the major killers and causes of decreased quality of life in the modern era and include diseases such as atherosclerosis, hypertension, and schizophrenia. Asthma and COPD fulfill the criteria for complex genetic diseases.

It is clear, however, that the distinction between simple single-gene and complex genetic disorders is blurred; even single-gene mendelian disorders show marked phenotypic heterogeneity, with some patients showing early-onset severe disease and others showing late-onset and more slowly progressing disease. This heterogeneity can be due to environmental factors, which in the case of CF include access to and quality of care, but there is good evidence that the severity of disease is in itself controlled by genetic factors. Some families affected by CF show a severe phenotype, whereas others with the identical *CFTR* mutations show a much more benign phenotype, and this familial concordance cannot be solely attributed to shared environment. A similar effect of "modifier" genes may explain the observation that some patients who are homozygous for the α_1-antitrypsin deficiency genotypes (ZZ or SS) may be completely free of pulmonary dysfunction, whereas others who have the same genotype (and similar smoking history) develop advanced COPD at an early age. Modifier genes are probably the main reason why many single-gene disorders show variable penetrance; the single genes manifest themselves preferentially on a specific genetic background.

GENERAL APPROACHES TO GENE MAPPING: LINKAGE ANALYSIS AND ASSOCIATION STUDIES

The variations in DNA sequence that cause or contribute to disease are called mutations or polymorphisms, based solely on their frequency in the population; by convention, any DNA sequence variant with a frequency of more than 1% is termed a polymorphism, whereas those that occur in fewer than 1% of individuals are called mutations. The most common type of DNA sequence variant is the single-nucleotide polymorphism (SNP), in which a single base in the sequence is replaced by a different nucleotide in more than 1% of chromosomes. There are SNPs approximately every 500 to 1,000 base pairs in the human genome. Since the genome contains about three billion base pairs, this means that there are between three and six million sites at which more than 1% of the population differ from the majority. Although this would seem to provide a large potential for diversity, simple calculations show that even the most genetically diverse people are at least 99.8 to 99.9% identical. If the SNPs were evenly spaced over the entire genome, this would mean that there would be ~300,000 to 600,000 SNPs within the ~30,000 human genes, and it is this variation that, in combination with environmental factors and stochastic events, accounts for all of human phenotypic diversity, including disease susceptibility.

Two major strategies have been employed to identify the genes and the mutations/polymorphisms that contribute to the development of pulmonary diseases, linkage analysis and candidate gene association studies (Table 29-1). Linkage analysis requires recruitment of affected families, whereas candidate genes are tested by association studies of unrelated subjects.

Linkage Analysis

Linkage analysis (sometimes referred to as positional cloning or genomic scanning) is the classic methodology for randomly searching the entire human genome for disease-causing genes. It usually requires affected families of at least two generations, although single-generation sib pairs can also be used. Each family member is typed for DNA markers (polymorphisms) that are scattered throughout the genome. Linkage analysis determines whether any of the markers are inherited with the disease more than predicted by chance. The genes are identified solely on the basis of their position in the genome (thus "positional cloning"). The *CFTR* gene and the mutations within this gene that are the cause of CF were the first severe disease-causing gene and mutations to be identified with positional cloning.[1,2] The advantage of this approach is that completely novel genes can be implicated in disease pathogenesis; one is not limited to a search for disease-causing polymorphisms in candidate genes known or suspected to be involved in the disorder.

A variant of linkage analysis that has been extensively employed in complex genetic diseases is the affected sib-pair method. In the affected sib-pair approach, it is assumed that siblings who are both affected by a disease share susceptibility genes. DNA from affected siblings, and if possible their parents, is genotyped for hundreds of polymorphisms scattered evenly throughout the genome. By chance, sibs should share specific alleles passed on from their parents 50% of the time; if allele sharing is significantly more than 50%, then that polymorphism must be, or be close to, a disease-causing polymorphism. Although classic linkage analysis has not proved as successful in definitively identifying disease-causing polymorphisms in complex genetic diseases as in single-gene disorders, an example of the recent success of the sib-pair approach was the finding of the *ADAM33* gene for asthma, which is discussed later in this chapter.[3]

Linkage analysis has the additional advantage that large regions of the genome can be efficiently screened for disease-causing polymorphisms. However, once a linked region is discovered, linkage analyses usually do not have sufficient resolution to identify the causal gene and polymorphisms, especially in complex genetic diseases. Therefore, association studies are ultimately required, even with the positional cloning approach. A final advantage of linkage analysis is that it is immune to confounding due to population admixture, which is a major potential problem with association studies (see below).

Genetic Association Studies

The second major gene-hunting strategy is the candidate gene association approach, in which polymorphisms in individual genes thought to be important in disease pathogenesis are tested for their involvement in a disease. In association studies, one first identifies candidate genes that are hypothesized or known to be important in the pathogenesis of a condition. In an attempt to increase the hit rate for candidates, a "positional candidate" approach is an option; biologically plausible candidates that are located in regions previously implicated by linkage analysis are given precedence. The next step is to identify polymorphisms within or close to the gene that could affect its regulation or

Table 29-1 Methods of Finding Disease-Causing Genes

Linkage analysis (families and sib pairs)	*Association studies (case–control and cohorts)*
Provides unbiased, genome-wide search	Limited to candidate genes known or suspected to be involved in pathogenesis
Locates large linked regions harboring many potential candidate genes	Allows relatively precise localization of disease-associated polymorphisms
Immune to spurious results caused by population stratification/admixture	Prone to spurious results based on population stratification/admixture
Impractical in late-onset disease when parents may be deceased and environmental factors are important	Relatively easy study design and control of known environmental factors

function. Finally, one examines whether the specific alleles occur more frequently in individuals who have a disease than in an appropriate control population or predict the development of disease in a cohort study. There are several criteria to be considered in choosing the most likely candidate genes.[4] First, the gene product must be a protein likely to be relevant to disease pathophysiology. Second, genes that lie within or close to linked loci should be given priority. Finally, the gene must contain SNPs or other types of genetic variation capable of producing functional differences in either the level of expression or the function of the gene product (occurring within coding or regulatory regions).

Case–Control versus Cohort Design The two basic designs of association study are cohort studies and case–control studies. In the former, cohorts of individuals are identified who have, or do not have, the disease allele. The cohorts are examined to determine whether the presence of a specific allele affects the risk of disease. The strength of the disease-causing allele in predicting the phenotype is indicated by the relative risk (RR). The RR is the probability of disease when the allele is present divided by the probability when the allele is absent:

$$\mathrm{RR} = \frac{a/(a+b)}{c/(c+d)}$$

where a is the number of individuals with the allele who have the disease, b is the number of individuals with the allele without the disease, and c and d are the corresponding numbers for individuals without the allele.

In a case–control study, subjects are identified by disease status, and the frequency of an allele is determined. A disadvantage of this design is that the investigator determines how many cases and controls to sample, so the risk that a person with the allele will become a case cannot be determined; that is, the RR cannot be calculated. Instead, the strength of the effect of the disease-causing allele on the phenotype is indicated by the odds ratio (OR). The OR is the odds of having the allele if the disease is present divided by the odds of having the allele if the disease is absent:

$$\mathrm{OR} = \frac{a/c}{b/d}$$

The OR is often used to approximate the RR. The OR gives an overestimate of RR when the prevalence of a disease is high. Although the design and implementation of association studies are relatively straightforward, there are several potential sources of error. A large sample size and relatively high allele frequency are necessary to power studies sufficiently since each gene polymorphism is likely to have a small effect in complex genetic diseases.

One of the major advantages of association studies is that one uses knowledge of biologically plausible pathogenetic mechanisms to focus the search for genes on relatively few candidates, although obviously only genes of known function can be examined. Another advantage is that the study subjects are usually unrelated individuals, so that genotypic and phenotypic data from multiple generations are not required. This is especially important in diseases such as COPD, where the late age at onset makes it very difficult to ascertain DNA and phenotypic data from parents of affected individuals. Unfortunately, a major complication in association studies is that a positive association may not always be due to a causative role for the polymorphism in disease pathogenesis.

Major Pitfall of Association Studies—Population Stratification The major challenge in association studies is obtaining a control group in whom there is no potential for bias in the distribution of genotypes. One of the major confounding factors in this regard is population stratification (admixture) according to genetic background. This happens when a particular subgroup of the population has increased frequencies of both a specific SNP and the disease (although for unrelated reasons). Such population stratification (ie, a population that has not fully equilibrated genetically) may confound our efforts to identify true associations between genotype and phenotype. False-positive associations can occur if the frequencies of genetic markers and of the disease of interest vary across different populations or ethnic groups.

For example, consider a population formed from two subpopulations that have recently mixed. In each subpopulation, allele A is not associated with the disease, but the disease and allele frequencies differ between the subpopulations, as shown in Table 29-2. The frequency of allele A in the combined population is $[(1{,}000 \times 0.5) + (10{,}000 \times 0.1)]/11{,}000 = 0.136$. Similarly, the frequency of the disease is $[(1{,}000 \times 0.4) + (10{,}000 \times 0.05)]/11{,}000 = 0.082$. Therefore, the expected frequency of allele A among those with the disease is $0.136 \times 0.082 = 0.011$. However, the observed frequency of allele A among those with the disease is $[(1{,}000 \times 0.20) + (10{,}000 \times 0.005)]/11{,}000 = 0.023$. Therefore, allele A is positively associated with the disease in the combined population, with an OR of ~2.5. If one was not aware of the population stratification, one might conclude that allele A (or a nearby allele) was contributing to the disease. However, since the association does not exist in either subpopulation, it is entirely spurious. In fact, the disease could be entirely nongenetic and would still be associated with allele A.

A graphic example of differing prevalence of a disorder between population groups for a genetic lung disease is CF. The prevalence of CF varies from 1 in 500 in Scotland[5] to 1 in 2,000 to 3,500 in the general northern European Caucasian population,[6] 1 in 17,000 among African Americans and 1 in 90,000 in First Nations and Asians.[7] Therefore, any mixing of those populations within an association study could lead to false-positive gene association. Another example is diffuse panbronchiolitis (DPB), a disease

Table 29-2 Population Stratification

Population size	*Frequency of allele A*	*Frequency of disease*	*Frequency of allele A with disease*
1,000	0.5	0.4	0.20
10,000	0.1	0.05	0.005

found only in Japanese, Chinese, and Korean individuals. Two Japanese studies have shown a strong association of DPB with HLA type B54.[8,9] Since this HLA type is only found in East Asians, it may explain the susceptibility of these ethnic groups to DPB. One might assume that the population stratification of disease-causing mutations would correspond to the stratification of the prevalence of the disease. However, the same disease-causing mutation may have a greater or lesser effect, depending on the genetic background of the specific population or on environmental factors that are influenced by ethnic or regional differences (eg, diet, occupational exposures). Particularly in complex genetic disorders, the presence of a specific mutation may not be sufficient to produce clinical disease. The clinical expression of the gene may only be apparent when it acts synergistically with additional genetic variants (which could be enriched in specific population samples) or in concert with specific environmental factors that may be confined to population subsets. For example, the Z mutation of the α_1-antitrypsin gene causes a severe deficiency of α_1-antitrypsin. Homozygosity for the Z mutation is known to increase the risk for the development of COPD. However, the risk of developing COPD is modulated by other factors, with cigarette smoking being the most important.

Family-Based Controls To avoid problems due to population stratification in association studies, both the cases and controls should be selected from the same population group and geographic area. Since population background is difficult to measure, is it impossible to guarantee genetic homogeneity. Therefore, alternative strategies based on the use of families have been employed. In the haplotype relative risk (HRR) and the similar affected family-based controls (AFBAC) methods, the parents of an affected child are used to form an alternative control.[10,11] The two alleles not transmitted from parents to their affected children are combined to form an artificial control genotype. Therefore, the cases and "controls" are matched for ethnic background. The strength of any association of the disease with the marker alleles is then assessed as with the traditional case–control method. However, under certain circumstances, these techniques may still produce false-positive associations due to population stratification.[12]

Transmission/Disequilibrium Test An alternative method of analysis is the transmission/disequilibrium test (TDT).[13] The TDT evaluates the frequency of transmission of specific alleles at a single locus from heterozygous parents to their affected children. In the absence of association, each allele is expected to be transmitted with a mendelian frequency of 50%. If a marker allele is transmitted significantly more often than 50% of the time, this implies that the allele must be linked to and associated with the disease-causing allele. The main advantage of the TDT is that it does not involve comparison of groups of cases and controls and therefore is not susceptible to population stratification. The TDT is a test of linkage since it looks for co-inheritance of a genetic marker and a disease. However, it differs because only specific alleles of a locus are considered, whereas in traditional linkage analysis the specific allele that is inherited is irrelevant. Note that the TDT is also a type of association analysis since a positive result must mean that the tested allele is associated with the disease-causing allele. An example of this approach is the finding of an association between the IL4-590 polymorphism and asthma.[14] The T allele of this polymorphism was transmitted from a heterozygous parent to an affected child 64% of the time, whereas chance alone predicts a 50% transmission rate. However, a major drawback with the TDT method is that it requires parental DNA, which is often unobtainable in studies of late-onset disease such as COPD.

Genomic Controls A more recent and powerful statistical method with which to test for spurious associations induced by population stratification or substructure has been developed by Devlin and Roeder.[15] In essence, genomic control (GC) uses markers throughout the genome to adjust for any inflation in test statistics due to population admixture. This strategy measures the degree of statistically identified genotype–phenotype association for up to 100 randomly chosen "null" SNPs. If there is an association of a disease with "null" GC SNPs, this suggests that there is a population subset with a different genetic background plus different disease susceptibility. Such a spurious association must be corrected in order to derive true gene–disease associations. GC has the advantages of simplicity, robustness, and wide applicability and is rapidly becoming an accepted method of choice for population stratification control in gene association studies.[16]

RECENT GENETIC STUDIES OF RESPIRATORY DISEASE

Cystic Fibrosis

A great deal has been learned about the molecular biology of CF since the cloning of the CF transmembrane conductance regulator (*CFTR*) gene in 1989.[1,2,17] Although the major CF mutation is a 3-bp deletion, known as ΔF508,[17] more than 1,000 additional *CFTR* mutant alleles and over 300 DNA sequence polymorphisms have been reported to the CF Genetic Analysis Consortium and listed in the CF Mutation Database (<www.genet.sickkids.on.ca/cftr/>).

Genotype–Pulmonary Phenotype Correlations There is a lack of direct correlation between *CFTR* genotype and CF lung phenotype,[18,19] and it is becoming clear that, despite its classification as a single-gene mendelian disorder, CF is affected by other "modifier" genes. The situation is further confounded by the fact that there is no direct measurement, other than transmucosal potential difference, for the airway epithelial abnormality that occurs in CF. The forced expiratory volume in 1 second (FEV_1) percent predicted (age, height, and sex adjusted) is often used to describe the severity of airway disease. Other markers are forced expiratory vital capacity (FVC) values, first detection of bacterial colonization, and types of bacteria. However, these can only be

considered as surrogate markers of the basic underlying abnormality. In addition, they are strongly influenced by environmental factors, including treatment and intervention. Nevertheless, data from the CF sibling studies show that FEV_1 and FVC can be used as surrogate lung function markers to study the effect of modifier genes.[20]

Candidate CF Modifier Genes Based on physiologic and pathologic findings among CF patients, it is possible to identify classes of candidate genes that may modulate the severity of various CF phenotypes. Owing to the great complexity of the pulmonary CF phenotype, the candidate genes are expected to influence the severity of CF lung disease through a variety of mechanisms. These include modulation of susceptibility to infection, variations in the intensity of the inflammatory response, different efficiency of mucociliary clearance, and variation in epithelial damage and repair. Another group of candidate genes is postulated to influence the presence and severity of gastrointestinal injury (liver, pancreas, intestine) and may act through different mechanisms of modulation, such as proteolysis (pancreatic proteases, protease inhibitors) and fibrosis (transforming growth factors). Finally, there are genes that may modulate the severity of the CF phenotype by acting at the basic molecular level: providing alternative Cl^- conductance or regulating the splicing and expression of CFTR. A list of some of the genes that have been implicated as modifier genes in CF lung disease is given in Table 29-3. It is recommended that the reader consult the references contained therein for further information.

A recent publication by Arkwright and colleagues describes one such example of research into other genetic factors that modulate CF.[21] Briefly, the authors of this study examined the hypothesis that polymorphisms of certain inflammatory mediator and regulatory genes affect clinical outcome in CF by influencing the degree of end-organ damage. It was shown that there is an association between SNPs in the coding region of the gene for angiotensin-I–converting enzyme and the development of portal hypertension and cirrhosis, showing that the SNPs significantly affect outcome.

Asthma

The contribution of heredity to asthma and other complex genetic diseases can be estimated by comparing the prevalence or incidence of the disease in first-degree relatives of affected individuals with the prevalence or incidence in the general population. Estimates of heritability of asthma and other allergic disorders suggest a major genetic contribution (heritability [H] = 0.6–1.0).[22–24] Of course, first-degree relatives usually share the same environment as well as 50% of their genes. To separate the effects of shared genes and environment, Hanson and colleagues compared twins reared apart with twins reared together.[25] The concordance for asthma and rhinitis and the correlation coefficient for the increased levels of total IgE were not higher in twins reared together than in those reared apart. These data suggest that there is a major genetic contribution to these phenotypes and a negligible environmental contribution.

Numerous whole genome linkage analyses have been performed for asthma and atopy phenotypes.[3,26–33] Several studies have implicated highly significant asthma-linked loci on chromosomes 3q21–22, 11p13, 14q24, and 17q12–21 (reviewed by Cookson[34]). Candidate asthma gene studies have involved many genes from chromosome 5q. For example, a polymorphism (−589T) in the interleukin-4 (IL-4) promoter was associated with increased gene transcription in vitro and with increased total IgE in vivo.[35] The −589T allele has been associated with other asthma-related phenotypes.[14,36–38] Two polymorphisms of *IL13* (C-1112T and G2044A) have been associated with asthma-related phenotypes.[39,40] CD14 is a receptor for lipopolysaccharide (LPS), and binding to CD14 elicits a strong IL-12 response from antigen-presenting cells. A promoter polymorphism in the CD14 gene (C-159T) was associated with total serum IgE and with higher soluble CD14 levels.[41] These results were supported by data showing that homozygotes for the C allele had a higher number of positive skin test findings and higher total IgE levels than subjects with CT and TT genotypes.[42] The Toll-like receptors (TLRs) mediate the cellular response to endotoxin and can influence the Th1–Th2 balance. The results of a recent study from the laboratories of Weiss and Martinez suggest that specific polymorphisms in TLR9 (mapped to chromosome 3p21.3) impart increased risk for asthma among Caucasians but not among African Americans.

There are two common polymorphisms of the β_2-adrenergic receptor (*ADRB2*) in the extracellular N-terminus at positions 16 (Arg16Gly) and 27 (Gln27Glu). Data from in vitro studies suggest that receptors containing Gly16 display greater down-regulation in response to agonists than cells that are Arg16/Arg16.[43] Asthmatic patients who had Gly16 showed significantly more desensitization to formoterol[44] and less response to albuterol.[45] The Gln27 allele was associated with bronchial hyperresponsiveness in asthmatic patients[46] and with increased prevalence of asthma in children.[47] Similar results were found in a separate study, in which homozygotes for Glu27 were significantly less responsive to histamine than Gln27 homozygotes.[48] Asthma candidates from other regions of the genome include the β-subunit of the high-affinity receptor for IgE (*FCER1B*),[49–52] the α-subunit of the IL-4 receptor (*IL4RA*),[38,53–55] and tumor necrosis factor.[36,56–60]

One of the most recent and exciting developments in our understanding of the genetics of asthma has been the identification of the *ADAM33* gene.[3,34] Not only did the researchers involved find linkage to chromosome 20 in a genome screen, but they also found positive disease associations with SNPs in the *ADAM33* gene within that locus. *ADAM33* codes for a membrane-anchored zinc-dependent metalloproteinase, hinting at possible roles of this protein in proteolysis, adhesion, intracellular signaling, and/or cell fusion.

COPD/Emphysema

The link between COPD and cigarette smoking is well established,[61] but only 10 to 20% of chronic heavy smokers will ever develop symptomatic COPD.[62,63] COPD is more prevalent

Table 29-3 Candidate Genes in Respiratory Disease

Gene class	*Gene*	*Name*	*References*				
			Asthma	*COPD*	*Cystic fibrosis*	*PPH*	*IPF*
Protease and antiprotease genes	α_1-Antitrypsin	*α_1-AT*		66, 73, 105			
	Tissue inhibitors of metalloproteinases	*TIMPs*		106			
	α_1-Antichymotrypsin	*α_1-ACT*		107			
	Matrix metalloproteinases	*MMP1*		108			
		MMP12		108			
		MMP9		108, 109			
		MMP7 (matrilysin)					104
	ADAM33	*ADAM33*	3				
	α_2-Macroglobulin	*α_2-MG*		110			
Antioxidant and xenobiotic metabolizing enzyme genes	Heme oxygenase-1	*HMOX-1*		78, 111			
	Microsomal epoxide hydrolase	*mEPHX*		73, 74, 112			
	Glutathione-*S*-transferases	*GST-M, GST-T, GST-P*		111–115			
	Cytochrome P4501A1	*CYP1A1*		116			
Inflammatory mediator genes	Tumor necrosis factor-α	*TNF-α*	56–59, 79	73, 80–82, 117, 118	79, 119–121		
	Vitamin D binding protein	*VDBP*		73, 122			
	Interleukin-1α, interleukin-1β	*IL1A, IL1B*		82, 123, 124	124		
	Interleukin-1 receptor, type 1	*IL1R1*		123			
	Interleukin-1 receptor, type 2	*IL1R2*		123			
	Interleukin-13	*IL13*	39, 100	125, 126			
	Nitric oxide synthase	*NOS1, NOS2*			127		
	Interleukin-1 receptor antagonist	*IL1RN*		82, 124	124		
	Interleukin-6	*IL6*			128		
	Interleukin-8	*IL8*			129, 130		
	Lymphotoxin-α	*LTA*	56–59		131		
	Interleukin-4	*IL4*	14, 35–38				
	Interleukin-4 receptor	*IL-4Rα*	38, 53–55, 132, 133				
	Interleukin-5	*IL5*	134, 135				
	Toll-like receptor 9	*TLR9*	136				
	High-affinity receptor for IgE	*FcεRIβ*	49, 51, 52				
	T-cell antigen receptor	*TCRα, TCRβ*	137, 138				
	5-Lipoxygenase	*ALOX5*	139				
Genes involved in airway defense	Human leukocyte antigens	*HLA class II (DP, DQ, DR)*	22	8, 9, 140			
	Cystic fibrosis transmembrane conductance regulator	*CFTR*	141	141, 142	1, 2		
	Defensins (β-defensin-1, defensin-2)	*hBD-1, DEFβ2*		143	144–146		
	Surfactant proteins	*SP-A, SP-B, SP-D*		147	148–150		
	Mucins	eg, *MUC2, MUC7, MUC1, 2, 5AC, 5B*	151, 152		153		
	Mannose-binding lectin	*MBL*			154–156		
	Tyrosine kinase	*c-SRC*			153		
	Leukotriene C_4 synthase	*LTC4*	157		158		
	CD14	*CD14*	41, 42				
Genes associated with tissue damage and repair	Transforming growth factor-β_1	*TGFβ1*			159		160
	Bone morphogenic protein receptor	*BMPR-2*				83–85	
	Glutathione-*S*-transferases	*GSTMP1, M1, M3*	161, 162		120, 163		
	Interferon-γ	*IFNG*	164				165
	Platelet-activating factor acetylhydrolase	*PAFAH*	166, 167				
	Plasminogen activator inhibitor-1		101				
	Angiotensin-I			21			
	Complement factor-5	*C5*	168				
Genes involved in other pathways	β_2-Adrenergic receptor	*β2-AR*	45, 47,		174		
	Human transformer-2α	*hTRA2α*	169–173		175		
	Ca^{2+}-dependent Cl^- channel 3	*CLCA3*			176		
	HOX genes			96		96	

in the relatives of cases than in the relatives of controls, supporting a role for genetic factors in the development of this disease.[64–66] Furthermore, the prevalence of COPD and similarity in lung function decrease with increased genetic distance.[67,68] The results of twin studies show that the proportion of the variability due to genetic factors (ie, the heritability, H) of lung function ranges from 0.5 to 0.8.[69,70] These studies support the idea that there is a considerable genetic contribution to the susceptibility to COPD.

The α_1-antitrypsin (*AAT*) gene was the first to be implicated in the pathogenesis of COPD. Although there is overwhelming evidence that homozygosity for α_1-antitrypsin deficiency alleles causes early-onset COPD in smokers, there are also data supporting a contribution of the intermediate deficiency imparted by the heterozygous state. In a recent large cohort study, the RR for COPD was increased in *AAT* MZ individuals in comparison with controls (RR = 2).[71] Dahl and colleagues showed that among COPD patients, FEV_1 was 655 mL less in MZ individuals than in MM individuals.[72] We recently confirmed the same magnitude of RR for COPD, using rate of decline of lung function as the phenotype.[73] Other COPD candidate genes have been identified (see Table 29-3). Microsomal epoxide hydrolase (EPHX1) plays an important role in the metabolism of highly reactive epoxide intermediates formed in cigarette smoke. Two common polymorphisms occur in the *EPHX1* gene: $Tyr^{113} \rightarrow His$ and $His^{139} \rightarrow Arg$. The slow-metabolizing form of EPHX1 was associated with emphysema and COPD,[74] with more severe COPD[75] and with rate of decline of lung function in smokers.[73] Heme oxygenase-1 (HMOX1) provides cellular protection against heme- and non–heme-mediated oxidant injury.[76,77] A $(GT)_n$ repeat within the *HMOX1* promoter was associated with emphysema in Japanese smokers (OR = 2),[78] but this polymorphic site was not associated with a more rapid decline of lung function in a Caucasian population.[73] Tumor necrosis factor (TNF) is a proinflammatory cytokine that causes neutrophil activation and release from the bone marrow. A *TNF* polymorphism (*TNF* G-308A) was associated with the level of TNF production in vitro[79] and with COPD in a Taiwanese population (OR = 11).[80] This association has been confirmed in a Japanese population[81] but not in other studies.[73,82]

Primary Pulmonary Hypertension

Primary pulmonary hypertension (PPH) was first described in 1951, in a report of three young women who had severe exertional dyspnea, radiographic and clinical evidence of pulmonary hypertension, and right ventricular hypertrophy. The disorder is very uncommon, having an incidence of only about 1 per 1,000,000 of the general population. In the Pulmonary Hypertension Registry of the National Institutes of Health, the mean age of the patients is 36 ± 15 years, with a female-to-male predominance of 1.7 to 1. Although the majority of cases appear to be sporadic, there is a definite subset in which PPH is clearly familial; it has been reported in twins and in members of three-generation families. The inheritance most closely conforms to an autosomal dominant pattern.

A gene on chromosome 2 that appears to be responsible for PPH in many families was recently identified by two independent groups using linkage analysis. Thomson and colleagues and Morse and colleagues studied large families with familial primary pulmonary hypertension (FPPH) and found linkage to bone morphogenetic protein receptor-2 (BMPR)-2.[83,84] Defects in this gene appear to account for more than half of the cases of FPPH and may also be involved in a sizable percentage (up to one-third) of cases of sporadic PPH,[83] as well as in other diseases associated with PPH, such as anorexia-induced PPH.[85]

BMPR-2 is a member of the transforming growth factor-β (TGF-β) receptor family and has been previously implicated in various developmental processes. Although at least 46 different germline mutations in the BMPR-2 gene have been described in both FPPH and sporadic PPH, it remains unclear how mutations in BMPR-2 lead to the clinical disease of PPH.[83,86–88] It is also unclear why mutations in such an important gene, which is expressed in multiple tissues, lead to lesions in only very specific regions of the pulmonary vascular system. FPPH families also show a pattern of incomplete penetrance, in which only 10 to 20% of family members actually develop overt disease, which is suggestive of a requirement for additional environmental and/or genetic events.

Another intriguing set of observations suggests that there may be somatic mutations in the pulmonary endothelial cells from patients who develop PPH. Tuder and colleagues performed microdissection of the plexiform lesions found in the lungs of these patients and showed that there was monoclonal proliferation of endothelial cells with "microsatellite instability" and overexpression of certain growth factors, including vascular endothelial growth factor.[89,90] This raises the possibility that in PPH a loss-of-function mutation could occur in the remaining BMPR-II alleles in the affected pulmonary vasculature, giving rise to a more complete defect in BMP receptor signaling. Such a combination of germline and somatic mutations has recently been shown to be involved in another variably penetrant dominant disorder, polycystic kidney disease.[91]

Interestingly, in one study of 24 families with 429 members, of whom 124 were known to carry the gene for PPH, the age at death was significantly lower (36 ± 13 vs 46 ± 15 years) in the younger generation than in the parental generation. This phenomenon (ie, younger age at onset and more rapid progression in successive generations) is termed *genetic anticipation*.[92] Genetic anticipation has been described in other inherited diseases, including Huntington's disease,[93] and is associated with the progressive accumulation of trinucleotide repeats at selected loci in the genome. Although there is currently no evidence for trinucleotide repeats in the BMPR-II gene in FPPH, it is possible that an alternative locus is affected by this phenomenon.

MICROARRAY ANALYSES

Microarrays are beginning to form the basis of powerful new tools for clinical research and diagnostics, with the potential

to establish novel correlations between genetic changes and disease progression as well as response to the environment and therapy. DNA arrays are fabricated with the use of high-speed robotics on glass or nylon substrates, and labeled patient nucleic acid is used to determine complementary binding, allowing massively parallel gene expression and gene discovery studies. Oligonucleotide probe microarrays are fabricated either by in situ light-directed combinational synthesis (the Affymetrix GeneChips) or by conventional synthesis followed by immobilization on glass substrates. Sample RNA is reverse transcribed into cDNA, with incorporation of a fluorescent label, and the cDNA is hybridized to the microarray probes. This technology has been successfully applied to the simultaneous expression of tens of thousands of genes and to large-scale gene discovery, as well as polymorphism screening and mapping of genomic DNA clones. The use of microarrays is becoming widespread in the field of research into the genetics of respiratory disease, and examples of several array-based studies are described below. As you might imagine, however, just as the amount of data is increased with microarray studies, so is the amount of experimental noise and false positives, and it is extremely important to validate the results of any array experiments and to use sound bioinformatics tools to analyze the original data.

Lung Development

Mammalian lung development is a complex morphogenetic process, which begins near midgestation and continues through early postnatal life. Further understanding of lung development is vital if we are to obtain clearer insights into respiratory disease pathogenesis. Mariani and colleagues undertook comprehensive gene expression profiling of the entire process of mouse lung development, using oligonucleotide-based microarrays; the expression patterns of 11,000 genes were followed throughout the morphologic stages of lung development.[94] In addition to identifying novel genes with undefined functions, the authors found known genes with previously unappreciated pulmonary expression.

Chambers and colleagues used microarrays to study TGF-β_1, which plays a central role in promoting extracellular matrix protein deposition by promoting the transformation of fibroblasts to myofibroblasts.[95] Global gene expression in human fetal lung fibroblasts was followed for up to 24 hours after treatment with TGF-β_1. Data were collected for approximately 150 genes that were up-regulated at least twofold at two time points. These genes were grouped into several major functional categories, including genes involved in gene transcription, metabolism and protein biosynthesis, cytoskeletal reorganization, matrix formation, cell signaling, proliferation, and survival. For more than half of these genes, this was the first report that they are TGF-β_1 responsive.

HOX genes belong to the large family of homeodomain genes, which function as transcription factors. Previous animal studies have indicated that such genes play an essential role in lung development, and Golpon and colleagues recently investigated the expression pattern of HOX genes in human lung tissue by using microarray techniques, showing altered HOX gene expression in PPH and emphysema.[96]

Cystic Fibrosis

An early example of the use of microarrays to study pharmacogenomics and pharmacotherapy was published by Srivastava and colleagues.[97] The protein encoded by the principal *CFTR* mutation, ΔF508-CFTR, fails to traffic efficiently from the endoplasmic reticulum to the plasma membrane and is the pathogenic basis for the missing cAMP-activated plasma membrane Cl^- channel. The xanthine drug CPX acts by binding to the mutant ΔF508-CFTR and correcting the trafficking deficit. Srivastava and colleagues used cDNA microarrays to study global gene expression in human cells permanently transfected with either wild-type or mutant *CFTR*. They also tested the effects of CPX on global gene expression when it was incubated with cells expressing either mutant or wild-type CFTR. Wild-type and mutant ΔF508-CFTR were shown to induce distinct and differential changes in the cDNA microarrays, significantly affecting up to 5% of the total genes in the array. CPX also induced substantial mutation-dependent and mutation-independent changes in gene expression. Some of these changes involved gene expression in mutant cells becoming like that in wild-type cells. The studies clearly demonstrated that cDNA array analysis of CF cells can yield useful pharmacogenomic information with relevance to both gene and pharmacologic therapy.

For individuals with CF, recurrent infections with the bacterium *Pseudomonas aeruginosa* contribute enormously to morbidity and mortality. Many microarray-based studies have been undertaken to decipher the interactions between this pathogen and the host airway.[98,99] Although there are no definitive results to date, such studies have the potential to provide useful information about the pathogenesis of lung disease in CF and may also reveal potential drug targets in the *Pseudomonas* pathogen.

Asthma

The proinflammatory cytokine IL-13 is released by T lymphocytes during the immediate hypersensitivity response and is a central mediator of asthma. Because IL-13 induces phenotypic features of asthma in mouse models that are deficient in T and B lymphocytes, it has been hypothesized that this cytokine contributes to the development of asthma by acting directly on resident airway cells. To analyze the global effects of IL-13 on gene expression in airway cells that could contribute to the phenotypic features of asthma, Lee and colleagues used GeneChip HuGene FL arrays (Affymetrix, Santa Clara, CA, USA) that contain probes for approximately 6,500 human genes.[100] Interestingly, despite activating a common signaling pathway, IL-13 was found to induce dramatically different patterns of gene expression in primary cultures of airway epithelial cells, airway smooth muscle cells, and lung fibroblasts, with little overlap among cell types.

Microarray studies by Cho and colleagues have demonstrated that activated human mast cells release a striking

amount of functionally active plasminogen activator inhibitor-1 (PAI-1).[101] These results suggest that PAI-1 could play an important role in airway remodeling of asthma, and inhibition of PAI-1 activity could represent a novel therapeutic approach in the management of airway remodeling.

Pulmonary Fibrosis

Idiopathic pulmonary fibrosis (IPF) is a progressive and largely untreatable disorder that affects up to 100,000 people in the United States alone. Most cases of IPF are sporadic, but there is clearly some familial clustering, and hence it is likely that there is a genetic component in some cases. Although no strong candidate susceptibility genes have yet been identified for pulmonary fibrosis, several studies have implicated modifier genes. Katsuma and colleagues used cDNA microarray-based gene expression profiling to monitor bleomycin-induced pulmonary fibrosis (bleomycin is a drug that causes lung inflammation and fibrosis).[102] Microarray studies in the Heller laboratory have suggested several genes as candidate modifiers for pulmonary fibrosis. Oligonucleotide arrays were used to analyze the gene expression patterns that underlie pulmonary fibrosis in response to bleomycin in two strains of susceptible mice (129 and C57BLy6). The gene expression patterns in these mice were then compared with those in mice carrying a null mutation in the epithelium-restricted integrin b6 subunit, which develop inflammation but are protected from pulmonary fibrosis. Two distinct groups of genes involved in the inflammatory and fibrotic responses were identified, with sequential induction of subsets of genes that characterize each response being revealed.[103] In subsequent array experiments by the same group, Zuo and colleagues analyzed samples from patients with histologically proven pulmonary fibrosis.[104] Gene expression patterns clearly distinguished normal from fibrotic lungs, and many of the genes whose expression was significantly increased in fibrotic lungs encoded proteins associated with extracellular matrix formation and degradation and proteins expressed in smooth muscle. Matrilysin (matrix metalloproteinase-7), a metalloproteinase not previously associated with pulmonary fibrosis, was the most convincingly up-regulated gene and therefore has been identified as a possible mediator of pulmonary fibrosis and a potential therapeutic target.

SUMMARY AND CONCLUSIONS

The study of the genetics of single-gene pulmonary diseases is well advanced, and although specific, highly effective therapies based on this knowledge have yet to be developed, the research has shed considerable light on disease pathogenesis and is likely to substantially alter diagnosis and management in the near future. For the much more common complex genetic diseases of the lung and airways, genetic studies are at an earlier stage, but the explosion in technologic and analytic capacity that has accompanied the human genome project has allowed impressive progress, and it is likely that a combination of linkage, association, and gene expression studies will completely transform our approach to the diagnosis and management of these conditions over the next decade.

ACKNOWLEDGMENT

This work was supported by grants from the Canadian Institutes of Health Research.

REFERENCES

1. Rommens JM, Iannuzzi MC, Kerem B, et al. Identification of the cystic fibrosis gene: chromosome walking and jumping. Science 1989;245:1059–65.
2. Riordan JR, Rommens JM, Kerem B, et al. Identification of the cystic fibrosis gene: cloning and characterization of complementary DNA. Science 1989;245:1066–73.
3. Van Eerdewegh P, Little RD, Dupuis J, et al. Association of the ADAM33 gene with asthma and bronchial hyperresponsiveness. Nature 2002;418:426–30.
4. Hall IP. Genetic factors in asthma severity. Clin Exp Allergy 1998;28 Suppl 5:16–20; discussion 6–8.
5. FitzSimmons SC. The changing epidemiology of cystic fibrosis. J Pediatr 1993;122:1–9.
6. Bye MR, Ewig JM, Quittell LM. Cystic fibrosis. Lung 1994; 172:251–70.
7. Rosenstein BJ, Langbaum TS, Metz SJ. Cystic fibrosis: diagnostic considerations. Johns Hopkins Med J 1982;150: 113–20.
8. Sugiyama Y, Kudoh S, Maeda H, et al. Analysis of HLA antigens in patients with diffuse panbronchiolitis. Am Rev Respir Dis 1990;141:1459–62.
9. Keicho N, Tokunaga K, Nakata K, et al. Contribution of HLA genes to genetic predisposition in diffuse panbronchiolitis. Am J Respir Crit Care Med 1998;158:846–50.
10. Falk CT, Rubinstein P. Haplotype relative risks: an easy reliable way to construct a proper control sample for risk calculations. Ann Hum Genet 1987;51:227–33.
11. Thomson G. Mapping disease genes: family-based association studies. Am J Hum Genet 1995;57:487–98.
12. Spielman RS, Ewens WJ. The TDT and other family-based tests for linkage disequilibrium and association. Am J Hum Genet 1996;59:983–9.
13. Spielman RS, McGinnis RE, Ewens WJ. The transmission/disequilibrium test detects cosegregation and linkage. Am J Hum Genet 1994;54:559–60.
14. Noguchi E, Shibasaki M, Arinami T, et al. Association of asthma and the interleukin-4 promoter gene in Japanese. Clin Exp Allergy 1998;28:449–53.
15. Devlin B, Roeder K. Genomic control for association studies. Biometrics 1999;55:997–1004.
16. Baron RM, Palmer LJ, Tantisira K, et al. DNA sequence variants in epithelium-specific ETS-2 and ETS-3 are not associated with asthma. Am J Respir Crit Care Med 2002; 166:927–32.
17. Kerem B, Rommens JM, Buchanan JA, et al. Identification of the cystic fibrosis gene: genetic analysis. Science 1989;245: 1073–80.
18. Zielenski J, Tsui L-C. Cystic fibrosis: genotypic and phenotypic variations. Annu Rev Genet 1995;29:777–807.
19. Zielenski J. Genotype and phenotype in cystic fibrosis. Respiration 2000;67:117–33.
20. Santis G, Osborne L, Knight R, et al. Genetic influences on pulmonary severity in cystic fibrosis. Lancet 1990;335:294.

21. Arkwright PD, Pravica V, Geraghty PJ, et al. End-organ dysfunction in cystic fibrosis—association with angiotensin I converting enzyme and cytokine gene polymorphisms. Am J Respir Crit Care Med 2003;167:384–9.
22. Sandford A, Weir T, Paré P. The genetics of asthma. Am J Respir Crit Care Med 1996;153:1749–65.
23. Duffy DL, Martin NG, Battistutta D, et al. Genetics of asthma and hay fever in Australian twins. Am Rev Respir Dis 1990;142:1351–8.
24. Nieminen MM, Kaprio J, Koskenvuo M. A population-based study of bronchial asthma in adult twin pairs. Chest 1991;100:70–5.
25. Hanson B, McGue M, Roitman-Johnson B, et al. Atopic disease and immunoglobulin E in twins reared apart and together. Am J Hum Genet 1991;48:873–9.
26. Daniels SE, Bhattacharrya S, James A, et al. A genome-wide search for quantitative trait loci underlying asthma. Nature 1996;383:247–50.
27. Hizawa N, Collins G, Rafnar T, et al. Linkage analysis of D*ermatophagoides pteronyssinus*-specific IgE responsiveness with polymorphic markers on chromosome 6p21 (HLA-D region) in Caucasian families by the transmission/disequilibrium test. Collaborative Study on the Genetics of Asthma (CSGA). J Allergy Clin Immunol 1998; 102:443–8.
28. Mathias RA, Freidhoff LR, Blumenthal MN, et al. Genome-wide linkage analyses of total serum IgE using variance components analysis in asthmatic families. Genet Epidemiol 2001;20:340–55.
29. Xu J, Meyers DA, Ober C, et al. Genomewide screen and identification of gene–gene interactions for asthma-susceptibility loci in three US populations: Collaborative Study on the Genetics of Asthma. Am J Hum Genet 2001;68:1437–46.
30. Xu X, Fang Z, Wang B, et al. A genome-wide search for quantitative-trait loci underlying asthma. Am J Hum Genet 2001;69:6.
31. Wjst M, Immervoll T. An Internet linkage and mutation database for the complex phenotype asthma. Bioinformatics 1998;14:827–8.
32. Ober C, Tsalenko A, Willadsen S, et al. Genome-wide screen for atopy susceptibility alleles in the Hutterites. Clin Exp Allergy 1999;29:11–5.
33. Yokouchi Y, Nukaga Y, Shibasaki M, et al. Significant evidence for linkage of mite-sensitive childhood asthma to chromosome 5q31–q33 near the interleukin 12 B locus by a genome-wide search in Japanese families. Genomics 2000; 66:152–60.
34. Cookson W. A new gene for asthma: would you ADAM and Eve it? Trends Genet 2003;19:169–72.
35. Rosenwasser LJ, Klemm DJ, Dresback JK, et al. Promoter polymorphisms in the chromosome 5 gene cluster in asthma and atopy. Clin Exp Allergy 1995;25:74–8.
36. Zhu S, Chan-Yeung M, Becker AB, et al. Polymorphisms of the IL-4, TNF-α, and FcεRIβ genes and the risk of allergic disorders in at-risk infants. Am J Respir Crit Care Med 2000;161:1655–9.
37. Burchard EG, Silverman EK, Rosenwasser LJ, et al. Association between a sequence variant in the IL-4 gene promoter and FEV_1 in asthma. Am J Respir Crit Care Med 1999;160: 919–22.
38. Sandford AJ, Chagani T, Zhu S, et al. Polymorphisms in the IL4, IL4RA, and FCERIB genes and asthma severity. J Allergy Clin Immunol 2000;106:135–40.
39. Graves PE, Kabesch M, Halonen M, et al. A cluster of seven tightly linked polymorphisms in the IL-13 gene is associated with total serum IgE levels in three populations of white children. J Allergy Clin Immunol 2000;105:506–13.
40. Howard TD, Whittaker PA, Zaiman AL, et al. Identification and association of polymorphisms in the interleukin-13 gene with asthma and atopy in a Dutch population. Am J Respir Cell Mol Biol 2001;25:377–84.
41. Baldini M, Lohman IC, Halonen M, et al. A polymorphism in the 5′ flanking region of the CD14 gene is associated with circulating soluble CD14 levels and with total serum immunoglobulin E. Am J Respir Cell Mol Biol 1999;20: 976–83.
42. Koppelman GH, Reijmerink NE, Colin Stine O, et al. Association of a promoter polymorphism of the CD14 gene and atopy. Am J Respir Crit Care Med 2001;163:965–9.
43. Green SA, Turki J, Bejarano P, et al. Influence of β2-adrenergic receptor genotypes on signal transduction in human airway smooth muscle cells. Am J Respir Cell Mol Biol 1995;13: 25–33.
44. Tan S, Hall IP, Dewar J, et al. Association between β2-adrenoceptor polymorphism and susceptibility to bronchodilator desensitization in moderately severe stable asthmatics. Lancet 1997;350:995–9.
45. Martinez FD, Graves PE, Baldini M, et al. Association between genetic polymorphisms of the β2-adrenoceptor and response to albuterol in children with and without a history of wheezing. J Clin Invest 1997;100:3184–8.
46. Hall IP, Wheatley A, Wilding P, et al. Association of Glu 27 β2-adrenoceptor polymorphism with lower airway reactivity in asthmatic subjects. Lancet 1995;345:1213–4.
47. Hopes E, McDougall C, Christie G, et al. Association of glutamine 27 polymorphism of β_2 adrenoceptor with reported childhood asthma: population based study. BMJ 1998; 316:664.
48. Ramsay CE, Hayden CM, Tiller KJ, et al. Polymorphisms in the β2-adrenoreceptor gene are associated with decreased airway responsiveness. Clin Exp Allergy 1999;29:1195–203.
49. Sandford AJ, Shirakawa T, Moffatt MF, et al. Localisation of atopy and β subunit of high-affinity IgE receptor (FcεRI) on chromosome 11q. Lancet 1993;341:332–4.
50. Palmer LJ, Rye PJ, Gibson NA, et al. Association of Fc epsilon R1-beta polymorphisms with asthma and associated traits in Australian asthmatic families. Clin Exp Allergy 1999;29: 1555–62.
51. Trabetti E, Cusin V, Malerba G, et al. Association of the FcεRI-β gene with bronchial hyper-responsiveness in an Italian population. J Med Genet 1998;35:680–1.
52. Hizawa N, Yamaguchi E, Jinushi E, Kawakami Y. A common FCER1B gene promoter polymorphism influences total serum IgE levels in a Japanese population. Am J Respir Crit Care Med 2000;161:906–9.
53. Deichmann KA, Heinzmann A, Forster J, et al. Linkage and allelic association of atopy and markers flanking the IL4-receptor gene. Clin Exp Allergy 1998;28:151–5.
54. Hershey GK, Friedrich MF, Esswein LA, et al. The association of atopy with a gain-of-function mutation in the α subunit of the interleukin-4 receptor. N Engl J Med 1997;337:1720–5.
55. Ober C, Leavitt SA, Tsalenko A, et al. Variation in the interleukin 4-receptor α gene confers susceptibility to asthma and atopy in ethnically diverse populations. Am J Hum Genet 2000;66:517–26.
56. Albuquerque RV, Hayden CM, Palmer LJ, et al. Association of polymorphisms within the tumour necrosis factor (TNF) genes and childhood asthma. Clin Exp Allergy 1998;28: 578–84.
57. Moffatt MF, Cookson WOCM. Tumour necrosis factor haplotypes and asthma. Hum Mol Genet 1997;6:551–4.
58. Moffatt MF, James A, Ryan G, et al. Extended tumour necrosis factor/HLA-DR haplotypes and asthma in an Australian population sample. Thorax 1999;54:757–61.

59. Trabetti E, Patuzzo C, Malerba G, et al. Association of a lymphotoxin α gene polymorphism and atopy in Italian families. J Med Genet 1999;36:323–5.
60. Winchester EC, Millwood IY, Rand L, et al. Association of the TNF-alpha-308 (G→A) polymorphism with self-reported history of childhood asthma. Hum Genet 2000;107:591–6.
61. Snider GL. Chronic obstructive pulmonary disease: risk factors, pathophysiology and pathogenesis. Annu Rev Med 1989;40:411–29.
62. Fletcher C, Peto R, Tinker C, et al. The natural history of chronic bronchitis. An eight-year study of chronic obstructive lung disease in working men in London. Oxford: Oxford University Press; 1976.
63. US Department of Health and Human Services. The health consequences of smoking. Chronic obstructive lung disease: a report of the surgeon general. Rockville, MD: DHHS Publications; 1984.
64. Speizer FE, Rosner B, Tager I. Familial aggregation of chronic respiratory disease: use of National Health Interview Survey data for specific hypothesis testing. Int J Epidemiol 1976;5:167–72.
65. Cohen BH, Diamond EL, Graves CG, et al. A common familial component in lung cancer and chronic obstructive pulmonary disease. Lancet 1977;2:523–6.
66. Silverman EK. Genetics of chronic obstructive pulmonary disease. Novartis Found Symp 2001;234:45–58; discussion 64.
67. Tager I, Tishler PV, Rosner B, et al. Studies of the familial aggregation of chronic bronchitis and obstructive airways disease. Int J Epidemiol 1978;7:55–62.
68. Redline S, Tishler PV, Rosner B, et al. Genotypic and phenotypic similarities in pulmonary function among family members of adult monozygotic and dizygotic twins. Am J Epidemiol 1989;129:827–36.
69. Hubert HB, Fabsitz RR, Feinleib M, et al. Genetic and environmental influences on pulmonary function in adult twins. Am Rev Respir Dis 1982;125:409–15.
70. Redline S, Tishler PV, Lewitter FI, et al. Assessment of genetic and non-genetic influences on pulmonary function: a twin study. Am Rev Respir Dis 1987;135:217–22.
71. Seersholm N, Wilcke JTR, Kok-Jensen A, et al. Risk of hospital admission for obstructive pulmonary disease in alpha (1)-antitrypsin heterozygotes of phenotype PiMZ. Am J Respir Crit Care Med 2000;161:81–4.
72. Dahl M, Nordestgaard BG, Lange P, et al. Molecular diagnosis of intermediate and severe alpha(1)-antitrypsin deficiency: MZ individuals with chronic obstructive pulmonary disease may have lower lung function than MM individuals. Clin Chem 2001;47:56–62.
73. Sandford AJ, Chagani T, Weir TD, et al. Susceptibility genes for rapid decline of lung function in the Lung Health Study. Am J Respir Crit Care Med 2001;163:469–73.
74. Smith CA, Harrison DJ. Association between polymorphism in gene for microsomal epoxide hydrolase and susceptibility to emphysema. Lancet 1997;350:630–3.
75. Yoshikawa M, Hiyama K, Ishioka S, et al. Microsomal epoxide hydrolase genotypes and chronic obstructive pulmonary disease in Japanese. Int J Mol Med 2000;5:49–53.
76. Otterbein LE, Lee PJ, Chin BY, et al. Protective effects of heme oxygenase-1 in acute lung injury. Chest 1999;116:61S–3S.
77. Choi AM, Alam J. Heme oxygenase-1: function, regulation, and implication of a novel stress-inducible protein in oxidant-induced lung injury. Am J Respir Cell Mol Biol 1996; 15:9–19.
78. Yamada N, Yamaya M, Okinaga S, et al. Microsatellite polymorphism in the heme oxygenase-1 gene promoter is associated with susceptibility to emphysema. Am J Hum Genet 2000;66:187–95.
79. Bouma G, Crusius JB, Oudkerk Pool M, et al. Secretion of tumour necrosis factor α and lymphotoxin α in relation to polymorphisms in the TNF genes and HLA-DR alleles. Relevance for inflammatory bowel disease. Scand J Immunol 1996;43:456–63.
80. Huang SL, Su CH, Chang SC. Tumor necrosis factor-α gene polymorphism in chronic bronchitis. Am J Respir Crit Care Med 1997;156:1436–9.
81. Sakao S, Tatsumi K, Igari H, et al. Association of tumor necrosis factor alpha gene promoter polymorphism with the presence of chronic obstructive pulmonary disease. Am J Respir Crit Care Med 2001;163:420–2.
82. Ishii T, Matsuse T, Teramoto S, et al. Neither IL-1beta, IL-1 receptor antagonist, nor TNF-alpha polymorphisms are associated with susceptibility to COPD. Respir Med 2000;94:847–51.
83. Thomson JR, Machado RD, Pauciulo MW, et al. Sporadic primary pulmonary hypertension is associated with germline mutations of the gene encoding BMPR-II, a receptor member of the TGF-beta family. J Med Genet 2000; 37:741–5.
84. Morse JH, Jones AC, Barst RJ, et al. Familial primary pulmonary hypertension locus mapped to chromosome 2q31–q32. Chest 1998;114(1 Suppl):57S–8S.
85. Humbert M, Deng Z, Simonneau G, et al. BMPR2 germline mutations in pulmonary hypertension associated with fenfluramine derivatives. Eur Respir J 2002;20:518–23.
86. Machado RD, Pauciulo MW, Thomson JR, et al. Heterozygous germline mutations in BMPR2, encoding a TGF-beta receptor, cause familial primary pulmonary hypertension. The International PPH Consortium. Nat Genet 2000;26:81–4.
87. Machado RD, Pauciulo MW, Thomson JR, et al. BMPR2 haploinsufficiency as the inherited molecular mechanism for primary pulmonary hypertension. Am J Hum Genet 2001;68: 92–102.
88. Deng Z, Morse JH, Slager SL, et al. Familial primary pulmonary hypertension (gene PPH1) is caused by mutations in the bone morphogenetic protein receptor-II gene. Am J Hum Genet 2000;67:737–44.
89. Lee SD, Shroyer KR, Markham NE, et al. Monoclonal endothelial cell proliferation is present in primary but not secondary pulmonary hypertension. J Clin Invest 1998;101:927–34.
90. Yeager ME, Halley GR, Golpon HA, et al. Microsatellite instability of endothelial cell growth and apoptosis genes within plexiform lesions in primary pulmonary hypertension. Circ Res 2001;88:E2–11.
91. Pei Y. A "two-hit" model of cystogenesis in autosomal dominant polycystic kidney disease? Trends Mol Med 2001;7: 151–6.
92. Loyd JE, Butler MG, Foroud TM, et al. Genetic anticipation and abnormal gender ratio at birth in familial primary pulmonary hypertension. Am J Respir Crit Care Med 1995;152:93–7.
93. Lanska DJ. George Huntington (1850–1916) and hereditary chorea. J Hist Neurosci 2000;9:76–89.
94. Mariani TJ, Reed JJ, Shapiro SD. Expression profiling of the developing mouse lung—insights into the establishment of the extracellular matrix. Am J Respir Cell Mol Biol 2002; 26:541–8.
95. Chambers RC, Leoni P, Kaminski N, et al. Global expression profiling of fibroblast responses to transforming growth factor-beta(1) reveals the induction of inhibitor of differentiation-1 and provides evidence of smooth muscle cell phenotypic switching. Am J Pathol 2003;162:533–46.
96. Golpon HA, Geraci MW, Moore MD, et al. HOX genes in human lung: altered expression in primary pulmonary hypertension and emphysema. Am J Pathol 2001;158: 955–66.

97. Srivastava M, Eidelman O, Pollard HB. Pharmacogenomics of the cystic fibrosis transmembrane conductance regulator (CFTR) and the cystic fibrosis drug CPX using genome microarray analysis. Mol Med 1999;5:753–67.
98. Lory S, Ichikawa JK. Pseudomonas–epithelial cell interactions dissected with DNA microarrays. Chest 2002;121(3 Suppl): 36S–9S.
99. Saavedra M, Vasil M, Randell S, et al. P*seudomonas aeruginosa*–human airway epithelial cell interaction: effects of iron on inflammation and apoptosis. Chest 2002;121 (3 Suppl):40S–1S.
100. Lee JH, Kaminski N, Dolganov G, et al. Interleukin-13 induces dramatically different transcriptional programs in three human airway cell types. Am J Respir Cell Mol Biol 2001;25: 474–85.
101. Cho SH, Tam SW, Demissie-Sanders S, et al. Production of plasminogen activator inhibitor-1 by human mast cells and its possible role in asthma. J Immunol 2000;165:3154–61.
102. Katsuma S, Nishi K, Tanigawara K, et al. Molecular monitoring of bleomycin-induced pulmonary fibrosis by cDNA microarray-based gene expression profiling. Biochem Biophys Res Commun 2001;288:747–51.
103. Kaminski N, Allard JD, Pittet JF, et al. Global analysis of gene expression in pulmonary fibrosis reveals distinct programs regulating lung inflammation and fibrosis. Proc Natl Acad Sci U S A 2000;97:1778–83.
104. Zuo F, Kaminski N, Eugui E, et al. Gene expression analysis reveals matrilysin as a key regulator of pulmonary fibrosis in mice and humans. Proc Natl Acad Sci U S A 2002;99:6292–7.
105. Larsson C. Natural history and life expectancy in severe alpha1-antitrypsin deficiency, Pi Z. Acta Med Scand 1978; 204:345–51.
106. Hirano K, Sakamoto T, Uchida Y, et al. Tissue inhibitor of metalloproteinases-2 gene polymorphisms in chronic obstructive pulmonary disease. Eur Respir J 2001;18:748–52.
107. Ishii T, Matsuse T, Teramoto S, et al. Association between alpha-1-antichymotrypsin polymorphism and susceptibility to chronic obstructive pulmonary disease. Eur J Clin Invest 2000;30:543–8.
108. Joos L, He JQ, Shepherdson MB, et al. The role of matrix metalloproteinase polymorphisms in the rate of decline in lung function. Hum Mol Genet 2002;11:569–76.
109. Minematsu N, Nakamura H, Tateno H, et al. Genetic polymorphism in matrix metalloproteinase-9 and pulmonary emphysema. Biochem Biophys Res Commun 2001;289:116–9.
110. Poller W, Barth J, Voss B. Detection of an alteration of the alpha 2-macroglobulin gene in a patient with chronic lung disease and serum alpha 2-macroglobulin deficiency. Hum Genet 1989;83:93–6.
111. He JQ, Ruan J, Connett J, et al. Antioxidant gene polymorphisms and susceptibility to a rapid decline in lung function in smokers. Am J Respir Crit Care Med 2002;166:323–8.
112. Yim JJ, Park GY, Lee CT, et al. Genetic susceptibility to chronic obstructive pulmonary disease in Koreans: combined analysis of polymorphic genotypes for microsomal epoxide hydrolase and glutathione S-transferase M1 and T1. Thorax 2000;55:121–5.
113. Yim JJ, Yoo CG, Lee CT, et al. Lack of association between glutathione S-transferase P1 polymorphism and COPD in Koreans. Lung 2002;180:119–25.
114. Gilliland FD, Gauderman WJ, Vora H, et al. Effects of glutathione-S-transferase m1, t1, and p1 on childhood lung function growth. Am J Respir Crit Care Med 2002;166:710–6.
115. Ishii T, Matsuse T, Teramoto S, et al. Glutathione S-transferase P1 (GSTP1) polymorphism in patients with chronic obstructive pulmonary disease. Thorax 1999;54:693–6.
116. Cantlay AM, Lamb D, Gillooly M, et al. Association between the CYP1A1 gene polymorphism and susceptibility to emphysema and lung cancer. J Clin Pathol Mol Pathol 1995; 48:M210–4.
117. Sakao S, Tatsumi K, Igari H, et al. Association of tumor necrosis factor-alpha gene promoter polymorphism with low attenuation areas on high-resolution CT in patients with COPD. Chest 2002;122:416–20.
118. Kucukaycan M, Van Krugten M, Pennings HJ, et al. Tumor necrosis factor-alpha +489G/A gene polymorphism is associated with chronic obstructive pulmonary disease. Respir Res 2002;3:29.
119. Eidelman O, Srivastava M, Zhang J, et al. Control of the proinflammatory state in cystic fibrosis lung epithelial cells by genes from the TNF-alphaR/NFkappaB pathway. Mol Med 2001;7:523–34.
120. Hull J, Thomson AH. Contribution of genetic factors other than CFTR to disease severity in cystic fibrosis. Thorax 1998;53: 1018–21.
121. Zielenski J, Corey M, Markiewicz D, et al. Mapping of cystic fibrosis modifier (CFM) loci in the human genome. Am J Hum Genet 1998;63 Suppl:42.
122. Ishii T, Keicho N, Teramoto S, et al. Association of Gc-globulin variation with susceptibility to COPD and diffuse panbronchiolitis. Eur Respir J 2001;18:753–7.
123. Hurme M, Santtila S. IL-1 receptor antagonist (IL-1Ra) plasma levels are co-ordinately regulated by both IL-1Ra and IL-1beta genes. Eur J Immunol 1998;28:2598–602.
124. Joos L, McIntyre L, Ruan J, et al. Association of IL-1beta and IL-1 receptor antagonist haplotypes with rate of decline in lung function in smokers. Thorax 2001;56:863–6.
125. Van Der Pouw Kraan TC, Kucukaycan M, Bakker AM, et al. Chronic obstructive pulmonary disease is associated with the −1055 IL-13 promoter polymorphism. Genes Immun 2002;3:436–9.
126. He JQ, Connett J, Anthonisen N, Sandford A. Polymorphisms in the IL13, IL13ra1 and IL4RA genes and rate of decline in lung function in smokers. Am J Respir Cell Mol Biol 2003; 28:379–85.
127. Meng QH, Polak JM, Edgar AJ, et al. Neutrophils enhance expression of inducible nitric oxide synthase in human normal but not cystic fibrosis bronchial epithelial cells. J Pathol 2000;190:126–32.
128. Kube D, Sontich U, Fletcher D, Davis PB. Proinflammatory cytokine responses to *P. aeruginosa* infection in human airway epithelial cell lines. Am J Physiol Lung Cell Mol Physiol 2001;280:L493–502.
129. Renzoni E, Lympany P, Sestini P, et al. Distribution of novel polymorphisms of the interleukin-8 and CXC receptor 1 and 2 genes in systemic sclerosis and cryptogenic fibrosing alveolitis. Arthritis Rheum 2000;43:1633–40.
130. Hull J, Ackerman H, Isles K, et al. Unusual haplotypic structure of IL8, a susceptibility locus for a common respiratory virus. Am J Hum Genet 2001;69:413–9.
131. Staugas RE, Harvey DP, Ferrante A, et al. Induction of tumor necrosis factor (TNF) and interleukin-1 (IL-1) by *Pseudomonas aeruginosa* and exotoxin A-induced suppression of lymphoproliferation and TNF, lymphotoxin, gamma interferon, and IL-1 production in human leukocytes. Infect Immun 1992; 60:3162–8.
132. Noguchi E, Shibasaki M, Arinami T, et al. Lack of association of atopy/asthma and the interleukin-4 receptor alpha gene in Japanese. Clin Exp Allergy 1999;29:228–33.
133. Risma KA, Wang N, Andrews RP, et al. V75R576 IL-4 receptor α is associated with allergic asthma and enhanced IL-4 receptor function. J Immunol 2002;169:1604–10.

134. Martinez FD, Solomon S, Holberg CJ, et al. Linkage of circulating eosinophils to markers on chromosome 5q. Am J Respir Crit Care Med 1998;158:1739–44.
135. Rioux JD, Stone VA, Daly MJ, et al. Familial eosinophilia maps to the cytokine gene cluster on human chromosomal region 5q31–q33. Am J Hum Genet 1998;63:1086–94.
136. Lazarus R, Klimecki WT, Raby BA, et al. Single-nucleotide polymorphisms in the Toll-like receptor 9 gene (TLR9): frequencies, pairwise linkage disequilibrium, and haplotypes in three US ethnic groups and exploratory case–control disease association studies. Genomics 2003;81:85–91.
137. Moffatt MF, Hill MR, Cornelis F, et al. Genetic linkage of T-cell receptor alpha/delta complex to specific IgE responses. Lancet 1994;343:1597–600.
138. Noguchi E, Shibasaki M, Arinami T, et al. Evidence for linkage between the development of asthma in childhood and the T-cell receptor beta chain gene in Japanese. Genomics 1998;47:121–4.
139. Drazen JM, Yandava CN, Dube L, et al. Pharmacogenetic association between ALOX5 promoter genotype and the response to anti-asthma treatment. Nat Genet 1999;22: 168–70.
140. Kauffmann F, Kleisbauer JP, Cambon-De-Mouzon A, et al. Genetic markers in chronic air-flow limitation: a genetic epidemiologic study. Am Rev Respir Dis 1983;127:263–9.
141. Tzetis M, Efthymiadou A, Strofalis S, et al. CFTR gene mutations—including three novel nucleotide substitutions—and haplotype background in patients with asthma, disseminated bronchiectasis and chronic obstructive pulmonary disease. Hum Genet 2001;108:216–21.
142. Cuppens H, Lin W, Jaspers M, et al. Polyvariant mutant cystic fibrosis transmembrane conductance regulator genes. The polymorphic (Tg)m locus explains the partial penetrance of the T5 polymorphism as a disease mutation. J Clin Invest 1998;101:487–96.
143. Matsushita I, Hasegawa K, Nakata K, et al. Genetic variants of human beta-defensin-1 and chronic obstructive pulmonary disease. Biochem Biophys Res Commun 2002; 291:17–22.
144. Smith JJ, Travis SM, Greenberg EP, Welsh MJ. Cystic fibrosis airway epithelia fail to kill bacteria because of abnormal airway surface fluid. Cell 1996;85:229–36.
145. Linzmeier R, Ho CH, Hoang BV, Ganz T. A 450-kb contig of defensin genes on human chromosome 8p23. Gene 1999;233:205–11.
146. Bals R, Wang X, Wu Z, et al. Human beta-defensin 2 is a salt-sensitive peptide antibiotic expressed in human lung. J Clin Invest 1998;102:874–80.
147. Guo X, Lin HM, Lin Z, et al. Surfactant protein gene A, B, and D marker alleles in chronic obstructive pulmonary disease of a Mexican population. Eur Respir J 2002;18: 482–90.
148. Floros J, DiAngelo S, Koptides M, et al. Human SP-A locus: allele frequencies and linkage disequilibrium between the two surfactant protein A genes. Am J Respir Cell Mol Biol 1996;15:489–8.
149. Ramet M, Haataja R, Marttila R, et al. Human surfactant protein—a gene locus for genetic studies in the Finnish population. Dis Markers 2000;16:119–24.
150. Choi E, Ehrmantraut ME, Foster C, et al. Association of alleles of surfactant proteins A1 and A2 genes with severity of lung disease in 135 adults with cystic fibrosis (CF). Pediatr Pulmonol Suppl 2000;20:211.
151. Kirkbride HJ, Bolscher JG, Nazmi K, et al. Genetic polymorphism of MUC7: allele frequencies and association with asthma. Eur J Hum Genet 2001;9:347–54.
152. Vinall LE, Fowler JC, Jones AL, et al. Polymorphism of human mucin genes in chest disease: possible significance of MUC2. Am J Respir Cell Mol Biol 2000;23:678–86.
153. Gonzalez-Guerrico AM, Cafferata EG, Radrizzani M, et al. Tyrosine kinase Src constitutes a bridge between MUC1 overexpression and the CFTR channel failure in cystic fibrosis. Pediatr Pulmonol Suppl 2001;22:197.
154. Garred P, Pressler T, Madsen HO, et al. Association of mannose-binding lectin gene heterogeneity with severity of lung disease and survival in cystic fibrosis. J Clin Invest 1999;104:431–7.
155. Gabolde M, Hubert D, Guilloud-Bataille M, et al. The mannose binding lectin gene influences the severity of chronic liver disease in cystic fibrosis. J Med Genet 2001;38:310–1.
156. Zielenski J, Pereira L, Corey M, et al. Analysis of mannose binding lectin (MBL) haplotypes in a large cohort of cystic fibrosis patients. Am J Hum Genet 2001;69 Suppl:650.
157. Sanak M, Simon HU, Szczeklik A. Leukotriene C4 synthase promoter polymorphism and risk of aspirin-induced asthma. Lancet 1997;350:1599–600.
158. Spencer DA, Sampson AP, Green CP, et al. Sputum cysteinyl-leukotriene levels correlate with the severity of pulmonary disease in children with cystic fibrosis. Pediatr Pulmonol 1992;12:90–4.
159. Arkwright PD, Laurie S, Super M, et al. TGF-beta(1) genotype and accelerated decline in lung function of patients with cystic fibrosis. Thorax 2000;55:459–62.
160. Yi ES, Bedoya A, Lee H, et al. Radiation-induced lung injury in vivo: expression of transforming growth factor-beta precedes fibrosis. Inflammation 1996;20:339–52.
161. Fryer AA, Bianco A, Hepple M, et al. Polymorphism at the glutathione S-transferase GSTP1 locus. A new marker for bronchial hyperresponsiveness and asthma. Am J Respir Crit Care Med 2000;161:1437–42.
162. Sundberg K, Johansson AS, Stenberg G, et al. Differences in the catalytic efficiencies of allelic variants of glutathione transferase P1-1 towards carcinogenic diol epoxides of polycyclic aromatic hydrocarbons. Carcinogenesis 1998;19: 433–6.
163. Henrion A, Flamant C, Roussey M, et al. Severity of cystic fibrosis is associated with gene polymorphism of anti-oxidizing enzymes. Pediatr Pulmonol Suppl 2001;22:215.
164. Barnes KC, Freidhoff LR, Nickel R, et al. Dense mapping of chromosome 12q13.12–q23.3 and linkage to asthma and atopy. J Allergy Clin Immunol 1999;104:485–91.
165. Aggarwal AN, Behera D. Interferon-gamma 1b: impact of new indications (idiopathic pulmonary fibrosis). Expert Opin Pharmacother 2000;1:1423–7.
166. Stafforini DM, Numao T, Tsodikov A, et al. Deficiency of platelet-activating factor acetylhydrolase is a severity factor for asthma. J Clin Invest 1999;103:989–97.
167. Kruse S, Mao X-Q, Heinzmann A, et al. The Ile198Thr and Ala379Val variants of plasmatic PAF-acetylhydrolase impair catalytical activities and are associated with atopy and asthma. Am J Hum Genet 2000;66:1522–30.
168. Karp CL, Grupe A, Schadt E, et al. Identification of complement factor 5 as a susceptibility locus for experimental allergic asthma. Nat Immunol 2000;1:221–6.
169. Moore PE, Laporte JD, Abraham JH, et al. Polymorphism of the beta(2)-adrenergic receptor gene and desensitization in human airway smooth muscle. Am J Respir Crit Care Med 2000;162:2117–24.
170. Scott MG, Swan C, Wheatley AP, Hall IP. Identification of novel polymorphisms within the promoter region of the human beta2 adrenergic receptor gene. Br J Pharmacol 1999;126:841–4.

171. Xie HG, Stein CM, Kim RB, et al. Frequency of functionally important beta-2 adrenoceptor polymorphisms varies markedly among African-American, Caucasian and Chinese individuals. Pharmacogenetics 1999;9:511–6.
172. Weir TD, Mallek N, Sandford AJ, et al. Beta2-adrenergic receptor haplotypes in mild, moderate and fatal/near fatal asthma. Am J Respir Crit Care Med 1998;158:787–91.
173. Holloway JW, Dunbar PR, Riley GA, et al. Association of beta2-adrenergic receptor polymorphisms with severe asthma. Clin Exp Allergy 2000;30:1097–103.
174. Buescher R, Grasemann H, Eilmes KJ, et al. Disease modifying genes in cystic fibrosis: β2-adrenergic receptor. Pediatr Pulmonol Suppl 2000;20:211.
175. Aznarez I, Zielenski J, Chan E, Tsui LC. Cis and trans regulation of the CFTR gene splicing in CF. Pediatr Pulmonol Suppl 2001;22:216.
176. Chung C, Fang I, Nguyen V, et al. Investigation of mCLCA3 as a modifier of CF disease in mice. Pediatr Pulmonol Suppl 2001;22:217.

CHAPTER 30

NEUROHUMORAL CONTROL OF THE AIRWAYS

Marie-Claire Michoud

The innervation of the airways is entirely supplied by the autonomic nervous system; there are no somatic afferent or efferent nerves in the airways. The autonomic nerves contribute to the regulation of airway smooth muscle tone and modulate secretions from the submucosal glands and the transport of fluid across the bronchial epithelium. Capillary permeability, bronchial bloodflow, and the release of mediators by mast cells and other inflammatory cells are also regulated by the autonomic nervous system.[1]

Although the physiologic role of sympathetic (adrenergic) and parasympathetic (cholinergic) nerves has been fairly well established in human and animal airways, the relatively recent discovery of both inhibitory and excitatory nonadrenergic noncholinergic nervous systems has prompted a considerable amount of interest. Extensive research has shown that these nerve fibers can release a variety of nonclassic neurotransmitters, such as neuropeptides, which, in turn, modulate smooth muscle tone and vascular permeability and reactivity. It also appears that interactions between inflammatory mediators and afferent nerve endings are more complex and numerous than previously thought. Thus, although it was concluded in the past that anomalies of the autonomic nervous system were not responsible for the airway hyperresponsiveness observed in asthma and chronic obstructive pulmonary disease (COPD), it appears that they might contribute to it, albeit not directly.

AIRWAY INNERVATION

Afferent Nerve Fibers

Several types of receptors of afferent nerves are found in the airways. In the trachea and the bronchi, there are the slowly adapting receptors (SARs) and rapidly adapting receptors (RARs), C-fiber endings, and sensory receptors in neuroepithelial bodies.[2] The SARs are myelinated nerve fiber endings localized in the smooth muscle of conducting airways. They respond to changes in the airway wall tone, as well as to the contractile mediators histamine and acetylcholine, and are inhibited by carbon dioxide.[2] Reflex activation of these receptors produces an inhibition of parasympathetic output resulting in changes in the pattern of respiration (shortening of inspiration and lengthening of expiration), bronchodilatation, tachycardia, and systemic vasodilatation.

The RARs, also known as irritant receptors, are Aδ myelinated fibers localized between and below epithelial cells. In the presence of a stimulus, they fire rapidly, but they quickly accommodate if the stimulus is maintained. They respond to chemical stimuli, noxious gases, inflammatory and immunologic mediators, and inhaled particles. The nerve fibers travel in the vagus nerve to the central nervous system, and efferent parasympathetic fibers travel back in the vagus nerve. Activation of these receptors results in reflex bronchoconstriction and cough, thus protecting to some extent the airways from further exposure to noxious stimuli.[3]

The C-fiber receptors are the nerve endings of nonmyelinated nerve fibers and contain the following neuropeptides: substance P (SP), neurokinin-A (NKA), and calcitonin gene–related peptide (CGRP). They are subdivided into two types based on their location: the bronchial C-fibers are present within the airway mucosa, and the pulmonary C-fibers are located in the lung parenchyma. Pulmonary C-fibers are sensitive to changes in lung volume, and an increase in lung volume results in reflex apnea followed by rapid shallow breathing, bradycardia, and hypotension. Stimulation of the bronchial C-fibers results in reflex bronchoconstriction, cough, an increase in vascular permeability, and an increase in mucus production.[4] These receptors are sensitive to various chemical stimuli, such as hypertonic saline, ozone, bradykinin, cigarette smoke, and capsaicin, the pungent extract of red pepper. The bronchial C-fibers have been the subject of extensive research as their activation releases various neuropeptides, in particular NKA, SP, and CGRP.[3,5] These substances have powerful biologic effects, such as inducing smooth muscle contraction, increasing vascular permeability, resulting in airway edema, and increasing mucus secretion. The release of these neuropeptides can be triggered locally by retrograde conduction of the afferent nerve impulses along the C-fibers, the so-called axon reflex.[1,6] Because the effects of these neuropeptides are similar to those observed with inflammatory mediators, they are

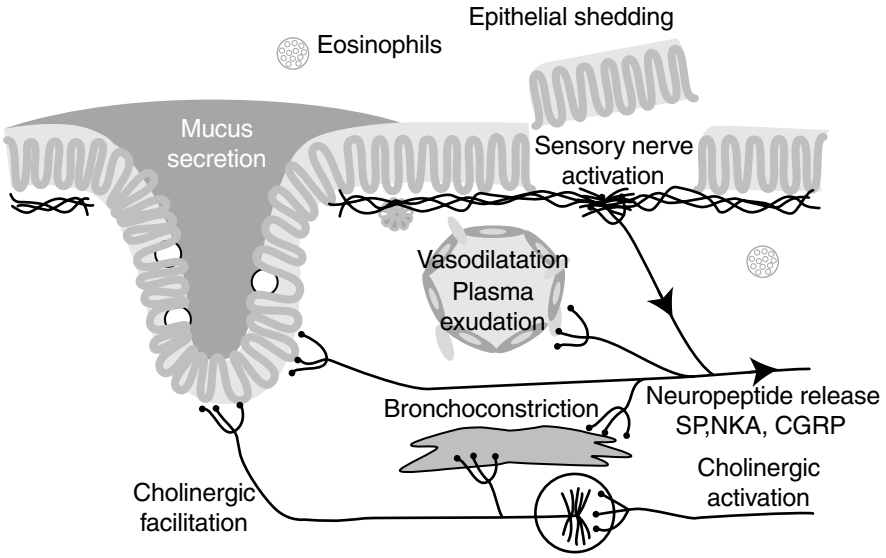

FIGURE 30-1 Postulated mechanisms of neurogenic inflammation and its pathophysiologic consequences.[10] CGRP = calcitonin gene–related peptide. NKA = neurokinin-A; SP = substance P. Adapted from Barnes PJ.[7]

often referred to collectively as "neurogenic inflammation."[7] Thus, unlike the RARs, which appear to have a mainly protective role, the C receptors have potentially deleterious effects on the airways, and their activation by inflammatory mediators can lead to a worsening of the inflammatory reaction through the release of neuropeptides.

Of further interest are the findings that the C-fibers can be sensitized by various agents, such as ozone, platelet-activating factor, prostaglandins, histamine, interleukin-1β (IL-1β), and nerve growth factor.[5,8,9] These observations have led to the hypothesis that neurogenic inflammation could be an important factor in airway diseases such as asthma and COPD, in which inflammation is an important contributor (Figure 30-1).[7,10] However, this hypothesis has been somewhat weakened by the fact that few neuropeptide-containing nerve fibers have been found in human airways (unlike in other animal species, such as guinea pigs, rats, and ferrets)[11] and by the observation that the number of nerve fibers is not increased in the airways of patients with asthma and COPD.[11,12] On the other hand, morphologic and functional studies have shown that neurokinin-1 (NK-1) and/or NK-2 receptors are present in submucosal glands and endothelial and smooth muscle cells[13–17] and that the amounts of SP and NKA recovered from the sputum and/or the bronchoalveolar lavage fluid of asthmatic patients are increased in comparison with the amounts recovered from normal, healthy volunteers.[18–20] A possible source of these neuropeptides could be immune cells—monocytes, macrophages, lymphocytes, eosinophils, and dendritic cells—that have been shown to produce SP.[21]

Efferent Innervation

Parasympathetic Nervous System The parasympathetic nervous system constitutes the predominant neural bronchoconstrictor system in humans and other animals.

Cholinergic Parasympathetic Nerves Efferent nerve fibers originate from the vagal motor nuclei of the brainstem and travel down the vagus nerve to the parasympathetic ganglia located within the bronchial wall. Ganglion cells are found along the peribronchial plexus all the way down to the level of small bronchi (Figure 30-2).[4,22] From these cells, postganglionic cholinergic fibers innervate the smooth muscle and the submucosal glands. The density of the innervation decreases from the trachea to the terminal bronchioles, and in humans there is no innervation of the airway epithelium and of the alveoli.[1,23,24] There is also no evidence that airway blood vessels are innervated.[24] The acetylcholine released from the preganglionic and postganglionic nerve fibers acts on the target cells through three types of muscarinic receptor: M_1, M_2, and M_3 (two other types of muscarinic receptor have been cloned and are expressed in rabbit lungs but not in humans[25]). The postjunctional M_3 receptors are found on bronchial airway smooth muscle and submucosal glands, and possibly on endothelial cells and vascular smooth muscle.[26,27] They are G protein–coupled receptors, and their stimulation induces an increase in intracellular Ca^{2+} and smooth muscle contraction. Activation of M_3 receptors also mediates mucus, water, and electrolyte secretion from submucosal glands and vasodilatation of the tracheobronchial blood vessels. M_2 receptors are also found on airway smooth muscle and submucosal glands; their activation does not cause smooth muscle contraction but inhibits β-adrenoceptor–induced smooth muscle relaxation by preventing the activation of adenylate cyclase and the opening of Ca^{2+}-activated K^+ channels.[27] Prejunctional M_2 receptors are also present on cholinergic nerve endings in the airways, and their activation inhibits the further release of acetylcholine, thus providing negative feedback control of acetylcholine release. M_1 receptors can be found on the cell bodies of preganglionic neurons and on submucosal glands (the M_1/M_3 ratio is 1:2 in human bronchi,[28,29] where they appear to modulate water and electrolyte secretion[27]). M_1 receptors located on preganglionic cell neurons facilitate parasympathetic neurotransmission through the ganglion.

Airway cholinergic nerves play an important role in the control of airway tone. Even at rest, there is a mild degree of continuous parasympathetic activity maintaining a certain

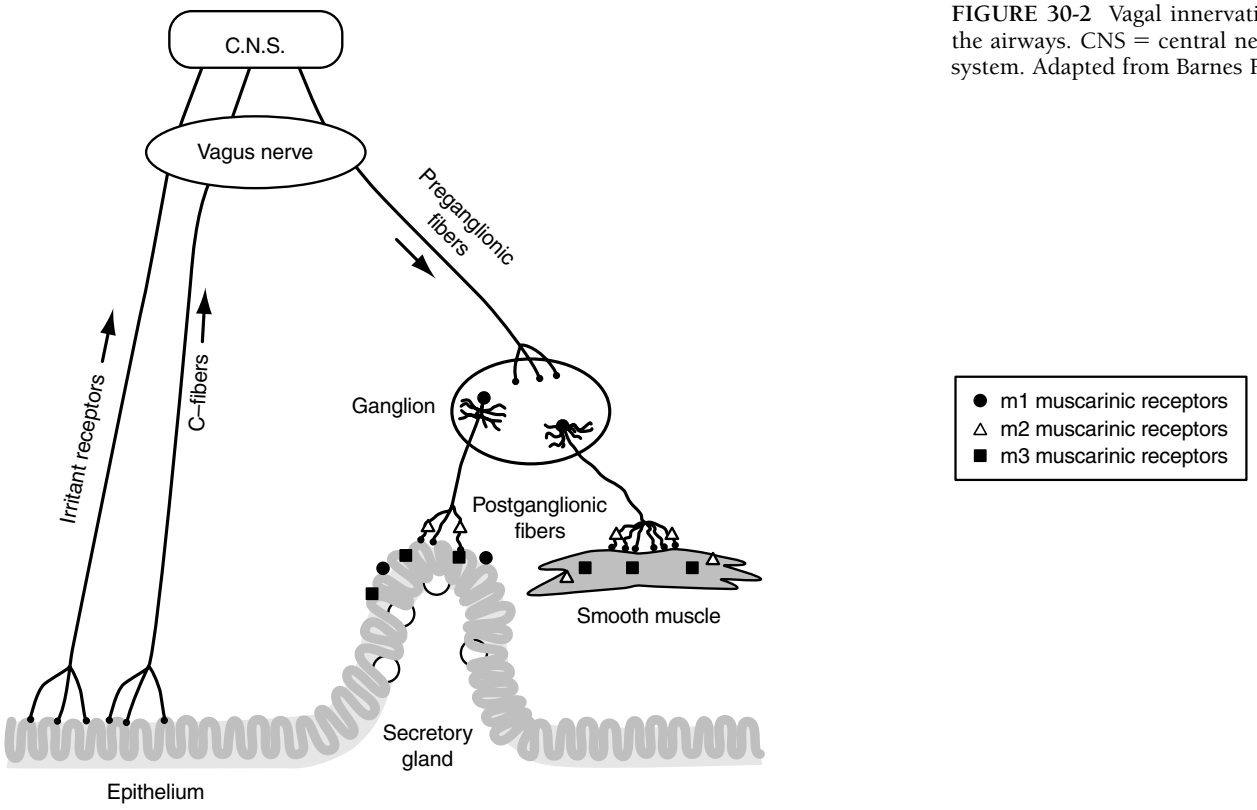

FIGURE 30-2 Vagal innervation to the airways. CNS = central nervous system. Adapted from Barnes PJ.[10]

level of smooth muscle contraction. In the presence of noxious stimuli such as sulfur dioxide, carbon dust, or ozone, reflex parasympathetic activation induces bronchoconstriction, thus protecting the lower airways.

Noncholinergic Parasympathetic Nerves In the presence of muscarinic blockade, vagal stimulation causes dilatation of preconstricted airways that can be abolished by vagotomy or ganglionic blockade. This reflex dilatation has been demonstrated in several species, including humans, in vitro by electric field stimulation,[30–32] and in vivo by laryngeal stimulation or stimulation of bronchial C-fibers.[33–35] Putative neurotransmitters are the vasoactive intestinal peptide (VIP), the structurally related peptide pituitary adenylate cyclase–activating peptide (PACAP), and nitric oxide (NO; formed from arginine by neuronal NO synthase).[4] Both VIP and NO synthase have been localized to nerve fibers innervating airway smooth muscle and to parasympathetic ganglia in the airways. Whether these transmitters are co-released with acetylcholine at postganglionic nerve endings or released from distinct parasympathetic nerves is not entirely clear.[36–38] The relative importance of NO, VIP, and the structurally related PACAP in promoting smooth muscle relaxation is still being debated. In the airways of humans and guinea pigs, pretreatment with the NO synthase inhibitor nitro-L-arginine methyl ester hydrochloride (L-NAME) considerably reduces the relaxation induced by electric field stimulation,[39–41] whereas other researchers have shown that VIP and PACAP are 100 to 1,000 times more potent than NO as airway relaxant agonists.[36]

Sympathetic Nervous System Sympathetic nerve fibers supplying the lungs originate from the upper six thoracic segments of the spinal cord and synapse in the cervical ganglia and the upper four thoracic ganglia.[10] Postganglionic fibers enter the lungs at the hilum. Adrenergic innervation of the airway varies greatly with the species studied. In cats, for example, there is a rich supply of adrenergic fibers, whereas they are very sparse in humans and guinea pigs (Figure 30-3).[42] Ultrastructural studies have shown that in humans, adrenergic nerve fibers are found in close proximity to submucosal glands, blood vessels, and airway ganglia but are practically nonexistent in airway smooth muscle.[10,43] However, despite the lack of sympathetic innervation, β-adrenergic receptors are numerous on airway smooth muscle, and their stimulation, presumably by circulating catecholamines, produces bronchodilatation.

α-Adrenoceptors are localized on pulmonary and bronchial blood vessels and on bronchial epithelial cells. α-Adrenoceptors are also found on submucosal glands, in parasympathetic ganglia, and on cholinergic and C afferent nerve fibers.[22]

In vitro, α-adrenergic stimulation increases mucus secretion and induces smooth muscle contraction. However, in humans and dogs, this last effect could be demonstrated only on preconstricted smooth muscle or tissue originating from diseased lungs.[44] In vivo, α-adrenergic stimulation has no effect on bronchomotor tone in healthy individuals but induces bronchoconstriction in asthmatic patients.[45–47] As the effect of the α-adrenergic stimulation could be reversed by anticholinergic agents as well as by an α-adrenergic

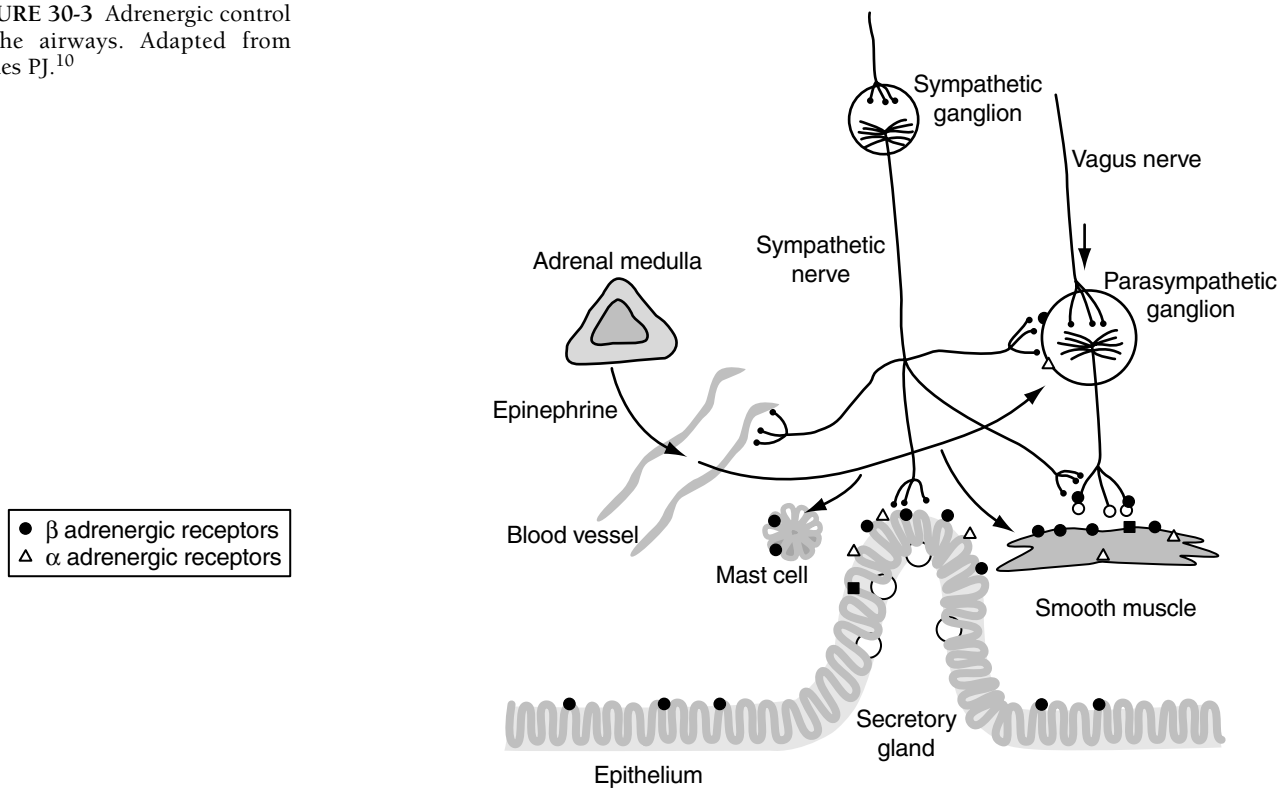

FIGURE 30-3 Adrenergic control of the airways. Adapted from Barnes PJ.[10]

antagonist, it is not clear whether the bronchoconstriction was due to a direct effect of the α-adrenergic agonist on airway smooth muscle or to an indirect effect via the modulation of parasympathetic neurotransmission in the parasympathetic ganglia. Indeed sympathetic nerve fibers are found in airway ganglia and could potentially modulate bronchomotor tone indirectly by inhibiting or decreasing the release of acetylcholine from preganglionic and postganglionic cholinergic nerves.[22]

The β-adrenoceptors are divided into two subtypes, based on their affinity for norepinephrine (β_1-adrenoceptors) and epinephrine (β_2-adrenoceptors). The β_2-adrenoceptors are present on airway smooth muscle cells, epithelial cells, mast cells, and endothelial and vascular smooth muscle cells. These receptors are also found in parasympathetic ganglia located within the airway wall and on postganglionic cholinergic nerve fibers.[22,48] Stimulation of these receptors induces relaxation of the airway smooth muscle, increases the secretion of mucus, and increases the production of surfactant. It also modulates cholinergic neurotransmission and inhibits the release of mediators from mast cells. In humans, in whom the sympathetic innervation is very sparse, these effects are presumably mediated mostly by circulating epinephrine. In other animal species, such as dogs, cats, and ferrets, however, sympathetic stimulation inhibits vagally induced bronchoconstriction. Depending on the species and the type of preparation, the site of modulation may be postganglionic nerves or the parasympathetic ganglia.[22]

ROLE OF NEUROHUMORAL FACTORS IN AIRWAY HYPERRESPONSIVENESS AND ASTHMA

Airway Sensory Nerves: Neurogenic Inflammation

Several stimuli known to cause bronchoconstriction in asthmatic subjects, such as bradykinin, sulfur dioxide, distilled water, and adenosine, have been shown to activate afferent nerves, resulting in reflex cough and bronchoconstriction.[49] Furthermore, it was postulated[22] that activation of these nerves by various inflammatory mediators could cause the release of neuropeptides via an axon reflex (the so-called excitatory nonadrenergic, noncholinergic nervous system.[6,10] Neuropeptide release would, in turn, produce vasodilatation, plasma exudation, smooth muscle contraction, and an increase in mucus production (Figure 30-1). In addition, there is increasing evidence that neuropeptides can be synthesized by inflammatory and other cells[21,50] and that inflammatory cytokines can increase the expression of neuropeptides in inflammatory cells, suggesting that their production may be increased in pathologic conditions. Thus, a possible role of neuropeptides in airway hyperresponsiveness and asthma has been extensively investigated.[49] It was reported that SP-containing nerves were more abundant in the lungs of asthmatic subjects than in those of healthy individuals,[51] although later studies could not confirm this observation,[52] and that the bronchoalveolar lavage fluid of asthmatic patients contained elevated levels of SP-like immunoreactivity, both at rest and following antigen challenge, in comparison with that of healthy control

subjects.[18] It has also been shown that two types of tachykinin receptor, NK-1 (activated by SP) and NK-2 (activated by NKA), are present in human lungs and that NK-2 expression is increased in asthmatic subjects.[53] NK-2 activation produces smooth muscle constriction in vitro, and this effect is more marked in small bronchi. In addition, inhalation of NKA produces bronchoconstriction in asthmatic patients. SP stimulates mucus secretion and induces vasodilatation and plasma exudation. It also stimulates angiogenesis, and both SP and NKA enhance eosinophil and lung fibroblast chemotaxis, suggesting that they could contribute to the airway remodeling observed in asthma.[11] Finally, tachykinins can also contribute to airway bronchoconstriction by facilitating ganglionic transmission and the release of acetylcholine from postganglionic nerves.[54,55] Tachykinins are degraded by angiotensin-converting enzyme present in the vascular endothelium and by neutral endopeptidase (NEP) located in the airway epithelium.[7] Indirect evidence for the role of tachykinins in asthma includes the facts that inactivation of these enzymes by phosphoramidon or thiorphan potentiates bronchoconstriction and that many inflammatory stimuli known to induce bronchoconstriction in asthmatic subjects, including viral infections and allergen exposure, inhibit or reduce the activity of NEP.[11]

CGRP is colocalized with SP in afferent nerves. In human airways, CGRP receptors are found mostly in blood vessels, and it has been postulated that CGRP might mediate hyperemia in asthma.

Extensive research over the last 10 years has shown that neuropeptides can be important mediators of airway inflammation and bronchoconstriction in rodents. Evidence of their role in human asthma and airway hyperresponsiveness is less clear. One of the strategies used to evaluate the possible role of neurogenic inflammation in airway responsiveness and asthma was the use of inhibitors of NEP. NEP is a membrane-bound metallopeptidase present at the surface of epithelial and smooth muscle cells, submucosal glands, and fibroblasts. Its activation leads to the degradation of tachykinins, thus limiting neurogenic inflammation. Administration of phosphoramidon, an NEP inhibitor, potentiates the dose–response curves for NKA, SP, and bradykinin in isolated human airways and also potentiates the bronchoconstriction induced by exogenous tachykinin in both control and asthmatic subjects,[11,56] supporting the hypothesis that a breakdown in the elimination of neuropeptides could lead to airway hyperresponsiveness and asthma. However, another study has shown that inhibitors of NEP have no effects on baseline resistance, nor do they affect the responsiveness to histamine or the degree of bronchoconstriction induced by allergen challenge in asthmatic subjects,[57] indicating that the increase in bronchomotor tone in asthmatic patients is not due to a tonic release of tachykinins. In addition, the observation that NEP inhibitors enhance the response to NKA in asthmatic patients suggests that NEP is present and functional in these patients.[7] Indeed, in situ hybridization and immunocytochemical studies have confirmed that NEP is expressed in the bronchi of both nonasthmatic and asthmatic individuals.[7] Interestingly, a difference in NEP expression has been found between the biopsy specimens of asthmatic patients taking steroids and asthmatic patients not taking steroids, suggesting that one of the antiinflammatory effects of steroids could be mediated by the up-regulation of NEP.[58] Furthermore, morphologic studies of human lungs could not confirm the early study showing an increase in SP-containing nerves from autopsied lungs of asthmatic patients, and it appears that, in fact, innervation of human airways is very sparse and is not increased in asthma. Finally, tachykinin receptor antagonists have not been very useful in the treatment of asthma.[9] Indeed, it has been reported that administration of the potent and specific NK-1 blocker CP-99,994 has no effects on either baseline airway resistance or bronchoconstriction induced in asthmatic patients by inhalation of hypertonic saline.[59] It remains possible that treatment with more powerful and/or dual tachykinin receptor antagonists will be more effective. Furthermore, neurokinins released from non-neural tissues may prove to have important biologic effects, unrelated to neural control.

Role of the Parasympathetic System in Airway Hyperresponsiveness

Airway resistance is often increased in asthmatic patients, even during periods of remission, and there is evidence that this increase in basal tone is, at least partially, mediated by an increase in parasympathetic tone as anticholinergic drugs inhibit it. Anticholinergic treatment also decreases airway hyperreactivity to a number of irritants, such as bradykinin, histamine, capsaicin, or distilled water, indicating that the parasympathetic system is implicated in airway reactivity.[27,36] There is no evidence to suggest that this increased parasympathetic activity is mediated by an increase in the number or a decrease in the threshold for the response of postjunctional M_1 or M_3 muscarinic receptors. There is, on the other hand, increasing evidence that M_2 receptor function on parasympathetic nerves is altered.[27] In human airways, M_2 receptors have been localized to parasympathetic nerve endings, and their activation by acetylcholine leads to the inhibition of further transmitter release.[27,60] A decrease in the number of M_2 receptors, or an increase in their threshold for activation, would lead to an increase in acetylcholine release and bronchoconstriction. Interesting indirect evidence corroborating the role of M_2 muscarinic receptors in parasympathetic tone in human airway comes from epidemiologic studies of diabetic patients, showing that there is a low incidence of asthma in these patient populations and that diabetic patients have decreased bronchomotor tone and parasympathetic reflexes.[27] Furthermore, it has been shown that, in animal models of diabetes, the decrease in airway parasympathetic activity was not due to alteration of M_3 muscarinic receptors but to an increase in M_2 receptor activity.[61–63] At present, anticholinergic drugs are not selective and therefore inhibit M_2 receptors as well as M_1 and M_3 receptors. The development of more specific blockers of the M_1 and M_3 receptors should provide more effective treatment of airway bronchoconstriction, as well as help elucidate the role of the parasympathetic nervous system in asthma and bronchoconstriction.

Role of the Sympathetic Nervous System in Airway Hyperresponsiveness

β-Adrenergic agonists have a powerful effect in reversing asthmatic bronchoconstriction, and it was suggested by Szentivanyi in 1968[64] that asthma could result from a defect in β-adrenergic receptors. Since then, extensive work has been carried out to verify this hypothesis. There is both in vivo and in vitro evidence that β-adrenergic receptors are less responsive in asthmatic than in healthy individuals.[65–67] It is not clear, however, whether this decreased responsiveness is the cause of asthma or the byproduct of therapy with β-adrenergic agonists leading to desensitization of the β-adrenergic receptors. Another possible reason is that the decreased responsiveness is a consequence of the inflammatory processes occurring in asthmatic airways. It has been shown that the cytokines IL-1β, tumor necrosis factor-α (TNF-α), IL-5, and IL-13, all of which are found in increased concentrations in the bronchoalveolar lavage fluid of asthmatic patients, decrease the ability of airway smooth muscle to generate cyclic AMP.[68] The mechanism appears to involve COX-2 activation and prostaglandin E_2 (PGE_2) release. Indeed, Laporte and colleagues[69] reported that the inhibitory effects of IL-1β on the isoproterenol-induced response are abolished by COX-2 inhibitors and that exposure of human airway smooth muscle cells to IL-1β increases the expression of COX-2 and the release of PGE_2.[69] Thus, it appears more likely that β-adrenergic hyporesponsiveness is a consequence of the disease process rather than its cause. A powerful argument against the hypothesis of Szentivanyi is that administration of β-blockers to healthy individuals does not increase bronchoconstriction or modulate airway responsiveness. Propranolol administration has, on the other hand, been shown to cause bronchoconstriction in asthmatic patients. It is believed that the mechanism responsible for this effect is the increased release of acetylcholine resulting from the blockade of the adrenergic receptors localized on postganglionic nerve endings.

Although the inhalation of α-adrenergic agonists has been shown to produce bronchoconstriction in some asthmatic patients, the effects of α-adrenergic antagonists on bronchomotor tone have been variable. Prazosin, a specific α-adrenergic antagonist that has no effect on resting bronchomotor tone or on histamine-induced bronchoconstriction,[70–72] partially reversed exercise-induced bronchoconstriction.[72] Other authors, in contrast, have reported that inhalation of an α-adrenergic agonist decreases exercise-induced bronchoconstriction and have postulated that this effect was secondary to the vasoconstrictive effect of the drug leading to a decrease in hyperemia and mucosal edema, believed to be among the factors involved in exercise-induced asthma.[73] As there is no sympathetic innervation in the airway smooth muscle, it is difficult to conceive how α-adrenergic receptors could be activated. In addition, infusion of norepinephrine in asthmatic patients failed to increase airway resistance or histamine-induced bronchoconstriction.[74] Thus, the evidence that has accumulated over the years does not indicate that α-adrenergic receptors are a factor in airway hyperresponsiveness.

CONCLUSIONS

There is considerable evidence that neurohumoral factors contribute to asthmatic airway bronchoconstriction and airway hyperresponsiveness. Extensive research in animals, both in vivo and in vitro, has underlined the potential importance of the interactions between inflammatory mediators, neurogenic inflammation, and the muscarinic and adrenergic nervous systems in inducing bronchoconstriction. However, few studies have been conducted directly on human airways, and the paucity of studies, as well as the lack of specific inhibitors, particularly for tachykinins and other neuropeptides, continues to hamper research on the role of neural mechanisms in asthma and airway hyperresponsiveness.

REFERENCES

1. Barnes PJ. Neural control of human airways in health and disease. Am Rev Respir Dis 1986;134:1289–314.
2. Widdicombe J. Airway receptors. Respir Physiol 2001;125:3–15.
3. Belvisi MG. Sensory nerves and airway inflammation: role of A delta and C-fibres. Pulm Pharmacol Ther 2003;16:1–7.
4. Belvisi MG. Overview of the innervation of the lung. Curr Opin Pharmacol 2002;2:211–5.
5. Lee LY, Pisarri TE. Afferent properties and reflex functions of bronchopulmonary C-fibers. Respir Physiol 2001;125:47–65.
6. Barnes PJ. Asthma as an axon reflex. Lancet 1986;1:242–5.
7. Barnes PJ. Neurogenic inflammation in the airways. Respir Physiol 2001;125:145–54.
8. Lee LY, Widdicombe JG. Modulation of airway sensitivity to inhaled irritants: role of inflammatory mediators. Environ Health Perspect 2001;109 Suppl 4:585–9.
9. Spina D, Page CP. Pharmacology of airway irritability. Curr Opin Pharmacol 2002;2:264–72.
10. Barnes PJ. Neural control of airway function: new perspectives. Mol Aspects Med 1990;11:351–423.
11. Di Maria GU, Bellofiore S, Geppetti P. Regulation of airway neurogenic inflammation by neutral endopeptidase. Eur Respir J 1998;12:1454–62.
12. Howarth PH, Springall DR, Redington AE, et al. Neuropeptide-containing nerves in endobronchial biopsies from asthmatic and nonasthmatic subjects. Am J Respir Cell Mol Biol 1995;13:288–96.
13. Castairs JR, Barnes PJ. Autoradiographic mapping of substance-P receptors in lung. Eur J Pharmacol 1986;127:295–6.
14. Auberson S, Lundberg JM. Lactic acid-induced plasma protein extravasation in rat airways by stimulation of sensory nerves and NK1 receptor activation. Pharmacol Toxicol 1993;73:305–10.
15. Satoh H, Lou YP, Lundberg JM. Inhibitory effects of capsazepine and SR 48968 on citric acid-induced bronchoconstriction in guinea-pigs. Eur J Pharmacol 1993;236:367–72.
16. Sheppard MN, Kurian SS, Henzen-Logmans SC, et al. Neurone-specific enolase and S-100: new markers for delineating the innervation of the respiratory tract in man and other mammals. Thorax 1983;38:333–40.
17. Maghni K, Michoud MC, Alles M, et al. Airway smooth muscle cells express functional neurokinin-1 receptors and the nerve-derived preprotachykinin-a gene: regulation by passive sensitization. Am J Respir Cell Mol Biol 2003;28:103–10.
18. Nieber K, Baumgarten CR, Rathsack R, et al. Substance P and beta-endorphin-like immunoreactivity in lavage fluids of subjects with and without allergic asthma. J Allergy Clin Immunol 1992;90(4 Pt 1):646–52.

19. Heaney LG, Cross LJ, McGarvey LP, et al. Neurokinin A is the predominant tachykinin in human bronchoalveolar lavage fluid in normal and asthmatic subjects. Thorax 1998;53:357–62.
20. Tomaki M, Ichinose M, Miura M, et al. Elevated substance P content in induced sputum from patients with asthma and patients with chronic bronchitis. Am J Respir Crit Care Med 1995;151(3 Pt 1):613–7.
21. Joos GF, De Swert KO, Schelfhout V, Pauwels RA. The role of neural inflammation in asthma and chronic obstructive pulmonary disease. Ann N Y Acad Sci 2003;992:218–30.
22. Barnes PJ. Modulation of neurotransmission in airways. Physiol Rev 1992;72:699–729.
23. Mann SP. The innervation of mammalian bronchial smooth muscle: the localization of catecholamines and cholinesterases. Histochem J 1971;3:319–31.
24. Partanen M, Laitinen A, Hervonen A, et al. Catecholamine- and acetylcholinesterase-containing nerves in human lower respiratory tract. Histochemistry 1982;76:175–88.
25. Mak JC, Baraniuk JN, Barnes PJ. Localization of muscarinic receptor subtype mRNAs in human lung. Am J Respir Cell Mol Biol 1992;7:344–8.
26. Walch L, Brink C, Norel X. The muscarinic receptor subtypes in human blood vessels. Therapie 2001;56:223–6.
27. Coulson FR, Fryer AD. Muscarinic acetylcholine receptors and airway diseases. Pharmacol Ther 2003;98:59–69.
28. Mak JC, Barnes PJ. Autoradiographic visualization of muscarinic receptor subtypes in human and guinea pig lung. Am Rev Respir Dis 1990;141:1559–68.
29. Rogers DF. Motor control of airway goblet cells and glands. Respir Physiol 2001;125:129–44.
30. Palmer JB, Cuss FM, Barnes PJ. VIP and PHM and their role in nonadrenergic inhibitory responses in isolated human airways. J Appl Physiol 1986;61:1322–8.
31. Richardson JB. Noradrenergic inhibitory innervation of the lung. Lung 1981;159:315–22.
32. Taylor SM, Pare PD, Schellenberg RR. Cholinergic and nonadrenergic mechanisms in human and guinea pig airways. J Appl Physiol 1984;56:958–65.
33. Ichinose M, Inoue H, Miura M, Takishima T. Nonadrenergic bronchodilation in normal subjects. Am Rev Respir Dis 1988;138:31–4.
34. Lammers JW, Minette P, McCusker MT, et al. Nonadrenergic bronchodilator mechanisms in normal human subjects in vivo. J Appl Physiol 1988;64:1817–22.
35. Michoud MC, Amyot R, Jeanneret-Grosjean A, Couture J. Reflex decrease of histamine-induced bronchoconstriction after laryngeal stimulation in humans. Am Rev Respir Dis 1987; 136:618–22.
36. Canning BJ, Fischer A. Neural regulation of airway smooth muscle tone. Respir Physiol 2001;125:113–27.
37. Canning BJ, Undem BJ. Evidence that distinct neural pathways mediate parasympathetic contractions and relaxations of guinea-pig trachealis. J Physiol 1993;471:25–40.
38. Fischer A, Hoffmann B. Nitric oxide synthase in neurons and nerve fibers of lower airways and in vagal sensory ganglia of man. Correlation with neuropeptides. Am J Respir Crit Care Med 1996;154:209–16.
39. Tucker JF, Brave SR, Charalambous L, et al. L-NG-nitro arginine inhibits non-adrenergic, non-cholinergic relaxations of guinea-pig isolated tracheal smooth muscle. Br J Pharmacol 1990;100:663–4.
40. Belvisi MG, Stretton CD, Yacoub M, Barnes PJ. Nitric oxide is the endogenous neurotransmitter of bronchodilator nerves in humans. Eur J Pharmacol 1992;210:221–2.
41. Bai TR, Bramley AM. Effect of an inhibitor of nitric oxide synthase on neural relaxation of human bronchi. Am J Physiol 1993;264(5 Pt 1):L425–30.
42. Doidge JM, Satchell DG. Adrenergic and non-adrenergic inhibitory nerves in mammalian airways. J Auton Nerv Syst 1982;5:83–99.
43. Richardson JB. Nerve supply to the lungs. Am Rev Respir Dis 1979;119:785–802.
44. Kneussl MP, Richardson JB. Alpha-adrenergic receptors in human and canine tracheal and bronchial smooth muscle. J Appl Physiol 1978;45:307–11.
45. Simonsson BG, Svedmyr N, Skoogh BE, et al. In vivo and in vitro studies on alpha-receptors in human airways. Potentiation with bacterial endotoxin. Scand J Respir Dis 1972;53:227–36.
46. Snashall PD, Boother FA, Sterling GM. The effect of alpha-adrenoreceptor stimulation on the airways of normal and asthmatic man. Clin Sci Mol Med 1978;54:283–9.
47. Black JL, Salome CM, Yan K, Shaw J. Comparison between airways response to an alpha-adrenoceptor agonist and histamine in asthmatic and non-asthmatic subjects. Br J Clin Pharmacol 1982;14:464–6.
48. Michoud MC, Fajac I, Frossard N. Bronchial hyperreactivity: neurogenic factors. Rev Mal Respir 1994;11:131–40.
49. Spina D, Shah S, Harrison S. Modulation of sensory nerve function in the airways. Trends Pharmacol Sci 1998;19:460–6.
50. Maggi CA. The effects of tachykinins on inflammatory and immune cells. Regul Pept 1997;70:75–90.
51. Ollerenshaw SL, Jarvis D, Sullivan CE, Woolcock AJ. Substance P immunoreactive nerves in airways from asthmatics and nonasthmatics. Eur Respir J 1991;4:673–82.
52. Chanez P, Springall D, Vignola AM, et al. Bronchial mucosal immunoreactivity of sensory neuropeptides in severe airway diseases. Am J Respir Crit Care Med 1998;158:985–90.
53. Bai TR, Zhou D, Weir T, et al. Substance P (NK1)- and neurokinin A (NK2)-receptor gene expression in inflammatory airway diseases. Am J Physiol 1995;269(3 Pt 1):L309–17.
54. Myers AC. Transmission in autonomic ganglia. Respir Physiol 2001;125:99–111.
55. House A, Celly C, Hey JA. Role of cholinergic reflexes on the bronchoconstrictor reactivity to neurokinin a in allergic dogs. Pulm Pharmacol Ther 2002;15:169–73.
56. Naline E, Devillier P, Drapeau G, et al. Characterization of neurokinin effects and receptor selectivity in human isolated bronchi. Am Rev Respir Dis 1989;140:679–86.
57. Diamant Z, van d, V, Kuijpers EA, et al. The effect of inhaled thiorphan on allergen-induced airway responses in asthmatic subjects. Clin Exp Allergy 1996;26:525–32.
58. Sont JK, van Krieken JH, van Klink HC, et al. Enhanced expression of neutral endopeptidase (NEP) in airway epithelium in biopsies from steroid- versus nonsteroid-treated patients with atopic asthma. Am J Respir Cell Mol Biol 1997; 16:549–56.
59. Fahy JV, Wong HH, Geppetti P, et al. Effect of an NK1 receptor antagonist (CP-99,994) on hypertonic saline-induced bronchoconstriction and cough in male asthmatic subjects. Am J Respir Crit Care Med 1995;152:879–84.
60. Ten Berge RE, Zaagsma J, Roffel AF. Muscarinic inhibitory autoreceptors in different generations of human airways. Am J Respir Crit Care Med 1996;154:43–9.
61. Belmonte KE, Jacoby DB, Fryer AD. Increased function of inhibitory neuronal M2 muscarinic receptors in diabetic rat lungs. Br J Pharmacol 1997;121:1287–94.
62. Belmonte KE, Fryer AD, Costello RW. Role of insulin in antigen-induced airway eosinophilia and neuronal M2 muscarinic receptor dysfunction. J Appl Physiol 1998;85:1708–18.
63. Coulson FR, Bigg CS, O'Donnell SR. Antagonism by NKP608 of substance P-induced plasma protein exudation in a novel preparation of perfused trachea in rats and guinea-pigs in vivo. Inflamm Res 2002;51:317–23.

64. Szentivanyi A. Beta adrenergic theory of atopic abnormality in bronchial asthma. J Allergy 1968;42:203–32.
65. Bai TR. Abnormalities in airway smooth muscle in fatal asthma. Am Rev Respir Dis 1990;141:552–7.
66. Bai TR, Mak JC, Barnes PJ. A comparison of beta-adrenergic receptors and in vitro relaxant responses to isoproterenol in asthmatic airway smooth muscle. Am J Respir Cell Mol Biol 1992;6:647–51.
67. Barnes PJ, Pride NB. Dose–response curves to inhaled beta-adrenoceptor agonists in normal and asthmatic subjects. Br J Clin Pharmacol 1983;15:677–82.
68. Shore SA. Cytokine regulation of beta-adrenergic responses in airway smooth muscle. J Allergy Clin Immunol 2002;110 (6 Suppl):S255–60.
69. Laporte JD, Moore PE, Panettieri RA, et al. Prostanoids mediate IL-1beta-induced beta-adrenergic hyporesponsiveness in human airway smooth muscle cells. Am J Physiol 1998; 275(3 Pt 1):L491–501.
70. Baudouin SV, Aitman TJ, Johnson AJ. Prazosin in the treatment of chronic asthma. Thorax 1988;43:385–7.
71. Chodosh S, Tuck J, Pizzuto D. Prazosin in hypertensive patients with chronic bronchitis and asthma: a brief report. Am J Med 1989;86:91–3.
72. Barnes PJ, Wilson NM, Vickers H. Prazosin, an alpha 1-adrenoceptor antagonist, partially inhibits exercise-induced asthma. J Allergy Clin Immunol 1981;68:411–5.
73. Dinh Xuan AT, Chaussain M, Regnard J, Lockhart A. Pretreatment with an inhaled alpha 1-adrenergic agonist, methoxamine, reduces exercise-induced asthma. Eur Respir J 1989;2:409–14.
74. Larsson K, Hjemdahl P. No influence of circulating noradrenaline on bronchial reactivity to histamine in asthmatic patients. Eur J Respir Dis 1986;69:16–23.

CHAPTER 31

MECHANICS OF AIRWAY NARROWING

Peter D. Paré, Peter T. Macklem, Chun Y. Seow, Brent E. McParland

In this chapter we review the structural alterations that occur in the airway wall in chronic airway disease and discuss how these structural changes in the airways can alter airway function. The details of the structural changes come from morphometric analyses of the airways of patients who have airway disease. Although it has been recognized for some time that the airway walls are thickened in asthmatic subjects[1–5] and patients who have chronic obstructive pulmonary disease (COPD),[6] it was not possible to perform a systematic study of the quantitative changes in airway wall dimensions because a yardstick of airway size was not available to allow a valid comparison between control and diseased subjects. A similar problem was overcome in the cardiovascular field by normalizing cross-sectional areas of vascular wall structures to the internal elastic lamina, which was found to be a constant over a wide range of physiologic pressures.[7] James and colleagues[8,9] found that, like the internal elastic lamina of vessels, the airway basement membrane perimeter is also relatively constant, despite narrowing the airway by contracting airway smooth muscle (ASM) or distending the airway by increasing lung volume. This finding has allowed a number of investigators to examine the relationship between airway wall compartment areas and airway size in lungs affected by diseases such as asthma,[10–16] COPD,[14,16–19] Eisenmenger's syndrome,[20] and cystic fibrosis.[21] Although McParland and colleagues have challenged the concept that the airway basement membrane is relatively indistensible,[22] its measurement has allowed comparison of airways in lungs that were fixed with or without inflation and in the presence of terminal bronchoconstriction. This is most easily done by examining the relationships between airway internal perimeter (P_i) or basement membrane perimeter (P_{bm}) and the areas occupied by the respective tissue components (Figure 31-1). The slopes and intercepts of these relationships can be constructed and compared by using valid techniques for pooling data.[17] These results confirm that the airways of patients with fatal asthma,[10,11,13–15,23] and to a lesser extent nonfatal asthma,[11,14] COPD,[14,17–19] and cystic fibrosis,[21] show an increase in airway wall thickness that involves all layers of the airway wall. No increase in wall compartment areas was found in airways from patients with Eisenmenger's syndrome.[20] The airway wall remodeling that occurs in these disorders can cause functional alterations because of quantitative changes in airway wall compartments and/or because of changes in the biochemical composition or material properties of the various constituents of the airway wall. We review the quantitative changes in the dimensions and organization of the airway wall compartments, as well as the biochemical alterations that have been described. In addition, we review the studies in which modeling of the tracheobronchial tree has been used in an attempt to predict how these structural and biochemical changes might affect the mechanical properties of the airways and, ultimately, their ability to narrow.

STRUCTURAL CHANGES IN THE AIRWAY WALLS IN ASTHMA AND COPD

An increase in maximal inducible airway resistance, which is often interpreted as maximal airway narrowing, constitutes the most fundamental pathophysiologic abnormality in airway diseases. In normal subjects, very high concentrations of bronchoconstricting substances can be inhaled with only mild-to-moderate airway narrowing; in fact, most normal subjects develop a plateau on the dose–response curve for inhaled pharmacologic agonists,[24–26] whereas in moderate-to-severe asthma, a plateau does not develop.[24,26] In COPD, a plateau often occurs after an exaggerated amount of airway narrowing.[27,28] In some cases of COPD, as in severe asthma, the plateau does not appear to occur.[29] Exaggerated airway narrowing in asthma can be caused by exogenous or endogenous mediators, with the latter causing spontaneous airflow obstruction during attacks. Figure 31-2 shows the pathophysiologic mechanisms that lead to the exaggerated airway narrowing in these diseases.

Both asthma and COPD fulfill the criteria for complex genetic diseases, which include an increased risk in first-degree relatives of affected individuals and the requirement for interaction with environmental factors. In both disorders, this interaction causes inflammation of the airways, and it is the consequences of this inflammation, coupled with attempts at repair, that lead to the structural and mechanical changes in the airways of affected individuals.

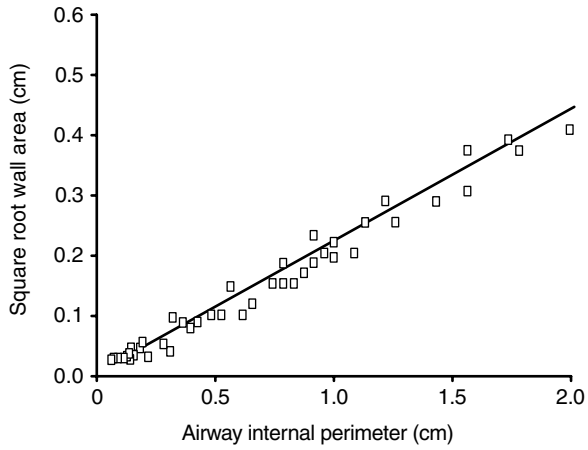

FIGURE 31-1 An example of the linear relationship between airway internal perimeter and the square root of airway wall area. This relationship provides a useful way to compare airway dimensions between individuals and groups of individuals.

The airway wall can be divided into three compartments: (1) the inner wall, consisting of epithelium, basement membrane, and lamina propria; (2) the outer wall, consisting of cartilage and the loose connective tissue between the muscle layer and the surrounding parenchyma; and (3) the smooth muscle layer. The proposed nomenclature by Bai and colleagues[30] usually includes the smooth muscle layer with the inner wall. Structural changes in the three layers can contribute to exaggerated airway narrowing in independent ways.

Inner Wall

Moreno and colleagues mathematically modeled the effect of thickening of the inner airway wall to show how it can amplify the degree of luminal narrowing for a given degree of ASM shortening.[31] In the model, thickening of the inner wall has the effect of shifting the inhaled methacholine (MCh) dose–response relationship upward. This upward shift occurs for geometric reasons because with a thicker inner wall there is greater luminal narrowing for a given degree of smooth muscle shortening. Only modest increases in thickness are required for a large effect on airway resistance because resistance is proportional to the fourth power of luminal diameter. Although inner wall thickening could explain increased maximal airway narrowing, it cannot explain the increased "sensitivity" of the airways seen in asthma and COPD. When actual measured values for the thickness of this layer in normal and diseased lungs[13] were used in a computational schema by Lambert and colleagues,[32] the results confirmed the predictions of Moreno and colleagues.[31] In the analysis by Lambert and colleagues, encroachment into the lumen by thickening of the inner wall, which would cause an increase in baseline resistance, was not taken into account. Brown and colleagues[33] used high-resolution computed tomography (HRCT) to measure airway caliber in asthmatic and normal subjects and found that the frequency distribution for airway size was shifted leftward, indicating that airways in asthmatic subjects may have a smaller internal diameter, possibly because of encroachment by the airway wall into the luminal space, which in part accounts for the higher baseline airway resistance in asthmatic subjects.[34] However, their results could also be explained on the basis of an increase in airway wall stiffness due to an increase in either passive (structural) or active (ASM tone) elements, which would shift the distending pressure (lung volume)–airway diameter relationship rightward, thereby resulting in a smaller internal diameter at functional residual capacity for airways in asthmatic lungs. An increased volume of intraluminal secretions or dilatation of the mucosal vessels can similarly amplify the effects of ASM shortening, in addition to decreasing baseline airway luminal area.

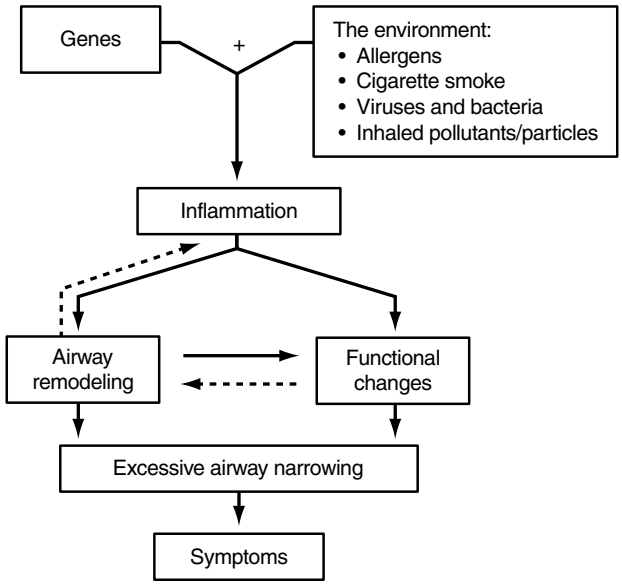

FIGURE 31-2 The interaction of susceptibility genes and environmental factors that underlies the pathogenesis of airway diseases. Inflammation, in its broadest sense, is central to the structural and functional changes, which are, in turn, responsible for the excessive airway narrowing that is the fundamental abnormality leading to symptoms.

Outer Wall

The degree of airway narrowing caused by ASM shortening in response to a stimulus is dependent on the load applied to the ASM. Contributions to this load as the airway narrows are provided by the structural elements in the airway wall, which undergo compression or strain, and the surrounding parenchyma, which is tethered to the outer airway wall. The parenchyma resists deformation if the airway attempts to become smaller than the "hole" in which it is embedded. The size of the hole in which the airway is embedded increases as lung volume is increased, and vice versa. During inspiration, the airway hole will effectively increase in size in response to parenchymal recoil. Thickening of the adventitia can act to decrease the transmission of this load to the muscle. When the ASM shortens, the outer diameter changes by a smaller amount than the luminal diameter. This geometric effect was discovered by Huber and Koessler[4] and led them to use the outer wall diameter as a yardstick of airway size, so that constricted airways could be compared with relaxed airways. Thickening of the outer wall thus decreases the change in outer airway wall diameter for

a given degree of airway narrowing. This smaller change in the outer wall diameter means that there is less distortion of the surrounding parenchyma, and this decreases the forces of interdependence, such that greater smooth muscle shortening can occur for the same force generation by the ASM.[32,35–37] A thicker airway with a greater external diameter may create a situation in which the airway is too big for its "hole" within the parenchyma, leading to unloading of the ASM and promoting airway narrowing. Factors that could thicken this airway layer include edema, inflammatory exudate, deposition of "loose connective tissue" within the peribronchial space, or thickening due to bronchial vascular dilatation. Whatever thickens the layer will allow the airway to recoil inward and the parenchyma to recoil outward, making the peribronchial pressure less negative and the elastic load on ASM less. The functional consequences are similar to the effect of decreasing lung volume. The importance of static and dynamic loads on the degree of airway narrowing has been amply demonstrated by the observation that lung volume and tidal volume have such a large effect on airway narrowing.[38–41]

An increase in end-expiratory lung volume provides a protective mechanism that attenuates airway narrowing. This mechanism operates during the dynamic hyperinflation that occurs in acute attacks of asthma and exacerbations of COPD. However, much of the hyperinflation in COPD is a consequence of loss of lung recoil, and there is some evidence that hyperinflation can actually induce loss of lung elastic recoil in asthma, undermining this "defense" mechanism.[42–45] Loss of recoil has been suggested as a contributing factor in life-threatening asthma attacks.[34,46] It is possible that acute loss of parenchymal recoil can occur during an asthma attack induced as a result of ASM activation generating large stresses that can only be counteracted by breathing at very high lung volume. During a period of lung hyperinflation, there may be sufficient creep of the alveolar attachments to effectively decrease parenchymal recoil and allow further airway narrowing. This hypothesis could be tested by comparing the responses to a single bolus dose of MCh before and after breathing at a high lung volume for a period equivalent to an asthma attack.

The importance of lung parenchyma–airway interaction is demonstrated by the dramatic changes in airway narrowing that can be induced by deep inspiration (DI). Fish and colleagues were the first to suggest that a different response to DI in asthmatic and nonasthmatic subjects might provide important clues to the mechanism of airway hyperresponsiveness in asthma.[47] They studied the response of patients with asthma and allergic rhinitis to inhaled MCh by measuring partial flow–volume curves and airway conductance before and after a DI. Both measures showed greater airway narrowing in asthmatic subjects, but the difference between the individuals with asthma and those with rhinitis was much less before than after DI. Based on this observation, they proposed that one of the important causes of airway hyperresponsiveness in asthma is a failure of the airways to dilate with DI. Skloot and colleagues confirmed and extended the findings of Fish and colleagues by obtaining complete dose–response curves for inhaled MCh in both normal and asthmatic subjects; the subjects were permitted to take DIs for the first dose–response curve, but DI was prohibited for the second dose–response curve.[48] Their results showed that inhibition of DIs during the challenge had little or no effect on the asthmatic subjects' dose–response curves but dramatically shifted the normal subjects' curves leftward with respect to sensitivity to the inhaled MCh and upward with respect to maximal response. Without periodic DI, normal subjects resembled asthmatic subjects (ie, appeared hyperresponsive).

One possible explanation for these observations is a failure of asthmatic airways to distend to the same extent as do normal airways in response to a DI. As suggested above, thickening of the outer airway wall would act to reduce the effectiveness of parenchymal recoil. Distention of an airway in response to a DI should stress the contracted ASM. The stress, if sufficient to cause strain, would disrupt the actin–myosin crossbridges and decrease the force developed by the ASM at any level of activation.[49] The transmission of stress to the ASM, in response to a DI, would be hindered by any process that promotes increased stiffness of the airway wall. There are considerable data suggesting that asthmatic airways are less distensible than those of normal subjects.[50,51] Lim and colleagues[52,53] showed that DI was ineffective in reversing bronchoconstriction during an acute spontaneous attack of asthma but became progressively more effective with intensive treatment of the disease with corticosteroids. Understanding the effect(s) of corticosteroid therapy is important if we are to elucidate the mechanism(s) responsible for the lack of airway dilatation in response to a DI in asthmatic patients. A progressive decrease in peribronchial edema during antiinflammatory therapy could cause a progressive increase in the effectiveness of DI in transmitting strain to the muscle.

Although this is an attractive explanation, the results of Brown and colleagues, who used HRCT to directly measure airway caliber before and during a DI, do not support the hypothesis that DI-induced dilatation in asthmatic airways is absent due to inadequate distention during DI.[33] They found that DI distended the airways of healthy and asthmatic subjects to similar extents. The dilatation was transient in asthmatic subjects. As a result of their findings, they suggested that an abnormality in ASM excitation or contraction counteracted the normal bronchodilating effect of a DI in asthma. In contrast, Jensen and colleagues,[54] using airway resistance as the measure of airway caliber, found that asthmatic subjects failed to dilate their airways to the same extent as normal subjects and had much more rapid redevelopment of airway narrowing after DI. It is unclear whether these differences were related to methodology or to differences in the severity of asthma in the subjects studied. A very interesting observation by Skloot and colleagues[48] was that the effectiveness of DI in decreasing bronchoconstriction in normal subjects diminishes with the time spent in the constricted state at or near residual volume before the DI occurs. This implies that ASM activation and adaptation to the shorter length could be an important determinant of whether a DI will decrease the stress developed by ASM.

Smooth Muscle Layer

A consistent pathologic finding in asthma is an increase in ASM mass.[1–5,10,11,13–15,23,55] A smaller but consistent increase in smooth muscle has been reported in COPD.[14,56] Lambert and colleagues[32] concluded from biomechanical modeling that "for a given maximal muscle stress, greater muscle thickness allows the development of greater tension and thus more contraction of the lumen." If the smooth muscle in asthma and COPD is capable of generating the same stress as normal ASM, then the greater cross-sectional area of muscle will lead to greater force development and allow the muscle to more easily overcome the preloads and afterloads that normally attenuate smooth muscle shortening and airway narrowing. Armour and colleagues[57] demonstrated that isometric force generated by human bronchial ring preparations in vitro is directly related to the ASM mass in the tissues. If exaggerated airway narrowing in asthmatic subjects is significantly dependent on an increase in ASM mass, one would predict that in vitro bronchial preparations from asthmatic subjects would demonstrate exaggerated force production. With a few exceptions,[58–61] this prediction has not proved true; force production in asthmatic tissues was not increased.[62–67] The reason for this finding is not known but may be related to the quality of the tissue. The most convincing data showing an increase in force generation by asthmatic tissues come from the studies of Bai,[58,59] in which tracheal tissues were examined. It is possible that it is easier to obtain functional tissue from the trachea than from the bronchus. When bronchi and trachea are used to examine ASM contraction, it would appear that tracheal tissues remain viable during storage for longer periods of time than bronchial tissue (personal observation). Another possible explanation for why few investigators find an increase in force generation by asthmatic tissues is that the ASM in asthma patients could be of an altered (less contractile) phenotype. There is increasing evidence that proliferating smooth muscle can change from a contractile to a synthetic phenotype[68]; an increased amount of muscle may not result in greater contractile capacity. In addition, the thickening of the ASM layer in asthma is not only due to an increase in the amount of the muscle but is also attributable to accumulation of matrix between smooth muscle cells and bundles.[61] To the extent that this increased area is included in estimates of muscle area, it will lead to an apparent decrease in smooth muscle stress. The connective tissue between smooth muscle cells and bundles has been postulated to constrain ASM shortening.[69,70] If the ability of this connective tissue to constrain muscle is disrupted, it could lead to greater smooth muscle shortening without an increase in smooth muscle isometric force or mass.

Another explanation for the relatively normal force generated by asthmatic airways in vitro could be that force generation in vitro may not reflect the ability of ASM to shorten, which is what causes airway narrowing in vivo.[71] Jiang and colleagues[72] observed that ASM from antigen-sensitized dogs that exhibit in vivo hyperresponsiveness had an increased velocity and degree of ASM shortening without a concomitant increase in isometric force production. Solway and Fredberg have postulated that increased ASM shortening velocity, without increased force production, could account for exaggerated airway narrowing.[73]

Although there have been fewer studies of ASM in COPD, Opazo-Saez and colleagues[56] demonstrated a modest increase in the amount of ASM as well as in the force and stress generated by airway rings from obstructed smokers in comparison with those from nonobstructed smokers. The most significant finding was that ASM stress was positively correlated with the degree of obstruction as assessed by the forced expiratory volume in 1 second/forced vital capacity ratio. Airways from patients with Eisenmenger's syndrome develop more force, but the reason for the apparent increase in force was not an increased amount of ASM but that intrinsic ASM tone, which is determined by endogenous contractile mediators, was absent in the tissues.[20] Intrinsic tone in human airways in vitro contributes more than 50% of the total active tone developed in response to a maximal dose of exogenous agonist.[74] Therefore, although the force developed by airways from patients with Eisenmenger's syndrome in response to contractile agonists was increased by approximately twofold compared with control airways, the total amount of force, intrinsic plus exogenously induced, was not different from that developed by control airways. Another problem with interpreting stress developed by airways is that the stress developed may depend on the length at which the tissues are adapted.[75] A tissue adapted at a longer length may develop the same force, but since the cross-sectional area is reduced with lengthening of the tissue, the apparent stress is increased. A tissue that is more distensible may appear to develop more stress simply because ASM length is allowed to increase more than in an airway that is not distensible.

BIOMECHANICAL CHANGES

Changes in airway geometry, as documented by morphometric measurements, do not fully take into account the potential effect of airway wall thickening on the mechanical properties of the airway. In addition to the amount, the organization and mechanical properties of the airway wall constituents could have a profound effect on airway mechanics. In fact, changes in extracellular matrix structure could have effects on cellular functions and may themselves modulate the physiologic process of inflammation.[76] Although deposition of connective tissue in the adventitia could "uncouple" the smooth muscle from the surrounding parenchyma, the thickening could also decrease the ability of the ASM to narrow the airway if the newly deposited material was stiff. Similarly, thickening of the inner airway wall, although it has the potential to amplify the effect of ASM shortening,[31] could also stiffen the airway. During ASM shortening, the airway tissue both internal and external to the ASM layer becomes distorted.[77] The airway does not narrow by collapsing, but rather the mucosal membrane buckles and is thrown into folds. The force required to distort the tissue and form the folds provides a serial elastic load that could attenuate ASM shortening.[16] Since the bending stiffness of a layer is directly related to its thickness cubed, airway wall thickening alone, without a change in the

mechanical properties of the tissue, could be protective. Furthermore, if the inner wall becomes stiffer, then even more work is required to distort the inner wall layer during activated ASM shortening.

Wiggs and colleagues[78] attempted to model the potential importance of mucosal folding by using finite element analysis in a computer model of the process. By doubling the thickness of the subepithelial collagen layer, mimicking the increased thickness observed in asthmatic airways, they found that a substantially greater force would be required to induce an equivalent degree of folding and narrowing (see below). In a different computer simulation, Seow and colleagues[79] demonstrated, from a geometric point of view, that if the material between the basement membrane and the ASM layer (ie, the lamina propria) is incompressible and confined during airway constriction, and if there are radial tethers (presumably collagen fibers) connecting the basement membrane and the muscle layer, narrowing of the airway (due to constriction of the muscle layer) will lead to an increase in pressure in the lamina propria, which, in turn, will further resist shortening of the ASM layer. The simulation also demonstrated that the thicker the lamina propria, the more effective it is in resisting narrowing of the airway caused by ASM contraction. These computer simulations predict a similar relationship between the thickness of the lamina propria and its protective effect on airway narrowing, although the underlying mechanisms are entirely different. The model proposed by Wiggs and colleagues[78] relies on a crucial assumption that the flexural rigidity of the mucosal layer is sufficiently large that there is a substantial resistance to folding; this assumption is not required in the model proposed by Seow and colleagues.[79] The results of a recent study by Niimi and colleagues[80] support a potential protective role for airway wall thickening. They used HRCT to measure the dimensions of the right apical segmental bronchus and compared these measures with indices of airway responsiveness in asthmatic subjects. They found that the thickening of this airway was inversely related to airway reactivity; the thicker the bronchus, the less reactive were the airways. To the extent that thickening of this large airway is a measure of "airway remodeling" in the remainder of the bronchial tree, this result suggests that "geometry is not everything."[81]

Airway wall thickening in asthma and COPD involves increased collagen deposition. Roche and colleagues have shown that the thickened subepithelial "basement membrane" in asthma consists of a dense layer rich in fibrillar collagens, under a normal subepithelial basal lamina.[82] This distinct collagenous matrix layer is typically doubled in thickness from 5 to 8 μm (normal) to 10 to 15 μm (asthma) and contains types I, III, and V collagen and fibronectin but not basal lamina components (type IV collagen, laminin). This collagenous matrix may be synthesized by its associated myofibroblasts since myofibroblast number correlates with the magnitude of subepithelial thickening.[83] Similar structural changes have been observed in patients with mild asthma and with occupational asthma associated with exposure to a variety of chemicals.[84] In some individuals with asthma induced by toluene di-isocyanate (TDI), cessation of exposure to TDI leads, after 6 to 20 months, to decreased subepithelial collagen thickness and decreased numbers of subepithelial fibroblasts associated with decreased numbers of mast cells and lymphocytes.[85] This suggests that these changes are potentially reversible, but the mechanism of this reversal is unknown.

The mechanical effects of changes in the abundance and types of collagen in the subepithelial matrix are unknown but are likely to depend on the precise architecture and chemistry of the collagens deposited. The collagen fibrils in the subepithelial collagen layer in the airways of asthmatic subjects appear to be more densely packed than in normal subjects,[82] and although the significance of this is unknown, it is probable that both increased collagen fibril density and thickening of this layer would increase both the tensile stiffness and resistance to deformation of the airway wall, thus tending to oppose smooth muscle contraction and airway narrowing. On the other hand, Lee and colleagues[86] found that the basement membrane thickness of biopsy tissues from asthmatic subjects showed a significant positive correlation with airway reactivity to inhaled MCh. In addition to collagen, the adhesive glycoprotein fibronectin and the antiadhesive glycoprotein tenascin appear to be deposited in the airway wall in asthmatic subjects.[87] These may be synthesized by epithelial cells in response to inflammatory mediators, including transforming growth factor-β,[88] tumor necrosis factor-α, and interferon-γ.[89]

The airway walls contain proteoglycans with their characteristic polysaccharides, the glycosaminoglycans. Specific proteoglycans and glycosaminoglycans of the extracellular matrix influence tissue biomechanics, fluid balance, cellular functions, and growth factor and cytokine biologic activities. Changes in glycosaminoglycan metabolism occur early in a number of animal models of inflammation,[90] suggesting that changes in proteoglycan metabolism may contribute to altered extracellular matrix properties in asthma. The long-chain glycosaminoglycan hyaluronan and the proteoglycans versican and decorin are localized in and around the smooth muscle bundles in the airways.[91] Although the functional correlates of proteoglycan deposition in the airway wall are unknown, hydrated proteoglycans may contribute to the increased volume of the submucosa in asthmatic subjects[23] and may influence airway mechanics. The deposition of proteoglycans in the submucosal region between the ASM and basement membrane could contribute to exaggerated airway narrowing by inhibiting the radial constraint provided by collagen bundles. On the other hand, the increased amount of matrix could increase tissue turgor and the resistance of the airway wall to deformation.

The mechanisms underlying changes in extracellular matrix composition in asthma and COPD are incompletely understood but are the subject of intense investigation. Several growth factors and cytokines released by inflammatory cells, or released by epithelial cells secondary to stimulation by cigarette smoke, oxygen radicals, or allergic inflammation, have the capacity to drive altered extracellular matrix metabolism by mesenchymal cells in the airway wall.

The airway wall remodeling that occurs in chronic asthma and COPD is almost certainly accompanied by degradation of matrix components in addition to synthesis

and deposition of new matrix. Elastin degradation has been described in asthma.[92] Proteolysis and reorganization of the matrix could free smooth muscle from constraints imposed by connective tissue and allow greater shortening.[79] Incubation of canine ASM strips[70] or human airway preparations[69] with collagenase, or injection of elastase into the ASM layer of pig airways,[93] has been shown to increase the shortening of ASM in vitro.

MODELING AIRWAY FUNCTION

Both Wiggs and colleagues[16] and Lambert and colleagues[32] attempted to determine which of the structural changes that occur in the airway wall of asthmatic subjects are most important in the development of exaggerated airway narrowing. They developed a computerized model of the tracheobronchial tree, in which ASM shortening occurred in a dose–response fashion. ASM shortening was allowed to proceed until the force generated by the ASM was equal and opposite to the force occurring in the surrounding lung parenchyma. The authors assumed that the contractile function and the length–tension relationship of the asthmatic ASM were the same as in normal subjects but that the force-generating capacity was increased in proportion to the increase in ASM mass. They found that all three of the structural changes that occur in asthma (increased mucosal thickness, increased ASM thickness, and increased adventitial thickness) could contribute to increased maximal airway narrowing in asthma. However, the analysis showed that, of these factors, the increase in ASM thickness was the most important abnormality. The increased submucosal and adventitial thickness could increase the maximal airway narrowing by a factor of 2 to 10, whereas the increased ASM thickness had the potential to increase maximal airway narrowing by two orders of magnitude. In this analysis, several assumptions were made that remain to be completely tested. The most important of these was that the increase in ASM mass that occurs in asthma is accompanied by a parallel increase in the ability of the ASM to generate force (ie, maximal ASM stress remains constant). However, as described above, there is reason to believe that when ASM proliferates, there could be a decrease in the contractility of the muscle.

In these analyses, it was also assumed that the only load that the ASM has to overcome to contract is the elastic recoil of the lung. However, the folding of the mucosal membrane that occurs during ASM contraction means that there is an additional load that impedes ASM shortening. Excised airways isolated from the surrounding parenchyma do not close. This means that there are elements within the airway wall that maintain airway patency. Okazawa and colleagues[77] measured the luminal patency of rabbit airways at zero transpulmonary pressure. The average luminal area of unconstricted airways at a transpulmonary pressure (P_L) of 0 cm H_2O was approximately one-quarter of the luminal area at a transpulmonary pressure of 10 cm H_2O. To narrow the airways beyond this equilibrium point, ASM is faced with an additional load that is required to deform the mucosal membrane.

Lambert[94] was the first to recognize that the magnitude of this load will be related to the number of folds that develop during ASM shortening as well as to the thickness and the mechanical properties of the tissue. More recently, Lambert and colleagues[95] described the effect of mucosal buckling on the maximal amount of ASM shortening. By considering the airway wall as a thin-layered material, Lambert and colleagues showed that as the number of folds in the airway mucosa increases, a greater transmural pressure difference is required to collapse the airway. Also, as the number of folds increases, a smaller reduction in luminal cross-sectional area results following ASM constriction. In a model proposed by Seow and colleagues,[79] increasing the number of folds also led to greater resistance to narrowing of the lumen by ASM constriction.

Wiggs and colleagues[78] developed a computational model of the airway as two concentric cylinders to analyze geometric and mechanical influences on airway wall buckling. A thicker outer cylinder (layer 1, elastic modulus E1) represented the lamina propria, and a thinner inner cylinder (layer 2, elastic modulus E2) represented the subepithelial reticular layer and epithelium. It was assumed that the airways are composed of incompressible material and that the contracting ASM exerts a uniform hoop stress. Finite element analysis showed that the "multilobed" folding similar to that seen in asthmatic airways only occurred when the ratio E2/E1 was between 8 and 30, that is, when the inner layer was significantly stiffer than the outer layer. This laminated design was chosen because no other regular structure could be found to exhibit multilobed buckling when loaded in this manner. These results, although based on theoretical models, highlight several interesting factors. First, the airway wall is primarily compressed as the ASM shortens. Therefore, compressive tests rather than length–tension-style experiments are required to obtain the information needed for an understanding of airway mechanics during constriction. Second, the relative elastic moduli of successive layers within the airway wall constitute a determinant of the folding pattern. Third, organization and the relative mechanical properties of the airway wall matrix molecules are important.

This modeling showed that the three factors contributing to the load that the ASM must overcome to shorten are the number of folds, the thickness of the two layers, and the elastic moduli of the two layers. The fewer the folds, the thinner the membrane, and the less elastic the membrane, the easier it will be to narrow the lumen. There is a paucity of information regarding these factors. The number of longitudinal bundles of elastin appears to be related to the number of mucosal folds, and the number of folds was not increased or decreased in airways of asthma patients.[96] There are no studies of the tensile or compressive properties of the airway inner wall in either normal or asthmatic subjects. If there are no changes in the mechanical properties of the inner wall, then one would predict that thicker airways will impart an increased load since the bending stiffness of a substance increases as the cube of its thickness. Thus, the wall thickening observed in asthma and COPD could cause a stiffening of the airway and protect from excessive narrowing. However, as discussed above, it is likely that there are changes in mechanical properties of the airway wall in

asthma secondary to altered architecture and increased collagen, proteoglycan, and elastin deposition. It is difficult to predict the nature of these changes. The increased deposition of type I and III collagen in the lamina reticularis might increase the stiffness of the airway, at least in response to tensile stresses. The work of Colebatch and colleagues[97] and Wilson and colleagues[51] supports the notion that the airways of asthmatic subjects are less distensible. Theory suggests that this should increase the resistance of the wall to buckling. However, there is reason to believe that there could be alterations in the airway wall that make it less elastic and more easily deformable. Both Bousquet and colleagues[98] and Mauad and colleagues[92] reported fragmentation of elastic fibers in asthmatic airways, which might decrease airway wall distention. Mauad and colleagues also noticed that elastin is arranged in two distinct layers: one in a superficial network that was attached to the basement membrane and a deeper network that lies close to the ASM. Digestion of connective tissue elements by proteases released from mast cells and other inflammatory cells could cause a decrease in the stiffness in the wall despite the increased thickness. The studies of Wiggs and colleagues[78] illustrated that it is the compressive stiffness of the wall that will have the greatest influence on the ease with which ASM can deform and fold the mucosal membrane. It is unclear what the relative roles of the different connective tissue proteins will be in response to compressive stress. These findings indicate an important future direction for airway mechanics research. With newly developed testing devices, the soft tissue compressive mechanics of airways in both control subjects and those with disease can be investigated. In these investigations, not only the viscoelastic behavior of the solid tissues but also the hydraulic flow of water through these tissues must be considered. With new techniques to determine the fractional content of airway matrix and the mechanical function of these components and theoretical models, we should be able to develop a more complete description of airway mechanics in normal subjects and in those with disease.

AIRWAY SMOOTH MUSCLE ADAPTATION

Smooth muscle can function over a much greater range of length than skeletal and cardiac muscle. This ability is vital for the normal action of hollow organs such as the bladder, bowel, and uterus, where large volume changes within the hollow organ are required for normal physiologic function. The first systematic study examining ASM tetanic force, shortening velocity, and compliance in relation to length was reported by Pratusevich and colleagues.[75] They proposed a new theory, smooth muscle plasticity (or adaptation), which could explain why force is (relatively) independent of length and velocity is proportional to muscle length. The theory states that the smooth muscle adapts to length changes by varying the number of contractile units in series. Functional studies indicate that adaptation of ASM to a length change occurs in two steps.

First, there is a decrease in the ability of ASM to generate force immediately after a length change. If the length of an adapted smooth muscle preparation is acutely reduced[75,99] or increased,[100,101] the maximal force achievable by the muscle immediately after the length change decreases. It is likely that the mechanism of the decrease in force involves a rearrangement in the contractile filaments, partial dissolution or fragmentation of the labile myosin thick filaments, and/or disruption of the actin-anchoring sites (ie, dense bodies, dense plaques). Kuo and colleagues[100] showed that in relaxed tracheal smooth muscle, there is a reduction in myosin thick filament density after a brief period of oscillation that stretches the muscle by 30% beyond its in situ length. The magnitude of the reduction in force and the myosin thick filament density were closely related. This close relationship between force developed and density of the myosin thick filaments at rest suggests that the resting density of thick filaments affects the density at the end of contraction, which was shown to be increased by 20 to 90% in rat anococcygeus smooth muscle[102,103] and by 63 to 144% in swine tracheal smooth muscle.[104] A close correlation between the thick filament density of activated ASM and its mechanical and energetic properties (isometric force, shortening velocity, power output, and rate of ATP consumption) at different muscle lengths was later demonstrated by Kuo and colleagues[105] and Herrera and colleagues.[106] It is unknown whether the increased density is due to lengthening of myosin thick filaments or to the formation of new filaments in parallel. Increased filament density due to contractile activation is not observed in all smooth muscle types, for example, guinea pig taenia coli smooth muscle preparations,[103] and this finding is thought to be related to the normally continuous cyclic activation of the muscle. It is unknown whether thick filament density changes in bronchial smooth muscle; however, plastic adaptation has recently been reported in a swine bronchial smooth muscle (BSM) preparation[107] and a canine BSM preparation.[108]

Second, the reduction of contractile capacity is followed by a period of force recovery, during which the muscle adapts to its new length in the absence of further perturbation. Force recovery follows an exponential course over a period of about 30 minutes, but the majority of recovery occurs within 5 minutes.[99–101]It is possible that if asthmatic airways are maintained in a narrower state due to increased activation of the ASM or decreased loads that normally help to maintain the airways patent, the smooth muscle will undergo plastic adaptation at the reduced length and will develop the same force as that previously generated at a greater length prior to adaptation. This sequence of events would mean that the newly adapted ASM at a reduced length would be poised to cause even further airway narrowing when next stimulated by contractile agonists. DI could reverse this adaptation process, but in the thickened, remodeled airways of asthmatic subjects, the effects of DI, especially during sleep, may be attenuated.[47,48,53,109,110]

There is evidence that a DI in asthma can effectively dilate airways, but an increase in shortening velocity makes the dilatation last for such a short time that it is difficult to measure.[33,111,112] In the time it takes to measure airway resistance or forced expiratory flow, the effect may be over. Furthermore, if shortening velocity is increased in asthma, it

could counteract the potent bronchodilatory effects of tidal stretches as the crossbridges broken during the stretch reform during expiration. Increased shortening velocity could also explain, at least in part, the increase in variability of airways obstruction that characterizes asthma.[113] If the variability is a fractal, an increase in velocity of shortening of ASM could be an important cause of volatility of airways obstruction.[114] The resulting instability, as evidenced by daily variability of peak expiratory flow, is thought to be a risk factor for serious asthma attacks. Why should shortening velocity be increased? The most obvious explanation would be ASM unloading, but increased ASM force development or alterations in the content of myosin light-chain kinase might also account for it.[72]

CONCLUSIONS

In summary, we have made major advances in our understanding of the mechanics of airway narrowing, based on careful studies of the morphology, biochemistry, and mechanical properties of airways and their constituent tissue types. In particular, the increased understanding of ASM cell plasticity and the cellular and molecular mechanisms that underlie contraction, relaxation, and adaptation have aided our understanding of normal and abnormal function. Much work remains to be done, however, if we are to have a complete understanding of why airways narrow excessively in disease, and fundamental advances in prevention and therapy are dependent on this knowledge.

REFERENCES

1. Dunnill M, Massarella G, Anderson J. A comparison of the quantitative anatomy of the bronchi in normal subjects, in status asthmaticus, in chronic bronchitis, and in emphysema. Thorax 1969;24:176–9.
2. Hossain S. Quantitative measurement of bronchial muscle in men with asthma. Am Rev Respir Dis 1973;107:99–109.
3. Housten JC, de Nevasquez S, Trounce JR. A clinical and pathological study of fatal cases of status asthmaticus. Thorax 1953;8:207–13.
4. Huber H, Koessler K. The pathology of bronchial asthma. Arch Intern Med 1922;30:689–760.
5. Takizawa T, Thurlbeck WM. Muscle and mucous gland size in the major bronchi of patients with chronic bronchitis, asthma, and asthmatic bronchitis. Am Rev Respir Dis 1971; 104:331–6.
6. Matsuba K, Wright JL, Wiggs BR, et al. The changes in airways structure associated with reduced forced expiratory volume in one second. Eur Respir J 1989;2:834–9.
7. Cook TA, Salmo NA, Yates PO. The elasticity of the internal lamina. J Pathol 1975;117:253–8.
8. James AL, Hogg JC, Dunn LA, Pare PD. The use of the internal perimeter to compare airway size and to calculate smooth muscle shortening. Am Rev Respir Dis 1988;138:136–9.
9. James AL, Pare PD, Hogg JC. Effects of lung volume, bronchoconstriction, and cigarette smoke on morphometric airway dimensions. J Appl Physiol 1988;64:913–9.
10. Bai TR, Cooper J, Koelmeyer T, et al. The effect of age and duration of disease on airway structure in fatal asthma. Am J Respir Crit Care Med 2000;162:663–9.
11. Carroll N, Elliot J, Morton A, James A. The structure of large and small airways in nonfatal and fatal asthma. Am Rev Respir Dis 1993;147:405–10.
12. Ebina M, Takahashi T, Chiba T, Motomiya M. Cellular hypertrophy and hyperplasia of airway smooth muscles underlying bronchial asthma. A 3-D morphometric study. Am Rev Respir Dis 1993;148:720–6.
13. James AL, Pare PD, Hogg JC. The mechanics of airway narrowing in asthma. Am Rev Respir Dis 1989;139:242–6.
14. Kuwano K, Bosken CH, Pare PD, et al. Small airways dimensions in asthma and in chronic obstructive pulmonary disease. Am Rev Respir Dis 1993;148:1220–5.
15. Saetta M, Di Stefano A, Rosina C, et al. Quantitative structural analysis of peripheral airways and arteries in sudden fatal asthma. Am Rev Respir Dis 1991;143:138–43.
16. Wiggs BR, Bosken C, Pare PD, et al. A model of airway narrowing in asthma and in chronic obstructive pulmonary disease. Am Rev Respir Dis 1992;145:1251–8.
17. Bosken CH, Wiggs BR, Pare PD, Hogg JC. Small airway dimensions in smokers with obstruction to airflow. Am Rev Respir Dis 1990;142:563–70.
18. Riess A, Wiggs B, Verburgt L, et al. Morphologic determinants of airway responsiveness in chronic smokers. Am J Respir Crit Care Med 1996;154:1444–9.
19. Tiddens HA, Pare PD, Hogg JC, et al. Cartilaginous airway dimensions and airflow obstruction in human lungs. Am J Respir Crit Care Med 1995;152:260–6.
20. McKay KO, Johnson PR, Black JL, et al. Airway structure and function in Eisenmenger's syndrome. Am J Respir Crit Care Med 1998;158:1245–52.
21. Tiddens HA, Koopman LP, Lambert RK, et al. Cartilaginous airway wall dimensions and airway resistance in cystic fibrosis lungs. Eur Respir J 2000;15:735–42.
22. McParland BE, Pare PD, Johnson PR, et al. Airway basement membrane perimeter in human airways is not a constant; potential implications for airway remodeling in asthma. J Appl Physiol 2004;97:556–63.
23. Ebina M, Yaegashi H, Chiba R, et al. Hyperreactive site in the airway tree of asthmatic patients revealed by thickening of bronchial muscles. A morphometric study. Am Rev Respir Dis 1990;141:1327–32.
24. James A, Lougheed D, Pearce-Pinto G, et al. Maximal airway narrowing in a general population. Am Rev Respir Dis 1992;146:895–9.
25. Moore BJ, King GG, D'Yachkova Y, et al. Mechanism of methacholine dose–response plateaus in normal subjects. Am J Respir Crit Care Med 1998;158:666–9.
26. Woolcock AJ, Salome CM, Yan K. The shape of the dose–response curve to histamine in asthmatic and normal subjects. Am Rev Respir Dis 1984;130:71–5.
27. Du Toit JI, Woolcock AJ, Salome CM, et al. Characteristics of bronchial hyperresponsiveness in smokers with chronic airflow limitation. Am Rev Respir Dis 1986;134:498–501.
28. Verhoeven GT, Verbraak AF, Boere-van der Straat S, et al. Influence of lung parenchymal destruction on the different indexes of the methacholine dose–response curve in COPD patients. Chest 2000;117:984–90.
29. Bel EH, Zwinderman AH, Timmers MC, et al. The protective effect of a beta 2 agonist against excessive airway narrowing in response to bronchoconstrictor stimuli in asthma and chronic obstructive lung disease. Thorax 1991; 46:9–14.
30. Bai A, Eidelman DH, Hogg JC, et al. Proposed nomenclature for quantifying subdivisions of the bronchial wall. J Appl Physiol 1994;77:1011–4.
31. Moreno RH, Hogg JC, Pare PD. Mechanics of airway narrowing. Am Rev Respir Dis 1986;133:1171–80.

32. Lambert RK, Wiggs BR, Kuwano K, et al. Functional significance of increased airway smooth muscle in asthma and COPD. J Appl Physiol 1993;74:2771–81.
33. Brown RH, Scichilone N, Mudge B, et al. High-resolution computed tomographic evaluation of airway distensibility and the effects of lung inflation on airway caliber in healthy subjects and individuals with asthma. Am J Respir Crit Care Med 2001;163:994–1001.
34. Irvin CG, Pak J, Martin RJ. Airway–parenchyma uncoupling in nocturnal asthma. Am J Respir Crit Care Med 2000;161:50–6.
35. Lambert RK, Pare PD. Lung parenchymal shear modulus, airway wall remodeling, and bronchial hyperresponsiveness. J Appl Physiol 1997;83:140–7.
36. Macklem PT. Bronchial hyporesponsiveness. Chest 1987;91: 189S–91S.
37. Pare PD, Bai TR. The consequences of chronic allergic inflammation. Thorax 1995;50:328–32.
38. Ding DJ, Martin JG, Macklem PT. Effects of lung volume on maximal methacholine-induced bronchoconstriction in normal humans. J Appl Physiol 1987;62:1324–30.
39. Moreno RH, Lisboa C, Hogg JC, Pare PD. Limitation of airway smooth muscle shortening by cartilage stiffness and lung elastic recoil in rabbits. J Appl Physiol 1993;75:738–44.
40. Shen X, Gunst SJ, Tepper RS. Effect of tidal volume and frequency on airway responsiveness in mechanically ventilated rabbits. J Appl Physiol 1997;83:1202–8.
41. Shen X, Ramchandani R, Dunn B, et al. Effect of transpulmonary pressure on airway diameter and responsiveness of immature and mature rabbits. J Appl Physiol 2000;89: 1584–90.
42. Finucane KE, Colebatch HJ. Elastic behavior of the lung in patients with airway obstruction. J Appl Physiol 1969;26: 330–8.
43. Gold WM, Kaufman HS, Nadel JA. Elastic recoil of the lungs in chronic asthmatic patients before and after therapy. J Appl Physiol 1967;23:433–8.
44. Peress L, Sybrecht G, Macklem PT. The mechanism of increase in total lung capacity during acute asthma. Am J Med 1976;61:165–9.
45. Woolcock AJ, Read J. The static elastic properties of the lungs in asthma. Am Rev Respir Dis 1968;98:788–94.
46. Gelb AF, Licuanan J, Shinar CM, Zamel N. Unsuspected loss of lung elastic recoil in chronic persistent asthma. Chest 2002;121:715–21.
47. Fish JE, Peterman VI, Cugell DW. Effect of deep inspiration on airway conductance in subjects with allergic rhinitis and allergic asthma. J Allergy Clin Immunol 1977;60:41–6.
48. Skloot G, Permutt S, Togias A. Airway hyperresponsiveness in asthma: a problem of limited smooth muscle relaxation with inspiration. J Clin Invest 1995;96:2393–403.
49. Gunst SJ. Contractile force of canine airway smooth muscle during cyclical length changes. J Appl Physiol 1983;55:759–69.
50. Colebatch HJ, Ng CK. A longitudinal study of pulmonary distensibility in healthy adults. Respir Physiol 1986;65:1–11.
51. Wilson JW, Li X, Pain MCF. The lack of distensibility of asthmatic airways. Am Rev Respir Dis 1993;148:806–9.
52. Lim TK, Ang SM, Rossing TH, et al. The effects of deep inhalation on maximal expiratory flow during intensive treatment of spontaneous asthmatic episodes. Am Rev Respir Dis 1989;140:340–3.
53. Lim TK, Pride NB, Ingram RH Jr. Effects of volume history during spontaneous and acutely induced air-flow obstruction in asthma. Am Rev Respir Dis 1987;135:591–6.
54. Jensen A, Atileh H, Suki B, et al. Selected contribution: airway caliber in healthy and asthmatic subjects: effects of bronchial challenge and deep inspirations. J Appl Physiol 2001;91:506–15.
55. Benayoun L, Druilhe A, Dombret M-C, et al. Airway structural alterations selectively associated with severe asthma. Am J Respir Crit Care Med 2003;167:1360–8.
56. Opazo Saez AM, Seow CY, Pare PD. Peripheral airway smooth muscle mechanics in obstructive airways disease. Am J Respir Crit Care Med 2000;161:910–7.
57. Armour CL, Diment LM, Black JL. Relationship between smooth muscle volume and contractile response in airway tissue. Isometric versus isotonic measurement. J Pharmacol Exp Ther 1988;245:687–91.
58. Bai TR. Abnormalities in airway smooth muscle in fatal asthma. Am Rev Respir Dis 1990;141:552–7.
59. Bai TR. Abnormalities in airway smooth muscle in fatal asthma. A comparison between trachea and bronchus. Am Rev Respir Dis 1991;143:441–3.
60. de Jongste JC, Mons H, Bonta IL, Kerrebijn KF. In vitro responses of airways from an asthmatic patient. Eur J Respir Dis 1987;71:23–9.
61. Thomson RJ, Bramley AM, Schellenberg RR. Airway muscle stereology: implications for increased shortening in asthma. Am J Respir Crit Care Med 1996;154:749–57.
62. Cerrina J, Labat C, Haye-Legrande I, et al. Human isolated bronchial muscle preparations from asthmatic patients: effects of indomethacin and contractile agonists. Prostaglandins 1989;37:457–69.
63. Cerrina J, Le Roy Ladurie M, Labat C, et al. Comparison of human bronchial muscle responses to histamine in vivo with histamine and isoproterenol agonists in vitro. Am Rev Respir Dis 1986;134:57–61.
64. Goldie RG, Spina D, Henry PJ, et al. In vitro responsiveness of human asthmatic bronchus to carbachol, histamine, beta-adrenoceptor agonists and theophylline. Br J Clin Pharmacol 1986;22:669–76.
65. Roberts JA, Raeburn D, Rodger IW, Thomson NC. Comparison of in vivo airway responsiveness and in vitro smooth muscle sensitivity to methacholine in man. Thorax 1984;39:837–43.
66. Schellenberg RR, Foster A. In vitro responses of human asthmatic airway and pulmonary vascular smooth muscle. Int Arch Allergy Appl Immunol 1984;75:237–41.
67. Whicker SD, Armour CL, Black JL. Responsiveness of bronchial smooth muscle from asthmatic patients to relaxant and contractile agonists. Pulm Pharmacol 1988;1:25–31.
68. Halayko AJ, Solway J. Molecular mechanisms of phenotypic plasticity in smooth muscle cells. J Appl Physiol 2001;90: 358–68.
69. Bramley AM, Roberts CR, Schellenberg RR. Collagenase increases shortening of human bronchial smooth muscle in vitro. Am J Respir Crit Care Med 1995;152:1513–7.
70. Meiss RA. Influence of intercellular tissue connections on airway muscle mechanics. J Appl Physiol 1999;86:5–15.
71. Macklem PT. A theoretical analysis of the effect of airway smooth muscle load on airway narrowing. Am J Respir Crit Care Med 1996;153:83–9.
72. Jiang H, Rao K, Halayko AJ, et al. Bronchial smooth muscle mechanics of a canine model of allergic airway hyperresponsiveness. J Appl Physiol 1992;72:39–45.
73. Solway J, Fredberg JJ. Perhaps airway smooth muscle dysfunction contributes to asthmatic bronchial hyperresponsiveness after all. Am J Respir Cell Mol Biol 1997;17:144–6.
74. Ellis JL, Undem BJ. Role of cysteinyl-leukotrienes and histamine in mediating intrinsic tone in isolated human bronchi. Am J Respir Crit Care Med 1994;149:118–22.
75. Pratusevich VR, Seow CY, Ford LE. Plasticity in canine airway smooth muscle. J Gen Physiol 1995;105:73–94.
76. Black JL, Roth M, Lee J, et al. Mechanisms of airway remodeling. Airway smooth muscle. Am J Respir Crit Care Med 2001; 164:S63–6.

77. Okazawa M, Pare PD, Lambert RK. Compliance of peripheral airways deduced from morphometry. J Appl Physiol 2000;89:2373–81.
78. Wiggs BR, Hrousis CA, Drazen JM, Kamm RD. On the mechanism of mucosal folding in normal and asthmatic airways. J Appl Physiol 1997;83:1814–21.
79. Seow CY, Wang L, Pare PD. Airway narrowing and internal structural constraints. J Appl Physiol 2000;88:527–33.
80. Niimi A, Matsumoto H, Takemura M, et al. Relationship of airway wall thickness to airway sensitivity and airway reactivity in asthma. Am J Respir Crit Care Med 2003;168: 983–8.
81. Pare PD. Airway hyperresponsiveness in asthma: geometry is not everything! Am J Respir Crit Care Med 2003;168:913–4.
82. Roche WR, Beasley R, Williams JH, Holgate ST. Subepithelial fibrosis in the bronchi of asthmatics. Lancet 1989;1:520–4.
83. Brewster CE, Howarth PH, Djukanovic R, et al. Myofibroblasts and subepithelial fibrosis in bronchial asthma. Am J Respir Cell Mol Biol 1990;3:507–11.
84. Boulet LP, Boutet M, Laviolette M, et al. Airway inflammation after removal from the causal agent in occupational asthma due to high and low molecular weight agents. Eur Respir J 1994;7:1567–75.
85. Saetta M, Maestrelli P, Turato G, et al. Airway wall remodeling after cessation of exposure to isocyanates in sensitized asthmatic subjects. Am J Respir Crit Care Med 1995; 151:489–94.
86. Lee SY, Kim SJ, Kwon SS, et al. Relation of airway reactivity and sensitivity with bronchial pathology in asthma. J Asthma 2002;39:537–44.
87. Laitinen LA, Laitinen A. Modulation of bronchial inflammation: corticosteroids and other therapeutic agents. Am J Respir Crit Care Med 1994;150:S87–90.
88. Romberger DJ, Beckmann JD, Claassen L, et al. Modulation of fibronectin production of bovine bronchial epithelial cells by transforming growth factor-beta. Am J Respir Cell Mol Biol 1992;7:149–55.
89. Harkonen E, Virtanen I, Linnala A, et al. Modulation of fibronectin and tenascin production in human bronchial epithelial cells by inflammatory cytokines in vitro. Am J Respir Cell Mol Biol 1995;13:109–15.
90. Blackwood RA, Cantor JO, Moret J, et al. Glycosaminoglycan synthesis in endotoxin-induced lung injury. Proc Soc Exp Biol Med 1983;174:343–9.
91. Roberts CR. Is asthma a fibrotic disease? Chest 1995; 107:111S–7S.
92. Mauad T, Xavier AC, Saldiva PH, Dolhnikoff M. Elastosis and fragmentation of fibers of the elastic system in fatal asthma. Am J Respir Crit Care Med 1999;160:968–75.
93. Gray PR, Mitchell HW. Intramural elastase injection increases responsiveness of isolated bronchial segments. Pulm Pharmacol 1996;9:239–43.
94. Lambert RK. Role of bronchial basement membrane in airway collapse. J Appl Physiol 1991;71:666–73.
95. Lambert RK, Codd SL, Alley MR, Pack RJ. Physical determinants of bronchial mucosal folding. J Appl Physiol 1994; 77:1206–16.
96. Carroll NG, Perry S, Karkhanis A, et al. The airway longitudinal elastic fiber network and mucosal folding in patients with asthma. Am J Respir Crit Care Med 2000;161:244–8.
97. Colebatch HJH, Greaves IA, Ng CKY. Pulmonary mechanics in diagnosis. In: de Kock MA, Nadel JA, Lewis CM, editors. Mechanisms of airways obstruction in human respiratory disease. Cape Town: AA Balkema; 1979. p. 25–47.
98. Bousquet J, Lacoste JY, Chanez P, et al. Bronchial elastic fibers in normal subjects and asthmatic patients. Am J Respir Crit Care Med 1996;153:1648–54.
99. Wang L, Pare PD, Seow CY. Selected contribution: effect of chronic passive length change on airway smooth muscle length–tension relationship. J Appl Physiol 2001;90:734–40.
100. Kuo KH, Wang L, Pare PD, et al. Myosin thick filament lability induced by mechanical strain in airway smooth muscle. J Appl Physiol 2001;90:1811–6.
101. Wang L, Pare PD, Seow CY. Effects of length oscillation on the subsequent force development in swine tracheal smooth muscle. J Appl Physiol 2000;88:2246–50.
102. Gillis JM, Cao ML, Godfraind-De Becker A. Density of myosin filaments in the rat anococcygeus muscle, at rest and in contraction. II. J Muscle Res Cell Motil 1988;9:18–29.
103. Xu JQ, Gillis JM, Craig R. Polymerization of myosin on activation of rat anococcygeus smooth muscle. J Muscle Res Cell Motil 1997;18:381–93.
104. Herrera AM, Kuo KH, Seow CY. Influence of calcium on myosin thick filament formation in intact airway smooth muscle. Am J Physiol Cell Physiol 2002;282:C310–6.
105. Kuo KH, Herrera AM, Wang L, et al. Structure–function correlation in airway smooth muscle adapted to different lengths. Am J Physiol Cell Physiol 2003;285:C384–90.
106. Herrera AM, Martinez EC, Seow CY. Electron microscopic study of actin polymerization in airway smooth muscle. Am J Physiol Lung Cell Mol Physiol 2004;286;L1161–8.
107. McParland BE, Pare PD, Seow CY. Plasticity is not just a phenomenon of tracheal smooth muscle. Am J Respir Crit Care Med 2003;167:A713.
108. Stephens NL, Zhang C, Cheng ZQ. Plasticity theory in bronchial smooth muscle. Am J Respir Crit Care Med 2003;167:A712.
109. Burns CB, Taylor WR, Ingram RH Jr. Effects of deep inhalation in asthma: relative airway and parenchymal hysteresis. J Appl Physiol 1985;59:1590–6.
110. Moore BJ, Verburgt LM, King GG, Pare PD. The effect of deep inspiration on methacholine dose–response curves in normal subjects. Am J Respir Crit Care Med 1997;156:1278–81.
111. Jackson AC, Rassulo J, Marquina J, Celli B. Influence of deep inspiration on methacholine induced bronchoconstriction. Am J Respir Crit Care Med 1999;159:A468.
112. Parham WM, Shepard RH, Norman PS, Fish JE. Analysis of time course and magnitude of lung inflation effects on airway tone: relation to airway reactivity. Am Rev Respir Dis 1983; 128:240–5.
113. Que CL, Kenyon CM, Olivenstein R, et al. Homeokinesis and short-term variability of human airway caliber. J Appl Physiol 2001;91:1131–41.
114. Mandelbrot BB. A multifractal walk down Wall Street. Sci Am 1999;280:70–3.

CHAPTER 32

AIRWAY SMOOTH MUSCLE: THE CONTRACTILE PHENOTYPE

Elizabeth D. Fixman, Barbara Tolloczko, Anne-Marie Lauzon

Airway smooth muscle is a tissue whose physiologic function is quite uncertain. It is usually in a state of low tone. In this state, it contributes to maintaining the stiffness of the airways, which may help stabilize the airways in the face of large swings in transmural pressure caused by exercise or other states in which changes in intrapleural pressures are augmented. It may also help fine-tune the distribution of ventilation. The interest in smooth muscle in the airways is promoted by the pathophysiology resulting from excessive airway narrowing in diseases such as asthma, cystic fibrosis, and chronic obstructive pulmonary disease. Airway smooth muscle contraction contributes to the airway narrowing that characterizes acute exacerbations of these diseases. In this chapter we discuss the properties of airway smooth muscle and the contractile apparatus so as to provide a basis for understanding the potential mechanisms by which the properties of smooth muscle may be altered in disease.

AIRWAY SMOOTH MUSCLE: GROSS STRUCTURE IN THE AIRWAYS

In the posterior wall of the trachea and main bronchi, a sheet of smooth muscle runs between the two ends of the U-shaped cartilage rings. In the subsequent bronchial generation, discontinuous bands of smooth muscle lie between the outside extremities of each cartilage ring. Throughout the medium-sized bronchi, as diameter decreases, muscle bundles move from outside the cartilage toward the inside, their final location being between the cartilage plates and behind the epithelium. Contraction of these smooth muscle bundles decreases the diameter of the large and medium-sized airways. From the bronchioles down, the smooth muscle lies between the adventitial tissue and the epithelium only. From the medium bronchi all the way down to the alveolar ducts, the muscle bundles describe helical patterns (Figure 32-1), and contraction of these spiraling fibers decreases both the diameter and the length of the small airways.

SMOOTH MUSCLE CELL STRUCTURE

When observed under the electron microscope, smooth muscle cells do not have the well-organized striated appearance of the better known skeletal and cardiac muscles. This striated appearance is due to the alignment of thick and thin filaments. Instead, smooth muscle has a more random organization of filaments, giving it a smooth appearance. Smooth muscle thin filaments are anchored in dense bodies, which are similar structures to the z-lines of skeletal muscle and are also principally composed of α-actinin. Like striated muscle contraction, however, smooth muscle contraction is achieved by the crossbridge formation and interaction between myosin and actin (Figure 32-2).

REGULATION OF AIRWAY SMOOTH MUSCLE CONTRACTION

Airway smooth muscle contraction is regulated at many levels. For example, the contractile state of airway smooth muscle is regulated by the types of agonist present in the extracellular milieu, the transmembrane receptors that relay the contraction or relaxation information to the cell, the intracellular signaling molecules that transmit the extracellular signal to the contractile apparatus, and the structure of the contractile apparatus itself. Herein, we focus on the regulation of smooth muscle contraction at the cellular level by discussing mechanisms by which contractile agonists regulate the phosphorylation and subsequent activation of myosin. We also discuss how the structure of the thin and thick filaments regulates smooth muscle contraction. Finally, we conclude with a summary of how these signaling pathways and contractile proteins may participate in the pathogenesis of human lung disease.

G Protein–coupled Receptors

Smooth muscle contraction is induced primarily by agonists that activate transmembrane receptors, most of which belong to the G protein–coupled receptor (GPCR) superfamily.[1]

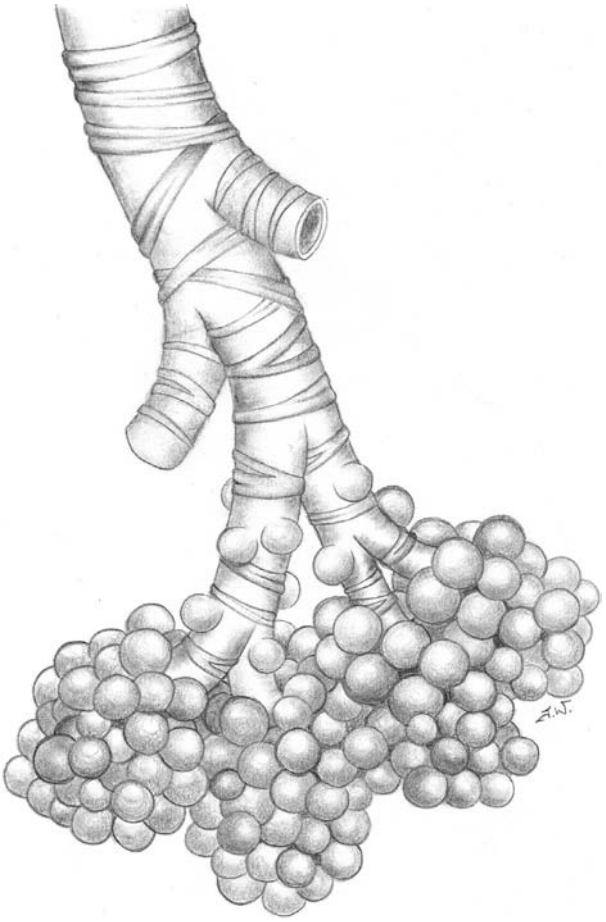

FIGURE 32-1 Smooth muscle bundles spiraling down from the medium bronchi to the alveolar ducts.

For example, the basal tone of airway smooth muscle is mediated primarily by parasympathetic cholinergic innervation-dependent activation of m3 muscarinic acetylcholine receptors. Moreover, exaggerated bronchoconstriction, as is found in asthma, for example, is induced by agonists that activate GPCRs, such as histamine via the H1 receptor and cysteinyl (Cys) leukotrienes (LTs) via Cys LT-1 receptors. On the other hand, stimulation of the sympathetic system produces bronchodilatation via activation of airway smooth muscle β-adrenergic receptors, which also belong to the GPCR superfamily. As such, the primary treatment to relieve acute bronchoconstriction in asthma is the administration of β_2-agonists. Some of the neurotransmitters of the nonadrenergic noncholinergic system, such as substance P and other neurokinins, also induce smooth muscle contraction via GPCR receptors.

GPCRS comprise the largest family of cell surface proteins expressed in the mammalian genome.[2,3] Members of this receptor superfamily are composed of seven stretches of hydrophobic amino acids, each of which is predicted to span the plasma membrane. The intracellular surface of the GPCR contacts a heterotrimeric protein complex, in which a high-molecular-weight GTP-binding protein, the α-subunit, interacts with and inhibits the βγ-subunits. Prior to stimulation, the intracellular face of the GPCR contacts the GDP-bound form of the Gα-subunit. The outcome of receptor activation is regulated initially by the Gα-subunit(s) that the receptor contacts. The majority of Gα-proteins, which are subdivided into four classes (G_s, $G_{i/o}$, $G_{12/13}$, and $G_{q/11}$) based on sequence similarity, are ubiquitously expressed. Whereas some GPCRs associate with only one Gα-subunit class, others activate multiple classes of Gα-subunits. Following ligand binding, the receptor induces exchange of GDP for GTP on the Gα-subunit and its subsequent dissociation from the βγ-subunits. The Gα–GTP and free βγ-subunits then modify the activity of diverse effector systems. Smooth muscle contraction is regulated by G_q-dependent Ca^{2+} release from intracellular stores and activation of myosin light-chain kinase (MLCK), as well as by $G_q/G_i/G_{12/13}$-dependent inhibition of myosin light-chain phosphatase (MLCP).[4–6]

Ca^{2+} Regulation and Activation of Myosin Light-chain Kinase

Activation of G_q-coupled GPCRs results in activation of phospholipase Cβ (PLCβ), which subsequently hydrolyzes the membrane phospholipid phosphatidylinositol 4,5-biphosphate (PIP_2) (Figure 32-3). PLCβ1, PLCβ3, and

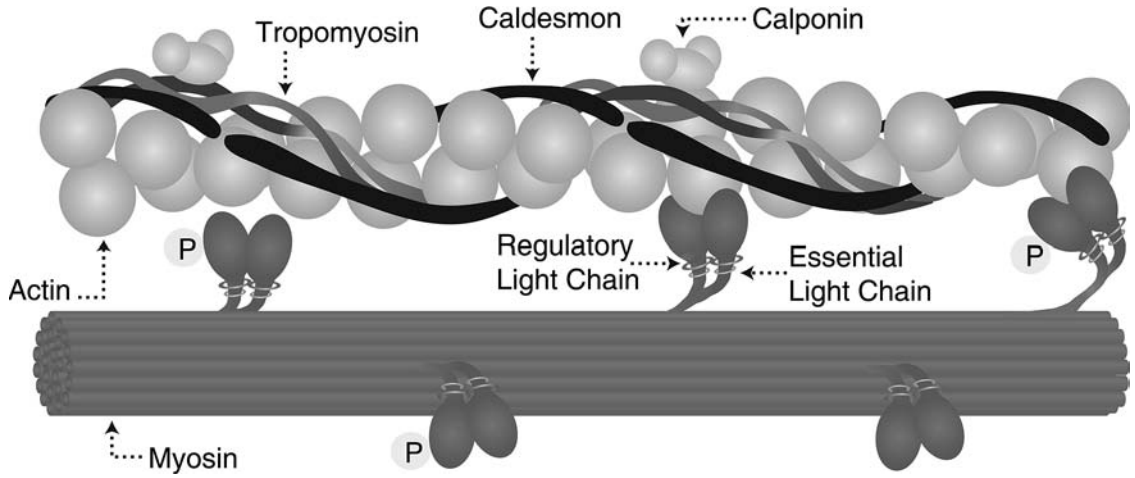

FIGURE 32-2 Smooth muscle myosin thick filament composed of myosin heavy chains and light chains (essential and regulatory) and thin filament composed of actin, tropomyosin, caldesmon, and calponin. P = phosphorylated myosin head.

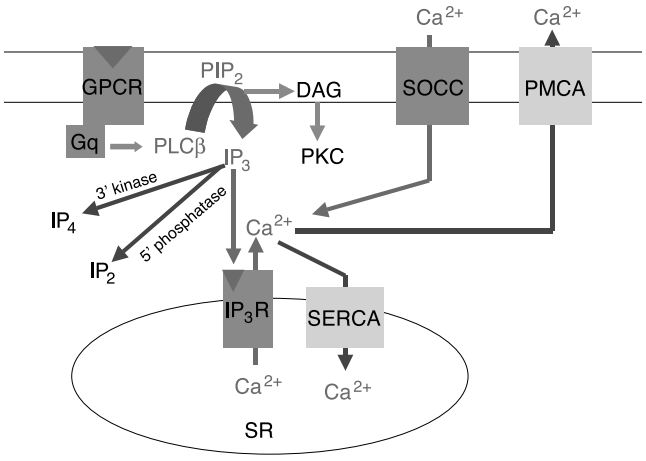

FIGURE 32-3 Main pathways regulating contractile agonist-induced Ca^{2+} signaling in airway smooth muscle. DAG = 1,2-diacylglycerol; GPCR = G protein–coupled receptor; IP_2 = inositol 1,4-biphosphate; IP_3 = inositol 1,4,5-triphosphate; IP_3R = IP_3 receptor; IP_4 = inositol 1,3,4,5-tetrakisphosphate; PIP_2 = phosphatidylinositol 4,5-biphosphate; PKC = protein kinase C; PLCβ = phospholipase Cβ; PMCA = plasma membrane Ca^{2+}-ATPase; SERCA = sarcoplasmic/endoplasmic reticulum Ca^{2+}-ATPase; SOCC = store-operated Ca^{2+} channel; SR = sarcoplasmic reticulum.

PLCβ4 isoforms are activated upon binding to the G_q α-subunit, whereas PLCβ2 is thought to be activated by the free βγ-subunits. The products of PIP_2 hydrolysis are inositol 1,4,5-trisphosphate (IP_3) and 1,2-diacylglycerol (DAG). DAG activates protein kinase C (PKC), and IP_3 induces release of Ca^{2+} from intracellular stores. The activity of PLCβ not only depends on G-protein subunit binding but also requires a normal Ca^{2+} gradient across the plasma membrane and therefore high levels of extracellular Ca^{2+}. In addition, the activity of PLCβ is down-regulated by PKC, providing negative feedback by DAG.[5] Following release by PLCβ, IP_3 is rapidly metabolized by two enzymes: IP_3 is dephosphorylated by a specific 5′-phosphatase or, alternatively, phosphorylated by a specific 3′-kinase (see Figure 32-3).[6]

A series of protein–protein interactions converts the initial Ca^{2+} signal into contraction of the muscle cell.[7] The newly released Ca^{2+} first interacts with calmodulin, an abundant cytoplasmic Ca^{2+}-binding protein. Each molecule of calmodulin binds with high affinity to four Ca^{2+} ions, after which the calmodulin undergoes a conformational change, enabling it to associate with its downstream target proteins. One of the first targets of Ca^{2+}–calmodulin to be identified was MLCK. Upon association with Ca^{2+}–calmodulin, MLCK is activated, after which it phosphorylates the 20 kDa regulatory light chain (LC_{20}) of myosin, thus activating myosin and initiating crossbridge cycling and smooth muscle contraction (see Figure 32-2).

Intracellular Ca^{2+} Stores and Ca^{2+} Release

Ca^{2+} is stored mainly in the sarcoplasmic reticulum, where it is buffered by proteins such as calreticulin and calsequestrin. These proteins can bind large amounts of Ca^{2+}, with estimated Ca^{2+} concentrations in sarcoplasmic reticulum reaching 10 to 15 mmol/L. Release of Ca^{2+} into the cytosol occurs through two types of structurally similar channels in the membrane of sarcoplasmic reticulum: IP_3 receptors (IP_3R), activated by IP_3, and ryanodine receptors (RyR). IP_3Rs are ubiquitously expressed in airway smooth muscle from many mammalian species. Each channel is composed of four subunits that form homotetrameric or heterotetrameric channels. Activation of IP_3R by IP_3 is regulated by cytoplasmic Ca^{2+}. A rise in cytoplasmic Ca^{2+} concentration from basal levels of ~100 nmol/L to ~300 nmol/L increases the potency of IP_3 in activating channel openings, but higher concentrations reduce the effectiveness of IP_3. Thus, high levels of IP_3 provide negative feedback for the release of more Ca^{2+}.[8] RyRs are activated by Ca^{2+} and cyclic ADP–ribose. However, the contribution of RyRs to Ca^{2+} signaling in airway smooth muscle is still debated.

Ca^{2+} Entry

The increase in intracellular Ca^{2+} concentration arises also from Ca^{2+} influx from the extracellular milieu. Two models of Ca^{2+}entry have been proposed: (1) capacitative Ca^{2+} entry, which is stimulated by emptying of intracellular stores, and (2) noncapacitative entry, which is independent of store emptying but dependent upon activation of specific Ca^{2+} channels. In airway smooth muscle cells, the increased Ca^{2+} influx that follows Ca^{2+} release triggered by GPCR stimulation is mainly due to capacitative entry, whereby the release of Ca^{2+} from sarcoplasmic reticulum stores triggers the opening of Ca^{2+} channels in plasma membranes and Ca^{2+} influx from the extracellular milieu.[9] The mechanism by which intracellular store depletion activates conductance in the plasma membrane is unclear. The molecular identity of the store-operated Ca^{2+} channels involved in capacitative Ca^{2+} entry is unknown. Several plasma membrane channels may control noncapacitative Ca^{2+} entry. Depending on the mechanisms of their activation, they are classified as follows:

1. Voltage operated channels (VOCs), activated by changes in transmembrane potential
2. Receptor-operated channels (ROCs), where the receptor acts as a channel and is activated by ligand binding
3. Second messenger–operated channels (SMOCs), activated by second messengers, such as arachidonate-operated channels or cyclic nucleotide–operated channels

Airway smooth muscle cells express purinergic P2X ROC-type receptors. Although VOCs are expressed in airway smooth muscle and are activated by cholinergic stimulation, their contribution to Ca^{2+} influx mediated by GPCRs seems to be small.[10]

Ca^{2+} Extrusion and Store Refilling

To offset the increase in cytoplasmic Ca^{2+} concentration, the combined action of buffers, pumps, and exchangers restores basal levels of Ca^{2+}.[8] There are two types of ATP-dependent pump actively removing Ca^{2+} from the cytoplasm: sarcoplasmic/endoplasmic reticulum Ca^{2+}-ATPase (SERCA) in the

sarcoplasmic reticulum membrane and plasmalemmal Ca^{2+}-ATPase (PMCA) in the plasma membrane (see Figure 32-3). SERCA pumps are activated by protein kinase A (PKA)-mediated or protein kinase G (PKG)-mediated phosphorylation of phospholamban, a small transmembrane protein that, when nonphosphorylated, inhibits SERCA activity. SERCAs generate and maintain about a 10,000-fold Ca^{2+} gradient between the sarcoplasmic reticulum lumen and the cytoplasm. PMCAs pump Ca^{2+} up the steep electrochemical gradient from cytosol to extracellular space. PMCAs are activated by binding of calmodulin to their C-termini, preventing autoinhibition and increasing the affinity for Ca^{2+} and subsequently the transport rate of Ca^{2+} to the extracellular space. Phosphorylation of PMCAs by other kinases may also reduce inhibition and facilitate Ca^{2+} transport.

Role of Cyclic Nucleotides in Ca^{2+} Regulation

Among the drugs that are known to relax smooth muscle are agents that elevate cyclic AMP (cAMP) and cyclic GMP (cGMP). Airway smooth muscle cells express at least two types of GPCR that activate adenylyl cyclase via G_s, namely β_2-adrenoceptors and prostanoid receptors (probably prostaglandin E receptor, subtype EP_2). There may be, in addition, a small population of vasoactive intestinal peptide receptors. Following activation by G_s-coupled GPCRs, adenylyl cyclase catalyzes the breakdown of ATP to cAMP, which, in turn, activates PKA. Similarly, guanylyl cyclase mediates production of cGMP, which stimulates cGMP-dependent PKG. Potential stimulators of guanylyl cyclase in vivo include atrial natriuretic peptide and nitric oxide.

It is well accepted that a reduction in Ca^{2+} mobilization is a critical event involved in cyclic nucleotide–dependent smooth muscle relaxation.[11] Virtually all of the steps in Ca^{2+} homeostasis may be affected by cAMP and/or cGMP. The proposed mechanisms for the PKA-dependent decrease in IP_3 formation include phosphorylation of the Ca^{2+}-mobilizing receptor, G proteins, and PLCβ itself. Inhibition of Ca^{2+} release from the sarcoplasmic reticulum may result from PKA-mediated and PKG-mediated phosphorylation of IP_3 receptors. Cyclic nucleotides may also promote Ca^{2+} uptake and/or extrusion by stimulating SERCA and PMCA, as well as by inhibiting Ca^{2+} entry.

Inhibition of Myosin Light-chain Phosphatase

Increases in Ca^{2+} concentration and activation of MLCK are essential for the induction of LC_{20} phosphorylation and smooth muscle contraction. In addition, phosphorylation of LC_{20} is also regulated by a myosin-specific phosphatase (MLCP).[4] The importance of phosphatase activity in the regulation of smooth muscle contraction has been appreciated for many years,[12] but the mechanism by which the myosin phosphatase is regulated by contractile agonists has only recently been defined, as discussed below.

One way of investigating the contraction of smooth muscle is to quantify force generation following ex vivo stimulation of smooth muscle strips.[12–14] The smooth muscle strips can be readily manipulated experimentally by treating them with agents that permeabilize the cells and tissue, such as α-toxin or β-escin.[15] One can then control the concentration of Ca^{2+} within the cells and also introduce different regulatory molecules or inhibitors into the muscle. Using this methodology, Kitazawa and colleagues demonstrated that whereas contraction of smooth muscle is absolutely dependent upon an increase in cytoplasmic Ca^{2+} concentration and activation of MLCK, for a given experimentally determined concentration of cytoplasmic Ca^{2+} the level of LC_{20} phosphorylation and force generation can be increased following incubation of the smooth muscle strip with contractile agonists.[12] This phenomenon is referred to as Ca^{2+} sensitization to indicate that contractile agonists have the unique ability to increase the sensitivity of the contractile machinery to Ca^{2+}. Similar to contractile agonist stimulation of permeabilized muscle in which the Ca^{2+} concentration is "clamped," contraction of smooth muscle strips can also be evoked by GTPγS, a nonhydrolyzable form of GTP.[13,14] This indicates that contraction of smooth muscle and Ca^{2+} sensitization are regulated by a GTP-binding protein, although it does not differentiate between GTP-binding proteins that mediate GPCR-dependent responses (ie, G_s, G_q, G_i, etc.) and GTP-binding proteins of the Ras superfamily, which regulate a variety of cellular responses (such as vesicular trafficking) but do not associate directly with GPCRs. Evidence that Ca^{2+} sensitization is mediated by Rho, which is a member of the Ras superfamily of GTP-binding proteins, was provided by data demonstrating that contraction of Ca^{2+}-clamped smooth muscle strips could be induced by addition of recombinant Rho.[13,14] Kimura and colleagues defined the mechanism by which Rho regulated Ca^{2+} sensitization and smooth muscle contraction when they demonstrated that Rho kinase, a protein activated by Rho, phosphorylated the 120 kDa myosin-targeting subunit of myosin phosphatase (MYPT1).[16] Phosphorylated MYPT1 inhibits the 37 kDa catalytic subunit. Altogether, these data demonstrate that GPCRs induce activation of Rho, which, in turn, inhibits MLCP; the overall effect of this is to increase phosphorylation of LC_{20} and smooth muscle contraction (Figure 32-4).

The mechanisms by which GPCR contractile agonists regulate Rho, and its targets Rho kinase and MLCP, have now been explored in detail. In different systems, activation of Rho is regulated by GPCR-induced activation of $G_{i/o}$, G_q and $G_{12/13}$.[4,17,18] A significant role for Rho kinase–dependent MLCP inhibition in smooth muscle contraction is further supported by data demonstrating dramatic inhibition of smooth muscle contraction, both in vivo and ex vivo, by a potent inhibitor of Rho kinase, Y-27632.[19] This inhibitor was originally isolated by Uehata and colleagues in a screen for compounds having the ability to inhibit smooth muscle contraction.[19] Y-27632 was isolated, and its target was identified as Rho kinase. Significantly, Y-27632 effectively decreases hypertension in several different rat models of hypertension but does not affect blood pressure in normal animals.[19] Y-27632 has since proven to be effective in inhibiting agonist-induced contraction of airway smooth muscle,[19–21] as well as in inhibiting airway hyperresponsiveness in a murine model of experimental asthma.[22] In addition to Rho kinase, other kinases may also phosphorylate

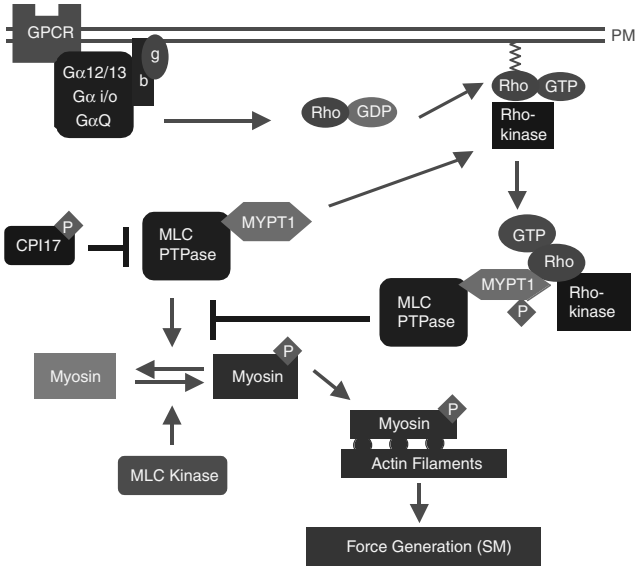

FIGURE 32-4 Regulation of myosin light-chain phosphatase activity by Rho kinase and CPI17. CPI17 = protein kinase C (PKC)-dependent phosphatase inhibitor of 17 kDa; GPCR = G protein–coupled receptor; MLC kinase = myosin light-chain kinase; MLC PTPase = myosin light-chain phosphatase; MYPT1 = myosin-targeting subunit of myosin phosphatase; SM = smooth muscle.

the myosin-targeting subunit of MLCP and inhibit the activity of the catalytic subunit. These include integrin-linked kinase and a zipper interacting protein (ZIP)-like kinase.[23,24] Whereas Rho kinase is established as an important regulator of smooth muscle contraction, the effects of other MYPT1 kinases on basal levels of smooth muscle tone or on smooth muscle disease pathogenesis are less well understood.

Rho kinase regulates Ca^{2+} sensitization and smooth muscle contraction through indirect inhibition of MLCP activity mediated by the MYPT1 subunit of the phosphatase enzyme. The catalytic subunit of MLCP is directly targeted by another protein that also regulates smooth muscle contraction and Ca^{2+} sensitization. CPI17 (PKC-dependent phosphatase inhibitor of 17 kDa) is a 17 kDa peptide that, when phosphorylated, potently inhibits MLCP.[25] Although it was originally thought to be phosphorylated by PKC, more recent data indicate that Rho kinase phosphorylates CPI17.[26] These data therefore suggest that inhibition of MLCP is regulated by Rho kinase via two different mechanisms, one in which MYPT1 is phosphorylated and the one in which the catalytic subunit itself is targeted by CPI17.

Myosin

The final effector of muscle contraction is crossbridge formation between myosin and actin. Myosin is composed of two globular heads that join together in the neck region to form a coiled-coil α-helix tail (see Figure 32-2). Each head contains an ATP-binding pocket and an actin-binding site. To each neck is attached a set of light chains, consisting of one regulatory light chain (LC_{20}) and one essential light chain (LC_{17}). The essential light chain is important for maximal rate of contraction and force production, as shown by in vitro motility and microneedle force assays.[27,28] As discussed above, LC_{20} must be phosphorylated via the Ca^{2+}–calmodulin–MLCK mechanism for smooth muscle myosin to be activated. The myosin molecule tails assemble together into the myosin thick filament. Evidence is now accumulating to suggest that smooth muscle myosin thick filaments form only after LC_{20} phosphorylation.[29–31] In relaxed smooth muscle cells, myosin would therefore exist, at least partially, as monomers.[31]

Smooth Muscle Myosin Heavy-chain Isoforms

On the basis of electrophysiologic measurements, smooth muscle has been divided into two categories: tonic, slowly contracting, and tone maintaining, as in most blood vessels, and phasic and rapidly contracting, as in the intestine.[32] It is still unclear how airway smooth muscle should be classified because in the literature it has been referred to as both a tonic[33] and a phasic[34] muscle. However, tonic and phasic smooth muscles have quite different mechanical properties,[35,36] possibly because of differences in myosin isoform expression.[37]

Two isoforms of the smooth muscle myosin heavy chain are generated following alternative splicing of RNA encoding the N-terminus (head region).[38,39] These two isoforms differ by the absence [(−)insert] or presence [(+)insert] of a seven–amino acid insert near the ATPase site. The expression of these isoforms is tissue specific. Tonic muscle is composed mostly of the (−)insert isoform, whereas phasic muscle is predominantly composed of the (+)insert isoform.[40,41] The presence of the insert doubles the activity of actin-activated ATPase and the rate of actin filament movement in the in vitro motility assay.[42–45] Two other isoforms of smooth muscle (SM1 and SM2) are generated by alternative splicing of RNA encoding the C-terminus (tail region),[38,39] but no differences in their molecular mechanical properties have been reported.[46] A recent study,[47] however, demonstrated that these two isoforms have different modes of assembly into thick filaments, which might ultimately lead to mechanical differences at the whole muscle level.

Actin and Thin Filament–Associated Proteins

Whole smooth muscle thin filaments are composed of actin, tropomyosin, caldesmon, calponin, and possibly SM22 (see Figure 32-2) (see Morgan and Gangopadhyay[48] for a review). The α-vascular and the γ-enteric actin isoforms are contractile.[49,50] Filamentous actin has a double-helical structure comprising two polymers of globular actin. The exact function of the thin filament-associated proteins is still being debated. That is, the regulation of actin–myosin crossbridge formation is known to be achieved by LC_{20} phosphorylation, but evidence is accumulating to suggest that the actin-decorating proteins also contribute to this regulation. Tropomyosin and caldesmon form continuous strands in the groove of the actin helices. Tropomyosin may serve, as in striated muscle, to transmit regulatory information simultaneously to multiple crossbridges. This would allow the myosin crossbridges to behave in a cooperative manner. The results of some studies have suggested that upon muscle activation, smooth muscle tropomyosin moves away from

the myosin-binding sites in a similar manner to that previously described in striated muscle.[48] Caldesmon has an inhibitory effect on MgATP hydrolysis. This inhibitory effect might be reversed by the binding of Ca^{2+}–calmodulin to caldesmon or by phosphorylation of caldesmon.[48] The N-terminus of caldesmon also binds to myosin, perhaps serving to join actin and myosin together. The role of calponin is still unclear. It has been suggested that it inhibits MgATP hydrolysis.[51] Furthermore, because it contains domains that bind extracellular signal regulated kinase (ERK) and protein kinase C (PKC), it may serve to bring signaling molecules in close proximity to actin, thereby favoring signal transduction.[48] The function of calponin may actually depend on whether the muscle is of the phasic or tonic type.[48,52] SM22 is also ubiquitously and specifically expressed in smooth muscle, but its function remains unknown.[48] The binding of SM22 to actin, however, remains controversial.[53]

CONCLUSIONS

In this chapter we have highlighted some of the important concepts in the regulation of smooth muscle contraction at the cellular and molecular levels. These signaling pathways and contractile proteins may be considered targets for drug development in diseases such as asthma, cystic fibrosis, and chronic obstructive pulmonary disease, where altered contraction of airway smooth muscle contributes to airway hyperresponsiveness and disease pathogenesis. The exploration of abnormalities of airway smooth muscle in human disease have been hampered by the lack of tissue for study. However, asthma has been extensively modeled in animals. Significantly, the changes in activation or expression of the signaling pathways and smooth muscle contractile proteins discussed above have all been shown to contribute to airway hyperresponsiveness in animal models of human asthma. For example, smooth muscle cells cultured from innately hyperresponsive rats (Fisher 344) have more robust Ca^{2+} responses when stimulated with contractile agonists than do normoresponsive Lewis strain rats.[54,55] In addition, Fisher rats also have higher levels of the (+)insert myosin isoform in the airway smooth muscle than do normoresponsive Lewis rats.[56] Moreover, rats with experimentally induced asthma also express higher levels of the proteins that couple contractile agonist stimulation with activation of MLCK and inactivation of MLCP, including $G\alpha_q$, Rho, and $G\alpha_{12/13}$.[57–59] Finally, MLCK protein levels and the phosphorylation of LC_{20} are both increased in airway smooth muscle from allergen-sensitized dogs,[60] consistent with data demonstrating that MLCK mRNA levels are increased in freshly isolated human asthmatic smooth muscle cells.[61] Thus, an understanding of the molecular mechanisms by which smooth muscle contracts may increase our understanding of airway hyperresponsiveness and provide novel targets for drug development for the treatment of human lung disease.

ACKNOWLEDGMENT

We thank Julie Wang for the artwork of Figures 32-1 and 32-2.

REFERENCES

1. Billington CK, Penn RB. Signaling and regulation of G protein-coupled receptors in airway smooth muscle. Respir Res 2003;4:2.
2. Gudermann T, Kalkbrenner F, Schultz G. Diversity and selectivity of receptor–G protein interaction. Annu Rev Pharmacol Toxicol 1996;36:429–59.
3. Cabrera-Vera TM, Vanhauwe J, Thomas TO, et al. Insights into G protein structure, function, and regulation. Endocr Rev 2003;24:765–81.
4. Somlyo AP, Somlyo AV. Ca^{2+} sensitivity of smooth muscle and nonmuscle myosin II: modulated by G proteins, kinases, and myosin phosphatase. Physiol Rev 2003;83:1325–58.
5. Rhee SG. Regulation of phosphoinositide-specific phospholipase C. Annu Rev Biochem 2001;70:281–312.
6. Chilvers ER, Lynch BJ, Challiss RA. Phosphoinositide metabolism in airway smooth muscle. Pharmacol Ther 1994;62: 221–45.
7. Kamm KE, Stull JT. Dedicated myosin light chain kinases with diverse cellular functions. J Biol Chem 2001;276:4527–30.
8. Berridge MJB, Bootman MD, Roderick HL. Calcium signaling: dynamics, homeostasis and remodeling. Mol Cell Biol 2003; 4:517–29.
9. Marthan R. Store-operated calcium entry and intracellular calcium release channels in airway smooth muscle. Am J Physiol Lung Cell Mol Physiol 2004;286:L907–8.
10. Janssen LJ. Ionic mechanisms and Ca(2+) regulation in airway smooth muscle contraction: do the data contradict dogma? Am J Physiol Lung Cell Mol Physiol 2002;282:L1161–78.
11. Abdel-Latif A. Cross talk between cyclic nucleotides and polyphosphoinositide hydrolysis, protein kinases and contraction in smooth muscle. Exp Biol Med 2001;226:153–63.
12. Kitazawa T, Masuo M, Somlyo AP. G protein-mediated inhibition of myosin light-chain phosphatase in vascular smooth muscle. Proc Natl Acad Sci U S A 1991;88:9307–10.
13. Hirata K, Kikuchi A, Sasaki T, et al. Involvement of rho p21 in the GTP-enhanced calcium ion sensitivity of smooth muscle contraction. J Biol Chem 1992;267:8719–22.
14. Gong MC, Iizuka K, Nixon G, et al. Role of guanine nucleotide-binding proteins—ras-family or trimeric proteins or both—in Ca^{2+} sensitization of smooth muscle. Proc Natl Acad Sci U S A 1996;93:1340–5.
15. Kitazawa T, Kobayashi S, Horiuti K, et al. Receptor-coupled, permeabilized smooth muscle. Role of the phosphatidylinositol cascade, G-proteins, and modulation of the contractile response to Ca^{2+}. J Biol Chem 1989;264: 5339–42.
16. Kimura K, Ito M, Amano M, et al. Regulation of myosin phosphatase by Rho and Rho-associated kinase (Rho-kinase). Science 1996;273:245–8.
17. Croxton TL, Lande B, Hirshman CA. Role of G proteins in agonist-induced Ca^{2+} sensitization of tracheal smooth muscle. Am J Physiol 1998;275:L748–55.
18. Gohla A, Schultz G, Offermanns S. Role for G(12)/G(13) in agonist-induced vascular smooth muscle cell contraction. Circ Res 2000;87:221–7.
19. Uehata M, Ishizaki T, Satoh H, et al. Calcium sensitization of smooth muscle mediated by a Rho-associated protein kinase in hypertension. Nature 1997;389:990–4.
20. Setoguchi H, Nishimura J, Hirano K, et al. Leukotriene C(4) enhances the contraction of porcine tracheal smooth muscle through the activation of Y-27632, a rho kinase inhibitor sensitive pathway. Br J Pharmacol 2001;132:111–8.
21. Yoshii A, Iizuka K, Dobashi K, et al. Relaxation of contracted rabbit tracheal and human bronchial smooth muscle by Y-27632 through inhibition of Ca^{2+} sensitization. Am J Respir Cell Mol Biol 1999;20:1190–200.

22. Hashimoto K, Peebles RS Jr, Sheller JR, et al. Suppression of airway hyperresponsiveness induced by ovalbumin sensitisation and RSV infection with Y-27632, a Rho kinase inhibitor. Thorax 2002;57:524–7.
23. Kiss E, Muranyi A, Csortos C, et al. Integrin-linked kinase phosphorylates the myosin phosphatase target subunit at the inhibitory site in platelet cytoskeleton. Biochem J 2002; 365:79–87.
24. MacDonald JA, Borman MA, Muranyi A, et al. Identification of the endogenous smooth muscle myosin phosphatase-associated kinase. Proc Natl Acad Sci U S A 2001;98:2419–24.
25. Eto M, Senba S, Morita F, Yazawa M. Molecular cloning of a novel phosphorylation-dependent inhibitory protein of protein phosphatase-1 (CPI17) in smooth muscle: its specific localization in smooth muscle. FEBS Lett 1997;410:356–60.
26. Koyama M, Ito M, Feng J, et al. Phosphorylation of CPI-17, an inhibitory phosphoprotein of smooth muscle myosin phosphatase, by Rho-kinase. FEBS Lett 2000;475:197–200.
27. VanBuren P, Waller GS, Harris DE, et al. The essential light chain is required for full force production by skeletal muscle myosin. Proc Natl Acad Sci U S A 1994;91:12403–7.
28. Lowey S, Waller GS, Trybus KM. Skeletal muscle myosin light chains are essential for physiological speeds of shortening. Nature 1993;365:454–6.
29. Godfraind-De Becker A, Gillis JM. Analysis of the birefringence of the smooth muscle anococcygeus of the rat, at rest and in contraction. I. J Muscle Res Cell Motil 1988;9:9–17.
30. Gillis JM, Cao ML, Godfraind-De Becker A. Density of myosin filaments in the rat anococcygeus muscle, at rest and in contraction. II. J Muscle Res Cell Motil 1988;9:18–29.
31. Herrera AM, Kuo KH, Seow CY. Influence of calcium on myosin thick filament formation in intact airway smooth muscle. Am J Physiol Cell Physiol 2002;282:310–6.
32. Somlyo AV, Somlyo AP. Electromechanical and pharmacomechanical coupling in vascular smooth muscle. J Pharmacol Exp Ther 1968;159:129–45.
33. Horiuti K, Somlyo AV, Goldman YE, Somlyo AP. Kinetics of contraction initiated by flash photolysis of caged adenosine triphosphate in tonic and phasic smooth muscles. J Gen Physiol 1989;94:769–81.
34. Malmqvist U, Arner A. Correlation between isoform composition of the 17 kDa myosin light chain and maximal shortening velocity in smooth muscle. Pflugers Arch 1991;418:523–30.
35. Fuglsang A, Khromov A, Torok K, et al. Flash photolysis studies of relaxation and cross-bridge detachment: higher sensitivity of tonic than phasic smooth muscle to MgADP. J Muscle Res Cell Motil 1993;14:666–77.
36. Himpens B, Matthijs G, Somlyo AV, et al. Cytoplasmic free calcium, myosin light chain phosphorylation, and force in phasic and tonic smooth muscle. J Gen Physiol 1988;92:713–29.
37. Somlyo AP. Myosin isoforms in smooth muscle: how may they affect function and structure? J Muscle Res Cell Motil 1993;14:557–63.
38. Eddinger TJ, Murphy RA. Two smooth muscle myosin heavy chains differ in their light meromyosin fragment. Biochemistry 1988;27:3807–11.
39. Nagai R, Kuro-o M, Babij P, Periasamy M. Identification of two types of smooth muscle myosin heavy chain isoforms by cDNA cloning and immunoblot analysis. J Biol Chem 1989;264:9734–7.
40. Hamada Y, Yanagisawa M, Katsuragawa Y, et al. Distinct vascular and intestinal smooth muscle myosin heavy chain mRNAs are encoded by a single-copy gene in the chicken. Biochem Biophys Res Commun 1990;170:53–8.
41. White S, Martin AF, Periasamy M. Identification of a novel smooth muscle myosin heavy chain cDNA: isoform diversity in the S1 head region. Am J Physiol 1993;264:1252–8.
42. Kelley CA, Adelstein RS. Characterization of isoform diversity in smooth muscle myosin heavy chains. Can J Physiol Pharmacol 1994;72:1351–60.
43. Lauzon AM, Tyska MJ, Rovner AS, et al. A 7-amino-acid insert in the heavy chain nucleotide binding loop alters the kinetics of smooth muscle myosin in the laser trap. J Muscle Res Cell Motil 1998;19:825–37.
44. Lauzon AM, Trybus KM, Warshaw DM. Molecular mechanics of two smooth muscle heavy meromyosin constructs that differ by an insert in the motor domain. Acta Physiol Scand 1998;164:357–61.
45. Rovner AS, Freyzon Y, Trybus KM. Chimeric substitutions of the actin-binding loop activate dephosphorylated but not phosphorylated smooth muscle heavy meromyosin. J Biol Chem 1995;270:30260–3.
46. Kelley CA, Sellers JR, Goldsmith PK, Adelstein RS. Smooth muscle myosin is composed of homodimeric heavy chains. J Biol Chem 1992;267:2127–30.
47. Rovner AS, Fagnant PM, Lowey S, Trybus KM. The carboxyl-terminal isoforms of smooth muscle myosin heavy chain determine thick filament assembly properties. J Cell Biol 2002;156:113–23.
48. Morgan KG, Gangopadhyay SS. Invited review: cross-bridge regulation by thin filament-associated proteins. J Appl Physiol 2001;91:953–62.
49. Herman IM. Actin isoforms. Curr Opin Cell Biol 1993;5:48–55.
50. North AJ, Gimona M, Lando Z, Small JV. Actin isoform compartments in chicken gizzard smooth muscle cells. J Cell Sci 1994;107(Pt 3):445–55.
51. Winder SJ, Walsh MP. Smooth muscle calponin. Inhibition of actomyosin MgATPase and regulation by phosphorylation. J Biol Chem 1990;265:10148–55.
52. Walsh MP. Calponin—knocked out but not down! J Physiol 2000;529(Pt 3):517.
53. Kobayashi R, Kubota T, Hidaka H. Purification, characterization, and partial sequence analysis of a new 25-kDa actin-binding protein from bovine aorta: a SM22 homolog. Biochem Biophys Res Commun 1994;198:1275–80.
54. Tao FC, Tolloczko B, Mitchell CA, et al. Inositol (1,4,5)trisphosphate metabolism and enhanced calcium mobilization in airway smooth muscle of hyperresponsive rats. Am J Respir Cell Mol Biol 2000;23:514–20.
55. Tao FC, Tolloczko B, Eidelman DH, Martin JG. Enhanced Ca(2+) mobilization in airway smooth muscle contributes to airway hyperresponsiveness in an inbred strain of rat. Am J Respir Crit Care Med 1999;160:446–53.
56. Lauzon AM, Azoulay E, Maghi K. Smooth muscle myosin heavy chain isoform expression in airway hyperresponsiveness. Am J Respir Crit Care Med 2001;163:A539.
57. Chiba Y, Misawa M. Increased expression of G12 and G13 proteins in bronchial smooth muscle of airway hyperresponsive rats. Inflamm Res 2001;50:333-6.
58. Chiba Y, Sakai H, Arimoto T, et al. Gq protein level increases concurrently with antigen-induced airway hyperresponsiveness in rats. Respir Physiol 2000;121:75–83.
59. Chiba Y, Takada Y, Miyamoto S, et al. Augmented acetylcholine-induced, Rho-mediated Ca^{2+} sensitization of bronchial smooth muscle contraction in antigen-induced airway hyperresponsive rats. Br J Pharmacol 1999;127: 597–600.
60. Jiang H, Rao K, Liu X, et al. Increased Ca^{2+} and myosin phosphorylation, but not calmodulin activity in sensitized airway smooth muscles. Am J Physiol 1995;268:L739–46.
61. Ma X, Cheng Z, Kong H, et al. Changes in biophysical and biochemical properties of single bronchial smooth muscle cells from asthmatic subjects. Am J Physiol Lung Cell Mol Physiol 2002;283:1181–9.

CHAPTER 33

CYTOKINES AND AIRWAY SMOOTH MUSCLE

Stephanie A. Shore

Asthma is an inflammatory disease characterized by reversible airway narrowing, airway hyperresponsiveness (AHR), and increased numbers of eosinophils and activated $CD4^+$ T cells in the airways. Until recently, the role of the airway smooth muscle cell in asthma was assumed to be as a passive downstream target of spasmogens derived from the inflammatory process. However, that view is rapidly changing. An increasing body of evidence indicates that cytokines produced in the asthmatic airway act directly on airway smooth muscle cells, leading to increased responses to contractile agonists and reduced β-agonist responsiveness, events that favor AHR. Moreover, in the presence of certain cytokines, the smooth muscle cell also appears to be capable of initiating and amplifying the inflammatory cascade by expressing adhesion molecules that permit interactions between smooth muscle cells, eosinophils, and T cells and by producing additional cytokines and chemokines. Finally, cytokine actions on airway smooth muscle also appear to be important in the airway remodeling that is characteristic of asthma, in that they lead to smooth muscle proliferation and altered matrix production.

The purpose of this chapter is to summarize the data regarding the effects of cytokines on (1) airway smooth muscle contractile responses, (2) airway smooth muscle relaxant responses, and (3) the ability of airway smooth muscle cells to produce cytokines, chemokines, and growth factors. Data from human airway smooth muscle are emphasized. Because of the importance of β-agonists and glucocorticoids in the treatment of asthma, wherever possible we indicate the impact of these agents on the smooth muscle function described. The reader is directed to other reviews on the capacity of smooth muscle cells to proliferate, express adhesion molecules, and modify extracellular matrix.[1–3]

EFFECTS OF CYTOKINES ON RESPONSES TO CONTRACTILE AGONISTS

Agonists that contract airway smooth muscle, such as histamine, acetylcholine (ACh), and leukotriene D_4 (LTD_4), act on seven transmembrane domain receptors that are coupled to G proteins of the G_q family. Receptor activation leads to dissociation of the α-subunit of G_q from the β-subunit and the γ-subunit and subsequent activation of phospholipase C (PLC). PLC hydrolyzes phosphatidylinositol 4,5-biphosphate, resulting in inositol 1,4,5-triphosphate (IP_3) production. IP_3 leads to an increased intracellular Ca^{2+} concentration as a result of Ca^{2+} release from the sarcoplasmic reticulum. Ca^{2+} binds calmodulin and activates myosin light-chain kinase, resulting in phosphorylation of the 20 kDa myosin light chain (MLC). In smooth muscle, MLC phosphorylation is required for actin–myosin interactions and muscle contraction.

Several different cytokines have been reported to increase Ca^{2+} signaling or contraction in airway smooth muscle (Table 33-1). The effects vary with the cytokine used, the contractile agonist, and the species examined. To date, there have been no studies examining the impact of corticosteroids on these changes in contractility.

Tumor Necrosis Factor-α

Levels of tumor necrosis factor-α (TNF-α) are increased in the airways of asthmatic subjects, and this cytokine has been reported to increase airway responsiveness, in both humans and other species. TNF-α also increases the contractile responses of isolated airways from a variety of species, including humans, guinea pigs, sheep, mice, and cows, suggesting that the role of TNF-α in AHR may be the result of its direct effects on smooth muscle. The ability of a variety of contractile agonists, including bradykinin (BK), carbachol, and thrombin,[4–6] to increase $[Ca^{2+}]_i$ in human airway smooth muscle (HASM) cells in culture is also augmented by TNF-α. The observation that responses to multiple agonists are affected by TNF-α is consistent with the nonspecific AHR that is characteristic of asthma in humans.

The mechanistic basis for the effects of TNF-α on the responses of airway smooth muscle to contractile agonists varies with the species studied. In HASM cells, the effects of TNF-α on agonist-induced changes in $[Ca^{2+}]_i$ are accompanied by increases in IP_3 formation, suggesting that the action

Table 33-1 Effects of Cytokines on Contractile Responses of Airway Smooth Muscle

Cytokine	*Species*	*Effect*
TNF-α	Human	Increases agonist-evoked increases in IP_3 and $[Ca^{2+}]_i$ in cultured cells and increases contractile responses of isolated bronchi
	Mouse, sheep, guinea pig, cow	Increases contractile responses of isolated airways
IL-1β	Human	Variable effects on contractile responses of isolated airways or changes in $[Ca^{2+}]_i$ in cultured cells, depending on the agonist
	Sheep	Increases contractile responses of isolated airways
LIF	Guinea pig	Increases tachykinin release and NK-2 receptor–mediated contraction in tracheal explants
IL-13	Human	Increases cell stiffness responses of cultured cells to LTD_4 but not to BK
	Mouse, rabbit	Increases contractile responses of isolated airways
IL-5, IL-10, GM-CSF	Rabbit	Increases contractile responses of isolated airways
IFN-γ	Human	Enhances LTD_4-induced changes in cell stiffness in cultured cells

BK = bradykinin; GM-CSF = granulocyte–macrophage colony-stimulating factor; IFN-γ = interferon-γ; IL-1β = interleukin-1β; IP_3 = inositol 1,4,5-triphosphate; LIF = leukemia inhibitory factor; LTD_4 = leukotriene D_4; NK-2 = neurokinin-2; TNF-α = tumor necrosis factor-α.

of TNF-α is upstream of IP_3, at the level of G_q, PLC, or their coupling. Indeed, Hotta and colleagues[7] demonstrated an increase in G_q expression in conjunction with an increase in carbachol-induced IP_3 formation in TNF-α–treated HASM cells. The observation that TNF-α increases the changes in $[Ca^{2+}]_i$ induced by thapsigargin,[6] which directly releases Ca^{2+} from internal stores, suggests that TNF-α also appears to affect the Ca^{2+} pools activated by these agonists. In contrast, in guinea pig and in bovine airway smooth muscle, the effect of TNF-α appears to be mediated through changes in the Ca^{2+} sensitivity of the myofilaments.[8,9] For excellent reviews on the capacity of TNF-α to augment contractile responses in airway smooth muscle, see Amrani and colleagues.[10,11]

Interleukin-1β

Levels of interleukin-1β (IL-1β) are also increased in asthmatic airways, and this cytokine has been shown to play a role in the AHR that is observed in animal models of asthma. However, the effect of IL-1β on airway smooth muscle responses to contractile agonists is much less consistent than the effect of TNF-α, and appears to depend on the contractile agonist used. For example, in isolated human bronchi, IL-1β increases contractile responses to a neurokinin-1 receptor agonist, has no effect on contractile responses to ACh, and decreases contractile responses to histamine.[12–14] In cultured HASM cells, IL-1β increases IP_3 accumulation and/or the Ca^{2+} transients that occur in response to BK and thrombin[5,14] but decreases IP_3 accumulation induced by histamine.[14] The effect of IL-1β on responses to histamine is abolished by cyclooxygenase-2 (COX-2) inhibitors and mimicked by prostaglandin E_2 (PGE_2), suggesting that this effect is induced by COX-2–generated prostanoids. One potential explanation for these observations is that the increased PGE_2 generated in response to IL-1β causes increased cAMP formation and consequent protein kinase A (PKA) activation, phosphorylating the H_1 receptor and uncoupling it from G_q.[14] A similar mechanism has been postulated to account for the β_2-adrenergic desensitization that occurs in response to IL-1β.[15] In contrast, BK or thrombin receptors may not be subject to phosphorylation by PKA.

Th1 Cytokines

Although interferon-γ (IFN-γ) is generally believed to play an inhibitory role in the induction of allergy, levels of IFN-γ are dramatically increased after viral infections, a common trigger for asthma exacerbations. Even in nonasthmatic subjects, viral infections may induce AHR and cough that can persist for weeks or months. The role of IFN-γ in the AHR induced by viral infections is still uncertain. However, it has recently been reported that IFN-γ augments the ability of LTD_4, an important bronchoconstrictor in asthma, to increase HASM cell stiffness.[16] Cell stiffness, as measured by magnetic twisting cytometry, is a proxy for force generation in these cells. The effect appears to be restricted to LTD_4 since responses to BK are not affected. This is consistent with the observation that IFN-γ augments cysteinyl leukotriene receptor 1 ($CysLT_1$) receptor expression in these cells.

Th2 Cytokines

It is now well established that cytokines derived from Th2 lymphocytes play a critical role in asthma. IL-13 and IL-5, in particular, appear to have an important role in the AHR of asthma. For example, exogenous administration of IL-13 or overexpression of IL-13 in the lungs results in increased airway responsiveness, whereas inhibiting IL-13 activity decreases the AHR observed in animal models of allergic asthma. Similarly, transgenic mice that constitutively express IL-5 in the lung epithelium have hyperresponsive airways, whereas in a mouse model of allergen-induced asthma, AHR was prevented in IL-5-deficient mice in comparison with wild-type mice. In contrast to the inflammatory cytokines IL-1β and TNF-α, there have been few reports on the effects of Th2 cytokines on airway smooth muscle, although it is known that these cells express the receptors for these cytokines and that Th2 cytokines activate JAK/STAT signaling cascades in these cells.[17,18] Moore and colleagues[19] reported that IL-13 augmented the changes in cell stiffness induced by LTD_4, but not BK, in HASM cells, possibly through effects of IL-13 on $CysLT_1$ expression. In contrast, IL-4 has no effect, even though IL-13 and IL-4 use the same receptor, a dimer composed of IL-13Rα1 and IL-4Rα, for signaling in these cells. Similarly, others have reported differences in the patterns of gene expression

induced by these two cytokines in human bronchial smooth muscle cells in culture.[20] The mechanistic basis for these differences remains to be established, but it is possible that when IL-13 is bound, the conformation of the receptor is not the same as when IL-4 is bound, leading to differences in the signal transduction pathways activated by the two cytokines. IL-13 and other Th2 cytokines, including IL-5, IL-10, and granulocyte–macrophage colony-stimulating factor (GM-CSF), have also been reported to increase contractile responses to cholinergic agonists in isolated rabbit airways.[21–24]

EFFECT OF CYTOKINES ON RESPONSES TO DILATOR AGONISTS

In HASM cells, β-agonists exert their effects by binding to the β_2-adrenergic receptor (β_2AR), a seven-transmembrane domain receptor that couples to the stimulatory G protein G_s. Activation of $G_{s\alpha}$ leads to adenylyl cyclase activation, cyclic AMP (cAMP) formation, and consequent PKA activation. The targets of PKA that ultimately induce cell relaxation include K^+ channels, Na^+/K^+-ATPases, Ca^{2+} sequestration, Ca^{2+} sensitivity of myosin, and IP_3 formation. β-Receptors can also activate the mitogen-activated protein (MAP) kinase pathway via a c Src–dependent pathway. Receptor activation leads to G protein–coupled receptor kinase (GRK) phosphorylation of the receptor, consequent β-arrestin binding, and recruitment of c-Src to β-arrestin.[25] The functional significance of this pathway for airway smooth muscle relaxation has not been addressed. β-Agonist–induced activation of PKA also causes phosphorylation of the transcription factor cAMP response element (CRE)-binding protein (CREB). PKA phosphorylation of CREB at serine-133 permits CREB bound to CREs in the regulatory region of genes to interact with CREB-binding protein (CBP) and p300 (Figure 33-1). The latter proteins interact with the basal transcriptional apparatus to initiate gene transcription, as described later in this chapter.

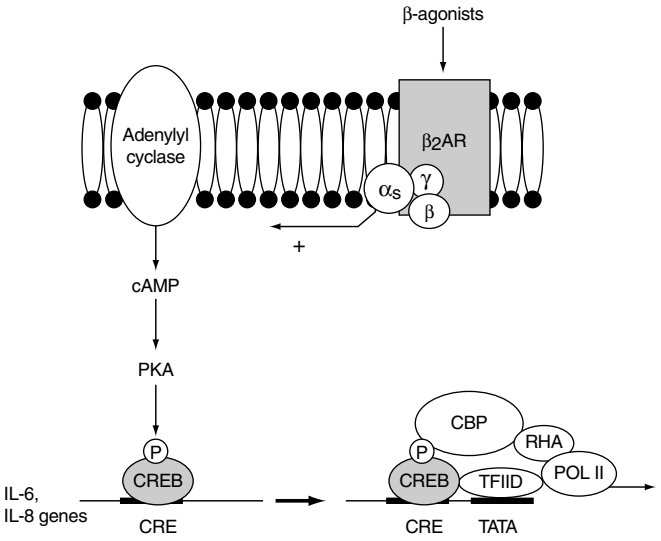

FIGURE 33-1 Mechanism of action of β-agonists on gene expression. Binding of a β-agonist to the β_2-adrenergic receptor (β_2AR) results in activation of adenylyl cyclase through a G_s-coupled mechanism. Adenylyl cyclase causes formation of the second messenger cAMP, which activates protein kinase A (PKA). PKA phosphorylates cAMP response element (CRE)-binding protein (CREB), which results in its binding to CREB-binding protein (CBP). CBP binding leads to recruitment of the basal transcriptional apparatus, resulting in gene transcription. Phosphorylation is indicated by a circled P. POL II = RNA polymerase II; RHA = RNA helicase A; TFIID = a multiprotein transcription factor, which includes TATA-binding protein (TBP) and TBP-associated factor (TAF).

Many cytokines have been reported to attenuate β-agonist–induced changes in HASM cell stiffness, cAMP formation, and relaxation of airways in tissue baths (Table 33-2). Of these, the most potent is IL-1β.

IL-1β

IL-1β causes a marked concentration and time-dependent inhibition of isoproterenol-induced changes in cell stiffness

Table 33-2 Effects of Cytokines on β-Adrenergic Responses of Airway Smooth Muscle

Cytokine	*Species*	*Preparation*	*Effect*
IL-1β	Human	Cultured cells	Attenuates ISO-induced changes in cAMP and cell stiffness through a COX-2–dependent mechanism
	Guinea pig, rabbit	Isolated trachea	Attenuates ISO-induced relaxation through effects on G_i
	Rat	Whole animal	Decreases bronchodilatation via down-regulation of β-receptors, increased G_i expression, and increased expression of G-protein receptor kinases
TNF-α	Human	Cultured cells	No effect alone, but enhances effects of IL-1β via a COX-2–dependent mechanism
	Guinea pig, rabbit	Isolated trachea	Attenuates ISO-induced relaxation through effects on Gi
	Dog	Cultured cells	Attenuates ISO-induced changes in cAMP levels in cultured cells
TGF-β	Human	Cultured cells	Attenuates ISO-induced changes in cAMP levels
IL-13	Human	Cultured cells	Attenuates ISO-induced changes in cAMP levels and cell stiffness through an ERK-dependent mechanism
	Rabbit	Isolated trachea	Attenuates ISO-induced relaxation through an autocrine loop involving IL-5 release
IL-5, IL-10, GM-CSF	Rabbit	Isolated trachea	Attenuate ISO-induced relaxation through autocrine loops leading to IL-1β expression

COX-2 = cyclooxygenase-2; GM-CSF = granulocyte–macrophage colony-stimulating factor; IL-1β = interleukin-1β; ISO = isoproterenol; TGF-β = transforming growth factor-β; TNF-α = tumor necrosis factor-α.

in HASM cells. The effect of IL-1β is dependent on COX-2 expression and mimicked by PGE_2. Similar results have been obtained using cAMP as the indicator of β_2-responsiveness, whereas IL-1β does not affect responses to dibutryl-cAMP, which directly activates PKA, or to forskolin, which directly activates adenylyl cyclase. IL-1β also has no effect on β_2AR or G_s expression in these cells. The results are consistent with the hypothesis that IL-1β–induced COX-2 expression results in increased PGE_2 levels, causing increased basal cAMP levels, and that the resultant increased PKA activity causes a decrease in β-adrenergic responsiveness by phosphorylating the β_2AR, uncoupling it from G_s.[15,26] IL-1β also inhibits isoproterenol-induced relaxation in airway smooth muscle from guinea pigs, rabbits, and dogs,[27–30] although the mechanistic basis for the effect of IL-1β appears to differ from that in humans, probably because of differences in experimental protocol.[31]

The effect of IL-1β on β-adrenergic responsiveness in HASM is abolished by glucocorticoids,[32] an effect that is probably related to the ability of glucocorticoids to inhibit IL-1β–induced COX-2 expression. Cytoplasmic glucocorticoid receptors (GRs) are normally kept inactive by binding to molecular chaperones. When they interact with glucocorticoids, GRs dissociate from these chaperones, uncovering nuclear localization signals and causing nuclear translocation. The GRs then either bind to glucocorticoid response elements (GREs) in the promoter regions of target genes or interact with other transcription factors to impact upon transcription.[33] For example, GRs have been shown to interact with nuclear factor kappa B (NFκB) and activator protein 1 (AP-1) in some cell types and inhibit the activity of these transcription factors.[34] There are no GREs in the COX-2 promoter, suggesting that glucocorticoids must be acting in some other fashion to inhibit COX-2 expression in HASM cells. Because IL-1β causes activation of both NFκB and AP-1 in HASM cells,[32] and because both transcription factors have been demonstrated to be important in COX-2 expression in other cell types, we examined the effect of dexamethasone on the binding of nuclear proteins isolated from IL-1β–stimulated HASM cells to NFκB or AP-1 consensus binding sequences. No effect of the glucocorticoid was observed.[32] Similarly, glucocorticoids do not have any impact on luciferase activity in HASM cells transfected with a luciferase reporter driven by multiple NFκB elements.[35] These results suggest that the ability of glucocorticoids to ablate IL-1β effects on COX-2 and β_2-responsiveness is not at the level of interference with NFκB or AP-1 activation. IL-1β causes only a weak increase in COX-2 promoter activity in HASM cells,[36] even though it can markedly increase levels of COX-2 mRNA,[37] suggesting that the effect of IL-1β may be mediated at the level of COX-2 mRNA stability[38] and that glucocorticoids may act at this level.

Glucocorticoids may also synergize directly with β-agonists. For example, glucocorticoids have been reported to increase β_2AR expression.[39] GR can also interact with other transcription factors, such as CCAAT enhancer binding protein alpha (C/EBPα), and it has been reported that co-stimulation of HASM cells with β-agonists and glucocorticoids leads to simultaneous activation of GR and C/EBPα. Subsequent formation of GR-C/EBPα complexes results in enhanced binding to elements in the promoter of the $p21^{(Waf1/Cip1)}$ gene, which inhibits airway smooth muscle proliferation.[40] Whether or how such complexes affect the expression of other genes that may be important for smooth muscle function remains to be determined.

The impact of IL-1β on β-adrenergic responsiveness is also observed in vivo in rats and is also reversed by glucocorticoid therapy.[41] In the rat, the effect of IL-1β appears to occur through multiple mechanisms, including down-regulation of β-receptors, increased G_i expression, and increased expression of GRKs, which are involved in receptor desensitization. Glucocorticoids do not alter the effects of IL-1β on β-receptor expression or G_i expression but do prevent the increases in GRK that are induced by IL-1β.

TNF-α

In contrast to the very potent effects of IL-1β, TNF-α has little effect on β-adrenergic responsiveness in HASM cells,[36,42] probably because TNF-α does not induce COX-2 expression in these cells. However, TNF-α is able to very markedly potentiate the effects of IL-1β: IL-1β, at a concentration that is ineffective on its own, causes marked suppression of isoproterenol-induced changes in cell stiffness if the same concentration of IL-1β is administered with an equally low concentration of TNF-α.[36] COX-2 inhibitors abolish the effects of combined treatment with IL-1β and TNF-α, suggesting that COX-2–induced prostanoids mediate these effects. Moreover, the same concentrations of IL-1β and TNF-α also synergize in the induction of COX-2 expression and PGE_2 release, through effects on COX-2 promoter activity. The results suggest that even very small amounts of IL-1β can interfere with β-adrenergic signaling in airway smooth muscle if the cytokine is released in conjunction with TNF-α.

Th1 and Th2 Cytokines

There are no studies on the effects of the Th1 cytokine IFN-γ on β-adrenergic responsiveness in human airway smooth muscle. However, in isolated guinea pig and rabbit airways studied in vitro, IFN-γ appears to augment rather than attenuate responses to isoproterenol.[22,43] In contrast, Th2 cytokines do appear to alter β-adrenergic relaxation of airway smooth muscle. For example, IL-13 attenuates isoproterenol-induced changes in cell stiffness and isoproterenol-induced cAMP formation in HASM cells, although the effect of IL-13 is not as marked as that observed with IL-1β.[18] The effect of IL-13 is likely to be at the level of β_2AR-G_s interaction since IL-13 has no effect on responses to direct stimulation of adenylyl cyclase with forskolin. IL-13 activates extracellular signal regulated kinase (ERK) in HASM cells,[17,18] and inhibition of ERK with U0126 restores the ability of isoproterenol to decrease cell stiffness in IL-13–treated cells.[18] Taken together, the results suggest that IL-13 exerts its effects on β-adrenergic responsiveness through an ERK-dependent pathway. In contrast, IL-4 has no effect. Th2 cytokines also have an effect on β-adrenergic responsiveness in airway smooth muscle from other species.[21–24] To date, there have been no studies on

the effects of glucocorticoids on changes in β-adrenergic responsiveness that are mediated by Th2 cytokines.

EFFECTS OF CYTOKINES ON EXPRESSION OF CYTOKINES, CHEMOKINES, AND GROWTH FACTORS

It is increasingly apparent that the function of airway smooth muscle is not limited to contraction and relaxation. Instead, a growing body of evidence indicates that airway smooth muscle participates in initiating and perpetuating airway inflammation through its capacity to release chemokines that recruit neutrophils, eosinophils, and mononuclear cells and through its capacity to release cytokines that are potent in activating these cells. Airway tissue from asthmatic subjects is difficult to obtain, and airway biopsy specimens usually do not contain smooth muscle. Consequently, most of the data regarding the ability of airway smooth muscle to generate cytokines, chemokines, and growth factors have come from studies in which smooth muscle cells in culture have been used. In many cases, cytokine release is at least partially regulated by the MAP kinase pathway.

IL-1β AND TNF-α

Multiple cytokines and chemokines are induced in HASM cells following stimulation with IL-1β and TNF-β (Table 33-3). It is of interest that IL-1β stimulates its own synthesis,[44,45] an event that is partially attenuated by inhibiting the ERK MAP kinase pathway. Given the prominent ability of this cytokine to induce the synthesis of a large spectrum of other cytokines, these results suggest a key role for IL-1β in a positive feedback loop promoting airway inflammation, an amplification cascade with the smooth muscle cell at its center.

IL-1β and TNF-α each induce the expression by HASM cells of a number of cytokines and chemokines that promote the recruitment, activation, and/or survival of eosinophils. These include eotaxin, RANTES, and GM-CSF.[46–51] In chemotaxis assays, supernatants from HASM cells stimulated with IL-1β or TNF-α have been demonstrated to express chemotactic activity for human eosinophils that is blocked by antibodies against eotaxin or RANTES.[48] The expression of eotaxin by these cells is notable even without cytokine stimulation and has been confirmed by immunostaining for eotaxin in sections from asthmatic airways.[48] The expression of eotaxin, RANTES, and GM-CSF occurs at both the message and protein levels and for each cytokine is very strongly inhibited by blocking either the ERK or p38 MAP kinase pathways.[46,47] RANTES promoter–reporter constructs also indicate an important role for AP-1 in the transcriptional regulation of RANTES by TNF-α,[49] and it is possible that the role of ERK in the induction of RANTES[46] is through phosphorylation of Elk-1, a transcription factor that leads to the induction of c-fos, one of the components of AP-1.

IL-1β and/or TNF-α also induce the expression of IL-8, a potent neutrophil chemoattractant and activator, in HASM cells. Although the presence of eosinophils in the airways of asthmatic subjects is perhaps better appreciated during acute exacerbations of the disease, increased numbers of neutrophils are also observed in status asthmaticus and in patients who die suddenly of asthma. Mice

Table 33-3 Cytokine and Growth Factor Expression in Human Airway Smooth Muscle Cells

Cytokine/growth factor	*Stimuli that induce expression*	*Effect of β-agonists*	*Effect of glucocorticoids*
Eotaxin	IL-1β, TNF-α, IL-4, IL-13	Inhibit release	Inhibit release
GM-CSF	IL-1β, TNF-α, atopic asthmatic serum	Inhibit release, particularly in the presence of indomethacin	Inhibit release
IL-1β	IL-1β, TNF-α, rhinovirus, IL-5	NA	Inhibit release
IL-5	IL-13, IL-10, atopic asthmatic serum, rhinovirus	NA	NA
IL-6	IL-1β, TNF-α, PGE_2, TGF-β	Increase release	Little effect
IL-8	IL-1β, TNF-α, PGE_2, TGF-β, bradykinin	Increase release on their own but have no effect on IL-1β–induced and TNF-α–induced release	Inhibit release
IL-10	Atopic asthmatic serum	NA	NA
IL-11	IL-1β, TGF-β, respiratory syncytial virus and parainfluenza virus	NA	NA
IL-13	Atopic asthmatic serum	NA	NA
LIF	IL-1β, IL-6, TGF-β	NA	NA
MCP-1, MCP-2, MCP-3	IL-1β, TNF-α, IFN-γ	NA	Inhibit release
NGF	IL-1β	NA	NA
RANTES	IL-1β, TNF-α, PAF	Inhibit release, particularly in the presence of indomethacin	Inhibit release
TGF-β	Angiotensin-II	NA	NA
VEGF	Bradykinin	NA	NA

GM-CSF = granulocyte–macrophage colony-stimulating factor; IL-1β = interleukin-1β; LIF = leukemia inhibitory factor; MCP = monocyte chemoattractant protein; NA = data not available; PAF = platelet-activating factor; PGE_2 = prostaglandin E_2; RANTES = regulated on activation normal T cells expressed and secreted; TGF-β = transforming growth factor-β; TNF-α = tumor necrosis factor-α; VEGF = vascular endothelial growth factor.

genetically deficient in the IL-8 receptor have fewer neutrophils in their airway lavage fluid upon sensitization and challenge with allergen than do wild-type control mice,[52] suggesting that IL-8 participates in recruitment of neutrophils during asthmatic attacks. Recent work in which IL-8 promoter–reporter constructs mutated at the putative NFκB-binding sites were used indicates that this transcription factor is important in the transcriptional regulation of IL-8 by TNF-α in HASM cells,[53] and we have observed similar effects with IL-1β–induced IL-8 expression (unpublished observations). IL-8 expression by IL-1β and/or TNF-α is also partially inhibited by blocking either the ERK or p38 MAP kinase pathways.[44,54] It is possible that the role of ERK or p38 in these events is at the level of NFκB activation since binding of nuclear extracts from IL-1β–stimulated HASM cells to NFκB consensus sequences is partially attenuated by inhibitors of the ERK or p38 pathways.[55]

IL-1β and/or TNF-α also lead to the expression of members of the IL-6 family of cytokines, including IL-6, IL-11, and leukemia inhibitory factor (LIF), but not oncostatin M.[49,56–59] TNF-α–induced IL-6 gene expression occurs via an NFκB-dependent pathway.[49] IL-6 and IL-11 are also induced by viruses.[56] It is not clear whether the effect of IL-1β on LIF release is a direct one or involves autocrine effects since IL-6, which is potently released by IL-1β, also induces the release of LIF.[59] The release of LIF and IL-6 by airway smooth muscle may have important functional consequences since LIF and IL-6 receptors are also expressed by these cells.[58,59] Furthermore, in guinea pig airways, LIF augments the capsaicin-induced release of endogenous tachykinins, as well as contractile responses to tachykinins.[60] IL-6 also causes STAT-3 and ERK phosphorylation in HASM cells and increases IL-1β–induced PGE_2 formation without altering COX-2 expression, suggesting that IL-6 may activate phospholipase A_2.[58]

Th1 Cytokines

There are limited data regarding the effects of IFN-γ on airway smooth muscle.[1] In general, this cytokine has been administered along with IL-1β and TNF-α, and it is often not possible to assess its separate contribution. However, IFN-γ has been shown to potentiate release of RANTES but not IL-8 induced by TNF-α without inducing any effect by itself.[50,61]

Th2 Cytokines

IL-4 and IL-13 do not induce either RANTES or IL-8 production in HASM cells, but both cytokines inhibit the release of RANTES and IL-8 induced by IL-1β.[50,61] In contrast, IL-13 and IL-4 enhance TNF-α–induced IL-8 release in a concentration-related fashion (unpublished observations), suggesting that the effect of these cytokines depends on the context in which they are administered. Furthermore, the effects of these two cytokines are not always the same. For example, IL-4 inhibits IL-1β–induced monocyte chemoattractant protein-1 (MCP-1) and MCP-2 expression, but IL-13 does not,[62] although it is possible that the latter is the result of differences in efficacy since IL-4 is about 10 times more potent in inducing eotaxin release than IL-13.[17,47] The effects of IL-4 and IL-13 on eotaxin expression are markedly enhanced by coadministration of IL-1β and TNF-α and are attenuated by inhibitors of the ERK MAP kinase pathway,[17,47] consistent with the ability of IL-4 and IL-13 to activate ERK.[18]

Effect of β-Agonists

In addition to relaxing HASM cells, β-agonist stimulation of airway smooth muscle induces changes in the transcription of several genes, including many of the cytokines and chemokines discussed above. These effects are summarized in Table 33-3. Note that some cytokines are induced by β-agonists, whereas release of other cytokines is inhibited.

β-Agonist Inhibition of Gene Expression The mechanistic basis for the ability of β-agonists to inhibit gene expression in airway smooth muscle is largely unexplored, despite the potential importance of these effects in β-agonist therapy for asthma. However, for most of the genes whose expression in airway smooth muscle is attenuated by β-agonists, expression is modified only if the cells are first activated, for example, by IL-1β or TNF-α. The induced expression of many of these genes is dependent on NFκB activation. In a monocytic cell line, β-agonists reduced NFκB activation via effects on IκB expression.[63] However, in HASM cells, agents that increase cAMP levels, such as β-agonists, do not alter the NFκB DNA-binding activity induced by TNF-α.[57] Another way in which β-agonists may inhibit the expression of NFκB-dependent genes is by activation of CREB. CREB and NFκB both require interaction with CBP for gene transcription, and there may be competition between these transcription factors for limiting amounts of CBP, resulting in their mutual repression[64] (Figure 33-2). Consistent with this hypothesis, TNF-α inhibits the ability of β-agonists to induce CRE-mediated gene expression in HASM cells without altered β-agonist–induced CREB phosphorylation.[65]

IL-1β appears to inhibit the ability of β-agonists to negatively regulate gene expression in HASM cells by a COX-2–dependent mechanism. For example, the β-agonist fenoterol has no effect on IL-1β–induced GM-CSF release. When COX-2 inhibitors are introduced prior to IL-1β stimulation, fenoterol causes a robust inhibition of GM-CSF release.[66] Very similar results are obtained with RANTES: induction of RANTES release stimulated by a mixture of cytokines, including IL-1β, is inhibited by fenoterol only in the presence of COX-2 inhibitors.[67] However, β-agonists do inhibit RANTES release from HASM cells stimulated with TNF-α rather than IL-1β, even in the absence of COX-2 inhibitors.[49,57] These data are consistent with the lack of effect of TNF-α on β_2AR responsiveness.[36]

β-Agonist-Induced Gene Expression It is likely that β-agonists induce gene expression through PKA-mediated CREB phosphorylation and activation of CRE elements in these genes (see Figure 33-1). For example, in HASM cells expression of both IL-6 and IL-8 is increased by β-agonists

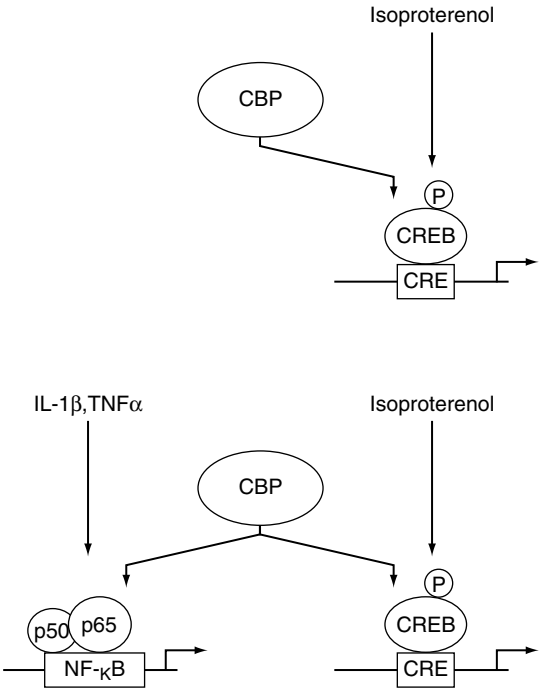

FIGURE 33-2 Potential mechanism by which activation of cytokines, such as IL-1β or TNF-α, and concurrent activation of β_2ARs by β-agonists, such as isoproterenol, lead to mutual repression of gene expression. Nuclear factor kappa B and cAMP response element-binding protein (CREB) compete for limiting amounts of CREB-binding protein (CBP). CRE = cAMP response element p50 and p65, nuclear factor kappa B subunits; NFκB = nuclear factor kappa B-binding sites on genes.

and other agents that increase cAMP levels. Both of these genes contain CRE elements in their promoter regions. Furthermore, β-agonist–induced IL-6 promoter activity is ablated in an IL-6 promoter–reporter construct that lacks a CRE element.[49]

IL-1β suppresses isoproterenol-induced IL-6 promoter activity, an event that occurs via both COX-2–dependent and COX-2–independent effects.[65] The latter are possibly the result of competition by IL-1β–induced NFκB with CREB for limiting amounts of CBP, as described above (see Figure 33-2). Similarly, β-agonists are unable to induce IL-8 expression in IL-1β–pretreated cells.[68] There are no data regarding the effects of Th1 or Th2 cytokines on the ability of β-agonists to induce gene expression.

Effect of Glucocorticoids

The induction by IL-1β and TNF-α of a variety of cytokines and chemokines, including eotaxin, RANTES, IL-8, MCP-1, MCP-2, MCP-3, and GM-CSF, is inhibited by dexamethasone (see Table 33-3). As discussed above, the transcription factor NFκB is required for the induced expression of many of these cytokines, but dexamethasone does not appear to interfere with binding of IL-1β–induced or TNF-α–induced NFκB to DNA, at least in HASM cells.[32,35] Furthermore, dexamethasone has very little effect on TNF-α–induced IL-6 expression, even though transcription of the IL-6 gene is dependent on NFκB.[49] GRs have the capacity to interact with many other transcription factors, including AP-1, C/EBPβ, and Myc, as well as CBP,[33,40,69] and interactions with these factors may be important for the effects of dexamethasone on cytokine and chemokine expression. Alternatively, glucocorticoids may induce moieties that interact with these genes in their 3′-untranslated regions, leading to changes in mRNA stability.

SUMMARY AND CONCLUSIONS

In summary, it is increasingly apparent that airway smooth muscle cells express receptors for cytokines and that these cytokines can induce marked changes in the phenotype of the cell, including alterations in contractility, responsiveness to β-agonists, and expression of cytokines, chemokines, and growth factors. It is likely that these changes contribute to the AHR observed in asthma. It is also apparent that the airway smooth muscle is at the center of a dynamic asthmatic response. It has been appreciated for many years that the smooth muscle cell contributes importantly to the airway narrowing of asthma, but only recently has it been established that this cell also participates in initiating and amplifying the airway inflammation of asthma.

ACKNOWLEDGMENT

This work was supported by the United States National Heart, Lung, and Blood Institute grants HL67664 and HL33009 and the United States National Institute for Environmental Health and Safety grant ES00002.

REFERENCES

1. Chung KF. Airway smooth muscle cells: contributing to and regulating airway mucosal inflammation? Eur Respir J 2000;15:961–8.
2. Panettieri RA Jr. Airway smooth muscle: an immunomodulatory cell. J Allergy Clin Immunol 2002;110:S269–74.
3. Hirst SJ, Walker TR, Chilvers ER. Phenotypic diversity and molecular mechanisms of airway smooth muscle proliferation in asthma. Eur Respir J 2000;16:159–77.
4. Amrani Y, Martinet N, Bronner C. Potentiation by tumour necrosis factor-alpha of calcium signals induced by bradykinin and carbachol in human tracheal smooth muscle cells. Br J Pharmacol 1995;114:4–5.
5. Amrani Y, Krymskaya V, Maki C, Panettieri RA Jr. Mechanisms underlying TNF-alpha effects on agonist-mediated calcium homeostasis in human airway smooth muscle cells. Am J Physiol 1997;273:L1020–8.
6. Amrani Y, Panettieri RA Jr, Frossard N, Bronner C. Activation of the TNF alpha-p55 receptor induces myocyte proliferation and modulates agonist-evoked calcium transients in cultured human tracheal smooth muscle cells. Am J Respir Cell Mol Biol 1996;15:55–63.
7. Hotta K, Emala CW, Hirshman CA. TNF-alpha upregulates Gialpha and Gqalpha protein expression and function in human airway smooth muscle cells. Am J Physiol 1999;276:L405–11.
8. Nakatani Y, Nishimura Y, Nishiuma T, et al. Tumor necrosis factor-alpha augments contraction and cytosolic Ca(2+) sensitivity through phospholipase A(2) in bovine tracheal smooth muscle. Eur J Pharmacol 2000;392:175–82.
9. Parris JR, Cobban HJ, Littlejohn AF, et al. Tumour necrosis factor-alpha activates a calcium sensitization pathway in

guinea-pig bronchial smooth muscle. J Physiol 1999;518: 561–9.
10. Amrani Y, Panettieri RA Jr. Cytokines induce airway smooth muscle cell hyperresponsiveness to contractile agonists. Thorax 1998;53:713–6.
11. Amrani Y, Chen H, Panettieri RA Jr. Activation of tumor necrosis factor receptor 1 in airway smooth muscle: a potential pathway that modulates bronchial hyper-responsiveness in asthma? Respir Res 2000;1:49–53.
12. Sukkar MB, Hughes JM, Armour CL, Johnson PR. Tumour necrosis factor-alpha potentiates contraction of human bronchus in vitro. Respirology 2001;6:199–203.
13. Barchasz E, Naline E, Molimard M, et al. Interleukin-1beta-induced hyperresponsiveness to [Sar9,Met(O2)11]substance P in isolated human bronchi. Eur J Pharmacol 1999; 379:87–95.
14. Pype JL, Xu H, Schuermans M, et al. Mechanisms of interleukin 1beta-induced human airway smooth muscle hyporesponsiveness to histamine. Involvement of p38 MAPK NF-kappaB. Am J Respir Crit Care Med 2001;163:1010–7.
15. Shore SA, Laporte J, Hall IP, et al. Effect of IL-1 beta on responses of cultured human airway smooth muscle cells to bronchodilator agonists. Am J Respir Cell Mol Biol 1997;16: 702–12.
16. Amrani Y, Moore PE, Hoffman R, et al. Interferon-gamma modulates cysteinyl leukotriene receptor-1 expression and function in human airway myocytes. Am J Respir Crit Care Med 2001;164:2098–101.
17. Hirst SJ, Hallsworth MP, Peng Q, Lee TH. Selective induction of eotaxin release by interleukin-13 or interleukin-4 in human airway smooth muscle cells is synergistic with interleukin-1beta and is mediated by the interleukin-4 receptor alpha-chain. Am J Respir Crit Care Med 2002;165: 1161–71.
18. Laporte JC, Moore PE, Baraldo S, et al. Direct effects of interleukin-13 on signaling pathways for physiological responses in cultured human airway smooth muscle cells. Am J Respir Crit Care Med 2001;164:141–8.
19. Moore PE, Calder M, Amrani Y, et al. Effect of Th2 cytokines on human airway smooth muscle responses to LTD4. Am J Respir Crit Care Med 2002;165:A116.
20. Lee JH, Kaminski N, Dolganov G, et al. Interleukin-13 induces dramatically different transcriptional programs in three human airway cell types. Am J Respir Cell Mol Biol 2001; 25:474–85.
21. Grunstein MM, Hakonarson H, Leiter J, et al. IL-13-dependent autocrine signaling mediates altered responsiveness of IgE-sensitized airway smooth muscle. Am J Physiol Lung Cell Mol Physiol 2002;282:L520–8.
22. Hakonarson H, Maskeri N, Carter C, Grunstein MM. Regulation of TH1- and TH2-type cytokine expression and action in atopic asthmatic sensitized airway smooth muscle. J Clin Invest 1999;103:1077–87.
23. Grunstein MM, Hakonarson H, Leiter J, et al. Autocrine signaling by IL-10 mediates altered responsiveness of atopic sensitized airway smooth muscle. Am J Physiol Lung Cell Mol Physiol 2001;281:L1130–7.
24. Hakonarson H, Maskeri N, Carter C, et al. Autocrine interaction between IL-5 and IL-1beta mediates altered responsiveness of atopic asthmatic sensitized airway smooth muscle. J Clin Invest 1999;104:657–67.
25. Cao W, Luttrell LM, Medvedev AV, et al. Direct binding of activated c-Src to the beta 3-adrenergic receptor is required for MAP kinase activation. J Biol Chem 2000;275: 38131–4.
26. Laporte JD, Moore PE, Panettieri RA, et al. Prostanoids mediate IL-1beta-induced beta-adrenergic hyporesponsiveness in human airway smooth muscle cells. Am J Physiol 1998; 275:L491–501.
27. Wills-Karp M, Uchida Y, Lee JY, et al. Organ culture with proinflammatory cytokines reproduces impairment of the beta-adrenoceptor-mediated relaxation in tracheas of a guinea pig antigen model. Am J Respir Cell Mol Biol 1993; 8:153–9.
28. Hakonarson H, Herrick DJ, Serrano PG, Grunstein MM. Mechanism of cytokine-induced modulation of beta-adrenoceptor responsiveness in airway smooth muscle. J Clin Invest 1996;97:2593–600.
29. Koto H, Mak JC, Haddad EB, et al. Mechanisms of impaired beta-adrenoceptor-induced airway relaxation by interleukin-1beta in vivo in the rat. J Clin Invest 1996;98:1780–7.
30. Emala CW, Kuhl J, Hungerford CL, Hirshman CA. TNF-alpha inhibits isoproterenol-stimulated adenylyl cyclase activity in cultured airway smooth muscle cells. Am J Physiol 1997;272:L644–50.
31. Shore SA, Moore PE. Effects of cytokines on contractile and dilator responses of airway smooth muscle. Clin Exp Pharmacol Physiol 2002;29:859–66.
32. Moore PE, Laporte JD, Gonzalez S, et al. Glucocorticoids ablate IL-1beta-induced beta-adrenergic hyporesponsiveness in human airway smooth muscle cells. Am J Physiol 1999;277:L932–42.
33. Adcock IM, Maneechotesuwan K, Usmani O. Molecular interactions between glucocorticoids and long-acting beta2-agonists. J Allergy Clin Immunol 2002;110:S261–8.
34. Adcock IM, Ito K. Molecular mechanisms of corticosteroid actions. Monaldi Arch Chest Dis 2000;55:256–66.
35. Amrani Y, Lazaar AL, Panettieri RA Jr. Up-regulation of ICAM-1 by cytokines in human tracheal smooth muscle cells involves an NF-kappa B-dependent signaling pathway that is only partially sensitive to dexamethasone. J Immunol 1999;163:2128–34.
36. Moore PE, Lahiri T, Laporte JD, et al. Synergism between TNF-alpha and IL-1beta in airway smooth muscle cells: implications for beta-adrenergic responsiveness. J Appl Physiol 2001;91:1467–74.
37. Belvisi MG, Saunders MA, el Haddad B, et al. Induction of cyclo-oxygenase-2 by cytokines in human cultured airway smooth muscle cells: novel inflammatory role of this cell type. Br J Pharmacol 1997;120:910–6.
38. Tamura M, Sebastian S, Yang S, et al. Interleukin-1beta elevates cyclooxygenase-2 protein level and enzyme activity via increasing its mRNA stability in human endometrial stromal cells: an effect mediated by extracellularly regulated kinases 1 and 2. J Clin Endocrinol Metab 2002;87:3263–73.
39. Mak JC, Nishikawa M, Barnes PJ. Glucocorticosteroids increase beta 2-adrenergic receptor transcription in human lung. Am J Physiol 1995;268:L41–6.
40. Roth M, Johnson PR, Rudiger JJ, et al. Interaction between glucocorticoids and beta2 agonists on bronchial airway smooth muscle cells through synchronised cellular signalling. Lancet 2002;360:1293–9.
41. Mak JC, Hisada T, Salmon M, et al. Glucocorticoids reverse IL-1beta-induced impairment of beta-adrenoceptor-mediated relaxation and up-regulation of G-protein-coupled receptor kinases. Br J Pharmacol 2002;135:987–96.
42. Pang L, Holland E, Knox AJ. Role of cyclo-oxygenase-2 induction in interleukin-1beta induced attenuation of cultured human airway smooth muscle cell cyclic AMP generation in response to isoprenaline. Br J Pharmacol 1998;125:1320–8.
43. Chen H, Munakata M, Amishima M, et al. Gamma-interferon modifies guinea pig airway functions in vitro. Eur Respir J 1994;7:74–80.

44. Hedges JC, Singer CA, Gerthoffer WT. Mitogen-activated protein kinases regulate cytokine gene expression in human airway myocytes. Am J Respir Cell Mol Biol 2000;23:86–94.
45. Hakonarson H, Halapi E, Whelan R, et al. Association between IL-1beta/TNF-alpha-induced glucocorticoid-sensitive changes in multiple gene expression and altered responsiveness in airway smooth muscle. Am J Respir Cell Mol Biol 2001;25:761–71.
46. Hallsworth MP, Moir LM, Lai D, Hirst SJ. Inhibitors of mitogen-activated protein kinases differentially regulate eosinophil-activating cytokine release from human airway smooth muscle. Am J Respir Crit Care Med 2001;164:688–97.
47. Moore PE, Church TL, Chism DD, et al. IL-13 and IL-4 cause eotaxin release in human airway smooth muscle cells: a role for ERK. Am J Physiol Lung Cell Mol Physiol 2002; 282:L847–53.
48. Ghaffar O, Hamid Q, Renzi PM, et al. Constitutive and cytokine-stimulated expression of eotaxin by human airway smooth muscle cells. Am J Respir Crit Care Med 1999; 159:1933–42.
49. Ammit AJ, Lazaar AL, Irani C, et al. Tumor necrosis factor-alpha-induced secretion of RANTES and interleukin-6 from human airway smooth muscle cells: modulation by glucocorticoids and beta-agonists. Am J Respir Cell Mol Biol 2002;26:465–74.
50. John M, Hirst SJ, Jose PJ, et al. Human airway smooth muscle cells express and release RANTES in response to T helper 1 cytokines: regulation by T helper 2 cytokines and corticosteroids. J Immunol 1997;158:1841–7.
51. Saunders MA, Mitchell JA, Seldon PM, et al. Release of granulocyte–macrophage colony stimulating factor by human cultured airway smooth muscle cells: suppression by dexamethasone. Br J Pharmacol 1997;120:545–6.
52. De Sanctis GT, MacLean JA, Qin S, et al. Interleukin-8 receptor modulates IgE production and B-cell expansion and trafficking in allergen-induced pulmonary inflammation. J Clin Invest 1999;103:507–15.
53. Zhu YM, Sowter D, Knox AJ. The mechanism of IL-8 induction by TNFalpha in HASMC. Am J Respir Crit Care Med 2002; 165:A619.
54. Baraldo S, Faffe DS, Moore PE, et al. Interleukin 9 influences chemokine release in airway smooth muscle: role of ERK. Am J Physiol Lung Cell Mol Physiol 2003;284:L1093–102.
55. Laporte JD, Moore PE, Lahiri T, et al. p38 MAP kinase regulates IL-1 beta responses in cultured airway smooth muscle cells. Am J Physiol Lung Cell Mol Physiol 2000;279:L932–41.
56. Elias JA, Wu Y, Zheng T, Panettieri R. Cytokine- and virus-stimulated airway smooth muscle cells produce IL-11 and other IL-6-type cytokines. Am J Physiol 1997;273:L648–55.
57. Ammit AJ, Hoffman RK, Amrani Y, et al. Tumor necrosis factor-alpha-induced secretion of RANTES and interleukin-6 from human airway smooth-muscle cells. Modulation by cyclic adenosine monophosphate. Am J Respir Cell Mol Biol 2000;23:794–802.
58. Lahiri T, Laporte JD, Moore PE, et al. Interleukin-6 family cytokines: signaling and effects in human airway smooth muscle cells. Am J Physiol Lung Cell Mol Physiol 2001;280: L1225–32.
59. Knight DA, Lydell CP, Zhou D, et al. Leukemia inhibitory factor (LIF) and LIF receptor in human lung. Distribution and regulation of LIF release. Am J Respir Cell Mol Biol 1999;20: 834–41.
60. Knight D, McKay K, Wiggs B, et al. Localization of leukaemia inhibitory factor to airway epithelium and its amplification of contractile responses to tachykinins. Br J Pharmacol 1997; 120:883–91.
61. John M, Au BT, Jose PJ, et al. Expression and release of interleukin-8 by human airway smooth muscle cells: inhibition by Th-2 cytokines and corticosteroids. Am J Respir Cell Mol Biol 1998;18:84–90.
62. Pype JL, Dupont LJ, Menten P, et al. Expression of monocyte chemotactic protein (MCP)-1, MCP-2, and MCP-3 by human airway smooth-muscle cells. Modulation by corticosteroids and T-helper 2 cytokines. Am J Respir Cell Mol Biol 1999;21: 528–36.
63. Farmer P, Pugin J. Beta-adrenergic agonists exert their "anti-inflammatory" effects in monocytic cells through the IkappaB/NF-kappaB pathway. Am J Physiol Lung Cell Mol Physiol 2000;279:L675–82.
64. Sheppard KA, Phelps KM, Williams AJ, et al. Nuclear integration of glucocorticoid receptor and nuclear factor-kappaB signaling by CREB-binding protein and steroid receptor coactivator-1. J Biol Chem 1998;273:29291–4.
65. Lahiri T, Moore PE, Baraldo S, et al. Effect of IL-1beta on CRE-dependent gene expression in human airway smooth muscle cells. Am J Physiol Lung Cell Mol Physiol 2002;283: L1239–46.
66. Lazzeri N, Belvisi MG, Patel HJ, et al. Effects of prostaglandin E2 and cAMP elevating drugs on GM-CSF release by cultured human airway smooth muscle cells. Relevance to asthma therapy. Am J Respir Cell Mol Biol 2001;24:44–8.
67. Lazzeri N, Belvisi MG, Patel HJ, et al. RANTES release by human airway smooth muscle: effects of prostaglandin E(2) and fenoterol. Eur J Pharmacol 2001;433:231–5.
68. Hallsworth MP, Twort CH, Lee TH, Hirst SJ. Beta(2)-adrenoceptor agonists inhibit release of eosinophil-activating cytokines from human airway smooth muscle cells. Br J Pharmacol 2001;132:729–41.
69. Tseng YT, Wadhawan R, Stabila JP, et al. Molecular interactions between glucocorticoid and catecholamine signaling pathways. J Allergy Clin Immunol 2002;110:S247–54.

CHAPTER 34

IMMUNOGLOBULINS AND THE LUNG

Salem al-Tamemi, Bruce Mazer

The airways consist of a series of organs lined by a mucosa that is exposed to the outside world. The function of exchanging air many times a minute continuously opens the nose, nasopharynx, sinuses, and, ultimately, the lungs to the external environment. As a consequence, the lung and upper airway must be equipped to cope with repeated invasion of its territory by a wide variety of potential pathogenic substances, including bacteria, viruses, fungi, toxins, and pollens, as well as large amounts of particulate matter. The consequences of infiltration by organisms, foreign proteins, or organic material can range from inert deposition into the lungs and subsequent clearance to infection and initiation of an inflammatory response. In order for their integrity to be maintained, the lungs are protected by a sophisticated system of defenses, which includes both innate and adaptive immunity. Examples of innate defenses include mucus, cilia, dendritic cells, macrophages, and other phagocytic cells. The adaptive immune system includes B and T lymphocytes, cells that are crucial for the production of immunoglobulins. In this chapter we review the role of the humoral immune system in pulmonary defenses and inflammatory reactions. We discuss antibody production, and the cells and molecules responsible for production of immunoglobulins. We also develop the concept of local versus systemic immunoglobulin production and review the consequences for the airways of deficiencies in antibody production.

STRUCTURE OF ANTIBODIES

Antibodies are composed of proteins known as immunoglobulins. These complex proteins are secreted in large quantities by differentiated B lymphocytes in response to antigen stimulation. Immunoglobulins are composed of four chains, two heavy and two light chains (Figure 34-1), both bound together by disulfide bonds. There are two light chains, known as κ-chains and λ-chains; only one light chain will associate with a heavy chain at any one time, and each B-cell clone will only express one of the light chains.[1] The two light chains and the proximal portions of the two heavy chains form the variable region, or the antigen-binding site, of the immunoglobulin molecule. This is the area of the molecule that interacts with the myriad of antigens that exist; it is postulated that there are at least 10^9 possible antigen-binding sites coded for by antibodies.[1] In contrast to T-cell receptors, antibodies recognize three-dimensional structures and not simply peptide fragments. Thus, antigens that are recognized by the variable region of the immunoglobulin molecule can consist of proteins, polysaccharides, or complex glycoproteins, again different from the situation with T cells. The antigen-binding site is important for antigen recognition and neutralization, a key action in the first line of defense. The efficacy of vaccines is based on the ability of primed or memory B lymphocytes to rapidly produce large amounts of circulating antibodies in order to trap and initiate the elimination of a foreign protein.

The distal portions of the heavy chains form the constant region or the effector region (see Figure 34-1). This part of the molecule is involved in two other functions of antibodies, namely opsonization and complement fixation. The constant region, which differs with the specific isotype of the molecule, acts as a stabilization site for the interaction of immunoglobulin molecules, which function as multimers, or can interact with specific receptors on the surface of phagocytic cells and other cells in the host defense system (Figure 34-2). There are five isotypes of immunoglobulin, classified according to differences in the constant regions of the heavy chains: IgG, IgM, IgA, IgE, and IgD. IgG is the most abundant form found in the serum and has four subclasses (IgG_1 to IgG_4, named for their relative abundance in the serum). IgG circulates as single molecules, whereas IgA functions as a dimer and IgM circulates as a pentamer.

PRODUCTION OF IMMUNOGLOBULINS

B lymphocytes develop from a common multipotent precursor stem cell population that originates in the paraaortic

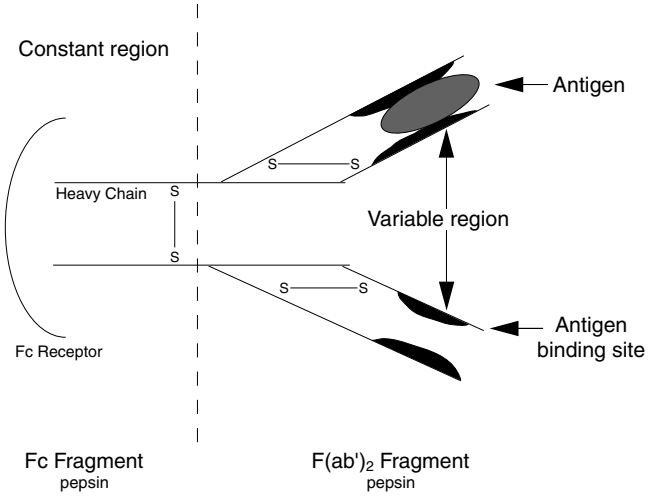

FIGURE 34-1 Basic structure of an immunoglobulin molecule.

splanchnopleural region of the embryo. The primary sites where B cells differentiate from precursors are the bone marrow and the fetal liver. Postnatally, the bone marrow then becomes the major site of B-cell maturation. This phase of B-cell growth is independent of antigens but is influenced by the rich cytokine milieu in the bone marrow. After the initial stages of maturation, B cells travel to secondary lymphoid organs, including lymph nodes, spleen, Peyer's patches in the gastrointestinal tract, and bronchus-associated lymphoid tissue (BALT).[2]

Primary or naive B lymphocytes can produce antibodies of the IgM isotype. Antigen may induce maturation of B cells in two ways, known as T-cell–independent and T-cell–dependent humoral responses. Polysaccharide antigens can be recognized directly by surface immunoglobulin receptors on the B cell; this activates B cells and can drive synthesis of antibodies of the IgM and IgG isotypes. T-cell–independent humoral responses produce low-affinity antibodies and facilitate memory B-cell development inadequately. In the T-cell–dependent humoral response, B cells use T-cell help to produce antibodies against protein antigens, as well as memory B lymphocytes. B lymphocytes and activated $CD4^+$ T cells are bridged by co-stimulatory molecules such as CD40 and B7 on B cells and CD40 ligand (CD40L) and CD28 on activated cells (Figure 34-3). These obligatory contacts initiate the genetic switching from the IgM isotype to more specialized immunoglobulins. In addition, activated $CD4^+$ T cells produce cytokines, which dictate which immunoglobulin isotype will be synthesized. This is elaborated upon below. In general, immunoglobulins produced by T-cell–dependent mechanisms are of higher affinity and engender the production of long-lasting memory B cells.[3]

Circulating IgG is extremely efficient at neutralizing pathogens and coating them with antibody to facilitate their uptake by phagocytic cells, a process known as opsonization (see Figure 34-2). When IgG molecules encounter specific pathogens, antibodies with high affinity will coat the antigen, creating an immune complex. Antibody–antigen complexes are taken up on specific IgG receptors (FcγR), a process that activates phagocytic cells (neutrophils, dendritic cells, or macrophages) and encourages phagocytes to engulf pathogens and initiate oxidative radical formation that ultimately leads to elimination of the foreign pathogen. IgG complexes (but not single IgG molecules) can also fix complement proteins and initiate either complement-mediated opsonization (due to specific complement receptors on phagocytes, such as CD21) or complement-mediated bacterial cell lysis (see Figure 34-2). Whereas IgG is only moderately efficient at complement fixation, the large pentameric structure of circulating IgM provides an excellent substrate for the C1qrs complex, the first component of the complement cascade (see Figure 34-2). In contrast, the structure of IgM precludes it from being efficient at opsonizing molecules or interacting with phagocytes. Although IgG is primarily active against blood-borne pathogens, it is present in measurable quantities in the pulmonary mucosa.[4] The

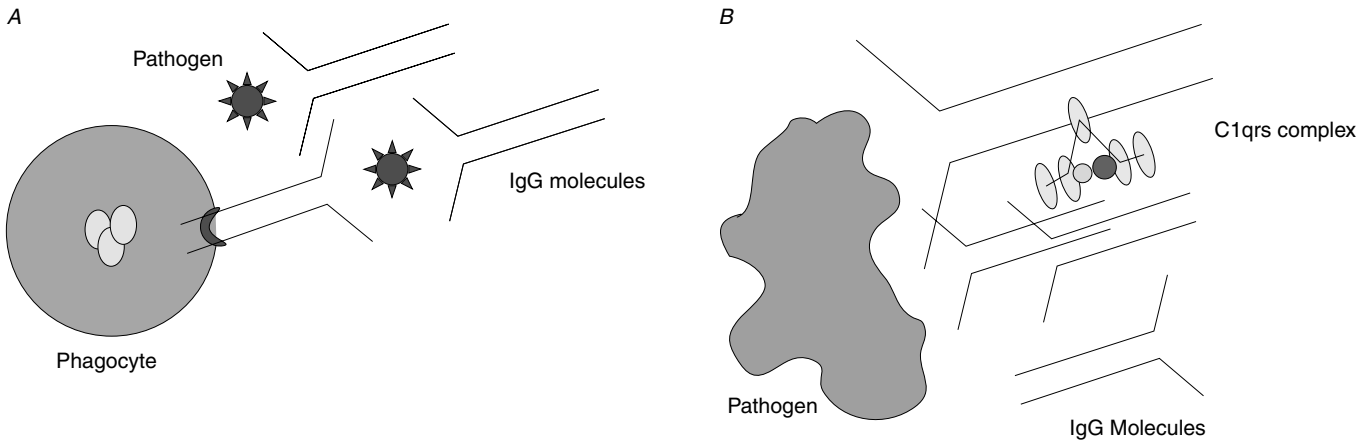

FIGURE 34-2 *A*, Antibody neutralization and opsonization. Multiple IgG molecules trap (neutralize) a pathogen, and the resulting complexes are taken up on Fcγ receptors to enhance phagocytosis. *B*, Opsonization and complement fixation: multiple IgG molecules coat a pathogen, and the resulting immune complex allows the initiator of the complement cascade, the C1qrs complex, to bind and become activated. The opsonized bacteria are taken up by phagocytes via Fcγ receptors as in *A*.

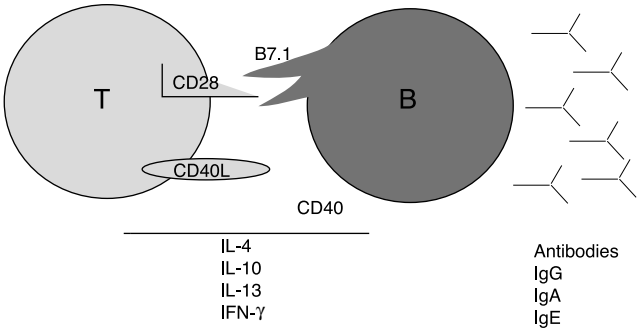

FIGURE 34-3 Immunoglobulin isotype switching: B and T cells interact via the bridging molecules CD40 ligand (CD40L) and B7.1 and CD28, on the B and T cells, respectively. This, plus elaboration of cytokines by T lymphocytes, initiates the switching of immunoglobulin isotypes from IgM to IgG, IgA, or IgE.

amount of mucosa-secreted IgG may increase in pathologic conditions in proportion to the increased presence of BALT during infection or in chronic inflammation.[5]

IgA is the primary immunoglobulin lining the respiratory tract and intestines. It has two subtypes, IgA_1 and IgA_2, based on their relative abundance in serum. IgA can be found as a monomer-like IgG or more frequently as a dimer or polymer, with two or more molecules linked together by a joining (J) chain. Most of the IgA in respiratory secretions is polymeric, whereas serum IgA is primarily monomeric.[6] Dimeric and polymeric IgA is associated with a protein known as secretory component, which allows IgA to be efficiently transported in secretions. IgA is produced by plasma cells in bone marrow and in specialized collections of plasma cells within the respiratory and intestinal mucosa. The environment drives the type of IgA molecule that is produced; 80% of bone marrow–produced IgA is monomeric, whereas 80% of pulmonary mucosa–derived IgA is polymeric. There is good evidence suggesting that almost all the IgA in the lungs is locally produced. The repertoire of IgA is replete with "natural antibodies"; these recognize common patterns encountered by the immune system over evolution and are present without there being preexisting antigen-primed cells. An example is the presence of IgA that binds *Streptococcus pneumoniae* via a bacterial surface protein called SpsA (Strep pneumo surface protein A).[6]

In pulmonary defense, the most important role that IgA plays is that of pathogen neutralization, intercepting organisms within the lumen, on epithelial cells, and in the lamina propria of the airway mucosa. Neutralization by IgA can take place without subsequent phagocytosis or engendering an inflammatory response and is thus protective for the mucosal surfaces. In addition, immune complexes containing IgA and antigens can be taken up by IgA receptors (FcαR). The distribution of the sites of expression of these receptors includes monocytes, macrophages, eosinophils, and basophils. Immune complexes taken up on FcαR activate the phagocyte and lead to engulfment of the pathogen and initiation of killing and production of reactive oxygen intermediates.[6]

ANATOMY OF BRONCHIAL LYMPHOID TISSUE

In addition to the systemic immunoglobulin synthesis that occurs in the bone marrow, mucosal lymphoid tissues are major sites for the production of immunoglobulin molecules. These regionally organized lymphoid tissues include the bronchial lymph nodes, which drain the upper and lower airways, and mucosal collections of lymphoid tissue such as nasal-associated lymphoid tissue in the nose and BALT in the lower airway. B lymphocytes are also commonly found in lung interstitium; their presence may be important in resistance to infections and the pathogenesis of airway hyperresponsiveness.[7] These structures are the main focus of this section.

The primary lymph nodes of the lung follow the trachea and large bronchi (Figure 34-4).[8] There are multiple paratracheal lymph nodes: tracheobronchial nodes at the bifurcation of the right and left mainstem bronchi and at the carina, hilar nodes, and intrapulmonary lymph nodes. These have classic lymph node architecture, with a capsule, high endothelial venules to facilitate blood supply and antigen presentation, and lymphoid vessels. Cross-sections of these lymph nodes reveal zones of T and B lymphocytes, as well as germinal centers, which are the primary sites of B-cell isotype switching. Antigens traffic to these nodes, where dendritic cells present them to T lymphocytes in the first 24 hours after antigen enters the body.[1] The activated T cells then migrate to the B-cell follicles of the lymph node, probably through elaboration of chemokines in the environment, such as secondary lymphoid tissue chemokine (SLC) and B-lymphocyte chemokine (SLC). The B cells, which have also encountered and processed the foreign antigen, then present the antigen to the $CD4^+$ helper T cells on the edges of the B-cell follicle. This is a major histocompatibility complex (MHC)-restricted process, involving class II MHC–T-cell receptor interactions.[9] The antigen-stimulated T cells up-regulate CD40L and elaborate cytokines such as interleukin-2 (IL-2), IL-10, IL-4, and IL-13. Depending on the cytokines released in the environment, B cells will produce particular immunoglobulin isotypes. Classically, the main isotype produced in the lung is IgA, which is under the control of transforming growth factor-x (TGF-β), IL-5, and IL-10. However, IgG and IgE are both detectable in the lung (see below). IgE synthesis is under the control of IL-4 and IL-13, and IgG can be induced by IL-10, IFN-γ, and IL-4. Although T cells are the primary sources of the cytokines that drive B-cell isotype switching, other sources of cytokines in the environment may play an equally important role. For example, TGF-β is produced in large amounts by fibroblasts and epithelium,[10] and mast cells in lung tissue produce IL-4 and IL-13. Even B cells themselves can secrete cytokines following antigen or T-cell activation and contribute to the process of isotype switching.[11–13] Thus, the lung is not only responsible for innate defenses via mucociliary clearance and other barriers but also plays a role in the provision of antibodies in the adaptive humoral immune response.[4]

In addition to the organized lymphoid tissue present in the paratracheal and bronchial regions, there are areas of lymphoid aggregates within the subepithelial layers of the

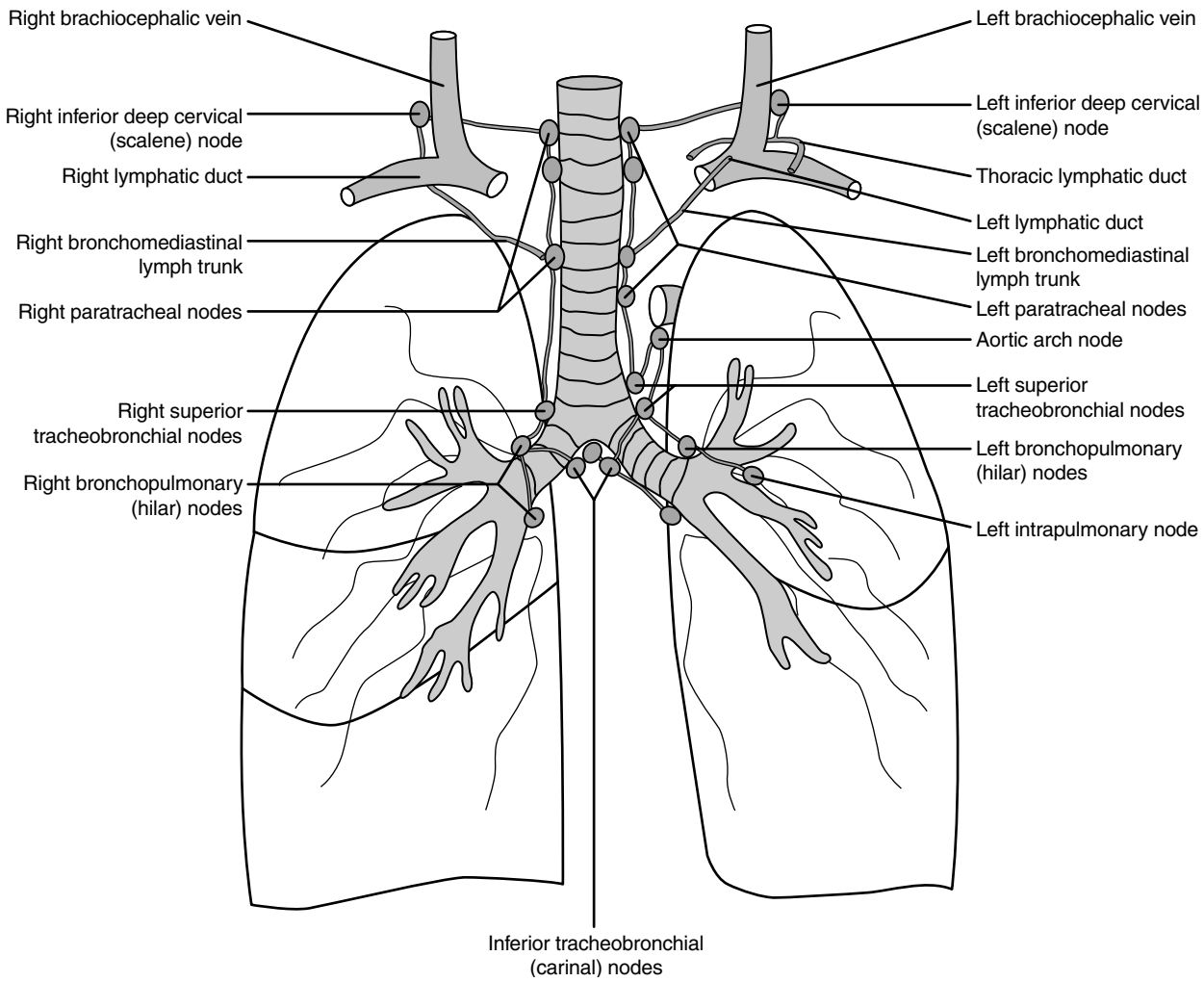

FIGURE 34-4 Distribution of the lymph nodes in the tracheobronchial tree.

bronchi. These collections of lymphocytes, known as BALT, are the bronchial equivalent of gut-associated lymphoid tissue (GALT), such as Peyer's patches. BALT is defined as an aggregate of lymphoid tissue with a follicle-like structure that is demarcated by an overlying epithelium and is fed by high endothelial venules similar to those that feed other lymphoid tissues.[14] However, the role of BALT is less well defined than that of GALT. The main reason why the role of BALT in normal defense remains controversial is the fact that little, if any, BALT is seen in normal adult lungs. However, it is observed in patients who have died of pulmonary infection, in severe smokers, and in people with chronic illness, such as rheumatoid arthritis.[8,15] Several investigators have attempted to isolate the distribution and pattern of BALT in human lungs. Hiller and colleagues studied 98 lungs and 51 specimens of epiglottis from autopsies of subjects representing a wide range of ages. There was no BALT or laryngeal-associated lymphoid tissue (LALT) in fetal specimens, and in children (aged 2 to 20 years) BALT was detected in 42% of specimens. It was found in only 3 of 24 adult specimens. In contrast, LALT was present much more frequently; it was present in 84% of specimens from subjects aged less than 20 years and in 56% of those from subjects aged over 20 years. Another important finding was that BALT, when present, was not focally distributed in sites of infection or inflammation but was homogeneously distributed throughout the lung.[14] In comparison with animal tissues, foci of BALT were smaller and had less active germinal centers.

BALT formation appears to be dependent on the presence of normal peribronchial lymph nodes. Tirouvanziam and colleagues, using mice with severe combined immunodeficiency (SCID), developed a system that allowed for development of BALT.[16] Implantation of bronchi into the flanks of SCID mice did not induce development of lymphoid tissue, but implantation of a bronchus with the associated peribronchial lymph nodes led to the appearance of BALT, including B and T lymphocytes, monocytes, and mast cells within the transplanted bronchus. The B lymphocytes were functional and able to secrete IgA. There appeared to be a need for interaction between the peribronchial lymph nodes and the bronchial mucosa, and if they were not transplanted contiguously, there was no BALT development.[16] Thus, BALT may be rudimentary in normal adults unless the lung is challenged or immunologically stimulated. In contrast, the paratracheal and parabronchial lymph nodes are present

consistently and probably represent the most important source of IgA for the airways.

SECRETION OF IMMUNOGLOBULINS IN THE LUNG AND RESPIRATORY MUCOSA

Specialized tissues in the lung can secrete immunoglobulins and contribute to all aspects of host defense. Although it has been known for some time that IgA can be secreted onto airway mucosa, the regulation of this local secretion is not well understood. In addition, other isotypes contribute to both host defense and pathology, thus necessitating the search for local production of antibodies of the IgG and IgE isotypes. This has been performed with the use of both direct measurement of lung immunoglobulins from bronchoalveolar lavage (BAL) fluid and cultures of respiratory mucosa.

It is possible to measure all immunoglobulin isotypes in BAL fluid, and their presence may reflect different intrapulmonary processes such as infection or inflammation.[17] Peebles and colleagues standardized a method of detecting IgG, IgA, and IgM in BAL fluid to enhance the sensitivity of detection of these proteins in the dilute milieu of the recovered BAL fluid.[4] BAL fluid immunoglobulins were detectable in the μg/mL range, whereas serum immunoglobulins were a 1,000-fold more concentrated. As expected, both serum IgA and uncomplexed IgA were present in the highest concentrations (10 to 13 μg/mL), although IgG was detectable at a similar concentration (9 to 10 μg/mL). Little IgM was detected, probably because of the difficulty of actively transporting this large molecule into the lung milieu. Interestingly, serum IgA and IgA levels in asthma and allergic rhinitis patients were 50 to 100% higher than in normal individuals; similar increases in IgG levels were not found.

Immunoglobulin levels in the lung change with disease processes. In sarcoidosis, pulmonary fibrosis, and other autoimmune lung processes, IgG or IgA level increases significantly.[18,19] Local and specific IgA production also increases in states of infection[20–22] or vaccination[23,24] but not in lung transplantation rejection.[20] In mouse models of infection and vaccination, IgG and/or IgA detected in respiratory secretions conferred protection against organisms, including influenza virus, *Mycoplasma*, and other common respiratory pathogens.[23,25–28]

A large amount of attention has been focused on the local IgE response as a marker of allergy. Indeed, although IgE is detectable in ng/mL quantities in serum (concentration 1,000 times less than those of the other immunoglobulin isotypes), the concentration of IgE in BAL fluid can be within 1/10 of the concentrations of other isotypes, including IgA.[29] Local IgE may be produced in response to a viral infection[30] or to antigen inhalation, naturally or in laboratory challenges.[29,31] In sensitized individuals, local IgE levels rise rapidly after antigen challenge, with increases being detectable within 24 hours of exposure to substances such as ragweed.[29] In general, the level of IgE specific to the allergen rises rapidly and disproportionately to the total IgE level detected in BAL fluid or to serum IgE level.[31] This suggests that the respiratory mucosa more readily produces IgE in response to inhaled allergen.[26]

These data, indicating increases in local allergen-specific IgE levels following exposure, suggest that the respiratory mucosa has resident memory B cells that rapidly respond to the presence of allergen by increasing the rate of IgE release. The detection of germinal center–like structures that secrete IgE in the lungs of sensitized animals was first described by Chvatchko and colleagues.[32] In human nasal epithelium tissue, IgE transcripts were detected within the B cells of allergic individuals who had undergone biopsies. These tissues can secrete IgE soon after exposure to antigen and can continue to secrete for up to 14 days without recruitment of cells from the systemic circulation.[33] In the lung, IgE can be found on mast cells, and circulating IgE has also been found in respiratory secretions.[34] Circulating IgE can persist in animals for 15 days or more after allergen challenge, and this IgE can form immune complexes with inhaled antigens. Although the role of antigen-specific IgE immune complexes in humans has not been explored, in a murine model of asthma, IgE–ovalbumin immune complexes caused a fourfold greater secretion of IL-4, as well as more prominent eosinophilia, in comparison with animals receiving ovalbumin alone.[35] Anti-IgE molecules that bind the Fc portion of IgE have been recently developed and are undergoing clinical trials for the treatment of asthma and other allergic diseases. The results of the trials suggest that this compound is effective, especially in severe asthma.[36–39] Because it targets the Fc portion of the IgE molecule, it cannot interact with IgE already bound on mast cells, but it can complex with circulating IgE. Inhibition of IgE immune complexes in the airways may explain, in part, the effectiveness of anti-IgE in clinical trials. These intriguing findings also suggest that more research into the role of locally secreted IgE in airway disease is needed.[36–40]

IMMUNE DEFICIENCY

When the immune system fails to fight infections adequately, such as in antibody deficiencies or primary ciliary dyskinesia, the airways are the prime portal of entry for pathogens. Because of the reliance on immunoglobulins for host defense in the lung, antibody deficiency can have important pulmonary sequelae if inadequately treated. In general, antibody-deficient patients present with recurrent sinus and pulmonary infections. However, if the condition is not recognized early and treated aggressively, these infections can ultimately lead to the development of bronchiectasis and impaired lung function.

Selective IgA Deficiency

The most common form of antibody deficiency is selective IgA deficiency. This disease affects 1 in 600 individuals in the Western world; the inheritance pattern is unknown, but there is variability between different ethnic groups, with IgA deficiency being one-third less frequent in Asian populations. The condition is asymptomatic in two-thirds of affected individuals, whereas the remaining patients suffer from a variety of viral and bacterial infections of both the upper and lower respiratory tracts.[41] Absolute IgA deficiency is defined as a serum value < 0.05 g/L, which is

generally considered undetectable by most standard clinical assays. There is a wide variability in normal values, based on current detection systems, but patients with low yet detectable levels of serum IgA are rarely symptomatic. IgA deficiency can be associated with other conditions, such as specific antibody deficiencies or IgG subclass deficiency, that may exacerbate the predisposition to infection. Patients with selective IgA deficiency also have an increased incidence of allergies, gastrointestinal tract diseases, and autoimmune diseases.

Deficiencies of IgG

There are several well-described diseases that are characterized by poor IgG antibody production and recurrent infections. It is important to note that simply having a decreased IgG value does not qualify a patient as immunodeficient or as a candidate for immunoglobulin therapy. All patients with suspected IgG antibody deficiencies should have a thorough evaluation, assessing their capacity to make normal B and T lymphocytes and to produce antibodies to pathogens or to recently administered vaccines.

X-Linked Agammaglobulinemia X-Linked agammaglobulinemia (XLA) affects male patients and is characterized by absent B cells and normal T cells. The disease was first described by Bruton in 1952—hence the eponym Bruton's agammaglobulinemia. The gene for XLA has been identified on the long arm of the X chromosome at Xq22; it encodes for a B-cell progenitor enzyme, Bruton tyrosine kinase, essential for B-cell differentiation. The prevalence is about 1 in 100,000. Infants usually present after 5 to 6 months of age, when passively acquired maternal IgG degrades. However, some patients are not diagnosed until later in childhood or even in young adulthood.[42] They usually present with recurrent otitis media, sinusitis, pneumonia, sepsis, or meningitis, most often due to encapsulated organisms such as *Streptococcus pneumoniae* or *Haemophilus influenzae*. They also can develop infections with unusual organisms such as *Mycoplasma pneumoniae*. Viral infections are frequent, and meningoencephalitis due to enteroviruses and paralysis related to live virus vaccination have been reported. Fatalities have occurred following enteroviral infections.

Hyper-IgM Syndrome The second most common IgG deficiency with an inherited pattern is the hyper-IgM syndrome. This disease is characterized by normal circulating B lymphocytes and T lymphocytes but unusually high IgM levels and absent serum IgG and IgA. The defect is associated with two genetic conditions. X-Linked hyper-IgM is due to a defect in the gene for CD-40L; this T-cell molecule is essential for the interaction with the CD40 molecule on the surface of B cells that leads to the initiation of isotype switching from IgM to IgG, IgA, or IgE.[43] The second genetic defect is in the gene for activation-induced cytidine deaminase (AID), coded for on chromosome 12.[44] AID is crucial for the initiation of isotype switching. The clinical manifestations are similar to those of XLA, but individuals with X-linked hyper-IgM often present with *Pneumocystis carinii* infection early in life and have an increased incidence of malignancies, such as lymphomas.

Common Variable Immunodeficiency Common variable immunodeficiency (CVID) is actually a heterogeneous group of humoral immunodeficiencies characterized by hypogammaglobulinemia, recurrent bacterial infections, and a wide spectrum of other immunologic abnormalities.[45] The prevalence of CVID ranges from 1 in 10,000 to 1 in 50,000.[46–48] The genetic defect has not yet been clearly identified, but a familial inheritance pattern can be seen in up to 25% of cases.[41] Different mechanisms have been suggested to explain the inability of these patients to produce antibodies, including dysregulation of gene expression involved in immunoglobulin production, abnormal IL-2 synthesis, and suboptimal interaction between T cells and B cells. There are two peaks for the age at onset of the disease: one at 1 to 5 years and a second at 16 to 25 years.[49]

The hallmarks of the disease include decreased levels of serum immunoglobulin; IgG < 3.0 g/L, decreased IgA level, and decreased serum IgM level are observed in half of the patients. Recurrent upper respiratory infections were the presenting feature in 100% of patients in one study[50]; pneumonia was present in 74%, sinusitis in 63%, otitis media in 63%, bronchiectasis in 58%, chronic obstructive pulmonary disease in 47%, pulmonary tuberculosis in 5%, and asthma in 5%. Other complications include a high predisposition for immune cytopenias, arthritis, gastrointestinal overgrowth, and diarrhea and an elevated incidence of lymphoid malignancy.[49]

Specific Antibody Deficiency There is a subset of patients with normal serum IgG levels who are unable to respond appropriately to vaccines or infection with certain organisms. Most commonly, these individuals cannot make antibodies against polysaccharide antigens, such as pneumococcal bacteria or unconjugated *Haemophilus influenzae* vaccines. These individuals suffer from recurrent sinus and pulmonary disease and can be susceptible to recurrent infections, such as sepsis or meningitis. This disorder is primarily seen in young children and may be a maturational dysfunction in immunoglobulin synthesis. Treatment should be reserved for those who have significant pulmonary complications or significant morbidity, such as hospitalizations and dependence on intravenous antibiotics for the treatment of their infections. Impaired polysaccharide antibody responses may have been responsible for the defect in patients labeled as having IgG_2 subclass deficiency; not all reported patients with IgG subclass deficiencies were evaluated for the ability to elicit normal vaccine responses. IgG subclasses are not always included in immune evaluations at present, but if they are included in an evaluation, depression of an immunoglobulin subclass alone is not indicative of a need for treatment; inadequate responses to vaccines also need to be demonstrated.

There are many other diseases that have IgG deficiency as a manifestation. These diseases include Wiskott–Aldrich syndrome, ataxia–telangiectasia, Nezelof's syndrome (cellular immunodeficiency with abnormal Ig synthesis), severe

combined immunodeficiency syndromes, and milder combined immunodeficiencies.[45]

Asthma and Immunoglobulin Deficiency

Patients with asthma frequently have infection-induced exacerbations. This has led to a number of studies in which asthmatic patients have been evaluated for humoral immunodeficiencies. Patients with severe steroid-dependent asthma experience repeated episodes of bronchitis and acute episodes of sinusitis, but these problems are rarely associated with impairment with specific antibody production.[51] Occasionally, hypogammaglobulinemia has been identified in asthmatic patients, attributed largely to corticosteroid therapy.[52] Young children with severe asthma were found to have isolated IgG_2 subclass deficiency,[53] but more recent studies have demonstrated an incidence similar to that in nonasthmatic children.[54] Page and colleagues treated a small cohort of asthmatic children with intravenous immunoglobulin (IVIG) and found an improvement in exacerbations, due to a decrease in infections.[55] Because of the high cost of IVIG, the cost/benefit ratio for this approach is not favorable. Thus, although true immunodeficiency in asthmatic patients is uncommon, individuals with difficult-to-control asthma and recurrent infections should be evaluated for immunodeficiency. There is also an increased risk of asthma in patients with IgA deficiency. Several investigators have used IVIG as a steroid-sparing therapy for severe asthma in otherwise immunocompetent patients. Clinical trials of IVIG in severe asthma, although promising, have not conclusively proven its efficacy.[56–61]

Evaluation of Immunoglobulin Deficiency

A classic history of recurrent sinus and pulmonary infections, septicemia, osteomyelitis, or meningitis is highly suggestive of humoral immunodeficiency.[41] Infections with bacteria, such as *Streptococcus pneumoniae*, *Haemophilus influenzae*, *Branhamella*, or *Moraxella catarrhalis*, are also important clues. Severe infections with *Mycoplasma* species, including *Mycoplasma pneumoniae* and *Mycoplasma hominis*, and *Ureaplasma urealytica* are more common in patients with poorly functioning humoral immune systems. [41,62]

The diagnosis is usually based on the absence or marked deficiency of an immunoglobulin class or classes, with an impairment in the ability to make antibodies. Careful evaluation of the patient's immune function is crucial. Low immunoglobulin levels may have no functional significance in fighting infections, and trials of IVIG have only been found to be useful in patients who have demonstrated poor humoral immune function.[63] This is best assessed with the use of vaccination booster responses for diphtheria and tetanus[64] or pneumococcus.[65–67] Optimal responses to vaccines suggest that the low immunoglobulin level may not be amenable to treatment with IVIG. Evaluation of B cells and T cells in the circulation with flow cytometry can reveal the presence of XLA or SCID. For several of these diseases, molecular diagnosis is now also possible.[45] A complete pulmonary and sinus assessment at baseline is crucial, due to the high incidence of preexisting upper and lower airway disease and long-term pulmonary complications.[50,68–70]

Patients with IgG deficiencies receive immunoglobulin replacement therapy, in the form of IVIG at doses that will achieve adequate levels to prevent the recurrence of infections. Early initiation of replacement therapy in patients with XLA has been shown to be effective in preventing severe bacterial infections, diffuse bronchiectasis, and pulmonary insufficiency when a residual IgG level above 5 g/L is maintained.[71] Patients, especially those with chronic chest disease or bronchiectasis, may also require prophylactic broad-spectrum antibiotic therapy,[70,72] as do individuals with symptomatic IgA deficiency who do not benefit from IVIG replacement therapy. Although the outcome of patients with severe antibody deficiencies has improved greatly since the institution of IVIG therapy, patients can still develop pulmonary complications, such as bronchiectasis; therefore, close monitoring and follow-up are essential.

CONCLUSIONS

The humoral immune system in the lung involves complex interactions between cells, lymphatics, lymph nodes, and secreted proteins. All of these work together to ensure optimal protection against external invaders. Our understanding of this adaptive immune network has led to attempts at exploiting its power in order to improve pulmonary health. Improved vaccine development, including direct mucosal vaccine administration and vaccines modified to increase IgA responses, can impact on how the lungs handle pathogens. In contrast, elevated levels of IgE in asthma and allergic rhinitis contribute to the pathogenesis of the disease. Monoclonal antibody therapy directed against IgE is an exciting new development that can be used to treat the dysregulated antibody production causing allergic diseases within the respiratory tree. B lymphocytes in lymph nodes and BALT can thus contribute to both respiratory health and disease, and research into their ultimate contributions will impact greatly on our understanding of pulmonary pathology.

REFERENCES

1. Janeway C, Traverse P, Walport M, Shlomchick M. Immunobiology. 5th ed. 2001.
2. Rich R, Fleisher T, Shearer W, Kotzin B, editors. Clinical immunology: principles and practices. 2nd ed. 2001.
3. Moore BB, Moore TA, Toews GB. Role of T- and B-lymphocytes in pulmonary host defences. Eur Respir J 2001;18:846–56.
4. Peebles RS Jr, Liu MC, Lichtenstein LM, Hamilton RG. IgA, IgG and IgM quantification in bronchoalveolar lavage fluids from allergic rhinitics, allergic asthmatics, and normal subjects by monoclonal antibody-based immunoenzymetric assays. J Immunol Meth 1995;179:77–86.
5. Pabst R. Is BALT a major component of the human lung immune system? Immunol Today 1992;13:119–22.
6. Pilette C, Ouadrhiri Y, Godding V, et al. Lung mucosal immunity: immunoglobulin-A revisited. Eur Respir J 2001;18:571–88.
7. Crapo JD, Harmsen AG, Sherman MP, Musson RA. Pulmonary immunobiology and inflammation in pulmonary diseases. Am J Respir Crit Care Med 2000;162:1983–6.
8. Pabst R, Gehrke I. Is the bronchus-associated lymphoid tissue (BALT) an integral structure of the lung in normal mammals, including humans? Am J Respir Cell Mol Biol 1990;3:131–5.

9. Garside P, Ingulli E, Merica RR, et al. Visualization of specific B and T lymphocyte interactions in the lymph node. Science 1998;281:96–9.
10. Salvi S, Holgate ST. Could the airway epithelium play an important role in mucosal immunoglobulin A production? Clin Exp Allergy 1999;29:1597–605.
11. Bastien Y, Toledano BJ, Mehio N, et al. Detection of functional platelet-activating factor receptors on human tonsillar B lymphocytes. J Immunol 1999;162:5498–505.
12. Cerutti A, Zan H, Schaffer A, et al. CD40 ligand and appropriate cytokines induce switching to IgG, IgA, and IgE and coordinated germinal center and plasmacytoid phenotypic differentiation in a human monoclonal IgM + IgD + B cell line. J Immunol 1998;160:2145–57.
13. Harris DP, Haynes L, Sayles PC, et al. Reciprocal regulation of polarized cytokine production by effector B and T cells. Nat Immunol 2000;1:475–82.
14. Hiller AS, Tschernig T, Kleemann WJ, Pabst R. Bronchus-associated lymphoid tissue (BALT) and larynx-associated lymphoid tissue (LALT) are found at different frequencies in children, adolescents and adults. Scand J Immunol 1998; 47:159–62.
15. Tschernig T, Pabst R. Bronchus-associated lymphoid tissue (BALT) is not present in the normal adult lung but in different diseases. Pathobiology 2000;68:1–8.
16. Tirouvanziam R, Khazaal I, N'Sonde V, et al. Ex vivo development of functional human lymph node and bronchus-associated lymphoid tissue. Blood 2002;99:2483–9.
17. Gorin AB, Stewart P, Gould J. Concentrations of immunoglobulin classes in subcompartments of the sheep lung. Res Vet Sci 1979;26:126–8.
18. Rankin JA, Naegel GP, Schrader CE, et al. Air-space immunoglobulin production and levels in bronchoalveolar lavage fluid of normal subjects and patients with sarcoidosis. Am Rev Respir Dis 1983;127:442–8.
19. Sato T, Kitajima A, Ohmoto S, et al. Determination of human immunoglobulin A and secretory immunoglobulin A in bronchoalveolar lavage fluids by solid phase enzyme immunoassay. Clin Chim Acta 1993;220:145–56.
20. Bastian A, Tunkel C, Lins M, et al. Immunoglobulin A and secretory immunoglobulin A in the bronchoalveolar lavage from patients after lung transplantation. Clin Transplant 2000;14:580–5.
21. von Hertzen L, Leinonen M, Surcel HM, et al. Measurement of sputum antibodies in the diagnosis of acute and chronic respiratory infections associated with Chlamydia pneumoniae. Clin Diagn Lab Immunol 1995;2:454–7.
22. Grubek-Jaworska H, Zwolska Z, Droszcz P, et al. Serum and bronchoalveolar IgG against A60 and 38 kDa antigens in the diagnosis of tuberculosis. Int J Tuberc Lung Dis 1997;1:556–62.
23. Ruedl C, Fruhwirth M, Wick G, Wolf H. Immune response in the lungs following oral immunization with bacterial lysates of respiratory pathogens. Clin Diagn Lab Immunol 1994; 1:150–4.
24. Rudin A, Riise GC, Holmgren J. Antibody responses in the lower respiratory tract and male urogenital tract in humans after nasal and oral vaccination with cholera toxin B subunit. Infect Immun 1999;67:2884–90.
25. Hodge LM, Simecka JW. Role of upper and lower respiratory tract immunity in resistance to Mycoplasma respiratory disease. J Infect Dis 2002;186:290–4.
26. Hodge LM, Marinaro M, Jones HP, et al. Immunoglobulin A (IgA) responses and IgE-associated inflammation along the respiratory tract after mucosal but not systemic immunization. Infect Immun 2001;69:2328–38.
27. McGhee JR, Kiyono H, Michalek SM, Mestecky J. Enteric immunization reveals a T cell network for IgA responses and suggests that humans possess a common mucosal immune system. Antonie Van Leeuwenhoek 1987;53:537–43.
28. Balkovic ES, Six HR. Pulmonary and serum isotypic antibody responses of mice to live and inactivated influenza virus. Am Rev Respir Dis 1986;134:6–11.
29. Peebles RS Jr, Hamilton RG, Lichtenstein LM, et al. Antigen-specific IgE and IgA antibodies in bronchoalveolar lavage fluid are associated with stronger antigen-induced late phase reactions. Clin Exp Allergy 2001;31:239–48.
30. Nadal D, Ogra PL. Development of local immunity: role in mechanisms of protection against or pathogenesis of respiratory syncytial viral infections. Lung 1990;168:379–87.
31. Wilson DR, Merrett TG, Varga EM, et al. Increases in allergen-specific IgE in BAL after segmental allergen challenge in atopic asthmatics. Am J Respir Crit Care Med 2002;165:22–6.
32. Chvatchko Y, Kosco-Vilbois MH, Herren S, et al. Germinal center formation and local immunoglobulin E (IgE) production in the lung after an airway antigenic challenge. J Exp Med 1996;184:2353–60.
33. Smurthwaite L, Walker SN, Wilson DR, et al. Persistent IgE synthesis in the nasal mucosa of hay fever patients. Eur J Immunol 2001;31:3422–31.
34. Crimi E, Scordamaglia A, Crimi P, et al. Total and specific IgE in serum, bronchial lavage and bronchoalveolar lavage of asthmatic patients. Allergy 1983;38:553–9.
35. Zuberi RI, Apgar JR, Chen SS, Liu FT. Role for IgE in airway secretions: IgE immune complexes are more potent inducers than antigen alone of airway inflammation in a murine model. J Immunol 2000;164:2667–73.
36. Busse W, Corren J, Lanier BQ, et al. Omalizumab, anti-IgE recombinant humanized monoclonal antibody, for the treatment of severe allergic asthma. J Allergy Clin Immunol 2001;108:184–90.
37. Corren J, Casale T, Deniz Y, Ashby M. Omalizumab, a recombinant humanized anti-IgE antibody, reduces asthma-related emergency room visits and hospitalizations in patients with allergic asthma. J Allergy Clin Immunol 2003;111:87–90.
38. Milgrom H, Berger W, Nayak A, et al. Treatment of childhood asthma with anti-immunoglobulin E antibody (omalizumab). Pediatrics 2001;108:E36.
39. Soler M, Matz J, Townley R, et al. The anti-IgE antibody omalizumab reduces exacerbations and steroid requirement in allergic asthmatics. Eur Respir J 2001;18:254–61.
40. Barnes PJ. Anti-IgE therapy in asthma: rationale and therapeutic potential. Int Arch Allergy Immunol 2000;123:196–204.
41. Ochs H, Conely ME, editors. Primary immunodeficiency diseases. 1999.
42. Hashimoto S, Miyawaki T, Futatani T, et al. Atypical X-linked agammaglobulinemia diagnosed in three adults. Intern Med 1999;38:722–5.
43. Notarangelo LD, Hayward AR. X-Linked immunodeficiency with hyper-IgM (XHIM). Clin Exp Immunol 2000;120: 399–405.
44. Revy P, Muto T, Levy Y, et al. Activation-induced cytidine deaminase (AID) deficiency causes the autosomal recessive form of the hyper-IgM syndrome (HIGM2). Cell 2000; 102:565–75.
45. Ballow M. Primary immunodeficiency disorders: antibody deficiency. J Allergy Clin Immunol 2002;109:581–91.
46. Group WS. Primary immunodeficiency diseases. Clin Exp Immunol 1999;118:S1–28.
47. Cunningham-Rundles C, Bodian C. Common variable immunodeficiency: clinical and immunological features of 248 patients. Clin Immunol 1999;92:34–48.
48. Cunningham-Rundles C. Clinical and immunologic analyses of 103 patients with common variable immunodeficiency. J Clin Immunol 1989;9:22–33.

49. Hermaszewski RA, Webster AD. Primary hypogammaglobulinaemia: a survey of clinical manifestations and complications. QJM 1993;86:31–42.
50. Martinez Garcia MA, de Rojas MD, Nauffal Manzur MD, et al. Respiratory disorders in common variable immunodeficiency. Respir Med 2001;95:191–5.
51. Hamilos DL, Young RM, Peter JB, et al. Hypogammaglobulinemia in asthmatic patients. Ann Allergy 1992;68:472–81.
52. Posey WC, Nelson HS, Branch B, Pearlman DS. The effects of acute corticosteroid therapy for asthma on serum immunoglobulin levels. J Allergy Clin Immunol 1978;62: 340–8.
53. Loftus BG, Price JF, Lobo-Yeo A, Vergani D. IgG subclass deficiency in asthma. Arch Dis Child 1988;63:1434–7.
54. de Moraes Lui C, Oliveira LC, Diogo CL, et al. Immunoglobulin G subclass concentrations and infections in children and adolescents with severe asthma. Pediatr Allergy Immunol 2002;13:195–202.
55. Page R, Friday G, Stillwagon P, et al. Asthma and selective immunoglobulin subclass deficiency: improvement of asthma after immunoglobulin replacement therapy. J Pediatr 1988;112:127–31.
56. Mazer BD, Gelfand EW. An open-label study of high-dose intravenous immunoglobulin in severe childhood asthma. J Allergy Clin Immunol 1991;87:976–83.
57. Salmun LM, Barlan I, Wolf HM, et al. Effect of intravenous immunoglobulin on steroid consumption in patients with severe asthma: a double-blind, placebo-controlled, randomized trial. J Allergy Clin Immunol 1999;103:810–5.
58. Rabinovitch N, Gelfand EW, Leung DY. The role of immunoglobulin therapy in allergic diseases. Allergy 1999; 54:662–8.
59. Schwartz HJ, Berger M. Intravenous gamma-globulin therapy in bronchial asthma. Allergy Asthma Proc 2002;23:15–8.
60. Shearer WT, Abramson SL, Adelman DC, et al. Letter to the editor regarding the use of intravenous immunoglobulin (IVIG) in asthma. Clin Immunol 1999;93:184–6.
61. Vrugt B, Wilson S, van Velzen E, et al. Effects of high dose intravenous immunoglobulin in two severe corticosteroid insensitive asthmatic patients. Thorax 1997;52:662–4.
62. Hermans PE, Diaz-Buxo JA, Stobo JD. Idiopathic late-onset immunoglobulin deficiency. Clinical observations in 50 patients. Am J Med 1976;61:221–37.
63. Jaffe E, Lejtenyi MC, Noya FJD, Mazer BD. Secondary hypogammaglobulinemia. Immunol Clin North Am 2001; 21: 141–63.
64. McCusker C, Somerville W, Grey V, Mazer B. Specific antibody responses to diphtheria/tetanus revaccination in children evaluated for immunodeficiency. Ann Allergy Asthma Immunol 1997;79:145–50.
65. Sorensen RU, Leiva LE, Javier FC 3rd, et al. Influence of age on the response to Streptococcus pneumoniae vaccine in patients with recurrent infections and normal immunoglobulin concentrations. J Allergy Clin Immunol 1998; 102:215–21.
66. Javier FC 3rd, Moore CM, Sorensen RU. Distribution of primary immunodeficiency diseases diagnosed in a pediatric tertiary hospital. Ann Allergy Asthma Immunol 2000;84:25–30.
67. Gagnon R, Bedard PM, Cote L, et al. Recurrent acute epiglottitis in adults: defective antibody response. Ann Allergy Asthma Immunol 2002;88:513–7.
68. Kainulainen L, Varpula M, Liippo K, et al. Pulmonary abnormalities in patients with primary hypogammaglobulinemia. J Allergy Clin Immunol 1999;104:1031–6.
69. Thickett KM, Kumararatne DS, Banerjee AK, et al. Common variable immune deficiency: respiratory manifestations, pulmonary function and high-resolution CT scan findings. QJM 2002;95:655–62.
70. Curtin JJ, Webster AD, Farrant J, Katz D. Bronchiectasis in hypogammaglobulinaemia—a computed tomography assessment. Clin Radiol 1991;44:82–4.
71. Quartier P, Debre M, De Blic J, et al. Early and prolonged intravenous immunoglobulin replacement therapy in childhood agammaglobulinemia: a retrospective survey of 31 patients. J Pediatr 1999;134:589–96.
72. Dalal I, Reid B, Nisbet-Brown E, Roifman CM. The outcome of patients with hypogammaglobulinemia in infancy and early childhood. J Pediatr 1998;133:144–6.
73. Busse PJ, Razvi S, Cunningham-Rundles C. Efficacy of intravenous immunoglobulin in the prevention of pneumonia in patients with common variable immunodeficiency. J Allergy Clin Immunol 2002;109:1001–4.
74. Roifman CM, Lederman HM, Lavi S, et al. Benefit of intravenous IgG replacement in hypogammaglobulinemic patients with chronic sinopulmonary disease. Am J Med 1985;79:171–4.

CHAPTER 35

MUCUS AND ITS ROLE IN AIRWAY CLEARANCE AND CYTOPROTECTION

Malcolm King

Mucus is a nonhomogeneous, viscoelastic fluid containing glycoproteins, proteins, and lipids in a watery matrix. Airway mucus is the secretory product of mucous cells—the goblet cells of the pseudostratified columnar surface layer of the airway epithelium and the mucous cells of the submucosal glands. The mucous secretion, along with serous fluid, forms the airway surface fluid (ASF), which provides a protective milieu for the airways. The composition and physical characteristics of ASF allow for normal ciliary activity and airway hygiene.[1] The mucus is transported from the lower respiratory tract into the pharynx by mucociliary clearance and by airflow. When disruption of normal secretory or mucociliary clearance processes occurs, respiratory secretions can accumulate and impair pulmonary function, reduce lung defenses, and increase the risk for infection and possibly neoplasia.[2–4]

ASF consists of two phases: a superficial gel or mucous layer and a liquid or periciliary fluid layer that bathes the epithelial cilia; these two layers are probably separated by a thin layer of surfactant.[5] In health, the mucous layer is about 2 to 5 μm thick in the trachea and extends from the bronchioles to the upper airway. The serous layer lies between the cellular surface and the mucous layer at a depth that is just less than the height of a fully extended cilium. The depth and composition of normal ASF depend on secretion from airway glands, goblet cell discharge, and active ion transport across the epithelial surface as a mechanism for modulating hydration.[6]

Expectorated sputum is a sign of respiratory disease and indicates excessive production (hypersecretion) and/or retention (impaired clearance); these conditions occur in patients with respiratory infection, bronchitis, asthma, bronchiectasis, and cystic fibrosis. Mucoactive medications are treatments designed to enhance the clearance of mucus from the respiratory tract. Mucoactive medications include mucolytics, designed to disrupt the structural macromolecules that give respiratory tract mucus its physical characteristics, and other agents designed to increase mucous flow by stimulating ciliary activity or improving periciliary fluid hydration. Mucokinetic therapy combating mucous retention is a major consideration in the treatment of cystic fibrosis and other chronic lung diseases in which mucous hypersecretion and impaired airway clearance produce symptoms.[7–9]

ROLE OF MUCUS IN MUCOCILIARY CLEARANCE

Airway mucus is cleared by two major mechanisms—mucociliary clearance and airflow interaction (cough); the latter assumes increasing importance as lung disease develops.[10] According to model studies, mucociliary clearance is critically dependent on maintaining the depth of periciliary fluid.[11,12] The depth of mucus does not appear to vary a great deal within the bronchi, but the mucous layer may become discontinuous in the smaller airways.[13,14] The normal daily volume of respiratory secretion arriving at the larynx is estimated to be about 10 mL/day. The total amount of ASF produced throughout the airway system is not known but is probably much higher than the volume actually reaching the larynx; this apparent reduction in airway fluid volume is believed to be due to absorption of water through the lower bronchi via active ion transport mechanisms.[15,16] Microaerosolization of ASF from peripheral airways during expiration may also contribute to reducing the airway fluid load as it converges on the central airways.[17]

The mucociliary clearance rate (MCR) is affected by ciliary, serous fluid, and mucous factors. Ciliary factors that affect the MCR are mainly ciliary beat amplitude and frequency, which together determine the maximal velocity at the tips of the cilia and hence the maximal forward velocity of the mucous layer. In principle, the faster the cilia beat, the higher the MCR, although there is little direct evidence for this in the literature. Also, longer cilia should be able to clear mucus faster because they can generate greater forward velocities. The density or spacing between cilia will also affect the MCR because the greater the distance between the cilia, the more energy will be dissipated in the mucus,

reducing the net forward velocity. In smaller airways, cilia are generally shorter than in the large bronchi, and even though the cilia beat frequency may be comparable, the rate of momentum transfer to the mucus will be proportionately reduced.

Serous factors that affect the MCR include serous fluid viscosity and serous fluid depth. If the serous fluid is too viscous, the cilia will not be able to move very well within it, and the decreased ciliary tip velocity will lead to a reduction of the MCR. This principle is well established for water-propelling cilia, but for the periciliary fluid in the two-layer mucociliary system, the serous fluid viscosity is unknown. Active ion transport and its associated transepithelial water flux[17] are probably of critical importance in modulating serous fluid viscosity. Transepithelial protein fluxes may also reasonably be expected to contribute to serous fluid viscosity.[18] The efficient transfer of momentum between the cilia and the mucous layer requires that the cilia firmly contact the mucus during their forward stroke while minimally interacting with it during the return stroke. If the serous fluid is too deep or too shallow, the MCR will also decrease.[12]

Mucous factors affecting the MCR are the mucous depth and mucous viscoelastic properties.[1,19] When the mucous layer is too thick and clearance by the cilia is hindered, clearance by coughing takes over.[20] Mucus needs to be both viscous and elastic. The elasticity of mucus is important for clearance by cilia because it efficiently transmits energy, with little energy loss. The viscosity of mucus results in energy loss, but this is necessary for mucus to be displaced and either expectorated or swallowed. A balance between these factors must be maintained for optimal MCR.

COUGH CLEARANCE

In various lung diseases characterized by mucous hypersecretion and impaired airway clearance, elimination of the excess mucus by coughing becomes of paramount importance. Cough clearance derives from the high-velocity interaction between airflow and mucus, leading to wave formation in the mucous layer, a temporary reduction in crosslinking within the mucous gel, and, ultimately, shearing and forward propulsion of portions of the mucous layer. The depth of mucus and the airflow linear velocity are critical determinants of cough clearance.[21] Mucous physical properties that are important to cough clearance are the viscosity or resistance to flow of the mucus, the elastic component, which impedes forward motion and results in recoil after the cough event, and the surface properties, both on the air–mucus interface and at the interface with the periciliary layer.[22] Adhesivity or surface tension inhibits cough clearance by suppressing mucus–airflow interaction, which manifests itself as wave formation in the mucous layer during the cough.

The dependence of cough clearance on mucous viscosity, elasticity, and adhesivity is shown in Figure 35-1. In addition, Zahm and colleagues[23] demonstrated that mucous thixotropy, the reduction in apparent viscosity with applied shear, is important in describing the movement of mucus in multiple rapid coughs and, by extension, high-frequency oscillation.

Mucus that is elastic may be efficient for mucociliary clearance, but it is inefficient for cough clearance,[20] and thus a dynamic balance between mucous viscosity and elasticity may be determined by nature. The effects of mucolytic treatments on both forms of clearance should be considered in evaluating their efficacy. In the design of therapeutic measures to modify the rheology of secretions, the initial state of the mucus should be considered; the monitoring of the viscoelastic properties of the mucus should be an essential part of any potential mucotropic therapy.

MUCUS AS A CYTOPROTECTIVE BARRIER

Mucus plays a crucial role in protecting the conducting airways from inhaled bacterial, fungal, and viral pathogens, as well as from the noxious particles and gases that we inhale. Some of this protection is physical—mucus forms a three-dimensional, crosslinked network that inhibits the migration of pathogens. Some of the protection is dilutional, particularly if inhalation stimulates secretory mechanisms,[24] and some of the protection is chemical or immunologic. Mucus presents a vast array of antigenically active oligosaccharides that serve as recognition sites for surface receptors on bacteria and viruses.[25] Indeed, mucus has probably evolved as a universal soluble receptor to deal with a variety of invaders, and enhancement of soluble receptor capacity is a possible strategy to combat viral infection. For example, administration of a soluble virus adhesion receptor to the nasal mucosa resulted in reduced experimental rhinovirus infection in a randomized clinical trial.[26] On the other hand, some viruses (eg, reovirus) appear to have evolved mucinolytic mechanisms to facilitate their penetration through the protective barrier of the mucous layer.[27] For some bacteria, such as *Campylobacter jejuni*, the penetration is also enhanced through motile mechanisms.[28]

In the gastrointestinal tract, mucus acts mainly as a barrier since it does not migrate laterally as it does along the airways. In fact, stomach mucus appears to be exquisitely equipped to resist dislocation since its viscoelasticity is primarily elastic.[29] Also, stomach mucus has a high capacity to resist gastric acid.[30] The buffer capacity of mucus against inhaled acids may also be important in the respiratory tract.[31] In viral uptake by shellfish mucus, the attachment of viruses is primarily ionic and involves the binding of viral particles to sulfated residues on the mucus.[32] Such mechanisms might be related to the well-known shift to sulfated mucins that commonly occurs in chronic bronchitis and cystic fibrosis.[33,34]

RHEOLOGY OF MUCUS

The *rheology* of mucus is its capacity to undergo flow and deformation in response to the forces applied to it. The proper evaluation of mucous rheology is essential for a complete understanding of mucociliary and cough clearance, for monitoring the action of medications that might affect mucous behavior, and for determining the role of mucus in epithelial function. Since the rheologic behavior of mucus involves the crosslinking and entanglement of glycoproteins, it is described as "viscoelastic." In other words,

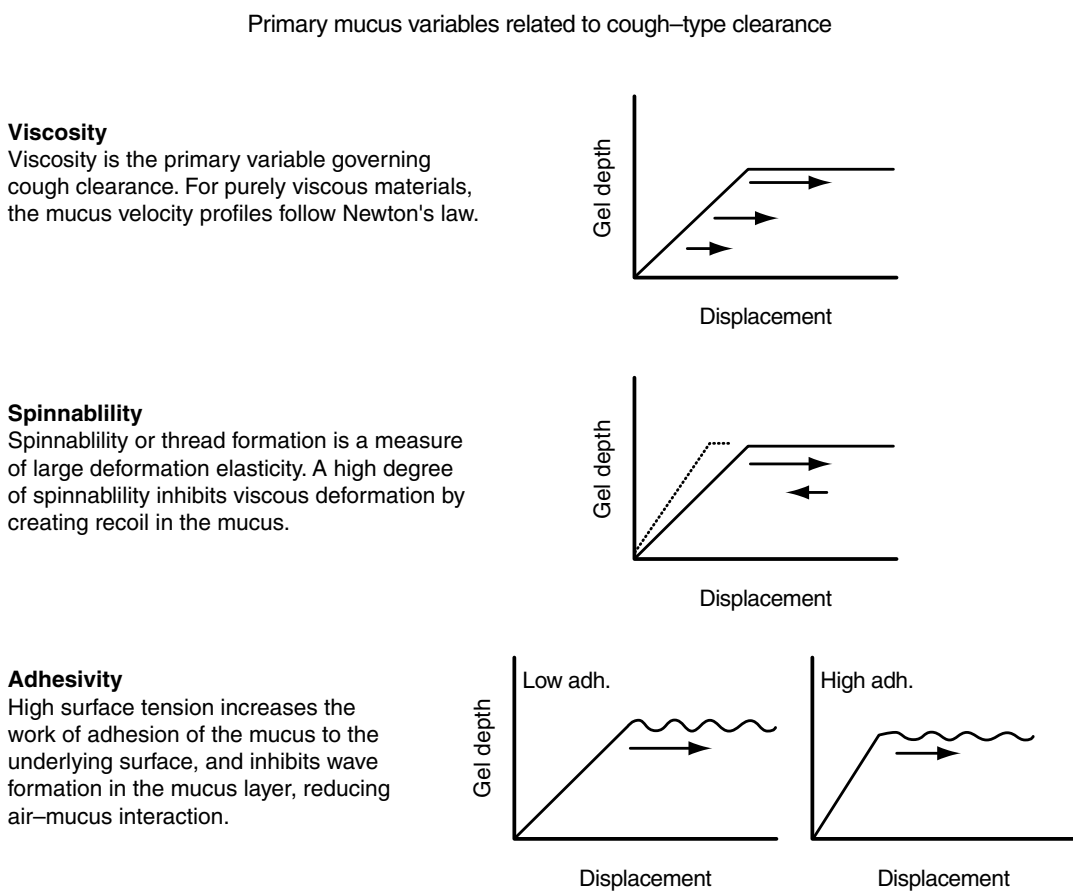

FIGURE 35-1 Cough clearance, based on the results of studies involving the simulated cough machine,[16] depends on three primary biophysical variables: (1) viscosity, (2) elasticity, and (3) adhesivity.

mucus has the characteristics of both a liquid and a solid.[1,19] *Viscosity* is resistance to flow, reflecting the absorption of energy from an object such as a solid particle moving through a substance. In ideal fluids, viscosity is independent of the applied stress. *Elasticity* (elastic modulus) is the capacity of the material to transmit recoil energy back to the object. The elasticity of a mucous gel is a measure of the density of crosslink points within a given time frame. At high measurement frequencies or within short times, the effective number of crosslinks is greater than for longer times, where the gel network has more opportunity to rearrange in response to the applied stress.

The viscosity of viscoelastic liquids such as mucus decreases with increasing stress or rate of strain (shear rate). Mucus responds to stress with an initial solid-like deformation followed by a viscoelastic deformation and finally by a period of steady flow with a constant rate of deformation. After the stress is removed, there is only partial recovery of the strain. This indicates that there has been a permanent deformation of the gel structure. This type of viscoelastic behavior is illustrated in Figure 35-2.

Many factors contribute to the viscoelasticity of mucus. Among these are the type of mucous glycoprotein, the hydration of the secretions, and the degree of mucous crosslinking and entanglement. The latter, in turn, is influenced by the pH and ion content of the secretions, as well as the presence of inflammatory mediators and enzymes. Mucolytics reduce viscosity by disrupting polymer networks in the secretion (Figure 35-3). Classic mucolytic agents work by severing disulfide bonds, binding Ca^{2+}, depolymerizing mucopolysaccharides, and liquefying proteins. Newer, peptide mucolytics degrade pathologic filaments of DNA and actin.

Breakage or reduction of the bonds within the mucous gel can be achieved through disruption of the gel network—the process known as mucolysis. Mucolysis can be achieved either through physical intervention, such as high-frequency oscillation,[35] or by biochemical or pharmacologic agents, such as *N*-acetylcysteine or dornase-α.[9] Thus, by breaking the macromolecular bonds, mucolysis will reduce the viscoelasticity of the mucous gel. If this process is carried out to a sufficient extent, it will facilitate mucous clearance.

Alternative strategies for reducing the concentration of crosslinks in the mucous gel (see Figure 35-1) include hydration or swelling, an attractive goal in theory but difficult to achieve, and rearrangement of the macromolecules to reduce their size and degree of interpenetration, as with hypertonic saline or oligosaccharide treatments (see below).

MOLECULAR BASIS OF MUCOLYTIC THERAPY

In the normal state, that is, in the absence of infection or inflammation, the respiratory mucous gel is composed primarily of a three-dimensional, crosslinked network of mucous glycoproteins or mucins. Mucins are encoded by several different genes; at least 14 human MUC gene products have been described,[36] and several of them are significantly expressed in airway tissue (notably MUC2,

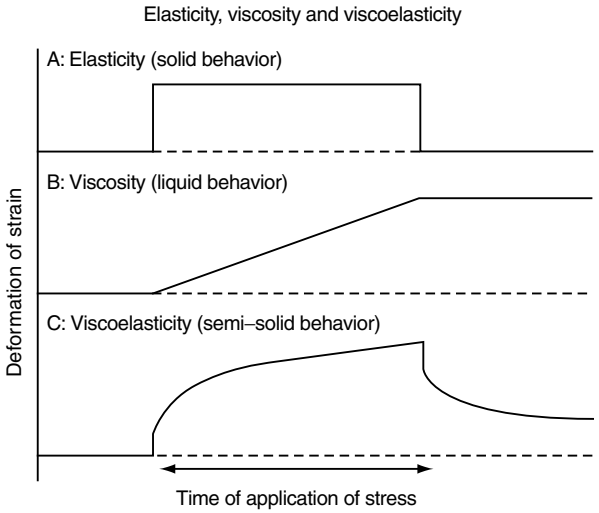

FIGURE 35-2 The viscoelastic behavior of a mucous gel. Stress–strain relationships are illustrated for idealized materials, namely (A) an elastic solid, where the displacement or strain is proportional to the applied force or stress; (B) a viscous liquid, where the rate of strain (displacement/time) is proportional to the stress; and (C) a viscoelastic semisolid, such as mucus. This responds instantaneously as a solid, with a very rapid displacement in response to an applied force. This is followed by a transition to a liquid-like response, where the rate of strain is constant with time. Finally a zone of viscous response is reached, where the rate of displacement is constant with time. After release of the applied force, the mucous gel only partially recoils to its initial position.

MUC5AC, and MUC5B).[37] Of the two major airway mucins, MUC5AC appears to be preferentially associated with goblet cells,[38] whereas MUC5B may be predominantly glandular. MUC1 is also expressed in airway tissue but as a surface mucin rather than in a soluble form (as are other mucin gene products, such as MUC3 and MUC4). The MUC genes all produce a similar product, namely a protein with tandem repeat units rich in serine, threonine, and proline and heavily glycosylated; these glycosylated regions are interspersed with largely nonglycosylated units that contain cysteine residues. The structure of soluble mucins is represented in Figure 35-4.[8,39]

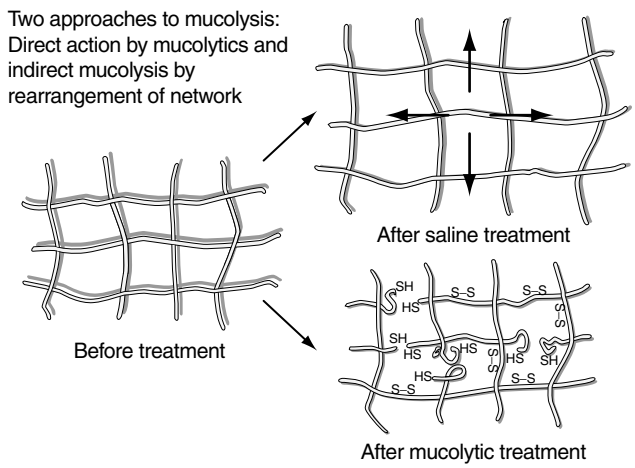

FIGURE 35-3 Two approaches to mucolysis: direct-acting mucolytics work by disrupting network bonds; indirect mucolytic action involves rearrangement of the crosslink network.

As indicated in Figure 35-4, the three-dimensional structure that forms the mucous gel is dependent upon a number of forms of bonding. The main elements include the following: (1) disulfide bonds—the intramolecular, covalent links that join glycoprotein subunits into extended macromolecular chains known as mucins; (2) because of their extended size, these mucin polymers readily form entanglements with neighboring macromolecules, and these act as time-dependent crosslinks, which are susceptible to mechanical degradation; (3) the sugar units that make up the oligosaccharide side chains (about 80% of the mucin weight) form hydrogen bonds with complementary units on neighboring mucins—although each bond is weak and easily broken, the numbers of bonds make this type of bonding potentially very important; (4) much stronger bonds due to van der Waals forces can potentially occur between complementary saccharide moieties on neighboring chains—however, the diversity of mucin oligosaccharides[25] may make such strong interactions uncommon; (5) mucins are also ionized, containing both positively charged amino acid residues and negatively charged sugar units, principally sialic acid and sulfated residues, and these increase in airway disease in general—in cystic fibrosis, the proportion of sulfated residues is particularly elevated,[40] and the ionic interactions between fixed negative charges result in a stiffer, more extended macromolecular conformation, effectively increasing the polymer size and adding to the numbers of entanglements; and (6) added to this in airway diseases characterized by infection and inflammation, especially cystic fibrosis, are the extra networks of high-molecular-weight (HMW) DNA and actin filaments released by dying leukocytes, exopolysaccharides secreted by bacteria, and glycosaminoglycans such as chrondroitin sulfate.[41]

GENERAL APPROACHES TO MUCOLYSIS

To change the physical properties of the viscous and rigid mucous gel, the direct strategy is mucolysis. Mucolysis refers to the disruption of the mucous gel, generally by altering the degree of crosslinking or the interactions between the macromolecules that form the gel. Normally, it is desirable to reduce the crosslinking and viscoelasticity in the mucous gel, in order to improve clearance, but occasionally, the mucus will be too thin for effective transport[42,43]; hence, increasing the crosslinking of the mucus with a mucospissic agent could be appropriate. Mucolytics and mucospissics are known collectively as mucotropic agents or mucomodulators.

DIRECT-ACTING MUCOLYTICS

The most important form of crosslinking in the mucous gel is due to the physical entanglements between neighboring mucin macromolecules as their broadly coiled spheres interpenetrate at the usual mucin concentrations (~1% by weight). A typical mucin molecule (molecular weight 2 to 3 MDa) in aqueous isotonic medium is randomly coiled,

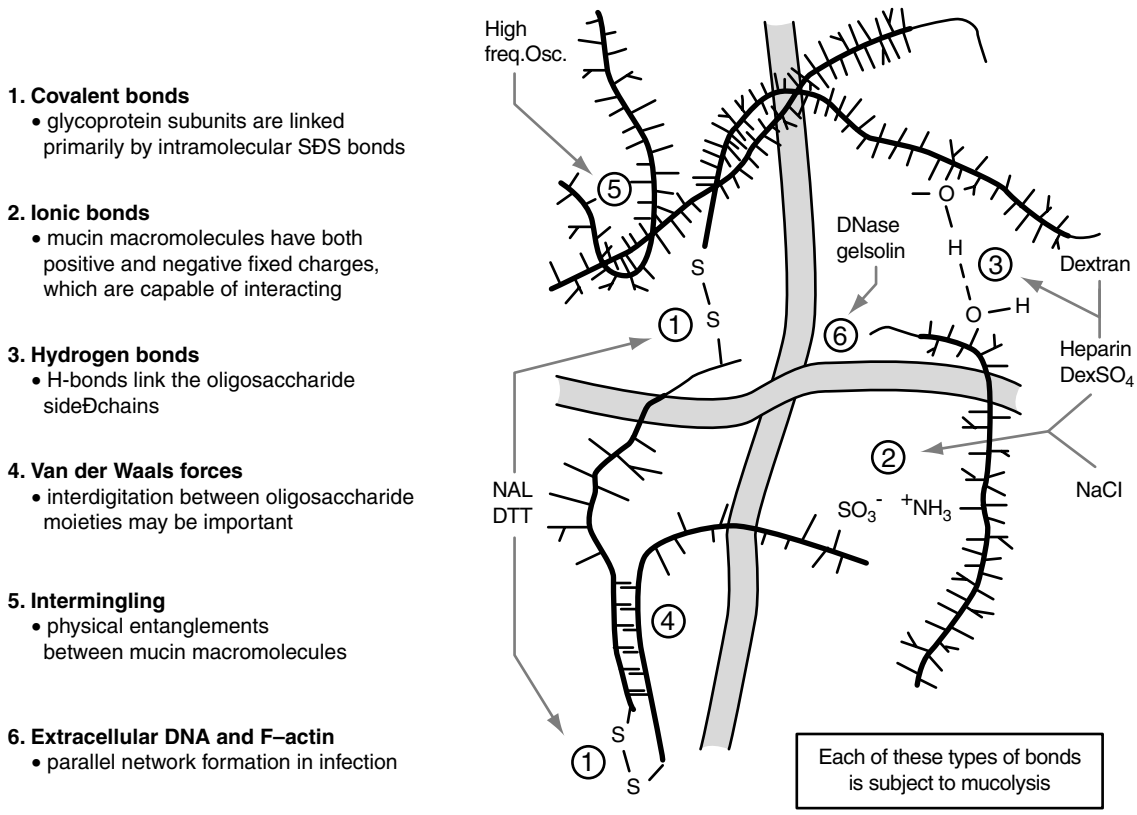

FIGURE 35-4 Types of bonds occurring in a mucous gel and the sites of interaction with various mucolytic treatments. DTT = dithiothreitol; NAC = *N*-acetylcysteine; rhDNase = recombinant human DNase. The mucous glycoproteins (mucins) consist of highly glycosylated subunits of ~500 kDa linked by nonglycosylated regions containing cysteines, which stabilize the structure via intramolecular bonds. The oligosaccharide side chains are composed mainly of *N*-acetylglucosamine, *N*-acetylgalactosamine, galactose, fucose, and sialic acid. These glycosidic units contain numerous sites for hydrogen bonds, as well as ionic interactions. In infection, additional large macromolecules, such as undegraded DNA and actin filaments released from leukocytes and bacteria, participate extensively in the three-dimensional structure of the gel. Adapted from Dasgupta B and King M.[39]

forming an extended, fuzzy sphere about 400 to 600 nm in diameter (radius of gyration (250 nm),[33] and at a concentration of 1% by weight (4.3×10^6 mol/L), the center of each molecule lies about 70 to 75 nm from its nearest neighbors. Hence, mucins at physiologic concentration exist as highly interpenetrating polymer coils, and the main form of crosslinking is through intermolecular entanglements that act as time-dependent crosslinks (Figure 35-5).

The basic mucin gene products consist of long, heavily glycosylated peptide units with shorter segments of largely nonglycosylated units containing cysteine residues.[33,37] Mucins are generally secreted as dimers or oligomers, held together by disulfide bridges derived from unpaired cysteine units near the nonglycosylated C-terminus of the mucin peptide, and stabilized by intramolecular disulfide bonds that form the so-called cystine knot.[44,45] Classic mucolytics, such as *N*-acetylcysteine[46] and other thiol reducing agents, degrade the three-dimensional network that forms the mucous gel by breaking the macromolecular backbone units that hold the polypeptide core together. For example, if the disulfide bridging unit that polymerizes a mucin dimer is reduced, the average length of the coiled mucin polymer is reduced by half, reducing its sphere of influence by perhaps a similar amount, and greatly decreasing the degree of entanglement with its neighboring macromolecules.

As indicated above, mucin macromolecules typically have molecular weights of 2 to 3 MDa, and in dilute solution they are 400 to 600 nm in size. At physiologic concentration (~1% mucoprotein by weight), the concentration of such a mucin would be 4.3×10^{-6} mol/L, that is, 2.6×10^{12} molecules/mm^3. The space available for each molecule is therefore about 73 nm before entanglement begins to occur. Given the typical size of the mucin (~500 nm), each mucin polymer will therefore interpenetrate (become entangled) with several neighboring molecules. Reducing the molecular length by 50% will greatly reduce the degree of interpenetration (from 6.8 to about 4.9 in the above example) and therefore reduce the crosslink density, which characterizes the viscoelasticity (resistance to deformation) of the gel. It is clear that it is not necessary to completely degrade the mucin molecule to greatly reduce the degree of crosslinking—only one break per mucin unit can produce a major effect (decreasing viscoelasticity to 36% of the initial value—$(4.9/6.8)^3$—in the above example, based on the number of crosslink points in a three-dimensional model).[47]

OPTIMIZING THE PROPERTIES OF MUCUS FOR CLEARANCE AND BARRIER FUNCTION

Little attention has been paid to maintaining or enhancing the barrier function of mucus in the process of developing

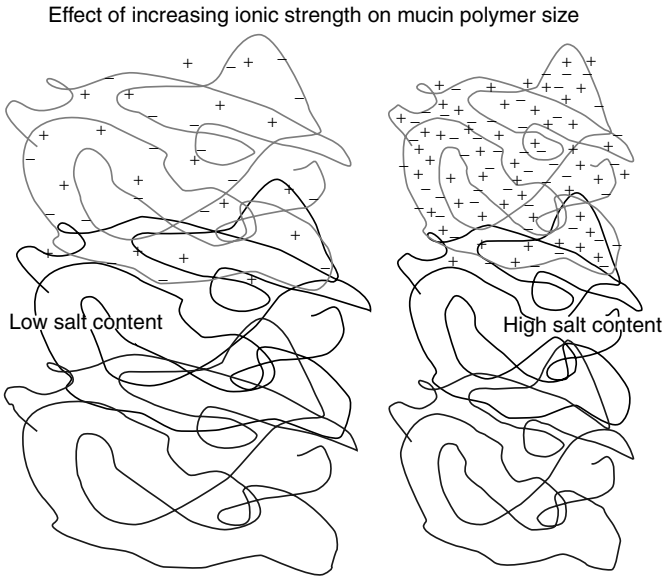

FIGURE 35-5 A model for intermolecular penetration in mucin gels. In the example shown, the mean size of each macromolecule is decreased by the addition of salt, which shields the fixed charges along the polymer backbone. This decreases the degree of penetration into neighboring molecules, thereby reducing the number of gel-forming crosslinks. The excess of fixed negative charges along the macromolecular chain is indicated by the *solid bars*. Mobile ions are indicated by + and − symbols.

mucokinetic therapies. Clearly, removing the mucous layer can lead to greatly improved access for airborne pathogens. This was shown by Ferrari and colleagues,[48] in a study in which mucolytic treatments allowed for better access of vectors for gene therapy, although the transfer of certain viral vectors appeared to be unaffected by mucus.[49] Intestinal mucins have been shown to inhibit rotavirus infection.[50] The results of this latter study suggest that mucin's capacity to inhibit viral infection may relate to specific binding between terminal oligosaccharides on the mucins. Mucolytics, especially those that could remove these specific binding sites, could reduce the effectiveness of this protective effect.

It may be possible to minimize or reduce bacterial transfer by *antimucolytic* or *mucomodulator* therapy. The principle is to increase the concentration of crosslinking sites in the mucin glycoprotein gel network, thereby raising mucin gel viscoelasticity and/or forming poorly soluble mucin complexes. The result would be a less aerosolizable respiratory secretion, which could decrease the transmission of airborne pathogens. The mucomodulation would have to be carried out in such a way as to minimize the change in mucociliary clearability.

One approach would be to increase the concentration of divalent cations in the mucus through the administration of Ca^{2+} and/or Mg^{2+} solutions. Conceptually, this is the opposite of what occurs in nature during mucin exocytosis, where the Ca^{2+} crosslinks that hold intracellular mucin granules tightly together give way to much looser interactions as Na^{+} exchanges for Ca^{2+} during fusion with the apical membrane.[51] Using an ex vivo frog palate model, we were able to increase mucous clumping with Ca^{2+} administration while maintaining mucociliary clearance.[52] A second approach could involve the administration of HMW dextran, which has approximately the same molecular weight (~500 kDa) as the subunits of mucin macromolecules. HMW dextran tends to raise elasticity relative to viscosity[53]; its use would therefore tend to favor mucociliary clearability at the expense of cough clearability and aerosolizability.[1] Other mucomodulator approaches could include the use of sodium tetraborate,[22] which causes reversible crosslink formation between the galactose units, the major neutral sugar component of mucins, and polycationic peptides, such as poly-L-lysine or poly-L-arginine, which would interact with the negative charges along the mucous glycoprotein, producing additional crosslinks.

Mucomodulator therapy directed against virus uptake may be more complex than for limiting the spread of bacteria because of the much smaller dimensions of viruses and could require modulation or enhancement of recognition sites to inhibit viral transfer.

CONCLUSIONS

Mucus forms a protective barrier for the airway epithelium and represents the first line of defense against inhaled irritants and pathogens. Normal airway hygiene is maintained by mucociliary clearance, and when this mechanism breaks down or is overloaded, cough clearance takes over. The unique viscoelastic and adhesive properties of mucus are important determinants of these two protective mechanisms. The physical properties of mucus derive largely from its content of highly glycosylated mucous glycoproteins, the degree of hydration of which is related to transepithelial ion and water transport.

Therapeutic modification of mucous viscoelasticity can be achieved with a variety of mucolytic approaches, which involve disrupting the intermolecular interactions that give mucus its gel-like properties. In the design of mucolytic therapies to improve airway clearance, attention should be paid to preserving the important barrier function of the mucous layer.

REFERENCES

1. King M, Rubin BK. Rheology of airway mucus: relationship with clearance function. In: Takashima T, Shimura S, editors. Airway secretion: physiological bases for the control of mucous hypersecretion. New York: Marcel Dekker; 1994. p. 283–314.
2. Wanner A. Clinical aspects of mucociliary transport. Am Rev Respir Dis 1977;116:73–109.
3. Zayas JG, Man GCW, King M. Tracheal mucus rheology in patients undergoing diagnostic bronchoscopy: interrelations with smoking and cancer. Am Rev Respir Dis 1990; 141:1107–13.
4. Wanner A, Salathé M, O'Riordan TG. Mucociliary clearance in the airways. Am J Respir Crit Care Med 1996;154:1868–902.
5. Morgenroth K, Bolz J. Morphological features of the interaction between mucus and surfactant on the bronchial mucosa. Respiration 1985;47:225–31.
6. Widdicombe JH, Bastacky SJ, Wu DXY, Lee CY. Regulation of depth and composition of airway surface liquid. Eur Respir J 1997;10:2892–7.

7. Rubin BK, Tomkiewicz RP, King M. Mucoactive agents: old and new. In: Wilmott RW, editor. The pediatric lung. Basel: Birkhäuser; 1997. p. 155–79.
8. King M, Rubin BK. Mucus controlling agents: past and present. Respir Care Clin North Am 1999;5:575–94.
9. King M, Rubin BK. Pharmacological approaches to discovery and development of new mucolytic agents. Advanced Drug Delivery Rev 2002;54:1475–90.
10. King M, Rubin BK. Mucus physiology and pathophysiology: therapeutic aspects. In: Derenne JP, Whitelaw WA, Similowski T, editors. Acute respiratory failure in COPD. Lung Biology in Health and Disease Series. New York: Marcel Dekker; 1996. p. 391–411.
11. Blake JR. On the movement of mucus in the lung. J Biomechanics 1975;8:179–90.
12. King M, Agarwal M, Shukla JB. A planar model for mucociliary transport: effect of mucus viscoelasticity. Biorheology 1993;30:49–61.
13. Gil J, Weibel ER. Extracellular lining of bronchioles after perfusion–fixation of rat lungs for electron microscopy. Anat Rec 1971;169:185–200.
14. Van As A. Pulmonary airway clearance mechanisms: a reappraisal. Am Rev Respir Dis 1977;115:721–6.
15. Boucher RC, Stutts MJ, Bromberg PA, Gatzy JT. Regional differences in airway surface liquid composition. J Appl Physiol 1981;50:613–20.
16. Dwyer TM. Urea: an estimate of airway surface liquid dilution in expired breath condensate. Am J Respir Crit Care Med 2003;167:A425.
17. Boucher RC. State of the art: human airway ion transport. Am J Respir Crit Care Med 1994;150:271–81.
18. Govindaraju K, Cowley EA, Eidelman DH, Lloyd DK. Analysis of proteins in micro samples of rat airway surface fluid by capillary electrophoresis. J Chromatogr Biomed Sci Applic 1998;705:223–30.
19. King M. Mucus, mucociliary clearance and coughing. In: Bates DV, editor. Respiratory function in disease. 3rd ed. Philadelphia: Saunders; 1989. p. 69–78.
20. King M. Role of mucus viscoelasticity in cough clearance. Biorheology 1987;24:589–97.
21. King M, Brock G, Lundell C. Clearance of mucus by simulated cough. J Appl Physiol 1985;58:1776–82.
22. King M, Zahm JM, Pierrot D, et al. The role of mucus gel viscosity, spinnability, and adhesive properties in clearance by simulated cough. Biorheology 1989;26:737–45.
23. Zahm JM, King M, Duvivier C, et al. Role of simulated repetitive coughing in mucus clearance. Eur Respir J 1991; 4:311–5.
24. King M, Wight A, De Sanctis GT, et al. Mucus hypersecretion and viscoelasticity changes in cigarette-smoking dogs. Exp Lung Res 1989;15:375–89.
25. Klein A, Strecker G, Lamblin G, Roussel P. Structural analysis of mucin-type O-linked oligosaccharides. Meth Mol Biol 2000;125:191–209.
26. Turner RB, Wecker MT, Pohl G, et al. Efficiency of tremacamra, a soluble intercellular adhesion molecule 1, for experimental rhinovirus infection: a randomized clinical trial. JAMA 1999;19:1797–804.
27. Bisaillon M, Senechal S, Bernier L, Lemay G. A glycosyl hydrolase activity of mammalian reovirus sigma1 protein can contribute to viral infection through a mucus layer. J Mol Biol 1999;286:759–73.
28. Szymanski CM, King M, Haardt M, Armstrong GD. Camphylobacter jejuni motility and invasion of Caco-2 cells. Infect Immun 1995;65:4295–300.
29. Mantle M, Stewart G, Zayas G, King M. The disulphide-bond content and rheological properties of intestinal mucins from normal subjects and patients with cystic fibrosis. Biochem J 1990;266:597–604.
30. Bhaskar KR, Garik P, Turner BS, et al. Viscous fingering of HCl through gastric mucin. Nature 1992;360:458–61.
31. Holma B, Hegg PO. pH- and protein-dependent buffer capacity and viscosity of respiratory mucus: their interrelationships and influence on health. Sci Total Environ 1989;84: 71–82.
32. Di Girolamo R, Liston J, Matches J. Ionic bonding, the mechanism of viral uptake by shellfish mucus. Appl Environ Microbiol 1977;33:19–25.
33. Thornton DJ, Davies JR, Carlstedt I, Sheehan JK. Structure and biochemistry of human respiratory mucins. In: Rogers DF, Lethem MI, editors. Airway mucus: basic mechanisms and clinical perspectives. Basel: Birkhäuser; 1997. p. 19–39.
34. Puchelle E, Zahm JM, de Bentzmann S, Gaillard D. Mucus and airway epithelium alterations in cystic fibrosis. In: Rogers DF, Lethem MI, editors. Airway mucus: basic mechanisms and clinical perspectives. Basel: Birkhäuser; 1997. p. 301–26.
35. Dasgupta B, Tomkiewicz RP, Boyd WA, et al. Effects of combined treatment with rhDNase and airflow oscillations on spinnability of cystic fibrosis sputum in vitro. Pediatr Pulmonol 1995;20:78–82.
36. Rogers DF. Mucoactive drugs for asthma and COPD: any place in therapy? Expert Opin Investig Drugs 2002:11:15–35.
37. Rose MC, Gendler SJ. Airway mucin genes and gene products. In: Rogers DF, Lethem MI, editors. Airway mucus: basic mechanisms and clinical perspectives. Basel: Birkhäuser; 1997. p. 41–66.
38. Hovenberg HW, Davies JR, Carlstedt I. Different mucins are produced by the surface epithelium and the submucosa in human trachea: identification of MUC5AC as a major mucin from the goblet cells. Biochem J 1996;318:319–24.
39. Dasgupta B, King M. Molecular basis for mucolytic therapy. Can Respir J 1995;2:223–30.
40. Chace KV, Leahy DS, Martin R, et al. Respiratory mucous secretions in patients with cystic fibrosis: relationship between levels of highly sulfated mucin component and severity of the disease. Clin Chim Acta 1983;132:143–55.
41. Rahmoune H, Lamblin G, Lafitte JJ, et al. Chondroitin sulfate in sputum from patients with cystic fibrosis and chronic bronchitis. Am J Respir Cell Mol Biol 1991;5:315–20.
42. Puchelle E, Zahm JM, Polu JM, Sadoul P. Drug effects on viscoelasticity of mucus. Eur J Respir Dis 1980;61:195–208.
43. Rubin BK, MacLeod PM, Sturgess J, King M. Recurrent respiratory infections in a child with fucosidosis: is the mucus too thin for effective transport? Pediatr Pulmonol 1991;10: 304–9.
44. Bell SL, Khatri IA, Xu G, Forstner JF. Evidence that a peptide corresponding to the rat Muc2 C-terminus undergoes disulphide-mediated dimerization. Eur J Biochem 1998; 253:123–31.
45. Perez-Vilar J, Hill RL. The structure and assembly of secreted mucins. J Biol Chem 1999;274:31751–4.
46. Sheffner AL, Medler EM, Jacobs LW, Sarrett HP. The in vitro reduction in viscosity of human tracheobronchial secretions by acetylcysteine. Am Rev Respir Dis 1964;90: 721–9.
47. Ferry JD. Viscoelastic properties of polymers. 2nd ed. New York: Wiley; 1970. p. 268–70.
48. Ferrari S, Kitson C, Farley R, et al. Mucus altering agents as adjuncts for nonviral gene transfer to airway epithelium. Gene Ther 2001;8:1380–6.
49. Yonemitsu Y, Kitson C, Ferrari S, et al. Efficient gene transfer to airway epithelium using recombinant Sendai virus. Nat Biotechnol 2000;18:970–3.

50. Chen CC, Baylor M, Bass DM. Murine intestinal mucins inhibit rotavirus infection. Gastroenterology 1993;105: 84–92.
51. Verdugo P. Molecular biophysics of mucin secretion. In: Takashima T, Shimura S, editors. Airway secretion: physiological bases for the control of mucous hypersecretion. New York: Marcel Dekker; 1994. p. 101–21.
52. King M, Zayas JG. Mucomodulator therapy in cystic fibrosis: balancing mucus leavability against the spread of airborne pathogens. Pediatr Pulmonol 2004;37 Suppl 126:77–9.
53. Feng W, Speert DP, King M. Effect of dextran molecular weight on CF sputum rigidity: further evidence for the mechanism of action. Pediatr Pulmonol 1997;14S:273.

CHAPTER 36

MUCOCILIARY CLEARANCE AND CYSTIC FIBROSIS

Mark R. Elkins, Peter T. P. Bye

Several defense mechanisms operate within the human airways to protect against the potentially damaging effects of inhaled particles. These include mucociliary clearance, cough clearance, and antimicrobial factors in the airway surface fluid.[1,2] Mucociliary clearance is often considered the primary physical mechanism, with cough serving to augment clearance when mucociliary clearance is abnormal or insufficient.[2] Cough clearance, however, appears to be effective only in the proximal generations of airways.[2–4]

Mucociliary clearance operates through the action of ciliated cells lining the airway epithelium. These cells beat within a layer of fluid known as the sol layer. The tips of the cilia just contact an overlying mucous layer. The cilia beat in synchrony to continuously move the mucous layer up the bronchial tree. Some evidence exists that the two layers might be separated by a thin layer of surfactant,[5] but others have suggested that the two layers are, in fact, a continuum, with a gradient of glycosylated macromolecule concentration from the air–liquid interface down to the epithelial surface.[6,7] In this chapter, two separate layers are recognized. Inhaled particles become trapped in the moving mucous layer and are transported into progressively more proximal airways until, they can be cleared from the bronchial tree.

Mucociliary clearance applies much lower shear forces to the mucous layer than those that occur with coughing. For the forces applied during mucociliary clearance to be effective, several physiologic parameters are required to be within their normal ranges: the depth and chemical composition of the airway surface liquid layer, the rheology of the mucous layer, and the synchrony and beat frequency of the ciliated cells.

The use of mucociliary clearance as an outcome measure is increasing in clinical trials on therapeutic interventions for use in patients with cystic fibrosis (CF). There are several reasons for this. It is able to demonstrate a mechanism of action of therapeutic agents designed to reverse mucous stasis. It circumvents the problems of swallowed secretions and expectorated saliva inherent in expectorated sputum measures. It is also able to provide some information about clearance rates in different regions of the lung.

There is considerable variation in the methods used by different investigators to measure mucociliary clearance. This variation can have a major impact on results and can make comparisons between studies meaningless. It is therefore important that scientific, medical, and allied health professionals understand how mucociliary clearance studies have been performed, so that the results can be interpreted correctly. Using CF as an example, this chapter summarizes the existing literature on mucociliary clearance measurement. It also reviews the various interventions that have been studied in controlled trials to improve airway clearance in this patient group.

MEASUREMENT OF MUCOCILIARY CLEARANCE

Quantification of mucociliary clearance can be reported as a linear velocity or as a percentage clearance rate. The velocity of mucous movement in the trachea has been studied in healthy subjects on seven occasions (Table 36-1). The mean tracheal mucous velocity (TMV) in the studies ranged from 3.6 to 8.9 mm/min. Metaanalysis of these results with a random effects model provides an overall estimate of 5 mm/min, with a 95% confidence interval (95% CI) of 4 to 6 for TMV in healthy adults.

It is generally accepted that mucociliary clearance in the periphery of the lung is slow, with progressive increases in speed through the airway generations to the trachea.[8] Comparisons of mucous transport rates in various airway generations support this.[9,10] Although measurement of TMV has the virtue of simplicity and ease of application, the variation in mucous transport velocity along the airway has led researchers to examine clearance of mucus from the whole lung. This generally involves the inhalation of a radioaerosol and subsequent measurement of the rate at which the radioactivity is cleared from the lung.[11]

The delivery of the radioaerosol to the airways must be carefully controlled to ensure that it deposits in both central

Table 36-1 Studies of Tracheal Mucous Velocity (TMV) in Healthy Adults

			TMV (mm/min)	
Author	*Year*	*N*	*Mean*	*SD*
Yeates et al[126]	1975	42	3.6	2.7
Friedman et al[127]	1977	5	8.0	1.8
Goodman et al[128]	1978	6	8.9	1.8
Foster et al[9]	1980	7	5.5	0.4
Yeates et al[10]	1981	22	5.1	2.9
Mussatto et al[129]	1988	6	4.9	1.3
Li et al[130]	2000	18	3.9	0.9

and peripheral airways and that this distribution is reproducible. This is essential for interpreting the results, regardless of whether mucociliary clearance is calculated for defined regions or only for the lung as a whole. The breathing pattern adopted during inhalation of the radioaerosol must be closely controlled to achieve an appropriate distribution of the deposited radioactivity.[12] The required breathing pattern will vary according to the nature of the aerosol, namely, the mass median aerodynamic diameter, and the amount of variability within the range of particle sizes produced.[12,13]

For the quantification of clearance of radioactivity from the lung, the margins of the lung must also be identified objectively and reproducibly. This has been achieved using inhaled radioactive gases[14–16] or transmission images of the thorax.[13,17–19] Transmission images may be affected by attenuation from the liver and by diaphragmatic motion, but the patient is exposed to less radiation, and the images may be recorded simultaneously with the emission images. Within the identified margins, some investigators have defined somewhat arbitrary regions of interest, such as upper, middle, and lower zones.[13,19,20] A distinction between central and peripheral lung fields has also been made,[14,15,21–26] although without three-dimensional imaging of the lung, this remains an approximation.

The differences that arise due to variation in measurement methodology may explain the lack of consistency in reported mucociliary clearance measurements in healthy subjects even when the same index of clearance is used. For example, eight authors have used the percentage of inhaled radioactivity cleared in 60 minutes (%C60) as an outcome measure in healthy subjects (Table 36-2). Metaanalysis of these results with a random effects model provides an overall estimate of 21% (95% CI, 14 to 28), although proposal heterogeneity is acknowledged.

Comparisons between studies are further confounded when different outcome measures are used. The time point specified for the outcome %C60 is arbitrary, and others (eg, %C20, %C90, and %C120) have been reported.[18,27,28] Some authors have calculated instead the average percentage cleared per minute over a given period.[29] Instead of reporting the percentage clearance at a given time point, other authors have reported the time taken to clear a given percentage of the initially deposited radioactive tracer activity from the lung.[30] Others have plotted the retained activity against time and reported the area under the curve as an indirect measure of mucociliary clearance.[31]

Table 36-2 Studies of Mucociliary Clearance in Healthy Adults, Using the Percentage of Inhaled Radioactivity Cleared in 60 minutes (%C60) as an Outcome Measure

			Mucociliary clearance (%C60)	
Author	*Year*	*N*	*Mean*	*SD*
Sanchis et al[131]	1973	9	0.5	7.2
Thomson et al[132]	1973	15	10.0	8.0
Pavia et al[133]	1983	9	15.0	7.0
Vastag et al[36]	1985	80	36.9	12.6
Del Donno et al[34]	1988	33	41.0	NS
Regnis et al[13]	1994	12	28.0	4.0
Mortensen et al[39]	1994	62	19.8	9.9
Bennett et al[15]	1996	12	26.2	10.5
Robinson[19]	2000	17	28.0	3.7

NS = not stated.
Unpublished data for one study were obtained directly from the authors.[15] Data from two studies were measured from the graph.[124,125]

Although variation occurs when different methods of measuring mucociliary clearance are used, results are usually highly repeatable within subjects. For example, where %C60 has been measured in healthy subjects, the absolute percentage difference between the results of repeat studies has been reported to be 5.4% or less,[13,19] and the coefficient of variation has been reported to be 15.6% or less.[32,33] Similar good repeatability has been reported for subjects with respiratory disease.[13,19,34,35] This level of repeatability is suitable for gauging the effect of respiratory pathologies on mucociliary clearance, as well as the effects of therapeutic interventions designed to accelerate removal of secretions from the airways.

FACTORS AFFECTING MUCOCILIARY CLEARANCE IN HEALTH

Age and Gender

There have been three reported studies on the effect of age on mucociliary clearance in healthy subjects.[32,36,37] Puchelle and colleagues noted significantly slower mucociliary clearance in subjects aged 55 to 67 years than in those aged 21 to 37 years, with mean (SD) %C60 values of 21.8% (7.8%) and 34.1% (14.1%), respectively.[32] A linear association between age and mucociliary clearance was also identified. This was later confirmed in a much larger study ($n = 80$) by Vastag and colleagues, who demonstrated a 3.7% reduction in %C60 for each decade increase in age from 20 to 80 years.[36] Similar results were reported by Incalzi and colleagues, extending up to 90-year-old subjects.[37] This effect may be due to an age-related decline in ciliary beat frequency.[38]

Unlike age, gender probably does not have an effect on mucociliary clearance. Studies in which %C60 has been examined in healthy subjects have not shown a difference in mucociliary clearance between the genders.[19,33,39] Among healthy nonsmokers used as a control group, Svartengren and colleagues noted significantly faster mucociliary clearance after 2 hours in the females than in the males.[40] However, in a subsequent study conducted specifically to examine this difference, mucociliary clearance was measured

for 6 hours, and no statistically significant difference was found between healthy males and females of comparable age.[24]

Gravity

Isawa and colleagues studied mucociliary clearance in 11 healthy subjects in the supine and right lateral decubitus positions. They found no effect of gravity on mucociliary clearance.[41] Similarly, in 7 healthy subjects, no difference in mucociliary clearance was noted between the upright position and 25° head-down tilt.[42]

Arousal from Sleep and Exercise

Mucociliary clearance in healthy subjects while awake and during sleep has been compared in two studies.[43,44] Both identified a sleep-related reduction in mucociliary clearance in healthy subjects. Exercise has been shown to increase mucociliary clearance in healthy subjects in comparison to quiet resting breathing while awake.[45]

Neural Control

Isolated elements of the mucociliary system have been extensively studied with respect to their susceptibility to autonomic regulation, including submucosal glands,[46,47] epithelial cells,[48] and cilia.[49] Less is known about autonomic control of overall mucociliary clearance in health. However, studies of overall mucociliary clearance in healthy subjects have shown that it is increased by cholinergic and β-adrenergic agonists[14,50,51] and by neuropeptides.[52] Conversely, mucociliary clearance is reduced by the cholinergic antagonist atropine.[50,53]

CYSTIC FIBROSIS

CF occurs as a result of mutations in the cystic fibrosis transmembrane conductance regulator (CFTR) gene. In the lung, this defect results in excessive airway Na^+ absorption and defective Cl^- secretion.[6] Other mechanisms may also contribute to the pathophysiologic changes in the CF lung, such as aberrant regulation of bicarbonate secretion. Epithelial Na^+ conductance is variable in other epithelial tissues, being decreased in the sweat duct and increased in the intestine. Epithelial tissue in the pancreas and reproductive organs may also be affected.

CFTR is a cyclic AMP-regulated epithelial Cl^- channel and may regulate several other transport proteins. Aberrant epithelial ion transport in CF therefore appears to result from a combination of defective Cl^- channel function and an impaired regulatory function of CFTR, which, in turn, is linked to impaired mucociliary clearance and development of chronic lung disease. Some aspects of how these defects produce the characteristic lung disease have been investigated,[54–59] although many details remain unclear. Two major models have been put forward to explain the mechanism by which abnormal CFTR disrupts mucociliary clearance. In the *isotonic volume depletion model*,[60] Cl^- secretion is reduced and Na^+ absorption is increased across the CF airway epithelium. This net loss of salt from the airway lumen involves loss of water, dehydrating airway secretions and depleting the sol layer. These changes disrupt the mucociliary mechanism, with retained mucus becoming a nidus for infection. The *compositional model*,[54,61] however, is based on Na^+ and Cl^- absorption being in excess of water absorption in the healthy airway, creating a hypotonic sol layer. The ion transport abnormalities in CF tend to increase the salt concentration in the sol layer, thus impairing the bactericidal activity of salt-sensitive antimicrobial peptides. Infection of airway mucus alters its rheology, so that the mucociliary mechanism is less effective. Currently, the weight of evidence favors the former model.

CF-affected persons characteristically produce excess tenacious secretions in their airways. These secretions are frequently unable to be cleared by mucociliary clearance, even with the assistance of cough clearance. The prolonged retention of secretions can result in airway obstruction, further compounding poor clearance and providing a nidus for infection. Typically, colonization by *Haemophilus influenzae* and *Staphylococcus aureus* occurs early. Colonization by *Pseudomonas aeruginosa* tends to occur later. This is the most common pathogen[62] (Figure 36-1).

There is evidence that infants with CF exhibit inflammation and bacterial colonization of the airways as early as 1 or 2 months of age.[63,64] Lung disease in CF is rarely evident at birth but develops progressively with age. The progressive lung disease in CF appears to be due to chronic airway infection and neutrophil-dominated airway inflammation,[65,66] although the complex interaction between these factors remains incompletely understood.[67]

AIRWAY SECRETIONS

The causes of the abnormal rheologic and chemical properties of CF secretions are complex. Chronic colonization of the airways by pathogenic bacteria in CF leads to the influx of large numbers of neutrophils. When these neutrophils degenerate, their cellular contents are released. The large amounts of proteases, elastases, and other proteolytic enzymes released are believed to damage the epithelium and underlying airway wall. This appears to be the major cause of bronchiectatic changes in CF.[67] Neutrophils also contain large quantities of nuclear DNA and cytoskeletal actin, both

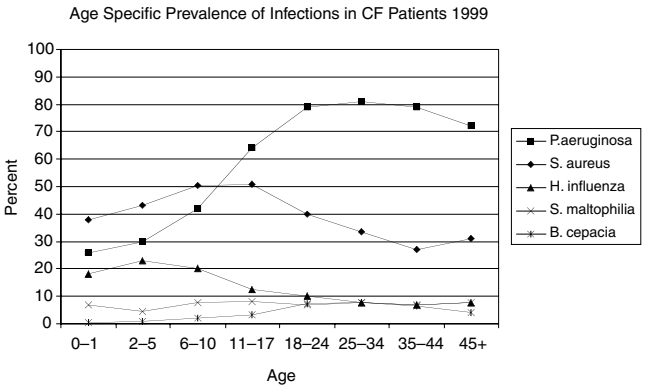

FIGURE 36-1 Prevalence of infectious organisms in the sputum of CF patients in the United States in 1999, by age group. Reproduced with permission from the US Cystic Fibrosis Foundation.[62]

of which markedly increase the viscosity of airway mucus.[68] Also present in purulent CF sputum are large amounts of polymerized, polyanionic DNA. These strands of DNA copolymerize with actin and interact with polyionic mucin molecules.[69] The resulting tangled networks are resistant to degradation by deoxyribonuclease. Filamentous actin also forms long protease-resistant filaments that become entangled in the mucous gel, increasing rigidity.[70] All of these interactions contribute to the increased viscosity of CF sputum.

Hypertrophy of the mucus-secreting glands and proliferation of goblet cells are other sequelae of chronic infection and inflammation.[71] These increased populations of secretory cells, as well as the increased basal rate of secretion of mucus by individual cells and the greater response to cholinergic stimulation, all contribute to the hypersecretion that occurs in the CF airway.[72]

The rheologic abnormalities of mucus in CF are not, however, related only to purulence. The viscosity has also been demonstrated to correlate with the sulfate concentration in sputum.[73] Mucins from CF-affected persons are hypersulfated as a result of posttranslational modification. This hypersulfation is also known to increase with the severity of disease,[74] and this appears to be independent of the effects of both infection and inflammation.[75,76] It could also facilitate colonization of the airways by organisms such as *P. aeruginosa*.[77]

The adhesivity of CF mucus is increased, due to abnormal ratios of various phospholipid subclasses. Increased adhesion of CF mucus to the respiratory mucosa subsequently promotes mucous stasis and airway obstruction.[78] The cleavage of DNA by recombinant human deoxyribonuclease alters the glycoprotein–DNA interaction in CF sputum. This is likely to unmask the associated lipids, allowing them to play a surface-active role at the interface between the airway mucosa and mucus. Presumably this is why in vitro incubation of CF mucus with recombinant human deoxyribonuclease was found to significantly improve the surface properties of the mucus, accelerating its transport by ciliary activity.[79] In that study, the increased recovery of phosphatidylglycerol was significantly associated with the improvements in mucous gel surface properties and transport capacity of ciliary activity.[79]

Finally, the rheologic properties of CF mucus are affected by abnormal exocytosis—the secretion of mucins from goblet cells and submucosal glands and the resultant swelling of mucous plaques.[80]

AIRWAY CILIA

The cilia of persons with CF have been shown to be normal in both structure and function.[81,82] Although some ultrastructural changes have been observed with electron microscopy, these changes are usually minor, nonspecific, and indicative of chronic infection.[81,83–86] Areas of epithelial desquamation are sequelae of chronic infection in the CF airway. However, these areas are usually not sufficient to alter the mucociliary clearance rate of the lung as a whole. Despite an intact epithelium and normal ciliary structure, infection and inflammation are known to slow the frequency at which the cilia beat.[87,88] For example, pyocyanin and 1-hydroxyphenazine are toxins produced by *P. aeruginosa* that appear to cause the reduction in ciliary beat frequency. Human neutrophil elastase has a similar effect and also disrupts the epithelium.

AIRWAY HYDRATION

The ion transport abnormality in CF leads to osmotic movement of water out of the airway lumen.[59,89] The total volume and therefore the depth of the sol layer are reduced, supporting the isotonic model discussed above. In health, the overlying mucous layer is supported by the sol layer, so that it just touches the tips of the cilia. The depletion of the sol layer in CF allows the mucous layer to come into full contact within the cilia and adhere directly to them, thus disrupting the normal mucociliary clearance mechanism.[59]

The osmotic movement of water out of the airway lumen also decreases the water content of the mucus itself.[90] This increases the concentration of mucin molecules within the mucous gel. Adjacent mucin molecules subsequently alter their interaction, increasing the repulsion between like-charged regions of the molecules. This results in mucin molecules that are more extended in aqueous solution. Entanglements and hence viscosity are therefore increased.

MUCOCILIARY CLEARANCE IN CF

Abnormally slow mucociliary clearance is a central tenet of the development of lung pathology in the current, predominant working hypotheses for CF lung disease.[55,56] Although slower clearance in subjects with CF than in healthy subjects has been demonstrated, not all studies have shown a difference, and some have shown the converse. It has therefore been suggested that the literature is inconclusive on this issue.[11] However, metaanalysis of the results of these studies supports slower clearance in subjects with CF than in healthy subjects, whether measured by TMV or mucociliary clearance. Metaanalysis with a random effects model provides an overall estimate that TMV is 8 mm/min slower in subjects with CF than in healthy subjects (95% CI, 0 to 15) (Table 36-3). A similar analysis of mucociliary clearance studies indicates that the %C60 is 3% less in subjects with CF than in healthy subjects (95% CI, −3 to 9) (Table 36-4).

The heterogeneity in the results of these studies may be due to the differences in measurement techniques discussed above. An additional confounder is that the subjects of these studies are generally adults with CF, in whom the effects of chronic infection are superimposed on the underlying disease process. It is uncertain to what extent the slower clearance could be due to chronic infection rather than cause it. Alternatively, both could be directly caused by the primary genetic defect or some other factor. Regardless of its cause, the slow mucociliary clearance in this population can be improved, and interventions that are shown to do so can be further examined to find whether this effect is clinically beneficial, for example, hypertonic saline.[91]

Table 36-3 Metaanalysis of Tracheal Mucous Velocity Studies Comparing Healthy Subjects and Subjects with Cystic Fibrosis

		Healthy		*CF*				
Study	*Year*	N	*Mean (SD)*	N	*Mean (SD)*	*Weighted mean difference (95% CI)*	*Weight (%)*	*Weighted mean difference (95% CI)*
Wood[134]	1975	20	20.10 (6.30)	14	2.60 (3.30)		32.48	17.50 (14.24, 20.76)
Yeates[135]	1976	42	4.70 (2.70)	20	3.42 (3.58)		33.83	1.28 (−0.49, 3.05)
Wong[136]	1977	7	4.36 (1.31)	13	−0.37 (3.16)		33.69	4.73 (2.76, 6.70)
Total		69		47			100.0	7.71 (−0.07, 15.49)

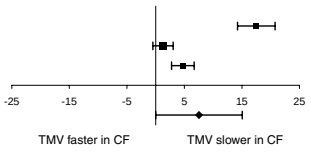

Table 36-4 Metaanalysis of Mucociliary Clearance Studies Comparing Healthy Subjects and Subjects with Cystic Fibrosis

	Healthy		*CF*				
Study	N	*Mean (SD)*	N	*Mean (SD)*	*Weighted mean difference (95% CI)*	*Weight (%)*	*Weighted mean difference (95% CI)*
Sanchis et al[131]	9	0.50 (7.2)	13	15.20 (11.98)		13.09	−14.70 (−22.74, −6.66)
Thomson et al[132]	15	22.00 (15)	2	36.50 (9.19)		8.95	−14.50 (−29.33, 0.33)
Kollberg et al[83]	63	62.00 (22)	5	60.20 (30.23)		3.89	1.80 (−25.25, 28.85)
Vastag et al,[36] App et al[104]	80	36.90 (12.6)	23	29.10 (8.2)		15.63	7.80 (3.46, 12.14)
Matthys and Kohler[134]	8	38.33 (9.4)	14	30.09 (10.56)		12.71	8.24 (−0.31, 16.79)
Regnis et al[13]	12	28.00 (4)	30	13.00 (2)		16.55	15.00 (12.63, 17.37)
Bennett et al[15]	12	26.21 (10.5)	14	31.83 (10.8)		12.95	−5.62 (−13.85, 2.61)
Robinson et al[19]	17	28.00 (3.7)	59	14.20 (1.40)		16.73	13.80 (12.01, 15.59)
Total	216		160			100.0	3.25 (−2.83, 9.33)

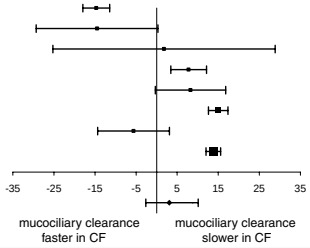

Unpublished data for one study were obtained directly from the authors.[15] Data for three studies were measured from graphs.[83,132,134]

Intrasubject reproducibility (9%) and intersubject variability (12%) have also been reported to be very acceptable in subjects with CF,[19] further supporting the use of mucociliary clearance rate as a useful outcome measure in future clinical trials.

PHARMACOLOGIC THERAPIES TO ENHANCE MUCOCILIARY CLEARANCE IN CF

Several pharmacologic agents have been shown to increase mucociliary clearance in subjects with CF when compared with placebo.[15,92,93] Differences in methodology between laboratories again confound comparisons of the relative effectiveness of pharmacologic interventions in different studies. Not all agents with the apparent potential to improve mucociliary clearance in CF in vitro have proven to do so on in vivo testing.

Terbutaline

The β_2-agonist terbutaline sulfate rapidly and significantly accelerates mucociliary clearance in healthy subjects.[33] It is also effective in subjects with asthma and bronchiectasis, although to a lesser degree. Mortensen also examined the effect of terbutaline in 10 subjects with CF.[33] Subjects inhaled 1 mg of terbutaline via a pressurized, metered dose inhaler and spacer, and mucociliary clearance was monitored for 3 hours. No significant difference in mucociliary clearance was evident between the placebo and terbutaline days. Terbutaline appears to increase mucociliary clearance in healthy subjects via increases in ciliary beat frequency[94,95] and Cl^- secretion with water cotransport.[96–98] β-Agonists are unable to stimulate the defective Cl^- secretion mechanism in the CF airway,[96,98,99] which may be why they do not improve mucociliary clearance in this population.

Recombinant Human Deoxyribonuclease

Recombinant human deoxyribonuclease (rhDNase) reduces the viscosity of sputum by cleaving extracellular DNA.[69] Therapy with rhDNase is associated with improvement in lung function and a nonsignificant reduction in the risk of infective exacerbations in subjects with CF.[100,101] It could be hypothesized that the reduction in sputum viscosity induced by rhDNase reverses mucous stasis, thus reducing infection and preserving lung function. However, no improvement in mucociliary clearance from the whole lung in subjects with CF was demonstrated following a 6-day course of rhDNase.[20] In a second study, mucociliary clearance was examined after a 6-day course of rhDNase.[102] On the seventh day, mucociliary clearance was measured immediately after a seventh dose of rhDNase. Again, no significant improvement in mucociliary clearance from the whole lung was demonstrated.

Amiloride

Amiloride is an Na^+ channel blocker that, when delivered to the CF airway, may reduce the osmotic water loss associated with excessive Na^+ absorption. In a pilot study of subjects with CF, amiloride improved sputum viscosity, elasticity, and indirect indices of mucociliary clearance.[103] App and colleagues conducted an acute intervention study in which 23 children and adults with CF inhaled nebulized amiloride, 10^{-3} mol/L, in normal saline solution.[104] Amiloride improved mucociliary clearance measured at 30 and 60 minutes: mean (SD) %C60 on the control day was 29.1%

(8.2%), whereas on the amiloride day it was 35.8% (10.4%), $p < .001$. Six of these subjects subsequently inhaled 3 mL of the same solution (equating to 0.07 mg of amiloride over 10 minutes) and placebo, each twice daily for 3 weeks in a crossover design. Although the baseline rate of mucociliary clearance was not improved after 3 weeks of amiloride administration, the acute effect of the final amiloride dose was greater than that of the initial dose.

A higher dose of amiloride, approximately 16 times that used in the study by App and colleagues, was examined in a subsequent study of 12 adults with CF.[18] No significant acceleration of mucociliary clearance occurred.

Uridine 5′-Triphosphate

Uridine 5′-triphosphate (UTP) induces Cl^- secretion through apical-membrane purinergic receptors in the CF airway[105] and stimulates the cilia.[106] The subsequent airway hydration and higher cilia beat frequency could potentially facilitate mucociliary clearance in the CF airway. Bennett and colleagues administered UTP and amiloride in combination to 14 adults with CF.[15] Mucociliary clearance from the central region of the lung appeared to be markedly affected by cough clearance, so these investigators concentrated their analysis on the peripheral region. UTP and amiloride improved mucociliary clearance in the peripheral region from a mean (SD) of 0.30% (0.05%)/min to 0.51% (0.09%)/min, $p = .04$, over 40 minutes. Although this clearance rate approached that measured in healthy subjects, 0.54% (0.07%)/min, over the same period, the difference was no longer significant after 80 minutes.[15]

Hypertonic Saline

There are several mechanisms by which hypertonic saline may improve mucociliary clearance in subjects with CF. The Na^+ and Cl^- ions in hypertonic saline could allow separation of the ionic bonds within the mucous gel, reducing crosslinking and entanglements and lowering viscosity and elasticity.[107] The increased ionic concentration of the mucus may cause a conformational change by shielding the negative charges and thereby reducing repulsion. This may reduce the dimensions of the mucin macromolecule and allow more effective clearance.[108] Finally, the hypertonicity causes osmotic flow of water into the airway lumen, restoring the airway surface liquid layer and rehydrating secretions.[93]

Robinson and colleagues examined the effect of nebulized 7% hypertonic saline on mucociliary clearance in 12 adults with CF.[18] Nebulized normal (0.9%) saline was used as a control to establish the baseline mucociliary clearance rate. Delivery of 7% hypertonic saline increased the percentage of radiolabeled secretions cleared immediately after the intervention from a mean (SD) of 14.7% (3.8%) to 26.5% (5.7%), $p < .01$. The significant difference seen immediately after inhalation was maintained 30 minutes later. Preceding the delivery of the hypertonic saline with 3 mg/mL of amiloride did not induce any further increase in mucociliary clearance (Figure 36-2).

In a subsequent study, Robinson and colleagues examined the effect of increasing doses of hypertonic saline by increasing the concentration of hypertonic saline inhaled by 10 subjects with CF.[93] Nebulized normal (0.9%) saline was again used as a control. Nebulized 3%, 7%, and 12% hypertonic saline each induced an immediate and significant increase in mucociliary clearance, with evidence of a concentration–response relationship (Figure 36-3). The significant differences seen immediately after inhalation were maintained 60 minutes later. Hypertonic saline frequently causes airway narrowing in persons with CF.[109] Premedication with 5 mg of albuterol was sufficient to prevent any significant bronchoconstriction with any strength of hypertonic saline in this study.[93]

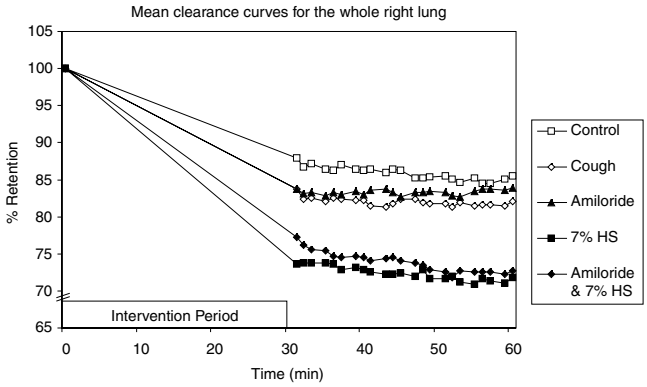

FIGURE 36-2 Time-activity curves for nine subjects with CF. The intervention period included a 15 = minute inhalation of nebulized amiloride, hypertonic saline (HS) or both. Postintervention clearance was measured for a further 30 mintues. Interventions containing HS were significantly different from the isotonic saline and cough controls ($p < .01$). Reproduced with permission from Robinson et al.[18]

Mannitol

Dry-powder mannitol is a nonionic, osmotic agent that also improves mucociliary clearance in subjects with CF. Twelve adults with CF inhaled 300 mg of mannitol as a dry powder, and the improvement in mucociliary clearance over the next 90 minutes approximated that seen with 6% hypertonic

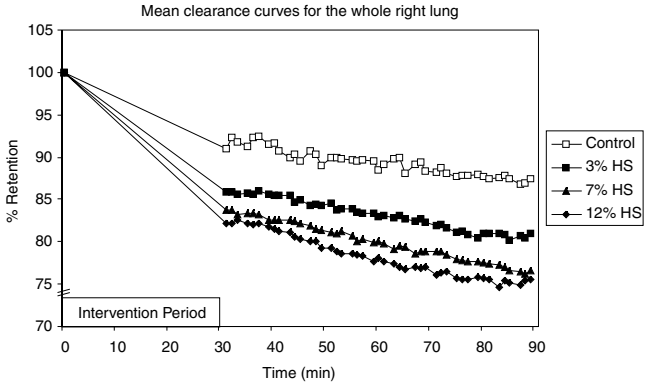

FIGURE 36-3 Time-activity curves for 40 subjects with CF. The intervention period included inhalation of 3%, 7%, or 12% saline. Postintervention clearance was measured for a further 60 minutes. Mucociliary clearance was significantly faster with all hypertonic saline (HS) concentrations than the isotonic saline control ($p = .003$). Reproduced with permission from Robinson et al.[93]

saline.[92] In this study, 1 g of terbutaline was inhaled prior to the mannitol in an attempt to prevent osmotically induced airway narrowing. Despite this premedication, there was a 7.3% fall in forced expiratory volume in 1 second (FEV_1) immediately after the inhalation of the mannitol. FEV_1 values returned to baseline 95 minutes later.

PHYSICAL TREATMENTS TO ENHANCE MUCOCILIARY CLEARANCE IN CF

Many researchers have examined the effects of physical therapies on mucociliary clearance in subjects with CF, and most have compared combinations of physical therapy techniques. Although this is how the techniques are applied in clinical practice, such comparisons provide relatively little evidence of the effectiveness of individual techniques.

Postural Drainage

Using TMV as an index of clearance, Wong and colleagues reported that positioning with 25° head-down tilt increased TMV in the majority of their 13 subjects with CF.[42] This effect of positioning was later confirmed by using rate of clearance of radiotracer as the measure of mucociliary clearance.[110] Six subjects with CF adopted both head-down and bed-flat positions with the left lung dependent over 40 minutes. This regimen significantly improved mucociliary clearance from the right lung in comparison with upright control subjects.

Percussion and Vibration

The addition of mechanical percussion to the above regimen of postural drainage did not significantly enhance mucociliary clearance.[110] However, the addition of manual percussion and manual vibration of the chest wall applied during the expiratory phase of deep breaths did improve mucociliary clearance from the whole lung, primarily through an effect on clearance in the central region.[110]

Positive Expiratory Pressure

Positive expiratory pressure (PEP) devices provide a constant back-pressure to the airways during expiration. One theory is that PEP devices are able to improve clearance by increasing the gas pressure behind mucus via collateral ventilation, thus making expiratory maneuvers more effective.[111,112] It has also been hypothesized that PEP may stabilize airways by splinting them open during expiration, which may facilitate airway clearance.[113] Falk and colleagues examined the effect of PEP on mucociliary clearance in subjects with CF. After 20 minutes of PEP with huffing, relaxed breathing, and coughing, mucociliary clearance was significantly greater than when the PEP component was omitted from the treatment.[114] However, in a separate study, coughing alone was found to be as effective as PEP with coughing.[115]

Combined Therapies

Several investigators have compared treatment regimens that are combinations of multiple physical therapy techniques. As discussed in relation to pharmacologic interventions, comparisons between studies may be heavily influenced by the differences in measurement techniques used by various research groups. Within single studies, most regimens have been shown to increase mucociliary clearance over that seen with rest or spontaneous coughing only, and few differences between one regimen and another have been identified.

Darbee and colleagues compared two regimens in 13 adults with CF: postural drainage, percussion, vibration, and deep breathing and breathing through a PEP mask, followed by exhalations to a low lung volume.[116] No significant difference in clearance was identified between these two regimens. Mortensen and colleagues compared two regimens in 10 adolescents and adults with CF: PEP, huffing, relaxed breathing, and coughing and alternation between deep and relaxed breathing in postural drainage positions, followed by huffing, relaxed breathing, and coughing.[117] No significant difference in mucociliary clearance was noted between the two regimens. This lack of difference was confirmed by Lannefors and Wollmer, who found no significant difference when they examined a third regimen—intermittent exercise, huffing, relaxed breathing, and coughing.[25]

Rossman and colleagues examined another combination of techniques: alternation between deep and relaxed breathing in postural drainage positions with percussion and vibration, followed by huffing, relaxed breathing, and coughing.[110] It was found to be more effective than either postural drainage alone or postural drainage with mechanical percussion. However, it was no more effective than vigorous directed coughing.

CHALLENGES

Currently, planar imaging is used to quantify mucociliary clearance within the three-dimensional lung structure. This two-dimensional analysis reduces our ability to discriminate between lung parenchyma, large airways, and small airways.[118–120] This lack of discrimination is particularly relevant in CF research since the peripheral airways are affected at an earlier stage and with greater severity than the central airways.[121] The imaging needs to be more relevant to the anatomy and pathology. Single-photon emission computed tomography (SPECT) allows three-dimensional imaging of radioisotopes in the lung. In studies of radioaerosol deposition, SPECT provided better discrimination of radioisotope distribution than did planar imaging.[122–125] This improved discrimination may allow objective separation of the true central and peripheral regions of the lung for mucociliary clearance measurement.

Very few mucociliary clearance studies have been performed with pediatric subjects, and none have been performed in children under 10 years of age. Techniques requiring minimal radiation exposure of the subject are needed for this population.

Although accelerating the clearance of secretions from the airway appears to be a logical treatment strategy in persons with CF, it is not known whether the normalization of mucociliary clearance improves their prognosis. Mucociliary

clearance impairment has been reported to correlate with disease severity,[13] but a larger case series did not confirm this relationship.[11] Because of possible confounders, such as the healthy survivor effect, this question may be more adequately answered by longitudinal studies.

It is also unclear whether interventions that increase mucociliary clearance do so for an adequate time period to have an effect on microbiologic or respiratory outcome measures. The interventions discussed in this chapter that have a beneficial effect on mucociliary clearance all show rapid dissipation of their effects. Even with the longest-lasting of these interventions, the few hours of improved mucociliary clearance per day may not be sufficient to have any long-term impact on the health of patients with CF.

CONCLUSIONS

Extensive research into the pathogenesis of CF lung disease has highlighted the fact that other factors besides mucociliary clearance impairment may play a more important role in disease progression than was previously believed. Regardless of the relative importance of the causative factors, one feature of the disease process remains the production of excess, infected, tenacious mucus that is not cleared at a normal rate. Until the relationship between mucociliary clearance and outcomes such as quality of life and mortality is established, interventions that improve mucociliary clearance should be examined further for evidence of a tangible effect on the disease process.

REFERENCES

1. Travis SM, Singh PK, Welsh MJ. Antimicrobial peptides and proteins in the innate defense of the airway surface. Curr Opin Immunol 2001;13:89–95.
2. Pavia D, Agnew JE, Lopez-Vidriero MT, Clarke SW. General review of tracheobronchial clearance. Eur J Respir Dis Suppl 1987;153:123–9.
3. Leith DE. Cough. Physiol Ther 1968;48:439–47.
4. Scherer PW. Mucus transport by cough. Chest 1981;80:830–3.
5. Yoneda K. Mucous blanket of rat bronchus: an ultrastructural study. Am Rev Respir Dis 1976;114:837–42.
6. Boucher RC. Human airway ion transport. Part one. Am J Respir Crit Care Med 1994;150:271–81.
7. Verdugo P. Mucin exocytosis. Am Rev Respir Dis 1991;144:S33–7.
8. Houtmeyers E, Gosselink R, Gayan-Ramirez G, Decramer M. Regulation of mucociliary clearance in health and disease. Eur Respir J 1999;13:1177–88.
9. Foster WM, Langenback E, Bergofsky EH. Measurement of tracheal and bronchial mucus velocities in man: relation to lung clearance. J Appl Physiol Respir Environ Exercise Physiol 1980;48:965–71.
10. Yeates DB, Pitt BR, Spektor DM, et al. Coordination of mucociliary transport in human trachea and intrapulmonary airways. J Appl Physiol Respir Environ Exercise Physiol 1981;51:1057–64.
11. Robinson M, Bye PT. Mucociliary clearance in cystic fibrosis. Pediatr Pulmonol 2002;33:293–306.
12. Laube BL, Jashnani R, Dalby RN, Zeitlin PL. Targeting aerosol deposition in patients with cystic fibrosis: effects of alterations in particle size and inspiratory flow rate. Chest 2000;118:1069–76.
13. Regnis JA, Robinson M, Bailey DL, et al. Mucociliary clearance in patients with cystic fibrosis and in normal subjects. Am J Respir Crit Care Med 1994;150:66–71.
14. Mortensen J, Groth S, Lange P, Hermansen F. Effect of terbutaline on mucociliary clearance in asthmatic and healthy subjects after inhalation from a pressurised inhaler and a dry powder inhaler. Thorax 1991;46:817–23.
15. Bennett WD, Olivier KN, Zeman KL, et al. Effect of uridine 5′-triphosphate plus amiloride on mucociliary clearance in adult cystic fibrosis. Am J Respir Crit Care Med 1996; 153:1796–801.
16. King GG, Eberl S, Salome CM, et al. Airway closure measured by a technegas bolus and SPECT. Am J Respir Crit Care Med 1997;155:682–8.
17. Bailey DL, Robinson M, Meikle SR, Bye PT. Simultaneous emission and transmission measurements as an adjunct to dynamic planar gamma camera studies. Eur J Nuclear Med 1996;23:326–31.
18. Robinson M, Regnis JA, Bailey DL, et al. Effect of hypertonic saline, amiloride, and cough on mucociliary clearance in patients with cystic fibrosis. Am J Respir Crit Care Med 1996;153:1503–9.
19. Robinson M, Eberl S, Tomlinson C, et al. Regional mucociliary clearance in patients with cystic fibrosis. J Aerosol Med 2000;13:73–86.
20. Laube BL, Auci RM, Shields DE, et al. Effect of rhDNase on airflow obstruction and mucociliary clearance in cystic fibrosis. Am J Respir Crit Care Med 1996;153:752–60.
21. Oldenburg FA Jr, Dolovich MB, Montgomery JM, Newhouse MT. Effects of postural drainage, exercise, and cough on mucus clearance in chronic bronchitis. Am Rev Respir Dis 1979;120:739–45.
22. Baum GL, Zwas ST, Katz I, Roth Y. Mucociliary clearance from central airways in patients with excessive sputum production with and without primary ciliary dyskinesia. Chest 1990;98:608–12.
23. Daviskas E, Anderson SD, Eberl S, et al. Inhalation of dry powder mannitol improves clearance of mucus in patients with bronchiectasis. Am J Respir Crit Care Med 1999;159:1843–8.
24. Hasani A, Vora H, Pavia D, et al. No effect of gender on lung mucociliary clearance in young healthy adults. Respir Med 1994;88:697–700.
25. Lannefors L, Wollmer P. Mucus clearance with three chest physiotherapy regimes in cystic fibrosis: a comparison between postural drainage, PEP and physical exercise. Eur Respir J 1992;5:748–53.
26. Agnew JE, Pavia D, Clarke SW. Mucus clearance from peripheral and central airways of asymptomatic cigarette smokers. Bull Eur Physiopathol Respir 1986;22:263–7.
27. Sood N, Bennett WD, Zeman K, et al. Increasing concentration of inhaled saline with or without amiloride: effect on mucociliary clearance in normal subjects. Am J Respir Crit Care Med 2003;167:158–63.
28. Daviskas E, Anderson SD, Eberl S, et al. Effects of terbutaline in combination with mannitol on mucociliary clearance. Eur Respir J 2002;20:1423–9.
29. Bennett WD, Zeman KL, Foy C, et al. Effect of aerosolized uridine 5′-triphosphate on mucociliary clearance in mild chronic bronchitis. Am J Respir Crit Care Med 2001;164: 302–6.
30. Olseni L, Wollmer P. Immediate effects of ethanol on mucociliary clearance in healthy men. Respiration 1992;59:151–4.
31. Hasani A, Toms N, O'Connor J, et al. Effect of salmeterol xinafoate on lung mucociliary clearance in patients with asthma. Respir Med 2003;97:667–71.
32. Puchelle E, Zahm JM, Bertrand A. Influence of age on bronchial mucociliary transport. Scand J Respir Dis 1979;60:307–13.

33. Mortensen J. Bronchoscintigraphy and pulmonary clearance of 99mTc-albumin colloid in the study of mucociliary clearance. Danish Med Bull 1998;45:195–209.
34. Del Donno M, Pavia D, Agnew JE, et al. Variability and reproducibility in the measurement of tracheobronchial clearance in healthy subjects and patients with different obstructive lung diseases. Eur Respir J 1988;1:613–20.
35. Ericsson CH, Svartengren K, Svartengren M, et al. Repeatability of airway deposition and tracheobronchial clearance rate over three days in chronic bronchitis. Eur Respir J 1995;8:1886–93.
36. Vastag E, Matthys H, Kohler D, et al. Mucociliary clearance and airways obstruction in smokers, ex-smokers and normal subjects who never smoked. Eur J Respir Dis Suppl 1985;139:93–100.
37. Incalzi RA, Maini CL, Fuso L, et al. Effects of aging on mucociliary clearance. Comp Gerontol [A] Clin Lab Sci 1989;3:65–8.
38. Yager J, Chen TM, Dulfano MJ. Measurement of frequency of ciliary beats of human respiratory epithelium. Chest 1978;73:627–33.
39. Mortensen J, Lange P, Nyboe J, Groth S. Lung mucociliary clearance. Eur J Nuclear Med 1994;21:953–61.
40. Svartengren M, Mossberg B, Philipson K, Camner P. Mucociliary clearance in relation to clinical features in patients with bronchiectasis. Eur J Respir Dis 1986;68:67–78.
41. Isawa T, Teshima T, Anazawa Y, et al. Effect of respiratory phases and gravity on mucociliary transport in the normal lungs. Sci Rep Res Inst Tohoku University [C] Med 1991; 38:43–50.
42. Wong JW, Keens TG, Wannamaker EM, et al. Effects of gravity on tracheal mucus transport rates in normal subjects and in patients with cystic fibrosis. Pediatrics 1977;60:146–52.
43. Bateman JR, Pavia D, Clarke SW. The retention of lung secretions during the night in normal subjects. Clin Sci Mol Med Suppl 1978;55:523–7.
44. Pavia D. Lung mucociliary clearance. In: Clarke S, Pavia D, editors. Aerosols and the lung: clinical and experimental aspects. London: Butterworth; 1984. p. 127–55.
45. Wolff RK, Dolovich MB, Obminski G, Newhouse MT. Effects of exercise and eucapnic hyperventilation on bronchial clearance in man. J Appl Physiol Respir Environ Exercise Physiol 1977;43:46–50.
46. Laitinen A, Partanen M, Hervonen A, Laitinen LA. Electron microscopic study on the innervation of the human lower respiratory tract: evidence of adrenergic nerves. Eur J Respir Dis 1985;67:209–15.
47. Laitinen A. Ultrastructural organisation of intraepithelial nerves in the human airway tract. Thorax 1985;40:488–92.
48. Mak JC, Baraniuk JN, Barnes PJ. Localization of muscarinic receptor subtype mRNAs in human lung. Am J Respir Cell Mol Biol 1992;7:344–8.
49. Ingels KJ, Meeuwsen F, Graamans K, Huizing EH. Influence of sympathetic and parasympathetic substances in clinical concentrations on human nasal ciliary beat. Rhinology 1992;30:149–59.
50. Foster WM, Bergofsky EH, Bohning DE, et al. Effect of adrenergic agents and their mode of action on mucociliary clearance in man. J Appl Physiol 1976;41:146–52.
51. Lafortuna CL, Fazio F. Acute effect of inhaled salbutamol on mucociliary clearance in health and chronic bronchitis. Respiration 1984;45:111–23.
52. Wong LB, Miller IF, Yeates DB. Stimulation of tracheal ciliary beat frequency by capsaicin. J Appl Physiol 1990;68: 2574–80.
53. Groth ML, Langenback EG, Foster WM. Influence of inhaled atropine on lung mucociliary function in humans. Am Rev Respir Dis 1991;144:1042–7.
54. Smith J, Travis S, Greenberg E, Welsh M. Cystic fibrosis airway epithelia fail to kill bacteria because of abnormal airway surface fluid. Cell 1996;85:229–36.
55. Matsui H, Grubb BR, Tarran R, et al. Evidence for periciliary liquid layer depletion, not abnormal ion composition, in the pathogenesis of cystic fibrosis airways disease. Cell 1998;95:1005–15.
56. Zabner J, Smith JJ, Karp PH, et al. Loss of CFTR chloride channels alters salt absorption by cystic fibrosis airway epithelia in vitro. Mol Cell 1998;2:397–403.
57. Wine JJ. The genesis of cystic fibrosis lung disease. J Clin Invest 1999;103:309–12.
58. Guggino WB. Cystic fibrosis salt/fluid controversy: in the thick of it. Nat Med 2001;7:888–9.
59. Tarran R, Grubb BR, Parsons D, et al. The CF salt controversy: in vivo observations and therapeutic approaches. Mol Cell 2001;8:149–58.
60. Stutts MJ, Boucher RC. Cystic fibrosis gene and functions of CFTR. In: Yankaskas JR, Knowles MR, editors. Cystic fibrosis in adults. Philadelphia: Lippincott-Raven; 1999. p. 3–25.
61. Goldman MJ, Anderson GM, Stolzenberg ED, et al. Human beta-defensin-1 is a salt-sensitive antibiotic in lung that is inactivated in cystic fibrosis. Cell 1997;88:553–60.
62. US Cystic Fibrosis Foundation (USCFF). Patient Registry Annual Data Report. Bethesda (MD): Cystic Fibrosis Foundation; 1999. p. 17.
63. Balough K, McCubbin M, Weinberger M, et al. The relationship between infection and inflammation in the early stages of lung disease from cystic fibrosis. Pediatr Pulmonol 1995; 20:63–70.
64. Khan TZ, Wagener JS, Bost T, et al. Early pulmonary inflammation in infants with cystic fibrosis. Am J Respir Crit Care Med 1995;151:1075–82.
65. Konstan MW, Berger M. Current understanding of the inflammatory process in cystic fibrosis: onset and etiology. Pediatr Pulmonol 1997;24:137–42; discussion 159–61.
66. Conese M, Assael BM. Bacterial infections and inflammation in the lungs of cystic fibrosis patients. Pediatr Infect Dis J 2001;20:207–13.
67. Davis PB, Drumm M, Konstan MW. Cystic fibrosis. Am J Respir Crit Care Med 1996;154:1229–56.
68. Perks B, Shute JK. DNA and actin bind and inhibit interleukin-8 function in cystic fibrosis sputa: in vitro effects of mucolytics. Am J Respir Crit Care Med 2000;162:1767–72.
69. Shak S, Capon DJ, Hellmiss R, et al. Recombinant human DNase I reduces the viscosity of cystic fibrosis sputum. Proc Natl Acad Sci U S A 1990;87:9188–92.
70. Vasconcellos CA, Allen PG, Wohl ME, et al. Reduction in viscosity of cystic fibrosis sputum in vitro by gelsolin. Science 1994;263:969–71.
71. Rogers DF. Airway goblet cells: responsive and adaptable front-line defenders. Eur Respir J 1994;7:1690–706.
72. Sturgess J, Reid L. An organ culture study of the effect of drugs on the secretory activity of the human bronchial submucosal gland. Clin Sci 1972;43:533–43.
73. Puchelle E, Jacquot J, Beck G, et al. Rheological and transport properties of airway secretions in cystic fibrosis—relationships with the degree of infection and severity of the disease. Eur J Clin Invest 1985;15:389–94.
74. Chace KV, Leahy DS, Martin R, et al. Respiratory mucous secretions in patients with cystic fibrosis: relationship between levels of highly sulfated mucin component and severity of the disease. Clin Chim Acta 1983;132: 143–55.
75. Cheng PW, Boat TF, Cranfill K, et al. Increased sulfation of glycoconjugates by cultured nasal epithelial cells from patients with cystic fibrosis. J Clin Invest 1989;84:68–72.

76. Zhang Y, Doranz B, Yankaskas JR, Engelhardt JF. Genotypic analysis of respiratory mucous sulfation defects in cystic fibrosis. J Clin Invest 1995;96:2997–3004.
77. Boat TF, Cheng PW. Epithelial cell dysfunction in cystic fibrosis: implications for airways disease. Acta Paediatr Scand Suppl 1989;363:25–9; discussion 29–30.
78. Girod S, Galabert C, Lecuire A, et al. Phospholipid composition and surface-active properties of tracheobronchial secretions from patients with cystic fibrosis and chronic obstructive pulmonary diseases. Pediatr Pulmonol 1992;13: 22–7.
79. Zahm JM, Galabert C, Chaffin A, et al. Improvement of cystic fibrosis airway mucus transportability by recombinant human DNase is related to changes in phospholipid profile. Am J Respir Crit Care Med 1998;157:1779–84.
80. Verdugo P. Polymer biophysics of mucus in cystic fibrosis. In: Baum G, Priel Z, Roth Y, et al, editors. Cilia, mucus, and mucociliary interactions. New York: Marcel Dekker; 1998. p. 167–90.
81. Rossman CM, Lee RM, Forrest JB, Newhouse MT. Nasal cilia in normal man, primary ciliary dyskinesia and other respiratory diseases: analysis of motility and ultrastructure. Eur J Respir Dis Suppl 1983;127:64–70.
82. Rutland J, Cole PJ. Nasal mucociliary clearance and ciliary beat frequency in cystic fibrosis compared with sinusitis and bronchiectasis. Thorax 1981;36:654–8.
83. Kollberg H, Mossberg B, Afzelius BA, et al. Cystic fibrosis compared with the immotile-cilia syndrome. A study of mucociliary clearance, ciliary ultrastructure, clinical picture and ventilatory function. Scand J Respir Dis 1978;59:297–306.
84. Simel DL, Mastin JP, Pratt PC, et al. Scanning electron microscopic study of the airways in normal children and in patients with cystic fibrosis and other lung diseases. Pediatr Pathol 1984;2:47–64.
85. Gilljam H, Motakefi AM, Robertson B, Strandvik B. Ultrastructure of the bronchial epithelium in adult patients with cystic fibrosis. Eur J Respir Dis 1987;71:187–94.
86. Armengot M, Escribano A, Carda C, et al. Nasal mucociliary transport and ciliary ultrastructure in cystic fibrosis. A comparative study with healthy volunteers. Int J Pediatr Otorhinolaryngol 1997;40:27–34.
87. Amitani R, Wilson R, Rutman A, et al. Effects of human neutrophil elastase and Pseudomonas aeruginosa proteinases on human respiratory epithelium. Am J Respir Cell Mol Biol 1991;4:26–32.
88. Del Donno M, Bittesnich D, Chetta A, et al. The effect of inflammation on mucociliary clearance in asthma: an overview. Chest 2000;118:1142–9.
89. Tarran R, Grubb BR, Gatzy JT, et al. The relative roles of passive surface forces and active ion transport in the modulation of airway surface liquid volume and composition. J Gen Physiol 2001;118:223–36.
90. Smith A. Pathogenesis of bacterial bronchitis in cystic fibrosis. Pediatr Infect Dis J 1997;16:91–5; discussion 95–6, 123–6.
91. Wark PA, McDonald V. Nebulised hypertonic saline for cystic fibrosis. In: Cochrane Database of Systematic Reviews. New Jersey: John Wiley & Sons, Ltd; 2003. CD001506.
92. Robinson M, Daviskas E, Eberl S, et al. The effect of inhaled mannitol on bronchial mucus clearance in cystic fibrosis patients: a pilot study. Eur Respir J 1999;14:678–85.
93. Robinson M, Hemming AL, Regnis JA, et al. Effect of increasing doses of hypertonic saline on mucociliary clearance in patients with cystic fibrosis. Thorax 1997;52:900–3.
94. Wong LB, Miller IF, Yeates DB. Stimulation of ciliary beat frequency by autonomic agonists: in vivo. J Appl Physiol 1988;65:971–81.
95. Sanderson MJ, Dirksen ER. Mechanosensitive and beta-adrenergic control of the ciliary beat frequency of mammalian respiratory tract cells in culture. Am Rev Respir Dis 1989;139:432–40.
96. Boucher RC, Stutts MJ, Knowles MR, et al. Na^+ transport in cystic fibrosis respiratory epithelia. Abnormal basal rate and response to adenylate cyclase activation. J Clin Invest 1986;78:1245–52.
97. Boucher RC, Cotton CU, Gatzy JT, et al. Evidence for reduced Cl^- and increased Na^+ permeability in cystic fibrosis human primary cell cultures. J Physiol 1988;405:77–103.
98. Welsh MJ, Liedtke CM. Chloride and potassium channels in cystic fibrosis airway epithelia. Nature 1986;322:467–70.
99. Yamaya M, Finkbeiner WE, Widdicombe JH. Altered ion transport by tracheal glands in cystic fibrosis. Am J Physiol 1991;261:L491–4.
100. Jones AP, Wallis CE. Recombinant human deoxyribonuclease for cystic fibrosis.[update of Cochrane Database of Systematic Reviews 2000;(2):CD001127; PMID: 10796748]. Cochrane Database of Systematic Reviews. New Jersey: John Wiley & Sons, Ltd; 2003. CD001127.
101. Fuchs HJ, Borowitz DS, Christiansen DH, et al. Effect of aerosolized recombinant human DNase on exacerbations of respiratory symptoms and on pulmonary function in patients with cystic fibrosis. The Pulmozyme Study Group. N Engl J Med 1994;331:637–42.
102. Robinson M, Hemming AL, Moriarty C, et al. Effect of a short course of rhDNase on cough and mucociliary clearance in patients with cystic fibrosis. Pediatr Pulmonol 2000;30:16–24.
103. Knowles MR, Church NL, Waltner WE, et al. A pilot study of aerosolized amiloride for the treatment of lung disease in cystic fibrosis. N Engl J Med 1990;322:1189–94.
104. App EM, King M, Helfesrieder R, et al. Acute and long-term amiloride inhalation in cystic fibrosis lung disease. A rational approach to cystic fibrosis therapy. Am Rev Respir Dis 1990;141:605–12.
105. Knowles MR, Clarke LL, Boucher RC. Activation by extracellular nucleotides of chloride secretion in the airway epithelia of patients with cystic fibrosis. N Engl J Med 1991;325: 533–8.
106. Lansley AB, Sanderson MJ, Dirksen ER. Control of the beat cycle of respiratory tract cilia by Ca^{2+} and cAMP. Am J Physiol 1992;263:L232–42.
107. Ziment I. Respiratory pharmacoogy and therapeutics. Philadelphia: WB Saunders; 1978.
108. King M, Eisenberg A. Viscoelastic properties of polyelectrolyte solutions at high concentrations. Am Chem Soc Org Coatings Plast Chem 1972;32:327–35.
109. Rodwell LT, Anderson SD. Airway responsiveness to hyperosmolar saline challenge in cystic fibrosis: a pilot study. Pediatr Pulmonol 1996;21:282–9.
110. Rossman CM, Waldes R, Sampson D, Newhouse MT. Effect of chest physiotherapy on the removal of mucus in patients with cystic fibrosis. Am Rev Respir Dis 1982;126:131–5.
111. Andersen JB, Qvist J, Kann T. Recruiting collapsed lung through collateral channels with positive end-expiratory pressure. Scand J Respir Dis 1979;60:260–6.
112. Groth S, Stafanger G, Dirksen H, et al. Positive expiratory pressure (PEP-mask) physiotherapy improves ventilation and reduces volume of trapped gas in cystic fibrosis. Bull Eur Physiopathol Respir 1985;21:339–43.
113. Oberwaldner B, Evans JC, Zach MS. Forced expirations against a variable resistance: a new chest physiotherapy method in cystic fibrosis. Pediatr Pulmonol 1986;2:358–67.
114. Falk M, Mortensen J, Kelstrup M, et al. Short-term effects of positive expiratory pressure and the forced expiration

technique on mucus clearance and lung function in CF. Pediatr Pulmonol 1993;Suppl 9:241.
115. van der Schans CP, van der Mark TW, de Vries G, et al. Effect of positive expiratory pressure breathing in patients with cystic fibrosis. Thorax 1991;46:252–6.
116. Darbee J, Dadparvar S, Bensel K, et al. Radionuclide assessment of the comparative effects of chest physical therapy and positive expiratory pressure mask in cystic fibrosis. Pediatr Pulmonol 1990;Suppl 5:251.
117. Mortensen J, Falk M, Groth S, Jensen C. The effects of postural drainage and positive expiratory pressure physiotherapy on tracheobronchial clearance in cystic fibrosis. Chest 1991; 100:1350–7.
118. Snell NJ, Ganderton D. Assessing lung deposition of inhaled medications. Respir Med 1999;93:123–33.
119. Berridge MS, Lee Z, Heald DL. Regional distribution and kinetics of inhaled pharmaceuticals. Curr Pharmaceut Design 2000;6:1631–51.
120. Fleming JS, Sauret V, Conway JH, et al. Evaluation of the accuracy and precision of lung aerosol deposition measurements from single-photon emission computed tomography using simulation. J Aerosol Med 2000;13:187–98.
121. Tomashefski JF, Abramowsky CR, Dahms BB. The pathology of cystic fibrosis. In: Davis PB, editor. Cystic fibrosis. New York: Marcel Dekker; 1993. p. 435–89.
122. Phipps PR, Gonda I, Bailey DL, et al. Comparisons of planar and tomographic gamma scintigraphy to measure the penetration index of inhaled aerosols. Am Rev Respir Dis 1989;139:1516–23.
123. Chan HK. Use of single photon emission computed tomography in aerosol studies. J Aerosol Med 1993;6:23–36.
124. Chan HK, Phipps PR, Gonda I, et al. Regional deposition of nebulized hypodense nonisotonic solutions in the human respiratory tract. Eur Respir J 1994;7:1483–9.
125. Chan HK, Daviskas E, Eberl S, et al. Deposition of aqueous aerosol of technetium-99m diethylene triamine penta-acetic acid generated and delivered by a novel system (AERx) in healthy subjects. Eur J Nuclear Med 1999;26:320–7.
126. Yeates DB, Aspin N, Levison H, et al. Mucociliary tracheal transport rates in man. J Appl Physiol 1975;39:487–95.
127. Friedman M, Dougherty R, Nelson SR, et al. Acute effects of an aerosol hair spray on tracheal mucociliary transport. Am Rev Respir Dis 1977;116:281–6.
128. Goodman RM, Yergin BM, Sackner MA. Effects of S-carboxymethylcysteine on tracheal mucus velocity. Chest 1978;74:615–8.
129. Mussatto DJ, Garrard CS, Lourenco RV. The effect of inhaled histamine on human tracheal mucus velocity and bronchial mucociliary clearance. Am Rev Respir Dis 1988;138:775–9.
130. Li L, Deng H, Tian R, et al. The measurement of tracheobronchial mucociliary clearance by technetium-99m DTPA aerosol scintigraphy. Hua-Hsi i Ko Ta Hsueh Hsueh Pao 2000;31:174–6.
131. Sanchis J, Dolovich M, Rossman C, et al. Pulmonary mucociliary clearance in cystic fibrosis. N Engl J Med 1973;288:651–4.
132. Thomson ML, Pavia D, Short MD, Norman AP. Lung clearance in two patients with cystic fibrosis. N Engl J Med 1973; 289:749–50.
133. Pavia D, Sutton PP, Agnew JE, et al. Measurement of bronchial mucociliary clearance. Eur J Respir Dis Suppl 1983;127: 41–56.
134. Wood RE, Wanner A, Hirsch J, Farrell PM. Tracheal mucociliary transport in patients with cystic fibrosis and its stimulation by terbutaline. Am Rev Respir Dis 1975;111:733–8.
135. Yeates DB, Sturgess JM, Kahn SR, et al. Mucociliary transport in the tracheas of patients with cystic fibrosis. Arch Dis Child 1976;51:28–33.
136. Wong JW, Keens TG, Wannamaker EM, et al. Effects of gravity on tracheal mucus transport rates in normal subjects and in patients with cystic fibrosis. Pediatrics 1977;60:146–52.
137. Matthys H, Kohler D. Bronchial clearance in cystic fibrosis. Eur J Respir Dis Suppl 1986;146:311–8.

CHAPTER 37

FLUID AND ELECTROLYTE TRANSPORT IN THE AIRWAYS

John W. Hanrahan

Epithelial ion and fluid transport processes determine the composition and volume of airway surface liquid (ASL), the thin layer of fluid that covers epithelial cells of the conducting airways. ASL is crucial for mucociliary clearance, innate defense against pathogens, and humidification of inspired air. Transepithelial fluid movement is secondary to the active transport of ions, particularly Na^+, Cl^-, and bicarbonate. In the fetus, fluid secreted into the airways serves as a template for normal lung development[1]; however, different mechanisms must predominate in adult lung because early lung development is normal in individuals with cystic fibrosis (CF), although reduced secretion is a hallmark of that disease. The goal of this chapter is to provide a concise summary of current knowledge regarding epithelial salt and water movements in adult airways, including locations and rates of transport, and their mechanisms and regulation. Transport defects in CF and other diseases are used to illustrate basic concepts. This is a vast topic and space is limited; therefore, the reader is directed to useful review articles for more detailed information.

COMPOSITION AND VOLUME OF ASL

ASL consists of a "sol" or periciliary layer, which contacts the epithelium and has a depth approximately equal to the height of outstretched cilia, and an overlying, discontinuous blanket of mucus, called the "gel" layer. Periciliary fluid has low viscosity, whereas the mucous layer is a tangled network of mucin macromolecules, antibacterial factors, water, and ions. Estimates of ASL depth vary; however, low-temperature scanning electron microscopy of rapidly frozen bovine trachea suggests a resting depth of about 23 μm, which increases transiently to 78 μm after 2 minutes of exposure of submucosal glands to the cholinergic agonist methacholine.[2] Thus, ASL depth depends on the rate of fluid transport across the epithelium, evaporative losses, and axial fluid movements, which are driven by ciliary beating and cough.

The composition of ASL has been hotly debated since it was suggested that ASL ionic strength is elevated in CF and that this salt inhibits antibacterial factors and therefore plays a central role in CF pathogenesis.[3] Studies of ASL are technically difficult in vivo because sample collection is susceptible to artifacts. Collecting fluid with absorbent filter paper can draw submucosal fluid through the epithelium, and all collection methods can potentially cause irritation that triggers submucosal gland secretion.[4] However, recent measurements obtained with fluorescent dyes and ion-sensitive electrodes indicate that Na^+ and Cl^- concentrations in ASL are similar to those in plasma and are not dramatically altered in CF.[5–7] Thus, although salt-sensitive antibacterial peptides such as β-defensin-2 are present in airway epithelium[8], it is unlikely that salt concentration is altered sufficiently in CF to affect antibacterial defenses.[5,9] The pH of ASL is near 7 in normal and CF mice when measured in situ using a fluorescent dye, as are secretions from submucosal glands from control subjects and CF patients,[6] although small reductions in pH and buffering capacity were detected in fluid covering cultured CF bronchial epithelial cells.[10] Interestingly, the depth of ASL measured optically is similar in normal and CF mice, although defective mucociliary clearance in CF has been ascribed to reduced ASL volume[5] (but see Verkman and colleagues[6]). These apparent discrepancies may be due to the different analytic methods used, or they may reflect the limitations of CF mice and cell cultures as experimental models. Liquid on the surface of epithelial cultures probably differs from ASL present in vivo because monolayer cultures lack submucosal glands. In vivo studies can be carried out using CF mice, which are less resistant to infection by *Pseudomonas* than normal mice, especially when bred into a particular genetic background (C57BL/6),[11] and have more lumen-negative electric potential differences in their nasal epithelium, consistent with those in CF patients. Nevertheless, CF mice have predominantly gastrointestinal rather than airway disease, and this has motivated the development of "gut-corrected" CF mice, in which human cystic fibrosis transmembrane conductance regulator (CFTR) is selectively expressed in the intestine.[12] Several reviews of ASL volume and composition have appeared.[6,13–15]

ELECTROLYTE TRANSPORT BY AIRWAY EPITHELIA: MECHANISMS AND REGULATION

Cell Models for Ion Secretion and Absorption

Epithelial fluid secretion is driven by active anion transport, as illustrated in Figure 37-1A. Cl^- enters the epithelial cell through basolateral cotransporters (Na^+–K^+–Cl^- cotransporter type 1; NKCC1), which carry these ions with a stoichiometry of 1:1:2.[16] Cotransport is thus electroneutral and driven by inward transmembrane concentration gradients for Na^+ and Cl^- and against an opposing concentration gradient for K^+. The cotransporter elevates Cl^- concentration above electrochemical equilibrium, which allows Cl^- ions to exit through apical membrane channels during secretagogue stimulation, but only in dog and bovine trachea[17]; Cl^- secretion has not been observed across human nasal, tracheal, and bronchiolar epithelia, which are predominantly absorptive.[18,19] In cultured nasal epithelial cells, Cl^- secretion does not occur because Na^+ absorption depolarizes the apical membrane and prevents apical Cl^- efflux unless a favorable voltage is generated, for example, by blocking Na^+ entry with the diuretic amiloride.[20] Several Cl^- channel types may coexist in the apical membrane of airway epithelia. One important secretory Cl^- channel is the CFTR, which is activated by secretatogues that elevate cAMP levels.[21–23] Ca^{2+}-activated Cl^- channels (CaCCs) have also been implicated, especially in transient secretory responses such as those elicited by activation of muscarinic receptors and various Ca^{2+}-mobilizing agonists such as bradykinin, which probably trigger Ca^{2+} release from stores near the apical membrane, as in other exocrine cells.[24] Exposure to the Na^+ pump inhibitor ouabain abolishes Cl^- secretion by dog trachea[25] because basolateral Na^+–K^+ pumps (Na^+/K^+-ATPase) are needed to generate the inward Na^+ gradient that is used by NKCC1 and other Na^+-coupled transporters. One basolateral cotransporter that uses the Na^+ gradient is called NBC1. It carries Na^+, bicarbonate, and carbonate ions into the cell and thus contributes to bicarbonate secretion.[26] Apical bicarbonate exit is mediated by CFTR channels, which carry both Cl^- and bicarbonate, and by the anion exchanger "down-regulated in adenoma" (DRA1), which is expressed by tracheal epithelium in a CFTR-dependent manner and is implicated in the secretory defect in CF.[27] Low rates of K^+ and Ca^{2+} secretion by airway epithelia have also been reported (eg, Al-Bazzaz and Jayaram[28]), but their physiologic significance is uncertain. Other transporters in airway epithelia include Na^+–H^+ and Na^+–Ca^{2+} exchangers, which regulate intracellular pH and Ca^{2+}, respectively. They are not discussed in detail here, although there is evidence that the anion exchanger AE2 is expressed at the basolateral membrane and contributes to transepithelial Cl^- secretion.[29]

The prevailing model for electrolyte reabsorption by proximal airways (Figure 37-1B) is based on radiotracer flux and microelectrode studies of nasal, tracheal, and bronchial surface cells and is essentially that proposed for frog skin by Koefoed-Johnson and Ussing.[30] Na^+ ions enter through an apical, amiloride-sensitive Na^+ channel called the epithelial Na^+ channel (ENaC). Other cation channels that are less sensitive to amiloride and less selective for Na^+ may also contribute to Na^+ absorption in the distal airways. Na^+ is extruded from the cells by basolateral Na^+/K^+-ATPase pumps in exchange for two K^+ ions, which are recycled to the interstitium through K^+-selective channels. Since net transepithelial Na^+ reabsorption is electrogenic, Cl^- ions must normally follow to maintain electroneutrality. This electrical coupling has been demonstrated by comparing net Na^+ and Cl^- radiotracer fluxes under open-circuit and short-circuit conditions. Under open-circuit conditions, the

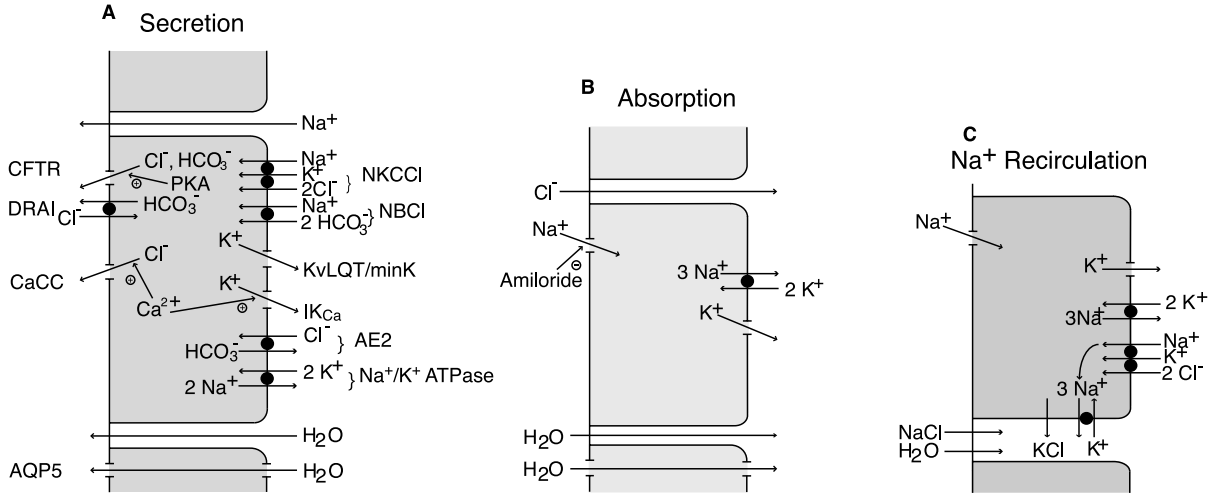

FIGURE 37-1 Cell models for ion secretion and absorption. *A*, Summary of channels and transporters implicated in salt and water secretion by airway epithelia. The relative contributions of Cl^+ and bicarbonate to transepithelial secretion depend on basolateral membrane potential. The contribution of NBC1, which carries a net negative charge, increases at depolarized potentials. *B*, Classic model of Koefoed–Johnsen and Ussing applied to Na^+ absorption by airway epithelium. *C*, The Na^+ recirculation hypothesis used to explain nearly isotonic fluid reabsorption by leaky epithelia. Note that much of the water flows paracellularly through tight junctions and that Na^+ is taken up at the basal membrane (probably by NKCC1) and recycled to the lateral intercellular space. This recirculation raises the osmolality of fluid in the lateral intercellular space by about 6 mOsm, which is sufficient to drive transepithelial fluid absorption. AE2 = anion exchanger 2; AQP5 = aquaporin 5; CaCC = Ca^{2+} activated CT channel; CFTR = cystic fibrosis transmembrane conductance regulator; DRA1 = down-regulated in adenoma; IK_{Ca} = intermediate-conductance Ca^{2+}-activated K^+ channel; NKCC1 = Na^+–K^+–Cl^- cotransporter type 1.

cell monolayer is allowed to generate a spontaneous (lumen-negative) transepithelial electric potential (V_t), which drives net Cl^- absorption. However, under short-circuit conditions, that is, when current is passed through the epithelium from an external circuit to keep the transepithelial potential at 0 mV, net Na^+ absorption is elevated and independent of Cl^- since a counterion is not required under these conditions.[18] Short-circuit current (I_{sc}) provides a measure of net active ion transport.

The transepithelial voltage in vivo is between −20 and −30 mV in proximal airways and is reduced by more than half by the Na^+ channel blocker amiloride. A predominant role of Na^+ transport in proximal airways was confirmed by comparing the net flux of radioisotopic Na^+ with the short-circuit current across nasal epithelial cell cultures and by demonstrating amiloride-induced hyperpolarization of the apical membrane potential and Cl^- secretion under short-circuit conditions (see reviews[18,31]). Thus, some Cl^- absorption by surface epithelia of the proximal airways may occur paracellularly, whereas Cl^- secretion by submucosal glands is mostly transcellular. To explain how the fluid remains isotonic during transepithelial absorption, a general "recirculation theory" has been proposed in which Na^+, K^+, and Cl^- ions are taken up by NKCC transporters at the basal membrane and recycled to the basolateral side with reabsorbed fluid (Figure 37-1C).[32]

Channels, Transporters, and Pumps Mediating Salt Transport across Airway Epithelia

Channels

CFTR Ion and fluid secretion by airway epithelia in adults is mediated in part by CFTR, the regulated Cl^- channel that, when mutated, causes the disease CF. CFTR is a glycoprotein of approximately 170 kDa and is most highly expressed in ciliated surface cells and submucosal glands, consistent with a role in cAMP-stimulated secretion.[33] It belongs to the "ATP-binding cassette" (ABC) superfamily of membrane transporters, members of which are present in organisms ranging from bacteria to humans. ABC transporters perform diverse functions, including transport of metabolic substrates, peptides, xenobiotics, and phospholipids, and antigen presentation, but CFTR is unique in being the only known Cl^- channel in the superfamily.[34] Figure 37-2A shows the two membrane domains (TMD1 and TMD2) of CFTR, each comprising six membrane-spanning helical segments, which are thought to line a transmembrane pore. The CFTR pore is selective for monovalent anions over divalent anions and cations, can hold more than one anion simultaneously, and is about three times more permeable to Cl^- than to bicarbonate. Transmembrane segments 1, 5, 6, 11, and 12 have been implicated in anion permeation. Each membrane domain in the linear amino acid sequence is followed by a nucleotide-binding domain (NBD1 and NBD2, respectively). ATP binding and hydrolysis at NBD2 serve as a "timer" that regulates channel opening and closing (gating); however, hydrolysis is not strictly required, and the channel can still gate as long as ATP is bound. ATP also binds at NBD1, but this interaction is stable, and ATP is not hydrolyzed significantly during many open–closed cycles.[35,36] In general, CFTR channel activity is observed when the regulatory (R) domain of CFTR becomes phosphorylated at multiple sites by protein kinase A (PKA) and protein kinase C (PKC); however, recent evidence suggests that organic acids such as glutamate[37] and ascorbate[38] can also stimulate channel activity independently of phosphorylation under some conditions. Mutagenesis studies have revealed that phosphorylation of the 15 predicted PKA sites and 9 predicted PKC sites is redundant, with no single site being essential for activation. PKA phosphorylation is the primary activating stimulus; however, PKC phosphorylation enhances PKA activation, in addition to having a small stimulatory effect of its own.

CF is caused by mutations in the CFTR gene, many of which cause misfolding and retention of the protein in the endoplasmic reticulum, where it is targeted for degradation.[39–41] The most common example of such mutations is ΔF508, which is found on ~70% of CF chromosomes worldwide. Other less frequent mutations cause synthesis of a truncated CFTR protein, loss of PKA regulation, reduced Cl^- conductance, or a shorter protein life span due to instability at the cell surface. Expression of CFTR influences the functions of diverse proteins, including K^+, Na^+, and other Cl^- channels and Na^+–H^+ and anion exchangers, to name only a few. The mechanisms that underlie these functional interactions are not known and are likely to be nonspecific; however, they may contribute to the pathogenesis of CF. In particular, normal CFTR is reported to down-regulate the function of ENaC and up-regulate expression of DRA1. Loss of these CFTR effects in CF is proposed to increase Na^+ and fluid absorption[42] and decrease bicarbonate secretion,[27] leading to airway and pancreatic disease, respectively. Comprehensive reviews of CFTR and CF can be found elsewhere.[34,43–45]

ENaC The epithelial Na^+ ch`annel ENaC is a functional tetramer comprising two α-subunits, one β-subunit, and one γ-subunit[46] (Figure 37-2B). Each subunit has two membrane-spanning segments (TM1, TM2), which are joined by a large extracellular loop containing many cysteine residues.[47] The distal end of the extracellular loop contains residues that line the channel pore and bind the positively charged guanidinium moiety of amiloride, thereby blocking Na^+ entry. The ENaC pore is highly selective for Na^+ over K^+ and most other ions, although it does pass protons, which are present at low concentrations (~10^{-7} mol/L) at physiologic pH, and the clinically relevant ion lithium. The C-termini of the ENaC β-subunit and γ-subunit have proline (P)-rich and tyrosine(Y)-rich motifs (PPPxYxxL) that interact with specialized "WW" domains of Nedd4, a protein with both scaffolding and enzymic (ie, ubiquitin protein ligase) activities.[48] Nedd4 down-regulates the number of associated ENaC channels at the cell surface by catalyzing ligation of a protein called ubiquitin to lysine residues near the N-termini of the ENaC subunits. This ubiquitination is the first step in ENaC channel degradation and causes it to have a relatively short half-life at the cell surface. Liddle syndrome is a genetic disease of Na^+ hyperabsorption, in which the interaction of the ENaC β-subunit and γ-subunit

with Nedd4 is lost and ENaC channels are allowed to accumulate in the plasma membrane. This leads to hypertension but does not produce any airway pathology,[49] although ENaC overexpression in mouse airways does produce CF-like symptoms.[50] Loss of amiloride-sensitive Na^+ absorption in pseudohypoaldosteronism type 1 (PHA1) (associated with hyponatremia, hyperkalemia, and volume depletion due to loss-of-function mutations in the ENaC Na^+ channel) has the opposite effect, increasing the volume of ASL in proximal airways.[51] The very survival of PHA1 patients indicates that human airway epithelia can compensate for the loss of ENaC channel function at birth, when rapid fluid absorption allows the transition to breathing. It is intriguing that such compensation for lost ENaC channels does not occur in mice lacking the ENaC α-subunit, which essentially drown at birth.[52] As mentioned above, ENaC channel activity is downregulated by CFTR in normal airways[42,53] (but see Nagel and colleagues[54]). But the mechanisms mediating this interaction

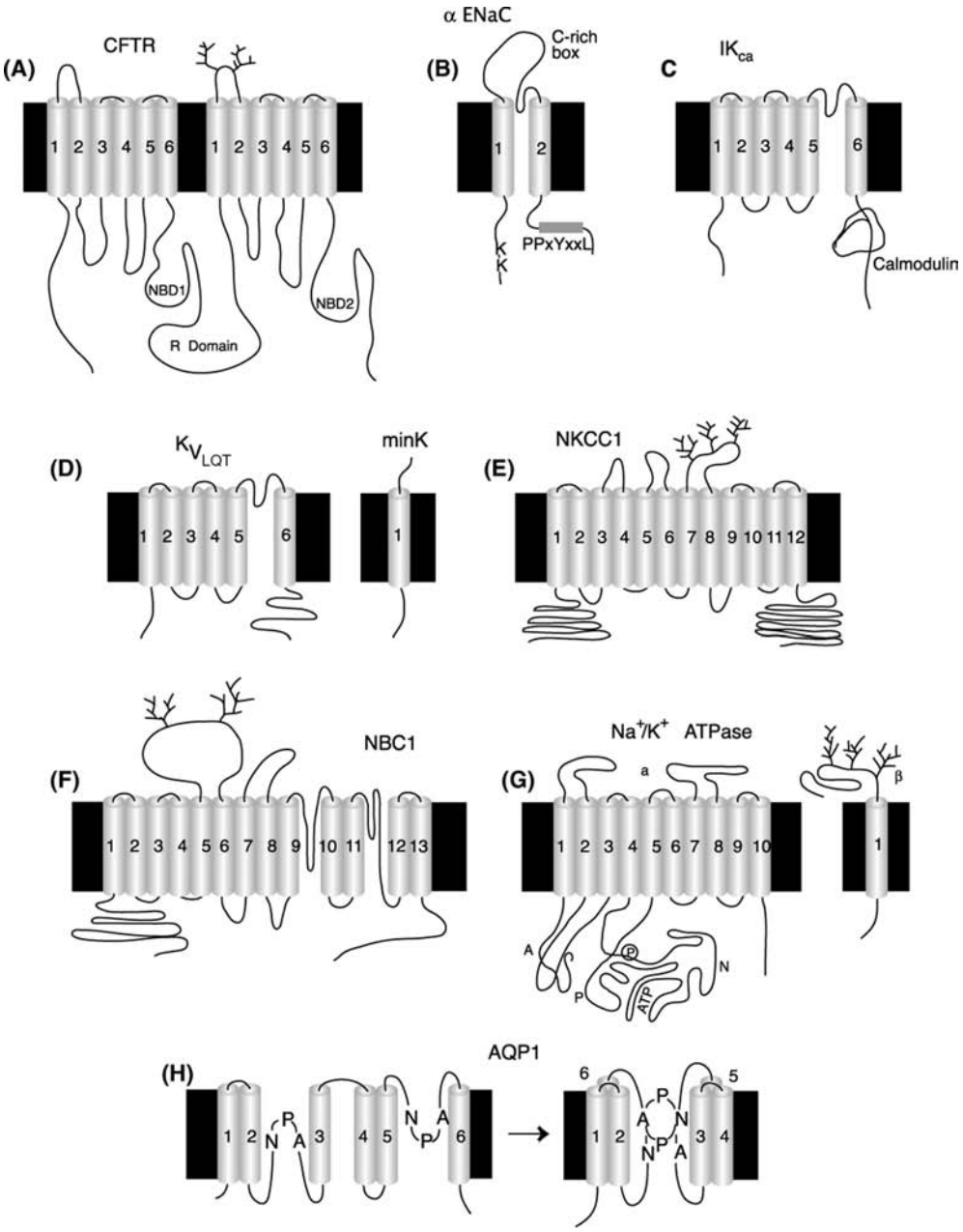

FIGURE 37-2 Gallery of transporters that mediate transport across airway epithelia. *A*, Cystic fibrosis transmembrane conductance regulator (CFTR), showing glycosylation, 12 membrane-spanning segments, two nucleotide-binding domains, and a regulatory (R) domain. *B*, The α-subunit of the epithelial Na^+ channel (ENaC) resembles the β- and γ-subunits in having two transmembrane domains: a large, extracellular loop with a cysteine-rich box and pore-lining residues and a C-terminal PY motif that binds to ubiquitin ligase NEDD4. *C*, The intermediate-conductance Ca^{2+}-activated K^+ channel (IK_{Ca}) binds calmodulin at the C-terminus as its Ca^{2+} sensor. *D*, Kv_{LQT} coassembles with MinK to form a cAMP-responsive basolateral K^+ channel. *E*, The Na^+–K^+–Cl^- cotransporter type 1 (NKCC1) has a large C-terminal domain. *F*, The topology of the Na^+–bicarbonate cotransporter remains uncertain, and there are alternative models with fewer transmembrane segments. *G*, The Na^+ pump (Na^+/K^+-ATPase) consists of α- and β-subunits. It has cytoplasmic actuator (A), phosphorylation (P), and nucleotide (N) domains that undergo large movements during the pump cycle, based on biochemical studies and analogy with Ca^{2+}-ATPase, the structure of which has been solved.

are obscure and apparently tissue specific since CFTR up-regulates ENaC channel activity in the sweat duct.[55]

One mode of ENaC regulation is through the action of extracellular serine proteases. Channel-activating protease type 1 (CAP1) is a glycosylphosphatidylinositol-anchored enzyme, first identified in frog kidney cells, that increases ENaC activity ~8-fold when coexpressed in frog oocytes with ENaC channel subunits. Part of this regulation in epithelia occurs at the cell surface since exposure to trypsin stimulates Na^+ conductance and exposure of cells to the protease inhibitor aprotonin inhibits it by ~50%. A serine protease called prostasin, which is somewhat less potent in stimulating ENaC (<2-fold), has been demonstrated in alveoli and in surface epithelium and submucosal gland cells and thus may function in the airways.[56] Another stimulatory serine protease called TMPRSS3 (for transmembrane protease, serine 3) was first identified as the product of a gene that is mutated in some forms of heritable deafness.[57] It is localized in the endoplasmic reticulum and has a large catalytic C-terminal region that contains a potential cleavage site for proteolytic activation. A related protease, TMPRSS2, is also expressed in airways but reportedly has opposite effects on Na^+ transport, drastically inhibiting ENaC activity when coexpressed with channel subunits in frog oocytes.[56] Membrane-bound and secreted serine proteases probably play a role in controlling Na^+ reabsorption by the surface epithelium of the airways, but their mechanisms of action remain to be established and may be complex. Extensive reviews of ENaC cell biology,[58] channel structure–function relationships, and regulation have recently appeared.[59,60]

IK_{Ca} and Kv_{LQT}/KCNE Basolateral K^+ channels play an essential role in transepithelial ion transport. K^+ efflux generates a current that flows through the paracellular pathway in a circuit and ultimately hyperpolarizes the apical membrane, thereby promoting apical Na^+influx during absorption and Cl^- efflux during secretion. The presence of multiple K^+ channel types was initially inferred from their differential activation by Ca^{2+} or cAMP and from their distinct pharmacologies. cDNA cloning has revealed an enormous diversity of K^+ channels, some of which have been identified recently in airway epithelia. One is activated by intracellular Ca^{2+} and is called IK_{Ca} (intermediate-conductance Ca^{2+}-activated K^+ channel).[61] It is encoded by the gene *KCNN4* (Figure 37-2C),[62] has six transmembrane segments, and is complexed with calmodulin, which binds Ca^{2+} and serves as a Ca^{2+} sensor.[63] IK_{Ca} channels are stimulated by 1-ethyl-2-benzimidazolinune (1-EBIO), inhibited by the drug clotrimizole, and weakly stimulated by PKA and PKC.[64] The main cAMP-stimulated K^+ conductance in airway epithelia is mediated by Kv_{LQT}/MinK, a channel complex originally identified in heart and found to be mutated in the cardiac disorder "long-QT" syndrome.[65,66] Kv_{LQT}/MinK carries a current (called I_{sK}) during sustained, cAMP-stimulated Cl^- secretion by tracheal epithelium[66] and Calu-3 cells.[67] Kv_{LQT} is the pore-forming subunit and is the product of the *KCNQ1* gene. It coassembles with one of several smaller subunits that are encoded by *KCNE1* to *KCNE3* (Figure 37-2D). *KCNN4*, *KCNQ1*, *KCNE2*, and *KCNE3* (MinK) are all expressed in the airway epithelial cell line Calu-3.[67] The Kv_{LQT}/KCNE channel complex also contributes to volume regulation in freshly isolated tracheal cells.[65] These basolateral K^+ channels and their functions in secretory epithelia have been reviewed.[70]

Transporters

NKCC1 Basolateral Cl^- entry during secretion is mediated by NKCC1, the first cloned member of a protein family that also includes K^+–Cl^- and Na^+–Cl^- cotransporters. NKCC1 is a >130 kDa glycoprotein with 12 membrane-spanning regions (Figure 37-2E). Like its absorptive cousin NKCC2 (which is expressed exclusively in the kidney), NKCC1 in airway epithelium is strongly inhibited by the loop diuretics bumetanide and furosemide. Mutagenesis of human NKCC1 protein and chimeras between human and shark NKCC1 have been used to identify determinants of drug and ion binding. Ion binding involves mainly transmembrane segments 2 to 7, whereas bumetanide binding depends on the same region and also on residues in transmembrane segment 11 or 12. In airway epithelia, NKCC1 becomes phosphorylated in response to β-adrenergic agonists (probably mediated by PKA) and to apical UTP (probably mediated by PKC). Stimulation of the cotransporter by secretagogues occurs secondarily to the fall in intracellular Cl^- concentration that accompanies Cl^- exit through the apical membrane. It is mediated by a type 1 protein phosphatase, which binds in a Cl^--dependent manner near the N-terminus of the cotransporter under resting conditions but not during stimulated secretion.[70] The contribution of NKCC1 to transepithelial secretion may be minor in some species, such as mouse, since the inhibitor bumetanide has little effect on basal transport by trachea or the stimulation induced by cAMP, although it does inhibit purinoceptor-stimulated secretion in young animals. This minor role in secretion, along with compensating mechanisms, may explain the lack of airway pathology in NKCC1 gene-knockout mice.[71] The properties of NKCC1 have been reviewed in detail.[16]

NBC1 Na^+ and bicarbonate are taken up through the basolateral membrane during secretion, in part by NBC1, a cotransporter that belongs to the same gene family as anion exchangers (AE1 to AE3) (Figure 37-2F) NBC1 has a molecular mass of 112 kDa, and its 1035 amino acids are predicted to pass through the membrane 10 times. In kidney, NBC1 cotransports one Na^+ and three base equivalents (ie, one bicarbonate ion and one carbonate ion); however, in secretory epithelia such as pancreatic ducts and probably airway submucosal glands, it is believed to carry one Na^+ and one bicarbonate ion. This variable stoichiometry may be controlled by PKA phosphorylation of serine-982 near the C-terminus. The NBC family has been comprehensively reviewed elsewhere.[72]

Pumps

Na^+/K^+-ATPase Basolateral Na^+ pumps generate the inward Na^+ gradient that helps drive Na^+ entry through apical ENaC channels, basolateral NKCC1 cotransporters, and various other Na^+ transporters involved in housekeeping functions such as Na^+–Ca^{2+} and Na^+–H^+exchangers

(Figure 37-2G). The Na^+ pump is a "P-type" ATPase because it becomes phosphorylated and dephosphorylated during each pump cycle; that is, three Na^+ are pumped out of the cell in exchange for two K^+. The unequal translocation of charge means that the Na^+ pump is electrogenic and contributes to the membrane potential. The pump consists of a catalytic α-subunit of 110 kDa with 10 membrane-spanning segments and a highly glycosylated accessory β-subunit of 55 kDa, which spans the membrane only once. Ions are translocated by the α-subunit, whereas the tightly associated β-subunits stabilize and enhance the enzymic activity of the α-subunit, as well as also enhance its trafficking to the plasma membrane. A γ-subunit may also play a regulatory role in some tissues.

Chemical cleavage studies of the Na^+ pump and its similarity to the Ca^{2+}-ATPase (the high-resolution structure of which has been solved by x-ray crystallography) indicate three major domains: N (nucleotide binding), P (phosphorylation), and A (actuator). These undergo large movements as the pump protein alternates between its inward-facing "E_1" and outward-facing "E_2" conformations. Pump rate is dependent on the intracellular Na^+ concentration and increases dramatically with cellular Na^+ load. Many other pathways regulating the pump have also been described, but most are tissue specific. Regulation of the pump has not been studied in detail in airway epithelial cells.[69,73] The reader is directed to recent reviews of Na^+ pump structure and function.[74–76]

Regulation of Salt Transport across Airway Epithelia

Activation of apical Cl^- channels is the rate-limiting step during transepithelial Cl^- secretion; however, basolateral Cl^- entry via NKCC1-mediated cotransport and the electrical effect of basolateral K^+ exit (ie, recycling) on entry through NBC1 are also regulated, as discussed above (see Figure 37-1A, B). Activation of basolateral K^+ channels serves an important function besides allowing K^+ that enters through NKCC1 and Na^+ pumps to recycle. It limits the extent of membrane depolarization that would otherwise occur when apical Cl^- conductance is increased and therefore helps maintain the driving force favoring apical Cl^- exit or Na^+ entry.[17,77] Such electrical coupling between basolateral and apical membranes is crucial for understanding transepithelial transport and is illustrated in Figure 37-3.

Vasoactive intestinal peptide (VIP) is present in parasympathetic ganglia and in nerves that contact the surface epithelium and form a dense network around submucosal glands. VIP stimulates fluid (ie, Cl^-) secretion from serous cells by elevating cAMP but appears to be even more potent in stimulating mucous secretion.[78,79] It is co-released with acetylcholine during strong stimulation of the nerves and may serve as a brake on further neurotransmitter release, as well as potentiating cholinergic responses in the target cell. In any case, since VIP and acetylcholine are released simultaneously, they may function as a single stimulus for ion transport under physiologic conditions, increasing both Cl^- permeability (cAMP-activated CFTR channels) and the driving force favoring Cl^- secretion (IK_{Ca}-induced hyperpolarization). Sympathetic stimulation may lead to similar dual regulation, increasing fluid and mucin secretion through preferential activation of Ca^{2+}/phospholipase C–coupled α-adrenoceptors and cAMP-coupled β-adrenoceptors, respectively.[80,81] Cholinergic agonists that activate muscarinic receptors are potent stimuli of airway ion secretion; however, other agonists that mobilize Ca^{2+} from intracellular stores, such as tachykinins, are also effective secretagogues and may be important for local regulation.[82]

PKA activation can be localized within the cell by A-kinase anchoring protein (AKAPs), which tether it near particular substrates. In airway epithelia this local signaling occurs at the apical membrane when apically released ATP is metabolized extracellularly to adenosine, which subsequently binds to A_{2B} adenosine receptors.[83] Secretion induced by PKA is usually sustained, whereas Ca^{2+} mobilization leads to only transient stimulation of Cl^- transport. Ca^{2+}-activated Cl^- conductance has been described in the apical membrane of airway epithelial cells[84,85] and probably mediates purinoceptor-stimulated secretion in most, but not all, cells.[86] Submucosal glands are innervated by parasympathetic and sensory afferent fibers that release acetylcholine and neuropeptides, respectively; however, the site of purinergic regulation has not been established. ATP can also be released from airway epithelium,[87] which expresses P_{2Y2} purinoceptors (activated by ATP and UTP), P_{2Y1} and P_{2X} (ATP) receptors, and receptors for adenosine (A_{2B}). Nucleotides are metabolized extracellularly and may be interconverted to other nucleotides.[88] Finally, receptors apparently form regulatory complexes with channels either through direct protein–protein interactions or via specialized scaffolding proteins, and these complexes may contain other regulatory proteins such as kinases and phosphatases. The organization and regulation of these complexes in airway

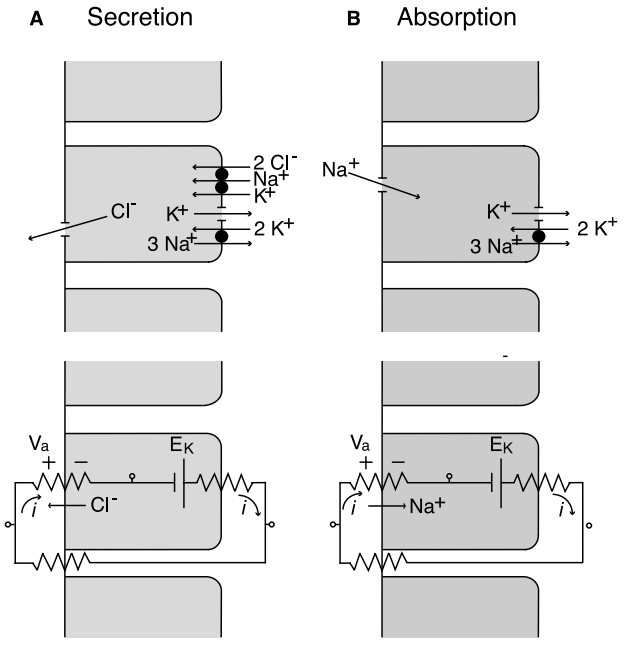

FIGURE 37-3 Electrical coupling of the apical and basolateral membranes of airway epithelia through the paracellular pathway. Apical Cl^- exit during secretion (*A*) and apical Na^+ entry during reabsorption (*B*) are both enhanced by the activation of basolateral K^+ conductance and the increased apical membrane voltage produced by current flowing in a loop through the paracellular pathway.

epithelial cells have become an active area of research. Compared with Cl^- secretion, less is known regarding the regulation of Na^+ reabsorption in the airways. The level of ENaC channel subunit expression in the airways is regulated by glucocorticoids; see, for example, Nakamura and colleagues.[89] Acute regulation of Na^+ transport may be mediated by mucosal nucleotides, which inhibit amiloride-sensitive Na^+ absorption in freshly excised human nasal epithelium.[90] This inhibition does not involve PKC but is mediated by a local decrease in phosphatidylinositol 4,5-biphosphate, which is induced by purinoceptor activation of phospholipase C.[91]

FLUID TRANSPORT BY AIRWAY EPITHELIA

Sites and Cellular Mechanisms of Fluid Secretion and Absorption

Only small osmotic gradients (eg, 1 to 4 mOsm) need to be generated by electrolyte secretion or absorption to drive fluid transport across airway epithelium. Fluid can traverse the epithelium by two routes: one that is "transcellular" and requires diffusion through the apical and basolateral membranes and a "paracellular" pathway, which consists of lateral intercellular spaces and tight junctions between cells. The relative contribution of each pathway to transepithelial salt and water movements in the airways is not yet established.

Figure 37-4A summarizes fluid secretion, using the submucosal gland as an example. Most fluid is secreted by serous cells located in the terminal acini, although some serous cells are found in proximal regions of the gland and on the surface of bronchioles, bronchi, and trachea. Fluid is thought to be secreted by the surface epithelium lining the small-diameter distal airways; demonstration of this and identification of the cells responsible remain elusive.[92] Bronchioles from humans,[19] pigs,[93] and sheep[94,95] are reabsorptive when studied in vitro, and net secretion is only observed if Na^+ channels are blocked by using amiloride. Nonciliated Clara cells from rabbit bronchioles[96] and alveolar type II cells from rat lung (see Chapter 38, "Epithelial Function in Lung Injury") are absorptive when studied in primary culture. Some fluid may seep into distal airways by transudation, driven by subepithelial hydrostatic pressure; however, the extent to which this contributes to ASL in healthy airways is uncertain. Above the respiratory bronchioles, ASL is transported cephalad by ciliary beating, and this movement is assisted by the frictional drag created by movement of the overlying mucus.[97] Reabsorption by the proximal airways helps maintain ASL at a constant depth as fluid moves up the respiratory tree and the area of airway surfaces declines by ~10,000-fold.

Aquaporins

Efficient fluid movement across membranes requires water channel proteins called aquaporins (AQPs). There are 11 human AQP genes, several of which are expressed in airway epithelium. AQP1 is expressed in the apical and basolateral membranes of bronchial epithelium and throughout the pulmonary vasculature. AQP3 is expressed in the basolateral membrane of proximal airways. AQP4 channels are found basolaterally throughout the airways, whereas AQP5 is found in alveolar and submucosal gland epithelial cells. AQP1 is illustrated in Figure 37-2H and is likely to be representative of other members of the AQP family. Each monomer of 28 kDa consists of six tilted transmembrane helices in an "hourglass" shape, which forms a pore for water permeation. The functional importance of AQPs in the airways has been studied with the use of gene-knockout mice. Water permeability of the pleura is reduced by 97% in mice lacking AQP5 or AQP1, yet humidification of the lower airways is diminished by only 6%, and fluid clearance at birth is not significantly affected when both genes are knocked out.[98] AQP3/AQP4 double-knockout mice do have reduced water permeability in the upper airways (by ~35%), but this has little impact on humidification and does not affect ASL depth or Na^+ concentration. Thus, AQPs contribute to water permeability but, at least in mice, are not essential for humidifying air or maintaining ASL volume. Interestingly, the only AQP knockout resulting in a significant airway phenotype is AQP5, which in normal mice is expressed at high levels in the apical membrane of submucosal gland serous cells. Knocking out this channel impairs fluid secretion by the glands, indicating that apical water permeability is a rate-limiting step for fluid secretion by these cells. Since the various AQP-knockout mice have fairly normal airway function, other (ie, compensatory) routes for water flux must be adequate, unlike the situation in kidney, where knocking out the AQP2 gene causes nephrogenic diabetes insipidus. The role of AQPs in airway fluid transport has been reviewed.[99,100]

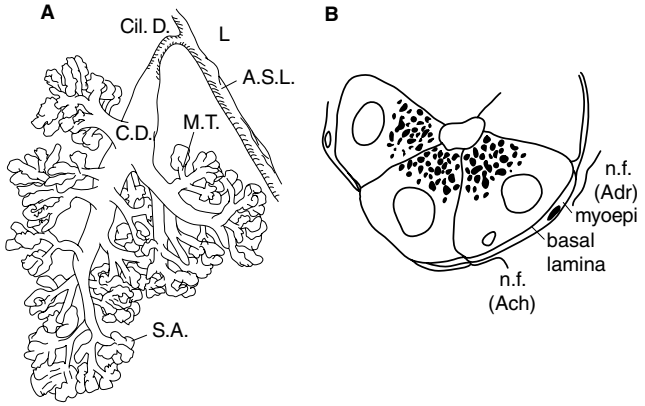

FIGURE 37-4 Schematic representation of the submucosal gland. *A*, Gland, showing the secretory acini (S.A.), mucus-secreting tubules (M.T.), collecting duct (C.D.), and ciliated duct (Cil.D.) and airway space liquid (A.S.L.) lining the luman (L). *B*, Serous cells with lysozyme-containing dense core vesicles, contractile myoepithelial cells, and cholinergic (Ach) and adrenergic (Adr) nerve fibers (n.f.).

Submucosal Glands are Major Sites of Fluid and Mucous Secretion

Some ASL arises from submucosal glands,[101] which become several-fold larger and more elaborate when inflamed. In humans, approximately 12 secretory tubules (each with multiple branches) carry fluid and mucus to a collecting duct, which opens to the airway surface through a narrow ciliated duct (see Figure 37-4A). Most cells lining the secretory tubules contain mucous granules, whereas serous cells with abundant electron-dense secretory vesicles are more prevalent in acini. Fluid that is secreted distally by the serous cells

may help flush mucus from the gland, assisted by contractions of surrounding myoepithelial cells. Submucosal gland secretions have similar compositions irrespective of secretion rate,[80] suggesting that there is little modification of acinar fluid during passage through the collecting and ciliated ducts. Nevertheless, homeostatic mechanisms regulating the pH of secretions have been suggested.[81] When studied in primary culture, some human submucosal gland cell monolayers secrete spontaneously, whereas others absorb.[102] Since CF submucosal glands yield only absorptive monolayers, this suggests a balance between secretory and absorptive fluid movements, such that absorption predominates in CF. Indeed, loss of CFTR-dependent Cl^- and bicarbonate secretion (and associated fluid transport) in CF causes early mucous impaction in glands, and similar impaction can be observed in vitro if fluid secretion is prevented pharmacologically.[101,103] Submucosal glands are found only in the cartilaginous airways down to bronchial diameters of >1 mm, so abnormal submucosal gland secretions would not explain plugging of smaller, aglandular bronchioles in CF patients.

Regulation of Submucosal Gland Secretion

Physiologic regulation of submucosal glands involves multiple agonists and coordinated activation of PKA, PKC, Ca^{2+} mobilization, and perhaps other signaling pathways. Little fluid is produced under resting conditions; however, secretion increases >30-fold during stimulation by acetylcholine or α-adrenergic agonists and to a lesser extent in response to VIP.[79,80,104] Secretory responses of the glands to β-adrenergic agonists are negligible. VIP responses are sustained and mediated by elevation of cAMP levels.[105,106] By contrast, the increases in secretion elicited by acetylcholine, histamine, bradykinin, nucleotides, and other Ca^{2+}-mobilizing agonists are transient, probably involving a temporary increase in Ca^{2+} concentration and short-lived activation of apical Cl^- channels and basolateral K^+ channels.[86,102] As mentioned above, co-release of VIP and acetylcholine would allow coordinated activation of CFTR and basolateral K^+ channels; however, some coordination may also result from shared signaling by PKC. Activating PKC leads to stimulation of salt and fluid secretion by ferret submucosal glands (~50% increase) without elevating intracellular Ca^{2+} concentration, whereas inhibiting PKC leads to a reduction in cholinergic-stimulated fluid secretion by a similar amount.[107] PKC phosphorylation of CFTR enhances its responses to PKA; thus, PKC may act as a coincidence detector and up-regulate secretion during periods of maximal stimulation. It should be noted, however, that a substantial fraction (up to 70%) of acetylcholine-stimulated submucosal gland secretion may be driven by electroneutral ion transport,[108] the basis of which is completely unknown. Submucosal gland function and regulation have recently been reviewed.[6,103,109]

SUMMARY AND CONCLUSIONS

New information has been obtained recently concerning salt and water transport by airway epithelia; however, many important questions remain. If large volumes of fluid enter the distal airways as the first step in mucociliary clearance, what is the source of that fluid and what is the mechanism of secretion? Are the functional interactions that have been described between CFTR and various channels and transporters physiologically significant, and what is the molecular basis of these interactions? How do CFTR mutations lead to chronic infection and other CF symptoms, particularly in the distal airways? Answering these important physiologic and pathophysiologic questions will require more extensive in vivo studies and characterization of freshly excised airway tissues.

REFERENCES

1. Strang LB. Fetal lung liquid: secretion and reabsorption. Physiol Rev 1991;71:991–1016.
2. Wu DX-Y, Lee CYC, Uyekubo SN, et al. Regulation of the depth of surface liquid in bovine trachea. Am J Physiol Lung Cell Mol Physiol 1998;274:L388–95.
3. Smith JJ, Travis SM, Greenberg EP, Welsh MJ. Cystic fibrosis airway epithelia fail to kill bacteria because of abnormal airway surface fluid. Cell 1996;85:229–36.
4. Landry JS, Eidelman DH. Airway surface liquid: end of the controversy? J Gen Physiol 2001;117:419–22.
5. Matsui H, Grubb BR, Tarran R, et al. Evidence for periciliary liquid layer depletion, not abnormal ion composition, in the pathogenesis of cystic fibrosis airways disease. Eur J Pharmacol 1998;95:1005–15.
6. Verkman AS, Song Y, Thiagarajah JR. Role of airway surface liquid and submucosal glands in cystic fibrosis lung disease. Am J Physiol Cell Physiol 2003;284:C2–15.
7. Caldwell RA, Grubb BR, Tarran R, et al. In vivo airway surface liquid Cl^- analysis with solid-state electrodes. J Gen Physiol 2002;119:3–14.
8. Bals R, Weiner DJ, Wilson JM. The innate immune system in cystic fibrosis lung disease. J Clin Invest 1999;103:303–7.
9. Jayaraman S, Joo NS, Reitz B, et al. Submucosal gland secretions in airways from cystic fibrosis patients have normal Na^+ and pH but elevated viscosity. Proc Natl Acad Sci U S A 2001;98:8119–23.
10. Coakley RD, Grubb BR, Paradiso AM, et al. Abnormal surface liquid pH regulation by cultured cystic fibrosis bronchial epithelium. Proc Natl Acad Sci U S A 2003;100:16083–8.
11. Stotland PK, Radzioch D, Stevenson MM. Mouse models of chronic lung infection with *Pseudomonas aeruginosa*: models for the study of cystic fibrosis. Pediatr Pulmonol 2000;30: 413–24.
12. Zhou L, Dey CR, Wert SE, et al. Correction of lethal intestinal defect in a mouse model of cystic fibrosis by human CFTR. Science 1994;266:1705–8.
13. Widdicombe JH. Regulation of the depth and composition of airway surface liquid. J Anat 2002;201:313–8.
14. Widdicombe JH, Widdicombe JG. Regulation of human airway surface liquid. Respir Physiol 2000;99:3–12.
15. Boucher RC. Regulation of airway surface liquid volume by human airway epithelia. Pflügers Arch 2003;445:495–8.
16. Haas M, Forbush BI. The Na–K–Cl cotransporter of secretory epithelia. Annu Rev Physiol 2000;62:515–34.
17. Shorofsky SR, Field M, Fozzard HA. Electrophysiology of Cl^- secretion in canine trachea. J Membr Biol 1983;72:105–15.
18. Boucher RC. Human airway ion transport. Part One. Am J Respir Crit Care Med 1994;150:271–81.
19. Blouquit S, Morel H, Hinnrasky J, et al. Characterization of ion and fluid transport in human bronchioles. Am J Respir Cell Mol Biol 2002;27:503–10.
20. Willumsen NJ, Davis CW, Boucher RC. Intracellular Cl^- activity and cellular Cl^- pathways in cultured human airway epithelium. Am J Physiol Cell Physiol 1989;256:C1033–44.
21. Kartner N, Hanrahan JW, Jensen TJ, et al. Expression of the cystic fibrosis gene in non-epithelial invertebrate cells produces a regulated anion conductance. Cell 1991;64:681–91.

22. Anderson MP, Sheppard DN, Berger HA, Welsh MJ. Chloride channels in the apical membrane of normal and cystic fibrosis airway and intestinal epithelia. Am J Physiol Lung Cell Mol Physiol 1992;263:L1–14.
23. Berger HA, Anderson MP, Gregory RJ, et al. Identification and regulation of the cystic fibrosis transmembrane conductance regulator-generated chloride channel. J Clin Invest 1991;88:1422–31.
24. Ashby MC, Camello-Almaraz C, Gerasimenko OV, et al. Long distance communication between muscarinic receptors and Ca^{2+} release channels revealed by carbachol uncaging in cell-attached patch pipette. J Biol Chem 2003;278: 20860–4.
25. Widdicombe JH, Ueki IF, Bruderman I, Nadel JA. The effects of sodium substitution and ouabain on ion transport by dog tracheal epithelium. Am Rev Respir Dis 1979;120: 385–92.
26. Devor DC, Singh AK, Lambert LC, et al. Bicarbonate and chloride secretion in Calu-3 human airway epithelial cells. J Gen Physiol 1999;113:743–60.
27. Wheat VJ, Shumaker H, Burnham C, et al. CFTR induces the expression of DRA along with Cl^-/HCO_3^- exchange activity in tracheal epithelial cells. Am J Physiol Cell Physiol 2000; 279:C62–71.
28. Al-Bazzaz FJ, Jayaram T. Calcium transport across canine tracheal mucosa. J Appl Physiol 1985;59:1191–5.
29. Loffing J, Moyer BD, Reynolds D, et al. Functional and molecular characterization of an anion exchanger in airway serous epithelial cells. Am J Physiol Cell Physiol 2000;279: C1016–23.
30. Koefoed-Johnsen V, Ussing HH. The nature of the frog skin potential. Acta Physiol Scand 1958;42:298–308.
31. Boucher RC. Human airway ion transport. Part Two. Am J Crit Care Med 1994;150:581–93.
32. Larsen EH, Sørensen JB, Sørensen JN. A mathematical model of solute coupled water transport in toad intestine incorporating recirculation of the actively transported solute. J Gen Physiol 2000;116:101–24.
33. Engelhardt JF, Zepeda M, Cohn JA, et al. Expression of the cystic fibrosis gene in adult human lung. J Clin Invest 1994; 93:737–49.
34. Hanrahan JW, Gentzsch M, Riordan JR. The cystic fibrosis transmembrane conductance regulator (ABCC7). In: Holland B, Higgins CF, Kuchler K, Cole SPC, editors. ABC proteins: from bacteria to man. New York: Elsevier Science; 2003. p. 589–618.
35. Aleksandrov L, Aleksandrov AA, Chang X-B, Riordan JR. The first nucleotide binding domain of CFTR is a site of stable nucleotide interaction whereas the second is a site of rapid turnover. J Biol Chem 2002;277:15419–25.
36. Basso C, Vergani P, Nairn AC, Gadsby DC. Prolonged nonhydrolytic interaction of nucleotide with CFTR's NH_2-terminal nucleotide binding domain and its role in channel gating. J Gen Physiol 2003;122:333–48.
37. Reddy MM, Quinton PM. Control of dynamic CFTR selectivity by glutamate and ATP in epithelial cells. Nature 2003;423: 756–60.
38. Fischer H, Schwarzer C, Illek B. Vitamin C controls the cystic fibrosis transmembrane conductance regulator chloride channel. Proc Natl Acad Sci U S A 2004;101:3691–6.
39. Kerem B-S, Rommens JM, Buchanan JA, et al. Identification of the cystic fibrosis gene: genetic analysis. Science 1989;245: 1073–80.
40. Riordan JR, Rommens JM, Kerem B-S, et al. Identification of the cystic fibrosis gene: cloning and characterization of complementary DNA. Science 1989;245:1066–73.
41. Rommens JM, Iannuzzi MC, Kerem B-S, et al. Identification of the cystic fibrosis gene: chromosome walking and jumping. Science 1989;245:1059–65.
42. Stutts MJ, Canessa CM, Olsen JC, et al. CFTR as a cAMP-dependent regulator of sodium channels. Science 1995; 269:847–50.
43. Sheppard DN, Welsh MJ. Structure and function of the CFTR chloride channel. Physiol Rev 1999;79:S23–45.
44. Gadsby DC, Nairn AC. Control of CFTR channel gating by phosphorylation and nucleotide hydrolysis. Physiol Rev 1999; 79:S77–107.
45. Quinton PM. Physiological basis of cystic fibrosis: a historical perspective. Physiol Rev 1999;79:S3–22.
46. Firsov D, Gautschi I, Merillat A-M, et al. The heterotetrameric architecture of the epithelial sodium channel (ENaC). EMBO J 1998;17:344–52.
47. Canessa CM, Schild L, Buell G, et al. Amiloride-sensitive epithelial Na^+ channel is made of three homologous subunits. Nature 1994;367:463–7.
48. Staub O, Dho S, Henry P, et al. WW domains of Nedd4 bind to the proline-rich PY motifs in the epithelial Na^+ channel deleted in Liddle's syndrome. EMBO J 1996;15: 2371–80.
49. Hansson JH, Schild L, Lu Y, et al. A *de novo* missense mutation of the b subumit of the epithelial sodium channel causes hypertension and Liddle syndrome, identifying a proline-rich segment critical for regulation of channel activity. Proc Natl Acad Sci U S A 1995;92:11495–9.
50. Mall M, Grubb BR, Harkema JR, et al. Increased airway epithelial Na^+ absorption produces cystic fibrosis-like lung disease in mice. Nat Med 2004;10:487–93.
51. Prince LS, Lauunspach JL, Geller DS, et al. Absence of amiloride-sensitive sodium absorption in the airway of an infant with pseudohypoaldosteronism. J Pediatr 1999;135:786–9.
52. Hummler E, Barker P, Gatzy J, et al. Early death due to defective neonatal lung liquid clearance in *alpha*EN*a*C-deficient mice. Nat Genet 1996;12:325–8.
53. König J, Schreiber R, Voelcker T, et al. The cystic fibrosis transmembrane conductance regulator (CFTR) inhibits ENaC through an increase in the intracellular Cl^- concentration. EMBO Rep 2001;21:1–5.
54. Nagel G, Szellas T, Riordan JR, et al. Non-specific activation of the epithelial sodium channel by the CFTR chloride channel. EMBO Rep 2001;21:249–54.
55. Reddy MM, Light MJ, Quinton PM. Activation of the epithelial Na^+ channel (ENaC) requires CFTR Cl^- channel function. Nature 1999;402:301–4.
56. Donaldson SG, Hirsh A, Li DC, et al. Regulation of the epithelial sodium channel serine proteases in human airways. J Biol Chem 2002;277:8338–45.
57. Guipponi M, Vuagniaux G, Wattenhofer M, et al. The transmembrane serine protease (TMPRSS3) mutated in deafness DFNB8/10 activates the epithelial sodium channel (ENaC) in vitro. Hum Mol Genet 2002;11:2829–36.
58. Rotin D, Kanelis V, Schild L. Trafficking and cell surface stability of ENaC. Am J Physiol Renal Fluid Electrol Physiol 2001;281:F391–9.
59. Kellenberger S, Schild L. Epithelial sodium channel/degenerin family of ion channels: a variety of functions for a shared structure. Physiol Rev 2003;82:735–67.
60. Gormley K, Dong Y, Sagnella GA. Regulation of the epithelial sodium channel by accessory proteins. Biochem J 2003;371: 1–14.
61. Welsh MJ, McCann JD. Intracellular calcium regulates basolateral potassium channels in a chloride-secreting epithelium. Proc Natl Acad Sci U S A 1985;82:8823–6.
62. Ishii TM, Silvia C, Hirschberg B, et al. A human intermediate conductance calcium-activated potassium channel. Proc Natl Acad Sci U S A 1997;94:11651–6.
63. Fanger CM, Ghanshani S, Logsdon NJ, et al. Calmodulin mediates calcium-dependent activation of the intermediate conductance K_{Ca} channel, $IKCa_1$. J Biol Chem 1999;274:5746–54.
64. Tabcharani JA, Boucher A, Eng JWL, Hanrahan JW. Regulation of an inwardly rectifying K channel in the T_{84} cell line by calcium, nucleotides and kinases. J Membr Biol 1994;142: 255–66.

65. Mall M, Wissner A, Schreiber R, et al. Role of K_{vLQT1} in cyclic adenosine monophosphate-mediated Cl^- secretion in human airway epithelia. Am J Physiol Lung Cell Mol Physiol 2000;23:283–9.
66. Hwang T-H, Suh D-J, Bae H-R, et al. Characterization of K^+ channels in the basolateral membrane of rat tracheal epithelia. J Membr Biol 1996;154:251–7.
67. Cowley EA, Linsdell P. Characterization of basolateral K^+ channels underlying anion secretion in the human airway cell line Calu-3. J Physiol 2002;538:747–57.
68. Lock H, Valverde MA. Contribution of the IsK (MinK) potassium channel subunit to regulator volume decrease in murine tracheal epithelial cells. J Biol Chem 2000;275: 34849–52.
69. Bleich M, Warth R. The very small-conductance K^+channel K_{vLQT1} and epithelial function. Pflügers Arch 2000;440: 202–6.
70. Darman RB, Flemmer A, Forbush B. Modulation of ion transport by direct targeting of protein phosphatase type 1 to the Na–K–Cl cotransporter. J Biol Chem 2001;276: 34359–62.
71. Grubb BR, Pace AJ, Lee E, et al. Alterations in airway ion transport in NKCC1-deficient mice. Am J Physiol Cell Physiol 2001;281:C615–23.
72. Gross E, Kurtz I. Structural determinants and significance of regulation of electrogenic Na^+–HCO_3^- cotransporter stoichiometry. Am J Physiol Renal Fluid Electrol Physiol 2002;283:F876–87.
73. Therien AG, Blostein R. Mechanisms of sodium pump regulation. Am J Physiol Cell Physiol 2000;279:C541–66.
74. Scheiner-Bobis G. The sodium pump. Its molecular properties and mechanics of ion transport. Eur J Biochem 2002;269: 2424–33.
75. Kaplan JH. Biochemistry of Na,K-ATPase. Annu Rev Biochem 2004;71:511–35.
76. Jorgensen PL, Håkansson KO, Karlish SJD. Structure and mechanism of Na,K-ATPase: functional sites and their interactions. Annu Rev Physiol 2003;65:817–49.
77. Welsh MJ, Smith PL, Frizzell RA. Chloride secretion by canine tracheal epithelium: III. Membrane resistances and electromotive forces. J Membr Biol 1983;71:209–18.
78. Barnes PJ, Baraniuk JN, Belvisi MG. Neuropeptides in the respiratory tract. Am Rev Respir Dis 1991;144:1187–98.
79. Joo NS, Saenz Y, Krouse ME, Wine JJ. Mucus secretion from single submucosal glands of pig. Stimulation by carbachol and vasoactive intestinal peptide. J Biol Chem 2002;277: 28167–75.
80. Quinton PM. Composition and control of secretion from tracheal bronchial submucosal glands. Nature 1979;279: 551–2.
81. Nadel JA. Neural control of airway submucosal gland secretion. Eur J Respir Dis 1983;64 Suppl 128:322–6.
82. Tamaoki J, Ueki I, Widdicombe JH, Nadel JA. Stimulation of Cl secretion by neurokinin A and neurokinin B in canine tracheal epithelium. Am Rev Respir Dis 1988;137:899–902.
83. Huang P, Lazarowski ER, Tarran R, et al. Compartmentalized autocrine signaling to cystic fibrosis transmembrane conductance regulator at the apical membrane of airway epithelial cells. Proc Natl Acad Sci U S A 2001;98:14120–5.
84. Willumsen NJ, Boucher RC. Activation of an apical Cl^- conductance by Ca^{2+} ionophores in cystic fibrosis airway epithelia. Am J Physiol Cell Physiol 1989;256:C226–33.
85. Anderson MP, Welsh MJ. Calcium and cAMP activate different chloride channels in the apical membrane of normal and cystic fibrosis epithelia. Proc Natl Acad Sci U S A 1991;88:6003–7.
86. Moon S, Singh M, Krouse ME, Wine JJ. Calcium-stimulated Cl^- secretion in Calu-3 human airway cells requires CFTR. Am J Physiol Lung Cell Mol Physiol 1997;273:L1208–19.
87. Grygorczyk R, Hanrahan JW. CFTR-independent ATP release from epithelial cells triggered by mechanical stimuli. Am J Physiol Cell Physiol 1997;272:C1058–66.
88. Lazarowski ER, Boucher RC, Harden TK. Constitutive release of ATP and evidence for major contribution of ecto-nucleotide pyrophosphatase and nucleoside diphosphokinase to extracellular nucleotide concentrations. J Biol Chem 2000; 275:31061–8.
89. Nakamura K, Stokes JB, McCray P Jr. Endogenous and exogenous glucocorticoid regulation of ENaC mRNA expression in developing kidney and lung. Am J Physiol Cell Physiol 2002;283:C762–72.
90. Mall M, Wissner A, Gonska T, et al. Inhibition of amiloride-sensitive epithelial Na^+ absorption by extracellular nucleotides in human normal and cystic fibrosis airways. Am J Respir Cell Mol Biol 2000;23:755–61.
91. Ma H-P, Saxena S, Warnock DG. Anionic phospholipids regulate native and expressed epithelial sodium channel (ENaC). J Biol Chem 2004;277:7641–4.
92. Kilburn KH. A hypothesis for pulmonary clearance and its implications. Am Rev Respir Dis 1968;98:449–63.
93. Ballard ST, Taylor AE. Bioelectric properties of proximal bronchiolar epithelium. Am J Physiol Lung Cell Mol Physiol 1994;267:L79–84.
94. Al-Bazzaz FJ, Tarka C, Farah M. Microperfusion of sheep bronchioles. Am J Physiol Lung Cell Mol Physiol 1991;260: L594–602.
95. Al-Bazzaz FJ, Gailey C. Ion transport by sheep distal airways in a miniature chamber. Am J Physiol Lung Cell Mol Physiol 2001;281:L1028–34.
96. Van Scott MR, Hester S, Boucher RC. Ion transport by rabbit nonciliated bronchiolar epithelial cells (Clara cells) in culture. Proc Natl Acad Sci U S A 1987;84:5496–500.
97. Matsui H, Randell SH, Peretti SW, et al. Coordinated clearance of periciliary liquid and mucus from airway surfaces. J Clin Invest 1998;102:1125–31.
98. Song Y, Jayaraman S, Yang B, et al. Role of aquaporin water channels in airway fluid transport humidification, and surface liquid hydration. J Gen Physiol 2001;117:573–82.
99. Verkman AS, Matthay MA, Song Y. Aquaporin water channels and lung physiology. Am J Physiol Lung Cell Mol Physiol 2000;278:L867–79.
100. Borok Z, Verkman AS. Role of aquaporin water channels in fluid transport in lung and airways. J Appl Physiol 2002; 93:2199–206.
101. Ballard ST, Trout L, Mehta A, Inglis SK. Liquid secretion inhibitors reduce mucociliary transport in glandular airways. Am J Physiol Lung Cell Mol Physiol 2002;283:L329–35.
102. Jiang C, Finkbeiner WE, Widdicombe JH, Miller SS. Fluid transport across cultures of human tracheal glands is altered in cystic fibrosis. J Physiol 1997;501:637–47.
103. Ballard ST, Inglis SK. Liquid secretion properties of airway submucosal glands. J Physiol 2003;556:1–10.
104. Ueki I, German VF, Nadel JA. Micropipette measurement of airway submucosal gland secretion. Autonomic effects. Am Rev Respir Dis 1980;121:351–7.
105. Joo NS, Irokawa T, Wu JV, et al. Absent secretion to vasoactive intestinal peptide in cystic fibrosis airway glands. J Biol Chem 2004;277:50710–5.
106. Tabcharani JA, Low W, Elie D, Hanrahan JW. Low-conductance chloride channel activated by cAMP in the epithelial cell line T_{84}. FEBS Lett 1990;270:157–64.
107. Shimura S, Ishihara H, Nagaki M, et al. A stimulatory role of protein kinase C in feline tracheal submucosal gland secretion. Respir Physiol 1993;93:239–47.
108. Trout L, Gatzy JT, Ballard ST. Acetylcholine-induced liquid secretion by bronchial epithelium: role of Cl^- and HCO_3^- transport. Am J Physiol Lung Cell Mol Physiol 2004;272: L1095–9.
109. Shimura S. Signal transduction of mucous secretion by bronchial gland cells. Cell Signal 2000;12:271–7.

CHAPTER 38

EPITHELIAL FUNCTION IN LUNG INJURY

Yves Berthiaume

Acute lung injury and the acute respiratory distress syndrome (ARDS) are syndromes in which widespread damage of the alveolar–capillary membrane leads to major physiologic dysfunction in gas exchange. Acute lung injury and ARDS are major causes of acute respiratory failure in critically ill patients. Although there is evidence that over the last decade the mortality from these syndromes has declined, it nevertheless remains high (30 to 40%). Many therapies have recently emerged that target the inflammatory response accompanying these syndromes. This is important because the development of the diffuse alveolar damage (DAD) associated with this disease is mainly dependent on the destruction of the alveolar–capillary membrane by inflammatory cells. However, the severity of and recovery from these injuries also depend on alveolar epithelial cell function. In this chapter I emphasize the importance of modulating the functions of the alveolar epithelium, which I consider to be strategically necessary for more rapid recovery from ARDS. After discussing the importance of surfactant in the recovery process, I elaborate on the mechanisms by which edema clearance and epithelial repair are enhanced.

LUNG ALVEOLAR EPITHELIAL CELLS: PLURIPOTENT CELLS OF THE DISTAL AIRSPACES?

Like any form of inflammation, acute lung injury represents a complex process in which multiple pathways propagate or inhibit the injury. The acute phase of acute lung injury is characterized by the influx of protein-rich edema fluid into the airspaces as a consequence of increased permeability of the alveolar–capillary membrane.[1] This membrane is composed of two barriers, the microvascular endothelium and the alveolar epithelium. Although the development of lung injury is mainly dependent on damage caused to endothelial cells by inflammatory cells,[2] the severity of and recovery from injury also depend on the function of epithelial cells of the alveolar barrier[3] (Figure 38-1). In fact, the predominant pathologic finding in acute lung injury is diffuse alveolar epithelial damage.[4,5] Damage to the alveolar type I cells is predominant because these cells seem to be more sensitive to injury than alveolar type II cells.[6] Endothelial cell injury is subtle and seems insufficient to explain the rapid and continuous escape of protein-rich fluid from the microcirculation.[4] Why there is such a disparate appearance of lesions between the epithelial and endothelial cells is still a mystery, but one hypothesis is that the repair phase of endothelial cells is much quicker than that of epithelial cells.

Physiologically, it has also been shown that the function of the alveolar epithelium is an important determinant of lung injury.[7] The chronic stage of acute lung injury (>7 days) is marked by its variability. In certain patients, there is, in fact, rapid reabsorption of alveolar edema fluid and repair of the injured region of the alveolar epithelium, followed by clinical recovery from respiratory failure. However, in a number of cases, alveolar edema persists, and the organization of hyaline membranes and the gradual appearance of intraalveolar fibrosis are observed[4,5] (Figure 38-2). The development of this intraalveolar and interstitial fibrosis distorts the normal architecture of the lung and impedes the recovery of patients because such an abnormal structure is incapable of performing adequate gas exchange. Thus, the key factors involved in recovery from lung injury are the abilities to clear edema fluid, reconstitute a normal alveolar structure, and resume surfactant secretion.

The cells involved in this process are the cells forming the alveolar epithelial barrier. This epithelium is lined by two morphologically distinct cells, type I and type II alveolar epithelial cells (Figure 38-3). Type I cells are squamous cells (diameter 50 to 100 μm and volume 2,000 to 3,000 μm^3). Type II cells are smaller, cuboidal cells (approximate diameter 10 μm and volume 450 to 900 μm^3). Both tight junctions and gap junctions couple type I and type II cells, providing barrier functions and pathways for intercellular communication.[8] Although the precise function of the alveolar type I cells remains largely speculative, this cell must play a role in gas exchange and possibly also has a role in

liquid movement. Twenty years ago, Mason and Williams described the alveolar type II cells as a crenated tower defending the alveolus.[9] At that time, virtually nothing was known about the functional abilities of these cells, and their in vitro story was just beginning. Almost a quarter of a century later, it can be asserted that alveolar type II cells are not passive bystanders but are pluripotent cells involved in surfactant secretion, ion transport, and epithelial repair.

ROLE OF SURFACTANT IN LUNG INJURY

Surfactant Metabolism

Surfactant has a vital role in maintaining alveolar homeostasis. Surface-active materials reduce surface tension in the lungs, preventing their collapse at resting transpulmonary pressures.[10,11] Furthermore, it has been shown that this low alveolar surface tension is essential to keep the alveolus dry and to prevent pulmonary edema.[10]

Surfactant is a complex mixture of lipids and proteins, whose composition is fairly constant among mammalian species[12] (Tables 38-1 and 38-2). Surfactant is synthesized, secreted, and recycled by alveolar type II cells. Its major components are lipids and surfactant-specific proteins. Lipids account for approximately 90% of surfactant, and phospholipids form the bulk of the lipids (see Table 38-1). Phosphatidylcholine is the most abundant component of surfactant and represents 70 to 80% of the total amount of lipid. Approximately 50 to 70% of the phosphatidylcholine is saturated in dipalmitoylated form (DPPC). DPPC is the main surface-active component of surfactant. Although most surfactant consists of lipids, approximately 10% consists of proteins. Four surfactant-associated proteins have been described[13,14] (see Table 38-2). These proteins can be divided into two groups: the hydrophilic proteins, surfactant protein-A (SP-A) and surfactant protein-D (SP-D), and the hydrophobic proteins, surfactant protein-B (SP-B) and surfactant protein-C (SP-C). Whereas SP-B and SP-C have been shown to directly participate in surfactant metabolism and turnover, SP-A and SP-D seem to have a role as immunologic modulators.

Surfactant metabolism has been well characterized over the past two decades (see Figure 38-3). Surfactant phosphatidylcholine is synthesized in the endoplasmic reticulum of type II cells and transferred to lamellar bodies, which are, in turn secreted with SP-B and SP-C into the hypophase that lines the alveolus. Surfactant is then transformed into tubular myelin, from which the monolayer is formed. The formation of this monolayer is dependent on the presence of SP-B and SP-C (absorption rate at the air–liquid interface) and on the presence of a carboxylesterase, termed convertase, that facilitates the transformation of tubular myelin in the monolayer.[10] Surfactant may then be recycled by the type II cells, catabolized, especially by macrophages, or cleared from the lungs by as yet unknown mechanisms. Whereas 90% of the surfactant cleared from the alveoli of developing lung is recycled, only 50% of it is recycled in the adult lung.[11]

Table 38-1 Composition of Pulmonary Surfactant

Component	*Percentage mass*
Lipid	90–95
Phospholipid	78
Saturated phosphatidylcholine	45
Unsaturated phosphatidylcholine	20
Phosphatidylglycerol	8
Other phospolipids	5
Neutral lipids	10
Other lipids	2
Protein	5–10
Surfactant-associated proteins	5
Loosely associated, mainly serum	0–5

Table 38-2 Surfactant-Associated Proteins

Name	*Possible functions*
SP-A (collectin)	Immunomodulatory role in host defense Might act cooperatively with SP-B in the formation of surfactant surface film
SP-B	Tubular myelin formation Formation of surfactant surface film
SP-C	Tubular myelin formation Formation of surfactant surface film
SP-D (collectin)	Immunomodulatory role in host defense

Surfactant in Lung Injury

Because of the observed similarities between infant respiratory distress syndrome, caused by surfactant deficiency,[12] and ARDS, it was postulated that surface-active material was abnormal at the time when the syndrome was first described.[15] Since then, it has been confirmed that there is surfactant dysfunction in ARDS and acute lung injury.[11,12] Lung injury can interfere with surfactant metabolism in many ways. It can promote the depletion of functional surfactant pools by altering the composition and quantity of phospholipids being secreted, as well as by depleting surfactant-associated proteins.[12] Furthermore, inflammatory mediators, especially oxygen radicals and proteases, may attack surfactant proteins and exert phospholipolytic activity that degrades surfactant lipids[12] (see Figure 38-1). Plasma proteins found in the edema fluid, especially fibrinogen but also, to a lesser degree, albumin and globulin, can also inhibit surfactant activity.[10] Finally, surfactant metabolism in the hypophase by convertases is also altered in lung injury, leading to a greater pool of inactive surfactant.[10] The alteration in surfactant metabolism and function in lung injury will contribute directly to the lung dysfunction observed.

Given the role of SP-A and SP-D as modulators of immune function, one has to wonder if alterations in their function and quantity might have a role to play in the defense mechanisms during acute lung injury. It is well known that there is an increased frequency of nosocomial pneumonia in injured lungs.[16] SP-A and SP-D are members of a group of important host defense proteins known as collectins. These proteins can interact with microorganisms and act as opsonins to facilitate microorganism uptake by phagocytic cells.[14] Mice deficient in SP-A have been shown

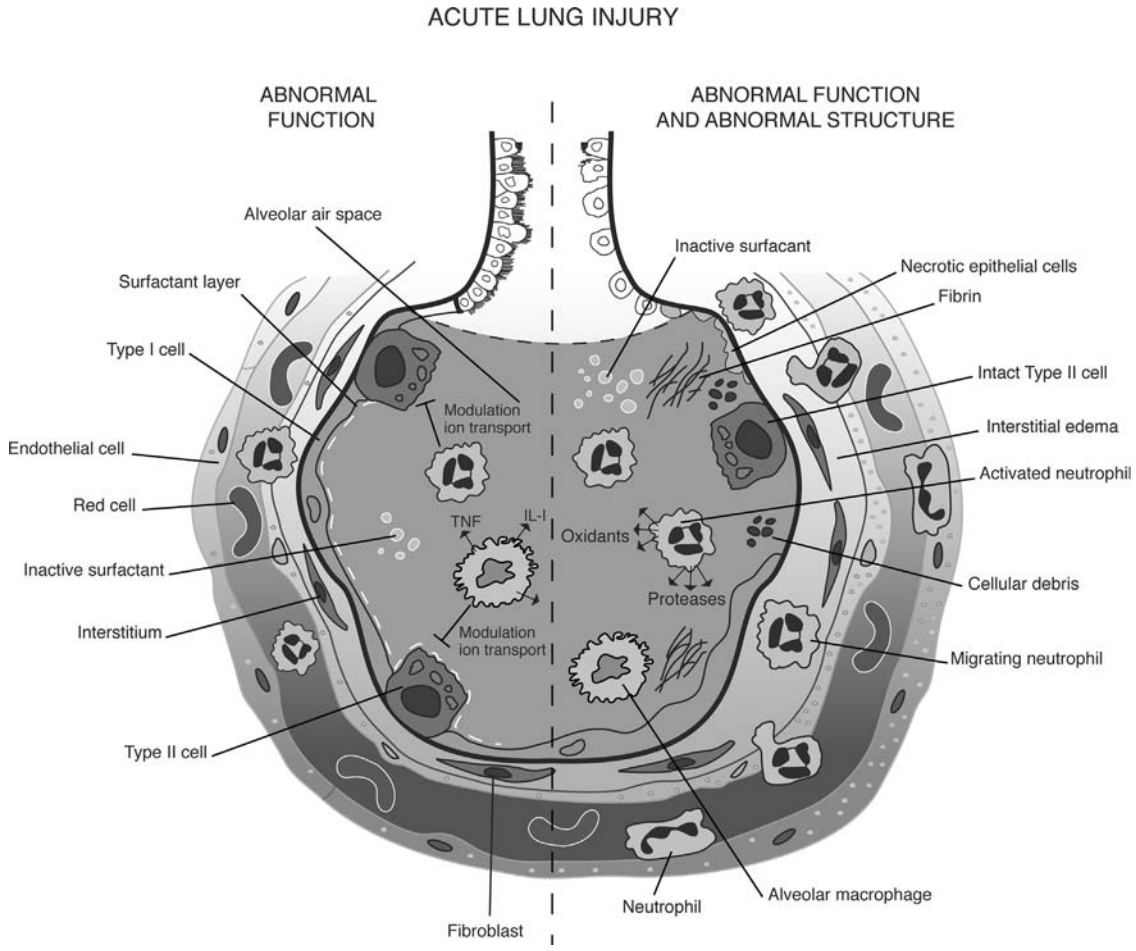

FIGURE 38-1 Lung injury is not a homogeneous process. Different types of injury can be present at the same time in the lung. Some areas may show no structural damage to the epithelium, but there is a decrease in surfactant secretion and an inhibition of surfactant function, as well as a decrease in the capacity of the epithelium to transport ions. These dysfunctions are probably influenced by inflammatory mediators released by macrophages or neutrophils. In other areas of the lung, the injury is associated with structural damage secondary to the sloughing of the alveolar epithelial cells. This leads to the formation of a protein-rich hyaline membrane. Interestingly, the same area may contain endothelial cell injury, which is more subtle (more vesicles, cells swelling). The degree of injury seems insufficient to explain the severity of the edema. This process involves macrophages and neutrophils. The macrophages, by releasing chemotactic factors, stimulate the migration of activated neutrophils from the microcirculation to the airspaces. By releasing different proinflammatory molecules (oxidants, proteases), these neutrophils mediate epithelial damage. IL = interleukin; TNF = tumor necrosis factor.

to be more susceptible to infection, and reduced levels of SP-A and SP-D have been found in ARDS.[17] It is thus possible that abnormal function of these surfactant proteins may contribute to the increased incidence of nosocomial pneumonia in injured lungs.

Surfactant Therapy in Lung Injury

Because of the obvious anomalies in surfactant function in injured lungs, surfactant replacement therapy has been proposed for patients with acute lung injury. Multiple pilot studies have been performed with various surfactant preparations and have indicated that surfactant replacement therapy might be useful.[12] The efficacy of an aerosolized synthetic surfactant preparation (Exosurf) in ARDS was investigated in one large, randomized, multicenter trial. However, this trial did not show any patient benefit.[18] There are several possible explanations for these negative results. Exosurf is a synthetic surfactant preparation lacking surfactant proteins, which are essential for surfactant function. In vitro, although Exosurf is reasonably surface active, it is less active than natural surfactant and is more sensitive to inhibition by proteins. Finally, the preparation was delivered as an aerosol, and less than 5% may have reached the distal airspaces. This dose is well below the level that would be necessary to be effective in lung injury.[12] Hence, although surfactant abnormalities contribute to the pathophysiology of lung injury, and surfactant therapy might help compensate for this surfactant dysfunction, further studies will be needed to determine its role in the therapeutic arsenal for ARDS. Furthermore, since acute lung injury is a complex pathologic process, it will be necessary to combine different treatment strategies to accelerate the resolution of injury. In this regard, we need to understand the other functions of the alveolar epithelium to guide us in the development of these strategies.

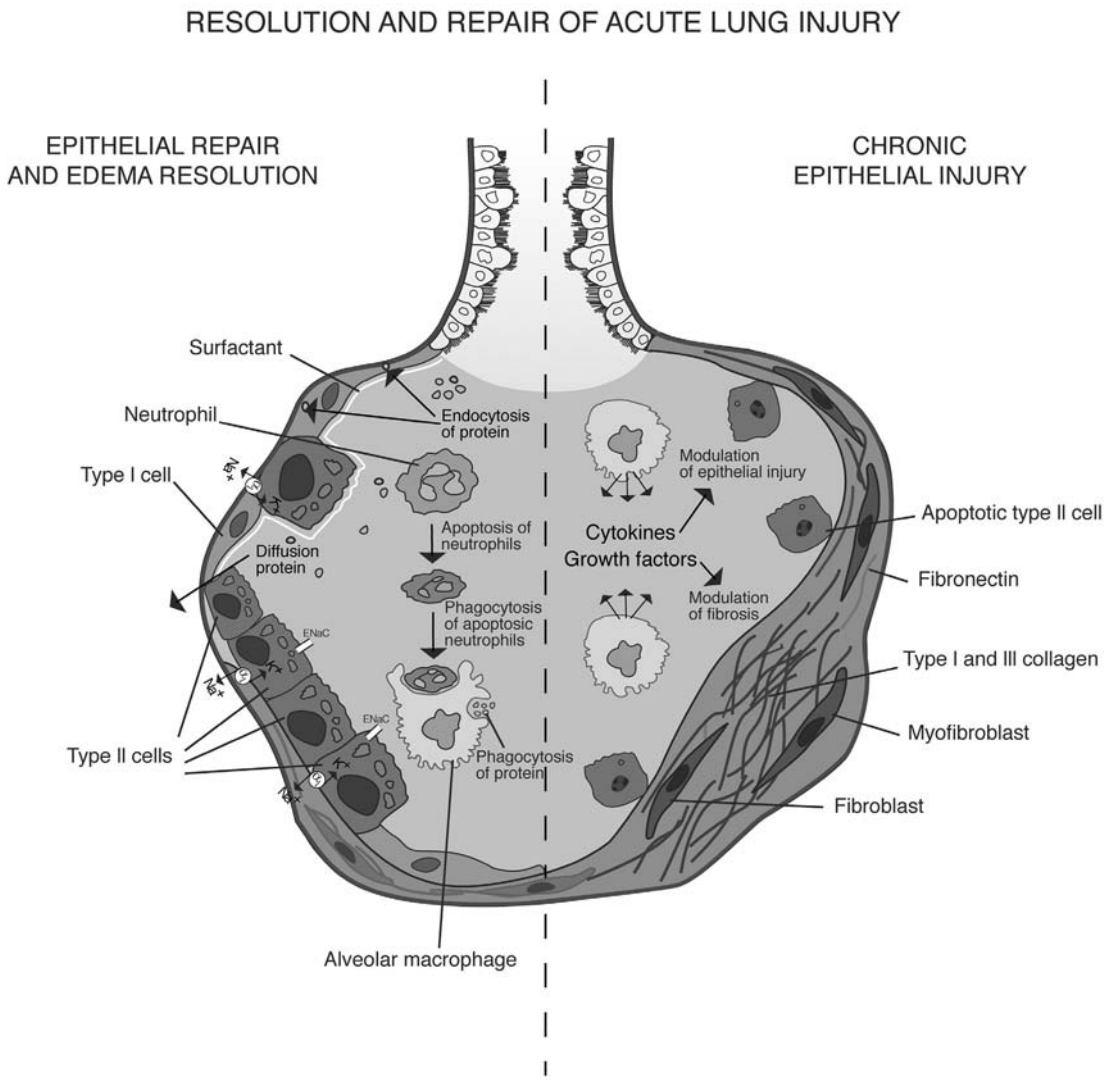

FIGURE 38-2 Acute injury of the lung is followed either by repair of the alveolar epithelium or persistence of the epithelial injury, leading to fibrosis. The repair process involves the proliferation and differentiation of alveolar type II cells. The resolution of alveolar edema is secondary to the activation of Na^+ transport across the alveolar epithelial cells. The soluble proteins present in the edema fluid are cleared by paracellular diffusion and endocytosis, whereas macrophages remove insoluble proteins and apoptotic cells present in the fluid. When the epithelial cells cannot proliferate, and apoptosis of the alveolar type II cells persists, there is a gradual proliferation of fibroblasts and myofibroblasts, leading to gradual interstitial and intraalveolar fibrosis. This process is partially modulated by cytokines and growth factors released into the injured alveoli by macrophages.

EDEMA RESOLUTION: THE ROLE OF ION TRANSPORT

Edema Clearance in Normal Lungs

Reabsorption of alveolar edema fluid is also an essential aspect of lung injury resolution. It has been shown that it may have a significant impact on the prognosis of patients with pulmonary edema.[19] The alveolar epithelium is a key element in the process of edema clearance. In fact, the alveolar epithelium is not only a tight epithelial barrier that prevents the movement of edema fluid into the alveoli but is also actively involved in the transport of ions and solutes, a process that is essential for edema clearance[20] (see Figure 38-3).

To study alveolar edema resolution, many investigators have used a model of alveolar flooding in which an isotonic fluid containing albumin is instilled into the lung airspaces. Fluid clearance is then measured by determining the amount of excess water in the experimental lung in comparison with that in a control lung.[21,22] With such an experimental approach, it was established that liquid clearance was faster than protein clearance, so that the solution remaining in the airspaces became more concentrated as the liquid was removed.[21,23] Since water clearance in the face of rising osmotic pressure could not be explained by changes in hydrostatic or osmotic forces across the alveolar epithelium, it was proposed that active transport of ions was responsible[21,23] (see Figure 38-3). This liquid clearance with rising protein concentration has been seen in the lungs of many species apart from humans.[24] Multiple experimental data suggest that the mechanism is located in the alveolar region,[25,26] although distal airway epithelial cells can also actively reabsorb Na^+.[27]

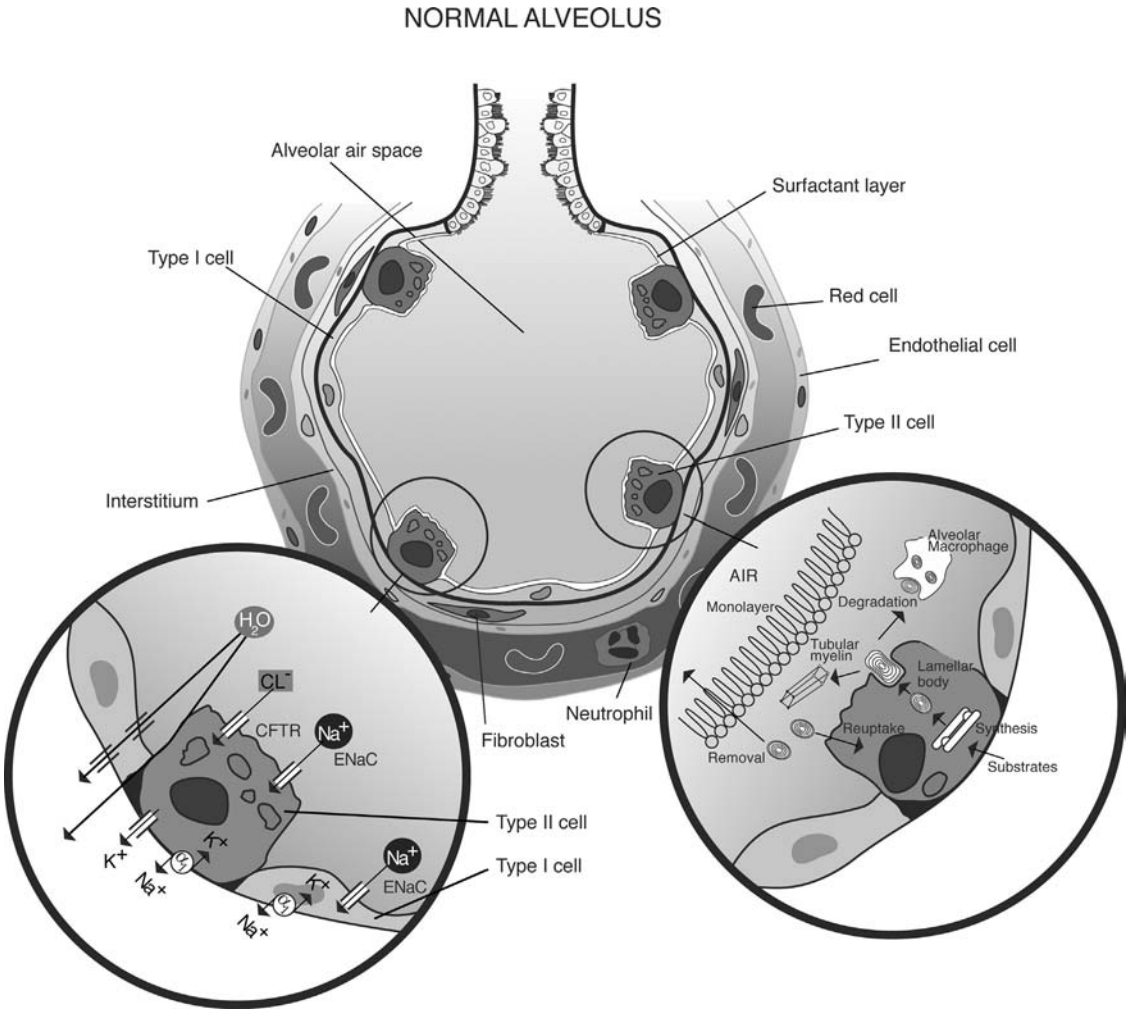

FIGURE 38-3 The alveolar epithelium is not only a tight epithelium but is also actively involved in surfactant secretion, as well as the transport of ions and solutes. Surfactant metabolism is a complex system involving synthesis, secretion, and recycling of phospholipid and surfactant-associated protein. The predominant ion transport present in the alveolar epithelium is Na^+ transport. Transepithelial Na^+ transport involves an Na^+ channel (ENaC) located at the apical surface of type II and type I cells, as well as the Na^+/K^+-ATPase located at the basolateral side of the cells. Na^+ is absorbed at the apical surface through the Na^+ channel and is extruded at the basolateral side by the Na^+ pump (Na^+/K^+-ATPase). The role of Cl^- transport in this response is still unclear. Water has been shown to move by the paracellular route, although it might also move through water channels. CFTR = cystic fibrosis transmembrane conductance regulator.

Much experimental evidence suggests that active Na^+ transport is the dominant ion transport mechanism involved in alveolar liquid clearance. The cellular mechanism responsible for this vectorial transport of Na^+ from alveoli to the interstitium has been better defined recently. Na^+ enters the cell by the amiloride-sensitive epithelial Na^+ channel (ENaC) or by other cationic channels located at the apical surface and is extruded by Na^+/K^+-ATPase located at the basolateral surface[28] (see Figure 38-3). Using drugs that interfere with the function of these molecules (amiloride–ENaC, ouabain–Na^+/K^+-ATPase), many laboratories have shown that Na^+ transport across the alveolar epithelium is important for edema resolution.[24]

Recent experimental data have allowed us to better characterize the structure and function of the major system involved in this transepithelial transport. ENaC is the first constituent of the Na^+ transport system. It has been cloned recently and is composed of three subunits, α-ENaC, β-ENaC, and γ-ENaC, which are able to reconstitute a functional channel.[29] In situ hybridization and immunohistochemical staining have shown that the ENaC subunits are expressed along the epithelium of the respiratory system[30,31] and are found in alveolar type II[31] and type I cells.[32] The physiologic role of α-ENaC in the lungs has been demonstrated in a mouse in which the α-ENaC gene was deleted by targeting a transgene by homologous recombination.[33] Unable to clear liquid from their lungs, these mice die shortly after birth.[33] Furthermore, another animal model with reduced α-ENaC expression was shown recently to be more susceptible to pulmonary edema.[34] ENaC activity and expression are regulated by a complex control system. ENaC function is dependent not only on direct modulation of channel activity[35] but also on channel degradation and membrane stability[36,37] (Figure 38-4). The second messenger cAMP is thought to play a major role in the modulation of the channel activity, although the cellular mechanism leading to this channel activation has not been completely

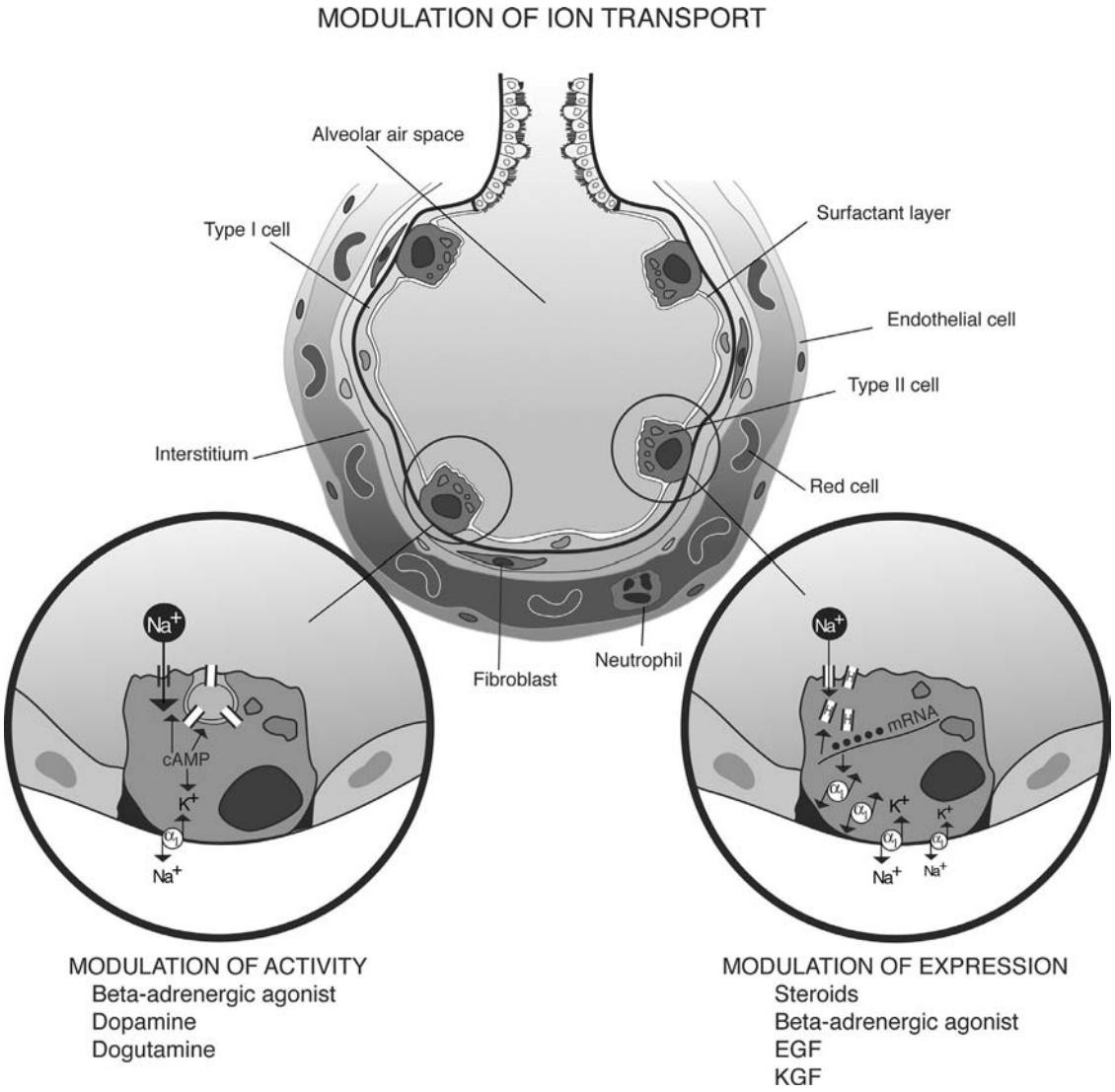

FIGURE 38-4 Ion transport in the lung is mediated by active transport of Na^+. Na^+ transport can be regulated by modulating either the activity or the expression of molecules involved in this transcellular transport system (epithelial Na^+ channel [ENaC], Na^+/K^+-ATPase). Different drugs have been shown to modulate either the activity or the expression of these molecules. EGF = epidermal growth factor; KGF = keratinocyte growth factor.

identified.[35] Increased Na^+ transport could also be associated with heightened channel gene expression (see Figure 38-4). The two major hormone groups that are thought to modulate ENaC expression in the lung are catecholamines[38] and steroids.[39] The regulation of expression of ENaC is particularly important around the time of birth, when the lung must clear the lung fetal liquid.[39] Also at this time, there is a transient rise in ENaC expression,[40] and liquid reabsorption in the lung is enhanced. Besides ENaC, a multitude of other cation channels, which could be involved in Na^+ transport, have been identified in alveolar type II cells.[35] The exact role of these channels in edema clearance remains to be elucidated.

Na^+/K^+-ATPase, which is composed of two subunits, is another major component of the transepithelial Na^+ transport system (see Figure 38-3). The α-subunit is the catalytic component of the complex and is involved in Na^+ extrusion, K^+ intrusion, and ATPase activity.[41] The β-subunit is a highly glycosylated protein whose role is not well understood. It is speculated to be an important regulatory component of the Na^+ pump. Although it is mainly the α_1- and β_1-subunits that have been detected in the lungs,[41] more recently it has been suggested that alveolar type I cells might express the α_2 Na^+/K^+-ATPase.[42] Na^+/K^+-ATPase inhibition with ouabain greatly decreases solute transport in alveoli[43] and reduces the short-circuit current across alveolar type II cells.[44] Changes in intracellular Na^+ concentration and the levels of various hormones, such as mineralocorticoids, adrenergic agonists, and thyroid hormones, have been found to modulate Na^+/K^+-ATPase activity[45,46] (see Figure 38-4). Like that of ENaC, modulation of Na^+/K^+-ATPase activity is complex and also involves the modulation of the trafficking of the protein to the membrane.[41] Furthermore, as with ENaC, heightened Na^+/K^+-ATPase expression could also be an important tactic to augment transepithelial Na^+ transport. Again, it is well known that Na^+/K^+-ATPase expression is increased around the time of birth[39,40] when fetal lung liquid needs to be cleared. Many major hormonal systems, such as the thyroid, mineralocorticoid, and gluco-

corticoid systems,[45,46] have been reported to modulate Na^+/K^+-ATPase expression (see Figure 38-4). In the lungs, the α-subunit does not seem to be modulated by corticosteroids,[47] but the β-subunit appears to be affected.[48] The β-adrenergic system is also a potent stimulator of Na^+/K^+-ATPase expression in alveolar epithelial cells.[38]

Until recently, it was generally accepted that liquid movement across the alveolar epithelium was an intercellular process secondary to the osmotic gradient generated by transepithelial Na^+ transport across the alveolar epithelium (see Figure 38-3). However, many laboratories have now demonstrated the presence of specialized water-transporting proteins (aquaporins) in the lungs. Water movement may then occur not only through paracellular pathways but also by a transcellular route[49] (see Figure 38-1). Although four different aquaporins are expressed in lung tissue, aquaporin 5 is the predominant form in alveolar type I cells,[50] the site where edema is believed to be cleared. Since this cell type has one of the highest cellular permeability coefficients for water, it could be postulated that some water movement across the alveolar epithelium goes through type I cells.[51] Transgenic mouse models of aquaporin deletion have provided information on the potential physiologic role of aquaporins in edema clearance. The data available at present suggest that alveolar liquid clearance in the neonatal and adult lung is not affected by aquaporin deletion.[50] The lack of apparent functional importance for aquaporins in edema clearance does not eliminate the possibility that they play a role under conditions of stress or injury.

Although the primary barrier to alveolar liquid clearance is epithelial, it is important to identify the major clearance pathways once the liquid has reached the interstitial space. Initially, it was thought that the lung lymphatics would provide the major route for fluid clearance; however, experimental data have now shown that the increase in lymph flow accounts for only 10 to 20% of the alveolar liquid transported to the interstitium.[20,22] The most likely clearance pathway for alveolar edema liquid is therefore the pulmonary circulation. Indeed, in experiments in which the pulmonary and bronchial circulations are occluded, alveolar liquid clearance continues at a normal rate, but lung liquid clearance is completely inhibited.[52,53] From these experiments, we can conclude that a minimal amount of bloodflow is necessary for alveolar liquid clearance and that most of the liquid is cleared from the lungs by bulk flow into the pulmonary vascular space. Under some pathologic conditions, the pleural space could also serve as an important clearance pathway for pulmonary edema.[54]

Edema Clearance in Injured Lungs

Although there are substantial data supporting the concept that lung liquid clearance is mediated by active Na^+ transport and that multiple pathways can be stimulated to enhance its efficiency in the normal lung, we have to wonder if this system is functional in pathologic conditions. Interestingly, the alveolar and distal airway epithelia are remarkably resistant to injury, particularly in comparison to the adjacent lung endothelium.[7,28] When lung endothelial injury occurs, the alveolar–epithelial barrier may retain its normal impermeability to proteins and its normal fluid transport capacity. For example, when intravenous or intraalveolar endotoxin is used to produce lung endothelial injury, passage of proteins through the lung epithelial barrier is not altered.[28,55] Furthermore, histologically, the ultrastructural appearance of alveolar epithelial cells is normal, whereas there are signs of endothelial cell injury, as indicated by the increased number of pinocytic vesicles. In these models of injury, where the alveolar epithelium is intact, there is no impairment of alveolar fluid clearance.

Interestingly, in mild-to-moderate lung injury, the capacity of the alveolar epithelium to transport salt and water is not only preserved but may even be up-regulated by stress hormones (Figure 38-5). When septic shock was induced in rats,[55] even though endothelial injury and interstitial pulmonary edema occurred, alveolar epithelial fluid transport was increased by 32%. This enhanced fluid clearance was inhibited by amiloride or propranolol, demonstrating that the augmented fluid clearance depended on endogenous β-adrenergic agonist stimulation of alveolar epithelial Na^+ transport.[55] After short-term hemorrhagic shock, alveolar fluid clearance can also be enhanced by catecholamine-dependent mechanisms.[56] Although catecholamines can stimulate the activity of Na^+ channels, through either increased levels of cAMP[35] or the activity[57] or membrane insertion[41] of the Na^+/K^+-ATPase, it has been reported recently that catecholamines, mainly β-adrenergic agonists, can modulate ENaC as well as Na^+/K^+-ATPase expression.[38] Glucocorticoids are other potent stress hormones that can change Na^+ channel and Na^+/K^+-ATPase expression[58] and stimulate alveolar fluid clearance.[24]

Lung fluid clearance can also be stimulated in lung injury by catecholamine-independent mechanisms (see

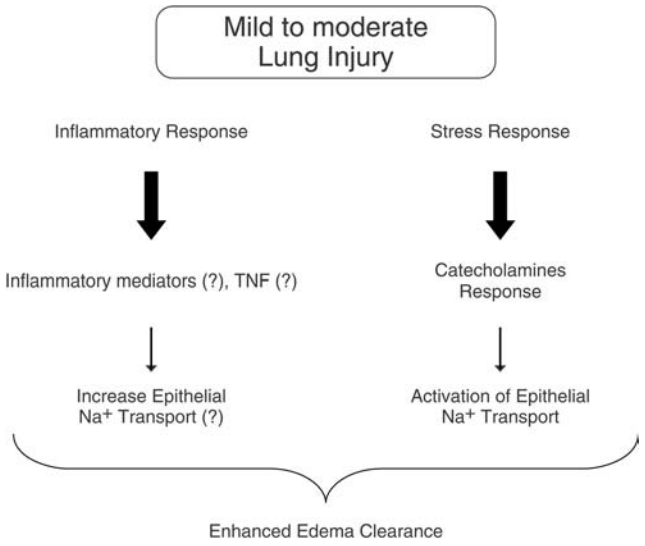

FIGURE 38-5 Mild-to-moderate lung injury can lead to enhanced edema clearance. This response is due to activation of epithelial Na^+ transport resulting from the catecholamine response associated with the lung injury. However, in certain types of injury, other pathways seem to be involved. It has been suggested that certain inflammatory mediators, such as tumor necrosis factor (TNF), might participate in this response.

Figure 38-5). Alveolar fluid clearance is increased in bleomycin-induced subacute lung injury, and this increased Na^+ transport occurs in the presence of decreased expression and function of amiloride-sensitive Na^+ channels (probably primary ENaC) in alveolar type II cells.[59] An increased number of alveolar type II cells was primarily responsible for the twofold increase in alveolar fluid clearance. In bacterial pneumonia induced by the instillation of *Pseudomonas* into the distal airways, there was a 48% increase in alveolar fluid clearance, which could be inhibited by amiloride but not by propranolol.[55] Interestingly, this effect was suppressed by an anti–tumor necrosis factor-α (TNF-α) antibody.[55] TNF-α is also important in stimulating alveolar fluid clearance after intestinal ischemia–reperfusion.[55] Although these results suggest that TNF can stimulate alveolar liquid clearance, the mechanism involved is still unknown, and it is possible that it is not a direct effect of TNF on Na^+ transport since TNF is also known to decrease Na^+ transport in alveolar epithelial cells. Alveolar fluid clearance can also be stimulated in subacute models of hyperoxic lung injury[55] by up-regulating Na^+ transport in the lungs, potentially by modulating Na^+/K^+-ATPase activity.[55] These experimental results suggest that when the integrity and function of the alveolar epithelium are preserved, alveolar liquid clearance can be stimulated even in the presence of lung interstitial or mild alveolar edema. The mechanism involved in this up-regulation of alveolar liquid clearance could involve some inflammatory mediators, but their exact role remains to be defined.

However, other experimental data indicate that the Na^+ transport mechanism may be down-regulated in severe forms of lung injury, and that this can be explained by the impact of inflammatory mediators on either the integrity or function of the alveolar epithelium (Figure 38-6). Reactive oxygen and nitrogen species can inhibit Na^+ transport and Na^+ channel activity.[55] There are also conflicting data regarding the modulation of Na^+/K^+-ATPase expression and activity in some models of lung injury,[55,60] suggesting that the response of the alveolar epithelium to injury is quite heterogeneous and that modulation of Na^+ transport depends on the severity of the injury[61] (see Figure 38-1). Recently, transforming growth factor-β (TGF-β)and TNF have been shown to decrease the activity and expression of Na^+ channels.[62,63] Furthermore, in the more severely injured lungs, a marked increase in paracellular permeability leads to significant alveolar epithelial damage and, subsequently, to a loss of salt and water transport capacity of the alveolar epithelial cells[28,55,60,64] (Figures 38-1 and 38-6).

One has to wonder whether alveolar liquid clearance mechanisms are intact in other types of pulmonary edema, such as hydrostatic pulmonary edema. Since the pulmonary circulation is not essential for alveolar fluid clearance,[28] it would not be expected that left heart failure could influence edema clearance. However, alveolar fluid clearance can be modulated by perfusion pressure. Although alveolar fluid clearance is normal in the presence of a moderate increase in left atrial pressure,[65] β-adrenergic stimulation did not stimulate alveolar fluid clearance when there was a persistent elevation of left atrial pressure.[65] This inhibitory effect has been attributed to atrial natriuretic factor (ANF), which has been shown to modulate Na^+/K^+-ATPase in vitro[65] and to decrease Na^+ transport in the lungs.[66] However, other mechanisms may also be involved. For example, since this effect has been seen in isolated perfused lungs, which have no functional lymphatics,[67] it is possible that augmented interstitial volume and pressure could slow alveolar fluid clearance. In fact, it has been reported recently that an increase in interstitial volume can limit alveolar fluid clearance.[68] Thus, although alveolar fluid clearance depends primarily on active ion transport in the distal lung epithelium,

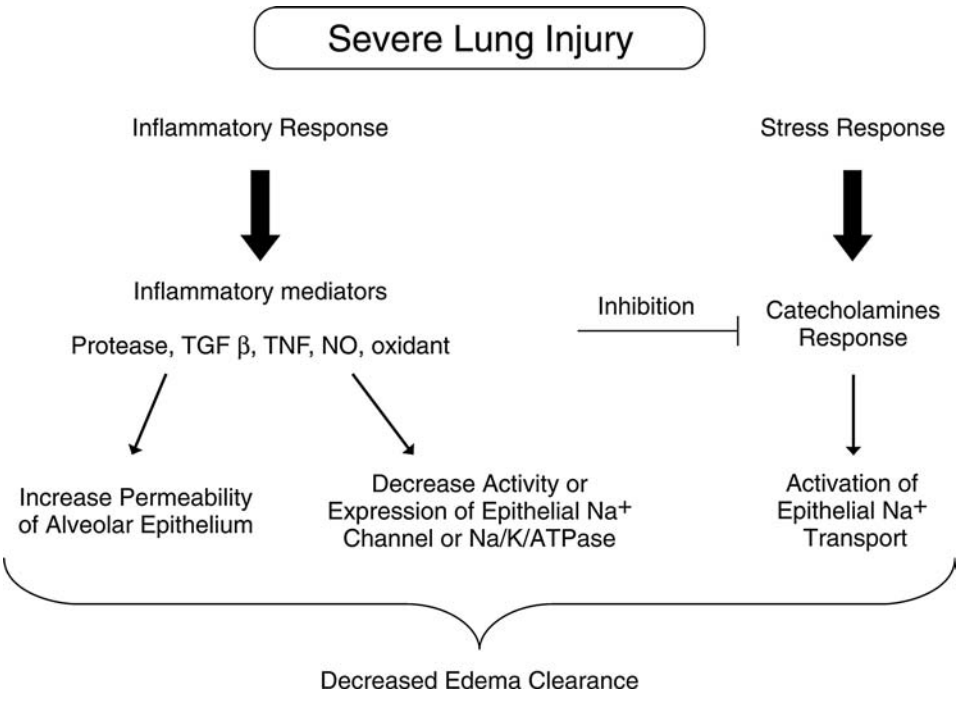

FIGURE 38-6 Severe lung injury can be associated with decreased edema clearance. This process is mainly due to the enhanced permeability of the alveolar epithelium, as well as decreased epithelial Na^+ transport. Various inflammatory molecules are involved in this response, such as proteases, transforming growth factor-β (TGF-β), tumor necrosis factor (TNF), nitric oxide (NO), and oxidants. Furthermore, oxidants might inhibit the catecholamine response, which is known to enhance Na^+ transport. It is therefore possible that the intensity of the inflammatory response may transform a mild form of lung injury into a severe form by inducing changes in the function of the alveolar epithelium.

it can be modulated by the pulmonary circulation and the interstitial pressure generated by interstitial edema fluid.

Collectively, these observations suggest that there could be either significant activation or significant inhibition of the Na^+ transport mechanism in lung injury. Since the alterations of alveolar liquid clearance vary between different models of lung injury, different mechanisms appear to lead to alveolar epithelial cell dysfunction. Furthermore, based on the heterogeneous responses observed, we can hypothesize that the variability of the systemic response to injury could also be a determinant of alveolar liquid clearance.

Clinical Relevance of Alveolar Liquid Clearance

Does alveolar liquid clearance have clinical significance? There is accumulating evidence that this process is highly relevant to patients with pulmonary edema. Investigators have demonstrated a link between the prognosis of lung injury and alveolar liquid clearance.[19] They found that 56% of patients with lung injury had impaired alveolar liquid clearance, and only 13% of them had a maximal alveolar liquid clearance rate. In contrast, they reported that 75% of patients with hydrostatic edema had submaximal to maximal alveolar liquid clearance.[19] Interestingly, the survival of patients with lung injury and maximal alveolar clearance rates was improved in comparison with that of patients with abnormal clearance rates. Furthermore, there was also a decrease in the number of days on a ventilator in patients with better edema resolution. A similar observation was also made in post–lung transplant patients; those with the best alveolar liquid clearance had the best clinical outcome.[69] Patients with hydrostatic pulmonary edema and altered alveolar liquid clearance capacity also have decreased arterial pH, suggesting that systemic hypoperfusion and systemic factors might have important regulatory influences on alveolar liquid clearance.[70] Recently, it has even been shown that manipulation of Na^+-driven alveolar fluid clearance could represent an appropriate target for therapy.[71] In this study, patients susceptible to high-altitude pulmonary edema had lower levels of Na^+ transport in the respiratory epithelium, and prophylatic inhalation of salmeterol decreased the incidence of pulmonary edema by more than 50%. Overall, there is now both physiologic and clinical evidence that this transport system is important in the pathogenesis of lung injury.

Treatment Strategies to Increase Alveolar Fluid Clearance in the Injured Lung

Since the mortality rate is lower in patients with maximal alveolar fluid clearance,[19] we can hypothesize that improving alveolar liquid clearance could potentially modify the evolution of lung injury. Various pharmacologic and molecular tools could be used to stimulate alveolar fluid clearance.

The best studied agents are cAMP agonists, that is, β-adrenergic receptor agonists. β-Adrenergic agonist therapy enhances alveolar fluid clearance in several models of lung injury, including hyperoxic lung injury and ventilator-induced lung injury, and can even stimulate alveolar fluid clearance when the agent is administered as an aerosol.[55] More recently, it has also been shown that aerosolized salmeterol, a lipid-soluble β_2 agonist, can stimulate lung liquid clearance at a clinically relevant dose.[24] Furthermore, as already discussed, β-adrenergic agonists have been proposed as prophylactic agents for the treatment of high-altitude pulmonary edema.[71] However, the use of β-adrenergic agonists to enhance the resolution of pulmonary edema might be limited by several factors[55] or ineffective in some types of lung injury.[64] First, prolonged stimulation by endogenous catecholamines may desensitize the β-adrenergic receptors or decrease their density and prevent effective stimulation by exogenous catecholamines. However, since stimulation of alveolar fluid clearance with β-adrenergic agonists rapidly returns to normal after circulating catecholamine levels revert to baseline, this limitation seems unlikely, except in patients with prolonged, unstable shock. Other circulating factors could, however, limit the action of β-adrenergic agonists. For example, in the presence of left atrial hypertension, it is possible that ANF could inhibit the stimulatory effect of β-adrenergic agonists on alveolar fluid clearance.[55] In prolonged hemorrhagic shock and resuscitation, cAMP agonists may not stimulate alveolar fluid clearance because oxidant-mediated injury down-regulates the response of the alveolar epithelium to β_2-agonists.[55] Finally, β-adrenergic agonists have also been associated with the induction of pulmonary edema in some pathologic conditions. One of the best known situations in which β-adrenergic agonists induce pulmonary edema is when they are used to inhibit preterm labor (tocolytic therapy).[72,73] In this clinical condition, β-adrenergic agonists are administered by continuous intravenous perfusion to stop the uterine contraction. Although the pathophysiologic mechanism has not been completely elucidated, it is unlikely that pulmonary edema is directly associated with the action of the β-adrenergic agonists. In fact, it is believed that pulmonary edema in this condition is multifactorial. One of the major contributing factors is the iatrogenic fluid overload associated with the therapy in patients who already have, because of the pregnancy, an increase in their plasma volume. The incidence of tocolytic pulmonary edema also seems to be greater in patients who have an ongoing infectious process. The most convincing evidence against a direct action of β-adrenergic agonists comes from the observation that, with careful choice of the intravenous solution and the volume administered, the incidence of pulmonary edema decreases. Therefore, although β-adrenergic agonists are potentially interesting therapeutic agents for modulating edema clearance, other therapeutic targets and agents might be necessary in some clinical conditions to enhance alveolar fluid clearance.

Vasoactive agents, such as dobutamine and dopamine, have been shown to augment alveolar fluid clearance.[8] Growth factors, such as epidermal growth factor (EGF), TGF-α, and keratinocyte growth factor (KGF), can also stimulate vectorial Na^+ transport.[8] Since KGF has been shown to stimulate alveolar fluid clearance and to have effects additional to those of β-adrenergic agonists,[74] even showing protective action in some models of lung injury, it may be an excellent alternative to β-adrenergic agonist therapy.[55,60] However, it still remains to be shown that these

agents can modulate alveolar fluid clearance and lung injury if they are administered after the insult.

One final approach that could be used to manipulate alveolar fluid clearance is gene therapy. Overexpression of the β-subunit of Na^+/K^+-ATPase[75]or β_2-adrenergic receptor[76] in the lung can stimulate alveolar fluid clearance and improve the survival of animals with hyperoxic lung injury.[77] Overexpression of both the α- and β-subunits of Na^+/K^+-ATPase also decreased edema formation in a model of thiourea-induced lung injury.[78] However, more data will be needed to determine if this therapeutic approach is effective only as a pretreatment or if it could also modulate alveolar fluid clearance and lung injury.

ALVEOLAR EPITHELIUM REPAIR: THE ROLE OF ALVEOLAR TYPE II CELLS

Although edema liquid removal is important in the resolution of lung injury, one of the most essential functions of the alveolar epithelium is its participation in the repair of alveolar structures. Residual type II alveolar epithelial cells, which are more resistant to injury than type I alveolar epithelial cells, are the source of cells for regeneration of the epithelium of the airspaces (see Figure 38-2). The turnover rate of type II alveolar epithelial cells in the normal adult lung is remarkably low, at ~4%/day but is boosted after acute lung injury.[6,60,79–81] However, proliferation of alveolar epithelial cells needs several hours to take place and at least 1 or 2 days to be significant.[79,80] So, in the early stages of repair, the adhesion, spreading, and migration of epithelial cells are prerequisites for optimal alveolar repair.[6,82–84] This repair process requires communication of the cells with their environment. Epithelial cells will interact with either a provisional matrix rich in fibronectin, fibrinogen, and plasma proteins containing multifolded or fragmented remnants of basal membranes[4,5] or with the extracellular matrix synthesized by alveolar epithelial cells.[85] Cell–matrix interactions are mediated by epithelial integrins.[86] The expression of these integrins is especially induced by normal wound healing.[86,87] Interestingly, hyaline-charged alveolar epithelial cells in areas of early DAD with intraalveolar fibrosis fail to express these integrins. In this respect, epithelial cell shedding has been commonly observed in acute lung injury and chronic fibrosing alveolitis with desquamative interstitial pneumonitis.[88,89] Most of these processes can be retrospectively related to apoptosis (or programmed cell death) since loss of contact between epithelial cells and their matrix environment can induce apoptosis.[90] Furthermore, pathologic investigations of acute DAD have revealed up-regulation of the apoptosis facilitators p53, WAF-1 (wild-type p53-activated fragment), and Bax in alveolar epithelial cells.[91,92] Finally, Fas–Fas ligand interactions, which constitute one of the major systems controlling the apoptosis of epithelial cells,[93] can elicit widespread alveolar epithelial cell apoptosis with subsequent pulmonary fibrosis.[93] Thus, it is reasonable to postulate that the failure of alveolar epithelial cell adhesion, spreading, and migration, and excessive apoptosis, can delay repair and favor fibrosis (see Figure 38-5).

This epithelial repair process needs modulators. Nearly all cytokines identified recently as promoters of alveolar epithelial cell migration are heparin sulfate–binding proteins (eg, EGF, TGF-α, KGF, hepatocyte growth factor [HGF], fibroblast growth factor [FGF]).[80,94] KGF, HGF, and FGF are paracrine fibroblast-derived polypeptides, whereas EGF and TGF-α can act in an autocrine–paracrine manner on alveolar epithelial cells bearing receptors.[80] These cytokines are now well recognized and are clearly omnipresent in the lung during development and after lung injury,[94] processes that are associated with significant remodeling of the alveolar epithelium. TGF-β is another cytokine involved in epithelial repair. Early after the induction of lung injury, there is a significant decrease in the secretion of biologically active TGF-β3,[95,96] and the expression of TGF-β receptors I and II is also diminished.[97] Since TGF-β is a powerful growth inhibitor of cells of epithelial origin, this initial nadir of TGF-β3 after lung injury could potentially facilitate alveolar epithelial cell proliferation. TGF-βs also up-regulate the production of matrix protein components[98] and are important regulators of integrin expression on epithelial cells,[99,100] physiologic phenomena that are vital in the repair process, particularly for cell migration. The lymphomonokines interleukin-2 (IL-2) and interferon-γ (IFN-γ) might also play an unexpected role in epithelial repair in the lungs. IFN-γ increases IL-2 receptor (IL-2R) expression on alveolar epithelial cells[101] and promotes IL-2–induced alveolar epithelial cell growth activity.[83,102]

Although many cytokines have been shown to be important in repair of the alveolar epithelium, there have been few studies on their potential in lung injury treatment. Recent animal experiments have indicated that HGF and KGF could have significant roles as new therapeutic agents. HGF administration to animals with lung injury can stimulate alveolar epithelial cell proliferation.[94] Furthermore, KGF treatment of rats prior to lung injury leads to a decrease in its severity.[94] However, it is still unclear whether this protective effect of KGF is linked to its impact on the proliferative capacity of alveolar epithelial cells or its impact on the ion transport capacity of these cells.[94] Although growth factors could have some therapeutic potential in ARDS, much work is needed to better define their therapeutic value since manipulation of this system could have a negative impact as well. In fact, it is known that overexpression of certain growth factors could lead to pulmonary fibrosis.[103] Thus, as with the development of therapeutic strategies for enhancing edema clearance, strategies for promoting epithelial repair are still at an early stage.

CONCLUSION

Although much has been learned about the mechanisms leading to acute lung injury, mortality—which is mainly related to sepsis or associated nonpulmonary organ dysfunction—remains high in ARDS patients.[1] Many new therapeutic approaches aimed at controlling the inflammatory response or surfactant dysfunction associated with the disease have been evaluated. However, these treatments have had no impact on mortality stemming from the dis-

ease.[1] The reason for the lack of success with these new interventions is probably multifactorial. It is also probably unrealistic to hope that a single treatment will modify the evolution of all ARDS patients, who represent a heterogeneous population with varying severity of lung injury. Thus, it is unlikely that therapy for mild lung injury will be as efficient in patients with severe lung injury. Also, most of the therapies tested recently have been targeted at controlling the inflammatory response,[104] whereas the severity of and recovery from lung injury also depend on epithelial cell function.[3] Therefore, combination therapy aimed at controlling the inflammatory response and at restoring normal epithelial function (edema clearance, alveolar epithelium repair, surfactant function) will be necessary to reduce the mortality rate and accelerate the recovery process of patients with lung injury. The challenge in the future will be to identify specific targets that will improve epithelial function in lung injury. It is, however, likely that more than one treatment strategy will be necessary since the injury process varies from one patient to another or even in the same patient.

REFERENCES

1. Ware LB, Matthay MA. Medical progress: the acute respiratory distress syndrome. N Engl J Med 2000;342:1334–9.
2. Donnelly SC, Haslett C. Cellular mechanisms of acute lung injury: implications for future treatment in the adult respiratory distress syndrome. Thorax 1992;47:260–3.
3. Matthay MA, Wiener-Kronish JP. Intact epithelial barrier function is critical for the resolution of alveolar edema in humans. Am Rev Respir Dis 1990;142:1250–7.
4. Albertine KH. Histopathology of pulmonary edema and the acute respiratory distress syndrome. In: Matthay MA, Ingbar DH, editors. Pulmonary edema. 1st ed. New York: Marcel Dekker; 1998. p. 37–83.
5. Bachofen M, Weibel ER. Structural alterations of lung parenchyma in the adult respiratory distress syndrome. Clin Chest Med 1982;3:35–56.
6. Adamson IY, Bowden DH. The type 2 cell as progenitor of alveolar epithelial regeneration. A cytodynamic study in mice after exposure to oxygen. Lab Invest 1974;30:35–42.
7. Montaner JSG, Tsang J, Evans KG, et al. Alveolar epithelial damage. A critical difference between high pressure and oleic acid-induced low pressure pulmonary edema. J Clin Invest 1986;77:1786–96.
8. Crandall ED, Matthay MA. Alveolar epithelial transport. Basic science to clinical medicine. Am J Respir Crit Care Med 2001;163:1021–9.
9. Mason RJ, Williams MC. Type II alveolar cell—defender of the alveolus. Am Rev Respir Dis 1977;115:81–91.
10. Jobe AH, Ikegami M. Surfactant and acute lung injury. Proc Assoc Am Physicians 1998;110:489–95.
11. Lewis JF, Jobe AH. Surfactant and the adult respiratory distress syndrome. Am Rev Respir Dis 1993;147:218–33.
12. Frerking I, Gunther A, Seeger W, Pison U. Pulmonary surfactant: functions, abnormalities and therapeutic options. Intensive Care Med 2001;27:1699–717.
13. Creuwels LA, van Golde LM, Haagsman HP. The pulmonary surfactant system: biochemical and clinical aspects. Lung 1997;175:1–39.
14. Wright JR. Immunomodulatory functions of surfactant. Physiol Rev 1997;77:931–62.
15. Ashbaugh DG, Bigelow DB, Petty TK, Levine BE. Acute respiratory distress in adults. Lancet 1967;2:319–23.
16. Markowicz P, Wolff M, Djedaini K, et al. Multicenter prospective study of ventilator-associated pneumonia during acute respiratory distress syndrome. Incidence, prognosis, and risk factors. ARDS Study Group. Am J Respir Crit Care Med 2000;161:1942–8.
17. Greene KE, Wright JR, Steinberg KP, et al. Serial changes in surfactant-associated proteins in lung and serum before and after onset of ARDS. Am J Respir Crit Care Med 1999;160:1843–50.
18. Anzueto A, Baughman RP, Guntupalli KK, et al. Aerosolized surfactant in adults with sepsis-induced acute respiratory distress syndrome. Exosurf Acute Respiratory Distress Syndrome Sepsis Study Group. N Engl J Med 1996; 334:1417–21.
19. Ware LB, Matthay MA. Alveolar fluid clearance is impaired in the majority of patients with acute lung injury and the acute respiratory distress syndrome. Am J Respir Crit Care Med 2001;163:1376–83.
20. Berthiaume Y. Mechanisms of edema clearance. In: Weir EK, Reeves JT, editors. Pulmonary edema. 1st ed. Armonk: Futura Publishing Company; p. 77–94.
21. Matthay MA, Landolt CC, Staub NC. Differential liquid and protein clearance from the alveoli of anesthetized sheep. J Appl Physiol 1982;53:96–104.
22. Berthiaume Y, Staub NC, Matthay MA. Beta-adrenergic agonists increase lung liquid clearance in anaesthetized sheep. J Clin Invest 1987;79:335–43.
23. Matthay MA, Berthiaume Y, Staub NC. Long-term clearance of liquid and protein from the lungs of unanesthetized sheep. J Appl Physiol 1985;59:928–34.
24. Matthay MA, Clerici C, Saumon G. Invited review: active fluid clearance from the distal air spaces of the lung. J Appl Physiol 2002;93:1533–41.
25. Berthiaume Y, Broaddus VC, Gropper MA, et al. Alveolar liquid and protein clearance from normal dog lungs. J Appl Physiol 1988;65:585–93.
26. Ballard ST, Gatzy JT. Volume flow across the alveolar epithelium of adult rat lung. J Appl Physiol 1991;70:1665–76.
27. Van Scott MR, Davis WC, Boucher RC. Na^+ and Cl^- transport across rabbit nonciliated bronchiolar epithelial (clara) cells. Am J Physiol 1989;256:C893–901.
28. Matthay MA, Folkesson HG, Verkman AS. Salt and water transport across alveolar and distal airway epithelia in the adult lung. Am J Physiol 1996;270:L487–503.
29. Alvarez DLR, Canessa CM, Fyfe GK, Zhang P. Structure and regulation of amiloride-sensitive sodium channels. Annu Rev Physiol 2000;62:573–94.
30. Burch LH, Talbot CR, Knowles MR. Relative expression of the human epithelial Na^+ channel subunits in normal and cystic fibrosis airways. Am J Physiol 1995;269:C511–8.
31. Farman N, Talbot CR, Boucher R, et al. Noncoordinated expression of a-, b-, and g-subunit mRNAs of epithelial Na^+ channel along rat respiratory tract. Am J Physiol 1997; 272:C131–41.
32. Johnson MD, Widdicombe JH, Allen L, et al. Alveolar epithelial type I cells contain transport proteins and transport sodium, supporting an active role for type I cells in regulation of lung liquid homeostasis. Proc Natl Acad Sci U S A 2002;99:1966–71.
33. Hummler E, Barker P, Gatzy J, et al. Early death due to defective neonatal lung liquid clearance in aENaC-deficient mice. Nat Genet 1996;12:325–8.
34. Olivier R, Scherrer U, Horisberger JD, et al. Limiting Na(+) transport rate in airway epithelia from alpha-ENaC transgenic mice: a model for pulmonary edema. J Appl Physiol 2002;93:1881–7.

35. Matalon S, Lazrak A, Jain L, Eaton DC. Biophysical properties of sodium channels in lung alveolar epithelial cells. J Appl Physiol 2002;93:1852–9.
36. Staub O, Gautschi I, Ishikawa T, et al. Regulation of stability and function of the epithelial Na^+ channel (ENaC) by ubiquitination. EMBO J 1997;16:6325–36.
37. Kamynina E, Staub O. Concerted action of ENaC, Nedd4-2, and Sgk1 in transepithelial Na(+) transport. Am J Physiol Renal Physiol 2002;283:F377–87.
38. Minakata Y, Suzuki S, Grygorczyk C, et al. Impact of b-adrenergic agonist on Na^+ channel and Na^+-K^+-ATPase expression in alveolar type II cells. Am J Physiol 1998;275:L414–22.
39. Barker PM, Olver RE. Clearance of lung liquid during the perinatal period. J Appl Physiol 2002;93:1542–8.
40. Dagenais A, Kothary R, Berthiaume Y. The a subunit of the epithelial sodium channel in the mouse: developmental regulation of its expression. Pediatr Res 1997;42:327–34.
41. Sznajder JI, Factor P, Ingbar DH. Lung edema clearance: role of Na(+)-K(+)-ATPase. J Appl Physiol 2002;93:1860–6.
42. Ridge KM, Olivera WG, Saldias F, et al. Alveolar type 1 cells express the alpha2 Na,K-ATPase, which contributes to lung liquid clearance. Circ Res 2002;92:453–60.
43. Basset G, Crone C, Saumon G. Significance of active ion transport in transalveolar water absorption: a study on isolated rat lung. J Physiol 1987;384:311–24.
44. Cheek JM, Kim KJ, Crandall ED. Tight monolayers of rat alveolar epithelial cells: bioelectric properties and active sodium transport. Am J Physiol 1989;256:C688–93.
45. Ingbar DH, Wendt CH, Crandall ED. Na,K-ATPase and the clearance of pulmonary edema fluid. In: Matthay MA, Ingbar DH, editors. Pulmonary edema. 1st ed. New York: Marcel Dekker; 1998. p. 477–99.
46. Ewart HS, Klip A. Hormonal regulation of the Na^+-K^+-ATPase: mechanisms underlying rapid and sustained changes in pump activity. Am J Physiol 1995;269:C295–311.
47. Tchepichev S, Ueda J, Canessa C, et al. Lung epithelial Na^+ channel subunits are differentially regulated during development and by steroids. Am J Physiol 1995;269:C805–12.
48. Barquin N, Ciccolella DE, Ridge KM, Sznajder JI. Dexamethasone upregulates the Na-K-ATPase in rat alveolar epithelial cells. Am J Physiol 1997;273:L825–30.
49. Verkman AS. Water transport and molecular water channels in lung. In: Matthay MA, Ingbar DH, editors. Pulmonary edema. 1st ed. New York: Marcel Dekker; 1998. p. 525–47.
50. Borok Z, Verkman AS. Role of aquaporin water channels in fluid transport in lung and airways. J Appl Physiol 2002; 93:2199–206.
51. Dobbs LG, Gonzalez R, Matthay MA, . Highly water-permeable type I alveolar epithelial cells confer high water permeability between the airspace and vasculature in rat lung. Proc Natl Acad Sci U S A 1998;95:2991–6.
52. Sakuma T, Pittet JF, Jayr C, Matthay MA. Alveolar liquid and protein clearance in the absence of blood flow or ventilation in sheep. J Appl Physiol 1993;74:176–85.
53. Jayr C, Matthay MA. Alveolar and lung liquid clearance in the absence of pulmonary blood flow in sheep. J Appl Physiol 1991;71:1679–87.
54. Matthay MA, Berthiaume Y, Jayr C, Hasting RH. Alveolar liquid and protein clearance: in vivo studies. In: Effros RM, Chang HK, editors. Fluid and solute transport in the airspaces of the lungs. New York: Marcel Dekker; 1994. p. 249–79.
55. Berthiaume Y, Folkesson HG, Matthay MA. Alveolar edema fluid clearance in the injured lung. J Appl Physiol 2002; 93:2207–13.
56. Modelska K, Matthay MA, McElroy MC, Pittet JF. Upregulation of alveolar liquid clearance after fluid resuscitation for hemorrhagic shock in rats. Am J Physiol 1997;273:L305–14.
57. Suzuki S, Zuege D, Berthiaume Y. Sodium-independent modulation of Na^+-K^+-ATPase activity by b-adrenergic agonist in alveolar type II cells. Am J Physiol 1995;268:L983–90.
58. Dagenais A, Denis C, Vives MF, et al. Modulation of alpha-ENaC and alpha(1)-Na(+)-K(+)-ATPase by cAMP and dexamethasone in alveolar epithelial cells. Am J Physiol Lung Cell Mol Physiol 2001;281:L217–30.
59. Folkesson HG, Nitenberg G, Oliver BL, et al. Upregulation of alveolar epithelial fluid transport after subacute lung injury in rats from bleomycin. Am J Physiol 1998;275:L478–90.
60. Berthiaume Y, Lesur O, Dagenais A. Treatment of adult respiratory distress syndrome: plea for rescue therapy of the alveolar epithelium. Thorax 1999;54:150–60.
61. Carter EP, Wangensteen OD, Dunitz J, Ingbar DH. Hyperoxic effects on alveolar sodium resorption and lung Na-K-ATPase. Am J Physiol 1997;273:L1191–202.
62. Frank J, Roux J, Kawakatsu H, et al. TGF-beta 1 decreases expression of the epithelial sodium channel alpha ENaC and alveolar epithelial vectorial sodium and fluid transport via an ERK 1/2-dependent mechanism. J Biol Chem 2003;278:43939–50.
63. Dagenais A, Frechette R, Yamagata Y, et al. Downregulation of ENaC activity and expression by TNFα in alveolar epithelial cells. Am J Physiol Lung Cell Mol Physiol 2003;286:L301–11.
64. Sugita M, Ferraro P, Dagenais A, et al. Alveolar liquid clearance and sodium channel expression are decreased in transplanted canine lungs. Am J Respir Crit Care Med 2003; 167:1440–50.
65. Campbell AR, Folkesson HG, Berthiaume Y, et al. Alveolar epithelial fluid clearance persists in the presence of moderate left atrial hypertension in sheep. J Appl Physiol 1999; 86:139–51.
66. Olivera W, Ridge K, Wood LD, Sznajder JI. ANF decreases active sodium transport and increases alveolar epithelial permeability in rats. J Appl Physiol 1993;75:1581–6.
67. Saldias FJ, Azzam ZS, Ridge KM, et al. Alveolar fluid reabsorption is impaired by increased left atrial pressures in rats. Am J Physiol Lung Cell Mol Physiol 2001;281:L591–7.
68. Fukuda N, Folkesson HG, Matthay MA. Relationship of interstitial fluid volume to alveolar fluid clearance in mice: ventilated vs. in situ studies. J Appl Physiol 2000;89:672–9.
69. Ware LB, Golden JA, Finkbeiner WE, Matthay MA. Alveolar epithelial fluid transport capacity in reperfusion lung injury after lung transplantation. Am J Respir Crit Care Med 1999; 159:980–8.
70. Verghese GM, Ware LB, Matthay BA, Matthay MA. Alveolar epithelial fluid transport and the resolution of clinically severe hydrostatic pulmonary edema. J Appl Physiol 1999; 87:1301–12.
71. Sartori C, Allemann Y, Duplain H, et al. Salmeterol for the prevention of high-altitude pulmonary edema. N Engl J Med 2002;346:1631–6.
72. Lamont RF. The pathophysiology of pulmonary oedema with the use of beta-agonists. BJOG 2000;107:439–44.
73. Hourdequin P, Bednarczyk L, Gabriel R, et al. Maternal complications from tocolytic treatment with beta-mimetics. Three cases of pulmonary edema. J Gynecol Obstet Biol Reprod (Paris) 1996;25:528–32.
74. Wang YB, Folkesson HG, Jayr C, et al. Alveolar epithelial fluid transport can be simultaneously upregulated by both KGF and beta-agonist therapy. J Appl Physiol 1999; 87:1852–60.
75. Factor P, Saldias F, Ridge K, et al. Augmentation of lung liquid clearance via adenovirus-mediated transfer of a Na,K-ATPase b_1 subunit gene. J Clin Invest 1998;102:1421–30.

76. Dumasius V, Sznajder JI, Azzam ZS, et al. b_2-Adrenergic receptor overexpression increases alveolar fluid clearance and responsiveness to endogenous catecholamines in rats. Circ Res 2001;89:907–14.
77. Factor P, Dumasius V, Saldias F, et al. Adenovirus-mediated transfer of an Na^+/K^+-ATPase beta1 subunit gene improves alveolar fluid clearance and survival in hyperoxic rats. Hum Gene Ther 2000;11:2231–42.
78. Stern M, Ulrich K, Robinson C, et al. Pretreatment with cationic lipid-mediated transfer of Na^+-K^+-ATPase pump in an animal model in vivo augments resolution of high dermeability pulmonary edema. Gene Ther 2000;7:960.
79. Adamson IY, Young L, Bowden DH. Relationship of alveolar epithelial injury and repair to the induction of pulmonary fibrosis. Am J Pathol 1988;130:377–83.
80. Panos RJ. Cytokines and alveolar type II cells. In: Kelley J, editor. Cytokines of the lung. 1st ed. New York: Marcel Dekker; 1993. p. 417–56.
81. Tanswell AK, Byrne PJ, Han RN, et al. Limited division of low-density adult rat type II pneumocytes in serum-free culture. Am J Physiol 1991;260:L395–402.
82. Adamson IY, Hedgecock C, Bowden DH. Epithelial cell-fibroblast interactions in lung injury and repair. Am J Pathol 1990;137:385–92.
83. Lesur O, Arsalane K, Lane D. Lung alveolar epithelial cell migration in vitro: modulators and regulation processes. Am J Physiol 1996;270:L311–9.
84. Kheradmand F, Folkesson HG, Shum L, et al. Transforming growth factor-a enhances alveolar epithelial cell repair in a new in vitro model. Am J Physiol 1994;267:L728–38.
85. Dunsmore SE, Rannels DE. Extracellular matrix biology in the lung. Am J Physiol 1996;270:L3–27.
86. Sheppard D. Epithelial integrins. Bioessays 1996;18:655–60.
87. Kim HJ, Henke CA, Savik SK, Ingbar DH. Integrin mediation of alveolar epithelial cell migration on fibronectin and type I collagen. Am J Physiol 1997;273:L134–41.
88. Stanley MW, Henry-Stanley MJ, Gajl-Peczalska KJ, Bitterman PB. Hyperplasia of type II pneumocytes in acute lung injury—cytologic findings of sequential bronchoalveolar lavage. Am J Clin Pathol 1992;97:669–77.
89. Katzenstein AA, Myers JL. Idiopathic pulmonary fibrosis—clinical relevance of pathologic classification. Am J Respir Crit Care Med 1998;157:1301–15.
90. Levkau B, Herren B, Koyama H, et al. Caspase-mediated cleavage of focal adhesion kinase $pp125^{FAK}$ and disassembly of focal adhesions in human endothelial cell apoptosis. J Exp Med 1998;187:579–86.
91. Guinee D Jr, Brambilla E, Fleming M, et al. The potential role of BAX and BCL-2 expression in diffuse alveolar damage. Am J Pathol 1997;151:999–1007.
92. Guinee D Jr, Fleming M, Hayashi T, et al. Association of p53 and WAF1 expression with apoptosis in diffuse alveolar damage. Am J Pathol 1996;149:531–8.
93. Fine A, Janssen-Heininger Y, Soultanakis RP, et al. Apoptosis in lung pathophysiology. Am J Physiol Lung Cell Mol Physiol 2000;279:L423–7.
94. Ware LB, Matthay MA. Keratinocyte and hepatocyte growth factors in the lung: roles in lung development, inflammation, and repair. Am J Physiol Lung Cell Mol Physiol 2002;282:L924–40.
95. Khalil N, O'Connor RN, Flanders KC, et al. Regulation of type II alveolar epithelial cell proliferation by TGF-b during bleomycin-induced lung injury in rats. Am J Physiol 1994;267:L498–507.
96. Buckley S, Bui KC, Hussain M, Warburton D. Dynamics of TGF-b3 peptide activity during rat alveolar epithelial cell proliferative recovery from acute hyperoxia. Am J Physiol 1996;271:L54–60.
97. Zhao Y, Gilmore BJ, Young SL. Expression of transforming growth factor-b receptors during hyperoxia-induced lung injury and repair. Am J Physiol 1997;273:L355–62.
98. Jakowlew SB, Mariano JM, You L, Mathias A. Differential regulation of protease and extracellular matrix protein expression by transforming growth factor-beta 1 in non-small cell lung cancer cells and normal human bronchial epithelial cells. Biochim Biophys Acta 1997;1353:157–70.
99. Zambruno G, Marchisio PC, Marconi A, et al. Transforming growth factor-b1 modulates b1 and b5 integrin receptors and induces the de novo expression of the avb6 heterodimer in normal human keratinocytes: implications for wound healing. J Cell Biol 1995;129:853–65.
100. Sheppard D, Cohen DS, Wang A, Busk M. Transforming growth factor b differentially regulates expression of integrin subunits in guinea pig airway epithelial cells. J Biol Chem 1992; 267:17409–14.
101. Lesur O, Arsalane K, Bérard J, et al. Functional IL-2 receptors are expressed by rat lung type II epithelial cells. Am J Physiol 1997;273:L495–503.
102. Ciacci C, Mahida YR, Dignass A, et al. Functional interleukin-2 receptors on intestinal epithelial cells. J Clin Invest 1993;92:527–32.
103. Korfhagen TR, Swantz RJ, Wert SE, et al. Respiratory epithelial cell expression of human transforming growth factor-a induces lung fibrosis in transgenic mice. J Clin Invest 1994;93:1691–9.
104. Berthiaume Y, Ware LB, Matthay MA. Treatment of acute pulmonary edema and the acute respiratory distress syndrome. In: Matthay MA, Ingbar DH, editors. Pulmonary edema. 1st ed. New York: Marcel Dekker; 1998. p. 575–631.

CHAPTER 39

CYTOKINES AND CHEMOKINES IN ASTHMA: AN OVERVIEW

Meri K Tulic, Pierre-Olivier Fiset, Zöe Müller,
Qutayba Hamid

Cytokines are a family of small glycosylated proteins involved in cell–cell signaling, cellular growth, differentiation, proliferation, chemotaxis, immunomodulation, immunoglobulin isotype switching, and apoptosis. The actions of cytokines are mediated through specific cytokine receptors on the surfaces of target cells. Although cytokines usually have effects on adjacent cells, they can act at a distance or have effects on the cell producing the cytokine itself. Many of these cytokines exhibit pleiotropy and have overlapping functions, making their individual roles in the pathogenesis of asthma and allergic disease difficult to unravel.

Until recently, T lymphocytes and eosinophils were considered to be the major sources of cytokines in allergic inflammation, but it is now recognized that cytokines are produced not only by other inflammatory cells but also by structural cells, including epithelial, endothelial and airway smooth muscle (ASM) cells, and fibroblasts (Figure 39-1). To date, more than 30 different cytokines have been described, and this list continues to grow (Table 39-1). Among these cytokines are T-cell–derived molecules that include so-called T-helper (Th)1 (interleukin-2 [IL-2], interferon-γ [IFN-γ], IL-12), Th2 (IL-4, IL-5, IL-9, IL-13, IL-17, IL-25), and Th3 or T regulatory cytokines [IL-10, transforming growth factor-β [TGF-β]), all of which are involved in the regulation of cell-mediated and humoral immunities. Although the distinction between Th1 and Th2 cells in humans is not as clear as in mice, there is overwhelming support in the literature for the notion that allergic inflammation is driven by an imbalance between Th1 and Th2 cytokines, favoring the Th2 arm of the immune response (see Figure 39-1). Other cytokines include proinflammatory cytokines (IL-1β, IL-6, IL-11, tumor necrosis factor-α [TNF-α], granulocyte–macrophage colony-stimulating factor [GM-CSF]) involved in innate host defense, antiinflammatory cytokines [IL-10, IFN-γ, IL-12, IL-18], growth factors platelet-derived growth factor [PDGF], TGF-β, fibroblast growth factor, epidermal growth factor), and chemotactic cytokines or chemokines (RANTES, monocyte chemoattractant protein-1 [MCP-1] to MCP-5, eotaxin, IL-8). For the purpose of this chapter, which is particularly focused on the role of cytokines and chemokines in asthma, cytokines and chemokines are broadly grouped on the basis of their functional activity and subdivided into (1) eosinophil-associated cytokines, (2) IgE-mediated cytokines, (3) remodeling-associated cytokines, and (4) immunomodulatory cytokines.

IgE-ASSOCIATED CYTOKINES

Asthma is clinically categorized into occupational, intrinsic, and atopic (allergic) forms; the vast majority of asthmatic patients have the atopic form. A central mediator in atopic asthma is IgE antibody, which is produced by sensitized allergen-specific B cells (Figure 39-2A). Allergens are antigens that elicit hypersensitivity or allergic reactions and that by themselves can increase IgE levels in the serum in susceptible subjects subsequent to stimulation. B cells, by presenting the allergen fragments in conjunction with the major histocompatibility complex (MHC), can activate specific Th2 helper cells to produce numerous cytokines, leading to further B-cell activation and antibody release. IgE antibodies bind to the high-affinity IgE receptor Fc epsilon receptor (FcεRI), present on mast cells and basophils, sensitizing these cells to antigen exposure (see Figure 39-2A). Subsequently, crosslinking of adjacent IgE–FcεRI complexes by allergens triggers the degranulation of cytoplasmic vesicles, containing histamine, and the de novo formation of eicosanoids and reactive oxygen species (Figure 39-2B). This results in smooth muscle contraction, mucous secretion, and vasodilatation, all of which are hallmarks of asthma. IgE-producing B cells play a critical role in allergic inflammation, and therefore factors responsible for their activation, namely IgE-associated cytokines such as IL-4, IL-9, and IL-13, are of considerable interest.

IL-4

IL-4 is vital for the regulation of growth, differentiation, activation, and function of B cells[1] (see Figure 39-1). IL-4 exerts its activities through a specific cell surface receptor

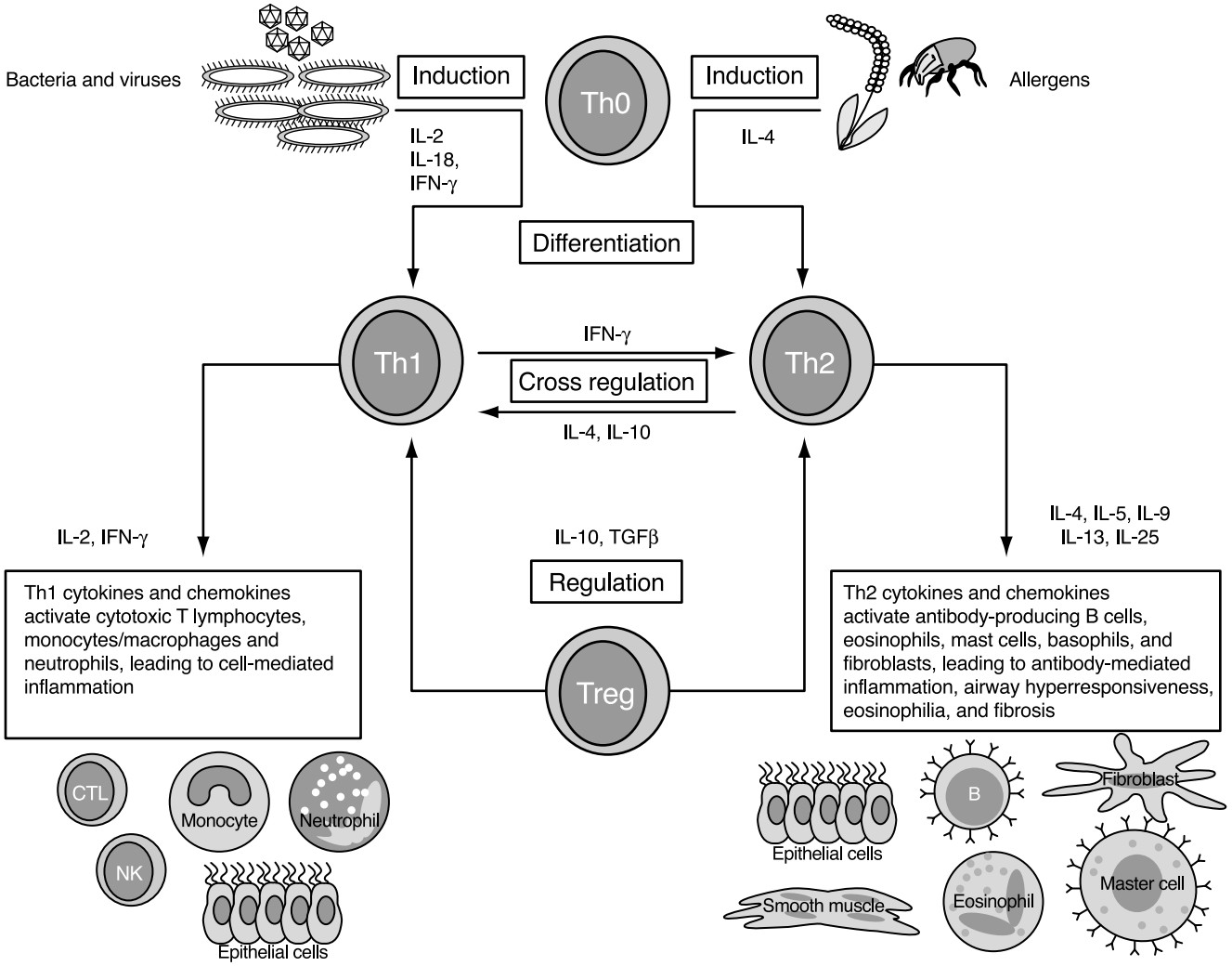

FIGURE 39-1 The Th1/Th2 paradigm. The two types of immune response are the cell-mediated immune response and the humoral or antibody-mediated immune response. Cytokines can be grouped on the basis of the types of T-helper (Th) cell that produce them and the types of immune response that they trigger. Th1 cells produce interleukin-2 (IL-2), interferon-γ (IFN-γ), and IL-12, which regulate cell-mediated inflammation, and Th2 cells produce IL-4, IL-5, IL-9, IL-13, IL-17, and IL-25, which regulate antibody-mediated inflammation. Bacteria and viruses can induce the innate immune system to produce cytokines that induce differentiation of Th0 cells to Th1; allergens induce Th2 cytokines, which promote Th0 cell differentiation to Th2. Th1 cytokines can crossregulate the production of Th2 cytokines and vice versa. T-regulatory cells (Treg) can regulate both arms of the immune system, through IL-10 and transforming growth factor-β (TGF-β). There is much evidence that allergic inflammation is driven by an imbalance between Th1 and Th2 cytokines, favoring the Th2 arm of the immune response.

composed of the IL-4Rα chain and the gamma common (γc) chain. IL-4 increases expression of the antigen-presenting proteins, MHC class II molecules, on B cells, resulting in increased capacity of allergen presentation to Th2 cells.[2] In the vasculature, IL-4 promotes expression of vascular cell adhesion molecule-1 (VCAM-1) on endothelium, thereby allowing for recruitment of eosinophils and other inflammatory cells, such as T cells, monocytes, and basophils, from the blood into sites of inflammation.[3] IL-4 also induces isotype switching, a process leading to the production of IgE by B cells, and after switching occurs, IL-4 potentiates IgE production. Furthermore, IL-4 enhances the IgE-mediated response by up-regulating IgE receptors on inflammatory cells within the airway.[4] Conversely, activation of IgE by IL-4 can be diminished by crossregulation from Th1 cytokines (see Figure 39-1). IFN-γ, a Th1 cytokine, can suppress isotype switch recombination to the IgE isotype in B cells activated by IL-4.[5] Additionally, IFN-γ inhibits IL-4–induced expression of the low-affinity IgE receptor.[6] IL-4Rα–deficient mice are more resistant to the development of features of asthma than are IL-4–deficient mice.[7] However, these mice still develop airway hyperresponsiveness (AHR), pointing to the existence of other cytokines sharing partial sequence homology with IL-4.

IL-13

IL-13 has 70% sequence homology with IL-4 and binds a heterodimer composed of the IL-4Rα chain and an IL-13Rα chain.[8] Like IL-4, IL-13 is produced by Th2 cells and is found in high concentrations within allergic tissues.[9,10] Because of the redundancy in IL-4Rα binding, both IL-4 and IL-13 exhibit some degree of functional overlap. As with

Table 39-1 Cytokines Involved in Asthma Pathogenesis

Cytokine	*Expression*	*Major actions*	*Cellular source*
IL-1β	Increased	Epithelial activation, mucin secretion, growth factor for Th2 cells	Macrophages, epithelium
IL-2	Increased	Proliferation of T cells	Th0 cells, eosinophils
IL-3	Increased	Hematopoietic growth factor for granulocytes and monocytes	Th1 and Th2 cells, mast cells
IL-4	Increased	IgE production, eosinophil recruitment, Th2 switching, AHR	Th0 and Th2 cells, mast cells, eosinophils
IL-5	Increased	Eosinophil priming, production, differentiation, activation, and survival, AHR	Eosinophils, Th2 cells, mast cells
IL-6	Increased	T- and B-cell growth factor, IgE production, ASM proliferation, fibrosis	Macrophages, T and B cells, eosinophils, epithelial cells, mast cells, and ASM cells
IL-7	Unknown	Lymphocyte proliferation, B-cell growth and differentiation	Thymus stromal cells
IL-8	Increased	Neutrophil chemoattractant, recruits primed eosinophils	Epithelial cells, eosinophils
IL-9	Increased	IgE and mucous production, airway hyperreactivity, primes mast cells, synergizes with IL-4 and IL-13	Th2 cells, eosinophils, neutrophils, mast cells
IL-10	Decreased	Inhibits Th1 cell differentiation, eosinophil survival, AHR	T cells, mast cells, macrophages
IL-11	Increased	Airway remodeling, activates fibroblasts, AHR	Eosinophils, epithelial cells, ASM cells, T cells, fibroblasts
IL-12	Decreased	Promotes Th1 and inhibits Th2 differentiation, inhibits IgE	Macrophages, T cells, B cells, dendritic cells
IL-13	Increased	IgE production, mucous secretion, eosinophilia, AHR, IFN-γ and IL-12 down-regulation	Epithelial cells, fibroblasts, eosinophils, ASM cells, T cells
IL-14	Unknown	B-cell growth factor	Endothelial cells
IL-15	Unknown	T-cell growth factor	NK cells, $CD34^+$ cells
IL-16	Increased	$CD4^+$ T-cell chemoattractant, eosinophil migration	Epithelial cells
IL-17	Increased	Macrophage activation, T-cell proliferation, neutrophilia	$CD4^+$ T cells
IL-18	Decreased	Induces IFN-γ production from Th1 cells, inhibition of IgE	Macrophages
IL-25	Unknown	IgE production, eosinophilia, enhances production of IL-4, IL-5, and IL-13	Th2 cells, mast cells
IFN-γ	Normal	Inhibits Th2 cell development and IgE, IL-4, and IL-13 production	Th1 cells, NK cells
GM-CSF	Increased	Eosinophil priming, survival, proliferation and differentiation, fibrosis	Epithelial cells, Th1 and Th2 cells
TGF-β	Increased	Fibroblast proliferation, collagen deposition	Fibroblasts, epithelial cells, eosinophils, ASM cells, macrophages
TNF-α	Increased	Granulocyte recruitment, primes inflammatory cells, fibroblast proliferation, AHR	Macrophages, epithelial cells
PDGF	Increased	Fibroblast, ASM cell, vascular smooth muscle cell and epithelial cell proliferation, collagen release	Eosinophils, platelets, fibroblasts, ASM cells, macrophages

AHR = airway hyperresponsiveness; ASM = airway smooth muscle; GM-CSF = granulocyte–macrophage colony-stimulating factor; IFN-γ = interferon-γ; IL = interleukin; NK = natural killer; PDGF = platelet-derived growth factor; TGF-β = transforming growth factor-β; TNF-α = tumor necrosis factor-α.

IL-4, overexpression of IL-13 within the lungs results in IgE production, inflammation, mucous hypersecretion, eosinophilia, and up-regulation of VCAM-1. However, the unique nature of IL-13 is seen in its effects on airway sensitivity to contractile agonists, whereby blocking IL-13 prevents AHR in mice following antigen challenge.[11] Accordingly, it is hypothesized that IL-13 is the primary factor involved in the expression and induction of allergen-induced AHR. Both IL-4 and IL-13 are critical in the induction and regulation of allergic asthma through their production of IgE. Interestingly, the effect of exogenous IL-13 is dependent on when it is given in relationship to allergen exposure as its administration after initial allergen sensitization in mice has no effect on serum IgE levels.[11] The emerging paradigm is that IL-13 induces features of the allergic response through its actions on epithelial and smooth muscle cells rather than through traditional effector pathways involving eosinophils and IgE-mediated events.[12]

IL-9

IL-9 also has actions relevant to IgE-dependent host responses. IL-9 is a Th2 cytokine, and its expression is regulated by a variety of mediators, in particular IL-2, which stimulates its production. Although IL-9 is produced by a variety of cell types, including mast cells, eosinophils, and neutrophils, the major source of this cytokine is the Th lymphocyte. Transgenic mice overexpressing IL-9 were found to have increased serum levels of all immunoglobulin isotypes, including IgE, and an associated accumulation of B cells in the lungs.[13,14] In vitro, IL-9 enhances IL-4–mediated IgE production by both human and murine B cells.[15] IL-9 also stimulates protease production by mast cells and induces their expression of FcεRI. This suggests that, in addition to potentiating IgE production, IL-9 primes mast cells to respond to allergen challenge through increased cell surface expression of FcεRI and the production of proinflammatory mediators. Other than its effects on IgE-mediated immunity, IL-9 is capable of coordinating a multitude of responses associated with asthma, through direct, indirect, and synergistic means. IL-9 has been identified as a T-cell growth factor, capable of stimulating the proliferation of activated T cells.[16–18] IL-9 transgenic mice demonstrate, in vivo, increased AHR, marked eosinophilia, mucous overproduction,[13,19] and increased expression of

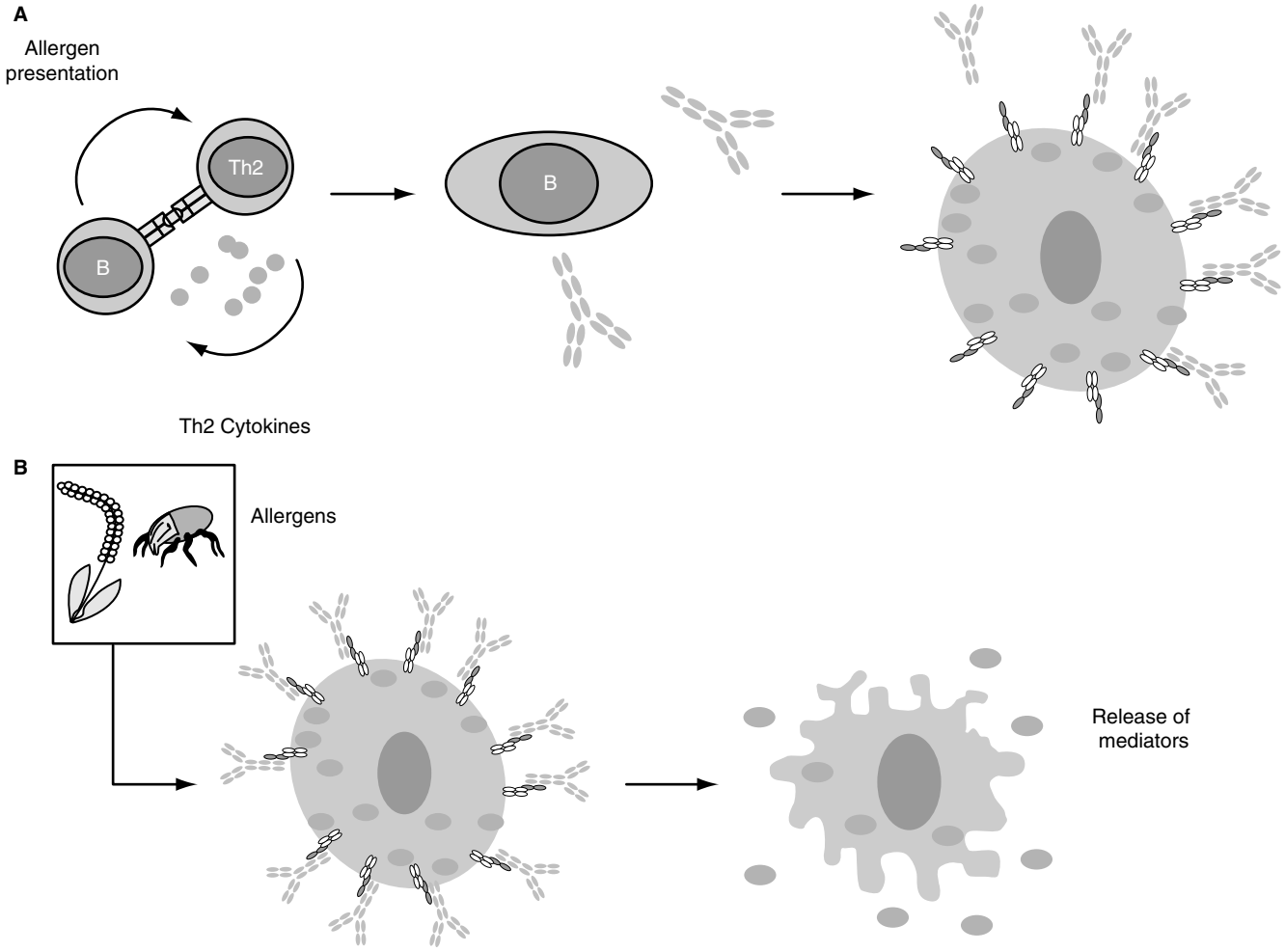

FIGURE 39-2 Mast cell sensitization: IgE and B cells. *A*, Allergen presentation by B cells can activate specific Th2 helper cells to produce cytokines, leading to B-cell activation and IgE release. IgE antibodies can bind to the high-affinity IgE receptor FcεRI on mast cells and basophils, sensitizing these cells to allergen exposure. *B*, Crosslinking of adjacent IgE–FcεRI receptor complexes by allergens triggers the production and release of many inflammatory mediators, such as histamine and leukotrienes.

eotaxin and MCP-1, MCP-3, and MCP-5 in airway epithelial cells.[20]

IL-25

The newly described cytokine IL-25 (IL-17E) also seems to have a role in the regulation of IgE-mediated responses. IL-25 stimulates IgE synthesis and eosinophilia in mouse models of allergic inflammation by stimulating the release of IL-4 and IL-5 cytokines.[21] As the roles of novel cytokines, such as IL-25, especially in the regulation of IgE-mediated inflammation, are clarified, it is evident that the cytokine network regulating inflammation is broad and complex. Nonetheless, insofar as these cytokines prove to be critical mediators of the inflammatory process, their stimulatory effects make them obvious targets in the treatment of allergic diseases.

EOSINOPHIL-ASSOCIATED CYTOKINES

Eosinophils are prominent in allergic airway disease, and the eosinophil is still considered by many to be the hallmark of asthma. Increased numbers of eosinophils in the bronchial mucosa, as well as the bronchoalveolar lavage (BAL) fluid and sputum, are consistent features of asthma, and BAL eosinophilia has even been linked to development of the late airway response (LAR) and asthma severity. Increased eosinophilia in asthmatic patients is observed not only in the large or central airways but also in the peripheral parts of the lungs.[22] Although terminal differentiation of eosinophils occurs within the bone marrow, recent evidence indicates that they can also differentiate locally at the site of inflammation and that the presence of eosinophils within allergic mucosal tissue is not solely due to infiltration of mature cells.[23]

Teleologically, eosinophils form part of the host defense against parasitic infestation. The biologic activity exerted by these cells is largely attributed to their release of prestored granular proteins, including eosinophil cationic protein, eosinophil peroxidase, and major basic protein (MBP). These potent cytotoxic proteins have been found in high concentrations in the sputum of asthmatic patients and are thought to play an important role in the epithelial damage seen in these patients. In addition to cytotoxic proteins, eosinophils can synthesize and release oxygen radicals, lipid mediators (leukotriene B_4, leukotriene C_4, platelet-activating factor), and numerous cytokines (IL-1, IL-2, IL-3, IL-4, IL-5, IL-6, IL-10, IL-12, IL-13, TNF-α, GM-CSF) and

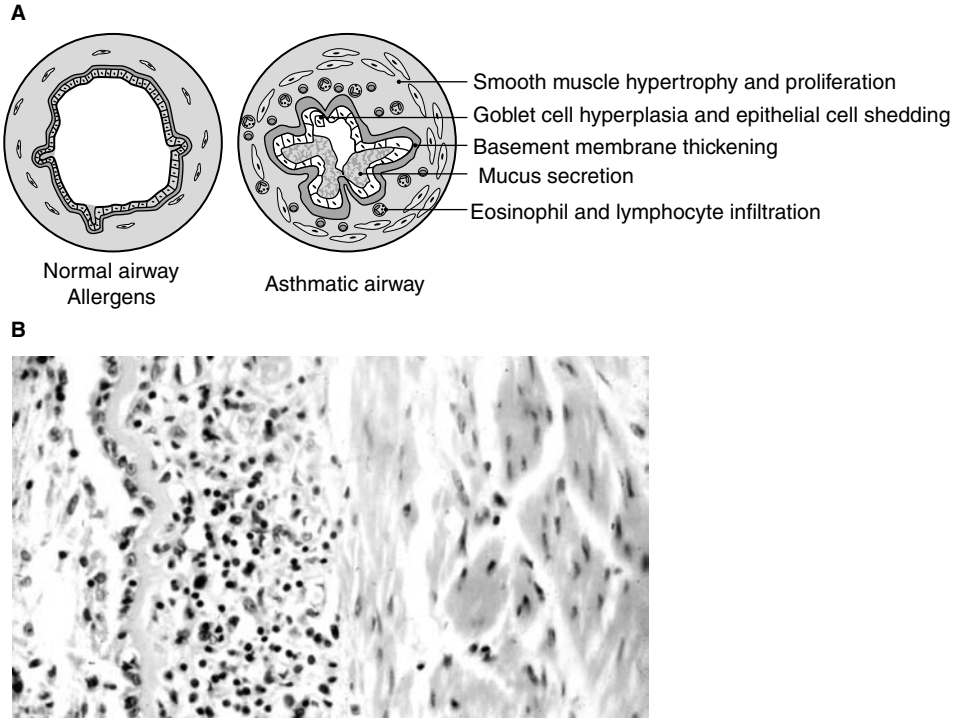

FIGURE 39-3 Airway remodeling. *A*, Remodeling causes many changes in the airways, including increased extracellular matrix deposition, thickening of the subepithelial basement membrane, goblet cell hyperplasia, increased smooth muscle mass and size, angiogenesis, and fibrosis. A consequence of this is increased mucous secretion and hyperresponsiveness. *B*, High levels of airway remodeling can be observed in postmortem airway sections from subjects with status asthmaticus, also known as fatal asthma.

chemokines (IL-8, RANTES and macrophage inflammatory protein-1α [MIP-1α]). Recently, it has been suggested that eosinophils may play a role in airway remodeling because they have the ability to synthesize and release fibrogenic cytokines, including TGF-β, IL-11, IL-17, and IL-25.[24] Together, these eosinophil-associated cytokines are responsible for the tissue-destroying potency of this proinflammatory cell.

IL-5

IL-5 is the most important Th2 cytokine associated with eosinophils, and it can regulate most aspects of eosinophil behavior, including eosinophil growth, maturation, differentiation, survival, and activation (see Figure 39-1). Although IL-5 is produced by T-helper cells, cytotoxic T lymphocytes, and mast cells, eosinophils are the predominant source of this cytokine. Human eosinophils express IL-5 mRNA and release IL-5 protein in vitro, and allergen challenge in the bronchial segments results in increased IL-5 mRNA expression in eosinophils in BAL fluid, with a 300-fold increase in IL-5 protein concentrations.[25] IL-5 plays a central role in accumulation and activation of eosinophils in the lungs, an effect readily seen in IL-5-overexpressing transgenic mice, which have lifelong eosinophilia.[26] Moreover, it is a potent eosinophil chemoattractant,[3] and it up-regulates integrin receptor expression on eosinophils, thereby promoting adherence of eosinophils to VCAM-expressing endothelial cells and eosinophil accumulation.

Studies with IL-5 monoclonal antibodies in animal models of allergic inflammation clearly support a role for IL-5 in allergic disease; however, similar studies in humans have proved disappointing. Although blocking IL-5 was effective in abolishing blood and sputum eosinophilia, it did not protect against the allergen-induced LAR or have any effect on baseline AHR in patients with mild asthma.[27] These latest results bring into question the role of eosinophils in airway responsiveness in humans and suggest that alternative mechanisms and/or factors are responsible for airway narrowing in asthmatic patients.

GM-CSF

Although secondary in importance to IL-5, IL-3 and GM-CSF are also typically viewed as eosinophil-associated cytokines. IL-3 and GM-CSF are pluripotent hematopoietic growth factors that stimulate the formation of not only eosinophil lineages but also neutrophil, erythroid, and monocytic lineages. Increased expression of GM-CSF has been documented in the bronchial epithelium and in the eosinophils of asthmatic patients following endobronchial allergen challenge. GM-CSF is involved in the priming of eosinophils and accounts for increased eosinophil survival in the BAL fluid of asthmatic patients. In addition, GM-CSF may be involved in development of chronic eosinophilia and airway remodeling of asthma (see below) as insertion of the GM-CSF gene into the epithelium of rats caused eosinophil accumulation in their lungs and irreversible fibrosis.[28,29]

REMODELING-ASSOCIATED CYTOKINES

It has been known for a long time that architectural and structural changes occur in the airways of asthmatic patients. These changes, which include collagen (types III and IV) and fibronectin deposition, increased thickness of subepithelial basement membrane, goblet cell hyperplasia, increased ASM mass and size, angiogenesis, and fibrosis,

collectively contribute to the phenomenon termed airway remodeling (Figure 39-3). Some of these changes were first described in postmortem airway sections from status asthmaticus victims in the 1960s, and, more recently, airway remodeling has been reported even in patients with mild asthma and in children with difficult asthma.[30] The functional consequences of airway remodeling include persistent AHR and mucous hypersecretion, contributing to increased susceptibility to asthma exacerbations. The mechanisms involved in airway remodeling are poorly understood, but research done in the last 3 to 5 years suggests that the balance between matrix metalloproteinases and tissue inhibitors of metalloproteinases (TIMPs) may play a role in this process. Moreover, the increase in ASM content, along with a change in the phenotype of fibroblasts to contractile myofibroblasts, may explain the permanent reduction in airway caliber, which is steroid insensitive and typical in patients with severe forms of the disease. The predominant remodeling-associated cytokines include TGF-β, PDGF, IL-6, IL-11, IL-13, IL-17, and IL-25 (IL-17E).

TGF-β

TGF-β is a potent profibrotic cytokine. The major sources of TGF-β include fibroblasts, eosinophils, and epithelial cells. However, macrophages, monocytes, neutrophils, ASM cells, and lymphocytes are also known to produce this cytokine. TGF-β is detected in increased concentrations in baseline BAL fluid from asthmatic patients before allergen challenge, and the concentration increases even more after allergen challenge. Furthermore, TGF-β exerts an important influence on the turnover of extracellular matrix proteins. In tissue culture systems, TGF-β exhibits a pleiotropic nature, depending on the cell type, culture conditions, and presence of other cytokines. TGF-β induces proliferation and release of profibrotic and proinflammatory cytokines in fibroblasts and ASM cells, whereas in monocytes, lymphocytes, and epithelial cells, TGF-β inhibits cytokine proliferation and release.[31,32] TGF-β is also a potent chemoattractant for many cell types, including monocytes, fibroblasts, and mast cells.

Recently, eosinophils have been recognized as one of the most abundant sources of TGF-β, not only in asthmatic airways but also in the nasal tissues of patients with nasal polyposis and in hypereosinophilic patients. In our laboratory, by use of in situ hybridization and immunocytochemistry, we have demonstrated TGF-β to be significantly elevated in both mildly and severely asthmatic patients in comparison with normal subjects and have shown levels of TGF-β expression to correlate with basement membrane thickness and disease severity in these patients.[33] Approximately 65% of all TGF-β-positive cells were activated eosinophils, which were localized within the reticular lamina. The local production of TGF-β by eosinophils may be responsible for the subepithelial fibrosis observed in asthmatic patients. However, TGF-β can also inhibit eosinophil survival and function and may be involved in the repair process of airway epithelial cells. Such effects of TGF-β illustrate the complex actions of this cytokine in asthma.

PDGF

PDGF is not only a major mitogen but also a remodeling-associated cytokine. The ability of PDGF to stimulate proliferation of tissue structural cells, including fibroblasts, epithelial cells, and vascular smooth muscle cells, is well accepted, and this cytokine has been implicated in the alterations of lung function in several chronic lung diseases. Fibroblasts from asthmatic patients show enhanced responsiveness to PDGF, and it is known to activate fibroblasts to proliferate, secrete collagen, and contract collagen lattices.[34] Eosinophils, once again, are the predominant cellular sources of this cytokine; however, platelets, macrophages, airway epithelial and endothelial cells, vascular smooth muscle cells, and fibroblasts themselves are known to secrete PDGF. PDGF can be induced by both mechanical and oxidative stress, as well as by exposure of cells to various cytokines, including IFN-γ, TNF-α, IL-1, and TGF-β. Although PDGF plays an important role in airway remodeling, it is thought that this growth factor is likely to be acting in concert with other remodeling cytokines, in particular TGF-β, to alter the structural makeup of the airway wall in asthmatic airways.

IL-6

IL-6 is another remodeling-associated cytokine. Originally, IL-6 was known for its antiviral activity and its growth-promoting effects on B cells. IL-6 is produced by macrophages, monocytes, T and B cells, fibroblasts, epithelial and endothelial cells, ASM cells, and eosinophils. This cytokine is consistently found in high concentrations in biologic fluids and tissues from both animal models of allergic disease and asthmatic patients, but its exact role in asthma remains unclear. IL-6 has the ability to stimulate T- and B-cell production of Th2 cytokines,[35] thereby contributing to the generation and/or the perpetuation of Th2-driven inflammation. In addition, IL-6 is a potent stimulant of the acute-phase allergic response and has recently been shown to be a potent smooth muscle mitogen. Mice overexpressing IL-6 in their airways have subepithelial fibrosis, collagen deposition, and increased accumulation of α-actin–containing smooth muscle cells, without eosinophilia, mucous cell metaplasia, or AHR.[36]

IL-11 and IL-13

IL-11 and IL-13 have recently received much attention as key remodeling-associated cytokines. The reason for this is that they are thought to not only cause fibrosis and collagen deposition but also induce myofibroblast hyperplasia, airway obstruction, and AHR. Much of what is known about the role of these cytokines in airway remodeling comes from studies using transgenic mice. Histologic analysis of mice in which IL-11 or IL-13 was constitutively overexpressed in the lungs showed airway wall thickening, enlarged alveoli, subepithelial and adventitial tissue fibrosis, collagen I and III deposition, and increased numbers of contractile and proinflammatory cells in comparison with littermate controls.[37–39] In addition, IL-11 and IL-13 transgenic mice had baseline airway obstruction and were more responsive to methacholine challenge.[40]

Sources of IL-11 and IL-13 include epithelial cells, fibroblasts, eosinophils, and smooth muscle cells. Recent evidence suggests that one mechanism by which IL-13 induces tissue fibrosis is by selectively stimulating and activating TGF-β production.[37]

We have recently found the results obtained in IL-11 transgenic mice to hold true for human asthma. Using immunocytochemistry and in situ hybridization, we have demonstrated increased expression of IL-11 mRNA and protein in the epithelial and subepithelial layers of the airway wall in patients with severe asthma but not in those with mild asthma or in healthy control subjects.[41] Furthermore, IL-11 expression was inversely correlated with forced expiratory volume in 1 second (FEV_1) in patients with severe asthma, and the IL-11 mRNA-positive cells were localized to epithelial cells and MBP-positive eosinophils.[42] One proposed mechanism by which IL-11 can induce these structural changes in the airways may be promotion of the synthesis of TIMP-1, the levels of which have been shown to be elevated in sputum and biopsy samples from asthmatic patients and to correlate with asthmatic airway obstruction.[43] Although these studies clearly support a role for IL-11 in airway remodeling, other studies suggest that IL-11 levels may, in fact, be increased as a result of normal airway repair. IL-11 transgenic mice exhibited selective inhibition of antigen-induced airway and parenchymal eosinophilia, Th2 inflammation, Th2 cytokine production, and VCAM-1 gene expression.[39] These conflicting data point to the dual nature of IL-11, which acts as both a cytokine that promotes healing and a cytokine capable of inducing local tissue fibrosis.

IL-17 Family

The newly emerging remodeling-associated cytokines recently described in the literature include IL-17 and IL-17E (IL-25). These are potent proinflammatory cytokines. IL-17, or IL-17A, is produced exclusively by activated Th lymphocytes, whereas Th2 cells and mast cells secrete IL-25. Expression of IL-17 is markedly increased in asthmatic subjects.[44] In mice, systemic overexpression of IL-17 induces neutrophilia via direct in vivo stimulation of IL-6 and IL-8, whereas overexpression of IL-25 results in increased Th2 cytokine gene expression (in particular, IL-4, IL-5, IL-10, and IL-13), increased mucous production, elevated serum levels of IgE and IgG_1, and tissue eosinophilia.[24] These pathologic changes can be observed in several tissues and are not restricted to the lungs.

IMMUNOMODULATORY CYTOKINES

It is now generally accepted that adult atopic disease is characterized by expression of T-cell immunity to common airborne environmental allergens that is polarized toward the Th2 cytokine profile; Th1-skewed immunity is observed among nonatopic subjects. As a result, attempts to shift the balance from Th2 to Th1 immunomodulatory cytokines, such as IL-10, IL-12, and IFN-γ, may be important in the treatment of allergic inflammation.

IL-10 Family

IL-10 is largely known as an inhibitory cytokine; however, it can have either immunosuppressive or immunostimulatory effects. IL-10 was originally identified as a product of murine Th2 cells, but in humans IL-10 is produced by Th0, Th1 and Th2 cells and also by activated monocytes, mast cells and macrophages.[21] In normal lungs, alveolar macrophages are the major source of IL-10, but its expression is significantly reduced in asthmatic individuals.[45,46] The effects of IL-10 are as follows: (1) it is capable of curtailing the effects of proinflammatory cytokines (TNF-α, IL-1β, IL-6, IL-8, MIP-1α) released during an allergic reaction; (2) it is able to inhibit eosinophil survival and migration by preventing the release of chemoattractants such as RANTES and IL-8 from human ASM cells[46]; (3) it inhibits allergen-induced eosinophilia in sensitized mice and dampens their late-phase response to allergen challenge[47]; (4) it down-regulates the IL-4–induced isotype switching of activated B cells,[3] thus preventing IgE synthesis; (5) it may inhibit Th2-driven inflammation, but it is also known to inhibit the differentiation of Th1 cells, thereby preventing the release of IFN-γ and IL-2; (6) it has the ability to interfere with monocyte and macrophage function as it can inhibit MHC class II expression on the surfaces of antigen-presenting cells (APCs)[3] and prevent superoxide and nitric oxide (NO) release from inflammatory cells.[48]

Included in the IL-10 family of cytokines are IL-19, IL-20, IL-22, and IL-24. Like IL-10, they are considered to be antiinflammatory cytokines, and are produced by a variety of cell types, including monocytes, keratinocytes, mast cells, and lymphocytes. However, unlike IL-10, these cytokines are unable to inhibit the effects of proinflammatory mediators involved in the allergic response. IL-19, IL-20, and IL-24 have not been extensively studied; however, studies on IL-22 have shown this cytokine to be involved in the induction of IgE-independent acute-phase response signals.[49]

IFN-γ

IFN-γ is the most important cytokine in cell-mediated immunity, controlling the balance of Th1/Th2 development (see Figure 39-1). IFN-γ is produced by Th1 cells and has an inhibitory effect on Th2 cells. IFN-γ inhibits allergic responses by preventing isotype switching of IgE and IgE production in B cells.[50] The main sources of IFN-γ are the Th cells. However, it can also be produced by cytotoxic T cells and natural killer (NK) cells. In addition to its potent inhibitory effect on Th2 cells, IFN-γ stimulates de novo expression of MHC class II molecules on epithelial and endothelial cells and up-regulates their expression on macrophages–monocytes and dendritic cells. Importantly, IFN-γ stimulates monocytes, NK cells, and neutrophils to increase their cytokine production, phagocytosis, adherence, respiratory burst, and NO production, thereby promoting cell-mediated cytotoxic responses at the site of inflammation.[3]

In sensitized and allergen-challenged mice, nebulized IFN-γ prevents allergen-induced increases in Th2 cytokine production, AHR, and lung eosinophilia.[51] This has been proposed to occur via up-regulation of IL-10. In the BAL fluid of asthmatic patients, there is reduced T-cell production of IFN-γ, and this correlates closely with disease

severity.[52] Clinical trials with IFN-γ in humans have proved disappointing as no significant improvement in lung function was observed in steroid-dependent asthmatic patients, despite reduced number of eosinophils in their blood.[53]

IL-12

IL-12 is produced by APCs, including B cells, monocytes, macrophages, Langerhans cells, and dendritic cells, as well as neutrophils and mast cells. IL-12 promotes T-cell differentiation toward a Th1-mediated response by stimulating NK and T cells to produce IFN-γ while suppressing the expansion and differentiation of IL-4–secreting Th2 cells.[54] The biologically active form of IL-12 is a heterodimer consisting of a p40 subunit and a p35 subunit, expressed by different genes. The effects of IL-12 have been extensively studied in small animal models of allergic inflammation, which have consistently demonstrated this cytokine to be involved in reduction of allergen-specific IgE production and abolition of AHR and airway eosinophilia.[55,56] However, this effect of IL-12 is critically dependent on the timing of its administration. The most effective protection against allergen-induced inflammation is seen when IL-12 is administered early during the active sensitization process and can act in synergy with IL-18.[57] IL-18, otherwise known as IFN-γ–inducing factor, is a potent inducer of IFN-γ production by T cells, NK cells, and B cells.[58] In asthmatic patients, IL-12 level is significantly reduced in peripheral blood and in airway biopsy specimens in comparison with healthy controls. IL-12 mRNA levels have been shown to be increased in biopsy specimens from asthmatic patients following treatment with corticosteroids,[9] and although the administration of IL-12 has failed to show any effects on AHR or the LAR in patients with mild asthma, IL-12 was effective in suppressing blood and sputum eosinophilia in these patients.[59]

CHEMOKINES

Chemokines are small cytokines (8 to 10 kDa) that are primarily involved in attracting and regulating leukocyte trafficking into the tissues, in a process called chemotaxis, by binding specifically seven membrane-spanning G protein–coupled receptors (Figure 39-4). To date, more than 40 chemokines have been described, and they are classified into four subclasses according to their structure: CXC, CC, C, and CX3C. The two main groups are CXC (α-chemokines) and CC (β-chemokines). CXC chemokines include IL-8 and IFN-induced protein-10 (IP-10), which

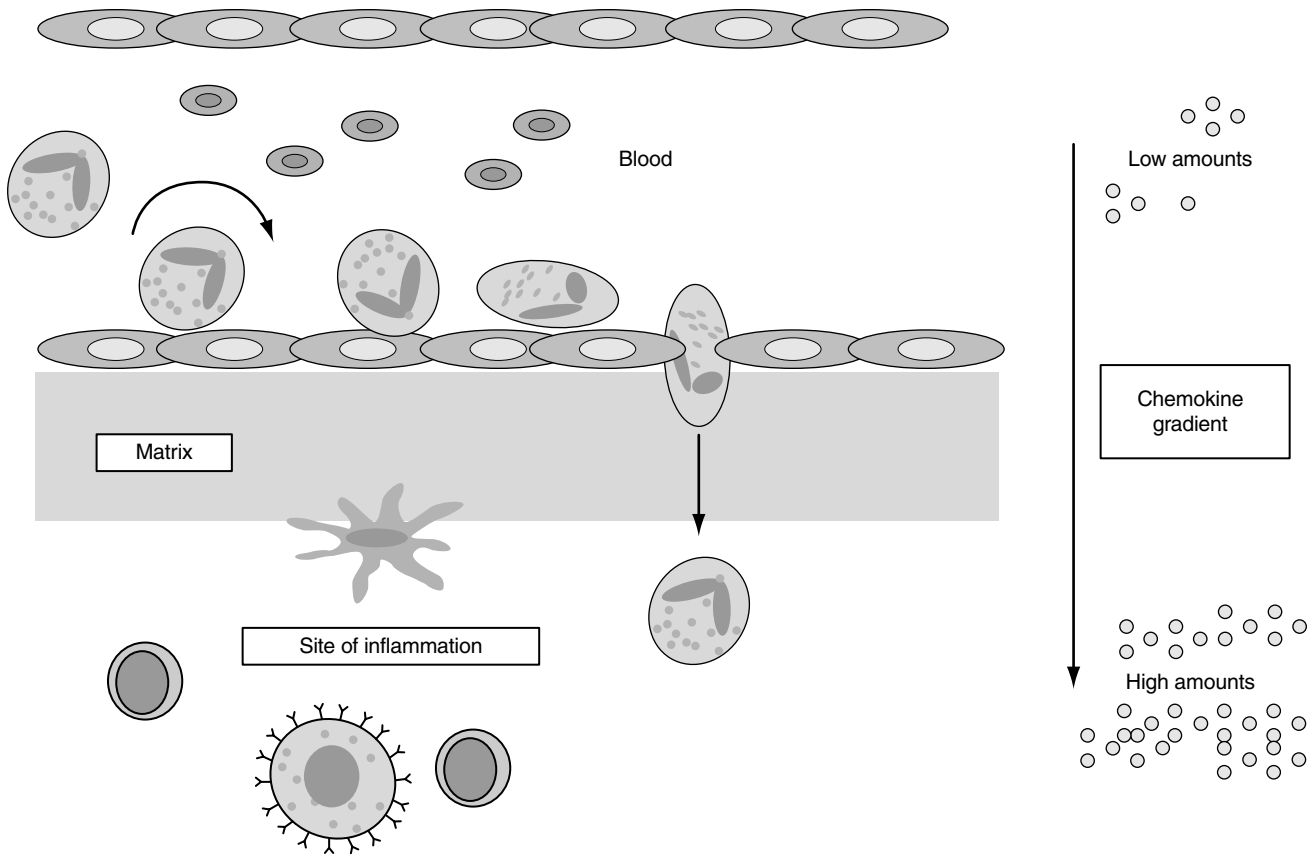

FIGURE 39-4 Chemokines and chemotaxis. Cytokines and chemokines regulate the entry of inflammatory cells into sites of inflammation by increasing the expression of adhesion proteins on endothelial cells and on the inflammatory cell. This causes the rolling of the inflammatory cell on the vasculature, followed by firm adhesion and transmigration between the endothelial cells and through the matrix to the site of inflammation, following a chemokine gradient.

Table 39-2 Chemokines Involved in Asthma Pathogenesis

Chemokine	*Expression*	*Major actions*	*Cellular source*
Eotaxin	Increased	Eosinophil chemoattractant	Epithelial cells, T cells, macrophages, eosinophils, endothelial cells
RANTES	Increased	Lymphocyte and eosinophil chemoattractant	Epithelial cells, T cells, ASM cells
MCP-1	Increased	Monocyte chemoattractant, promotes Th2 response	Macrophage, monocytes, epithelial cells, eosinophils
MCP-2	Unknown	Monocyte and eosinophil chemoattractant, promotes Th2 response	Fibroblasts
MCP-3	Increased	Eosinophil chemottractant, promotes Th2 response	T lymphocytes, eosinophils
MCP-4	Increased	Eosinophil, monocyte, lymphocyte, and basophil chemoattractant, promotes Th2 response	Epithelium, macrophages, eosinophils, T cells
MIP-1α	Increased	Eosinophil and basophil chemoattractant, stimulates IFN-γ production by Th1 cells	T cells, epithelial cells, eosinophils
MIP-1β	Unknown	Stimulates IFN-γ production by Th1 cells	Monocytes, T cells, eosinophils
IL-8	Increased	Neutrophil chemoattractant, recruits primed eosinophils	Macrophages, eosinophils, epithelial cells, T cells, neutrophils, and fibroblasts
IP-10	Increased	Neutrophil chemoattractant	T cells, epithelial cells

ASM = airway smooth muscle; IFN-γ = interferon-γ; IL = interleukin; IP-10 = IFN-induced protein-10; MCP = monocyte chemoattractant protein; MIP = macrophage inflammatory protein.

primarily target neutrophils, whereas eotaxin, RANTES, MCP-1 to MCP-4, MIP-1α, and MIP-1β are typical CC chemokines, targeting monocytes, T cells, and eosinophils (Table 39-2). For this reason, CC chemokines are thought to have the greatest relevance in the pathogenesis of asthma. Increased levels of chemokines in comparison with control subjects have been measured in both BAL fluid and biopsy samples from asthmatic patients.[21]

Eotaxin and RANTES

Eotaxin and RANTES, acting in synergy with IL-5, are the most important eosinophil chemoattractants in allergic inflammation. These chemokines are produced by the majority of inflammatory cells, and more recently their expression has been described in ASM cells and fibroblasts. Unlike RANTES, which binds many CC chemokine receptors (CCRs), including CCR1, CCR3, and CCR5, eotaxin binds specifically to CCR3, which is highly expressed on eosinophils and has selective chemoattractant activity for eosinophils.[60] In addition, eotaxin induces α_4- and β_1-integrin expression on eosinophils, allowing for firm adhesion of eosinophils to the endothelium and transmigration into the site of inflammation (see Figure 39-4). More importantly, eotaxin and RANTES are produced at high concentrations in the lungs of asthmatic patients.

MCPs and MIPs

MCP and MIP are monocyte–macrophage chemoattractants and activating factors. To date, four MCPs (MCP-1 to MCP-4) and two MIPs (MIP-1α and MIP-1β) have been described. Increased levels of MCP-1 and MCP-3 have been detected in BAL fluid of asthmatic patients,[61] and increased expression of MCP-4 has been reported in the sputum,[62] BAL fluid,[61,63] bronchial mucosa,[61] and small airways[64] of asthmatic patients, as well as in the nose of patients with allergic rhinitis.[65] MCP-1 binds CCR2, MCP-2 binds CCR3, MCP-3 binds CCR1 and CCR3, and MCP-4 binds CCR2, CCR3, and CCR5. MCP-1 immunoreactivity has been demonstrated in human eosinophils, whereas MCP-2, MCP-3, and, in particular, MCP-4 are also thought to be potent eosinophil chemoattractants.[63] Furthermore, MCP-4 attracts not only eosinophils and monocytes but also lymphocytes and basophils. MIP-1α binds CCR1 and CCR5, whereas MIP-1β binds CCR5 exclusively.

Although the primary role of chemokines is chemotaxis, they have a variety of other functions. These include direct effects on T-cell differentiation. MIP-1α, MIP-1β, and RANTES can promote the development of IFN-γ–producing Th1 cells by stimulating IL-12 production by APCs. In contrast, MCP-1, MCP-2, MCP-3, and MCP-4 can increase T-cell production of IL-4 and decrease APC production of IL-12, resulting in a Th2 phenotype.

CYTOKINE AND CHEMOKINE RECEPTORS

Cytokines function by binding to specific cytokine receptors, which may be either membrane bound or in soluble form. Cytokine receptors are grouped according to the degree of common structural homology of their extracellular regions. They include the immunoglobulin superfamily (IL-1R, IL-6R, and PDGFR), the cytokine receptor superfamily (IL-2R, IL-3R, IL-4R, IL-5R, IL-12R, and GM-CSFR), and the IFN receptor superfamily (IFN-γR and IL-10R) (Table 39-3). Some of the subunits of these receptors may be shared by more than one cytokine receptor, resulting in the formation of heterodimeric structures. Such examples include IL-3R, IL-5R, and GM-CSFR, which share the common GM-CSF receptor β-chain, and IL-2R, IL-4R, and IL-13R, which share the IL-2 receptor γ-chain. Receptors for IL-1, IL-2, IL-4, IL-5, IL-6, IL-10, and GM-CSF have all been reported to show increased expression in asthma (see Table 39-3).

Some cytokine receptors exist also in a soluble form in the serum, and these are produced by alternative mRNA splicing, leading to proteins that lack the region of the receptor required for membrane anchoring. The soluble cytokine receptor interacts with its target cytokine, reducing the effective levels of cytokine available for target cells. In

Table 39-3 Cytokine and Chemokine Receptors in Asthma Pathogenesis

Receptor	*Form*	*Expression*	*Cellular source*
IL-1R	Soluble	Increased	Most inflammatory and structural cells
IL-2R	MB	Increased	$CD4^+$ T cells
IL-3R	MB	Increased	Endothelial cells
IL-4R	Soluble and MB	Increased	Epithelium, T and B cells
IL-5R	Soluble and MB	Increased	Eosinophils
IL-6R	Soluble	Increased	Macrophages, T and B cells, epithelial cells
IL-10R	MB	Decreased	Lymphoid and myeloid cells, NK cells
IL-12R	MB	Decreased	T cells and NK cells
IL-13R	Soluble and MB	Decreased	Unknown
IFN-γR	MB	Decreased	T and B cells, macrophages, dendritic cells
GM-CSFR	MB	Increased	Macrophages, eosinophils, fibroblasts
PDGFR	MB	Increased	Fibroblasts and ASM cells
TNF-αR	Soluble and MB	Increased	Macrophages, T cells, epithelial cells, mast cells
CCR3	MB	Increased	Eosinophils, basophils, Th2 cells, mast cells
CCR4	MB	Increased	Th2 cells, eosinophils, mast cells, monocytes
CCR8	MB	Increased	Eosinophils, Th2 cells, and mast cells

ASM = airway smooth muscle; CCR = chemokine receptor; GM-CSF = granulocyte–macrophage colony-stimulating factor; IFN-γ = interferon-γ; IL = interleukin; MB = membrane-bound; NK = natural killer; PDGF = platelet-derived growth factor; TNF-α = tumor necrosis factor-α.

murine experimental models of asthma, soluble IL-4R, which binds and sequesters free IL-4, reduces allergen-induced IgE production, AHR, and eosinophil accumulation.[66] We have previously demonstrated that in patients with atopic and intrinsic asthma, there are not only increased levels of membrane-bound IL-5R mRNA but also increased soluble IL-5R mRNA levels in bronchial biopsy specimens and that this expression is directly correlated with FEV_1.[67] These results suggest that the soluble form of IL-5R may play an important role in the development of airflow obstruction. Studies such as these prompt interest in the potential use of receptors as therapeutic targets.

The chemokine receptors are a large family of G protein–coupled receptors. These have generated considerable interest because of the possibility of using receptor antagonists to block eosinophil trafficking and degranulation in asthma. CCR3, CCR4, and CCR8 are preferentially expressed by Th2 cells, mast cells, and eosinophils and therefore represent therapeutic targets for allergy and asthma. Of these, CCR3 has received the most attention. CCR3 not only binds eotaxin, RANTES, MCP-3, and MCP-4, but it is also considered to be the major CC chemokine receptor on eosinophils and basophils. Increased CCR3 expression has been found in bronchial biopsy specimens of asthmatic patients,[68] and monoclonal antibody selective for CCR3 inhibits eosinophilia.[69] CCR3 receptor is involved in eosinophil differentiation and is up-regulated by Th2 cytokines in $CD34^+$ progenitor cells.[68] For these reasons, the most recent research has been focused on identifying CCR3 antagonists that are capable of preventing allergic inflammation.[70,71]

CYTOKINES, ASTHMA, AND INFECTION

The reasons for the increased prevalence of allergic respiratory diseases in developed countries remain unclear. For many years, lower respiratory tract infections in early life have been recognized as primary triggers of asthma exacerbations in young children. Using both epidemiologic and virology data, prospective studies have convincingly shown that viral, not bacterial, respiratory infections precipitate reactive airway symptoms.[72] It is now believed that the development of bacteria-induced, nonwheezing lower respiratory tract infection in childhood may protect against the development of atopy and asthma in later life. This line of thought comes from experimental evidence suggesting that the principal trigger for normal postnatal maturation of the immune system is the commensal microbial flora, particularly that of the gastrointestinal tract. Microbial exposure helps skew the immune response away from the allergic phenotype and toward the normal adult nonatopic immune response,[73] and the longer the immune system takes to adapt postnatally to its functionally mature state, the greater the risk of allergic sensitization.[74]

Hygiene Hypothesis

The hygiene hypothesis suggests that decreasing levels of exposure to infections and/or commensal microbial stimuli in developed countries, particularly during the induction of primary Th1/Th2 responses to allergens in early life, may be responsible for the increased prevalence of asthma (Figure 39-5). There is ample epidemiologic evidence to support this hypothesis.[75] The reported increase in atopy inversely correlates with a steady decline in the extent to which Western society is exposed to infectious diseases such as whooping cough, measles, tuberculosis, and influenza.[76] The incidence of allergic diseases appears to increase with advancing socioeconomic development, they occur more frequently in industrialized countries than in developing areas,[77] and the farming environment is thought to be protective against the development of allergies.[78,79]

Bacterial lipopolysaccharide (LPS), or endotoxin, has been suggested as a potential mediator of these effects. LPS is a major component of the outer membrane of ubiquitous gram-negative bacteria. It has been reported that LPS makes up a significant proportion of the weight of common house dust, and a significant correlation has been reported

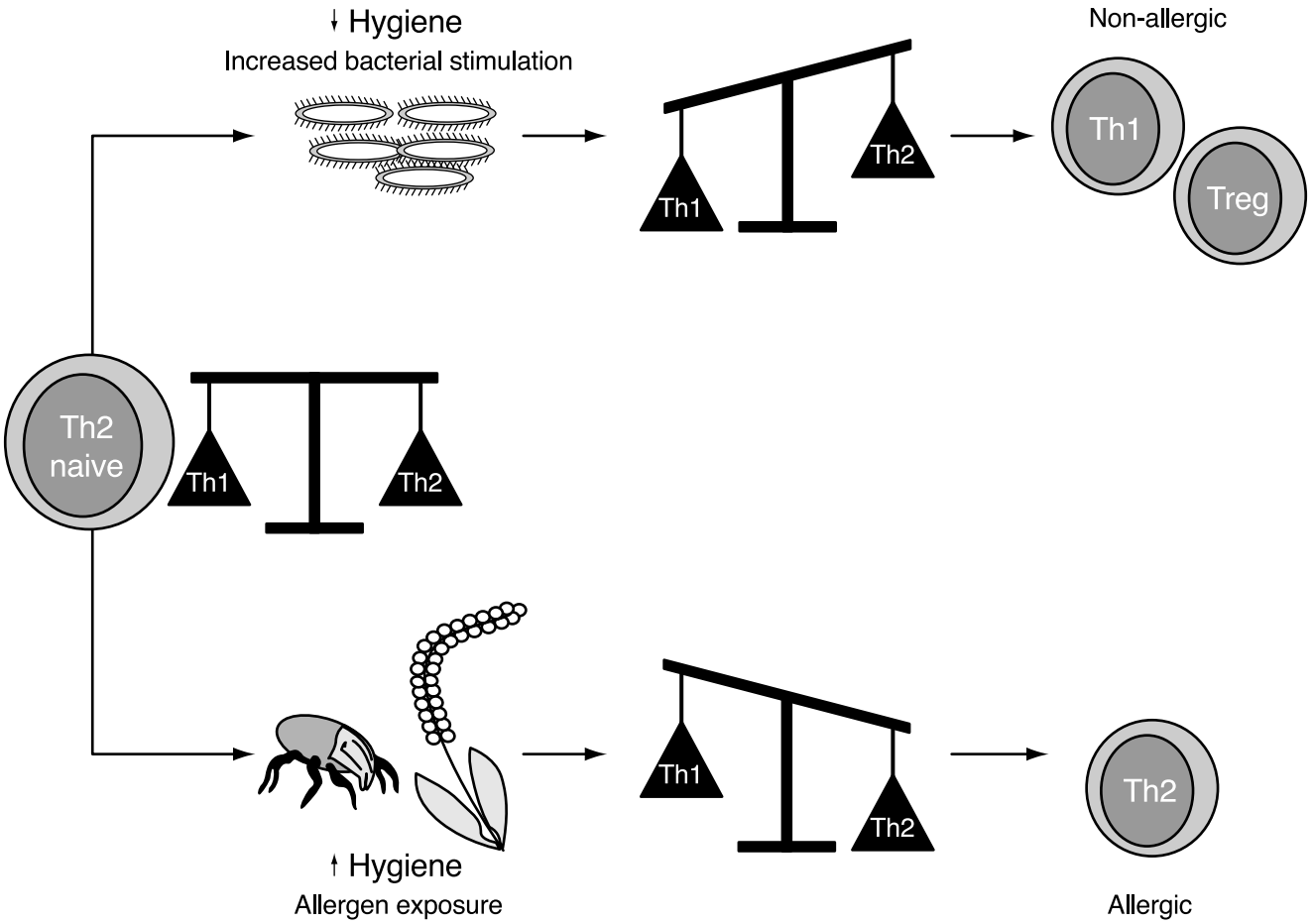

FIGURE 39-5 Hygiene hypothesis. The hygiene hypothesis suggests that infections and/or commensal microbial stimuli are important during the maturation of the immune system. Lack of exposure may lead to an unbalanced Th2 response to allergens, causing allergic disease. Treg = T-regulatory cells.

between domestic LPS exposure and clinical severity of asthma in adults.[80] The first direct in vivo evidence that environmental exposure to LPS early in life (before polarized Th cell responses are established) protected against allergen sensitization was reported by Gereda and colleagues, who demonstrated that the homes of allergen-sensitive infants (9 to 24 months of age) contained lower concentrations of LPS in house dust than those of nonsensitive infants, and the lower concentrations were associated with reduced proportions of IFN-γ–producing Th cells.[81] In line with this hypothesis, three distinct LPS phenotypes in humans have been described (namely, sensitive, intermediate, and hyporesponsive), based on reduction in FEV_1 following inhalation of increasing doses of LPS and in vitro production of IL-6 and IL-8 by peripheral blood monocytes and alveolar macrophages.[82]

Experimental results in animal models of asthma have supported the hygiene hypothesis. They have shown that treatment with microbes (eg, BCG[83] and *Lactobacillus*[84]) or microbial products (LPS[47,85] and CpG DNA[86,87]) inhibits allergic sensitization, eosinophilic inflammation, and AHR in these animals. In a similar animal model of allergic disease, we previously showed that the timing of exposure and the dose were critical to the in vivo effect of LPS.[85] That study demonstrated that whereas LPS exposure during early sensitization protects against increased production of IgE and consequent allergic inflammation, in marked contrast, LPS exposure after allergen challenge further exacerbates the allergic response as demonstrated by increased inflammation and reduced lung function.

TLR4

Toll is a receptor in *Drosophila* involved in antifungal immune responses. Toll-like receptors (TLRs) are a large family of evolutionarily conserved receptors originating from Toll, which sense invasion by microorganisms through the recognition of specific pathogen-associated molecule patterns and produce immediate innate responses (Figure 39-6). To date, 10 TLRs have been identified in humans and mice (TLR1 to TLR10).[88] TLRs are single transmembrane domain receptors that have a cytoplasmic signaling portion homologous to IL-1R. Although the TLRs differ in their extracellular domain structure, similar cytoplasmic domains allow TLRs to use the same signaling molecules. All TLRs signal through an adaptor protein named myeloid differentiation factor 88 (MyD88) (see Figure 39-6). Following activation, MyD88 recruits the IL-1R/IL-1R–associated protein kinase (IRAK) complex to the TLR; IRAK becomes

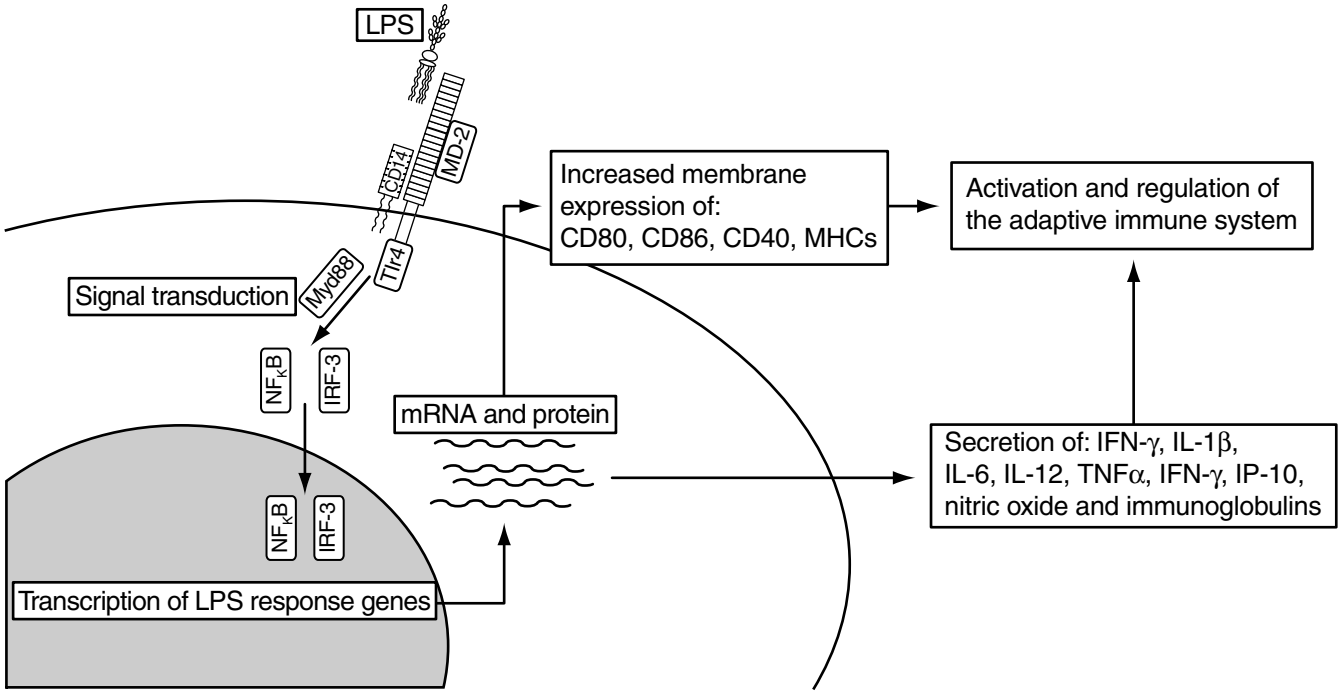

FIGURE 39-6 Toll family. Toll-like receptors (TLRs) are a large family of evolutionarily conserved receptors recognizing specific pathogen-associated molecule patterns. TLR4, with cluster determination 14 (CD14) and MD-2, recognizes bacterial lipopolysaccharide (LPS), initiating intracellular signaling by myeloid differentiation factor 88 (MyD88). MyD88 signaling ultimately leads to activation of the transcription factors nuclear factor kappa B (NFκB) and interferon regulatory factor-3 (IRF-3). These factors activate the transcription of many proinflammatory genes involved in inflammation, including genes involved in antigen presentation, promotion of Th1 responses by cytokines and chemokines, antibody production, and nitric oxide production. IFN = interferon; IL = interleukin; IP-10 = IFN-induced protein-10; MHC = major histocompatibility complex; TNF-α = tumor necrosis factor-α.

phosphorylated and is then able to activate the TNF receptor–associated factor 6 (TRAF6). This process leads to activation of c-Jun N-terminal kinase (JNK), mitogen-activated protein kinase (MAPK), and nuclear factor kappa B (NFκB) pathways, leading to a cascade of events, including the release of cytokines and activation of APCs.

Different TLRs recognize different ligands. TLR3 is a cell surface receptor for double-stranded RNA and hence may be implicated in viral recognition. TLR5 is specific for bacterial flagellin, whereas TLR9 is a receptor for unmethylated CpG motifs, which are abundant in bacterial DNA. In mammals, TLR4 is the principal receptor responsible for LPS-induced signal transduction.[89] Recognition of LPS by TLR4 is aided by two accessory proteins: CD14 and MD-2 (see Figure 39-6). TLR4 is expressed at particularly high levels by cells of the innate immune system, such as monocytes, dendritic cells, macrophages, and endothelial cells.[90–93] TLR4 expression is thought to be related to LPS sensitivity,[94] and it was recently demonstrated in murine macrophages that TLR expression and function decline with age.[95]

More recently, we have shown the ability of bacterial LPS to prevent local allergen-induced allergic inflammation in the nasal mucosa of atopic children. This occurs through down-regulation of local Th2 cytokines and up-regulation of Th1 cytokines in the tissue proliferation and activation of $TLR4^{+}IL\text{-}10^{+}$ and $CD25^{+}$ Th cells, and increased expression of the antiinflammatory cytokine IL-10.[96] These events occur locally without systemic recruitment of inflammatory cells and are orchestrated through the TLR4-dependent pathway. TLR4 is an important bridge between innate and adaptive immunity, potentially driving the molecular mechanisms governing the hygiene hypothesis and helping to explain why reduced exposure to bacterial products may lead to delayed or skewed development of the immune system and more atopic disease.

CONCLUSIONS

Bronchial asthma is a complex, chronic disease of the airways that is characterized by reversible AHR, airway remodeling, and inflammation. Furthermore, these pathologic and physiologic changes occur even in patients with mild asthma and can be detected in asthmatic children. In the last decade, one of the most striking advances in the study of asthma has been the recognition that cytokines and chemokines play integral roles in orchestrating, perpetuating and amplifying the underlying processes in this disease. Future therapy for asthma may involve specific targeting of cytokine and chemokine receptors rather than global immunosuppression. Additionally, it has become clearer that bacterial products play a role in the maturation of early immune responses and can modulate allergic inflammation in young children. Only by understanding the principal regulatory mechanisms involved in asthma can we begin to provide a rational basis for novel drug design and make progress in identifying those individuals at risk for its development.

REFERENCES

1. Tangye SG, Ferguson A, Avery DT, et al. Isotype switching by human B cells is division-associated and regulated by cytokines. J Immunol 2002;169:4298–306.
2. Seder RA, Paul WE. Acquisition of lymphokine-producing phenotype by CD4+T cells. Annu Rev Immunol 1994;12: 635–73.
3. Chung KF, Barnes PJ. Cytokines in asthma. Thorax 1999;54: 825–57.
4. Vercelli D, Jabara HH, Lee BW, et al. Human recombinant interleukin 4 induces Fc epsilon R2/CD23 on normal human monocytes. J Exp Med 1988;167:1406–16.
5. Xu L, Rothman P. IFN-gamma represses epsilon germline transcription and subsequently down-regulates switch recombination to epsilon. Int Immunol 1994;6:515–21.
6. Denoroy MC, Yodoi J, Banchereau J. Interleukin 4 and interferons alpha and gamma regulate Fc epsilon R2/CD23 mRNA expression on normal human B cells. Mol Immunol 1990;27: 129–34.
7. Gavett SH, O'Hearn DJ, Karp CL, et al. Interleukin-4 receptor blockade prevents airway responses induced by antigen challenge in mice. Am J Physiol 1997;272:L253–61.
8. Schleimer RP, Sterbinsky SA, Kaiser J, et al. IL-4 induces adherence of human eosinophils and basophils but not neutrophils to endothelium. Association with expression of VCAM-1. J Immunol 1992;148:1086–92.
9. Naseer T, Minshall EM, Leung DY, et al. Expression of IL-12 and IL-13 mRNA in asthma and their modulation in response to steroid therapy. Am J Respir Crit Care Med 1997;155:845–51.
10. Humbert M, Durham SR, Kimmitt P, et al. Elevated expression of messenger ribonucleic acid encoding IL-13 in the bronchial mucosa of atopic and nonatopic subjects with asthma. J Allergy Clin Immunol 1997;99:657–65.
11. Wills-Karp M, Luyimbazi J, Xu X, et al. Interleukin-13: central mediator of allergic asthma. Science 1998;282:2258–61.
12. Wills-Karp M, Chiaramonte M. Interleukin-13 in asthma. Curr Opin Pulm Med 2003;9:21–7.
13. McLane MP, Haczku A, van de Rijn M, et al. Interleukin-9 promotes allergen-induced eosinophilic inflammation and airway hyperresponsiveness in transgenic mice. Am J Respir Cell Mol Biol 1998;19:713–20.
14. Vink A, Warnier G, Brombacher F, Renauld JC. Interleukin 9-induced in vivo expansion of the B-1 lymphocyte population. J Exp Med 1999;189:1413–23.
15. Dugas B, Renauld JC, Pene J, et al. Interleukin-9 potentiates the interleukin-4-induced immunoglobulin (IgG, IgM and IgE) production by normal human B lymphocytes. Eur J Immunol 1993;23:1687–92.
16. Uyttenhove C, Simpson RJ, Van Snick J. Functional and structural characterization of P40, a mouse glycoprotein with T-cell growth factor activity. Proc Natl Acad Sci U S A 1988; 85:6934–8.
17. Houssiau FA, Renauld JC, Stevens M, et al. Human T cell lines and clones respond to IL-9. J Immunol 1993;150:2634–40.
18. Schmitt E, Van Brandwijk R, Van Snick J, et al. TCGF III/P40 is produced by naive murine CD4+T cells but is not a general T cell growth factor. Eur J Immunol 1989;19:2167–70.
19. Louahed J, Toda M, Jen J, et al. Interleukin-9 upregulates mucus expression in the airways. Am J Respir Cell Mol Biol 2000;22:649–56.
20. Dong Q, Louahed J, Vink A, et al. IL-9 induces chemokine expression in lung epithelial cells and baseline airway eosinophilia in transgenic mice. Eur J Immunol 1999;29: 2130–9.
21. Borish LC, Steinke JW. Cytokines and chemokines. J Allergy Clin Immunol 2003;111:S460–75.
22. Minshall EM, Hogg JC, Hamid QA. Cytokine mRNA expression in asthma is not restricted to the large airways. J Allergy Clin Immunol 1998;101:386–90.
23. Cameron L, Christodoulopoulos P, Lavigne F, et al. Evidence for local eosinophil differentiation within allergic nasal mucosa: inhibition with soluble IL-5 receptor. J Immunol 2000;164:1538–45.
24. Hurst SD, Muchamuel T, Gorman DM, et al. New IL-17 family members promote Th1 or Th2 responses in the lung: in vivo function of the novel cytokine IL-25. J Immunol 2002;169: 443–53.
25. Ohnishi T, Kita H, Weiler D, et al. IL-5 is the predominant eosinophil-active cytokine in the antigen-induced pulmonary late-phase reaction. Am Rev Respir Dis 1993;147: 901–7.
26. Mould AW, Ramsay AJ, Matthaei KI, et al. The effect of IL-5 and eotaxin expression in the lung on eosinophil trafficking and degranulation and the induction of bronchial hyperreactivity. J Immunol 2000;164:2142–50.
27. Leckie MJ, ten Brinke A, Khan J, et al. Effects of an interleukin-5 blocking monoclonal antibody on eosinophils, airway hyper-responsiveness, and the late asthmatic response. Lancet 2000;356:2144–8.
28. Xing Z, Ohkawara Y, Jordana M, et al. Transfer of granulocyte–macrophage colony-stimulating factor gene to rat lung induces eosinophilia, monocytosis, and fibrotic reactions. J Clin Invest 1996;97:1102–10.
29. Adach K, Suzuki M, Sugimoto T, et al. Granulocyte colony-stimulating factor exacerbates the acute lung injury and pulmonary fibrosis induced by intratracheal administration of bleomycin in rats. Exp Toxicol Pathol 2002;53:501–10.
30. Payne DN, Rogers AV, Adelroth E, et al. Early thickening of the reticular basement membrane in children with difficult asthma. Am J Respir Crit Care Med 2003;167:78–82.
31. Wahl SM, Hunt DA, Wakefield LM, et al. Transforming growth factor type beta induces monocyte chemotaxis and growth factor production. Proc Natl Acad Sci U S A 1987;84:5788–92.
32. Kehrl JH, Wakefield LM, Roberts AB, et al. Production of transforming growth factor beta by human T lymphocytes and its potential role in the regulation of T cell growth. J Exp Med 1986;163:1037–50.
33. Minshall EM, Leung DY, Martin RJ, et al. Eosinophil-associated TGF-beta1 mRNA expression and airways fibrosis in bronchial asthma. Am J Respir Cell Mol Biol 1997;17:326–33.
34. Clark RA, Folkvord JM, Hart CE, et al. Platelet isoforms of platelet-derived growth factor stimulate fibroblasts to contract collagen matrices. J Clin Invest 1989;84:1036–40.
35. Akira S, Taga T, Kishimoto T. Interleukin-6 in biology and medicine. Adv Immunol 1993;54:1–78.
36. DiCosmo BF, Geba GP, Picarella D, et al. Airway epithelial cell expression of interleukin-6 in transgenic mice. Uncoupling of airway inflammation and bronchial hyperreactivity. J Clin Invest 1994;94:2028–35.
37. Lee CG, Homer RJ, Zhu Z, et al. Interleukin-13 induces tissue fibrosis by selectively stimulating and activating transforming growth factor beta(1). J Exp Med 2001;194:809–21.
38. Chen LC, Zhang Z, Myers AC, Huang SK. Cutting edge: altered pulmonary eosinophilic inflammation in mice deficient for Clara cell secretory 10-kDa protein. J Immunol 2001;167: 3025–8.
39. Wang J, Homer RJ, Hong L, et al. IL-11 selectively inhibits aeroallergen-induced pulmonary eosinophilia and Th2 cytokine production. J Immunol 2000;165:2222–31.
40. Zhu Z, Homer RJ, Wang Z, et al. Pulmonary expression of interleukin-13 causes inflammation, mucus hypersecretion, subepithelial fibrosis, physiologic abnormalities, and eotaxin production. J Clin Invest 1999;103:779–88.

41. Zhu Z, Lee CG, Zheng T, et al. Airway inflammation and remodeling in asthma. Lessons from interleukin 11 and interleukin 13 transgenic mice. Am J Respir Crit Care Med 2001; 164:S67–70.
42. Minshall E, Chakir J, Laviolette M, et al. IL-11 expression is increased in severe asthma: association with epithelial cells and eosinophils. J Allergy Clin Immunol 2000;105: 232–8.
43. Hermann JA, Hall MA, Maini RN, et al. Important immunoregulatory role of interleukin-11 in the inflammatory process in rheumatoid arthritis. Arthritis Rheum 1998;41:1388–97.
44. Molet S, Hamid Q, Davoine F, et al. IL-17 is increased in asthmatic airways and induces human bronchial fibroblasts to produce cytokines. J Allergy Clin Immunol 2001;108:430–8.
45. Borish L, Aarons A, Rumbyrt J, et al. Interleukin-10 regulation in normal subjects and patients with asthma. J Allergy Clin Immunol 1996;97:1288–96.
46. John M, Lim S, Seybold J, et al. Inhaled corticosteroids increase interleukin-10 but reduce macrophage inflammatory protein-1alpha, granulocyte–macrophage colony-stimulating factor, and interferon-gamma release from alveolar macrophages in asthma. Am J Respir Crit Care Med 1998;157:256–62.
47. Tulic MK, Knight DA, Holt PG, Sly PD. Lipopolysaccharide inhibits the late-phase response to allergen by altering nitric oxide synthase activity and interleukin-10. Am J Respir Cell Mol Biol 2001;24:640–6.
48. Cunha FQ, Moncada S, Liew FY. Interleukin-10 (IL-10) inhibits the induction of nitric oxide synthase by interferon-gamma in murine macrophages. Biochem Biophys Res Commun 1992;182:1155–9.
49. Lecart S, Morel F, Noraz N, et al. IL-22, in contrast to IL-10, does not induce Ig production, due to absence of a functional IL-22 receptor on activated human B cells. Int Immunol 2002;14:1351–6.
50. Stirling RG, Chung KF. New immunological approaches and cytokine targets in asthma and allergy. Eur Respir J 2000; 16:1158–74.
51. Lack G, Bradley KL, Hamelmann E, et al. Nebulized IFN-gamma inhibits the development of secondary allergic responses in mice. J Immunol 1996;157:1432–9.
52. Koning H, Neijens HJ, Baert MR, et al. T cell subsets and cytokines in allergic and non-allergic children. I. Analysis of IL-4, IFN-gamma and IL-13 mRNA expression and protein production. Cytokine 1997;9:416–26.
53. Boguniewicz M, Schneider LC, Milgrom H, et al. Treatment of steroid-dependent asthma with recombinant interferon-gamma. Clin Exp Allergy 1993;23:785–90.
54. Manetti R, Parronchi P, Giudizi MG, et al. Natural killer cell stimulatory factor (interleukin 12 [IL-12]) induces T helper type 1 (Th1)-specific immune responses and inhibits the development of IL-4-producing Th cells. J Exp Med 1993; 177:1199–204.
55. Lee YL, Fu CL, Ye YL, Chiang BL. Administration of interleukin-12 prevents mite Der p 1 allergen-IgE antibody production and airway eosinophil infiltration in an animal model of airway inflammation. Scand J Immunol 1999;49:229–36.
56. Kips JC, Brusselle GJ, Joos GF, et al. Interleukin-12 inhibits antigen-induced airway hyperresponsiveness in mice. Am J Respir Crit Care Med 1996;153:535–9.
57. Hofstra CL, Van Ark I, Hofman G, et al. Prevention of Th2-like cell responses by coadministration of IL-12 and IL-18 is associated with inhibition of antigen-induced airway hyperresponsiveness, eosinophilia, and serum IgE levels. J Immunol 1998;161:5054–60.
58. Nakanishi K, Yoshimoto T, Tsutsui H, Okamura H. Interleukin-18 is a unique cytokine that stimulates both Th1 and Th2 responses depending on its cytokine milieu. Cytokine Growth Factor Rev 2001;12:53–72.
59. Bryan SA, O'Connor BJ, Matti S, et al. Effects of recombinant human interleukin-12 on eosinophils, airway hyperresponsiveness, and the late asthmatic response. Lancet 2000;356: 2149–53.
60. Ponath PD, Qin S, Post TW, et al. Molecular cloning and characterization of a human eotaxin receptor expressed selectively on eosinophils. J Exp Med 1996;183:2437–48.
61. Miotto D, Christodoulopoulos P, Olivenstein R, et al. Expression of IFN-gamma-inducible protein; monocyte chemotactic proteins 1, 3, and 4; and eotaxin in TH1- and TH2-mediated lung diseases. J Allergy Clin Immunol 2001; 107:664–70.
62. Taha RA, Laberge S, Hamid Q, Olivenstein R. Increased expression of the chemoattractant cytokines eotaxin, monocyte chemotactic protein-4, and interleukin-16 in induced sputum in asthmatic patients. Chest 2001;120: 595–601.
63. Lamkhioued B, Garcia-Zepeda EA, Abi-Younes S, et al. Monocyte chemoattractant protein (MCP)-4 expression in the airways of patients with asthma. Induction in epithelial cells and mononuclear cells by proinflammatory cytokines. Am J Respir Crit Care Med 2000;162:723–32.
64. Taha RA, Minshall EM, Miotto D, et al. Eotaxin and monocyte chemotactic protein-4 mRNA expression in small airways of asthmatic and nonasthmatic individuals. J Allergy Clin Immunol 1999;103:476–83.
65. Christodoulopoulos P, Wright E, Frenkiel S, et al. Monocyte chemotactic proteins in allergen-induced inflammation in the nasal mucosa: effect of topical corticosteroids. J Allergy Clin Immunol 1999;103:1036–44.
66. Henderson WR Jr, Chi EY, Maliszewski CR. Soluble IL-4 receptor inhibits airway inflammation following allergen challenge in a mouse model of asthma. J Immunol 2000;164: 1086–95.
67. Yasruel Z, Humbert M, Kotsimbos TC, et al. Membrane-bound and soluble alpha IL-5 receptor mRNA in the bronchial mucosa of atopic and nonatopic asthmatics. Am J Respir Crit Care Med 1997;155:1413–8.
68. Lamkhioued B, Abdelilah SG, Hamid Q, et al. The CCR3 receptor is involved in eosinophil differentiation and is up-regulated by Th2 cytokines in CD34+progenitor cells. J Immunol 2003;170:537–47.
69. Senechal S, Fahy O, Gentina T, et al. CCR3-blocking antibody inhibits allergen-induced eosinophil recruitment in human skin xenografts from allergic patients. Lab Invest 2002;82: 929–39.
70. Erin EM, Williams TJ, Barnes PJ, Hansel TT. Eotaxin receptor (CCR3) antagonism in asthma and allergic disease. Curr Drug Targets Inflamm Allergy 2002;1:201–14.
71. Warrior U, McKeegan EM, Rottinghaus SM, et al. Identification and characterization of novel antagonists of the CCR3 receptor. J Biomol Screen 2003;8:324–31.
72. Johnston SL, Pattemore PK, Sanderson G, et al. Community study of role of viral infections in exacerbations of asthma in 9–11 year old children. BMJ 1995;310:1225–9.
73. Sudo N, Sawamura S, Tanaka K, et al. The requirement of intestinal bacterial flora for the development of an IgE production system fully susceptible to oral tolerance induction. J Immunol 1997;159:1739–45.
74. Holt PG. Environmental factors and primary T-cell sensitisation to inhalant allergens in infancy: reappraisal of the role of infections and air pollution. Pediatr Allergy Immunol 1995;6:1–10.
75. Liu AH, Redmon AH Jr. Endotoxin: friend or foe? Allergy Asthma Proc 2001;22:337–40.

76. Cookson WOCM, Moffatt MF. Asthma: an epidemic in the absence of infection? Science 1997;275:41.
77. Yemaneberhan H, Bekele Z, Venn A, et al. Prevalence of wheeze and asthma and relation to atopy in urban and rural Ethiopia. Lancet 1997;350:85–90.
78. Von Ehrenstein OS, Von Mutius E, Illi S, et al. Reduced risk of hay fever and asthma among children of farmers. Clin Exp Allergy 2000;30:187–93.
79. Riedler J, Eder W, Oberfeld G, Schreuer M. Austrian children living on a farm have less hay fever, asthma and allergic sensitization. Clin Exp Allergy 2000;30:194–200.
80. Michel O, Kips J, Duchateau J, et al. Severity of asthma is related to endotoxin in house dust. Am J Respir Crit Care Med 1996;154:1641–6.
81. Gereda JE, Leung DYM, Thatayatikom A, et al. Relation between house-dust endotoxin exposure, type 1 T-cell development, and allergen sensitisation in infants at high risk of asthma. Lancet 2000;355:1680–3.
82. Kline JN, Cowden JD, Hunninghake GW, et al. Variable airway responsiveness to inhaled lipopolysaccharide. Am J Respir Crit Care Med 1999;160:297–303.
83. Erb KJ, Holloway JW, Sobeck A, et al. Infection of mice with Mycobacterium bovis–bacillus Calmette-Guerin (BCG) suppresses allergen-induced airway eosinophilia. J Exp Med 1998;187:561–9.
84. Murosaki S, Yamamoto Y, Ito K, et al. Heat-killed Lactobacillus plantarum L-137 suppresses naturally fed antigen-specific IgE production by stimulation of IL-12 production in mice. J Allergy Clin Immunol 1998;102:57–64.
85. Tulic MK, Wale JL, Holt PG, Sly PD. Modification of the inflammatory response to allergen challenge after exposure to bacterial lipopolysaccharide. Am J Respir Cell Mol Biol 2000;22:604–12.
86. Broide D, Schwarze J, Tighe H, et al. Immunostimulatory DNA sequences inhibit IL-5, eosinophilic inflammation, and airway hyperresponsiveness in mice. J Immunol 1998;161:7054–62.
87. Kline JN, Waldschmidt TJ, Businga TR, et al. Modulation of airway inflammation by CpG oligodeoxynucleotides in a murine model of asthma. J Immunol 1998;160:2555–9.
88. Beutler B, Rietschel ET. Innate immune sensing and its roots: the story of endotoxin. Nat Rev Immunol 2003;3: 169–76.
89. Chow JC, Young DW, Golenbock DT, et al. Toll-like receptor-4 mediates lipopolysaccharide-induced signal transduction. J Biol Chem 1999;274:10689–92.
90. Medzhitov R, Preston-Hurlburt P, Janeway CA Jr. A human homologue of the Drosophila Toll protein signals activation of adaptive immunity. Nature 1997;388:394–7.
91. Rock FL, Hardiman G, Timans JC, et al. A family of human receptors structurally related to Drosophila Toll. Proc Natl Acad Sci U S A 1998;95:588–93.
92. Muzio M, Natoli G, Saccani S, et al. The human toll signaling pathway: divergence of nuclear factor kappaB and JNK/SAPK activation upstream of tumor necrosis factor receptor-associated factor 6 (TRAF6). J Exp Med 1998;187: 2097–101.
93. Zhang FX, Kirschning CJ, Mancinelli R, et al. Bacterial lipopolysaccharide activates nuclear factor-kappaB through interleukin-1 signaling mediators in cultured human dermal endothelial cells and mononuclear phagocytes. J Biol Chem 1999;274:7611–4.
94. Nomura F, Akashi S, Sakao Y, et al. Cutting edge: endotoxin tolerance in mouse peritoneal macrophages correlates with down-regulation of surface toll-like receptor 4 expression. J Immunol 2000;164:3476–9.
95. Renshaw M, Rockwell J, Engleman C, et al. Cutting edge: impaired Toll-like receptor expression and function in aging. J Immunol 2002;169:4697–701.
96. Tulic MK, Fiset PO, Manoukian JJ, et al. Protective role of bacterial lipopolysaccharide in the nasal mucosa of atopic children but not adults: role for Toll-like receptor-4. Lancet 2004;363:1689–97.

CHAPTER 40

NITRIC OXIDE AND THE LUNG

Jennifer S. Landry, David H. Eidelman

NITRIC OXIDE

The free radical nitric oxide (NO), an important mediator in biologic processes, is a colorless, odorless, highly reactive gas that is produced in many organs of the body, including the lung. Since being recognized in 1977 as having biologic activity, NO has provoked an enormous amount of research activity, culminating in a Nobel Prize for the discovery that NO is a smooth muscle relaxant and a signaling molecule.[1] Clinically, NO is of interest both because asthma is associated with high levels of NO in exhaled breath and because of the widespread therapeutic use of inhaled NO in the critical care setting. The physiologic activity of NO depends on many local factors, including the amount and activity of the enzymes responsible for producing NO, the level of oxidant stress, and its rate of uptake by molecules such as hemoglobin and glutathione. In the lung, NO is produced by a wide variety of cell types, including epithelial, inflammatory, and vascular endothelial cells, as well as airway nerves, and acts as both a bronchodilator and a vasodilator. Although NO-derived oxidants are important weapons against invading pathogens, they probably also play a role in the pathogenesis of asthma and other inflammatory disorders by modulating cellular function and possibly by contributing to airway damage.

PRODUCTION OF NO BY NO ISOFORMS

NO is one of the smallest molecular mediators in biology. It is formed, along with L-citrulline, from molecular oxygen and L-arginine in a reaction catalyzed by the enzyme nitric oxide synthase (NOS) in the presence of a variety of cofactors (Figure 40-1). Three isoforms of NOS have been described, based on the tissue in which they were originally described: neuronal NOS (nNOS or NOS-I), cytokine-inducible NOS (iNOS or NOS-II), and endothelial cell NOS (ecNOS or NOS-III). Each of the isoforms is encoded by distinct genes on different chromosomes, and they differ with regard to their capacity to produce NO, their capacity for up-regulation by inflammatory stimuli, and their distribution among the various tissues of the body (Table 40-1). These isoforms are divided in two classes: constitutive (nNOS and ecNOS) and inducible (iNOS). An important generic difference between the constitutive NOS isoforms and iNOS is the relative efficiency with which NO production takes place. For both nNOS and ecNOS, the rate of NO production is regulated by changes in intracellular Ca^{2+} levels. In contrast, NO production by iNOS is both independent of Ca^{2+} levels and occurs at much higher rates than with the other isoforms, suggesting a very different biologic role for this enzyme. Although constitutive NOS activity is usually thought to be accounted for by nNOS and ecNOS, there is also some evidence to support the existence of NOS activity specific to the mitochondria.[2]

nNOS

Called neuronal NOS because it was first identified in neurons, nNOS is strongly associated with the nervous system. Within the lung, nNOS is primarily expressed in airway nerves, although it may also be detected in other airway tissues, such as smooth muscle.[3] nNOS is encoded by one of the largest genes known, with about 30 exons,[4] and is produced in several variants, based on a complex system of transcriptional control involving both multiple promoters and alternative splicing. One form of nNOS, termed nNOS-μ, is an important structural protein in skeletal muscle, where it is attached to dystrophin.[5] Duchenne muscular dystrophy, the severe X-linked recessive disorder that results in progressive muscle degeneration, is due to a lack of dystrophin, a membrane cytoskeletal protein. Utrophin and dystrophin form part of a complex of proteins and glycoproteins that links the basal lamina to the cytoskeleton, thus ensuring the stability of the muscle membrane. One protein of the complex, syntrophin, is associated with the muscular isoform of the nNOS.[5] Other nNOS variants have been reported to exhibit tissue-specific expression; for example, there is regional variation along the gastrointestinal tract.[6] Although generally classified as a constitutive enzyme, nNOS may be up-regulated in inflammatory states,[7] and it is possible that different transcriptional variants are favored under different conditions.

The biologic role of nNOS in the lung is unclear. nNOS in airway nerves contributes to the activity of the nonadrenergic noncholinergic (NANC) nervous system.[8] Evidence obtained in nNOS-knockout mice suggests that as much as 40% of basal NO production may be accounted for by nNOS,[9] although it is unknown whether production of NO by nNOS is as important in humans. Although it has long been believed that the NO produced by nNOS primarily serves as a bronchodilator of airway smooth muscle, there is

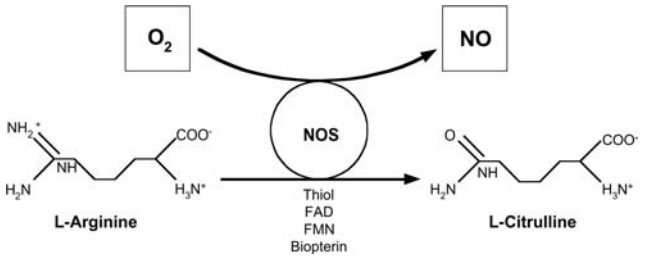

FIGURE 40-1 Formation of nitric oxide (NO). Conversion of molecular oxygen (O_2) and the amino acid L-arginine by the different isoforms of nitric oxide synthase (NOS) to form NO and L-citrulline. Cofactors of the NOS enzyme include thiol, riboflavin adenosine diphosphate (FAD), riboflavin 5′-dihydrogenphosphate (FMN), and biopterin.

recent evidence in mice suggesting that nNOS somehow contributes to the bronchial hyperresponsiveness induced by repeated allergen challenge.[10] Furthermore, population studies suggest that nNOS may be associated with bronchial hyperreactivity in humans[11] and that polymorphisms in the nNOS gene may account from some of the variability in exhaled NO concentrations among individuals. There is also some suggestion that nNOS exerts an important influence on airway obstruction in asthmatic patients who have already been treated with inhaled corticosteroids.[12] The mechanisms by which nNOS contributes to these phenomena remain to be elucidated.

ecNOS

It was the discovery that NO produced by ecNOS is the endothelial relaxing factor[13] that inaugurated the entire field of NO biology. Within the lung, the ecNOS isoform is largely restricted to endothelial cells of both the pulmonary and bronchial circulations. Although, like nNOS, ecNOS has been thought of as a constitutive enzyme responsible for NO production only under resting conditions, it is clear that ecNOS can be up-regulated under some circumstances. Of particular relevance in pulmonary diseases are the observations that ecNOS expression can be altered by hypoxia[14] and by sepsis,[15] potentially contributing to vascular dysregulation in these conditions.

Table 40-1 Nitric Oxide Synthase Isoforms

Isoform types	*Traditional name*	*Sites of production*	*Roles*
NOS-I	nNOS (neuronal)	Airway nerves Smooth muscles	Neurotransmitter Regulates airway smooth muscle tone
NOS-II	iNOS (inducible)	Immune effector cells Airway epithelium	Mediator of inflammation Production increased in asthma
NOS-III	ecNOS (endothelial cells)	Endothelial cells of pulmonary and bronchial circulation	Regulation of vascular smooth muscle tone Effects on blood pressure

iNOS

Originally described in macrophages, iNOS is widely expressed, particularly in inflammatory disorders, in which the transcription of iNOS is increased by the action of proinflammatory cytokines such as tumor necrosis factor-α and interferon-γ (IFN-γ). In the lung, increased iNOS expression has been described in a variety of conditions, including asthma,[16] pneumonia,[17] and sepsis.[18] Although substrate availability and the presence of sufficient quantities of essential cofactors may also modulate iNOS activity, increased transcription of iNOS mRNA is the principal mechanism by which NO production is up-regulated in inflammation. The regulation of iNOS expression in the lung has perhaps been best studied in epithelial cells, where IFN-γ and interleukin-4 have been shown to induce its expression.[19] IFN-γ is thought to induce gene expression through the Janus kinase (Jak)–STAT 1 (signal transducer and activator of transcription) pathway, which involves a tyrosine phosphorylation cascade.[20,21] (Figure 40-2). There is also evidence that pathways involving the transcription factor nuclear factor kappa B (NFκB) may be involved in up-regulation of epithelial iNOS gene expression, but this seems to be more prominent in rodents. Despite increased expression of cytokines that signal through the NFκB pathway in asthma, NFκB activation is low in asthmatic airway epithelial cells.[22] Since iNOS has a high capacity to produce NO and does not depend on changes in intracellular Ca^{2+} levels for its activity, increases in the amount of iNOS protein result in very large increases in NO production that are sustained until the inflammatory signal ends.

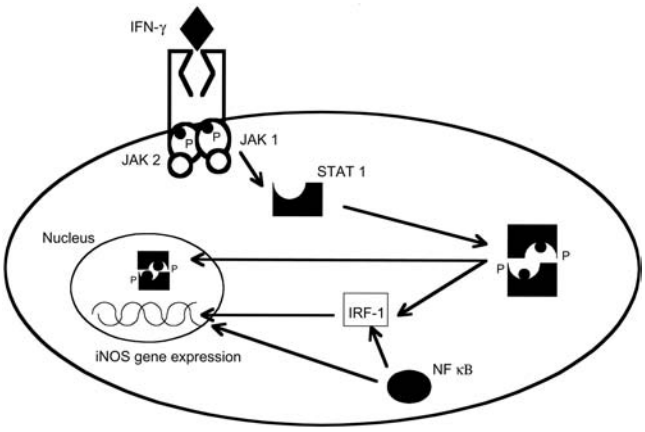

FIGURE 40-2 Induction of iNOS gene expression. The iNOS promoter has several regulatory components that are essential for complete expression of iNOS, including nuclear factor kappa B (NFκB), STAT 1, and interferon regulatory factor-1 (IRF-1) binding sites. STAT 1 and IRF-1 are components of the interferon-γ (IFN-γ) signaling pathway, both having an influence on iNOS expression. NFκB alters iNOS expression either via IRF-1 or directly.[56] Shown here is an example of STAT-mediated activation of gene expression by IFN-γ. When ligand binds to the receptor, the receptors form dimers. The dimers for IFN-γ bind Jak1 and Jak2. The receptors and the Jaks become phosphorylated, forming the complex that is the catalyst for phosphorylation of STATs. The IFN-γ–receptor complex recognizes STAT 1. The phosphorylated STATs dimerize and, in turn, enter the nucleus and activate the gene expression of iNOS. Jak = Janus kinase; P = phosphorylation; STAT = signal transducer and activator of transcription.

Airway epithelial cells express iNOS constitutively as well as when inflamed and are therefore important sources of NO production in the bronchial tree, even in healthy individuals. NO production by iNOS may be an important component of defense against infectious agents, some of which are susceptible to the antimicrobial actions of NO.[23]

HOW DOES NO WORK?

Understanding the role of NO in the lung is made difficult by the broad range of biologic activities that have been described for it. These activities may be grouped into two broad categories: those that result from the production of cGMP and those caused by the generation of reactive nitrogen species (RNS).

NO AND cGMP

The first described biologic function of NO was as an endothelial smooth muscle relaxant, the endothelium-derived relaxing factor.[13] NO was subsequently shown to relax other smooth muscles, including airway smooth muscle,[24] suggesting that in the lung NO acts primarily as a bronchodilator as part of the NANC inhibitory nervous system of the airways.[25] The smooth muscle–relaxant effects of NO are dependent on its ability to bind to the heme group of guanylate cyclase, resulting in increased cellular concentrations of cGMP, which, in turn, lead to smooth muscle relaxation.[26] The generation of intracellular cGMP underlies many of the biologic effects of NO in tissues other than smooth muscle, accounting for at least some of its action as a neurotransmitter, as well as effects on lymphocytes.[27]

Reactive Nitrogen Species

In recent years, increasing attention has been paid to actions of NO that do not involve cGMP but instead depend on reactive derivatives of NO, termed reactive nitrogen species. NO may exert an oxidative influence both directly through reactions with a variety of biomolecules and indirectly through its interactions with glutathione (GSH) and other thiols. Although NO itself is a radical with the capacity to participate in oxidative reactions, much of the oxidant activity of NO is mediated by derivatives formed under conditions of oxidative stress. Of these, the best known is peroxynitrite ($ONOO^-$), a highly reactive intermediate formed at high rates from reaction of molecular NO with superoxide ion (O_2^-), which can nitrate proteins, lipids, and DNA (Figure 40-3). Peroxynitrite can cause oxidative nitration of tyrosine residues on proteins, leading to the formation of 3-nitrotyrosine (3NT), which can be detected by immunologic methods and has been described in many inflammatory disorders of the lung, including asthma,[28] chronic obstructive pulmonary disease (COPD),[29] and cystic fibrosis (CF).[30] Among the many proteins that have been found to be susceptible to nitration, a key group of proteins that are potentially important are the tyrosine kinases involved in signaling pathways.[31] Initial interest was focused on the importance of tyrosine residues in these enzymes, but it now appears that peroxynitrite can act at multiple levels, including the G protein–coupled receptors receptor-activated kinases and even receptor-independent kinases, such as the Src family of kinases.[32] Nitration has been described as both increasing and decreasing kinase function, depending on the circumstances. Moreover, peroxynitrite has been reported to oxidize the phosphatases responsible for limiting the activity of various kinases, thereby indirectly increasing signaling activity.[33]

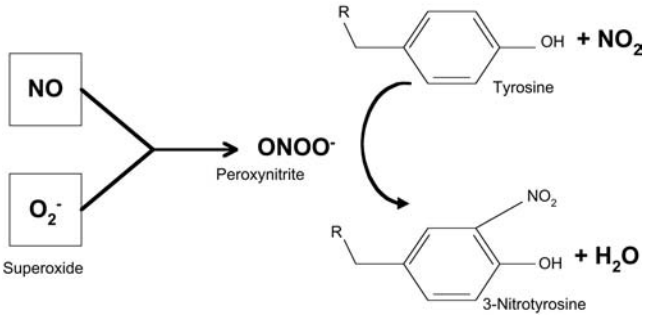

FIGURE 40-3 Oxidant properties of nitric oxide (NO): formation of peroxynitrite ($ONOO^-$) through the exposure of NO to superoxide species (O_2^-), and the role of peroxynitrite in the formation of 3-nitrotyrosine in the presence of tyrosine residues.

The peroxynitrite mechanism may not be the only important means by which protein nitration occurs in asthma and other inflammatory disorders. There is a close association between the detection of 3NT and the presence of granulocytes such as neutrophils or eosinophils. These cells are rich in peroxidases that have the capacity to promote protein nitration even in the absence of peroxynitrite formation.[34] In eosinophil peroxidase–deficient mice, we observed a substantial decrease in 3NT detection following antigen challenge in comparison with controls.[35] The lack of eosinophil peroxidase resulted in much less 3NT than did the lack of iNOS in iNOS-knockout mice. This suggests that peroxidase activity may be an important source of 3NT in allergic inflammation and asthma, raising the possibility that eosinophil peroxidase may play an important role in the pathogenesis of these disorders. Nevertheless, this phenomenon was largely restricted to the eosinophils themselves rather than involving the airways generally. Recently, in nasal biopsy specimens from patients with chronic sinusitis, another condition associated with 3NT formation, we again found that 3NT level was very closely related to the eosinophils.[36] It thus remains an open question as to whether the formation of 3NT by peroxidases such as eosinophil peroxidase is a factor outside of eosinophils themselves.

The possibility that NO acts through oxidant mechanisms is of particular importance in the lung, an environment rich in oxygen. As part of their antimicrobial function, inflammatory cells such as macrophages, lymphocytes, and granulocytes may produce large quantities of superoxide and other reactive oxidant species, which are helpful in killing bacteria or other parasites. Under these conditions, a variety of highly reactive NO derivatives are produced with the potential to attack structural proteins, enzymes, lipids, and even DNA. Production of NO in the context of a vigorous inflammatory response thus has the potential to contribute

to tissue damage and cellular dysfunction. In asthma, evidence of NO-mediated oxidative damage in the form of 3NT has been found prior to treatment with inhaled corticosteroids.[28] Clinically, this type of oxidant stress contributes to fibrotic remodeling of the lung in patients with acute respiratory distress syndrome (ARDS) exposed for long periods of time to high inspired fractions of oxygen. It is therefore of interest that administration of inhaled corticosteroids to asthmatic patients is associated not only with decreases in NO production but also with decreased levels of 3NT,[28] suggesting the possibility that antiinflammatory treatment that blocks excessive NO production or minimizes oxidative stress may be able to prevent the long-term development of irreversible airway obstruction in asthmatic patients by minimizing tissue damage.

NO and Thiols

Another potentially important activity of NO relates to its capacity to combine with thiol groups to form *S*-nitrosothiols (SNOs). The most important interaction is with GSH, leading to the formation of *S*-nitrosylglutathione (GSNO), a compound that has biologic activity independent of molecular NO.[37] As well as being the principal intracellular antioxidant, GSH is also present in high concentrations in the airway lining liquid, where it presumably contributes to defense against the high oxygen concentrations faced by this compartment. The formation of SNOs thus potentially contributes to disease pathogenesis in several ways. Inside the cell, where the oxidative health of the cell depends on the relative amounts of oxidized and reduced GSH, the production of GSNO may decrease the availability of GSH, potentially increasing oxidative stress.[38] There is also some suggestion that *S*-nitrosylation of molecules, including signaling proteins, may modulate their function, raising the possibility that *S*-nitrosylation could act as a signaling mechanism analogous to phosphorylation.[39]

In the extracellular compartment, SNO formation probably has a different significance from that inside cells. Our data suggest that in the airway lining liquid, at least, most of the nitrosothiol formation is associated with proteins, particularly albumin, rather than with low-molecular-weight compounds such as GSH.[40] Thus, extracellular SNO formation may help buffer increases in NO production, decreasing the oxidative activity of NO by preventing its reaction with superoxide and providing a reservoir of molecular NO.

NO AND PULMONARY DISEASES

Asthma

Much of the interest in NO in the lung has been focused on asthma, a disease that is associated with marked increases in NO concentrations in exhaled air and in which iNOS is markedly up-regulated, most notably in epithelial cells.[28] In experimental models in which sensitized rodents are exposed to inhaled allergens, iNOS expression correlates with airway eosinophilia and other measures of the inflammatory response.[41,42] In bronchial biopsy specimens from patients with uncontrolled asthma,[28] both iNOS mRNA and protein levels are increased in airway epithelial cells, macrophages, and other inflammatory cells. Treatment with inhaled corticosteroids leads to decreased iNOS expression as well as decreases in exhaled NO.[43] Despite the prominence of iNOS expression in asthma and other inflammatory diseases of the lung, the pathophysiologic role of NO in these disorders is incompletely understood.

Early studies of NO in asthma focused on the possibility that NO is an endogenous bronchodilator, decreasing bronchial responsiveness by relaxing smooth muscle. Given that, as asthma severity worsens, both bronchial hyperresponsiveness and NO production increase, this seems too simplistic. Nevertheless, there is both a physiologic and genetic basis for believing that NO, particularly that produced by nNOS, may influence bronchial reactivity.[9,11,12] Whereas in mice, nNOS somehow promotes excessive bronchial tone,[9] data in humans suggest that residual airway obstruction after steroid therapy in asthma is associated with an apparent decrease in nNOS activity.[12] As nNOS is primarily expressed in the nerves of the airway wall, where it can exert a direct influence on airway smooth muscle, it is intriguing to speculate that NO production by nNOS is a regulator of airway tone. Indeed, it has been proposed that the elevated NO diffusing capacity of the airways in asthma may reflect up-regulation of NANC NO-producing nerves in airways in compensation for decreased sensitivity of airway smooth muscles to the relaxant effects of endogenous NO.[44] Its effects are thus separate from, and potentially opposite to, those of NO produced by iNOS in epithelial and inflammatory cells.

NO may also be a potent modulator of the inflammatory response itself. Inhibition of NO production can block the development of eosinophilic inflammation in animal models of asthma.[42,45,46] Although this has not yet been definitively demonstrated in humans, administration of inhaled corticosteroids leads to down-regulation of iNOS at the same time as symptoms improve and airway eosinophilia is suppressed.[28] Many inflammatory cells in the asthmatic airway are capable of producing NO, and NO has also been reported to promote programmed cell death (apoptosis) in several types of cell.[47] In mice, NO promotes the production of chemotactic factors (chemokines) for eosinophils,[48] suggesting the possibility that NO acts as part of a positive feedback loop in which inflammatory cells produce NO and thereby promote their further recruitment through the action of chemokines.

There is evidence that the level of exhaled NO correlates well with the level of airway inflammation in asthma, as documented by sputum eosinophilia and methacholine responsiveness,[49] as well as the degree of protein nitration and tissue damage.[28] Exhaled NO has been shown to be a sensitive marker of the dose-dependent effect of steroid treatment and has been proposed as a surrogate measurement of airway inflammation and therapeutic compliance. Furthermore, persistent elevation of exhaled NO level in treated patients may suggest the need to intensify therapy for their asthma, based on the premise that their asthma control, defined as the degree of airway inflammation, is suboptimal.[50] The level of NO has also been found to be increased in atopic subjects with seasonal rhinitis and/or

asthma in comparison with nonatopic subjects, suggesting that it is the allergic nature of airway inflammation that is mainly responsible for higher NO production in the lower airways.[51] It is important to note that nasal NO concentrations are high relative to those in the lower respiratory tract in humans, with the highest levels being found in the paranasal sinuses, and NO may have physiologic roles, such as preserving sinus sterility and modulating ciliary motility.[52]

NO in COPD and Chronic Bronchitis

The level of exhaled NO has not been found to be consistently increased in patients with stable COPD, but a positive relationship has been established between the reversibility of airflow limitation with corticosteroid treatment and an elevated exhaled NO level. Since high numbers of sputum eosinophils and other inflammatory cells, and some degree of reversibility of airflow obstruction, were found in subjects with elevated exhaled NO levels, these patients may form a subgroup that responds differently to treatment from those without reversible airflow limitation.[53] Exhaled NO level has also been shown to be increased in patients with chronic bronchitis, although it is possible that this study may have included some patients with asthma.[54]

NO in CF and Bronchiectasis

Previous studies in children with CF have shown that exhaled NO level is reduced despite the presence of severe airway inflammation, bacterial colonization, and chronic infection. Several explanations have been proposed for this paradoxical finding. Most importantly, iNOS expression by the epithelial cells of patients with CF is reduced[55,56] (see Figure 40-2). The absence of iNOS expression in CF epithelial cells appears to be related to a defect in cell signaling.[56] This does not appear to be specific to CF, however, as iNOS expression has been reported to be decreased in patients with immotile cilia syndromes.[57] In bronchiectasis, exhaled NO levels are unaffected unless there is concomitant *Pseudomonas aeruginosa* infection.[58] Since iNOS expression in inflammatory cells is normal in CF, other factors may also contribute to low exhaled NO levels in this disorder. GSH, the predominant intracellular antioxidant, is an organic anion whose efflux depends on the cystic fibrosis transmembrane conductance regulator. As NO production is profoundly affected by GSH, this may contribute to decreased expression of iNOS. Other possibilities remain: poor diffusion of NO across increased and viscous airway secretions and consumption of NO by its rapid reaction with superoxide to form peroxynitrite. These diminished levels of exhaled NO were not correlated with genotype or infection status and, given the known bacteriostatic effects of NO and its possible effect on mucociliary clearance, this may be of clinical importance since NO has been shown to modulate airway ciliary beating through an NO-dependent mechanism that up-regulates ciliary motility in response to stimuli.[59] In this regard, it has been hypothesized that absence of iNOS expression in CF epithelial cells[56] may contribute to host susceptibility in this disorder.

Table 40-2 Summary of Findings of Exhaled NO (eNO) Level in Selected Pulmonary Diseases

Disease	*Findings of exhaled NO level*	*Interpretation*
Normal	eNO levels less than 10 ppb	No correlation between eNO, gender and age[78]
Asthma	Increased eNO level	Marker of airway inflammation; correlates with asthma control; eNO level is elevated in acute asthma, in steroid-resistant severe asthma, or when the maintenance dose of inhaled corticosteroids is reduced. eNO level is quickly reduced with steroid treatment.[44,49,50,60,61]
Atopy	Increased eNO level in atopic asthmatic and allergic rhinitis	Increased levels of eNO seen in atopic patients with asthma and rhinitis, but no difference between atopic and nonatopic control subjects without asthma or rhinitis[51]
COPD	Normal eNO level	Increased eNO level in patients with bronchodilator response; these patients may have different responses to treatment from those without reversible airflow limitation[53,54]
CF	Reduced nasal NO and eNO	No association between genotypes and exhaled NO levels. Despite the airway inflammation that is characteristic of CF, both nasal and exhaled NO levels are reduced[59]
Acute lung allograft rejection	eNO level is elevated in fulminant acute rejection Reduction in eNO level after partial immunosuppression	eNO level correlates with the degree of acute lung allograft rejection and may serve as a noninvasive measure of acute lung transplant rejection in the clinical setting[68]
Chronic lung allograft rejection (BOS)	eNO level is positively correlated with iNOS expression in bronchial epithelium and the percentage of neutrophils in BAL fluid in stable chronic rejection	eNO levels appear to reflect the degree of airway neutrophilia in both stable chronic rejection and BOS. Serial eNO measurements may be able to predict the early development of BOS.[69]
Scleroderma	Inverse correlation between eNO level and the presence of pulmonary hypertension	Increased level of eNO in patients with scleroderma may reflect respiratory tract infection. The negative correlation between eNO level and pulmonary hypertension suggests an important role of NO in regulating pulmonary vascular resistance[79]

BOS = bronchiolitis obliterans syndrome; CF = cystic fibrosis; COPD = chronic obstructive pulmonary disease.

EXHALED NO AND ITS MEASUREMENT

Based on the observation that NO production is greatly increased in asthmatic airways, there has been interest in using exhaled NO as a noninvasive marker of airway inflammation, disease activity, and response to treatment (Table 40-2). As first described in the early 1990s, the level of exhaled NO is related to the presence of sputum eosinophils and the degree of airway hyperresponsiveness as measured by the provocative concentration (PC_{20}),[60] suggesting that it is a suitable candidate for a noninvasive measure of asthmatic airway inflammation. Exhaled NO, however, is nonspecific, and it has been argued that it is inferior to sputum eosinophilia for monitoring asthma activity.[61] Nevertheless, in the appropriate context, exhaled NO measurements may prove very useful for monitoring asthma patients provided that they are carried out appropriately. In particular, exhaled NO measurements may represent an excellent tool for following patient compliance with inhaled corticosteroids and for monitoring asthma in young children.

Although relatively easy to carry out, the measurement of exhaled NO is very sensitive to the technique used to harvest exhaled air. Commercial instruments for the detection of NO are usually based on chemiluminescence, with results expressed in parts per billion (ppb), equivalent to nanoliters per liter (nL/L). Chemiluminescence detection is a highly sensitive but potentially noisy technique, and care has to be taken to ensure standardization of the measurement technique as well as careful interpretation of results. In particular, the manner in which the exhalation is carried out must be carefully controlled[62–64] to avoid contamination from the nose and to ensure test reproducibility. The pattern of exhalation, particularly the rate of exhalation, influences the dilution of NO as gas passes through the airways and thus may alter the final measured concentration. This variation in exhaled NO with the expiratory flow has been attributed to faster flows minimizing the transit time of alveolar gas in the airway, and for this reason, the use of constant expiratory flow rates is emphasized in standardized techniques. Interpretation of the results therefore requires standardized maneuvers. Laboratories may choose to measure exhaled NO either during a single expiration or during tidal breathing. Although both are acceptable, the results of these two methods are not directly comparable.[65] Similarly, slightly different approaches are appropriate for measurements in children and adults. To address the need for standardization, the American Thoracic Society has issued guidelines for procedures to be used for the on-line and off-line measurement of exhaled NO in both adults and children[52] (Table 40-3). Most commercially available NO-monitoring systems are now compliant with these standards.

Table 40-3 General Aspects of the Measurement of Exhaled NO Level[52]

NO measurements
On-line measurement: exhaled NO testing with a real-time display of exhaled NO breath profiles
Off-line testing: collection of exhalate into suitable receptacles for later analysis
Terminology and units
On-line measurement: The fractional exhaled NO concentration (F_ENO) is expressed in parts per billion (ppb), which is equivalent to nanoliters per liter (nL/L). The exhalation flow rate employed for a particular test can be expressed as a subscript of the flow in liter/s, for example, $F_ENO_{0.05}$.
Off-line NO collection: F_ENO refers to the fractional NO concentration in exhalate from a vital capacity collection. If the exhalation is at a constant flow, this should be added as a subscript, for example, $F_ENO_{0.35}$, with the flow rate in liters per second.
Nasal: The fractional concentration of nasal NO is termed nasal F_ENO
Nasal NO contamination
Nasal NO can accumulate to high concentrations relative to the lower respiratory tract, so techniques should be adapted accordingly in order to avoid contamination
Ambient NO levels
Environmental NO can reach high levels relative to those in exhaled breath, so standardized techniques must prevent the contamination of biologic samples with ambient NO, and ambient NO level at the time of each test should be recorded
Expiratory flow rate dependence
The concentration of exhaled NO from the lower respiratory tract exhibits significant expiratory flow dependence; in view of this flow dependency, the use of constant flow rates must be emphasized
Breath-holding
Breath-holding results in NO accumulation in the nasal cavity and lower airways. For this reason, the use of breath-holding is discouraged in the standard techniques proposed.

NO AND VARIOUS PULMONARY DISEASES

High-altitude pulmonary edema (HAPE) is a life-threatening condition that occurs in predisposed subjects at altitudes above 2,500 m. It is thought to be multifactorial in its causation and involves hemodynamic changes such as an increase in the pulmonary artery pressure and defective alveolar fluid clearance. It has been postulated that pulmonary NO synthesis is altered in this syndrome.[66] In HAPE-prone subjects, reduced levels of exhaled NO have been documented, leading to the speculation that this contributes to exaggerated hypoxic vasoconstriction, leading to pulmonary edema. The low level of exhaled NO also suggests that the onset of HAPE is not preceded by airway inflammation.

It has also been proposed that NO plays a role in the hepatopulmonary syndrome; elevated levels of exhaled NO and increased expression of iNOS have been documented as part of this syndrome, in which pulmonary vascular dilatation and liver cirrhosis are combined. In an experimental cirrhosis model in the rat, increased production of NO was correlated with pulmonary vasodilatation. These findings were reversible after treatment with a nonselective NOS inhibitor for 6 weeks.[67]

Exhaled NO has also been found to correlate with the presence and severity of acute rejection of lung transplants and has been proposed as a noninvasive measure of this complication. This remains experimental and has so far been restricted to animal models.[68] In chronic pulmonary allograft rejection or bronchiolitis obliterans syndrome (BOS), increased levels of exhaled NO appear to reflect the degree of airway neutrophilia, and early reports suggest that exhaled NO measurements may be able to predict the early development of BOS.[69]

ALTERNATIVES TO EXHALED NO

Even when performed well, it is debatable whether measurements of NO concentrations in exhaled air actually reflect those at the level of the tissues.[70] Because NO has a short half-life and high tissue solubility, interpretation of exhaled NO level is intrinsically problematic. Moreover, it has been suggested that exhaled NO may reflect the chemistry of the airway lining liquid, particularly its pH, more than endogenous NO production.[71] Several alternative approaches have been proposed. The concentrations of NO metabolites in expectorated sputum or in bronchoalveolar lavage fluid have been measured. Most recently, breath condensate, which holds promise as a noninvasive alternative to exhaled NO, has also been used for these measurements. When exhaled gas is passed over a cooling coil or its temperature is otherwise reduced, the liquid content of exhaled gas is easily captured.[72] The resulting condensate can be shown to contain measurable levels of NO metabolites as well as a variety of other properties or compounds of interest,[72,73] particularly pH.[74] It remains to be seen whether the breath condensate technique will prove sufficiently useful to be introduced into clinical practice. A weakness of all these techniques is that it is hard to know where in the tracheobronchial tree the condensate is coming from. To date, none of them has been demonstrated to be superior to exhaled NO.

INHALED NO THERAPY

ARDS

In addition to its importance in disease pathogenesis, NO has been applied therapeutically (Table 40-4). ARDS is characterized by intrapulmonary shunting that results in arterial hypoxemia and by acute pulmonary arterial hypertension due to vasoconstriction and widespread occlusion of the pulmonary vasculature. Inhaled NO, at concentrations varying between 5 and 80 ppm, has been used to successfully reduce the degree of pulmonary arterial hypertension and relieve hypoxic vasoconstriction of the pulmonary capillaries, resulting in improved oxygenation and hemodynamics in the setting of ARDS. This beneficial effect is believed to be due to a redistribution of the pulmonary bloodflow away from the nonventilated region of the lung, thus improving the ventilation–perfusion mismatch. Although high concentrations of NO have been associated with fatal acute pulmonary edema, there is little evidence of toxicity below a concentration of 50 ppm.[75] Unfortunately, despite its usefulness in improving hypoxemic respiratory failure and pulmonary vasoconstriction in the short term, inhaled NO has not so far been shown to improve clinical outcomes and is not currently recommended as a routine therapeutic agent in the treatment of ARDS.[76]

Pulmonary Hypertension

By virtue of its importance as an endogenous vasodilator in the pulmonary circulation, there has been interest in the use of inhaled NO as a therapeutic agent in pulmonary hypertension. In practice, the principal application of inhaled NO is in the evaluation of patients with primary and secondary causes of pulmonary hypertension. The demonstration of a reduction in pulmonary artery pressures in response to inhaled NO predicts which patients with primary pulmonary hypertension are likely to respond to therapy with Ca^{2+} channel blockers.[77] In addition, inhaled NO has been applied to the acute management of pulmonary hypertension in recipients of heart and lung transplants. The safety of long-term use of NO as a therapy for primary pulmonary hypertension has not yet been documented, except in a small number of case reports.

Table 40-4 Potential Therapeutic Applications of NO and Its Derivatives by Modulation of Endogenous NO Production or Activity

Disease	*Agents*	*Possible effects of these agents*
ARDS	Inhaled NO	Pulmonary vasodilatation
Asthma	NO donor cNOS activators iNOS inhibition Antioxidants	Pulmonary vasodilatation; improved lung function; bronchodilatation; improved mucociliary clearance; reduced inflammation and airway hyperreactivity
COPD	NO donor iNOS inhibition Antioxidants	Pulmonary vasodilatation; antibacterial effects; reduced inflammation
CF	NO donor cNOS activators	Improved lung function; improved mucociliary clearance; bronchodilatation
Pulmonary hypertension	Inhaled NO cNOS activators	Pulmonary vasodilatation

ARDS = acute respiratory distress syndrome; CF = cystic fibrosis; COPD = chronic obstructive pulmonary disease.

CONCLUSIONS

There has been intensive research into the role of NO in the pathophysiology of asthma, CF, ARDS, and other lung diseases over the last several years. Although there is strong evidence that production of NO within the airway tree contributes to the development of airway inflammation, there is also reason to believe that NO acts to relax bronchial smooth muscle. Thus, NO probably plays several roles, acting less as a sole mediator than as part of one or several cascades of events in respiratory diseases. Given the prominence of NO in pulmonary inflammatory disorders, it is tempting to consider the development of therapeutic strategies aimed at controlling its production. The development of such strategies requires better understanding of the ways in which NO modulates bronchial tone and contributes to the regulation of the inflammatory response in the airways.

REFERENCES

1. Williams N. NO news is good news—but only for three Americans. Science 1998;282:610–1.
2. Piantadosi CA, Tatro LG, Whorton AR. Nitric oxide and differential effects of ATP on mitochondrial permeability transition. Nitric Oxide 2002;6:45–60.
3. Patel HJ, Belvisi MG, Donnelly LE, et al. Constitutive expressions of type I NOS in human airway smooth muscle cells: evidence for an antiproliferative role. FASEB J 1999;13: 1810–6.

4. Wang Y, Newton DC, Marsden PA. Neuronal NOS: gene structure, mRNA diversity, and functional relevance. Crit Rev Neurobiol 1999;13:21–43.
5. Chaubourt E, Voisin V, Fossier P, et al. Muscular nitric oxide synthase (muNOS) and utrophin. J Physiol Paris 2002;96: 43–52.
6. Saur D, Paenge H, Shusdziarra V, Allescher HD. Distinct expression of splice variants of neuronal nitric oxide synthase in the human gastrointestinal tract. Gastroenterology 2000;118:849–58.
7. Callsen-Cencic P, Hoheisel V, Kaske A, et al. The controversy about spinal neuronal nitric oxide synthase: under which conditions is it up- or downregulated? Cell Tissue Res 1999;295:183–94.
8. Bredt DS. Endogenous nitric oxide synthesis: biological functions and pathophysiology. Free Radic Res 1999;31:577–96.
9. De Sanctis GT, Mehta S, Kobzik L, et al. Contribution of type I NOS to expired gas NO and bronchial responsiveness in mice. Am J Physiol 1997;273(4 Pt 1):L883–8.
10. Chiba Y, Arimoto T, Yoshikawa T, Misawa M. Elevated nitric oxide synthase activity concurrent with antigen-induced airway hyperresponsiveness in rats. Exp Lung Res 2000;26:535–49.
11. Ricciardolo FL, Timmers MC, Geppetti P, et al. Allergen-induced impairment of bronchoprotective nitric oxide synthesis in asthma. J Allergy Clin Imunol 2001;108:198–204.
12. Silkoff PE, Sylvester JT, Zamel N, Permutt S. Airway nitric oxide diffusion in asthma: role in pulmonary function and bronchial responsiveness. Am J Respir Crit Care Med 2000;161(4 Pt 1):1218–28.
13. Sessa WC, Harrison JK, Barber CM, et al. Molecular cloning and expression of a cDNA encoding endothelial cell nitric oxide synthase. J Biol Chem 1992;267:15274–6.
14. Arnet UA, McMillan A, Dinerman JL, et al. Regulation of endothelial nitric oxide synthase during hypoxia. J Biol Chem 1996;271:15069–73.
15. Javeshghani D, Magder S. Regional changes in constitutive nitric oxide synthase and the hemodynamic consequences of its inhibition in lipopolysaccharide-treated pigs. Shock 2001;16:232–8.
16. De Sanctis GT, MacLean JA, Hamada K, et al. Contribution of nitric oxide synthases 1, 2, and 3 to airway hyperresponsiveness and inflammation in a murine model of asthma. J Exp Med 1999;189:1621–30.
17. Goodrum KJ, Poulson-Dunlap J. Cytokine responses to group B streptococci-induced nitric oxide production in respiratory epithelial cells. Infect Immunol 2002;70:49–54.
18. Bailey TC, Cavanagh C, Mehta S, et al. Sepsis and hyperoxia effects on the pulmonary surfactant system in wild-type and iNOS knockout mice. Eur Respir J 2002;20:177–82.
19. Guo FH, Uetani K, Haque SJ, et al. Interferon-γ and interleukin-4 stimulate prolonged expression of inducible nitric oxide synthase in human airway epithelium through synthesis of soluble mediators. J Clin Invest 1997;100:829–38.
20. Haque SJ, Williams BR. Signal transduction in the interferon system. Semin Oncol 1998;21(1 Suppl 1):14–22.
21. Hill CS, Treisman R. Transcriptional regulation by extracellular signals: mechanisms and specificity. Cell 1995; 80:199–211.
22. Guo FH, Comhair SAA, Zheng S, et al. Molecular mechanisms of increased nitric oxide (NO) in asthma: evidence for transcriptional and post-translational regulation of NO synthesis. J Immunol 2000;164:5970–80.
23. Alam MS, Akaike T, Okamoto T, et al. Role of nitric oxide in host defense in murine salmonellosis as a function of its antibacterial and antiapoptosis activities. Infect Immunol 2002; 70:3130–42.
24. Belvisi MG, Stretton D, Barnes PJ. Nitric oxide as an endogenous modulator of cholinergic neurotransmission in guinea-pig airways. Eur J Pharmacol 1991;198:219–21.
25. Ali S, Metzger WJ, Olanrewaju HA, Mustafa SJ. Adenosine receptor-mediated relaxation of rabbit airway smooth muscle: a role for nitric oxide. Am J Physiol 1997;273(2 Pt 1):L581–7.
26. Tamaoki J, Nakata J, Kawatani K, et al. Ginsenoside-induced relaxation of human bronchial smooth muscles via release of nitric oxide. Br J Pharmacol 2000;130:1859–64.
27. Roozendaal R, Kauffman HF, Dijkhuis AJ, et al. Interaction between nitric oxide and subsets of human T lymphocytes with differences in glutathione metabolism. Immunology 2002;107:334–9.
28. Saleh D, Ernst P, Lim S, et al. Increased formation of the potent oxidant peroxynitrite in the airways of asthmatic patients is associated with induction of nitric oxide synthase: effect of inhaled glucocorticoid. FASEB J 1998;12:929–37.
29. Ichinose M, Sugiura H, Yamagata S, et al. Increase in reactive nitrogen species production in chronic obstructive pulmonary disease airways. Am J Respir Crit Care Med 2000; 162(2 Pt 1):701–6.
30. Morrisey BM, Schilling K, Weil JV, et al. Nitric oxide and protein nitration in the cystic fibrosis airway. Arch Biochem Biophys 2002;406:33–9.
31. Gow AJ, Duran D, Malcom S, Ischiropoulos H. Effects of peroxynitrite-induced protein modifications on tyrosine phosphorylation and degradation. FEBS Lett 1996;385: 63–6.
32. MacMillan-Crow LA, Greendorfer JS, Vickers SM, Thompson JA. Tyrosine nitration of c-SRC tyrosine kinase in human pancreatic ductal adenocarcinoma. Arch Biochem Biophys 2000;377:350–6.
33. Klotz LO, Schroeder P, Sies H. Peroxynitrite-signaling: receptor tyrosine kinases and activation of stress-responsive pathways. Free Radic Biol Med 2002;33:737–43.
34. Iijima H, Duguet A, Eum SY, et al. Nitric oxide and protein nitration are eosinophil dependent in allergen-induced mice. Am J Respir Crit Care Med 2001;163:1233–40.
35. Duguet A, Iijima H, Eum SY, et al. Eosinophil peroxidase mediates protein nitration in allergic airway inflammation in mice. Am J Respir Crit Care Med 2001;164:1119–26.
36. Bernardes JF, Tewfik M, Shan J, et al. Protein nitration in chronic sinusitis and human nasal polyposis: role of eosinophils. Am J Respir Crit Care Med 2002;165:A324.
37. Gaston B. Nitric oxide and thiol groups. Biochim Biophys Acta 1999;1411:323–33.
38. Rosenberg PA, Li Y, Ali S, et al. Intracellular redox state determines whether nitric oxide is toxic or protective to rat oligodendrocytes in culture. J Neurochem 1999;73:476–94.
39. Park SW, Li J, Loh HH, Wei LN. A novel signaling pathway of nitric oxide on transcriptional regulation of mouse kappa opioid receptor gene. J Neurosci 2002;22:7941–7.
40. Govindaraju K, Iijima H, Eidelman DH. Nitrosothiols exist mostly as nitrosoproteins in rodent airway lining liquid and are increased following allergic challenge. Am J Respir Crit Care Med 2002;165:A210.
41. Feder LS, Stelts D, Chapman RW, et al. Role of nitric oxide on eosinophilic lung inflammation in allergic mice. Am J Respir Cell Mol Biol 1997;17:436–42.
42. Xiong Y, Karupiah G, Hogan SP, et al. Inhibition of allergic airway inflammation in mice lacking nitric oxide synthase 2. J Immunol 1999;162:445–52.
43. Redington AE, Meng QH, Spingall DR, et al. Increased expression of inducible nitric oxide synthase and cyclo-oxygenase-2 in the airways epithelium of asthmatic subjects and regulation by corticosteroid treatment. Thorax 2001; 56:351–7.

44. Silkoff PE, Sylvester JT, Zamel N, Permutt S. Airway nitric oxide diffusion in asthma: role in pulmonary function and bronchial responsiveness. Am J Respir Crit Care Med 2000; 161:1218–28.
45. Kuo HP, Liu S, Barnes PJ. The effect of endogenous nitric oxide on neurogenic plasma exudation in guinea-pig airways. Eur J Pharmacol 1992;221:385–8.
46. Xiong Y, Karupiah G, Hogan SP, et al. Inhibition of allergic airway inflammation in mice lacking nitric oxide synthase 2. J Immunol 1999;162:445–52.
47. Hashimoto S, Kobayashi A, Kooguchi K, et al. Upregulation of two death pathways of perforin/granzyme and FasL/Fas in septic acute respiratory distress syndrome. Am J Respir Crit Care Med 2000;161:237–43.
48. Trifilieff A, Fujitani Y, Mentz F, et al. Inducible nitric oxide synthase inhibitors suppress airway inflammation in mice through down-regulation of chemokine expression. J Immunol 2000;165:1526–33.
49. Stirling RG, Kharitonov SA, Campbell D, et al. Increase in exhaled nitric oxide levels in patients with difficult asthma and correlation with symptoms and disease severity despite treatment with oral and inhaled corticosteroids. Thorax 1998;53:1030–4.
50. Sippel JM, Holden WE, Tilles SA, et al. Exhaled nitric oxide levels correlate with measures of disease control in asthma. J Allergy Clin Immunol 2000;106:645–50.
51. Gratziou G, Lignos M, Dassiou M, Roussos C. Influence of atopy on exhaled nitric oxide in patients with stable asthma and rhinitis. Eur Respir J 1999;14:897–901.
52. American Thoracic Society. Recommendations for standardized procedures for the on-line and off-line measurement of exhaled lower respiratory nitric oxide and nasal nitric oxide in adults and children—1999. Am J Respir Crit Care Med 1999;160:2104–17.
53. Papi A, Romagnoli M, Baraldo S, et al. Partial reversibility of airflow limitation and increased exhaled nitric oxide and sputum eosinophilia in chronic obstructive pulmonary disease. Am J Respir Crit Care Med 2000;162:1773–7.
54. Delen FM, Sippel JM, Osborne ML, et al. Increased exhaled nitric oxide in chronic bronchitis: comparison with asthma and COPD. Chest 2000;117:695–701.
55. Kelley TJ, Drumm ML. Inducible nitric oxide synthase expression is reduced in cystic fibrosis murine and human airway epithelial cells. J Clin Invest 1998;102:1200–7.
56. Kelley TJ, Elmer HL. In vivo alterations of IFN regulatory factor-1 and PIAS1 protein levels in cystic fibrosis epithelium. J Clin Invest 2000;106:403–10.
57. Horrath I, Lonkides S, Wodehouse T, et al. Comparison of exhaled and nasal nitric oxide and exhaled carbon monoxide levels in bronchiectatic patients with and without primary ciliary dyskinesia. Thorax 2003;58:68–72.
58. Tsang KW, Leung R, Fung PC, et al. Exhaled and sputum nitric oxide in bronchiectasis: correlation with clinical parameters. Chest 2002;121:88–94.
59. Thomas SR, Kharitonov SA, Scott SF, et al. Nasal and exhaled nitric oxide is reduced in adult patients with cystic fibrosis and does not correlate with cystic fibrosis genotype. Chest 2000;117:1085–9.
60. Jatakanon A, Lim S, Kharitonov SA, et al. Correlation between exhaled nitric oxide, sputum eosinophils, and methacholine responsiveness in patients with mild asthma. Thorax 1998; 53:91–5.
61. Berlyne GS, Parameswaran K, Kamada D, et al. A comparison of exhaled nitric oxide and induced sputum as markers of airway inflammation. J Allergy Clin Immunol 2000;106:638–44.
62. Paredi P, Loukides S, Ward S, et al. Exhalation flow and pressure-controlled reservoir collection of exhaled nitric oxide for remote and delayed analysis. Thorax 1998;53:775–9.
63. Jobsis Q, Schellekens SL, Kroesbergen A, et al. Sampling of exhaled nitric oxide in children: end-expiratory plateau, balloon and tidal breathing methods compared. Eur Respir J 1999;13:1406–10.
64. Silkoff PE, Stevens A, Pak J, et al. A method for the standardized offline collection of exhaled nitric oxide. Chest 1999; 116:754–9.
65. Rutgers SR, Meijer RJ, Kerstjens HA, et al. Nitric oxide measured with single-breath and tidal-breathing methods in asthma and COPD. Eur Respir J 1998;12:816–19.
66. Sartori O, Allemann Y, Trueb L, et al. Exaggerated pulmonary hypertension is not sufficient to trigger high-altitude pulmonary oedema in humans. Schweiz Med Wochenschr 2000;130:385–9.
67. Nunes H, Lebrec D, Mazmanian M, et al. Role of nitric oxide in hepatopulmonary syndrome in cirrhotic rats. Am J Respi Crit Care Med 2001;164:879–85.
68. Mora BN, Boasquovisque CH, Uy G, et al. Exhaled nitric oxide correlates with experimental lung transplant rejection. Ann Thorac Surg 2000;69:210–15.
69. Gabbay E, Walters EH, Orsida B, et al. Post-lung transplant bronchiolitis obliterans syndrome (BOS) is characterized by increased exhaled nitric oxide levels and epithelial inducible nitric oxide synthase. Am J Respir Crit Care Med 2000;162:2182–7.
70. Marshall HE, Stamler JS. NO waiting to exhale in asthma. Am J Respir Crit Care Med 2000;161(3 Pt 1):685–7.
71. Hunt JF, Fang K, Malik R, et al. Endogenous airway acidification. Implications for asthma pathophysiology. Am J Respir Crit Care Med 2000;161(3 Pt 1):694–9.
72. Hanazawa T, Kharitonov SA, Barnes PJ. Increased nitrotyrosine in exhaled breath condensate of patients with asthma. Am J Respir Crit Care Med 2000;162(4 Pt 1):1273–6.
73. Ho LP, Innes JA, Greening AP. Nitrite levels in breath condensate of patients with cystic fibrosis is elevated in contrast to exhaled nitric oxide. Thorax 1998;53:680–4.
74. Kostikas K, Papatheodorou G, Ganas K, et al. pH in expired breath condensate of patients with inflammatory airway diseases. Am J Respir Crit Care Med 2002;165:1364–70.
75. Rossaint R, Falke KJ, Lopez F, et al. Inhaled nitric oxide for adult respiratory distress syndrome. N Engl J Med 1993;328:399–405.
76. Klinger JR. Inhaled nitric oxide in ARDS. Crit Care Clin 2002;18:45–68.
77. Sitbon O, Humbert M, Simonneau F. Primary pulmonary hypertension: current therapy. Prog Cardiovasc Dis 2002;45:115–28.
78. Ekroos H, Tuomien J, Sovijarvi AR. Exhaled nitric oxide and its long-term variation in healthy non-smoking subjects. Clin Physiol 2000;20:434–9.
79. Rolla G, Colagrande P, Scappaticci E, et al. Exhaled nitric oxide in systemic sclerosis: relationship with lung involvement and pulmonary hypertension. J Rheumatol 2000;27:1693–8.

CHAPTER 41

VIRAL INFECTIONS AND AIRWAY RESPONSIVENESS

Paolo Renzi

Viral infections and airway hyperresponsiveness (AHR) in atopic asthmatic individuals are independently associated with complex sequences of immunologic events. When they co-occur, viral infections and atopic asthma can dramatically influence the progression and severity of one another, often in unpredictable ways. Three overlapping classes of interaction are currently the focus of intensive research:

1. The effect of viral infections on AHR in asthmatic individuals
2. The potential for infection by certain viruses to protect against the development of asthma and allergies
3. The potential for other, mainly respiratory, viruses to trigger or even induce the development of asthma

In patients with existing asthma, respiratory infections often precipitate acute episodes of wheezing and airway obstruction.[1,2] There have been investigations on the extent to which viruses are responsible for asthma exacerbations and the impact of asthma on the course of viral infections.

An intriguing hypothesis, supported by some epidemiologic studies (but not others), is that exposure to certain pathogens during early childhood may steer the development of the immune system away from a pattern of responses that mediate allergic reactions such as asthma.[3] Recent evidence for and against this "hygiene hypothesis" is described.

Conversely, some viruses have been implicated as precipitating—not protecting against—the development of AHR. In most children, virus-induced wheezing is self-limiting and has no long-term consequences, but in others, virus-induced wheezing is associated with asthma development and allergic sensitization.[4] Respiratory syncytial virus (RSV) is a prime suspect in this regard. It remains controversial whether viral infection in infancy induces atopic asthma or merely triggers asthma development in children with a genetic predisposition to atopy.

Describing, interpreting, and managing the interactions between viruses and asthma or other allergic diseases require an understanding of underlying immunologic processes; this understanding remains only partially complete. The implications for treatment of current knowledge about these processes and interactions are discussed.

ROLE OF VIRAL INFECTIONS IN ASTHMA EXACERBATIONS

Incidence

The capacity of viral infections to trigger exacerbations in patients with asthma is well established. Most lower respiratory tract illnesses accompanied by wheezing in the first years of life are caused by viruses,[5] and viral infection coincides with 80 to 85% of exacerbations in asthmatic individuals 9 to 11 years of age.[6] Predictably, respiratory viruses are the main culprits. In a study in which PCR was used to detect viruses in nasal aspirates from children 3 months to 14 years of age who were hospitalized for severe asthma attacks, rhinovirus was found in 46.9% and RSV in 21.2% of cases.[7] Among adult asthmatic individuals, viral upper respiratory infections are associated with half of all asthma episodes.[8]

Role of Inflammation

Although patients with atopic asthma appear to be no more likely to contract colds than are healthy people, in response to rhinoviral infection they experience more frequent, more severe, and prolonged lower respiratory tract involvement.[9] This relationship is somewhat surprising, given that rhinovirus has traditionally been considered a pathogen of the upper airways.[10] In fact, in both asthmatic and healthy subjects, during active rhinoviral infection there is an increase in the numbers of lymphocytes and eosinophils in bronchial mucosa.[11] This sets the stage in asthmatic subjects for inflammation to progress from the upper respiratory tract to the lower airways, leading to symptom exacerbation.

The greater impact of respiratory viral infections in atopic individuals appears to be due to dysregulation of the immune system.[6] In response to infection, type 1 T-helper (Th1) cells predominantly produce cytokines associated with cell-mediated immunity, including interleukin-12 (IL-12) and interferon-γ (IFN-γ). On the other hand, type 2 T-helper (Th2) cells synthesize cytokines associated with humoral immunity, including IL-4, IL-5, IL-10, and IL-13, which are implicated in the promotion of allergic inflammation. Individuals with asthma and allergic diseases are disposed toward a Th2-type response. Individuals

who develop strong Th2 responses may not be able to clear viruses efficiently, leading to persistent infection and thus exacerbation of the inflammation associated with asthma.[12]

Among people with asthma or allergic rhinitis, those who produce higher levels of IFN-γ and lower levels of IL-5 tend to have fewer symptoms during the peak of a cold and a shorter duration of illness than individuals who show a more extreme Th2-type response.[6] In addition, rhinoviral infection in subjects who have asthma or allergic rhinitis leads to neutrophilia in blood and nasal secretions and increased levels of granulocyte colony-stimulating factor and IL-8, suggesting that these proinflammatory cytokines also contribute to rhinovirus-induced inflammation in atopic individuals (Figure 41-1).[13]

During virus-induced asthma exacerbations in children, nasal secretions show increased levels of the toxic eosinophil granule product major basic protein, as well as the chemokines regulated upon activation, normal T cell–expressed and secreted (RANTES), and macrophage inflammatory protein-1α.[14] These and other eosinophil chemoattractants have been shown to promote AHR in mice.[15] Activation of eosinophils by RSV has been seen in vitro, leading to elevated superoxide production and increased leukotriene C_4 release.[4]

The pathways by which respiratory viruses can lead to inappropriate immune responses in atopic individuals are becoming better understood. For example, rhinovirus infection of respiratory epithelial cells induces elevated expression of intercellular adhesion molecule-1 (ICAM-1), a cell surface glycoprotein that binds to ligands on eosinophils and $CD4^+$ and $CD8^+$ T cells and that may play a central role in the infiltration of these inflammatory cells into the lower airways of asthmatic individuals.[16]

Wheezing in asthmatic individuals may also be exacerbated by direct binding of rhinovirus to the ICAM-1 receptor, which induces enhanced expression and activation of G_i protein in the airway smooth muscle.[17] A recent study has demonstrated that even UV-irradiated rhinovirus, which is unable to replicate within cells, is still able to bind to ICAM-1 and thereby elicit airway smooth muscle hyperresponsiveness.[18]

Other Mechanisms for Viral-Induced Asthma Exacerbations

Other noninflammatory mechanisms might also contribute to the wheezing associated with viral respiratory tract infection. In rodents, RSV infection of respiratory epithelium leads to decreased production of nitric oxide, a bronchodilator agonist of the nonadrenergic, noncholinergic inhibitory system, resulting in AHR.[4] The generality of this result across respiratory viruses and its applicability to humans are complicated by the finding that exhaled nitric oxide levels in humans with asthma increase following rhinoviral infection, possibly limiting asthma exacerbations.[19]

Enhanced stimulation of sensory C-fibers during infection may provoke release of substance P and neurokinin-A, which are both agonists of the nonadrenergic, noncholinergic activating system, inducing a brainstem reflex leading to bronchoconstriction. Neuropeptides released by sensory C-fibers can cause increased leukotriene synthesis, release of mast cell mediators, and increased mucous secretion.[4] However, the role of sensory C-fibers in virus-associated asthma exacerbations in humans remains unclear.

Following viral infection, an inflammatory immune response and AHR linger in atopic individuals. In a guinea pig model of AHR, RSV infection causes hyperresponsiveness that lasts for at least 5 weeks, and viral antigen remains detectable during this period.[20] In allergic human patients, nasal eosinophil influx following common cold infection is prolonged in comparison with nonallergic patients.[14] Eosinophilia is also prolonged in asthmatic individuals in comparison with nonasthmatic individuals,[11] as is enhancement of airway narrowing in response to methacholine, a bronchoconstrictor stimulus.[21]

Viruses may persist in the airways of asthmatic individuals even after clinical resolution of symptoms. In a comparison of 50 asthmatic but currently asymptomatic children with 20 healthy control children, nasopharyngeal swabs revealed the presence of rhinovirus RNA and coronavirus RNA in 32.4% and 2.7% of asthmatic children, respectively, but in none of the control children.[22] Adenovirus DNA was found in 78.4% of asthmatic children but in only 1 (5%) of the 20 control children.[22]

Viral persistence in patients with asthma may have important consequences for the treatment of acute asthma episodes. In a study of 34 asthmatic children who responded poorly to standard corticosteroid and bronchodilator therapy, 31 (94%) tested positive for adenovirus.[23] A possible mechanism underlying this observation is suggested by the finding that in the guinea pig, latent adenoviral infection causes the eosinophilic component of allergen-induced lung inflammation to become steroid resistant.[24]

Taken together, these results highlight the value of protecting against respiratory viral infections in atopic individuals. For example, asthma management may benefit from wider application of influenza vaccination; a recent study showed that, after adjustment for asthma severity, the incidence of asthma exacerbations among patients 1 to 6 years of age was reduced by up to 41% following influenza vaccination in comparison with before vaccination.[25] Furthermore, in a 1-year study of 57 asthmatic individuals, exacerbation of asthma symptoms by colds was positively correlated with levels of sulfur dioxide and nitrogen oxide,[26] providing another reason to adhere to asthma guidelines that recommend reducing exposure to air pollutants.

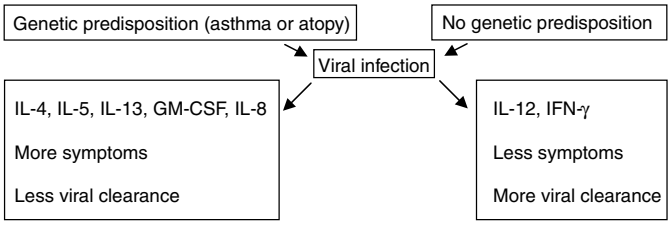

FIGURE 41-1 Immune response to viral infection in patients with allergic rhinitis or asthma. GM-CSF = granulocyte–macrophage colony-stimulating factor; IFN-γ = interferon-γ; IL = interleukin.

CAN VIRAL INFECTIONS PROTECT AGAINST THE DEVELOPMENT OF ASTHMA?

Hygiene Hypothesis

Early allergic sensitization is linked to delayed maturation of normal immune responses.[5] Although, as seen above, certain viruses provoke asthma exacerbations, early exposure of the immune system to other viruses and bacteria has been suggested to prevent the development of atopy. However, Strachan's hygiene hypothesis, which originally proposed that early childhood infections might prevent allergic disease later in life, has received mixed support in the case of asthma.[3]

Results Suggesting a Role for Viral Infection in Protecting Against the Development of Asthma

In a study of Italian air force cadets, subjects with no antibodies against the foodborne or orofecal pathogens *Toxoplasma gondii*, *Helicobacter pylori*, and hepatitis A virus were 2.7 times as likely to be highly atopic as were subjects with antibodies to two or three of these microbes.[27] However, this study showed no relationship between risk of atopy and exposure to six other pathogens, including measles, that are transmitted by other routes. Indeed, a cross-sectional study in Finland that included more than half a million subjects showed a positive, not negative, correlation between natural measles infection and atopy; subjects who had previously had measles were 1.67 times as likely to have asthma as were those who had not.[28]

The recently published results of a longitudinal birth cohort study of 1,314 German children suggest that repeated viral (but not bacterial, fungal, or gastrointestinal) infections in early childhood, other than lower respiratory tract infections (LRTIs), may reduce the risk of developing asthma by the age of 7 years.[29] Recurrent runny nose in the first year of life and herpes-type viral infections were associated with half the risk of being diagnosed with asthma, current wheeze, or bronchial hyperresponsiveness at age 7 years.[29] These results support the hypothesis that repeated viral infections other than LRTIs early in life may stimulate the immature immune system to adopt the Th1 phenotype.[29]

These findings imply that vaccinating against common childhood diseases may have unintended negative consequences for asthma incidence. For example, in a survey of 1,265 children born in New Zealand in 1977, the 23 who received no immunizations against diphtheria, pertussis, tetanus, or polio had no recorded asthma or medical consultation for allergic illness by 10 years of age. In contrast, of the remaining immunized children, 23% experienced asthma attacks and 30% saw a doctor because of other allergic illnesses.[30] Clearly, however, it would be premature to discontinue such immunization programs on the basis of the equivocal data gathered thus far.

Timing of Exposure May Be Crucial

It is noteworthy that the same pathogen might exert opposite effects on AHR, depending on the timing of exposure and atopic status of the exposed individual. An example is posed by endotoxin, a cell wall component of gram-negative bacteria. In children, endotoxin exposure is inversely related to the risk for atopic asthma, hay fever, allergic sensitization, and atopic wheeze.[31] Production by leukocytes of the cytokines tumor necrosis factor-α (TNF-α), IFN-γ, IL-10, and IL-12 is inversely related to the endotoxin level in children's bedding, indicating that during childhood, immune responses to natural allergens are decreased by exposure to microbial products.[31] However, in older patients with existing asthma, endotoxin promotes release of cytokines that lead to inflammation, including IL-1, TNF-α, and IL-8. In asthmatic individuals, therefore, airborne endotoxin increases AHR, increases susceptibility to rhinoviral infection, and can cause chronic bronchitis, emphysema, and irreversible airway obstruction.[32]

CAN VIRAL INFECTIONS INDUCE ASTHMA?

Potential Causative Viruses

Far from exerting a protective effect against the development of AHR, certain viruses may be intimately involved in precipitating atopic asthma. Parainfluenza viruses, coronavirus, adenovirus, influenza virus, and enteroviruses have all been suggested not only to trigger exacerbations but also to contribute to the development of allergic asthma.[4] A link may also exist for Epstein–Barr virus as antibody titers are higher in atopic individuals than in nonatopic controls.[33]

This potential link is strongest, however, for RSV, which infects 70% of children during their first year and essentially 100% of children by 3 years of age (Figure 41-2). Of those infected, 20 to 30% will develop bronchiolitis, a disease of the lower respiratory tract.[33] In tissue biopsy specimens from children with RSV bronchiolitis, mucous membranes are inflamed, and cellular debris and fibrin plug bronchioles, causing atelectasis and hyperinflation. Premature infants are more likely to be infected with RSV than infants born at term because they have incomplete passage of maternal IgG in utero. They also have more severe RSV infection because of their small airways, which are more readily obstructed by edema and necrotic debris.[34]

Severe bronchiolitis is accompanied by wheezing and prolonged airway obstruction and is strongly correlated with the development of childhood asthma and AHR, which may persist for many years.[33,35] Children hospitalized during infancy for RSV bronchiolitis are nearly 13 times as likely to have asthma at 7 years of age as are children who were not.[36] The sequelae of RSV bronchiolitis over a 2- to 13-year follow-up period were investigated in a review of controlled studies between 1978 and 2000.[35] In all nine qualifying studies, postbronchiolitis subjects had a significantly higher incidence of bronchial obstructive symptoms, diminished lung function, or increased bronchial reactivity to exercise or histamine challenge than did control subjects. The link is strongest for bronchiolitis cases severe enough to require hospitalization and remains after correction for family history of asthma and/or atopy.

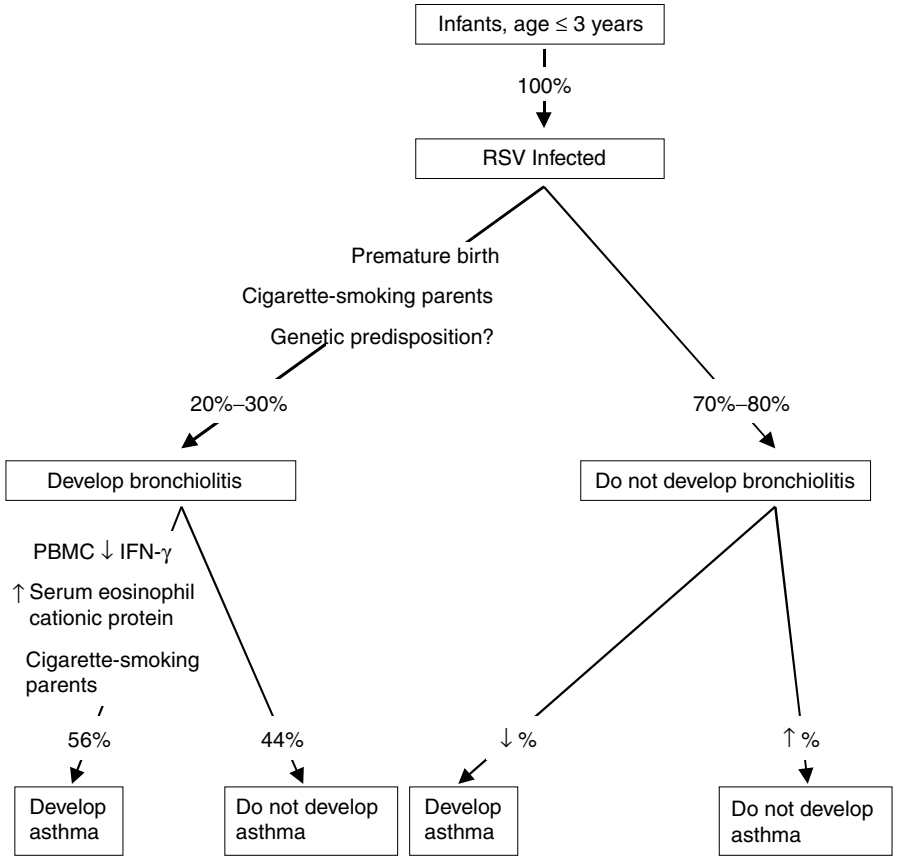

FIGURE 41-2 Link between RSV infection and the development of childhood asthma. Italics indicate risk factors. PBMC = peripheral blood mononuclear cell.[33,34,40]

Mechanism of Action: Predisposition and/or Skewing to a Th2 Response?

The inflammatory response in bronchiolitis includes high numbers of submucosal lymphocytes and epithelial eosinophils in the lower airways.[4] Levels of soluble IL-2 receptor (sCD25) remain elevated for as long as 150 days after bronchiolitis, although they are not as high as during the acute stage. This indicates a persistent inflammatory process after bronchiolitis, contrasting with the rapid decline in sCD25 levels after acute measles or dengue fever.[37] Patients who have suffered from RSV bronchiolitis during infancy show higher numbers of RSV-specific IL-4–producing cells 7.5 years later than do patients who experienced only mild RSV infection.[12] This suggests either that RSV bronchiolitis causes proliferation of RSV-specific Th2 memory cells or that the symptoms of RSV infection are simply more severe in individuals predisposed to a Th2 response.[12]

Strong evidence exists of a link between abnormal cellular immunity and wheezing following bronchiolitis. Five months after acute bronchiolitis, infants show high counts of $CD4^+$, $CD25^+$, and $CD23^+$ cells, suggesting activation of cellular immunity.[38] Among those infants who wheeze the most, production of IL-4 from peripheral blood lymphocytes in response to dust mite antigen is elevated 5 months later in comparison with those who wheeze less. There is also a positive correlation between the number of days of wheezing and blood eosinophil count (Figure 41-3). Predisposition toward a greater Th2 response in infants who suffer severe wheezing due to bronchiolitis is supported by the finding that during bronchiolitis their lymphocytes produce less INF-γ and more IL-4 upon stimulation with IL-2.[38] Furthermore, there is a significant inverse correlation between IFN-γ production during bronchiolitis and pulmonary function at 4.9 months, as well as a significant positive correlation between pulmonary function at 4.9 months and a diagnosis of asthma 2 years later.[39] Similarly, among infants with RSV bronchiolitis, those who have higher serum eosinophil cationic protein levels during the initial infection are at increased risk for developing persistent wheezing, detected at 5-year follow-up.[40] Infants with serum eosinophil cationic protein levels of at least 8 μg/L are almost 10 times as likely to develop persistent wheezing as are infants with levels lower than 8 μg/L.

Although clinical studies have not yet shown whether lower IFN-γ production is present before bronchiolitis or is induced by bronchiolitis,[39] epidemiologic studies suggest a genetic predisposition for asthma following viral infection. In the German birth cohort study discussed above,[29] the number of LRTIs with wheezing in the first 3 years of life was positively associated with a diagnosis of asthma and current wheeze and bronchial hyperreactivity at age 7 years. The results of the same study, however, suggest that children predisposed to asthma might simply be more likely to develop symptoms of the lower respiratory tract. The

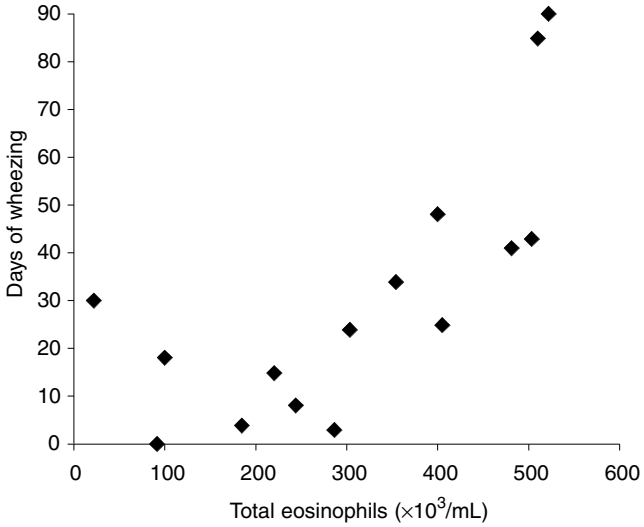

FIGURE 41-3 Correlation between blood eosinophil level and number of days of wheezing in 15 infants during the 90-day period ending 5 months after hospitalization for bronchiolitis. Adapted from Renzi PM et al.[38]

frequency of repeated LRTIs in this cohort was higher in children with a family history of atopy than in those with no atopic family member.[29] Similar results were obtained by Angelakou and colleagues, who reported that a positive family history of atopy was associated with the development of severe wheezing.[41]

Viral Infections and Allergic Sensitization

In a birth cohort stratified by the type of virus detected during respiratory tract infections before 3 years of age, children with RSV infection had an increased risk for wheezing at 6 years, but the risk diminished with age and was not significant by 13 years.[42] The prevalence of allergic sensitization at any age did not differ between children with or without respiratory tract infections, suggesting that RSV infection did not lead to allergic sensitization but rather that RSV infection and atopy were independent risk factors for asthma development.[42]

In the absence of large, prospective, controlled trials in which infants are experimentally infected with RSV to identify a causal connection with atopy, whether or not RSV infection induces allergic sensitization in humans remains unclear. Of seven epidemiologic studies of RSV bronchiolitis serious enough to require hospitalization, three showed an increased risk of sensitization, whereas four did not.[35] The balance of evidence suggests that mild RSV infection either does not increase the risk of sensitization or does so only within the first year of life.

RODENT MODELS OF VIRAL INFECTION AND AHR

Role for a Combination of Viral Infection and Allergic Sensitization

Because of the ethical difficulties inherent in manipulating the sequence of viral infection and allergic sensitization in human infants, much of our current understanding derives from animal models, in which infection, allergic sensitization, and components of the immune response can be perturbed. Recently, a mouse model for the exploration of the role of viral infection (particularly by RSV) in respiratory illness has been developed, in which the respiratory function of infected BALB/c mice is measured in a plethysmograph.[43] These mice show heightened airway responsiveness to methacholine challenge.[43] RSV or influenza A virus infection alone is insufficient to cause chronic AHR in mice.[44,45] Sensitization to ovalbumin (OVA) without RSV infection leads to AHR that resolves shortly after discontinuation of OVA aerosol administration, but RSV infection during OVA aerosol treatment leads to AHR that lasts for more than 2 weeks following the infection.[44] The combination of influenza A infection and OVA sensitization also increases AHR in mice.[45]

In mice, inhalation of nebulized OVA 4 to 10 days after infection with either RSV or influenza A virus induced specific serum antibodies, and intradermal skin challenge with OVA on day 18 caused acute systemic illness and collapse. By contrast, in uninfected mice, inhalation of OVA did not induce production of specific serum antibodies, and skin challenge on day 18 elicited no response.[37] This suggests that infection with respiratory viruses affects lung permeability and enhances allergy development.

The outcome of the interaction between viral exposure and allergic sensitization depends upon the timing of these events. In a mouse model of asthma, intranasal administration of OVA led to $CD4^+$ T-cell tolerance to OVA. However, infection with influenza A virus 3 days before OVA administration disrupted the normal development of immunologic tolerance to the allergen, leading to the development of AHR and the production of IgE, IL-4, IL-5, IL-13, and IFN-γ upon subsequent OVA challenge.[46] On the other hand, when OVA was administered 15 or 30 days after influenza A virus infection, subsequent OVA challenge caused a predominantly IFN-γ response, protecting against the development of AHR.[46]

Roles of Cells and Cytokines

The mouse RSV model has clarified the relative roles of various immunologic components in the development of AHR following allergic sensitization and infection. For example, discrimination of the roles of different T cells in RSV-induced lung eosinophilia and AHR was facilitated by transplanting CD4 or CD8 T cells from mice that had been infected with RSV into naive mice that were subsequently sensitized to OVA. When the mice were challenged with methacholine, AHR developed in the naive mice that had received CD8 but not CD4 T-cell transplants.[47]

The mouse model has been particularly useful for dissecting the effects of various cytokines and chemokines. In IL-10–deficient mice, AHR does not develop in response to inhaled methacholine following OVA sensitization and challenge, as it would in IL-10–competent mice. AHR does develop in IL-10–deficient mice, however, if they are infected with RSV following OVA sensitization but before OVA challenge.[48] Epithelial cells produce more IL-11 following infection by RSV, parainfluenza virus, and rhinovirus.[49]

Although the role of IL-11 in viral infection is not yet clear, administration of IL-11 in the lungs of mice leads to increased airway responsiveness to methacholine challenge.[4]

In mice that show only mild disease in response to RSV infection, IL-12 titer quadruples.[50] Treatment of RSV-infected mice with anti–IL-12 leads to increased AHR, mucus production, and eosinophilia. When mice with a deficiency in the Stat-4 intracellular signal transducer are infected with RSV, they show similarly severe disease. As IL-12 activation is Stat-4 dependent, these results indicate that IL-12 plays an important role in clearing RSV infection and protecting against inappropriate inflammatory responses.[50]

Conversely, in this model there is an increase in IL-13 level as the AHR progresses, and treatment of mice with anti–IL-13 during RSV infection decreases allergen-induced AHR.[51,52] Neutralization of IL-13 is followed by an increase in IL-12 production in the lungs. Stat-6–deficient mice show a decreased response, similar to that seen with anti–IL-13 treatment. In mice sensitized to cockroach allergen, production of IL-13 during a previous RSV infection exacerbates asthma-like symptoms produced by later exposure to cockroach allergen. These results imply that increased production of IL-13 could interfere with an effective antiviral response and lead to chronic RSV-induced AHR.[51]

Experiments in rodents have highlighted the dominating influence of IL-5 on the eosinophilic component of inflammation following RSV infection and the subsequent development of AHR to methacholine challenge.[4] RSV infection leads to airway eosinophilia and AHR in response to methacholine challenge in IL-4–deficient and IFN-γ–deficient mice but not in IL-5–deficient mice, indicating that IL-5, but not IFN-γ or IL-4, is necessary for infiltration of eosinophils into the lung and the development of AHR.[53] The timing of these events, however, is critical; mice treated with anti–IL-5 during acute RSV infection but not during later sensitization to OVA show reduced AHR and lung eosinophilia in response to methacholine challenge.[54] Administration of IL-5 to both IL-5–deficient and IL-4–deficient mice during RSV infection is sufficient to restore strong responses to allergen. IL-5 administration only during sensitization restores responses in IL-4–deficient mice but not in IL-5–deficient mice.[54]

In the guinea pig, virus-induced AHR also depends on IL-5, but eosinophil influx does not.[4] Cationic proteins released by eosinophils bind to presynaptic M2 muscarinic receptors on postganglionic parasympathetic airway nerves, blocking an inhibitory feedback mechanism and resulting in increased acetylcholine release and airway muscle tone and reactivity. This mechanism occurs in allergic sensitization and following acute viral infection. Parainfluenza virus neuraminidase can bind directly to M2 muscarinic receptors and may trigger the mechanism just described, even in the absence of eosinophils.[4] Viral neuraminidase may deglycosylate the M2 receptor, decreasing its affinity for acetylcholine, whereas viruses and IFN-γ decrease M2 receptor gene expression.[55]

In humans with asthma, eosinophil numbers in airway mucosa are often elevated even during asymptomatic periods. Experiments in mice show that although IL-5 and the chemokine eotaxin promote airway eosinophilia, they do not themselves cause eosinophil degranulation and AHR.[56] Allergen challenge in the presence of eosinophilia results in degranulation and AHR. The mouse data suggest a pathway in asthmatic individuals whereby eosinophils that have infiltrated into airways in response to IL-5 and eotaxin can become activated by allergen provocation, leading to AHR.[56]

IMPLICATIONS FOR ASTHMA TREATMENT

Prevention

The results summarized here demonstrate the importance of considering viral infection and its sequelae for the effective management of asthma and other allergic diseases. These results also suggest possible preventive and treatment strategies for AHR with viral involvement. The strategies fall into two categories: prevention of viral infections or use of antiviral agents to treat infections in their early stages and inhibiting proinflammatory immune responses to viral infection.

Because certain viruses are known to provoke AHR and may even induce or at least trigger the development of atopic asthma, avoiding infection by these pathogens holds out the promise of significantly reducing the medical burden of asthma. Both RSV and parainfluenza virus are spread by direct contact with infected secretions or contaminated objects, highlighting the importance of hand washing to decrease transmission.[34,57] Adoption in hospitals of stringent hygiene protocols, including cohorting of patients, staff, or medical equipment by patient RSV status, has been shown to significantly reduce nosocomial RSV infection rates.[34]

Unfortunately, there are few effective vaccines for the viruses chiefly implicated in asthma development and exacerbations. A notable exception is influenza; as noted above, asthmatic individuals immunized against influenza A virus experience significantly fewer exacerbations.[25] Furthermore, a prospective, randomized, double-blind study involving over 2,000 patients revealed that influenza vaccination itself does not exacerbate asthma symptoms and is safe in both children and adults with asthma.[58]

The apparently key role of RSV infection in the development of AHR argues strongly for effective vaccination against RSV. An intramuscular formalin-inactivated RSV vaccine was developed in the 1960s, but this did not protect against subsequent RSV infection. On the contrary, vaccinated infants had more severe disease in the next season,[34] with even more lower respiratory tract involvement than in natural RSV bronchiolitis and evidence of pneumonia.[33] Mice immunized with formalin-inactivated RSV vaccine showed increased Th2 cytokine production and AHR.[59] Although it does not offer full protection against re-infection either, live RSV vaccine administered parenterally does not lead to enhanced illness in subsequent RSV infection.[33] Mice immunized with live RSV, then sensitized with OVA, and later infected with RSV, showed no increase in airway response to methacholine challenge in comparison with control mice.[59]

Prophylaxis of RSV with intravenous RSV immunoglobulin (RSV-IVIG) is an alternative strategy that may reduce the risk for developing reactive airway disease in childhood. In a small study of children with chronic lung disease who had received RSV-IVIG 5 to 9 years earlier, pulmonary function was significantly better than in matched controls, and there was less atopy and a lower frequency of asthma attacks in the treated group.[60] This supports the hypothesis that RSV prophylaxis may have long-term benefit in reducing the risk of AHR.

Palivizumab, a neutralizing monoclonal antibody to RSV fusion protein, may be a better choice than RSV-IVIG. Palivizumab prophylaxis opposes the penetration of infectious particles into the lower respiratory tract epithelium, inhibiting up-regulation of the neurokinin-1 receptor gene and its associated inflammatory effects.[60] In the rat, palivizumab is twice as effective as RSV-IVIG at preventing the proinflammatory effects of substance P released from sensory nerves.[34] Prophylaxis with palivizumab prevents acute neurogenic inflammatory changes in the rat lower respiratory tract infected with RSV and protects against the development of long-term susceptibility to neurogenic-mediated inflammation after the infection.[60] Although it may be too expensive for widespread use, palivizumab for the prevention of severe infections is potentially cost-effective in infants with chronic lung disease.[34]

Therapy

A fundamental problem with using antiviral agents is that once infections are recognized, it is usually at a late stage in the illness, and many of these agents, such as neuramidase, are only effective if used early in the course of illness.[1] As prophylactic use of neuramidase can prevent about 80% of influenza cases, it may be effective to extend this approach to high-risk individuals for protection against rhinoviruses, which present too many serotypes for vaccination to be practical.[1] Antirhinoviral agents include soluble ICAM-1 and capsid-binding agents, and new compounds, such as inhibitors of rhinovirus 3C protease, are potential treatments.

An alternative strategy to reduce AHR due to viral infection is to target, during infection, specific signaling pathways, proinflammatory cytokines, and other mediators of inflammation. In mice treated with type 4 phosphodiesterase inhibitors during RSV infection, for example, AHR and eosinophil infiltration into the lung in response to methacholine challenge were reduced in comparison with RSV-infected control mice.[61] Anti–TNF-α treatment might also reduce the severity of RSV bronchiolitis associated with either an eosinophilic response or with activated $CD8^+$ T cells.[37]

Antiinflammatory therapy, already in widespread use, may be an effective treatment approach. Systemic glucocorticoids administered at the first sign of cold have been shown to reduce airway obstruction and risk of hospitalization for acute asthma exacerbations.[1] In a study in which budesonide was administered to asthmatic subjects 2 weeks prior to experimental rhinovirus 16 infection, AHR was improved and eosinophil levels were lowered prior to infection in comparison with controls who did not receive budesonide. The improvement persisted after rhinovirus infection, even though budesonide did not significantly affect the accumulation of T cells seen after rhinovirus infection in both groups.[62]

The utility of antiinflammatory agents against RSV is equivocal. Sixteen weeks of antiinflammatory therapy (budesonide or cromolyn sodium) given to 89 infants under 2 years of age hospitalized for RSV infection with wheezing had no effect on the occurrence of asthma 3 years later.[63] Conversely, in a study of 117 infants with a mean age of 2.6 months who were hospitalized for RSV bronchiolitis, prevalence of asthma at 2 years was inversely related to the duration of budesonide therapy: asthma developed in 37% of children who did not receive budesonide at initial hospitalization, in 18% of those who received 7 days of therapy, and in 12% of those who received 2 months of therapy.[64]

CONCLUSIONS

Epidemiologic data indicate that viral respiratory tract infection in infancy may cause transient asthma symptoms or may trigger the development of persistent asthma in children with a predisposition to atopy but does not directly induce allergic sensitization itself.[4] For medical management purposes, in either case, effective therapies to prevent or suppress infection by viruses linked to AHR are desirable. Treatment would also be desirable in asthma patients of all ages to reduce the high burden of virus-induced exacerbations. Whether certain pathogens may play a beneficial role in protecting against AHR remains unclear, and medical strategies for AHR based on the hygiene hypothesis would be premature.

ACKNOWLEDGMENT

This article was prepared with the assistance of BioMedCom Consultants Inc., Montreal, Canada.

REFERENCES

1. Gern JE, Busse WW. Relationship of viral infections to wheezing illnesses and asthma. Nat Rev Immunol 2002;2:132–8.
2. Grunberg K, Timmers MC, de Klerk EP, et al. Experimental rhinovirus 16 infection causes variable airway obstruction in subjects with atopic asthma. Am J Respir Crit Care Med 1999;160:1375–80.
3. Strachan DP. Family size, infection and atopy: the first decade of the "hygiene hypothesis." Thorax 2000;55 Suppl 1:S2–10.
4. Schwarze J, Gelfand EW. The role of viruses in development or exacerbation of atopic asthma. Clin Chest Med 2000; 21:279–87.
5. Martinez FD. Viruses and atopic sensitization in the first years of life. Am J Respir Crit Care Med 2000;162(3 Pt 2):S95–9.
6. Gern JE. Rhinovirus respiratory infections and asthma. Am J Med 2002;112 Suppl 6A:19S–27S.
7. Freymuth F, Vabret A, Brouard J, et al. Detection of viral, Chlamydia pneumoniae and Mycoplasma pneumoniae infections in exacerbations of asthma in children. J Clin Virol 1999;13:131–9.
8. Micillo E, Bianco A, D'Auria D, et al. Respiratory infections and asthma. Allergy 2000;55 Suppl 61:42-5.
9. Corne JM, Marshall C, Smith S, et al. Frequency, severity, and duration of rhinovirus infections in asthmatic and non-asthmatic individuals: a longitudinal cohort study. Lancet 2002;359:831–4.

10. Gern JE, Calhoun W, Swenson C, et al. Rhinovirus infection preferentially increases lower airway responsiveness in allergic subjects. Am J Respir Crit Care Med 1997;155:1872–6.
11. Fraenkel DJ, Bardin PG, Sanderson G, et al. Lower airways inflammation during rhinovirus colds in normal and in asthmatic subjects. Am J Respir Crit Care Med 1995;151(3 Pt 1):879–86.
12. Folkerts G, Walzl G, Openshaw PJ. Do common childhood infections 'teach' the immune system not to be allergic? Immunol Today 2000;21:118–20.
13. Gern JE, Vrtis R, Grindle KA, et al. Relationship of upper and lower airway cytokines to outcome of experimental rhinovirus infection. Am J Respir Crit Care Med 2000;162:2226–31.
14. van Benten IJ, KleinJan A, Neijens HJ, et al. Prolonged nasal eosinophilia in allergic patients after common cold. Allergy 2001;56:949–56.
15. Gerard C, Rollins BJ. Chemokines and disease. Nat Immunol 2001;2:108–15.
16. Papi A, Johnston SL. Rhinovirus infection induces expression of its own receptor intercellular adhesion molecule 1 (ICAM-1) via increased NF-kappaB-mediated transcription. J Biol Chem 1999;274:9707–20.
17. Hakonarson H, Maskeri N, Carter C, et al. Mechanism of rhinovirus-induced changes in airway smooth muscle responsiveness. J Clin Invest 1998;102:1732–41.
18. Grunstein MM, Hakonarson H, Whelan R, et al. Rhinovirus elicits proasthmatic changes in airway responsiveness independently of viral infection. J Allergy Clin Immunol 2001; 108:997–1004.
19. de Gouw HW, Grunberg K, Schot R, et al. Relationship between exhaled nitric oxide and airway hyperresponsiveness following experimental rhinovirus infection in asthmatic subjects. Eur Respir J 1998;11:126–32.
20. Riedel F, Oberdieck B, Streckert HJ, et al. Persistence of airway hyperresponsiveness and viral antigen following respiratory syncytial virus bronchiolitis in young guinea-pigs. Eur Respir J 1997;10:639–45.
21. Cheung D, Dick EC, Timmers MC, et al. Rhinovirus inhalation causes long-lasting excessive airway narrowing in response to methacholine in asthmatic subjects in vivo. Am J Respir Crit Care Med 1995;152(5 Pt 1):1490–6.
22. Marin J, Jeler-Kacar D, Levstek V, Macek V. Persistence of viruses in upper respiratory tract of children with asthma. J Infect 2000;41:69–72.
23. Macek V, Sorli J, Kopriva S, Marin J. Persistent adenoviral infection and chronic airway obstruction in children. Am J Respir Crit Care Med 1994;150:7–10.
24. Hogg JC. Role of latent viral infections in chronic obstructive pulmonary disease and asthma. Am J Respir Crit Care Med 2001;164(10 Pt 2):S71–5.
25. Kramarz P, Destefano F, Gargiullo PM, et al. Does influenza vaccination prevent asthma exacerbations in children? J Pediatr 2001;138:306–10.
26. Tarlo SM, Broder I, Corey P, et al. The role of symptomatic colds in asthma exacerbations: influence of outdoor allergens and air pollutants. J Allergy Clin Immunol 2001;108:52–8.
27. Matricardi PM, Rosmini F, Riondino S, et al. Exposure to foodborne and orofecal microbes versus airborne viruses in relation to atopy and allergic asthma: epidemiological study. BMJ 2000;320:412–7.
28. Paunio M, Heinonen OP, Virtanen M, et al. Measles history and atopic diseases: a population-based cross-sectional study. JAMA 2000;283:343–6.
29. Illi S, von Mutius E, Lau S, et al. Early childhood infectious diseases and the development of asthma up to school age: a birth cohort study. BMJ 2001;322:390–5.
30. Kemp T, Pearce N, Fitzharris P, et al. Is infant immunization a risk factor for childhood asthma or allergy? Epidemiology 1997;8:678–80.
31. Braun-Fahrländer C, Riedler J, Herz U, et al. Environmental exposure to endotoxin and its relation to asthma in school-age children. N Engl J Med 2002;347:869–77.
32. Reed CE, Milton DK. Endotoxin-stimulated innate immunity: a contributing factor for asthma. J Allergy Clin Immunol 2001;108:157–66.
33. Graham BS, Johnson TR, Peebles RS. Immune-mediated disease pathogenesis in respiratory syncytial virus infection. Immunopharmacology 2000;48:237–47.
34. Greenough A. Respiratory syncytial virus infection: clinical features, management, and prophylaxis. Curr Opin Pulm Med 2002;8:214–7.
35. Sigurs N. Epidemiologic and clinical evidence of a respiratory syncytial virus-reactive airway disease link. Am J Respir Crit Care Med 2001;163(3 Pt 2):S2–6.
36. Sigurs N, Bjarnason R, Sigurbergsson F, Kjellman B. Respiratory syncytial virus bronchiolitis in infancy is an important risk factor for asthma and allergy at age 7. Am J Respir Crit Care Med 2000;161:1501–7.
37. Openshaw PJ. Potential mechanisms causing delayed effects of respiratory syncytial virus infection. Am J Respir Crit Care Med 2001;163(3 Pt 2):S10–3.
38. Renzi PM, Turgeon JP, Yang JP, et al. Cellular immunity is activated and a TH-2 response is associated with early wheezing in infants after bronchiolitis. J Pediatr 1997;130: 584–93.
39. Renzi PM, Turgeon JP, Marcotte JE, et al. Reduced interferon-gamma production in infants with bronchiolitis and asthma. Am J Respir Crit Care Med 1999;159(5 Pt 1):1417–22.
40. Pifferi M, Ragazzo V, Caramella D, Baldini G. Eosinophil cationic protein in infants with respiratory syncytial virus bronchiolitis: predictive value for subsequent development of persistent wheezing. Pediatr Pulmonol 2001;31:419–24.
41. Angelakou V, Bitsori M, Galanakis E. Asthma and early childhood infectious disease. Infection is trigger rather than cause. BMJ 2001;323:164.
42. Stein RT, Sherrill D, Morgan WJ, et al. Respiratory syncytial virus in early life and risk of wheeze and allergy by age 13 years. Lancet 1999;354:541–5.
43. van Schaik SM, Enhorning G, Vargas I, Welliver RC. Respiratory syncytial virus affects pulmonary function in BALB/c mice. J Infect Dis 1998;177:269–76.
44. Peebles RS Jr, Sheller JR, Johnson JE, et al. Respiratory syncytial virus infection prolongs methacholine-induced airway hyperresponsiveness in ovalbumin-sensitized mice. J Med Virol 1999;57:186–92.
45. Suzuki S, Suzuki Y, Yamamoto N, et al. Influenza A virus infection increases IgE production and airway responsiveness in aerosolized antigen-exposed mice. J Allergy Clin Immunol 1998;102:732–40.
46. Tsitoura DC, Kim S, Dabbagh K, et al. Respiratory infection with influenza A virus interferes with the induction of tolerance to aeroallergens. J Immunol 2000;165:3484–91.
47. Schwarze J, Makela M, Cieslewicz G, et al. Transfer of the enhancing effect of respiratory syncytial virus infection on subsequent allergic airway sensitization by T lymphocytes. J Immunol 1999;163:5729–34.
48. Mäkelä MJ, Kanehiro A, Dakhama A, et al. The failure of interleukin-10-deficient mice to develop airway hyperresponsiveness is overcome by respiratory syncytial virus infection in allergen-sensitized/challenged mice. Am J Respir Crit Care Med 2002;165:824–31.
49. Einarsson O, Geba GP, Zhu Z, et al. Interleukin-11: stimulation in vivo and in vitro by respiratory viruses and induction of airways hyperresponsiveness. J Clin Invest 1996;97: 915–24.
50. Tekkanat KK, Maassab H, Berlin AA, et al. Role of interleukin-12 and Stat-4 in the regulation of airway inflammation and

hyperreactivity in respiratory syncytial virus infection. Am J Pathol 2001;159:631–8.
51. Tekkanat KK, Maassab HF, Cho DS, et al. IL-13-induced airway hyperreactivity during respiratory syncytial virus infection is STAT6 dependent. J Immunol 2001;166:3542–8.
52. Lukacs NW, Tekkanat KK, Berlin A, et al. Respiratory syncytial virus predisposes mice to augmented allergic airway responses via IL-13-mediated mechanisms. J Immunol 2001;167:1060–5.
53. Schwarze J, Cieslewicz G, Hamelmann E, et al. IL-5 and eosinophils are essential for the development of airway hyperresponsiveness following acute respiratory syncytial virus infection. J Immunol 1999;162:2997–3004.
54. Schwarze J, Cieslewicz G, Joetham A, et al. Critical roles for interleukin-4 and interleukin-5 during respiratory syncytial virus infection in the development of airway hyperresponsiveness after airway sensitization. Am J Respir Crit Care Med 2000;162(2 Pt 1):380–6.
55. Jacoby DB, Fryer AD. Interaction of viral infections with muscarinic receptors. Clin Exp Allergy 1999;29 Suppl 2:59–64.
56. Mould AW, Ramsay AJ, Matthaei KI, et al. The effect of IL-5 and eotaxin expression in the lung on eosinophil trafficking and degranulation and the induction of bronchial hyperreactivity. J Immunol 2000;164:2142–50.
57. Hall CB. Respiratory syncytial virus and parainfluenza virus. N Engl J Med 2001;344:1917–28.
58. Castro M, Dozor A, Fish J, et al. The safety of inactivated influenza vaccine in adults and children with asthma. N Engl J Med 2001;345:1529–36.
59. Peebles RS Jr, Sheller JR, Collins RD, et al. Respiratory syncytial virus (RSV)-induced airway hyperresponsiveness in allergically sensitized mice is inhibited by live RSV and exacerbated by formalin-inactivated RSV. J Infect Dis 2000;182:671–7.
60. Piedimonte G. The association between respiratory syncytial virus infection and reactive airway disease. Respir Med 2002;96 Suppl B:S25–9.
61. Ikemura T, Schwarze J, Makela M, et al. Type 4 phosphodiesterase inhibitors attenuate respiratory syncytial virus-induced airway hyper-responsiveness and lung eosinophilia. J Pharmacol Exp Ther 2000;294:701–6.
62. Grünberg K, Sharon RF, Sont JK, et al. Rhinovirus-induced airway inflammation in asthma: effect of treatment with inhaled corticosteroids before and during experimental infection. Am J Respir Crit Care Med 2001;164(10 Pt 1):1816–22.
63. Reijonen TM, Kotaniemi-Syrjanen A, Korhonen K, Korppi M. Predictors of asthma three years after hospital admission for wheezing in infancy. Pediatrics 2000;106:1406–12.
64. Kajosaari M, Syvanen P, Forars M, Juntunen-Backman K. Inhaled corticosteroids during and after respiratory syncytial virus-bronchiolitis may decrease subsequent asthma. Pediatr Allergy Immunol 2000;11:198–202.

CHAPTER 42

ROLES OF LIPID MEDIATORS IN ACUTE LUNG INJURY AND PULMONARY FIBROSIS

Takahide Nagase

Platelet-activating factor (PAF) and metabolites of arachidonic acid, that is, eicosanoids, are lipid mediators that have various biologic effects, including cell adhesion, endothelial cell activation, and the production of cytokines. PAF is a proinflammatory phospholipid mediator that has various biologic effects, including cell adhesion, endothelial cell activation, and the production of cytokines and eicosanoids through activation of the G protein–coupled PAF receptor (PAFR).[1–13] Thromboxanes (TXs) and leukotrienes (LTs) are also potent mediators that are generated from arachidonic acid by cyclooxygenase and 5-lipoxygenase, respectively. TXA_2 may increase lung permeability, whereas LTB_4 is a potent neutrophil chemoattractant. A key enzyme for the production of these inflammatory mediators, including eicosanoids and PAF, is phospholipase A_2 (PLA_2). The cytosolic isoform of PLA_2 ($cPLA_2$) is of particular importance since it is activated by submicromolar concentrations of Ca^{2+} and by phosphorylation by mitogen-activated protein kinases.[14–16] These lipid mediators have various roles in the respiratory system (Figure 42-1) (see Chapter 43, "Eicosanoids and the Lung").

In respiratory diseases, there are several inflammatory disorders for which no pharmaceutical agents are presently effective. For example, adult respiratory distress syndrome (ARDS) is an acute lung injury with a high mortality rate, despite current best care.[17–19] Idiopathic pulmonary fibrosis (IPF) is a progressive and fatal disorder of the lung parenchyma,[20–22] for which there are also no particularly effective drugs currently available. However, their mechanisms still remain to be elucidated.

The focus of this chapter is on the recent novel findings regarding the role of PAF and $cPLA_2$ in lung inflammatory diseases, especially acute lung injury and pulmonary fibrosis. To address this question, studies have been performed on a variety of genetically engineered mice, namely, PAFR transgenic mice, PAFR gene–disrupted mice, and $cPLA_2$ gene–disrupted mice.

ARDS

ARDS is an acute lung injury with a mortality rate that ranges from 40 to 70%, despite intensive care and the use of all currently available drugs. Severe sepsis and acid aspiration are the most important causes of ARDS.[17–19] Potential mechanisms for ARDS include (1) damage to the alveolar–capillary membrane[17] and (2) polymorphonuclear neutrophil (PMN) adhesion, activation, and sequestration,[18] leading to pulmonary edema and deterioration of gas exchange.

PAF and metabolites of arachidonic acid are potentially involved in the development of ARDS.[19] To elucidate the roles of PAF and eicosanoids in the molecular mechanisms underlying ARDS, mutant mice and specific pharmacologic interventions have been recently exploited.

Effects of PAFR Gene Modulation in Acute Lung Injury

PAF is a proinflammatory phospholipid mediator with various biologic effects that follow the activation of a G protein–coupled PAFR. Given its potent biologic activity, PAF is potentially involved in the development of inflammatory disorders, including acute lung injury. To examine the pathophysiologic role of PAF in the pathogenesis of diseases, previous studies have depended on various types of PAFR antagonists. In such studies there are often significant problems arising from the issue of the specificity of these agents. For elucidation of the pathophysiologic role of PAF in vivo without being subject to the uncertainties arising from the use of potentially nonspecific PAFR antagonists, genetically engineered mice have been recently developed.[12,13]

To investigate the exact role of PAF in a murine model of acid aspiration–induced lung injury, we used two different mutant mice: (1) transgenic mice overexpressing the PAFR gene[12] and (2) mice with disruption of the PAFR gene.[13] Overexpression of the PAFR gene enhanced lung injury,

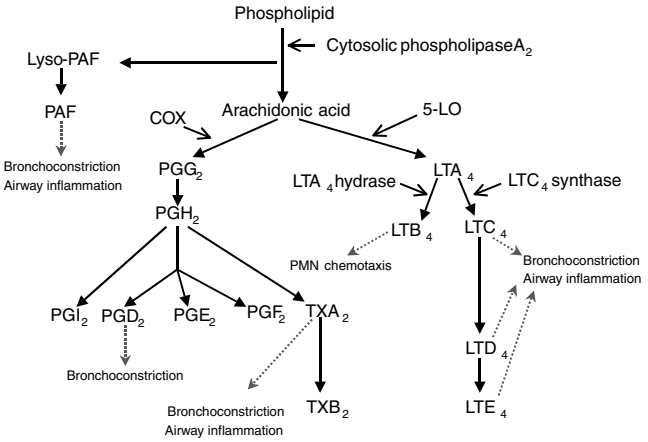

FIGURE 42-1 Physiologic roles of PAF and arachidonic acid metabolites in lungs. 5-LO = 5-lipoxygenase; COX = cyclooxygenase; LT = leukotriene; PAF = platelet-activating factor; PG = prostaglandin; PMN = polymorphonuclear neutrophil; TX = thromboxane.

pulmonary edema, and deterioration of gas exchange caused by hydrochloric acid aspiration. Disruption of the PAFR gene significantly attenuated the acid-induced injury, edema, and respiratory failure. PMN sequestration was, however, unaffected by the modulation of the PAFR gene.[23] This study indicates that a specific intervention at the level of the PAF receptor could make an important contribution to management of acid-induced lung injury. Previous studies have also shown that antagonism of the PAF receptor might be effective in acute lung injury.[24,25] Moreover, it has been recently demonstrated that PAF acetylhydrolase, which abolishes PAF activity, could be a potential therapeutic agent in the setting of severe acute inflammation.[26]

Oxidized phospholipids, lysophosphatidylcholine, or bacterial endotoxin can activate the PAF receptor.[27] Acid aspiration could potentially induce the formation of these compounds, providing a mechanism for the generation of PAF and PAF-like ligands and the involvement of this pathway in lung injury, leading to pulmonary edema and respiratory failure. These observations suggest that an intervention to reduce or antagonize the biologic activity of PAF is a plausible therapeutic strategy for acute lung injury.

Effects of cPLA$_2$ Gene Disruption in Acute Lung Injury

A key enzyme for the production of inflammatory lipid mediators, including eicosanoids and PAF, is cPLA$_2$. Therefore, it is likely that cPLA$_2$ participates in the development of acute lung injury. To investigate the role of cPLA$_2$ in different types of acute lung injury induced by (1) septic syndrome or (2) acid aspiration, we used mutant mice established in our laboratory,[28] namely, cPLA$_2$ gene–disrupted mice (*cpla2*$^{-/-}$) and their littermate controls (*cpla2*$^{+/+}$). Disruption of the cPLA$_2$ gene significantly attenuated different types of acute lung injury induced by either endotoxemia or acid aspiration, confirming the importance of the cPLA$_2$ gene in mediating acute lung injury, probably through production of inflammatory mediators, including TXs and LTs.

The sepsis syndrome is the most frequent cause of ARDS and is associated with a 35 to 45% incidence of ARDS development.[18,19] It has been postulated that endotoxemia and phagocytosis of bacteria are involved in the pathogenesis of ARDS associated with septic syndrome.[29] Therefore, the model of acute lung injury induced by combined administration of lipopolysaccharide (LPS) and zymosan was studied.[30] In this model, circulating LPS and phagocytosis of microbial particles by LPS-primed PMNs elicit acute lung injury, mimicking sepsis-associated acute lung injury. In *cpla2*$^{+/+}$ mice, we observed increases in lung elastance, lung edema, PMN infiltration, and severe worsening of gas exchange following LPS and zymosan administration. Consistently, marked increases in TX and LT levels were detected in the bronchoalveolar (BAL) fluid. These findings were markedly attenuated by cPLA$_2$ gene disruption. Potential mechanisms by which cPLA$_2$ mediates sepsis-induced acute lung injury include the release of proinflammatory mediators. The present results also suggest that the major mediator of PMN infiltration is a cPLA$_2$ product, most probably LTB$_4$.[31] Recent evidence from lung injury models in which the LTB$_4$ receptor is overexpressed shows that LTB$_4$ is an important mediator of neutrophil-mediated lung injury.[32] Not only infiltration but also activation of PMN in lungs is required to induce the development of acute lung injury. Triggered by the sepsis syndrome, cPLA$_2$-initiated pathways may mediate both the infiltration and activation of PMNs, resulting in sepsis-associated ARDS. Indeed, in human neutrophils during sepsis, elevated cPLA$_2$ expression and activity have been recently reported.[33]

Aspiration of gastric contents is reported to be associated with a 26 to 36% incidence of ARDS. A high incidence of acid aspiration–associated lung injury has been reported to occur during and following surgery.[34,35] Acute lung injury induced by massive acid aspiration is characterized by increases in lung elastance and permeability, enhanced PMN sequestration, and respiratory failure. Aspirated hydrochloric acid may cause direct damage to the alveolar–capillary membrane and promote PMN adhesion, activation, and sequestration. TX synthesis associated with PMN activation is a potential mechanism for the induction of pulmonary edema and respiratory failure. After acid aspiration, eicosanoids, including TX, are generated by activated tissues.[36] It is speculated that activation and adhesion of PMNs might be the initiating events leading to generation of reactive oxygen species and increases in microvascular permeability. The current findings suggest that cPLA$_2$ has a dominant role in PMN sequestration, possibly through the generation of LTB$_4$ and TXA$_2$. Interactions among mediators, including PAF and eicosanoids, may further accentuate the development of acute lung injury.[37]

In summary, the disruption of the cPLA$_2$ gene significantly attenuates the lung damage and respiratory failure induced by (1) LPS/zymosan treatment or (2) acid aspiration. cPLA$_2$ products may be involved in the pathogenesis of acute lung injury caused by septic syndrome or acid aspiration, and the inhibition of cPLA$_2$-initiated pathways may provide a novel and potentially useful therapeutic approach to ARDS, for which no pharmaceutical agents are currently effective.[38]

Effects of Pharmacologic Intervention in Acute Lung Injury

Several distinct types of PLA_2 have been characterized, but $cPLA_2$ is thought to be particularly important.[39,40] This PLA_2 preferentially hydrolyzes phospholipids containing arachidonic acid and is activated by submicromolar concentrations of Ca^{2+} and by phosphorylation of a serine residue.[41] Recently, it has been reported that an analog of arachidonic acid in which the –COOH functional group is replaced by $–COCF_3$, named arachidonyl trifluoromethyl ketone (ATK), is a potent and selective slow-binding inhibitor of $cPLA_2$.[42] The effects of ATK in a murine model of LPS-induced acute lung injury have been recently examined. The treatment of animals with ATK significantly attenuated lung injury, PMN sequestration, and deterioration of gas exchange caused by LPS/zymosan administration,[43] supporting the concept that pharmacologic intervention to inhibit $cPLA_2$ may be valuable in the acute lung injury caused by sepsis syndrome.

The effects of ATK administration are similar to those of $cPLA_2$ gene disruption in terms of inhibiting lung injury. However, there are also differences between the results of these two studies. Although ATK administration significantly reduced LPS/zymosan-induced production of TXB_2, LTB_4 and cysteinyl LTs by 73%, 47%, and 27%, respectively,[43] it was not as effective as $cPLA_2$ gene disruption, which reduced the production of each eicosanoid by $>90\%$ in this model in comparison with the LPS/zymosan-treated wild-type mice.[38] This finding suggests that ATK administration was still insufficient to completely inhibit $cPLA_2$. Since it is postulated that pharmacologic intervention against $cPLA_2$ may be useful in managing ARDS, the development of novel $cPLA_2$ inhibitors warrants future research.

PULMONARY FIBROSIS

Pulmonary fibrosis is a disorder of the lung parenchymal interstitium.[20–22] IPF is the most common disorder characterized by alveolar inflammation and the development of a progressive process associated with fibroblast proliferation and collagen deposition. The pathophysiologic features of IPF are increased lung elasticity, restrictive ventilation impairment, and respiratory failure.[20] No effective drugs are currently available for its treatment, and IPF is a progressive and fatal disease. At present, medical intervention for IPF includes only lung transplantation or supportive treatment, for example, oxygen therapy. The molecular mechanisms underlying the development of pulmonary fibrosis remain to be elucidated, but potential mechanisms leading to pulmonary fibrosis might be (1) the infiltration of inflammatory cells into the lungs and (2) the generation of proinflammatory and proliferative mediators, leading to fibroblast proliferation and accumulation of extracellular collagen.[20,21]

Potentially, PAF and metabolites of arachidonic acid could be involved in the pathogenesis of pulmonary fibrosis, but little attention has thus far been paid to this possibility. PAF is a proinflammatory phospholipid mediator whose biologic effects include cell proliferation and the production of cytokines and eicosanoids. TXA_2 may induce lung inflammation, and LTB_4 is a potent neutrophil chemoattractant. The cysteinyl LTs, LTC_4, LTD_4, and LTE_4, are among the most important mediators in inflammatory lung diseases. A crucial enzyme for the generation of these proinflammatory mediators, including eicosanoids and PAF, is $cPLA_2$.

Effects of $cPLA_2$ Gene Disruption in Pulmonary Fibrosis

To elucidate the role of $cPLA_2$ in the experimental model of pulmonary fibrosis induced by bleomycin, $cPLA_2$ gene–disrupted mice ($cpla2^{-/-}$) and their littermate controls ($cpla2^{+/+}$) were used.[28] The effects of $cPLA_2$ gene disruption in bleomycin-induced pulmonary fibrosis are summarized in Table 42-1 and Figure 42-2. Disruption of the $cPLA_2$ gene significantly attenuated pulmonary fibrosis and inflammation induced by bleomycin. These observations indicate that the $cPLA_2$ gene may be involved in pulmonary fibrosis through overproduction of inflammatory mediators, including TXs and LTs.[44]

Fibrotic lung disorders, including IPF, are characterized by chronic lung parenchymal injury and inflammation, that is, alveolitis.[20] The inflammation of pulmonary fibrosis is associated with infiltration of leukocytes, including macrophages, lymphocytes, and neutrophils. It is thought that these inflammatory cells might generate and release chemical mediators, leading to proliferation of mesenchymal cells and deposition of extracellular matrix protein. This pathologic process is associated with clinical findings that include reduced vital capacity and impaired gas exchange.[20] Investigation of the pathogenesis of pulmonary fibrosis with the use of pharmacologic approaches is limited since the

Table 42-1 Roles of $cPLA_2$ in Bleomycin-Induced Pulmonary Fibrosis: Physiologic and Biochemical Data after Saline or Bleomycin Treatment

Mouse type/ treatment	E_L *(cm H_2O/mL)*	*BAL fluid total protein (mg)*	*BAL fluid total cell counts ($\times 10^4$)*	*BAL fluid total TXB_2 (ng)*	*BAL fluid total LTB_4 (ng)*	*BAL fluid total $LTC_4/LTD_4/LTE_4$ (ng)*
$cpla2^{+/+}$Saline	14.5 ± 0.2	0.122 ± 0.006	9.9 ± 0.8	0.011 ± 0.011	0.000 ± 0.000	1.103 ± 0.144
$cpla^{-/-}$Saline	15.4 ± 0.8	0.129 ± 0.011	8.5 ± 0.8	0.000 ± 0.000	0.000 ± 0.000	0.281 ± 0.169
$cpla2^{+/+}$Bleomycin	33.0 ± 3.0*	0.703 ± 0.142†	63.1 ± 6.1*	0.077 ± 0.018*	0.026 ± 0.005*	23.400 ± 5.201*
$cpla2^{-/-}$Bleomycin	20.0 ± 1.1‡	0.224 ± 0.073‡	23.4 ± 1.3‡	0.015 ± 0.009‡	0.000 ± 0.000‡	1.838 ± 0.643‡

Reproduced with permission from Nagase T et al.[44]

BAL, bronchoalveolar lavage; EL = lung elastance; LT = leukotriene; TX = thromboxane.

*$p<.01$, †$p<.05$, versus saline-treated groups; ‡$p<.01$ versus bleomycin-treated $cpla2^{+/+}$ group ($n=4$ to 7, respectively).

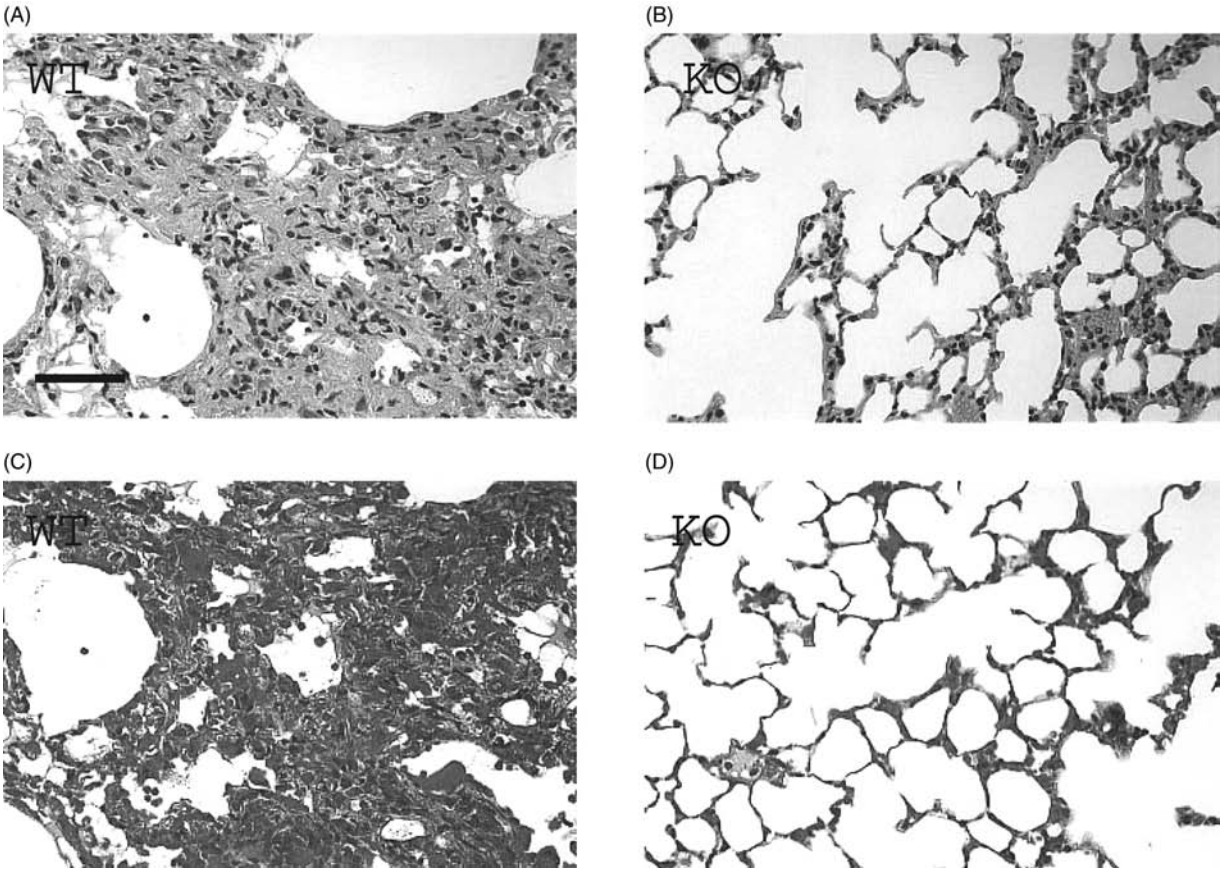

FIGURE 42-2 Photomicrographs of lung tissues from *cpla2*$^{+/+}$ (*A*, *C*) and *cpla2*$^{-/-}$ (*B*, *D*) mice 14 days after bleomycin administration. In *cpla2*$^{+/+}$ mice, marked accumulation of neutrophils and collagen is observed (*A*, *C*), whereas there are few histologic changes in *cpla2*$^{-/-}$ mice (*B*, *D*). Stains: hematoxylin and eosin (*A*, *B*), and Masson's trichrome stain (*C*, *D*). Scale bar: 50 μm. Reproduced with permission from Nagase T et al.[44]

progression of this disease is a chronic and continuous process. We therefore chose to use a mutant murine model to test the hypothesis that $cPLA_2$ mediates the development of pulmonary fibrosis.

In bleomycin-treated *cpla2*$^{+/+}$ mice, we observed increases in lung elastance, pulmonary fibrosis, protein leakage, and infiltration of inflammatory cells, including macrophages, lymphocytes, and neutrophils. Increases in TXs and LTs were consistently found in the BAL fluid of bleomycin-treated *cpla2*$^{+/+}$ mice. These responses to bleomycin were markedly attenuated by $cPLA_2$ gene disruption. Clearly, $cPLA_2$ products are related to infiltration of various leukocytes, which may lead to fibrosis. Indeed, increases in numbers of leukocytes, especially PMNs, are found in BAL fluid of patients with IPF,[20] and it has been reported that lung homogenates from IPF patients contain much higher levels of LTB_4 and LTC_4 in comparison with controls.[21] Recently, it has been shown that LTB_4 is an important mediator of neutrophil-mediated inflammation, including lung injury.[32] It has been speculated that not only PMNs, but also macrophages and lymphocytes, may be important in the induction of bleomycin-induced lung inflammation. $cPLA_2$-initiated pathways may mediate both infiltration and activation of these leukocytes triggered by bleomycin, resulting in pulmonary fibrosis. These findings suggest that $cPLA_2$-derived products have a dominant role in leukocyte sequestration. Potential interactions between mediators, including PAF and eicosanoids, may further up-regulate the development of the fibrotic process. Taken together, these results show that the disruption of the $cPLA_2$ gene significantly attenuates lung inflammation and fibrosis induced by bleomycin treatment, indicating the importance of $cPLA_2$ pathways in the pathogenesis of pulmonary fibrosis caused by bleomycin.

Relative Contribution of Downstream Mediators of $cPLA_2$ in Pulmonary Fibrosis

To assess the relative contribution of $cPLA_2$ downstream mediators, the role of PAF in bleomycin-induced pulmonary fibrosis was examined with the use of PAFR gene–disrupted mice (*pafr*$^{-/-}$) and their littermate controls (*pafr*$^{+/+}$). As shown in Table 42-2, although disruption of the PAFR gene significantly reduced the score of fibrotic lesions, there was still a marked difference between bleomycin-treated *pafr*$^{-/-}$ mice and saline-treated groups. However, there was no significant difference in either lung elastance or hydroxyproline content between bleomycin-treated *pafr*$^{+/+}$ and *pafr*$^{-/-}$ mice. These findings suggest that PAF, a downstream mediator of $cPLA_2$, may be involved in the development of bleomycin-induced pulmonary fibrosis. However, the relative contribution of PAF is only partial and limited when compared with the crucial role of $cPLA_2$. It is therefore

Table 42-2 Roles of Platelet-Activating Factor in Bleomycin-Induced Pulmonary Fibrosis

Mouse type/ treatment	E_L *(cm H_2O/mL)*	*Hydroxyproline value (μg/left lung)*	*Score of fibrotic lesions*
$pafr^{+/+}$ Saline	14.8 ± 1.1	43.2 ± 3.3	0.0 ± 0.0
$pafr^{-/-}$ Saline	14.1 ± 1.1	43.0 ± 3.7	0.0 ± 0.0
$pafr^{+/+}$ Bleomycin	32.5 ± 2.2*	82.0 ± 7.2†	2.8 ± 0.2*
$pafr^{-/-}$ Bleomycin	26.9 ± 2.3†	59.8 ± 12.1	2.0 ± 0.0*‡

Reproduced with permission from Nagase T et al.[44]
*$p < .001$, †$p < .05$, versus saline-treated groups; ‡$p < .05$ versus bleomycin-treated $pafr^{+/+}$ group ($n = 4$ to 5, respectively).

speculated that other downstream mediators of $cPLA_2$, such as eicosanoids produced by cyclooxygenase and/or lipoxygenase, may also contribute to the development of bleomycin-induced pulmonary fibrosis. This would be consistent with the recent finding that 5-lipoxygenase gene-disrupted mice demonstrate significant protection from bleomycin-induced pulmonary fibrosis,[45] suggesting that LTs have important roles in the pathogenesis of pulmonary fibrosis.

SUMMARY AND CONCLUSIONS

Recent studies have shown that PAF and eicosanoids, downstream mediators of $cPLA_2$, may be involved in the pathogenesis of various inflammatory diseases, including bronchial asthma, ARDS, and IPF.[46–50] Although there are extreme differences in clinical features between ARDS and IPF, both diseases are frequently fatal disorders for which no useful drugs are currently available. On the basis of recent findings in mutant mice, $cPLA_2$ might be a potential target for the development of drugs to treat pulmonary fibrosis and acute lung injury.

REFERENCES

1. Ishii S, Shimizu T. Platelet-activating factor (PAF) receptor and genetically engineered PAF receptor mutant mice. Prog Lipid Res 2000;39:41–82.
2. Prescott SM, Zimmerman GA, McIntyre TM. Platelet-activating factor. J Biol Chem 1990;265:17381–4.
3. Chao W, Olson MS. Platelet-activating factor: receptors and signal transduction. Biochem J 1993;292:617–29.
4. Izumi T, Shimizu T. Platelet-activating factor receptor: gene expression and signal transduction. Biochim Biophys Acta 1995;1259:317–33.
5. Honda Z, Nakamura M, Miki I, et al. Cloning by functional expression of platelet-activating factor receptor from guinea-pig lung. Nature 1991;349:342–6.
6. Nakamura M, Honda Z, Izumi T, et al. Molecular cloning and expression of platelet-activating factor receptor from human leukocytes. J Biol Chem 1991;266:20400–5.
7. Ye RD, Prossnitz ER, Zou AH, Cochrane CG. Characterization of a human cDNA that encodes a functional receptor for platelet activating factor. Biochem Biophys Res Commun 1991;180:105–11.
8. Kunz D, Gerard NP, Gerard C. The human leukocyte platelet-activating factor receptor. cDNA cloning, cell surface expression, and construction of a novel epitope-bearing analog. J Biol Chem 1992;267:9101–6.
9. Sugimoto T, Tsuchimochi H, McGregor CG, et al. Molecular cloning and characterization of the platelet-activating factor receptor gene expressed in the human heart. Biochem Biophys Res Commun 1992;189:617–24.
10. Bito H, Honda Z, Nakamura M, Shimizu T. Cloning, expression and tissue distribution of rat platelet-activating-factor-receptor cDNA. Eur J Biochem 1994;221:211–8.
11. Ishii S, Matsuda Y, Nakamura M, et al. A murine platelet-activating factor receptor gene: cloning, chromosomal localization and up-regulation of expression by lipopolysaccharide in peritoneal resident macrophages. Biochem J 1996;314:671–8.
12. Ishii S, Nagase T, Tashiro F, et al. Bronchial hyperreactivity, increased endotoxin lethality and melanocytic tumorigenesis in transgenic mice overexpressing platelet-activating factor receptor. EMBO J 1997;16:133–42.
13. Ishii S, Kuwaki T, Nagase T, et al. Impaired anaphylactic responses but intact sensitivity to endotoxin in mice lacking a platelet-activating factor receptor. J Exp Med 1998; 187:1779–88.
14. Leslie CC. Properties and regulation of cytosolic phospholipase A_2. J Biol Chem 1997;272:16709–12.
15. Clark JD, Lin LL, Kriz RW, et al. A novel arachidonic acid-selective cytosolic PLA_2 contains a Ca^{2+}-dependent translocation domain with homology to PKC and GAP. Cell 1991; 65:1043–51.
16. Lin LL, Wartmann M, Lin AY, et al. $cPLA_2$ is phosphorylated and activated by MAP kinase. Cell 1993;72:269–78.
17. Pittet JF, Mackersie RC, Martin TR, Matthay MA. Biological markers of acute lung injury: prognostic and pathogenetic significance. Am J Respir Crit Care Med 1997;155:1187–205.
18. Fowler AA, Hamman RF, Good JT, et al. Adult respiratory distress syndrome: risk with common predispositions. Ann Intern Med 1983;98:593–7.
19. Hudson LD, Milberg JA, Anardi D, Maunder RJ. Clinical risks for development of the acute respiratory distress syndrome. Am J Respir Crit Care Med 1995;151:293–301.
20. American Thoracic Society. Idiopathic pulmonary fibrosis: diagnosis and treatment; international consensus statement. Am J Respir Crit Care Med 2000;161:646–64.
21. Wilborn J, Bailie M, Coffey M, et al. Constitutive activation of 5-lipoxygenase in the lungs of patients with idiopathic pulmonary fibrosis. J Clin Invest 1996;97:1827–36.
22. Lan Tran P, Weinbach J, Opolon P, et al. Prevention of bleomycin-induced pulmonary fibrosis after adenovirus-mediated transfer of the bacterial bleomycin resistance gene. J Clin Invest 1997;99:608–17.
23. Nagase T, Ishii S, Kume K, et al. Platelet-activating factor mediates acid-induced lung injury in genetically engineered mice. J Clin Invest 1999;104:1071–6.
24. Chang SW, Feddersen CO, Henson PM, Voelkel NF. Platelet-activating factor mediates hemodynamic changes and lung injury in endotoxin-treated rats. J Clin Invest 1987;79: 1498–509.
25. Miotla JM, Jeffery PK, Hellewell PG. Platelet-activating factor plays a pivotal role in the induction of experimental lung injury. Am J Respir Cell Mol Biol 1998;18:197–204.
26. Tjoelker LW, Wilder C, Eberhardt C, et al. Anti-inflammatory properties of a platelet-activating factor acetylhydrolase. Nature 1995;374:549–53.
27. Smiley PL, Stremler KE, Prescott SM, et al. Oxidatively fragmented phosphatidylcholines activate human neutrophils

through the receptor for platelet-activating factor. J Biol Chem 1991;266:11104–10.
28. Uozumi N, Kume K, Nagase T, et al. Role of cytosolic phospholipase A_2 in allergic response and parturition. Nature 1997;390:618–22.
29. Donnelly SC, Haslett C. Cellular mechanisms of acute lung injury: implications for future treatment in the adult respiratory distress syndrome. Thorax 1992;47:260–3.
30. Miotla JM, Williams TJ, Hellewell PG, Jeffery PK. A role for the beta2 integrin CD11b in mediating experimental lung injury in mice. Am J Respir Cell Mol Biol 1996;14:363–73.
31. Yokomizo T, Izumi T, Chang K, et al. A G-protein-coupled receptor for leukotriene B_4 that mediates chemotaxis. Nature 1997;387:620–4.
32. Chiang N, Gronert K, Clish CB, et al. Leukotriene B_4 receptor transgenic mice reveal novel protective roles for lipoxins and aspirin-triggered lipoxins in reperfusion. J Clin Invest 1999;104:309–16.
33. Levy R, Dana R, Hazan I, et al. Elevated cytosolic phospholipase A_2 expression and activity in human neutrophils during sepsis. Blood 2000;95:660–5.
34. Hardman JG, O'Connor PJ. Predicting gastric contents following trauma: an evaluation of current practice. Eur J Anaesthesiol 1999;16:404–9.
35. Marion DW. Complications of head injury and their therapy. Neurosurg Clin North Am 1991;2:411–24.
36. Nagase T, Fukuchi Y, Teramoto S, et al. Intravenous bolus of prednisolone decreases 15-hydroxyeicosatetraenoic acid formation in the rat model of acid aspiration. Crit Care Med 1991;19:950–4.
37. Stewart AG, Dubbin PN, Harris T, Dusting GJ. Platelet-activating factor may act as a second messenger in the release of eicosanoids and superoxide anions from leukocytes and endothelial cells. Proc Natl Acad Sci U S A 1990;87:3215–9.
38. Nagase T, Uozumi N, Ishii S, et al. Acute lung injury by sepsis and acid aspiration: a key role for cytosolic phospholipase A_2. Nat Immunol 2000;1:42–6.
39. Shindou H, Ishii S, Uozumi N, Shimizu T. Roles of cytosolic phospholipase A_2 and platelet-activating factor receptor in the Ca-induced biosynthesis of PAF. Biochem Biophys Res Commun 2000;271:812–7.
40. Wong DA, Kita Y, Uozumi N, Shimizu T. Discrete role for cytosolic phospholipase A_2 alpha in platelets: studies using single and double mutant mice of cytosolic and group IIA secretory phospholipase A_2. J Exp Med 2002;196:349–57.
41. Riendeau D, Guay J, Weech PK, et al. Arachidonyl trifluoromethyl ketone, a potent inhibitor of 85-kDa phospholipase A_2, blocks production of arachidonate and 12-hydroxyeicosatetraenoic acid by calcium ionophore-challenged platelets. J Biol Chem 1994;269:15619–24.
42. Street IP, Lin HK, Laliberte F, et al. Slow- and tight-binding inhibitors of the 85-kDa human phospholipase A_2. Biochemistry 1993;32:5935–40.
43. Nagase T, Uozumi N, Aoki-Nagase T, et al. A potent inhibitor of cytosolic phospholipase A_2, arachidonyl trifluoromethyl ketone, attenuates LPS-induced lung injury in mice. Am J Physiol Lung Cell Mol Physiol 2003;284:L720–6.
44. Nagase T, Uozumi N, Ishii S, et al. A pivotal role of cytosolic phospholipase A_2 in bleomycin-induced pulmonary fibrosis. Nat Med 2002;8:480–4.
45. Peters-Golden M, Bailie M, Marshall T, et al. Protection from pulmonary fibrosis in leukotriene-deficient mice. Am J Respir Crit Care Med 2002;165:229–35.
46. Figueroa DJ, Breyer RM, Defoe SK, et al. Expression of the cysteinyl leukotriene 1 receptor in normal human lung and peripheral blood leukocytes. Am J Respir Crit Care Med 2001;163:226–33.
47. Nagase T, Ishii S, Katayama H, et al. Airway responsiveness in transgenic mice overexpressing platelet-activating factor receptor: roles of thromboxanes and leukotrienes. Am J Respir Crit Care Med 1997;156:1621–7.
48. Nagase T, Ishii S, Shindou H, et al. Airway hyperresponsiveness in transgenic mice overexpressing platelet-activating factor receptor is mediated by an atropine sensitive pathway. Am J Respir Crit Care Med 2002; 165:200–5.
49. Stimler-Gerard NP. Parasympathetic stimulation as a mechanism for platelet-activating factor-induced contractile responses in the lung. J Pharmacol Exp Ther 1986;237:209–13.
50. Zhu X, Munoz NM, Kim KP, et al. Cytosolic phospholipase A_2 activation is essential for beta 1 and 2 integrin-dependent adhesion of human eosinophils. J Immunol 1999;163:3423–9.

CHAPTER 43

EICOSANOIDS AND THE LUNG

William S. Powell

Eicosanoids are 20-carbon fatty acids derived principally from arachidonic acid.[1] This polyunsaturated fatty acid is oxidized by many enzymes, the most important of which are the cyclooxygenases and 5-lipoxygenase (5-LO) (Figure 43-1). Many eicosanoids are potent inflammatory mediators, although in some cases they also have antiinflammatory effects. In asthma, cysteinyl-leukotrienes (cysLTs) are of particular importance because of their bronchoconstrictor and proinflammatory effects. 5-Oxo-6,8,11,14-eicosatetraenoic acid (5-oxo-ETE) and prostaglandin D_2 (PGD_2) are potent eosinophil chemoattractants that may play significant roles in pulmonary inflammation in asthma, whereas PGE_2 may play an antiinflammatory role. In lung diseases involving neutrophilic inflammation, as well as in bacterial infection, LTB_4 appears to play an important physiologic role.

BIOSYNTHESIS AND METABOLISM OF EICOSANOIDS

Release of Arachidonic Acid

The initial step in the production of eicosanoids is the release of arachidonic acid from membrane phospholipids, which is catalyzed by phospholipase A_2 (PLA_2). Of the many forms of this enzyme, the only one that is highly selective for phospholipids containing arachidonic acid is cytosolic PLA_2 ($cPLA_2$).[2] This enzyme is found in the cytosol of resting cells but translocates to internal membranes (mainly the Golgi, endoplasmic reticulum, and nuclear envelope) in response to agents that elevate cytosolic Ca^{2+} levels, for example, by activation of PLC. This is due to the presence in $cPLA_2$ of a Ca^{2+}-dependent phospholipid-binding domain (C2 domain). The enzymic activity of $cPLA_2$ is further increased by phosphorylation, principally of serine-505 in response to mitogen-activated protein kinase, and also of serine-707. $cPLA_2$ is transcriptionally regulated by various cytokines and growth factors, including interleukin-1 (IL-1), tumor necrosis factor-α (TNF-α), and interferon-γ (IFN-γ), and is negatively regulated by glucocorticoids. In addition to initiating the synthesis of eicosanoids, $cPLA_2$ concomitantly releases the lysophospholipid precursor for platelet-activating factor (PAF), which is converted to PAF by an acetyltransferase. Besides $cPLA_2$, certain secretory PLA_2 enzymes, in particular $sPLA_2$ group IIa, contribute to the release of arachidonic acid, especially in pathologic conditions. These enzymes act at the extracellular surface, require millimolar concentrations of Ca^{2+}, and are not selective for phospholipids containing arachidonic acid.

Biosynthesis and Metabolism of Prostanoids

Once released from the membrane, arachidonic acid is rapidly converted into prostaglandins (PGs) by cells containing cyclooxygenase (COX; prostaglandin H synthase). There are constitutive (COX-1) and inducible (COX-2) isoforms of this enzyme.[3] COX-1 is expressed in many cell types in the lung and elsewhere, whereas COX-2 is expressed under conditions of stress and inflammation and is transcriptionally regulated by mediators that act through protein kinases A and C, as well as nuclear factor kappa B (NFκB). It is thus induced by a variety of proinflammatory cytokines and growth factors, as well as by one of its products, PGE_2. Conversely, COX-2 expression is inhibited by glucocorticoids and IL-4. Both COX-1 and COX-2 are present in the active state in the endoplasmic reticulum and the nuclear envelope. These enzymes convert arachidonic acid to the unstable endoperoxide PGH_2, which is converted by specific synthases to five biologically active prostanoids: PGD_2, PGE_2, $PGF_{2\alpha}$, PGI_2 (prostacyclin), and thromboxane A_2 (TXA_2).[1] There are several PGE synthases, one of which (mPGES-1) is a highly inducible microsomal enzyme that is associated with inflammation.[4]

Prostacyclin and TXA_2 are unstable and are rapidly degraded nonenzymically to biologically inactive products (6-keto-$PGF_{1\alpha}$ and TXB_2, respectively), whereas other prostanoids are inactivated by metabolic enzymes. PGE_2 and $PGF_{2\alpha}$ are rapidly oxidized to biologically inactive 15-keto metabolites by 15-hydroxyprostaglandin dehydrogenase, and this is followed by reduction of the 13,14-double bond by PG Δ^{13}-reductase. PGD_2 is enzymically reduced to 11β-$PGF_{2\alpha}$ and can also be degraded nonenzymically in the presence of albumin to PGJ_2 and its derivatives, including 15-deoxy-$\Delta^{12,14}$-PGJ_2. The last-mentioned product has a variety of antiinflammatory properties, but its physiologic relevance is somewhat controversial.

In addition to the above enzymic pathways for the synthesis of prostanoids, a complex array of isoprostanes is

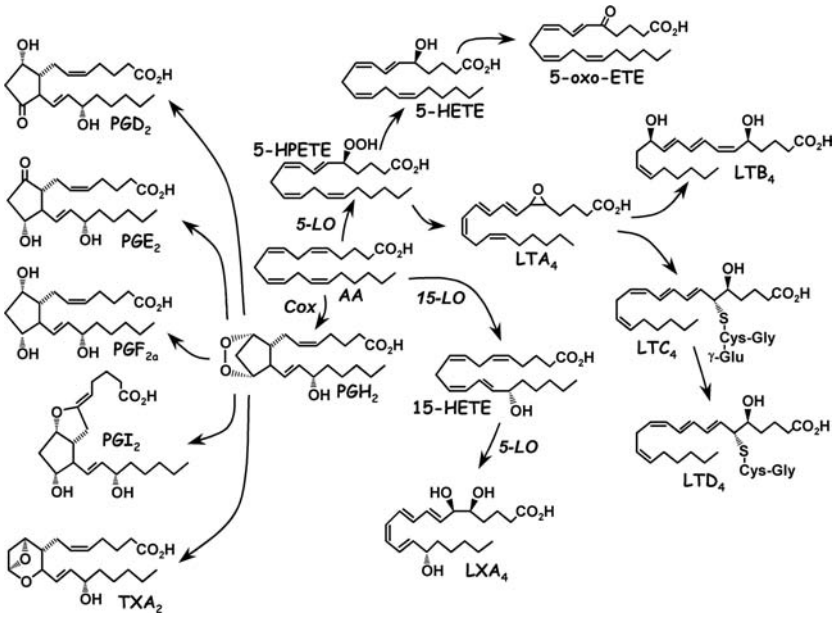

FIGURE 43-1 Biosynthesis of products of the cyclooxygenase (COX) and 5-lipoxygenase (5-LO) pathways. Note that lipoxin A_4 (LXA_4) can be produced by several pathways, including the one shown. AA = arachidonic acid; 5-HETE = 5-hydroxy-6,8,11,14-eicosatetraenoic acid; 5-HPETE = 5-hydroperoxy-6,8,11,14-eicosatetraenoic acid; 5-oxo-ETE = 5-oxo-6,8,11,14-eicosatetraenoic acid; 15-HETE = 15-hydroxy-5,8,11,13-eicosatetraenoic acid; 15-LO = 15-lipoxygenase; LT = leukotriene; PG = prostaglandin; TX = thromboxane.

formed by the nonenzymic oxidation of arachidonic acid. These products are similar in structure to PGs but consist of complex mixtures of stereoisomers. They are end products of lipid peroxidation and serve as markers of oxidative stress. Elevated levels of isoprostanes have been reported in urine[5] and condensate from exhaled air[6] from asthmatic subjects. Certain isoprostanes have been reported to have biologic activities.

Biosynthesis and Metabolism of 5-LO Products

Expression of 5-LO is mainly restricted to inflammatory cells. This enzyme is present in the cytosol or, in some cells, within the nucleus.[1] Unlike cyclooxygenases, 5-LO must be activated by mobilization of intracellular Ca^{2+}, which stimulates its translocation to the nuclear membrane. It also requires an accessory protein, 5-LO-activating protein (FLAP), which serves to bind arachidonic acid released by PLA_2. 5-LO converts arachidonic acid to 5-hydroperoxy-6,8,11,14-eicosatetraenoic acid (5-HPETE) and an unstable epoxide intermediate, LTA_4, which is converted by LTA_4 hydrolase to LTB_4 and by the LTC_4 synthase-catalyzed addition of glutathione to LTC_4. The latter substance is converted by γ-glutamyl leukotrienase to LTD_4, which is then metabolized by a dipeptidase to LTE_4, which has considerably lower biologic activity. Together, LTC_4 LTD_4 and LTE_4 are known as the cysLTs. LTE_4 is excreted in the urine and serves as a marker for the in vivo synthesis of cysLTs. LTE_4 is further metabolized by β- and ω-oxidation. In the rat (but not in humans), *N*-acetyl-LTE_4 is a major urinary metabolite of cysLTs.

LTB_4 is rapidly inactivated by LTB_4 20-hydroxylase, which is very active in neutrophils. The initially formed 20-hydroxy-LTB_4 is further metabolized to the corresponding ω-carboxy compound, which is further metabolized by β-oxidation. LTB_4 is also metabolized by oxidation of its 12-hydroxyl group by two distinct 12-hydroxyeicosanoid dehydrogenases. One of these is a microsomal NAD^+-dependent enzyme found in leukocytes,[7] whereas the other is a cytosolic $NADP^+$-dependent dehydrogenase present in hepatocytes and epithelial cells in a variety of tissues, including the lung.[8] Interestingly, the latter enzyme also catalyzes the reduction of 15-keto-PGs to their 13,14-dihydro derivatives, which are the major circulating metabolites of PGs.

5-HPETE, an intermediate in the formation of LTA_4, is released from 5-LO and is rapidly reduced by a peroxidase to 5-hydroxy-6,8,11,14-eicosatetraenoic acid (5-HETE). 5-HETE is oxidized to the potent granulocyte chemoattractant 5-oxo-ETE by 5-hydroxyeicosanoid dehydrogenase, a microsomal $NADP^+$-dependent enzyme present in most inflammatory cells,[9] as well as epithelial cells. 5-Oxo-ETE is inactivated by ω-oxidation, as well as by reduction of its 6,7-double bond.

Biosynthesis and Metabolism of Eicosanoids in the Lung

Because the lung contains a large variety of both structural and inflammatory cell types, it has the capability to produce all of the major eicosanoids. The nature and amounts of eicosanoids synthesized can change dramatically, depending on health status and the numbers of leukocytes migrating into the lung from the circulatory system. In general, structural cells tend to produce predominantly prostanoids, whereas inflammatory cells tend to produce more 5-LO products (Table 43-1). The major sites for the production of cysLTs in humans are mast cells, basophils, eosinophils, and macrophages, whereas neutrophils, monocytes, and macrophages are the major sources of LTB_4 and 5-oxo-ETE. Unlike human eosinophils, which form large amounts of LTC_4 but very little LTB_4, rodent eosinophils produce LTB_4 rather than LTC_4.[10]

TXA_2 is produced by macrophages, blood monocytes, and platelets. It is a major product of arachidonic acid metabolism in the lungs, particularly in the guinea pig. PGD_2 is synthesized principally by mast cells and by

Table 43-1 Major Cellular Sources of Eicosanoids in the Lung

Cell type	*Major products*
Airway epithelial cells	PGE_2, 15-HETE
Vascular endothelial cells	PGI_2, PGE_2
Macrophages	TXA_2, PGE_2, LTB_4, 5-oxo-ETE, LTC_4
Monocytes	TXA_2, PGE_2, LTB_4, 5-oxo-ETE
Mast cells	PGD_2, LTC_4
Basophils	LTC_4
Neutrophils	LTB_4, 5-oxo-ETE
Eosinophils	LTC_4, 15-HETE

15-HETE = 15-hydroxy-5,8,11,13-eicosatetraenoic acid; 5-oxo-ETE = 5-oxo-5,8,11,13-eicosatetraenoic acid; LT = leukotriene; PG = prostaglandin; TX = thromboxane.

Th2 cells.[11] Epithelial cells and macrophages produce large amounts of PGE_2. Lung fibroblasts normally release low levels of PGE_2, but its synthesis can be dramatically increased following treatment with IL-1α, IL-1β, or TNF-α.[12] Vascular endothelial cells synthesize both PGI_2 and PGE_2, with microvascular cells producing more PGE_2, and endothelial cells from larger blood vessels making more PGI_2.[13]

Mast cells are major sites for the synthesis of both LTC_4 and PGD_2 in the lung and are responsible for the rapid release of these eicosanoids following allergen challenge of asthmatic subjects. Although all mast cells can synthesize PGD_2, their ability to synthesize LTC_4 is more restricted and appears to be related to the tissue environment.[14] Lung mast cells synthesize comparable amounts of LTC_4 and PGD_2, whereas skin mast cells synthesize primarily PGD_2. The synthesis of LTC_4 is regulated by Th2 cytokines as LTC_4 synthase is strongly induced by IL-4. In contrast to mast cells, basophils do not synthesize PGD_2 but produce amounts of LTC_4 comparable to the amounts produced by mast cells.

The lung plays a critical role in the metabolism of PGs. Because of the rapid termination of their biologic activities due to conversion to 13,14-dihydro-15-keto metabolites in the pulmonary circulation, these compounds do not function as circulating hormones but instead act locally, at the sites of their production. Over 90% of PGs are metabolized in a single pass through the perfused lung,[15] and 97% of intravenously administered PGE_2 is removed from the blood after only 1.5 minutes.[16]

Production of Eicosanoids by Transcellular Metabolism

Intermediates produced in the synthesis of eicosanoids (eg, PGH_2 and LTA_4) can be released into the extracellular milieu and converted by other cells to biologically active products. This process may be of particular relevance in the case of LTB_4 and cysLTs as the expression of 5-LO is more or less restricted to inflammatory cells, whereas the enzymes required to convert LTA_4 to LTB_4 and LTC_4 are more widely distributed. For example, platelets and endothelial cells, both of which lack significant amounts of 5-LO, can convert LTA_4, released by neutrophils, to LTC_4.[17] The importance of transcellular biosynthesis for the formation of LTB_4 has recently been demonstrated in vivo in a study in which bone marrow cells from LTA hydrolase$^{-/-}$ mice were transferred to irradiated 5-LO$^{-/-}$ mice.[18] The donor cells could synthesize LTA_4 but not LTB_4, whereas the recipient mice could not synthesize LTA_4 but could convert donor cell–derived LTA_4 to LTs by transcellular biosynthesis. These authors showed that the 5-LO$^{-/-}$ recipient mice were able to synthesize LTB_4 at inflammatory loci, although at a lower level than normal mice, thus demonstrating the potential contribution of transcellular biosynthesis of LTs in vivo.

The complexity of the lung provides abundant opportunities for the formation of eicosanoids by transcellular biosynthesis. This has been demonstrated in experiments in which human neutrophils have been injected into blood-free perfused rabbit lungs, and this has been followed by stimulation with either Ca^{2+} ionophore or monoclonal antibodies in the presence of complement.[19] Although neither neutrophils nor perfused lungs by themselves synthesized appreciable amounts of cysLTs under these conditions, large amounts were formed by perfused lungs containing sequestered human neutrophils. Upon stimulation, these neutrophils release LTA_4, which is then converted to LTC_4 and other cysLTs by lung vascular or perivascular cells. Lungs contain high levels of LTC_4 synthase, whereas endothelial cells contain microsomal glutathione (GSH) *S*-transferase-II, which also catalyzes the formation of LTC_4.[20]

An important example of transcellular metabolism is the production of lipoxins by the combined actions of leukocyte 5-LO and either 15-LO, 12-LO, or COX-2 present in other cell types. In addition to PGs, cyclooxygenase converts arachidonic acid to small amounts of 11-HETE and 15-HETE. However, when COX-2 is treated with aspirin, unlike COX-1, it remains catalytically active and converts arachidonic acid to 15R-HETE rather than PGH_2.[21] The 15R-HETE can then be converted by 5-LO in other cell types to 15R-lipoxin A_4 (15R-LXA_4, 15-epi-LXA_4), which has the opposite configuration at C-15 to that of LXA_4 generated by other mechanisms. For example, co-incubation of neutrophils with aspirin-treated endothelial cells or A549 airway epithelial cells in which COX-2 has been induced leads to the formation of "aspirin-triggered lipoxins."[17] As the LXA_4 receptor (ALX) interacts similarly with 15R- and 15S-LXA_4, the aspirin-triggered 15R-LXA_4 has high biologic potency. Lipoxins can thus be produced by several pathways involving transcellular biosynthesis in the lung, and increased levels of these substances are found in bronchoalveolar lavage (BAL) fluid from subjects with asthma and other lung diseases.[22]

EICOSANOID SIGNALING

The effects of eicosanoids are normally mediated by G protein–coupled receptors situated on the plasma membrane. Once released from cells, eicosanoids are rapidly metabolized in vivo, and for this reason they usually act locally, in close proximity to their sites of production. Their actions are thus limited not only by the distribution of their receptors but also by the localization of the enzymes responsible for their synthesis.

Prostanoid Receptors

There are nine prostanoid receptors, including one each for $PGF_{2\alpha}$, PGI_2, and TXA_2, two for PGD_2, and four for PGE_2 (Figure 43-2). These receptors are named according to the letter designating their target (D, E, F, I, or T) followed by "P" for prostanoid.[23] Four of these receptors (DP_1, EP_2, EP_4, and IP) are coupled to G_s and hence tend to be associated with inhibitory responses, smooth muscle relaxation, and immunomodulatory effects. The EP_1, FP, and TP receptors are coupled to G_q and tend to induce stimulatory responses such as smooth muscle contraction associated with Ca^{2+} mobilization. The EP_3 receptor signals primarily through G_i and acts principally by inhibiting adenylyl cyclase and to a lesser extent by activating PLC. Alternatively spliced variants (six in humans) of the EP_3 receptor exist and have alterations in the cytoplasmic tail of the molecule. These differences result in altered coupling of these isoforms to G proteins and differences in their desensitization. Similarly, the TP and FP receptors each have two different variants, formed by multiple splicing.[24]

Although all of the above receptors are localized on the plasma membrane, there is evidence that some, including all of the EP receptor subtypes, are also present on the nuclear membrane and may be involved in gene regulation. For example, activation of the nuclear membrane EP_3 receptor by intracellular PGE_2 results in increased endothelial cell nitric oxide (NO) synthase expression in endothelial cells.[25]

The sequences of the eight prostanoid receptors described above are closely related to one another, indicating that they are members of the same family. In contrast, the sequence of the DP_2 receptor is more closely related to receptors for LTB_4, formyl-Met-Len-Phe (fMLP), and other chemoattractants.[26] Prior to the identification of the ligand for this receptor, it was identified and cloned as a selective marker for Th2 cells as it was not expressed by other lymphocyte subsets. Because of its resemblance to chemoattractant receptors, it was named "chemoattractant receptor-homologous molecule expressed on Th2 cells" (CRTH2). Subsequently, the ligand for CRTH2 was determined to be PGD_2. About the same time, using a pharmacologic approach, we independently identified a second receptor for PGD_2, which we named the "DP_2" receptor.[27] Based on substrate selectivities and distribution, it would appear that CRTH2 and the DP_2 receptor are identical. This receptor has so far been identified on Th2 cells, eosinophils, and basophils.[26,27] It is coupled through either G_i[26] or G_q,[28] depending on the cell type.

Receptors for 5-LO Products

There are six known receptors for products of the 5-LO pathway. LTB_4 and LTD_4 each have two receptors, whereas 5-oxo-ETE and LXA_4 each have their own selective receptors. As with prostanoid receptors, these are all G protein– coupled receptors located on the plasma membrane. With the exception of the LXA_4 receptor, they are all

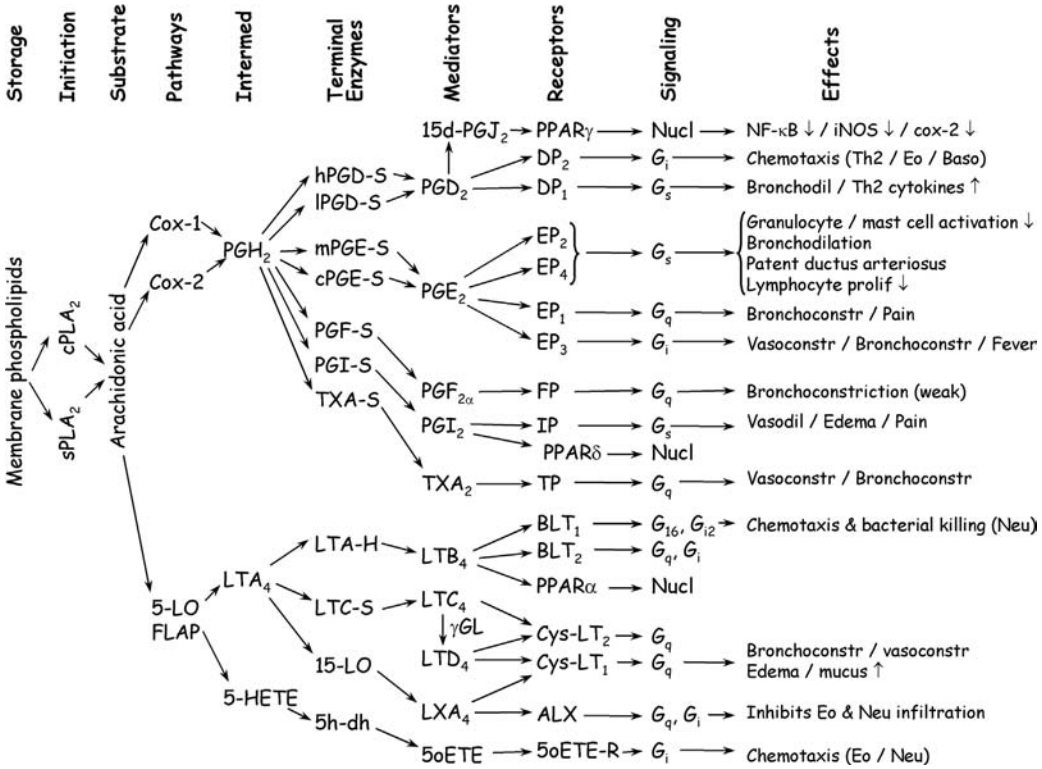

FIGURE 43-2 Biosynthesis, mechanisms of action and biologic effects of cyclooxygenase (COX) and 5-lipoxygenase (5-LO) products. Arachidonic acid, released by phospholipase A_2 (PLA_2), is converted to the intermediates prostaglandin H_2 (PGH_2), leukotriene A_4 (LTA_4), and 5-hydroxy-6,8,11,14-eicosatetraenoic acid (5-HETE), which are then converted to various biologically active products by a series of "terminal enzymes." The products act on selective receptors, most of which act through G proteins to induce various biologic responses; only those relevant to the lung are shown here. BLT = leukotriene B_4 receptor; 15d-PGJ_2 = 15-deoxy-$\Delta^{12,14}$-PGJ_2; FLAP = 5-lipoxygenase-activating protein; γGL = γ-glutamyl leukotrienase; 5h-dh = 5-hydroxyeicosanoid dehydrogenase; iNOS = inducible nitric oxide synthase; LTA-H = LTA hydrolase; NFκB = nuclear factor kappa B; 5oETE = 5-oxo-6,8,11,14-eicosatetraenoic acid; Nucl (in the cases of PPARs) act in nucleus as transcription factors; PPAR = peroxisome proliferator-activated receptor; S (in the case of terminal enzymes) = synthase; TX = thromboxane.

"stimulatory" receptors, associated with Ca^{2+} mobilization and cell activation.[29]

The two receptors for LTB_4 are known as the BLT_1 and BLT_2 receptors.[29] The BLT_1 receptor has a very high affinity and selectivity for LTB_4 and is responsible for most of its biologic effects. This receptor is found in high abundance on neutrophils, monocytes, macrophages, and eosinophils. It signals through G_{16} and G_{i2}. The BLT_2 receptor has a lower affinity than the BLT_1 receptor for LTB_4 and is less selective as it also has significant affinity for 12S-HETE. It is highly expressed in the spleen, but its precise role is not yet well understood.

The biologic effects of the cysLTs are mediated by their interaction with the $cysLT_1$ and $cysLT_2$ receptors. The $cysLT_1$ receptor is abundant in airway smooth muscle and mediates cysLT-induced bronchoconstriction.[30] It is also present on eosinophils, on monocytes, and in the spleen. It is highly selective for LTD_4, having 200- to 300-fold lower affinities for LTC_4 and LTE_4. The $cysLT_1$ receptor is up-regulated in monocytes and macrophages by IL-4 and IL-13, in eosinophilic cells by IL-5, and in airway smooth muscle cells by IL-13 and transforming growth factor-β.[31] A variety of cysLT antagonists have been developed for use in asthma, and all are selective for this receptor. The $cysLT_2$ receptor is present in lung macrophages, peripheral leukocytes, heart, and brain.[32] Unlike the $cysLT_1$ receptor, it binds LTC_4 and LTD_4 equally well. It has very little affinity for LTE_4. There are as yet no selective antagonists for this receptor, although the LTE_4 analog BAY u9773 acts as an antagonist at both the $cysLT_1$ and $cysLT_2$ receptors.

5-Oxo-ETE acts through a unique receptor that is expressed on eosinophils, neutrophils, and monocytes.[33] This receptor is highly selective for 5-oxo-ETE and is activated to a much lesser extent by 5-HETE and a variety of closely related metabolites. It is not stimulated significantly by any of the LTs. The 5-oxo-ETE receptor is coupled to G_i and has recently been cloned.[34]

LXA_4 interacts with the ALX receptor, which is highly homologous with the fMLP receptor.[35] It was first cloned based on its homology with the latter receptor and was initially known as the FPRL1 (formyl peptide receptor like-1) receptor. The ALX receptor has high affinity for LXA_4 but little affinity for LXB_4, fMLP, or LTB_4. LTD_4 has some activity at this receptor, having a K_i about 50 times higher than that of LXA_4. The ALX receptor is present on neutrophils, monocytes, and eosinophils and is coupled to G_i and G_q.[29] In addition to the latter receptor, an LXA_4 analog has been shown to interact strongly in an antagonistic manner with the $cysLT_1$ receptor, resulting in inhibition of the response to LTD_4.[36]

Nuclear Peroxisome Proliferator–activated Receptors for Eicosanoids

Peroxisome proliferator–activated receptors (PPARs) are members of the nuclear hormone receptor superfamily and include three isoforms, PPARα, PPARβ/δ, and PPARγ.[37] As well as having a variety of metabolic effects, they inhibit inflammatory responses and suppress the production of various cytokines and other proinflammatory molecules. Their actions are mediated in part by inhibition of the transcription factors NFκB, STATs, and NFAT. Although their endogenous ligands are not known with certainty, certain eicosanoids have been implicated. The PGD_2 degradation product 15-deoxy-$\Delta^{12,14}$-PGJ_2 stimulates PPARγ and thereby inhibits a variety of proinflammatory responses, including expression of certain cytokines, inducible NO synthase, and COX-2. Many of these effects are mediated by inhibitory effects on transcription factors such as NFκB. 15-Deoxy-$\Delta^{12,14}$-PGJ_2 has also been shown to inhibit the NFκB pathway directly, by the formation of covalent bonds with proteins due to its highly nucleophilic character.[38] Although 15-deoxy-$\Delta^{12,14}$-PGJ_2 clearly has anti-inflammatory effects, its potential physiologic role is somewhat controversial[39] as the concentrations required to induce these effects are rather high (low micromolar), and only very small amounts appear to be formed biologically. On the other hand, we found that this substance is a potent activator of human eosinophils (EC_{50}, ~10 nM), acting through the DP_2 receptor, suggesting that at lower concentrations, it may have proinflammatory effects.[39]

Other PPARs can also respond to eicosanoids. LTB_4 stimulates PPARα but is about 100 times less potent at this receptor than at the BLT_1 receptor. Furthermore, PPARα is not selective for LTB_4 as it has higher affinity for various C_{18} unsaturated fatty acids.[40] PGI_2 is a potent stimulator of PPARδ.[41]

EFFECTS OF EICOSANOIDS ON THE LUNG AND INFLAMMATORY CELLS

Airway Smooth Muscle

Leukotrienes CysLTs were discovered because of their ability to contract smooth muscle following their release from perfused lungs challenged with antigen or snake venom.[42] LTC_4 and LTD_4 are highly potent stimulators of airway smooth muscle from both humans and other species,[43] being about 1,000 times more potent than histamine (Figure 43-3A). These actions are mediated by the $cysLT_1$ receptor, which is highly expressed on airway smooth muscle cells.[30] The high potency of LTC_4 is presumably due to its rapid conversion to LTD_4. Although LTE_4 also elicits airway smooth muscle contraction, it is considerably less potent than LTD_4, as expected from its much lower affinity for the $cysLT_1$ (and $cysLT_2$) receptor.[30,32] Asthmatic subjects are more sensitive to all of the cysLTs than control subjects. However, there is a disproportionate increase in the potency of LTE_4 in asthmatic subjects for reasons that are presently unclear,[44] although possible explanations could be different rates of metabolism of cysLTs in asthmatic subjects or the presence of an additional cysLT receptor subtype. LTB_4 has potent constrictor effects on guinea pig airway parenchymal strips, but these responses are dependent on TXA_2 release.[45] This mechanism appears to be particular to the guinea pig, the lungs of which have a very high capacity to synthesize TXA_2, and does not appear to play an important role in humans.

In addition to their contractile effects, cysLTs also stimulate airway smooth muscle cell proliferation. LTD_4 enhances the proliferative response of human airway smooth muscle cells to epidermal growth factor, although by itself it has no effect.[46] There is also evidence that cysLTs promote smooth muscle cell hyperplasia following antigen challenge in animal models of asthma.[47,48]

Prostanoids Among the cyclooxygenase products, TXA_2 is the most potent bronchoconstrictor (see Figure 43-3A).[49]

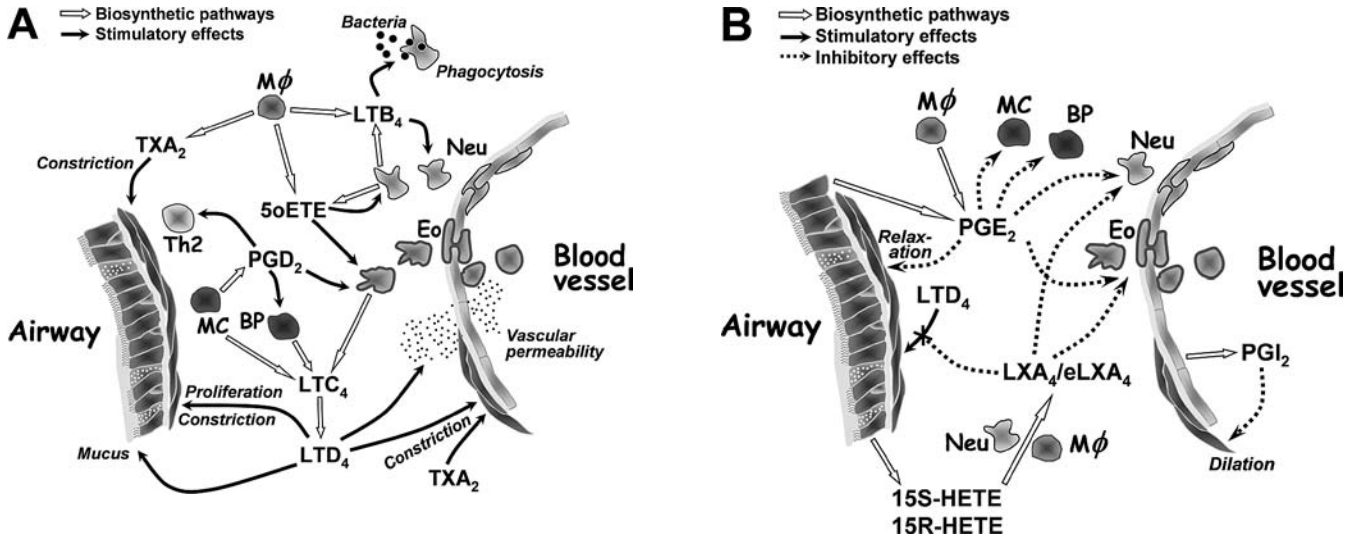

FIGURE 43-3 Biosynthesis and biologic effects of eicosanoids in the lung. Stimulatory (*A*) and inhibitory (*B*) effects of eicosanoids on the lung and inflammatory cells. Biosynthetic pathways are indicated by *open arrows*. Stimulatory and inhibitory effects and mediators are shown in *solid and broken arrows*, respectively. BP = basophils; Eo = eosinophils; LT = leukotriene; LX = lipoxin; MC = mast cells; Mø = macrophage; Neu = neutrophils; 5oETE = 5-oxo-ETE, 5-oxo-6,8,11,14-eicosatetraenoic acid; PG = prostaglandin; 15R-HETE = 15R-hydroxy-5,8,11,13-eicosatetraenoic acid; 15S-HETE = 15S-hydroxy-5,8,11,13-eicosatetraenoic acid; TXA_2 = thromboxane A_2.

Because of its instability, it has been difficult to conduct biologic studies directly on TXA_2, but, fortunately, there are several stable TXA_2 analogs that are potent TP receptor agonists, being active at low nanomolar concentrations. PGs, including PGD_2, $PGF_{2\alpha}$, and $11\beta\text{-}PGF_{2\alpha}$, have also been shown to have bronchoconstrictor activity, but they are active only at relatively high (low micromolar) concentrations and appear to act through TP rather than FP or DP receptors as their effects can be blocked by a TP receptor antagonist.[49] PGD_2 can also elicit relaxation of airway smooth muscle through the DP_1 receptor.[50] Thus, from a physiologic perspective, LTD_4 and TXA_2 are the most important bronchoconstrictors among eicosanoids.

In contrast to the constrictor effects of many eicosanoids, PGE_2 is unique among this group of compounds in primarily eliciting bronchodilatation due to its stimulatory effect on adenylyl cyclase through the EP_2 receptor.[51] PGE_2 is released by epithelial cells and appears to contribute to "epithelium-derived relaxing factor" activity (along with NO). However, PGE_2 can also induce neurally mediated coughing and bronchoconstriction due to the activation of afferent vagal C-fibers. These effects are mediated by EP_1 and EP_3 receptors and are not observed in mice in which the genes for these receptors have been disrupted.[52]

Pulmonary Vasculature

Most eicosanoids induce constrictor responses in the pulmonary circulation. TXA_2 was first discovered because of its potent vasoconstrictor effect on rabbit aorta, and TP receptor agonists have similar effects on the pulmonary circulation.[53] Although PGE_2 is a vasodilator of other vascular beds and lowers blood pressure in vivo, it is generally a pulmonary vasoconstrictor, due to its interaction with vascular EP_3 receptors.[54] However, in some situations, presumably depending on receptor distribution, vasodilatation can also occur and is probably mediated by EP_2 receptors.[54] PGD_2 can induce vasodilatation through the DP_1 receptor.[55]

Although cysLTs have direct vasoconstrictor effects on the pulmonary vasculature, they induce NO-dependent relaxation in the guinea pig.[56] In humans, cysLTs constrict the pulmonary artery, but this effect is attenuated by the release of PGI_2. There is some evidence that this effect may be mediated by a novel cysLT receptor as it is resistant to both $cysLT_1$ receptor antagonists and the cysLT½ antagonist BAY u9773.[57]

In contrast to other eicosanoids, PGI_2 is a potent pulmonary vasodilator. In addition to its role in the adult, it appears to contribute (along with NO) to the dramatic reduction in pulmonary resistance that occurs following initiation of breathing after birth, being released in response to stretch.[58] Because of its potent dilatory effect on the pulmonary vasculature, PGI_2 (epoprostenol) is used to treat pulmonary hypertension. Unfortunately, because of its instability, it must be administered by continuous intravenous infusion with an indwelling catheter, which entails considerable risk when done over a long period of time. The use of longer-acting PGI_2 analogs administered by inhalation may reduce the risks and side effects considerably, as demonstrated in a recent clinical trial with iloprost.[59]

PGE_2 plays a critical role in regulating the fetal circulation through its EP_4-mediated dilatory effect on the ductus arteriosus.[60] During fetal life, the patent ductus arteriosus permits 90% of the blood entering the pulmonary artery to bypass the lungs, allowing circulating PGs to avoid pulmonary metabolism and thereby reach levels that are consistent with biologic activity. High levels of circulating PGE_2 are required to maintain the patency of the ductus arteriosus

in the fetus as the ductus itself converts arachidonic acid to PGI_2 rather than PGE_2. After birth, PGE_2 levels drop dramatically because of the redistribution of blood flow to the lungs, due to the decrease in pulmonary resistance that occurs after the initiation of breathing, permitting closure of the ductus. If this does not happen, pulmonary hypertension and death will ensue, due to a reversal of flow through the ductus caused by the lower pulmonary resistance after birth. The importance of pulmonary metabolism of PGE_2 in the newborn for closure of the ductus arteriosus has recently been demonstrated in a study using mice, in which the gene for 15-hydroxy PG dehydrogenase was deleted, resulting in failure of closure after birth and death of all of the neonates within 2 days.[61] This effect could be reversed by treatment of the dehydrogenase-deficient mice with indomethacin to lower PGE_2 levels.

Inflammatory Cells and Leukocyte Infiltration

Although chemokines are clearly important regulators of the infiltration of all classes of leukocytes into tissues, lipid mediators also play important roles in this process, especially with respect to neutrophils, eosinophils, monocytes, and basophils, because of their chemotactic effects on these cells. The most important chemoattractants among the eicosanoids are LTB_4, 5-oxo-ETE, and PGD_2.

Neutrophils Shortly after its discovery, LTB_4 was shown to be a highly potent in vitro neutrophil chemoattractant.[62] Early studies using intravital microscopy to examine a hamster cheek pouch preparation demonstrated the high potency of LTB_4 in inducing the adherence of leukocytes to vessel walls in vivo.[63] Consistent with this finding, intravenous injection of LTB_4 into rabbits was reported to induce a dramatic neutropenia, presumably due to increased adherence of neutrophils to the endothelium.[64] LTB_4 also elicits a dramatic infiltration of neutrophils into the skin following intradermal injection in humans and neutrophil infiltration into the lungs in guinea pigs.[65] 5-Oxo-ETE has effects on neutrophils similar to those of LTB_4 but is less potent. It is also active in vivo, inducing neutrophil infiltration into the skin.[66]

LTB_4 plays an important role in host defense against bacterial infection in vivo, through its effects on neutrophils. Mice lacking 5-LO are considerably more susceptible than wild-type mice to pulmonary bacterial infection.[67] This effect is due principally to a failure of neutrophils to adequately phagocytose bacteria and can be prevented by administration of LTB_4.

Eosinophils Among eicosanoids, the most potent chemoattractants for human eosinophils are 5-oxo-ETE and PGD_2. CysLTs appear to contribute to the infiltration of these cells into the lungs in asthma, but this effect appears to be indirect, possibly mediated by increased IL-5 production[68] or by some other mechanism,[69] as they have only very modest effects on human eosinophil migration in vitro.[70] LTB_4 is a potent chemotaxin for rodent eosinophils but has only weak effects on human cells.[10] PAF is also an eosinophil chemoattractant but is not as potent as 5-oxo-ETE.[70]

Eosinophils express high levels of the 5-oxo-ETE receptor,[33] and 5-oxo-ETE is a potent activator of these cells, inducing a variety of responses, including actin polymerization, Ca^{2+} mobilization, CD11b expression, and L-selectin shedding, in addition to chemotaxis.[33,71] It also stimulates eosinophil degranulation, which is enhanced by priming wth granulocyte–macrophage colony-stimulating factor.[71] 5-Oxo-ETE is also active in vivo. It elicits infiltration of eosinophils into the lungs of rats following intratracheal administration[73] and into human skin after intradermal injection, with asthmatic subjects responding more strongly than control subjects.[66] As well as being a potent eosinophil chemoattractant in its own right, 5-oxo-ETE can act synergistically with the chemokines eotaxin and RANTES,[33] as well as with the lipid mediator PAF,[70] in inducing eosinophil migration in vitro.

Human eosinophils also express high levels of the DP_2 receptor (CRTH2). PGD_2 is a potent chemoattractant for these cells and also stimulates a variety of responses similar to those elicited by 5-oxo-ETE.[26,27] Unlike 5-oxo-ETE, PGD_2 is selective for eosinophils over neutrophils as the latter do not express the DP_2 receptor. Although at higher concentrations ($\geq$100 nM), 5-oxo-ETE elicits a much stronger chemotactic response in eosinophils than PGD_2, at low nanomolar concentrations these two eicosanoids have similar effects.[39] Intravenous infusion of PGD_2 induces a reduction in the level of circulating eosinophils, presumably due to activation and sequestering of these cells by interaction with the endothelium. Superfusion of dog trachea with PGD_2 has been shown to induce the tissue accumulation of eosinophils.[74]

Th2 Cells Among lymphocytes, the DP_2 receptor is selectively expressed on Th2 cells, and PGD_2 is a potent chemoattractant for these cells.[26] Relatively little is known about other effects of PGD_2 on Th2 cells, although antigen-challenged mice lacking the DP_1 receptor display reduced levels of Th2 cytokines,[50] suggesting that PGD_2 could have a stimulatory effect on their production. There is also evidence that PGD_2 can promote a Th2 response through a DP_1 receptor–mediated effect on dendritic cells.[75]

Basophils Because of the small numbers of circulating basophils and the lack of good basophil markers in the past, less is known about the roles of eicosanoids in regulating the function of these cells. However, human basophils were recently shown to express the DP_2 receptor and to undergo chemotaxis in response to PGD_2.[26] Furthermore, we recently found that PGD_2 is by far the most potent eicosanoid in stimulating the surface expression of basophil activation markers. 5-Oxo-ETE and LTB_4 are less potent, and LTD_4 is virtually inactive.[76] In spite of its potent effect on the expression of the selective basophil activation marker CD203c, PGD_2 does not induce basophil degranulation.

Vascular Permeability

LTD_4 is a very potent stimulator of vascular permeability in vivo, as shown in the hamster cheek pouch with the use of

intravital microscopy.[63] Studies with knockout mice indicate that both LTC_4 synthase and the $cysLT_1$ receptor[77] play important roles in the increase in vascular permeability induced by zymosan in the mouse. CysLTs are also involved in allergen-induced microvascular permeability changes in animal models of asthma[78] and mediate the increase in vascular permeability observed following viral-induced neurogenic inflammation in the lungs.[79] LTB_4 and PGE_2 do not by themselves enhance plasma leakage but can enhance the response to other agonists through their effects on neutrophils and blood flow, respectively.

Mucous Secretion

LTC_4 and LTD_4 increase mucous secretion by the airways of humans and other species.[80] CysLTs appear to play a role as physiologic mediators of this response as mucous secretion in response to allergen challenge can be blocked by $cysLT_1$ receptor antagonists. Moreover, cysLTs are released in response to IL-13 and various cytokines and mediate at least part of their effects on mucous secretion.[81] PGD_2 may also be involved in regulating mucous production as high levels of the DP_1 receptor are present on goblet cells.[82]

EFFECTS OF GLUCOCORTICOIDS ON EICOSANOID PATHWAYS

Glucocorticoids can interact with the biosynthesis and actions of eicosanoids at multiple levels. They have inhibitory effects on the expression of a number of enzymes required for eicosanoid synthesis, including both $cPLA_2$ and $sPLA_2$,[2] and could therefore potentially inhibit the formation of all eicosanoids. The induction of COX-2 by various cytokines and growth factors is also inhibited by glucocorticoids, at both the transcriptional level and at the level of mRNA stability. Similarly, expression of the inducible mPGES-1, which converts PGH_2 to PGE_2, is inhibited by glucocorticoids.[83] In contrast, glucocorticoids stimulate the expression of some of the enzymes/proteins involved in the formation of 5-LO products, including 5-LO and FLAP in monocytes,[84] and γ-glutamyl transpeptidase–related enzyme, which converts LTC_4 to LTD_4, in bronchial epithelial cells.[85]

Despite their in vitro inhibitory effects on some of the enzymes required for the formation of eicosanoids, in vivo inhibition of eicosanoid formation by glucocorticoids has been more difficult to demonstrate. For example, treatment with steroids did not reduce the levels of cysLT metabolites in urine following challenge of asthmatic subjects.[86] Furthermore, the levels of LTE_4 and PGD_2 in BAL fluid from asthmatic subjects following allergen challenge were not affected by prior treatment with oral prednisone, in spite of its ability to inhibit eicosanoid production by BAL fluid macrophages from these individuals in vitro.[87] This variability may be due to differing effects of steroids on eicosanoid synthesis among different cell types, with some cells, such as macrophages and basophils, exhibiting substantial inhibition, and others, such as neutrophils, mast cells, and monocytes, being unaffected.[88] In contrast to the lack of effect of steroids on eicosanoid formation in human subjects, we found that dexamethasone substantially reduced the levels of urinary cysLT metabolites in Brown Norway rats following antigen challenge.[89] This may be because cysLTs originate from different cell types in the two species. In humans, they appear to be synthesized primarily by mast cells and eosinophils. In contrast, rat eosinophils produce little LTC_4, whereas rat macrophages may be a major site for the formation of this substance.[90]

Glucocorticoids can also affect responses to eicosanoids. Dexamethasone reduces the responsiveness of Brown Norway rat airways to LTD_4 in vivo.[89] In contrast, this steroid increases the responsiveness of neutrophils to LTB_4 by increasing the expression of the BLT_1 receptor.[91] This may contribute to the paradoxical inhibitory effect of glucocorticoids on neutrophil apoptosis as the effect of dexamethasone could be blocked by the BLT_1 receptor antagonist U75302.

CONTRIBUTION OF EICOSANOIDS TO ASTHMA

5-LO Products

CysLTs The association of eicosanoids with asthma goes back over 60 years to the initial discovery in Australia of the biologic activity now attributed to the cysLTs and initially referred to as "slow-reacting substance of anaphylaxis."[42] Although there was considerable evidence for a role for this substance in asthma, substantial progress in this area did not occur until the structural elucidation of the cysLTs by Samuelsson's group in Sweden in 1979.[92] Following the chemical synthesis of LTC_4, LTD_4, and LTE_4, it became clear that these substances are highly potent bronchoconstrictors and proinflammatory agents.

There is abundant evidence for the rapid release of eicosanoids in response to challenge of asthmatic subjects. High levels of LTC_4 are found in BAL fluid following allergen challenge of atopic asthmatic subjects (Table 43-2).[93] Although its concentrations are ~15 times lower than those of histamine, the amount of cysLTs released would be much more significant biologically because of their much greater potency. Elevated levels of cysLTs are also present in urine,[94] sputum,[95] and exhaled breath condensate[96] from asthmatic subjects following challenge.

Because of their production by the lung and their potent bronchoconstrictor and proinflammatory effects, cysLTs present an attractive target for the development of antiasthma drugs. A substantial number of agents have been developed that either block the synthesis of the cysLTs along with other 5-LO products (5-LO inhibitors) or prevent their

Table 43-2 Levels of Eicosanoids and Histamine in Bronchoalveolar Lavage Fluid Following Allergen Challenge of Atopic Asthmatic Subjects

Mediator (pg/mL)	*Baseline*	*Challenge*
PGD_2	90 ± 20	1,400 ± 400
LTC_4	60 ± 20	620 ± 190
TXB_2	50 ± 10	180 ± 30
Histamine	1,100 ± 500	8,800 ± 1,300

Data from Wenzel SE et al. 1990.[93]
LTC_4 = leukotriene C_4; PGD_2 = prostaglandin D_2; TXB_2 = thromboxane B_2.

Table 43-3 Anti–Eicosanoid Drugs Used in the Treatment of Asthma

Target	*Drug*	*Other names*	*Company*
$CysLT_1$ receptor	Singulair	Montelukast, MK-0476	Merck
$CysLT_1$ receptor	Accolate	Zafirlukast, ICI 204,219	Astra-Zeneca
$CysLT_1$ receptor	Onon, Ultair*	Pranlukast, ONO-1078	Ono
5-LO	Zyflo	Zileuton, Leutrol, A-64077	Abbott
TP receptor	Bronica*	Seratrodast, A-2414	Takeda
TXA synthase	Domenan*	Ozagrel, OKY-046	Kissei

*Available in Japan but not in North America.
LT = leukotriene; TXA = thromboxane A.

actions ($cysLT_1$ receptor antagonists). This area has been extensively reviewed[97,98] and is not addressed in detail here. The results of early experiments in which these agents were used in both humans and animal models supported an important role for cysLTs in asthma. For example, MK-571, one of the early $cysLT_1$ antagonists developed by Merck, completely blocked antigen-induced bronchoconstriction in both Brown Norway rats and squirrel monkeys. Many studies in humans have provided strong evidence for a critical role of cysLTs in asthmatic responses induced by allergen, exercise, and nonsteroidal antiinflammatory drug (NSAIDs). In addition to their inhibitory effects on airway resistance following challenge of asthmatic subjects, both $cysLT_1$ antagonists and 5-LO inhibitors also inhibit pulmonary eosinophilia and Th2 cytokine production.[99] $CysLT_1$ antagonists have also been shown to block smooth muscle hyperplasia and mucous secretion associated with airway remodeling following exposure to allergen.[47,48]

Further evidence for a central role for cysLTs as mediators in asthma comes from studies with knockout mice. 5-LO–deficient mice did not develop hyperresponsiveness to methacholine following exposure to antigen, as occurred in control wild-type mice.[100] The knockout mice were also protected from antigen-induced eosinophilia and had much lower serum IgE levels in comparison wild-type controls.[100]

There are currently three anti-LT drugs on the North American market, all orally active, that are used in the treatment of asthma (Table 43-3). Zileuton is a 5-LO inhibitor that is relatively short-acting and must be given four times a day. Although its use is somewhat restricted because of a possible effect on liver enzymes, its efficacy is comparable to those of $cysLT_1$ receptor antagonists.[101] There are two $cysLT_1$ receptor antagonists available in North America, montelukast[102] and zafirlukast,[103] administered once a day and twice a day, respectively. A third $cysLT_1$ antagonist, pranlukast,[104] is available in Japan and Latin America. Not all asthmatic subjects respond to the above LT modifiers, and they are not as efficacious as glucocorticoids.[105] However, they clearly have beneficial effects in a substantial proportion of patients and have additive effects with glucocorticoids in asthmatic subjects incompletely controlled with the latter drugs.[106]

Pharmacogenetics and Responses to LT-Modifying Drugs The individual variability in the responses of individuals to drugs designed to prevent the actions of cysLTs could be due in part to genetic differences. The promoter region of the 5-LO gene (ALOX5) normally contains five tandem repeats of the Sp1-binding motif GGGCGG (allele frequency 0.77), but some individuals possess three, four, or six repeats of this motif.[107] Replacement of the wild-type five tandem repeats with either a greater or lesser number of repeats in *both* alleles is associated with lower promoter activity and, in asthmatic subjects, with lack of improvement following treatment with the 5-LO inhibitor ABT-761.[107] A reduced ability of these asthmatic subjects to synthesize cysLTs would mean that their disease would be less dependent on these mediators, and hence they would be less susceptible to LT-modifying drugs. However, only about 6% of asthmatic subjects fall into this category, so this would explain the lack of response to LT modifiers of only a relatively small number of subjects.

A single-nucleotide polymorphism exists in the promoter region of the LTC_4 synthase gene, in which cytosine has replaced adenine 444 bases upstream from the translation start site. The allelic frequency of the $A_{-444}C$ polymorphism was originally reported to be higher in aspirin-intolerant asthmatic subjects,[108] but this has not been confirmed in later studies.[109] It has been reported that subjects with the $A_{-444}C$ polymorphism respond better to the $cysLT_1$ antagonists zafirlukast[110] and pranlukast.[111]

Other 5-LO Products Although the cysLTs appear to be the most important proinflammatory mediators among 5-LO products in asthma, other 5-LO products could also be involved as their synthesis would also be blocked by 5-LO inhibitors. For example, there is evidence that 5-LO products other than LTs may be involved in the induction of pulmonary eosinophilia in response to antigen challenge[112] or Sephadex beads,[113] raising the possibility that 5-oxo-ETE could be involved in this phenomenon. It is also possible that LTB_4 and 5-oxo-ETE could be involved in the neutrophilic inflammation seen in severe asthma.

Cyclooxygenase Products

TXA_2 TXA_2 is a potent bronchoconstrictor, and the levels of its degradation product TXB_2 in BAL fluid are elevated following allergen challenge of atopic asthmatic subjects (see Table 43-2). Guinea pig lungs have a very high capacity to synthesize TXA_2, and this substance could play an important role in allergen-induced airway narrowing in this animal model. However, the evidence is less clear in humans, although two drugs that interfere with either the synthesis (Ozagrel) or the action (Seratrodast) of TXA_2 are available on the Japanese market (see Table 43-3).[114] It would appear that only a subgroup of patients respond to these agents. For example, in one study, only 40% of the subjects responded to Seratrodast. This group was characterized by higher levels of a urinary TXA_2 metabolite (11-dehydro-TXB_2), suggesting that anti-TX drugs may be useful in a subgroup of patients with high levels of TXA synthase activity.

PGD_2 The presence of high levels of hematopoietic-type PGD synthase in mast cells places PGD_2 in an ideal position

to play an important role in atopic asthma. Consistent with this, dramatically increased amounts of PGD_2 are found in BAL fluid following allergen challenge of asthmatic subjects (see Table 43-2).[93,115] Although the role of PGD_2 in asthma in humans is not yet clear, a number of animal studies suggest that this PG may be an important inflammatory mediator in this disease. Although high doses of PGD_2 can induce airway constriction, these effects appear to be mediated by interaction with TP receptors, and the main role of PGD_2 is probably due to its proinflammatory effects. Overexpression of lipocalin-type PGD synthase in mice results in increased numbers of eosinophils and lymphocytes in BAL fluid following antigen challenge, as well as increased levels of Th2 cytokines (IL-4 and IL-5) and eotaxin.[113]

Two recent findings have focused attention on PGD_2 as a possible drug target in asthma therapy. An elegant study using DP_1 receptor knockout mice showed that these animals exhibit reduced asthma-like symptoms following antigen challenge.[50] The numbers of eosinophils and lymphocytes in BAL fluid were dramatically lower in $DP_1^{-/-}$ mice than in wild-type controls, and hyperresponsiveness to acetylcholine was reduced, suggesting that activation of DP_1 receptors by PGD_2 following antigen challenge contributes to the resulting airway inflammation and hyperresponsiveness. The mechanism for these effects is uncertain as this receptor is coupled to adenylyl cyclase, and elevation of cAMP levels in eosinophils leads to reduced responsiveness to inflammatory mediators. However, the levels of Th2 cytokines (IL-4, IL-5, and IL-13) were much lower in BAL fluid from the $DP_1^{-/-}$ mice in comparison with wild-type mice following antigen challenge,[50] suggesting that PGD_2 may favor a Th2 response. This could possibly be explained, at least in part, by a DP_1 receptor–mediated inhibitory effect of PGD_2 on the production of IL-12 by dendritic cells,[75] thus favoring a Th2 response and eosinophil infiltration. Another possibility is that stimulation of DP_1 receptors results in increased eosinophil survival as DP_1 receptor agonists,[117] like other agents that elevate cAMP levels in eosinophils, including PGE_2, promote the survival of these cells. Further evidence for a role for the DP_1 receptor in airway inflammation is the finding that antigen-induced pulmonary eosinophilia is reduced following treatment of sensitized guinea pigs with an antagonist of this receptor.[118]

The second recent advance implicating PGD_2 in allergy and asthma was the discovery of a second receptor for this PG, termed either the DP_2 receptor[27] or CRTH2.[26] As this receptor is expressed on eosinophils, Th2 cells, and basophils and mediates the chemotactic effect of PGD_2 on these cells, it could potentially be important in asthma. However, there are as yet no selective DP_2 receptor antagonists, and its physiologic role has not yet been fully evaluated.

BENEFICIAL ROLES OF EICOSANOIDS IN ASTHMA

In spite of the potential detrimental roles of PGD_2 and TXA_2 in asthma, studies in animal models suggest that, on balance, prostanoids play a beneficial role. Interestingly, disruption of the gene for the constitutive COX-1 rather than that for the inducible COX-2 results in exacerbation of asthma-like responses in C57B/6 mice. Thus, COX-$1^{-/-}$ mice that had been sensitized to ovalbumin (OVA) exhibited increased baseline airway resistance, hyperresponsiveness to methacholine, and epithelial permeability, whereas COX-$2^{-/-}$ mice exhibited only increased epithelial permeability.[119] However, in another study, the results of treatment of BALB/c mice with selective COX-1 and COX-2 inhibitors suggested that both enzymes play a role in limiting OVA-induced airway hyperresponsiveness and that COX-2 is more important in limiting expression of IL-5, IL-13, and several chemokine receptors in the lung.[120] In any case, these studies suggest that, on balance, cyclooxygenase products play a protective role in limiting asthma-like responses in these animal models. There is also evidence in humans that prostanoids act as endogenous inhibitory mediators in exercise-induced asthma and are responsible for the fact that airways become refractory to exercise following an initial exercise challenge.[121] It would seem likely that the cyclooxygenase product responsible for these effects is PGE_2.

PGE_2

Although most eicosanoids exert proinflammatory or bronchoconstrictor effects in asthma, PGE_2 stands out as a mediator with potent antiinflammatory and bronchodilator effects (Figure 43-3B). As PGE_2 can increase cAMP levels through its effects on EP_2 and EP_4 receptors, it could potentially induce airway relaxation in a manner similar to β-agonists. Indeed, it has long been known that PGE_2 has bronchodilator effects, particularly in asthmatic subjects. However, PGE_2 occasionally induces bronchoconstrictor responses in some subjects and has irritant effects on the upper airways, resulting in coughing.

PGE_2 attenuates airway constriction following exercise challenge of individuals with exercise-induced asthma[122] and inhibits both the early and late responses as well as airway hyperresponsiveness and eosinophilia induced by allergen challenge of atopic asthmatic subjects.[123] It has similar effects in OVA-challenged Brown Norway rats, inhibiting early and late responses as well as pulmonary eosinophilia.[124] Although the bronchodilator properties of PGE_2 could potentially contribute to its inhibitory effect on the early response, this effect would not persist long enough to affect the late response. The beneficial effect of PGE_2 is therefore due principally to its antiinflammatory properties, including its inhibitory effects on cell activation and mediator release. In Brown Norway rats, PGE_2 completely blocked the increase in BAL fluid cysLT levels following OVA challenge and reduced the numbers of BAL cells expressing the Th2 cytokines IL-4 and IL-5.[124] In contrast, it had no effect on the numbers of cells expressing the Th1 cytokine IFN-γ. In human asthmatic subjects, PGE_2 significantly reduced the levels of both PGD_2 and cysLTs in BAL fluid following allergen challenge.[125] The reduction in mediator release by PGE_2 is consistent with its inhibitory effects on the activation of many inflammatory cells in vitro, including mast cells, neutrophils, eosinophils, and basophils, resulting from its stimulatory effects on adenylyl cyclase.

Because of its potent inhibitory effects in asthmatic subjects and animal models of asthma, PGE_2 could potentially be a useful therapeutic agent in asthma, especially as its effects are complementary to those of steroids and β-agonists. Its mechanism of action is quite different from that of steroids, and it is much more effective in inhibiting the formation of cysLTs. Although it acts similarly to β-agonists in elevating intracellular cAMP levels and can induce bronchodilatation, unlike the latter agents, its effectiveness is principally due to its antiinflammatory properties. However, the usefulness of PGE_2 has been limited by its effect on neurally mediated coughing through stimulation of EP_1 and EP_3 receptors.[52] Selective EP_2 or EP_4 agonists that can be administered directly into the airways to avoid systemic side effects and rapid metabolism may offer a promising therapeutic approach in the future.

Lipoxins

LXA_4 reduces LTC_4-induced bronchoconstriction in humans, probably due to its antagonistic effect at the $cysLT_1$ receptor,[36] and inhibits PAF-induced migration of human eosinophils (see Figure 43-3B).[126] A recent study in mice demonstrated that a 15-epi-LXA_4 analog inhibits OVA-induced hyperresponsiveness and pulmonary infiltration of eosinophils and lymphocytes and reduces the levels of cysLTs, PGE_2, IL-13, and IL-5 in BAL fluid.[127] Selective overexpression of the human ALX receptor in mouse leukocytes had similar antiinflammatory effects but did not affect hyperresponsiveness.[127] Thus, metabolically resistant LXA_4 analogs such as the one used in this study [15-epi-16-(p-fluoro)-phenoxy-LXA_4 methyl ester] may potentially be of use in the treatment of asthma and other inflammatory diseases.

ASPIRIN-INDUCED ASTHMA

The interrelationship of stimulatory cysLTs and inhibitory PGs is dramatically illustrated in aspirin-induced asthma, which affects about 5 to 10% of asthmatic subjects.[128] Subjects with aspirin-induced asthma have elevated basal levels of urinary LTE_4 and respond acutely to ingestion of aspirin and other NSAIDs with airway narrowing and inflammation accompanied by increased urinary excretion of LTE_4. These responses can be inhibited by treatment with both anti-LT drugs and PGE_2. Aspirin-intolerant asthmatic subjects are characterized by very high levels of LTC_4 synthase in the lung in comparison with aspirin-tolerant asthmatic subjects, and it would seem that the inhibitory effects of prostanoids (presumably PGE_2) are particularly important in limiting cysLT production in these individuals.[129] It would appear that it is COX-1 that is responsible for the production of PGE_2 in these subjects as the selective COX-2 inhibitors rofecoxib[130] and celecoxib[131] are well tolerated by aspirin-intolerant asthmatic subjects.

CONCLUSIONS

The eicosanoids are a complex group of mediators that have wide-ranging effects on the lungs. 5-LO products are synthesized primarily by inflammatory cells and are involved in host defense in the lung. However, they also contribute to the pathology of inflammatory diseases, such as asthma, because of their potent bronchoconstrictor properties and their stimulatory effects on inflammatory cells and cytokine production. Drugs that prevent the synthesis or actions of cysLTs have proven useful in the treatment of asthma. It is possible that the development of second-generation 5-LO inhibitors could also be of some benefit because they would also inhibit the synthesis of 5-oxo-ETE and LTB_4, which are also potent proinflammatory mediators. Cyclooxygenase products are synthesized by both structural and inflammatory cells in the lung and elicit a large array of responses, depending on the target. TXA_2 is a potent smooth muscle constrictor, whereas PGD_2 is a potent proinflammatory mediator. PGI_2 is a pulmonary vasodilator that is useful in the treatment of pulmonary hypertension, and PGE_2 has antiinflammatory effects that are important in limiting asthmatic responses.

REFERENCES

1. Funk CD. Prostaglandins and leukotrienes: advances in eicosanoid biology. Science 2001;294:1871–5.
2. Kudo I, Murakami M. Phospholipase A2 enzymes. Prostaglandins Other Lipid Mediat 2002;68–69:3–58.
3. Smith WL, DeWitt DL, Garavito RM. Cyclooxygenases: structural, cellular, and molecular biology. Annu Rev Biochem 2000;69:145–82.
4. Jakobsson PJ, Thoren S, Morgenstern R, Samuelsson B. Identification of human prostaglandin E synthase: a microsomal, glutathione-dependent, inducible enzyme, constituting a potential novel drug target. Proc Natl Acad Sci U S A 1999;96:7220–5.
5. Dworski R, Murray JJ, Roberts LJ, et al. Allergen-induced synthesis of F_2-isoprostanes in atopic asthmatics. Evidence for oxidant stress. Am J Respir Crit Care Med 1999;160:1947–51.
6. Montuschi P, Corradi M, Ciabattoni G, et al. Increased 8-isoprostane, a marker of oxidative stress, in exhaled condensate of asthma patients. Am J Respir Crit Care Med 1999;160:216–20.
7. Wainwright SL, Powell WS. Mechanism for the formation of dihydro metabolites of 12-hydroxyeicosanoids. Conversion of leukotriene B_4 and 12-hydroxy-5,8,10,14-eicosatetraenoic acid to 12-oxo intermediates. J Biol Chem 1991;266:20899–906.
8. Yamamoto T, Yokomizo T, Nakao A, et al. Immunohistochemical localization of guinea-pig leukotriene B4 12-hydroxydehydrogenase/15-ketoprostaglandin 13-reductase. Eur J Biochem 2001;268:6105–13.
9. Powell WS, Gravelle F, Gravel S. Metabolism of 5(S)-hydroxy-6,8,11,14-eicosatetraenoic acid and other 5(S)-hydroxy-eicosanoids by a specific dehydrogenase in human polymorphonuclear leukocytes. J Biol Chem 1992;267:19233–41.
10. Sun FF, Crittenden NJ, Czuk CI, et al. Biochemical and functional differences between eosinophils from animal species and man. J Leukoc Biol 1991;50:140–50.
11. Tanaka K, Ogawa K, Sugamura K, et al. Differential production of prostaglandin D_2 by human helper T cell subsets. J Immunol 2000;164:2277–80.
12. Elias JA, Gustilo K, Baeder W, Freundlich B. Synergistic stimulation of fibroblast prostaglandin production by recombinant interleukin 1 and tumor necrosis factor. J Immunol 1987;138:3812–6.

13. Carley WW, Niedbala MJ, Gerritsen ME. Isolation, cultivation, and partial characterization of microvascular endothelium derived from human lung. Am J Respir Cell Mol Biol 1992;7:620–30.
14. Boyce JA. Mast cells: beyond IgE. J Allergy Clin Immunol 2003; 111:24–32.
15. Piper PJ, Vane JR, Wyllie JH. Inactivation of prostaglandins by the lungs. Nature 1970;225:600–4.
16. Hamberg M, Samuelsson B. On the metabolism of prostaglandins E_1 and E_2 in man. J Biol Chem 1971;246:6713–21.
17. Gronert K, Clish CB, Romano M, Serhan CN. Transcellular regulation of eicosanoid biosynthesis. Methods Mol Biol 1999;120:119–44.
18. Fabre JE, Goulet JL, Riche E, et al. Transcellular biosynthesis contributes to the production of leukotrienes during inflammatory responses in vivo. J Clin Invest 2002;109: 1373–80.
19. Grimminger F, Kreusler B, Schneider U, et al. Influence of microvascular adherence on neutrophil leukotriene generation. Evidence for cooperative eicosanoid synthesis. J Immunol 1990;144:1866–72.
20. Scoggan KA, Jakobsson PJ, Ford-Hutchinson AW. Production of leukotriene C_4 in different human tissues is attributable to distinct membrane bound biosynthetic enzymes. J Biol Chem 1997;272:10182–7.
21. Lecomte M, Laneuville O, Ji C, et al. Acetylation of human prostaglandin endoperoxide synthase-2 (cyclooxygenase-2) by aspirin. J Biol Chem 1994;269:13207–15.
22. Lee TH, Crea AE, Gant V, et al. Identification of lipoxin A4 and its relationship to the sulfidopeptide leukotrienes C_4, D_4, and E_4 in the bronchoalveolar lavage fluids obtained from patients with selected pulmonary diseases. Am Rev Respir Dis 1990;141:1453–8.
23. Coleman RA, Smith WL, Narumiya S. International Union of Pharmacology classification of prostanoid receptors: properties, distribution, and structure of the receptors and their subtypes. Pharmacol Rev 1994;46:205–29.
24. Breyer RM, Bagdassarian CK, Myers SA, Breyer MD. Prostanoid receptors: subtypes and signaling. Annu Rev Pharmacol Toxicol 2001;41:661–90.
25. Gobeil F Jr, Vazquez-Tello A, Marrache AM, et al. Nuclear prostaglandin signaling system: biogenesis and actions via heptahelical receptors. Can J Physiol Pharmacol 2003;81: 196–204.
26. Hirai H, Tanaka K, Yoshie O, et al. Prostaglandin D_2 selectively induces chemotaxis in T helper type 2 cells, eosinophils, and basophils via seven-transmembrane receptor CRTH2. J Exp Med 2001;193:255–61.
27. Monneret G, Gravel S, Diamond M, et al. Prostaglandin D_2 is a potent chemoattractant for human eosinophils that acts via a novel DP receptor. Blood 2001;98:1942–8.
28. Stubbs VE, Schratl P, Hartnell A, et al. Indomethacin causes prostaglandin D_2-like and eotaxin-like selective responses in eosinophils and basophils. J Biol Chem 2002;277: 26012–20.
29. Brink C, Dahlen SE, Drazen J, et al. International Union of Pharmacology XXXVII. Nomenclature for leukotriene and lipoxin receptors. Pharmacol Rev 2003;55:195–227.
30. Lynch KR, O'Neill GP, Liu Q, et al. Characterization of the human cysteinyl leukotriene $CysLT_1$ receptor. Nature 1999; 399:789–93.
31. Espinosa K, Bosse Y, Stankova J, Rola-Pleszczynski M. CysLT1 receptor upregulation by TGF-beta and IL-13 is associated with bronchial smooth muscle cell proliferation in response to LTD_4. J Allergy Clin Immunol 2003;111:1032–40.
32. Heise CE, O'Neill BF, Figueroa DJ, et al. Characterization of the human cysteinyl leukotriene 2 receptor. J Biol Chem 2000; 275:30531–6.
33. Jones CE, Holden S, Tenaon L, et al. Expression and characterization of a 5-oxo-6E, 8Z, 11Z, 14Z-eicosatetraenoic acid receptor highly expressed on human eosinophils and neutrophils. Mol Pharmacol 2003;63:471–7.
34. Hosoi T, Koguchi Y, Sugikawa E, et al. Identification of a novel eicosanoid receptor coupled to $G_{i/o}$. J Biol Chem 2002;277: 31459–65.
35. McMahon B, Mitchell S, Brady HR, Godson C. Lipoxins: revelations on resolution. Trends Pharmacol Sci 2001;22: 391–5.
36. Gronert K, Martinsson-Niskanen T, Ravasi S, et al. Selectivity of recombinant human leukotriene D_4, leukotriene B_4, and lipoxin A_4 receptors with aspirin-triggered 15-epi-LXA_4 and regulation of vascular and inflammatory responses. Am J Pathol 2001;158:3–9.
37. Daynes RA, Jones DC. Emerging roles of PPARs in inflammation and immunity. Nat Rev Immunol 2002;2:748–59.
38. Straus DS, Glass CK. Cyclopentenone prostaglandins: new insights on biological activities and cellular targets. Med Res Rev 2001;21:185–210.
39. Powell WS. A novel PGD_2 receptor expressed in eosinophils. Prostaglandins Leukot Essent Fatty Acids 2003;69:179–85.
40. Lin Q, Ruuska SE, Shaw NS, et al. Ligand selectivity of the peroxisome proliferator-activated receptor alpha. Biochemistry 1999;38:185–90.
41. Lim H, Dey SK. A novel pathway of prostacyclin signaling—hanging out with nuclear receptors. Endocrinology 2002; 143:3207–10.
42. Kellaway CH, Trethewie ER. The liberation of a slow-reacting smooth muscle-stimulating substance in anaphylaxis. Q J Exp Physiol 1940;30:121–45.
43. Dahlén SE, Hedqvist P, Hammarström S, Samuelsson B. Leukotrienes are potent constrictors of human bronchi. Nature 1980;288:484–6.
44. Arm JP, O'Hickey SP, Hawksworth RJ, et al. Asthmatic airways have a disproportionate hyperresponsiveness to LTE_4, as compared with normal airways, but not to LTC_4, LTD_4, methacholine, and histamine. Am Rev Respir Dis 1990; 142:1112–8.
45. Sirois P, Chagnon M, Borgeat P, Vallerand P. Role of cyclooxygenase products in the lung action of leukotrienes A_4, B_4, C_4, D_4 and E_4. Pharmacology 1985;31:225–36.
46. Panettieri RA, Tan EM, Ciocca V, et al. Effects of LTD_4 on human airway smooth muscle cell proliferation, matrix expression, and contraction in vitro: differential sensitivity to cysteinyl leukotriene receptor antagonists. Am J Respir Cell Mol Biol 1998;19:453–61.
47. Henderson WR Jr, Tang LO, Chu SJ, et al. A role for cysteinyl leukotrienes in airway remodeling in a mouse asthma model. Am J Respir Crit Care Med 2002;165:108–16.
48. Wang CG, Du T, Xu LJ, Martin JG. Role of leukotriene D_4 in allergen-induced increases in airway smooth muscle in the rat. Am Rev Respir Dis 1993;148:413–7.
49. Coleman RA, Sheldrick RL. Prostanoid-induced contraction of human bronchial smooth muscle is mediated by TP-receptors. Br J Pharmacol 1989;96:688–92.
50. Matsuoka T, Hirata M, Tanaka H, et al. Prostaglandin D_2 as a mediator of allergic asthma. Science 2000;287:2013–7.
51. Sheller JR, Mitchell D, Meyrick B, et al. EP_2 receptor mediates bronchodilation by PGE_2 in mice. J Appl Physiol 2000;88: 2214–8.
52. Tilley SL, Hartney JM, Erikson CJ, et al. Receptors and pathways mediating the effects of prostaglandin E2 on airway tone. Am J Physiol Lung Cell Mol Physiol 2003;284: L599–606.
53. Kaye AD, Nossaman BD, Ibrahim IN, et al. Analysis of thromboxane receptor-mediated responses in the feline pulmonary vascular bed. Crit Care Med 1995;23:164–70.
54. Jones RL, Qian Y, Wong HN, et al. Prostanoid action on the human pulmonary vascular system. Clin Exp Pharmacol Physiol 1997;24:969–72.

55. Walch L, Labat C, Gascard JP, et al. Prostanoid receptors involved in the relaxation of human pulmonary vessels. Br J Pharmacol 1999;126:859–66.
56. Sakuma I, Gross SS, Levi R. Peptidoleukotrienes induce an endothelium-dependent relaxation of guinea pig main pulmonary artery and thoracic aorta. Prostaglandins 1987;34: 685–96.
57. Walch L, Norel X, Back M, et al. Pharmacological evidence for a novel cysteinyl-leukotriene receptor subtype in human pulmonary artery smooth muscle. Br J Pharmacol 2002;137: 1339–45.
58. Heymann MA. Control of the pulmonary circulation in the fetus and during the transitional period to air breathing. Eur J Obstet Gynecol Reprod Biol 1999;84:127–32.
59. Olschewski H, Simonneau G, Galie N, et al. Inhaled iloprost for severe pulmonary hypertension. N Engl J Med 2002;347: 322–9.
60. Smith GC. The pharmacology of the ductus arteriosus. Pharmacol Rev 1998;50:35–58.
61. Coggins KG, Latour A, Nguyen MS, et al. Metabolism of PGE_2 by prostaglandin dehydrogenase is essential for remodeling the ductus arteriosus. Nat Med 2002;8:91–2.
62. Ford-Hutchinson AW, Bray MA, Doig MV, et al. Leukotriene B, a potent chemokinetic and aggregating substance released from polymorphonuclear leukocytes. Nature 1980;286: 264–5.
63. Dahlén SE, Björk J, Hedqvist P, et al. Leukotrienes promote plasma leakage and leukocyte adhesion in postcapillary venules: in vivo effects with relevance to the acute inflammatory response. Proc Natl Acad Sci U S A 1981;78: 3887–91.
64. Marleau S, Fortin C, Poubelle PE, Borgeat P. In vivo desensitization to leukotriene B_4 (LTB_4) in the rabbit. Inhibition of LTB_4-induced neutropenia during intravenous infusion of LTB_4. J Immunol 1993;150:206–13.
65. Silbaugh SA, Stengel PW, Williams GD, et al. Effects of leukotriene B_4 inhalation. Airway sensitization and lung granulocyte infiltration in the guinea pig. Am Rev Respir Dis 1987;136:930–4.
66. Muro S, Hamid Q, Olivenstein R, et al. 5-Oxo-6,8,11,14-eicosatetraenoic acid induces the infiltration of granulocytes into human skin. J Allergy Clin Immunol 2003;112: 768–74.
67. Bailie MB, Standiford TJ, Laichalk LL, et al. Leukotriene-deficient mice manifest enhanced lethality from Klebsiella pneumonia in association with decreased alveolar macrophage phagocytic and bactericidal activities. J Immunol 1996;157:5221–4.
68. Underwood DC, Osborn RR, Newsholme SJ, et al. Persistent airway eosinophilia after leukotriene (LT) D_4 administration in the guinea pig: modulation by the LTD4 receptor antagonist, pranlukast, or an interleukin-5 monoclonal antibody. Am J Respir Crit Care Med 1996;154:850–7.
69. Eum SY, Maghni K, Hamid Q, et al. Involvement of the cysteinyl-leukotrienes in allergen-induced airway eosinophilia and hyperresponsiveness in the mouse. Am J Respir Cell Mol Biol 2003;28:25–32.
70. Powell WS, Chung D, Gravel S. 5-Oxo-6,8,11,14-eicosatetraenoic acid is a potent stimulator of human eosinophil migration. J Immunol 1995;154:4123–32.
71. Powell WS, Ahmed S, Gravel S, Rokach J. Eotaxin and RANTES enhance 5-oxo-6,8,11,14-eicosatetraenoic acid-induced eosinophil chemotaxis. J Allergy Clin Immunol 2001;107: 272–8.
72. O'Flaherty JT, Kuroki M, Nixon AB, et al. 5-Oxo-eicosatetraenoate is a broadly active, eosinophil-selective stimulus for human granulocytes. J Immunol 1996;157:336–42.
73. Stamatiou P, Hamid Q, Taha R, et al. 5-Oxo-ETE induces pulmonary eosinophilia in an integrin-dependent manner in Brown Norway rats. J Clin Invest 1998;102:2165–72.
74. Emery DL, Djokic TD, Graf PD, Hadel JA, Prostaglandin D_2 causes accumulation of eosinophils in the lumen of the dog trachea. J Appl Physiol 1989;67:959–62.
75. Gosset P, Bureau F, Angeli V, et al. Prostaglandin D2 affects the maturation of human monocyte-derived dendritic cells: consequence on the polarization of naive Th cells. J Immunol 2003;170:4943–52.
76. Monneret G. Boumiza R, Gravel S, et al. Effects of prostaglandin D(2) and 5-lipoxygenase products on the expression of CD203C and CD11b by basophils. J Pharmacol Exp Ther 2005;312:627–34.
77. Maekawa A, Austen KF, Kanaoka Y. Targeted gene disruption reveals the role of cysteinyl leukotriene 1 receptor in the enhanced vascular permeability of mice undergoing acute inflammatory responses. J Biol Chem 2002;277:20820–4.
78. Evans TW, Rogers DF, Aursudkij B, et al. Inflammatory mediators involved in antigen-induced airway microvascular leakage in guinea pigs. Am Rev Respir Dis 1988;138:395–9.
79. Wedde-Beer K, Hu C, Rodriguez MM, Piedimonte G. Leukotrienes mediate neurogenic inflammation in lungs of young rats infected with respiratory syncytial virus. Am J Physiol Lung Cell Mol Physiol 2002;282:L1143–50.
80. Marom Z, Shelhamer JH, Bach MK, et al. Slow-reacting substances, leukotrienes C_4 and D_4, increase the release of mucus from human airways in vitro. Am Rev Respir Dis 1982;126:449–51.
81. Vargaftig BB, Singer M. Leukotrienes mediate murine bronchopulmonary hyperreactivity, inflammation, and part of mucosal metaplasia and tissue injury induced by recombinant murine interleukin-13. Am J Respir Cell Mol Biol 2003;28:410–9.
82. Wright DH, Nantel F, Metters KM, Ford-Hutchinson AW. A novel biological role for prostaglandin D_2 is suggested by distribution studies of the rat DP prostanoid receptor. Eur J Pharmacol 1999;377:101–15.
83. Stichtenoth DO, Thoren S, Bian H, et al. Microsomal prostaglandin E synthase is regulated by proinflammatory cytokines and glucocorticoids in primary rheumatoid synovial cells. J Immunol 2001;167:469–74.
84. Riddick CA, Ring WL, Baker JR, et al. Dexamethasone increases expression of 5-lipoxygenase and its activating protein in human monocytes and THP-1 cells. Eur J Biochem 1997; 246:112–8.
85. Zaitsu M, Hamasaki Y, Aoki Y, Miyazaki S. A novel pharmacologic action of glucocorticosteroids on leukotriene C_4 catabolism. J Allergy Clin Immunol 2001;108:122–4.
86. O'Shaughnessy KM, Wellings R, Gillies B, Fuller RW. Differential effects of fluticasone propionate on allergen-evoked bronchoconstriction and increased urinary leukotriene E_4 excretion. Am Rev Respir Dis 1993;147: 1472–6.
87. Dworski R, FitzGerald GA, Oates JA, Sheller JR. Effect of oral prednisone on airway inflammatory mediators in atopic asthma. Am J Respir Crit Care Med 1994;149:953–9.
88. Peters-Golden M, Sampson AP. Cysteinyl leukotriene interactions with other mediators and with glucocorticosteroids during airway inflammation. J Allergy Clin Immunol 2003; 111:S37–42.
89. Powell WS, Xu LJ, Martin JG. Effects of dexamethasone on leukotriene synthesis and airway responses to antigen and leukotriene D_4 in rats. Am J Respir Crit Care Med 1995;151: 1143–50.
90. Yu W, Xu LJ, Martin JG, Powell WS. Cellular infiltration and eicosanoid synthesis in Brown Norway rat lungs after allergen challenge. Am J Respir Cell Mol Biol 1995;13:477–86.

91. Stankova J, Turcotte S, Harris J, Rola-Pleszczynski M. Modulation of leukotriene B_4 receptor-1 expression by dexamethasone: potential mechanism for enhanced neutrophil survival. J Immunol 2002;168:3570–6.
92. Murphy RC, Hammarström S, Samuelsson B. Leukotriene C: a slow-reacting substance from murine mastocytoma cells. Proc Natl Acad Sci U S A 1979;76:4275–9.
93. Wenzel SE, Larsen GL, Johnston K, et al. Elevated levels of leukotriene C_4 in bronchoalveolar lavage fluid from atopic asthmatics after endobronchial allergen challenge. Am Rev Respir Dis 1990;142:112–9.
94. Manning PJ, Rokach J, Malo JL, et al. Urinary leukotriene E_4 levels during early and late asthmatic responses. J Allergy Clin Immunol 1990;86:211–20.
95. Macfarlane AJ, Dworski R, Sheller JR, et al. Sputum cysteinyl leukotrienes increase 24 hours after allergen inhalation in atopic asthmatics. Am J Respir Crit Care Med 2000;161: 1553–8.
96. Montuschi P, Barnes PJ. Exhaled leukotrienes and prostaglandins in asthma. J Allergy Clin Immunol 2002;109:615–20.
97. Peters SP. Leukotriene receptor antagonists in asthma therapy. J Allergy Clin Immunol 2003;111:S62–70.
98. Drazen JM, Israel E, O'Byrne PM. Treatment of asthma with drugs modifying the leukotriene pathway. N Engl J Med 1999;340:197–206.
99. Holgate ST, Peters-Golden M, Panettieri RA, Henderson WR Jr. Roles of cysteinyl leukotrienes in airway inflammation, smooth muscle function, and remodeling. J Allergy Clin Immunol 2003;111:S18–34.
100. Irvin CG, Tu YP, Sheller JR, Funk CD. 5-Lipoxygenase products are necessary for ovalbumin-induced airway responsiveness in mice. Am J Physiol 1997;272:L1053–8.
101. Leff AR. Regulation of leukotrienes in the management of asthma: biology and clinical therapy. Annu Rev Med 2001; 52:1–14.
102. Young RN. Discovery of montelukast: a once-a-day oral antagonist of leukotriene D4 for the treatment of chronic asthma. Prog Med Chem 2001;38:249–77.
103. Calhoun WJ. Summary of clinical trials with zafirlukast. Am J Respir Crit Care Med 1998;157:S238–45.
104. Keam SJ, Lyseng-Williamson KA, Goa KL. Pranlukast: a review of its use in the management of asthma. Drugs 2003;63:991–1019.
105. Ducharme FM. Inhaled glucocorticoids versus leukotriene receptor antagonists as single agent asthma treatment: systematic review of current evidence. BMJ 2003;326:621–3.
106. Laviolette M, Malmstrom K, Lu S, et al. Montelukast added to inhaled beclomethasone in treatment of asthma. Montelukast/Beclomethasone Additivity Group. Am J Respir Crit Care Med 1999;160:1862–8.
107. Drazen JM, Yandava CN, Dube L, et al. Pharmacogenetic association between ALOX5 promoter genotype and the response to anti-asthma treatment. Nat Genet 1999;22:168–70.
108. Sanak M, Szczeklik A. Genetics of aspirin induced asthma. Thorax 2000;55 Suppl 2:S45–7.
109. Van Sambeek R, Stevenson DD, Baldasaro M, et al. 5′ Flanking region polymorphism of the gene encoding leukotriene C_4 synthase does not correlate with the aspirin-intolerant asthma phenotype in the United States. J Allergy Clin Immunol 2000;106:72–6.
110. Sampson AP, Siddiqui S, Buchanan D, et al. Variant LTC_4 synthase allele modifies cysteinyl leukotriene synthesis in eosinophils and predicts clinical response to zafirlukast. Thorax 2000;55 Suppl 2:S28–31.
111. Asano K, Shiomi T, Hasegawa N, et al. Leukotriene C_4 synthase gene A(-444)C polymorphism and clinical response to a CYS-LT_1 antagonist, pranlukast, in Japanese patients with moderate asthma. Pharmacogenetics 2002;12:565–70.
112. Seeds EA, Kilfeather S, Okiji S, et al. Role of lipoxygenase metabolites in platelet-activating factor- and antigen-induced bronchial hyperresponsiveness and eosinophil infiltration. Eur J Pharmacol 1995;293:369–76.
113. Namovic MT, Walsh RE, Goodfellow C, et al. Pharmacological modulation of eosinophil influx into the lungs of Brown Norway rats. Eur J Pharmacol 1996;315:81–8.
114. Dogné JM, de Leval X, Benoit P, et al. Therapeutic potential of thromboxane inhibitors in asthma. Expert Opin Investig Drugs 2002;11:275–81.
115. Murray JJ, Tonnel AB, Brash AR, et al. Release of prostaglandin D_2 into human airways during acute antigen challenge. N Engl J Med 1986;315:800–4.
116. Fujitani Y, Kanaoka Y, Aritake K, et al. Pronounced eosinophilic lung inflammation and Th2 cytokine release in human lipocalin-type prostaglandin D synthase transgenic mice. J Immunol 2002;168:443–9.
117. Gervais FG, Cruz RP, Chateauneuf A, et al. Selective modulation of chemokinesis, degranulation, and apoptosis in eosinophils through the PGD_2 receptors CRTH2 and DP. J Allergy Clin Immunol 2001;108:982–8.
118. Arimura A, Yasui K, Kishino J, et al. Prevention of allergic inflammation by a novel prostaglandin receptor antagonist, S-5751. J Pharmacol Exp Ther 2001;298:411–9.
119. Gavett SH, Madison SL, Chulada PC, et al. Allergic lung responses are increased in prostaglandin H synthase-deficient mice. J Clin Invest 1999;104:721–32.
120. Peebles RS Jr, Hashimoto K, Morrow JD, et al. Selective cyclooxygenase-1 and -2 inhibitors each increase allergic inflammation and airway hyperresponsiveness in mice. Am J Respir Crit Care Med 2002;165:1154–60.
121. Manning PJ, Watson RM, O'Byrne PM. Exercise-induced refractoriness in asthmatic subjects involves leukotriene and prostaglandin interdependent mechanisms. Am Rev Respir Dis 1993;148(Pt 1):950–4.
122. Melillo E, Woolley KL, Manning PJ, et al. Effect of inhaled PGE_2 on exercise-induced bronchoconstriction in asthmatic subjects. Am J Respir Crit Care Med 1994;149:1138–41.
123. Gauvreau GM, Watson RM, O'Byrne PM. Protective effects of inhaled PGE_2 on allergen-induced airway responses and airway inflammation. Am J Respir Crit Care Med 1999;159: 31–6.
124. Martin JG, Suzuki M, Maghni K, et al. The immunomodulatory actions of prostaglandin E_2 on allergic airway responses in the rat. J Immunol 2002;169:3963–9.
125. Hartert TV, Dworski RT, Mellen BG, et al. Prostaglandin E_2 decreases allergen-stimulated release of prostaglandin D_2 in airways of subjects with asthma. Am J Respir Crit Care Med 2000;162:637–40.
126. Soyombo O, Spur BW, Lee TH. Effects of lipoxin A_4, on chemotaxis and degranulation of human eosinophils stimulated by platelet-activating factor and N-formyl-L-methionyl-L-leucyl-L-phenylalanine. Allergy 1994;49:230–4.
127. Levy BD, De Sanctis GT, Devchand PR, et al. Multi-pronged inhibition of airway hyper-responsiveness and inflammation by lipoxin A_4. Nat Med 2002;8:1018–23.
128. Szczeklik A, Stevenson DD. Aspirin-induced asthma: advances in pathogenesis, diagnosis, and management. J Allergy Clin Immunol 2003;111:913–21.
129. Cowburn AS, Sladek K, Soja J, et al. Overexpression of leukotriene C_4 synthase in bronchial biopsies from patients with aspirin-intolerant asthma. J Clin Invest 1998;101:834–46.
130. Martin-Garcia C, Hinojosa M, Berges P, et al. Safety of a cyclooxygenase-2 inhibitor in patients with aspirin-sensitive asthma. Chest 2002;121:1812–7.
131. Woessner KM, Simon RA, Stevenson DD. The safety of celecoxib in patients with aspirin-sensitive asthma. Arthritis Rheum 2002;46:2201–6.

CHAPTER 44

LUNG TRANSPLANTATION

Tom Kotsimbos

Human lung transplantation has now reached the stage of being regarded as an established therapy for end-stage lung disease in selected patients.[1,2] Indeed, for patients with severe functional impairment and limited life-expectancy, lung transplantation offers the possibility of marked improvements in survival and quality of life. The development of lung transplantation as a viable therapeutic option has been achieved in a remarkably short period of time when one considers that the first successful heart–lung transplant was only performed in 1981 for end-stage lung disease caused by pulmonary hypertension.[3]

Following the initial breakthroughs associated with successful en bloc heart–lung transplantation, single-lung transplantation and bilateral sequential lung transplantation (BSLTx) were rapidly developed for obstructive and restrictive end-stage lung disease and severe pulmonary vascular disease and soon became the procedures of choice for most forms of advanced lung disease where transplantation was an option.[4–6] Currently, the most common indications for lung transplantation are chronic obstructive pulmonary disease (COPD) (including emphysema due to α_1-antitrypsin deficiency), cystic fibrosis–related end-stage bronchiectasis, idiopathic pulmonary fibrosis (IPF), primary pulmonary hypertension, and Eisenmenger's syndrome.[2,7]

The 1980s and early 1990s were associated with many technical successes in the field of lung transplantation.[8] This was followed by a period of consolidative growth in the middle to late 1990s, during which time both the number of lung transplantation procedures and the number of potential recipients on lung transplantation waiting lists increased significantly. It is beyond doubt that over the last 20 years there have been dramatic improvements in early survival, largely due to advances in organ preservation, surgical techniques, and postoperative care.[9,10] Despite these early improvements, however, there has been no real impact on long-term survival. The major causes of long-term morbidity and mortality after lung transplantation remain chronic allograft rejection in the form of bronchiolitis obliterans syndrome (BOS) and infection.[9] BOS is characterized by chronic airflow limitation progressing from months to years. The risk has been estimated to be between 30 and 50% within 2 years, with a mortality rate approaching 50% within 3 years of developing BOS, emphasizing the major human and financial burden from this disease.[2] Infection in lung transplant recipients often occurs in the lung allograft itself and is frequently aggravated by a course of augmented immunosuppression for BOS.

LUNG TRANSPLANT RECIPIENT SELECTION

General Considerations

Lung transplantation is considered to be the last management option for advanced lung disease for which all standard therapies have been tried and have failed. Potential lung transplantation candidates should have untreatable end-stage pulmonary disease, a limited life-expectancy, and no other significant medical comorbidity. The major indications for lung transplantation are shown in Table 44-1. Typical age criteria include <65 years for single-lung transplantation, <60 years for BSLTx, and <55 years for heart–lung transplantation.[11,12]

In general, a patient should be referred for lung transplantation at the stage in the course of their disease at which death is considered likely within 1 to 2 years. More specifically, listing for lung transplantation should occur when it would enhance life expectancy (this assessment takes into account the risk of dying on the waiting list and transplantation procedure–related mortality rates). Indeed, the available prognostic indicators have formed the basis of the disease-specific guidelines for lung transplantation referral and its appropriate timing that have now been formulated.[13] Although group prognostic data are of major importance in deciding who should be further assessed for lung transplantation, other critical factors that need to be integrated into the decision-making process include individual rates of deterioration in lung function status, the patient's current quality-of-life status, the anticipated time on the lung transplantation waiting list, and the presence of any significant comorbidities that may greatly increase the risk of posttransplantation complications.[11]

Although transplantation should be offered only to patients with end-stage lung disease for whom there are no alternative options, careful selection criteria are used so that, usually, inappropriate candidates are not transplanted simply because of the desperate nature of their situation. Moreover, although patients on the lung transplantation waiting list are functionally disabled and have a high risk of death within a few years, they should still be ambulatory

Table 44-1 Main Indications for Lung Transplantation

Obstructive lung disease
Cystic fibrosis/bronchiectasis
COPD secondary to α_1-antitrypsin deficiency
COPD secondary to cigarette smoking
Restrictive lung disease
Idiopathic pulmonary fibrosis
Sarcoidosis
Lymphangioleiomyomatosis
Histiocytosis X
Systemic connective tissue disease (primarily limited to the lung)
Pulmonary vascular disease
Eisenmenger's syndrome
Primary pulmonary hypertension

COPD = chronic obstructive pulmonary disease.

Table 44-2 International Guidelines for Lung Transplantation Referral

Obstructive lung disease
Post-bronchodilator FEV_1 <30% predicted (without reversibility)
Resting hypoxemia and hypercapnia (PO_2 < 60 mm Hg, PCO_2 > 50 mm Hg)
Pulmonary hypertension
Progressive deterioration
Frequent hospitalizations
Restrictive lung disease
TLC or VC < 60% predicted
DLco < 40%
Resting hypoxemia
Secondary pulmonary hypertension
Progressive deterioration
Pulmonary hypertension
NYHA Class III or IV (despite optimal medical treatment)
Mean pulmonary artery pressure >55 mm Hg (<25 mm Hg at rest)
Cardiac index < 2 L/min/^{2}
Progressive deterioration

Adapted from the American Society for Transplant Physicians (ASTP)/American Thoracic Society (ATS)/European Respiratory Society (ERS)/International Society for Heart and Lung Transplantation (ISHLT).[11]
DLco = diffusing capacity for carbon monoxide; FEV_1 = forced expiratory volume in 1 second; PCO_2 = partial pressure of carbon dioxide; PO_2 = partial pressure of oxygen; TLC = total lung capacity; VC = vital capacity.

and free of any other clinical significant end-organ disease when transplanted. The option of lung transplantation is generally discouraged for patients receiving mechanical ventilation, both for logistic reasons (primarily unacceptably long waiting times for donor lungs) and because it is recognized that these patients generally have a much higher mortality rate posttransplantation, which is also unacceptable in the setting of limited donor resources. The term "transplant window" had been used to refer to the period of time during which the patient is sick enough to require lung transplantation but healthy enough to have a reasonable probability of success. Finally, as well as lung transplantation candidates ideally being ambulatory with rehabilitation potential, they should also be psychologically stable, committed to the idea of transplantation, and willing to comply with posttransplantation medical protocols.[11,12]

Studies useful in evaluating potential lung transplantation candidates include tests of lung disease severity, tests for technical operative procedure and donor–recipient matching evaluations, and tests to assess comorbidities. These tests include pulmonary function tests (spirometry and lung volumes), arterial blood gases, high-resolution computed tomography scan of the chest, quantitative ventilation–perfusion scan (particularly helpful with respect to single-lung transplants), electrocardiography, echocardiography, dobutamine thallium scan/coronary angiography (if at risk for coronary artery disease), exercise performance testing (usually a 6-minute walk[14]), routine biochemical, hematologic, and microbiologic screening tests, 24-hour urine assessment of renal status, and bone densitometry assessment.

Specific Indications and Contraindications

The overall goal of recipient selection is to identify individuals whose pulmonary disease prognosis justifies lung transplantation and whose comorbid health problems will not significantly increase the risk of the operation or reduce the potential for long-term success. Although general guidelines for specific disease indications have been provided[15–18] (Table 44-2), these are meant to serve as a guide to which specific individual important information needs to be added, including the natural history of the underlying disease process, any recent acceleration in deterioration of lung function in an individual, current quality of life, likely waiting list times, and the individual's approach to lung transplantation as a medical intervention.

Contraindications to lung transplantation include extrapulmonary or multiorgan disease, including active infectious processes (human immunodeficiency virus infection, hepatitis B, and hepatitis C) and active malignancy within the last 2 years. Dysfunction of major organs that includes significant coronary disease, left ventricular dysfunction, significant liver disease with portal hypertension and renal dysfunction (creatinine clearance <50 mg/mL/min), and symptomatic osteoporosis is also a contraindication. Additional contraindications include psychological instability and active substance abuse, including tobacco use in the prior 6 months.[12,19]

Lung Transplantation Waiting List

The likely waiting time for a suitable donor lung is also an important consideration that needs to be factored into the decision-making process regarding the recommendation of lung transplantation to a potential candidate. Of particular importance is the organ allocation system being used, which may prioritize strictly according to time on the waiting list, according to the severity of lung disease, or according to some combination of the two, with donor–recipient matching then being optimized within the constraints chosen. Although waiting list times are often difficult to predict, they are generally a function of donor–recipient matching protocols, specific recipient-related factors such as thoracic size, blood group, and immunologic status, and the transplant center's lung transplantation activity profile.

Once patients are accepted for lung transplantation, renewed efforts should be made to maximize their pulmonary function and physical condition prior to the procedure. These efforts include optimizing bronchodilator

therapy in COPD patients, a lower threshold for using appropriate antibiotic therapy for acute and chronic bacterial respiratory tract infections, the use of vasodilator therapy for pulmonary hypertension, a lower threshold for using anticoagulation prophylaxis unless this is specifically contraindicated, optimizing nutritional status (aim for within 30% of ideal body weight, thereby avoiding the negative impact of both malnutrition and obesity), participation in a cardiopulmonary rehabilitation program, psychosocial supportive intervention, and optimal management of any depression/anxiety that may be present.[20] In addition, as respiratory failure worsens, high-flow supplemental oxygen (eg, using oxygen-conserving devices or transtracheal oxygen delivery) and/or nasal noninvasive positive pressure ventilation may be required to help "bridge" a patient to transplantation. Although there are reports of successful lung transplantation being performed on patients requiring full mechanical ventilation, this is generally not routinely encouraged as it is considered to be extremely high risk in the best of circumstances.

Unlike for patients with kidney disease (dialysis) and heart disease (mechanical circulatory support), an alternative bridge to transplantation does not exist for people with end-stage lung disease. In the setting of lung transplantation waiting list times that would result in almost certain death while the patient was awaiting lung transplantation, living-donor bilateral lobar lung transplantation has been used in a few centers, primarily for desperately ill patients with cystic fibrosis; in these cases, lung lobes are most usually donated by healthy parents or close relatives of the recipient.[21,22] The outcomes of established living-donor lobar lung transplantation programs are generally acceptable for both recipients and donors in highly selected cases, although there is always the very important risk of significant morbidity and mortality in a healthy donor.[23]

CADAVERIC LUNG DONOR ASSESSMENT CRITERIA

Once brain death has been confirmed in an intensive care unit, cadaveric lung donation becomes a possibility. Guidelines for the selection of an acceptable donor lung are listed in Table 44-3. The clinical history and radiologic assessment are generally used to identify factors that may preclude the donor lung being acceptable. The current physiologic status of the donor lungs is primarily assessed on the basis of gas exchange criteria (generally aim for stable arterial partial pressure of oxygen [P_aO_2] > 300 mm Hg on 100% fractional inspired oxygen [F_IO_2] and 5 cm H_2O positive end-expiratory pressure).[20,24] Should gas exchange be unexpectedly low or decrease during the time of assessment, it is important to identify the underlying explanation for this in order to avoid rejecting potentially useful lungs. This is particularly important because the lung is perhaps the most fragile organ in a patient who is brain-dead and is subject to damage by excessive fluid administration, aspiration, ventilator-associated pneumonia, and even subtle thromboemboli, all of which may be potentially reversible. After careful assessment, donor lungs that may be partly compromised according to standard criteria can often be safely used. This is especially so if transplant coordination logistics are optimized and both lungs are transplanted, thereby increasing the recipient's respiratory reserve after transplantation.[25–28]

Table 44-3 International Guidelines for Donor Lung Assessment

Donor age <65 years
Limited cumulative cigarette-smoking history (<20 pack-years)
No past/current history of significant lung disease or systemic disease
Clear chest radiograph
Stable gas exchange (P_aO_2 > 300 mm Hg on 100% F_IO_2 and 5 cm H_2O PEEP)
Satisfactory bronchoscopic examination results and gross appearance of donor lung(s)
Negative routine microbiologic screening tests for HIV, hepatitis B, and hepatitis C

Adapted from the American Society for Transplant Physicians (ASTP)/American Thoracic Society (ATS)/European Respiratory Society (ERS)/International Society for Heart and Lung Transplantation (ISHLT).[11]
F_IO_2 = fractional inspired oxygen; P_aO_2 = arterial partial pressure of oxygen; PEEP = positive end-expiratory pressure.

LUNG TRANSPLANTATION

Recipient–Donor Matching

Donor and recipients are generally matched for ABO blood group, size, and, in some programs, serologic status for cytomegalovirus (CMV). Size matching is usually performed on the basis of donor and recipient height measurements, thoracic dimensions measured from a chest radiograph, and predicted lung volume estimates. The predicted total capacity of the donor lung(s) should approach the recipient's predicted value, although a modest size discrepancy is generally well tolerated.[29,30]

In clinical lung transplantation, prospective human leukocyte antigen (HLA) matching is considered ideal but is not routinely feasible because of waiting list constraints, donor lung shortages, and ischemic time limitations.[31] In Australia, a prospective crossmatch between donor blood and recipient serum is routinely performed to identify any preexisting antibodies to donor class I or II antigens.[32] These results are then used in the decision-making process regarding donor–recipient matching, so that the risk of hyperacute rejection can be minimized.

Lung Transplantation Surgery

There are three major surgical approaches to lung transplantation:

- Single-lung transplantation
- Bilateral sequential lung transplantation
- Heart–lung transplantation

Although heart–lung transplantation was the first procedure to be successfully implemented, it is now primarily used in patients in whom irreversible severe injury has occurred to both the heart and lungs (eg, Eisenmenger's syndrome secondary to congenital heart damage that cannot be repaired). Optimal use of the very limited pool of organs can be best achieved by using "lung-only" transplants when possible,

thus reserving hearts for those patients needing heart or heart–lung transplants. The presence of cor pulmonale does not mandate heart–lung transplantation since the recovery of right ventricular function is generally rapid and complete following lung transplantation alone.[33] BSLTx using a transverse thoracosternotomy and separate and sequential lung implantation is now the preferred method for transplanting two lungs. This procedure allows for excellent exposure of the pleural spaces, uses bronchial anastomoses, which are less prone to complications than a tracheal anastomosis, and can usually avoid the need for cardiopulmonary bypass as the recipient can be supported on the contralateral lung.[6,34] BSLTx is primarily used for patients with cystic fibrosis–associated bronchiectasis because of sepsis-related considerations. Single-lung transplantation is now the most commonly used lung transplantation procedure; it is primarily used in patients with nonseptic obstructive or restrictive lung disease and is also used in some patients with primary pulmonary hypertension. The main advantages of single-lung transplantation are the fact that one donor can be used for two recipients and the relative technical ease of this operation.

BSLTx may also be used in younger patients with α_1-antitrypsin–related emphysematous lung disease and in patients with pulmonary hypertension to minimize the risk of immediate postoperative complications. Dynamic hyperinflation of the native lung following single-lung transplantation for emphysema is a major concern, particularly if ventilatory requirements are increased due to early ischemic reperfusion injury and/or infection in the lung allograft. Indeed, native lung dynamic hyperinflation may persist as a significant problem after single-lung transplantation for emphysema and require subsequent lung volume reduction surgery.[35] On the other hand, single-lung transplantation for pulmonary hypertension may be complicated by exaggerated pulmonary edema in the lung allograft for any given degree of ischemic perfusion injury (due to the high vascular resistance in the native lung causing the lung allograft to handle nearly the entire cardiac output). In addition, although right ventricular function usually improves quickly after single-lung transplantation for primary pulmonary hypertension, postoperative management is complex because of the imbalance between ventilation, which is evenly distributed between the native and transplanted lungs, and cardiac output, which is directed almost exclusively to the allograft. Hence, in both emphysema and primary pulmonary hypertension, the advantages of single-lung transplantation mentioned previously have to be weighed against the potential benefits of bilateral lung transplantation.[36–39]

In the transition from donor to recipient, the lung is exposed to two major injuries, ischemia and reperfusion. Although current methods are acceptable for an ischemic time of 6 to 9 hours, they are far from optimal, and ischemia–reperfusion remains a significant clinical problem, especially if the integrity of the lung allograft is complicated by any associated lung trauma or sepsis.[40–43] Indeed, intensive research is currently being done on ischemia–reperfusion injury in an attempt to improve both short- and long-term outcomes after lung transplantation.

Postoperative Supportive Management

The development of primary graft failure magnifies any limitation to physiologic reserve after lung transplantation, and, as already discussed, this is particularly the case following single-lung transplantation.

Mild, transient pulmonary edema is a common feature of the newly transplanted allograft. The causes of this are multifactorial and include surgical trauma, ischemia–reperfusion injury, disruption of lymphatic drainage mechanisms, elevated left ventricular end-diastolic pressure due to cardiac dysfunction, and fluid overload, particularly in the setting of renal dysfunction. In approximately 20% of cases, the injuries are sufficiently severe to cause a form of acute respiratory distress syndrome termed "primary graft failure."[44,45] The diagnosis of primary graft failure rests on the presence of widespread infiltrate on a chest radiograph, severe hypoxemia within 72 hours of transplantation, and the exclusion of other causes of graft dysfunction, such as aspiration pneumonitis, pneumonia, hyperacute rejection, occlusion of the venous anastomosis, and volume overload. Thrombosis of the pulmonary venous anastomosis is an important diagnosis that can masquerade as primary graft failure, which may be asymmetric between the upper and lower lobes of the lung allograft. This complication is often technical in nature, is usually apparent within the first few hours after transplantation, and is best diagnosed with the use of transesophageal echocardiography.[46]

The management of primary graft failure is generally supportive, relying on prolonged mechanical ventilation. Independent lung ventilation (in the setting of single-lung transplantation for emphysema), inhaled nitric oxide, surfactant replacement, and extracorporeal membrane oxygenation have all been used as adjunctive procedures.[47–50]

Major airway complications and venous anastomotic complications are now much rarer, due to improvements in surgical techniques.[10,51,52] Bronchial anastomotic stenosis due to granulation tissue, fibrosis, or bronchomalacia, however, can still occur weeks to months after transplantation and generally results from prolonged ischemic injury, either before or after implantation. These complications usually present with focal wheezing, recurrent lower respiratory tract infections, and suboptimal pulmonary function test results. Interventional bronchoscopy and stent placement have proved useful in this situation.

It is also noteworthy that denervation of the allograft lung is associated with clinically relevant impaired sensation below the anastomosis and increased propensity to gastroesophageal reflux, two problems that can easily compound each other, particularly in patients with cystic fibrosis. More subtle changes to physiologic responses in the denervated lung no doubt also exist but have not been systematically elucidated. Anecdotal evidence suggests that lung donors with mild-to-moderate asthma can be used with no significant impact on early outcomes. This issue is currently under more focused investigation as efforts are being made to increase the available lung donor pool. From the opposite perspective, the transplantation of a healthy lung into a recipient who is α_1-antitrypsin deficient raises the important issue of α_1-antitrypsin replacement therapy. In the absence

of any data either way, α_1-antitrypsin is not replaced after lung transplantation.

In addition to a specific focus on the respiratory status of the lung transplant recipient early after transplantation, there is a parallel focus on their overall conditioning, with specific emphasis on nutritional status, physiotherapy, and exercise rehabilitation programs. Routinely, patients are discharged from hospital within 2 weeks following surgery, with regular clinical review in the transplantation outpatient clinic and a program of educational/psychosocial support. Initially, weekly studies include immunosuppressant drug levels, routine hematologic and biochemical testing, routine spirometry, and chest radiography when indicated. Most institutions perform surveillance bronchoscopy on a routine schedule within the first year after transplantation, and thereafter this procedure is generally reserved for episodes of clinical deterioration in the lung allografts. In general, there is a low threshold for investigating any new respiratory symptomatology and any significant fall in lung function status as measured by spirometry or oxygen saturation.

IMMUNOSUPPRESSION AND ALLOGRAFT REJECTION

Immunosuppression

The unrivalled polymorphism of the major histocompatibility complex (MHC) is primarily responsible for alloreactivity and provides the biggest hurdle to routine success in organ transplantation. The development of modern immunosuppressive regimens based on the calcineurin inhibitor cyclosporin A (CyA) was therefore critical to the success of clinical solid-organ transplantation in general and lung transplantation specifically.[53,54] Although experimental and clinical evidence has confirmed that the lung allograft is particularly prone to rejection,[55–58] the number of HLA mismatches in the setting of current immunosuppression protocols has only a modest effect on outcomes.[59] This suggests that other factors, such as specific HLA mismatches and infection, may also be very important.

Rejection of solid-organ allografts can be divided into three major categories: hyperacute, acute, and chronic. Hyperacute rejection occurs within minutes of organ perfusion with recipient blood. It is humorally mediated by the action of preformed antibodies to blood group, HLA, or other antigens. This form of rejection is rare in lung transplantation and can be avoided by pretransplantation crossmatch screening.[56] Acute and chronic allograft rejection are characterized clinically according to specific histopathologic criteria and the temporal pattern post–lung transplantation. The reliable diagnosis and classification of acute and chronic lung allograft rejection by well-accepted international criteria are central to both our understanding of these conditions and to the success of well-conducted trials of immunosuppressive regimens in lung transplantation.

In general, pharmacologic immunosuppression for lung transplantation is used to prevent acute and chronic rejection while avoiding the complications of immunodeficiency and nonimmune drug effects. Current immunosuppression protocols for heart and lung transplantation are derived from the early lung transplantation experiences at Stanford[3] and Toronto,[4] whose protocols had themselves been extrapolated from those used primarily in renal transplantation. Given the suboptimal long-term outcomes from lung transplantation, it is imperative that these protocols be continually critically reviewed as new agents and strategies become available.[60] Randomized control trials in the field of solid-organ transplantation are usually performed in renal transplant recipients (much more common by factors of 10 to 20, depending on region), and the benefits are extrapolated to lung transplant recipients. Given the significant increases in infection and rejection risk in the latter and the likely marked differences in risk/benefit ratio of various immunosuppression protocols, it is crucial that we formally evaluate new therapies and competing regimens in lung transplantation as much as possible.

Strategically, the immunosuppression protocols are composed of three main phases: induction, maintenance immunosuppression, and treatment of rejection.

Induction Regimens

Calcineurin-dependent pathways are critical in specific T-cell activation processes, particularly in relation to interleukin-2–driven clonal expansion of potentially alloreactive T cells (Table 44-4). Therefore, calcineurin inhibition, most often with CyA, is commenced either prior to or immediately after transplantation. The reason for this is based on experimental evidence suggesting that the maximum effectiveness of CyA is at the time of antigen presentation[61] and theoretical considerations regarding the induction of a permanent state of immunologic tolerance at the time of engraftment, which is the "holy grail" of transplantation immunobiology. Administration of a nucleoside inhibitor (azathioprine or mycophenolate mofetil) and corticosteroids is commenced shortly after transplantation. Alternative induction regimens have used ATGAM polyclonal antilymphocyte preparations, which result in rapid T-cell depletion and variable but significant effects on platelets and granulocytes. These regimens have fallen out of favor due to increased toxicity and no proven benefit.[62,63] In contrast, the new interleukin-2 (IL-2) receptor antagonists have been well received as additional induction agents as they have minimal side effects to detract from their potential efficacy.[64]

Standard Maintenance Regimen

In the absence of permanent tolerance induction, maintenance therapy is usually achieved using a combination of calcineurin inhibitor (CyA or tacrolimus), nucleoside synthesis inhibitor, and corticosteroids. The dose of corticosteroids is gradually reduced after transplantation to approximately 5 to 7.5 mg/day (physiologic replacement levels). Although acute rejection is unlikely in the first 4 days after transplantation, most lung transplant recipients will have at least one episode of significant acute rejection within the first 3 months. More careful monitoring of drug levels,[65] or better still, the effects of immunosuppressive drugs on their target enzymes and pharmacodynamic parameters may prove to be clinically useful in avoiding

Table 44-4 Actions and Side Effects of the Main Immunosuppressive Drugs

	Main actions	*Main side effects*
1. Calcineurin inhibitors Cyclosporin Tacrolimus	Bind to the cytosolic immunophilins cyclophilin and FK-binding protein-12, respectively, and inhibit calcineurin. Dependent T-cell activation. Primarily target adaptive immune responses and have little effect on nonspecific immunity—hence a high immunosuppressive index. Dosing depends on drug levels.	Opportunistic infection and nephrotoxicity are major effects. Also potentially problematic are migraine headaches, seizures, excess hair growth, and gum hyperplasia, all of which are less frequent with tacrolimus.
2. Nucleoside synthesis inhibitors Azathioprine Mycophenolate mofetil	Azathioprine and mycophenolate mofetil (a prodrug) inhibit nucleoside and DNA synthesis by competitive inhibition of guanosine monophosphate production and noncompetitive inhibition of inosine monophosphate dehydrogenase production, respectively. Lymphocytes are more dependent on new nucleoside synthesis than other rapidly dividing cells because of their low levels of nucleoside salvage pathways.	Nonspecific actions. Bone marrow depression and leukopenia, hepatotoxicity, and gastrointestinal tract disturbance are often the dose-limiting effects—the last of these being a particular problem with mycophenolate. Extreme caution needs to be used with xanthine oxidase inhibitors such as allopurinol.
3. Corticosteroids	These drugs act at many levels by binding to cytoplasmic and nuclear receptors, which interact with glucocorticoid reactive elements to exert a broad immunosuppressive effect that is not specific.	Side effects are a major problem and include infections, osteopenia, myopathy, glucose intolerance, and gastrointestinal bleeding.
4. Antibody therapies Monoclonal IL-2 receptor antagonists (basiliximab/daclizumab)	Bind to IL-2 receptor and inhibit T-cell activation and subsequent clonal expansion. Primarily used as induction therapy.	Minimal side-effect profile. Cost is a major consideration.
Polyclonal (anti–T cell) ATGAM (horse derived) Thymoglobulin (rabbit derived)	Nonspecifically reduce circulating and possibly tissue T cells. Dosing is titrated to reduce peripheral blood $CD2/3^+$ cells to approximately 10% of baseline.	Hypersensitivity reactions and increased risk of opportunistic infections are the major side effects.
5. Rapamycin/RAD Sirolimus (Rapamune) Everolimus (Certican)	Binds to FK-binding protein-12, but unlike tacrolimus, it does not cause inhibition of calcineurin-dependent pathways. Instead, the rapamycin–FK-binding protein-12 complex inhibits target proteins critical for cell cycle regulation.	Adverse effects include reversible marrow suppression, increased risk of opportunistic infection, hyperglycemia, hyperlipidemia, and myositis.

IL-2 = interleukin-2.

under- or overtreatment, but this is only now beginning to be systematically studied.

Augmented and Alternative Immunosuppression Treatment

Pulse intravenous corticosteroids are used as first-line therapy if there is evidence that maintenance immunosuppression has been insufficient to avoid acute allograft rejection. Methylprednisolone is usually given in a dose of 500 mg to 1 g for approximately 3 days. This regimen usually results in rapid resolution of symptoms. If rejection is resistant to steroids, antilymphocyte preparations are used; these briefly augment baseline immunosuppression to combat increased rejection. These preparations are usually given for 5 days, with the aim of significantly reducing the numbers of circulating T cells (and possibly tissue T cells).

Alternative maintenance regimens are used if there has been recurrent rejection or significant drug toxicity. Currently, tacrolimus and mycophenolate mofetil are used as alternatives to CyA and azathioprine, respectively, in the setting of recurrent acute rejection or progressive BOS, although preliminary studies suggest that they be beneficial as first-line agents.[66–68] Rapamycin is a relatively new agent, and clinical trials are currently under way to define its role in clinical transplantation. It is hoped that this agent may be effective in chronic rejection because of its potent immunosuppressive and antiproliferative effects.[69]

Acute Allograft Rejection

Acute rejection can develop in up to 75% of patients within the first 12 months after transplantation, with most episodes occurring within the first 3 months.[70,71]

Acute vascular rejection is primarily T cell mediated and occurs as a result of recognition of the allograft by the recipient as foreign.[72] T cells are essential in the process of graft rejection, as it has been shown that T cell–deprived animals fail to reject allografts. Vascular endothelial cells in the graft are usually the first foreign encounter for the host's immune system. Nonspecific up-regulation of MHC and adhesion molecule expression secondary to ischemia and injury are soon followed by specific interactions between host T cells and foreign "MHC–antigen" complexes on the endothelial cell surface. This leads to progressive infiltration of the graft by host mononuclear cells, particularly $CD8^+$ cytotoxic T cells. Hence, acute allograft rejection tends to be angiocentric, with increasing grades of rejection sequentially encroaching on interstitial and alveolar spaces (Figures 44-1–3).[72,73]

The clinical diagnosis of acute vascular rejection (based on symptoms of dry cough, fever, and dyspnea plus signs of low-grade temperature in association with a fall in forced expiratory flow in 1 second [FEV_1]) and bronchoalveolar lavage (BAL) were shown to have relatively poor sensitivity and specificity from the outset of lung transplantation.[73] Hence, the histopathologic assessment of transbronchial biopsy specimens quickly became the gold standard for the

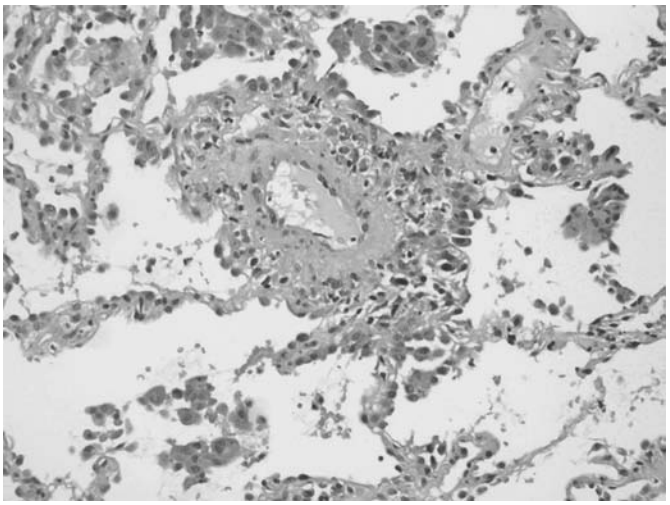

FIGURE 44-1 Acute rejection: grade A2 (transbronchial biopsy, low power). The characteristic cuff of perivascular lymphocytes without alveolar infiltration is shown. (Hematoxylin and eosin stain, ×100)

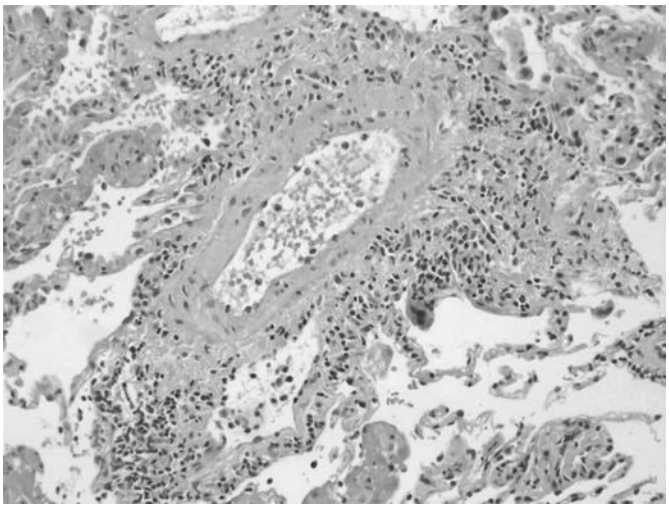

FIGURE 44-3 Acute rejection: grade A3 (transbronchial biopsy, medium power). Perivascular lymphocytic infiltration spills over and involes the alveolar structures. (Hematoxylin and eosin stain, ×200)

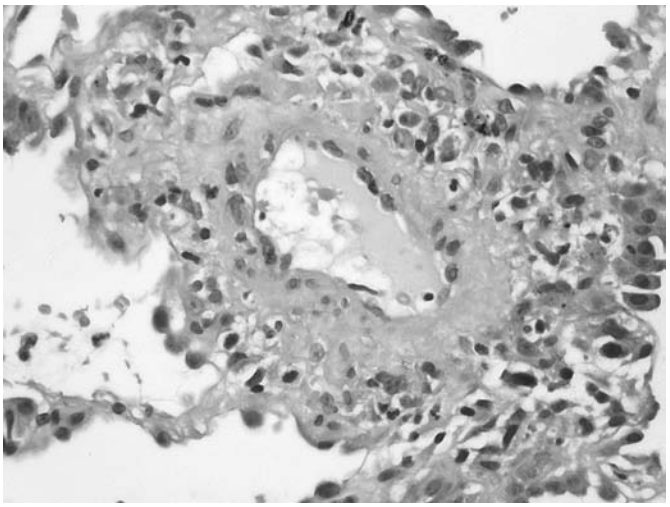

FIGURE 44-2 Acute rejection: grade A2 (transbronchial biopsy, high power). Lymphocyte infiltration completely surrounds the vessel shown.

diagnosis of acute rejection in the lung allograft, despite its inaccuracies.[74,75] A working formulation that standardized the diagnostic criteria and grading system for lung allograft rejection was first published in 1990 and later revised in 1996.[76]

Chronic Rejection

Chronic rejection of the lung allograft has been equated with the histologic findings of obliterative bronchiolitis (OB).[77] Chronic rejection in other solid-organ transplants is characterized by fibroobliteration of tubular structures. OB is histologically a chronic fibrosing process in the terminal and respiratory bronchioles that may be accompanied by a mononuclear infiltrate (Figures 44-4–5).[78,79] The process is inhomogeneous, with normal bronchioles often found near areas of severe OB. Hence, although bronchoscopy, including transbronchial biopsy, is the standard technique used in allograft surveillance, a persistent deterioration in lung function can frequently occur in the absence of abnormal results of this test.[80] Indeed, the major use of bronchoscopic sampling in this setting is to exclude infection or late acute allograft rejection as the cause of any significant decrease in lung function.[75] Open-lung biopsy may show evidence of classic OB more often but also has diagnostic limitations that, when combined with the significant morbidity associated with this procedure, make it an impractical test for OB. As a result of the lack of consistent histopathologic findings, bronchiolitis obliterans syndrome was defined by the International Society for Heart and Lung Transplantation as a persistent decline in FEV_1 of greater than 20% from the best achieved after transplant in the absence of an alternative explanation[81] (Table 44-5). Recent studies have shown that bronchiolar airflow ($FEF_{25–75\%}$) impairment often precedes the decrease in FEV_1 in BOS, although the predictive utility of this test was only modest.[82]

The immune response plays a major role in chronic rejection as this problem is not seen in all allografts (thereby excluding ischemia–reperfusion injury as a sole cause) and is rarely seen in syngeneic grafts. In addition, chronic rejection is enhanced by immunization of recipients before grafting and is much more likely to occur in the setting of inadequate immunosuppression. Although recent reviews have identified acute rejection (frequency, timing, intensity, and duration) as the single most important risk factor for the development of BOS, they have also stressed the likely importance of alloantigen-independent factors.[79,83–85] This is in keeping with the modest benefits, at best, associated with augmented immunosuppression strategies in BOS.[86]

Current evidence suggests that BOS arises as the result of ongoing, partially suppressed immune activation,[87,88] with CMV infection in particular and acute, persistent, or multiple recurrent infections in general, significantly amplifying these processes.[79,83,85,89,90] Lymphocytic bronchiolitis can

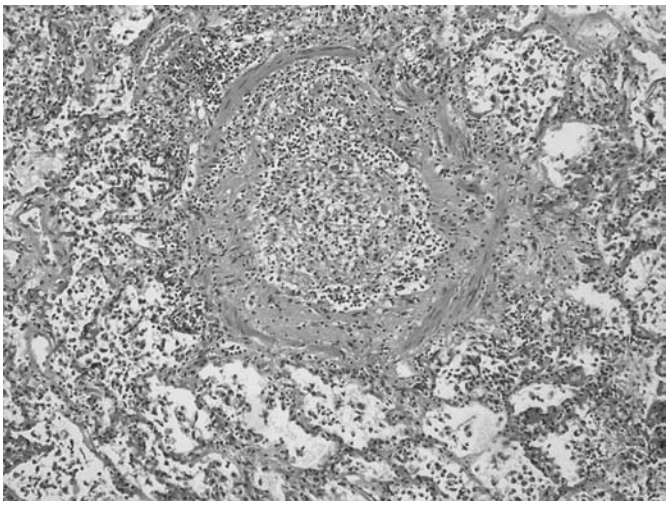

FIGURE 44-4 Obliterative bronchiolitis (active) (transbronchial biopsy). The typical broncholiolar infiltration by mononuclear cells and patchy fibroobliteration are shown. (Hematoxylin and eosin stain, ×200)

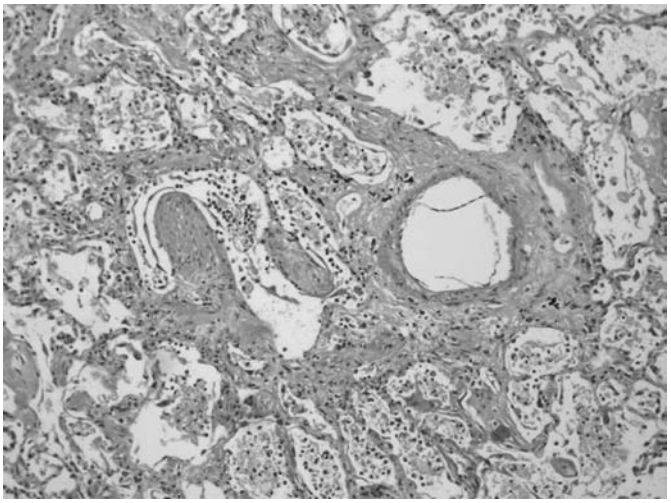

FIGURE 44-5 Obliterative bronchiolitis (inactive) (transbronchial biopsy). The typical fibroobliteration of bronchioles adjacent to patent arteioles is shown. (Hematoxylin and eosin stain, ×100)

occur in the presence or absence of the perivascular lymphocytic infiltration characteristic of acute rejection.[91] It is postulated that the presence of a chronic mononuclear cell infiltrate in the lung allograft may, in turn, increase the activation and survival of both recruited inflammatory cells and resident airway cells, thereby stimulating the subsequent release of growth factors, fibrogenic cytokines, and extracellular matrix components.[92–94] In addition, it is possible that the loss of antiproliferative and antifibrogenic signals (particularly from a damaged epithelium) may lead to excess proinflammatory and profibrogenic signals, with the final result being a complex process of airway "remodeling" and airway obliteration by scar collagen.[93,95] Interestingly, there is some evidence to suggest that bronchial hyperresponsiveness after lung transplantation may be associated with the subsequent development of BOS.[96] The exact mechanism underlying this association has not been determined.

Table 44-5 Bronchiolitis Obliterans Syndrome (BOS) as Defined by the International Society for Heart and Lung Transplantation

Baseline FEV_1 defined as the average of the two previous highest consecutive measurements after lung transplantation
Current FEV_1 is compared to baseline
Grade 0: FEV_1 > 90% of baseline
Grade 0 potential: FEV_1 80–89% of baseline ± decreased $FEF_{25–75\%}$
Grade 1: FEV_1 66–79% of baseline
Grade 2: FEV_1 51–65% of baseline
Grade 3: FEV_1 < 50% of baseline
Assess histopathology
a = No obliterative bronchiolitis (or no biopsy)
b = Obliterative bronchiolitis

FEF 25–75% = forced expiratory flow between 25% and 75% of the expired vital capacity; FEV_1 = forced expiratory volume in 1 second.

Although the definitions of alloantigen-dependent and alloantigen-independent factors for chronic rejection/BOS have been accompanied by a general description of inflammatory cell infiltrates and cytokine profiles, these data remain largely cross-sectional in nature and are often not well controlled with respect to key confounders. This is perhaps particularly the case regarding cytokine profiles in stable lung transplant recipients and lung transplant recipients with BOS. Nevertheless, it remains extremely likely that certain cytokines involved in both immune–inflammatory cell interactions (eg, IL-2, IL-4, IL-5, IL-10, IL-12, interferon-γ, IL-1, IL-6, IL-8) and interactions with the lung epithelial–mesenchymal unit (eg, epidermal growth factor, granulocyte colony-stimulating factor, transforming growth factor-β [TGF-β], platelet-derived growth factor, and fibroblast growth factor) play pivotal roles in the various stages of BOS pathogenesis.[97] Of particular interest is the linking of persistent cytokine profiles and their downstream effects to the known alloantigen-dependent and alloantigen-independent risk factors that may be driving BOS development through specific T-cell subsets.

To help elucidate some of the mechanisms involved in BOS pathogenesis, small animal (murine heterotopic tracheal and rat allograft models) and large animal (genetically defined miniature swine) models are being increasingly used.[97–99] Although these animal models are extremely advantageous with respect to providing relevant longitudinal information that is both controlled and amenable to specific intervention, the ultimate utility of the experimental results obtained can only be tested in well-conducted human clinical trials that take into account all the complexity of clinical lung transplantation.

INFECTION AND ANTIMICROBIAL INTERVENTION

General Considerations

Infection is a major problem in lung transplant recipients.[63,100,101] Several factors influence the susceptibility of lung transplant recipients to serious infections.

Open-chest surgery results in open wounds, which may constitute a site of entry for bacterial organisms. Although the thoracic wound, intravenous lines, and intercostal catheters are all potential sites of entry for bacterial

pathogens, the most common cause of morbidity and mortality from early bacterial infections is the development of pneumonia in the lung allograft. The factors that may immediately impair host defense mechanisms in the lung allograft include reduced cough reflexes, anastomotic narrowing, denervated airways and decreased mucociliary clearance, allograft reimplantation injury, and disrupted lymphatic drainage.[102] Early bacterial pneumonia in this setting may be of donor, recipient, or nosocomial origin. The timing of intubation in relation to the event causing brain death and the duration of intubation reflect the risk of aspiration or colonization in the donor lung. Recipient factors such as primary disease, nutritional status, and preoperative steroid dose contribute significantly to the risk of early bacterial pneumonia after lung transplantation. Donors are therefore screened by bronchial washings or tracheal aspiration, and the recipients are fully assessed in terms of airway microbiology. Appropriate antibiotic prophylaxis is used to cover any organisms isolated from the donor BAL fluid, known colonizers of the recipient's airway (particularly important in cystic fibrosis patients), and any prevalent nosocomial pathogens specific to the transplant center.[102]

Pharmacologic immunosuppression further predisposes the lung allograft to increased infection complications resulting from opportunistic, nosocomial, and typical community-acquired pathogens[71,100,101] (Table 44-6). Hence, infection is a major cause of early *and* late morbidity and mortality following lung transplantation.[71,101] Bacterial pneumonia is probably the most common infection reported and peaks during the first 6 months after lung transplantation and again later during the period of augmented immunosuppression for the treatment of chronic rejection/BOS.[100] The ubiquitous DNA herpesvirus CMV is the most frequent cause of viral infection in lung transplant recipients and has been associated with both direct and indirect effects on the lung allograft.[71,83,101,103,104] Fungal infections, in particular those caused by *Aspergillus*, can be major causes of morbidity and mortality after lung transplantation.[105,106] *Aspergillus* is a relatively frequent airway colonizer of the lung allograft and can cause tracheobronchitis, focal parenchymal disease, or widely disseminated angioinvasive disease.[105,107] In general, *Aspergillus fumigatus* isolated from BAL fluid from the lung transplant recipient is very likely to be significant, and hence a low threshold for prophylactic/preemptive therapy with oral itraconazole or the newer voriconazole is advised, although care should be taken to adjust CyA dosage and monitor liver function tests because of the side-effect profile of these agents. Locally invasive *Aspergillus* disease is most commonly seen in the setting of augmented immunosuppression with agents such as ATGAM or in conjunction with clinical CMV disease. Treatment of semi-invasive disease is rarely successful at clearing *Aspergillus* from the airways; however, adequate use of liposomal amphotericin and reduced immunosuppression strategies offer the best hope for long-term control.[108,109] *Pneumocystis carinii* pneumonia was a major problem prior to the use of trimethoprim-sulfamethoxazole prophylaxis but is now extremely rare.[110]

Table 44-6 Main Infectious Complications after Lung Transplantation

Bacterial
Gram positive
Staphylococcus aureus
Streptococcus pneumoniae
Gram negative
Pseudomonas aeruginosa
Stenotrophomonas maltophilia
Haemophilus influenzae
Atypical bacteria
Legionella pneumophila
Nocardia
Mycobacterium
Chlamydia pneumoniae
Mycoplasma pneumoniae
Viral
Cytomegalovirus
Other herpesviruses
Epstein–Barr virus
Varicella zoster
Herpes simplex
Respiratory RNA viruses
Respiratory syncytial virus
Parainfluenza virus
Influenza virus
Fungal
Aspergillus fumigatus

Specific DNA Virus Reactivation

CMV is a ubiquitous herpesvirus with the ability to remain latent in host tissues and become reactivated in those patients who are immunosuppressed. It causes the most common (>75% of lung transplant recipients are at risk) and often most serious viral infection seen after organ transplantation, and this is particularly so in recipients of lung transplants.[103,111] There is a wide spectrum of manifestations of CMV infection, ranging from asymptomatic infection to severe pneumonitis and widespread dissemination. Prior to routine ganciclovir prophylaxis, CMV disease was common and was associated with high morbidity and mortality, particularly in the primary mismatch setting.[103,111]

Although ganciclovir prophylaxis has reduced the incidence of CMV disease, the direct and indirect effects of subclinical CMV reactivation in the lung allograft remain largely unsurmounted obstacles.[112,113] It has recently been shown that CMV adopts a specific strategy of blocking cell surface expression of class I antigens in infected cells[114,115] and that specific CD8 T-cell control is critical in defense against CMV.[116,117] This complex virus–host interaction leads to significant increases in local immunosuppression while at the same time enhancing MHC class I and II expression on surrounding uninfected donor allograft cells, thereby increasing the probability of allograft rejection. Hence, CMV pneumonitis is paradoxically associated with both other opportunistic infections and allograft rejection and therefore overall lower long-term survival rates.[90,118,119] It is hoped that newer, more sensitive and quantitative methods for detecting CMV in the peripheral blood and in the lung allograft will yield new insights into this problem and allow for the optimization of anti-CMV strategies after transplantation.[120–123]

Human herpesvirus 6 is a recently described β-herpesvirus that is epidemiologically and biologically similar to CMV.[124–126] The implications of the reactivation of this virus in the lung allograft are only now beginning to be systematically examined.[127] Unlike the β-herpesviruses, Epstein–Barr virus (EBV) has cell-transforming properties and is associated with lymphoproliferative disease, particularly in the primary mismatch setting. Indeed, EBV posttransplantation lymphoproliferative disease (PTLD) occurs in 5 to 10% of lung transplant recipients and in 30% of EBV donor seropositive/recipient seronegative lung transplant recipients, particularly in the setting of augmented immunosuppression or CMV disease.[128,129] It is therefore a major cause of malignancy after lung transplantation. Lymphocytic proliferation ranges from reactive B-cell hyperplasia to large cell lymphoma. PTLD may regress after a reduction in immunosuppression as the EBV-induced B-cell proliferation is kept in check by cytotoxic T lymphocytes in immunocompetent individuals. Antiviral therapy with ganciclovir and the recent use of monoclonal antibody therapy have proven to be useful adjunctive therapeutic interventions in many cases.[129–131] Herpes simplex virus and varicella zoster reactivation also occur relatively commonly after lung transplantation. When these viruses reactivate in the setting of stable immunosuppression, the response to treatment is usually good; however, both primary infection and reactivation in the patient who has recently undergone augmented immunosuppression pose a major problem.

Specific Respiratory RNA Virus Infection

Respiratory RNA viruses are the most common pathogens of humans, and as such they pose a particular risk to lung transplant recipients. Common viral pathogens such as respiratory syncytial virus (RSV), parainfluenza virus, and influenza A and B viruses can cause frequent, recurrent, and persistent infection in the lung allograft and hence may be associated with significant morbidity and mortality after lung transplantation.[132,133] Unlike the herpesviruses, which can reactivate from a latent state in most recipients, these viruses pose a threat after each new encounter. The role of RSV and other respiratory viruses in acute and chronic allograft rejection is unclear, but there is anecdotal evidence of increased immune activation and rejection in the setting of viral respiratory tract infections. Although newer diagnostic techniques are only now beginning to be systematically used, it is widely believed that these difficult-to-diagnose pathogens are the precipitants of many episodes of acute deterioration in previously stable lung transplant recipients and may, in part, explain the winter peaks in BOS development.[79,132,134,135] Treatment with antiviral agents should always be considered, although the therapeutic options for these viruses are currently very limited.

LUNG TRANSPLANTATION OUTCOMES

General Considerations

The magnitude of improvement after lung transplantation is the product of many factors, including pretransplantation diagnosis and status, operative outcomes, and postoperative complications, none of which are necessarily independent.[13,136,137] Acute 30-day mortality rates in experienced centers are generally below 5 to 10%, with 1-year and 5-year survival rates varying between 60 and 85% and 40 and 60%, respectively.[2,138,139] Early mortality in the first 3 months is mostly due to primary graft failure and infection, whereas late mortality (>3 months) is most often related to chronic rejection and its complications.[71] In an uncomplicated lung transplant recipient, there is gradual improvement in lung function and functional status during the first 6 to 12 months after transplantation. Even though exercise testing usually reveals a reduction in maximum oxygen consumption in stable, long-term lung transplant recipients, the majority of recipients are able to enjoy marked improvements in their performance of activities of daily living, general exercise capacity, and overall quality of life.[138,140]

Survival

Mortality outcomes after lung transplantation relate principally to posttransplantation complication rates, which are at least in part a function of recipient selection practices, transplant center activity profiles, clinical protocols, and the availability of clinical support services. The advanced age of recipients (55 years or older), a diagnosis of IPF, and significant systemic comorbidities are usually associated with poor long-term survival. According to the Registry of the International Society for Heart–Lung Transplantation, 1-, 3, and 5-year actuarial survival rates after lung transplantation are 75%, 59%, and 46%, respectively, with a median survival of 4.1 years.[2]

Whether lung transplantation truly increases survival over the natural history of the underlying disease remains difficult to ascertain in the absence of a randomized trial. A disease-specific comparison of survival after transplantation with the survival of patients awaiting transplantation showed that transplantation offered a survival benefit to patients with cystic fibrosis and pulmonary fibrosis, whereas no such advantage could be demonstrated in patients with emphysema (a disease that typically follows a protracted course even in the advanced stages).[13] In both single-lung and bilateral lung transplant recipients, long-term survival is limited principally by the development of BOS.[141–143] The poorer long-term survival rates for lung transplantation in comparison with heart and liver transplantation (approximately 70% 5-year survival) are generally related to the higher incidence of chronic rejection/BOS in the lung allograft and the greater propensity for this organ to suffer infectious complications related to both the magnitude of immunosuppression used and its exposure to the environment.

Pulmonary Function, Hemodynamics, and Exercise Capacity

The maximum improvement in lung function after lung transplantation is typically achieved within 6 months, at which point the limiting effects of thoracic surgery and postoperative pain, respiratory muscle dysfunction, and acute lung injury have dissipated. In patients undergoing BSLTx for chronic obstructive lung disease, the FEV_1 can be

expected to improve 60 to 70% predicted, whereas BSLTx for pulmonary fibrosis leads to a marked but incomplete improvement in lung volumes, with persistence of a mild restrictive pattern.[138,144] In both of these cases, following BSLTx the majority of the ventilation and perfusion goes to the transplanted lung, although ventilation–perfusion matching is not perfect, as shown by a widened alveolar–arterial oxygen gradient. Nevertheless, arterial oxygenation rapidly improves following an uncomplicated procedure, and supplemental oxygen should not be required by the time of hospital discharge. BSLTx procedures usually result in normal spirometry findings and lung volumes, with a normal distribution of ventilation and perfusion and a normal alveolar–arterial oxygen gradient.[138,145] Although hypercapnia may persist for several weeks in those with preoperative hypercapnia and blunted ventilatory responses to carbon dioxide, persistent hypercapnia in the setting of a well-functioning allograft should alert the physician to the possibility of diaphragmatic dysfunction due to phrenic nerve injury.[146]

Patients undergoing BSLTx for primary pulmonary hypertension have no significant change in pulmonary function, marked improvements in gas exchange, and near-normal hemodynamics. In these patients, the normalizations of pulmonary vascular resistance and pulmonary arterial pressures are accompanied by an immediate increase in cardiac output and a more gradual reversal of the right ventricular hypertrophy.[33]

Following lung transplantation, exercise capacity improves sufficiently in the majority of lung recipients for them to pursue an active lifestyle. By the end of the first year after transplantation, approximately 85% of survivors report minimal limitations in daily activity.[2] At the other extreme, approximately 2 to 3% require total assistance. Postoperatively, the 6-minute walk test result typically doubles and tends to be better in bilateral lung transplant recipients than in single-lung transplant recipients (a function, perhaps, of both selection bias and increased respiratory reserve).[138] Interestingly, although progressive cardiopulmonary exercise testing in stable lung transplant recipients reveals some responses (especially cardiac) that may vary between single, bilateral, and heart–lung transplant recipients, there remains a stereotypic pattern of exercise limitation, characterized by decreased peak work rate, decreased peak oxygen consumption (typically only 40 to 60% of the predicted value), and early anaerobic (lactate) thresholds. In addition, ventilatory responses are usually normal, and there is no gas exchange abnormality.[147,148] This pattern of exercise limitation persists after transplantation and is independent of the underlying disease or the type of transplantation procedure.[147,148] The finding of an abnormally low anaerobic threshold in association with evidence of impaired peripheral oxygen utilization suggests a defect at the level of the skeletal muscle. It has been postulated that skeletal muscle dysfunction after transplantation may result from CyA-induced impairment in muscle mitochondrial respiration,[149,150] but this hypothesis has not yet been systematically examined across the various solid-organ transplants for which CyA is the core immunosuppressant used.

Quality of Life

Quality of life after lung transplantation is largely determined by the degree of functional improvement associated with the lung allograft and the development of either respiratory or nonrespiratory posttransplantation complications.

The available studies suggest that there is a dramatic global improvement in all quality-of-life measures within several months after lung transplantation, which tends to mirror the improvements seen in performance status.[151–153] Despite these improvements, however, fewer than 30% of lung transplant recipients work either full time or part time.[2] The reasons for this are likely to be complex and include the assignment of a lower priority to employment than to other posttransplantation goals, the potential loss of disability income or medical benefits as a result of employment, and the potential reluctance of employers to hire someone with a complex medical condition.[154] In addition to the well-recognized respiratory complications, such as allograft rejection and infection, impacting on quality-of-life status after lung transplantation, nonrespiratory complications, such as CyA-related nephrotoxicity,[155] osteoporosis,[156] and malignancy, are increasing causes of significant morbidity in long-term survivors.[157]

CONCLUSIONS AND FUTURE DIRECTIONS

Lung transplantation currently provides great hope for patients with end-stage lung disease wishing to increase their life expectancy and quality of life. Current 5-year survival rates dictate that these procedures continue to be regarded as palliative rather than as curative interventions. The major obstacle to improved long-term outcomes remains the problem of chronic allograft rejection/BOS. It is hoped that future immunosuppression strategies using newer immunosuppressants,[60,158] co-stimulatory blockade of T-cell activation[159] and/or immunomodulatory stem cells[160,161] will limit alloreactive responses without significant infection- and toxicity-related side effects, thereby maximizing the prognostic, functional, and quality-of-life benefits that may be derived from this procedure. However, any significant improvements in long-term outcomes following lung transplantation will put further pressure on donor organ supplies, which will ultimately always be a major limitation to the broad applicability of this procedure. Xenotransplantation and tissue-engineering approaches offer potential solutions to the shortage of donor organs, but as yet they are a long way from becoming a clinical reality.[162]

ACKNOWLEDGMENTS

The author would like to acknowledge Associate Professors Trevor J. Williams, MD, and Gregory I. Snell, MD, for their critical review of the manuscript and many helpful comments. I also wish to acknowledge financial support from NHMRC Australia, The Alfred Hospital Whole Time Medical Specialists Fund, The Margaret Pratt Foundation, and Novartis Pharmaceuticals.

REFERENCES

1. American Thoracic Society, Medical Section of the American Lung Association. Lung transplantation. Report of the ATS workshop on lung transplantation. Am Rev Respir Dis 1993;147:772–6.
2. Hertz MI, Taylor DO, Trulock EP, et al. The registry of the international society for heart and lung transplantation: nineteenth official report—2002. J Heart Lung Transplant 2002;21:950–70.
3. Reitz BA, Wallwork JL, Hunt SA, et al. Heart–lung transplantation: successful therapy for patients with pulmonary vascular disease. N Engl J Med 1982;306:557–64.
4. Toronto Lung Transplant Group. Unilateral lung transplantation for pulmonary fibrosis. N Engl J Med 1986;314:1140–5.
5. Cooper JD, Pearson FG, Patterson GA, et al. Technique of successful lung transplantation in humans. J Thorac Cardiovasc Surg 1987;93:173–81.
6. Cooper JD, Patterson GA, Trulock EP. Results of single and bilateral lung transplantation in 131 consecutive recipients. Washington University Lung Transplant Group. J Thorac Cardiovasc Surg 1994;107:460–70.
7. Arcasoy SM, Kotloff RM. Lung transplantation. N Engl J Med 1999;340:1081–91.
8. Patterson GA, Cooper JD. Status of lung transplantation. Surg Clin North Am 1988;68:545–58.
9. Stewart KC, Patterson GA. Current trends in lung transplantation. Am J Transplant 2001;1:204–10.
10. Meyers BF, Patterson GA. Technical aspects of adult lung transplantation. Semin Thorac Cardiovasc Surg 1998;10:213–20.
11. American Society for Transplant Physicians (ASTP)/American Thoracic Society (ATS)/European Respiratory Society (ERS)/International Society for Heart and Lung Transplantation (ISHLT). International guidelines for the selection of lung transplant candidates. Am J Respir Crit Care Med 1998;158:335–9.
12. Maurer JR. Patient selection for lung transplantation. JAMA 2001;286:2720–1.
13. De Meester J, Smits JM, Persijn GG, Haverich A. Listing for lung transplantation: life expectancy and transplant effect, stratified by type of end-stage lung disease, the Eurotransplant experience. J Heart Lung Transplant 2001;20:518–24.
14. Kadikar A, Maurer J, Kesten S. The six-minute walk test: a guide to assessment for lung transplantation. J Heart Lung Transplant 1997;16:313–9.
15. Conte JV, Borja MJ, Patel CB, et al. Lung transplantation for primary and secondary pulmonary hypertension. Ann Thorac Surg 2001;72:1673–9.
16. Noone PG, Egan TM. Cystic fibrosis: when to refer for lung transplantation—is the answer clear? Am J Respir Crit Care Med 2002;166(12 Pt 1):1531–2.
17. Patterson GA, Cooper JD. Lung transplantation for emphysema. Chest Surg Clin North Am 1995;5:851–68.
18. Sulica R, Teirstein A, Padilla ML. Lung transplantation in interstitial lung disease. Curr Opin Pulm Med 2001;7: 314–22.
19. Smith CM. Patient selection, evaluation, and preoperative management for lung transplant candidates. Clin Chest Med 1997;18:183–97.
20. Craven JL, Bright J, Dear CL. Psychiatric, psychosocial, and rehabilitative aspects of lung transplantation. Clin Chest Med 1990;11:247–57.
21. Liou TG, Cahill BC, Adler FR, Marshall BC. Selection of patients with cystic fibrosis for lung transplantation. Curr Opin Pulm Med 2002;8:535–41.
22. Starnes VA, Barr ML, Cohen RG, et al. Living-donor lobar lung transplantation experience: intermediate results. J Thorac Cardiovasc Surg 1996;112:1284–90.
23. Woo MS, MacLaughlin EF, Horn MV, et al. Living donor lobar lung transplantation: the paediatric experience. Paediatr Transplant 1998:2:185–90.
24. Weill D. Donor criteria in lung transplantation: an issue revisited. Chest 2002;121:2029–31.
25. Gabbay E, Williams TJ, Griffiths AP, et al. Maximizing the utilization of donor organs offered for lung transplantation. Am J Respir Crit Care Med 1999;160:265–71.
26. Frost AE. Donor criteria and evaluation. Clin Chest Med 1997;18:231–7.
27. Snell GI, Griffiths A, Macfarlane L, et al. Maximizing thoracic organ transplant opportunities: the importance of efficient coordination. J Heart Lung Transplant 2000;19:401–7.
28. Studer SM. Active donor management strategies may increase organ availability in lung transplantation. J Heart Lung Transplant 2001;20:925.
29. Noirclerc M, Shennib H, Giudicelli R, et al. Size matching in lung transplantation. J Heart Lung Transplant 1992;11(4 Pt 2):S203–8.
30. Park SJ, Houck J, Pifarre R, et al. Optimal size matching in single lung transplantation. J Heart Lung Transplant 1995; 14:671–5.
31. McGee C, Fox MD, Loyd JE. The feasibility of HLA matching for lung transplantation. Clin Transplant 1996;10(6 Pt 1):564–7.
32. Schneider HG, Rutherford D, Kotsimbos T. Provision of laboratory services for heart and lung transplantation in Australia. Clin Chim Acta 2001;313:221–9.
33. Kramer MR, Valantine HA, Marshall SE, et al. Recovery of the right ventricle after single-lung transplantation in pulmonary hypertension. Am J Cardiol 1994;73:494–500.
34. Esmore DS, Brown R, Buckland M, et al. Techniques and results in bilateral sequential single lung transplantation. The National Heart & Lung Replacement Service. J Card Surg 1994;9:1–14.
35. Anderson MB, Kriett JM, Kapelanski DP, et al. Volume reduction surgery in the native lung after single lung transplantation for emphysema. J Heart Lung Transplant 1997;16: 752–7.
36. Gammie JS, Keenan RJ, Pham SM, et al. Single- versus double-lung transplantation for pulmonary hypertension. J Thorac Cardiovasc Surg 1998;115:397–402.
37. Sundaresan RS, Shiraishi Y, Trulock EP, et al. Single or bilateral lung transplantation for emphysema? J Thorac Cardiovasc Surg 1996;112:1485–94.
38. Bando K, Armitage JM, Paradis IL, et al. Indications for and results of single, bilateral, and heart–lung transplantation for pulmonary hypertension. J Thorac Cardiovasc Surg 1994;108:1056–65.
39. Bando K, Paradis IL, Keenan RJ, et al. Comparison of outcomes after single and bilateral lung transplantation for obstructive lung disease. J Heart Lung Transplant 1995;14:692–8.
40. Egan TM. Lung preservation. Semin Thorac Cardiovasc Surg 1992;4:83–9.
41. Gammie JS, Stukus DR, Pham SM, et al. Effect of ischemic time on survival in clinical lung transplantation. Ann Thorac Surg 1999;68:2015–9.
42. Thabut G, Vinatier I, Brugiere O, et al. Influence of preservation solution on early graft failure in clinical lung transplantation. Am J Respir Crit Care Med 2001;164:1204–8.
43. Thabut G, Brugiere O, Leseche G, et al. Preventive effect of inhaled nitric oxide and pentoxifylline on ischemia/reperfusion injury after lung transplantation. Transplantation 2001;71:1295–300.
44. Christie JD, Bavaria JE, Palevsky HI, et al. Primary graft failure following lung transplantation. Chest 1998;114:51–60.
45. Thabut G, Vinatier I, Stern JB, et al. Primary graft failure following lung transplantation: predictive factors of mortality. Chest 2002;121:1876–82.

46. Schulman LL, Anandarangam T, Leibowitz DW, et al. Four-year prospective study of pulmonary venous thrombosis after lung transplantation. J Am Soc Echocardiogr 2001;14: 806–12.
47. Ardehali A, Laks H, Levine M, et al. A prospective trial of inhaled nitric oxide in clinical lung transplantation. Transplantation 2001;72:112–5.
48. Meade M, Granton JT, Matte-Martyn A, et al. A randomized trial of inhaled nitric oxide to prevent reperfusion injury following lung transplantation. J Heart Lung Transplant 2001;20: 254–5.
49. Meyers BF, Sundt TM III, Henry S, et al. Selective use of extracorporeal membrane oxygenation is warranted after lung transplantation. J Thorac Cardiovasc Surg 2000;120:20–6.
50. Struber M. What is the role of surfactant and inhaled nitric oxide in lung transplantation? Crit Care 2002;6:186–7.
51. Date H, Trulock EP, Arcidi JM, et al. Improved airway healing after lung transplantation. An analysis of 348 bronchial anastomoses. J Thorac Cardiovasc Surg 1995;110: 1424–32.
52. Griffith BP, Magee MJ, Gonzalez IF, et al. Anastomotic pitfalls in lung transplantation. J Thorac Cardiovasc Surg 1994;107: 743–53.
53. Blumenstock DA, Lewis C. The first transplantation of the lung in a human revisited. Ann Thorac Surg 1993;56:1423–4.
54. Maurer JR. Therapeutic challenges following lung transplantation. Clin Chest Med 1990;11:279–90.
55. Cooper DK, Novitzky D, Rose AG, Reichart BA. Acute pulmonary rejection precedes cardiac rejection following heart–lung transplantation in a primate model. J Heart Transplant 1986;5:29–32.
56. Frost AE, Jammal CT, Cagle PT. Hyperacute rejection following lung transplantation. Chest 1996;110:559–62.
57. McGregor CG, Baldwin JC, Jamieson SW, et al. Isolated pulmonary rejection after combined heart–lung transplantation. J Thorac Cardiovasc Surg 1985;90:623–6.
58. Glanville AR, Baldwin JC, Hunt SA, Theodore J. Long-term cardiopulmonary function after human heart–lung transplantation. Aust N Z J Med 1990;20:208–14.
59. Quantz MA, Bennett LE, Meyer DM, Novick RJ. Does human leukocyte antigen matching influence the outcome of lung transplantation? An analysis of 3,549 lung transplantations. J Heart Lung Transplant 2000;19:473–9.
60. Briffa N, Morris RE. New immunosuppressive regimens in lung transplantation. Eur Respir J 1997;10:2630–7.
61. Kahan BD, Ghobrial R. Immunosuppressive agents. Surg Clin North Am 1994;74:1029–54.
62. Cooper JD, Pohl MS, Patterson GA. An update on the current status of lung transplantation: report of the St Louis International Lung Transplant Registry. Clin Transplant 1993;95–100.
63. Kramer MR, Marshall SE, Starnes VA, et al. Infectious complications in heart–lung transplantation. Analysis of 200 episodes. Arch Intern Med 1993;153:2010–6.
64. Garrity ER Jr, Villanueva J, Bhorade SM, et al. Low rate of acute lung allograft rejection after the use of daclizumab, an interleukin 2 receptor antibody. Transplantation 2001;71:773–7.
65. Dumont RJ, Partovi N, Levy RD, et al. A limited sampling strategy for cyclosporine area under the curve monitoring in lung transplant recipients. J Heart Lung Transplant 2001;20: 897–900.
66. Garrity ER Jr, Hertz MI, Trulock EP, et al. Suggested guidelines for the use of tacrolimus in lung-transplant recipients. J Heart Lung Transplant 1999;18:175–6.
67. Horning NR, Lynch JP, Sundaresan SR, et al. Tacrolimus therapy for persistent or recurrent acute rejection after lung transplantation. J Heart Lung Transplant 1998;17:761–7.
68. Treede H, Klepetko W, Reichenspurner H, et al. Tacrolimus versus cyclosporine after lung transplantation: a prospective, open, randomized two-center trial comparing two different immunosuppressive protocols. J Heart Lung Transplant 2001;20:511–7.
69. Selman M. From anti-inflammatory drugs through antifibrotic agents to lung transplantation: a long road of research, clinical attempts, and failures in the treatment of idiopathic pulmonary fibrosis. Chest 2002;122:759–61.
70. Hopkins PM, Aboyoun CL, Chhajed PN, et al. Prospective analysis of 1,235 transbronchial lung biopsies in lung transplant recipients. J Heart Lung Transplant 2002;21:1062–7.
71. Bando K, Paradis IL, Komatsu K, et al. Analysis of time-dependent risks for infection, rejection, and death after pulmonary transplantation. J Thorac Cardiovasc Surg 1995; 109:49–57.
72. King-Biggs MB. Acute pulmonary allograft rejection. Mechanisms, diagnosis, and management. Clin Chest Med 1997;18:301–10.
73. Lawrence EC. Diagnosis and management of lung allograft rejection. Clin Chest Med 1990;11:269–78.
74. Trulock EP, Ettinger NA, Brunt EM, et al. The role of transbronchial lung biopsy in the treatment of lung transplant recipients. An analysis of 200 consecutive procedures. Chest 1992;102:1049–54.
75. Sibley RK, Berry GJ, Tazelaar HD, et al. The role of transbronchial biopsies in the management of lung transplant recipients. J Heart Lung Transplant 1993;12:308–24.
76. Yousem SA, Berry GJ, Cagle PT, et al. Revision of the 1990 working formulation for the classification of pulmonary allograft rejection: Lung Rejection Study Group. J Heart Lung Transplant 1996;15(1 Pt 1):1–15.
77. Yousem SA, Burke CM, Billingham ME. Pathologic pulmonary alterations in long-term human heart–lung transplantation. Hum Pathol 1985;16:911–23.
78. Boehler A, Chamberlain D, Kesten S, et al. Lymphocytic airway infiltration as a precursor to fibrous obliteration in a rat model of bronchiolitis obliterans. Transplantation 1997;64: 311–7.
79. Boehler A, Kesten S, Weder W, Speich R. Bronchiolitis obliterans after lung transplantation: a review. Chest 1998;114: 1411–26.
80. Kramer MR, Stoehr C, Whang JL, et al. The diagnosis of obliterative bronchiolitis after heart–lung and lung transplantation: low yield of transbronchial lung biopsy. J Heart Lung Transplant 1993;12:675–81.
81. Cooper JD, Billingham M, Egan T, et al. A working formulation for the standardization of nomenclature and for clinical staging of chronic dysfunction in lung allografts. International Society for Heart and Lung Transplantation. J Heart Lung Transplant 1993;12:713–6.
82. Ouwens JP, van der Mark TW, Koeter GH, et al. Bronchiolar airflow impairment after lung transplantation: an early and common manifestation. J Heart Lung Transplant 2002;21:1056–61.
83. Estenne M, Maurer JR, Boehler A, et al. Bronchiolitis obliterans syndrome 2001: an update of the diagnostic criteria. J Heart Lung Transplant 2002;21:297–310.
84. Bando K, Paradis IL, Similo S, et al. Obliterative bronchiolitis after lung and heart–lung transplantation. An analysis of risk factors and management. J Thorac Cardiovasc Surg 1995;110:4–13.
85. Tullius SG, Tilney NL. Both alloantigen-dependent and -independent factors influence chronic allograft rejection. Transplantation 1995;59:313–8.
86. Date H, Lynch JP, Sundaresan S, et al. The impact of cytolytic therapy on bronchiolitis obliterans syndrome. J Heart Lung Transplant 1998;17:869–75.

87. Haque MA, Mizobuchi T, Yasufuku K, et al. Evidence for immune responses to a self-antigen in lung transplantation: role of type V collagen-specific T cells in the pathogenesis of lung allograft rejection. J Immunol 2002;169:1542–9.
88. Yousem SA. Significance of clinically silent untreated mild acute cellular rejection in lung allograft recipients. Hum Pathol 1996;27:269–73.
89. Heng D, Sharples LD, McNeil K, et al. Bronchiolitis obliterans syndrome: incidence, natural history, prognosis, and risk factors. J Heart Lung Transplant 1998;17:1255–63.
90. Husain S, Singh N. Bronchiolitis obliterans and lung transplantation: evidence for an infectious etiology. Semin Respir Infect 2002;17:310–4.
91. Yousem SA. Lymphocytic bronchitis/bronchiolitis in lung allograft recipients. Am J Surg Pathol 1993;17:491–6.
92. Ward C, Snell GI, Zheng L, et al. Endobronchial biopsy and bronchoalveolar lavage in stable lung transplant recipients and chronic rejection. Am J Respir Crit Care Med 1998; 158:84–91.
93. Yousem SA, Suncan SR, Ohori NP, Sonmez-Alpan E. Architectural remodeling of lung allografts in acute and chronic rejection. Arch Pathol Lab Med 1992;116:1175–80.
94. Zheng L, Walters EH, Ward C, et al. Airway neutrophilia in stable and bronchiolitis obliterans syndrome patients following lung transplantation. Thorax 2000;55:53–9.
95. Zheng L, Ward C, Snell GI, et al. Scar collagen deposition in the airways of allografts of lung transplant recipients. Am J Respir Crit Care Med 1997;155:2072–7.
96. Stanbrook MB, Kesten S. Bronchial hyperreactivity after lung transplantation predicts early bronchiolitis obliterans. Am J Respir Crit Care Med 1999;160:2034–9.
97. Belperio JA, Keane MP, Strieter RM. Cytokines during the pathogenesis of bronchiolitis obliterans. Curr Opin Organ Transplant 2003;8:228–38.
98. Neuringer IP, Mannon RB, Coffman TM, et al. Immune cells in a mouse airway model of obliterative bronchiolitis. Am J Respir Cell Mol Biol 1998;19:379–86.
99. Yamada K, Gianello PR, Ierino FL, et al. Role of the thymus in transplantation tolerance in miniature swine. J Exp Med 1997;186:497–506.
100. Maurer JR, Tullis DE, Grossman RF, et al. Infectious complications following isolated lung transplantation. Chest 1992;101:1056–9.
101. Speich R, van der Bij W. Epidemiology and management of infections after lung transplantation. Clin Infect Dis 2001;33 Suppl 1:S58–65.
102. Chaparro C, Kesten S. Infections in lung transplant recipients. Clin Chest Med 1997;18:339–51.
103. Wreghitt T. Cytomegalovirus infections in heart and heart–lung transplant recipients. J Antimicrob Chemother 1989;23 Suppl E:49–60.
104. Wreghitt TG, Abel SJ, McNeil K, et al. Intravenous ganciclovir prophylaxis for cytomegalovirus in heart, heart–lung, and lung transplant recipients. Transplant Int 1999;12:254–60.
105. Kubak BM. Fungal infection in lung transplantation. Transplant Infect Dis 2002;4 Suppl 3:24–31.
106. Westney GE, Kesten S, De Hoyos A, et al. Aspergillus infection in single and double lung transplant recipients. Transplantation 1996;61:915–9.
107. Soubani AO, Chandrasekar PH. The clinical spectrum of pulmonary aspergillosis. Chest 2002;121:1988–99.
108. Gordon SM, Avery RK. Aspergillosis in lung transplantation: incidence, risk factors, and prophylactic strategies. Transplant Infect Dis 2001;3:161–7.
109. Birsan T, Taghavi S, Klepetko W. Treatment of aspergillus-related ulcerative tracheobronchitis in lung transplant recipients. J Heart Lung Transplant 1998;17:437–8.
110. Kramer MR, Stoehr C, Lewiston NJ, et al. Trimethoprim–sulfamethoxazole prophylaxis for Pneumocystis carinii infections in heart–lung and lung transplantation—how effective and for how long? Transplantation 1992;53:586–9.
111. Smyth RL, Scott JP, Borysiewicz LK, et al. Cytomegalovirus infection in heart–lung transplant recipients: risk factors, clinical associations, and response to treatment. J Infect Dis 1991;164:1045–50.
112. Rubin RH. Cytomegalovirus in solid organ transplantation. Transplant Infect Dis 2001;3 Suppl 2:1–5.
113. Tolkoff-Rubin NE, Fishman JA, Rubin RH. The bidirectional relationship between cytomegalovirus and allograft injury. Transplant Proc 2001;33:1773–5.
114. Farrell HE, Vally H, Lynch DM, et al. Inhibition of natural killer cells by a cytomegalovirus MHC class I homologue in vivo. Nature 1997;386:510–4.
115. Gilbert MJ, Riddell SR, Plachter B, Greenberg PD. Cytomegalovirus selectively blocks antigen processing and presentation of its immediate-early gene product. Nature 1996;383:720–2.
116. Reddehase MJ, Koszinowski UH. Significance of herpesvirus immediate early gene expression in cellular immunity to cytomegalovirus infection. Nature 1984;312:369–71.
117. Zeevi A, Morel P, Spichty K, et al. Clinical significance of CMV-specific T helper responses in lung transplant recipients. Hum Immunol 1998;59:768–75.
118. Duncan SR, Paradis IL, Yousem SA, et al. Sequelae of cytomegalovirus pulmonary infections in lung allograft recipients. Am Rev Respir Dis 1992;146:1419–25.
119. Estenne M, Hertz MI. Bronchiolitis obliterans after human lung transplantation. Am J Respir Crit Care Med 2002;166:440–4.
120. Kotsimbos AT, Sinickas V, Glare EM, et al. Quantitative detection of human cytomegalovirus DNA in lung transplant recipients. Am J Respir Crit Care Med 1997;156(4 Pt 1):1241–6.
121. Michaelides A, Liolios L, Glare EM, et al. Increased human cytomegalovirus (HCMV) DNA load in peripheral blood leukocytes after lung transplantation correlates with HCMV pneumonitis. Transplantation 2001;72:141–7.
122. Riise GC, Andersson R, Bergstrom T, et al. Quantification of cytomegalovirus DNA in BAL fluid: a longitudinal study in lung transplant recipients. Chest 2000;118:1653–60.
123. Gerna G, Zavattoni M, Baldanti F, et al. Human cytomegalovirus (HCMV) leukodnaemia correlates more closely with clinical symptoms than antigenemia and viremia in heart and heart–lung transplant recipients with primary HCMV infection. Transplantation 1998;65:1378–85.
124. Cone RW, Hackman RC, Huang ML, et al. Human herpesvirus 6 in lung tissue from patients with pneumonitis after bone marrow transplantation. N Engl J Med 1993;329:156–61.
125. Hall CB, Long CE, Schnabel KC, et al. Human herpesvirus-6 infection in children. A prospective study of complications and reactivation. N Engl J Med 1994;331:432–8.
126. Morris DJ, Littler E, Arrand JR, et al. Human herpesvirus 6 infection in renal-transplant recipients. N Engl J Med 1989; 320:1560–1.
127. Michaelides A, Glare EM, Spelman DW, et al. Beta-herpesvirus (human cytomegalovirus and human herpesvirus 6) reactivation in at-risk lung transplant recipients and in human immunodeficiency virus-infected patients. J Infect Dis 2002;186:173–80.
128. Aris RM, Maia DM, Neuringer IP, et al. Post-transplantation lymphoproliferative disorder in the Epstein–Barr virus-naive lung transplant recipient. Am J Respir Crit Care Med 1996;154(6 Pt 1):1712–7.
129. Wong JY, Tait B, Levvey B, et al. EBV mismatching and HLA matching post lung transplantation: key risk factors

for post transplant lymphoproliferative disease (PTLD). Transplantation 2004;78:205-10.
130. Cook RC, Connors JM, Gascoyne RD, et al. Treatment of post-transplant lymphoproliferative disease with rituximab monoclonal antibody after lung transplantation. Lancet 1999;354:1698–9.
131. Holmes RD, Sokol RJ. Epstein–Barr virus and post-transplant lymphoproliferative disease. Pediatr Transplant 2002;6: 456–64.
132. Billings JL, Hertz MI, Wendt CH. Community respiratory virus infections following lung transplantation. Transplant Infect Dis 2001;3:138–48.
133. Weinberg A, Zamora MR, Li S, et al. The value of polymerase chain reaction for the diagnosis of viral respiratory tract infections in lung transplant recipients. J Clin Virol 2002;25:171–5.
134. Billings JL, Hertz MI, Savik K, Wendt CH. Respiratory viruses and chronic rejection in lung transplant recipients. J Heart Lung Transplant 2002;21:559–66.
135. Vilchez RA, McCurry K, Dauber J, et al. The epidemiology of parainfluenza virus infection in lung transplant recipients. Clin Infect Dis 2001;33:2004–8.
136. Hayden AM, Robert RC, Kriett JM, et al. Primary diagnosis predicts prognosis of lung transplant candidates. Transplantation 1993;55:1048–50.
137. Pochettino A, Kotloff RM, Rosengard BR, et al. Bilateral versus single lung transplantation for chronic obstructive pulmonary disease: intermediate-term results. Ann Thorac Surg 2000;70:1813–8.
138. Williams TJ, Grossman RF, Maurer JR. Long-term functional follow-up of lung transplant recipients. Clin Chest Med 1990;11:347–58.
139. Snell GI, Shiraishi T, Griffiths A, et al. Outcomes from paired single-lung transplants from the same donor. J Heart Lung Transplant 2000;19:1056–62.
140. Williams TJ, Snell GI. Early and long-term functional outcomes in unilateral, bilateral, and living-related transplant recipients. Clin Chest Med 1997;18:245–57.
141. Cassivi SD, Meyers BF, Battafarano RJ, et al. Thirteen-year experience in lung transplantation for emphysema. Ann Thorac Surg 2002;74:1663–9.
142. Egan TM, Detterbeck FC, Mill MR, et al. Long term results of lung transplantation for cystic fibrosis. Eur J Cardiothorac Surg 2002;22:602–9.
143. Liou TG, Adler FR, Cahill BC, et al. Survival effect of lung transplantation among patients with cystic fibrosis. JAMA 2001;286:2683–9.
144. Chacon RA, Corris PA, Dark JH, Gibson GJ. Comparison of the functional results of single lung transplantation for pulmonary fibrosis and chronic airway obstruction. Thorax 1998;53:43–9.
145. Chacon RA, Corris PA, Dark JH, Gibson GJ. Respiratory mechanics after heart–lung and bilateral lung transplantation. Thorax 1997;52:718–22.
146. Maziak DE, Maurer JR, Kesten S. Diaphragmatic paralysis: a complication of lung transplantation. Ann Thorac Surg 1996;61:170–3.
147. Levy RD, Ernst P, Levine SM, et al. Exercise performance after lung transplantation. J Heart Lung Transplant 1993;12(1 Pt 1):27–33.
148. Williams TJ, Patterson GA, McClean PA, et al. Maximal exercise testing in single and double lung transplant recipients. Am Rev Respir Dis 1992;145:101–5.
149. Evans AB, Al Himyary AJ, Hrovat MI, et al. Abnormal skeletal muscle oxidative capacity after lung transplantation by 31P-MRS. Am J Respir Crit Care Med 1997;155:615–21.
150. Tirdel GB, Girgis R, Fishman RS, Theodore J. Metabolic myopathy as a cause of the exercise limitation in lung transplant recipients. J Heart Lung Transplant 1998;17:1231–7.
151. Gross CR, Savik K, Bolman RM III, Hertz MI. Long-term health status and quality of life outcomes of lung transplant recipients. Chest 1995;108:1587–93.
152. Gross CR, Raghu G. The cost of lung transplantation and the quality of life post-transplant. Clin Chest Med 1997;18: 391–403.
153. Chaparro C, Scavuzzo M, Winton T, et al. Status of lung transplant recipients surviving beyond five years. J Heart Lung Transplant 1997;16:511–6.
154. Paris W, Diercks M, Bright J, et al. Return to work after lung transplantation. J Heart Lung Transplant 1998;17:430–6.
155. Zaltzman JS, Pei Y, Maurer J, et al. Cyclosporine nephrotoxicity in lung transplant recipients. Transplantation 1992;54: 875–8.
156. Aris RM, Neuringer IP, Weiner MA, et al. Severe osteoporosis before and after lung transplantation. Chest 1996;109: 1176–83.
157. Maurer JR, Tewari S. Nonpulmonary medical complications in the intermediate and long-term survivor. Clin Chest Med 1997;18:367–82.
158. Hausen B, Morris RE. Review of immunosuppression for lung transplantation. Novel drugs, new uses for conventional immunosuppressants, and alternative strategies. Clin Chest Med 1997;18:353–66.
159. Chambers CA, Allison JP. Costimulatory regulation of T cell function. Curr Opin Cell Biol 1999;11:203–10.
160. Pham SM, Mitruka SN, Youm W, et al. Mixed hematopoietic chimerism induces donor-specific tolerance for lung allografts in rodents. Am J Respir Crit Care Med 1999;159:199–205.
161. Pham SM, Rao AS, Zeevi A, et al. Effects of donor bone marrow infusion in clinical lung transplantation. Ann Thorac Surg 2000;69:345–50.
162. Dorling A, Riesbeck K, Warrens A, Lechler R. Clinical xenotransplantation of solid organs. Lancet 1997;349:867–71.

CHAPTER 45

PHYSIOLOGIC RESPONSES TO EXERCISE

Hans C. Haverkamp, Jerome A. Dempsey, Jordan D. Miller,
Lee M. Romer, Marlowe W. Eldridge

The exchange of gas by the lung represents the first critical link in the transport of oxygen and carbon dioxide between the atmosphere and tissue mitochondria. The increases in muscular oxygen consumption ($\dot{V}O_2$) and carbon dioxide production ($\dot{V}CO_2$) accompanying whole body exercise present a greater challenge to the maintenance of pulmonary gas exchange than any other physiologic stressor. In this chapter we discuss the responses of the healthy respiratory system to exercise, with an emphasis on the following problems. What neurochemical mechanisms regulate the ventilatory response to exercise, and what are the consequences of this hyperpnea for the work and fatigue of the respiratory muscles? What mechanisms underlie the widening of the alveolar–arterial partial pressure of oxygen (PO_2) difference during exercise? How do the unique characteristics of the pulmonary circulation determine its response to exercise? We consider these problems primarily in the healthy, young, normally fit adult, with occasional reference to special cases of the highly trained athlete and to the effects of healthy aging.

EXERCISE HYPERPNEA—THE FIRST LINE OF DEFENSE

During exercise, increases in alveolar ventilation must parallel the increased tissue oxygen consumption and carbon dioxide production by the exercising muscles, both of which rise in direct proportion to the increase in power output. These relationships are governed by the following equations,* which dictate the regulation of alveolar PO_2 (P_AO_2) and PCO_2 (P_ACO_2):

$$P_AO_2 = \text{inspired } PO_2 - (\dot{V}O_2/\dot{V}_A)K$$

where $\dot{V}O_2$ is oxygen consumption/min and $\dot{V}_A$ is alveolar ventilation/min.

$$P_ACO_2 = (\dot{V}CO_2/\dot{V}_A)K$$

where $\dot{V}CO_2$ is carbon dioxide production/min.

As shown by the mean values for healthy young subjects in Table 45-1, the matching of 5- to 10-fold increases in $\dot{V}CO_2$ above rest with proportional increases in alveolar ventilation ($\dot{V}_A$) during mild through moderate exercise intensities is extremely precise; accordingly, alveolar PCO_2 (and arterial PO_2 and pH) is maintained very close to resting levels. One might predict that the mechanisms controlling these very large increases in ventilation must be linked to the muscle carbon dioxide production. However, intense searches over the last century for receptors with appropriately high sensitivity on the venous side of the circulation, including the lung, which might respond to some element of "carbon dioxide flow" (ie, mixed venous carbon content [$C\bar{v}CO_2$] or cardiac output [CO]) have not proven fruitful. There have been very enticing data presented—such as the extracorporeal circulation studies in unanesthetized resting animals, which showed near-perfect tracking of $\dot{V}_A$ to $CO \times C\bar{v}CO_2$,[1] but even these beautifully designed experiments did not always produce these tight relationships, especially with substantial increases in carbon dioxide flow.[2] Since the 1980s, this strictly "metabolic" hypothesis has been set aside by most investigators in favor of strong neural "feedforward" and "feedback" drives to breathe, which are only indirectly associated with $\dot{V}CO_2$ but directly linked to the act of locomotion. Analogous mechanisms are also purported to be responsible for the linear increases in cardiac output in relation to $\dot{V}O_2$ during exercise.

The first of these mechanisms is "central command," a strong feedforward neural drive originating in locomotor areas of the higher central nervous system (CNS) (hypothalamus, cerebellum, diencephalon), whose axons project to

*Calculation of alveolar gases may be done from these equations if both $\dot{V}O_2$ and alveolar ventilation ($\dot{V}_A$) are expressed in liters per minute. The constant K then becomes 863. For example, if inspired PO_2 is 150 mm Hg, $\dot{V}O_2$ is 0.240 L/min STPD, and $\dot{V}_A$ is 4.0 L/min BTPS, alveolar PO_2 is 98 mm Hg. The same applies to carbon dioxide exchange between alveoli and atmosphere, except that the equation is simplified because carbon dioxide is virtually absent in inspired air.

the medullary respiratory rhythm-generating neurons. As activation of these motor pathways commands spinal motor neuron activation, limb muscle contraction, and locomotion, they also cause parallel activation of respiratory motor output. Landmark studies produced "fictive locomotion" by using pharmacologic or electrical stimulation methods to activate central command in paralyzed, decorticated cats.[3] Phrenic nerve activity increased in proportion to this central locomotor command without any need for raised metabolic carbon dioxide production or any type of feedback from contracting locomotor muscles. These remarkable responses of ventilation (and of cardiac output and blood pressure) have been verified in several subsequent studies.[3] Of course, it is questionable exactly how closely these experimental simulations of central command actually mimic the complex, coordinated output that occurs during whole body exercise. Attempts have been made to increase central locomotor command (ie, effort) in humans independently of muscle force output by using spinal blockade, partial muscle paralysis, patients with selected spinal cord lesions, or hypnotic suggestion of exercise in normal, intact subjects.[4] Inferences have been drawn about the role of central command during actual exercise on the basis of the substantial hyperpnea and tachycardia observed under these conditions of increased central motor output. However, we cannot be sure how closely, if at all, these changes in so-called central locomotor command mimic those normally occurring during exercise. For example, it seems unlikely that the increased locomotor "effort" under these nonphysiologic conditions originates from the same motor areas of the higher CNS and travels along the same descending neural pathways as are normally used during whole body exercise.

The second type of neural pathway underlying the cardioventilatory response to exercise originates in the mechanical and chemical receptors in the working locomotor muscles. Until recently, these muscle receptors were only thought to increase their activity in response to experimental perturbations such as ischemia, vessel distention, or electrical stimulation of motor nerves. However, Kaufman and Forster, in their comprehensive review, concluded that locomotion induced by electrical stimulation of central command in the higher CNS increases type III and IV afferent nerve activity in the muscle in response to the "exercise stimulus" per se.[5] The presence of these feedback effects is much more difficult to demonstrate in humans, although increases in ventilation can be produced by local muscle ischemia, lower body positive pressure, vascular distention, or electrical stimulation of muscle.[6] Stimulating these muscle receptors does not always elicit comparable ventilatory and cardiovascular responses. Quite often, an increase in blood pressure and sympathetic vasoconstrictor outflow in response to muscle metabolic stimuli are not accompanied by significant changes in ventilation.[5]

It seems remarkable that these very large and precise increases in ventilation accompanying exercise are governed primarily by mechanisms that have no direct link to the regulated variable (ie, carbon dioxide). Perhaps, then, we should view the two types of locomotor-linked neural drive as only the "primary" stimuli for exercise hyperpnea, which serve only to increase ventilation within the desired range. Thereafter, we depend on fast-responding peripheral and central chemoreceptors to detect errors or mismatches of $\dot{V}_A$ to $\dot{V}CO_2$ and to provide fine-tuning for more precise respiratory motor output and ventilation. This arrangement sounds feasible, but exactly how all these mechanisms are able to communicate with one another in an integrative fashion during exercise remains elusive.

Finally, in heavy exercise at metabolic rates requiring more than 75 to 85% of $\dot{V}O_{2MAX}$, hyperventilation occurs ($\uparrow\dot{V}_A > \uparrow\dot{V}CO_2$), commensurate with the onset of arterial acidosis (Table 45-1). The mechanisms involved here appear to be more straightforward as the carotid bodies are now exposed to high levels of several known stimuli—acidosis, norepinephrine, and K^+.[7] On the other hand, reports of a normal hyperventilatory response following prevention of lactic acidosis (through glycogen depletion) in humans, or even removal of the carotid bodies in animal models, show that these humoral mechanisms are not necessary for the hyperventilatory response.[5,7] Theoretically, both primary mechanisms of hyperpnea could also be involved in this hyperventilatory response. For example, curvilinear increases in the feedback stimulus from the working muscle may occur as lactic acid and heat accumulate in working limb muscles. Furthermore, curvilinear increases in the feedforward central command stimulus are likely in heavy exercise as more motor units are recruited in an attempt to maintain force output in the face of limb muscle fatigue.[7] We favor a combination of the following three mechanisms to explain the hyperventilatory response to heavy exercise: (1) carotid body stimulation, (2) nonlinear metabolite production and afferent stimulation, and (3) increased central motor output as fatigue nears.

BREATHING PATTERN DURING EXERCISE

The precise matching of $\dot{V}_A$ with metabolic rate during exercise is achieved by an increase in minute ventilation ($\dot{V}_E$), while at the same time the mechanical work performed by the respiratory muscles is minimized. The increase in $\dot{V}_E$ during exercise is accomplished by increases in both tidal volume ($\dot{V}_T$) and breathing frequency (f_b) (see Table 45-1). The increased V_T does result in a slight increase in conducting airway dead space, due to the tethering effects of the lung parenchyma on airway lumen size; however, the relative increase in $\dot{V}_T$ is much greater than this effect. Thus, the ratio of dead space volume to tidal volume (V_D/V_T) decreases during exercise from normal resting values of ~0.35 to values of ~0.20 or slightly less and translates into more efficient alveolar ventilation. During low- to moderate-intensity exercise, both V_T and f_b increase roughly in proportion to intensity, whereas at higher intensities, V_T reaches a plateau, and further increases in $\dot{V}_E$ are accomplished by increases in f_b alone. The increase in f_b is accomplished by decreases in both inspiratory time (T_I) and expiratory time (T_E). However, the ratio of T_I to total breath cycle duration (T_{TOT}), known as the duty cycle (T_I/T_{TOT}), increases only slightly during exercise (~0.40 at rest to ~0.50 during high-intensity exercise). The fact that the inspiratory duty cycle remains low is important and beneficial because prolonged diaphragmatic contractions

Table 45-1 Ventilation, Pulmonary Gas Exchange and the Pulmonary Circulation During Exercise in Healthy Young Adults (body mass 70 kg; $\dot{V}O_{2MAX}$ 40 to 45 mL/kg/min)

	% $\dot{V}O_{2MAX}$							
	Rest	*15*	*30*	*45*	*60*	*75*	*90*	*100*
Breathing pattern								
$\dot{V}O_2$ (L/min)	0.30	0.45	0.90	1.35	1.8	2.25	2.7	3.0
$\dot{V}CO_2$ (L/min)	0.24	0.40	0.77	1.21	1.71	2.31	3.0	3.3
$\dot{V}_E$ (L/min)	8	14	22	35	51	75	100	115
$\dot{V}_A$ (L/min)	5.3	9	18	28	41	60	81	94
$\dot{V}_T$ (L)	0.65	0.9	1.2	1.6	2.2	2.5	2.6	2.6
f_b (breaths/min)	12	15	18	22	23	30	38	44
V_D/V_T	0.35	0.28	0.21	0.20	0.19	0.18	0.18	0.18
EELV (% TLC)	0.50	0.49	0.46	0.45	0.44	0.43	0.42	0.42
Gas exchange and blood gases								
P_aO_2 (mm Hg)	91	95	93	93	92	94	94	95
P_AO_2 (mm Hg)	96	100	101	103	107	112	114	117
P_aCO_2 (mm Hg)	40	40	37	37	36	34	33	31
$P_{A-a}O_2$ (mm Hg)	5	5	8	10	15	18	20	22
pH	7.4	7.4	7.38	7.36	7.34	7.30	7.29	7.28
S_aO_2 (%)	97	97	97	97	96.5	96	95.5	95
$\dot{V}_A/\dot{Q}$	1.1	1.3	2.0	2.5	2.9	3.5	4.1	4.5
Pulmonary circulation								
CO (L/min)	5	7	9	11	14	17	20	21
PCBV (mL)	83	95	107	119	137	155	173	180
Transit time (s)	1.00	0.81	0.71	0.65	0.59	0.55	0.52	0.51
P_{pa} (mm Hg)	11.8	13.8	15.8	17.8	20.8	23.9	26.9	27.9
PVR (mm Hg/L/min)	2.4	1.97	1.76	1.62	1.49	1.41	1.35	1.33

PCBV calculated from Hsia CCW, McBrayer DG, Ramanathan M. Reference values of pulmonary diffusing capacity during exercise by a rebreathing technique. Am J Respir Crit Care Med 1995;152:658–65.

P_{pa} calculated from Reeves JT, Dempsey JA, Grover RF. Pulmonary circulation during exercise. In: Weir EK, Reeves JT, editors. Pulmonary vascular physiology and pathophysiology. Vol 38. New York: Marcel Dekker; 1988. p. 107–33.

CO calculated from Rowell LB. Human cardiovascular control. New York: Oxford University Press; 1993. p. 162–203.

All other data compiled from authors' laboratory.

CO = cardiac output; EELV = end-expiratory lung volume; f_b = breathing frequency; P_{pa} = pulmonary artery pressure; P_aCO_2 = partial pressure of arterial carbon dioxide; P_aO_2 = partial pressure of arterial oxygen; P_AO_2 = partial pressure of alveolar oxygen; PCBV = pulmonary capillary blood volume; PVR = pulmonary vascular resistance; S_aO_2 = saturation of hemoglobin with oxygen; $\dot{V}_A$ = alveolar ventilation; $\dot{V}_A/\dot{Q}$ = alveolar ventilation–perfusion relationship; $\dot{V}_E$ = minute ventilation; V_D/V_T = dead space to tidal volume fraction; V_T = tidal volume.

hinder bloodflow to this muscle and may precipitate and result in excessive diaphragmatic fatigue.[8]

The increase in V_T at the onset of exercise is accomplished by both an increase in end-inspiratory lung volume (EILV) and a decrease in end-expiratory lung volume (EELV). However, as exercise intensity increases, EILV does not normally increase beyond 85 to 90% of total lung capacity (TLC) since beyond this point lung compliance decreases markedly, and the respiratory pressure production required for a given change in volume is very large. This inefficiency at high operating lung volumes leads to neuromechanical uncoupling, in that a mismatch develops between the required "effort" to inspire and the actual volume of air inhaled. EELV decreases at the onset of all levels of exercise, due to active recruitment of the expiratory muscles, and its decrease is proportional to exercise intensity.[9] This reduction serves to place the diaphragm on a more optimal point of its length–tension relationship and also reduces inspiratory muscle work during the ensuing inspiration, due to outward recoil of the rib cage at the onset of inspiration. The drop in EELV also helps keep operating lung volumes within the linear portion of the pressure–volume relationship, which helps minimize the reduction in respiratory system compliance and associated dyspnea that develop at high lung volumes.

Tidal exercise flow–volume curves plotted within the maximal volitional flow–volume envelope provide a simple and useful method for the analysis of alterations in flow rates, tidal volume, and operating lung volumes during exercise (Figure 45-1). In normal, healthy humans the maximal attainable flow rates at any given lung volume are usually much greater than the spontaneous flow rates reached during exercise of all intensities. Thus, there is usually a large reserve for increasing $\dot{V}_E$, even at maximal exercise. However, endurance-trained individuals with high maximal exercise $\dot{V}_E$ may intersect the boundary of the expiratory portion of the maximal flow–volume envelope and thus become "flow-limited."[†] This may also occur in untrained

[†]True expiratory flow limitation is only present when expiratory flow fails to increase in response to further increases in transpulmonary pressure at a given lung volume.[10] Thus, the intersection of the tidal and maximal volitional flow–volume envelopes does not necessarily represent true expiratory flow limitation and may be partially due to artifact created by gas compression during the maximal expiratory maneuver. There are, however, physiologic consequences that occur when the maximal and exercise flow–volume loops intersect, as described in the text.

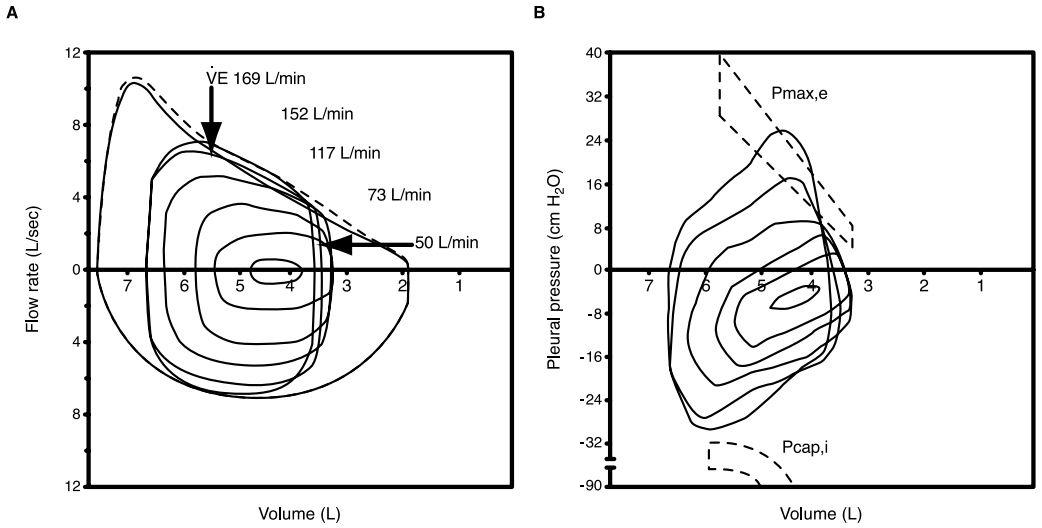

FIGURE 45-1 Spontaneous exercise tidal flow–volume curves plotted within the maximal volitional flow–volume envelope performed before (*solid line*) and immediately after (*dotted line*) exercise of increasing intensity to maximum. Also shown are corresponding pressure–volume loops. $P_{max,e}$ is the pleural pressure at which expiratory flow becomes limited at different lung volumes, and $P_{cap,i}$ is the maximal capacity of the inspiratory muscles for pressure generation. Note the reduction in end-expiratory lung volume (EELV) during exercise and the slight rise in EELV as expiratory flow limitation occurs at the higher ventilation rates. Also note that the $\dot{V}_E$ of 117 L/min corresponds to a maximal exercise $\dot{V}_E$ for sedentary males, whereas the higher minute ventilation rates are for trained male athletes. Reproduced with permission from Harms CA, Wetter TJ, Dempsey JA. Breathing in exercise. In: Cherniak NS, Altose MD, Homma I, editors. Rehabilitation of the patient with respiratory disease. New York: McGraw-Hill; 1999. p. 87–96.

individuals with abnormally small airways or in those with a compromised lung elastic recoil and ability to produce high flow rates, due to dynamic airway collapse, such as in obstructive lung disease. Expiratory flow limitation during exercise appears to occur more often in women, primarily because of smaller airways and lower maximal expiratory flow rates, than in age- and height-matched men.[11]

The outcomes of expiratory flow limitation are twofold and include (1) a limiting of V_T and $\dot{V}_E$ with even moderate amounts of overlap between the tidal exercise and maximal volitional flow–volume curves since inspiratory and expiratory time are limited because of increased f_b at higher workloads and also an inability to increase EILV, due to mechanical constraints[11,12] and (2) an increase in EELV (ie, dynamic hyperinflation), sometimes to lung volumes greater than resting functional residual capacity (FRC).[12] The rise in EELV has the beneficial consequence of lessening the expiratory flow limitation; however, it may also increase the elastic component of the work of breathing (see "Work of Breathing During Exercise").

CONTROL OF AIRWAY CALIBER DURING EXERCISE

Upper Airway Caliber

The upper airway comprises the nose, mouth, pharynx, and larynx and provides the majority of resistance to airflow at rest and during exercise. Additionally, each region of the upper airway has the potential to independently contribute to alterations in airway resistance during exercise. The work required to produce the large increases in airflow during exercise would become excessively large during even low-intensity exercise if several mechanisms were not in place to reduce resistance to airflow in the upper airway during exercise.

First, the route of airflow switches from predominantly nasal to oronasal breathing when $\dot{V}_E$ reaches approximately 30 L/min.[13] Second, nasal resistance decreases during exercise in an intensity- and duration-dependent manner, secondary to sympathetically mediated vasoconstriction of the nasal mucosal vasculature.[14] Third, the nasal dilator muscles and presumably the skeletal muscles of the pharyngeal and laryngeal regions contract in phase with, but slightly preceding, inspiratory muscle recruitment, and this drive to the upper airway muscles is increased at increasing $\dot{V}_E$, resulting in decreased resistance and a less collapsible airway.[15] Finally, the glottic narrowing that normally occurs during expiration is attenuated during exercise by laryngeal abductor muscle activation, in addition to a widened mean glottic aperture throughout the respiratory cycle.[16] Thus, the work required to produce the increased airflow that occurs during whole body exercise is minimized by a variety of adjustments that occur in the upper airway, all of which act to decrease resistance to airflow.

Bronchial Caliber

Bronchial dilatation in response to exercise has been well documented in healthy humans.[17] Furthermore, this bronchodilator influence is very powerful, as evidenced by the prevention of an increase in pulmonary resistance during exercise after histamine inhalation in asthmatic subjects who exhibited large increases in resistance during histamine inhalation at rest.[18] Additionally, forced expiratory volume in 1 second (FEV_1) is increased immediately after exercise in both normal[19] and asthmatic subjects.[20] There are several potential mechanisms contributing to the bronchodilator

effect of exercise, including neural, mechanical, and locally released mediator mechanisms.

A primary component of the exercise-induced increase in airway caliber is withdrawal of vagal parasympathetic tone to the airways, which occurs at the immediate onset of exercise, resulting in bronchial smooth muscle relaxation.[17] The withdrawal of cholinergic tone is thought to be mediated in part by the stimulation of muscle mechanosensitive and chemosensitive afferents (ie, the same muscle afferents believed to be involved in the pressor and ventilatory response to exercise).[21] Increased lung stretch and activation of slowly adapting pulmonary stretch receptors (which occurs as EILV is increased during exercise) may contribute to this withdrawal of vagal tone.[22] It has also been suggested that a feedforward (ie, central command) component may explain a portion of the diminished vagal tone during exercise. However, the data do not support this contention since electrical or chemical stimulation of the mesencephalic and hypothalamic locomotor regions in cats does not result in bronchodilatation.[23] Finally, circulating catecholamines released from the adrenal medulla have a bronchodilator influence on the airways at rest; however, they are not necessary for the bronchodilator response during exercise since airway resistance still decreases in humans after β-receptor blockade.[17]

Mechanical influences may also play a substantial role in increasing airway caliber during exercise. The airways are tethered open by the lung parenchyma, and the increase in EILV and operating lung volumes during exercise will enlarge airway diameter simply as a result of this airway–parenchymal interdependence.

The increased outward radial force exerted by the parenchyma on the airways during exercise may induce bronchodilatation by a separate mechanism operating at the level of the crossbridges of bronchial smooth muscle.[24] Isolated bovine tracheal smooth muscle strips subjected to sinusoidal stretches (which mimicked a range of tidal volume excursions) exhibited a progressive decrease in both force and stiffness as the excursions from optimal length increased. Additionally, only very small-length fluctuations (in the range of normal tidal breathing) were necessary to cause force and stiffness to fall appreciably,[24] which suggests that even small volume excursions may have potent bronchial smooth muscle–relaxing effects. These findings suggest that airway stretch may modulate bronchial smooth muscle crossbridge formation, resulting in decreased bronchial smooth muscle force and stiffness and relaxation of airway smooth muscle. Thus, increased operating lung volumes during exercise may result in decreased smooth muscle force production independently of neural reflex–mediated mechanisms.

The final postulated controller of bronchial airway caliber during exercise is the local release of chemical mediators from airway resident and nonresident cells. Airway mast cells, macrophages, neutrophils, eosinophils, epithelial cells, and smooth muscle cells all have the potential to release a variety of chemical mediators that may alter airway caliber. Consequently, it has been suggested that some bronchodilator mediators are released that would in part explain the increase in airway caliber during exercise.[25] Locally released mediators would probably not contribute to the immediate bronchodilatation upon exercise commencement but might contribute to reductions in airway resistance as exercise continues. This is a relatively new area of research, and thus far only nitric oxide and prostaglandin E_2 (PGE_2), both endogenous bronchodilators, have been studied. However, neither one appears to be necessary for exercise- or hyperpnea-induced bronchodilatation.[26,27] The possibility of other locally released chemical mediators (eg, PGI_2, calcitonin gene–related peptide, *S*-nitrosothiol) interacting with other mechanisms determining airway smooth muscle caliber during exercise is an exciting area for future research.

WORK OF BREATHING DURING EXERCISE

Work Performed on the Lung

The work performed by any given muscle is defined as the product of the force it produces and the change in distance between its origin and insertion points ($W = F \times D$). As the insertions, origins, and geometric configurations of the respiratory muscles preclude accurate, quantitative analyses of their changes in length, a common surrogate for the work performed by the respiratory muscles is the work performed on the lung (W_L). When examined in such a manner, the change in lung volume now serves as the change in length, and transpulmonary pressure (P_{TP}) is the force applied to the lung. The work performed on the lung can then be divided into two main components: elastic work and flow-resistive work. The properties of the lung and chest wall contributing to the work of breathing are only discussed briefly here; for a more detailed treatment of the static and dynamic properties of the lung, the reader is referred to elsewhere in this book (see Chapter 3, "Statics of the Lung," and Chapter 4, "Act of Breathing: Dynamics").

The elastic work performed on the lung ($W_{L,EL}$) is defined as the amount of work required to overcome the combined static recoil properties of the lung and chest wall. The $W_{L,EL}$ during inspiration can be calculated from a tidal pressure–volume plot, such as that in Figure 45-2A, and is represented as the integrated area ABCDA.[28] Upon examination of Figure 45-2A, it should become clear that $W_{L,EL}$ is a function of both tidal volume (AB) and lung compliance (slope of line ADC).

The flow-resistive work performed on the lung ($W_{L,FR}$), by definition, is the amount of work required to overcome the resistance to gas movement provided by the airways, which is a function of both airway caliber and the viscosity of the gas moving through the airways. As shown in Figure 45-2A, this is quantified as the integrated area ADCEA during inspiration and area AFCDA during expiration.[28] The two primary factors affecting $W_{L,FR}$ are airway caliber and airflow rate, with the contribution of airway caliber to the $W_{L,FR}$ during exercise being minimized by a consistent drop in airway resistance as a result of bronchodilatation (see "Control of Airway Caliber During Exercise").

The work performed on the lung per unit of time $W_{L,TOT}$ is defined as the sum of the elastic work and flow-resistive work. At rest (see Figure 45-2A), this is defined as the sum of the integrated areas ABCEA (inspiratory $W_{L,FR}$ and $W_{L,EL}$)

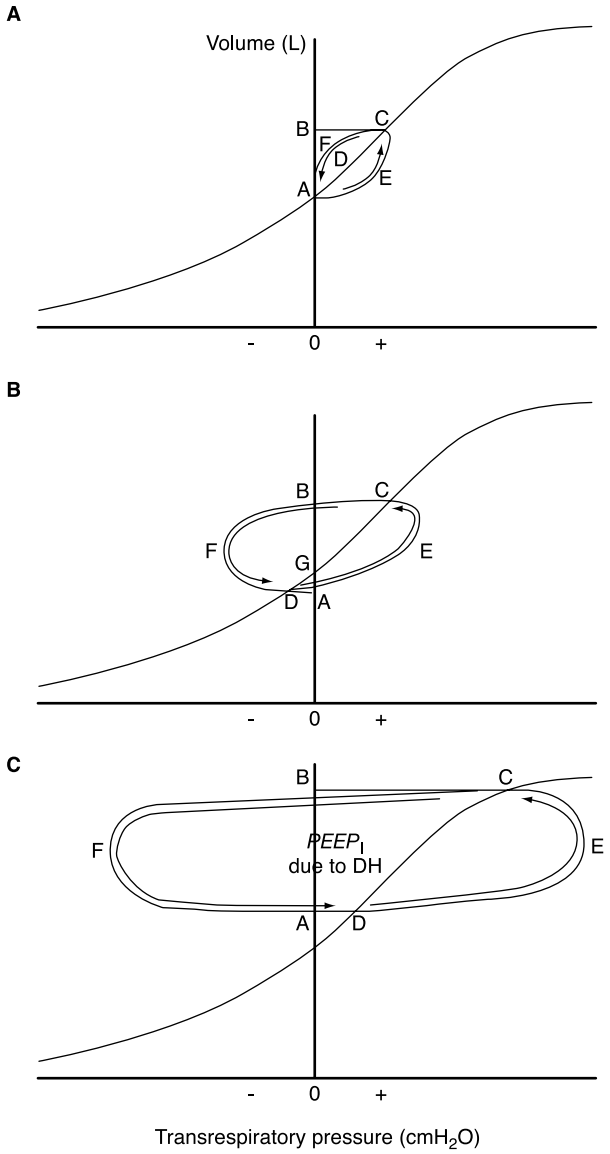

FIGURE 45-2 Work performed on the lung at rest (*A*), during moderate-intensity exercise (*B*) and during exercise with dynamic hyperinflation and intrinsic positive end-expiratory pressure ($PEEP_i$) present (*C*). The quantitative analysis of these figures is discussed in the text.

and AFCDA (expiratory $W_{L,FR}$).[28] During expiration at rest, the energy stored in the elastic tissues in the lung from the preceding inspiration is used to overcome the $W_{L,FR}$, and expiration is passive (ie, ABCDA > AFCDA). However, during moderate-intensity exercise (Figure 45-2B), it can now be seen that the expiratory $W_{L,FR}$ (DGCBFD) is greater than the elastic energy (GBCG) stored by the lung during the preceding inspiration, and the *active* work performed on the lung is defined as area DFBGD.[28] This is in part due to active expiration, which reduces EELV below FRC. The reduction of EELV below FRC also allows for the storing of elastic energy in the respiratory system during expiration (in the amount of area DGAD), which can be used to overcome a portion of the $W_{L,FR}$ (area DGCED) done during the ensuing inspiration.

As exercise intensity increases (Figure 45-2C), EELV may shift upward slightly in the absence of true flow limitation (ie, an increase in intrathoracic pressure without a further increase in airflow), in an attempt to minimize $W_{L,FR}$ (due to increased airway caliber at higher operating lung volumes).[10] Although this increase in EELV reduces $W_{L,FR}$ and avoids impending flow limitation, the reductions in $W_{L,FR}$ must be balanced with the increases in $W_{L,EL}$ at higher lung volumes. However, when EELV is forced upward, as is the case with dynamic hyperinflation (see Figure 45-2C), the combination of an increased expiratory $W_{L,FR}$ (due to the dynamic airway compression inciting the dynamic hyperinflation, area AFCDA) and increases in $W_{L,EL}$ (due to the increased lung recoil at higher lung volumes, area ABCDA) can result in substantial increases in $W_{L,TOT}$.[29] When dynamic hyperinflation becomes severe, subjects may be forced to breathe on the nonlinear portion of their pressure–volume relationship, that is, where large changes in P_{TP} translate into small changes in lung volume, and $W_{L,EL}$ (area ABCDA) for any given tidal volume is substantially increased.[29,30] Also, a "threshold" for the generation of inspiratory flow (commonly called intrinsic positive end-expiratory pressure, or $PEEP_i$) is present when EELV exceeds the normal lung and chest wall relaxation volume. In patients with obstructive pulmonary disease and substantial dynamic hyperinflation, $PEEP_i$ can comprise up to 50% of $W_{L,EL}$ during exercise.[31] The "unsatisfied" inspiratory efforts produced under these conditions are a major source of dyspnea in these patients.

Work Performed on the Abdomen and Rib Cage

Although the calculation of the work performed on the lung does provide a great deal of insight into the work done by the respiratory muscles, it also neglects a large portion of the work of breathing, namely, the work performed on the abdominal wall and rib cage.[32] This is in large part due to the difficulties associated with the accurate partitioning of the volume excursions between the pulmonary-apposed rib cage, the abdominal-apposed rib cage, and the abdominal compartment. Despite this limitation, the studies examining the work performed on the abdomen and rib cage do provide useful estimates of the respiratory muscle work left unmeasured by the work performed on the lung alone.

A substantial component of the work performed by the respiratory muscles comes from the work performed on the abdominal wall.[32] As the diaphragm descends during inspiration, the work done on the abdominal compartment is a function of both the compressibility of the abdominal contents and the compliance of the abdominal wall. Assuming that the compressibility of the abdominal contents remains relatively constant over the range of normal tidal volumes, the work done on the abdominal compartment now becomes a function of abdominal wall compliance. Although this is usually minimized by abdominal muscle relaxation during inspiration,[33] the work performed on the abdominal wall can comprise up to 25% of the total work of breathing during exercise.[32] Furthermore, the presence of expiratory flow limitation can elicit decreases in abdominal wall compliance, due to abdominal muscular tension lasting

well into inspiration,[33] which can markedly increase the amount of work done by the diaphragm on the abdominal compartment.

The remaining work performed by the respiratory muscles is that which is performed on the rib cage. Spontaneous breathing at rest does not usually deform the rib cage from its relaxed configuration (ie, the shape of the rib cage at any given lung volume when there is no force applied by the respiratory muscles).[32,34] Even at exercise intensities of up to 70% $\dot{V}O_{2MAX}$, the distortion of the rib cage from its relaxed configuration appears to be minimized (<1% distortion) by the coordinated recruitment of the respiratory muscles.[34] Thus, the vast majority of the work performed by the respiratory muscles on the rib cage during moderate-intensity exercise is a function of the undistorted elastic properties of the rib cage (as derived from static pressure–volume relationships). Whether or not greater degrees of rib cage distortion substantially increase the work performed on the rib cage at workloads greater than 70% $\dot{V}O_{2MAX}$ is unknown, but it is unlikely, because of the relatively low pressure cost of the distortion to the respiratory muscles.[35]

Energy Cost of the Work of Breathing During Dynamic Exercise

The work performed per liter of ventilation increases fairly linearly from rest to maximal exercise, from approximately 0.5 J/L up to >4 J/L in normal, healthy humans.[32] Given a normal resting minute ventilation of 6 L/min and a peak exercise ventilation of 150 L/min in trained endurance athletes, this translates into a 200-fold increase in the work of breathing (from 3 J/min at rest to 600 J/min at peak exercise).[32] The oxygen cost of the work of breathing (when expressed per liter of ventilation) also increases linearly with increasing levels of ventilation to a maximum of ~2.85 mL oxygen/L.[36] However, when work is expressed per unit time (ie, J/min), respiratory muscle work increases nonlinearly with increasing levels of ventilation (Figure 45-3). Thus, respiratory muscle $\dot{V}O_2$ can reach ~15% of the total body $\dot{V}O_2$ during maximal exercise in trained athletes, and, in turn, ~15% of total CO must be directed to the respiratory muscles.[36] In the untrained young adult working at $\dot{V}O_{2MAX}$, about 10% of the $\dot{V}O_2$ and CO are directed to the respiratory muscles. To ensure that this proportion of blood is diverted to the respiratory muscles (to maintain adequate perfusion), autonomic reflexes originating from the respiratory muscles are thought to be enacted.[37]

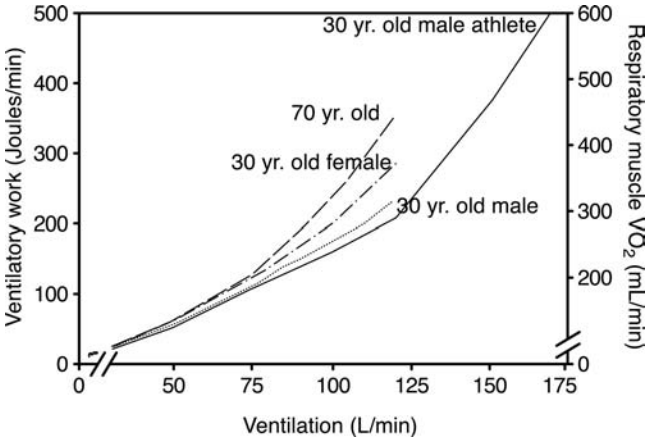

FIGURE 45-3 Ventilatory work and respiratory muscle $\dot{V}O_2$ during exercise of increasing intensity plotted as a function of $\dot{V}_E$ for sedentary men, active young females, and trained young and older men. In young adult males, the oxygen cost of exercise hyperpnea was determined by having subjects mimic the pressure–volume curve, breathing frequency, duty cycle, and ventilation that they experienced during submaximal and maximal exercise and measuring the change in $\dot{V}O_2$ from resting eupnea.[37] Reproduced with permission from Harms CA, Dempsey JA. Cardiovascular consequences of exercise hyperpnea. Exerc Sport Sci Rev 1999;27:37–62.

PULMONARY HEMODYNAMICS AND LUNG FLUID HOMEOSTASIS DURING EXERCISE

The pulmonary vascular bed is unique. Being in series with the left heart and the systemic circulation, the pulmonary vascular bed must accommodate the entire CO. In health, high-intensity exercise can raise CO and thus pulmonary bloodflow to four or five times the resting levels (see Table 45-1). This dramatic increase in bloodflow is necessary to accomplish a massive increase in gas exchange, where $\dot{V}O_2$ and $\dot{V}CO_2$ can be 10 to 20 times greater than resting values. Remarkably, the lung vascular response to exercise does not appear to depend on extrinsic neural or humoral control. The dominant mechanism regulating pulmonary hemodynamic responses during exercise is left ventricular filling pressure. Left ventricular filling pressure, which climbs during exercise, both recruits and distends the delicate thin-walled vessels of the lung, and thus expands the capillary surface area and volume. Another challenge is keeping the alveolar surface intact and dry in the face of high bloodflow and rising capillary pressures. Fortunately, alveolar edema is minimized during exercise because both capillary absorptive pressure and lymph flow increase. In this section, these ideas are explored in more detail, and the concepts are integrated to provide a comprehensive understanding of how the pulmonary circulation copes with the demands of exercise.

Pulmonary Circulation During Exercise

Right heart catheterization has allowed hemodynamic measurements to be made in both men and women during both supine and upright exercise.[38–43] These studies have shown that both pulmonary arterial pressure (P_{pa}) and pulmonary bloodflow increase with muscular exercise (see Table 45-1). Interestingly, pulmonary bloodflow increases proportionally more than P_{pa}. Thus, either the left ventricular end-diastolic pressure (LV_{EDP}) or pulmonary vascular resistance (PVR) must fall during exercise.

Exercise increases venous return to both the right and left ventricles. The increased left ventricular filling volume and pressure allow increased myocardial work and augmented stroke volume through the Starling mechanism. If the Starling mechanism is in operation, then LV_{EDP} is likely to increase from rest to exercise. Although it is rarely done, Luepker and colleagues used transseptal cardiac catheterization to show

that LV_{EDP} increased with supine exercise.[44] More recently, Reeves and colleagues showed that end-diastolic pressure rises in both ventricles during upright exercise.[39] LV_{EDP} can be estimated from the pulmonary artery occlusion pressure, also called the wedge pressure (P_w). The P_w is obtained when a balloon-tip catheter is wedged into a lobar branch of the pulmonary artery. The measured downstream pressure should approximate the LV_{EDP}. Thadani and Parker measured LV_{EDP} and P_w simultaneously during both supine and upright exercise.[43] P_w closely approximated LV_{EDP}, with the rise in pressure being independent of exercise position. Subsequently, numerous studies have shown that P_w increases with both upright and supine exercise.[39,45,46] Moreover, the increase in P_w accounts for 80% of the increase in P_{pa}. As exercise intensity increases, P_w continues to climb, whereas stroke volume levels off.[39,45,46] The dissociation between filling volume and filling pressure remains unexplained, but pericardial restriction, limited diastolic filling time, changes in intrathoracic pressure (eg, during expiratory flow limitation), and a decrease in left ventricular compliance have all been implicated.

PVR falls during exercise. Neural, humoral, and mechanical factors have been implicated as regulators of the vascular tone during exercise. The role of the sympathoadrenal system has been evaluated in exercising sheep.[47] Blockade of β-adrenergic receptors results in increased resting pulmonary vascular tone and prevents the exercise-induced fall in PVR. With α-adrenergic blockade, resting tone is unaffected, and the fall in resistance during exercise is augmented. Interestingly, with both α- and β-blockade, the hemodynamic response to exercise is similar to that with no intervention. It appears that during exercise, any increase in distal α-adrenergic vasoconstrictor tone is balanced by β-adrenergic vasodilatation. In contrast, measurements in exercising humans suggest that the densely innervated main pulmonary artery and its major branches stiffen with the onset of exercise. The result is improved impedance matching of the right ventricle and the pulmonary circulation. The stiffening of the large pulmonary vessels results in increased pulsatile flow in the capillary circulation, which, in turn, will increase vascular endothelial shear stress.

Shear stress has been shown to induce endothelial release of potent vasodilators, including prostacyclin and nitric oxide (NO).[48] Endogenous NO clearly plays a role in modulating the pulmonary vascular tone at rest, but its role during exercise appears to be minimal. In both sheep[47] and thoroughbred horses,[49] inhibition of NO synthase with *N*-nitro-L-arginine (L-NAME) results in a rise in left atrial pressure, P_{pa}, and pulmonary vascular tone at rest. However, during exercise, PVR falls in the same way as in control animals, suggesting that NO is not an essential modulator of pulmonary vascular tone during exercise. Similarly, cyclooxygenase inhibition in both dogs[50] and sheep[51] increased resting PVR but had no impact on the pulmonary response to exercise. Since vasodilator agents appeared not to influence pulmonary vascular tone during exercise, control of the pulmonary vascular bed must be regulated by mechanical forces.

The predominant mechanism regulating pulmonary hemodynamic responses to exercise is left ventricular filling pressure. At the onset of exercise, increasing bloodflow and left ventricular filling pressure appear to fully recruit the pulmonary microcirculation. As exercise intensity increases, bloodflow and LV_{EDP} continue to rise, resulting in maximal distention of the pulmonary vascular bed. The transit time (TT) for a red blood cell traversing a pulmonary capillary is dependent on the relationship between pulmonary capillary blood volume (PCBV) and CO (TT = PCBV/CO). Vascular distention and recruitment expand the pulmonary capillary surface area and volume, thus minimizing any reduction in red blood cell TT. This sequential strategy is supported by carbon monoxide diffusing capacity measurements during exercise, which show that both gas exchange surface area and PCBV increase progressively with exercise intensity.[52]

Lung Fluid Homeostasis During Exercise

Pulmonary bloodflow, P_{pa}, and left atrial pressure all increase with exercise. In combination, these forces should augment transvascular fluid filtration and promote edema formation. However, significant extravascular lung water accumulation appears not to occur because both the osmotic pressure gradient and lymph flow increase to oppose edema formation.[53] Furthermore, exercise hyperpnea appears to both augment microvascular filtration and dramatically increase lymph flow. Thus, interstitial and alveolar edema is minimized during exercise because both capillary absorptive pressure and lymph flow increase.

In summary, with exercise, pulmonary bloodflow and P_{pa} rise whereas PVR falls. The dominant mechanism regulating pulmonary hemodynamic responses during exercise is left ventricular filling pressure. Left ventricular filling pressure, which climbs during exercise, both recruits and distends the pulmonary capillaries and veins, thus contributing to the fall in PVR. Furthermore, vascular distention and recruitment expand the capillary surface area and volume, thus minimizing any fall in red blood cell TT within the pulmonary capillaries in the face of an increasing CO. Interstitial and alveolar edema is minimized because both capillary absorptive pressure and lymph flow increase during exercise.

GAS EXCHANGE DURING EXERCISE

The efficiency of gas exchange for oxygen within the lung is defined and quantitated as the difference in PO_2 between the alveolar gas and the arterial blood and is known as the alveolar to arterial PO_2 difference ($P_{A-a}O_2$). If gas exchange within the lung were perfect, $P_{A-a}O_2$ would be equal to zero. However, $P_{A-a}O_2$ normally amounts to 5 to 10 mm Hg at rest in young, healthy subjects.[54] During exercise, the efficiency of gas exchange worsens in an intensity-dependent manner, and $P_{A-a}O_2$ increases to values of 15 to 25 mm Hg or more at maximal exercise (see Table 45-1). In contrast, fixed-workload endurance exercise does not result in a time-dependent worsening of gas exchange in comparison to the first minute of exercise,[55] indicating that the magnitude of $P_{A-a}O_2$ is determined primarily by metabolic rate as opposed to exercise duration.

$P_{A-a}O_2$ is a complex physiologic variable and as such is determined by a variety of mechanisms during rest and exercise. The worsening of gas exchange during exercise is primarily due to an exaggeration of mechanisms present at rest. The principal contributor to $P_{A-a}O_2$ during both rest and exercise is the imperfect matching of the distributions of alveolar ventilation ($\dot{V}_A$) and pulmonary bloodflow ($\dot{Q}$), otherwise known as the $\dot{V}_A/\dot{Q}$ ratio. The ratio of $\dot{V}_A$ to $\dot{Q}$ can be partitioned into that occurring *among* lung regions (ie, interregional, primarily dependent on gravity) and to that *within* an isogravitational plane of the lung (ie, intraregional, or independent of the effects of gravity). The distributions for $\dot{V}_A$ and $\dot{Q}$ were once thought to be dominated by gravity; however, recent studies suggest that there is a great deal of pulmonary bloodflow heterogeneity within an isogravitional plane of the lung.[56] Presumably, much intraregional heterogeneity exists for alveolar ventilation as well.

During exercise, overall $\dot{V}_A/\dot{Q}$ nonuniformity increases slightly as measured by the multiple inert gas elimination technique (MIGET) (a technique that is not able to partition $\dot{V}_A/\dot{Q}$ into separate interregional and intraregional distributions).[46,57] Despite this, both $\dot{V}_A$ and $\dot{Q}$ become more uniform from lung apex to base, resulting in a more uniform interregional $\dot{V}_A/\dot{Q}$ distribution.[58] Thus, the increased overall $\dot{V}_A/\dot{Q}$ nonuniformity observed during exercise can be attributed almost entirely to a more maldistributed intraregional $\dot{V}_A/\dot{Q}$, which contributes to the decreased efficiency of gas exchange (ie, widening of $P_{A-a}O_2$) at increasing exercise intensities.

Counteracting the greater nonuniformity of $\dot{V}_A/\dot{Q}$ during exercise is the fact that $\dot{V}_A$ increases out of proportion to $\dot{Q}$ at increasing exercise intensities (see Table 45-1).[57] Thus, even though the distribution for $\dot{V}_A/\dot{Q}$ becomes more nonuniform, the higher overall $\dot{V}_A/\dot{Q}$ ensures that little if any of the lung will be markedly underventilated (ie, $\dot{V}_A/\dot{Q} < 0.8$). P_AO_2 is therefore kept high throughout the lung, and this ensures maintenance of end-capillary PO_2 near resting levels, even in the face of a progressive reduction in mixed venous oxygen content.

The mechanisms underlying the greater $\dot{V}_A/\dot{Q}$ maldistribution during exercise are largely unknown, although several possibilities exist. A mild interstitial edema could develop during exercise if the rate of lymphatic drainage was overwhelmed by the leakage of plasma across the pulmonary capillary endothelium. This could cause changes in local compliance or resistance of the bronchial airways or pulmonary vessels, which would affect the distributions for both $\dot{V}_A$ and $\dot{Q}$. This situation could arise under two conditions. First, pulmonary capillary stress failure could occur if pulmonary capillary pressure were to increase to the extent that the integrity of the blood–gas barrier was compromised.[59] Indeed, exercise-induced pulmonary hemorrhage is well documented in thoroughbred horses,[60,61] in which huge increases in both P_{pa} (120 mm Hg)[62,63] and left atrial pressure (70 mm Hg) occur with exercise.[64] The estimated pulmonary capillary pressure of 100 mm Hg results in capillary disruption and bleeding into the alveolar space. Does capillary stress failure occur in exercising humans? Bronchoalveolar lavage performed after high-intensity exercise in trained athletes has revealed increases in red blood cell numbers and protein levels in comparison with nonexercised control subjects, indicating that the integrity of the blood–gas barrier may be compromised during exercise, resulting in a transient alveolar hemorrhage and interstitial fluid accumulation.[65] However, no evidence for stress failure of the blood–gas barrier has been found in healthy but untrained humans. Second, capillary permeability could be increased secondary to the release of inflammatory mediators if the combination of minute ventilation and the condition of the inspired air were such that the airway surface lining osmolarity increased appreciably. It is also possible that shear or mechanical stress during exercise due to high airflow rates per se may induce inflammatory mediator release from the epithelium or other lung cells.[66] Again, however, inflammatory mediators do not appear to play a role in gas exchange abnormality during exercise in young, healthy subjects.[66] Finally, the fact that the amount of $\dot{V}_A/\dot{Q}$ mismatch correlates with P_{pa} in both normobaric and hypobaric hypoxia supports a role for fluid accumulation in causing greater $\dot{V}_A/\dot{Q}$ heterogeneity.[46]

A second contributing factor to $P_{A-a}O_2$ is the mixing of shunted blood (ie, venous blood that does not pass a ventilated alveolus) with arterial blood. There are two types of shunt that may contribute to $P_{A-a}O_2$ in health. The first type is known as an extrapulmonary shunt and primarily consists of thebesian venous drainage from the coronary circulation, which drains deoxygenated blood directly into the left ventricle.[67] The bronchial circulation also contributes to the extrapulmonary shunt and contains direct anastomoses between the bronchial veins and pulmonary veins.[68] Collectively, extrapulmonary shunts as small as 1 to 2% of the cardiac output have been calculated to account for about half of $P_{A-a}O_2$ during moderate-intensity exercise.[57] Importantly, these shunts would be expected to increase total venous admixture during exercise of increasing intensity because of the decreased oxygen content of thebesian effluent (as a result of increased myocardial oxygen extraction)[69] as well as increased total thebesian flow.

A second type of shunt that may contribute to $P_{A-a}O_2$ is commonly referred to as an intrapulmonary shunt and is the result of direct anatomic connections between pulmonary arterial and venous vessels. These arteriovenous connections have been shown to exist in perfused whole human lungs[70] and would have a greater influence on P_aO_2 during exercise of increasing intensity as $P\bar{v}O_2$ falls. This would be true even if the fraction of total CO traversing these connections remained constant. Thus, venous admixture from both intrapulmonary and extrapulmonary shunt sources must contribute significantly to $P_{A-a}O_2$ during exercise. However, further investigation is needed to accurately quantify the total shunt fractions during exercise and how exactly these contribute to $P_{A-a}O_2$.

A final potential contributor to the widened $P_{A-a}O_2$ during exercise is a disequilibrium for diffusion of oxygen across the blood–gas barrier and its reaction with hemoglobin in the pulmonary capillaries. For this to occur, the TT of a red blood cell in the pulmonary capillary would have to be shortened to the extent that equilibration of oxygen between

the alveoli and red blood cell does not occur. The TT is ~0.75 seconds at rest and does decrease during exercise (see Table 45-1); however, the concomitant expansion of the PCBV as CO increases attenuates this decrease. Thus, even in well-trained athletes during high-intensity exercise, TT does not fall below ~0.45 seconds.[71] Additionally, in an isolated rabbit lung preparation with a near homogeneous $\dot{V}_A/\dot{Q}$ distribution and perfused with desaturated blood ($P\bar{v}O_2$ ~22 mm Hg), a TT of 0.18 seconds resulted in no measurable $P_{A-a}O_2$.[72] This finding highlights both the rapidity with which diffusion across the blood–gas barrier occurs and the importance of $\dot{V}_A/\dot{Q}$ mismatch in determining $P_{A-a}O_2$. Thus, a disequilibrium between alveolar and end pulmonary capillary PO_2 cannot explain $P_{A-a}O_2$ in most healthy but untrained humans, even at maximal exercise.

A diffusion limitation could occur if CO continued to rise after PCBV had reached its maximal morphologic limits of ~220 mL,[73] a situation that could arise in highly trained athletes with very high $\dot{V}O_{2MAX}$ and maximal CO (ie, >35 L/min). In this case, TT may decrease enough so that full equilibration does not occur. Also, the critical TT necessary for complete equilibration of oxygen between alveoli and pulmonary capillaries is not fixed but depends upon the alveolar and mixed venous PO_2.[74] That is, the linear slope formed by the oxyhemoglobin dissociation curve between P_AO_2 and $P\bar{v}O_2$ is a critical determinant of the time necessary for equilibration (ie, steeper slope = longer equilibration time). Thus, during exercise, the lowered $P\bar{v}O_2$ increases the TT necessary for equilibration, but critical TT can be more or less at a given $P\bar{v}O_2$, depending on the diffusion gradient determined by the level of alveolar ventilation. This is important because, in highly trained athletes with high oxygen extraction and low $P\bar{v}O_2$, in combination with a potentially less than adequate hyperventilatory response to the exercise, critical TT may be lengthened even further.

The MIGET has been used to provide evidence that a diffusion limitation for oxygen exists during exercise in healthy humans.[46,75] The MIGET estimates the amount of $\dot{V}_A/\dot{Q}$ inequality and assumes complete equilibration for oxygen and no extrapulmonary shunts. It is argued that any difference between the actual $P_{A-a}O_2$ and that predicted from the measured amount of $\dot{V}_A/\dot{Q}$ mismatch given by the inert gases can be attributable to diffusion limitation. With the use of this technique, significant amounts of diffusion limitation (up to two-thirds of the total $P_{A-a}O_2$) have been found at metabolic rates of 2.5 to 3.0 L/min.[46,75] However, it is unlikely that a diffusion limitation would occur at these moderate metabolic rates, when PCBV and CO are submaximal and mean TT is still greater than 0.5 seconds. The MIGET is also prone to spurious results, as evidenced by the occasional impossible findings of a wider predicted $P_{A-a}O_2$ than actually measured.[75] Thus, we think it highly unlikely that a disequilibrium between alveolar and end pulmonary capillary PO_2 can explain the widened $P_{A-a}O_2$ or even a part thereof during exercise in healthy but untrained humans, but it may contribute during high-intensity exercise in trained athletes.

EXERCISE-INDUCED RESPIRATORY MUSCLE FATIGUE

The structural and functional properties of the respiratory muscles appear to be well suited to the ventilatory requirements of exercise. For example, the human at rest can sustain up to six to eight times the resting diaphragmatic pressure production for 10 to 15 minutes without inducing significant fatigue or task failure of the diaphragm.[76] Furthermore, pressures and velocities of shortening sustained by the diaphragm that are 1.5 to 2 times greater than those attained during exhaustive exercise are required to cause diaphragm fatigue when the subject is in the resting state and increases ventilation voluntarily.[76] Nevertheless, significant 15 to 50% reductions in the transdiaphragmatic pressure response to bilateral phrenic nerve stimulation, across a wide range of stimulation frequencies (1 to 100 Hz) and lung volumes residual volume to TLC, have been observed following constant-load, whole body endurance exercise.[77–80] The magnitude of exercise-induced diaphragm fatigue is determined in part by the amount of diaphragm work contributing to the exercise hyperpnea. Thus, reducing the pressures produced by the diaphragm during endurance exercise with the use of a proportional assist ventilator prevented diaphragm fatigue.[80] Popular predictors of fatigue, such as the pressure–time index of the diaphragm[8] and the ratio of transdiaphragmatic pressure to maximal transdiaphragmatic pressure,[81] were unable to show consistently whether the diaphragmatic force output during exercise was sufficient to cause diaphragm fatigue. Indeed, exercise-induced diaphragm fatigue occurred most often when the values of these indices were only one-half to two-thirds those required to produce fatigue under resting conditions.[76] Thus, although these indices are adequate predictors of task failure during sustained voluntary efforts against an inspiratory resistive load in resting subjects, they are not during whole body exercise. Whole body exercise itself appears to lower the threshold of force output by the diaphragm required for its fatigue (Figure 45-4), probably because a finite bloodflow must be distributed to both locomotor and respiratory muscles.[82] Such a disparity between oxygen supply and demand appears to occur in subjects of varying fitness levels, but only at workloads exceeding 85% of $\dot{V}O_{2MAX}$[77] or when arterial oxygen content is decreased.[83]

Respiratory Muscle Fatigue and Exercise Performance

Theoretically, respiratory muscle fatigue could limit exercise performance through alveolar hypoventilation (and reduced systemic oxygen transport and carbon dioxide elimination) if either "pump failure" occurs or a tachypneic breathing pattern causes high dead space ventilation and, therefore, reduces alveolar ventilation. However, exercise-induced respiratory muscle fatigue probably does not compromise the adequacy of alveolar ventilation because hyperventilation usually occurs over time.[77–80]

There is evidence that respiratory muscle recruitment is altered by diaphragm fatigue, which, in turn, might negatively influence exercise performance. Johnson and

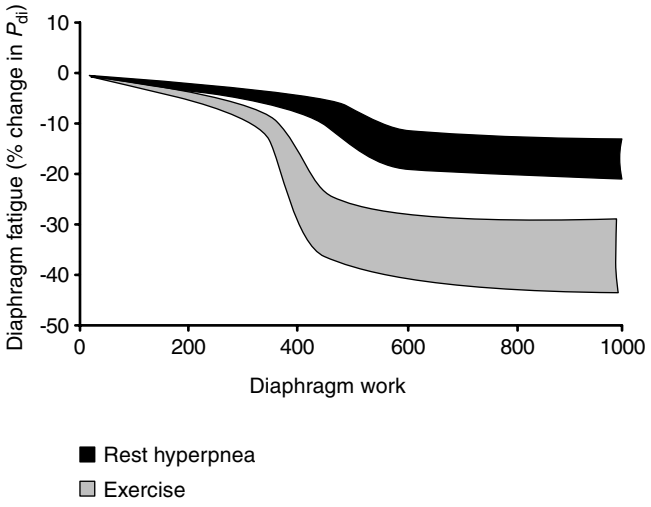

FIGURE 45-4 Diaphragm work versus diaphragm fatigue (determined by bilateral phrenic nerve stimulation) for whole body, high-intensity exercise (*shaded area*) and resting hyperpnea (*filled area*). During the resting-hyperpnea trials, subjects mimicked at rest the diaphragm pressure (P_{di}), breathing frequency, and duty cycle that elicited exercise-induced diaphragm fatigue for a similar time period. Much greater diaphragm pressures had to be produced at rest relative to those produced with exercise to obtain significant diaphragmatic fatigue. This implies that factors other than diaphragmatic pressure generation (ie, work) are necessary to produce the fatigue observed during exercise. Based upon data from Johnson and colleagues[77] and Babcock and colleagues.[78]

colleagues observed that, beginning at the fifth to the tenth minute of constant-load exercise to exhaustion, transdiaphragmatic pressure reached a plateau even though minute ventilation, inspiratory flow, and esophageal pressure integrated over time all continued to rise substantially.[77] Those subjects who decreased or minimized the relative contribution of the diaphragm to total ventilatory work the most for the duration of exercise showed the least diaphragm fatigue in the postexercise period. These findings suggest that diaphragm fatigue may occur during the early period of a prolonged bout of heavy exercise and that this fatigue inhibits further diaphragmatic recruitment. Moreover, diaphragm fatigue may result in the recruitment of additional inspiratory muscles in an attempt to spare this primary inspiratory muscle. Evidence that exercise-induced diaphragm fatigue affects the recruitment of accessory respiratory muscles comes from a study in which the respiratory muscles were partially unloaded during exercise with the use of mechanical ventilation.[80] The reduction in transdiaphragmatic pressure over time was prevented with unloading, and there was an attendant decrease in exercise-induced diaphragmatic fatigue. A change in respiratory muscle recruitment may result in chest wall distortion, mechanical inefficiency of breathing, and increased metabolic and bloodflow demand by the respiratory muscles (see below). This fatigue-induced increase in respiratory muscle work would be perceived directly, through central corollary discharge, as an increased sense of respiratory muscle effort or dyspnea.[84]

Fatiguing the respiratory muscles prior to subsequent whole body exercise, using either sustained maximal isocapnic hyperpnea[85,86] or resistive loading,[87,88] has been used to determine whether respiratory muscle fatigue influences whole body exercise performance. With this approach, either a decrease[86–88] or no change[85] in time-to-exhaustion during subsequent short-term, high-intensity exercise has been found. Unfortunately, these divergent findings are difficult to interpret since none of the studies used an objective measure of respiratory muscle fatigue. It is also difficult to separate the effects of prior fatigue of the respiratory muscles from exercise-induced respiratory muscle fatigue upon exercise performance.

Another approach used to determine whether respiratory muscle work/fatigue influences exercise performance is to partially unload the respiratory muscles and to reduce the work of breathing during exercise. Breathing of reduced-density gas mixtures (He/O_2) did not affect either time-to-exhaustion or whole body $\dot{V}O_2$ at moderate work intensities, although during high-intensity exercise (greater than 85 to 90% of $\dot{V}O_{2MAX}$), time-to-exhaustion increased by 40%, and $\dot{V}O_2$ was reduced near the end of exercise.[89] However, studies in which reduced-density gas mixtures have been used are subject to criticism, in that these gas mixtures have effects other than simply unloading the respiratory muscles.[89] For example, He/O_2 can expand the maximal flow–volume envelope and eliminate the expiratory flow limitation that occurs in many endurance-trained individuals. Furthermore, He/O_2 may act by unloading the external respiratory apparatus, which often provides significant resistance to breathing.

In more recent studies, pressure-assist has been used to partially unload the respiratory muscles.[90–93] Mechanical unloading of the respiratory muscles by over 50% of their total inspiratory and expiratory work during heavy-intensity exercise (~90% of $\dot{V}O_{2MAX}$) prevented diaphragm fatigue[80] and resulted in a 14% increase in exercise capacity in trained male cyclists, with a reduction in $\dot{V}O_2$ and the rate of rise in perceptions of respiratory and limb discomfort (Figure 45-5).[90] Studies that have not shown a significant effect of respiratory muscle unloading upon exercise capacity have generally been conducted with less fit subjects at lower relative exercise intensities (about 70 to 80% of $\dot{V}O_{2MAX}$).[91–93] Differences in the oxygen cost of breathing between moderately fit (~10% of $\dot{V}O_{2MAX}$) and highly fit subjects (~15% of $\dot{V}O_{2MAX}$) during near-maximal exercise suggest that the effect of reducing the work of breathing would be most noticeable in the highly fit subjects exercising at higher work rates with greater ventilatory requirements.[36] Furthermore, bloodflow redistribution between the respiratory muscles and the locomotor muscles occurs with loading and unloading at work rates requiring greater than 85% of $\dot{V}O_{2MAX}$[37] but not during exercise at 50 or 75% of $\dot{V}O_{2MAX}$.[94] Thus, it is perhaps not surprising that exercise capacity was not increased with respiratory muscle unloading during the moderate-intensity exercise studies. Moreover, studies showing no effect of unloading may be confounded by the fact that the respiratory muscles may not have been unloaded sufficiently since $\dot{V}O_2$ remained

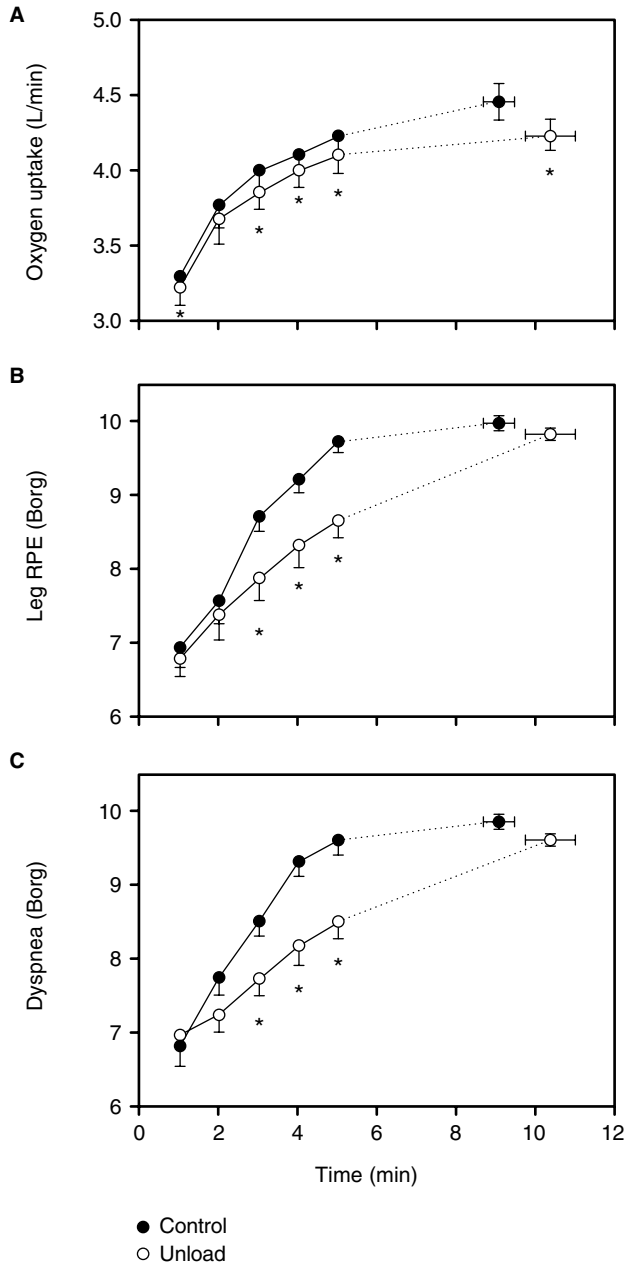

FIGURE 45-5 Effects of respiratory muscle unloading through mechanical ventilation on endurance exercise capacity at a workload requiring ~90% of $\dot{V}O_{2MAX}$ in trained male cyclists ($n = 7$). Group mean data are shown for minutes 1 to 5 of exercise and at exhaustion. Absolute time-to-exhaustion under control conditions averaged 9.1 minutes. Unloading normal work of breathing by 50% from control increased time-to-exhaustion in 76% of trials by a mean of 1.3 minutes (+14.0%). Respiratory muscle unloading caused reductions in oxygen uptake and the rate of rise in perceptions of limb and respiratory discomfort throughout the duration of exercise. Based upon data from Harms and colleagues.[90] *Significantly different from control, $p < .05$.

unchanged during the unloaded conditions.[91–93] In contrast to previous studies, Harms and colleagues used several practice trials and multiple, randomized performance trials in an attempt to reduce the effect of random variability on performance time.[90]

A limitation of the aforementioned unloading studies is that it is impossible to differentiate between the effects of the work of breathing and of respiratory muscle fatigue upon exercise performance. Alternative mechanisms to explain the increase in time-to-exhaustion with unloading include the relief of locomotor muscle fatigue, which would decrease limb discomfort as a result of there being less type IV afferent activity (peripheral mechanism), and a decreased central motor command to the respiratory muscles, which would be perceived directly as a decreased sense of respiratory effort (central mechanism). In view of previous findings,[37] it is likely that increases in limb vascular conductance and bloodflow occurred with unloading. These local changes would probably have important effects on oxygen transport to and carbon dioxide removal from the working locomotor muscles and therefore on their fatigability. Unloading would also be expected to influence the perceptions of both respiratory and peripheral muscle effort. Indeed, unloading ameliorated exertional dyspnea, and these changes were correlated significantly with changes in time-to-exhaustion.[90] The magnitude of respiratory effort sensation increases in proportion to the developed inspiratory muscle tension.[95] Thus, unloading the respiratory muscles would be expected to reduce the fraction of maximum tension generated with each breath, improve dyspnea, and thereby increase exercise tolerance. Preventing diaphragm fatigue with unloading[80] might also attenuate the dyspneic response to exercise through a decrease in central motor output,[84] a decrease in respiratory metaboreceptor afferent feedback,[96] or both.

In summary, the work of breathing during heavy-intensity endurance exercise in healthy subjects appears to be a significant determinant of exercise performance. Whether this effect is attributable to locomotor muscle fatigue and/or to associated perceptions of effort and discomfort remains unknown and difficult to determine in the exercising human. Also unknown is whether respiratory muscle fatigue, per se, contributes significantly to this effect of the normal respiratory muscle load upon exercise performance.

LIMITATIONS TO THE RESPONSE OF THE HEALTHY LUNGS TO EXERCISE

We have emphasized in our brief review that the young, healthy, untrained lung is near ideally designed and regulated to meet the demands for increased ventilation and gas exchange imposed by exercise—even maximum exercise.[‡]

Accordingly, it is only very rare that arterial blood gas homeostasis or mechanical efficiency of breathing is compromised in the healthy pulmonary system. One example is the widened $P_{A-a}O_2$ experienced during exercise, but even this is of little consequence for systemic oxygen transport because the hyperventilatory response to heavy exercise raises alveolar PO_2 sufficiently to completely compensate for the widened $P_{A-a}O_2$, and P_aO_2 (and C_aO_2) are maintained near resting lev-

[‡]The healthy "overbuilt" lung contrasts with the respiratory muscles, which do experience fatigue even in untrained subjects—albeit at very high exercise intensities (see "Exercise-Induced Respiratory Muscle Fatigue").

els. However, there are some other notable exceptions with more serious consequences for exercise performance.

First, at high altitudes (especially > 3,000 m), alveolar–capillary diffusion limitation becomes a problem because of decreased driving pressure for diffusion within the lung; thus, exercise-induced arterial hypoxemia (EIAH) commonly occurs. Even at sea level, many highly trained young athletes with high $\dot{V}O_{2MAX}$ experience significant reductions in P_aO_2 and arterial hemoglobin saturation (S_aO_2), due to a combination of an excessively widened $P_{A-a}O_2$ (30 to 50 mm Hg) and only a minimal hyperventilatory response.[97] A diffusion limitation is suspected, but not proven, to be the reason for this excessive $P_{A-a}O_2$, whereas mechanical limitation to expiratory flow at high ventilatory demand (see Figure 45-1) explains a significant portion of the constrained hyperventilatory response.[29] Anecdotal clinical observations have uncovered other explanations for EIAH and/or expiratory flow limitation in healthy, athletic subjects. These conditions include upper airway obstruction—often mistakenly diagnosed as asthma[98]—and intraseptal cardiac shunt, both of which are manifested only in heavy exercise. Even a few cases of multiple pulmonary emboli have been diagnosed by clinicians in highly trained, young endurance athletes, who suddenly experience decrements in performance and show marked oxygen desaturation during exercise. How frequently these conditions actually occur in the otherwise healthy population of young athletes remains to be seen. In all of these cases of EIAH, the lung's limited gas exchange capability becomes a significant limiting factor to oxygen transport and the maximum arteriovenous oxygen difference (a-$\bar{v}O_2$), and therefore to maximal exercise capacity and $\dot{V}O_{2MAX}$.[99,100] We emphasize that at sea level, EIAH does not occur in all, or probably even a majority of, healthy endurance-trained athletes and is limited to decrements in S_aO_2, which are at most 10 to 12% below resting levels (ie, 85 to 90% S_aO_2), causing at most a 10 to 15% reduction in $\dot{V}O_{2MAX}$. Thus, in health, maximum CO and stroke volume remain the dominant determinants of $\dot{V}O_{2MAX}$.

Normal healthy aging is another circumstance in which the lung may pose a significant limitation to exercise performance. With normal aging (even in nonsmokers), substantial progressive losses occur in the alveolar–capillary surface area, diffusion capacity, and the lung's elastic recoil, the last of these leading to high closing volume of the airways, increased dead space ventilation, and a reduced maximum flow–volume envelope. These age-dependent changes vary widely in magnitude, even among healthy, nonsmoking subjects. Habitual physical training throughout the aging process has marked effects on slowing the aging process in the cardiovascular system[101] but has no apparent effect on age-dependent deterioration of lung structure.[102] Accordingly, during exercise, the older healthy subject (at and beyond about the sixth decade) experiences expiratory flow limitation and its sequelae of dynamic hyperinflation and increased ventilatory work at lower exercise ventilations than in younger subjects and must also produce greater overall ventilation to achieve the amount of alveolar ventilation required to maintain normocapnia during exercise.[102] In summary, the opportunities for the lung to present as a significant limiting factor to exercise performance, through an increased work of breathing and/or dyspnea, or through exercise-induced hypoxemia, are significantly enhanced by the normal aging process.

CONCLUSIONS

During exercise, pulmonary ventilation must rise in proportion to the increase in metabolic rate so that arterial blood gas homeostasis is maintained. In the healthy person, multiple neural feedforward and feedback mechanisms act to increase alveolar ventilation in proportion to metabolic rate. The rise in pulmonary ventilation results in substantial increases in the work of breathing and thus the energy cost of breathing. However, the work of breathing is minimized, due to decreased resistance of the intrathoracic and extrathoracic airways during exercise, along with the maintenance of lung volume on the linear portion of the pressure–volume relationship. Despite the efficient mechanics of breathing during exercise in healthy subjects, sustained high-intensity aerobic exercise does result in respiratory muscle fatigue. However, the implications of this fatigue for exercise performance are unclear. As pulmonary bloodflow increases during exercise, increases in pulmonary vascular pressures are minimized by concomitant decreases in PVR, which helps prevent large increases in pulmonary capillary pressures and accumulation of extravascular lung water. Nonetheless, the high bloodflow achieved during maximal exercise can result in a two- to threefold increase in pulmonary arterial pressure. Exercise also results in a worsening of the efficiency of alveolar to arterial gas exchange (ie, widened $P_{A-a}O_2$), but a disproportionate rise in alveolar ventilation relative to metabolic rate during high-intensity exercise prevents arterial hypoxemia from occurring. Thus, the demands placed on the lung and respiratory muscles during whole body aerobic exercise are indeed extreme. However, the lungs' alveolar capillary surface area, airways, and the respiratory muscles are sufficiently overbuilt, and the neurochemical control system for ventilation is sufficiently precise that appropriate ventilation and gas exchange are not compromised even during high-intensity exercise. Thus, only in the highly fit young athlete, the older athlete, or in those with structural or functional impairment does the pulmonary system become a "weak link" in determining oxygen transport and exercise performance.

Despite years of innovative research, many questions concerning the physiologic response of the healthy pulmonary system to exercise remain unanswered. Key questions requiring new and innovative approaches include the following:

- The relative contributions of neural feedforward and feedback mechanisms to the exercise hyperpnea—including the potential role of "learning" and "experience"
- The specific neural feedforward and feedback mechanisms responsible for the precise regulation of breathing pattern and the order of inspiratory and expiratory muscle recruitment during exercise

- The factors responsible for the worsening of the $\dot{V}_A/\dot{Q}$ distribution
- The relative roles of diffusion limitation and extrapulmonary and intrapulmonary shunts in causing exercise-induced widening of $P_{A-a}O_2$ and hypoxemia
- The mechanisms regulating cardiopulmonary interactions during exercise and the effect of sympathetic efferent outflow and respiratory muscle work and fatigue on the distribution of systemic vascular conductance and bloodflow during exercise. How and why do the large changes in intrathoracic pressure during both inspiration and expiration influence stroke volume and CO during exercise?

REFERENCES

1. Phillipson EA, Duffin J, Cooper JD. Critical dependence of respiratory rhythmicity on metabolic CO_2 load. J Appl Physiol 1981;50:45–54.
2. Bennett FM, Tallman RD Jr, Grodins FS. Role of $\dot{V}CO_2$ in control of breathing of awake exercising dogs. J Appl Physiol 1984;56:1335–7.
3. Waldrop TG, Eldridge FL, Iwamoto GA, Mitchell JH. Central neural control of respiration and circulation during exercise. In: Rowell LB, Shepherd JT, editors. Handbook of physiology: exercise: regulation and integration of multiple systems. New York: Oxford University Press; 1996. p. 333–80.
4. Williamson JW, McColl R, Mathews D, et al. Hypnotic manipulation of effort sense during dynamic exercise: cardiovascular responses and brain activation. J Appl Physiol 2001;90:1392–9.
5. Kaufman MP, Forster HV. Reflexes controlling circulatory, ventilatory, and airway responses to exercise. In: Rowell LB, Shepherd JT, editors. Handbook of physiology: exercise: regulation and integration of multiple systems. New York: Oxford University Press; 1996. p. 381–447.
6. Adams L, Frankel H, Garlick J, et al. The role of spinal cord transmission in the ventilatory response to exercise in man. J Physiol (Lond) 1984;355:85–97.
7. Dempsey JA, Forster HV, Ainsworth DM. Regulation of hyperpnea, hyperventilation, and respiratory muscle recruitment during exercise. In: Dempsey JA, Pack AI, editors. Regulation of breathing. New York: Marcel Dekker; 1995. p. 1065–133.
8. Bellemare F, Grassino J. Effect of pressure and timing of contraction on human diaphragm fatigue. J Appl Physiol 1982;53:1190–5.
9. Henke KG, Sharratt M, Pegelow D, Demspey JA. Regulation of end-expiratory lung volume during exercise. J Appl Physiol 1988;64:135–46.
10. Mota S, Casan P, Drobnic F, et al. Expiratory flow limitation during exercise in competition cyclists. J Appl Physiol 1999; 86:611–6.
11. McClaran SR, Harms CA, Pegelow DF, Dempsey JA. Smaller lungs in women affect exercise hyperpnea. J Appl Physiol 1998;84:1872–81.
12. McClaran SR, Wetter TJ, Pegelow DF, Dempsey JA. Role of expiratory flow limitation in determining lung volumes and ventilation during exercise. J Appl Physiol 1999;86:1357–66.
13. Dempsey JA, Adams L, Ainsworth D, et al. Airway, lung and respiratory muscle function during exercise. In: Rowell LB, Shepherd JT, editors. Handbook of physiology: exercise: regulation and integration of multiple systems. New York: Oxford University Press; 1996. p. 448–514.
14. Forsyth RD, Cole P, Shephard RJ. Exercise and nasal patency. J Appl Physiol 1983;55:860–5.
15. Connel DC, Fegosi RF. Influence of nasal airflow and resistance on nasal dilator muscle activities during exercise. J Appl Physiol 1993;74:2529–36.
16. England SJ, Bartlett DJ. Changes in respiratory movements of the human vocal cords during hypernea. J Appl Physiol 1982;52:780–5.
17. Warren JB, Jennings SJ, Clark TJ. Effect of adrenergic and vagal blockade on the normal human airway response to exercise. Clin Sci 1984;66:79–85.
18. Stirling DR, Cotton DJ, Graham BL, et al. Characteristics of airway tone during exercise in patients with asthma. J Appl Physiol 1893;54:934–42.
19. Cordain L, Rode EJ, Gotshall RW, Tucker A. Residual lung volume and ventilatory muscle strength changes following maximal and submaximal exercise. Int J Sports Med 1994;15:158–61.
20. Gauvreau GM, Ronnen GM, Watson RM, O'Byrne PM. Exercise-induced bronchoconstriction does not cause eosinophilic inflammation or airway hyperresponsiveness in subjects with asthma. Am J Respir Crit Care Med 2000;162:1302–7.
21. Kaufman MP, Rybicki KJ, Mitchell JH. Hindlimb muscular contraction reflex decreases total pulmonary resistance in dogs. J Appl Physiol 1985;59:1521–6.
22. Bowes G, Shakin EJ, Phillipson EA, Zamel N. An efferent pathway mediating reflex tracheal dilation in awake dogs. J Appl Physiol 1984;57:413–8.
23. Beyaert CA, Hill JM, Lewis BK, Kaufman MP. Effect on airway caliber of stimulation of the hypothalamic locomotor region. J Appl Physiol 1998;84:1388–94.
24. Fredberg JJ, Inouye D, Miller B, et al. Airway smooth muscle, tidal stretches, and dynamically determined contractile states. Am J Respir Crit Care Med 1997;156:1752–9.
25. Beck KC. Control of airway function during and after exercise in asthmatics. Med Sci Sports Exerc 1999;31:S4–11.
26. Suman OE, Beck KC. Role of airway endogenous nitric oxide on lung function during and after exercise in mild asthma. J Appl Physiol 2002;93:1932–8.
27. Suman OE, Marrow JD, O'Malley KA, Beck KC. Airway function after cyclooxygenase inhibition during hyperpnea-induced bronchoconstriction in guinea pigs. J Appl Physiol 2000;89:1971–8.
28. Otis AB. The work of breathing. In: Fenn WO, Rahn H, editors. Handbook of physiology: respiration. Vol 1. Baltimore: Waverly Press; 1969. p. 463–76.
29. Johnson BD, Saupe KW, Dempsey JA. Mechanical constraints on exercise hyperpnea in endurance athletes. J Appl Physiol 1992;73:874–86.
30. O'Donnell DE. Ventilatory limitations in chronic obstructive pulmonary disease. Med Sci Sports Exerc 2001;33:S647–55.
31. Sliwinski P, Kaminski D, Zielinski J, Yan S. Partitioning of the elastic work of inspiration in patients with COPD during exercise. Eur Respir J 1998;11:416–21.
32. Goldman MD, Grimby G, Mead J. Mechanical work of breathing derived from rib cage and abdominal V–P partitioning. J Appl Physiol 1976;41:752–63.
33. Aliverti A, Iandelli I, Duranti R, et al. Respiratory muscle dynamics and control during exercise with externally imposed expiratory flow limitation. J Appl Physiol 2002; 92:1953–63.
34. Kenyon CM, Cala SJ, Yan S, et al. Rib cage mechanics during quiet breathing and exercise in humans. J Appl Physiol 1997;83:1242–55.
35. Boynton BR, Barnas GM, Dadmun JT, Fredberg JJ. Mechanical coupling of the rib cage, abdomen, and diaphragm through their area of apposition. J Appl Physiol 1991;70:1235–44.

36. Aaron EA, Seow KC, Johnson BD, Dempsey JA. Oxygen cost of exercise hyperpnea: implications for performance. J Appl Physiol 1992;72:1818–25.
37. Harms CA, Babcock MA, McClaran SR, et al. Respiratory muscle work compromises leg blood flow during maximal exercise. J Appl Physiol 1997;82:1573–83.
38. Hickam JB, Cargill WH. Effect of exercise on cardiac output and pulmonary arterial pressure in normal persons and in patients with cardiovascular disease and pulmonary emphysema. J Clin Invest 1948;27:10–23.
39. Reeves JT, Groves BM, Cymerman A, et al. Operation Everest II: cardiac filling pressures during cycle exercise at sea level. Respir Physiol 1990;80:147–54.
40. Riley RL, Himmelstein A, Motley HL, et al. Studies of the pulmonary circulation at rest and during exercise in normal individuals and in patients with chronic pulmonary disease. Am J Physiol 1948;152:372–80.
41. Slonim NB, Ravin A, Balchum OJ, Dressler SH. The effect of mild exercise in the supine position on the pulmonary arterial pressure of five normal human subjects. J Clin Invest 1954;33:1022–30.
42. Sullivan MJ, Cobb FR, Higgenbotham MB. Stroke volume increases by similar mechanisms during upright exercise in normal men and women. Am J Cardiol 1991;67:1405–12.
43. Thadani U, Parker JO. Hemodynamics at rest and during supine and sitting bicycle exercise in normal subjects. Am J Cardiol 1978;41:52–9.
44. Luepker R, Holmberg S, Varnauskas E. Left atrial pressure during exercise in hemodynamic normals. Am Heart J 1971; 81:494–7.
45. Eldridge MW, Podolsky A, Richardson RS, et al. Pulmonary hemodynamic response to exercise in subjects with prior high-altitude pulmonary edema. J Appl Physiol 1996; 81:911–21.
46. Wagner P, Gales G, Moon R, et al. Pulmonary gas exchange in humans exercising at sea level and simulated exercise. J Appl Physiol 1986;61:260–70.
47. Kane DW, Tesauro T, Gupta R, Newman JH. Exercise induced vasoconstriction during combined blockade of nitric oxide (NO) synthase and beta adrenergic receptors. J Clin Invest 1994;93:677–83.
48. Davies P. Flow-mediated endothelial mechanotransduction. Physiol Rev 1995;75:519–60.
49. Manohar M, Goetz T. L-NAME does not affect exercise-induced pulmonary hypertension in thoroughbred horse. J Appl Physiol 1998;84:1902–8.
50. Lindenfeld J, Reeves JT, Horwitz LD. Low exercise pulmonary resistance is not dependent on vasodilator prostaglandins. J Appl Physiol 1983;55:558–61.
51. Newman JH, Butka BJ, Brigham KL. Thromboxane A_2 and prostacyclin do not modulate pulmonary hemodynamics during exercise in sheep. J Appl Physiol 1986;61:1706–11.
52. Johnson RL, Spicer WS, Bishop JM, Forster RE. Pulmonary capillary blood volume, flow, and diffusing capacity during exercise. J Appl Physiol 1960;15:893–902.
53. Coates G, O'Brodovich H, Jefferies AL, Gray GW. Effects of exercise on lung lymph flow in sheep and goats during normoxia and hypoxia. J Clin Invest 1984;74:133–41.
54. Dempsey JA, Hanson PG, Henderson KS. Exercise-induced arterial hypoxaemia in healthy human subjects at sea level. J Physiol 1984;355:161–75.
55. Wetter TJ, St Croix CM, Pegelow DF, et al. Effects of exhaustive endurance exercise on pulmonary gas exchange and airway function in women. J Appl Physiol 2001;91:847–58.
56. Glenny RW, Bernard S, Robertson HT, Hlastala MP. Gravity is an important but secondary determinant of regional pulmonary blood flow in upright primates. J Appl Physiol 1999;86:623–32.
57. Gledhill N, Froese AB, Dempsey JA. Ventilation to perfusion distribution during exercise in health. In: Dempsey JA, Reed CE, editors. Muscular exercise and the lung. Wisconsin: University of Wisconsin Press; 1977. p. 325–44.
58. Bryan AC, Bentivoglio LG, Beerel F, et al. Factors affecting regional distribution of ventilation and perfusion in the lung. J Appl Physiol 1964;19:395–402.
59. West JB. Pulmonary capillary stress failure. J Appl Physiol 2000; 89:2483–9.
60. Manohar M, Goetz T. Pulmonary vascular pressures of exercising thoroughbred horses with and without endoscopic evidence of EIPH. J Appl Physiol 1996;81:1589–93.
61. West JB, Mathieu-Costello O, Jones JH, et al. Stress failure of pulmonary capillaries in racehorses with exercise-induced pulmonary hemorrhage. J Appl Physiol 1993;75:1097–109.
62. Erickson BK, Erickson HH, Coffman JR. Pulmonary, aortic and oesophageal pressure changes during high intensity treadmill exercise in the horse: a possible relation to exercise-induced hemorrhage. Equine Vet 1990;9:47–52.
63. Manohar M. Pulmonary artery wedge pressure increases with high intensity exercise in horses. Am J Vet Res 1993;54:142–6.
64. Jones J, Smith B, Birks E, et al. Left atrial and pulmonary arterial pressures in exercising horses. FASEB J 1992;6:A2020.
65. Hopkins SR, Schoene RB, Henderson WR, et al. Intense exercise impairs the integrity of the pulmonary blood–gas barrier in elite athletes. Am J Respir Crit Care Med 1997; 155:1090–4.
66. Wetter TJ, Xiang Z, Sonetti DA, et al. Role of lung inflammatory mediators as a cause of exercise-induced arterial hypoxemia in young athletes. J Appl Physiol 2002;93:116–26.
67. Ravin MB, Epstein RM, Malm JR. Contribution of thebesian veins to the physiologic shunt in anesthetized man. J Appl Physiol 1965;20:1148–52.
68. Agostoni P, Godden DJ, Baile EM. Measurement of bronchial blood flow in humans. In: Butler J, editor. Lung biology in health and disease: the bronchial circulation. Vol 57. New York: Marcel Dekker; 1992. p. 181–96.
69. Kitamura K, Jorgensen CR, Gobel FL, et al. Hemodynamic correlates of myocardial oxygen consumption during upright exercise. J Appl Physiol 1972;32:516–22.
70. Tobin CE. Arteriovenous shunts in the peripheral pulmonary circulation in the human lung. Thorax 1966;21:197–204.
71. Warren GL, Cureton KJ, Middendort WF, et al. Red blood cell pulmonary capillary transit time during exercise in athletes. Med Sci Sports Exerc 1991;23:1353–61.
72. Ayappa I, Brown LV, Wang PM, et al. Effect of blood flow on capillary transit time and oxygenation in excised rabbit lung. Respir Physiol 1996;105:203–16.
73. Reuschlein PS, Reddan WG, Burpee J, et al. Effect of physical training on the pulmonary diffusing capacity during submaximal work. J Appl Physiol 1968;24:152–8.
74. Wagner PD. Influence of mixed venous PO_2 on diffusion of O_2 across the pulmonary blood:gas barrier. Clin Physiol 1982;2:105–15.
75. Hammond MD, Gale GE, Kapitan KS, et al. Pulmonary gas exchange in humans during exercise at sea level. J Appl Physiol 1986;60:1590–8.
76. Babcock MA, Pegelow DF, McClaran SR, et al. Contribution of diaphragmatic power output to exercise-induced diaphragm fatigue. J Appl Physiol 1995;78:1710–9.
77. Johnson BD, Babcock MA, Suman OE, Dempsey JA. Exercise-induced diaphragmatic fatigue in healthy humans. J Physiol 1993;460:385–405.
78. Babcock MA, Pegelow DF, Johnson BD, Dempsey JA. Aerobic fitness effects on exercise-induced low-frequency diaphragm fatigue. J Appl Physiol 1996;81:2156–64.

79. Babcock MA, Pegelow DF, Taha BH, Dempsey JA. High frequency diaphragmatic fatigue detected with paired stimuli in humans. Med Sci Sports Exerc 1998;30:506–11.
80. Babcock MA, Pegelow DF, Harms CA, Dempsey JA. Effects of respiratory muscle unloading on exercise-induced diaphragm fatigue. J Appl Physiol 2002;93:201–6.
81. Roussos CS, Macklem PT. Diaphragmatic fatigue in man. J Appl Physiol 1977;43:189–97.
82. Harms CA, Wetter TJ, McClaran SR, et al. Effects of respiratory muscle work on cardiac output and its distribution during maximal exercise. J Appl Physiol 1998;85:609–18.
83. Babcock MA, Johnson BD, Pegelow DF, et al. Hypoxic effects on exercise-induced diaphragmatic fatigue in normal healthy humans. J Appl Physiol 1995;78:82–92.
84. Gandevia SC, Killian KJ, Campbell EJ. The effect of respiratory muscle fatigue on respiratory sensations. Clin Sci (Colch) 1981;60:463–6.
85. Dodd SL, Powers SK, Thompson D, et al. Exercise performance following intense, short-term ventilatory work. Int J Sports Med 1989;10:48–52.
86. Martin B, Heintzelman M, Chen HI. Exercise performance after ventilatory work. J Appl Physiol 1982;52:1581–5.
87. Mador MJ, Acevedo FA. Effect of respiratory muscle fatigue on subsequent exercise performance. J Appl Physiol 1991; 70:2059–65.
88. Mador MJ, Acevedo FA. Effect of respiratory muscle fatigue on breathing pattern during incremental exercise. Am Rev Respir Dis 1991;143:462–8.
89. Johnson BD, Aaron EA, Babcock MA, Dempsey JA. Respiratory muscle fatigue during exercise: implications for performance. Med Sci Sports Exerc 1996;28:1129–37.
90. Harms CA, Wetter TJ, St Croix CM, et al. Effects of respiratory muscle work on exercise performance. J Appl Physiol 2000;89:131–8.
91. Gallagher CG, Younes M. Effect of pressure assist on ventilation and respiratory mechanics in heavy exercise. J Appl Physiol 1989;66:1824–37.
92. Krishnan B, Zintel T, McParland C, Gallagher CG. Lack of importance of respiratory muscle load in ventilatory regulation during heavy exercise in humans. J Physiol 1996; 490:537–50.
93. Marciniuk D, McKim D, Sanii R, Younes M. Role of central respiratory muscle fatigue in endurance exercise in normal subjects. J Appl Physiol 1994;76:236–41.
94. Wetter TJ, Harms CA, Nelson WB, et al. Influence of respiratory muscle work on $\dot{V}O_2$ and leg blood flow during submaximal exercise. J Appl Physiol 1999;87:643–51.
95. El-Manshawi A, Killian KJ, Summers E, Jones NL. Breathlessness during exercise with and without resistive loading. J Appl Physiol 1986;61:896–905.
96. Balzamo E, Lagier-Tessonnier F, Jammes Y. Fatigue-induced changes in diaphragmatic afferents and cortical activity in the cat. Respir Physiol 1992;90:213–26.
97. Dempsey JA, Wagner PD. Exercise-induced arterial hypoxemia. J Appl Physiol 1999;87:1997–2006.
98. McFadden ER II, Zawadski DK. Vocal cord dysfunction masquerading as exercise-induced asthma: a physiologic cause for "choking" during athletic activities. Am J Respir Crit Care Med 1996;153:942–7.
99. Powers SK, Lawler J, Dempsey JA, et al. Effects of incomplete pulmonary gas exchange on $\dot{V}O_2$max. J Appl Physiol 1989;66:2491–5.
100. Harms CA, McClaran SR, Nickele GA, et al. Effect of exercise-induced arterial O_2 desaturation on $\dot{V}O_2$max in women. Med Sci Sports Exerc 2000;32:1101–8.
101. Dempsey JA, Seals DR. Aging, exercise and cardiopulmonary function. In: Lamb DR, Gisolfi CV, Nadel E, editors. Perspectives in exercise science and sports medicine. Vol 8. Exercise in older adults. Carmel, IN: Cooper Publishing Group; 1995. p. 237–304.
102. McClaran SR, Babcock MA, Pegelow DF, et al. Longitudinal effects of aging on lung function at rest and exercise in the healthy, active, fit, elderly adult. J Appl Physiol 1995;78:1957–68.

CHAPTER 46

VENTILATORY FACTORS IN EXERCISE PERFORMANCE IN PATIENTS WITH CHRONIC OBSTRUCTIVE PULMONARY DISEASE

Carmen Lisboa, Orlando Díaz, Gisella Borzone

Impaired exercise performance is a common complaint among patients with chronic obstructive pulmonary disease (COPD). During a progressive exercise test, they usually stop because of dyspnea, leg fatigue, or a combination of both.[1,2] Although it has been shown that exercise intolerance in patients with COPD is multifactorial, reflecting abnormalities of both ventilatory and peripheral muscles and abnormalities in metabolic and cardiovascular systems in variable combinations, it is dyspnea, and therefore ventilatory impairment, that is the most important factor limiting exercise performance during everyday activities.[3–8]

The main pathophysiologic feature of patients with COPD is expiratory airflow limitation, which in severe disease can be present even during resting breathing.[9,10] Patients with COPD often breathe tidally along their maximal expiratory flow–volume curve, whereas normal subjects do not exhibit expiratory flow limitation (EFL), even during maximal exercise.

EFL determines dynamic hyperinflation (DH), one of the most important ventilatory factors leading to exercise limitation in these patients.[11] As exercise progresses, EFL worsens, and DH increases. As exercise capacity is not closely related to the results of conventional pulmonary function tests, it is not surprising that recent investigations have shown a poor relationship between exercise capacity and the degree of airway obstruction when both variables are expressed as percent predicted values. In fact, forced expiratory volume in 1 second (FEV_1) explains only about 25% of the variability of exercise capacity, assessed by $\dot{V}O_{2max}$.[12] These findings have motivated the search for variables more closely related to DH, which could predict more accurately the reduced exercise capacity in COPD.

As a consequence of EFL, patients with COPD exhibit a reduced ventilatory reserve, defined as the ratio of maximal exercise ventilation ($\dot{V}_{Emax}$) to the maximal voluntary ventilation (MVV),[13,14] which is further reduced as COPD progresses.

Unlike normal subjects performing a maximal exercise test, who use about 65% of their MVV, patients with COPD use ~95% of their MVV.[15] On the one hand, their ventilation is disproportionate for the level of $\dot{V}O_{2,12}$, and on the other, MVV is reduced due to EFL. However, the ratio $\dot{V}_{Emax}$/MVV does not give specific information on the underlying mechanisms of ventilatory impairment during exercise in COPD, particularly the roles of EFL, DH, and elastic load.[16]

EFL can be detected by comparing the flow–volume ($\dot{V}$–V) curves at rest with the corresponding maximal $\dot{V}$–V curve. Flow limitation exists when resting flow equals maximal flow.[10] The presence of EFL during exercise is evaluated by comparing the exercise $\dot{V}$–V curves with the maximal curve obtained during rest.[16–18] In normal subjects, even during maximal exercise, the flows are less than maximal, and consequently there is no flow limitation. In contrast, in patients with COPD, maximal expiratory flows are reached even at rest or at some point after the beginning of exercise, indicating the presence of flow limitation. Because maximal flows depend on the volume and time history of the preceding inspiration, measurements performed at rest and during exercise require the estimation of the lung volumes at which the curves are being compared.[9] Another approach to assessing EFL consists in applying a negative expiratory pressure (NEP) at the mouth during a tidal expiration and comparing the ensuing expiratory flow–volume curve with that of the previous control expiration.[19] If the application of NEP increases flow over the whole range of the control tidal expiration, there is no EFL. In contrast, if NEP does not elicit an increase in flow over part or all of the control tidal

expiration, the subject is considered to be flow limited. The NEP technique has the advantage of comparing $\dot{V}$–V curves obtained at rest or exercise during tidal breaths. Consequently, the volume and time history during the expiration with NEP are the same as in the preceding control breath, and there is no need to determine the lung volume at which measurements were performed. Figure 46-1 shows the three above-mentioned ways of assessing EFL.

The assessment of EFL is not possible in most pulmonary function laboratories, and it has been studied mainly for research purposes. However, its consequence, that is, the magnitude of DH, can be easily evaluated at rest by measuring inspiratory capacity (IC). As a result of DH, end-expiratory lung volume (EELV) increases, and since total lung capacity (TLC) does not change significantly,[20] IC decreases proportionally. The advantage of this method of detecting hyperinflation at rest over other methods is that IC can be serially measured during exercise.

EFFECTS OF EFL AND DH ON EXERCISE TOLERANCE

Three of the most deleterious effects of EFL and DH on exercise performance are (1) constraint of exercise tidal volume (V_T), (2) mechanical disadvantage of respiratory muscles, and (3) increase in the work of breathing, with dyspnea being the clinical consequence.

Constraint of Exercise V_T

To augment ventilation during exercise, COPD patients need to increase their expiratory flow, and they do this by breathing at a higher lung volume. As expiratory time decreases during exercise, due to the increase in respiratory rate, dynamic air trapping increases in exercise, with a consequent reduction in IC. In this situation, progressive reduction of an already reduced IC means that V_T becomes positioned near TLC, and a further increase in V_T is not possible (Figure 46-2). As observed by O'Donnell and colleagues, at the end of a maximal exercise, patients with COPD breathe close to TLC.[15] In contrast, in normal subjects V_T increases progressively on exercise but does not reach TLC, even at maximal exercise. The impact of a reduction in exercise V_T in COPD patients during a progressive exercise test limited by symptoms has been demonstrated by Díaz and colleagues[21] and by O'Donnell and colleagues,[15] who found a close relationship between V_{Tmax} and $\dot{V}O_{2max}$ ($r = 0.70$ and 0.68, respectively). In addition, V_{Tmax} was related to both resting and exercise IC. These findings confirmed the importance of DH in exercise intolerance in patients with COPD.

Interestingly, not only high-intensity exercise elicits DH. It has also been found with the 6-minute walking test (6MW). Marín and colleagues[22] found a significant fall in IC at the end of the 6MW test and a close correlation between the fall in IC and the magnitude of dyspnea assessed by the Borg scale. Similarly, Reid and colleagues[23] studied the behavior of IC during the 6MW test in COPD patients with and without EFL. They observed a significant fall in IC in patients with EFL in comparison with those without EFL. An additional finding in the study of Reid and colleagues was that arterial oxygen saturation (S_aO_2) fell significantly at the end of exercise in EFL patients, whereas no changes were observed in patients who did not have EFL, illustrating the role of EFL in determining gas exchange abnormalities.

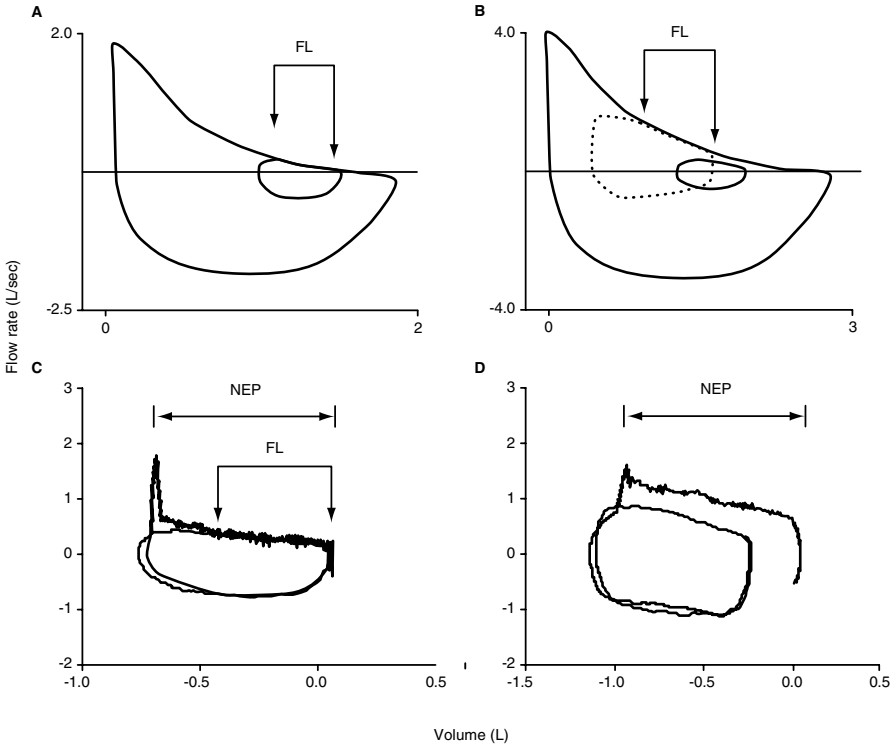

FIGURE 46-1 Two different ways of assessing expiratory flow limitation. *A* and *B*, Tidal flow–volume curves at rest (*solid lines*) and during exercise (*dotted lines*) compared with maximal flow–volume curves. A corresponds to a patient with flow limitation (FL) at rest and *B* to a patient with FL only during exercise. *C* and *D*, Flow–volume curves obtained with the negative expiratory pressure (NEP) technique; test breath and preceding control breath in a patient with FL (*C*) and in a patient without FL (*D*). *Horizontal arrows* indicate the volume range over which NEP was applied. Zero volume corresponds to the end-expiratory lung volume of control breaths.

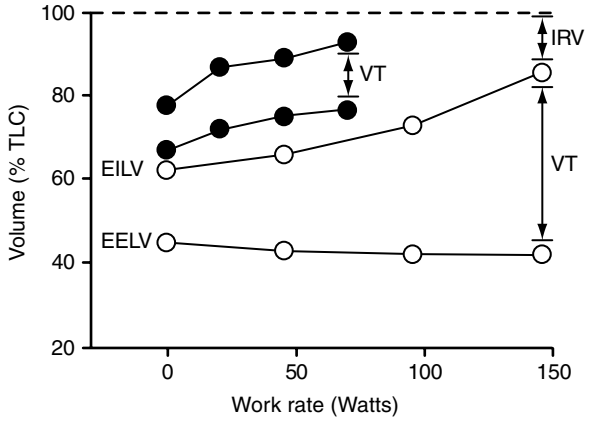

FIGURE 46-2 Changes in tidal volume (V_T) with increasing work rate during a symptom-limited progressive exercise in a normal subject and in a patient with severe chronic obstructive pulmonary disease (COPD). The normal subject (*open circles*) maintains baseline end-expiratory lung volume (EELV), and V_T increases with increasing work rate. The patient with severe COPD has an increased baseline EELV, and changes in V_T are limited.

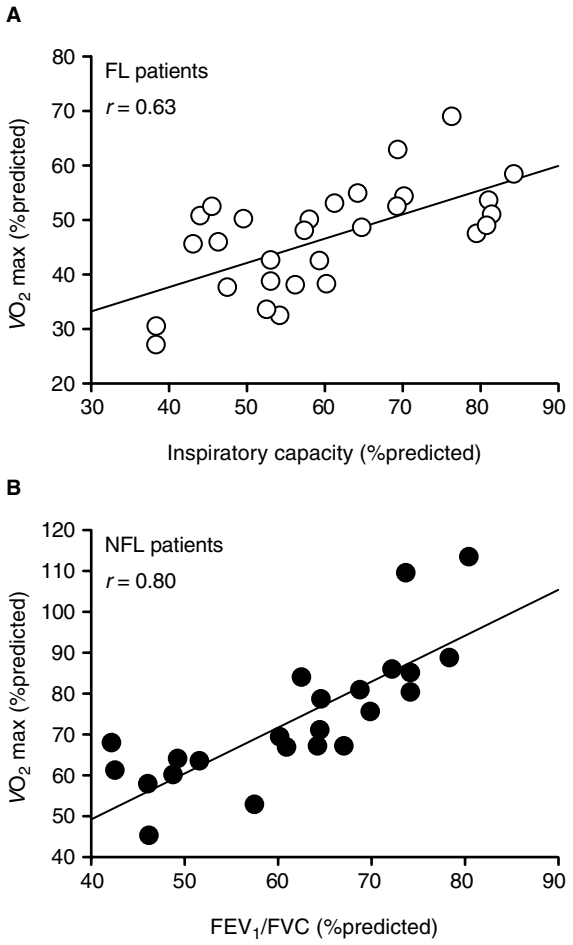

FIGURE 46-3 Relationships between $\dot{V}O_{2max}$ and inspiratory capacity at rest in patients with expiratory flow limitation (FL) (*A*) and between $\dot{V}O_{2max}$ and forced expiratory volume in 1 second (FEV_1)/forced vital capacity (FVC) in non-FL patients at rest (NFL) (*B*). Values are expressed as percent predicted. Adapted from Díaz O et al.[24]

Díaz and colleagues[24] studied the effect of DH on exercise capacity, separating patients with COPD according to the presence or absence of EFL. They showed that IC was lower in patients with EFL than in those without ($60 \pm 3\%$ vs $93 \pm 3\%$ of their predicted value). Similarly, $\dot{V}O_{2max}$ was lower in patients with EFL (47 ± 2 vs $73 \pm 23\%$ predicted). A significant correlation between IC and $\dot{V}O_{2max}$ was found in patients with EFL ($r = 0.63$), whereas for patients without EFL, the FEV_1/forced vital capacity ratio, expressed as percent predicted, showed the best correlation with $\dot{V}O_{2max}$ ($r = 0.80$) (Figure 46-3). Resting IC was the best predictor of V_{Tmax}, showing that patients with a low IC were unable to generate a large enough V_T during exercise. As dead space increased with DH, there was a consequent decrease in alveolar ventilation ($\dot{V}_A$), which could explain why these patients develop hypercapnia and hypoxemia at the end of exercise.

These results show that EFL at rest promotes DH, limits V_T, and impairs gas exchange during exercise, reducing exercise tolerance.

Inspiratory Muscle Function Impairment

Inspiratory muscle function is impaired in some patients with COPD, mainly due to DH and the contribution of other factors, such as malnutrition[25,26] and hypoxemia.[27] Reduction in muscle strength is reflected in low maximal inspiratory mouth (P_{Imax}) and transdiaphragmatic (P_{dimax}) pressures. Factors impairing inspiratory muscle function due to hyperinflation are as follows:

1. Shortening of the diaphragm, affecting its length–tension properties and decreasing force generation
2. Abolition of the zone of apposition of the costal portion of the diaphragm with the rib cage, resulting in less lateral expansion of the thoracic cage during inspiration
3. Inward motion of the lateral rib cage, which occurs during diaphragmatic contractions with severe DH, when diaphragm fibers become oriented radially rather than axially
4. Inward recoil of the chest wall, which means that inspiratory muscles work not only against the lung elastic recoil but also against the elastic recoil of the chest wall[28]

There is evidence showing that the capacity of the diaphragm for generating tension at rest is reduced in COPD, mainly as a result of hyperinflation.[29–31] On the other hand, DH not only decreases the capacity of the inspiratory muscles but also imposes a larger demand on these muscles, which have to overcome the increased elastic load and the intrinsic positive end-expiratory pressure (PEEPi) by generating an abnormally higher proportion of P_{Imax} in terms of pleural pressure (P_{pl}) swings for a given V_T.

There have been few studies on the function of inspiratory muscles during exercise in COPD.[32–35] Yan and colleagues[35] showed that most of the diaphragmatic pressure contribution to breathing occurs before the beginning of the

inspiratory flow, in order to overcome PEEPi, whereas rib cage muscle contraction provides almost all the inspiratory pressure needed to overcome the elastic load caused by increasing V_T. Thus, rib cage muscles compensate for the progressive reduction in the diaphragmatic contribution to inspiration as exercise increases. These authors also found that P_{dimax} remained constant during exercise, despite a progressive increase in the amplitude of P_{pl} swings. In healthy subjects, EELV is reduced during exercise, improving the performance of the diaphragm as a pressure generator. In contrast, as previously discussed, the increase in EELV in patients with COPD severely reduces diaphragmatic performance.

Increase in the Work of Breathing

In patients with severe COPD, the work of breathing is high even at rest and increases further during exercise, mainly because of the increment in its elastic component.

The relationship between ventilation and work rate or its equivalent, oxygen uptake ($\dot{V}O_2$), often shows the same slope in COPD patients as in normal subjects. However, minute ventilation ($\dot{V}_E$) is higher in COPD patients than in normal subjects at any given workload (or $\dot{V}O_2$).[36]

The mechanical work of breathing has been studied by Sliwinski and colleagues[37] and others[38,39] in COPD patients during an incremental symptom-limited exercise test. The elastic work of inspiration in healthy subjects increases with exercise, mainly because of an increase in V_T. This effect is partly compensated by the fall in EELV as a result of exercise-induced recruitment of expiratory muscles. In patients with COPD, the increase in inspiratory work is larger than what would be predicted for the increase in V_T during exercise. At least two factors play a crucial role in this increment caused by flow limitation. First, EELV is above the relaxation volume of the respiratory system, resulting in PEEPi, which behaves as an inspiratory threshold load that needs to be overcome before inspiratory flow can be generated, significantly increasing inspiratory work for a given ventilation. Second, patients now have a decreased static compliance and consequently breathe along a flatter portion of the static pressure–volume curve. According to Sliwinski and colleagues,[37] inspiratory work due to PEEPi accounted for over 50% of total work at peak exercise.

Figure 46-4 summarizes the mechanical factors involved in exercise intolerance in COPD. Patients with this disease must develop higher respiratory pressures than normal subjects during exercise, whereas their maximal capacity to generate pressure is reduced. Thus, they have a severe reduction in inspiratory muscle reserve and a consequent increase in P_{pl}/P_{Imax}. As these patients are unable to increase V_T during exercise, their V_T expressed as a percentage of predicted vital capacity (VC) (V_T/VC) is reduced. O'Donnell and colleagues[7] proposed the concept of "ventilatory effort," which is the proportion of P_{Imax} necessary to generate a given V_T expressed as a percentage of predicted VC ($P_{pl}/P_{Imax}/V_T$/VC). Ventilatory effort is large in these patients as a result of both the higher percentage of P_{Imax} used during exercise and a small V_T. The same group of investigators[8] has demonstrated a significant relationship between ventilatory effort and both DH and dyspnea.

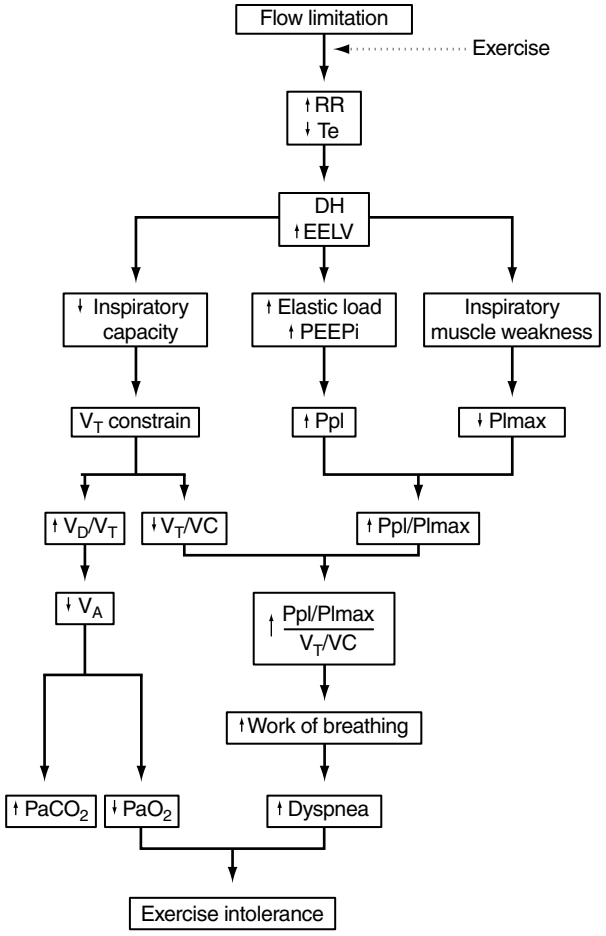

FIGURE 46-4 Integrated view of ventilatory factors limiting exercise in chronic obstructive pulmonary disease (COPD). DH = dynamic hyperinflation; EELV = end-expiratory lung volume; P_aCO_2 = arterial partial pressure of carbon dioxide; $PEEP_i$ = intrinsic positive end-expiratory pressure; P_aO_2 = arterial partial pressure of oxygen; P_{Imax} = maximal inspiratory mouth pressure; P_{pl} = pleural pressure; RR = respiratory rate; Te = expiratory time; V_A = alveolar ventilation; VC = vital capacity; V_D = dead space volume; V_T = tidal volume;

Increase in Ventilatory Demands

In addition to the already discussed altered mechanical properties of the respiratory system, patients with COPD have to cope with increased ventilatory demands, mainly because of a disproportionate ventilation for $\dot{V}O_2$ in exercise. Factors that have been implicated in this excess ventilation by increasing ventilatory drive are (1) the increase in ventilation–perfusion abnormalities, (2) early lactic acidosis during exercise,[40] and (3) hypoxemia and hypercapnia due to hypoventilation during exercise.

CLINICAL RELEVANCE

Because of the physiologic alterations discussed above, COPD limits the ability of patients to increase ventilation, reducing exercise tolerance. Although the mechanisms of exercise intolerance in COPD are complex and multifaceted,

EFL is the hallmark of the disease and imposes increased inspiratory muscle demands, particularly when ventilation must increase, thus contributing to dyspnea.

Interestingly, although most of the new data regarding the effect of EFL on exercise performance have been obtained with the use of exercise testing under controlled laboratory conditions, it is now known that DH also develops during walking and probably other everyday activities.

Exercise intolerance and dyspnea are major complaints of patients with COPD, affecting their quality of life. Studies designed to improve exercise tolerance in COPD have shown that reduction in DH plays a pivotal role in improving exercise performance. In that sense, the effects of bronchodilators and oxygen supplementation during exercise are good examples.[41–43] Unfortunately, changes in DH have been largely ignored in the process of evaluating different therapies in COPD patients. It should be stressed that reduction in DH is probably one of the best tools with which to adequately evaluate the benefits of available therapies and new interventions. With the availability of spirometric measures of hyperinflation, this can be done easily, allowing the prediction of exercise intolerance in these patients.

ACKNOWLEDGMENT

This work was funded in part by Fondecyt Grants nos. 198/0937 and 1010/993.

REFERENCES

1. Killian KJ, Inman KD, Jones NL. The thorax in exercise. In: Roussos C, editor. The thorax. 2nd ed. Part B: Applied physiology. New York: Marcel Dekker; 1995. p. 1355–72.
2. Killian KJ, Leblanc P, Martin DH, et al. Exercise capacity and ventilatory, circulatory, and symptom limitation in patients with chronic airflow limitation. Am Rev Respir Dis 1992;146:935–40.
3. Hamilton AL, Killian KJ, Summers E, Jones NL. Muscle strength, symptom intensity and exercise capacity in patients with cardiorespiratory disorders. Am J Respir Crit Care Med 1995;152:2021–31.
4. Neder JA, Jones PW, Nery LE, Whipp BJ. Determinants of the exercise endurance capacity in patients with chronic obstructive pulmonary disease. Am J Respir Crit Care Med 2000;162:497–504.
5. Gosselink R, Troosters T, Decramer M. Peripheral muscle weakness contributes to exercise limitation in COPD. Am J Respir Crit Care Med 1996;153:976–80.
6. Muriari C, Ghezzo H, Milic-Emili J, Gauthier H. Exercise limitation in obstructive lung disease. Chest 1998;114:965–8.
7. O'Donnell DE, Bertley JC, Chau LKL, Webb KA. Qualitative aspects of exertional breathlessness in chronic airflow limitation. Am J Respir Crit Care Med 1997;155:109–15.
8. O'Donnell DE, Webb KA. Exertional breathlessness in patients with chronic airflow limitation: the role of lung hyperinflation. Am Rev Respir Dis 1993;148:1351–7.
9. Hyatt RE. The interrelationship of pressure, flow and volume during various respiratory maneuvers in normal and emphysematous patients. Am Rev Respir Dis 1961;83:676–83.
10. Hyatt RE. Expiratory flow limitation. J Appl Physiol 1983;55:1–8.
11. Pride NB, Macklem PT. Lung mechanics in disease. In: Macklem PT, Mead J, editors. The handbook of physiology. Section 3. The respiratory system. Vol III. Part 2. Bethesda (MD): American Physiological Society; 1986. p. 659–92.
12. Bauerle O, Chrusch CA, Younes M. Mechanisms by which COPD affects exercise tolerance. Am J Respir Crit Care Med 1998;157:57–68.
13. Dillard TA, Piantadosi S, Rajagopal KR. Prediction of ventilation at maximal exercise in chronic airflow obstruction. Am Rev Respir Dis 1985;132:230–5.
14. Jensen I, Lyager S, Pedersen OF. The relationship between maximal ventilation, breathing pattern and mechanical limitation of ventilation. J Physiol 1980;309:521–32.
15. O'Donnell DE, Revill SM, Webb KA. Dynamic hyperinflation and exercise tolerance in chronic obstructive pulmonary disease. Am J Respir Crit Care Med 2001;164:770–7.
16. Grimby G, Stiksa J. Flow–volume curves and breathing pattern during exercise in patients with obstructive lung disease. Scand J Clin Lab Invest 1970;25:303–13.
17. Johnson BD, Reddan WG, Pegelow DF, et al. Flow limitation and regulation of functional residual capacity during exercise in a physically active aging population. Am Rev Respir Dis 1991;143:960–7.
18. Leaver DG, Pride NB. Flow volume curves and expiratory pressures during exercise in patients with chronic airway obstruction. Scand J Respir Dis 1971;77 Suppl:S23–7.
19. Koulouris NG, Valta P, Lavoie A, et al. A simple method to detect expiratory flow limitation during spontaneous breathing. Eur Respir J 1995;8:306–13.
20. Stubbing DG, Pengelly LD, Morse JLC, Jones NL. Pulmonary mechanics during exercise in subjects with chronic airflow obstruction. J Appl Physiol 1980;49:511–5.
21. Díaz O, Villafranca C, Ghezzo H, et al. Breathing pattern and gas exchange at peak exercise in COPD patients with and without flow limitation at rest. Eur Respir J 2001; 17: 1120–7.
22. Marín JM, Carrizo SJ, Gascon M, et al. Inspiratory capacity, dynamic hyperinflation, breathlessness and exercise performance during the six minute-walk test in chronic obstructive pulmonary disease. Am J Respir Crit Care Med 2001;163:1395–9.
23. Reid R, Díaz O, Jorquera J, Lisboa C. Efecto de la caminata de seis minutos sobre la hiperinflación pulmonar en pacientes con enfermedad pulmonar obstructiva crónica avanzada. Rev Med Chile 2001;129:1171–8.
24. Díaz O, Villafranca C, Ghezzo H, et al. Role of inspiratory capacity on exercise tolerance in COPD patients with and without tidal expiratory flow limitation at rest. Eur Respir J 2000;16:269–75.
25. Arora NS, Rochester DF. Respiratory muscle strength and maximal voluntary ventilation in undernourished patients. Am Rev Respir Dis 1982;126:5–8.
26. Gray-Donald K, Gibbons L, Shapiro SH, et al. Nutritional status and mortality in chronic obstructive pulmonary disease. Am J Respir Crit Care Med 1996;153:961–6.
27. Jardim JR, Farkas G, Prefaut C, et al. The failing inspiratory muscles under normoxic and hypoxic conditions. Am Rev Respir Dis 1981;124:274–9.
28. Decramer M, Gosselink R, Derom E. Respiratory muscle mechanics in chronic obstructive pulmonary disease and acute respiratory failure. In: Derenne JP, Whitelaw WA, Similowski T, editors. Acute respiratory failure in chronic obstructive pulmonary disease. New York: Marcel Dekker; 1996. p. 47–64.
29. Newell SZ, McKenzie DK, Gandevia SC. Inspiratory and skeletal muscle strength and endurance and diaphragmatic activation in patients with chronic airflow limitation. Thorax 1989;44:903–12.
30. Polkey MI, Kyroussis D, Hamnegard CH, et al. Diaphragm strength in chronic obstructive pulmonary disease. Am J Respir Crit Care Med 1996;154:1310–7.

31. Similowski T, Yan S, Gauthier AP, et al. Contractile properties of the human diaphragm during chronic hyperinflation. N Engl J Med 1991;325:917–23.
32. Kyroussis D, Polkey MI, Keilty SEJ, et al. Exhaustive exercise slows inspiratory muscle relaxation rate in chronic obstructive pulmonary disease. Am J Respir Crit Care Med 1996; 153:787–93.
33. Polkey MI. Muscle metabolism and exercise tolerance in COPD. Chest 2002;121:131S–5S.
34. Montes de Oca M, Rasullo J, Celli BR. Respiratory muscle and cardiopulmonary function during exercise in very severe COPD. Am J Respir Crit Care Med 1996;154:1284–9.
35. Yan S, Kaminski D, Sliwinski P. Inspiratory muscle mechanics of patients with chronic obstructive pulmonary disease during incremental exercise. Am J Respir Crit Care Med 1997; 156:807–13.
36. Bauerle O, Younes M. Role of ventilatory response to exercise in determining exercise capacity in COPD. J Appl Physiol 1995;79:1870–7.
37. Sliwinski P, Kaminski D, Zielinski J, Yan S. Partitioning of elastic work of inspiration in patients with COPD during exercise. Eur Respir J 1998;11:416–21.
38. Grimby G, Elgefors B, Oxhoj H. Ventilatory levels and chest wall mechanics during exercise in obstructive lung disease. Scand J Respir Dis 1973;54:45–52.
39. Dodd DS, Brancatisano T, Engel LA. Chest wall mechanics during exercise in patients with severe chronic airflow limitation. Am Rev Respir Dis 1984;129:33–8.
40. Casaburi R, Patessio A, Ioli F, et al. Reductions in exercise lactic acidosis and ventilation as a result of exercise training in patients with obstructive lung disease. Am Rev Respir Dis 1991;143:9–18.
41. Belman MJ, Botnick WC, Shin JW. Inhaled bronchodilators reduce dynamic hyperinflation during exercise in patients with chronic obstructive pulmonary disease. Am J Respir Crit Care Med 1996;153:967–75.
42. Boni E, Corda L, Franchini D, et al. Volume effect and exertional dyspnoea alter bronchodilator in patients with COPD with and without expiratory flow limitation at rest. Thorax 2002;57:528–32.
43. O'Donnell DE, D'Arsigny C, Webb KA. Effects of hyperoxia on ventilatory limitation during exercise in advanced chronic obstructive pulmonary disease. Am J Respir Crit Care Med 2001;163:892–8.

CHAPTER 47

PRACTICAL ASSESSMENT OF EXERCISE LIMITATION

Nicholas C. Duffy, Peter M. A. Calverley

This chapter describes ways in which performance during exercise can be assessed in the clinical setting, what we expect to see in the normal subject, and how different disease states impact on exercise performance with some examples of typical exercise tests in different conditions.

During exercise, oxygen needs to be delivered to the exercising muscles and carbon dioxide removed in greater quantities than are necessary at rest. The mechanisms involved in this task are complex and involve many different body systems, of which the cardiorespiratory system is only a part; the oxygen-carrying capacity of the blood is also important, as are the cellular processes involved in oxygen use. Exercise limitation, which occurs at maximal exercise in disease and in health, arises because one or more of the processes involved is working at capacity or because symptoms become intolerable at levels below this. There are a number of mechanisms that may lead to limitation. To understand which processes predominate in respiratory disease it is useful to consider the integrated responses of the cardiorespiratory system during exercise. This is best done by performing an exercise test.

EXERCISE TESTING

Several different approaches to assessing exercise capacity have been developed ranging in complexity from simple field tests that require no special equipment but give relatively limited information to a complex cardiorespiratory exercise test that gives breath-by-breath data on a wide range of physiologic variables and can be considered as the "gold standard."

Cardiopulmonary Exercise Test

Cardiopulmonary exercise test assesses cardiovascular function—heart rate, blood pressure response, electrocardiogram (ECG) changes, and, if using invasive measurements of arterial and venous gas concentrations, cardiac output. Pulmonary variables now commonly assessed include breath-by-breath measurement of oxygen uptake of the lungs ($\dot{V}O_2$), carbon dioxide output ($\dot{V}CO_2$), minute ventilation ($\dot{V}E$) and breathing pattern from information given from tidal volume (V_T), respiratory frequency (f), oxygen saturation (S_aO_2), and expiratory and inspiratory times (T_e and T_i). In addition, measures of symptom intensity (typically a category scale like the modified Borg score) are recorded.

The test can be performed either on a treadmill or an electrically braked cycle ergometer in which the impedance of the ergometer can be progressively increased in either a stepped or ramped fashion. The treadmill has the disadvantage that it is harder to quantify workload and it can be difficult to perform in subjects with balance problems; on the other hand it involves a form of exercise that is more familiar, and the maximal $\dot{V}O_2$ tends to be higher on the treadmill; in practice, differences between the two forms of test are not important.[1]

Several different types of flow meter are available for use during exercise. Pneumotachographs incorporate either a number of parallel tubes or wire mesh screens of known resistance to airflow; by knowing the pressure, either side of this resistor flow can be calculated. Flow is normally integrated electrically to produce a volume signal, but a series of technical limitations including integrator drift prevents absolute volume measurement during exercise. Instead the integrator is rezeroed after each breath, which allows tidal volume to be measured but not end-expiratory lung volume relative to the resting values. If this is to be measured, a different approach is required. Pneumotachographs depend on the airflow being laminar. Pitot tubes are an alternative way of measuring flow that does not depend on laminar airflow and also does not add any resistance to the breathing circuit. Flow when using a pitot tube is calculated from Bernoulli's law by measuring pressure at openings directly facing and perpendicular to the airflow.[2]

Guidelines have been produced covering the indications interpretation and standardization of cardiopulmonary exercise testing.[3,4]

Field Tests

Field tests are relatively simple forms of exercise tests that can be easily performed with a minimum of equipment and have the advantage of testing in a manner that is easily performed and is familiar to the subject. They offer reliable measures of exercise capacity but are not suitable for the detailed assessment of the cause of exercise limitation. The following field tests are among the commonest to be performed.

6-Minute Walk Test The 6-minute walk test has evolved from the 12-minute walk test.[5] It involves walking as quickly as the subject is able along a level corridor; the total distance covered in 6 minutes is recorded. Subjects are allowed to stop during this time if they cannot go any farther, although most patients pace themselves to avoid this after they have completed the initial practice test. Six minutes appears to be as sensitive as 12-minute testing, although shorter duration walks are less reproducible. The test has been shown to have good repeatability within and between days and has now been extensively used. It has been shown to predict survival in chronic obstructive pulmonary disease (COPD)[6] and heart failure.[7] Oxygen uptake plateaus during the second half of the 6-minute walk, and the values are similar to those reached during an incremental cycle exercise test in COPD.[8]

The disadvantages of the test are that the pace is not standardized and the walking speed is influenced by the degree of motivation and encouragement; as a result there is wide variation between different centers in the walking distance for similar groups of patients, and therefore valid comparisons cannot be made between them. Practice walks are generally performed with an adequate period of rest between walks as there has been shown to be some learning effect, although this is generally not large.[9] Recent data suggest that the design of the walking course can influence the distance covered more than does this practice effect, longer distances being recorded on circular courses without a stop.[10] Despite these difficulties in standardization, there is agreement that a change of 54 meters represents a clinically recognizable improvement in walking distance.[11] Guidelines have been produced to aid in the standard performance of the procedure.[12]

Shuttle Walk Tests Shuttle walk tests have been devised in which subjects walk in response to an auditory cue that increases in frequency to indicate a change in speed. Thus, the investigator imposes an external pacing not present in the 6-minute walk test. The first of the shuttle walk tests to be developed was the incremental shuttle walk test (ISWT),[13] in which the walking speed progressively increases. The distance walked in this test correlates well with the maximal oxygen uptake (VO_2max) measured during a cardiorespiratory exercise test.[14] The endurance shuttle walk test (ESWT)[15] is a complementary test to the ISWT that examines the response to submaximal exercise with a constant walking speed determined from the distance walked in the preceding ISWT. The ESWT has been shown to be both repeatable and sensitive to change. This test requires the patient to walk at a constant pace approximately 85% of the maximum achieved in the ISWT.

Step Tests Paced step tests have been used as a measure of exercise capacity, but a marked learning effect has been demonstrated and stepping is a less familiar activity for subjects than walking. They have the advantage of simplicity. However, the test is not standardized or readily comparable to other forms of test. A study comparing step testing with walking tests and cycle ergometry found that a steady state for VO_2 and ventilation was not achieved for the step tests, whereas it was for the other testing modalities.[16]

RESPONSES TO EXERCISE

Exercise limitation can occur for a number of reasons: a limit to oxygen transport may have been reached within the cardiorespiratory system; mitochondrial oxygen use may be maximal (in both cases VO_2max is achieved) or exercise may be limited by severe symptoms (dyspnea, leg fatigue, or pain) when maximal VO_2 may not have been achieved.

Normal Responses to Exercise

In health, the limiting factors vary from person to person and have been mainly analyzed in fit athletes of varying ages. Exercise performance can usefully be analyzed under several headings.

Cardiovascular Response The normal cardiovascular response to exercise requires the cardiac output to increase, a change expressed in a familiar formula as:

$$\text{Cardiac output (Q)} = \text{Heart rate (HR)} \times \text{Stroke volume (SV)} \quad (47\text{-}1)$$

At the start of exercise the stroke volume almost immediately increases,[17,18] owing to the increased venous return caused by contracting muscles and the increased cardiac inotropy associated with exercise. As exercise proceeds, the cardiac output rises due to an increased heart rate with relatively little change in stroke volume. The pulmonary vascular bed dilates at the start of exercise, leading to a lowered pulmonary vascular resistance. Lung units that were underperfused at rest receive an increased blood flow leading to an improved ventilation/perfusion (V/Q) matching. Another consequence of the fall in pulmonary vascular resistance is that the afterload on the right ventricle is decreased, and this increases venous return to the left ventricle.

Gas Exchange Gas exchange variables change at different stages of exercise. The ratio of the whole-body carbon dioxide output to the oxygen consumption—respiratory exchange ratio (RER)—depends on the substrate being metabolized to produce energy. At rest proportionately more lipid is metabolized compared with carbohydrate than occurs during exercise (as carbohydrate requires less oxygen use). Metabolism of lipid generates less carbon dioxide than it uses oxygen—therefore, at steady state the respiratory exchange ratio ($RER = VCO_2/VO_2$) is less than 1 (typically 0.8)—whereas metabolism of carbohydrate produces the same amount of carbon dioxide as oxygen consumed. During aerobic exercise a predominance of carbohydrate is metabolized, and the RER therefore approaches 1. The uptake of oxygen during exercise is proportional to the work rate during aerobic exercise; the absolute value of VO_2 at any given work rate depends on body size—the heavier the subject the more oxygen is required.[19] There is an upper limit at which the body's oxygen uptake and utilization processes are working at capacity; if this point is reached the

VO_2 will plateau, that is, there is no further increase in VO_2 despite an increasing work rate. This is the true VO_2max, although this point may not be reached if unbearable symptoms cause cessation of exercise. In many clinical situations the exercise test is technically submaximal; the maximum VO_2 in this situation is reported as the symptom-limited VO_2max.

Before VO_2max is reached, the exercising muscle's need for energy exceeds the capacity of the cardiorespiratory transport system to deliver sufficient oxygen to sustain aerobic metabolism. The resulting lactate production increases carbon dioxide production. During aerobic exercise VCO_2 is less than VO_2 (ie, RER <1). Once lactate is produced, after an initial period when it is buffered within the cells, it relies on bicarbonate ions for its buffering, leading to additional CO_2 production in accordance with the Henderson-Hasselbach equilibrium. The onset of anaerobic respiration is termed the lactate threshold and can be estimated graphically as the time during exercise when there is a relatively excessive VCO_2 (Figure 47-1).

Ventilatory Changes In health, alveolar ventilation is tightly regulated to keep arterial partial pressure of carbon dioxide (P_aCO_2) constant in the face of increasing CO_2 production. Only during very heavy exercise does P_aCO_2 fall if a metabolic acidosis is induced by lactate. Above the lactate threshold, ventilation increases at a faster rate than previously, mirroring the VCO_2. Ventilation is also influenced by the size of the physiologic dead space as this is "wasted ventilation" in terms of gas exchange. Alveolar ventilation is responsible for gas exchange, with the difference between it and VE being made of the dead space; clearly, the larger the dead space, the larger the VE that is needed to maintain P_aCO_2 within the set limits.

Ventilation can be calculated from the alveolar ventilation equation as follows:

$$VE = \frac{863 \times VCO_2}{P_aCO_2(1 - V_D/V_T)} \qquad (47\text{-}2)$$

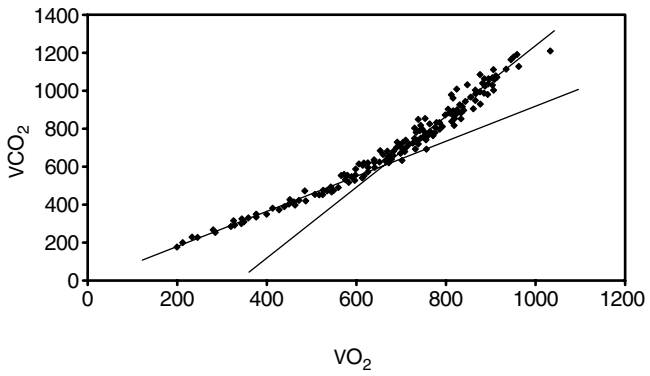

FIGURE 47-1 CO_2 output (VCO_2 mL/min) plotted against oxygen uptake (VO_2 mL/min) during an exercise test in a subject with COPD. Estimated lactate threshold is achieved as shown by the increase in VCO_2 relative to the VO_2, as shown by the change in gradient seen on the graph. This has occurred at a lower level than would be expected in normal subjects.

863 being a factor to account for barometric pressure, temperature, and water vapor to correct the volume measurement and with P_aCO_2 measured in mm Hg. VD/VT is the ratio of physiologic dead space to tidal volume. VE is minute ventilation, which is the volume of expired air measured at the mouth over 1 minute.

The maximal ventilatory capacity can be estimated at rest by measuring the maximal voluntary ventilation (MVV). In normal subjects, generally VEmax when exercising reaches 50 to 80% of the MVV,[17] the difference between VEmax and the MVV being the breathing reserve, which is usually 20 to 50% of the MVV. The MVV maneuver is affected by the subject's effort and can be estimated indirectly as forced expiratory volume in 1 second (FEV_1) $\times 40$. This provides a useful estimate of maximal exercise ventilation in both normal subjects and those with obstructive lung disease.[20,21]

Breathing Pattern Ventilation initially increases by changing both tidal volume and respiratory frequency; tidal volume usually reaches a value of 50 to 60% of vital capacity. Further increases in minute ventilation occur by an increase in respiratory frequency. In healthy younger subjects tidal volume is increased by a combination of a higher end-inspiratory lung volume and a reduction in the end-expiratory lung volume (EELV) owing to the recruitment of expiratory respiratory muscles, especially the abdominals. As a consequence, the respiratory system continues to operate on the steep part of the pressure-volume curve, which is mechanically advantageous and therefore energetically more efficient. Similar changes are also seen in older subjects at lower intensity exercise, although the changes in EELV are less marked, as mechanical ventilatory responses are progressive with aging. These changes are most marked in the more elderly (85–95 years old). EELV may increase on exercise in this group, although whether this occurs at levels of exercise normally achieved by people of this age, generally leading sedentary lifestyles, is less clear.[22] The increase in respiratory frequency involves a fall in both expiratory and inspiratory times, with a proportionately larger fall during expiration. Thus, the proportion of total breath duration (T_{tot}) that is inspiratory (T_i)—or the duty cycle (T_i/T_{tot})—increases, although to a minor degree only.

Response to Exercise in COPD

COPD is characterized by a persistent airflow limitation owing to a combination of an increased peripheral airflow resistance and loss of pulmonary elastic recoil due to emphysema. Many different factors interact to reduce the maximum exercise capacity in this common condition, and these are typical of the problems posed by chronic airflow obstruction of any cause. Although there is a general relationship between the degree of spirometric impairment and the duration or intensity of exercise, there are large differences between the amount of exercise that can be performed by individuals with apparently similar degrees of airflow limitation. The reasons for this are reported in detail elsewhere (see Chapter 46, "Exercise Limitation in Disease" and Chapter 58, "Spirometirc Predictions of Exercise Limitation in Patients with Chronic Obstructive Pulmonary Disease"). Here we

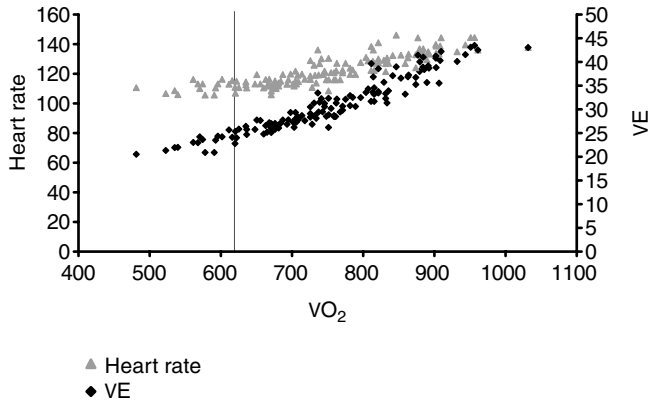

FIGURE 47-2 Heart rate and minute ventilation plotted against VO_2. Heart rate increases relatively little during exercise, and as a consequence there is a high heart rate reserve at end exercise. The increase in heart rate is linear with increases in VO_2; initially, this is the case with VE, but above lactate threshold this linearity is lost. The estimated lactate threshold is indicated by the *vertical line*.

focus on the typical exercise-related responses that can be readily identified in the laboratory.

Cardiovascular Response Subjects with COPD tend to increase their cardiac output by increasing the heart rate to a greater degree than in normal subjects, even in mild disease (Figure 47-2). In more severe disease, tachycardia may result from increasing right ventricular dysfunction, decreasing the stroke volume, or the presence of occult cardiac dysfunction. COPD patients are at greater risk of these problems due to their tobacco exposure and sedentary lifestyle secondary to their respiratory condition.

Gas Exchange The relationship between VO_2 and external work in subjects with COPD is normal when exercising below the lactate threshold.[23–25] However, patients with COPD have a reduced VO_2max and reach their lactate threshold at a lower work rate (see Figure 47-1). This may be partly owing to deconditioning but also reflects impaired oxygen metabolism at a mitochondrial level.[26–28] Typically, subjects with COPD have a degree of resting hypoxia that is exacerbated by exercise, especially in severe disease (Figure 47-3A). A minority of patients with resting hypoxemia improve ventilation perfusion mismatching on exercise, leading to an increase in arterial partial pressure of oxygen (P_aO_2).

Ventilatory Changes Subjects with COPD have an increased physiologic dead space and need a higher minute ventilation to maintain the same alveolar ventilation and P_aCO_2 (Equation 47-2). When they exceed the lactate threshold, which tends to happen soon after exercise begins, they may be unable to increase minute ventilation sufficiently to maintain alveolar ventilation in the face of an increased carbon dioxide output. The resultant rise in P_aCO_2 contributes to the increasing sensation of breathlessness. Maximal ventilatory capacity is reduced in COPD because of the altered lung and chest wall mechanics that cause the inspiratory muscles to work at a disadvantage. As a consequence, maximal VE in exercise approaches maximal ventilatory capacity much more closely than in normal subjects.[29–31] Expiratory flow limitation leads to dynamic hyperinflation as demonstrated by a reduced inspiratory capacity, which can be measured during exercise. Although not routinely performed in most laboratories at present, this useful test should become much easier to do now that simpler software algorithms have become available.

Breathing Pattern Tidal volume increase is limited in COPD patients who develop dynamic hyperinflation and ventilation increases by an increase in respiratory frequency. The resultant decrease in expiratory time (T_e) further worsens lung emptying and promotes dynamic hyperinflation. As noted elsewhere, this is a potent cause of exercise limitation.

Response to Exercise in Interstitial Lung Disease

A wide range of disorders fall under the umbrella of interstitial lung disease (ILD), and there is some variation in the behavior of the cardiorespiratory system during exercise between diseases. The major physiologic changes seen are reduced lung volumes, decreased lung compliance, and impaired gas exchange as shown by a reduced lung diffusing capacity (DL_{CO}). These features have a major impact on the lungs' ability to respond normally during exercise.

Cardiovascular Response The cardiac status is rarely normal in subjects with ILD; there is a high incidence of right ventricular hypertrophy and pulmonary hypertension due to the high pulmonary vascular resistance evident in advanced disease.[32] Thus, it is often difficult to increase cardiac output by increasing stoke volume to the same degree as in normal subjects, and cardiac output is disproportionately dependent on the increasing heart rate. In addition, hypoxemia is frequently seen on exercise in subjects with ILD, and this will have a direct inhibitory effect on the myocardial contractility.

Gas Exchange Subjects with ILD typically become hypoxemic on exercise (Figure 47-3B), particularly if DL_{CO} is reduced. The causes of the hypoxia are multifactorial; the major reasons are V/Q mismatch and shunting, but diffusion limitation, which is compounded by reduced mixed venous oxygen content, is also important. The ability of the normal lung to reduce V/Q mismatch by opening up previously underperfused lung segments is lost in ILD. In addition, the reduced red blood transit time through the lungs on exercise leads to less time for equilibration between alveolar gas and the blood to occur. Striking changes in oxygen saturation can be readily detected using even field exercise testing. Oxygen desaturation on exercise can occur, even when spirometry is relatively preserved.

Ventilatory Changes In ILD, minute ventilation is often increased at rest and rises rapidly with exercise; this is because of the relatively large physiologic dead space and the inability to increase the tidal volume on exercise owing to the low pulmonary compliance. As a result the VD/VT is increased, and a higher total ventilation is required to achieve the necessary alveolar ventilation. The altered mechanics in ILD means that

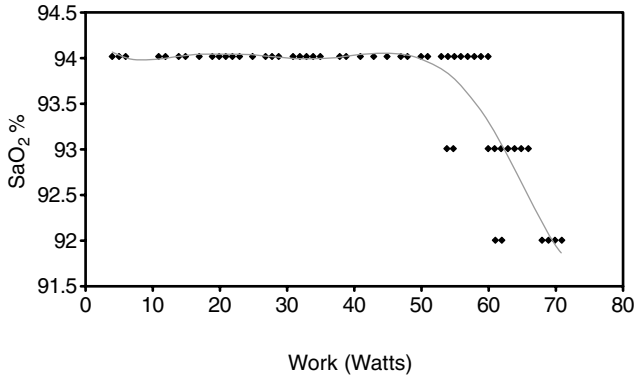

FIGURE 47-3A Oxygen saturation plotted against work rate in COPD. Initially, oxygen saturation is maintained at around 94%, but as exercise proceeds desaturation was observed in this subject.

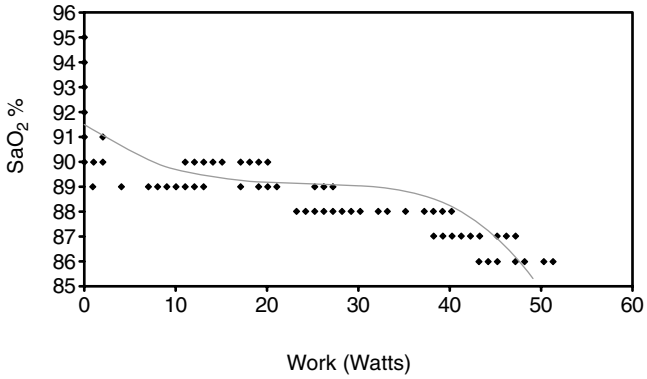

FIGURE 47-3B Oxygen saturation plotted against work rate in ILD. Oxygen desaturation was observed in this subject on exercise, which occurred even when freewheeling against no resistance.

maximal ventilatory capacity is markedly reduced and VEmax may approach this value during exercise.

Breathing Pattern The significant elastic load to breathing and resultant increase in work of breathing lead to a rapid, shallow breathing pattern that serves to minimize the peak inspiratory pressure developed. The increased respiratory frequency is achieved by decreases in both inspiratory and expiratory times.

Response to Exercise with Coexisting Cardiac Disease

Cardiac function is a major determinant of exercise capacity, and coexisting cardiac disease is common in subjects with respiratory disease. In this situation, field exercise tests are relatively insensitive, and more complex cardiorespiratory exercise testing is needed to study the cardiac component of exercise limitation. The abnormalities seen on cardiorespiratory exercise test depend on the balance between underlying respiratory and cardiac conditions causing exercise limitation. When significant coronary artery disease is present, initially there may be few abnormalities, but as workload increases cardiac ischemia may develop, which can be identified if an ECG is continuously recorded during testing. If cardiac ischemia impairs left ventricular function, VO_2 increases more slowly as a function of work rate and may plateau well before the predicted maximum value is attained; heart rate frequently increases disproportionately as stroke volume is affected by myocardial ischemia. As a result of the reduced VO_2 the lactate threshold is low. If cardiac impairment predominates, then some of the ventilatory changes that might otherwise be expected to be present may not be observed because exercise ends before these changes can occur.

Responses to Exercise in Obesity or Deconditioning Clearly, subjects with no disease exercise to different levels and achieve different VO_2max. Obese subjects have different responses to the nonobese; at a given work rate the VO_2 will be higher than in a lean subject, although the graphed slope of VO_2 against work rate will be normal. The increased VO_2 is because of the increased energy that is needed to move heavier limbs during exercise. In very obese subjects resting cardiac output is increased owing to the increased demands for oxygen supply; during exercise the increase in cardiac output is limited. Extrinsic compression of the chest wall and abdomen means that at rest there is atelectasis of peripheral lung units; this may result in resting hypoxia, which on exercise is abolished as the atelectasis improves, leading to improved gas exchange. A similar change might be anticipated in the expiratory tidal flow limitation observed in these patients, but this has yet to be tested experimentally.

In subjects who are deconditioned, the pattern of the cardiorespiratory variables described in the above settings is that of a normal subject; that is, there is no evidence of ventilatory impairment and the VEmax does not approach the maximal ventilatory capacity, and the cardiac response will be appropriate. Compared with an athlete, however, the VO_2max is lower and the lactate threshold occurs earlier in exercise.

PRACTICAL APPLICATIONS OF EXERCISE TESTING

There are many applications of cardiopulmonary exercise testing; it can assess the cardiovascular and respiratory responses to exercise and provide much more insight into the mechanisms limiting exercise than can be provided by testing at rest. Cardiopulmonary exercise testing can be useful in assessing a subject with unexplained dyspnea; in this situation symptoms often occur on exertion and resting pulmonary function testing may be unhelpful. Different disease processes demonstrate different patterns as described above; exercise testing can be useful in demonstrating deconditioning (with an otherwise normal response to exercise) and also the disordered respiratory response to exercise seen in subjects with idiopathic hyperventilation. To illustrate the responses to exercise, typical cardiorespiratory exercise tests in subjects with COPD, interstitial lung disease, and idiopathic hyperventilation are shown.

Table 47-1A Resting Data for Subject with Chronic Obstructive Pulmonary Disorder

Measurement	*Predicted*	*Measured*
Age		49 yr
Sex		Female
Weight		47.0 kg
Height		150 cm
FEV_1	2.39 L	0.90 L (37.7% predicted)
FVC	2.86 L	2.07 L (72.6% predicted)

FEV_1 = forced expiratory volume in 1 second; FVC = forced vital capacity.

Table 47-1B Exercise Data for Subject with Chronic Obstructive Pulmonary Disorder

Measurement	*Predicted*	*Measured*
Maximal VO_2 (mL/min)	1,298	887
Maximal heart rate	171	136
Heart rate reserve		35
Maximal VE (L/min)	36	41.3
Breathing reserve		−5.3
VD/VT (rest, max exercise)		0.41, 0.24

VD = dead space; VE = minute ventilation; VO_2 = oxygen uptake; VT = tidal volume.

Chronic Obstructive Pulmonary Disease

Table 47-1A shows resting data and 47-1B a summary of the exercise data for a subject with COPD. Resting lung function measurements show evidence of severe airway obstruction; and on exercise there is a reduced maximal VO_2. There is evidence of ventilatory limitation as shown by a maximal VE that exceeds the prediction of maximal ventilation, which is estimated as forced expiratory volume in 1 second (FEV_1) multiplied by 40. This compares with the normal subject whose maximal minute ventilation (VEmax) is usually around 50 to 80% of maximal ventilatory capacity (MVV). As a consequence of the ventilatory limitation, the breathing reserve is low (in this case zero). The heart rate at maximal exercise is lower than predicted, leading to a high heart rate reserve. The ratio of physiologic dead space to tidal volume (VD/VT) is increased compared with normal subjects, although it falls during exercise as VT increases, but this is not always the case. The VD/VT ratio is calculated noninvasively in this situation. This method has important flaws as it involves an estimation of arterial partial pressure of carbon dioxide (P_aCO_2) by using measured end-tidal CO_2 rather than determining it accurately by using arterial blood sampling; particularly in the presence of lung disease, these measurements are not accurate.[33]

Interstitial Lung Disease

Table 47-2A shows resting data and Table 47-2B a summary of exercise data. Baseline spirometry reveals a restrictive defect, and on exercise there is marked oxygen desaturation. The maximal oxygen uptake (VO_2) attained during exercise is lower than that predicted. Minute ventilation is increased predominantly by an increase in respiratory rate, increasing to 63 breaths a minute with relatively little change in tidal volume (see Table 47-2B) as a consequence of the reduction in lung volumes. At maximum workload, ventilation exceeds the predicted level, leaving no breathing reserve.

Table 47-2A Resting Data for Subject with Interstitial Lung Disease

Measurement	*Predicted*	*Measured*
Age		72 yr
Sex		Female
Weight		59.0 kg
Height		158 cm
FEV_1	2.04 L	0.93 L (45.5% predicted)
FVC	2.58 L	1.13 L (43.6% predicted)
RR	–	20
VT	–	0.50 L

FEV_1 = forced expiratory volume in 1 second; FVC = forced vital capacity.

Table 47-2B Exercise Data for Subject with Interstitial Lung Disease

Measurement	*Predicted*	*Measured*
Maximal VO_2 (mL/min)	1,268	887
Maximal heart rate	148	122
Heart rate reserve		26
Maximal VE (L/min)	37.2	40.8
Breathing reserve		0
VD/VT (rest, max exercise)		0.33, 0.33
Max RR	–	63
Max VT	–	0.64 L

RR = respiratory rate; VD = dead space; VE = minute ventilation; VO_2 = oxygen uptake; VT = tidal volume;

With little change in tidal volume, there is as a consequence little change in the ratio of physiologic dead space to tidal volume (VD/VT).

Idiopathic Hyperventilation

Table 47-3A shows resting data, demonstrating spirometric results within the normal range. The summary of important

Table 47-3A Resting Data for Subject with Idiopathic Hyperventilation

Measurement	*Predicted*	*Measured*
Age		26 yr
Sex		Male
Weight		66.7 kg
Height		173 cm
FEV_1	4.21 L	3.67 L (87% predicted)
FVC	5.02 L	4.27 L (85% predicted)

FEV_1 = forced expiratory volume in 1 second; FVC = forced vital capacity.

Table 47-3B Exercise Data in Subject with Idiopathic Hyperventilation

Measurement	*Predicted*	*Measured*
Maximal VO_2 (mL/min)	2737	1983
Maximal heart rate	194	168
Heart rate reserve		26
Maximal VE (L/min)	146.8	93.1
Breathing reserve		53.7
VD/VT (rest, max exercise)		0.29, 0.13
Mean S_aO_2 exercise		99%
Mean end tidal CO_2 exercise (mm Hg)		20

S_aO_2 = saturation of oxygen; VD = dead space; VE = minute ventilation; VO_2 = oxygen uptake; VT = tidal volume.

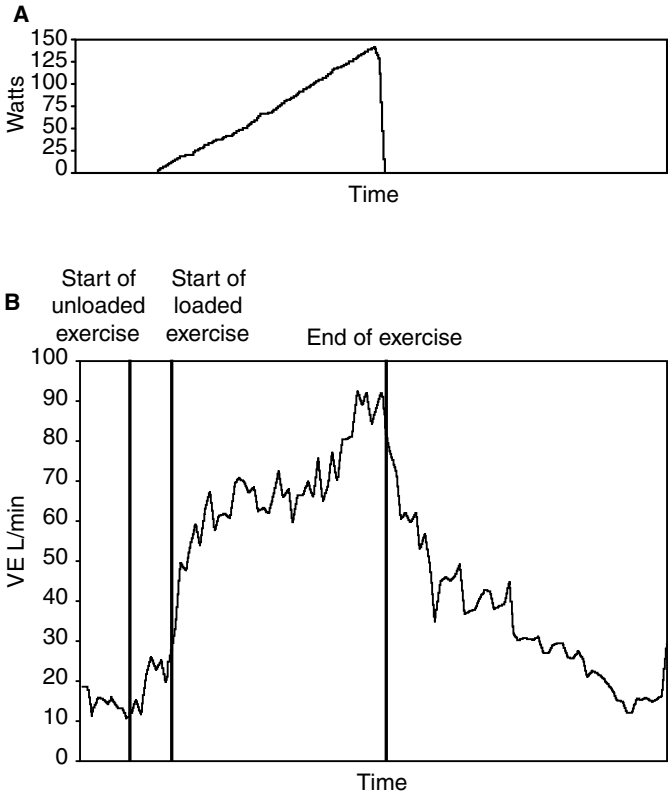

FIGURE 47-4 Exercise test for a subject with idiopathic hyperventilation with work rate *A* and minute ventilation *B*.

exercise data (Table 47-3B) shows a good oxygen uptake (VO_2) response, achieving 72.5% of predicted maximal VO_2 with a breathing reserve suggesting no ventilatory limitation, and a low end-tidal CO_2 with no evidence of oxygen desaturation, which may stimulate a degree of hyperventilation. The pattern of ventilation throughout the exercise test is shown, with work load (Figure 47-4A). The pattern of breathing is disorganized, with an immediate increase in ventilation as soon as loaded work commences. Toward the end of exercise the pattern is more normal, but no respiratory compensation as demonstrated by an accelerated increase in minute ventilation (VE) at anaerobic threshold is seen (Figure 47-4B). During the recovery stage of the exercise test, VE reduces but does so in an erratic fashion.

REFERENCES

1. Wasserman K, Hansen JE, Sue DY, et al. In: Principles of exercise testing and interpretation. 2nd ed. Baltimore: Lea & Febiger; 1994. p 102–3.
2. Porszasz J, Barstow T, Wasserman K. Evaluation of symmetrical disposed pitot tube flowmeter for measuring gas flow during exercise. J Appl Physiol 1994;77:2659–65.
3. ERS Task Force. Clinical exercise testing with reference to lung diseases: indications, standardization and interpretation strategies. Eur Repir J 1997;10:2662–89.
4. American Thoracic Society. ATS/ACCP Statement on cardiopulmonary exercise testing. Am J Respir Crit Care Med 2003; 167:211–77.
5. Butland RJ, Pang J, Gross ER, et al. Two-, six-, and twelve minute walk tests in respiratory disease. BMJ 1982;284:1607–8.
6. Gerardi DA, Lovett L, Benoit-Connors ML, et al. Variables related to increased mortality following outpatient pulmonary rehabilitation. Eur Respir J 1996;110:325–32.
7. Cahalin LP, Mathier MA, Semigran MJ, et al. The six minute walk test predicts peak oxygen uptake and survival in patients with advanced heart failure. Chest 1996;110:325–32.
8. Troosters T, Villaro J, Rabinovich R, et al. Physiological responses to the 6-min walk test in patients with chronic obstructive lung disease. Eur Respir J 2002;20:564–9.
9. Knox AJ, Morrison JF, Muers MF. Reproducibility of walking test results in chronic obstructive airways disease. Thorax 1988; 43:388–92.
10. Sciurba F, Criner GJ, Lee SM, et al. Six-minute walk distance in chronic obstructive pulmonary disease. Reproducibility and effect of walking course layout and length. Am J Respir Crit Care Med 2003;167:1522–7.
11. Redelmeier DA, Bagoumi AM, Goldstein RS, Guyatt GH. Interpreting small differences in functional status: the six minute walk test in chronic lung disease. Am J Respir Crit Care Med 1997;155:1278–82.
12. American Thoracic Society. ATS statement: guidelines for the six-minute walk test. Am J Respir Crit Care Med 2002;166: 111–7.
13. Singh SJ, Morgan MDL, Scott S, et al. Development of a shuttle walk test of disability in patients with chronic airways obstruction. Thorax 1992;47:1019–24.
14. Singh SJ, Morgan MDL, Hardman AE, et al. Comparison of oxygen uptake during a conventional treadmill test and the shuttle walk test in chronic airflow limitation. Eur Respir J 1994;7:2016–20.
15. Revill SM, Morgan MDL, Singh SJ, et al. The endurance shuttle walk: a new field test for the assessment of endurance capacity in chronic obstructive pulmonary disease. Thorax 1999;54:213–22.
16. Swinburn CR, Wakefield JM, Jones PW. Performance, ventilation, and oxygen consumption in three different types of exercise test in patients with chronic obstructive lung disease. Thorax 1985;40:581–6.
17. Rowell LB. Human circulation regulation during physical stress. New York: Oxford University Press; 1986. p. 215.
18. Loeppky JA, Greene ER, Hoekanga DE, et al. Beat by beat stroke volume assessment by pulsed Doppler in upright and supine exercise. J Appl Physiol 1981;50:1173–82.
19. Wasserman K, Whipp BJ. Exercise physiology in health and disease. Am Rev Respir Dis 1975;112:219–49.
20. Hansen JE, Sue DY, Wasserman K. Predicted values for clinical exercise testing. Am Rev Respir Dis 1984;129 Suppl: S49–55.
21. Campbell SC. A comparison of the maximum voluntary ventilation with forced expiratory volume in one second: an assessment of subject cooperation. J Occup Med 1982;24: 531–3.
22. Delorey DSBL, Birkley PS, Palumbo BD, et al. Progressive mechanical ventilatory limitations with aging. Med Sci Sports Exerc 1998;30:S41.
23. Levison H, Cherniack RM. Ventilatory costs of exercise in chronic obstructive pulmonary disease. J Appl Physiol 1968; 25:21–7.
24. Nery LE, Wasserman K, Andrews JD, et al. Ventilatory and gas exchange kinetics during exercise in chronic airways obstruction. J Appl Physiol 1982;53:1594–602.
25. Shuey CB, Pierce AK, Johnson RL. An evaluation of exercise tests in chronic obstructive lung disease. J Appl Physiol 1969;27:256–61.

26. Maltais F, Jobin J, Sullivan MJ, et al. Metabolic and hemodynamic responses of lower limb during exercise in normal subjects and in COPD. J Appl Physiol 1998;84:1573–80.
27. Maltais F, Simard AA, Simard C, et al. Oxidative capacity of the skeletal muscle and lactic acid kinetics during exercise in normal subjects and in patients with COPD. Am J Respir Crit Care 1996;153:288–93.
28. Maltais F, Leblanc P, Simard C, et al. Skeletal muscle adaptation to endurance training in patients with chronic obstructive pulmonary disease. Am J Respir Crit Care 1996;154: 442–7.
29. Clark TJ, Freedman S, Campbell EJ, Winn RR. The ventilatory capacity of patients with chronic airways obstruction. Clin Sci 1969;36:307–16.
30. Mahler DA, Harver A. Prediction of peak oxygen consumption in obstructive airways disease. Med Sci Sports Exerc 1988; 20:574–8.
31. Matthews JL, Bush BA, Ewald FW. Exercise responses during incremental and high intensity and low intensity steady state exercise in patients with obstructive lung disease and normal control subjects. Chest 1987;92:696–703.
32. Packe GE, Cayton RM, Edwards CW. Comparison of right ventricular size at necroscopy in interstitial pulmonary fibrosis and in chronic bronchitis and emphysema. Thorax 1980;40:712.
33. Lewis D, Sietsama KE, Casaburi R, Sue DY. Inaccuracy of noninvasive estimates of VD/VT in clinical exercise testing. Am Rev Respir Dis 1993;147:A185.

CHAPTER 48

REGULATION OF SKELETAL MUSCLE BLOOD FLOW DURING EXERCISE

Sabah N. A. Hussain, Alain S. Comtois

Since blood flow is essential for the delivery of nutrients, maintenance of fluid balance, and the removal of metabolites, the delivery of adequate blood flow to skeletal muscle is an essential requirement for maintaining physical exercise. The pattern and time course of changes in skeletal muscle blood flow in response to physical exercise are determined to a large extent by the intensity and the type of exercise being performed. In this respect, two categories of exercise should be considered, namely, isometric exercise, in which the contracting muscle generates high tension and little shortening, and dynamic exercise, in which the contracting muscle shortens significantly but generates little tension. In both types, skeletal muscle blood flow rises substantially in response to increased muscle metabolic demands. For example, whereas most skeletal muscles receive between 5 and 10 mL of blood for each 100 g of tissue per minute at rest, limb muscle blood flow can reach 500 mL/100 g/min during high-intensity dynamic exercise.

Important differences exist between species and among various muscles in a given species with respect to the degree of blood flow augmentation in response to exercise. For example, relatively higher levels of skeletal muscle blood flow have been observed in response to exercise in quadrupeds than in humans. Within a species, blood flow to muscles rich in oxidative fibers (red muscles) tends to be significantly greater during exercise than blood flow to muscles rich in glycolytic fibers (white muscles) (Figure 48-1).[1,2]

It should also be pointed out that dynamic whole body exercise, which is associated with substantial increases in minute ventilation, also elicits significant elevations in the ventilatory muscles, particularly the diaphragm and intercostal muscles. For instance, diaphragm blood flow reaches 265 mL/100 g/min during maximum dynamic exercise in ponies, which is comparable to that of the gluteus medius and biceps femoris in the same animals.[3]

Providing sufficient blood flow to skeletal muscles during high-intensity exercise is considered to be the greatest stress on the cardiovascular system. The delivery of high blood flow to active skeletal muscles during dynamic exercise requires complex and coordinated cardiovascular adaptive responses, including a rise in cardiac output (reaching approximately four- to fivefold of resting values); redistribution of blood flow away from nonmuscle tissues such as kidney, viscera, and skin; and maintenance of elevated blood flow to cardiac muscles. Combined heart and skeletal muscle blood flow may account for about 85 to 90% of cardiac output during high-intensity exercise compared with only 15 to 20% of cardiac output at rest. Throughout this chapter, augmentation of skeletal muscle blood flow in response to isometric or dynamic exercise designated as active or functional hyperemia.

ISOMETRIC EXERCISE

The influence of muscle contractile force on skeletal muscle active hyperemia was first described more than 130 years ago. The earliest studies revealed that both mechanical compression during muscle contraction and the local release of chemical substances influence the venous outflow of contracting limb muscles. In 1933, Anrep and colleagues[4,5] described a significant decline in skeletal muscle blood flow during the contraction phase of intermittent contractions. They concluded that this was due to compression of vessels undergoing muscle contraction. It has now been well established, using isolated muscle preparations, that during exercise, skeletal muscle undergoes rhythmic changes in length and tension, giving rise to mechanical perturbations within the tissue that intermittently affect muscle blood flow.

Four distinct phases of blood flow alteration can be observed in response to intermittent isometric contractions of skeletal muscles. The initial phase is manifested as backthrust, observed immediately after the initiation of muscle contraction. The second phase is characterized by reduction in blood flow during muscle contraction as muscle force rises. Immediately upon muscle relaxation, there is a blood flow overshoot. This constitutes the third phase. It is followed by sustained hyperemia throughout the fourth phase,

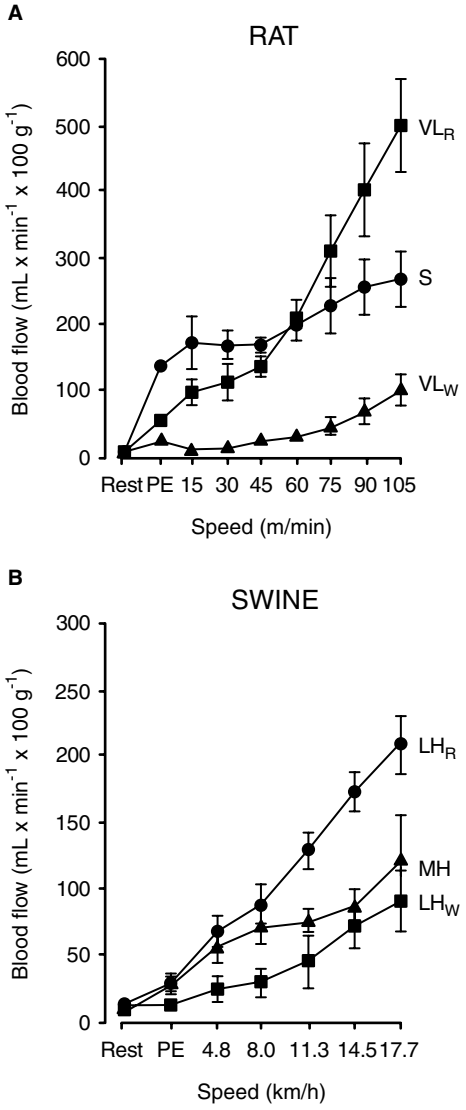

FIGURE 48-1 Relationship between blood flow and exercise intensity in skeletal muscles of different fiber-type composition in rats and miniature swine. LH_R = lateral head of the triceps brachii (deep red); LH_W = lateral head of the triceps brachii (superficial white); MH = medial head of the triceps brachii; PE = preexercise (rats standing on treadmill); S = soleus; VL_R = vastus lateralis red; VL_W = vastus lateralis white. Reproduced with permission from Laughlin MH et al.[2]

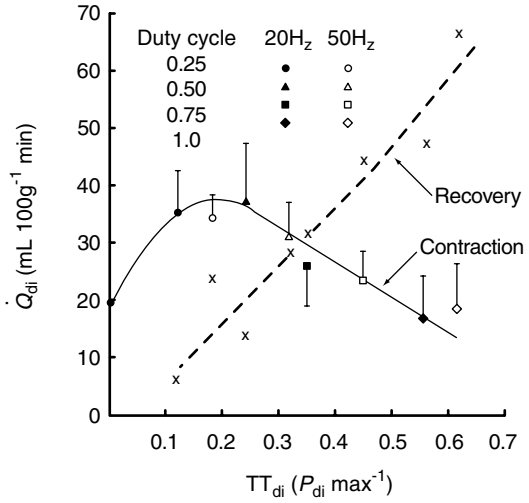

FIGURE 48-2 Relationship between final diaphragm blood flow ($\dot{Q}_{di}$) during a contraction period (*solid line*), debt measured during recovery (*dashed line*), and diaphragmatic tension–time index (TT_{di}) in 4 animals during periodic contractions with duty cycles of 0.25, 0.5, 0.75, and 1.0. Results obtained at 20 and 50 Hz are shown. Bars indicate ±SE for the contraction: during recovery, SE is 5.85 at 20 Hz and 17.4 at 50 Hz. P_{di} = transdiaphragmatic pressure. Best-fitted lines are drawn by eye. Reproduced with permission from Bellemare F et al.[6]

the relaxation period. It is noteworthy that these four phases are observed mainly when the muscle is generating relatively high levels of force. Indeed, arterial blood flow declines during the contraction phase when muscle force reaches about 40 to 50% of maximum. By comparison, compression of blood vessels during the contraction phase of sustained or intermittent contraction may not be evident when muscle force is relatively low (15 to 30% of maximum voluntary force).

DETERMINANTS OF MUSCLE BLOOD FLOW

Vascular Geometry and Muscle Anatomy

The relationship between contractile force and muscle blood flow is highly influenced by vascular geometry and the shape of the muscle. For instance, fusiform-shaped muscles such as the soleus are able to withstand greater degrees of muscle force with little hindrance of arterial blood flow during muscle contraction in comparison with pennate and cylindrical muscles.

Intensity and Duration of Contraction

Bellemare and colleagues[6] provided the best description of the influence of the intensity and the duration of isometric contractions on skeletal muscle blood flow by studying diaphragmatic isometric contractions elicited by artificial phrenic nerve stimulation in dogs. These authors introduced the concept of the diaphragmatic tension–time index (TT_{di}), which is the product of normalized force (transdiaphragmatic pressure, P_{di}) and the duty cycle (ratio of contraction time to total duration of contraction–relaxation cycle). They described a parabolic relationship between TT_{di} and diaphragmatic blood flow, with the latter increasing as TT_{di} rises, until a TT_{di} of 0.2 is reached (Figure 48-2). With further increases in TT_{di}, diaphragmatic blood flow begins to decline and postcontraction hyperemia begins to increase, indicating significant impedance of blood flow during the contraction phase at TT_{di} values equal to and higher than 0.2.

The equation of Bellemare and colleagues also predicts that during sustained isometric contractions, blood flow to the diaphragm is impeded at a force equivalent to and higher than 20% of maximum values, a prediction that holds true mainly during artificial diaphragm stimulation. A major weakness of this research is that only a limited number of duty cycles (0.25, 0.5, 0.75, and 1) and levels of muscle force were studied. Subsequent investigations, in which several combinations of duty cycles and muscle force were generated, have revealed a more complex relationship

between muscle blood flow and TT_{di}, particularly when the latter has a value greater than 0.2.[7]

Contraction Frequency

Another factor that influences the degree of exercise hyperemia during repeated contractions is the contraction frequency (number of intermittent trains of contractions per minute). In dogs in which the diaphragm was maximally stimulated at duty cycles of 0.25 and 0.75, increasing the contraction frequency elicited a significant rise in diaphragm blood flow until a frequency of 80 contractions/min was reached, when blood flow to the diaphragm declined with increasing frequency, particularly at a duty of cycle of 0.75.[8] Although the exact mechanism behind this effect has not been identified, it has been suggested that increasing frequency of stimulation augments muscle metabolic demand by elevating the heat of activation.[8]

Intramuscular Pressure

Most investigators agree that the direct influence of muscle contractile force on blood flow is mediated through changes in intramuscular pressure (IMP), the sum of solid and fluid pressures within the muscle.[9,10] Measurements of IMP with miniature transducers, balloon catheter, or fluid catheter systems have revealed substantial augmentation of IMP during isometric, concentric, and eccentric contractions of skeletal muscles in various species. For example, mean IMP has been shown to reach 269 mm Hg and 151 mm Hg, respectively, in the soleus and tibialis anterior muscles of normal humans during treadmill running.[11] Much lower IMP values have been described in flat muscles such as the diaphragm.[12,13] However, it should be emphasized that IMP values are not uniform along the length and depth of a given muscle. Regional variations in IMP have been proposed as the main factor responsible for inhomogeneous blood flow within various regions of active skeletal muscles.[14]

Another important point regarding IMP is that although it is linearly related to the force of contraction during isometric contractions, the speed of contraction rather than muscle force appears to determine the IMP generated during isotonic contractions.[15] Moreover, despite the linear relationship between IMP values and blood flow impedance during isometric contractions, the slope of this relationship is unique to each muscle, as is the value of IMP at which cessation of blood flow during the contraction phase occurs. For instance, Hussain and Magder observed a significant reduction in diaphragm blood flow during intermittent phrenic nerve stimulation in dogs when intradiaphragmatic IMP reached a mean value of only 50 mm Hg.[16]

External Forces

In addition to IMP generated within the muscle itself, external forces applied to muscle surfaces also influence basal muscle blood flow and the degree of active hyperemia. This is particularly applicable to the diaphragm, which is exposed to pleural and abdominal pressure swings. Buchler and colleagues[17] measured diaphragm blood flow in response to sustained diaphragmatic contractions generated under two conditions. When the abdomen was bound and the chest was opened (highly positive abdominal pressure), significantly lower diaphragm active hyperemia was provoked than when the abdomen was opened and the chest was closed (highly negative pleural pressure). These results suggest that positive abdominal pressure may be transmitted to the diaphragmatic vasculature, resulting in impedance of arterial flow, whereas strong negative pleural pressure may actually facilitate diaphragm blood flow. This facilitatory effect of pleural pressure is reversed when the pressure in the pleural space becomes positive, as during positive end-expiratory pressure (PEEP). Indeed, Kawagoe and colleagues[18] compared diaphragm blood flow measured during hyperinflation generated by intrinsic PEEP with that elicited by inspiratory resistive loading. At a given level of muscle metabolism, intrinsic PEEP generated significantly lower blood flow than resistive loading, suggesting that positive pleural pressure impedes diaphragm blood flow.

MECHANISMS OF CONTRACTILE FORCE AND BLOOD FLOW REGULATION

Two mechanisms have been proposed to explain the influence of the contractile force on muscle blood flow during isometric contractions or during dynamic shortening. The first proposed mechanism is that flow is limited during strong contractions as a result of passive reductions in vessel diameter (due to compression and axial stretch) and kinking and pinching of vessels (due to shear forces generated between muscle fibers and fiber bundles).[19] This mechanism has been implicated in the reduction of blood flow when muscle length is changed acutely beyond its optimal length (L_O) (the length at which active isometric tension is maximum). Indeed, in isolated dog diaphragmatic strips in situ, blood flow at rest and during near-maximum rhythmic contractions fell by 59% and 36%, respectively, when muscle fiber length was extended from 92 to 107% of L_O.[20] Intravital visualization of skeletal muscle capillaries has confirmed that capillary diameter actually declines and red cell velocities are significantly reduced when muscle fiber is stretched beyond L_O.[21]

The second proposed mechanism is based on evidence that changes in muscle length alter the output of the sympathetic nervous system to the skeletal muscle vasculature, resulting eventually in changes to the diameter of arterioles and feed arteries. Vasoconstriction of these vessels due to sympathetic nerve activation accounts for approximately two-thirds of the reduction in muscle blood flow when muscle length approaches 130% of L_O.[22]

DYNAMIC EXERCISE

Although the use of isolated muscle preparations has contributed significantly to our understanding of the mechanisms regulating muscle blood flow in isometric conditions, the extent to which findings obtained with these preparations relate to the in vivo condition in humans is not always obvious. A clear example in this respect is peak muscle blood flow, which may reach 50 to 60 mL/100 g/min in isolated muscle preparations but reaches more than fivefold

higher values when measured in humans or animals performing dynamic exercise. The majority of data on the response of skeletal muscle blood flow to dynamic exercise are obtained by the use of ultrasound Doppler flow probes placed around the major arteries that supply skeletal muscles. These probes measure blood flow velocity, which can then be translated into blood flow at a constant arterial diameter.

The time course and magnitude of skeletal muscle functional hyperemia during dynamic exercise are influenced by many factors, such as the type of exercise being performed, the intensity and the timing of muscle contraction, and the type of muscle being activated. The general view is that dynamic exercise performed at mild-to-moderate workloads in humans and animals elicits a biphasic active hyperemic response (Figure 48-3). The first part of the response (phase 1) is marked by an initial rise in blood flow that develops immediately (1 to 2 seconds) after initiation of muscle contraction and then reaches a plateau within 5 to 7 seconds. This is followed by a second response (phase 2) that is evident within 15 to 20 seconds of initiation of muscle contraction and is characterized by a slow increase to a new steady-state level (see Figure 48-3).[23] Some authors have described a variation of phase 1, manifested as an initial overshoot of blood flow in the hind limb muscles of rats and dogs.[24,25] The fact that the initial rise in blood flow is more rapid than muscle oxygen utilization suggests that phase 1 of active hyperemia is not dependent on muscle metabolism. In comparison, numerous studies have shown linear relationships between the magnitude of phase 2 and muscle work and oxygen utilization during dynamic exercise, indicating that muscle metabolism is a major determinant of this phase of the active hyperemic response.

In addition to the classic biphasic hyperemic response described above, a few studies have shown a triphasic hyperemic response during dynamic exercise at workloads exceeding 75% of maximum. Under these conditions, a still a very rapid phase 1 can be detected but is followed by a slower second phase, which peaks after 50 to 60 seconds of exercise initiation. The third, and slowest, phase reaches a plateau 150 seconds after initiation of exercise.[26] Furthermore, others have explored active hyperemic responses elicited by dynamic exercise in terms of the time needed for the blood flow to reach 50% of the final plateau level, which has been estimated to be between 2.2 and 8.9 seconds in limb muscles.[26]

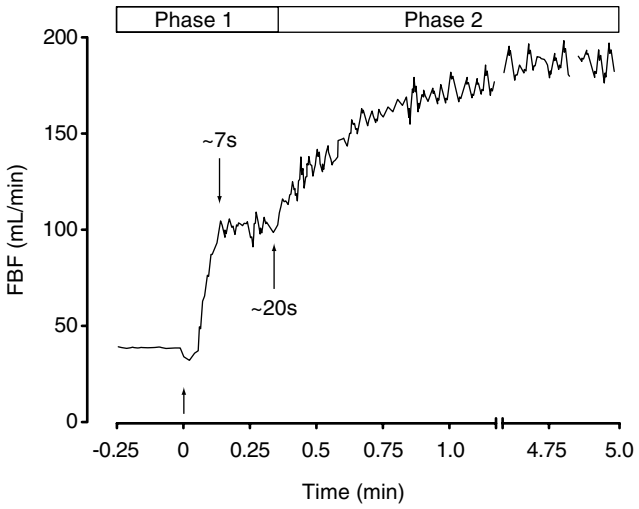

FIGURE 48-3 Limb blood flow in healthy humans increases rapidly at the onset of dynamic exercise in a biphasic manner. An initial plateau following 5 to 7 seconds of exercise (phase 1) gives way after ~20 seconds (phase 2) to a slow increase toward a new steady-state level. FBF = forearm blood flow. Reproduced with permission from Shoemaker JK and Hughson RL.[23]

DETERMINANTS OF MUSCLE BLOOD FLOW

Perfusion Pressure and Metabolic Activity of the Muscle

Blood flow to any organ is determined by the ratio of perfusion pressure to vascular resistance. The importance of perfusion pressure as a regulator of skeletal muscle blood flow is not clearly obvious when muscle metabolic demands are low, such as during rest and when perfusion pressure changes within a relatively narrow range. This is simply because, as with other organs, skeletal muscle vasculature exhibits the phenomenon of autoregulation, which is defined as the intrinsic tendency of an organ to maintain constant blood flow despite changes in perfusion pressure. In resting limb muscles, studies have revealed that blood flow is maintained independent of mean arterial pressure when the latter increases or decreases between 40 and 120 mm Hg.[27] However, the range of mean arterial pressure over which muscle blood flow is autoregulated is much narrower in the diaphragm. Hussain and colleagues reported that diaphragm blood flow in spontaneously breathing dogs is autoregulated between mean arterial pressure values of 90 and 120 mm Hg.[28] This difference between limb muscle and the diaphragm is attributed, in part, to the fact that the diaphragm is not at rest in spontaneously breathing dogs. Indeed, many studies have shown that the range of mean arterial pressure over which effective autoregulation of skeletal muscle blood flow occurs is highly dependent on the metabolic status of the muscle.[27]

There are two different interpretations of the relationship between muscle metabolic activity and the effectiveness of blood flow autoregulation. In an absolute sense, changes in muscle blood flow for given alterations in mean arterial pressure are greater in contracting muscles than in resting ones, implying poor blood flow autoregulation in active versus resting muscles. In comparison, when viewed in a relative sense, the percent change in blood flow for a given alteration in mean arterial pressure diminishes as metabolic demands increase, indicating that autoregulation actually improves when muscle is recruited. Despite these contradictory interpretations of how changes in arterial pressure influence muscle blood flow, there is little disagreement as to the importance of arterial pressure in determining muscle blood flow when the muscle is maximally activated. Accumulated evidence from several muscles indicates that at maximum metabolic activity, muscle blood flow becomes a function of mean arterial pressure. A clear example of this is seen in dogs undergoing maximal phrenic nerve stimulation.

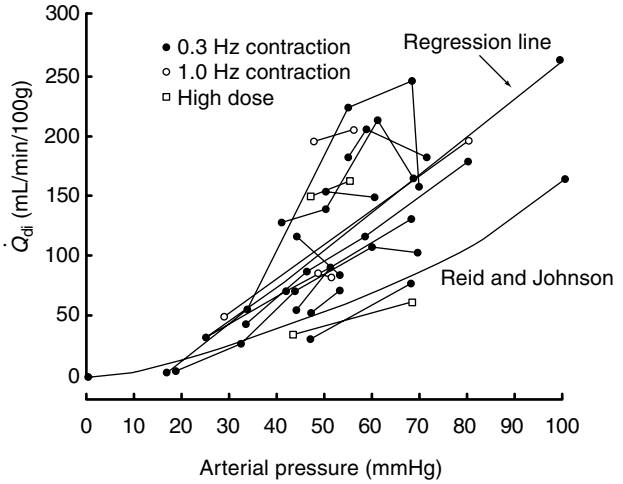

FIGURE 48-4 Pressure (arterial pressure)–flow ($\dot{Q}_{di}$) relation of diaphragm with stimulated contraction and maximal vasodilatation induced by nitroprusside. Lines connect points for the same animal. There was a linear relation between flow and pressure ($r = .71$). Also included are points obtained with a higher frequency of stimulation (1 Hz) and increased dose of nitroprusside. "Reid and Johnson" refers to equation from Reid and Johnson.[30] Reproduced with permission from Magder S.[29]

In these animals, diaphragm blood flow is linearly related to mean arterial pressure (Figure 48-4).[29] This linear function contrasts with a parabolic relationship between mean arterial pressure and diaphragmatic blood flow in dogs exposed to hypoxia and inspiratory resistive loading, suggesting that diaphragm metabolic demands might not have reached maximum values in these animals and that factors other than mean arterial pressure are still able to influence diaphragm vascular resistance.[30]

In addition to metabolic status, the degree to which arterial pressure regulates skeletal muscle blood flow is strongly influenced by the pattern and intensity of contractions. This is simply because, at a given muscle vascular resistance, arterial blood flow to the muscle during the contraction phase will be determined by perfusion pressure and the contractile force, so that at low perfusion pressure values, blood flow will become limited at much lower levels of contractile forces than at high perfusion pressure values. This interplay between perfusion pressure and contractile force in determining skeletal muscle flow is clearly evident during diaphragm contractions in dogs. At a duty cycle of 0.5 and a mean arterial pressure of 116 mm Hg, diaphragm blood flow becomes limited when muscle force exceeds 30% of maximum. In comparison, when mean arterial pressure is reduced to 75 mm Hg, blood flow limitation is evident when muscle force reaches only 10% of maximum.[7] These findings clearly underscore the importance of maintaining normal arterial pressure to achieve optimal skeletal muscle perfusion during exercise.

Sympathetic Adrenergic Activation

One of the most important adaptive responses in the cardiovascular system to dynamic exercise is an increase in mean arterial pressure.[31] This pressor response is mediated by an increased sympathetic adrenergic neural drive to resistance arterioles of peripheral vascular beds, including those of splanchnic, renal, and nonactive skeletal muscles. Despite the fact that enhanced sympathetic adrenergic neural discharge also targets resistance vessels of exercising skeletal muscles, local metabolic and flow-dependent vasodilatory mechanisms are triggered by muscle activation. These are able to selectively attenuate the influence of elevated sympathetic adrenergic activity on vascular conductance in the exercising muscle, a concept known as functional sympatholysis.[2]

The exact mechanism behind activation of the sympathetic nervous system during exercise remains under investigation. Four pathways have been proposed thus far.

First, it is suggested that increased neural discharge from the posterior hypothalamic area, in response to increased effort, activates the sympathetic nervous system in a feedforward control manner.[32]

Second, many authors have proposed that activation of the sympathetic nervous system during exercise is mediated by alterations in arterial and cardiopulmonary baroreflexes.[33] There have been many reports that dynamic exercise is associated with resetting of the arterial baroreflex in such a way that it operates at higher pressure values than those at rest. The degree of this resetting is directly related to the intensity of exercise and is not associated with alterations in the gain of the reflex, thereby allowing the reflex to respond to changes in arterial pressure during exercise as effectively as it does at rest.

Third, it has been suggested that the activation of peripheral reflexes, triggered by afferent nerve endings in the skeletal muscles that are sensitive to mechanical activation (type III and IV afferents), is also involved in activating the sympathetic nervous discharge to the peripheral circulation during exercise. Activation of these reflexes could result from active increases in IMP inside skeletal muscles during muscle contraction or from external compression of muscle tissues.[34]

Fourth, the rise in arterial pressure during exercise has been attributed to the activation of a muscle metaboreflex, which is triggered by a mismatch between blood flow and metabolism in the exercising muscle. This mismatch causes changes in the concentrations of metabolites that are detected by metabolite-sensitive nerve endings within the skeletal muscle interstitium. Many agents, including lactic acid, arachidonic acid, H^+, K^+, phosphate, and adenosine, have been suggested as stimulants that increase the discharge of group IV (metaboreceptor) afferent fibers, eventually resulting in the potent reflex that increases sympathetic nerve activity.[35] The importance of this metaboreflex in relation to blood flow regulation lies in the fact that it is initiated in response to a mismatch between blood flow and metabolic activity. Thus, the reflex provides an important feedback mechanism by which insufficient blood flow to active skeletal muscle during exercise triggers sympathetic nerve activation. Sympathetic activation, in turn, elevates mean arterial pressure and, consequently, increases blood flow to the muscle and correction of the mismatch between muscle blood flow and metabolic activity.[31] The degree to

which this metaboreflex operates to regulate skeletal muscle blood flow has been evaluated in exercising dogs[36] and humans[37] in which active skeletal muscles were rendered ischemic as a means of augmenting the rise in arterial pressure. These studies revealed that elevations in mean arterial pressure, triggered by muscle ischemia, are able to restore about 50% of blood flow error.

MECHANISMS OF ACTIVE HYPEREMIA

Skeletal muscle vascular resistance, and hence its blood flow, is determined to a large extent by the caliber of resistance arteries, which is, in turn, a function of vascular smooth muscle contractility (often referred to as vasomotor or vascular tone). Vascular resistance of skeletal muscles both at rest and during exercise is regulated by two main control mechanisms: central cardiovascular and local vascular. The relative importance of these mechanisms varies with the intensity and the duration of skeletal muscle activation during exercise.

In resting skeletal muscles, vascular tone is set by two main factors: the inherent contractility of vascular smooth muscles (local control mechanism) and the activity of the sympathetic adrenergic nervous system (central control mechanism). The latter regulates smooth muscle contractility of resistance vessels through the release of norepinephrine from postganglionic neurons. The importance of the sympathetic adrenergic neural drive in regulating the blood flow of resting skeletal muscle is clear when it is observed that blood flow is doubled when sympathetic adrenergic nerves are physically interrupted or pharmacologically blocked.[38] When skeletal muscle is activated during exercise, the relatively high vascular tone in resting muscle allows local control mechanisms to regulate capillary perfusion in a precise and measured fashion to meet increasing metabolic demands. Thus, skeletal muscle blood flow during exercise is regulated primarily by local vascular control mechanisms, particularly at the onset of exercise. Central cardiovascular control mechanisms are superimposed on the dominant local factors when exercise duration is relatively long.

Central Control Mechanisms

Central cardiovascular control mechanisms, which consist of neural and hormonal pathways, exert their influence on skeletal muscle blood flow during exercise directly by acting on muscle vasculature and indirectly through changes in cardiac activity and vascular tone of other organs. Central control mechanisms help divert blood away from nonexercising organs such as intestine and kidney toward the vasculature of exercising skeletal muscles.

Neural pathways (the sympathetic nervous system) represent the main mechanisms through which central control mechanisms influence muscle blood flow during exercise. The rapid onset of exercise hyperemia and the poor relationship between exercise intensity and the magnitude of phase 1 of active hyperemia during dynamic exercise have led several investigators to propose neural mechanisms as major regulators of muscle vascular resistance during the transition from rest to exercise. This proposal is supported by the observations that procaine and cocaine (local anesthetics) are capable of attenuating exercise hyperemia and by the fact that muscle blood flow can increase in anticipation of exercise.[39]

One form of neural mechanism, which was initially proposed by Hilton,[40] is an intrinsic dilatory neural network located in muscle resistance vessels, which, when activated through a direct link with α motor neurons or muscle afferents, leads to vasodilatation and increased blood flow. Honig[41] used a bioassay preparation in dogs in which the venous effluent of a donor contracting muscle was infused into the arterial supply of a resting recipient skeletal muscle. He noticed that, whereas the blood flow of the donor muscle rose significantly in response to nerve stimulation, the vasculature of the recipient muscle failed to respond to the effluent of the contracting muscle, suggesting that exercise hyperemia in the donor muscle is generated by the involvement of local vasodilatory nerve networks. However, the existence of such networks in skeletal muscle vasculature has not been confirmed. Moreover, Honig's bioassay experiments do not rule out the contribution to exercise hyperemia of the donor muscle of locally acting metabolites or mechanical factors, such as a muscle pump.

Another neural pathway that has been proposed to regulate exercise hyperemia is the autonomic nervous system, which can reduce skeletal muscle vascular tone and increase muscle blood flow through either a rise in parasympathetic cholinergic nerve activity or a withdrawal of sympathetic adrenergic nerve activity. Regarding the contribution of the parasympathetic cholinergic nervous system, several experiments conducted on humans, rats, and dogs have revealed that administration of atropine (cholinergic muscarinic receptor blocker) has no significant effect on the pattern of muscle blood flow augmentation during dynamic exercise.[42] Sanders and colleagues[43] described an interesting experiment in normal humans, in which isometric handgrip contractions elicited a small but significant atropine-sensitive vasodilatation in the contralateral forearm. These results suggest the existence of an atropine-sensitive pathway that has a small influence on skeletal muscle vascular tone; however, it remains unclear whether this cholinergic pathway is neural in nature or is mediated through the release of acetylcholine in the venous effluent of the exercising muscle.

Although the suggestion that withdrawal of sympathetic adrenergic nerve activity from skeletal muscle resistance vessels may contribute to exercise-induced hyperemia is attractive and plausible, there is little experimental evidence supporting this suggestion. In fact, both dynamic and isometric exercise elicit a significant elevation of sympathetic adrenergic nerve activity to various organs, including the exercising skeletal muscles. Moreover, the findings in experimental animals that lumbar sympathectomy or pharmacologic blockade of autonomic nerves has little effect on the initial rise in blood flow but increases the magnitude of steady-state hyperemia of exercising hind limb muscles suggest that sympathetic neural activity exerts a vasoconstrictor effect that opposes local vasodilatory control mechanisms.[44]

Local Control Mechanisms

The importance of local control mechanisms in exercise hyperemia is underscored by the fact that isolated skeletal muscles are capable of achieving substantial rises in their blood flow upon nerve stimulation or direct muscle activation. Local control mechanisms involved in the regulation of exercise hyperemia include the myogenic mechanism, metabolic factors, endothelium-derived factors, and the muscle pump.

Myogenic Mechanism The role of intrinsic properties of vascular smooth muscle (independent of hormonal, neural and metabolic influences) in regulating skeletal muscle vascular tone was first described in 1902 by Bayliss, who reported that smooth muscle contractility and vascular resistance are sensitive to changes in transmural pressure.[45] According to Bayliss's theory, elevation of transmural pressure elicits vascular smooth muscle contraction and increases vascular resistance, whereas a reduction in transmural pressure causes smooth muscle relaxation and a decline in vascular resistance.[45] This myogenic response is most pronounced in arterioles but can be demonstrated occasionally in arteries, venules, veins, and lymphatics. In the vascular system, the myogenic response has been proposed as a central feature in a number of physiologically important functions, the two most important of which are the establishment of basal vascular tone and autoregulation of blood flow and capillary hydrostatic pressure. The development of spontaneous tone in response to physiologic transmural pressure in isolated arteries in vitro with an internal diameter of less than 150 μm is a strong indication of the importance of myogenic tone in these vessels. It should be emphasized that the myogenic response is elicited not only by static but also by pulsatile alterations in transmural pressure.

The fact that IMP increases substantially during tetanic and rhythmic contractions of skeletal muscles has led to the proposal that the myogenic response also contributes to active hyperemia. According to this proposal, elevation of extravascular pressure during muscle contractions leads to a reduction in transmural pressure across resistance arteries and arterioles, leading to a reduction in vascular wall tension and dilatation of these vessels. Direct evidence supporting this notion was provided by Mohrman and Sparks,[46] who used an inflatable cuff to artificially increase the IMP in the calf muscles of dogs to a similar extent and in the same way as the increases generated by tetanic muscle contraction. These authors concluded that the myogenic response contributes about one-third to one-half of the vasodilatation produced by brief tetanic contractions. Similarly, Grande and colleagues[47] reported that changes in vascular transmural pressure of 40 mm Hg maintained for 15 to 120 seconds can elicit a myogenic response in cat skeletal muscle. However, other investigators who have studied twitch contractions of limb muscles have described an absence of or very little contribution of the myogenic response to vasodilatation elicited by these contractions in other animals.[48]

Metabolic Mechanisms The metabolic control hypothesis states that muscle metabolism provides a local mechanism through which the nutritional requirements of muscle fibers are tightly coupled to blood flow. Accordingly, increased muscle metabolism during exercise causes the release into the interstitium of metabolites, which, in turn, elicit significant relaxation of smooth muscles of resistance vessels and precapillary sphincters, leading eventually to a decline in muscle vascular resistance and an increase in blood flow.[2] Augmentation of blood flow and increased oxygen extraction by muscle fibers will then provide an adequate oxygen supply to meet the increasing oxygen demands during exercise. Thus, the metabolic control hypothesis emphasizes the importance of muscle oxygen supply as the primary variable responsible for exercise hyperemia.[2]

Alterations in local levels of several metabolites have been proposed as important modulators of skeletal muscle blood flow during increased metabolic activity. These alterations include increased partial pressure of carbon dioxide (PCO_2), a decline in partial pressure of oxygen (PO_2) and pH, and elevation of lactate, adenosine, and K^+ levels and osmolarity. None of these alterations by itself can reduce muscle vascular resistance and increase blood flow to the levels observed during exercise. It has been suggested that these alterations may act in a cooperative manner to dilate muscle vasculature and that the contribution of each of these alterations to the overall rise in muscle blood flow is determined by the pattern and the duration of muscle activation, as well as by the type of muscle fibers being recruited.

Although the primary importance of metabolic control mechanisms in muscle hyperemia during sustained exercise is not in dispute, it has been proposed that the rapid phase of exercise hyperemia during dynamic exercise is not mediated by metabolites. This notion is based on the observations that the magnitude of phase 1 of exercise hyperemia during dynamic exercise is not influenced by the intensity of exercise (hence muscle metabolic rate) and that the arteriolar dilatation observed after the initiation of muscle contraction occurs more slowly than the rapid rise in muscle blood flow.[49]

Reductions in tissue and blood PO_2 and elevations of PCO_2 and inorganic phosphate (P_i), H^+ and lactate concentrations were among the earliest proposed mechanisms to explain active hyperemia during sustained exercise. However, direct measurements of tissue PO_2 showed that rapid arteriolar dilatation in active skeletal muscle precedes the decline in muscle PO_2, thereby excluding local hypoxia as an important modulator of the rapid phase of exercise hyperemia. However, the role of tissue hypoxia as an important contributor to augmentation of muscle blood flow during sustained exercise is not disputed since the magnitude of muscle hyperemia during the steady-state phase of exercise correlates very well with tissue PO_2. With regard to CO_2, H^+, P_i, and lactate, many reports have documented that, even when administrated at relatively high concentrations, these metabolites are not capable of augmenting blood flow in a resting muscle to levels similar to those observed during exercise. In addition, the fact that exercise hyperemia in McArdle syndrome patients (inborn lack of glycogen phosphorylase), who are incapable of producing lactate, is

normal, despite no evidence of any changes in lactate level, pH, or PCO_2 in their venous blood, argues against direct involvement of these metabolites in regulating skeletal muscle vascular tone during sustained exercise. More recently, it has been proposed that PO_2, PCO_2, H^+, lactate, and P_i may be sensed within arterioles, venules, red cells, and muscle tissues and that the resulting vasodilatation elicited by these compounds is mediated through indirect mechanisms, such as the release of ATP and enhanced nitric oxide (NO) and prostaglandin production.[50,51]

Another metabolite that has also been proposed to mediate exercise hyperemia is K^+, primarily because its concentration in the venous effluents of exercising muscle, as well as inside muscle fibers, increases significantly during exercise in humans.[52] In addition, depletion of K^+ in dogs has been shown to result in attenuation of exercise hyperemia, although muscle tension is also reduced significantly in these animals.[53] These results contrast with the findings that leg or forearm exercise in humans is associated with a very small rise in venous K^+ concentration in the systemic circulation or the venous effluent of forearm muscles.[54] Finally, the fact that the vasodilatation elicited by exogenously administered K^+ occurs much more slowly than the vascular dilatation elicited by exercise suggests that this metabolite is not likely to be an important modulator of the rapid phase of exercise hyperemia during dynamic exercise.

Adenosine Adenosine is derived from the reaction of AMP with 5′-nucleotidase, an enzyme localized in the vascular endothelium and muscle fiber cell membrane. Adenosine activates two main receptor types (A1 and A2), which are abundantly expressed at the surface of vascular smooth muscles of resistance arterioles. These receptors, when activated by adenosine, trigger a rise in intracellular cyclic AMP concentration and activation of protein kinase A, resulting eventually in depression of myosin phosphorylation and smooth muscle relaxation. There are several experimental results that support an important role for adenosine in modulating skeletal muscle vascular resistance during exercise. First, infusion of even minute amounts of adenosine into femoral arteries of humans elicits a very rapid vasodilatation that lasts for as long as the infusion is maintained[55] (Figure 48-5). Second, adenosine accumulates inside skeletal muscles of humans during exercise. Levels as high as 800 μg/L have been detected with the use of microdialysis techniques in leg muscles during dynamic knee extension exercises.[56] At these concentrations, adenosine is capable of producing significant dilatation of resistance arterioles of skeletal muscles. The cellular source of adenosine production during exercise remains unclear; however, vascular cells, nerve fibers, myocytes, and erythrocytes have all been implicated. Third, pharmacologic blockade of adenosine receptors by theophylline attenuates exercise hyperemia by 20 to 40%, suggesting that endogenous adenosine is an important mediator of active hyperemia, particularly during sustained dynamic exercise.[55] However, animal experiments using dipyridamole, a compound that prevents cellular adenosine uptake, thereby causing an increase in local adenosine concentration, have revealed that the contribution of adenosine to exercise hyperemia is only evident in muscles rich in type I (highly oxidative) fibers, such as the soleus and the ventilatory muscles; muscles rich in type II (highly glycolytic) fibers do not depend on adenosine to reduce vascular resistance and increase blood flow during exercise.[57]

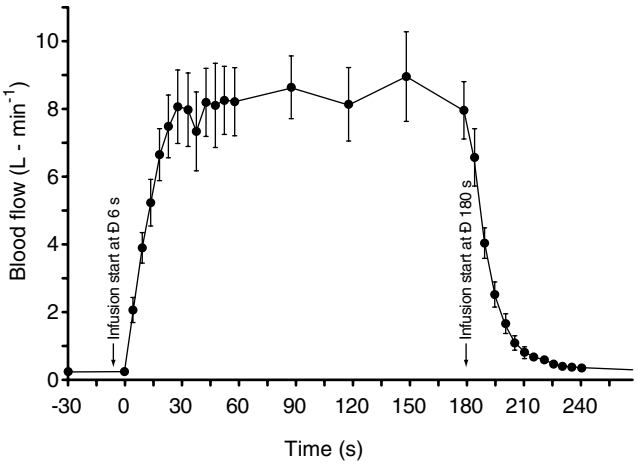

FIGURE 48-5 The time course for the change in femoral arterial inflow (ultrasound Doppler) when adenosine is infused at a rate of 2 mg/min/L thigh volume. Reproduced with permission from Radegran G and Calbet JA.[55]

Endothelium-Derived Mediators It has been well established over the past 20 years that the vascular endothelium is not merely a physical barrier between the blood and the vascular smooth muscles but is capable of sensing both physical forces exerted on blood vessels and chemical substances released into the blood. In response, the endothelium may elicit vasodilatation or vasoconstriction by synthesizing vasoactive substances, which diffuse toward smooth muscles in the immediate vicinity of the endothelium and elicit relaxation of these muscles. In this respect, two important substances, NO and prostacyclin (prostaglandin I_2, PGI_2), are released by the endothelium and are considered to be important modulators of muscle blood flow both at rest and during exercise.

Nitric Oxide NO is synthesized by three isoforms of nitric oxide synthase (NOS).[58] Endothelial NOS (eNOS) is mainly expressed in endothelial cells and is involved in the regulation of vascular resistance in all vascular beds, whereas neuronal NOS (nNOS) is mainly expressed in neurons and is involved in neurotransmission. A specific form of the nNOS isoform known as nNOSμ is selectively expressed inside skeletal muscle fibers and associates with the dystrophin complex.[59] Inducible NOS (iNOS) is expressed in the vasculature and inflammatory cells in response to proinflammatory stimulants, and its contribution to the regulation of skeletal muscle vascular tone under normal conditions is negligible. Endothelium-derived NO diffuses from the endothelium toward vascular smooth muscles and activates soluble guanylate cyclase to form cyclic GMP, which, in turn, activates protein kinase G, resulting eventually in reduction

of smooth muscle cell Ca^{2+} flux and vascular relaxation. NO also regulates vascular smooth muscle contractility by inhibiting the release of norepinephrine from sympathetic adrenergic neurons.

It is now well recognized that the endothelium continuously releases relatively low levels of NO, which provide a tonic vasodilatory effect that counteracts the vasoconstrictor effect of myogenic tone and establishes the basal vascular tone in all organs, including resting skeletal muscles. This is evident from the observation that administration of pharmacologic inhibitors of NOS induces vasoconstriction in resting skeletal muscles in various mammalian species.[60–62] Direct visualization of muscle vasculature has confirmed that arteriolar vasoconstriction develops in response to NOS inhibition. In resting normal humans, systemic administration of NOS inhibitors elicits a significant rise in total vascular resistance and arterial pressure,[63] and intraarterial injection of an NOS inhibitor into the brachial arteries of resting humans produces a greater than 50% increase in basal forearm blood flow.[64]

The involvement of NO in exercise hyperemia remains controversial. Experimental support for a role for NO emanates from the fact that NO production increases significantly in response to muscle activation in incubated rat skeletal muscle preparations, as well as in human skeletal muscle interstitium.[65] Furthermore, both acute bouts of exercise and chronic exercise training have been shown to result in augmentation of limb and ventilatory muscle NO production and NOS expression.[66] An important stimulus for enhanced NO production in response to skeletal muscle activation during exercise is increased intracellular Ca^{2+} concentration inside endothelial cells, which is brought about by physical factors such as increased shear stress, and by receptor–signal transduction pathways, such as that of bradykinin and ATP.

Evaluation of the NO contribution to exercise hyperemia in animals and humans has generally been evaluated with the use of pharmacologic inhibitors such as N^G-nitro-L-arginine, N^G-nitro-L-arginine methyl ester (L-NAME), and N^G-monomethyl-L-arginine. On the one hand, administration of these inhibitors, or inhibitors of guanylate cyclase, results in significant attenuation of skeletal muscle exercise hyperemia during isometric or dynamic exercise in dogs.[67,68] In contracting hamster cremaster muscles, L-NAME infusion inhibited the dilatory response of first-order and second-order but not third-order arterioles.[69] The contribution of NO to active hyperemia in the canine diaphragm was assessed by Hussain and colleagues, who reported that 25 to 41% of the vascular diaphragm vasodilatation elicited by phrenic nerve stimulation could be accounted for by increased NO production.[70] On the other hand, several investigators failed to find a significant influence of NOS inhibitors on limb muscle active hyperemia in cats, dogs, and rabbits.[71–73] Similarly, contradictory results have been reported regarding the contribution of NO to exercise hyperemia in humans. For instance, intraarterial infusion of NOS inhibitors into the forearm vasculature of normal humans revealed that the NO contribution to exercise hyperemia elicited by intermittent handgrip exercise ranges between 11 and 30% of peak blood flow[74–76] (Figure 48-6). Other

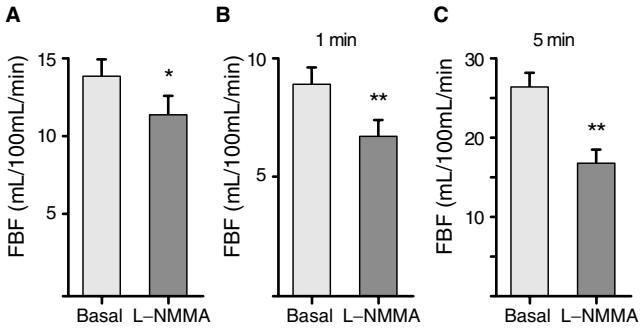

FIGURE 48-6 The effect of N^G-monomethyl-L-arginine (L-NMMA) (inhibitor of nitric oxide synthases) on forearm blood flow (FBF) (measured by venous occlusion plethysmography). The rise in FBF in response to 2 minutes of isotonic exercise was significantly attenuated by intraarterial infusion of L-NMMA (2 mg/min). *A*, Peak FBF. *B* and *C*, Volume repaid. $*p < .01$; $**p < .0001$. Reproduced with permission from Duffy SJ et al.[76]

investigators have failed to show a significant reduction in exercise hyperemia of limb muscles after NOS inhibitions in humans.[77–79] These variations in results are probably due to differences in experimental designs, the type of muscle involved, the selectivity and dosage of NOS inhibitors, and the type and duration of exercise being investigated. There is also the confounding issue of the methodology used to measure muscle blood flow in humans. For instance, plethysmography measurements are restricted to rest and to pauses after the termination of exercise, whereas thermodilution and ultrasound Doppler measurements provide information regarding muscle blood flow changes during muscle contraction.

Prostaglandins In addition to NO, the endothelium is capable of synthesizing vasoactive prostaglandins, with PGI_2 being the best characterized endothelium-derived vasodilator. Prostaglandin synthesis inside the endothelium is initiated through the activation of G protein–coupled receptors by increasing shear stress. These receptors, in turn, activate the enzyme phospholipase A_2, which liberates arachidonic acid from cell membrane phospholipids. Oxidation of arachidonic acid by the cyclooxygenases results in the release of vasoactive prostaglandins. PGI_2 induces smooth muscle relaxation by both increasing cAMP levels and inhibiting phospholipase C activity. Both effects lead to a reduction in intracellular Ca^{2+} concentration and smooth muscle relaxation. In support of the involvement of prostaglandins in the regulation of exercise hyperemia is a significant (fourfold) rise in the forearm venous concentration of prostaglandin metabolites (PGF_1 and PGE_2) in response to wrist flexion exercise in humans.[80] Direct measurements of these metabolites inside the gastrocnemius and vastus lateralis muscles with the use of microdialysis have confirmed an approximate fourfold rise in response to dynamic, but not static, exercise.[81] Blockade of prostaglandin synthesis by indothemacin or aspirin has been shown to reduce resting forearm blood flow by 23 to 41%.[76,80] In the rat diaphragm, selective blockade of prostaglandin synthesis by mafenamic acid (cyclooxygenase inhibitor) reduced

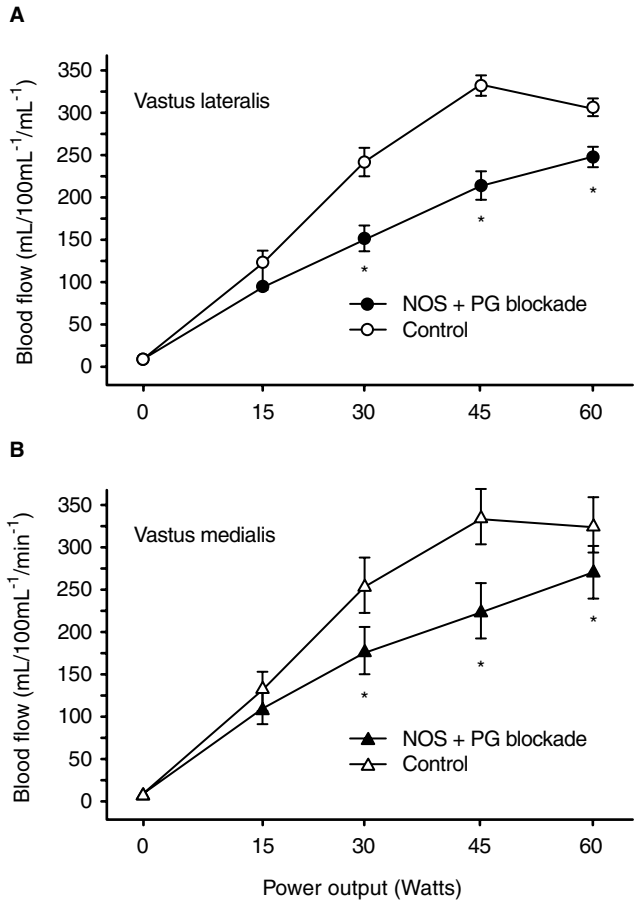

FIGURE 48-7 Quadriceps microvascular blood flow during exercise. Regional microvascular blood flow in the quadriceps muscles during incremental dynamic knee extension. Blood flow in the vastus lateralis (*upper panel*) and vastus medialis (*lower panel*) in control knee extension (*open symbols*) and during combined nitric oxide synthase (NOS) and prostaglandin (PG) (*filled symbols*). *Asterisks* indicate difference between control and blockade conditions ($p < .05$). Reproduced with permission from Boushel R et al.[84]

arteriolar diameter by only 4%, whereas blockade of NO synthesis reduced the diameter by 15%.[82] These results suggest that the degree to which prostaglandins contribute to the regulation of resting skeletal muscle blood flow is dependent on the type of muscle and the species involved. The involvement of prostaglandins in active hyperemia has also been evaluated, using indomethacin and aspirin as pharmacologic inhibitors of cyclooxygenases. Administration of these compounds during mild-to-moderate recruitment of forearm muscles revealed that prostaglandins contribute 15 to 32% of the total rise in blood flow.[76,80,83] When inhibitors of NOS and prostaglandin synthesis were combined, their inhibitory effects on exercise hyperemia in humans appeared to be synergistic[84] (Figure 48-7).

Muscle Pump The muscle pump, which consists of contraction-induced rhythmic propulsion of blood from skeletal muscle vasculature that facilitates both venous return to the heart and inflow of blood into muscle arterioles, is an important mechanism responsible for the rapid rise in muscle blood flow during the transition from rest to exercise. This mechanism, which is selective for skeletal muscles, operates only during rhythmic contractions since sustained tetanic contractions impede rather than promote muscle blood flow. The concept of the muscle pump, first proposed by Folkow and colleagues,[85] implies that during muscle contraction, the blood is ejected unidirectionally through the venules and deep veins because of the orientation of valves in these vessels. Upon sudden muscle relaxation, the pressure inside venules and deep veins becomes negative, and this, in turn, facilitates inflow into the muscle vasculature. Thus, the muscle pump facilitates blood flow by at least two mechanisms: decreased venous pressures during the relaxation phase and increased total kinetic energy to force blood through the muscle vascular bed during the contraction phase. Laughlin[86] estimated that the muscle pump mechanism contributes as much as 60% of the total energy required for perfusion of limb muscles in rats undergoing treadmill exercise. The efficacy of this mechanism in promoting muscle blood flow is strongly influenced by the maximal pressure developed during contraction, precontraction vascular volume, and the type of muscle and contractile activity. This is clearly evident from the significantly greater blood flow of the soleus muscles and the red portion of gastrocnemius muscles when these muscles undergo dynamic locomotive exercise than when they undergo tetanic or twitch contractions.[87] This observation suggests that sequential recruitment of muscle fibers during locomotive exercise renders the muscle pump mechanism more efficient than during simultaneous activation of fibers by artificial stimulation.

SUMMARY

Many different factors are involved in regulating muscle blood flow at different stages of muscle metabolism. At rest, muscle metabolic activity is relatively low, and the vascular tone is regulated by the balance between vasoconstrictor factors, namely, smooth muscle myogenic tone and the sympathetic adrenergic nervous system, and vasodilator factors, which are mainly endothelial-derived NO and PGI_2. The rapid rise in muscle blood flow observed within seconds of the initiation of muscle contraction is mediated mainly by the muscle pump, which increases muscle blood flow by reducing the pressure in the venous compartment and enhancing endothelial-derived NO and PGI_2 production as a result of increased shear stress inside conducting and resistance vessels. As muscle metabolism increases during sustained exercise, local metabolites and endothelial-derived factors become the dominant mechanisms responsible for exercise hyperemia.

REFERENCES

1. Armstrong RB, Delp MD, Goljan EF, Laughlin MH. Distribution of blood flow in muscles of miniature swine during exercise. J Appl Physiol 1987;62:1285–98.
2. Laughlin MH, Korthius RJ, Duncker DJ, Bache RJ. Control of blood flow to cardiac and skeletal muscle during exercise. In: Rowell LB, Shepherd JT, editors. Handbook of physiology. Exercise: regulation and integration of multiple systems. Bethesda, MD: American Physiological Society; 1996. p. 705–69.

3. Manohar M. Vasodilator reserve in respiratory muscles during maximal exertion in ponies. J Appl Physiol 1986;60:1571–7.
4. Anrep GV, Cerqua S, Samaan A. The effect of muscular contraction upon the blood flow in the skeletal muscle, in the diaphragm and in the small intestine. Proc R Soc Lond B Biol Sci 1933;114:245–57.
5. Anrep GV Saalfeld EV. The blood flow through the skeletal muscle in relation to its contraction. J Physiol Lond 1935;85: 375–99.
6. Bellemare F, Wight D, Lavigne CM, Grassino A. Effect of tension and timing of contraction on the blood flow of the diaphragm. J Appl Physiol 1983;54:1597–606.
7. Hussain SN, Roussos C, Magder S. Effects of tension, duty cycle, and arterial pressure on diaphragmatic blood flow in dogs. J Appl Physiol 1989;66:968–76.
8. Buchler B, Magder S, Roussos C. Effects of contraction frequency and duty cycle on diaphragmatic blood flow. J Appl Physiol 1985;58:265–73.
9. Korner L, Parker P, Almstrom C, et al. Relation of intramuscular pressure to the force output and myoelectric signal of skeletal muscle. J Orthop Res 1984;2:289–96.
10. Aratow M, Ballard RE, Crenshaw AG, et al. Intramuscular pressure and electromyography as indexes of force during isokinetic exercise. J Appl Physiol 1993;74:2634–40.
11. Ballard RE, Watenpaugh DE, Breit GA, et al. Leg intramuscular pressures during locomotion in humans. J Appl Physiol 1998;84:1976–81.
12. Decramer M, Jiang TX, Reid MB. Respiratory changes in diaphragmatic intramuscular pressure. J Appl Physiol 1990;68:35–43.
13. Supinski GS, DiMarco AF, Altose MD. Effect of diaphragmatic contraction on intramuscular pressure and vascular impedance. J Appl Physiol 1990;68:1486–93.
14. Wisnes A, Kirkebo A. Regional distribution of blood flow in calf muscles of rat during passive stretch and sustained contraction. Acta Physiol Scand 1976;96:256–66.
15. Degens H, Salmons S, Jarvis JC. Intramuscular pressure, force and blood flow in rabbit tibialis anterior muscles during single and repetitive contractions. Eur J Appl Physiol Occup Physiol 1998;78:13–9.
16. Hussain SN, Magder S. Diaphragmatic intramuscular pressure in relation to tension, shortening, and blood flow. J Appl Physiol 1991;71:159–67.
17. Buchler B, Magder S, Katsardis H, et al. Effects of pleural pressure and abdominal pressure on diaphragmatic blood flow. J Appl Physiol 1985;58:691–7.
18. Kawagoe Y, Permutt S, Fessler HE. Hyperinflation with intrinsic PEEP and respiratory muscle blood flow. J Appl Physiol 1994;77:2440–8.
19. Nakao M, Segal SS. Muscle length alters geometry of arterioles and venules in hamster retractor. Am J Physiol 1995;268: H336–44.
20. Supinski GS, Bark H, Guanciale A, Kelsen SG. Effect of alterations in muscle fiber length on diaphragm blood flow. J Appl Physiol 1986;60:1789–96.
21. Poole DC, Musch TI, Kindig CA. In vivo microvascular structural and functional consequences of muscle length changes. Am J Physiol 1997;272:H2107–14.
22. Welsh DG, Segal SS. Muscle length directs sympathetic nerve activity and vasomotor tone in resistance vessels of hamster retractor. Circ Res 1996;79:551–9.
23. Shoemaker JK, Hughson RL. Adaptation of blood flow during the rest to work transition in humans. Med Sci Sports Exerc 1999;31:1019–26.
24. Laughlin MH, Armstrong RB. Rat muscle blood flows as a function of time during prolonged slow treadmill exercise. Am J Physiol 1983;244:H814–24.
25. Donald DE, Rowlands DJ, Ferguson DA. Similarity of blood flow in the normal and the sympathectomized dog hind limb during graded exercise. Circ Res 1970;26:185–99.
26. Radegran G, Saltin B. Muscle blood flow at onset of dynamic exercise in humans. Am J Physiol 1998;274:H314–22.
27. Goodman AH, Einstein R, Granger HJ. Effects of changing metabolic rate on local blood flow control in the canine hind limb. Circ Res 1978;43:769–76.
28. Hussain SNA, Roussos Ch, Magder S. Autoregulation of diaphragmatic blood flow in dogs. J Appl Physiol 1988;64: 329–36.
29. Magder S. Pressure–flow relations of diaphragm and vital organs with nitroprusside-induced vasodilatation. J Appl Physiol 1986;61:409–16.
30. Reid MB, Johnson RL Jr. Efficiency, maximal blood flow, and aerobic work capacity of canine diaphragm. J Appl Physiol 1983;54:763–72.
31. Rowell LB, O'Leary DS. Reflex control of the circulation during exercise: chemoreflexes and mechanoreflexes. J Appl Physiol 1990;69:407–18.
32. Eldridge FL, Millhorn DE, Waldrop TG. Exercise hyperpnea and locomotion: parallel activation from the hypothalamus. Science 1981;211:844–6.
33. DiCarlo SE, Bishop VS. Central baroreflex resetting as a means of increasing and decreasing sympathetic outflow and arterial pressure. Ann N Y Acad Sci 2001;940:324–37.
34. McCloskey DI, Mitchell JH. Reflex cardiovascular and respiratory responses originating in exercising muscle. J Physiol 1972;224:173–86.
35. Victor RG, Bertocci LA, Pryor SL, Nunnally RL. Sympathetic nerve discharge is coupled to muscle cell pH during exercise in humans. J Clin Invest 1988;82:1301–5.
36. O'Leary DS, Sheriff DD. Is the muscle metaboreflex important in control of blood flow to ischemic active skeletal muscle in dogs? Am J Physiol 1995;268:H980–6.
37. Rowell LB, Savage MV, Chambers J, Blackmon JR. Cardiovascular responses to graded reductions in leg perfusion in exercising humans. Am J Physiol 1991;261: H1545–53.
38. Hudlicka O. Regulation of muscle blood flow. Clin Physiol 1985;5:201–29.
39. Armstrong RB, Hayes DA, Delp MD. Blood flow distribution in rat muscles during preexercise anticipatory response. J Appl Physiol 1989;67:1855–61.
40. Hilton SM. Experiments on the post contraction hyperaemia of skeletal muscle. J Physiol 1953;120:230–45.
41. Honig CR. Contributions of nerves and metabolites to exercise vasodilation: a unifying hypothesis. Am J Physiol 1979; 236: H705–19.
42. Armstrong RB, Laughlin MH. Atropine: no effect on exercise muscle hyperemia in conscious rats. J Appl Physiol 1986; 61:679–82.
43. Sanders JS, Mark AL, Ferguson DW. Evidence for cholinergically mediated vasodilation at the beginning of isometric exercise in humans. Circulation 1989;79:815–24.
44. Peterson DF, Armstrong RB, Laughlin MH. Sympathetic neural influences on muscle blood flow in rats during submaximal exercise. J Appl Physiol 1988;65:434–40.
45. Bayliss WM. On the local reactions of the arterial wall to changes of internal pressure. J Physiol Lond 1902;28: 220–31.
46. Mohrman DE, Sparks HV. Myogenic hyperemia following brief tetanus of canine skeletal muscle. Am J Physiol 1974;227: 531–5.
47. Grande PO, Lundvall J, Mellander S. Evidence for a rate-sensitive regulatory mechanism in myogenic microvascular control. Acta Physiol Scand 1977;99:432–47.

48. Bacchus A, Gamble G, Anderson D, Scott J. Role of the myogenic response in exercise hyperemia. Microvasc Res 1981; 21:92–102.
49. Sheriff DD, Rowell LB, Scher AM. Is rapid rise in vascular conductance at onset of dynamic exercise due to muscle pump? Am J Physiol 1993;265:H1227–34.
50. Ellsworth ML, Forrester T, Ellis CG, Dietrich HH. The erythrocyte as a regulator of vascular tone. Am J Physiol 1995;269:H2155–61.
51. Gonzalez-Alonso J, Richardson RS, Saltin B. Exercising skeletal muscle blood flow in humans responds to reduction in arterial oxyhaemoglobin, but not to altered free oxygen. J Physiol 2001;530:331–41.
52. Juel C, Pilegaard H, Nielsen JJ, Bangsbo J. Interstitial K(+) in human skeletal muscle during and after dynamic graded exercise determined by microdialysis. Am J Physiol Regul Integr Comp Physiol 2000;278:R400–6.
53. Hazeyama Y, Sparks HV. Exercise hyperemia in potassium-depleted dogs. Am J Physiol 1979;236:H480–6.
54. Wilson JR, Kapoor SC, Krishna GG. Contribution of potassium to exercise-induced vasodilation in humans. J Appl Physiol 1994;77:2552–7.
55. Radegran G, Calbet JA. Role of adenosine in exercise-induced human skeletal muscle vasodilatation. Acta Physiol Scand 2001;171:177–85.
56. MacLean DA, Radegran G, Hellsten Y, Bangsbo J. Measurements of muscle interstitial adenosine levels by microdialysis during incremental dynamic exercise in humans. J Physiol 1996;491:160P.
57. Laughlin MH, Klabunde RE, Delp MD, Armstrong RB. Effects of dipyridamole on muscle blood flow in exercising miniature swine. Am J Physiol 1989;257:H1507–15.
58. Knowles RG, Moncada S. Nitric oxide synthases in mammals. Biochem J 1994;298:249–58.
59. Silvagno F, Xia H, Bredt DS. Neuronal nitric-oxide synthase-m, an altneratively spliced isoform expressed in differentiated skeletal muscle. J Biol Chem 1996;271:11204–8.
60. Gardiner SM, Compton AM, Kemp PA, Bennett T. Regional and cardiac haemodynamic effects of NG-nitro-L-arginine methyl ester in conscious, Long Evans rats. Br J Pharmacol 1990;101:625–31.
61. White DG, Drew GM, Gurden JM, et al. The effect of N^G-nitro-L-arginine methyl ester based upon basal blood flow and endothelium-dependent vasodilation in the dog hindlimb. Br J Pharmacol 1993;108:763–8.
62. Ward ME, Hussain SNA. Regulation of baseline vascular resistance in the canine diaphragm by nitric oxide. Br J Pharmacol 1994;112:65–70.
63. Sander M, Chavoshan B, Victor RG. A large blood pressure-raising effect of nitric oxide synthase inhibition in humans. Hypertension 1999;33:937–42.
64. Vallance P, Collier J, Moncada S. Effects of endothelium-derived nitric oxide on peripheral arteriolar tone in man. Lancet 1989;2:997–1000.
65. Balon TW, Nadler JL. Nitric oxide release is present from incubated skeletal muscle preparations. J Appl Physiol 1994;77:2519–21.
66. Vassilakopoulos T, Dechman G, Kebbewar M, et al. Regulation of nitric oxide production in limb and ventilatory muscles during chronic exercise training. Am J Physiol Lung Cell Mol Physiol 2003;284:L452–7.
67. Sagach VF, Kindybalyuk AM, Kovalenko TN. Functional hyperemia of skeletal muscle: role of endothelium. J Cardiovasc Pharmacol 1992;20 Suppl 12:S170–5.
68. Shen W, Lundborg M, Wang J, et al. Role of EDRF in the regulation of regional blood flow and vascular resistance at rest and during exercise in conscious dogs. J Appl Physiol 1994;77:165–72.
69. Hester RL, Eraslan A, Saito Y. Differences in EDNO contribution to arteriolar diameters at rest and during functional dilation in striated muscle. Am J Physiol 1993;265:H146–51.
70. Hussain SNA, Stewart D, Ludeman J, Magder S. The role of endothelium-derived relaxing factor in active hyperemia of the canine diaphragm. J Appl Physiol 1992;72:2393–401.
71. Persson MG, Gustafsson LE, Wiklund NP, et al. Endogenous nitric oxide as a modulator of rabbit skeletal muscle microcirculation. Br J Pharmacol 1990;10:463–6.
72. Ekelund U, Bjornberg J, Grande PO, et al. Myogenic vascular regulation in skeletal muscle in vivo is not dependent on endothelium-derived nitric oxide. Acta Physiol Scand 1992;144:199–207.
73. O'Leary DS, Dunlap RC, Glover KW. Role of endothelium-derived relaxing factor in hindlimb reactive and active hyperemia in conscious dogs. Am J Physiol 1994;266: R1213–9.
74. Gilligan DM, Panza JA, Kilcoyne CM, et al. Contribution of endothelium-derived nitric oxide to exercise-induced vasodilation. Circulation 1994;90:2853–8.
75. Dyke CK, Proctor DN, Dietz NM, Joyner MJ. Role of nitric oxide in exercise hyperaemia during prolonged rhythmic handgripping in humans. J Physiol 1995;488(Pt 1):259–65.
76. Duffy SJ, New G, Tran BT, et al. Relative contribution of vasodilator prostanoids and NO to metabolic vasodilation in the human forearm. Am J Physiol 1999;276:H663–70.
77. Endo T, Imaizumi T, Tagawa T, et al. Role of nitric oxide in exercise-induced vasodilation of the forearm. Circulation 1994;90:2886–90.
78. Shoemaker JK, Halliwill JR, Hughson RL, Joyner MJ. Contributions of acetylcholine and nitric oxide to forearm blood flow at exercise onset and recovery. Am J Physiol 1997;273:H2388–95.
79. Wilson JR, Kapoor S. Contribution of endothelium-derived relaxing factor to exercise-induced vasodilation in humans. J Appl Physiol 1993;75:2740–4.
80. Wilson JR, Kapoor SC. Contribution of prostaglandins to exercise-induced vasodilation in humans. Am J Physiol 1993; 265:H171–5.
81. Karamouzis M, Langberg H, Skovgaard D, et al. In situ microdialysis of intramuscular prostaglandin and thromboxane in contracting skeletal muscle in humans. Acta Physiol Scand 2001;171:71–6.
82. Boczkowski J, Vicaut E, Danialou G, Aubier M. Role of nitric oxide and prostaglandins in the regulation of diaphragmatic arteriolar tone in the rat. J Appl Physiol 1994;77: 590–6.
83. Kilbom A, Wennmalm A. Endogenous prostaglandins as local regulators of blood flow in man: effect of indomethacin on reactive and functional hyperaemia. J Physiol 1976;257: 109–21.
84. Boushel R, Langberg H, Gemmer C, et al. Combined inhibition of nitric oxide and prostaglandins reduces human skeletal muscle blood flow during exercise. J Physiol 2002;543: 691–8.
85. Folkow B, Gaskell P, Waaler BA. Blood flow through limb muscles during heavy rhythmic exercise. Acta Physiol Scand 1970;80:61–72.
86. Laughlin MH. Skeletal muscle blood flow capacity: role of muscle pump in exercise hyperemia. Am J Physiol 1987;253: H993–1004.
87. Laughlin MH, Schrage WG. Effects of muscle contraction on skeletal muscle blood flow: when is there a muscle pump? Med Sci Sports Exerc 1999;31:1027–35.

CHAPTER 49

PERIPHERAL MUSCLE DYSFUNCTION IN CHRONIC OBSTRUCTIVE PULMONARY DISEASE

Richard Debigaré, François Maltais

Cough, dyspnea, and exercise intolerance are among the early clinical manifestations of chronic obstructive pulmonary disease (COPD).[1] As the disease progresses, several extrathoracic organs are affected, such that COPD is now recognized as a multisystem disease. Altered kidney and endothelial function,[2] endocrine abnormalities,[3] osteoporosis,[4] and peripheral muscle dysfunction[5] are now commonly reported in COPD. Among these extrathoracic manifestations of COPD, the involvement of the peripheral muscles is the subject of intense research because it may influence quality of life, functional status, and survival independently of the alteration in lung function. Thus, the improvement in peripheral muscle function represents a potential and valid therapeutic target for many patients with COPD.

Our understanding of the mechanisms underlying the alteration in peripheral muscle function in COPD is in its early stages. Although promising pathophysiologic concepts are emerging from experimental models, such as cultured muscle cells and cachectic animals, the precise mechanisms of the alterations in peripheral muscle function seen in chronic diseases such as COPD have yet to be elucidated.

In this chapter, we discuss the evidence for and clinical consequences of peripheral muscle dysfunction in COPD and review potential mechanisms of muscle wasting. Finally, actual and future therapies that stop muscle proteolysis or increase muscle mass are discussed.

EVIDENCE OF PERIPHERAL MUSCLE DYSFUNCTION

Body weight loss and muscle wasting in COPD-affected subjects have long been recognized by clinicians,[6] and many reports have confirmed the high prevalence of this phenomenon.[7] Furthermore, the peripheral muscles in patients with COPD are affected not only quantitatively (wasting) but also qualitatively, as illustrated by the marked alterations in fiber-type distribution and decreased metabolic capacity. The quadriceps is the most commonly studied peripheral muscle, not only because it is readily accessible but also because it is a primary effector muscle of ambulation. Since most studies have included patients with moderate-to-severe disease, the muscle changes reported herein pertain to this patient population.

Muscle Mass

Peripheral muscle wasting is an important consequence of COPD (Figure 49-1), with an overall estimated prevalence of 30%.[7] The prevalence of this problem increases with the degree of airflow obstruction. A key concept is that muscle mass may be low despite the preservation of total body weight.[7] The implication of this is that the prevalence of muscle wasting is likely to be underestimated if one relies only on measurements of body weight. Another implication is that in patients with COPD, there is a preferential loss of muscle tissue in comparison with other body compartments.[8,9]

Muscle Fiber Type, Size, and Capillarization

Human skeletal muscle fibers can be grouped into separate categories on the basis of their physiologic and metabolic characteristics. Type I fibers are characterized by low contractile velocity and high oxidative capacity (which account for their relative resistance to fatigue), whereas type IIb (or IIx) fibers have a high contractile velocity and a lower oxidative capacity (and therefore are more prone to fatigue).[5] Type IIa fibers are intermediate between types I and IIb.[5] The fiber-type profile, an important determinant of muscle metabolic capacity, has been assessed in patients with COPD by using both classic histochemical fiber typing and analysis of myosin heavy-chain isoform expression. In patients with mild-to-moderate airflow obstruction, the

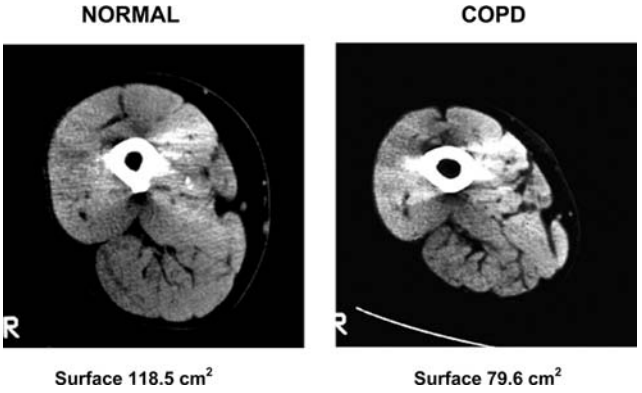

FIGURE 49-1 Computed tomography scans of one healthy subject (*left panel*) and one patient with chronic obstructive pulmonary disease (COPD) (*right panel*) of the same age group. The thigh muscle cross-sectional area was considerably reduced in the COPD patients in comparison with normal subject. Reproduced with permission from Bernard S et al.[8]

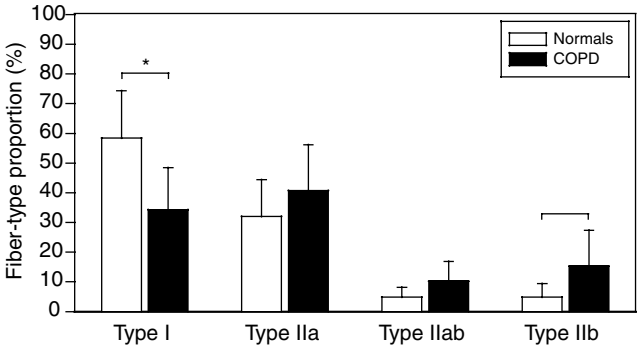

FIGURE 49-2 Fiber-type proportions of the vastus lateralis muscle found in normal subjects and in patients with chronic obstructive pulmonary disease (COPD). As can be seen, a significant reduction in the proportion of type I fibers was found, with a corresponding increase in the proportion of type IIb fibers, in patients with COPD in comparison with normal subjects. Values are mean ±SD. $*p < .0005$, $**p < .015$. Reproduced with permission from Whittom F et al.[11]

proportion of type I fibers is preserved.[10] In patients with more advanced airflow obstruction, there is a reduction in the proportion of type I fibers (17 to 29% vs 45 to 50% in COPD and normal subjects, respectively), with a reciprocal increase in type IIb fibers[11] (Figure 49-2). In COPD, type I and IIa fibers are atrophic, and the number of capillaries in contact with them is reduced in comparison with age-matched healthy subjects.[11] The reduction in type I and IIa fiber cross-sectional area is proportional to the reduction in midthigh cross-sectional area, suggesting that the loss in vastus lateralis muscle mass is mostly due to specific type I–IIa fiber atrophy.

Muscle Metabolic Capacity

In line with the fiber-type profile described above, low activity of two mitochondrial enzymes, citrate synthase[12,13] and 3-hydroxyacyl-CoA dehydrogenase,[13] has been reported in needle biopsy specimens of the vastus lateralis muscle in COPD. These two enzymes, which are involved in the citric acid cycle and β-oxidation of fatty acids, respectively, are good markers of muscle oxidative capacity. In contrast to the above findings, Sauleda and colleagues have reported higher activity of cytochrome *c* oxidase, a key enzyme of the electron transport chain (the last step of the oxidative pathway), in COPD patients than in healthy controls.[14] This finding is unexpected, given that the activities of all mitochondrial enzymes usually vary in a coordinated fashion. The significance of this apparently uncoordinated expression of mitochondrial enzymes in patients with COPD needs to be further investigated.

Peripheral Muscle Metabolism at Rest and During Exercise

In keeping with the morphologic and enzymic muscle changes, muscle energy metabolism is modified at rest and during exercise in COPD. At rest, low intracellular pH, reduced phosphocreatine (PCr) and ATP concentrations, and increased lactate and inosine monophosphate concentrations have been found in the vastus lateralis muscle.[15] When nuclear magnetic resonance spectroscopy (^{31}P-NMR) was used to study the oxidative metabolism of skeletal muscle during exercise (reviewed by Levy and colleagues[16]), greater declines in muscle intracellular pH and PCr/inorganic phosphate ratio were observed during exercise in patients with COPD than in normal subjects. These findings are indicative of impaired oxidative phosphorylation and ATP resynthesis, with a high reliance on anaerobic glycolysis within the contracting muscles. Although these exercise-induced peripheral muscle metabolic abnormalities are worsened by hypoxemia and can be partially reversed with oxygen supplementation, they have also been reported in patients with little or no reduction in peripheral oxygen delivery,[17] suggesting that altered muscle metabolism during exercise is related, at least in part, to poor muscle oxidative capacity or abnormal metabolic regulation.

Upper Extremity and Respiratory Muscles versus Lower Limb Muscles

Interestingly, all peripheral muscles are not affected to the same extent in patients with COPD. For instance, the strength of the upper extremity muscles is relatively preserved in comparison with that of the lower extremities,[8,18] and the activity of citrate synthase in the deltoid muscle was found to be preserved in patients with severe COPD in comparison with subjects with normal respiratory function.[19] The adaptation of the diaphragm in COPD is also different to that of the vastus lateralis muscle.[20,21] Whereas the vastus lateralis muscle shows a low capacity for aerobic metabolism and increased susceptibility to fatigue,[13] the diaphragm is characterized by an increased proportion of fatigue-resistant fibers.[20,21] The observation of differential adaptation of the respiratory, upper limb, and lower limb muscles is intriguing and may lead to insights into the mechanisms responsible for peripheral muscle dysfunction in COPD (see below). For instance, differential adaptive responses of the different muscle groups do not support the presence of a generalized myopathic disorder but would be

consistent with involvement of local muscular events in the deterioration of lower limb muscle function.

PERIPHERAL MUSCLE DYSFUNCTION AND CLINICAL STATUS

Functional peripheral muscle tissue is necessary for activities of daily living and vital functions such as breathing and eating. Moreover, muscle tissue can serve as an important reservoir from which amino acids can be drawn to support intense protein synthesis, such as during the systemic inflammatory response to infections or injuries.[22] The interactions between actin and myosin, which are responsible for force production and movement, require a continuous supply of energy, which is ensured by ATP production by either glycolytic or oxidative metabolism.[5] The relative proportions of the different myosin isoforms determine the speed of contraction, whereas the magnitude of force production is proportional to the muscle cross-sectional area. It is thus evident that alterations in muscle mass, morphologic characteristics, and enzymic characteristics will have negative influences at numerous levels.

Muscle Weakness and Endurance

In patients with moderate-to-severe airflow obstruction, the quadriceps muscle strength is reduced by approximately 30%.[8,18] The strength of the quadriceps muscle is an important determinant of exercise capacity in COPD.[18] This may be related to the influence of muscle strength on the perception of leg effort during exercise, the main limiting symptom in 40 to 45% of patients with COPD.[23] The question of whether muscle weakness is merely the consequence of muscle atrophy or contractile dysfunction and/or abnormal neural recruitment may contribute to loss of strength has been recently addressed. In patients with COPD, the quadriceps muscle strength/midthigh cross-sectional area ratio is similar to that of normal subjects.[8] To further address this question, in vitro contractile properties of the vastus lateralis muscle were studied in 16 patients with COPD and 9 control subjects.[24] Muscle bundles from the vastus lateralis muscle obtained by open biopsy were vertically suspended in an organ bath, and their contractile properties were measured. This experimental setup is interesting because under such conditions the maximal force production is totally independent of motivational factors. The maximal isometric peak forces, both in absolute values and normalized for the muscle bundle cross-sectional area, were similar for COPD and control subjects. On the basis of the in vivo and in vitro data, it is concluded that the contractile properties of the vastus lateralis muscle are preserved in patients with COPD. Therefore, the reduction in quadriceps muscle strength in patients with COPD can be explained not on the basis of an alteration of the contractile apparatus but rather on the basis of a loss in muscle mass. However, the loss in strength may be out of proportion to the loss of muscle mass in patients exposed to systemic corticosteroids.[8,25] This is in accordance with previous animal studies showing that corticosteroids may alter muscle function without causing muscle atrophy.[26]

In line with the histochemical and enzymic changes, the resistance to fatigue of the vastus lateralis muscle, measured during isometric contractions, is reduced in patients with COPD.[27]

Exercise Intolerance

Exercise intolerance is a major consequence of COPD, and this fact cannot be explained solely on the basis of limitations in ventilation and gas exchange. For instance, the degree of impairment in lung function is a poor predictor of exercise capacity.[28] Perhaps the most striking clinical observation pointing to a peripheral component of exercise limitation in COPD is that exercise capacity remains abnormally low in most lung transplant recipients despite normalization of lung function.[29]

In patients with COPD, exercise termination usually occurs before a true plateau in oxygen consumption (VO_2) is reached. In many patients, psychological factors such as anxiety, fear of dyspnea, and poor motivation may contribute to exercise intolerance. As a result, the physiologic contribution of individual factors to reduced peak VO_2 is difficult to assess. The contribution of peripheral muscle abnormalities to exercise limitation in COPD has been challenged by Richardson and colleagues.[30] These authors showed that the aerobic capacity of the lower limb muscle was not reached during cycling exercise (when a large muscle mass was involved) because of the early occurrence of central limitation to exercise. The implication of this is that the aerobic capacity of the exercising muscles of the lower limbs, even if reduced, is not overwhelmed during whole body exercise in patients with COPD. It must be remembered, however, that patients with COPD stop exercising because of exertional discomfort and not necessarily because of physiologic constraints. Leg fatigue is commonly perceived at peak exercise in patients with COPD[23]; this could be related to the fact that peripheral muscle alterations increasing susceptibility to contractile fatigue, such as poor oxidative capacity, atrophy, and weakness, are common in this disease. In line with these observations, Mador and colleagues[31] confirmed that contractile fatigue of the quadriceps muscle might occur during exercise in patients with COPD. We recently evaluated the impact of leg fatigue on the exercise response to acute bronchodilatation in patients with COPD in order to test the hypothesis that the improvement in airflow obstruction should not translate into greater exercise capacity in patients with higher susceptibility to leg fatigue.[32] Patients with COPD performed two constant-work-rate cycling exercises up to exhaustion. These tests were preceded by nebulization of placebo or 500 μg of ipratropium bromide. Muscle fatigue was defined as a postexercise reduction in quadriceps muscle twitch force >15% of the resting value. Nine patients developed contractile fatigue after placebo exercise. In these patients, ipratropium bromide did not increase endurance time, despite an 11% improvement in forced expiratory volume in 1 second. In the nine patients who did not show fatigue after placebo exercise, endurance time was increased by ipratropium bromide. There was a significant correlation between the improvement in endurance time with ipratropium bromide and quadriceps

muscle twitch force at 10 minutes after placebo exercise. In summary, improved exercise response after bronchodilatation may be prevented by concomitant leg fatigue, providing direct evidence of the role of peripheral muscle dysfunction in exercise intolerance in COPD.

Lower capacity for muscle aerobic metabolism may influence exercise tolerance in several ways. Increased lactic acidosis for a given exercise work rate, which is a common finding in COPD,[13,33,34] increases ventilatory needs by increasing nonaerobic carbon dioxide production.[33] This imposes an additional burden on the respiratory muscles, which are already facing increased impedance to breathing. In addition, the resulting acidemia may act as a breathing stimulus through the carotid bodies. Premature muscle acidosis, a contributory factor to muscle fatigue and early exercise termination in healthy subjects, may be an important mechanism contributing to exercise intolerance in COPD.[17] This may be exacerbated by a tendency to retain carbon dioxide (respiratory acidosis) during exercise.[33]

Our interpretation of the current literature is that although muscle oxidative potential may not be fully used during a maximal exercise test, the muscle atrophy and weakness and the alterations in muscle metabolism during exercise that have been repeatedly reported in COPD are likely to influence the capacity to perform exercise by increasing the perception of leg effort and the ventilatory requirements and by contributing to the development of contractile fatigue of the peripheral muscles.

Other Consequences of Muscle Dysfunction

Other likely consequences of muscle wasting and poor peripheral muscle function in COPD include reduction in quality of life,[35] greater utilization of health care resources,[36] and poor survival.[37]

ETIOLOGY OF PERIPHERAL MUSCLE DYSFUNCTION IN COPD

Several factors have been suggested to explain the occurrence of muscle dysfunction in COPD, and their relative importance is likely to vary among patients. Peripheral muscle dysfunction is probably multifactorial in origin and is unlikely to be explained by one mechanism in all patients. Chronic inactivity,[38] nutritional imbalance,[39] systemic corticosteroid use,[25] hypoxemia,[40] systemic inflammation with increased circulating levels of proinflammatory cytokines,[41] electrolyte disturbances,[42] and low anabolic hormone levels[43,44] have all been suggested as potential contributors to the development of poor peripheral muscle function in COPD. However, a causal link between these abnormal states and the deterioration in muscle function has not been established.

It is often supposed that muscle wasting in COPD is due to an imbalance between caloric intake and energy expenditure, leading to a reduction in protein synthesis.[39,45] However, attempts to increase nutritional intake have resulted in only modest and inconsistent improvements in body weight and muscle mass and strength (reviewed by Ferreira and colleagues[46]). As in many chronic disorders,[47] increased muscle proteolysis is likely to be present in COPD and could explain the lack of efficacy of nutritional interventions in ameliorating muscle dysfunction in COPD.

A similar conclusion was reached with regard to several other illnesses,[22,48,49] leading to the development of the concept of cachexia. Cachexia (Greek: bad condition), in contrast to starvation, is characterized by preferential loss in the muscle tissue compartment associated with systemic inflammation and lack of response to nutritional supplementation.[22] The preferential loss of muscle tissue,[8,9] the lack of response to nutritional supplementation, and the presence of low-grade systemic inflammation[41] with increased blood levels of proinflammatory cytokines[50] strongly suggest that the loss in body weight and muscle mass in patients with COPD can be considered to constitute a state of cachexia.

Regulation of Muscle Protein Synthesis and Degradation

The muscle tissue is a primary reservoir of amino acids in the body. In response to disease or fasting, amino acids released from muscle tissue are mobilized to sustain liver protein synthesis (acute-phase protein synthesis) or immune cell replication, as well as for energy production (gluconeogenesis).[22] The amount of muscle tissue (ie, its protein content) in a given individual is the result of a tight balance between protein synthesis and breakdown. Increased protein degradation is a hallmark of many diseases, such as cancer,[22] sepsis,[51] and chronic renal failure.[49] For COPD, there have been only two studies in which protein metabolism was assessed, and their conclusions conflict.[45,52] In comparison with healthy subjects, one study found decreased protein synthesis in COPD patients,[45] whereas the other[52] found simultaneous increases in protein synthesis and degradation, reflecting increased whole body protein turnover. Lack of agreement between these studies may be explained by the use of different techniques to measure protein metabolism, in addition to the disparity in the subjects studied. Further studies of protein metabolism will be needed to clarify this issue.

Muscle Proteolysis

There are different pathways for degrading proteins. Lysosomes contain proteases that have optimal activity at an acidic pH (eg, cathepsins) and degrade membrane or endocytosed proteins. Traditionally, degradation by this pathway has been thought to be nonspecific, but there is growing evidence that some intracellular proteins can be specifically targeted by the lysosome for degradation.[53] A second proteolytic pathway involves Ca^{2+}-dependent proteases (eg, calpains). These proteases are believed to play a role in cytoskeletal reorganization.[54] A third intracellular proteolytic system is even more obscure and involves proteolysis that does not require energy. The specific enzymes involved and the mechanisms that regulate their activities are poorly understood, but this category may include metalloproteases and proteases involved in apoptosis. Finally, there are energy-requiring proteolytic systems. The fourth and best-described system for muscle proteolysis is the

ubiquitin–proteasome pathway, which requires ATP and degrades the bulk of cellular and some membrane proteins.[55]

Activation of the ubiquitin–proteasome system has been well established in a wide range of animal models[47] and to a lesser extent in human muscle tissues in association with diverse illnesses such as cancer,[56] sepsis,[57] head trauma,[58] and AIDS.[59] However, the role of the ubiquitin–proteasome system in the wasting process in patients with COPD has not been established. In most animal models of cachexia, the genes encoding for different components of the ubiquitin–proteasome system are up-regulated two- to fourfold during muscle atrophic processes.[47] This system is complex and consists of a highly organized cascade of enzymic reactions, which select, mark, and degrade proteins (Figure 49-3).[55] Proteins destined for degradation by this system are first modified by the attachment of a small protein, ubiquitin. Ubiquitin is abundantly expressed in all higher eukaryotic cells and is one of the most evolutionarily conserved proteins known. In most cases, ubiquitin is linked to the substrate protein through an isopeptide bond between the ε-amino groups of lysines in the target protein and the C-terminal glycine of ubiquitin. Cycles of these reactions link additional ubiquitins to lysines with ubiquitins added previously.[55]

The conjugation of ubiquitin and protein substrates involves a series of complex steps. Initially, an ubiquitin-activating E1 enzyme uses ATP to form an E1–ubiquitin thioester adduct with the C-terminal glycine of ubiquitin. A single E1 enzyme is responsible for ubiquitin activation in all mammalian cells. After ubiquitin activation, members of the E2 ubiquitin-carrier protein family (also called ubiquitin-conjugating enzymes) participate in the transfer of the activated ubiquitin to protein substrates. In the vast majority of cases, a member of the E3 ubiquitin–protein ligase family also participates in the conjugation process. The purpose of the various E3 ubiquitin ligases is to provide selectivity to the ubiquitination process by serving as docking proteins that bring the substrate protein and the E2 carrier protein with activated ubiquitin together. In some instances, accessory proteins required for ubiquitin conjugation interact with E3 ubiquitin ligases. The E3 ubiquitin ligases are grouped into three major families, on the basis of structural similarities and the functional classes of substrates that they recognize. These three groups are the HECT domain ubiquitin ligases, and the two groups comprising the RING finger ubiquitin ligases, the single-unit and multisubunit enzymes.[55] Recently, two groups have identified new ubiquitin ligases that are expressed specifically and robustly in wasting muscles of animals in catabolic states. MuRF1 (muscle RING finger-1) is a single-subunit RING finger E3 ligase.[60] Atrogin-1 (atrophy gene-1),[61] also known as MAFbx (muscle atrophy F-box),[60] is an F-box–containing protein that is a member of the family of the multisubunit E3 ubiquitin ligases.

Clearly, activation of the ubiquitin–proteasome system is necessary for muscle wasting. However, muscle proteolysis does not directly depend on activation of this system. For instance, actomyosin complexes and myofibrils are resistant to degradation by this system.[62] In order to undergo ubiquitination and eventually degradation by the proteasome, contractile proteins must be released from the myofibril and cleaved. One appealing hypothesis is that activation of proapoptotic proteases that could cleave actomyosin complexes and actin into fragments is necessary to trigger their degradation by the ubiquitin–proteasome system.[63] Other investigators have suggested that the role played by the Ca^{2+}-dependent proteolytic enzyme calpain is a key step in the release of actin and myosin from the sarcomere.[64] It has also been suggested that the oxidation of contractile proteins as a consequence of muscle oxidative stress could be one mechanism triggering the ubiquitination and degradation of myofibril proteins (see below).

Although muscle proteolysis and activation of the ubiquitin–proteasome system are thought to be of the utmost importance in the development of cachexia in various conditions, the signals that trigger this process seem to differ from one pathologic state to another. For instance,

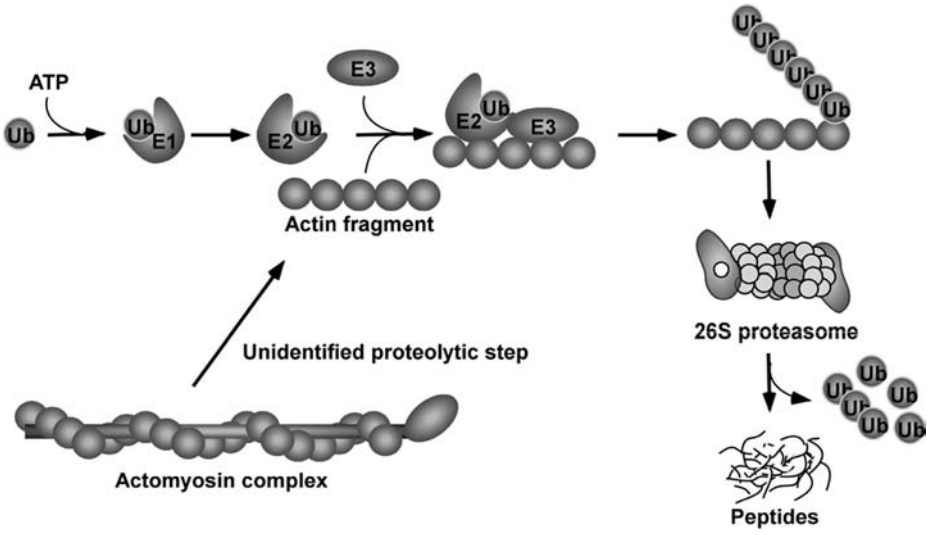

FIGURE 49-3 The ubiquitin (Ub)–proteasome pathway. Initially, a Ub-activating enzyme (E1) uses ATP to form an E1–Ub thioester adduct with the C-terminal glycine of Ub. After Ub activation, members of the Ub-carrier protein family (E2) participate in the transfer of the activated Ub to protein substrates such as actin fragment, which is provided by unidentified proteolytic steps. In the majority of cases, a member of the Ub–protein ligase family (E3) also participates in the conjugation process. When a chain of four or more Ub molecules is formed, the chain is recognized by the 26S proteasome, and the substrate protein is degraded into short peptides.

glucocorticoids and low insulin levels are essential for the enhanced proteolysis and muscle wasting in diabetes, whereas tumor necrosis factor-α (TNF-α), prostaglandins, and glucocorticoids play important roles in muscle wasting in sepsis and cancer-induced cachexia.[22,47] Finally, acidosis and glucocorticoids have been shown to play important roles in the muscle cachexia observed in uremic animals.[47]

Inflammation and Oxidative Stress

A common finding in different wasting conditions is the elevated blood levels of proinflammatory cytokines. The role of these cytokines in the wasting process is based on the following observations: (1) cultured myoblasts exposed to TNF-α or other cytokines do not undergo normal differentiation[65] and (2) muscle cachexia can be induced in small animals by systemic injection of proinflammatory cytokines,[66] and this can be prevented by inhibiting the activity of these cytokines[67] or their receptors.[66] Although proinflammatory cytokines such as TNF-α and interleukin-6 (IL-6) can activate the ubiquitin–proteasome pathway, they do not reduce lean body mass directly. In this regard, the activation of nuclear factor kappa B (NFκB) seems to be a key intermediate step.[68] NFκB is a ubiquitous transcription factor, present in the cytosol in an inactive form when coupled to its natural inhibitor, IκB. Inflammatory cytokines can activate NFκB by initiating the degradation of IκB by the proteasome. Free of its inhibitor, NFκB can then translocate into the nucleus, bind to target DNA elements, and regulate the transcription of several genes coding for inflammatory and growth molecules. In muscle, NFκB can inhibit the expression of MyoD, which is a transcription factor that is essential and specific for skeletal muscle differentiation and repair.[65] Direct inhibition of NFκB prevents muscle wasting in animal models.[65] The negative action of NFκB on muscle growth and repair is subject to tight counterregulatory mechanisms. For instance, NFκB can also suppress the transcription of the proteasome C3 subunit in muscle cells, thus blocking muscle protein degradation.[69] Interestingly, glucocorticoids exert their catabolic effect by opposing the NFκB proteasome suppression.[69]

Inflammation may also induce an oxidant–antioxidant imbalance in patients with chronic disorders by providing a continuous source of oxidative stress,[70] which may contribute to poor muscle performance[71] and impaired muscle regeneration because oxidative stress also inhibits myogenic differentiation.[72] It was recently shown that mild oxidative stress increases protein degradation in skeletal muscle by causing increased expression of the major components of the ubiquitin–proteasome pathway.[73] In addition, skeletal muscle proteins modified by reactive oxygen species (ROS) can be easily degraded by the proteasome.[74] Interestingly, antioxidants may prevent muscle wasting in a murine model of cachexia induced by TNF-α.[75] Thus, inflammation and ROS may have interrelated actions and act synergistically in inducing muscle proteolysis.

COPD is characterized by low-grade systemic inflammation (reviewed by Debigaré and colleagues[50]), which is often accompanied by low blood levels of anabolic hormones.[43,44,76] Elevated blood levels of IL-6, IL-8, TNF-α, and C-reactive protein in COPD patients have been associated with low muscle mass, increased resting energy expenditure, and unresponsiveness to nutritional interventions, giving support to the concept that these cytokines play a role in COPD-associated cachexia. In addition, levels of adhesion molecules are increased in bronchoalveolar fluids and plasma of COPD patients in comparison with healthy subjects. The presence of adhesion molecules in the blood is necessary for the initiation of bronchial inflammatory cell infiltration. In theory, these adhesion molecules could also induce inflammatory cell infiltration in other tissues, such as skeletal muscle, but this has yet to be verified. Accordingly, it is conceivable that a low-grade and chronic systemic inflammatory process may participate in the development of peripheral muscle wasting and dysfunction in COPD[76,77] (reviewed by Debigaré and colleagues[50]).

In view of the possible interaction between proinflammatory cytokines and ROS, it is interesting that there is increased generation of ROS, originating from the contractile muscles, after low-intensity exercise[78] and after local exercise of the quadriceps muscle in patients with COPD.[79] As a result, local muscle exercise induces an imbalance between oxidant and antioxidant defenses in patients with COPD. Thus, repeated bursts of ROS occurring within the peripheral muscles of patients with COPD during activities of daily living may be involved in triggering the cachexic cascade. Muscle oxidative stress may also reduce muscle endurance, as suggested by one study that showed an inverse and significant relationship between markers of exercise-induced muscle oxidative stress and quadriceps muscle endurance.[79] These findings support the role of cytotoxic oxidant and oxidative stress in the development of muscle fatigue and altered endurance capacity in patients with COPD. Indeed, muscle oxidative stress causes noticeable damage to myocyte organelles, DNA, proteins, and lipids and results in excessive rises in intracellular free Ca^{2+} level, mitochondrial dysfunction, and bioenergetic enzyme down-regulation.[71]

Decreased Anabolism

Although increased catabolism is a hallmark of muscle wasting, there is also support for the hypothesis that anabolic factors are equally important for muscle mass homeostasis. A mechanistic link between anabolic factors and the maintenance of muscle mass is emerging.[76] For instance, it was recently demonstrated that insulin and insulin-like growth factors (IGFs) stimulate myofibril synthesis.[80] Conversely, insulin and IGFs can decrease protein degradation by reducing the activity of the ubiquitin–proteasome pathway.[81,82] Interestingly, proinflammatory cytokines can exert a suppressive action on IGF-1 by up-regulating the expression of its circulating inhibitor, insulin-like growth factor binding protein-1.[83] This indicates that there is a close relationship between the catabolic and anabolic pathways. Other factors regulating muscle growth, such as myostatin and myogenin, have been recently identified, and their role in wasting disorders is currently being investigated.[84,85]

Concurrently with the low-grade systemic inflammation, patients with COPD also show a higher prevalence of low

plasma levels of testosterone[44,76] and IGF-1[43] than healthy subjects of a similar age. The clinical relevance of this finding remains to be elucidated as correlations between body weight or muscle mass and plasma levels of these hormones, taken individually, are weak,[44,76] and supplementation with anabolic steroids[39] or growth hormone[86] had only a modest effect on lean mass and functional status. However, a significant relationship has been described between IL-6/DHEAS (dehydroepiandosterone, DHEAS sulfate) ratio and midthigh muscle cross-sectional area in patients with COPD, supporting the concept that the balance between catabolic and anabolic factors is more relevant to muscle wasting than either category of factors taken individually.[76] This finding also suggests that there is an intimate relationship between the catabolic and anabolic pathways in regulating muscle mass.

Nutritional Imbalance

Increased total daily and resting energy expenditure is common in patients with COPD and could contribute to body weight and muscle mass loss.[87,88] In many patients, the greater energy expenditure is compensated for by increases in caloric intake, so that body weight is maintained. However, this adaptation is progressively lost in patients with severe COPD, as indicated by Schols and colleagues, who reported a decrease in caloric intake with increasing severity of airflow obstruction.[88] Although nutritional imbalance may play a role in muscle wasting in some patients, the absent or modest improvement in peripheral muscle function associated with nutritional supplementation suggests that a negative energetic balance is not the primary mechanism of muscle wasting in most cases.[46]

Hypoxemia

In healthy subjects, chronic hypoxia decreases muscle mass, lowers the oxidative capacity of skeletal muscle, and reduces the cross-sectional area of type I fibers.[89] In keeping with this, a positive correlation between the arterial partial pressure of oxygen (P_aO_2) and percentage of type I fibers in the vastus lateralis muscle has been reported in patients with COPD.[40] Although such a relationship should be interpreted with caution, since hypoxemia only occurs in patients with advanced disease and severe functional impairment, it raises the possibility that chronic hypoxemia may play a role in patients with low resting P_aO_2 or in those with repeated oxygen desaturation occurring during sleep and/or exercise.[90] Hypoxemia may also contribute to wasting in COPD by decreasing anabolic hormone levels[91] and increasing proinflammatory cytokine levels.[92] The presence of hypoxemia is also associated with the generation of ROS, which contribute to oxidative stress.[78] Overall, hypoxemia may contribute to wasting by shifting the balance between anabolic and catabolic factors in favor of the latter.

Chronic Inactivity and Deconditioning

Chronic inactivity leading to muscle deconditioning is the most often quoted cause of peripheral muscle dysfunction in COPD. It is a common observation that patients with COPD often reduce their level of activity to avoid the dyspnea that ambulation engenders. Furthermore, the similarity between the histochemical and enzymic muscle changes associated with chronic inactivity in healthy humans and those reported in patients with COPD[5] is another indication that muscle deconditioning is likely in COPD. The different degrees of activation of the lower limb muscles and upper limb and diaphragmatic muscles may be responsible for the different levels of abnormalities in these three muscle groups.[8,20] In comparison with lower limb muscles, those of the upper limb probably remain more active in daily living, explaining why their function is relatively maintained.[8,19] Furthermore, in COPD, the pectoralis major and latissimus dorsi muscles may also act as accessory inspiratory muscles, another potential source of stimulation.[93] The level of activation of the diaphragm is also greater than that of the lower limb muscles in COPD, and the chronic increase in work of breathing faced by the diaphragm is, in fact, a continuous training stimulus. The increased proportion of type I fibers in the emphysematous diaphragm is likely to represent an adaptation to training, reinforcing the role of deconditioning in peripheral muscle dysfunction in these individuals.[20] Finally, the improvement in skeletal muscle oxidative capacity observed after training also supports a role for deconditioning.[38]

Systemic versus Local Factors in Peripheral Muscle Dysfunction

The finding that diaphragmatic function is preserved or even better than expected in COPD[20,21,94] is inconsistent with the possibility that muscle wasting is entirely due to systemic factors. Therefore, local factors must be involved in the development of peripheral muscle cachexia in COPD. The most obvious candidate is decreased level of activity. Inactivity may increase the activity of the ubiquitin–proteasome pathway[95] and reduce the production of IGF-1, one of the main muscle growth factors.[96] More recently, IGF-2, but not IGF-1, was shown to be down-regulated in muscle atrophy induced by weightlessness in rats.[97] Peripheral muscles and the liver are major sources of IGF.[96] Because of differences in the level of muscle activation, we therefore speculate that IGF-1 and IGF-2 are down-regulated in the vastus lateralis muscle but not in the diaphragm in patients with COPD. In contrast to inactivity, exercise training should improve the balance between catabolism and anabolism by increasing the levels of muscle growth factors.

Other local factors, yet to be identified, are likely to be involved in muscle wasting, as indicated by the marked modifications in the myosin heavy-chain profile of the vastus lateralis muscle in patients with COPD in comparison with healthy subjects, despite modest differences in physical fitness.[98] Perhaps the most provocative observation in this regard is the decreased hindlimb muscle oxidative capacity found in the emphysematous hamster despite there being no reduction in the level of activity in comparison with control animals.[99] We can only speculate about the factors that could also contribute at the local level to the induction of muscle wasting. The results of some animal studies suggest that muscle acidosis may be involved in protein degradation.[47] This may be relevant to patients with COPD, in whom mild exercise, such as that performed in daily

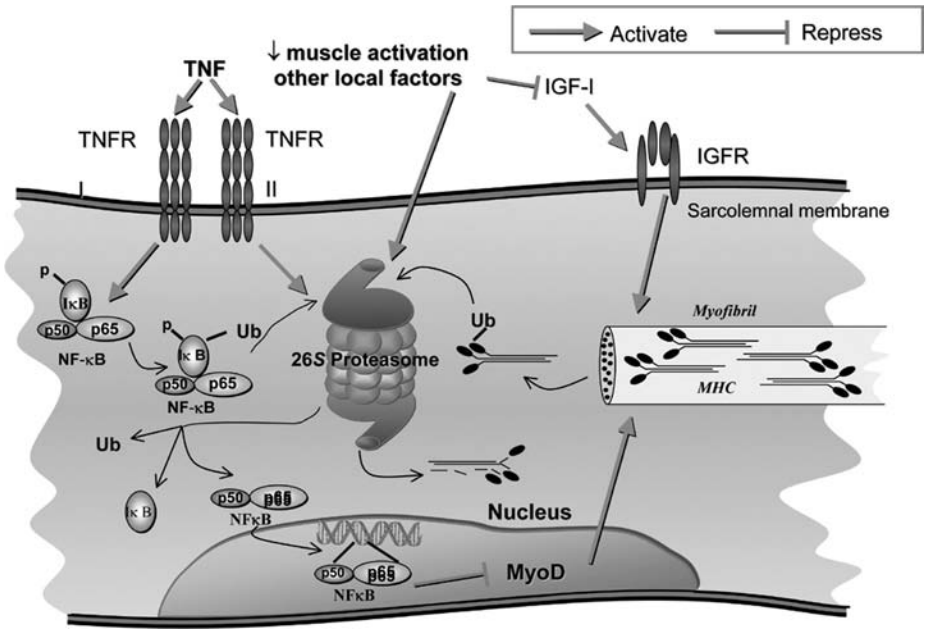

FIGURE 49-4 Schematic representation of the possible mechanisms of cachexia in chronic obstructive pulmonary disease. Growth factors such as insulin-like growth factor-1 (IGF-1) and MyoD exert their anabolic effects by activating myofibril synthesis. Myofibrillar proteins are marked for degradation by ubiquitin (Ub) and are then processed through the 26S proteasome. This protein degradation pathway can be activated by muscle inactivity. Proinflammatory cytokines such as tumor necrosis factor (TNF) (shown here), interleukin-1 (IL-1), and IL-6 exert their catabolic effects by activating nuclear factor kappa B (NFκB), which can enter the nucleus after dissociating from its inhibitor (IκB). One catabolic action of NFκB is to repress the gene expression of MyoD. Proinflammatory cytokines may also activate the ubiquitin–proteasome pathway. A reasonable hypothesis is that systemic (TNF, growth factors) as well as local (inactivity, acidosis) factors interact in the development of cachexia. IGFR = insulin-like growth factor receptor; MHC = myosin heavy chain; TNFR I and II = TNF receptors I and II. Reproduced with permission from Debigaré R et al.[50]

living, induces early and exaggerated muscle acidosis in comparison with healthy subjects.[17] As indicated above, ROS may act locally to trigger muscle wasting. The exciting hypothesis that muscle wasting could occur without a decrease in muscle activation will be extremely difficult to show in humans, in whom the level of physical activity cannot be adequately controlled.

Apoptosis

The results of recent studies on apoptosis suggest that an increased frequency and/or intensity of this phenomenon could be responsible for the segmental loss of muscle mass in many different conditions, such as inactivity, aging, and congestive heart failure (reviewed by Sandri[100]). Although similar findings have also been obtained in COPD,[101] it is not clear how apoptosis is triggered in skeletal muscle. Death signals originate in some foci and are translated into apoptotic events through the cell by mitochondria-related pathways. It has been suggested that apoptosis occurs in only part of the multinucleated muscle fiber as a segmental process in order to maintain the right cytoplasm/nucleus ratio.[100] Perhaps, in atrophying muscle, apoptosis acts as a regulatory mechanism, maintaining a vital degree of function in the affected muscle group.

A reasonable integrative hypothesis is that cachexia in COPD is the result of an interplay of systemic factors (eg, cytokines, growth factors) that, although not remarkably elevated, may synergize with local factors (eg, inactivity, ROS, acidosis), leading to a disequilibrium between anabolism and catabolism.[50] A simplified but useful schematic representation of the cellular mechanisms of muscle wasting in COPD is given in Figure 49-4. Further studies are warranted to determine the relative importance of all the potential factors involved in this complex process.

Corticosteroids

Muscle wasting and weakness characterize steroid-induced myopathy and preferentially affect type IIb fibers.[102] The potential role of corticosteroids in the development of muscle weakness should not be overlooked in some individuals submitted to chronic or even intermittent systemic corticosteroid treatment.[25,102] In patients with COPD, subtle muscle weakness may appear with low doses of corticosteroids (<10 mg/day), perhaps because of greater susceptibility to the development of corticosteroid-induced myopathy.[25]

TREATMENT OF PERIPHERAL MUSCLE DYSFUNCTION IN COPD

The treatment of peripheral muscle dysfunction is likely to remain suboptimal as long as our understanding of this problem is incomplete. Because the etiology of peripheral muscle dysfunction in COPD appears to be multifactorial, one isolated therapeutic strategy is unlikely to completely resolve the problem. A global approach, with correction of all possible contributing factors, should have a better chance of success.

Although no cure is available for muscle wasting in COPD patients, it is important to recognize the potential therapeutic consequences of peripheral muscle wasting. Gains in muscle mass and strength have been associated with

better exercise tolerance and survival.[103] Thus, improving peripheral muscle function is an important therapeutic target in patients with COPD.

Exercise Training

Probably the best available therapeutic modality for increasing and/or preserving muscle mass is exercise training, which has been shown to increase muscle mass, strength, and aerobic capacity.[38,104,105] Several studies have indicated that patients with severe COPD can sustain the necessary training intensity and duration for skeletal muscle adaptation to training to occur.[11,38,106] After 12 weeks of leg-cycling exercise, increases were found in the activity of two mitochondrial enzymes (Figure 49-5), type I fiber size of the vastus lateralis muscle, and capillary density.[11,38] As a consequence of the improvement in muscle oxidative capacity with training, changes in muscle metabolism also occur, leading to a reduction in lactic acid efflux during exercise.[105] Other investigators have reported increased quadriceps muscle endurance during voluntary contractions after 3 weeks of endurance training.[107] Strength training also appears to be worthwhile in patients with COPD[108] as this type of training has more potential to improve muscle mass and strength than does aerobic training.[104] In addition, strength training causes less dyspnea during the exercise period, making this strategy easier to tolerate by patients with severe COPD than aerobic training.[108]

Nutritional Intervention

Nutritional support has been used with the hope that restoring nutritional balance will increase body weight, muscle mass and, ultimately, functional status. Comparison between studies is difficult because of the variety of nutritional interventions (reviewed by Ferreira and colleagues[46]). Weight gain can be achieved with oral or enteral nutritional supplementation for 2 to 12 weeks, although the results are often modest and inconsistent. Patients in whom body weight increases following a nutritional intervention show a somewhat better prognosis than those in whom this intervention does not modify body weight.[103] However, it is unclear whether the survival advantage in the responders is related to the gain in body weight per se or simply reflects the presence of more favorable patient characteristics.

Typically, the increase in body weight resulting from nutritional supplementation is due to an increase in fat, with there being little or no increase in muscle mass.[39] It is therefore not surprising that the magnitude of improvement in muscle strength and functional status following nutritional supplementation is often disappointing. There are also important limitations to aggressive nutritional intervention in patients with severe COPD. Gastrointestinal symptoms, such as bloating, early satiety, meal-related oxygen desaturation, and postprandial dyspnea, are common side effects.[109] Despite the lack of strong evidence for beneficial effects of nutritional intervention on muscle function, it is nevertheless advisable to restore a positive energetic balance for patients with low body weight. The first step in achieving this goal is dietetic counseling.[109]

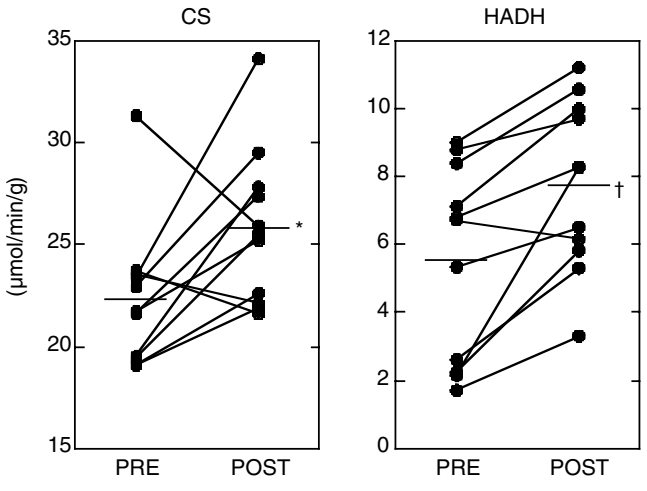

FIGURE 49-5 Individuals' values for the activity of citrate synthase (CS) and 3-hydroxyacyl-CoA-dehydrogenase (HADH) in 11 patients with COPD before and after 12 weeks of exercise training. These values increased significantly after training. $^{*}p < .05$, $^{\dagger}p < .01$. Reproduced with permission from Maltais F et al.[38]

Anabolic Hormone Supplementation

The results of anabolic steroid[39,110] and growth hormone[86] supplementation have been disappointing so far. However, the doses used were probably subtherapeutic, and further studies are needed to determine optimal dosages for these anabolic hormones. The use of these drugs should also be studied in conjunction with exercise training as synergy may be observed.[111]

Oxygen Therapy

Although short-term oxygen therapy enhances exercise tolerance and muscle aerobic metabolism in hypoxemic patients with COPD,[16] little is known of the effects of long-term oxygen therapy on muscle function. Six to nine months of home oxygen therapy has been shown to facilitate the formation of muscle ATP but does not appear to improve skeletal muscle enzyme activity.[12] It seems possible that long-term oxygen supplementation might allow an increased level of activity and therefore improved muscle function. This possibility deserves to be investigated.

Novel Therapeutic Strategies

Based on our current knowledge of muscle homeostasis, several novel therapeutic avenues can be proposed to reverse the wasting. One way to intervene is to increase protein synthesis with the use of growth factors such as IGF-1, which can suppress ubiquitin–proteasome activities[81] and induce hypertrophy.[80] Novel forms of nutritional intervention, involving branched amino acid supplementation (leucine, isoleucine, and valine), are of interest as they may inhibit proteolysis in skeletal muscle by acting as a negative feedback regulator of the lysosomal proteolytic system and by decreasing ubiquitin–proteasome system gene expression.[112] In rats, clenbuterol, a β_2-adrenergic agonist, normalizes protein breakdown and prevents skeletal muscle wasting.[113]

However, equivocal results have been obtained with this drug in humans.[114] The efficacies of new antiinflammatory drugs, such as cytokine inhibitors or muscle-specific proteasome inhibitors, alone or together, in blocking muscle proteolysis and increasing muscle mass are likely to be evaluated in the near future.[115] Finally, antioxidants could also represent another promising therapeutic target. Clearly, research on muscle wasting in patients with COPD and other chronic diseases will help identify new therapeutic strategies for this important problem that can reverse its adverse clinical effects.

CONCLUSION

Modern medicine faces the challenge of improving the care of patients with chronic diseases such as COPD. Despite all the efforts of preventive medicine, the burden of COPD is expected to increase in the coming decades. Unless a cure for the disease is found, physicians will have to deal with the systemic consequences of COPD. It will therefore be important to better address the problem of peripheral muscle dysfunction as an appropriate treatment for this condition should result in a better life for our patients in terms of both quality and duration.

ACKNOWLEDGMENT

The research discussed in this chapter was supported by CIHR grant no. MOP-53135.

REFERENCES

1. American Thoracic Society. Standards for the diagnosis and care of patients with chronic obstructive pulmonary disease. Am J Respir Crit Care Med 1995;152:S77–120.
2. Sharkey RA, Mulloy EM, Kilgallen IA, O'Neill SJ. Renal functional reserve in patients with severe chronic obstructive pulmonary disease. Thorax 1997;52:411–5.
3. Gow SM, Seth J, Beckett GJ, Douglas G. Thyroid function and endocrine abnormalities in elderly patients with severe chronic obstructive lung disease. Thorax 1987;42:520–5.
4. Biskobing DM. COPD and osteoporosis. Chest 2002;121: 609–20.
5. American Thoracic Society/European Respiratory Society. Skeletal muscle dysfunction in chronic obstructive pulmonary disease. Am J Respir Crit Care Med 1999;159:S1–40.
6. Sadoul P. Les cachexies respiratoires. Bull Physiopathol Respir 1969;5:3–11.
7. Schols AMWJ, Soeters PB, Dingemans MC, et al. Prevalence and characteristics of nutritional depletion in patients with stable COPD eligible for pulmonary rehabilitation. Am Rev Respir Dis 1993;147:1151–6.
8. Bernard S, Leblanc P, Whittom F, et al. Peripheral muscle weakness in patients with chronic obstructive pulmonary disease. Am J Respir Crit Care Med 1998;158:629–34.
9. Engelen MP, Schols AM, Does JD, Wouters EF. Skeletal muscle weakness is associated with wasting of extremity fat-free mass but not with airflow obstruction in patients with chronic obstructive pulmonary disease. Am J Clin Nutr 2000;71:733–8.
10. Satta A, Migliori GB, Spanevello A, et al. Fibre types in skeletal muscles of chronic obstructive pulmonary disease patients related to respiratory function and exercise tolerance. Eur Respir J 1997;10:2853–60.
11. Whittom F, Jobin J, Simard PM, et al. Histochemical and morphological characteristics of the vastus lateralis muscle in COPD patients. Comparison with normal subjects and effects of exercise training. Med Sci Sports Exerc 1998;30: 1467–74.
12. Jakobsson P, Jorfeldt L, Henriksson J. Metabolic enzyme activity in the quadriceps femoris muscle in patients with severe chronic obstructive pulmonary disease. Am J Respir Crit Care Med 1995;151:374–7.
13. Maltais F, Simard AA, Simard C, et al. Oxidative capacity of the skeletal muscle and lactic acid kinetics during exercise in normal subjects and in patients with COPD. Am J Respir Crit Care Med 1996;153:288–93.
14. Sauleda J, García-Palmer F, Wiesner RJ, et al. Cytochrome oxidase activity and mitochondrial gene expression in skeletal muscle of patients with chronic obstructive pulmonary disease. Am J Respir Crit Care Med 1998;157:1413–7.
15. Pouw EM, Schols AMWJ, van der Vusse GJ, Wouters EFM. Elevated inosine monophosphate levels in resting muscle of patients with stable chronic obstructive pulmonary disease. Am J Respir Crit Care Med 1998;157:453–7.
16. Levy P, Wuyam B, Pepin JL, et al. Skeletal muscle abnormalities in chronic obstructive lung disease with respiratory insufficiency. Value of P31 magnetic resonance spectroscopy. Rev Mal Respir 1997;14:183–91.
17. Maltais F, Jobin J, Sullivan MJ, et al. Metabolic and hemodynamic responses of the lower limb during exercise in patients with COPD. J Appl Physiol 1998;84:1573–80.
18. Gosselink R, Troosters T, Decramer M. Peripheral muscle weakness contributes to exercise limitation in COPD. Am J Respir Crit Care Med 1996;153:976–80.
19. Gea J, Pasto M, Carmona MA, et al. Metabolic characteristics of the deltoid muscle in patients with chronic obstructive pulmonary disease. Eur Respir J 2001;17:939–45.
20. Levine S, Kaiser L, Leferovich J, Tikunov B. Cellular adaptation in the diaphragm in chronic obstructive pulmonary disease. N Engl J Med 1997;337:1799–806.
21. Mercadier JJ, Schwartz K, Schiaffino S, et al. Myosin heavy chain gene expression changes in the diaphragm of patients with chronic lung hyperinflation. Am J Physiol 1998; 274:L527–34.
22. Tisdale MJ. Cachexia in cancer patients. Nat Rev Cancer 2002;2:862–71.
23. Killian KJ, Leblanc P, Martin DH, et al. Exercise capacity and ventilatory, circulatory, and symptom limitation in patients with airflow limitation. Am Rev Respir Dis 1992; 146:935–40.
24. Debigaré R, Cote CH, Hould FS, et al. In vitro and in vivo contractile properties of the vastus lateralis muscle in males with COPD. Eur Respir J 2003;21:273–8.
25. Decramer M, Lacquet LM, Fagard R, Rogiers P. Corticosteroids contribute to muscle weakness in chronic airflow obstruction. Am Rev Respir Dis 1994;150:11–6.
26. Dekhuijzen PNR, Gayan-Ramirez G, Dom R, et al. Triamcinolone and prednisolone affect contractile properties and histopathology of rat diaphragm differently. J Clin Invest 1993;92:1534–42.
27. Serres I, Gautier V, Varray AL, Préfaut CG. Impaired skeletal muscle endurance related to physical inactivity and altered lung function in COPD patients. Chest 1998;113:900–5.
28. Jones NL, Killian KJ. Limitation of exercise in chronic airway obstruction. In: Cherniack NS, editor. Chronic obstructive pulmonary disease. Philadelphia: WB Saunders; 1991. p. 196–206.
29. Williams TJ, Patterson GA, Mcclean PA, et al. Maximal exercise testing in single and double lung transplant recipients. Am Rev Respir Dis 1992;145:101–5.

30. Richardson RS, Sheldon J, Poole DC, et al. Evidence of skeletal muscle metabolic reserve during whole body exercise in patients with chronic obstructive pulmonary disease. Am J Respir Crit Care Med 1999;159:881–5.
31. Mador MJ, Deniz O, Aggarwal A, Kufel TJ. Quadriceps fatigability after single muscle exercise in patients with COPD. Am J Respir Crit Care Med 2003;168:102–8.
32. Saey D, Debigare R, Leblanc P, et al. Contractile leg fatigue after cycle exercise: a factor limiting exercise in patients with COPD. Am J Respir Crit Care Med 2003;168:425–30.
33. Casaburi R, Patessio A, Ioli F, et al. Reductions in exercise lactic acidosis and ventilation as a result of exercise training in patients with obstructive lung disease. Am Rev Respir Dis 1991;143:9–18.
34. Maltais F, Bernard S, Jobin J, et al. Lactate kinetics during exercise in chronic obstructive pulmonary disease. Can Respir J 1997;4:251–7.
35. Mostert R, Goris A, Weling-Scheepers C, et al. Tissue depletion and health related quality of life in patients with chronic obstructive pulmonary disease. Respir Med 2000;94:859–67.
36. Decramer M, Gosselink R, Troosters T, et al. Muscle weakness is related to utilization of health care resources in COPD patients. Eur Respir J 1997;10:417–23.
37. Marquis K, Debigare R, Lacasse Y, et al. Midthigh muscle cross-sectional area is a better predictor of mortality than body mass index in patients with chronic obstructive pulmonary disease. Am J Respir Crit Care Med 2002;166: 809–13.
38. Maltais F, Leblanc P, Simard C, et al. Skeletal muscle adaptation to endurance training in patients with chronic obstructive pulmonary disease. Am J Respir Crit Care Med 1996;154:442–7.
39. Schols AMWJ, Soeters PB, Mostert R, et al. Physiologic effects of nutritional support and anabolic steroids in patients with chronic obstructive pulmonary disease. A placebo-controlled randomized trial. Am J Respir Crit Care Med 1995;152:1268–74.
40. Jakobsson P, Jorfeldt L, Brundin A. Skeletal muscle metabolites and fibre types in patients with advanced chronic obstructive pulmonary disease (COPD), with and without chronic respiratory failure. Eur Respir J 1990;3:192–6.
41. Schols AMWJ, Buurman WA, Staal-van den Brekel AJ, et al. Evidence for a relation between metabolic derangements and increased levels of inflammatory mediators in a subgroup of patients with chronic obstructive pulmonary disease. Thorax 1996;51:819–24.
42. Fiaccadori E, Coffrini E, Ronda N, et al. Hypophosphatemia in course of chronic obstructive pulmonary disease. Prevalence, mechanisms, and relationships with skeletal muscle phosphorus content. Chest 1990;97:857–68.
43. Casaburi R, Goren S, Bhasin S. Substantial prevalence of low anabolic hormone levels in COPD patients undergoing rehabilitation. Am J Respir Crit Care Med 1996;153: A128.
44. Kamischke A, Kemper DE, Castel MA, et al. Testosterone levels in men with chronic obstructive pulmonary disease with or without glucocorticoid therapy. Eur Respir J 1998;11:41–5.
45. Morrison WL, Gibson JNA, Scrimgeour C, Rennie MJ. Muscle wasting in emphysema. Clin Sci 1988;75:415–20.
46. Ferreira IM, Brooks D, Lacasse Y, Goldstein RS. Nutritional support for individuals with COPD: a meta-analysis. Chest 2000;117:672–8.
47. Mitch WE, Goldberg AL. Mechanism of muscle wasting. N Engl J Med 1996;335:1897–905.
48. Anker SD, Coats AJS. Cardiac cachexia. Chest 1999;115:836–47.
49. Goodship TH, Lloyd S, Clague MB, et al. Whole body leucine turnover and nutritional status in continuous ambulatory peritoneal dialysis. Clin Sci (Lond) 1987;73:463–9.
50. Debigaré R, Cote CH, Maltais F. Peripheral muscle wasting in chronic obstructive pulmonary disease. Clinical relevance and mechanisms. Am J Respir Crit Care Med 2001;164: 1712–7.
51. Fischer D, Gang G, Pritts T, Hasselgren PO. Sepsis-induced muscle proteolysis is prevented by a proteasome inhibitor in vivo. Biochem Biophys Res Commun 2000;270: 215–21.
52. Engelen MPKJ, Deutz NEP, Wouters EFM, Schols AMW. Enhanced levels of whole-body protein turnover in patients with chronic obstructive pulmonary disease. Am J Respir Crit Care Med 2000;162:1488–92.
53. Cuervo AM, Dice JF, Knecht E. A population of rat liver lysosomes responsible for the selective uptake and degradation of cytosolic proteins. J Biol Chem 1997;272:5606–15.
54. Goll DE, Thompson VF, Li H, et al. The calpain system. Physiol Rev 2003;83:731–801.
55. Glickman MH, Ciechanover A. The ubiquitin–proteasome proteolytic pathway: destruction for the sake of construction. Physiol Rev 2002;82:373–428.
56. Williams A, Sun X, Fischer JE, Hasselgren PO. The expression of genes in the ubiquitin–proteasome proteolytic pathway is increased in skeletal muscle from patients with cancer. Surgery 1999;126:744–9.
57. Tiao G, Hobler S, Wang JJ, et al. Sepsis is associated with increased mRNAs of the ubiquitin–proteasome proteolytic pathway in human skeletal muscle. J Clin Invest 1997;99: 163–8.
58. Mansoor O, Beaufrere B, Boirie Y, et al. Increased mRNA levels for components of the lysosomal, Ca^{2+}-activated, and ATP–ubiquitin-dependent proteolytic pathways in skeletal muscle from head trauma patients. Proc Natl Acad Sci U S A 1996;93:2714–8.
59. Llovera M, Garcia-Martinez C, Agell N, et al. Ubiquitin and proteasome gene expression is increased in skeletal muscle of slim AIDS patients. Int J Mol Med 1998;2:69–73.
60. Bodine SC, Latres E, Baumhueter S, et al. Identification of ubiquitin ligases required for skeletal muscle atrophy. Science 2001;294:1704–8.
61. Gomes MD, Lecker SH, Jagoe RT, et al. Atrogin-1, a muscle-specific F-box protein highly expressed during muscle atrophy. Proc Natl Acad Sci U S A 2001;98:14440–5.
62. Solomon V, Goldberg AL. Importance of the ATP–ubiquitin–proteasome pathway in the degradation of soluble and myofibrillar proteins in rabbit muscle extracts. J Biol Chem 1996;271:26690–7.
63. Debigare R, Meireles C, Price SR. Impaired insulin activity initiates muscle proteolysis by activating caspases 3 to breakdown actomyosin. FASEB J 2003;17:A183.
64. Williams AB, Decourten-Myers GM, Fischer JE, et al. Sepsis stimulates release of myofilaments in skeletal muscle by a calcium-dependent mechanism. FASEB J 1999;13:1435–43.
65. Guttridge DC, Mayo MW, Madrid LV, et al. NF-κB-induced loss of MyoD messenger RNA: possible role in muscle decay and cachexia. Science 2000;289:2363–6.
66. Llovera M, Garcia-Martinez C, Lopez-Soriano J, et al. Role of TNF receptor I in protein turnover during cancer cachexia using gene knockout mice. Mol Cell Endocrinol 1998;142: 183–9.
67. Tsujinaka T, Fujita J, Ebisui C, et al. Interleukin 6 receptor antibody inhibits muscle atrophy and modulates proteolytic systems in interleukin 6 transgenic mice. J Clin Invest 1996; 97:244–9.
68. Li YP, Reid MB. NF-kappaB mediates the protein loss induced by TNF-alpha in differentiated skeletal muscle myotubes. Am J Physiol Regul Integr Comp Physiol 2000;279: R1165–70.

69. Du J, Mitch WE, Wang X, Price SR. Glucocorticoids induce proteasome C3 subunit expression in L6 muscle cells by opposing the suppression of its transcription by NF-kappa B. J Biol Chem 2000;275:19661–6.
70. Repine JE, Bast ALI. Oxidative stress in chronic obstructive pulmonary disease. Am J Respir Crit Care Med 1999;156: 341–57.
71. Reid MB. Redox modulation of skeletal muscle contraction: what we know and what we don't. J Appl Physiol 2001;90: 724–31.
72. Langen RC, Schols AM, Kelders MC, et al. Tumor necrosis factor-alpha inhibits myogenesis through redox-dependent and -independent pathways. Am J Physiol Cell Physiol 2002;283:C714–21.
73. Gomes-Marcondes MC, Tisdale MJ. Induction of protein catabolism and the ubiquitin–proteasome pathway by mild oxidative stress. Cancer Lett 2002;180:69–74.
74. Nagasawa T, Hatayama T, Watanabe Y, et al. Free radical-mediated effects on skeletal muscle protein in rats treated with Fe-nitrilotriacetate. Biochem Biophys Res Commun 1997;231:37–41.
75. Buck M, Chojkier M. Muscle wasting and dedifferentiation induced by oxidative stress in a murine model of cachexia is prevented by inhibitors of nitric oxide synthesis and antioxidants. EMBO J 1996;15:1753–65.
76. Debigaré R, Marquis K, Cote CH, et al. Catabolic/anabolic balance and muscle wasting in patients with COPD. Chest 2003;124:83–9.
77. Eid AA, Ionescu AA, Nixon LS, et al. Inflammatory response and body composition in chronic obstructive pulmonary disease. Am J Respir Crit Care Med 2001;164:1414–8.
78. Heunks LM, Viña J, van Herwaarden CLA, et al. Xanthine oxidase is involved in exercise-induced oxidative stress in chronic obstructive pulmonary disease. Am J Physiol 1999; 277:R1697–704.
79. Couillard A, Maltais F, Saey D, et al. Exercise-induced quadriceps oxidative stress and peripheral muscle dysfunction in COPD patients. Am J Respir Crit Care Med 2003;167: 1664–9.
80. Musaro A, McCullagh K, Paul A, et al. Localized Igf-1 transgene expression sustains hypertrophy and regeneration in senescent skeletal muscle. Nat Genet 2001;27:195–200.
81. Fang CH, Li BG, Sun X, Hasselgren P-O. Insulin-like growth factor I reduces ubiquitin and ubiquitin-conjugating enzyme gene expression but does not inhibit muscle proteolysis in septic rats. Endocrinology 2000;141:2743–51.
82. Solomon V, Madihally S, Yarmush M, Toner M. Insulin suppresses the increased activities of lysosomal cathepsins and ubiquitin conjugation system in burn-injured rats. J Surg Res 2000;93:120–6.
83. Benbassat CA, Lazarus DD, Cichy SB, et al. Interleukin-1 alpha (IL-1 alpha) and tumor necrosis factor alpha (TNF alpha) regulate insulin-like growth factor binding protein-1 (IGFBP-1) levels and mRNA abundance in vivo and in vitro. Horm Metab Res 1999;31:209–15.
84. Langley B, Thomas M, Bishop A, et al. Myostatin inhibits myoblast differentiation by down-regulating MyoD expression. J Biol Chem 2002;277:49831–40.
85. Zimmers TA, Davies MV, Koniaris LG, et al. Induction of cachexia in mice by systemically administered myostatin. Science 2002;296:1486–8.
86. Burdet L, de Muralt B, Schutz Y, et al. Administration of growth hormone to underweight patients with chronic obstructive pulmonary disease. A prospective, randomized, controlled study. Am J Respir Crit Care Med 1997; 156:1800–6.
87. Baarends EM, Schols AMWJ, Pannemans DLE, et al. Total free living energy expenditure in patients with severe chronic obstructive pulmonary disease. Am J Respir Crit Care Med 1997;155:1549–54.
88. Schols AMWJ, Mostert R, Soeters PB, et al. Energy balance in patients with chronic obstructive pulmonary disease. Am Rev Respir Dis 1991;143:1248–52.
89. Kayser B, Hoppeler H, Claassen H, Cerretelli P. Muscle structure and performance capacity of Himalayan Sherpas. J Appl Physiol 1991;70:1938–42.
90. Fletcher EC, Luckett RA, Miller T, Fletcher JG. Exercise hemodynamics and gas exchange in patients with chronic obstruction pulmonary disease, sleep desaturation, and a daytime PaO_2 above 60 mm Hg. Am Rev Respir Dis 1989; 140:1237–45.
91. Semple PD, Beastall GH, Watson WS, Hume R. Serum testosterone depression associated with hypoxia in respiratory failure. Clin Sci (Colch) 1980;58:105–6.
92. Takabatake N, Nakamura H, Abe S, et al. The relationship between chronic hypoxemia and activation of the tumor necrosis factor-α system in patients with chronic obstructive pulmonary disease. Am J Respir Crit Care Med 2000;161:1179–84.
93. Orozco-Levi M, Gea J, Sauleda J, et al. Structure of the latissimus dorsi muscle and respiratory function. J Appl Physiol 1995;78:1132–9.
94. Similowski T, Yan S, Gauthier AP, et al. Contractile properties of the human diaphragm during chronic hyperinflation. N Engl J Med 1991;325:917–23.
95. Medina R, Wing SS, Goldberg AL. Increase in levels of polyubiquitin and proteasome mRNA in skeletal muscle during starvation and denervation atrophy. Biochem J 1995;307: 631–7.
96. Adams GR. Autocrine/paracrine IGF-I and skeletal muscle adaptation. J Appl Physiol 2002;93:1159–67.
97. Lalani R, Bhasin S, Byhower F, et al. Myostatin and insulin-like growth factor-I and -II expression in the muscle of rats exposed to the microgravity environment of the Neurolab space shuttle flight. J Endocrinol 2000;167:417–28.
98. Maltais F, Sullivan MJ, Leblanc P, et al. Altered expression of myosin heavy chain in the vastus lateralis muscle in patients with COPD. Eur Respir J 1999;13:850–4.
99. Mattson JP, Poole DC. Pulmonary emphysema decreases hamster skeletal muscle oxidative enzyme capacity. J Appl Physiol 1998;85:210–4.
100. Sandri M. Apoptotic signaling in skeletal muscle fibers during atrophy. Curr Opin Clin Nutr Metab Care 2002;5: 249–53.
101. Agusti AG, Sauleda J, Miralles C, et al. Skeletal muscle apoptosis and weight loss in chronic obstructive pulmonary disease. Am J Respir Crit Care Med 2002;166:485–9.
102. Decramer M, de Bock V, Dom R. Functional and histologic picture of steroid-induced myopathy in chronic obstructive pulmonary disease. Am J Respir Crit Care Med 1996;153: 1958–64.
103. Schols AMWJ, Slangen J, Volovics L, Wouters EFM. Weight loss is a reversible factor in the prognosis of chronic obstructive pulmonary disease. Am J Respir Crit Care Med 1998; 157:1791–7.
104. Bernard S, Whittom F, Leblanc P, et al. Aerobic and strength training in patients with COPD. Am J Respir Crit Care Med 1999;159:896–901.
105. Sala E, Roca J, Marrades RM, et al. Effects of endurance training on skeletal muscle bioenergetics in chronic obstructive pulmonary disease. Am J Respir Crit Care Med 1999;159: 1726–34.

106. Maltais F, Leblanc P, Jobin J, et al. Intensity of training and physiologic adaptation in patients with chronic obstructive pulmonary disease. Am J Respir Crit Care Med 1997;155: 555–61.
107. Serres I, Varray A, Vallet G, et al. Improved skeletal muscle performance after individualized exercise training in patients with chronic obstructive pulmonary disease. J Cardiopulm Rehab 1997;17:232–8.
108. Simpson K, Killian K, McCartney N, et al. Randomised controlled trial of weightlifting exercise in patients with chronic airflow limitation. Thorax 1992;47:70–5.
109. Donahoe M. Nutritional support in advanced lung disease. Clin Chest Med 1997;18:547–61.
110. Ferreira IM, Verreschi IT, Nery LE, et al. The influence of 6 months of oral anabolic steroids on body mass and respiratory muscles in undernourished COPD patients. Chest 1998;114:19–28.
111. Bhasin S, Storer TW, Berman N, et al. The effects of supraphysiologic doses of testosterone on muscle size and strength in normal men. N Engl J Med 1996;335:1–7.
112. Busquets S, Alvarez B, Llovera M, et al. Branched-chain amino acids inhibit proteolysis in rat skeletal muscle: mechanisms involved. J Cell Physiol 2000;184:380–4.
113. Costelli P, Garcia-Martinez C, Llovera M, et al. Muscle protein waste in tumor-bearing rats is effectively antagonized by a β_2-adrenergic agonist (clenbuterol). J Clin Invest 1995;95: 2367–72.
114. Meeuwisse WH, McKenzie DC, Hopkins SR, Road JD. The effect of salbutamol on performance in elite nonasthmatic athletes. Med Sci Sports Exerc 1992;24:1161–6.
115. Fang CH, Wang J-J, Hobler SC, et al. Proteasome blockers inhibit protein breakdown in skeletal muscle after burn injury in rats. Clin Sci 1998;95:225–33.

CHAPTER 50

PHYSIOLOGY OF THE UPPER AIRWAYS AND UPPER AIRWAY OBSTRUCTION IN DISEASE

R. John Kimoff

The upper airway is a complex structure that serves as the conduit from the external environment to the intrathoracic airways and lungs. The anatomic regions of the upper airway (Figure 50-1) include the nasal cavity, nasopharynx, velopharynx behind the soft palate, oropharynx, hypopharynx, and larynx. This conduit has a variety of functions, including the filtering and conditioning of air, olfaction, mastication and deglutition, phonation, coughing, and protection of the lower airways and lungs from large particulate material.[1–6] This chapter focuses on the physiology and pathophysiology of the respiratory-related functions of the upper airway. The discussion of other upper airway functions is limited to their interaction with respiratory function.

ANATOMY AND PHYSIOLOGY OF THE UPPER AIRWAY

Nose

To enter the upper airway, air flows rapidly upward through the anterior nares or nasal vestibules, which are 1 cm–diameter channels in the anterior portion of the nose. Coarse hairs or vibrissae within the vestibules serve to filter larger particulate matter. The air then encounters the nasal septum, which divides the nasal passage into two fossae. The lateral walls of the fossae contain irregular projections known as the turbinates, which create turbulent flow and reduce flow rate. This prolongs contact of the inspired air with the nasal mucosa, which at this level is richly supplied with a system of subepithelial capillaries and venous sinusoids, along with submucosal glands and goblet cells. The rich vascularization of the mucosa provides for humidification and temperature conditioning of the inspired air. Production of a mucous layer by glandular structures provides for trapping of particulate matter. Nasal secretions produced by the highly vascular mucosa are rich in immunoglobulins, cytokines, and other cytolytic substances, and there is extensive mucosal production of nitric oxide by the nose and paranasal sinuses; all of these have potent antimicrobial activity. There is thus considerable filtering, temperature conditioning, and humidification of the air traversing the nasal fossae, which have an important protective function for the lower airways.

Although the nose accounts for over 50% of upper airway flow resistance in normal, awake persons, it is the preferred route of breathing during resting ventilation. As ventilatory drive increases, some dilatation of the nares and vasoconstriction of the nasal mucosa may help to reduce airflow resistance, but as demands increase, the mouth opens and the lower-resistance oropharyngeal route is recruited, although at the cost of reduced conditioning of the inspired air. Other functions of the nose include olfaction and a contribution to phonation, in that the nose acts as a resonating chamber for some components of speech.

Pharynx

This structure consists of the nasopharynx, oropharynx, and hypopharynx. Inspired air exits the nasal passages posteriorly through 2.5×1.5 cm openings known as the choanae and enters the nasopharynx. The nasopharynx extends from the choanae down to the lower margin of the soft palate. The segment of the nasopharynx immediately behind the soft palate has been termed the velopharynx. The mucosa of the posterior nasopharyngeal wall contains a collection of lymphoid tissue termed the single pharyngeal or adenoid tonsil. This structure can hypertrophy and produce nasal obstruction, which often contributes to obstructive sleep apnea (OSA) in children. As with the palatine tonsils between the anterior and posterior tonsillar pillars lower down, the adenoid tends to involute after puberty.

The muscular structures in the wall of the nasopharynx and soft palate play a major role in speech, swallowing, and breathing. These muscles act to partition airflow between the oral and nasal routes, particularly under conditions of increased ventilatory drive. The palatal muscles are also important in the maintenance of airway patency.

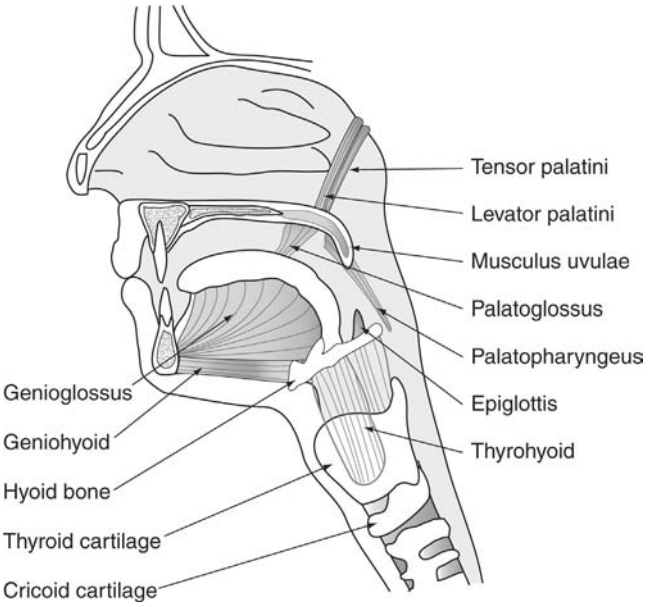

FIGURE 50-1 Anatomy of the upper airway.

The oropharynx lies behind the oral cavity and extends from the soft palate superiorly to the tip of the epiglottis inferiorly. The lateral walls include the anterior (palatoglossal) and posterior (palatopharyngeal) tonsillar pillars, which merge superiorly into the soft palate and between which lie the fossae of the palatine tonsils. The posterior pharyngeal wall is largely composed of the pharyngeal constrictor muscles, whereas the posterior aspect or base of the tongue lies anteriorly. This structure serves as the main conduit for both solids and liquids from the mouth to the esophagus and for the flow of air through to the larynx. The coordination of these various neuromuscular functions is achieved through reflex control involving neural afferents in the pharyngeal mucosa; these project to pontomedullary centers, which integrate this information and regulate swallowing and respiratory functions.

Swallowing is characterized by initial elevation of the larynx, followed by active contraction of the oropharynx, leading to shortening and constriction of the pharynx to actively propel food toward the esophagus. The normal coordination of this action in humans is such that swallowing occurs almost exclusively during late expiration in seated humans and is accompanied by respiratory inhibition, that is, prolongation of expiratory time, and other processes, such as vocal cord closure and laryngeal elevation, that assist in protecting the laryngeal aperture.[7–9]

In contrast to the passage of food during swallowing, airflow through the oropharynx is passive, being driven by the negative intrathoracic pressure generated by the respiratory pump muscles. However, whereas the nasal and laryngeal segments of the upper airway are supported by bony and cartilaginous structures, the pharynx is a collapsible muscular tube. There is clear evidence that the stability and patency of this structure during breathing depend upon tonic and phasic activation of muscles surrounding the airway, which act to stiffen and dilate the pharynx during inspiration.[10–13] These muscles include the genioglossus muscle, which positions and stabilizes the tongue, palatal muscles such as the tensor and levator palatini and the palatoglossus and palatopharyngeus muscles, and muscles that stablilize the hyoid bone, such as the geniohyoid and sternohyoid muscles. If the dilating musculature is not sufficiently activated, collapse of this segment will occur during inspiration, due to a suction effect of the negative intraluminal pressure associated with inspiratory airflow. Thus, in generating inspiratory impulses, the brainstem respiratory controller produces a sequential wave of respiratory muscle activation, with initial activation of pharyngeal dilators, which stiffen and dilate this conduit. Subsequently, laryngeal activation leads to opening of the glottic aperture, chest wall muscle activation that stiffens and expands the chest wall, and diaphragmatic activation.[14–16] Pharyngeal caliber is also modulated by important reflex mechanisms that regulate within-breath levels of phasic muscle activation. Both tonic and phasic activity of pharyngeal dilators and the protective reflexes are reduced during sleep, which leads to increased airflow resistance during sleep in normal subjects and can contribute to collapse of the upper airway in patients with OSA.

The hypopharynx extends downward from the upper margin of the epiglottis to the lower border of the cricoid cartilage, serving as the conduit from the oropharynx to the laryngeal inlet and esophagus. The piriform recesses lie on each side of the hypopharynx. These recessess serve to direct food boluses down and away from the larynx in transit to the esophagus. During swallowing, as noted above, there is laryngeal constriction and a movement of the epiglottis in order to protect the laryngeal aperture.

Larynx

The structure of the larynx, and in particular the cartilaginous skeleton and musculature, is illustrated in Figure 50-2, which also illustrates the action of the musculature on glottic patency.[3,17–19] In addition to the thyroid, cricoid, and arytenoid cartilages, the epiglottic cartilage, which descends to protect the laryngeal aperture during swallowing, is also considered to be part of the laryngeal apparatus. The larynx plays an integral role in all upper airway functions, including respiration, phonation, cough, swallowing, and vomiting. As with the pharyngeal structures, these activities are initiated and coordinated by brainstem centers, with modulation by afferent neural inputs from the airway itself. In the case of the larynx, there is a rich sensory array of mucosal sensory receptors, which respond to changes in airflow, pressure, temperature, and laryngeal position. Impulses from these receptors are conveyed centrally through the superior laryngeal nerve to modulate laryngeal function and breathing pattern. Motor innervation of the laryngeal musculature is conveyed through the recurrent laryngeal nerves, with the exception of the cricothyroid muscle, which is supplied by the external branch of the superior laryngeal nerve. The recurrent laryngeal nerves arise from the vagus nerve within the thorax and travel superiorly along the mediastinal structures to the larynx. On the right, the recurrent laryngeal nerve arises at the level of the subclavian artery,

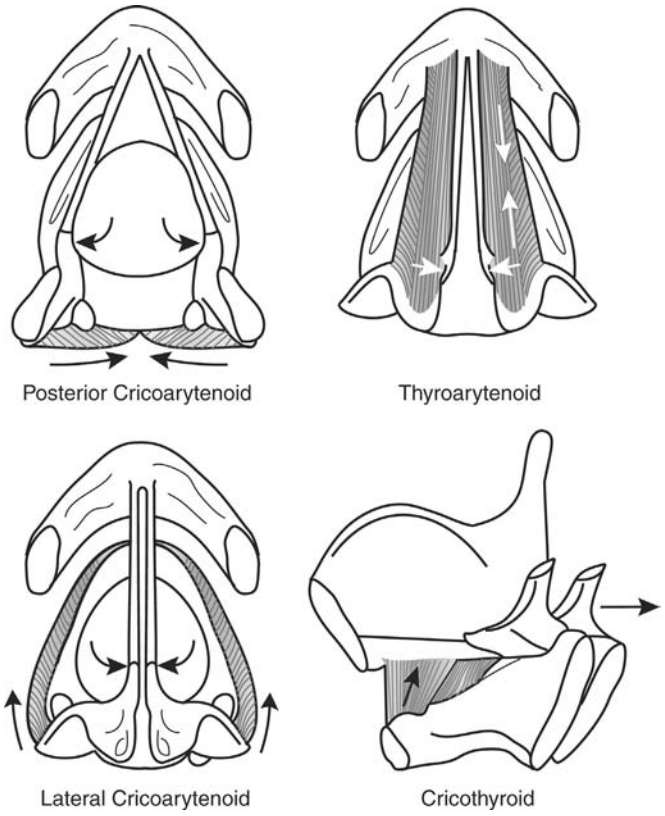

FIGURE 50-2 Laryngeal skeleton and musculature, illustrating the actions of the major muscles.

and on the left, the nerve arises at the level of the aortic arch. Disease processes, including intrathoracic disease, that disrupt the recurrent laryngeal nerve therefore lead to vocal cord paralysis and laryngeal dysfunction, which has implications for all of the other functions of the larynx.

Although protective closure of the larynx during swallowing is part of the integrated deglutition process, there is also a more basic laryngeal protective response called the "glottic closure reflex." This is characterized by a short-latency activation of the adductor muscles to rapidly close the glottic aperture in response to stimulation of the laryngeal mucosa by tactile or chemical stimuli. This is therefore a critical response that protects against aspiration of foreign material into the upper airway. It is of note that, in contrast to the situation in many mammalian species, the human reflex is not crossed, so that damage to the superior laryngeal nerve on one side can result in failure of ipsilateral vocal fold closure, thereby increasing the risk of aspiration.[17] Although the glottic closure reflex represents a crucial protective mechanism, the response may become exaggerated in some disease conditions, leading to laryngospasm or prolonged glottic closure following withdrawal of the inciting stimulus.

With respect to the respiratory function of the larynx, during inspiration the posterior cricoarytenoid muscle, the only vocal cord abductor muscle, is activated to widen the glottic aperture.[18,19] There is simultaneous activation of the cricothyroid muscle, which acts to lengthen the vocal fold. The concurrent lengthening and abduction of the folds lead to an increase in glottic cross-sectional area, thus reducing resistance to inspiratory airflow. The posterior cricoarytenoid muscle relaxes during expiration, whereas the cricothyroid muscle may remain active, to maintain the length of the cords. Under some conditions, there is active contraction of the adductor muscles to narrow the aperture and produce expiratory "braking." This strategy is adopted in an attempt to maintain end-expiratory lung volume. This occurs, for example, in neonates with respiratory distress syndrome and is manifested as expiratory grunting due to glottic closure. An extreme instance of prolonged glottic closure appears to occur in apnea of prematurity, in which experimental evidence has demonstrated that apneas are associated with active glottic closure.[20]

In some patients, laryngeal function becomes disturbed such that there is intermittent inspiratory closure of the vocal cords. This condition has been variously termed vocal cord dysfunction syndrome, paradoxical vocal cord motion, and laryngismus stridulus.[21–23] The clinical presentation may mimic both asthma and organic upper airway obstruction and may be acute and lead to endotracheal intubation. Spirometric flow–volume curves are very helpful in making the diagnosis (see below). A substantial proportion of affected individuals also have asthma; patients without asthma are often women who have been misdiagnosed as asthmatic. This syndrome typically occurs in the absence of any evident structural laryngeal disease, and the mechanisms responsible are unclear. However, psychogenic factors appear to play a role as the dysfunction is intermittent, may be worse in times of emotional stress, and, even if sustained during wakefulness, tends to disappear during sleep. Furthermore, psychiatric disorders are common among affected individuals. Treatment approaches include patient education, psychotherapy as needed, and referral to a speech pathologist.

The larynx also plays a major role in phonation. Although sound can be produced passively by creating airflow through the larynx, the generation of speech or song requires finely controlled activation of laryngeal muscles. These muscles act to shape and position the vocal cords to generate speech and modulate the spatial relationship between the cricoid and thyroid cartilages to vary the pitch of the sound produced. Further modulation of sound is produced superiorly in the pharynx and nasal cavity. Breathing during speech is characterized by rapid inspiration, followed by prolonged expiration, during which the subglottic pressure is maintained relatively constant as the fine motor actions of the laryngeal apparatus produce sound.[24] Stuttering appears to represent an example of an altered interaction between laryngeal and respiratory function during speech, the mechanisms for which remain poorly understood.[25]

CLINICAL PHYSIOLOGY OF UPPER AIRWAY OBSTRUCTION

Clinical Description

Obstruction of the upper airway can occur in various clinical contexts and disease states, although it is much less

Table 50-1 Causes of Upper Airway Obstruction

Infectious
Acute epiglottitis
Laryngotracheobronchitis (croop)
Ludwig's angina
Retropharyngeal abscess
Allergic/immune
Edema associated with anaphylaxis
Angioneurotic edema
Relapsing polychondritis
Rheumatoid arthritis
Sjögren's syndrome (adenopathy)
Wegener's granulomatosis
Tumors
Benign
Malignant
Laryngeal carcinoma
Bronchogenic carcinoma
Lymphoma
Other metastatic disease
Vascular
Right-sided aortic arch
Double aortic arch
Innominate artery syndrome
Aberrant left pulmonary artery
Tracheal abnormalities
Neuromuscular
Vocal cord dysfunction
Foreign body aspiration
Trauma
Inhalation
Smoke/burn
Chemical

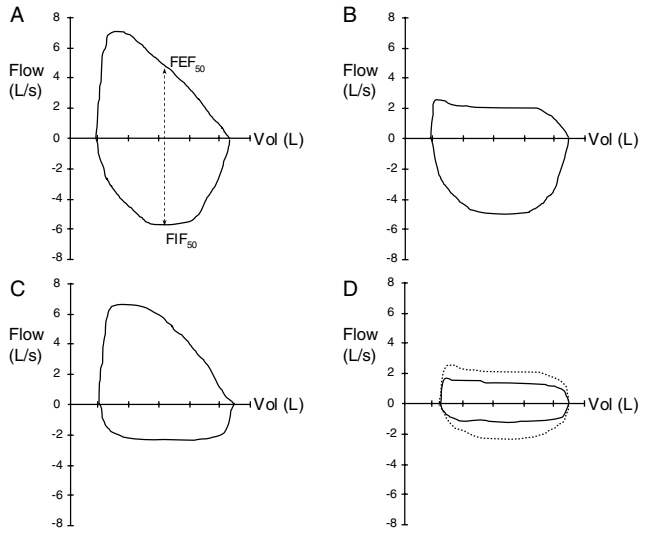

FIGURE 50-3 Flow–volume curves: upper airway obstruction. *A*, Normal flow–volume curve. *B*, Variable intrathoracic obstruction due to a tracheal tumor. *C*, Variable extrathoracic obstruction due to a laryngeal tumor. *D*, Fixed upper airway obstruction due to large tracheal tumor. Solid line = air; dotted line = helium. Note the improvement in both inspiratory and expiratory flow with helium.

common than obstructive disease of the lower airway, such as asthma or chronic obstructive pulmonary disease (COPD). Unfortunately, the clinical presentation of the two may be very similar (dyspnea and noisy breathing), so that the less common diagnosis of upper airway obstruction may be missed if a careful clinical evaluation and appropriate testing are not performed. A missed diagnosis, particularly in the context of acute or severe upper airway obstruction, may have devastating consequences for the patient as appropriate treatment may be delayed beyond the point of severe airway compromise and respiratory arrest.

A hallmark clinical feature of upper airway obstruction is dyspnea with stridor, a loud, constant-pitch inspiratory sound that indicates obstruction of the extrathoracic airway. Severe extrathoracic or variable intrathoracic large airway obstruction may also cause expiratory prolongation and a wheeze-like sound, making it difficult to distinguish from disease of the lower airways. Other symptoms associated with upper airway obstruction include cough, hoarseness, dysphagia, and orthopnea, depending upon the location and nature of the obstructing lesion. Although it is beyond the scope of this chapter to provide an exhaustive description of causes of upper airway obstruction, a list of common pathologies is provided in Table 50-1.

Physiologic Testing for Upper Airway Obstruction

Forced expiratory and inspiratory spirometry with recording of the flow–volume curve is the most important physiologic tool for the diagnosis of upper airway obstruction.[26–35] Examples of normal and pathologic flow–volume curves are shown in Figure 50-3. Normally, there is an initial rapid rise in expiratory flow to a peak value that is dependent on effort, lung elastic recoil, and flow in the large airways. As lung volume decreases, flow becomes effort-independent and determined by the balance between lung recoil and flow resistance in progressively smaller airways. During forced inspiration, flow is effort dependent throughout, with the peak value occurring at midinspiration. Peak expiratory flow rate is considerably larger than peak inspiratory flow rate because of the effects of lung elastic recoil. However, at 50% of vital capacity, forced inspiratory flow (FIF_{50}) is somewhat greater than forced expiratory flow (FEF_{50}), due in part to normal expiratory dynamic compression of the airways. Thus, the normal FIF_{50}/FEF_{50} ratio is slightly greater than 1.

Obstructing lesions of the upper airways may be either fixed or variable; that is, lesions produce narrowing that varies with pressures acting across the airways during inspiration and expiration (Figure 50-4). In the case of variable intrathoracic large airway obstruction (see Figure 50-3B), during expiration, pleural pressure is more positive than intratracheal pressure, leading to dynamic compression of the airway and thereby increased airway narrowing and reduced expiratory flow. However, during inspiration, there is a net distending pressure across the large airway, so that patency of the lumen tends to increase, yielding a relative preservation of inspiratory flow rate. The FIF_{50}/FEF_{50} ratio will therefore be well above 1, typically in the range of 2 to 3.

In the case of variable extrathoracic upper airway obstruction (see Figure 50-3C), the pressure surrounding the airway is atmospheric, so that during inspiration, there is a net negative transmural pressure, which tends to worsen

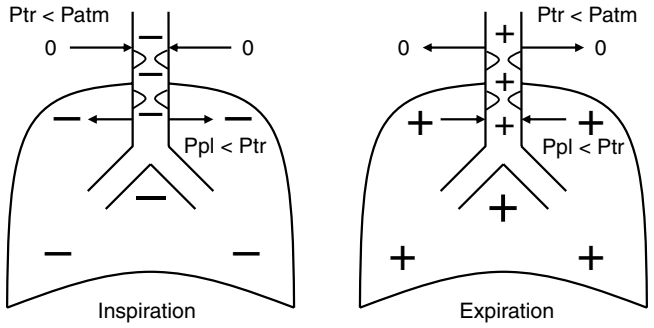

FIGURE 50-4 Forces acting across the airways that determine spirographic patterns in cases of variable intrathoracic and extrathoracic upper airway obstruction. P_{atm} = atmospheric pressure; P_{pl} = pleural pressure; P_{tr} = tracheal pressure.

airway narrowing and reduce inspiratory flow. In contrast, during expiration, the positive pressure within the airway produces a transmural distending pressure and reduces the extent of narrowing, resulting in increased expiratory relative to inspiratory flow. Thus, the FIF_{50}/FEF_{50} ratio will be less than 1.

The anatomy of many upper airway lesions, however, is such that the degree of obstruction is not materially influenced by the pressures acting across the airway, with resultant comparable reductions in both inspiratory and expiratory flow (see Figure 50-3D). In this case, the FIF_{50}/FEF_{50} ratio may be close to 1.

From Figure 50-3, it can be seen that inspection of the flow–volume curve and recognition of the characteristic changes in pattern are crucial to the recognition of upper airway obstruction. It is important to emphasize that one cannot rely solely upon tabular data from simple spirometry to exclude the diagnosis of upper airway obstruction. Because flow in the medium and small airways contributes significantly to forced expiratory volume in 1 second (FEV_1), substantial large airway obstruction may be present before significant changes in FEV_1 occur. When concomitant airway disease, such as COPD, is present, the sensitivity of spirometry for the detection of upper airway obstructing lesions is even lower. Peak expiratory flow rate is much more sensitive for the presence of expiratory large airway obstruction, and a hallmark finding in tabular data is a reduction in peak expiratory flow rate (as percent predicted) that is out of proportion to other changes in flow rates, particularly FEV_1. However, assessment of the inspiratory flow pattern is also crucial.

The characteristic flattening of the flow–volume curve in upper airway obstruction reflects the presence of pathologic flow limitation. Flow limitation is defined as a state in which increasing effort does not result in increasing airflow. Thus, flow is reduced and constant over a range of lung volumes, producing the flattened shape of the curves depicted in Figure 50-3. The turbulent flow occurring in the context of a high driving pressure during inspiration is responsible for producing the sound of stridor in extrathoracic airway obstruction. As noted above, intrathoracic obstruction can result in prolonged expiratory flow and low-pitched wheeze, and increased breath sounds can be heard during both inspiration and expiration, again due to turbulent flow resulting from fixed airway obstruction.

Turbulence due to airway narrowing can be reduced by administration of a helium–oxygen (Heliox) mixture, which is less dense than air. This can be used diagnostically in cases where it is unclear whether changes in flow–volume curves are due to large airway obstruction. The standard criterion for identifying a large airway component is the detection of an increase with helium of more than 50% in either peak expiratory or inspiratory flow.[34] Heliox administration is also a useful, albeit temporary, therapeutic adjunct in the clinical management of upper airway obstruction.

Mediastinal masses may cause intrathoracic large airway obstruction that varies with body position. Owing to gravitational factors, intrathoracic large airway obstruction resulting from anterior mediastinal masses may be more prominent when the patient is supine. Airway obstruction can worsen with the chest wall relaxation that occurs on the induction of anesthesia, so that preoperative and postoperative airway management in such patients requires careful attention. The positional variation of large airway obstruction can be evaluated by assessing changes in peak flow rates during seated versus supine spirometry.[36]

In the context of acute, severe extrathoracic upper airway obstruction (eg, epiglottitis, foreign body aspiration, or acute laryngeal injury), inspiratory intrathoracic driving pressures may become extremely negative, and this, in turn, may lead to the development of "negative-pressure pulmonary edema."[37,38] This is believed to be due to a combination of increased venous return leading to increased pulmonary blood volume and negative pericapillary interstitial tissue pressure caused by large negative intrapleural pressures, resulting in forces that favor fluid transudation into the interstitium. In some patients, left ventricular (LV) dysfunction is believed to also contribute because of increased LV wall transmural pressure, that is, afterload, resulting from the negative intrapleural pressure. Management of this condition primarily involves management of the upper airway obstruction.

PATHOPHYSIOLOGY OF UPPER AIRWAY COLLAPSE DURING SLEEP: OBSTRUCTIVE SLEEP APNEA

Clinical Description

OSA is characterized by repeated episodes of upper airway obstruction during sleep. This important condition is highly prevalent in the adult population, being estimated to affect 2 to 9% of women and 4 to 15% of men, depending on the precise definitions used and the population under study.[39,40] OSA also occurs in the pediatric age group, although with considerably lower prevalence. OSA is associated with considerable morbidity, increased health care resource utilization, and, probably, increased mortality.[12,13,40–42] Apneic episodes are characterized by upper airway closure and progressively increasing respiratory efforts driven by chemoreceptor and mechanoreceptor stimuli, which then provoke arousal from sleep and reopening of the

airway. These events result in sleep fragmentation, repetitive hypoxemia, and swings in heart rate, blood pressure, and cardiac output, which are responsible for the clinical sequelae of OSA. The latter include excessive daytime sleepiness, impaired concentration, cognitive functions and memory, and mood disturbances. There is a rapidly growing body of data linking OSA to increased cardiovascular risk, including hypertension, cardiac ischemic events, arrhythmia, cerebrovascular accidents, congestive heart failure, and pulmonary hypertension. Severe OSA can also be associated with changes in ventilatory control and hypoventilation during wakefulness, typically in the context of underlying lung dysfunction. There is also growing evidence of a link between OSA and asthma. These issues are discussed further below and in a subsequent chapter.

OSA should be suspected clinically in patients with a history of heavy habitual snoring and excessive daytime sleepiness. Sleep testing is performed to establish the diagnosis. The current "gold standard" test is complete overnight polysomnography performed in a sleep laboratory. This test involves recording of the electroencephalogram, electrooculogram and submental electromyogram for sleep–wake staging, pulse oximetry, determination of airflow with an oronasal thermistor or through nasal pressure (currently the method of choice), determination of respiratory effort with inductance plethysmography, piezoelectric sensors or mercury strain gauges around the thorax and abdomen or with an esophageal balloon (typically reserved for research studies or special clinical cases), determination of body position with mercury switch or video recording, recording of sound (snoring) with a microphone, and detection of periodic limb movements with leg electromyographic electrodes. A typical polysomnographic tracing from a patient with severe OSA is shown in Figure 50-5.

The raw data tracings from the sleep study are scored by a technologist to identify sleep–wake state for each consecutive 30-second period (epoch) of the night, according to standard criteria.[43] The respiratory signals are scored to identify apneas (>10 seconds of complete cessation of airflow) and hypopneas (event lasting >10 seconds, with reduced airflow associated with oxygen desaturation and/or brief arousal from sleep), and whether these are obstructive or central in nature (associated or not with ongoing respiratory effort during events).[44] Summary data are generated in both tabular and graphic form to describe the physiology of sleep, breathing, and other events through the night (Figure 50-6). Although

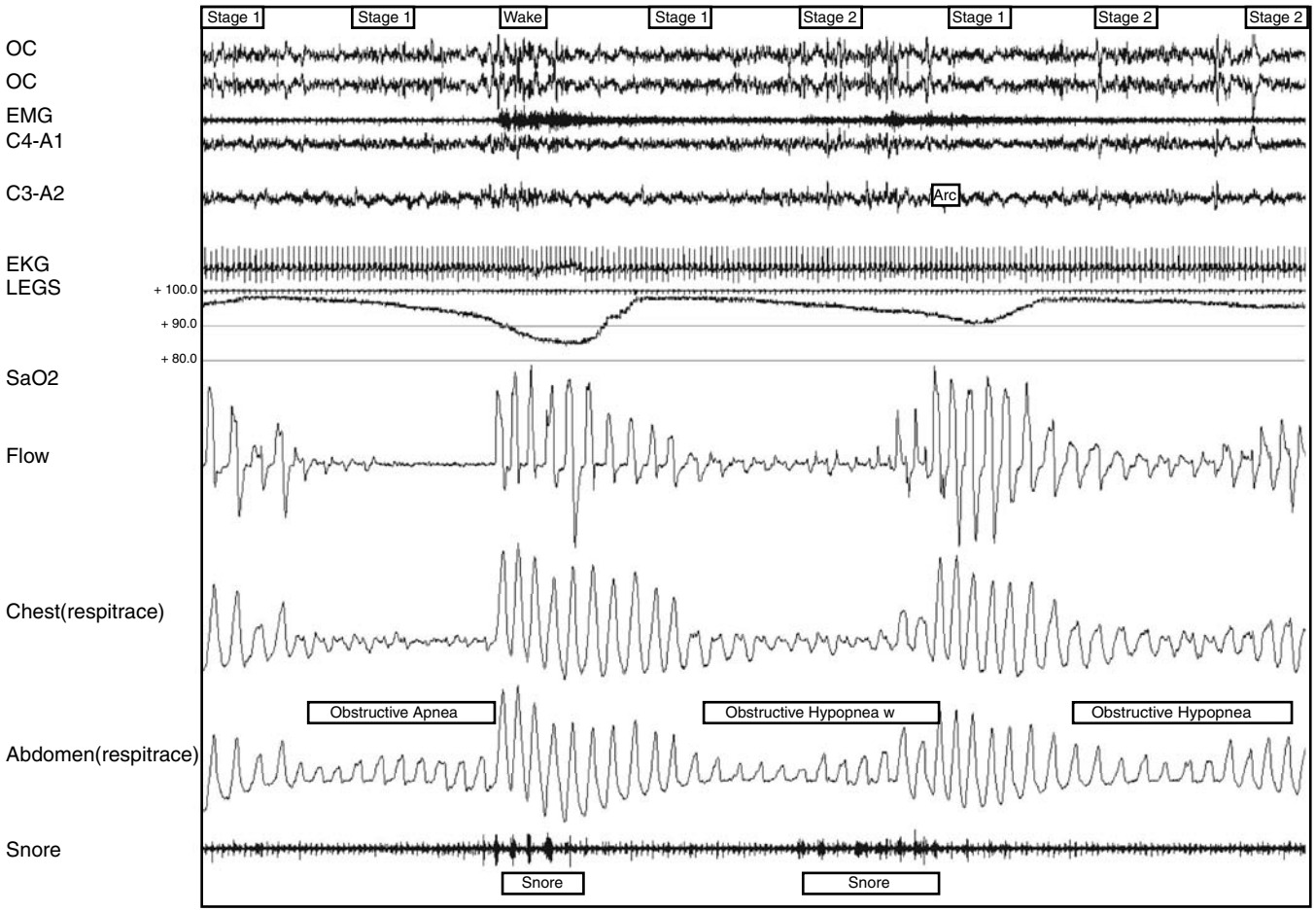

FIGURE 50-5 Representative tracing from a polysomnographic recording in a patient with obstructive sleep apnea, showing three sequential obstructive events, one apnea and two hypopneas. Note that the severity of event-associated oxygen desaturation correlates with the extent of flow reduction during these events. The flow signal is a nasal pressure recording, with inspiration in the upward direction, and illustrates the upper airway flow limitation (flattening) during hypopneas. Note the partial rib cage paradox in the thoracic respiratory inductance plethysmography signal.

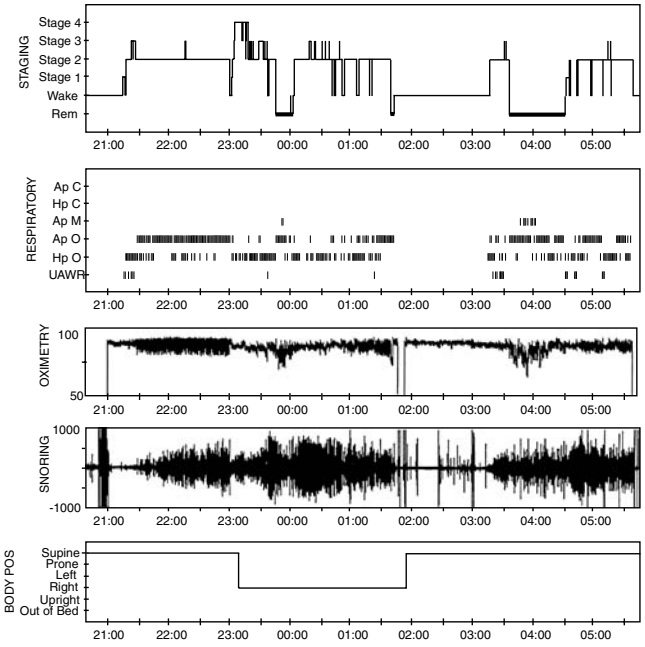

FIGURE 50-6 Composite hypnogram from a patient with severe obstructive sleep apnea and hypopnea. Individual apneas and hypopneas are indicated by vertical bars on the "Respiratory" graph. The patient was awake from 1:45 am to 3:15 am, so that no respiratory disturbance occurred during that time. Note that in this patient the severity of respiratory disturbance is influenced by sleep stage and body position. Oxygen desaturation is more severe during rapid eye movement (REM) than during non-REM sleep, in part due to increased length of events related to increased arousal threshold during REM. During stage 2, non-REM sleep apneas predominate when the patient is supine (eg, 10 pm), whereas hypopneas predominate when the patient is on the side (eg, 1 am), due to gravitational effects on upper airway caliber. This results in positional effects on event-associated oxygen desaturation.

the polysomnogram therefore provides extensive physiologic information, which is useful in the clinical setting, this is a time- and cost-intensive testing procedure of limited availability. Owing to the prevalence of OSA and issues of limited access to full polysomnography, there is a growing reliance on simplified tests that record oximetry alone, or oximetry with airflow and respiratory effort channels, to establish the diagnosis.

Mechanisms of Upper Airway Collapse during Sleep

As described above, the pharyngeal airway can be considered as a collapsible tube, the patency of which is determined by a balance between forces tending to close the airway, such as intraluminal suction pressure during breathing, and forces acting to maintain airway patency, notably the activation of upper airway dilator muscles. The current broad conception of OSA pathophysiology is that upper airway anatomic dimensions are reduced in affected patients, leading to compensatory activation of upper airway dilators. Muscle activity is therefore adequate during wakefulness to maintain airway patency, but at sleep onset, when upper airway tonic and phasic activity are reduced and protective reflexes are inhibited, airway closure supervenes.[12,13,42] The evidence supporting these concepts, as well as other potential factors contributing to the pathophysiology of OSA, is considered in the following sections. A schematic of the mechanisms contributing to upper airway collapse during sleep is shown in Figure 50-7.

Upper Airway Anatomy in OSA Upper airway collapse during sleep in OSA occurs predominantly in the retropalatal and retroglossal airway, that is, the velopharynx and oropharynx.

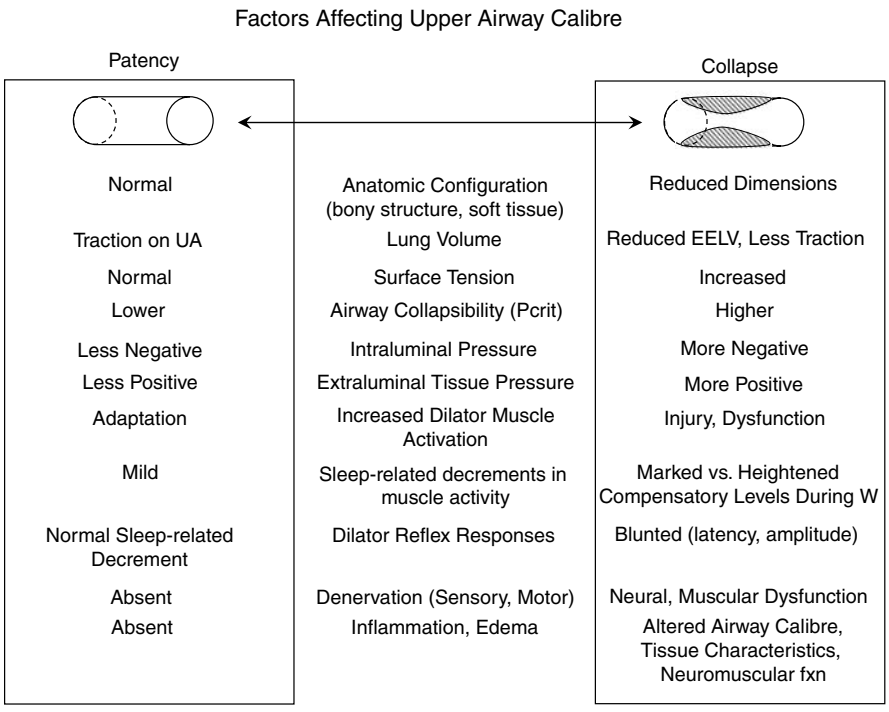

FIGURE 50-7 Schematic of mechanisms contributing to upper airway collapse during sleep in obstructive sleep apnea.

There is abundant evidence that the airway dimensions are reduced in OSA patients in comparison with normal control subjects. Techniques that have been used to study airway size include cephalometry, fluoroscopy, acoustic reflection, videoendoscopy, computed tomography, and magnetic resonance imaging (MRI). The accumulated data indicate that both reductions in the dimensions of the bony craniofacial framework and increases in the size of soft tissue structures surrounding the airway may contribute to reduced airway dimensions. Alterations in craniofacial proportions that have been described include reduced length of the mandibular ramus, inferior positioning of the hyoid bone, and retroposition of the maxilla.[45] In addition to circumferential narrowing, increased airway length may also be a factor. Increased distance between the hyoid bone and the mandibular plane found in cephalometric studies and increased airway length found in a recent MRI modeling analysis appear to be associated with an increased likelihood of upper airway collapse.[46]

Increases in soft tissue dimensions that have been found in imaging studies include enlargement of the soft palate, tongue, parapharyngeal fat pads, and lateral pharyngeal walls. These increases contribute to anatomic narrowing and may also contribute to increased tissue pressure, which favors airway collapse. The increased tissue volume probably reflects changes that also affect mechanical characteristics of the tissues, leading to altered airway biomechanics (see below). Several mechanisms appear to contribute to these soft tissue changes. Upper airway edema has been found clinically, histologically, and by MRI scanning.[47–49] This may result from upper airway trauma during obstructive events, hypoxemia, systemic inflammation, or a combination of factors. Mucosal edema improves with nasal continuous positive airway pressure (CPAP) treatment of OSA.[48] Increased deposition of fat in the upper airway in obese patients contributes to narrowing, particularly in the region of the parapharyngeal fat pads, but elsewhere in the upper airway as well.[45] Weight gain is also associated with increased amounts of fat-free tissue, some of which is muscle, such that obesity may contribute to increased upper airway muscle mass. The latter may also be due to loading with hypertrophy or muscle injury and edema, which is discussed further below. Genetic factors probably also play a role in determining soft-tissue volume, in a manner analogous to craniofacial structure.

Lung Volume Effects on Upper Airway Size Studies in both humans and animals have shown that upper airway caliber is influenced by changes in lung volume, such that decreased lung volume is associated with decreased upper airway dimensions and increased airflow resistance.[50–52] This appears to be due to effects of tracheal tug on upper airway length and/or wall characteristics.[51,52] OSA patients appear to have greater lung volume dependence of upper airway caliber than normal subjects.[53] Assumption of the recumbent position is associated with reduced end-expiratory lung volume, and obese patients have particularly marked reductions in supine functional residual capacity. Furthermore, lung volume may also decrease during the course of obstructive apnea. These reductions in lung volume would therefore contribute to reduced upper airway caliber, further increasing the predisposition to collapse.

Mechanical Properties of the Upper Airway The cross-sectional area of the pharynx is determined by the interaction between the mechanical characteristics of this structure, that is, compliance of the wall, and the transmural pressure.[12,13] The passive mechanical properties of the upper airway in OSA have received considerable attention. Schwartz and colleagues[54,55] have modeled the upper airway as a Starling resistor and produced an extensive literature assessing the collapsibility of the pharyngeal airway under passive conditions. This typically involves the application of a range of positive and negative airway pressures, with extrapolation from steady-state pressure–flow relationships to determine the pressure associated with airway closure, or critical pressure, P_{crit}. During sleep, P_{crit} values are about $-13\,cm\,H_2O$ in normal subjects, about $-6\,cm\,H_2O$ in snorers, and about $-2\,cm\,H_2O$ in patients with predominantly obstructive hypopnea; in apneic patients, the upper airway closing pressure is positive, often in the range $+10$ to $+15\,cm\,H_2O$. Isono and colleagues[56] have studied the static properties of the human pharynx under conditions of general anesthesia and muscle paralysis. These authors found that for OSA versus control subjects, the average and maximal velopharyngeal cross-sectional areas were smaller, closing pressures were higher, and area–pressure compliance curves were shifted down and to the right, indicative of increased collapsibility. Other authors have also shown reduced distensibility of the upper airway in OSA. Collectively, these data point to the presence of a smaller, more collapsible, and less distensible, that is, less compliant, airway in OSA.

During active breathing, the transmural pressure across the pharynx is another major determinant of cross-sectional area. The transmural pressure is determined by the balance between the intraluminal pressure, which is negative during inspiration, and the extraluminal or tissue pressure. The latter is determined by the volume and mechanical characteristics of tissues surrounding the airways and by the level of activation of surrounding constrictor and dilator muscles. Muscle activation will be considered in the following section. No direct measurements have been made of interstitial tissue pressure in humans, although measurements in anesthetized pigs showed positive extraluminal pressures that correlated with airway obstructive events. The occurrence of airway collapse under passive conditions without negative intraluminal pressure[54,55] suggests that positive tissue pressures probably also exist in humans.

Surface tension contributes to pharyngeal collapsibility.[12,57,58] This may be particularly important at the point where generation of an opening pressure is required to separate mucosal surfaces that have come into contact during complete airway collapse. However, surface forces will also influence the distensibility of the rounded pharyngeal structure throughout the respiratory cycle. Upper airway surface lining fluid from OSA subjects shows increased surface tension in comparison with that of fluid

from control subjects.[58] Topical application of artificial surfactant renders the upper airway less collapsible and can produce reductions in the severity of obstructive events during sleep in OSA patients.[57]

Neural Control of Pharyngeal Motor Activity As discussed earlier in this chapter, the tonic and phasic activation of dilatory musculature surrounding the pharyngeal airway is critical to the prevention of airway collapse as negative intraluminal pressure during inspiration causes a decrease in transmural pressure. Results from several groups have indicated that the activity of upper airway dilators is greater in OSA patients than in normal subjects, and this is believed to represent a compensatory mechanism for the inherent anatomic compromise of the airway in such patients.[59,60]

There are several major inputs influencing the activation of pharyngeal dilator muscles by the brainstem respiratory controller.[13,61–63] As noted above, the normal integrated pattern of central respiratory output is such that there is preactivation of upper airway musculature before activation of the lower pump muscles occurs.[14,15] Perturbations in this pattern, with delayed activation of upper airway dilators in relation to chest wall and diaphragm activation, have been reported in some patients with OSA, and this is believed to contribute to upper airway instability.[15] Central output to upper airway motor neurons is also influenced by chemoreceptor stimulation, so that fluctuations in carbon dioxide level may destabilize output to the dilator muscles.

Most important for sleep apnea, however, is the influence of sleep-related decrements in pharyngeal motor output. Whereas the upper airway may be narrowed during wakefulness in OSA, obstruction occurs only during sleep, emphasizing the importance of state-dependent influences on upper airway control. Sleep onset in normal subjects is initially associated with reduced tonic and phasic activity of the genioglossus, geniohyoid, and palatal muscles. However, phasic muscle activity tends to recover as sleep is established, whereas muscles with a predominantly tonic pattern of activation tend to show further losses of activity as sleep deepens.[13,42] It is therefore believed that reduced tonic activation is an important factor contributing to upper airway collapse. However, both phasic and tonic muscle activity may be potently inhibited during rapid eye movement (REM) sleep,[64] accounting in part for the increased severity of OSA during REM versus non-REM sleep. A key observation in OSA patients is that the fall in upper airway dilator electromyographic activity associated with sleep onset appears to be substantially greater than in controls.[65] Thus, upper airway dilator activity is greater during wakefulness, representing a compensation for upper airway size and mechanics, but appears to be lost at sleep onset.

The activity of upper airway dilators is also modulated by reflex inputs. The available evidence indicates that the most important local stimulus for activation of these muscles is intrapharyngeal negative pressure.[13,66] Reflex activation by pulses of negative pressure applied to the upper airway has been described for the genioglossus, levator palatini, and palatoglossus muscles. This negative pressure reflex is impaired for the levator palatini and palatoglossus muscles in OSA versus control subjects. Furthermore, even in normal individuals, there is a decrease in the activity of this reflex at sleep onset. Thus, an important modulating influence on upper airway caliber is attenuated during sleep, and this is believed to predispose to upper airway collapse.

The afferent inputs to the negative pressure reflex arise from the mucosa of the oropharynx and larynx.[66–68] The importance of mucosal afferents to upper airway motor control has been demonstrated in studies involving topical application of anesthetic to interfere with mucosal sensory receptor activity. Topical upper airway anesthesia leads to reduced dilator muscle activity and increased pharyngeal airflow resistance during wakefulness and sleep and can induce apnea and hypopnea in normal subjects, increase the frequency of obstructive events in snorers, and lead to delayed end-apneic arousal and increased apnea duration in OSA subjects.[67–69] Recently, we showed the presence of an impairment in mucosal mechanosensory function in the oropharynx of snorers and OSA patients, which partially improved in OSA patients following CPAP treatment.[67] The severity of oropharyngeal sensory impairment correlates with the latency of the palatoglossus and genioglossus muscle reflex responses to pulses of negative pressure delivered to the upper airway, as described by Mortimore and Douglas.[70] Therefore, the afferent neural impairment appears to contribute to impaired dilator reflex responsiveness, which probably has important implications for upper airway function. Additional studies using endoscopic sensory testing have also demonstrated impaired laryngeal sensation in OSA patients versus controls.[68] Within the OSA group, there appeared to be two subgroups, one with normal sensation and another with abnormal sensation, the severity of which correlated with the apnea–hypopnea index. Thus, in some patients, an impairment of mucosal sensory function appears to contribute to OSA pathophysiology.

Although the mechanisms underlying impaired upper airway sensation remain unclear, histologic studies have demonstrated neural changes consistent with injury and repair that could represent the basis for mucosal sensorineural dysfunction.[49,68] An accumulating body of data points to the presence of significant cellular inflammation in upper airway tissue.[49,68] As noted above, this may be related to tissue injury resulting from vibration-associated trauma, hypoxemia, or other factors, including the state of systemic inflammation, which has been associated with both OSA and obesity. Inflammatory mechanisms or mechanical trauma may account for the neural injury observed in the upper airway mucosa, although further investigation is required to establish the precise mechanisms involved.

Pharyngeal Muscle Function in OSA There is accumulating evidence that OSA is associated with changes in the structure and function of the upper airway dilator muscles. Some of these changes appear to be adaptive in nature, whereas others are more consistent with injury and may lead to impaired contractile function, thus contributing to upper airway dysfunction. As noted above, upper airway dilator

activity is increased in OSA patients during wakefulness. Whereas sleep-related decrements in upper airway muscle activity contribute to upper airway collapse, the termination of obstructive events is associated with massive activation of upper airway dilators, which, it should be noted, occurs under hypoxic conditions. Thus, the evidence suggests that, overall, upper airway muscle activity is substantially increased in OSA. This raises the possibility that these muscles could undergo secondary changes as a direct consequence of their increased activity level.[71] Skeletal muscle is well recognized to alter its phenotype in order to adapt to the prevailing demands placed upon it, thereby maximizing muscle efficiency. Properties such as muscle fiber size, contractile protein isoform profile, and metabolic enzyme content can be readily modified, with resultant changes in muscle performance. However, when excessive contractile demands are placed upon muscle, it is well documented that the structural integrity of the muscle cell can be physically disrupted by the forces produced during muscle contraction. This activity-induced injury is particularly prominent when the forces opposing muscle contraction result in muscle lengthening during activation, or so-called eccentric contraction.[71,72]

Eccentric contractions of upper airway dilator muscles have been demonstrated during airway occlusion and progressive hypercapnia in anesthetized cats.[73] Because similar events occur in human OSA, it has been hypothesized that eccentric contractions also occur in pharyngeal dilators in this condition,[71] through at least two possible mechanisms: (1) muscles that are mechanically linked could contract against one another, as has been demonstrated for the sternohyoid and geniohyoid muscles during airway occlusion in anesthetized animals, and (2) large negative intraluminal pressures associated with pharyngeal obstruction, which could act to forcibly lengthen the opposing dilator muscles.[71,72]

Petrof and colleagues,[72] using the English bulldog, which suffers from OSA, found that the sternohyoid muscle, an important upper airway dilator muscle, showed evidence of fiber-type shift but also changes consistent with activity-induced muscle injury, consisting of abnormal fiber morphology (central nucleation, fissured and moth-eaten appearance), inflammatory cell infiltrates, and increased amounts of connective tissue. Muscle injury was also found in the geniohyoid muscle, another pharyngeal dilator. A subsequent MRI study using the bulldog model[74] showed changes consistent with muscle edema or fibrosis in four of five pharyngeal muscles examined. These changes were not seen in limb muscles or in control animals. Thus, there is compelling evidence for muscle injury in this animal model of OSA.

Studies on human OSA tissues have also shown evidence of both adaptation and injury. Several smaller studies have shown histologic changes consistent with injury.[71] However, studies by Series and colleagues[75,76] on the musculus uvulae muscle did not show pathologic evidence of injury but demonstrated an increase in the proportion of fast-twitch (type IIa) fibers and the activity of enzymes of anaerobic metabolism in OSA patients. The force-generating capacity of the muscle was the same in OSA patients and control subjects when normalized for muscle cross-sectional area, but in a subsequent study, changes in the musculus uvulae muscle correlated with upper airway collapsibility. Patients with the most easily collapsible upper airway also showed the greatest increases in force production, type IIa fiber prevalence, anaerobic metabolism, and susceptibility to muscle fatigue. Carrera and Barbé[77] studied genioglossus muscles from OSA patients and from controls; they also reported a shift to type II fiber type and specifically demonstrated increased fatigability of the genioglossus muscle in OSA. Thus, even in the absence of morphologic injury, adaptive changes induced by the contraction history of the upper airway muscles may also have adverse functional consequences.

In the discussion on pharyngeal motor control in the preceding section, it was noted that there is evidence for an upper airway afferent neuropathy in OSA, based on both sensory testing data and pathologic findings. There is evidence to suggest that there may, in fact, be a more diffuse upper airway neuropathy in OSA that also affects efferent nerves and may lead to muscle denervation. Woodson and colleagues[47] reported demyelination in upper airway tissue specimens. Histologic evidence of motor denervation, such as fiber type grouping and grouped atrophy, has also been found in several recent studies.[50,78] In a recent study of human upper airway surgical specimens from OSA and control subjects, we demonstrated increased nerve tissue proliferation within the muscle compartment, revealed by specific antibody to neural tissue (PGP 9.5), and also found groups of myocytes expressing neural cell adhesion molecule, a sensitive marker of muscle denervation.[49] These findings suggest that denervation-related changes may contribute to upper airway muscle function in OSA.

As discussed above, the edema and inflammatory cell infiltration of the upper airway mucosa described by several groups suggest that inflammatory mechanisms may contribute to upper airway dysfunction in OSA, leading, for example, to neuropathic changes.[49] In the study just cited from the author's laboratory,[49] we demonstrated increased inflammatory cell infiltration in OSA upper airway muscle. Furthermore, preliminary data from our laboratory have revealed increased expression of tumor necrosis factor-α and interleukin-1α in muscle tissue from patients with severe OSA versus those with mild OSA. It is now well established that cytokines can lead directly to muscle dysfunction.[79] Thus, inflammatory changes in the upper airway may alter muscle function directly by this means or conceivably by contributing to neuropathy, which, in turn, may lead to muscle denervation. It is likely that muscle adaptation and injury are ongoing in a dynamic process in OSA, that different muscle groups within the upper airway may be affected differently, and that the extent of change and physiologic consequences for muscle function may vary between OSA patients. Further work will be required to further elucidate the contribution of upper airway muscle denervation and injury to the pathophysiology of this disorder, as well as to determine whether muscle changes may represent a potential therapeutic target in OSA.

OSA and Ventilatory Control There is a growing understanding of the effects of chemoreceptor sensitivity and ventilatory control instability on the pathogenesis of periodic breathing and central apnea.[80,81] Differences in the control of breathing between wakefulness and sleep (eg, the higher ventilatory setpoint and ventilatory chemosensitivity during wakefulness) lead to respiratory instability during the transition from wakefulness to sleep, accounting for apneas and hypopneas, which may be seen at sleep onset in normal subjects. Furthermore, recent work has shown that ventilatory responses are heightened at the instant of arousal from sleep in comparison to stable wakefulness.[62] Thus, instability of the sleep–wake state per se may destabilize breathing. The state changes associated with apneas and hypopneas, that is, microarousal at the termination of events, followed by the rapid return to sleep, therefore represent a situation of inherently unstable respiratory control. Numerous investigators have postulated that altered chemoreceptor sensitivity or instability of other respiratory control mechanisms may therefore contribute to the pathogenesis of OSA. An early observation in support of this hypothesis was the occurrence of periodic breathing during sleep immediately following tracheostomy for OSA.[82]

A large body of data has been generated concerning changes in classic chemoreceptor responses in OSA, although there have been rather inconsistent findings. Some authors have reported heightened hypoxic sensitivity, which was postulated to contribute to respiratory instability, whereas others have reported blunted hypoxic sensitivity.[83] Hypercapnic ventilatory responsiveness has been reported to be normal or decreased in OSA and, if reduced, may improve following treatment with nasal CPAP.[83]

Recently, Younes and colleagues used proportional assist ventilation (PAV) to evaluate ventilatory control stability in OSA patients.[84] With the upper airway stabilized during sleep by nasal CPAP, increasing levels of PAV (controller gain) were applied up to the point at which periodic breathing was elicited. It was found that patients with severe OSA were much more susceptible to the development of periodic breathing than patients with mild-to-moderate OSA, indicating increased endogenous loop gain in the severe group. The mechanisms underlying this ventilatory instability, and its precise role in the pathogenesis of OSA, remain to be established.

Although the role of changes in chemoreceptor sensitivity in the pathogenesis of OSA remains unclear, there is strong evidence that severe OSA may produce secondary changes in ventilatory control, namely hypoventilation during wakefulness. This occurs in a subset of OSA patients who appear to be the group at risk for decompensation and respiratory failure in the context of intercurrent medical illness, or in some cases simply because of inexorable progression of the changes associated with sleep-disordered breathing. Most patients with OSA and daytime hypoxemia and/or hypercapnia have some underlying lung dysfunction, such as COPD or obesity-related or neuromuscular restrictive impairment.[83,85,86] OSA patients with hypercapnia have been described as demonstrating impaired ventilatory recovery after apnea.[87] This may represent a blunting or failure of load compensation mechanisms in such patients and may contribute to a "resetting" of the chemoreceptors, leading to awake hypoventilation. Daytime blood gases typically improve dramatically or normalize following effective treatment of OSA, supporting the concept that the nocturnal respiratory disturbance leads to the development of awake hypoventilation.

OSA and Asthma There is growing evidence of a link between OSA and asthma. In a recent study at McGill,[88] 26 consecutive refractory asthmatic subjects were evaluated in comparison with 21 age-matched and gender-matched control subjects with moderate asthma. The prevalence of OSA in both groups was dramatically increased over population normal values, with a tendency for OSA to be more prevalent among subjects with severe asthma (16/26, 62%) than among those with moderate asthma (10/21, 48%) and for OSA to be somewhat more severe among the refractory asthma group. These findings, together with evidence from other case series, suggest that OSA may contribute to worsened asthma control. For example, Chan and colleagues[89] studied nine patients with severe asthma and snoring or OSA who suffered frequent nocturnal asthma attacks despite maximum bronchodilator therapy. CPAP treatment of upper airway obstruction during sleep improved asthma control, as reflected in asthma symptoms, bronchodilator use, and peak flow rates.

There are several mechanisms by which OSA and asthma could interact. There is evidence that stimulation of upper airway mechanoreceptors during snoring and apneas can lead to reflex bronchoconstriction. Alternatively, gastroesophageal reflux occurs frequently in OSA patients and is a well-recognized exacerbating factor in asthma. Treatment of asthma with corticosteroids may contribute to OSA by increasing obesity and/or pharyngeal myopathy.[90] Finally, as noted above, there are considerable data documenting upper airway inflammation in OSA and growing evidence that this plays a role in OSA pathophysiology. The links between rhinosinus inflammation and lower airway inflammation in asthma are well documented (termed the "united airway hypothesis"). It may therefore be that pharyngeal involvement represents part of a continuum of airway inflammatory involvement. There may thus be a reciprocal interaction between these disease processes, such that worsening of OSA may contribute to worsened asthma control and vice versa. This concept is supported by the clinical data cited above concerning the effects of OSA treatment on asthma control. Research efforts are ongoing to further evaluate the mechanisms of the OSA–asthma interaction and to more systematically assess the effects of OSA treatment on asthma control.

Physiologic Aspects of Diagnostic Testing for OSA

In recent years, recording of nasal pressure has emerged as a sensitive indicator of upper airway narrowing. Introduction of a standard nasal oxygen cannula into the nares, with connection of the tubing end to a differential pressure transducer referenced to atmosphere, provides for

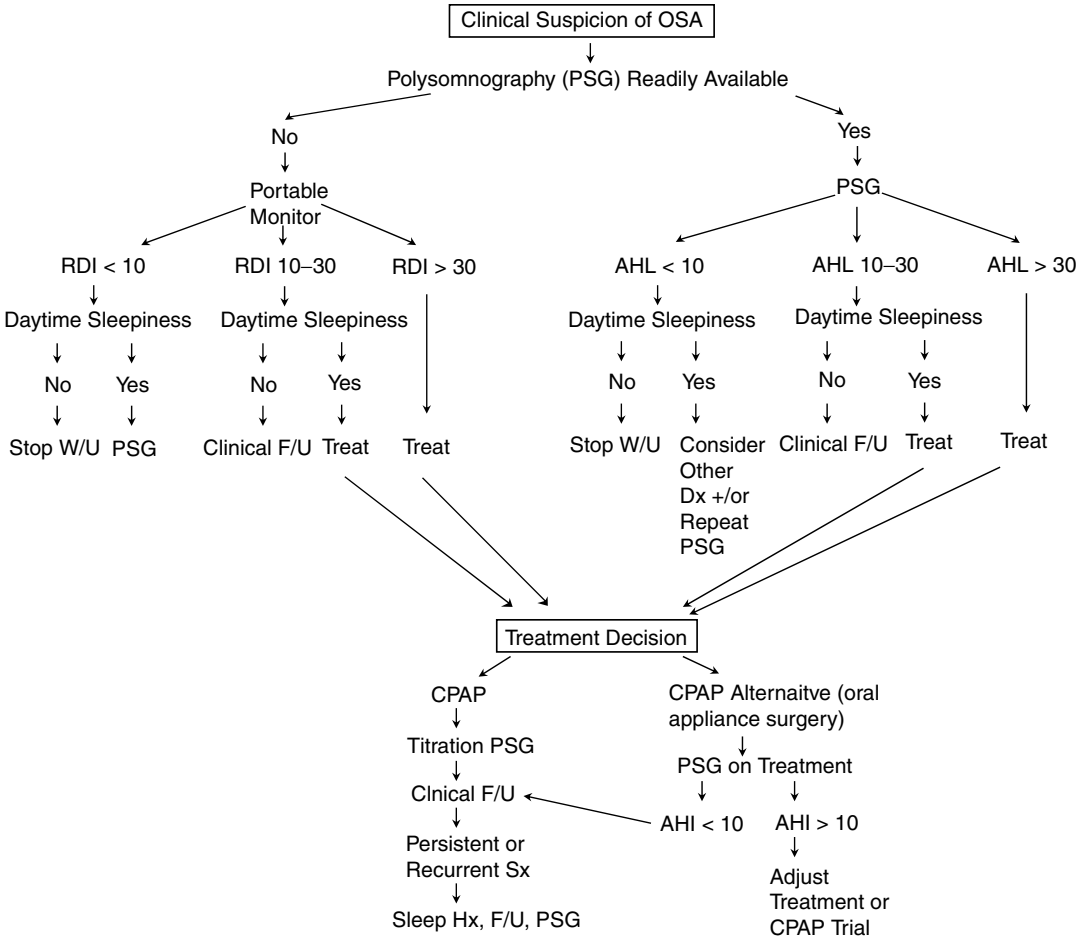

FIGURE 50-8 Approach to diagnosis and management of obstructive sleep apnea.

a semiquantitative assessment of nasal airflow. Of greater interest is the fact that the shape of the inspiratory pressure curve during tidal respiratory cycles shows flattening indicative of flow limitation as upper airway narrowing occurs, in the same way that forced maximal curves reveal extrathoracic upper airway obstruction, as discussed earlier in this chapter.[91,92] This technique provides for the detection of subtle episodes of upper airway narrowing.

Respiratory effort was traditionally measured by using an esophageal catheter to estimate pleural pressure. This invasive approach has largely been replaced by techniques involving the use of sensors on the rib cage and abdomen to detect respiratory effort and movement. The most sensitive of these is respiratory inductance plethysmography, which provides data on changes in thoracoabdominal motion resulting from partial or complete upper airway obstruction. Partial or complete rib cage paradoxical motion is often seen during apneas and hypopneas and can provide confirmatory evidence of increasing respiratory effort in the context of upper airway obstruction.

Physiology of Treatment Approaches to OSA

There are several treatments aimed at compensating for the anatomic predisposition to upper airway collapse. Mandibular advancement splints, for example, act to advance the lower jaw in relation to other craniofacial structures, thereby increasing the anteroposterior oropharyngeal dimension.[93] This approach does not compensate for other factors contributing to upper airway collapse during sleep, and there are limitations to its anatomic effects. Oral appliances are therefore effective in mild-to-moderate apnea but typically do not alleviate moderate-to-severe OSA. Surgical interventions are also aimed at compensating for reduced upper airway dimensions. In childhood OSA, hypertrophy of the adenoid and, to a lesser extent, the palatine tonsils is often a major factor contributing to airway compromise, so that adenoidectomy–tonsillectomy is a mainstay of treatment for OSA in the child. Maxillomandibular advancement surgery may be beneficial in the context of craniofacial insufficiency, for example, the marked micrognathia associated with Pierre–Robin syndrome. This approach may also be useful for nonobese adults with similar but more subtle craniofacial disproportion. Surgical intervention in general, however, has a much more limited role in adult OSA.[94] Tracheostomy is highly effective as it bypasses the site of airway obstruction. However, there are adverse social as well as medical aspects of chronic tracheostomy, which severely limit the applicability of this intervention. A variety of approaches directed at reducing or stiffening soft palate tissue have been applied to adult OSA. These include conventional uvulopalatopharyngoplasty, laser-assisted uvuloplasty, radiofrequency-controlled

thermoablation (somnoplasty), and other procedures. Overall, the results of these interventions have been highly disappointing in the context of moderate-to-severe OSA. This is undoubtedly due to the limited anatomic effects of these interventions, combined with the role of factors other than anatomic predisposition to upper airway collapse during sleep.

The treatment of choice for OSA is nasal CPAP.[95,96] CPAP functions as a pneumatic splint for the upper airway. A sealed mask is applied over the nose, and a continuous positive pressure is applied to the mask from a blower unit to distend the airway. The pressure required to maintain airway patency is determined by anatomic, mechanical, neuromuscular, and state-dependent factors, such that a greater pressure may be required for the supine position than for the lateral decubitus position and during REM than during non-REM sleep. Traditionally, CPAP titration has been performed in the sleep laboratory, with manual adjustment to determine the minimum pressure required to maintain airway patency in all sleep stages and body positions. This pressure is then prescribed for home treatment. More recently, automated CPAP devices have become available, which continuously monitor the amplitude and contour of airflow with a pneumotachograph in the CPAP unit. A microprocessor then evaluates the adequacy of these signals and adjusts the pressure to respond to inspiratory flow limitation and/or reduced airflow. The concept is that this is a more physiologic approach that should match the treatment delivered to the dynamic changes in upper airway caliber determined by the factors described above. An algorithm for the diagnosis and management of OSA is shown in Figure 50-8.

UPPER AIRWAY IN CENTRAL SLEEP APNEA

Central sleep apnea is encountered in a variety of clinical conditions. It may be present as part of primary or secondary hypoventilation syndromes (hypercapnic central apnea) due to central nervous system (CNS) lesions or neuromuscular disease involving the respiratory muscles. Alternatively, nonhypercapnic forms of central apnea include idiopathic central sleep apnea and Cheyne–Stokes respiration (CSR) during sleep, which may occur in the setting of congestive heart failure, renal failure, or CNS lesions.[97]

Although the upper airway is not believed to play a primary role in most of these conditions, there is evidence that upper airway instability and collapse are associated with central apnea and may contribute to its pathophysiology. Badr and colleagues have shown, using video-endoscopy, that upper airway collapse occurs in the context of hyperventilation-induced central apnea during sleep, even in normal subjects.[98] Thus, the loss of respiratory drive due to induced hypocapnia leads to airway closure, confirming the importance of respiratory drive to upper airway muscles in maintaining airway patency. Conversely, there is evidence that upper airway collapse may induce central apneas. The clinical correlate of this is that patients with snoring and some obstructive apneas or hypopneas during REM sleep may demonstrate central events during non-REM sleep. Furthermore, some patients with predominant central apnea respond to nasal CPAP treatment, suggesting that upper airway closure contributes to these events.[99] These findings may in part be explained by evidence indicating that stimulation of upper airway mechanoreceptors may result in reflex inhibition of inspiratory drive. Thus, stimulation of laryngeal receptors in experimental animals has been reported to induce apnea.[97,100] Furthermore, we found that inhibition of upper airway mucosal receptors with the use of topical anesthesia resulted in increased respiratory effort during obstructive apneas in OSA patients. This points to the loss of an inhibitory influence on respiratory drive, with attenuation of airway sensory receptor function.[69]

There has been considerable recent interest in CSR during sleep in the setting of chronic congestive heart failure. Sleep-disordered breathing is common among stable heart failure patients, occurring in up to 40%,[101,102] with CSR representing the most common form. CSR is believed to both result from and lead to worsening of heart failure through complex mechanisms and has been shown to be associated with reduced survival for a given level of cardiac dysfunction. Treatment with nasal CPAP in this group leads to improvements in CSR, ventricular function, and quality of life.[102] A multicenter trial (CANPAP) is currently under way to determine the effects of CPAP on mortality in heart failure patients with CSR. The mechanisms by which CPAP leads to improvement in CSR remain unclear. However, recent work at McGill, involving the forced oscillation technique to assess upper airway patency, has demonstrated that upper airway closure is frequent even during pure central events in heart failure patients with CSR.[103] Furthermore, overlap between OSA and CSR has been described in this population.[104] Thus, upper airway instability may also contribute to the pathogenesis of CSR.

SUMMARY AND CONCLUSIONS

This chapter has examined the normal structure and function of the upper airway, with an emphasis on the physiologic aspects of the integration of breathing with the variety of other upper airway functions. The most serious clinical disturbance of upper airway function is anatomic or functional obstruction with airflow compromise. We have considered the physiologic basis for both the clinical presentation and approach to diagnostic testing for the various forms of upper airway obstruction. Finally, we have considered sleep-disordered breathing and in particular OSA, a very common but, for many individuals, no less serious form of variable extrathoracic upper airway obstruction occurring during sleep. The research that has been directed at understanding the mechanisms underlying OSA has led to major advances in our knowledge of upper airway structure and function. Although considerable progress has been made, ongoing work aimed at further elucidating the mechanisms of OSA will undoubtedly broaden our understanding of upper airway function in general.

REFERENCES

1. Proctor D. Form and function of the upper airways and the larynx. In: Macklem P, Mead J, editors. Handbook of physiology. Section 3. The respiratory system, mechanics of breathing. Bethesda, MD: American Physiological Society; 1986. p. 63–74.
2. Isaacs RS, Sykes JM. Anatomy and physiology of the upper airway. Anesthesiol Clin North Am 2002;20:733–45, v.
3. Proctor DF. The upper airways. II. The larynx and trachea. Am Rev Respir Dis 1977;115:315–42.
4. Doyle DJ, Arellano R. Upper airway diseases and airway management: a synopsis. Anesthesiol Clin North Am 2002;20: 767–87, vi.
5. Cauna N. Blood and nerve supply of the nasal lining. In: Proctor DF, Anderson IB, editors. The nose. Oxford: Elsevier Biomedical Press; 1982. p. 44–69.
6. Thach B, Brouillette R. The respiratory function of pharyngeal musculature: relevance to clinical obstructive apnea. In: Euler C, Lagercrantz H, editors. Central nervous control mechanisms in breathing. Oxford: Pergamon Press; 1979. p. 483–94.
7. McFarland DH, Lund JP. Modification of mastication and respiration during swallowing in the adult human. J Neurophysiol 1995;74:1509–17.
8. McFarland DH, Lund JP, Gagner M. Effects of posture on the coordination of respiration and swallowing. J Neurophysiol 1994;72:2431–7.
9. Broussard DL, Altschuler SM. Central integration of swallow and airway-protective reflexes. Am J Med 2000;108 Suppl 4a:62S–7S.
10. Remmers JE, DeGroot WJ, Sauerland EK, Anch AM. Pathogenesis of upper airway occlusion during sleep. J Appl Physiol 1978;44:931–8.
11. Kuna ST, Sant'Ambrogio G. Pathophysiology of upper airway closure during sleep. JAMA 1991;266:1384–9.
12. Wheatley JR, Amis TC. Mechanical properties of the upper airway. Curr Opin Pulm Med 1998;4:363–9.
13. Fogel RB, Malhotra A, White DP. Sleep. 2: pathophysiology of obstructive sleep apnoea/hypopnoea syndrome. Thorax 2004;59:159–63.
14. Strohl KP, Hensley MJ, Hallett M, et al. Activation of upper airway muscles before onset of inspiration in normal humans. J Appl Physiol 1980;49:638–42.
15. Hudgel DW, Harasick T. Fluctuation in timing of upper airway and chest wall inspiratory muscle activity in obstructive sleep apnea. J Appl Physiol 1990;69:443–50.
16. Patrick GB, Strohl KP, Rubin SB, Altose MD. Upper airway and diaphragm muscle responses to chemical stimulation and loading. J Appl Physiol 1982;53:1133–7.
17. Sasaki CT, Weaver EM. Physiology of the larynx. Am J Med 1997;103:9S–18S.
18. Suzuki M, Kirchner JA. The posterior cricoarytenoid as an inspiratory muscle. Ann Otol Rhinol Laryngol 1969;78:849–64.
19. Wyke B. Respiratory activity of intrinsic laryngeal muscles. An experimental study. In: Wyke BD, editor. Ventilatory and phonatory control systems. London: Oxford University Press; 1974. p. 408–21.
20. Fortier PH, Reix P, Arsenault J, et al. Active upper airway closure during induced central apneas in lambs is complete at the laryngeal level only. J Appl Physiol 2003;95:97–103.
21. Cormier YF, Camus P, Desmeules MJ. Non-organic acute upper airway obstruction: description and a diagnostic approach. Am Rev Respir Dis 1980;121:147–50.
22. Newman KB, Mason UG III, Schmaling KB. Clinical features of vocal cord dysfunction. Am J Respir Crit Care Med 1995;152 (4 Pt 1):1382–6.
23. Macklem P, Rector W, Wang K. Upper airway obstruction in asthma. Johns Hopkins Med J 1980;147:233–7.
24. Proctor DF. Modifications of breathing for phonation. In: Macklem PT, Mead J, editors. Handbook of physiology. Bethesda (MD): American Physiological Society; 1986. p. 597–604.
25. Johnston S, Yan S, Sliwinski P, Macklem PT. Modified Campbell diagram to assess respiratory muscle action in speech. Respirology 1999;4:213–22.
26. Kryger M, Bode F, Antic R, Anthonisen N. Diagnosis of obstruction of the upper and central airways. Am J Med 1976;61: 85–93.
27. Miller RD, Hyatt RE. Evaluation of obstructing lesions of the trachea and larynx by flow–volume loops. Am Rev Respir Dis 1973;108:475–81.
28. Hyatt RE. Evaluation of major airway lesions using the flow–volume loop. Ann Otol Rhinol Laryngol 1975;84 (5 Pt 1):635–42.
29. Gibson GJ, Pride NB, Empey DW. The role of inspiratory dynamic compression in upper airway obstruction. Am Rev Respir Dis 1973;108:1352–60.
30. Owens GR, Murphy DM. Spirometric diagnosis of upper airway obstruction. Arch Intern Med 1983;143:1331–4.
31. Kashima HK. Documentation of upper airway obstruction in unilateral vocal cord paralysis: flow–volume loop studies in 43 subjects. Laryngoscope 1984;94:923–37.
32. Vincken WG, Gauthier SG, Dollfuss RE, et al. Involvement of upper-airway muscles in extrapyramidal disorders. A cause of airflow limitation. N Engl J Med 1984;311:438–42.
33. Vincken W, Elleker G, Cosio MG. Detection of upper airway muscle involvement in neuromuscular disorders using the flow–volume loop. Chest 1986;90:52–7.
34. Orr JB. Helium–oxygen gas mixtures in the management of patients with airway obstruction. Ear Nose Throat J 1988; 67:866–9.
35. Ernst A, Feller-Kopman D, Becker HD, Mehta AC. Central airway obstruction. Am J Respir Crit Care Med 2004;169: 1278–97.
36. Hnatiuk OW, Corcoran PC, Sierra A. Spirometry in surgery for anterior mediastinal masses. Chest 2001;120:1152–6.
37. Kanter RK, Watchko JF. Pulmonary edema associated with upper airway obstruction. Am J Dis Child 1984;138: 356–8.
38. Kollef MH, Pluss J. Noncardiogenic pulmonary edema following upper airway obstruction. 7 cases and a review of the literature. Medicine (Baltimore) 1991;70:91–8.
39. Young T, Peppard PE, Gottlieb DJ. Epidemiology of obstructive sleep apnea: a population health perspective. Am J Respir Crit Care Med 2002;165:1217–39.
40. Flemons WW. Clinical practice. Obstructive sleep apnea. N Engl J Med 2002;347:498–504.
41. Cistulli PA, Sullivan CE. Pathophysiology of sleep apnea. In: Saunders NA, Sullivan CE, editors. Sleep and breathing. New York: Marcel Dekker; 1994. p. 405–48.
42. Ayappa I, Rapoport DM. The upper airway in sleep: physiology of the pharynx. Sleep Med Rev 2003;7:9–33.
43. Rechtschaffen A, Kales A. A manual of standardized terminology, technique and scoring system for sleep stages of human sleep. Los Angeles: Los Angeles Brain Information Service, Brain Information Institute, UCLA; 1968.
44. Sleep-related breathing disorders in adults: recommendations for syndrome definition and measurement techniques in clinical research. The Report of an American Academy of Sleep Medicine Task Force. Sleep 1999;22: 667–89.
45. Schwab RJ. Pro: sleep apnea is an anatomic disorder. Am J Respir Crit Care Med 2003;168:270–1.

46. Malhotra A, Huang Y, Fogel RB, et al. The male predisposition to pharyngeal collapse: importance of airway length. Am J Respir Crit Care Med 2002;166:1388–95.
47. Woodson BT, Garancis JC, Toohill RJ. Histopathologic changes in snoring and obstructive sleep apnea syndrome. Laryngoscope 1991;101:1318–22.
48. Ryan CF, Lowe AA, Li D, Fleetham JA. Three-dimensional upper airway computed tomography in obstructive sleep apnea. A prospective study in patients treated by uvulopalatopharyngoplasty. Am Rev Respir Dis 1991;144: 428–32.
49. Boyd JH, Petrof BJ, Hamid Q, et al. Upper airway muscle inflammation and denervation changes in obstructive sleep apnea. Am J Respir Crit Care Med 2004;170:541–6.
50. Series F, Cormier Y, Desmeules M. Influence of passive changes of lung volume on upper airways. J Appl Physiol 1990;68:2159–64.
51. Van de Graaff WB. Thoracic traction on the trachea: mechanisms and magnitude. J Appl Physiol 1991;70:1328–36.
52. Rowley JA, Permutt S, Willey SJ, et al. Effect of tracheal and tongue displacement on upper airway airflow dynamics. J Appl Physiol 1996;80:2171–8.
53. Hoffstein V, Zamel N, Phillipson EA. Lung volume dependence of pharyngeal cross-sectional area in patients with obstructive sleep apnea. Am Rev Respir Dis 1984;130:175–8.
54. Schwartz AR, Smith PL, Wise RA, et al. Induction of upper airway occlusion in sleeping individuals with subatmospheric nasal pressure. J Appl Physiol 1988;64:535–42.
55. Gleadhill IC, Schwartz AR, Schubert N, et al. Upper airway collapsibility in snorers and in patients with obstructive hypopnea and apnea. Am Rev Respir Dis 1991;143:1300–3.
56. Isono S, Remmers JE, Tanaka A, et al. Anatomy of pharynx in patients with obstructive sleep apnea and in normal subjects. J Appl Physiol 1997;82:1319–26.
57. Jokic R, Klimaszewski A, Mink J, Fitzpatrick MF. Surface tension forces in sleep apnea: the role of a soft tissue lubricant: a randomized double-blind, placebo-controlled trial. Am J Respir Crit Care Med 1998;157(5 Pt 1):1522–5.
58. Kirkness JP, Madronio M, Stavrinou R, et al. Relationship between surface tension of upper airway lining liquid and upper airway collapsibility during sleep in obstructive sleep apnea hypopnea syndrome. J Appl Physiol 2003;95: 1761–6.
59. Mezzanotte WS, Tangel DJ, White DP. Waking genioglossal electromyogram in sleep apnea patients versus normal controls (a neuromuscular compensatory mechanism). J Clin Invest 1992;89:1571–9.
60. Suratt PM, McTier RF, Wilhoit SC. Upper airway muscle activation is augmented in patients with obstructive sleep apnea compared with that in normal subjects. Am Rev Respir Dis 1988;137:889–94.
61. Horner RL. Motor control of the pharyngeal musculature and implications for the pathogenesis of obstructive sleep apnea. Sleep 1996;19:827–53.
62. Horner RL. Impact of brainstem sleep mechanisms on pharyngeal motor control. Respir Physiol 2000;119:113–21.
63. Horner RL. The neuropharmacology of upper airway motor control in the awake and asleep states: implications for obstructive sleep apnoea. Respir Res 2001;2:286–94.
64. Wiegand L, Zwillich CW, Wiegand D, White DP. Changes in upper airway muscle activation and ventilation during phasic REM sleep in normal men. J Appl Physiol 1991;71: 488–97.
65. Mezzanotte WS, Tangel DJ, White DP. Influence of sleep onset on upper-airway muscle activity in apnea patients versus normal controls. Am J Respir Crit Care Med 1996;153 (6 Pt 1):1880–7.
66. Malhotra A, Fogel RB, Edwards J, et al. Local mechanisms drive genioglossus activation in obstructive sleep apnea. Am J Respir Crit Care Med 2000;161:1746–9.
67. Kimoff RJ, Sforza E, Champagne V, et al. Upper airway sensation in snoring and obstructive sleep apnea. Am J Respir Crit Care Med 2001;164:250–5.
68. Nguyen ATD, Jobin V, Payne R, et al. Laryngeal and velopharyngeal sensory impairment in obstructive sleep apnea. Sleep. [In press]
69. Cala SJ, Sliwinski P, Cosio MG, Kimoff RJ. Effect of upper airway anesthesia on apnea lengthening across the night in obstructive sleep apnea. J Appl Physiol 1996;81: 2618–26.
70. Mortimore IL, Douglas NJ. Palatal muscle EMG response to negative pressure in awake sleep apneic and control subjects. Am J Respir Crit Care Med 1997;156:867–73.
71. Petrof BJ, Hendricks JC. Muscle factors in obstructive sleep apnea. In: Pack AI, editor. Sleep apnea: pathogenesis, diagnosis, and treatment. New York: Marcel Dekker; 2002. p. 217–34.
72. Petrof BJ, Pack AI, Kelly AM, et al. Pharyngeal myopathy of loaded upper airway in dogs with sleep apnea. J Appl Physiol 1994;76:1746–52.
73. van Lunteren E, Haxhiu MA, Cherniack NS. Effects of tracheal airway occlusion on hyoid muscle length and upper airway volume. J Appl Physiol 1989;67:2296–302.
74. Schotland HM, Insko EK, Panckeri KA, et al. Quantitative magnetic resonance imaging of upper airway musculature in an animal model of sleep apnea. J Appl Physiol 1996;81: 139–46.
75. Series F, Cote C, Simoneau J-A, et al. Physiologic, metabolic, and muscle fiber type characteristics of musculus uvulae in sleep apnea hypopnea syndrome and in snorers. J Clin Invest 1995;95:20–5.
76. Series F, Simoneau JA, St Pierre S. Muscle fiber area distribution of musculus uvulae in obstructive sleep apnea and non-apneic snorers. Int J Obes Relat Metab Disord 2004;24: 410–5.
77. Carrera M, Barbé F, Savelda J, et al. Patients with obstructive sleep apnea exhibit genioglossus dysfunction that is normalized after treatment with continuous positive airway pressure. Am J Respir Crit Care Med 1999;159:1960–6.
78. Edstrom L, Larsson H, Larsson L. Neurogenic effects on the palatopharyngeal muscle in patients with obstructive sleep apnoea: a muscle biopsy study. J Neurol Neurosurg Psychiatry 1992;55:916–20.
79. Wilcox P, Milliken C, Bressler B. High-dose tumor necrosis factor α produces an impairment of hamster diaphragm contractility. Am J Respir Crit Care Med 1996;153:1611–5.
80. Phillipson EA, Bowes G. Control of breathing during sleep. In: Cistulli PA, Widdicombe JG, editors. Handbook of physiology. Vol 2. The respiratory system, control of breathing. Section 3. Part 1. Bethesda, MD: American Physiological Society; 1986. p. 649–80.
81. Dempsey JA, Smith CA, Eastwood PR, et al. Sleep-induced respiratory instabilities. In: Pack AI, editor. Sleep apnea: pathogenesis, diagnosis and treatment. New York: Marcel Dekker; 2002. p. 57–98.
82. Onal E, Lopata M. Periodic breathing and the pathogenesis of occlusive sleep apnea. Am Rev Respir Dis 1982;126:676–80.
83. Kimoff RJ, Brooks D, Horner RL, et al. Ventilatory and arousal responses to CO_2 and hypoxia during application of a canine model of obstructive sleep apnea. Am J Respir Crit Care Med 1997;156:886–94.
84. Younes M, Ostrowski M, Thompson W, et al. Chemical control stability in patients with obstructive sleep apnea. Am J Respir Crit Care Med 2001;163:1181–90.

85. Bradley TD, Rutherford R, Lue F, et al. Role of diffuse airway obstruction in the hypercapnia of obstructive sleep apnea. Am Rev Respir Dis 2004;134:920–4.
86. Krieger J, Sforza E, Apprill M, et al. Pulmonary hypertension, hypoxemia, and hypercapnia in obstructive sleep apnea patients. Chest 1989;96:729–37.
87. Ayappa I, Berger KI, Norman RG, et al. Hypercapnia and ventilatory periodicity in obstructive sleep apnea syndrome. Am J Respir Crit Care Med 2002;166:1112–5.
88. Shannon J, Pepe C, Ernst P, et al. High prevalence of obstructive sleep apnea (OSA) in severe and moderate asthma. Am J Respir Crit Care Med 2004;169:A542.
89. Chan CS, Woolcock AJ, Sullivan CE. Nocturnal asthma: role of snoring and obstructive sleep apnea. Am Rev Respir Dis 1988;137:1502–4.
90. Yigla M, Tov N, Solomonov A, et al. Difficult-to-control asthma and obstructive sleep apnea. J Asthma 2003;40: 865–71.
91. Montserrat JM, Farre R, Ballester E, et al. Evaluation of nasal prongs for estimating nasal flow. Am J Respir Crit Care Med 1997;155:211–5.
92. Condos R, Norman RG, Krishnasamy I, et al. Flow limitation as a non-invasive assessment of residual upper-airway resistance during continuous positive airway pressure therapy of obstructive sleep apnea. Am J Respir Crit Care Med 1994;150:475–80.
93. Ferguson KA. The role of oral appliance therapy in the treatment of obstructive sleep apnea. Clin Chest Med 2003;24:355–64.
94. Li KK. Surgical management of obstructive sleep apnea. Clin Chest Med 2003;24:365–70.
95. Sullivan CE, Issa FG, Berthon-Jones M, Eves L. Reversal of obstructive sleep apnoea by continuous positive airway pressure applied through the nares. Lancet 1981;1:862–5.
96. Verse T, Pirsig W, Stuck BA, et al. Recent developments in the treatment of obstructive sleep apnea. Am J Respir Med 2003;2:157–68.
97. Bradley TD, Phillipson EA. Central sleep apnea. Clin Chest Med 1992;13:493–505.
98. Badr MS, Toiber F, Skatrud JB, Dempsey J. Pharyngeal narrowing/occlusion during central sleep apnea. J Appl Physiol 1995;78:1806–15.
99. Hoffstein V, Slutsky AS. Central sleep apnea reversed by continuous positive airway pressure. Am Rev Respir Dis 1987;135:1210–2.
100. Lee JC, Stoll BJ, Downing SE. Properties of the laryngeal chemoreflex in neonatal piglets. Am J Physiol 1977;233: R30–6.
101. Bradley TD, Floras JS. Sleep apnea and heart failure: part II: central sleep apnea. Circulation 2003;107:1822–6.
102. Sin DD, Logan AG, Fitzgerald FS, et al. Effects of continuous positive airway pressure on cardiovascular outcomes in heart failure patients with and without Cheyne–Stokes respiration. Circulation 2000;102:61–6.
103. Jobin V, Rigau J, Farre R, et al. Evaluation of upper airway patency during Cheyne–Stokes respiration using the forced oscillation technique. Am J Respir Crit Care Med 2002;165: A247.
104. Tkacova R, Niroumand M, Lorenzi-Filho G, Bradley TD. Overnight shift from obstructive to central apneas in patients with heart failure: role of PCO2 and circulatory delay. Circulation 2001;103:238–43.

CHAPTER 51

CARDIOVASCULAR CONSEQUENCES OF SLEEP-DISORDERED BREATHING

Steven R. Coughlin, Peter M. A. Calverley

The last 20 years have seen a revolution in our understanding of the role of the upper airway in producing significant physiologic dysfunction and clinical disease. Traditionally, the upper airway was viewed as a conduit through which gas, fluid, and solid passed. Its coordinated function was recognized as essential in the protection of the lower respiratory tract from aspiration and in phonation. However, clinicians and physiologists alike have been slow to recognize that the major impact of upper airway dysfunction occurred when there was a fall in skeletal muscle tone with the onset of sleep. In this state the upper airway may behave as a Starling resistor, in which inspiratory flow limitation and ultimately complete collapse occur if the cross-sectional area falls below a critical value.

The reasons for this happening and the immediate physiologic and clinical consequences are discussed in detail elsewhere in this volume. Suffice it to say here that this problem has proven to be much more widespread than initially thought, affecting at the most conservative estimates 1 to 1.5% of middle-aged adult males.[1] Apart from the social impact of the penetrating snoring that characterizes these obstructive episodes, the major consequences for the patient and partner relate to the characteristically disrupted sleep that results from the usual cycle of upper airway obstruction and arousal, which is needed to restore airway patency.[2] The patient is excessively sleepy during the day, especially when placed in an unstimulating environment. It is no surprise that patients with obstructive sleep apnea syndrome (OSAS) perform poorly during driving simulator testing and are significantly more likely to be involved in road traffic accidents than other drivers of a similar age.[3,4]

A subtler and potentially even more important problem has now been identified, this time relating to the cardiovascular system. Once significant numbers of patients with sleep apnea were identified, the clinicians seeing them became aware that many of them had been already diagnosed as being hypertensive or had elevated blood pressure when seen in the clinic.[5] Moreover, epidemiologic studies suggested that cardiovascular death was more common among patients who declined treatment for their OSAS.[6] This has led to the proposal that OSAS may produce changes in waking blood pressure. The significant increases in blood pressure that accompany the termination of an apnea leant credence to this concept,[7,8] but it was rejected by those who felt that the association was a spurious one that failed to allow for the coexisting obesity seen in many OSAS patients.[9]

More recent data have begun to change this view again, and this forms the substance of this chapter, in which we discuss the relationship between nocturnal respiratory events and both cardiovascular and metabolic control in waking OSAS patients. Its inclusion in this volume is intended to illustrate the many and complex interactions that occur between normal respiratory and cardiovascular control systems and how their disturbance by disease can lead to unanticipated complications that are not immediately predictable from the acute respiratory event.

SLEEP-DISORDERED BREATHING

Breathing disorders during sleep form a spectrum of severity that correlates with increasing weight. The mildest form of sleep-disordered breathing, intermittent snoring, does not appear to have any adverse effects on health. Loud persistent snoring, upper airway resistance syndrome (where snoring is associated with microarousals without apnea), and OSAS are more severe forms of sleep-disordered breathing, which have progressively greater effects on morbidity and mortality from cardiovascular events. Obesity-hypoventilation syndrome, in which patients present with daytime respiratory failure, represents a different but severe form of sleep-disordered breathing where airway patency is maintained. It is associated with a high morbidity and mortality, but less is known about this disorder and its relationship to cardiovascular and metabolic problems.

OSAS is the most common form of sleep-disordered breathing, affecting approximately 4% of the general

population in the Western world, most of whom are obese, with a short, fat neck.[10] It is characterized by repetitive episodes of apnea and hypopnea during sleep, each terminating with an arousal. The cessation in airflow is associated with a period of hypoxia and hypercapnia that is corrected by a short period of hyperventilation upon arousal. These repetitive arousals result in sleep fragmentation and chronic sleep deprivation, which cause the patient to be hypersomnolent during the daytime. Other common symptoms include loud persistent snoring, nocturnal choking, unrefreshing and restless sleep, personality changes, nocturia, and an increased incidence of road traffic accidents.[4]

Recent evidence suggests that OSAS may have adverse effects on physiologic systems, especially during wakefulness. These include a number of acute changes in hemodynamic and cardiovascular systems occurring during and upon the termination of each apnea and a number of chronic cardiovascular changes that will be explored further. The majority of work in this area has focused on the effect of OSAS on daytime blood pressure and the resulting risk of cardiovascular and cerebrovascular events. Some well-controlled studies have also investigated the cardiovascular and metabolic abnormalities that may underpin this risk (Figure 51-1). Whether OSAS is causal in these relationships is uncertain because of possible confounding factors such as obesity and the use of different techniques to establish the diagnosis and severity of OSAS. The night-to-night variability of the apnea–hypopnea index also questions their use of one night of polysomnography to diagnose and estimate the severity of OSAS.[11] Despite this, a small number of intervention studies using continuous positive airway pressure (CPAP) therapy have provided evidence that OSAS contributes to the development of these cardiovascular and metabolic changes.

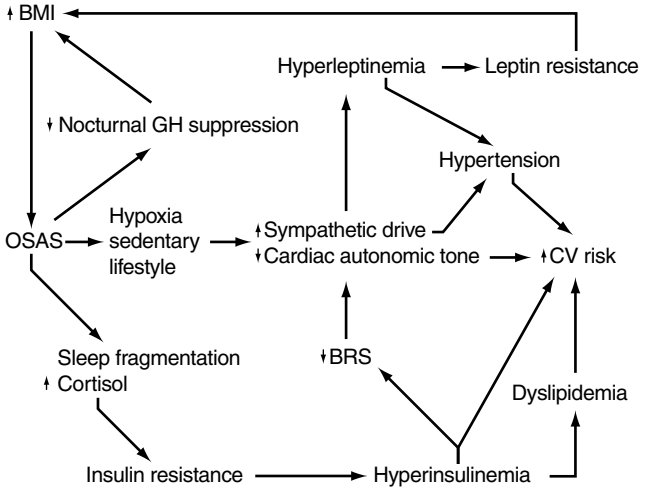

FIGURE 51-1 Pathophysiology of hypertension in obstructive sleep apnea syndrome. Obstructive sleep apnea syndrome leads to weight gain by reducing nocturnal growth hormone suppression, further driving its development. Hypoxia and a sedentary lifestyle cause an increase in sympathetic activity and a decrease in cardiac autonomic tone, both risk factors for hypertension and an increased cardiovascular risk. The increase in sympathetic activity could also increase leptin production from adipocytes, further driving hypertension. A resistance to the weight-reducing effects of this leptin may then lead to further weight gain. Sleep fragmentation and excess cortisol production cause insulin resistance and a resulting hyperinsulinemia. This hyperinsulinemia may have direct atherosclerotic effects on the vascular wall, causing an increase in cardiovascular risk and a reduction in baroreceptor sensitivity. The reduction in baroreceptor sensitivity could lead to an increase in sympathetic drive, possibly causing hypertension through the mechanisms discussed previously. The increase in blood pressure may then cause the baroreceptors to reset to higher pressures, further reducing their sensitivity. Insulin resistance may also have indirect atherosclerotic effects on the vasculature through its influence on dyslipidemia, a known cardiovascular risk factor. BMI = body mass index; BRS = baroreceptor sensitivity; CV = cardiovascular; GH = growth hormone; OSAS = obstructive sleep apnea syndrome.

ACUTE CARDIOVASCULAR AND HEMODYNAMIC EFFECTS

Ineffective inspiratory efforts occurring during apneic events reduce intrathoracic pressures, which can in themselves substantially alter cardiac function.[12] Firstly, venous return to the right ventricle is increased, leading to distention of this chamber. The resulting leftward shift of the interventricular septum decreases left ventricular (LV) compliance and LV end-diastolic volume.[13] Decreases in intrathoracic pressure also impair LV relaxation and, therefore, LV diastolic filling.[14] Furthermore, there is evidence that it can delay blood leaving the intrathoracic aorta, causing an increase in LV afterload.[15] The combination of these changes results in decreased stroke volume and cardiac output, which abruptly increases following arousal.

During the initial phase of an apneic episode a decrease in stroke volume causes blood pressure to fall, suppressing carotid sinus baroreceptors and increasing sympathetic activity. Simultaneous increases in aortic transmural pressure, arising because of exaggerated negative intrathoracic pressure, activate the aortic baroreceptors, reducing sympathetic activity.[16,17] As the aortic baroreceptors predominate, there is an overall decrease in sympathetic activity. The sympathoexcitatory response to hypoxia does not occur until several seconds after the apnea begins. Accordingly, most of the sympathetic response to hypoxia occurs postapnea and may be mediated by blunting of baroreceptor sensitivity.[18] The carotid chemoreceptors when stimulated by the reduced partial pressure of arterial O_2 rise in the partial pressure of arterial CO_2 and rise in arterial hydrogen ions cause an initial decrease in heart rate and an increase in the secretion of catecholamines and sympathetically mediated vasoconstriction, which results in cyclical surges in mean arterial blood pressure.[19–21]

The arousal response is a critical event, activating upper airway dilator muscles to restore airway patency and terminate an apnea. However, it also contributes to surges in sympathetic output to other vascular beds and increases heart rate, thereby increasing pulmonary and systemic blood pressure, independently of the effects of hypoxia.[22–24] How much of this rise in blood pressure is due to the arousal response is unclear.

The evidence suggests that pulmonary artery pressure rises during each apnea, with a further brief rise upon

termination of apnea that gradually increases over many cycles.[25] These rises in pulmonary artery pressure can be attributed to hypoxia-induced constriction of the pulmonary arterioles. Furthermore, subatmospheric pleural pressures lead to an increased venous return, providing an added preload to the right ventricle, increasing pulmonary artery pressures. A reduced LV ejection fraction may also contribute.

CHRONIC CARDIOVASCULAR EFFECTS

The observation that many patients with OSAS are hypertensive has led some to suggest that OSAS may be causal. This was supported by Davies and colleagues in a case control study of 24-hour ambulatory blood pressure in patients with OSAS and normal control subjects matched for age and obesity[26] and two large-scale epidemiologic studies. The Sleep Heart Health Study demonstrated that after controlling for all potential confounders there was a weak dose-response relationship between the presence of OSAS (mild to moderate) and hypertension.[27] Similarly, the Wisconsin Sleep Cohort Study demonstrated a dose-response relationship between the severity of OSAS at baseline and the presence of hypertension after 4 years, even after adjusting for all confounding factors.[28] This increase in blood pressure is partly responsible for the increase in cardiovascular risk reported in this group.

Abnormalities of the autonomic nervous system have also been associated with OSAS; however, whether these occur as a direct result of the acute changes outlined above has been the subject of much speculation. Transient increases in sympathetic activity during apneic episodes have been demonstrated to persist during wakefulness independent of obesity and may contribute to hypertension.[29] The mechanism behind this is unknown, although chronic responses to cyclical hypoxia during apnea and movement arousals may play a central role.[30] It has been suggested that the increased sympathetic nerve response to hypoxia and hypercapnia may persist after the stimulus has been removed,[31] resulting in higher tonic levels of sympathetic activity, even during normoxia.[32] This effect appears to be attributable to a reduced peripheral hypoxic chemosensitivity from hypoxia rather than hypercapnia.[33] Furthermore, repetitive increases in blood pressure may cause baroreceptors to reset to a higher pressure, permitting higher levels of sympathetic activation. Finally, a sedentary lifestyle, a major consequence of daytime hypersomnolence, could lead to sympathetic overactivity by reducing the inhibitory influence of cardiac efferents on renal sympathetic activity.[34,35]

Heart rate variability is an indirect measure of cardiac autonomic tone, which can be assessed by the power spectral analysis of continuous electrocardiographic recordings. When performing this analysis it is widely accepted that the high-frequency component is mediated primarily through vagal cardiac control and the power of the high-frequency band has been used to quantify parasympathetic activity.[36] On the other hand, power in the low-frequency component can be due to both sympathetic and parasympathetic activity. Studies using this technique in OSAS have demonstrated

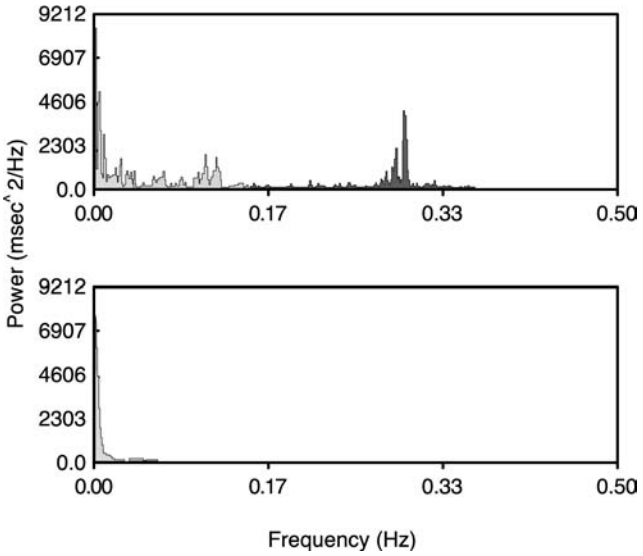

FIGURE 51-2 Power spectral analysis of continuous electrocardiogram data. The *top frame* is from a normal healthy subject and the *bottom frame* from a subject with obstructive sleep apnea syndrome who was similar for body mass index, fat distribution, and adiposity. The very low-frequency component of heart rate variability is measured in the 0 to 0.04 Hz frequency band, the low-frequency component in the 0.04 to 0.15 Hz frequency band, and the high-frequency component in the 0.15 to 0.40 Hz frequency band. The low-frequency component is thought to be a marker of cardiac sympathetic activity and the high-frequency component of cardiac parasympathetic activity.

a withdrawal of cardiac autonomic nervous system activity, especially in the vagal component, independent of body mass index.[37] Unpublished data obtained in our laboratory from subjects with OSAS and control subjects with similar body mass index, fat distribution, and adiposity support this idea (Figure 51-2). However, the mechanism by which this occurs is unknown. Withdrawal of vagal efferent activity, especially from the myocardium, is known to have adverse cardiovascular consequences.[38–40]

Baroreceptors, stretch receptors found in major vessel walls, are important in maintaining short-term blood pressure homeostasis by altering heart rate up or down accordingly and have been shown to be less sensitive to changes in blood pressure during the daytime in OSAS patients, independent of coexisting obesity.[41] The mechanism for this is unresolved, but it may be that repetitive nocturnal surges in blood pressure chronically downregulate the baroreceptors, reducing their capacity to buffer long-term changes in blood pressure. Alternatively, evidence from canine models suggests that chronic increases in daytime blood pressure cause baroreceptors to reset to higher pressures,[42] dampening their capacity to buffer further rises in blood pressure[43] and maintaining increased sympathetic activation.

CHRONIC METABOLIC EFFECTS

There are a number of chronic metabolic changes aside from the well-defined abnormalities in cortisol and growth hormone secretion that occur in OSAS. These include insulin

resistance with its profound implications for hypertension, dyslipidemia, and hyperleptinemia. Whether these occur due to sleep fragmentation or the direct effect of hypoxia on neurotransmitters, which, in turn, affects the hypothalamic-pituitary axis, remains uncertain.

Insulin resistance has been implicated in the pathogenesis of hypertension. It may also increase cardiovascular risk independent of this through its effects on lipids, coronary artery disease, and vascular wall responsiveness. Conflicting data have been reported regarding the relationship between OSAS and insulin resistance.[44–46] However, a number of small population studies have recently shown that although body mass index has a significant influence, there is an independent association between insulin resistance, hyperinsulinemia, and indices of OSAS.[47–49] Furthermore, a recent unpublished study carried out in our laboratory in which subjects with OSAS were matched to control subjects for body mass index, fat distribution, and adiposity confirms this relationship (Figure 51-3).

Evidence suggests that sleep fragmentation has a role in the development of insulin resistance[50] by activating the hypothalmic-pituitary axis, leading to the release of cortisol and other hormones that are important in the pathogenesis of insulin resistance.[51] Furthermore, cortisol production may also be influenced by the chronic elevation of sympathetic nervous system activity. Hypoxia could have similar actions, triggering the release of hormones that result in gluconeogenesis and interference with insulin action.[52] If chemosensitivity is heightened in OSAS, this could occur during periods of relative normoxia.

Although not a direct effect of OSAS, evidence suggests that insulin resistance may lead to dyslipidemia, a known risk factor for cardiovascular disease.[53] Accordingly dyslipidemia has been demonstrated in OSAS patients independent of obesity.[54,55] Abnormal vascular function could lead to chronic hypertension and has been reported in hypertensive OSAS patients.[56] It is thought that this may arise due to the effects of intermittent hypoxia and abrupt decreases and increases in cardiac output provoking elaboration of oxygen free radicals and ischemia-reperfusion injury of the vascular wall,[57] which could, in turn, precipitate or accelerate the formation of atherosclerotic plaques and vascular smooth muscle proliferation.[58] Sleep disturbances may also contribute,[59] as could hyperlipidemia and hyperinsulinemia, both common features in OSAS.

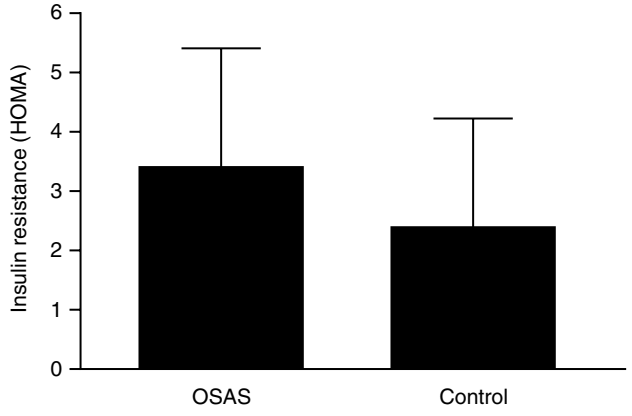

FIGURE 51-3 Insulin resistance in subjects with obstructive sleep apnea syndrome and control subjects similar for body mass index, fat distribution, and adiposity. $p < .01$ when comparing OSAS and control subjects using an unpaired *t*-test. HOMA = homeostasis model assessment; OSAS = obstructive sleep apnea syndrome. Bars denote the standard deviation.

Leptin, synthesized and secreted from adipocytes, decreases appetite and increases energy expenditure, protecting us from the adverse effects of overeating. Studies have demonstrated increased leptin in OSAS patients matched for body mass index and adiposity.[60] Although the mechanism for this is unclear, it is possible that an increased sympathetic activity contributes, although the direction of this association is unclear.[61] Despite having increased circulating leptin, these patients gained weight in the year prior to investigation, suggesting that they were resistant to its weight-reducing effects.[57] This hypersecretion of leptin may have other chronic effects on health, such as increasing blood pressure by raising sympathetic activity.[62]

The mechanisms by which OSAS leads to hyperleptinemia are unclear; however, adipocyte β_3-receptor downregulation on adipocytes as a result of OSAS-induced sympathetic activation is possible.[63] Conversely, hyperleptinemia and leptin resistance may be important in the development of OSAS through their effects on weight gain and ventilatory control.[64]

INTERVENTION STUDIES

Intervention studies have provided the most robust evidence of a causal role of OSAS in the development of chronic cardiovascular and metabolic changes. To date most of the work has focused on the effects of CPAP on 24-hour ambulatory blood pressure; however, a number of small uncontrolled intervention studies have demonstrated that short-term CPAP treatment probably normalizes the abnormalities of sympathetic activity,[65] cardiac autonomic nervous system function,[66] insulin resistance,[45] dyslipidemia, hyperleptinemia,[54] and vascular function.[59] In contrast, no data on the effect of CPAP on baroreceptor sensitivity during wakefulness have been presented.

Intervention studies using CPAP confirm a causal role for OSAS in increasing blood pressure. A small study using subtherapeutic CPAP, the most robust placebo control, demonstrated a significant reduction in 24-hour blood pressure after 6 weeks of CPAP treatment.[67] This effect was larger in those with more severe OSAS and those using antihypertensive medications. Likewise, a 4-week placebo-controlled crossover trial, using an oral placebo as a control intervention, demonstrated similar changes in the mean 24-hour and systolic blood pressure profiles.[68] In contrast, a placebo-controlled parallel group study of nonsleepy apneics, also using subtherapeutic CPAP, showed no effect of CPAP on 24-hour mean arterial blood pressure.[69] This suggested that the increased blood pressure and sleepiness observed in OSAS may share a causal pathway.

CARDIOVASCULAR AND CEREBROVASCULAR DISEASE

It is thought that cardiovascular and cerebrovascular events may occur more often in OSAS as a consequence of the associated hypertension; however, there is no reason why cyclical surges in blood pressure may not contribute to this increased cardiovascular risk. Furthermore, pathophysiologic changes, such as hyperinsulinemia, hyperleptinemia, and dyslipidemia, may have direct cardiovascular effects independent of their influence on blood pressure. However, studying this association is difficult as cardiovascular and cerebrovascular disease may take years to develop as a result of exposure to OSAS. Also, stroke and heart failure can cause sleep-disordered breathing.[70,71] Despite this, the Sleep Heart Health Study has now demonstrated a relationship between OSAS and cardiovascular and cerebrovascular events, independent of obesity. In the absence of intervention studies, however, this evidence is not considered robust enough to establish a causal relationship.

A further cross-sectional analysis of the Sleep Heart Health Study demonstrated that OSAS was a modest independent risk factor for coronary artery disease.[72] Furthermore, in patients with confirmed coronary artery disease, the presence of relatively mild OSAS was a poor prognostic indicator. This was significantly predicted by the respiratory disturbance index.[73] This analysis also demonstrated that the presence of OSAS was associated with an increase in the risk of congestive heart failure independent of other known risk factors.[72] However, this association may represent the role of congestive heart failure in destabilizing the upper airway as a result of an increased chemosensitivity, hyperventilation, and possibly prolonged circulation time, which predispose it to collapse.[74,75] Also, patients with congestive heart failure may experience edema in the soft tissues of the neck and pharynx, narrowing the upper airway and making it more collapsible.[76] Finally, the presence of OSAS was associated with a clear but modestly increased prevalence of stroke.[72] However, as sleep apnea is extremely common among subjects following a self-reported stroke,[77] this did not allow them to establish cause and effect. However, as the frequency of obstructive apneas does not decline between the period immediately after stroke to 3 months later,[78] OSAS is most likely to present first.

In the first intervention study of its kind, Peker and colleagues have provided the most robust evidence of a causal role of OSAS in cardiovascular disease. In this study they demonstrated that efficient treatment of OSAS over 7 years was associated with a significant cardiovascular risk reduction independent of disease severity and daytime sleepiness in 182 middle-aged men recruited from a sleep clinic.[79]

SUMMARY AND CONCLUSIONS

OSAS is associated with a cascade of acute and chronic changes that possibly give rise to hypertension and a subsequent increase in cardiovascular and cerebrovascular risk. However, in the absence of well-controlled intervention studies, the role of OSAS in these chronic changes cannot be considered conclusive and should be the subject of further research.

REFERENCES

1. Davies RJ, Stradling JR. The epidemiology of sleep apnoea. Thorax 1996;51:S65–70.
2. Douglas NJ, Polo O. Pathogenesis of obstructive sleep apnoea/hypopnoea syndrome. Lancet 1994;344:653–5.
3. Barbe F, Pericas J, Munoz A, et al. Automobile accidents in patients with sleep apnea syndrome. An epidemiological and mechanistic study. Am J Respir Crit Care Med 1998;158:18–22.
4. Findley L, Unverzagt M, Guchu R, et al. Vigilance and automobile accidents in patients with sleep apnea or narcolepsy. Chest 1995;108:619–24.
5. Wilcox I, McNamara SG, Collins FL, et al. Syndrome Z: the interaction of sleep apnoea, vascular risk factors and heart disease. Thorax 1998;53:S25–8.
6. Partinen M, Jamieson A, Guilleminault C. Long-term outcome for obstructive sleep apnea syndrome patients. Chest 1988;94:1200–4.
7. Davies RJ, Crosby J, Prothero A, Stradling JR. Ambulatory blood pressure and left ventricular hypertrophy in subjects with untreated obstructive sleep apnoea and snoring, compared with matched control subjects, and their response to treatment. Clin Sci (Lond) 1994;86:417–24.
8. Rees K, Spence DP, Earis JE, Calverley PM. Arousal responses from apneic events during non-rapid-eye-movement sleep. Am J Respir Crit Care Med 1995;152:1016–21.
9. Wright J, Johns R, Watt I, et al. Health effects of obstructive sleep apnoea and the effectiveness of continuous positive airways pressure: a systematic review of the research evidence. BM J 1997;314:851–60.
10. Young T, Palta M, Dempsey J, et al. The occurrence of sleep-disordered breathing among middle-aged adults. N Engl J Med 1993;328:1230–5.
11. Chediak AD, Acevedo-Crespo JC, Seiden DJ, et al. Nightly variability in the indices of sleep-disordered breathing in men being evaluated for impotence with consecutive night polysomnograms. Sleep 1996;19:589–92.
12. Virolainen J, Ventila M, Turto H, Kupari M. Influence of negative intrathoracic pressure on right atrial and systemic venous dynamics. Eur Heart J 1995;16:1293–9.
13. Shiomi T, Guilleminault C, Stoohs R, Schnittger I. Leftward shift of the interventricular septum and pulsus paradoxus in obstructive sleep apnea syndrome. Chest 1991;100: 894–902.
14. Brinker JA, Weiss JL, Lappe DL, et al. Leftward septal displacement during right ventricular loading in man. Circulation 1980;61:626–33.
15. Buda AJ, Pinsky MR, Ingels NB, et al. Effect of intrathoracic pressure on left ventricular performance. N Engl J Med 1979;301:453–9.
16. Morgan BJ, Denahan T, Ebert TJ. Neurocirculatory consequences of negative intrathoracic pressure vs. asphyxia during voluntary apnea. J Appl Physiol 1993;74:2969–75.
17. Somers VK, Dyken ME, Skinner JL. Autonomic and hemodynamic responses and interactions during the Mueller maneuver in humans. J Auton Nerv Syst 1993;44:253–9.
18. Ziegler MG, Nelesen RA, Mills PJ, et al. The effect of hypoxia on baroreflexes and pressor sensitivity in sleep apnea and hypertension. Sleep 1995;18:859–65.
19. Shepard JW. Cardiopulmonary consequences of obstructive sleep apnea. Mayo Clin Proc 1990;65:1250–9.

20. Sajkov D, Cowie RJ, Thornton AT, et al. Pulmonary hypertension and hypoxemia in obstructive sleep apnea syndrome. Am J Respir Crit Care Med 1994;149:416–22.
21. Laks L, Lehrhaft B, Grunstein RR, Sullivan CE. Pulmonary artery pressure response to hypoxia in sleep apnea. Am J Respir Crit Care Med 1997;155:193–8.
22. Horner RL, Brooks D, Kozar LF, et al. Immediate effects of arousal from sleep on cardiac autonomic outflow in the absence of breathing in dogs. J Appl Physiol 1995;79: 151–62.
23. Ziegler MG, Nelesen R, Mills P, et al. Sleep apnea, norepinephrine-release rate, and daytime hypertension. Sleep 1997;20:224–31.
24. Davies RJ, Belt PJ, Roberts SJ, et al. Arterial blood pressure responses to graded transient arousal from sleep in normal humans. J Appl Physiol 1993;74:1123–30.
25. Marrone O, Bonsignore MR, Romano S, Bonsignore G. Slow and fast changes in transmural pulmonary artery pressure in obstructive sleep apnoea. Eur Respir J 1994;7:2192–8.
26. Davies CW, Crosby JH, Mullins RL, et al. Case-control study of 24 hour ambulatory blood pressure in patients with obstructive sleep apnoea and normal matched control subjects. Thorax 2000;55:736–40.
27. Nieto FJ, Young TB, Lind BK, et al. Association of sleep-disordered breathing, sleep apnea, and hypertension in a large community-based study. JAMA 2000;283:1829–36.
28. Young T, Peppard P, Palta M, et al. Population-based study of sleep disordered breathing as a risk factor for hypertension. Arch Intern Med 1997;157:1746–52.
29. Marrone O, Riccobono L, Salvaggio A, et al. Catecholamines and blood pressure in obstructive sleep apnoea syndrome. Chest 1993;103:722–7.
30. Loredo JS, Ziegler MG, Ancoli-Israel S, et al. Relationship of arousals from sleep to sympathetic nervous system activity and BP in obstructive sleep apnea. Chest 1999;116:655–9.
31. Morgan BJ, Crabtree DC, Palta M, Skatrud JB. Combined hypoxia and hypercapnia evokes long-lasting sympathetic activation in humans. J Appl Physiol 1995;79:205–13.
32. Narkiewicz K, van de Borne PJ, Pesek CA, et al. Selective potentiation of peripheral chemoreflex sensitivity in obstructive sleep apnea. Circulation 1999;99:1183–9.
33. Mahamed S,.Duffin J. Repeated hypoxic exposures change respiratory chemoreflex control in humans. J Physiol 2001; 534:595–603.
34. Dicarlo SE, Stahl LK, Bishop VS. Daily exercise attenuates the sympathetic nerve response to exercise by enhancing cardiac afferents. Am J Physiol 1997;273:H1606–10.
35. Meredith IT, Friberg P, Jennings GL, et al. Exercise training lowers resting renal but not cardiac sympathetic activity in humans. Hypertension 1991;18:575–82.
36. Task Force of the European Society of Cardiology and the North American Society of Pacing and Electrophysiology. Heart rate variability: standards of measurement, physiological interpretation and clinical use. Circulation 1996;93: 1043–65.
37. Hilton MF, Chappell MJ, Bartlett WA, et al. The sleep apnoea/hypopnoea syndrome depresses waking vagal tone independent of sympathetic activation. Eur Respir J 2001;17:1258–66.
38. Takahashi N, Zipes DP. Vagal modulation of adrenergic effects on canine sinus and atrioventricular nodes. Am J Physiol 1983;244:H775–81.
39. Schwartz PJ, Pagani M, Lombardi F, et al. A cardiocardiac sympathovagal reflex in the cat. Circ Res 1973;32:215–20.
40. Muscholl E. Peripheral muscarinic control of norepinephrine release in the cardiovascular system. Am J Physiol 1980;239: H713–20.
41. Narkiewicz K, Pesek CA, Kato M, et al. Baroreflex control of sympathetic nerve activity and heart rate in obstructive sleep apnea. Hypertension 1998;32:1039–43.
42. Brooks D, Horner RL, Floras JS, et al. Baroreflex control of heart rate in a canine model of obstructive sleep apnea. Am J Respir Crit Care Med 1999;159:1293–7.
43. Sleight P, Robinson JL, Brooks DE, Rees PM. Characteristics of single carotid sinus baroreceptor fibers and whole nerve activity in the normotensive and the renal hypertensive dog. Circ Res 1977;41:750–8.
44. Tiihonen M, Partinen M, Narvanen S. The severity of obstructive sleep apnoea is associated with insulin resistance. J Sleep Res 1993;2:56–61.
45. Brooks B, Cistulli PA, Borkman M, et al. Obstructive sleep apnea in obese noninsulin-dependent diabetic patients: effect of continuous positive airway pressure treatment on insulin responsiveness. J Clin Endocrinol Metab 1994;79: 1681–5.
46. Stoohs RA, Fachinni F, Guilleminault C. Insulin resistance and sleep-disordered breathing in healthy humans. Am J Respir Crit Care Med 1996;154:174–9.
47. Strohl KP, Novak RD, Singer W, et al. Insulin levels, blood pressure and sleep apnoea. Sleep 1994;17:614–8.
48. Ip M, Lam B, Ng M, et al. Obstructive sleep apnoea is independently associated with insulin resistance. Am J Respir Crit Care Med 2002;165:670–6.
49. Punjabi NM, Sorkin JD, Katzel LI, et al. Sleep-disordered breathing and insulin resistance in middle-aged and overweight men. Am J Respir Crit Care Med 2002;165:677–82.
50. Spiegel K, Leproult R, Van Cauter E. Impact of sleep debt on metabolic and endocrine function. Lancet 1999;354:1435–9.
51. Rosmond R, Dallman MF, Bjorntorp P. Stress-related cortisol secretion in men: relationships with abdominal obesity and endocrine, metabolic and hemodynamic abnormalities. J Clin Endocrinol Metab 1998;83:1853–9.
52. Landsberg L,.Krieger DR. Obesity, metabolism, and the sympathetic nervous system. Am J Hypertens 1989;2: 125S–32S.
53. Howard BV. Insulin resistance and lipid metabolism. Am J Cardiol 1999;84:28J–32J.
54. Ip MS, Lam KS, Ho C, et al. Serum leptin and vascular risk factors in obstructive sleep apnea. Chest 2000;118:580–6.
55. Zgierska A, Gorecka D, Radzikowska M, et al. Obstructive sleep apnea and risk factors for coronary artery disease. Pneumonol Alergol Pol 2000;68:238–46.
56. Carlson JT, Rangemark C, Hedner JA. Attenuated endothelium-dependent vascular relaxation in patients with sleep apnoea. J Hypertens 1996;14:577–84.
57. Dean RT, Wilcox I. Possible atherogenic effects of hypoxia during obstructive sleep apnea. Sleep 1993;16:S15–21.
58. Faller DV. Endothelial cell responses to hypoxic stress. Clin Exp Pharmacol Physiol 1999;26:74–84.
59. Imadojemu VA, Gleeson K, Quraishi SA, et al. Impaired vasodilator responses in obstructive sleep apnea are improved with continuous positive airway pressure therapy. Am J Respir Crit Care Med 2002;165:950–3.
60. Phillips BG, Kato M, Narkiewicz K, et al. Increases in leptin levels, sympathetic drive, and weight gain in obstructive sleep apnea. Am J Physiol Heart Circ Physiol 2000;279: H234–7.
61. Shimizu K, Chin K, Nakamura T, et al. Plasma leptin levels and cardiac sympathetic function in patients with obstructive sleep apnoea-hypopnoea syndrome. Thorax 2002;57: 429–34.
62. Haynes WG. Interaction between leptin and sympathetic nervous system in hypertension. Curr Hypertens Rep 2000; 2:311–8.

63. Klaus S, Muzzin P, Revelli JP, et al. Control of beta 3-adrenergic receptor gene expression in brown adipocytes in culture. Mol Cell Endocrinol 1995;109:189–95.
64. Phipps PR, Starritt E, Caterson I, Grunstein RR. Association of serum leptin with hypoventilation in human obesity. Thorax 2002;57:75–6.
65. Narkiewicz K, Kato M, Phillips BG, et al. Nocturnal continuous positive airway pressure decreases daytime sympathetic traffic in obstructive sleep apnea. Circulation 1999;100: 2332–5.
66. Khoo MC, Belozeroff V, Berry RB, Sassoon CS. Cardiac autonomic control in obstructive sleep apnea: effects of long-term CPAP therapy. Am J Respir Crit Care Med 2001;164: 807–12.
67. Pepperell JC, Ramdassingh-Dow S, Crosthwaite N, et al. Ambulatory blood pressure after therapeutic and subtherapeutic nasal continuous positive airway pressure for obstructive sleep apnoea: a randomised parallel trial. Lancet 2002;359:204–10.
68. Faccenda JF, Mackay TW, Boon NA, Douglas NJ. Randomized placebo-controlled trial of continuous positive airway pressure on blood pressure in the sleep apnea-hypopnea syndrome. Am J Respir Crit Care Med 2001;163:344–8.
69. Barbe F, Mayoralas LR, Duran J, et al. Treatment with continuous positive airway pressure is not effective in patients with sleep apnea but no daytime sleepiness. Ann Intern Med 2001;134:1015–23.
70. Bassetti C, Aldrich MS, Quint D. Sleep-disordered breathing in patients with acute supra- and infratentorial strokes. A prospective study of 39 patients. Stroke 1997;28:1765–72.
71. Kryger MH, Hanly PJ. Cheyne-Stokes respiration in cardiac failure. Prog Clin Biol Res 1990;345:215–24.
72. Shahar E, Whitney CW, Redline S, et al. Sleep-disordered breathing and cardiovascular disease: cross-sectional results of the Sleep Heart Health Study. Am J Respir Crit Care Med 2001;163:19–25.
73. Peker Y, Hedner J, Kraiczi H, Loth S. Respiratory disturbance index: an independent predictor of mortality in coronary artery disease. Am J Respir Crit Care Med 2000;162:81–6.
74. Ponikowski P, Chua TP, Piepoli M, et al. Chemoreceptor dependence of very low frequency rhythms in advanced chronic heart failure. Am J Physiol 1997;272:H438–47.
75. Sun SY, Wang W, Zucker IH, Schultz HD. Enhanced peripheral chemoreflex function in conscious rabbits with pacing-induced heart failure. J Appl Physiol 1999;86:1264–72.
76. Shepard JW, Pevernagie DA, Stanson AW, et al. Effects of changes in central venous pressure on upper airway size in patients with obstructive sleep apnea. Am J Respir Crit Care Med 1996;153:250–4.
77. Wessendorf TE, Teschler H, Wang YM, et al. Sleep-disordered breathing among patients with first-ever stroke. J Neurol 2000;247:41–7.
78. Parra O, Arboix A, Bechich S, et al. Time course of sleep-related breathing disorders in first-ever stroke or transient ischemic attack. Am J Respir Crit Care Med 2000;161: 375–80.
79. Peker Y, Hedner J, Norum J, et al. Increased incidence of cardiovascular disease in middle-aged men with obstructive sleep apnea. Am J Respir Crit Care Med 2002;166: 159–65.

CHAPTER 52

COMPLEXITY AND RESPIRATION: A MATTER OF LIFE AND DEATH*

Peter T. Macklem

LIFE AND THE SECOND LAW OF THERMODYNAMICS

It is a curious fact that, until recently, very few physicians or physiologist have asked the question, "What is life?" Claude Bernard, the founder of experimental medicine, was a remarkable exception. His lifelong goal was to determine those characteristics that distinguished life from nonlife. As we all know, he discovered that one of the distinguishing features was the *fixité du milieu intérieur*. He did this at a time when European physics was fascinated by the emerging field of thermodynamics, in particular the extraordinary implications of the second law of thermodynamics, which states that "the entropy of the universe tends toward a maximum." Unfortunately, the vast majority of physicians and physiologists had no idea what this meant (and still do not). Thus, to the detriment of our profession, we have largely been unable to apply this fundamental law to health and disease.

Not so Claude Bernard. He understood that, according to the second law, inanimate things must eventually come into equilibrium† with their environment. In contrast, his greatest discovery was that in life "Le corps vivant . . . ne tombe jamais en indifférence chimico-physique avec le milieu extérieur."[1] This idea, combined with the *fixité du milieu intérieur*, was subsequently taken up by Walter Cannon in the United States, who coined the term "homeostasis" to describe it. But what Bernard almost certainly meant by this statement is that living things do not appear to obey the second law of thermodynamics. This to him was a profound mystery because he firmly believed that the laws of physics governed biologic systems as well as nonbiologic ones.

Unfortunately, medicine and physiology lost sight both of this mystery and the real purpose of Bernard's enquiries, namely to discover what distinguishes life from nonlife. Because we failed to realize what Bernard was trying to uncover, his legacy to us has been largely limited to homeostasis. Although this is certainly important, what he was really trying to solve was even more important.

To understand the implications of our oversight we need to rephrase the second law in a way that we can all understand. Here is another way of stating it: Systems tend to evolve from ordered, statistically improbable configurations to less ordered, statistically more probable ones. Take your average cigarette smoker, who on exhaling blows a smoke ring. The smoke particles are in a highly ordered, statistically improbable configuration in the shape of a doughnut. With the passage of time the smoke particles diffuse away and become randomly distributed through the room; the smoke ring disappears and never reappears spontaneously. If we were sitting in a smoky room and all of a sudden the smoke particles all by themselves came together to form a smoke ring, we would not believe our eyes. And the reason we would not is that such an extraordinary event would violate the second law of thermodynamics.

But spontaneous development of stunning order is exactly what has happened over several billion years in the case of Darwinian evolution or what happens daily in the development of a baby after fertilization of an ovum by a sperm. In both instances the system has evolved from less ordered, statistically more probable configurations to highly ordered statistically incredible states. Where has all this order come from? We see it everywhere we look: the beauty of birds, flowers, and butterflies; the grandeur of trees, the lion, and the eagle; the incredible complexity of a human resulting from the simple union of two cells and the richness and diversity of

---

*Translated with modifications from Macklem PT. Une question de vie ou de mort. Rev Francaise Mal Respir 2002;19(2 Pt 1):135–9 by permission of the publisher.

†Here we must distinguish between thermodynamic equilibrium, which is the sense in which Bernard used the word, and physiologic equilibrium. In the former, equilibrium means that in a closed system there is no change of heat or matter with the environment; there are no thermal gradients, all chemical reactions go equally in both directions, and the mechanical forces acting on a system all balance so that motion is impossible. Physiologic equilibrium is equivalent to a steady state, with constancy of the *milieu intérieur* in spite of variations in environmental conditions. It is ironic that Bernard discovered physiologic equilibrium while realizing that living things were never in thermodynamic equilibrium. His discovery changed the word "equilibrium" to a meaning in physiology almost diametrically opposite to its meaning in thermodynamics!

life and its ecosystems starting billions of years ago in some primeval soup. Where is the second law in all this?

It was physicists who asked this question. Embarrassingly, because we failed to understand what Claude Bernard was really asking, the Nobel laureate Erwin Schrödinger took up the quest and wrote the classic *What is Life?* He realized that life seemed to violate the second law, and he wanted to know how it was done. He did not get the answer, but one of his students, another Nobel Prize–winning physicist, Ilya Prigogine, did.

Prigogine asked the question, "How can Darwinian evolution, the selection of rare and unexpected configurations, be reconciled with the disappearance of all such rare configurations according to the second law of thermodynamics? Can Carnot and Darwin both be right?"[2] To answer these questions he experimented with simple physical and chemical systems and showed that by putting energy into them (for example, by simply heating them) order could spontaneously appear as if by magic. A simple example is familiar to us all. Whenever we pull the plug in a bathtub to let the water drain out, a little whirlpool appears in which an inverted cone of air, defying the laws of gravity, extends well below the surface of the water toward the drain. This is a highly ordered state in which the cone of air is surrounded by billions of water molecules all spiraling in unison together, whereas a few moments previously they were all involved in doing their own thing in isolated random motion. If someone were to turn on the tap so that water ran into the tub at the same rate it left, the whirlpool would become permanent.

The whirlpool appears when we pull the plug because we convert the potential energy of the water into kinetic energy. The water entering the tub adds a continuous supply of energy to replace that dissipated by the water leaving by the drain. Just as we would be astonished if a smoke ring appeared spontaneously, we would not believe it if the whirlpool appeared without the water draining out somewhere. What Prigogine showed was that when a system moves away from thermodynamic equilibrium by consuming and dissipating energy, the rate of entropy production decreases. As entropy is a measure of the disorder of the system, when its production rate decreases the system becomes more ordered. Order can develop spontaneously if a system, by consuming and dissipating energy, moves sufficiently far from thermodynamic equilibrium. Prigogine won the Nobel Prize for quantifying the relationships between energy consumption and dissipation, distance from thermodynamic equilibrium, and the rate of entropy production.

All living things function far from thermodynamic equilibrium.[2,3] We dissipate energy continuously, by consuming oxygen and burning foodstuffs in a process we call metabolism. This is why we are so highly ordered. For us, thermodynamic equilibrium is the ultimate disease, a state we only reach after we die. If life requires that we be far from thermodynamic equilibrium and death occurs when we move too close to equilibrium, it would seem likely that for health we must be just the right distance from equilibrium. This is not a very original conclusion because we know that conditions that increase or decrease our metabolic rate (or the amount of energy we dissipate and therefore our distance from thermodynamic equilibrium), like thyrotoxicosis, myxedema, or inflammation, make us unhealthy.

HEALTH, HOMEOKINESIS, AND THE SECOND LAW OF THERMODYNAMICS

How can we tell if a tissue or organ is just the right distance from equilibrium and is therefore healthy or sick? We could measure the metabolic rate, but for individual organs or tissues this poses serious problems. There may be an easier way. Let us return to the bathtub whirlpool. If "health" requires a whirlpool of just the right size, then the rate of water inflow must not only equal the rate of water outflow, it must also be adjusted to produce a "healthy" whirlpool. If the rate is too small the whirlpool is too small, whereas if it is too large the whirlpool is too large. Note that if one were to examine the water pathologically to find out why the whirlpool is "unhealthy," one would find that the water molecules were entirely normal. The structural abnormality does not result from a molecular abnormality but from an abnormal amount of energy dissipation.

But there is another feature of the whirlpool that gives us a clue as to whether the amount of energy being consumed is "healthy" or not. The whirlpool, while remaining at the same size for a given rate of energy dissipation, is not static. It fluctuates continuously. If the water drains slowly from our bathtub, the whirlpool is smaller and so are its fluctuations. In rivers and oceans, whirlpools and their fluctuations can be much larger, in fact, dangerously so if we happen to be swimming near them. The size of the fluctuations seems to be a function of how much energy is being consumed and dissipated.

Spontaneously ordered systems, such as whirlpools, have emergent properties that can neither be predicted nor understood by studying their component parts in isolation. They are called complex systems and have given birth to the science of complexity.[3] There are many such systems, and, surprisingly, they share many characteristics with the features that distinguish life from nonlife. They include groups of organisms struggling to survive in their environment (eg, ecosystems or extinctions in Darwinian evolution) and totally nonliving systems manipulated by humans (eg, economic and political systems or the stock market).[4] The principles of supply and demand, natural selection, and survival of the fittest appear to apply to such systems. Thus, understanding their behavior may have profound implications for understanding the behavior and misbehavior of our bodies.

More specifically, the ordered fluctuations that all these systems undergo may help us predict the future. In many if not all of such systems the fluctuations follow a power law. Take earthquakes. In every region in the world there are a lot of little earthquakes and a few bigger ones in a given period of time. When the frequency distribution of the power released by earthquakes is plotted on a log-log scale it is a straight line with a negative slope.[4] In Japan or the Pacific coast of North America, this line is above but parallel to regions where the risk of large earthquakes is minimal. A big earthquake is unlikely to hit Winnipeg in a given decade but

could certainly hit San Francisco. The relative chance that this will occur in one city or the other is given by the distance between the two parallel lines. If the cities are two orders of magnitude apart, the risk of the big earthquake hitting San Francisco is 100 times greater than it is for Winnipeg. In any given region the ratio of big to little earthquakes is independent of where it is on the surface of the earth.[4] This tells us that if we wait long enough, no matter where we are, some day a really big earthquake is going to hit our region. Although the probabilities can be calculated with a high degree of accuracy, the precise time when it will occur cannot be predicted. Because we do not know when they are going to happen and we do not know how to prevent them, this does little more than stir up fear.

The point is that big earthquakes are an intrinsic property of the system. They are to be expected. Similarly, large extinctions are expected in Darwinian evolution, and large fluctuations are bound to occur in the stock market and the economy.[4]

Just as the probability that a Richter scale 8 earthquake is unlikely to hit Winnipeg in a given decade, perhaps health depends upon the probability of a huge fluctuation in a physiologic parameter being vanishingly small in our lifetime. We have a lot of little fluctuations but only a few big ones. Thus, healthy, homeostatically controlled systems functioning far from equilibrium generally fluctuate within acceptable limits. But they are not static. This is true for heart rate,[5] ventilation and its parameters,[6] blood pressure,[7] renal blood flow,[8] leukocyte counts,[9] and airway resistance,[10] to name a few. Homeostasis is the wrong word. It should be called *homeokinesis*,[11] tentatively defined as "the ability of an organism functioning in a variable external environment to maintain a highly organized internal environment fluctuating within acceptable limits by dissipating energy in a far-from-equilibrium state."[10] Given that physiologic fluctuations should be kept within acceptable limits, can the size of fluctuations measured in physiologic systems give us information about energy consumption, metabolic rate, and our state of health?

Living things must adapt to varying environmental conditions. Adaptability is one of the essential features of life. It seems likely that systems that do not vary, or only fluctuate minimally, are frozen, and lack adaptability. This is failure of homeokinesis, and it would result from inadequate energy dissipation. On the other hand, excessive energy dissipation would make us unstable and put us at risk of large, damaging fluctuations.

FLUCTUATIONS AND ASTHMA

To the extent that analysis of fluctuations allows prediction of future events, the risk of a life-threatening attack of asthma might be compared with the risk of a Richter scale 8 earthquake in San Francisco, whereas the risk of such an attack occurring in a healthy subject might be compared with the risk of a similar-sized earthquake in Winnipeg. The former might occur tomorrow, but the latter is unlikely to occur in a lifetime. But in contrast to earthquakes, a serious attack of asthma might well be preventable.

In asthma, when airway smooth muscle is activated and its metabolic rate increases, energy dissipation becomes excessive. This displaces the system further from thermodynamic equilibrium, and, as a result, fluctuations in the degree of airways obstruction increase. Indeed, excessive variability of airway caliber is a characteristic feature of this disease.[10,12]

Let us see what can be learned from measuring the variability of respiratory system impedance (Zrs) in health and asthma. First, the frequency distributions of Zrs in both states are nearly log normal.[10] That is, the variability of Zrs in both normal and asthmatic lungs extends over a range of values of impedance. Values for asthmatic lungs overlap slightly with those for normal lungs, but most values of Zrs are well outside the normal range and thus are statistically highly improbable. This is illustrated in Figure 52-1, which shows the log normal frequency distributions of Zrs in both normal and asthmatic subjects measured by the forced oscillation technique at 6 Hz while breathing quietly for 15 minutes in the seated posture.

Each value of Zrs presumably represents a set of tracheobronchial configurations that give rise to that particular value of Zrs. If so, the configurations in the asthmatic lung are statistically highly unlikely in the normal lung. Asthmatic patients live with configurations rarely, if ever, seen normally. If asthma is an alteration in lung structure that goes from the commonplace to a statistically improbable shape, then its entropy production should decrease. This is exactly what one would predict from the excessive energy dissipation resulting from activation of airway smooth muscle. This moves the system farther from thermodynamic equilibrium, so we should expect rare and unusual configurations: this is what we find.

This process can be modeled in normal lungs. This is illustrated in Table 52-1, which gives the mean values for

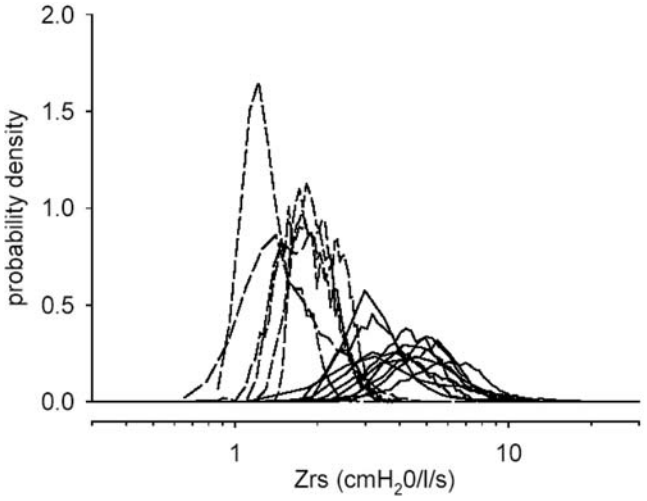

FIGURE 52–1 Log normal frequency distributions of respiratory impedance (Zrs) measured by the forced oscillation technique at 6 Hz while breathing quietly in the seated position for 15 minutes in normal subjects (*dashed lines*) and asthmatics (*solid lines*). The ordinate is frequency expressed as probability density, so that the area under each curve equals 1. See text for further description. Reproduced with permission from Que C et al.[10]

Tabel 52-1 Mean and SD of lnZrs

Normals	μ *(mean ± SEM)*	*p vs A**	σ *(mean ± SEM)*	*p vs A**	r^2 *(mean ± SEM)***
Upright	0.89 ± 0.06	< .001	0.24 ± 0.03	< .05	0.933 ± 0.021
Supine	1.07 ± 0.09	< .005	0.29 ± 0.09	N S	0.981 ± 0.004
Mch U	1.27 ± 0.19	N S	0.22 ± 0.03	< .02	0.970 ± 0.015
Mch S	1.47 ± 0.20	N S	0.32 ± 0.06	N S	0.966 ± 0.014
Asthmatics	1.59 ± 0.06		0.34 ± 0.03		0.981 ± 0.005

Mch = methacholine; NS = not significant; S = supine; U = upright.
**p* values for significance of difference vs. asthmatics
**r^2 values for least squares fit of pdd's to log-normal distribution function.
Reproduced with permission from Que C et al.[10]

log-normally distributed values of Zrs (μ) and their standard deviation (σ) as a measure of variability, under control conditions seated upright (U), in the supine posture (S), and following administration of methacholine (Mch) upright and supine. Administration of Mch activates the smooth muscle and increases mean μ to a value not significantly different from that for asthmatic patients, but it does not increase the variability as assessed by σ as much. Changing from the upright to the supine position increases the σ to a degree similar to that found in asthmatic patients but not μ. Combining Mch with the supine position converts normal airway smooth muscle into behavior as assessed by μ and σ, not signicantly different from that found in asthmatic patients.

The supine position decreases lung volume and lung elastic recoil pressure. When airway smooth muscle contracts, an important part of the load it acts against is lung elastic recoil. Thus, the supine position unloads smooth muscle. Unloading causes smooth muscle to shorten faster for a given degree of activation, according to the muscles' force velocity characteristics; it also leads to increased shortening. These two factors account for the increased variability in normal subjects supine. Combining activation with unloading converts the behavior of normal airway smooth muscle to behavior similar to that found in asthmatic patients[10] (see Table 52-1).

Thus, in asthma, airway smooth muscle could be entirely normal but both activated and unloaded by the inflammatory process. If so, the greater the degree of activation and unloading, the greater should be both the degree of obstruction and the variability. The frequency distribution of Zrs would be shifted to the right, and the probability of assuming a configuration of the tracheobronchial tree that could lead to a very severe, even fatal, asthmatic attack would increase.

An attractive feature of frequency distribution curves is that they have predictive properties. Properly interpreted, the frequency distribution of Zrs should allow a calculation of the probability that a dangerous value of Zrs will occur in a particular time period, the next 24 hours, say. As measurement of the frequency distribution is easy and could be done at home on awakening, it is conceivable that a daily measurement of Zrs distribution might allow for better prognosis and for appropriate preventive therapy to be instituted. Randomized controlled prospective studies will be necessary to determine if this prediction is true or not.

HOMEOKINETIC CODE

At present, the clinical and prognostic significance of variability in physiologic parameters is largely unknown. We do know that excessive variability of peak expiratory flow rates measured over a period of weeks is a measure of asthma severity.[12] Variability in ventilatory parameters in patients receiving mechanical ventilation appears to produce better gas exchange,[13,14] and spontaneous variation in ventilatory parameters is substantial.[6] On the other hand, in congestive heart failure when energy consumption is too low, so that energy delivery may be inadequate to meet tissue demands, heart rate variability is also too low. This is now a recognized risk factor for sudden cardiac death.[15] Similarly, variability in respiratory rate in coma is less than normal and becomes more regular as coma deepens.[16]

At the very least, fluctuations of homeokinetically controlled parameters contain information about the state of the system that we should try to decipher. We need to understand what the body is trying to tell us. Fluctuations are ordered variations. Things that fluctuate move together. They therefore imply a decrease in entropy and thus greater energy dissipation and displacement further from equilibrium. In biologic systems they would appear to be an index of a system's metabolic rate.

However, it is evident from studying Zrs that variability can be affected by factors other than metabolic rate. There is a great need to study variability as a function of energy dissipation or metabolic rate and thus distance from thermodynamic equilibrium.

If we could understand the information contained within the variability of a homeokinetically controlled system, prognosis and prevention might make a quantum leap forward. What we know so far is that big fluctuations outside acceptable limits imply excessive energy dissipation, lesser entropy, and unhealthy instability. Too little fluctuations signify a move toward thermodynamic equilibrium, too much entropy, a failure of adaptability, and thus an inability of the body to maintain its highly ordered state. Here is where a unique opportunity lies for the study of the respiratory system. In contrast to most other organ systems, we can measure fluctuations of important respiratory variables much easier than the possible measurements of variability available to nephrologists, gastroenterologists, endocrinologists, and so forth. They are largely limited to biochemical measurements that cannot

be made repeatedly over short periods of time. Most of our measurements are physical and can be measured often. Exercise circuits already do this for us automatically, but they are not usually analyzed in terms of variability. Yet measurement of variability of cardiorespiratory parameters during exercise should provide valuable information on the effect of metabolic rate on variability.

In spite of growing scientific interest in variability, the information encoded in variation is poorly understood, particularly the information it tells us about disease. In general, variation in parameters has been used to uncover previously unrecognized control mechanisms. Respirologists can become world leaders in deciphering the message contained in the homeokinetic code. However, we will have to cope with uncertainty because although size of fluctuations may contain information about tissue or organ metabolic rates, the prognostic information can only be expressed in terms of probability, never certainty.

The mathematics of uncertainty and probability is statistical mechanics. Statistical mechanics provides the mathematical tools by which the science of complexity is analyzed. They include power laws,[17] analysis of frequency distributions,[10] fractal properties,[18] detrended fluctuation analysis,[19] and calculation of approximate entropy,[20] to name a few. A detailed description of these tools is beyond the scope of this chapter, but if we are to understand the complex nature of our bodies and know whether we are just the right distance from thermodynamic equilibrium or not, we will have to learn statistical mechanics. Although this may be a difficult challenge, if Claude Bernard were around today, would jump at the chance.

REFERENCES

1. Bernard C. La fixité du milieu intérieur est la condition de la vie libre. Oeuvres. xvi, 113.
2. Prigogine I, Stengers I. Order out of chaos. New York: Bantam Books; 1984.
3. Kauffman S. Origins of order. New York: Oxford University Press; 1993.
4. Bak P. How nature works. New York: Copernicus; 1996.
5. Kobayashi M, Krusha T. 1/f fluctuations of heartbeat period. IEEE Trans Biomed Eng 1982;29:456–7.
6. Bruce E. Temporal variations in the pattern of breathing. J Appl Physiol 1996;80:1079–87.
7. Wagner CD, Persson PB. Two ranges in blood pressure power spectrum with different 1/f characteristics. Am J Physiol Heart Circ Physiol 1994;267:H449–54.
8. Wagner CD, Persson PB. Nonlinear, chaotic dynamics of arterial blood pressure and renal blood flow. Am J Physiol Heart Circ Physiol 1995;268:H621–27.
9. Goldberger AL, Kobalter K, Bhargava V. 1/f-like scaling in normal neutrophil dynamics: implications for hematologic monitoring. IEEE Trans Biomed Eng 1986;33:874–8.
10. Que C, Kenyon CM, Olivenstein R, et al. Homeokinesis and short term variability of human airway caliber. J Appl Physiol 2001;91:1131–41.
11. Yates FE. Outline of a physical theory of physiological systems. Can J Physiol Pharmacol 1982;60:217–48.
12. Quanjer PH, Lebowitz MD, Gregg I, et al. Peak expiratory flow: conclusions and recommendations of a Working Party of the European Respiratory Society. Eur Respir J 1997; Suppl 10:2S–8S.
13. Mutch WAC, Eschun GM, Kowalski SE, et al. Biologically variable ventilation prevents deterioration of gas exchange during prolonged anaesthesia. Br J Anaesth 2000;84:197–203.
14. Suki B, Alencar AM, Sujeer MK, et al. Life-support system benefits from noise. Nature 1998;393:127–8.
15. Kleiger RE, Muller JP, Bigger JT Jr, Moss AJ. Decreased heart rate variability and its association with increased mortality after myocardial infarction. Am J Cardiol 1987; 59:256–62.
16. Leigh RJ, Shaw DA. Rapid regular respiration in unconscious patients. Arch Neurol 1976;33:356–61.
17. Suki B. Fluctuations and power laws in pulmonary physiology. Am J Respir Crit Care Med 2002;166:133–7.
18. Francis DP, Willson K, Georgiadou P, et al. Physiological basis of fractal complexity properties of heart rate variability. J Physiol 2002;542(P2):619–29.
19. Peng CK, Havlin S, Stanley HE, Goldberger AL. Quantification of scaling exponents and crossover phenomena in unstationary heartbeat time series. Chaos 1995;5:82–7.
20. Engoran M. Approximate entropy of respiratory ate and tidal volume during weaning from mechanical ventilation. Crit Care Med 1998;26:1773–4.

CHAPTER 53

SEX AND GENDER DIFFERENCES IN AIRWAY BEHAVIOR ACROSS THE HUMAN LIFE SPAN

Margaret R. Becklake, Joanne Shannon

The airway behavior of girls and women is different from that of boys and men, and these differences vary in strength and in direction across different ages and time windows.[1–4] Physiologists interested in structure–function relationships have, in general, explored these differences more thoroughly than have clinicians, despite the fact that airway behavior is an important determinant of the clinical manifestations of airway disease. In this review we examine the determinants of airway behavior, focusing on sex differences, and propose an approach to analyzing their relevance for clinical and public health practice as well as for research into the origins of airway disease.

BACKGROUND

Interest in sex and gender differences in airway behavior and disease is not new. This is illustrated by three remarkable documents published in the nineteenth century. The first, published in 1846 by a London surgeon, J. Hutchinson,[5] was entitled "On the Capacity of the Lungs and on the Respiratory Function with a View of Establishing a Precise and Easy Method of Detecting Disease by the Spirometer" (Figure 53-1). The spirometer is an instrument that he developed to measure "vital capacity" (VC), a term he introduced to describe the maximum amount of air that could be blown out after the deepest possible breath in. Based on his observations of over 2,000 men aged 15 to 65 years drawn from all walks of life (including soldiers and guardsmen, gentlemen, giants, and dwarfs) and 26 young girls, he identified height, weight, and age as determinants of VC in what was probably the first epidemiologic study of lung function. Although his spirometer was not useful for the purpose for which he developed it—to "distinguish disease"—it was put to good use by others.

In 1894, Havelock Ellis,[6] a London writer, published a remarkably well-referenced book entitled *Man and Woman: A Study of Human Secondary Sexual Characters*, which he described as "an anthropological and psychological study of those secondary sexual differences which recent investigations have shown to exist among civilized human races." He classified sex characters as *primary* (essential for reproduction), *secondary* (those that distinguish the sexes, the breast being the main example), and *tertiary* (only perceptible when averages are taken into account). Referring to the latter, he cited studies that showed that VC (the breathing power indicated by the Hutchinson spirometer) was "decidedly less in women than in men, the maximum differences being at the ages of 20–40," and that "men produce more carbonic acid than women." These differences he attributed in part to biologic (size) differences (given their lower carbonic acid production, he argued that "women have a less keen need of air") and partly to cultural factors ("artificial constriction due to dress"). He also cited studies showing sex differences in susceptibility to the various medical interventions. For instance, men were more susceptible to the effects of chloroform ("the overwhelming majority of deaths from chloroform are in males") and to alcohol (delirium tremens was only rarely seen in women), whereas women were more susceptible to the effects of opium, mercury, antimony, and antipyrine, all accepted treatments in his day.

In his text, Havelock Ellis also referred to a study published in 1890 by Professor Ott and conducted in La Charité Hospital, Berlin.[7] Ott set out to measure the physiologic as opposed to the psychological and emotional processes that accompanied menstrual bleeding in 60 women in good health studied over a 3-month period covering 68 cycles. He combined measurements of body temperature, muscular force, VC using Hutchinson's spirometer, and reflex action into a composite index that he called the "*fonction physiologique de l'organisme feminin*" (the physiologic function of the female organism), which was expressed on a scale of 0 to 100% (Figure 53-2). This index was about 52% at midcycle, peaked at about 80% 3 days before menstrual bleeding started, began to fall immediately prior to the onset of bleeding, and fell to a low of about 35% during bleeding

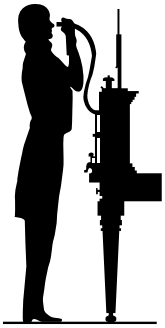

Hutchinson J. On the capacity of the lung and the respiratory function with a view to establishing a precise and easy method of detecting disease by the spirometer. Med Clin Trans 1846;29:137–252

FIGURE 53-1 The spirometer designed by Mr John Hutchinson, surgeon. This figure is reproduced from page 284 of Hutchinson's 1846 paper and[1] shows the spirometer that he designed for the purpose implicit in the title of his paper. Although it was not successful for this purpose, it was used for other purposes in the United Kingdom and in Europe to document, among other things, the differences in vital capacity between men and women, varyingly reported as between 350 and 750 cubic centimeters.

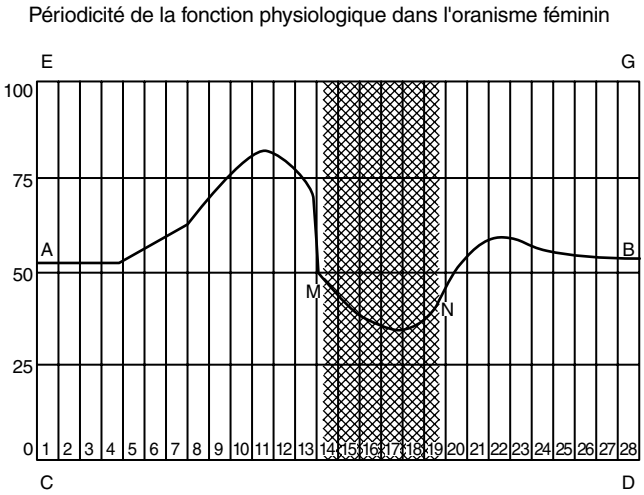

FIGURE 53-2 *La périodicité de la fonction physiologique dans l' organism feminin.* (The periodicity of the physiological function of the female organism). This figure is reproduced from page 505 in Professor Ott's 1894 paper.[7] Line A-B represents the oscillations of the physiologic processes over a month. The shaded area M and N denotes the days on which menstrual bleeding occurred. The lined C to D marks the days of the monthly cycle. The line D to E is the scale (from 0 to 100%) registering the intensity of Ott's index of the "functional energy of the feminine organism."

before returning to its midcycle level. He cited evidence that such fluctuations were not seen in prepubertal girls or in postmenopausal women and interpreted his results as evidence that his index was driven by the female organs of reproduction during a woman's reproductive years. Of interest to the chest physician or physiologist is the fact that Ott's composite index included a measure of lung function, suggesting that sex hormones influence airway behavior.

More than a century later, questions about sex differences in the nonreproductive area of biology continue to challenge this field of research. In 2001, the Institute of Medicine in a report entitled "Exploring the Biological Contributions to Human Health: Does Sex Matter?" noted that many normal physiologic functions "are influenced directly or indirectly by sex-based differences in biology," and the authors reminded their readers that "every cell has sex."[8] In their view, appreciation of this fact had been slow in coming because of the recent emphasis on differences between women and men at the societal level (in Havelock Ellis's terms "tertiary characters"[6]), and the terms *sex* and *gender* have been used interchangeably. Their report defines *sex* as "the classification of living things as male or female according to their organs of reproduction" and *gende*r as "a person's self representation as male or female or how that person is responded to by social institutions on the basis of the individual's gender presentation."

DEFINITIONS

The definitions of the terms *sex* and *gender* used in this chapter are those used in the 2001 Institute of Medicine report,[8] definitions that are also in conformity with those used by Ellis in 1894.[6] *Airway behavior* refers to "the dimensions, structure and functions of the lung, their relationship to each other and to the mechanical properties of the lung" and *determinant* to "any factor, event, characteristic or other definable entity that brings about change in a health characteristic or other defined entity."[9] Determinants may increase or decrease risk; they may also be established or putative.

Much of the material published on sex and gender differences in airway behavior and disease is limited to specific ages or time windows. Studies of children usually reflect the methods of study used in pediatrics and the clinical experience of pediatricians, studies of adolescents those of physicians in sports medicine, studies of adults those of internists, and studies of the elderly those of geriatricians. Since this chapter focuses on changes across the human life span, the material cited relies heavily on the findings from the few population-based studies in which sex- and gender-based differences in airway behavior and disease have been examined using the same methodology to gather information over the human life span.[1,10–12]

BIOLOGIC DETERMINANTS OF AIRWAY BEHAVIOR

The biologic determinants of airway behavior include (1) *dimensional factors*, which are described in morphometric and physiologic terms and yield information on lung structure–function relationships, and generally favor the female lung; (2) *immunologic factors*, of particular importance in diseases such as asthma; and (3) *hormonal factors* attributable to the cyclical changes in female sex hormones that occur during the reproductive years of a woman's life. Because these factors contribute to different degrees and often in different directions over different age and time windows, they are considered separately below.

Dimensional Determinants of Airway Behavior

The dimensional determinants of airway behavior are summarized for different ages in Table 53-1.[13–30] The structure of the lungs is an important determinant of their ventilatory

Table 53-1 Sex Differences in Airway Behavior across the Human Life Span, Reflected in Lung Structure–Function Relationships

Period	*Lung growth, development, and aging*	*Sex differences in lung structure–function relationships*
Prenatal: since conception	Muscle seen in trachea at 6–8 wk. Airway development completed ~15 wk. Alveoli appear at ~30 wk.	No sex differences in relationship of lung to somatic growth. Mouth movements reflecting fetal breathing more advanced in female than in male fetuses. Phospholipid profiles more mature in female than male fetuses from 32 wk.
Infancy: peri- and postnatal up to 1 yr	Alveolar multiplication occurs from ~36 wk through 1 yr or more. Lung vasculature develops in relation to the bronchial tree before birth and to multiplying alveoli after birth	Female neonates less likely than male neonates to develop transient hyperpnea or respiratory distress syndrome and more responsive to hormone accelerators of surfactant. Lungs of infant girls are smaller then those of infant boys but have higher absolute and size-corrected flow rates.
Childhood: age 1–10 yr	Alveolar multiplication continues up to ~2 yr; somatic growth is more or less linear with age up to ~10 yr. Airway-parenchyma-somatic growth is complex and exhibits dysanapsis.	Based on morphometry, lungs of girls remain smaller than those of boys, yet they have lower specific airway resistance at any given height. Maximum forced expiratory volume is higher in girls than boys and increases after a deep inspiration in girls but not in boys. Large airways grow proportionately to lung volumes in girls but lag in boys, whereas smallairways grow faster than lung volumes in girls but proportionately in boys.
Early adolescence: from 10 yr to midteens	Somatic and lung growth accelerate with age. Peak velocity for somatic growth precedes that for lung growth by 1–2 yr. FVC and TLC do not grow at the same rate.	Peak velocity for height growth in girls precedes that of boys by ~2 yr. Height ceases to increase at ~16 yr in girls but only slows at ~18 yr in boys. FEV_1 and FEV_1/FVC% remain higher in girls than in boys, but not peak flow rates. Adolescent girls generate lower respiratory pressures than adolescent boys at all lung volumes.
Late adolescence: from mid-to late teens	Duration of adolescent growth spurt similar whether onset of maturity is early, middle, or late.	Growth velocity in adolescent girls plateaus after height ceases to increase but continues at a slower pace in adolescent boys until the mid-20s. This is attributed to a "muscularity effect" in boys, in particular of the shoulder girdle, caused by male sex hormones; growth of TLC and of flow rates relative to TLC are slower in adolescent girls than boys; specific airway resistance decreases up to ~18 yr in girls but not boys, while FEV_1 in relation to height and FEV_1/FVC % remains higher in adolescent girls than boys.
Early adulthood: from late teens to mid-20s	Linear age-related increase in lung function slows with the end of the adolescent growth spurt. Height stabilizes, but weight increases.	Growth velocity for adolescent young men continues at a slower pace until the mid-20s, attributed to "muscularity effect" (see late adolescence). Once height stabilizes, weight becomes a determinant of lung volumes and flow rates in young men and women. Sex differences in tracheal area (measured by acoustic reflection) vs lung volume suggest that the configuration of the adult female lung is the result of proportional growth of airways vs parenchyma, but in the adult male lung growth of the airways has lagged behind that of the parenchyma, ie, has been dysanaptic.
Adulthood through old age: from ~30 yr	Age-related loss of lung function is linear up to ~50 yr and accelerates thereafter. With age, alveolar air volume decreases, and alveolar duct air and lung connective tissue increase, altering the lungs' mechanical properties.	Changes related to aging of the lungs' mechanical properties develop later and proceed more slowly in women than men. Age-related changes result in increases in lung compliance, decreases in maximal expiratory flow rates, and airway closure at higher lung volumes. With increasing age, the large airways of men also lose elastic recoil, which may counteract the loss of parenchymal recoil and explain the relative preservation of their peak flow rates.

FEV_1 = forced expiratory volume in 1 second; FVC% = forced vital capacity; TLC = total lung capacity.
Adapted from Kauffman F et al,[1] Becklake MR and Kauffmann F[2] and Kauffmann F and Becklake MR.[3]

function through its effects on the lungs' mechanical properties. These, in turn, are reflected in the relationships of flow, volume, and time during a forced expiratory maneuver. Thus, the relationship of lung volume (a measure of lung size) to forced expiratory volume (a measure of airway size) is also a measure of the structure–function relationship. Despite the lungs of girls and women being smaller than those of boys and men of the same height, they exhibit higher values for forced expiratory flow (FEF) rates and for forced expiratory volume in 1 second (FEV_1)/forced vital capacity (FVC)% over the human life span. These sex-based differences in airway dimensions are thought to be the consequence of disproportionate growth between the airways, whose number is fixed by about 16 weeks gestation, and the air spaces (alveoli), which continue to multiply up to the age of about 2 years and perhaps longer, a phenomenon characterized by Mead as *dysanapsis*.[17] Mead also pointed out that this loose coupling between airways and air spaces favors the smaller lungs of girls and women compared with the larger lungs of boys and men whose gas drainage systems are, relatively speaking, both narrower and longer.[17] These dimensional advantages of female over male lungs are also reflected in the reference (predicted) values used routinely by clinical laboratories. For instance FEV_1/FVC% prediction formulae generated from the study of different populations in different countries on different continents are consistent in showing higher values in girls and women than in boys and men.[31–34]

Sex differences in lung structure– function relationships by age are described in greater detail in Table 53-1. For the readers convenience, it is summarized here.

1. Prenatal (from conception): Mouth movements, reflecting fetal breathing,[18] are more advanced and phospholipid profiles[19] more mature in female than male fetuses.
2. Infancy (peri- and postnatal period to age 1 year): Female neonates are less likely than male neonates to develop transient tachypnea[35] or the respiratory distress syndrome of the newborn, and they are more responsive to hormone accelerators of surfactant production.[19]
3. Childhood (from age 1 to 10 years): Based on morphometry, the lungs of girls remain smaller than those of boys, yet they have lower values for specific airway resistance at any given height.[22] Large airways grow proportionately to lung volumes in girls but lag in boys, whereas small airways grow faster than lung volumes in girls but proportionately in boys.[22]
4. Early adolescence (from age 10 years to midteens): FEV_1 and FEV_1/FVC% remain higher in girls than in boys, but not peak flow rates.[29] Adolescent girls generate lower maximal respiratory pressures than adolescent boys at all lung volumes. These sex differences, described as a "muscularity effect" involving the muscles of the shoulder girdle, start with the onset of puberty and have been attributed to the puberty-associated increases in male sex hormones.[29]
5. Late adolescence (from mid-to late teens): Growth of total lung capacity (TLC) and of flow rates relative to TLC is slower in adolescent girls than in adolescent boys.[27,30] Specific airway resistance decreases up to about age 18 years in girls but not in boys,[22] differences attributed to a muscularity effect (see early adolescence above).[29]
6. Early adulthood (from late teens to midtwenties): After height stabilizes, weight becomes a determinant of lung volumes in young men and women. Sex differences in tracheal area (measured by acoustic reflection) vis-à-vis lung volumes[36] suggest that configuration of the adult female lung is the result of proportional growth of airways and parenchyma, but in the adult male lung, growth of the airways has lagged behind that of the parenchyma (ie, has been dysanaptic).[17,36]
7. Adulthood through old age (from about age 30 years): Aging of the lungs' mechanical properties occurs later and proceeds more slowly in women than in men.[32] Age-related changes in lung structure and function result in increases in lung compliance, decreases in maximal expiratory flow rates, and airway closure at higher lung volumes. With increasing age, the large airways of men (measured by acoustic techniques) lose elastic recoil. This may counteract the loss of parenchymal recoil and explain the relative preservation of their peak flow rates.[36,37]

Immunologic Determinants of Airway Behavior

Sex-based differences in the immune system are reflected in the manifestations of allergy,[2] and atopy, a marker of allergic status, is an important determinant of airway behavior as well as an important host risk factor for asthma.[38] Atopy has been defined as that form of immunologic activity in which "IgE antibody is readily produced in response to common allergens of the subject's environment."[2] Phenotype markers of atopy used in population-based studies include skin prick reactivity to common allergens, total or specific serum immunoglobulin (IgE), blood eosinophil counts, and, in children up to 2 years of age, mononuclear proliferative and cytokine responses to specific allergens and tetanus toxoid.[2] These biomarkers of atopy differ in their evolution with age, their relationship to each other is complex, and, although sex-based differences in the immune system have long been recognized, there have been few studies that have examined specific time windows by sex and age. In addition, account needs to be taken of between-study differences in methodology, for instance, in the test batteries of allergens used for assessing skin prick reactivity and in the criteria for reading a skin test as positive.

Total and Allergen-Specific Serum IgE Sex differences in the manifestations of allergy assessed by total serum IgE have been reported across the human life span, with levels in girls and women being lower than those in boys and men in most, but not all, studies.[2] In the Tucson study, one of few community-based cohort studies covering the human life span using the same methodology, the differences in IgE levels were consistent from childhood through old age (lower in girls and women than in boys and men) and followed a similar pattern over time in both sexes (Table 53-2).[10,12] These differences are obviously biologically determined, although for reasons that are not clear.[38] By contrast,

Table 53-2 Sex Differences in Markers of Atopy over the Human Life Cycle

Age (yrs)	*IgE**		*Skin test positive† (%)*	
	Male	*Female*	*Male*	*Female*
>5	NA	NA	40.0	**50.0**
5	**86.7**	71.1	**61.9**	55.7
15–34	**54.1**	37.1	62.5	**66.6**
35–54	**36.3**	26.6	50.7	**60.9**
55–74	**29.9**	16.5	**38.3**	30.0
75+	**25.1**	12.6	26.7	**28.0**
Overall	**42.1**	25.5	51.2	50.3

NA, not available.

Date are presented as %. Based on data gathered in the Tucson, AZ, USA, community study of obstructive lung diseases at the fifth and sixth surveys carried out in 1971 and 1972.[9–11] For each age stratum, figures in bold indicate the higher prevalence level for the two markers of atopy. For IgE, prevalence levels are consistently higher in males than in females for all age strata, and the overall level correctly reflects the pattern by age. This is not the case for skin test positivity, where the prevalences vary by age strata yet the overall level implies that values are similar for both sexes at all age strata.

*$n = 2{,}699$; †$n = 1333$.

sex-based differences in allergen-specific IgE are less consistent across studies and are likely to be related to local differences in prevalent outdoor and indoor antigens.[38] For instance, in a community-based Norwegian study of 1,512 adults aged 18 to 78 years, prevalence odds ratios, adjusted for potential confounders, were significantly higher in men than women for only one of three serum-specific IgE antibodies to the indoor allergens tested (the house dust mite) and not to the two others (cat and mold) or to the two outdoor allergens tested (birch and timothy grass).[39] A plausible explanation is that allergen-specific T-cell memory develops prenatally or in early infancy.[40,41] Thus, in the Norwegian study, sensitization to house dust mite likely occurred in the first year of life, when infant boys are more at risk for sensitization than are infant girls.

Skin Test Reactivity In contrast to the sex-based differences in total serum IgE that are consistent in direction from childhood through old age (lower in girls and women than in boys and men), sex-based differences in the prevalence of skin test reactivity to a panel of allergens differ in direction in different time windows. In the Tucson study, rates in childhood up to the midteens were higher in boys than girls, but throughout their reproductive years women exhibited higher rates than men, although not after the menopause (see Table 53-2).[10,12] Because these sex differences in rates for total serum IgE were consistent across the age strata studied, the average differences (25.5% vs 42.1% in females vs males, respectively) are an accurate reflection of the sex differences. However, although the average sex differences for the prevalence of skin test positivity are similar (50.3% vs 51.2% for females vs males, respectively), they are clearly not an accurate reflection of the complexity of the relationship of skin test positivity with age. The authors concluded that "the (skin) reaction rate in men and women is virtually identical" but that "depending on the age and the number of subjects, an apparent, but probably spurious sex difference may be noted."[10] In other words, the authors failed to recognize this evidence of important interactions between the immune and reproductive systems of women in their childbearing years. Subsequently published data confirmed that these sex differences were indeed not spurious.[41–43]

Immune Status of Fetus and Mother during Pregnancy Pregnancy involves two physiologies, that of the fetus and that of the mother. Although the placenta is a barrier to most blood constituents, transfer of IgG is a normal feature of pregnancy. There is also a bidirectional interaction between the mother's immune and reproductive systems, the mother's immune response either enhancing or inhibiting the development of the fetal-placental unit,[44] and the success of the pregnancy depends on the maternal immune system to facilitate ovule implantation and to develop tolerance to the fetus, a semiallograft. Thus, the mother's immune system is biased toward humoral (T helper cell type 1; ie, Th1) responsiveness and the fetal–placental immune system toward a cell-mediated (T helper type 2; ie, Th2) responsiveness, due to cytokines produced by the amnion and placenta, and spontaneous abortion is likely to occur if this immune profile does not develop in time.[44,45] T cells from the cord blood of babies born to atopic mothers respond to food and inhaled antigens to which the mother was exposed during pregnancy.[44–46] In addition, estrogen levels, as they increase during pregnancy, have been shown to have multiple effects on cytokine production and on the fetal–maternal immune system. Whether the sex of the fetus affects these relationships does not appear to have been studied.

Early Life Events as Primers of the Immune System Pre- and early postnatal events appear to be important as primers of the human immune system when it hangs in the balance between Th2 and Th1 responsiveness, that is, between developing atopy and the asthma phenotype or not.[40] Besides a family history, early life events associated with a decreased risk of developing childhood allergy or asthma include breast-feeding, having older siblings, having recurrent early childhood respiratory or gastrointestinal infections, and having been inoculated with certain vaccines, such as BCG.[40] By contrast, migration and urbanization are associated with an increased risk of developing atopy and asthma.[47–50] Only one study commented on sex differences in immune programming by the mother, in 777 newborn infants in Detroit, Michigan. An association between a maternal history of asthma and an elevated cord blood IgE was found for newborn girls but not for the newborn boys.[51]

Hormonal Determinants of Airway Behavior

Despite the evidence cited by Havelock Ellis[6] over 100 years ago that female sex hormones influence airway behavior, and despite the recognition by physiologists in the early twentieth century that the hyperventilation of pregnancy was largely driven by progesterone,[52] the role of hormonal factors as determinants of airway behavior is still poorly understood. There is, however, compelling evidence that, during their reproductive years, the airways of women respond to the cyclical variations in sex hormones. This has been demonstrated in the context of circadian and menstrual rhythms and the use of oral contraceptives, as well as

in pregnancy and the menopause and postmenopausal hormone replacement therapy (HRT).[1] Much of the information comes from studies of subjects with asthma, although a few, such as the classic study by Ott,[7] included nonasthmatic subjects.[53,54] Many studies did not, however, distinguish whether the cycles studied were natural or experienced by women on oral contraceptives. Research interest also is now shifting to understanding the role of sex hormones in the genesis of other respiratory diseases, such as chronic obstructive pulmonary disease, lung cancer, and obstructive sleep apnea (OSA).[55]

Circadian and Menstrual Rhythms and Contraceptive Use

Studies in Nonasthmatic Subjects There is increasing evidence supporting the hypothesis that hormones exert important biologic effects on the respiratory tract. Progesterone has long been identified as a potent stimulant of ventilatory drive.[52,56,57] In addition, progesterone and estrogen have been shown to act by decreasing bronchial smooth muscle tone.[58–60] Circadian rhythms affect airway responsiveness to inhaled challenges, as well as skin prick reactivity, in diurnally active nonasthmatic men and women, both being least at about noon and greatest around midnight.[61] Skin reactivity also exhibits marked menstrual variability. Other cyclical variations that occur over the menstrual cycle include airway responsiveness to methacholine, which has been shown to increase in the luteal compared with the follicular phase of the cycle,[62] and diffusing capacity for carbon monoxide, which has been shown to be reduced by about 8% in the pre- or perimenstrual period compared with midcycle levels.[63] Clearance of theophylline has also been shown to be significantly higher in the luteal than the follicular phase of the cycle.[64] The expired level of nitric oxide (NO), reflecting the biologic level of the endothelial relaxing factor, is also significantly higher during the luteal than the follicular phase of the cycle.[53]

Studies in Asthmatic Subjects The level of expired NO has been interpreted as a marker of allergen-induced inflammation and may explain premenstrual exacerbations of asthma.[53] Increased clearance of theophylline in the luteal phase could have the same effect. Premenstrual aggravation of asthma symptoms, which occurs in 30 to 40% of asthmatic women, may be severe, even life threatening.[65] In some studies of women whose asthma is exacerbated premenstrually, modest parallel decreases in spirometric lung functions and increases in airway responsiveness have been shown.[66] The physiologic fall in progesterone and estradiol production by the corpus luteum in the late luteal phase may be responsible for the premenstrual worsening of asthma symptoms.[67,68] Secretion of progestins and estradiol by the corpus luteum peaks at 5 to 7 days after ovulation and then drops to baseline levels shortly before the onset of menses. There is also some evidence that menstrual rhythmicity in airway behavior is reduced or suppressed by intramuscular progesterone[69] or by the use of oral contraceptives.[53,64] Premenstrual exacerbation of asthma has been attributed[1–4] to (1) an increase in allergen-induced airway inflammation, (2) a decrease in smooth muscle contractility, (3) microvascular leak, (4) direct action of progesterone on the airways, and (5) in a speculative paper entitled "Is Asthma an Endocrine Disease?"[70] to changing "Western lifestyles, including increasing use of oral contraceptives, which, when withdrawn, still delays the success of subsequent efforts at conception."

Pregnancy Pregnancy is accompanied by changes in chest wall and lung mechanics, increases in the diffusing capacity that stabilize at about 26 weeks,[71] and an increase in ventilation at rest and on effort of about 30%, attributable to increased progesterone levels.[3] Progesterone levels are estimated to be approximately 900% higher by the end of gestation and estradiol levels are 100 times higher compared with levels at conception.[60] During pregnancy, asthma may remain stable, improve, or get worse, in roughly similar proportions.[72–74] Acute attacks are more likely to be experienced at 17 to 24 weeks,[73] particularly in women at the end of the reproductive period of their lives, whereas worsening of asthma symptoms is more likely to occur at 29 to 32 weeks.[74] The variability of the effect of pregnancy on asthma can be attributed to a number of factors. In the group of patients with reduced exacerbations, the high level of circulating progesterone may be the dominant influence. In the subgroup of patients in whom symptoms worsen, the beneficial effects of the circulating hormones on the airways may be attenuated by the reduced functional residual capacity and residual volume. Furthermore, gastroesophageal reflux is not uncommon during pregnancy and may also be a factor in triggering exacerbations in certain patients. In none of the studies cited above was the sex of the fetus reported or apparently considered as potentially important on influencing the mother's asthma. However, in one study carried out in London on 34 pregnant asthmatic women, asthma symptoms improved if the fetus was male and remained unchanged or increased if the fetus was female (Table 53-3).[67] Overall, few studies have objectively examined asthmatic subjects who were pregnant, and to our knowledge, none have followed patients from conception to delivery. In future such studies will hopefully also control for other confounding factors, such as physiologic changes in pulmonary function during pregnancy, gastroesophageal reflux, medication use, and access to health care.

Menopause and HRT Menopause is characterized by significant reductions in circulating serum hormone levels. Few studies have investigated the effect of menopause or of HRT on the airways and pulmonary function. However,

Table 53-3 Asthma Status in 34 Women during Pregnancy in Relation to the Sex of the Fetus

	Sex of fetus	
Asthma status	*Boy*	*Girl*
Improved	8	1
Unchanged	5	6
Worse	5	9

Table shows the number of woman in each group. Based Beecroft N et al.[75]

some data suggest that hormonal changes in menopause may have important pathophysiologic consequences in diseases such as asthma and OSA.

HRT and Asthma The Nurses Health Study reported that postmenopausal women who were never-users of HRT had a lower risk of asthma than premenopausal women (relative risk = 0.65; 95% confidence interval [CI] = 0.46 to 0.92). In addition, past and current users of HRT demonstrated increased risk of asthma when compared with women who never used HRT.[68] The Cardiovascular Health Study reported different findings. In this longitudinal population-based study of 2,353 women aged 65 and older, FEV_1 and FVC values were higher among current HRT users compared with noncurrent users. In addition, women with asthma using HRT had a trend toward higher FEV_1 and FVC values than women with asthma who were not using HRT.[77] To our knowledge, no prospective studies examining the influence of HRT on asthma control have included a preparation with a progesterone component. Furthermore, the actual doses of estrogen in the HRT preparations, which are significantly lower than in oral contraceptive pills, may be too low to exert a potent clinical effect on asthma control.

HRT and OSA Early epidemiologic studies of OSA suggested that this was a disease primarily confined to men. More recent data confirm that men are two to three times more likely to have sleep-disordered breathing than women[78] and that the majority of women affected by OSA are postmenopausal, among whom the prevalence is at least double that in premenopausal women.[79] The increased ventilatory chemoresponsiveness triggered by progesterone may be responsible for these phenomena. Female hormones may also promote activity of the dilator upper airway muscles.[80] In a study of 14 morbidly obese subjects (7 men and 7 women) referred for gastric bypass surgery, none of the women desaturated during sleep, whereas 6 of the men had apneic episodes with desaturation. The one man in whom apneic events were not recorded had hypogonadism. These findings suggest that testosterone may also play an important role in the pathophysiology of this disorder in men.[81]

ENVIRONMENTAL AND SOCIOCULTURAL DETERMINANTS OF AIRWAY BEHAVIOR

The environmental and sociocultural determinants of airway behavior, like the biologic determinants, may act with varying strength and on occasion in opposite directions within different ages. Their impact is likely to vary between communities, cultures, and countries, reflecting differences in environmental factors such as climate, natural resources, and levels of urbanization, industrialization, and affluence or poverty, as well as differences in sociocultural factors, such as acceptability of smoking among women and the degree to which they participate in the commercial, sporting, and entertainment life of their communities.[1,3] There is also increasing evidence of complex interactions between the biological (sex-based) and sociocultural (gender-based) determinants of airway behavior (see below).

Environmental Exposures

In industrialized countries and increasingly in industrializing countries, exposures common to both genders include environmental (secondhand) tobacco smoke and alcohol use, usually more and less frequent in women than in men, respectively.[1–3] On the other hand, for active smoking, rates have in the past been lower in girls and women than in boys and men, although this is fast changing as women and now adolescent girls take up the smoking habit. Workplace exposure to dusts, fumes, and vapors is likely to show similar trends as women move into traditionally male jobs. On the other hand, women are more likely than men to be exposed to home cleaning materials and to nitrogen dioxide fumes from gas cookers (potentially harmful to small airway function), as are young children in the home.[82] There is also increasing evidence that women are more susceptible to the harmful effects of certain inhaled pollutants, tobacco smoke probably being the most important.[3] The lung structures targeted by tobacco smoke may also be different in girls and women (lung vasculature) than in boys and men (airways in general, small airways in particular).[83]

Sociocultural Factors

Gender-based differences in the perception, reporting, and interpretation of respiratory symptoms have usually been attributed to sociocultural factors.[2] For instance, shortness of breath is more commonly reported by women (and may be more socially acceptable to them than men), whereas cough, raising sputum, and snoring are less commonly reported by women (and may be less socially acceptable to them than to men).[1] However, some markers of airway behavior attributed to gender (sociocultural differences) may in fact be sex based (biologically determined). This is illustrated in Figure 53-3, which shows that at all levels of FEV_1 (an objective marker of airway function), age-standardized, shortness of breath (a subjective marker of airway function) is more frequently reported by women than men. A plausible explanation is that their perception of breathlessness has been enhanced by the cyclical fluctuation of their airway caliber in response to the cyclical fluctuation of their sex hormones throughout their reproductive lives.[1] As far as the symptoms of cough and raising sputum are concerned, women have consistently been shown to have a lower threshold to cough challenge tests than men, and this threshold is lower in pre- than postmenopausal women.[4,84–86] These findings also illustrate the complexity of the potential interactions between the biologic and sociocultural determinants of airway behavior in women in their reproductive years.

Methodologic Issues

Studies of sex and gender differences in airway behavior are subject to methodologic sources of bias, which are particularly challenging to handle.[2] For instance, inferences about sex or gender differences in susceptibility to tobacco smoke derived from epidemiologic studies are potentially subject to underestimation as a result of (1) selection bias from the "healthy" smoker effect (those whose airways are less able to sustain the habit remain nonsmokers)[87]; (2) information

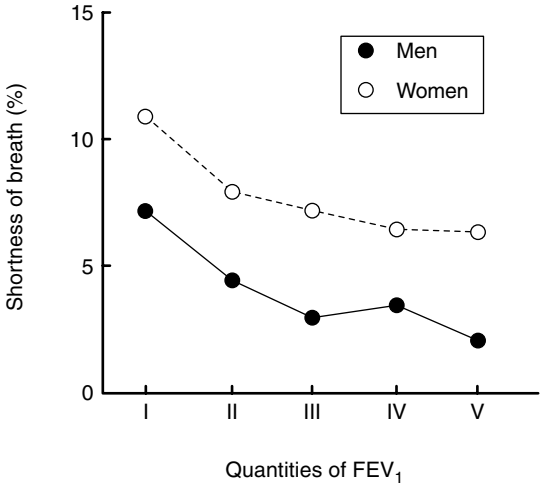

FIGURE 53-3 Sex differences in reported shortness of breath (prevalence %) by quintiles of cc. Based on data gathered in the *PARRC (Pollution Atmosphériques et Affections Respiratoires Chroniques)*, a cross-sectional population based study conducted in 1975 on over 20,000 adults aged 25 to 59 years, excluding subjects with reported respiratory or cardiovascular disease. The quintiles of FEV_1 were defined separately for women and men, age taking into account. Reproduced with permission from Kauffmann and Becklake.[1]

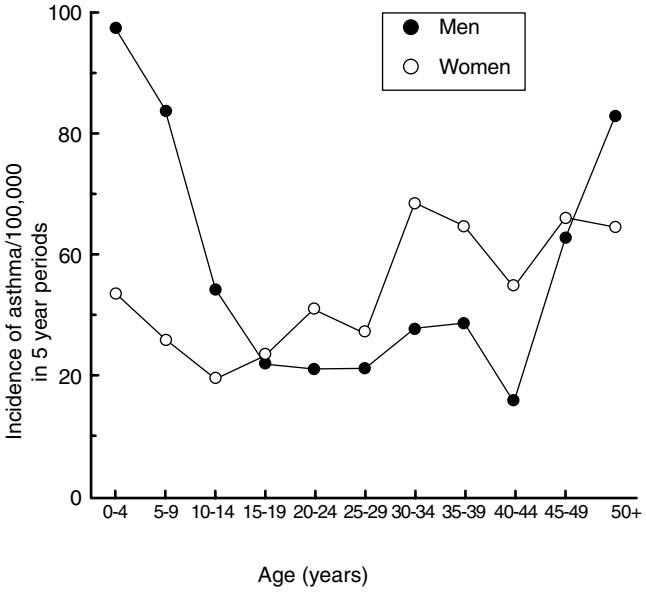

FIGURE 53-4 Incidence of asthma per 100,000 in 5-year age periods in girls and women compared with boys and men. Based on data gathered in the *PAARC (Pollution Atmosphériques et Affections Respiratoires Chroniques)*, a cross-sectional population-based study conducted in 1975 on over 20,000 adults aged 25 to 59 years, excluding subjects with reported respiratory or cardiovascular disease. Incidence of asthma was estimated retrospectively from age at onset as reported by the subjects. Reproduced with permission from Kauffmann and Becklake.[1]

bias (although reported levels of smoking may be similar for men and women, the effects of passive smoking, which are likely to be higher in women than in men, are not always taken into account in analysis)[3,88]; (3) diagnostic bias (symptoms such as shortness of breath and wheezing may attract a different diagnosis when reported by women than by men)[89]; (4) confounding bias (inferences are crucially dependent on how the reference, nonsmoking group is constituted, which, in turn, depends on the definition of "nonsmoker" and the reasons, usually very different, why men and women do not smoke). These and other methodologic issues will, for the most part, underestimate the effects of environmental and sociocultural determinants on airway behavior and disease in women and hence of the associated sex or gender differences.

SUMMARY AND CONCLUSIONS

To what extent are sex- and gender-based differences in airway behavior reflected in the clinical manifestations of airway disease? We addressed this question using, as the example, asthma based on data gathered in the *PAARC* (*Pollution Atmospherique et Affections Respiratoires Chroniques*) study,[1] one of few in which the same methodology was used to estimate the incidence of asthma (within 5-year age periods) across the human life span (Figure 53-4). Up to the age of 5 years, incidence rates in girls were less than one-half that of boys, attributable to their dimensional advantages in lung structure and function. Between the ages of 5 and 15 years, the sex-based differences in incidence rates decreased, probably in part because the dysanaptic growth patterns seen in younger boys are replaced by more linear growth patterns, similar to those seen in girls. Between the ages of 15 and 19 years, the incidence rates started to reverse, and from the age of 20 through 44 years (ie, throughout their reproductive years) incidence rates in women exceeded those in men. During this period, although women retained their dimensional advantages over men, their higher rates can be attributed to hormonal factors as well as interactions between immunologic and hormonal factors. From the age of 45 years, incidence rates again reversed; the rates in men increased, whereas those in women remained stable. The reasons for this are not clear but may be methodologic. After menopause, the airways of women appear to remain responsive to their sex hormones. Almost three decades after the PAARC study was carried out, the sex reversal rates of asthma during the reproductive period of women's lives was confirmed by data gathered in the European Community Respiratory Health Survey (ECRHS) on a comparable number of subjects (18,000 to 19,000), although over a more limited age span (20 to 45 years of age). The pattern of distribution of asthma was similar within the 16 countries studied and was not affected by smoking.[90] In other studies, late-onset asthma was found to be largely confined to women and usually started around menopause.

Biologic (sex-based) and sociocultural (gender-based) differences in the airway behavior of girls and women compared with those of boys and men occur across the human life span. These differences, which vary in both strength and direction for different age spans, interact in a complex way to affect the clinical manifestations of airway disease. The biologic determinants of these differences include dimensional (lung structure–function relationships), immunologic, and hormonal factors. In childhood, the lungs of girls,

although smaller than those of boys, exhibit dimensional advantages compared with those of boys, measurable as higher flow rates in relation to lung size. From adolescence and throughout their child-bearing years, immunologic and hormonal factors exert important and interacting roles on the airway behavior of women and are probably responsible for the higher rates of asthma in women during the reproductive period of their lives. In addition, from late childhood through adolescence and into their adult life, airway behavior in women is influenced by environmental and sociocultural (gender-related) factors, some shared with men, some not. These act to modify how the symptoms of lung disease are perceived and reported by women compared with men, as well as how they are managed by their physicians. Results of studies on the effects of airway behavior on the manifestations of airway disease, whether clinical or epidemiologic, should be analyzed separately by sex and stratified by age prior to being combined, for instance, in clinical trials. In addition, the mechanisms of these sex-based differences should be the focus of research studies in the early years of the twenty-first century. We fully concur with the conclusion expressed by the authors of the 2001 Institute of Medicine report[8]: "Understanding [the] sex differences in health and illness merits serious scientific inquiry in all aspects of biomedical and health related research."

REFERENCES

1. Kauffmann F, Becklake MR, Saurel-Cubizolles MJ, Blondell B, editors. La santé des femmes. Paris: Flammarion, Médecine et Sciences, 1996; 11. Maladies obstructives pulmonaires: un paradigme de la complexité des différences de santé entre hommes et femmes. p. 209–33.
2. Becklake MR, Kauffmann F. Gender differences in airway behaviour over the human life span. Thorax 1999;54:1119–38.
3. Kauffmann F, Becklake MR. Sex and gender. Eur Respir Mon 2000;5:288–304.
4. Becklake MR. Gender differences in airway behaviour (physiology) over the human lifespan. Eur Respir Mon 2003;25:8–25.
5. Hutchinson J. On the capacity of the lungs and on the respiratory function with a view of establishing a precise and easy method of detecting disease by the spirometer. Med Clin Trans 1846;29:137–252.
6. Ellis H. Man and woman: a study of human secondary sexual characters. New York: Charles Scribner's Sons; 1894. p. 200–57.
7. Ott O. Les lois de la périodicité de la fonction physiologique dans l'organisme féminin. Nouvelles archives d'obstétrique et de gynécologie 1890;502–6.
8. Institute of Medicine. Wizeman TM, Pardue M-L, editors. Exploring the biological contributions to human health: does sex matter? Washington (DC): National Academy Press; 2001.
9. Last JM, editor. A dictionary of epidemiology. 4th ed. New York: Oxford University Press; 2001.
10. Barbee RA, Kaltenborn W, Lebowitz MD, et al. Longitudinal changes in allergen skin test reactivity in a community population sample. J Allergy Clin Immunol 1987;79:16–24.
11. Sapigni T, Biayati P, Simoni M, et al. The Po River Delta respiratory epidemiological survey: an analysis of factors related to level of total serum IgE. Eur Respir J 1998;11:278–83.
12. Cline MG, Burrows B. Distribution of allergy in a population sample residing in Tucson, Arizona. Thorax 1989;44:425–31.
13. Thurlbeck WM. Postnatal growth and development of the lung. Am Rev Respir Dis 1975;111:803–44.
14. Jeffrey PK. The development of large and small airways. Am J Respir Crit Care Med 1998;157(5 Pt 2):S174–80.
15. Thurlbeck WM. Postnatal human lung growth. Thorax 1982;37:564–71.
16. Langston C, Kida K, Reed M, et al. Human lung growth in late gestation and in the neonate. Am Rev Respir Dis 1984;129:607–13.
17. Mead J. Dysanapsis in normal lungs assessed by the relationship between maximal flow, static recoil, and vital capacity. Am Rev Respir Dis 1980;121:339–42.
18. Hepper PG, Shannon EA, Dornan JC. Sex differences in fetal mouth movements. Lancet 1997;350:1820.
19. Torday JS, Nielsen HC. The sex difference in fetal lung surfactant production. Exp Lung Res 1987;12:1–19.
20. Martin TR, Feldman HA, Fredberg JJ, et al. Relationship between maximal expiratory flows and lung volumes in growing humans. J Appl Physiol 1988;65:822–8.
21. Hibbert H, Lannigan A, Raven J, et al. Gender differences in lung growth. Pediatr Pulmonol 1995;19:129–34.
22. Doershuk CF, Fisher BJ, Matthews LW. Specific airway resistance from the perinatal period into adulthood. Alterations in childhood disease. Am Rev Respir Dis 1974; 109:452–7.
23. Pagtakhan RD, Bjelland JC, Landau LI, et al. Sex differences in growth patterns of the airways and lung parenchyma in children. J Appl Physiol 1984;56:1204–10.
24. Taussig LM, Cota K, Kaltenborn W. Different mechanical properties of the lung in boys and girls. Am Rev Respir Dis 1981;123:640–3.
25. Schwartz JD, Katz SA, Fegley RW, et al. Analysis of spirometric data from a national sample of healthy 6- to 24-year-olds (NHANES II). Am Rev Respir Dis 1988;138:1405–14.
26. Schwartz J, Katz SA, Fegley RW, et al. Sex and race differences in the development of lung function. Am Rev Respir Dis 1988;138:1415–21.
27. Merkus PJFM, Borsboom GJJM, Van Pelt W, et al. Growth of airways and air spaces in teenagers is related to sex but not to symptoms. J Appl Physiol 1993;75:2045–53.
28. Wang X, Dockery DW, Wypij D, et al. Pulmonary function growth velocity in children 6 to 18 years of age. Am Rev Respir Dis 1993;148:1502–8.
29. Schrader PC, Quanjer PH, Olivier ICW. Respiratory muscle force and ventilatory function in adolescents. Eur Respir J 1988;1:368–75.
30. Merkus PJFM, ten Have-Opbroek AAW, Quanjer PH. Human lung growth: a review. Pediatr Pulmonol 1996;21:383–97.
31. American Thoracic Society. Lung function testing: selection of reference values and interpretative strategies. Am Rev Respir Dis 1991;144:1202–18.
32. Development, growth and ageing of the lung. Brody JS, Thurlbeck WM, Macklem PT, Mead J, editors. Volume III: Mechanics of breathing, Part 1. Fishman AP, editor. Section 3: The respiratory system. Handbook of physiology. A critical comprehensive presentation of physiologic knowledge and concepts. Bethesda (MD): American Physiological Society; 1986. p. 355–86.
33. Quanjer PH, Borsboom GJ, Brunekreef B, et al. Spirometric reference values for white European children and adolescents: Polgar revisited. Pediatr Pulmonol 1995;19: 135–42.
34. Stocks J, Quanjer PH. Reference values for residual volume, functional residual capacity and total lung capacity. ATS workshop on lung volume measurements. Official statement of the European Respiratory Society. Eur Respir J 1995;8:492–506.

35. Demissie K, Marcella SW, Breckenridge MB, et al. Maternal asthma and transient tachypnea of the newborn. Pediatrics 1998;102:84–90.
36. Hoffstein V. Relationship between lung volume, maximal expiratory flow, forced expiratory volume in one second, and tracheal area in normal men and women. Am Rev Respir Dis 1986;134:956–61.
37. Gibellino F, Osmanliev DP, Watson A, et al. Increase in tracheal size with age. Implications for maximal expiratory flow. Am Rev Respir Dis 1985;132:784–7.
38. Holgate ST. The cellular and mediator basis of asthma in relation to natural history. Lancet 1997;350 Suppl II:SII5–9.
39. Omenaas E, Bakke P, Elsayed S, et al. Total and specific serum IgE levels in adults: relationship to sex, age and environmental factors. Clin Exp Allergy 1993;24:530–9.
40. Bjorksten B. Allergy priming early in life. Lancet 1999;353:167–8.
41. Prescott SL, Mccaubas C, Smallacombe T, et al. Development of allergen-specific T-cell memory in atopic and normal children. Lancet 1999;353:196–200.
42. Sears MR, Burrows B, Flannery EM, et al. Atopy in childhood. I. Gender and allergen related risks for development of hay fever and asthma. Clin Exp Allergy 1993;23:941–8.
43. Schuurs AHWM, Verheul HAM. Effects of gender and sex steroids on the immune response. J Steroid Biochem 2002;35:157–72.
44. Wegmann T, Lin H, Gulbert L, et al. Bidirectional cytokine interactions in the maternal-fetal relationship: is successful pregnancy a Th2 phenomenon? Immunol Today 1993;14:353–6.
45. Cookson WOCM, Moffatt MF. Asthma: an epidemic in the absence of infection. Science 1997;275:41–2.
46. Holt PG, Sly PD. Allergic respiratory disease: strategic targets for primary prevention during childhood. Thorax 1997;52:1–4.
47. Chan-Yeung MJL. Occupational asthma. N Engl J Med 1995;333:107–12.
48. von Mutius E, Martinez FD, Fritzsch C, et al. Skin test reactivity and number of siblings. BMJ 1994;308:692–5.
49. von Mutius E, Martinez FD, Fritzsch C, et al. Prevalence of asthma and atopy in two areas of west and east Germany. Am J Respir Crit Care Med 1994;149:358–64.
50. Platts-Mills TAE, Carter MC. Asthma and indoor exposure to allergens. N Engl J Med 1997;336:1382–4.
51. Johnson CC, Ownby DR, Peterson DL. Parental history of allergy and concentration of cord blood IgE. Clin Exp Allergy 1996;26:624–9.
52. Dempsey JA, Olson EBJ, Skatrud JB. Hormones and neurochemicals in the regulation of breathing. Cherniak NS, Widdicombe JG, editors. Section 3: The respiratory system. Handbook of physiology. Bethesda (MD): American Physiological Society; 1986. p. 181–222.
53. Kharitonov SA, Logan-Sinclair RB, Busset CM, et al. Peak expiratory nitric oxide differences in men and women: relation to the menstrual cycle. Br Heart J 1994;72:243–5.
54. Weinmann GG, Zakur H, Fish JE. Absence of changes in airway responsiveness to methacholine during the menstrual cycle and the effect of oral contraceptives. J Allergy Clin Immunol 1987;79:634–8.
55. Saaresranta T, Polo O. Hormones and breathing. Chest 2002;122:2165–82.
56. Zwillich CW, Natalino MR, Suttton FD, Weil JV. Effects of progesterone on chemosensitivity in normal men. J Lab Clin Med. 1978;92:262–9.
57. Sutton FD, Zwillich CW, Creagh CE, et al. Progesterone for outpatient treatment of Pickwickian syndrome. Ann Intern Med 1975;83:476.
58. Kumar D. In vitro inhibitory effect of progesterone on extrauterine human smooth muscle. Am J Obstet Gynecol 1962;84:1300–4.
59. Moawad AH, River LP, Kilpatrick SJ. The effect of estrogen and progesterone on beta-adrenergic receptor activity in rabbit lung tissue. Am J Obstet Gynecol 1982;144:608–13.
60. Haggerty CL, Ness RB, Kelsey S, Waterer W. The impact of estrogen and progesterone on asthma. Ann Allergy Asthma Immunol 2003;90:284–91.
61. Smolensky MH, Reinberg A. Clinical chronobiology: relevance and applications to the practice of occupational medicine. Occupational Medicine: State of the Art Reviews 1990;5: 239–72.
62. Juniper EF, Kline PA, Roberts RS, et al. Airway responsiveness to methacholine during the natural menstrual cycle and the effect of oral contraceptives. Am Rev Respir Dis 1987;135: 1039–42.
63. Bilancia R, Caputo G, Posca A, et al. CO diffusing capacity (DLCO) during menstruation cycle. Chest 1996;110 (4 Suppl):61S.
64. Nagata K, Ishitobi K, Yamamoto Y, et al. Increase theophylline metabolism in the menstrual phase of health women. J Allergy Clin Immunol 1997;100:39–43.
65. Edwards AL, Rose MS, Donovan LE, et al. Premenstrual exacerbation of life-threatening asthma: effect of gonadotropin releasing hormone analogue therapy. Can Respir J 1996;3:203–6.
66. Eliasson O, Scherzer HH, DeGraff ACJ. Morbidity in asthma in relation to the menstrual cycle. J Allergy Clin Immunol 1986;77:87–94.
67. Eliasson O, Scherzer HH, DeGraff AC Jr. Morbidity in asthma in relation to the menstrual cycle. J Allergy Clin Immunol 1986;77:87–94.
68. Gibbs CJ, Coutts II, Lock R, et al. Premenstrual exacerbation of asthma. Thorax 1984;39:833–6.
69. Benyon HLC, Garnett ND, Barnes PJ. Severe premenstrual exacerbations of asthma: effects of intramuscular progesterone. Lancet 1988;332:370–2.
70. Wjst M, Dold S. Is asthma an endocrine disease? Pediatr Allergy Immunol 1997;8:200–4.
71. Bates DV. Respiratory function in disease. 3rd ed. Philadelphia (PA): W.B. Saunders; 1998; p. 106–51.
72. Juniper EF, Daniel EE, Roberts RS, et al. Improvement in airway responsiveness and asthma severity during pregnancy: a prospective study. Am Rev Respir Dis 1989;140:924–31.
73. Stenius-Aarniala BSM, Hedman J, Teramo KA. Acute asthma during pregnancy. Thorax 1996;51:411–4.
74. Stenius-Aarniala B, Piirila P, Teramo K. Asthma and pregnancy: a prospective study of 198 pregnancies. Thorax 1988;43:12–8.
75. Beecroft N, Cochrane GM, Milburn J. Effect of sex of foetus on asthma during pregnancy: blind prospective study. BMJ 1998;317:856–7.
76. Troisi RJ, Speizer FE, Willett WC, et al. Menopause, postmenopausal estrogen preparations, and the risk of adult-onset asthma. Am J Respir Crit Care Med 1995;152: 1183–8.
77. Carlson CL, Cushman M, Enright PL, et al. Hormone replacement therapy is associated with higher FEV_1 in elderly women. Am J Respir Crit Care Med 2001;163:423–8.
78. Kapsimalis F, Kryger MH. Gender and obstructive sleep apnea syndrome, part 1: clinical features. Sleep 2002;25:409–16.
79. Dancey DR, Hanly PJ, Soong C, et al. Impact of menopause on the prevalence and severity of sleep apnea. Chest 2001; 120:151–5.
80. Popovic RM, White DP. Upper airway muscle activity in normal women: influence of hormonal status. J Appl Physiol 1998;84:1055–62.
81. Harman E, Wynne JW, Block AJ, Malloy-Fisher L. Sleep disordered breathing and oxygen desaturation in obese patients. Chest 1981;79:256–60.

82. Jarvis D, Chinn S, Luczynska C. Association of respiratory symptoms and lung function in young adults with use of domestic gas appliances. Lancet 1996;347:426–31.
83. Masi MA, Hanley JA, Ernst P, et al. Environmental exposure to tobacco smoke and lung function in young adults. Am Rev Respir Dis 1988;138:296–9.
84. Morice A, Kastelik JA, Thompson RH. Gender differences in airway behaviour. Thorax 2000;55:629.
85. Diepinigaitis PV, Khalid R. The influence of gender on cough reflex sensitivity. Chest 1998;113:1319–21.
86. Fujimura M, Kasahara K, Kamio Y, et al. Female gender as a determinant of cough threshold to inhaled capsaicin. Eur Respir J 1996;9:1624–6.
87. Becklake MR, Lalloo U. The "healthy smoker": a phenomenon of health selection. Respiration 1990;57:137–44.
88. Xu X, Weiss ST, Rijcken B, et al. Association of smoking and changes in smoking habits with rate of decline in FEV_1: new insight into gender differences. Eur Respir J 1994; 7:477–83.
89. Dodge R, Cline MG, Burrows B. Comparisons of asthma, emphysema, and chronic bronchitis diagnoses in a general population sample. Am Rev Respir Dis 1986;133: 981–6.
90. de Marco R, Locatelli F, Sunyer J, et al. Differences in incidence of reported asthma related to age in men and women. Am J Respir Crit Care Med 2000;162:68–74.

CHAPTER 54

MEASUREMENT TECHNIQUES IN RESPIRATORY MECHANICS

Jason H. T. Bates

The assessment of respiratory mechanics begins with the measurement of variables whose correlations contain information about the mechanical functioning of the respiratory system. These variables are usually pressures and flows, or volumes, of gas made at appropriate sites. The amount of detail that can be gleaned about the mechanical function of the respiratory system depends on which particular variables are measured and the conditions under which they are measured. Although the modern history of measurement in respiratory mechanics extends back at least 100 years, novel methods and approaches are still being developed as advances in instrumentation and computer technology continue to extend the boundaries of what is possible.

This review of measurement in respiratory mechanics begins with the general theory of measurement as it applies to modern electronic transducers and the acquisition of data by digital computer. It then proceeds to consider how this theory is applied to the measurement of respiratory pressures, flows, and volumes. Finally, it is shown how these measurements are used in combination to collect information from which respiratory mechanics are determined.

MEASUREMENT THEORY

The general measurement situation is depicted in Figure 54-1, which shows the steps involved in converting a biologic signal into a string of numbers stored on a computer. At each step we have the potential for errors to occur, represented as additive noise. First we consider the issues involved in transducing the biologic signal into an electrical signal. This is performed by a transducer. We then consider the process of digitizing the electrical signal so that it can be manipulated in digital form on a computer, which is how any subsequent data analysis is carried out.

TRANSDUCERS

A *transducer* is something that converts energy from one form to another, although for the present purposes we restrict ourselves to the more particular definition of the conversion being between some biologic quantity we are interested in and a *voltage*. Ideally, we would like the voltage to be a perfect representation of the biologic quantity, but this is never the case in practice. It is therefore crucial to understand the imperfections of the transducer to be used in any particular application and whether or not these imperfections are going to limit the amount of information that can be extracted from the measured signals.

Static Properties of Transducers We first consider the various *static properties* that characterize a transducer's performance. These are properties that do not depend on how rapidly the measured signal is varying, which is equivalent to saying that the transducer has no trouble keeping up with the signal. One such property is *linearity*, which refers to the extent to which the voltage v produced by a transducer can be represented in terms of the biologic signal s by an equation of the form

$$v = as + b \tag{54-1}$$

where a and b are constants (solid line in Figure 54-2). Manufacturers of transducers usually specify the linearity of a transducer in terms of its full-scale output. A value of 1% is typical. Although linearity is a desirable trait, with the availability of digital computers it is not essential. Suppose, for example, that v is not a linear function of s as in Equation 54-1 but is instead a curvilinear function of s that can be accurately represented as a polynomial (dashed line in Figure 54-2). If the polynomial coefficients are known (say, from a prior calibration experiment) it is a simple matter to use a computer to invert the equation to obtain s as a function of v, allowing the recorded voltage to be related back to the value of the original biologic signal.

Another important static property of a transducer is *hysteresis*, which refers to the extent to which the voltage corresponding to a biologic signal differs depending on whether the immediately preceding value was below or above the current value (Figure 54-3). Hysteresis is obviously a bad thing and is unfortunately extremely difficult to correct for, so one should always try to select a transducer with minimal hysteresis.

In selecting a transducer for a particular application, it is important to make sure it has the appropriate *resolution* and *dynamic range*, which determine the smallest and largest changes in the biologic signal that can be accurately

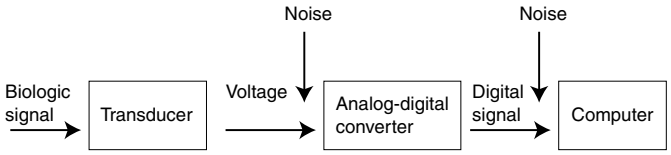

FIGURE 54-1 The general measurement scenario.

measured. Related to the issue of resolution is the *signal-to-noise ratio*. What the transducer in Figure 54-1 actually records in response to a biologic signal is a voltage plus noise. The latter must be substantially lower than any important changes that are to be recorded in the biologic signal (by preferably at least an order of magnitude).

Dynamic Properties of Transducers We now consider the somewhat more complicated issue of *dynamic properties* of transducers. These refer to those characteristics that determine how well a transducer can respond to a changing biologic signal. Most transducers are *low-pass* systems because they can respond faithfully to slowly varying signals but have increasing difficulty keeping up as the signal increases in frequency. Some transducers are *high-pass* systems because they faithfully record high frequencies but do not respond when frequency is very low. Transducers are characterized in general by the way in which they respond to input signals that vary sinusoidally. Provided that the transducers are linear, their voltage outputs to an input sine wave will also be sinusoidal with the same frequency but will in general be altered in amplitude by a factor A and shifted in phase by an amount ϕ. That is, if the input sine wave is $\sin(2\pi ft)$, then the output will be $A\sin(2\pi ft + \phi)$ (Figure 54-4). The values of A and ϕ depend on frequency and together constitute the *frequency response* of the transducer.

Digital Data Acquisition

Once a transducer has converted a biologic signal into a voltage, it must be recorded in some permanent medium for subsequent analysis and display. In the early days of physiology (ie, until about 20 years ago), physiologic recording was achieved by have a writing instrument move laterally

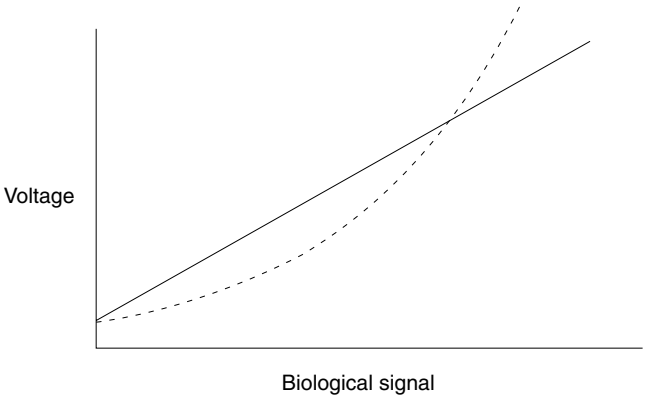

FIGURE 54-2 Characteristics of a linear (*solid line*) and nonlinear (*dashed line*) transducer.

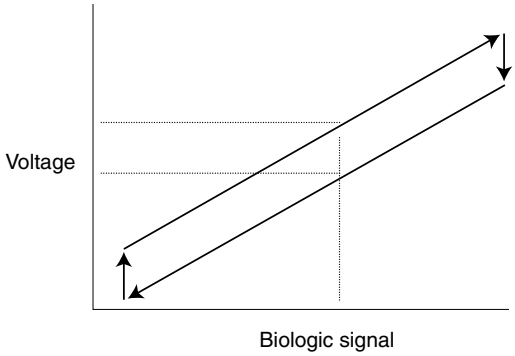

FIGURE 54-3 Hysteresis. The voltage output by a transducer in response to a particular value of the input biologic signal depends on whether the value was approached from above or below.

over a suitable recording medium as it scrolled by. In the early part of the twentieth century, the writing instrument was a rigid pointer and the scrolling medium was a cylindrical drum covered in soot. This was eventually replaced by the electronic chart recorder, consisting of one or more ink pens writing on a roll of paper moving past at constant speed. Each experiment produced a (frequently large) stack of paper that then had to be analyzed manually if calculations were to be made from the recorded signals.

Since the advent of the modern laboratory digital computer, however, these earlier analog recording devices have been replaced by digital computers that both record and analyze experimental data. The speed and flexibility of computers, together with their universal availability, have revolutionized the way that physiologic research is done.

Everything is thus now done digitally, beginning with the recording of the analog voltage signal arriving from the transducer. Conversion of an analog signal to digital form is known as *digitization* and is accomplished with an *analog-to-digital (A-D) converter*. Figure 54-5 shows what is involved. The analog (continuous) voltage signal is sampled at regularly spaced intervals by the A-D converter, and the resulting set of voltage values is stored in the computer as a set of numbers. These numbers and their locations in time then constitute our representation of the original signal.

Resolution and Discretization Error A major consideration when digitizing signals is the resolution of the A-D converter, which defines the smallest difference in voltage level that it can distinguish in the incoming analog signal. A-D

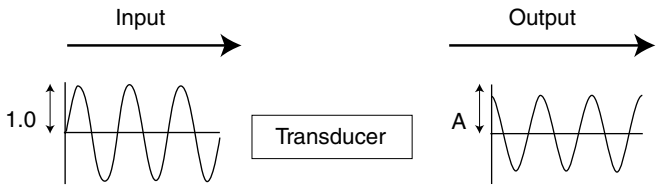

FIGURE 54-4 If an input to a linear transducer is $\sin(2\pi ft)$, its output in general will be $A\sin(2\pi ft + \phi)$, where the values of A and ϕ characterize the frequency response of the transducer.

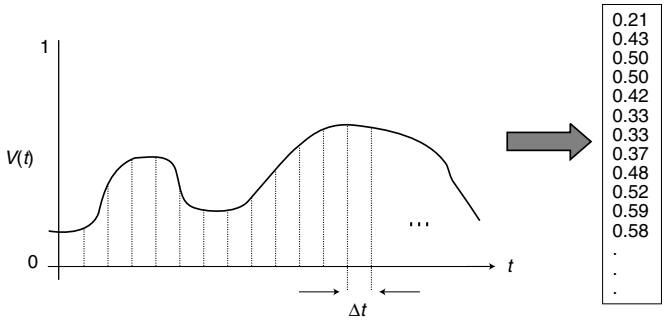

FIGURE 54-5 Digitization. An analog voltage signal $V(t)$ is sampled every Δt seconds to produce a series of numbers that are stored in a computer for subsequent analysis.

converters are set up to receive voltages within a specified range, such as −10 to +10 volts. This voltage range is divided into N equally spaced bins numbered 0 to $N-1$ (Figure 54-6). N is determined by the number of *bits* in the A-D converter. A 12-bit A-D converter has $2^{12} = 4{,}096$ bins, a 16-bit converter has $2^{16} = 65{,}536$ bins, and so on. Thus, for example, a 12-bit converter with a ±10-volt input range can resolve voltage differences of 20/4,096 = 0.0049 volts.

The finite resolution of an A-D converter means that care must be taken to ensure that it is able to resolve the smallest differences in voltage required by the experimenter. For example, suppose one is measuring flow of gas entering a patient's lungs during mechanical ventilation. If the flow reaches 2,000 mL.s^{-1} during both inspiration and expiration, then the range of flows encountered is 4,000 mL.s^{-1}. If this flow signal is recorded on a 12-bit A-D converter, the resulting digitized signal has a maximum resolution of 4,000/4,096 = 0.98 mL.s^{-1}. However, it only achieves this resolution if the entire dynamic range of the A-D converter is used. This only occurs if the analog signal produced by the flow transducer is amplified so that a flow of −2,000 mL.s^{-1} produces the lowest voltage the A-D converter can receive (eg, −10 volts), and similarly a flow of +2,000 mL.s^{-1} produces the highest receivable voltage (eg, +10 volts).

This may not be the case. A common error in the laboratory occurs when the voltage signal coming in from the transducer is not amplified enough to make use of many of the discrete bins in the A-D converter. As an example, suppose that the flow signal of −2,000 to +2,000 mL.s^{-1} results in a voltage signal that only occupies the range of −0.1 to +0.1 volts. Now only the middle 1% of the available bins (numbers 2,028 to 2,069) of the A-D converter are used, giving a 100-fold reduction in flow resolution. In extreme examples of this situation, the discrete levels of the A-D converter will be apparent in a plot of the resulting voltage signal (Figure 54-7). The errors incurred in having insufficient vertical resolution in an A-D converter are called *discretization errors*.

Sampling Theorem and Aliasing Another major question that arises when digitizing analog signals is how frequently to sample the signal. A continuous signal is composed of an infinite number of infinitesimally spaced points yet must somehow be represented by a finite number of digitized values. Obviously, if a signal is changing rapidly, then sampling its value infrequently will cause the detail between the samples to be lost. On the other hand, sampling a long signal too rapidly might result in an unmanageably large number of data points. Thus, one might be inclined to think that the choice of sampling rate represents a tradeoff between capturing detail in the original signal on the one hand and avoiding being overwhelmed by the volume of data on the other. Fortunately, however, we are saved by something known as the *sampling theorem* (often associated with engineers Shannon and Nyquist).

To understand the sampling theorem, it is necessary to first understand what is meant by the *frequency content* of a signal. Any analog signal can be expressed as the sum of a series of sine wave functions of appropriate frequency, amplitude, and phase. Furthermore, this collection of frequencies, amplitudes, and phases is unique to that signal, which means they define it distinctly from all other possible signals. A signal can be decomposed into its individual sine wave components by the *Fourier transform*. A simple example is given in Figure 54-8, which shows the four sine waves making up a signal that looks considerably more complex than any of its individual components. The frequency content of a signal thus refers to the unique spectrum of

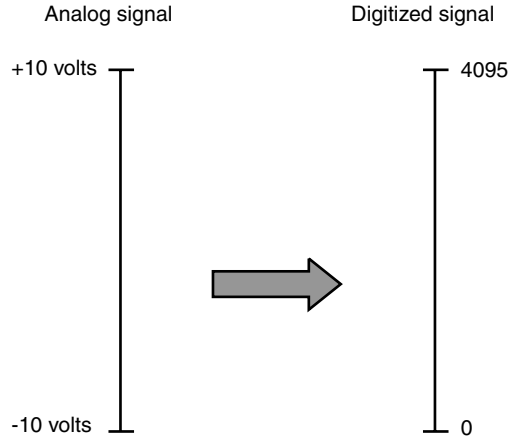

FIGURE 54-6 Digitization of the ±10 volt analog range by a 12-bit A-D converter. The 20-volt span of possible input signals is assigned to 4,096 numbers representing successive increments of 4.9 millivolts.

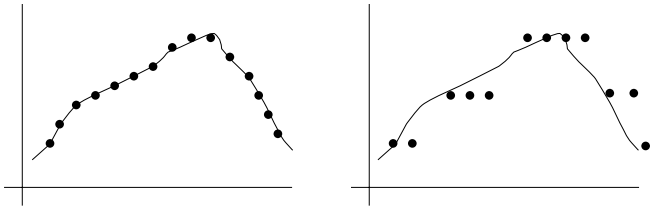

FIGURE 54-7 Discretization error. The *left panel* shows an analog signal faithfully captured by a set of digitized points. The *right panel* shows points occupying discrete levels corresponding to adjacent bins of the A-D converter.

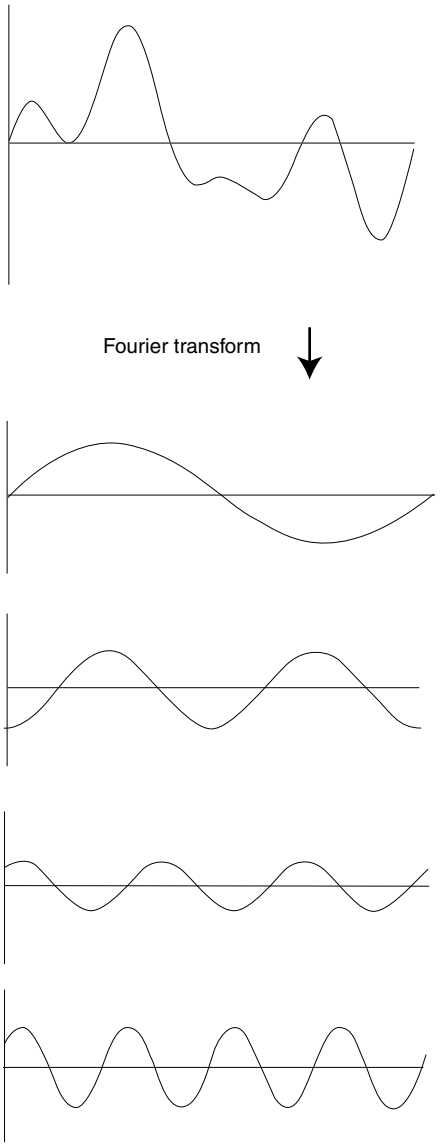

FIGURE 54-8 An analog signal can be decomposed (by the Fourier transform) into its component sine waves, each with its own frequency, amplitude, and phase.

sinusoidal components from which it is composed. In particular, if the frequency content of a signal is such that none of its sinusoidal components has a frequency greater than some maximum frequency, then the signal is said to be *band limited*.

The sampling theorem says that it is possible to capture all the information in a band-limited analog signal by sampling the signal at a rate at least twice the highest frequency in the signal itself. Thus, for example, if Fourier analysis of a signal reveals that it contains no components with frequencies greater than f_0, then we need not sample the signal any faster than $2f_0$ (known as the *Nyquist rate*). Intuitively, this makes sense because sampling a sine wave at its Nyquist frequency means collecting another sample from the signal every time it changes direction. If we know we are sampling a sine wave, then from this set of points we can reconstruct the intervening continuous signal segments by fitting a sine wave to the points. Thus, by sampling an analog signal at or above the Nyquist rate, we lose no information—the entire original continuous signal can be reconstructed from the sampled points alone.

The sampling theorem in principle means we lose nothing in moving from a continuous to a digital environment. However, there is a practical issue—what if f_0 is so high that we still end up with an unmanageably large number of data points when we satisfy the sampling theorem? Unfortunately, we cannot drop the sampling rate below $2f_0$ and hope to merely sacrifice some detail in the retained samples. The high frequencies in the analog signal do not simply disappear—they turn up in the digitized data but at wrong (much lower) frequencies! This is a particularly insidious problem known as *aliasing*, and experimenters must always be careful to avoid it, especially if the power spectra of the collected data are of interest. Aliasing can lead to completely erroneous spectral characterization of a signal and at the very least degrades the signal-to-noise ratio of a measurement. Figure 54-9 shows how aliasing occurs; a sine wave is sampled at a frequency below the Nyquist rate to yield a set of points that look as if they represent a different sine wave of a much lower frequency. Obviously, aliasing can be avoided by sampling at or above the Nyquist rate. However, in practice it is usually necessary to force the analog signal to be band limited to some manageable f_0. This is done by passing the signal through a high-quality low-pass electronic filter before it is digitized. Such filters are known as *antialiasing filters*. It is important to remember that filtering for antialiasing must be done prior to digitization of the signal. Once aliasing occurs, no amount of digital filtering after the fact can fix the problem.

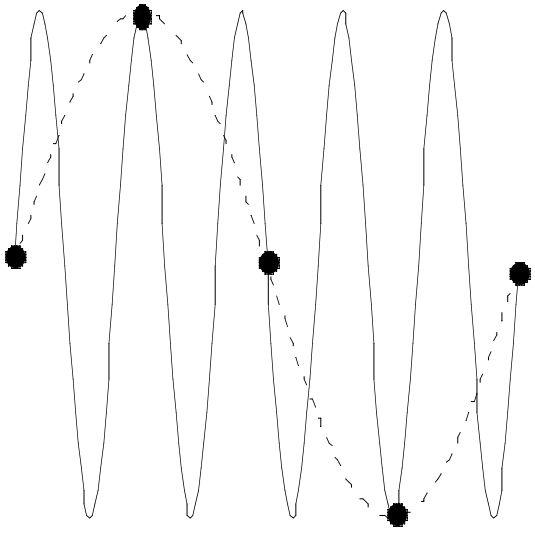

FIGURE 54-9 A sine wave (*solid line*) is sampled (*dots*) below the Nyquist rate, yielding a set of data points defining a different sine wave (*dashed line*) at a lower frequency.

MEASUREMENT OF RESPIRATORY SIGNALS

Having established the general considerations for measuring signals in the laboratory, we now move on to consider those signals specific to the study of mechanical lung function.

PRESSURE

The measurement of pressure is central to the study of respiratory physiology because it is pressure that generates the flow of gas needed to ventilate the lungs.

Pressure Transducers Pressure transduction is based on the graded deformation of some mechanical element whose altered configuration is read by some electronic means (Figure 54-10). Until about 15 years ago, the mainstay of pressure measurement in the respiratory physiology laboratory was the *variable reluctance transducer* in which a thin metal disk is placed between the primary and secondary coils of a transformer excited by several kHz of alternating electric current. A pressure difference either side of the disk causes it to deform in a way that alters the magnetic flux linkage between the transformer coils, thereby changing the induced voltage in the secondary coil. The change in voltage is then transformed into a DC voltage proportional to the pressure difference. These transducers are sensitive and accurate. They also typically have a frequency response that is flat to 20 Hz or more, depending on the length of the tubing connecting its ports to the sites of pressure measurement.[1] However, they are somewhat cumbersome and can be damaged by over pressurization.

In recent years, respiratory pressure measurement has been taken over by the piezoresistive transducer,[2] in which the pressure-sensitive element changes its electrical resistance as it deforms. If a constant voltage (or current) is passed through the piezoresistive element when it is configured to be one of the four arms of a suitably balanced Wheatstone bridge, the voltage across the bridge is then proportional to the change in the element's resistance. A medium-gain amplifier followed by an antialiasing filter are the only remaining elements required to produce an electrical signal proportional to pressure that is ready for digitization. When piezoresistive pressure transducers were first used in respiratory physiology in the 1980s, they tended to suffer from baseline drift, were affected by orientation and temperature, and were not very sensitive. These problems have now been essentially overcome allowing piezoresistive transducers to be exploited for their several advantages. These include an extremely high-frequency response (typically flat to several hundred Hz), robustness (they can be pressurized to many times their nominal full-scale range without damage), and the fact that they can be manufactured using solid-state technology to be very small and light. Piezoresistive transducers are also much cheaper than their variable reluctance counterparts and require simpler electronic signal conditioning circuitry.

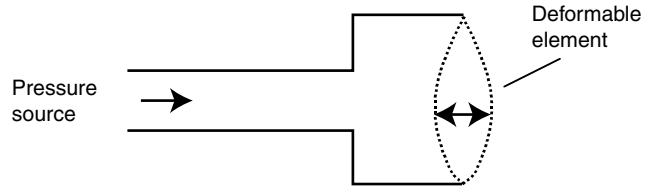

FIGURE 54-10 Pressure transducer. The application of a pressure deforms an element whose configuration is converted into an electrical signal proportional to the degree of deformation.

Measuring Pressure at the Airway Opening The assessment of pulmonary function frequently requires that the pressure in a flowing stream of gas be measured, such as at the entrance to the endotracheal tube in a mechanically ventilated patient. Gas always flows down a pressure gradient, so at each point along the stream of flowing gas there is a driving pressure pushing the gas downstream of it. The goal is to determine this driving pressure. The easiest way is to insert a perpendicular tap into the tube and connect it to a pressure transducer (Figure 54-11). This provides what is known as lateral pressure (P_{lat}), and it corresponds to the pressure exerted perpendicular to the direction of flow as the gas moves past the point of measurement. It turns out, however, that P_{lat} is less than the pressure driving the gas along the tube because of a phenomenon known as the Bernoulli effect, which occurs because of the principle of conservation of energy; the faster gas is moving along the tube, and consequently the larger its kinetic energy, the more it loses in potential energy, manifest as a drop in P_{lat}. P_{lat} underestimates true driving pressure, in a tube of cross-sectional area A with flow $\dot{V}$, by an amount ΔP_b given by the formula

$$\Delta Pb = \frac{\beta \rho \dot{V}^2}{2A^2} \qquad (54\text{-}2)$$

where ρ is the density of the gas and β is a factor determined by the flow velocity profile. For example, if the profile is flat (the linear velocity of the gas molecules is the same at every point in the tube cross section) then $\beta = 1$ and $\beta = 2$ if the profile is parabolic.

If the gas in the tube were stationary, then P_{lat} would equal driving pressure, a condition that can always be achieved by connecting a pressure transducer to a small tube

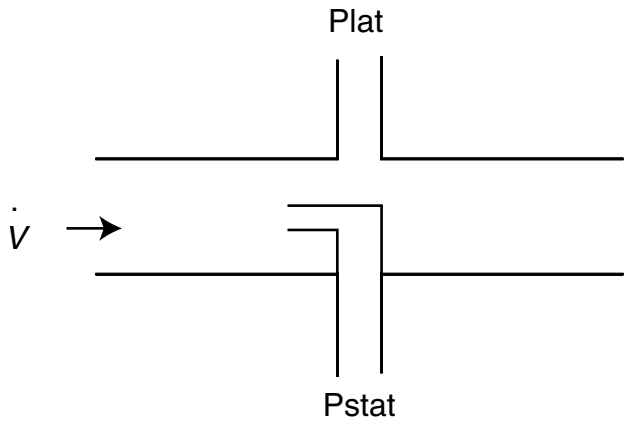

FIGURE 54-11 Lateral pressure (P_{lat}) measured through a lateral tap, and static pressure (P_{stat}) measured with a Pitot tube.

that enters the flow stream laterally and then bends until its open end faces directly into the oncoming flow (see Figure 54-11). Such a device, called a Pitot tube, measures the static pressure (P_{stat}) in a small parcel of gas that has been brought to rest by abutting up against the tube opening. ΔP_b is the difference between P_{stat} and P_{lat}. That is,

$$P_{lat} = P_{stat} - \Delta P_b \quad (54\text{-}3)$$

The problem for respiratory pressure measurement caused by the Bernoulli effect is apparent from Equation 54-2, which shows that ΔP_b depends on the square of flow divided by cross-sectional area. When the area is large enough, ΔP_b is negligible. However, as the area decreases there comes a point at which ΔP_b starts to become important, compared with P_{stat}. Indeed, Equation 54-3 shows that for small tube areas P_{lat} may even become negative. Thus, it is important in any application in which lateral pressures are measured to be sure that the Bernoulli effect is not significantly affecting the measurement of the desired quantity, namely driving pressure.[3] The Bernoulli effect may also be an important factor influencing the measurement of pressures at the distal end of an endotracheal tube in an intubated patient.[4]

Esophageal and Gastric Pressures Two other pressures of great practical importance in the study of respiratory physiology are those in the esophagus and stomach. Esophageal pressure (P_{es}) is a useful surrogate for pleural pressure, the esophageal lumen being separated from the pleural space by only soft tissue. Gastric pressure (P_{ga}) measures the pressure exerted on the diaphragm by the abdominal contents, which is important for understanding active expiration. The difference between P_{es} and P_{ga} is the pressure across the diaphragm, which is important in studies of respiratory muscle function.[5]

Both P_{es} and P_{ga} can be measured using a balloon-tipped catheter (Figure 54-12). A thin-walled latex balloon, a few centimeters in length, is sealed over a thin plastic catheter, typically about 100 cm long. The balloon is passed into the esophagus, usually via the nose. Once in place in either the esophagus or stomach, a small volume of air is injected into the balloon and a pressure transducer is connected to the proximal end of the catheter. The volume of air in the balloon must be sufficient to prevent the walls of the balloon from occluding all the multiple holes in the end of the catheter, but not so much that there is tension in the balloon walls. The correct placement of the balloon is gauged from the nature of the recorded pressure signals. When the balloon is in the stomach, spontaneous inspiration produces a positive deflection in the recorded P_{ga}. As the balloon is withdrawn and enters the esophagus, the inspiratory pressure swings will suddenly become negative. At this point, when inspiratory efforts are made against an occluded airway (the so-called occlusion test), the deflections in P_{es} should match those in pressure measured at the airway opening (P_{ao}). Thus, a regression of P_{es} versus P_{ao} should yield a slope of unity.[6] In practice, slopes that differ from 1.0 by up to 10% are common. Although the occlusion test requires that the subject be able to breathe spontaneously, it has been shown that the esophageal balloon also works well during paralysis.[7] The frequency response of the esophageal balloon is obviously somewhat compromised by the fact that pressure changes in the esophageal lumen must be transmitted through the air inside a long thin catheter to a pressure transducer some distance away. However, a reasonably good response to 30 Hz has been observed.[8] P_{es} has also been measured using catheter-tip piezoresistive transducers, which have been shown to perform well[9] and have a much better frequency response than balloon catheter systems. In small animals, P_{es} can be measured using a water-filled catheter.[10]

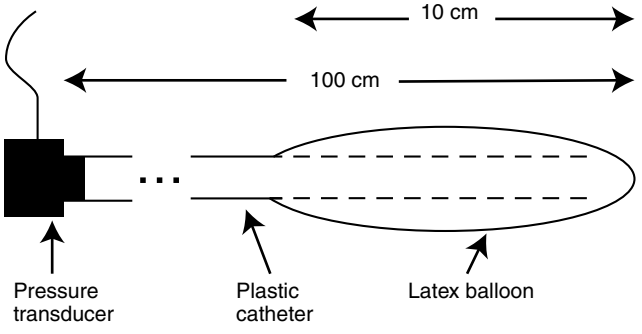

FIGURE 54-12 An esophageal balloon catheter. Note the multiple holes in the walls of the catheter inside the balloon.

Alveolar Pressure In experimental animals it is possible to measure alveolar pressure directly using a technique known as the alveolar capsule.[11] The chest is opened and retracted to expose the pleural surface of the lung to which a small plastic capsule is fixed (Figure 54-13). The capsule has a cylindrical chamber leading down to a small window on the pleural surface encircled by a flange. If the pleural surface is first swabbed with alcohol and dried, the flange can be secured to it with cyanoacrylate glue. Small puncture holes are then made in the pleural surface within the capsule window. If the holes are made carefully to a depth of 1 to

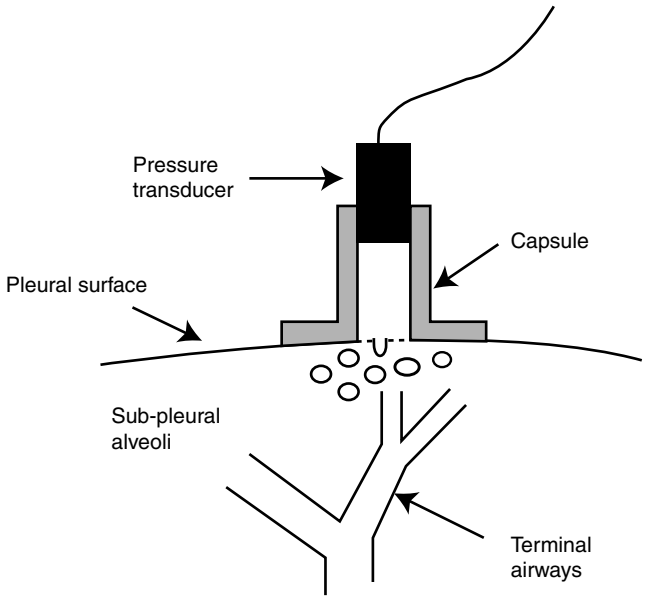

FIGURE 54-13 The alveolar capsule.

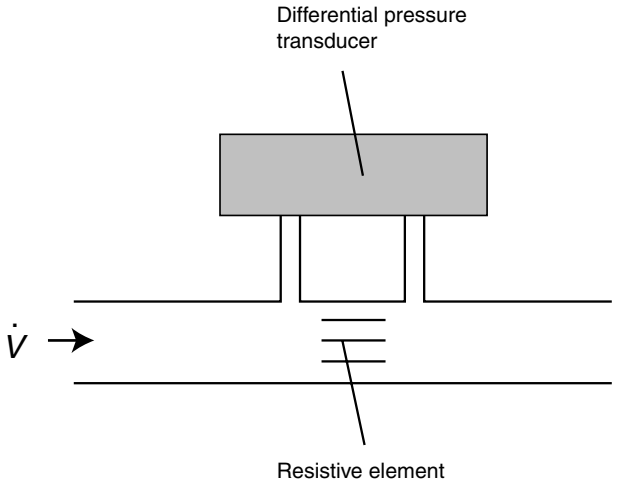

FIGURE 54-14 The pneumotachograph.

2 mm, preferably with a cautery needle, bleeding is minimal and the subpleural alveoli are brought into contact with the capsule chamber. A small piezoresistive pressure transducer can then be lodged in the chamber to give a direct recording of subpleural pressure. In large animals, such as dogs, several alveolar capsules can be installed at different sites over the lung surface.[12–14] A single alveolar capsule can even be used in an animal as small as a mouse.[15]

Flow

Pneumotachographs The mainstay of flow measurement in respiratory physiology is the pneumotachograph, which is a calibrated resistance (R) across which a differential pressure is measured (Figure 54-14). When gas flows through the pneumotachograph, there is a pressure drop (ΔP) from the upstream side of the resistance to the downstream side that increases as flow ($\dot{V}$) increases, thus

$$\Delta P = R\dot{V} \tag{54-4}$$

If R is independent of $\dot{V}$ over the range of flows of interest then the pneumotachograph is said to be linear. Manufacturers strive for linearity and always quote the linear range of a pneumotachograph. However, if the device is nonlinear, so that R depends on $\dot{V}$, it is a simple matter to invert Equation 54-4 on a computer and calculate $\dot{V}$ from a measurement of ΔP, provided that the relationship of R to $\dot{V}$ is known.

The frequency response of a pneumotachograph depends on the construction of its resistive element. Some consist of a honeycomb arrangement of conduits, whereas others consist of a wire screen. The honeycomb type is less likely to become partially blocked by secretions but has a poorer frequency response than the screen type. Either type should be heated to above body temperature during prolonged use to avoid breath condensate from settling on the resistive element and changing its resistance (and hence altering the calibration of the device). Pneumotachographs can have a good frequency response above 20 Hz with a resonance occurring at around 70 Hz, provided that the associated differential transducer has a response at least that good and is connected with the shortest possible lengths of tubing.[1] The frequency response of a pneumotachograph degrades rapidly as the tubing connecting the transducer to the lateral taps either side of the resistance element increases in length. Inadequate frequency response can be corrected for to a significant extent by digital compensation, giving an effectively flat frequency response to more than 100 Hz.[16]

Another consideration for pneumotachographs concerns their dynamic common-mode rejection characteristics. If the two ports of the pneumotachograph are both subjected to the same change in pressure, ideally the device should register a flow of zero. This is not always the case, however, particularly if the physical dimensions of the two ports are different and if the input impedance of the pressure transducer is not very large compared with that of the system under investigation when flow oscillates at a high frequency. Digital compensation methods can improve the situation to a certain extent.[17] Poor dynamic common-mode rejection is a significant problem for pneumotachographs used with very small animals.[18]

Other Devices for Measuring Flow Although the resistive pneumotachograph is the mainstay for measuring flow in respiratory applications, other devices have been used. For example, ultrasonic transducers based on differences in time-of-flight of sound propagating into the direction flow versus away from it have an excellent frequency response and avoid the problems of a resistive element becoming clogged with secretions.[19] Devices based on the rate of cooling of a heated wire are also in use.[20]

Volume

Direct Measurement of Volume The volume of gas entering the lungs can be measured directly with a spirometer attached to the mouth or from the pressure or flows emanating from a whole body plethysmograph when the subject breathes through a conduit connected to outside the plethysmograph. A more convenient but less accurate plethysmographic method is provided by the changes in trunk volume assessed with an inductance plethysmograph.[21] Recently, a more accurate but expensive optical plethymograph has been developed that allows the detailed measurement of thoracic movement during breathing.[22] However, for many applications requiring the assessment of lung function, the easiest way to assess changes in lung volume is to integrate the flow measured at the mouth with a pneumotachograph.

Integration of Flow Before the advent of the modern laboratory digital computer, integration was typically achieved in real time using an electronic circuit based on the charging of a capacitor. Nowadays, integration is performed digitally on a computer. The digitized flow signal consists of a series of data points $\{\dot{V}_1, \dot{V}_2, \dot{V}_3, \cdots\}$ separated by equal time intervals Δt. A simple formula for numerical integration is the trapezoidal rule, which involves approximating the area under a section of a curve by a trapezoid. This means approximating the curve between $\dot{V}_1$ and $\dot{V}_2$ by a straight line (Figure 54-15) and calculating the area ΔA under it as

$$\Delta A \approx \frac{\dot{V}_1 + \dot{V}_2}{2}\,\Delta t \tag{54-5}$$

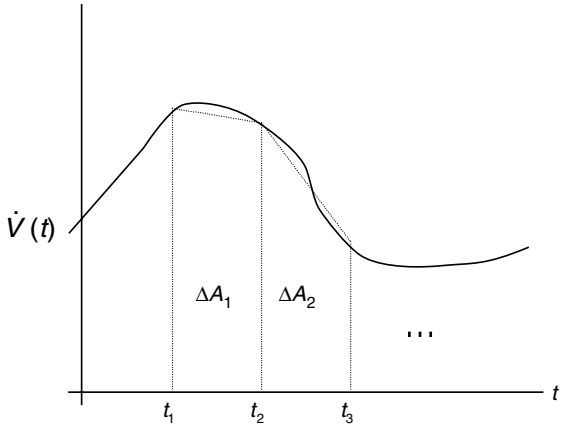

FIGURE 54-15 Trapezoidal integration of flow involves connecting each sampled flow value by straight line and summing the areas under each trapezoid.

The area A under a section of curve is then simply the sum of all the individual ΔAs, thus

$$A \approx \sum_{i=1}^{n} \Delta A_i = \left(\frac{\dot{V}_1}{2} + \dot{V}_2 + \dot{V}_3 + \cdots + \dot{V}_{n-1} + \frac{\dot{V}_n}{2} \right) \Delta t \quad (54\text{-}6)$$

There are other more accurate, and more complicated, numerical integration schemes. However, the key thing is that Δt should be small enough so that the errors involved in approximating the true curve between points is negligible. This can be tested for by integrating the data using progressively smaller values for Δt, until the results do not change.

MEASUREMENT OF LUNG FUNCTION

Now that a set of respiratory data has been collected and stored on a computer, as described above, we are faced with the task of having to interpret it. How this is done depends very much on the nature of the data collected. In most cases, however, the assessment of lung function from respiratory data is based on some model idealization of the real system under study. The model is only useful if it behaves like the real system to a satisfactory degree. It is therefore crucial to understand what model is being invoked whenever lung function is being assessed so that the suitability of the model can be evaluated. In most applications, the model concerned is very simple, typically involving only a single compartment. In some cases, the model may be very complicated with multiple alveolar compartments and airway branches represented. Regardless of the level of model complexity, however, it is crucial that any investigation of mechanical lung function begin with an understanding of the mathematical model being invoked.

Forced Expired Flow

Having just expounded on the importance of models in the analysis of lung function data, it turns out that the traditional mainstay of clinical pulmonary function testing, the forced expiration, yields quantities that are usually treated as purely empirical. The forced vital capacity (FVC) and the forced expiratory volume in 1 second (FEV_1) are widely used either individually or as a ratio to diagnose a variety of common lung pathologies. The great advantage of the forced expiration is that it can be performed easily in an outpatient setting, requiring nothing more than a device for measuring flow (or volume) and some cooperation from the subject. The measuring device must be able to measure flows of greater than 10 $L.s^{-1}$ with a frequency response that captures the rapid onset of flow at the start of a maximal forced expiration beginning from total lung capacity. There are commercially available systems designed specifically for this task, either by direct spirometric measurement of exhaled volume or by pneumotachograph measurement of flow.

The clinical utility of forced expired flows arises from the phenomenon of flow limitation, whereby exhaled flow reaches a maximum value independent of further increases in expiratory muscle activity. Subjects with normal muscle function can reach this limiting flow over most of the vital capacity range. The limiting flow is reduced in obstructive lung disease, and the relationship of flow to exhaled volume assumes shapes that are characteristic of various lung pathologies. Detailed accounts of the flow-volume curve and its relation to pulmonary disease can be found in standard texts.[23] Unfortunately, the underlying mechanical mechanisms in the lung responsible for producing the flow-volume loop are complex and nonlinear, so parameters such as FVC and FEV_1 are not easily related to a model of the respiratory system. Consequently, making the link between function and lung structure from forced expired flows has not been straightforward. In other words, although parameters such FVC and FEV_1 are sensitive to both obstructive and restrictive lung disease, it is unclear how to deduce the site or nature of an abnormality from the values of these parameters, although some sophisticated computer modeling studies have attempted to elucidate the relationships between the forced expired flow-volume loop and the physical properties of the lungs.[24] Nevertheless, the convenience of measuring forced expired flows and their diagnostic utility make this technique the most clinically important of all lung function measurements.

Methods Based on the Single-Compartment Model

The model of respiratory or pulmonary mechanics most frequently employed as the basis for lung function measurements is that of a single elastic compartment served by a single flow-resistive airway (Figure 54-16). This model assumes that the lungs are homogeneously ventilated and that all alveolar pressures are equal to each other at all times.

Plethysmography Whole-body plethysmography complements the measurement of forced expired flows as the other major methodology for measuring lung function in current clinical use. Plethysmography is used to measure two important parameters of lung function, thoracic gas volume (TGV) and airway resistance (R_{aw}), both under the assumption of the single-compartment linear model. The

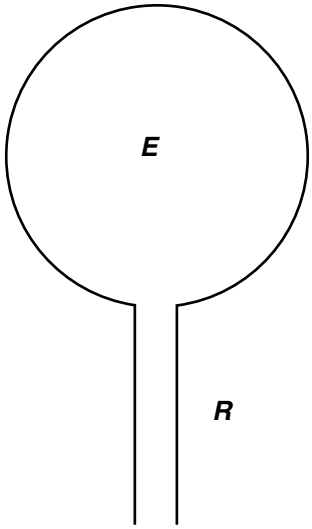

FIGURE 54-16 The single-compartment model of the respiratory system. *R* is resistance and *E* is elastance (see Equation 54-8).

calculation of TGV and R_{aw} using a body plethysmograph is covered in numerous other articles and books[23] and so is described only briefly here.

TGV is measured first by having the subject make breathing efforts against a closed airway while the change in airway opening pressure (ΔP_{ao}) is measured (Figure 54-17A). At the same time, the pressure in the plethysmograph or the flow leaving it (depending on whether it is a pressure or flow box) provides a measure of changes in total body volume (ΔV). Assuming that the only compressive part of the body is the gas in the lungs, ΔV is equal to the compression of the thoracic gas. Applying Boyle's law gives

$$\frac{\Delta P_{ao}}{1000} = \frac{-\Delta V}{TGV} \qquad (54\text{-}7)$$

where we have equated 1 atmosphere to 1,000 cm H_2O in the denominator on the left side of Equation 54-7, which can be rearranged to give a measure of TGV.

Next, this measurement of TGV is used to estimate R_{aw} by having the subject pant while completely enclosed inside the plethysmograph. Flow ($\dot{V}$) is measured at the subject's mouth with a pneumotachograph while pressure (P_{box}) inside the plethysmograph is measured (Figure 54-17B). P_{box} varies because of two factors. One of these is that gas inspired from the plethysmograph becomes humidified and heated to body temperature, thereby increasing in volume. This increases the combined volume of the remaining plethysmographic gas and the subject's body and so compresses the plethysmographic gas. The other factor is that a negative pressure in the thorax is required for inspiration and the converse for expiration. This results in compressive volume changes in the thoracic gas that are again manifest as changes in the combined volume of plethysmographic gas and subject. To the extent that the first source of changes in P_{box} can be ignored, the changes in P_{box} can be equated to compressive changes in thoracic gas volume, which can then be used, again via Boyle's law, to infer the changes in alveolar pressure (P_{alv}). The difference between P_{alv} and P_{ao} divided by $\dot{V}$ then yields a measure of R_{aw}.

The plethysmographic measurement of TGV and R_{aw} assumes that the lungs are a homogeneously ventilated (ie, effectively single-compartment) system. This works well in normal lungs but may not in severely diseased lungs in which obstructed airways can lead to marked differences between P_{alv} and P_{ao} when panting against a closed airway.[25]

An unrestrained version of plethysmography has been used in an attempt to assess lung function in infants[26] and small animals.[27] This technique involves merely measuring variations in P_{ao} as the subject breathes while inside the box. Although these pressure swings arguably give information about the pattern of breathing,[28] they cannot provide meaningful information about respiratory mechanical function,[29] despite recent claims to the contrary.[30,31]

Resistance and Elastance The single-compartment model of respiratory mechanics (see Figure 54-16) is described by a simple and extremely useful mathematical equation if it is linear. If the resistive pressure drop between one end of the airway and the other is considered to be proportional to the flow of gas ($\dot{V}$) through it, then the constant of proportionality (*R*) is termed *resistance*. Similarly, the elastic recoil pressure inside the compartment is taken as

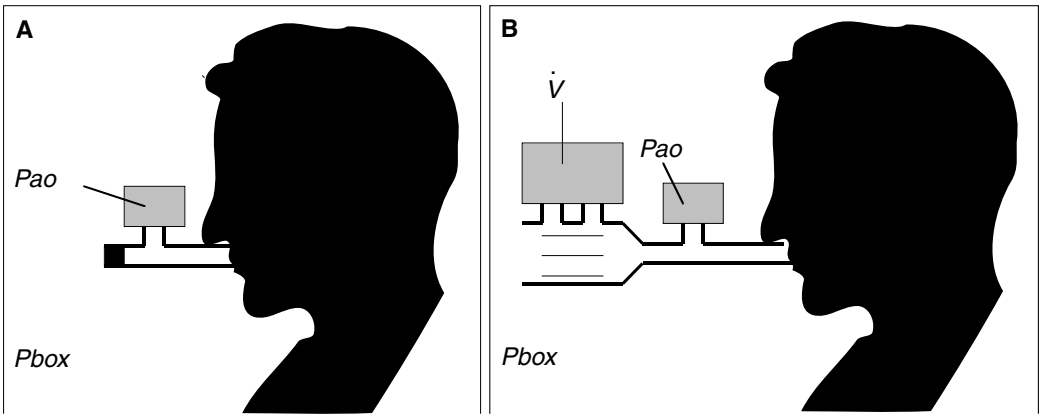

FIGURE 54-17 Body plethysmograph used to measure *A*, TGV and *B*, R_{aw}. P_{ao} is airway opening pressure, P_{box} is pressure inside the plethysmograph, and $\dot{V}$ is mouth flow.

proportional to the volume of the compartment above some elastic equilibrium volume, with its constant of proportionality (E) termed *elastance*. Finally, we must account for the possibility that the pressure (P) applied across the model (from the entrance to the airway through to the outside of the elastic compartment) has some finite value P_0 when $\dot{V}$ and V are both zero. Simple addition of pressures shows that P is the sum of the resistive and elastic pressures, thus,

$$P(t) = R\dot{V}(t) + EV(t) + P_0 \qquad (54\text{-}8)$$

where we have written the variables $P, \dot{V}$, and V explicitly as functions of time (t) to remind us that they all vary during breathing.

Equation 54-8 is used in respiratory investigations to estimate R, E, and P_0 via multiple linear regression. This provides those values of P, $\dot{V}$, and V that, when used in the right side of Equation 54-8, provide the closest approximation to the measured P in the left side. "Closest" here means in the least squares sense, which means that the sum of the squared differences between the measured value of P and the model values is minimal. R and E are taken as measures of the resistance and elastance of the lung or respiratory system, which in a sense they are. Strictly speaking, however, R and E are nothing more than the parameters of a simple model (see Figure 54-16) that has been forced to match the measured signals as well as possible. The usefulness of R and E as reflections of physiology thus lies in the degree to which the single-compartment linear model accurately describes the behavior of the system under study. In many cases, this accuracy is acceptable, such as the example shown in Figure 54-18 of a patient with chronic obstructive lung disease being mechanically ventilated in the intensive care unit.

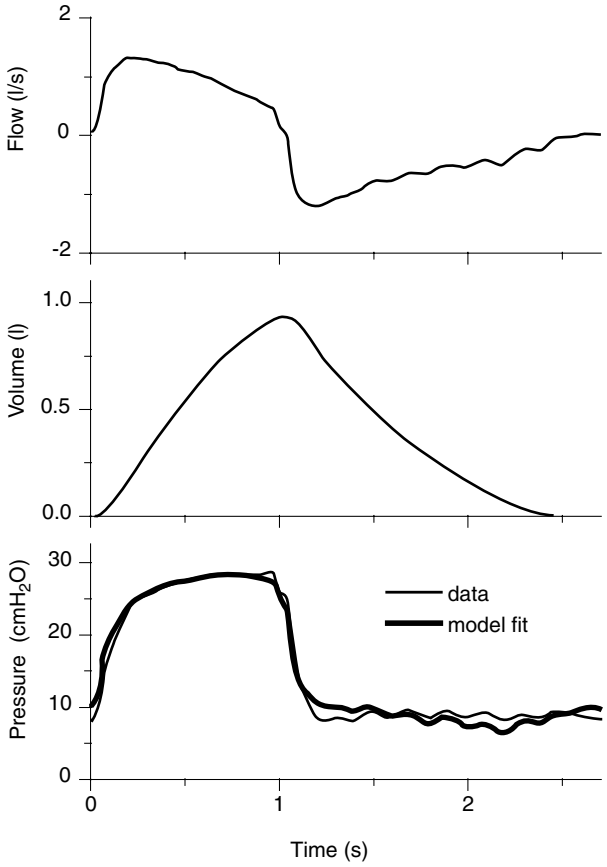

FIGURE 54-18 Example of pressure, flow, and volume data over a single breath from a mechanical ventilated patient in the intensive care unit. The *lower panel* also shows the fit to pressure produced by Equation 54-8.

When the single-compartment linear model does describe a set of respiratory data to an acceptable degree of accuracy, one is then faced with the task of assigning a physiologic interpretation to the values of R and E it provides. It might seem obvious, for example, that R would correspond to the flow resistance of the airway tree. However, this turns out not to be the case, at least not entirely. Studies with the alveolar capsule in dogs and other animals have allowed total lung resistance (ie, R) to be partitioned into airway resistance and tissue resistance.[11,32] The latter has been shown to depend greatly on the frequency at which the lungs are oscillated and, at normal breathing frequencies, may constitute the great majority of R.[13] It is not until frequency gets well above the range of normal breathing (above about 2 Hz) that the tissue component of R decreases to the point where R is a good reflection of airway resistance alone.[33–35] In the intact animal, R also contains a significant contribution from the chest wall.[36]

Nonlinear Single-Compartment Models There are situations in which the single-compartment linear model does not describe a set of respiratory data with acceptable accuracy. The model must then be replaced by a more realistic (and invariably more complex) model. An example typically occurs when the volume excursions of the lungs become large or when the stiffness of the lung tissue increases in certain diseases. In this case, one often finds that the dynamic elastic behavior of the tissues is significantly better described by a curvilinear function of volume rather than a straight line, as in the linear model. For example, it has been shown in both humans[37] and animals[38] that a nonlinear model with the equation

$$P(t) = R\dot{V}(t) + E_1V(t) + E_2V^2(t) + P_0 \qquad (54\text{-}9)$$

sometimes fits the data significantly better than the linear model above (see Equation 54-8). The nonlinear model is structurally the same as the linear model in that it still has only a single compartment being ventilated through a single airway. The difference is that the elastic properties of the tissues surrounding the compartment are nonlinear. Similarly, the linear resistance term in Equation 54-8 can be replaced by two terms representing a flow-dependent resistance as originally proposed by Rohrer.[38] Which of these models should be used to describe a given set of respiratory data can be decided using, for example, the F-ratio test applied to the mean squared differences between measured P and P predicted by the various models.[38]

Another use of the single-compartment model of respiratory mechanics arises when the stiffness of the lung or respiratory system is assessed from the quasistatic pressure-volume (P-V) curve. The P-V curve is obtained by inflating

and deflating the lungs, either continuously or in steps, slowly enough that the resistive pressure drop across the airways can be neglected. The result is a relationship that embodies the elastic properties of the pulmonary or respiratory tissues, viewed as a single compartment. The model invoked to account for the P-V curve is thus again a single-compartment model, but now it is nonlinear because the elastic recoil pressure inside the compartment increases disproportionately as volume approaches total lung capacity. A commonly used equation for describing the descending limb of the P-V curve is the exponential expression[39]

$$V = A - Be^{-KP} \qquad (54\text{-}10)$$

where A, B, and K are constants chosen to make the right side of the equation match the left side as closely as possible.

The ascending limb of the P-V curve lies to the right of the descending limb (Figure 54-19), reflecting a phenomenon known as *hysteresis*. The amount of hysteresis depends on the volume range over which V is cycled and is caused by a number of factors. One of the most important is recruitment of closed airspaces during inspiration that remain open during expiration. Hysteresis may become markedly enhanced in pathologies such as acute lung injury.[40]

Methods Based on Multicompartment Models

The single-compartment linear model (see above) generally describes respiratory pressure-flow data well when volume excursions are modest and the volume oscillations are concentrated around a single frequency, such as pertains, for example, during normal breathing or mechanical ventilation. However, the values of R and E obtained using this model vary with frequency. In particular, R decreases markedly as frequency is increased over the range of normal breathing, whereas E correspondingly increases. The main reason for this frequency dependence of R and E in normal lungs is the fact that the respiratory tissues are *viscoelastic*, that is, they exert a recoil pressure that is a function not only of volume but also of volume history.[41] In diseased lungs, additional variation of R and E with frequency may be caused by regional variations in mechanical function throughout the lung, leading to transient redistribution of gas as the lungs are dynamically inflated and deflated.[42,43] In any case, the single-compartment linear model no longer suffices as a description of pulmonary or respiratory mechanics when multiple frequencies are involved. Instead, we need to invoke models featuring two or more compartments to account for regional differences in mechanical function throughout the lung.[44]

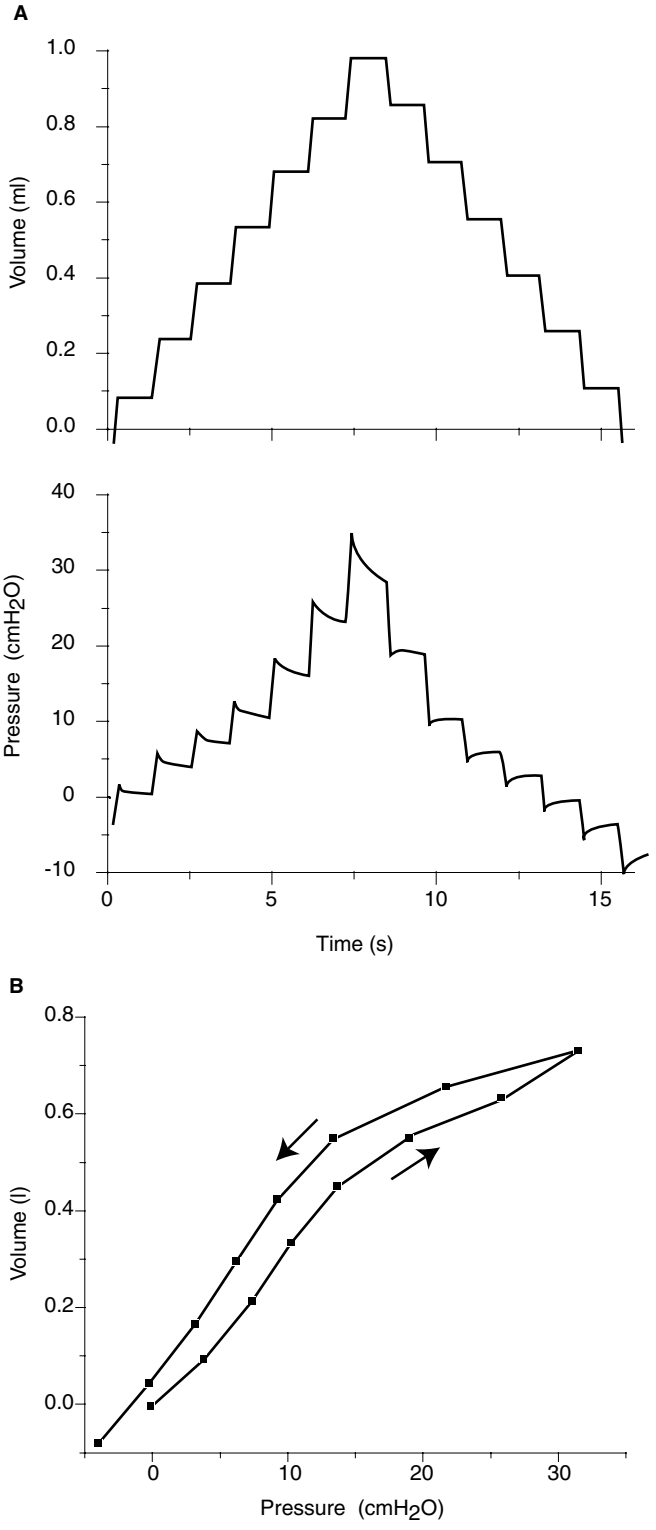

FIGURE 54-19 *A*, Pressure and volume data obtained from a mouse during stepwise inflation and deflation of the lungs. *B*, Ascending and descending limbs of the quasistatic pressure-volume (*P-V*) curve derived from the plateaus of the data in Figure 54-19A.

Interrupter Technique A technique for assessing lung function that was first introduced nearly a century ago involves the rapid interruption of airflow at the airway opening, while pressure just behind the point of interruption is measured. Initially, it was thought that this maneuver would simply obliterate any resistive pressure drop across the airways, so that the observed sudden change in pressure would reflect R_{aw}. However, work over the past two decades has shown that the sudden change in pressure occurring with interruption of flow is accompanied by some rapid damped oscillations and a subsequent further transient change in pressure to a stable plateau (Figure 54-20). The oscillations are mainly owing to ringing of the gas in the central airways,[45] whereas the secondary slow pressure change is due

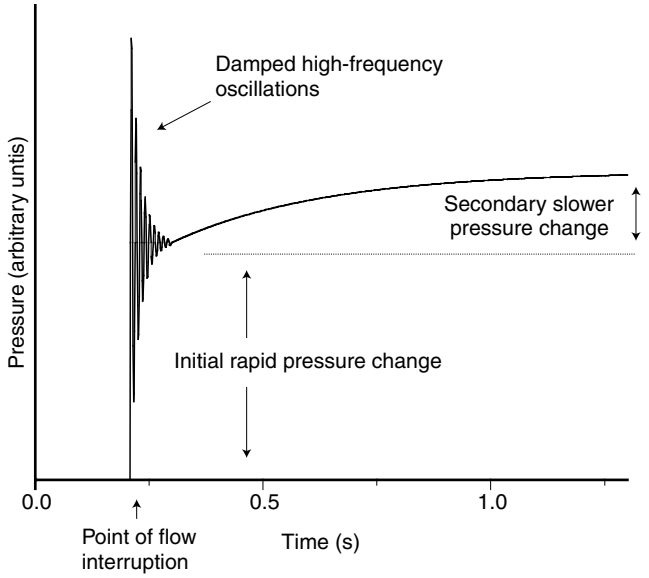

FIGURE 54-20 Schematic representation of airway opening pressure recorded during interruption of expiratory flow. An initial almost instantaneous jump in pressure is accompanied by rapid damped oscillations, which are followed by a slower further pressure change.

to the viscoelastic properties of the respiratory tissues when the lung is normal[12] and may be accentuated by gas redistribution in pathologic situations.[46] Interpreting the initial rapid and secondary slower pressure changes has been done on the basis of two-compartment models of respiratory mechanics.[44,47,48]

The interrupter technique is currently gaining interest among pediatricians,[49] who face a particular challenge in trying to assess lung function in young children and infants unable to perform the voluntary maneuvers necessary to generate forced expired flows. However, the interruption of flow is merely a specialized kind of flow perturbation. Understanding the information obtained by applying general flow perturbations to the lungs is best done in the context of the forced oscillation technique and impedance.

Input Impedance The frequency dependence of R and E has led respiratory researchers to move to a more global assessment of mechanics based on a quantity known as input impedance (Z_{in}). Z_{in} can be determined over a range of frequencies by subjecting the lungs to an oscillatory $\dot{V}$ signal that contains multiple frequencies. Z_{in} is then determined by taking the ratio of the Fourier transform of P to the Fourier transform of $\dot{V}$. This yields a complex function of frequency

$$Z_{in}(f) = R(f) + iX(f) \tag{54-11}$$

with a real part $R(f)$ and an imaginary part $X(f)$, where $i = \sqrt{-1}$. The value of R at each value of f is equal to the resistance of an equivalent single-compartment linear model, so the $R(f)$ is called the resistance. $X(f)$ is called the reactance and at each f is related to the elastance of the equivalent single-compartment model by

$$X(f) = \frac{-E(f)}{2\pi f} \tag{54-12}$$

Z_{in} is thus nothing more than a description of how R and E vary over a range of frequencies. Z_{in} still requires that the system under study be linear. This assumes that whatever values of R and E are obtained at a particular frequency, their values do not depend on the amplitudes of the $P, \dot{V}$, and V signals used to measure them (which, of course, is never precisely the case in practice).

Forced Oscillation Technique The measurement of Z_{in} is achieved by the so-called forced oscillation technique in which a flow generator (such as a loudspeaker or piston pump) is used to drive an oscillatory flow into the lungs via the airway opening.[50] The frequency range over which the signal oscillates determines the kind of information that will be obtained about respiratory mechanical function. At frequencies below about 2 Hz, much of Z_{in} is determined by the rheologic properties of the tissues, as well as regional mechanical heterogeneities throughout the lung should they exist. Regional heterogeneities can affect the shape of Z_{in} above 2 Hz as well.[42,43] At frequencies of hundreds of Hz one obtains information about the acoustic characteristics of the airways.[51]

Whatever the frequency range, the interpretation of Z_{in} in physiologic terms requires some kind of model of the system under investigation. For example, normal respiratory or pulmonary Z_{in} is described very accurately below about 20 Hz by a model consisting of a uniformly ventilated compartment surrounded by viscoelastic tissue. The compartment is served by a single airway having a newtonian resistance R_N, whereas the viscoelastic tissue has an impedance with real and imaginary parts that both decrease hyperbolically with f. The equation for the impedance of this construct, which is frequently referred to as the constant-phase model, is[35]

$$Z_{in}(f) = R_N + i2\pi fI + \frac{G_{ti} - iH_{ti}}{(2\pi f)^{\alpha}} \tag{54-13}$$

where the parameter α is related to the two tissue parameters via the relation

$$\alpha = \frac{2}{\pi} \tan^{-1} \frac{H_{ti}}{G_{ti}} \tag{54-14}$$

G_{ti} characterizes the viscous dissipation of energy in the tissues and so is related (but not equivalent to) tissue resistance. H_{ti} characterizes the storage of elastic energy in the tissues and is closely related to E. I is an inertance reflecting the mass of the gas in the central airways. The four parameters R_N, I, G_{ti}, and H_{ti} together account for the entire frequency spectrum of Z_{in} below 20 Hz in a convenient and compact way. They also allow Z_{in} to be partitioned into a component pertaining to the airways (ie, R_N and I) and a component pertaining to the lung periphery (ie, G_{ti} and H_{ti}). Figure 54-21 shows an example of the fit to Z_{in} provided by Equation 54-13.

Other Respiratory Impedances The calculation of respiratory impedance is not limited to Z_{in} obtained from P and $\dot{V}$ at the airway opening. Any relevant pressure and flow signals will do, although the impedance obtained will

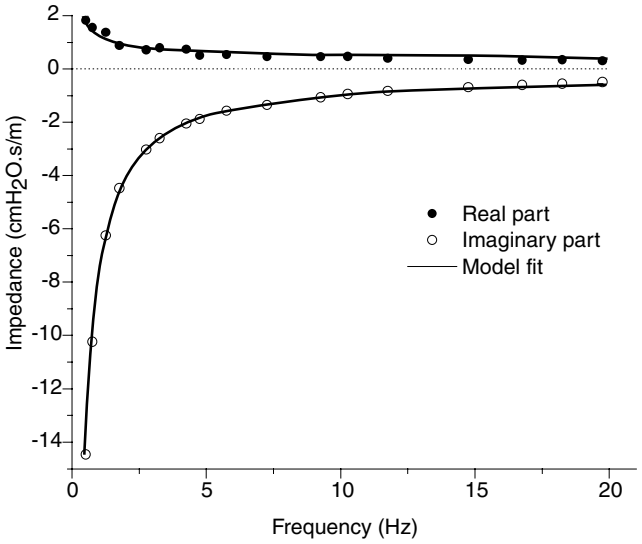

FIGURE 54-21 Fit of constant-phase model (Equation 54-13) to Z_{in} data from a mouse.

be different in each case. For example, if pressure is oscillated around the body surface while flow is measured at the mouth, the impedance obtained is known as transfer impedance (Z_{tr}). Z_{tr} has been used in numerous studies in both animals[52] and humans.[53–55] Although in principle Z_{tr} should give similar information about lung function to Z_{in}, its measurement may be associated with some practical advantages. First, when the distal airways of the lung become significantly constricted, the flow oscillations applied at the mouth to measure Z_{in} may become shunted to a large degree into the central airways that have a finite compliance.[43] If the amount of flow reaching the lungs becomes small to the point that it approaches the noise level of flow measurements at the mouth, then one effectively loses the ability to probe the lung periphery. In contrast, when pressure oscillations are applied at the body surface, flow is driven from the lung periphery toward the trachea, and shunting into the central airway compartment is minimized. This means that all flow measured at the mouth comes from the lung periphery, giving Z_{tr} a signal-to-noise advantage over Z_{in} for the investigation of severely constricted lungs.

Another recently developed variant of respiratory impedance uses the heart as the oscillatory source, producing what has been termed output impedance.[56] When a subject relaxes with an open glottis, the beating heart perturbs the lungs sufficiently to generate a small flow that can be measured at the mouth. When the airway opening is occluded, corresponding pressure oscillations are measured just behind the point of occlusion. The impedance determined from these two signals was found to have an essentially zero imaginary part and a real part that corresponded closely to the resistance of the conducting airways, as measured by Z_{in}.[56]

Yet a further type of respiratory impedance has been obtained by applying forced oscillations in flow to the lungs of dogs through an alveolar capsule.[57] The resulting alveolar input impedance (Z_A) between 26 and 200 Hz was found to be well described by a simple model consisting of a subpleural alveolar compartment connecting to the rest of the lungs by a terminal airway compartment. The magnitude of Z_A was found, on the basis of an anatomically accurate computer model of the dog lung,[58] to correspond to that expected of a single lung acinus. When Z_A was followed during the development of bronchoconstriction, the response of the lung periphery was demonstrated to be extremely heterogeneous both spatially and temporally.[59,60]

The information obtained about lung mechanical function thus depends on the site at which flow perturbations are applied and where pressures and flows are measured. It also depends to a great extent on the nature of the flow perturbations themselves. Measuring lung mechanics during normal breathing in a conscious subject using an esophageal balloon has the advantage of allowing the subject to remain in a reasonably natural state. However, it suffers from the disadvantage that the subject is free to choose the breathing pattern, which may change with an intervention. This itself will affect the measurement of mechanics regardless of any true changes in the intrinsic mechanical properties of the airways or tissues. Thus, one faces a trade-off between minimizing the interventional nature of the measurement and controlling for confounding variables. This situation has been likened to the uncertainty principle of quantum mechanics.[61]

SUMMARY

The quantitative study of respiratory mechanics involves measurement at two levels, namely the measurement of the raw signals that carry the mechanical information and the measurement of key physiologic parameters that embody this information. Measurement of signals requires the use of transducers for recording pressure, flow, and volume and computers for capturing and storing the data. Measurement of physiologic parameters involves matching the measured signals to a suitable mathematical model of respiratory mechanics. There are many decisions to be made in achieving these ends, such as which type of transducer to use, how fast to sample the signals, what resolution of analog-to-digital converter is required, what kind of perturbation should be applied to the respiratory system, and what mathematical model should be invoked to interpret the data. There is no universally correct decision for any of these issues because the appropriate action to be taken depends on the physiologic questions being addressed. These questions, whatever they are, will determine what mathematical model of respiratory mechanics should be invoked, what frequency response characteristics are required of the transducers, what data sampling rate is needed, and so on. It is therefore important for the respiratory scientist to understand the basics of measurement theory as it applies to both the collection of physiologic signals and their interpretation through mathematical models. Such an understanding minimizes the risk, for example, of being misled by measurement artifact from a transducer that is not up to the task required of it or of being confused by the apparently bizarre behavior of a calculated parameter obtained using a model that does not apply to the situation at hand.

REFERENCES

1. Jackson AC, Vinegar A. A technique for measuring frequency response of pressure, volume, and flow transducers. J Appl Physiol 1979;47:462–7.
2. Duvivier C, Rotger M, Felicio da Silva J, et al. Static and dynamic performances of variable reluctance and piezoresistive pressure transducers for forced oscillation measurements. Eur Respir J 1991;1:146–50.
3. Bates JHT, Sly PD, Sato J, et al. Correcting for the Bernoulli effect in lateral pressure measurements. Pediatr Pulmonol 1992;12:251–6.
4. Navalesi P, Hernandez P, Laporta D, et al. Influence of site of tracheal pressure measurement on in situ estimation of endotracheal tube resistance. J Appl Physiol 1994;77:2899–906.
5. Couture JG, Chartrand D, Gagner M, Bellemare F. Diaphragmatic and abdominal muscle activity after endoscopic cholecystectomy. Anesth Analg 1994;78:733–9.
6. Baydur A, Behrakis PK, Zin WA, et al. A simple method for assessing the validity of the esophageal balloon technique. Am Rev Respir Dis 1982;126:788–91.
7. Dechman G, Sato J, Bates JHT. Factors affecting the accuracy of esophageal balloon measurement of pleural pressure in dogs. J Appl Physiol 1992;72:383–8.
8. Peslin R, Navajas D, Rotger M, Farre R. Validity of the esophageal balloon technique at high frequencies. J Appl Physiol 1993;74:1039–44.
9. Panizza JA. Comparison of balloon and transducer catheters for estimating lung elasticity. J Appl Physiol 1992;72:231–5.
10. Wang CG, DiMaria G, Bates JH, et al. Methacholine-induced airway reactivity of inbred rats. J Appl Physiol 1986;61:2180–5.
11. Fredberg JJ, Keefe DH, Glass GM, et al. Alveolar pressure nonhomogeneity during small-amplitude high-frequency oscillation. J Appl Physiol 1984;57:788–800.
12. Bates JH, Ludwig MS, Sly PD, et al. Interrupter resistance elucidated by alveolar pressure measurement in open-chest normal dogs. J Appl Physiol 1988;65:408–14.
13. Ludwig MS, Dreshaj I, Solway J, et al. Partitioning of pulmonary resistance during constriction in the dog: effects of volume history. J Appl Physiol 1987;62:807–15.
14. Ludwig MS, Romero PV, Bates JH. A comparison of the dose-response behavior of canine airways and parenchyma. J Appl Physiol 1989;67:1220–5.
15. Tomioka S, Bates JH, Irvin CG. Airway and tissue mechanics in a murine model of asthma: alveolar capsule vs. forced oscillations. J Appl Physiol 2002;93:263–70.
16. Renzi PE, Giurdanella CA, Jackson AC. Improved frequency response of pneumotachometers by digital compensation. J Appl Physiol 1990;68:382–6.
17. Farre R, Peslin R, Navajas D, et al. Analysis of the dynamic characteristics of pressure transducers for studying respiratory mechanics at high frequencies. Med Biol Eng Comput 1989;27:531–6.
18. Schuessler TF, Maksym GN, Bates JHT. Estimating tracheal flow in small animals. Proceedings of the 15th Annual International Meeting of the I.E.E.E. Engineering in Medicine and Biology Society; 1993 October 28–31; San Diego, California. p. 560–1.
19. Schibler A, Hall GL, Businger F, et al. Measurement of lung volume and ventilation distribution with an ultrasonic flow meter in healthy infants. Eur Respir J 2002;20:912–8.
20. Clary AL, Fouke JM. Fast-responding automated airway temperature probe. Med Biol Eng Comput 1991;29:501–4.
21. Cohen KP, Ladd WM, Beams DM, et al. Comparison of impedance and inductance ventilation sensors on adults during breathing, motion, and simulated airway obstruction. IEEE Trans Biomed Eng 1997;44:555–66.
22. Aliverti A, Dellaca R, Pelosi P, et al. Compartmental analysis of breathing in the supine and prone positions by opto-electronic plethysmography. Ann Biomed Eng 2001; 29:60–70.
23. Gold WM. Pulmonary function testing. In: Murray JF, Nadel JA, editors. Textbook of respiratory medicine. Philadelphia (PA): W.B. Saunders; 2000. p. 781–882.
24. Lambert RK, Wilson TA, Hyatt RE, Rodarte JR. A computational model for expiratory flow. J Appl Physiol 1982;52:44–56.
25. Shore S, Milic-Emili J, Martin JG. Reassessment of body plethysmographic technique for the measurement of thoracic gas volume in asthmatics. Am Rev Respir Dis 1982;126:515–20.
26. Drorbaugh J, Fenn W. A barometric method for measuring ventilation in newborn infants. Pediatrics 1955;16:81–7.
27. Hamelmann E, Schwarze J, Takeda K, et al. Noninvasive measurement of airway responsiveness in allergic mice using barometric plethysmography. Am J Respir Crit Care Med 1997;156:766–75.
28. Epstein RA, Epstein MA, Haddad GG, Mellins RB. Practical implementation of the barometric method for measurement of tidal volume. J Appl Physiol 1980;49:1107–15.
29. Lundblad LK, Irvin CG, Adler A, Bates JH. A reevaluation of the validity of unrestrained plethysmography in mice. J Appl Physiol 2002;93:1198–207.
30. Finotto S, Neurath MF, Glickman JN, et al. Development of spontaneous airway changes consistent with human asthma in mice lacking T-bet. Science 2002;295:336–8.
31. Chong BT, Agrawal DK, Romero FA, Townley RG. Measurement of bronchoconstriction using whole-body plethysmograph: comparison of freely moving versus restrained guinea pigs. J Pharmacol Toxicol Methods 1998;39:163–8.
32. Fredberg JJ, Ingram RH Jr, Castile RG, et al. Nonhomogeneity of lung response to inhaled histamine assessed with alveolar capsules. J Appl Physiol 1985;58:1914–22.
33. Sato J, Davey BL, Shardonofsky F, Bates JH. Low-frequency respiratory system resistance in the normal dog during mechanical ventilation. J Appl Physiol 1991;70:1536–43.
34. Hantos Z, Daroczy B, Suki B, Nagy S. Low-frequency respiratory mechanical impedance in the rat. J Appl Physiol 1987; 63:36–43.
35. Hantos Z, Daroczy B, Suki B, et al. Input impedance and peripheral inhomogeneity of dog lungs. J Appl Physiol 1992;72:168–78.
36. Bates JH, Abe T, Romero PV, Sato J. Measurement of alveolar pressure in closed-chest dogs during flow interruption. J Appl Physiol 1989;67:488–92.
37. Bersten AD. Measurement of overinflation by multiple linear regression analysis in patients with acute lung injury. Eur Respir J 1998;12:526–32.
38. Wagers S, Lundblad L, Moriya HT, et al CG. Nonlinearity of respiratory mechanics during bronchoconstriction in mice with airway inflammation. J Appl Physiol 2002;92:1802–7.
39. Salazar E, Knowles JH. An analysis of pressure-volume characteristics of the lungs. J Appl Physiol 1964;19:97–104.
40. Hickling KG. The pressure-volume curve is greatly modified by recruitment. A mathematical model of ARDS lungs. Am J Respir Crit Care Med 1998;158:194–202.
41. Bates JH, Brown KA, Kochi T. Respiratory mechanics in the normal dog determined by expiratory flow interruption. J Appl Physiol 1989;67:2276–85.
42. Kaczka DW, Ingenito EP, Israel E, Lutchen KR. Airway and lung tissue mechanics in asthma. Effects of albuterol. Am J Respir Crit Care Med 1999;159:169–78.
43. Lutchen KR, Greenstein JL, Suki B. How inhomogeneities and airway walls affect frequency dependence and separation of airway and tissue properties. J Appl Physiol 1996;80: 1696–707.

44. Similowski T, Bates JHT. Two compartment modelling of respiratory system mechanics at low frequencies: gas redistribution or tissue rheology? Eur Respir J 1991;4:353–8.
45. Romero PV, Sato J, Shardonofsky F, Bates JH. High-frequency characteristics of respiratory mechanics determined by flow interruption. J Appl Physiol 1990;69:1682–8.
46. Ludwig MS, Romero PV, Sly PD, et al. Interpretation of interrupter resistance after histamine-induced constriction in the dog. J Appl Physiol 1990;68:1651–6.
47. Bates JH, Baconnier P, Milic-Emili J. A theoretical analysis of interrupter technique for measuring respiratory mechanics. J Appl Physiol 1988;64:2204–14.
48. Bates JH, Rossi A, Milic-Emili J. Analysis of the behavior of the respiratory system with constant inspiratory flow. J Appl Physiol 1985;58:1840–8.
49. Frey U, Silverman M, Kraemer R, Jackson AC. High-frequency respiratory input impedance measurements in infants assessed by the high speed interrupter technique. Eur Respir J 1998;12:148–58.
50. MacLeod D, Birch M. Respiratory input impedance measurement: forced oscillation methods. Med Biol Eng Comput 2001;39:505–16.
51. Dorkin HL, Lutchen KR, Jackson AC. Human respiratory input impedance from 4 to 200 Hz: physiological and modeling considerations. J Appl Physiol 1988;64:823–31.
52. Sobh JF, Lilly CM, Drazen JM, Jackson AC. Respiratory transfer impedance between 8 and 384 Hz in guinea pigs before and after bronchial challenge. J Appl Physiol 1997;82:172–81.
53. Marchal F, Bouaziz N, Baeyert C, et al. Separation of airway and tissue properties by transfer respiratory impedance and thoracic gas volume in reversible airway obstruction. Eur Respir J 1996;9:253–61.
54. Peslin R, Gallina C, Duvivier C. Respiratory transfer impedances with pressure input at the mouth and chest. J Appl Physiol 1986;61:81–6.
55. Peslin R, Gallina C, Teculescu D, Pham QT. Respiratory input and transfer impedances in children 9-13 years old. Bull Eur Physiopathol Respir 1987;23:107–12.
56. Bijaoui E, Baconnier PF, Bates JH. Mechanical output impedance of the lung determined from cardiogenic oscillations. J Appl Physiol 2001;91:859–65.
57. Davey BL, Bates JH. Regional lung impedance from forced oscillations through alveolar capsules. Respir Physiol 1993; 91:165–82.
58. Mishima M, Balassy Z, Bates JH. Assessment of local lung impedance by the alveolar capsule oscillator in dogs: a model analysis. J Appl Physiol 1996;80:1165–72.
59. Balassy Z, Mishima M, Bates JH. Changes in regional lung impedance after intravenous histamine bolus in dogs: effects of lung volume. J Appl Physiol 1995;78:875–80.
60. Mishima M, Balassy Z, Bates JH. Acute pulmonary response to intravenous histamine using forced oscillations through alveolar capsules in dogs. J Appl Physiol 1994;77:2140–8.
61. Bates JH, Irvin CG. Measuring lung function in mice: the phenotyping uncertainty principle. J Appl Physiol 2003; 94:1297–306.

CHAPTER 55

ESOPHAGEAL PRESSURE MEASUREMENT

Walter Araujo Zin, Joseph Milic-Emili

The measurement of esophageal pressure (Pes) is a practical approach to measuring changes in intrathoracic pressure for the evaluation of respiratory system mechanics in the assessment of pulmonary physiology and pathophysiology. Pes yields an indirect measure of pleural pressure (Ppl), or, more precisely, the changes in Pes (ΔPes) correspond to pleural pressure (Ppl) oscillations (ΔPpl). Thus, the pressures across the lung and chest wall can be measured, and these measurements, together with volume and flow, allow the respiratory system resistance and compliance to be partitioned into their pulmonary and chest wall components. The measurement of Pes has many uses. The changes in Pes reflect the magnitude of the effort to breathe during spontaneous or machine-aided ventilation and can be used to compute the work of breathing across the lung and external circuit or to calculate the product of pressure developed by the inspiratory muscles and the duration of inspiratory effort. ΔPes also help in the interpretation of the end-expiratory wedge pressure under conditions of vigorous hyperpnea or elevated alveolar pressures. Transdiaphragmatic pressure and transmural cardiac pressures can also be calculated from Pes. As examples of recent diverse uses of Pes, it has been demonstrated that (1) a Pes-based strategy resulted in faster patient weaning (1.7 days) than when standard clinical parameters were used[1]; (2) it was possible to initiate pressure-support ventilation based on Pes values[2]; (3) assessment of obstructive sleep apnea-hypopnea syndrome by conventional indices may underestimate the risk of highly negative Pes[3]; and (4) ΔPes measured with a water-filled catheter reflects accurately ΔPpl in preterm infants under positive end-expiratory pressure.[4]

The indirect measurement of Ppl through a balloon placed into the esophagus was proposed in 1878 by Luciani and was subsequently popularized by the work of Buytendijk,[5] published in 1949. Several approaches can be used to make measurements, including air-filled balloon catheters, liquid-filled catheters,[6] and small transducers placed in the esophagus.[7] In addition, ΔPpl can also be estimated from measurement of pressure in the vena cava and over the suprasternal fossa.[8] Finally, although relatively simple and well standardized,[9,10] the technique for measuring Pes requires special attention to avoid errors and artifacts.

PRINCIPLES OF MEASUREMENT

Although not difficult to accomplish, the precise measurement of Pes requires full understanding of certain methodological and theoretical concepts.

Frequency Response of the Measuring Assembly

The dynamic characteristics of measuring instruments may be described by their frequency response.[11] Consider a signal represented by a square wave (Figure 55-1). Under ideal circumstances the recording apparatus should provide a true representation of the original signal. An overdamped recording device modifies the signal, smoothing out sharp corners and delaying the rise and fall of the input wave. On the other hand, for the same input signal an underdamped apparatus generates an output wave that oscillates disproportionately after each transient.[13] When the catheter is connected to a pressure transducer and the input and output signals are compared, the two should follow each other faithfully up to a frequency of at least 15 Hz. Stated otherwise, the entire system should have a flat response up to 15 Hz.[14] The measuring assembly should not delay the pressure signal. In other words, Pes should not lag behind the pressure measured at the airway opening (Pao) and vice versa (Figure 55-2). One should be able to achieve signals that are in phase up to frequencies as high as 32 Hz.[16]

Another important aspect of a pressure measuring device is represented by its common mode rejection ratio.[13] When a differential pressure transducer has both its chambers identically pressurized, the resulting signal should be nil. No pressure transients should be observed when the chambers of the transducer are compressed or decompressed simultaneously to the same degree.

Both the frequency response and common mode rejection characteristics need to be determined in order to ensure that an adequate measuring system is being used to register Pes.

Compliance and Resistance of the Measuring Assembly

In addition to the above-mentioned factors, the compliance and resistance of the experimental circuit may also serve to distort the measurements. For instance, a very compliant

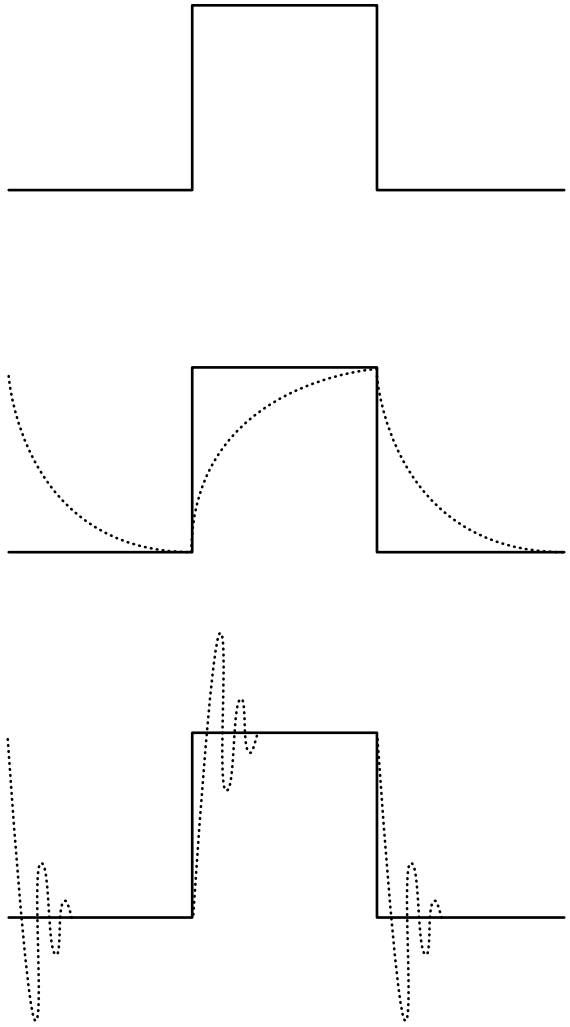

FIGURE 55-1 Frequency response of measuring assembly. The true signal is represented by the *solid lines*, whereas the *dotted lines* depict the output provided by the equipment. From top to bottom: in the ideal system the input and the output signals should be identical, and hence, the two lines are superimposed; in the overdamped assembly the sharp corners are rounded, and the rise and fall of the input signal are delayed; the underdamped system generates an output signal that oscillates after transient changes in the input wave. Reproduced with permission from Zin WA and Milic-Emili J.[12]

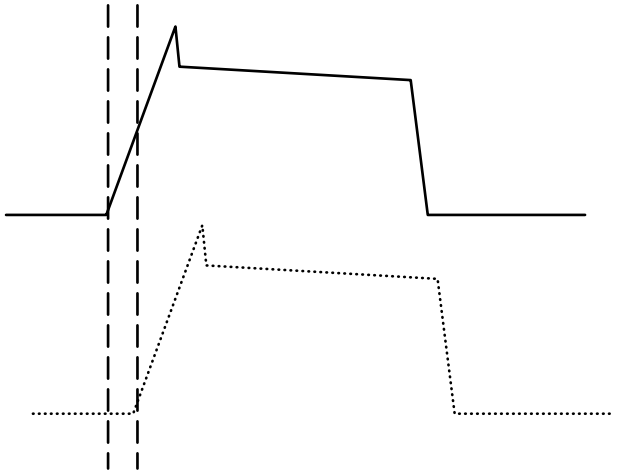

FIGURE 55-2 Phase lag. The pressure variation was simultaneously measured by two different assemblies, as represented by the *solid* and *dotted lines*. Note that the pressure changes recorded lag a certain amount of time behind the other, represented by the distance between the two vertical *broken lines*. Reproduced with permission from Zin.[15]

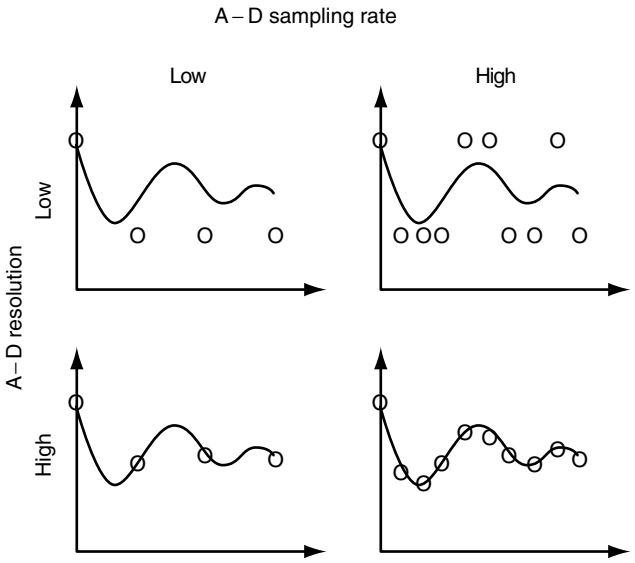

FIGURE 55-3 Different analog-to-digital resolutions and sampling rates of the digitalized data points. With a high resolution the points are more closely spaced on the ordinate, whereas with a high sampling rate the spaces are more closely spaced on the abscissa. Reproduced with permission from Zin WA.[15]

piece of rubber tubing or connection added in series to the esophageal balloon catheter or air bubbles in the liquid-filled catheter will dampen the pressure signal. The tubing and connectors should not be too narrow because the increased resistance may also impair the rapid transmission of pressure at the site of measurement to the recording device.

Analog-to-Digital Conversion

The output of the transducer is in the form of an analog signal, which is usually either a change in voltage or current. With the aid of an analog-to-digital (A-D) converter, a continuous electrical signal can be converted to a discrete digital format in order to be processed by computer. Ideally, the interval between each sample should be as small as possible so that the digital data points closely approximate the analog signal. The faster the changes in the input signal, the higher the sampling frequency needs to be.[17] Likewise, the better the resolution of the A-D converter, the closer the points will be spaced on the y-axis (Figure 55-3). Basically, the resolution improves as the number of bits of the A-D converter increases.

SETTING UP THE MEASURING SYSTEM

Once the investigator is assured that the recording system is working properly, there are a number of important considerations related to instrumenting the subject. As is discussed

in detail below, there are three most commonly used methods to determine esophageal pressure—esophageal balloon, liquid-filled catheter, and microtip transducer—and all require adequate positioning within the esophagus. This section reviews the care of the experimental subject and the methods to assess proper positioning of the device. The esophageal balloon catheter is discussed because it is the most frequently used device and is the largest of the three devices.

Preparing for the Test

If infants and children are to be examined, the physical and psychological preparation depends on the age, interests, previous experience, and level of trust. The subject must be told how the test is performed, that is, that a tube will be passed through his or her mouth or nose into the stomach and then pulled slowly back into the esophagus, and that it will remain there for a certain amount of time. Additionally, he or she must be advised that a gagging sensation may be experienced when the tube is inserted. At this point the subject should swallow a mouthful of water through a straw from a glass, as previously instructed. If the gagging sensation is excessive, topical anesthesia should be applied to the oropharynx. Care may need to be taken in some cases to avoid the risk of aspiration of saliva, food, or fluids.

Finally, the common causes of swallowing difficulty may require physician supervision of the balloon placement. Disorders of the mouth and pharynx, such as obstruction to the passage of food or liquid (eg, emotional or anxiety disorder, tumors, cervical spine disease, or pharyngoesophageal diverticulum), and neuromuscular problems (eg, stroke, Parkinson's disease, Huntington's disease, multiple sclerosis, myasthenia gravis, muscular dystrophy, polymyositis, or amyotrophic lateral sclerosis) may cause problems. Esophageal pathology, such as to cause obstruction to the passage of food or liquid (eg, tumor, strictures secondary to radiation or chemical burns, medications or ulcers, Schatzki's ring, or foreign bodies), or neuromuscular problems (eg, achalasia, diffuse esophageal spasm, hypertensive lower esophageal sphincter, or scleroderma) may also make balloon passage difficult.

Introducing the Measuring Device into the Esophagus

When the subject is relaxed and understands the instructions, a rough estimate of the length of the catheter from the nostril to the stomach is taken, and a mark is placed on the catheter with a marker pen. About 3 mL of topical anesthetic is administered with a syringe into the more patent of the two nostrils, and the subject is asked to sniff deeply and repeatedly. After a while he or she is expected to report that the nasopharynx is anesthetized. The balloon should be emptied with a glass syringe. To the balloon (catheter or microtip transducer) more topical anesthetic is applied, and the measuring device is slowly and carefully inserted through the nostril. When the subject feels that the tip of the device is touching his or her lower pharynx, a mouthful of water should be swallowed. If an extra amount is required, he or she can drink through a straw from a glass or plastic cup already in his or her hand. While the subject is swallowing, the measuring device is introduced into the esophagus and advanced until it is in the stomach, based on the previously placed mark on the catheter.

Balloon Positioning

Once the empty balloon catheter is in the stomach, 0.5 mL of air should be injected into the system, and the catheter is connected to a pressure transducer. During spontaneous breathing, positive pressure swings during inspiratory efforts confirm that the balloon is located in the stomach. The catheter is then withdrawn slowly until a negative pressure deflection is identified; the upper part of the balloon is now in the thoracic esophagus. The catheter is then withdrawn a further 10 cm, at which point the whole balloon should be in the esophagus, at a distance ranging from 35 to 45 cm from the nares. In this site, the top of the balloon is about midway between the apex and the base of the lung.[18]

Balloon volume should be checked again before proceeding further. For such purpose the balloon is emptied either by gently pulling on a glass syringe or more adequately by having the subject perform a Valsalva maneuver or a series of coughs. Five milliliters of air is injected into the balloon via a syringe, and 4.5 mL is subsequently withdrawn. Following maneuvers resulting in large changes in intraesophageal pressure, it is a good idea to recheck balloon volume to ensure that leaks in the system have not allowed the balloon to deflate.

To validate the measurement of ΔPes as a reflection of ΔPpl, a comparison of changes in Pes (ΔPes) and the changes in airway opening pressure (ΔPao) is made during voluntary static Valsalva and Müller maneuvers while keeping the glottis open. The position of the esophageal catheter is considered acceptable when there is good agreement between the two pressure swings. In many patients and untrained volunteers, this maneuver may be difficult to perform because of glottic closure, poor coordination, and so on. Furthermore, this procedure cannot be used in children, during anesthesia, or in very sick patients. An alternative is to compare ΔPes and ΔPao during spontaneous efforts made against a closed airway.[19] This dynamic "occlusion test" has been validated in normal awake adults in different body positions.[20] The test consists of occluding a subject's airway at end-expiration while measuring Pes and Pao during three to five spontaneous inspiratory efforts (Figure 55-4). When the balloon is ideally positioned, the ratio between ΔPes and ΔPao should be close to unity throughout the inspiratory efforts, that is, no net change in the transpulmonary pressure should occur since no flow and change in volume are permitted by the closed airway, and hence, pressure losses across the lungs are negligible. In addition, when ΔPes is plotted against ΔPao, a closed loop indicates that there is no phase lag between the two signals (see Figure 55-4). Baydur and colleagues studied 10 healthy seated subjects, each of whom swallowed a balloon 5 cm long positioned in the middle and lower esophagus.[20] The mean ΔPes/ΔPao ratio amounted to 1.04 (range 0.99–1.10). When examined in various postures, the ratio remained close to unity in both right (mean 1.02; range 0.94–1.10) and left (mean 0.98;

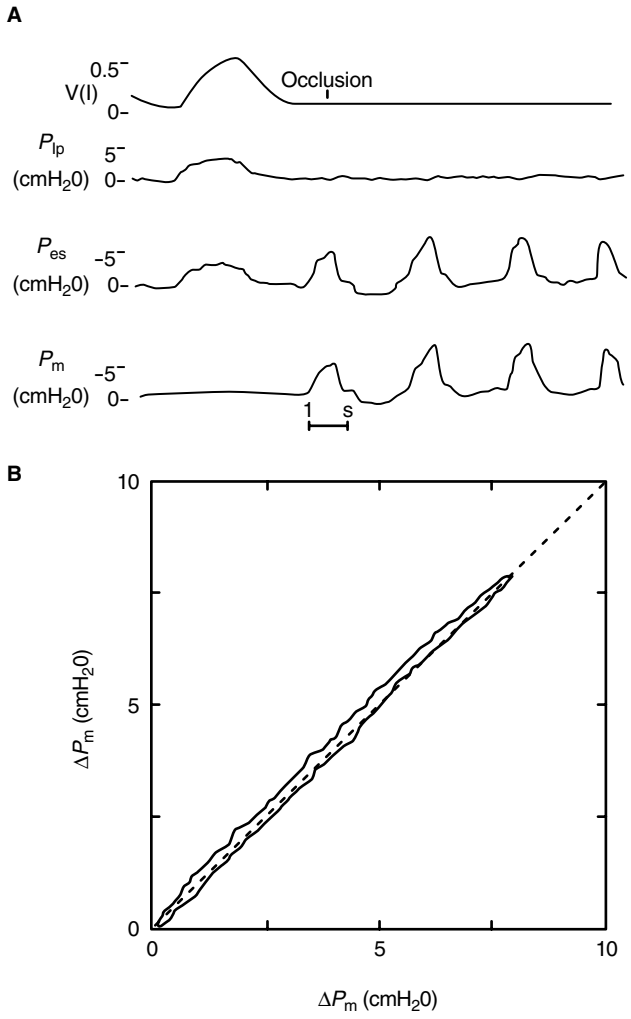

FIGURE 55-4 *A*, Tracing of volume (V), transpulmonary (Ptp), esophageal (Pes), and mouth pressures (Pm) during a dynamic "occlusion test" in a seated normal subject. *B*, Plot of ΔPes versus ΔPm for the first occluded inspiratory effort in *A*. Line of identity is indicated by the *broken line*. Reproduced with permission from Baydur A et al.[20]

range 0.86–1.08) lateral decubitus. In the supine position this was not always the case, although a satisfactory ΔPes/ΔPao ratio (between 0.86 and 1.10) could be obtained in all supine subjects by repositioning the balloon at different levels of the esophagus (5–15 cm from the cardioesophageal junction). Similar results have been found in 10 supine patients undergoing general anesthesia,[21] as well as in semirecumbent patients with chronic obstructive pulmonary disease (COPD) in acute respiratory failure.[22] In both of these latter studies the patients were intubated, and hence there were no problems of transmission of alveolar pressure to the airway opening. This is not always the case, and, accordingly, the static Valsalva and Müller maneuvers must substitute for the dynamic occlusion test.

The dynamic occlusion test has also been carried out in neonates.[19,23] Using a balloon catheter system with an adequate frequency response, Beardsmore and colleagues were able to obtain a satisfactory ΔPes/ΔPao ratio in the lateral position.[23] However, they emphasized the necessity to use an "ideal" balloon to obtain satisfactory recordings and described the painstaking procedures and difficulties in achieving good performance of their balloon system in neonates. Milner and colleagues found that in the supine position ΔPes tended to be smaller than ΔPao by an average of about 20% and showed an intrasubject variability of 20%.[19] However, a 1 mm–wide esophageal catheter was used, which may have made the frequency response of their esophageal balloon catheter system inadequate (overdampening ΔPes).[23]

The occlusion test can be applied even in paralyzed subjects because, although unable to generate respiratory efforts, they can be subjected to external applied pressure changes around the thorax.[24] As with spontaneously breathing human subjects, the airway is occluded and the body surface pressure is varied while recording Pes and Pao. When studies involving partitioning of respiratory mechanics are envisaged in patients that will necessitate administration of neuromuscular blocking agents, the positioning of an esophageal balloon catheter should be performed before neuromuscular blockade, while the patient is still breathing spontaneously.

In conclusion, since 1982, the dynamic occlusion test has been used in patients requiring mechanical ventilation,[22,25,26] in anesthetized patients,[21,27] in normal volunteers,[28,29] and in awake[30] and anesthetized animals.[31–34]

ESOPHAGEAL BALLOON METHOD

Air-containing latex balloons sealed over catheters, which, in turn, transmit the balloon pressure to transducers, are the most widely used means for measuring Pes. Details for constructing such balloon catheter systems have been published.[35,36] Ideally, the balloon perimeter should correspond to that of the esophagus (4–4.8 cm for human adults). In practice, 0.1 mm–thick, 5 to 10 cm–long latex balloons with perimeters varying between 3.2 and 4.8 cm have been found to be adequate.[9,10,20] In adult studies, polyethylene catheters with an internal diameter of 1.4 mm (PE-200) and a length of 100 cm are conventionally used.[9,20] When the speed of pressure changes is very high, such as occurs in the determination of frequency dependence of respiratory compliance,[37] the frequency response of the balloon catheter system can be improved by increasing the internal diameter of the catheter to 1.7 mm or by filling the balloon catheter system with a gas of lower density than air (helium, for instance).

Although respiratory frequencies are higher in newborns than in adults, catheters of smaller internal diameters (1–1.2 mm) have been commonly used in the former,[19,38] which may have led to the underestimation of Pes.[23] At high respiratory frequencies the catheter should have a relatively high internal diameter (1.4–1.7 mm) but be as short as possible.[39]

Finally, spirally arranged holes should be made over the entire portion of the catheter covered by the balloon because the gas in the balloon tends to the site of most negative pressure. If there is no hole in this location, there will be no communication between the gas in the balloon and the

catheter-manometer system, and the measurement of Pes will not be correct.

The optimal volume of gas in the esophageal balloon has been determined to be around 0.5 mL of air, but the range of working gas volumes must be determined. For such determination, a three-way stopcock is connected to the distal end of the catheter and left open to the atmosphere. A pressure transducer is attached to the other port of the stopcock. The balloon is emptied by submerging it in water. Thereafter, the stopcock is positioned to connect the pressure transducer to the balloon catheter assembly. With a calibrated syringe gas is introduced into the system in 0.1 mL steps and a volume-pressure curve is constructed. One observes a range of volumes over which balloon pressure does not change appreciably. In most instances the balloon working range encompasses the 0.5 mL volume, the amount of gas generally used.

LIQUID-FILLED CATHETER METHOD

The liquid-filled catheter method has been used for many years, mainly in neonates and small animals,[40] and it has the advantage of a high-frequency response because of rapid pressure transmission through a noncompressible fluid (usually water or saline solution). It thus follows that catheters narrower (internal diameter 1 mm) than those onto which esophageal balloons are mounted can be used without loss of fidelity of measurements. The discomfort for the baby is minimized by such small-bore tubes.

There are some disadvantages associated with liquid-filled catheters, such as the difficulty in obtaining absolute values of Pes because of hydrostatic factors. Additionally, its distal end must be provided with several holes to avoid mucus plugging of the catheter. For the same reason, intermittent flushing of the catheter is required. A constant infusion of liquid at a slow rate (10 mL/h) from a syringe pump can be used, which also serves to keep the catheter free of gas bubbles that might overdamp the recorded pressure.

Validation of the liquid-filled catheter method[40,41] has been performed[42] using the dynamic occlusion test in healthy full-term newborns. Measurements were made during quiet sleeping or resting wakefulness in right lateral, prone, and supine positions. The group average ΔPao was less than ΔPes by only 1.6% (range 0–3.3%). During the occlusion test, preterm neonates studied with the water-filled catheter system also had a finite region of the esophagus where ΔPes equaled ΔPao.[43] Using an "ideal" balloon catheter system, a decrease in ΔPes relative to ΔPao of up to 6% has been observed.[23] Using the same test, the results of Asher and colleagues were confirmed on supine healthy full-term babies during quiet sleep,[42] whereas during rapid eye movement (REM) sleep, agreement between ΔPes and ΔPao was not assured.[44] The latter applied in all instances to preterm babies.[44] The discrepancies between occluded ΔPes and ΔPao were attributed to uneven distribution of Pes swings as a result of distortion caused by the highly compliant chest wall of newborns.[45] The liquid-filled catheter method also has application in small animals.[39,46,47] As predicted, both narrow and wide short (30 cm long) catheters are reliable, and the correct catheter placement can be established using the dynamic occlusion test.[20]

SMALL TRANSDUCER METHOD

Microtransducers placed directly into the esophagus also provide reliable assessments of Pes.[6] A comparison of a 5F catheter-tip pressure transducer in the esophagus and a solid-state pressure transducer measuring Pao, both systems sharing a high-frequency response, has shown close concordance of ΔPes/ΔPao during an occlusion test. The slope of the relationship averaged 0.999, indicating that the microtip transducer was adequately recording Pes up to a frequency of 50 Hz.[48]

CONTRAINTS IN MEASURING ESOPHAGEAL PRESSURE

Cardiac Artifacts

Changes in intrathoracic pressure caused by the beating of the heart appear on recordings of esophageal pressure, irrespective of the devices used to make the measurements. The noise, termed "cardiac artifact," is particularly prominent in normal subjects during resting breathing. Cardiac artifact can be minimized by using balloons shorter than 10 cm and with a large perimeter (4.8 cm) and by choosing a suitable locus in the esophagus.[20] Alternatively, the pressures may be measured at fixed times of the cardiac cycle[49] and ensemble averaged using a personal computer (Figure 55-5).[50] When the artifact results from the use of a catheter-tip pressure transducer it can be markedly reduced by rotating the catheter.[48]

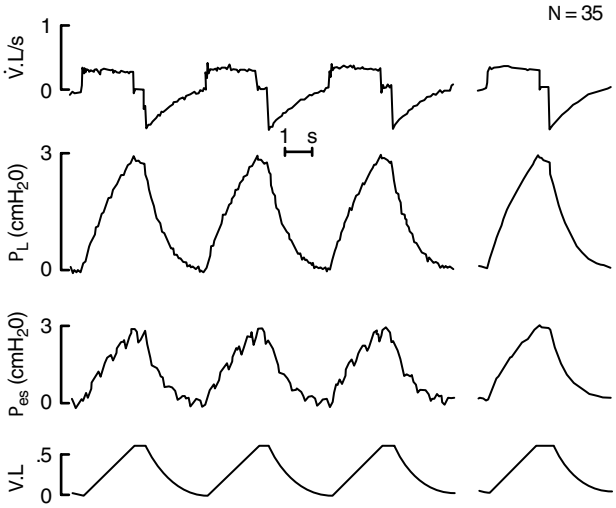

FIGURE 55-5 *Left*, tracing of flow (V), transpulmonary (PL) and esophageal (Pes) pressures, and volume (V) obtained during three consecutive breaths in an anesthetized paralyzed subject. *Right*, ensemble average of records form 35 consecutive breaths gathered under the same conditions as in *Left*. Reproduced with permission from D'Angelo E et al.[50]

Uneven Distribution of Pleural Surface Pressure

Pleural pressure is not uniform but has a gradient from top to bottom reflecting gravity and chest wall configuration.[51] Despite this fact, Pes, as sampled at a single site in the esophagus, provides a reasonable estimate of pressure for the assessment of the mechanical properties of the lung and chest wall because swings in pressure are similar over the entire pleural surface. In the upright position, the esophageal balloon technique measures Pes from a site near the midlevel of the lung.[52] This region is close to the point where the changes in regional lung volume are equal to those in overall lung volume. In fact, it has been demonstrated that at lung volumes greater than functional residual capacity (FRC), the regional and overall volume-pressure curves of the lung are virtually superimposed, indicating that at these lung volumes Pes measured with the esophageal balloon closely reflects the static mechanical properties of the lung.[53] Below FRC, where small airway closure is known to occur in dependent lung zones,[54] Pes cannot be interpreted as reflecting the intrinsic elastic properties of the lung. At low lung volumes, compression of the esophagus by the mediastinal structures may cause Pes to deviate from the true Ppl (see below).[53,55,56] Although measurement of Pes in body postures other than the upright may be subject to similar problems to the supine, the shape of the *V-P* curves of the lungs is virtually identical in all postures.[57] Consequently, it can be concluded that independent of body posture, measurements of Pes can provide accurate values of the changes in overall static Ppl with lung volume.

The dynamic occlusion test indicates that in general during spontaneous breathing the dynamic changes of Pes closely reflect the corresponding changes in Ppl, even in different postures. In addition, it has been found that ΔPes reflects ΔPpl after muscle paralysis.[24] Therefore, it is not necessary to repeat the occlusion test after paralysis if its result is acceptable in the nonparalyzed state.

Esophageal Distortion and Contraction

If the tissues interposed between the pleural space and the esophageal lumen are flaccid, ΔPpl should be transmitted without attenuation to the esophageal lumen, and ΔPes/ΔPao would equal 1.0 during an occlusion test. Thus, some investigators attribute their difficulty in properly recording Pes in the supine position to esophageal compression by the mediastinal contents.[20,55,56,58] However, if changes in posture alter the pressures acting on the rib cage and distort the esophageal and mediastinal soft tissues, the estimate of ΔPpl may be affected.[24]

Esophageal contraction (peristalsis) may not only affect the baseline value of Pes, but the amplitude of ΔPes may also be altered. However, these contractions are easily detected, and no data should be obtained until Pes returns to its baseline value. Nevertheless, esophageal contractions may occur following the administration of certain drugs, such as methacholine, and may hinder the recording of Pes.

Transmission of Alveolar Pressure to the Airway Opening

Poor transmission of the changes in alveolar pressure (Palv) to the airway opening is a potential major source of time delay between ΔPpl and ΔPao.[14,19,43] The speed with which Palv is conveyed to the airway opening depends on the flow resistance offered by the airways and the compliance of the extrathoracic airways (equipment included). The latter depends partly on the compressibility of the gas in the extrathoracic airways (including mouthpiece, tracheal tube, etc), as well as on the structural (tissue) compliance of the upper airways (cheeks, pharynx, base of the oral cavity, etc). In practice, the compressibility of the gas in the extrathoracic airways causes essentially no problems in terms of transmission of Palv to the airway opening. The tissue compliance of the upper airway is considerably greater than that of gas, especially when cheeks or other structures are not supported,[59] but again essentially no problem of transmission of Palv to the airway opening can be detected.[60,61] However, in patients with severe airways obstruction there is often a considerable delay in the transmission of Palv to the mouth. Under these circumstances ΔPao underestimates ΔPalv, and dynamic occluded ΔPao underestimates the concomitant ΔPes.[62]

The delay in the transmission of Palv to the mouth resulting from incorrect assembly setup is a different entity from the difference between Palv and Pao caused by "intrinsic"[63] or "auto positive end-expiratory pressure"[64] (PEEPi). The latter condition is most likely to occur in clinical situations of increased resistance or compliance (less elastic recoil) and short expiratory times. Thus, airflow does not cease at the end of expiration but continues slowly as increased alveolar pressure decompresses through dynamically narrowed airways, and hence there is not enough time for the equilibration between Palv and Pao. Under these conditions, the initiation of a spontaneous breath requires the patient to generate sufficient inspiratory force to counterbalance dynamic PEEPi.[65] Under these circumstances, if the dynamic occlusion test fails one can ask the patient to slow down his or her breathing frequency and repeat the test. If the occlusion test is still inaccurate, the static Valsalva and Müller maneuvers should be used, as discussed above.

COMPARISON BETWEEN PLEURAL AND ESOPHAGEAL PRESSURES

Studies comparing Ppl and Pes have produced conflicting results. Some of these discrepancies may result from differences between the pleural and esophageal catheters used, adequate placement of the esophageal balloon, or the measurements of Ppl in regions distant from the periesophageal pleural space.[66–69]

Several studies using air-filled needles introduced into the lateral pleural space found significant differences between absolute Pes and Ppl. Cherniack and colleagues found more negative pressures in the pleural space than in the esophagus, although inspiratory ΔPpl and ΔPes were similar.[70] Daly and Bondurant reported that ΔPpl in most regions of the rib cage were not equal to ΔPes until a small

amount of air was introduced intrapleurally.[71] When Ppl was recorded directly from an air-filled catheter system, it was higher than Pes in the lateral decubitus, but no significant difference was found in either prone or supine dogs.[72] However, when air-filled catheters or needles are used, recorded Ppl may be distorted by the presence of an air–liquid interface between the measuring device and the pleural liquid.[73] In addition, pressures measured by means of liquid-filled catheters may represent liquid rather than surface pressures.[74,75]

An assortment of liquid- and air-filled balloon-like devices have been used to measure Ppl in a manner approximating the esophageal balloon technique.[76–79] Hurewitz and colleagues used perfectly matched pleural and esophageal latex balloons and were able to demonstrate an excellent correlation between Pes and Ppl, as well as between ΔPes and ΔPpl.[77] Wohl and colleagues employed mushroom catheters in paralyzed ventilated dogs and reported only a small difference between Pes and Ppl.[79] Nevertheless, the discrepancies between direct determinations of pleural and esophageal pressures have not been as yet completely resolved. On the other hand, there is good evidence that ΔPpl is accurately tracked by ΔPes.[20,21–24,42,48]

CONCLUSIONS

The indirect determination of changes in pleural pressure via the esophageal pressure forms the basis for the assessment of respiratory system mechanics in the pulmonary function laboratory and in experimental physiology. Several methods for measuring changes in esophageal pressure can be safely employed in both human subjects of all ages and experimental animals. Although the assessment of respiratory mechanics in patients is usually accomplished by noninvasive means, the evaluation of certain pathologies, in particular those associated with restrictive ventilatory impairment and mixed restrictive and obstructive impairment as well as suspected occupational lung disease, may still require direct assessment of the mechanical properties of the lungs. A thorough knowledge of the methodology involved is essential so that reliable measurements are obtained.

REFERENCES

1. Gluck EH, Barkoviak MJ, Balk RA, et al. Medical effectiveness of esophageal balloon pressure manometry in weaning patients from mechanical ventilation. Crit Care Med 1995;23:504–9.
2. Barnard M, Shukla A, Lovell T, Goldstone J. Esophageal-directed pressure support ventilation in normal volunteers. Chest 1999;115:482–9.
3. Watanabe T, Kumano-Go T, Suganuma N, et al. The relationship between esophageal pressure and apnea hypopnea index in obstructive sleep apnea-hypopnea syndrome. Sleep Res Online 2000;3:169–72.
4. Seddon PC, Dasvis GM. Validity of esophageal pressure measurements with positive end-expiratory pressure in preterm infants. Pediatr Pulmonol 2003;36:216–22.
5. Buytendijk HJ. Oesophagusdruck en Longelasticiteit [Dissertatie]. The Netherlands: University of Groningen; 1949.
6. Dornhorst AC, Leathart GL. A method of assessing the mechanical properties of lungs and air-passages. Lancet 1952;263:09–11.
7. Gilbert R, Peppi D, Auchinloss JH Jr. Measurement of transdiaphragmatic pressure with a single gastric-esophageal probe. J Appl Physiol 1979;47:628–30.
8. Tobin MJ, Jenouri GA, Watson H, Sackner MA. Noninvasive measurement of pleural pressure by surface inductive plethysmography. J Appl Physiol 1983;55:267–75.
9. Milic-Emili J, Mead J, Turner JM, Glauser EM. Improved technique for estimating pleural pressure from esophageal balloons. J Appl Physiol 1964;19:207–11.
10. Macklem PT. Procedures for standardized measurements of lung mechanics. Bethesda (MD): Division of Lung Diseases of the National Heart and Lung Institute; 1975.
11. Fry DL. Physiologic recording by modern instruments with particular reference to pressure recording. Physiol Rev 1960;40:753–88.
12. Zin WA, Milic-Emili J. Esophageal pressure measurement. In: Tobin MJ, editor. Principles and practice of intensive care monitoring. New York: McGraw-Hill, Inc.; 1998. p. 545–52.
13. Butler JP, Leith DE, Jackson AC. Principles of measurement: applications to pressure, volume, and flow. In: Macklem PT, Mead J, editors. Handbook of physiology. The respiratory system. Mechanics of breathing. Bethesda (MD): American Physiological Society; 1986; p. 15–33.
14. Milic-Emili J. Measurement of pressures in respiratory physiology: techniques in the life sciences. Shannon (Ireland): Elsevier Scientific; 1984. p. 1–22.
15. Zin WA. Principles of laboratory research on respiratory mechanics. In: Gullo A, editor. Proceedings of the 14th Postgraduate Course in Critical Care Medicine. Milan: Springer-Verlag; 2000. p. 23–34.
16. Peslin R, Navajas D, Rotger M, Farré R. Validity of the esophageal balloon technique at high frequencies. J Appl Physiol 1993;74:1039–44.
17. Beauchamp KG, Yuen CK. Digital methods for signal analysis. London: Chapman & Hall; 1979.
18. Mead J, Milic-Emili J. Theory and methodology in respiratory mechanics with glossary of symbols. In: Fenn WO, Rahn H, editors. Handbook of physiology. Respiratory system. Washington (DC): American Physiological Society; 1964. p. 363–76.
19. Milner AD, Saunders RA, Hopkin IE. Relationship of intra-oesophageal pressure to mouth pressure during the measurement of thoracic gas volume in the newborn. Biol Neonate 1978;33:314–9.
20. Baydur A, Behrakis PK, Zin WA, et al. Simple method for assessing the validity of the esophageal balloon technique. Am Rev Respir Dis 1982;126:788–91.
21. Higgs BD, Behrakis PK, Bevan DR, Milic-Emili J. Measurement of pleural pressure with esophageal balloon in anesthetized humans. Anesthesiology 1983;59:340–3.
22. Fleury B, Murciano D, Talamo C, et al. Work of breathing in patients with chronic obstructive pulmonary disease in acute respiratory failure. Am Rev Respir Dis 1985;131:822–7.
23. Beardsmore CS, Helms P, Stocks J, et al. Improved esophageal balloon technique for use in infants. J Appl Physiol 1980; 49:735–42.
24. Dechman G, Sato J, Bates JHT. Factors affecting the accuracy of esophageal balloon measurement of pleural pressure in dogs. J Appl Physiol 1992;72:383–8.
25. Marini JJ, Rodriguez M, Lamb V. Bedside estimation of the inspiratory work of breathing during mechanical ventilation. Chest 1986;89:56–63.
26. Swartz MA, Marino PL. Diaphragmatic strength during weaning from mechanical ventilation. Chest 1985;88:736–9.

27. D'Angelo E, Robatto FM, Calderini E, et al. Pulmonary and chest wall mechanics in anesthetized paralyzed humans. J Appl Physiol 1991;70:2602–10.
28. Clarysse I, Demedts M. Human esophageal pressures and chest wall configuration in upright and head-down posture. J Appl Physiol 1985;59:401–7.
29. Dahlqvist M, Hedenstierna G. Lung volumes measured by He dilution and by body-plethysmograph with mouth and esophageal pressures. Clin Physiol 1985;5:179–87.
30. Sadoul N, Bazzy AR, Akabas SR, Haddad GG. Ventilatory response to fatiguing and nonfatiguing resistive load in awake sheep. J Appl Physiol 1985;59:969–78.
31. Bates JHT, Brown KA, Kochi T. Respiratory mechanics in the normal dog determined by expiratory flow interruption. J Appl Physiol 1989;67:2276–85.
32. Kochi T, Okubo S, Zin WA, Milic-Emili J. Chest wall and respiratory system mechanics in cats: effects of flow and volume. J Appl Physiol 1988;64:2636–46.
33. Similowski T, Levy P, Corbeil C, et al. Viscoelastic behavior of lung and chest wall in dogs determined by flow interruption. J Appl Physiol 1989;67:2219–29.
34. Zin WA, Böddener A, Silva PRM, et al. Active and passive respiratory mechanics in anesthetized dogs. J Appl Physiol 1986;61:164–75.
35. Mead J, McIlroy MB, Selverstone NJ, Kriete BC. Measurement of intraesophageal pressure. J Appl Physiol 1955;7:491–5.
36. Schilder DP, Hyatt RE, Fry DL. An improved balloon system for measuring intraesophageal pressure. J Appl Physiol 1959;14:1057–8.
37. Macklem PT. Airway obstruction and collateral ventilation. Physiol Rev 1971;51:368–436.
38. Senterre J, Geubelle F. Measurement of endoesophageal pressure in the newborns. Biol Neonate 1970;16:47–53.
39. Saldiva PHN, Cardoso WV, Caldeira MPR, Zin WA. Mechanics in rats by the end-inflation occlusion and single breath methods. J Appl Physiol 1987;63:1711–8.
40. Cook CD, Sutherland JM, Segal S, et al. Studies of respiratory physiology in the newborn infant. III. Measurements of mechanics of respiration. J Clin Invest 1957;36:440–8.
41. Karlberg P, Cherry RB, Escardo F, Koch G. Respiratory studies in newborn infants. Acta Paediatr Stockholm 1960;49: 345–57.
42. Asher MI, Coates AL, Collinge JM, Milic-Emili J. Measurement of pleural pressure in neonates. J Appl Physiol 1982; 52:491–4.
43. Coates AL, Davis GM, Vallinis P, Outerbridge EW. Liquid-filled esophageal catheter for measuring pleural pressure in preterm neonates. J Appl Physiol 1989;67:889–93.
44. LeSouëf PN, Lopes JM, England SJ, et al. Influence of chest wall distortion on esophageal pressure. J Appl Physiol 1983; 55:353–8.
45. LeSouëf PN, Lopes JM, England SJ, et al. Effect of chest wall distortion on occlusion pressure and the preterm diaphragm. J Appl Physiol 1983;55:359–64.
46. Rodrigues ACM, Moreira LFP, Souza CL, et al. Effects of thoracotomy on respiratory system, lung, and chest wall mechanics. Chest 1993;104:1882–6.
47. Sousa AS, Moll RJ, Pontes CF, et al. Mechanical and morphometrical changes in progressive bilateral pneumothorax and pleural effusion in normal rats. Eur Respir J 1995; 8:99–104.
48. Chartrand DA, Ye TH, Maarek JM Chang HK. Measurement of pleural pressure at low and high frequencies in normal rabbits. J Appl Physiol 1987;63:1142–6.
49. Trop D, Peeters R, Van De Woestijne KP. Localization of recording site in the esophagus by means of cardiac artifacts. J Appl Physiol 1970;29:283–7.
50. D'Angelo E, Prandi E, Tavola M, et al. Chest wall interrupter resistance in anesthetized paralyzed humans. J Appl Physiol 1994;77:883–7.
51. Agostoni E. Mechanics of the pleural space. Physiol Rev 1972;52:75–128.
52. Milic-Emili J, Henderson JAM, Dolovich MB, et al. Regional distribution of inspired gas in the lung. J Appl Physiol 1966;21:749–59.
53. Sutherland PW, Katsura T, Milic-Emili J. Previous volume history of the lung and regional distribution of gas. J Appl Physiol 1968;25:566–74.
54. Anthonisen NR. Closing volume. In: West JB, editor. Regional differences in the lung. New York: Academic Press; 1977. p. 451–82.
55. Ferris BG Jr, Mead J, Frank NR. Effect of body position on esophageal pressure and measurement of pulmonary compliance. J Appl Physiol 1959;14:521–4.
56. Knowles JH, Hong SK, Rahn H. Possible errors using esophageal balloon in determination of pressure-volume characteristics of the lung and thoracic cage. J Appl Physiol 1959;14:525–30.
57. Milic-Emili J, Mead J, Turner JM. Topography of esophageal pressure as a function of posture in man. J Appl Physiol 1964;19:212–6.
58. Mead J, Gaensler EA. Esophageal and pleural pressures in man, upright and supine. J Appl Physiol 1959;14:81–3.
59. Jaeger MJ. Effect of the cheeks and the compliance or alveolar gas on the measurement of respiratory variables. Respir Physiol 1982;47:325–40.
60. Rodenstein DO, Stanescu DC, Francis C. Demonstration of failure of body plethysmography in airway obstruction. J Appl Physiol 1982;52:949–54.
61. Shore S, Milic-Emili J, Martin JG. Reassessment of body plethysmographic technique for the measurement of thoracic gas volume in asthmatics. Am Rev Respir Dis 1982;126:515–20.
62. Marazzini L, Cavestri R, Gori D, et al. Difference between mouth and esophageal occlusion pressure during CO_2 rebreathing in chronic obstructive pulmonary disease. Am Rev Respir Dis 1978;118:1027–33.
63. Rossi A, Gottfried SB, Zocchi L, et al. Measurement of static compliance of the total respiratory system in patients with acute respiratory failure during mechanical ventilation: the effect of intrinsic positive end-expiratory pressure. Am Rev Respir Dis 1985;131:672–7.
64. Pepe PE, Marini JJ. Occult positive end-expiratory pressure in mechanically ventilated patients with airflow obstruction. The auto-PEEP effect. Am Rev Respir Dis 1982;126:166–70.
65. Petrof BJ, Legaré M, Goldberg P, et al. Continuous positive airway pressure reduces the work of breathing and dyspnea during weaning from mechanical ventilation in severe chronic obstructive pulmonary disease. Am Rev Respir Dis 1990;141:281–9.
66. Brookhart JM, Boyd TE. Local differences in intrathoracic pressure and their relation to cardiac filling pressure in the dog. Am J Physiol 1947;148:434–44.
67. Coleridge JCG, Linden RJ. The measurement of effective atrial pressure. J Physiol 1954;126:304–18.
68. Duomarco JL, Rimini R, Migliaro JP. Intraesophageal pressure and the local differences in pleural pressure. Acta Physiol Latino-Am 1954;4:133–40.
69. Wiggers CJ, Levy MN, Graham G. Regional intrathoracic pressures and their bearing on calculation of effective venous pressures. Am J Physiol 1947;151:1–12.
70. Cherniack RM, Fahri LF, Armstrong RW, Proctor DF. A comparison of esophageal and intrapleural pressures in man. J Appl Physiol 1955;8:203–11.

71. Daly WJ, Bondurant S. Direct measurements of respiratory pleural changes in normal man. J Appl Physiol 1963;18:513–8.
72. Gillespie DJ, Lai Y, Hyatt RE. Comparison of esophageal and pleural pressures in anesthetized dogs. J Appl Physiol 1973;35:709–13.
73. Rutishauser WJ, Banchero S, Tsakiris AG, et al. Pleural pressures at dorsal and ventral sites in supine and prone body positions. J Appl Physiol 1966;21:1500–10.
74. Miserocchi G, Agostoni E. Pleural liquid and surface pressure at various lung volumes. Respir Physiol 1980;39:315–26.
75. Permutt S, Caldini P, Bane HN, et al. Liquid pressure versus surface pressure of the esophagus. J Appl Physiol 1967;23: 927–33.
76. Hoppin FG Jr, Green ID, Mead J. Distribution of pleural surface pressure in dogs. J Appl Physiol 1969;27:863–73.
77. Hurewitz AN, Sidhu U, Bergofsky EH, Chanana AD. How alterations in pleural pressure influence esophageal pressure. J Appl Physiol 1984;56:1162–9.
78. Marini JJ, Culver BH, Butler J. Effect of positive end-expiratory pressure on canine ventricular function curves. J Appl Physiol 1981;51:1367–74.
79. Wohl MEB, Turner J, Mead J. Static volume-pressure curve of dog lungs *in vivo* and *in vitro*. J Appl Physiol 1968;24: 348–54.

CHAPTER 56

GUIDE TO THE EVALUATION OF PULMONARY FUNCTION

Charles G. Irvin

The measurement of lung function is a key but often overlooked part of the work-up of the patient with lung disease. In fact, pulmonary function tests (PFTs) are often not performed even though the patient in question clearly has lung disease. One of the striking deficiencies observed among fellows in training for respiratory or pulmonary medicine is the paucity of training in and knowledge of pulmonary physiology and pulmonary function testing as well as the integration of both topics into clinical practice.

This chapter provides the reader a perspective on the interpretation of PFTs that is based on clinical experience. Some may also find this information useful in the interpretation of results derived from research projects and clinical trials. The interested reader is also referred to previous reviews and book chapters for further insights and more detail on certain topics, including various technical issues.[1–7]

Lung function tests can be invaluable in the assessment of patients with any disease and lung disease in particular. As an example, the measurement of the forced vital capacity (FVC) has been shown to predict heart disease and death due to all causes.[8,9] The forced expiratory volume in 1 second (FEV_1) is known to be correlated with mortality attributable to chronic lung disease.[10] Indeed, spirometry may be among the most useful clinical tests that we have.[11]

Lung function testing serves many purposes and is performed so as to answer a variety of important clinical questions (Table 56-1). All these questions are significant to the patient, and the answers can and do have an impact on clinical management. The only time that lung function evaluation is not helpful is if the patient fails to provide a minimum of adequate effort or cooperation. In many such cases, further testing and follow-up testing may be warranted if the results are equivocal or if clinically indicated.

Although there is a vast array of books, chapters, and reviews on respiratory physiology and on the technical aspects of performing tests, the literature is nearly devoid of guidelines for interpretation or examples of lung function results. It is with this shortcoming in mind that an attempt is made to provide a framework for interpreting PFTs.

CONCEPTS OF NORMALITY: PREDICTED EQUATIONS VERSUS REFERENCE VALUES

The first issue that must be addressed is normality—in other words, "What constitutes normal lung function?" For this question there is no firm answer of what "normal" lung function is exactly, but the usual practice is to compare an individual's test results with a "predicted" value derived from a reference population and to express this comparison as a percentage of the predicted value.[12–14] An alternative, and perhaps better, approach is to present data as a standard deviation score that takes into account variation in sex, age, and standing height.[12] In the interpretation of PFTs it is common practice to assess lung function results solely in regard to a percentage of predicted value, a practice that is flawed. The problem one encounters with this approach is illustrated by the following example. Suppose that a patient had an FEV_1 that was 110% of that predicted a year ago and now it is 90% of predicted value. For a man 50 years of age, using the National Health and Nutrition Examination Survey (NHANES) III data,[15] that would mean a fall of greater than 50 mL in FEV_1, more than twice the normal rate of 25 mL/year decline in FEV_1. If coupled with an increase in symptoms this might represent significant worsening in his disease status. Yet if one only had a single measurement of lung function at one point in time, one would conclude that the patient's lung function (90% of predicted value) was normal. This example also illustrates the importance of periodic measurement of lung function; however, many experts object to this practice. This seems surprising as health practitioners frequently do not have any problem in ordering serial determinations of blood pressures, radiographs, or other similar studies.[16]

The factors that influence lung function are multiple, but some factors are of particular importance (Table 56-2). These include age, sex, race, and standing height.[12,17]

Table 56-1 Questions in Interpreting Pulmonary Function Tests

Key questions
1. Is lung function within normal limits?
2. Is lung function abnormal?
3. Are the results borderline and therefore a prelude to further testing?
4. Are the patterns of results suggestive of a specific abnormality?
5. What is the severity of the disease?
6. Has there been (or not been) a deterioration in lung function?
7. Has there been (or not been) a response to therapy?

Other questions
1. Is the person at risk?
2. Is the patient suitable for surgery?
3. Is a drug affecting the lung (eg, bleomycin)?
4. Is the transplanted lung rejecting?
5. Has the exposure to chemical or other pollutants altered lung function?
6. Is there evidence of functional impairment or disability?
7. Has health status changed since the last time?

Table 56-2 Factors Influencing Lung Function

Factor	*Approximate effect*
Sex	30%
Age	8%
Height	20%
Weight	2%*
Race	10%
Technical	3–10%
Biology	30%

Adapted from Becklake M.[25]
*Weight becomes a more important factor for lung volumes (especially functional residual capacity) and if kg/cm > 1.0.[40]

The first of these factors, age, has a complex effect on lung function. During the first decades of life, lung volume and airway size increase in a more or less linear fashion. Although lung function assessment with traditional measures is limited to those aged 5 years and older, newer techniques of forced oscillation are possible in those of about 2 years of age.[18] Pediatric populations present further problems because of fewer high-quality studies, limited size of the study populations, and issues stemming from growth spurts. With the exception of spirometry, the measures of lung function require at least two equations to determine predicted values, one for patients who are younger than 18 to 20 years or so and another for those who are older.[12] Often this creates difficulties in interpretation as a person transfers from one predictive equation to another. The other end of the spectrum can also be problematic as most studies have a paucity of subjects beyond 65 years of age; however, it has been shown that extrapolations to older ages for spirometry, at least, are acceptable.[19]

The factor of ethnicity is more problematic because few studies have large numbers of ethnic groups other than Caucasians.[12,14] The one exception is for basic spirometry.[15] One general rule of thumb is that if one cannot trace a person's ethnic origins back to northern Europe, then a variable reduction of 5 to 15% in the predicted values is indicated.[12,14,16] A fixed reduction (eg, 12%) is not recommended. For persons of mixed ancestry the ethnic group that the person lays claim to should be used.

Standing height is the single most important variable that must be measured with each office visit as people are well known to misreport their height and height changes as they age. For persons with spine or thorax deformities or confined to wheelchairs, arm span is used. A misreport of height by 2 inches translates into 200 mL or about 8 years of lung aging, so do not rely on stated height; measure a patient's height with a stadiometer.

Lastly, the sex of the patient is an important factor. Women have smaller lung volumes and hence maximum expiratory airflows that are less than that for men. As many computer programs default to male sex, one should check each time to see that a female patient is not mistakenly identified as male, resulting in a misdiagnosis of restrictive disease. This is a common error.

When all is said and done, age, sex, race, and height account for only about 70% of the variance in lung function (see Table 56-2). The remaining 30% is attributed to biologic variation, which makes the diagnosis of lung disease as a cross-sectional determination difficult, particularly in a primary practice setting.[17] With the exception of spirometry, limited studies are available for other measures of lung function, and this becomes increasingly problematic as each generation is taller. As a result, the comparison of a current set of PFT results with previous studies is almost always more useful than the cross-sectional comparison to a reference equation.

Assess the patient relative to the predicted equations.[20] For example, a white patient 56 years of age of average height has a more predictable lung function than a short Asian of advancing years. In the former case one is more certain of the ability of a predicted equation to predict, whereas in the latter this ability is dubious, which is why some prefer to refer to predicted equations as reference values.[12] One should state that a patient's age, height, or race is outside the range or not covered by the subjects in the reference study used by the laboratory performing the testing.

PATIENT

The next step in evaluating a set of PFT results is to assess test quality. The guidelines for acceptable test quality have been extensively codified and so will not be repeated here.[12,16,21–24] Although getting good test results is always a laudable goal, there is perhaps too much attention paid to obtaining "publishable" data. It should be stressed that even tests of poor quality contain information because patients who do not provide reproducible data or cannot perform the maneuvers are likely to be sick or have lung disease.[12,16,25]

The key elements are, first, reproducibility and, second, maximal patient cooperation and effort. For spirometry, the FEV_1 should be reproducible within 200 mL, and patient effort should be carefully documented by the person performing the test. If patient effort is judged to be suboptimal, then more weight should be given to those measures that are less effort dependent, for example, functional residual capacity (FRC) and specific airway conductance (S_{gaw}) or diffusion capacity (DL_{co}).

For the interpretation to provide the best information to the physician caring for the patient, the interpreter should first ascertain why the patient was referred for testing. In all cases, but especially when asthma is in the differential diagnosis, consider the current disease status in interpreting results. Specifically, patients with asthma may have altogether normal function at the time of testing yet quickly deteriorate if exposed to a relevant antigen or other trigger.

SPIROMETRY

Spirometry is typically the first PFT to be performed in a patient. This is because the indications for performing spirometry are extensive (Table 56-3). The indications are so numerous, in fact, that it is a surprise that spirometry is so greatly underused.[8,11,26] There are several perceived and real barriers to its use, but these can be easily overcome by studying spirometry interpretation guides and by getting the right equipment and good training.[11,27] There are now excellent documents that provide knowledge and practice guidelines for performance of these tests.[16,28]

The first factor to consider is test quality. For the most part, spirometry results assume the patient made a maximal effort, in particular, that the patient inhaled all the way to total lung capacity (TLC). One should assess whether at least three acceptable traces are obtained, and even if only one trace is reported one should be sure the graphs or data selected are representative of the others. Next FEV_1 or FVC should be reported and compared with reference data values using the NHANES III reference[15,28] equations unless there is reason not to.

What constitutes an abnormal result? Although any values less than 80% and FEV_1 or FVC of less than 90% of predicted are common criteria for abnormality and are perhaps the easiest to remember (Table 56-4), such an approach increases the chance of misclassifications. A more scientific approach is to assess whether the patient's values fall below (or above) the 95% CI, hence forward referred to as lower limits of normal (LLN), or the SD score, which is essentially equivalent.[12] If either FEV_1 or FVC is abnormal, the results are abnormal.[12,28] Another useful measure, long known to be a sensitive indication of airflow limitation, is the FEV_1 or FVC expressed as a ratio with or as a percentage of predicted value; less than 90% of predicted or 70% of absolute value is abnormal.[12,28]

Table 56-3 Indications for Spirometry

To diagnose chronic obstructive pulmonary disease
To diagnose asthma
To monitor smokers who may develop chronic obstructive pulmonary disease
For staging of asthma or chronic obstructive pulmonary disease
To monitor dyspnea
To monitor restrictive lung disease
To detect hyperresponsiveness
To assess bronchodilator response
To assess workplace exposures
To assess preoperative risk of complications
To assess degree of impairment
To assess risk of mortality owing to all causes

Table 56-4 Approximate Limits of Normality for Common Pulmonary Function Tests

Test	*Lower limits of normal*	*Coefficient of variation*
FEV_1	≥80%	5%
FVC	≥80%	5%
FEV_1/FVC	≥90%	<5%
PEF	65–135%	20%
TLC	80–120%	10%
FRC	70–130%	10%
RV	60–140%	15%
S_{gaw}	≥70–80%	10%
DL_{CO}	75–125%	15%
PC_{20}	8–16 mg/mL	One doubling dose

Adapted in part from Pennock et al.[20]
DL_{CO} = diffusion capacity of carbon monoxide; FEV_1 = forced expiratory volume in 1 second; FRC = functional residual capacity; FVC = forced vital capacity; PC_{20} = provocative concentration of methacholine that drops FEV_1 20%; PEF = peak expiratory flow; RV = residual volume; S_{gaw} = specific airway conductance; TLC = total lung capacity.

Peak flow is often used as a surrogate for spirometry (ie, FEV_1, FVC, etc), but it has limited usefulness.[29,30] Two major shortcomings include its dependence on maximal effort by the patient and a lower sensitivity to airflow obstruction of smaller airways. Accordingly, a reduction in peak expiratory flow (PEF), in isolation from FEV_1 or FVC, is suggestive of either muscle weakness or, if the test is adequately performed, a central airways defect. As discussed below, inspection of the flow-volume trace will assist in the interpretation of such a finding.

BRONCHODILATOR RESPONSE

After baseline spirometry is determined, the patient should be given a bronchodilator unless there is a compelling reason not to do so because if the patient has lung function within normal limits the patient can still have a significant bronchodilator response.[31] Patients must be properly informed and instructed when medications need to be withdrawn, especially if the patient is on a long-acting bronchodilator, as a false-negative may otherwise result. A change of 12% or an absolute change of 200 mL represents a significant response.[12,32] A significant bronchodilator response indicates an underlying elevated cholinergic tone or an inflammatory process.

FORCED EXPIRATORY FLOW FROM 25 TO 75% OF FVC

The forced expiratory flow from 25 to 75% of FVC (FEF 25–75) is often, and inappropriately, used to assess small airways function. A low FEF 25–75 is interpreted as "small airways disease"—this is wrong. No conclusions regarding the site of disease can be drawn from this measurement. The FEF 25–75 is highly variable and very sensitive to differences in lung volume and other measurement artifact. By the time the FEF 25–75 is significantly decreased (<65% predicted),

the FEV_1/FVC ratio is also decreased.[12] Accordingly, the use of this index to determine small airways disease is strongly discouraged.

FLOW-VOLUME RELATION

One of the most useful measurements of lung function that can be made is the flow-volume relationship or "loop" (Figure 56-1). The flow-volume loop has a characteristic shape or configuration that takes on characteristic forms in certain forms of lung disease (Figures 56-2 and 56-3). As such, this gestalt or "inkblot" analogy forms the principal utility of this approach.[26,33] Visual evaluation of the flow-volume loop also provides an efficient and rapid approach to both the adequacy of the forced expiratory maneuver and functional assessment.[26]

To interpret upper airways obstruction, good patient effort and a reproducible flow–volume curve are required. Inspiratory airflow truncation is indicative of an extrathoracic upper airways obstruction, whereas a truncation of the expiratory flow is indicative of intrathoracic, lower airway obstruction (see Figure 56-2). If both inspiratory and expiratory flows are truncated a fixed central airways obstruction should be suspected. These patterns, and especially the extrathoracic (inspiratory truncation) pattern, are frequently missed[34] and is the reason to spend time reviewing all the graphical data.

LUNG VOLUMES

Recall that lung disease can be crudely separated into obstructive and restrictive processes; lung volumes usually increase in the former and decrease in the latter (Figure 56-4). The values of lung volume and capacity are a complex reflection of chest wall and lung recoil, respiratory muscle actions, and airway closure (Figure 56-5).[1,4,7,35,36] Moreover, lung volumes often give insight into severity and chronicity of the disease process. So, for example, in the case of the patient with asthma, the degree of hyperinflation measured as residual volume (RV) or FRC is related to disease severity. In severe cases or during an acute attack the TLC can become elevated.[1] Also, lung volumes give an indirect estimate of lung elastic recoil if one concludes that the chest wall is not involved, as is usually the case.[21,35–37] Lastly, lung volumes influence airflow because of airway–parenchymal interdependence, and, accordingly, measurement of airways resistance needs to be "corrected" for the lung volume at which it is determined and reported as specific conductance (Figure 56-6). After simple spirometry and examination of the flow-volume loops, the measurement of lung volumes provides the most information.[36] Lung volumes are especially informative and important to measure in exploring the patient who has a disease process causing a restrictive or a mixed pattern of abnormality of lung function (see Figure 56-3).

Of the various lung volumes and capacities (see Figure 56-4), the three boundaries of lung volume—FRC, RV, and TLC—yield the most insight into the disease process present.[1] The boundaries of lung volume are the maximal volume of air present after a full inspiration (TLC), the minimal amount of air remaining after a full expiration (RV), and the equilibrium point (FRC), the amount of air in the lung at the end of a normal exhalation (see Figure 56-4).

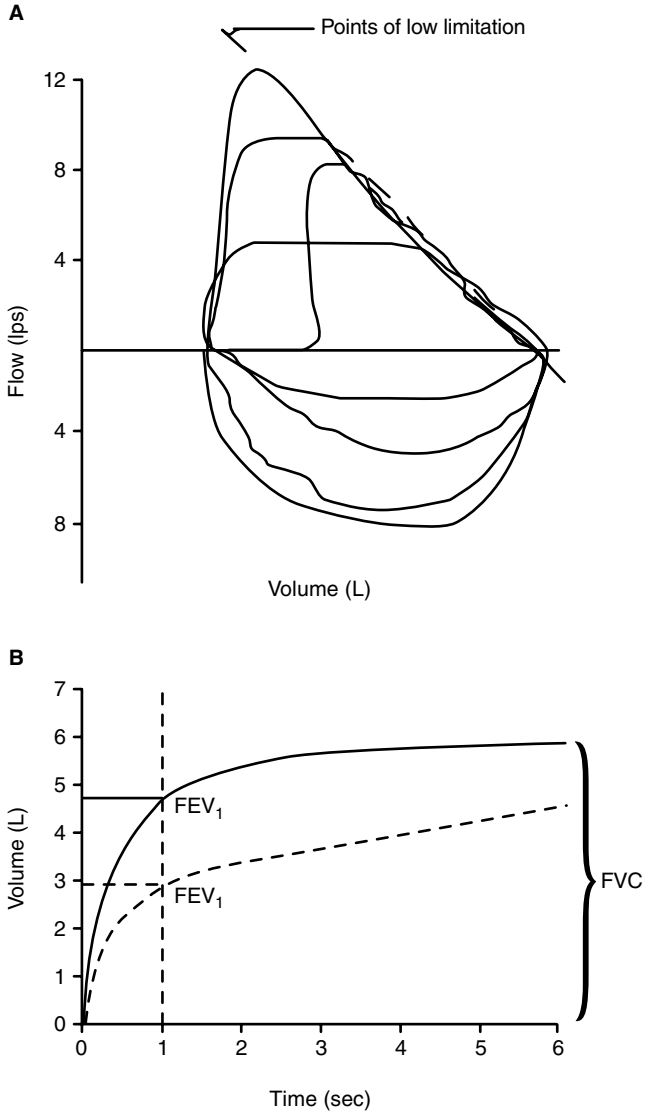

FIGURE 56-1 *A*, The *upper panel* depicts the flow-volume loop of a normal person. Flow is plotted against volume with the various "loops" representing different degrees of effort by a single patient. Whereas the inspiratory loop shows increasing flow with each increased effort, the expiratory loops show flow limitation. Even with a submaximal effort one can sometimes detect the existence of airflow limitation by reproducible shapes of the loop. The usefulness of the flow-volume loop comes in assessing various patterns and is the best display to assess patient effort. The early part of the expiration is emphasized by this presentation. *B*, The *lower panel* depicts the volume–time trace. The *solid curve* is a normal person, and the *dashed curve* is a patient with chronic obstructive pulmonary disease (COPD). Both curves show good starts with adequate expiratory times. Note that for the patient with COPD the "real" forced vital capacity (FVC) is never reached. The volume–time trace is most useful to measure the forced expiratory volume in 1 second (FEV_1), but it also assesses and emphasizes the later part of expiration. In short, these two displays are complementary.

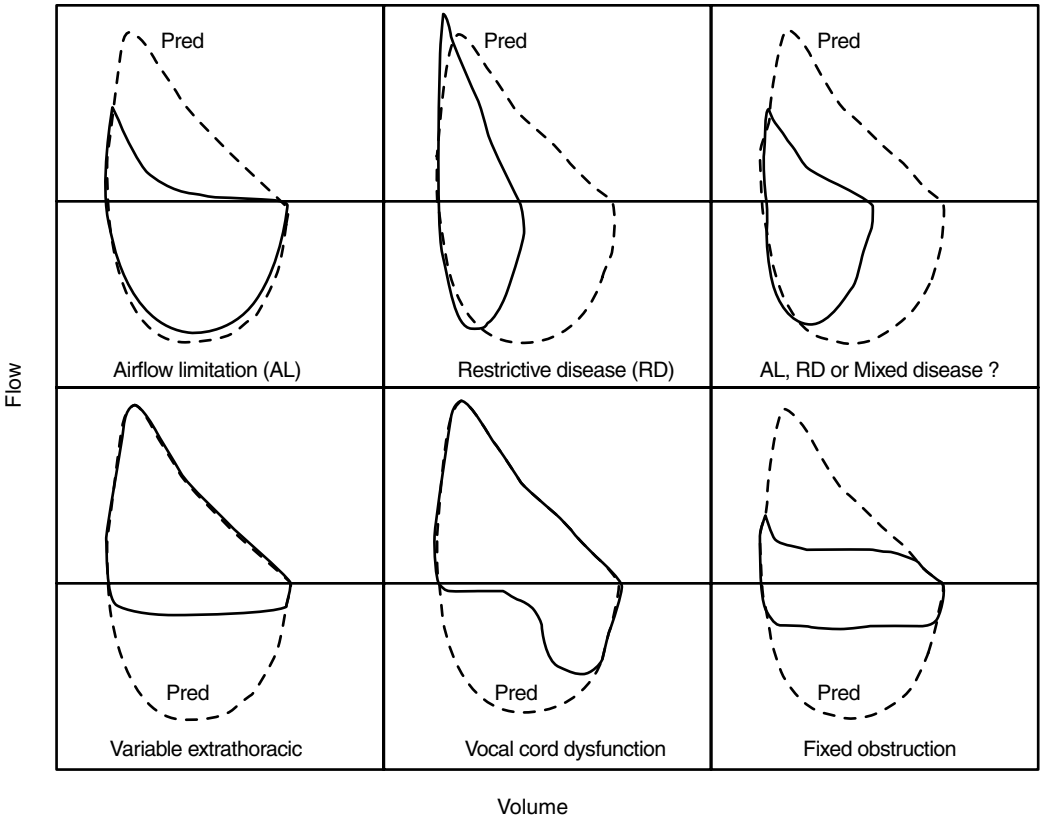

FIGURE 56-2 Schematic flow-volume loop from six different clinical situations that illustrate the utility of the flow-volume relationship for pattern recognition. The *dashed loops* are the predicted (Pred) normal flow-volume relationship. *Airflow limitation* (AL): Note the fall in flows and reduced flow in the later part of this pattern. Also referred to as variable intrathoracic obstruction. *Restrictive pattern* (RD): Note the reductions in forced vital capacity (FVC) and preservation of peak flow. This pattern is characterized by the steep expiratory flow pattern. *Mixed pattern*: This pattern shows a loss of flow and volume, the genesis of which is often unclear and requires further investigation (see Figure 56-3). *Variable extrathoracic*: Consistent truncation of the inspiratory flow characterizes the patient with variable extrathoracic obstruction (eg, collapse of the trachea). *Vocal chord dysfunction* (VCD): Often characterized by inspiratory flow that starts normally but then truncates as the chords adduct. *Fixed obstruction*: Relatively rare, the pattern of fixed obstruction shows truncation of both inspiratory and expiratory limbs of the flow-volume loops. Adapted from Irvin CG.[26]

FUNCTIONAL RESIDUAL CAPACITY

FRC is largely determined by the balance between the outward recoil of the chest and the inward recoil of the lung and unlike RV or TLC is not dependent on maximal voluntary maneuvers.[1,2] This is a useful thing to remember in a patient who cannot or will not perform maximal maneuvers. A decrease in the FRC/TLC ratio in a patient without an apparent chest wall restrictive process is very suggestive of a lung restrictive process, whereas an increase in the FRC/TLC ratio can be the result of either anxiety or hyperinflation, both commonly associated with airflow obstruction (see Figure 56-5).

RESIDUAL VOLUME AND TOTAL LUNG CAPACITY

In a normal adult the RV is determined by airway closure as the consequence of the instability of lung and airway patency as one expires to RV.[1] RV is more variable than TLC (see Table 56-4) but has been shown to rise even in patients with mild obstructive disorders. TLC is determined by chest wall elastic recoil and the ability of respiratory muscles to maximally distort the thorax; as such, adequate patient effort is needed to correctly assess this boundary. Expression of RV and FRC as a ratio with TLC helps deal with the uncertainty of the predicted values for various populations and is commonly used to assess hyperinflation (see Figure 56-5).

AIRWAYS RESISTANCE AND SPECIFIC CONDUCTANCE

As measurements of lung volumes are best performed with body plethysmography, an additional variable can be obtained, that of airways resistance (R_{aw}). Recall, however, that R_{aw} is highly lung volume dependent. Lung volume changes in disease and also changes during the performance of the R_{aw} panting maneuver, so the R_{aw} measurement is of little value (see Figure 56-6). Correction of these effects by calculating specific airway conductance (S_{gaw}) in large part corrects for this volume effect.[2,3,7] Accordingly, only use S_{gaw} in interpreting such results.[37] In adults S_{gaw} has a coefficient of variation (COV) of about 10% (see Table 56-4) but in spite of this shows good sensitivity. A decrease in S_{gaw} occurs in obstruction and can be

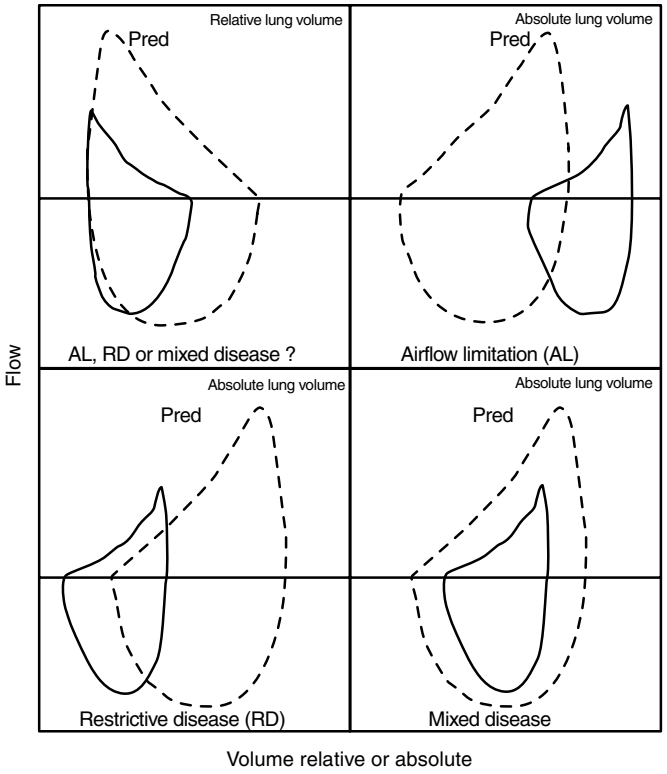

FIGURE 56-3 Schematic flow-volume loops of three possibilities to explain the mixed disease pattern from Figure 56-2. The *dashed line* is the predicted (Pred) relationship for a normal person. Three of the panels are the loops plotted at absolute lung volume where a measurement of functional residual capacity (FRC) (TGV) is first made in a body plethysmograph and then volume tracked throughout the maneuver. If the total lung capacity (TLC) is elevated then the patient has airflow limitation (eg, asthma or chronic obstructive pulmonary disease); if the TLC is decreased then the patient could have restriction or mixed disease as depicted. These examples show the importance of measuring lung volume. Adapted from Irvin CG.[26]

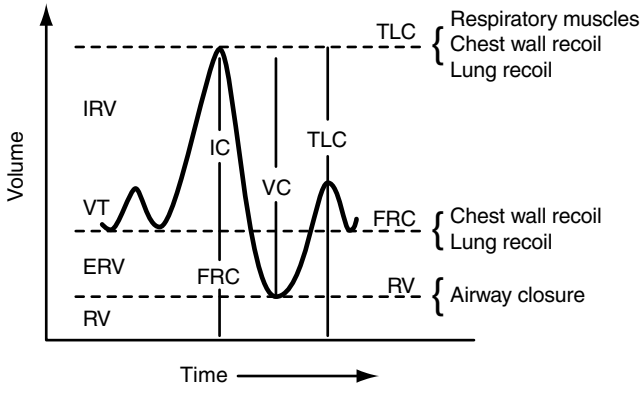

FIGURE 56-4 A plot of lung volume versus time of a typical spirogram where the efforts are slow but maximal. Lung volumes (tidal volume [VT]), expiratory reserve volume (ERV), inspiratory reserve volume (IRV), and residual volume (RV) are combined into lung capacities: vital capacity (VC), functional reserve capacity (FRC), inspiratory capacity (IC), and total lung capacity (TLC). Of these, TLC, FRC, and RV are the most useful and are determined by the factors listed. Hence, RV rises with airway closure, whereas a change in TLC is a complex relationship between respiratory muscles, chest wall recoil, and lung recoil. Modified from Irvin CG and Cherniack RM.[1]

independent of changes in volumes or FEV_1.[20] An increase in S_{gaw} is suggestive of a restrictive process, although the genesis of this increase is not altogether clear.

DIFFUSION CAPACITY

Of the battery of tests commonly ordered, the most illusive is the DL_{CO}. It is important to remember that the DL_{CO} measures the total area available for gas exchange at TLC and is unrelated to blood gas determinations of gas exchange.[2,3,8,23] In the determination of the DL_{CO}, a single breath maneuver of helium (or other inert gas) dilution is performed during which the alveolar volume (V_A) is determined. Ascertain that the DL_{CO} has been corrected for hemoglobin (Hb) or CO Hb if it is greater than 5%.[23,39,40] Although expressed as standard temperature and pressure, dry (STPD), for calculation of the DL_{CO}, V_A can also be expressed as body temperature and pressure saturated (BTPS), where in a normal person it should agree with TLC $\pm$ 200 mL.[2,4,35] In patients with large trapped-gas regions, the V_A (BTPS) will be much smaller than the TLC.[35] A high V_A relative to the TLC by body plethysmography is most suggestive of a leak in the DL_{CO} system, poor mouth seal, or a perforated eardrum. Coupled with spirometry results and clinical history, the DL_{CO} is very useful in distinguishing between different causes of airflow obstruction if the diagnosis is in doubt.[2,7] Low DL_{CO} is observed in emphysema, little change in bronchitis, and often raised DL_{CO} in asthma (Table 56-5).[39]

If the patient presents with unremarkable spirometry and values but a low DL_{CO}, strongly consider a vascular process (eg, pulmonary embolus); a high DL_{CO} with normal spirometry may be indicative of alveolar hemorrhage (eg, Goodpasture's syndrome). The DL_{CO} is also commonly used to assess possible rejection of a transplanted lung or resolution of a hemorrhagic process.

MIXED DISEASE PROCESSES

Patients often do not fit simple patterns of obstruction and restriction. This is particularly true of patients with interstitial lung disease (ILD) where there is often a significant involvement of the airways.[41] As a result, most patients presenting with ILD show a mixed pattern of restriction and obstruction. The obese patient (kg/cm $>$ 0.5 kg/cm) presents a situation where the chest wall is restricted[42] and coupled with airflow limitation will present a confusing picture of findings. In this regard simple spirometry is inadequate and more extensive investigations are indicated; in particular the measurement of lung volumes is often required. Remember that anytime a patient has a reduced FEV_1/FVC and in particular a reduced FVC, a restrictive or mixed process cannot be ruled out (see Figure 56-3).

AN APPROACH TO INTERPRETATION

There is nothing more controversial than to propose a hard and fast approach to interpretation of a battery of lung function tests. What follows is a somewhat simplistic and

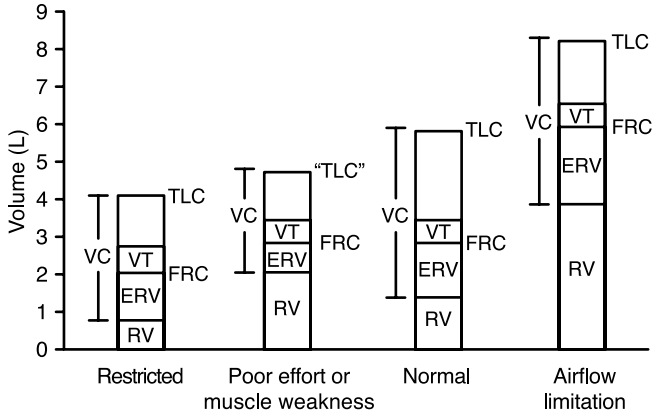

FIGURE 56-5 The division of lung volume is normal, restricted, poor effort or muscle weakness or in patients with airflow limitation or obstruction. *Restricted*: characterized by a fall in lung volumes, especially the total lung capacity (TLC) and residual volume (RV). *Effort or weakness*: depicted as a fall in TLC and rise in RV as the patient fails to maximally inspire or expire; it could also be a mixed process. Note that the functional residual capacity (FRC) is normal, which therefore is the only correct value. Accordingly, in patients in whom effort is suboptimal the FRC is the most reliable lung volume variable to assess. *Airflow limitation or obstruction*: characterized by a rise in first RV, then FRC, and finally TLC as shown.

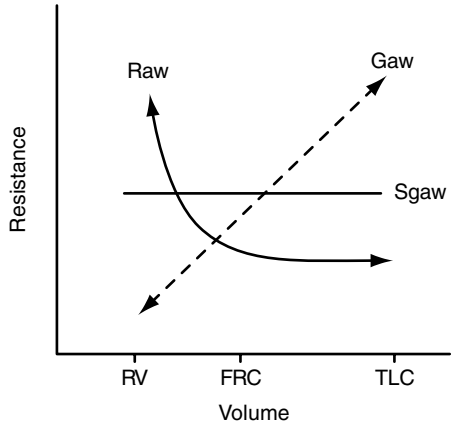

FIGURE 56-6 The relationship of total airway resistance (R_{aw}) to lung volume where R_{aw} rises as lung volume falls. On the other hand, a rise in lung volume causes R_{aw} to fall. The relationship between lung volume and resistance becomes linear when expressed as the reciprocal ($1/R_{aw}$) and reported as conductance (G_{aw}). To better account for lung volume changes that occur during its determination, R_{aw} is "corrected" for volume by dividing G_{aw} by TGV or function residual capacity (FRC) to obtain specific airway conductance (S_{gaw}). This measurement is the only meaningful measurement to be interpreted. Modified from Kaminsky DA and Irvin CG.[3]

incomplete discussion of the factors and considerations that go into an interpretation. Nevertheless, the following outline serves to introduce the reader to the rudiments of interpreting PFT results:

1. *Patient characterization*. The first thing to do is assess age and increase the lower limits of normal (LLN) if the patient is younger (age <15 years or so) or older (>65 years). Be sure the patient's sex has not been misidentified, especially as computer programs often default to male. Check that the height has been determined correctly. If the race cannot be linked to northern Europe then adjust the reference values accordingly (eg, for African Americans decrease by about 12%). Use race-specific reference equations wherever possible. Assess the patient's smoking status and determine if he or she is exposed to particulates, either of which would be expected to cause nonspecific mild airflow limitation.
2. *Test quality*. Assess all the data, including more than just the best effort reported; especially look at each of the flow-volume loops. Assess test–retest reproducibility (see Table 56-4); although achieving American Thoracic Society or European Respiratory Society criteria for reproducibility is a laudable goal, remember that the patient who has poor reproducibility or poor test quality may have an active disease process.[25] Accordingly, even poor quality data may still hold useful information. Be sure to read and understand any subjective evaluation by technicians of patient cooperation and effort.[43,44] One suggestion is that the report should rate test quality as one of three levels: *acceptable* (meets official society guidelines for quality), *suboptimal* (does not exactly meet guidelines but still appears to be useful or interpretable), and *questionable* (data are of limited usefulness).
3. *Lung volumes*. Consider the patient's ethnicity as well as weight-to-height ratio; kg/cm >0.5 would be expected to decrease FRC and kg/cm >1.0 will result in a decrease of TLC.[42] Assess RV and FRC ratios; where an elevated RV/TLC in isolation is suggestive of peripheral airway disease,[1,45] an elevated FRC/TLC is hyperinflation, as is an elevated TLC. Reduced lung volumes not explained by race or weight are interpreted as restriction.
4. *Airflows*. Assess spirometry, flow-volume loops, and specific airway conductance. Be sure to review all efforts and loops—data as well as graphics—for consistency and patterns of response. Avoid the use of terms such as mild, moderate, or severe as two patients with the same low FEV_1 can have radically different clinical presentations.[2] As such, terms such as mild, moderate, and severe are not nearly as helpful as just indicating that the patient does or does not have airflow limitation. However, such terms may be needed if the patient is being evaluated for disability. Interpretation of severe is acceptable in patients in whom FEV_1 is <1 L or 35% of predicted as mortality is likely within the next 5 years.[12,28] Be sure to note any patterns consistent with

Table 56-5 Patterns of Pulmonary Function Tests and the Clinical Utility of DL_{CO}

Clinical condition	*FEV_1*	*DL_{CO}*
Obstruction		
Emphysema	↓	↓
Bronchitis	↓	WNL
Asthma	↓	↑ or WNL
Normal spirometry		
Vascular process	WNL	↓
Hemorrhage	WNL	↑

DL_{CO} = diffusion capacity of carbon monoxide; FEV_1 = forced expiratory volume in 1 second; WNL = within normal limits.

fixed or extrathoracic obstruction (see Figure 56-2). Be alert for consistent, partial truncations of the inspiratory loop, indicative of vocal chord dysfunction (see Figure 56-2).

5. *Bronchodilator response*. If the S_{gaw} improves 25%, FEV_1 or FVC improves 12% and 200 mL, or there is a significant change in lung volumes (eg, FRC) of 15 to 20% or 500 mL, the patient has a significant bronchodilator effect.[31,38] However, the absence of significant bronchodilation in response to just two inhalations of salbutamol does not exclude acute bronchospasm as a cause of the reduced maximal expiratory airflows.
6. *Diffusion capacity*. If the DL_{CO} is outside the limits of normality, an abnormality may exist. High DL_{CO} with obstruction is consistent with asthma or obesity[39] and without obstruction is indicative of hemorrhage. Blood abnormalities such as anemia or elevated carboxyhemoglobin levels decrease the DL_{CO}, about 1.2% per percentage point increase carboxyhemoglobin and 4% per g/dL difference in hemoglobin.[23] Low DL_{CO} is consistent with emphysema if airflow limitation and hyperinflation coexist, whereas a low DL_{CO} with normal airflows is suggestive of a pulmonary vascular process. The DL_{CO}/V_A is of little clinical usefulness and should not factor into the interpretation.
7. *Comparison with previous results*. Compare the current set of findings with previous data. If the previous study was performed in another laboratory one can still compare the FEV_1 and FVC, but other variables are less reliable, especially the DL_{CO}.[46] Assess whether the lung function of the patient has significantly changed by assessing each variable and then give an overall impression of the trend (ie, better, worse, or unchanged). This is important as physicians often send patients home for a period of observation and follow-up. The signal-to-noise ratio or variability for a single test can be quite large, so long follow-up periods may be needed so a clear trend can be determined.[8,30,46]
8. *Additional testing*. Suggest further testing if clinically indicated. This might include pressure-volume relationships for patients with suspected restrictive process, bronchial challenge testing for patients suspected of having asthma but with a normal bronchodilator response (12%) or borderline airflow limitation,[47,48] and control of breathing determinations in patients with hyper- or hypoventilation.

Remember to provide answers to the questions that the referring physician is asking (see Table 56-1). Avoid merely stating which values are low or high. Be conservative in regard to a specific diagnosis unless you have access to all the clinical information. Lastly, expertise in interpretation is a skill that results from practice and a firm grasp of the physiologic principles involved.

CONCLUSIONS

The major limitation of the use and application of PFT results is how the results are interpreted. PFTs can identify the pattern and severity of lung disease and uncover processes not suspected when the tests were ordered. Before interpreting any PFT results, ascertain that the tests were of acceptable technical performance. A careful step-by-step assessment of all the tests will result in an accurate and useful interpretation that when coupled with the history, imaging, and other laboratory tests will provide diagnostic and prognostic utility to the treatment of the patient with respiratory disease. The cornerstone to making the most out of PFT results is a firm grasp of physiology and the physiologic principles upon which they are based.

ACKNOWLEDGMENTS

The author thanks Ted Marcy, MD, David Kaminsky, MD, and Muireann Ni Chroinin, MD, for their review of this material and their helpful suggestions and comments. The skilled preparation of this chapter is credited to Jean Hood.

REFERENCES

1. Irvin CG, Cherniack RM. Pathophysiology assessment of the asthmatic patient. Sem Resp Med 1987;8:201–15.
2. Corbridge T, Irvin CG. Pathophysiology of obstructive lung disease with emphasis on abnormalities of structure and function. In: Casaban R, Petty Th, editors. Principles and practice of pulmonary rehabilitation. Philadelphia (PA): W.B. Saunders Co; 1993. p. 18–32.
3. Kaminsky DA, Irvin CG. Lung function in asthma. In: Barnes PJ, Granstein MM, Leff AR, Woolcock AJ, editors. Asthma. New York: Lippincott-Raven Publishers; 1997. p. 1277–300.
4. Eidelman DH, Irvin CG. Airway mechanics. In: Busse WW, Wolgate ST, editors. Asthma and rhinitis. 2nd ed. Oxford: Blackwell Science; 2000. p. 1237–47.
5. Kaminsky DA, Irvin CG. New insights from lung function. Curr Opin Allergy Clin Immunol 2001;1:205–9.
6. Larsen GL, Kerby GS, Irvin CG. Pulmonary physiology in children and adults. In: Szefler SJ, Leung DYM, editors. Severe asthma: pathogenesis and clinical management. 2nd ed. New York: Marcel Dekker; 2001. p. 39–66.
7. Wagers S, Jaffe EF, Irvin CG. Development, structure and physiology in normal and asthmatic lung. In: Adkinson NF Jr, Younginger JW, Busse WW, et al, editors. Allergy principles and practice. 6th ed. 2003. Philadelphia: Mosby; p. 727–40.
8. Ferguson GT, Enright PL, Buist AS, Higgins MW. Office spirometry for lung health assessment in adults. Chest 2000;117: 1146–61.
9. Kannel WB, Lew EA. Vital capacity as a predictor of cardiovascular disease: the Farmingham study. Am Health J 1983;105: 311–5.
10. Burrows B, Lebowitz MD, Camilli AE, Knudsen RJ. Longitudinal changes in forced expiratory volume in one second in adults. Methodological considerations and findings in healthy smokers. Am Rev Respir Dis 1986;133:974–80.
11. Irvin CG. To blow or not to blow—that is the question. Respir Care 2002;47:1145–6.
12. American Thoracic Society. Lung function testing: selection of reference values and interpretive strategies. Am Rev Respir Dis 1991;144:1202–18.
13. Ghio AJ, Crapo RO, Elliott CG. Reference equations used to predict pulmonary function at institutions with respiratory disease training programs in the United States and Canada: a survey. Chest 1990;97:400–3.

14. Wanger J, Irvin CG. Appropriate predicted equations: race and ethnic issues. Respir Care 1984;29:765–7.
15. Hankinson JL, Odencratz JR, Fedan KB. Spirometric reference values from a sample of the general US population. Am J Respir Crit Care Med 1999;159:179–87.
16. American Thoracic Society. Standardization of spirometry: 1994 update. Am J Respir Crit Care Med 1995;152:1107–36.
17. Becklake M. Concepts of normality applied to the measurement of lung function. Am J Med 1986;80:1158–63.
18. Ducharme F. Davis G. Respiratory resistance in emergency department: reproducible and responsive measure of asthma severity. Chest 1998;113:1566–72.
19. Enright PL, Kronmal RA, Higgins M, et al. Spirometry reference values for women and men 65–85 years of age. Cardiovascular health study. Am Rev Respir Dis 1993;147: 125–33.
20. Pennock BF, Cottrell JS, Rodgers RM. Pulmonary function testing: what is normal? Arch Intern Med 1983;143:2123–6.
21. Quanjer PH, Tammeling GJ, Cotes JE, et al. Lung volumes and forced ventilatory flows. Report Working Party Standardization of Lung Function Tests, European Community for Steel and Coal. Official Statement of the European Respiratory Society. Eur Respir J Suppl 1993;16:5–40.
22. Stocks J, Quanjer PH. Reference values for residual volume, functional residual capacity and total lung capacity. ATS Workshop on Lung Volume Measurements. Official Statement of the European Respiratory Society. Eur Respir J 1995;8:492–506.
23. ATS Committee on Proficiency Standards for Clinical Pulmonary Laboratories. Single-breath carbon monoxide diffusing capacity (Transfer factor). Am J Respir Crit Care Med 1995;152:2185–98.
24. Wanger J, Crapo RO, Irvin CG, editors. Pulmonary function laboratory management and procedure manual. New York: American Thoracic Society; 1998.
25. Becklake M. Epidemiology of test failure. Br J Ind Med 1990; 4:73–4.
26. Irvin CG. Asthma: pulmonary function tests. UpToDate in Pulm Dis and CC [CD-ROM module]. Wellesley (MA): UpToDate; 1996.
27. Wanger J, Irvin CG. Office spirometry: equipment selection and training of staff in the private practice setting. J Asthma 1997;34:93–104.
28. Petty TL, Enright PL. Simple office spirometry for primary core practitioners. National Lung Health Education Program; 2003. Available at: http://www.nlhep.org/resources.html.
29. Irvin CG. Throwing the baby out with the bath water. J Asthma 1996;33:275–6.
30. Sly PD. Peak expiratory flow monitoring in pediatric asthma: is there a role? J Asthma 1996;33:277–8.
31. Nicolls MD, Wanger J, Irvin CG. Bronchodilator response in the "borderlands." Respir Care 1997;42:230–2.
32. Eliasson O, Degraff AC Jr. The use of criteria for reversibility and obstruction to define patient groups for bronchodilator trials: influence of clinical diagnosis, spirometric and anthropometric values. Am Rev Respir Dis 1985;132: 858–64.
33. Miller RD, Hyatt RE. Obstructing lesions of the larynx and trachea. Mayo Clin Proc 1969;58:1305–13.
34. Hnatiuk O, Moores L, Loughney T, Torrington K. Evaluation of internists' spirometric interpretations. J Gen Intern Med 1996;11:204–8.
35. Wade J, Mortenson R, Irvin CG. Physiological evaluation of bullous emphysema. Chest 1991;100:1151–4.
36. Irvin CG. Lung volume: a principle determinant of airway smooth muscle function. Eur Respir J 2003;22:3–5.
37. Wagers SS, Bouder TG, Kaminsky DA, Irvin CG. The invaluable pressure-volume curve. Chest 2000;117:578–83.
38. Smith HR, Irvin CG, Cherniack RM. The utility of spirometry in the diagnosis of reversible airways obstruction. Chest 1991;101:1577–81.
39. Saydain G, Beck KC, Decker PA, et al. Clinical significance of elevated diffusing capacity. Chest 2004;125:446–52.
40. Wanger J, Irvin CG. Importance of correcting diffusing capacity for hemoglobin and alveolar volume. Respir Care 1984;29: 1240–3.
41. Kreiss K, Greenburg L, Kogut S, et al. Hardrock mining exposures affect smokers and nonsmokers differently: results of a community prevalence study. Am Rev Respir Dis 1989;139:1487–93.
42. Ray CS, Sue DY, Bray G, et al. Effect of obesity on respiratory function. Am Rev Respir Dis 1983;128:501–9.
43. McDonnell TJ, Irvin CG. Reduced lung volume: muscle impairment or lung disease? Respir Care 1985;30:202–5.
44. Wanger J, Irvin CG. Can't or won't. Respir Care 1994;39:67–9.
45. Kraft M, Pak J, Martin RJ, et al. Distal lung dysfunction at night in nocturnal asthma. Am J Respir Crit Care Med 2001;163: 1551–6.
46. Wanger J, Irvin CG. Comparability of pulmonary function results from 13 laboratories in a metropolitan area. Respir Care 1991;36:1375–82.
47. Matz J, Irvin CG. A bronchodilator response does not asthma make. Respir Care 1991;36:53–5.
48. Irvin CG. Asthma: bronchial challenge. UpToDate in Pulm Dis and CC [CD-ROM module]. Wellesley (MA): UpToDate; 1996.

CHAPTER 57

SINGLE-BREATH CARBON MONOXIDE DIFFUSING CAPACITY OR TRANSFER FACTOR

David J. Cotton, Brian L. Graham

In 1915 Marie Krogh first described the single-breath diffusing capacity of the lung for carbon monoxide (DL_{CO}^{SB}), proving that passive diffusion alone could explain gas transport across the air-blood barrier and putting to rest the once popular belief that the alveolar epithelium functioned like a gland, actively secreting oxygen (O_2) into capillary blood.[1] Today, the test is recognized as a unique screening tool to examine the integrity of the air-blood barrier. In the United States, the average pulmonary function laboratory performs >800 DL_{CO}^{SB} tests per year.[2] The "diffusing capacity" is not the best choice of term since it is a conductance (the inverse of resistance) rather than a "capacity," and CO uptake involves not only passive diffusion but also chemical binding with hemoglobin (Hb). Outside North America it is called the *transfer factor*.

PRINCIPLES OF DIFFUSION

DL_{CO}^{SB} measures the overall ability of the lung to transfer CO from air to blood and, by inference, is a surrogate measure of O_2 diffusion. In a steady state, Fick's law states:

$$\text{Gas transfer} \propto A \cdot D \cdot (P_2 - P_1)/T \qquad (57\text{-}1)$$

The flux or mass transfer of gas molecules across the air-blood barrier is directly proportional to the surface area of the membrane (A), inversely proportional to its thickness (T), and directly proportional to the driving pressure, or difference in partial pressure, of the gas across the membrane ($P_2 - P_1$). The diffusivity (D) of the gas species is its solubility, divided by the square root of its molecular weight. Gas diffusion for CO is the flux (mL/min) of CO molecules across the air-blood barrier, divided by the driving pressure (mm Hg) of CO between the alveolar air and capillary blood. Krogh chose CO rather than O_2 because the affinity of CO for Hb is 225 times greater than the affinity of O_2 for Hb, so the effective capillary CO pressure is assumed to be zero.[1] Hence, the driving pressure for CO is determined by measuring only the fractional CO in the alveolar gas and the barometric pressure (P_B).

PHYSIOLOGIC FACTORS AFFECTING DL_{CO}^{SB}

Components of DL_{CO}^{SB}

The pathway for CO from air to blood (Figures 57-1 and 57-2) classically consists of two resistances in series.[3] The first is $1/D_M$, or the "extra-Hb resistance," due to the diffusing capacity of the alveolar membrane (D_M). This resistance is the result of passive diffusion through an astonishingly thin minimal tissue barrier (<0.6 μm), consisting of the alveolar epithelial type 1 cell, a fused basement membrane, and a capillary endothelial cell. Additionally, there is an intracapillary component consisting of an "unstirred" plasma layer surrounding the red cell,[4] the red cell membrane, and cytoplasm.

The second resistance ($1/\theta V_C$), or the "intra-Hb resistance," is owing to the CO conductance within the red cells in the pulmonary capillary blood.[3] The rate (mL/min/mm Hg) of chemical combination of CO with Hb (θ), per mL of whole blood, measured in vitro using venous blood at a standard Hb concentration, estimates the finite reaction rate of CO binding with Hb. Knowing the total volume of capillary blood exposed to alveolar air (V_C), the overall conductance of the blood for CO transfer (θV_C) can be calculated (see Figures 57-1 and 57-2). Hence,

$$1/DL_{CO} = 1/D_M + 1/(\theta V_C) \qquad (57\text{-}2)$$

The extra-Hb resistance ($1/D_M$) is independent of alveolar [O_2], whereas the intra-Hb resistance ($1/\theta V_C$) changes with alveolar [O_2] because O_2 competes with CO for the same Hb binding sites, causing θ to decrease with increasing [O_2]. D_M and V_C are estimated from at least two measurements of DL_{CO}^{SB} and θ at different alveolar [O_2]. A plot of $1/DL_{CO}^{SB}$ (y axis) versus $1/\theta$ (x axis) yields a straight line where the y intercept is $1/D_M$ and the slope is $1/V_C$.[3] The measurement of V_C depends critically on accurate measurements of θ, which must be indirectly estimated using in vitro mixing chambers.[3] Furthermore, θ depends directly on the capillary hematocrit (Hct), which is assumed to be the same as systemic venous values but is actually substantially lower in

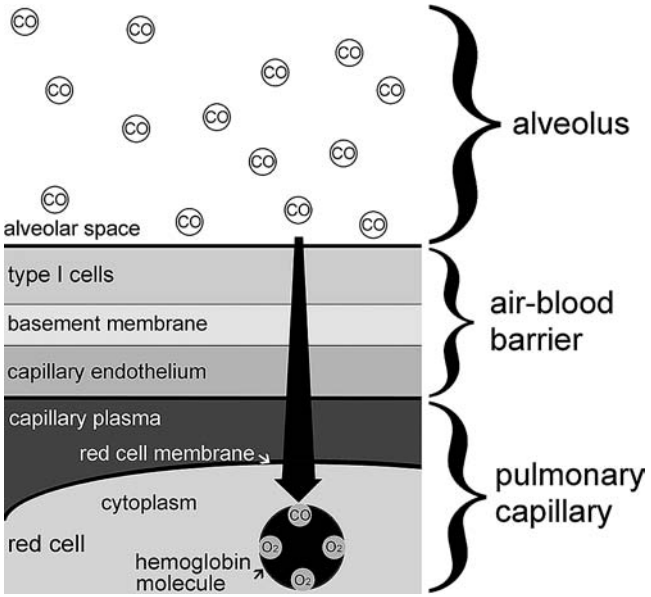

FIGURE 57-1 The pathway for CO: The extra-Hb ($[O_2]$ independent) component ($1/D_M$) is represented by the *arrow*. It consists of a thin (<6 μm) tissue barrier (air-blood barrier), the capillary plasma, the red cell membrane, and the red cell cytoplasm. The intra-Hb ($[O_2]$-dependent) resistance ($1/\theta V_c$) is due to the finite time for the chemical binding of CO with the Hb molecule, within the red cell. Structures are not drawn to scale.

the pulmonary capillaries than in the systemic circulation.[5] In normal subjects D_M is very large, so most of the diffusive resistance is a result of the chemical combination of CO with Hb (see Figure 57-1). Diseases that damage the alveolar-capillary membrane likely reduce both D_M and V_C because the alveolar epithelium and pulmonary capillaries are anatomically in such close proximity. Measuring the components of DL_{CO}^{SB} (D_M and V_C) usually adds little additional, useful clinical information, particularly because of inaccuracies in estimating θ.

Although ignored in the classic analysis, part of the CO pathway involves gas-phase transport, by both convection and gas diffusion, from the more proximal airways to the more distal gas-exchanging bronchioles and alveoli (see Figure 57-2). The mixing of a gas rich in CO and a tracer gas, helium (He), is neither instantaneous nor complete during inhalation and short periods of breath holding (t_{BH}). Time-dependent gradients in CO and He concentration ([CO] and [He], respectively) develop in the lung periphery, distal to terminal bronchioles.[6] This lowers the [CO] at the air-blood interface and, by reducing the effective driving pressure for CO, lowers DL_{CO}^{SB}. The simultaneously created, time-dependent gradients for He result in worsening of ventilation inhomogeneity. This incomplete gas-phase mixing creates a third "gas-mixing" conductance, called G_{MIX},[7] which is normally so large that it does not affect the pathway for CO.[8] However, when gas-phase mixing worsens, G_{MIX} decreases.[9,10] In this case, the pathway for CO becomes

$$1/DL_{CO} = 1/G_{MIX} + 1/D_M + 1/(\theta V_C) \qquad (57\text{-}3)$$

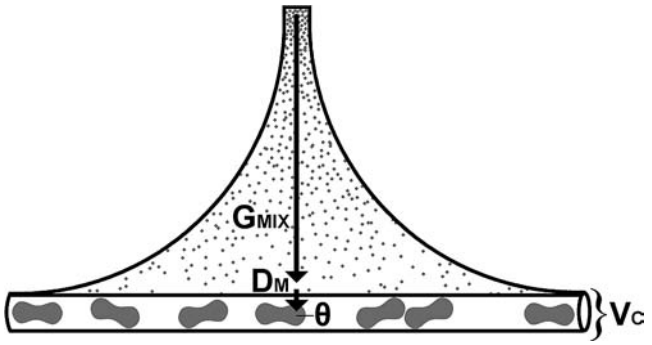

FIGURE 57-2 Gas-mixing resistance ($1/G_{MIX}$): The cumulative cross-sectional area of the airways and alveoli is represented by a single trumpet and the pulmonary capillaries by a volume of blood (V_C) containing red cells (biconcave disks). The classic components are the two resistances: $1/D_M$ and $1/\theta V_C$. The decreasing density of dots within the trumpet depicts a transient gradient for [CO] and [He] during inhalation and breath holding, caused by incomplete mixing of inspired gas with resident gas. This creates a third "gas mixing" resistance ($1/G_{MIX}$), in series with $1/D_M$ and $1/\theta V_C$.

Pulmonary Capillary Recruitment

DL_{CO}^{SB} is not maximal in normal, seated subjects at rest because the pulmonary capillary bed is not fully recruited, that is, open or distended. Capillaries behave like millions of highly collapsible tubes connected in parallel and stacked in sheets one above the other. Gravitational forces create a gradient in pulmonary perfusion and, hence, also in diffusion that is greater in the base than the apex of the lung.[11] There are three zones of perfusion that are not only influenced by the prevailing alveolar pressure (P_A) but are also affected by pulmonary artery pressure (P_a) and pulmonary venous pressure (P_v). In zone III, at the bottom of the lung where P_a and P_v exceed P_A, capillaries are mostly recruited and distended. With distance down this zone, capillaries become more distended, thus increasing regional V_C. In zone II in the midlung region, where P_a is higher than P_v, but P_A exceeds P_v, a waterfall or sluice effect develops whereby capillary blood flow depends on the difference between P_a and P_A. For capillaries situated gravitationally lower down this zone, there is progressively greater recruitment or distention, thus increasing regional V_C and D_M. In zone I at the lung apex, where P_A exceeds both P_a and P_v, there is minimal blood flow, so the capillaries are nearly empty, and regional V_C and D_M approach zero. These factors determine the degree of pulmonary capillary recruitment in response to physiologic stimuli and in lung diseases.

Hemoglobin

DL_{CO}^{SB} increases with increasing Hb concentration ([Hb])[12] and decreases with decreasing [Hb][13] because θ is directly proportional to [Hb]. Although adjustment of DL_{CO}^{SB} to a standard [Hb] (146 g/L for men and 134 g/L for women) is recommended,[14] the precise effect of changes in Hb on DL_{CO}^{SB} is controversial. A commonly recommended theoretical adjustment,[14] which assumes that D_M/V_C is 0.7 (or 230 in SI units), underestimates the effect of anemia on DL_{CO}^{SB}. In patients recovering from severe anemia DL_{CO}^{SB}

increases 1.4 mL/min/mm Hg for every 10 g/L increase in [Hb].[13] Empiric observations in anemic patients reveal that DL_{CO}^{SB} decreases 7% for every 10 g/L decrease in [Hb],[15] but the effect in a general (nonanemic) population is only about 2% per 10 g/L.[16]

Carboxyhemoglobin

Carboxyhemoglobin (COHb) is present in small concentrations (≤1%) in nonsmokers but increases with repeated DL_{CO}^{SB} testing[17] and also increases up to 10% or higher in chronic smokers. Failure to adjust DL_{CO}^{SB} for increasing COHb causes two separate effects. First a portion of the Hb becomes bound by CO and, hence, is no longer available for further CO uptake, thus reducing the effective [Hb]. This is called the "anemia effect." Empirically increasing DL_{CO}^{SB} by 1% for every 1% increase in COHb[18] approximates the adjustment for this effect. Second DL_{CO}^{SB} is still underestimated unless adjustment is also made for the ambient alveolar [CO], or "back-pressure," in the lung prior to each single breath. This is assumed to be zero but is actually increased in smokers.[17] When ignored, the decay of CO during t_{BH} is underestimated and, hence, DL_{CO}^{SB} is reduced. For a COHb of 10%, DL_{CO}^{SB} is still spuriously decreased by approximately 6 to 10% if adjusted for COHb but not for CO back-pressure.[17] Abstaining from smoking for 24 hours prior[14] eliminates any COHb and CO back-pressure, but this is not practical in heavy smokers.

Alveolar Volume

If the normal lung were a collection of spheres and if DL_{CO}^{SB} were directly proportional to the surface area of the spheres, then DL_{CO}^{SB} would vary with alveolar volume $(V_A)^{2/3}$. In reality, capillary surface area, and hence DL_{CO}^{SB}, is preserved with decreasing V_A because the alveolar-capillary membrane tends to fold, rather than shrink, as lung volume decreases. Partitioning of the longitudinal distribution of pulmonary vascular resistance reveals that the resistance of the "alveolar segment" decreases with decreasing V_A from total lung capacity (TLC) to functional residual capacity (FRC)[19] because pulmonary capillaries widen, thus increasing V_C with decreasing V_A. Hence, decreasing V_A from TLC to 50% of inspiratory capacity (IC) decreases DL_{CO}^{SB} minimally.[17] DL_{CO}^{SB} is also affected by volume history because alveolar surface tension is lower on deflation versus inflation. Alveolar capillaries therefore bulge more into the alveolus on deflation than on inflation at the same absolute V_A,[20] so DL_{CO}^{SB} is higher when the same absolute V_A is achieved by deflation from TLC versus inflation from FRC.[21] A deep breath immediately prior to testing therefore increases DL_{CO}^{SB} by at least 10%.[22]

CONVENTIONAL MEASUREMENTS OF DL_{CO}^{SB}

Historical Development of Conventional DL_{CO}^{SB} Testing

Krogh had subjects inhale a vital capacity (VC) breath of CO-rich gas, at which time two alveolar samples were collected.[1] The first was collected during an immediate exhalation to about 1/2 VC, to measure the [CO] (F_ACO_{t0}) at the beginning of breath holding (t_0). After breath holding (t_{BH}) for 6 seconds, the second sample was collected, to measure the [CO] (F_ACO_{t1}) at the end of breath holding (t_1). V_A was determined separately using the dilution of hydrogen. Assuming exponential CO decay, the "Krogh equation" accurately describes diffusion of CO into the blood for t_{BH} during apnea:

$$DL_{CO}^{SB} = V_A \cdot \ln(F_ACO_{t0} / F_ACO_{t1}) / t_{BH} / (P_B - 47) \quad (57\text{-}4)$$

P_B is the ambient, barometric pressure in dry gas. V_A is TLC–dead space (V_D). The units, standard temperature, and pressure, dry (STPD), are mL/min/mm Hg. To convert to SI units (mmol/min/kPa), divide the value by 2.986.

Krogh's DL_{CO}^{SB} method was ignored until 1957, when Ogilvie[23] proposed eliminating the first alveolar sample by incorporating an inert gas, He, in the test gas. Ogilvie's[23] standardized DL_{CO}^{SB} test, still in use today (Figure 57-3), had subjects rapidly inhale test gas containing 0.3% CO, 10% He, and 21% O_2, balance N_2 from residual volume (RV) to TLC. After an arbitrary t_{BH} of 10 seconds, subjects exhaled to RV. After exhaling sufficient gas to clear V_D, a single alveolar sample was collected to measure the alveolar [CO] (F_ACO_{t1}) and [He] (F_AHe_{t1}) (see Figure 57-3). Instead of directly measuring the [CO] at time zero (F_ACO_{t0}), Ogilvie's major modification[23] was to use the simultaneously measured dilution of He to estimate the [CO] at the onset of breath holding, where

$$F_ACO_{t0} = F_ICO \cdot F_AHe_{t1} / F_IHe \quad (57\text{-}5)$$

The [CO] and [He] in the inspired gas are F_ICO and F_IHe, respectively. Ogilvie collected all of the alveolar gas, except the first liter (to clear V_D), and measured t_{BH} from onset of inhalation (t_0) to the beginning of sample collection (t_1) (see Figure 57-3).[23] DL_{CO}^{SB} was

$$DL_{CO}^{SB} = V_A \cdot \ln(F_ACO_{t0} / F_ACO_{t1}) / (t_1 - t_0) / (P_B - 47) \quad (57\text{-}6)$$

In 1961, Jones and Meade[24] recognized that errors were caused by applying the Krogh breath-holding equation (see Equation 57-3), valid only for the portion of t_{BH} during apnea, to Ogilvie's method.[23] Errors could be minimized by measuring an "adjusted" t_{BH}, from 3/10 of the time of inhalation to the time for one-half of the alveolar sample collection, and by collecting a small (85 mL) alveolar gas sample (see Figure 57-3).[24]

Conventional DL_{CO}^{SB} Method in Current Practice

Current recommendations (see Figure 57-3) for a standardized method[14,25] use modifications of Ogilvie's method to calculate DL_{CO}^{SB} (see Equation 57-6). Ogilvie[23] used an independent method to measure V_A, but today V_A (converted to STPD) is measured from the single breath dilution of He, as proposed by McGrath and Thompson,[26] where

$$V_A = VC \cdot F_IHe/F_AHe_{t1} - V_D \quad (57\text{-}7)$$

The Jones and Meade[27] method (see Figure 57-3) of measuring the adjusted t_{BH} is preferred,[24] but alternate methods remain in common use. Many lung function testing systems

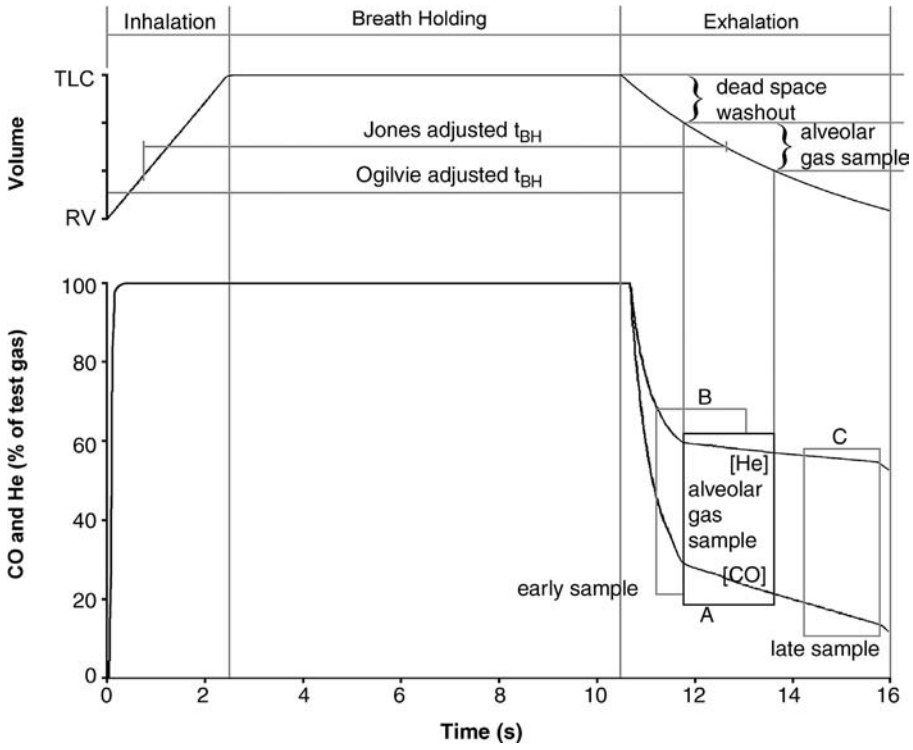

FIGURE 57-3 Conventional (standardized) DL_{CO}^{SB}.[14] Changes in volume (*upper graph*) and continuous analysis of [CO] and [He] (*lower graph*) are plotted versus time (s) on the x axis. At RV, seated subjects rapidly inhale test gas to TLC and, after breath holding, exhale smoothly. Recommendations include inhalation time <2.5 s (<4 s in COPD patients); inspired volume >90% of VC; adjusted t_{BH} of 9–11 s (Jones adjusted t_{BH} preferred rather than Ogilvie's method; see text); P_A not measured, but changes minimized by the patient relaxing against a closed glottis or valve during t_{BH}; smooth exhalation, but not necessarily forced; dead space washout of 0.75–1.0 L (reduced to 0.5 L if VC < 2.0 L); collection of an alveolar gas sample of 0.5–1.0 L (sample A) with sample collection time <4.0 s); no smoking for 24 hr prior to testing. Use of rapidly responding analyzers prevents collecting the sample too early (sample B), which causes contamination of the alveolar sample with dead space gas, lowering DL_{CO}^{SB},[30] whereas collecting alveolar gas later in exhalation (sample C) increases DL_{CO}^{SB}[28] (see text).

still allow washout of a fixed volume (0.75–1.0 L) during the initial phase of exhalation, assuming that V_D is smaller than this value. Thereafter, a fixed alveolar sample (0.5–1.0 L) is collected to measure alveolar [CO] and [He]. More recently, use of rapidly responding analyzers for both CO and a tracer gas (methane) improves testing by more accurately defining the dead space washout of CO, so that the timing of the alveolar sample is appropriate (see Figure 57-3, sample A).

PITFALLS IN CONVENTIONAL DL_{CO}^{SB}

Computational Errors

Since the Krogh equation is valid only when inhalation and exhalation are infinitely fast, conventional methods are accurate only when single breath approaches this ideal. Deviations from the ideal cause computational errors in DL_{CO}^{SB} because the Krogh equation does not accurately describe the changes in alveolar [CO] during either inhalation or exhalation, even assuming a homogeneous lung model. This is an important pitfall because only about 70% of the adjusted t_{BH} actually occurs during apnea at TLC, even under optimal conditions. At least 10% of the adjusted t_{BH} occurs during inhalation, whereas at least an additional 20% usually occurs during exhalation (see Figure 57-3). Rapid exhalation is not mandated because of limitations in testing equipment and patient cooperation or capability.[14,25] Decreasing the exhaled flow rate increases DL_{CO}^{SB}[23,24,28,29] because a greater proportion of CO uptake occurs at lung volumes below TLC when CO is disappearing from the lung, not only by diffusion into the blood but also by exhalation. When the inhaled flow rate decreases, DL_{CO}^{SB} decreases because the adjusted t_{BH} is represented mostly by inhalation, during which time CO has had insufficient time to reach the air-blood barrier.[29] Decreasing t_{BH} markedly reduces the proportion of time that actually occurs during apnea, and, hence, the Krogh equation is no longer mathematically accurate. Its use has variable effects on DL_{CO}^{SB}, depending on the measurement of the adjusted t_{BH}, the amount of time spent during inhalation and exhalation, and the details of alveolar sample collection. DL_{CO}^{SB} increases with decreasing t_{BH} using Ogilvie's method,[23] whereas Jones and Meade's method, using small (85 mL) alveolar samples, is less affected by decreasing t_{BH} in normal subjects.[27]

The size and timing of the alveolar sample collection cause further variability. Collecting the sample too early will include V_D in the alveolar gas, causing DL_{CO}^{SB} to be grossly underestimated because CO-rich dead space gas contaminates the alveolar sample (see Figure 57-3, sample B).[30] DL_{CO}^{SB} is slightly overestimated if V_D is not subtracted from V_A. In the conventional DL_{CO}^{SB} method a fixed washout volume is used (0.75–1.0 L),[14] which assumes that this volume is adequate to wash out V_D. However, the washout volume actually exceeds 1.0 L in 26% of cases when measured using a rapidly responding analyzer.[31] Furthermore, DL_{CO}^{SB} is progressively overestimated the later in exhalation that an alveolar sample of fixed size is collected because a greater proportion of the adjusted t_{BH} occurs during exhalation (see Figure 57-3).[28,29] When the entire alveolar sample is collected, DL_{CO}^{SB} is overestimated[32] because Ogilvie's adjusted t_{BH} (see Figure 57-3), which stops at the onset of sample collection,[23] ignores CO diffusion into the blood during sample collection.

Lung Volume

Measuring DL_{CO}^{SB}/V_A, the so-called Krogh's constant, does not compensate for the effect of changing V_A because this ratio is not constant as lung volume decreases. With decreasing V_A, DL_{CO}^{SB} decreases far less than V_A, so DL_{CO}^{SB}/V_A actually increases, and the increase is much greater when the single breath is immediately preceded by a deep breath or sigh.[33] For maneuvers preceded by a deep breath, DL_{CO}^{SB}/V_A increases by 15% when IC decreases from 100 to 50%.[33] The practice of using DL_{CO}^{SB}/V_A to "correct" DL_{CO}^{SB} for variations in lung volume is therefore not recommended.

Inert Gas Dilution

The principle of inert gas dilution[23,26] assumes homogeneous mixing of inspired gas with alveolar gas. When the distribution of ventilation is nonuniform, computational errors occur in measuring V_A (see Equation 57-7) and F_ACO_{t0} (see Equation 57-5) because the phase III slope for the tracer gas (He), rather than being horizontal, is negative (Figure 57-4) and the slope is steeper with shorter t_{BH}, with smaller inspired volumes, and in patients with airway disease. This causes F_AHe_{t1} to be higher both when an alveolar sample is collected early versus late in exhalation (see Figure 57-3, sample A vs C) and when a smaller versus larger alveolar gas sample is collected after a fixed washout volume. Whenever F_AHe_{t1} increases, V_A decreases (see Equation 57-7) and F_ACO_{t0} increases (see Equation 57-5).[31] In patients with airflow obstruction, V_A is underestimated by 7 to 9% when measured from a 1.0 L alveolar sample and by 9 to 13% when measured from a 0.2 L alveolar sample.[9] The two errors (measuring V_A and F_ACO_{t0}) have opposite effects on DL_{CO}^{SB}, but if F_ACO_{t1} (see Equations 57-4 and 57-6) were the same in the calculation, the net effect is an increase in DL_{CO}^{SB} because the CO decay term is logarithmic (see Equation 57-6). In practice, the overall effect is complicated since the [CO] in the alveolar gas sample (F_ACO_{t1}) also varies with the size and timing of sample collected (see Figure 57-3).

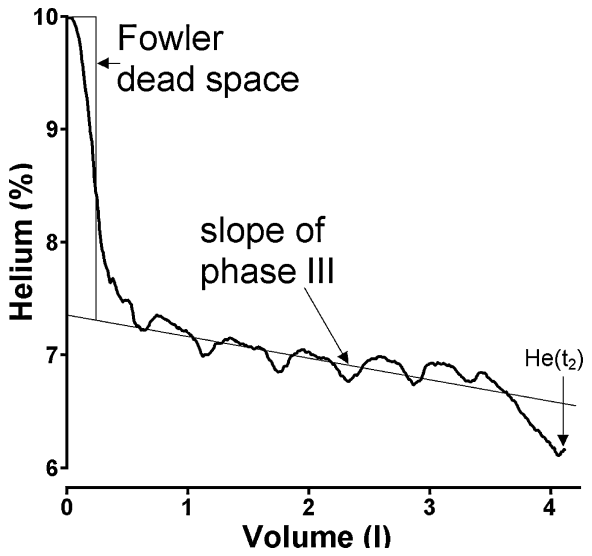

FIGURE 57-4 Single breath distribution of an inert gas; Plot of a tracer gas (He) (y axis) versus exhaled volume (x axis) in a normal subject for a single breath consisting of slow (0.5 L/s) inhalation of test gas (10% He) from RV to TLC and slow (0.5 L/s) continuous exhalation back to RV, with no breath holding. The Fowler method measures anatomic dead space (V_D). The phase III slope for He, measured by linear regression through the middle third of the exhaled volume, is an index of ventilation inhomogeneity. V_A is measured using a mass balance equation applied at end-exhalation (time = t_2), which in this example is RV:

$$RV = \int_{t_0}^{t_2} \frac{He(t)\,dV(t)}{He(t_2)} \quad \text{and} \quad V_A(t_2) = RV - V_D$$

which assumes that the mass of He entering the lung during inhalation beginning at t_0 is equal to the mass of He leaving the lung during exhalation, plus the mass left in the lung at end-expiration. The method assumes that average He concentration of the gas remaining in the lung at RV is the [He] measured at end-exhalation, that is, $He(t_2)$.[9,31,81]

Alveolar Pressure

P_A, not routinely monitored, is assumed to be atmospheric P_B (see Equation 57-6). When the actual mean P_A differs from P_B, computational errors occur (about 5–10%), which spuriously increase DL_{CO}^{SB} when P_A is higher than P_B (Valsalva's maneuver) and decrease DL_{CO}^{SB} when P_A is lower than P_B (Müller's maneuver). However, the dominant effect of changes in P_A on DL_{CO}^{SB} is in the opposite direction and is caused by a direct effect on the pulmonary capillaries. A Müller maneuver creates subatmospheric P_A, which increases DL_{CO}^{SB} by increasing pulmonary capillary recruitment. DL_{CO}^{SB} (corrected for changes in P_B) increases by 10 to 20% if P_A is reduced only during slow constant VC inhalation[34,35] and by 6% if subjects actively inspire against a closed glottis or valve near TLC during breath holding.[36] Alternatively, increasingly positive P_A (Valsalva's maneuver) during breath holding decreases cardiac output[37] and V_C,[36] thus decreasing DL_{CO}^{SB} by about 20%.[36] Highly positive P_A during rapid, forced exhalation also lowers DL_{CO}^{SB}, particularly with increasing airflow obstruction.[38]

Reproducibility

Large variability in the conventional DL_{CO}^{SB} exists, despite rigid standardization,[14,25] which, in practice, is not achieved in one-third of healthy subjects,[39] and success is even less likely in patients with lung disease. Predicted values for DL_{CO}^{SB} vary markedly and need to be chosen to match results from a locally studied healthy population. The limits for "normality" should be based on the 95% confidence limits, which result in a wide range for normality (about 70–130% predicted). The source of this wide variability is threefold. First, there is biologic variability resulting from the effects of changes in Hb, P_A, cardiac output, COHb, and CO back-pressure, as well as the effects of the circadian rhythm and variations during the normal menstrual cycle in women. DL_{CO}^{SB} decreases by 9% by the third day of menses compared with the week preceding menses.[14] Second, there is variability related to how the single breath is performed, that is, variations in the inhaled and exhaled flow rates, V_A, volume history, t_{BH}, and the speed, size,

and timing of alveolar sample collection. However, this type of variability is disease specific, that is, in patients with airflow obstruction the reduced flow rates prolong exhalation, whereas in patients with restrictive lung disease, V_A is reduced. Third, there are technical factors related to calibration procedures, instrument linearity, measurement errors, algorithms for measuring t_{BH}, and $[O_2]$ in the test gas, which in Europe is 17% O_2 but in North America is 21% O_2.[14] Although DL_{CO}^{SB} is routinely used, along with spirometry, to classify respiratory impairment and disability, the wide variability in DL_{CO}^{SB} limits its usefulness in this regard.[40]

VALUE OF CONVENTIONAL DL_{CO}^{SB} TESTING IN CLINICAL PRACTICE

Obstructive Lung Diseases

A low DL_{CO}^{SB} may help in establishing a diagnosis of emphysema since loss of overall alveolar surface area reduces DL_{CO}^{SB}, and the decrease correlates with emphysema severity, detected by high-resolution computed tomography (HRCT).[41] In the seated position, DL_{CO}^{SB} is more sensitive to lower lobe and diffuse emphysema but does not reliably detect bullous emphysema in the lung apex.[42] A very low DL_{CO}^{SB}, along with a low forced expiratory volume in 1 second (FEV_1), predicts poor survival for chronic obstructive pulmonary disease (COPD) patients after lung volume reduction surgery.[43] DL_{CO}^{SB} testing plays a limited role in detecting emphysema in patients with severe airflow obstruction because the test may be low in patients with little emphysema (by HRCT)[44] but can be normal in patients with a substantial degree of emphysema.[45] The test is either normal or low[46] in patients with cystic fibrosis (CF). It may help to separate asthma patients from COPD patients since DL_{CO}^{SB} in asthma patients is either normal[9] or may be increased[47] as a result of either computational errors caused by the decreased exhaled flow[31] or more negative inspiratory pressure during forced inhalation.[35]

Interstitial Lung Disease

DL_{CO}^{SB} is reduced early in the course of chronic interstitial lung diseases (ILD) when the chest radiograph may still be normal,[48] presumably because the disease process both thickens the air-blood barrier and decreases the number of capillaries participating in gas diffusion. The decrease in DL_{CO}^{SB} correlates with overall lung involvement by HRCT[49] and appears more sensitive than changes in lung volume in screening patients at risk for pneumoconiosis.[40] DL_{CO}^{SB} decreases in acute ILD, such as *Mycoplasma* pneumonia, early lung transplant rejection, and bronchiolitis obliterans, and also decreases in chronic ILD, which occurs in scleroderma, rheumatoid arthritis, systemic lupus erythematosus, idiopathic pulmonary fibrosis, sarcoidosis, hypersensitivity pneumonitis, lymphangioleiomyomatosis, and ILD induced by drugs, such as nitrofurantoin, bleomycin, or amiodarone. DL_{CO}^{SB} may be useful in the detecting and following the progression of drug-induced lung disease.[50]

Pulmonary Vascular Obstruction

DL_{CO}^{SB} is decreased by pulmonary vascular obstruction (PVO), which occurs following lymhangiography,[51] talc emboli in talc granulomatosis,[52] recurrent leukocyte sequestration as a result of chronic hemodialysis,[53] and pulmonary emboli (PE) of either thrombotic[54] or tumor origin. Although the test has no current role in the investigation of suspected PE, a low value should raise the suspicion of this diagnosis. DL_{CO}^{SB} is decreased more in PE, the greater the PVO,[54] and is also decreased in patients with chronic unresolved PE and primary pulmonary hypertension.[55] However, in the seated position at rest, the reduction in DL_{CO}^{SB} may be masked by compensatory recruitment or distention of the pulmonary capillaries in lung zones spared from vascular occlusion.[56] "Static pulmonary capillary blood," distal to obstructed pulmonary vascular segments, could cause the diffusing capacity to decrease from the first to the fifth of five sequential single breaths,[57] but this method of PE detection needs further validation.

Cardiovascular Disease

When pulmonary vascular resistance (PVR) is normal, DL_{CO}^{SB} changes according to the principles that govern pulmonary capillary recruitment. DL_{CO}^{SB} increases when cardiac output or inflow pressure (P_a) increases (exercise, left-to-right shunt) or when outflow pressure (P_v) increases (mild congestive heart failure [CHF] or early mitral stenosis).[58] However, DL_{CO}^{SB} decreases when P_a decreases (pulmonary stenosis,[59] or systemic venodilation following administration of nitroglycerin[60]). When mitral stenosis or CHF becomes chronic, pulmonary vascular remodeling increases PVR, leading to a decrease in DL_{CO}^{SB}.[59] The vascular remodeling appears fixed in CHF since the low DL_{CO}^{SB} does not improve following heart transplantation.[61]

"Isolated" Low DL_{CO}^{SB}

When DL_{CO}^{SB} is low, but lung function is otherwise normal, consider the following possibilities: anemia,[13] focal emphysema,[62] early interstitial lung disease,[48] pulmonary vascular diseases, or undetected PE.[54] Unlikely factors include a decreased P_a due to pulmonary stenosis[59] or systemic venodilatation, such as occurs with administration of a systemic vasodilator.[60] Rule out testing errors, including contamination of the alveolar sample with V_D, slowing of inhaled flow, excessively long t_{BH}, undetected Valsalva's maneuver, underestimation of V_A, or increases in COHb or CO backpressure due to smoking or repeated DL_{CO}^{SB} testing.

"Isolated" High DL_{CO}^{SB}

When lung function is otherwise normal, but DL_{CO}^{SB} is increased, consider polycythemia[12]; anxiety or exercise immediately preceding testing; "static" alveolar red cells, which occurs in patients with pulmonary hemorrhagic syndromes[63]; increased body mass index, seen in obstructive sleep apnea[64]; mild asthma[47]; left-to-right shunts[59]; or transiently increased P_v (mild left heart failure or left atrial myxoma). Rule out testing errors including decreased exhaled flow rate; shortened t_{BH}; collection of the alveolar sample late in exhalation; undetected Müller's maneuver; overestimation

of F_ACO_{to} by underestimating the tracer gas dilution; or overestimation of V_A.

Stress Testing to Recruit V_C

Most airway narrowing is patchy, so regional ventilation in more affected lung zones decreases, causing regional hypoxic pulmonary vasoconstriction (HPV), which diverts blood flow to more normal lung zones with relatively preserved regional ventilation. In the seated position at rest, compensatory capillary recruitment increases regional V_C in relatively normal lung zones and, hence, limits the reduction in DL_{CO}^{SB}. However, HPV decreases the potential for further capillary recruitment, so the increase in DL_{CO}^{SB}, in response to interventions that normally fully recruit pulmonary capillaries, is reduced or abolished. Interventions that recruit Vc include the 15° head-down position,[34] exercise,[23] and negative inspiratory pressure.[35] In patients with CF, the increase in DL_{CO}^{SB} on assuming the 15° head-down position or in response to high negative inspiratory pressure is reduced breathing room air.[34] However, when HPV is eliminated by breathing 100% O_2 for 20 minutes, the positional change in DL_{CO}^{SB} is restored.[34] The positional increase in DL_{CO}^{SB} is also reduced in smokers with apical emphysema[65] and in patients with scleroderma,[66] sarcoidosis,[67] CHF, [68] and insulin-dependent diabetes.[69] The supine DL_{CO}^{SB} may therefore be more sensitive in the early detection of changes in the pulmonary vasculature, but few normal regressions for supine DL_{CO}^{SB} exist.[70]

ALTERNATIVE DL_{CO}^{SB} TESTING METHODS

Steady-State DL_{CO}

The flow or uptake of CO is measured during steady-state tidal breathing and divided by the driving pressure, measured from the mean alveolar [CO] (P_ACO).[71] The method, not in common use today, is usually measured during exercise because substantial errors in P_ACO occur during resting tidal breathing.

Rebreathing DL_{CO}

During rapid rebreathing, the decrease in [CO] from a rebreathing bag, measured using a rapidly responding CO analyzer, is assumed to reflect the uptake of CO from the lungs. The test, used mostly in normal subjects during exercise,[72] requires considerable subject cooperation, and the high airflow rate and lack of t_{BH} actually impair diffusive gas mixing in the lung periphery (see Figure 57-2).[73]

"Intrabreath" DL_{CO}, or $DL_{CO}^{(exhaled)}$

This method[24,38] assumes that the decrease in CO, measured only during constant flow, slow exhalation using rapidly responding analyzers,[74–76] represents the diffusion of CO across the air-blood barrier. However, the decrease in CO (Figure 57-5) during exhalation is not only due to ongoing diffusion of CO into the blood but is also influenced both by transient, t_{BH}-dependent gradients in [CO] within peripheral gas-exchanging units (see Figure 57-2)[77] and by differences in [CO] among larger parallel lung units (due to regional differences in specific ventilation), which empty sequentially.[78] Therefore, ventilation inhomogeneity alone changes the slope for CO, and this effect is superimposed on true change in [CO] during exhalation owing to diffusion of CO into the blood.[77] The strategy of "correcting" the observed CO slope for the simultaneously measured slope of He ($F_ACO_{t1\ (corrected)} = F_ACO_{t1} \cdot F_AHe_{t1} / F_AHe_{t0}$) does not satisfactorily eliminate the effects of ventilation inhomogeneity on the slope of the CO decay curve because ongoing CO diffusion into the blood causes the regional ratios

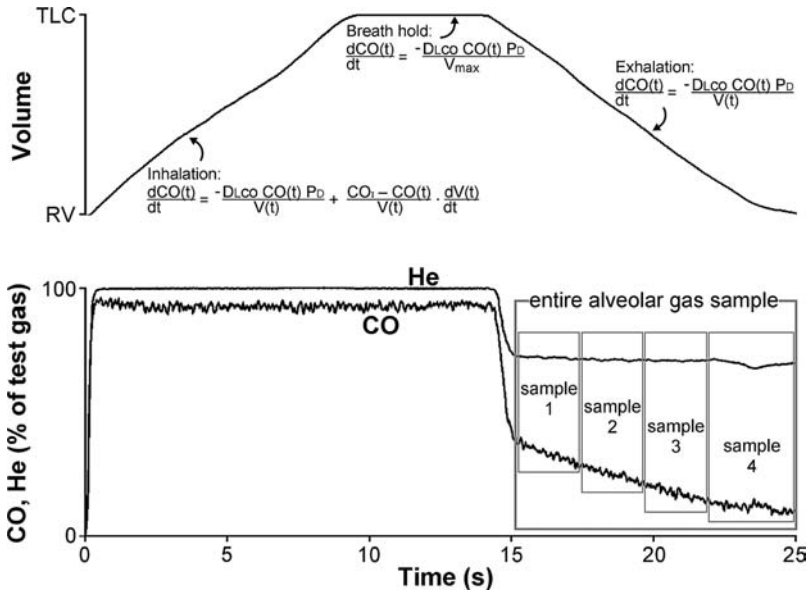

FIGURE 57-5 Three-equation method ($DL_{CO}^{SB\text{-}3EQ}$). The single breath consists of slow (0.5 L/s) VC inhalation of test gas, variable breath holding at TLC (5 s in the example), and slow (0.5 L/s) exhalation to RV. Since the factors that determine the change in [CO] in the alveolar space are actually different in the three different phases of the single breath, three separate mass balance equations are used. During inhalation CO enters the alveolar space through the mouth as it simultaneously leaves the alveolar space by diffusion. CO leaves the alveolar space only by diffusion during breath holding (Krogh equation). During exhalation, CO simultaneously leaves the alveolar space by both exhalation and by diffusion. The three equations (*upper graph*) are solved using an iteration technique that finds the single value of $DL_{CO}^{SB\text{-}3EQ}$ that best predicts the observed amount of CO exhaled. Digital recording eliminates the need for physically collecting a gas sample because any "virtual" gas sample can be constructed. The entire alveolar gas sample provides the best estimate of DL_{CO}^{SB} of the average diffusion characteristics for the entire lung. To calculate an index of diffusion nonuniformity, D_I (see Figure 57-6), $DL_{CO}^{SB\text{-}3EQ}$ is calculated from each of four equal alveolar samples (Sample 1, 2, 3, 4), expressed as a percentage of the $DL_{CO}^{SB\text{-}3EQ}$ from the entire alveolar gas sample.

of alveolar [CO]/[He] to become dramatically different over time, particularly when diffusion inhomogeneity coexists.[77,78] The $DL_{CO}^{(exhaled)}$ method is therefore not suitable for measuring lung diffusion in the presence of increased ventilation inhomogeneity.

Diffusing Capacity Using Nitric Oxide

Nitric oxide (NO) binds tightly with Hb with an affinity that is 400 times greater than that of CO. Diffusing capacity using nitric oxide (DL_{NO}) can be measured simultaneously with DL_{CO}^{SB}. It is fourfold larger than DL_{CO}^{SB}, independent of $[O_2]$, and measures primarily D_M in normal subjects.[79] However, in patients with lung disease, NO may, itself, alter lung diffusion because it is a potent pulmonary vasodilator, which inhibits HPV.

Three-Equation Single-Breath Diffusing Capacity

The three-equation single-breath diffusing capacity ($DL_{CO}^{SB\text{-}3EQ}$) method, which is a significant advance over conventional methods,[14] takes advantage of rapidly responding analyzers to continuously measure airflow rates, volume, CO, and a tracer gas, such as He or methane, throughout the single breath. By digitally recording all the data, the need to physically collect an alveolar gas sample is eliminated. A "virtual" sample of any size can be constructed and analyzed for either CO or He for any time period (see Figure 57-5). Rather than using the single Krogh equation, three separate mass balance equations, each valid for the respective phases of inhalation, breath holding, and exhalation, are used to accurately describe the instantaneous changes in CO in the alveolar space throughout the entire single breath (see Figure 57-5).[29] The equations are solved using a standard iteration technique,[80] which matches the predicted alveolar [CO] to that measured in "virtual" sample, consisting of all the exhaled alveolar gas (see Figure 57-5). Successive iterations (usually <12) converge to a single $DL_{CO}^{SB\text{-}3EQ}$, which predicts the measured alveolar [CO] to within a tolerance of 0.1%.[80] The method assumes a homogeneous lung with a constant DL_{CO}^{SB}; a single Fowler V_D, measured for each breath (see Figure 57-4); a single homogeneously mixed alveolar space; and the same instantaneous changes in flow rate and V_A, observed in the actual maneuver (see Figure 57-5).[80] To measure V_A more accurately [He] is monitored continuously, and a mass balance equation is used to describe the behavior of He throughout the entire single breath (see Figure 57-4).[9,80] Subjects perform a slow deep breath of room air from FRC to TLC, with 5 seconds of t_{BH}, immediately before the DL_{CO}^{SB} test to eliminate variations in DL_{CO}^{SB} due to previous volume history,[22,33] and the mean alveolar [CO] during the exhalation phase of the deep breath is used to adjust $DL_{CO}^{SB\text{-}3EQ}$ for CO back-pressure and for COHb.[17]

Since $DL_{CO}^{SB\text{-}3EQ}$ is accurate for a homogeneous lung, despite changes in the way the single breath is performed or the way the alveolar sample is collected,[32] measurements can be obtained not only during large VC single breaths but also during submaximal "near-tidal" breaths with slow flow rates.[22,33,81] Since it is not necessary to strictly standardize t_{BH}, as is the case using the conventional method, $DL_{CO}^{SB\text{-}3EQ}$ is more precise and accurate in both normal subjects and patients with lung disease[31,32,46] and is independent of t_{BH} in normal subjects.[9,32,81,82]

$DL_{CO}^{SB\text{-}3EQ}$ could potentially decrease with decreasing t_{BH} if worsening ventilation inhomogeneity increases $1/G_{MIX}$. In patients with significant airflow obstruction and ventilation inhomogeneity (COPD, asthma, and emphysema), $DL_{CO}^{SB\text{-}3EQ}$, measured from the entire alveolar sample, actually decreased with decreasing t_{BH} during slow VC breaths, suggesting that the pathway for CO was significantly affected by an increase in $1/G_{MIX}$ (see Figure 57-2) during short periods of t_{BH}.[9] When submaximal single breaths are performed near the tidal volume range, t_{BH}-dependent inhomogeneity in gas mixing in the lung periphery increases dramatically, even in normal subjects,[73,81] thus potentially increasing $1/G_{MIX}$. However, no effect of decreasing t_{BH} was found in either normal subject nonsmokers or smokers with normal forced exhaled flow rates when $DL_{CO}^{SB\text{-}3EQ}$ was measured from the entire alveolar sample during slow inhalation-exhalation "near-tidal" breaths, performed from FRC to one-half IC with exhalation to RV.[10,81,82] In contrast, t_{BH}-dependent ventilation inhomogeneity did affect $DL_{CO}^{SB\text{-}3EQ}$ in normal subjects during near-tidal breaths when $DL_{CO}^{SB\text{-}3EQ}$ was measured

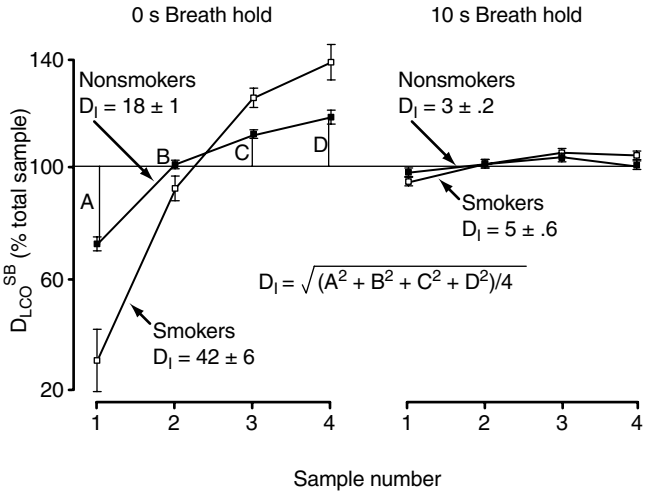

FIGURE 57-6 Diffusion nonuniformity (D_I): Mean values (±SE) for $DL_{CO}^{SB\text{-}3EQ}$, measured from each of four equal alveolar gas samples (Sample 1, 2, 3, 4; Figure 5) and expressed as a percentage of $DL_{CO}^{SB\text{-}3EQ}$ measured from the entire alveolar sample, for normal nonsmokers (*closed circles*) and asymptomatic smokers with otherwise normal lung function (*open circles*). Single breaths were preceded by a deep breath and consisted of slow (0.5 L/s) constant inhalation of test gas from FRC to ½ IC and slow (0.5 L/s) exhalation back to RV with a t_{BH} of either 0 s (*left graph*) or 10 s (*right graph*)[10,83] $DL_{CO}^{SB\text{-}3EQ}$ for sample 1 was underestimated, relative to $DL_{CO}^{SB\text{-}3EQ}$ from the whole sample, but progressively increased in subsequent samples, so that it became relatively overestimated in sample 4. This effect is t_{BH} dependent since it is greatest for single breaths without breath holding. D_I is an index to quantify the degree to which $DL_{CO}^{SB\text{-}3EQ}$ from each of the four samples deviates from $DL_{CO}^{SB\text{-}3EQ}$, measured from the entire sample (A, B, C, D). This variation is expressed as the root mean square difference of the four normalized $DL_{CO}^{SB\text{-}3EQ}$ values. At a t_{BH} of 0 s, D_I is larger (42) in smokers versus nonsmokers (18) (*left graph*), but this difference is less after a t_{BH} of 10 s (*right graph*). Data replotted from Cotton DJ et al.[10]

separately from each of four equal alveolar samples, revealing temporal changes in $DL_{CO}^{SB\text{-}3EQ}$ from early versus late samples.[82] $DL_{CO}^{SB\text{-}3EQ}$ was reduced in the first alveolar sample, early in exhalation, but increased for alveolar samples later in exhalation (Figure 57-6).[82] An index of diffusion nonuniformity (D_I) quantified how each of the four normalized $DL_{CO}^{SB\text{-}3EQ}$ values deviated from $DL_{CO}^{SB\text{-}3EQ}$, measured from the entire alveolar sample and was measured using the root mean square difference.[10,80] In normal, nonsmokers D_I was exquisitely sensitive to t_{BH}-dependent ventilation inhomogeneity in the lung periphery since D_I was highest for single breaths without t_{BH} and decreased dramatically with as little as 6 seconds of t_{BH} (see Figure 57-6).[82]

For "near-tidal" breaths without t_{BH}, the normalized phase III He slope was also increased in smokers, even although both the forced exhaled flows and the phase III slope of the standard, vital capacity and single-breath nitrogen washout were normal.[83] In this same group of smokers, D_I was markedly increased for near-tidal breaths without t_{BH} (see Figure 57-6) and correlated with both age and pack-years of smoking,[10] D_I decreased with increasing t_{BH}, in both smokers and nonsmokers, but the change was much greater in smokers. With increasing t_{BH} the change in D_I also correlated with the improvement of the phase III He slope.[10] The change in D_I with t_{BH} therefore quantifies an effect of an increase in $1/G_{MIX}$ for single breaths within the tidal volume range and, may, along with changes in the phase III He slope, be useful in detecting smoke-induced inflammation in small airways.[10,83]

SUMMARY

The conventional DL_{CO}^{SB} is a clinically useful, noninvasive tool to assess the integrity of the air-blood barrier but lacks sensitivity and specificity because it is affected by a number of physiologic variables and because, even for a homogeneous lung, the single, Krogh breath-holding equation causes maneuver-related computational errors that are disease specific. $DL_{CO}^{SB\text{-}3EQ}$ avoids the computational errors of the conventional DL_{CO}^{SB} method because the mass balance equations accurately describe the behavior of both CO and He throughout a single breath. $DL_{CO}^{SB\text{-}3EQ}$ is equally valid for maneuvers with varying flow rates, V_A, and t_{BH}. The advantages of slow inhalation–exhalation single breaths are that the distribution of an inert tracer gas can be measured simultaneously, the effects of wide swings in P_A are minimized, and the maneuvers with short t_{BH} can be performed equally well by both normal subjects and patients alike. The best estimate of $DL_{CO}^{SB\text{-}3EQ}$ for the whole lung is obtained using the entire alveolar gas sample. When $1/G_{MIX}$ increases, the pathway for CO is altered, causing changes, with t_{BH}, both in $DL_{CO}^{SB\text{-}3EQ}$ measured from the entire alveolar sample in patients with airflow obstruction and in D_I in smokers with normal lung function.

REFERENCES

1. Krogh M. The diffusion of gases through the lungs of man. J Physiol 1915;49:271–300.
2. MacIntyre NR III, Davies J, MacIntyre NR, Crapo R. For the ATS Pulmonary Function Laboratory Standards Committee. Characteristics of pulmonary function laboratories in North America. Am J Respir Crit Care Med 2002;165:A200.
3. Forster RE. Chapter 5. Diffusion of gases across the alveolar membrane. In: Farhi LE, Tenney SM, editors. Handbook of physiology. Section 3. The respiratory system. Vol IV. Gas exchange. Bethesda (MD): American Physiological Society; 1987. p 71–88.
4. Holland RAB, Shibata H, Scheid P, Piiper J. Kinetics of O_2 uptake and release by red cells in stopped-flow apparatus: effects of unstirred layer. Respir Physiol 1985;59:71–91.
5. Brudin LH, Valind SO, Rhodes CG, et al. Regional lung hematocrit in humans using positron emission tomography. J Appl Physiol 1986;60:1155–63.
6. Engel LA. Gas mixing within the acinus of the lung. J Appl Physiol 1983;54:609–18.
7. Piiper J, Scheid P. Chapter 4. Diffusion and convection in intrapulmonary gas mixing. In: Farhi LE, Tenney SM, editors. Handbook of physiology. Section 3. The respiratory system. Vol IV. Gas exchange. Bethesda (MD): American Physiological Society; 1984. p. 51–69.
8. Sikand RS, Magnussen H, Scheid P, Piiper J. Convective and diffusive gas mixing in human lungs: experiments and model analysis. J Appl Physiol 1976;40:362–71.
9. Graham BL, Mink JT, Cotton DJ. Effect of breath-hold time on $D_{Lco}^{(SB)}$ in patients with airway obstruction. J Appl Physiol 1985;58:1319–25.
10. Cotton DJ, Mink JT, Graham BL. Nonuniformity of diffusing capacity from small alveolar gas samples is increased in smokers. Can Respir J 1998;5:101–8.
11. West JB, Dollery CT, Naimark A. Distribution of blood flow in isolated lung; relation to vascular and alveolar pressures. J Appl Physiol 1964;19:713–24.
12. Burgess JH, Bishop JM. Pulmonary diffusing capacity and its subdivisions in polycythemia vera. J Clin Invest 1963; 42:997–1005.
13. Marrades RM, Diaz O, Roca J, et al. Adjustment of DL_{co} for hemoglobin concentration. Am J Respir Crit Care Med 1997;155:236–41.
14. Official statement of the American Thoracic Society. Single-breath carbon monoxide diffusing capacity (transfer factor). Recommendations for a standard technique-1995 update. Am J Respir Crit Care Med 1995;152:2185–98.
15. Dinakara P, Blumenthal WS, Johnston RF, et al. The effect of anemia on pulmonary diffusing capacity with derivation of a correction equation. Am Rev Respir Dis 1970;102:965–9.
16. Gulsvik A, Bakke P, Humerfelt S, et al. Single breath transfer factor for carbon monoxide in an asymptomatic population of never smokers. Thorax 1992;47:167–73.
17. Graham BL, Mink JT, Cotton DJ. Effects of increasing carboxyhemoglobin on the single breath carbon monoxide diffusing capacity. Am J Respir Crit Care Med 2002;165:1504–10.
18. Mohsenifar Z, Tashkin DP. Effect of carboxyhemoglobin on the single breath diffusing capacity: derivation of an empirical correction factor. Respiration 1979;37:185–91.
19. Fishman AP. Chapter 3. Pulmonary circulation. In: Fishman AP, Fisher AB, editors. Handbook of physiology. Section 3. The respiratory system. Vol 1. Circulation and non-respiratory functions. Bethesda (MD): American Physiological Society; 1985. p 93–165.
20. Bachofen H, Schurch S, Urbinelli M, Weibel ER. Relations among alveolar surface tension, surface area, volume, and recoil pressure. J Appl Physiol 1987;62:1878–87.
21. Cassidy SS, Ramanathan M, Rose GL, Johnson RL Jr. Hysteresis in the relation between diffusing capacity of the lung and lung volume. J Appl Physiol 1980;49:566–70.

22. Prabhu MB, Mink JT, Graham BL, Cotton DJ. Effect of a deep breath on gas mixing and diffusion in the lung. Respir Physiol 1990;79:195–204.
23. Ogilvie CM, Forster RE, Blakemore WS, Morton JW. A standardized breath holding technique for the clinical measurement of the diffusing capacity of the lung for carbon monoxide. J Clin Invest 1957;36:1–17.
24. Jones RS, Meade F. A theoretical and experimental analysis of anomalies in the estimation of pulmonary diffusing capacity by the single breath method. Q J Exp Physiol 1961;46: 131–43.
25. Cotes JE, Chinn DJ, Quanjer PH, et al. Standardization of the measurement of transfer factor (diffusing capacity). Report working party standardization of lung function tests. European community for steel and coal. Official statement of the European Respiratory Society. Eur Respir J 1993;16 Suppl:41–52.
26. McGrath MW, Thompson ML. The effect of age, body size and lung volume change on alveolar-capillary permeability and diffusing capacity in man. J Physiol London 1959; 146:572–82.
27. Jones RS, Meade F. Pulmonary diffusing capacity. An improved single breath method. Lancet 1960;1:94–5.
28. Cotton DJ, Newth CJL, Portner PM, Nadel JA. Measurement of single-breath CO diffusing capacity by continuous rapid CO analysis in man. J Appl Physiol 1979;46:1149–56.
29. Graham BL, Dosman JA, Cotton DJ. A theoretical analysis of the single breath diffusing capacity for carbon monoxide. IEEE Trans Biomed Eng 1980;BME 27:221–7.
30. Huang Y-CT, MacIntyre NR. Real-time gas analysis improves the measurement of single-breath diffusing capacity. Am Rev Respir Dis 1992;146:946–50.
31. Graham BL, Mink JT, Cotton DJ. Overestimation of the single breath carbon monoxide diffusing capacity in patients with air-flow obstruction. Am Rev Respir Dis 1984;129: 403–8.
32. Graham BL, Mink JT, Cotton DJ. Improved accuracy and precision of single-breath CO diffusing capacity measurements. J Appl Physiol 1981;51:1306–13.
33. Cotton DJ, Taher F, Mink JT, Graham BL. Effect of volume history on changes in $D_{Lco}^{SB\text{-}3EQ}$ with lung volume in normal subjects. J Appl Physiol 1992;73:434–9.
34. Cotton DJ, Graham BL, Mink JT. Pulmonary diffusing capacity in adult cystic fibrosis: reduced positional changes are partially reversed by hyperoxia. Clin Invest Med 1990;13: 82–91.
35. Cotton DJ, Mink JT, Graham BL. Effect of high negative inspiratory pressure on single breath CO diffusing capacity. Respir Physiol 1983;54:19–29.
36. Smith TC, Rankin J. Pulmonary diffusing capacity and the capillary bed during Valsalva and Muller maneuvers. J Appl Physiol 1969;27:826–33.
37. Gotshall RW, Davrath LR. Cardiovascular effects of the breathhold used in determining pulmonary diffusing capacity. Aviat Space Environ Med 1999;70:471–4.
38. Newth CJL, Cotton DJ, Nadel JA. Pulmonary diffusing capacity measured at multiple intervals during a single exhalation in man. J Appl Physiol 1977;43:617–25.
39. Welle I, Eide GE, Bakke P, Gulsvik A. Applicability of the single-breath carbon monoxide diffusing capacity in a Norwegian community study. Am J Respir Crit Care Med 1998;158:1745–50.
40. Taiwo OA, Cain HC. Pulmonary impairment and disability. In: Redlich CA, Rose CS, editors. Clinics in chest medicine. Occupational and environmental lung disease. Vol 23. 4th ed. Philadelphia (PA): W.B. Saunders Co; 2003. p. 841–51.
41. Baldi S, Miniati M, Bellina CR, et al. Relationship between extent of pulmonary emphysema by high-resolution computed tomography and lung elastic recoil in patients with chronic obstructive pulmonary disease. Am J Respir Crit Care Med 2001;164:585–9.
42. Gurney JW, Jones KK, Robbins RA, et al. Regional distribution of emphysema: correlation of high-resolution CT with pulmonary function tests in unselected smokers. Radiology 1992;183:457–63.
43. Fishman A, Fessler H, Martinez F, et al. For the National Emphysema Treatment Trial. Patients at high risk of death after lung-volume-reduction surgery. N Engl J Med 2001;345:1075–83.
44. Gelb AF, Schein M, Kuel J, et al. Limited contribution of emphysema in advanced chronic obstructive pulmonary disease. Am Rev Respir Dis 1993;147:1157–61.
45. Wilson JS, Galvin JR. Normal diffusing capacity in patients with PiZ α_1-antitrypsin deficiency, severe airflow obstruction, and significant radiographic emphysema. Chest 2000;118:867–71.
46. Cotton DJ, Graham BL, Mink JT, Habbick BF. Reduction of the single breath CO diffusing capacity in cystic fibrosis. Chest 1985;87:217–22.
47. Collard P, Njinou B, Nejadnik B, et al. Single breath diffusing capacity for carbon monoxide in stable asthma. Chest 1994;105:1426–29.
48. Epler GR, McCloud MD, Gaensler AE, et al. Normal chest roentgenograms in chronic diffuse infiltrative lung disease. N Engl J Med 1978;298:934–9.
49. Xaubet A, Agustí C, Luburich P, et al. Pulmonary function tests and CT scan in the management of idiopathic pulmonary fibrosis. Am J Respir Crit Care Med 1998;158:431–6.
50. Ngan HY, Liang RH, Lam WK, Chan TK. Pulmonary toxicity in patients with non-Hodgkin's lymphoma treated with bleomycin-containing combination chemotherapy. Cancer Chemother Pharmacol 1993;32:407–9.
51. Gold WM, Youker J, Anderson S, Nadel JA. Pulmonary function abnormalities after lymphangiography. N Engl J Med 1965;273:519–24.
52. Radow SK, Nachamkin I, Morrow C, et al. Foreign body granulomatosis: clinical and immunologic findings. Am Rev Respir Dis 1983;127:575–80.
53. Herrero JA, Alvarez-Sala JL, Coronel F, et al. Pulmonary diffusing capacity in chronic dialysis patients. Respir Med 2002;96:487–92.
54. Wimalaratna HS, Farrell J, Lee HY. Measurement of diffusing capacity in pulmonary embolism. Respir Med 1989; 83:481–5.
55. Steenhuis LH, Groen HJ, Koeter GH, Van der Mark TW. Diffusion capacity and haemodynamics in primary and chronic thromboembolic pulmonary hypertension. Eur Respir J 2000;16:276–81.
56. Gold WM. Pulmonary function testing. In: Murray JF, Nadel JA, Mason RJ, Boushey HA, editors. Textbook of respiratory medicine. 3rd ed. Philadelphia (PA): W.B. Saunders Co; 2000. p. 781–881.
57. Hallenborg C, Holden W, Menzel T, et al. The clinical usefulness of a screening test to detect static pulmonary blood using a multiple-breath analysis of diffusion capacity. Am Rev Respir Dis 1979;119:349–56.
58. Burgess JH, Gillespie J, Graf PD, Nadel JA. Effect of pulmonary vascular pressures on single-breath CO diffusing capacity in dogs. J Appl Physiol 1968;24:692–6.
59. Burgess JH. Pulmonary diffusing capacity in disorders of the pulmonary circulation. Circulation 1974;XLIX:541–50.
60. Nemery B, Piret L, Brasseur L, Frans A. Effect of nitroglycerin on DL of normal subjects at rest and during exercise. J Appl Physiol 1982;52:851–6.

61. Mettauer B, Lampert E, Charloux A, et al. Lung membrane diffusing capacity, heart failure, and heart transplantation. Am J Cardiol 1999;83:62–7.
62. Klein JS, Gamsu G, Webb WR, et al. High-resolution CT diagnosis of emphysema in symptomatic patients with normal chest radiographs and isolated low diffusing capacity. Radiology 1992;182:817–21.
63. Lipscomb DJ, Patel K, Hughes JMB. Interpretation of increases in the transfer coefficient for carbon monoxide (TLco/Va or Kco). Thorax 1978;33:728–33.
64. Collard P, Wilputte JY, Aubert G, et al. The single-breath diffusing capacity for carbon monoxide in obstructive sleep apnea and obesity. Chest 1996;110:1189–93.
65. Hyland RH, Krastins IRB, Aspin N, et al. Effect of body position on carbon monoxide diffusing capacity in asymptomatic smokers and nonsmokers. Am Rev Respir Dis 1978; 117:1045–53.
66. Ettinger WH, Wise RA, Stevens MB, Wigley FM. Absence of positional change in pulmonary diffusing capacity in systemic sclerosis. Am J Med 1983;75:305–12.
67. Sharma OP, Mohler JG. The effect of postural change on the coefficient of diffusion in sarcoidosis patients. Sarcoidosis 1991;8:125–8.
68. Faggiano P, D'Aloia A, Simoni P, et al. Effects of body position on the carbon monoxide diffusing capacity in patients with chronic heart failure: relation to hemodynamic changes. Cardiology 1998;89:1–7.
69. Fuso L, Cotroneo P, Basso S, et al. Postural variations of pulmonary diffusing capacity in insulin-dependent diabetes mellitus. Chest 1996;110:1009–13.
70. Huang Y-CT, Helms MJ, MacIntyre NR. Normal values for single exhalation diffusing capacity and pulmonary capillary blood flow in sitting, supine positions and during mild exercise. Chest 1994;105:501–8.
71. Bates DV, Boucot NG, Dormer AE. The pulmonary diffusing capacity in normal subjects. J Physiol 1955;129:237–52.
72. Hsia CCW, Mcbrayer DG, Ramanathan M. Reference values of pulmonary diffusing capacity during exercise by a rebreathing technique. Am J Respir Crit Care Med 1995; 152:658–65.
73. Paiva M, Engel LA. Gas mixing in the lung periphery. In: Chang HK, Paiva M, editors. Respiratory physiology. An analytic approach. Lung biology in health and disease. Vol 40. New York: Marcel Dekker, Inc.; 1989. p. 245–76.
74. Huang Y-CT, O'Brien SR, MacIntyre NR. Intrabreath diffusing capacity of the lung in healthy individuals at rest and during exercise. Chest 2002;122:177–85.
75. Wilson AF, Hearne J, Brenner M, Alfonso R. Measurement of transfer factor during constant exhalation. Thorax 1994;49:1121–6.
76. Graham BL, Mink JT, Cotton DJ. Dynamic measurements of CO diffusing capacity using discrete samples of alveolar gas. J Appl Physiol 1983;54:73–9.
77. Cotton DJ, Prabhu MB, Mink JT, Graham BL. Effect of ventilation inhomogeneity on "intrabreath" measurements of diffusing capacity in normal subjects. J Appl Physiol 1993; 75:927–32.
78. Cotton DJ, Graham BL. Effect of ventilation and diffusion nonuniformity on DLco (exhaled) in a lung model. J Appl Physiol 1980;48:648–56.
79. Borland CDR, Higenbottam TW. A simultaneous single breath measurement of pulmonary diffusing capacity with nitric oxide and carbon monoxide. Eur Respir J 1989;2:56–63.
80. Graham BL, Mink JT, Cotton DJ. Implementing the three-equation method of measuring single breath carbon monoxide diffusing capacity. Can Respir J 1996;3:247–57.
81. Cotton DJ, Prabhu MB, Mink JT, Graham BL. Effects of ventilation inhomogeneity on $DL_{CO}^{SB\text{-}3EQ}$ in normal subjects. J Appl Physiol 1992;73:2623–30.
82. Soparkar GR, Mink JT, Graham BL, Cotton DJ. Measurement of temporal changes in $DL_{CO}^{SB\text{-}3EQ}$ from small alveolar samples in normal subjects. J Appl Physiol 1994;76: 1494–501.
83. Cotton DJ, Mink JT, Graham BL. Detection of peripheral ventilation inhomogeneity in smokers. Can Respir J 1997;4: 27–33.

CHAPTER 58

SPIROMETRIC PREDICTIONS OF EXERCISE LIMITATION IN PATIENTS WITH CHRONIC OBSTRUCTIVE PULMONARY DISEASE

Joseph Milic-Emili, Nickolaos G. Koulouris, Claudio Tantucci

During the last 40 years the correlation of exercise tolerance to routine pulmonary function tests in patients with chronic obstructive pulmonary disease (COPD) has been investigated in many studies. In almost all instances, however, pulmonary function was assessed in terms of forced expiratory volume in 1 second (FEV_1). Since a weak correlation was found between exercise tolerance and FEV_1, it was concluded that factors other than lung function impairment play a predominant role in limiting exercise capacity in COPD patients. Recent studies, however, have shown that in patients with moderate-to-very severe COPD the inspiratory capacity, a surrogate marker of hyperinflation, is a better predictor of exercise tolerance than FEV_1 and forced vital capacity (FVC), suggesting that the main cause of exercise intolerance in these patients is dynamic pulmonary hyperinflation due to tidal expiratory flow limitation.

DYNAMIC HYPERINFLATION

In normal individuals at rest, the end-expiratory lung volume, or functional residual capacity (FRC), corresponds to the relaxation volume (V_r) of the respiratory system—that is, the lung volume at which the elastic recoil pressure of the respiratory system is zero.[1] Pulmonary hyperinflation, which is defined as an increase in FRC above the predicted normal range, may be due to increased V_r as a result of loss of lung recoil (eg, emphysema) or dynamic pulmonary hyperinflation, which is said to be present when the FRC exceeds V_r. Dynamic hyperinflation exists whenever the duration of expiration is insufficient to allow the lungs to deflate to V_r prior to the next inspiration. This may occur when expiratory flow is impeded (eg, increased airway resistance) or expiratory time is shortened (eg, increased breathing frequency). Expiratory flow may also be reduced by other mechanisms, such as persistent contraction of the inspiratory muscles during expiration and expiratory narrowing of the glottic aperture. In COPD patients, dynamic hyperinflation is very common and is mainly due to tidal expiratory flow limitation.[2–4]

EXPIRATORY FLOW LIMITATION

The term expiratory flow limitation (EFL) should be used only to describe a condition in which expiratory flow cannot be augmented at a given lung volume. Thus, EFL reflects effort independence of flow, that is, the incapacity to increase expiratory flow by further increasing pleural and, therefore, alveolar pressure at that lung volume. It is exhibited by both normal subjects and patients with respiratory disorders during correctly performed maximal forced expiratory maneuvers in which, from peak expiratory flow, isovolumic (at the same lung volume) expiratory flow rates cannot be increased by increasing the expiratory effort and, thus, are maximal.[5,6]

Most normal subjects do not exhibit EFL even during maximal exercise.[5,7] In contrast, in COPD patients EFL may be present even at rest. Tidal EFL is said to occur when tidal expiratory flow rates are maximal under the prevailing conditions, either at rest or during exercise.[2–4]

MECHANISMS CAUSING EFL

Two main mechanisms promote the occurrence of tidal EFL, namely a reduction in expiratory flow reserve and an increase in ventilatory requirements.

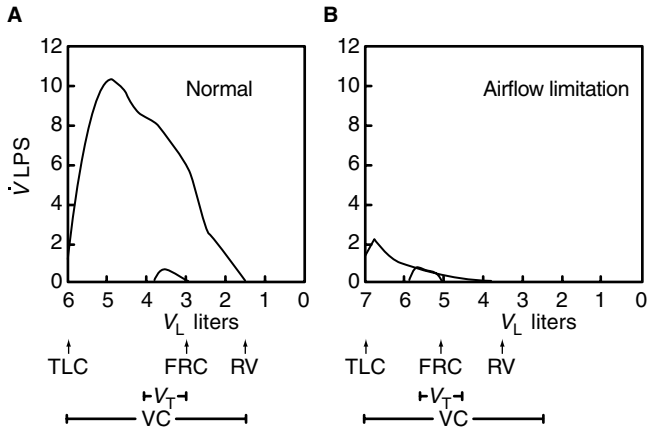

FIGURE 58-1 Flow-volume curves during quiet and forced expiration in a normal subject (*left*) and a patient with severe chronic obstructive pulmonary disease (COPD) (*right*). Whereas in the normal subject there is considerable expiratory flow reserve in the resting tidal volume range, in the patient the tidal expiratory flow is maximal, that is expiratory flow limitation is present. The latter promotes an increase in FRC with concomitant reduction of inspiratory capacity (IC) (IC = TLC − FRC). FRC = functional residual capacity; RV = residual volume; TLC = total lung capacity; V_T = tidal volume during quiet breathing; VC = vital capacity. Reproduced with permission from Bates DV et al.[8]

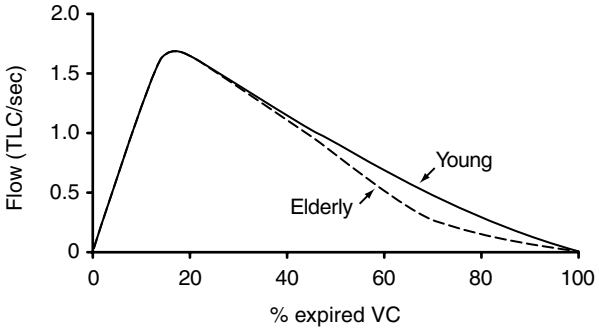

FIGURE 58-2 Maximal expiratory flow-volume curves for young and old subjects, aged 25 to 35 and 65 to 75 years, respectively. To allow for different size of subjects, the axes have been standardized for lung volume. Reproduced with permission from Knudson RJ.[13]

The expiratory flow reserve in the tidal volume range is given by the difference between the maximal flows available and the actual tidal flows developed during expiration. In normal individuals at rest the expiratory flow reserve is very high (Figure 58-1, left), whereas in patients with severe COPD there may not be any flow reserve left (see Figure 58-1, right). In the latter condition ventilation can only be increased by increasing the operating lung volume with a concurrent increase in maximal expiratory flows or by decreasing the duration of inspiration with a concurrent increase in time available for expiration.

The expiratory flow reserve can be reduced by airway obstruction, a term that implies a reduction in maximal flow rates below the predicted normal range at a given lung volume (see Figure 58-1, right). Reduced FRC, as occurs in gross obesity, restrictive disorders, congestive heart failure, and so on, is usually associated with decreased expiratory flow reserve in the tidal volume range.[8–11]

In the supine position, the V_r is lower than upright, and hence the FRC tends to decrease in recumbency.[1,2] Since the maximal expiratory flow volume (MEFV) curve shows little postural variation,[12] recumbency promotes EFL because tidal breathing occurs at a lower lung volume.[2] This explains why EFL in the supine position occurs earlier than in the sitting position, the latter reflecting a more advanced stage of the disease.[3]

With aging, there is a decrease in maximal expiratory flows, which is more evident at low lung volumes (Figure 58-2).[13] This makes elderly individuals susceptible to develop EFL more readily, particularly in the supine position. In the early stages of COPD, which are characterized by abnormalities in the peripheral airways, there is also a preferential reduction of maximal expiratory flows at low lung volume,[14] promoting tidal EFL. Furthermore, it should be noted that COPD patients are in general older, and hence their high prevalence of EFL is often owing to the combined effect of old age and of the disease per se.

Increased ventilatory requirements augment the expiratory flows because of greater tidal volume and faster respiratory frequency, promoting tidal EFL. In COPD patients who do not exhibit EFL at rest but have little expiratory flow reserve, EFL will occur at low levels of exercise, whereas patients with larger flow reserve at rest should be able to achieve greater exercise levels without developing EFL.[4] Since the FEV_1/FVC ratio is a marker of the shape of the MEFV curve and hence of the expiratory flow reserve at rest, a high FEV_1/FVC ratio in COPD patients heralds greater exercise tolerance (see below).[15]

EFFECTS OF DYNAMIC HYPERINFLATION ON RESPIRATORY WORK

Figure 58-3 illustrates the pressure required to overcome the elastic recoil of the respiratory system for the same tidal volume—20% of vital capacity (VC)—inhaled from V_r (34% VC) and from an increased end-expiratory lung volume corresponding to 67% VC. As shown by the hatched areas, the elastic work increases approximately fivefold when the breath is inhaled from 67% VC (see Figure 58-3B) relative to the breath taken from the V_r (see Figure 58-3A). Clearly, dynamic hyperinflation implies an increase in both work of breathing (WOB) and inspiratory muscle effort. Furthermore, as the lung volume increases, there is a decreased effectiveness of the inspiratory muscles as pressure generators because their fibers become shorter (force-length relationship) and their geometric arrangement changes. Thus, in COPD patients there is a vicious cycle: the inspiratory flow-resistive WOB is invariably increased because of airway obstruction, but more importantly, as a result of hyperinflation, there is increase in WOB owing to intrinsic positive end-expiratory pressure ($PEEP_i$) (see below) and impairment of the mechanical performance of the inspiratory muscles. This promotes dyspnea and exercise

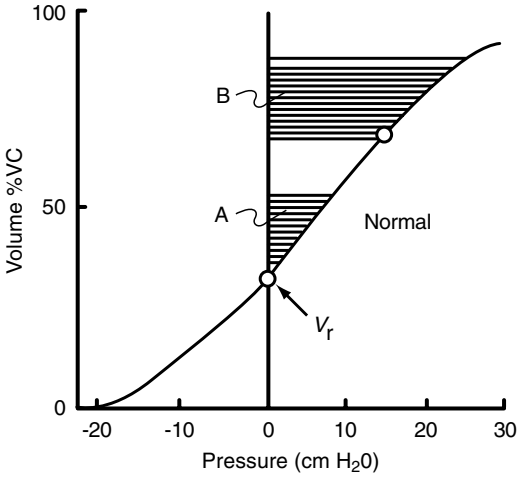

FIGURE 58-3 Static volume-pressure diagram of relaxed respiratory system showing the increase in elastic work caused by dynamic hyperinflation. *A*, Elastic work of breath starting from the relaxation volume (normal). *B*, Elastic work of similar breath to *A* but starting from a higher volume than V_r. In *B*, the intrinsic positive end-expiratory pressure is 15 cm H_2O. V_r = relaxation volume of the respiratory system; VC = vital capacity.

limitation and eventually leads to hypercapnic ventilatory failure and inspiratory muscle fatigue.[2,14,16]

INTRINSIC POSITIVE END-EXPIRATORY PRESSURE

Under normal conditions, the end-expiratory elastic recoil pressure of the respiratory system is zero (see Figure 58-3A). In this case, the alveolar pressure becomes subatmospheric, and gas flows into the lungs as soon as the inspiratory muscles contract. When breathing takes place at lung volumes greater than V_r, the end-expiratory elastic recoil pressure of the respiratory system is positive (15 cm H_2O in Figure 58-3B). The elastic recoil pressure present at end-expiration has been termed auto- or intrinsic positive end-expiratory pressure ($PEEP_i$). When $PEEP_i$ is present, onset of inspiratory muscle activity and inspiratory flow are not synchronous: inspiratory flow starts only when pressure developed by the inspiratory muscles exceeds $PEEP_i$, and subsequently the alveolar pressure becomes subatmospheric. In this respect, $PEEP_i$ acts as an inspiratory threshold load, which increases the inspiratory effort as well as WOB. This places a further burden on the inspiratory muscles, which, in hyperinflated patients, operate under disadvantageous force length and geometric conditions.

Since the static volume-pressure relationship of the respiratory system is approximately linear (see Figure 58-3), $PEEP_i$ is approximated by the product of the static elastance of the respiratory system (Est, rs, the reciprocal of the slope in Figure 58-3) and the magnitude of dynamic hyperinflation, that is, the increase of FRC above V_r:

$$PEEP_i = \text{Est, rs } (FRC - V_r).$$

This implies that dynamic hyperinflation and $PEEP_i$ are closely related indices. However, in spontaneously breathing subjects it is very difficult to determine $PEEP_i$,[16] whereas the degree of dynamic hyperinflation can be readily assessed (see below).

METHODS FOR ASSESSING EFL

Comparison between full (or partial) maximal and tidal flow-volume loops has been widely used in the past to detect EFL, which is assumed to be present when the tidal expiratory flows impinge on or exceed the maximal expiratory flows at the same lung volume (see Figure 58-1, right).[5] This method, however, is inaccurate because of the different volume and time history between resting breathing and the FVC maneuver.[17] In fact, since the inflation volume and speed of inspiration during resting breathing are necessarily different from those obtained during the FVC maneuver, it is axiomatic that detection of flow limitation based on comparison of tidal with maximal flow-volume curves is problematic.

Recently, the negative expiratory pressure (NEP) method has been introduced to detect EFL.[2–4,18,19] It consists of applying a small negative pressure during tidal expiration (usually between −3 and −5 cm H_2O), thus widening the pressure gradient between the alveoli and the airway opening. In the earlier studies, NEP was generated with a vacuum cleaner,[3,18] whereas more recently a Venturi device is in general used instead.[2] In the absence of EFL, with NEP there is an increase in expiratory flow compared with the preceding control breath (Figure 58-4, left). In contrast, in the presence of EFL the expiratory flow does not increase throughout the entire or part of the tidal expiration over that of the preceding control expiration (see Figure 58-4, right).

With the NEP method the volume and time history are not a problem because these are necessarily the same during the control and NEP test breaths. Furthermore, the NEP method does not require either a body plethysmograph or the

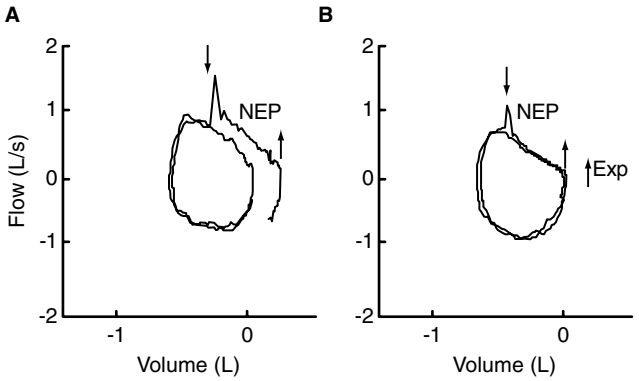

FIGURE 58-4 Flow-volume curves during tidal breathing in two representative patients. In *A*, where expiratory flow with negative pressure (NEP) increases throughout expiration relative to preceding control breath, there is no expiratory flow limitation (left). In *B*, where expiratory flow did not increase with NEP during part of expiration compared with the preceding control breath, expiratory flow limitation (EFL) is present (*right*). *Arrows* indicate when NEP was applied and removed. Reproduced with permission from Koulouris NG et al.[19]

patient's cooperation and coordination and can be used not only in sitting patients but in any desired posture, both at rest and during exercise.[4] The NEP method has been validated using isovolume flow-measure curves.[18]

However, assessing the expiratory flow in response to a negative pressure applied at the airway opening (as opposed to the response to a positive alveolar pressure) has a potential drawback, namely, that it can result in the partial or complete collapse of the extrathoracic airways, except in tracheostomized and intubated patients. This phenomenon, which is very common in patients with obstructive sleep apnea–hypopnea syndrome (OSAHS),[20,21] occurs rarely and inconsistently in patients without OSAHS.[22,23] Accordingly, valid assessment of EFL can be performed in almost all non-OSAHS patients. In the few non-OSAHS patients in whom there is consistent upper airway collapse in response to the application of NEP, EFL can be assessed by squeezing the abdomen during expiration[24] or by maximal or submaximal expiratory maneuvers initiated immediately from end-tidal inspiration, using submaximal expiratory effort.[25] To correct for the thoracic compression artifact, the maximal maneuvers should be performed in a body plethysmograph.[26] The same strategies can be used to assess EFL in OSAHS patients who exhibit consistently upper airway collapse in the face of NEP application.

METHODS FOR ASSESSING PULMONARY HYPERINFLATION

Pulmonary hyperinflation is commonly assessed through the measurement of the FRC with body plethysmography. In patients with severe airway obstruction, this method may overestimate the actual FRC because during the panting maneuver the transmission of alveolar pressure to the mouth is delayed by increased airway resistance.[27] On the other hand, measurements with the nitrogen washout or helium dilution methods may underestimate the FRC because of gas trapping in the lung. However, in patients with resting tidal EFL the increase of FRC is in general accompanied by a reduction in inspiratory capacity (IC).[4,15,28] In contrast to FRC, measurement of IC is simple, cheap, and reliable.[29] Thus, IC testing provides a useful tool for the indirect assessment of pulmonary hyperinflation. Indeed, in such patients a reduction in IC implies dynamic hyperinflation with concurrent decrease in exercise tolerance[15,28,30] and increase in chronic dyspnea.[2]

IC AND EXERCISE TOLERANCE

Most normal subjects and endurance athletes do not exhibit EFL even during maximal exercise.[5,7] In contrast, in COPD patients EFL is commonly present even at rest,[2,4,15,31,32] as first suggested by Hyatt.[5] Tidal EFL promotes dynamic hyperinflation with a concomitant decrease in IC (see Figure 58-1, right). In fact, Diaz and coworkers have recently shown that in most COPD patients with EFL at rest, the IC (% predicted) is lower than normal, whereas in the patients without EFL at rest the IC is usually within normal limits (Figure 58-5).[15]

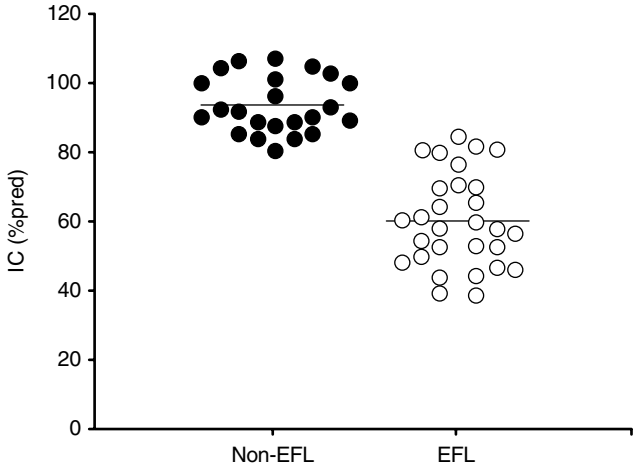

FIGURE 58-5 Inspiratory capacity (IC), expressed as percentage predicted (%pred), in 52 ambulatory chronic obstructive pulmonary disease (COPD) patients with (EFL) and without (non-EFL) tidal expiratory flow limitation at rest. In almost all patients with EFL, IC was decreased, whereas in the non-EFL patients IC was within normal limits. The difference in IC between patients with and without EFL is significant ($p < .002$). Reproduced with permission from Diaz O et al.[15]

In normal subjects there is a large expiratory flow reserve at lung volumes both above and below the FRC, as demonstrated by the fact that the maximal expiratory flow rates available are much higher than the flow rates used during resting breathing (see Figure 58-1, left). As a result, in normal subjects the tidal volume during exercise can increase both at the expense of the inspiratory and expiratory reserve volumes.[4] In contrast, in COPD patients who exhibit EFL at rest, the flows available at lung volumes below FRC are insufficient to sustain even resting ventilation (see Figure 58-1, right), and thus the tidal volume during exercise can increase only at the expense of the inspiratory reserve volume. Since in such patients IC is decreased because of dynamic hyperinflation at rest, the potential for an exertional increment of tidal volume is limited. As a result, in COPD patients with EFL at rest the maximal tidal volume during exercise ($V_{T\,max}$) and hence exercise tolerance should be reduced.

Based on these considerations, Murariu and colleagues were the first to show that in patients with COPD the resting IC is a much better predictor of exercise tolerance than either FEV_1 or FVC.[28] This has been subsequently confirmed by several studies.[4,15] Furthermore, it has been shown that in patients with COPD the resting IC is a good predictor of $V_{T\,max}$ and, hence, of maximal exercise ventilation and exercise tolerance.[32]

Figure 58-6 illustrates the relationship of maximal oxygen uptake ($\dot{V}O_{2max}$) during incremental, symptom-limited exercise on a cycle ergometer and IC in stable patients with COPD reported by Diaz and colleagues.[15] The patients were stratified according to the presence or absence of EFL during resting breathing in the sitting position. The coefficient of determination (r^2) of $\dot{V}O_{2max}$ to IC is 0.56, indicating that IC can explain 56% of the variance in $\dot{V}O_{2max}$. Using stepwise multiple regression analysis, Diaz and colleagues showed that the FEV_1/FVC ratio also plays a significant role

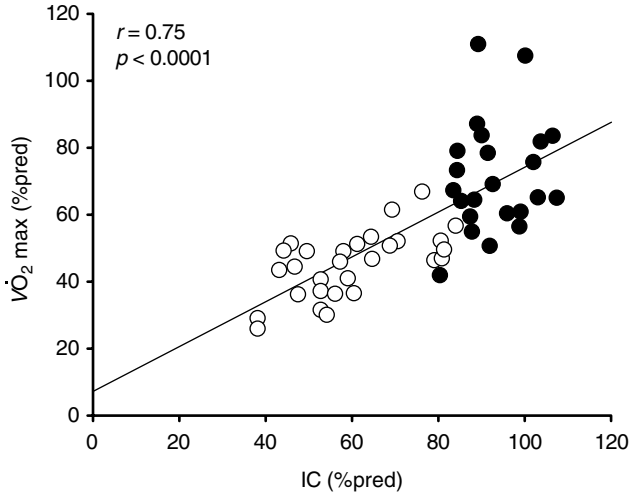

FIGURE 58-6 Relationship of maximal O_2 uptake during exercise ($\dot{V}O^2_{max}$) to resting inspiratory capacity (IC) in 23 chronic obstructive pulmonary disease (COPD) patients without (•) and 29 COPD patients with (◦) tidal expiratory flow limitation (EFL) at rest. Same patients as in Figure 58-5. Reproduced with permission from Diaz O et al.[15]

in predicting $\dot{V}O_{2max}$. Together, IC and the FEV_1/FVC ratio could account for 72% of the variance of $\dot{V}O_{2max}$ ($r^2 = .72$). However, when stepwise multiple regression analysis was performed separately for patients with EFL and without EFL, only IC was identified as a significant contributor for patients with EFL, whereas only the FEV_1/FVC ratio was selected for subjects without EFL. The fact that $\dot{V}O_{2max}$ correlates significantly with IC only in patients with EFL can be seen by visual inspection of Figure 58-6. The significant correlation of $\dot{V}O_{2max}$ with FEV_1/FVC ratio in patients without EFL is mainly owing to the fact that a high FEV_1/FVC ratio reflects an MEFV curve with an upward convexity (Figure 58-1, left), which implies a large flow reserve over the resting tidal volume range, whereas a low FEV_1/FVC ratio reflects a curve with an upward concavity (Figure 58-1, right) with little expiratory flow reserve over the resting tidal volume range. Thus, patients without EFL at rest but with a low FEV_1/FVC ratio are more prone to develop EFL during exercise than are patients in whom this ratio is high. Development of EFL during exercise limits $V_{T\,max}$ and hence maximal exercise ventilation and exercise tolerance.[32] Accordingly, in COPD patients without EFL at rest, $\dot{V}O_{2max}$ correlates directly with FEV_1/FVC ratio (% predicted).

Since in COPD patients reduced exercise capacity shows only a weak link to lung function impairment measured in terms of FEV_1 and FVC,[2,15,28] it has been suggested that factors other than lung function impairment (eg, deconditioning and peripheral muscle dysfunction) were the predominant contributors to reduced exercise tolerance.[33–35] The recent studies based on assessment of IC and FEV_1/FVC ratio, however, indicate that lung function impairment is in general the major contributor to reduced exercise tolerance in COPD.[15,36] In fact, since in COPD patients the IC and FEV_1/FVC ratio together account for 72% of the $\dot{V}O_{2max}$ variance, only the remaining 28% can be ascribed to other factors, such as deconditioning and peripheral muscle dysfunction or decreased cardiac output as a result of intrinsic PEEP.[32] These considerations pertain to average values. In any given patient, however, the contribution of these factors may be entirely different.

In a study on 96 stable COPD patients, a significant correlation ($r = .60$) was found between arterial partial pressure of carbon dioxide (P_aCO_2) and $PEEP_i$.[16] Since both $PEEP_i$ and reduced IC reflect DH, a significant correlation of $PaCO_2$ to IC would be expected. In fact, in COPD patients with EFL at rest, the P_aCO_2 is significantly higher than in patients without EFL ($p < .04$) and correlates significantly ($r = .62$) with IC (% predicted).[15] Thus, hypercapnic COPD patients (the so-called *blue bloaters*) are characterized by a reduction in IC owing to dynamic hyperinflation elicited by tidal EFL at rest. These patients also exhibit a further significant ($p < .002$) increase in P_aCO_2 at peak exercise ($p < .002$) associated with a significant ($p < .05$) reduction in arterial partial pressure of oxygen (P_aO_2) relative to rest.[32] This essentially reflects reduced $\dot{V}_{E\,max}$ owing to a lower V_{Tmax} in patients with EFL than in those without EFL. In fact, V_{Tmax} is significantly correlated with IC ($p = .0001$).[32] In contrast, in *pink puffers* the P_aCO_2 tends to be normal at rest and does not increase even during exercise. Furthermore, at peak exercise the P_aO_2 is not decreased. This discrepant behavior probably reflects the increased burden placed on the respiratory muscles by $PEEP_i$ and dynamic hyperinflation in patients with EFL.

DYSPNEA

Together with decreased exercise tolerance, dyspnea is the predominant complaint of patients with COPD and is commonly the reason for seeking medical attention. Because dyspnea ratings correlate poorly with FEV_1 and FVC, it has been suggested that dyspnea and lung function should be considered as separate factors, which independently characterize the severity of COPD.[36] In reality, however, this is probably because of the fact that FEV_1 and FVC are poor predictors of dynamic hyperinflation, which is the major cause of dyspnea.[2] In fact, there is a good correlation between the degree of chronic dyspnea measured with the modified Medical Research Council (MRC) scale to various indices of dynamic hyperinflation,[2] including IC.[31]

A close correlation ($r = -.86$) was recently also found between maximal exercise power ($\dot{W}_{max}$) and the modified MRC score in stable patients with COPD[37] and diffuse bronchiectasis.[19] This suggests that the MRC dyspnea scale is designed to assess exercise capacity rather than the severity of dyspnea per se. Further studies are required to confirm these observations, which suggest that when ergometry is not available or contraindicated, the maximum exercise capacity can be predicted to a good approximation with the modified MRC scale.

ASSESSMENT OF SEVERITY OF COPD

The severity of COPD is commonly judged from the value of FEV_1, expressed as percentage predicted.[2] To the extent that

"severity" implies curtailment of exercise capacity and increased dyspnea, the choice of FEV_1 does not seem to be appropriate in view of the poor correlation of this parameter to both exercise capacity[15,28,34] and chronic dyspnea.[2] Assessment of severity of COPD according to IC (% predicted) appears to be more appropriate.[15,28,32]

Separation of COPD patients into two categories, namely with and without EFL while sitting at rest, appears to be clinically useful because the patients with resting EFL not only have curtailment of exercise capacity and increased chronic dyspnea but also tend to have increased P_aCO_2 and decreased P_aO_2 both at rest and during exercise.[15,32] Thus, this category of patients exhibits the altered blood gases, which categorizes the blue bloaters, as discussed above. It should also be noted that the two-point EFL classification according to presence or absence of EFL at rest in sitting position essentially reflects patients with and without a reduction of resting IC (see Figure 58-5).

The reduction in IC appears to be a good predictor of the decrease in exercise tolerance, which, together with dyspnea, is the main complaint of patients with COPD. As shown in Figure 58-6, the lower limit of resting IC found in ambulatory COPD patients is about 40% of predicted normal value. When the IC decreases below this limit the patient requires domiciliary oxygen therapy because of markedly reduced P_aO_2 at rest or during exercise. Supplemental oxygen elicits a decrease in dynamic hyperinflation, as reflected by increased resting IC, with a concurrent improvement of dyspnea.[38] This is mainly owing to a reduction of ventilation caused by removal of hypoxic stimulus, although removal of bronchoconstriction due to hypoxemia probably also plays a role.[39] Another way to decrease dynamic hyperinflation is by bronchodilator administration.

ASSESSMENT OF BRONCHODILATOR RESPONSE

The effect of bronchodilators in patients with obstructive lung disease is commonly assessed in terms of the change in FEV_1 seen after bronchodilator administration relative to the control values. According to the American Thoracic Society's recommended criteria, a change in FEV_1 of more than 12% and 200 mL as relative to baseline represents a significant response.[40] Although most COPD patients do not exhibit a significant change in FEV_1 after bronchodilator administration, many of them claim improvement in symptoms.[41] Since pulmonary hyperinflation plays a paramount role in determining the intensity of dyspnea,[2] it is likely that in such patients there should be a decrease in the degree of dynamic hyperinflation (decreased FRC and increased IC) after bronchodilator administration. Indeed, Belman and colleagues have shown that the decrease in dynamic hyperinflation during exercise with the concurrent improvement in inspiratory flow reserve, inspiratory pressure reserve, and neuroventilatory coupling was the key determinant of the reduced breathlessness claimed at peak exercise by COPD patients after bronchodilator administration.[42]

Tantucci and colleagues, however, were the first to assess the effect of a bronchodilator (salbutamol) on resting IC.[31] Subsequently, it has been shown that the increase in IC after anticholinergic therapy best reflected the improvement in exercise tolerance.[43] The improvement of IC after bronchodilator administration, which is mainly limited to patients with EFL at rest and exhibit a reduction of baseline IC, entails reduction in dyspnea both at rest and during light exercise.[44,45] Thus, in obstructive lung disease, the benefit of bronchodilator therapy should be assessed not only in terms of changes in FEV_1 but, more importantly, also in terms of increases in IC. In this connection it should be noted that, since performance of IC precedes the FVC maneuver, FEV_1 and IC are in general recorded together during bronchodilator testing.

Although bronchodilator testing has traditionally focused on changes in FEV_1, the scrutiny of changes in IC should be mandatory because it provides more useful information than FEV_1 pertaining to dyspnea and exercise tolerance. The fact that after bronchodilator administration there is a significant reduction in DH only in patients with EFL at rest in the sitting position further supports the usefulness of stratifying COPD patients in subgroups with and without EFL.

Assessment of IC and EFL has also provided useful information on the effects of surgical treatment in COPD patients.[46] Furthermore, a recent study has shown that in COPD patients the IC but not FEV_1 was significantly correlated with health-related quality of life (HRQL) (St. George's Respiratory Questionnaire) and dyspnea (ATS scale).[47]

ORTHOPNEA

As shown in Figure 58-7, in stable COPD patients with tidal EFL in sitting or supine position there is a high prevalence of orthopnea,[48] which probably results in part from increased inspiratory efforts owing to dynamic hyperinflation and the concomitant increase in inspiratory threshold

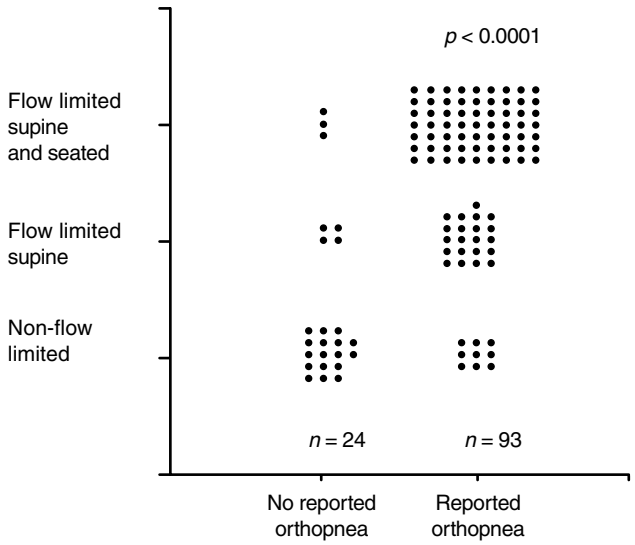

FIGURE 58-7 Prevalence of orthopnea in 117 stable chronic obstructive pulmonary disease (COPD) patients without and with tidal expiratory flow limitation (EFL) in sitting or supine posture. *P* value pertains to difference between the two orthopnea groups. Reproduced with permission from Eltayara L et al.[48]

load form $PEEP_i$. Increased airway resistance in the supine position probably also plays a role in the genesis of orthopnea. A similar mechanism for orthopnea is also found in obesity [9] and acute left heart failure.[11]

WHY ARE FEV_1 AND FVC POOR PREDICTORS OF EXERCISE TOLERANCE IN COPD?

Although it has been long established that FEV_1 and FVC are poor predictors of exercise capacity, no plausible explanations have been provided. Inspection of Figure 58-1 (right), however, readily explains the reason for this lack of correlation between exercise capacity and FVC. In fact, over the entire range of expiratory reserve volume (FRC-RV), the maximal expiratory flows are insufficient to sustain even resting ventilation. Accordingly, a large part of vital capacity is irrelevant in terms of ventilation at rest and during exercise. In Figure 58-1 (right) this nonphysiologic volume, namely the expiratory reserve volume, amounts to 43% of VC.

The poor correlation of exercise tolerance to FEV_1 is probably the result of two main factors: (1) in patients with severe COPD the FEV_1 is in general smaller than the IC; hence, it does not encompass the entire volume range where ventilation can take place at rest and during exercise, that is, between FRC and total lung capacity (TLC) (Figure 58-1, right); and (2) there is no single MEFV curve, as implied in Figure 58-1, because the maximal flows depend on the previous volume and time history[17] (Figure 58-8). In this connection it should be noted that, in most lung function laboratories, the FVC maneuver is preceded by a relatively slow inspiration to TLC with a variable breath hold, which should yield relatively low flows as shown by the lower MEFV curve in Figure 58-8. In reality, during maximal exercise the inspirations are fast and without end-inspiratory pause, which should correspond to the fast maneuver in Figure 58-8. In fact, with the fast maneuver the FEV_1 is higher than with the slow maneuver.[17]

The above mechanisms probably also explain in part the observation that in many patients with severe COPD the maximal breathing capacity (MBC) computed according to the conventional formula ($MBC = 35 \times FEV_1$) is less than the actual ventilation measured during maximal exercise. In fact, in patients with severe COPD the difference in FEV_1 between the fast and slow maneuvers illustrated in Figure 58-8 averages 23%.[17] Clearly, in predicting MBC, FEV_1 should be obtained with the fast maneuver, which yields higher values and is more closely related to respiratory timing during peak exercise. It should be stressed, however, that as a result of bronchodilatation the FEV_1 increases during exercise in COPD patients,[49] which also explains in part the finding that the MBC computed according to the resting FEV_1 may be lower than the ventilation observed during maximal exercise.

The fact that FEV_1 and FVC are not good predictors of exercise tolerance and dyspnea is not surprising because neither reflects DH or EFL, which are the main abnormalities in moderate to severe COPD. Figure 58-9 depicts the relationship between FEV_1 and EFL in 117 stable COPD patients.

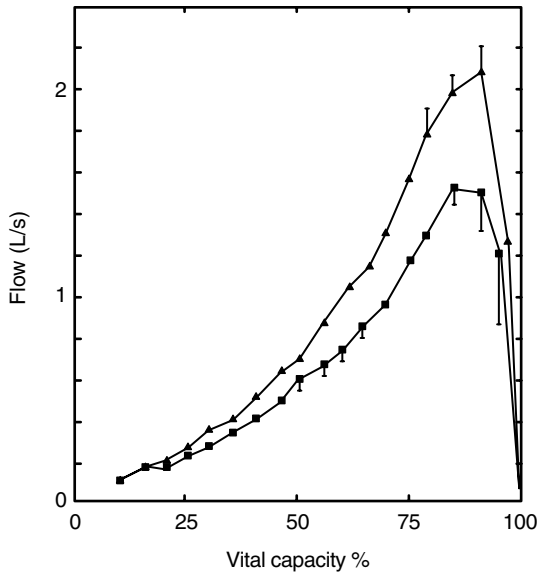

FIGURE 58-8 Mean values of expiratory flow obtained in a chronic obstructive pulmonary disease (COPD) patient at 5% intervals between 10 and 95% forced vital capacity (FVC) during forced expired vital capacity maneuvers following slow inspiration with end-inspiratory pause (*squares*) and rapid inspiration without end-inspiratory pause (*triangles*). Each point is the mean of four or five measures: bars are SD. The continuous lines joining data points represent the corresponding maximal expiratory flow-volume (MEFV) curves. Reproduced with permission from D'Angelo E et al.[17]

EFL was determined during resting breathing in sitting and supine positions. Although, on average, the patients with EFL both seated and supine had significantly lower FEV_1 (% predicted) than those without EFL ($p < .001$), there was a very marked scatter of the data. Indeed, 60% of the patients without EFL had an $FEV_1 < 49\%$ predicted and would be classified as having severe to very severe airway obstruction. Thus, FEV_1 is not a good predictor of tidal EFL.

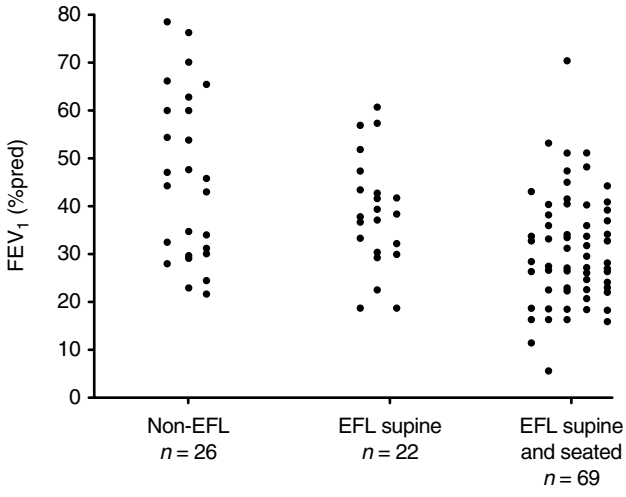

FIGURE 58-9 Individual values of forced expiratory volume in 1 second (FEV_1) (%pred) and tidal expiratory flow limitation (EFL) in 117 chronic obstructive pulmonary disease (COPD) patients while seated and supine at rest. Twenty-six patients had no EFL both seated and supine (non-EFL); 23 had EFL only supine (EFL supine); and 69 had EFL both seated and supine (EFL supine and seated). Reproduced with permission from Eltayara L.[2]

The choice of the appropriate predictors of exercise limitation and dyspnea requires understanding of the underlying pathophysiologic abnormalities, which may differ among COPD patients (eg, with EFL and without EFL). This also implies that the resting ventilatory function tests, which should best predict exercise intolerance and dyspnea, may be different for different etiologies. For example, in diffuse bronchiectasis the IC is not a useful marker of either chronic dyspnea or exercise tolerance.[19]

In conclusion, measurement of IC is useful for monitoring the status and progress of COPD patients and for assessing the efficacy of their treatment. It is time for IC, the Cinderella of pulmonary function testing, to take pride of place with her two stepsisters, FEV_1 and FVC. It should be stressed that this applies to COPD but not necessarily to other respiratory diseases.

REFERENCES

1. Agostoni E, Mead J. Statics of the respiratory system. In: Macklem PT, Mead J, editors. Handbook of physiology. Section 3. Volume I. The respiratory system: mechanics of breathing. Bethesda (MD): American Physiological Society; 1964. p 387–409.
2. Eltayara L, Becklake MR, Volta CA, Milic-Emili J. Relationship between chronic dyspnea and expiratory flow-limitation in patients with chronic obstructive pulmonary disease. Am J Respir Crit Care Med 1996;154:1726–34.
3. Koulouris NG, Valta P, Lavoie A, et al. A simple method to detect expiratory flow limitation during spontaneous breathing. Eur Respir J 1995;8:306–13.
4. Koulouris NG, Dimopoulou I, Valta P, et al. Detection of expiratory flow limitation during exercise in COPD patients. J Appl Physiol 1997;82:723–31.
5. Hyatt RE. The interrelationship of pressure, flow and volume during various respiratory maneuvers in normal and emphysematous patients. Am Rev Respir Dis 1961; 83:676–83.
6. Volta CA, Ploysongsang Y, Eltayara L, et al. A simple method to monitor performance of forced vital capacity. J Appl Physiol 1996;80:693–8.
7. Mota S, Casan P, Drobnic F, et al. Expiratory flow limitation during exercise in competition. J Appl Physiol 1999;86:611–6.
8. Bates DV, Macklem PT, Christie RV. Respiratory function in disease. Philadelphia (PA): W.B. Saunders Co.; 1971.
9. Ferretti A, Giampiccolo P, Cavalli A, et al. Expiratory flow limitation and orthopnea in massively obese subjects. Chest 2001;119:1401–8.
10. Baydur A, Milic-Emili J. Expiratory flow limitation during spontaneous breathing. Comparison of patients with restrictive and obstructive respiratory disorders. Chest 1997;112: 1017–23.
11. Duguet A, Tantucci C, Lozinguez O, et al. Expiratory flow limitation as a determinant of orthopnea in acute left heart failure. J Am Coll Cardiol 2000;35:690–700.
12. Castile R, Mead J, Jackson A, et al. Effect of posture on flow-volume curve configuration in normal humans. J Appl Physiol 1982;53:1175–83.
13. Knudson RJ. Physiology of the aging lung. In: Crystal RG, West JB, et al, editors. The lung: scientific foundations. New York: Raven Press Ltd; 1991. p. 1749.
14. Pride NB, Milic-Emili J. Lung mechanics. In: Calverley PMA, Pride NB, editors. Chronic obstructive pulmonary disease. London: Chapman & Hall; 1995. p. 135–60.
15. Diaz O, Villafranca C, Ghezzo H, et al. Exercise tolerance in COPD patients with and without tidal expiratory flow limitation at rest. Eur Respir J 2000;16:269–75.
16. Haluszka J, Chartrand DA, Grassino AE, Milic-Emili J. Intrinsic PEEP and arterial PCO_2 in stable patients with chronic obstructive pulmonary disease. Am Rev Respir Dis 1990;141:1194–7.
17. D'Angelo E, Prandi E, Marazzini L, Milic-Emili J. Dependence of maximal flow-volume curves on time course of preceding inspiration in patients with chronic obstructive lung disease. Am J Respir Crit Care Med 1994;150:1581–6.
18. Valta P, Corbeil C, Lavoie A, et al. Detection of expiratory flow limitation during mechanical ventilation. Am J Respir Crit Care Med 1994;150:1131–317.
19. Koulouris NG, Retsou S, Kosmas E, et al. Tidal expiratory flow limitation, dyspnoea, and exercise capacity in patients with bilateral bronchiectasis. Eur Respir J 2003;21:743–8.
20. Liistro G, Veritier C, Dury M, et al. Expiratory flow limitation in awake sleep-disordered breathing subjects. Eur Respir J 1999;14:185–90.
21. Verin E, Tardif C, Portier F, et al. Evidence for expiratory flow limitation of extrathoracic origin in patients with obstructive sleep apnoea. Thorax 2002;57:423–8.
22. Tantucci C, Mehiri S, Duguet A, et al. Application of negative expiratory pressure during expiration and activity of genioglossus in humans. J Appl Physiol 1998;84:1076–82.
23. Tantucci C, Duguet A, Ferretti A, et al. Effect of negative expiratory pressure on respiratory system flow resistance in awake snorers and non-snorers. J Appl Physiol 1999;87: 969–76.
24. Ninane V, Leduc D, Kafi SA, et al. Detection of expiratory flow limitation by manual compression of the abdominal wall. Am J Respir Crit Care Med 2001;163:1326–30.
25. Pellegrino R, Brusasco V. Lung hyperinflation and flow limitation in chronic airway obstruction. Eur Respir J 1997; 10:543–9.
26. Ingram RH Jr, Schilder DP. Effect of gas compression on pulmonary pressure, flow, and volume relationship. J Appl Physiol 1966;21:1821–6.
27. Shore SA, Milic-Emili J, Martin JG. Reassessment of body plethysmographic technique for the measurement of thoracic gas volume in asthmatics. Am Rev Respir Dis 1982; 126:515–20.
28. Murariu C, Ghezzo H, Milic-Emili J, Gauthier H. Exercise limitation in obstructive lung disease. Am Rev Respir Dis 1987;135:1069–74.
29. Yan S, Kaminski D, Sliwinski P. Reliability of inspiratory capacity for estimating end-expiratory lung volume changes during exercise in patients with chronic obstructive pulmonary disease. Am J Respir Crit Care Med 1997;156:55–9.
30. Jones NG, Jones G, Edwards, RHT. Exercise tolerance in chronic airway obstruction. Am Rev Respir Dis 1971;103:477–91.
31. Tantucci C, Duguet A, Similowski T, et al. Effect of salbutamol on dynamic hyperinflation in chronic obstructive pulmonary disease patients. Eur Respir J 1998;12:799–804.
32. Diaz O, Villafranca C, Ghezzo H, et al. Breathing pattern and gas exchange at peak exercise in COPD patients with and without tidal flow limitation at rest. Eur Respir J 2001; 17:1120–7.
33. Maltais F, Simard AA, Simard C, et al. Oxidative capacity of the skeletal muscle and lactic acid kinetics during exercise in normal subjects and in patients with COPD. Am J Respir Crit Care Med 1996;153:288–93.
34. Hamilton N, Killian KJ, Summers E, Jones NL. Muscle strength, symptom intensity, and exercise capacity in patients with cardio-respiratory disorders. Am J Respir Crit Care Med 1995;152:2021–31.

35. Gosselink R, Troosters T, Decramer M. Peripheral muscle weakness contributes to exercise limitation in COPD. Am J Respir Crit Care Med 1996;153:976–80.
36. Mahler DA, Harver A. A factor analysis of dyspnea ratings, respiratory muscle strength, and lung function in patients with chronic obstructive pulmonary disease. Am Rev Respir Dis 1992;145:467–70.
37. Kontogiorgi M, Kosmas EN, Gaga M, et al. Exercise capacity, tidal expiratory flow limitation, and chronic dyspnea in patients with stable COPD. Am J Respir Crit Care Med 2003;167:A293.
38. Alvisi V, Mirkovic T, Nesme P, et al. Acute effects of hyperoxia on dyspnea in hypoxemic patients with chronic airway obstruction at rest. Chest 2003;123:1038–46.
39. Coe CL, Pride NB. Effects of correcting arterial hypoxaemia on respiratory resistance in patients with chronic obstructive pulmonary disease. Clin Sci (Lond) 1993;84:325–9.
40. American Thoracic Society. Standards for the diagnosis and care of patients with chronic obstructive pulmonary disease (COPD) and asthma. Am Rev Respir Dis 1987;136:225–44.
41. Guyatt GH, Townstead M, Pugsley SO, et al. Bronchodilators in chronic airflow limitation. Effects on airway function, exercise capacity, and quality of life. Am Rev Respir Dis 1987; 135:1069–74.
42. Belman, MJ, Botnick WC, Shin JW. Inhaled bronchodilators reduce dynamic hyperinflation during exercise in patients with chronic obstructive pulmonary disease. Am J Respir Crit Care Med 1996;153:967–75.
43. O'Donnell DE, Lam M, Webb KA. Spirometric correlates of improvement in exercise performance after anti-cholinergic therapy in chronic obstructive pulmonary disease. Am J Respir Crit Care Med 1999;160:542–9.
44. Boni E, Corda L, Franchini D, et al. Volume effect and exertional dyspnea after bronchodilator in COPD patients with and without expiratory flow limitation at rest. Thorax 2002;57:528–31.
45. Di Marco F, Milic-Emili J, Boveri B, et al. Effect of inhaled bronchodilators on inspiratory capacity and dyspnea at rest in COPD. Eur Respir J 2003;21:86–94.
46. Murciano D, Pichot M, Boczkowki J, et al. Expiratory flow limitation in COPD patients after single lung transplantation. Am J Respir Crit Care Med 1997;155:1036–41.
47. Soicher JS, Mayo NE, Bourbeau J. Clinical indicators of health-related quality of life in COPD based on a rehabilitation model (unpublished observations).
48. Eltayara L, Ghezzo H, Milic-Emili J. Orthopnea and tidal expiratory flow limitation in patients with stable COPD. Chest 2001;119:99–104.
49. Raimondi AC, Edwards RHT, Denison DM, et al. Exercise tolerance breathing a low density gas mixture, 35% oxygen and air in patients with chronic obstructive bronchitis. Clin Sci 1970;39:675–85.

CHAPTER 59

DETERMINANTS OF DECLINE IN LUNG FUNCTION

Nicholas R. Anthonisen, Jure Manfreda

The most extensively studied and most significant aspect of lung function decline is that of the forced expiratory volume in 1 second (FEV_1), for two reasons. First, the FEV_1 is the most reproducible lung function test and therefore is best adapted to the assessment of large groups of people. Second, excessive decline of FEV_1 is the hallmark of obstructive lung disease, especially chronic obstructive pulmonary disease (COPD), and most studies of age-related decline in lung function have been done in this context. For this reason we confine our discussion to decline of FEV_1.

DECLINE OF FEV_1 IN NORMAL SUBJECTS

In normal adults, the FEV_1 declines with age. Whether this is a result of changes intrinsic to the lung or a response to inhalants with adverse effects on the lung is unknown and probably unknowable. The rate of decline in normal subjects, that is, people who have never smoked and do not have respiratory symptoms, has been estimated in both cross-sectional and longitudinal studies. Cross-sectional studies have largely been used for the development of normal values; the most recent and probably the best of these is that of Hankinson and colleagues, who studied a random sample of the U.S. population.[1] Table 59-1 shows illustrative examples of annual decline of FEV_1 from these data. Generally, decline increased with age, although this was not the case in African American and Mexican American males, and decline was larger in men than in women.

In general, longitudinal studies of FEV_1 decline in normal subjects agree with cross-sectional estimates, although agreement is not entirely consistent. In particular, Burrows and colleagues found that FEV_1 tended to plateau in early adulthood, beginning to decline in the midthirties in both sexes.[2] Longitudinal studies, by definition, examine data from a particular cohort and measure events occurring during the study, whereas cross-sectional studies examine the effects of events that occurred before the study, so failure to have exact agreement is explicable.

CHRONIC OBSTRUCTIVE PULMONARY DISEASE

COPD is defined as chronic airways obstruction that cannot be completely reversed with therapy and is not explained by another more specific pathology. In the developed world, it is strongly related to smoking.[3,4] COPD includes three specific pathologies: chronic bronchitis, peripheral airways disease, and emphysema. Chronic bronchitis is usually defined as cough and sputum present more than 3 months of the year for 2 consecutive years and is accompanied by pathologic changes in large airways. Peripheral airways disease involves obstruction of bronchioles. Emphysema is defined as destruction of peripheral lung units with loss of gas-exchanging area. Chronic bronchitis, peripheral airways disease, and emphysema are all related to tobacco use, and all three are present in many but not all patients with severe COPD. Peripheral airways disease and emphysema cause chronic airways obstruction, but this is not necessarily true of chronic bronchitis. Although related to smoking, most heavy smokers do not develop clinically apparent COPD, so there must be additional determinants or risk factors. Most information on decline of FEV_1 is related to the development of COPD and risk factors involved, and this is the context for the remainder of this chapter.

Relationship to Asthma

Asthma is also characterized by airways obstruction but is regarded as different from COPD because asthma and COPD generally present different clinical pictures, have different epidemiologic features, and have different natural histories. On the other hand, some asthmatics pursue an unremitting course and some develop nonreversible airways obstruction,[5] but the mechanisms involved in the chronic obstruction of asthma probably differ from those in smoking-related COPD.

Some patients with progressive airways obstruction and significant smoking histories resemble asthmatics in that they demonstrate substantial reversibility of their obstruction with inhaled bronchodilators.[6] It has not been shown that these individuals differ in any important way from COPD patients with less reversibility, and it should be noted that reversibility is not a very reproducible test.[6]

Natural History of COPD

COPD is commonly characterized as an abnormally rapid decline in FEV_1 in response to inhaled toxins: in the developed world, by far the most important of these is tobacco smoke. Figure 59-1 shows a model of the effects of smoking

Table 59-1 Average Decline in FEV_1 (mL/yr)

	Male (height 175 cm)			*Female (height 165 cm)*		
Age (yr)	*Caucasian*	*African American*	*Mexican American*	*Caucasian*	*African American*	*Mexican American*
20–40	23.4	23.1	29.3	15.3	18.7	18.6
41–60	30.4	23.1	29.3	23.2	22.6	23.2
61–80	37.3	23.1	29.3	31.0	26.5	27.7

Adapted from Hankinson JL et al.[1]
FEV_1 = forced expiratory capacity in 1 second.

on lung function, adapted from the classic work of Fletcher and colleagues[7] and validated in many subsequent studies.[8] The decline in FEV_1 is shown as linear functions starting at age 30 years. Disability occurs at a value of 1.5 to 2.0 L and severe disability at 1.0 L. In the average nonsmoker, FEV_1 declines at a rate approximating 30 mL/yr, so disability does not occur during the normal life span. In the average smoker, the FEV_1 declines approximately twice as fast, at a rate of about 60 mL/yr, and disability will not occur until quite late in life. A subgroup of smokers is unusually "sensitive" to the effects of tobacco smoke and declines much more rapidly, at rates of 100 mL/yr and more. These people develop severe disability in late middle age. This "sensitive" subgroup is thought to consist of 15 to 20% of all smokers.

The effect of smoking cessation in middle age is also illustrated in Figure 59-1. With cessation, the rate of decline reverts to that of the normal nonsmoker. This effect was observed in people who spontaneously quit smoking[7] and in a randomized trial of smoking cessation.[8] Smoking cessation in middle age will either prevent or greatly delay the onset of symptomatic disease (see Figure 59-1). Once disability has developed, the benefit of cessation is not as clear.

RISK FACTORS FOR ACCELERATED DECLINE OF FEV_1

Airways Hyperreactivity

In the 1960s Dutch investigators proposed that the degree of airways reactivity was an important determinant of the development of COPD.[9] According to this argument, smokers with highly reactive airways would be much more likely to develop chronic airways obstruction than would those with less reactivity. The "Dutch hypothesis" proved difficult to test for several reasons. First, airways hyperreactivity is a hallmark of asthma, and Dutch investigators tended to lump together patients with asthma and those with COPD, so many Dutch studies of the influence of airways reactivity included asthmatics. Second, it was clear that the degree of airways reactivity was inversely proportional to the FEV_1 in people with airways obstruction[10] and that the reactivity might be a consequence rather than a cause of the obstruction. For this reason, cross-sectional studies of reactivity in people with COPD were of little value in testing the Dutch hypothesis.

Prospective studies of the influence of airways reactivity on the rate of decline of lung function have been carried out in a number of populations at relatively low risk of symptomatic COPD and indicated that reactivity did predict decline. However, the Lung Health Study provided the best support for the Dutch hypothesis.[11] In nonasthmatic smokers aged 35 to 59 years with a ratio of FEV_1 to forced vital capacity (FVC) <0.70, the degree of methacholine responsiveness was the second most important predictor (after smoking status) of subsequent decline in FEV_1. Reactivity was strongly interactive with smoking; in continuing smokers it had a powerful effect on decline, whereas it had much less effect in people who stopped smoking.

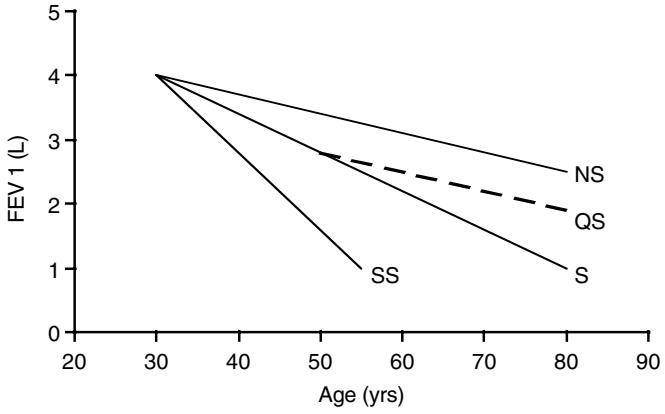

FIGURE 59-1 Schematic model of rate of decline of FEV_1 in adult men. Trajectories are shown for nonsmokers (NS), "average" smokers (S), "sensitive" smokers (SS), and men who quit smoking (QS).

Atopy

Two manifestations of atopy have been thought to be risk factors for loss of lung function and, by implication, for COPD. These are serum total immunoglobulin E (IgE) levels and skin test reactivity to common allergens. Both are associated with asthma and airways hyperreactivity in healthy people.[12] Of the two, IgE levels have received the most attention. Smoking is also associated with increased IgE levels.[13] Given the associations of IgE levels with both smoking and asthma, it is not surprising that the IgE level is inversely related to lung function in cross-sectional studies.[14] However, most longitudinal studies of lung function have not found a relationship between IgE levels and rate of decline of lung function in smokers.[15] IgE is probably not a risk factor for the development of smoking-related COPD.[16]

If asthmatics are excluded, atopy as assessed by skin tests is apparently not related to decline in lung function in either smokers or nonsmokers.[17]

Episodes of Acute Bronchitis: Exacerbations

The "British hypothesis" explaining the pathogenesis of COPD was that chronic bronchitis predisposed individuals to repeated episodes of respiratory tract infection and that these episodes led to irreversible lung damage and airways obstruction.[18] The hypothesis rested on the observation that many COPD patients had chronic cough and sputum production associated with periodic chest infections occurring prior to the onset of dyspnea and disability. Further, even when clinically stable, these patients had bacteria in their sputum that were similar to those recovered during acute episodes.

The landmark study of Fletcher and colleagues tested the British hypothesis by evaluating 792 male London transit workers (both smokers and nonsmokers) for 8 years, with regular assessment of sputum, chest infections, and FEV_1.[7] They found that neither symptomatic chronic bronchitis nor chest infections correlated with the decline of lung function. Acute chest infections were more common in people with chronic bronchitis but did not relate to the development of chronic airways obstruction. Their results were confirmed by other long-term studies.[19]

For many years, it was thought that the presence or absence of chronic bronchitis with or without acute episodes had no long-term effect on the course of the disease, although exacerbations undeniably caused short-term decreases in lung function and were important causes of hospitalization and death. However, two carefully done long-term studies have demonstrated that the rate of decline of FEV_1 is higher in smokers with chronic cough and sputum production than in those without symptomatic chronic bronchitis.[20,21]

Recently, new light has been shed on the problem. Seemungal and colleagues carefully followed a cohort of COPD patients, characterizing their exacerbations, including peak flows measured before, during, and after the illness.[22] Not all patients recovered completely. Indeed, in about 7% of patients peak flows were lower 90 days after an exacerbation than they were before. Thus, exacerbations may have a long-term deleterious effect on lung function in COPD. Retrospective analysis of data from the Lung Health Study supported this argument.[23] Participants were asked at annual visits if they had seen a doctor for bronchitis, pneumonia, influenza, or chest colds. Positive responses were classified as lower respiratory infections (LRIs). Participants with chronic cough and sputum production had about twice as many LRIs as those without. People who quit smoking had fewer LRIs than those who continued. In continuing smokers, a single LRI was associated with a loss of 7 mL of FEV_1 during the year of the event, and there was a clear dose-response effect, with more LRIs associated with greater losses. This was true whether or not chronic cough and sputum production were present. In people who stopped smoking, LRIs had no effect on the rate of decline of FEV_1. Thus, exacerbations of symptoms had a long-term negative effect on lung function, which would be significant if several episodes occurred per year.

Sex

COPD has been considered to be largely a disease of men; this sex distribution reflected differences in smoking habits between men and women, and as the prevalence of female smokers has increased over the last 50 years, so has the prevalence of COPD in women. There is little question that the COPD prevalence in women will continue to increase in the foreseeable future.

If sex were an independent risk factor for COPD, men and women with the same smoking habits would develop COPD at different rates. The effect of smoking on sex-specific lung function has been examined on a number of occasions with conflicting results. The Lung Health Study followed a substantial number of women with airways obstruction, and data from 11 years of follow-up have recently been examined to look for sex-specific functional differences.[24] Among continuing smokers, rates of decline of FEV_1 were quite similar between sexes when expressed as a percentage of the predicted normal value (Table 59-2). Men were heavier smokers than women, so these results could be interpreted as indicating that women might be more sensitive than men to cigarette smoke, but differences are probably minor and are not evident given sex-related differences in smoking habit.

Genetic or Hereditary Risk Factors

The observation that only 15 to 20% of smokers develop COPD is a strong indication that genetically controlled susceptibility to the disease may be involved in the development of COPD. Familial aggregation has been documented in COPD; more cases than expected have been found in the families of index cases. However, it has been difficult to separate the presumed hereditary effect from the sharing of environmental exposures or lifestyle. In North America, the effects of familial aggregation and heredity on lung function were examined in a number of cross-sectional studies. Heritability was estimated as the proportion of the variance in lung function owing to hereditary factors. Most such studies showed such an influence.[25] Only a modest effect of family history has been shown in longitudinal analysis,[26] probably because of methodological problems in conducting such studies that tend to dilute associations. Lung function must be hereditary to some extent, but the effect is difficult to quantify.

The only genetic factor that is strongly correlated with the development of COPD is that of the homozygous ZZ phenotype of α_1-antitrypsin (AAT) deficiency.[27] Although this phenotype is associated with the premature development of severe emphysema, it leads to substantially reduced life expectancy largely in smokers; the effects in people who

Table 59-2 Sex Effects in the Lung Health Study: Change of FEV_1 over 11 Years

	Women		*Men*		
	N	*FEV_1% predicted*	*N*	*FEV_1% predicted*	p
Sustained quitter	253	−0.05	462	−0.27	<.0001
Intermittent quitter	906	−0.86	1,423	−0.88	.697
Continuous smoker	396	−1.31	644	−1.27	.532

FEV_1 = forced expiratory capacity in 1 second.

never smoked and in those not exposed to environmental hazards are relatively small.[28] Because the ZZ phenotype is rare, it accounts for only a small proportion of individuals with COPD. Among heterozygous AAT phenotypes, only the more common MZ and SZ phenotypes might interact with smoking and environmental exposure to produce the disease; however, the evidence for their role is not consistent. Sandford and colleagues reviewed seven case-control studies that showed a 1.5 to 5.0 times higher risk of COPD for MZ than for normal MM control subjects.[29] There was no excess risk for MS and SZ phenotypes. On the other hand, in cross-sectional population studies, there is little difference between MZ or SZ and MM phenotypes with respect to FEV_1, particularly between nonsmoking subjects.[30] In the absence of smoking and environmental exposures, these phenotypes probably do not result in COPD, but the MZ phenotype may well increase the rate of decline of FEV_1 in smokers.

It is unlikely that there is one gene responsible for COPD susceptibility. COPD is likely a disease of complex genetic origin, with many genes involved in mediating different steps in the disease and influencing the response to different environmental exposures, including smoking. The number of new candidate genes is increasing quickly and is briefly reviewed.

α_1-Antichymotrypsin α_1-Antichymotrypsin (ACT) is a serine protease inhibitor.[31] Deficiency is inherited in an autosomal dominant pattern. In one study, the deficiency was found in 4 of 100 individuals with COPD and in no control subjects.[32]

Matrix Metalloproteinases Matrix metalloproteinases (MMPs) are a family of proteolytic enzymes whose substrate is connective tissue. There are a number of naturally occurring polymorphisms of human MMP gene promoters, and polymorphisms in the *MMP1* and *MMP12* genes, but not *MMP9*, have been found to be associated with rapid decline of FEV_1.[33] A tissue inhibitor of MMP (TIMP) has been described, and two polymorphisms of the *TIMP2* gene have been found to be overrepresented in COPD patients.[34]

Vitamin D Binding Protein Vitamin D binding protein (VDBP), group-specific component, is a serum α_2-globulin encoded by a gene with substantial variability. There have been conflicting reports regarding the frequency of this variation in COPD patients, the best evidence favoring no effect.[35]

ABO Blood Group Antigens Early findings of variations of FEV_1 with different blood groups have not been borne out by longitudinal study.[36] Similarly, the ability to secrete antigen into body fluids (ABH secretor status) was found to be related to cross-sectional lung function, but this was not the case in longitudinal study.[37]

Microsomal Epoxide Hydrolase The enzyme microsomal epoxide hydrolase (mEPHX) is involved in the metabolism of reactive epoxide intermediates produced in oxidative stress. An Exon-3 mutation of the controlling gene reduces the enzyme activity by 50% and has been associated with COPD in case-control studies.[38]

Heme Oxygenase-1 Heme Oxygenase-1 (HO-1) is a lung antioxidant. Carriers of some alleles have been characterized as likely to have emphysema.[39]

Tumor Necrosis Factor Alpha Tumor necrosis factor alpha (TNF-α) is a multifunctional cytokine, a proinflammatory mediator that is released by epithelial cells and macrophages. The bulk of the evidence does not support a role for TNF-α polymorphisms with rapid decline of FEV_1.[35]

Interleukin 1 Interleukin 1 (IL-1), which exists in two forms, is a proinflammatory cytokine associated with airways disease. Both the IL-1β (IL-1β) form and the IL-1 receptor antagonist (IL-1RN) have naturally occurring genetic polymorphisms. Although specific genotypes were not associated with rapid decline of lung function, the distribution of IL-1β and IL-1RN haplotypes differed between smokers with rapid decline and those without.[40]

Occupational Exposures

It has long been known that occupational exposure to dusts can be associated with symptoms and abnormalities of lung function. However, assessments of the contribution of occupational exposures to the rapid decline of FEV_1 and COPD have been difficult and often inconclusive. It should also be noted that over the past 30 years, the levels of occupational exposure to a variety of dusts have decreased as a result of legislation aimed at workers' protection, so the current applicability of much of the data in older workers is questionable.

Cross-sectional studies have repeatedly shown occupational exposure to mineral dusts to be associated with chronic cough and sputum production and reductions in lung function.[41] Longitudinal studies of workers exposed to mineral dusts have also shown deleterious effects. Both coal miners and hard rock miners have higher rates of lung function loss than control subjects after correction for the effects of smoking.[42,43] The most recent estimates in coal miners indicate a risk that is at most one-half that imposed by smoking.[44,45]

Other occupational dust exposures have been associated with increased loss of lung function over time. A particularly well-documented instance is cotton dust exposure in textile workers,[46] and relatively low levels of cotton dust exposure may interact with smoking, in that exposure-related loss of lung function was evident only in smokers.[47] In cross-sectional studies, dust exposure has had a more pronounced effect on lung function than exposure to gases and fumes, but the latter were associated with relatively minor deficits.

In summary, it is likely that occupation-related exposures to dusts and, to some extent, noxious fumes and gases accelerate loss of lung function. With the possible exception of people exposed to cadmium, which causes emphysema in animal models, and a previous generation of coal miners, it is unlikely that occupational exposure alone causes much COPD, at least in Europe and North America.

Air Pollution

Adverse effects of ambient air pollution on health have been recognized for a long time. There is good evidence that current pollutants, derived from the combustion of fossil fuels, photochemical reactions, and automotive exhaust, are associated with excess mortality and hospitalizations.[48] Rises in pollution levels have been associated with exacerbations of asthma and COPD.

It is, however, less well established whether chronic exposure to air pollution affects the decline of FEV_1. This is owing to difficulties in interpreting cross-sectional studies, in conducting appropriate longitudinal studies, in estimating personal exposure levels in large numbers of individuals, and in controlling the effects of potential confounders, such as smoking. In addition, people are frequently exposed to several air pollutants concurrently. The issue has been intensely studied with inconsistent results, in that specific pollutants had varying effects or effects that varied with the age or sex of the people exposed. Two very large American studies found that FEV_1 was lower in people exposed to oxides of nitrogen, ozone, and particulates after adjustment for confounding variables.[49,50] The effects were small compared with those of smoking.

Environmental Tobacco Smoke

Environmental tobacco smoke (ETS) is other people's cigarette smoke and contains most of the toxins that the original smoker inhaled. It is difficult to estimate ETS exposure in other than a semiquantitative way, such as the number of smokers in the immediate environment and the fraction of time in the suspect environment. Most studies compare nonsmokers who are exposed to smokers with those who are not. There is an increased risk of dying from emphysema or bronchitis in nonsmoking women exposed to ETS but not in men.[51] Most other evidence relating ETS and lung function has been obtained from cross-sectional studies comparing FEV_1 between ETS-exposed and nonexposed nonsmokers. The results of these studies are inconsistent but taken together indicate that long-term exposure to ETS is associated with a decrease of approximately 0.1 L, too small to cause clinical illness.

Indoor Air Pollution

Indoor air pollution may be an important determinant of health because people spend a substantial proportion of their life indoors and because, under some circumstances, pollutant levels can be very high. Evidence from developing countries is accumulating to suggest that smoke from wood and other biomass fuels may be an important determinant of airflow obstruction. This is typified by a recent study from Mexico.[52]

Childhood Conditions

Events in childhood could predispose to reduced lung function in adults by a number of mechanisms. It is extremely difficult to study childhood influences on a disease that develops gradually and becomes apparent only in late adult life, and no such longitudinal studies are available. Nevertheless, the influences of childhood respiratory infections and exposures to ETS have been intensely investigated. To summarize, both appear to cause small reductions in lung function, at least in children. Although these changes per se are not large enough to pose a credible COPD risk factor, it is conceivable that these childhood events increase the susceptibility of smokers to tobacco products.

A specific and promising hypothesis regarding childhood infection and COPD has emerged from the work of Hogg, who demonstrated that pieces of the adenoviral genome were commonly present in autopsied lung specimens from smokers with and without COPD.[53] This genetic material was presumably due to previous infection with this agent that might have occurred during childhood. They also demonstrated that the E1A viral segment is present much more often in smokers with airways obstruction than in those without and have developed evidence that this viral segment could be a cause of chronic inflammation.

Dietary Factors

Three groups of dietary factors have been investigated as potential contributors to chronic obstructive disease: (1) antioxidants, (2) ω-3 fatty acids, and (3) electrolytes. Such studies are plagued with methodological problems, and the resulting evidence is far from conclusive but is worthy of consideration because dietary factors apply to large populations.

Antioxidants Cross-sectional studies have related the estimated intake of specific antioxidants to the FEV_1. In several, higher intake of vitamin C was associated with slightly higher values of FEV_1. Similar but less consistent associations have been developed for vitamin E and β-carotenoid intake.

ω-3 Fatty Acids ω-6 Fatty acids are proinflammatory; ω-3 fatty acids, largely derived from fish, are protective. People who eat fish regularly tend to have a slightly higher level of FEV_1 than those who do not.

Electrolytes There are some studies suggesting that bronchial responsiveness is higher in people with a higher intake of sodium, and a higher intake of magnesium may have a protective effect. Bronchial reactivity is associated with rapid decline of FEV_1 in smokers.

SUMMARY AND CONCLUSIONS

Lung function—FEV_1—declines in normal people, but the decline is so slow that they do not develop dyspnea in the absence of disease. Tobacco smoking causes accelerated decline of FEV_1, the hallmark of COPD. However, only a minority of smokers develop symptomatic COPD, so other "host factors" must be involved, and several have been identified. Airways reactivity, as assessed by methacholine, is associated with relatively rapid loss of lung function in smokers, as is repeated respiratory infection. It is well known that homozygous ZZ α_1-antitrypsin deficiency combined with smoking causes severe, premature COPD, and the role of other genes is under intense investigation. Results are promising but not conclusive. Occupational exposure to

certain dusts is also associated with accelerated loss of lung function. Other putative risk factors, including ambient air pollution, environmental tobacco smoke, and dietary components, are probably not important. At present it is still impossible to predict which smokers will develop symptomatic COPD.

REFERENCES

1. Hankinson JL, Odenkrantz JR, Fedan KB. Spirometric reference values from a sample of the general U.S. population. Am J Respir Crit Care Med 1999;159:179–87.
2. Burrows B, Lebowitz MD, Camilli AE, Knudson RJ. Longitudinal changes in forced expiratory volume in one second in adults. Methodologic considerations and findings in healthy nonsmokers. Am Rev Respir Dis 1986;133:974–80.
3. Palmer KNV. The role of smoking in bronchitis. BMJ 1954; 1:1473–4.
4. US Department of Health, Education and Welfare. Smoking and health: a report to the Advisory Committee to the Surgeon General of the Public Health Service. Washington (DC): US Department of Health, Education and Welfare; 1964. Public Health Service Publication No. 1103.
5. Lange P, Parner J, Vestbo J, Schnohr P, Jensen G. A 15-year follow-up study of ventilatory function in adults with asthma. N Engl J Med 1998;339:1194–2000.
6. Anthonisen NR, Wright EC, the IPPB Trial Group. Bronchodilator response in chronic obstructive pulmonary disease. Am Rev Respir Dis 1986;133:814–9.
7. Fletcher C, Peto R, Tinker C, Speizer FE. The natural history of chronic bronchitis and emphysema. Oxford: Oxford University Press; 1976.
8. Anthonisen NR, Connett JE, Kiley JP, et al. Effects of smoking intervention and the use of an inhaled anticholinergic bronchodilator on the rate of decline of FEV_1. The Lung Health Study. JAMA 1994;272:1497–505.
9. Orie NGM, Sluiter HJ, de Vries K, et al. The host factor in chronic bronchitis. In: Orie NGM, Sluiter HJ, editors. Bronchitis, an International Royal Symposium. Assen (The Netherlands): Royan Van Gorcum; 1961. p. 43–59.
10. Ramsdell JW, Nachtwey FJ, Moser KM. Bronchial hyperreactivity in chronic obstructive bronchitis. Am Rev Respir Dis 1982;126:829–32.
11. Tashkin DP, Altose MD, Connett JE, et al. For the Lung Health Study Research Group. Methacholine reactivity predicts changes in lung function over time in smokers with early chronic obstructive pulmonary disease. Am J Respir Crit Care Med 1996;153:1802–11.
12. O'Connor GT, Sparrow D, Weiss ST. The role of allergy and nonspecific airway hyperresponsiveness in the pathogenesis of chronic obstructive pulmonary disease. Am Rev Respir Dis 1989;140:225–52.
13. Gerrard JW, Heiner DE, Ko CG, et al. Immunoglobulin levels in smokers and non-smokers. Ann Allergy 1980;44:261–2.
14. Burrows B, Lebowitz MD, Barbee RA, et al. Interactions between smoking and immunologic factors in relation to airways obstruction. Chest 1983;84:657–61.
15. Taylor RG, Joyce H, Gross E, et al. Bronchial reactivity to inhaled histamine and annual rate of decline in male smokers and ex-smokers. Thorax 1985;40:9–16.
16. Burrows B, Knudson RJ, Cline MG, Lebowitz MD. A reexamination of risk factors for ventilatory impairment. Am Rev Respir Dis 1988;138:829–36.
17. Annesi I, Neukirch F, Orvoen-Frija E, et al. The relevance of hyperresponsiveness but not of atopy to FEV_1 decline. Bull Eur Pathophys Respir 1987;23:397–400.
18. Fletcher CM. Chronic bronchitis: its prevalence, nature and pathogenesis. Am Rev Respir Dis 1959;80:483–94.
19. Howard P. A long-term follow-up of respiratory symptoms and ventilatory function in a group of working men. Br J Industr Med 1970;27:326–33.
20. Sherman CB, Xu X, Speizer FE, et al. Longitudinal lung function decline in subjects with respiratory symptoms. Am Rev Respir Dis 1992;146:855–9.
21. Vestbo J, Prescott E, Lange P. The Copenhagen City Heart Study Group. Association of chronic mucus hypersecretion with FEV_1 decline and chronic obstructive pulmonary disease morbidity. Am J Respir Crit Care Med 1996;153:1530–5.
22. Seemungal TA, Donaldson GC, Bhowmik A, et al. Time course and recovery of exacerbations in patients with chronic obstructive pulmonary disease. Am J Respir Crit Care Med 2000;161:1608–13.
23. Kanner RE, Anthonisen NR, Connett JE. For the Lung Health Study Research Group. Lower respiratory illnesses promote FEV_1 decline in current smokers but not in ex-smokers with mild chronic obstructive pulmonary disease. Am J Respir Crit Care Med 2001;164:358–64.
24. Anthonisen NR, Connett JC, Murray RP. For the Lung Health Study Research Group. Smoking and lung function of Lung Health Study [LHS] participants after 11 years. Am J Respir Crit Care Med 2002;166:675–9.
25. Givelber RJ, Couromitree NN, Gottlieb DJ, et al. Segregation analysis of pulmonary function among families in the Framingham study. Am J Respir Crit Care Med 1998;157: 1445–51.
26. Gottlieb DJ, Wilk JB, Harmon M, et al. Heritability of longitudinal change in lung function. The Framingham Study. Am J Respir Crit Care Med 2001;164:1655–9.
27. Laurell CB, Erickson S. The electrophoretic α_1-globulin pattern of serum in α_1-antitrypsin deficiency. Scand J Clin Lab Invest 1963;15:132–40.
28. Seersholm N, Kok-Jensen A, Dirksen A. Survival of patients with severe α_1-antitrypsin deficiency with special reference to non-index cases. Thorax 1994;94:695–8.
29. Sandford AJ, Weir TD, Pare PD. Genetic risk factors for chronic obstructive pulmonary disease. Eur Respir J 1997;10: 1380–91.
30. Turino GM, Barker AF, Brantly ML, et al. Clinical features of individuals with PI* SZ phenotype of α_1 anti-trypsin deficiency. Am J Respir Crit Care Med 1996;154:1718–25.
31. Eriksson S, Lindmark B, Lilja H. Familial α_1 antichymotrypsin deficiency. Acta Med Scand 1986;220:447–53.
32. Poller W, Faber J-P, Scholz S, et al. Missense mutation of α_1 antichymotrypsin gene associated with chronic lung disease. Lancet 1992;339:1538.
33. Joos L, He J-Q, Shepherdson MB, et al. The role of matrix metalloproteinase polymorphisms in the rate of decline in lung function. Hum Mol Genet 2002;11:569–76.
34. Hirano K, Sakamoto T, Uchida Y, et al. Tissue inhibitor of metalloproteinases-2 gene polymorphisms in chronic obstructive pulmonary disease. Eur Respir J 2001;18:748–52.
35. Sandford AJ, Chagani T, Weiss TD, et al. Susceptibility genes for rapid decline of lung function in the Lung Health Study. Am J Respir Crit Care Med 2001;163:469–77.
36. Horne SL, Cockcroft DW, Lovegrove A, Dosman JA. ABO, Lewis and secretor status and relative incidence of air flow obstruction. Disease Markers 1985;3:55–62.
37. Abboud RT, Yu P, Chan-Yeung M, Tan F. Lack of relationship between ABH secretor status and lung function in pulp mill workers. Am Rev Respir Dis 1982;126:1089–91.
38. Smith CAD, Harrison DJ. Association between polymorphism in gene for microsomal epoxide hydrolase and susceptibility to emphysema. Lancet 1997;350:630–3.

39. Yamada N, Yamaya M, Okinaga S, et al. Microsatellite polymorphism in the heme oxygenase-1 gene promoter is associated with susceptibility to emphysema. Am J Hum Genet 2000;66:187–95.
40. Joos L, McIntyre L, Ruan J, et al. Association of IL-1β and IL-1 receptor antagonist haplotypes with rate of decline in lung function in smokers. Thorax 2001;56:863–6.
41. Becklake MR. Chronic airflow limitation: its relation to work in dusty occupations. Chest 1985;88:608–17.
42. Love RG, Miller BG. Longitudinal study of lung function in coal miners. Thorax 1982;37:193–7.
43. Manfreda J, Johnson B, Cherniack RM. Longitudinal changes of lung function: comparison of employees of hard rock mining industry and general population. Am Rev Respir Dis 1984;129:A142.
44. Oxman AD, Muir DC, Shannon HS, et al. Occupational dust exposure and chronic obstructive pulmonary disease. A systematic overview of the evidence. Am Rev Respir Dis 1993;148:38–48.
45. Burge PS. Occupation and chronic obstructive pulmonary disease [COPD]. Eur Respir J 1994;7:1032–4.
46. Zuskin E, Ivankovic D, Schachter EN, Witek TJ Jr. A ten year follow-up study of cotton textile workers. Am Rev Respir Dis 1991;143:301–5.
47. Glindmeyeer HW, Lefante JJ, Jones RN, et al. Exposure-related declines in the lung function of cotton textile workers. Relationship to current workplace standards. Am Rev Respir Dis 1991;144:675–83.
48. Brunekreef B, Holgate ST. Air pollution and health. Lancet 2002;360:1233–42.
49. Schwartz J. Lung function and chronic exposure to air pollution: a cross-sectional analysis of NHANES II. Environ Res 1989;50:309–21.
50. Chestnut LG, Schwarz J, Savitz DA, Burchfiel CM. Pulmonary function and ambient particulate matter: epidemiological evidence from NHANES I. Arch Environ Health 1991;46:135–44.
51. Sandler DP, Comstock GW, Helsing KJ, Shore DL. Deaths from all causes in non-smokers who lived with smokers. AJPH 1989;79:163–7.
52. Pérez-Padilla R, Regalado J, Vedal S, et al. Exposure to biomass smoke and chronic airway disease in Mexican women. A case control study. Am J Respir Crit Care Med 1996;154:701–6.
53. Matsuse T, Hayashi S, Kuwano K, et al. Latent adenoviral infection in the pathogenesis of chronic airways obstruction. Am Rev Respir Dis 1992;146:177–84.

CHAPTER 60

ASSESSMENT OF RESPIRATORY MUSCLES

Guy Czaika, Alejandro E. Grassino

The intracellular environment of the membrane-bound eukaryotic cell contains a vast network of rods composed of highly conserved proteins (actin filaments, tubulin microtubules, intermediate filaments, and fibrous proteins such as vimentin and laminin). Some of these hydrolyze adenosine triphosphate (ATP) and are able to tap the energy contained in the phosphate bonds in order to produce molecular movement. The eons-long evolution within these cells has given rise to the specialized molecules of myosin, whose heads march along actin filaments, the basic mechanism still at play in skeletal muscle cells today.

Should evolution be considered the essence of life, or is evolution the result of random chemical reactions? It does not seem so. After all, in its early stages, evolution gave rise to specialized intracellular structures, such as the Golgi apparatus, the nucleus, and mitochondria, and, most importantly, the ability for cells to divide. These structures were retained and have become part of the most evolved cells in complex organisms. In this way life could be preserved and improved. Thus, from the housekeeping chores of intracellular molecular trafficking to the flight of the condor, movement represents a major attribute of life that is expressed by muscles. The skeletal muscle cell is a marvel in micromechanics. We now examine the structural components of the muscle cell. The functional motor unit of the muscle cells is the sarcomere.

SKELETAL MUSCLE STRUCTURE

Skeletal muscle cells are endowed with a specialized design. The greater part of their cell body is occupied by long fibrous proteins. These are mainly composed of well-aligned long filaments reminiscent of a stack of pencils, with the capacity to slide along each other. The functional unit of the muscle cell is the sarcomere, an elaborate structure about 3 μ long (Figure 60-1).[1] The sarcomere length is shorter than a lymphocyte diameter (5 μ). A 10 cm–long muscle cell may have over 100,000 sarcomeres assembled in series to cover the distance between insertion on bone or cartilage structures.

Each sarcomere is comprised of two z disks (see Figure 60-1), structures to which actin filaments are attached. Between successive z disks are molecules of myosin interspersed with actin and nebulin (thin filaments). The latter are surrounded by thick "floating" filaments (myosin) that are held in line by long filaments of titin, which are attached to z disks on one end and attached to myosin fibers on the other end. The myosin fibers are the contractile components of the sarcomeres, whereas actin is not. The myosin molecules slide along the actin filaments, bringing the z disks closer. In so doing they shorten the distance between adjacent z disks to which they are attached. This is the action that provides muscular movement. If motion is impeded, the sarcomere generates isometric force. During muscle relaxation, sarcomeres return to their optimal length of about 2 to 2.2 μ, mainly by passive stretch caused by antagonistic muscles. There is recent evidence that myosin may be able to actively backtrack, that is, undergo active lengthening. This would make the sarcomeres a unit with forward and backward active power.[2]

FUNCTIONAL ASPECTS OF SARCOMERES

The myosin filaments slide along the actin filaments through the rotary action of the head of the myosin molecules. Sarcomere lengths and numbers of overlapping actin–myosin filaments at the beginning of contraction are the main factors that dictate the force developed by sarcomeres. Force–length measurements in diaphragm muscle strips 20 to 30 mm in length (as used in physiologic tests in vitro) show similar force–length ratios as a single sarcomere. There is an optimal sarcomere length at which force generation is maximal. Force rapidly decreases when the muscle is lengthened or shortened beyond optimal length (Figure 60-2).[3]

When a maximal force is developed by inspiring against an occluded airway (MIP), we notice that the most negative pressure at the airway is obtained at a lung volume corresponding to forced residual capacity (FRC) or slightly below

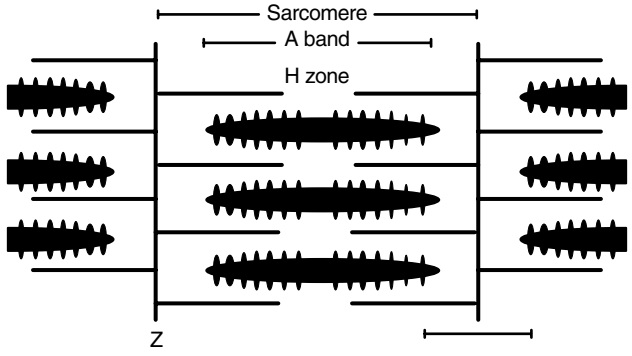

FIGURE 60-1 Molecular structure of the sarcomere. The organization of the major protein components between two z disks is shown. Reproduced with permission from Jerusalem F.[1]

it (about 100 cm H_2O). In doing so, the sarcomere length is optimal to generate force. On the other hand, MIP measured at total lung capacity (TLC) is just enough to overcome the elastic recoil of the lungs and chest wall (ie, approximately 40 cm H_2O). Maximum expiratory pressure (MEP) occurs at the highest lung volume where all the expiratory muscles seem to be at the most advantageous length, such as occurs during coughing when a maximum pressure of 200 cm H_2O can be developed (Table 60-1B). It is rather remarkable that a sarcomere, a diaphragm muscle strip, or the full array of inspiratory or expiratory muscles makes the chest wall behave quite similarly. There is an optimal sarcomere length at which force is maximal, and departure from this optimal length results in decreased force. The maximal force is exerted when sarcomeres do not shorten. If shortening is allowed, there is an inverse exponential relationship between the force developed and the velocity of muscle shortening (Figure 60-3).[3]

With the basic principles of muscle physiology restated, it is possible to construct the boundaries of maximal force

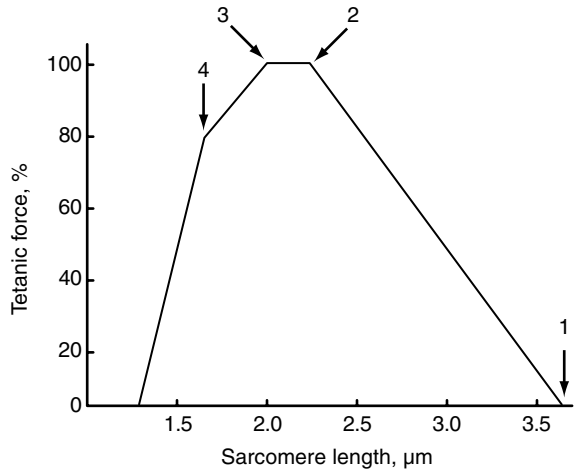

FIGURE 60-2 Variation in isometric tetanic tension with sarcomere length in single fibers from frog striated muscle. *Arrows* indicate striation spacings at which critical overlaps occur. Optimal overlap occurs at 2 μ. Reproduced with permission from Jerusalem F.[1]

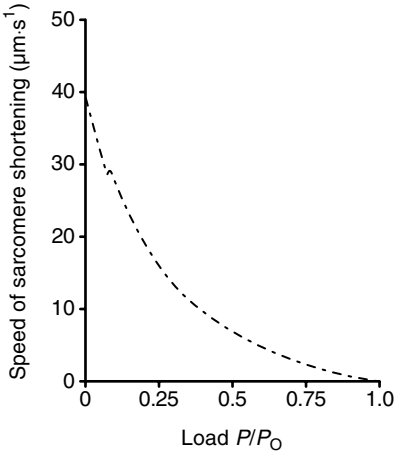

FIGURE 60-3 Force-velocity curve for the mouse diaphragm. Speed of sarcomere shortening related to isotonic load is expressed as a fraction of the maximum isometric tension. Adapted from Luff AR.[3]

exerted by inspiratory muscles, their length, and the velocity of shortening within a single figure.[4] Figure 60-4 is a three-dimensional graphic representation that encompasses the main characteristics of inspiratory muscle function in humans: force, as transdiaphragmatic pressure (Pdi), is plotted as a function of inspiratory muscle length (lung volume) and velocity of shortening (airflow at the mouth) as a function of length. However, from a functional viewpoint, force (intrathoracic pressure) can be sustained at only about 40% of its maximum if the duty cycle is about 40%; the duty cycle is the fraction of the contraction time (Ti) between successive contractions (Tt). Hence, the inner walls of this tent-like structure represent the limits within which a sustainable pattern of force in time is possible (nonfatigue zone, Figure 60-4). The outermost walls represent maximal static force (pressure), velocity of shortening (flow), and muscle length (lung volume). Under conditions of high-force contractions held at shortened muscle length (high FRC), fatigue develops rapidly. Fatigue is defined as a loss of maximal muscle force that is recoverable by rest.

MUSCLE CELL FUNCTION

Although the above description of the muscle cell is mainly that of the "engine" aspect of the muscle fiber, there is also an underlying and quite complex intracellular support structure that governs the metabolic aspects of muscle cell function (Figure 60-5). Briefly, bundles of sarcomeres are enveloped within a membrane that surrounds them. This envelope includes an extensive sarcoplasmic reticulum (SR) as well as mitochondria. The external cell membrane is connected to the SR by the so-called transverse tubes.[5] The tubes open in flat, glove-like structures called lateral sacs. The SR possesses membrane tubes that are deployed along the fibers. The SR is a large reservoir of Ca^{++} ions (see Figure 60-5).

A muscle fiber has one neuromuscular junction, a point at which nerves depolarize the membrane through liberation of acetylcholine in the cleft. Depolarization is then transmitted

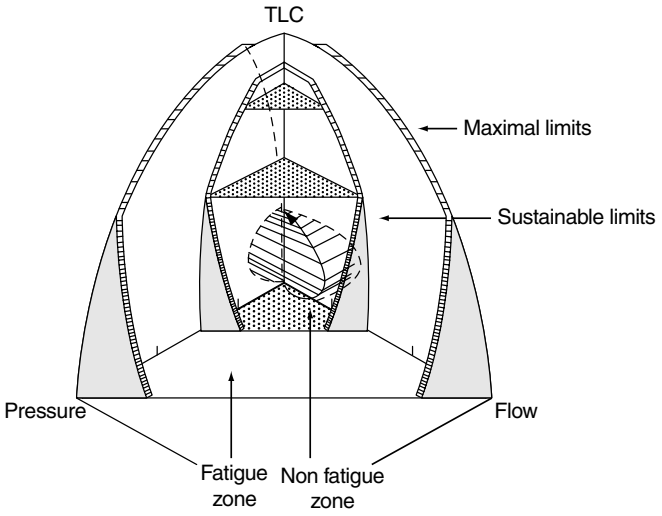

FIGURE 60-4 Maximal and sustainable limits of pressure and flow at various lung volumes. The outside "walls" represent maximal limits of flow, pressure, and volume. The smaller "igloo" represents maximal values of sustainable pressure and flow at various lung volumes when Ti/Tt is equal to 0.4. The loop in the corner is an inspiratory effort where flow and pressure are developed. Reproduced with permission from Grassino A.[4]

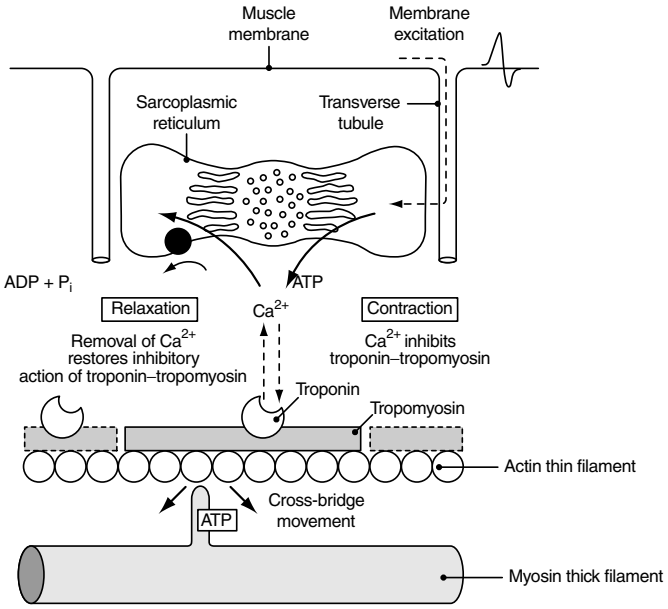

FIGURE 60-5 Summary of the sarcomere activation process and the role of calcium and the sarcoplasmic reticulum in excitation–contraction coupling. Reproduced with permission from Vander AJ et al.[5]

to the transverse tubules and to the SR, where Ca^{++} is released into the cytoplasm and links to troponin. In the presence of Ca^{++}, the myosin heads then attach to the actin fibers, and changes occur to the three-dimensional configuration of the myosin head in such a way that it allows the sliding of myosin along the actin filaments. Calcium is rapidly recaptured into the SR. Prolonged exposure to calcium in the cytoplasm activates lipases and proteases that can disintegrate intracellular structural elements such as mitochondria and membrane systems. Prolonged exercise results in injury of muscle fibers. Repair of muscle cells is guided by a time-based sequence of gene expression of molecular factors, which reconstruct the injured portion of the muscle cell. Following a lesion, it takes about 10 days to repair both structure and function.

Activated muscles prevented from shortening do generate tension (tension twitch). If the load to the muscle is less than the active tension generated, the stimulus produces a shortening on the muscle.

The length of individual muscle fibers varies widely from a few millimeters up to 10 cm. However, muscle fibers are activated through neuromuscular junctions in such a way that the stimuli can reach all parts of the fiber. If instead of a single twitch, there is a succession of stimuli (eg, 20–100/s), the muscle will fuse the twitches and remains contracted permanently, until stimulation ceases. This phenomenon is known as summation, and the resulting contraction is termed "tetanic."

The length of time that a tetanic contraction can be maintained depends on the supply of ATP to the contractile proteins (via muscle perfusion). If ATP becomes depleted, force decreases. The drop in maximal tension with prolonged stimulation is known as muscle fatigue. Loss of force during contraction is largely owing to a reduced blood flow passing through the muscle vasculature, which causes hypoxia as well as accumulation of catabolites in the muscle fiber (see Table 60-1H and I). It was established experimentally in dogs' diaphragms that force more than 40% of the maximum limits of perfusion. As well, duty cycle (Ti/Tt) above .4 does not allow complete washout of the muscle catabolites. Hence the functional threshold for sustainable contractility is given by the equation

$$\text{Ttdi} = (\text{Pi}/\text{Pmax}) \cdot (\text{Ti}/\text{Tt})$$

where Ttdi is tension-time index (DI is force developed as a percentage of maximum), Ti is contraction time, and Tt is the total cycle duration.

RESPIRATORY MUSCLE FUNCTION ASSESSMENT IN HUMANS

This chapter provides a brief guide on the hows and whys of evaluating the functional status of the respiratory muscles in both healthy humans and in subjects with muscle dysfunction secondary to disease states. A combined American Thoracic Society and European Respiratory Society statement on respiratory muscle testing was recently published.[6] This document contains a detailed explanation of a broad variety of tests and an extensive literature about their relevance to specific clinical situations.

Figure 60-6 is a diagram in which the main components of the respiratory control system and the anatomic organization of the muscle in inspiratory and expiratory groups are shown.

Respiratory muscles, whose continuous activity is required to provide ventilation throughout life, have similar physiologic properties to limb muscles that have prolonged periods of rest (as in sleep). Respiratory muscles are activated

Table 60-1 Summary of Tests Assessing Respiratory Muscle Function*

Test	*Parameter evaluated*	*Typical graphical report*	*Information obtained*
A Measure of static lung volumes.	The measure of lung volume components evaluates the muscle force used to expand the chest wall and lungs.	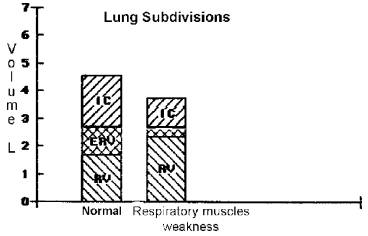	Respiratory muscle weakness decreases vital capacity.
B Maximal static inspiratory and expiratory muscle force.	MIP and MEP measured at various lung volumes from TLC to RV.	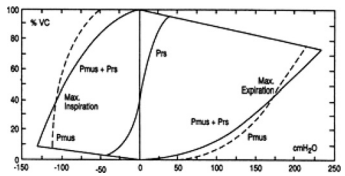	†The diagram describes the maximal force-generating capacity of inspiratory and expiratory muscles under isometric contractions from RV to TLC.
C Dynamic spirometry. Maximal inspiratory and expiratory flow/volume.	Maximum flow generated by forced inspirations and expirations from TLC to RV.	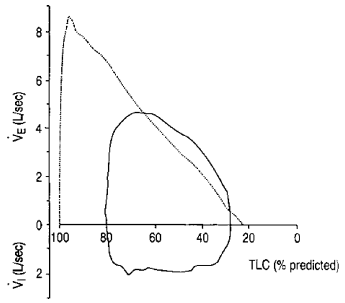	†Shows alterations in volume and flows. The reduction in vital capacity (small loop) points to muscle weakness in this neuromuscular patient.
D Sniff test.	Maximal pressure measured at the blocked nostril following a short maximal inspiratory effort from FRC. Shows dynamic pressure generated at the nose, thorax, Pab, Pdi.	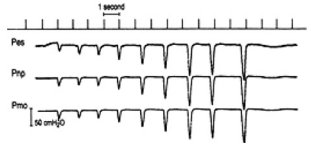	‡Sniff is a maneuver that is easy to perform. Results are comparable to swing in esophageal pressure. A practical and reliable test of inspiratory muscle's strength.
E Cough test.	Pes measured during cough. Test to assess dynamic muscle strength of expiratory muscles.	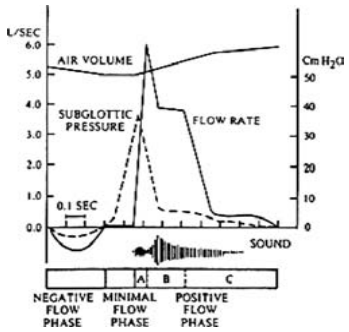	§Strength of expiratory muscles near TLC. An easy maneuver to perform. Pes is measured at its peak, before glottis opens. Useful to assess capacity to expectorate secretions.

F Pdi obtained via phrenic nerve electrical or magnetic stimulation.	Pressures measured with esophageal and gastric balloons. Evaluates strength of the diaphragm to twitches or short tetanic stimuli applied to the phrenic nerves at the neck.	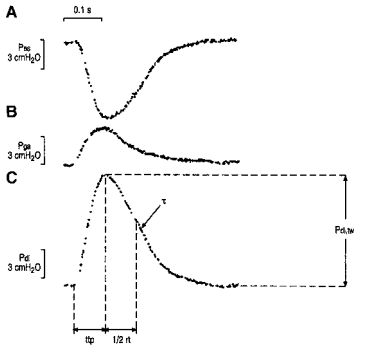	†Functional status of the diaphragm. COPD patients have a reduced twitch caused by a shorter diaphragm (*B*). Slow relaxation of Pdi is a sign of fatigue.
G Tension-time index of inspiratory muscles in humans.	Product of mean pressure swing (% of maximum) multiplied by Ti/Tt. Each point is the breathing pattern of COPD during resting breathing. Some patients are close to the fatigue area. • = normocapnic; x= hypercapnic.	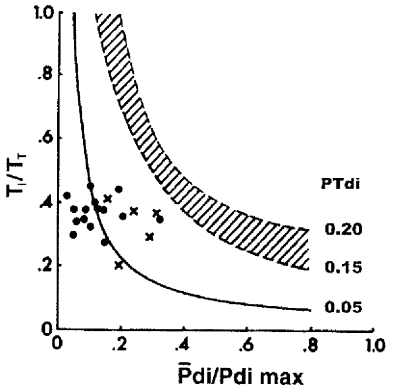	‡‡Level of P time. Assess the risk of developing fatigue. If threshold is exceeded for a period of time at an index of 0.18 or higher, it forecasts muscle fatigue and failure.
H Diaphragm blood perfusion measured in live dogs in experimental setup.	Blood flow of the diaphragm driven by electrical stimulation from prefatigue to fatigue tension-time indexes. Ttdi above 0.16 to 0.18 limits blood flow (Q).	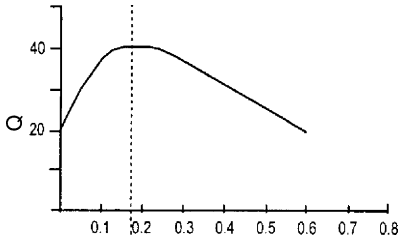	#Increase in Pdi increases perfusion of the diaphragm up to a tension-time index of up to 0.16–0.18. Beyond this, it causes hypoperfusion that leads to fatigue.
I Maximal sustainable inspiratory force.	Time that an inspiratory force can be sustained. Pressure of about 40% is sustainable for over 1 h. Ti/Tt about 0.4.	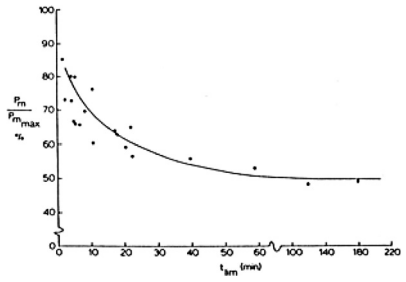	**Indicates endurance to sustain a pressure as a function of time. There is a progressive loss of maximum force during contraction. Sustainable pressure is about 40% maximum, at a Ti/Tt of 0.4.

(*Continued*)

Table 60-1 (*Continued*)

Test	*Parameter evaluated*	*Typical graphical report*	*Information obtained*
J Phrenic nerve stimulation. It could be done by electrical or magnetic stimulation.	Pdi twitch. Pressure swing is measured with esophageal or gastric balloons or at the mouth with closed airway.	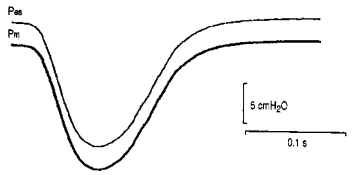	†Diaphragm capability to generate dynamic force. Useful to evaluate Pdi in COPD or in myopathies suspected of having a weaker diaphragm.
K Rahn diagram. Assessment of relaxed pressure–volume relation of the chest wall lungs and total respiratory system.	The pressure–volume relationship of the relaxed chest wall, respiratory system, and lungs.	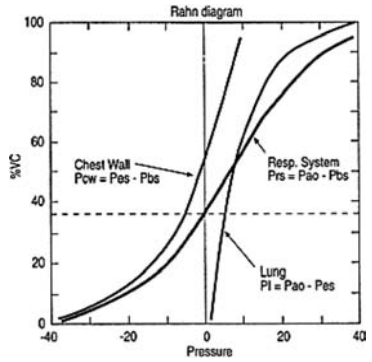	†Provides information on the status of the elastic properties of the components of the respiratory system, chest wall, lung muscles.
L Campbell diagram. Assessment of the active chest wall undergoing changes in lung volume.	Swings in pleural pressure during breathing are plotted against changes in lung volume at isotime. This yields the work of breathing, both dynamic (airways) and static (elastic).	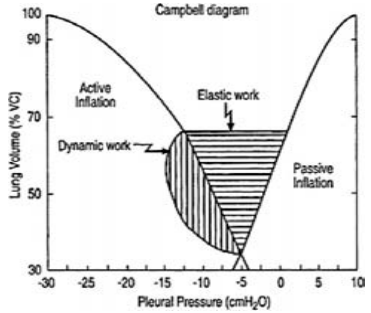	†Allows calculation of the elastic and resistive work of breathing.
M Konno-Mead diagram. Rib cage and abdomen contribution to tidal volume.	Plot of the relative motion of rib cage and abdomen measured as diameter displacement (magnetometer) or as circumference changes (Respitrace). Shows the contribution of the diaphragm and rib cage motion to ventilation.	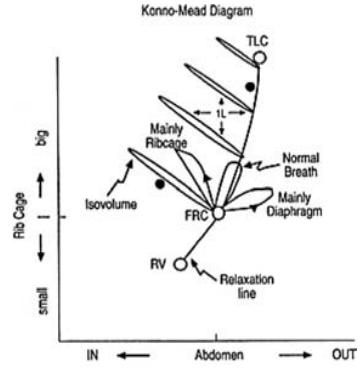	†Detects paradoxical motion of rib cage or abdominal wall due to discoordination. Measures minute VE noninvasively once the Respitrace is calibrated.

N Edi/Pdi. "Gain" of force as a function of increased activation. At high lung volumes (85% VC) the diaphragm generates lower force for the same Edi.	Integrated EMG from esophageal electrode against Pdi during static progressive isometric voluntary efforts.	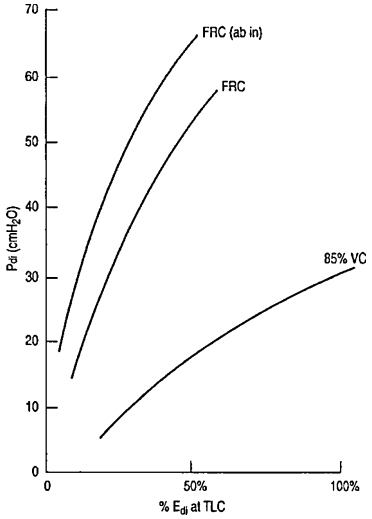	§The shape of Edi/Pdi changes with the length of the diaphragm. For example, when FRC vs 85% of vital capacity, the shorter diaphragm then requires more Edi to obtain a given force.
O Macklem diagram.	Plots esophageal and gastric pressure. Similar to the Konno-Mead diagram, which plots rib cage/abdominal displacements. Shows the dominant use of rib cage or diaphragm.	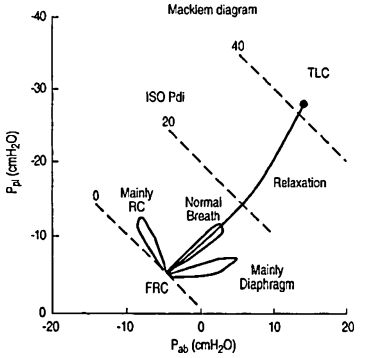	†Use of rib cage muscles is visualized as a shift to the left (diaphragm weakness). Use of the diaphragm shows a displacement to the right. Combined use shows an increase in Pab/Ppl along relaxation line.

*Tests are presented from the simplest and least specific to the most invasive and specific.
†Figure reproduced with permission from American Thoracic Society/European Respiratory Society.[6]
‡Figure reproduced with permission from Lance JW et al.[12]
§Figure adapted from Yanagihara N et al.[13]
||Figure reproduced with permission from Bellemare F et al.[9]
#Figure adapted from Bellemare F et al.[10]
**Figure reproduced with permission from Clanton TL.[7]
COPD = chronic obstructive pulmonary disease; Edi = electromyographic activity of diaphragm; EMG = electromyogram; FRC = forced residual capacity; MEP = maximal intrathoracic expiratory pressure; MIP = maximal intrathoracic inspiratory pressure; Pab = pressure, abdominal; Pdi = pressure, transdiaphragmatic; Pes= pressure, esophageal; Ppl = pleural pressure; RV = residual volume; Ti/Tt = contraction time/total cycle time; TLC = total lung capacity; Ttdi = tension-time index; $\dot{V}_E$ = minute ventilation.

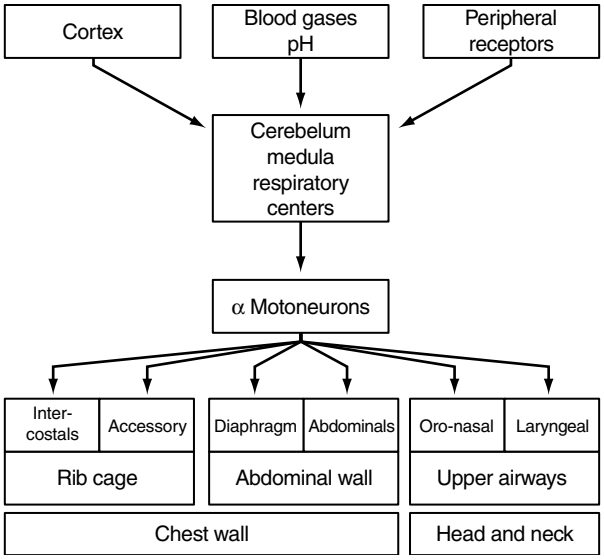

FIGURE 60-6 Schematic representation of respiratory neuromuscular control system for each muscle group.

either voluntarily or by default, and activation occurs through the respiratory centers that are responsible for maintaining ventilation pH and blood oxygenation levels within a desirable range. Throughout most of our life, breathing occurs at the subconscious level. Ventilation is regulated by V_T/f, arterial partial pressure of carbon dioxide (P_aCO_2), arterial partial pressure of oxygen (P_aO_2), and pH. The so-called respiratory centers integrate the neurochemical signals (input) and regulate ventilation to correct output. Even during moderate bouts of exercise, ventilation is perceived as a pleasant and satisfying sensation. In these situations, the function of respiratory muscles remains well within physiologic limits. However, in circumstances in which there is disruption of the normal anatomy of the respiratory muscles (such as in COPD patients) or where the lungs become more rigid (such as in pulmonary fibrosis), breathing is then sensed as a labored process. Force-generated increases for a given level of ventilation and the accompanying sensation of effort are usually called dyspnea. Dyspnea is a sensation whose intensity is related to the neural activation of respiratory muscles, measured as integrated electromyographic activity of the diaphragm (Edi), and the force generated by respiratory muscles (Pdi) (dyspnea = Edi/Pdi).

If the breathing pattern or the effort is carried beyond well-established limits of muscle tidal force or maximum force of about 40% and a ratio of inspiratory duration to total cycle time (Ti/Tt) of 0.4, this leads to alterations in muscle cell metabolism and subsequent loss of force. Table 60-1G shows the resting tension-time product in a group of COPD patients at rest. If minute ventilation increases and pressure swing goes beyond the threshold (dashed area), it then rapidly reverses to a lower Ttdi pattern, mainly by decreasing tidal pressure. This loss of force is termed "fatigue," a condition that is recoverable by rest. Force developed is related to the number of sarcomeres acting in parallel, like in the biceps, whereas the amount of shortening is reflected by the number of sarcomeres acting in series (as in the diaphragm).

The boundaries of sustainable muscle function are determined by the force developed, by the speed of shortening, and by the contraction time expressed as a function of breathing cycle duration (Ti/Tt). Most skeletal muscles that work at pressure-time indices above 0.15 to 0.18 (see Table 60-1G, dashed band) are unable to sustain the imposed load, mainly because of limitations in muscle blood flow that affect cellular metabolism (see Table 60-1H). This figure shows blood flow of the diaphragm on the vertical plotted against PTdi, in progressive exercise. When PTdi increases beyond 0.16 to 0.18, perfusion of the diaphragm becomes limited, leading to loss of force, which, in turn, leads to hypoventilation.[7] Below this critical pressure-time index, respiratory muscles do sustain breathing for life (see Table 60-1G and I). Resting breathing requires a pressure-time index of 0.02 to 0.04. Some severe COPD or lung fibrosis patients require pressure-time indices that range from 0.10 to 0.14. In Table 60-1G, each dot defines the steady breathing pattern of a normocapnic COPD patient at rest. Crosses show hypercapnic COPD patients. Bicycle exercise brought to a level of 90% of maximal VO_2 requires a pressure-time index close to 0.15. An important clinical situation arises when patients being mechanically ventilated cannot be weaned. Although many factors play a role in weaning, the load imposed on the muscles may be too great and lead to ventilatory failure. A prospective study by Vassilakopoulos studied patients who were unsuccessfully weaned on a first try of weaning from a ventilator but subsequently succeeded.[8] Each patient was his or her own control. Patients who failed to wean had developed tension-time indices of 0.12 to 0.20. Patients who weaned successfully on the first attempt had tension-time indices between 0.05 and 0.12 (Figure 60-7). This suggests that the ratio of the respiratory load to available force was too high, leading to muscle fatigue and ventilation failure.

Dyspnea has always been related to the level of load and pleural pressure swing that the respiratory muscles developed. Quantification of dyspnea by the Borg scale is found to be related linearly to the pressure-time index or to the work of breathing or simply the pleural pressure swings. Most specifically, dyspnea seems to be related to the level of the neural activation to the chest wall muscles (ie, diaphragm or intercostal integrated EMG). The force generated to shorten the diaphragm of COPD patients required a larger neural activation (measured as integrated EMG of the diaphragm) in order to generate the same pressure as in normal subjects (see Table 60-1N). Dyspnea is an index of neural output sent to muscles and muscle force developed; otherwise stated, dyspnea is a sensation that seems to be related to EMG/Pdi. A high numeric index indicates poor efficiency in transducing stimulation into muscle force. Such a situation is typically seen in subjects with COPD during exercise, particularly because dynamic hyperinflation further shortens inspiratory muscles.

Assessment of respiratory muscle function is done by (1) monitoring clinical signs and symptoms; (2) measurement of the pressure-time index; (3) measurement of static maximal

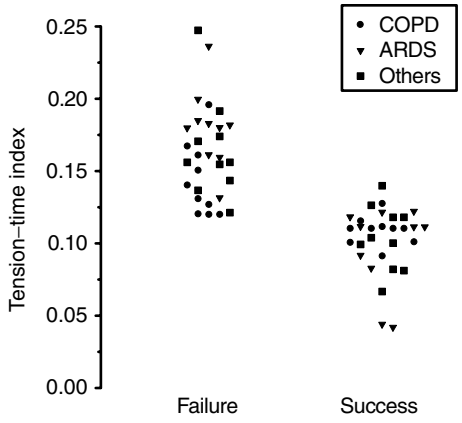

FIGURE 60-7 The tension-time index during weaning failure and success. Each symbol represents one patient. ARDS = adult respiratory distress syndrome; COPD = exacerbated chronic obstructive pulmonary disease. Reproduced with permission from Clanton TL.[7]

force of the diaphragm; (4) measurement of endurance to sustain a given load; (5) measurement of integrated EMG and pleural, abdominal, and Pdi swings; and (6) magnetic or electrical maximal Pdi elicited by phrenic nerve stimulations.

It is well known that different muscles do not have the same force–length relationship, which is mainly owing to the different fiber types that cause muscle to behave differently (cell type I: endures aerobic activity; cell type II: can sustain anaerobic metabolism for short intervals).

The relative contributions of the different compartments of the chest wall (rib cage and diaphragm or abdomen) to tidal volume can be measured with devices that register movements of the rib cage and abdominal wall anteroposterior (AP) displacements (magnetometers or Respitrace). The Konno-Mead method consists of displaying chest wall movements of the rib cage AP diameter (or its circumference displacement on the y-axis) and abdominal AP or circumference displacements on the x-axis (see Table 60-1M). Normalization of the axes is achieved by adjusting the respective gains of RC and Ab in such a way as to make both signals corresponding to the displacements of the two compartments equal, that is, a straight line at 45° to both axes. This is done by performing maneuvers involving reciprocal displacements of the rib cage and abdomen with a closed glottis (isovolume displacements) and by setting the slope of the volume changes of rib cage against abdomen at -1 ($-45°$). Then, while breathing with an open glottis, the relative contribution of rib cage or diaphragm abdomen to

Table 60-2 Clinical Evaluation of Respiratory Muscle Dysfunction

Symptom or sign	*Disease*	*Putative mechanism*
Dyspnea on exertion. Tachypnea.	Chronic heart failure.	Weak respiratory muscles, disused because of sedentary life. Low blood perfusion to the muscles.
Abdominal paradoxing during inspiration. Shortness of breath.	Diaphragm paresis. Paralysis of the diaphragm. Post–upper abdominal surgery.	Weak muscle that cannot generate the force to overcome the pleural pressure swing.
Intercostals and supraclavicular space are withdrawn during inspiration.	Increase in the pleural pressure swing because of airway obstruction or low lung compliance.	Subatmospheric pleural pressures overcome the compliance of tissues.
Alternans, ie, shifts from predominant rib cage to predominant abdominal breathing.	Elasticity or resistive loaded breathing.	May be a central mechanism whose purpose is to unload either group of muscles. It can be done voluntarily.
Hiccups.	Neurologic: CNS local lesion.	Mediastinal infection or tumor. A short activation of the phrenic nerve.
Paradoxical movements of the rib cage during an inspiration without air flow.	Sleep apnea during REM stage.	Closing of the upper airway with a predominantly active diaphragm.
Small VC, tachypnea. Shortness of breath.	Obesity, lung fibrosis, neuromuscular disease, OAP, steroid treatment, polymyositis, malnourishment, postpolio syndrome.	Any form of muscle weakness relative to respiratory system compliance.
Cheyne-Stokes breathing.	Neurologic, stroke. Congestive heart failure.	Unknown. Effect on patterns of breathing generation (CNS).
Weak, ineffective cough to clear bronchial secretions.	Chest pain, flail chest, COPD kyphoscoliosis, quadriplegia, Guillain-Barré syndrome. Central airway obstruction.	Insufficient expiratory muscle force to create a peak expiratory flow above 5 L/s.
Rapid loss of ventilation during MVV. Sensation of fatigue and weakness.	Myasthenia gravis.	Lack of acetylcholine receptors on the muscles. Neuromuscular junction fatigue.
Hypercapnea with normal lungs.	Neuromuscular weakness caused by disease. For example, muscular dystrophy or postpolio syndrome.	Loss of muscle fibers. The remaining ones cannot generate enough force even if activation is high. They could be derecruited.
Muscle stiffness. Slow relaxation rigor.	After heavy exercise. Severe acidosis.	Lack of ATP to recapture Ca^{++} back into the sarcoplasmic reticulum.
A saw-toothed pattern in the flow-volume curve.	Parkinson's disease. Upper airway weakness.	Instability of the upper airway's dynamics. Starling resistor effect.
EMG and pleural pressure swings preceding mouth flow.	Intrinsic PEEP. In COPD. High threshold load in a ventilator.	Neural output builds up pressure over 50–250 ms before overcoming PEEP. The same for overcoming threshold pressure in a ventilator.

ATP = adenosine triphosphate; EMG = electromyogram; CNS = central nervous system; COPD = chronic obstructive pulmonary disease; MVV = maximum voluntary ventilation; OAP = pulmonary edema; PEEP = positive end-expiratory pressure; REM = rapid eye movement.

V_T can be calculated.[7,9–11] The Macklem diagram allows one to infer the relative activity of rib cage and diaphragm or the abdominal muscles by measuring their departure from passive expiration (see Table 60-1O). The relaxation line is the relationship between the change in volume of rib cage and abdomen during deflation of the respiratory system from TLC while all the respiratory muscles are relaxed.

Table 60-1 lists other important tests that can be used to assess various aspects of respiratory muscle function, what parameters they explore, the standard way to express their results, and the information they provide. Items in Table 60-1 are referenced so the reader can acquire complete information on each test.

Table 60-2 is a complementary set of data obtainable mainly by bedside clinical evaluation of respiratory muscle dysfunction and the underlying pathology causing respiratory muscle dysfunction.

CONCLUSIONS

1. Evaluation of respiratory muscles provides information on their strength and endurance and allows one to assess their capacity to sustain adequate alveolar ventilation.
2. Tests have been developed to measure maximal respiratory force, both by voluntary maximal static efforts or by performing semistatic maneuvers and easy to perform acts such as coughing and sniffing (see Table 60-1D and E).
3. Electrical or magnetic phrenic nerve stimulation can indicate the functional status of the diaphragm (see Table 60-1F)
4. Calculations of areas of pressure–volume values yield information on the work of breathing. However, such calculations are seldom made in clinical evaluation (see Table 60-1L).
5. Intrathoracic or transdiaphragmatic pressure and amount of neural stimulation are linked to the sensation of dyspnea. A short diaphragm with high neural stimulation results in severe dyspnea, as happens to COPD with increased ventilation (see Table 60-1I and N).
6. Endurance of respiratory muscles can be tested by using incremental inspiratory loads, each minute until task failure results. This test is similar to incremental whole body exercise (see Table 60-1I)
7. Measure of EMG center frequency is a noninvasive test that detects shifts in the center frequency toward lower frequency, heralding muscle fatigue.
8. The EMG signal from the diaphragm is now being used to trigger a mechanical ventilator. The old method required a swing in pleural pressure beyond an established threshold, that is, the ventilator is triggered with a delay in relation to the neural output. This concept is being developed and tested in humans.
9. Relative use of rib cage inspiratory muscle and diaphragm can be measured noninvasively by use of Respitrace (see Table 60-1I and M). This signal allows detecting paradoxical movements of abdominal wall, compatible with diaphragm paralysis (see Table 60-1M).

REFERENCES

1. Jerusalem F. The cross-bridge cycle and energetics of contraction. In: Enger AE, Franzini-Armstrong C, editors. Myology. New York: McGraw-Hill; 1994.
2. Tsiavaliaris G, Fujita-Becker S, Manstein DJ. Molecular engineering of a backwards-moving myosin motor. Nature 2004; 427:558–61.
3. Luff AR. Dynamic properties of the inferior rectus, extensor digitorum longus, diaphragm and soleus muscles of the mouse. J Physiol 1981;313:161–71.
4. Grassino A. Limits of maximal inspiratory muscle function. In: Breathlessness: The Campbell Symposium. Hamilton (ON): CME-Boehringer-Ingelheim; 1992.
5. Vander AJ, Sherman JH, Luciano DS, editors. Human physiology: The mechanisms of body function. 2nd ed. New York: McGraw-Hill; 1975.
6. American Thoracic Society/European Respiratory Society. ATS/ERS statement on respiratory muscle testing. Am J Respir Crit Care Med 2002;166:518–624.
7. Clanton TL. Respiratory muscle endurance in humans. In: Roussos C, editor. The thorax. Part B: Applied physiology. New York: Marcel Dekker; 1995. p 1199–230.
8. Vassilakopoulos T, Zakynthinos S, Roussos C, The tension-time index and the frequency/tidal volume ratio are the major pathophysiologic determinants of weaning failure and success. Am J Respir Crit Care Med 1998;158:378–85.
9. Bellemare F, Grassino F. Evaluation of human diaphragm fatigue. J Appl Physiol 1983;55:8–15.
10. Bellemare F, et al. Effect of tension and timing of contraction on the blood flow of the diaphragm. J Appl Physiol 1983; 54:1597–606.
11. Grassino A, et al. Mechanics of the human diaphragm during voluntary contraction: statics. J Appl Physiol 1978;44: 829–39.
12. Lance JW, et al. Harlequin syndrome: the sudden onset of unilateral flushing and sweating. J Neurol Neurosurg Psychiatry 1988;51:635–42.
13. Yanagihara N, Von Leden H, Werner-Kukuk E. The physical parameters of cough: the larynx in a normal single cough. Acta Otolaryngol (Stockh) 1966;61:495–510.

CHAPTER 61

ASSESSMENT OF ACID–BASE BALANCE: A PHYSICAL-CHEMICAL APPROACH

Sheldon Magder

The management of acid–base disorders is one of the most fundamental aspects of the management of critically ill patients and especially those with respiratory disorders. At the bedside, clinicians commonly use sets of rules for interpreting acid–base disorders and determining management plans. However, to properly manage unusual situations and to properly evaluate treatment options, one must have a clear understanding of the principles of acid–base regulation.

Traditional teaching of acid–base regulation is based on the Henderson-Hasselbalch equation, which is a statement of the mass-action equation of the equilibrium relationship of partial pressure of carbon dioxide (PCO_2), carbonic acid (H_2CO_3), hydrogen ion (H^+), and bicarbonate (HCO_3-). The equation is

$$pH = 6.1 + \log([HCO_3-]/[0.0301 \times PCO_2]) \quad (61\text{-}1)$$

where 0.031 is a constant to account for the solubility of CO_2 in water and the equilibrium constant between PCO_2 and carbonic acid and 6.1 is the pK_a of the dissociation of carbonic acid and the dissociation of carbonate ion. In the classic approach, one first determines if there is an acid–base disturbance by observing whether there is a deviation of the pH from the physiologically neutral value of 7.4. Increases or decreases in the PCO_2 are used to determine if there is a respiratory component, and variations in HCO_3^- are used to determine if there is a metabolic component. A complex set of equations can then be used to determine if the changes are acute or chronic and compensated or uncompensated. This approach has by and large served clinicians adequately. However, although the respiratory part of the classic analysis gives a mechanistic understanding of the processes that are disturbing the normal acid–base balance, the metabolic component provides no insight into physiologic mechanisms and potentially produces some very faulty reasoning.

The limitations of the metabolic component of the conventional approach were pointed out by Peter Stewart who presented a physical-chemical approach to acid–base balance.[1] The most important point of Stewart's analysis is that in water solutions, H^+ and HCO_3- are dependent variables and not independent variables as they are traditionally treated in biochemical analysis. This means that the addition of H^+ or HCO_3- to a solution does not necessarily result in a change in the concentration of $[H^+]$ or $[HCO_3-]$ that is equal to the amount added. In fact, as is shown below, all solutions in the body, with the exception of gastric juices, are actually alkaline, that is $[H^+] < [\text{hydroxide ion } (OH)^-]$ (the notation [ ] is used to refer to concentration), and in alkaline solutions, the addition of H^+ never produces a change in its concentrations that is equal to what was given. Stewart pointed out that the three independent variables that determine $[H^+]$ (and $[HCO_3-]$) are the PCO_2, strong ion difference [SID], and the concentration of weak proteins $[A_{Total}]$ (Figure 61-1). The significance of each of these is discussed in the next sections.

NEUTRAL PH

We begin with some definitions. An acid solution is defined as one in which $[H^+] > [OH^-]$, a neutral solution is one in which $[H^+] = [OH^-]$, and an alkaline solution is one in which $[H^+] < [OH^-]$.[1] Pure water at body temperature of 37°C has a pH of 6.68 but is pH neutral because $[H^+] = [OH^-]$. The pH of pure water decreases with decreases in temperature because the dissociation constant of water increases with temperature (Figure 61-2A) and results in increasing amounts of both $[H^+]$ and $[OH^-]$, but the solution is neutral from the acid–base point of view (Figure 61-2B). The addition of other components to pure water can change the pH, but if $[H^+]$ is equal to $[OH^-]$, the solution is still neutral.

Blood pH is tightly regulated over a narrow range in all organisms because the conformation and thus function of enzymes and structural proteins are highly pH dependent. For physiologic studies and clinical purposes, pH 7.4 is called "normal," for this is the normal value in the blood, although intracellular pH is usually somewhat lower.[1–3]

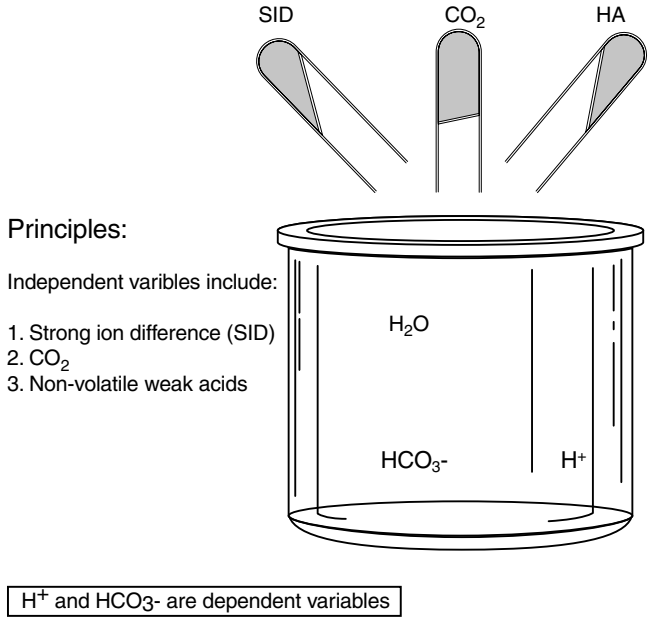

FIGURE 61-1 Principles of the physical-chemical approach to acid-base analysis. The three independent variables are the SID, PCO_2, and concentration of weak acids (HA). H^+ and HCO_3- are dependent variables.

However, it is important to appreciate that blood at a pH of 7.4 is not a "neutral" solution and that when the pH is below 7.4, blood is not actually an acidic solution. This is because in all of the solutions in the body, with the exception of the gastric contents after fasting, $[H^+] < [OH^-]$ and the solutions are thus alkaline. The definition of 7.4 as normal is thus just a useful reference point in the same way that one calls the freezing point of water 0°C even though true "zero" is a much lower value. Thus, as in the traditional approach, in the physical-chemical analysis of acid–base balance, a blood pH below 7.4 is still called an acidemia and pH greater than 7.4 an alkalemia even though what is called acidemia is really just a less alkaline solution and what is called alkalemia a more alkaline solution.

PARTIAL PRESSURE OF CARBON DIOXIDE

PCO_2 is an independent variable because CO_2 production is determined by metabolic activity, and PCO_2 in the blood is determined by ventilation, which is normally tightly controlled by the brain. As in the conventional approach, PCO_2 is an important determinant of $[H^+]$, and it defines the respiratory component of acid–base disorders. The Henderson-Hasselbach equation presented in Equation 61-1 was derived from the mass-action relationship of the PCO_2 to carbonic acid in the blood and the dissociation of H_2CO_3 into $[H^+]$ and HCO_3-:

$$PCO_2 \overset{K1}{\rightleftharpoons} H_2CO_3 \overset{K2}{\rightleftharpoons} H^+ + HCO_3- \qquad (61\text{-}2)$$

where K1 is a constant that relates the solubility of CO_2 in plasma and the equilibrium relationship with H_2CO_3 and K2 is the equilibrium constant for the relationship of H_2CO_3, H^+, and HCO_3-.

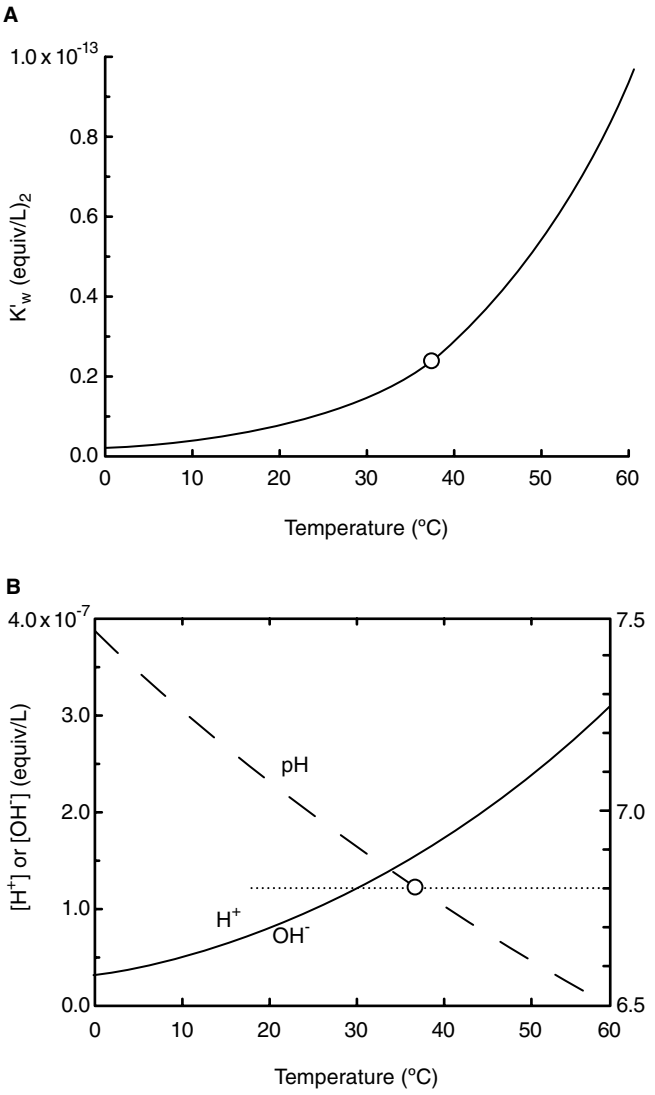

FIGURE 61-2 The effect of temperature on the K′w, the product of the dissociation constant of water and the water concentration, is shown in *A*. Increasing temperature increases the dissociation of water. The effect of the temperature dependent change in K′w on pH, H^+, and OH^- is shown in *B*. Increasing temperature increases H^+ and decreases the pH. However, the solution is still acid base neutral, because H^+ equals OH^-.

However, it needs to be appreciated that once the value of PCO_2 is fixed by a well-functioning ventilatory center, the dissociation of H_2CO_3 is determined by the rate constants of the reaction and by other factors in the solution, including the [SID] and $[A_{Total}]$, which are discussed below. Since one side of Equation 61-2, the PCO_2, is fixed by ventilation, the products of this equilibrium reaction, H^+ and HCO_3-, are dependent variables. An interesting historical point made by Stewart is that the emphasis on the importance of HCO_3- in acid–base physiology occurred because it became possible to measure total CO_2 in a solution before it was possible to measure PCO_2.[1] This was done by making the SID of a CO_2-containing solution negative, which drives all the HCO_3- into H_2CO_3 and dissolved CO_2. The dissolved CO_2 is then converted to the gas phase by placing the sample in an evacuated container. A close approximation of the

PCO_2 can then be made by using the Henderson-Hasselbach equation to calculate PCO_2 with the measured pH and the total CO_2 as an estimate of the HCO_3–. Ironically, today, the actual HCO_3– is calculated from the measured PCO_2 and the pH.

In the physical-chemical approach, as in the traditional approach, a $PCO_2 > 40$ mm Hg is called a respiratory acidosis and a $PCO_2 < 40$ mm Hg a respiratory alkalosis. The suffix "-osis" refers to an acidifying or alkalinizing process. These definitions are true even if the pH is not acidemic or alkalemic relative to the normal value of 7.4. In the physical-chemical analysis, it is not necessary to refer to compensated or uncompensated conditions but rather to the metabolic or respiratory processes that are actually occurring. As will be seen, the physical-chemical approach allows quantification and mechanistic understanding of the processes involved in metabolic acid–base disturbances and the compensatory mechanisms, without having to resort to empiric rules.

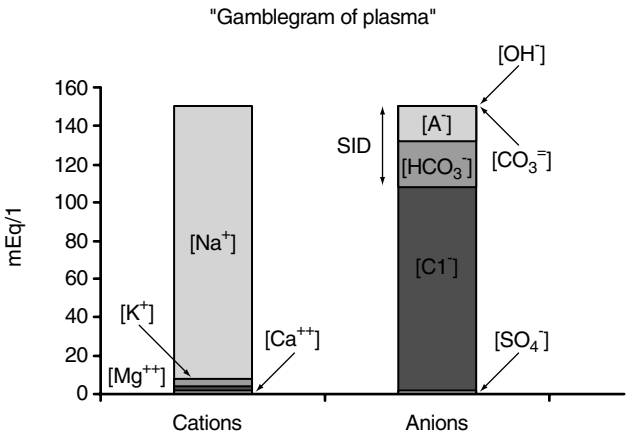

FIGURE 61-3 A "gamblegram" of plasma. The dominant strong cation Na^+ and the dominant strong anion is Cl^-. The strong ion difference (SID) is positive and is accounted for primarily by the concentration of HCO_3– and A^-, the concentration of weak anions.

STRONG ION DIFFERENCE

A very important regulator of the metabolic component of acid–base balance that is not considered in the traditional approach is the [SID]. SID is the difference in concentrations (measured in equivalents) of the strong cations and strong ions in the solution. A strong ion is an ion that exists in essentially a dissociated form in solution. Examples of strong cations are Na^+, K^+, Mg^{++}, and Ca^{++}. Examples of strong anions are Cl^-, SO_4^{2+}, and lactate. On the other hand, as will be seen later, phosphate behaves as a weak acid. The key principle that makes the [SID] of the solution so important is the principle of electrical neutrality, which says that in a macrosolution all positive charges must equal all negative charges. To consider the significance of electrical neutrality, consider a sphere of 1 mm in diameter with a charge difference between the positive and negative ions of 1×10^{-7} Eq/L. Using Coulomb's law it can be calculated that the net charge would be 400,000 volts. Thus, even a small charge difference in a solution produces a very strong force that affects other molecules in the solution that are not totally dissociated for the charge must be balanced. In a solution with only strong electrolytes in water, the only other source of ions is water. The electrical charge from the [SID] thus alters the dissociation of water and the final $[H^+]$ and $[OH^-]$.

The predominant strong ions in plasma are Na^+ and Cl^-, and because the concentration of the strong cations (mainly Na^+ in the extracellular space) is much greater than the concentration of the strong anions (mainly Cl^- in the extracellular space), the [SID] is positive in almost all biologic solutions. The normal [SID] of plasma is about +42 mEq/L. The relative magnitude of the ions in plasma can be seen by examining a "Gamblegram" of the plasma electrolytes (Figure 61-3). The other strong ions in plasma, such as K^+, Mg^{++}, Ca^{++}, and SO_4^{2-}, are found in much smaller quantities, that is, 1 to 4 mEq/L. Since small deviations of their concentrations from the normal values have major physiologic effects, they do not play a significant role in changes in the plasma [SID], and changes in $[Na^+]$ and $[Cl^-]$ dominate the regulation of the [SID]. Furthermore, $[Na^+]$ is very important for the regulation of plasma osmolality and volume status of the extracellular space. Therefore, changing plasma and extracellular $[Na^+]$ is not a very viable option for the maintenance of the normal [SID]. Thus, the only electrolyte that can be readily altered to regulate plasma [SID] is Cl^-, and it becomes clear that regulation of $[Cl^-]$ is critical for maintenance of the normal [SID] and normal acid–base balance.

DISORDERS OF THE STRONG ION DIFFERENCE

PRINCIPLES

It often seems that H^+ is directly added to a solution and that H^+ is thus an independent determinant of acid–base balance. This misconception likely occurs because the distinction between the dependent and independent behavior of $[H^+]$ is not evident in solutions with a negative [SID]. Take, for example, a solution in which the only two ions are Na^+ and Cl^- and $[Cl^-]$ is greater than $[Na^+]$. The [SID] of this solution is thus negative. When an acid, such as HCl, is added to this solution, the Cl^- must remain in the solution as an ion for it is a strong ion. The change in $[H^+]$ in this solution will equal the change in $[Cl^-]$ for there are no other cations in the solution to balance the change in Cl^-. It thus appears as if $[H^+]$ was directly added to the solution and is an independent variable for $[H^+]$ increased by the same amount as that added. However, the dependent behavior of $[H^+]$ becomes evident when HCl is added to a solution with a positive [SID]. Take, for example, a solution in which $[Na^+]$ is greater than $[Cl^-]$ as occurs in extracellular fluid. When HCl is added to a solution with a positive [SID], the Cl^- again must remain dissociated for it is a strong ion. However, this time the change in $[H^+]$ will be smaller than the change in $[Cl^-]$. This is because the addition of

Cl^- decreases the electrical force that had altered the dissociation of water. If this electrical force had not been present, $[H^+]$ would have been equal to $[OH^-]$ instead of being much lower (and the pH very high). However, in contrast to Cl^-, H^+ is a very weak ion and does not have to remain dissociated. Therefore, some of the added H^+ associates with OH^- and forms water. To determine the final concentration of H^+ in the new solution, one must take into account two laws of nature, the mass-action equation for the dissociation of water and the principle of electrical neutrality, which accounts for all the charges in the solution. The solution of these two equations determines the final $[H^+]$. Since nearly all major biologic fluids have a positive SID, the addition of an acid to these fluids never produces an increase in H^+ that is equal to the increase in the anion and the true dependent nature of H^+ becomes evident.

Consider what happens to the same solution with $[Na^+]$ greater than $[Cl^-]$ and $[Na^+]$ is increased by the addition of $NaOH^-$. The principle of electrical neutrality requires that there must be a negative ion to balance the increase in $[Na^+]$. Since OH^- is the only available anion to balance the increase in Na^+ from the dissociation of water and the OH^- added with the Na^+, the change in the charge difference of strong ions will alter the dissociation equilibrium of water and increase the $[OH^-]$ in the solution. A very small amount of the OH^- will react with H^+ and decrease the H^+ and increase the pH and thus produce an alkalinizing effect. However, the magnitude of the OH^- concentration is orders of magnitude higher than that of the H^+ so that it will seem that OH^- increased by an equal amount to the increase in Na^+. It will appear that the addition of OH^- had the alkalinizing effect when, in fact, it was the addition of Na^+ that was responsible for the change in $[H^+]$. In summary, the narrowing of the SID of plasma has an acidifying effect and looks like the addition of HCl. The widening of the SID has an alkalinizing effect and looks like the addition of NaOH.

The SID can be altered by changes in the amount of water or by the gain or loss of a strong ion. Let us first consider changes in water.

Changes in Water

Figure 61-4 shows a beaker with 1 liter of water, $[Na^+] = 140 \times 10^{-6}$ Eq/L and $[Cl^-] = 100 \times 10^{-6}$ Eq/L. The [SID] is thus 40×10^{-6} Eq/L, and the pH of the solution is 10.6. If 1 liter of water is added, $[Na^+]$ decreases to 0.70×10^{-6} Eq/L, $[Cl^-]$ to 0.50×10^{-6} Eq/L, and the [SID] to 0.20×10^{-6} Eq/L. This gives a pH of 10.1. Thus, just adding water changed the pH, and this demonstrates a dilutional acidosis. In contrast, a loss of water will increase the [SID], which has an alkalinizing effect.

Changes in Chloride

As already noted, the primary strong anion in blood is Cl^-, and Cl^- is thus the most important strong anion available for the regulation of acid–base balance. A good example of the role that Cl^- plays in acid–base balance is the metabolic acidemia commonly seen after resuscitation with normal saline. This is easily explained by the physical-chemical approach by considering the effect of saline resuscitation on the [SID] and blood pH. Since normal saline has equal $[Na^+]$ and $[Cl^-]$, the [SID] is 0. Thus, the administration of normal saline narrows the [SID] of blood, which is an acidifying effect. The kidney counters increases in $[Na^+]$ faster than it counters increases in $[Cl^-]$, so the excretion of Cl^- lags behind the excretion of Na^+, which further contributes to the smaller [SID] and the acidifying effect. This is seen as a hyperchloremic acidemia.

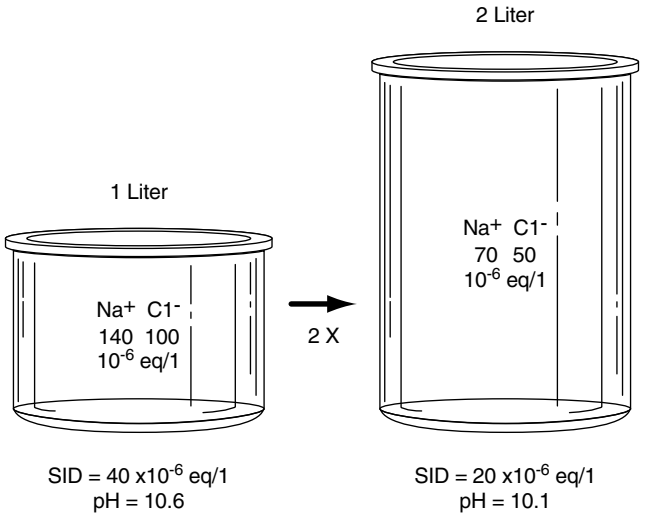

FIGURE 61-4 The effect of changes in water on the SID. Doubling the amount of water without changing the amount of electrolytes reduces the SID by half. This decreases the force that affects the dissociation of water and the pH falls eventhough no "acid" was added to the solution.

The role of Cl^- is central in the pathophysiology of renal tubular acidosis. In the traditional approach, the explanation for renal tubular acidosis is that there is a failure to reabsorb HCO_3^-, but HCO_3^- is a dependent variable and is determined by the PCO_2 and [SID]. From a physical-chemical approach, there is a failure to excrete Cl^-, which is a common problem in renal disease.[4] For the kidney to excrete Cl^-, to satisfy the principle of electrical neutrality a cation is needed to balance the negative charge of Cl^- in the urine. The cation cannot be Na^+ for, besides the consequent decrease in plasma osmolality, the equal loss of Na^+ and Cl^- would produce a steady decrease in the [SID] of blood, which would have an acidifying effect. Normally, the kidney balances the negative charge of Cl^- in the urine by producing ammonia (NH_3), which freely moves across the tubular membranes into the urine, where it forms NH_4^+, a weak base. NH_3 must be produced from metabolism of amino acids. The diseased kidney is unable to do so and is thus only left with Na^+ to balance Cl^- and fails to correct the academia.

Another situation where the [SID] is narrowed because of hyperchloremia is diarrhea. In the upper bowel, the fluid is normally alkaline with a low $[Cl^-]$ compared with plasma and a large [SID]. When diarrhea is present, the more rapid transit in the bowel results in a failure to reabsorb Na^+ and loss of water (possibly also owing to a failure to excrete Cl^-) in the distal bowel. The loss of volume and decrease in

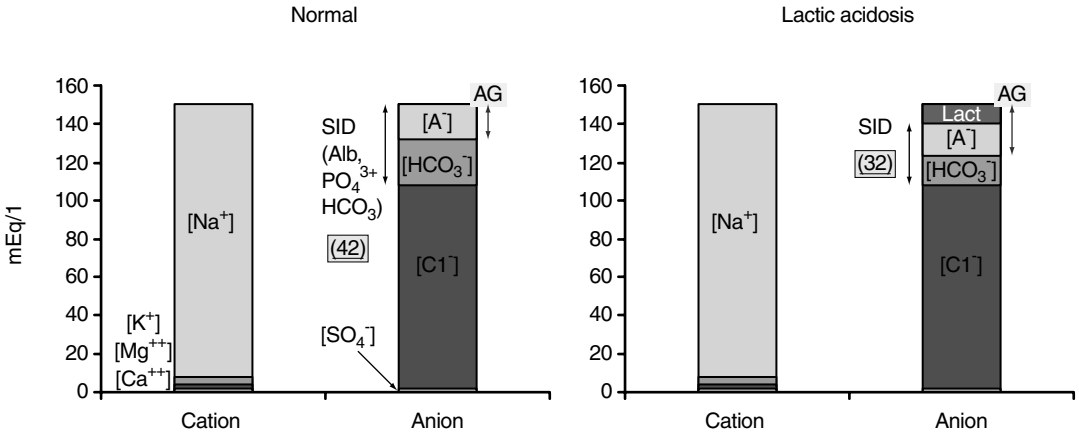

FIGURE 61-5 A gamblegram of normal plasma and plasma of a patient with lactic acidosis. Because the pKa of lactic acid is low, lactic acid is essentially dissociated in the solution and acts like a strong ion. An increase in lactate narrows the SID (in this case from 42 to 32 meq/l), and thus has an acidifying effect.

$[Na^+]$ has an acidifying effect by narrowing the [SID]. Retention of Cl^- by the kidneys as part of the compensation for the salt loss would narrow the [SID] further and increase the acidosis. The situation also is made worse when normal saline is used as the resuscitation fluid because, in contrast to the normal extracellular fluid, the $[Na^+]$ and $[Cl^-]$ of this solution are equal and will further narrow the [SID], as discussed above for the metabolic acidosis associated with saline resuscitation.

The opposite occurs when there is gastric suction. In this situation there is a loss of Cl^- without a loss of Na^+, and thus [SID] widens and there is an alkalosis. It needs to be appreciated that this will only occur when the stomach contents are acidic for otherwise the loss of Na^+ could be greater than the loss of Cl^-, in which case acidosis could even occur. Note again that it is the loss of Cl^- that is important and not the loss of H^+. The H^+ is derived from the dissociation of water, and concentration of water is 10^9 times greater that that of H^+ (the concentration of H_2O at 37°C is 55.3 M and the concentration of H^+ is 40×10^{-9} M.)

Addition of Other "Strong" Ions

Another way the [SID] can be changed is by the addition of ions that are not strong ions, but at the pH of plasma they are fully dissociated and thus act in the solution like strong ions. These are usually anions, and examples of effectively strong anions that can accumulate in pathologic conditions include lactate, formate, oxylate, β-hydroxybutyrate, acetoacetate, and salicylate. These will be recognized as the ion in classic "wide anion gap" acidosis.[5] It is important to appreciate that for acid–base balance, the effect of the addition of a strong ion, such as lactate, has the same effect as the addition of Cl^-. The only difference is that lactate can be metabolized, whereas Cl^- has to be excreted.

The understanding that these substances produce an acidosis by narrowing the [SID] helps explain why the administration of $NaHCO_3$ cannot successfully treat an acidosis that results from the production or absorption of a strong anion (Figures 61-5 and 61-6). The addition of $NaHCO_3$ corrects the acidemia by the addition of Na^+, which widens the [SID], and not by the addition of HCO_{3-}. $[HCO_{3-}]$ is a dependent variable and, in an open system, is controlled by the excretion of carbon dioxide by ventilation. Thus, to correct a lactic acidemia of 10 mmol/L, $[Na^+]$ would have to increase by 10 mEq/L, which would produce severe hypernatremia with consequent effects on cellular volumes. Furthermore, it is likely that the kidney or bowel will excrete the excess Na^+ or water will be retained so that normal osmolality is maintained, and therefore the body will not even allow the Na^+ to increase.

The use of $NaHCO_3$ solutions can, however, be of help in patients with renal failure and acidosis that is related to a failure to clear Cl^-. The infusion of $NaHCO_3$ provides a cation, Na^+, that can be excreted with Cl^-, whereas based on Equation 61-2, HCO_{3-} is in equilibrium with H_2CO_3, which is in equilibrium with PCO_2, and the PCO_2 is regulated by ventilation.

The administration of $NaHCO_3$ to patients with severe lung injury who are being managed with permissive hypercapnia and thus have a respiratory acidosis seems to be of clinical benefit. A possible explanation is that in these patients ventilation is relatively constant and does not change with changes in PCO_2. Thus, CO_2 no longer behaves as an independent variable and with the addition of HCO_{3-} can act as a dependent variable and be increased by the addition of $NaHCO_3$. In this situation, the HCO_{3-} could combine with H^+ in plasma and decrease $[H^+]$.

An interesting observation and application of Stewart's principles was recently made by Prange and coworkers, who showed that the decrease in partial pressure of oxygen (PO_2) in venous blood results in increased binding of Cl^- to hemoglobin.[6] This reduces the oxygen affinity of oxyhemoglobin and partly explains the Haldane effect. It also accounts for the increase in red blood count (RBC)-ICF $[Cl^-]$ that occurs in venous blood by what is known as the chloride shift. The binding of Cl^- to hemoglobin means that there is less free Cl^- in the intracellular fluid than expected and therefore less of a decrease in intracellular [SID] of the red cells on the venous side of the circulation than would otherwise have

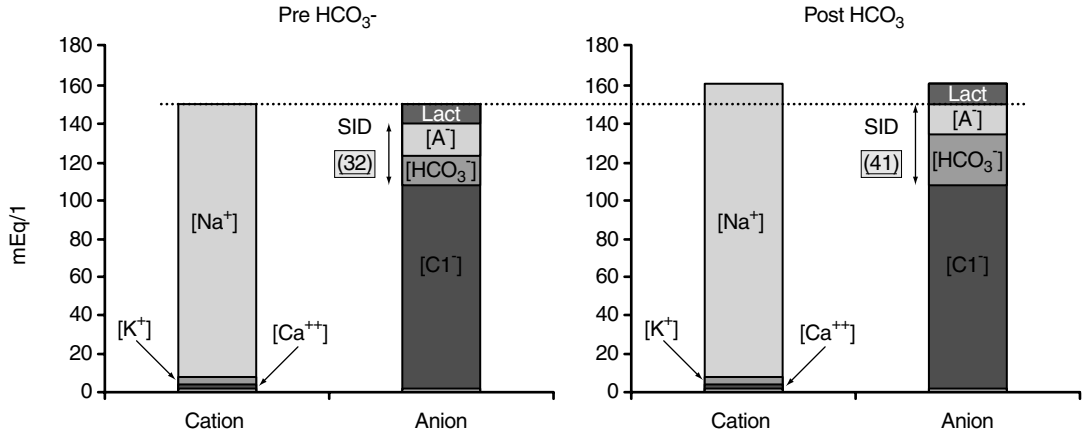

FIGURE 61-6 The gamblegram on the left is that of the patient with lactic acidosis shown in Figure 61-5, and the gamblegram on the right shows the effect of an infusion of $NaHCO_3$. The $NaHCO_3$ restores the SID increasing the Na^+ which also results in a small increase in HCO_3-. The primary event was the widening of the SID.

occurred from the influx of Cl^-. Because the influx of Cl^- does not narrow the SID as much as would otherwise have occurred, there is less of an acidifying effect from the influx of Cl^-. The authors propose that this binding of Cl^- to hemoglobin explains why $[H^+]$ is lower (and pH higher) and $[HCO_3-]$ higher than predicted in venous blood.

WEAK ACIDS

Principles

Weak acids are substances that only partially dissociate in a solution. The two important variables for determining their effect on $[H^+]$ are the total amount added (referred to as A_{Total}) and the pK_a of the reaction for this defines how much of the substance is dissociated at a given pH. Weak acids that are particularly important for acid–base balance have pK_as within an order of magnitude of the pH of normal plasma. If the pK_a is much below the pH of plasma, the substance will be mainly dissociated and function more like a strong ion in the solution. If the K_a is much higher than the pH of plasma, it will be largely associated at normal pH and have no effect on acid-base balance.

Weak acids with pK_a close to the pH of blood are often considered "buffers," but the concept of a buffer first needs to be reviewed. A buffer is defined as a substance that reduces the change in pH or $[H^+]$ when a base or acid is added to a solution.[2] This is defined mathematically as:

$$\beta = \frac{d\beta}{dpH} \qquad (61\text{-}3)$$

where β is the buffer strength, dB is the amount of base added, and dpH is the change in pH. A potentially confusing point that can lead to erroneous predictions is the standard definition of a base as a proton acceptor. Thus, Cl^- is defined as a base because it "accepts" a proton, H^+. However, nothing of the sort happens. Cl^- is a strong anion, which means that it binds minimally with cations in the solution, and its charge is balanced by H^+, but it is not bound to it. As already discussed, the dependent behavior of $[H^+]$ becomes obvious when HCl is added to a solution with a positive [SID] for in a solution with a positive [SID], the addition of HCl results in a smaller change in $[H^+]$ than the change in $[Cl^-]$. This occurs even without a weak acid, or so-called buffer, being present. It is the change in [SID] that determines the change in $[H^+]$, and what really happens when buffer strength is tested is that the addition of a strong cation or anion changes the [SID] and the change in [SID] changes pH.

Weak acids are either volatile, which is the case for H_2CO_3 in biologic solutions, or nonvolatile. In a solution with strong electrolytes, a positive [SID], and essentially no nonvolatile weak acids (ie, no protein), for example, interstitial fluid, the addition of a strong acid or base only produces a small change in pH, and the solution seems to be "buffered." The addition of a nonvolatile weak acid to create a solution similar to plasma or the intracellular environment has some important consequences. There are now two important variables that determine $[H^+]$, the [SID] and $[A_{Total}]$, where $[A_{Total}]$ is the total concentration of weak acids, which are classically viewed as "buffers." Over the range of [SID] from 0 to $[A_{Total}]$, $[H^+]$ actually increases more rapidly than is the case in a solution where there is no weak acid—the opposite of what a buffer should do.[1] What the weak acid does, though, is markedly lower the pH and thus lower the pH of the solution observed for a given change in [SID] over the range of $[SID] = 0$ to $[SID] = [A_{Total}]$. If the dissociation constant of the weak acid is within an order of magnitude of normal plasma, which is the case for what are usually considered to be physiologically important buffers, and [SID] is increased, negative ions are needed to balance the positive charge difference, and this drives the dissociation of the weak acid. When the [SID] equals $[A_{Total}]$, the weak acid is almost completely dissociated and no longer affects the solution.

Albumin

The most important normal weak acid in plasma is albumin. The pK_a of the histidine side chains is close to the value of normal plasma pH, and therefore changes in plasma [SID] have a major effect on their dissociation. These ions account for most of the normal "anion gap," so a decrease in albumin

is associated with a decrease in the anion gap.[7–9] This effect of albumin on the pH of the solution is traditionally referred to as buffering, but as already noted, what this weak acid really does is set a range over which there are small changes in pH for given changes in SID. A major difficulty for the application of the physical-chemical approach to clinical acid–base analysis is assigning an "equivalents" value to the anion of albumin. This problem was dealt with empirically by Figge and coworkers,[9,10] who performed titration curves on blood with different albumin concentrations and different SID. They thus were able to provide a formula for the anion equivalence of albumin at different values of pH that can be used to obtain the "charge effect" of weak acids that are dominated by albumin as follows:

$$\text{Albumin equivalence} = (0.123 \times \text{pH} - 0.631) \times ([\text{albumin}]) \quad (61\text{-}4)$$

where albumin is in g/L.

A decrease in albumin concentration is very common in critically ill patients.[7,8,11] The reduction in this weak acid has an alkalinizing effect, and an increase in the albumin concentration has an acidifying effect. For example, with a constant PCO_2, a decrease in albumin from 42 to 20 g/L has the same alkalinizing effect as a decrease in a strong anion of 6 mEq/L. This means that this decrease in albumin would have the same effect on $[H^+]$ as a decrease in lactate from 8 mEq/L to 2 mEq/L.

A decrease in water with dehydration increases the albumin concentration, which has an acidifying effect. On the other hand, as discussed above, dehydration can widen the [SID], which has an alkalinizing effect. The final effect will depend upon how normal regulatory mechanisms respond to the increase in $[Na^+]$ and $[Cl^-]$. Since $[Na^+]$ is normally well regulated, it is likely that the increase in $[Na^+]$ will be regulated first, and that would narrow the [SID] and lead to acidemia. Indeed, this has been observed during a cholera outbreak.[12]

The second weak acid of potential clinical importance is phosphate (PO_4^{3+}). The dissociation of phosphoric acid to PO_4^{3+} has three steps with three pK_a. At 37°C the first pK_a is only 1.91, and therefore this component acts as a strong anion and is essentially totally dissociated. The second pK_a is 6.66, which is close to normal pH and is very much affected by the other components of plasma. The third pK_a is very high, 11.8, and is therefore only minimally dissociated in the plasma.[10] Normal $[PO_4^{3+}]$ in plasma is only around 1 mmol/L, and therefore changes in its dissociation actually have little effect on $[H^+]$, but $[PO_4^{3+}]$ can play a role when the concentration increases with disease. The relationship, again from Figge and colleagues,[10] is

$$(\text{Pi}-) = (\text{Pi}) \times (0.309 \times \text{pH} - 0.469) \quad (61\text{-}5)$$

where Pi− is the ionized portion and Pi is the total phosphate.

CLINICAL APPROACHES AT THE BEDSIDE

Stewart's Original Presentation

The first physical-chemical approach to the analysis of acid–base balance was presented by Stewart, who gave a comprehensive analysis of the regulation of $[H^+]$ in the body. His approach was further developed by Figge and colleagues[9,10] and Fencyl and Rossing.[13] Stewart provided six equations that could be solved simultaneously by combining them into a quadratic equation to calculate $[H^+]$.[1] He then calculated the effect of changes in PCO_2 and [SID] at a fixed A_{Total} and plotted these together. This is shown in Figure 61-7. The analysis is begun by plotting the pH (or H^+) and PCO_2 and determining the expected [SID]. For example, if a patient's PCO_2 is increased and pH is normal and the [SID] is the normal value of 42 mEq/L, then the problem is purely respiratory, and the clinical solution is to treat the respiratory problem. In contrast, if there is a decrease in pH with a decrease in PCO_2 and a decrease in the SID, there is a metabolic problem.

The next step is to determine why the [SID] is abnormal. This is done by determining the sum of $[Na^+] + [K^+] - [Cl^-]$, the common major strong ions in the plasma, for this gives the inorganic [SID]. If this value is not the same as that given by the nomogram, then the next step is to determine whether this is because of an increase in $[Cl^-]$ or a decrease in $[Na^+]$. If $[Na^+]$ and $[K^+]$ are normal, and [SID] differs from the value predicted by the nomogram, unidentified anions must be present. These anions are the same as those that explain the traditional wide anion gap acidosis.

Stewart also pointed out that if the nomogram is not available, then the expected [SID] can be estimated by $[\text{SID}] = HCO_3^- + [\text{A}-]$, and $[\text{A}-]$ can be estimated from the $[\text{SID}] - [HCO_3^-]$, that is, $[Na^+] + [K^+] - [Cl^-] - [HCO_3^-]$, which is the anion gap. This estimate, however, leaves out the variability of $[\text{A}-]$ with changes in pH as demonstrated in Figge and colleagues' equation.[10]

A weakness in the simple approach first presented by Stewart[1] is that it did not factor in changes in $[A_{Total}]$ or give a process for quantitatively analyzing them for the assumption in the nomogram in Figure 61-7 is that $[A_{Total}]$ is constant, which usually is not the case in critically ill patients.

Presentation by Jones

An early advocate of the Stewart approach was Norman Jones.[14,15] He used essentially the same approach as Stewart but elaborated on the relationship of the measured and predicted [SID] and introduced the concept of a [SID] gap. Building on Stewart's work, he used the nomogram in Figure 61-7 to predict the [SID] and compared it with [SID] obtained from the measurement of plasma electrolytes. He also pointed out that since $[\text{SID}] - [HCO_3] - [\text{A}-] = 0$ one can assess the role of each of these three factors in the acid–base disorder.

CONCEPT OF STRONG ION GAP

The concept of strong ion gap (SIG) was further elaborated by Kellum and colleagues, who built on concepts presented by Fencl and Leith.[16] Based on the work of Stewart[1] and Figge and colleagues,[10] SIG is defined as the difference

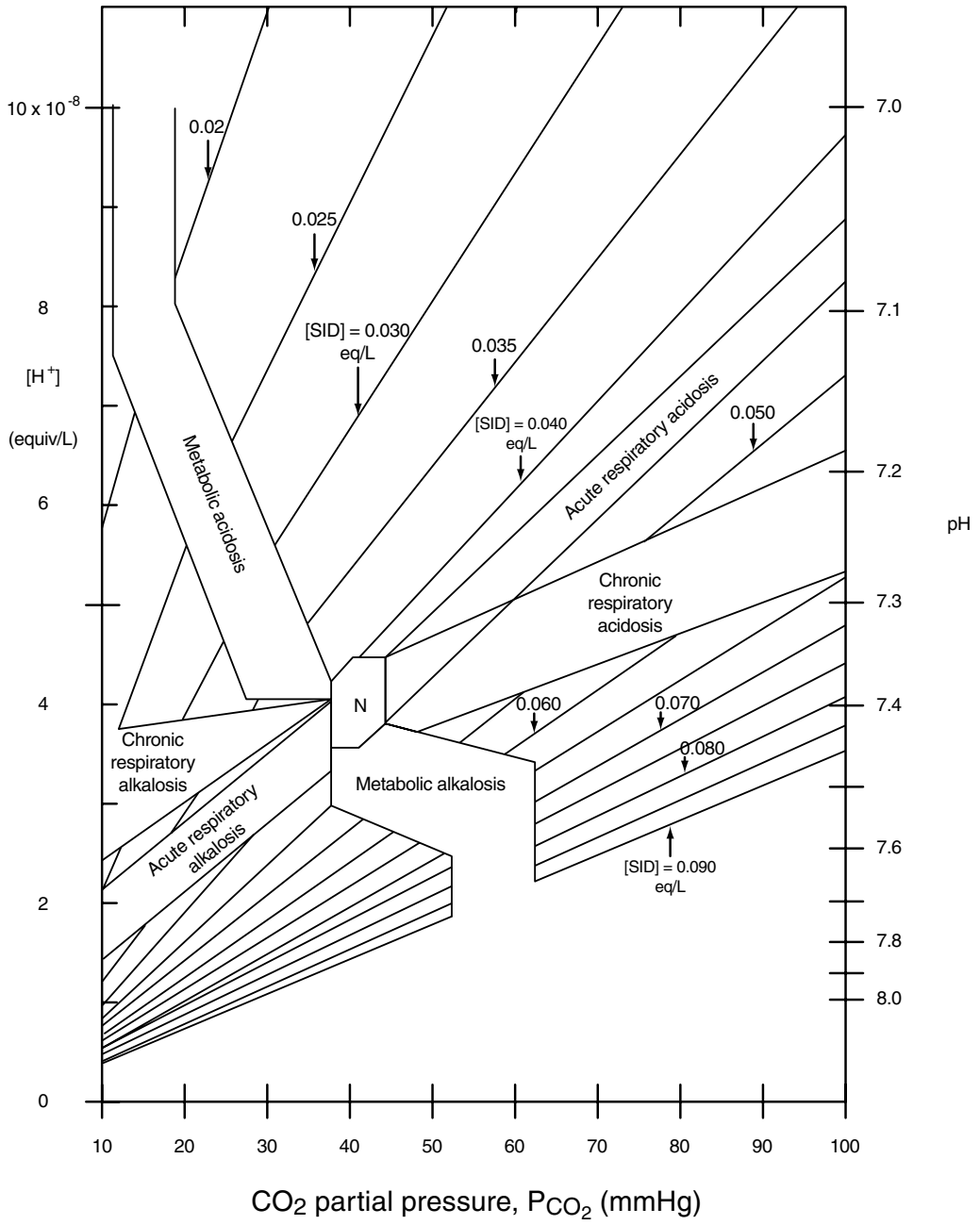

FIGURE 61-7 Stewart's nomogram for effects of changes in CO_2 and [SID] on H^+ or pH. See text for details. Reproduced with permission from Roos A and Boron WF[2].

between the apparent strong ion difference [SID]a and the effective strong ion difference [SID]e where

$$[SID]a = [Na^+] + [K^+] + [Mg^{++}] + [Ca^{++}] - [Cl^-] - [lactate] - [urate]$$

(all ionized concentrations are in mEq/L) and

$$[SID]e = 1{,}000 \times (2.46 \times 10^{-11}) \times (PCO_2/(10^{-pH})) + \{[albumin] \times (0.123\ pH - 0.631)\} + \{[PO_4] \times (0.309\ pH - 0.469)\}$$

($[PO_4]$ is in mmol/L and albumin is in g/L). The formula for calculating all the components of the analysis are given at a Web site created by Kellum called The Acid Base pHorum: <http://www.ccm.upmc.edu/education/resource/phorum.html>.

The SIG should normally be zero. If it is not, there are unexplained anions. By using the formula provided by Figge and colleagues, this approach accounts for changes in albumin concentration. Thus, Kellum and colleagues proposed that the SIG should be used instead of the anion gap for evaluating patients.[16] An unexpected observation in their studies was that there are often large amounts of unknown anions in patients with sepsis and liver disease.

A number of investigators have now used this approach to evaluate the abnormalities of various conditions,[13,17–22] as

well as the effect of interventions.[23–25] The basic approach is to first examine whether the [SID] deviates from the normal value of 42 mEq/L. If it is abnormal, the next question is what measured ions are abnormal to account for the abnormality. For example, is the lactate increased? If there is a SIG with a [SID]e less than the [SID]a, unmeasured anions are present that are greater in number than the unmeasured cations and if SIG is positive, there must be unexplained cations.

BASE EXCESS AND BASE EXCESS GAP

Magder and colleagues introduced another approach, which classifies metabolic abnormalities into those owing to water, Cl^-, albumin, and "other" factors.[26] The "other" factors are calculated by using the base excess (BE) rather than the SIG. This approach is based on one used by Fencyl and Leith but never published (personal communication).

In this approach, and in all of the physical-chemical approaches, the first step in evaluating acid–base balance is to determine if there is an acidemia or alkalemia, and this is done by simply determining if there is a deviation in pH from the physiologic normal value of 7.40. If the pH is greater than 7.40 there is an alkalemia, and if the pH is less than 7.40 there is an acidemia. However, it must be remembered that a pH in plasma <7.40 does not actually mean that the blood is an acid solution in the chemical sense for $[H^+]$ is still much less than $[OH^-]$. It is really just less alkaline. However, this terminology is common usage and convenient for interpreting deviations from normal.

The next step is to evaluate the respiratory component. This is done by examining the deviation of PCO_2 from the standard value of 40 mm Hg. If the PCO_2 is >40 mm Hg, by definition there is a respiratory acidosis regardless of the pH for the PCO_2 defines a process. If the PCO_2 is <40 mm Hg, there is a respiratory acidosis regardless of the pH.

The metabolic components are examined next. First one examines the role of changes in the concentrations of electrolytes that are a result of changes in "water." Since the amount of extracellular water is determined primarily by the $[Na^+]$, $[Na^+]$ is used to assess water effects. This is done by comparing the measured $[Na^+]$ with the $[Na^+]$ reference value, which is 140 mEq/L, and by assuming normal [SID] of 42 mEq/L as follows:

$$\text{Water effect (mEq/L)} = \{(Na - 140)/140\} \times 42 = 0.3\ \{[Na^+] - 140\}$$

As discussed above, the major mechanism available to the body to regulate the [SID] is the regulation of $[Cl^-]$. Therefore, an important step is the evaluation of the change in $[Cl^-]$. To do this, one must first account for the effect of changes in water on $[Cl^-]$ for this was already accounted for in the previous step. This is done by correcting the measured $[Cl^-]$ by the ratio of the standard value of $[Na^+]$ of 140 mEq/L, and the measured $[Na^+]$:

$$[Cl^-] - \text{corrected (mEq/L)} = [Cl^-] \times 140/[Na^+]$$

The effect of the change in $[Cl^-]$ can then be calculated from

$$\text{Chloride effect (mEq/L)} = 102 - \{[Cl^-] - \text{corrected (mEq/L)}\}$$

where 102 mEq/L is the standard $[Cl^-]$ value.

The third metabolic factor is the effect of changes in albumin for albumin is the major determinant of the effect of weak acids and the one to have a change in concentration in pathologic conditions. The ionic equivalents of a change in albumin can be determined by an adaptation of the empiric formula developed by Figge and colleagues[10]:

$$\text{Albumin effect (mEq/L)} = 42 - \{[\text{albumin}] \times (0.123 \times \text{pH} - 0.631)\}$$

where albumin is in g/L and 42 represents the standard value of albumin.

Once the effect of these three factors—water, $[Cl^-]$, and albumin—is accounted for, the presence of any "other" factors can be determined by the use of the SIG as described above. Alternatively, we found that it is very convenient to use the base excess (BE), which is given with the outputs from most blood gas machines. To do so, one adds the value in mEq/L of the water effect, chloride effect, and albumin effect and subtracts this sum from the calculated BE, which is also in the units of mEq/L:

$$\text{"Other" (mEq/L)} = \text{BE} - (\text{water effect} + \text{chloride effect} + \text{albumin effect})$$

To understand the rationale for this last step it is necessary to understand the concept of BE. BE is a concept that was developed in the early part of the century to account for the nonrespiratory component of an acid–base disturbance and was best elaborated by Siggaard-Andersen.[27] He first restored the PCO_2 back to 40 mm Hg to eliminate the respiratory contribution to any alteration in the pH. Next he performed titrations with a strong base or strong acid to restore the pH to 7.40. This was essentially a titration of the [SID] and is thus an empiric assessment of the SIG. Indeed, there is a tight relationship between measurements of "other" by this method (or as it could also be called the BE gap) and the SIG.[26]

The BE reported on blood gases today comes from a nomogram created empirically by Siggaard-Andersen to determine the BE. Because the electrolytes in plasma are in equilibrium with the interstitial space, a titration in a test tube of blood is not the same as a titration on whole blood or, for that matter, on serum. This has often been viewed as being due to a greater "buffering effect" of hemoglobin in the test tube, and because of this, BE is often given as "standard base excess," which is based on a hemoglobin value of 50 g/L, which takes into account the distribution of electrolytes throughout the extracellular space.[28,29] However, the differences are really quite small, and we have used the BE based on a hemoglobin of 150 g/L. The reason why the effect is small is that hemoglobin does not actually "buffer" the plasma because it is not in contact with it. The only way red cells in the plasma can affect $[H^+]$ is by electrolyte shifts between the intracellular space and the plasma, which then

can alter plasma [SID]. However, the RBC intracellular volume is small compared with that of plasma. In the body, the intracellular compartment of RBC interacts with the whole extracellular volume and therefore has only a minimal effect on electrolyte concentrations.

The analysis based on the effects of water, chloride, albumin, and BE has the advantage of indicating which major regulator is causing the acid–base abnormality. It is also easier to calculate than the full equation for determining the apparent $[H^+]$. The disadvantage to this approach, however, is that it introduces another empiric measurement, that is, the BE, and therefore has the potential for other confounding factors that may not have been accounted for in the original titration experiments that were used to obtain the BE nomogram. The effects of other factors, such as phosphate, also become more of a problem at the extremes of the range of phosphate values, but this can also be accounted for by the formula introduced by Figge and colleagues[10] as given above.

SUMMARY

Appreciation of the physical-chemical factors that determine $[H^+]$ is essential for understanding the mechanisms behind acid–base disorders. Once one understands the basic processes, an examination of the electrolytes can give a quick, but not quantitative, insight into the basic mechanism. For example, a low $[Na^+]$ indicates a major water effect, a high $[Cl^-]$ indicates a "non-anion gap" metabolic acidosis, and a low albumin indicates a metabolic alkalosis. An abnormal BE in the absence of major $[Cl^-]$ abnormalities means that there are very likely abnormal anions present. When a more quantitative analysis is desired, one can calculate the SIG or use the calculations given above to quantify the water effect, chloride effect, albumin effect, and "other."

REFERENCES

1. Stewart PA. How to understand acid-base. a quantitative acid-base primer for biology and medicine. New York: Elsevier North Holland; 1981.
2. Roos A, Boron WF. Intracellular pH. Physiol Rev 1981;61:296–434.
3. Kowalchuk J, Heigenhauser G, Sutton J, Jones N. Effect of chronic acetazolamide administration on gas exchange and acid-base control after maximal exercise. J Appl Physiol 1994;76:1211–9.
4. Magder S. Pathophysiology of metabolic acid-base disturbances in patients with critical illness. Crit Care Nephrol 1998;279–96.
5. Emmett M, Narins RG. Clinical use of the anion gap. Medicine 1977;56:38–54.
6. Prange HD, Shoemaker JLJ, Westen EA, et al. Physiological consequences of oxygen-dependent chloride binding to hemoglobin. J Appl Physiol 2001;91:33–8.
7. Rossing TH, Maffeo N, Fencl V. Acid-base effects of altering plasma protein concentration in human blood in vitro. J Appl Physiol 1986;61:2260–5.
8. Rossing TH, Boixeda D, Maffeo N. Hyperventilation with hypoproteinemia. J Lab Clin Med 1986;117:453–67.
9. Figge J, Rossing TH, Fencl V. The role of serum proteins in acid-base equilibria. J Lab Clin Med 1991;117:453–67.
10. Figge J, Mydosh T, Fencl V. Serum proteins and acid-base equilibria: a follow-up. J Lab Clin Med 1992;120:713–9.
11. Wilkes P. Hypoproteinemia, strong-ion difference, and acid-base status in critically ill patients. J Appl Physiol 1998;84: 1740–8.
12. Wang F, Butler T, Rabbani GH. The acidosis of cholera: contributions of hyperproteinemia, lactic acidemia and hyperphosphatemia to an increased serum anion gap. N Engl J Med 1986;315:1591–5.
13. Fencl V, Rossing TH. Acid-base disorders in critical care medicine. Annu Rev Med 1989;40:17–29.
14. Jones NL. A quantitative physiochemical approach to acid-base physiology. Clin Biochem 1990;23:189–95.
15. Jones NL. Should we change our approach to acid-base physiology? Ann RCPSC 1990;23:235–40.
16. Kellum JA, Kramer DJ, Pinsky MR. Strong ion gap: a methodology for exploring unexplained anions. J Crit Care 1995; 10:51–5.
17. Fencl V. Acid-base balance in cerebral fluids. Handbook of physiology – the respiratory system II. 1997.
18. Fencl V, Jabor A, Kazda A, Figge J. Diagnosis of metabolic acid-base disturbances in critically ill patients. Am J Respir Crit Care Med 2000;162:2246–51.
19. Kellum JA, Bellomo R, Kramer DJ, Pinksy MR. Hepatic anion flux during acute endotoxemia. J Appl Physiol 1995;78:2212–7.
20. Kellum JA, Kramer DJ, Pinsky MR. Strong ion gap: a methodology for exploring unexplained anions. J Crit Care 1995;10:51–5.
21. Kellum JA. Metabolic acidosis in the critically ill: Lessons from physical chemistry. Kidney Int 1998;53:S81–6.
22. Waters JH, Scanlon TS, Howard RS, Leivers D. Role of minor electrolytes when applied to Stewart's acid-base approach in an acidotic rabbit model. Anesth Analg 1995;81:1043–51.
23. Hayhoe M, Bellomo R, Lui G, et al. Role of the splanchnic circulation in acid-base balance during cardiopulmonary bypass. Crit Care Med 1999;27:2671–7.
24. Liskaser FJ, Bellomo R, Hayhoe M, et al. Role of pump prime in the etiology and pathogenesis of cardiopulmonary bypass-associated acidosis. Anesthesiology 2000;93:1170–3.
25. Rehm M, Orth V, Scheingraber S, et al. Acid-base changes caused by 5% albumin versus 6% hydroxyethyl starch solution in patients undergoing acute normovolemic hemodilution. Anesthesiology 2000;93:1174–87.
26. Gilfix BM, Bique M, Magder SA. A physiological approach to the analysis of acid-base balance in the clinical setting. J Crit Care 1993;8:187–97.
27. Siggaard-Andersen O. The acid-base status of the blood. 2nd ed. Baltmore (MD): Williams and Wilkins; 1964.
28. Mizock BA. Utility of standard base excess in acid-base analysis. Crit Care Med 1998;26:1146–7.
29. Schlichtig R, Grogono AW, Severinghaus JW. Human Paco2 and standard base excess compensation for acid-base imbalance. Crit Care Med 1998;26:1173–9.

CHAPTER 62

AIRWAY HYPERRESPONSIVENESS

Ron Olivenstein, Rame Taha

The term "airway responsiveness" refers to the capacity of the airways to narrow after exposure to constrictor agonists. Airway hyperresponsiveness describes an exaggerated capability of an individual to develop this response and is termed nonspecific when triggered by chemical or physical stimuli. The term "specific" hyperresponsiveness is reserved for provocation by allergens. Nonspecific airway hyperresponsiveness is a characteristic feature of asthma and has been included in the defining characteristics of the condition,[1] although it should be noted that it is not specific for that disease. Nevertheless, measurements of airway hyperresponsiveness have been found to be useful in confirming the diagnosis of asthma, particularly in individuals who have symptoms consistent with asthma but no spirometric evidence of airflow obstruction. These measurements commonly are referred to as bronchoprovocation tests and can be performed safely and reproducibly in the pulmonary function laboratory. The measurement of airway hyperresponsiveness is performed using standardized inhalational challenges with airway constrictor agonists, usually histamine or methacholine.

BRONCHOCONSTRICTOR DOSE-RESPONSE CURVES

An excessive response to inhaled bronchoconstrictor agents is one of the key features of asthma. When direct-acting bronchoconstrictors such as histamine or methacholine are used, airway hyperresponsiveness can be defined as both an increase in the ease and magnitude of the induced bronchoconstriction.[2] Airway responses to bronchoconstrictor stimuli are performed using challenge tests in the laboratory that expose subjects to stepwise increases in doses of the stimulus while measuring some index of lung function,[3] so as to construct a bronchoconstrictor dose-response curve. Three characteristics of the dose-response curve need to be distinguished since they describe phenomena that may vary independently[4] and likely are the result of different pathophysiologic mechanisms.

The bronchoconstrictor dose-response curve is sigmoid in shape and can be characterized from (1) position (sensitivity), (2) slope (reactivity), and (3) plateau (maximal response).[5] Figure 62-1 illustrates examples of these characteristics in methacholine dose-response curves obtained in human subjects in vivo.

Hyperresponsiveness is the term most often used to describe the phenomenon of irritability in general. Hypersensitivity refers specifically to a leftward shift from the normal dose-response curve position so that a given decrease in the measured lung function (ie, fall in forced expiratory volume in 1 second [FEV_1] from baseline) occurs at a lower dose of bronchoconstrictor compared with normal. Hyperreactivity refers specifically to an increase in slope of the dose-response curve. The term is often mistakenly misused as a synonym for hypersensitivity. An increase in the maximal bronchoconstrictor-induced response leads to an unmeasurable plateau level and reflects the phenomenon of excessive airway narrowing. Since the terminology is used interchangeably, it is important to specifically define outcome measurements of bronchoconstrictor challenge tests.

Hypersensitivity of the Airways

Strictly speaking, it is not really known whether the airways in asthma are hypersensitive to bronchoconstrictor stimuli in vivo. The provocative concentration causing a 20% decrease in FEV_1 (PC_{20}) has been interpreted in this way. The leftward shift of a dose-response curve is usually expressed as the reduction in the dose of bronchoconstrictor causing a half-maximal response ED_{50}. This can be measured precisely only if the complete curve has been recorded, that is, a plateau is present.[4] Since often the plateau cannot be measured in vivo in many asthmatics,[5] the PC_{20} but not the ED_{50} is measured and the former may not adequately reflect the position of the dose-response curve. The more than 1,000-fold range in PC_{20} observed in nature among individuals makes it likely, however, that PC_{20} reflects, at least in part, real differences in airway sensitivity.

Examples of the mechanisms that determine airway hypersensitivity are those that amplify the effective stimulus to the airways,[6] such as epithelial damage (loss), opening of

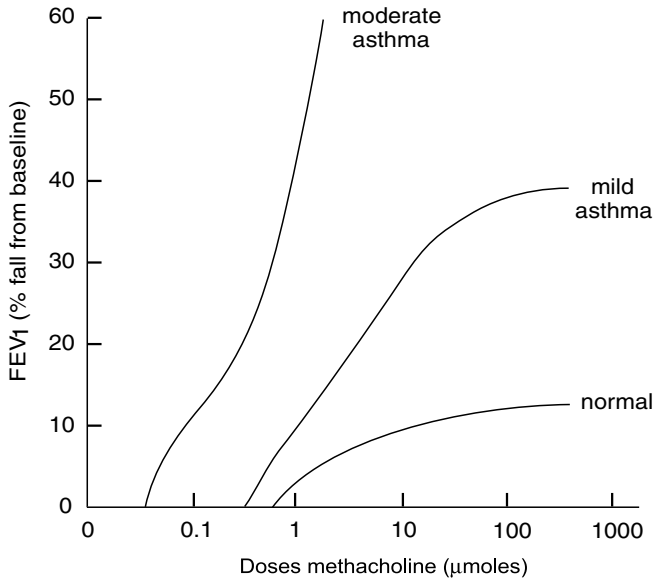

FIGURE 62-1 Characteristics of methacholine dose-response curves in asthmatic and nonasthmatic individuals. Leftward shift and increased maximal response in mild asthmatic individuals. Excessive sensitivity and excessive airway narrowing after methacholine in individuals with more severe asthma.

tight junctions (increased permeability), and increased inflammatory infiltrate within the airways.[7,8]

Excessive Airway Narrowing

It is still not well understood what mechanisms protect nonasthmatic subjects from excessive airway narrowing following a bronchoconstrictor stimulus.[6,9] Nonasthmatics demonstrate a reproducible maximal response plateau on the dose-response curve at mild degrees of airway narrowing,[5,10] usually at 10 to 30% decrease in FEV_1.[11] Neither humoral or neurogenic inhibition of maximal airway narrowing has been demonstrated in humans in vivo.[12] Factors that can be postulated to limit maximum airway narrowing include the intrinsic properties of the muscle itself,[13] deviation from the optimal resting length of airway smooth muscle under physiologic conditions,[14] nonoptimal resting smooth muscle length,[15] and smooth muscle orientation within the airway walls.[16] Interdependence between the airway and the surrounding parenchyma and cartilage likely limits excessive airway narrowing in nonasthmatics by mechanically counterbalancing muscle shortening.[6,13,14,17]

In asthmatics, an increase in maximal response to bronchoconstrictor stimuli is a result of responses in the smooth muscle itself, that is, smooth muscle shortening and mechanisms potentiating the effect of muscle shortening on airway resistance.[6,18] The in vivo plateau can be lost if smooth muscle shortens by 40% of its resting length.[13]

Increased smooth muscle contractility has been shown in hyperresponsive guinea pigs as a result of increased intrinsic contractility[19] or an increase in smooth muscle owing to hyperplasia[20] or hypertrophy.[21] Increased intrinsic smooth muscle contractility could be caused by increased actomyosin adenosine triphosphatase (ATPase) activity in smooth muscle cells as observed following active sensitization in dogs[22] and passive sensitization in human airways.[23] Increased smooth muscle thickening may be even a more important determinant of excessive airway narrowing[24,25] and could result from the effect of mechanical strain[26] or growth factors.[20,21]

Increased muscle shortening could also result from decreased elastic loads. Variations in the elastic recoil pressure change the maximal response to bronchoconstrictors in vivo[27] and thus create disturbances in the mechanical protection provided by the airway–parenchymal interdependence.[7]

Factors that increase airway wall thickening lead to increased airway narrowing as well[6] either on mucosal or submucosal[9] surfaces internal to the smooth muscle or on adventitious surfaces external to the smooth muscle.[7] Inflammatory processes, including plasma exudation, edema, and microvascular congestion,[28] can decrease luminal patency, lead to filling of the interstices between luminal epithelial projections,[29] decrease airway elastance,[30] and reduce epithelial folds owing to submucosal swelling or to collagen deposition in the subepithelial reticular layer in asthma.[31,32]

BRONCHOPROVOCATION TESTING

Rationale

There are several potentially useful reasons to perform bronchoprovocation testing when asthma is suspected as a clinical diagnosis. Asthmatics in general have a provocative concentration of an inhaled agonist (usually histamine or methacholine) that causes a 20% fall in FEV_1 (PC_{20}) of less than 8 mg/mL, whereas in most nonasthmatics the PC_{20} exceeds 16 mg/mL. There is, however, considerable overlap, and this measurement cannot be used to definitively distinguish asthmatics from nonasthmatics. Failure to show airway hyperresponsiveness strongly argues against the diagnosis of asthma since this feature appears to distinguish most individuals with symptomatic asthma. In asymptomatic individuals, airway hyperresponsiveness may be the only evidence of airway dysfunction.[2] This finding may have predictive value for the future development of symptomatic asthma as it appears that such individuals may be at increased risk of developing the disease.[2,33] Furthermore, the severity of airway hyperresponsiveness generally correlates with the severity of asthma.[3–6] Also the degree of airway hyperresponsiveness correlates with other measurements of asthma severity, such as the improvement in FEV_1 to bronchodilator administration and variations in peak expiratory flow.[34] In most individuals, both asthma symptoms and airway hyperresponsiveness vary over time, possibly reflecting cyclic inflammation within the airways.[1]

Direct-Acting and Indirect-Acting Stimuli

Airway hyperresponsiveness can be demonstrated to a variety of chemical and physical stimuli. Agonists that cause bronchoconstriction by acting directly on receptors that are present on airway smooth muscle include inhaled histamine, cholinergic agonists, notably methacholine and acetylcholine, and chemical mediators such as cysteinyl leukotrienes C_4 and D_4[35] and prostaglandins D_2 and $F_{2\alpha}$.[36,37] These are designated as direct-acting measurements of

airway responsiveness. Indirect stimuli cause bronchoconstriction through the release of constrictor mediators that are preformed or synthesized de novo by cells within the airways. Indirect stimuli include adenosine,[38] exercise,[39] hyperventilation of cold dry air,[40] and hypotonic or hypertonic aerosols.[41] Indirect-acting stimuli are used only exceptionally in clinical practice.

Methacholine Challenge Testing

Methacholine, an acetylcholine derivative, is the most commonly used pharmacologic agent to perform bronchial challenge. The longer duration of bronchospasm induced by methacholine facilitates measurement of the bronchoconstrictive response compared with acetylcholine. Histamine is now used less than methacholine because of side effects such as flushing and headaches. Results with methacholine and histamine seem to be equivalent in asthmatics,[42,43] even if the two agonists stimulate different receptors. Only histamine activates airway neural reflexes, but the magnitude of this contribution to bronchoconstriction seems to be relatively minor compared with the direct effect on airway smooth muscle.

Indications

Asthma Diagnosis Methacholine inhalation testing is the most widely used method for the assessment of airway hyperresponsiveness. The nonspecificity of the nature of symptoms in asthma, combined with the long-term social and therapeutic implications of a diagnosis of a chronic disease such as asthma, necessitates objective confirmation of the diagnosis. Methacholine inhalational testing is indicated in clinical situations where the diagnosis of asthma is considered and usual objective methods, notably spirometry, fail to establish the diagnosis. Such situations include (1) individuals with symptoms consistent with asthma but with normal spirometry and no improvement in airflow after administration of a bronchodilator, a situation encountered in individuals with mild or well-managed asthma[44]; (2) individuals with nonspecific symptoms, such as chronic cough, that could be due to asthma or other disease states. The absence of airway hyperresponsiveness in this clinical setting usually suggests an alternative diagnosis to asthma[45]; and (3) atypical symptoms of bronchospasm such as chest pains or insomnia.

Assessment of Therapeutic Response Abnormal airway hyperresponsiveness may be the only objective outcome measurement in some individuals with asthma. Since improvement in the clinical severity of asthma is associated with improvement in airway hyperresponsiveness,[46] some clinical studies have used changes in this parameter as an objective outcome measure.[47,48] The routine use of serial methacholine challenges to direct treatment in individuals with asthma awaits further assessment.

Evaluation of Occupational Asthma Bronchoprovocation testing with specific occupational agents is done using specific protocols in centers that are specialized to perform such tests when there is a clinical suspicion that a particular occupational agent, food additive, or environmental antigen may be responsible for asthma-like symptoms. Facilities for 24-hour monitoring of individuals may be required. The evaluation of the patient with occupational asthma is discussed in Chapter 64, "Evaluation of the Patient with Occupational Asthma."

Contraindications

The contraindications to methacholine inhalation testing are summarized in Table 62-1 and include conditions that may compromise the quality of the test or place the individual at a greater risk or discomfort.

Low FEV_1 Methacholine inhalation testing should be performed in the absence of signs and symptoms of significant airflow obstruction since occasional dramatic falls in FEV_1 may occur during the test and the risk of such events is increased in individuals with low baseline lung function. However, the level of lung function at which methacholine inhalation testing is contraindicated is controversial since the risk is small even in individuals with relatively severe airway obstruction.[49] In a report of 88 individuals with $FEV_1 < 60\%$ predicted who underwent methacholine inhalation testing, all but four individuals returned to >90% baseline FEV_1 after a single treatment with inhaled short-acting β_2-agonist, and those initial "nonresponders" improved adequately with a second bronchodilator treatment. A baseline FEV_1 of < 1.5 L or $< 60\%$ predicted in adults has been proposed as a relative contraindication to methacholine inhalation testing by Sterk and colleagues[2] and Tashkin and colleagues.[50] The Second National Asthma Expert Panel Report used an $FEV_1 < 65\%$ predicted.[51] In a recent survey, one-half of the investigators polled considered an $FEV_1 < 70\%$ predicted to be a contraindication, whereas 20% each used cutoffs of 60 and 80% of predicted FEV_1.[52] Severe airflow limitation with an $FEV_1 < 1.0$ L or $< 50\%$ predicted is usually considered an absolute contraindication to methacholine inhalation testing. It is certainly prudent to insist on increased medical supervision if testing is considered to be necessary in individuals with an increased degree of airway obstruction.

Table 62-1 Contraindications for Methacholine Challenge Inhalation Testing

Absolute
Pulmonary
Severe airflow limitation ($FEV_1 < 50\%$ predicted or < 1.0 L)
Cardiac
Heart attack or stroke in last 3 months
Uncontrolled hypertension, systolic BP > 200 mm Hg, or diastolic BP > 100 mm Hg
Known aortic aneurysm
Relative
Pulmonary
Moderate airflow limitation ($FEV_1 < 60\%$ predicted or < 1.5 L)
Inability to perform acceptable-quality spirometry
Others
Pregnancy
Nursing mothers
Current use of cholinesterase inhibitor medication (for myasthenia gravis)

BP = blood pressure; FEV_1 = forced expiratory volume in 1 second.

Airway Obstruction Airway hyperresponsiveness is also found in individuals with chronic obstructive pulmonary disease (COPD) and correlates strongly with the degree of baseline airway obstruction. Therefore, increased airway responsiveness, that is, a "positive" methacholine inhalation test, is more likely to be found when baseline spirometry shows a low FEV_1 to forced vital capacity (FVC) ratio and a low FEV_1. The interpretation as to whether this individual has COPD, asthma, or both diagnoses remains problematic. In these individuals with severe airway obstruction in whom the clinical suspicion for asthma is good and significant improvement ($>12\%$ and >0.2 L) in FEV_1 can be demonstrated with bronchodilator administration, the diagnosis of asthma can usually be confirmed, precluding the necessity for a methacholine challenge test.

Spirometry Quality The acceptability of a methacholine inhalation test depends on the ability of individuals to perform acceptable and reproducible spirometric maneuvers. Persons who cannot must be rescheduled or tested using another outcome measure.

Cardiovascular Problems A history of cardiovascular problems should always be determined since some may constitute contraindications to performing the maneuvers. Induced bronchospasm causes increased ventilation-perfusion mismatching, which can result in arterial hypoxemia[53,54] leading to compensatory changes in blood pressure, heart rate, and cardiac output,[55,56] increasing cardiovascular stress. This, in turn, may precipitate cardiovascular events in individuals with uncontrolled hypertension (systolic blood pressure [BP] >200 mm Hg, or diastolic BP >100 mm Hg) or recent (ie, less than 3 months) heart attack or stroke.

Pregnancy and Nursing Mothers Methacholine is a pregnancy category C drug, which indicates that animal reproductive studies have not been performed, so the effect on fetal abnormalities remains to be determined. It is not known whether methacholine is excreted in breast milk. In general, methacholine inhalation testing should be avoided during pregnancy and nursing.

Cholinesterase Inhibitor Medication Current use of cholinesterase inhibitor medication, such as neostigmine given to patients with myasthenia gravis, is a contraindication to methacholine inhalation testing.

Safety of Methacholine Testing

Since methacholine can cause bronchoconstriction, it is important to ensure the safety of patients and technicians during the testing procedures. Resuscitation equipment and medications to treat severe bronchospasm, including epinephrine and atropine for subcutaneous administration, as well as oxygen, salbutamol, and ipratropium, must be available in the testing area.

Thousands of methacholine inhalational challenges have been performed with no serious side effects, although transient side effects such as cough, wheeze, chest tightness, and mild dyspnea are common.[49,50,57–62] For example, fewer than 20% of 700 subjects undergoing histamine challenge for occupational lung disease reported cough, chest tightness, or flushing.[63] Delayed responses to methacholine have not ben reported with usual clinical testing. There have been no reports of fatality during or following a methacholine inhalation test, although fatalities have occurred with specific antigen challenge[64] and distilled water challenge.[65] Technician exposure to methacholine can be minimized by adequate room ventilation (at least two complete air exchanges per hour), use of fume hoods, or by using the dosimeter technique. Technicians with known active asthma should not perform methacholine tests.

Patient Preparation

Individuals should be given a list of items and medications to avoid prior to testing (Table 62-2). It is important also to take into account factors that may increase airway hyperresponsiveness when determining the timing of methacholine inhalation tests. Respiratory infections in particular may increase airway hyperresponsiveness for up to 6 weeks.[66,67]

Methacholine Preparation

Methacholine (acetyl-β-methylcholine chloride) is available as a dry, crystalline powder and is the agent of choice for nonspecific bronchoprovocation testing. A US Food and Drug Administration–approved formulation (Provocholine) is also available in prepackaged vials that do not require refrigeration. Methacholine powder is very hydroscopic and should be stored with a desiccator in the freezer. Phenol is sometimes added to the sterile saline diluent as a preservative to reduce bacterial contamination, but there is no evidence that this is necessary.[68] Methacholine solutions with concentrations greater than 0.3 mg/mL ($pH<6$) remain stable for at least 3 months when stored in the refrigerator (4°C),[68–70] but this is not necessarily the case for lower concentrations of methacholine, which have a higher pH. Methacholine solutions should be warmed to room temperature prior to testing. Since the concentration will change during nebulization,[71] the nebulizer output should be calibrated and adjusted.

Procedure for Methacholine Inhalation Testing

The basic procedures for methacholine testing have been published by the American Thoracic Society[2,72] and the Canadian Thoracic Society.[42,73] The two most widely used techniques are described briefly.

Two-Minute Tidal Breathing Dosing Protocol A series of 10 methacholine solutions prepared in twofold concentrating intervals ranging from 0.03 to 16 mg/mL are prepared in sterile vials. Baseline spirometry is performed and a target FEV_1 indicating a 20% fall in FEV_1 is calculated. The solutions (3 mL) are administered via a Wright Nebulizer with an output of 0.13 mL/min ± 10%. The subject breathes in the solution (tidal breathing) for 2 minutes via a mouthpiece. Alternatively, a face mask with a nose clip may be used and may be easier for some individuals.[74] FEV_1 is measured at 30 seconds and 90 seconds after completion of nebulization, using a maximum of three to four

maneuvers to obtain an acceptable FEV_1 and taking no more than 3 minutes to perform the maneuvers. The highest FEV_1 from an acceptable maneuver is reported. The time interval between the start of subsequent concentrations should be less than 5 minutes to keep the cumulative effect of methacholine concentrations constant.

Increasing twofold concentrations of methacholine are administered until the FEV_1 falls more than 20% from baseline or the highest concentration is given. Salbutamol is then administered to reverse any bronchoconstriction.

Five-Breath Dosimeter Protocol Five doses of methacholine solution (2 mL) are prepared in fourfold concentration intervals ranging from 0.0625 to 16 mg/mL. Subjects are instructed to inhale slowly at the end of tidal breathing exhalation (functional residual capacity) to total lung capacity over a 5-second interval and then to breath-hold for another 5 seconds. Five such inspiratory capacity inhalations are performed at each concentration during a maximum of 2 minutes.

Determination of the dose that provokes a 20% drop in FEV_1 is performed as described above and is referred to as the PD_{20}. Generally, a PD_{20} of 8 mg/mL methacholine or less is considered a positive test. Nebulizers used for this technique should deliver 9 μL ±10% of solution per 0.6 s activation during inhalation.[75] The DeVilbiss model 646 nebulizer is commonly used, but the interunit output variability is high,[76,77] so each unit's output must be checked. The extra vent on this nebulizer should be permanently closed for the methacholine inhalation test to ensure unit output.[78] The two methods appear to give similar results, perhaps as much by chance as by design.

The 2-minute tidal breathing protocol may be shortened by starting at a high initial concentration of methacholine. For a diagnostic test in a subject with normal lung function and no response to diluent, a starting dose of 1 mg/mL is safe.[73] Also, if the FEV_1 has fallen less than 5% after a dose of methacholine, a fourfold increase in dosage is safe.

The use of a diluent step is controversial.[72] Most current protocols start with a diluent step. Advantages of this step include the opportunity for the subject to learn the testing technique and better comparison with reference data, which are generally performed with a diluent step. However, the use of a diluent does not improve test safety, adds 5 minutes to the test, and does not affect the PC_{20}.[79] Only 1% of subjects demonstrate a fall in FEV_1 of greater than 20%, and the clinical significance is unknown.[80] When a diluent step is used, the postdiluent FEV_1 is the reference point for comparison.

Outcome Measures

Change in FEV_1 is the primary outcome measure for methacholine inhalational challenge testing. Measures of airway resistance (R_{aw}) or specific conductance (S_{gaw}) are alternatives when subjects cannot perform acceptable spirometric measurements.[81,82] These measurements parallel changes in FEV_1 but are much more variable, so that a 45% change is required for a positive test.

Forced oscillation techniques have been assessed more recently[83,84] and do not require patient effort but should be restricted to laboratories with expertise in their use. In healthy or mildly asthmatic persons, the deep inhalation preceding a forced expiratory maneuver causes transient bronchodilatation lasting up to 6 minutes,[85–87] which may mask underlying bronchial hyperresponsiveness. Forced oscillation techniques may eventually prove useful in this clinical setting. FEV_1 still remains the best parameter for discriminating healthy persons from those with asthma.[88,89] A decrease in FVC during methacholine challenge testing correlates with asthma severity.[90]

Table 62-2 Items to Avoid Prior to Methacholine Testing

Items	*Time interval prior to study*	*Reference*
Medications		
Short-acting inhaled bronchodilators:		
metaproterenol, albuterol, or terbutaline	8 h	137, 138
Medium-acting bronchodilators:		
ipratropium	24 h	139, 140
Long-acting inhaled bronchodilators:		
salmeterol, formoterol, tiotropium	48 h (perhaps 1 wk)	141, 142
Oral bronchodilators		
Theophylline:		143, 144
Liquid	12 h	
Intermediate-acting	24 h	
Long-acting	48 h	
β_2-Agonist tablets		
Standard	12 h	
Long-acting	24 h	
Cromolyn sodium	8 h	
Nedocromil	48 h	
Hydroxazine, cetirizine	3 d	
Leukotriene antagonists	24 h	
Foods		145
Coffee, tea, cola drinks, chocolate	Day of study	

Oral or inhaled corticosteroids should not be routinely withheld, but their antiinflammatory effect may decrease bronchial responsiveness.

Interpretation of Methacholine Inhalational Challenge Tests

The percent change in FEV_1 compared with the reference value is plotted on the ordinate versus the log concentration of methacholine on the abscissa. Whether the degree of airway responsiveness can determine if an individual has asthma depends on whether the methacholine test is properly performed, whether the test is not affected by modifiers (medications, respiratory infections, allergen exposure, etc), and on whether the individual's pretest probability of having asthma can be reasonably estimated.[91–93] The pretest probability is the clinical estimate of asthma, based on a patient's medical history, physical examination, and laboratory data and expressed in fractional terms. The difference between the probability of having asthma before and after the bronchoprovocation test is called the final diagnostic gain and represents the contribution of the test to the diagnosis. The maximal positive diagnostic gain is achieved when the pretest probability is 0.48 and the maximum negative diagnostic gain occurs with a pretest probability of 0.7. For example, if the pretest probability of asthma is less than 70% and the PC_{20} is >16 mg/mL, there is a high degree of certainty that the individual does not currently have asthma.

In general, the sensitivity of a positive methacholine inhalation test to confirm a diagnosis of asthma is 86%.[94] The positive predictive value of a methacholine challenge test is limited by false-positive results in allergic rhinitis, COPD, bronchitis, congestive heart failure, and cystic fibrosis.[72]

In asthmatic subjects it is difficult to use the degree of severity of airway hyperresponsiveness to determine the degree of asthma severity because although these parameters correlate significantly, the relationship is not strong enough to predict asthma severity in individuals.[95–99] The significance of a change in PC_{20} is also difficult to interpret once there is a change in baseline FEV_1, that is, after successful therapy.

ASYMPTOMATIC INDIVIDUALS WITH A POSITIVE TEST

There are individuals who have a positive test without asthma symptoms, either because they are "poor perceivers" of symptoms, do not recognize such symptoms as abnormal, have another airway abnormality (post–viral respiratory infection, cigarette smoking), or have subclinical asthma that may develop into clinical asthma in the future.[100,101] Asymptomatic BHR may develop into asthma in 15 to 45% of persons during 2- to 3-year follow-up.[102,103]

SYMPTOMATIC INDIVIDUALS WITH A NEGATIVE TEST

Subjects who develop a late asthmatic response to antigen inhalation have hyperresponsive airways that return to normal gradually and may therefore be nonresponsive at the time of testing.

Persons with vocal cord dysfunction or central airway obstruction can mimic asthma but generally have negative methacholine inhalation tests.

ADENOSINE AIRWAY RESPONSIVENESS

Recently there has been interest in the role of adenosine in mediating airway hyperreactivity, particularly since the finding in 1983 that atopic and nonatopic asthmatics had airway hyperresponsiveness to inhaled adenosine.[38] Hyperresponsiveness to adenosine is also found in individuals with COPD[104] and allergic rhinitis without asthma.[105] Individuals with atopic asthma respond to much lower doses of adenosine than do healthy individuals, individuals with allergic rhinitis,[106] smokers,[107] or individuals with COPD.[108]

Adenosine is a purine nucleoside that mediates a variety of cellular responses relevant to asthma and COPD through interaction with specific receptors in lung tissue.[109,110] Adenosine is released as a result of hydrolysis of adenosine nucleotides whenever lung tissues are damaged. It is normally rapidly phosphorylated and metabolized in the lung, but if tissue damage is extensive, high levels of adenosine can accumulate in the lung tissues of asthmatics.

Adenosine is believed to act predominantly indirectly through the release of inflammatory mediators or stimulation of neural pathways through activation of purinergic receptors expressed on intermediary inflammatory cells such as mast cells or on afferent nerve endings, leading to smooth muscle contraction.

Although methacholine and histamine have become gold standards as provocation agents used to measure airway hyperresponsiveness, the airway response to adenosine appears to more closely reflect the degree of airway inflammation and in particular has been correlated with the presence of sputum eosinophilia in asthma and COPD.[111] Adenosine airway reactivity improves after effective antiinflammatory treatment in asthma but not in COPD,[112] suggesting that it may correlate better than direct stimuli such as methacholine and histamine with airway inflammation.

In children, bronchoprovocation tests with inhaled adenosine monophosphate appear to be considerably more specific and sensitive than methacholine at discriminating asthma from pediatric chronic obstructive lung disorders such as cystic fibrosis, bronchiolitis, and bronchiectasis.[113] Adenosine bronchoprovocation testing is more specific than histamine in establishing allergic factors in preschool children with wheeze. Furthermore, regular treatment of asthmatic children with inhaled corticosteroids results in a significant reduction in responsiveness to adenosine monophosphate but not to methacholine or bradykinin responsiveness.[114] Two recent studies suggest, however, that adenosine responsiveness is a more general marker for airway mucosal injury rather than a reflection of allergic asthma inflammation specifically.[104,115]

At this juncture, standardized dose-response criteria with specific cutoff points for adenosine PC_{20} are not available, so

the role of adenosine challenge remains in the realm of investigation of disease mechanisms rather than in clinical practice.

EUCAPNIC VOLUNTARY HYPERVENTILATION AND AIRWAY HYPERRESPONSIVENESS

Eucapnic voluntary hyperventilation (EVH) is an indirect airway stimulus that can be used to measure airway responsiveness. The test involves inhaling dry air containing 5% carbon dioxide (to maintain isocapnic conditions) while breathing levels of ventilation comparable to exercise. A variety of protocols have been proposed, and results vary with the duration and intensity of the ventilation challenge. A recent study has shown that the bronchoconstriction obtained from an uninterrupted EVH challenge of 6 minutes duration at a target minute ventilation of $30 \times FEV_1$ is safe and reproducible[116] and it has been proposed that this protocol be adopted as a standard.

Recently this technique has been proposed as an alternative to exercise testing in the field or in the laboratory to identify individuals with exercise-induced bronchoconstriction, in particular, elite athletes. In contradistinction to exercise testing in the field or laboratory, the EVH technique has the advantages of reproducibility and the ability to reach the high levels of ventilation required to induce bronchoconstriction with dry air.[116] Another study suggests that more individuals who are hyperresponsive to dry air can be identified by EVH compared with exercise challenge tests in the field and thus have the potential advantage to identify individuals with exercise-induced asthma who escape detection by standard or field exercise protocols.[40] Nevertheless, there is as yet no commonly accepted standardized technique, and EVH remains largely a research tool at this time.

EXERCISE CHALLENGE

Exercise can induce airway narrowing in people with asthma, which is known as exercise-induced bronchoconstriction (EIB) and occurs through a mechanism caused by water loss or dehydration of the airways.[117–120] Thermal or osmotic effects of dehydration stimulate the release of inflammatory mediators such as histamine and cysteinyl leukotrienes.[121–124]

The exercise challenge test is used to diagnose EIB in people with asthma with a history of dyspnea after exercise. Exercise testing can be used as well to determine the effectiveness of medications designed to prevent EIB.

Contraindications to exercise testing are the same as for methacholine inhalation testing and, in addition, persons with unstable cardiac ischemia or malignant arrhythmias should not undergo testing. Vigorous exercise should not be done for at least 4 hours prior to testing as such exercise may render a subject refractory to subsequent challenge.

The test proceeds in the following general manner. Bronchodilators are withheld as per methacholine inhalation tests and antihistamines are withheld for 48 hours. Baseline spirometry is determined and the individual is then exercised on a treadmill or cycle ergometer to about 85% of the predicted maximum heart rate, which is sustained for 6 to 8 minutes. The target heart rate should be reached within 4 minutes because the determining factor for the induction of EIB is the rate of water loss from the airways. A refractory response may occur if the exercise is prolonged at submaximal work loads.

MANNITOL AND AIRWAY HYPERRESPONSIVENESS

The inhalation of dry powder mannitol has been developed as a novel indirect stimulus for assessing AHR in people with asthma.[125] From a practical point of view, it does not require a nebulizer and can be performed outside the laboratory environment using a simple handheld inhaler device. The test is a cumulative dose challenge that is performed by asking the patient to inhale increasing doses consisting of 0 (empty capsule acting as placebo), 5, 10, 20, 40, 80, and 160 mg of mannitol. The doses of 80 mg and 160 are administered in multiple doses of 40 mg capsules, and the total number of capsules containing mannitol required for the challenge test is 18.[126] Moreover, when compared with another indirect challenge, such as exercise, mannitol results in a more controlled sequential reduction in lung function. The challenge is completed when a 15% fall in FEV_1 is documented or a cumulative dose of 635 mg has been administered, reducing the chance of excessive airway narrowing.

Mannitol responsiveness is effective at identifying asthmatic subjects who are also responsive to hypertonic saline, eucapanic hyperpnea, and exercise and those who will respond to inhaled steroids. Mannitol responsiveness is attenuated following treatment with inhaled steroid. Responsiveness to mannitol can be used to predict risk of exacerbation during steroid withdrawal trials.[127]

OBESITY AND AIRWAY HYPERRESPONSIVENESS

There may be an association between the rising prevalence of asthma in developed nations and the rising prevalence of obesity. Several reports have found a relationship between obesity and asthma in children and women.[128-130] A recent study also has a strong relationship between obesity in men and development of airway hyperresponsiveness.[131] The airway hyperresponsiveness developed particularly in adult males who gained weight during the period of observation.

Various theories have been proposed to explain the association between obesity and airway hyperresponsiveness and asthma. Obesity results in reductions in lung volumes resulting in decreased airway caliber, which is a known determinant of airway hyperresponsiveness.[132,133] Breathing at lower tidal volume as a consequence of obesity leads to higher contractile responses of airway smooth muscle. Furthermore, there is mounting evidence to suggest that systemic inflammation can occur in obese subjects, as indicated by increased levels of proinflammatory cytokines in

the circulation. These proinflammatory cytokines provide a possible explanation by which obesity may predispose to airway hyperresponsiveness or asthma.[134–136]

CONCLUSIONS

The ability to measure airway responsiveness to inhaled bronchoconstrictor agonists, such as methacholine, remains an important tool for the diagnosis of asthma, particularly in individuals suspected to have asthma but in whom airflow obstruction is not found on spirometric assessment. Methacholine challenge testing is standardized, is reproducible, and can be safely performed in pulmonary function laboratories.

Indirect tests of airway responsiveness, including adenosine, exercise, and eucapnic voluntary hyperventilation with dry air, have allowed for a better understanding of the pathophysiology of airway hyperresponsiveness but have not yet been standardized or tested in large enough populations to be applicable to common clinical practice.

The role of airway inflammation in the development of asymptomatic, variable, and persistent airway hyperresponsiveness is primordial, but the factors responsible for the range of such responses are not fully understood and require further investigation.

REFERENCES

1. Cockcroft DW. Airway responsiveness. In: Barnes PJ, Grustein MM, Leff AR, Woolcock AJ, editors. Asthma. New York: Lippincott-Raven Publishers; 1997.
2. Sterk PJ, Fabbri LM, Quanjer PH, et al . Airway responsiveness: standardized challenge testing with pharmacological, physical and sensitizing stimuli in adults. Statement of the European Respiratory Society. Eur Respir J 1994;6 Suppl 16:52–83.
3. Sterk PJ, Bel EH. The shape of the dose response curve to inhaled bronchoconstriction agents in asthma and in chronic obstructive pulmonary disease (COPD) and asthma. Am Rev Respir Dis 1991;143:1433–7.
4. Jubber AS, Foster RW, Hassan NACM, et al. Airway response to inhaled methacholine in normal human subjects. Pulm Pharmacol 1993;6:177–84.
5. Woolcock AJ, Salome CM, Yan K. The shape of the dose response curve to histamine in asthmatic and normal subjects. Am Rev Respir Dis 1984;130:71–5.
6. Moreno RH, Hogg JC, Pare PD. Mechanics of airway narrowing. Am Rev Respir Dis 1986;133:1171–80.
7. Macklem PT. A theoretical analysis of the effect of airway smooth muscle load on airway narrowing. Am J Respir Crit Care Med 1996;153:83–9.
8. Pare PD, Bai TR. The consequences of chronic allergic inflammation. Thorax 1995;50:328–32.
9. James A. Limited airway narrowing: why does not everyone have asthma? Eur Respir J 1994;7:1210–2.
10. Sterk PJ, Daniel EE, Zand N, Hargreave FE. Limited bronchoconstriction to methacholine using partial flow-volume curves in non-asthmatic subjects. Am Rev Respir Dis 1985;132:272–7.
11. Sterk PJ, Timmers MC, Bel EH, Dijkman JH. The combined effects of histamine and methacholine on the maximal degree of airway narrowing in normal humans in vivo. Eur Respir J 1988;1:34–40.
12. Sterk PJ, Daniel EE, Zamel N, Hargreave FE. Limited maximal airway narrowing in nonasthmatic subjects. Role of neural control and prostaglandin release. Am Rev Respir Dis 1988;132:865–70.
13. Wiggs BR, Moreno R, Hogg JC, et al. A model of the mechanics of airway narrowing. J Appl Physiol 1990;69:849–60.
14. Macklem PT. Mechanical factors determining minimum bronchoconstriction. Eur Respir J 1989;2 Suppl 6;516S–9S.
15. Okazawa M, Pare P, Road J. Tracheal smooth muscle mechanics in vivo. J Appl Physiol 1990;68:209–19.
16. Bates JHT, Martin JG. A theoretical study of the effect of airway smooth muscle orientation on bronchoconstriction. J Appl Physiol 1990;69:995–1001.
17. Hoppin FG. Parenchymal mechanics and asthma. Chest 1995;107 Suppl 3:140S–4S.
18. Sterk PJ, Bel EH. Bronchial hyperresponsiveness: the need for a distinction between hypersensitivity and excessive airway narrowing. Eur Respir J 1989;2:267–74.
19. Ishida K, Pare PD, Thomson RJ, Schellenberg RR. Increased in vitro responses of tracheal smooth muscle from hyperresponsive guinea pigs. J Appl Physiol 1990; 68:1216–320.
20. Hirst SJ, Twart CHC. The proliferative response of airway smooth muscle. Clin Exp Allergy 1992;22:907–15.
21. Knox AJ. Airway re-modeling in asthma: role of airway smooth muscle. Clin Sci 1994;86:647–52.
22. Jiang E, Rao K, Halayko AJ, et al. Ragweed sensitization-induced increase of myosin light-chain kinase content in canine airway smooth muscle. Am J Respir Cell Mol Biol 1992;7:567–73.
23. Mitchel RW, Ruhlmann E, Magnussen H, et al. Passive sensitization of human bronchi augments smooth muscle shortening velocity and capacity. Am J Physiol 1994;267:L218–L22.
24. Lambert RK, Wiggs BR, Kuwano K, et al. Functional significance of increased airway smooth muscle in asthma and COPD. J Appl Physiol 1993;74:2771–81.
25. Ebina M. Takahashi T, Chiba T, Motomiya M. Cellular hypertrophy and hyperplasia of airway smooth muscles underlying bronchial asthma. A 3-D morphometric study. Am Rev Respir Dis 1993;148:720–6.
26. Smith PG, Janiga KE, Bruce MC. Stain increases airway smooth muscle cell proliferation. Am J Respir Cell Mol Biol 1994;10:85–90.
27. Ding DJ, Martin JG, Macklem PT. Effects of lung volume on maximal methacholine-induced bronchoconstriction in normal humans. J Appl Physiol 1987;62:1324–30.
28. Persson CGA. Plasma exudation in the airways: mechanism and function. Eur Respir J 1991;4:1268–74.
29. Yayo D, Butler JP, Bastacky J, et al. Amplification of airway constriction due to liquid filling of airway interstices. J Appl Physiol 1990;69:2873–84.
30. Bramley AM, Thomson RJ, Roberts CR, et al. Hypothesis: excessive bronchoconstriction in asthma is due to decreased airway elastance. Eur Respir J 1994;7:337–41.
31. Lambert RK, Codd SL, Alley MR, et al. Physical determinants of bronchial mucosol folding. J Appl Physiol 1994;77: 1206–16.
32. Beasley R, Roche WR, Roberts JA, Holgate ST. Cellular events in the bronchi in mild asthma and after bronchial provocation. Am Rev Respir Dis 1989;139:306–17.
33. Boulet LP. Asymptomatic airways hyperresponsiveness: a curiosity or an opportunity to prevent asthma. Am J Respir Crit Care Med 2003;167:371–8.
34. Ryan G, Latimer KM, Dolovich J et al. Bronchial response to histamine: relationship to diurnal variation of peak flow rate, improvement after bronchodilator, and airway caliber. Thorax 1982:37:423–9.

35. Barnes PJ. Anti-leukotrienes: here to stay? Curr Opin Pharmacol 2003;3:257–63.
36. Powell WS. A novel PGD(2) receptor expressed in eosinophils. Prostaglandins Leukot Essent Fatty Acids 2003;69:179–85.
37. Alexis N, Urch B, Tarlo S, et al. Cyclooxygenase metabolites play a different role in ozone-induced pulmonary function decline in asthmatics compared to normals. Inhal Toxicol 2000;12:1205–24.
38. Cushley MJ, Tattersfield AE, Holgate ST. Inhaled adenosine and guanosine on airway resistance in normal and asthmatic subjects. Br J Clin Pharmacol 1983;15:161–5.
39. Eliasson AH, Phillips YY, Rajagopal KR, Howard RS. Sensitivity and specificity of bronchial provocation testing. An evaluation of four techniques in exercise-induced bronchospasm. Chest 1992;102:347–55.
40. Rundell KW, Anderson SD, Spiering BA, Judelson MA. Field exercise vs. laboratory eucapnic voluntary hyperventilation to identify airway hyperresponsiveness in elite cold weather athletes. Chest 2004;125:909–15.
41. Anderson SD, Brannan JD. Methods for "indirect" challenge tests including exercise, eucapnic voluntary hyperpnea, and hypertonic aerosols. Clin Rev Allergy Immunol 2003;24:27–54.
42. Hargreave FE, Ryan G, Thomson NC. Bronchial responsiveness to histamine or methacholine in asthma: measurement and clinical significance. J Allergy Clin Immunol 1981;68:347.
43. Chatham M, Blacker ER, Smith PL, et al. A comparison of histamine, methacholine, and exercise airway reactivity in normal and asthmatic patient. Am Rev Respir Dis 1982;126:235.
44. Cockcroft DW, Hargreave FE. Airways hyperresponsiveness: definition, measurement and clinical relevance. In: Kaliner MA, Barnes PJ, C. G, editors. 1991.
45. Postma DS, Kerstjens HA. Characteristics of airway hyperresponsiveness in asthma and chronic obstructive pulmonary disease. Am J Respir Crit Care Med 1998;158 Suppl: S187–92.
46. Juniper EF, Frith PA, Hargreave FE. Airways responsiveness to histamine and methacholine: relationship to minimum treatment to control symptoms of asthma. Thorax 1991;36:575–9.
47. Kraan J, Koeter GH, van der Mark TW, et al. Changes in bronchial hyperreactivity induced by 4 weeks of treatment with antiasthmatic drugs in patients with allergic asthma: a comparison between budesonide and terbutaline. J Allergy Clin Immunol 1985;76:628–36.
48. Kerrebijn KF, van Essen-Zandvliet EE, Neijens HJ. Effect of long-term treatment with inhaled corticosteroids and beta-agonists on the bronchial responsiveness in children with asthma. J Allergy Clin Immunol 1987;79:653–9.
49. Martin RJ, Wanger JS, Irvin CG, Bartelson BB, and the Asthma Clinical Research Network (ACRN). Methacholine challenge testing: safety of low starting FEV_1. Chest 1997;112:53–6.
50. Tashkin DP, Altose MD, Bleecker ER, et al, and the Lung Health Research Group. The Lung Health Study: airway responsiveness to inhaled methacholine in smokers with mild to moderate airflow limitation. Am Rev Respir Dis 1992;145:301–10.
51. National Asthma Education and Prevention Program. Expert Panel Report 2: guidelines for the diagnosis and management of asthma. Washington DC: US Government Printing Office; 1997. NHLBI Publication No. 97-4051.
52. Scott GC, Braun SR. A survey of the current use and methods of analysis of bronchoprovocational challenges. Chest 1991;100:322–8.
53. Rodriquez-Roisin R, Ferrer A, Navajas D, et al. Ventilation-perfusion mismatch after methacholine challenge in patients with mild bronchial asthma. Am Rev Respir Dis 1991;144:88–94.
54. Roca J, Rodriguez-Roisin R. Editorial: asthma, allergen challenge and gas exchange. Eur Respir J 1992;5:1171–2.
55. Goldman MD, Mathieu M, Montely JM, et al. Inspiratory fall in systolic pressure in normal and asthmatic subjects. Am J Respir Crit Care Med 1995;151:743–50.
56. Stewart IC, Parker A, Catterall JR, et al. Effect of bronchial challenge on breathing patterns and arterial oxygenation in stable asthma. Chest 1989;95:65–70.
57. Shapiro GG, Simon RA, and for the American Academy of Allergy and Immunology Bronchoprovocation Committee. Bronchoprovocation committee report. J Allergy Clin Immunol 1992;89:775–8.
58. Scott GC, Braun SR. A survey of the current use and methods of analysis of bronchoprovocational challenges. Chest 1991;100:322–8.
59. Weiss ST, Tager IB, Weiss JW, et al. Airways responsiveness in a population sample of adults and children. Am Rev Respir Dis 1984;129:898–902.
60. Rijcken B, Schouten JP, Weiss ST, et al. The relationship between airway responsiveness to histamine and pulmonary function level in a random population sample. Am Rev Respir Dis 1988;137:826–32.
61. Baake PS, Baste V, Gulsvik A. Bronchial responsiveness in a Norwegian community. Am Rev Respir Dis 1991;143:317–22.
62. Peat JK, Salome CM, Xuan W. On adjusting measurements of airway responsiveness for lung size and airway caliber. Am J Respir Crit Care Med 1996;154:870–5.
63. Kremer AM, Pal TM, Oldenziel M, et al. Use and safety of a shortened histamine challenge test in an occupational study. Eur Respir J 1995;5:737–41.
64. Fish JE. Bronchial challenge testing. In: Middleton E, editor. Allergy: principles and practice. 4th ed. St. Louis (MO): Mosby-Year Book; 1993.
65. Seatta M, Di Stefano A, Turato G, et al. Fatal asthma attack during an inhalation challenge with ultrasonically nebulized distilled water. J Allergy Clin Immunol 1995;95:1285–7.
66. Empey DW, Laitinen LA, Jac L, et al. Mechanisms of bronchial hyperreactivity in normal subjects after upper respiratory tract infection. Am Rev Respir Dis 1976;113:131–9.
67. Cheung D, Dick EC, Timmers EC, et al. Rhinovirus inhalation causes long-lasting excessive airway narrowing in response to methacholine in asthmatic subjects in vivo. Am J Respir Crit Care Med 1995;152:1490–6.
68. Hayes RD, Beach JR, Rutherford DM, Sim MR. Stability of methacholine chloride solutions under different storage conditions over a 9 month period. Eur Respir J 1998;11:946–8.
69. Watson BL, Cormier RA, Harbeck RJ. Effect of pH on the stability of methacholine chloride in solution. Respir Med 1998;92:588–92.
70. Pratter MR, Woodman TF, Irwin RS, Johnson B. Stability of stored methacholine chloride solutions: clinically useful information. Am Rev Respir Dis 1982;126:717–9.
71. MacDonald NC, Whitmore CK, Makoid MC, Cobby J. Stability of methacholine chloride in bronchial provocation test solutions. Am J Hosp Pharmacy 1981;38:868–71.
72. Crapo RO, Casaburi R, Coates AL, et al. Guidelines for methacholine and exercise challenge testing-1999. This official statement of the American Thoracic Society was adopted by the ATS Board of Directors, July 1999. Am J Respir Crit Care Med 2000;161:309–29.
73. Juniper EF, Cockcroft DW, Hargreave FE. Tidal breathing method. In: Histamine and methacholine inhalation tests: laboratory procedure and standardization. 2nd ed. Lund (Sweden): Astra Draco AB; 1994.
74. Juniper EF, Syty-Golda M, Hargreave FE. Histamine inhalation tests: inhalation of aerosol via a facemask versus a valve box with mouthpiece. Thorax 1984;39:556–7.

75. Ryan G, Dolovich MB, Obminski G, et al. Standardization of inhalation provocation tests: influence of nebulizer output, particle size, and method of inhalation. J Allergy Clin Immunol 1981;67:156–61.
76. Massey DG, Miyauchi D, Massey GF. Nebulizer function. Bull Eur Physiopathol Respir 1982;18:665–71.
77. Hollie MC, Malone RA, Skufca RM, Nelson HS. Extreme variability in aerosol output of the DeVilbiss 646 jet nebulizer. Chest 1991;100:1339–44.
78. Dolovich MB. Technical factors influencing response to challenge aerosols. In: Hargreave FE, Woolcock AJ, editors. Airway responsiveness: measurement and interpretation. Mississauga (ON): Astra Pharmaceuticals; 1985.
79. Connolly MJ, Avery AJ, Walters EH, Hendrick DJ. The use of sequential doses of inhaled histamine in the measurement of bronchial responsiveness: cumulative effect and distortion produced by shortening the protocol. J Allergy Clin Immunol 1988;82:863–8.
80. Wanger J, Irvin CG. Responses to diluent inhalation in clinical methacholine challenges [abstract]. Am J Respir Crit Care Med 1998;157(Suppl):A672.
81. Cockcroft DW, Berscheid BA. Measurement of responsiveness to inhaled histamine: comparison of FEV_1 and sGaw. Ann Allergy 1983:51:374–7.
82. Habib MP, Paré PD, Engel LA. Variability of airways response to inhaled histamine in normal subjects. J Appl Physiol Respir Environ Exercise Physiol 1979:47:51–8.
83. Wilson NM, Bridge P, Phagoo SB, Silverman M. The measurement of methacholine responsiveness in 5 year old children: three methods compared. Eur Respir J 1995;8: 364–70.
84. Klug B, Bisgaard H. Measurement of lung function in awake 2-4 year old asthmatic children during methacholine challenge and acute asthma: a comparison of the impulse oscillation technique, the interrupter technique and transcutaneous measurement versus whole-body plethysmograph. Pediatr Pulmonol 1996;21:290–300.
85. Parham WM, Shepard RH, Norman PS, Fish JE. Analysis of the time course and magnitude of lung inflation effects on airway zone: relation to airway reactivity. Am Rev Respir Dis 1983;128:240–5.
86. Malmberg P, Larsson K, Sundblad BM, Zhiping W. Importance of the time interval between FEV_1 measurements in a methacholine provocation test. Eur Respir J 1993;6:680–6.
87. Pellegrino R, Sterk PJ, Sont JK, Brusasco V. Assessing the effect of deep inhalation on airway calibre: a novel approach to lung function in bronchial asthma and COPD. Eur Respir J 1998;12:1219–27.
88. Michoud MC, Ghezzo H, Amyot R. A comparison of pulmonary function tests used for bronchial challenges. Bull Eur Physiopathol Respir 1982;18:609–21.
89. Fish JE, Kelley JF. Measurements of responsiveness in bronchoprovocation testing. J Allergy Clin Immunol 1979;64:592–6.
90. Gibbons WJ, Sharma A, Lougheed D, Macklem PT. Detection of excessive bronchoconstriction in asthma. Am J Respir Crit Care Med 1996;153:582–9.
91. Perpiña M, Pellicer C, deDiego A, et al. Diagnostic value of the bronchial provocation test with methacholine in asthma: bayesian analysis approach. Chest 1993;104:149–54.
92. Gilbert R, Auchincloss JH. Post-test probability of asthma following methacholine challenge. Chest 1990;97:562–5.
93. Cockcroft DW, Murdock KY, Berscheid BA, Gore BP. Sensitivity and specificity of histamine PC_{20} determination in a random selection of young college students. J Allergy Clin Immunol 1992;89:23–30.
94. Simon RA. Sulfite challenge for the diagnosis of sensitivity. Allergy Proc 1989;10:357.
95. Cockcroft DW, Killian DN, Mellon JJ, Hargreave FE. Bronchial reactivity to inhaled histamine: a method and clinical survey. Clin Allergy 1977;7:235–43.
96. Woolcock AJ, Peat JK, Salome CM, et al. Prevalence of bronchial hyperresponsiveness and asthma in a rural adult population. Thorax 1987;42:361–8.
97. Josephs LK, Gregg I, Mullee MA, Holgate ST. Nonspecific bronchial reactivity and its relationship to the clinical expression of asthma: a longitudinal study. Am Rev Respir Dis 1989;140:350–7.
98. Chabra SK, Gaur SN, Khanna AK. Clinical significance of nonspecific bronchial hyperresponsiveness in asthma. Chest 1989;96:596–600.
99. Avital A, Noviski N, Bar-Yishay E, et al. Nonspecific bronchial reactivity in asthmatic children depends on severity but not on age. Am Rev Respir Dis 1991;144:36–8.
100. Hopp RJ, Townley RG, Biven RE, et al. The presence of airway reactivity before the development of asthma. Am Rev Respir Dis 1990;141:2–8.
101. Jansen DF, Timens W, Kraan J, et al. Asymptomatic bronchial hyperresponsiveness and asthma. Respir Med 1997;91: 121–13.
102. Zhong NS, Chen RC, Yang MO, et al. Is asymptomatic bronchial hyperresponsiveness an indication of potential asthma? A two year follow-up of young students with bronchial hyperresponsiveness. Chest 1992;102:1104–9, 158.
103. Laprise C, Boulet LP. Asymptomatic airway hyperresponsiveness: a three year follow-up. Am J Respir Crit Care Med 1997;156:403–9.
104. Oosterhoff Y, Jansen MA, Postma DS, Koeter GH. Airway responsiveness to adenosine 5'-monophosphate in smokers and nonsmokers with atopic asthma. J Allergy Clin Immunol 1993;92:773–6.
105. Polosa R, Ciamarra I, Mangano G, et al. Bronchial hyperresponsiveness and airway inflammation markers in nonasthmatics with allergic rhinitis. Eur Respir J 2000;15:30–5.
106. Prieto L, Gutierrez V, Uixera S, Bruno L. Concentrations of exhaled nitric oxide in asthmatics and subjects with allergic rhinitis sensitized to the same pollen allergen. Clin Exp Allergy 2002;32:1728–33.
107. Rutgers SR, Koeter GH, Van Der Mark TW, Postma DS. Protective effect of oral terfenadine and not inhaled ipratropium on adenosine 5'-monophosphate-induced bronchoconstriction in patients with COPD. Clin Exp Allergy 1999;29:1287–92.
108. Spicuzza L, Polosa R. Curr Opin Allergy Clin Immunol 2003;3: 65–9.
109. Meade CJ, Dumont I, Worrall L. Why do asthmatic subjects respond so strongly to inhaled adenosine? Life Sci 2001;69:1225–40.
110. Polosa R, Rorke S, Holgate ST. Evolving concepts on the value of adenosine hyperresponsiveness in asthma and chronic obstructive pulmonary disease. Thorax 2002;57:649–54.
111. Van Den Berge M, Meijer RJ, Kerstjens H, et al. PC_{20} adenosine 5'-monophosphate is more closely associated with airway inflammation in asthma than PC_{20} methacholine. Am J Respir Crit Care Med 2001;163:1546–50.
112. Van Den Berge M, Kerstjens HA, Meijer RJ, et al. Corticosteroid-induced improvement in the PC_{20} of adenosine monophosphate is more closely associated with reduction in airway inflammation than improvement in the PC_{20} of methacholine. Am J Respir Crit Care Med 2001;164: 1127–32.
113. Avital A, Springer C, Bar-Yishay E, Godfrey S. Adenosine, methacholine, and exercise challenges in children with asthma or paediatric chronic obstructive pulmonary disease. Thorax 1995;50:511–6.

114. Doull J, Sandall D, Smith S, et al. Differential inhibitory effect of regular inhaled corticosteroid on airway responsiveness to adenosine 5' monophosphate, methacholine, and bradykinin in symptomatic children with recurrent wheeze. Pediatr Pulmonol 1997;23:404–11.
115. Prieto L, Gutierrez V, Uixera S, Berto JM. Effect of cigarette smoking on airway responsiveness to adenosine 5'-monophosphate in subjects with allergic rhinitis. Chest 2003;123:993–7.
116. Argyros GJ, Roach JM, Hurwitz KM, et al. Eucapnic voluntary hyperventilation as a bronchoprovocation technique: development of a standard dosing schedule in asthmatics. Chest 1996;109:1520–4.
117. Chen WY, Horton DJ. Heat and water loss from the airways and exercise-induced asthma. Respiration 1977;34:305–13.
118. Strauss RH, McFadden ER, Ingram RH, et al. Influence of heat and humidity on the airway obstruction induced by exercise in asthma. J Clin Invest 1978;61:433–40.
119. McFadden ER, Ingram RH. Exercise-induced asthma. Observations on the initiating stimulus. N Engl J Med 1979;301:763–9.
120. Anderson SD, Schoeffel RE, Follet R, et al. Sensitivity to heat and water loss at rest and during exercise in asthmatic patients. Eur J Respir Dis 1982;63:459–71.
121. Finnerty JP, Holgate ST. Evidence for the roles of histamine and prostaglandins as mediators in exercise-induced asthma: the inhibitory effect of terfenadine and flurbiprofen alone and in combination. Eur Respir J 1990;3:540–7.
122. Randolph C. Exercise-induced asthma: update on pathophyiology, clinical diagnosis, and treatment. Curr Probl Pediatr 1997;27:53–77.
123. Reiss TF, Hill JB, Harman E, et al. Increased urinary excretion of LTE_4 after exercise and attenuation of exercise-induced bronchospasms by montelukast, a cysteinyl leukotreiene receptor antagonist. Thorax 1997;52:1030–5.
124. Leff JA, Busse WW, Pearlman D, et al. Montelukast, a leukotriene-receptor antagonist, for the treatment of mild asthma and exercise-induced bronchoconstriction. N Engl J Med 1998;339:147–52.
125. Anderson SD, Brannan J, Spring J, et al. A new method for bronchial-provocation testing in asthmatic subjects using a dry powder of mannitol. Am J Respir Crit Care Med 1997;156(3 Pt 1):758–65.
126. Leuppi JD, Brannan JD, Anderson SD. Bronchial provocation tests: the rationale for using inhaled mannitol as a test for airway hyperresponsiveness. Swiss Med Wkly 2002;132:151–8.
127. Brannan JD, Koskela H, Anderson SD, Chan HK. Budesonide reduces sensitivity and reactivity to inhaled mannitol in asthmatic subjects. Respirology 2002;7:37–44.
128. Gennuso J, Epstein LH, Paluch RA, Cerny F. The relationship between asthma and obesity in urban minority children and adolescents. Arch Pediatr Adolesc Med 1998;152:1197–200.
129. Luder E, Melnik TA, DiMaio M. Association of being overweight with greater asthma symptoms in inner city black and hispanic children. J Pediatr 1998;132:699–703.
130. Seidell JC, de Groot LC, van Sonsbeek JL, et al. Associations of moderate and severe overweight with self-reported illness and medical care in Dutch adults. Am J Public Health 1986;76:264–9.
131. Litonjua AA, Sparrow D, Celedon JC, et al. Association of body mass index with the development of methacholine airway hyperresponsiveness in men: the Normative Aging Study. Thorax 2002;57:581–5.
132. Chen Y, Horne SL, Dosman JA. Body weight and weight gain related to pulmonary function decline in adults: a six year follow up study. Thorax 1993;48:375–80.
133. Fredberg JJ. Airway smooth muscle in asthma: flirting with disaster. Eur Respir J 1998;12:1252–6.
134. Mohamed-Ali V, Goodrick S, Bulmer K, et al. Production of soluble tumor necrosis factor receptors by human subcutaneous adipose tissue in vivo. Am J Physiol 1999;277 (6 Pt 1):E971–5.
135. Bastard JP, Jardel C, Delattre J, et al. Evidence for a link between adipose tissue interleukin-6 content and serum C-reactive protein concentrations in obese subjects. Circulation 1999;27:2221–2.
136. Chung KF, Barnes PJ. Cytokines in asthma. Thorax 1999;54:825–57.
137. Ahrens RC, Bonham AC, Maxwell GA, Weinberger MM. A method for comparing the peak intensity and duration of action of aerosolized bronchodilators using bronchoprovocation with methacholine. Am Rev Respir Dis 1984;129:903–6.
138. Greenspon LW, Morrissey WL. Factors that contribute to inhibition of methacholine-induced bronchoconstriction. Am Rev Respir Dis 1986;133:735–9.
139. Crimi N, Palermo F, Oliveri R, et al. Protective effects of inhaled ipratropium bromide on bronchoconstriction induced by adenosine and methacholine in asthma. Eur Respir J 1992;5:560–5.
140. Wilson NM, Green S, Coe C, Barnes PJ. Duration of protection by oxitropium bromide against cholinergic challenge. Eur J Respir Dis 1987;71:455–8.
141. Derom EY, Pauwels RA, Van Der Straeten ME. The effect of inhaled salmeterol on methacholine responsiveness in subjects with asthma up to 12 hours. J Allergy Clin Immunol 1992;89:811–5.
142. Cockcroft DW, Swystun VA. Effect of single doses of S-salbutamol, R-salbutamol, racemic salbutamol, and placebo on the airway response to methacholine. Thorax 1997;52:845–8.
143. McWilliams BC, Menendez R, Kelley HW, Howick J. Effects of theophylline on inhaled methacholine and histamine in asthmatic children. Am Rev Respir Dis 1984;130:193–7.
144. Magnussen H, Reuss G, Jörres R. Theophylline has a dose-related effect on the airway response to inhaled histamine and methacholine in asthmatics. Am Rev Respir Dis 1987;136:1163–7.
145. Henderson JC, O'Connell F, Fuller RW. Decrease of histamine induced bronchoconstriction by caffeine in mild asthma. Thorax 1993;48:824–6.

CHAPTER 63

ASSESSMENT OF FORCED EXPIRATORY FLOWS IN INFANTS

Robert S. Tepper, Debra Turner

HISTORICAL BACKGROUND

Forced expiratory maneuvers are the most frequently used method for assessing the pulmonary function of adults. The development of this methodology and the concepts of flow limitation were a central focus of pulmonary research from 1950 to 1980.[1–4] During this period, investigators and clinicians interested in the evaluation of children also applied this methodology to older cooperative children. However, infants and toddlers, who have a high incidence of respiratory disease, could not be evaluated because of a lack of subject cooperation, as well as the absence of an adaptation of this methodology to this very young age group. However, the difficulty presented by the absence of active cooperation can at least be partially overcome by using the infant's passive cooperation, evaluating pulmonary function during anesthesia or sleep. In 1977, Motoyama reported the initial assessment of forced expiratory flows in anesthetized, intubated infants,[5] whereas in 1978 Adler and Wohl first described the assessment of forced expiratory maneuvers in sleeping newborn infants.[6] Measurements of resistances, as well as lung volumes, have also been obtained in sleeping infants[7–9]; however, forced expiratory flow is the measurement most frequently used and more closely reflects the properties of the intrathoracic airways as it is not dominated by nasal and upper airway resistance. Forced expiratory maneuvers have the advantage of longitudinal assessment using a similar methodology in infancy through adulthood.

METHODOLOGY

Pressure Generation

In sleeping infants, forced expiration is produced by the rapid application of pressure to the body surface so as to cause thoracoabdominal compression. The applied pressure increases pleural pressure and generates a forced expiration. In the initial studies by Adler and Wohl, the infant was placed in a neck-out body plethysmograph, and the pressure in the plethysmograph was rapidly increased by using the output from a vacuum cleaner motor.[6] Taussig and colleagues modified this approach by placing the infant into an invaginated plastic bag that was loosely secured at the neck; rapidly inflating the bag from large-volume pressurized drums resulted in a more rapid compression of the chest and abdomen.[10] Tepper and colleagues replaced the invaginated bag by an inflatable cuff wrapped around the infant's chest and abdomen, which significantly reduced the volume and the response time of the system.[11] Current systems employ jackets that encircle the infant's chest and abdomen, and there is an inflatable bladder in the anterior portion of the jacket. The efficiency of the pressure transmission from within the jacket to the body surface and the pleural space depends upon the physical characteristics of the jacket and how it is placed on the infant, as well as the lung volume and compliance of the infant's respiratory system.[12,13]

Tidal Volume Maneuvers

Inspiratory and expiratory flows are measured using a calibrated pneumotachometer, which is linear over the flow range of interest. Volumes are obtained by integration of the flow signal with respect to time. The pneumotachometer is fitted to a low dead-space facemask that covers the infant's nose and mouth while the sleeping infant lies in the supine position. Tidal breathing is monitored until there is a stable end-expiratory level, which reflects functional residual capacity (FRC). Forced expiratory maneuvers over the tidal volume range of lung volume are generated by rapidly inflating the compression jacket at end-tidal inspiration and maintaining the applied pressure until lung volume is below FRC, which requires less than 2 seconds.[14] A partial expiratory flow volume curve is illustrated in Figure 63-1. Since forced expiratory flows are dependent upon the lung volume at which flow is measured, the curve is quantified by the forced expiratory flow at FRC ($\dot{V}'_{FRC}$).

To confirm that maximal forced expiratory flow has been achieved requires fulfilling the criterion that flow limitation is achieved. Under these conditions, increasing driving pressure does not produce an increase in flow when assessed at the same lung volume. In cooperative older children and

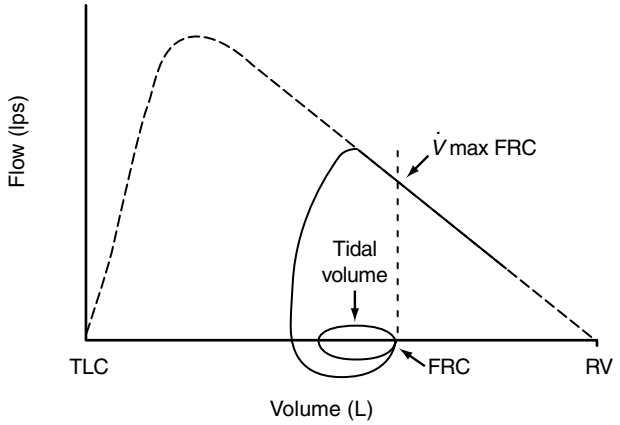

FIGURE 63-1 A partial flow volume maneuver (*solid line*) is illustrated with a full forced expiratory maneuver from total lung capacity (TLC) to residual volume (RV) (*dashed line*). For the partial maneuver, a stable end-expiratory level at functional residual capacity (FRC) is obtained followed by forced expiration, which is initiated at end-tidal inspiration and proceeds past FRC. The partial curve is quantified by the maximal flow obtained at FRC (V′FRC).

adults, flow limitation is achieved with easily attainable expiratory effort, and increasing effort does not produce an increase in flow. The reproducibility of multiple maneuvers is used as indirect evidence that flow limitation is achieved. For infants, the applied jacket compression pressure is an indirect measure of the driving pressure. If the infant remains passive, increasing jacket compression pressure will produce an increase in pleural pressure. Forced expiratory maneuvers in sleeping infants are obtained at increasing jacket compression pressures until maximal and reproducible partial expiratory flow volume (PEFV) maneuvers and V′FRC are obtained. Standardization for this methodology has recently been described in detail by a joint European Respiratory Society and American Thoracic Society task force.[15]

The use of PEFV maneuvers for assessing infants has significantly increased our understanding of lung function in this age group, as is reviewed below; however, there are important limitations to PEFV maneuvers in infants. First, as inspiratory effort is not inhibited, infants can inspire even while forced expiration is generated by the application of pressure to the body surface. Inspiration can potentially decrease the net driving pressure below that required to achieve flow limitation, even with increasing jacket compression pressure.[16] Second, flows are volume referenced to FRC, which may not be stable and thus increase intrasubject variability. Changes in FRC occur with sleep state, as well as with changes in airways constriction. Last, assessment of airway function is restricted to the tidal volume range. These limitations to PEFV maneuvers stimulated the development of the raised lung volume technique.

Raised Lung Volume Maneuvers

For this maneuver, forced expiration is initiated from a defined lung volume above the tidal volume range, instead of end-tidal inspiration. In addition, by rapidly inflating the respiratory system several times to the elevated lung volume, inspiratory effort is inhibited by recruiting the Hering-Breuer reflex and producing a mild decrease in carbon dioxide. Lung volumes at airway inflation pressures of 20 and 30 cm H_2O have been used; however, 30 cm H_2O, which is closer to total lung capacity, is used more commonly.[14,17–19] Tracings of a raised volume maneuver are illustrated in Figure 63-2. Studies have demonstrated that flow limitation is achieved during the raised lung volume maneuver. Using an esophageal catheter to assess changes in pleural pressure, Feher and colleagues constructed isovolume pressure flow curves, and flow limitation occurred at lung volumes of 50% FVC and below in healthy infants (Figure 63-3).[18] In a study by Jones and colleagues, the transient application of negative expiratory pressure to the

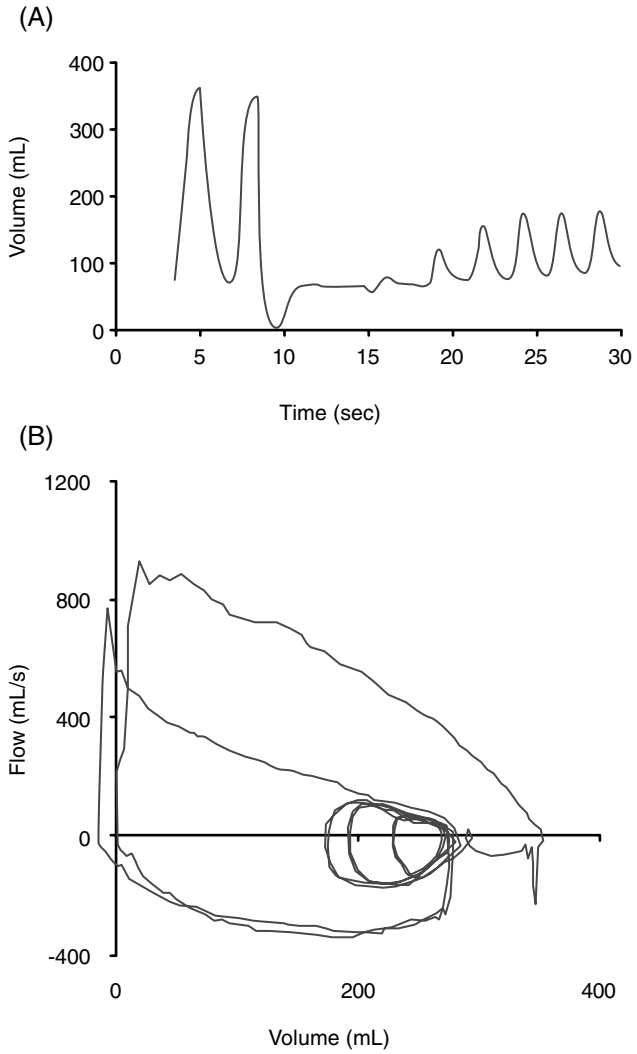

FIGURE 63-2 Raised volume maneuver. *A*, Volume versus time. *B*, Flow versus volume. The respiratory system is inflated several times to a lung volume at an airway pressure of 30 cm H_2O, which inhibits respiratory effort. The compression jacket is rapidly inflated to generate forced expiration that proceeds from V30 to residual volume. Following release of the jacket pressure at residual volume (RV), the lung volume recoils to functional residual capacity (FRC) and inspiratory effort resumes after several seconds.

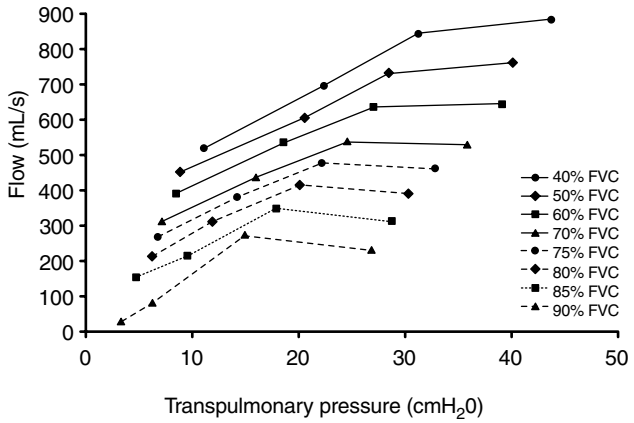

FIGURE 63-3 Forced expiratory flow versus transpulmonary pressure measured at different isovolumes (%FVC) during raised volume thoracic-abdominal compression maneuvers in a healthy infant. The plateau in flow with increased transpulmonary pressure illustrates that flow limitation is achieved.[18]

airway opening during the forced expiratory maneuver also demonstrated that flow limitation is achieved in healthy infants.[20]

APPLICATIONS

Lung Growth

The early studies using PEFV maneuvers demonstrated that when forced expiratory flows were adjusted for lung volume, the lung size-corrected flows expressed as V′maxFRC/FRC(s^{-1}) were higher for infants than older children and adults.[10,11] Although the absolute size of the infant airway is smaller than that of older children and adults, the airway size relative to the lung volume it serves is large. This concept of dysanaptic growth between airway size and lung volume was also demonstrated with forced maneuvers from raised lung volumes.[21,22] In contrast to FEFV maneuvers in adults, which are primarily quantified by the FEV_1, forced maneuvers initiated from a lung volume at an airway pressure of 30 cm H_2O, which is near TLC, proceed to residual volume in less than 1 second in healthy infants; FEV_1 equals FVC.[18,20] Therefore, the more rapid emptying of the infant lung requires that shorter-timed volumes, such as $FEV_{0.5}$, be used to quantify forced expiration in infants. Calculation of the rate constant (s^{-1}) for forced emptying yields the highest values for neonates and a progressive decline in the rate constant during the first 2 years of life.[23]

The term "dysanaptic growth" has also been used to describe the relative size of the central to the peripheral airways. In older children and adults, the relationship between the peripheral and the central airways has been assessed by measuring the change in forced expiratory flows when subjects breathe air compared with a less dense gas mixture of 80% helium and 20% oxygen. In healthy children and adults, forced expiratory flows are higher over most of the forced vital capacity (FVC) when breathing the less dense gas mixture. However, older children and adults with peripheral airway disease have less density dependence of maximum flows than healthy subjects because of increased frictional resistance and less convective acceleration. Using retrograde catheters in normal lungs obtained at autopsy, Hogg and colleagues reported that peripheral airway resistance relative to central airway resistance was significantly higher in the first few years of life compared with older children and adults.[24] A higher ratio of peripheral to central airway resistance should result in less convective accelerative and greater viscous frictional losses in the infants. However, Davis and colleagues have reported that healthy infants have values of density dependence similar to those reported in older children and adults.[25] Therefore, this finding does not support the hypothesis that the ratio of peripheral to central airway resistance is significantly greater in infants than in older children and adults.

Studies using forced expiratory maneuvers have found that female infants have higher flows than male infants when assessed by partial and full maneuvers.[11,26,27] This sex difference in forced expiratory flows may reflect relatively larger airways in females than males, which may contribute to the lower incidence of respiratory illnesses in female infants.

Airway Obstruction

Infants have limited activity and ability to communicate; therefore, it is difficult to determine whether an infant has normal airway function and significant respiratory reserve when the evaluation is limited to a physical examination and a chest radiograph. Measurements of forced expiratory flow in infants have significantly increased our ability to assess airway function in this age group and evaluate factors that contribute to the development of respiratory disease early in life.

Pre- and postnatal exposure to tobacco smoking has long been associated with an increased risk for the development of airway disease early in life. However, it was not until forced expiratory flows were measured early in life that tobacco exposure was associated with lower airway function, even in asymptomatic infants.[27,28] In addition, cohort studies of healthy infants have demonstrated that the presence of lower forced expiratory flows prior to the occurrence of any lower respiratory illness significantly increases the risk of a subsequent wheezy respiratory illness early in life.[29–32]

Patients with cystic fibrosis do not have respiratory symptoms at birth; however, they often develop recurrent respiratory symptoms within the first few years of life. Measurements of forced expiratory flow have demonstrated the presence of unsuspected airways obstruction in asymptomatic infants with cystic fibrosis.[33,34] Decreased airway function in asymptomatic infants with cystic fibrosis is consistent with the presence of increased inflammatory cells and cytokines found in the bronchoalveolar lavage fluid obtained from this patient population.[35–37] The ability to detect low airway function in asymptomatic infants maximizes our ability to evaluate the efficacy of early therapeutic interventions designed to maintain normal lung function early in life.

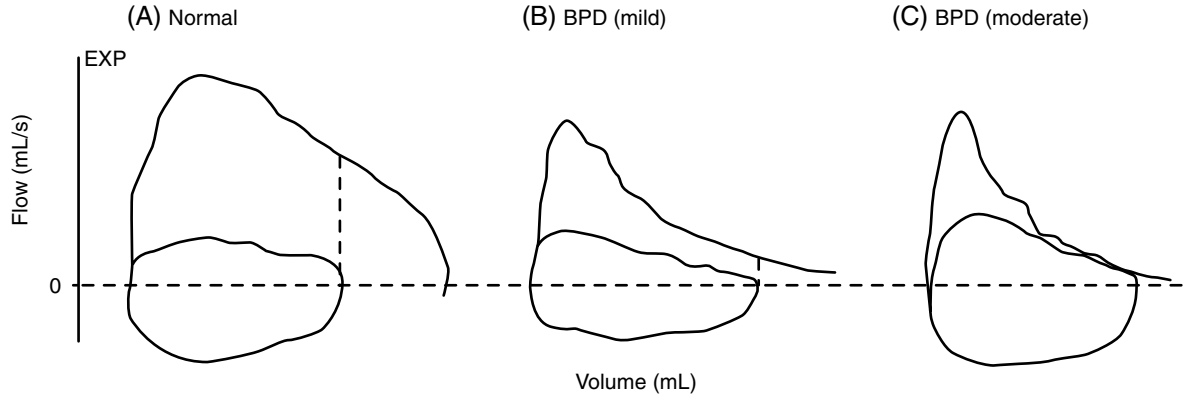

FIGURE 63-4 Partial expiratory flow-volume curves obtained from a healthy normal infant, an asymptomatic infant with mild severity of bronchopulmonary dysplasia (BPD), and a symptomatic infant with moderate severity of BPD. The healthy infant demonstrates a significant increase in forced expiratory flow relative to tidal breathing. The infants with mild BPD had significantly lower forced expiratory reserve, whereas the infant with moderate BPD was flow limited during a portion of tidal breathing.[39]

In contrast to the progression of airway disease in infants with cystic fibrosis, infants with bronchopulmonary dysplasia (BPD) develop chronic lung disease in the neonatal period, which is modified by the subsequent growth and maturation of the lung. Forced expiratory flows can be used in this patient population to demonstrate the presence of airway disease in asymptomatic infants and to quantify the severity of the airway disease (Figure 63-4), as well as track individuals longitudinally with lung growth.[38,39]

Airway Reactivity (Responsiveness)

Lower respiratory illnesses (LRIs) in infants are often associated with wheezing; however, for many years it was assumed that airway reactivity developed in infants only following an LRI. Bronchial challenge tests of healthy infants using forced expiratory maneuvers to assess changes in airway function have demonstrated that airway reactivity is present early in life, even in healthy infants with no prior LRI or family history of asthma.[40,41] Bronchial challenge testing has been able to demonstrate that healthy infants are more reactive than older children and adults and that reactivity declines with lung growth and maturation.[42–44] Healthy infants not only respond to inhaled bronchoconstrictive agonists, but under baseline conditions, there are healthy asymptomatic infants who exhibit increased baseline airway tone; they demonstrate an increase in forced expiratory flows following inhalation of a bronchodilator.[45]

Although healthy infants exhibit airway reactivity, those infants with a family history of asthma and who are exposed to maternal smoking have heightened airway reactivity compared with those infants without a family history of asthma and no exposure to maternal smoking.[32,41] In addition, heightened airway reactivity very early in life is associated with an increased risk for developing asthma as an older child.[32] Infants with a history of an episode of bronchiolitis not only have heightened airway reactivity compared with infants without prior LRI, those infants with prior bronchiolitis demonstrate a persistence of heightened airway reactivity, which does not decline with increasing age.[46]

Heightened airway responsiveness during infancy is not limited to infants with asthma. Infants with cystic fibrosis also have a greater increase in forced expiratory flow following an inhaled bronchodilator compared with age-matched controls, as well as greater sensitivity to inhaled agonists.[47,48] These findings are consistent with the presence of increased inflammatory cells and cytokines in the bronchoalveolar lavage fluid obtained from infants with cystic fibrosis.[35–37]

SUMMARY

The assessment of lung function in infants using forced expiratory maneuvers has significantly contributed to our understanding of lung growth early in life, determination of factors that contribute to the development of lung disease, and quantification of the degree of airway dysfunction in this age group. Although these measurements have proven to be very useful for clinical research studies, several significant issues still need to be addressed. The measurements for raised volume measurements have not yet been standardized, and there is a paucity of data from healthy infants for defining reference values to characterize the lung function, bronchodilator response, and airway reactivity of an individual infant.

REFERENCES

1. Hyatt RE, Schilder DP, Fry DL. Relationship between maximum expiratory flow and degree of lung inflation. J Appl Physiol 1958;13:331–6.
2. Hyatt RE, Rodarte JR, Wilson TA, Lambert RK. Mechanisms of expiratory flow limitation. Ann Biomed Eng 1981;9:489–99.
3. Hyatt RE. Expiratory flow limitation. J Appl Physiol 1983;55:1–8.
4. Mead J, Turner JM, Macklem PT, Littler JB. Significance of the relationship between lung recoil and maximum expiratory flow. J Appl Physiol 1967;22:95–108.
5. Motoyama E. Pulmonary mechanics during early postnatal years. Pediatr Res 1977;11:220–3.

6. Adler S, Wohl M. Flow-volume relationship at low lung volumes in healthy term newborn infants. Pediatrics 1978;61:636–40.
7. Polgar G, String ST. The viscous resistance of the lung tissues in new born infants. J Pediatr 1966;69:787–92.
8. Doershuk CF, Fisher BJ, Matthews LW. Specific airway resistance from the perinatal period into adulthood. Am Rev Respir Dis 1974;109:452–7.
9. Stocks J, Levy NM, Godfrey S. A new apparatus for the accurate measurement of airway resistance in infancy. J Appl Physiol 1977;43:155–9.
10. Taussig LM, Landau LI, Godfrey S, Arad I. Determinants of forced expiratory flows in newborn infants. J Appl Physiol 1982;53:1220–7.
11. Tepper RS, Morgan WJ, Cota K, et al. Physiologic growth and development of the lung during the first year of life. Am Rev Respir Dis 1986;134:513–9.
12. Lum S, Hoo AF, Stocks J. Influence of jacket tightness and pressure on raised lung volume forced expiratory maneuvers in infants. Pediatr Pulmonol 2002;34:361–8.
13. Stick S, Turner D, Lesouef P. Transmission of pressure across the chest wall during the rapid thoracic compression technique in infants. J Appl Physiol 1994;76:1411–6.
14. Lesouef PN, Castile R, Turner DJ, et al. Forced expiratory maneuvers. In: Stocks J, Sly PD, Tepper RS, Morgan WJ, editors. Infant respiratory function testing. New York: Wiley-Liss; 1996. p 379–409.
15. Sly PD, Tepper R, Henschen M, et al. Tidal forced expirations. ERS/ATS Task Force on Standards for Infant Respiratory Function Testing. European Respiratory Society/American Thoracic Society. Eur Respir J 2000;16:741–8.
16. Hoskyns EW, Milner AD, Hopkin IE. Validity of forced expiratory flow volume loops in neonates. Arch Dis Child 1987;62:895–900.
17. Turner DJ, Stick SM, Lesouef KL, et al. A new technique to generate and assess forced expiration from raised lung volume in infants. Am J Respir Crit Care Med 1995;151:1441–50.
18. Feher A, Castile R, Kisling J, et al. Flow limitation in normal infants: a new method for forced expiratory maneuvers from raised lung volumes. J Appl Physiol 1996;80:2019–25.
19. Castile R, Filbrun D, Flucke R, et al. Adult-type pulmonary function tests in infants without respiratory disease. Pediatr Pulmonol 2000;3:215–27.
20. Jones MH, Davis SD, Kisling JA, et al. Flow limitation in infants assessed by negative expiratory pressure. Am J Respir Crit Care Med 2000;161(3 Pt 1):713–7.
21. Green M, Mead J, Turner JM. Variability of maximum expiratory flow-volume curves. J Appl Physiol 1974;37:67–74.
22. Mead J. Dysanapsis in normal lungs assessed by the relationship between maximal flow, static recoil, and vital capacity. Am Rev Respir Dis 1980;121:339–42.
23. Tepper RS, Jones M, Davis S, et al. Rate constant for forced expiration decreases with lung growth during infancy. Am J Respir Crit Care Med 1999;160:835–8.
24. Hogg JC, Williams J, Richardson JM, et al. Age as a factor in the distribution of lower-airway conductance and in the pathologic anatomy of obstructive lung disease. N Engl J Med 1970;282:1283–7.
25. Davis S, Jones M, Kisling J, et al. Density dependence of forced expiratory flows in healthy infants and toddlers. J Appl Physiol 1999;87:1796–801.
26. Hoo AF, Dezateux C, Hanrahan JP, et al. Sex-specific prediction equations for Vmax(FRC) in infancy—a multicenter collaborative study. Am J Respir Crit Care Med 2002;165: 1084–92.
27. Jones M, Castile R, Davis S, et al. Forced expiratory flows and volumes in infants. Normative data and lung growth. Am J Respir Crit Care Med 2000;161(2 Pt 1):353–9.
28. Hanrahan JP, Tager IB, Segal MR, et al. The effect of maternal smoking during pregnancy on early infant lung function. Am Rev Respir Dis 1992;145:1129–35.
29. Martinez FD, Morgan WJ, Wright AL, et al. Diminished lung function as a predisposing factor for wheezing respiratory illness in infants. N Engl J Med 1988;319:1112–7.
30. Martinez FD, Morgan WJ, Wright AL, et al. Initial airway function is a risk factor for recurrent wheezing respiratory illnesses during the first three years of life. Group Health Medical Associates. Am Rev Respir Dis 1991;143:312–6.
31. Dezateux C, Stocks J, Dundas I, Fletcher ME. Impaired airway function and wheezing in infancy. Am J Respir Crit Care Med 1999;159:403–10.
32. Palmer LJ, Rye PJ, Gibson NA, et al. Airway responsiveness in early infancy predicts asthma, lung function, and respiratory symptoms by school age. Am J Respir Crit Care Med 2001;163:37–42.
33. Tepper RS, Hiatt P, Eigen H, et al. Pulmonary function at diagnosis in infants with cystic fibrosis. Pediatr Pulmonol 1988;5:15–8.
34. Turner DJ, Lanteri CJ, Lesouef PN, Sly PD. Improved detection of abnormal respiratory function using forced expiration from raised lung volume in infants with cystic fibrosis. Eur Respir J 1994;7:1995–9.
35. Kirchner KK, Wagener JS, Khan TZ, et al. Increased DNA levels in bronchoalveolar lavage fluid obtained from infants with cystic fibrosis. Am J Respir Crit Care Med 1996;154:1426–9.
36. Khan TZ, Wagener JS, Bost T, et al. Early pulmonary inflammation in infants with cystic fibrosis. Am J Respir Crit Care Med 1995;151:1075–82.
37. Balough K, McCubbin M, Weinberger M, et al. The relationship between infection and inflammation in the early stages of lung disease from cystic fibrosis. Pediatr Pulmonol 1995;20:63–70.
38. Baraldi E, Filippone M, Trevisanuto D, et al. Pulmonary function until two years of life in infants with bronchopulmonary dysplasia. Am J Respir Crit Care Med 1997;155:149–55.
39. Tepper RS, Morgan W, Cota K, Taussig L. Flow limitation in infants with bronchopulmonary dysplasia. J Pediatr 1986; 109:1040–6.
40. Tepper RS. Airway reactivity in infants: a positive response to methacholine and metaproterenol. J Appl Physiol 1987; 62:1155–9.
41. Young S, Lesouef PN, Geelhoed GC, et al. The influence of a family history of asthma and parental smoking on airway responsiveness in early infancy. N Engl J Med 1991;324:1168–73.
42. Montgomery GL, Tepper RS. Changes in airway reactivity with age in normal infants and young children. Am Rev Respir Dis 1990;142:1372–6.
43. Weist A, Williams T, Kisling J, et al. Volume history and effect on airway reactivity in infants and adults. J Appl Physiol 2002;93:1069–74.
44. Lesouef PN, Geelhoed GC, Turner DJ, et al. Response of normal infants to inhaled histamine. Am Rev Respir Dis 1989;139:62–6.
45. Goldstein AB, Castile RG, Davis SD, et al. Bronchodilator responsiveness in normal infants and young children. Am J Respir Crit Care Med 2001;164:447–54.
46. Tepper RS, Rosenberg D, Eigen H. Airway responsiveness in infants following bronchiolitis. Pediatr Pulmonol 1992;13:6–10.
47. Ackerman V, Montgomery GL, Eigen H, Tepper RS. Assessment of airway responsiveness in infants with cystic fibrosis. Am Rev Respir Dis 1991;144:344–6.
48. Hiatt P, Eigen H, Yu P, Tepper RS. Bronchodilator responsiveness in infants and young children with cystic fibrosis. Am Rev Respir Dis 1988;137:119–22.

CHAPTER 64

EVALUATION OF THE PATIENT WITH OCCUPATIONAL ASTHMA

Catherine Lemière

Occupational asthma (OA) is defined as "a disease characterized by variable airflow limitation and/or airway hyperresponsiveness due to causes and conditions attributable to a particular occupational environment and not to stimuli encountered outside the workplace."[1] Occupational asthma has been divided into OA with a latency period, which implies that an underlying immunologic mechanism has been identified, and OA without a latency period, which refers to irritant-induced asthma or reactive airways dysfunction syndrome (RADS). In the current review, we refer only to OA with a latency period and not address the question of irritant-induced asthma or RADS.

OA is the most frequent occupational respiratory ailment according to several sentinel self-declaration studies.[2] A population-based study recently carried out in six communities in Canada (Vancouver, Montreal, Winnipeg, Halifax, Hamilton, and Prince Edward Island) has estimated that the prevalence of probable and possible OA was 36.1% (31.3 to 41.0%, 95% CI) among all asthmatics.[3] Even if the definition chosen by the authors is likely to overestimate the prevalence of OA,[4] the proportion of asthma attributable to the workplace represents a significant proportion of the asthmatic population.

The major prognostic factors for persistent asthma are the duration of exposure after occurrence of respiratory symptoms and the severity of asthma at the time of removal from exposure.[5] Therefore, an early and accurate diagnosis after the onset of respiratory symptoms is critical to decrease the number of individuals who will have persistent asthma after removal from exposure.

DIAGNOSIS OF OCCUPATIONAL ASTHMA: CURRENT DIAGNOSTIC TOOLS

Clinical and Occupational History

The diagnosis of OA is often difficult to make and includes several steps.[6,7] A thorough clinical and occupational history must be recorded carefully. The improvement of respiratory symptoms over weekends or holidays is consistent with OA but is not confirmatory. Indeed, the positive predictive value of a history suggestive of OA, which includes features such as worsening of dyspnea, cough, wheezing, or chest tightness at work with improvement during weekends or holidays, is only 63%, whereas the negative predictive value of a history not suggestive of OA is 83%.[4] Rhinitis is associated with respiratory symptoms in the majority of cases of OA and often precedes the occurrence of respiratory symptoms, especially with high-molecular-weight agents, of which flour and latex, both proteins, are two examples,[8] as opposed to low-molecular-weight agents, which are nonprotein chemicals.

Identification of direct or even indirect exposure to a known respiratory sensitizer in the workplace is also an important aspect of the history but is often not readily apparent to the worker or the clinician. Information provided by material safety data sheets (MSDSs), which are documents listing the chemical composition of compounds, may be useful to identify a known sensitizer, but these MSDSs are unfortunately often incomplete as most components at a concentration of $<1\%$ are not mentioned. More than 250 agents have been identified as being responsible for OA. The list of these agents can be found on the Web site of the Réseau de référence pour l'asthme professionnel (RRAP) (<www.asthme.csst.qc.ca>).

After the history is obtained, one must confirm the diagnosis of asthma by documenting significant bronchodilation by spirometry, consisting of an improvement in forced expiratory volume in 1 second (FEV_1) of 12% or greater, with an absolute increase of at least 200 mL from the baseline after the administration of a β-adrenergic agonist or significant airway responsiveness to methacholine, defined by a concentration of methacholine inducing a 20% fall in FEV_1 (PC_{20}) lower or equal to 8 mg/mL. However, the lack of airway hyperresponsiveness does not exclude the diagnosis of OA in a subject who has been removed from exposure. One then needs to establish the relationship of these parameters to the workplace exposure.

Immunologic Assessment

Immunologic assessment can be done in vivo by performing skin-prick tests or in vitro using methods such as the radioallergo sorbent test (RAST) or enzyme immunoassay (EIA) to detect specific immunoglobulin E (IgE) or G (IgG). In the case of high-molecular-weight agents, increased levels

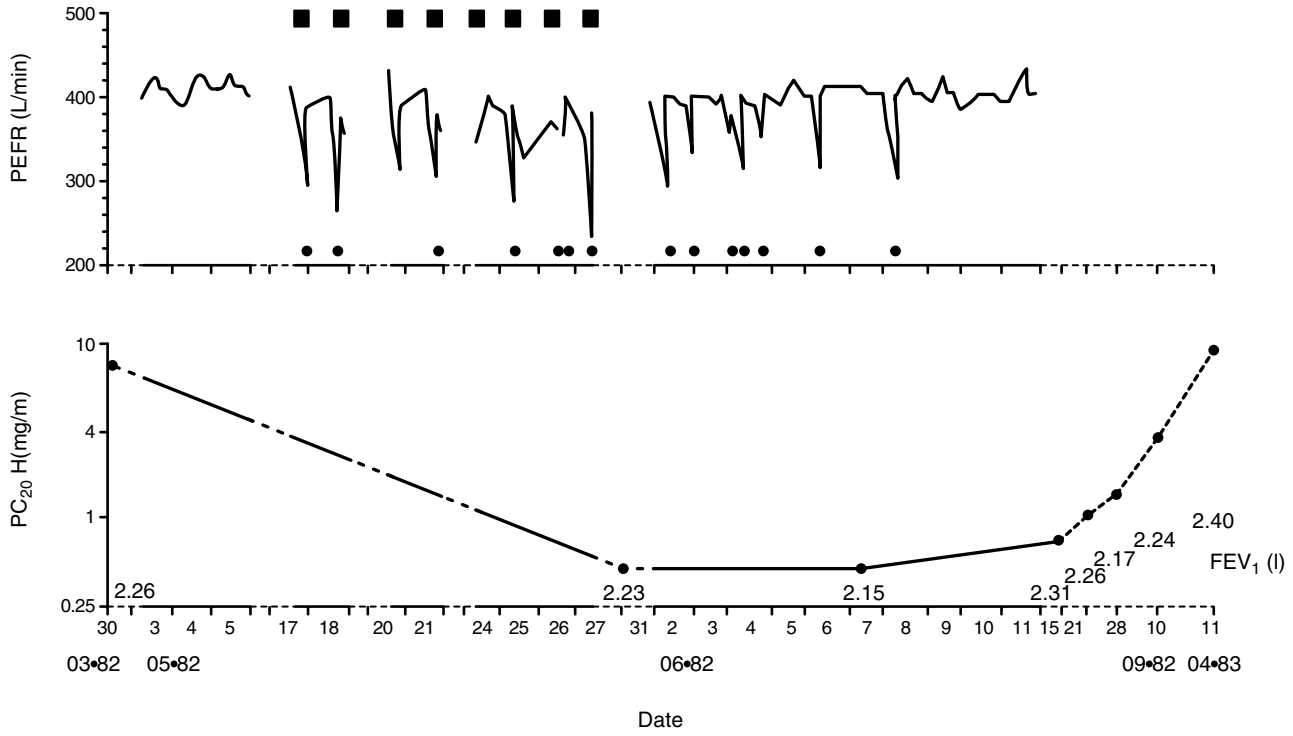

FIGURE 64-1 The serial peak expiratory flow (PEF) monitoring in a patient with occupational asthma during periods off work and at work. *Black squares* represent periods at work; *black* circles represent use of short β-2-agonists.

of IgE may reflect exposure or sensitization but do not indicate that the subject has OA. However, negative skin-prick tests to high-molecular-weight agents make the diagnosis of OA due to these agents unlikely.[9] Specific IgE and IgG to isocyanates, the chemicals most frequently responsible for OA, have been found in some subjects with OA due to isocyanates. Specific IgE were found in 31% of subjects with OA due to isocyanates and only in 0.03% of subjects without OA. IgG had a better sensitivity than specific IgE since 72.3% of subjects with OA due to isocyanates had increased specific IgG compared with 25% without OA.[10] However, neither increased specific IgE nor IgG to isocyanates confirms or refutes the diagnosis of OA to isocyanates.

Serial Monitoring of Peak Expiratory Flows

Peak expiratory flow (PEF) is the maximum flow achieved during a forced expiration starting from a maximal lung inflation. It is usually considered to be an indirect index of airway caliber. It can be measured with portable devices that are inexpensive and readily available. Serial monitoring of PEF at work and off work has been proposed as a method to confirm the diagnosis of OA.[11] This investigation entails the serial measurement of PEF at least four times a day[12] for a minimum period of 15 days at work (unless a significant change in symptoms or PEF occurs sooner), followed by the same measurements for a similar period of time out of the workplace. These measurements have several advantages: they are easy to perform, they make it possible to assess the patient's lung function outside the laboratory in a natural setting, and they are useful in differentiating between personal and occupational asthma.[11] Further, they can be performed in centers where specific inhalation challenges are not available. Although computer analysis of graphs is possible,[13] its sensitivity and specificity need to be assessed compared with a gold standard such as specific inhalation challenges and compared with the sensitivity and specificity of visual analysis of PEF monitoring. Indeed, visual analysis of PEF monitoring has been shown to be one of the best methods to evaluate PEF variability at and away from work[14] (Figure 64-1)[15] However, the reading of PEF plots is often not objective. Some results are borderline and difficult to interpret. When compared with the reference test-specific inhalation challenges in the laboratory, PEF monitoring has a sensitivity of 86 to 81% and a specificity of 89 to 74% in subjects with OA caused by red cedar.[15,16] In another study investigating subjects with OA caused by low- and high-molecular-weight agents, the specificity of PEF monitoring was 53% when inclusive of undetermined interpretations.[17] The suboptimal specificity can be explained by several pitfalls of PEF monitoring summarized in a statement manuscript.[11] Compliance is one of the main factors that can affect the interpretation of PEF monitoring[18] as it is usually low, around 50%,[19] especially with subjects seeking compensation.[20] PEF may also under- or overestimate changes in airway caliber.[21] Monitoring of PEF is more useful in confirming the diagnosis than in excluding the diagnosis of OA.[22] It is also impossible to determine the causal agent of OA in the workplace, particularly if the subject is exposed to several sensitizers. Therefore, although it can be a useful tool, when used on its own, it can often lead to the misdiagnosis of OA.

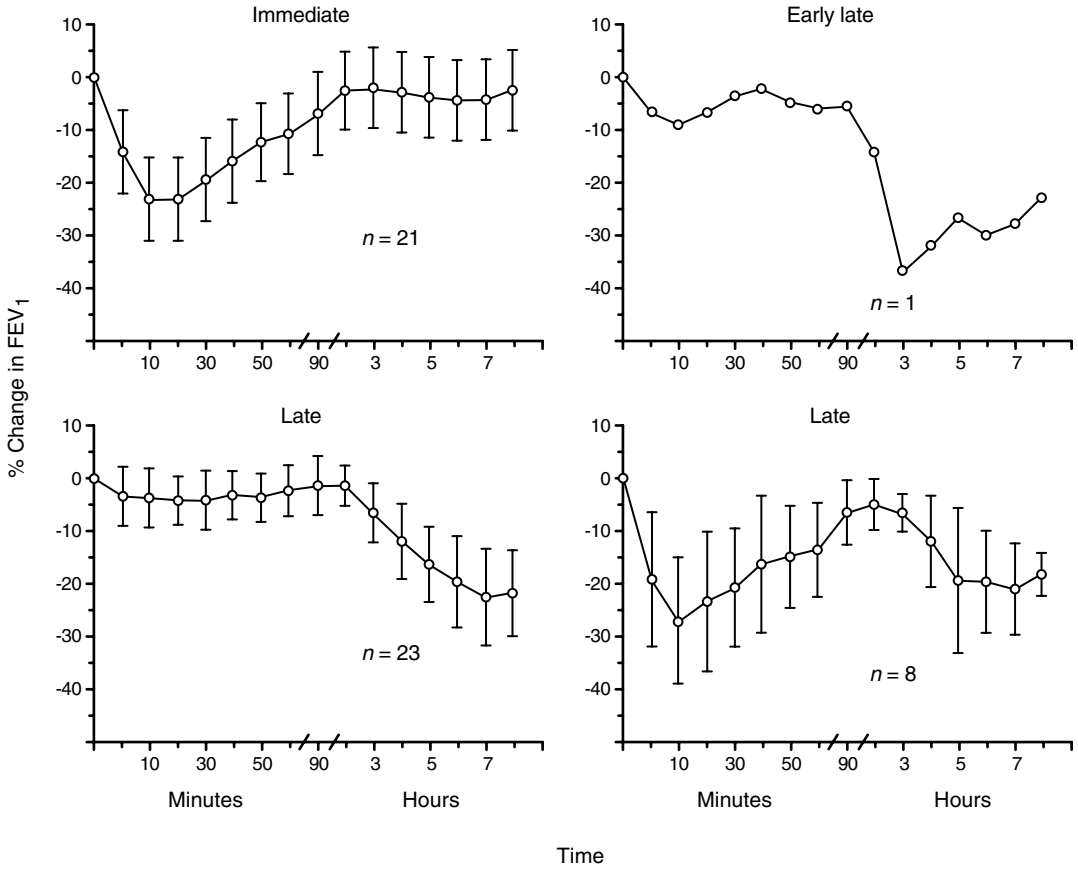

FIGURE 64-2 Typical patterns of asthmatic reactions as proposed by Zammit-Tabona M et al.[42]

The serial monitoring of airway responsiveness alone during periods at work and away from work shows neither a good sensitivity nor specificity for diagnosing OA.[16]

Specific Inhalation Challenges

The gold standard for diagnosing OA is still the performance of specific inhalational challenges in the laboratory or workplace.[7,23] These tests entail exposing the subjects to the suspected occupational agent in a safe and controlled fashion. The tests can be done in a realistic manner by exposing the subject in a provocation chamber to the product he or she is exposed to at work. The subjects are asked to mix powders like flour or to inhale chemicals (isocyanates, acrylates, etc). The exposure can also be performed using a closed-circuit apparatus from which the subject inhales a predetermined concentration of the agent accurately delivered by the machine. This concentration is measured constantly and can be modified if needed.[24–26] The exposure is progressive, and FEV_1 is checked every 10 minutes for the hour following the exposure, then every 30 minutes for the second hour, and then hourly until 7 to 8 hours after the end of exposure. Forced vital capacity is measured hourly.[23]

Different patterns of asthmatic reactions can be induced by the exposure to occupational agents: Immediate reactions occur 10 to 20 minutes after exposure ends and last 1 to 2 hours. Late reactions develop either 1 to 2 hours (early-late) or 4 to 8 hours after the end of exposure. Dual reactions combine an immediate and a late reaction (Figure 64-2). Immediate, late, and dual reactions are the patterns most frequently observed, but atypical patterns have also been described.[23]

Specific inhalational challenges do have some limitations. They require expensive and technically sophisticated equipment and well-trained personnel and are time consuming. One must realize also that a negative test does not entirely rule out the diagnosis of OA as results may be misinterpreted if the wrong agent or process is used, the patient has undergone desensitization, or the patient is exposed to a medication inhibiting an asthmatic reaction.

DIAGNOSIS OF OCCUPATIONAL ASTHMA: FUTURE DIAGNOSTIC TOOLS

There are some promising additional tools that might be added in the future to the investigation of OA when the role of these tests is validated in the investigation of OA.

Induced Sputum

Airway inflammation is one of the main characteristics of asthma and OA. Induced-sputum analysis is a reproducible, valid, and noninvasive method for studying airway inflammation. Induced sputum is increasingly used in the investigation of asthma.

The analysis of induced sputum in subjects with OA has allowed us to study the changes in airway inflammation

during periods at work and off work as well as after exposure to occupational agents in the laboratory. Subjects with OA have higher eosinophil counts when at work[27] compared with periods away from work. Changes in sputum cell counts after exposure to various occupational agents during specific inhalational challenges have also been studied and described in a number of case reports. As in asthma, the eosinophils are the cells that are most often increased in the sputum of subjects with OA. Sputum eosinophilia can be induced by exposure to both high-[28,29] and low-molecular-weight agents.[30,31] However, sputum neutrophilia has also been reported, especially after exposure to low-molecular-weight agents and more specifically after exposure to isocyanates.[32] The factors influencing a neutrophilic or an eosinophilic inflammation are unknown. Changes in airway inflammation may be worth studying in the investigation of OA. It is likely that the presence of sputum eosinophilia when at work, resolving after a period away from work, will provide further evidence for a diagnosis of OA. Performance of sputum induction in addition to serial PEF monitoring and airway responsiveness monitoring during periods at work and away from work may increase the sensitivity and specificity of the latter tests. This would be useful in particular for centers that are unable to perform specific inhalational challenges. The exact role of induced sputum in the investigation of OA is currently under investigation and needs to be established.

Exhaled Nitric Oxide

Exhaled nitric oxide (ENO) has been proposed as a convenient, safe noninvasive surrogate marker of airway inflammation. Exhaled breath nitric oxide levels are high in adults and children with untreated asthma and fall after corticosteroid therapy.[33,34] Furthermore, the change in ENO is rapid, occurring a few days after the start of inhaled corticosteroids and even faster after oral steroids. Moreover, it has been shown that ENO increases during the late response to inhaled allergens.[35] These findings indicate that ENO measurement is a promising tool for the investigation of OA.

However, relatively few studies have investigated the changes in ENO in OA. Adiesh and colleagues found higher ENO levels in subjects with OA due to laboratory animals compared with asymptomatic exposed subjects.[36] In that study, however, the definition of OA was based upon the positivity of skin-prick tests or RAST to laboratory animals and the presence of respiratory symptoms in the workplace. In reality, the standard methods for diagnosing OA are specific inhalational challenges and serial peak-flow monitoring at work and off work, and these were not described.

ENO has been assessed after specific inhalational challenges to red cedar in two groups of subjects: one group with positive specific inhalational challenges (responders) and one with negative specific challenges (nonresponders).[37] Surprisingly, there was a significant increase in ENO 24 hours after specific inhalational challenges only in the nonresponder group. In another study performed by the same investigator's group among subjects with OA due to red cedar, there was a significant positive correlation between sputum eosinophils and ENO.[38] However, ENO did not correlate with the functional parameters (FEV_1, PC_{20}) or the respiratory impairment.

Tan and colleagues failed to show any difference in ENO after work exposure to latex in latex-sensitive subjects.[39] The changes in ENO did not seem very consistent after inhalational challenges.

Exhaled NO may have some value for the early detection of OA in the workplace, but the factors affecting its measurement, such as smoking, inhaled steroid treatment, or suboptimal bronchodilation, are likely to limit its usefulness in clinical practice.

Biologic Markers

Increased secretion of monocyte chemoattractant protein-1 (MCP-1) by peripheral blood mononuclear cells after coincubation with diisocyanate-human serum albumin (DIISO-HSA) has been shown to be associated with OA to isocyanates.[40] More recently, Bernstein and colleagues showed a sensitivity and specificity of DIISO-HSA–stimulated production of MCP-1 by peripheral blood monocytes of 79 and 91%, respectively, compared with specific inhalational challenge to isocyanates.[41] In the same study the sensitivity and specificity for specific IgG were 47% and 74% and 21%

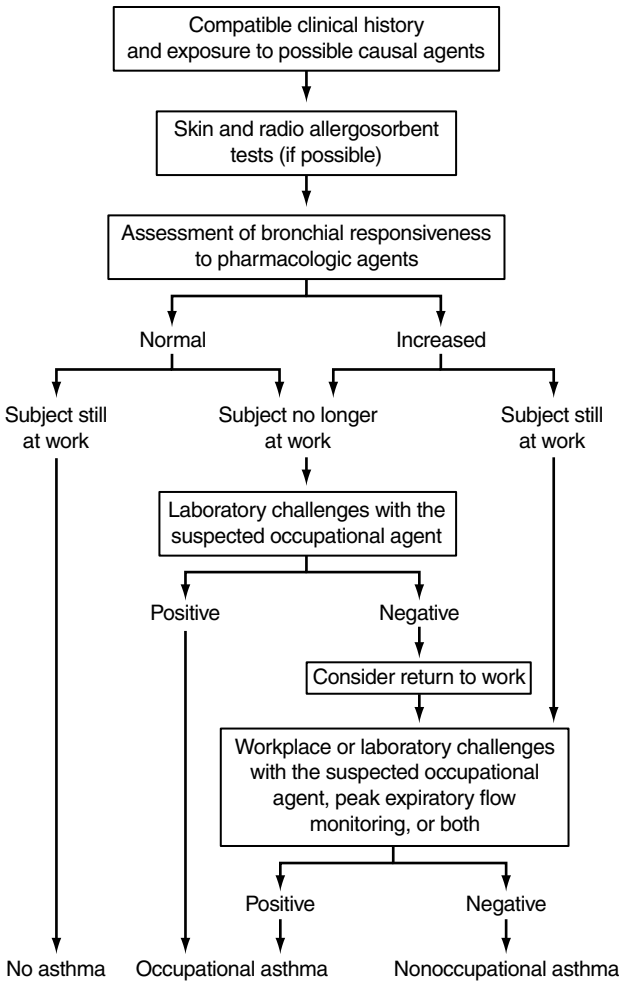

FIGURE 64-3 Algorithm proposed for the investigation of occupational asthma by Chan-Yeung M and Malo J.[2]

and 89% for specific IgE to isocyanates. Therefore, the in vitro assay of MCP-1 production may be a useful diagnostic tool in the investigation of OA but is restricted to OA due to isocyanates.

EVALUATION OF SUBJECTS WITH OCCUPATIONAL ASTHMA

A proposed algorithm for the investigation of OA is shown in Figure 64-3.[2] In a subject who reports a history suggestive of OA, the first step is to perform skin-prick tests to the suspected agent when possible. This is usually the case with high-molecular-weight agents, as well as with some low-molecular-weight agents such as platinum salts. The diagnosis of asthma must then be established. Methacholine challenge is usually performed after a period at work when possible. A $PC_{20} > 16$ mg/mL in a subject with suspected OA who has already been removed from the workplace cannot exclude the diagnosis of OA; indeed, return to work may then be associated with significant increase in methacholine bronchial responsiveness. However, a $PC_{20} > 16$ mg/mL in a subject still exposed and who complains of his or her usual respiratory symptoms makes the diagnosis of OA most unlikely. When an increased airway responsiveness has been established at work, the performance of serial PEF monitoring for periods at work and away from work can be performed. It can be combined with the monitoring of airway responsiveness and eventually, in the centers where the appropriate set-up is available, with the monitoring of airway inflammation by performing methacholine challenges and sputum induction after periods at work and away from work. In some cases, documentation of airway responsiveness at work and PEF variability at work and away from work can be used to establish the diagnosis of OA. This method of investigation is probably valid when there are major functional changes between periods at work and away from work, but when the changes are minor, the diagnosis becomes much more difficult. Specific inhalational challenges should then be performed when possible to prove the diagnosis of OA and identify the causal agent of the disease. In the province of Quebec, these tests are almost always performed to confirm the diagnosis of OA. In Finland and in Quebec, the worker compensation boards require objective evidence such as specific inhalational challenges for the diagnosis of OA and for compensating the workers. Specific inhalational challenges are therefore almost always performed in these places. In other provinces in Canada and elsewhere in the world, these challenges are not always performed. The diagnosis is often based upon a suggestive history of OA combined with serial monitoring of PEF at work and away from work. Some centers mainly consider a suggestive history, which can be misleading.

CONCLUSION

Establishing the diagnosis of OA is difficult, and the patients with suspected OA need to be assessed carefully. Although specific inhalational challenges are costly and time consuming, the alternative approach with PEF monitoring has not proven to be an equivalent tool. The development of additional tools in the investigation of OA may provide in the future an interesting alternative to the performance of specific inhalational challenges in a number of cases. In the meantime, the specific challenge remains the gold standard for making a diagnosis of OA with a high level of confidence.

ACKNOWLEDGMENTS

The author thanks Mr James Hatch and Dr André Cartier for reviewing the manuscript.

REFERENCES

1. Berstein IL, Chan-Yeung M, Malo JL, Bernstein DI. Definition and classification of asthma. In: Berstein IL, Chan-Yeung M, Malo JL, Bernstein DI, editors. Asthma in the workplace. New-York: Marcel Dekker; 1993. p. 1–3.
2. Chan-Yeung M, Malo J. Occupational asthma. N Engl J Med 1995;333:107–12.
3. Johnson AR, Dimich-Ward HD, Manfreda J, et al. Occupational asthma in adults in six Canadian communities. Am J Respir Crit Care Med 2000;162:2058–62.
4. Malo J, Ghezzo H, L'Archevêque J, et al. Is the clinical history a satisfactory means of diagnosing occupational asthma? Am Rev Respir Dis 1991;143:528–32.
5. Chan-Yeung M, MacLean L, Paggiaro P. Follow-up study of 232 patients with occupational asthma caused by western red cedar (Thyja plicata). J Allergy Clin Immunol 1987;79:792–6.
6. Cartier A, Bernstein I, Burge P, et al. Guidelines for bronchoprovocation on the investigation of occupational asthma. Report of the subcommittee on bronchoprovocation for occupational asthma. J Allergy Clin Immunol 1989;84:823–9.
7. Tarlo SM, Boulet LP, Cockcroft DW, et al. Directives de la Société canadienne de thoracologie pour l'asthme professionnel Canadian Thoracic Society guidelines for occupational asthma. Can Respir J 1998;5:397–410.
8. Malo JL, Lemiere C, Desjardins A, Cartier A. Prevalence and intensity of rhinoconjunctivitis in subjects with occupational asthma. Eur Respir J 1997;10:1513–5.
9. Cartier A. Definition and diagnosis of occupational asthma. Eur Respir J 1994;7:153–60.
10. Cartier A, Grammer L, Malo J, et al. Specific serum antibodies against isocyanates: association with occupational asthma. J Allergy Clin Immunol 1989;84:507–14.
11. Moscato G, Godnic-Cvar J, Maestrelli P, et al. Statement on self-monitoring of peak expiratory flows in the investigation of occupational asthma. J Allergy Clin Immunol 1995;96:295–301.
12. Malo J, Côté J, Cartier A, et al. How many times per day should peak expiratory flow rates be assessed when investigating occupational asthma? Thorax 1993;48:1211–7.
13. Gannon P, Newton D, Belcher J, et al. Development of OASYS-2: a system for the analysis of serial measurement of peak expiratory flow in workers with suspected occupational asthma. Thorax 1996;51:484–9.
14. Côté J, Kennedy S, Chan-Yeung M. Quantitative versus qualitative analysis of peak expiratory flow in occupational asthma. Thorax 1993;48:48–51.
15. Côté J, Kennedy S, Chan-Yeung M. Sensitivity and specificity of PC 20 and peak expiratory flow rate in cedar asthma. J Allergy Clin Immunol 1990;85:592–8.
16. Perrin B, Lagier F, L'Archevêque J, et al. Occupational asthma: validity of monitoring of peak expiratory flow rates and non-allergic bronchial responsiveness as compared to specific inhalation challenge. Eur Respir J 1992;5:40–8.

17. Liss GM, Tarlo SM. Peak expiratory flow rates in possible occupational asthma. Chest 1991;100:63–9.
18. Malo J, Cartier A, Ghezzo H, Chan-Yeung M. Compliance with peak expiratory flow readings affects the within- and between-reader reproducibility of interpretation of graphs in subjects investigated for occupational asthma. J Allergy Clin Immunol 1996;98:1132–4.
19. Quirce S, Contreras G, Dybuncio A, Chan-Yeung M. Peak expiratory flow monitoring is not a reliable method for establishing the diagnosis of occupational asthma. Am J Respir Crit Care Med 1995;152:1100–2.
20. Malo J, Trudeau C, Ghezzo H, et al. Do subjects investigated for occupational asthma through serial PEF measurements falsify their results? J Allergy Clin Immunol 1995;96:601–7.
21. Bérubé D, Cartier A, L'Archevêque J, et al. Comparison of peak expiratory flow rate and FEV1 in assessing bronchomotor tone after challenges with occupational sensitizers. Chest 1991;99:831–6.
22. Leroyer C, Perfetti L, Trudeau C, et al. Comparison of serial monitoring of peak expiratory flow and FEV1 in the diagnosis of occupational asthma. Am J Respir Crit Care Med 1998;158:827–32.
23. Cartier A, Malo J. Occupational challenge tests. In: Bernstein IL, Chan-Yeung M, Malo JL, Bernstein DI, editors. Asthma in the workplace. New York: Marcel Dekker; 1993. p. 215–47.
24. Cloutier Y, Lagier F, Cartier A, Malo J. Validation of an exposure system to particles for the diagnosis of occupational asthma. Chest 1992;102:402–7.
25. Vandenplas O, Malo J, Cartier A, et al. Closed-circuit methodology for inhalation challenge test with isocyanates. Am Rev Respir Dis 1992;145:582–7.
26. Lemière C, Cloutier Y, Perrault G, et al. Closed-circuit apparatus for specific inhalation challenges with an occupational agent, formaldehyde, in vapor form. Chest 1996;109:1631–5.
27. Lemiere C, Pizzichini MM, Balkissoon R, et al. Diagnosing occupational asthma: use of induced sputum. Eur Respir J 1999;13:482–8.
28. Alvarez MJ, Castillo R, Rey A, et al. Occupational asthma in a grain worker due to Lepidoglyphus destructor, assessed by bronchial provocation test and induced sputum. Allergy 1999;54:884–9.
29. Lemiere C, Chaboillez S, Malo JL, Cartier A. Changes in sputum cell counts after exposure to occupational agents: What do they mean? J Allergy Clin Immunol 2001;107:1063–8.
30. Quirce S, Baeza ML, Tornero P, et al. Occupational asthma caused by exposure to cyanoacrylate. Allergy 2001;56:446–9.
31. Maestrelli P, Calcagni P, Saetta M, et al. Sputum eosinophilia after asthmatic responses induced by isocyanates in sensitized subjects. Clin Exp Allergy 1994;24:29–34.
32. Park H, Jung K, Kim H, et al. Neutrophil activation following TDI bronchial challenges to the airway secretion from subjects with TDI-induced asthma. Clin Exp Allergy 1999;29:1395–401.
33. Massaro A, Gaston B, Kita D, et al. Expired nitric oxide levels during treatment of acute asthma. Am J Respir Crit Care Med 1995;152:800–3.
34. Alving K, Weitzberg E, Lundberg J. Increased amount of nitric oxide in exhaled air of asthmatics. Eur Respir J 1993;6:1368–70.
35. Kharitonov S, O'Connor B, Evans D, Barnes P. Allergen-induced late asthmatic reactions are associated with elevation of exhaled nitric oxide. Am J Respir Crit Care Med 1995;151:1894–9.
36. Adisesh LA, Kharitonov SA, Yates DH, et al. Exhaled and nasal nitric oxide is increased in laboratory animal allergy. Clin Exp Allergy 1998;28:876–80.
37. Obata H, Dittrick M, Chan H, Chan-Yeung M. Sputum eosinophils and exhaled nitric oxide during late asthmatic reaction in patients with Western red cedar asthma. Eur Respir J 1999;13:489–95.
38. Chan-Yeung M, Obata H, Dittrick M, et al. Airway inflammation, exhaled nitric oxide, and severity of asthma in patients with Western red cedar asthma. Am J Respir Crit Care Med 1999;159:1434–8.
39. Tan K, Bruce C, Birkhead A, Thomas PS. Nasal and exhaled nitric oxide in response to occupational latex exposure. Allergy 2001;56:627–32.
40. Lummus ZL, Alam R, Bernstein JA, Bernstein DI. Diisocyanate antigen-enhanced production of monocyte chemoattractant protein-1, IL-8, and tumor necrosis factor-alpha by peripheral mononuclear cells of workers with occupational asthma. J Allergy Clin Immunol 1998;102:265–74.
41. Bernstein DI, Cartier A, Cote J, et al. Diisocyanate antigen-stimulated monocyte chemoattractant protein-1 synthesis has greater test efficiency than specific antibodies for identification of diisocyanate asthma. Am J Respir Crit Care Med 2002;166:445–50.
42. Zammit-Tabona M, Sherkin M, Kijek K, et al. Asthma caused by diphenylmethane diisocyanate in foundry workers. Clinical, bronchial provocation, and immunologic studies. Am Rev Respir Dis 1983;128:226–30.

CHAPTER 65

PHYSIOLOGIC BASIS FOR PULMONARY REHABILITATION OF CHRONIC OBSTRUCTIVE PULMONARY DISEASE

Jean Bourbeau, Hélène Perrault

Chronic obstructive pulmonary disease (COPD) is a major cause of disability and mortality throughout the world[1] and is a disease that is characterized by complex and diverse pathophysiologic manifestations. The inflammatory pulmonary process that is principally triggered by cigarette smoke induces expiratory flow limitation with dynamic collapse of the airways, air trapping, and lung hyperinflation. Increases in respiratory rate, such as occurs during exercise, further amplify lung hyperinflation, leading to "dynamic hyperinflation" as a result of airflow limitation, with mechanical and sensory consequences for the affected individual. Despite breathing strategies that develop over time, adaptations are quickly overwhelmed during exercise when there is an acute increase in ventilatory demand. Acute and chronic hyperinflation have been shown to contribute to exertional breathlessness, reduced ventilatory capacity, and exercise limitation in COPD.[2,3] Wasted ventilation also leads to high ventilatory demands to maintain blood gas homeostasis. Although the initial pathology is confined to the lung in COPD, as the disease progresses, the associated reduction in physical activity and emotional problems increasingly contribute to the patient's disability and poor health-related quality of life. Official organizations across the world have recommended pulmonary rehabilitation as an integral part of the long-term management of COPD.[4–7] In the last few years, the medical literature has provided evidence that pulmonary rehabilitation favorably affects outcomes in COPD.[8]

In this chapter, we review how pulmonary rehabilitation has evolved over time from an art to an evidence-based practice with the application of sound scientific principles. We review the effectiveness and physiologic basis of existing models of pulmonary exercise rehabilitation and the pieces of the puzzle that are still missing. Finally, we explore the potential for biologic adaptations to physical exercise training with a more global approach, a biopsychosocial model that integrates a multidimensional view of different perspectives of health: biologic, individual, and social.

DEFINING PULMONARY REHABILITATION OVER TIME

The definition of rehabilitation is not specific for any single disease, and rehabilitation programs have been developed for persons affected with a variety of diseases. The word rehabilitation is derived from the Latin *habilitare*, which means to make fit, via the French word *habilité*, which translates into capability. Rehabilitation was and still is a clinical science requiring a multidisciplinary approach.

In 1974, the introduction of rehabilitation to patients with chronic respiratory disease led to the development of a definition for pulmonary rehabilitation by the American College of Chest Physicians[9]: "Pulmonary rehabilitation may be defined as an art of medical practice wherein an individually tailored, multidisciplinary program is formulated which through accurate diagnosis, therapy, emotional support, and education, stabilizes or reverses both the physio- and psychopathology of pulmonary diseases and attempts to return the patient to the highest possible functional capacity allowed by his pulmonary handicap and overall life situation." This definition was endorsed by the American Thoracic Society in 1981.[10] This early definition underlined several aspects of today's pulmonary rehabilitation, although it was primarily considered as an art of medical practice.

The scientific evidence for the efficacy of pulmonary rehabilitation with an exercise training program was illustrated in 1996, in a landmark metaanalysis paper that showed that rehabilitation decreases dyspnea and fatigue and improves exercise capacity. Since that time, other well-designed, randomized, and controlled trials have confirmed these results.[11] In 1997, a joint panel of the American College of Chest Physicians and the American Association of Cardiovascular and Pulmonary Rehabilitation published evidence-based guidelines on pulmonary rehabilitation.[8] This article showed that, among the components of pulmonary rehabilitation program, the highest grade of evidence was achieved for lower-extremity training, resulting

in significant improvement of exercise tolerance and dyspnea. The last decade has seen an increase in studies specifically addressing the underlying physiologic consequences of physical exercise training in patients with COPD.[12–14]

New definitions have been proposed in North America and Europe. The most recent definition proposed by the American Thoracic Society (1999) reads as follows[4]: "Pulmonary rehabilitation is a multidisciplinary program of care for patients with chronic respiratory impairment that is individually tailored and designed to optimize physical and social performance and autonomy." In 1997, the European Respiratory Society provided a definition highlighting the concept that pulmonary rehabilitation represents an intervention founded upon sound scientific data[15]: "Pulmonary rehabilitation is a process which systematically uses scientifically based diagnostic and treatment options to achieve the optimal daily functioning and health related quality of life of individual patient suffering from impairment and disability due to chronic respiratory disease as measured by clinically and/or physiologically relevant outcome measures."

PHYSIOLOGIC BASIS OF EXISTING MODELS OF EXERCISE REHABILITATION

Despite clear evidence that pulmonary rehabilitation with exercise training is an effective therapeutic strategy in patients with COPD, it remains largely underused.[16] Skepticism often comes from a belief that because exercise training does not impact on pulmonary function, it has no impact on patient disability and quality of life. In addition, the medical community has a poor understanding of the physiologic basis to explain how exercise training improves patients' dyspnea, exercise capacity, and functional status. Although our understanding of the physiologic basis is far from complete, we have made important progress in the last decade.

Effects of Exercise Training on the Lower Extremities

Results from a metaanalysis of randomized trials with comparable patient selection and training modalities conducted over the last 40 years clearly show that pulmonary rehabilitation improves the functional capacity and the health-related quality of life of patients with COPD.[11,17] In addition to an educational component, rehabilitation programs generally include a component that focuses on breathing strategies to minimize breathlessness and optimize breathing mechanics in addition to a large muscle mass exercise training component. The exercise training programs have typically been structured around supervised institutional programs ranging from 4 weeks up to 1 year in duration (mode: 8 weeks) consisting of treadmill walking, stationary cycling, and free-walking. Over the last decade, strength training of either lower or upper extremities has also been introduced as a valuable adjunctive exercise rehabilitation modality in patients with COPD. Similarly, an increasing number of studies have addressed the long-term effectiveness of home-based exercise training on functional status, quality of life, and the long-term adherence to physical activity training.[4,18,20] Outcome measures of the effectiveness of the exercise training programs on functional or physical performance indicators have been obtained from direct open-circuit spirometry measurements during incremental maximal exercise tests but more often from exercise tests using a fixed absolute submaximal power output or using a timed-distance field test. Most studies have assessed subjects with mild or moderate disease severity; however, improvements in exercise tolerance have also been observed in severely impaired patients. Table 65-1 summarizes the effects of exercise rehabilitation on submaximal and maximal exercise variables. As can be seen, results generally show that patients exhibit reduced dyspnea and leg fatigue for an identical submaximal power output after an exercise rehabilitation program. This is also generally associated with decreases in heart rate, minute ventilation, and plasma lactate concentration reflecting concurrent physiologic adaptations.

Measures of Maximal Aerobic Power and Submaximal Exercise

Results from randomized and nonrandomized control trials of combined respiratory training and aerobic exercise show average improvements in peak work rate of approximately 15%.[19,21–23] As is the case in healthy humans, the magnitude of the improvement in peak power is related to the overall exercise load such that greater improvements are observed following higher exercise intensity and duration. Although significant changes in peak oxygen consumption (VO_2) are often not measured or not observed following a structured aerobic exercise training program in COPD, improvements of up to 10% were observed following rigorous controlled training programs.[21–23] Quantitative changes on many parameters related to endurance training–induced physiologic adaptations have been shown after structured aerobic exercise training (Figure 65-1).[13] In addition to increases in exercising peak power and associated decreases in the submaximal exercise circulatory (heart rate), metabolic (plasma lactate concentration), and respiratory (minute ventilation and carbon dioxide consumption) responses seen in patients with COPD, results also show increases in the activity of citrate synthase (CS) and 3-hydroxyacyl-coA (HADH) of exercise-trained muscles. This may be taken to reflect metabolic adaptation to the regular endurance exercise training.

Table 65-1 Change Usually Measured after Exercise Rehabilitation for Chronic Obstructive Pulmonary Disease

Variable	*Submaximal exercise**	*Maximal exercise*
Leg fatigue score	↓	=
Dyspnea score	↓	=
Heart rate (bpm)	↓	=
Minute ventilation (L/min)	↓	=
Tidal volume (L)	↑	=
Breathing frequency (cycles/min)	↓	=
Oxygen consumption	↑=	=↑
Plasma lactate	↓	=↑

*A given absolute work rate.

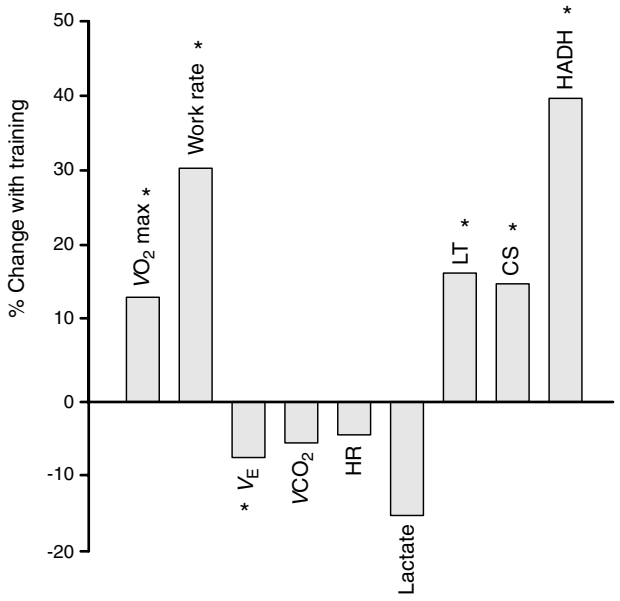

FIGURE 65-1 The effects of endurance training on maximal oxygen consumption (VO_2) and work rate achieved during exercise on VE, carbon dioxide consumption (VCO_2), heart rate (HR), and lactic acid concentration for identical exercise work rate, on lactate threshold (LT), and on the activity of citrate synthase (CS) and 3-hydroxyacyl-coA (HADH). Significant changes are indicated by an *asterisk*. Reported values represent changes (%) from baseline values that occurred after training. Adapted from Maltais F et al.[13]

The most frequently reported submaximal exercise indicators following exercise rehabilitation are an increase in the 6-minute walking distance or in submaximal endurance time. Improvements between 40 and 85% have been reported in the exercise time completed during cycling or walking sessions at a set intensity of 75 to 90% peak VO_2, whereas an average 30% increase is generally reported in the 6-minute walking distance. The 6-minute walking test (6MWT) is a useful measure of the functional response to a medical intervention and can be used as a one-time measure of functional status or to help predict morbidity and mortality in patients with COPD.[24] Although the reproducibility of the test appears satisfactory in patients with COPD with a coefficient of variation of approximately 8%, there is little information about the validity of this test for prediction of maximal aerobic capacity. In end-stage lung disease, a modest relationship between the 6-minute walking distance and peak VO_2 was found, such that 49% of the variance in the 6MWT was explained by the variance in peak VO_2.[25] The physiologic significance of the test, however, remains unclear since it does not provide information on any specific organ or systemic response but rather reflects a general physical response, which may be greatly affected by test instructions and motivational factors.[24] Guyatt and colleagues found the magnitude of increase in performance on the 6MWT in patients with chronic airflow limitation or congestive heart failure resulting from simple verbal encouragement to be the same as that use seen after therapeutic interventions such as exercise rehabilitation.[26] The overall functional character of this test is also illustrated by the fact that, contrary to that expected from the well-known principle of training specificity in the physiologic adaptations to physical training, improvements in 6-minute walking distance are most often reported following supervised cycle-ergometry training. The most significant factor in training-induced increases in 6MWT appears to be the improvement in self-reported dyspnea,[24] which may be related to improved skeletal muscle metabolic function resulting in less reflex stimulation of breathing, although psychological factors may affect the perception of breathing and leg fatigue discomfort.

Effects of Weight Training

Peripheral muscle strength is considerably reduced in patients with COPD, and irrespective of lung function, impairment is negatively related to overall exercise capacity.[21,22,27] It therefore seems reasonable that weight training be recommended in patients in COPD. Nonetheless, there are, to date, a relatively small number of randomized trials of weight lifting in COPD. Most trials have used a training modality consisting of three series of 10 movement repetitions of low or moderate intensity with respect to the maximal strength of the target muscle group, including both lower and upper limb muscle masses. Similar to healthy individuals, significant gains in the strength of the exercised muscle groups may be observed following strength training,[19] indicating that the disease process does not impair muscle tissue trainability in COPD. In fact, improvements in muscle endurance have also been reported following unloaded callisthenic-type exercises,[28] which may be explained by the relatively weak baseline status. Although strength gains are specifically associated with strength rather than aerobic training,[29] programs using combined strength and aerobic exercise training lead to improvements in strength of a magnitude similar to that of strength training alone.[29,30] It is interesting that contrary to observations in healthy populations, increases in peripheral muscle strength transfer to improvements in submaximal endurance time[29,30] and quality of life. This may be related to the fact that some patients with COPD are so low on the exercise fitness continuum that a small initial gain in peripheral muscle strength or endurance may make a difference to their ability to sustain longer bouts of physical activity using this muscle mass.

Weight training is associated with distinct advantages in patients with chronic diseases such as COPD, coronary heart disease, or congestive heart failure because the metabolic demands of segmental or localized muscle contractions and thus the related circulatory and ventilatory requirements remain significantly lower than for large muscle group exercise training. Patients can therefore perform substantial exercise without experiencing adverse symptoms such as pain or breathlessness. Circuit training is a training modality that combines both weight lifting and aerobic training as subjects successively move two or three times through a circuit consisting of 6 to 10 stations and performing series of 10 to 12 repetitions of a given exercise at each weight lifting station using several upper and lower limb muscle groups.

This approach has been used safely and successfully in cardiac rehabilitation programs, resulting in significant increases in both aerobic endurance and musculoskeletal strength. The use of this training modality in patients with COPD is restricted to series of consecutive arm exercises in upper extremity training but otherwise remains relatively unexplored.

Effects of Exercise Training on the Upper Extremities

The oxygen cost per $kg \cdot min^{-1}$ of arm ergometry is higher during arm cycling ($3\,mL \cdot kg^{-1} \cdot min^{-1}$) compared with leg cycling ($2\,mL \cdot kg^{-1} \cdot min^{-1}$)[31] on account of the additional involvement of upper body stabilizing muscles during arm exercise. In addition, in untrained individuals, the maximal work capacity achieved using arm ergometry is approximately 64 to 80% of that achieved using lower extremities. Thus, for a given absolute work rate, the relative demands when performed with the upper limb muscles are much greater, leading to greater cardiorespiratory responses. Given these factors, it is difficult to determine the appropriate grounds for comparison of arm and leg exercise responses following a given therapeutic intervention. In a recent study, investigators examined the efficiency of energy expenditure during peak and submaximal arm and leg cycling in patients with COPD.[32] In agreement with the known effects of arm exercise, in the healthy control subjects, the VO_2 per watt of peak external work was higher during arm ($15.5 \pm 0.7\,mL\ O_2 \cdot min^{-1}/W^{-1}$) than leg ($10.0 \pm 0.3\,mL\ O_2 \cdot min^{-1}/W^{-1}$) ergometry. In patients, however, the VO_2 per watt of peak external work was the same during arm ($17.3 \pm 0.6\,mL\ O_2 \cdot min^{-1}/W^{-1}$) and leg ($17.3 \pm 0.7\,mL\ O_2 \cdot min^{-1}/W^{-1}$) ergometry. The mechanical efficiency (%), measured at an intensity of work corresponding to 50% of the specific arm or leg peak exercise performance, was significantly lower in patients than control subjects for legs (15.6 ± 0.6 vs 22.5 ± 0.6) but not for arm ergometry, for which a normal mechanical efficiency was observed (18.3 ± 0.9 vs 21 ± 1.2). This suggests that upper and lower limbs are not comparably affected in COPD, although a clear explanation remains to be determined. Evidence indicating that muscles of the upper limbs are equally affected by disuse or chronic hypoxemia was published by Sato and colleagues,[33] showing type II fiber atrophy in the biceps muscle of patients with severe emphysema as is reported in the lower limb muscles of patients with COPD.[21,34] On the other hand, recent results from biopsies of deltoid muscles in COPD patients indicate comparable and even higher oxidative enzyme activity than that of age-matched control subjects when only severe patients were considered.[35] The deltoid muscle, however, is responsible for arm elevation and abduction, as well as fixation of the shoulder joint, but may also be recruited upon increased respiratory efforts. Similar to the recent report of a "supranormal" oxidative capacity of the costal diaphragm and external intercostal muscles of emphysematous patients,[36] the higher citrate synthase activity observed in the deltoid muscle of severe COPD patients could be explained by an enhanced recruitment of the deltoid in light of the exaggerated work of breathing.

Patients also report increased dyspnea when completing daily tasks involving arm movement, to displace objects or to raise arms above head level, referred to as "unsupported arm exercise," compared with leg exercise. The main problem in studying the physiologic responses to unsupported arm exercise and the potential related benefits of therapeutic interventions on responses to this exercise is the lack of standardization of the mechanical work and the resulting energy requirements. Because in unsupported arm exercise the amount of force displaced is not known, there cannot be a valid computation of the mechanical work. In addition, unsupported arm exercise involves the participation of accessory inspiratory muscles for stabilization of the torso to different degrees depending on the type of movement, which further complicates the bioenergetics assessment.

Upper extremity training using arm ergometry, weight lifting, or rhythmic unsupported arm movements using a wooden dowel have been successfully used in patients with COPD to improve dyspnea and arm working capacity. These studies show significant improvements in maximal arm work capacity or endurance following upper extremity training and support the principle of exercise-induced specificity of training since crossover effects of leg exercise training alone on arm exercise performance were not observed.[37–39] Additional randomized controlled trials are required in these patients to further examine the added benefits of upper extremity training on functional ability, ventilatory discomfort, and the resulting skeletal muscle metabolic or circulatory adaptations.

PHYSIOLOGIC MECHANISMS FOR EXERCISE-INDUCED IMPROVEMENTS

Exercise challenges the appropriate delivery and utilization of oxygen to the exercising muscles. In healthy individuals, the end result of exercise training is an improvement in all of the processes involved in the oxygen transport system, whether it is in the delivery, uptake, or utilization by the exercising muscles. The oxygen transport capacity is best expressed by the Fick equation:

$$VO_2\ (L \cdot min^{-1}) = (Qs \times HR) \cdot (CaO_2 - CvO_2)$$

where VO_2 reflects whole body oxygen consumption, Qs is stroke volume (mL/beat), HR is heart rate in $beat \cdot min^{-1}$, and CaO_2 and CvO_2 are, respectively, the arterial and mixed venous oxygen content. The cardiac output and the outcome of the diffusion of oxygen in the lung, CaO_2, reflect the central components of the oxygen transport system, whereas the oxygen extraction by peripheral tissue (primarily working skeletal muscles during exercise) resulting from peripheral oxygen delivery and utilization reflects the peripheral component.

The weakest link in the oxygen transport system may be the result of an alteration in either the central or peripheral components of the system owing to a genetic limitation for the expression of this component, disease, or deconditioning. Thus, in the presence of a chronic disease, improvements of the maximal oxygen flux capacity will be mostly found in those components that are less directly affected by

the disease process and thus may respond to the training stimulus.[40] The advantage of the multisystemic organization of the oxygen transport system is therefore that improvements in components that are not affected by the disease process may at least partially compensate for the disease-imposed limitation, resulting in an overall improvement in the maximal aerobic capacity. For example, although patients with COPD exhibit a clear limitation in their pulmonary contribution to oxygen transport owing to a reduced lung oxygen transfer and resulting arterial hypoxemia, an increase in working muscle capillarization or oxidative enzyme activity may nevertheless lead to improved aerobic capacity because of an enhanced ability of peripheral muscles to access and use oxygen. The improvements in the functional status and physical performance status of patients with COPD following exercise rehabilitation have been related to several factors, such as (1) general physiologic adaptations to endurance training; (2) improved respiratory muscle function and reduced impedance to breathing, increased symptom tolerance, or desensitization; and (3) enhanced mechanical efficiency. Table 65-2 presents an overview of the physiologic mechanisms for exercise rehabilitation-related improvement in exercise tolerance. In the following section, we review the potential causes of improvement in functional status and examine their relationship and contribution to the oxygen transport system.

Table 65-2 Physiologic Mechanisms for Exercise Rehabilitation–Related Improvement in Exercise Tolerance

Proposed cause	*Potential mechanism**	*Clinical sign or symptom*
↑ VO_2 maximal	↑ Peripheral muscle capillarization ↑ Peripheral muscle angiogenesis (?) ↑ Substrate oxidation ↑ Peripheral muscle oxidative enzymatic activity ↑ Mitochondrial density ↑ Peripheral muscle fiber size	↑ Work capacity and exercise tolerance
↓ VO_2 submaximal or ↑ mechanical efficiency	↑ Peripheral muscle mitochondrial coupling (?) ↓ Respiratory muscle VO_2 (?) ↑ Motor coordination (?)	↓ Leg fatigue ↓ Breathlessness
↓ Heart rate submaximal	↓ Peripheral muscle chemoreceptor activation	↓ Breathlessness
↓ VE submaximal	↓ Peripheral muscle chemoreceptor activation ↑ Neuromuscular coupling	↓ Breathlessness ↑ Exercise endurance

*Where (?) is indicated, the explanation for the mechanism is tentative and not proven.
VE = minute ventilation; VO_2 = volume of oxygen consumption.

General Physiologic Adaptations to Endurance Training

Physiologic adaptations to aerobic training are multiple, involving central and peripheral circulatory responses, salt and water regulation, metabolic hormonal responses, and respiratory, neuromuscular, and immune responses.[31] In healthy humans, a sustained program of moderate or intense regular endurance exercise training will cause increases in plasma volume (12–20%), resulting in an increased maximal stroke volume and cardiac output and increases in glucose uptake by trained muscles, leading to enhanced insulin sensitivity as well as enhanced heat dissipation and water conservation mechanisms. Central circulatory adaptations include a reduction in resting and submaximal heart rate, whereas an increase in capillarization of exercise-trained muscles contributes to improving peripheral circulation. Neuromuscular adaptations may be seen at various levels, including the motor end plate, neuronal transport, and skeletal muscle structural, and regulatory adaptations at both the cellular and subcellular levels.

Evidence for Central and Peripheral Circulatory Exercise-Training Responses in COPD An impairment in peak exercise cardiac output (Qc) and stroke volume (Qs) measured during incremental exercise testing has been observed in subjects with COPD, and a relationship between severity of expiratory obstruction and the exercise-induced changes in stroke volume has been reported.[41,42]

There are relatively few reports of central and peripheral blood flow during steady-state submaximal exercise in COPD, and except for one study[43] of hemodynamics of patients with COPD following exercise training, there are no studies investigating the effects of pulmonary rehabilitation on central and peripheral blood flow distribution. In the above-mentioned study, 12 COPD and emphysema patients were trained three times 20 minutes daily on a cycle ergometer at a self-selected intensity, for a total of 18 weeks. Right heart catheterization was performed before and after training, cardiac output was measured by the Fick technique, and pulmonary capillary wedge, pulmonary artery, right ventricular, and right atrial pressures were recorded. Although a small decrease in resting and exercise VO_2 was observed, the results failed to show any change in exercising cardiac index or in right or left stroke work following training, suggesting that the improved oxygen transport resulted from peripheral rather than central adaptations. However, measurements were reported only for one exercise condition, which was also not clearly described. Thus, the effects of exercise rehabilitation on exercise cardiac output and its distribution to the periphery remain incompletely documented. A potential relationship between ventilatory mechanics and stroke volume has been suggested by several authors, including Montes de Oca and colleagues,[44] who observed pleural pressure swings during exercise to be the best predictor of O_2 pulse (VO_2/HR). Although significant knowledge has been gained over the last decade regarding the role of dynamic hyperinflation on dyspnea and exercise limitation in COPD,[3] the extent to which exercise ventilatory mechanics may contribute to a central circulatory limitation and the effects of endurance training to reverse such a potential effect have not been examined.

Evidence for a Peripheral Training Response in COPD Subjects with COPD have low percentages of type I fibers and corresponding myosin heavy chain type I and associated

increases in the percentage of myosin heavy chain type IIa and smaller type II fibers. In addition, they have reduced mitochondrial volume density and enzymatic activities as well as skeletal muscle bioenergetics indicative of a lower phosphate potential ([ATP]/[ADP] [Pi]),[21,27,34] which reflects the reduced work output capability of the cell. Muscle capillarization, however, appears to be preserved as similar numbers of capillary-to-fiber contact points may be found in lower limb muscles of patients with COPD when expressed relative to the skeletal muscle cross-sectional area.[45] Large muscle group endurance exercise training reverses the adverse effects of skeletal muscle disuse and deconditioning. This is illustrated by the increases in mitochondrial volume and density as well as oxidative enzyme activities and improvement in muscle bioenergetics, which have been reported in well-controlled investigations of COPD patients[21]. The effects of endurance exercise training on peripheral muscle blood flow, however, are not clear. Using thermodilution to measure femoral blood flow during cycling exercise, Sala and colleagues found no effect of an intensive 8-week cycling program on femoral blood flow in COPD patients;[14] however, peripheral oxygen extraction was significantly enhanced after training. In their investigation of the vastus lateralis using skeletal muscle biopsies before and after training, Whittom and colleagues found no change in the capillary-to-fiber ratio but observed the number of capillary contacts to increase in proportion to the increase in type I and IIa cross-sectional area in patients with COPD.[45] Angiogenesis is a common skeletal muscle adaptation in response to exercise training, which may be particularly stimulated by exercise-related reduction in oxygen tension or related metabolic alterations in the skeletal muscle. Vascular endothelial growth factor (VEGF) has to date been identified as the major putative angiogenic factor since it seems to increase to a greater extent and more consistently than other measured angiogenic factors, such as transforming growth factor-β1 (TGF-β1), basic fibroblast growth factor (bFGF), and angiopoietin 1 and 2, in response to increased skeletal muscle physical training.[46] Evidence from studies in both animals and humans indicates the expression of VEGF to be enhanced by rigorous exercise training, especially when conducted in hypoxia or in conditions leading to a relative local hypoxia since a hypoxia-inducible factor (HIF subunit 1) appears to be involved in the exercise-related up-regulation of VEGF. An increase in the skeletal muscle VEGF gene expression has indeed been reported in patients with chronic heart failure after 8 or 12 weeks of endurance training. This gene expression may be a response to their reduced ability for peripheral oxygen delivery,[47,48] leading to conditions of hypoperfusion and localized relative hypoxemia in peripheral muscles during large muscle mass exercise. Whether neovascularization is enhanced in COPD patients exhibiting significant exercise-induced hypoxemia or following exercise training remains to be investigated.

Respiratory Muscle Function, Impedance to Breathing, and Symptom Tolerance

The improved exercise tolerance observed in patients with COPD following a program of supervised endurance training is mostly explained by a decrease in dyspnea or breathlessness for any level of submaximal exercise. Consistent with respiratory disease being a major limitation in their maximal working capacity, maximal ventilation or peak heart rate generally remains unchanged following training, inasmuch as a true maximal effort is imposed. On the other hand, endurance exercise training generally results in a decrease in minute ventilation as well as a fall in the ventilatory equivalent for oxygen for submaximal exercise work rates, suggesting that less respiratory muscle work is required for a given exercise level. As discussed in the next section, it is not known whether these adaptations translate into lower total body oxygen cost of work or enhanced mechanical efficiency. The decrease in minute ventilation is most commonly explained by a decrease in breathing frequency with minor changes in tidal volume, leading to lower dead space ventilation[12,49,50] and improved ventilatory efficiency. The physiologic mechanism involved in the training-induced ventilatory response of patients with COPD remains incompletely documented, as is our current understanding of factors regulating ventilation during dynamic exercise.

The improvement in ventilatory efficiency may be related to enhanced gas exchange and a reduction in the breathing stimulus. It is generally accepted that inadequate skeletal muscle oxygen delivery related to either decreased perfusion, as is the case in chronic heart failure or reduced arterial oxygen tension, as may be seen in exercising COPD, may cause excessive afferent chemoreflex activation leading to an excess ventilatory drive.[31] Changes in skeletal muscle oxidative potential and presumably also mitochondrial function observed after supervised exercise training may thus act to reduce the level of afferent chemoreflex activation triggered at any given submaximal exercise load. Alternately, given the fact that the perception of breathlessness for any given level of ventilation is also reduced following exercise training in COPD, factors related to better neuromuscular respiratory coupling or improved ventilatory muscle function may also be involved in the improved exercise tolerance. Using a multimodality upper and lower limb exercise training program of three sessions per week over a 6-week period, O'Donnell and colleagues observed significant improvements in static inspiratory and expiratory muscle strength and endurance following high-level ventilation exercise training.[50] These improvements were, however, not associated with changes in exercise operational lung volumes, which remained unaltered after training. Correlational analyses suggested that the improved dyspnea was primarily explained by reduced ventilatory requirements and not by more favorable ventilatory mechanics. Finally, because the reduced post-training ventilatory requirements explained only a portion of the variance in symptom sensation, it has been suggested that exercise training in these patients may be associated with the development of a better tolerance of the stimuli associated with exercise-induced symptoms, leading to a reduced perception of symptoms.[50]

Thus, although skeletal muscle metabolic adaptations to training may explain the reduced ventilatory requirements during submaximal exercise following training, a clear

explanation for the alleviation of exercise symptoms for a given level of ventilation following training remains to be provided.

Enhanced Mechanical Efficiency

Mechanical efficiency refers to the ratio of the external mechanical work to the metabolic energy expenditure. The external mechanical work usually recorded as kilogram meters (kg·m) is the product of force acting through a distance. The metabolic energy expenditure is inferred from the steady-state work or exercise oxygen consumption (VO_2), which is referred to as "gross energy expenditure" since it includes the resting energy expenditure as well as the oxygen cost related to the internal work of skeletal muscles throughout the motion. Thus, "gross mechanical efficiency" is calculated as mechanical power (watts)/exercise metabolic power (watts) 100%.

Studies in bioenergetics indicate that the gross mechanical efficiency of steady-state cycling is approximately 20% in healthy humans, whereas that for walking on a slight incline is 15% and decreases by only 1 or 2% with aging. There are, however, few data on the mechanical efficiency of exercising COPD patients. Using the VO_2 and corresponding power output values from 10 studies of COPD patients in which steady-state measurements were provided, values of gross mechanical efficiency are found to vary between 11 and 23%, which is not much different from the 13 to 23% values calculated for age-matched control subjects.[51] In a recent study, conducted specifically to assess the mechanical efficiency of cycling at 50% of peak load in 30 patients with moderate to severe COPD, Baarends and colleagues found values of net mechanical efficiency to range between 8.5 and 22.7%, with 13 of 23 men exhibiting a "low" (<17%) and 10 exhibiting a "high" (>17%) mechanical efficiency.[51] Interestingly, however, the difference between groups was unaccounted for by differences in resting energy expenditure, static lung hyperinflation, pulmonary function, or blood gas tensions.

Although a decrease in submaximal exercise ventilation is a common observation following exercise training, decreases in the VO_2 for given submaximal work rates or increased mechanical efficiency have only been sporadically reported following exercise training programs in COPD.[43,52] The physiologic basis for this increase in efficiency remains to be determined. Theoretically, a training-induced decrease in the oxygen cost at a given absolute work rate or an increased mechanical efficiency may result from two distinct or related phenomena: (1) the energy demands associated with the exercise are actually decreased as reflected by a decrease in resting VO_2, in the cost of the internal work of movement, or in the cost of external work and (2) mitochondrial respiration is enhanced leading to a higher ratio of moles of adenosine triphosphate (ATP) produced per mole of atomic oxygen processed through the mitochondria (P:O coupling) and lower O_2 requirement for the same external work-related ATP requirement.

Mitochondrial Respiration in COPD Markers of skeletal muscle mitochondrial respiration have been recently reported in respiratory but not ambulatory muscles of patients with COPD.[36] Results indicate mitochondrial respiration of costal diaphragm and external intercostal muscles to be significantly enhanced in emphysematous patients compared with age-matched control subjects, with a significant positive correlation between the maximal oxidative capacity and the degree of pulmonary obstruction. These findings have been explained by an adaptive response of these muscles to the chronic resistive and elastic overloads in a manner analogous to that imposed by exercise training. There is to date, however, no report on the effects of exercise training on peripheral muscle mitochondrial function.

Decreased Energy Cost of Work Following Exercise Training in COPD Similar to what is observed in healthy individuals, there is no evidence of a training-induced decrease in resting metabolic rate in patients with COPD following exercise training. Differences in the cost of the internal work of movement, however, may be related to factors such as joint stiffness, limb size, abnormalities in gait, or poor motor coordination. Although the internal work of movement has not been reported in COPD, it is possible that improvements in motor coordination and joint stiffness occur as a result of the repeated exercise, which could to a small extent decrease the total oxygen cost of work. A decrease in the oxygen cost of breathing seems a plausible explanation for a post-training reduction in whole-body oxygen uptake since a decrease in submaximal exercise ventilation is commonly seen. The extent to which the changes in ventilation will lower whole body oxygen consumption depends on the mechanical efficiency of the respiratory muscles. Using resistive breathing at 40% of the maximal inspiratory pressure, Baarends and colleagues recently established the range of respiratory efficiency for patients with COPD to be similar (1.4–8.7%) to that of the healthy elderly subjects under resting conditions.[53] Similar measurements have not been obtained during exercise, and too few measurements on the mechanical work or respiratory muscles and the cost of breathing for various exercise modalities and intensities have been obtained to clearly understand how breathing efficiency will affect the total oxygen cost of mechanical work. For example, exercise-induced hyperinflation has been associated with enhanced diaphragm activation in COPD, which could decrease the respiratory muscle efficiency[54] and lead to an exaggerated cost of breathing, with repercussions for whole body oxygen uptake during exhaustive exercise. The few results on the mechanical efficiency of lower or upper body exercise, however, are inconsistent in clearly establishing whether patients with COPD indeed exhibit a lower mechanical efficiency and how exercise training impacts on this work characteristic. The discrepancy in findings may be related to the very limited set of data as well as to variations in the exercise intensity at which measurements are made; indeed, few studies have examined the impact of increasing exercise intensities on the mechanical work efficiency in this population. The interpretation of these findings is also often further complicated by the fact that comparable data on age-matched healthy control subjects are not provided. Further investigations are therefore

required to establish the impact of pulmonary rehabilitation or exercise training on the oxygen cost of work or mechanical efficiency.

Remaining Questions

Scientific evidence shows that exercise training impacts not only on symptoms but also on physiologic function, as seen from the improvements in skeletal muscle oxidative capacity. On the other hand, an increase in maximal aerobic capacity is not systematically reported after exercise training in COPD. This raises the question why training induces adaptations in the skeletal muscle oxidative potential that are not in evidence during maximal aerobic exercise.

One explanation may be related to the fact that since there is only a small number of studies in which maximal aerobic power is specifically assessed after exercise training, it is therefore only in a relatively small number of studies in which an increase in maximal VO_2 is reported. A second explanation is that a factor impinging on a component of the oxygen transport system, whose importance is minimal at submaximal work rates, becomes so important at maximal exercise that it masks or even counters any exercise-induced adaptation in another portion of the oxygen transport system. It is now well established that respiratory muscle energy requirements may compromise exercising leg blood flow when demands for respiratory blood flow are such that there is a competition with locomotor muscles for blood flow. Results from Harms and colleagues clearly established that upon intensive respiratory muscle loading, during dynamic exercise involving a large muscle mass such as cycling, leg perfusion to the working locomotor muscles may be reduced on account of the exaggerated respiratory flow requirements.[55] Findings by Sheel and colleagues recently showed in healthy subjects that the reflex increase in leg vascular resistances or fall in leg blood flow could be triggered by fatiguing respiratory muscle work, causing significant reduction in diaphragm force production.[56]

The extent to which blood flow requirements of respiratory muscles "steal" blood flow from the working muscles during maximal exercise in patients with COPD has not been clearly established. This factor may also be compounded by a limitation in ensuring appropriate central blood flow. How much exercise-induced dynamic hyperinflation affects ventricular filling and thus exercise cardiac output remains to be determined, but it is likely to cause or worsen preexisting pulmonary hypertension. Nevertheless, it follows that any training-induced improvement in the oxygen extraction potential of trained skeletal muscles will not have a chance to be expressed fully if peripheral skeletal muscles remain underperfused because of a limited cardiac output distribution. Alternately, as shown in Figure 65-2, an improvement in skeletal muscle capillarization and oxidative potential resulting from exercise rehabilitation may allow the patient to optimize his aerobic exercise capacity to the extent that it is only limited by the severity of the underlying respiratory limitation. Thus, as a result of endurance exercise training, a patient may achieve a greater work capacity for a similar level of acceptably tolerable ventilation.

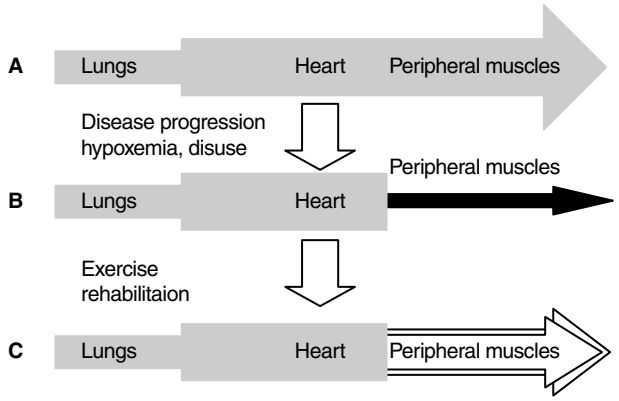

FIGURE 65-2 Effect of disease stage and exercise rehabilitation on sites of maximal oxygen flux limitation in patients with chronic obstructive pulmonary disease (COPD). Sites of maximal oxygen flux limitation in patients with COPD. *A*, The bottle-neck occurs at the site of disease involvement in early stages of the disease. *B*, With disease progression and related disuse and hypoxemia peripheral muscle dysfunction also appears, which may further reduce the O_2 flux capacity and thus become the limiting factor. *C*, Aerobic exercise training may enhance peripheral muscle O_2 flux capacity to such an extent that it equals or exceeds the degree of limitation imposed from the lungs.

ONE SIZE DOES NOT FIT ALL IN EXERCISE REHABILITATION

Several unanswered questions complicate the interpretation of physiologic adaptations to physical training in COPD. For one, the disease appears with advancing age, which in itself is associated with decreases in the physiologic determinants of exercise performance. To date there are still too few studies in which physiologic evidence has been obtained in patients and in age-matched healthy control subjects under comparable conditions to clearly establish the extent to which the disease contributes to physiologic dysfunction.

In addition, the disease is evolving, which means that the impact of the disease on physiologic function or the physiologic repercussions of an intervention such as exercise training may vary according to the disease stage. A still unanswered question is the extent to which the observed deviations from "normal" in muscle physiologic markers reflect "dysfunction," "disuse," or "adaptation." The fact that some of the observed "abnormal" muscle characteristics, such as the reduction in oxidative enzymes activity or skeletal muscle fiber atrophy, are reversed with aerobic training points to a major role of deconditioning and disuse. On the other hand, the observation that the capillary-to-fiber ratio was not lower in COPD patients than in age-matched control subjects[45] and was only affected by aerobic training in a way to preserve the capillary-to-fiber ratio provides an example of cellular plasticity and adaptive response to adverse conditions of bioenergetics. It has been clearly established that the potential to physiologically adapt to physical training or "exercise-induced trainability" is maintained throughout the life span.[31] However, the extent to which disease or staging of disease interacts with trainability has not been examined.

Furthermore, the extent to which contextual factors (environmental and personal factors) interact or contribute to "exercise-induced trainability" cannot be ignored. Exercise training and the improved skeletal muscle function in pulmonary rehabilitation undoubtedly result in improved exercise tolerance and quality of life. Yet, the relationship between the degree of physiologic change and patient's disabilities or activity limitations and patient's handicap or participation restriction (health-related quality of life) has not been demonstrated. This missing link might reflect in part our incomplete understanding of the physiologic responses to exercise as previously discussed. Alternatively, it might be related to the commonly made mistake of reducing the complex notion of disability to consideration of a single component. Looking at the biologic and physiologic aspects as the only explanatory factor to functional and health status improvement after pulmonary exercise rehabilitation is simplistic and unrealistic. The International Classification of Functioning, Disability and Health (ICF) has been proposed by the World Health Organization to help describe changes in body function and structure, patient activities in a standard environment (their level of capacity), and patient participation (their level of performance).[57] The "biopsychosocial model" is a useful model of disability, which represents a coherent view of different perspectives of health: biologic, individual, and social. A simple representation of this model is illustrated in Figure 65-3.

Disability and functioning are viewed as outcomes of interactions between health condition and contextual factors (environmental and personal factors). Little is known about the impact of internal personal factors such as sex, age, disease severity, coping styles, social background, education, past and current experience, and overall behavior pattern, which might influence how disability is experienced by the individual. Environmental factors such as social attitudes, legal and social structures, physical characteristics of the environment, climate, and so forth might equally affect this experience. When pulmonary rehabilitation is carried out in a supervised setting, for example, in hospital, the environment is standardized to such an extent that it will neutralize the varying impact of environmental diversity on the individual's ability. The capacity construct as measured by various testing procedures such as exercise tests will reflect the environmentally adjusted ability of the individual in a specific domain. This is called the "capacity qualifier." However, it does not provide any measure of what an individual is capable of doing in his or her current environment. In contrast, the current environment always includes the overall societal context as it represents ongoing life situations or the lived experience of people in their actual context. This is called the "performance qualifier." This is what we try to measure when using testing procedures or questionnaires such as activities of daily living (for example, using the London Chest Activity of Daily Living[58]) or health-related quality of life (for example, using the SF-36,[59] a generic questionnaire, or the St George's Respiratory Questionnaire,[60] a disease-specific questionnaire).

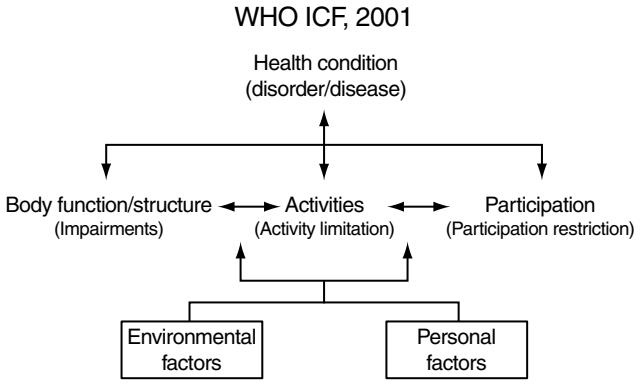

FIGURE 65-3 The biopsychosocial model proposed by the World Health Organization International Classification of Functioning, Disability and Health.[61]

The gap between both capacity and performance qualifiers is important to understand. A person's current environment can enable one to perform better than what might be predicted from the exercise "testing" capacity construct. On the other hand, the person can possess the inherent biologic capacity, but some aspect of the environment may act as a barrier to performance. At this time, we do not know to what extent the measured exercise capacity of a patient will translate into specific activities of daily living or to any given scores of health-related quality of life. Further studies are thus required to identify environmental factors, which may act as barriers and facilitators of the exercise training response and of its translation into the well-being of patients with COPD.

SUMMARY AND CONCLUSIONS

Although still incomplete, an answer is now emerging for the long-time query of health professionals as to how a COPD patient can have improved dyspnea and exercise capacity after a pulmonary rehabilitation program, despite no associated improvement in pulmonary function. In the above sections, we have provided scientific evidence for potential physiologic mechanisms such as skeletal muscle adaptations, improved respiratory muscle function, and enhanced mechanical efficiency, through which exercise training can and does contribute to the improved exercise tolerance of patients with COPD. However, several additional factors need to be considered before claiming a complete understanding of the physiologic basis of exercise responses or training in COPD.

An adaptation of the model to exercise training is required to emphasize the multiple intricacies surrounding exercise rehabilitation as a clinical management tool to optimize function and symptom relief. In the face of such an intricate and complicated model, it becomes obvious that the one-size-fits-all approach to exercise training can only result in a simplistic and loosely fitting outcome, be it in terms of clinical management or of physiologic expectations. Further efforts must therefore be devoted to establish better matching of patients and exercise rehabilitation

modality. Prescriptions of exercise modalities and practice clearly should be reviewed to address the interactions between physical and psychosocial environments and global function as it relates to disease status and evolution. With the development of a biopsychosocial model, rehabilitation professionals will be able to target not only the specific impairments but also those activity limitations and participation restrictions that are modifiable by intervention, and this on a more individual basis.

REFERENCES

1. Hurd S. The impact of COPD on lung health worldwide. Epidemiology and incidence. Chest 2000;117:1S–4S.
2. O'Donnell DE, Webb KA. Exertional breathlessness in patients with chronic airflow limitation: the role of lung hyperinflation. Am Rev Respir Dis 1993;148:1351–7.
3. O'Donnell DE, Revill SM, Webb KA. Dynamic hyperinflation and exercise intolerance in chronic obstructive pulmonary disease. Am J Resp Crit Care Med 2001;164:770–7.
4. American Thoracic Society. Pulmonary rehabilitation. Official statement of the American Thoracic Society Board of Directors. Am J Respir Crit Care Med 1999;159:1666–82.
5. O'Donnell DE, Hernandez P, Aaron S, et al. Canadian Thoracic Society COPD Guidelines: summary of highlights for family doctors. Can Respir J 2003;10:183–5.
6. Pauwels RA, Buist AS, Calverley MP, et al. Global strategy for the diagnosis, management, and prevention of chronic obstructive pulmonary disease: National Heart, Lung, and Blood Institute and World Health Organization Global Initiative for Chronic Obstructive Lung Disease (GOLD): executive summary. Respir Care 2001;46:798.
7. Donner CF, Decramer M. Pulmonary rehabilitation. Eur Respir Mon 2000;13.
8. ACCP/AACVPR. Pulmonary rehabilitation guidelines panel. Pulmonary rehabilitation. Joint ACCP/AACVPR evidence-based guidelines. Chest 1997;112:1363–96.
9. Petty TL. Pulmonary rehabilitation. Respir Care 1977;22:68–78.
10. Hodgkin JE, Farrell MJ, Gibson SR, et al. American Thoracic Society. Medical Section of the American Lung Association. Pulmonary rehabilitation. Am Rev Respir Dis 1981;124: 663–6.
11. Lacasse Y, Wong E, Guvatt GH, et al. Metaanaylsis of respiratory rehabilitation in chronic obstructive pulmonary disease. Lancet 1996;348:1115–9.
12. Casaburi R, Patessio A, Iioli F, et al. Reductions in exercise lactic acidosis and ventilation as a result of exercise training in patients with obstructive lung disease. Am Rev Respir Dis 1991;143:9–18.
13. Maltais F, Leblanc P, Simard C, et al. Skeletal muscle adaptation to endurance training in patients with chronic obstructive pulmonary disease. Am J Respir Crit Care Med 1996; 154:442–7.
14. Sala E, Roca J, Marrades RM, et al. Effects of endurance training on skeletal muscle bioenergetics in chronic obstructive pulmonary disease. Am J Respir Crit Care Med 1999;159: 1726–34.
15. Donner CF, Muir JF. Selection criteria and programmes for pulmonary rehabiliation in COPD patients. Rehabilitation and Chronic Care Scientific Group of the European Respiratory Society. Eur Respir J 1997;10:744–57.
16. Brooks D, Lacasse Y, Goldstein RS. Pulmonary rehabilitation programs in Canada: national survey. Can Respir J 1999;6: 55–63.
17. Lacasse Y, Brosseau L, Milne S, et al. Pulmonary rehabilitation for chronic obstructive pulmonary disease. Cochrane Database Syst Rev 2002(3):CD003793.
18. Salman G, Mosier MC, Besley BW, Calkins DR. Rehabilitation for patients with chronic obstructive pulmonary disease. J Gen Intern Med 2003;18:213–21.
19. Giglioti F, Romagnoli I, Scano G. Breathing retraining and exercise condition in patients with chronic obstructive pulmonary disease (COPD): a physiological approach. Respir Med 2003;97:197–204.
20. Troosters T, Gosselink R, Decramer M. Short and long-term effects of outpatient rehabilitation in patients with chronic obstructive pulmonary disease: a randomized trial. Am J Med 2000;109:207–12.
21. Casaburi R. Skeletal muscle dysfunction in chronic obstructive pulmonary disease. Med Sci Sports Exerc 2001;33(7 Suppl): S662–70.
22. Gosselink R, Troosters T, Decramer M. Exercising training in COPD patients: the basic questions. Eur Respir J 1997;10: 2884–91.
23. Güell R, Casan P, Belda J, et al. Long-term effects of outpatient rehabilitation of COPD. A randomized trial. Chest 2000; 117:976–83.
24. American Thoracic Society. ATS statement: Guidelines for the six-minute walk test. Am J Respir Crit Care Med 2002; 166:111–7.
25. Cahalin L, Papagionopoulos P, Prevost S, Wain J, Ginns L. The relationship of the 6-minute walk test to maximal oxygen consumption in transplant candidates with end-stage lung disease. Chest 1995;108:452–9.
26. Guyatt GH, Pugsley SO, Sullivan MJ, et al. Effect of encouragement on walking test performance. Thorax 1984;39:818–22.
27. Gosker HR, Wouters EF, van der Vusse GJ, Schols AM. Skeletal muscle dysfunction in chronic obstructive pulmonary disease and heart failure: underlying mechanisms and therapy perspectives. Am J Clin Nutr 2000;71:1033–47.
28. Clark CJ, Cochrane L, Mackay E. Low intensity peripheral muscle conditioning improves exercise tolerance and breathlessness in COPD. Eur Respir J 1996;9:2590–6.
29. Ortega F, Toral J, Cejudo P, et al. Comparision of effects of strength and endurance training in patients with chronic obstructive pulmonary disease. Am J Respir Crit Care Med 2002;166:669–74.
30. Bernard S, Whittom F, Leblanc P, et al. Aerobic and strength training in patients with COPD. Am J Respir Crit Care Med 1999;159:896–901.
31. Brooks GA, Fahey TD, White TP, Baldwin KM, editors. Exercise testing and prescription. In: Exercise physiology. Human bioenergetics and its applications 3rd ed. Mayfield Publishing; 2001. p. 639–82.
32. Franssen FM, Wouters EF, Baarends EM, et al. Arm mechanical efficiency and arm exercise capacity are relatively preserved in chronic obstructive pulmonary disease. Med Sci Sports Exerc 2002;34:1570–6.
33. Sato Y, Asoh T, Honda Y, et al. Morphologic and histochemical evaluation of muscle in patients with chronic pulmonary emphysema manifesting generalized emaciation. Eur Neurol 1997;37:116–21.
34. Maltais F, LeBlanc P, Jobin J, Casaburi R. Peripheral muscle dysfunction in chronic obstructive pulmonary disease. Clin Chest Med 2000;21:665–77.
35. Gea JG, Pasto M, Carmona MA, et al. Metabolic characteristics of the deltoid muscle in patients with chronic obstructive pulmonary disease. Eur Respir J 2001;17:939–45.
36. Ribera F, N'Guessan B, Zoll J, et al. Mitochondrial electron transport chain function is enhanced in inspiratory muscles of patients with chronic obstructive pulmonary disease. Am J Respir Crit Care Med 2003;167:873–9.
37. Lake FR, Henderson K, Briffa T, et al. Upper-limb and lower-limb exercise training in patients with chronic airflow obstruction. Chest 1990;97:1077–82.

38. Ries AL, Ellis B, Hawkins RW. Upper extremity exercise training in chronic obstructive pulmonary disease. Chest 1988;93: 688–92.
39. Martinez FJ, Vogel PD, Dupont DN, et al. Supported arm exercise vs unsupported arm exercise in the rehabilitation of patients with severe chronic airflow obstruction. Chest 1993;103:1397–402.
40. Hsia CC. Coordinated adaptation of oxygen transport in cardiopulmonary disease. Circulation 2001;104:963–9.
41. Oelberg DA, Kacmarek RM, Pappagianopoulos PP, et al. Ventilatory and cardiovascular responses to inspired He-O_2 during exercise in chronic obstructive pulmonary disease. Am J Respir Crit Care Med 1998;158:1876–82.
42. Bogaard HJ, Dekker BM, Arntzen BW, et al. The haemodynamic response to exercise in chronic obstructive pulmonary disease; assessment by impendance cardiography. Eur Respir J 1998;12:374–9.
43. Alpert JS, Bass H, Szucs MM, et al. Effects of physical training on hemodynamics and pulmonary function at rest and during exercise in patients with chronic obstructive pulmonary disease. Chest 1974;66:647–251.
44. Montes de Oca M, Rassulo J, Celli BR. Respiratory muscle and cardiopulmonary function during exercise in very severe COPD. Am J Respir Crit Care Med 1996;154:1284–9.
45. Whittom F, Jobin J, Simard PM, et al. Histochemical and morphological characteristics of the vastus lateralis muscle in patients with chronic obstructive pulmonary disease. Med Sci Sport Exerc 1998;30:1467–74.
46. Gustafsson T, Kraus WE. Exercise-induced angiogenesis-related growth and transcription factors in skeletal muscle, and their modification in muscle pathology. Front Biosci 2001;6:D75–89.
47. Gustafsson T, Bodin K, Sylven C, et al. Increased expression of CEGF following exercise training in patients with heart failure. Eur J Clin Invest 2001;31:362–6.
48. Testa M, Ennezat PV, Vikstrom KL, et al. Modulation of vascular endothelial gene expression by physical training in patients with chronic heart failure. Ital Heart J 2000;1:426–30.
49. Casaburi R, Porszasz J, Burns MR, et al. Physiolological benefits of exercise training in rehabilitation of patients with severe chronic obstructive pulmonary disease. Am J Respir Crit Care Med 1997;155:1541–51.
50. O'Donnell DE, McGuire M, Samis L, Webb KA. General exercise training improves ventilatory and peripheral muscles strength and endurance in chronic airflow limitation. Am J Resp Crit Care Med 1998;157:1489–97.
51. Baarends EM, Schols AM, Akkermans MA, Wouters EF. Decreased mechanical efficiency in clinically stable patients with COPD. Thorax 1997;52:981–6.
52. O'Donnell DE, McGuire M, Samis L, Webb KA. The impact of exercise reconditioning on breathlessness in severe chronic airflow limitation. Am J Respir Crit Care Med 1995; 152:2005–13.
53. Baarends EM, Schols AM, Nusmeier CM, et al. Breathing efficiency during inspiratory threshold loading in patients with chronic obstructive pulmonary disease. Clin Physiol 1998; 18:235–44.
54. Sinderby C, et al. Diaphragm activation during exercise in chronic obstructive pulmonary disease. Am J Respir Crit Care Med 2001;163:1637–41.
55. Harms C, Harms CA, Wetter, et al. Effects of respiratory muscle work on cardiac output and its distribution during maximal exercise. J Appl Physiol 1998;85: 609–18.
56. Sheel AW, Derchak PA, Morgan BJ, et al. Fatiguing inspiratory muscle work causes reflex reduction in resting leg blood flow in humans. J Physiol 2001;537:277–89.
57. World Health Organization. International classification of impairment, disabilities and handicaps: a manual classification relating to the consequences of disease. Geneva: World Health Organization; 1980.
58. Garrod R, Bestall JC, Paul EA, et al. Development and validation of a standardized measure of activity of daily living in patients with severe COPD: the London Chest Activity of Daily Living scale (LCADL). Respir Med 2000;94:589–96.
59. Harper R, Brazier JE, Waterhouse JC, et al. Comparison of outcome measures for patients with chronic obstructive pulmonary disease. Thorax 1997;52:879–87.
60. Jones PW, Quirk FH, Baveystock CM, Littlejohns P. A self-complete measure of health status for chronic airflow limitation. The St. George's Respiratory Questionnaire. Am Rev Respir Dis 1992;145:1321–7.
61. World Health Organization. Resolution of the Executive Board of the WHO: international classification of functioning, disability and health. 2001:18.

CHAPTER 66

LUNG VOLUME REDUCTION SURGERY

Koji Chihara

The finding that the expanded rib cage and flattened diaphragm of patients with end-stage emphysema adapted to the size of the transplanted lungs, which were of normal size, soon after surgery and a description of an innovative surgical approach for patients with emphysema by Brantigan and Muller in 1950s[1] prompted Cooper and colleagues to perform a procedure to reduce the overall volume of each lung by 20 to 30% in patients with advanced emphysema.[2] The most destroyed areas of both lungs as gauged by preoperative computed tomography (CT) scan and quantitative nuclear scans, which they called target areas, were excised by successive applications of linear stapling devices through a median sternotomy. The procedure was termed pneumectomy (volume reduction) and revealed marked benefits, such as increase in forced expiratory volume in 1 second (FEV_1), decrease in residual volume (RV), increase in 6-minute walk distance (6MWD), decrease in dyspnea, and improvement of quality of life, that could not be obtained by any other means except lung transplantation.[2] Following this striking report in 1995, lung volume reduction surgery (LVRS) spread widely and rapidly to other surgical centers.[3–6]

OPERATIVE OUTCOMES

The inclusion and exclusion criteria for LVRS generally accepted in the early period of this surgical intervention are shown in Table 66-1.[7,8] LVRS has been performed either by a median sternotomy[2–4] or by video-assisted thoracoscopic surgery (VATS).[5,6] Needless to say, it is a procedure for patients with poor pulmonary reserve and carries a substantial risk of operative mortality and morbidity. A systematic review of LVRS revealed that 30-day and 3- to 6-month mortalities ranged from 0 to 6% and 0 to 8%, respectively.[9] Air leak of more than 7 days duration was the most common postoperative complication, occurring in about 50% of cases.[10] Other postoperative complications included pneumonia, respiratory failure, gastrointestinal perforation, and the need for reoperation because of intractable air leak or hemorrhage.[2,10]

Both procedures showed similar results with 75 to 85% patients benefiting from LVRS. Early reports of LVRS showed that FEV_1 as a percentage of the predicted value (FEV_1% predicted) increased from 24 to 28% to 35 to 41% and 6MWD increased from a range of 241 to 290 m to 306 to 434 m 3 to 6 months after LVRS. Although the favorable short-term results of LVRS gained broad acceptance,[11] questions were raised about the mechanisms of improvement, risk–benefit ratio, magnitude and duration of benefit, optimal technique for LVRS, and optimal candidates for LVRS. In the United States, to answer these questions a multicenter, randomized control trial of medical therapy versus medical therapy plus LVRS for the treatment of patients with severe bilateral emphysema (National Emphysema Treatment Trial) was conducted from 1998 to 2002.[12]

EARLY PHYSIOLOGIC CHANGES FOLLOWING LVRS

Pulmonary Function and Mechanics

Although improvement in the FEV_1 may not be the main goal of LVRS, it is certainly an important outcome measure so that the mechanisms accounting for an improvement on spirometric measures of function after LVRS have received attention.

Gelb and colleagues measured pulmonary function, lung elastic recoil pressure (P_{el}), and airway conductance of airways between the alveoli and the flow-limiting segment (G_s) according to the expiratory flow-limitation model of Pride and colleagues.[13,14] Accordingly, maximal expiratory flow ($\dot{V}_{max}$) = ($P_{el} - P_{tm'}$) G_s, where $P_{tm'}$ is the critical transmural pressure at the site of the collapsible segment within the airway tree. They showed that lung compliance (C_L) near functional residual capacity (FRC) did not change following LVRS, whereas lung elastic recoil at total lung capacity ($P_{el,TLC}$) significantly increased from 10.3 to 14.6 cm H_2O, although it was still less than normal. Almost all patients showed a positive $P_{tm'}$ before LVRS, and the mean $P_{tm'}$ was significantly decreased by surgery from 3.1 to 2.4 cm H_2O. They concluded that the improvement in $\dot{V}_{max}$

Table 66-1A Indications for Surgery

Inclusion criteria	*Exclusion criteria*
End-stage emphysema, refractory to medical therapy	Age > 75 years
Severe dyspnea	Cigarette use within 3–6 months prior to surgery
FEV_1 < 35% of predicted	Severe obesity or cachexia
Hyperinflated lungs by chest x-ray and body plethysmography	Severe comorbid illness, or rapidly fatal medical illness
Able to complete pre-operative pulmonary rehabilitation program	Severe pulmonary hypertension
	Inability to participate in rehabilitation
	Severe hypercapnia ($P_aCO_2 \geq 50$ mm Hg)
	Ventilator dependence

FEV_1 = forced expiratory volume in 1 second; P_aCO_2 = arterial partial pressure of carbon dioxide.

Table 66-1B Common Relative Exclusion Criteria

Diffuse homogeneous lung involvement (usually assessed with CT scan or $\dot{V}/\dot{Q}$ scan)
Age > 75 years
CO_2 retention ($P_aCO_2 > 50$ mm Hg)
Pulmonary hypertension (mean pulmonary arterial pressure > 35 mm Hg or systolic pulmonary arterial pressure > 45 mm Hg*)
End-stage disease with severe disability (FEV_1 < 20% predicted, 6-minute walk < 600 feet)
Malnutrition
Inability to comply with pulmonary rehabilitation

CT = computed tomography; FEV_1 = forced expiratory volume in 1 second; $PaCO_2$ = arterial partial pressure of carbon dioxide; $\dot{V}/\dot{Q}$ = ventilation/perfusion.
*Modified according to the text.

could be primarily attributed to an increase in P_{el} and its secondary effect of enlarging airway diameter, causing an increase in G_s. Scuiba and colleagues also showed that the maximal static recoil pressure increased after LVRS.[15] These studies support the hypothesis proposed by Brantigan and Muller,[1] in which the improvement of pulmonary function after multiple wedge resections of useless lung tissues could contribute to the restoration of airway caliber. In contrast, Ingenito and colleagues studied the changes in spirometry and pulmonary mechanics in patients undergoing bilateral LVRS and used the same model of flow limitation expanded in the Taylor series. Among responders whose FEV_1 increased more than 12% over baseline, $P_{el,TLC}$ increased and the time constant for expiration ($\tau = C_L/G_s$) decreased, whereas $P_{tm'}$, C_L, and G_s did not change. Among nonresponders, τ increased significantly, contributing to a decline of the ratio of FEV_1 to forced vital capacity (FVC). They concluded that improvement in expiratory flows after LVRS was largely owing to an increase in $P_{el,TLC}$ rather than by improving small airway conductance or by decreasing air trapping during forced expiration.[16]

There are theoretical reports that have examined the effect of lung volume reduction on the maximal expiratory flow-volume curves of the lung from the viewpoint of interaction between the lung and chest wall.[17,18] Fessler and Permutt developed an important physiologic model to answer the question of why removing a part of the lung in a patient with emphysema caused improvements in spirometry.[18] As vital capacity (VC) is determined by an interaction between the mechanical properties of the lung and chest wall, the two static pressure-volume (P-V) lines are plotted simultaneously. Plotting static lung volume (V) against pleural pressure (P_{pl}) allows the estimation of P_{el} and C_L during inspiration. Plotting static lung volume against maximal inspiratory pleural pressure during airway occlusion gives the mechanical properties of the chest when the inspiratory muscles act on it maximally. In these plots, total lung capacity (TLC) is determined by the intersection of the two lines at the point where P_{el} is equal and opposite to the maximally negative pleural pressure that the inspiratory muscles can generate. VC is the difference between TLC and residual volume (RV). Assuming linear approximations, the effects of LVRS on VC are solved algebraically from graphic representations as follows:

$$VC = (P_{el,TLC} - P_{tm'})\ C_L = P_{el,TLC}\ C_L - P_{tm'}C_L$$

and

$$RV = RV_0 + P_{tm'}C_L$$

where $P_{tm'}$ is the transmural pressure of airway closure and RV_0 is the residual volume when $P_{tm'}$ is zero. $P_{tm'}C_L$ is the volume of trapped gas resulting from airway closure. If one assumes that the removal of lung does not alter the P-V characteristics of the chest wall or the intrinsic ability of the respiratory muscles to generate force at a given chest wall volume, the maximal inspiratory P-V curve of the chest wall and compliance of the active chest wall (C_{wmax}) should not change. The effects of LVRS are shown graphically in Figure 66-1. If pure bullae with little elastic recoil were removed and C_L did not change, VC after surgery would increase by the amount of the decrease in RV (response A). If the emphysematous changes were homogeneous through the lung, LVRS would result in a proportional reduction in both RV and C_L. VC would therefore increase slightly less than in response A (response B). In a patient with less hyperinflation and homogeneous emphysema, preoperative RV/TLC and C_L would be lower than in the previous two cases. Thus, VC could decrease after LVRS (response C). Although the amount of trapped gas ($P_{tm'}C_L$) is a determinant of the change in VC, $P_{tm'}$ is neglected in all figures for simplicity. Their analysis yielded the conclusion that the ratio of RV to TLC was the single most important determinant of the improvement in pulmonary function after LVRS (see Figure 66-1).

The validity of their predictions was tested in a group that underwent bilateral LVRS and another group that underwent bilateral or unilateral LVRS.[19] In the former group, RV/TLC was the only preoperative independent predictor of the increase in FVC. Seventy percent of the increase in FEV_1 was attributable to an increase in FVC, with the remainder owing to increases in FEV_1/FVC. A significant increase both in FEV_1 and FVC and a decrease in RV were found in the subgroup, with a preoperative RV/TLC more than 0.67, whereas there was no significant improvement in these parameters in

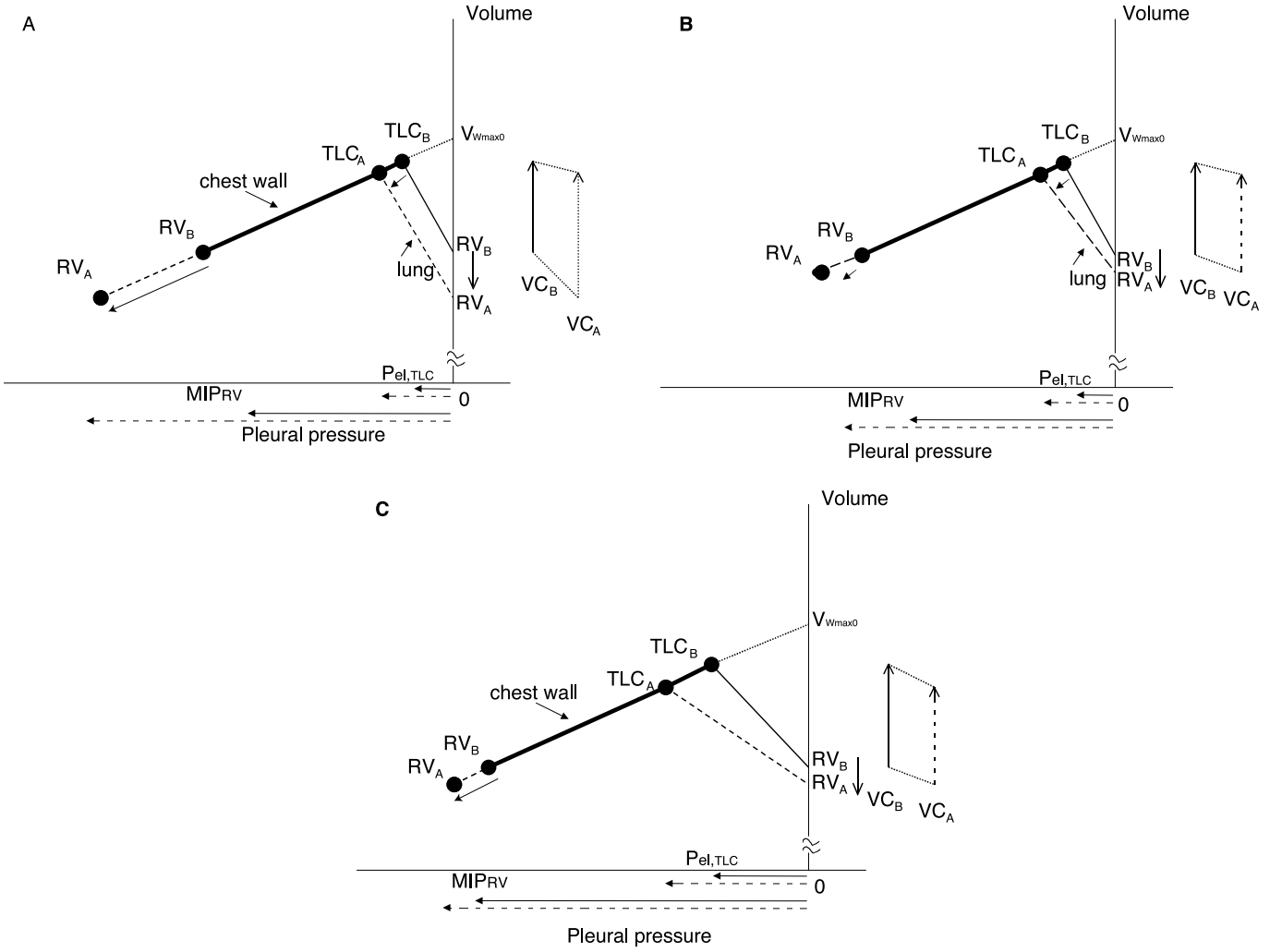

FIGURE 66-1 Graphic descriptions of the effects of lung volume reduction surgery (LVRS) on vital capacity (VC) (Fessler and Permutt). Pressure-volume (P-V) relationships of the lung and chest wall are depicted. In these descriptions, it is assumed that LVRS does not change the chest wall determinants (V_{wmax0} and C_{wmax}). *A*, The effects of removal of pure bullae, which are assumed to be completely nonfunctional space-occupying legions, are shown by the *dotted line*. There is a parallel downward shift of the lung P-V relationship. It is assumed that the P-V relationship of the chest wall shifts downward on the same line. As the vertical difference between residual volume (RV) before surgery (RV_B) and RV after surgery (RV_A) is larger than that of total lung capacity (TLC) ($TLC_B \rightarrow TLC_A$), VC increases after surgery ($VC_B \rightarrow VC_A$). Lung elastic recoil pressure at TLC ($P_{el,TLC}$) and maximal inspiratory pressure at RV during airway closure (MIP_{max}) increase after surgery (*straight line*: before surgery; *dotted line*: after surgery). *B*, The effects of LVRS on a patient with homogeneous distribution of emphysema. In this case, compliance of the lung (C_L) decreases according to resection, which results in a higher position of RV_A than that in model *A*. As a result, increase in VC is smaller than that in model A. *C*, In a patient with less hyperinflated emphysema, the preoperative RV is smaller than that of models *A* and *B*, and the preoperative compliance of the lung is more normal than that of *A* and *B*. LVRS now decreases VC because the change in TLC is larger than that in RV. Note $P_{el,TLC}$ and MIP_{max} increase in all three models because of decrease in RV. The model anticipates that RV decreases and C_L does not change or decreases after surgery. However, an opposite response happens if one removes more normal lung instead of functionless tissue, or if one performs LVRS on a patient whose remaining lung is easily hyperinflated after surgery.

the other patients with RV/TLC less than this cutoff value. Interestingly, compliance increased and inspiratory resistance decreased after LVRS in the high RV/TLC subgroup, whereas these parameters showed opposite changes in the low RV/TLC subgroup. The authors found in the latter group that RV/TLC again correlated with the increase in FVC, and changes in FEV_1 were also largely attributable to change in FVC. However, RV/TLC was not predictive of the increase in FEV_1 overall because FEV_1/FVC in patients with a low preoperative RV/TLC often increased despite little change in FVC.

Subsequently, Ingenito and colleagues clarified the difference in physiologic characteristics between responders and nonresponders to LVRS by no-cut thoracoscopic lung plication using the same flow-limitation model and the model proposed by Fessler and Permutt.[20] Among responders, improvement in FEV_1 was primarily due to increase in FVC, not to increase in FEV_1/FVC—in other words, not to improvement in the expiratory time constant. In contrast, small changes in RV were accompanied by equivalent changes in TLC resulting in no changes in FEV_1, FVC, and RV/TLC in nonresponders. $P_{el,TLC}$ increased in nonresponders

as much as in responders. Thurnheer and colleagues also found that the preoperative RV/TLC was significantly correlated with increase in FVC.[21] These results have provided support for the hypothesis of Fessler and Permutt that LVRS improves pulmonary function by resizing the lung relative to the chest wall.

As FVC in patients with emphysema is often smaller than VC, and LVRS is not a procedure for patients with bullae but for patients with emphysema, there would be some limitations in the prediction of FEV_1 or FVC after LVRS using the model proposed by Fessler and Permutt. However, it provides a framework for understanding how LVRS works in patients with different preoperative characteristics. The model predicts that the higher the RV and C_L preoperatively, the greater the increase in VC and in P_{el} after LVRS, and that the change in the slope of the static lung P-V curve after surgery is an important determinant of the change in VC. Furthermore, RV/TLC, a reflection of the size mismatch between the hyperinflated lungs and the chest wall, is the best predictor of improvement in airflow limitation after LVRS. It is also important to note that an improvement in VC may be expected in patients with a homogeneous distribution of disease if preoperative RV is high.[19]

Chest Wall Function, Dyspnea, and Exercise Capacity

Effects of Chronic Hyperinflation on Static Chest Wall Function The chest wall and the lung affect each other through the amount of air in the lung. The excessive volume of air in chronic obstructive pulmonary disease (COPD) patients increases the work of breathing for the muscles of the chest wall. Chronic hyperinflation in patients with advanced emphysema displaces both the inspiratory and the expiratory muscles of the chest wall far from their original configurations. As a result, the mechanical properties of the respiratory muscles and the interactions among them have been changed. The diaphragmatic length has shortened because of chronic hyperinflation of the lungs. One might expect that the ability of the diaphragm to generate pressure at any given length would be reduced if the length–tension relationship of the muscle were unchanged. However, recent studies on patients with stable COPD[22] and patients with end-stage emphysema undergoing lung transplantation[23] showed that although the length of diaphragm of the patients was short, its ability to generate pressure was the same as or greater than normal at the same high lung volumes. This suggests that length adaptation of the human diaphragm occurs as it does in emphysematous hamsters.[24] Even so, a shorter diaphragm impairs the function of the ventilatory pump because a lesser degree of shortening of the diaphragm displaces the lungs in the craniocaudal direction less than normal. In addition, the shorter diaphragm expands the lower rib cage less than normal because both appositional and insertional components of the diaphragm[25] are decreased by the configurational changes of the diaphragm and the lower rib cage. Impairment of the diaphragmatic action on the lower rib cage increases the relative contribution of the upper rib cage and the neck muscles to the performance of inspiratory work. In addition, the work of inspiration is greater than normal because of an increase in elastic load by an excessive residual volume and intrinsic positive end-expiratory pressure ($PEEP_i$) that serves as an additional inspiratory load.[26] The work of expiration for the expiratory muscles increases because of an increased resistive load caused by severe expiratory flow limitation. Indeed, expiratory muscles are recruited even at rest.[27,28] The physiologic implication of this recruitment of the abdominal expiratory muscles in COPD is not well understood, but it has been suggested that it pushes the diaphragm to a more favorable position at the onset of inspiration, when the diaphragm starts to contract. As the anteroposterior (AP) diameter of the lower rib cage increases in patients with severe COPD,[29] it is possible that the shift of the lower rib cage may stretch the abdominal wall, creating passive tension in the abdominal muscles. Such an effect might be expected to promote abdominal muscle activation.

Effects of Chronic Hyperinflation on Dynamic Chest Wall Function During quiet breathing, the respiratory muscles in patients with emphysema may compensate for the impairment in ventilatory function. However, this can result in severe dyspnea during ordinary activities such as walking and dressing. During exercise, patients increase ventilation, but because exhalation needs a longer time than in normal subjects because of expiratory flow limitation, there is a gradual increase in end-expiratory lung volume (EELV) or so-called dynamic hyperinflation.[26] The length of the diaphragm at the beginning of each contraction becomes shorter with each breath as EELV increases gradually. As a result, the diaphragmatic active tension decreases progressively, and the upper rib cage and neck muscles are progressively recruited to overcome the increased work of breathing. Recent experimental studies on normal subjects and findings in patients with COPD showed that the degree of recruitment of the upper rib cages and the neck muscles corresponded to the severity of dyspnea.[30–32] The stronger the recruitment of these muscles, the more severe was the dyspnea, resulting in limitation exercise. O'Donnell and colleagues showed that inspiratory effort estimated as the ratio of esophageal pressure during tidal breathing to the maximal esophageal pressure at the same lung volume in patients with COPD correlated strongly with dynamic EELV/TLC at isotime during cycle-exercise testing. They concluded that the sensation of dyspnea may have its origins in thoracic hyperinflation and the resultant disparity between inspiratory effort and ventilatory output[33] (Figure 66-2).

Effects of LVRS on Static Chest Wall Function Lando and colleagues measured AP and transverse diameters at multiple sites of the rib cage with chest roentgenograms while standing upright and supine with CT scans.[34] They showed that postoperative reductions of AP diameters of the lower rib cage were most likely the result of reduction in lung volume and were correlated with an increase in 6MWD. The ability of the diaphragm to generate pressure isdetermined by three factors: (1) length– tension relationship,

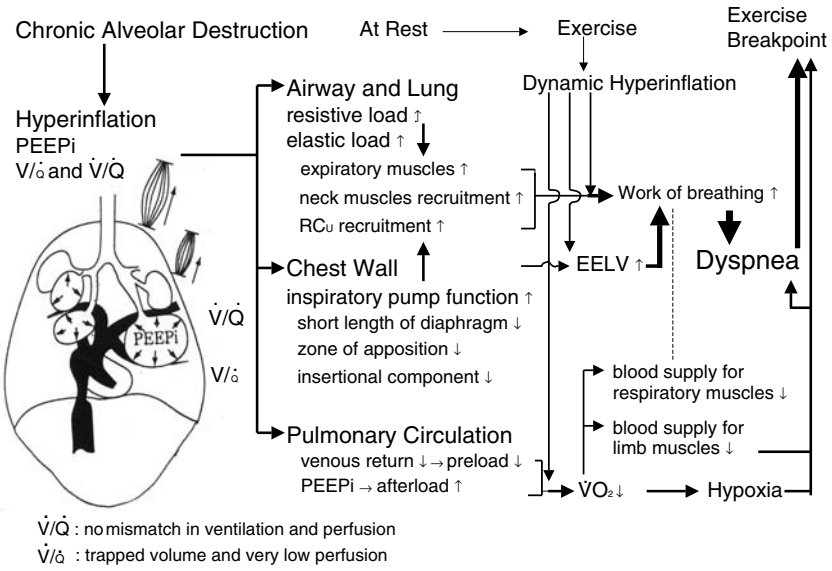

FIGURE 66-2 A proposed schematic representing hyperinflation and dyspnea in chronic obstructive pulmonary disease. An unusual symbolic expression (V/Q̇) is used for a part of air-trapped lung with very low perfusion.

(2) force–velocity relationship, and (3) radius of curvature and diaphragmatic tension according to Laplace's law.[35] In addition, the size of the zone where the diaphragm is directly apposed to the inner surface of the rib cage is an important determinant of the diaphragm's action on the rib cage. Cassart and colleagues found that LVRS made the diaphragm dome move upward and increased the zone of apposition without a change in diaphragm dimensions at FRC. A significant increase in the total diaphragm length, especially in the zone of apposition, was observed with chest roentgenograms 3 to 6 months after LVRS.[36] This suggests that both the increase in diaphragmatic fiber length and in the area of apposition may have improved diaphragmatic function. These factors are known to be important in determining diaphragmatic action in normal subjects. Consistent with these measurements, the diaphragmatic strength assessed by transdiaphragmatic pressure (P_{di}) during a Müller maneuver, maximum sniff, phrenic nerve stimulation, or maximal inspiratory mouth pressure increased significantly after LVRS.[37,38] In the evaluation of changes in these pressures, it is necessary to remember that comparison of the pressures before and after LVRS should be performed at the same lung volume because these pressures are volume dependent.

Effects of LVRS on Dynamic Chest Wall Function

Abnormal motions such as a biphasic motion of the abdomen during inspiration or a phase difference between the rib cage and the abdomen have been observed in patients with COPD by body surface measurements.[39,40] The factors contributing to these abnormal chest wall motions in patients with COPD are increased airway resistance[41] and hyperinflation. Block and colleagues measured rib cage and abdominal volume changes with respiratory inductive plethysmography during normal breathing at rest before and after LVRS.[42] The contribution of abdominal volume change to tidal volume increased and the fraction of inspiratory time associated with abdominal paradoxical motion decreased postoperatively. The phase shift between rib cage and abdominal motion was reduced postoperatively. As abdominal motion should reflect diaphragmatic motion, we analyzed the diaphragm and rib cage motions with serial lateral chest roentgenograms during one breathing cycle while the patients continued effort breathing in the supine posture.[43] We found that the diaphragm did not move as a unit but showed a small and delayed motion of the anterior part of the diaphragm in the craniocaudal direction before LVRS compared with the central and posterior parts of the diaphragm. The phase shifts among the three parts of the diaphragm were improved after surgery. The plots of posteroanterior motion of the upper rib cage (RC_U) and craniocaudal motion of the center part of the diaphragm (D_{ic}), which was similar to the Konno-Mead diagram, showed loops because D_{ic} lagged behind RC_U before LVRS, and the phase shifts were improved after surgery. More recently, magnetic resonance imaging during breathing (dynamic MRI) has allowed researchers to analyze, noninvasively, diaphragmatic motion and has provided insights into the chest wall mechanics of patients with emphysema.[44–46] These studies on patients undergoing LVRS showed improvements in configuration of the chest wall and in diaphragmatic motion, which resulted in better coordination of the chest wall compartments. The improvement in diaphragmatic function and restoration of the lower rib cage and the abdominal wall to a more normal position by LVRS should have an important role in improving the act of breathing.[46]

Benditt and colleagues studied the effects of LVRS on ventilatory muscle recruitment by measuring pleural pressure (P_{pl}) and gastric pressure (P_{ga}) during rest and during exercise.[47] The P_{ga}–P_{pl} diagram at isowatt exercise after LVRS returned to a more normal pattern, which suggested better function of the diaphragm. Interestingly, the change in P_{pl} and P_{ga} correlated with the degree of FRC reduction but not the increase in FEV_1.

In summary, LVRS improves the configurations of the diaphragm and the lower rib cage, which ensures better

inspiratory reserve and better coordination of the compartments of the chest wall during breathing. As inspiratory capacity (IC) is an important determinant of exercise endurance in patients with COPD, an increase in IC can be associated with improvement in exercise capacity after LVRS.[48–51]

Effects of LVRS on Exercise Capacity and Dyspnea
Dyspnea is an expression of the sense of respiratory effort.[52] There are four management strategies for dyspnea: reducing ventilatory work, improving respiratory muscle function, reducing ventilatory demand, and altering central perception. LVRS reduces dyspnea in patients with emphysema by reducing elastic and resistive loads and by improving chest wall pump function through alleviation of the adverse effects of hyperinflation. A lower EELV after LVRS enables a patient with emphysema to do exercise with less dyspnea. As a result, exercise endurance times become longer because dynamic hyperinflation occurs later in exercise than before LVRS. A decrease in central respiratory drive was also found following LVRS[51,53,54].

WHO BENEFITS FROM LVRS?

What is the benefit of LVRS for patients with end-stage emphysema? Improvements in exertional dyspnea and exercise capacity must be important benefits for patients who have been suffering from discomfort and restricted activities for years. As the sensation of dyspnea in patients with emphysema is a perception of the ventilatory load caused by hyperinflation, reducing RV and lowering EELV should be of primary significance. In other words, preoperative hyperinflation is the essential criterion of LVRS.

Hyperinflation

How much preoperative hyperinflation is required so that one can expect a favorable outcome of LVRS? Weder and colleagues showed that almost all patients with RV/TLC greater than 0.5 preoperatively had an increase in FEV_1 and had a decrease in dyspnea 3 months after LVRS, as long as the indication for LVRS was severe hyperinflation.[55] The same group later performed a detailed statistical analysis to investigate the independent effect of several potential factors on outcomes after LVRS in 70 patients and found that the preoperative RV/TLC ratio was significantly correlated with changes in FVC and postoperative RV/TLC; the higher the preoperative RV/TLC, the greater the increase in FVC. They showed that the cutoff value of the preoperative RV/TLC corresponding to 75 and 95% specificity was 67 and 77%, respectively, when one predicted postoperative gain in FVC more than 1 L.[21] In the other cited study,[19] patients with RV/TLC <0.67 did not achieve a statistically significant increase in FVC or decrease in RV after surgery. Thus, this value might be an important predictor for patient selection for LVRS.

There are some patients who experience decreases in dyspnea but have no improvement in FEV_1. Martinez and collegues found that one-half of their patients showed a less than 20% improvement in FEV_1 but experienced a decrease in breathlessness at equivalent workload after LVRS. The decrease in Borg score for dyspnea was strongly correlated with the decrease in EELV.[50] In their study, the preoperative mean RV/TLC of 64% corresponds to a value between 50 and 75% specificity for expectation of improvement by more than 1 L in FVC according to the analysis of Thurnheer and colleagues.[21] As a patient with a lower RV/TLC might have less severe emphysema, the configurational change in the chest wall and the degree of dynamic hyperinflation during exercise would be less preoperatively than in a patient with a higher RV/TLC. A decrease in lung volume in such patients could result in a decrease in dyspnea without significant improvement in maximum expiratory flows. However, some objective indices, such as a minimum cutoff value in RV and RV/TLC or landmarks for hyperinflation of the chest wall, by which one could expect benefits following LVRS, remain unresolved issues.

After LVRS, a patient with greater air trapping before LVRS should obtain a greater improvement in ventilatory reserve than another patient with a lesser degree of air trapping. Tschernko and colleagues found that preoperative dynamic intrinsic positive end-expiratory pressure ($PEEP_{i,dyn}$) predicted postoperative increases in FEV_1% predicted and exercise capability and decrease in dyspnea. They noted that a threshold value for preoperative $PEEP_{i,dyn}$ ≥ 5 cm H_2O resulted in the best combination of sensitivity (93%) and specificity (88%) of all examined threshold values when a good functional result was defined as an increase in FEV_1% predicted $\geq 40\%$.[56]

These cutoff values of pulmonary function and mechanics as described above surely have an important role in patient selection for LVRS. However, these values represent the global respiratory system, and other potential indices regarding the distribution pattern or the severity of emphysema are necessary for better prediction of outcome following LVRS.

Heterogeneity and Severity of Emphysema

It has been shown that a heterogeneous distribution of emphysema estimated by CT scan, perfusion scan, and roentgenograph is the most important predictor of surgical outcome.[2,55,57–59] Weder and colleagues determined homogeneous, moderately heterogeneous, and markedly heterogeneous types of emphysema based on the subjective analysis of CT scan and showed that a mean increase in FEV_1 in these three groups 3 months after LVRS was 34%, 44%, and 81%, respectively.[55] Others found that better outcomes following LVRS occurred in patients with a heterogeneous distribution of emphysema, in other words, in patients in whom identification of the target areas was easy. Some patients with homogeneous emphysema and severe hyperinflation also benefited from LVRS, although improvement in pulmonary function was less than that in patients with heterogeneous emphysema.[55] The role of perfusion scintigraphy in prediction of outcome of LVRS is controversial. Thurnheer and colleagues claimed that it had a limited role in outcome prediction, but it might help select target areas with relative hypoperfusion for resection in emphysema that is homogeneously

distributed on the chest CT.[21] On the other hand, others found that the ability of the perfusion scan to predict outcome of LVRS was the same as the CT scans.[60,61]

There are few reports of the relationship between morphologic severity of emphysema and outcome of LVRS.[62,63] Rogers and colleagues measured severity of emphysema with CT morphometry, which converted the radiographic attenuation values into a measurement of volume of gas per gram of tissue.[63] They found that the maximal cardiopulmonary exercise performance following surgery correlated significantly with baseline values of severe emphysema, and a decrease in severe emphysema correlated positively with an increase in watts on a cycle ergometer, as well as with improvement in pulmonary function. They studied the relationship between morphologic severity of emphysema and diffusing capacity of carbon monoxide (DL_{CO}) as the standard marker of physiologic severity of emphysema. They showed that the higher the ratio of volume of severe emphysema to total lung volume (TLV) preoperatively, the more the DL_{CO} improved postoperatively. In contrast, the higher the ratio of moderate emphysema to TLV preoperatively, the more likely DL_{CO} was to decrease. The authors suggested that pulmonary capillary volume could increase or decrease according to the balance between the changes in regional lung mechanics and physical removal of capillaries in severe or moderate emphysema. Weg and colleagues found pulmonary hypertension in six of nine patients after LVRS. This was attributed to an increase in pulmonary vascular resistance.[64] On the other hand, Kubo and colleagues suggested the possibility for pulmonary capillary recruitment to occur after LVRS by the finding of a lack of change in pulmonary artery pressure, despite a significant increase in cardiac output.[65]

There are no doubts about the value of assessing the morphologic heterogeneity of emphysema by the static imaging modalities as described above under patient selection for LVRS. However, if parts of the lung showing air trapping during breathing could be identified dynamically, it would provide information on functional heterogeneity in the emphysematous lung. To select patients for LVRS we have been using findings regarding the prediction of symptoms and pulmonary function after giant bullectomy.[46] Briefly, patients in whom the motion of the diaphragm and a bulla were in phase during forceful breathing preoperatively had a decrease in FEV_1 and were more breathless 6 months after bullectomy. In contrast, other patients whose preoperative bulla motion was completely paradoxical with respect to the motion of the diaphragm had an increase in FEV_1 and an improvement in dyspnea 1 to 3 months after surgery.[66] A potential target area in LVRS does not have as clear a boundary as a bulla has, but using magnetic resonance imaging it can be approximated during breathing. Based on the assumption that a widening or narrowing of the vascular markings during breathing is proportional to regional ventilation, we determined an emphysematous part with little changes in vascular geometry during breathing as a target area of emphysema that we called a tumor of air or airoma. Twenty-five patients underwent bilateral or unilateral resection of airomas irrespective of their location in the upper or lower lobes. All patients experienced decreases in the sensation of dyspnea, and 22 of 25 showed increases in FEV_1 after surgery. The 3-year survival rate of the patients was 91%. Although this method is based on a critical assumption and a subjective analysis performed on a limited number of slices of the lung, it might have a role in patient selection and delineation of target areas in LVRS.

Unilateral or Bilateral LVRS

Bilateral LVRS has been instituted as the standard procedure in many centers since improvement in FEV_1 following bilateral LVRS is almost twice that following unilateral LVRS.[2] Furthermore, long-term survival rates in patients after bilateral LVRS are better than those of unilateral LVRS.[67] However, unilateral LVRS also results in symptomatic improvement, improved walking distance, and increase in FEV_1 and decrease in RV.[68] It is still an important therapeutic option for patients with an asymmetric distribution of emphysema or poor pulmonary reserve.

Upper or Lower Lobes

Many reports support the claim that improvement following LVRS is better in patients whose target areas are in the upper lobes than in patients with lower-lobe targets.[2,5,58–60] A high ratio of emphysema in the upper lobe to the lower lobe on CT or perfusion scan predicted short-term functional improvements well. However, others found that even if the areas most affected by emphysema were found in the lower lobe, LVRS resulted in similar improvements in pulmonary function, exercise, quality of life, or other outcome measurements of LVRS.[55,69] Recently, it has been shown that LVRS yields a survival advantage for patients with both predominantly upper-lobe emphysema and low baseline exercise capacity, whereas it does not afford patients with non–upper-lobe emphysema and high exercise capacity the benefit.[70]

High-Risk Patients

The NETT study recently revealed that a subgroup of patients with FEV_1 equal to or less than 20% of predicted value and either with a homogeneous distribution of emphysema on CT scan or with DL_{CO} equal to or less than 20% predicted showed a 30-day mortality of 16% in surgically treated patients but 0% in medically treated patients. Furthermore, as survivors of surgery had small improvements at 6 months compared with medically treated patients, authors warned that patients with these characteristics should not be considered as candidates for LVRS.[71] This is an important set of findings. First, one should be mindful that patients with too far advanced emphysema—in other words, with poor pulmonary vascular beds—are at high risk for surgery even if ventilatory improvement could be expected theoretically. Second, as one of the primary outcomes of NETT is a comparison of survival rates between the LVRS group and the medical treatment group, patients with unacceptable predicted mortality should obviously not undergo surgery. Otherwise, high early postoperative mortality and morbidity in any subgroups of patients could offset the positive results in other patients who would benefit from LVRS (Figure 66-3).

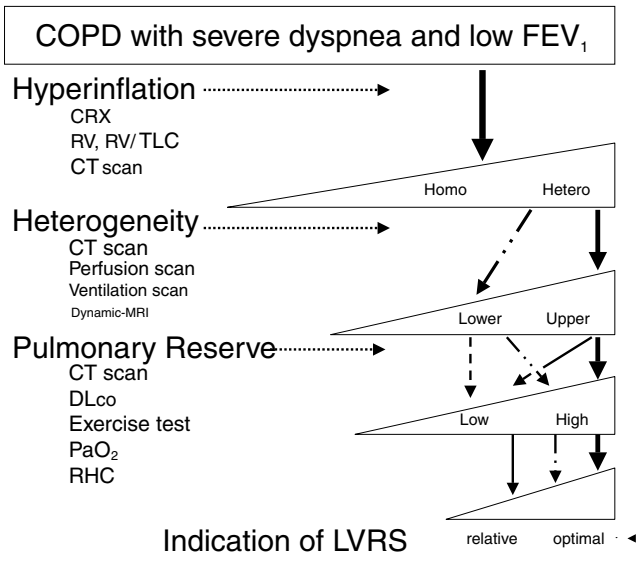

FIGURE 66-3 A proposed flowchart in patient selection for lung volume reduction surgery.

DURATION OF BENEFITS AND LONG-TERM RESULTS

There are a few reports regarding long-term results of LVRS. Cooper and Lefrak showed that improvements in FEV_1 and RV, reduction of dyspnea, and 6MWD were well maintained for 3 years after LVRS.[72] Gelb and colleagues showed that improvements in pulmonary function, dyspnea sensation, and oxygen independence reached peaks levels at different points after surgery, and each parameter declined gradually thereafter to the preoperative level for 4 to 5 years.[73] The time courses of functional decline may be inevitable because the remaining lung after LVRS is not normal but only near normal or with moderately emphysematous lung tissue, which might be abnormally stretched by the increases in lung recoil following LVRS. The absolute amount of normal lung preoperatively might be an important determinant of more sustained benefit.

With respect to long-term survival rate, Gelb and colleagues reported 1- through 5-year mortality of 26 patients who underwent thoracoscopic lung volume reduction as 4, 19, 31, 46, and 58%, respectively.[73] Interestingly, the same group found there was a correlation between the amount of tissue resected and improvement in FEV_1 and FVC after bilateral LVRS, but there did not appear to be greater long-term survival with larger lung resections, despite greater improvement in spirometry.[74] Yusen and colleagues showed that annual survival from Kaplan-Meier curves in 200 patients 1 through 5 years after LVRS was 93, 88, 83, 74, and 63%, respectively. In addition, they remarked that the duration of improvement was at least 5 years in the majority of survivors.[75]

CONCLUSION

Respiratory discomfort and dyspnea during ordinary activities of daily living cripple patients with severe emphysema. These functional consequences are caused by the pathologic anatomy of the lung and chest wall following chronic destruction of alveoli with resulting "airomas." The airomas, by causing excessive hyperinflation and gas trapping, are responsible for much of the disability in patients with emphysema. LVRS can result in functional improvement by removal of the airomas. The optimal candidate for LVRS remains an issue to be resolved; however, the evidence indicates that patients with severe hyperinflation and heterogeneous distribution of emphysema are most likely to have the greatest benefits from surgery. The degree and duration of improvement after LVRS might be determined by the amount of the normal or near-normal lung parenchyma remaining after surgery. Variation in this amount might cause variable responses to surgery among patients. LVRS is an intervention not only for ventilation but also for pulmonary circulation. Achieving maximal reduction of excessive air from the lung and minimum loss of the pulmonary vascular beds of the lung based on applied physiology and functional imaging modalities is the crucial objective. Ideally, resizing an emphysematous lung to normal by air reduction without loss of normal parenchyma by any means should provide better outcomes than LVRS as currently practiced.

REFERENCES

1. Brantigan OC, Muller E. Surgical treatment of pulmonary emphysema. Am Surg 1957;23:789–804.
2. Cooper JD, Trulock EP, Triantafillou AN et al. Bilateral pnemectomy (volume reduction) for chronic obstructive pulmonary disease. J Thorac Cardiovasc Surg 1995;109:106–19.
3. Daniel TM, Truwit JD, Redder J, et al. Lung volume reduction surgery: case selection, operative technique and clinical results. Ann Surg 1996;223:526–31.
4. Miller JI Jr, Mansour KA, Lee RB. Lung-volume reduction surgery: lessons learned. Ann Thorac Surg 1996;61:1464–8.
5. McKenna RJ Jr, Brenner M, Fischel RJ, et al. Should lung-volume reduction surgery be unilateral or bilateral. J Thorac Cardiovascular Surg 1996;112:1331–9.
6. Bingisser R, Weder W, Russi EW, et al. Bilateral volume reduction surgery for diffuse pulmonary emphysema by video-assisted thoracoscopy. J Thorac Cardiovascular Surg 1996; 112:875–82.
7. American Thoracic Society Medical Section of the American Lung Association. Lung volume reduction surgery. Am J Respir Crit Care Med 1996;154:1151–2.
8. NHLBI Workshop Summary. Evaluation and research in lung volume reduction surgery. Am J Respir Crit Care Med 1996;1913–8.
9. Young J, Fry-Smith A, Hyde C. Lung volume reduction surgery (LVRS) for chronic obstructive pulmonary disease (COPD) with underlying severe emphysema. Thorax 1999;54: 779–89.
10. Stirling GR, Babidge WJ, Peacock MJ, et al. Lung volume reduction surgery in emphysema: a systematic review. Ann Thorac Surg 2001;72:330–3.
11. Berger RL, Bartolome RC, Meneghetti AL, et al. Limitations of randomized clinical trials for evaluating emerging operations: the case of lung volume reduction. Ann Thorac Surg 2001;72:649–57.
12. The National Emphysema Treatment Trial Research Group. Rationale and design of the National Emphysema Treatment Trial. A prospective randomized trial of lung volume reduction surgery. Chest 1999;116:1751–61.

13. Gelb AF, Zamel N, McKenna RJ Jr, et al. Mechanism of short-term improvement in lung function after emphysema resection. Am J Respir Crit Care Med 1996;154:945–51.
14. Pride NB, Permutt S, Riley RL, Bromberger-Barnea B. Determinants of maximum expiratory flow from the lungs. J Appl Physiol 1967;23:646–62.
15. Scuiba FC, Roger RM, Keenan RJ, et al. Improvement in pulmonary function and elastic recoil after lung-reduction surgery for diffuse emphysema. N Engl J Med 1996;334: 1095–9.
16. Ingenito EP, Loring SH, Moy ML, et al. Interpreting improvement in expiratory flows after lung volume reduction surgery in terms of limitation theory. Am J Respir Crit Care Med 2001;163:1074–80.
17. Hoppin FG Jr. Theoretical basis for improvement following reduction pneumoplasty in emphysema. Am J Respir Crit Care Med 1997;155:520–5.
18. Fessler H, Permutt S. Lung volume reduction surgery and airflow limitation. Am J Respir Crit Care Med 1998;157: 715–22.
19. Fessler HE, Scharf SM, Permutt S. Improvement in spirometry following lung volume reduction surgery: application of a physiologic model. Am J Respir Crit Care Med 2002;165: 34–40.
20. Ingenito Scuiba FC, Roger RM, Keenan RJ, et al. Improvement in pulmonary function and elastic recoil after lung-reduction surgery for diffuse emphysema. N Engl J Med 1996;334:1095–9.
21. Thurnheer R, Engel H, Weder H, et al. Role of lung perfusion scintigraphy in relation to chest computed tomography and pulmonary function in the evaluation of candidates for lung volume reduction surgery. Am J Respir Crit Care Med 1999; 158:301–10.
22. Similowski T, Yan S, Gauthier A, et al. Contractile properties of the human diaphragm during chronic hyperinflation. N Engl J Med 1991;325:917–23.
23. Wanke T, Merkel M, Formanek D, et al. Effect lung transplantation on diaphragmatic function in patients with chronic obstructive pulmonary disease. Thorax 1994;49:459–64.
24. Farkas GA, Roussos C. Adaptability of the hamster diaphragm to exercise and/or emphysema. J Appl Physiol 1982;53: 1262–272.
25. Loring SH, DeTroyer A. Action of the respiratory muscles. In: Roussos C, Macklem PT, editors. The Thorax. New York: Marcel Dekker; 1985. p 327–45.
26. Younes M. Load responses, dyspnea, and respiratory failure. Chest 1990;97:59S–68S.
27. Ninane V, Yernault JC, DeTroyer, Intrinsic PEEP in patients with chronic obstructive pulmonary disease. Am Rev Respir Dis 1993;148:1037–42.
28. Celli B, Martinez F, Courser J, Rassulo J. Factors determining the pattern of ventilatory muscle recruitment (VMR) in patients with chronic obstructive pulmonary disease (COPD). Chest 1990;97:68S.
29. Cassart M, Gevenois PA, Estenne M. Rib cage dimensions in hyperinflated patients with severe chronic obstructive pulmonary disease. Am J Respir Crit Care Med 1996; 154:800–5.
30. Ward ME, Eidelman D, Stubbing DG, et al. Respiratory sensation and pattern of respiratory muscle activation during diaphragm fatigue. J Appl Physiol 1988;2181–9.
31. Breslin EH, Garoutte BC, Kohlman-Carrieri V, Celli BR. Correlation between dyspnea, diaphragm and sternomastoid recruitment during inspiratory resistance breathing in normal subjects. Chest 1990;98:298–302.
32. Sharp JT, Druz WS, Moisan T, et al. Postural relief of dyspnea in severe COPD. Am Rev Respir Dis 1980;122:201–11.
33. O'Donnell, Bertley JC, Laurence KL, Katherine AW. Qualitative aspects of exertional breathlessness in chronic airflow limitation. Pathophysiologic mechanisms. Am J Respir Crit Care Med 1997;155:109–15.
34. Lando Y, Boiselle P, Shade D, et al. Effects of lung volume reduction surgery on bony thorax configuration in severe COPD. Chest 1999;116:30–9.
35. Gauthier AP, Verbanck S, Estenne M, et al. Three-dimensional reconstruction of the in vivo human diaphragm shape at different lung volumes. J Appl Physiol 1994;76:495–506.
36. Cassart M, Hamacher J, Verbandt Y, et al. Effects of lung volume reduction surgery for emphysema on diaphragm dimensions and configuration. Am J Respir Crit Care Med 2001;163:1171–5.
37. Teschler H, Stamatis G, El-Raouf Farhat AA, et al. Effect of surgical lung volume reduction on respiratory muscle in pulmonary emphysema, Eur Respir J 1996;9:1778–84.
38. Criner G, Cordova FC, Leyenson V, et al. Effect of lung volume reduction surgery on diaphragm strength. Am J Respir Crit Care Med 1998;157:1578–85.
39. Ashutosh K, Gilbert R, Auchincloss JH, et al. Asynchronous breathing movements in patients with chronic obstructive pulmonary disease. Chest 1975;67:553–7.
40. Gillemartin JJ, Gibson GJ. Mechanisms of paradoxical rib cage motion in patients with chronic obstructive pulmonary disease. Am Rev Respir Dis 1986;134:683–7.
41. Jubran A, Tobin MJ. The effect of hyperinflation on rib cage-abdominal motion. Am Rev Respir Dis 1992;148:1378–82.
42. Block KE, Li Y, Zhang J, et al. Effect of surgical lung volume reduction on breathing patterns in severe pulmonary emphysema. Am J Respir Crit Care Med 1997;156:553–60.
43. Sahara H, Nakai S, Tsuda T, et al. Diaphragm—rib cage motion before and after lung volume reduction surgery. Chest 1998;114:351S.
44. Gierada DS, Hakimian S, Slone RM, et al. MR analysis of lung volume and thoracic dimensions in patients with emphysema before and after lung volume reduction surgery. AJR Am J Roentgenol 1998;170:707–14.
45. Suga K, Tsukuda T, Awaya H, et al. Interactions of regional respiratory mechanics and pulmonary ventilatory impairment in pulmonary emphysema assessment with dynamic MRI and xenon-133 single-photon emission CT. Chest 2000;117: 1646–55.
46. Chihara K, Hidaka A. Dynamic magnetic resonance imaging—a powerful modality in diagnosis and management of patients with emphysema. In: Mechanics of breathing, pathophysiology, diagnosis, and treament. Milan: Springer; 2002. p 60–9.
47. Benditt J, Wood D, McCooL F, et al. Changes in breathing and ventilatory muscle recruitment patterns induced by lung volume reduction surgery. Am J Respir Crit Care Med 1997; 155:279–84.
48. Ferguson GT, Fernandez E, Zamora M, et al. Improved exercise performance following lung volume reduction surgery for emphysema. Am J Respir Crit Care Med 1998;157: 1195–203.
49. Benditt JO, Lewis S, Wood DE, et al. Lung volume reduction surgery improves maximal O_2 consumption, maximal minute ventilation, O_2 pulse, and dead space-to-tidal volume ratio during leg cycle ergometry. Am J Respir Crit Care Med 1997;156:561–6.
50. Martinez FJ, de Oca MM, Whyte RI, et al. Lung-volume reduction improves dyspnea, dynamic hyperinflation, and respiratory muscle function. Am J Respir Crit Care Med 1997;155:1984–90.
51. O'Donnell DE, Webb KA, Bertley JC, et al. Mechanisms of relief of exertional breathlessness following unilateral

bullectomy and lung volume reduction surgery in emphysema. Chest 1996;110:18–27.
52. Killian KJ, Jones NL. Respiratory muscle and dyspnea. Clin Chest Med 1988;9:237–48.
53. Celli BR, Montes de Oca M, Mendez R, et al. Lung reduction surgery in severe COPD decreases central drive and ventilatory response to CO_2. Chest 1997;112:902–6.
54. Lahrmann II, Wild M, Wanke T, et al. Neural drive to the diaphragm after lung volume reduction surgery. Chest 1999; 116:1593–600.
55. Weder W, Thurnheer R, Stammberger Uz, et al. Radiologic emphysema morphology is associated with outcome after surgical lung volume reduction. Ann Thorac Surg 1997;64: 313–20.
56. Tschernko EM, Kritzinger M, Gruber EM, et al. Lung volume reduction surgery: preoperative functional predictors for postoperative outcome. Anesth Analg 1999;88:28–33.
57. Baldwin JC, Miller CC 3rd, Prince RA, Espada R. Chest radiograph heterogeneity predicts functional improvement with volume reduction surgery. Ann Thorac Surg 2000;70: 1208–11.
58. Wisser W, Senvaklavaci O, Ozepker, et al. Is long-term functional outcome after lung volume reduction surgery predictable? Eur J Cardiothoracic Surg 2000;17:666–72.
59. Flaherity KR, Kazerooni EA, Curtis JL, et al. Short-term and long-term outcome after bilateral lung volume reduction surgery: prediction by quantitative CT. Chest 2001;119: 1337–46.
60. Kotloff RM, Hansen-Flaschen, J, Lipson DA, et al. Apical perfusion fraction as a predictor of short-term functional outcome following bilateral lung volume reduction surgery. Chest 2001;120:1609–15.
61. Hunsaker AR, Ingenito EP, Reilly JJ, Costello P. Lung volume reduction surgery for emphysema: correlation of CT and V/Q imaging with physiologic mechanisms of improvement in lung function. Radiology 2002;222:491–8.
62. Becker MD, Berkmen YM, Austin JHM, et al. Lung volume before and after lung volume reduction surgery. Am J Respir Crit Care Med 1998;157:1593–9.
63. Rogers RM, Coxson HO, Scuiba FC, et al. Preoperative severity of emphysema predictive of improvement after lung volume reduction surgery. Use of CT morphometry. Chest 2000;118:1240–7.
64. Weg IL, Rossoff L, McKeon K, et al. Development of pulmonary hypertension after lung volume reduction surgery. Am J Respir Crit Care Med 1999;159:552–6.
65. Kubo K, Koizumi K, Fujimoto K, et al. Effects of volume reduction surgery on exercise pulmonary hemodynamics in severe emphysema. Chest 1998;114:1575–82.
66. Chihara K, Hitomi S. Classification for bullous emphysema based on analysis of chest wall motion and pulmonary function before and after bullectomy. Jpn J Thorac Dis 1990; 28:239–45.
67. Serna DL, Brenner M, Osann KE, et al. Survival after unilateral versus bilateral lung volume reduction surgery for emphysema. J Thorac Cardiovasc Surg 1999;118:1109–19.
68. Geiser T, Schwizer B, Krueger T, et al. Outcome after unilateral lung volume reduction surgery in patients with severe emphysema. Eur J Cardiothorac Surg 2001; 20:674–8.
69. Travaline JM, Furukawa S, Kuzma AM, et al. Bilateral apical vs nonapical stapling resection during lung volume reduction surgery. Chest 1998;114:981–7.
70. National Emphysema Treatment Trial Research Group. A randomized trial comparing lung-volume-reduction surgery with medical therapy for severe emphysema. N Engl J Med 2003;348:2059–73.
71. National Emphysema Treatment Trial Research Group. Patients at high risk of death after lung-volume-reduction-surgery. N Engl J Med 2001;345:1075–83.
72. Cooper JD, Lefrak SS Lung-reduction surgery: 5 years on. Lancet 1999;353:26–7.
73. Gelb A, McKenna RJ Jr, Brenner M. Lung function 5 yr after lung volume reduction surgery for emphysema. Am J Respir Crit Care Med 2001;163:1562–6.
74. Brenner M, McKenna RJ Jr, Chen JC, et al. Relationship between amount of lung resected and outcome after lung volume reduction surgery. Ann Thorac Surg 2000;69: 388–93.
75. Yusen RD, Lefrak SS, Gierada DS, et al. A prospective evaluation of lung volume reduction surgery in 200 consecutive patients. Chest 2003;123:1026–37.

CHAPTER 67

DIAPHRAGM RESPONSES TO STIMULATION

François Bellemare, Claude Poirier

The response of the diaphragm to stimulation has long been used to study its mechanisms of action and as a means of providing ventilatory assistance in high cervical cord–injured patients or in patients with central alveolar hypoventilation.[1] The major clinical application of the technique, however, has been in the evaluation of phrenic nerve function and diaphragm paralysis.[2] Since 1981, phrenic nerve stimulation has gained in popularity in various laboratories for the evaluation of diaphragm contractility and fatigue.[3] Recently, the technique has also found interesting applications in the evaluation of central conducting pathways to the phrenic motor nucleus[4,5] and of upper airway stability.[6] This chapter reviews the techniques available to stimulate the phrenic nerves in humans and their principal applications in the evaluation of phrenic nerve and diaphragm function. The different pathways that can be activated and the various sites where the stimuli can be applied that activate the phrenic nerves are listed in Table 67-1, along with the principal pathologies that may affect the recorded responses at each of those sites.

TECHNIQUES FOR PHRENIC NERVE STIMULATION IN THE EVALUATION OF DIAPHRAGM FUNCTION

The phrenic nerves can be stimulated by either electrical or pulsed magnetic fields. Electric fields depolarize nerve fibers directly, whereas rapidly changing magnetic fields initiate local currents in the vicinity of nerves that, in turn, activate nerve fibers. The diaphragm is innervated by the *C*3–*C*5 phrenic nerve roots, and all three branches are accessible to either form of stimulation. Stimuli can be delivered in the neck area laterally or over the cervical spine to activate the phrenic nerve roots and trunk directly or over the scalp near the vertex to activate the phrenic nerves indirectly via corticofugal pathways. The choice of the method largely depends on investigator experience or preference and the type of investigation being performed. Electrical stimulation is more tedious, requires greater skill, and may cause more discomfort and is more suitable for superficial than for deep nerves. When stimulating through bones, large voltages (up to 1,000 volts) are required, which are painful. Magnetic stimulation is easier to perform and essentially painless, and in contrast to electric stimulation, magnetic fields cross the scalp and spine unchanged, which makes this technique most suitable for cortical or cervical stimulation. When evaluating phrenic nerve conduction and diaphragm function, electrical stimulation may be preferred as the site of stimulation is more precisely defined and the responses less affected by the coactivation of other chest wall muscles. With magnetic stimulation, the stimulus is less specific and other chest wall muscles are coactivated with the diaphragm complicating the interpretation of electrical and mechanical responses. This chapter starts with a description of the different methods used to stimulate the phrenic nerves in humans. This is followed by a description of the various applications of these techniques.

Electrical Stimulation

For electrical stimulation, electric shocks can be delivered at the inferior and posterior border of the sternocleidomastoid muscle at the level of the cricoid cartilage either transcutaneously with surface electrodes of various sizes (preferably 5 mm cathode)[2,7] or percutaneously with needles[8,9] or fine wires[10] inserted at this site and positioned close to the phrenic nerves. In all these instances, a large plate over the manubrium sterni or over the upper thoracic spine can be used as an anode. When needles and fine wires are used for stimulation, the same type of electrode can also serve as an anode. These are simply inserted subcutaneously at a convenient location in relation to the cathode, that is, anteriorly to the sternocleidomastoid muscle. Selective and reproducible stimulation of the phrenic nerves and activation of the diaphragm can be achieved with any of these methods. Some investigators have used double-pronged electrodes, with prongs about 1.5 to 2 cm apart, to stimulate the phrenic nerves in the neck area.[11] With this type of electrode, however, higher voltages or currents are invariably required, neck

Table 67-1 Nervous Pathways to Diaphragm Activation

Level	*Pathologies*	*Specific stimulation*
Corticofugal pathways	Stroke, multiple sclerosis Central alveolar hypoventilation	Stimulation over the vertex (central conduction time; cortical facilitation)
Spinal cord	Spinal cord transection (C3-C4-C5) Cervical chiropractic manipulation Cervical spondylosis Amyotrophic lateral sclerosis Poliomyelitis	Stimulation over C6–C7 (peripheral conduction time and determination of central conduction time)
Phrenic nerve	Thoracic surgery Cardiac surgery (cooling)[87] Tumor compression Postviral Radiation therapy Guillain-Barré syndrome Idiopathic	Stimulation in neck area (peripheral conduction time: demyelination vs axonal degeneration and determination of central conduction time)
Neuromuscular junction	Myasthenia gravis Monitor response to curare-like neuromuscular blocking drugs	Repeated stimulation in neck area (decrement of the response)
Diaphragm	Muscular dystrophy Dysthyroidism Systemic lupus erythematosus Idiopathic Diaphragm fatigue	Stimulation in the neck area (amplitude and decrement of the response)

accessory muscles are almost invariably recruited, and a stable stimulation is very difficult to achieve. This technique is not recommended. Fine wire electrodes are particularly well suited when the test involves strong coactivation, by volitional efforts, of accessory muscles, which tend to displace the stimulating electrodes.[12] Because of its safety and ease of installation, a transcutaneous approach is recommended for most clinical and research applications. In all instances selectivity is greatly influenced by the level of experience of the investigator manipulating the cathode or inserting the needle. Once proper placement of the cathode is achieved, graded responses up to maximum can be obtained with any of these methods by increasing the current or voltage applied. To this end, the electrical responses or compound motor action potentials from the diaphragm to each nerve shock can be recorded with surface electrodes over the lower intercostal spaces on the ipsilateral side[2] or with esophageal electrodes placed at the gastroesophageal junction.[7] The stimulation is considered maximal when further increasing the stimulus intensity produces no further increase in the size of the compound motor action potential. Usually, currents or voltages 20 to 30% greater than those producing maximal responses are employed to ensure constancy of maximal stimulation, a condition referred to as "supramaximal" stimulation.[12]

For cervical stimulation of the phrenic nerve roots, high-voltage electric shocks (at least 750 volts) can be delivered through 10 mm surface gel electrodes placed over the spinal process of the 4th cervical vertebra (cathode) and over the external occipital protuberance (anode).[4] Because it is painful and maximal stimulation may not be achieved, and because special equipment is required, the technique is of limited application. The same considerations apply to cortical stimulation by electric shocks that requires the same equipment. In this case, a cathode is placed over the vertex and an anode some 5 cm anterior to the vertex.[4] With this arrangement and with condenser discharges of at least 750 volts, both phrenic nerves can be activated simultaneously. The shocks must be delivered during ongoing inspiratory efforts, which reduce the threshold for cortical stimulation. When delivered during relaxation, responses are very small or absent.

With any form of stimulation when applied in the neck area, there is always a possibility of stimulating the vagus nerve, although no side effects have been reported. In particular, the heart rate was found to be unaffected.[13] With insertion of needles in the neck there is always a risk of damaging the phrenic nerve and of inducing a pneumothorax, although again no side effects have been reported. Another advantage of needle or fine wire techniques for clinical application is that once in place, the electrodes need not be held by the investigator, although readjustments may be required from time to time. However, neck braces have been described that can be used to stabilize transcutaneous electrodes[14,15] and may help free the hands of the investigator or allow stimulation to be effected at a distance.

Magnetic Stimulation

For magnetic stimulation, a large quantity of static energy stored in a capacitor (typically 500 J) is rapidly transferred (in about 100 μs) to a coil made of insulated wires and is appropriately positioned over the structure to be stimulated. The rate at which the energy can be transferred determines the magnitude of the magnetic field. For a given capacitive energy, this will depend on the size and geometry of the coils. Circular and double figure-eight coils of various sizes

are available. The intensity of the magnetic field decreases rapidly with distance and is thus maximal at the coil surface. Small coils can generate greater magnetic fields than larger ones, but their depth of penetration is smaller. Figure of eight coils provide a greater selectivity than circular coils and are most suitable for anterior phrenic nerve stimulation. For bilateral stimulation two such coils are required. Circular coils are more suitable for cervical and cortical stimulation as these coils can activate both phrenic nerves simultaneously.

For anterior stimulation, figure-eight coils can be positioned unilaterally or bilaterally over the sternocleidomastoid muscles.[16,17] The stimulation, however, is not selective as the sternocleidomastoid, brachial plexus, and upper rib cage muscles are coactivated. Furthermore, during unilateral stimulation, the contralateral phrenic nerve is also activated, although not maximally.[17]

Cervical bilateral phrenic nerve stimulation can also be achieved by magnetic stimulation using a single 90 mm circular coil centered on the spinous process of the 7th cervical vertebra.[10,18–20] Higher coil positions result in lower electrical and mechanical responses. The exact site of nerve stimulation is unknown at this time as the latency of the electrical responses is shorter, not longer, than with electrical stimulation in the neck, suggesting an even more distal site and possibly an intrathoracic site of stimulation.[21] A contamination of the compound motor action potentials by coactivated muscles, however, cannot be excluded, even with esophageal electrodes.[22] Neck accessory muscles, the intercostal muscles of the upper five intercostal spaces, the muscles of the shoulder girdle including the pectoralis muscles, and some of the back muscles are also activated.[18–24] For optimal stimulation, the neck of the subject must be flexed, which in some circumstances may limit the application of this technique as it may be difficult to study intubated or supine patients this way. The technique, however, is simple and apparently well tolerated by subjects, which explains its popularity.

The criteria for a maximal stimulation using either the anterior or the cervical approach are less clear than with electrical stimulation. Diaphragm electrical and mechanical responses are initiated at around 40% of maximum power output, and in most subjects a leveling off of these responses can be demonstrated at greater than 90% of maximum power output, suggesting a maximal stimulation.[10,20] However, it is not clear whether the output of the stimulator remains linear in this range. A leveling off of the responses is not seen in all subjects, so maximal stimulation may not always be achieved. A major advantage of the magnetic stimulation technique is that the phrenic nerves can be stimulated without even touching the skin, that is, over subjects' garments, a feature that may be particularly useful in some cases, particularly in intensive care unit patients, who often have catheters inserted in the neck area, and burn patients, in whom it may not be otherwise possible to stimulate their phrenic nerves. As for electrical stimulation, magnetic stimulation in the neck area also carries the risk of vagal stimulation, although no adverse events have been reported to date. Magnetic stimulation techniques are contraindicated in patients with implanted cardiac pacemakers.

For transcortical magnetic stimulation, 70 mm figure-eight coils[25] or 90 mm circular coils[5,26] are placed over the vertex or a few centimeters lateral to the vertex. The position of the coil is not as critical as for electrical stimulation. The power output is set to maximal. As for electric stimulation, the threshold is greatly reduced when the stimuli are delivered during moderate inspiratory efforts. This likely results from facilitation of the motoneurons by the descending voluntary motor drive, a useful feature that helps in locating the appropriate site of the stimulation and improves selectivity. Several trunk muscles are activated in addition to the diaphragm. The exact site of intracranial stimulation is unknown at this time.

In summary, electrical stimulation in the neck area represents the most selective and reproducible way of stimulating the phrenic nerves in humans. Criteria for maximal stimulation are clearly defined. A transcutaneous approach is usually preferred, although the insertion of needles in the neck has not been linked to any complication. The use of electric stimulation at cervical and cortical levels is limited by pain and requires special equipment not commercially available. Magnetic stimulation provides a less selective stimulation since several trunk muscles are coactivated along with the phrenic nerves, contaminating the responses. The method is essentially painless and thus most suitable for cortical and cervical stimulation. However, the exact sites of cortical and cervical magnetic stimulation and the criteria for maximal stimulation are not precisely defined.

DIAPHRAGMATIC RESPONSES TO PHRENIC NERVE STIMULATION

The most frequently recorded electrical and mechanical responses to phrenic nerve stimulation are illustrated in Figures 67-1 and 67-2.

Electrical Responses

The measurement of peripheral nerve conduction velocity is useful in distinguishing muscle weakness caused by demyelinating peripheral neuropathies (eg, Guillain-Barré syndrome, chronic liver disease, and paraneoplastic disease) from those resulting from axonal degeneration (eg, critical illness, vitamin B_{12} deficiency, and human immunodeficiency virus infection) or nerve trauma. However, conduction velocity of the phrenic nerves cannot be measured in intact humans. In 1967, Newsom Davis introduced the measurement of phrenic nerve conduction time in the evaluation of phrenic nerve function.[2] This was defined as the time elapsed between the application of an electrical stimulus in the neck and the onset of the compound motor action potential recorded with surface electrodes over the lower chest wall (eighth intercostal space; anterior axillary line). He showed prolonged latencies in patients with peripheral neuropathies but not in patients with local lesions of the contralateral nerve. In the former, he also showed an inverse relationship between phrenic nerve conduction time and forearm conduction velocity, thus establishing the

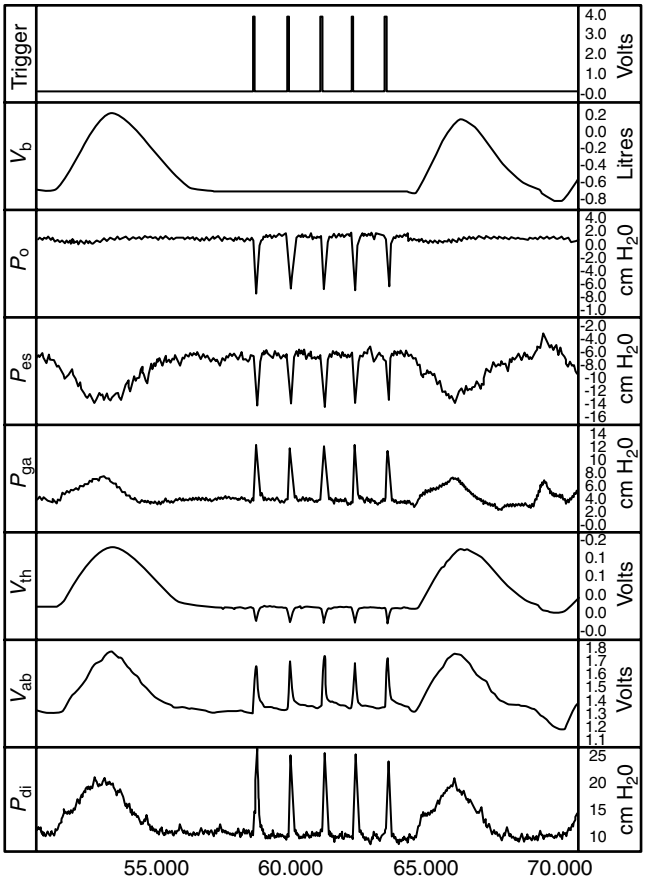

FIGURE 67-1 Mechanical responses to supramaximal bilateral phrenic nerve stimulation with single electric shocks at end-expiratory lung volume in a normal seated subject. *From top to bottom*: trigger pulses to stimulator; volume measured at the mouth with pneumotachograph; mouth pressure; esophageal pressure; gastric pressure; lung-apposed rib cage cross-section (Respitrace); abdominal cross-section (Respitrace); transdiaphragmatic pressure. Recordings were obtained after 10 minutes of quiet breathing and stimulations delivered during an expiratory pause at end-expiratory lung volume in a normal female subject in the seated erect posture.

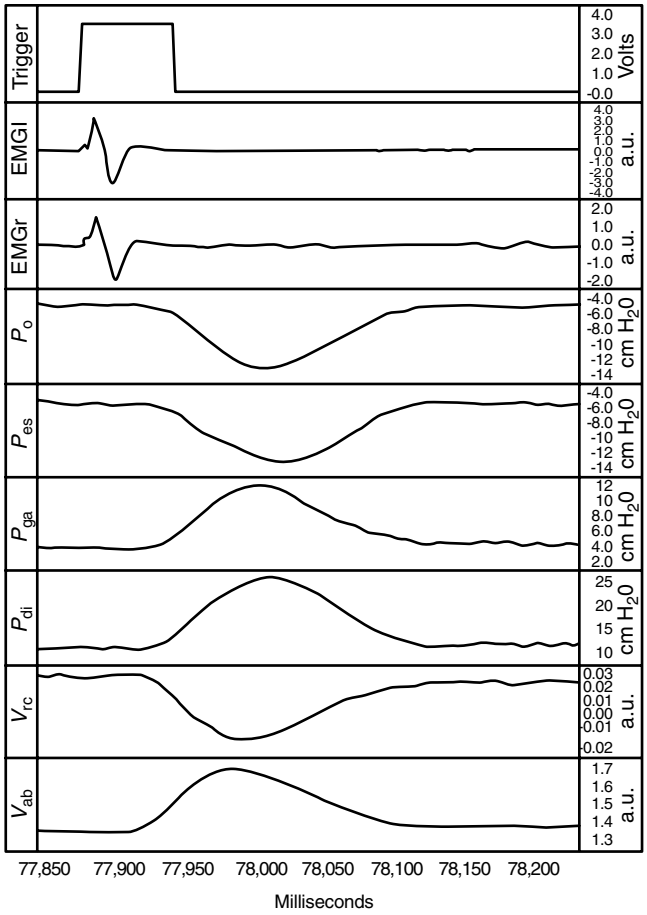

FIGURE 67-2 Electrical and mechanical responses to supramaximal bilateral phrenic nerve stimulation with single electric shocks. *From top to bottom*: trigger pulse to stimulator; compound muscle action potential from left hemidiaphragm recorded with surface electrodes in left eighth intercostal space; compound muscle action potential from right hemidiaphragm recorded with surface electrodes in right eighth intercostal space; twitch mouth pressure; twitch esophageal pressure; twitch gastric pressure; twitch transdiaphragmatic pressure; twitch lung-apposed rib cage cross-section (Respitrace); twitch abdominal cross-section (Respitrace).

diagnostic value of the test. Furthermore, in patients with peripheral neuropathies, prolongation of phrenic nerve latencies preceded the onset of respiratory failure, thus establishing the clinical utility of this simple test. Compound motor action potential amplitude was of lesser value as this varied considerably among normal subjects and was uncorrelated to conduction time. Thus, the technique is less useful in the diagnosis of axonal degeneration unless this is very severe and the compound motor action potential is very low or absent, as in unilateral or bilateral diaphragm paralysis. In the latter patients, conduction times, when they can be measured, are within the normal range. All these findings have been largely confirmed in subsequent studies.[27,28]

Published values for phrenic nerve conduction time in normal subjects using electrical stimulation are remarkably consistent in different studies[2,7,29–36] (Table 67-2). The accepted upper limit of the normal range is 10 ms. Variability among studies is largely attributable to differences in recording techniques and electrode placement and explained by differences in conduction distances of the phrenic nerve branches, including their intramuscular course to the recording sites.[34] It is important, therefore, that the recording technique be standardized and normal values selected accordingly.

Phrenic nerve conduction times increase with age.[32,34–36] A positive relationship with height has also been found by some authors[32] but not by others.[29,30,33] In our laboratory we also find height and age to be significant cofactors.[36] However, when sex was entered in a stepwise regression model together with age and height, height was rejected and only age and sex were found to be significant cofactors. The reason for this is unclear but is unlikely to be solely explained by the shorter stature of the females. The following equations predict phrenic nerve conduction time based on age and sex. They were derived from a set of 40 normal subjects (21 males, 19 females; age range 21–78 years) studied in the seated erect posture with chest surface electrodes

Table 67-2 Phrenic Nerve Conduction Time in Normal Subjects Using Electric Stimulation

						Eesophageal		*Chest wall*	
Author	*Year*	*n*	*Sex*	*Age (yr)*	*Height (cm)*	*Left*	*Right*	*Left*	*Right*
Delhez[7]	1965	30	16 M, 13 F	21–27	165–178	8.2 ± 0.71	7.5 ± 0.53		
Davis[2]	1967	18	?	20–61	?			7.7 ± 0.8	
Shaw[29]	1980	16	10M	22–53	?			8.35 ± 0.83	8.64 ± 0.76
			6F	22–53	?			8.27 ± 0.87	8.22 ± 0.72
MacLean[32]	1981	30	?	18–74	152–186			7.44 ± 0.59	
DeTroyer[33]	1982	31	?	30–85	?			7.1 ± 0.8	6.9 ± 0.9
McKenzie[34]	1985	20	M	20–66	163–190	7.93 ± 0.85	6.82 ± 0.64	7.92 ± 0.92	7.68 ± 0.56
Mier[50]	1989	20	10 M, 10 F	24–73	153–183			6.8 ± 0.75	
Swenson[30]	1992	20	?	24–38	?			6.72 ± 1.15	6.87 ± 1.37
Chen[35]	1995	25	14 M, 11 F	22–80	169 ± 10			6.54 ± 0.77	
Bellemare[36]		40	21 M	21–78	161–182			6.76 ± 0.68	7.12 ± 0.75
			19 F	21–73	150–173			6.16 ± 0.63	6.27 ± 0.81

Values are means ± SD.

in the eighth intercostal space and anterior axillary line (age is in years; male = 0, female = 1)[36]:

$$\text{Left conduction time (ms)} = 6.823 - (0.634 * \text{sex}) + (0.0125 * \text{age})\ r = 0.535;\ \text{SEE} = 0.691$$

$$\text{Right conduction time (ms)} = 7.107 - (0.906 * \text{sex}) + (0.0203 * \text{age})\ r = 0.649;\ \text{SEE} = 0.622$$

The measure of phrenic nerve conduction finds interesting applications in the early detection of phrenic nerve involvement in the setting of peripheral neuropathies, as in thyroid dysfunction,[37] tumor compression,[38] or chronic renal failure.[39] Although normal values for phrenic nerve conduction time have also been published for cervical magnetic stimulation,[26] this method needs to be further standardized before it can be recommended for clinical use. For example, with cervical magnetic stimulation, phrenic nerve conduction times are typically 1 to 2 ms shorter than with electrical stimulation, whereas they should be longer.[21] Furthermore, the difference increases with increasing intensity of stimulation and presumably the depth of penetration of the magnetic field. With electric shocks, phrenic nerve latencies are independent of stimulation intensity. Comparable values are obtained with electric and magnetic stimulation when the output of the magnetic stimulator is set to 50 to 60% of maximum, that is, just above the threshold for recruitment.[21] For magnetic stimulation, an esophageal electrode is required as the signals recorded from chest wall surface electrodes are contaminated by the activity of other chest wall muscles. Even esophageal electrode recordings may be contaminated.[22] Thus, predictably, normal values will depend not only on the recording site but also on the type of stimulator, the type of coil employed, and the power output selected. Thus, until a consensus can be reached as to the most appropriate settings, it is recommended that when using magnetic stimulation, each laboratory, after standardization of its methods, should establish its own set of normal values.

Central Conduction Time The difference in compound motor action potential latency between transcortical and cervical stimulation provides a measure of central conduction time between the two stimulation sites. For electric stimulation, Gandevia and Rothwell reported a central conduction time of 4.3 ms in three normal subjects, a value comparable to that obtained for the deltoid muscle.[4] For magnetic stimulation at 50% of power output at the peripheral site and maximum output at the central site, Zifko and colleagues reported a value of 5.3 ± 1.1 ms in 35 normal subjects.[26] With maximum power output at both sites, Kheder and Trakhan reported much longer values (8.8 ms for the left side and 8.9 ms for the right side recordings).[25] As for peripheral latencies, central conduction latencies are more difficult to interpret with magnetic stimulation. However, the short latencies obtained with electrical stimulation are suggestive of the activation of rapidly conducting oligosynaptic pathways and possibly even monosynaptic pathways[4] and of more complex pathways when using magnetic stimulation. The central conduction times have been studied in patients with stroke (capsular-type hemiplegia). After cortical magnetic stimulation, diaphragm electromyographic response (EMG) was abolished or markedly reduced on the plegic side.[40] This indicates that the two hemidiaphragms do not have a bilateral cortical motor representation.

Amplitude and Shape of Compound Motor Action Potential As mentioned above, the amplitude of the compound motor action potential is of limited value in the evaluation of phrenic nerve function as normal values typically vary over a 10-fold range. However, for a given electrode placement, the shape and amplitude of the compound motor action potential are highly reproducible, even on several consecutive days. Thus, when a subject or patient serves as his or her own control, the amplitude of the compound motor action potential provides a reliable measure of diaphragm motor unit recruitment. Useful applications of this technique have been found in the evaluation of diaphragm resistance to curare-like neuromuscular blocking drugs,[41] of diaphragm involvement in myasthenia gravis,[42,43] of phrenic nerve or diaphragm injury during surgical procedures,[44,45] and of the contribution of neuromuscular transmission failure to diaphragm fatigue.[46,47]

Table 67-3 Summary of Electrical Responses

Electrical response	*Clinical applications*	*Preferred method*
Phrenic nerve conduction time	Neuropathies of the phrenic nerves: surgical trauma, Guillain-Barré syndrome, herpes-zoster virus, tumor compression, etc	Transcutaneous electric stimulation
Central conduction time	Central nervous system dysfunction: encephalitis, stroke, cerebral anoxia, etc	Transcortical and cervical magnetic stimulation or transcortical magnetic and peripheral electric or magnetic stimulation in neck area
Compound motor action potential amplitude	Myasthenic syndromes, diaphragm fatigue (low or high frequency); action of curare-like neuromuscular blocking drugs	Electric or magnetic stimulation in neck area with intraindividual comparison

In summary, the measurement of phrenic nerve conduction time can be useful in several diseases (Table 67-3) as it enables physicians to detect abnormalities when only subtle clinical changes are perceived. In the setting of peripheral neuropathies, it can predict oncoming respiratory failure. The measurement of central conduction time should also be useful in evaluating repercussions of multilacunar diseases or central demyelinating pathologies (eg, multiple sclerosis). Standardization of the method, mostly for magnetic stimulation, is advocated for each laboratory.

Mechanical Responses

The tension developed by the diaphragm cannot be directly measured. However, diaphragmatic tension changes are converted into pressure changes, which can be recorded with conventional pressure transducers. The contraction of the diaphragm lowers pleural (Ppl) and esophageal (Pes) pressures and increases abdominal (Pab) and transdiaphragmatic (Pdi) pressures. The latter provides the closest approximation of diaphragmatic tension generation. Furthermore, when the extrathoracic airways are closed and stabilized and when the glottis is opened, pleural pressure changes that are then equal to alveolar pressures changes can be transmitted unchanged to the airway opening (Pao) and can be measured as mouth or tracheal pressure changes, providing a noninvasive means to evaluate the mechanical output of the diaphragm.[48] During the build-up of diaphragmatic tension, the diaphragmatic fibers vibrate laterally, producing muscular sounds (phonomyograms) that can be recorded by microphones or accelerometers placed over the lower chest wall, providing yet another noninvasive means of evaluating the mechanical output of the diaphragm during phrenic nerve stimulation.[49]

Because of unavoidable distortions of the diaphragm during unilateral stimulation, the pressure responses are about 2.5 times greater during bilateral than during unilateral stimulation.[12,50] Furthermore, the time course of single twitches differs markedly between unilateral and bilateral stimulation.[51] It is thus important that both phrenic nerves be stimulated simultaneously when recording pressure responses. However, phonomyograms, like compound motor action potentials, are the same during unilateral and bilateral stimulation.[52] Thus unilateral stimulation is sufficient when recording these responses.

For all electrical and mechanical responses, the consideration of the effect of lung volume changes is paramount.[10,14,53–57] The degree of overlap of actin and myosin filaments within each sarcomere determines the strength of the muscle mechanical responses. The degree of overlap varies with muscle fiber length and thus with lung volume. There is also possibly a relationship between the position and degree of curvature of the diaphragm and its capacity to generate pressure (Laplace's law). This factor, therefore, must be carefully controlled when evaluating diaphragm function with any of these methods. The simplest way to control for lung volume changes is to obtain measurements at end-expiratory lung volume. If variations in end-expiratory lung volume are expected, the relationship with lung volume can be established by repeating measurements at different lung volumes.

Pressure responses have a different meaning depending on whether an electrical or a magnetic stimulation technique is employed. With electrical stimulation, the mechanical responses are essentially confined to the diaphragm. The isolated diaphragmatic contraction produces an expansion of the anterior abdominal wall and of the lower, diaphragm-apposed rib cage but a depression of the upper, lung-apposed rib cage.[19,58] These distortions are exaggerated when the airways are closed and result in a shortening of the diaphragm and, because of the force–length and force–velocity properties, result in a smaller transdiaphragmatic pressure (Pdi) change than if the normal geometry of the chest wall were retained. These distortions can be reduced but not prevented by fitting a tight binder around the lower rib cage and abdomen, a procedure that increases Pdi changes by about 30 to 35%.[51,59]

With magnetic stimulation, the situation is quite different as the responses are not confined to the diaphragm. Both cervical and anterior magnetic stimulation in the neck activate several upper rib cage muscles, both inspiratory and expiratory, in addition to the diaphragm. These muscles contribute directly to Ppl changes and, by virtue of their action on the upper rib cage, contribute indirectly to Pdi changes. At ordinary and lower lung volumes in normal subjects, the action of inspiratory rib cage muscles predominates, causing an expansion, not a depression, of the upper, lung-apposed rib cage, a greater fall in Ppl, and greater Pdi changes.[19] At higher lung volumes, the opposite occurs as the contribution of expiratory rib cage muscles eventually

predominates, causing a compression of the upper, lung-apposed rib cage, smaller falls or even increases in Ppl, and lower Pdi changes than with electrical stimulation.[19] Although only limited comparisons are available, these effects seem to be substantially greater for cervical than for anterior magnetic stimulation, suggesting a greater selectivity for phrenic nerve stimulation with the latter.[17] However, in a study by Mador and colleagues,[60] Pdi responses to cervical and bilateral magnetic stimulation were not different, and both were significantly greater than with electrical stimulation. Thus, with either approach, the fact that other chest wall muscles can contribute to pressure changes can lead to errors in interpretation as changes in Pdi may not reflect actual changes in diaphragm contractility. For example, when the inspiratory rib cage muscles are selectively fatigued, the Pdi response to cervical magnetic stimulation is reduced, but the response to electric stimulation is unchanged.[23] In this case, cervical magnetic stimulation yields a false-positive test result for the diaphragm. A false-negative test result for the diaphragm may also be anticipated in cases of selective diaphragm weakness, although this is a rare condition since a compensatory increase in the strength of the extradiaphragmatic muscles may be expected to occur under those conditions. Thus, whenever magnetic stimulation is employed alone, extreme care must be exercised when interpreting Pdi changes. For instance, whereas a decrease in twitch Pdi has been found to occur with age when measured in response to cervical magnetic stimulation,[61] no change was found when measured in response to electric stimulation.[36] The only way to discriminate false-positive and false-negative test results for the diaphragm when using magnetic stimulation is to compare the responses with those obtained by electric stimulation, which is the gold standard.[19,20,23]

In summary, several techniques are available to record the mechanical output of the diaphragm in response to phrenic nerve stimulation, including transdiaphragmatic and mouth or tracheal pressure changes and the muscular sound that are summarized in Table 67-4. These responses are dependent on lung volume, which must be controlled. When using magnetic stimulation, these mechanical responses are contaminated by the cocontraction of other trunk muscles that are costimulated. These contaminations can lead to false-negative and false-positive test results, which can only be managed by comparing the responses to both magnetic and electrical stimulation.

Tetanic Responses Pdi–frequency relationships of the diaphragm can be constructed using brief (0.5–1 s) tetani at different frequencies.[3] The shape of the relationships thus obtained resembles the classic force–frequency relationship reported for other human muscles having a mixed fiber-type composition and intermediate contractile properties such as the quadriceps femoris.[3,62] Fusion of successive twitches typically starts at a frequency of stimulation of about 7 to 8 Hz, and complete fusion occurs at frequencies between 50 and 100 Hz. Currently available magnetic stimulators cannot deliver trains of tetanic stimulation and therefore cannot be used for this purpose.

Pdi–frequency relationships are particularly useful in distinguishing different types of peripheral fatigue.[3,62,63] A selective depression of Pdi at high stimulation frequencies (50–100 Hz: high-frequency fatigue) signals an excitation defect distal to the point of nerve stimulation, that is, either at the neuromuscular junction (as exemplified by myasthenia gravis), along the sarcolemmal fiber membrane, or in the triads. By contrast, a selective depression of Pdi at low-stimulation frequencies (10–20 Hz: low-frequency fatigue) signals a defect of the excitation–contraction coupling mechanism caused by a reduction in the amount of calcium released by the sarcoplasmic reticulum per impulse.[3,62–64] This distinction is important as high-frequency fatigue recovers quickly, generally within 30 minutes,[3] whereas low-frequency fatigue may require 24 to 48 hours to recover[65] and may thus require a different therapeutic strategy. Maximal tetanic phrenic nerve stimulation is difficult to achieve at rates greater than 35 Hz, particularly during bilateral stimulation.[50,51] If repeated measurements are required, the test can eventually be painful.

High-frequency fatigue has been shown to occur after an endurance exercise at high intensity (88–92% maximal oxygen consumption [VO_2]) in trained individuals.[66] However, low-frequency fatigue, because it recovers more slowly and because of its predominant effects at low rates of stimulation, as in normal breathing, could be of greater clinical importance. Low-frequency fatigue has been difficult to observe in pathologic states. Laghi and colleagues have shown, using bilateral magnetic stimulation, that this pattern of diaphragmatic fatigue was not implicated in the difficult-to-wean patient.[67] However, the recent demonstration of a selective depression of the Pdi response to single phrenic nerve shocks (the lowest possible stimulation frequency) in patients with cystic fibrosis, in the presence of a normal maximal voluntary response (equivalent to stimulation at high frequencies), is suggestive of chronic low-frequency diaphragm fatigue in these patients.[68] This may be important as low-frequency diaphragm fatigue may contribute to hypercapnic respiratory failure during wakefulness and sleep in these patients and may be an indication for the institution of noninvasive mechanical ventilation. Phrenic nerve stimulation is the only way this form of fatigue can be detected.

In summary, although tetanic stimulation of the phrenic nerves may be an ideal test to evaluate the function of the diaphragm, it is clearly too difficult and painful to be recommended for routine use in patients or naive subjects. This test, therefore, is essentially restricted to research and has little or no clinical utility. Recording of the single response as described below is more applicable clinically and can be used to detect low-frequency diaphragm fatigue, although it cannot be used to detect high-frequency fatigue.[67,68]

Paired Phrenic Nerve Stimulation

Reproducible Pdi–frequency relationships of the diaphragm can be constructed using paired shocks instead of trains of shocks and by varying the interval between the two stimuli. Both electrical[69] and magnetic[70] stimulation techniques can be used for this purpose. In the latter instance, two magnetic

Table 67-4 Summary of Mechanical Responses

Recorded response	*Examples of clinical conditions*	*Preferred method*
Transdiaphragmatic pressure (Pdi)	Pdi: Any condition affecting diaphragm contractility: comparison with normal values.	Bilateral electrical or magnetic stimulation (diaphragm alone)
Airway opening pressure (Pao: opened glottis)	Pao: Any condition when patient serves as his control (ie, treatment effects).	Cervical magnetic stimulation (diaphragm and trunk muscles)
Phonomyograms	Serial measurements on the same subject (treatment effects)	Unilateral electrical stimulation in neck area
Tetanic responses	High-frequency fatigue as in myasthenia gravis Low-frequency fatigue with chronic loading as in cystic fibrosis Little or no clinical application	Bilateral electrical stimulation in neck area
Paired phrenic nerve stimulation	As for tetanic responses. Little or no clinical application.	Bilateral electrical or magnetic stimulation in neck area
Single responses (gold standard for evaluation of diaphragm contractility and fatigue)	Obstructive lung diseases Chronic heart failure Malnutrition, etc	Bilateral electrical or magnetic stimulation in neck area
Repeated stimulation (4 Hz)	Effects of neuromuscular blocking drugs	Unilateral (phonomyogram) or bilateral (Pdi) electrical stimulation
Maximal diaphragm strength	Obstructive lung diseases Drugs Muscular dystrophy	Twitch occlusion method Bilateral electric or magnetic stimulation in neck area (Pdi) Magnetic cervical stimulation (Pao)

stimulators appropriately synchronized are required. With either technique, the amplitude of the Pdi response to the second impulse of each pair is measured after subtraction of the first response (which is equal to a single twitch: T1) from the total response. The amplitude of this second response (T2) declines as the interval between the stimuli decreases, that is, as the instantaneous frequency of stimulation increases. A computer is required to compute T2. This method is much easier to perform than tetanic stimulation and is well tolerated by normal subjects. It provides similar information as the tetanic responses concerning the evaluation of high- versus low-frequency diaphragmatic fatigue. The shape of the Pdi–frequency relationships is about the same with either electric or magnetic stimulation techniques, but no direct comparison has been made. The ratio of the second twitch at 10 Hz over that at 100 Hz ($T2_{10/100Hz}$) in the fresh, nonfatigued state, a measure of the shape of the pressure–frequency relationship, is nearly the same with electrical stimulation (1.33 ± 0.05)[69] and magnetic stimulation (1.33 ± 0.36).[70] Intersubject variability is, however, considerably greater with the latter technique. With electrical stimulation, a value of this ratio less than 1.0 was diagnostic of low-frequency diaphragm fatigue.[69] With electrical stimulation, however, it was necessary to restrict the motion of the lower rib cage and abdomen by rigid binding, which limits the clinical application of this test. This precaution was not required in the study with magnetic stimulation,[70] presumably because rib cage and diaphragm distortions were minimized by the costimulation of upper rib cage muscles (see above). As for any test of diaphragm function, lung volume at which measurements are made must be controlled as the $T2_{10/100Hz}$ ratio decreases with increasing lung volume, owing to a shift of the Pdi–frequency relationship to higher frequencies.[70] This test, although simpler than tetanic phrenic nerve stimulation, is also difficult to standardize and thus, like tetanic stimulation, largely restricted to research applications.

Single Responses

As an alternative to tetanic or paired phrenic nerve stimulation, recording of single muscle twitches during relaxation can be employed to evaluate the strength of the diaphragm.[8,12] The recording of single twitches is the gold standard in the evaluation of diaphragm contractility and fatigue.[71] This approach is virtually painless and well accepted by patients and naive subjects. It is particularly well suited for repeated measurements. It does not require any effort on the part of the patient. Published values for twitch Pdi in normal subjects from the largest series are remarkably consistent when using either electrical or magnetic stimulation (Table 67-5). For reasons already discussed, normal values of twitch Pdi are consistently and significantly greater for magnetic than for electrical stimulation. Less consistent comparisons have been reported for bilateral magnetic and electrical stimulation of the phrenic nerves. In one study, twitch Pdi was found to be essentially the same with these two techniques,[16] whereas in the other twitch Pdi with bilateral magnetic stimulation was essentially the same as with cervical magnetic stimulation, both values being significantly greater than with electrical stimulation.[60] Additional comparisons are therefore required as the bilateral magnetic stimulation technique is easier to apply in difficult settings.[67]

In contrast to maximal voluntary Pdi, twitch Pdi using electrical stimulation at end-expiratory lung volume is independent of age and sex, at least in normal subjects, a feature that may prove particularly useful in the clinical evaluation of diaphragm function.[36] However, a decrease with age has been found when using cervical magnetic

Table 67-5 Diaphragm Twitch Pressure in Normal Subjects

Reference	*Year*	*n*	*Sex*	*Age (yr)*	*BES*	*CMS*	*BMS*
Mier[50]	1989	20	10 M, 10 F	24–73	20.7 ± 5.3		
Johnson[73]	1992	11	M	33 ± 3 (SE)	24.9 ± 1.8(SE)		
Bellemare[36]	2003	20	M	21–78	23.3 ± 6.4		
		18	F	21–73	22.8 ± 5.7		
Mador[20]	1996	10	9 M, 1 F	27.6 ± 0.7 (SE)	27.4 ± 2.3 (SE)	39.3 ± 3 (SE)	
Laghi[19]	1996	16	M	25–35	32.3 ± 2.2 (SE)	37.7 ± 1.9 (SE)	
Mador[60]	2002	12	8 M, 4 F	27.7 ± 2 (SE)	25.6 ± 2.2 (SE)	32 ± 2.1 (SE)	31.6 ± 1.8 (SE)
Luo[93]	2002	32	?	?			28 ± 5

Unless otherwise indicated values are means ± SD.
BES = bilateral electrical stimulation; BMS = bilateral magnetic stimulation; CMS = cervical magnetic stimulation.

stimulation,[60] which may be explained by a variable contribution of the extradiaphragmatic rib cage muscles with the cervical magnetic stimulation technique in young and old subjects. Useful applications of the electrical stimulation technique have been found in the evaluation of diaphragm fatigue during respiratory loading[8,46,72] or exercise in normal subjects,[73] in the evaluation of pharmacologic agents,[74,75] in the evaluation of the effects of chronic lung hyperinflation[76–78] or chronic heart failure[79] on diaphragm function, in the evaluation of diaphragm weakness[50] or malnutrition,[80] and in the evaluation of difficult-to-wean patients.[67]

However, some precautions are required when recording single Pdi twitches from the relaxed diaphragm. Because coactivation of abdominal muscles or rib cage muscles can independently alter twitch Pdi, it is important that these other muscles be relaxed as much as possible. If these extradiaphragmatic muscles are costimulated, as with cervical magnetic stimulation and possibly with bilateral magnetic stimulation, their level of activation may be difficult to control. Because of the twitch occlusion phenomenon (see below), it is also important that the diaphragm be relaxed, as can be inferred from Pdi and Pga baseline tracings. Because lung volume is important, measurements should be obtained at end-expiratory lung volume. For longitudinal studies in the same subject and if end-expiratory lung volume is expected to change, measurements can be repeated at different lung volumes and the linear relationship between twitch Pdi and lung volume employed to estimate twitch Pdi at any volume by interpolation. Although only limited comparisons are available, twitch Pdi was found to be nearly the same in seated erect and supine postures.[81] This suggests that the same set of normal values may be used in both postures. Changes in chest wall configuration produced by external forcing were also shown to have trivial effects on twitch Pdi in comparison with those produced by lung volume changes.[10] Again, however, only limited comparisons are available. Caution is therefore advised, particularly since distortions produced by internal forcing can have marked effects on twitch Pdi.[82] Twitch Pdi can be importantly affected by twitch potentiation when preceded by moderate (>25% maximum) to strong voluntary contractions.[47,83,84] It is important, therefore, that contraction history of the diaphragm also be controlled. Potentiated twitches return to control levels after 3 to 15 minutes. Thus, a good practice is to allow at least 10 minutes of quiet breathing before recording Pdi twitches. Some investigators also advocate the use of a stimulation frequency not exceeding 0.3 Hz when recording successive twitches to avoid twitch potentiation caused by the staircase phenomenon, although this has not been formally studied.[19] In our experience, packets of three to five consecutive twitches at a rate of 0.5 to 1 Hz can be delivered at intervals of 1 to 2 minutes without appreciable changes in twitch amplitude (see Figure 67-1). When these precautions are taken, reproducible twitches can be recorded from the relaxed diaphragm at end-expiratory lung volume over extended periods of time both with bilateral electrical[8,12] and magnetic[19] stimulation.

Mouth pressure twitches can also be employed when a subject serves as his or her own control.[48,85–88] For faithful pressure transmission from the alveoli to the mouth, it is important that the glottis is open and the upper airway stabilized either by applying positive pressure at the airway opening[48,88] or by asking the subject to perform gentle inspiratory efforts.[87]

In summary, twitch Pdi is a reproducible, well-described, and studied method to evaluate diaphragm contractility and fatigue that is independent of age and sex, at least when the electrical stimulation technique is employed. Lung volume setting and abdominal and rib cage muscle relaxation are obviously important to obtain reproducible results. With the glottis opened, mouth pressure twitches can also be used as a noninvasive measure of diaphragm strength, but only when a subject serves as his or her own control.

Muscular Sound of the Diaphragm

Like other skeletal muscles, the diaphragm vibrates laterally during the build-up of tension. These vibrations or sounds can be recorded with microphones or accelerometers positioned over the lower chest wall in the zone of apposition of the diaphragm with the rib cage. These are called phonomyograms or acoustic myograms. Their amplitude is proportional to the size of Pdi twitches during bilateral stimulation and to the size of the compound motor action potentials recorded ipsilaterally during unilateral or bilateral stimulation. Because of rapid attenuation as a function of distance, the muscular sound of the diaphragm is the same during unilateral and bilateral stimulation, and there is essentially no contamination from the contralateral

hemidiaphragm.[52] Thus, it is only necessary to stimulate one phrenic nerve to evaluate changes in diaphragm contractility, which simplifies the examination. However, the acoustic response is highly sensitive to lung volume changes and the changes are difficult to predict.[55] Therefore, it is particularly important that lung volume be carefully controlled when using this technique. Provided that sufficient control can be exercised over lung volume and the microphone and EMG electrode placements remain the same, reproducible measures of diaphragm excitation–contraction coupling can be obtained over several hours and even days (Figure 67-3). The technique may thus be useful clinically when a subject serves as his or her own control.

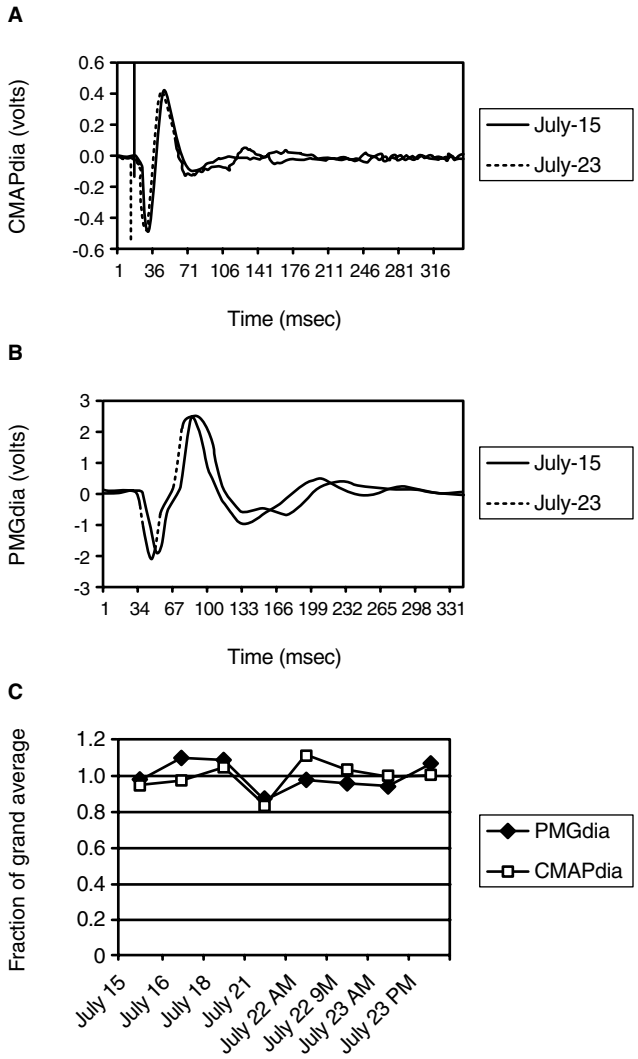

FIGURE 67-3 Reproducibility of compound muscle action potential (CMAPdia: *top*) and phonomyogram (PMGdia: *middle*) of the diaphragm during unilateral supramaximal right phrenic nerve stimulation at end-expiratory lung volume in a normal male subject studied on different days as indicated. To facilitate between-days comparison, a small delay was introduced between the two signals. The *bottom panel* shows the mean value of 15 consecutive responses to stimulation on each occasion, measured as peak to peak and expressed as a fraction of the grand average over all days.

ESTIMATION OF DIAPHRAGM ACTIVATION AND MAXIMAL STRENGTH

Because of high intersubject variability in twitch Pdi in relation to maximal Pdi, the latter cannot be reliably estimated from single twitches. When an objective estimate of maximal Pdi or of the level of diaphragmatic activation by the voluntary effort is required, the twitch occlusion method can be employed. When phrenic nerve shocks are superimposed to ongoing voluntary contractions, the twitch amplitude declines almost linearly as a function of the voluntary Pdi developed (twitch occlusion; Figure 67-4).[12] When all phrenic motor units are recruited and fully activated by natural activity, the extra phrenic nerve shocks superimpose no additional twitch Pdi on the voluntary Pdi record. The amplitude of the superimposed Pdi twitch thus detects the force reserve left for full diaphragm activation by the central nervous system. Extrapolation of the relationship from submaximal levels to the abscissa yields an objective estimate of maximal Pdi that is independent of the voluntary effort developed. Because of a slight nonlinearity at Pdi greater than 70% maximum, this extrapolation underestimates the true maximal Pdi by about 10%. The extent of diaphragm activation for any breathing effort can also be calculated from the ratio of the superimposed to relaxed twitches:

$$\%\ \text{diaphragm activation} = (1 - (\text{superimposed twitch Pdi} / \text{relaxed twitch Pdi})) \times 100 \quad (67\text{-}3)$$

Because of the underestimation of the maximal Pdi alluded to above, diaphragm activation tends to be overestimated with this technique. The technique of twitch occlusion has been used in a number of studies to investigate the

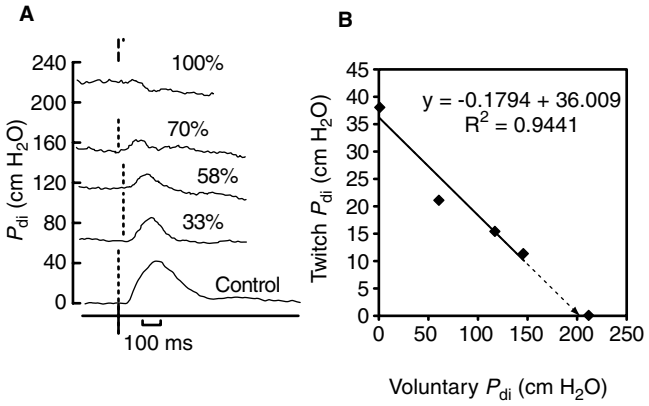

FIGURE 67-4 *A*, Illustration of twitch occlusion in one normal subject during voluntary contractions at the relative intensities indicated. Note the progressive decrease in twitch transdiaphragmatic pressure (Pdi) and twitch duration as the level of inspiratory effort increases. At the highest level of effort achieved, no superimposed twitch can be detected, indicating that all diaphragm motor units were recruited and fully activated by the voluntary effort. *B*, Twitch occlusion diagram using data presented on the left panel. A linear regression line is drawn through the data obtained at submaximal voluntary efforts and extrapolated (*dotted line* and *arrow*) to the abscissa to estimate maximal Pdi. Maximal Pdi estimated this way was about 10% smaller than measured maximal Pdi.

effect of fatigue,[46,72,75] of pharmacologic agents, of different respiratory maneuvers,[9,12,50,89] and of chronic hyperinflation[78] and asthma[91] on the maximum strength of the diaphragm and the extent of diaphragm activation by voluntary effort. It has also been employed in the investigation of difficult-to-wean patients.[67] In this setting, the twitch occlusion technique revealed submaximal diaphragm activation during attempted maximum voluntary efforts against an occlusion performed at the end of the weaning trial. Single Pdi twitches recorded at end-expiration also showed marked diaphragmatic weakness in several patients but no further decline during the weaning trial. Indeed, twitch Pdi was 8.9 ± 2.2 cm H_2O before the weaning trials and 9.4 ± 2.4 cm H_2O after their completion in the weaning-failure patients. The corresponding values in the weaning-success patients were 10.3 ± 1.5 and 11.2 ± 1.8 cm H_2O.

Although no direct comparison has been made, the twitch occlusion diagrams for the diaphragm appear to be similar whether the phrenic nerves are stimulated transcutaneously with surface electrodes,[12,89] percutaneously with fine wire electrodes,[9] or with cervical magnetic stimulation.[92]

Twitch occlusion diagrams can also be constructed using twitch Pao instead of twitch Pdi and using voluntary Pao as a measure of inspiratory effort instead of Pdi changes.[85,87,90] This is possible because the twitch Pao-to-twitch Pdi ratio remains constant at different levels of effort.[87] The twitch occlusion diagram, however, can have a different meaning when using electrical and magnetic stimulation. With electrical stimulation, twitch Pao reflects changes in diaphragm activation alone, whereas voluntary Pao reflects changes in the recruitment of all chest wall muscles being recruited. As a result, the twitch occlusion diagram does not solely reflect diaphragm activation, and the twitch occlusion diagram may depart from linearity.[87,90] With magnetic stimulation, chest wall muscles other than the diaphragm contribute to both twitch Pao and voluntary Pao. In the only study in which this was examined, the twitch occlusion diagram was linear.[85] Thus, when Pao is employed, the twitch occlusion diagram may more closely reflect the activation of all chest wall muscles with magnetic than with electrical stimulation. However, the level of recruitment of all these muscles may be difficult to control.

In summary, the maximal strength of the diaphragm is better studied by the twitch occlusion technique, a way to detect the force reserve left for full diaphragm activation during any type of breathing effort. Twitch occlusion can also be performed when using Pao instead of Pdi as a non-invasive way to estimate diaphragm recruitment during volitional efforts. Because the volitional efforts reflect the contribution of all inspiratory muscles, when recording Pao a magnetic stimulation technique may be preferred.

CONCLUSION

In conclusion, there are two methods to stimulate the phrenic nerves in humans, electrical and magnetic. Each can be applied peripherally in the neck area or centrally over the cortex. For cortical stimulation the magnetic stimulation technique is preferred. For the evaluation of phrenic nerve function and when recordings of the electrical and mechanical responses from the diaphragm that are free from contamination from other chest wall muscles are desired, the electrical stimulation technique is recommended. When the technique is well controlled, these responses are highly reproducible in the same subject. When performed at different levels of the neuraxis, these stimulations can provide valuable information on the function of the entire neuromuscular network from the cortex to the diaphragm and eventually serve to better characterize the pathologic state and evaluate its severity.

REFERENCES

1. Sarnoff SJ, Maloney JV, Sarnoff LC, et al. Electrophrenic respiration in acute bulbar poliomyelitis. JAMA 1950;143:1383–90.
2. Davis JN. Phrenic nerve conduction in man. J Neurol Neurosurg Psychiatry 1967;30:420–6.
3. Aubier M, Farkas G, De Troyer A, et al. Detection of diaphragmatic fatigue in man by phrenic stimulation. J Appl Physiol 1981;50:538–44.
4. Gandevia SC, Rothwell JC. Activation of the human diaphragm from the motor cortex. J Physiol 1987;384:109–18.
5. Similowski T, Catala M, Rancurel G, Derenne J-P. Impairment of central motor conduction to the diaphragm in stroke. Am J Respir Crit Care Med 1996;154:436–41.
6. Series F, Straus C, Demoule A, et al. Assessment of upper airway dynamics in awake patients with sleep apnea using phrenic nerve stimulation. Am J Respir Crit Care Med 2000; 162:795–800.
7. Delhez L. Modalités, chez l'homme normal, de la réponse électrique des piliers du diaphragme à la stimulation électrique des nerfs phréniques par des chocs uniques. Arch Int Physiol Biochim 1965;73:832–9.
8. Aubier M, Murciano D, Lecocguic Y, et al. Bilateral phrenic stimulation: a simple technique to assess diaphragmatic fatigue in humans. J Appl Physiol 1985;58:58–64.
9. Hershenson MB, Kikuchi Y, Loring SH. Relative strengths of the chest wall muscles. J Appl Physiol 1988;65:852–62.
10. Hubmayr RD, Litchy WJ, Gay PC, Nelson SB. Transdiaphragmatic twitch pressure. Effects of lung volume and chest wall shape. Am Rev Respir Dis 1989;139:647–52.
11. Wragg S, Aquilina R, Moran J, et al. Comparison of cervical magnetic stimulation and bilateral percutaneous electrical stimulation of the phrenic nerves in normal subjects. Eur Respir J 1994;7:1788–92.
12. Bellemare F, Bigland-Ritchie B. Assessment of human diaphragm strength and activation using phrenic nerve stimulation. Respir Physiol 1984;58:263–277.
13. Sarnoff SJ, Sarnoff LC, Whittenberger JL. Electrophrenic respiration. VII. The motor point of the phrenic nerve in relation to external stimulation. Surg Gynecol Obstet 1951;93:190–6.
14. Gandevia SC, McKenzie DK. Human diaphragmatic EMG: changes with lung volume and posture during supramaximal phrenic stimulation. J Appl Physiol 1986;60:1420–8.
15. Eastwood PR, Panizza JA, Hillman DR, Finucane KE. Application of a cervical stimulating apparatus for bilateral transcutaneous phrenic nerve stimulation. J Appl Physiol 1995;79:632–7.
16. Mills GH, Kyroussis D, Hamnegard C-H, Polkey MI. Bilateral magnetic stimulation of the phrenic nerves from an anterolateral approach. Am J Respir Crit Care Med 1996;154: 1099–105.
17. Mills GH, Kyroussis D, Hamnegard C-H, et al. Unilateral magnetic stimulation of the phrenic nerve. Thorax 1995;50:1162–72.

18. Similowski T, Fleury B, Launois S, et al. Cervical magnetic stimulation: a new painless method for bilateral phrenic nerve stimulation in conscious humans. J Appl Physiol 1989;67:1311–8.
19. Laghi F, Harrison MJ, Tobin MJ. Comparison of magnetic and electrical phrenic nerve stimulation in assessment of diaphragmatic contractility. J Appl Physiol 1996;80:1731–42.
20. Mador MJ, Rodis A, Magalang UJ, Ameen K. Comparison of cervical magnetic and transcutaneous phrenic nerve stimulation before and after threshold loading. Am J Respir Crit Care Med 1996;154:448–53.
21. Similowski T, Mehiri S, Duguet A, et al. Comparison of magnetic and electrical phrenic nerve stimulation in assessment of phrenic nerve conduction time. J Appl Physiol 1997;82:1190–9.
22. Luo Y, Polkey M, Johnson L, et al. Diaphragm EMG measured by cervical magnetic and electrical phrenic nerve stimulation. J Appl Physiol 1998;85:2089–99.
23. Similowski T, Straus C, Attali V, et al. Cervical magnetic stimulation as a method to discriminate between diaphragm and rib cage muscle fatigue. J Appl Physiol 1998;84:1692–700.
24. Attali V, Mehiri S, Straus C, et al. Influence of neck muscles on mouth pressure response to cervical magnetic stimulation. Am J Respir Crit Care Med 1997;156:509–14.
25. Kheder E, Trakhan M. Localization of diaphragm motor cortical representation and determination of corticodiaphragmatic latencies by using magnetic stimulation in normal adult human subjects. Eur J Appl Physiol 2001;85:560–6.
26. Zifko U, Remtulla H, Power K, et al. Transcortical and cervical magnetic stimulation with recording of the diaphragm. Muscle Nerve 1996;19:614–20.
27. Macia F, Le Masson G, Rouanet-Larrivière M, et al. A prospective evaluation of phrenic nerve conduction in multifocal motor neuropathy and chronic inflammatory demyelinating polyneuropathy. Muscle Nerve 2003;3:319–23.
28. Zifko U, Chen R, Remtulla H, et al. Respiratory electrophysiological studies in Guillain-Barre syndrome. J Neurol Neurosurg Psychiatry 1996 ;60:191–4.
29. Shaw RK, Glenn WWL, Hogan JF, Phelps ML. Electrophysiological evaluation of phrenic nerve function in candidates for diaphragm pacing. J Neurosurg 1980;53:345–54.
30. Swenson MR, Rubenstein RS. Phrenic nerve conduction studies. Muscle Nerve 1992;15:597–603.
31. Markand ON, Kincaid JC, Pourmand RA, et al. Electrophysiologic evaluation of diaphragm by transcutaneous phrenic nerve stimulation. Neurology 1984;34:604–14.
32. MacLean IC, Mattioni TA. Phrenic nerve conduction studies: a new technique and its application in quadriplegic patients. Arch Phys Med Rehabil 1981;62:70–3.
33. De Troyer A, Vanderhoeft P. Phrenic nerve function after pneumonectomy. Chest 1982;81:212–4.
34. McKenzie DK, Gandevia SC. Phrenic nerve conduction times and twitch pressures of the human diaphragm. J Appl Physiol 1985;58:1496–504.
35. Chen R, Collins S, Remtulla H, et al. Phrenic nerve conduction study in normal subjects. Muscle Nerve 1995;18:330–5.
36. Bellemare F, Jeanneret A, Couture J. Assessment of respiratory muscle strength using volitional efforts and phrenic nerve stimulation. Am J Respir Crit Care Med 2003;167:A412.
37. Laroche CM, Cairns T, Moxham J, Green M. Hypothyroidism presenting with respiratory muscle weakness. Am Rev Respir Dis 1988;138:472–4.
38. Zegers de Beyl D, De Troyer A. Phrenic nerve conduction time measurement in pulmonary disorders. Acta Neurol Belg 1982;82:91–8.
39. Zifko U, Auinger M, Albrecht G, et al. Phrenic neuropathy in chronic renal failure. Thorax 1995;50:793–4.
40. Similowski T, Catala M, Rancurel G, Derenne JP. Impairment of central motor conduction to the diaphragm in stroke. Am J Respir Crit Care Med 1996;154:436–41.
41. Donati F, Antzaka C, Bevan D. Potency of pancuronium at the diaphragm and adductor pollicis muscle in humans. Anesthesiology 1986;65:1–5.
42. Zifko UA, Nicolle MW, Grisold W, Bolton. Repetitive phrenic nerve stimulation in myathenia gravis. Neurology 1999;53: 1083–7.
43. Mier A, Brophy C, Moxham J, Green M. Repetitive stimulation of the phrenic nerves in myasthenia gravis. Thorax 1992;47: 640–4.
44. Estenne M, Yernault J-C, De Smet J-M, De Troyer A. Phrenic and diaphragm function after coronary artery bypass grafting. Thorax 1985;40:293–9.
45. Dimopoulou I, Daganou M, Dafni U, et al. Phrenic nerve dysfunction after cardiac operations: electrophysiologic evaluation of risk factors. Chest 1998;113:8–14.
46. Bellemare F, Bigland-Ritchie B. Central components of diaphragmatic fatigue assessed by phrenic nerve stimulation. J Appl Physiol 1987;62:1307–16.
47. McKenzie DK, Bigland-Ritchie B, Gorman RB, Gandevia SC. Central and peripheral fatigue of human diaphragm and limb muscles assessed by twitch interpolation. J Physiol 1992;454:643–56.
48. Yan S, Gauthier AP, Similowski T, et al. Evaluation of human diaphragm contractility using mouth pressure twitches. Am Rev Respir Dis 1992;145:1064–9.
49. Petitjean M, Ripart J, Couture J, Bellemarre F. Diaphragmatic fatigue investigated by phonomyography. Am J Respir Crit Care Med 1997;155:1162–6.
50. Mier A, Brophy C, Moxham J, Green M. Twitch pressures in the assessment of diaphragm weakness. Thorax 1989;44:990–6.
51. Bellemare F, Bigland-Ritchie B, Woods JJ. Contractile properties of the human diaphragm in vivo. J Appl Physiol 1986;61:1153–61.
52. Petitjean M, Bellemare F. Phonomyogram of the diaphragm during unilateral and bilateral phrenic nerve stimulation and changes with fatigue. Muscle Nerve 1994;17:1201–9.
53. Hamnegard C-H, Wragg S, Mills G, et al. The effect of lung volume on transdiaphragmatic pressure. Eur Respir J 1995;8:1532–6.
54. Mier A, Brophy C, Moxham J, Green M. Influence of lung volume and rib cage configuration on transdiaphragmatic pressure during phrenic nerve stimulation in man. Respir Physiol 1990;80:193–202.
55. Petitjean M, Ripart J, Couture J, Bellemarre F. Effects of lung volume and fatigue on evoked diaphragmatic phonomyogram in normal subjects. Thorax 1996;51:705–10.
56. Smith J, Bellemarre F. Effect of lung volume on in vivo contraction characteristics of human diaphragm. J Appl Physiol 1987;62:1893–900.
57. Yan S, Similowski T, Gauthier AP, et al. Effect of fatigue on diaphragmatic function at different lung volumes. J Appl Physiol 1992;72:1064–7.
58. Ward ME, Ward JW, Macklem PT. Analysis of human chest wall motion using a two-compartment rib cage model. J Appl Physiol 1992;72:1338–47.
59. Koulouris N, Mulvey DA, Laroche CM, et al. The effect of posture and abdominal binding on respiratory pressures. Eur Respir J 1989;2:961–5.
60. Mador JM, Khan S, Kufel TJ. Bilateral anterolateral magnetic stimulation of the phrenic nerves can detect diaphragmatic fatigue. Chest 2002;121:452–8.
61. Polkey MI, Harris EH, Hughes PD, et al. The contractile properties of the elderly human diaphragm. Am J Respir Crit Care Med 1997;155:1560–4.
62. Moxham J, Morris A, Spiro S, et al. Contractile properties and fatigue of the diaphragm in man. Thorax 1981;36:164–8.

63. Edwards RHT, Young A, Hosking GP, Jones D. Human skeletal muscle function: description of tests and normal values. Clin Sci Mol Med 1977;52:283–90.
64. Efthimiou J, Fleming J, Edwards RHT, Spiro SG. Effect of aminophylline on fatigue of the sternomastoid muscle in man. Thorax 1986;41:122–7.
65. Laghi F, D'Alfonso N, Tobin MJ. Pattern of recovery from diaphragmatic fatigue over 24 hours. J Appl Physiol 1995;79:539–46.
66. Babcock MA, Pegelow DF, Taha BH, Dempsey JA. High frequency diaphragmatic fatigue detected with paired stimuli in humans. Med Sci Sports Exerc 1997;30:506–11.
67. Laghi F, Cattapan SE, Jubran A, et al. Is weaning failure caused by low-frequency fatigue of the diaphragm? Am J Respir Crit Care Med 2003;167:120–7.
68. Bellemare F, Jeanneret-Grosjean A, Lands L. Chronic diaphragm fatigue in adult patients with cystic fibrosis. Am J Respir Crit Care Med 2003;167:A913.
69. Yan S, Gauthier AP, Similowski T, et al. Force-frequency relationship of in vivo human and in vitro rat diaphragm using paired stimuli. Eur Respir J 1993;6:211–8.
70. Polkey MI, Kyroussis D, Hamnegard C-H, et al. Paired phrenic nerve stimuli for the detection of diaphragm fatigue in humans. Eur Respir J 1997;10:1859–64.
71. NHLBI Workshop Summary. Respiratory muscle fatigue. Am Rev Respir Dis 1990;142:474–80.
72. McKenzie DK, Bigland-Ritchie B, Gorman RB, Gandevia SC. Central and peripheral fatigue of human diaphragm and limb muscles assessed by twitch interpolation. J Physiol 1992;454:643–56.
73. Johnson BD, Babcock MA, Suman OE, Dempsey JA. Exercise-induced diaphragmatic fatigue in healthy humans. J Physiol 1993;460:385–405.
74. Aubier M, Murciano D, Virès N, et al. Effects of digoxin on diaphragmatic strength generation in patients with chronic obstructive pulmonary disease during acute respiratory failure. Am Rev Respir Dis 1987;135:544–8.
75. Levy RD, Nava S, Gibbons L, Bellemarre F. Aminophylline and human diaphragm strength in vivo. J Appl Physiol 1990; 68:2591–6.
76. Bellemare F, Cordeau M, Couture J, et al. Effects of emphysema and lung volume reduction surgery on transdiaphragmatic pressure and diaphragm length. Chest 2002;121: 1898–910.
77. Polkey MI, Kyroussis D, Hamnegard C-H, et al. Diaphragm strength in chronic obstructive pulmonary disease. Am J Respir Crit Care Med 1996;154:1310–7.
78. Similowski T, Yan S, Gauthier AP, et al. Contractile properties of the human diaphragm during chronic hyperinflation. N Engl J Med 1991;325:917–23.
79. Hughes P, Polkey M, Harris M, et al. Diaphragm strength in chronic heart failure. Am J Respir Crit Care Med 1999;160:529–34.
80. Murciano D, Rigaud D, Pingleton S, et al. Diaphragmatic function in severely malnourished patients with anorexia nervosa. Am J Respir Crit Care Med 2002;150:1569–74.
81. Koulouris N, Mulvey DA, Laroche CM, et al. The effect of posture and abdominal binding on respiratory pressures. Eur Respir J 1989;2:961–5.
82. Chen R, Kayser B, Yan S, Macklem P. Twitch transdiaphragmatic pressure depends critically on thoracoabdominal configuration. J Appl Physiol 2000;88:54–60.
83. Wragg S, Hamnegard C, Road J, D. et al. Potentiation of diaphragmatic twitch after voluntary contraction in normal subjects. Thorax 1994;49:1234–7.
84. Mador M, Magalang U, Kyfel T. Twitch potentiation following voluntary diaphragmatic contraction. Am J Respir Crit Care Med 1994;149:739–43.
85. De Bruin P, Watson R, Khalil N, Pride N. Use of mouth pressure twitches induced by cervical magnetic stimulation to assess voluntary activation of the diaphragm. Eur Respir J 1998;12:672–8.
86. Hamnegard C-H, Wragg S, Kyroussis D, et al. Mouth pressure in response to magnetic stimulation of the phrenic nerves. Thorax 1995;50:620–4.
87. Similowski T, Gauthier AP, Yan S, et al. Assessment of diaphragm function using mouth pressure twitches in chronic pulmonary disease patients. Am Rev Respir Dis 1993;147:850–6.
88. Laghi F, Tobin MJ. Relationship between transdiaphragmatic and mouth twitch pressures at functional residual capacity. Eur Respir J 1997;10:530–6.
89. Gandevia SC, McKenzie DK, Plassman BL. Activation of human respiratory muscles during different voluntary manoeuvres. J Physiol 1990;428:387–403.
90. Gandevia SC, McKenzie DK. Activation of the human diaphragm during maximal static efforts. J Physiol 1985;367:45–56.
91. Allen GA, McKenzie DK, Gandevia SC. Reduced voluntary drive to breathe in asthmatic subjects. Respir Physiol 1993; 93:29–40.
92. Similowski T, Duguet A, Starus C, et al. Assessment of voluntary activation of the diaphragm using cervical and cortical magnetic stimulation. Eur Respir J 1996;9:1224–31.
93. Luo YM, Hart N, Mustfa N, et al. Reproducibility of twitch and sniff transdiaphragmatic pressures. Respir Physiol Neurobiol 2002;132:301–6.

CHAPTER 68

AN INTRODUCTION TO LUNG MORPHOMETRY

R. Heberto Ghezzo

HISTORY

Morphometry is the study of forms in general. Stereology is defined as the body of mathematical methods that relates parameters defining three-dimensional structures to measurements obtainable on two-dimensional sections. This definition was proposed at the First International Congress of Stereology in Vienna (1963), where the science of stereology officially came into existence. In stereology we are concerned with the estimation of some geometric properties of the whole based on a small sample using the principles of statistical geometry. Morphometry is based on stereologic principles but goes further, using methods usually tailored to the question being investigated.

Stereology is simply the practical application of the principles of geometric probability and, as such, is completely intertwined with the science of statistics.

The beginnings of geometric probability can be traced to the Count de Buffon, who in 1777 asked what the probability was that a randomly tossed needle of length l would intersect a grid of parallel lines of distance d.[1] He found the answer: $p = 2/\pi\ l/d$. This formula is now the basis for the estimation of the surface area of particles.

Geology, trying to estimate the amount of metal in rock formations from a sample of pieces of the rock, was the engine that motivated the earlier development of stereology. In 1847 a French geologist, Delesse, in his paper "Procédé mécanique pour déterminer la composition des roches," demonstrated that the area density in a section was the same as volume density in the whole body.[2] Rosiwal, also a geologist, demonstrated in 1898 that segment density (the length of the intersection of a line with the structure over the total length of the line) was the same as volume density, thus confirming and simplifying the principle put forward by Delesse.[3] Glagoleff in 1933 went further, demonstrating that the number of points falling on a structure over the total points used was similar to volume density (point counting)[4] (Figure 68-1). Crofton already introduced this method in rigorous mathematical terms in an article on mathematical probability in the *Encyclopaedia Britannica* in 1885.[5]

In 1945 the Russian Saltikov demonstrated that the surface area of embedded particles could be estimated from the intersections of the boundary with test lines.[6] An application of the old Buffon formula was now redeveloped with a different objective.

From a different perspective in 1925 Wicksell derived the size distribution of spherical and ellipsoidal particles from their profiles in a section.[7]

In 1943 Chalkley introduced the point-counting method in biologic research[8]; up to this point stereology was used only in geology or metallurgy and systematically developed by mathematicians and statisticians.

PRINCIPLES OF STEREOLOGY

Stereology is concerned with estimating geometric properties of structures embedded in a referent space by studying the intersections of the structures with a probe. These properties can be shape, volume, surface area, number, connectivity, etc.

A structure is "something made up of interdependent parts." It can be a mineral embedded in a different rock, cells inside a tissue, or organelles within a cell.

The referent space is the space containing the structures of interest. It could be all the three-dimensional space as in a rock or another larger structure, such as a special type of tissue.

A probe, a geometric entity used to intersect the structure, can be a volume (dimension = 3), a plane (dimension = 2), a line (dimension = 1), or a set of points (dimension = 0). The fundamental principle of stereology states that the dimension of the probe to be used for any measurement should be the difference of the dimensions of the referent space minus the dimension of the structure (ie, for the estimation of the volume of the structure over the volume of the referent space—dimension 3–dimension 3—the dimension of the probe must be 0; this is point counting).

SAMPLING

Stereology deals with very small samples, such as a microscopic slide. For example, in lung stereology the dimensions of a slide are 20 mm × 20 mm × 0.005 mm, that is, 2 mm^3 for estimating a lung with a volume of 6 L, an extrapolation of 3,000,000:1; this ratio is similar to sampling only one

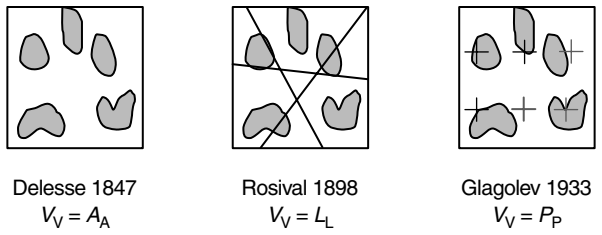

FIGURE 68-1 Evolution of the measurement of volume density.

individual to estimate some characteristic of the population of a large city such as Montreal. Thus, careful sampling is necessary; generally a combination of stratified and multiple-step sampling is needed in order to achieve representativeness. Otherwise, bias toward one type of structure or another may occur.

Generally, stereology deals with multistage sampling. This means that sampling is performed several times in pieces of tissue each time smaller. For example, we fix and inflate a lung; a first stage of sampling is effected when we choose how to cut the lung and then which slices of lung to use. Then on each slice a second sampling is realized by the random placement of the cutting template. Once this block is embedded in paraffin a third sampling is produced when we choose the cut to stain and mount, and finally the fourth sampling step is in the choosing of the fields in the microscope to be measured.

These sampling steps can be completely random or stratified. Stratified sampling means, for example, that we select three slices of lung: one peripheral, one medial, and one central. The placement of the template in each slice could also be stratified, one at the top, one central, and one at the bottom, or two at each site. The selection of sections to mount could be sequential, choosing a random one from the first five sections and then choosing sequentially each of the five sections of the microtome.

Samples to be used for stereology must be uniform isotropic random (UIR); this means that not only the position of the sample within the whole must be completely random but also the orientation of the block (ie, the cut surface) must be random. In our example, the positioning of the templates on the lung slice cannot all be parallel.

For some structures that are definitely stratified, such as sedimentary rocks or the walls of blood vessels or the digestive tract (ie, when the object has a definitive "vertical" axis in its structures), the vertical isotropic random (VIR) must be used. Here we define the vertical direction, the axis perpendicular to the stratification, and randomize the angle of rotation around the vertical. The cutting surface must include the vertical axis.

If proper care is not applied to the sampling process, the results obtained are not valid. One must remember that stereology and statistics go hand in hand; stereology needs statistics to claim validity for its results. Proper sampling, often ignored, is an obligatory step to ensure the validity of the results obtained.

How large a sample is needed? This eternal question can only be answered after a pilot study is performed. Then a nested analysis of variance for random effects can estimate the variance components for the between-slides, between-blocks, and between-subjects factors. In this way one may decide on the best allocation of resources in order to minimize the observed variance of the estimators.

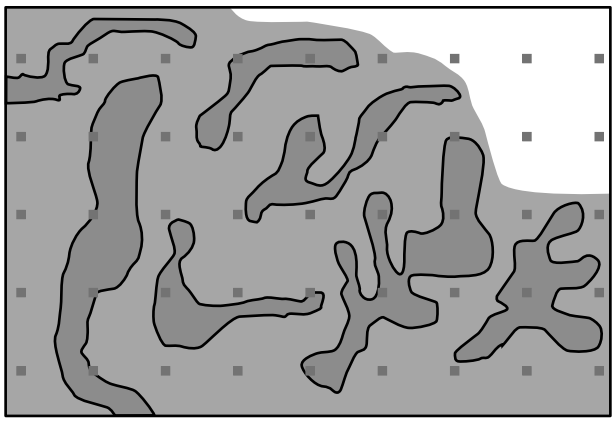

FIGURE 68-2 In this image we count 15 points in the structure and 40 on the referent space. Note that 5 points are not in the referent space. In this case Vv = 15/40 = 0.375, or 37.5%.

ESTIMATORS

Most values estimated from stereology are ratios of the structure measurement over the referent space. Below we provide the formulas for the different kinds of estimators.

Volume Density

Volume density (Vv) or volume fraction or "porosity" is the ratio between the volume of the structure and the volume of the referent space. The probes to be used must be points because the difference between the dimensions of the object and referent space is zero.

The method is generally called point counting and the estimator (Vv) is a dimensionless number, formulated as follows:

$$Vv = \frac{\Sigma P_i}{\Sigma Q_i} \qquad (68\text{–}1)$$

where P_i is points in structure in image i and Q_i is points in referent space in the image i (Figure 68-2).

Surface Density

Surface density (Sv) is the ratio of surface area of the structure to the volume of the referent space. The difference between dimensions is one, so the probes must be lines (dimension = 1). Each line segment should have an associated point, not necessarily on the line. All the intersections between the line and the structure of interest are counted, as are the associated points that fall on either the structure or the referent space. The estimator has the dimension of 1/length:

$$Sv = \frac{2I_L i}{dl \cdot \Sigma P_i}$$

where $I_L i$ is the number of intercepts between line and surface of interest, dl is the length of a line segment, and P_i is

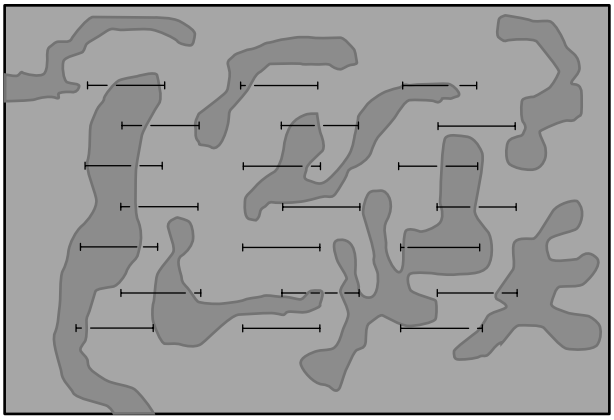

FIGURE 68-3 In this image we count $(1+1+2)+(2+3+0)+(2+2+1)+(1+0+1)+(1+0+1)+(2+3+1)+(2+0+1)$; if each line is, say, 0.0032 mm long and the associated point is the right end of the bars, we have 9 bars in the structure and 12 on the referent space. The surface area per unit of volume is

$$Sv = \frac{2 \cdot 27}{(0.0032 \cdot 21)} = 803.57 \text{ mm}^{-1}$$

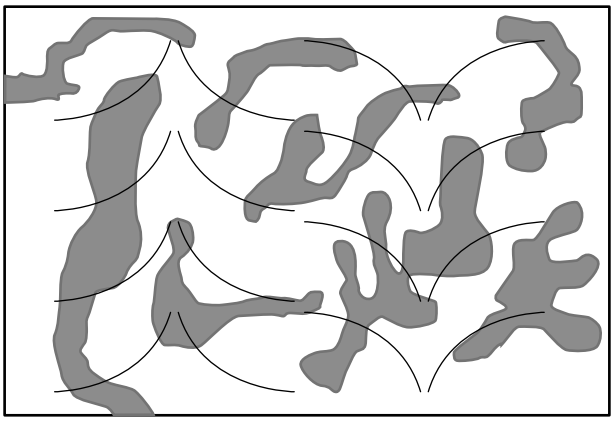

FIGURE 68-4 In this case, if the length of each cycloid arc is 0.063 we have a surface area per unit volume as follows:

$$Sv = \frac{2 \cdot 47}{(0.063 \cdot 16)} = 93.25 \text{ mm}^{-1}$$

the number of associated points that fall in the referent space and the structure.

One should use isotropic lines in UIR sections (Figure 68-3) or cycloid lines in VIR sections (see sampling) with the small axis parallel to the vertical direction (Figure 68-4). This ensures the statistical requirement of uniform sampling.

Length Density

Length density (Lv) is the length of the structure per volume of the referent space (ie, estimation of the length of a vessel in an organ). The difference in dimensions is 2, so the probes are areas. The dimension of the estimator is 1/area or 1/length squared:

$$Lv = \frac{2\Sigma P_i}{dx \cdot dy \Sigma Q_i}$$

where P_i is the number of profiles in a counting frame, dx and dy the dimensions of the counting frame, and Q_i the number of counting frames used.

The counting frame is a square with the vertical sides extending to infinity at the top in the left and to the bottom at the right. The whole left side and extension, the bottom side, and the extension at the right are called the forbidden lines, and intersections of structures with forbidden lines even outside of the counting frame disqualify the structure as a countable one (Figure 68-5).

In the second image for Figure 68-5, we have counted three intersections in the countable area; of the others, two touch one of the forbidden sides of the counting frame. If the counting frame measures, say, 0.1 mm per side, the estimated length of the structure per unit volume is as follows:

$$Lv = \frac{2 \cdot 3}{(0.1 \cdot 0.1)} = 600 \text{ mm}^{-2}$$

Numerical Density

Numerical density (Nv) is the number of structures per volume of the referent space (ie, number of T cells per unit volume of lung); the difference in dimensions is 3, so the probes are volumes. The dimension of the estimator is 1/volume or 1/length cubed.

How to measure a volume? There are several methods depending on the quality of the referent space.

Dissector The most common is the method called "dissector."[9] Two consecutive slices of the organ or sample of interest are used. The thickness of the slice must be known. The structures of interest present in a counting frame (see Lv) in one slice but not in the other are counted; if the same structure is present in both slices, it is not counted. The resulting number divided by the volume of the counting frame, defined as the area of the counting frame times the thickness of the slide, is the ratio sought. The slides can be used in the reverse, so using both images twice. If the structures to be counted are big, the slices need not be consecutive, provided that the distance between the slices is known. The dimension of the estimator is 1/volume or 1/length cubed:

$$Nv = \frac{\Sigma P_i}{dx \cdot dy \cdot dz \, \Sigma Q_i}$$

where P_i is the number of profiles in a counting frame, dx and dy the dimensions of the counting frame, dz the thickness of the slide or the distance between the two slides used, and Q_i the number of counting frames used (Figure 68-5).

Optical Dissector First proposed in confocal microscopy as the "unbiased brick" by Howard[10] and then generalized to conventional microscopy as the optical dissector by Gundersen,[11] this method has the advantage over the simple dissector that only one slide needs to be used. The use of a narrow focus lens is necessary.

The counting frame is the same as in Lv, but instead of lines per side we consider surfaces defined by the sides across the thickness of the slide plus two other surfaces, the

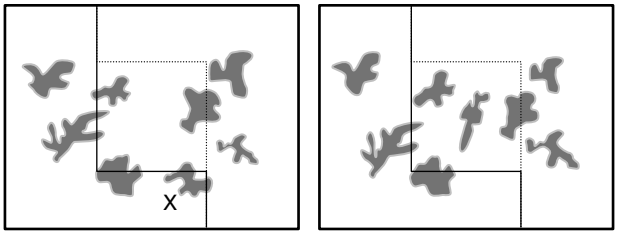

FIGURE 68-5 In the first image we have one valid count, which is also present in the second image, so the total count is zero. In the second image we have two counts, of which one is not in the first image. If the distance between the two images is 0.025 (five cuts of the microtome at 0.005 each cut), the number of structures per unit volume is as follows:

$$Nv = \frac{1}{(0.1 \cdot 0.1 \cdot 0.025 \cdot 2)} = 2000 \text{ mm}^{-3}$$

top and the bottom slightly below (above) the physical top and bottom of the slide. Here, intersections with three surfaces in the counting frame are acceptable (front, top, and right), and three surfaces are forbidden (bottom, back, and left). This method provides an advantage in assessing structures in the edges of the counting box. The thickness of the measuring box is the thickness of the histologic section.

The method consists in focusing at the top surface and counting the structures as they appear in focus while moving the focus down into the slide. Remember that the bottom surface is a forbidden surface.

Obviously the referent space must be somewhat translucid or made so by the mounting substance in order to visualize structures throughout the thickness of the slide without interference of images above or below the image in focus at the time of counting. In the case of lung tissue the slides can be really thick since the alveoli provide for seeing through the structures.

As air and tissue have different refractive indices (1.0 and 1.5, respectively), the measurement of the vertical distance is biased. It is better to use oil immersion objectives, which match the refractive indices, and thus avoid the complications of correcting the measurement of the box thickness.

Counting of Ellipsoidal Shapes In cases in which the structures to be counted are of similar sizes and ellipsoidal in shape (most cells in tissue), a simpler method that approximates closely the actual numbers as obtained by the dissector method can be used. The method is as follows:

1. Using a counting frame, Na (the number of structures per unit area) is computed.
2. The volume ratio of the structure to the referent space V/v is then obtained by point counting.
   a. The shape constant β can be obtained from available tables; the shape factor β has been determined from the mean curvature of the particles by integral geometry by Hadwiger[12] in 1955 and runs from 1.38 for the sphere to 1.86 for an octahedron, being 1.55 for the dodecahedron and oblate spheroids.
   b. The numerical density (Nv) number/volume can then be computed by the formula $Nv = (1/\beta)\ N_A^{3/2} / V_V^{1/2}$.

Another approximation is based on the equation $N_V = N_A/H$, where H is the mean tangent diameter of the particles and N_A is the number of particles per area. We must consider the "missing cap" problem—particles cut close to the top will not be seen; then if h_0 is the maximum height that remains invisible and t is the thickness of the slice, $N_V = N_A/(t + H - 2 \cdot h_0)$. This formula was developed by Floderus in 1944.[13]

Estimation of the Volume of the Referent Space

If the referent space is the whole organ, volume can be estimated by immersion in liquid, but if the referent space is embedded in the organ, the only way of estimating its volume is by the method of Cavalieri.[14]

Cavalieri The whole organ must by sectioned. It is not necessary to measure all slices, but a sequential sampling schema can be used, with a random start, and then sequentially choosing slices. We need to measure the area of the referent space in each slice; this can be obtained by tracing the perimeter or more easily by point counting. The estimator of the total volume of the referent space when using point counting is as follows:

$$V = T\,dx \cdot dy\,\Sigma P_i$$

$$\text{Variance (V)} = \frac{3a + c - 4b}{12} + \frac{0.0543B}{\sqrt{A}} \cdot \sqrt{m\Sigma P_i}$$

where T is thickness, dx is distance on x-axis between points, dy is distance on y-axis between points, and P_i is points that fell on the structure to be measured in slab "i"; $a = \Sigma\ P_i \cdot P_i$, $b = \Sigma\ P_i \cdot P_{i+1}$, $c = \Sigma\ P_i \cdot P_{i+2}$, and $B/\sqrt{A}$ is a shape factor.[15,16]

Mean Volume of Structures

This refers to the calculation of the volume of a structure within a referent space. Here again sampling becomes a crucial issue: how is the structure to be measured sampled? Is the sampling to be proportional to the size of the structure (volume weighted) or do all the structures have the same probability of being selected (number weighted) or something in between, where the probability is proportional to the surface area (surface area weighted). The volume is always estimated as $\pi/3 \cdot l_0^3$, with l_0 being a chord length drawn from a random point in an isotropic direction. To increase precision, three or four isotropic lines from the same point should be drawn.

Volume Weighted The referent space is sampled with a point-counting grid, and the structures under the point are identified; thus, it is volume weighted, the larger particles having more chance of being selected. Through the point, isotropic lines are drawn, and the length of the segment is measured

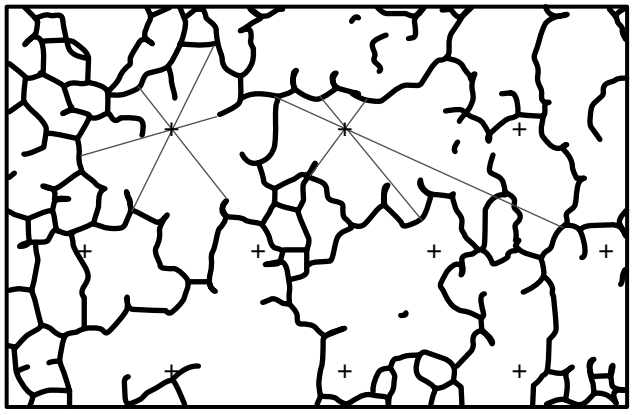

FIGURE 68-6 In this image we have 10 points in a staggered grid; from the first two we have traced three diameters in random directions. Note that in the second point one of the diameters has two sections. The l_0 must be computed as ${l_1}^3 + ({l_3}^3 - {l_2}^3)$ or, say, $40^3 + (50^3 - 42^3) = 115,012\ \mu$; the others of length, say, 23 μ, 32 μ, 22 μ, 15 μ, and 26 μ will give a volume-weighted estimation of area volume as follows:

$$\begin{aligned} Vv &= \frac{3.14}{3} \cdot \frac{23^3 + 32^3 + 22^3 + 15^3 + 26^3 + 115,012}{6} \\ &= 33414\,\mu^2 \end{aligned}$$

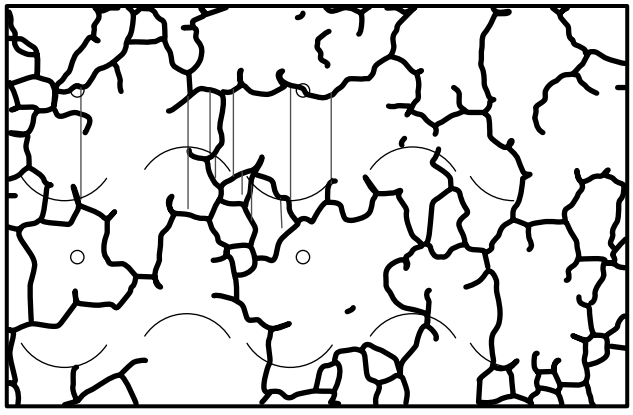

FIGURE 68-7 Here we started drawing the vertical chords, assuming their lengths are 19, 21, 11, 14, 4, 5, 20, and 13 μ, the estimated surface-weighted volume is

$$\begin{aligned} Vs &= \frac{\left[\begin{array}{l}(2 \cdot 3.14/3) \\ \times (19^3 + 21^3 + 11^3 + 14^3 + 4^3 + 5^3 + 20^3 + 13^3)\end{array}\right]}{8} \\ &= 2.09 \cdot 3822.6 \\ &= 7989.3\,\mu^3 \end{aligned}$$

(Figure 68-6). The mean volume weighted particle volume is given by

$$Vv = \frac{\pi}{3} \cdot \frac{\Sigma {l_0}^3}{n}$$

Number Weighted The structures are "selected" with the dissector method, and then a point is randomly placed on each selected structure; through this point three isotropic lines are drawn, and the previous formula can then be used for the estimation of Vv.

Surface Area Weighted The structures to be measured are selected by a cycloid line and chord lengths are drawn in the direction of the minor axis of the cycloid as before. The point to draw the chords from is given by the intersections of the cycloid and the particle (Figure 68-7). A similar formula as before is used to calculate Vv replacing π by 2. π.

Errors in Stereology

The estimators are, in general, a ratio of two counts; their variance can be approximated as follows:

$$\text{Var}\,(Vv) = \sqrt{\frac{k}{(k-1)}\left[\frac{\Sigma {P_i}^2}{\Sigma P_i \cdot \Sigma P_i} + \frac{\Sigma {Q_i}^2}{\Sigma Q_i \cdot \Sigma Q_i} - \frac{2\Sigma P_i Q_i}{\Sigma P_i \cdot \Sigma Q_i}\right]}$$

where P_i is points in structure in image i, Q_i is points in referent space in the image i, and k is the number of images.

This is the variance of the estimator in one slide. This should be differentiated from the variance of the estimation, which includes the between-slides variation, between-blocks variation, and the between-individuals variation. Contrary to expectations, the larger source of variation is the between-individuals variation, then the heterogeneity between the blocks, which depends on the tissue being studied, and lastly between the slices. A rule of thumb is that 200 points per subject are enough. Mathieu found that grids with 64 points are as good as tracing to evaluate volume ratios.[17]

As already said, for each study a pilot should be conducted to estimate the variances between subjects, blocks, and slices in order to reduce the larger variances.

MORPHOMETRY OF THE LUNG

Preparation of the Lung

The lung behaves as a sponge, changing volume depending on the surrounding pressures. Thus, measurements of volumes, areas, and so on must be made in relation to a certain total lung volume; otherwise the measurements have no real scale either absolute or relative to another structure. It has become standard to fix the lung in inflation to an estimated total lung capacity (TLC) at 25 cm water pressure (25 pascals). This is easy to achieve in formalin-fixed lungs and slightly more complicated in frozen lungs as these must be inflated with OCT before fast freezing. The tissue samples from a formalin-fixed lung have to be cut while the lung is floating in water in order to attain the true volume of fixation, TLC. Templates of known size should be used to be able to correct for tissue shrinkage.

During the preparation of histologic sections, dehydration and deparaffinization shrink the tissue in a nonhomogeneous fashion owing to the heterogeneity of the lung tissue. Resins such as methacrylate minimize shrinkage. Ratio estimators are not affected by shrinkage, but absolute measurements, such as the volume of a counting cell, are and must be corrected.

The degree of shrinkage in the tissue on a slide is estimated from the original dimensions of the block from which it was cut and the corresponding dimensions in the final stained slide. Every slide should be corrected individually. The formula used for shrinkage correction is as follows:

$$\text{Factor} = \frac{\text{Total area of the tissue on the slide}}{\text{Area of the template}}$$

The shrinkage factor is an average value since the shrinkage is not uniform. If it is used to correct linear measurements, the square root of the factor is used; it represents the linear shrinkage averaged over all directions.

Size of Airspaces

Stereologic measurements are used in the study of the lung parenchyma to determine size of alveoli, total alveolar volume, alveolar duct volume, and emphysematous space volume. To quantify the degree of emphysema we can use the Lm (mean linear interalveolar wall distance, or mean linear intercept),[18] the destructive index (DI),[19] or the star volume of the alveoli.[20]

The Lm is equal to the length of a test line divided by the number of its intercepts with alveolar walls. This number estimates twice the inverse of the alveolar surface area per unit of lung volume[18]:

$$\text{Lm} = \frac{\Sigma \text{dl}}{\Sigma \text{N}} = \frac{2}{\text{Sv}}$$

Also, we can have

$$\text{Total alveolar surface area} = \frac{2 \cdot \text{ Lung volume} \cdot \text{\% tissue}}{\text{Lm}}$$

where % tissue is obtained by point counting and lung volume by immersion, so the product of these two terms represents the volume of the airspaces in the lung.

If we compute the Lm of a collection of equal spheres, the Lm will be equal to two-thirds of the spheres' diameter. The alveoli are not spheres and are of different sizes, plus the alveolar ducts can have convoluted shapes, but, on average, Lm can give an idea of the alveolar size.

The Lm is generally calculated at the subject level, that is, averaging over slides and images on each slide. A derived measure is to calculate the Lm per image and then compute the standard deviation between all the images of a subject. This SD (Lm) is supposed to increase in heterogeneous tissue like in centrilobular emphysema.[19] Another variation on the study of airspaces is to measure not the mean value per subject but the distribution of sizes per subject. This distribution is supposed to be a mixture of the distribution of alveolar sizes and the distribution of alveolar duct sizes. Tracing the areas has showed some promise,[21] but estimation with the star volume technique is in progress.

However, for phases that consist of complex and convoluted systems of tunnels and cavities, the total volume and surface area are of little use.[22] The star volume measures the mean volume of the airspaces. The ideal weighting schema to use would be number weighted, but given the size of the airspaces, the dissector method cannot be applied, so we must choose between volume- or surface area–weighted estimation.

If the objective of the exercise is to compare two groups in the amount of emphysema, the volume-weighted approach, which emphasizes the larger structures, is probably more sensitive to small increments in large structures.

The DI was conceived to measure not size but the integrity of the alveoli, thus being a more specific as well as more sensitive measure of early parenchyma lung destruction.

Other Measurements of Emphysema

The DI is a method specific for the recognition and measurement of emphysema and not a truly stereologic method. The integrity of the alveolar wall is the measurement of interest and is obtained by randomly selecting air spaces with a point-counting grid and then counting the breaks in the walls (holes) of the selected airspaces. The absolute or relative size of the alveoli is not measured. In this method, lung inflation becomes critical: with little inflation pressure, holes in the wall collapse; with a large inflation pressure, fenestrae could become holes.

Airway Measurements

Structure of Airways The size and shape of airways can be measured directly on a slide. A caveat is that since the section is UIR, the airways intersect the cutting plane in all directions. A general technique is to measure the two main diameters of the airways; if their ratio is greater than, say, 3:2 it is considered that the cut is too tangential and the other measurements will be too distorted; a ratio of 3:2 will imply a cut at 45 degrees to the long axis of the airway. If the ratio is less than 3:2 we can consider that we have a VIR and testing with cycloids can provide us with the estimates of the surface area per volume of the different interfaces, epithelial, base membrane, muscle, fibrosis, and so on. Point-counting techniques will give the relative volume of the layers, or we can use direct planimetry. If not enough airways with ratios of 3:2 or less are obtained, we can still proceed with the analysis but using only the portions of the airway wall corresponding to the intersections of the small diameter with the airway wall; here the cut of the airway is almost perpendicular, and we can assume a VIR structure.

Number and Integrity of Alveolar Attachment to a Bronchi The number of alveolar wall attachments in a bronchi is a function of its diameter, or better internal perimeter. Emphysema and inflammation in the airway wall destroy these attachments, decreasing their number.[23] The number of normal and abnormal attachments (present but broken) around the circumference of the airway are counted, and their numbers are correlated with the degree of disease in the airways and parenchyma in chronic obstructive pulmonary disorder. The number of attachments has to be stratified by the size—perimeter or diameter—of the airway.

Cellularity

There are two basic methods to study the cellularity in the lung: the in situ method with specific staining of the cells in the tissue and the extraction of the cells, from the tissue followed by a cytospin fluorescent-activated cell sorting (FACS) and specific staining. Both methods have their pros and cons. The cell extraction method gives a large number of cells, easy to count, for example, using flow cytometry, but the localization of the cells in the lung tissue is unknown; whether they are intraalveolar, parenchymal, or peribronchial is not known. The only result obtained is the differential cell count and the total cell count per weight of lung. This last result is of doubtful usefulness because of the nonuniform destruction of cells during the extraction process.

The in situ method allows determination of the exact location of the cells in the tissue and offers the possibility of colocalization of two or more types of cells, but the total number of cells counted per slide is small, requiring several slides at high magnification to obtain reproducible results.

With this method, there is also the possibility of expressing the number of cell per mm of alveolar wall. This is not an estimation of the absolute number of cells per unit volume of tissue, such as obtained with the dissector method, but will in some way express the cellularity "corrected" by the degree of alveolar wall destruction, given a better index of hypercellularity in inflammation. Also, the dissector can be used on the nuclei of the cells to express the number of cells per volume of alveolar wall.

If the cells under study are lymphocytes, their nucleus can be considered ellipsoidal, and the approximate method can be used to estimate the actual load of cells in the lung.

With this method there is also the possibility of expressing the number of cells per millimeter of alveolar wall.

FINAL TIPS

The morphometric analysis of the lung offers a varied collection of options to the researcher in lung structure. It is paramount that the tissue under the microscope be really representative of the whole; this can be achieved only with a carefully designed sampling procedure.

Also the precision required of the measurements should be established a priori since this will constitute the basis on which the sampling procedure will be designed, how many fields per slide, how many slides per block, how many blocks per subject, and finally how many subjects per group under study.

The measurements, as we have seen, can be relative, as percentage of emphysema, or can be absolute, as alveolar volume. In this latter case, the total volume of the lung is needed. If the subject is a mouse, total volume by either the Cavalieri method or volume displacement is easy to obtain, but if the subject is a human being, even volume displacement is difficult because of the deformation of the lung when submerged in water. In these cases the total gas volume can be measured and the alveolar volume then calculated as a percentage of gas volume and not of total lung volume.

Computerized methods are slow to come into general use, mainly owing to the difficulties in deciding whether a white space is an alveolus or a bronchus. Artificial intelligence techniques are being explored to facilitate these morphometric techniques but are still in the future.

REFERENCES

1. Buffon GLL Comte de. Essai d'arithmetique morale. In: Supplement a l'Histoire Naturelle. Vol 4. Paris: Imprimerie Royale; 1777.
2. Delesse MA. Procédé méchanique pour déterminer la composition des roches. C R Acad Sci Paris 1847;25:544–5.
3. Rosiwal A. Ueber geometrische Gesteinsanalysen. Verb K. K. Geol. Reichsanst. Wein 1898; 143.
4. Glagoleff AA. On the geometrical methods of quantitative mineralogic analysis of rocks. Trans Inst Econ Min Moscow 1933;59:1.
5. Crofton MW. Probability. In: Encyclopedia Britannica. 9th ed. Volume 19. p. 768.
6. Saltikov SA. Zavodskaya Laboratorija 1946;12:816.
7. Wicksell SD. The corpuscule problem II. Biometrika 1925; 18:152.
8. Chalkley HW. Methods for quantitative morphological analysis of tissue. J Natl Cancer Inst 1943;4:47.
9. Sterio DC. The unbiased estimation of number and sizes of arbitrary particles using the dissector. J Microsc 1984;134: 127–36.
10. Howard CV, Reid S, Baddeley A, Boyde A. Unbiased estimation of particle density in the tandem scanning reflected light microscope. J Microsc 1985;138:203–12.
11. Gundersen HJG. Stereology of arbitrary particles. A review of unbiased number and size estimators and the presentation of some new ones, in the memory of W.R. Thompson. J Microsc 1986;138:127–42.
12. Harwiger H. Altes und Neues uber konvexe Korper. Basel: Birkhauser; 1955.
13. Floderus S, Untersuchungen uber den Bau der menschlichen Hypophyse mit besonderer Berucksichtigung der quantitativen mikromorphologischen Verhaltnisse. Acta Pathol Microbial Scand 1944;53:1.
14. Cavalieri B. Geometria Indivisibilius Continuorum. Typis Clementis Feronij. Bononi. 1635.
15. Roberts N, Garden AS, Cruz-Orive LM, et al. Estimation of fetal volume by MRI and stereology. Br J Radiol 1994; 67:1067–77.
16. Cruz-Orive LM. Systematic sampling in stereology. Bull Int Statis Inst. Proceedings of the 49th session, Florence; 1993. 1993;52:451–68.
17. Mathieu O, Cruz-Orive LM, Hoppeler H, Weibel ER. Measuring error and sampling variation in stereology. J Microsc 1981; 121:75–88.
18. Dunnill MS. Quantitative methods in the study of pulmonary pathology. Thorax 1962;17:320–8.
19. Saetta M, Shiner RJ, Angus GE, et al. Destructive index: a measurement of lung parenchymal destruction in smokers. Am Rev Respir Dis 1985;131:764–9.
20. Reed MG, Howard CV. Surface-weighted star volume: concept and estimation. J Microsc 1998;190:350–6.
21. Zhu E, Ghezzo H, Ma H, Cosio MG. A morphometric technique to diagnose the type and extent of microscopic emphysema. Am Rev Respir Dis 1993;147:A864.
22. Serra J. Image analysis and mathematical morphology. London: Academic Press; 1982.
23. Saetta M, Kim WD, Shiner R, et al. Alveolar attachments in the lung of smokers: relationship to morphology and function. Am Rev Respir Dis 1983.

INDEX

Note: Page numbers followed by *f* refer to figures and page numbers followed by *t* refer to tables.